

Volume 12 Issue 1

January 2021



ISSN 2156-5570(Online)

ISSN 2158-107X(Print)



Editorial Preface

From the Desk of Managing Editor...

It may be difficult to imagine that almost half a century ago we used computers far less sophisticated than current home desktop computers to put a man on the moon. In that 50 year span, the field of computer science has exploded.

Computer science has opened new avenues for thought and experimentation. What began as a way to simplify the calculation process has given birth to technology once only imagined by the human mind. The ability to communicate and share ideas even though collaborators are half a world away and exploration of not just the stars above but the internal workings of the human genome are some of the ways that this field has moved at an exponential pace.

At the International Journal of Advanced Computer Science and Applications it is our mission to provide an outlet for quality research. We want to promote universal access and opportunities for the international scientific community to share and disseminate scientific and technical information.

We believe in spreading knowledge of computer science and its applications to all classes of audiences. That is why we deliver up-to-date, authoritative coverage and offer open access of all our articles. Our archives have served as a place to provoke philosophical, theoretical, and empirical ideas from some of the finest minds in the field.

We utilize the talents and experience of editor and reviewers working at Universities and Institutions from around the world. We would like to express our gratitude to all authors, whose research results have been published in our journal, as well as our referees for their in-depth evaluations. Our high standards are maintained through a double blind review process.

We hope that this edition of IJACSA inspires and entices you to submit your own contributions in upcoming issues. Thank you for sharing wisdom.

Thank you for Sharing Wisdom!

Kohei Arai
Editor-in-Chief
IJACSA
Volume 12 Issue 1 January 2021
ISSN 2156-5570 (Online)
ISSN 2158-107X (Print)

Editorial Board

Editor-in-Chief

Dr. Kohei Arai - Saga University

Domains of Research: Technology Trends, Computer Vision, Decision Making, Information Retrieval, Networking, Simulation

Associate Editors

Alaa Sheta

Southern Connecticut State University

Domain of Research: Artificial Neural Networks, Computer Vision, Image Processing, Neural Networks, Neuro-Fuzzy Systems

Domenico Ciuonzo

University of Naples, Federico II, Italy

Domain of Research: Artificial Intelligence, Communication, Security, Big Data, Cloud Computing, Computer Networks, Internet of Things

Dorota Kaminska

Lodz University of Technology

Domain of Research: Artificial Intelligence, Virtual Reality

Elena Scutelnicu

"Dunarea de Jos" University of Galati

Domain of Research: e-Learning, e-Learning Tools, Simulation

In Soo Lee

Kyungpook National University

Domain of Research: Intelligent Systems, Artificial Neural Networks, Computational Intelligence, Neural Networks, Perception and Learning

Krassen Stefanov

Professor at Sofia University St. Kliment Ohridski

Domain of Research: e-Learning, Agents and Multi-agent Systems, Artificial Intelligence, e-Learning Tools, Educational Systems Design

Renato De Leone

Università di Camerino

Domain of Research: Mathematical Programming, Large-Scale Parallel Optimization, Transportation problems, Classification problems, Linear and Integer Programming

Xiao-Zhi Gao

University of Eastern Finland

Domain of Research: Artificial Intelligence, Genetic Algorithms

CONTENTS

Paper 1: A Novel Traffic Shaping Algorithm for SDN-Sliced Networks using a New WFQ Technique

Authors: Ronak Al-Haddad, Erika Sanchez Velazquez, Arooj Fatima, Adrian Winckles

PAGE 1 – 9

Paper 2: Human-Robot Interaction and Collaboration (HRI-C) Utilizing Top-View RGB-D Camera System

Authors: Tariq Tashtoush, Luis Garcia, Gerardo Landa, Fernando Amor, Agustin Nicolas Laborde, Damian Oliva, Felix Safar

PAGE 10 – 17

Paper 3: Application-based Evaluation of Automatic Terminology Extraction

Authors: Marija Brkic Bakaric, Nikola Babic, Maja Matetic

PAGE 18 – 27

Paper 4: Deep Learning Architectures and Techniques for Multi-organ Segmentation

Authors: Valentin Ocrean, Alexandru Dorobantiu, Remus Brad

PAGE 28 – 35

Paper 5: Development of a Physical Impairment Prediction Model for Korean Elderly People using Synthetic Minority Over-Sampling Technique and XGBoost

Authors: Haewon Byeon

PAGE 36 – 41

Paper 6: Data-Forensic Determination of the Accuracy of International COVID-19 Reporting: Using Zipf's Law for Pandemic Investigation

Authors: Aamo Iorliam, Anthony T S Ho, Santosh Tirunagari, David Windridge, Adekunle Adeyelu, Samera Otor, Beatrice O. Akumba

PAGE 42 – 49

Paper 7: Clustering K-Means Algorithms and Econometric Lethality Model by Covid-19, Peru 2020

Authors: Javier Pedro Flores Arocutipa, Jorge Jinchuña Huallpa, Gamaniel Carbajal Navarro, Luís Delfín Bermejo Peralta

PAGE 50 – 57

Paper 8: Optimize the Cost of Resources in Federated Cloud by Collaborated Resource Provisioning and Most Cost-effective Collated Providers Resource First Algorithm

Authors: V Pradeep Kumar, Kolla Bhanu Prakash

PAGE 58 – 65

Paper 9: Impact of Artificial Intelligence-enabled Software-defined Networks in Infrastructure and Operations: Trends and Challenges

Authors: Mohammad Riyaz Belgaum, Zainab Alansari, Shahrulniza Musa, Muhammad Mansoor Alam, M. S. Mazliham

PAGE 66 – 73

Paper 10: Predicting the Depression of the South Korean Elderly using SMOTE and an Imbalanced Binary Dataset

Authors: Haewon Byeon

PAGE 74 – 79

Paper 11: Validation of the Components and Elements of Computational Thinking for Teaching and Learning Programming using the Fuzzy Delphi Method

Authors: Karimah Mohd Yusoff, Noraidah Sahari Ashaari, Tengku Siti Meriam Tengku Wook, Noorazean Mohd Ali

PAGE 80 – 88

Paper 12: Ground Control Point Generation from Simulated SAR Image Derived from Digital Terrain Model and its Application to Texture Feature Extraction

Authors: Kohei Arai

PAGE 89 – 94

Paper 13: Modeling of the Factors Affecting e-Commerce Use in Turkey by Categorical Data Analysis

Authors: Ömer Alkan, Hasan Küçükoğlu, Gökhan Tutar

PAGE 95 – 105

Paper 14: Customer Profiling for Malaysia Online Retail Industry using K-Means Clustering and RM Model

Authors: Tan Chun Kit, Nurulhuda Firdaus Mohd Azmi

PAGE 106 – 113

Paper 15: Amalgamation of Machine Learning and Slice-by-Slice Registration of MRI for Early Prognosis of Cognitive Decline

Authors: Manju Jain, C.S. Rai, Jai Jain, Deepak Gambhir

PAGE 114 – 130

Paper 16: Full Direction Local Neighbors Pattern (FDLNP)

Authors: Maher Alrahal, Supreethi K.P

PAGE 131 – 141

Paper 17: Stanza Type Identification using Systematization of Versification System of Hindi Poetry

Authors: Milind Kumar Audichya, Jatinderkumar R. Saini

PAGE 142 – 153

Paper 18: Detection and Recognition of Moving Video Objects: Kalman Filtering with Deep Learning

Authors: Hind Rustum Mohammed, Zahir M. Hussain

PAGE 154 – 157

Paper 19: Performance Evaluation of Different Mobile Ad-hoc Network Routing Protocols in Difficult Situations

Authors: Sultan Mohammed Alkahtani, Fahd Alturki

PAGE 158 – 167

Paper 20: The Design and Implementation of Mobile Heart Monitoring Applications using Wearable Heart Rate Sensor

Authors: Ummi Namirah Hashim, Lizawati Salahuddin, Raja Rina Raja Ikram, Ummi Rabaah Hashim, Ngo Hea Choon, Mohd Hariz Naim Mohayat

PAGE 168 – 173

Paper 21: A Survey on Junction Selection based Routing Protocols for VANETs

Authors: Irshad Ahmed Abbasi, Elfatih Elmubarak Mustafa

PAGE 174 – 181

Paper 22: Design of a Rule-based Personal Finance Management System based on Financial Well-being

Authors: Alhanoof Althnian

PAGE 182 – 187

Paper 23: Robust Control Approach of SISO Coupled Tank System

Authors: Mohd Hafiz Jali, Ameelia Ibrahim, Rozaimi Ghazali, Chong Chee Soon, Ahmad Razif Muhammad

PAGE 188 – 193

Paper 24: Text Coherence Analysis based on Misspelling Oblivious Word Embeddings and Deep Neural Network

Authors: Md. Anwar Hussien Wadud, Md. Rashadul Hasan Rakib

PAGE 194 – 203

Paper 25: Comprehensive Multilayer Convolutional Neural Network for Plant Disease Detection

Authors: Radhika Bhagwat, Yogesh Dandawate

PAGE 204 – 211

Paper 26: Personalized Book Recommendation System using Machine Learning Algorithm

Authors: Dhiman Sarma, Tanni Mitra, Mohammad Shahadat Hossain

PAGE 212 – 219

Paper 27: Learning Management System based on Machine Learning: The Case Study of Ha'il University - KSA

Authors: Mohamed Hédi Maîloul, Younès Bahou

PAGE 220 – 224

Paper 28: Using IndoWordNet for Contextually Improved Machine Translation of Gujarati Idioms

Authors: Jatin C. Modh, Jafinderkumar R. Saini

PAGE 225 – 232

Paper 29: "ISAY": Blockchain-based Intelligent Polling System for Legislative Assistance

Authors: Deshan Wattegama, Pasindu S.Silva, Chamika R. Jayathilake, Kalana Elapatha, Kavinga Abeywardena, N. Kuruwitaarachchi

PAGE 233 – 239

Paper 30: Modeling the Estimation Errors of Visual-based Systems Developed for Vehicle Speed Measurement

Authors: Abdulrazzaq Jawish Alkherref, Musab AbuAddous

PAGE 240 – 251

Paper 31: Characterization of Quaternary Deposits in the Bou Ahmed Coastal Plain (Chefchaouen, Morocco): Contribution of Electrical Prospecting

Authors: Yassyr Draoui, Fouad Lahlou, Imane Al Mazini, Jamal Chao, Mohamed Jalal El Hamidi

PAGE 252 – 258

Paper 32: BiDETS: Binary Differential Evolutionary based Text Summarization

Authors: Hani Moetque Aljahdali, Ahmed Hamza Osman Ahmed, Albaraa Abuobieda

PAGE 259 – 271

Paper 33: Semi-Direct Routing Approach for Mobile IP

Authors: Basil Al-Kasasbeh

PAGE 272 – 279

Paper 34: An Automated Convolutional Neural Network Based Approach for Paddy Leaf Disease Detection

Authors: Md. Ashiqul Islam, Md. Nymur Rahman Shuvo, Muhammad Shamsojjaman, Shazid Hasan, Md. Shahadat Hossain, Tania Khatun

PAGE 280 – 288

- Paper 35: Quantification of Surface Water-Groundwater Exchanges by GIS Coupled with Experimental Gauging in an Alluvial Environment**
Authors: Yassyr Draoui, Fouad Lahlou, Jamal Chao, Lhoussaine El Mezouary, Imane Al Mazini, Mohamed Jalal El Hamidi
PAGE 289 – 294
- Paper 36: Simplified Framework for Benchmarking Standard Downlink Scheduler over Long Term Evolution**
Authors: Srinivasa R K, Hemanth Kumar A.R
PAGE 295 – 306
- Paper 37: The Cognizance of Green Computing Concept and Practices among Secondary School Students: A Preliminary Study**
Authors: Shafinah Kamarudin, Siti Munirah Mohd, Nurul Nadwa Zulkifli, Rosli Ismail, Ribka Alan, Philip Lepun, Muhd Khaizer Omar
PAGE 307 – 312
- Paper 38: Recognizing Activities of Daily Living using 1D Convolutional Neural Networks for Efficient Smart Homes**
Authors: Sumaya Alghamdi, Etimad Fadel, Nahid Alowidi
PAGE 313 – 323
- Paper 39: A Cryptocurrency-based E-mail System for SPAM Control**
Authors: Shafiya Afzal Sheikh, M. Tariq Banday
PAGE 324 – 333
- Paper 40: Discovery Engine for Finding Hidden Connections in Prose Comprehension from References**
Authors: Amal Babour, Javed I. Khan, Fatema Nafa, Kawther Saeedi, Dimah Alahmadi
PAGE 334 – 347
- Paper 41: Impact of the Mining Activity on the Water Quality in Peru Applying the Fuzzy Logic with the Grey Clustering Method**
Authors: Alexi Delgado, Anabel Fernandez, Brigitte Chirinos, Gabriel Barboza, Enrique Lee Huamani
PAGE 348 – 357
- Paper 42: The Role of Electronic Means in Enhancing the Intellectual Security among Students at the University of Jordan**
Authors: Mohammad Salim Al-Zboun, Mamon Salim Al-Zboun, Hussam N. Fakhouri
PAGE 358 – 364
- Paper 43: Enhancement of 3D Seismic Images using Image Fusion Techniques**
Authors: Abrar Alotaibi, Mai Fadel, Amani Jamal, Ghadah Aldabbagh
PAGE 365 – 372
- Paper 44: Multi-beam Antenna Array Operating Over Switch On/Off Element Condition**
Authors: Julian Imami, Elson Agastra, Aleksandër Biberaj
PAGE 373 – 378
- Paper 45: A Survey on Image Encryption using Chaos-based Techniques**
Authors: Veena G, Ramakrishna M
PAGE 379 – 384
- Paper 46: Classification of Arabic-Speaking Website Pages with Unscrupulous Intentions and Questionable Language**
Authors: Haya Mesfer Alshahrani
PAGE 385 – 391

Paper 47: Cyber Situation Awareness Perception Model for Computer Network

Authors: Olofintuyi Sunday Samuel

PAGE 392 – 397

Paper 48: Visualization of Arabic Entities in Online Social Media using Machine Learning

Authors: Khowla Mohammed Alyamani, Abdul Khader Jilani Saudagar

PAGE 398 – 409

Paper 49: Systematic Review of Methodologies for the Development of Embedded Systems

Authors: Kristina Blašković, Sanja Čandrić, Alen Jakupović

PAGE 410 – 420

Paper 50: B-droid: A Static Taint Analysis Framework for Android Applications

Authors: Rehab ALmotairy, Yassine Daadaa

PAGE 421 – 430

Paper 51: HoloLearn: An Interactive Educational System

Authors: Shorooq Alghamdi, Samar Aloufi, Layan Alsalea, Fatma Bouabdullah

PAGE 431 – 436

Paper 52: Prototype of Web System for Organizations Dedicated to e-Commerce under the SCRUM Methodology

Authors: Ventocilla Gomero-Fanny, Aguila Ruiz Bengy, Laberiano Andrade-Arenas

PAGE 437 – 444

Paper 53: Blockchain in Insurance: Exploratory Analysis of Prospects and Threats

Authors: Anokye Acheampong AMPONSAH, Adebayo Felix ADEKOYA, Benjamin Asubam WEYORI

PAGE 445 – 466

Paper 54: Dual Frequencies Usage by Full and Incomplete Ring Elements

Authors: Kamarulzaman Mat, Norbahiah Misran, Mohammad Tariqul Islam, Mohd Fais Mansor

PAGE 467 – 472

Paper 55: An Efficient Data Replication Technique with Fault Tolerance Approach using BVAG with Checkpoint and Rollback-Recovery

Authors: Sharifah Hafizah Sy Ahmad Ubaidillah, A. Noraziah, Basem Alkazemi

PAGE 473 – 480

Paper 56: Evaluation of Water Quality in the Lower Huallaga River Watershed using the Grey Clustering Analysis Method

Authors: Alexi Delgado, Diego Cuadra, Karen Simon, Katya Bonilla, Katherine Tineo, Enrique Lee Huamaní

PAGE 481 – 492

Paper 57: A Comparative Analysis of Machine Learning Models for First-break Arrival Picking

Authors: Mohammed Ayub, SanLinn I. Kaka

PAGE 493 – 502

Paper 58: Olive Oil Ripening Time Prediction Model based on Image Processing and Neural Network

Authors: Mutasem Shabeb Alkhasawneh

PAGE 503 – 509

Paper 59: A New Discretization Approach of Bat and K-Means

Authors: Rozlini Mohamed, Noor Azah Samsudin

PAGE 510 – 516

Paper 60: Development of a System to Manage Letters of Recommendation

Authors: Reham Alabduljabbar

PAGE 517 – 523

Paper 61: Conceptual Temporal Modeling Applied to Databases

Authors: Sabah Al-Fedaghi

PAGE 524 – 534

Paper 62: Towards a Real Time Distributed Flood Early Warning System

Authors: EL MABROUK Marouane

PAGE 535 – 548

Paper 63: Modelling Health Process and System Requirements Engineering for Better e-Health Services in Saudi Arabia

Authors: Fuhid Alanazi, Valerie Gay, Mohammad N. Alanazi, Ryan Alturki

PAGE 549 – 559

Paper 64: Comparison of Deep and Traditional Learning Methods for Email Spam Filtering

Authors: Abdullah Sheneamer

PAGE 560 – 565

Paper 65: Mobile Application Design with IoT for Environmental Pollution Awareness

Authors: Anthony Ramos-Romero, Brighitt Garcia-Yataco, Laberiano Andrade-Arenas

PAGE 566 – 572

Paper 66: An Integrated Imbalanced Learning and Deep Neural Network Model for Insider Threat Detection

Authors: Mohammed Nasser Al-Mhiqani, Rabiah Ahmed, Z Zainal Abidin, S.N Isnin

PAGE 573 – 577

Paper 67: A Systematic Study of Duplicate Bug Report Detection

Authors: Som Gupta, Sanjai Kumar Gupta

PAGE 578 – 589

Paper 68: A Blockchain-based Crowdsourced Task Assessment Framework using Smart Contract

Authors: Linta Islam, Syada Tasmia Alvi, Mafizur Rahman, Ayesha Aziz Prova, Md. Nazmul Hossain, Jannatul Ferdous Sorna, Mohammed Nasir Uddin

PAGE 590 – 600

Paper 69: Fake Reviews Detection using Supervised Machine Learning

Authors: Ahmed M. Elmogy, Usman Tariq, Ammar Mohammed, Atef Ibrahim

PAGE 601 – 606

Paper 70: An Adaptive Genetic Algorithm for a New Variant of the Gas Cylinders Open Split Delivery and Pickup with Two-dimensional Loading Constraints

Authors: Anouar Annouch, Adil Bellabdaoui

PAGE 607 – 619

Paper 71: Study of Post-COVID-19 Employability in Peru through a Dynamic Model, Between 2020 and 2025

Authors: Richard Ronny Arias Marreros, Keyla Vanessa Nalvarte Dionisio, Luis Alberto Romero Tuanama, Juber Alfonso Quiroz Gutarra, Laberiano Andrade-Arenas

PAGE 620 – 625

Paper 72: Topic based Sentiment Analysis for COVID-19 Tweets

Authors: Manal Abdulaziz, Alanoud Alotaibi, Mashail Alsolamy, Abeer Alabbas

PAGE 626 – 636

Paper 73: Building a Personalized Fitness Recommendation Application based on Sequential Information

Authors: Manal Abdulaziz, Bodor Al-motairy, Mona Al-ghamdi, Norah Al-qahtani

PAGE 637 – 648

Paper 74: Inventory Management Analysis under the System Dynamics Model

Authors: Shal´om Adonai Huaraz Morales, Laberiano Andrade-Arenas

PAGE 649 – 653

Paper 75: Cuckoo-Neural Approach for Secure Execution and Energy Management in Mobile Cloud Computing

Authors: Vishal, Bikrampal Kaur, Surender Jangra

PAGE 654 – 663

Paper 76: An Improved Biometric Fusion System of Fingerprint and Face using Whale Optimization

Authors: Tajinder Kumar, Shashi Bhushan, Surender Jangra

PAGE 664 – 671

Paper 77: Implementation of an e-Commerce System for the Automation and Improvement of Commercial Management at a Business Level

Authors: Anthony Tupia-Astoray, Laberiano Andrade-Arenas

PAGE 672 – 678

Paper 78: Heuristic Evaluation of Peruvian Government Web Portals, used within the State of Emergency

Authors: Flores Quispe Percy Santiago, Mamani Condori Kevin Alonso, Paniura Huamani Jose Maykol, Anampa Chura Diego David, Escobedo Quispe Richart Smith

PAGE 679 – 684

Paper 79: k-Integer-Merging on Shared Memory

Authors: Ahmed Y Khedr, Ibrahim M Alseadoon

PAGE 685 – 691

Paper 80: An Accessibility Evaluation of the Websites of Top-ranked Hospitals in Saudi Arabia

Authors: Obead Alhadreti

PAGE 692 – 698

A Novel Traffic Shaping Algorithm for SDN-Sliced Networks using a New WFQ Technique

Ronak Al-Haddad¹, Dr. Erika Sanchez Velazquez², Dr. Arooj Fatima³, Adrian Winckles⁴

Computing and Technology Department
Anglia Ruskin University, Cambridge
United Kingdom

Abstract—Managing traditional networks comes with number of challenges due to their limitations, in particular, because there is no central control. Software-Defined Networking (SDN) is a relatively new idea in networking, which enables networks to be centrally controlled or programmed using software applications. Novel traffic shaping (TS) algorithms are proposed for the implementation of a Quality of Service (QoS) bandwidth management technique to optimise performance and solve network congestion problems. Specifically, two algorithms, namely “Packet tagging, Queueing and Forwarding to Queues” and “Allocating Bandwidth”, are proposed for implementing a Weighted Fair Queuing (WFQ) technique, as a new methodology in an SDN-sliced testbed to reduce congestion and facilitate a smooth traffic flow. This methodology aimed at improving QoS that does two things simultaneously, first, making traffic conform to an individual rate using WFQ to make the appropriate queue for each packet. Second, the methodology is combined with buffer management, which decides whether to put the packet into the queue according to the proposed algorithm defined for this purpose. In this way, the latency and congestion remain in check, thus meeting the requirements of real-time services. The Differentiated Service (DiffServ) protocol is used to define classes in order to make network traffic patterns more sensitive to the video, audio and data traffic classes, by specifying precedence for each traffic type. SDN networks are controlled by floodlight controller(s) and FlowVisor, the slicing controller, which characterise the behaviour of such networks. Then, the network topology is modelled and simulated via the Mininet Testbed emulator platform. To achieve the highest level of accuracy, The SPSS statistical package Analysis of Variance (ANOVA) is used to analyse particular traffic measures, namely throughput, delay and jitter as separate performance indices, all of which contribute to QoS. The results show that the TS algorithms do, indeed, permit more advanced allocation of bandwidth, and that they reduce critical delays compared to the standard FIFO queueing in SDN.

Keywords—Network congestion; SDN; slicing; QoS; queueing; OpenFlow (OF); Weighted Fair Queuing (WFQ); SPSS Analysis of Variance (ANOVA)

I. INTRODUCTION

Traditional computer networks are implemented using various hardware devices, including switches, routers, and different middleboxes that implement several complex algorithms and protocols [1]. Middleboxes are networking devices that can alter network traffic for purposes other than packet forwarding. Typically, network administrators need to configure network policies to deal with different situations.

Often, the administrators need to accomplish their goals using limited essential resources, while ensuring that the devices have sufficient flexibility to address inconsistent conditions. They need to configure devices individually often using low-level commands, which can lead to a high error rate. Because of the complexity of traditional networks, network maintenance, reconfiguring and reorienting processes continue to be problematic. Moreover, traditional networking components do not have the dynamic characteristics for addressing the various types of packets or their different content. As noted by [2], this results owing to the rigidity of the routing protocols that do not allow for any adaptability. This results in significant restrictions for the traditional network operations that cannot be easily reprogrammed or re-tasked [3].

Software-Defined Network (SDN) technology [4] has emerged as an effective way for programming networking devices as well as providing higher scalability by distinguishing the control plane from the data forwarding plane. The new separation concept means that the control plane can reside outside the networking device and can be developed from one or multiple controllers, where their number can be defined by the user to establish the network size. Furthermore, this separation would allow for them to treat network protocols and services as software. The data plane aims to receive information and requests from the control plane and implement them in the hardware as needed [5] [6].

In this paper, a new model for SDN networks is proposed that introduces two Traffic Shaping (TS) algorithms. The main purpose of the proposed model is to provide good quality of service (QoS). To achieve this purpose, we introduce a new system, to handle network traffic aimed at improving the network throughput, reducing end-to-end delay and dealing with traffic issues, such as bottlenecks and congestion. We present statistical results to show the accuracy of the proposed system.

The rest of this paper describes the proposed system and demonstrates its effectiveness. Initially, Section II discusses related work and then, Section III presents the proposed methodologies and TS algorithms. Section IV provides analysis and results. Finally, the conclusion is presented in Section V along with suggested avenues for future work.

II. RELATED WORK

A. Quality of Service (QoS) in SDN

Ensuring QoS has been a persistent issue in traditional networks due to their limitations. This can lead to additional operational expenses as well as the risk of degraded network performance, consequently providing unreliable quality to the end-users [7]. Commercial systems, such as Cisco [8], provide adequate overall QoS, i.e. taking all different types of traffic into account and implementing higher priority for specific traffic flows. However, there are still scalability and congestion issues in these systems. There have been numerous research studies proposing different congestion-management methods, e.g. Priority Queueing (PQ), Custom Queueing (CQ), Weighted Fair Queueing (WFQ), and Class-Based Weighted Fair Queueing (CBWFQ) [9] [10]. In theory, most of these methods can manage the delivery of packets when there is the need for more bandwidth than a link can handle. But in practice, they need re-evaluation and validation within the new expanded network systems, such as SDN. It is possible for SDN to address various network QoS issues by providing complete network visibility to collect and analyse flows of traffic so as to ensure that networking devices are programmable.

QoS in basic switching systems is increasingly being investigated and one method to ensure a high level is to utilise advanced queueing algorithms. Regarding which, First In First Out (FIFO) standard queueing in traditional and SDN networks is limited. The limitations of FIFO affect the QoS when there is more than one type of traffic involved. SDN systems (control planes and data planes) are independent of FIFO, managing the FIFO queueing between the controllers and the switches via the communications protocol OpenFlow (OF). The general behaviour of the FIFO algorithm in the SDN framework is derived from the limited queueing property in FIFO (outbound) [11]. The first packet to enter is the first to leave. In other words, there is no prioritisation of traffic and hence, no attention is paid to the Quality of Service (QoS) aims and criteria. FIFO is an ordinary queueing algorithm that has been widely adopted and used by researchers in order to evaluate network characteristics or behaviour of SDN and QoS frameworks. Accordingly, it has been used to establish the baseline condition for quantitative performance in this research so as to compare it with our proposed TS algorithms in terms of performance.

B. Analysis of Approaches to Network Performance in Software-Defined Networks

QoS illustrates the network's ability to deliver improved services to selected traffic across a range of IP, LAN and WAN technologies. There are several factors involved in network performance measurement rules that affect QoS, i.e. bandwidth, network congestion, latency (delay), packet delay variation (PDV) / jitter, and error rate. Researchers have analysed the protocols available for traditional networks and suggested new solutions to support a broad range of applications, including voice, video and file transfers. Their solutions involve combining traditional protocols with the latest technologies, such as, virtualisation, SDN's latest

paradigms and slicing mechanisms. Below is the summary of the most relevant works.

The authors in [12] propose a system for monitoring queues at each link through SDN. Their system extends the Floodlight controller, which uses OpenFlow as a southbound protocol. The proposed system is also built into the network controller, which allows the QoS and other traffic monitoring/engineering applications to access and use device reports to manage traffic. The bandwidth of the available queue is monitored using network switch polling queue statistics. The difference between two transmitted byte readings is determined by using a queue bandwidth over the time frame. The limitation in their study is the lack of extensive bandwidth management evaluation.

In [13], CORONET is introduced, which is a device that evaluates network congestion and is extremely fast in responding to errors. Due to the VLAN components attached to its local switches, it is very suitable for large and extensive networks. The benefit of CORONET is that it can rebound with a minimum downtime. It is also compatible with dynamic networks, which can be changed. It uses multi-path routine strategies, if necessary and can be combined with virtually any form of network topology. CORONET is characterised by a set of modules designed to map routes, traffic control, exploration of topology, and to find the best (fastest) packet path. One of the key elements in CORONET modules is the use of VLANs, for this is an efficient means of standardising packet movement that does not over-complicate processes. They also help monitor the volume of flow controls and promote the maintenance of a completely adaptable and scalable system.

Another approach, as proposed by [14], involves deriving a model of queue delay from network parameters, i.e. queue buffer size, queue bandwidth, number of flows, and the tested mini-net propagation delay. Approximate queue time is ascertained from the model and used to monitor the delay of end-to-end traffic. Their study shows that a flow may be shifted into a separate queue when an upper delay limit reaches a specific delay level. The most interesting part of this work is the end-to-end delay control application, which helps to retain control by monitoring the parameters used in the model and switches flows to a suitable queue, when needed. Injecting sample packets earlier when no traffic occurs, will estimate the propagation delay on a network connection. The authors believe that the delay in a queue is the primary explanation for the latency of the network, since packet processing is negligible, and propagation is constant.

OpenNetMon [15] is a POX OpenFlow controller module that helps to monitor per-flow throughput, packet loss and delay metrics. It enables fine-grained traffic engineering for reducing overhead and improve throughput: The tool tracks statistics from the ingress-and-go to measure the byte number transmitted during the flow. Other research by [16] proposes monitoring methods for SDN controllers using the OpenFlow protocol. Their method involves collecting statistics and calculating the throughput of the traffic, with the key goals being to cut total costs and increase accuracy. They measure the current transmission rate of each link by counting bytes

that move through the link over time. These determined values are used by the monitoring module to manage loads when a new connection is made. When connection usage reaches 80%, a different path is selected instead of the shortest one, to prevent packet loss [16, 17]. A survey on managing QoS in SDN Networks [17] involved reviewing various methods to monitor and manage QoS. The authors concluded that there is a lack of extensive analysis on the network performance parameters, including delay, throughput and jitter, particularly when dealing with variety of network applications, such as video, audio, and data, in one testbed framework.

During the SDN era, DiffServ protocol has been tested by several scientists within various contexts. For instance, authors in [18] used queue-based classification strategies to provide QoS support for floodlight-controlled SDN networks. They used DiffServ DSCP and common queuing techniques in Open vSwitch to approach topology management and software-defined QoS. The authors identified various groups of services (e.g. Expedited Forwarding and Best Effort) along with rate-limiting paths. They introduced a QoS module inside a floodlight controller, which covers packet matching, classification, and flow operations, such as input and deletion. This module allows just two types of policies, i.e. Queuing Policy and a ToS/DSCP Policy. The other main part of the architecture is the QoSPath application, which allows the addition of both policies using a "circuitpusher" based application. The authors hold that to measure QoS metrics, their work requires extensive assessment and evaluation.

III. PROPOSED METHODOLOGIES AND ITS ALGORITHMS

We propose a new model as a bandwidth management technique aimed at improving Quality of Service (QoS). The model utilises the FIFO queuing technique as the baseline condition. We introduce two new Traffic Shaping algorithms called Algorithm I and Algorithm II.

A. FIFO Model Implementation

Fig. 1 presents the proposed system, which utilises an SDN FIFO queuing model. A Mininet Testbed emulator was used to control the virtual environment represented by the virtual machine with virtual switches using Floodlight and FlowVisor controllers (to control slices) as well as OpenFlow (OF) switches, which is characteristic behaviour of SDN [19]. As shown in Fig. 1, the input flows from each host (H1, H2, H3) are aggregated after each packet is transmitted through the switch (S1). This switch is configured specifically to decide the packet routing towards the switches S2, S3 and S5 in predefined paths in the custom topology. The different flow types (represented as X1, X2, X3) are queued as a result of the aggregation and propagation functions of the traffic flows through the proposed SDN model. S1 and S4 function as pipeline-based switches, while S2, S3 and S5 serve as forwarding plane-based OpenFlow protocol specifications. S1 performs the routing management as an ingress bound interface to decide what to do with the arriving packets by looking up in the flow table the information needed to determine the routing path, which it then sends to the outbound interface (S4) passing through S2, S3 and S5. In this model, the FIFO algorithm can be configured in two ways to set the queue length, i.e. by choosing between (i) "Packet

FIFO", which is based on the number of packets or (ii) "Byte FIFO", which is based on the number of bytes in the FIFO scheduler. To implement the FIFO algorithm in a sliced-template SDN, "Byte FIFO" is adopted as the FIFO scheduler, since it is less complex and compatible with the slice configuration [20]. FIFO describes the conditions used in this evaluation study, where the output traffic flows are converted into capacity units (bytes) and stored in a FIFO Queue (FQ) with a capacity of k bytes. It defines various capacities for output channels for three different test scenarios. The servers process the queued data at a rate of 40, 70 and 100 (b/s) as the limiting speed of the outbound interface. In the experimental system used for the study, the flow (Y) leaving the queueing system can be divided into m output traffic flows, based on the testing scripts created for this purpose, to allow for configuring the proportion of traffic to be forwarded to every single output. Flow separation is computed according to (a) the designed slicing mechanism in the SDN system, (b) the measured magnitude of every input flow and (c) the output configuration. Finally, the queueing modules store traces of the traffic flows, measured at every single input and output in the database, with time granularity. The data is stored separately for different types of files, i.e. video, audio and data.

The performance of the network is continuously monitored for analysis purposes using the D-ITG tool [21]. The differentiated service code point protocol (DiffServ) (DSCP) [22] has been used to assign classes to each queue within the slices. It also provides soft and dynamic QoS guarantees by the use of queueing, which enables the routers to classify packets. The packets are classified using the Differentiated Services Code Point (DSCP), which assigns the value of the best-effort to the packet headers.

Three flows (i.e. video, audio, and data) are directed to switch S4, where they compete for the maximum resources available in the bottleneck link between this switch and the hosts, due to the limited queueing under FIFO. Video, which requires the highest channel capacity (bandwidth), will suffer most degradation over the long term, although exceptions are seen where it has arrived first. So, control over the switches (S2, S3, S5) is manipulated to ensure that the principles of limited FIFO queueing are followed. The simulation was run for different timescale parameters across the defined stress test conditions 1, 5 and 15 minutes for 10 replicates each. The mean results for 10 trials in each combination of design variables were pre-extracted for each of the three performance measures: throughput, delay, and jitter.

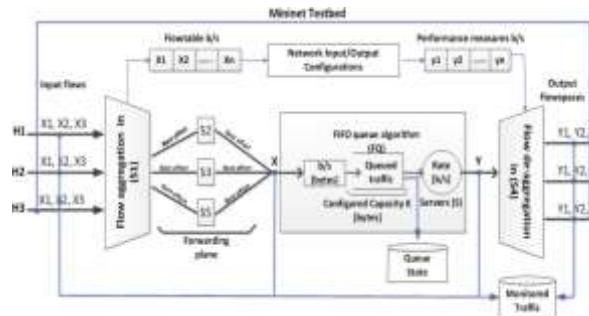


Fig. 1. The Data Plane for the FIFO Queueing SDN Model.

B. Traffic Shaping Algorithms based the New WFQ Model

A novel Traffic Shaping (TS) algorithm is proposed to tackle the single queueing limitation in the FIFO algorithm, which is aimed at solving congestion problems, and providing multimedia applications a reasonable QoS level using WFQ disciplines in an SDN-sliced context, especially when large flows fill the buffer quickly and cause packet dropping in other flows. We developed the experimental system for the TS algorithm using multiple weighted queues as demonstrated in Algorithm 1 below. The proposed algorithm performs packet tagging, queueing and forwarding.

Algorithm 1: Packet Tagging and Forwarding

```

Input:
P: packets received from the hosts
Bandwidth: maximum bandwidth for the queue

Output:
SP: sorted list of packets
EF_q: list of EF packets
AF_q: list of AF packets
BE_q: list of BE packets

while P ≠ ∅
    for each packet pi in P do
        SP→weight:= 0
        SP→port:= 0
        Ip←getPacketInfo(pi)
        SP→ID = Ip→ID
        if Ip→type == video then
            SP→weight = 46
            SP→port = 9999
            SP→tag = video
            SP→device = S3
            SP→length = Ip→length
            add_to_queue(pi, EF_q)
            sort_queue(EF_q, DSC)
        else if Ip→type == audio then
            SP→weight = 18
            SP→port = 8888
            SP→tag = audio
            SP→device = S5
            SP→length = Ip→length
            add_to_queue(pi, AF_q)
            sort_queue(AF_q, DSC)
        else
            SP→weight = 0
            SP→port = 1111
            SP→tag = data
            SP→device = S2
            SP→length = Ip→length
            add_to_queue(pi, BE_q)
            sort_queue(BE_q, DSC)
        end if
        store_in_DB(SP)
        forward_packet(SP, Bandwidth)
    end for
end while
    
```

The model utilises Algorithm 1 to create three different queues, each with a specific weight assigned to it, such that delay-sensitive classes of traffic are taken into consideration.

In order to provide high QoS, the TS algorithm enforces an assignment of weights to each flow and queues the resources using WFQ techniques. It defines three queues for each type of traffic, i.e. AF (Assured Forwarding), EF (Expedite forwarding) and BE (Best Effort). BE is given weight=0, EF is given a weight=46 and AF is given a weight=18. The customised model topology uses five switches, as shown in Fig. 2.

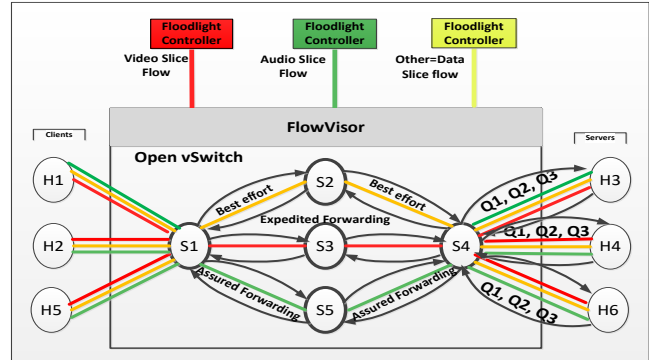


Fig. 2. Traffic-Shaping Algorithm: Template Design Linking the Data and Control Planes.

Fig. 2 represents the specific setup of the SDN system implemented for this study. Below is description of the various modules built into the model.

Topology Links: The links in the three different colours are intended to show the three flows that have been previously configured. The figure shows the different packets arriving from different ports to the switch (S1), which will handle the flow rule actions and hence, the flow statistics to match the packets.

Matching: The matching and routing process is based on the port numbers. Port 9999 is set up for video flow, whilst port 8888 is used for audio and the data flow is listed on port 1111. Each host (H1, H2, H5) in the network edge works as a client, sending a mixture of flow packets of video, audio and data. The packets arrive at the switch (S1), where these are forwarded by the class selector [23], according to Per-Hop-Behaviour (PHB).

Buffer and Access Permission: The arriving packet is buffered and the packet header is checked each time against the rules in the flow table for matching purposes. The access permission for each slice in the flow space is assigned based on the permission number (7-bitmask value) between FlowVisor and the switches, whilst the bitmasked-set is used to select metadata updates [24]. The individual permissions are READ, WRITE, AND DELEGATE (2+4+1=7, respectively). Based upon the configurations between the switches and controllers, these permissions allow the controllers to read, write and delegate slices in the flow space.

Forwarding: Packet forwarding can be done according to these rules for the slices that belong to the flow. If it does not match, the packet will either be dropped or it will be sent to the Floodlight controller for processing, according to the flow rules. The Floodlight controller will send the packet to the switch. The action for the scenario will be stored in the flow

table to be used again. The stored actions in the flow table are used for similar packets in the future without needing to pass the packet to the Floodlight controller for a decision [25].

Routing: The switch S1 decides the routing, depending upon the predefined routing paths for the port number for each arriving flow, and this is based on their OpenFlow specification. Data flows between S1-S2-S4 as the routing path, while the video flow is assigned between S1-S3-S4, and finally, the audio flow between S1-S5-S4.

Queueing: To implement minimal queue management, a minimum buffering rate is defined for each queue. In switch S4 three queues for each output interface between S4 and the three hosts H3, H4 and H6 are configured. Algorithm 2 proposes implementation of a WFQ variant that is used on the three slices, with weights configured proportional to the allocated bandwidth for each slice. EF traffic receives higher bit weight by giving the highest bandwidth allocation to video and then, AF receives the second highest bit weight, with the BE flow being allocated the lowest. Hence, the scheme works according to a ratio principle, the ratio of 20 Mega/2Mega/200Kilo bytes being used for a 40Mbps link capacity. Similarly, for 70Mbps the ratio is 45 Mega /4.5 Mega /450Kilo, while for 100Mbps, it is 50Mega/5Mega/500Kilo.

Algorithm 2: Allocate Bandwidth

```

Input:
  QT: queue type
  Bandwidth: maximum bandwidth for the queue

Output:
  Allocated_bandwidth: bandwidth in Bs (bits)

if Bandwidth == 40 then
  if QT == video then
    Allocated_bandwidth = 20000000
  else if QT == audio then
    Allocated_bandwidth = 2000000
  else if QT == data then
    Allocated_bandwidth = 200
  end if
else if Bandwidth == 70 then
  if QT == video then
    Allocated_bandwidth = 45000000
  else if QT == audio then
    Allocated_bandwidth = 4500000
  else if QT == data then
    Allocated_bandwidth = 450000
  end if
else if Bandwidth == 100 then
  if QT == video then
    Allocated_bandwidth = 50000000
  else if QT == audio then
    Allocated_bandwidth = 5000000
  else if QT == data then
    Allocated_bandwidth = 500000
  end if
end if

return Allocated_bandwidth

```

The objective of TS algorithms (1 and 2) is to measure the delay for a video slice (EF flow) without specifying any particular priority scheme. In other words, the EF flow will experience less delay than AF and BE, with the queuing delay being distributed, while the bandwidth allocation remains fixed. This scheme works as a conservation (sparing) scheme, whereby the AF flow can use the remaining bandwidth that is left from the EF flow, as long as the traffic is within the maximum capacity of the link. One of the technical contributions of this study is the devised set of measurements (parameters) for each algorithm. To evaluate the parameters' performance, a testbed was developed as a proof of concept that implements the algorithms and records the test results. The results have been used for statistical analysis using SPSS software.

C. Managing Queueing Time at the Network Nodes

For all classes of traffic, as previously discussed, the average delay time in the switch, throughput for performance and jitter are the most important considerations, for these will result in minimising the queue length at the network nodes. Equations 1, 2, 3 (presented below) are used to express the functional relationships of traffic flows over time for the queueing approach implemented in the TS algorithm using WFQ. Fig. 3 shows the model developed and adopted for this study, illustrating how queues are handled schematically as they arrive at a downstream server host.

The scheduling involved underlies the equations, which express the delay times inevitably accruing and this more sophisticated algorithm avoids delays and jitter, consequently improving QoS.

The model in Fig. 3 was developed in 2006 by a group of software engineering researchers [26] in order to ensure QoS for real time services. It is generally used as a method to describe delay time in the queues for network nodes using WFQ for video and other types of applications.

The theory description for the WFQ queueing method is expressed as follows.

t_i^R is the time in seconds when the last bit of a packet pRi (R packet of i flow) arrives at the queue; L_i^R is the length of packet pRi; and $\epsilon_{R i}$ is the time in seconds, when the last served bit of packet pR i has been sent [26].

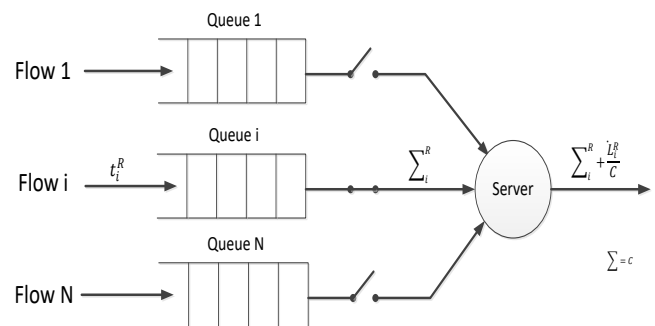


Fig. 3. Model of the Network Nodes used to Manage Queueing Time in the SDN System Design [26].

In this case, the queueing time of packet p_{Ri} can be expressed as:

$$W_i^R = \sum_i^R t_i^R \quad (1)$$

Depending on the queueing scheduling discipline, the delay time in the whole system of packets from flow i [EF, AF, BE] can be expressed by:

$$W_i^R(t) = \sum_{R=0}^{\infty} L_i^R \cdot \int (t - L_i^R) \quad (2)$$

here: $\delta(t)$ – Dirac’s delta function [27]. Then, the function of the common queueing time in the network node is:

$$W_i(s; t) = \int_s^t w_i(t)\delta(t) \quad (3)$$

IV. ANALYSIS AND RESULTS

To achieve the highest level of accuracy, a novel comparative approach for evaluating FIFO queueing and TS systems in packet switching in SDN has been proposed. The SPSS statistical package Analysis of Variance (ANOVA) [28] was used to perform the first level of analysis of the data with various tests of hypotheses. The analyses involve the means of 10 repeated measures (replicates) for three levels of stress test durations of 15, 5 and 1 minutes, three bandwidth levels of 40, 70 and 100 Mbps, and three traffic types, namely video, audio, and data, all of them defined as independent variables, while the performance indices throughput, delay and jitter are defined as dependent variables. The interaction terms all have * in their tables’ row titles. For this study, pairwise comparisons involve the computation of a p-value of < 0.05 for each pair of the compared groups.

A. Throughput Results Analysis

1) *Throughput analysis for test duration 15 minutes:* In Table I, it can be seen that the relative throughput of audio and video is pretty similar, with a slight influence of bandwidth on this traffic class (Traffic Type) effect; it is about 2- fold at both 40 and 70 Mbps, but about 4-fold at 100 Mbps. This pattern discussed because the bandwidth* traffic type interaction is significant (P= 0.005 in the Table) for Between-Subjects Effects.

In Table II, the interaction between traffic type and algorithms is significant, with a p-value = 0.001, whilst the throughput of audio, data and video is similar for FIFO to that for the TS algorithm. This is a direct consequence of the algorithms being programmed with the bit rate weight policy higher for audio than for data in TS.

2) *Throughput analysis for test duration 5 minutes:* In Table III, the interaction between traffic type and algorithms is also significant, with a p-value =0.001. The entry for data traffic type in the TS algorithm appears substantially out of line with the corresponding adjusted mean entries in the separate tables for the longer and shorter durations, having a value of 25733.105, which is because of the properties of TS using WFQ.

3) *Throughput analysis for test duration 1 minute:* From Table IV, it can be seen that the Traffic Type * Algorithm

interaction is similar in form at 1 minute to what is seen at the other durations, but it is somewhat stronger and distinctive in form (p-value = 0.001) for the mean throughput measure.

TABLE I. RESULTS OF THROUGHPUT IN MEGABITS PER SECOND (MBPS) MEASURES OF BANDWIDTH*TYPE OF TRAFFIC FOR 15 MINUTES DURATION

Dependent Variable: Throughput traffic averaged across 10 tests					
Bandwidth	Traffic Type	Mean Throughput	Std. Error	95% Confidence Interval	
				Lower Bound	Upper Bound
40	Video	23087.984	4655.968	12943.501	33232.466
	Audio	11914.602	4655.968	1770.119	22059.084
	Data	5092.873	4655.968	-5051.609	15237.356
70	Video	35017.427	4655.968	24872.944	45161.909
	Audio	16520.710	4655.968	6376.228	26665.193
	Data	10223.169	4655.968	78.687	20367.651
100	Video	66591.740	4655.968	56447.258	76736.223
	Audio	16837.987	4655.968	6693.504	26982.469
	Data	9887.850	4655.968	-256.633	20032.332

TABLE II. RESULTS OF THROUGHPUT IN MEGABITS PER SECOND (MBPS) MEASURES OF TRAFFIC TYPE*ALGORITHM FOR 15 MINUTES DURATION

Dependent Variable: Throughput traffic averaged across 10 tests					
Traffic type	Algorithm	Mean throughput	Std. Error	95% Confidence Interval	
				Lower Bound	Upper Bound
Video	FIFO	21847.142	4655.968	11702.659	31991.624
	Traffic Shaping	46375.872	4655.968	36231.389	56520.354
Audio	FIFO	20697.995	4655.968	10553.513	30842.477
	Traffic Shaping	17043.173	4655.968	6898.691	27187.656
Data	FIFO	20532.508	4655.968	10388.026	30676.990
	Traffic Shaping	3245.114	4655.968	-6899.369	13389.596

TABLE III. RESULTS OF THROUGHPUT IN MEGABITS PER SECOND (MBPS) MEASURES OF TRAFFIC TYPE*ALGORITHM FOR 5 MINUTES DURATION

Dependent Variable: Throughput					
Traffic type	Algorithm	Mean Throughput	Std. Error	95% Confidence Interval	
				Lower Bound	Upper Bound
Video	FIFO	16536.844	7375.332	901.838	32171.850
	Traffic Shaping	34465.388	7375.332	18830.383	50100.394
Audio	FIFO	17434.975	7375.332	1799.969	33069.981
	Traffic Shaping	20498.615	7375.332	4863.609	36133.621
Data	FIFO	17998.648	7375.332	2363.643	33633.654
	Traffic Shaping	25733.105	7375.332	10098.099	41368.110

TABLE IV. RESULTS OF THROUGHPUT IN MEGABITS PER SECOND (MBPS) MEASURES OF TRAFFIC TYPE*ALGORITHM FOR 1 MINUTE DURATION

Dependent Variable: Throughput					
Traffic type	Algorithm	Mean Throughput	Std. Error	95% Confidence Interval	
				Lower Bound	Upper Bound
Video	FIFO	21815.346	4015.542	13302.778	30327.915
	Traffic Shaping	38837.933	4015.542	30325.364	47350.501
Audio	FIFO	21606.774	4015.542	13094.206	30119.343
	Traffic Shaping	20899.601	4015.542	12387.032	29412.170
Data	FIFO	21728.523	4015.542	13215.954	30241.091
	Traffic Shaping	6608.666	4015.542	-1903.903	15121.235

B. Delay Results Analysis

1) Delay analysis for test duration 15 minutes: In Table V, the overall difference between bandwidth levels in the transmission delay experienced is significant (p-value = 0.002) and it is apparently non-monotonic. Regarding the Standard Error (SE), only the difference between BW 100 and the other two 40 and 70 Mbps is shown to be significant. These findings are unsurprising and represent the natures of all the algorithms that have been implemented.

2) Delay analysis for test duration 5 minutes: In Table VI, at test duration 5 minutes, the overall effect of the algorithms on transmission delay is significant (p-value = 0.008) and the effect is significantly clear between the FIFO and TS algorithms.

In Table VII, the delay of the bandwidth overall effects is significant, with a p-value = 0.002 at duration 5 minutes.

3) Delay analysis for test duration 1 minute: Table VIII shows Traffic type*Algorithm largely independent of bandwidth, with a significant p-value = 0.001 as the overall effect.

TABLE V. RESULTS OF DELAY IN MILLISECONDS (MS) MEASURES OF BANDWIDTH FOR 15 MINUTES DURATION

Dependent Variable: Delay traffic averaged across 10 tests				
Bandwidth	Mean delay	Std. Error	95% Confidence Interval	
			Lower Bound	Upper Bound
40	6.194	11.938	-18.444	30.833
70	0.164	11.938	-24.475	24.802
100	43.809	11.938	19.171	68.448

TABLE VI. RESULTS IN MILLISECONDS (MS) FOR DELAY MEASURES OF THE ALGORITHMS FOR 5 MINUTES DURATION

Dependent Variable: Delay				
Algorithm	Mean delay	Std. Error	95% Confidence Interval	
			Lower Bound	Upper Bound
FIFO	5.731	2.596	0.348	11.114
Traffic Shaping	0.845	2.596	-4.538	6.228

TABLE VII. RESULTS OF DELAY IN MILLISECONDS (MS), FOR THE DIFFERENT BANDWIDTHS AT 5 MINUTES DURATION. THE IDENTITY OF THE STANDARD ERROR (SE) TO THAT IN THE PREVIOUS TABLE IS NOT A MISTAKE, BUT RATHER, A COINCIDENCE FAVOURED BY THE PRESENCE OF LOW VALUES AND THE LIMITED DISTRIBUTION OF ERRORS

Dependent Variable: Delay				
Bandwidth	Mean delay	Std. Error	95% Confidence Interval	
			Lower Bound	Upper Bound
40	2.969	2.596	-2.414	8.352
70	1.508	2.596	-3.875	6.891
100	13.656	2.596	8.273	19.039

TABLE VIII. RESULTS FOR DELAY IN MILLISECONDS (MS) MEASURES EXPRESSING TRAFFIC TYPE*ALGORITHM INTERACTION FOR 1-MINUTE DURATION

Dependent Variable: Delay					
Traffic type	Algorithm	Mean delay	Std. Error	95% Confidence Interval	
				Lower Bound	Upper Bound
Video	FIFO	0.002	0.114	-0.237	0.241
	Traffic Shaping	0.001	0.114	-0.239	0.240
Audio	FIFO	0.002	0.114	-0.237	0.241
	Traffic Shaping	0.004	0.114	-0.235	0.243
Data	FIFO	0.002	0.114	-0.237	0.241
	Traffic Shaping	0.322	0.114	0.083	0.561

C. Jitter Results Analysis

1) Jitter analysis for test duration 15 minutes: In Table IX, the results for jitter in milliseconds (ms) are largely independent of traffic type. The Bandwidth*Algorithm interaction deleted at (p-value = 0.969). With an interaction so far from significant it is not meaningful to state its effect size. This is the result aggregated across all traffic types and there is very little jitter overall. The effect of the algorithms is seen only at the widest bandwidth, but the other bandwidths have values so low that they do not emerge from the error. The reason for this is that the ordinal predictions for jitter from the FIFO algorithm are limited, as the patterns of jitter are being driven primarily by the partly random properties of the input. All types of traffic compete for the available bandwidth and the average waiting times will be longer as the process is the same for all traffic types within the repeated traffic samples.

2) Jitter analysis for test duration 5 minutes: In Table X, the bandwidth*algorithm interaction is significant. The jitter values are variable and the differences among them below 2SE, except that at bandwidths 70 and 100 FIFO stands out from TS algorithm, and at 100 bandwidth the jitter is greater overall with (5.451 ms) mean jitter.

3) Jitter analysis for test duration 1 minute: In Table XI, for 1-minute duration and jitter as the dependent variable, the interaction Bandwidth*Traffic Type (p-value = 0.005) and (petasq= 0.685) shows that the jitter suffered under any algorithm depends on the bandwidth available.

TABLE IX. RESULTS OF JITTER IN MILLISECONDS (MS) MEASURES OF BANDWIDTH*ALGORITHM FOR 15 MINUTES DURATION

Dependent Variable: Jitter traffic averaged across 10 tests					
Bandwidth	Algorithm	Mean jitter	Std. Error	95% Confidence Interval	
				Lower Bound	Upper Bound
40	FIFO	0.000	1.925	-4.045	4.046
	Traffic Shaping	0.001	1.925	-4.044	4.047
70	FIFO	0.000	1.925	-4.045	4.045
	Traffic Shaping	0.001	1.925	-4.045	4.046
100	FIFO	11.593	1.925	7.548	15.639
	Traffic Shaping	0.015	1.925	-4.030	4.060

TABLE X. RESULTS OF JITTER IN MILLISECONDS (MS) MEASURES OF BANDWIDTH*ALGORITHM FOR 5 MINUTES DURATION

Dependent Variable: Jitter					
Bandwidth	Algorithm	Mean jitter	Std. Error	95% Confidence Interval	
				Lower Bound	Upper Bound
40	FIFO	0.070	0.147	-0.251	0.391
	Traffic Shaping	0.001	0.147	-0.320	0.322
70	FIFO	0.485	0.147	0.164	0.806
	Traffic Shaping	0.071	0.147	-0.250	0.392
100	FIFO	5.451	0.147	5.130	5.772
	Traffic Shaping	0.657	0.147	0.336	0.978

TABLE XI. RESULTS OF JITTER IN MILLISECONDS (MS) MEASURES OF BANDWIDTH*TRAFFIC TYPE FOR 1 MINUTE DURATION

Dependent Variable: Jitter					
Bandwidth	Traffic type	Mean jitter	Std. Error	95% Confidence Interval	
				Lower Bound	Upper Bound
40	Video	0.002	0.147	-0.319	0.323
	Audio	0.002	0.147	-0.319	0.323
	Data	0.076	0.147	-0.245	0.397
70	Video	0.295	0.147	-0.026	0.616
	Audio	0.261	0.147	-0.060	0.582
	Data	0.002	0.147	-0.319	0.323
100	Video	1.593	0.147	1.272	1.914
	Audio	1.820	0.147	1.499	2.141
	Data	3.056	0.147	2.735	3.377

V. CONCLUSION AND FUTURE WORK

In this paper, a novel Traffic Shaping (TS) algorithm has been proposed as a new contribution for the implementation of a Quality of Service (QoS) bandwidth management technique to optimise performance in an SDN-sliced network. Two algorithms, namely “Packet Tagging, Queueing, Forwarding

to Queues” and “Allocating Bandwidth” have been proposed for implementing a Weighted Fair Queuing (WFQ) technique as a new methodology in an SDN-sliced testbed to reduce congestion problem and facilitate smooth traffic flow. The proposed methodology contributes to improving QoS by performing two actions: (i) making traffic conform to an individual rate using WFQ to make the appropriate queue for each packet; and (ii) combining the methodology with buffer management, which decides the queue the packet should be assigned to. In this way, the latency and congestion remain in check, thus meeting the requirements of real-time services. The Differentiated Service (DiffServ) protocol is used to define classes, in order to make network traffic patterns more sensitive to traffic classes by specifying precedence for each traffic type, i.e. video, audio and data. The proposed SDN model utilises floodlight controllers, FlowVisor controller and OpenFlow (OF) switches. It has been modelled and simulated via the Mininet Testbed emulator platform.

To validate the proposed approach, a FIFO has been implemented and tested to establish the baseline condition for quantitative performance. In this research, the result obtained from FIFO is used to compare it with our proposed TS algorithms to show a characteristic qualitative pattern of performance. To achieve the highest level of accuracy, The SPSS statistical package has been used to analyse and evaluate the traffic measures of throughput, delay and jitter. These parameters are used as metrics to evaluate the QoS for each switch. We evaluated the proposed TS algorithms against FIFO queuing model. These algorithms permit the more advanced allocation of bandwidth, and reduce critical delays significantly, specifically for delay sensitive traffic, such as video and audio, as compared with data traffic. Up until the early 2020, the deficiencies in package switching for audio, video and data were largely unknown. This changed when the COVID-19 pandemic occurred. As social distancing increased, people needed to find new ways to communicate, for instance, through video chat, as every school child needed communication technologies, like Skype for classes (also, Zoom, Slack and Cisco Webex Teams, and other apps). During this process, users experienced significant failures and video asynchronies, leading to user frustration. In addition, big institutions like the NHS also rely on patient video calls. Universities, business and non-governmental organisations (NGOs) also require these technologies. The pandemic disrupted all previous expectations and projections, changing how traffic generation and distribution impact on existing networks, consequently detrimentally affecting application performance. Hence, there is a real need for improved QoS and new systems to handle network traffic with statistical results that enhance network throughput and (or) reduce end-to-end delay, whilst also dealing with traffic issues like bottlenecks and congestion.

To conclude, this research demonstrates that the implemented algorithms not only minimises the delay and traffic congestion, but also, improves network performance by overcoming the limitations of the FIFO model. A new more advanced queueing agent based on the Packet Tagging and Forwarding, with the proposal of a comparative evaluation with TS and FIFO will be the subject of future work, another

significant research path that requires serious investigation is Machine Learning (ML) for the SDN-based traffic classification system. Classification of traffic requires encrypted flow packets that mask flow features. For this classification, advanced deep-learning methods are required to generate patterns using large quantities of training data and to predict the host's bandwidth behaviour.

REFERENCES

- [1] Nunes, B.A.A., Mendonca, M., Nguyen, X.N., Obraczka, K. and Turletti, T., (2014). A survey of software-defined networking: Past, present, and future of programmable networks. *IEEE Communications Surveys & Tutorials*, 16(3), pp.1617-1634.
- [2] Kim, H. and Feamster, N., (2013). Improving network management with software defined networking. *IEEE Communications Magazine*, 51(2), pp.114-119.
- [3] Bakshi, K., (2013), March. Considerations for software defined networking (SDN): Approaches and use cases. In 2013 IEEE Aerospace Conference (pp. 1-9). IEEE.
- [4] Bakshi, T., (2017). State of the art and recent research advances in software defined networking. *Wireless Communications and Mobile Computing*.
- [5] Rowshanrad, S., Namvarasl, S., Abdi, V., Hajizadeh, M. and Keshtgari, M., (2014). A survey on SDN, the future of networking. *Journal of Advanced Computer Science & Technology*, 3(2), pp.232-248.
- [6] Al-Haddad, R. and Velazquez, E.S., (2018), July. A Survey of Quality of Service (QoS) Protocols and Software-Defined Networks (SDN). In *Science and Information Conference* (pp. 527-545). Springer, Cham.
- [7] Jarraya, Y., Madi, T. and Debbabi, M., (2014). A survey and a layered taxonomy of software-defined networking. *Communications Surveys & Tutorials*, IEEE, 16(4), pp.1955-1980.
- [8] Szilágyi, S. and Almási, B., (2012). A review of congestion management algorithms on cisco routers. *Journal of Computer Science and Control Systems*, 5(1), p.103.
- [9] Thakur, S. and Shukla, A., (2013). A Survey on Quality of Service and Congestion Control. *International Journal of Computer Science & Engineering Technology (IJCSSET)*.
- [10] Szilágyi, S. and Almási, B., (2012). A review of congestion management algorithms on cisco routers. *Journal of Computer Science and Control Systems*, 5(1), p.103.
- [11] Englert, M. and Westermann, M., (2009). Lower and upper bounds on FIFO buffer management in QoS switches. *Algorithmica*, 53(4), pp.523-548.
- [12] Rowshanrad, S., Namvarasl, S. and Keshtgari, M., (2017). A queue monitoring system in openflow software defined networks. *Journal of Telecommunications and Information Technology*.
- [13] Kim, H., Schlansker, M., Santos, J.R., Tourrilhes, J., Turner, Y. and Feamster, N., (2012), October. Coronet: Fault tolerance for software defined networks. In 2012 20th IEEE international conference on network protocols (ICNP) (pp. 1-2). IEEE.
- [14] Haiyan, M., Jinyao, Y.A.N., Georgopoulos, P. and Plattner, B., (2016). Towards SDN based queuing delay estimation. *China Communications*, 13(3), pp.27-36.
- [15] Van Adrichem, N.L., Doerr, C. and Kuipers, F.A., (2014), May. Opennetmon: Network monitoring in openflow software-defined networks. In 2014 IEEE Network Operations and Management Symposium (NOMS) (pp. 1-8). IEEE.
- [16] Luong, D.H., Outtagarts, A. and Hebbbar, A., (2016), June. Traffic monitoring in software defined networks using opendaylight controller. In *International Conference on Mobile, Secure, and Programmable Networking* (pp. 38-48). Springer, Cham.
- [17] Binsahaq, A., Sheltami, T.R. and Salah, K., (2019). A survey on autonomic provisioning and management of QoS in SDN networks. *IEEE Access*, 7, pp.73384-73435.
- [18] Wallner, R. and Cannistra, R., (2013). An SDN approach: quality of service using big switch's floodlight open-source controller. *Proceedings of the Asia-Pacific Advanced Network*, 35(14-19), pp.10-7125.
- [19] Maugendre, M., (2015). Development of a performance measurement tool for SDN (Master's thesis, Universitat Politècnica de Catalunya).
- [20] Ishimori, A., Farias, F., Cerqueira, E. and Abelém, A., (2013), October. Control of multiple packet schedulers for improving QoS on OpenFlow/SDN networking. In 2013 Second European Workshop on Software Defined Networks (pp. 81-86). IEEE.
- [21] Ruiz, M., Coltraro, F. and Velasco, L., (2018). CURSA-SQ: a methodology for service-centric traffic flow analysis. *Journal of Optical Communications and Networking*, 10(9), pp.773-784.
- [22] Baker, F., Black, D., Blake, S. and Nichols, K., (1998). Definition of the Differentiated Services Field (DS field) in the IPv4 and IPv6 headers. *RFC 2474*, Dec.
- [23] Kulhari, A. and Pandey, A.C., (2016), February. Traffic shaping at differentiated services enabled edge router using adaptive packet allocation to router input queue. In 2016 Second International Conference on Computational Intelligence & Communication Technology (CICT) (pp. 242-247). IEEE.
- [24] Bosshart, P., Gibb, G., Kim, H.S., Varghese, G., McKeown, N., Izzard, M., Mujica, F. and Horowitz, M., (2013). Forwarding metamorphosis: Fast programmable match-action processing in hardware for SDN. *ACM SIGCOMM Computer Communication Review*, 43(4), pp.99-110.
- [25] Kuźniar, M., Perešini, P. and Kostić, D., (2015), March. What you need to know about SDN flow tables. In *International Conference on Passive and Active Network Measurement* (pp. 347-359). Springer, Cham.
- [26] Dekeris, B., Adomkus, T. and Budnikas, A., (2006), June. Analysis of QoS assurance using weighted fair queueing (WQF) scheduling discipline with low latency queue (LLQ). In 28th International Conference on Information Technology Interfaces, 2006. (pp. 507-512). IEEE.
- [27] Khuri, A.I., (2004). Applications of Dirac's delta function in statistics. *International Journal of Mathematical Education in Science and Technology*, 35(2), pp.185-195.
- [28] Rutherford, A., (2001). *Introducing ANOVA and ANCOVA: a GLM approach*. Sage.

Human-Robot Interaction and Collaboration (HRI-C) Utilizing Top-View RGB-D Camera System

Tariq Tashtoush^{1*}, Luis Garcia², Gerardo Landa³
School of Engineering
Texas A&M International University
Laredo, TX, 78041 USA

Fernando Amor⁴, Agustin Nicolas Laborde⁵,
Damian Oliva⁶, Felix Safar⁷
Department of Science and Technology
National University of Quilmes
Quilmes, Argentina

Abstract—In this study, a smart and affordable system that utilizes an RGB-D camera to measure the exact position of an operator with respect to an adjacent robotic manipulator was developed. This developed technology was implemented in a simulated human operation in an automated manufacturing robot to achieve two goals; enhancing the safety measures around the robot by adding an affordable smart system for human detection and robot control and developing a system that will allow the between the human-robot collaboration to finish a predefined task. The system utilized an Xbox Kinect V2 sensor/camera and Scorbobot ER-V Plus to model and mimics the selected applications. To achieve these goals, a geometric model for the Scorbobot and Xbox Kinect V2 was developed, a robotics joint calibration was applied, an algorithm of background segmentation was utilized to detect the operator and a dynamic binary mask for the robot was implemented, and the efficiency of both systems based on the response time and localization error was analyzed. The first application of the Add-on Safety Device aims to monitor the working-space and control the robot to avoid any collisions when an operator enters or gets closer. This application will reduced and remove physical barriers around the robots, expand the physical work area, reduce the proximity limitations, and enhance the human-robots interaction (HRI) in an industrial environment while sustaining a low cost. The system was able to respond to human intrusion to prevent any collision within 500 ms on average, and it was found that the system's bottleneck was PC and robot inter-communication speed. The second application was developing a successful collaborative scenario between a robot and a human operator, where a robot will deposit an object on the operator's hand, mimicking a real-life human-robot collaboration (HRC) tasks. The system was able to detect the operator's hand and it's location then command the robot to place an object on the hand, the system was able to place the object within a mean error of 2.4 cm, and the limitation of this system was the internal variables and data transmitting speed between the robot controller and main computer. These results are encouraging and ongoing work aims to experiment with different operations and implement gesture detection in real-time collaboration tasks while keeping the human operator safe and predicting their behavior.

Keywords—Robotics manipulator; robot end-effector; computer vision; human-robot interaction (HRI); human-robot collaboration (HRC); robotics safety; scorbobot; Kinect; RGB camera; industrial system modeling; manufacturing systems design

I. INTRODUCTION

The demands and trends of the current market require enhanced manufacturing systems with reduced delivery times, mass production, and product customization, which impose a greater need for system flexibility and adaptability. Collaboration between humans and robots is considered a promising

technique to increase productivity and decrease the cost of production by combining both the robot's fast repetition and high production capabilities, and a human operator's ability to judge, react and plan. Collaborative robots (Co-bots) represent an evolution that can resolve a few challenges presented in the manufacturing and assembly environments. Co-bots allow physical interaction with humans within the work-space. Matheson and his team [1] described different ways a robot and an operator can work together, (1) *Co-existence*: the operator and robot are in the same work-space, but no interaction, (2) *Synchronized*: the operator and robots work within the same work-space, but at different times, (3) *Cooperation*: the operator and robots work together in the same work-space but have independent tasks, (4) *Collaboration*: the operator and robots work together to complete an assigned task. In a collaboration environment, it is important to note that any action will have immediate consequences for the other entity.

According to the International Standard ISO 10218 (1 and 2), and more extensively in Technical Specification ISO/TS 15066:2016, [2–5] four classes of safety requirements for collaborative robots are required:

- *Supervised stop*: The movement of the robot is stopped before an operator enters the collaborative work-space to interact with the robot and complete the desired task.
- *Manual guide*: The operator uses a manually operated device located on or near the robot's end-effector to transmit movement commands to the robot's system.
- *Monitoring speed and separation*: The robot and operator can move within the collaborative work-space simultaneously. The reduction of risk is achieved by always maintaining a distant separation between the operator and robot.
- *Power and force limitation*: Where the system must be designed to adequately reduce the risk for an operator by not exceeding the threshold as defined by the risk assessment.

Additionally, it is important to note that collaborative methods can be adopted even when using traditional robots. However, this requires the use of several and expensive safety devices such as laser sensors or visual systems. For these reasons, the team started to work on evaluating and developing affordable and accurate sensory systems that can measure the distance between the operator and the robot. This study utilizes

a lowcost RGBD camera to measure the position of an operator with respect to the robotic manipulator. While this configuration of specific measurement was utilized to track human beings [6], to our knowledge and based on the conducted literature review, it was not previously studied in the context of human-robot interaction and collaboration. Some researcher [7–15] analyzed the literature review and found that most of the RGB-D use was meant for human identification and tracking, human activity recognition, human behavior analysis for shopping and security purposes, intelligent health care systems, detecting defects in produce and animal recognition, also a data-based had been developed to summarize all these uses and algorithms. It was proven that the top-view RGB-D cameras can be utilized successfully in several applications where behaviors and interactions can be analyzed and they are very attractive due to their affordability and the sufficient information extracted from the provided pictures or live feed.

The paper is organized as follows: Section II is a literature review about robotics and their application in the industrial system, robotics safety regulations and standards, and collaboration and interaction between human and robots, Section III is a description of the robot and sensory system developed in this research, Section IV describes the followed methodology including the geometric model of the robot-sensor system, the process of calibration, and the detection of the operator, while in Section V, we evaluate the two methods of interaction between human and robot and reporting our findings and Section VI concludes the paper and describes the future plan.

II. LITERATURE REVIEW

The world has come to a point of many technological innovations where the presence and use of robotics are growing. Robots had been presented in manufacturing, hospitals, personal-use robots, service robots, etc. These robots aid the productivity of several tasks depending on their surrounding environment. In general, robotics could be used in many different settings where their intended purpose is to aid on a specific goal, complete a set of tasks that is difficult/tedious for a human to achieve, or simply make processes faster. Expedite services in systems such as Industrial/manufacturing, Health, or personal use, is a great enhancement to all current systems as their efficiency will increase. Therefore, safety standards are essentially required and must be implemented to achieve a safe operation of robotics in certain areas and or near human beings. Traditional robots have been separated from humans in workplaces trying to avoid any risk, injuries, or fatal incidents. This separation was implemented in the form of physical barricades or shut off robots whenever a human is present. However, technological improvements have shown great results where robotics no longer need to be separated and robots can be collaborative by working closely with humans, by developing new safety standards to design collaborative robotics to ensure humans' safety.

The Existence of robots in industrial settings enhances the production to meet the required demands while keeping the cost low. Robotics is considered as a flexible cell within a manufacturing line as they can be programmed to conduct different processes when needed. Safety is of utmost priority when designing robots and placing them in such environments and because of the rapid rise of robotics presence, safety

standards are to be frequently developed and improved to meet the new technology trends.

Few researchers and their teams [3, 16–21] discussed different industrial environments, the safety approaches that should be followed, and some real-life case studies. It was showed that lead designers must develop and evaluate safe, human-centered, ergonomics, and efficient collaborative assembly workstations, where the operator's feedback was provided in regards to occupational health and safety. Additionally, the Human Industrial Robot Collaboration (HIRC) workstation design process was evaluated through computer-based simulations based on the performance and safety characteristics such as Ergonomics, Operation time, operational costs, Maximum contact forces, and maximum energy density, this research illustrated how difficult is to evaluate safety and performance characteristics due to lack of physical workstations.

Parigi-Polverini [18], developed a new safety assessment tool "*Kinetostatic Safety Field*" which identifies *sources of danger* which could be an obstacle, human body part, or another robot link. The main advantage of this tool is the real-time applications and real-time collision avoidance with the use of a reactive control strategy. Another researcher suggested that robotics no longer need to be separated from humans, as robots can enforce safety by proposing a kinematic control strategy and maintain the robots' max level of productivity by reduced when humans are present in a working area.

Incorporating the industrial regulations such as the International Standard ISO 10218, Technical Specification ISO/TS 15066:2016, the American ANSI/RIA R15.06, the European EN 775 ISO 10218, and the national standards Spanish Association of Normalization and Certification, is the main procedure that is followed by manufacturing systems. These standards are outdated and have not been improved in the last five years, therefore some researchers introduced new concepts to cover techniques for estimation and evaluation of injuries focusing on various areas of the human body and the importance of developing new devices to detect impact, and minimize the human-robot impact.

Risk assessment is a crucial tool that must be used to enhance safety for both humans and robot systems. From literature review [22–27] discussed some history of operators and robots and how industrial robots have been evolved, differences between collaborative and non-collaborative robot cell safeguarding, voluntary industry consensus standards, and the risk assessment. Risk assessment should include quantitative head injury index for service robots as mechanical risk and incidents such as robot throws or drops and trapping and crushing are more to happen with such robots. Another proposed method to address safety in the human-Robot collaboration setting is Cooperative Collision Avoidance in dynamic environments [25]. This method computes a collision-free local motion for a short time horizon, which restricts the actuator motion but allows a smooth and safe control. Modeling human behavior and errors is another proposed method [28]. This formal verification methodology was developed to analyze the safety of collaborative robotic applications with a rich non-deterministic formal model of operator behaviors that captures the hazardous situations, which allows safety engineers to refine their designs until all plausible erroneous behaviors are considered and mitigated.

Other researchers [29–31] discussed different aspects of robotics design and their relationship to their safety ranking. Robot design principles should include robustness, fast reaction time, context awareness, energy, and power limitations. These principles will facilitate the following features as speech processing, vision processing, and robot control that also follow guidelines that will allow the robot to recognize speech, gestures, and correlations which eventually learns in the long run while also keeping humans safe. Predicting human behaviors, collision avoidance, collision reduction by data analysis, collisions reduction by design, perceptions affecting design, boundaries, sensors, adaptability to the surrounding environment, path planning, statistical probability, and robotic decision making are some of the safeguards that can be implemented in a high speeds and payload levels industrial settings.

III. SYSTEM DETAILS AND SETUP

The system is developed based on available educational and off-the-shelf components to model real-life robotics tasks, which are explained below.

A. Robotic Manipulator

The robotic manipulator selected for this project was the Scorbot ER-V Plus show in Fig. 1. This robot has five degrees of freedom, the Fig. 2 shows the length of the links and the degree of rotation and operation range determining the work-space of the robot. The direct kinematics of this robot determine the pose of tool $\{T\}$ with respect to the base $\{B\}$ is resolved using equation (2) based on Fig. 3. The base of the robot is at a fixed position on a workbench.

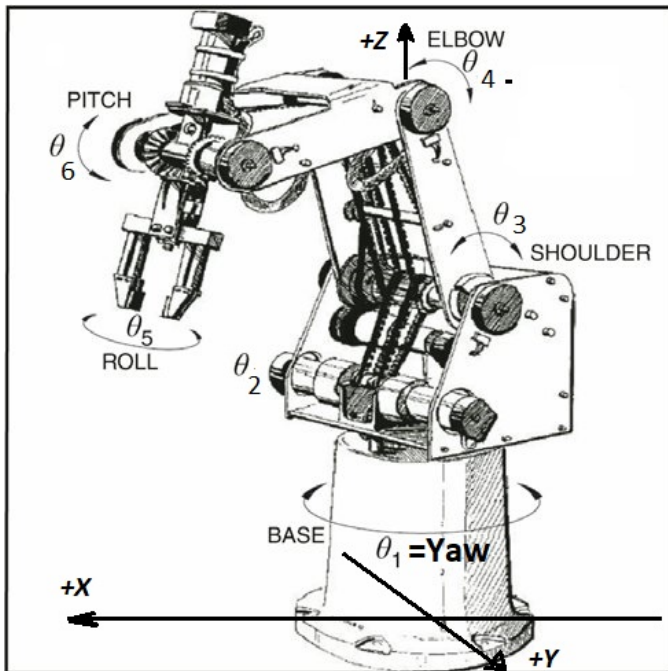
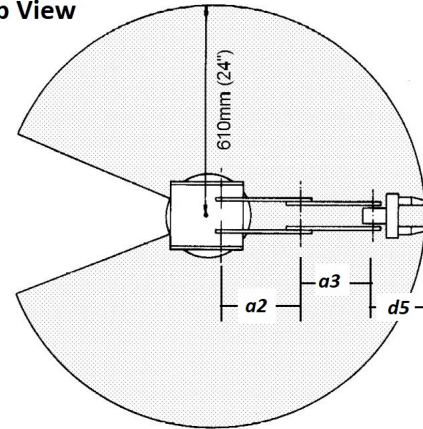


Fig. 1. Scorbot ER-V Plus Robot Details of Angles and Conventions.
Note: the arm occupies a plane coinciding with the z-axis of its base [32].

The robot is controlled using ACL, which is a language that can be used as a multitask robotic programming environment

A: Top View



B: Side View

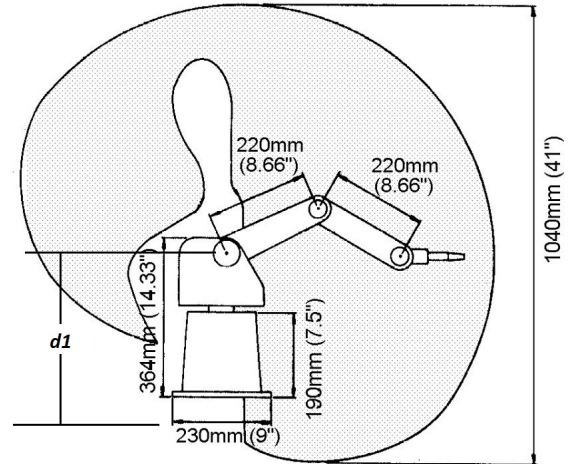


Fig. 2. The Operation Range that Defines the Space and Parameters of the Robot used in the Kinematics [32].

[33, 34]. MATLAB functions were created to establish bidirectional serial communication with the Scorbot controller. Both systems (robot and Computer Vision systems) are running in MATLAB, and give ACL commands which allowed the robot to execute specific tasks, read and load pose data into the controller, and modified the manipulator's movement speed. Fig. 3 also shows the flow of exchanging information between system components.

B. Vision Sensory System

The Kinect V2 sensor (RGB-D sensor) is composed of two cameras, the RGB and an infrared IR camera. The IR camera can be utilized to obtain depth maps, with a field of vision (70° horizontal and 60° vertical). The Kinect camera is capable of running at a rate of (30 fps) at a resolution of (512X424 pixels) and the operational range for the IR camera is between (0.5 m to 4.5 m). The sensor operates based on the time-of-flight principle [35]. The depth data obtained in each pixel corresponds to the Z_i coordinate measured on the optical axis of the IR camera as illustrated in Fig. 4.

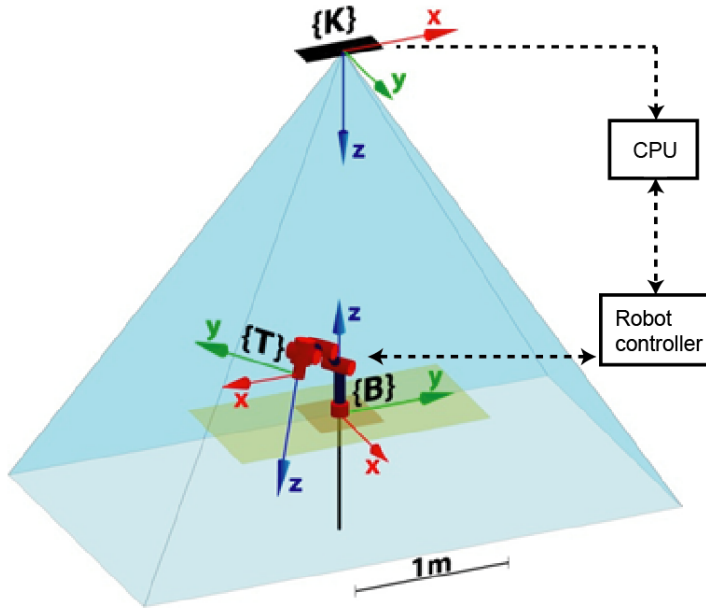


Fig. 3. The Frame Associated with the System Problem Modeling, $\{B\}$ is the base of the Robot, $\{K\}$ Represents the Kinect Sensor, $\{T\}$ Represent the Robot's Tool. The Dotted Line Indicates the Information Flow that is being Exchanged in the Systems.

IV. METHODOLOGY

A. Kinect-Robot Modeling and Calibrating

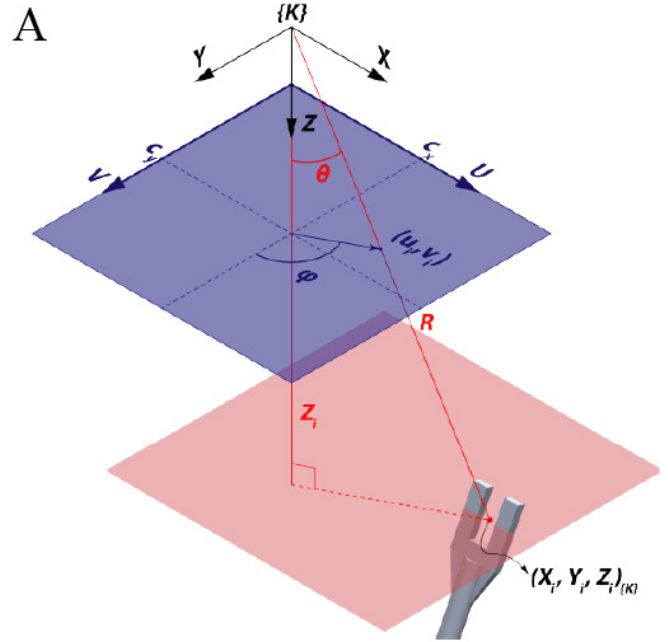
The objective of this work is to provide a system that allows the robot to sense its surroundings and act accordingly. It is necessary to represent the three-dimensional space around the manipulator. There are three important frames [36], the center base of the robot $\{B\}$, the robot's tool $\{T\}$, and the origin of the physical model of the Kinect's depth camera $\{K\}$ as shown in Fig. 3. The robot's task was defined in Cartesian coordinates referred to the base frame $\{B\}$.

For the geometric description of the system, a homogeneous coordinates based on the knowledge gained from [36] was used. The coordinates of a point p with respect to the frame $\{K\}$ is written as ${}^K p = (X_K, Y_K, Z_K, 1)^T$. To calculate the coordinates with respect to frame $\{B\}$ the expression ${}^B p = {}^B_K T \cdot {}^K p$ is used.

The homogeneous matrix T is given by equation (1) where ${}^B_K R$ is a rotation matrix that describes the orientation of the frame $\{K\}$ with respect to the base $\{B\}$, and ${}^B t_K$ corresponds to the coordinates of origin $\{K\}$ in frame $\{B\}$.

$${}^B_K T = \begin{bmatrix} {}^B_K R & {}^B t_K \\ 0_{1 \times 3} & 1 \end{bmatrix} \quad (1)$$

1) *Robot Geometric Model:* In a previous project [37], the direct and inverse kinematics of the Scorbot ER-V Plus were studied. The results presented allowed the calculating of position (${}^B p = (X_B, Y_B, Z_B, 1)^T$) and orientation ($\alpha = yaw, \beta = pitch, \gamma = roll$) of the tool $\{T\}$ in a function of the five rotational angles of the robot ($\theta_1, \theta_2, \theta_3, \theta_4, \theta_5$). Equations



B

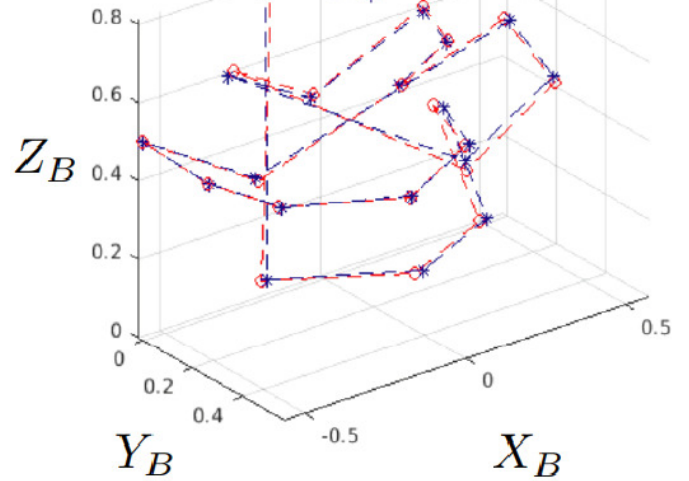


Fig. 4. (A) Geometric Model Utilized to Calibrate the Kinect-Scorbot. Z_i Results in the Intensity of the Pixel (u_i, v_i) . (B) Calibration of Kinect-Scorbot, the Blue Points Indicate the Coordinates of the tool's Position, while the Red Points Indicate the Prediction of the Positions after Calibrating the Parameters f and ${}^B_K T$ of the Model.

(2) and (3) represent the results while Fig. 1 represents the parameters of the robot.

$$\begin{aligned} X_B &= c_{\theta_1} (a_3 c_{\theta_S} + a_2 c_{\theta_2} + d_5 c_{\theta_W}) \\ Y_B &= s_{\theta_1} (a_3 c_{\theta_S} + a_2 c_{\theta_2} + d_5 c_{\theta_W}) \\ Z_B &= d_1 + a_3 s_{\theta_S} + a_2 s_{\theta_2} + d_5 s_{\theta_W} \end{aligned} \quad (2)$$

$$\begin{aligned} \theta_S &= \theta_2 + \theta_3 \\ \theta_W &= \theta_2 + \theta_3 + \theta_4 \end{aligned}$$

$$\begin{aligned}\alpha &= \theta_1 = \arctan(Y_B, X_B) \\ \beta &= -\theta_2 - \theta_3 - \theta_4 = -\theta_W \\ \gamma &= \theta_5\end{aligned}\quad (3)$$

Note that once θ_1 is defined, the robot is contained in a plane that coincides with the Z -axis of the first articulation. This observation is important because it allows the construction of a binary mask that allows the Scorbot detection when moving.

2) *RGB-D geometric model*: The camera model used was a *pinhole* type. The hypothesis is as follow: the origin of the frame $\{K\}$ coincides in XY with the center of the image (c_x, c_y) , and the focal distance f is the same in X as in XY . Spherical coordinates were employed to map the coordinates (u_i, v_i) and data Z_i with coordinates $(X_i, Y_i, Z_i, 1)_{\{K\}}^T$ as shown in equation (4)-(6).

$$\varphi_i = \text{atan}\left(\frac{v_i - c_y}{u_i - c_x}\right) \quad (4)$$

$$\theta_i = \text{atan}\left(\frac{\sqrt{(u_i - c_x)^2 + (v_i - c_y)^2}}{f}\right) \quad (5)$$

$$R_i = \frac{Z_i}{\cos(\theta_i)} \quad (6)$$

Thus, the three-dimensional point p_i has coordinates in frames $\{K\}$ and $\{B\}$ given by (7)-(8).

$${}^K p_i = (R \cos(\theta_i) \cos(\phi_i), R \cos(\theta_i) \sin(\phi_i), Z_i, 1)^T \quad (7)$$

$${}^B p_i = {}^B T \cdot {}^K p_i = ({}^K T)^{-1} \cdot {}^K p_i \quad (8)$$

3) *Geometric calibration of Kinect-Scorbot system*: The geometric calibration of the robot was accomplished in [38]. The only intrinsic parameter that was considered unknown in the Kinect was the focal distance of f . Also, the extrinsic parameter that represents the pose of the camera $\{K\}$ with respect to the robot $\{B\}$ needed to be calibrated.

The experiment had the robot take a wooden cube using its claw in a way that allows the center mass of the block to be aligned with the manipulator's tool frame. The Kinect was placed on the roof of the lab as seen in Fig. 3. Each measurement is represented by the index i , making a total of $N = 22$. As a pattern for the adjustment of the camera model, the coordinates were obtained from the robot driver (${}^B p_{exp,i}$) through serial port communication. Given the parameters $(f, {}^B T)$ coordinates can be predicted ${}^B p_{pred,i}$ and calculate a prediction error, defined by equation (9).

$$\epsilon = \frac{1}{N} \sum_{i=1}^N |{}^B p_{exp,i} - {}^B p_{pred,i}(f, {}^B T)| \quad (9)$$

To simplify the optimization problem, it was assumed that the optical axis of the Kinect camera was perpendicular to the XY plane of the plot $\{B\}$, and the Z axes of the two frames were parallel and opposite to each other. The optimized parameters resulted in the following values: the focal length, and the position of the camera $\{K\}$ with respect to the frame $\{B\}$: ${}^B t_K$.

First, f was adjusted so that ϵ equation (9) is minimal, starting with a ${}^B t_K = (0, 0, 2.40)^T m$. This resulted in a perfect alignment in XY of the camera and the robot in Fig. 3 with a value of Z_i taken from a depth image. With the focal distance optimized, the 22 points are re-projected and a mean error for each axis was computed. These deviations were introduced as corrections in ${}^B t_K$ to reduce the mean re-projection error. With the adjusted transformation, a new focal point was computed. With the mean error being negligible for each axis, the parametric adjustment at that point was finalized.

The optimized focal distance resulted in 362.8 *pixels*. The mean error of re-projection from the 22 coordinates was 1.70 *cm* and a standard deviation of 0.87 *cm* and a peak of 3.66 *cm*. The transformation that maps the frame $\{K\}$ with $\{B\}$ was determined by equation 10.

$${}^B T = \begin{pmatrix} 0 & 1 & 0 & -0,0142 \text{ m} \\ 1 & 0 & 0 & -0,0289 \text{ m} \\ 0 & 0 & -1 & 2,3907 \text{ m} \\ 0 & 0 & 0 & 1 \end{pmatrix} \quad (10)$$

B. Human Detection using Background-Foreground Technique

For human or foreign object detection in the scene, a Background-Foreground (B-F) technique [39] was used. 100 frames of depth images were captured within 10 *sec* and used to form images of the *background* making sure the scene stayed static.

As previously mentioned, rotating and fixed rectangular binary masks were generated to avoid the detection of the robot's movement by the *foreground*. A captured image was printed on the screen, and the mouse determined the vertices of the two rectangles and a fixed point for one of them to rotate. The non-rotating rectangle was used to hide the base of the robot from the *foreground*. The rotating rectangle did the same with the extension of the maximum possible arm. The fixed point corresponded approximately with the robot axis. The angle of rotation of this mask was computed by reading the status of the encoders of the robot, and applying direct kinematics as in (2) so that it could follow the movement of the plane occupied by the robot Fig. 2.

Human detection scenarios differ slightly for the applications selected, and they are described below.

1) *Collision prevention*: Three areas were determined to be evaluated in the depth images, which represent the severity of the collision. Starting from the robot base, and utilizing the Kinect sensor calibration, two sections were established to determine the *red* and *yellow* areas in the images. The sections were 660 *mm* which is 50 *mm* more than the maximum reach of the robot for the *red zone* and 1150 *mm* for the *yellow zone*. The *green zone* was considered outside the radius of the *yellow zone*. The behavior of the robot was modeled as

a machine of finite states. There were (1) *Green* is a normal speed, (2) *Yellow* is a medium speed, (3) *Red* is minimum/very slow speed, which is illustrated in Fig. 5.

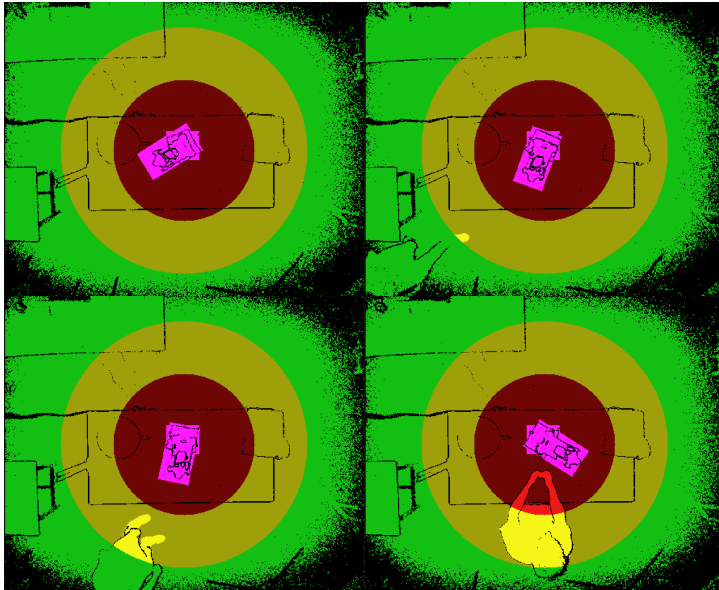


Fig. 5. Collision Prevention Scenario.

At the beginning of each iteration, a depth image will be captured, and the value of the robot's base encoder will be gathered. Then a binary mask will be added to the foreground where the captured image was subtracted from the background then a binary mask was applied to hide the robot. An opening was performed to the resulting image with a 5 pixels radius kernel disk to remove the noise. Finally, a 50 mm depth threshold was used to binarize the image.

The B-F results combined with the areas of interest to determine the behavior of the robot's speed. If the *foreground* binary area within the *red* zone exceeded 100 pixels, the state turns *red*. If the area is not exceeding 100 pixels in the *red* zone but reaching at least 500 pixels in the *yellow* zone, then the state turns *yellow*. If none of the above conditions are met, the state updates to *green*.

2) *Collaborative Scenario*: Each iteration started with the robot taking an object located at a pre-established location and a request that will appear on the user screen to guide the operator to position her/his hand where she/he wanted to receive the object from the robot. Subsequently, a binary mask will be generated for the *foreground*. The *background* image will be subtracted from the captured image and applied a 15 mm depth threshold to make it binary. It was decided to analyze a 200 pixels radius to avoid dealing with peripheral noise. The radius was equivalent to the calibration at 1.32 m at the height of the workbench. The *foreground* was cleaned by imposing an opening using a disk of 4 pixels radius like a kernel. After closing was imposed with a kernel disk with a radius of 3 pixels to remove any imperfections remaining in the *blobs*. The *blobs* with an area smaller than 800 pixels were discarded. A binary mask was generated with the remaining *blobs*. Two zones were separated by heights zones in the resulting *blobs* using Otsu's method [40].

Given the characteristics of the system, the system will be able to identify the head, torso, and arms. The portion of *blobs* that had the torso and arms inside the robot's work area will be isolated. The pixels within the radius of the work-space were filtered from the processed mask. Finally, the coordinate (u_i, v_i) of the pixel corresponding to the center of the hand was found. To find the center of the palm, a skeletonized binary image was obtained [39]. The team looked for the radius with the maximum circumference in pixels that could fit the binary mask. The coordinate of the pixel with the largest radius was preserved and the depth value Z_i assigned was that of greater repetition within the maximum circumference that could fit in the mask with center (u_i, v_i) , and applied to the originally captured image.

The coordinates (u_i, v_i) and Z_i obtained were transformed. First to coordinates $(X_i, Y_i, Z_i, 1)_{\{K\}}^T$ using equations (4)-(6), and then to $(X_i, Y_i, Z_i, 1)_{\{B\}}^T$, by using equation (10). At this position, a height increase, Z_B , of 7 cm was made to prevent collisions with the operator's hand. Then adjusted height was entered automatically by serial communication to an internal variable of the robot controller. This allowed the end effector to deposit the object at the desired position. As a result, the collaborative job will be completed as shown in Fig (6).

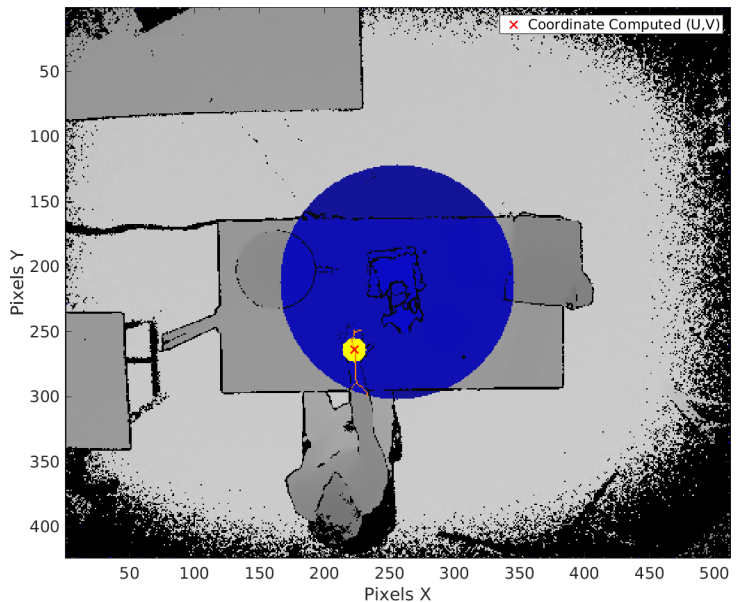


Fig. 6. Collaboration with an Operator Scenario.

V. RESULTS

This work is meant to develop an affordable prototype that can be added to industrial robots to increase robot safety, decrease the barriers between human operators and robots, and facilitate a collaboration system between them. The designed system addressed these goals as follow:

A. Collision Prevention System

The detection of an operator in the pre-established zones is exemplified in Fig. 5. To test the operation of the system, 10 tests were made in areas of interest, where a human operator will introduce his/her hand into the robot surroundings. The

system was used to detect the operator when first entering the yellow zone (Operator's leg) where the system forced the robot to move at half of its original operation speed. Then the operator introduced his/her hands within the red zone to force the robot to slow significantly to almost not moving. These actions were captured by the camera and highlighted by the associated colors shown in Fig. 5, which displays the areas of interest corresponds to the detection of the pixels as part of the foreground and the outline of the ScorBot is shown inside the binary mask.

In all test cases, the system behaved correctly as intended, by identify the existence of the human operator and change the robot speed according to the distance between the human and the robot. The robot response time to change the end-effector speed was recorded and the mean system update time was 0.45 s with a standard deviation of 0.30 s, which is a significantly fast response.

Modify the speed of the robot was accomplished through an ACL command called 'CLRBUF', which was introduced as an instant stop to the robot followed by an immediately a new movement speed was set, and a new trajectory was generated from the current pose until the next corresponding task resuming the job. the team implemented other methods to change the speed by changing the task priorities on the robot or send speed change commands during a test but all failed since these commands could only be utilized after completing the previous tasks.

B. Collaborative Scenario

Collaboration between the robot and human operator was simulated by having the automated system detect the operator's hand and estimate the spatial coordinate of the center of the hand then command the robot will move to pick up an object from a predefined location then place it on the operator's hand, this is illustrated in Fig. 6. The blue region represents the Scorbot work-space, the orange lines show the skeletonization of the operator's arm while the yellow area shows the mask's maximum circumference where the robot should place the object on.

Experiments with 20 different hand positions within the robot's work-space were conducted, the system gave satisfactory results, where the job was done correctly, and placement coordinates mean error was 2.4 cm.

VI. CONCLUSION

This work showed that an overhead low-cost RGB-D camera can measure the position of an operator with respect to a robotic manipulator, and thus improve human-robot interaction safety and increase the collaboration opportunities through 3D sensing of the robot surrounding environment. This proposed system will allow manufacturing and industrial companies to update their existing robotics and automation system by adding an affordable add-on safety and collaboration device without influencing their manufacturing lines with a lower cost of investment.

In the collision prevention scenario, the captured video analysis proved that the reaction times of the system was 500ms and the system's bottleneck was the PC and robot

inter-communication which required relatively longer times and added pauses and checkpoints to make sure it is reliable.

In the collaborative scenario, detecting the operator's hand and have the robot placing an object was achieved, and similar to the other scenario, the internal variables, and data transmitting speed between the robot controller and the main computer was the main factor to defined the speed of the system.

The team is working on a few improvements to the proposed system including enhancing the B-F algorithm internal variables and date, exploring the application of dynamics methods that can assimilate changes in the scene on slower times scales. Also, an RGB camera system development is being conducted to detect a particular color or clothing as an activator for robot tasks. Additionally, more sophisticated moving object classification techniques such as convolution neural networks will be explored.

ACKNOWLEDGMENT

This project was funded and supported by "100,000 Strong in the Americas Innovation Fund – Exxon Mobil", and the U.S. Department of Education - Minority Science and Engineering Improvement (MSEIP) Program (Grant # P120A170102), National University of Quilmes, and Texas A&M International University. With their support, this project was a successful collaboration between the two institutes.

REFERENCES

- [1] Matheson, E., Minto, R., Zampieri, E. G., Faccio, M., & Rosati, G. (2019). Human-Robot Collaboration in Manufacturing Applications: A Review. *Robotics*, 8(4), 100.
- [2] Ferraguti, F., Bertuletti, M., Landi, C. T., Bonfe, M., Fantuzzi, C., & Secchi, C. (2020). A control barrier function approach for maximizing performance while fulfilling to iso/ts 15066 regulations. *IEEE Robotics and Automation Letters*, 5(4). <https://doi.org/10.1109/LRA.2020.3010494>
- [3] Robla-Gomez, S., Becerra, V. M., Llata, J. R., Gonzalez-Sarabia, E., Torre-Ferrero, C., & Perez-Oria, J. (2017). Working together: a review on safe human-robot collaboration in industrial environments. *IEEE Access*, 5. <https://doi.org/10.1109/ACCESS.2017.2773127>
- [4] Harper, C., & Virk, G. (2010). Towards the development of international safety standards for human-robot interaction. *International Journal of Social Robotics*, 2(3), 229-234.
- [5] Anandan, T. M. (2013). Safety and control in collaborative robotics. Published on: Aug, 6, 1-4.
- [6] Paolanti, M., Romeo, L., Liciotti, D., Cenci, A., Frontoni, E., & Zingaretti, P. (2018). Person Re-Identification with RGB-D Camera in Top-View Configuration through Multiple Nearest Neighbor Classifiers and Neighborhood Component Features Selection. *Sensors*, 18(10), 3471. MDPI AG. <http://dx.doi.org/10.3390/s18103471>
- [7] Zhang, J., Li, W., Ogunbona, P. O., Wang, P., & Tang, C. (2016). RGB-D-based action recognition datasets: A survey. *Pattern Recognition*, 60, 86-105. <https://doi.org/10.1016/j.patcog.2016.05.019>.
- [8] Coupeté, E., Moutarde, F., & Manitsaris, S. (2015). Gesture recognition using a depth camera for human-robot collaboration on an assembly line. *Procedia Manufacturing*, 3, 518-525. <https://doi.org/10.1016/j.promfg.2015.07.216>.
- [9] Shukla, D., Erkent, Ö., & Piater, J. (2016, August). A multi-view hand gesture RGB-D dataset for human-robot interaction scenarios. In 2016 25th IEEE international symposium on robot and human interactive communication (RO-MAN) (pp. 1084-1091). IEEE. <https://doi.org/10.1109/ROMAN.2016.7745243>.
- [10] Lorenzo-Navarro J, Castrillón-Santana M, Hernández-Sosa D. On the Use of Simple Geometric Descriptors Provided by RGB-D Sensors for Re-Identification. *Sensors*. 2013; 13(7):8222-8238. <https://doi.org/10.3390/s130708222>
- [11] Lorenzo-Navarro J., Castrillón-Santana M., Hernández-Sosa D. (2012) An Study on Re-identification in RGB-D Imagery. In: Bravo J., Hervás

- R., Rodríguez M. (eds) Ambient Assisted Living and Home Care. IWAAL 2012. Lecture Notes in Computer Science, vol 7657. Springer, Berlin, Heidelberg. https://doi.org/10.1007/978-3-642-35395-6_28
- [12] Paolanti, M., Pietrini, R., Mancini, A., Frontoni, E., & Zingaretti, P. (2020). Deep understanding of shopper behaviours and interactions using RGB-D vision. *Machine Vision and Applications*, 31(7), 1-21. <https://doi.org/10.1007/s00138-020-01118-w>
- [13] Liciotti D., Paolanti M., Frontoni E., Zingaretti P. (2017) People Detection and Tracking from an RGB-D Camera in Top-View Configuration: Review of Challenges and Applications. In: Battiato S., Farinella G., Leo M., Gallo G. (eds) *New Trends in Image Analysis and Processing – ICIAP 2017*. ICIAP 2017. Lecture Notes in Computer Science, vol 10590. Springer, Cham. https://doi.org/10.1007/978-3-319-70742-6_20
- [14] Moallem, P., Razmjoo, N., & Ashourian, M. (2013). Computer vision-based potato defect detection using neural networks and support vector machine. *International Journal of Robotics and Automation*, 28(2), 137-145. <https://doi.org/10.2316/Journal.206.2013.2.206-3746>
- [15] Turarova, A., Zhanatkyzy, A., Telisheva, Z., Sabyrov, A., & Sandygulova, A. (2020, March). Child Action Recognition in RGB and RGB-D Data. In *Companion of the 2020 ACM/IEEE International Conference on Human-Robot Interaction* (pp. 491-492). <https://doi.org/10.1145/3371382.3378391>
- [16] Gualtieri, L., Rauch, E., Vidoni, R., & Matt, D. T. (2020). Safety, ergonomics, and efficiency in human-robot collaborative assembly: design guidelines and requirements. *Procedia Cirp*, 91, 367-372. <https://doi.org/10.1016/j.procir.2020.02.188>
- [17] Ore, F., Vemula, B., Hanson, L., Wiktorsson, M., & Fagerstrom Bjorn. (2019). Simulation methodology for performance and safety evaluation of human-industrial robot collaboration workstation design. *International Journal of Intelligent Robotics and Applications*, 3(3), 269-282. <https://doi.org/10.1007/s41315-019-00097-0>
- [18] Parigi Polverini, M., Zanchettin, A. M., & Rocco, P. (2017). A computationally efficient safety assessment for collaborative robotics applications. *Robotics and Computer Integrated Manufacturing*, 46, 25- 37. <https://doi.org/10.1016/j.rcim.2016.11.002>
- [19] Zanchettin, A. M., Ceriani, N. M., Rocco, P., Hao, D., & Matthias, B. (2016). Safety in human-robot collaborative manufacturing environments: metrics and control. *IEEE Transactions on Automation Science and Engineering*, 13(2). <https://doi.org/10.1109/TASE.2015.2412256>
- [20] Vicentini, F. (2020). Terminology in the safety of collaborative robotics. *Robotics and Computer Integrated Manufacturing*, 63. <https://doi.org/10.1016/j.rcim.2019.101921>
- [21] Vicentini, F., Askarpour, M., Rossi, M. G., & Mandrioli, D. (2020). Safety assessment of collaborative robotics through automated formal verification. *IEEE Transactions on Robotics*, 36(1), 42-61. <https://doi.org/10.1109/TRO.2019.2937471>
- [22] Franklin, C. S., Dominguez, E. G., Fryman, J. D., & Lewandowski, M. L. (2020). Collaborative robotics: a new era of human-robot cooperation in the workplace. *Journal of Safety Research*, 74, 153-160. <https://doi.org/10.1016/j.jsr.2020.06.013>
- [23] Echavarrí Javier, Ceccarelli, M., Carbone, G., Alen Cristina, Muñoz Jose Luis, Díaz Andres, & Muñoz-Guijosa, J. M. (2013). Towards a safety index for assessing head injury potential in service robotics. *Advanced Robotics*, 27(11), 831-844. <https://doi.org/10.1080/01691864.2013.791655>
- [24] Smit-Anseeuw, N., Remy, C. D., & Vasudevan, R. (2019). Walking with confidence: safety regulation for full order biped models. *IEEE Robotics and Automation Letters*, 4(4), 4177-4184. <https://doi.org/10.1109/LRA.2019.2931225>
- [25] Alonso-Mora, J., Beardsley, P., & Siegwart, R. (2018). Cooperative collision avoidance for nonholonomic robots. *IEEE Transactions on Robotics*, 34(2), 404-420. <https://doi.org/10.1109/TRO.2018.2793890>
- [26] Gurriet, T., Mote, M., Singletary, A., Nilsson, P., Feron, E., & Ames, A. D. (2020). A scalable safety-critical control framework for nonlinear systems. *IEEE Access*, 8. <https://doi.org/10.1109/ACCESS.2020.3025248>
- [27] Oyekan, J. O., Hutabarat, W., Tiwari, A., Grech, R., Aung, M. H., Mariani, M. P., & Dupuis, C. (2019). The effectiveness of virtual environments in developing collaborative strategies between industrial robots and humans. *Robotics and Computer Integrated Manufacturing*, 55, 41-54. <https://doi.org/10.1016/j.rcim.2018.07.006>
- [28] Askarpour, M., Mandrioli, D., Rossi, M., & Vicentini, F. (2019). Formal model of human erroneous behavior for safety analysis in collaborative robotics. *Robotics and Computer-Integrated Manufacturing*, 57, 465-476. <https://doi.org/10.1016/j.rcim.2019.01.001>
- [29] Giuliani, M., Lenz, C., Muller Thomas, Rickert, M., & Knoll, A. (2010). Design principles for safety in human-robot interaction. *International Journal of Social Robotics*, 2(3), 253-274. <https://doi.org/10.1007/s12369-010-0052-0>
- [30] Raiola, G., Cardenas, C. A., Tadele, T. S., de Vries, T., & Stramigioli, S. (2018). Development of a safety- and energy-aware impedance controller for collaborative robots. *IEEE Robotics and Automation Letters*, 3(2), 1237-1244.
- [31] Hull, T., & WCX™ 17: SAE World Congress Experience Detroit, Michigan, United States 2017-04-04. (2017). Intelligent robotics safeguarding. *SAE International Journal of Engines*, 10(2), 215-221. <https://doi.org/10.4271/2017-01-0293>
- [32] Intelitek Inc. Scrobot-ER V plus: User's Manual. Catalog #100016 Rev. C February 1996.
- [33] Siciliano, B. & Khatib, O. (Eds.). (2016). *Springer handbook of robotics*. Springer.
- [34] Robotec, E. (1994). *ACL-Advanced Control Language Versions 1.43, F1. 44 and ATS-Advanced Terminal Software Version 1.44*.
- [35] Villena Martínez, V. (2015). Comparative analysis of calibration methods for RGB-D sensors and their influence on the recording of multiple views.
- [36] Craig, J. J. (2005). *Introduction to Robotics*.
- [37] Del Vigo, L., Peyton, R., Bussi, U., & Oliva, D. E. (2018, November). Computer-aided design and simulation of a robotic manipulator for educational purposes. In *2018 Argentine Conference on Automatic Control (AADECA)* (pp. 1-6). IEEE.
- [38] Pessag, F., De Cristoforis, P., Perri, V. & Oliva, D. (2014). Implementación y validación de un modelo cinemático para el manipulador robótico SCORBOT ER-Vplus. *Argentina, CABA. VIII Jornadas Argentinas de Robotica*, ISBN-13. pp. 978-987-1087-19-9.
- [39] Russ, J. C. & Neal, F. B. (2016). *The image processing handbook*, 7th ed. CRC Press. pp. 381-391
- [40] Otsu, N. (1979). A threshold selection method from gray-level histograms. *IEEE transactions on systems, man, and cybernetics*, 9(1), 62-66.

Application-based Evaluation of Automatic Terminology Extraction

Marija Brkic Bakaric¹, Nikola Babic², Maja Matetic³

Department of Informatics
University of Rijeka
Rijeka, Croatia

Abstract—The aim of this paper is to evaluate performance of several automatic term extraction methods which can be easily utilized by translators themselves. The experiments are conducted on German newspaper articles in the domain of politics on the topic of Brexit. However, they can be easily replicated on any other topic or language as long as it is supported by all three tools used. The paper first provides an extensive introduction into the field of automatic terminology extraction. Next, selected terminology extraction methods are assessed using precision with respect to the gold standard compiled on the same corpus. Moreover, the corpus has been completely annotated to allow for the calculation of recall. The effects of using five cut-off points are examined in order to find an optimal value which should be used in translation practice.

Keywords—Terminology extraction; hybrid methods; evaluation; precision; recall; gold standard; language resources

I. INTRODUCTION

The aim of this paper is to provide an extensive introduction into the field of automatic terminology extraction (ATE) and to evaluate one statistical and two hybrid methods of extraction on German newspaper articles in the domain of politics on the topic of Brexit. The main highlights of the research are the following: (1) extensive introduction into the field of terminology extraction followed by the (2) creation of the gold standard on the Brexit-related German terminology and (3) evaluation of the selected methods on the Brexit-related jargon which shows abundance of creative coinages by (3a) conducting both manual and automatic extraction on the same corpus, and (3b) by annotating the corpus completely in order to allow for the calculation of recall.

The problem of the related work is that it is not directly comparable due to the differences in “corpus selection (e.g. domain, size), evaluation methodology (e.g. human judges, dictionary based, gold standard based), and scope (e.g. entire results, parts of results, top n best results)” [1]. With the above said in mind, this study does not propose a novel approach to ATE, but compares performance of well-known extraction methods under the same experimental settings. Since the use of the gold standard supports reproducibility of results and comparison between different methods, this paper opts for that approach. Although there are toolkits such as JATE 2.0 [2] or ATR4S [3] which implement more than ten automatic terminology extraction methods, these toolkits, as well as other related software toolkits are rather limited for several reasons – some of them lack the adequate language support,

some cannot be used by the users who need these tools in practice but do not have enough technical expertise, e.g. translators, and lastly, some are proprietary. Moreover, the evaluation of ATE is usually conducted in technical domains such as biology or medicine, as acknowledged by [1]. Therefore, evaluation in less technical domains is missing.

The following section not only presents the related work, but it can serve as an introduction for those who wish to enter the field of terminology extraction. The experimental study is presented in section three, which is subdivided into descriptions of corpus, and manual and automatic extraction tasks. The results and discussion are given in section four. Concluding remarks are provided in the last section.

II. BACKGROUND

A. Basic Concepts and Definitions

Terminology extraction aims at “structuring terminological knowledge from unstructured texts” [4] and identifying “the core vocabulary of a specialized domain” [5]. Terms can be defined as a “designation of a defined concept in a special language by a linguistic expression” (ISO 1087). Terms are usually nominal constructions, while collocations represent preferred ways of expressing things and thus contain more verbal parts [6]. For an overview of the existing definitions for the concepts “term” and “domain”, please refer to [7].

In the Traditional Manual Terminology Extraction (MTE), a terminologist first makes a list of potential term candidates (TCs) which are then discussed with domain experts. The resulting list contains all validated terms [5]. Automatic terminology extraction (ATE) is based on the computational analysis of a textual corpus. The process is carried out by the computer and is thus objective. The fact that ATE is based on objective corpus evidence compensates for possible human errors [8]. On the other hand, humans identify terms not only by form, but also according to extra-linguistic criteria, and the terms detected on the basis of semantics also have to fit domain. The automatic process can therefore only assist humans who must be engaged during the final verification or filtering stage [9]. As long as humans are needed at least in the verification stage, the process of ATE will be considered semi-automatic [10]. However, since MTE is error-prone, labor intensive, time-consuming, and subjective, ATE is useful even if used only as a “preliminary identification” of TCs [5].

This research was supported by the Erasmus+ grant number 19-203-060377 – KA2-HE-01/19 and the University of Rijeka grant number unirdrustv-18-122.

In terms of ATE, designation of a word or a phrase as a term is not a simple binary decision. ATE result is presented as a continuum, in the form of a list of candidates ranked according to the score [11].

There are two types of terminology extraction from unstructured texts – monolingual terminology extraction which processes and extracts terms from texts in one language, and bilingual or multilingual terminology extraction which extracts and aligns terms from texts in two or more languages [4]. This paper is concerned with the first, while the latter will be subject of our future work.

B. Applications of ATE

Three possible applications of ATE, which are identified in [6] and [9], refer to terminology, translation, and document management or retrieval (e.g. automatic keyword extraction [12]). This research has been conducted from the translation aspect. In terms of translation, the extracted terminology might be used as a preparation for interpreting, for the development and improvement of machine translation engines, for ensuring consistency, particularly if multiple translators work on the same project [13], etc. The practical requirement is usually to find everything the system does not know yet, so for this purpose term extraction is followed by term recognition, i.e. the comparison of the extraction results with some dictionary/term bank resource in order to identify known/unknown terms.

C. Approaches to ATE

According to the authors in [12], ATE methods can be analyzed according to two aspects. The first aspect is “unithood”, which is defined as “the degree of strength or stability of syntagmatic combinations and collocations” and refers to the internal coherence of language units [14] or to “the identification of linguistic elements that constitute a multiword unit and refer to one conceptual unit” [5]. The second aspect, termhood, on the other hand, refers to “the degree that a linguistic unit is related to domain-specific concepts” [12] or to the affiliation of a certain lexical unit or group to a terminology of a special purpose domain. In simple words, termhood detection is a method which ranks the extracted units according to the likelihood that they constitute a valid term for the specialized domain considered.

There are two basic approaches to the process of ATE – linguistic and statistical. Depending on the method used for ATE, the corpora might undergo pre-processing like lemmatization, part-of-speech (POS) tagging, chunking or full syntactic parsing [5]. Linguistic approaches are thus heavily language dependent. They use morpho-syntactic patterns, while statistical approaches use terms frequencies as evidence for unithood [5]. Co-occurrence measures for unithood include chi-square, t-score, log-likelihood ratio, mutual information, and the phi coefficient. The termhood can be measured by analyzing contextual usage of TCs, TCs’ internal structure, or distributional properties of TCs within the domain and the dispersion over different documents [5]. Most of the contemporary systems are hybrid, which means that they are based on the combination of two approaches [4]. This implies that the classification into statistical and linguistic is deprecated, and that linguistic methods are nowadays regarded as mere filters. Co-occurrence measures are therefore usually calculated for word combinations that have passed the linguistic filter. The filter can be either open-class and thus less restrictive, which results in huge lists abundant with false positives, or closed class, boosting precision at the cost of recall [5]. Beside representative domain specific corpus, contrastive approaches to ATE additionally require a general language corpus. Additionally, they should be coupled with word sense disambiguation, since many terms (‘belt’, ‘fault’, etc.) are homonymous between a term reading and a general reading [6]. The methods selected for this research can be roughly categorized into statistical (Rainbow), hybrid (Termsuite), and hybrid contrastive (Sketch Engine).

Majority of ATE methods follow the scheme given in Fig. 1, which is based on the work of [7]. For an extensive list of feature computation methods and their classification, please refer to [7].

D. Evaluation of ATE

ATE evaluation methods can be divided into direct (intrinsic) and indirect (extrinsic) methods, as asserted by [14]. While the first evaluate some intrinsic properties, the latter measure the improvement gained in another system which uses the results of term extraction.

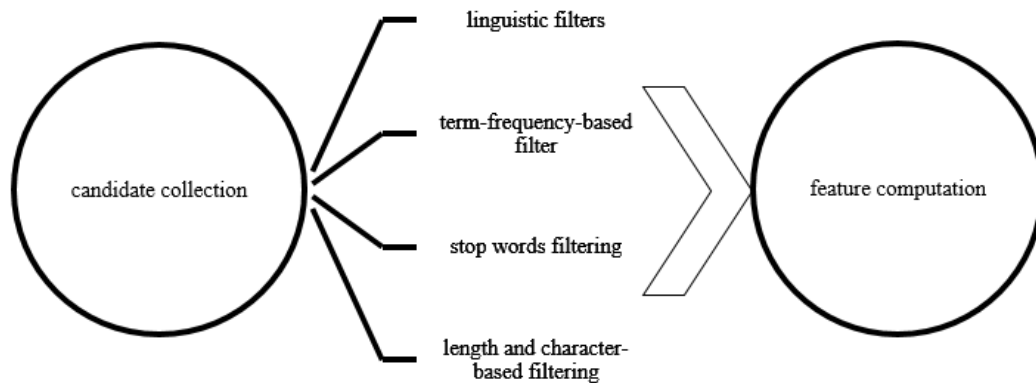


Fig. 1. General ATE Pipeline (based on [7]).

Furthermore, there are two direct approaches to ATE evaluation. The first approach is to have domain experts conduct a manual evaluation. This approach suffers from low inter-annotator agreement. It can be conducted in a strict mode in which all evaluators have to agree on the term, and lenient in which all candidates approved by at least one evaluator are counted [1]. The other approach is to use the “gold standard”, also known as Reference Term Lists (RTLs), which implies assessing the quality relative to a list of terms manually compiled by a domain specialist [5]. However, the main difficulty of the approach is that there are no objective rules to distinguish terms from non-terms [15]. RTLs “may be more or less detailed, depending on terminologists’ needs and preferences” [16], which significantly affects evaluation. Moreover, RTLs should contain not only reference terms, but also their variants. In relation to the gold standard, the authors in [17] differentiate between two types of true positives – actual true positives (ATP) which relate to all the terms in the gold standard, and recoverable true positives (RTP) which relate to the intersection of the filtered term candidates and the gold standard. In this research, in this paper the direct approach of using the gold standard is taken.

The approach of using the gold standard can be further subdivided, as the authors in [7] suggest, into labelling of a whole dataset, labelling of a subset, and, lastly, adaptation of available resources, which depends on the availability of domain thesauri, vocabularies, keywords or indexes.

The measures which are usually used for ATE evaluation are precision and recall, and, lately, average precision. These are the measures used also in this research. Precision (P) shows the percentage of correct terms out of the list of extracted terms (1). It is sometimes referred to as precision at level K (P@K). Recall (R) shows the percentage of correct terms out of the list of manually extracted terms (2). It is worth noting, as the authors in [7] emphasize, that the recall is usually implicitly evaluated because it is determined by the specified number of recognized terms. Average precision (AvgP), given in (3), is a standard ATE metric. If recall cannot be calculated as no gold standard exists, the union of all the correct terms predicted by methods which are being evaluated can be used for calculating at least a relative recall [18].

$$P@K = \frac{\text{correct} \cap \text{retrieved}}{K} \quad (1)$$

$$R@K = \frac{\text{correct} \cap \text{retrieved}}{\text{correct}} \quad (2)$$

$$\text{AvgP@K} = \frac{1}{K} \sum_{k=1}^K P@k \quad (3)$$

A slightly different measure of precision is sometimes used (e.g. [1]), which is taken over from [19]. It averages precision at the i^{th} correct term (with respect to how many candidate terms preceded the i^{th} term) out of the total K correct terms in the output. There is also a version which takes recall into account, as given in [3].

Since precision and recall have many underlying problems (e.g. there is no intuition as to which terms are considered relevant, or the system gives a term in its base form but the reference term bank has it in inflected form, should proper names be included or not, etc.), the work of [6] proposes the

evaluation measure which relies on the issue of usability, which is calculated as the ratio between really possible concepts (semantic units) and candidates which will never be used in any application, and are only noise.

The evaluation procedure is additionally burdened by the fact that two actors of different profiles are involved in the manual compilation. A terminologist is an expert on deciding whether an expression is a real term or belongs to the general language, while a domain expert uses a specific expression to refer to a concept in the domain [14]. Since it is not realistic to have a terminologist available for all the task types, two domain specialists are employed for the task. In general, it is difficult to obtain the complete set of terms in a given corpus (i.e. it is easier to ask a specialist about the termhood of a given TC than to ask him or her to compile the complete list of terms), which is why only precision is sometimes calculated [14]. If the gold standard is present, as in this research study, there is a possibility to accept the TCs listed in the standard and to ask human evaluators to judge the remaining TCs.

E. Thresholds

The authors in [7] list different scenarios regarding the number of terms to be recognized and distinguish between those with a predetermined number of terms (cut-off value) and those in which the number of terms is determined by the algorithm. A hard threshold means that candidates with scores less than a threshold are not accepted. A top list, on the other hand, takes a certain number of candidates into account, while there is also a top percentage version which takes a certain percentage of top candidates into account. The authors in [7] also enumerate scenarios based on the length of term candidates.

In this research, the length of the candidates is not restricted. Although different cut-off values are explored, the paper also reports results when the complete TC lists are taken into account.

F. Bilingual ATE

When it comes to bilingual ATE or bilingual glossary compilation, there are many more challenges that need to be tackled compared to the monolingual ATE, e.g. the usage of terms is often not harmonized, especially in case of more translators or authors, mostly due to the differences and particularities of two systems. However, ATE can serve a valuable purpose of highlighting terminology issues and facilitating harmonization of terminology [20]. The evaluation should be conducted by assessing whether a target phrase is the translation of a source term or not [6].

G. Related Work

Although there is a huge line of work on ATE, in this subsection only those that at least distinctly relate to this study are presented. One of the first limitations in conducting this type of study is appropriate language support. The existing tools or frameworks support only a handful of languages.

The authors in [21] evaluate nine terminology extraction tools from a translator’s perspective. They distinguish three classes of tools – standalone terminology extraction tools (e.g. Termsuite), web-based terminology extraction tools (e.g.

SketchEngine), and frameworks (e.g. Rainbow). This study is limited to a handful of tools since a massive approach would not contribute neither to comprehensibility nor to drawing clear conclusions. However, one tool representative of each category based on the criterion of user-friendliness is included. The clarity of making conclusions is affected even with such a limitation imposed, as shall be seen later in the paper.

By underlining the quality issues that ATE often exhibits, the results in [18] suggest that bare frequency may not be sufficient to extract even correct single-word terms (SWTs), but also that single words which occur frequently have a high chance of being identified as terms specific to that corpus. Furthermore, the performance of a POS tagger plays a great role in detecting terms, especially with regard to recall. While SWTs are usually too polysemous and too generic, multi-word terms (MWTs) often represent finer concepts in a domain [22]. Although MWTs might predominate in some languages thus making SWT extractors almost useless [6], [9], in some studies majority of domain specific terms turn out to be compound nouns [23]. The authors in [24] also acknowledge that in German texts the use of SWTs is frequent. More precisely, they report that the proportion of SWTs in three different subject domains of technical documents ranges from 57 to 94%. For that reason, the focus is put on hybrid tools, although one statistical tool is also included in this research for the sake of comparison.

Majority of the related work on German employs a hybrid approach. For example, the research presented in [24] combines linguistic filtering techniques with a statistical technique in order to extract noun-phrases from technical texts. The authors in [16] also combine a linguistic filter by using the list of pre-defined patterns with the weirdness ratio in the domains of chemical protection suits and of alcohol and drug detection. The authors in [25] extract nominal candidates in DIY domain. Statistical measures are combined to rank the TCs by the domain specificity after extracting TCs based on POS patterns and filtering out syntactically invalid ones and those occurring only embedded in other candidates. The comparison between the results of well-known statistical measures in the domain of grammar in [8] shows that measures based on corpus comparison outperform all others. The authors attribute this to the fact that German word formation allows for complex compound-unigrams (almost 83% of manually extracted terms are SWTs), which causes weaker performance of algorithms designed to identify MWTs. Three different approaches to ATE are compared, which are also representatives of three different categories of tools.

In this research study the same corpus is used both for manual and automatic term extraction, since one of the related works reveals that 35% of the false positives in the top 500 candidates qualify for the inclusion into the gold standard which is created without full access to the corpus used for automatic extraction [16]. While the authors in [8] manually extract the gold standard from a subset of the corpus and obtain best results for measures based on corpus comparison, the manual extraction in this study is conducted on the whole corpus.

There is little work on the effects that the domain has on ATE. The authors in [1] show that domain has an “impact on the performance of algorithms”, as exemplified by the comparative study in the domains of biology and medicine. Moreover, both, language and domain, affect term length as illustrated in [15]. However, according to the findings over 80% of all the terms irrespective of the language and the domain belong to one of eight POS patterns - single nouns (N), a noun and an adjective (N+A), a single adjective (A), a named entity (NE), two nouns (N+N), two nouns separated by a preposition (N+P+N), two adjectives and a noun (N+A+A) or a single verb (V). While there are many N and N+A patterns, substantial differences can be observed between different domains and, even more so, between different languages. The trade-off between precision and recall can be determined by applying a cut-off value since [16] find almost 50% of terms in the gold standard in the top 500. The author in [3] demonstrates that there is no method which performs best on all datasets.

The experimental study presented in the remainder of the paper is designed based on the aims set out in this section and on the findings of the related work presented.

III. EXPERIMENTAL STUDY

In this experimental study a black box evaluation of the selected terminology extraction tools is conducted from the translators’ point of view. Since bilingual term extraction is the most useful feature in the eyes of translators, one tool from each category distinguished in [21] is chosen but only if it supports bilingual term extraction. However, this study is limited to monolingual terminology extraction only. This is done purposefully in order to check what level of quality can be expected in a more simplistic scenario.

The topic chosen for this work is Brexit due to its relative novelty and creativity in word coinage. Its linguistic impact is recognized in [26].

The choice of tools is made logically by satisfying the criteria that the tool has support for German, that it supports bilingual term extraction, and that it has user friendly interface, where a user is considered to be a translator and not a developer. The gold standard list is lemmatized and after term extraction, the same procedure is repeated for each term candidate list. The lemmatized forms are obtained with the python package spaCy. The results are presented in terms of precision and recall at five different levels and in terms of total precision, recall, and average precisions.

A. Language and Corpus

In this study a monolingual German corpus is compiled on the topic of Brexit. A geopolitical change known under the term Brexit has occurred as of recent. The term itself first appeared almost ten years ago. As a result, a multitude of other creative coinages and compounds appeared [26]. German lies somewhere between configurational languages—which encode grammatical relations through the position of constituents—and case languages—which encode grammatical relations through morphological marking [27]. The leading way of word formation in the contemporary German language is compounding [28]. An example is

Meinungsforschungsinstitut, which consists of Meinung (opinion), Forschung (research) and Institut (institute) connected with the letter's'. The connecting letter makes it easier to see where one word ends and another begins. Another example of a compound is a German neologism Brexit-Schock (shock caused by Brexit), which is a hybrid made up of one English and one German noun connected with a hyphen. In general, such compounds are hard to translate into other languages and usually require paraphrasing.

The corpus is compiled from German newspaper articles from three different sources—Frankfurter Allgemeine Zeitung, Süddeutsche Zeitung and Zeit, and consists of 50 articles on Brexit in the period of one month. The corpus has 20.409 words in total. The topic of Brexit is chosen since it is very specific for the domain of political newspaper articles, as well as relatively novel. Moreover, as the authors in [29] warn, new or upcoming domains are usually characterized by terminological variation, which may affect the overall results. Due to its specificity and to the design of the experiment elaborated further on, the size of the corpus is relatively small compared to the usual size.

B. Manual Extraction Task

A Reference Term List is manually extracted to serve as the gold standard for the evaluation of monolingual TCs automatically extracted from German texts in the newspaper domain on the topic of Brexit. The extracted list consists of SWTs and MWTs. A terminologist is purposefully omitted from the task since the analysis focuses on the translation purposes. In that scenario, having domain experts compile the list is a more realistic scenario. Two experts are asked to extract all linguistic terms regardless of their structure, similarly to [8].

The experiments are conducted separately with the union and with the intersection of the obtained lists. Almost 79% of terms in the union of the lists are unigrams or SWTs (535 out of 681), and the remaining 21% are MWTs (bigrams 11%, trigrams 6%, fourgrams 3%, fivegrams and sixgrams both less than 1%; in counts 77, 43, 21, 2, and 2, respectively). The terms extracted manually from the above-described corpus cover nouns, verbs, and adjectives, and belong to different registers in the German language. Unlike the authors in [8], who do manual extraction on a subset of their corpus, in this paper a small-sized corpus is chosen in order to process the whole corpus manually, as this is considered beneficial according to [16]. A random sample of terms is shown in Table I. The manually extracted lists contain quite a big percentage (almost 77%) of terms which consist of nouns or nouns and adjectives (Table II). The top 10 patterns account for 92% of manually extracted terms.

C. Automatic Extraction Task

Three tools are used and evaluated in the task of ATE – Rainbow, which is part of the Okapi framework; Termsuite which is a tool developed within TTC project; and Sketch Engine, which is not a terminology extraction tool per se, but a leading web service for corpus analysis. The reference corpus used in the evaluation is the German web 2013 (deTenTen) corpus from the TenTen family [30], which consists of 16.5 billion words. In the first part of the

experiment, different cut-off values are applied to ATE results, similarly to [18]. The selected cut-off values are 50, 100, 200, 500, and 1000. In the second part of the experiment, no cut-off value is applied. The differentiation is made between the lists obtained without a minimum frequency threshold and those obtained with the minimum frequency threshold set to three.

Based on the Okapi Framework, Rainbow is an open-source platform-independent term extraction tool written in Java, which implements purely statistical methods, and can thus be applied to any language. Since a token grouping method is applied for the extraction, terms are not reduced to their stems. The only linguistic knowledge provided is a list of stop words. This means that a sequence of words is discontinued if a stop word is found in-between. Due to the fact that almost no linguistic knowledge is utilized, one experiment is conducted in which the corpus is lemmatized prior to the extraction to explore the effects that lemmatization has on the process.

Termsuite is an open-source tool developed within TTC project. Term extraction in Termsuite is a two-step procedure. A pattern-based candidate identification from the first step is followed by ordering by decreasing domain-specificity. Term candidates are, beside SWTs, restricted to bigrams and trigrams in accordance with previously identified POS patterns [29]. Since Termsuite enables also morphological compound detection and term variant processing, it is expected to be best suited for German.

TABLE I. A RANDOM SAMPLE OF MANUALLY EXTRACTED TERMS

German Terms
Austrittsdatum
Brexit-Gruppe des Europaparlaments
Brexit-Schock
Chaos-Brexit
EU-Botschafter
Gestaltung der Grenze
No-Deal-Szenario
Steuersenkung
Vereinigte Staaten
Zwangspause des Parlaments

TABLE II. TOP 10 POS PATTERNS IN MANUALLY EXTRACTED TERMS

Pattern	Frequency
N	484
ADJ N	40
V	28
ADJ	22
NN	15
N ART N	10
N PREP N	7
PREP N V	6
ART N	5
N V	4
PREP N	4

Sketch Engine is named after one of its key features—word sketches. It employs a contrastive two-step approach to terminology extraction—first the grammatical validity of a phrase (unithood) is assessed using the term grammar, next the normalized frequencies of TCs from the focus corpus are contrasted (termhood) with those in the reference corpus [31] by using the ‘Simple Math’ (with an add-N parameter of one) statistics [32]. Sketch Engine implements ATE as two separate processes, dependent on the user needs—keywords extraction and multiwords extraction. Keyword designates a word typical of a corpus in comparison to a general corpus and it is determined by the keyness score given in eq. 4, where $f_{pm_{focus}}$ stands for the normalized frequency (per one million words) of the word in the focus corpus, and $f_{pm_{ref}}$ for the normalized frequency (per one million words) of the word in the reference corpus. The default value of n is set to one. Terms are multiword expressions and the same score is used for their extraction, except that the absolute frequency counts are used. While keywords can be extracted from any corpus, a prerequisite for extracting terms is the existence of a term grammar since term extraction requires tagged and lemmatized corpora.

$$\frac{f_{pm_{focus}} + n}{f_{pm_{ref}} + n} \quad (4)$$

IV. RESULTS AND DISCUSSION

In this paper intrinsic evaluation is applied [14] and precision, recall, and average precision quality indicators are used. The comparison with the gold standard is implemented as a strict string matching of the list entries as well as a lemmatized string matching of entries. Only the latter scores are reported as these prove to be slightly superior. The counts of terms manually extracted and extracted by each tool are given in the Table III.

The overlaps between ATE results are given in Fig. 2. Please note that R stands for Rainbow, S for Sketch Engine

and T for Termsuite, and these labels will be used in figures henceforth. Furthermore, R(V1) is used when referring to the Rainbow results on the non-lemmatized corpus, and R(V2) when referring to the Rainbow results on the lemmatized corpus. Since R(V2) version results in a degradation, it is discarded from all further experiments. Although Sketch Engine and Rainbow give more similar lists, their scores differ greatly, as evident from Fig. 3 and Fig. 4, which give overall evaluation results. The overlaps between ATE results which are found in the gold union are shown in Fig. 5.

Termsuite results with the minimum frequency threshold set to 3 are superior up to the cut-off value of 200, after which it suddenly deteriorates and Sketch Engine gets better under the same settings. The results on the gold intersection follow the same pattern although the precisions are lower from the very beginning. Rainbow manages to recover a great number of terms in the gold intersection even with the minimum frequency threshold set to 3.

TABLE III. COUNTS OF LEMMATIZED TERMS IN THE GOLD STANDARD AND TERMS EXTRACTED AUTOMATICALLY BY EACH TOOL

	Number of terms					
	SWTs		MWTs		Total min=3	Total N/A
	min=3	N/A	min=3	N/A		
MTE union	536		145		N/A	681
MTE intersect	229		82		N/A	311
Rainbow	933	3655	343	6147	1276 (V1) 1217 (V2)	9802 (V1) 8731 (V2)
Sketch Engine	883	3222	14	317	897	3539
TermSuite	622	1384	134	359	756	1743

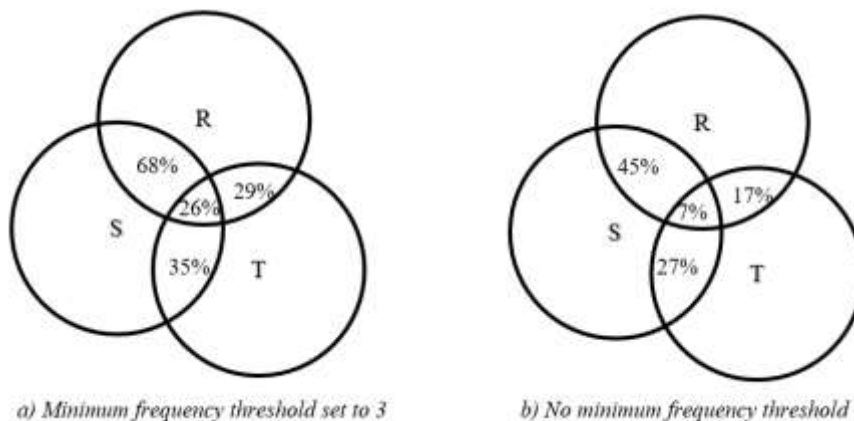


Fig. 2. Overlap between ATE Results.

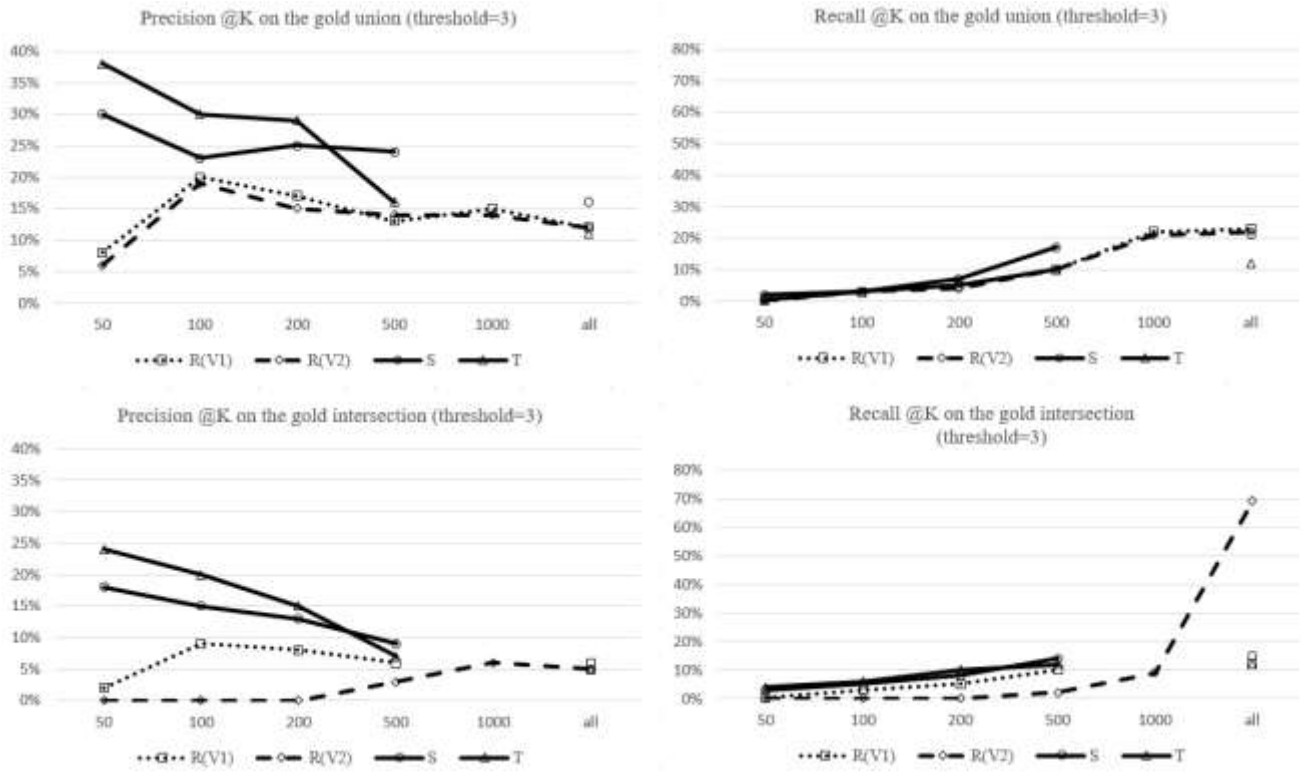


Fig. 3. Overall Lemmatized Evaluation Results on the Gold Union and Intersection.

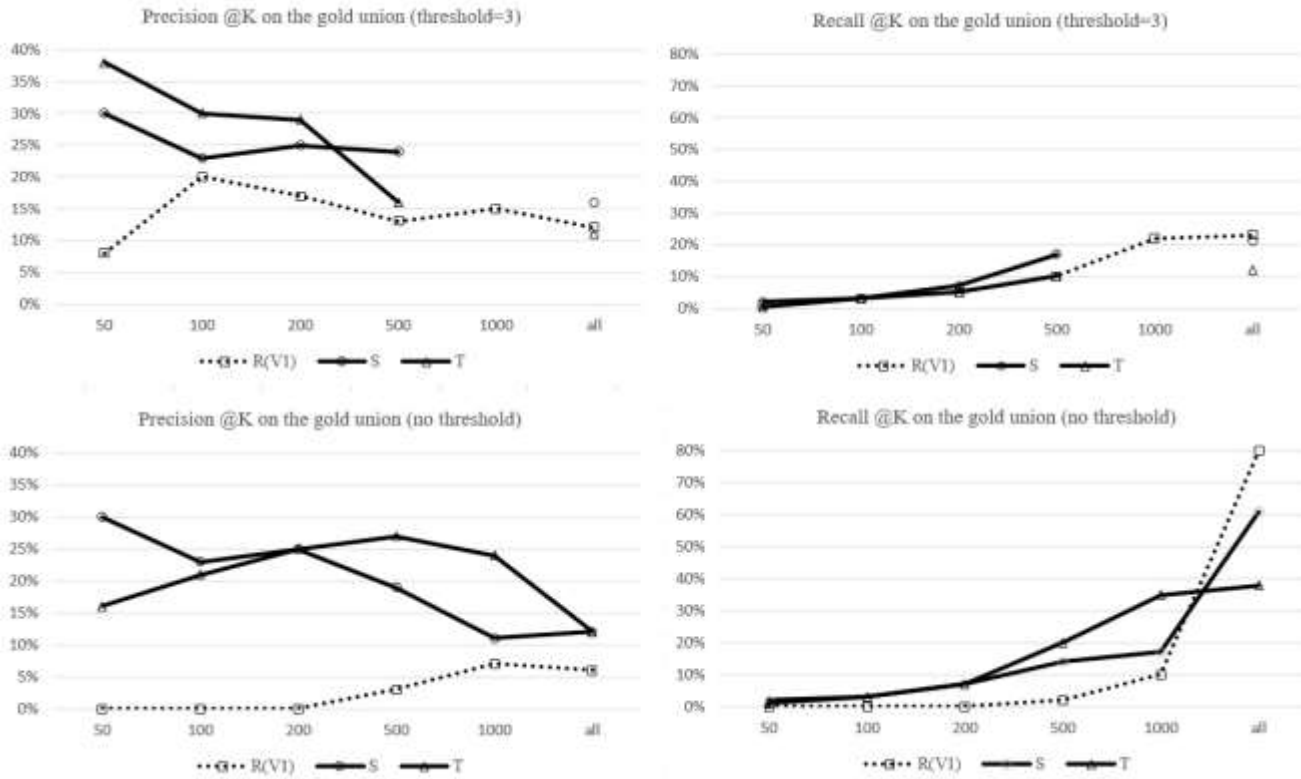


Fig. 4. Overall Lemmatized Evaluation Results on the Gold Union with and without Minimum Frequency Threshold.

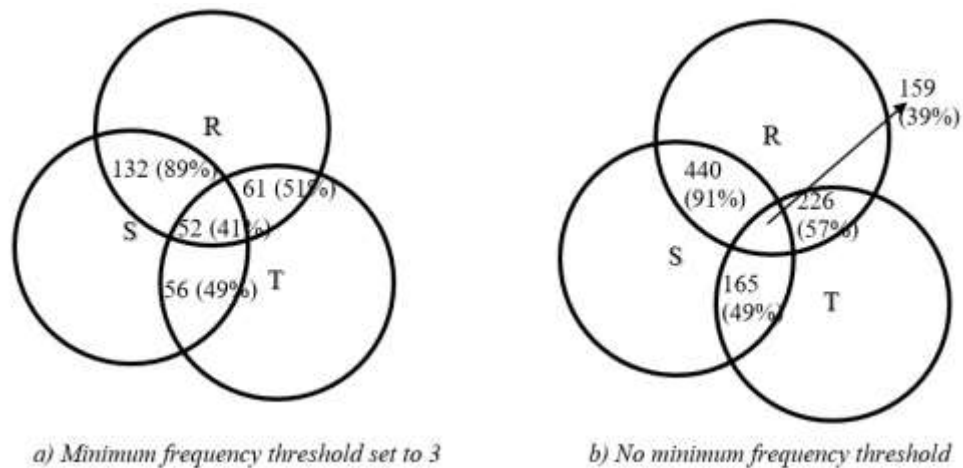


Fig. 5. Overlap between ATE Results per Tools and the Gold Standard.

Without the minimum frequency threshold, the situation with Sketch Engine and Termsuite gets somewhat reversed, i.e. the result is a draw at 200, while Termsuite beats Sketch Engine when the cut-off value is set to 500 or higher. While Sketch Engine performs similarly as in the scenario with the minimum frequency threshold, it can be concluded that Termsuite is affected by the threshold settings. Finally, when there is no cut-off value, the two tools perform the same. The results regarding recall are more stable when the minimum frequency threshold is set. When the minimum frequency threshold is removed, all the tools gain better recall scores at the expense of precision, except for Termsuite which has a 1% increase in precision alongside 26% increase in recall.

Since this paper presents an analysis of terminology extraction tools from a translator's perspective, and since Rainbow is, expectedly, the worst scoring tool regarding precision, average precisions are calculated only for the remaining two tools (Table IV).

Although the average precision at rank 1000 which takes recall into account is better for Termsuite (9%) than for Sketch Engine (4%), they both do the same, i.e. 9% according to the overall results.

Regarding MWUs, it is worth noting that in the scenario with the minimum frequency threshold applied, the number of recovered MWUs is 12, 7, and 5 for Rainbow, Sketch Engine, and Termsuite, respectively.

TABLE IV. AVERAGE PRECISIONS FOR SKETCH ENGINE AND TERMSUITE

	<i>avgP@500</i>	<i>avgP(+recall)@500</i>	<i>Total avgP(+recall)</i>
Sketch Engine	25%	4%	5%
Termsuite	28%	3%	3%
Sketch Engine (no threshold)	27%	3%	9%
Termsuite (no threshold)	28%	5%	9%

The average precisions at rank 500 are 25% and 28% for Sketch Engine and Termsuite, respectively. By looking at average precisions which take recall into account, it is evident that only 5% overall average precision is obtained for Sketch Engine versus 3% for Termsuite. In the scenario without the minimum frequency threshold, average precisions at rank 500 are 27% and 28% for Sketch Engine and Termsuite, respectively.

Another thing worth noting is that less than 2% of the terms extracted by Sketch Engine in the scenario with the threshold are MWUs, while that percentage goes up to 10% in the scenario with no threshold. Termsuite, on the other hand extracts pretty similar percentage of MWUs in both scenarios, i.e. 21% and 26%, respectively. Rainbow doubles the percentage from 37% in the first scenario to 63% in the second. On the other hand, even 50% of the MWU candidates extracted by Sketch Engine in the scenario with the threshold are correct, while those percentages are as low as 3.5 and 1.5% for Rainbow and Termsuite, respectively. The results on Rainbow assert the fact that due to data sparseness in small-sized specialized corpora statistical measures that use the candidate's frequency in a domain-specific corpus perform much better on SWTs than on MWTs [25]. A general conclusion can be made that linguistic approaches seem to be more suitable for translators as translators do not want to go through huge lists of term candidates and find only a handful of real terms. Although the performance of Sketch Engine and Termsuite is competitive, results speak slightly in favor of Termsuite with German as the language and Brexit as the domain. Regarding the overlap in the correct terms between Sketch Engine and Termsuite, there seems to be potential in combining their outputs.

V. CONCLUSION AND FUTURE WORK

The research described in this paper is conducted on the German corpora. The study does not propose a novel approach to automatic terminology extraction, but compares performance of three well-known extraction methods under the same experimental settings.

Due to the differences in corpus selection, evaluation methodology, and scope of TCs included in the evaluation, comparisons of various research results are often intractable. One of the goals set for this research was to create a gold standard and thus facilitate performance comparisons of various terminology extraction tools. One of the strengths of the study presented in this paper is the fact that the gold standard is compiled by two domain specialists as this is a more realistic setting than having a terminologist at hand when doing terminology extraction for translation purposes. Both the union and intersection of the two lists compiled by domain specialists are used in the experiments. Although having two evaluators approve the term in order to include it in the gold standard somewhat improves recall for lower levels, it reduces the size of the gold standard, and consequently precision for at least 6%. The analysis conducted on the gold union reveals that altogether only three POS tags for unigrams and two POS patterns for bigrams account for over 86% of the terms. These tags and patterns are included in the list of eight most important patterns provided by [15]. Precision could thus be potentially improved by restricting the rules. A cut-off value of 500 per category is opted for since ATE systems produce significant amounts of noise and users in the role of translators are mostly unwilling to scan through TC lists. Another strength of this research is the fact that the gold standard is based on the same corpus of the exact same size which is used for testing purposes.

To conclude, the results confirm that fully automatic terminology extraction is still out of reach for computers. The choice of method should therefore depend on whether the application puts more importance on the precision or recall. In general, if the extracted lists are to be checked manually, precision should be considered more important to avoid the task being too tedious. Since terms are inherently semantically defined, the final confirmation of an expression's term status still has to be done manually by domain specialists.

There are several directions which open up for future work. In order to get more meaningful results, the size of the focus corpus should be increased. This has not been done for the purpose of this research in order to have both manual and automatic extraction conducted on the same corpus, which would not be feasible with a corpus greater in size. Human evaluators could be asked to judge the TCs which are, perhaps mistakenly, not included in the gold standard. Furthermore, besides testing other tools, the combination of different ATE results or a voting mechanism could be employed. From the results presented in this paper, there exists some potential in combining Sketch Engine and Termsuite outputs. In the future, the work will be extended with domain-specific terminology in fast developing domains, e.g. the Information and Communication Technology (ICT) domain and different issues will be highlighted which occur when the corpus is compiled by different authors in languages which do not have a harmonized terminology and thus exhibit inconsistencies at the lexical level.

REFERENCES

- [1] Z. Zhang, J. Iria, C. Brewster, and F. Ciravegna, "A comparative evaluation of term recognition algorithms," *Proc. 6th Int. Conf. Lang. Resour. Eval. Lr.* 2008, pp. 2108–2113, 2008.
- [2] Z. Zhang, J. Gao, and F. Ciravegna, "JATE 2.0: Java Automatic Term Extraction with Apache Solr," *Proc. 10th Int. Conf. Lang. Resour. Eval. Lr.* 2016, pp. 2262–2269, 2016.
- [3] N. A. Astrakhantsev, "ATR4S: toolkit with state-of-the-art automatic terms recognition methods in Scala," *Lang. Resour. Eval.*, vol. 52, no. 3, pp. 853–872, 2018.
- [4] A. Repar, V. Podpečan, A. Vavpetič, N. Lavrač, and S. Pollak, "TermEnsembler: An ensemble learning approach to bilingual term extraction and alignment," *Int. J. Theor. Appl. Issues Spec. Commun.*, no. January, 2019.
- [5] K. Heylen and D. De Hertog, "Automatic Term Extraction," in *Handbook of Terminology*, 2015, pp. 276–287.
- [6] G. Thurmaier, "Making Term Extraction Tools Usable," in *Proceedings of EAMT-CLAW*, 2003.
- [7] N. Astrakhantsev, D. G. Fedorenko, and D. Y. Turdakov, "Methods for automatic term recognition in domain-specific text collections: A survey," *Program. Comput. Softw.*, vol. 41, no. 6, pp. 336–349, 2015.
- [8] C. Lang, R. Schneider, and K. Suchowolec, "Extracting Specialized Terminology from Linguistic Corpora," *Gramm. Corpora*, pp. 425–434, 2018.
- [9] M. L. Homme and L. Benali, "Definition of an evaluation grid for term-extraction software," *Terminology*, vol. 3, no. 2, pp. 291–312, 1996.
- [10] G. Dođru, "Automatic Term Extraction from Turkish to English Medical Corpus," in *Computational and Corpus-based Phraseology*, 2019, pp. 157–166.
- [11] R. Nazar, "Distributional analysis applied to terminology extraction," *Terminol. Int. J. Theor. Appl. Issues Spec. Commun.*, vol. 22, no. 2, pp. 141–170, 2016.
- [12] K. Kageura and B. Umino, "Methods of Automatic Term Recognition: A Review," *Terminol. Int. J. Theor. Appl. Issues Spec. Commun.*, vol. 3, no. 2, pp. 259–289, 1996.
- [13] G. Dođru, A. Martín, and A. Aguilar-amat, "Parallel Corpora Preparation for Machine Translation of Low-Resource Languages: Turkish to English Cardiology Corpora," in *Proceedings of the LREC 2018 Workshop 'Multilingual BIO: Multilingual Biomedical Text Processing'*, 2018, pp. 12–15.
- [14] J. Vivaldi, "Evaluation of terms and term extraction systems: A practical approach," *Terminology*, vol. 13, no. 2, pp. 225–248, 2007.
- [15] A. Rigouts Terry, V. Hoste, and E. Lefever, "A Gold Standard for Multilingual Automatic Term Extraction from Comparable Corpora: Term Structure and Translation Equivalents," in *11th International Conference on Language Resources and Evaluation (LREC 2018)*, 2018.
- [16] A. Gojun, U. Heid, B. Weissbach, C. Loth, and I. Mingers, "Adapting and evaluating a generic term extraction tool," *Proc. 8th Int. Conf. Lang. Resour. Eval. Lr.* 2012, pp. 651–656, 2012.
- [17] A. Šajatović, M. Buljan, J. Šnajder, and B. Dalbelo Bašić, "Evaluating Automatic Term Extraction Methods on Individual Documents," in *Proceedings of the Joint Workshop on Multiword Expressions and WordNet (MWE-WN 2019)*, 2019, vol. 0, pp. 149–154.
- [18] D. Inkpen, T. Sima Paribakht, F. Farahnaz, and A. Ehsan, "Term Evaluator: A Tool for Terminology Annotation and Evaluation," *Int. J. Comput. Linguist. Appl.*, vol. 7, no. 2, pp. 145–165, 2016.
- [19] P. Schone and D. Jurafsky, "Is knowledge-free induction of multiword unit dictionary headwords a solved problem?," *Proc. 2001 Conf. Empir. Methods Nat. Lang. Process.*, pp. 100–108, 2001.
- [20] M. Brkic Bakaric and I. Lalli Pacelat, "Parallel Corpus of Croatian-Italian Administrative Texts," in *2nd Workshop on Human-Informed Translation and Interpreting Technology (Hit-IT 2019)*, 2019, pp. 11–18.
- [21] H. Costa, A. Zaretskaya, G. Corpas, and M. Seghiri, "Nine terminology extraction tools Are they useful for translators?," *Multiling. #159*, vol. 27, no. 3, pp. 14–20, 2016.
- [22] D. Bourigault, M. De Recherche, A. Machado, and C. Jacquemin, "Term Extraction + Term Clustering: An Integrated Platform for Computer-Aided Terminology Components of the Platform for Computer-Aided Terminology," in *Ninth Conference of the European Chapter of the Association for Computational Linguistics*, 1999, pp. 15–22.

- [23] H. Nakagawa, "A Simple but Powerful Automatic Term Extraction Method," in COLING-02 on COMPUTERM 2002: second international workshop on computational terminology-Volume 14, 2002, pp. 1–7.
- [24] M. Hong, S. Fissaha, and J. Haller, "Hybrid filtering for extraction of term candidates from German technical texts," Conference TIA-2001, Nancy, 3 4 mai 2001 Hybrid, p. 10, 2001.
- [25] J. Schäfer, I. Rösiger, U. Heid, and M. Dorna, "Evaluating noise reduction strategies for terminology extraction," CEUR Workshop Proc., vol. 1495, pp. 123–131, 2015.
- [26] G. Lalić-Krstin and N. Silaški, "From Brexit to Bregret," English Today, vol. 34, no. 2, pp. 3–8, 2018.
- [27] K. Ivanova, U. Heid, S. S. I. Walde, A. Kilgarriff, and J. Pomikálek, "Evaluating a German sketch grammar: A case study on noun phrase case," Proc. 6th Int. Conf. Lang. Resour. Eval. Lr. 2008, pp. 2101–2107, 2008.
- [28] M. M. A. Gizi, "Word Formation in German Linguistics: Theoretical and Methodological Analysis," Open J. Mod. Linguist., vol. 08, no. 05, pp. 143–150, 2018.
- [29] U. Heid and A. Gojun, "Term candidate extraction for terminography and CAT : an overview of TTC," Proc. 15th EURALEX Int. Congr., pp. 585–594, 2012.
- [30] M. Jakubiček, A. Kilgarriff, V. Kovář, P. Rychlý, and V. Suchomel, "The TenTen Corpus Family," 7th Int. Corpus Linguist. Conf., pp. 125–127, 2013.
- [31] M. Jakubiček, A. Kilgarriff, V. Kovář, P. Rychlý, and V. Suchomel, "Finding Terms in Corpora for Many Languages with the Sketch Engine," pp. 53–56, 2015.
- [32] A. Kilgarriff, "Simple maths for keywords," in Proceedings of the Corpus Linguistics Conference, 2009.

Deep Learning Architectures and Techniques for Multi-organ Segmentation

Valentin Ogrea¹, Alexandru Dorobantiu², Remus Brad³

Faculty of Engineering
“Lucian Blaga” University
Sibiu, Romania

Abstract—Deep learning architectures used for automatic multi-organ segmentation in the medical field have gained increased attention in the last years as the results and achievements outweighed the older techniques. Due to improvements in the computer hardware and the development of specialized network designs, deep learning segmentation presents exciting developments and opportunities also for future research. Therefore, we have compiled a review of the most interesting deep learning architectures applicable to medical multi-organ segmentation. We have summarized over 50 contributions, most of which are more recent than 3 years. The papers were grouped into three categories based on the architecture: “Convolutional Neural Networks” (CNNs), “Fully Convolutional Neural Networks” (FCNs) and hybrid architectures that combine more designs - including “Generative Adversarial Networks” (GANs) or “Recurrent Neural Networks” (RNNs). Afterwards we present the most used multi-organ datasets, and we finalize by making a general discussion of current shortcomings and future potential research paths.

Keywords—Deep Learning; Multi-Organ Segmentation; Fully Convolutional Neural Networks (FCNs); Generative Adversarial Networks (GANs); Recurrent Neural Networks (RNNs)

I. INTRODUCTION

Medical imaging using Computed Tomography (CT), Magnetic Resonance (MR), ultrasound, X-ray, and so on, has become an essential part in detection, diagnosis, and treatment of diseases [1].

A new medicine branch, imaging and radiology was developed to train human experts that can interpret medical images and provide an accurate diagnosis. The training is challenging due to the complexity involved, but more importantly, the diagnosis process itself is a tedious and exhausting work that is further impacted by the large variations in pathology between different individuals. Therefore, the need for automated help grew larger as the medical imaging sector expanded, with use-cases like segmentation of medical images, delineating human organs or automated diagnosis being intensively studied using Deep Learning (DL) architectures.

Deep learning absorbs the feature engineering designed by human experts into a learning step [2]. Furthermore, deep learning needs only a set of training/testing data with minor pre-processing (if necessary), and then can extract the human body representations in an autonomous manner. Throughout different architectures, DL has demonstrated enormous potential in computer vision [3].

Multi-organ deep learning architectures could lend a helping hand in the field of radiation therapy, by the making the segmentation process faster and more robust [4]. Multi-organ segmentation also paves the way for automation processes that are generalized to the full body or to a large spectrum of diseases facilitating online adaptive radiotherapy and fulfilling medical image segmentation’s goal to become autonomous in reaching an accurate diagnosis in any medical imaging environment.

A. Segmentation Applications in the Medical Field

- Radiotherapy in cancer treatment. In radiotherapy, the need exists to control the radiation exposure of the target and healthy organs, so segmentation of organs at risk (OARs) could provide an important help to physicians [5].
- Automation. OARs and other clinical structures in the human body are manually segmented by physicians from medical images, which is difficult, tedious and time consuming [4]. Automating the segmentation process could help tremendously even if it will be only as a pre-step in the diagnosis (used for initial selection of cases or pathologies).
- Finding ROIs. Automatically finding regions could help while preparing for medical procedures or in applying specific procedures on highlighted regions.
- Computer Aided Diagnosis (CADx). To achieve this, a correct delineation of body structures is needed in the pipeline of any CADx systems. Accurate automatic segmentation could be used in non-invasive diagnosis scenarios and could be even deployed online.
- Mass detection. Detecting the mass of organs has as prerequisites a correct segmentation of the organ and the neighbouring surfaces
- Assistance in endoscopic procedures. Automatic segmentation provides help for physicians when executing endoscopic procedures and could be used also in the training phase of the human experts [6].

B. Summary of other Reviews in the same Knowledge Field

The deep learning knowledge base was described in papers written by Schmidhuber [2], LeCun et al. [3], Benuwa et al. [7] and Voulodimos et al. [8]. More recently, great articles were written by Serre et al. [9] and Alom et al. [10].

For a description of deep learning architectures specifically applied in the medical field, we would like to highlight works written by Litjens et al. [11], Shen et al. [1], Hesamian et al. [12], Zhou et al. [13], Ker et al. [14], Taghanaki et al. [15] and Lu et al. [16]. For details regarding GAN in medical image processing we have an article by Yi et al. [17] and for a review of unsupervised deep learning techniques we have a paper written by Raza et al. [18]. More recently, a comprehensive overview targeted towards multi-organ architectures was written by Lei et al. [4].

C. The Aim of this Study

This article discusses the most interesting deep learning architectures and techniques applicable to medical multi-organ segmentation. Targeted to DL-based medical image multi-organ segmentation, there are several objectives that we aimed to fulfil with this article:

- Categorize and summarize the latest research
- Present the most important contributions and identify the current challenges
- Provide an overview of existing medical benchmarks
- Indicate future trends and solutions for the identified challenges

D. Contents of the Survey

The paper summarizes over 50 contributions, most of which are more recent than 3 years.

In our process of data searching and gathering, we used several different sources which include arXiv, Google Scholar, PubMed, ISBI, MICCAI or SPIE Medical Imaging. Search keywords included medical segmentation, multi-organ, fully convolutional neural network, and other architectures related to deep learning. The final end-result contains at least 30 articles that describe architectures for single organ segmentation and over 60 articles that detail deep learning techniques for multi-organ delineation.

To make this survey as recent as possible, we have selected works that were mostly published after 2017, while still including older papers that had a big impact in the research field. The most recent date of publication was set to June 1st, 2020, which excluded papers newer than that date.

The bulk of the reviewed works are in Sections II, III and IV and are grouped into three categories – CNNs, FCNs, and

hybrid – according to the architecture and which network design is most prominent. The hybrid category has also 3 sub-sections: GANs, RNNs and fully hybrid approaches. For each architecture classification we presented a small description of the methods and highlighted the most relevant works that were related to multi-organ segmentation. For each included paper we listed the reference, the human structures that were used in training and a summary of their important features and achievements. In Section V we present the most used multi-organ datasets correlated to the human structures that they target. We finalize with a conclusion regarding the future of the research in this subject.

II. ARCHITECTURES APPLICABLE TO MEDICAL MULTI-ORGAN SEGMENTATION BASED ON CNNs

A CNN is a sub-genre of deep neural networks [12] that are based on fully connected layers. A layer is made up by more neurons, and each one of these is linked to every neuron from the subsequent layer. A CNN architecture applies a convolution in at least one of its layers. Except for the initial layer, which is linked to the medical image, the input of each layer represents the output of the subsequent layer. Each one of these can perform specific tasks like convolution, pooling, loss calculation while different architectures make use of these layers in differing techniques.

Considering the input image's proportions and the dimension of the convolutional kernels, CNNs can be grouped into three categories. In 2D architectures the medical image is sliced into several 2D images which are fed to the CNN. 2.5D architectures still use 2D kernels, but the network is fed with several patches that are cut from a 3D medical image along the three orthogonal axes. The final category boasts 3D kernels which can extract the full information from a 3D medical image. The major downside of 3D architectures is the computational and memory requirements which are considered large even using the most up-to-date hardware.

In Table I we present a list of papers that employ CNNs for segmentation in a multi-organ setup. Even though they do not result in a segmentation, papers that present object detection methods in multi-organ scenarios were included in this list. The reason is that they could be used as a pre-step to the actual segmentation by generating regions of interest used to improve the accuracy of the end-result.

TABLE I. CNN MULTI-ORGAN SEGMENTATION PAPERS

Ref.	Site	Important features
[19]	Brain, Breast and Cardiac	The authors demonstrate that a 2.5D CNN can be trained in a multi-modality (MRI and CT) scenario to segment tissues three different human structures. The results were comparable as in using three different architectures for each segmentation task.
[20]	Abdomen	The authors proposed an architecture that segments several abdominal organs using a two-step approach. Organ localization obtained via a multi-atlas technique followed by training a 3D CNN that classifies the voxels to the corresponding organ [20]. They also use thresholding as a pre-processing step.
[21]	Chest, cardiac, abdomen	The authors trained a 2.5D CNN that identifies if target human structures are present in input images (CT) [21]. Bounding boxes can also be placed around the found targeted structures.
[22]	Brain, abdomen	The authors propose several methods that can improve the segmentation accuracy: supervised or unsupervised image enhancement and a novel loss function [22].
[23]	Thorax-abdomen	This work presents a 2.5 CNN trained for localization of several human structures in CT images [23].
[24]	Pelvic organs	The authors propose a novel hierarchical dilated CNN. The novelty is that they propose a multi-scale architecture comprised of several modules working with different resolutions [24].
[25]	Torso – 17 organs	The authors propose an architecture for organ localization and 3D bounding boxes generation [25].
[26]	Head and neck	The article proposes a multi-organ segmentation architecture that cascades three CNNs followed by majority voting [26].
[27]	Head and body	The authors propose an architecture for organ localization based on a 3D CNN that also improves the localization performance on small organs [27].

III. ARCHITECTURES APPLICABLE TO MEDICAL MULTI-ORGAN SEGMENTATION BASED ON FCNS

CNNs can classify each individual voxel from a medical image, but this approach has a huge drawback. Because the neighbouring patches on which convolutions are calculated have overlapping voxels, the same calculations are done multiple times with performance penalties. To counter this major issue, Long et al. [28] proposed the “Fully convolutional network” where the size of the predicted image is increased to match the size of the input image by using a transposed

convolution layer. Ronneberger et al. [29] proposed the U-Net network that has a contracting path with layers that include convolutions, max pooling and Rectified Linear Unit (RELU) [30] and an expanding path that involves up-convolutions and concatenations with high-resolution features from the contracting path [29]. Çiçek et al. [31] implemented the first 3D U-Net design while Milletari et al. [32] improved the U-Net architecture by adding residual blocks and a dice loss layer.

In Table II we present a list of papers that employ FCNs for segmentation in a multi-organ setup.

TABLE II. FCN MULTI-ORGAN SEGMENTATION PAPERS

Ref.	Site	Important features
[33]	Liver and heart	The authors propose a 3D FCN enhanced by a deep supervision technique [33]. The architecture is validated against heart and liver datasets (not a full-blown multi-organ implementation).
[6]	Abdomen	The article proposed an approach on segmenting 4 abdominal organs using an FCN that employs “dilated convolution units with dense skip connections” [6].
[34]	Abdomen	In this article the authors prove that a “multi-class 3D FCN trained for seven abdominal structures can achieve competitive segmentation results, while avoiding the need training organ-specific models” [34]. They proposed an architecture comprised of two FCNs, with the first delineating a candidate region, while the later uses that as input for the final segmentation.
[35]	Esophagus, Trachea, Heart, Aorta	The authors propose “two collaborative architectures to jointly segment multiple organs” [35]. The first network will learn anatomical constraints employing also conditional random fields, while its output will be used by the second network for guiding and refining the segmentation.
[36]	Liver, spleen, kidneys	The authors propose a deep 3D FCN for organ segmentation that is enhanced using a “time-implicit multi-phase evolution method” [36].
[37]	Torso and special regions: lumen and stomach content	The authors propose a 2.5D FCN architecture trained on CTs. The algorithm uses a fusion method for the final 3D segmentation. They summarize the algorithm as “multiple 2D proposals followed by 3D integration” [37].
[38]	Liver, Left kidney	In this paper, the authors propose an improvement of their previous segmentation architectures by adding an organ localization module [38].
[39]	Gastro-intestinal tract	The authors present an implementation of a Dense V-Net architecture in a multi-organ setup while showing that their proposed “dense connections and the multi-scale structure” [39] produce better segmentation results.
[40]	Abdomen	The paper describes an implementation of a 3D U-Net for multi-organ CT segmentation [40]. The authors obtained a combined dice of 89.3% in testing 7 organs.

Ref.	Site	Important features
[41]	Abdomen	The authors present an architecture that is based on a “multi-scale pyramid of stacked 3D FCNs” [41]. The results are obtained by taking the predictions of a lower-resolution 3D FCN up-sampling, cropping them and afterwards concatenating them with the inputs of a 3D FCN that utilizes a higher resolution which will generate a final segmentation.
[42]	Abdomen	The authors argue that the results of multi-organ segmentation using FCNs depend on the architecture, but also are heavily influenced by the chosen loss function [42]. They also evaluate the loss function’s influence in multi-organ segmentation scenarios.
[43]	Abdomen	The authors propose a cascaded approach that uses two 3D FCNs. The first architecture defines a candidate region, while the second focuses on the details and provides the final segmentation. The authors argue that their “approach reduces the number of voxels the second FCN must classify to ~10%” [43].
[44]	Torso	The paper presents three 3D FCN architectures and surveys their results of multi-organ segmentation in the human torso. The dice scores average between 0.91 and 0.98 for 6 covered organs.
[45]	Head and neck	The authors present an architecture based on a 3D U-Net that is tested against a head and neck dataset. The results were mixed, with fair segmentation scores for 7 organs out of 11, but with low results for the other organs.
[46]	Brain, Abdomen	The authors propose an FCN architecture [46] that outperforms the initial U-Net implementation in several segmentation tasks for brain or abdomen. The results have a dice percentage between 83.42% and 96.57% for several abdomen organs.
[47]	Chest	The authors propose an architecture based on two cascaded networks.
[48]	Abdomen	The authors present a novel architecture that improves the segmentation using a transfer learning scheme. 3D U-Nets are used in a general approach or single organ approach with transfer learning between them. Furthermore, probabilistic atlases are used to estimate the location of the organs.
[49]	Abdomen	The authors present an architecture for segmentation in a multi-organ scenario consisting of a “2D U-Net localization network and a 3D U-Net segmentation network” [49]. Compared to other architectures, the authors results are better for several organs like prostate and bladder.
[50]	Abdomen	The authors propose a two-step architecture. The first step contains 2D networks with reverse connections that detect features. These features are afterwards merged with the original image to “enhance the discriminative information for the target organs” [50] and are used as input for the final segmentation network.
[51]	Gland	The paper describes two Dense U-Nets used for segmentation of several gland types.
[52]	Abdomen	The authors propose a multi-organ segmentation architecture based on 3D convolution [52]. Their design obtained an average Dice score of 83.7% for 6 abdominal organs in their targeted dataset.
[53]	Thorax	The authors propose an architecture where a 3D U-Net localizes each target organ. Afterwards, cropped images with one organ serve as input to several individual 3D U-Net segmentation networks and as a final step the individual results are merged for a global segmentation result.
[54]	Thorax and abdomen	The paper describes in detail the SegTHOR [54] multi-organ dataset and present a segmentation framework based on U-Net.
[55]	Thorax and abdomen	The paper proposes an architecture for segmentation of the SegTHOR [54] multi-organ dataset that consists of two 3D V-Net working on different resolutions (one for organ localization and one for segmentation refinement). Their approach ranked first in the initial phase of the SEGTHOR challenge.
[56]	Thorax and abdomen	The authors propose an improvement to the U-Net and obtain a “uniform U-like encoder-decoder segmentation architecture” [56]. The architecture ranked second on the initial phase of the SEGTHOR challenge.
[57]	Thorax and abdomen	The authors propose a simplified version of the Dense V-net model with postprocessing that improve the organ segmentation results.
[58]	Thorax	The paper proposes a multi-organ segmentation architecture that contains “dilated convolutions and aggregated residual connections in a U-Net styled network” [58].
[59]	Abdomen, torso	The paper proposes a 3D U-Net like architecture [59] that is validated on 5 different organs.
[60]	Abdomen	The authors propose a multi-class segmentation architecture based on U-Net [60]. Their design has similar results to other approaches on 4 organs but with superior dice scores for the intestine.
[61]	Abdomen	The authors propose a 3D U-Net architecture tested in a multi-organ segmentation scenario.
[62]	Abdomen	The authors propose an architecture consisting of a 3D U-Net that is enhanced by graph-cut post-processing [62] tested in a multi-organ segmentation scenario.
[63]	Abdomen	The authors present a “pyramid-input pyramid-output” [63] architecture that can be trained in a multi-scale and partially labeled scenario. In order to discriminate the features in differing scales, they designed an “adaptive weighting layer to fuse the outputs in an automatic fashion” [63]

IV. ARCHITECTURES APPLICABLE TO MEDICAL MULTI-ORGAN SEGMENTATION BASED ON HYBRID METHODS

As the DL field is expanding, new and exciting network architectures are developed. At the same time, the possibilities of improving the existing segmentation networks are shrinking. Therefore, to overcome these challenges, hybrid approaches are used more extensively. These hybrid methods involve using several network designs in the same architecture serving different functional purposes. We have divided the hybrid approaches into segmentation architectures enriched with GANs, enriched with RNNs and fully hybrid approaches.

A. Hybrid Methods Employing GANs

A GAN is a type of machine learning network designed by Goodfellow et al. [64]. These networks are taught to be able to generate new data that shares the same characteristics as a provided initial training set. In Table III we present a list of papers that propose GAN based hybrid multi-organ architectures.

B. Hybrid Methods Employing RNNs

A Recurrent Neural Network (RNN) is a type of machine learning network that generalizes the feedforward neural network architecture and has hidden states that act as an internal memory. Empowered with these connections the RNNs can memorize the patterns from previous inputs. These architectures are applied mostly to time series predictions or speech recognition. But because medical images are usually comprised of multiple adjacent slices with correlating information between them, RNNs can be employed in hybrid scenarios to improve the segmentation results. In Table IV we present a list of papers that propose RNN based hybrid multi-organ architectures.

TABLE III. GAN MULTI-ORGAN SEGMENTATION PAPERS

Ref.	Site	Important features
[65]	Brain, liver, cells	The authors propose an architecture made by “a generative, a discriminative, and a refinement network” [65] based on U-Net. The final semantic segmentation masks are composed by the output of the three networks.
[66]	Thorax	The paper describes an architecture that trains a set of generator networks (based on U-Net) and a set of discriminators (based on FCNs). “The generator and discriminator compete against each other in an adversarial learning process to produce the optimal segmentation map of multiple organs” [66].
[67]	Thorax	The authors propose a hybrid architecture that first generates a “global localization map by minimizing a reconstruction error within an adversarial framework [67]. Afterwards, the localization map guides an FNC for multi-organ segmentation.
[68]	Abdomen	The authors present a hybrid architecture that combines GAN based image synthesis methods with a deep attention strategy that learns discriminative features for organ segmentation.
[69]	Abdomen	The paper describes a hybrid architecture that combines cascaded convolutional networks with adversarial networks to alleviate data scarcity limitations.

TABLE IV. RNN MULTI-ORGAN SEGMENTATION PAPERS

Ref.	Site	Important features
[70]	Optic disc, cell nuclei, left atrium	The authors present a hybrid architecture that combines a CNN with an RNN.
[71]	Abdomen – small organs	This paper presents an architecture in which a recurrent module “repeatedly converts the segmentation probability map from the previous iteration as spatial weights and applies these weights to the current iteration” [71].
[72]	Blood vessel, skin cancer, lungs	The article presents a hybrid architecture based on U-Net and RNN where the “feature accumulation with recurrent residual convolutional layers” [72] provides better segmentation end results.
[73]	Abdomen	The paper proposes an attention gate model that can be integrated into neural networks.” Models trained with AGs implicitly learn to suppress irrelevant regions in an input image” [73].
[74]	Vertebrae, liver	The authors present a hybrid architecture that consists of a U-Net-like network enhanced with bidirectional C-LSTM [74].

C. Fully Hybrid and Generic Segmentation Improvement Methods

In Table V we present hybrid methods that do not fit in any previous category and generic segmentation improvement methods in multi-organ scenarios.

TABLE V. HYBRID MULTI-ORGAN SEGMENTATION PAPERS

Ref.	Site	Important features
[75]	Torso and abdomen	The authors present a sample selection method [75] that improves the training of neural networks. The method is tested in a multi-organ segmentation scenario.
[76]	Abdomen	The authors investigate the “effectiveness of learning from multiple modalities to improve the segmentation accuracy” [76].
[77]	Abdomen	The authors propose an architecture in which an initial model is trained on annotated data to generate pseudo labels that enrich the training data for a second model that will do a final segmentation.
[78]	Abdomen	The authors propose an architecture that incorporates anatomical domain knowledge on abdominal organ sizes to guide and improve the training process.
[79]	Retina, lungs	The paper describes an architecture that “embeds edge-attention representations to guide the process of segmentation” [79].
[80]	Heart, gland, lymph node	The authors propose an architecture that firstly decomposes the segmentation problem into several sub-problems, then applies DL modules onto each sub-problem and lastly integrates the results to obtain the final segmentation.
[81]	Abdomen, heart, brain	The authors present an architecture that tries “to integrate local features with their corresponding global dependencies” [81] by using a guided self-attention mechanism.

V. ARCHITECTURES APPLICABLE TO MEDICAL MULTI-ORGAN SEGMENTATION BASED ON HYBRID METHODS

There are multiple collaborative initiatives with medical organizations to obtain better and larger datasets usable for organ segmentation. But despite all these efforts, the amount of annotated data that is at the disposal of DL scientists is still low. There are solutions in combining several datasets of parts of the human body, but different modalities or scales reduce considerably their usage in multi-organ segmentation scenarios. In Table VI we present several datasets that try to overcome these challenges and are usable in multi-organ validation of segmentation architectures.

TABLE VI. MULTI-ORGAN DATASETS

Year	Dataset	Modality	Organ
2015	“MICCAI Multi-Atlas Labeling Beyond the Cranial Vault” [82]	CT	Abdomen
2015	“MICCAI Challenge - Head and Neck Auto Segmentation Challenge” [83]	CT	Head and Neck
2017	“AAPM Thoracic Auto-segmentation Challenge” [84]	CT	Thorax
2018	“Medical Segmentation Decathlon” [85]	CT & MRI	Head, Thorax and Abdomen
2019	“CHAOS - Combined (CT-MR) Healthy Abdominal Organ Segmentation” [86]	CT & MRI	Abdomen
2019	“SegTHOR Challenge: Segmentation of Thoracic Organs at Risk in CT Images” [54]	CT	Thorax
2019	“Annotations for Body Organ Localization based on MICCAI LITS Dataset” [87]	CT	Abdomen

VI. FINAL CONCLUSIONS

This paper is an overview of deep learning methods in medical multi-organ segmentation. Based on most of the surveyed works, FCNs are the most used architectures used to perform multi-organ automatic delineating. As the amount of research related to FCNs is huge, the possibilities to improve them is dwindling. So, more recently, hybrid methods, be it with the use of GANs, RNNs or completely new architectures are gaining much more attention. We speculate that in the future the number of available datasets will grow, so the usage of FCNs or hybrid networks will become more straightforward. Another un-charted territory is the usage of more intelligent semi-supervised methods, the usage of fully unsupervised methods or reinforcement learning.

REFERENCES

[1] D. Shen, G. Wu, and H.-I. Suk, “Deep learning in medical image analysis,” *Annu. Rev. Biomed. Eng.*, vol. 19, no. 1, pp. 221–248, Jun. 2017, doi: 10.1146/annurev-bioeng-071516-044442.

[2] J. Schmidhuber, “Deep learning in neural networks: An overview,” *Neural Networks*, vol. 61, pp. 85–117, Jan. 2015, doi: 10.1016/j.neunet.2014.09.003.

[3] Y. LeCun, Y. Bengio, and G. Hinton, “Deep learning,” *Nature*, vol. 521, no. 7553, pp. 436–444, May 2015, doi: 10.1038/nature14539.

[4] Y. Lei et al., “Deep learning in multi-organ segmentation,” arXiv:2001.10619 [physics], Jan. 2020. Available: <http://arxiv.org/abs/2001.10619>.

[5] B. Ibragimov and L. Xing, “Segmentation of organs-at-risks in head and neck CT images using convolutional neural networks,” *Med. Phys.*, vol. 44, no. 2, pp. 547–557, Feb. 2017, doi: 10.1002/mp.12045.

[6] E. Gibson et al., “Towards image-guided pancreas and biliary endoscopy: automatic multi-organ segmentation on abdominal CT with dense dilated networks,” in *Medical Image Computing and Computer Assisted Intervention – MICCAI 2017*, vol. 10433, M. Descoteaux, L. Maier-Hein, A. Franz, P. Jannin, D. L. Collins, and S. Duchesne, Eds. Cham: Springer International Publishing, 2017, pp. 728–736.

[7] B. B. Benuwa, Y. Z. Zhan, B. Ghansah, D. K. Wornyo, and F. Banaseka Kataka, “A review of deep machine learning,” *JERA*, vol. 24, pp. 124–136, Jun. 2016, doi: 10.4028/www.scientific.net/JERA.24.124.

[8] A. Voulodimos, N. Doulamis, A. Doulamis, and E. Protopapadakis, “Deep learning for computer vision: A brief review,” *Computational Intelligence and Neuroscience*, vol. 2018, pp. 1–13, 2018, doi: 10.1155/2018/7068349.

[9] T. Serre, “Deep learning: The good, the bad, and the ugly,” *Annu. Rev. Vis. Sci.*, vol. 5, no. 1, pp. 399–426, Sep. 2019, doi: 10.1146/annurev-vision-091718-014951.

[10] M. Z. Alom et al., “A state-of-the-art survey on deep learning theory and architectures,” *Electronics*, vol. 8, no. 3, p. 292, Mar. 2019, doi: 10.3390/electronics8030292.

[11] G. Litjens et al., “A survey on deep learning in medical image analysis,” *Medical Image Analysis*, vol. 42, pp. 60–88, Dec. 2017, doi: 10.1016/j.media.2017.07.005.

[12] M. H. Hesamian, W. Jia, X. He, and P. Kennedy, “Deep learning techniques for medical image segmentation: Achievements and challenges,” *J Digit Imaging*, vol. 32, no. 4, pp. 582–596, Aug. 2019, doi: 10.1007/s10278-019-00227-x.

[13] T. Zhou, S. Ruan, and S. Canu, “A review: Deep learning for medical image segmentation using multi-modality fusion,” *Array*, vol. 3–4, p. 100004, Sep. 2019, doi: 10.1016/j.array.2019.100004.

[14] J. Ker, L. Wang, J. Rao, and T. Lim, “Deep learning applications in medical image analysis,” *IEEE Access*, vol. 6, pp. 9375–9389, 2018, doi: 10.1109/ACCESS.2017.2788044.

[15] S. A. Taghanaki, K. Abhishek, J. P. Cohen, J. Cohen-Adad, and G. Hamarneh, “Deep semantic segmentation of natural and medical images: A review,” arXiv:1910.07655 [cs, eess], Jun. 2020. Available: <http://arxiv.org/abs/1910.07655>.

[16] L. Lu, X. Wang, G. Carneiro, and L. Yang, “Deep learning and convolutional neural networks for medical imaging and clinical informatics,” 2019.

[17] X. Yi, E. Walia, and P. Babyn, “Generative adversarial network in medical imaging: A review,” *Medical Image Analysis*, vol. 58, p. 101552, Dec. 2019, doi: 10.1016/j.media.2019.101552.

[18] K. Raza and N. K. Singh, “A tour of unsupervised deep learning for medical image analysis,” arXiv:1812.07715 [cs, eess], Dec. 2018. Available: <http://arxiv.org/abs/1812.07715>.

[19] P. Moeskops et al., “Deep learning for multi-task medical image segmentation in multiple modalities,” arXiv:1704.03379 [cs], vol. 9901, pp. 478–486, 2016, doi: 10.1007/978-3-319-46723-8_55.

[20] M. Larsson, Y. Zhang, and F. Kahl, “Robust abdominal organ segmentation using regional convolutional neural networks,” in *Image Analysis*, vol. 10270, P. Sharma and F. M. Bianchi, Eds. Cham: Springer International Publishing, 2017, pp. 41–52.

[21] B. D. de Vos, J. M. Wolterink, P. A. de Jong, T. Leiner, M. A. Viergever, and I. Išgum, “ConvNet-based localization of anatomical structures in 3-D medical images,” *IEEE Trans. Med. Imaging*, vol. 36, no. 7, pp. 1470–1481, Jul. 2017, doi: 10.1109/TMI.2017.2673121.

[22] G. Wang et al., “Interactive medical image segmentation using deep learning with image-specific fine-tuning,” *IEEE Trans. Med. Imaging*, vol. 37, no. 7, pp. 1562–1573, Jul. 2018, doi: 10.1109/TMI.2018.2791721.

[23] G. E. Humpire-Mamani, A. A. A. Setio, B. van Ginneken, and C. Jacobs, “Efficient organ localization using multi-label convolutional

- neural networks in thorax-abdomen CT scans,” *Phys. Med. Biol.*, vol. 63, no. 8, p. 085003, Apr. 2018, doi: 10.1088/1361-6560/aab4b3.
- [24] S. Zhou et al., “Fine-grained segmentation using hierarchical dilated neural networks,” in *Medical Image Computing and Computer Assisted Intervention – MICCAI 2018*, vol. 11073, A. F. Frangi, J. A. Schnabel, C. Davatzikos, C. Alberola-López, and G. Fichtinger, Eds. Cham: Springer International Publishing, 2018, pp. 488–496.
- [25] X. Zhou et al., “Automatic anatomy partitioning of the torso region on CT images by using a deep convolutional network with majority voting,” in *Medical Imaging 2019: Computer-Aided Diagnosis*, San Diego, United States, Mar. 2019, p. 34, doi: 10.1117/12.2512651.
- [26] T. Zhong, X. Huang, F. Tang, S. Liang, X. Deng, and Y. Zhang, “Boosting-based cascaded convolutional neural networks for the segmentation of CT organs-at-risk in nasopharyngeal carcinoma,” *Med. Phys.*, vol. 46, no. 12, pp. 5602–5611, Dec. 2019, doi: 10.1002/mp.13825.
- [27] X. Xu, F. Zhou, B. Liu, D. Fu, and X. Bai, “efficient multiple organ localization in ct image using 3d region proposal network,” *IEEE Trans. Med. Imaging*, vol. 38, no. 8, pp. 1885–1898, Aug. 2019, doi: 10.1109/TMI.2019.2894854.
- [28] J. Long, E. Shelhamer, and T. Darrell, “Fully convolutional networks for semantic segmentation,” in *2015 IEEE Conference on Computer Vision and Pattern Recognition (CVPR)*, Boston, MA, USA, Jun. 2015, pp. 3431–3440, doi: 10.1109/CVPR.2015.7298965.
- [29] O. Ronneberger, P. Fischer, and T. Brox, “U-Net: Convolutional networks for biomedical image segmentation,” arXiv:1505.04597 [cs], May 2015. Available: <http://arxiv.org/abs/1505.04597>.
- [30] V. Nair and G. E. Hinton, “Rectified linear units improve restricted boltzmann machines,” in *Proceedings of the 27th International Conference on International Conference on Machine Learning*, Madison, WI, USA, 2010, pp. 807–814.
- [31] Ö. Çiçek, A. Abdulkadir, S. S. Lienkamp, T. Brox, and O. Ronneberger, “3D U-Net: Learning dense volumetric segmentation from sparse annotation,” arXiv:1606.06650 [cs], Jun. 2016. Available: <http://arxiv.org/abs/1606.06650>.
- [32] F. Milletari, N. Navab, and S.-A. Ahmadi, “V-Net: Fully convolutional neural networks for volumetric medical image segmentation,” arXiv:1606.04797 [cs], Jun. 2016. Available: <http://arxiv.org/abs/1606.04797>.
- [33] Q. Dou et al., “3D deeply supervised network for automated segmentation of volumetric medical images,” *Medical Image Analysis*, vol. 41, pp. 40–54, Oct. 2017, doi: 10.1016/j.media.2017.05.001.
- [34] H. R. Roth et al., “Hierarchical 3D fully convolutional networks for multi-organ segmentation,” arXiv:1704.06382 [cs], Apr. 2017. Available: <http://arxiv.org/abs/1704.06382>.
- [35] R. Trullo, C. Petitjean, D. Nie, D. Shen, and S. Ruan, “Joint segmentation of multiple thoracic organs in ct images with two collaborative deep architectures,” in *Deep Learning in Medical Image Analysis and Multimodal Learning for Clinical Decision Support*, vol. 10553, M. J. Cardoso, T. Arbel, G. Carneiro, T. Syeda-Mahmood, J. M. R. S. Tavares, M. Moradi, A. Bradley, H. Greenspan, J. P. Papa, A. Madabhushi, J. C. Nascimento, J. S. Cardoso, V. Belagiannis, and Z. Lu, Eds. Cham: Springer International Publishing, 2017, pp. 21–29.
- [36] P. Hu, F. Wu, J. Peng, Y. Bao, F. Chen, and D. Kong, “Automatic abdominal multi-organ segmentation using deep convolutional neural network and time-implicit level sets,” *Int J CARS*, vol. 12, no. 3, pp. 399–411, Mar. 2017, doi: 10.1007/s11548-016-1501-5.
- [37] X. Zhou, R. Takayama, S. Wang, T. Hara, and H. Fujita, “Deep learning of the sectional appearances of 3D CT images for anatomical structure segmentation based on an FCN voting method,” *Med. Phys.*, vol. 44, no. 10, pp. 5221–5233, Oct. 2017, doi: 10.1002/mp.12480.
- [38] X. Zhou, R. Takayama, S. Wang, X. Zhou, T. Hara, and H. Fujita, “Automated segmentation of 3D anatomical structures on CT images by using a deep convolutional network based on end-to-end learning approach,” Orlando, Florida, United States, Feb. 2017, p. 1013324, doi: 10.1117/12.2254201.
- [39] E. Gibson et al., “Automatic multi-organ segmentation on abdominal CT with dense v-networks,” *IEEE Trans. Med. Imaging*, vol. 37, no. 8, pp. 1822–1834, Aug. 2018, doi: 10.1109/TMI.2018.2806309.
- [40] H. Roth et al., “Deep learning and its application to medical image segmentation,” *ArXiv*, vol. abs/1803.08691, 2018.
- [41] H. R. Roth et al., “A multi-scale pyramid of 3D fully convolutional networks for abdominal multi-organ segmentation,” arXiv:1806.02237 [cs], Jun. 2018. Available: <http://arxiv.org/abs/1806.02237>.
- [42] C. Shen et al., “On the influence of Dice loss function in multi-class organ segmentation of abdominal CT using 3D fully convolutional networks,” arXiv:1801.05912 [cs], Jan. 2018. Available: <http://arxiv.org/abs/1801.05912>.
- [43] H. R. Roth et al., “An application of cascaded 3D fully convolutional networks for medical image segmentation,” *Computerized Medical Imaging and Graphics*, vol. 66, pp. 90–99, Jun. 2018, doi: 10.1016/j.compmedimag.2018.03.001.
- [44] S. Chen et al., “Automatic multi-organ segmentation in dual energy CT using 3D fully convolutional network,” 2018.
- [45] W. van Rooij, M. Dahele, H. Ribeiro Brandao, A. R. Delaney, B. J. Slotman, and W. F. Verbakel, “Deep learning-based delineation of head and neck organs at risk: geometric and dosimetric evaluation,” *International Journal of Radiation Oncology*Biophysics*Physics*, vol. 104, no. 3, pp. 677–684, Jul. 2019, doi: 10.1016/j.ijrobp.2019.02.040.
- [46] L. Chen, P. Bentley, K. Mori, K. Misawa, M. Fujiwara, and D. Rueckert, “DRINet for medical image segmentation,” *IEEE Trans. Med. Imaging*, vol. 37, no. 11, pp. 2453–2462, Nov. 2018, doi: 10.1109/TMI.2018.2835303.
- [47] G. González, G. R. Washko, and R. San José Estépar, “Multi-structure segmentation from partially labeled datasets. Application to body composition measurements on CT scans,” in *Image Analysis for Moving Organ, Breast, and Thoracic Images*, vol. 11040, D. Stoyanov, Z. Taylor, B. Kainz, G. Maicas, R. R. Beichel, A. Martel, L. Maier-Hein, K. Bhatia, T. Vercauteren, O. Oktay, G. Carneiro, A. P. Bradley, J. Nascimento, H. Min, M. S. Brown, C. Jacobs, B. Lassen-Schmidt, K. Mori, J. Petersen, R. San José Estépar, A. Schmidt-Richberg, and C. Veiga, Eds. Cham: Springer International Publishing, 2018, pp. 215–224.
- [48] H. Kakeya, T. Okada, and Y. Oshiro, “3D U-JAPA-Net: Mixture of convolutional networks for abdominal multi-organ CT segmentation,” in *Medical Image Computing and Computer Assisted Intervention – MICCAI 2018*, vol. 11073, A. F. Frangi, J. A. Schnabel, C. Davatzikos, C. Alberola-López, and G. Fichtinger, Eds. Cham: Springer International Publishing, 2018, pp. 426–433.
- [49] A. Balagopal et al., “Fully automated organ segmentation in male pelvic CT images,” *Phys. Med. Biol.*, vol. 63, no. 24, p. 245015, Dec. 2018, doi: 10.1088/1361-6560/aaf11c.
- [50] Y. Wang, Y. Zhou, W. Shen, S. Park, E. K. Fishman, and A. L. Yuille, “Abdominal multi-organ segmentation with organ-attention networks and statistical fusion,” *Medical Image Analysis*, vol. 55, pp. 88–102, Jul. 2019, doi: 10.1016/j.media.2019.04.005.
- [51] T. Binder, E. M. Tantaoui, P. Pati, R. Catena, A. Set-Aghayan, and M. Gabrani, “Multi-organ gland segmentation using deep learning,” *Front. Med.*, vol. 6, p. 173, Aug. 2019, doi: 10.3389/fmed.2019.00173.
- [52] M. P. Heinrich, O. Oktay, and N. Bouteldja, “OBELISK-Net: Fewer layers to solve 3D multi-organ segmentation with sparse deformable convolutions,” *Medical Image Analysis*, vol. 54, pp. 1–9, May 2019, doi: 10.1016/j.media.2019.02.006.
- [53] X. Feng, K. Qing, N. J. Tustison, C. H. Meyer, and Q. Chen, “Deep convolutional neural network for segmentation of thoracic organs-at-risk using cropped 3D images,” *Med. Phys.*, vol. 46, no. 5, pp. 2169–2180, May 2019, doi: 10.1002/mp.13466.
- [54] Z. Lambert, C. Petitjean, B. Dubray, and S. Ruan, “SegTHOR: Segmentation of thoracic organs at risk in CT images,” arXiv:1912.05950 [cs, eess], Dec. 2019. Available: <http://arxiv.org/abs/1912.05950>.
- [55] M. Han et al., “Segmentation of CT thoracic organs by multi-resolution VB-nets,” 2019.
- [56] T. He, J. Hu, Y. Song, J. Guo, and Z. Yi, “Multi-task learning for the segmentation of organs at risk with label dependence,” *Medical Image Analysis*, vol. 61, p. 101666, Apr. 2020, doi: 10.1016/j.media.2020.101666.

- [57] M. Feng, W. Huang, Y. Wang, and Y. Xie, "Multi-organ segmentation using simplified dense V-net with post-processing," 2019.
- [58] S. Vesal, N. Ravikumar, and A. Maier, "A 2D dilated residual U-Net for multi-organ segmentation in thoracic CT," arXiv:1905.07710 [cs, eess], May 2019. Available: <http://arxiv.org/abs/1905.07710>.
- [59] C. Huang, H. Han, Q. Yao, S. Zhu, and S. K. Zhou, "3D U-Net: A 3D universal U-Net for multi-domain medical image segmentation," arXiv:1909.06012 [cs, eess], Sep. 2019. Available: <http://arxiv.org/abs/1909.06012>.
- [60] Z. Liu et al., "Segmentation of organs-at-risk in cervical cancer CT images with a convolutional neural network," *Physica Medica*, vol. 69, pp. 184–191, Jan. 2020, doi: 10.1016/j.ejmp.2019.12.008.
- [61] J. Léger, E. Brion, P. Desbordes, C. De Vleeschouwer, J. A. Lee, and B. Macq, "Cross-domain data augmentation for deep-learning-based male pelvic organ segmentation in cone beam CT," *Applied Sciences*, vol. 10, no. 3, p. 1154, Feb. 2020, doi: 10.3390/app10031154.
- [62] H. Kim et al., "Abdominal multi-organ auto-segmentation using 3D-patch-based deep convolutional neural network," *Sci Rep*, vol. 10, no. 1, p. 6204, Dec. 2020, doi: 10.1038/s41598-020-63285-0.
- [63] X. Fang and P. Yan, "Multi-organ segmentation over partially labeled datasets with multi-scale feature abstraction," arXiv:2001.00208 [cs], Jun. 2020. Available: <http://arxiv.org/abs/2001.00208>.
- [64] I. J. Goodfellow et al., "Generative adversarial networks," arXiv:1406.2661 [cs, stat], Jun. 2014. Available: <http://arxiv.org/abs/1406.2661>.
- [65] M. Rezaei, H. Yang, and C. Meinel, "Conditional generative refinement adversarial networks for unbalanced medical image semantic segmentation," arXiv:1810.03871 [cs], Oct. 2018. Available: <http://arxiv.org/abs/1810.03871>.
- [66] X. Dong et al., "Automatic multiorgan segmentation in thorax CT images using U-net-GAN," *Med. Phys.*, vol. 46, no. 5, pp. 2157–2168, May 2019, doi: 10.1002/mp.13458.
- [67] R. Trullo, C. Petitjean, B. Dubray, and S. Ruan, "Multiorgan segmentation using distance-aware adversarial networks," *J. Med. Imag.*, vol. 6, no. 01, p. 1, Jan. 2019, doi: 10.1117/1.JMI.6.1.014001.
- [68] Y. Lei et al., "Male pelvic multi-organ segmentation aided by CBCT-based synthetic MRI," *Phys. Med. Biol.*, vol. 65, no. 3, p. 035013, Feb. 2020, doi: 10.1088/1361-6560/ab63bb.
- [69] P.-H. Conze et al., "Abdominal multi-organ segmentation with cascaded convolutional and adversarial deep networks," arXiv:2001.09521 [cs, eess], Jan. 2020. Available: <http://arxiv.org/abs/2001.09521>.
- [70] A. Chakravarty and J. Sivaswamy, "RACE-Net: A recurrent neural network for biomedical image segmentation," *IEEE J. Biomed. Health Inform.*, vol. 23, no. 3, pp. 1151–1162, May 2019, doi: 10.1109/JBHI.2018.2852635.
- [71] Q. Yu, L. Xie, Y. Wang, Y. Zhou, E. K. Fishman, and A. L. Yuille, "Recurrent saliency transformation network: Incorporating multi-stage visual cues for small organ segmentation," arXiv:1709.04518 [cs], Apr. 2018. Available: <http://arxiv.org/abs/1709.04518>.
- [72] M. Z. Alom, C. Yakopcic, M. Hasan, T. M. Taha, and V. K. Asari, "Recurrent residual U-Net for medical image segmentation," *J. Med. Imag.*, vol. 6, no. 01, p. 1, Mar. 2019, doi: 10.1117/1.JMI.6.1.014006.
- [73] J. Schlemper et al., "Attention gated networks: Learning to leverage salient regions in medical images," arXiv:1808.08114 [cs], Jan. 2019. Available: <http://arxiv.org/abs/1808.08114>.
- [74] A. A. Novikov, D. Major, M. Wimmer, D. Lenis, and K. Buhler, "Deep sequential segmentation of organs in volumetric medical scans," *IEEE Trans. Med. Imaging*, vol. 38, no. 5, pp. 1207–1215, May 2019, doi: 10.1109/TMI.2018.2881678.
- [75] Y. Wang, Y. Zhou, P. Tang, W. Shen, E. K. Fishman, and A. L. Yuille, "Training multi-organ segmentation networks with sample selection by relaxed upper confident bound," arXiv:1804.02595 [cs], Apr. 2018. Available: <http://arxiv.org/abs/1804.02595>.
- [76] V. V. Valindria et al., "Multi-modal learning from unpaired images: application to multi-organ segmentation in CT and MRI," in 2018 IEEE Winter Conference on Applications of Computer Vision (WACV), Lake Tahoe, NV, Mar. 2018, pp. 547–556, doi: 10.1109/WACV.2018.00066.
- [77] Y. Zhou et al., "Semi-supervised multi-organ segmentation via deep multi-planar co-training," arXiv:1804.02586 [cs], Nov. 2018. Available: <http://arxiv.org/abs/1804.02586>.
- [78] Y. Zhou et al., "Prior-aware neural network for partially-supervised multi-organ segmentation," arXiv:1904.06346 [cs], Aug. 2019. Available: <http://arxiv.org/abs/1904.06346>.
- [79] Z. Zhang, H. Fu, H. Dai, J. Shen, Y. Pang, and L. Shao, "ET-Net: A generic edge-attention guidance network for medical image segmentation," arXiv:1907.10936 [cs], Jul. 2019. Available: <http://arxiv.org/abs/1907.10936>.
- [80] Y. Zhang, M. T. C. Ying, and D. Z. Chen, "Decompose-and-integrate learning for multi-class segmentation in medical images," arXiv:1906.02901 [cs, eess, stat], Jun. 2019. Available: <http://arxiv.org/abs/1906.02901>.
- [81] A. Sinha and J. Dolz, "Multi-scale self-guided attention for medical image segmentation," arXiv:1906.02849 [cs], Feb. 2020. Available: <http://arxiv.org/abs/1906.02849>.
- [82] (Author Name Not Available), "Segmentation outside the cranial vault challenge," 2015, doi: 10.7303/SYN3193805.
- [83] P. F. Raudaschl et al., "Evaluation of segmentation methods on head and neck CT: Auto-segmentation challenge 2015," *Med. Phys.*, vol. 44, no. 5, pp. 2020–2036, May 2017, doi: 10.1002/mp.12197.
- [84] J. Yang et al., "Autosegmentation for thoracic radiation treatment planning: A grand challenge at AAPM 2017," *Med. Phys.*, vol. 45, no. 10, pp. 4568–4581, Oct. 2018, doi: 10.1002/mp.13141.
- [85] A. L. Simpson et al., "A large annotated medical image dataset for the development and evaluation of segmentation algorithms," arXiv:1902.09063 [cs, eess], Feb. 2019. Available: <http://arxiv.org/abs/1902.09063>.
- [86] A. E. Kavur, M. A. Selver, O. Dicle, M. Barış, and N. S. Gezer, "CHAOS - Combined (CT-MR) healthy abdominal organ segmentation challenge data." Zenodo, Apr. 11, 2019, doi: 10.5281/ZENODO.3362844.
- [87] X. Xu, B. Liu, and F. Zhou, "Annotations for body organ localization based on MICCAI LiTS dataset." *IEEE DataPort*, Jul. 10, 2018, doi: 10.21227/DF8G-PQ27.

Development of a Physical Impairment Prediction Model for Korean Elderly People using Synthetic Minority Over-Sampling Technique and XGBoost

Haewon Byeon

Department of Medical Big Data
College of AI Convergence, Inje University
Gimhae 50834, Gyeongsangnamdo, South Korea

Abstract—The old people's 'physical functioning' is a key factor of active ageing as well as a major factor in determining the quality of life and the need for long-term care in old age. Previous studies that identified factors related to ADL mostly used regression analysis to predict groups of high physical impairment risk. Regression analysis is useful for confirming individual risk factors, but has limitations in grasping multiple risk factors. As methods for resolving this limitation of regression models, machine learning ensemble boosting models such as random forest and eXtreme Gradient Boosting (XGBoost) are widely used. Nonetheless, the prediction performances of XGBoost, such as accuracy and sensitivity, remain to be verified additionally by follow-up studies. This article proposes an effective method of dealing with imbalanced data for the development of ensemble-based machine learning, by comparing the performances of disease data sampling methods. This study analyzed 3,351 old people aged 65 or above who resided in local communities and completed the survey. As machine learning models to predict physical impairment in old age, this study compared the logistic regression model, XGBoost and random forest, with respect to the predictive performances of accuracy, sensitivity, and specificity. This study selected as the final model a model whose sensitivity and specificity were 0.6 or above and whose accuracy was highest. As a result, synthetic minority over-sampling technique (SMOTE)-based XGBoost whose accuracy, sensitivity, and specificity were 0.67, 0.81, and 0.75, respectively, was determined as the most excellent predictive performance. The results of this study suggest that in case of developing a predictive model using imbalanced data like disease data, it is efficient to use the SMOTE-based XGBoost model.

Keywords—Random forest; XGBoost; GBM; gradient boosting machine; physical impairment prediction model

I. INTRODUCTION

According as ageing progresses across the world, ageing-related new concepts such as 'healthy ageing' and 'successful ageing' have emerged [1]. There are several standards for successful ageing, but in general, successful ageing is defined as having the high levels of physical, psychological, and social functions and satisfaction with life, a step further from physically healthy ageing [2]. It has been reported that factors affecting the successful ageing include age, abstaining from smoking, disability, arthritis, and diabetes, and particularly that the better their subjective health, family support and physical activities, the higher their level of successful aging [1,3,4,5].

The World Health Organization (WHO) introduced the concept of active ageing in order to promote the development of policies to cope with the problem of ageing [6,7]. According to the definition of WHO [6], active ageing is the process of optimizing opportunities for health, participation and security in order to enhance quality of life as people age. That is, active ageing supports people with ADL functions so that they actively participate in social activities, and induces people with ADL dysfunction to actively perform daily life by enhancing their ADL functions with appropriate support [8].

On the other hand, old people's 'physical functioning' is a key factor of active ageing as well as a major factor in determining the quality of life and the need for long-term care in old age [9,10]. Old people's state of physical functioning is mostly assessed in terms of activities of daily living (ADL), with which it can be judged whether an elderly can lead an independent life or not [11,12]. For the assessment of ADL, Katz Index, Barthel Index, and MBI are usually used [13]; and in the Korea National Health and Nutrition Examination Survey, the Korean Activities of Daily Living scale(K-ADL), a standardized test tool for physical functioning developed by reflecting Korean old people's living environment and culture, was used [14]. Old age, low educational level, the beneficiary of medical benefits, non-subscriber of health insurance, stroke, urinary incontinence, diabetes, and lung cancer have been reported as risk factors affecting K-ADL [15-21].

Previous studies that identified factors related to ADL [15-21] mostly used regression analysis to predict groups of high physical impairment risk. Regression analysis is useful for confirming individual risk factors, but has limitations in grasping multiple risk factors [22,23]. In addition, regression models assume the independence and normality of variables; however, it is difficult to derive accurate results in case of data that violate the normality of distribution, as in disease [24]. As methods for resolving this limitation of regression models, machine learning ensemble boosting models such as random forest, gradient boosting machine (GBM), and eXtreme Gradient Boosting (XGBoost) are widely used [25,26]. Ensemble learning is a technique for deriving more accurate final prediction by generating several classifiers and combining their predictions, and some previous studies [27,28] have reported that XGBoost developed recently shows performance exceeding that of the existing random forest or gradient boosting. Nonetheless, the prediction performances of

XGBoost, such as accuracy and sensitivity, remain to be verified additionally by follow-up studies.

On the other hand, it is highly probable that the problem of imbalanced data will occur in the prediction of impairment using big data [29]. Particularly, in the case of disease data, data are highly probable to distribute unequally because generally the number of patients is very fewer than those without disease. These imbalanced data cause prediction error in the process of machine learning and deteriorate the performance of a model, and thus techniques for dealing with imbalanced data are required in order to resolve this problem [30].

Hence, first, this article prepares basic data for policy-making to respond to ageing by predicting and analyzing the tendencies of physical impairment risk among Korean old people in local communities, and second, this article proposes an effective method of dealing with imbalanced data for the development of ensemble-based machine learning, by comparing the performances of disease data sampling methods.

II. RESEARCH METHODS

A. Sources of Data

This study used and analyzed the raw data of Seoul Panel Study Data (SEPANS), which was carried out with Seoul citizens by the Seoul Welfare Foundation from June 1, 2016 to August 31, 2016. The SEPANS was conducted to grasp the welfare levels of households residing in Seoul, find out the actual state of vulnerable groups, and estimate demand for welfare service. Its population was households in Seoul as of the survey period among households subjected to 2005 Population and Housing Census, excluding foreigners and those in nursing homes, the military, and prisons. As for the sampling method, the stratified cluster sampling was used. As for the survey method, the computer-aided personal interview was used in which an interviewer visited households to be surveyed and inputted their responses to a structured questionnaire into a portable computer. This study analyzed 3,351 old people aged 65 or above who resided in local communities and completed the survey.

B. Measurement of Variables

The outcome variable was defined as physical impairment of the elderly measured by means of K-ADL, a standardized test. According to Won (2002) [14], reliability and validity were high according as the reliability coefficient of K-ADL was 0.7 or higher at the stage of test development (standardization) and the inter-item consistency of the questionnaire was 0.937. K-ADL consisted of 7 items of the most basic physical functions in daily life, including dressing, washing the face, bathing, self-feeding, moving out of bed, using the toilet, and relieving oneself. In the event of answering with partial help or complete dependence to any item of K-ADL, the respondent was classified into the group of physical impairment, and in the event of answering with complete independence to all the items, the respondent was classified into the group of non-physical impairment.

Explanatory variables included sex, age, educational background (elementary school or below, middle school, high school, college graduate or above), being insured or not, stroke, diabetes, arthritis, monthly total household income (below KRW 2 million, KRW 2-4 million, KRW 4 million or above), the presence of a spouse (cohabiting with a spouse, having but not cohabiting with a spouse, no spouse), smoking (non-smoking, smoking in the past, smoking at present), and the presence of depressive symptoms (yes, no), which were reported to have associations with Korean old people's ADL.

C. Predictive Model

As machine learning models to predict physical impairment in old age, this study compared the logistic regression model, XGBoost and random forest, with respect to the predictive performances of accuracy, sensitivity, and specificity. In testing the predictive performances, data were randomly divided into train data and test data in the proportion of 7:3; a predictive model was generated from the train data, and the performance of the model was tested with the test data. Random forest and XGBoost are models that include randomness, and the models were developed with the seed being fixed to 1234. The value of predictive performance for each model was predicted by means of the Area Under the Curve (AUC) of ROC curve (Fig. 1). As model performance assessment indices, the accuracy, sensitivity, and specificity of each model were obtained. Accuracy is the ratio of successful predictions to all predictions. Sensitivity is the ratio of a predictive model's predicting accurately old people to whom actual impairment will occur. Specificity is the ratio of a predictive model's predicting accurately that impairment will not occur to healthy old people to whom impairment will not occur actually. This study defined as the model of the best predictive performance a model whose sensitivity and specificity were 0.6 or above and whose accuracy was found to be highest after comparison with other models; and selected it as the final model for the prediction of physical impairment in old age. In all the analyses, R version 4.0.2 (Foundation for Statistical Computing, Vienna, Austria) was used.

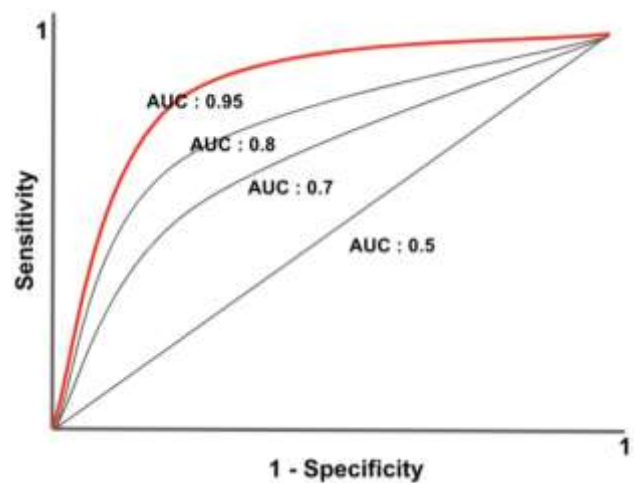


Fig. 1. Concepts of ROC Curve.

D. Ensemble Model

The ensemble model combines the prediction or classification results of several models, and use them in final decision-making, and a number of studies have shown that the model has better predictive performance than single decision tree models [31]. Ensemble methods are classified into boosting and bagging. Bagging is a method of generating several models through the sampling of source data and then making prediction by combining the outcomes of the models by voting or averaging; and reduces the variance of predicted values [32]. Boosting is a machine learning algorithm; is a method for better classifying observation values difficult to classify, by using more misclassified observation values; and reduces the bias of predictive values [33]. The concepts of boosting and bagging are presented in Fig. 2.

E. Random Forest

The forest ensemble is an ensemble form of decision trees. The decision tree is a model that divides the scope of variables in each branching, and can be used regardless of continuous/categorical target variables. It has the advantage of being capable of explaining a model easily, but its performance drops in the event that data has a structure not easily divided with horizontal partitioning or vertical partitioning [35]. A method developed to remedy this shortcoming is the random forest. The random forest samples data, generates several tree models, and then votes or averages the outcomes of the trees. It is similar to bagging, but is different from bagging in that it supplements the problem of multicollinearity by random selection of variables as well as sampling of data [36]. The concept of random forest is presented in Fig. 3.

F. XGBoost

XGBoost is one of boosting methods, and uses a misclassified observation value more in the next model when generating a tree [38]. That is, it is a boosting algorithm that trains with a method for improving performance as to misclassified observation values. XGBoost has the advantage of speedy calculation process owing to parallel computing that uses all CPU cores in learning, and is very useful because it supports various programming languages including Python and R [38]. The concept of XGBoost is presented in Fig. 4.

G. Sampling

Disease data generally have the problem of imbalance because the number of patients is fewer than healthy people. In the case of data used in this study, the ratio of normal old people was found to be 92%, and the ratio of old people with physical impairment only 8.0%, respectively, as a result of ADL assessment, which shows the problem of imbalance. To resolve the problem of imbalance, this study used the algorithms of under-sampling [40], over-sampling [41], and synthetic minority over-sampling technique (SMOTE) [30].

The under-sampling is a method of resolving the problem of data imbalance by randomly removing the major class among classes of response variables. The technique of under-sampling can reduce the speed of model construction by removing data amount, but has the shortcoming of information loss.

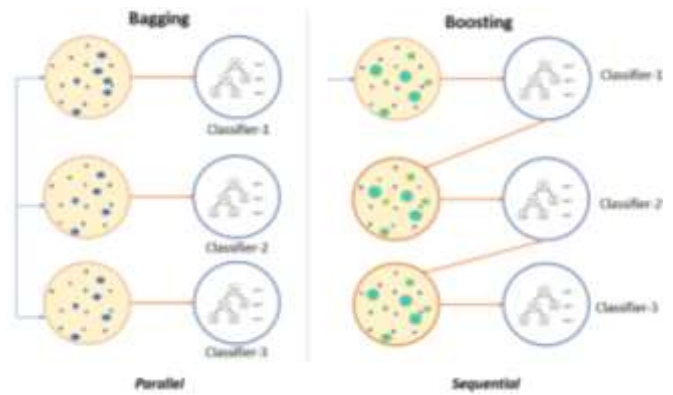


Fig. 2. Concepts of Bagging and Boosting Algorithm [34].

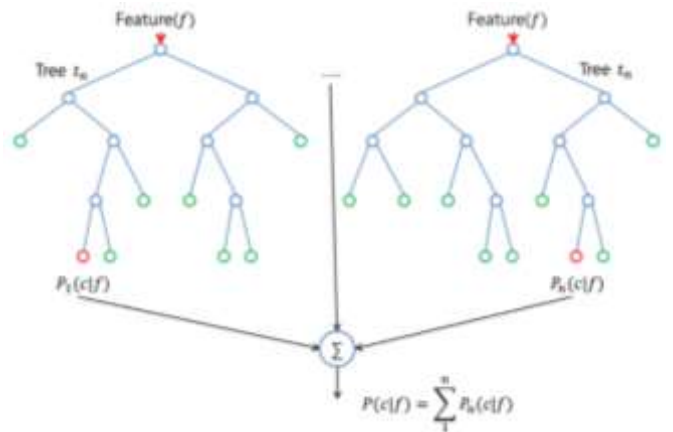


Fig. 3. Concepts of Random Forest Algorithm [37].

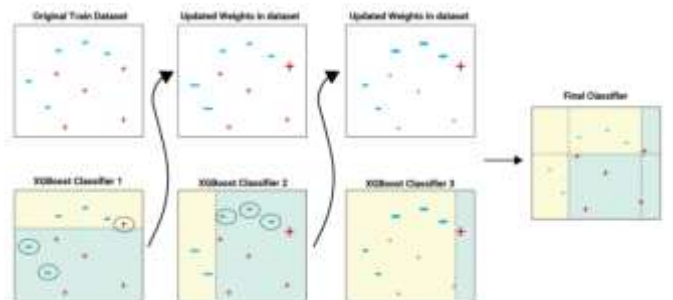


Fig. 4. Concepts of XGBoost Algorithm [39].

The over-sampling is a method of resolving the problem of imbalance by randomly copying the minor class among classes of response variables. The over-sampling technique may cause the problem of overfitting because the speed of model construction increases due to the increase in data amount and it copies a small number of categories.

SMOTE (Synthetic Minority Over-sampling Technique) is a method for supplementing overfitting, the shortcoming of over-sampling. One of minor classes among classes of response variables is randomly chosen, and then k nearest neighbors of this data is found. And the difference between this chosen sample and k neighbors is obtained, and the difference multiplied by any value between 0 and 1 is added to the existing sample, and then the resulting value is added to the training data. Lastly, this process is repeated. The SMOTE

algorithm is similar to over-sampling in that it increases data of a minor class of few categories, but it is known that it supplements overfitting, the shortcoming of over-sampling, through creating a new sample by properly combining the existing data, not copying the same data. The concepts of sampling types are presented in Fig. 5.

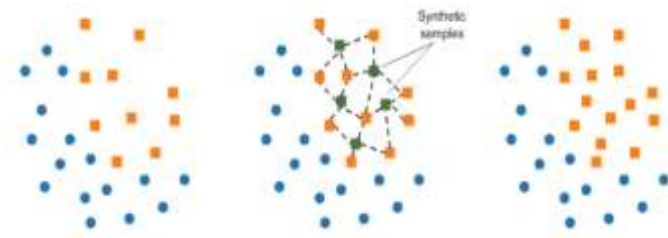


Fig. 5. Concepts of SMOTE Algorithm [42].

III. RESULTS

A. Accuracy of Predictive Models

The accuracy, sensitivity, and specificity of predictive models to which sampling methods were applied are presented in Table I. This study selected as the final model a model whose sensitivity and specificity were 0.6 or above and whose accuracy was highest. As a result, SMOTE-based XGBoost whose accuracy, sensitivity, and specificity were 0.67, 0.81, and 0.75, respectively, was determined as the final predictive model.

B. Results of XGBoost Model Development

The model to predict the physical impairment was developed through the Xgboost and the predictive power was compared with the results of random forest and logistic regression (Table II). Xgboost had higher classification accuracy than other predictive model in both training and test data. The analysis results of test data showed that the classification accuracy was 67.2% for Xgboost, 65.0% for logistic regression, and 62.1% for random forest.

TABLE I. PERFORMANCE (ACCURACY, SENSITIVITY, AND SPECIFICITY) OF PREDICTIVE MODELS TO WHICH SAMPLING METHODS WERE APPLIED

Model		Random Forest	Logistic regression	XGBoost
Raw data	Accuracy	0.73	0.65	0.75
	Sensitivity	0.50	0.43	0.63
	Specificity	0.85	0.94	0.90
Under-sampling	Accuracy	0.63	0.49	0.60
	Sensitivity	0.63	0.48	0.74
	Specificity	0.79	1.00	0.93
Over-sampling	Accuracy	0.54	0.62	0.77
	Sensitivity	0.52	0.63	0.65
	Specificity	0.80	0.91	0.93
SMOTE	Accuracy	0.62	0.65	0.67
	Sensitivity	0.68	0.70	0.81
	Specificity	0.81	0.78	0.75

TABLE II. RESULTS OF MODEL TO PREDICT THE PHYSICAL IMPAIRMENT

Model	Factors	Characteristics
Random forest	9	sex, age, educational background, being insured or not, stroke, diabetes, arthritis, the presence of a spouse, the presence of depressive symptoms
Logistic regression	6	sex, age, educational background, stroke, diabetes, arthritis
XGBoost	7	sex, age, educational background, being insured or not, stroke, diabetes, arthritis

IV. CONCLUSION

Sensitivity and specificity are in the relationship of trade-off. Therefore, the proportions of sensitivity and specificity are selected by the judgment of a researcher who uses a model. In this article, among random forest, logistic regression and XGBoost, the SMOTE-based XGBoost model, which showed the sensitivity and specificity of 0.6 or above and the highest accuracy, was derived as the final model of the most excellent predictive performance.

Similarly to the results of this study, previous studies also reported that XGBoost is more excellent than other ensemble models, such as GBM, in terms of accuracy [27,28]. It is presumed that XGBoost displayed excellent predictive performance in the areas of classification and regression because although it, one of tree-based ensemble learning algorithms, is based on GBM, it is equipped with its own functions of overfitting regularization and early stopping [27,28]. Further, previous studies [43,44] reported that XGBoost shows faster execution time than GBM. Therefore, the results of this study suggest that in case of developing a predictive model using imbalanced data like disease data, it is efficient to use the SMOTE-based XGBoost model.

ACKNOWLEDGMENT

This research was supported by Basic Science Research Program through the National Research Foundation of Korea (NRF) funded by the Ministry of Education (NRF-2018R1D1A1B07041091, NRF-2019S1A5A8034211).

REFERENCES

- [1] S. H. Kim, S. Park, A meta-analysis of the correlates of successful aging in older adults. *Research on Aging*, vol. 39, no. 5, pp. 657-677, 2017.
- [2] J. Woo, J. Leung, T. Zhang, Successful aging and frailty: opposite sides of the same coin?. *Journal of the American Medical Directors Association*, vol. 17, no. 9, pp. 797-801, 2016.
- [3] J. Mana, O. Bezdicek, Cognition in successful aging: Systematic review and future directions. *Clinical Gerontologist*, pp. 1-9, 2020.
- [4] B. Teater, J. M. Chonody, How do older adults define successful aging? A scoping review. *The International Journal of Aging and Human Development*, vol. 91, no. 4, pp. 599-625, 2020.
- [5] J. H. Cho, The Influence of Self-Efficacy, Self-Esteem, Aging Anxiety on Successful Aging in Middle-Aged Women. *Medico Legal Update*, vol. 20, no. 1, pp. 2265-2270, 2020.
- [6] A. I. Hijas-Gómez, A. Ayala, M. P. Rodríguez-García, C. Rodríguez-Blázquez, V. Rodríguez-Rodríguez, F. Rojo-Pérez, G. Fernández-Mayoralas, A. Rodríguez-Laso, A. Calderón-Larrañaga, M. J. Forjaz, The WHO active ageing pillars and its association with survival: Findings from a population-based study in Spain. *Archives of Gerontology and Geriatrics*, vol. 90, 104114, 2020.
- [7] E. Thalassinou, M. Cristea, G. G. Noja, Measuring active ageing within the European Union: implications on economic development.

- Equilibrium. Quarterly Journal of Economics and Economic Policy, vol. 14, no. 4, pp. 591-609, 2019.
- [8] D. Sánchez-González, F. Rojo-Pérez, V. Rodríguez-Rodríguez, G. Fernández-Mayoralas, Environmental and psychosocial interventions in age-friendly communities and active ageing: a systematic review. *International Journal of Environmental Research and Public Health*, vol. 17, no. 22, 8305, 2020.
- [9] L. Dipietro, W. W. Campbell, D. M. Buchner, K. I. Erickson, K. E. Powell, B. Bloodgood, T. Hughes, K. R. Day, K. L. Piercy, A. Vaux-Bjerke, R. D. Olson, 2018 Physical Activity Guidelines Advisory Committee, Physical Activity, Injurious Falls, and Physical Function in Aging: An Umbrella Review. *Medicine and Science in Sports and Exercise*, vol. 51, no. 6, pp. 1303-1313, 2019.
- [10] D. O'Neill, D. E. Forman, The importance of physical function as a clinical outcome: Assessment and enhancement. *Clinical Cardiology*, vol. 43, no. 2, pp. 108-117, 2020.
- [11] M. A. Sharkawi, S. M. Zulfarina, S. M. Z. Aqilah-SN, N. M. Isa, A. M. Sabarul, A. S. Nazrun, Systematic review on the functional status of elderly hip fracture patients using Katz Index of Activity of Daily Living (Katz ADL) score. *IJUM Medical Journal Malaysia*, vol. 15, no. 2, E-pub, doi:10.31436/ijm.v15i2.397, 2016.
- [12] F. Sharifi, M. Alizadeh-Khoei, H. Saghebi, L. Angooti-Oshnari, S. Fadaee, S. Hormozi, F. Taati, M. Haghi, H. Fakhrzadeh, Validation study of ADL-Katz scale in the Iranian elderly nursing homes. *Ageing International*, vol. 43, no. 4, pp. 508-523, 2018.
- [13] L. T. Y. D. Silveira, J. M. D. Silva, J. M. P. Soler, C. Y. L. Sun, C. Tanaka, C. Fu, Assessing functional status after intensive care unit stay: the Barthel Index and the Katz Index. *International Journal for Quality in Health Care*, vol. 30, no. 4, pp. 265-270, 2018.
- [14] C. W. Won, K. Y. Yang, Y. G. Rho, S. Y. Kim, E. J. Lee, J. L. Yoon, K. H. Cho, H. C. Shin, B. R. Cho, J. R. Oh, D. K. Yoon, H. S. Lee, Y. S. Lee, The development of Korean activities of daily living (K-ADL) and Korean instrumental activities of daily living (K-IADL) scale. *Journal of the Korean Geriatrics Society*, vol. 6, no. 2, pp. 107-120, 2002.
- [15] S. Y. Sohn, Factors Related to the Health Related Quality. of Life in Elderly Women. *Korean Journal of Women Health Nursing*, vol. 15, no. 2, pp. 99-107, 2009.
- [16] S. M. Bang, J. O. Lee, Y. J. Kim, K. W. Lee, S. Lim, J. H. Kim, Y. J. Park, H. J. Chin, K. W. Kim, H. C. Jang, J. S. Lee, Anemia and activities of daily living in the Korean urban elderly population: results from the Korean Longitudinal Study on Health and Aging (KLoSHA). *Annals of Hematology*, vol. 92, no. 1, pp. 59-65, 2013.
- [17] J. W. Noh, K. B. Kim, J. H. Lee, M. H. Kim, Y. D. Kwon, Relationship of health, sociodemographic, and economic factors and life satisfaction in young-old and old-old elderly: a cross-sectional analysis of data from the Korean longitudinal study of aging. *Journal of Physical Therapy Science*, vol. 29, no. 9, pp. 1483-1489, 2017.
- [18] H. M. Ku, J. H. Kim, H. S. Lee, H. J. Ko, E. J. Kwon, S. Jo, D. K. Kim, A study on the reliability and validity of Seoul-Activities of Daily Living (S-ADL). *Journal of the Korean Geriatrics Society*, vol. 8, no. 4, pp. 206-214, 2004.
- [19] H. Byeon, H. W. Koh, The relationship between communication activities of daily living and quality of life among the elderly suffering from stroke. *Journal of Physical Therapy Science*, vol. 28, no. 5, pp. 1450-1453, 2016.
- [20] H. Byeon, S. Cho, Association between Drinking Behavior and Activities of Daily Living in Community-dwelling Older Adults. *International Journal of Bio-Science and Bio-Technology*, vol. 7, no. 4, pp. 135-144, 2015.
- [21] K. S. Ahn, S. K. Park, Y. C. Cho, Physical Function (ADL, IADL) and Related Factors in the Elderly People Institutionalized in Long-term Care Facilities. *Journal of the Korea Academia-Industrial cooperation Society*, vol. 17, no. 3, pp. 480-488, 2016.
- [22] H. Byeon, Developing a model to predict the occurrence of the cardio-cerebrovascular disease for the Korean elderly using the random forests algorithm. *International Journal of Advanced Computer Science and Applications*, vol. 9, no. 9, pp. 494-499, 2018.
- [23] H. Byeon, S. Cha, K. Lim, Exploring Factors Associated with Voucher Program for Speech Language Therapy for the Preschoolers of Parents with Communication Disorder using Weighted Random Forests. *International Journal of Advanced Computer Science and Applications*, vol. 10, no. 5, pp. 12-17, 2019.
- [24] H. Byeon, Model development for predicting the occurrence of benign laryngeal lesions using support vector machine: focusing on South Korean adults living in local communities. *International Journal of Advanced Computer Science and Applications*, vol. 9, no. 10, pp. 222-227, 2018.
- [25] J. Nobre, R. F. Neves, Combining principal component analysis, discrete wavelet transform and XGBoost to trade in the financial markets. *Expert Systems with Applications*, vol. 125, pp. 181-194, 2019.
- [26] H. Nguyen, X. N. Bui, H. B. Bui, D. T. Cuong, Developing an XGBoost model to predict blast-induced peak particle velocity in an open-pit mine: a case study. *Acta Geophysica*, vol. 67, pp. 477-490, 2019.
- [27] E. K. Sahin, Assessing the predictive capability of ensemble tree methods for landslide susceptibility mapping using XGBoost, gradient boosting machine, and random forest. *SN Applied Sciences*, vol. 2, 1308, 2020.
- [28] T. Hengl, J. G. Leenaars, K. D. Shepherd, M. G. Walsh, G. B. Heuvelink, T. Mamo, H. Tilahun, E. Berkhout, M. Cooper, E. Fegraus, I. Wheeler, N. A. Kwabena, Soil nutrient maps of Sub-Saharan Africa: assessment of soil nutrient content at 250 m spatial resolution using machine learning. *Nutrient Cycling in Agroecosystems*, vol. 109, pp. 77-102, 2017.
- [29] A. Fernández, S. García, F. Herrera, N. V. Chawla, SMOTE for learning from imbalanced data: progress and challenges, marking the 15-year anniversary. *Journal of Artificial Intelligence Research*, vol. 61, pp. 863-905, 2018.
- [30] N. V. Chawla, K. W. Bowyer, L. O. Hall, W. P. Kegelmeyer, SMOTE: synthetic minority over-sampling technique. *Journal of Artificial Intelligence Research*, vol. 16, pp. 321-357, 2002.
- [31] M. Skurichina, R. P. Duin, Bagging, boosting and the random subspace method for linear classifiers. *Pattern Analysis and Applications*, vol. 5, pp. 121-135, 2002.
- [32] Y. Grandvalet, Bagging equalizes influence. *Machine Learning*, vol. 55, pp. 251-270, 2004.
- [33] A. Mayr, B. Hofner, E. Waldmann, T. Hepp, S. Meyer, O. Gefeller, An update on statistical boosting in biomedicine. *Computational and Mathematical Methods in Medicine*, vol. 2017, E-pub, 6083072, doi:10.1155/2017/6083072, 2017.
- [34] <https://www.pluralsight.com/guides/ensemble-methods:-bagging-versus-boosting>.
- [35] F. Tang, H. Ishwaran, Random forest missing data algorithms. *Statistical Analysis and Data Mining: The ASA Data Science Journal*, vol. 10, no. 6, pp. 363-377, 2017.
- [36] P. Thanh Noi, M. Kappas, Comparison of random forest, k-nearest neighbor, and support vector machine classifiers for land cover classification using Sentinel-2 imagery. *Sensors*, vol. 18, no. 1, 18, 2018.
- [37] <https://builtin.com/data-science/random-forest-algorithm>.
- [38] R. Mitchell, E. Frank, Accelerating the XGBoost algorithm using GPU computing. *PeerJ Computer Science*, vol. 3, E-pub, e127, doi:10.7717/peerj-cs.127, 2017.
- [39] <https://blog.thinknewfound.com/2020/05/defensive-equity-with-machine-learning/xg-boost-final-01/>.

- [40] S. J. Yen, Y. S. Lee, Cluster-based under-sampling approaches for imbalanced data distributions. *Expert Systems with Applications*, vol. 36, no. 3, pp. 5718-5727, 2009.
- [41] L. Abdi, S. Hashemi, To combat multi-class imbalanced problems by means of over-sampling techniques. *IEEE Transactions on Knowledge and Data Engineering*, vol. 28, no. 1, pp. 238-251, 2015.
- [42] <https://www.kaggle.com/rafjaa/resampling-strategies-for-imbalanced-datasets>.
- [43] Z. Ding, H. Nguyen, X. N. Bui, J. Zhou, H. Moayedi, Computational intelligence model for estimating intensity of blast-induced ground vibration in a mine based on imperialist competitive and extreme gradient boosting algorithms. *Natural Resources Research*, vol. 29, pp. 751-769, 2020.
- [44] A. Kadiyala, A. Kumar, Applications of python to evaluate the performance of decision tree - based boosting algorithms. *Environmental Progress and Sustainable Energy*, vol. 37, pp. 618-623, 2018.

Data-Forensic Determination of the Accuracy of International COVID-19 Reporting: Using Zipf's Law for Pandemic Investigation

Aamo Iorliam¹, Anthony T S Ho², Santosh Tirunagari³
David Windridge⁴, Adekunle Adeyelu⁵, Samera Otor⁶, Beatrice O. Akumba⁷
Department of Mathematics and Computer Science, BSU, Makurdi, Nigeria^{1, 5, 6, 7}
Faculty of Engineering and Physical Sciences, University of Surrey, Guildford, Surrey, United Kingdom GU2 7XH^{2, 4}
Tianjin University of Science and Technology, China²
Wuhan University of Technology, China²
Department of Computer Science, Middlesex University, London, UK^{3, 4}

Abstract—Severe outbreaks of infectious disease occur throughout the world with some reaching the level of international pandemic: Coronavirus (COVID-19) is the most recent to do so. In this paper, a mechanism is set out using Zipf's law to establish the accuracy of international reporting of COVID-19 cases via a determination of whether an individual country's COVID-19 reporting follows a power-law for confirmed, recovered, and death cases of COVID-19. The probability of Zipf's law (P-values) for COVID-19 confirmed cases show that Uzbekistan has the highest P-value of 0.940, followed by Belize (0.929), and Qatar (0.897). For COVID-19 recovered cases, Iraq had the highest P-value of 0.901, followed by New Zealand (0.888), and Austria (0.884). Furthermore, for COVID-19 death cases, Bosnia and Herzegovina had the highest P-value of 0.874, followed by Lithuania (0.843), and Morocco (0.825). China, where the COVID-19 pandemic began, is a significant outlier in recording P-values lower than 0.1 for the confirmed, recovered, and death cases. This raises important questions, not only for China, but also any country whose data exhibits P-values below this threshold. The main application of this work is to serve as an early warning for World Health Organization (WHO) and other health regulatory bodies to perform more investigations in countries where COVID-19 datasets deviate significantly from Zipf's law. To this end, this paper provide a tool for illustrating Zipf's law P-values on a global map in order to convey the geographic distribution of reporting anomalies.

Keywords—COVID-19; power-law; pandemic; Zipf's Law; WHO

I. INTRODUCTION

The Coronavirus Disease 2019 (COVID-19) broke out in 2019 in Wuhan, China and has caused alarming health crises, unemployment, unimaginable hunger, lockdown of the entire world, constant fear and in some cases death [1]. Up till now, several countries are accused of wrongly reporting the COVID-19 confirmed, recovered, and death cases globally [2,3].

Determining the accuracy of reporting COVID-19 cases internationally is important because it will assist health regulatory bodies to perform in depth investigations into country's suspected data [2]. Moreover, this has a potential to

aid these regulatory bodies in their planning, measures to curb this deadly pandemic, and save more lives [2,3].

The Zipf's law has proved over the years to be very effective in differentiating forged/fabricated data from authentic/original data [4]. Motivated by the capability of the Zipf's law, this paper investigates the COVID-19 datasets using the Zipf's law with the objective of determining the accuracy of international COVID-19 reporting. Any consistency of the COVID-19 datasets to the Zipf's law indicates that such data is reliable, whereas a deviation from the Zipf's law may indicate a wrong reporting of COVID-19 cases.

Results in this paper showed that most countries COVID-19 datasets followed the Zipf's law, whereas some countries COVID-19 datasets deviated from the Zipf's law. The rest of the paper is organized as follows. Related works are described in Section II. Section III explains the experimental setup. Results are presented in Section IV. Section V discusses the results. Conclusions and future work are presented in Section VI.

II. RELATED WORKS

A. Historical Perspective on Covid-19 Pandemic Investigations

The first recorded pandemic was in 165 AD to 180 AD. This pandemic was referred to as the Antonine Plague (also known as the plague of Galen) and resulted in about 5 million deaths across the globe. Analysis of symptomology and infection pattern suggest that this was likely smallpox or measles [5].

In around the 735 AD – 737AD, the Japanese smallpox epidemic erupted (believed to be a variola virus), killing up to 1 million persons [6]. Later, around 541 AD – 542 AD, the Plague of Justina killed between 30 – 50 million persons, believed to be the world's first bubonic plague [7]. Procopius described the plague as that “by which the whole human race was near to being annihilated [8 - 9].”

The most devastating pandemic, in terms of its impact of the global population, occurred between 1347 AD and 1352

AD; this is the pandemic referred to as ‘The Black Death’, which claimed between 75 – 200 million lives. It is believed to have been caused by the bubonic plague [10]; Benedictow in [11] described this plague as “the greatest catastrophe ever”; Michael of Piazza, a Franciscan friar wrote contemporaneously that: “the infection spread to everyone who had any intercourse with the disease” [12].

It is recorded that around 1520 AD there was an outbreak of the new world smallpox, believed to be a Variola virus, resulting in 25 to 55 million deaths. The New world smallpox caused so much damage that Noble David Cook [13-14] estimated that “in the end, the regions least affected lost 80 percent of their populations; those most affected lost their full populations, and a typical society lost 90 percent of its population.”

Around 1629-1631 AD, the Italian Plague erupted, believed to originate from Yersinia Pestis bacteria in rats/fleas. It claimed up to 1 million lives [15-16].

Around 1665 AD, the great plague of London claimed 75,000 to 100,000 lives, also believed to have its source from rats and fleas [17].

From 1817 to 1923 the Cholera Pandemic (caused by V. Cholera bacteria) killed more than 1 million people [18] in Europe. Around 1885, a third plague caused by Yersinia Pestis bacteria carried by rats and fleas resulted in around 12 million deaths in China and India [19]. Also in the late 1800s Yellow fever, its source is believed to be viruses/mosquitoes, resulted in more than 150,000 deaths. It targeted mostly South America and sub-Saharan Africa [20-21].

The Russian Influenza outbreak of around 1889 to 1890, transmitted via the H2N2 virus, claimed around 1 million lives [22-23]. The Spanish flu of 1918 to 1919, its source believed to be H1N1 virus, claimed about 40 to 50 million lives [22-23], by far the most deadly influenza pandemic. Asian flu, believed to be transmitted by the H2N2 virus, claimed around 2 million lives in 1968 – 1970 [23], while the 1968-1970 Hong Kong Flu, transmitted via the H3N2 virus claimed up to 1 million lives [24].

The HIV/AIDS epidemic, which commenced around 1981 has so far claimed 25 to 30 million lives [25-26]. From 2002 to 2003, Severe Acute Respiratory Syndrome (SARS) resulting from Coronavirus in Bats and Civets killed up to 770 people [27]. Later, between 2009 and 2010, Swine flu, its source believed to be the H1N1 virus in pigs, killed about 200,000 people [23].

Around 2012 – 2016, an outbreak of the Ebola virus disease (EVD) killed up to 11,000 persons; it is believed to have arisen from Ebola virus in wild animal. EVD was itself recorded as far back as 1976 [28-29].

From 2015 till the present time, the Middle East Respiratory Syndrome (MERS) believed to be caused by MERS corona-virus (MERS-CoV) in wild animals has so far killed 850 persons [30].

COVID-19 [1], the subject of the current study, erupted in 2019; according to [31], COVID-19 has claimed 146,201 lives as of 17/ 04/2020.

As is clear from the above historical account of pandemic spread, the potential for negative global impact is very substantial indeed if unchecked. In the majority of the above cases, the reporting and compilation of pandemic statistics was substantially after the fact (sometimes by many centuries) given the limited contemporaneous statistical capabilities. In the absence of such statistics, compiled while the outbreak was still live, it would have been very difficult or impossible for authorities to make well-informed policy decisions in order to combat the pandemic spread.

It is therefore critical in the current COVID-19 pandemic that accurate compilation of international reporting is undertaken. However, given the potential for countries/individuals to falsify records, for political, offensive or financial purposes, it is necessary to have methods in place to distinguish authentic from forged records. In this paper, the Zipf’s law is proposed as means to achieve this.

B. Motivation for the use of Zipf’s Law

Zipf’s law was proposed in 1935 by the US linguist George K Zipf [32] and may be stated succinctly as follows: given some corpus of natural language utterances, the frequency of any given word is inversely proportional to its rank in a frequency table.

Newman [33] made this explicitly stochastic; when considering the probability of measuring a particular quantity (in this case, COVID-19 cases), and it is found that the quantity varies inversely as a power of that value, then the quantity may be said to follow Zipf’s law [33]. Mathematically:

$$p(x) = cx^{-\alpha} \quad (1)$$

where $p(x)$ is the distribution of the quantity x , α is the Zipf’s law exponent and C is a constant [33].

Zipf’s law is hence a Power law with small occurrences relatively common and large occurrences very uncommon. The null hypothesis in applying Zipf’s law is hence that natural phenomena should follow a Power law and un-natural (or tampered-with) phenomena should deviate from this law [4,34]. Power laws have been applied to human language [4, 33], the city populations [4,33], intensity of earthquakes [4, 33], sizes of power outages [4], ranks of people watching a particular TV station at a given time [4, 35], stock market indices [35], gene expression [35], chess openings [35], the arts [35], paper citations [35], family names [35], personal donations [35], keystroke dynamics [4], the scales of Influenza A (H1N1) and Avian Influenza (H7N9) outbreaks [35, 36] amongst others.

The gap in the related works is that to the best of the researchers’ knowledge, the application of Zipf’s law to COVID-19 cases has not been done as at April, 2020 when this research was conducted. Hence, this paper proposes the investigation of *reported* COVID-19 datasets using Zipf’s law to establish veracity and accuracy, in particular because of presence of widespread allegations that countries may have hidden or systematically underreported the cases of COVID-19 [2,3].

Thus, the aim is to establish probability values (P-values) in relation to Zipf's law calculation for each country affected by COVID-19. Furthermore, the P-values of each country based on the Zipf's law calculation on a global map are presented. This is hence an ongoing work as more data is compiled throughout the current COVID-19 outbreak.

III. EXPERIMENTS

The primary goal is to investigate internationally reported cases of COVID-19 in order to determine consistency with Zipf's law. A secondary goal is to calculate the P-value for Zipf's law on each country's COVID-19 datasets. Lastly, Zipf's law P-values on a global map to convey the geographic distribution of reporting anomalies is illustrated.

The Power-law package developed by Clauset, Shalizi, and Newman [37] is used to obtain P-values for reported cases of COVID-19 per country. As methodologically reported in [37] and evaluated in [4], experiments are carried out 1000 times on the COVID-19 datasets in order to obtain P-values in each case. The steps followed to test whether COVID-19 datasets follow a Power-law are set out in [4] and [37]. It should be noted that the P-values are generated using the Kolmogorov-Smirnov (KS) statistic goodness-of-fit test as specified in [4] and [37]. The standard COVID-19 datasets available at: <https://github.com/CSSEGISandData/COVID-19> are used. The data consists in rows representing countries and columns representing the number of COVID-19 cases per each day from 22/1/2020 to 6/4/2020.

The evaluated hypotheses are thus:

- 1) Is Zipf's law applicable to COVID-19 case data?
- 2) How is Zipf's law behavior characterized if applicable?

IV. RESULTS

The P-values for all the countries/regions using COVID-19 confirmed cases based on the Power law calculation is performed. The complete P-values for the COVID-19 confirmed cases can be accessed at: <https://www.preprints.org/manuscript/202004.0531/v1>.

Furthermore, the distribution of P-values across countries/regions for COVID-19 confirmed cases is shown in Fig. 1. These P-values range from 0 to 1, with any country having a value of less than 0.1 deemed to deviate from Zipf's law.

Table I shows four countries'/regions' P-values to illustrate score dichotomy: Uzbekistan, Belize, Qatar have high P-values close to 1 while China has a P-value of 0 (to within the measured accuracy of the test). Countries/regions with the higher P-values indicate COVID-19 datasets in very close compliance with Zipf's law; China's reported statistics, along with those scoring similar P-values such as Australia, US, etc. are not possible to reconcile with Zipf's law.

Furthermore, P-values on all recovered cases of COVID-19 are calculated and are available at: <https://www.preprints.org/manuscript/202004.0531/v1>. Due to the number of recovered cases being small in some countries, Zipf's law is not statistically robust in such cases.

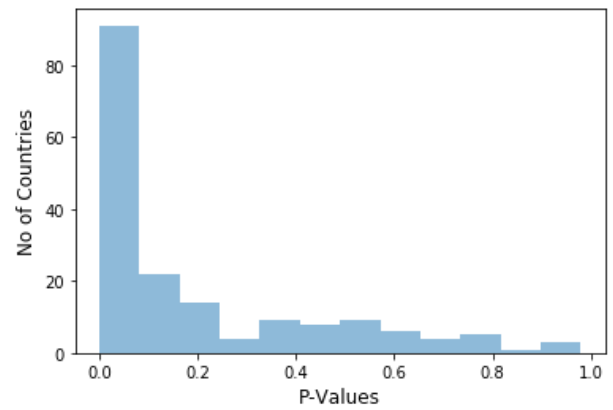


Fig. 1. Distribution of P-values across Countries / Regions for Confirmed Cases.

TABLE I. P-VALUES OF FOUR COUNTRIES / REGIONS FOR CONFIRMED CASES

Country	P-value
Uzbekistan	0.940
Belize	0.929
Qatar	0.897
China	0.000

The distribution of P-values across countries/regions for COVID-19 recovered cases are also illustrated in Fig. 2.

Again, Table II shows four external countries'/regions' P-values: Iraq, New Zealand, Austria and China (with China having an extremely low P-value of 0.002). It should however be noted that other countries such as Ghana, US, etc. have P-values of 0 which are lesser than China when considering P-values for recovered cases.

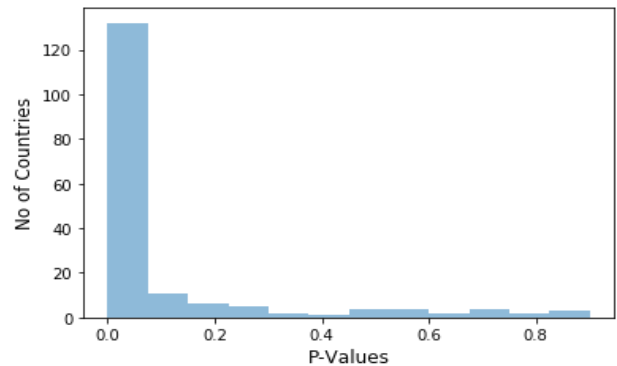


Fig. 2. Distribution of P-values across Countries / Regions for Recovered Cases.

TABLE II. P-VALUES OF FOUR COUNTRIES / REGIONS FOR RECOVERED CASES

Country	P-value
Iraq	0.901
New Zealand	0.888
Austria	0.884
China	0.002

The P-values of all death cases of COVID-19 across each country are also calculated and can be accessed at: <https://www.preprints.org/manuscript/202004.0531/v1>. In countries in which there are only a few recorded cases of COVID-19 deaths, power-law P-values are not presented.

The P-value distribution across countries/regions for COVID-19 death cases are indicated in Fig. 3.

Four extremal P-values are also shown in Table III; those for Bosnia and Herzegovina, Lithuania, Morocco and China; Bosnia and Herzegovina, Lithuania, Morocco have high P-values while China has a P-value of 0.000. Countries such as Costa Rica, Jordan, etc. have P-values of 0 similar to that of China.

Zipf's law power-law graph fits for each of the four countries identified in Tables I, II, and III are shown in Fig. 4, 5, and 6 for COVID-19 confirmed cases, recovered cases, and death cases, respectively.

Fig. 7a, b, and c indicate, on a global map, P-values per country for the COVID-19 confirmed cases, recovered cases, and death cases respectively. These maps are interactive and can also be viewed online for the COVID-19 confirmed cases¹, recovered cases², and death cases³ showing the P-values and country names when hovered on it.

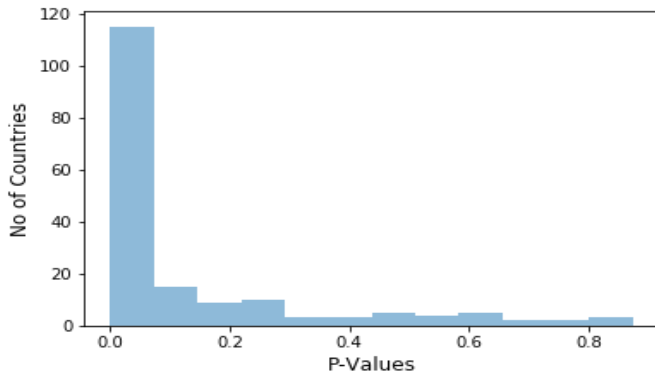


Fig. 3. Distribution of P-values across Countries / Regions for Death Cases.

TABLE III. P-VALUES OF FOUR COUNTRIES / REGIONS FOR DEATH CASES

Country	P-value
Bosnia and Herzegovina	0.874
Lithuania	0.843
Morocco	0.825
China	0.000

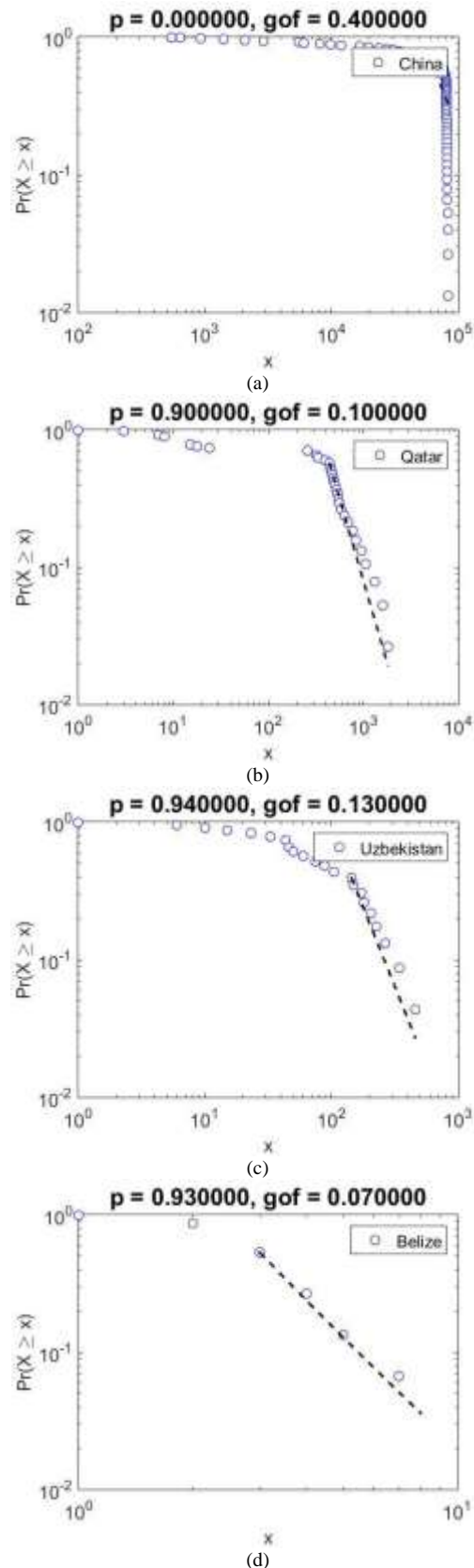


Fig. 4. Zipf's Law Power-Law Fits of COVID-19 Confirmed Cases for: (a) China, (b) Qatar, (c) Uzbekistan, (d) Belize.

¹ Confirmed Cases: <https://covid0.volitionlabs.xyz/zipfs/confirmed>

² Recovered Cases: <https://covid0.volitionlabs.xyz/zipfs/recovered>

³ Death Cases: <https://covid0.volitionlabs.xyz/zipfs/death>

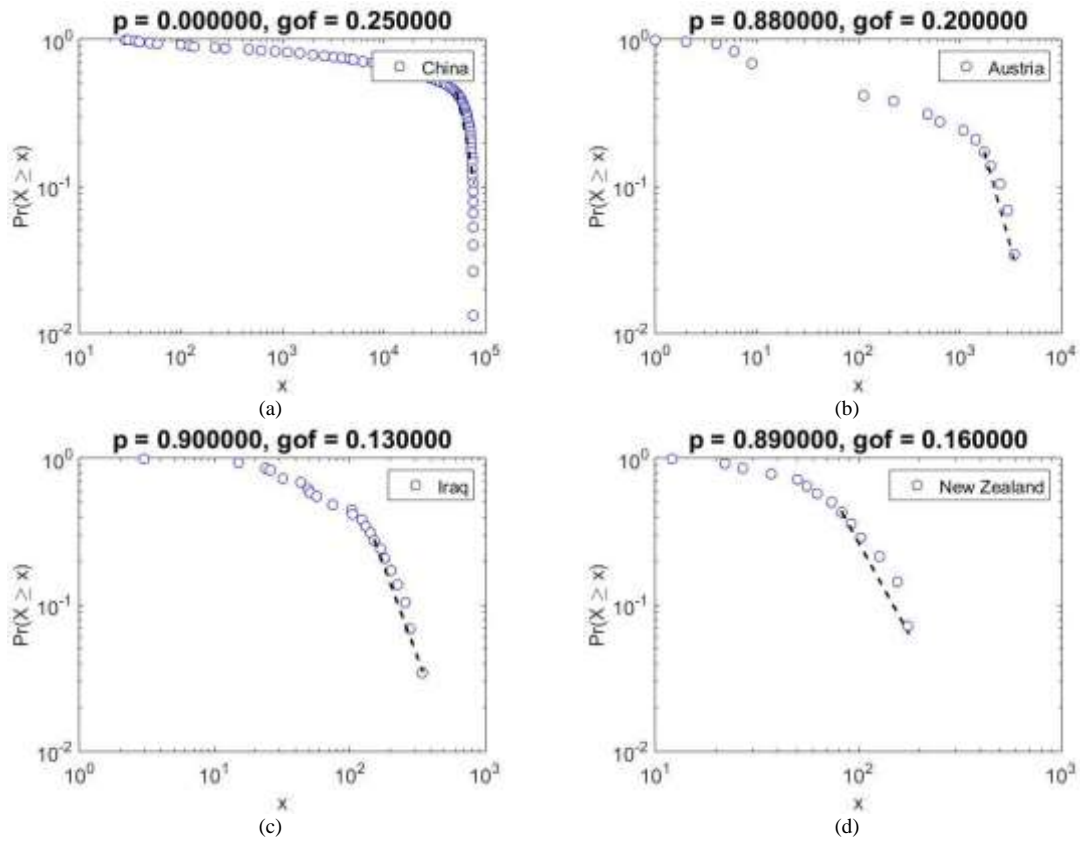


Fig. 5. Zipf's Law Power-Law Fits of COVID-19 Recovered Cases for: (a) China, (b) Austria, (c) Iraq, (d) New Zealand.

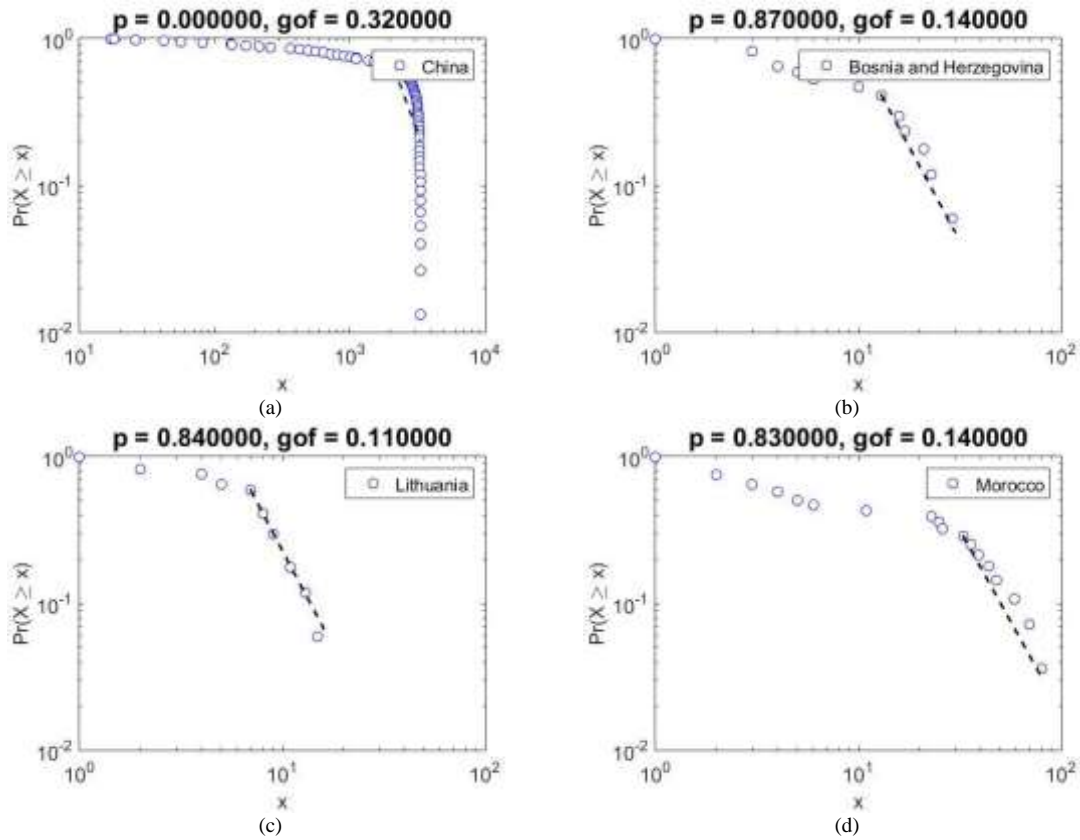


Fig. 6. Zipf's Law Power-Law Fits of COVID-19 Death Cases for (a) China, (b) Bosnia and Herzegovina, (c) Lithuania, (d) Morocco.

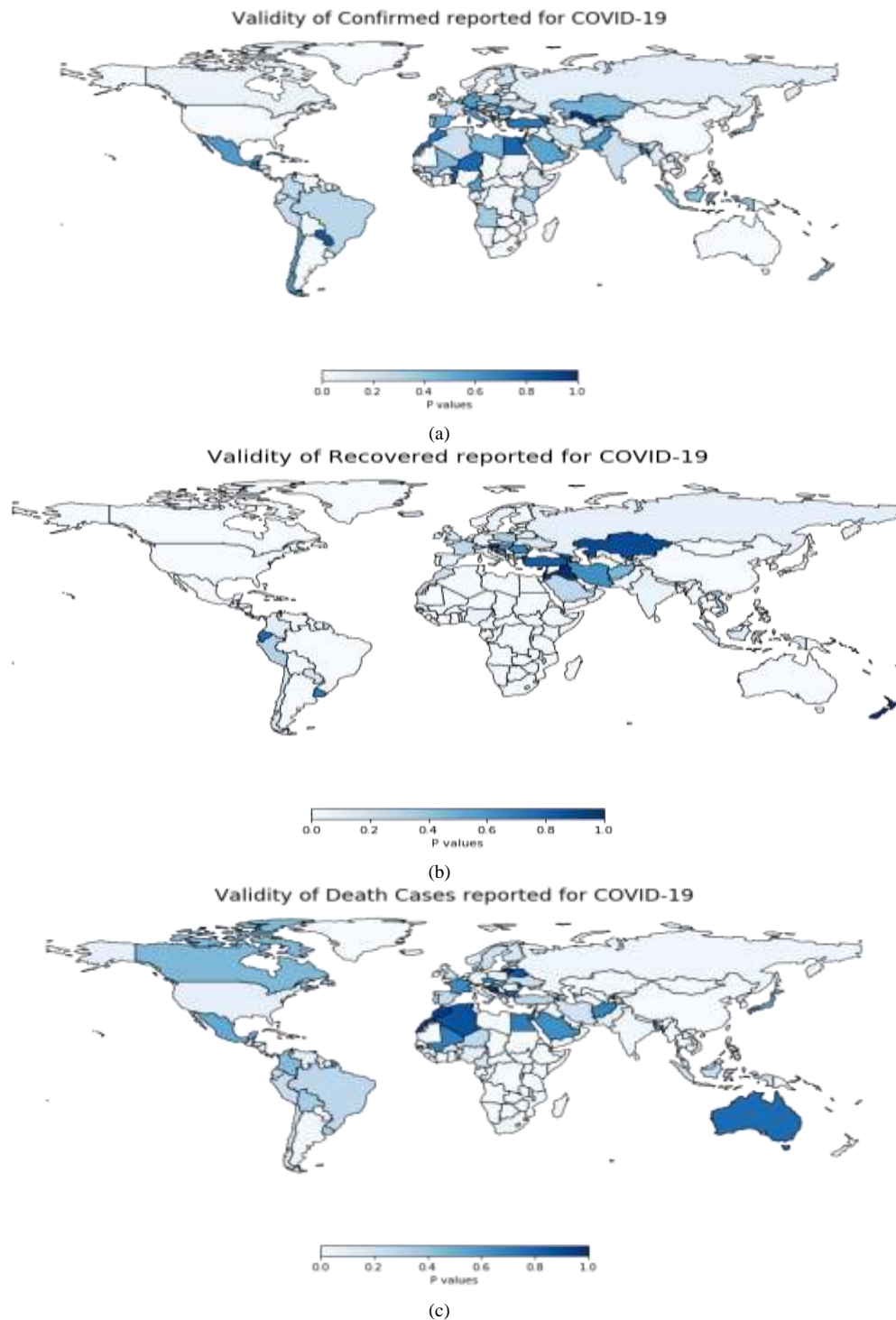


Fig. 7. Maps of: (a) COVID-19 Confirmed Cases, (b) COVID-19 Recovered Cases, (c) COVID-19 Death Cases.

V. DISCUSSION

Experiments indicate that many countries' COVID-19 datasets follow a consistent power law for confirmed cases of COVID-19, recovered cases of COVID-19, and death cases of COVID-19. (Table I indicates that Uzbekistan had the highest P-value of 0.94, followed by Belize with a P-value of 0.929, and Qatar with a P-Value of 0.897; Table II indicates that

Iraq's recovered cases data most closely follows Zipf's law with a P-value of 0.901, followed by New Zealand with a P-value of 0.888, and Austria with a P-value of 0.884; Table III indicates that Bosnia and Herzegovina had the highest P-value of 0.874, followed by Lithuania with a P-value of 0.843, and Morocco with a P-value of 0.825).

As can be seen in Fig. 4, 5 and 6, the CDF represented as $Pr(x)$ is plotted as a function of frequency (x) for the COVID-

19 dataset for confirmed, recovered, and death cases. The straight line (black line) shows the section of the plots where the Power law provided a good model fit [35] of the data considered.

From Fig. 1 to 6 and Tables I to III, however, it is observed that several countries have P-values that are less than 0.1. Notably, China's confirmed cases, recovered cases, and death cases of COVID-19 all failed to follow Zipf's law despite an earlier commencement of data recording than those of other countries (being the pandemic origin).

This has raised some questions, not only for China, but also every other country whose power-law P-values are less than 0.1 (this threshold being the one selected to establish compliance with Zipf's law according to the reasoning in [4, 37]).

Based on the above discussion, the paper can conclude that:

- 1) Zipf's law can be applied to COVID-19 case data with reliability monotonically improving in relation to dataset size.
- 2) This analysis can potentially be used as an 'early warning system' for further investigation into COVID-19 datasets not consistent with Zipf's law.

VI. CONCLUSIONS AND FUTURE WORK

In this paper, it is established that COVID-19 datasets for many countries can be shown to be consistent with Zipf's law. However, experiments also indicate that deviation of COVID-19 datasets from Zipf's law may be indicative of incorrect data reporting. The main application of this work is thus to serve as a potential early warning system for international health regulatory bodies such as the World Health Organization (WHO) in performing further investigations in countries where COVID-19 datasets have deviated from Zipf's law.

In future work, the plan is to:

- 1) Re-perform this experiment with complete statistics once the COVID-19 pandemic has ended.
- 2) Carry out experiments with other power laws variants (in particular Benford's law and Heap's law) both for COVID-19 and other pandemic datasets.

REFERENCES

- [1] Z. Y. Zu, M. D. Jiang, P. P. Xu, W. Chen, Q. Q. Ni, G. M. Lu, and L. J. Zhang, "Coronavirus disease 2019 (COVID-19): a perspective from China." *Radiology*, 200490, 2020.
- [2] L. Winter, Data fog: Why some countries' coronavirus numbers do not add up, Accessed on April, 30, 2020. [Online]. Available: <https://www.aljazeera.com/features/2020/6/17/data-fog-why-some-countries-coronavirus-numbers-do-not-add-up>.
- [3] A. Lachmann, "Correcting under-reported COVID-19 case numbers." *medRxiv*, 2020.
- [4] A. Iorliam, A. T. Ho, N. Poh, S. Tirunagari, and P. Bours, "Data forensic techniques using Benford's law and Zipf's law for keystroke dynamics." In *3rd Int. Workshop on Biometrics and Forensics (IWBF 2015)* pp. 1-6. IEEE, Mar., 2015.
- [5] R. P. Duncan-Jones, "The impact of the Antonine plague," *J. of Rom. Archeo.*, vol. 9, pp. 108-136, 1996.
- [6] A. M. Geddes, "The history of smallpox." *Clinics in dermatology*, vol. 24 no. 3, pp. 152-157, 2006.
- [7] F. M. Snowden, "Epidemics and Society: From the Black Death to the Present. Yale Uni. Press," 2019.
- [8] R. S. Bray, "Armies of pestilence: the impact of disease on history." James Clarke & Co., 2004.
- [9] R. Findlay, and M. Lundahl, "Demographic shocks and the factor proportions model: from the plague of Justinian to the Black Death." In *The Economics of the Frontier* (pp. 125-172). Palgrave Macmillan, London, 2017.
- [10] R. Horrox, "The black death." 2013.
- [11] O. J. Benedictow, "The Black Death: the greatest catastrophe ever." *History Today*, vol. 55, no. 3, pp. 42-49, 2005.
- [12] C. J. Duncan, and S. Scott, "What caused the black death?." *Postgraduate. Medical J.*, vol. 81, no. 955, pp. 315-320, 2005.
- [13] N. D. Cook, "Born to die: disease and New World conquest," pp. 1492-1650 vol. 1. Cambridge University Press, 1998.
- [14] N. Nunn, and N. Qian, "The Columbian exchange: A history of disease, food, and ideas." *J. of Econs. Perspective*, vol. 24, no. 2, pp. 163-88, 2010.
- [15] C. B. Vicentini, S. Manfredini, D. Mares, T. Bonacci, C. Scapoli, M. Chicca, and M. Pezzi, "Empirical 'integrated disease management' in Ferrara during the Italian plague" (1629-1631). *Parasitology Int.*, vol. 75, pp. 102046, 2020.
- [16] G. Alfani, and T. E. Murphy, "Plague and lethal epidemics in the pre-industrial world." *the J. of economic History*, vol. 77 no.1, pp. 314-343, 2017.
- [17] R. S. Roberts, "The place of plague in English history." *Proceedings of the Royal Society of Medicine*, 59(2), 101, 1966.
- [18] D. Barua, "History of cholera." In *Cholera* pp. 1-36. Springer, Boston, MA. 1992.
- [19] K. L. Kausrud, M. Begon, T. B. Ari, H. Viljugrein, J. Esper, U. Buntgen, and L. Xu, "Modeling the epidemiological history of plague in Central Asia: palaeoclimatic forcing on a disease system over the past millennium." *Bmc Biology*, vol. 8 no.1, pp. 112, 2010.
- [20] F. Delaporte, "History of yellow fever: an essay on the birth of tropical medicine." MIT Press, 1991.
- [21] A. J. Haddow, "X.—The Natural History of Yellow Fever in Africa." *Proceedings of the Royal Society of Edinburgh, Section B: Biological Sci.*, vol. 70 no. 3, pp. 191-227, 1969.
- [22] A. J. Valleron, S. Meurisse, and P. Y. Boelle, "Historical Analysis of the 1889-1890 Pandemic in Europe." *Int. J. of Infectious. Diseases.*, vol. 12, e95, 2008.
- [23] A. Choi, and A. García-Sastre, "Influenza forensics." In *Microbial. Forensic*, pp. 89-104. Academic Press, 2020.
- [24] W. G. Laver, and R. G. Webster, "Studies on the origin of pandemic influenza: II. Peptide maps of the light and heavy polypeptide chains from the hemagglutinin subunits of A2 influenza viruses isolated before and after the appearance of Hong Kong influenza." *Virology.*, vol. 48 no.2, pp. 445-455, 1972.
- [25] M. R. Ramogale, and J. Moodley, "HIV-associated maternal mortality—primary causes of death at King Edward VIII Hospital," *Durban. South Afric. Med. J.*, vol. 97 no. 5, pp. 363-366, 2007.
- [26] A. D. Grant, G. Djomand, and K. C. De, "Natural history and spectrum of disease in adults with HIV/AIDS in Africa." *AIDS (London, England)*, 11, S43-54, 1997.
- [27] C. C. Hon, T. Y. Lam, Z. L. Shi, A. J. Drummond, C. W. Yip, F. Zeng, and F. C. C. Leung, "Evidence of the recombinant origin of a bat severe acute respiratory syndrome (SARS)-like coronavirus and its implications on the direct ancestor of SARS coronavirus." *J. of Virology.*, vol. 82 no. 4, pp. 1819-1826, 2008.
- [28] J. Weyer, A. Grobbelaar, and L. Blumberg, "Ebola virus disease: history, epidemiology and outbreaks." *Current. Infectious. Disease. Report.*, vol. 17 no.5, pp. 21, 2015.
- [29] X. Pourrut, B. Kumulungui, T. Wittmann, G. Moussavou, A. Délicat, P. Yaba, and E. M. Leroy, "The natural history of Ebola virus in Africa." *Microbes and infection*, vol. 7 no. 7-8, pp. 1005-1014, 2005.
- [30] A. M. Ajlan, R. A. Ahyad, L. G. Jamjoom, A. Alharthy, and T. A. Madani, "Middle East respiratory syndrome coronavirus (MERS-CoV) infection:

- chest CT findings." American Journal of Roentgenology, vol. 203 no. 4, pp. 782-787, 2014.
- [31] Novel Coronavirus (COVID-19) Cases Data, Accessed on April, 17, 2020. [Online]. Available: <https://data.humdata.org/dataset/novel-coronavirus-2019-ncov-cases>.
- [32] C. D. Manning, and H. Schütze, "Foundations of statistical natural language processing." MIT press, 1999.
- [33] M. E. Newman, "Power laws, Pareto distributions and Zipf's law." Contemporary physics, vol. 46 no. 5, pp. 323-351, 2005.
- [34] L. R. Kalankesh, R. Stevens, and A. Brass, "The language of gene ontology: a zipf's law analysis." BMC bioinformatics, vol. 13 no. 1, pp. 127, 2012.
- [35] L. Wang, X. Li, Y. Q. Zhang, Y. Zhang, and K. Zhang, "Evolution of scaling emergence in large-scale spatial epidemic spreading." PloS one, vol. 6 no. 7, 2011.
- [36] Y. N. Pan, J. J. Lou, and X. P. Han, "Outbreak patterns of the novel avian influenza (H7N9)." Physica A: Statistical Mechanics and its Applications, vol. 401, pp. 265-270, 2014.
- [37] A. Clauset, C. R. Shalizi, and M. E. Newman, "Power-law distributions in empirical data." SIAM review, vol. 51 no. 4, pp. 661-703, 2009.

Clustering K-Means Algorithms and Econometric Lethality Model by Covid-19, Peru 2020

Javier Pedro Flores Arocutipa¹
Universidad Nacional de San
Agustín, Arequipa, Perú

Jorge Jinchuña Huallpa²
Universidad Nacional de Moquegua
Moquegua, Perú

Gamaniel Carbajal Navarro³
Luís Delfín Bermejo Peralta⁴
Universidad José Carlos Mariátegui
Moquegua, Perú

Abstract—Objective: The study looks at how the Covid-19 wave was in Peru, where and when it begins, where and when it culminates. As it faced, the shortcomings that were detected and especially that very little could be done to confront the disease as an emerging country. The wave began in May and ended in August with the greatest number of deaths and then fell. **Methodology:** Basic, explanatory level, with SINADEF data by region, of the situation room, to get the number of deaths, between January and September 2020/2019. **Results.** The relationship between infected and deceased was found a Pearson Rho of 0.94. The total death toll model depends on Lima, Huánuco, and Piura. The differences between the deaths of 2019 and 2020 were corroborated with the ANOVA, where a bilateral sig of 0.042 was got. The COVID cycle is found in the cluster algorithm model, of the nine months in 44.4% of them, it generated the highest lethality, between May and August. **Conclusion.** It is proven that COVID devastated regions of Peru. The model generated by the K-Means algorithm tells us that the COVID-19 cycle began in March and reached its highest peak of deceased and then descended.

Keywords—Infected; lethality; COVID 19 cycle; razing

I. INTRODUCTION

From March to October 2020, COVID-19 completed its cycle and showed the health crisis in Peru. The first wave would have passed, and it left 90 thousand dead according to SINADEF. Could anyone claim they existed, strategies with positive results against COVID-19? The answer is no. From Iquitos, Ucayali, Piura, Callao, Arequipa, Moquegua, Ica among other regions, allows us to compile what happened, since the MINSa, Essalud, and Diresas, [2] do not yet find the way, of what needs to be done in a holistic and holistic approach to prevention, diagnosis, treatment, and recovery.

The work of [3] also demonstrates the enormous number of deaths is in inverse relation to the shortage of doctors, beds, and Public expenditure per capita, in 30 countries of Europe. The car showed fewer inputs for the disease, more deceased. However, the investigation finds [4] that the greatest number of deaths are related to corruption rates, calling them risk factors.

There were little prevention and minimal targeted action. Although public policies propose that molecular testing is vital in diagnosis; it still uses rapid testing. They have caused more problems and are not blunt. The MINSa uses rapid antigen detection tests, erratic measurement since rapid tests are not useful for early diagnosis because such a test only finds

antibodies from day 10. Therefore, thousands of patients did not receive timely treatment, increasing the number of deaths in and outside the hospital, which reached its peak in May and then followed other regions, until August.

What did doctors learn from the experience between May and August in Peru?

In May 2020, they said that in Iquitos, Ucayali Piura, Callao; cases were decreasing. However, specialist and non-specialist people were focused on taking medicines to avoid reaching the third phase of the disease, a critical stage between life and death. Another is the lack of knowledge that COVID patients developed pneumonia, which led doctors in the regions to use very early tomography scans. The patient, on the third, fourth, and fifth day of illness, had a CT scan whose reports showed lung involvement (10% to 30%). The treatment showed apparently harmed the patient and sped up the path to the grave.

It can be concluded that from Iquitos to Tacna in Peru, they had the same problems because they used the same strategies even though they had 2, 3, or 4 months to prepare. And if they did, it did little good.

In Table I, the timeline of what happened between January and October in the world takes us that there is always a month or a “peak” day where there was the greatest number of deaths, it is infected who generate after days the number of deaths. For example, the highest number of deaths in China was on February 22, in Spain and Italy was the last third of March, the United Kingdom, and France reached the highest number of infected and deceased in April. Russia and Ecuador had in May, Peru had its hard month in June, Brazil in July, and Argentina with Colombia in August.

II. METHODOLOGY

It is a basic study of descriptive level, with the non-experimental design of the explanatory level. The analysis was mortality by regions in 2020. SINADEF, the Ministry of Health, and the regional health directorates of the regions of Peru were contacted. We tabulated the data of 24 regions in infected and deceased, included in some steps by districts to observe the difference between urban and rural. Pearson’s coefficient of determination and correlation and K-Means algorithm was applied. And variance analysis for related samples. Groups of regions have been defined by stages as they reached the maximum number of deaths in this PO.

III. RESULTS

The COVID 19 cycle in the world (Table I) shows peak dates. Thus, the maximum number of daily infected in the first wave (PO) in the United States, occurred on April 4 with 34582 daily, in the second wave was on July 2 with 79651 infected and in the third cusp that was on December 11 with 247414 infected. The highest number of daily deaths was on April 21 with 2743 deaths, on July 30 with 1853, and on December 9 with 3263. In France, in the first wave, it had a maximum of infected, on March 31 with 7578 infected and in the second wave on November 7 with 88790 daily. Those who died on April 15 were 1437, in the second wave (SO), on November 13, with 932 deaths. In Italy, on 21 March, the number of cases infected was 6554, while in the second wave, on 13 November, it was 40896. The deaths on March 27 of 921 died, in the second wave, December 3, with 993. In the UK in the PO the maximum arrived on April 10 with 7860 infected. In the OS on November 12 with 33470 infected. So also, in the PO, on April 21 with 1166 deaths while in the SO on November 25 with 696 deaths. In Spain, on March 20, in the PO the maximum daily was 10654, and in the OS on October 27 with 22641 infected, the maximum number of deaths in the PO was on April 2 with 996 deaths and in the OS the maximum daily was on November 24 with 537. This scenario leads us to ask how was the approach of COVID 19 in the world and especially in Peru by regions in the first wave (PO)?

In the PO, in January 2020, the OMS proclaimed to the world the disaster of the COVID-19 outbreak, which advanced at an indescribable speed, becoming the worst pandemic of this century. It started in China, crossed the countries of Europe, and reached Latin America in a few weeks. In Peru, according to medical specialists (infectologists, epidemiologists, among others) “raze” from Iquitos to Tacna, collapsing the supply of the health sector, exposing the deficiencies of infrastructure, its equipment, logistics of medicines, besides the competencies “in crisis” by health workers, expressed by fallacies in the treatment and use of medicines, who through ignorance and uncertainty used medicines - now withdrawn and outside the protocols of the MINSA - such as Azithromycin, Ivermectin, Hydroxychloroquine [1], including chlorine dioxide.

In the regions of Peru, what could be done? In Table II, we can observe it that the regions reached their highest peak of deaths during May, June, July, and August. In the first group are; Callao, Loreto, Ucayali, and Piura where the highest level of deceased, was in May (Fig. 1), then there is, Ancash, La Libertad, Lambayeque, Lima, Madre de Dios, San Martin, and Tumbes, here the highest ridge occurred in June (Fig. 2). In third place are the regions Amazonas, Arequipa, Cajamarca, Huánuco, Ica, Junín (Fig. 3) that had the highest number of deaths in July, and close with Ayacucho, Cusco, Huancavelica, Apurímac Moquegua Pasco, Puno, and Tacna in August (Fig. 4). Everything suggests that there was never a real strategy against Covid in Peru, or the impotence of not being able to do anything. Then COVID 19 will “walk” around the country. After sweeping the northern regions it enters the center and then to the south, for August raze Puno, Moquegua, and Tacna. The razing concept I use [5] when he tells us that in the middle of the nineteenth century the various global diseases demolished (cholera) Europe, is not that there is nothing left

but that anger did what it wanted with human beings in the West without problems that prevent it from being transnational (p.1). Table II shows that in Loreto, by March it had 211 dead, in April 474, and in May it reached the maximum of 1166 and then descend to 472 in June and in September to reach 229 dead. This is seen in all regions. Nothing prevented it from reaching the peak of death and then descending.

TABLE I. WORLD COVID-19 TIMELINE

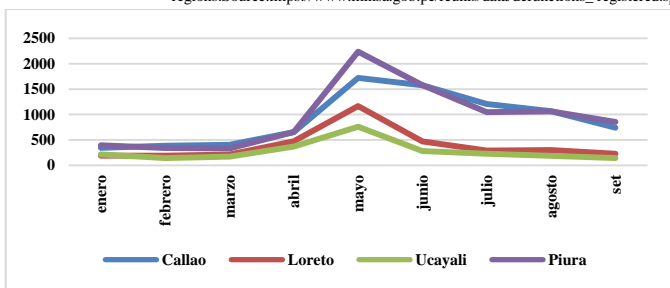
Countries	Jan	Feb	March	April	May	Jun - July	August	Sep	Oct
China	Jan-22	Feb-22	Mar22						
Infected	259	14108	40						
Deceased	8	142	22						
Spain		8-Mar	20-Mar	2-Abr	8-May	4-Jun			
Infected		2221	10856	4618	344	360			
Death		7	262	961	213	25			
Italy	25-Feb	21-Mar	27-Mar	30-May	30-Jun				
Infected	94	6554	5907	417	142				
Deceased	4	796	921	112	23				
UK		14-Mar	10-Abr	21-Abr		14-Jul			
Infected		310	7860	3896		398			
Deceased		18	1149	1166		46			
France		9-Mar	31-Mar	15-Abr	9-May				
Infected		203	7578	2633	433				
Deceased		3	498	1437	80				
Russia		27-Mar		15-Abr	29-May	1-Jul	15-Ago	6-Sep	22-Oct
Infected		196		3388	8572	6556	5061	5195	15971
Deceased		1		28	232	216	119	61	317
Ecuador		18-Mar	24-Abr	4-May	10-May	14-Jul	15-Ago	15-Sep	21-Oct
Infected		154	7059	2178	407	1033	1189	1972	1510
Deceased		2	25	301	640	105	55	41	47
Peru			22-Mar	19-May	31-May	17-Jun	5-Jul	16-Ago	22-Oct
Infected			32	4550	8805	3752	3638	10143	2991
Deceased			2	271	253	302	163	206	47
Brazil			1-Apr	4-Jun	19-Jun		29-Jul		22-Oct
Infected			1163	31890	55209		70869		31985
Deceased			41	1492	1221		1554		503
Argentina		31-Mar					29-Jul	22-Ago	22-Oct
Infected		159					8670	13056	8570
Deceased		2					380	400	172
Colombia				1-Abr	14-May	10-Jun	30-Jul	19-Aug	22-Oct
Infected				159	680	6803	9965	13056	8570
Deceased				4	21	61	380	400	192

Note: The cycle in the world was not uniform began in China, and reached its highest level and continued with the other countries until August, which reaches Colombia and Argentina. The virus passed through the world. Source: <https://www.worldometers.info/coronavirus/>

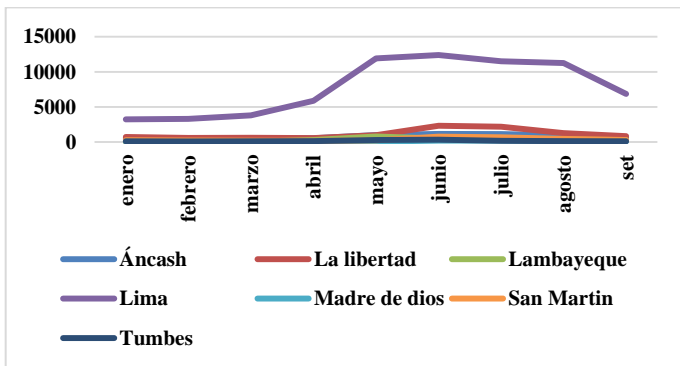
TABLE II. DEATHS TIMELINE BY REGION

Peru, deaths: Timeline by region-2020									
Region	Jan	Feb	Mar	Apr	May	Jun	Jul	Aug	Sep
Loreto	189	191	211	474	1166	472	292	301	229
Ucayali	215	144	171	369	761	282	229	186	143
Piura	395	341	331	657	2239	1581	1046	1064	854
Lambayeque	42	52	46	280	790	486	376	333	290
Callao	346	386	404	652	1722	1577	1209	1065	743
Ancash	473	465	492	531	1002	1160	1131	955	616
La libertad	719	574	597	569	972	2309	2183	1259	838
Lima	3220	3300	3792	5866	11910	12390	11508	11260	6851
Madre de Dios	88	51	59	43	69	194	193	121	77
San Martin	258	209	205	173	247	764	685	437	288
Tumbes	114	82	97	122	288	336	172	131	105
Amazonas	82	77	62	61	76	112	194	115	85
Arequipa	579	576	566	576	657	1208	2647	1889	828
Cajamarca	306	250	245	227	282	373	832	666	465
Huánuco	280	240	250	242	272	377	532	480	309
Ica	368	388	344	402	822	1231	1292	985	602
Junín	523	500	550	427	638	713	1390	1186	736
Ayacucho	174	155	135	135	177	174	251	317	229
Cusco	573	496	479	447	454	516	798	1415	687
Huancavelica	165	153	157	193	191	194	267	356	210
Apurímac	131	132	121	140	161	175	188	248	245
Moquegua	75	57	60	42	55	90	319	446	112
Pasco	99	78	81	63	103	86	148	170	106
Puno	377	414	358	347	385	406	715	1568	658
Tacna	108	93	95	74	101	106	240	477	202

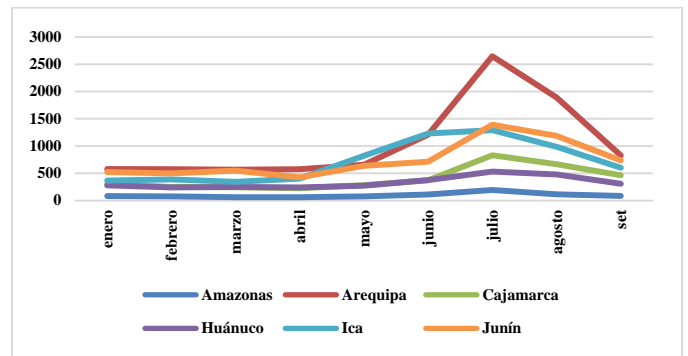
Note: The highest elevation started in May through August regions. Source: https://www.minsa.gob.pe/reunis/data/defuncions_registered.sp



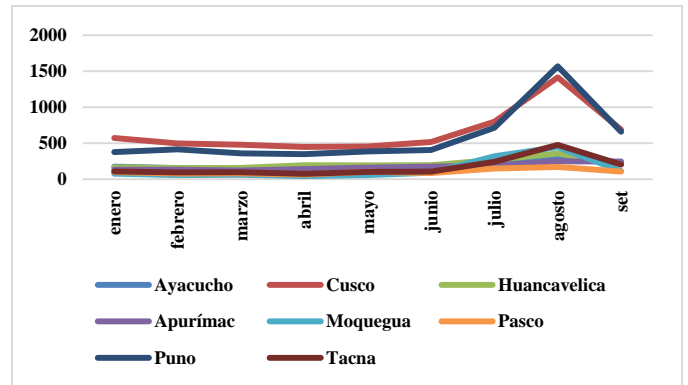
Note: The cycle reached its highest point in May, then fell.
Fig. 1. Regions with the Highest Deaths in May 2020.



Note: The cycle reached its peak in June, then descended.
Fig. 2. Regions with the Highest Deaths in June 2020.



Note: The cycle reached its peak in July, then descended.
Fig. 3. Regions with the Highest Deaths in July 2020.



Note: The cycle reached its peak in August, then descended.
Fig. 4. Regions with the Highest Deaths in August 2020.

Between January and September of the years 2019 and 2020 (Table III), it made a comparison of the number of deaths for all concept. This according to SINADEF data and globally in the analysis period in 2019 69 024 people died and in the year 2020, 167953, the difference, is an excess of 98926 deaths.

It is in Lima, where the greatest number of people died, from 22629 in the period January to September 2019 to 70097 in the period January to September 2020, a difference of 47418 people.

Then, the second region where more people died was Piura with 8508, there is an excess of 6431 people, in freedom the excess was 5262 people, in Arequipa with 4484 people in excess, also Ica with 3129 people in excess, Junín with 2826 people in excess, the silence that had 5292 people in excess, in Moquegua the excess was 667 people.

In 2020, 167950 people died between January and September. Of these, Lima concentrates 41.74%, freedom 5.97%, Arequipa 5.67%, Piura 5%, and Callao with 4.83%. They are the first five regions in the death ranking.

The difference between the deaths in 2020 and 2019 was a total of 98926. And of these, Lima concentrates 47.9%, La Libertad with 5.3%, Arequipa with 4.5%, Piura with 6.5%, and Callao with 5.3%. The percentage increase of the first five ranking regions leads us to point out that in the Lambayeque region the increase was 524%, five times more. It went from 432 deaths to 2695 in 2020.

TABLE III. DEAD TIME LINE ALL CONCEPT

All concept deaths, by region 2019-2020			
Region	Jan-Sep 2019	Jan-Sep 2020	Difference
Callao	2813	8104	5292
Loreto	1205	3525	2320
Ucayali	1190	2500	1310
Piura	2077	8508	6431
Ancash	3582	6825	3243
La Libertad	4758	10020	5262
Lambayeque	432	2695	2263
Lima	22679	70097	47418
Madre de Dios	498	895	397
San Martin	1380	3266	1886
Tumbes	705	1447	742
Amazonas	548	864	316
Arequipa	5042	9526	4484
Cajamarca	1637	3646	2009
Huánuco	1657	2982	1325
Ica	3305	6434	3129
Junín	3837	6663	2826
Ayacucho	678	1747	1069
Cusco	4383	5865	1482
Huancavelica	1097	1886	789
Apurímac	1101	1541	440
Moquegua	590	1256	667
Pasco	421	934	513
Puno	2739	5228	2489
Tacna	669	1496	827
TOTAL	69024	167950	98926

Note: The difference in deaths between January and September 2020 compared to 2019 was 98926.

In the same way Piura, with an increase of 310%. Passed from 2077 to 8508 deceased. In Lima, the number of deaths increased by 209%, from 22679 to 70097. In Callao, the number of deaths increased from 2813 to 8104, an increase of 188%. In the ranking, Loreto is in fifth place with an increase of 192%, from 1205 to 3525 deaths. The national average was 143%.

The average percentage lethality rate between May 15 and August 1, 2020, in Peru was 3.09%, meaning that for every 100 infected 3 had died.

The region with the highest rate was Ica with 6.81%, meaning for every 100 infected people 7 had died. In Lambayeque in the same way (6.8%). In Ancash, Piura, and Tumbes the deaths per 100 were 6. In the same way in the Loreto and Libertad region where it was 5 per 100.

In Amazonas, Callao and Ucayali are three people out of 100 who died. In Ucayali, Arequipa, Lima, San Martin, Junín, Pasco, Apurímac, Puno, Huánuco, Tacna, and Cajamarca had 2 per 100. And in Madre de Dios, Ayacucho, Huancavelica, Moquegua and Cusco was one person dead for every 100 infected.

Today, it can be stated based on empirical evidence that 98.5 percent of the deceased are adults and older adults [6], in the same way, they observe it in the relationship between infection and lethality. This is quite high. Calculations have been made for 75 days between May and August 2020. In the regions, determination and correlation coefficients have been found that exceed 0.70 and reach 0.996. The containment or self-containment measures have threatened mortality, as claimed [7], even though the infection did not stop. This should be investigated.

If the infected grow in proportion, the deceased will grow. This reality is definitively repeated in Ica, Ancash, La Libertad, Apurímac, San Martín, Moquegua, Pasco, Tacna, Huánuco, Callao that are above 0.97%, another high impact group is, Ayacucho, Lima, Madre de Dios, Tumbes, Piura, Lambayeque, Ucayali, Arequipa (Table IV), which are above 0.94 or 94%, in the third group are Loreto, Huancavelica, Cajamarca, Junín, Amazonas which are above 90% up to 94%. Cusco has a ratio of 0.845 that is significant and high, but not as high as that of the Ica region

Concerning the levels of explanation of deaths by the variable infected, it can be said that this ranges from 81.6% to 99.1%. All direct and meaningful.

There are differences (Table V) between those who died in 2019 and those who died in 2020. Sig. has been achieved, bilateral 0.042 denoting that the calculated t is greater than the table t. Differences between the data are accepted.

TABLE IV. HIGHER INFECTED COVID-19 HIGHER LETHALITY

Region	R ²	R
Ica	0.991	0.996
Ancash	0.984	0.992
La Libertad	0.983	0.991
Apurímac	0.981	0.990
San Martín	0.975	0.988
Moquegua	0.971	0.985
Pasco	0.963	0.981
Tacna	0.958	0.979
Huánuco	0.956	0.978
Puno	0.949	0.974
Callao	0.942	0.970
Ayacucho	0.935	0.967
Lima	0.934	0.966
Madre de Dios	0.926	0.962
Tumbes	0.926	0.962
Piura	0.925	0.962
Lambayeque	0.899	0.948
Ucayali	0.897	0.947
Arequipa	0.892	0.945
Amazonas	0.866	0.930
Junín	0.855	0.925
Cajamarca	0.850	0.922
Huancavelica	0.818	0.904
Loreto	0.816	0.903
Cusco	0.714	0.845

TABLE V. MATCHED SAMPLE TEST

Matched differences				t	Gl	Sig. (bilateral)	
Average	Standard deviation	Average of standard error	95% difference confidence Interval				
			Inferior	Superior			
-3957,0	9211,7	1842,35	7759,51	154,64	2,148	24	,042

The results of sig. (bilateral) is less than 0.05.

The econometric model that explains the total number of deaths by region is as follows:

$$\text{TOTAL DEATHS} = -2081.89357334 + 1.35125103834 * \text{LIMA} + 24.8222422247 * \text{HUANUCO} + 2.10959941364 * \text{PIURA}$$

$$R^2 = 0.9996, (0.0019) (0.0000) (0.0001) (0.0073) \text{ DW } (2.70)$$

And it can be concluded that in the period January to September of the year 2020, the regions of Lima, Huánuco, and Piura that are the independent variables, explain in an R2 of 0.9996 the total of deceased given that, probabilistic is less than 0.05 and obviously, the Durwin Watson is 2.70 that being around 2 shows us it is an acceptable model.

We would like to know what the impact of the deaths in Lima is on the total number of deaths. In practice, it can be said that for each percent that the deaths in Lima increase, it has an impact of 0.40% on the total number of deaths in the country. Likewise, in Huánuco, for each percent of those who die has an impact of 0.46% on the national total.

If in Piura increases by one percent, the number of deaths the impact on the total deaths is 0.2%. With certainty, we can say it that if the number of deaths in Lima increases by 10%, the number of deaths in Peru will increase by 4.3%. There's the regression model:

$$\text{LOG (TOTAL DEATHS)} = 1.83321127186 + 0.436468121477 * \text{LOG (LIMA)} + 0.465169428114 * \text{LOG (HUANUCO)} + 0.205749187226 * \text{LOG (PIURA)}$$

$$(0.0003) (0.0046) (0.0009) (0.0208) \text{ DW } (2.42)$$

Another observation got when analyzing the regions; Arequipa, Puno, Tacna, and Moquegua, is when the greatest number of deaths are concentrated in the urban part and mainly in the capital city. In Arequipa in July, there were 2647 deaths of that total, 2147 died in Arequipa, while in Islay 81, Caylloma with 75, in Camana 50, in Caravelí 19, in Castilla 19, in Condesuyos two and Union 5.

The same happened in Puno. Two cities, San Roman, which is Juliaca, and Puno the capital. In August there were 1,568 people dead. And in San Román-Juliaca there were 580 and in Puno 431 dead. The summation generates 1000 people, then Huancané 111, Azángaro 72, Collao 63, Melgar 62, and so on. With Moquegua, it should be stated that the two provinces concentrate almost the total of the deceased. They are Marshal Nieto 311 and Ilo 121 deceased.

In Tacna, in August 477 people died, and in the four provinces, in Tacna 448 other provinces died, Jorge Basadre 14, Candarave 6, Tarata 9.

In conclusion, it can be said that the greatest number of deaths are in urban areas and linked to the capitals of regions, while in rural areas the penetration of the COVID was in a smaller proportion and from there also the low number of deaths.

COVID-19 has questioned us on multiple aspects related to decision-making in public health, from health communication to the legal bases of prevention measures, monitoring of infection-related behaviors [8], or the application of epidemiological models.

The algorithm found by regions has variability and are concentrated in some 9 months analyzed, which allows us to observe that three clusters have formed (Fig. 5), three groups are observed. And that is one of them: it concentrates the last results, pointing out that there is correlate in the chain and with quite marked lethality peaks. It was the months of May, June, July, and August (Table VI). It contrasts with what reality presents. The article Mathematical Physical Modeling [9] showed that peaks can be found two weeks in advance.

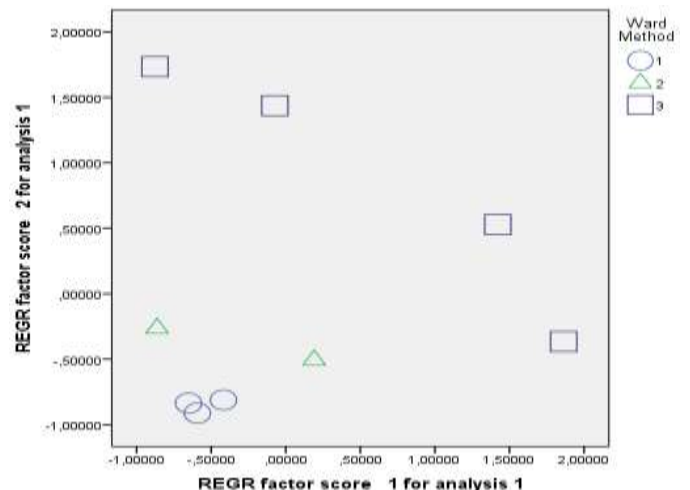


Fig. 5. Three Final Clusters.

TABLE VI. FINAL CLUSTER CENTERS: LETHALITY BY REGION

Regions	Cluster		
	1	2	3
Callao	378,67	697,50	1393,25
Loreto	197,00	351,50	557,75
Ucayali	176,67	256,00	364,50
Piura	355,67	755,50	1482,50
Áncash	476,67	573,50	1062,00
Libertad	630,00	703,50	1680,75
Lambayeque	46,67	285,00	496,25
Lima	3437,33	6358,50	11767,00
Madre de Dios	66,00	60,00	144,25
Martin	224,00	230,50	533,25
Tumbes	97,67	113,50	231,75
Amazonas	73,67	73,00	124,25
Arequipa	573,67	702,00	1600,25
Cajamarca	267,00	346,00	538,25
Huánuco	256,67	275,50	415,25
Ica	366,67	502,00	1082,50
Junín	524,33	581,50	981,75
Ayacucho	154,67	182,00	229,75
Cusco	516,00	567,00	795,75
Huancavelica	158,33	201,50	252,00
Apurímac	128,00	192,50	193,00
Moquegua	64,00	77,00	227,50
Pasco	86,00	84,50	126,75
Puno	383,00	502,50	768,50
Tacna	98,67	138,00	231,00

IV. DISCUSSION

In the papers analyzed, they show the cycle (Wave) of the COVID as can be seen in (Fig. 6) and its probable repetition, and perhaps in greater magnitude. It is known that the OMS pointed out in May that Brazil by August would have over 100 thousand dead, by the end of August this was 121 thousand dead [10]. It was said in the United States that the number of deaths would be 150,000 today reaches 400,000. It should be pointed out that the Ministry of Health does not yet determine the actual number of deaths in Peru, according to SINADEF. As of 31 December, there are 37680 deaths. From the above, we already know that the figure reaches almost 100,000 deaths from COVID in December.

Adults and older adults are the passive of deaths, in Spain, they show it is an aged country where the over 65 years are a percentage of 19% that in total are 8.7 million people [11] but is a product of life expectancy (EV) as a component of the Human Development Index. People in Europe have an 84-year-old EV just like France, Italy, and the UK.

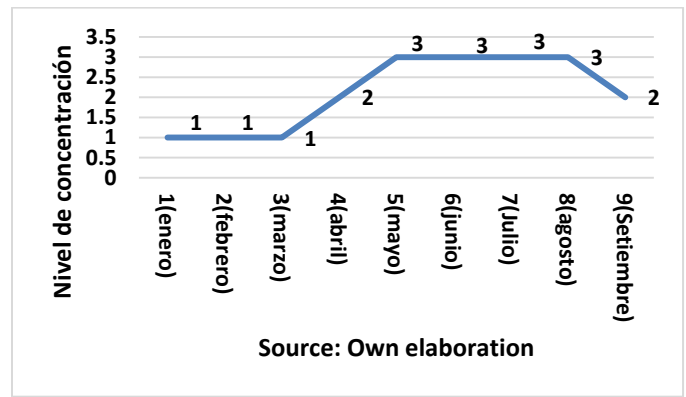


Fig. 6. Cluster De Pertinencia (3 Clusters). The Three Segments denote the behavior of Lethality.

In [12] the same way, it has been showed in Peru that in 98.5%, of the deceased are adults and older adults, other factors of death among the health sector’s own servants are the EPP, which, while aimed at administrative procedures but not at the prosecution of infections.

In [1] fact, as in Latin America, COVID-19 devastates the critical health situation in emerging countries and, of course, in Peru. The infrastructure teams are not prepared to face the COVID even from the perspective of human capital and its remunerations, which are those they face in the first phase. Although in this work it is not presented in a concatenated way. We state that from February to August 2020 it affected in maximum figures. Asia and Europe, then when entering Peru begins in regions of the east, then the north, from there the center and arrive in the Peruvian South. And gradually from May to August, sweep with death and infected too much, demonstrating the weak infrastructure of MINSA and ESSALUD.

As he tells us [5] in the middle of the 19th century, the different cholera viruses devastated Europe, not that nothing is left but that cholera did what it wanted with human beings in the world, without problems that prevent it from being transnational. In Peru, this expression is accommodated, however, we would add to it that the Wave came from Iquitos and ended in Tacna.

From now on, Lima and Callao are concerned about the levels of infected and deceased because of the urban population, but outside it the ones that have the greatest incidence are Loreto and Piura [1], meaning that the COVID appropriates the urban sector.

The deceased [1] correspond to a segment of the population, so we note that 85% of those are over 70 years old. For this reason, many Peruvians have been asking for the restructuring of the health system, that it serves Peruvian citizens [1] and in this modern world, we already know that they are linked to the sectors most affected [13], which are tourism and trade.

In [14] Latin America, analyzing the number of deaths about the number of infected reported (lethality of the disease), it was found that Ecuador, Brazil, and Argentina recorded the highest frequency of deaths by COVID-19, with percentages of

8.3%, 6.5%, and 4.4%, respectively. Chile 1%, Paraguay (1.3%) and Venezuela (1.3%) recorded the lowest frequencies in COVID-19 deaths.

The data suggest Chile is the South American country that presented the best coping strategy for COVID-19. [14], today is the best gains and implements the vaccine for its citizens.

Differences in [2], screening programs, as above, may underestimate the denominator and overestimate mortality rates if mild cases are not tested.

Age was associated with higher mortality, in our series, the highest proportion of deaths were in the age groups over 60 years, besides, that for every 10 years that the age increased, the risk of dying increased by 32%, This was described in [15], a large series of Chinese population data, in which the age groups 60 to 69, 70 to 79 and over 80 years had 3.6%, 8%, and 14.8% mortality respectively.

In conclusion, the largest series of patients hospitalized with COVID-19 in the country was reported; the population tested presented high mortality and was associated with age, comorbidities, [16] inflammatory markers, and respiratory involvement. These results could serve us to propose strategies for reorganizing the care system and to direct management differentiating in [15] patients with higher risk factors for mortality.

All this has led OMS to come up with formulas for carrying out global mortality estimates; [17] and that they are ratified by the work of [18] that the mathematical model SIR generates for Colombia teaches us that the quarantine, hygiene, distancing and budget for the EPP do not cease to allow the greatest lethality.

Or as I try [19], that is why the author got that the referred lethality was 0.9524%, is the average of 1.02%, between 0.65 and 1.34% with 149 countries.

80% of patients behave asymptomatic [20] as in Peru, and that in the absence of molecular evidence then becomes a factor of contagion and death.

The severity of COVID focuses on older adults in men rather than women and obviously, mechanical ventilation is a proportional aid. [21], [22], quarantine still influences the decrease in mortality.

If we point out that in Peru the case fatality rate was around 3% in China where the pandemic began, it was reported that the crude case fatality rate in [23] China was 2.3% in patients infected with SARS-CoV-2.

They are those over 40 years old, those who have a high risk of lethality [23], and that increases as the years go by. Dangerous is over 60 years of age.

V. CONCLUSIONS

COVID-19 demonstrated the precariousness of the health system in Peru, as in the countries of Asia and Europe, it toured the Peruvian east, then the north, it toured the center and devastated the Peruvian south and very little could be done to stop deaths. So, in May, he started in the east to end up in the south in the cycle of the highest number of deaths from

COVID-19 infection. The ratio between infected and deceased was on average quite high and direct 0.9. The total number of deaths is explained by what happens in the regions of Lima, Huánuco, and Piura. There are differences between the deaths of 2020 and 2019.

In the developed countries, the United Kingdom, Italy, Germany, France achieves levels of explanation (R2) on an average of 0.98 and finally China with 0.8184. Infection is a variable that influences and explains the behavior of deaths in the world.

The model generated by the K-Means algorithm shows the conglomerate is defined in the months of May-August, where the greatest lethality is concentrated. Above: March, April, or September.

The K-Means model shows us the behavior of lethality with fairly lofty peaks in the months mentioned.

VI. FUTURE WORK

Future work will focus on comparative analysis of the behavior of the first and second waves of covid-19, proposed model with reviews software and 2020-2021 algorithms.

Effects of the covid-19 coronavirus on employment, family income and digital education in Peru, 2020 - 2021 using econometric models.

Algorithms that explain the effects of COVID 19 on tax collection, private and public investment in Peru 2021.

REFERENCES

- [1] C. Maguiña Vargas, "Reflexiones sobre el COVID-19, el Colegio Médico del Perú y la Salud Pública Reflections on COVID-19 infection, Colegio Medico del Peru and the Public Health," *Acta Medica Peru.*, vol. 37, no. 1, pp. 8-10, 2020.
- [2] C. Maguiña, R. Gastelo, and A. Tequen, "El nuevo coronavirus y el desarrollo de la ciencia," *Rev Med Hered.*, vol. 9, no. 2, pp. 5-6, 2020.
- [3] E. Barrera-Algarin, J. L. Estepa-Maestre, Francisco Sarasola-Sanchez-Serrano, and A. Vallejo-Andrada, "COVID 19, neoliberalism and health systems in 30 countries in Europe: repercussions on the number of deaths.," *Rev. Esp. Salud Publica.*, vol. 94, p. 15, 2020.
- [4] R. Mazzucchelli, A. Agudo Dieguez, E. M. Dieguez Costa, and N. Crespi Villarias, "Democracia y mortalidad por Covid-19 en Europa," *Rev. Esp. Salud Publica.*, vol. 94, pp. 1-9, 2020.
- [5] F. Lizaraso Caparó and J. C. Del Carmen Sara, "Coronavirus and global health threats," *Horiz. Physician.*, vol. 20, no. 1, pp. 4-5, 2020, doi: 10.24265/horizmed.2020.v20n1.01.
- [6] J. P. Flores Arocutipa, J. Jinchuña Huallpa, and R. T. Condori Perez, "Validation of an Econometric Model of Lethality for Infected People COVID-19, Peru Mayo 2020," *Quipukamayoc.*, vol. 28, no. 57, pp. 17-23, 2020, doi: 10.15381/quipu.v28i57.18396.
- [7] Z. Yuan, Y. Xiao, Z. Dai, J. Huang, Z. Zhang, and Y. Chen, "Modelling the effects of wuhan's lockdown during covid-19, china," *Bull. World Health Organ.*, vol. 98, no. 7, pp. 484-494, 2020, doi: 10.2471/BLT.20.254045.
- [8] I. Hernández-Aguado and A. M. García, "Will public health be better after COVID-19?," *Gac. Sanit.*, No. xx, 2020, doi: 10.1016/j.gaceta.2020.06.004.
- [9] H. E. Sánchez Vargas, L. Beltrán Ramos Sánchez, P. Á. Galindo Llanes, and A. S. Rodríguez, Salgado, "Modelación fisico-matemática para la toma de decisiones frente a la COVID-19 en Cuba Physical-mathematical modeling for decision-making against COVID-19 in Cuba Luis Beltrán Ramos Sánchez Pablo Ángel Galindo Llanes Amyrsa Salgado Rodríguez Palabras clave," *Retos Dir.* 2020, vol. 14, No. 2, pp. 55-86, 2020.

- [10] N. Muñoz, "Covid-19 in Latin America: A first glance to the mortality," *Colomb. Med.*, vol. 51, no. 2, pp. 1-2, 2020, doi: 10.25100/cm.v51i2.4366.
- [11] R. Fernández-ballesteros and S. Alonso, "Clínica y Salud," vol. 31, pp. 165-169, 2020.
- [12] E. Galán-Rodas, A. Tarazona-Fernández, and M. Palacios-Celi, "Risk and death of doctors 100 days after the state of emergency by the COVID-19 in Peru," *Acta Medica Peru.*, vol. 37, no. 2, pp. 119-121, 2020, doi: 10.35663/amp.2020.372.1033.
- [13] N. Araújo Vila, "Economic impact of the pandemic caused by COVID-19 at the global level. Analysis of the most affected sectors," *Quipukamayoc*, vol. 28, no. 57, pp. 85-93, 2020, doi: 10.15381/quipu.v28i57.17903.
- [14] M. da C. N. Pinheiro, "Current situation of COVID-19 in South America," *Point of view*, p. 2, 2020, doi: 10.22354/in.v24i3.848.2.
- [15] M. A. Vences et al., "Factors associated with mortality in hospitalized patients with COVID-19: Prospective cohort at the Edgardo Rebagliati Martins National Hospital," *Scielo Prepr.*, no. 1, pp. 1-23, 2020, doi: 10.1590/SciELOPreprints.1241.
- [16] E. P. Beriso, "COINFECTION SARS-COV-2 AND OTHER PATHOGENS," *Rev. Esp. Salud Publica*, pp. 1-4, 2020.
- [17] WHO, "COVID-19 mortality estimation; scientific note. ," vol. 19, pp. 1-4, 2020.
- [18] J. Homero, W. Visbal, and M. C. Castillo Pedraza, "Mathematical approximation of the SIR epidemiological model for the understanding of containment measures against covid-19," *Rev. española Salud Pública*, vol. 94, no. 22, pp. 1-11, 2020.
- [19] Jesús I Simón Domínguez, Nadima Simón Domínguez, and Miguel A Reyes Núñez, "How to estimate the lethality of COVID-19," *Rev. Mex. Patol. Clínica y Med. Lab.*, vol. 67, no. 1, pp. 4-8, 2020, doi: 10.35366/93845.
- [20] M. Á. Serra Valdes, "COVID-19. From pathogenesis to high mortality in the elderly and with comorbidities," *Rev. Habanera Ciencias Médicas*, vol. 19, no. 3, pp. 1-12, 2020.
- [21] B. E. L. Manuel-Gamarra-villegas and K. E. Campos-correa, "Clinical-epidemiological characteristics and analysis of survival in deaths from COVID-19. attended in accommodation of the Red Sabogal-Callao 2020," *Horiz Med*, vol. 20, no. 2, p. e1229, 2020.
- [22] P. F. Grillo-Rojas, R. Romero Onofre, and J. Aldana-Carrasco, "Comparison of early non-pharmacological interventions in COVID-19 mortality from Peru and the United States of America," *Rev. la Fac. Med. Humana*, vol. 20, no. 3, pp. 425-432, 2020, doi: 10.25176/rfmh.v20i3.3114.
- [23] C. R. Aquino-Canchari, R. del C. Quispe-Arrieta, and K. M. Huaman Castillon, "COVID-19 and its relationship with vulnerable populations," *Rev. Habanera Ciencias Médicas*, vol. 19, pp. 1-18, 2020.

Optimize the Cost of Resources in Federated Cloud by Collaborated Resource Provisioning and Most Cost-effective Collated Providers Resource First Algorithm

V Pradeep Kumar¹, Kolla Bhanu Prakash²
Department of Computer Science and Engineering
Koneru Lakshmaiah Education Foundation
Vijayawada, India

Abstract—Cloud Computing works as the best solution for providing many of its services for cloud consumer agents with different requests for huge computational VM's with large storage capacity. The instance requests of cloud consumers will dynamically change as per their usage of application requirements with the demand for business growth, and single-vendor cloud becomes a constraint to satisfy these needs of the cloud consumers. Federated Cloud can contribute its solution approaches to meet these dynamic needs of cloud consumer requests of resource instances. The interoperability of clouds was made realistic with cloud federation. This paper provides an optimized solution approach where a set of collaborated cloud providers will provide services to satisfy consumer agents' multiple requests. It presents the two-phase collaborated resource provisioning (CCRP) approach and Most Cost-Effective Collated Providers Resources First (MCECPRF) algorithm. The algorithm's efficiency has been tested with specific data set for optimizing the cost for cloud consumer agents and analyzes the cancellation of requests, decision time for provisioning for different VM configurations within specific time slots.

Keywords—Cloud computing; federated cloud; collaborated resource provisioning; optimized cost

I. INTRODUCTION

Cloud computing has provided a wide range of computing services, which enabled business applications to utilize these services effectively in handling their client issues like on-demand access of resources [1], scaling the storage data, and fast access abilities [2]. The massive growth of cloud consumers who handle critical application services like online banking, shopping, and trading services requests resource instances that may not be taken by a single cloud provider [3]. The maintenance cost of making available a massive set of resources for cloud consumers' dynamic requests is typically tricky for a single cloud provider in meeting contractual agreement of quality of service (QoS) parameters as mentioned in Service Level Agreements (SLA).

Cloud provider agents need to enhance their computing services to satisfy the cloud consumer agent's requests at any instance. The dynamic resource provisioning leads to over-provisioning and under-provisioning resources as they get provisioned to cloud consumers, which leads to wastage of

resources and profit loss due to not meeting their contractual agreements. The inter-cloud concept [4] can meet the demand of dynamic resource provisioning by coordinating among a set of cloud providers and meeting all cloud consumers' service level agreements. Different flavours of inter-cloud mechanisms exist, Hybrid-cloud which makes all private cloud providers to get extended their services by making use of public clouds without any intimation; Multi-cloud utilizes the libraries of multiple cloud providers to enable the consumer applications to use resources without their knowledge, Sky computing provides a massive set of resources of various cloud provider agents without establishing any trust between them and federated cloud where the group of cloud providers agents provides resources by collaborating among themselves by forming a federated level agreement between them.

This paper presents a collaborative resource provisioning approach for forming coordination among cloud provider agents to share the resources using federated-level agreements [23] in the federated cloud. The cooperation among the cloud provider agent is realized in our work as a cooperative cloud market where resource provisioning is managed and generating optima profit for each cloud provider participating in the collaboration. Our significant contribution is supporting the cloud broker agent to deal with workloads' division according to dynamic resource instances' user requests.

The main contribution of this paper is a two-phase collaborated resource provisioning wherein one phase the consolidation of resource instances is done by the collated cloud service providers and second phase based on the type of requests of cloud consumer agents the consolidated resources are provisioned within an optimal cost using Most Cost-Effective Collated Providers Resources First (MCECPRF) algorithm. The paper's remaining sections are included a brief detail about related research in the Related work section. The section titled Collaborated Cloud providers Collation Formation with Resource Provisioning discusses the cooperative cloud providers effectively dealing with the consolidated resources. The detail about the two-phase approach and the MCECPRF algorithm, and the mathematical model were covered under the above section. The

Implementation and Results Evaluation section lists the different sampling data tested on the simulation tool is presented. Finally, Mentioned summarized findings with future work in the Conclusion section.

II. RELATED WORK

The computers' advancement rather than its improved computing ability in providing services as a utility like water usage and electricity usage bill was started long back in the year 1970s [28]. High technological advancements both at hardware and software level shifted the computing paradigm from single PC usage to considerable servers used for computing like utility, grid, and cloud with improved performance, reliability, scalability, and autonomy in varied services deployment, storage, processing. The mechanism of trading schemes was proposed by Buyya et al. [7] among the cloud providers in providing computing resources to cloud consumers within the specification of QoS parameters. The different schedules within approaches [8] were proposed based on the research advancement by building toolkits to demonstrate cloud providers and cloud consumers' interaction as the Cloud market.

The market-oriented nature of cloud, as proposed by Buyya et al. [9], has given significant functionality in managing admission control processes for different cloud consumer's requests. The QoS specification with available resources is used to accept or reject the suggestions based on their violation. The cloud broker model was proposed in [10] in which cloud service providers and cloud consumers are going to have interaction for meeting the demand-supply of resources with intermediate involvement in checking violations of Service Level Agreements (SLA). The E-Commerce paradigm is proposed in [11] with implementing cloud market model with four named entities like sellers, buyers, brokers acting as intermediaries with different policy mechanisms for gathering information about SLA, selection, and sharing of resources, negotiation and payment for the help as allocated [29].

Virtualization [12] is the unique feature of cloud computing methodology in realizing all its resources for allocation to meet the cloud user's requirements for managing their services at a different level of deployment of applications within the cloud. The share of resources is done in VM instances, including the composition of storage, computing machines, and bandwidth for cloud consumers by cloud providers. This mechanism of allocation of resources at runtime is termed as resource provisioning, as mentioned in [13]. Generally, cloud resources get provisioned dynamically to satisfy cloud users' workload requests based on several criteria mentioned in [14, 15] to group the set of VM's by cloud providers with single-server configurations. Meng et al. [16], Proposed a VM Multiplexing concept where a bunch of VM instances can be selected based on combined criteria as computed by intermediate broker systems. Zhan et al. [17] presents a resource provisioning mechanism that considers heterogeneous workloads for a single cloud provider sharing information of its configurations through a third party with other cloud providers to satisfy the cloud user's requests.

H. Wang et al. [18] presented a distributed system mechanism in managing the pricing options for cloud users with knowledge of cloud providers to provide the resources at the optimal price. Users can afford to use them for their application needs. Mazzucco et al. [19] worked on flexible pricing options for cloud consumers by considering good revenue collections for cloud providers. Menglan et al. [20] have studied the effects of reserved and on-demand instances based on achieving the minimum budget within the limitation of job allocation of cloud users. The formulations were made to perform jobs with a limited budget for cloud user varied requests. S. Khatua et al. [6] done work on formulating the pricing options that cloud users can pay for cloud services is treated as an integer programming problem with reserved and on-demand instances for gaining optimal cost. Quan et al. [21] implemented a stochastic method of integer programming model to optimize the cost for resource scheduling with SLA limitation. S. Chaisiri et al. [22] have dealt with many uncertainties to provide an optimal price for varied requests of cloud user demands for some time by using a stochastic linear integer programming. K. C. Okafor et al. [24] developed a distributed cloud computing network real-time model named spine-leaf to study the virtualization of resources with minimum SLA violations in a data center. The collaboration of automatic fog computing nodes with software-defined neural switch [25] shows the results of cooperation satisfying the massive workload requests made by cloud consumers. The scalability of fog computing nodes with spine-leaf network topology [26] shows can service effective management of different resource requests with low response time and less bandwidth.

Finally, the above-related work provides the list of research gaps which need to be addressed in the federated cloud. Cloud providers' collaboration for managing the request instances of type big data streaming needs to be provisioned. The formation of collation needs to be analyzed in terms of vulnerabilities faced during resource provisioning [27]. Providing the optimal cost for cloud consumers will lead to reasonable customer satisfaction, exploring the possibility of gaining good profits for cloud providers.

III. COLLABORATED CLOUD PROVIDERS RESOURCE PROVISIONING APPROACH

The Collaborated Cloud Providers Resource Provisioning approach is implemented by cloud Broker Agent to effectively handle the cloud market of provisioning resources within their optimal purchase cost. Initially, the Cloud Provider Agents (CPA) will analyze the type of requests of VM instances made by the cloud consumers and perform the Federated Level Agreement [23] with a set of (Quality of Service) QoS parameters like response time, process time, and availability and form collation and this collation formation will change as per the VM instances availability at the individual cloud providers who are involved in the collation. The cloud broker agent does handle the first phase of the CCPR approach by fixing the SLA parameters between the Collated Cloud Provider Agents (CCPA) and the request instance made by the Cloud Consumer Agent (CCA). The second phase involves the optimal computing cost [28] for a different type of requests serviced at CCPA. Fig. 1 gives clear pictures of the

CCPR approach with a neat block diagram mentioning its phase's operations [30]. Among the procedures, FLA monitoring and SLA monitoring are critical to managing by Cloud Broker Agent for handling the requested VM instances of CCA.

Our objective of the CCPR approach is to minimize the total cost spent by the cloud consumer agent in getting his request serviced from collated providers with the following constraints:

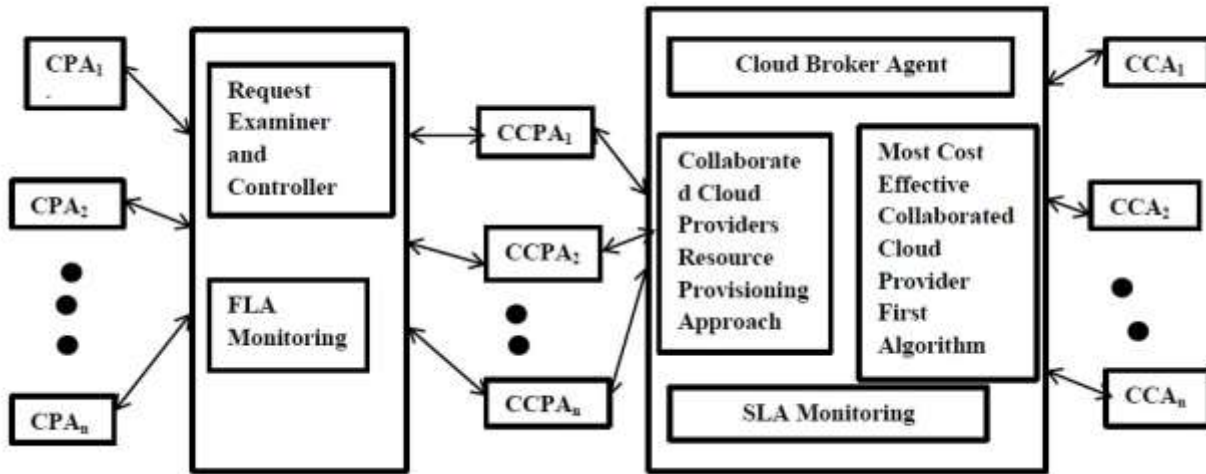


Fig. 1. Architecture Model for Collaborated Resource Provisioning Approach in Agent-Based Model for Federated Cloud.

Algorithm 1: ResourceAggregator (cpa,ca,ncpa,nca):

Input: objects of Cloud Provider Agents and Cloud Consumer Agents –CPA,ca,No of CCPA-ncpa, NoofCCA-nca
Global variable REQSTATUS=[‘Marked’, ‘Allocated’, ‘Marked for Allocation’]

Output: Requested VM instances status of Cloud Consumer Agents and return the TotalOptimalCost

```

// Initialized all types of request VM instances to zeros
UserReqVM, UserReservedVM, UserDemandVM, UserSpotVM=[0,0,0,0]
TotalReservedCost=0, TotalOptimalCost
// Aggregating the resources request of CCA depending on their request type
for i in 1: nca // for each Consumer Agent Object
  for j in 1:4 // for each requested Instance VM of type [SmallVM, MediumVM, LargeVM, ExtraLargeVM]
    UserReqVM [i][j]=ca[i].ResRe[j] // Intialize the user request array with consumer agent request array
    if ca[i].TypeofReq=='R' and ca[i].ResReq[j]!=0 // Checking the type of request for reserved instance
      UserReservedVM[i][j]=ca[i].ResReq[j]
    if ca[i].TypeofReq=='D' and ca[i].ResReq[j]!=0
      // Checking the type of request for On-Demand instance
      UserDemandVM[i][j]=ca[i].ResReq[j]
    if ca[i].TypeofReq=='R' and ca[i].ResReq[j]!=0
      // Checking the type of request for Spot instance
      UserSpotVM[i][j]=ca[i].ResReq[j]
// handling the reserved instances request by CCPA
for i in 1:ncpa
  for j in 1:nca
    for k in 1:4
//Checking the availability of requested reserved VM with CCPA and compute cost.
    if ((UserReservedVM[j][k]<=cpa[i].ARes[k]) and (ca[j].TypeofReq=='R')):
      cpa[i].ARes[k]=cpa[i].ARes[k]-UserReservedVM[j][k]
      TotalReserveCost += UserReservedVM[j][k]*cpa[i].CRes[k]
TotalCostDmdSpot=MostCostEffectiveCollatedProvidersResourceFristApproach(cpa,ca,ncpa,nca,UserDemandVM,UserSpotVM
)
  TotalOptimalCost=TotalCostDmdSpot+TotalReservedCost
for i 1:nca
  display the CCA requested resources status
return TotalOptimalCost

```

Algorithm 2: MostCostEffectiveCollatedProvidersResourceFristApproach(cpa,ca,ncpa,nca,dvm,svm):

Input: objects of Cloud Provider Agents and Cloud Consumer Agents –cpa,ca,No of CCPA-ncpa, NoofCCA-nca
dvm,svm Globalvariable REQSTATUS=['Marked','Allocated','Marked for Allocation']

Output: Requested VM instances and total cost for On-Demand and Spot are allocated for Cloud Consumer Agents

// Initialize local variables for total no of CCPA, Total demand and spot request and cost variables

```
maxCount=ncpa
totvm=[0,0,0,0]
rpcount,
TotDmdCost, TotSpotCost=0
for i in 1:ncpa
  for j in 1:4
    if(ca[i].TypeofReq=='D'):
      totdvm[i][j]=dvm[i][j]
      TotalDmdCost=ComputeTotalCost(cpa,ca,ncpa,nca,totvm,rpcount)
    if(ca[i].TypeofReq=='S'):
      totsvm[i][j]=svm[i][j]
      TotalSptCost=ComputeTotalCost(cpa,ca,ncpa,nca,totvm,rpcount)
  end for
end for
return(TotDmdCost+TotSpotCost)
```

Algorithm 3: ComputeTotalCost(cpa,ca,ncpa,nca,totvm,rpcount)

Input: objects of Cloud Provider Agents and Cloud Consumer Agents –cpa,ca,No of CCPA-ncpa, NoofCCA-nca
totvm Globalvariable REQSTATUS=['Marked','Allocated','Marked for Allocation']

Output: Requested VM instances and total cost for On-Demand /Spot are allocated for Cloud Consumer Agents

//Initialize local variables for computing the cost while allocating resources for On-Demand/Spot

```
xvm, xrp, sxvm, sxrp=[0,0,0,0]
rpcount, M, yrp, , ind, sind=0
Totcost=0
for j in range(nca):
  for k in range(4):
    if(M<ncpa):
      // Checking the minium VM requirements for On-Demand/Spot request with CCPA
      while((totvm[j][k]>0)and(cpa[M].ARes[k]!=0)):
        if(totvm[j][k]>=cpa[M].MinVm[k]):
          if (totvm[j][k]<=cpa[M].ARes[k]):
            //Initial matching of resources and getting allocated
            VMallocate(cpa[M],ca[j],totvm[j][k],M)
            cpa[M].ARes[k]=cpa[M].ARes[k]-totvm[j][k]
            ca[j].R=REQSTATUS[2]
            TotCost=TotCost+cpa[i].CRes[k]*totvm[j][k]
            totvm[j][k]=0
          else:
            // If required VM instances of On-Demand/Spot are available with CCPA after residue VM identified
            xvm[ind]=cpa[M].ARes[k]
            xrp[ind]=M
            totvm[j][k]=totvm[j][k]-cpa[M].ARes[k]
            ind=ind+1
            ca[j].ReqSt=REQSTATUS[3]
            rpcount=rpcount+1
        else:
          // if the Price requirements are agreed then the request status is updated
          if(ca[j].ReqPrice[k]>=cpa[M].CRes[k]):
            yrp=M
            ca[j].ReqSt=REQSTATUS[1]
```

```

M=M+1
if(totvm[j][k]==0):
    if(ca[j].ReqSt=="Allocated"):
        continue
    if((ca[j].ReqSt=="Marked for Allocation") and(rpcount<=maxCount)):
        //
        for j in range(ind):
            VMallocate(cpa[yrp],ca[j],xvm[k])
            cpa[yrp].ARes[k]=0
            totdvm[j][k]=0
            ca[j].ReqSt=REQSTATUS[2]
            TotCost=TotCost+cpa[i].CRes[k]*totvm[j][k]
        if(totvm[j][k]!=0):
            print("Unable to Provision consumer agent request")
            break
    end while
end for
end for
return(TotCost)

```

1) VM instances for all types of claims like Reservation, On-Demand, and Spot are nonnegative integers.
2) Cloud Consumer Agents need to follow a unique pricing model for a different type of request instances.

Table I notations are used to specify the formulate approach for understanding those above constraints:

Total reservation request VM instance cost is measured using the following:

$$\sum_{CCPA_{i=1}}^n \sum_{t=1}^T [Cost_f * ReqVM_r + Cost_r * ReqVM_r * TD] \quad (1)$$

Total On-Demand request VM instance cost is measured using the following:

$$\sum_{CCPA_{i=1}}^n \sum_{t=1}^T [Cost_o * ReqVM_o * TD] \quad (2)$$

Total Spot request VM instance cost is measured using the following:

$$\sum_{CCPA_{i=1}}^n [Cost_s * ReqVM_s * t] \quad (3)$$

Thus the optimal cost of operation from a Cloud Consumer Agents is specified as

$$\sum_{CCPA_{i=1}}^n \sum_{t=1}^T [Cost_f * ReqVM_r + Cost_r * ReqVM_r * TD] + [Cost_o * ReqVM_o * TD] + \sum_{CCPA_{i=1}}^n [Cost_s * ReqVM_s * t] \quad (4)$$

Subject to following constraints as mentioned

$$ReqVM_r, ReqVM_o, ReqVM_s \geq 0 \quad (5)$$

$$Cost_s + Cost_o + Cost_r \geq TotalCost_D \quad (6)$$

The equation (1) to (3) provides the formulae for computing reservation cost, on-demand cost and spot cost. Equation (4) gives the total optimal cost by meeting constraints as specified in equations (5) and (6). In Algorithm 1, all reserved requests were assigned for collated cloud providers who satisfy their exact match of a reserved right of VM instances. Table II and Table III specify the

Service level Agreement Parameters from the Cloud Consumer Agents and Cloud Provider Agents side. The Federated Level Agreement can be created based on those SLA of Cloud Provider Agents and form the corresponding Collated Cloud Provider Agents for satisfying the requests of VM instances of Cloud Consumer Agents. Algorithm 2 provides detail pseudo code for MCECPRF algorithm to which input of CCPA entity, CCA entity along with number of collated cloud providers and on-demand VM vector and spot VM vector. Depending on the request of VM vector type Algorithm 3 computes the total cost of resources for that respective request. The on-demand VM vector get provisioned for specific time duration and spot VM vector will be provisioned based on the availability of VM's for that time instance.

TABLE I. NOTATION SUMMARY

Parameter	Description
TD	Total time duration to handle the requests.
Cost	Reserved instance of Cost of resources
Cost _o	On-Demand instance of cost of resources per hour
Cost _s	Spot instance of resources cost at that instance.
ReqVM _r	Reserved Instance of the request of VMs
ReqVM _o	On-Demand Instance of the request of VMs
ReqVM _s	Spot instance of a request of VMs
TotalCost _D	Total Cost corresponding to demand vector for a duration D
Rev-Cost	Total reservation Cost for the entire contract period
Dem-Cost	Total on-demand cost for an entire-time slot
Spot-Cost	Total spot cost for that instance

TABLE II. CLOUD CONSUMER AGENTS REQUESTS SERVICE LEVEL AGREEMENTS

Type of VM	Requested VMs	Price(\$)	Availability (%)
Small VM	20	0.42	0.95
Medium VM	14	0.41	0.98
Large VM	15	0.35	0.96
Extra Large VM	10	0.46	0.98

TABLE III. CLOUD PROVIDER AGENTS SERVICE LEVEL AGREEMENTS

Type of VM	MaxVM's	Availability (%)	MinVM's	VMCost(\$)
Small VM	1000	0.98	50	0.45
Medium VM	1000	0.99	100	0.47
Large VM	1200	0.98	100	0.51
Extra Large VM	900	0.99	50	0.62

IV. IMPLEMENTATION AND RESULT ANALYSIS

Tested the proposed algorithms by simulation using Python3.7. Our execution's hardware platform is Intel I3 Processor with Core Duo Processor (1.5 MHz) and Windows 8.1 operating system. For simulation 5, cloud providers agents with random configurations, as stated in Table II for each type of VM instances, and four cloud consumer agents with random configurations as said for each VM instance as in Table III. The resource providers varying prices have been taken from Amazon EC2 [5].

Table IV and Table V are the results of MCECPRF algorithm of CCRP and stochastic results of Non-CCRP. Fig. 2 gives the details about slot-wise configurations for which collated cloud providers can handle the requests and provide the resources at an optimal cost to cloud consumers. The Fig. 3 graph provides a clear interpretation of the

percentage of cloud consumers' licenses cancelled in a particular timeslot for varied VM random configurations. The Fig. 4 shows the difference in milliseconds' decision time for provisioning resources for different time slots with various random VM configurations of collated cloud provider agents.

TABLE IV. CLOUD CONSUMERS UTILIZATION COST WITH COLLABORATED RESOURCE PROVISIONING (CCRP) APPROACH

Consumer Agents	Rev-Cost(\$)	Dem-Cost(\$)	Spot-Cost(\$)	Total Optimal Cost(\$)
CCA1	12.34	10.23	5.23	27.8
CCA2	10.26	15.23	8.26	33.75
CCA3	22.31	16.34	4.25	42.9
CCA4	15.26	13.24	8.23	36.23

TABLE V. CLOUD CONSUMERS UTILIZATION COST WITH NON-COLLABORATED RESOURCE PROVISIONING (NON-CCRP) APPROACH

Consumer Agents	Rev-Cost(\$)	Dem-Cost(\$)	Spot-Cost(\$)	Total Optimal Cost(\$)
CCA1	22.43	14.23	12.87	49.53
CCA2	18.45	17.43	18.26	54.14
CCA3	32.31	26.76	14.34	73.41
CCA4	20.26	17.24	18.23	55.73

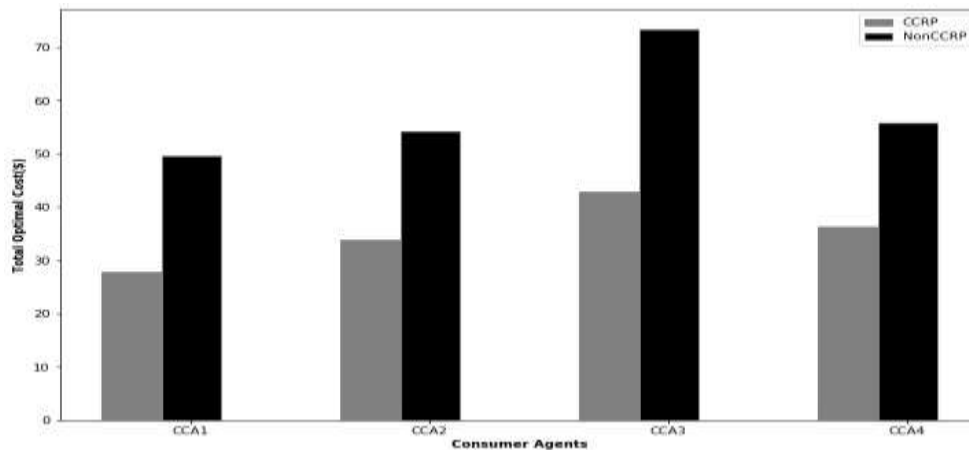


Fig. 2. Total Optimal Cost Comparison between CCRP vs. Non-CCRP Approach.

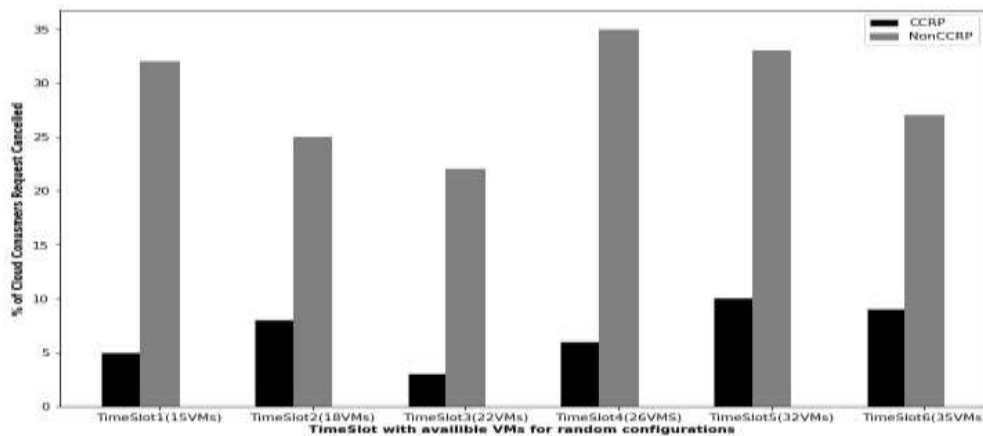


Fig. 3. Percentage of Cloud Consumers requests Cancelled.

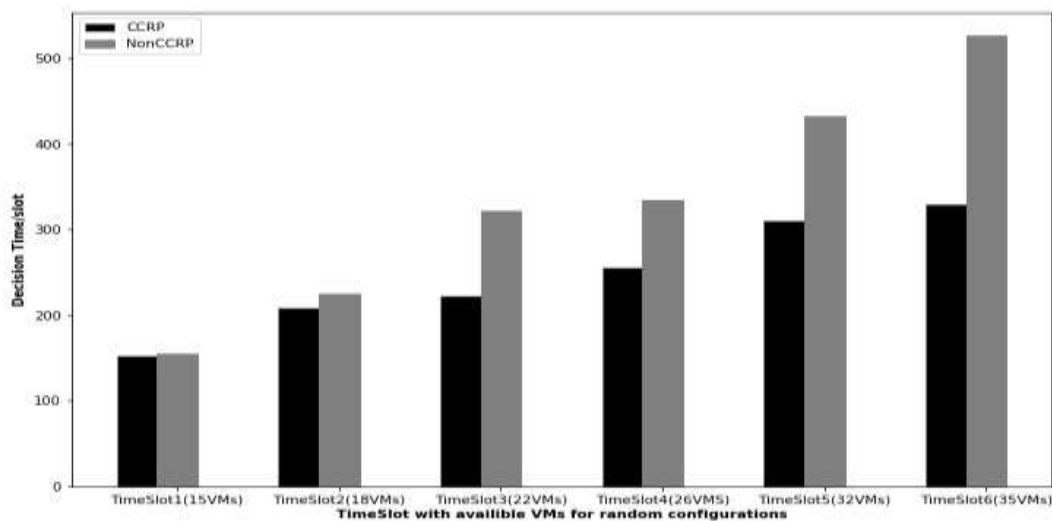


Fig. 4. Provisioning Decision Time in Milli-sec/slot.

V. CONCLUSION

Developed a useful cloud market model and managed federated cloud interactions among cloud provider agents and cloud consumer agents is realized through an Agent-Based Model. The Cloud Broker Agent is acting as an intermediary to meet the cloud user requirements and deliver services to them by using a collaborated resource provisioning approach (CCRP) where a different set of cloud providers are getting coordinated to provision VM instances at optimal cost for the other kind of requests like reservation, on-demand, and spot. The proposed MCECPRF algorithm provides the mechanism for checking VM instances with collated cloud provider agents and limiting resource provision for a particular period and samples. The future work would demonstrate this simulation on real-time setup to get the appropriate conclusions of generating optimal cost for cloud consumers for different VM configurations of cloud providers.

REFERENCES

- [1] Buyya, Rajkumar, Chee Shin Yeo, Srikumar Venugopal, James Broberg, and Ivona Brandic. "Cloud computing and emerging IT platforms: Vision, hype, and reality for delivering computing as the 5th utility." *Future Generation computer systems* vol. 25, 2009, pp. 599-616.
- [2] Kondo, Derrick, Bahman Javadi, Paul Malecot, Franck Cappello, and David P. Anderson. "Cost-benefit analysis of cloud computing versus desktop grids." In *2009 IEEE International Symposium on Parallel & Distributed Processing*, pp. 1-12. IEEE, 2009.
- [3] Campegiani, Paolo, and Francesco Lo Presti. "A general model for virtual machines resources allocation in multi-tier distributed systems." In *2009 Fifth International Conference on Autonomic and Autonomous Systems*, pp. 162-167. IEEE, 2009.
- [4] Grozev, Nikolay, and Rajkumar Buyya. "Inter-Cloud architectures and application brokering: taxonomy and survey." *Software: Practice and Experience* vol.44, 2014, pp. 369-390.
- [5] (2014) <http://aws.amazon.com/ec2/pricing/>.
- [6] Khatua, Sunirmal, Preetam K. Sur, Rajib K. Das, and Nandini Mukherjee. "Heuristic-based optimal resource provisioning in application-centric cloud." *arXiv preprint arXiv: 1403.2508* (2014).
- [7] Buyya, Rajkumar, Chee Shin Yeo, and Srikumar Venugopal. "Market-oriented cloud computing: Vision, hype, and reality for delivering it services as computing utilities." In *2008 10th IEEE international conference on high performance computing and communications*, pp. 5-13. IEEE, 2008.
- [8] Wu, Zhangjun, Xiao Liu, Zhiwei Ni, Dong Yuan, and Yun Yang. "A market-oriented hierarchical scheduling strategy in cloud workflow systems." *The Journal of Supercomputing* vol.63, 2013, pp.256-293.
- [9] Mudali, Geetika, Manas Ranjan Patra, K. Hemant K. Reddy, and Diptendu S. Roy. "Cooperative Resource Provisioning for Futuristic Cloud Markets." In *Computational Intelligence in Data Mining-Vol. 3*, pp. 607-616. Springer, New Delhi, 2015.
- [10] Ferrer, Ana Juan, Francisco HernáNdez, Johan Tordsson, Erik Elmroth, Ahmed Ali-Eldin, Csilla Zsigri, Raúl Sirvent et al. "OPTIMUS: A holistic approach to cloud service provisioning." *Future Generation Computer Systems* vol. 28, 2012, pp.66-77.
- [11] Li, Haifei, and Jun-Jang Jeng. "CCMarketplace: a marketplace model for a hybrid cloud." In *Proceedings of the 2010 Conference of the Center for Advanced Studies on Collaborative Research*, pp. 174-183. 2010.
- [12] Sotomayor, Borja, Rubén S. Montero, Ignacio M. Llorente, and Ian Foster. "Virtual infrastructure management in private and hybrid clouds." *IEEE Internet computing* vol.13, 2009, pp. 14-22.
- [13] Zhang, Qi, Lu Cheng, and Raouf Boutaba. "Cloud computing: state-of-the-art and research challenges." *Journal of internet services and applications* vol.1, 2010, pp. 7-18.
- [14] Padala, Pradeep, Kang G. Shin, Xiaoyun Zhu, Mustafa Uysal, Zhikui Wang, Sharad Singhal, Arif Merchant, and Kenneth Salem. "Adaptive control of virtualized resources in utility computing environments." In *Proceedings of the 2nd ACM SIGOPS/EuroSys European Conference on Computer Systems 2007*, pp. 289-302. 2007.
- [15] Bennani, Mohamed N., and Daniel A. Menasce. "Resource allocation for autonomic data centers using analytic performance models." In *Second international conference on autonomic computing (ICAC'05)*, pp. 229-240. IEEE, 2005.
- [16] Meng, Xiaoqiao, Canturk Isci, Jeffrey Kephart, Li Zhang, Eric Bouillet, and Dimitrios Pendarakis. "Efficient resource provisioning in compute clouds via VM multiplexing." In *Proceedings of the 7th international conference on Autonomic computing*, 2010, pp. 11-20.
- [17] Zhan, Jianfeng, Lei Wang, Xiaona Li, Weisong Shi, Chuliang Weng, Wenyao Zhang, and Xiutao Zang. "Cost-aware cooperative resource provisioning for heterogeneous workloads in data centers." *IEEE Transactions on Computers* vol.62, 2012, pp. 2155-2168.
- [18] Wang, Hongyi, Qingfeng Jing, Bingsheng He, Zhengping Qian, and Lidong Zhou. "Distributed systems meet economics: pricing in the Cloud.", 2010.
- [19] Mazzucco, Michele, and Marlon Dumas. "Reserved or on-demand instances? A revenue maximization model for cloud providers." In *2011 IEEE 4th International Conference on Cloud Computing*, pp. 428-435. IEEE, 2011.
- [20] Hu, Menglan, Jun Luo, and Bharadwaj Veeravalli. "Optimal provisioning for scheduling divisible loads with reserved cloud

- resources." In 2012 18th IEEE International Conference on Networks (ICON), pp.204-209. IEEE, 2012.
- [21] Li, Qiang, and Yike Guo. "Optimization of resource scheduling in cloud computing." In 2010 12th International Symposium on Symbolic and Numeric Algorithms for Scientific Computing, pp. 315-320. IEEE, 2010.
- [22] Chaisiri, Sivadon, Bu-Sung Lee, and Dusit Niyato. "Optimization of resource provisioning cost in cloud computing." *IEEE transactions on services Computing* vol.5, 2011, pp. 164-177.
- [23] Vadala, Pradeep Kumar, Bhanu Prakash Kolla, and Thinagaran Perumal. "FLA-SLA Aware Cloud Collation Formation Using Fuzzy Preference Relationship Multi-Decision Approach for Federated Cloud." *Pertanika Journal of Science & Technology* vol.28, 2020, pp. 117-140.
- [24] Okafor, K.C., Ugwoke, F.N., Obayi, A.A., Chijindu, V.C. and Oparaku, O.U., "Analysis of cloud network management using resource allocation and task scheduling services" *International Journal of Advanced Computer Science and Applications*, vol.7, 2016, pp.375-386.
- [25] Okafor, K.C., Ononiwu, G.C., Goundar, S., Chijindu, V.C. and Udeze, C.C., "Towards complex dynamic fog network orchestration using embedded neural switch." *International Journal of Computers and Applications*, 2018, pp.1-18.
- [26] Okafor, K.C., Achumba, I.E., Chukwudebe, G.A. and Ononiwu, G.C., "Leveraging fog computing for scalable IoT datacenter using spine-leaf network topology." *Journal of Electrical and Computer Engineering*, 2017, pp. 1-11.
- [27] Sultanpur, K.A. and Reddy, L.S.S., "Job Scheduling for Energy Efficiency Using Artificial Bee Colony through Virtualization.", *International Journal of Intelligent Engineering and Systems*, vol. 11, 2018, pp.138-148.
- [28] Praveen, S.P., Rao, K.T. and Janakiramaiah, B., "Effective allocation of resources and task scheduling in cloud environment using social group optimization.", *Arabian Journal for Science and Engineering*, vol. 43, 2018, pp.4265-4272.
- [29] Praveen, S.P. and Rao, K.T., 2019. An Effective Multi-faceted Cost Model for Auto-scaling of Servers in Cloud. In *Smart Intelligent Computing and Applications*, 2019, pp. 591-601. Springer, Singapore.
- [30] Sultanpur, K.A. and Reddy, L.S.S., "An Energy-Aware Resource Utilization Framework to Control Traffic in Cloud Network and Overloads." *International Journal of Electrical & Computer Engineering*, vol.8, 2018, pp.2088-8708.

Impact of Artificial Intelligence-enabled Software-defined Networks in Infrastructure and Operations: Trends and Challenges

Mohammad Riyaz Belgaum¹, Shahrulniza Musa^{3*}
Malaysian Institute of Information Technology
Universiti Kuala Lumpur
Kuala Lumpur, Malaysia

Muhammad Mansoor Alam⁴
Malaysian Institute of Information Technology
Universiti Kuala Lumpur, Kuala Lumpur, Malaysia
Institute of Business Management, Karachi, Pakistan

Zainab Alansari²
Faculty of Information Technology
Majan University College, Muscat, Oman
University of Malaya, Kuala Lumpur, Malaysia

M. S. Mazliham⁵
Malaysia France Institute
Universiti Kuala Lumpur
Kuala Lumpur, Malaysia

Abstract—The emerging technologies trending up in information and communication technology are tuning the enterprises for betterment. The existing infrastructure and operations (I&O) are supporting enterprises with their services and functionalities, considering the diverse requirements of the end-users. However, they are not free of the challenges and issues to address as the technology has advanced. This paper explains the impact of artificial intelligence (AI) in the enterprises using software-defined networking (SDN) in I&O. The fusion of artificial intelligence with software-defined networking in infrastructure and operations enables to automate the process based on experience and provides opportunities to the management to make quick decisions. But this fusion has many challenges to be addressed. This research aimed to discuss the trends and challenges impacting infrastructure and operations, and the role of AI-enabled SDN in I&O and discusses the benefits it provides that influence the directional path. Furthermore, the challenges to be addressed in implementing the AI-enabled SDN in I&O shows future directions to explore.

Keywords—Artificial intelligence; infrastructure and operations; software-defined network; virtualization

I. INTRODUCTION

Industry 4.0 puts together dynamic systems, which exist in several conflicting ways in their practical implementation within businesses. "4.0" is far from being a paradigm but composite geography which differentiates itself from the management culture, organizational growth, technical choices, the position of employees, regulatory structures, and the expectations of labour unions. Inside factories, it is the mixture of the physical world between manufacturing processes and the fictional environment of digital knowledge. Within the enterprise, the infrastructure and operations are adopting intelligent technologies in line with the vision of industry 4.0 [1]. The enabling technologies allowing for the smart environment are the Internet of Things (IoT), 5G networks [2], big data, cloud computing, virtual and augmented reality, artificial intelligence, and multi-access

edge computing [3] skills. Many new security and networking problems continue to emerge as IT systems are developed with these technologies. While these technologies have clear benefits, the ability of an organisation to support and sustain quick, high-demand supply chain operations is not therefore sufficient if traditional network technology is considered. Networking is the cornerstone of business growth in today's ever-connected world. For regular those complex supply-chain activities, producers, manufacturers, distributors, and consumers must be dynamic as company branches that rely on immediate communications for their offices. This is necessary if the supply chain is to have the needed management versatility and visibility. IoT devices, sensor connectivity, and other cyber-oriented systems are expanding, fostering development at the edge and on the network. The transformation from conventional networking to SDN brings efficiency, agility, and reduces costs [4].

Software-defined networking (SDN) is a modern paradigm in the field of networking, making it more agile by programming the network. This feature of customizing the network enables the infrastructure and operations to utilize better the resources based on the needs of enterprise and market demand. The end-user devices, storage data centres, and wide area networks are the players moving in a software-defined industry which enhances the control, programming, and response to business requirements of network operators. The motivation behind the move to SDN and Network Functions Virtualizations (NFV) has led to software and virtualization taking advantage that is based on agility, flexibility, and adaptability. This changes considerably the way networks are designed, managed and services delivered. Software, which becomes an increasingly important part of every network, embraces changing end-user criteria for greater programming and transparency. This level of business change requires significant restructuring of the network. Software-defined wide area networks [5] (SD-WANs) with a significant focus on SD security with many software platforms of

*Corresponding Author

companies is one of the most effective and efficient ways of achieving this milestone. The combination of various systems allows the manufacturers to operate more efficient, fast, and cost-effectively, while rising bandwidth. Also, synergies between SD-WAN and the multi-cloud architectures [6] offer several advantages to automation and virtualization and on-demand provisioning, while maintaining mobility and cost savings.

New technology deployment is not risk-free, and a company needs to evaluate its strategies for mitigating any threats to business continuity. To know where the threat comes from, first and foremost, it is essential to understand that any interruption to the company, regardless of how complicated, can be detrimental. Instead of a separate transportation line for enterprise-related networking, the use of cloud and SaaS can substitute the same reducing the security vulnerabilities [7]. Finally, it is essential to acknowledge that real innovation is not inherently the responsibility of existing vendors who have a crucial involvement in most companies. Organizations must also consider and depend on start-up innovation to take advantage of innovative solutions. Nevertheless, not all obstacles may be faced by SD-WAN. For instance, if there is a small business that only has one website, there is no need for SD-WAN if only a limited number of applications rely upon it. Moreover, when using the internet, it is still required to protect how the offices connect to the cloud or SaaS, consolidating multiple devices on the branch to create the software-defined branch. Currently, most organizations are using traditional networking and are ending up incurring huge expenses on administering the network management. Realizing the benefits of SDN they are transforming towards SDN to reduce the CAPEX and OPEX. The fusion of AI into SDN makes the process automated without human intervention. The basic purpose of this study is to explore some challenges faced in artificial intelligence-enabled SDN in I&O with a focus on the following.

- Trends impacting the I&O which play a significant role and are expected to accompany the commitments of organizations are discussed.
- The impact of AI on I&O with AI-enabled SDN in I&O along with the benefits are also discussed.
- Stepwise process of transforming a commoditized AI algorithm to a customized AI algorithm is presented.
- Challenges and future directions arising in merging these technologies.

The remaining paper is structured in the following way. Section 2 presents the related literature. Section 3 has a discussion part with the trends impacting I&O and the impact of AI on I&O. The challenges and future directions are presented in Section 4. In Section 5, the conclusion is presented.

II. RELATED LITERATURE

AI is a game-changing technology, which is integrated with various other technologies to give optimized results. In this section, some of the related studies have been discussed,

which shows how AI diffusion has impacted in improving the performance of different techniques in different domains.

Blockchain is a distributed technology that is currently being used to ensure secure and irreversible transactions. The authors in [8] have proposed a data-sharing mechanism with a focus on the network operations happening without human intervention. A trusted data-sharing framework was presented by designing a smart contract using DataChain and BehaviorChain. The smart contract grants permission to access considering the access methods and requirements. In [9], the authors have used AI in civil infrastructures to assess the visual quality of the constructions made. The authors proposed a smart mixed reality framework, by integrating it with a wearable device to detect the cracks. The mixed reality technology will help the investigators to assess and take decisions by improving the visual inspection.

Operations management (OM) is a field of management that converts raw materials and labour into products and services. The authors in [10] studied the feasibility of AI in OM considering various factors and proposed guidelines for the managers to take decisions. The results of the study present that the utilization of AI in OM increases efficiency, quality, and customer satisfaction. Also, they conclude that the adoption of AI in OM can be successful when the human and AI both function symbiotically. The digital transformation strategy (DTS) discussed in [11] is in a continually evolving state. A framework to transform from pre-digital organizations to a fully digital system has been proposed. A thorough study of this transformation has been discussed in a phase-wise manner until it is realized that DTS has been attained. The authors in [12] briefed how AI can improve business operations. Enterprises have been acquiring knowledge from experiences and by utilizing AI. Enterprise Cognitive Computing (ECC) with the help of AI has automated the process of information analysis to speed up the process with accuracy. The capabilities that companies should pose along with the key practices to follow for the organizations to be on the success path were discussed.

Reliable and robust network infrastructure is a challenging task that contributes to enhancing the user experience. The authors in [13] proposed an intelligent framework by utilizing the promising features of SDN and NFV focusing to reduce operational expenses (OPEX). The framework proposed was to fulfil three main requirements being automated network monitoring, autonomic network maintenance, and automated & dynamic service provisioning. But the proposed framework was not validated using real-time scenarios. The active use of virtualization technologies in organizations automate the management process by constructing modern network infrastructures. The tools used to manage the virtual components dynamically are discussed in [14]. The network infrastructure resources can be efficiently used by automating network equipment management. The authors in [15] have trained the network using an artificial neural network to handle the routing decisions considering the monitoring period. Varying the monitoring period from 3, 5, 10 seconds, various metrics were compared with static, dynamic, and artificial intelligence-enabled routing to prove that the network can learn from past experiences. Machine learning is

a stream of artificial intelligence, where it is also used to optimize multiple objectives and improve QoS in [16]. Also, this shows that artificial intelligence increases reliable links in the process of communication in terms of TCP and UDP.

III. DISCUSSION

A. Trends Impacting I & O

An important digital transformation has begun leading the enterprises with a massive I&O transformation. The theme is not about improving the hardware or software but providing delivery of the services to the organizations in an efficient way, matching their needs. The future of I&O is everywhere, as it is driven by business by nature. Various trends impacting the I&O can be seen from the following fig 1, which is adopted from [17].

1) *Serverless computing*: An emerging trend with the capability to provide a function platform as a service (FPaaS) is known as serverless computing [18]. There is no intervention of the user, and the functions to deliver and manage the infrastructure to the user is written as code. Rapid scaling and its granular billing are making FPaaS more exciting and attractive to the users. As the name says, it does not mean that the servers will be eliminated, but it supports utility logic, unpredictable demand, and event-driven requirements. In the coming decade, many organizations will follow this trend. Most of the cloud service providers are moving towards serverless computing by providing the functions abstracted. In a traditional data centre, the abstraction is provided in the physical environment. In contrast, with cloud services like IaaS and PaaS, the abstraction is done for hardware and operating system, respectively. Whereas in serverless computing, the abstraction is done at language runtime, and everything is provided using functions, so it gives function as a Service (FaaS) [19]. Fig 2 shows the user's control over the cloud services. From the figure, it is revealed that serverless computing comes before SaaS because, in SaaS, everything is delivered as software while in serverless, the applications are still in control of the user. Kubernetes is an open-source platform provided by Google for horizontal auto-scaling of applications in the infrastructure, based on resource usage. It is one of the microservice available as a function. The resources, like CPU / RAM, are valuable resources for any organization. Kubernetes implements Horizontal Pod Autoscaler (HPA), a pod is a basic unit of deployment to auto-scale the applications when the load increases. The threshold is fixed at the time of deployment, and the HPA gets triggered once the resource utilization reaches the limit. On the other hand, Amazon web services (AWS) implement the functions using Kinesis and Lambda.

2) *Artificial intelligence*: AI is a field of computer science, which has been successful in solving many real-time problems like failure recognition, predictive analysis, and others. Also, here AI can be used to perform faster with the growing I&O requirements, thereby reducing the need for

hiring staff. Various streams of AI are used in extracting data, classifying data, clustering, mapping, predicting, and optimizing.

3) *Network agility*: The changes in the networking field bring automation and orchestration with software-defined networks (SDN), and network function virtualization (NFV) that enables the business to rely on cloud services, IoT, edge services. The network performance affecting parameters like latency, bandwidth utilization, throughput, etc can be varied to make the network more agile.

4) *Death of data centre*: Realizing the fact that the traditional data centres are consuming a lot of physical resources, several organizations have started to shut down the data centres, and Gartner predicts that by 2025, this may go up to 80%. And the reason for this shutdown is not the technology but the business needs. This trend has put forth a challenge on how to satisfy the customer better by considering the increasing workloads and changing requirements.

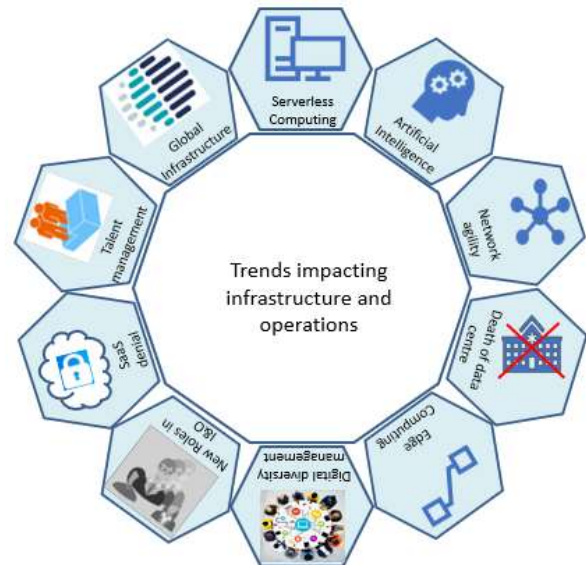


Fig. 1. Trends Impacting I & O.

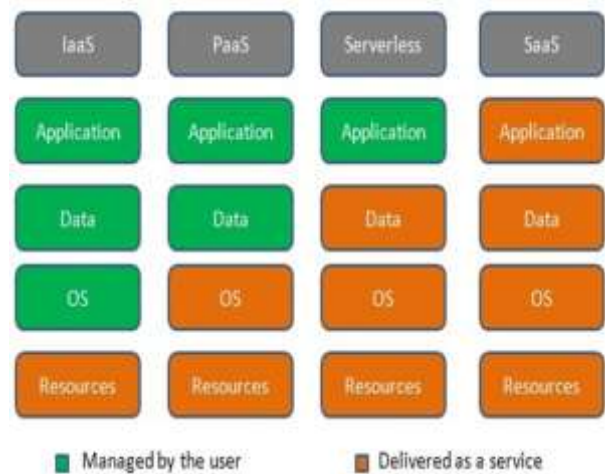


Fig. 2. Control over Cloud Services.

5) *Edge computing*: Most of the customers use latency-sensitive applications and, in no time, are always ready to shift to other providers if this latency increases. And edge computing is a technology that helps to reduce this latency by considering geographical locations and some laws of physics [20]. Moreover, most of the organizations are moving to industry 4.0, which supports digitization, edge computing helps in attaining better digital quality with increasing demands.

6) *Digital diversity management*: Diversity, here refers to the heterogeneous resources and different technologies used in digitization by enterprises. The wide use of digital devices in an organization utilizes the resources in distributing and managing digital assets. The management of these diverse resources is a challenge to avoid wastage and maintain accurate information as it directly impacts the business.

7) *New roles within I &O*: A significant concern is the lack of skills in maintaining cloud services with the personnel. With the increasing demand for I&O, the business must target on optimizing the costs and reducing the complexity in supporting new cloud services. The management of cloud services for customizing them according to the needs should be taken up by the new roles.

8) *SaaS denial*: I&O is all about maintaining, managing, and providing services to the customers. To better deliver the services with the existing infrastructure, the focus should be put on Software as a service (SaaS) because denial in SaaS may lead to disaster from a security, integrity, and delivery point of view for business.

9) *Talent management*: Normally, the IT personnel are placed in the organization chart vertically based on the expertise. However, this kind of organization keeps them bounded and restricted as the level moves towards the upward direction, resulting in limited output. Instead, if the IT personnel are horizontally exposed to different technologies, then the success of organizations will have no bounds.

10) *Global infrastructure*: As the customers access the services from different locations, I&O requires a global infrastructure to support them. The increase in the scalability of digital access helps the I&O groups and their supporters to provide infrastructure everywhere. Because the servers are located at different geographical locations, it requires global server load balancing, which extends to L4 and L7 of the Open System Interconnection (OSI) model. The load balancers are gaining significance as many enterprises are moving their applications to the data centres and clouds [21]. Therefore, the Infrastructure and Operations pioneers have come into focus as the trends mentioned above have put forth the challenges and opportunities.

B. Impact of Artificial Intelligence on I &O

Infrastructure and Operations is an umbrella with significant sections like helpdesk operations, infrastructure management, and application performance management. The enabler for the transformation in I&O is the artificial intelligence that interconnects the traditional approaches and

new business applications in a highly reliable way. It targets major cost savings, productivity, and performance improvements. It might also lead to the company's market transformation. Artificial intelligence is contributing a majority of spending in I&O to efficiently utilize the resources. According to International Data Corporation (IDC)¹, the Worldwide Semiannual Artificial Intelligence Systems Spending Guide expects that the AI systems to reach more than double in spending by 2022. Apart from spending the amount, there is a need for getting the fruit for the amount paid, and so the forecast says that the ground annual growth rate will be around 38% more during the mentioned period. The artificial intelligence learning process gets the experience from the function performed on the previous collection of input-output pairs and predicts output for upcoming inputs. It creates an environment to improve from the observation of the last contributions. Knowledge and feedback can be used to classify AI learning models.

1) *Knowledge-based classification*: Based on knowledge, AI learning models can be classified as inductive and deductive learning models. The inductive learning model is based entirely on the input-output pair of data collection. The deductive learning model continues with several regulations and frames new rules to improve efficiency with a particular AI algorithm.

2) *Feedback-based classification*: In terms of features, AI learning models can be classified as supervised, semi-supervised, unsupervised, and reinforced models based on feedback. Supervised learning models learn from the internal feedback to link the input with output observations. Semi-supervised models utilize a collection of compiled, numbered statistics to deduce new labels/attributes from existing databases of information. Semi-supervised models are a safe intermediate between supervised and unsupervised models. Unsupervised models investigate and analyze a sample that does not include any external feedback in attempting to enter statistics. Clustering is a typical case of the unsupervised model. The reinforcement learning model utilizes contrasting mechanisms such as incentives and punishment to "reinforce" special information. This form of mastering method in current AI solutions is increasing significantly. Fig 3 shows how AI is used in various sections of I&O. At the helpdesk and customer support where several tickets are handled, the organization can use machine language and natural language processing to handle tickets efficiently. And AI can be used in the infrastructure management section by efficiently managing the resources and predicts the long-term demand considering applications performance.

¹ https://www.idc.com/getdoc.jsp?containerId=IDC_P33198.

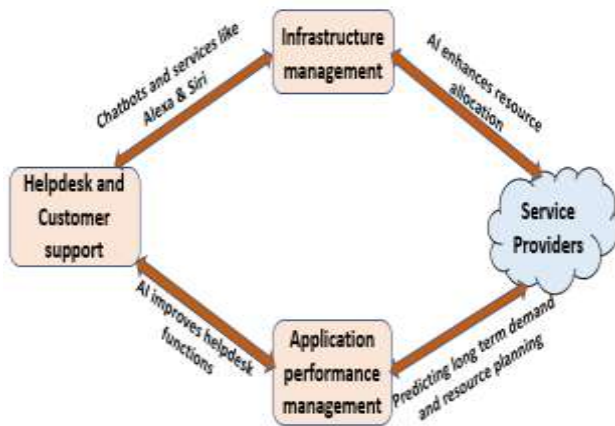


Fig. 3. AI-Driven Infrastructure and Operations.

Artificial intelligence is often debated, but many significant achievements are still in progress [22]. The most significant headwind of AI is its investment costs, which in the short term will skew returns. Nevertheless, if the change occurs, companies that make the investments should expect a significant performance gap to be unfairly rewarded. The AI techniques must address another essential element that every strategy needs: a code of ethics. Humans have developed artificial intelligence, and so it is not neutral and can be exposed to be biased [23]. Instances of such bias are already found in image searches, financial searches, etc. The technology providers must follow certain principles as shown in the following Table I, to ensure that AI is free of bias.

AI algorithms are readily available in the open-source environment or via cloud-based APIs, using a vast machine learning (ML) network [24]. Therefore, the availability of an AI algorithm designed for customization, optimization, search, or recommendation improves the customer experience by enhancing the quality of service (QoS). However, the commoditized AI algorithm lacks the following which is mentioned in Table II to match the user’s requirements.

TABLE I. PRINCIPLES TO BE FOLLOWED BY TECHNOLOGY PROVIDERS

Principle	Explanation
Utility	Ensure that the AI algorithms are clear, useful, and delightful for the user by using holistic metrics as the aim is not only to generate revenue but also to focus on social outcomes.
Empathy and respect	Evaluate the AI algorithms by satisfying the implicit and explicit needs of the population without having homogenous teams in the community and consider diversity.
Trust	Gaining trust is essential by being open, secure, and stable in behaviour.
Fairness and safety	In the real world, where these algorithms are used should not cause any harm either physically or digitally.
Accountability	A degree of responsibility must be set by measuring the performance and restructure it if the customers are unsatisfied.

TABLE II. DRAWBACKS OF COMMODITIZED AI ALGORITHMS

Drawback	Description
Lacks matching requirements	The truth is that commoditized algorithms are not readily available for competition. AI is just a commoditized tool without human intelligence to change algorithms. Humans must, therefore, incorporate technology to program algorithms as per requirements.
Human Intelligence only strengthens AI	Many technology firms are racing in the context of the AI revolution to harness AI, ML, and big data and drive further functionality and customization into individual client experiences. They can not only bear in mind the current needs of users but also function constructively to predict their customer’s tastes, moods, desires, and issues.
Lack of efficacy	The commoditized AI algorithms lack efficacy as the results generated may not match with the expected results.

The available commoditized AI algorithm needs to be seamlessly blended to match the requirements. The following framework should be followed in customizing the algorithms

- Step 1: Understand and define the goals you want your AI to achieve. This is achieved by introducing programmatic or visual methods for software-taking IT teams to see how the AI works in its present state.
- Step 2: The second stage is the implementation of the highest integrity criteria for the AI. IT managers and programmers should be able to explain what the AI is doing to personalize the AI. To understand what works and what is not in the algorithm, analytics is an integral part of the equation.
- Step 3: Then, program your intellectual property to map your specifications for the algorithms.

This is the best way to maximize the competitive edge that any algorithmic output can achieve and see if it aligns with or does not meet requirements.

The new algorithms proposed using AI technology use pattern matching techniques and implement them in the current scenario by customizing them according to the requirements. An unskilled person will ideally be able to focus on actual business outcomes through editing or augmenting the outputs in these AI algorithms sometime within the not-too-distant future and will not have to rely on the technical person to do so. This seamless combination of people and machines requires trust from above, which can be accomplished if proof and validations that their algorithm modification works are collected. Every day, algorithms get smarter, but alone somehow cannot do it. As the algorithms evolve, people are seeking to sharpen their intellect, to link the points, and to push towards a smarter future for business and beyond.

C. AI-enabled SDN in I & O

AI-enabled SDN helps the cloud companies to offer superior user interface application efficiency. The SDN enables application-conscious routing through the network via intelligence and the identification of apps. The required QoS and security policy enforcement is given to each class of requests, according to business requirements. Dynamism in resource distribution is an inevitable necessity to resolve the

issues in the I&O of any organization [25]. In other words, network services are delegated on request and released immediately after use. The various sections in I&O communicate and share the data through essential networking techniques. Rather when these sections communicate using AI-enabled SDN as shown in fig 4, then the resources can be intelligently used by improving the performance. AI-enabled SDN optimizes the distribution of requests across all servers to improve the QoS.

At present, SDN is the most appealing facilitator for the deployment of dynamic resources. The various streams of AI can be applied in SDN to optimize the performance in I&O. Using the inductive learning model, the managers can better extract the desired output as the inputs provided can be controlled. From the experiences of past behaviour, new rules can be discovered by implementing this model. The network administrators have centralized control over all the network operations. The deductive learning model is instruction-oriented learning. The concepts and rules are inducted to all employees in the organization by providing training. The SDN controller's global perspective of the usage of network services for all the participating users is part of the infrastructure sharing [26]. The controller functions as a broker between the tenants and the network owner and communicates each tenant to network service functionality (e.g. network use status) securely via authentication/authorization. This enables service trackers to dynamically ask the service manager for network support and agreements for SLAs through signals. Conventional networking is no longer appropriate mostly because of the rear-mounting of all traffic from branches to headquarters-including that for the cloud-contributes to latency and affects application efficiency. SDN offers network simplification, reduced costs, productivity in bandwidth, and seamless cloud-based on-ramps with substantial application performance, particularly for critical applications, with no privacy or protection. The works discussed in [15] and [16] are evidence of how artificial intelligence fusion with SDN has improved the results in terms of performance.

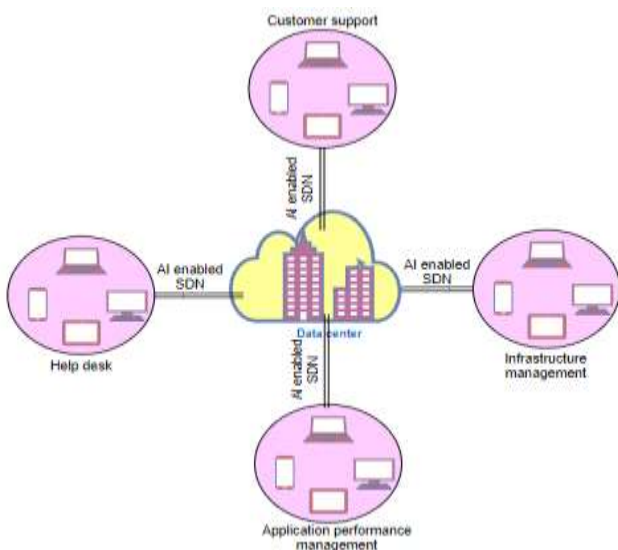


Fig. 4. AI-enabled SDN in Infrastructure and Operations.

1) *Combining SDN with 5G:* 5G networks spread across vertical and regional areas over the next decade are increasing. The service providers may provide the services at an increased bandwidth and minimize latency with a price costing less per bit than today. The parallel adoption of 5G and SD-WAN [27] makes it essential that organizations understand what these technologies can do for companies.:

- To achieve the agility, costs, and flexibility necessary for the digital age, all techniques are guided and applied with a disassembled model that separates hardware and software, and the data plane from the control plane.
- In deployments for improved customer experience, both technologies will be distributed. Organizations will offer completely new CX technologies such as AR / VR in retail.
- 5G can provide a high-performance connectivity underlay network that can be made more widely available in many areas where the high-speed broadband service wireline networks cannot deliver [28]. The integration of 5G in SDN improves network performance in terms of throughput, latency, energy efficiency, connectivity, service deployment, reliability, etc.

D. Benefits of AI-enabled SDN in I & O

- **Efficient:** The efficiency in terms of provisioning time is indisputable. It shortens the provisioning cycle from seconds to milliseconds and this significant reduction, in turn, has increased the efficiency.
- **Automated:** The integration of AI has enabled the process to be automated. The functions to be performed are triggered timely based on the actions programmed and does not need any human intervention.
- **Reduced human errors:** Manual operations result in misconduct of operations by making errors in network misconfiguration. But the automation reduces such errors.
- **Secure:** The transmission of data using AI-enabled SDN is secure. As it gives a centralized view of the whole network and easily detects anomalies and attacks.
- **Consistent:** A key benefit of AI-enabled SDN is to efficiently use various modes of network transport. A simple solution is to block the traffic coming from an underperforming link and redirect it to a better performing link to ensure consistency in providing the services.
- **Monitoring and better management:** An AI-enabled SDN intelligently monitors and manages to support the transport services. It improves network performance by enhancing the metrics used to measure the QoS (packet loss rate, latency, jitter, throughput).
- **Zero-touch provisioning:** The centralized orchestration and control over the network enable to configure the devices automatically without the intervention of the network administrator.

- Storage management: The storage resources can be optimally utilized by performing predictive analysis and the storage space can be adjusted based on necessity.

IV. CHALLENGES AND FUTURE DIRECTIONS

The following are the challenges faced by the organizations in the process of transforming from traditional networking to AI-enabled SDN from the I&O perspective.

- Deployment: Wi-Fi is today the most common connectivity used in the IT sector. SD-WAN plays a significant role in transforming the edge network in IT infrastructure, but the question arises on how sensors and devices are deployed and linked, which are so prevalent within production companies. The challenges concerned with coverage, intrusion, capability, and security are unaddressed.
- Threat Detection and Analysis: Several solutions are available in new generations of wireless internet access points to deal with this problem by extending the network or radio technology available. However, safety is the main challenge because establishing a safe and secure network is crucial to the operation of business-critical IT infrastructure along with managing them within the manufacturing company. Prevention of outages and disruptions is a major concern. The drastic changes in technology though it brings advancement yet comes with various open threats that have to be handled.
- Protection: Protection has increasingly been the focus when regulatory authorities and end-users want to have a free and fair exchange. It can be provided using a heuristic-based approach and intelligence-driven as protection in providing services requires tight integration at the system level. Many companies create AI advice engines so reliable that very little information is required about the individual who makes a choice, and that customization is a challenge to be addressed.
- Resource utilization: Another challenge concerned with the infrastructure is the communication between the representative and clients that consumes a lot of resources, time, and cost. So to minimize this, the AI technology system comprises of specialized software for a pre-check site and argument sheet, where the Automatic speech recognizing (ASR), converts audio into text, and by using natural language processing (NLP) the researchers have taken the task of reducing the consumption of resources and improving the performance.
- Next-generation implementation: With 5G implementations in the industry becoming more popular, 5G will provide an additional or alternative Wi-Fi solution. Based on various analogies, the key difference between 5G and Wi-Fi is with its implementation and management in terms of range and power consumption. Through 5G, a company can connect its sensors and devices through the network in a fully managed and secure environment. Globally,

mobile network providers aim to deliver 5G services operated to businesses in precisely such an area. The full implementation of this next-generation networking has many new challenges unaddressed.

- Cyber-security: In the present situation of the pandemic, most of the employees are performing their tasks by work from home using different networks. This has made it the attackers easy to penetrate the network. Most of the organizations are investing now in making this more secure and is an open area of research.

V. CONCLUSION

Infrastructure and Operations in any organization need to be efficient to benefit its stakeholders. The transformation of communication mode from traditional to SDN in various sections of I&O gives a centralized control. AI's role in the field of networking with a capacity to program the network in SDN has changed the perception of providers and users. Various trends impacting I&O are discussed with a focus on AI-enabled SDN in I&O. The softwarization of the networking provides the users with applications, data, and resources along with a platform to use them. This research contributes to putting forward a framework following a step-wise process of converting commoditized AI algorithms to customized algorithms matching the requirements. Also, the impact of AI on various sections of I&O highlights the benefits of integrating AI-enabled SDN in I&O. The challenges discussed in the process of implementing AI-enabled SDN, from the infrastructure and operations perspective put forward future directions for the researchers to explore more in the area.

REFERENCES

- [1] L. Agostini and R. Filippini, "Organizational and managerial challenges in the path toward Industry 4.0," *European Journal of Innovation Management*, vol. 22, no. 3, pp. 406-421, 2019.
- [2] N. Javaid, A. Sher, H. Nasir, and N. Guizani, "Intelligence in IoT-based 5G networks: Opportunities and challenges," *IEEE Communications Magazine*, vol. 56, no. 10, pp. 94-100, 2018.
- [3] Q.-V. Pham et al., "A survey of multi-access edge computing in 5G and beyond: Fundamentals, technology integration, and state-of-the-art," *IEEE Access*, vol. 8, pp. 116974-117017, 2020.
- [4] A. A. Barakabitze, A. Ahmad, R. Mijumbi, and A. Hines, "5G network slicing using SDN and NFV: A survey of taxonomy, architectures, and future challenges," *Computer Networks*, vol. 167, p. 106984, 2020.
- [5] D. Kim, Y.-H. Kim, C. Park, and K.-I. Kim, "KREONET-S: Software-defined wide area network design and deployment on KREONET," *IAENG International Journal of Computer Science*, vol. 45, no. 1, pp. 27-33, 2018.
- [6] K. Zkik, G. Orhanou, and S. El Hajji, "Secure mobile multi-cloud architecture for authentication and data storage," *International Journal of Cloud Applications and Computing (IJCAC)*, vol. 7, no. 2, pp. 62-76, 2017.
- [7] R. Buyya et al., "A manifesto for future generation cloud computing: Research directions for the next decade," *ACM computing surveys (CSUR)*, vol. 51, no. 5, pp. 1-38, 2018.
- [8] G. Zhang, T. Li, Y. Li, P. Hui, and D. Jin, "Blockchain-based data sharing system for ai-powered network operations," *Journal of Communications and Information Networks*, vol. 3, no. 3, pp. 1-8, 2018.
- [9] E. Karaaslan, U. Bagci, and F. N. Catbas, "Artificial intelligence assisted infrastructure assessment using mixed reality systems," *Transportation Research Record*, vol. 2673, no. 12, pp. 413-424, 2019.
- [10] P. Grover, A. K. Kar, and Y. K. Dwivedi, "Understanding artificial intelligence adoption in operations management: insights from the

- review of academic literature and social media discussions," *Annals of Operations Research*, pp. 1-37, 2020.
- [11] S. Chanias, M. D. Myers, and T. Hess, "Digital transformation strategy making in pre-digital organizations: The case of a financial services provider," *The Journal of Strategic Information Systems*, vol. 28, no. 1, pp. 17-33, 2019.
- [12] M. Tarafdar, C. M. Beath, and J. W. Ross, "Using AI to enhance business operations," *MIT Sloan Management Review*, vol. 11, 2019.
- [13] P. Neves et al., "Future mode of operations for 5G–The SELFNET approach enabled by SDN/NFV," *Computer Standards & Interfaces*, vol. 54, pp. 229-246, 2017.
- [14] A. Klimova, S. Kodolov, K. Aksyonov, and A. Y. Filimonov, "Implementing Dynamic Management Of Virtual Network Infrastructure Components," in *CEUR Workshop Proceedings*, 2019, vol. 2525: CEUR-WS.
- [15] Wu, Y. J., Hwang, P. C., Hwang, W. S., & Cheng, M. H., "Artificial Intelligence Enabled Routing in Software Defined Networking." *Applied Sciences*, vol. 10 no.18, 6564, 2020.
- [16] A. Akbar, M. Ibrar, M. A. Jan, A. K. Bashir, and L. Wang, "SDN-enabled Adaptive and Reliable Communication in IoT-Fog Environment Using Machine Learning and Multi-Objective Optimization," in *IEEE Internet of Things Journal*, doi: 10.1109/JIOT.2020.3038768.
- [17] Gartner, "Gartner IT Infrastructure, Operations & Cloud Strategies Conference," 2019. [Online]. Available: <https://www.gartner.com/en/newsroom/press-releases/2019-09-09-gartner-announces-it-infrastructure-operations-and-cloud-strategies-conference-2019>.
- [18] P. Castro, V. Ishakian, V. Muthusamy, and A. Slominski, "The rise of serverless computing," *Communications of the ACM*, vol. 62, no. 12, pp. 44-54, 2019.
- [19] A. Dakkak, C. Li, S. G. De Gonzalo, J. Xiong, and W.-m. Hwu, "Trims: Transparent and isolated model sharing for low latency deep learning inference in function-as-a-service," in *2019 IEEE 12th International Conference on Cloud Computing (CLOUD)*, 2019: IEEE, pp. 372-382.
- [20] H. Luo, H. Cai, H. Yu, Y. Sun, Z. Bi, and L. Jiang, "A short-term energy prediction system based on edge computing for smart city," *Future Generation Computer Systems*, vol. 101, pp. 444-457, 2019.
- [21] M. R. Belgaum et al., "A behavioral study of task scheduling algorithms in cloud computing," *International Journal of Advanced Computer Science and Applications*, vol. 10, no. 7, pp. 498-503, 2019.
- [22] R. Vinuesa et al., "The role of artificial intelligence in achieving the Sustainable Development Goals," *Nature Communications*, vol. 11, no. 1, pp. 1-10, 2020.
- [23] E. Ntoutsi et al., "Bias in data-driven artificial intelligence systems—An introductory survey," *Wiley Interdisciplinary Reviews: Data Mining and Knowledge Discovery*, vol. 10, no. 3, p. e1356, 2020.
- [24] N. Gift, *Pragmatic AI: An Introduction to Cloud-based Machine Learning*. Addison-Wesley Professional, 2018.
- [25] Chien, W.-C., C.-F. Lai, and H.-C. Chao, *Dynamic resource prediction and allocation in C-RAN with edge artificial intelligence*. *IEEE Transactions on Industrial Informatics*, 2019. 15(7): p. 4306-4314.
- [26] Chaudhary, R., et al., BEST: Blockchain-based secure energy trading in SDN-enabled intelligent transportation system. *Computers & Security*, 2019. 85: p. 288-299.
- [27] Z. Duliński, R. Stankiewicz, G. Rzym, and P. Wydrych, "Dynamic Traffic Management for SD-WAN Inter-Cloud Communication," *IEEE Journal on Selected Areas in Communications*, 2020.
- [28] Prerna, D., R. Tekchandani, and N. Kumar, Device-to-device content caching techniques in 5G: A taxonomy, solutions, and challenges. *Computer Communications*, 2020. 153: p. 48-84.

Predicting the Depression of the South Korean Elderly using SMOTE and an Imbalanced Binary Dataset

Haewon Byeon

Department of Medical Big Data
College of AI Convergence, Inje University
Gimhae 50834, Gyeongsangnamdo, South Korea

Abstract—Since the number of healthy people is much more than that of ill people, it is highly likely that the problem of imbalanced data will occur when predicting the depression of the elderly living in the community using big data. When raw data are directly analyzed without using supplementary techniques such as a sample algorithm for datasets, which have imbalanced class ratios, it can decrease the performance of machine learning by causing prediction errors in the analysis process. Therefore, it is necessary to use a data sampling technique for overcoming this imbalanced data issue. As a result, this study tried to identify an effective way for processing imbalanced data to develop ensemble-based machine learning by comparing the performance of sampling methods using the depression data of the elderly living in South Korean communities, which had quite imbalanced class ratios. This study developed a model for predicting the depression of the elderly living in the community using a logistic regression model, gradient boosting machine (GBM), and random forest, and compared the accuracy, sensitivity, and specificity of them to evaluate the prediction performance of them. This study analyzed 4,085 elderly people (≥ 60 years old) living in the community. The depression data of the elderly in the community used in this study had an unbalance issue: the result of the depression screening test showed that 87.5% of subjects did not have depression, while 12.5% of them had depression. This study used oversampling, undersampling, and SMOTE methods to overcome the unbalance problem of the binary dataset, and the prediction performance (accuracy, sensitivity, and specificity) of each sampling method was compared. The results of this study confirmed that the SMOTE-based random forest algorithm showing the highest accuracy (a sensitivity ≥ 0.6 and a specificity ≥ 0.6) was best prediction performance among random forest, GBM, and logistic regression analysis. Further studies are needed to compare the accuracy of SMOTE, undersampling, and oversampling for imbalanced data with high dimensional y-variables.

Keywords—Random forests; gradient boosting machine; SMOTE; undersampling; imbalanced data; oversampling

I. INTRODUCTION

Depression is one of the important mood disorders at senescence. It is very important to diagnose and treat depression at an early stage because it is possible to treat and cure depression using medication or psychosocial therapy even after its onset [1]. Depressive symptoms in old age differ from those in young age. First, it is difficult to clearly distinguish depressive symptoms from dementia symptoms

[2]. Pseudodementia, similar to dementia, shows a decline in cognitive ability in the dementia screening test, similar to the cognitive function test result of depression [3, 4]. In particular, the elderly accompanied by depression often express a subjectively recognized decrease in memory and cognitive function, which are not common with adolescents [5,6]. Moreover, the elderly with depression suffer from a decrease in memory and cognition more than the healthy elderly [5, 6].

Second, even though young patients complain about various physical symptoms, the key to diagnose depression, these physical symptoms are not very useful for diagnosing depression for elderly patients. For example, sleep disorder is a common symptom in adolescent depression, but elderly people frequently experience it regardless of depression [7,8]. Physical symptoms such as a normal decline in sexual function, constipation, and joint pain, associated with aging, are commonly found even in the elderly without depression [9]. Consequently, it is critical to accurately determine whether the depressive symptoms complained by the elderly are due to normal aging or depressive disorder.

Nevertheless, most of the studies that evaluated the depression of South Korean elderly were mainly regarding the factual survey for one city in terms of mental health, depression assessment, and the effectiveness of interventions for depression prevention and management. There are much fewer predictive model studies for identifying the factors associated with the depression of the elderly living in the community than patient-control group comparison studies. Previous studies [1,10,11,12,13] that evaluated the factors related to geriatric depression in South Korea local communities reported that health, socioeconomic status, education level, age, spouse, and social activities affected geriatric depression. Since regression analysis was mainly used as a modeling method to predict depression, they were efficient in identifying individual risk factors [14,15]. However, they were limited in identifying compound-risk factors (multivariate) such as sociodemographic variables and living habits [14,15]. Moreover, since regression analysis assumes independence, normality, and homoscedasticity, there is a possibility of producing biased results when the model is developed using data in violation of normality [16]. As a way to overcome the limitation of the regression model, big data-based analysis, called machine learning or data mining, has been widely used in various fields. Machine learning can

analyze data accurately even if the data somewhat violate the assumption of normality such as nonlinear data in the estimation process [17]. Especially, it has been known that gradient boosting machine (GBM), which generates many classifiers and combines the predictions to derive more accurate results, and ensemble learning models such as random forest have much higher sensitivity and accuracy than a single decision tree [18,19]. Nonetheless, since the predictive performance of the ensemble learning model has been mainly tested using simulation data [20], it is necessary to conduct additional validation and verification for confirming the predictive performance of the ensemble learning model for using it for disease data, which are mostly imbalanced data [21].

Since the number of healthy people is much more than that of ill people, it is highly likely that the problem of imbalanced data will occur when predicting the depression of the elderly living in the community using big data [22]. When raw data are directly analyzed without using supplementary techniques such as a sample algorithm for datasets, which have imbalanced class ratios, it can decrease the performance of machine learning by causing prediction errors in the analysis process [23]. Therefore, it is necessary to use a data sampling technique for overcoming this imbalanced data issue [24]. As a result, this study tried to identify an effective way for processing imbalanced data to develop ensemble-based machine learning by comparing the performance of sampling methods using the depression data of the elderly living in South Korean communities, which had quite imbalanced class ratios.

II. METHODS AND MATERIALS

A. Data Source

This study analyzed the raw data of the 2016 Seoul Panel Study (SEPANS) data. The SEPANS data was conducted from June 1 to August 31, 2016, for the purpose of estimating the welfare level of Seoul citizens and the actual status situation of socially vulnerable class. The population of this study was the households in Seoul at the time of the survey among the households subject to the 2005 Population and Housing Census. The stratified cluster sampling method was used for sampling households in 25 districts in Seoul. This study excluded foreigners and those admitted to retirement homes or nursing hospitals among the survey subjects. This study used the computer aided personal interview method that an interviewer visited the target households and entered the response to the structured questionnaire into a portable computer. This study analyzed 4,085 elderly people (≥ 60 years old) living in the community.

B. Variable Measurement

Depression, the outcome variable, was defined according to the Korean version of Center for Epidemiologic Studies Depression Scale-Revised (K-CESD) [25]. K-CES-D is a self-administered depression scale composed of 20 items and it was developed by the National Institute of Mental Health. It is a primary screening tool for depression. The maximum score is 60, and a higher score indicates more severe depression.

The cut-off score of K-CES-D, the threshold of depression, was defined as 25 points.

Explanatory variables were age, gender, educational level (elementary school graduate and below, middle school graduate, high school graduate, or college graduate or above), smoking (smokers or non-smokers), drinking (less than once a week or twice or more per week), economic activity (yes or no), social activities for the past month (yes or no), mean monthly household income (less than KRW 1.5 million, KRW 1.5-3 million, or KRW 3 million or more), spouse living together (living together, bereavement/separated, or single), disease/accident/addiction in the last two weeks (yes or no), subjective health status (good, fair, or bad), subjective stress (yes or no), days of walking for 30 minutes or more per day (less than 1 day per week or 2 days or more per week), the frequency of meetings neighbors (less than once a month or twice or more per month), and the frequency of meeting relatives (less than once a month or twice or more per month).

III. ANALYSIS

A. Model Development and Evaluation

This study developed a model for predicting the depression of the elderly living in the community using a logistic regression model, GBM, and random forest, and compared the accuracy, sensitivity, and specificity of them to evaluate the prediction performance of them. To test the prediction performance of them, the data were randomly divided into train dataset (70%) and test dataset (30%). Prediction models were developed using the training dataset and the accuracy, sensitivity, and specificity of them were calculated by using the test dataset. Since GBM and Random forest have random characteristics, models were developed while the seed was fixed as 123456 for repeated measurement. The predictive performance of each model was evaluated by the area under the curve (AUC) of the ROC curve, and the accuracy, sensitivity, and specificity of each model were calculated as evaluation indices for the model performance. Accuracy means the percentage of successful predictions in all data. Sensitivity indicates the rate of a model predicting a senior with depression as depression. Specificity is a true negative rate, indicating how accurately a model predicts a senior without depression and not depression. This study defined the best predictive performance model as a model with the highest accuracy while sensitivity and specificity were 0.6 or higher, and the model was selected as the final model for predicting the depression of the elderly living in the community. . All analyses were performed using R version 4.0.2 (Foundation for Statistical Computing, Vienna, Austria) and Python version 3.8.0 (<https://www.python.org>).

B. Random Forest

Random forest is an ensemble model and it generates a number of decision trees to calculate predictions. The ensemble model is a method of integrating the classification results of multiple decision trees and using them for making the final decision. A number of studies [26, 27, 28] reported that the ensemble model had higher predictive power than single decision tree models. The ensemble model can be divided into bagging and boosting. Bagging is a way to predict

by combining the results of each model through averaging or voting after generating multiple decision tree models by sampling raw data. It has the advantage of reducing the variance of predicted values [29]. Boosting is a machine learning method that enables better classification for the observation values that are difficult to classify by using more misclassified observations. It has the advantage of reducing the bias of predicted values [30]. The concepts of bagging and boosting are presented in Fig. 1.

These ensemble models supplement the poor performance of decision trees when handling data that are not divided well into horizontal or vertical division [31]. Random forest samples data to create multiple tree models and then vote or average the results of each tree. It is widely used in various fields because it can handle the multicollinearity problem of trees by randomly selecting variables as well as sampling data from each model [32, 33]. The concept of random forest is presented in Fig. 2.

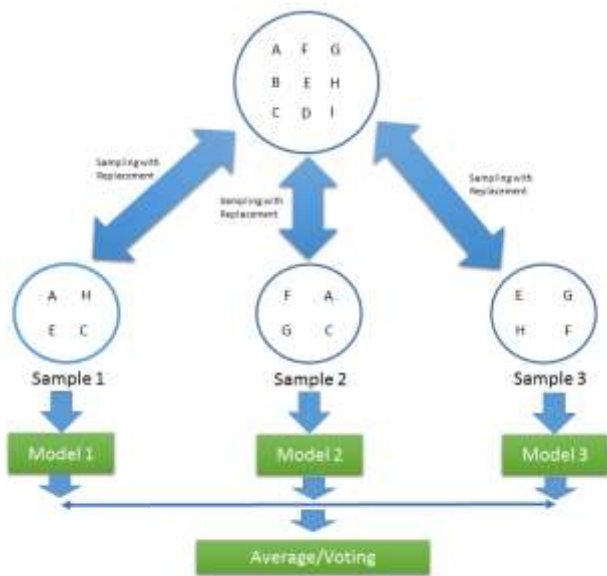


Fig. 1. The Concept of Bagging [34].

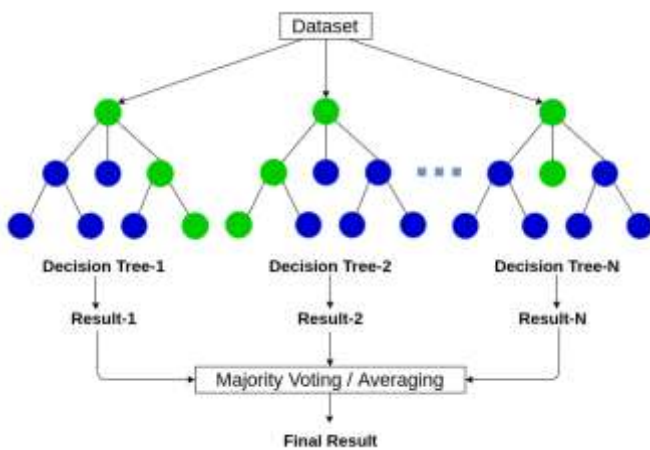


Fig. 2. Concept of Random Forest [35].

C. GBM

The GBM is a machine learning algorithm designed by Friedman (2001) [36] that generates a prediction model by combining weak learners of traditional decision trees using ensemble techniques. This model generalizes the model by generating models for each step and optimizing the loss function that can randomly differentiate, like other boosting methods. In machine learning, boosting refers to a method of generating strong learners by combining weak learners [36]. It generates a model even if the accuracy of it is low, and the error of this model is supplemented by the next model. A more accurate model is created through this process, and the basic principle of it is to increase accuracy by repeating this process. The prediction model learning is to find a parameter that minimizes the loss function. One of the ways to find the optimal parameter is gradient descent. When a slope is calculated by differentiating the loss function with parameters and moving the parameters in the direction of decreasing the value, it reaches the point where the loss function is minimized. In the gradient boosting process, this exploration process is carried out in the functional space. Therefore, it differentiates the loss function by the model function learned so far, instead of the parameter. GBM's algorithm is presented in Fig. 3.

Algorithm Gradient boosting algorithm	
Input:	Input data $(x, y)_{i=1}^N$
	Number of iterations M
	Choice of the loss-function $\Psi(y, f)$
	Choice of the base-learner model $h(x, \theta)$
1:	Initialize f_0 with a constant
2:	for $t = 1$ to M do
3:	Compute the negative gradient $y_t(x)$;
4:	Fit a new base-learner function $h(x, \theta_t)$;
5:	Find the best gradient descent step-size p_t
	$p_t = \underset{p}{\operatorname{argmin}} \sum_{i=1}^N \Psi(y_i, \tilde{f}_{t-1}(x_i) + p h(x_i, \theta_t))$;
6:	Update the function estimate:
	$\tilde{f}_t \leftarrow \tilde{f}_{t-1} + p_t h(x, \theta_t)$;
7:	end for

Fig. 3. The Algorithm of Gradient Boosting Machine [36].

D. Sampling Techniques for Resolving Imbalanced Data

Disease data generally poses the problem of imbalanced classes because the number of people with a disease is smaller than those without a disease. The depression data of the elderly in the community used in this study also had an unbalance issue: the result of the depression screening test showed that 87.5% of subjects did not have depression, while 12.5% of them had depression. This study used oversampling [37], undersampling [38], and SMOTE [24] methods to overcome the unbalance problem of the binary dataset, and the prediction performance (accuracy, sensitivity, and specificity) of each sampling method was compared.

The undersampling method is a technique of randomly deleting data of multiple classes to match with the number of data in a class with small data. It is the fastest because it deletes data without conducting separate calculations, but the variation of performance is large because it deletes data randomly [38]. When a pair of data belonging to different classes and there is no data closer to each other, it is called

Tomek link. The Tomek link technique is a way to exclude data belonging to a class with more data. It has the effect of pushing the boundary line toward the class with many data. The edited nearest neighbors (ENN) technique is a technique that deletes the nearest k data out of a class with many data unless all or several of them belong to the class with many data. In other words, this technique deletes data of a class with more data that are around a class with fewer data. Since these traditional undersampling techniques delete data, they incur a loss of data and weaken the representativeness of data.

The oversampling technique is to use the data of a class with fewer data repetitively and randomly, which increases the weight. Like the random undersampling technique, it is the fastest because it copies data without conducting separate calculations, but the performance varies greatly because it copies data randomly.

The SMOTE technique finds n nearest neighbors of a class with small data regarding certain data belonging to the same class with a small data size, draws a straight line with the neighbor, and generates points until the random points have a balanced ratio. The concept of sampling types is presented in Fig. 4. Moreover, the algorithm of SMOTE is presented in Fig. 5. The Python code for executing SMOTE is presented in Fig. 6.

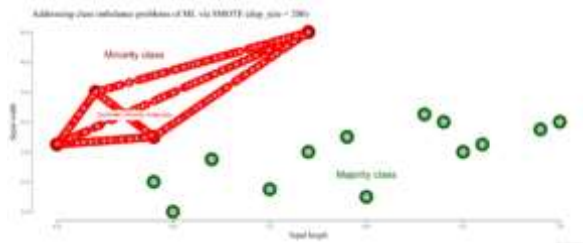


Fig. 4. Type of Sampling [39].

```

Algorithm SMOTE(T, N, k)
Input: Number of minority class samples T; Amount of SMOTE N%; Number of nearest neighbors k
Output: (N/100) * T synthetic minority class samples
1. (* If N is less than 100%, randomize the minority class samples as only a random percent of them will be SMOTEd. *)
2. if N < 100
3.   then Randomize the T minority class samples
4.     T = (N/100) * T
5.     N = 100
6.   endif
7. N = (int)(N/100) (* The amount of SMOTE is assumed to be in integral multiples of 100. *)
8. k = Number of nearest neighbors
9. nattrs = Number of attributes
10. Sample[]: array for original minority class samples
11. newindex: keeps a count of number of synthetic samples generated, initialized to 0
12. Synthetic[]: array for synthetic samples
    (* Compute k nearest neighbors for each minority class sample only. *)
13. for i = 1 to T
14.   Compute k nearest neighbors for i, and save the indices in the narray
15.   Populate(N, i, narray)
16.   endwhile

    Populate(N, i, narray) (* Function to generate the synthetic samples. *)
17. while N ≠ 0
18.   Choose a random number between 1 and k, call it rn. This step chooses one of the k nearest neighbors of i.
19.   for attr = 1 to nattrs
20.     Compute: dif = Sample[narray[rn][attr]] - Sample[i][attr]
21.     Compute: gap = random number between 0 and 1
22.     Synthetic[newindex][attr] = Sample[i][attr] + gap * dif
23.   endwhile
24.   newindex++
25.   N = N - 1
26. endwhile
27. return (* End of Populate. *)
    End of Pseudo-Code.
    
```

Fig. 5. The Algorithm of SMOTE.

```

from sklearn.datasets import make_classification
from sklearn.decomposition import PCA
from imblearn.over_sampling import SMOTE

# Generate the dataset
X, y = make_classification(n_classes=2, weights=[0.1, 0.9],
                          n_features=20, n_samples=5000)

# Apply the SMOTE over-sampling
sm = SMOTE(ratio='auto', kind='regular')
X_resampled, y_resampled = sm.fit_sample(X, y)
    
```

Fig. 6. Code for Executing SMOTE in Python.

IV. RESULTS

A. Comparing the Prediction Performance of the Model for Predicting Senile Depression

Table I shows the prediction performance (accuracy, sensitivity, and specificity) of oversampling, undersampling, and SMOTE. This study defined the final model with the best predictive performance as a model with the highest accuracy while sensitivity and specificity were 0.6 or higher. As a result, this study chose the SMOTE-based random forest algorithm, showing an accuracy of 0.68, a sensitivity of 0.83, and a specificity of 0.74, as the final model for predicting senile depression.

TABLE I. RESULTS OF THE PREDICTION PERFORMANCE (ACCURACY, SENSITIVITY, AND SPECIFICITY) OF OVERSAMPLING, UNDERSAMPLING, AND SMOTE

Type	Raw Data			Undersampling			Oversampling			SMOTE		
	Ac c	Se n	Sp e	Ac c	Se n	Sp e	Ac c	Se n	Sp e	Ac c	Se n	Sp e
LR	0.78	0.52	0.83	0.64	0.66	0.81	0.57	0.54	0.81	0.63	0.69	0.79
GBM	0.67	0.45	0.93	0.50	0.51	0.98	0.63	0.65	0.90	0.65	0.71	0.77
RF	0.73	0.65	0.88	0.61	0.75	0.92	0.78	0.64	0.91	0.68	0.83	0.74

Acc=accuracy; Sen=sensitivity; Spe=specificity; LR= Logistic regression; RF= Random forest

B. Major Predictors of Senile Depression

The model to predict the depression was developed through the GBM and the predictive power was compared with the results of random forest and logistic regression (Table II, Table III). Random forest had higher classification accuracy than other predictive model in both training and test data. The analysis results of test data showed that the classification accuracy was 63.0% for logistic regression, 65.1% for GBM, and 68.3% for random forest. Table III shows the major predictors of senile depression according to the SMOTE algorithm.

TABLE II. NUMBER OF MAJOR DEPRESSION PREDICTORS BY THE ALGORITHM

Model	Factors
Logistic regression-raw data	8
GBM-raw data	10
Random forest-raw data	12
Logistic regression-undersampling	7
GBM-undersampling	10
Random forest-undersampling	12
Logistic regression-oversampling	6
GBM-oversampling	9
Random forest-oversampling	11
Logistic regression-SMOTE	8
GBM-SMOTE	10
Random forest-SMOTE	12

TABLE III. RESULTS OF MAJOR PREDICTORS OF SENILE DEPRESSION

Model	Characteristics
Random forest-SMOTE	Age, gender, educational level, economic activity, social activities for the past month, mean monthly household income, spouse living together, disease/accident/addiction in the last two weeks, subjective health status, subjective stress, the frequency of meetings neighbors, the frequency of meeting relatives.
Logistic regression-SMOTE	Age, gender, educational level, mean monthly household income, spouse living together, disease/accident/addiction in the last two weeks, subjective health status, subjective stress
GBM-SMOTE	Age, gender, educational level, social activities for the past month, mean monthly household income, spouse living together, disease/accident/addiction in the last two weeks, subjective health status, subjective stress, the frequency of meetings neighbors

V. CONCLUSION

This study compared the performance of ensemble-based machine learning sampling methods using the depression data of the elderly in the community, which had an imbalanced class ratio. The results of this study confirmed that the SMOTE-based random forest algorithm showing the highest accuracy (a sensitivity ≥ 0.6 and a specificity ≥ 0.6) was the final model with the best prediction performance among random forest, GBM, and logistic regression analysis. Since specificity and sensitivity have a trade-off relationship (when one value increases, the other value decreases), the ratio of specificity and sensitivity is selected according to the judgment of the researcher using a model. This study proposes to compare the performance of machine learning suitable for the study objective by considering accuracy, specificity, and sensitivity instead of considering only accuracy when future studies on prediction models will compare models and evaluate predictive performance.

This study compared the prediction performance of ensemble models built on imbalanced data by sampling method and found that SMOTE showed the best performance.

Previous studies also reported that SMOTE had better predictive performance than undersampling and oversampling when analyzing imbalanced data [40]. The SMOTE technique has shown successful performance in various applied fields [41]. The ADASYN technique generates more realistic points deviated from the line by producing random points and adding random noise and it is a recently developed improved version of SMOTE. There have been continuous attempts to develop advanced algorithms that have better accuracy than SMOTE [42].

The results of this study suggest that using SMOTE as a sampling method to overcome the imbalance can be an efficient option when developing a prediction model using imbalanced binary data like disease data. SMOTE can alleviate the overfitting problem due to random oversampling and has the advantage of not losing useful data compared to undersampling or oversampling techniques [40]. However, it has also been reported that SMOTE may cause class overlapping, induce additional noise, and not be effective for treating imbalanced data with a high-dimensional y variable [42]. Therefore, although this study confirmed the effectiveness of SMOTE using an imbalanced binary dataset, the results cannot be generalized for all dimensions of data and the result should be interpreted with caution. Further studies are needed to compare the accuracy of SMOTE, undersampling, and oversampling for imbalanced data with high dimensional y-variables.

ACKNOWLEDGMENT

This research was supported by Basic Science Research Program through the National Research Foundation of Korea (NRF) funded by the Ministry of Education (NRF-2018R1D1A1B07041091, NRF-2019S1A5A8034211).

REFERENCES

- [1] H. Byeon, Relationship between physical activity level and depression of elderly people living alone. International journal of environmental research and public health, vol. 16, no. 20, pp. 4051, 2019.
- [2] H. Kang, F. Zhao, L. You, C. Giorgetta, D. Venkatesh, S. Sarkhel, and R. Prakash, Pseudo-dementia: A neuropsychological review. Annals of Indian Academy of Neurology, vol. 17, no. 2, pp. 147-154, 2014.
- [3] J. A. Sáez-Fonseca, J. A. Lee, and Z. Walker, Long-term outcome of depressive pseudodementia in the elderly. Journal of Affective Disorders, vol. 101, no. 1-3, pp. 123-129, 2006.
- [4] M. H. Connors, L. Quinto, and H. Brodaty, Longitudinal outcomes of patients with pseudodementia: a systematic review. Psychological Medicine, vol. 49, no. 5, pp. 727-737, 2019.
- [5] H. Byeon, Development of depression prediction models for caregivers of patients with dementia using decision tree learning algorithm. International Journal of Gerontology, vol. 13, no. 4, pp. 314-319, 2019.
- [6] S. M. McClintock, M. M. Husain, T. L. Greer, and C. M. Cullum, Association between depression severity and neurocognitive function in major depressive disorder: a review and synthesis. Neuropsychology, vol. 24, no. 1, pp. 9-34, 2010.
- [7] S. H. Kang, I. Y. Yoon, S. D. Lee, J. W. Han, T. H. Kim, and K. W. Kim, REM sleep behavior disorder in the Korean elderly population: prevalence and clinical characteristic. Sleep, vol. 36, no. 8, pp. 1147-1152, 2013.
- [8] S. Lerche, A. Gutfreund, K. Brockmann, M. A. Hobert, I. Wurster, U. Sünkel, G. W. Eschweiler, F. G. Metzger, W. Maetzler, and D. Berg, Effect of physical activity on cognitive flexibility, depression and RBD in healthy elderly. Clinical Neurology and Neurosurgery, vol. 165, pp. 88-93, 2018.

- [9] J. F. Gallegos-Orozco, A. E. Foxx-Orenstein, S. M. Sterler, and J. M. Stoa, Chronic constipation in the elderly. *American Journal of Gastroenterology*, vol. 107, no. 1, pp. 18-25, 2012.
- [10] S. K. Kahng, and B. K. Chung, Predictors of elderly depression using the andersen model. *Korean Journal of Gerontological Social Welfare*, vol. 49, no. 1, pp. 7-29, 2010.
- [11] S. D. Chung, and M. J. Koo, Factors influencing depression: a comparison among babyboomers, the pre-elderly, and the elderly. *Journal of Gerontological Social Welfare*, vol. 52, no. 1, pp. 305-324, 2011.
- [12] H. S. Jeon, and S. K. Kahng, Predictors of Depression trajectory among the elderly: using the Korean welfare panel data. *Journal of the Korea Gerontological Society*, vol. 29, no. 4, pp. 1611-1628, 2009.
- [13] H. K. Han, and Y. R. Lee, A study on factors impacting on the mental health level of the elderly people living alone. *Journal of the Korea Gerontological Society*, vol. 29, no. 3, pp. 805-822, 2009.
- [14] H. Byeon, Developing a model to predict the occurrence of the cardio-cerebrovascular disease for the Korean elderly using the random forests algorithm. *International Journal of Advanced Computer Science and Applications*, vol. 9, no. 9, pp. 494-499, 2018.
- [15] H. Byeon, S. Cha, K. Lim, Exploring factors associated with voucher program for speech language therapy for the preschoolers of parents with communication disorder using weighted random forests. *International Journal of Advanced Computer Science and Applications*, vol. 10, no. 5, pp. 12-17, 2019.
- [16] H. Byeon, Model development for predicting the occurrence of benign laryngeal lesions using support vector machine: focusing on South Korean adults living in local communities. *International Journal of Advanced Computer Science and Applications*, vol. 9, no. 10, pp. 222-227, 2018.
- [17] A. Iqbal, S. Aftab, U. Ali, Z. Nawaz, L. Sana, M. Ahmad, and A. Husen, Performance analysis of machine learning techniques on software defect prediction using NASA datasets. *International Journal of Advanced Computer Science and Applications*, vol. 10, no. 5, pp. 300-308, 2019.
- [18] J. Nobre, and R. F. Neves, Combining principal component analysis, discrete wavelet transform and XGBoost to trade in the financial markets. *Expert Systems with Applications*, vol. 125, pp. 181-194, 2019.
- [19] H. Nguyen, X. N. Bui, H. B. Bui, and D. T. Cuong, Developing an XGBoost model to predict blast-induced peak particle velocity in an open-pit mine: a case study. *Acta Geophysica*, vol. 67, no. 2, pp. 477-490, 2019.
- [20] L. Pourjafar, M. Sadeghzadeh, and M. Abdeyazdan, Combination of neural networks and fuzzy clustering algorithm to evaluation training simulation-based training. *International Journal of Advanced Computer Science and Applications*, vol. 7, no. 7, pp. 31-38, 2016.
- [21] H. Byeon, Application of machine learning technique to distinguish Parkinson's disease dementia and Alzheimer's dementia: predictive power of Parkinson's disease-related non-motor symptoms and neuropsychological profile. *Journal of Personalized Medicine*, vol. 10, no. 2, pp. 31, 2020.
- [22] H. Byeon, Is the random forest algorithm suitable for predicting Parkinson's disease with mild cognitive impairment out of Parkinson's disease with normal cognition?. *International Journal of Environmental Research and Public Health*, vol. 17, no. 7, pp. 2594, 2020.
- [23] A. Fernández, S. García, F. Herrera, and N. V. Chawla, SMOTE for learning from imbalanced data: progress and challenges, marking the 15-year anniversary. *Journal of Artificial Intelligence Research*, vol. 61, pp. 863-905, 2018.
- [24] S. Shrivastava, P. M. Jeyanthi, and S. Singh, Failure prediction of Indian Banks using SMOTE, Lasso regression, bagging and boosting. *Cogent Economics & Finance*, vol. 8, no. 1, e-pub. 1729569, 2020.
- [25] S. Lee, S. T. Oh, S. Y. Ryu, K. Lee, E. Lee, J. Y. Park, S. W. Yi, and W. J. Choi, Validation of the Korean version of Center for Epidemiologic Studies Depression Scale-Revised (K-CESD-R). *Korean Journal of Psychosomatic Medicine*, vol. 24, no. 1, pp. 83-93, 2016.
- [26] M. Skurichina, and R. P. Duin, Bagging, boosting and the random subspace method for linear classifiers. *Pattern Analysis and Applications*, vol. 5, no.2, pp. 121-135, 2002.
- [27] H. Byeon, Exploring the predictors of rapid eye movement sleep behavior disorder for Parkinson's disease patients using classifier ensemble. In *Healthcare*, vol. 8, no. 2, pp. 121, 2020.
- [28] B. Hyeon, Development of a depression in Parkinson's disease prediction model using machine learning. *World Journal of Psychiatry*, vol. 10, no. 10, pp. 234-244, 2020.
- [29] Y. Grandvalet, Bagging equalizes influence. *Machine Learning*, vol. 55, no. 3, pp. 251-270, 2004.
- [30] A. Mayr, B. Hofner, E. Waldmann, T. Hepp, S. Meyer, and O. Gefeller, An update on statistical boosting in biomedicine. *Computational and Mathematical Methods in Medicine*, vol. 2017, 6083072, E-pub, doi:10.1155/2017/6083072, 2017.
- [31] F. Tang, and H. Ishwaran, Random forest missing data algorithms. *Statistical Analysis and Data Mining: The ASA Data Science Journal*, vol. 10, no. 6, pp. 363-377, 2017.
- [32] P. T. Noi, and M. Kappas, Comparison of random forest, k-nearest neighbor, and support vector machine classifiers for land cover classification using Sentinel-2 imagery. *Sensors*, vol. 18, no. 1, pp. 18, 2018.
- [33] H. Byeon, Best early-onset Parkinson dementia predictor using ensemble learning among Parkinson's symptoms, rapid eye movement sleep disorder, and neuropsychological profile. *World Journal of Psychiatry*, vol. 10, no. 11, pp. 245-259, 2020.
- [34] R. Kumar, Machine Learning quick reference: quick and essential machine learning hacks for training smart data models. Packt Publishing, Birmingham, 2019.
- [35] A. Sharma, Decision Tree vs. Random Forest – Which Algorithm Should you Use?. *Analytics Vidhya*, Gurgaon, 2020.
- [36] J. H. Friedman, Greedy function approximation: a gradient boosting machine. *Annals of statistics*, vol. 29, no. 5, pp. 1189-1232, 2001.
- [37] L. Abdi, and S. Hashemi, To combat multi-class imbalanced problems by means of over-sampling techniques. *IEEE Transactions on Knowledge and Data Engineering*, vol. 28, no. 1, pp. 238-251, 2016.
- [38] S. J. Yen, and Y. S. Lee, Cluster-based under-sampling approaches for imbalanced data distributions. *Expert Systems with Applications*, vol. 36, no. 3, pp. 5718-5727, 2009.
- [39] R. Kunert, Smote explained for noobs-synthetic minority over-sampling technique line by line. *Rich Data*, Berlin, 2017.
- [40] N. V. Chawla, K. W. Bowyer, L. O. Hall, and W. P. Kegelmeyer, SMOTE: synthetic minority over-sampling technique. *Journal of Artificial Intelligence Research*, vol. 16, pp. 321-357, 2002.
- [41] B. Santoso, H. Wijayanto, K. A. Notodiputro, and B. Sartono, Synthetic over sampling methods for handling class imbalanced problems: a review. *IOP Conference Series: Earth and Environmental Science*, vol. 58, no. 1, pp. 012031, 2017.
- [42] M. Karajizadeh, M. Nasiri, M. Yadollahi, A. H. Zolfaghari, and A. Pakdam, Mortality prediction from hospital-acquired infections in trauma patients using an unbalanced dataset. *Healthcare Informatics Research*, vol. 26, no. 4, pp. 284-294, 2020.

Validation of the Components and Elements of Computational Thinking for Teaching and Learning Programming using the Fuzzy Delphi Method

Karimah Mohd Yusoff¹, Noraidah Sahari Ashaari², Tengku Siti Meriam Tengku Wook³, Noorazeen Mohd Ali⁴
Matriculation Division, Ministry of Education Malaysia, Putrajaya, Malaysia¹
Software Technology and Management System Universiti Kebangsaan Malaysia
Bangi, Selangor, Malaysia^{2, 3, 4}

Abstract—Computational Thinking is a phrase employed to explain the developing concentration on students' knowledge development regarding designing computational clarifications to problems, algorithmic Thinking, and coding. The difficulty of learning computer programming is a challenge for students and teachers. Students' ability in programming is closely related to their problem-solving skills and their cognitive abilities. Even though computational thinking is a problem-solving skill in the 21st century, its use for programming needs to be planned systematically taken into account the appropriate components and elements. Therefore, this study aims to validate the main components and elements of computational thinking for solving problems in programming. At the beginning of the study, researchers conducted a literature review to determine the components and the elements of computational thinking that could be used in teaching and learning programming. This validation involved the consensus of a group of experts using the Fuzzy Delphi method. The data were analysed using the Fuzzy Delphi technique, where the experts individually evaluated the components and elements agreed upon prior discussion. A group of experts consisting of 15 people validated 14 components and 35 elements. The results showed that all components and elements reached a threshold (d) value of less than 0.2, a percentage of agreement exceeded 75%, and the Fuzzy score (A) exceeded 0.5. The finding indicates that the main components and elements of the proposed computational thinking are suitable for problem-solving approaches in programming.

Keywords—Expert consensus; focus group; problem-solving; components; elements

I. INTRODUCTION

Teaching and learning methods have evolved globally, where various advancements have introduced over the years. Recently, computer programming is of growing interest in line with the efforts to enhance Science, Technology, Engineering and Mathematics (STEM) based education and career. Besides government and non-governmental agencies, industries also suggest learning institutions to prepare students who have knowledge, understanding, and skills in programming and problem-solving [1]. Indirectly, educators should continuously enrich their experience and skills to provide effective teaching and learning environment.

Programming is a subject that involves problem-solving skills starting from problem formulation to complete program development. Therefore, structured teaching and learning

methods for programming should be established by including all steps to solve the problem. Amongst the steps are formulating the problem, planning the solutions, designing the solutions, translating the solutions into programming codes and testing and evaluating the complete program. The main challenge faced by novice programmers in learning programming was related to the cognitive ability of an individual [2][3][4][5]. Based on the cognitive load theory, the teaching design is tailored to reduce the student's load during the thinking process to achieve optimal learning outcomes [6].

Computational thinking is gaining attention among educators, and it is often linked to problem-solving [7]. Computational thinking is considered as a 21st-century skill [8][9] that can build the essential cognitive skills of students [10]. Relationship between computational thinking implementation and students' cognitive level was reported in previous studies [11][12][13], for different purposes. A blended learning model is developed for students to acquire basic programming skills through activities tailored to students' cognitive levels [11]. The activity is designed by considering the three levels of computational thinking skills which is basic, intermediate, and advanced that could be used on the Moodle platform. In contrast, computational thinking is introduced in the context of creative programming activities using Scratch software [13]. Besides, a study to provide new instruments for the measurement of computational thinking and prove the nature of computational thinking through its relationship with cognitive psychological constructs consist of spatial ability, reasoning ability and problem-solving ability [12]. These studies shows the potential of computational thinking in education.

In this study, we proposed the components and elements of computational thinking for problem solving in programming. We believe that by involving appropriate components and elements, computational thinking is potentially to develop problem solving skills for programming. Hence, this article reports the validation process systematically of the components and elements of computational thinking for problem-solving approach in programming. The validation in performed by a group of experts through the Fuzzy Delphi Method (FDM).

The discussion of the following section as follows: Section II is a literature review that leads to the components of CT. Section III describes the validation process in this study.

Section IV discussing about data analysis. Section V details about findings and discussion. Section V conclude the study and further work.

II. LITERATURE REVIEW

Computational thinking skills that derived from computer science [14] is an approach to problem-based teaching and learning that meets the needs of problem-solving skills in the 21st century that has gained the attention among researchers and educators [15]. Computational thinking provides a set of cognitive skills to solve problems that are appropriate for all areas [16][17]. In 1980, Seymour Papert introduced the idea of computational thinking. Later, computational thinking was defined as the application of some basic concepts of Computer Science to solve the problems, designing systems, and understanding human behavior [18]. The computational thinking definition was revised as a thought process for formulating and solving problems in a form that information processing agents can effectively execute [19]. Apart from that, several definitions of computational thinking differ in meaning but generally focused on solving problems [20][21]. Latest, computational thinking is defined as the thinking skills and also the practice to design computation that enable computers to execute the instructions they receive. Computational thinking also explains and interprets what happens in reality as a complex processing of information that takes place in a computer [22]. Based on the proposed definitions, in this study, computational thinking is regarded as a thinking approach to develop problem-solving skills through computing to find solutions.

Computational thinking is the primary skills that are used in the problem-solving process. Various computational thinking skills have been suggested in previous studies [23-26] [19][7][27-29] as shown in Table I. As a pioneer of computational thinking, Jannette Wing proposed abstraction, decomposition, generalisation, algorithm and automation skills.

The computational thinking skills proposed by the researchers were almost similar with a few differences. However, the concepts presented in all areas are practically uniform [16]. Based on Table I, similar computational thinking skills include abstraction, decomposition, generalisation (pattern recognition) and algorithm incorporated in this study.

Computational thinking is a cognitive process that involves logical thinking, including the ability to perform abstraction, decomposition, identification of patterns through generalisation, solving the problems sequentially, and evaluation of the results. Therefore, logical reasoning identified as a new component of computational thinking for problem-solving [24]. In programming, programs need to be tested and evaluated; thus, evaluation skills among the best talents in programming [24][25]. As this study focuses on the use of problem-solving skill in programming, computational thinking skills should play a role in line with the problem-solving step in programming. Table II shows the description of computational thinking skills components identified for problem-solving in programming.

To date, there is no consensus on the exact components of computational thinking, but computational thinking can

involve multiple components and may not necessarily be cognitive [15]. Therefore, other than skills, dimension and approach were included in this study.

TABLE I. COMPUTATIONAL THINKING SKILLS SUGGESTED BY RESEARCHERS

Computational Thinking Skills	Reference
abstraction, decomposition, generalisation, algorithm, automation	Wing, 2006, 2008, 2011
abstraction, decomposition, generalisation (pattern recognition), algorithm, evaluation.	Selby & Wollard, 2013
logical reasoning, abstraction, decomposition, generalisation (pattern recognition), algorithm, evaluation.	Csizmadia et al., 2015
abstraction, decomposition, generalisation, algorithm, debugging.	Angeli et al., 2016
abstraction, decomposition, pattern recognition, algorithm	Shute, Sub & Asbell-Clarke, 2017
abstraction, decomposition, generalisation, algorithm	Denning, 2017
abstraction, decomposition, data representation, pattern recognition, algorithmic thinking	Rodriguez et al., 2017
abstraction, decomposition, pattern recognition, algorithm	Burbaite, Drasute & Stuiikys, 2018

TABLE II. DESCRIPTION OF COMPUTATIONAL THINKING SKILLS

Skills	Description
Abstraction	The skill to identify and retrieve relevant information to determine key ideas and to remove unnecessary details.
Decomposition	The skill to breakdown the problem to a small section and easy to manage for complex problems. The solution can be implemented part by part until the whole problem is solved.
Pattern Recognition	Skills in observing patterns, tendencies and regularity of data through similarities.
Algorithm	Skill to perform tasks or solve problems step by step.
Logical reasoning	Skill explain what happens by analysing and studying facts by thinking clearly and accurately.
Evaluation	Skill determines whether the algorithm, system or process is working correctly and following its purpose.

Beside skills, dimensions of computational thinking framework that consisted of computational concepts, practices and perspectives [30] is proposed to ensure the delivery and development of computational thinking skills as shown in Table III. The efforts include teaching delivery, student involvement practically and assessment of student performance.

Apart from dimensions, it is essential to stimulate the thinking processes that lead to computational thinking skills. In this study investigates computational thinking approach, which is a practice applied during teaching and learning session. There are five approaches of computational thinking, which are tinkering, creating, debugging, collaborating, and persevering [24] as presented in Table IV.

The idea of tinkering emerged since [31] introduced the concept of computational thinking in the 1980s. Tinkering is trying something new through exploration, trying repeatedly and making improvements. The problem-solving process involves thinking and tinkering to obtain the best solution [32]. The tinkering approach for adult learning implemented through exploring and building, which are carried out through trial leading to improve solutions [33]. Tinkering activities which are performed repeatedly can assist a novice in learning programming [34].

Creating refers to the planning, designing and evaluating, for example, a program [33]. Programming involves the process of developing algorithms in the form of flow charts or pseudo-codes and then followed by programs. One learning programming should undergo these steps and procedures. Therefore, the creating approach is in line with the learning of programming.

Debugging is a component of computational thinking by [23]. Debugging refers to the process of tracking and fixing errors [35] either an algorithm or a program [33]. However, debugging is usually related to improving programs because it involves syntax and semantics. This activity performed after testing programs as a programmer can identify the error and know how to fix it [36]. Novices need to expose with debugging approach to be on par with experienced programmers [37]. Therefore, students need to practice in debugging and evaluating programs while being monitored by the instructors [38].

Meanwhile, collaborative learning allows the process of knowledge acquisition, sharing, creation, and dissemination. Collaborating is one of the computational thinking approaches [24] to obtain the right solutions and motivate students to complete misleading assignments [33]. When students work together to solve problems or engage in activities, they also have the opportunity to apply new concepts they have learned, facilitates the application of concepts for the specific problem through exploration, critical thinking and analysis. Indirectly, collaborative learning can enhance assessment skills when group members use different approaches [39]. The collaborative approach is ideal for new programmers as they can build an understanding of problems, plan alternative solutions, learn with peers, build knowledge, and engage actively in programming learning [15]. Other than face-to-face collaboration approach in the classroom, this approach is also

implemented through different mediums such as online learning systems [40], online training tools [41] and networks such learning management system (moodles) [42]. Therefore, students who learn programming course collaboratively can develop computational thinking skills as reported by [15]. Besides that, opportunities to get ideas from their peers and explain the knowledge gained to other friends can help students develop logical skills and increase their perseverance [33].

Programming is difficult and challenging to produce effective programs. In addition to problem-solving skills, using computational thinking skills as a solution strategy and mastering a programming language, programmers have to be resilient. Persevering is a computational thinking approach introduced by [24] defined as never giving up, determined, resilient and persistent. For example, educators play a role to avoid an environment that can cause students to give up or lose motivation by interacting with them and always give feedback to students if necessary [43]. Teaching strategy or teaching aids should be able to motivate students and help them to learn interestingly. There are teaching aids introduced by past researchers to motivate students to learn programming such as simulations, games, visualizations and robotics. However, these teaching aids focuses on learning the concepts of programming. Current studies concern about the strategy for problem solving as well as program development. Hence, we suggest the use of computational thinking to be implemented as teaching strategy since it offers the components consisted of skills, dimensions and approaches as listed in Tables I to III. As the skill components play the primary role in problem-solving, a detailed element is required to implement it. Hence, 35 elements were proposed representing abstraction, decomposition, pattern recognition, algorithm, logical reasoning and evaluation. These components and elements are potentially integrated as teaching strategy. We believed that when students are able to master in learning they will be more motivated to learn and educators are considered effective if they can help and motivate students in learning.

TABLE III. DESCRIPTION OF COMPUTATIONAL THINKING DIMENSIONS

Computational Thinking Skills	Descriptions
Computational concepts	The concept used by programmers during programming activities.
Computational practices.	Problem-solving in programming practice that focuses on thinking and learning processes.
Computational perspectives	Students' knowledge of themselves, their relationships with others, and the ability to use technology around them.

TABLE IV. DESCRIPTION OF COMPUTATIONAL THINKING APPROACHES

Approaches	Descriptions
Tinkering	Trying something new through exploration, experimentation, and improvement.
Creating	Creating is related to planning, designing, and evaluating something like programs and animations.
Debugging	The process of finding and identifying mistakes.
Collaborating	Work with others to ensure the best results.
Persevering	Never despair, determination, resilience, and perseverance.

III. VALIDATION

This study used the Fuzzy Delphi method, a method improved from the Delphi method using Fuzzy theory. This method employed expert opinion and consensus to evaluate and validate each component and element of computational thinking for teaching and learning programming course as illustrated in Fig. 1. The verification process employed a focus group discussion involving 15 expert panels. Several steps were taken before validation using the Fuzzy Delphi method, to ensure that the components and elements are suitable for the problem-solving in a programming course and meet the needs of students. The processes involved were identifying the components of computational thinking for solving problems in programming, identification of components operational definitions, pre-evaluation of the operational definition, improvement of the operational definition and construction of elements for each component.

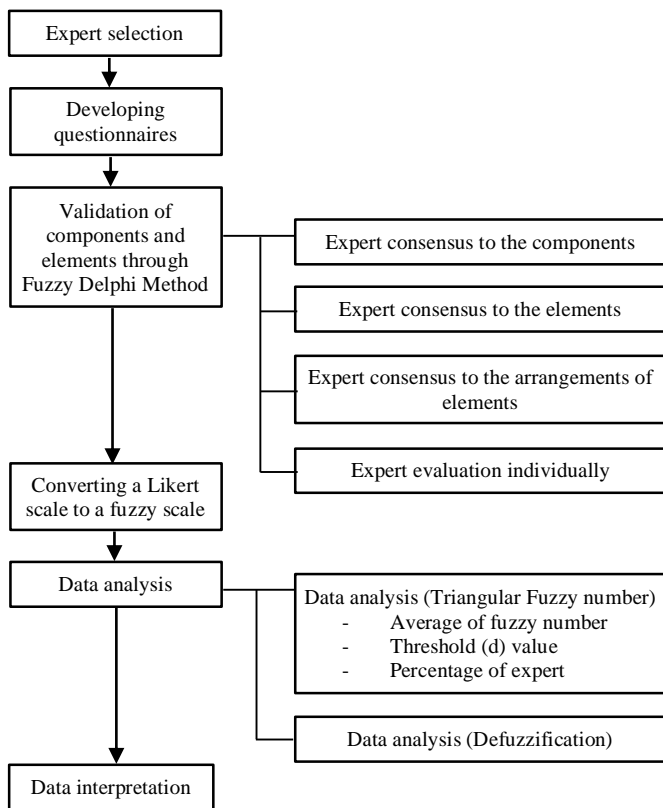


Fig. 1. Validation Procedures of the Computational thinking Components.

A. Expert Selection

Experts in the field of study were selected for validation of computational thinking components using the Fuzzy Delphi method. There are several perspectives in determining the number of experts. According to the Delphi method, the number of experts should be between 10 to 50 people [44]. In this study, 15 experts in the programming field were selected as there was a uniformity among experts and is sufficient, according to [45]. The panel of experts consisted of lecturers from pre-university, public and private higher education institutions, vocational college, and teachers. All the selected experts have more than ten years of experience in teaching and

learning programming. Instructors can also be considered as an expert if they have been in service for five to 10 years [44]. First, experts must give their consent to contribute their opinions within their expertise to evaluate and improve the proposed questionnaire that comprised of computational thinking components and elements for problem-solving in programming.

B. Development of Questionnaires

Based on the literature, 14 components of computational thinking that represented computational skills, dimensions and approaches as listed in Tables I to III were identified and characterised as 14 questionnaire items in this study. As the skill component plays a leading role in the problem-solving process or activity, the skill components are detailed with appropriate elements (Table V) to suit their use in the study context and included as 35 questionnaire items.

The questionnaire used a 7-point Likert scale representing strongly disagree to strongly agree.

TABLE V. DESCRIPTION OF ELEMENTS FOR EACH COMPUTATIONAL THINKING (COMPUTATIONAL THINKING) SKILLS

Skill Components	Elements Descriptions
Abstraction	There are five (5) elements related to the process of understanding and formulating problems as well as identifying relevant information.
Decomposition	There are five (5) elements related to the process of decomposing the problem.
Pattern recognition	There are five (5) elements to integrate existing knowledge and experience as a problem-solving strategy.
Algorithm	There are seven (7) elements to develop an algorithm and the consequences if the algorithm is not perfect.
Logical reasoning	There are seven (7) elements related to logic in programming.
Evaluation	There are six (6) elements related to evaluation to ensure that solutions are accurate, appropriate and meet its purpose.

C. Validation of Components and Elements using the Fuzzy Delphi Method

The validation of components and elements referring to the questionnaire items were done using the Fuzzy Delphi method, where focus group discussions took place involving expert panels. There are several steps in a validation process including validation of principal components and elements and arrangement of elements based on expert opinions and consensus; evaluation of components and elements by experts individually; and finally data were collected and analysed using the Fuzzy Delphi technique. The details of the processes are explained as follows:

1) *Expert consensus regarding main components*: The components and elements of computational thinking were provided to the experts using Google sheets and shared via email a week before the discussion to provide them with research information, comfortable period to understand the context of the study and to generate ideas to improve the questionnaire. The statements and views were presented during the discussion. During the discussion, each expert was

provided again with the details of computational thinking components. There were four worksheets used during the discussion. The first, second, and third worksheets were the

tables for the first, second, and third groups, respectively as shown in Fig. 2 while the fourth column is for list of suggested elements for the component as shown in Fig. 3.

	A	B	C	D
1	COMPUTATIONAL THINKING - SKILLS			
2	ABSTRACTION	1st Argument	2nd Argument	Consensus
3				
4	DECOMPOSITION	1st Argument	2nd Argument	Consensus
5				
6	PATTERN RECOGNITION	1st Argument	2nd Argument	Consensus
7				

Fig. 2. Google Drive Templates for each Group.

	A	B	C	D	E	F	G
1	PART 1: SKILLS						
2	1) ABSTRACTION						
3	Group 1	Group 2	Group 3	Consensus	As a teacher who teaches programm		
4					1st Element	2nd Element	3rd
5							
6	2) DECOMPOSITION						
7	Group 1	Group 2	Group 3	Consensus	As a teacher who teaches programm		
8					1st Element	2nd Element	3rd
9							
10	3) PATTERN RECOGNITION						
11	Group 1	Group 2	Group 3	Consensus	As a teacher who teaches programm		

Fig. 3. Google Drive Template for the Final Consensus.

During the discussion, experts were divided into three groups consisted of five people for each group. The component verification process was carried out in two stages. In the first stage, experts in each group evaluated and validated the components of the research based on the definitions provided. The opinions by experts were recorded in the Google Sheet document accordingly. The facilitator then transferred the consensus from each group to the fourth worksheet according to the group column. The second stage of the component verification process was a discussion for the consensus to evaluate and validate the components based on the suggestions from each group. The final consensus was filled in the fourth column. The validated components were used for the evaluation and validation of the proposed elements for the component. The focus group discussion procedure used is aimed at addressing the weakness of the iterative process identified when using the Delphi method (DM) [46], but at the same time retaining the features of Fuzzy Delphi method such as research time frame compared to DM. Fig. 1 and Fig. 2 shows the Google drive document for the validation process.

D. Expert Consensus to the Arrangement of Elements

After validating the skill components, the expert evaluated and validated the proposed element for each skill components. The list of elements was displayed next to the component, which was validated by the experts. The validation process involved a discussion among the experts to improve the suggested elements. Improvements included language structure to be clear and in line with the skills' definition and according to the context of the study; avoid repetitive, inappropriate, or unnecessary elements and suggest new elements as necessary to meet the skills' definition.

E. Expert Consensus to the Arrangement of Elements According to Priority

Questionnaire items for components and elements were transferred into Google forms for individual expert evaluation.

The use of Google forms allowed data to be transferred to Microsoft Excel and facilitated data analysis.

The questionnaire was then distributed to experts via email and Whatsapp using the Google form URL. The expert then answered the questionnaires individually to evaluate the components and elements by choosing the option on a 7-point Likert scale that represents strongly disagree to strongly agree. The answered questionnaire by all the experts through Google forms was saved directly in Google sheets. Fig. 3 shows the process of verifying components and elements.

The validated elements were then sorted in order of priority to fit the problem-solving approach in programming. The priority order considered the dimensions of their use during delivery, student engagement practically, development and evaluation of student performance. The arrangement process was performed together by all the experts.

F. Expert Evaluation Individually

Questionnaire items for components and elements were transferred into Google forms for individual expert evaluation. The use of Google forms allowed data to be transferred to Microsoft Excel and facilitated data analysis. The

questionnaire was then distributed to experts via email and Whatsapp using the Google form URL. The expert then answered the questionnaires individually to evaluate the components and elements by choosing the option on a 7-point Likert scale that represents strongly disagree to strongly agree. The answered questionnaire by all the experts through Google forms was saved directly in Google sheets. Fig. 4 shows the process of verifying components and elements.

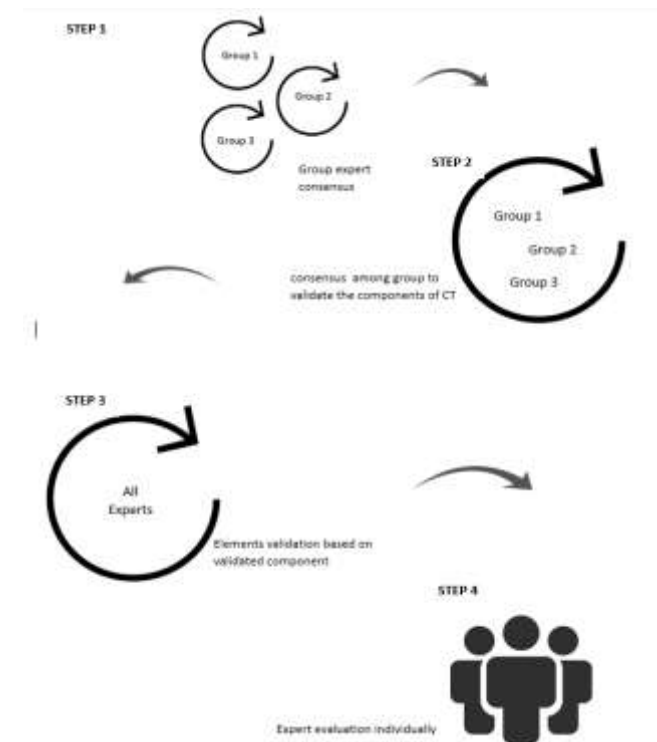


Fig. 4. Google Drive Template for the Final Consensus.

IV. DATA ANALYSIS

A. Converting Likert Scale to Fuzzy Scale

The Fuzzy scale was determined for each Likert scale, as shown in Table VI. Data in the Likert scale were converted to Fuzzy numbers through Microsoft Excel using the VLOOKUP function to be analysed using the Fuzzy Delphi (FDM) method. The Fuzzy set theory [47] allows the use of linguistic terms such as the level of agreement in Table VI by converting them to appropriate fuzzy sets and numbers. Respondents' answer on the Likert scale was translated into the Fuzzy scale, which was divided into three values: minimum value (m1), most reasonable value (m2) and maximum value (m3).

B. Data Analysis using the Fuzzy Delphi Method

In analysing the Fuzzy Delphi method, importance is given to the Triangular Fuzzy Number and the Defuzzification process. Both analyses aimed to determine whether a component or element is accepted or rejected based on the expert consensus [48]. Element acceptance was determined by the threshold (d) and per cent of consensus. The Defuzzification process aimed to obtain a Fuzzy score (A) to determine the acceptability of components and elements and its priority.

TABLE VI. QUESTIONNAIRE SCALE

Linguistic variables	Likert scale	Fuzzy scale (m ₁ , m ₂ , m ₃)		
Extremely agree	7	0.9	1	1
Strongly agree	6	0.7	0.9	1
Agree	5	0.5	0.7	0.9
Moderately agree	4	0.3	0.5	0.7
Disagree	3	0.1	0.3	0.5
Strongly disagree	2	0	0.1	0.3
Extremely disagree	1	0	0	0.1

The Likert scale data from Google sheets were transferred into Microsoft Excel worksheet template to analyse the Fuzzy Delphi method by expert numbers (1 - 15). The Triangular Fuzzy Number composed of minimum(m1), reasonable (m2), and maximum (m3) values were used. Data analysis involved the determination of (i) the average value of the Fuzzy scale (m1, m2, m3), (ii) the threshold (d) value (iii) the percentages of consensus on each component and element, and (iv) the Fuzzy score to determine the acceptability and the ranking of components and elements using defuzzification process. Data were analysed using Microsoft Excel software.

1) *Triangular fuzzy number: Average of Fuzzy Number* (m1, m2, m3).

Fig. 5 shows a triangular graph against triangular values. All the values (m1, m2, m3) are in the range 0 to 1 which refers to the Fuzzy number (0,1).

The average value of a Fuzzy number was determined using the following Formula 1:

$$\frac{m=\sum_1^n m_i}{n} \tag{1}$$

where n refers to the number of experts.

2) *Triangular fuzzy number: Threshold (d) Value:* The threshold value (d) was calculated to obtain the level of expert consensus for all questionnaire items [49]. Based on the Fuzzy numbering (0,1), the threshold value (d) for both Fuzzy numbers m (m1, m2, m3) and n = (n1, n2, n3) can be determined using the following Formula 2;

$$d(\tilde{m}, \tilde{n}) = \sqrt{\frac{1}{3}[(m_1 - n_1)^2 + (m_2 - n_2)^2 + (m_3 - n_3)^2]} \tag{2}$$

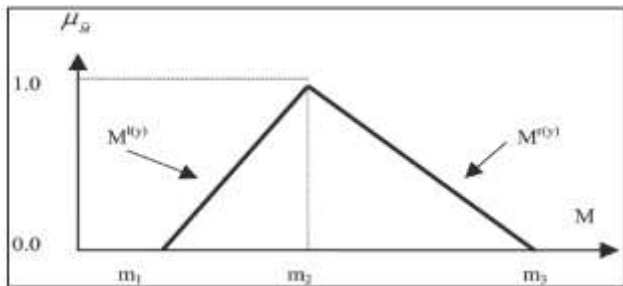


Fig. 5. Triangular Graph against Triangular Values.

If the distance between the mean value and the expert evaluation data is less than or equal to the threshold value (d) = 0.2, then all experts are considered to have reached an agreement [50]. Table VII shows the interpretation of the data based on the threshold value (d).

TABLE VII. INTERPRETATION OF THE DATA BASED ON THE THRESHOLD VALUE (D)

Threshold (d) value	Descriptions	Interpretation
$d \leq 0.2$	The threshold (d) value is less than or equal to 0.2	Accepted
$d \geq 0.2$	The threshold (d) value is greater than 0.2	Rejected OR conduct the second cycle, which involved only experts who disagreed.

To meet the conditions of acceptance for each item agreed upon by the experts, the percentage value of the expert's consensus must be equal to or greater than 75%. If the expert's consensus percentage is less than 75%, the item needs to be removed or a second round is conducted against the non-consenting expert.

C. *Defuzzification: The Fuzzy Score*

The Fuzzy score (A) obtained using the defuzzification process indicates whether an item is accepted based on the expert's consensus or not. An element is accepted when the Fuzzy score (A) equals or exceeds the median (α - cut) value of 0.5 [42]. The Fuzzy (A) score was calculated using the following Formula 3:

$$\text{Fuzzy score (A)} = (1/3) * (m1+m2+m3) \tag{3}$$

Apart from that, the Fuzzy score value (A) can determine the order and ranking of the questionnaire item. Since this study is about the problem-solving approach in programming, the arrangement of elements of each component based on the experts' discussion was followed. If the priority of the element is considered based on the defuzzification process, the results may not comply with the approach of problem-solving in programming. The expert will re-evaluate the order and priority of the element if any element is rejected after the analysis.

V. FINDINGS AND DISCUSSION

Focus group discussion was conducted, consisting of experts to evaluate and validate computational thinking components and elements. There are 14 main components of computational thinking and 35 elements representing computational thinking skill. All the components and elements evaluated by the experts were accepted. Based on a 7-point Likert scale, components and elements showed the average scores within 6 and 7 for all items, which strongly agree and extremely agree. For analysis, Likert scale scores were converted to Fuzzy scales. The results showed that all main components of computational thinking and skill elements of computational thinking met the first prerequisite of threshold (d) ≤ 0.2 based on the consensus of 15 experts. For the second prerequisite, the 14 components and 35 elements evaluated showed the percentage of consensus greater than

75%. Hundred percent consensus was achieved for the 14 components of computational thinking, while for the elements of computational thinking skill, the consensus are in the range from 86.6% to 100% was achieved. The third prerequisite was to obtain a Fuzzy score (A) to determine the acceptability of the questionnaire items. If the Fuzzy score (A) exceeds 0.5, then the questionnaire item is accepted. The Fuzzy score (A) in the range of 0.876 to 0.960 was obtained for all the components and elements evaluated. The findings confirmed the acceptance of all the components and elements of computational thinking tested and are suitable for teaching and learning programming.

Based on the analysis, FDM gives effective results in validating the components and elements of computational thinking. The results of the analysis in tandem with other research using FDM analysis for item-based validation [52-54]. The FDM analysis supported the suitability of the components and elements evaluated where all the questionnaires items were accepted, and pre-requisites met based on the threshold value (d), percentage of consensus and fuzzy score (A). The results of the analysis were influenced by the discussion method. All experts had the opportunity to give opinions and ideas to validate questionnaire through open discussion. Expert opinions were merged to get questionnaire items that fit the context of the study. The panel experts consisted of instructors who are curriculum developer and experienced programming lecturers where eight of them have followed trainees of trainers in computational thinking. The experts' evaluation was analysed to determine either the questionnaire items were accepted or rejected. The findings indicated similar responses from experts from the same institution for the items related to the program code. This similar view may be related to the common practices and approaches of teaching and learning used by the experts.

A. FDM Analysis Effectively

Generally, the focus group discussion method to get consensus is an effective method where researchers do not have to spend a lot of time to meet experts individually. Uploading materials in Google Drive and sharing with the experts involved in this study allowed retrieval of quick feedback from experts. Besides, this method provides an open discussion space and validated questionnaire items as a result of expert consensus can be updated online. However, expert group discussion requires a high level of commitment by the researchers and experts. The researcher should survey the available time of each expert, identify the appropriate date for all the experts to meet and discuss, and remind them through Google Calendar to ensure their attendance on the selected date. Besides, there are other preparations before the discussions such as preparation of expert invitation letters, printed materials and Google drives, and Google forms templates, a place with internet connections for discussions and refreshments for the experts.

The Fuzzy Delphi (FDM) method can avoid misinformation or loss of important information that can occur when using the Delphi method [36]. However, there are some limitations, even though FDM can give fast and reliable feedback. Researchers must have existing knowledge in the context of the study as relevant elements to be identified from

literature review besides the need to communicate with the experts in the field of study who are willing to participate in the study.

The FDM method can be applied in other studies that require an expert's opinion and consensus. The FDM is not only suitable to validate components and elements as used in this study, but it can also be used to validate pre-construction to determine components during the analysis and evaluation phase which involved the development of models, modules, frameworks and products. The data obtained in quantitative form has higher reliability since it undergoes several qualitatively implemented stages. Analysis through FDM can determine the validity of computational thinking components and elements for problem-solving in programming based on expert consensus. The findings from this study can be used to develop problem-solving models in programming as a guide for teaching and learning.

VI. CONCLUSION

This study aimed to validate computational thinking components and elements as a problem-solving approach in programming by obtaining expert consensus using the Fuzzy Delphi method (FDM). Analysis results showed that all components and elements are accepted based on expert consensus. Hence, these components and elements potentially applied in teaching and learning programming as well as model development as teachers' guide. In the further work of this study, a model as a teachers' guide for teaching and learning programming will be developed by applying the accepted components and elements.

ACKNOWLEDGMENT

This study was funded by the UKM Research Grant (GUP-2018-155). We would like to thank the fifteen experts and Matriculation Division, Ministry of Education Malaysia for their assistance and contribution to this study.

REFERENCES

- [1] C. C. Selby, "Relationships: Computational Thinking, Pedagogy of Programming, and Bloom's Taxonomy," *Proc. Work. Prim. Second. Comput. Educ.*, pp. 80–87, 2015.
- [2] B. Du Boulay, "Some Difficulties of Learning to Program," *J. Educ. Comput. Res.*, vol. 2, no. 1, pp. 57–73, 1986.
- [3] Y. Qian and J. Lehman, "Students' Misconceptions and Other Difficulties in Introductory Programming," *ACM Trans. Comput. Educ.*, vol. 18, no. 1, pp. 1–24, 2017.
- [4] A. Robins, J. Rountree, and N. Rountree, "Learning and Teaching Programming: A Review and Discussion," *Comput. Sci. Educ.*, vol. 13, no. 2, pp. 137–172, 2003.
- [5] L. E. Winslow, "Programming Pedagogy --A Psychological Overview," *ACM SIGCSE Bull.*, vol. 28, no. 3, pp. 17–22, 1996.
- [6] F. Paas and P. Ayres, "Cognitive Load Theory: A Broader View on the Role of Memory in Learning and Education," *Educ. Psychol. Rev.*, vol. 26, no. 2, pp. 191–195, 2014.
- [7] V. J. Shute, C. Sub, and J. Asbell-Clarke, "Demystifying computational thinking," *Educ. Res. Rev.*, vol. 22, no. September, pp. 142–158, 2017.
- [8] S. Bocconi et al., *Developing Computational Thinking: Approaches and Orientations in K-12 Education*, no. June. 2016.
- [9] A. Yadav, H. Hong, and C. Stephenson, "Computational Thinking for All: Pedagogical Approaches to Embedding 21st Century Problem Solving in K-12 Classrooms," *TechTrends*, vol. 60, no. 6, pp. 565–568, 2016.

- [10] A. D. F. Perez and G. M. Valladares, "Development and assessment of computational thinking: A methodological proposal and a support tool," *IEEE Glob. Eng. Educ. Conf. EDUCON*, vol. 2018-April, pp. 787–795, 2018.
- [11] A. R. Lopez and F. J. Garcia-Penalvo, "Personalized contents based on cognitive level of student's computational thinking for learning basic competencies of programming using an environment b-learning," *Proc. Fourth Int. Conf. Technol. Ecosyst. Enhancing Multicult. - TEEM '16*, pp. 1139–1145, 2016.
- [12] M. Roman-Gonzalez, J. C. Perez-Gonzalez, and C. Jimenez-Fernandez, "Which cognitive abilities underlie computational thinking? Criterion validity of the Computational Thinking Test," *Comput. Human Behav.*, vol. 72, pp. 678–691, 2017.
- [13] M. Romero, A. Lepage, and B. Lille, "Computational thinking development through creative programming in higher education," *Int. J. Educ. Technol. High. Educ.*, vol. 14, no. 1, 2017.
- [14] E. B. Witherspoon, R. M. Higashi, C. D. Schunn, E. C. Baehr, and R. Shoop, "Developing computational thinking through a virtual robotics programming curriculum," *ACM Trans. Comput. Educ.*, vol. 18, no. 1, pp. 1–20, 2017.
- [15] B. Wu, Y. Hu, A. R. Ruis, and M. Wang, "Analysing computational thinking in collaborative programming: A quantitative ethnography approach," *J. Comput. Assist. Learn.*, no. January, pp. 1–14, 2019.
- [16] F. K. Cansu and S. K. Cansu, "An Overview of Computational Thinking," *Int. J. Comput. Sci. Educ. Sch.*, vol. 3, no. 1, p. 17, 2019.
- [17] A. Yadav, C. Stephenson, and H. Hong, "Computational thinking for teacher education," *Commun. ACM*, vol. 60, no. 4, pp. 55–62, 2017.
- [18] J. M. Wing, "Computational thinking," *Commun. ACM*, vol. 49, no. 3, p. 33, 2006.
- [19] J. M. Wing, *Research Notebook: Computational Thinking-What and Why?* The Link magazine of Carnegie Mellon University. 2011.
- [20] P. J. Denning, "the Profession of It Beyond Computational thinking," no. 6, pp. 5–7, 2009.
- [21] A. Yadav, C. Mayfield, N. Zhou, S. Hambrusch, and J. T. Korb, "Computational Thinking in Elementary and Secondary Teacher Education," *ACM Trans. Comput. Educ.*, vol. 14, no. 1, pp. 1–16, 2014.
- [22] P. J. Denning and M. Tedre, *Computational Thinking*. London, England: The MIT Press, 2019.
- [23] C. Angeli et al., "A K-6 computational thinking curriculum framework: Implications for teacher knowledge," *Educ. Technol. Soc.*, vol. 19, no. 3, pp. 47–57, 2016.
- [24] A. Csizmadia et al., "Computational thinking - A guide for teachers," *Comput. Sch.*, 2015.
- [25] C. Selby and J. Woollard, "Computational Thinking: The Developing Definition," *Univ. Southampt.*, 2013.
- [26] J. M. Wing, "Computational thinking and thinking about computing," *Philos. Trans. R. Soc. A Math. Phys. Eng. Sci.*, vol. 366, no. 1881, pp. 3717–3725, 2008.
- [27] P. J. Denning, "Remaining trouble spots with computational thinking," *Commun. ACM*, vol. 60, no. 6, pp. 33–39, 2017.
- [28] B. Rodriguez, S. Kennicutt, C. Rader, and T. Camp, "Assessing computational thinking in CS unplugged activities," *Proc. Conf. Integr. Technol. into Comput. Sci. Educ. ITiCSE*, pp. 501–506, 2017.
- [29] R. Burbaitė, V. Stukys, and V. Drasute, "Integration of Computational Thinking Skills in STEM-Driven Computer Science Education," *IEEE Glob. Eng. Educ. Conf. EDUCON*, pp. 1824–1832, 2018.
- [30] K. Brennan and M. Resnick, "New frameworks for studying and assessing the development of computational thinking," *Proc. 2012 Annu. Meet. Am. Educ. Res. Assoc. Vancouver, Canada.*, vol. 1, pp. 1–25, 2012.
- [31] S. Papert, *Mindstorms: Children, computers and powerful ideas*, vol. 1. 1980.
- [32] F. Anna, Sabariah Sha'rif, W. Wong, and Muralindran Mariappan, "Computational Thinking and Tinkering : Exploration Study of Primary School Students' in Robotic and Graphical Programming," *Int. J. Assess. Eval. Educ.*, vol. 7, no. 1993, pp. 44–54, 2017.
- [33] CAS Barefoot, "Computational Thinking," 2014.
- [34] M. Berland, T. Martin, T. Benton, C. P. Smith, and D. Davis, "Journal of the Learning Using Learning Analytics to Understand the Learning Pathways of Novice Programmers," no. January 2014, pp. 564–599, 2013.
- [35] J. Krauss and K. Prottsman, *Computational Thinking and Coding for Every Student: The Teacher's Getting- Started Guide*. Corwin Press: Sage Publishing Company, 2016.
- [36] R. McCauley et al., "Debugging: A review of the literature from an educational perspective," *Comput. Sci. Educ.*, vol. 18, no. 2, pp. 67–92, 2008.
- [37] B. Özmen and A. Altun, "Undergraduate Students' Experiences in Programming: Difficulties and Obstacles Üniversite Öğrencilerinin Programlama Deneyimleri: Güçlükler ve Engeller," *Turkish Online J. Qual. Inq.*, vol. 5, no. 3, pp. 9–27, 2014.
- [38] K. Kwon and J. Cheon, "Exploring problem decomposition and program development through block-based programs," *Int. J. Comput. Sci. Educ. Sch.*, vol. 3, no. 1, p. 3, 2019.
- [39] M. Tom, "Five Cs framework: A student-centered approach for teaching programming courses to students with diverse disciplinary background," *J. Learn. Des.*, vol. 8, no. 1, pp. 21–37, 2015.
- [40] M. Othman, N. M. Zain, U. H. Mazlan, and R. Zainordin, "Assessing cognitive enhancements in introductory programming through online collaborative learning system," *2015 Int. Symp. Math. Sci. Comput. Res.*, vol. 2015, pp. 7–12, 2015.
- [41] M. Karyotaki and A. Drigas, "Online and other ICT-based training tools for problem-solving skills," *Int. J. Emerg. Technol. Learn.*, vol. 11, no. 6, pp. 35–39, 2016.
- [42] M. Tiantong and S. Teemuangjai, "The four scaffolding modules for collaborative problem-based learning through the computer network on moodle lms for the computer programming course," *Int. Educ. Stud.*, vol. 6, no. 5, pp. 47–55, 2013.
- [43] A. Gomes and A. Mendes, "A teacher's view about introductory programming teaching and learning: Difficulties, strategies and motivations," *Proc. - Front. Educ. Conf. FIE*, vol. 2015-Febru, no. February, 2015.
- [44] D. C. Berliner, "The Near Impossibility of Testing for Teacher Quality," *J. Teach. Educ.*, vol. 56, no. 3, pp. 205–213, 2005.
- [45] M. Adler and E. Ziglio, *Gazing into the oracle*. Bristol, PA: Jessica Kingsley Publishers, 1996.
- [46] N. Amira M. Saffie, Nur'Amirah Mohd Shukor, and Khairul A. Rasmani, "Fuzzy delphi method: Issues and challenges," pp. 1–7, 2017.
- [47] L. A. Zadeh, "Fuzzy set," *Inf. Control*, vol. 8, pp. 338–353, 1965.
- [48] Mohd Ridhuan Mohd Jamil, Saedah Siraj, Zaharah Hussin, Nurulrabihah Mat Noh, and Ahmad Ariffin Sapar, *Pengenalan Asas Kaedah Fuzzy Delphi Dalam Penyelidikan Reka Bentuk dan Pembangunan*. Minda Intellect, 2017.
- [49] N. S. Thomaidis, N. Nikitakos, and G. D. Dounias, "The evaluation of information technology projects: A fuzzy multicriteria decision-making approach," *Int. J. Inf. Technol. Decis. Mak.*, vol. 5, no. 1, pp. 89–122, 2006.
- [50] C.-H. Cheng and Y. Lin, "Evaluating the best main battle tank using fuzzy decision theory," *Eur. J. Oper. Res.*, vol. 142, pp. 174–186, 2002.

Ground Control Point Generation from Simulated SAR Image Derived from Digital Terrain Model and its Application to Texture Feature Extraction

Kohei Arai

Faculty of Science and Engineering
Saga University, Saga City
Japan

Abstract—Ground Control Point: GCP generation from simulated topographic map derived from Digital Terrain Model: DTM is proposed. Also, texture feature extraction is attempted from the simulated image. In this study, simulated image is derived from elevation data only, under assumptions of a simple scattering model without consideration of complex dielectric constant of the targets of interest. The performance of the acquired GCPs was evaluated by using several measures with texture features of GCP chip images. This paper describes the details about proposed method for acquisition of GCPs and simulated results on relationship between texture features and GCP matching success rate corresponding to the cross correlation between reference and distorted GCP chip images.

Keywords—Ground Control Point: GCP; Digital Terrain Model: DTM; scattering model; complex dielectric constant; texture feature; matching success rate; GCP chip

I. INTRODUCTION

Various researches have been conducted on the method of extracting [1]-[5] Ground Control Point: GCP from image data obtained by optical sensors. In particular, these days, the technology in optical sensors can be effectively applied to image data by SAR (synthetic aperture radar) [6]. Have been shown in a study by Dr. Guindon et al [1]. They have proposed an automatic matching method between real and simulated SAR images with distortion due to terrain effects.

Essentially, space-based SAR imagery data has distortions due to layover, foreshortening, shadowing and so on. Therefore, geometric fidelity of the SAR imagery data is still key issues. One of the problems of geometric fidelity improvement of the space-based SAR imagery data is GCP extraction from the SAR imagery data. GCP extraction is not so easy. Also, another problem is matching accuracy improvement. By using GCPs, geometric distortions have to be removed through GCP matching. This is not so easy either. In order to improve these GCP extraction and GCP matching processes, GCP extraction from digital elevation model, and chip image based GCP matching are proposed here.

In this study, simulated a SAR image is generated using digital terrain model (DTM) and tried to extract GCP. In addition, as an evaluation of the extracted GCP, matching was performed between the GCP chip image with some distortion and the original image, and the accuracy was examined.

Furthermore, in order to evaluate the matching accuracy of the GCP chip using only the chip image, the correlation between the texture features and the accuracy was examined [7].

In this paper, the author first describes the simulation method for the SAR image adopted in this study, and then introduce the features introduced as indices for GCP evaluation [8]. Finally, the extracted GCPs are evaluated using these characteristic quantities, and the conditions for the optimal GCP are examined.

In the following section, related research works are described. Then, the proposed method is described followed by experimental set-up together with experimental results. After that, concluding remarks and some discussions are described.

II. RELATED RESEARCH WORKS

Automated matching of real and simulated SAR image as a tool for GCP acquisition is proposed [1]. Image-scale and look direction effect on the detectability of lineaments in radar images is studied and well reported [2]. Studies on GCP matching of remote sensing image data is conducted [3]. Accuracy of digital elevation data by various interpolation methods is assessed [4].

A method for textural analysis of synthetic aperture radar images by Grey Level Co-occurrence Matrix: GLCM method is proposed [5]. Also, Synthetic Aperture Radar: SAR is well overviewed [6]. Landsat Thematic Mapper: TM image classification using seasonal change of texture information is proposed [7]. Outline of national land numerical information is well organized [8].

Some studies on GCP selection process and its accuracy is investigated [9] together with effects on GCP success rate [10]. On the other hand, experiment on GCP matching is conducted and well reported [11] together with studies on GCP matching of remote sensing imagery data [12].

GCP acquisition using simulated SAR derived from Digital Elevation Model: DEM is attempted [13] together with GCP acquisition using simulated SAR and evaluation of GCP matching accuracy with texture features [14].

Effect of planimetric correction with a few GCPs on terrain height estimation with stereo pair is evaluated [15].

Meanwhile, speckle noise removal of SAR images with DEM is proposed [16]. Then, a method of speckle noise reduction for SAR data is proposed and tested [17]. After that, a new method for SAR speckle noise reduction (Chi Square Filter) is proposed and evaluated its effectiveness [18].

Decomposition of SAR polarization signatures by means of eigen-space representation is proposed [19]. Also, SAR image classification based on Maximum Likelihood: MLH decision rule with texture features taking into account a fitness to the probability density function is well reported [20]. Meanwhile, polarimetric SAR image classification with maximum curvature of the trajectory in eigen space domain on the polarization signature is proposed [21] together with polarimetric SAR image classification with high frequency component derived from wavelet multi resolution analysis: MRA [22].

Comparative study of polarimetric SAR classification methods including proposed method with maximum curvature of trajectory of backscattering cross section in ellipticity and orientation angle space is conducted [23]. Multi-Resolution Analysis: MRA and its application to polarimetric SAR classification is proposed [24]. Recently, Sentinel 1A SAR data analysis for disaster mitigation in Kyushu is reported. [25]. Comparison of geometric features and color features for face recognition is conducted and discussed [26].

III. PROPOSED METHOD

A. Generation of SAR Image

The proposed method for simulation of SAR image is based on DTM or DEM. There are some sources of the DTM. It allows slope calculation in accordance with its mesh size or spatial resolution. Without consideration of geometric distortions derived from foreshortening, shadowing, layover, speckle noise, SAR image can be simulated using just slope calculated with DTM, satellite altitude and off-nadir angle (look angle).

In the proposed model, the backscattering coefficient is calculated according to the following procedure.

1) Calculate the slope between each point from DTM.

2) Calculate the angle of incidence of the radar wave from the positional relationship between the satellite and the observation point, and calculate the distribution of the backscattering cross section σ^0 assuming equation (1).

$$\sigma^0 \propto I_r = I_n \cos^2 \theta \quad (1)$$

where I_r , I_n , and θ are the scattering direction unit vector, the scattering plane normal vector, and the radar wave incident angle, respectively.

3) Since the observation point is distorted in the distance between pixels due to the terrain effect, Lissasoprisog is performed at right angles using the following equation.

$$P(i) = L_i \delta_i + L_{i-1} (1 - \delta_{i-1}) + L_{i+1} (1 - \delta_{i+1}) \quad (2)$$

$$\delta_i = (x - \frac{x}{2} - \delta x_i) / x$$

where $P(i)$: i-th pixel value, L_i : i-th pixel value before resampling, x : distance between pixels, δx_i : Pixel shift due to terrain effect.

Pixel shift δx_i due to the effect of layover, foreshortening, and shadowing was calculated from topographic information, and linear interpolation was performed by equation (2). However, the addition of a few terms in equation (2) was performed after judging whether or not $x / 2 - \delta x_i$ contributed to the i-th pixel value.

4) Convert the obtained values of $P_i(X, Y)$ $X, Y = 1$ to 320 into 8-bit gray level image data of 0 to 255.

B. Extraction of GCP

In order to extract GCP chip images from the simulated SAR image, the SAR image is divided with small size of sub-images as candidates of GCP. Then, variance of the candidates of GCP chip image is calculated. It is assumed that GCP chip image has a relatively large variance. The image obtained in this way was divided into chips of 32×32 pixels, and the variance of the pixel value of each chip was calculated.

The actual SAR image has a geometric distortion caused by the deviation of the position and attitude of the satellite or their estimation errors such as skew and rotation. In order to simulate them, a skew or rotation is applied to the original image obtained by extracting the GCP chip as geometric distortion, and the area correlation between the resulting distortion image and the original GCP chip image is calculated. Here, the skew and the rotation were given as the center of rotation of the GCP chip image as shown in Fig. 1.

C. GCP Matching

Detailed steps for matching are as follows,

1) A point corresponding to the center point of each GCP chip in the original image is defined as GCP, and skew distortion and rotation distortion are given around this point.

2) A search window of 48×48 pixels is provided on the original image side centering on GCP.

3) Shift the GCP chip by one pixel in the search window, calculate the area correlation of the overlapping part, and obtain the peak of the correlation coefficient.

Here, the peak of the correlation coefficient was obtained by extracting nine correlation coefficients centered on the pixel of interest and interpolating independently in the X and Y directions by a quadratic equation.

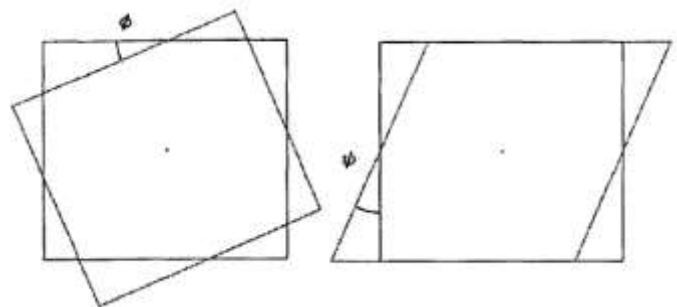


Fig. 1. Image Rotation (ϕ) and Skew (ψ).

D. Texture Feature Extraction

The author proposes a method for quantitatively evaluating the matching accuracy of GCP chips based on texture information. If the correlation between the matching accuracy and some feature amount of the chip image is strong, the GCP candidate with high automatic matching accuracy can be easily selected by evaluating the feature amount. In this study, feature extraction was performed using GLCM (Gray Level Co-occurrence Matrix) proposed by Haralick et. al (1973).

The 32 (PIXEL) x 32 (LINE) GCP chip consists of 256 gray levels, but for simplicity of calculation, this was integrated into 128 gray levels to calculate the GLCM. GLCM was obtained for four directions ($\theta = 0^\circ, 45^\circ, 90^\circ, 135^\circ$). GLCM was normalized by the following equations.

$$P(i,j,d,\theta) = P(i,j,d,\theta) / R \quad (3)$$

$$R = \sum_{i=0}^{Nq-1} \sum_{j=0}^{Nq-1} P(i,j,d,\theta) \quad (4)$$

where P is the normalized co-occurrence probability matrix, and P is the co-occurrence probability. The rate matrix (GLCM), d is the distance between pixels, and Nq is the number of gray levels.

Next, the following texture feature values were calculated from GLCM. Here, $P(i,j,d,\theta)$ is abbreviated as P_{ij} .

i) Angular Second Moment

$$ASM = \sum_i \sum_j P_{ij}^2 \quad (5)$$

ii) Homogeneity

$$HOM = \sum_i \sum_j P_{ij} / \{1 + (i-j)^2\} \quad (6)$$

iii) Contrast

$$CON = \sum_i \sum_j (i-j)^2 P_{ij} \quad (7)$$

iv) Dissimilarity

$$DIS = \sum_i \sum_j |i-j| P_{ij} \quad (8)$$

v) Entropy

$$ENT = -\sum_i \sum_j P_{ij} \log P_{ij} \quad (9)$$

vi) Correlation coefficient (Correlation)

$$COR = \{\sum_i \sum_j (ij) P_{ij} - \mu_x \mu_y\} / \sigma_x \sigma_y \quad (10)$$

vii) Chi-square

$$CHI = \sum_i \sum_j P_{ij}^2 / P_x(i) P_y(j) \quad (11)$$

where, P_{ij} is the average and standard deviation of the pixel values in the co-occurrence probability matrix direction, and $P_x(i) P_y(j)$ is the appearance probability in the matrix direction, respectively.

IV. EXPERIMENT

A. Generation of SAR Image

The DTM used for the simulation is a magnetic tape file (KS110) produced by the Geospatial Information Authority of Japan. In this file, altitude data is stored in m units according to a format called a standard area mesh system. The primary

area division mesh included in this data has a size of 80km by 80km, which is equivalent to one terrain map of 20 planes, and is large enough as an East area. The section of code No.5338 where all the data of the grid points were prepared was selected from these. This is the area that includes Mt. Fuji in the lower right as shown in Fig. 2. Fig. 3 shows the simulated SAR image (Full scene) derived from the DTM.

The data is divided into 320×320 primary partitions, and arranged in a complicated manner according to the mesh code system, and is converted into a two-dimensional image. Since the data is divided into primary partitions of 320×320 and arranged in a complicated manner according to the mesh code system, it is difficult to process it as a two-dimensional image. In addition, in this data, since there are several abnormal grid points without elevation value as inland waters, they were replaced with the average value of two points before and after. Fig. 4 shows an example of a sub scene of the simulated SAR image.

Furthermore, the altitude values from 0 to 3776 m were re-quantized to 255 gray levels for processing as monochromatic images. The grid point interval of this mesh is 250 m on the actual ground, but it is coarse compared to the resolution, so the upper left corner was cut out as a subscene (Northern Akaishi Mountains), and interpolation was performed at 50 m intervals with a cubic spline function.

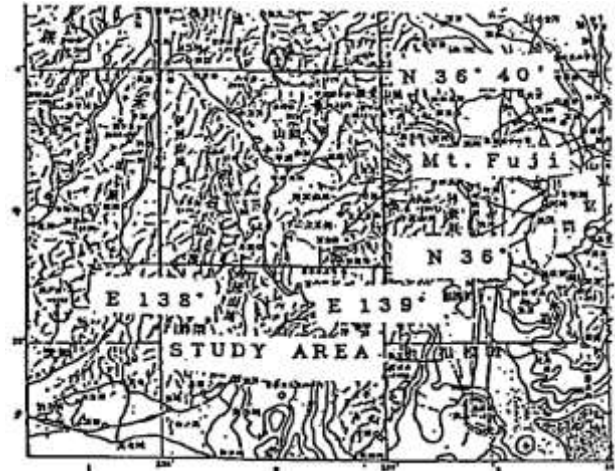


Fig. 2. Topographic Map of Intensive Study Area.

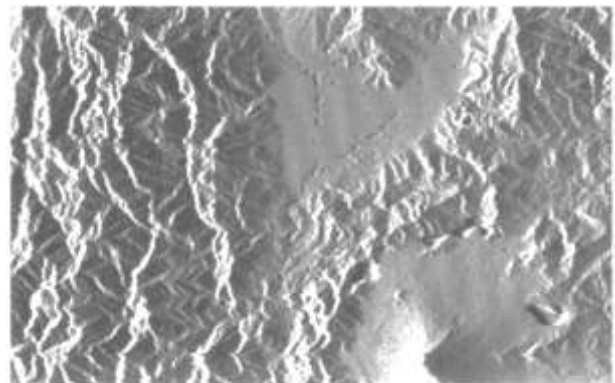


Fig. 3. Simulated SAR Image of Mt.Fuji and its Vicinity Derived from the DTM.



Fig. 4. Sub Scene of the Simulated SAR Image.

B. GCP Extraction

Since the observation area is a mountain area covered mostly by trees, it is considered to be a perfect diffusion surface, and it is assumed that the physical backscattering coefficient is uniform, and the reflected power obeys Rampart's cosine law. As the observation conditions from the satellite, as shown in Fig. 5.

It is assumed that observation is performed from west of the test site at an altitude of 570 km and an off-nadir angle of 35° while flying north-south.

The images obtained in this way are divided into chips of 32 x 32 pixels, and the results of calculating the variance of the pixel values of each chip are shown in Fig. 6, 7. Of these, 14 chips shown in Fig. 6, 7 with a tether were randomly selected as GCP candidates. Figure 8 shows three-dimensional images of these chips.

C. Texture Feature of GCP Chip Image

Table I shows the matching accuracy of each chip when the skew and rotation were changed every 1° from 1° to 4°, respectively. The matching accuracy is the Euclidean distance between the estimated GCP indicated by the peak of the correlation coefficient and the true position. Skew and rotation can occur simultaneously in the real image, respectively, but each case is treated independently to separate and evaluate. Miss-identification is defined as the sum up of distances, between GCP chip center and functional correlation peak point, for which skew or rotation distortions from 1 to 4 degrees with 1 deg. step are added to the original image. Here, R_1 and R_2 correspond to, respectively, skew and rotation.

Table II shows the relationship between GCP matching accuracy and each feature value by correlation coefficient.

As an example, Fig. 9 shows the relationship between the magnitude of GCP mismatch due to skew distortion and GLCM CON. Here, the sizes of the mismatches from 1 to 4 were added and evaluated. Clearly a negative correlation is

observed. Almost the same results were obtained for the other feature values. When the texture features in four directions were adjusted, it was found that there was a difference in the texture features in the 90° direction compared to the other three directions, as shown in Table III.

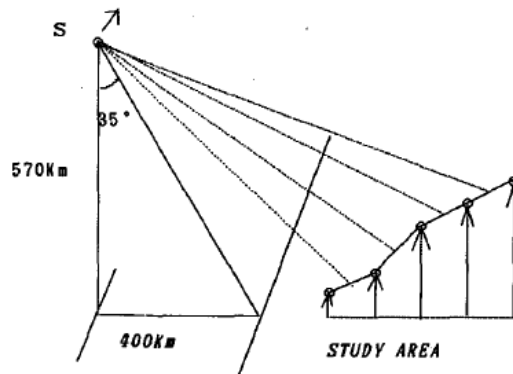


Fig. 5. Geometric Relationship between Satellite and Target.

171	93	25	382	25	145	188	273	280	211
824	325	79	74	100	223	296	284	387	528
198	623	343	31	142	215	225	308	275	346
346	848	336	126	84	246	139	280	254	225
406	844	752	281	81	103	131	124	276	238
709	1082	272	540	69	15	32	162	224	153
675	954	415	634	61	104	236	260	121	133
740	1032	529	585	127	269	263	167	177	204
1092	474	873	408	212	671	50	8	59	134
858	766	920	791	421	346	439	150	45	42

▨ This area is selected for subscene

Fig. 6. Gray Level Variance of each GCP Chip of Full Scene Divided into 10 by 10 Subsets.

165	32	25	80	191	165	64	3	5	95
58	61	141	189	119	198	81	48	13	235
106	150	214	112	166	130	163	28	42	251
131	162	265	185	206	252	82	65	41	265
124	227	292	253	301	122	169	98	41	249
183	179	340	305	139	85	179	118	137	406
78	254	174	137	242	131	218	201	190	535
58	208	234	93	149	112	291	104	155	508
58	167	285	165	81	178	318	140	130	1037
57	66	167	122	188	285	287	294	139	718

▨ This area is selected for GCP's

Fig. 7. Gray Level Variance of each GCP Chip of Sub Scene Divided into 10 by 10 Subsets.

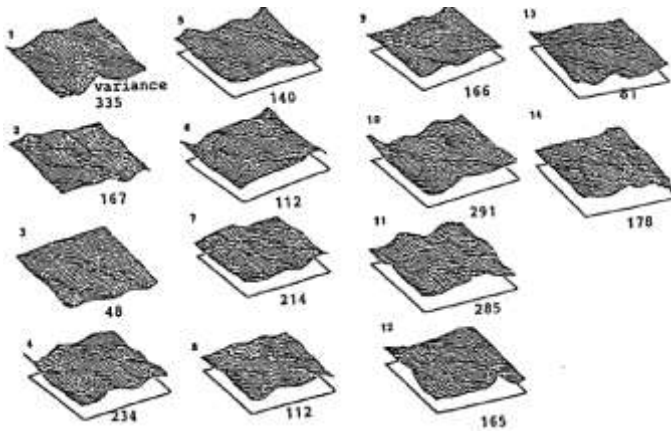


Fig. 8. Gray Level 30 Image and its Variance of GCP Chip.

TABLE I. MISS-IDENTIFICATION DUE TO THE GEOMETRIC DISTORTIONS IN TERMS OF SKEW AND ROTATION

GCP No.	Skew Angle (deg.)				Rotation Angle (deg.)			
	1	2	3	4	1	2	3	4
1	0.065	0.156	0.256	0.364	0.073	0.168	0.259	0.363
2	0.078	0.139	0.204	0.25	0.083	0.165	0.287	0.441
3	0.106	0.212	0.34	0.468	0.149	0.313	0.481	0.67
4	0.025	0.054	0.093	0.139	0.019	0.062	0.111	0.173
5	0.07	0.125	0.195	0.272	0.026	0.08	0.138	0.2
6	0.054	0.114	0.183	0.252	0.04	0.084	0.145	0.201
7	0.024	0.067	0.127	0.19	0.085	0.156	0.228	0.286
8	0.057	0.106	0.159	0.226	0.014	0.054	0.095	0.154
9	0.025	0.051	0.088	0.128	0.102	0.212	0.33	0.464
10	0.038	0.071	0.115	0.166	0.042	0.084	0.123	0.167
11	0.026	0.041	0.07	0.095	0.028	0.058	0.092	0.127
12	0.059	0.118	0.186	0.258	0.068	0.133	0.214	0.28
13	0.077	0.115	0.226	0.306	0.048	0.087	0.131	0.179
14	0.03	0.052	0.094	0.141	0.064	0.111	0.167	0.235

TABLE II. CORRELATION BETWEEN EACH TEXTURE FEATURE AND MIS-IDENTIFICATION OF GCPs' DUE TO SKEW OR ROTATION

	VAR	CON	CHI	ENT	ASM	HOM	DIS	COR
R1	-0.488	-0.706	-0.162	0.742	0.757	0.74	-0.728	0.732
R2	-0.29	-0.61	-0.323	0.562	0.626	0.627	-0.628	0.53

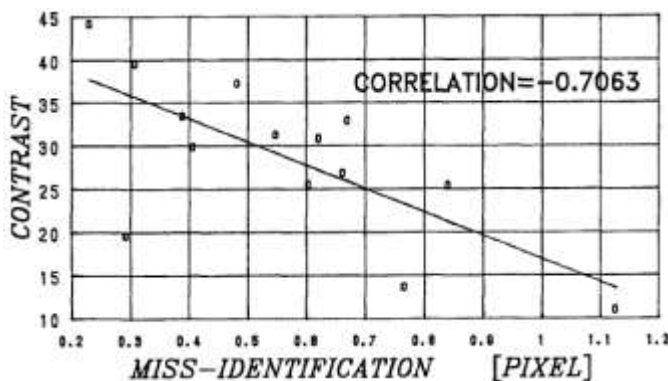


Fig. 9. Correlation between Contrast and Miss Identification (1-4 Degrees).

TABLE III. TEXTURE FEATURES OF GCP CHIPS

GCP No.	σ^2	CON	CHI	ENT	ASM	HOM	DIS	COR
1	335	25.33	30.43	-21.91	0.0227	1.79	7.07	0.0459
2	167	32.82	22.65	-21.5	0.0298	1.64	8.25	0.0854
3	48	10.98	14.66	-17.5	0.0784	2.2	4.76	0.29
4	234	39.5	20.82	-22.3	0.0224	1.52	8.94	0.0829
5	140	26.75	20.84	-21.13	0.03	1.57	7.87	0.103
6	112	25.5	22.11	-20.44	0.0342	1.72	7.27	0.13
7	214	28.78	19.81	-21.27	0.293	1.55	8.25	0.0694
8	112	31.15	25.71	-20.54	0.0358	1.61	7.98	0.123
9	166	19.56	20.83	-20.82	0.0306	1.84	6.44	0.0891
10	291	33.39	32.99	-22.17	0.0208	1.16	8.23	0.0518
11	285	44.13	18.92	-23.09	0.0152	1.24	10.39	0.515
12	165	30.81	27.09	-21.42	0.0248	1.52	8.32	0.0889
13	81	13.62	18.56	-19	0.0502	2	5.47	0.184
14	178	37.17	25.37	-21.57	0.0291	1.54	8.76	0.0839

V. REMARKS

From the experimental results, the following are remarks,

1) Table III shows that in this image, the 90 direction has less change than the other three directions. This is because the observation direction is 180. It can be seen that these features are highly dependent on the beam irradiation direction in the SAR image.

2) Skew distortion has a higher correlation between each feature and matching success rate than rotation distortion. This is considered to be due to the fact that the rotation has more distortion (larger loss (change) of the original information) than the skew that deforms only in one direction even at the same angle.

3) Variance and chi-square values have low correlation with GCP matching accuracy. This is because they do not always correspond to the complexity of terrain change (BUSYNESS).

4) The contrast, dissimilarity, entropy, angular second moment and homogeneity show relatively strong negative or positive correlation with GCP mismatch degree. Therefore, a regression equation can be obtained from these correlations to predict the degree of GCP mismatch.

5) HOM, COM and DIS have cross-correlation, and ASM and ENT have high cross-correlation. Furthermore, there is a negative correlation between these groups. Therefore, it is desirable to evaluate GCP by selecting an appropriate one.

VI. CONCLUSION

A method for extracting chip images suitable for GCP using simulated SAR images created from DTM was proposed. The followings are major results,

1) As a result of examining the relationship between the matching accuracy and the texture feature of the chip, the correlation with the index indicating the feature of GLCM of

contrast, second moment of moment, entropy, homogeneity, dissimilarity is high It turns out. From this, it was found that by examining only the very small amount of texture of the chip image, GCP which seems to have high matching accuracy can be selected.

2) In the central Japan area (around Mt. Fuji) studied this time, the correlation between the matching accuracy and the texture feature amount is 0.7 to 0.75 when considering skew distortion, and 0.06 to 0.62 when similarly considering rotation distortion.

3) Among texture features, the angular second moment has the highest correlation with matching accuracy, which is suitable for GCP candidate selection.

VII. FUTURE RESEARCH WORKS

The proposed system is adopted in the real earth observation satellite data, and it is a future subject to realize a more usable GCP acquisition method.

ACKNOWLEDGMENT

The author, also, would like to thank Professor Dr. Hiroshi Okumura and Professor Dr. Osamu Fukuda for their valuable discussions.

REFERENCES

- [1] B. Guindon, H. Maruyama, Automated Matching of Real and Simulated SAR Image as a Tool for GCP Acquisition. Canadian Journal of Remote Sensing, Vol 12.2 pp. 149/159, 1985.
- [2] Y. Yamaguchi, Image-Scale and Look Direction Effect on the Detectability of Lineaments in Rader Images. Remote Sensing of Environment. Vol 17 pp. 117/127, 1985.
- [3] K. Tsuchiya, K. Arai, K. Tanaka, Studies on Ground Control Points Matching of Remote Sensing Image Data. Proceedings of the 14th Symposium on Space Technology and Science. pp. 1321/1328, 1984.
- [4] Kuzumaki, Shuji, Yokoyama, Ryuzo, The 6th Lecture by the Japan Remote Sensing Society on the Accuracy of Digital Elevation Data by Various Interpolation Methods Proceedings of the Society, p. 55/58, 1986.
- [5] Hashimoto, G., Matsuo, Y., A method for textural analysis of synthetic aperture radar images by GCLM method. .7,4 pp. 25/35, 1987.
- [6] Nobuyoshi Raino, Synthetic Aperture Radar, Remote Sensing Society of Japan Vol1,1 pp. 49/107, 1981.
- [7] Kohei Arai, K., TM Image Classification Using Seasonal Change of Texture Information, Journal of the Japan Society of Photogrammetry, Vol. 26, 4, 1987.
- [8] Ministry of Construction, National Institute of Land and Geography, Department of Map Management, Outline of National Land Numerical Information, 1983.
- [9] K.Tsuchiya, and Kohei Arai, Some studies on GCP selection process and its accuracy, Proc.of the 2nd Australasian Conference on Remote Sensing, 6-14-1-6.14.6, 1980.
- [10] K.Tsuchiya and Kohei Arai, Effects on GCP success rate, Proc.of the 7th Canadian Symposium on Remote Sensing, No.17, 497-501, 1980.
- [11] K.Tsuchiya, Kohei Arai, and T.Tanaka, Experiment on GCP matching, Proc.of the ISPRS Commission II-3, and 4, B-18, 9-16 1983.
- [12] K.Tsuchiya Kohei Arai and T.Tanaka, Studies on GCP matching of remote sensing imagery data, Proc.of the ISTS, m-3-2,1321-1328, 1984.
- [13] Kohei Arai, and N.Fujimoto, GCP acquisition using simulated SAR derived from DEM, Proc.of the ISPRS Symposium, 33-40, 1988.
- [14] Kohei Arai, GCP Acquisition Using Simulated SAR and Evaluation of GCP Matching Accuracy with Texture Features, International Journal of Remote Sensing, Vol.12, No.11, pp.2389-2397, Oct.1991.

- [15] Kohei Arai, S.Mukai and Y.Terayama, Effect of planimetric correction with a few GCPs on terrain height estimation with stereo pair, Proc.of the ISPRS Committee-IV, PS-5-5, 1992.
- [16] H.Wakabayashi and Kohei Arai, Speckle noise removal of SAR images with Digital Elevation Model: DEM, Proc. of the 5th ISCOPS Symposium, 1993.
- [17] H. Wakabayashi and Kohei Arai, A method of Speckle Noise Reduction for SAR Data, International Journal of Remote Sensing, Vol.17, No.10, pp.1837-1849, May 1995.
- [18] H. Wakabayashi and Kohei Arai, A New Method for SAR Speckle Noise Reduction(Chi Square Filter), Canadian Journal of Remote Sensing, Vol.22, No.2, pp.190-197, Jun.1995.
- [19] Kohei Arai Decomposition of SAR Polarization Signatures by Means of Eigen-Space Representation, Proc. of the Synthetic Aperture Radar Workshop '98, 1998.
- [20] Kohei Arai and Y.Terayama, SAR image classification based on Maximum Likelihood Decision rule with texture features taking into account a fitness to the probability density function, Final Report of JERS-1/ERS-1 System Verification Program, J2, vol.II, pp.2-415 to 424, Munich, Mar., 1995.
- [21] Kohei Arai and J.Wang, Polarimetric SAR image classification with maximum curvature of the trajectory in eigen space domain on the polarization signature, Advances in Space Research, 39, 1, 149-154, 2007.
- [22] Kohei Arai, Polarimetric SAR image classification with high frequency component derived from wavelet multi resolution analysis: MRA, International Journal of Advanced Computer Science and Applications, 2, 9, 37-42, 2011.
- [23] Kohei Arai Comparative study of polarimetric SAR classification methods including proposed method with maximum curvature of trajectory of backscattering cross section in ellipticity and orientation angle space, International Journal of Research and Reviews on Computer Science, 2, 4, 1005-1009, 2011.
- [24] Kohei Arai, Wavelet Multi-Resolution Analysis and Its Application to Polarizatic SAR Classification, Proceeding of the SAI Computing Conference 2016.
- [25] Kohei Arai, Sentinel 1A SAR Data Analysis for Disaster Mitigation in Kyushu, Kyushu Brunch of the Japanese Society on Remote Sensing, Special Lecture for Young Engineers on Remote Sensing, Nagasaki University, 2018.
- [26] Cahya Rahmad, Kohei Arai, Rosa A. Asmara, Ekojono Dimas, R. H. Putra, Comparison of Geometric Features and Color Features for Face Recognition, International Journal of Intelligent Engineering and Systems, IJIES on Volume 14, Issue 1, 541-551, 2021 DOI: 10.22266/ijies.

AUTHOR'S PROFILE

Kohei Arai, He received BS, MS and PhD degrees in 1972, 1974 and 1982, respectively. He was with The Institute for Industrial Science and Technology of the University of Tokyo from April 1974 to December 1978 also was with National Space Development Agency of Japan from January, 1979 to March, 1990. During from 1985 to 1987, he was with Canada Centre for Remote Sensing as a Post Doctoral Fellow of National Science and Engineering Research Council of Canada. He moved to Saga University as a Professor in Department of Information Science on April 1990. He was a councilor for the Aeronautics and Space related to the Technology Committee of the Ministry of Science and Technology during from 1998 to 2000. He was a councilor of Saga University for 2002 and 2003. He also was an executive councilor for the Remote Sensing Society of Japan for 2003 to 2005. He is a Science Council of Japan Special Member since 2012. He is an Adjunct Professor of University of Arizona, USA since 1998. He also is Vice Chairman of the Science Commission "A" of ICSU/COSPAR since 2008 then he is now award committee member of ICSU/COSPAR. He wrote 55 books and published 620 journal papers as well as 450 conference papers. He received 66 of awards including ICSU/COSPAR Vikram Sarabhai Medal in 2016, and Science award of Ministry of Mister of Education of Japan in 2015. He is now Editor-in-Chief of IJACSA and IJISA.<http://teagis.ip.is.saga-u.ac.jp/index.html>.

Modeling of the Factors Affecting e-Commerce Use in Turkey by Categorical Data Analysis

Factors Affecting e-Commerce Use

Ömer Alkan¹

Associate Professor
Department of Econometrics
Ataturk University, Erzurum, Turkey

Hasan Küçüköğlü²

PhD Candidate, Department of
Management Information Systems
Ataturk University, Erzurum, Turkey

Gökhan Tutar³

Lecturer, Department of
Management Information Systems
Ataturk University, Erzurum, Turkey

Abstract—e-Commerce use is a subject of study that has been frequently discussed in recent years. The aim of this study was to detect the socio-demographic and economic factors affecting e-commerce use of individuals in Turkey. The micro dataset obtained from Information and Communication Technology (ICT) Usage Survey in Households performed by the Turkish Statistical Institute in 2014-2018 was employed in this study. Multinomial logistic and multinomial probit regression analyses were performed to detect the factors affecting e-commerce use of individuals in Turkey. The data of 129,643 individuals, who participated in ICT Usage Survey in Households in 2014-2018, were employed in the regression analyses. According to the analysis results, the variables of survey year, age, gender, educational level, occupation, income level, region and household size were detected to be effective on online shopping. The results of the study indicated that e-commerce use was gradually increasing. It was determined that more educated and young individuals and individuals living in relatively more developed regions were more inclined to online shopping. Policies should also be developed to increase e-commerce use of low educated individuals and individuals over middle age. In particular, small and medium-sized businesses (SMB) should pay more attention to the use of e-commerce in order to increase their activities by taking these situations into consideration. Indeed, how important e-commerce use is has been found out in epidemics/pandemics such as COVID-19, which causes people to lock themselves at home in the countries.

Keywords—Electronic commerce; online shopping; online purchase; e-commerce; Turkey; multinomial probit regression

I. INTRODUCTION

Various shopping techniques and methods have been employed according to needs throughout history. Nowadays, the final point these changes have reached is online shopping [1]. It is possible to say that today's technologies and the innovations brought by them have strong effects on this process of change. Along with the fact that information and internet technologies have become a part of life, individuals' motivations for online shopping are affected by this development [2].

In particular, the start of internet use has revolutionized commercial activities by enabling the shopping activities over the network called e-commerce [3]. e-Commerce use refers to shopping behaviors of consumers in an online store or on a website used for online purchasing [4]. Global shoppers get

tremendous benefits from purchasing products and services online. Internet allows product and service availability at minimum cost for 7/24 and 365 days [5]. Online shopping is one of the commonly used environments for easy shopping. Actually, it is a popular tool for shopping in the internet community in many parts of the world [6]. Through online shopping, detailed information and multiple options are also offered to customers so that they can compare the products and prices. With this diversity, it also becomes easier to find the products needed. Due to these opportunities, online shopping is becoming popular and the number of people who prefer this method is increasing day by day [7].

This method, which is beneficial for the companies that provide services over the network in addition to the advantages it offers to the consumer, reduces the transaction costs and provides companies with more global access [8]. Especially with the widespread use of the internet, consumers have the opportunity to access the product they desire at any time and from any location without being limited to any geographical region. Consumers can make choices for the product they will buy by making comparisons among more options. e-Commerce also offers advantages such as ease of use, time and energy savings. In the studies, it was observed that online shopping provided more satisfaction for the consumers looking for both comfort and speed [7]. e-Commerce is taking the place of traditional shopping methods and will become even more popular in the near future [9]. The demands for online shopping have increased so much that not only big companies but also small businesses and individuals sell handmade products over the Internet [10]. Online shopping is a new form of business, and this form of business supports the economic growth of underdeveloped regions [11].

As the contribution of online shopping to the economy has increased, the competition regarding this issue has also increased. Since online shopping has some advantages compared to traditional businesses, businesses are heading towards online shopping [12]. It is observed that there has been a great increase in both quantity and volume in individuals' online shopping through smart devices, such as mobile phones, personal digital assistants (PDAs), computers, and tablets, both in the world and in our country, especially in recent times [13]. Along with the continuous growth of global trade and the rapid advancement of digital society, consumers are increasingly heading towards shopping from abroad [14]. These tendencies

have promoted the increase of traditional foreign trade patterns at various dimensions of sustainability. Through competitive prices and a wide range of products, charming products can be offered to consumers and the time and space distance between consumers and suppliers can be shortened considerably [15]. Consumers use the internet to search for information about products, and they are expected to increase it in the future [16]. Unlike traditional shopping, online shopping has lower search costs because it reduces the time consumers spend on finding products and reduces the loss of energy to compare. Therefore, online shopping helps consumers to get price and product information from various sellers more quickly and easily [17].

Information seeking is a stage of the decision making process in which individuals actively collect information from both internal and external sources and include it before making a choice. Individuals adopt this behavior to meet their need for information [18]. Before purchasing products or services, consumers search and collect the relevant information and then compare the sellers based on this information to make the best purchasing decision [19]. Consumers are currently using the Internet to search for information and are expected to increase it in the future [16].

It is not surprising that the number of online shoppers has increased a lot over the past few years along with the increase in number of internet users. A global study on the trends in online shopping conducted by The Nielsen Company reveals that over 85% of internet users in the world perform a purchasing transaction over the internet. Online shopping is directly proportional to the increasing use of the internet. A study on world internet usage and population statistics in 2009 reveals that 26.6% of the total world population were internet users and there has been a growth rate of 399.3% over the past decade. While 230-billion dollar transactions were performed in cross-border online shopping from consumer to consumer all around the world in 2015, this figure is expected to increase to 1 trillion dollars a year in the near future [20]. In a comprehensive study on internet use and online shopping on a global scale, it was determined that the number of internet users increased from 5.233 billion to 5.530 billion in the last 5 years, that the number of people who had accessed the Internet at least once increased from 48.2% to 59.9% compared to the population, and that these people usually preferred desktop computers by 41%, mobile phones by 40%, tablets by 3% and other devices by 16% to use the internet. In terms of frequency of shopping, it was reported that while 31% of internet consumers around the world performed online shopping once a month, 24% of them performed online shopping every other week, 20% of them performed online shopping once a week, 15% of them performed online shopping 3-4 times in 3 months, and 10% of them performed online shopping every 3 months. On the basis of transaction volume, the volume of e-commerce, which was 1.3 trillion dollars in 2014, reached 3.5 trillion dollars in 2019, and it is predicted to increase to 4.9 trillion dollars in 2021 [21].

Although traditional shopping methods are still employed around the world, it is observed that online shopping transactions have increased rapidly. According to the Global e-Commerce Report, two shopping categories in which consumers do more online shopping compared to stores are

book, music, movie & video games (60%) and toys (39%) shopping. In general, while 43% of purchases in the electronics & computer category were made over the internet, 36% of purchases in the sport equipment & outdoor category, 37% of purchases in the health & beauty category, 40% of purchases in the clothing & footwear category, 32% of purchases in the jewelry/watches category, 33% of purchases in the household appliances category, 30% of purchases in the DIY/home improvement category, 30% of purchases in the furniture & homeware category, and 23% of purchases in the grocery category were made over the internet. In the same report, when the sectors in which purchases are made over the internet were analyzed on the basis of continents, it was reported that while the people in the Asia-Pacific region mostly (40%) purchased packaged foods, purchases were mostly made in the video games sector (31%) in North America, personal care sector in (28%) in South America, fashion sector (49%) in Eastern Europe, electronic appliances sector (36%) in Western Europe, and fashion sector (35%) in the Middle East and Africa [21].

In a study covering 28 countries including European countries and Turkey, the average internet usage of people who had ordered or purchased a product or service over the internet in the past year was calculated to be 87% in Europe and 72% in Turkey, and the average of people who had ordered or purchased a product or service was calculated to be 60% in Europe and 25% in Turkey [22].

Different dimensions were also discussed in the studies on e-commerce use. In a study investigating the determining factors in online shopping, it was indicated that the quality of the website over which services are provided had positive effects on consumers' satisfaction and loyalty behaviors [23]. In another study, online shoppers were evaluated in terms of five different shopping motivations such as convenience, searching brands, information search, shopping experience and social interaction [24]. In another study, it was determined that website design, convenience, information usability, payment system and security had significant positive effects on shopping motivations [25]. It is also emphasized that the price is an important shopping motivation that affects the purchase intention [26,27]. It is indicated that wide product availability and price comparison between similar products have led customers to online shopping [28]. In another study in which the factors affecting consumers' online shopping were analyzed, the variables of perceived value, ease of use, satisfaction, reliability of the website, secure payment, customization and interaction were observed to have quite directive effects on consumers [29]. In an empirical study in which individuals' purchasing behaviors for online shopping were investigated, it was concluded that internet access, website aesthetics, security, user experience, age and learning capacity were very important factors in exhibiting such behaviors [30]. In another recent study conducted on online purchasing preferences of university students in India, it was determined that the presence of too many options for the product intended to be purchased increased purchasing anxiety in consumers. Furthermore, it was indicated that consumers' characteristics, contextual factors, and perceived uncertainty had negative effects on their online purchasing preferences, and that the reliability of the website also had negative effects

on purchasing preferences [31]. The results of a study conducted in Thailand revealed that the perceived benefit had no significant effect on consumers' shopping over the internet, however, perceived ease of use, perceived security, perceived uncertainty, and online shopping experience played an effective role in online shopping [13].

Individual differences as well as technological developments are also effective on e-commerce use. To know the products purchased according to individual characteristics can be employed to detect the advertisements that will be provided to be viewed by individuals with certain characteristics, especially in social media. The aim of this study was to detect the socio-economic and demographic factors affecting online shopping of individuals in Turkey. In this study, multinomial logistic and multinomial probit regression analyses were employed to detect the factors affecting e-commerce use of individuals.

II. MATERIALS AND METHODS

A. Data

The micro dataset obtained from Information and Communication Technology (ICT) Usage Survey in Households performed by the Turkish Statistical Institute in 2014-2018 was employed in this study. In this study, the data of 129,643 individuals, who participated in ICT Usage Survey in Households in 2014-2018, were employed.

The aim of the ICT Usage Survey in Households is to detect the criteria of information society and to produce the relevant statistics. The scope of the study is households in all settlements located within the borders of Turkey. Those in school, dormitory, hotel, kindergarten, nursing home, hospital and prison, which are defined as institutional population, and those residing in barracks and military houses were not included. Furthermore, settlements, the population of which would not exceed 1% of the total population where it was considered that sufficient number of sample households (small villages, nomad groups, fields, etc.), could not be reached, were excluded. Individuals between the ages of 16 and 74 years were included according to the methodology of the research. A stratified two stage cluster sampling method was employed obtain the data. The first stage sampling unit was the blocks that were randomly selected proportionally to their size from among the clusters (blocks) containing an average of 100 household addresses, and the second stage sampling unit was the household addresses systematically randomly selected from each selected cluster [32].

B. Measures

The dependent variable of the study was e-commerce use measured by the question "When was the last time you purchased or ordered goods/services for personal use over the Internet (websites or mobile applications)?" (In the past three months; more than three months; more than a year; never used). The categories "more than three months" and "more than a year" were combined and a three-category dependent variable was generated in order to obtain more significant results.

The independent variables in the study were detected by performing a comprehensive literature review. Socio-demographic and economic factors that could be effective on e-commerce use were considered as independent variables. Independent variables were year of survey, age, gender, educational level, occupation, income level, and household size.

One of the independent variables was the region variable. The establishment of Nomenclature of Territorial Units for Statistics (NUTS) in Turkey is based on the necessity to establish Development Agencies. The national program prepared after the accession partnership agreement signed with the EU has made it necessary to establish NUTS regions, as they see NUTS regions as a prerequisite for the establishment of Development Agencies. The existing geographical regions were not taken into account in the establishment of NUTS regions in Turkey, and regional boundaries were detected depending on many different criteria. The most important of them is the amount of population. Except for the population, cultural structure and development status of the provinces were also taken into consideration [33]. Turkey was divided into 12 regions at Level 1 under the name of Nomenclature of Territorial Units for Statistics. Some regions were combined and expressed in 8 regions to obtain more significant results in the analysis [34]. These regions and the provinces in these regions are presented in Table I in detail.

C. Research Method

Survey statistics in Stata 15 (Stata Corporation) were used to account for the complex sampling design and weights. Weighted analysis was performed [35]. The frequency and percentages were first obtained according to the status of e-commerce use of the individuals who participated in the study. Chi-square test of independence was performed to examine the relationship between the status of e-commerce use and the independent variables. Then, the factors affecting e-commerce use were detected using the multinomial logistic regression and multinomial probit regression analyses.

TABLE I. STATISTICAL REGION UNITS CLASSIFICATION -LEVEL 1

Code	Level 1	Provinces
TR1	İstanbul	İstanbul
TR2/ TR4	West Marmara/ East Marmara	Tekirdağ, Edirne, Kırklareli, Balıkesir, Çanakkale, Bursa, Eskişehir, Bilecik, Kocaeli, Sakarya, Düzce, Bolu, Yalova
TR3	Aegean	İzmir, Aydın, Denizli, Muğla, Manisa, Afyonkarahisar, Kütahya, Uşak
TR5/ TR7	Western Anatolia/ Central Anatolia	Ankara, Konya, Karaman, Kırıkkale, Aksaray, Niğde, Nevşehir, Kırşehir, Kayseri, Sivas, Yozgat
TR6	Mediterranean	Antalya, Isparta, Burdur, Adana, Mersin, Hatay, Kahramanmaraş, Osmaniye
TR8/ TR9	West Blacksea/ East Blacksea	Zonguldak, Karabük, Bartın, Kastamonu, Çankırı, Sinop, Samsun, Tokat, Çorum, Amasya, Trabzon, Ordu, Giresun, Rize, Artvin, Gümüşhane
TRA/ TRB	Northeastern Anatolia/ East Anatolia	Erzurum, Erzincan, Bayburt, Ağrı, Kars, Iğdır, Ardahan, Malatya, Elazığ, Bingöl, Tunceli, Van, Muş, Bitlis, Hakkâri
TRC	Southeastern Anatolia	Gaziantep, Adıyaman, Kilis, Şanlıurfa, Diyarbakır, Mardin, Batman, Şırnak, Siirt

III. RESULTS

A. Descriptive Statistics and Chi-Square Tests

Socio-demographic and economic factors affecting e-commerce use of individuals are presented in Table II. The highest participation was in the 25-54 age group. The ratios of males and females were 48% and 52%, respectively. It was observed that 24.6% of the individuals lived in the household with 4 individuals, while 14.2% of them lived in the household

with 5 individuals. While 34.3% of the individuals were primary school graduates, 14.7% of them were university graduates. More than half (57.5%) of the individuals who participated in the survey consisted of those who did not work in any job. Approximately 23% of the individuals were at the 1st income level, 18% of them were at the 5th income level. Furthermore, it was observed in Table II that the rate of e-commerce use increased by years and that the highest rate of e-commerce use was 58% in 2018.

TABLE II. FREQUENCY AND PERCENTAGES OF INDIVIDUALS ACCORDING TO THEIR E-COMMERCE USE

Variables		e-Commerce use			n (%)	P
		In the past three months	Before three months	Never used		
Year	2014	1941 (12.1)	1514 (14.4)	20297 (19.7)	23752 (18.3)	0.000 ^a
	2015	2258 (14.0)	1640 (15.6)	18972 (18.4)	22870 (17.6)	
	2016	2949 (18.3)	1917 (18.2)	20192 (19.6)	25058 (19.3)	
	2017	3990 (24.8)	2682 (25.5)	22687 (22.0)	29359 (22.6)	
	2018	4963 (30.8)	2782 (26.4)	20859 (20.3)	28604 (22.1)	
Age	15-24	3821 (23.7)	2524 (24.0)	15325 (14.9)	21670 (16.7)	0.000 ^a
	25-34	6068 (37.7)	3403 (32.3)	16232 (15.8)	25703 (19.8)	
	35-44	4072 (25.3)	2714 (25.8)	21221 (20.6)	28007 (21.6)	
	45-54	1570 (9.8)	1293 (12.3)	21125 (20.5)	29388 (18.5)	
	55-64	474 (2.9)	510 (4.8)	17907 (17.4)	18891 (14.6)	
	65+	96 (0.6)	91 (0.9)	11197 (10.9)	11385 (8.8)	
Gender	Male	8794 (54.6)	6171 (58.6)	46591 (45.2)	61556 (47.5)	0.000 ^a
	Female	7307 (45.4)	4364 (41.4)	56416 (54.8)	68087 (52.5)	
Educational level	Did not finish a school	46 (0.3)	76 (0.7)	18693 (18.1)	18815 (14.5)	0.000 ^a
	Primary school	873 (5.4)	1225 (11.6)	42430 (41.2)	44528 (34.3)	
	Secondary school	2321 (14.4)	2017 (19.1)	19277 (18.7)	23615 (18.2)	
	High school	4890 (30.4)	3508 (33.3)	15241 (14.8)	23639 (18.2)	
	University	7971 (49.5)	3709 (35.2)	7366 (7.2)	19046 (14.7)	
Occupation	Executives	805 (5)	326 (3.1)	812 (0.8)	1943 (1.5)	0.000 ^a
	Professional occupation	3175 (19.7)	1328 (12.6)	2138 (2.1)	6641 (5.1)	
	Mechanists, technicians and assistant professional occupation	505 (3.1)	219 (2.1)	409 (0.4)	1133 (0.9)	
	Staff working in office services	1977 (12.3)	1000 (9.5)	2418 (2.3)	5395 (4.2)	
	Service and sales staff	1913 (11.9)	1344 (12.8)	6718 (6.5)	9975 (7.7)	
	Skilled agricultural, forestry and aquaculture workers	113 (0.7)	131 (1.2)	5314 (5.2)	5558 (4.3)	
	Artisans and employees in related jobs	467 (2.9)	368 (3.5)	2309 (2.2)	3144 (2.4)	
	Plant and machine operators and installers	342 (2.1)	292 (2.8)	1739 (1.7)	2373 (1.8)	
	Workers in elementary occupations	1348 (8.4)	1325 (12.6)	16289 (15.8)	18962 (14.6)	
	Unemployed	5456 (33.9)	4202 (39.9)	64861 (63)	74519 (57.5)	
Income	1 st income level (lowest)	843 (5.2)	956 (9.1)	27954 (27.1)	29753 (22.9)	0.000 ^a
	2 nd income level	1581 (9.8)	1498 (14.2)	22639 (22)	25718 (19.8)	
	3 rd income level	2811 (17.5)	2309 (21.9)	22890 (22.2)	28010 (21.6)	
	4 th income level	3498 (21.7)	2418 (23)	16839 (16.3)	22755 (17.6)	
	5 th income level (highest)	7368 (45.8)	3354 (31.8)	12685 (12.3)	23407 (18.1)	
Region	TR1	3263 (20.3)	1790 (17)	12662 (12.3)	17715 (13.7)	0.000 ^a
	TR2/TR4	2713 (16.8)	1644 (15.6)	15285 (14.8)	19642 (15.2)	
	TR3	1908 (11.9)	1410 (13.4)	11043 (10.7)	14361 (11.1)	
	TR6	1543 (9.6)	1338 (12.7)	10688 (10.4)	13569 (10.5)	
	TR5/TR7	2969 (18.4)	1721 (16.3)	16282 (15.8)	20972 (16.2)	
	TR8/TR9	1741 (10.8)	1259 (12)	13257 (12.9)	16257 (12.5)	
	TRC	795 (4.9)	535 (5.1)	10393 (10.1)	11723 (9)	

	TRA/TRB	1169 (7.3)	838 (8)	13397 (13)	15404 (11.9)	
Household size	2 and fewer	3372 (20.9)	1947 (18.5)	23577 (22.9)	28896 (22.3)	0.000 ^a
	3 people	4946 (30.7)	2916 (27.7)	20564 (20)	28426 (21.9)	
	4 people	4866 (30.2)	3271 (31)	23715 (23)	31852 (24.6)	
	5 people	1881 (11.7)	1448 (13.7)	15095 (14.7)	18424 (14.2)	
	6 and more	1036 (6.4)	953 (9)	20056 (19.5)	22045 (17)	

^ap<.01

According to the results of chi-square test of independence, a significant relationship was found between the status of e-commerce use of individuals and socio-economic and demographic variables in the study.

B. Estimation of Models

The multinomial logistic regression and multinomial probit regression analyses were employed to detect the factors affecting e-commerce use of individuals over the age of 15 years included in the study. Ordinal and nominal variables were defined as dummy variables to observed the effects of the categories of all variables to be included in multinomial logistic and multinomial probit regression models [35].

Whether there was multicollinearity between independent variables to be included in the multinomial logistic and multinomial probit regression model was tested. It was considered that those with a variance inflation factor (VIF) value of 5 and above led to moderate multicollinearity, and those with a VIF value of 10 and above led to higher multicollinearity [33]. As seen in Table III, none of the independent variable included in the model had 5 or more variance inflation factors. Accordingly, there was no variable that led to multicollinearity problem among the variables in the model.

The results of the estimated multinomial logistic regression and multinomial probit regression model are presented in Table III. In the models, the “never used” category of the dependent variable was considered as the reference category. According to test results, multinomial logistic regression model provides the assumption of independence of irrelevant alternatives.

When Table III was examined, it was observed that the variables of year (2015, 2016, 2017, 2018), age (15-24, 25-24, 35-44, 45-54, 55-64, 65+), educational level (primary school, secondary school, high school, university), occupation (executives; professional occupation members; mechanists, technicians and assistant professional occupation members; staff working in office services; service and sales staff; skilled agricultural, forestry and aquaculture workers; artisans and employees in related jobs; workers in elementary occupations), income level, region (TR1, TR2/TR4, TR3, TR/6, TR5/TR7 and TR8/TR9) and household size (2 and fewer, 3 people, 4 people, 5 people, 6 and more) were statistically significant.

C. Average Direct Elasticity

The average direct elasticities values of socio-demographic and economic factors affecting e-commerce use of individuals in Turkey are presented in Table IV.

The comparison criteria of the models used in the study are presented in Table V. According to Table V, it can be said that the multinomial probit regression model with the lowest AIC (Akaike Information Criterion) and BIC (Bayesian Information Criterion) values was the best model.

According to the multinomial probit regression model presented in Table IV, while other variables were fixed, an individual who participated in the study in 2018 was 135.6% more likely to use e-commerce in the past three months and 74.7% more likely to use e-commerce before three months compared to 2014. An individual who participated in the study in 2015, 2016 and 2017 was 31.5%, 57.6% and 92.7% more likely to use e-commerce in the past three months, respectively, compared to the reference category.

Individuals aged between 15 and 24 years were 389.3% more likely to use e-commerce in the past three months and 271.3% more likely to use e-commerce before three months compared to the 65+ age (reference category) group. The fact that the individual was in the 25-34, 35-44, 45-54 and 55-64 age group increased the possibility of using e-commerce in the past three months by 369%, 328.8%, 225.3% and 103.8%, respectively, compared to the reference group. Females were 19.7% less likely to use e-commerce in the past three months and 36.4% less likely to use e-commerce before three months compared to males.

University graduate individuals were 350.5% more likely to use e-commerce in the past three months and 260.5% more likely to use e-commerce before three months compared to those who did not finish a school (reference category). Having graduated from primary school, secondary school and high school increased the possibility of using e-commerce in the past three months by 130.9%, 208.1% and 292.8%, respectively, compared to the reference group.

Executive individuals were 112.1% more likely to use e-commerce in the past three months and 50.6% more likely to use e-commerce before three months compared to unemployed individuals (reference category). Professional occupation members, mechanists/technicians/assistant professional occupation members, staff working in office services, service/sales staff, artisans/employees in related jobs and plant and machine operators/installers increased the possibility of using e-commerce in the past three months by 80.4%, 94.1%, 78.7%, 36.9%, 38.3% and 4.2%, respectively, compared to the reference category. Skilled agricultural/forestry/aquaculture workers and the workers in elementary occupations decreased the possibility of using e-commerce in the past three months by 73.2% and 19.7%, respectively, compared to the reference category.

TABLE III. MULTINOMIAL LOGISTIC REGRESSION AND MULTINOMIAL PROBIT REGRESSION MODEL RESULTS

Variables	Multinomial Logistic Regression				Multinomial Probit Regression				VIF
	In the past three months		Before three months		In the past three months		Before three months		
	β	Std. Error	β	Std. Error	β	Std. Error	β	Std. Error	
Year (reference category: 2014)									
2015	0.265 ^a	0.041	0.182 ^a	0.043	0.202 ^a	0.030	0.135 ^a	0.030	1.63
2016	0.485 ^a	0.039	0.314 ^a	0.042	0.374 ^a	0.029	0.234 ^a	0.029	1.67
2017	0.831 ^a	0.037	0.607 ^a	0.039	0.631 ^a	0.028	0.447 ^a	0.027	1.75
2018	1.272 ^a	0.037	0.871 ^a	0.040	0.961 ^a	0.027	0.643 ^a	0.028	1.74
Age (reference category: 65+)									
15-24	3.376 ^a	0.117	2.733 ^a	0.123	2.447 ^a	0.077	1.899 ^a	0.076	3.47
25-34	3.149 ^a	0.116	2.641 ^a	0.122	2.278 ^a	0.076	1.829 ^a	0.075	3.51
35-44	2.726 ^a	0.117	2.372 ^a	0.123	1.953 ^a	0.077	1.619 ^a	0.075	3.64
45-54	1.734 ^a	0.118	1.605 ^a	0.123	1.226 ^a	0.078	1.054 ^a	0.075	2.98
55-64	0.794 ^a	0.123	0.898 ^a	0.127	0.529 ^a	0.081	0.559 ^a	0.078	2.35
Gender (reference category: male)									
Female	-0.208 ^a	0.026	-0.358 ^a	0.028	-0.161 ^a	0.019	-0.263 ^a	0.020	1.35
Educational level (reference category: did not finish a school)									
Primary school	1.324 ^a	0.172	1.245 ^a	0.137	0.753 ^a	0.091	0.693 ^a	0.072	2.60
Secondary school	2.153 ^a	0.171	1.848 ^a	0.139	1.274 ^a	0.090	1.102 ^a	0.073	2.59
High school	3.065 ^a	0.170	2.591 ^a	0.138	1.972 ^a	0.089	1.678 ^a	0.072	2.60
University	3.788 ^a	0.170	3.110 ^a	0.139	2.082 ^a	0.074	2.082 ^a	0.074	3.04
Occupation (reference category: unemployed)									
Executives	1.106 ^a	0.070	0.660 ^a	0.084	0.510 ^a	0.061	0.510 ^a	0.061	1.12
Professional occupation	0.741 ^a	0.046	0.493 ^a	0.055	0.390 ^a	0.040	0.390 ^a	0.040	1.55
Mechanists, technicians and assistant professional	0.894 ^a	0.089	0.614 ^a	0.105	0.478 ^a	0.076	0.478 ^a	0.076	1.07
Staff working in office services	0.740 ^a	0.046	0.534 ^a	0.052	0.426 ^a	0.038	0.426 ^a	0.038	1.21
Service and sales staff	0.334 ^a	0.040	0.286 ^a	0.044	0.227 ^a	0.031	0.227 ^a	0.031	1.22
Skilled agricultural, forestry and aquaculture workers	-0.688 ^a	0.113	-0.511 ^a	0.107	-0.343 ^a	0.068	-0.343 ^a	0.068	1.10
Artisans and employees in related jobs	0.341 ^a	0.070	0.257 ^a	0.072	0.208 ^a	0.051	0.208 ^a	0.051	1.09
Plant and machine operators and installers	0.035	0.078	0.109	0.081	0.090	0.058	0.090	0.058	1.08
Workers in elementary	-0.212 ^a	0.042	-0.095 ^b	0.042	-0.068 ^a	0.029	-0.068 ^b	0.029	1.30
Income level (reference category: 1st income level (lowest))									
2 nd income level	0.367 ^a	0.053	0.282 ^a	0.050	0.203 ^a	0.033	0.203 ^a	0.033	1.59
3 rd income level	0.746 ^a	0.049	0.574 ^a	0.047	0.419 ^a	0.032	0.419 ^a	0.032	1.70
4 th income level	1.002 ^a	0.049	0.68 ^a	0.048	0.504 ^a	0.033	0.504 ^a	0.033	1.72
5 th income level (highest)	1.543 ^a	0.049	0.937 ^a	0.050	0.700 ^a	0.034	0.700 ^a	0.034	2.10
Region (reference category: TRA/TRB)									
TR1	0.369 ^a	0.050	0.240 ^a	0.055	0.180 ^a	0.038	0.180 ^a	0.0381	2.08
TR2/TR4	0.336 ^a	0.052	0.185 ^a	0.056	0.139 ^a	0.038	0.139 ^a	0.0384	2.16
TR3	0.291 ^a	0.054	0.370 ^a	0.057	0.267 ^a	0.039	0.267 ^a	0.0394	1.88
TR6	0.253 ^a	0.055	0.435 ^a	0.057	0.308 ^a	0.040	0.308 ^a	0.0398	1.79
TR5/TR7	0.228 ^a	0.050	0.069	0.055	0.058 ^a	0.038	0.058	0.0377	2.15
TR8/TR9	0.297 ^a	0.054	0.323 ^a	0.058	0.233 ^a	0.040	0.233 ^a	0.0399	1.91
TRC	-0.062	0.064	-0.157 ^b	0.069	-0.099	0.047	-0.099 ^b	0.0469	1.62
Household size (reference category: 2 and fewer)									
3 people	-0.277 ^a	0.035	-0.227 ^a	0.038	-0.160 ^a	0.027	-0.160 ^a	0.0272	1.73
4 people	-0.533 ^a	0.035	-0.381 ^a	0.039	-0.278 ^a	0.027	-0.278 ^a	0.0274	1.96
5 people	-0.733 ^a	0.044	-0.525 ^a	0.047	-0.385 ^a	0.033	-0.385 ^a	0.0328	1.70
6 and more	-1.196 ^a	0.051	-0.830 ^a	0.053	-0.614 ^a	0.036	-0.614 ^a	0.0364	1.98

^ap<0.01; ^bp<0.05

TABLE IV. MULTINOMIAL LOGISTIC REGRESSION AND MULTINOMIAL PROBIT REGRESSION MODEL RESULTS AND MARGINAL EFFECTS

Variables	Multinomial Logistic Regression			Multinomial Probit Regression		
	In the past three months	Before three months	Never used	In the past three months	Before three months	Never used
	ey/dx (%)	ey/dx (%)	ey/dx (%)	ey/dx (%)	ey/dx (%)	ey/dx (%)
Year (reference category: 2014)						
2015	22.4 ^a	14.1 ^a	-4.1 ^a	31.5 ^a	17.6 ^a	-4.0 ^a
2016	40.7 ^a	23.6 ^a	-7.8 ^a	57.6 ^a	29.3 ^a	-7.7 ^a
2017	67.9 ^a	45.6 ^a	-15.2 ^a	92.7 ^a	55.3 ^a	-14.9 ^a
2018	102.0 ^a	61.9 ^a	-25.2 ^a	135.6 ^a	74.7 ^a	-24.7 ^a
Age (reference category: 65 +)						
15-24	293.6 ^a	229.3 ^a	-44.0 ^a	389.3 ^a	271.3 ^a	-43.2 ^a
25-34	275.9 ^a	225.1 ^a	-39.0 ^a	369.0 ^a	267.0 ^a	-38.3 ^a
35-44	242.8 ^a	207.3 ^a	-29.8 ^a	328.8 ^a	246.3 ^a	-29.0 ^a
45-54	159.8 ^a	146.9 ^a	-13.6 ^a	225.3 ^a	175.7 ^a	-13.2 ^a
55-64	74.6 ^a	85.0 ^a	-4.8 ^a	103.8 ^a	101.3 ^a	-4.6 ^a
Gender (reference category: male)						
Female	-14.9 ^a	-29.9 ^a	5.8 ^a	-19.7 ^a	-36.4 ^a	5.9 ^a
Educational level (reference category: did not finish a school)						
Primary school	124.8 ^a	116.8 ^a	-7.6 ^a	130.9 ^a	112.3 ^a	-7.2 ^a
Secondary school	198.3 ^a	167.7 ^a	-17.0 ^a	208.1 ^a	166.4 ^a	-15.6 ^a
High school	270.8 ^a	223.5 ^a	-36.7 ^a	292.8 ^a	229.2 ^a	-34.2 ^a
University	321.5 ^a	253.8 ^a	-57.3 ^a	350.5 ^a	260.5 ^a	-56.3 ^a
Occupation (reference category: unemployed)						
Executives	86.3 ^a	41.7 ^a	-24.3 ^a	112.1 ^a	50.6 ^a	-24.6 ^a
Professional occupation	58.6 ^a	33.8 ^a	-15.5 ^a	80.4 ^a	42.0 ^a	-16.2 ^a
Mechanists, technicians and assistant professional	69.8 ^a	41.8 ^a	-19.6 ^a	94.1 ^a	50.9 ^a	-20.3 ^a
Staff working in office services	58.1 ^a	33.8 ^a	-15.5 ^a	78.7 ^a	47.4 ^a	-16.6 ^a
Service and sales staff	26.5 ^a	21.6 ^a	6.9 ^a	36.9 ^a	27.7 ^a	-7.3 ^a
Skilled agricultural, forestry and aquaculture workers	-58.4 ^a	-40.6 ^a	10.4 ^a	-73.2 ^a	-45.2 ^a	9.4 ^a
Artisans and employees in related jobs	27.3 ^a	19.0 ^a	-6.8 ^a	38.3 ^a	24.6 ^a	-7.1 ^a
Plant and machine operators and installers	2.2	9.6	-1.4	4.2	12.9	-1.7
Workers in elementary	-18.0 ^a	-6.4 ^c	3.1 ^a	-19.7 ^a	-7.8 ^c	2.6 ^a
Income level (reference category: 1st income level (lowest))						
2 nd income level	31.5 ^a	23.1 ^a	-5.2 ^a	41.7 ^a	27.7 ^a	-4.9 ^a
3 rd income level	62.9 ^a	45.7 ^a	-11.7 ^a	82.7 ^a	54.9 ^a	-11.3 ^a
4 th income level	84.3 ^a	52.1 ^a	-15.9 ^a	109.3 ^a	63.1 ^a	-15.4 ^a
5 th income level (highest)	127.1 ^a	66.5 ^a	-27.2 ^a	163.1 ^a	80.0 ^a	-26.5 ^a
Region (reference category: TRA/TRB)						
TR1	30.1 ^a	17.2 ^a	-6.8 ^a	39.5 ^a	21.6 ^a	-6.6 ^a
TR2/TR4	27.7 ^a	12.6 ^b	-5.8 ^a	37.3 ^a	15.8 ^a	-5.7 ^a
TR3	22.2 ^a	30.1 ^a	-6.9 ^a	29.2 ^a	36.0 ^a	-6.7 ^a
TR6	18.2 ^a	36.4 ^a	-7.1 ^a	24.0 ^a	42.7 ^a	-6.9 ^a
TR5/TR7	19.4 ^a	3.5	-3.4 ^a	26.6 ^a	5.1	-3.4 ^a
TR8/TR9	23.2 ^a	25.8 ^a	-6.5 ^a	30.1 ^a	31.0 ^a	-6.3 ^a
TRC	-4.3	-13.9 ^b	1.9 ^a	-2.8	-15.2 ^b	1.5
Household size (reference: 2 and fewer)						
3 people	-20.9 ^a	-15.9 ^a	6.7 ^a	-27.2 ^a	-17.6 ^a	6.6 ^a
4 people	-41.5 ^a	-26.3 ^a	11.8 ^a	-54.3 ^a	-30.7 ^a	11.6 ^a
5 people	-57.8 ^a	-36.9 ^a	15.5 ^a	-74.2 ^a	-43.9 ^a	15.0 ^a
6 and more	-96.9 ^a	-60.3 ^a	22.7 ^a	-128.4 ^a	-73.2 ^a	22.1 ^a

^ap<0.01; ^bp<0.05; ^cp<0.10

TABLE V. COMPARISON OF MULTINOMIAL MODELS

Criteria	MLOGIT	MPROBIT
AIC	119786.06	119670.38
BIC	120548.32	120432.64
Log-likelihood	-59815.03	-59757.9
P-value	0.000	0.000
N	129,643	129,643

Individuals with the highest income were 163.1% more likely to use e-commerce in the past three months and 80% more likely to use e-commerce before three months compared to the lowest income group. Being at the 2nd, 3rd and 4th income levels increased the possibility of using e-commerce in the past three months by 41.7%, 82.7% and 109.3%, respectively, compared to the reference category. Individuals living in TR1 (Istanbul) region were 39.5% more likely to use e-commerce in the past three months and 21.6% more likely to use e-commerce before three months compared to TRA/TRB (Northeastern Anatolia/Middle East Anatolia) region.

Individuals with 3 people in their households were 27.2% less likely to use e-commerce in the past three months and 17.6% less likely to use e-commerce before three months compared to those with 2 and fewer people in their households (reference category). Individuals with 4 people, 5 people and 6 and more people in their households decreased the possibility of using e-commerce in the past three months by 54.3%, 74.2% and 128.4%, respectively, compared to the reference category.

IV. DISCUSSION

The shopping methods and habits of users have changed with the effect of digitalization all over the world. Especially because of its advantages such as product range, affordable prices, comparability offered by online shopping, the number of users who prefer this method is increasing day by day. Nevertheless, disadvantages of online shopping, such as inability to directly examine the product to be purchased, the fact that return and exchange may take time, sharing personal information (ID number, card number, account, address information etc.), security vulnerabilities of websites, and cheating with fake sites, may also affect the shopping preferences of users.

The aim of this study was to detect the socio-economic and demographic factors affecting online shopping of individuals in Turkey. Multinomial logistic and multinomial probit regression analyses were employed to detect the factors affecting e-commerce use of individuals in Turkey.

According to the analysis results, it was determined that the year of survey was an effective variable on e-commerce use. With the increasing compliance with technology and the widespread use of technology, individuals' expected possibility of using e-commerce also continuously increases as the year increases. In the study, it was determined that the age of the individuals also significantly affected e-commerce use. Individuals at a young age were more likely to use e-commerce than the elderly. Individuals' expected possibility of using e-commerce decreases as the age increases. Similar results were obtained in the literature [36-38]. In a study in which the consumer behaviors of online shoppers in Bangladesh were

examined, it was observed that most of the e-commerce users consisted of individuals under the age of 40 for reasons such as saving time, price flexibility and product range [39]. Another study confirming the results was conducted in Oman, and it was indicated that the young population had the most intensive e-commerce use and that their expectations were slightly different from other groups of people [40]. In a review conducted to find out how young consumers learned to do shopping, adolescence (9-14 years) was stated to be the most important time period in socialization [41]. Furthermore, it was stated that the increase in e-commerce preferences of users in this period resulted from the fact that children and young people, as online consumers, considered internet as an important means of socialization due to its two-way communication ability which helps them use their competence [42]. It is indicated that generations affect e-commerce attitudes according to the age range of individuals. In a study conducted in Malaysia, it was stated that e-commerce was mostly preferred by the individuals of the Y Generation (20-40 years old) and it was detected that the perceived trust in purchase intentions of this generation members was determinant [43]. In another study, the statistics of users who ordered or purchased a product over the internet between 2008 and 2018 were analyzed according to their age groups. In that study, it was indicated that the most e-commerce activities were between the ages of 25-54 according to average level of use, and the 16-24 age group increased above the average especially after 2014 [22].

In the study, it was detected that females were less likely to use e-commerce both in the past three months and before three months compared to males. Similar results were also obtained in the studies conducted in the literature [44-46]. In another study in which the effect of gender difference, age and occupational group on shopping methods was investigated, it was determined that e-commerce use was more preferred by men during the research period. It was stated that store shopping was mostly preferred by women. Furthermore, it was observed that male individuals generally changed their shopping methods due to service quality, product range and pricing [47].

One of the factors affecting e-commerce use is the educational levels of individuals. In the study, individuals' expected possibility of using e-commerce increased as the educational level increased. It was detected that similar results were found in some studies conducted in the literature [48-50]. In another study supporting the results, it was remarked that online consumers were more educated (university students) than the general population and therefore the educational level was effective on online shopping [51]. A similar study was conducted in Thailand, and according to the results obtained, it was determined that the segment who did the most shopping over the internet consisted of university students [52]. In another study in which the effects of educational level on online shopping habit were investigated, it was indicated that the fact that university students were further affected by family, friends and social media was decisive in their preference for this method more [53]. It was also observed that educational level was more effective on people purchasing tickets online compared to other factors [54].

The occupation of individuals is also an important factor affecting e-commerce use. Skilled agricultural/forestry/aquaculture workers and the workers in elementary occupations are less likely to use e-commerce than unemployed individuals. It was determined that the possibility of using e-commerce was higher in other occupational groups compared to unemployed individuals. In a study, it was detected that employed individuals were more inclined to use e-commerce compared to the unemployed [55]. In another study, it was reported that employees, self-employed individuals constituted the occupational group who mostly preferred e-commerce, followed by students, retired, other inactive and unemployed groups [22].

In the study, it was determined that the expected possibility of using e-commerce increased as the income increased. It is indicated that income positively affects online shopping. In the studies in the literature, it was determined that the increase in income increased the possibility of online shopping [56,57,55,58]. In a study in which it was stated that the effects on consumer behaviors often occurred between external and internal factors, it was reported that the improvement of socio-economic conditions, one of external factors, had a significant effect on e-commerce use [59]. In another study in which the factors affecting e-commerce motivation were investigated, it was stated that the fact that individuals living in Greece especially paid attention to pricing and promotion sensitivity in their online shopping was affected by income level and economic conditions [60].

The region of residence also affects online shopping. While those who mostly preferred online shopping were living in TR1 (İstanbul) and TR2/TR4 (West/East Marmara) region, those who least preferred it were living in TRC (Southeastern Anatolia) region. As a result of a study conducted with Thai online shoppers, it was observed that consumers did face-to-face shopping instead of online shopping because they found the products they desired in the areas where the population was relatively more intense [52].

Finally, the size of households that do online shopping is also an effective variable. It was determined that the possibility of using e-commerce decreased as household size increased. In a study, it was stated that the number of children was negative, small but insignificant in online shopping [48]. In another study, it was determined that the number of children had no effect on online shopping. In a study, contrary to that study, it was determined that the number of children had a positive effect on online shopping [50].

According to the results obtained in the study, it was determined that the year of survey, education and income level increased the possibility of online shopping. It was determined that age, household size and being a woman decreased the possibility of online shopping. One of the interesting results of the study was that the individuals residing in the TRC (Gaziantep, Adiyaman, Kilis, Şanlıurfa, Diyarbakır, Mardin, Batman, Şırnak, Siirt) region were less likely to do online shopping compared to the TRA/TRB (Erzurum, Erzincan, Bayburt, Ağrı, Kars, Iğdır, Ardahan, Malatya, Elazığ, Bingöl, Tunceli, Van, Muş, Bitlis, Hakkâri) region, which is a relatively less developed region. Another remarkable result

was that skilled agricultural, forestry and aquaculture workers and the workers in elementary occupations were less likely to do online shopping compared to the unemployed.

The results of the study indicated that e-commerce use was gradually increasing. It was determined that more educated and young individuals and individuals living in relatively more developed regions were more inclined to online shopping. Policies should also be developed to increase e-commerce use of low educated individuals and individuals over middle age. In particular, small and medium-sized businesses (SMB) should pay more attention to the use of e-commerce in order to increase their activities by taking these situations into consideration. Indeed, how important e-commerce use is has been found out in epidemics/pandemics such as COVID-19, which causes people to lock themselves at home in the countries.

Considering that e-commerce has become increasingly widespread and the transaction volume has increased, it can be said that studies to raise awareness of service providers and service recipients are important for adaptation to the digitalization process. As a result of the results, since it was observed that age, gender, educational level, average monthly income and the number of households were effective on online shopping, it is considered that it would be beneficial for service providers to develop advertising and marketing strategies based on this data. Moreover, the requests and complaints of the user can be received directly with real-time field studies in order to detect the preferred factors (price, promotion, time saving, diversity, comparability, change, return options etc.). Thus, competitive advantage can be offered for service providers, and a customizable shopping experience can be offered for users.

This study had some limitations. The dependent variable (status of e-commerce use) discussed in this study was not obtained as a result of any commercial registration. The procedure was performed completely considering the responses of the participants. Therefore, the answers may be biased. The variables required for statistical analysis were the variables included in the Information and Communication Technology (ICT) Usage Survey in Households microdata set. However, the variables such as marital status, race, use of social media, use of mobile/internet banking, may affect individuals' online shopping, could not be taken into account.

ACKNOWLEDGMENT

The authors would like to thank the Turkish Statistical Institute for the data. The views and opinions expressed in this manuscript are those of the authors only and do not necessarily represent the views, official policy, or position of the Turkish Statistical Institute.

REFERENCES

- [1] Barnes, S. J., & Vidgen, R. T. (2002). An integrative approach to the assessment of e-commerce quality. *Journal of Electronic Commerce Research*, 3(3), 114-127.
- [2] Corbitt, B. J., Thanasankit, T., & Yi, H. (2003). Trust and e-commerce: a study of consumer perceptions. *Electronic commerce research and applications*, 2(3), 203-215.
- [3] Zwass, V. (2003). Electronic commerce and organizational innovation: Aspects and opportunities. *International Journal of Electronic Commerce*, 7(3), 7-37.

- [4] Y Monsuwé, T. P., Dellaert, B. G., & De Ruyter, K. (2004). What drives consumers to shop online? A literature review. *International journal of service industry management*, 15(1), 102-121.
- [5] Jiradilok, T., Malisuwan, S., Madan, N., & Sivaraks, J. (2014). The impact of customer satisfaction on online purchasing: A case study analysis in Thailand. *Journal of Economics, Business and Management*, 2(1), 5-11.
- [6] Bourlakis, M., Papagiannidis, S., & Fox, H. (2008). E-consumer behaviour: Past, present and future trajectories of an evolving retail revolution. *International Journal of E-Business Research*, 4(3), 64-76.
- [7] Yu, T.-K., & Wu, G.-S. (2007). Determinants of internet shopping behavior: An application of reasoned behaviour theory. *International Journal of Management*, 24(4), 744-762,823.
- [8] Onyusheva, I., & Thongaim, J. (2018). Customer satisfaction in online shopping: A case study of Bangkok urban area. *The EUrASEANs: journal on global socio-economic dynamics*, 2(9), 13-23.
- [9] Jiang, L. A., Yang, Z., & Jun, M. (2013). Measuring consumer perceptions of online shopping convenience. *Journal of Service Management*, 24(2), 191-214.
- [10] Czaplewski, M. (2017). The use of e-commerce in the promotion and sale of hand made products. *Management*, 22(1), 154-162.
- [11] Zhang, X. (2019). Investigation of e - commerce in China in a geographical perspective. *Growth and Change*, 50(3), 1062-1084.
- [12] Lee, R. J., Sener, I. N., Mokhtarian, P. L., & Handy, S. L. (2017). Relationships between the online and in-store shopping frequency of Davis, California residents. *Transportation Research Part A: Policy and Practice*, 100, 40-52.
- [13] Changchit, C., Cutshall, R., Lonkani, R., Pholwan, K., & Pongwiritthon, R. (2019). Determinants of online shopping influencing thai consumer's buying choices. *Journal of Internet Commerce*, 18(1), 1-23.
- [14] Stoklosa, M. (2020). Prices and cross-border cigarette purchases in the EU: Evidence from demand modelling. *Tobacco control*, 29(1), 55-60.
- [15] Valarezo, Á., Pérez-Amaral, T., Garín-Muñoz, T., García, I. H., & López, R. (2018). Drivers and barriers to cross-border e-commerce: Evidence from Spanish individual behavior. *Telecommunications Policy*, 42(6), 464-473.
- [16] Afsar, B., Qureshi, J. A., Rehman, A., & Bangash, R. U. (2011). Consumer panacea over internet usage in Pakistan. *Management & Marketing Journal*, 9(1), 43-52.
- [17] Shin, D.-H., & Biocca, F. (2017). Explicating user behavior toward multi-screen adoption and diffusion. *Internet research*, 27(2), 338-361.
- [18] Hong, W., Tam, K. Y., & Yim, C. K. B. (2016). E-service environment: Impacts of web interface characteristics on consumers' online shopping behavior. In R. T. Rust, & P. K. Kannan (Eds.), *E-Service: New directions in theory and practice* (pp. 120-140): Routledge.
- [19] Park, J., Chung, H., & Yoo, W. S. (2009). Is the Internet a primary source for consumer information search?: Group comparison for channel choices. *Journal of Retailing and Consumer Services*, 16(2), 92-99.
- [20] Erickson, J., & Najberg, A. (2015). Cross-border e-commerce to reach \$1 trillion in 2020. <https://www.alizila.com/cross-border-e-commerce-to-reach-1-trillion-in-2020/>. Accessed 28.03.2020.
- [21] EcommerceFoundation (2019). 2018 Global Ecommerce Report. <https://www.ecommercefoundation.org/free-reports>. Accessed 23.01.2020.
- [22] Eurostatstatistics (2018). E-commerce statistics for individuals. https://ec.europa.eu/eurostat/statistics-explained/index.php?title=E-commerce_statistics_for_individuals#Context. Accessed 28.03.2020.
- [23] Lin, G. T., & Sun, C. C. (2009). Factors influencing satisfaction and loyalty in online shopping: an integrated model. *Online information review*, 33(3), 458-475.
- [24] Padmavathy, C., Swapana, M., & Paul, J. (2019). Online second-hand shopping motivation-Conceptualization, scale development, and validation. *Journal of Retailing and Consumer Services*, 51, 19-32.
- [25] Shin, J. I., Chung, K. H., Oh, J. S., & Lee, C. W. (2013). The effect of site quality on repurchase intention in Internet shopping through mediating variables: The case of university students in South Korea. *International Journal of Information Management*, 33(3), 453-463.
- [26] Kim, J., & Lennon, S. J. (2013). Effects of reputation and website quality on online consumers' emotion, perceived risk and purchase intention. *Journal of Research in Interactive Marketing*, 7(1), 33-56.
- [27] Wolfenbarger, M., & Gilly, M. C. (2001). Shopping online for freedom, control, and fun. *California management review*, 43(2), 34-55.
- [28] Park, E. J., Kim, E. Y., Funches, V. M., & Foxx, W. (2012). Apparel product attributes, web browsing, and e-impulse buying on shopping websites. *Journal of business research*, 65(11), 1583-1589.
- [29] Hamidzadeh, M. R., Haji, K. A. A., & Naeiji, M. J. (2011). Designing and explaining the model of persistent customer loyalty in e-commerce: A study in the e-retailer's web sites. *New Marketing Research Journal*, 1(2), 79-92.
- [30] Rahman, M. A., Islam, M. A., Esha, B. H., Sultana, N., & Chakravorty, S. (2018). Consumer buying behavior towards online shopping: An empirical study on Dhaka city, Bangladesh. *Cogent Business & Management*, 5(1), 1514940.
- [31] Nagar, K. (2016). Drivers of E-store patronage intentions: Choice overload, internet shopping anxiety, and impulse purchase tendency. *Journal of Internet Commerce*, 15(2), 97-124.
- [32] TÜİK (2018). Hanehalkı Bilişim Teknolojileri/ICT Usage Survey in Households. http://www.tuik.gov.tr/MicroVeri/HBT_2018/english/index.html. Accessed 03.04.2020.
- [33] Alkan, Ö., Oktay, E., & Genç, A. (2015). Determination of factors affecting the children's internet use. *American International Journal of Contemporary Research*, 5(6), 57-67.
- [34] Bilenkisi, F., Gungor, M. S., & Tapsin, G. (2015). The impact of household heads' education levels on the poverty risk: The evidence from Turkey. *Educational Sciences: Theory and Practice*, 15(2), 337-348.
- [35] Alkan, Ö., & Abar, H. (2020). Determination of factors influencing tobacco consumption in Turkey using categorical data analyses1. *Archives of environmental & occupational health*, 75(1), 27-35.
- [36] Alqahtani, A. S., Goodwin, R. D., & de Vries, D. B. (2018). Cultural factors influencing e-commerce usability in Saudi Arabia. *International Journal of Advanced and Applied Sciences*, 5(6), 1-10.
- [37] Law, M., & Ng, M. (2016). Age and gender differences: Understanding mature online users with the online purchase intention model. *Journal of Global Scholars of Marketing Science*, 26(3), 248-269.
- [38] Teo, T. S. (2006). To buy or not to buy online: adopters and non-adopters of online shopping in Singapore. *Behaviour & Information Technology*, 25(6), 497-509.
- [39] Constantinides, E. (2004). Influencing the online consumer's behavior: the Web experience. *Internet research*, 14 (2), 111-126.
- [40] Al-Jahwari, N. S., Khan, F. R., Al Kalbani, G. K., & Al Khansouri, S. (2018). Factors influencing customer satisfaction of online shopping in Oman: Youth perspective. *Humanities & Social Science Reviews*, 6(2), 64-73.
- [41] Niu, H. J. (2013). Cyber peers' influence for adolescent consumer in decision - making styles and online purchasing behavior. *Journal of Applied Social Psychology*, 43(6), 1228-1237.
- [42] Hill, W. W., & Beatty, S. E. (2011). A model of adolescents' online consumer self-efficacy (OCSE). *Journal of business research*, 64(10), 1025-1033.
- [43] San, L. Y., Omar, A., & Thurasamy, R. (2015). Online purchase: a study of generation Y in Malaysia. *International Journal of Business and Management*, 10(6), 1-7.
- [44] Doherty, N. F., & Ellis - Chadwick, F. E. (2003). The relationship between retailers' targeting and e - commerce strategies: an empirical analysis. *Internet research*, 13(3), 170-182.
- [45] Hashim, A., Ghani, E. K., & Said, J. (2009). Does consumers' demographic profile influence online shopping?: An examination using Fishbein's theory. *Canadian Social Science*, 5(6), 19-31.
- [46] Escobar-Rodríguez, T., Grávalos-Gastaminza, M. A., & Pérez-Calañas, C. (2017). Facebook and the intention of purchasing tourism products: moderating effects of gender, age and marital status. *Scandinavian Journal of Hospitality and Tourism*, 17(2), 129-144.

- [47] Lee, S. L., Ibrahim, M. F., & Hsueh-Shan, C. (2005). Shopping-centre attributes affecting male shopping behaviour. *Journal of Retail & Leisure Property*, 4(4), 324-340.
- [48] Stranahan, H., & Kosiel, D. (2007). E - tail spending patterns and the importance of online store familiarity. *Internet research*, 17(4), 421-434.
- [49] Koyuncu, C., & Lien, D. (2003). E-commerce and consumer's purchasing behaviour. *Applied Economics*, 35(6), 721-726.
- [50] Leong, L.-Y., Jaafar, N. I., & Ainin, S. (2018). Understanding facebook commerce (F-commerce) actual purchase from an artificial neural network perspective. *Journal of Electronic Commerce Research*, 19(1), 75-103.
- [51] Bellman, S., Lohse, G. L., & Johnson, E. J. (1999). Predictors of online buying behavior, association for computing machinery. *Communications of the ACM*, 42(12), 32-38.
- [52] Palvia, P. (2009). The role of trust in e-commerce relational exchange: A unified model. *Information & management*, 46(4), 213-220.
- [53] Aghdaie, S. F. A., Piraman, A., & Fathi, S. (2011). An analysis of factors affecting the consumer's attitude of trust and their impact on internet purchasing behavior. *International Journal of Business and Social Science*, 2(23).
- [54] Fernández, A. M. G. (2000). Los valores personales en el comportamiento del consumidor: Revisión de diversas metodologías aplicadas al marketing. *Esic Market*(107), 9-36.
- [55] Vicente, M. (2015). Determinants of C2C e-commerce: an empirical analysis of the use of online auction websites among Europeans. *Applied Economics Letters*, 22(12), 978-981.
- [56] Burkolter, D., & Kluge, A. (2011). Online consumer behavior and its relationship with socio-demographics, shopping orientations, need for emotion, and fashion leadership. *Journal of Business and Media Psychology*, 2(2), 20-28.
- [57] Cristóbal-Fransi, E., Martín-Fuentes, E., & Daries-Ramon, N. (2015). Behavioural analysis of subjects interacting with information technology: categorising the behaviour of e-consumers. *International Journal of Services Technology and Management*, 21(1-3), 163-182.
- [58] Akhter, S. H. (2003). Digital divide and purchase intention: Why demographic psychology matters. *Journal of Economic Psychology*, 24(3), 321-327.
- [59] Kumar, V., & Dange, U. (2012). A study of factors affecting online buying behavior: A conceptual model. *SSRN Electronic Journal*.
- [60] Rohm, A. J., & Swaminathan, V. (2004). A typology of online shoppers based on shopping motivations. *Journal of business research*, 57(7), 748-757.

Customer Profiling for Malaysia Online Retail Industry using K-Means Clustering and RM Model

Tan Chun Kit¹, Nurulhuda Firdaus Mohd Azmi²

Advanced Informatics Department
Razak Faculty of Technology and Informatics
Universiti Teknologi Malaysia, Kuala Lumpur, Malaysia

Abstract—Malaysia's online retail industry is growing sophisticated for the past years and is not expected to stop growing in the following years. Meanwhile, customers are becoming smarter about buying. Online Retailers have to identify and understand their customer needs to provide appropriate services/products to the demanding customer and attracting new customers. Customer profiling is a method that helps retailers to understand their customers. This study examines the usefulness of the LRFMP model (Length, Recency, Frequency, Monetary, and Periodicity), the models that comprised part of its variables, and its predecessor RFM model using the Silhouette Index test. Furthermore, an automated Elbow Method was employed and its usefulness was compared against the conventional visual analytics. As result, the RM model was selected as the finest model in performing K-Means Clustering in the given context. Despite the unusefulness of the LRFMP model in K-Means Clustering, some of its variables remained useful in the customer profiling process by providing extra information on cluster characteristics. Moreover, the effect of sample size on cluster validity was investigated. Lastly, the limitations and future research recommendations are discussed alongside the discussion to bridge for future works.

Keywords—Customer Profiling; LRFMP; RFM; Data Mining; K-Means Clustering

I. INTRODUCTION

The online retail industry in Malaysia is in its growth trajectory in the past decade and is likely to enjoy strong growth over the coming years [1-2]. While internet freeing up the geographical limitations, online retailer now has to compete with each other directly regardless of their location. To the local small and medium online retailers, the battlefield quickly levels to the international level when online retail giant with economies of scale such as Amazon and Taobao provides a wide range of product selections and reduced shipping fare. Furthermore, despite the benefits of being able to sell online, compared to traditional physical outlets, the lack of seller-buyer interaction leaving the seller confused about customer preference and trends. Moreover, customers are becoming smarter and selective with their spending given the wide range of selection [3].

Under such circumstances, one retailer could never fulfill every customer's needs and provide satisfiable service to every new customer. Hence it is important to identify the most profitable customer in the long-run, then provide tailored and customized service to these groups of customers to reduce the cost while maximizing profitability. Customer profiling is a

potential method of achieving it and resolve the described issues. Customer profiling is technique retailers or service providers used in analyzing consumer characteristics and needs. It increases retailers' understanding of consumers and provides a foundation to retailers in making an informed decision in many business aspects such as product selection or marketing tactics.

To conduct a customer profiling, two aspect has to be considered: The theoretical guidance where a theory that guided which variables to be used to create customer profiles and the technical calculation aspect focuses on methods and formulas to calculate the scoring for each variable and aggregate the result in creating customer profiles.

Theoretical-wise, apart from some grounded theory development that proposed unique domain-specific variables to use in customer profiling [4], RFM (Recency, Frequency, Monetary) analysis is used widely in performing customer profiling in many domains [5-6]. In the past decade, many modifications of the original RFM model, either to create a domain-specific RFM variation or to optimize the RFM model in general have been done. Some examples are RFQ (Quality) [7], and LRFMP (Length and Periodicity) [3].

Technical-wise, conventionally, analyst convert the entire RFM model's raw data into Likert-scale as it not only eases understanding but also simplify calculation [8]. Researchers such as Peker, Kocogit, and Eren [3] and Palaniappan, Mustapha, and Mohd Foozy [9] had used data mining techniques while conducting customer profiling due to its powerful capability and the benefit of no need to skimming down the data.

The research objectives (RO) are as follows:

- RO1: To identify the theoretical model and techniques that could be used in customer profiling within Malaysia's online retail industry.
- RO2: To develop a customer profiling model based on RFM's variation model and K-Means clustering within Malaysia's online retail industry.
- RO3: To compare and evaluate the developed customer profiling models to identify an optimal model for the given dataset.

The purpose of this paper is to examine the usefulness of the LRFMP model, and its predecessor RFM model using the

Silhouette Index (SI) test for customer profiling. In addition, the work explained in this paper examined the possibility of an automated customer profiling process where the K-value decision and optimal variables to be used could be decided without human intervention such as the conventional EM's visual analysis.

This paper is presented by the following sections: Section I will discuss the general context of the work explained in the paper. Next, in Section II, the literature review that presents the theoretical and conceptual of the study is explained. In Section III, the methodology of the experimentation and analysis is described. The experimental result is explained in Section IV and finally, Section V conclude the work discuss in the paper.

II. LITERATURE REVIEW

To identify the current method and technique of conducting customer profiling, a literature review was conducted and is summarized into the following subsections:

A. Theoretical Model in Customer Profiling

While some researcher employs grounded theory and proposed domain-specific variables in customer profiling [4] [10–13], most researchers favored the use of the RFM model. The popular usage of RFM or its various models covers many domains such as banking [14], Hotel industry [15], Small and Medium Enterprises (SME) [16], grocery retail industry [3], and online retail industry [5] [11] [17].

Due to the popular uses of the RFM model, many pieces of research had proposed a varied RFM model with additional or removal of certain variables, which claimed to improve its relatedness to a particular industry and better performance in customer profiling. For instance, Li [18] proposed the uses of the FM model with recency removed, the model remained effective in performing customer profiling in the retail industry. Li argues the uses of the only 2 important variables could effectively create a matrix of 4 distinctive groups of customer profiles. On the other hand, Liu, Zhao, and Li [7] argues the replacement of Quality over the original Monetary variable (RFQ model) is effective and more relevant in the mobile apps domain as most mobile apps are freemium oriented therefore no monetary aspect was involved. Moreover, Wei, Lin, and Weng [19] suggested the additional variable of Length (LRFM model) in the dental industry to improve the quality of customer profiling. They suggested the length in time a customer has visited since the first visitation indicates customer loyalty and is an important indicator in customer profiling. Recently, Peker, Kocyigit, and Eren [3] proposed the Periodicity variable on top of Wei, Lin, and Weng [19]'s model LRFM, creating a LRFMP model and was used in the grocery retail industry in Turkey.

B. Technical aspect in Customer Profiling

The technical aspect of customer profiling refers to the method and calculation used to aggregate data into useful insight. Conventionally, analyst tends to convert the RFM model's raw data into Likert-scale following by assigning customer into a certain group (for instance group that has high in R, low in F, and high in M, etc.) [8]. However, this is not

the case for the past decade. Recent research shows a trend of adopting a data mining technique in aggregating and clustering the consumer group [3] [19]. Given the nature of customer profiling is to cluster consumers into several comprehensible groups, the clustering technique from the data mining domain seems to be the best method of aggregating the customer data to provide useful insight.

Hung, Yen and Wang [10] employs a Decision Tree and Neural Network in conducting customer profiling in Taiwan's Telecom industry. Similarly, Sankar [11] also employed the Neural Clustering technique in the USA's Online retail industry. Another example of data mining used in customer profiling has been mentioned by Hu and Yeh [20], which used constraint-based mining in the food and beverage industry. Apart from that, the majority of the research had adopted the K-Means clustering technique in the conjunction with RFM model or its variation [3] [5-6] [14-15] [17] [18] [21–23].

Among the researchers used K-Means Clustering in customer profiling, Christy et. al. [23] had attempted to compare the performance of K-Means clustering with other clustering techniques. They compare the effect of K-Means Clustering and Fuzzy C-Means using the RFM model. Interestingly, they also attempted to include the RM model in the comparison. The result suggested Fuzzy C-Means gains better Silhouette width performance at the cost of runtime while the RM model K-Means Clustering achieved the lowest runtime and highest Silhouette width, indicating a proper implementation of K-Means Clustering can be effective in both clustering quality and runtime. However, their work did not include the RM model's Fuzzy C-Means analysis.

Evaluation on K-Means clustering customer profiling is another aspect that need to be addressed. While classification-related methods could be benchmarked through the use of confusion matrix, the K-Means clustering evaluation is benchmarked through the manipulation of K to measuring the cluster distances. The cluster distance indicates unique cluster characteristics and therefore, unique customer profiling result. Studies regarding validation on cluster distance was performed in many studies [6][13-14][21][23]. For instance, Dong, Zhang, and Ye [13] evaluated the consistency of cluster distances among iterations to justify validity. Another literature suggested the use of Self Organizing Maps analysis in identifying the best number of K [15]. Besides, more researches had employs a cluster distances-related analysis in justifying cluster validity [6][14][21][23]. For instance, Maryani and Riana [6] measures the Euclidean distance among clusters to justify each cluster contains unique characteristics and is not overlapping with other clusters. Similarly, both Walters and Bekker [21] and Christy et. al. [23] used SI in measuring inter-cluster distances while the former used it to identify the best number of K but the latter used it in inter-model comparison (FM vs. RFM model). In addition, Aryuni, Madyatmadja, and Miranda [14] used both Average Within Cluster (AWC) and Davies-Bouldin Index (DBI) in measuring cluster distances. Lastly, instead of employing cluster distance-related formulas in validating clusters, research such as Chen, Sain, and Guo [5] evaluate the characteristics of each cluster to justify its uniqueness and meaningful clustering result. Among the distance-based

analysis, SI is much more popular compared with other methods, mainly due to its better accuracy [24]. However, it is important to note that one of the disadvantages of using the SI is its complex and long computational runtime [24].

C. RFM Model for Customer Profiling

Theoretical wise, the uses of the RFM model is currently a popular method of conducting customer profiling. While some studies proposed the removal of some certain variables will not have a significant impact on cluster quality, some proposed number of new variables which were believed to be able to improve the quality of customer profiling. However, these researches are mostly containing little to no replica study. Furthermore, most of these studies did not compare the newly proposed model against its original RFM model, leaving its improvement in terms of quality beyond the original RFM model questionable.

Technical wise, K-Means clustering were used frequently among other data mining technique when it comes to customer profiling. While most of the studies did not tackle the evaluation of the clustering result, limited studies suggested the uses of techniques such as the SI, Davies-Bouldin Index (DBI) to validate the clustering results [14] [21]. Furthermore, it is possible to evaluate the quality and usefulness of the clustering result by directly evaluating the unique characteristics of each cluster, which is the combination of RFM variables in the given context, where unique clusters indicating successful clustering while similar cluster characteristics indicating low clustering quality.

To identify the optimal model among the vast proposed RFM variations in the online retail industry, RO2 and RO3 were coined. K-Means Clustering was implemented guided by the LRFMP model as proposed by Peker, Kocyigit, and Eren [3] due to its relatedness and the promising result beyond the original RFM model. Nevertheless, the LRFMP model contains all newly proposed variables as reviewed in the literature review except for Quality, which was created specifically for the mobile apps industry.

III. METHODOLOGY

This research is quantitatively oriented that employs a case study and experimental approach through data analysis. The data was provided by an anonymous online retailer located in Malaysia. The following descriptions record the methodology conducted in this study.

Step 1: Data Collection: Utilizing convenient sampling techniques and a list of data requirements as shown in Table I, a totally of 60 data acquisition approaches were done and one had accepted to participate in the study anonymously and the customer and company-related information have to be protected. Any data that could possibly reveals the company had been shielded by converting this information into unique ID prior to any data processing. The participating company is an online retailer performs sales solely on Facebook and Instagram and communication between salespersons and buyers was done through WeChat, WhatsApp, calling, or direct messenger within the platform. The data provider's company focuses on cosmetic product sales with minor

branches on clothing with about four years of company history.

TABLE I. DATA REQUIREMENT

Mandatory	
Data	Details
Customer ID	An identifier for a particular 1 customer, some alternative includes IC, numbers, name or mailing address
Date	Date of Purchase OR date of the recorded order
Expenses (MYR)	Total expenses in 1 receipt
Optional	
Demographical Information	Mailing Address, Gender, Age, etc.

Step 2: Data Pre-processing: Data aggregation was done to pivot the raw data table as in Table I into the new LRFMP table using the following formulas:

Length:

$$L=lv-fv \quad (1)$$

Where lv represents the date of the last visit, and fv represents the date of the first visit, and Length (L) measures in days. This variable reveals the length of history a customer spent with the company, measuring in day.

Recency:

$$R=od-lv \quad (2)$$

Where od represents observation date, and lv represents average days of all visit dates and observation day. This variable reflects whether a particular customer remained active recently.

Frequency: Counted in times, the total visit of a particular customer.

Monetary: The sum of all spending, which is different from [3] uses of average spending. While not affecting the pattern and distribution, using sum could directly reflect a particular customer's contribution to the company total revenue.

Periodicity:

$$P=\text{stdev}(IVT_1+IVT_2+\dots IVT_n) \quad (3)$$

Where:

$$IVT_i=\text{date_diff}(t_{i+1},t_i) \quad (4)$$

Where $I \geq 1$ and t_i refers to the date corresponding to the i th visit of a particular customer. This variable reflects the customer consistency in visiting the shop.

Then, both the standardized z-score and normalized value is calculated based on the output of the 5 formulas. While the standardized z-score is used to feed into the data mining pipeline, a normalized score is used in descriptive statistics to compare dispersion of each variable within the LRFMP model.

Step 3: Model Development and Evaluation Phase: Models are proposed based on the dispersion measurement. Using a normalized LRFMP score which all variables will have the same range between 0 and 1, each variable is compared using

standard deviation and the one with the lowest dispersion is removed one by one. This results in a list of models starting from LRFMP, following by a model with 1 less variable, and so on, down to when only 1 variable has remained. RFM model is added exclusively for the baseline comparison purposes. Then, K-Means Clustering is implemented on each model using the Scikit-Learn package on Python 3.5 with the settings as shown in Table II. The results are evaluated through an evaluation matrix as shown in Table III.

As shown in Table III, Elbow Method (EM) serves as the most important rule of thumb in deciding the best number of K, however, its method tends to be too naïve as stated by Buitinck et. al. [25]. Hence, further validity mechanism has been set to triangulate the results of the EM. Therefore, SI was used to justify the EM's results. The EM's formula is stated in the below cited from [26] :

$$W_k = \sum_{r=1}^k \frac{1}{n_r} D_r \quad (5)$$

Where k represents the number of clusters, n_r represents the total number of points in the cluster r and D_r is the sum of distances between all points in a particular cluster.

$$D_r = \sum_{i=1}^{n_r-1} \sum_{j=i+1}^{n_r} \|d_i - d_j\|_2 \quad (6)$$

The conventional EM requires human intervention in deciding the knee jerk through visual analysis of the graph. However, this can be sometimes confusing and inconsistent. Therefore, an automated method was suggested by Bertagnolli [27] and is adopted in this study. It involves calculating the closest distance of each point of scores to an imaginary straight line between the first and the last k value as shown in Fig. 1.

Furthermore, the SI was adopted and the formula is listed below as discussed by Perera [28]:

$$s(i) = \frac{b(i) - a(i)}{\max(a(i), b(i))} \quad (7)$$

TABLE II. CLUSTERING SETTINGS

Setting	Detail
No. of Cluster	2 - 10
Method for initialization	K-Means++
Max iteration	300
Max centroid iteration	10
Random seed	0

TABLE III. EVALUATION MATRIX

Validation technique	Range	Usage	Usage
EM	0 - ∞	K-value Selection	Decisional method
SI	-1 - 1	K-value Validation & Inter-model Comparison	Supportive method

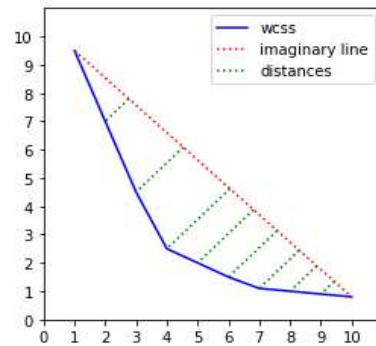


Fig. 1. Automated EM Illustration.

where $s(i)$ refers to the SI test score, $b(i)$ and $a(i)$ refer to 2 different clusters. The score of the SI test can range between -1 and 1 where -1 indicates the clusters are overlapping and 1 indicates the boundaries and distances between each cluster are clear and distant [28]. While similar to the EM, the SI test is known to provide a better result with its complex calculation. Furthermore, unlike the EM, the purpose of utilizing the SI is its advantage of extracting a standardized score (-1 to +1), which is comparable among models, while the EM could only be used for intra-cluster comparison which is related to the selection of the best number of K.

Step 4: Customer Profiling: Based on the result of K-Means Clustering, customer profiling was conducted and descriptive statistics of each cluster were extracted. Lastly, a theme was given to each cluster and cluster characteristics were discussed.

IV. FINDING AND RESULT

A. Descriptive Statistics

The result of the descriptive statistics serves the purpose of data exploration and suggesting models for the following K-Means clustering analysis. Table IV records both the summary statistics and the trimmed version of it on the right. It shows that with the outliers removed, Length, Frequency, and Periodicity presents a mean score of 0, 1, and 0 respectively with little to no deviation.

To investigate this in detail, the count of identical scores was conducted and is recorded in Table V, showing that 87%, 87%, and 96% of the variable Length, Frequency, and Periodicity are the same value (0 for Length and Periodicity, 1 for Frequency). This hinted the 3 variables might not be useful in K-Means Clustering analysis due to the lack of heterogeneity.

Furthermore, the standard deviation of normalized scores was calculated and recorded in Table VI, and model proposal for K-Means clustering analysis is created based on the standard deviation scoring, such that: variable with lower standard deviation values is excluded 1 by 1 in the next model, starting from the complete LRFMP model.

The complete model proposal is recorded in Table VII. Apart from that, model 6 which contains the original RFM model was added.

TABLE IV. SUMMARY STATISTICS

Summary Statistics								Summary Statistics (trimmed)					
Var.	Mean	Median	Range	SD	Variance	Skewness	Kurtosis	Mean	Range	SD	Variance	Skewness	Kurtosis
L	8.06	0	0-340	33.19	1101.65	5.83	40.00	0	0-0	0	0	0	0
R	109.15	89	32-389	70.11	4915.80	1.75	3.20	105.38	32-389	68.51	4693.38	1.89	3.96
F	1.43	1	1-74	3.48	12.11	16.50	306.01	1	1-2	0.06	0	17.58	307.99
M	151.76	110	1-4793	272.79	74413.42	11.78	173.44	116.99	0-1135	100.53	10105.54	4.65	36.06
P	0.81	0	0-76	5.47	29.94	8.95	91.22	0	0-0	0	0	0	0

TABLE V. DATA HOMOGENEITY STATISTICS

	Count (= 0)	Count (= 1)	Related Proportion
Length	621	N/A	0.87
Frequency	N/A	619	0.87
Periodicity	680	N/A	0.96

TABLE VI. STANDARD DEVIATION. OF NORMALIZED VARIABLES

Variable	S.D.
nfrequency	0.003790
nperiodicity	0.013200
nlength	0.085361
nmonetary	0.253688
nrecency	0.255671

TABLE VII. PROPOSED MODELS

Count	Model
Model 1	LRFMP
Model 2	LRMP
Model 3	LRM
Model 4	RM
Model 5	R
Model 6	RFM

B. K-Means Clustering – Cluster Evaluation

To identify the optimal K value, the proposed automated EM was implemented and Fig. 3, 4, and 5 were constructed where the green line indicating the optimal k-value as recommended by the automated EM while the red line/shade indicating the potential K values based on conventional visual analytics. These models with their respective best K value based on the automated EM are then compared with other models to identify the optimal model for the given dataset and is recorded in Table VIII. The comparison as shown in Table VIII shows that the RM model provides the highest SI scores among all following by the RFM model. Therefore, the RM model is selected as the most relevant model among all and was used to conduct customer profiling.

TABLE X. CLUSTER CHARACTERISTICS AND THEME

	Count	L	R*	F	M*	P	M(Sum)	Customer Profiling Tag
Cluster 0	581	4.26	81.73	1.17	131.35	0.27	76314.00	The One-Time buyer
Cluster 1	127	21.21	233.08	1.47	160.57	3.19	20393.00	The Loosen one
Cluster 2	3	187.33	175.00	50.67	3730.33	4.05	11191.00	The Loyal Buyer

Note: * are variables used in K-Means Clustering.

TABLE VIII. INTER-MODEL COMPARISON

	LRFMP	LRMP	LRM	RM	R	RFM
K value	4	4	4	3	3	3
SI	0.60	0.61	0.61	0.63	0.59	0.62

C. The Effect of Sample Size toward Cluster Validity

It is expected that as the business grows, the sample size could increase dramatically. To investigate its effect towards the proposed cluster validity, a t-test was carried out based on the SI scoring with the following Hypothesis:

H_0 : There is no significant difference between the full sample and half sample group in terms of the Silhouette Index scoring at a 95% confidence interval.

H_1 : There is a significant difference between the full sample and half sample group in terms of the Silhouette Index scoring at a 95% confidence interval.

The data was then split into half and only half of it was used in the testing. There were two methods used in splitting the dataset which is the random selection among all samples and only selects the first half of the dataset based on time order. The result in Table IX records the result where both sampling method returns the scoring of $p > 0.05$, indicates sample size could have a significant effect on the SI test scores. The result suggested SI test must be conducted periodically to ensure cluster validity as the business grow.

D. Customer Profiling based on RM Model

Customer profiling was conducted using the selected model RM due to its highest SI score among all models. The mean scores of the remaining variables: Length, Frequency, and Periodicity were recorded too for discussion purposes and is shown in Table X.

TABLE IX. HALF SAMPLE TESTS RESULT

Half Sample Method	p-value
Random	0.548
Time-based	0.573

Based on the result of the K-Means Clustering, 3 unique clusters (cluster 0, 1, and 2) were identified, and themes were given to each cluster: The one-time buyer, the loosen one, and the loyal buyer after analyzing the characteristics of each cluster. It can be seen that Cluster 0 and 1 are the typical one-time buyer, having a mean Frequency around 1 (Cluster 0 = 1.17 and Cluster 1 = 1.47). The obvious difference that distinguishes Cluster 1 from Cluster 0 is the high level of recency, showing that Cluster 1 may be the customers that are losing interest in the shop in the past 1 year. Cluster 2 is a very unique, yet important cluster to the shop, consisting of only 3 customers, but contributed a significant amount of income toward the shop. Fig. 2a and Fig. 2b compares the cluster's expenses on average and total levels. On average as in Fig. 2a, customers in Cluster 2 spent extremely more amount of money when compares with Cluster 0 and 1. On total level as in Fig. 2b, Cluster 2 contributed 35.3% sales toward the shop's total income. Furthermore, customers from Cluster 2 are themed as the loyal buyers due to its high Frequency and Length, indicating frequent visitations in a long period.

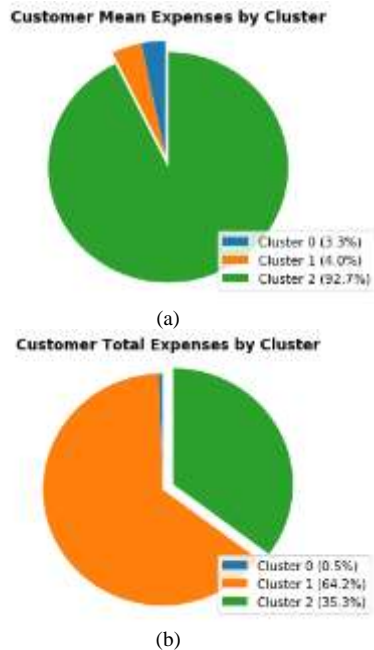


Fig. 2. Mean Expenses Pie Chart, (b) Total Expenses Pie Chart.

V. DISCUSSIONS

A. Automated Elbow Method vs Silhouette Index

Through the process of K value selection of all proposed models, the employed automated EM techniques seem to select a K-value with only acceptable SI scorings instead of the one with the highest SI scorings. This could be due to the fact that the EM seeks for maximum possible K-value by selecting the maximum number of K before the diminishing mean squared distance flattens as the K-value increases. SI, on the other hand, did not perceive such biases, each SI score for every K value was calculated independently, resulting in extremely high runtime when compare to the automated EM but much objective cluster evaluation [29]. Despite being not able to select the K-value with the highest SI scores, it is important to note that the SI scorings generally served as the validation and supportive technique in K-Means clustering to triangulate EM's decision. On a larger sample size, the benefit of using the EM quickly outrun the SI due to the runtime advantage [29]. However, due to the identified effect of sample size toward the SI scores, the customer profiling based on the automated EM approach has to be validate periodically using the SI tests to ensures cluster validity.

On the other hand, when evaluating the result of the automated EM through visual analysis in Fig. 3, Fig. 4 and Fig. 5, the automated K-value selection seems to work properly on the obvious model such as RM and LRM. On the model with more confusing curves such as LRFMP and LRMP, the automated EM selected the K-value somewhat between the possible K value based on visual analysis, indicating its consistency beyond conventional visual analysis due to the well-defined criteria for the automation. Lastly, the SI scorings of all selected K-value are around 0.6, with model R being the lowest at 0.59, indicating the acceptable quality of the proposed automated EM. Combining the result with the sample size testing, the automated EM is an acceptable method of K-Means selection in the long run with the aid of SI validity test periodically, instead of purely relying on the SI test, which is known to be computationally intensive.

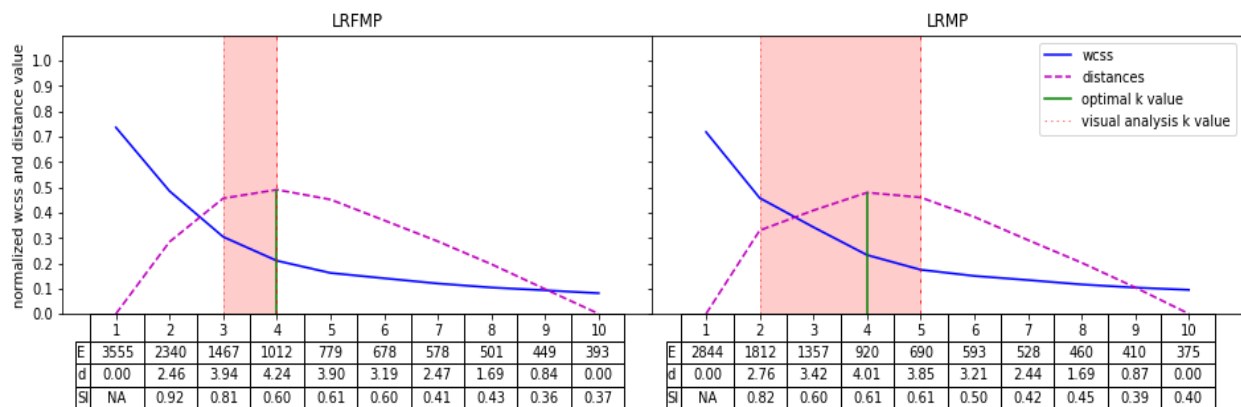


Fig. 3. K-Means Clustering Result for Model LRFMP and LRMP.

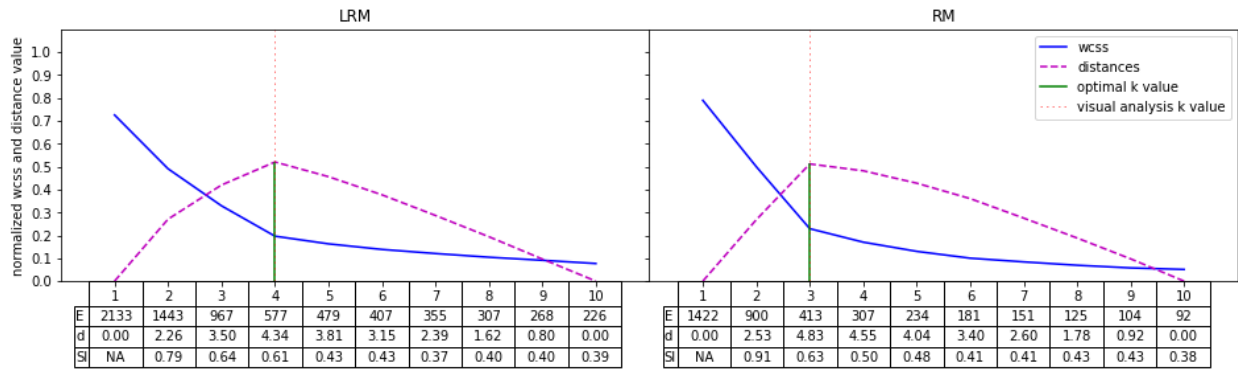


Fig. 4. K-Means Clustering Result for Model LRM and RM.

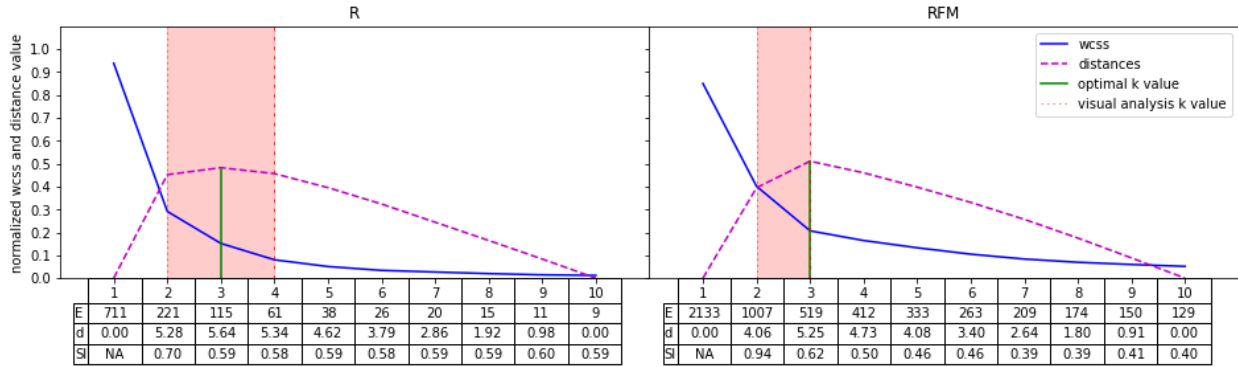


Fig. 5. K-Means Clustering Result for Model R and RFM.

B. Customer Profiling

In the process of conducting the analysis, due to the lack of dispersion on variable Length, Frequency, and Periodicity, it was expected these variables will not provide useful information in customer profiling due to the almost universal scorings as shown in Table V. This assumption was further supported by the fact that the SI scorings of the model including these variables were lower when comparing to RM model. However, during the customer profiling process, variables such as Length and Frequency were able to provide supportive numbers in justifying the differences between some clusters and providing insight regarding cluster characteristics.

C. LRFMP Model in Malaysia's Online Retail Industry

Based on the given dataset and testing, the finding indicates variable Periodicity may not be the best variable to be used in customer profiling in the online retail industry. This could be due to fact that most buyers are one-time buyers, resulting in identical scorings among customers. This is especially problematic as most clustering technique such as K-Means clustering requires dispersion to work with when creating clusters. Due to the same issue of one-time buyers, both Length and Frequency which utilizes date in calculation also results in high universal scoring, and only provided a supportive reference in the customer profiling process. Variables Recency and Monetary are the two variables that remained useful in both K-Means clustering and the customer profiling process. When comparing the SI scoring for both the LRFMP model and its original predecessor RFM model, the latter scores slightly higher than the LRFMP model, indicating the LRFMP model may not provide extra information beyond

the RFM model in the given dataset and assumingly, the online retail industry domain, but extensive research has to be done to test this assumption.

VI. CONCLUSION

In the study, we employed K-Means Clustering and LRFMP model in conducting customer profiling after the literature review. The usefulness of each variable in K-Means clustering was evaluated through descriptive statistics, following by some test model proposal. These models were then compared using the SI scoring, resulting in the RM model being the finest model in the given dataset.

The study demonstrated the automated customer profiling process where the K-value decision and optimal variables to be used could be decided without human intervention such as the conventional EM's visual analysis. Moreover, the outlined process is able to compare and evaluate if the variables are useful in any new dataset, and automatically select the model that fits the dataset. Furthermore, the process is expandable to cover more variables as variables are proposed in the future.

ACKNOWLEDGMENT

The authors would like to thank Ministry of Education, Malaysia and Razak Faculty of Technology and Informatics, Universiti Teknologi Malaysia for the support of the resources. This work is currently funded with vot. R.K130000.7856.5F229.

REFERENCES

- [1] S. Kemp and S. Moey, "Digital 2019 Spotlight: Ecommerce In Malaysia," Datareportal, 2019. <https://datareportal.com/reports/digital-2019-ecommerce-in-malaysia>.

- [2] Department of Statistics Malaysia, "Information and Communication Technology Satellite Account 2017," 2018.
- [3] S. Peker, A. Kocyyigit, and P. E. Eren, "LRFMP model for customer segmentation in the grocery retail industry: a case study," *Mark. Intell. Plan.*, vol. 35, no. 4, pp. 544–559, 2017, doi: 10.1108/MIP-11-2016-0210.
- [4] W. M. Lim, "How can challenger marketers target the right customer organization? The A-C-O-W customer organization profiling matrix for challenger marketing," *J. Bus. Ind. Mark.*, 2018, doi: 10.1108/JBIM-02-2017-0039.
- [5] D. Chen, S. L. Sain, and K. Guo, "Data mining for the online retail industry: A case study of RFM model-based customer segmentation using data mining," *J. Database Mark. Cust. Strateg. Manag.*, vol. 19, no. 3, pp. 197–208, 2012, doi: 10.1057/dbm.2012.17.
- [6] I. Maryani and D. Riana, "Clustering and profiling of customers using RFM for customer relationship management recommendations," 2017 5th Int. Conf. Cyber IT Serv. Manag. CITSM 2017, pp. 2–7, 2017, doi: 10.1109/CITSM.2017.8089258.
- [7] F. Liu, S. Zhao, and Y. Li, "How many, how often, and how new? A multivariate profiling of mobile app users," *J. Retail. Consum. Serv.*, vol. 38, no. December 2016, pp. 71–80, 2017, doi: 10.1016/j.jretconser.2017.05.008.
- [8] P. Makhija, "RFM Analysis for Customer Segmentation," *CleverTap*, 2020. <https://clevertap.com/blog/rfm-analysis/> (accessed Aug. 25, 2020).
- [9] S. Palaniappan, A. Mustapha, C. F. Mohd Foozy, and R. Atan, "Customer Profiling using Classification Approach for Bank Telemarketing," *JOIV Int. J. Informatics Vis.*, vol. 1, no. 4–2, p. 214, 2018, doi: 10.30630/joiv.1.4-2.68.
- [10] S. Y. Hung, D. C. Yen, and H. Y. Wang, "Applying data mining to telecom churn management," *Expert Syst. Appl.*, vol. 31, no. 3, pp. 515–524, 2006, doi: 10.1016/j.eswa.2005.09.080.
- [11] R. Sankar, "Customer Data Clustering Using Data Mining Technique," *Int. J. Database Manag. Syst.*, vol. 3, no. 4, pp. 1–11, 2011, doi: 10.5121/ijdms.2011.3401.
- [12] H. Ma and D. Gang, "The customer relationship management based on data mining," *WIT Trans. Eng. Sci.*, vol. 80, pp. 287–294, 2013, doi: 10.2495/aie120341.
- [13] D. Dong, J. Zhang, and J. Ye, "Research on Customer Segmentation Method of Commercial Bank Based on Data Mining," 2017 3rd Int. Conf. Innov. Dev. E-commerce Logist., no. Icidel, pp. 62–65, 2017.
- [14] M. Aryuni, E. Didik Madyatmadja, and E. Miranda, "Customer Segmentation in XYZ Bank Using K-Means and K-Medoids Clustering," *Proc. 2018 Int. Conf. Inf. Manag. Technol. ICIMTech 2018*, no. September, pp. 412–416, 2018, doi: 10.1109/ICIMTech.2018.8528086.
- [15] A. Dursun and M. Caber, "Using data mining techniques for profiling profitable hotel customers: An application of RFM analysis," *Tour. Manag. Perspect.*, vol. 18, pp. 153–160, 2016, doi: 10.1016/j.tmp.2016.03.001.
- [16] J. Silva, N. Varela, L. A. B. López, and R. H. R. Millán, "Association rules extraction for customer segmentation in the SMES sector using the apriori algorithm," *Procedia Comput. Sci.*, vol. 151, no. 2018, pp. 1207–1212, 2019, doi: 10.1016/j.procs.2019.04.173.
- [17] O. Dogan, E. Aycin, and Z. A. Bulut, "Customer Segmentation By Using Rfm Model and Clustering Methods: a Case Study in Retail Industry," *Int. J. Contemp. Econ. Adm. Sci.*, vol. 8, no. 1, pp. 1–19, 2018.
- [18] Z. Li, "Research on customer segmentation in retailing based on clustering model," 2011 Int. Conf. Comput. Sci. Serv. Syst. CSSS 2011 - Proc., pp. 3437–3440, 2011, doi: 10.1109/CSSS.2011.5974496.
- [19] J. T. Wei, S. Y. Lin, C. C. Weng, and H. H. Wu, "A case study of applying LRFM model in market segmentation of a children's dental clinic," *Expert Syst. Appl.*, vol. 39, no. 5, pp. 5529–5533, 2012, doi: 10.1016/j.eswa.2011.11.066.
- [20] Y. H. Hu and T. W. Yeh, "Discovering valuable frequent patterns based on RFM analysis without customer identification information," *Knowledge-Based Syst.*, vol. 61, pp. 76–88, 2014, doi: 10.1016/j.knsys.2014.02.009.
- [21] M. Walters and J. Bekker, "Customer Super-Profiling Demonstrator To Enable Efficient Targeting in Marketing Campaigns," *South African J. Ind. Eng.*, vol. 28, no. 3, pp. 113–127, 2017, doi: 10.7166/28-3-1846.
- [22] H. Takci, P. A. Sarvari, and A. Ustundag, "Performance evaluation of different customer segmentation approaches based on RFM and demographics analysis," *Kybernetes*, vol. 45, no. 7, pp. 1129–1157, 2016, doi: 10.1108/K-07-2015-0180.
- [23] A. J. Christy, A. Umamakeswari, L. Priyatharsini, and A. Neyaa, "RFM ranking – An effective approach to customer segmentation," *J. King Saud Univ. - Comput. Inf. Sci.*, 2018, doi: 10.1016/j.jksuci.2018.09.004.
- [24] S. Petrovic, "A Comparison Between the Silhouette Index and the Davies-Bouldin Index in Labelling IDS Clusters," 11th Nord. Work. Secur. IT-systems, pp. 53–64, 2006, [Online]. Available: https://xp-dev.com/svn/b_frydrych.../silhouetteIndexRegulaStopu.pdf.
- [25] K. Mahendru, "How to Determine the Optimal K for K-Means?," *Analytics Vidhya*, 2019. <https://medium.com/analytics-vidhya/how-to-determine-the-optimal-k-for-k-means-708505d204eb>.
- [26] N. Bertagnolli, "Elbow Method and Finding the Right Number of Clusters," 2015. <http://www.nbertagnolli.com/jekyll/update/2015/12/10/Elbow.html>.
- [27] A. Perera, "Finding the optimal number of clusters for K-Means through Elbow method using a mathematical approach compared to graphical approach," 2017. <https://www.linkedin.com/pulse/finding-optimal-number-clusters-k-means-through-elbow-asanka-perera#:~:text=So the most easiest way,the use of Elbow method.&text=Just like the name suggests,points against the cluster centroid>.
- [28] O. Arbelaitz, I. Gurrutxaga, J. Muguerza, J. M. Pérez, and I. Perona, "An extensive comparative study of cluster validity indices," *Pattern Recognit.*, vol. 46, no. 1, pp. 243–256, 2013, doi: 10.1016/j.patcog.2012.07.021.
- [29] C. Yuan and H. Yang, "Research on K-Value Selection Method of K-Means Clustering Algorithm," *J.*, vol. 2, no. 2, pp. 226–235, 2019, doi: 10.3390/j2020016.

Amalgamation of Machine Learning and Slice-by-Slice Registration of MRI for Early Prognosis of Cognitive Decline

Manju Jain¹

University School of Information
Communication and Technology, Guru Gobind Singh
Indraprastha University, Delhi India
Meerabai Institute of Technology, New Delhi, India

C.S. Rai²

University School of Information, Communication and
Technology, Guru Gobind Singh Indraprastha University
Delhi India

Jai Jain³

Media Agility India Ltd
New Delhi, India

Deepak Gambhir⁴

Galgotia College of Engineering and Technology
Utter Pradesh, India

Abstract—Brain atrophy is the degradation of brain cells and tissues to the extent that it is clearly indicative during Mini-Mental State Exam test and other psychological analysis. It is an alarming state of the human brain that progressively results in Alzheimer disease which is not curable. But timely detection of brain atrophy can help millions of people before they reach the state of Alzheimer. In this study we analyzed the longitudinal structural MRI of older adults in the age group of 42 to 96 of OASIS 3 Open Access Database. The nth slice of one subject does not match with the nth slice of another subject because the head position under the magnetic field is not synchronized. As a radiologist analyzes the MRI image data slice wise so our system also compares the MRI images slice wise, we deduced a method of slice by slice registration by driving mid slice location in each MRI image so that slices from different MRI images can be compared with least error. Machine learning is the technique which helps to exploit the information available in abundance of data and it can detect patterns in data which can give indication and detection of particular events and states. Each slice of MRI analyzed using simple statistical determinants and Gray level Co-Occurrence Matrix based statistical texture features from whole brain MRI images. The study explored varied classifiers Support Vector Machine, Random Forest, K-nearest neighbor, Naive Bayes, AdaBoost and Bagging Classifier methods to predict how normal brain atrophy differs from brain atrophy causing cognitive impairment. Different hyper parameters of classifiers tuned to get the best results. The study indicates Support Vector Machine and AdaBoost the most promising classifier to be used for automatic medical image analysis and early detection of brain diseases. The AdaBoost gives accuracy of 96.76% with specificity 95.87% and sensitivity 87.37% and receiving operating curve accuracy 96.3%. The SVM gives accuracy of 96% with 92% specificity and 87% sensitivity and receiving operating curve accuracy 95.05%.

Keywords—Brain atrophy; registration; Freesurfer; GLCM; texture features; FDR; decision support system; SVM; AdaBoost; Randomforest Bagging; KNN; Naive Bayes; classification; hyperparameters; GridsearchCV; Sklearn; Python

I. INTRODUCTION

The brain tissues degenerate due to aging a visual difference between normal and atrophied brain shown in Fig.1. Besides age many other factors viz. social and occupational conditions and family history plays a major role in the degradation process of brain tissues resulting in the cognitive skills of the person nosedive.

This effect is measurable during clinical judgment trials in the form of Clinical Dementia Rating (CDR) score. The CDR value zero means the person is cognitive normal but more than zero means the person is with brain atrophy making him cognitive abnormal.

Another biomarker of brain atrophy is the deterioration of medial temporal lobe structure of the brain which is a volumetric detection using Magnetic Resonance Imaging (MRI) a pathological test. The goal of this study and experimentation is to find mapping of clinical findings and corresponding pathological finds using MRI scans. Medial temporal lobe is that anatomic and physiological part of the brain which is responsible for memory retention and retrieval of information. It is that part of the brain where our short-term memories become long term memories. In a way we can say its non-volatile memory of the brain which becomes volatile because of brain atrophy state. That's why we only remember only current events and forget as we lose the reference just as the computer's volatile RAM loses its contents after power is switched off.

Next to find the reasons of dimensional loss, the brain atrophy is characterized by deposits of plaques and neurofibrillary tangles (NFTs), which cause loss of neurons and synapses. The loss and deposits are a simultaneous process which makes it difficult to distinguish and identify.

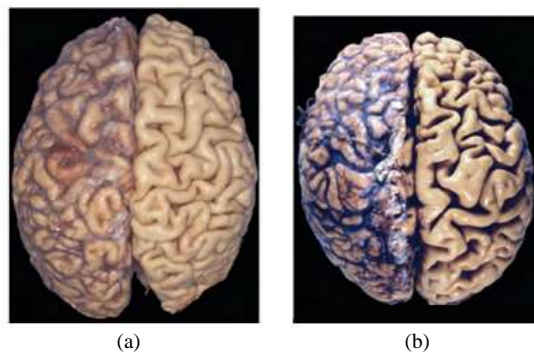


Fig. 1. (a) Normal Adult Brain, (b) Atrophied Brain with Narrow Gyri and Widened Sulci.

The extent of brain atrophy is determined by its anatomically distribution i.e. from stage I to stage VI [1], research and findings shows that major area affected as : stage I & II Entorhinal cortex a very small part behind hippocampus, stage III and IV hippocampus and amygdale stage V and VI neocortex., but the severity of disease is determined by NFTs. Hippocampus is a very compact area of the brain in the medial temporal lobe. It consists of cortical areas and main hippocampus. The cerebral cortex is highly folded as it has to be accommodated into a limited volume of brain skull.

Motivation to exploit the machine learning technology and computer based image processing is that radiologists sometimes find it very difficult to localize the degradation patterns because of many above said complicated and compact structures of the brain secondly Individuals show varied patterns. The MRI data itself is complicated 3D images. The 3D images consist of several slices of 2D images. It becomes very cumbersome for the radiologist to scan each slice and get the correlations. In this study we designed a computer aided decision support system of automatic detection using machine learning techniques which is useful for a radiologist for faster easy and accurate decisions.

II. LITERATURE REVIEW

The past few decades have proved to be promising in early experimentation and studies of detection of medical conditions using machine learning as a tool in combination of image processing.

The advancement in medical technology has led to providing data through various modalities of pathology like X Ray, MRI, fMRI, ultrasound scans and other advanced scans and availability of software to handle this data.

Image processing techniques play a significant role in the accuracy of a study. Some earlier studies used (VBM) voxel based morphometry [2][3][4]. These studies worked on T1 weighted MRI scans on very small groups of subjects, later they used voxel based relaxometry (VBR) on T2 weighted scans of same subjects. In VBM specific tissue templates were used to compare voxel by voxel and they segmented white, grey and cerebrospinal fluid by comparing with reference templates well defined by Montreal Neurologic Institute. The surface reconstruction was done voxel by voxel of size

1.5X1.5X1.5 mm each. But such procedures were too complicated and compromise accuracy.

Another voxel based morphometry study [5] used the comparisons of intensities of white matter, deep white matter and periventricular deep white matter voxel by voxel.

Another image processing technique, deformation based image analysis, was used in several studies [6][7][8]. These studies created a reference space and calculated the deformation required to transfer the individual image into reference space. The other deformation based studies[9] applied Jacobian determinant at each transformation to measure the volume change patterns. The study [7] applied Deformation based morphometry to detect brain changes, but they used the concept of longitudinal DBM where they tried to measure volume changes of same subjects over the period of study.

Tensor based morphometry is another image processing technique used in [10][11]. They designed 3D metrics of disease base differences in brain structures but again a very complicated and time consuming process. Other Tensor based morphometry [12][13] studies created difference tensors of diseased regions and a common anatomical template, at each pixel a colour coded Jacobin determinant calculated that gives a differential change in volumes at region of interest.

A study applied data mining [14] where millions of voxels are mined to select sufficient no of voxels to predict the hypothesis with high accuracy.

All the above studies performed on very small datasets, with changing lifestyle and growing no of cases in brain atrophy and other brain diseases, related data sets have increased manifolds giving researchers a wider domain to work on and yield better results in early detection of brain diseases using machine learning as a tool for both image processing and identification of diseases. The author in [15] applied Machine learning tools on ADNI (Alzheimer's Disease Neuroimaging initiative)database. They work on spatial patterns of abnormalities. It was a massive project and carried out on 16 CPU parallel processing as AD-PS scores computation needs overnight processing using parallel processors. It was extension study of earlier study [16].

The author in [17] used machine learning SVM (Support Vector Machine) combined with voxel based morphometry for early detection of brain atrophy using ADNI database. The classifier is used as an iterator to find the weights associated with each voxel. Voxels with particular weight values were selected as features rest are dropped hence voxels as features are redetermined at every training level. This study finds that study accuracy depends on number of subjects in the database.

Texture analysis may be defined as "the feel, appearance or consistency of a surface or a substance". In our study of Biomedical Image analysis image texture provides information about micro and macro structural changes in the tissues and cells. Radiologist with time train themselves to drive a relationship between visual patterns indicating molecular and cellular properties of tissues. Radiologist face many problems in evaluating and inference the biomedical images:

- Diversity in diseases and anatomy.
- Complicated operational physics behind acquisition tools and dependence on technical staff.
- Non Uniformity image acquisition, interpretation and Reporting.

Computer aided mathematical biomedical image texture analysis provides an aid to radiology by interpreting the image in terms of statistical features and signal variation algorithms giving a quantitative definition of image. List of latest texture based studies [18]-[24] on Brain atrophy MRI are listed in Table 1A.

Limitations of above studies are:

1) These were constrained to very small datasets subject numbers below 200 subjects except few. Most of the studies

are on ADNI1 and ADNI2, OASIS1, OASIS2, the latest published data set OASIS 3 a potential data to be explored.

2) Most of the studies used cross sectional MRI Database than longitudinal, while brain atrophy is a longitudinal study.

3) Most of the studies are ROI (Region of Interest) based. But such studies need a prior and in depth knowledge of the under study disease, means it becomes necessary that one of co-researcher must be from a medical background. Even when we segment the image to get ROI, the classification accuracy will depend on the accuracy of segmentation. Most studies used SPM or free surfer software to get ROI. Most of the above studies consider only the shrinkage of the hippocampus and cerebral cortex and enlargements of ventricles. But brain atrophy is not localized to some segments of the brain but it affects the brain as a whole, hence the whole brain MRI needs to be analyzed slice by slice as most Radiologists do.

TABLE I. (A) EARLIER STUDIES ON THE BRAIN DEGENERATION DISEASES CLASSIFICATION USING TEXTURE ANALYSIS FEATURES

Reference	Dataset	No. of Subjects	Method	Accuracy	Sensitivity	Specificity
Olfa Ben Ahmed 2014 [18]	ADNI	AD218 NC250	Content Based Visual Features from Hippocampus ROI SVM, 1.5 T1 Weighted	87%	Not Available	Not Available
	Bordeaux	AD16 NC21		85%		
Amulya E.R. 2017[19]	OASIS 2	235	Texture Base GLCM, SVM	75.5%	Not Available	Not Available
Tooba Altaf S Anwar, Feb 2018 [20]	ADNI		Hybrid features Texture + Clinical Data ROI and Complete Brain, KNN AdaBoost	79%	79%	92%
				97.8%	95.65%	100%
Loris Nanni May 2019 [21]	ADNI Salvator	AD 137 NC 162	Texture plus Voxel Based, ROI SVM, 1.5 T1 Weighted	78.8%	78.8%	77.4%
				87.6%	84%	90.3%
K W Kim June 2019 [22]	ADNI2		Texture Based GLCM, GLRLM, ROI, SVM 3T1 weighted	73%	65%	100%
Jia-Hui Cai Jan 2020 [23]	ADNI		ROI, Texture Based GLCM, GLRLM	Not Available	Not Available	Not Available
M. Gattu Feb 2020 [24]	ADNI	1167	Cortical Thickness Measurements left and right hippocampal	75%	Not Available	Not Available

III. DATA PRE-PROCESSING

The baseline of sustainable research and development is the infrastructure, data, software and algorithms. This work used the best image analysis environment which provided computational tools and facilitated the reproducible research and data. The Jupyter notebook is used to provide a flexible and well documented workflow. The Python 3.0 gives the very interesting and useful library modules, which make image processing implementation work very easy, like SimpleITK [25] and Nibable, Sklearn.

The study used OASIS-3 latest release December 2019 MRI dataset. Its retrospective data over the period of 15 years consists of 1098 subjects and more than 2000 sessions. The

link to the data is www.oasis-brains.org. The dataset is accompanied with clinical and cognitive assessments. The Table 1B lists the Demographic Details of the Subjects.

In our study we took the patients CDR status at a particular time stamp, and tried to classify for early prognosis of brain atrophy causing cognitive impairment which may lead to Alzheimer.

TABLE I. (B) DEMOGRAPHIC DETAILS

	Female Subjects	Male subjects	Total
Number	487	611	1098
Average Age	43-95	42 – 91	

Machine learning approach is data based approach accuracy of study strongly based on data clarity and details because data is the building block of such studies. Besides data acquisition process is not perfect, the MRI scanning results into images which have to pre-processed to improve the accuracy of final results, because the MRI scanning process got affected due to static magnetic field strength, coil variations, tissues penetration difference, eddy currents etc. in MRI machine. The study used Freesurfer [26] open access specialised software for neuroimaging analysis and interpretation of Brain MRI data. The study performed a set of scripts using Freesurfer software to implement preprocessing pipeline procedures as described in Fig. 2.

A. Skull Stripping

It is a process to remove non-skull tissues from the brain MRI Images to improve accuracy of brain image processing to be used for early diagnosis and prognosis of various brain related diseases. Many techniques of brain stripping are used in biomedical image studies.

- **Mathematical Morphometric Method:** This method uses edge detection and thresholding criteria to remove non skull tissues from brain MRIs. It is highly dependent on initial parameters like threshold values.
- **Intensity based Method:** This method uses the intensity of the basic feature of image that is pixel to differentiate non brain tissues from brain tissues by using histogram or region growing method.
- **Deformable surface based Method:** An active contour which works like self growing contour based on energy components of a desirable brain mask is used to separate out brain tissues. It's a very robust method.

B. Inhomogeneity Correction

Inhomogeneity means similar tissues of brain have different pixel intensity during MRI scan of brain, while similar tissues of brain should have approximate same pixel intensities hence this problem is known as inhomogeneity. It is because during MRI scanning process signal intensity is not uniform because different tissues of brain require different magnitude of signal to penetrate so signal is not kept uniform throughout the scan, but this change in signal may result into spikes and inhomogeneity in pixel intensities of same tissues, to correct it signal is convolved with a bias signal using two models additive or multiplicative model. This process is called inhomogeneity correction. If $T(x)$ is the observed image signal with bias field $b(x)$ and noise $n(x)$.

Then two models to represent the observed image signal are:

I Additive Model

$$T(x) = S(x) + b(x) + n(x) \quad (1)$$

II Multiplicative Model

$$T(x) = S(x).b(x) + n(x) \quad (2)$$

$$T(\widehat{x}) = \log S(x) + \log b(x)$$

$$\widehat{T}(x) = \widehat{S}(x) + \widehat{b}(x) \quad (3)$$

(multiplicative model transferred to logarithmic signal).

Inhomogeneity Corrections methods used in this study are:

1) *Modified fuzzy C means:* Modified Fuzzy C means segments the brain into three segments background, white matter and gray matter. To improve the quality of segmentation it adds two more parameters that is Spatial coherence of tissue classes t , tissues can be white matter, Gray matter, cerebrospinal fluid muscle, fat skin or skull or background (as signal penetration depends on type of tissue). And bias field \widehat{b} used to smooth the output image signal. Fuzzy C means jointly segments and estimate the bias field to minimize the inhomogeneity and the joint objective function is written as under.

$$O(k) = \sum_{k=1}^t \sum_{x \in \text{gridpoint}} S_{kx}^n |\widehat{T}(x) - \widehat{b}(x) - t_k|^2 + \frac{\alpha}{\#N_x} \sum_{k=1}^t \sum_{x \in \text{gridpoint}} S_{kx}^n \left(\sum_{r \in N_x} |\widehat{T}(r) - \widehat{b}(r) - t_k|^2 \right) \quad (4)$$

' t ' is the number of tissue classes, α is the neighbourhood influence and N_x is the number of neighbours, S_{kx} is the voxel X belonging to k^{th} tissue class. The parameters to be estimated for the minimization of $O(k)$ are the class centres $\{t_k\}$ and biasfield estimates $\{b_x\}$.

2) *Non parametric non uniform intensity normalization (N3):* Freesurfer scripts uses N3 method of inhomogeneity correction. N3 is a histogram based non uniform intensity correction method. If $S = (s_1, s_2, \dots, s_N)^T$ be intensities of N voxels of a MRI scan and $b = (b_1, b_2, \dots, b_N)^T$ are the corresponding bias field. The histogram of S will be blurred version of actual true image due to convolution of bias part b . The objective of this algorithm is to minimize this blurriness by de-convolution method using an iterative way to estimate a smooth bias model. The metric to be estimated is known as

$$CJV = \frac{\sigma_1 + \sigma_2}{|\mu_1 - \mu_2|} \quad (5)$$



Fig. 2. Data Preprocessing Pipeline.

where (μ_1, σ_1) and (μ_2, σ_2) are the mean and standard deviation of two different tissue types. This metric will be optimized if the standard deviation within in one class of tissues is minimum, hence the objective that one type of tissues should approximately should have same intensity values. It is done iteratively in particular value of bin $K = 200$, we try to estimate the CJV for the values.

$$\mu_1 = \min(S - b) \text{ to } \mu_k = \max(S - b) \quad (6)$$

C. Co-Registration

Registration is the most crucial stage of pre-processing because it helps to control the changes in data acquisition because of rotational transformational changes in brain position and even the size of brain may be different in different subjects. It helps to quantify the anatomical and morphometric alterations related to an individual (longitudinal studies) and a group of individual (both longitudinal as well as cross sectional studies). A common reference space or template is used to compare the source image and the template by applying optimal geometric transformations. The template can be the brain image of the same subject in case of longitudinal studies or common available templates.

D. Normalization

A technique to have uniform intensity distribution throughout the group of MRI images of a group to improve the accuracy of study using histogram equalization method.

E. Smoothing

It is a technique to remove unwanted noise from the MRI image which may result in incorrect results and affects accuracy of the study.

IV. PROPOSED METHOD

But during study we observed after applying Freesurfer scripts of registration, the slices of inter subjects does not

contain the similar information, means the slices of different subjects are not exactly parallel as shown in Fig 3, as our study is slice by slice study the Nth slice of X subject should contain almost same contents as the Nth slice of Y subject. Even the brain size of all subjects not same. We deduced a method to synchronize the inter subject slices. The steps of this method are listed below:

Mid_Slice_brainsize_Equalization_Method:

- Find the actual slice number of data acquisition, means first nonempty slice the actual start of MRI scan.
- Find the actual slice number of data acquisition ends, means first empty slice of MRI scan.
- Take the mid of first non-empty slice number and first empty slice of MRI scan., that is actual mid slice of each MRI scan, also calculate the length of scanning in each MRI scan, means Number of Nonempty slices in each MRI scan.
- From Mid Slice and actual size of brain which is actually the Number of Non empty slices we synchronize the Nth slice of X subject to the Nth slice of y subject as shown in Fig. 3.

A. SWMA Slice Wise Multivolume Analyse (SWMA) Design

Multivariate Approach considering Whole Brain Slices instead of Region of Interest (ROI). Earlier studies used ROI because of small sample size. As our sample set is sufficiently large so our study experimented with whole brain slices without compromising loss of information due to segmentation and approximation. Each MRI image is a volumetric representation which is flattened to 256 slices. In computation each slice is a two dimensional matrix of order 256X256. Slice Wise Multivolume Analysis described in Fig. 4.

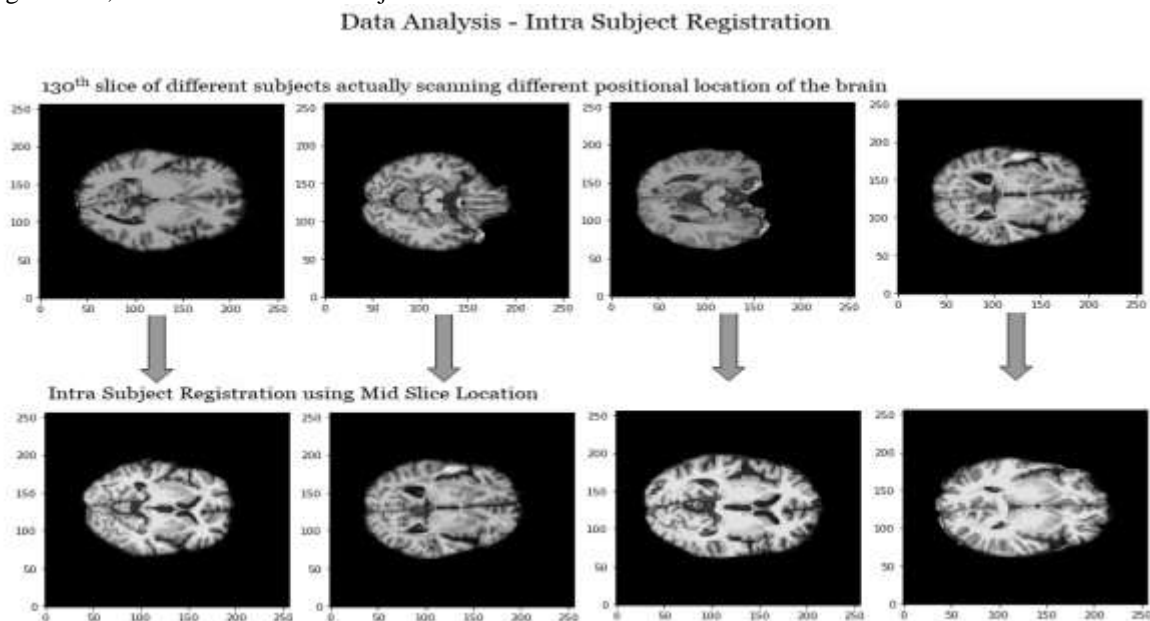


Fig. 3. Mid Slice Brain Size Equalization Method.

256 slices in each MRI Image for each subject

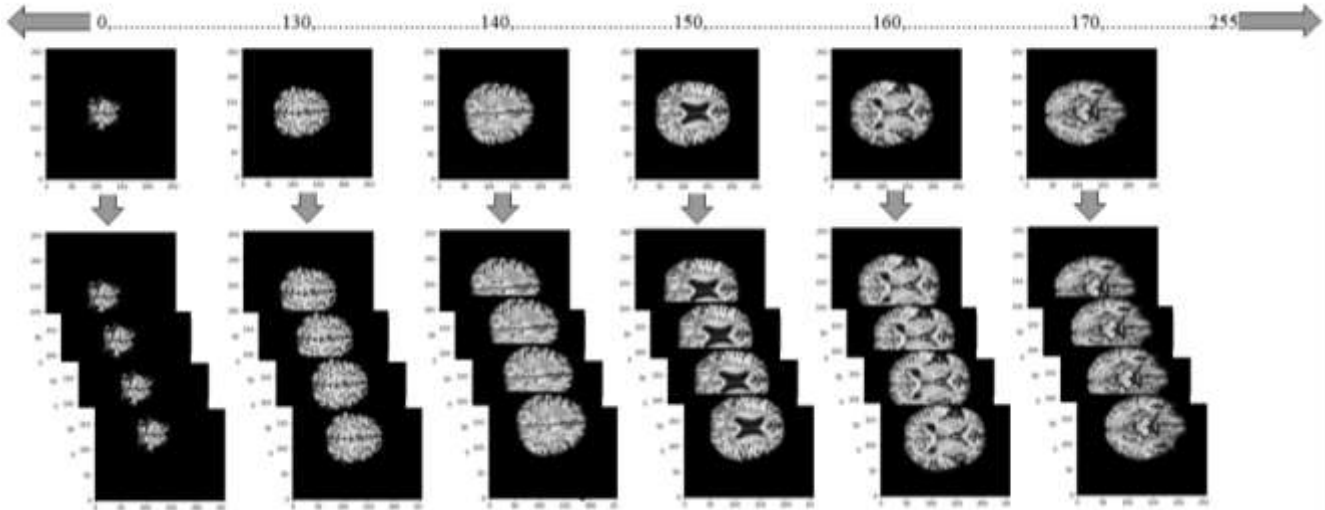


Fig. 4. Slice Wise Multivolume Analysis.

B. Feature Extraction

This study uses biomedical texture analysis for feature extraction. Texture analysis is a way of extracting image signatures pixel by pixel in terms of intensities, intra and inters pixel relationship and spectral properties. These can be calculated using mathematical statistical tools. Image analysis using this gives consistent, fast and accurate results. The features generated using texture based statistical distribution of pixel intensities give quantitative measures of image which are easily differentiable from each other hence helping image comparison easily. Each element of the matrix is the value of intensity at a particular pixel. We calculated the simple central tendencies statistics of these image slice matrices. These gross values are very much helpful in providing wide characteristics of image slice contents.

1) *Mean*: it gives a measure of concentration of data around the central distribution of data. But it is affected by extreme observations.

2) *Standard Deviation*: It is the measurement of how well the mean is able to represent the whole dataset. It gives the dispersion of the data.

3) *Skewness*: It is the measure of lack of symmetry. It helps us to determine the concentration of observation towards the higher and lower side of the observed data.

4) *Kurtosis*: It measures the convexity of the distribution curve.

These statistics give only intensity based information. These do not provide repeating nature of pixel values.

Gray Level CO-occurrence Matrix (GLCM) gives texture analysis of the image by measuring the spatial relationship among the pixels. At each pixel value we calculate a Gray Level co-occurrence matrix around it which calculates the number of pixels having the same pixel value. The GLCM matrix is calculated in four major directions. The directions are horizontal, vertical, diagonal up and diagonal down (at angles 0°, 90°, 45°, 135°, respectively).

Steps to create GLCM:

- Let x is the pixel under consideration.
- Let M is the set of pixels surrounding pixel x , which lie under the considered region M .
- Define each element mn of the GLCM as the number of times two pixels of intensity m and n occur in specified spatial relationship. Sum all the values with the specified intensity around that pixel x .
- To get symmetric GLCM make a transpose copy of GLCM and then add it to itself.
- Normalize the GLCM, divide each element by the sum of all elements.

If we have a slice of 256X256, GLCM will be too much data, we use some descriptive quantities from GLCM matrices. Each descriptor is calculated in four directions.

$$Energy = \sum_{m,n=0}^{N-1} (X_{mn})^2$$

$$Contrast = \sum_{m,n=0}^{N-1} X_{mn}(m-n)^2$$

$$Homogeneity = \sum_{m,n=0}^{N-1} \frac{X_{mn}}{1+(m-n)^2}$$

$$Correlation = \sum_{m,n=0}^{N-1} X_{mn} \frac{(m-\mu)(n-\mu)}{\sigma^2}$$

$$Entropy = \sum_{m,n=0}^{N-1} -\ln(X_{mn})X_{mn}$$

X_{mn} is the element of the normalized symmetrical GLCM

N is the number of gray levels

$$\mu = \sum_{m,n=0}^{N-1} iX_{mn} \sigma^2 = \sum_{m,n=0}^{N-1} X_{mn}(m - \mu)^2$$

Total Number of features from Texture analysis are 28. The most impotent and unique property of these statistical and GLCM features is that these are invariant to geometrical transformations of surfaces like translation horizontal or vertical, rotation, etc. The features should follow the rule of invariance. Features are volumetric signatures of microscopic structures of Brain: The most affected microstructures of the brain are hippocampus, amygdale and temporal horn. Studies show the volume of these structures decline with age but if the rate of change of the volumes over a certain time is more than normal change, it indicates some non-cognitive developments may cause brain diseases in future.

C. Feature Selection

Feature extraction and selection and classification share very thin line boundaries, a good feature extractor and selection technique surely makes the classification very easy and correct, but a good classifier would not need a good feature extractor or selection technique. As the features are the input to the classifiers so either we should have the best features so the classification should be with least error or the classification algorithm should be such that even the features provide least information but the algorithm is smart enough to extract the correct piece of information with least classification error.

Every classifier works on a discriminate function $F_{ci}(X)$, the classifier as described in Fig. 5 will assign a feature vector X to a said class c1 if $F_{ck}(X) > F_{cj}(X)$ for all $k <> j$.

Objective of this function is that create a boundary or hyper plane in feature space which distinguishes the n No of classes. The hyper plane can be represented with the equation

$$F_{ci}(X) = w_i^t X + w_{i0} \tag{7}$$

Where $w = \mu_j - \mu_k$

but the classifier function's discriminability gets affected by decision bias degrading Classification accuracy and other scores. The variance σ is also biased. The means the variance of a sample feature is not as expected.

Theoretically when we extract features we hope that each feature help up to some extent to the discrimination function means all are independent but practically it's not true many times. Table II shows discriminatory performance of basic statistical features in the concerned study and Table III shows the discriminatory performance of GLCM Features. The classification accuracy also depends on dimensionality. After applying a set of feature the accuracy performance may be inadequate we may think to add more no of features to improve the performance at the cost of computational cost but practically as we add the new features generally it increase the performance but up to some extent only after a point as we increase the features the performance decreases. Our study applied Fisher Linear Discriminant It is based on simple criteria if the mean of two sample space features differ than its

variance then it will definitely provide better discrimination ability to classify two sets of classes. The vector w in decision function is a scalar dot product with X as in equation vii, results into a vector the direction of this vector is important, not the magnitude. The FLD employs the linear function $W_i^t X$ such that

$$J(w) = \frac{|m_1 - m_2|^2}{\sigma_1^2 + \sigma_2^2} \tag{8}$$

Should be maximum where m_1 and m_2 are mean of the feature in two different classes and σ_1 and σ_2 are the standard deviation of features in two classes of the same feature. This is called Feature Discrimination Ratio (FDR). FDR is applied in each classifier, by keeping on adding the features if the classifier shows improved accuracy, if the accuracy or other scores decrease stop adding the features. By applying FDR on our extracted features we find that Mean, standard deviation, skewness, homogeineity in two directions and energy in all four directions are the best FDR values by adding other features the accuracy and specificity sensitivity decrease. But it's not true in all the classifiers. The AdaBoost, Randomforest and Bagging Classifier based on ensemble techniques are more efficient classifiers and almost give similar accuracy with or without feature selection but SVM and K neighbours accuracy increase a lot after applying FDR.

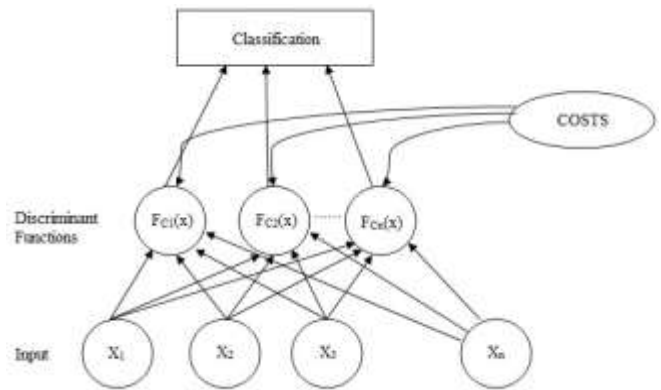


Fig. 5. A Generic Classifier.

TABLE II. BASIC STATISTICS SHOWING HIGH DISCRIMINARY PERFORMANCE

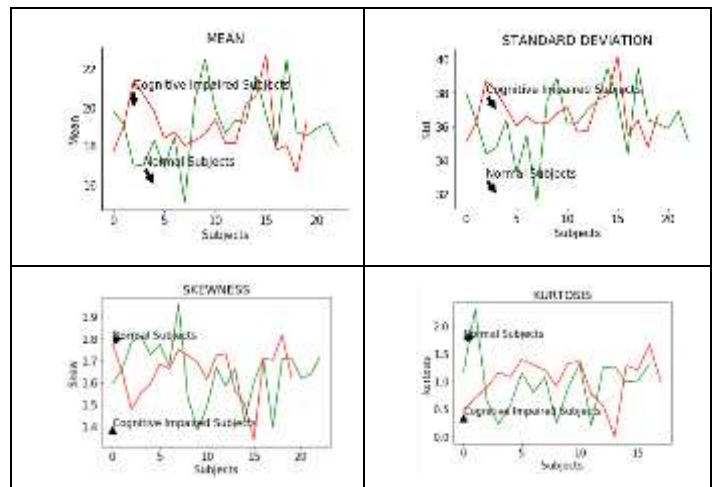
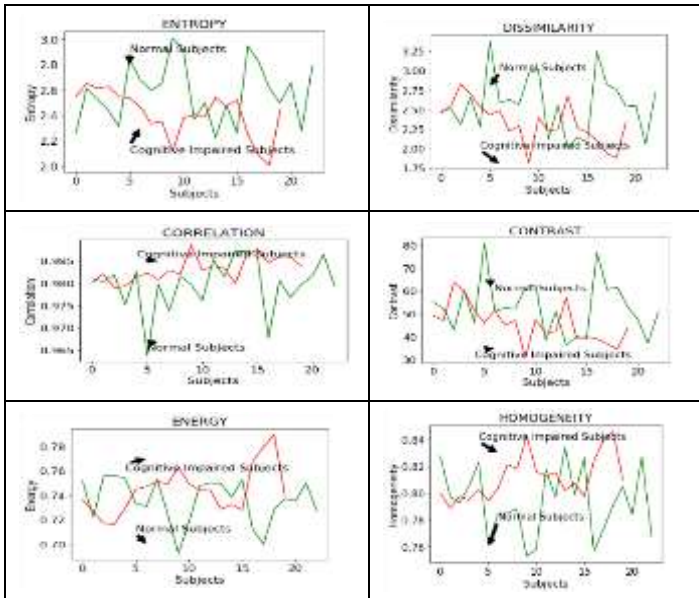


TABLE III. GLCM SHOWING HIGH DISCRIMINATORY PERFORMANCE



V. CLASSIFICATION

A. Support Vector Machine

As the objective of a classifier is to find a hyperplane which divides the sample space into desired set of classes with least error, SVM tries to find this hyperplane by processing the input data transferring into higher dimension plane using suitable kernel function so that sample data can be easily classified which cannot otherwise classified in lower dimension plane. The solution vector hyperplane may not be unique. The objective is to find the optimal hyperplane.

If L is the optimal hyperplane and two hyperplanes S and T passing through the nearest vectors in two classes from the optimal hyperplane. Then the distance between the optimal hyperplane L and S or L and T is called margin. The points on the hyperplane S and T are called support vectors, as shown in Fig. 6. These are the vectors which are the most informative for the classifier. The algorithm implements such that the controlling parameters are C and gamma and the kernel. Kernel is the function which converts the input features from lower dimensional plane to higher dimensional plane. C is a regularity parameter which changes the width of margin and gamma decides how much stringent is the classifier to the outliers. The training the data with SVM is that we want the hyperplane margin big enough to generalize the classifier. The C is the costing factor also, if C is large then it gives a large penalty and margin will be small but if C is small less penalty hence margin will be big. But the behavior change also depends on the particular size of sample set, the hyperparameter tuning results vary from model to model. The hyperparameter tuning do have limitations like, hyperparameters values change from dataset to datasets. The best parameters for one dataset may not work perfectly with other datasets. Moreover it is a time consuming process. But Data Processing and classification model evaluating scores really affected by hyperparameter tuning. It gives practical experience of algorithms. The classifier behaviour under various parameters gives an insight of its design. Fig. 7A

depicts the hyperparameter tuning C and Gamma to optimize accuracy, Fig. 7B depicts the hyperparameter tuning to optimize specificity and Fig. 7C depicts the hyperparameter tuning to optimize sensitivity.

1) SVM classification with full features: First the experimentation was carried out with full features, Table IV shows the results of GridsearchCV method, which internally applies 10 fold cross validation under a given set of parameters. The best value of accuracy is 92.95% with specificity 84.22% and sensitivity 79.28%. The results are again checked with 10 fold cross validation with hold out data, the results are comparable with receiving operating curve area showing accuracy as shown in Fig. 8.

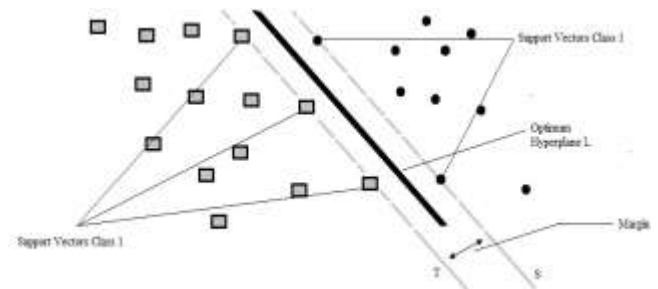
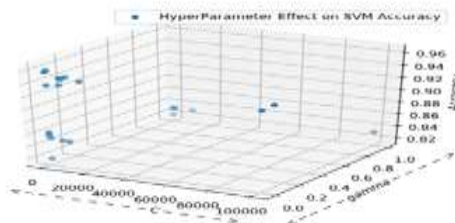
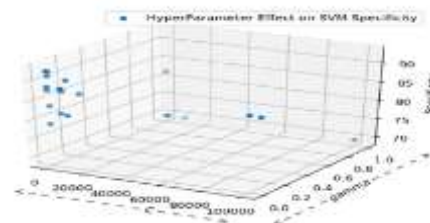


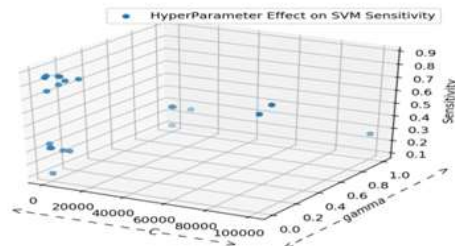
Fig. 6. SVM Hyperplane.



(a) Effect of C and Gamma in SVM Classifier Accuracy



(b) Effect of C and Gamma on SVM Classifier Specificity



(c) Effect of C and Gamma on SVM Classifier Sensitivity

Fig. 7. (a) Hyper Parameter Tuning to Optimize SVM Accuracy, (b) Hyper Parameter Tuning to Optimize SVM Specificity, (c) Hyper Parameter Tuning to Optimize Sensitivity.

2) *SVM Classification with FDR Selected Features:* The Table V are results of Gridsearch CV exploring SVM under varying C and gamma, using a subset of features after applying FDR. The highest value of Accuracy is 96.09% with specificity 92.63% and sensitivity 87.21%. The results are again checked with 10 fold cross validation with hold out data, the results are comparable with receiving operating curve area showing accuracy as shown in Fig. 9.

B. Random Forest

The Random Forest algorithm is a meta-process which internally works on N no of decision trees to keep the information. Unlike decision tree the result is based on a multiple decision trees, here the algorithm based on divide and conquer approach means it divides the samples among N no of decision trees randomly and then enumerates the decision of all these trees to give the final result. Its way of taking advice of N experts rather than single. It's an ensemble approach hence time consuming but because today the technology is advanced to handle parallel processing so mean time to fit is not that important criteria to evaluate a classifier. One more important thing the study observed, Feature selection process does not much affect accuracy as Random forest itself chooses both sample divides as well as feature vector divides. The results with FDR or without FDR are almost the same. The Random Forest classifier is a very stable classifier which the study found during the GridsearchCV method. The Accuracy range does not change much even after tuning hyper parameters.

1) *Randomforest classification with full features:* Table VI are results of GridsearchCV with all features, the best accuracy is 89.98% with specificity 88.23 and sensitivity 56.39%. The results are again cross validated with hold out data and compared with receiving operating accuracy as shown in Fig. 10.

2) *Randomforest classification with FDR selected features:* The random forest hyperparameters tuning after applying FDR, results are listed in Table VII, with maximum accuracy 90.6% with specificity 87.13% and sensitivity 61.55% with criterion entropy max_depth None and No of estimators 100. The results are cross validated on hold out data and results are comparable for receiving operating area accuracy using 10 fold cross_validation algorithm shown in Fig. 11.

C. AdaBoost

Boosting is a process which is designed to deal with the problem of weak learning classifiers. Weak learning results in higher detection errors and low decision accuracy of the classifier. Weak classifiers are the moderate classifiers which give a bit better insight of the problem than random guesses. AdaBoost is a classifier which deals with a set of weak classifiers iteratively. Logic of using same weak classifiers on same data does not lead to a better results, but AdaBoost is designed in such a way that during each iteration the weak classifiers work with subsets of data, not full data as whole, these subsets of data may give different results with weak classifiers, initially all the classifiers are assigned equal

weights, but after each iteration the classifiers are judged on the basis of classification error, the classifiers with less error is given higher weight. AdaBoost is a kind of greedy algorithm with the objective of minimizing the classification error by improving the learning model after each iteration. AdaBoost is an adaptive boosting algorithm because it has no error bound and no bounds on the number of weak classifiers.

1) *AdaBoost classification with full features:* The AdaBoost algorithm works better with full features. Table VIII shows results of AdaBoost with all parameters GridsearchCV results with maximum average accuracy 96.76% with specificity 95.87% and sensitivity 87.37% using learning rate 1 and No of estimators 150. AdaBoost wins over all the classification method. The results are cross validated on hold out data using ROC curves shown in Fig. 12.

2) *AdaBoost Classification with FDR Slected Features:* The FDR degrades the accuracy of AdaBoost. Table IX shows AdaBoost with Gridsearch CV results With 10 features the best accuracy is 91.6% with specificity 86.15% and sensitivity 68.59% using no of estimators 150, learning rate 1. The results are cross validated on hold out data using ROC curves shown in Fig. 13.

D. Bagging Classifier

It is also an ensemble technique classifier very similar to random forest classifier, as in such classifiers the subsets of samples are randomly chosen in random forest, in which the previously selected samples are replaced with new samples. This is also used to improve the accuracy and other performances of decision tree classifiers.

1) *Bagging classification with full features:* Gridsearch CV results for different parameters are tabulated in Table X. The best accuracy is 86.86% with specificity 87.25% and sensitivity 38.95% which is using maximum samples selected from the bag are 200 and No of estimators 200, which are cross verified using hold out data using receiving operating curve accuracy as shown in Fig. 14.

2) *Bagging classification with FDR slected features:* Table XI lists the results of GridsearchCV using FDR selected features the accuracy is 86.1% with accuracy sensitivity 38.95 and specificity 85.9%, the results are cross verified on hold out data using Receiving Operating Curve accuracy as shown in Fig. 15.

E. Nearest Neighbours

KNN is a non parametric classifier, it is a lazy algorithm but very simple. Like to predict a vector X, it will look k Vectors which are nearest to X, the distance is generally calculated using Euclidean or Manhattan metrics which measure the distance between two observations X_s and X_t for j features.

$$\sqrt{\sum_{j=1}^p (x_{sj} - x_{tj})^2} \text{ Euclidean Distance}$$

$$\sum_{j=1}^p |x_{sj} - x_{tj}| \text{ Manhattan Distance}$$

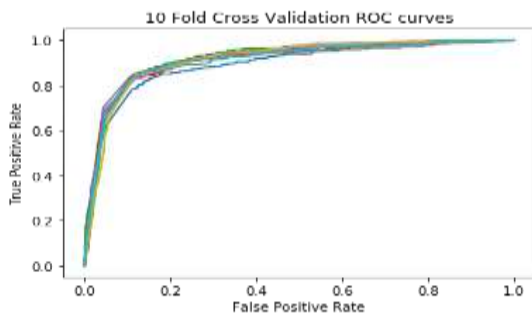
SVM Parameter Tuning

TABLE IV. SVM GRIDSEARCH CV: BEST RESULTS WITH C=1, GAMMA = 10, ACCURACY 92.9% WITH SPECIFICITY 84.22% AND SENSITIVITY 79.28% WITH ALL FEATURES

param_C	Param gamma	mean Specificity	mean_Sensitivity	mean_Accuracy
1	0.01	83.344442332466	0.2578847438557	0.8432073329718
1	0.1	83.853987796136	0.7178562638444	0.9168477040299
1	1	83.607909582329	0.7727646707218	0.9250390969494
1	10	84.223396084093	0.7928993354664	0.9295074469075
1	100	86.272333827734	0.6822210892725	0.9156894483427
10	0.001	80.241227828115	0.2457156921345	0.8390699034284
10	0.01	82.878571005636	0.7677437502197	0.9226396671760
10	0.1	83.314746871451	0.7845188284518	0.9262807503327
10	100	80.511885530581	0.7245385183362	0.9108060955636
100	0.0001	74.584867980930	0.1567930100910	0.8226860220531
100	0.001	81.966054078167	0.7610386413979	0.9195780542180
100	0.01	82.705260558913	0.7882880348792	0.9254527988212
100	100	78.643503364618	0.7148939910692	0.9051800376864
1000	1E-05	66.975494228749	0.1136176646390	0.8133371266275
1000	0.0001	80.486585304024	0.7350462360676	0.9122973257960
1000	0.001	82.692441319188	0.7891318870644	0.9255359226332
1000	100	78.568888719043	0.7148939910692	0.9050144747725
10000	1E-06	65.472364610713	0.1224359199746	0.8132545505836
10000	1E-05	77.250521741845	0.6331598748285	0.8905360047984
10000	0.0001	81.697496074876	0.7861836784923	0.9228044769088
10000	10	81.119868761615	0.8155233641573	0.9257005954239
10000	100	78.568888719043	0.7148939910692	0.9050144747725
100000	1E-06	72.383866822978	0.4713178158292	0.8597560925509
100000	1E-05	80.296232630667	0.7656569740867	0.9164344129842
100000	10	80.506045797683	0.8079726451249	0.9231350549685
100000	100	78.568888719043	0.7148939910692	0.9050144747725

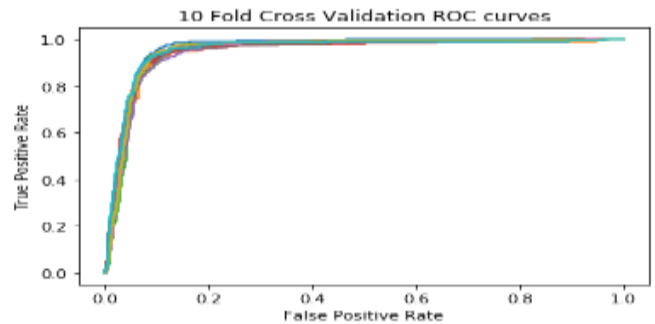
TABLE V. SVM GRIDSEARCH: BEST RESULTS WITH C 1000, GAMMA = 0.0001, ACCURACY 96.09%, SPECIFICITY 92.63% AND SENSITIVITY 87.21% AFTER APPLYING FDR FEATURE SELECTION

C	Gamma	Specificity	Sensitivity	Accuracy
1	0.01	78.829923692182	0.11613339896628	0.81879816935894
1	0.1	80.532799121772	0.26162054780071	0.84146940167288
1	1	81.817542579539	0.11196863682711	0.81979236849456
10	0.001	88.608313139021	0.32035793396856	0.85760425396721
10	0.01	91.338500106760	0.75266692451039	0.93703631428743
10	0.1	86.861630821078	0.76898843219296	0.93124339254706
10	1	69.457820713316	0.26581343834605	0.83137526772166
100	0.0001	87.785798941696	0.35392039661052	0.86256915572499
100	0.001	92.636598407176	0.85619703948525	0.95805075345504
100	0.1	87.117762600668	0.8310273900355	0.942247780169698
100	1	69.4578207133165	0.2658134383460	0.831375267721668
1000	1E-05	83.781206927729	0.32413768854822	0.85396365010763
1000	0.0001	92.634766545677	0.8721229914559	0.96094570796290
1000	0.1	86.32964031705	0.8314387679758	0.9405924933857
1000	1	69.457820713316	0.2658134383460	0.83137526772166
10000	1E-06	81.859571838812	0.3203614500193	0.85156380950815
10000	1E-05	90.934324474569	0.8540979571745	0.95424397044243
10000	0.1	86.32964031705	0.8314387679758	0.9405924933857
10000	1	69.457820713316	0.2658134383460	0.83137526772166
100000	1E-06	88.029537238048	0.8021166625646	0.93918527708850
100000	0.1	86.32964031705	0.83143876797581	0.9405924933857
100000	1	69.457820713316	0.26581343834605	0.83137526772166



Receiving operating Curve Accuracy: 0.8937792926314483
 Receiving operating Curve Accuracy: 0.9179476564187485
 Receiving operating Curve Accuracy: 0.9226346488033448
 Receiving operating Curve Accuracy: 0.9157707603773151
 Receiving operating Curve Accuracy: 0.9162423970273819
 Receiving operating Curve Accuracy: 0.9149871321207529
 Receiving operating Curve Accuracy: 0.9027465236824136
 Receiving operating Curve Accuracy: 0.913242903607333
 Receiving operating Curve Accuracy: 0.912467964860967
 Receiving operating Curve Accuracy: 0.9134321596900

Fig. 8. The Cross Validation of Table IV Results with Receiving Operating Curve with Hold out Data with SVM and All Parameters.



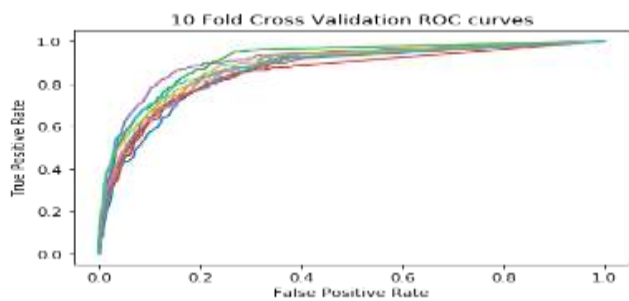
Receiver operating Curve accuracy:0.9617590965184548
 Receiver operating Curve accuracy: 0.942635941021788
 Receiver operating Curve accuracy: 0.949475534894809
 Receiver operating Curve accuracy: 0.947978539771402
 Receiver operating Curve accuracy: 0.9452122348088005
 Receiver operating Curve accuracy: 0.9480958157900996
 Receiver operating Curve accuracy: 0.9542638074464368
 Receiver operating Curve accuracy: 0.9523513244133015
 Receiver operating Curve accuracy: 0.9523604360217566
 Receiver operating Curve accuracy: 0.9549160237865637

Fig. 9. The Cross Validation of Table V Results with Receiving Operating Curve with Hold Out Data with SVM with Selected Features.

Random Forest Parameter Tuning

TABLE VI. RANDOM FOREST GRIDSEARCHCV RESULTS MAXIMUM ACCURACY IS 89.98% WITH SPECIFICITY 88.23% AND SENSITIVITY 56.39% USING CRITERION ENTROPY AND MAX_DEPTH NONE AND N ESTIMATORS 100

criterion	depth	estimator	specificity	sensitivity	Accuracy
gini	5	20	84.888824121	0.230188679245	0.839400708997
gini	5	30	85.850144850	0.234800838574	0.840972734829
gini	5	50	84.784164752	0.231027253668	0.839648984840
gini	5	100	84.905496091	0.218867924528	0.837828477838
gini	15	20	86.667233743	0.522012578616	0.889706767578
gini	15	30	87.691345970	0.540880503144	0.894257419101
gini	15	50	88.032210687	0.539203354297	0.894505626502
gini	15	100	88.341393086	0.543815513626	0.895664190068
gini	20	20	86.353249455	0.516142557651	0.888217694282
gini	20	30	87.101982059	0.529140461215	0.891527411466
gini	20	50	87.815480695	0.540880503144	0.894423118844
gini	20	100	88.034856531	0.538364779874	0.894340440079
gini	25	20	86.502917560	0.517400419287	0.888631430318
gini	25	30	87.233662182	0.529559748427	0.89177565308
gini	25	50	87.989689597	0.540880503144	0.894671360466
gini	25	100	88.215312778	0.538364779874	0.894588613258
gini	None	20	86.502917560	0.517400419287	0.888631430318
gini	None	30	87.233662182	0.529559748427	0.891775653088
gini	None	50	87.989689597	0.540880503144	0.894671360466
gini	None	100	88.215312778	0.538364779874	0.894588613258
entropy	5	20	86.565016992	0.179454926624	0.832533409441
entropy	5	30	85.625514909	0.198322851153	0.835015688774
entropy	5	50	85.087555336	0.198322851153	0.834850160138
entropy	5	100	85.445716966	0.189517819706	0.833443389172
entropy	15	30	88.583992309	0.566037735849	0.899966497305
entropy	25	20	88.823140395	0.563941299790	0.899883715876
entropy	None	20	88.823140395	0.563941299790	0.899883715876

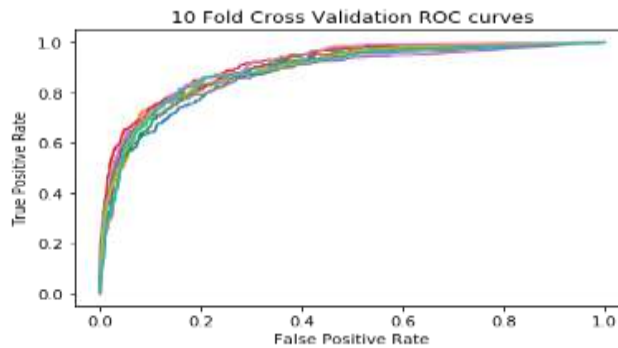


Receiving Operating Curve accuracy: 0.8635070069526353
 Receiving Operating Curve accuracy: 0.8768584331740022
 Receiving Operating Curve accuracy: 0.9081541453199207
 Receiving Operating Curve accuracy: 0.8475329655992669
 Receiving Operating Curve accuracy: 0.9046812480763313
 Receiving Operating Curve accuracy: 0.8626087454212453
 Receiving Operating Curve accuracy: 0.8753501140194329
 Receiving Operating Curve accuracy: 0.8639699552341596
 Receiving Operating Curve accuracy: 0.8887315511961502
 Receiving Operating Curve accuracy: 0.8852172129377727

Fig. 10. Random Forest the Cross Validation of Table VI Results with Hold out Data Results Comparable with ROC Area Accuracy.

TABLE VII. RANDOM FOREST CLASSIFIER WITH FDR FEATURES USING GRIDSEARCHCV, BEST ACCURACY 90.6% WITH SPECIFICITY 87.13% AND SENSITIVITY 61.55% USING ENTROPY CRITERION MAX_DEPTH NONE AND NO OF ESTIMATORS 100

criterion	depth	estimators	Specificity	Sensitivity	Accuracy
gini	5	20	82.405557662	0.281761006289	0.846102822131
gini	5	30	81.753935627	0.268343815513	0.843537761369
gini	5	50	82.324952592	0.278825995807	0.845440810251
gini	5	100	83.218901214	0.272955974842	0.84527555538
gini	15	20	85.672104091	0.594549266247	0.900131854834
gini	15	30	86.027370483	0.596226415094	0.900959224243
gini	15	50	86.273793287	0.592452830188	0.900793866714
gini	15	100	86.892389272	0.600838574423	0.903110377861
gini	20	20	85.894661091	0.596226415094	0.900793661385
gini	20	30	86.037359156	0.598742138364	0.901373234050
gini	20	50	86.312500959	0.594549266247	0.901207568529
gini	20	100	86.680282575	0.598742138364	0.90244829753
gini	25	20	85.894661091	0.596226415094	0.900793661385
gini	25	30	86.037359156	0.598742138364	0.901373234050
gini	25	50	86.312500959	0.594549266247	0.901207568529
gini	25	100	86.688653578	0.599161425576	0.902531044746
gini	None	20	85.894661091	0.596226415094	0.900793661385
gini	None	30	86.037359156	0.598742138364	0.901373234050
gini	None	50	86.312500959	0.594549266247	0.901207568529
gini	None	100	86.688653578	0.599161425576	0.902531044746
entropy	5	20	86.4218333770	0.220125786163	0.838656326345
entropy	5	30	84.4299042596	0.218448637316	0.837332644799
entropy	5	50	83.3893286936	0.222641509433	0.837415084015
entropy	5	100	82.6401550351	0.244444444444	0.840228009963
entropy	15	20	86.3301678223	0.599580712788	0.90195201962
entropy	15	30	86.7762836186	0.60377358490	0.90344116136
entropy	15	50	87.1423000822	0.607547169811	0.904682369472
entropy	15	100	87.3657096503	0.615094339622	0.906336766076
entropy	20	20	86.1350772246	0.603773584905	0.90236568721
entropy	20	30	86.4527911908	0.600838574423	0.902448160654
entropy	20	50	86.9335626954	0.607547169811	0.904351483307
entropy	20	100	87.1309161889	0.615513626834	0.906006051017
entropy	25	20	86.1350772246	0.603773584905	0.902365687217
entropy	25	30	86.4527911908	0.600838574423	0.902448160654
entropy	25	50	86.9335626954	0.607547169811	0.904351483307
entropy	25	100	87.1309161889	0.615513626834	0.906006051017
entropy	None	20	86.1350772246	0.603773584905	0.902365687217
entropy	None	30	86.4527911908	0.600838574423	0.902448160654
entropy	None	50	86.9335626954	0.607547169811	0.904351483307
entropy	None	100	87.1309161889	0.615513626834	0.906006051017



Area under the ROC curve: 0.8772840343735866
 Area under the ROC curve: 0.889214912760619
 Area under the ROC curve: 0.8947546991251121
 Area under the ROC curve: 0.9128083521162034
 Area under the ROC curve: 0.883718402186543
 Area under the ROC curve: 0.8945758258258258
 Area under the ROC curve: 0.9118374548334127
 Area under the ROC curve: 0.8821687953919359
 Area under the ROC curve: 0.8938542616531675
 Area under the ROC curve: 0.8887535609191084

Fig. 11. GridsearchCV Results of Random Forest Verified with Hold Out Data Results Verification with FDR Features.

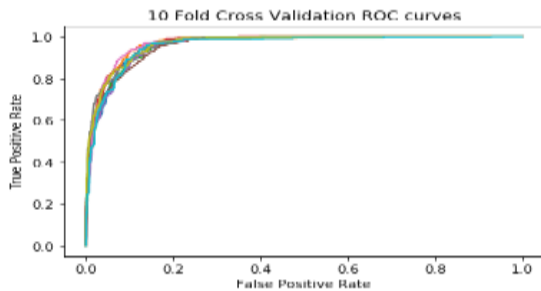
AdaBoost Parameter Tuning

TABLE VIII. ADABOOST WITH ALL PARAMETERS GRIDSEARCHCV RESULTS WITH MAXIMUM AVERAGE ACCURACY 96.76% WITH SPECIFICITY 95.87% AND SENSITIVITY 87.37% USING LEARNING RATE 1 AND NO OF ESTIMATORS 150

Learning rate	Estimators	Specificity	Sensitivity	Accuracy
0.001	20	100	0	0.80266
0.001	30	100	0	0.80266
0.001	50	100	0	0.80266
0.001	100	100	0	0.80266
0.001	150	100	0	0.80266
0.005	20	100	0	0.80266
0.005	30	100	0	0.80266
0.005	50	100	0	0.80266
0.005	100	100	0	0.80266
0.005	150	100	0	0.80266
0.01	20	100	0	0.80266
0.01	30	100	0	0.80266
0.01	50	100	0	0.80266
0.01	100	100	0	0.80266
0.01	150	100	0	0.80266
0.2	20	88.73902	0.05073	0.81094
0.2	30	79.53308	0.12075	0.81996
0.2	50	77.35336	0.19078	0.82914
0.2	100	78.42884	0.24780	0.83791
0.2	150	80.73031	0.29392	0.84660
0.3	20	76.08379	0.12872	0.81996
0.3	30	75.20920	0.18449	0.82682
0.3	50	76.16444	0.23438	0.83419
0.3	100	79.68608	0.31614	0.84883
0.3	150	84.43293	0.40084	0.86704
0.5	20	75.60548	0.19706	0.82873
0.5	30	75.98205	0.24235	0.83493
0.5	50	79.10773	0.30818	0.84726
0.5	100	86.60799	0.46289	0.87970
0.5	150	90.92653	0.58742	0.90692
0.9	20	74.20717	0.30734	0.84147
0.9	30	78.71854	0.36520	0.85454
0.9	50	86.59273	0.49853	0.88574
0.9	100	91.11120	0.70021	0.92727
0.9	150	93.94760	0.81426	0.95284
1	20	75.97621	0.34214	0.84759
1	30	81.68857	0.40545	0.86249
1	50	89.30735	0.53627	0.89566
1	100	91.18001	0.76394	0.93861
1	150	95.87176	0.87379	0.96765

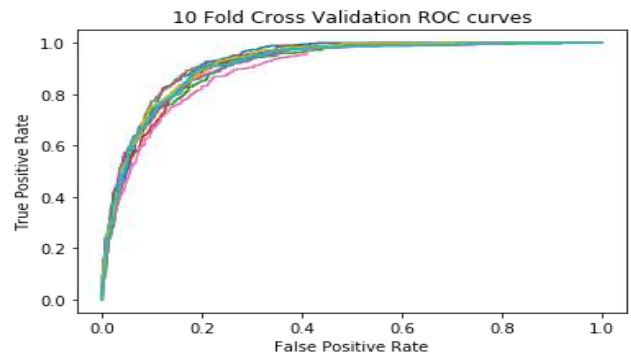
TABLE IX. ADABOOST WITH GRIDSEARCHCV RESULTS WITH 10 FEATURES THE BEST ACCURACY IS 91.6% WITH SPECIFICITY 86.15% AND SENSITIVITY 68.59% USING NO OF ESTIMATORS 150, LEARNING RATE 1

Learning rate	Estimators	Specificity	Sensitivity	Accuracy
0.001	20	100	0	0.80266
0.001	30	100	0	0.80266
0.001	50	100	0	0.80266
0.001	100	100	0	0.80266
0.001	150	100	0	0.80266
0.005	20	100	0	0.80266
0.005	30	100	0	0.80266
0.005	50	100	0	0.80266
0.005	100	100	0	0.80266
0.005	150	100	0	0.80266
0.01	20	100	0	0.80266
0.01	30	100	0	0.80266
0.01	50	100	0	0.80266
0.01	100	100	0	0.80266
0.01	150	100	0	0.80266
0.2	20	87.06042	0.05912	0.81193
0.2	30	76.39592	0.14046	0.82169
0.2	50	74.62386	0.19161	0.82749
0.2	100	75.31635	0.24570	0.83485
0.2	150	77.70321	0.29811	0.84420
0.3	20	75.59483	0.13962	0.82054
0.3	30	73.17302	0.20377	0.82790
0.3	50	75.07925	0.22683	0.83220
0.3	100	77.68116	0.30650	0.84528
0.3	150	79.09073	0.36646	0.85562
0.5	20	73.78344	0.20042	0.82798
0.5	30	75.12703	0.24277	0.83452
0.5	50	76.43679	0.28889	0.84180
0.5	100	80.70590	0.41216	0.86422
0.5	150	83.68746	0.48428	0.87936
0.9	20	74.64103	0.31572	0.84321
0.9	30	78.62295	0.36394	0.85396
0.9	50	80.12446	0.45241	0.86952
0.9	100	85.14953	0.58239	0.89740
0.9	150	85.99633	0.66373	0.91221
1	20	74.37228	0.32788	0.84478
1	30	79.05477	0.38365	0.85793
1	50	80.45211	0.48344	0.87457
1	100	85.07785	0.62558	0.90435
1	150	86.15287	0.68595	0.91618



Receiving Operating Curve Accuracy: 96.16587687161517
 Receiving Operating Curve Accuracy: 96.5823773693516
 Receiving Operating Curve Accuracy: 96.0141773646603
 Receiving Operating Curve Accuracy: 96.67279696025804
 Receiving Operating Curve Accuracy: 95.86224658961727
 Receiving Operating Curve Accuracy: 95.83158385817588
 Receiving Operating Curve Accuracy: 96.7128517189369
 Receiving Operating Curve Accuracy: 96.66772665818672
 Receiving Operating Curve Accuracy: 96.71101941785082
 Receiving Operating Curve Accuracy: 95.79305816277098
 Average Accuracy: 96.30137149714237

Fig. 12. GridsearchCV Results of adaBoost of Table VIII Verified with Hold out Data Results Verification with full Features with Average Accuracy 96.3.



Receiving Operating Curve Accuracy: 92.24488989792022
 Receiving Operating Curve Accuracy: 91.67784243641628
 Receiving Operating Curve Accuracy: 90.8119193588127
 Receiving Operating Curve Accuracy: 91.23084331888616
 Receiving Operating Curve Accuracy: 91.548607052406
 Receiving Operating Curve Accuracy: 92.37635017691973
 Receiving Operating Curve Accuracy: 89.59660719974514
 Receiving Operating Curve Accuracy: 92.29814330924668
 Receiving Operating Curve Accuracy: 92.1426847303852
 Receiving Operating Curve Accuracy: 91.57330098242107
 Average Accuracy: 91.55011884631591

Fig. 13. GridsearchCV Results of Table IX Cross Validated on Hold out Data Average Accuracy 91.55%.

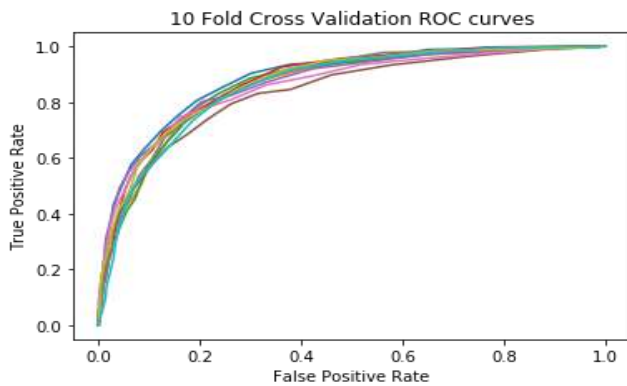
Bagging Classifier Parameter Tuning

TABLE X. BAGGING CLASSIFIER GRIDSEARCHCV RESULTS MAXIMUM ACCURACY 86.86% WITH SPECIFICITY 87.35% AND SENSITIVITY 39.16 USING MAX_SAMPLE FROM BAG 200 AND ESTIMATORS 50 WITH ALL FEATURES

max sam	estimator s	specificity	Sensitivity	accuracy
5	20	61.9225812999993	0.163941299790356	0.777922819236364
5	30	76.6148382202139	0.038993710691824	0.802995223042736
5	50	88.641975308642	0.014255765199162	0.801671267726228
5	100	100	0	0.802664234213609
5	200	100	0	0.802664234213609
10	20	57.3384277875513	0.075471698113208	0.799933507930625
10	30	72.9626890756303	0.049056603773585	0.803988189530117
10	50	84.7058823529412	0.015094339622642	0.803739776801557
10	100	82.1759259259259	0.015513626834382	0.804319144137901
10	200	79.1273054430949	0.035220125786164	0.806636031720447
20	20	54.7680693719426	0.153878406708595	0.804814737266674
20	30	56.1579806137808	0.158909853249476	0.805724751578716
20	50	62.5900805494047	0.121174004192872	0.809365902469857
20	100	61.3947033358798	0.130398322851153	0.810607247464455
20	200	62.4301942004478	0.12746312368973	0.811600453501237
30	20	58.7801119010948	0.20335429769392	0.811764715947454
30	30	64.798210923243	0.183228511530398	0.817226065849393
30	50	68.8224646380291	0.146750524109015	0.817805090972307
30	100	65.4505831704934	0.170649895178197	0.815654211124469
30	200	66.3242335725634	0.161844863731656	0.816647143390507
50	20	64.2439406993273	0.187421383647799	0.819293719391148
50	30	68.5296108891203	0.165199161425577	0.819873839597037
50	50	74.0037009529775	0.167295597484277	0.82376261612585
50	100	71.4577484693443	0.19874213836478	0.825252100078264
50	200	74.6157054563379	0.19832285115304	0.827072470195777
100	20	70.126649647095	0.228092243186583	0.828561577713419
100	30	71.4837866188963	0.238574423480084	0.83063046322352
100	50	75.0823274419283	0.259538784067086	0.836587988377063
100	100	79.7148769872991	0.252830188679245	0.839731184506766
100	200	81.2326043291691	0.258700209643606	0.841800001574182
200	20	85.3025104450034	0.368553459119497	0.862898554593137
200	30	86.8260797310868	0.390775681341719	0.868111286438458
200	50	87.3511737282356	0.391614255765199	0.868608111895578
200	100	87.2558236365198	0.389517819706499	0.868194273195141
200	200	87.8557218134902	0.381551362683438	0.867532158651515

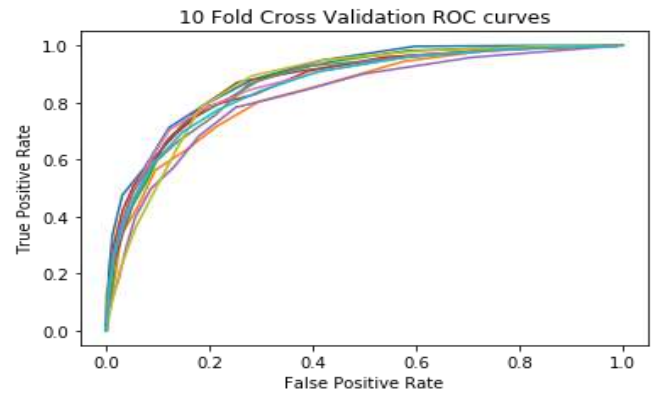
TABLE XI. BAGGING CLASSIFIER GRIDSEARCHCV RESULTS MAXIMUM ACCURACY 86.1% WITH SPECIFICITY 85.90% AND SENSITIVITY 35.72 USING MAX_SAMPLE FROM BAG 200 AND ESTIMATORS 100 WITH FDR FEATURES

max sam	estimators	specificity	Sensitivity	accuracy
5	20	76.9869281045752	0.023480083857442	0.802085790853525
5	30	80.952380952381	0.005031446540881	0.802664405320324
5	50	100	0	0.802664234213609
5	100	100	0	0.802664234213609
5	200	100	0	0.802664234213609
10	20	57.5746807492888	0.108176100628931	0.800346114662716
10	30	52.7995652542967	0.090146750524109	0.802498021150843
10	50	65.9676052770524	0.059538784067086	0.805394447176448
10	100	66.8473163105784	0.092662473794549	0.806221987691952
10	200	68.5488230149631	0.089727463312369	0.808621554039094
20	20	60.6883730203888	0.09601677148847	0.808455101426927
20	30	67.2984063572946	0.09727463312369	0.81019286122253
20	50	75.5615700089384	0.105241090146751	0.813088637042619
20	100	68.6563164386452	0.124947589098533	0.813585325614367
20	200	73.2714047214799	0.116981132075472	0.815074912230811
30	20	67.4581412473286	0.153039832285115	0.815736171240862
30	30	67.1873053086082	0.167295597484277	0.817060674098858
30	50	71.3315605294971	0.148846960167715	0.816729582605702
30	100	70.0808632215366	0.179874213836478	0.81896365453828
30	200	72.0420630600271	0.174842767295598	0.819956826353719
50	20	65.7035032574865	0.183228511530398	0.820700695685681
50	30	71.6890309539053	0.165199161425577	0.823100878016996
50	50	77.848966366415	0.135010482180293	0.821115321477007
50	100	76.7065896952809	0.178197064989518	0.825500512806824
50	200	76.6562019744781	0.184067085953878	0.825417834042228
100	20	73.3607674212325	0.238993710691824	0.832533717433687
100	30	74.5578503120475	0.241090146750524	0.833857604307509
100	50	79.7696255447569	0.212159329140461	0.833608780922833
100	100	80.6639735923208	0.242767295597484	0.838408187387861
100	200	79.3784316065887	0.256603773584906	0.839814376591506
200	20	84.2752589651809	0.341719077568134	0.857438984201032
200	30	83.8258450469914	0.321174004192872	0.853632304673985
200	50	84.6664830924616	0.29643605870021	0.850488081903993
200	100	85.9051302031996	0.357232704402516	0.861492502274864
200	200	84.017160828805	0.358490566037736	0.859755016250004



Receiving Operating Curve Accuracy: 88.6077212947019
 Receiving Operating Curve Accuracy: 86.13601530743381
 Receiving Operating Curve Accuracy: 86.47772069666797
 Receiving Operating Curve Accuracy: 87.59216258055226
 Receiving Operating Curve Accuracy: 86.9632627583638
 Receiving Operating Curve Accuracy: 83.67623048741638
 Receiving Operating Curve Accuracy: 85.90495419479267
 Receiving Operating Curve Accuracy: 86.5789072039072
 Receiving Operating Curve Accuracy: 87.16157031374424
 Receiving Operating Curve Accuracy: 85.93123904332582
 Average accuracy: 86.50297838809061

Fig. 14. Bagging Classifier GridSearchCV Results of Table X Verified using ROC on Holdout Data, Average Accuracy 86.5%.



Receiving Operating Curve Accuracy: 89.2582028251113
 Receiving Operating Curve Accuracy: 83.30865172606707
 Receiving Operating Curve Accuracy: 87.38146156666258
 Receiving Operating Curve Accuracy: 86.89730009557185
 Receiving Operating Curve Accuracy: 82.10881903855447
 Receiving Operating Curve Accuracy: 87.17537108726057
 Receiving Operating Curve Accuracy: 86.77546994821599
 Receiving Operating Curve Accuracy: 86.68428919178224
 Receiving Operating Curve Accuracy: 86.57772635034999
 Receiving Operating Curve Accuracy: 85.90527854724532
 Average accuracy: 86.20725703768213

Fig. 15. Bagging Classifier GridSearchCV Results of Table XI Verified using ROC on Holdout Data, Average Accuracy 86.2%.

First do the prediction for k nearest point, the predict of X point will be 1 if most of k nearest points predict as 1 otherwise -1. The k generally is odd.

1) *KNN classification with full features*: The Gridsearch results of KNN with Full features listed in Table XII maximum accuracy 82.65 % with specificity 60.01% and sensitivity 36.85%, same is verified using hold out data as shown in Fig. 16, with K equals to 5.

2) *KNN Classification with FDR Selected Features*: The accuracy is increased noticeably using FDR, the results are listed in Table XIII showing maximum accuracy 91.5% with specificity 81.54% and sensitivity 74.04% with K equal to 5. The results of Table XIII are verified in Fig. 17 using hold out data using ROC curve.

F. Gaussian Naive Bayes

It is a probability based classifier that works on Bayes theorem that states the outcome of an event can be measured from the past probability of events. It's a non parametric algorithm. As there are no major parameters to vary so GridsearchCV testing is not done for Naive Bays.

1) *Naive bayes classification with full features*: Naive Bayes results average accuracy 71.23614190687361specificity 85.95% sensitivity 32.78%.The results are cross validated with ROC accuracy on hold out data as shown in Table XIV.

2) *Naive Bayes Classification with FDR Selected Features*: FDR helped to improve average accuracy 74.86 specificity 86% sensitivity 37%. The results are cross validated with ROC accuracy on hold out data as shown in Table XV.

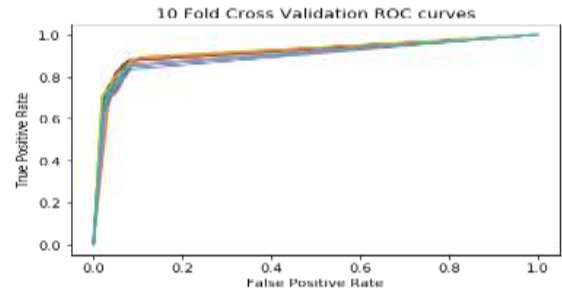
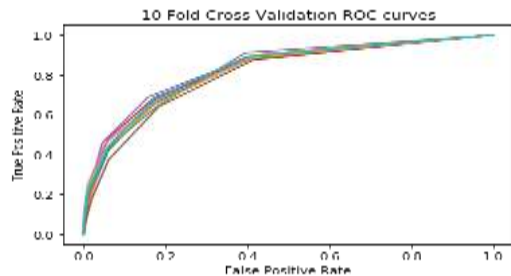
KNN Parameter Tuning

TABLE XII. KNN GRIDSEARCHCV RESULTS WITH ALL FEATURES MAXIMUM ACCURACY 82.65%, SPECIFICITY 60.01% AND SENSITIVITY 36.85%

param_n_neighbors	mean_test_spf	mean_test_recall	mean_test_accuracy
5	60.012901927092	0.368553459119497	0.826576089616115
9	61.358111609077	0.284696016771488	0.822934904503632
21	61.6474825441166	0.148427672955975	0.81317206867676
43	63.6911556294288	0.072536687631027	0.807959610602183
77	66.9705668401321	0.037735849056604	0.805890998862825
89	62.4337623814821	0.025576519916143	0.804401754459811

TABLE XIII. GRIDSEARCHCV RESULTS OF KNN USING FDR SELECTED FEATURES SHOWS GREAT ACCURACY OVER FULL FEATURES, ACHIEVED ACCURACY OF 91.56% WITH SPECIFICITY 81.54% AND SENSITIVITY 74.04%

param_n_neighbors	mean_test_spf	mean_test_recall	mean_test_accuracy
5	81.5485312602163	0.740461215932914	0.915604590177174
9	82.1180030569542	0.706918238993711	0.911715437213589
21	82.7013558282025	0.614675052410902	0.898477013352826
43	83.3771383841857	0.472117400419287	0.877047950603545
77	83.644701871265	0.293920335429769	0.849247010680139
89	85.1447572468791	0.254088050314465	0.843951326299478



Receiving Operating Curve Accuracy: 82.15695827072376
 Receiving Operating Curve Accuracy: 81.93653392513502
 Receiving Operating Curve Accuracy: 82.06034314209442
 Receiving Operating Curve Accuracy: 82.36647671448222
 Receiving Operating Curve Accuracy: 83.22803372846145
 Receiving Operating Curve Accuracy: 80.14621887137308
 Receiving Operating Curve Accuracy: 82.74669279949138
 Receiving Operating Curve Accuracy: 82.62315515141213
 Receiving Operating Curve Accuracy: 81.78181660072175
 Receiving Operating Curve Accuracy: 82.76304217006896
 Average Accuracy: 82.18092713739642

Receiving Operating Curve Accuracy: 91.94355482489823
 Receiving Operating Curve Accuracy: 91.51060955102596
 Receiving Operating Curve Accuracy: 91.51995101107273
 Receiving Operating Curve Accuracy: 91.61473850079078
 Receiving Operating Curve Accuracy: 89.30411280393969
 Receiving Operating Curve Accuracy: 91.84231716559303
 Receiving Operating Curve Accuracy: 90.42768397578847
 Receiving Operating Curve Accuracy: 90.06755508898804
 Receiving Operating Curve Accuracy: 92.16000862063807
 Receiving Operating Curve Accuracy: 90.09826182197293
 Average Accuracy: 91.04887933647078

Fig. 16. Table XII Results Cross Validated on Hold out Data using ROC Curves Average Accuracy 82.18%.

Fig. 17. Table XIII Results are Cross Validated on Hold out Data using ROC Curve Accuracy with Average Accuracy 91.04%.

Naïve Bayes Parameter Tuning

TABLE XIV. NAIVE BAYES RESULTS WITH FDR FEATURES

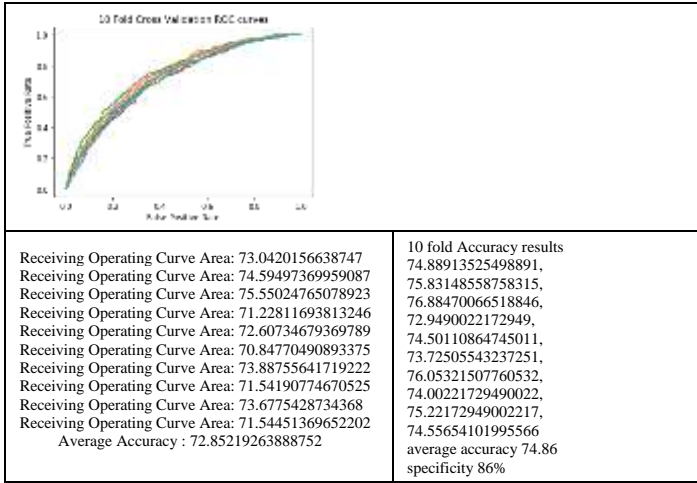
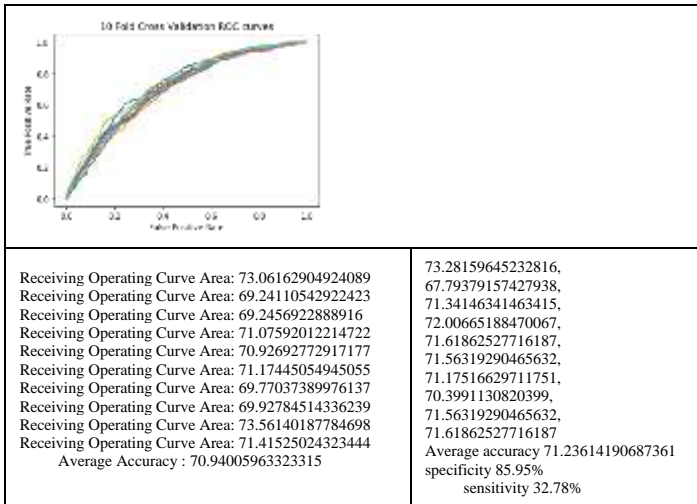


TABLE XV. NAIVE BAYES RESULTS WITH ALL FEATURES



VI. RESULTS AND MODEL EVALUATION

The Model is evaluated on the basis of Accuracy, Specificity and Sensitivity and accuracy from Receiving Operating Curve. It's a screening test so more priority is to optimize the Specificity than sensitivity. The formulations of these metrics are: The confusion matrix is defined as

$$\begin{bmatrix} \text{True Positive} & \text{False Positive} \\ \text{False Negatives} & \text{True Negatives} \end{bmatrix}$$

$$\text{Accuracy} = \frac{\text{True Positive} + \text{True Negatives}}{\text{True Positives} + \text{False Positive} + \text{False Negatives} + \text{True Negatives}}$$

$$\text{Specificity} = \frac{\text{True Positives}}{\text{True Positives} + \text{False Negatives}}$$

$$\text{Sensitivity} = \frac{\text{True Negatives}}{\text{True Negatives} + \text{False Positives}}$$

We tried to optimize the accuracy sensitivity and specificity using GridsearchCV method which applied 10 fold Stratified method for a given classifier with a given set of

input parameters. The evaluation results using different classifiers with GridsearchCV method are listed in following tables. The experiments are done twice using feature selection with Fisher Discriminate Ratio method.

VII. RESULT COMPARISONS CHARTS

The results of different classification models are compared in Fig. 18, 19 and 20.

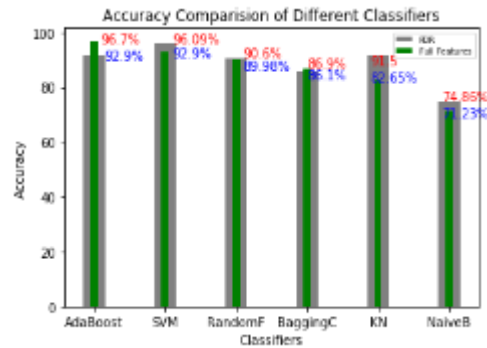
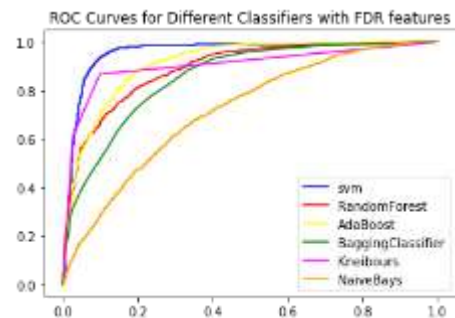
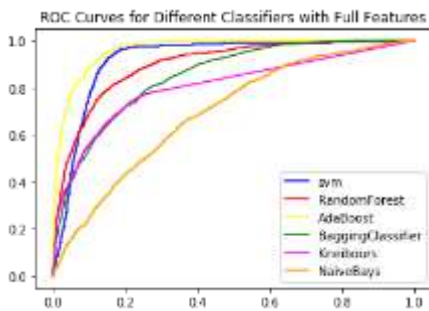


Fig. 18. Accuracy Comparison of different Classifiers with FDR as well as Full Features.



SVM ROC Accuracy 95.88491108807841 Random Forest ROC Accuracy 89.03526077312283 AdaBoost ROC Accuracy 91.3290828085577 Bagging ROC Accuracy 85.61042208468754 KNN ROC Accuracy 90.32602391010393 Naive Bayes ROC Accuracy 71.80806968262688
--

Fig. 19. ROC Accuracy Comparison of different Classifiers with FDR Features.



SVM ROC Accuracy 92.1662431476976 RandomForest ROC Accuracy 89.92557071323482 AdaBoost ROC Accuracy 96.39966479308009 Bagging ROC Accuracy 84.95671446702912 KNN ROC Accuracy 80.56178731319386 Naive Bayes ROC Accuracy 69.52003889699243

Fig. 20. ROC Accuracy Comparison of different Classifiers with Full Features.

VIII. CONCLUSION

The objective was to design a Decision support system for the Radiologist which help them for fast and correct predictions for the early detection of brain atrophy which can result into Alzheimer in future, we are able to deduce a system where radiologist can input the middle 25 slices from slice_no 110 to 140 of MRI to the system as input and on the basis of data in these slices the system can results the prediction about atrophy of brain. The accuracy of results can be achieved the best with AdaBoost classifier 96.7% and specificity and sensitivity. This study has achieved a better accuracy than the earlier research works because correct registration method and better classifiers that is AdaBoost. It will definitely going to support the radiologist for better decision of brain atrophy. This is a screening test so it's more important to have more specificity than sensitivity. This is an academic research with a purpose to explore machine learning classifiers and their parametric studies. The study also gives a hands out experiences for Image processing, how biomedical texture analysis helpful to extract image signatures which can be used for classification. It's a comparative study on the basis of different classifiers and further how classifiers results can be improved using feature selection criteria, but it also give an insight how some of classifiers are strong classifiers where feature selection criteria does not affect much its performance.

IX. FUTURE WORK

The Support system lacks the front end, in the future work we can design an automated system which automatically extract middle slices with proper frontend system where radiologist can feed the DICOM image slices and the system should give a report about the slices. Many other texture features can be explored to improve the performance. Many other feature extraction methods as well as classification techniques can be explored for better results. The study consumed much time in preprocessing of data, a fast and error data preprocessing steps can be explored in future work.

ACKNOWLEDGMENT

As the study is a practical study under the domain knowledge of Dr Ritesh Garg, Sr. Radiologist, who is owning MRI Diagnostic Center. The results had been verified under the supervision of radiologist. Our sincere thanks and gratitude to Dr Ritesh Garg for his unconditional support while analysing the data as without his help at every point of analysis, this study would have not completed.

REFERENCES

- [1] Braak and E. Braak, "Neuropathological staging of Alzheimer-related changes," *Acta Neuropathol.*, vol. 82, no. 4, pp. 239–259, Sep. 1991, doi: 10.1007/BF00308809.
- [2] G. B. Karas *et al.*, "A comprehensive study of gray matter loss in patients with Alzheimer's disease using optimized voxel-based morphometry," *Neuroimage*, vol. 18, no. 4, pp. 895–907, 2003, doi: 10.1016/S1053-8119(03)00041-7.
- [3] Z. Lao, D. Shen, Z. Xue, B. Karacali, S. M. Resnick, and C. Davatzikos, "Morphological classification of brains via high-dimensional shape transformations and machine learning methods," *Neuroimage*, vol. 21, no. 1, pp. 46–57, 2004, doi: 10.1016/j.neuroimage.2003.09.027.
- [4] K. Specht, M. Minnerop, J. Müller-Hübenthal, and T. Klockgether, "Voxel-based analysis of multiple-system atrophy of cerebellar type: Complementary results by combining voxel-based morphometry and voxel-based relaxometry," *Neuroimage*, vol. 25, no. 1, pp. 287–293, 2005, doi: 10.1016/j.neuroimage.2004.11.022.
- [5] W. Wen, P. S. Sachdev, X. Chen, and K. Anstey, "Gray matter reduction is correlated with white matter hyperintensity volume: A voxel-based morphometric study in a large epidemiological sample," *Neuroimage*, vol. 29, no. 4, pp. 1031–1039, 2006, doi: 10.1016/j.neuroimage.2005.08.057.
- [6] S. J. Teipel *et al.*, "Multivariate deformation-based analysis of brain atrophy to predict Alzheimer's disease in mild cognitive impairment," *Neuroimage*, vol. 38, no. 1, pp. 13–24, 2007, doi: 10.1016/j.neuroimage.2007.07.008.
- [7] V. A. Cardenas, C. Studholme, S. Gazdzinski, T. C. Durazzo, and D. J. Meyerhoff, "Deformation-based morphometry of brain changes in alcohol dependence and abstinence," *Neuroimage*, vol. 34, no. 3, pp. 879–887, 2007, doi: 10.1016/j.neuroimage.2006.10.015.
- [8] S. J. Teipel, T. Meindl, L. Grinberg, H. Heinsen, and H. Hampel, "Novel MRI techniques in the assessment of dementia," *Eur. J. Nucl. Med. Mol. Imaging*, vol. 35, no. SUPPL. 1, pp. 58–69, 2008, doi: 10.1007/s00259-007-0703-z.
- [9] V. A. Cardenas *et al.*, "Deformation-based morphometry reveals brain atrophy in frontotemporal dementia," *Arch. Neurol.*, vol. 64, no. 6, pp. 873–877, 2007, doi: 10.1001/archneur.64.6.873.
- [10] R. Stahl, O. Dietrich, S. J. Teipel, H. Hampel, M. F. Reiser, and S. O. Schoenberg, "White matter damage in Alzheimer disease and mild cognitive impairment: Assessment with diffusion-tensor MR imaging and parallel imaging techniques," *Radiology*, vol. 243, no. 2, pp. 483–492, 2007, doi: 10.1148/radiol.2432051714.
- [11] D. Sydykova *et al.*, "Fiber connections between the cerebral cortex and the corpus callosum in Alzheimer's disease: A diffusion tensor imaging and voxel-based morphometry study," *Cereb. Cortex*, vol. 17, no. 10, pp. 2276–2282, 2007, doi: 10.1093/cercor/bhl136.
- [12] P. M. THOMPSON *et al.*, "Tracking Alzheimer's Disease," *Ann. N. Y. Acad. Sci.*, vol. 1097, no. 1, pp. 183–214, Feb. 2007, doi: 10.1196/annals.1379.017.
- [13] X. Hua *et al.*, "Tensor-based morphometry as a neuroimaging biomarker for Alzheimer's disease: An MRI study of 676 AD, MCI, and normal subjects," *Neuroimage*, vol. 43, no. 3, pp. 458–469, 2008, doi: 10.1016/j.neuroimage.2008.07.013.
- [14] C. Plant *et al.*, "Automated detection of brain atrophy patterns based on MRI for the prediction of Alzheimer's disease," *Neuroimage*, vol. 50, no. 1, pp. 162–174, 2010, doi: 10.1016/j.neuroimage.2009.11.046.
- [15] R. Casanova *et al.*, "Using high-dimensional machine learning methods to estimate an anatomical risk factor for Alzheimer's disease across imaging databases," *Neuroimage*, vol. 183, pp. 401–411, 2018, doi: 10.1016/j.neuroimage.2018.08.040.
- [16] R. Casanova, F. C. Hsu, and M. A. Espeland, "Classification of Structural MRI Images in Alzheimer's Disease from the Perspective of Ill-Posed Problems," *PLoS One*, vol. 7, no. 10, 2012, doi: 10.1371/journal.pone.0044877.
- [17] S. Adaszewski, J. Dukart, F. Kherif, R. Frackowiak, and B. Draganski, "How early can we predict Alzheimer's disease using computational anatomy?," *Neurobiol. Aging*, vol. 34, no. 12, pp. 2815–2826, 2013, doi: 10.1016/j.neurobiolaging.2013.06.015.
- [18] O. Ben Ahmed, J. Benois-Pineau, M. Allard, C. Ben Amar, and G. Catheline, "Classification of Alzheimer's disease subjects from MRI using hippocampal visual features," *Multimed. Tools Appl.*, vol. 74, no. 4, pp. 1249–1266, 2014, doi: 10.1007/s11042-014-2123-y.
- [19] A. E.R., S. Varma, and V. Paul, "Classification of Brain MR Images using Texture Feature Extraction," *Int. J. Comput. Sci. Eng. Commun.*, vol. 5, no. 5, pp. 1722–1729, 2017.
- [20] T. Altaf, S. M. Anwar, N. Gul, M. N. Majeed, and M. Majid, "Multi-class Alzheimer's disease classification using image and clinical features," *Biomed. Signal Process. Control*, vol. 43, pp. 64–74, 2018, doi: 10.1016/j.bspc.2018.02.019.
- [21] L. Nanni, S. Brahnay, C. Salvatore, and I. Castiglioni, "Texture descriptors and voxels for the early diagnosis of Alzheimer's disease," *Artif. Intell. Med.*, vol. 97, no. May, pp. 19–26, 2019, doi: 10.1016/j.artmed.2019.05.003.

- [22] S. Lee, H. Lee, and K. W. Kim, "Magnetic resonance imaging texture predicts progression to dementia due to Alzheimer disease earlier than hippocampal volume," *J. Psychiatry Neurosci.*, vol. 45, no. 1, pp. 7–14, 2020, doi: 10.1503/jpn.180171.
- [23] J. H. Cai *et al.*, "Magnetic Resonance Texture Analysis in Alzheimer's disease," *Acad. Radiol.*, 2020, doi: 10.1016/j.acra.2020.01.006.
- [24] V. P. S. Rallabandi, K. Tulpule, and M. Gattu, "Automatic classification of cognitively normal, mild cognitive impairment and Alzheimer's disease using structural MRI analysis," *Informatics Med. Unlocked*, vol. 18, 2020, doi: 10.1016/j.imu.2020.100305.
- [25] Z. Yaniv, B. C. Lowekamp, H. J. Johnson, and R. Beare, "SimpleITK Image-Analysis Notebooks: a Collaborative Environment for Education and Reproducible Research," *J. Digit. Imaging*, vol. 31, no. 3, pp. 290–303, 2018, doi: 10.1007/s10278-017-0037-8.
- [26] B. Fischl, "FreeSurfer Authos Manuscript," *Neuroimage*, vol. 62, no. 2, pp. 774–781, 2012, doi: 10.1016/j.neuroimage.2012.01.021.FreeSurfer.

Full Direction Local Neighbors Pattern (FDLNP)

A Novel Method for Multimedia Image Retrieval System using Ensemble Classifiers on Distributed Framework

Maher Alrahhah¹

Ph.D. Scholar in Computer Science and Engineering Dept.
JNTUH College of Engineering, Hyderabad
Hyderabad, India

Supreethi K.P²

Professor in Computer Science and Engineering Dept.
JNTUH College of Engineering, Hyderabad
Hyderabad, India

Abstract—In this paper, we proposed the Full Direction Local Neighbor Pattern (FDLNP) algorithm, which is a novel method for Content-Based Image Retrieval. FDLNP consists of many steps, starting from generating Max and Min Quantizers followed by building two matrix types (the Eight Neighbors Euclidean Decimal Coding matrix, and Full Direction Matrixes). After that, we extracted Gray-Level Co-occurrence Matrix (GLCM) from those matrixes to derive the important features from each GLCM matrixes and finishing with merging the output of previous steps with Local Neighbor Patterns (LNP) histogram. For decreasing the feature vector length, we proposed five extension methods from FDLNP by choosing the specific direction matrixes. Our results demonstrate the effectiveness of our proposed algorithm on color and texture databases, comparing with recent works, with regard to the Precision, Recall, mean Average Precision (mAP), and Average Retrieval Rate (ARR). For enhancing the image retrieval accuracy, we proposed a novel framework that combined the image retrieval system with clustering and classification algorithms. Moreover, we proposed a distributed model that used our FDLNP method with Hadoop to get the ability to process a huge number of images in a reasonable time.

Keywords—Content-Based image retrieval; full direction local neighbor patterns; local neighbor pattern; gray-level co-occurrence matrix; ensemble classifiers; k-means clustering; hadoop

I. INTRODUCTION

In the latest decade, the number of digital photos and videos accessible has increased dramatically. Although software and hardware are available to digitize, archive, and compress multimedia data, there are no clear ways to retrieve the kept info. In traditional Text-Based Image Retrieval (TBIR), metadata that describes the image contents are manually added to image files. This metadata is used to retrieve similar images by word matching. TBIR has two major difficulties: (a) labeling the images manually, therefore, a significant volume of time is required, and (b) human sensitivity for images is not precise and unique. Content-based image retrieval (CBIR) [1-5] is an alternative to traditional TBIR that overcomes the above limitations because images are retrieved based on their content such as color, texture, shapes, and contour.

CBIR is a very vital area, specifically in the latest era due to the increasing essentials to retrieve images from a multimedia datasets. It intersects with many areas such as

image segmentation, machine learning for classification and clustering, big data for processing huge databases, and deep learning for extract semantic features. For that, CBIR has several applications in different areas. For example, CBIR systems are utilized in satellite imagery to discover ground natural resources, aerial surveys, monitor agriculture, and create climate reports and path surface objects. Medical imaging is a prominent area of CBIR application, which utilizes to monitor patient health reports, to assist in diagnosis by detecting related previous studies [6], etc. Fingerprint matching images that lead to a distinct verification is another domain that can use in the banking area, universities, business companies, and scientific laboratories [7-9].

A. Problem Statement

Image search engines are very important tools for searching similar images from huge databases, which depend on the CBIR field to automatically retrieve the best matching images by extracting the information from the query image. However, many studies in the CBIR focus on the low feature extraction from the images. Therefore, there is still a semantic gap between the low-features extracted using those algorithms and how the human can understand the images. This is the first problem of the CBIR domain, whereas the second main problem is retrieving similar images from a huge database in a reasonable time.

B. Contribution of our Work

To address the above problems, we proposed a new framework that combined image processing, machine learning, and big data, as the following:

First, we reduced the semantic gap between the low-level and high-level feature extraction by proposing a novel and efficient method for feature extraction, namely Full-Directions Local Neighbors Pattern that focused on the color changes of minimum and maximum image blocks, fused with the texture features that extract the relationships of the center pixel with its neighbors.

Second, to get the ability to process a huge number of images, we reduced the size of FDLNP's feature vector by proposing extended versions of our proposed method.

Third, we studied the importance of using the machine learning algorithms to enhance the effectiveness of the system,

by using our proposed FDLNP for training the classifier and retrieving the top k images from the classifier's output class.

Forth, we applied our proposed method in the Map Reduce framework to get the ability to process a large image database.

II. RELATED WORK

Low-level features are very popular in image representation and pattern recognition technologies that also proved powerful in image classification and retrieval [10-13]. Many methods discussed the using of the color feature in CBIR, some of them are color histogram, color moments [14], color correlogram [15], and color co-occurrence matrix [16].

Xiaoyin [14] proposed a new technique for improving color features extracted from the image that is color moment invariant. The color feature was extracted for each color component (red, green, and blue) to make an accurate features vector of the image. Color co-occurrence matrix (CCM) [17] is another approach that is interested in the spatial relationship between color channels. Where the image can be considered as an appropriate composition for "elementary structures". The elements of these pixels have visible properties of colors and relationships between the colors.

Jhanwar et al. [18] have employed another approach in the CBIR domain, known as motif co-occurrence matrix (MCM), which is conceptually near to the CCM. Where the image is subdivided into blocks, and each block replaced by a scan motif. Guoping [19] has proposed block truncation coding (BTC) which is a type of image compression method. The authors used the features extracted using BTC for retrieving the images. The main idea of BTC is to build two types of features used to retrieve both texture and color images. Those features are block color co-occurrence matrix and block pattern histogram. Many researchers used this idea to propose another BCT variants [20, 21]. The dominant color descriptor (DCD) [22] has proposed as one application of MPEG-7 to use it for extracting color features from the image with important merits that are small feature vector size with good performance.

The texture is another important feature in the CBIR domain that is interested in extracting the spatial arrangement from an image. Many researchers worked on the texture features for enhancing the image retrieval area, some of them are: Gabor filters, Wavelet transforms, gray-level co-occurrence matrix (GLCM) [23], Markov random field (MRF) [24], edge histogram descriptor (EHD) [25], steerable pyramid decomposition (SPD) [26], and Tamura features [27].

Some researchers have turned to merge feature types to make a robust descriptor of the image as Xingyuan and Zongyu [28] whose combined color and texture features in their proposed method namely a structure element descriptor (SED). Liu et al. [29] proposed a micro-structure descriptor (MSD) that extracts edge orientation and fused with color features to represent the image, whereas Chatzichristofis et al. [30] represented the image by fuse the fuzzy color and texture histograms. His method generally is suitable for dealing with large databases due to the small size of image representation. Lai et al. [31] proposed a framework that combined the features extracted from the image and genetic algorithm for

getting the robust features that rely on the fusion of both color and texture features.

Shape feature is another important descriptor of the images that is used in many fields like image segmentation, object detection, and image retrieval. Many researchers have a focus on extracting the shape descriptors that characterize rotation, translation, and scaling invariant. Some proposed methods proved an accurate shape descriptor such as shape context SIFT, HOG, and SURF descriptors [32-35]. The SIFT and SURF descriptors rely on extracting interest points from the image and extract the features from those points. And because of the large size of those descriptors, many researchers proposed methods for reducing the size of those features by using a bag of visual word techniques that used in many vision applications [36-39].

In recent years, deep learning domain has been proved a very efficient way to use in vision tasks like object detection, image recognition, image segmentation, and image analysis [40-47]. Convolutional neural networks (CNNs) had used in image retrieval to extract semantic features by training the network and using it to extract features that consider somehow high-level features in image retrieval [40, 43-45].

III. METHODOLOGY

The general architecture of CBIR system consists of several steps as shown in Fig.1:

Query Request: the user inputs an image as a query image.
Feature Extraction: extracts the features from the query image using our proposed method FDLNP.

Similarity Measures: measure the similarity between the feature vector of the query image and all feature vectors in the feature database; which made in the offline phase of the CBIR system by repeating the feature extraction step for all the image in the database, using this equation (1) [48]:

$$D_L(Q, DB) = \sum_{i=1}^L \left| \frac{f_{DB_{ji}} - f_{Q_i}}{1 + f_{DB_{ji}} + f_{Q_i}} \right| \quad (1)$$

Where $f_{DB_{ji}}$ is the i^{th} feature of the j^{th} image in the database, and f_{Q_i} is the feature vector of the query image.

Sorting and Retrieving: Sort the distance in a rising way and retrieve the top k images as the output of the system.

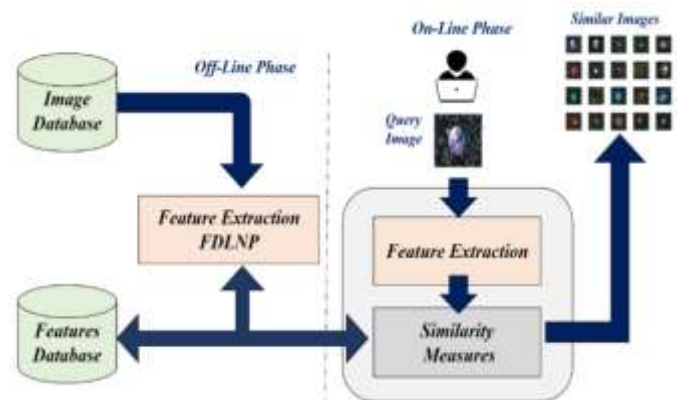


Fig. 1. The Architecture of CBIR System.

The feature extraction step considers the most important step in the whole system because the accuracy and effectiveness of the CBIR system depend mainly in this step. A novel and efficient visual feature descriptor, namely, Full Direction Local Neighbor Pattern is proposed for image representation and retrieval as shown in Fig.2, which consists of the following main steps:

Step 1: Min and Max Quantizers: Suppose a color image of size $M \times N$ is partitioned into multiple non-overlapping image blocks of size $m \times n$. Let $f(x, y) = \{f_R(x, y), f_G(x, y), f_B(x, y)\}$ be an image block, where $x = 1, 2 \dots m$ and $y = 1, 2 \dots n$. The minimum and maximum value of the image block for each RGB color space are computed as equation (2), (3):

$$q_{min}(x, y) = \{\min_{v,x,y} f_R(x, y), \min_{v,x,y} f_G(x, y), \min_{v,x,y} f_B(x, y)\} \quad (2)$$

$$q_{max}(x, y) = \{\max_{v,x,y} f_R(x, y), \max_{v,x,y} f_G(x, y), \max_{v,x,y} f_B(x, y)\} \quad (3)$$

Step 2: Right Neighbor Euclidean Coding (RNEC): For each pixel in min and max quantizers, we calculated the RNEC matrix using the right neighbors (RN_1, RN_2, RN_3) of the center pixel (cp) as shown in Fig.3, using this equation (4):

$$RNEC(cp) = \sqrt{(RN_1 - cp)^2 + (RN_2 - cp)^2 + (RN_3 - cp)^2} \quad (4)$$

Step 3: Eight Neighbors Euclidean Decimal Coding: Calculated Eight Neighbors Euclidean Decimal Coding (ENEDC) matrix using the equations (5), (6):

$$ENEDC = \sum_{p=1}^8 2^{(p-1)} \times f_1(g_p - g_c) \quad (5)$$

$$f_1(x) = \begin{cases} 1 & x \geq 0 \\ 0 & otherwise \end{cases} \quad (6)$$

Where g_c is the RNEC value of the center pixel, g_p is the RNEC value of its neighbors, and p is the number of neighbors.

Step 4: Directions Matrix: Calculated the direction of each pixel and stored it in dir_Matrix , by using the right neighbor pattern as illustrated in Fig.1. The direction of the center pixel defined as the direction from the smallest element in the pattern to the largest element in the pattern. In the case of the existing more than one minimum (maximum) element, we take the first minimum (maximum) element as the smallest (largest) value. Moreover, if the pattern has the same value, then we consider the direction of the pattern is "one". We have eight directions derived from right neighbor pattern as shown in Fig.4.

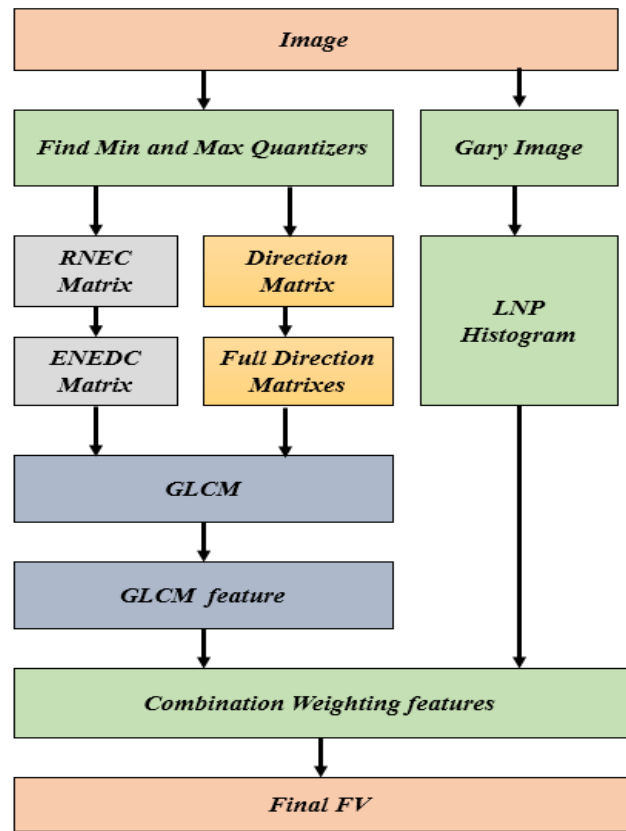


Fig. 2. Flow Chart of our Proposed Feature Extraction Method (FDLNP).

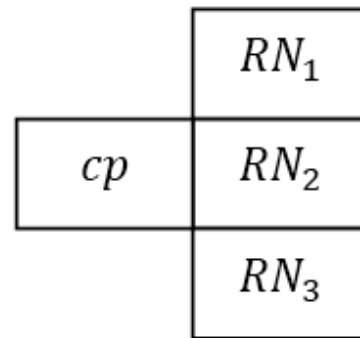


Fig. 3. Right Neighbor Pattern.

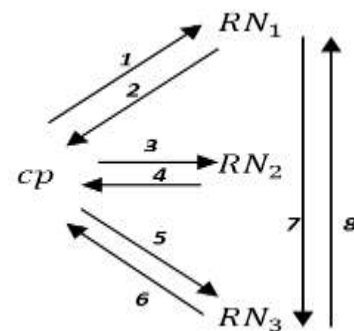


Fig. 4. Eight Directions in Neighbor Pattern.

Step 5: Full Directions Matrixes

From *dir_matrix*, derive *Full Directions Matrixes*, which is a set of 64 matrixes corresponding to the pair (*dir_value*, *Nbr_value*) where:

dir_value is the direction value of the center pixel of 3 × 3, and its value ranges from one to eight.

Nbr_value is the direction value of the 3 × 3 neighbors around *dir_value*, and their values range from 1 to 8.

To illustrate the calculation of the *Full Directions Matrixes*, we use this example like the following:

Suppose we want to derive the matrix corresponding to *dir_value* = 5, and *Nbr_value* = 2.

First, we found each pixel in *dir_value* = 5. Second, look at *Nbr_value* = 2 in the eight neighbors around the center pixel, and if it is found, replace its location by one, otherwise zero. Third, replaced the center pixel by the decimal value of the eight neighbors starting from the top-left pixel, using these equations (7), (8):

$$decimal_Value = \sum_{p=1}^8 2^{p-1} f_{dir_value}(i) \tag{7}$$

$$f_{dir_value}(i) = \begin{cases} 1 & ; i = Nbr_value \\ 0 & \text{Otherwise} \end{cases} \tag{8}$$

Where the value of *f_{dir_value}* determines if the value of the neighbor pixels equals *Nbr_value* or not.

At the end of the fifth step, we have 65 matrixes (1 for *ENEDC*, and 64 matrixes for Full Directions Matrixes) for each Min quantizer and Max quantizer. Fig.5 is an illustrating example of *step 2 to step 5* in our proposed method.

Step 6: Gray-Level Co-occurrence Matrix (GLCM): This step is for deriving the GLCM matrix for each of the 65 matrixes, where we calculated the GLCM [49] matrix with distance *d* = 1, and direction $\theta = 0^\circ$. From each GLCM matrix, we extracted 10 feature values [49] as follows: Contrast, Cluster prominence, Entropy, Sum of Square Variance, Sum Average, Sum Entropy, Difference Variance, Difference Entropy, Information Measure of Correlation, and Inverse Difference Moment Normalized. Finally, we combined those values to get the first feature vector *FV₁* whose size is 1300.

Step 7: Local Neighbor Pattern (LNP): This step starts with converting the query image to a grayscale image and then finds the Local Neighbor Pattern (LNP) histogram [48] to get the second feature vector *FV₂*, whose size is 256. Fig.6 illustrates the mechanism of building the LNP matrix.

Step 8: Fusion Features: For getting the final feature vector of our proposed method, we fused *FV₁* with *FV₂* using the equation (9) as follows:

$$FV = \alpha \times FV_1 + \beta \times FV_2 \tag{9}$$

Knowing that, we used $\alpha = 1$, and $\beta = 0.1$, and the size of the final feature vector is $1300 + 256 = 1556$, where “+” represents the concatenating operator.

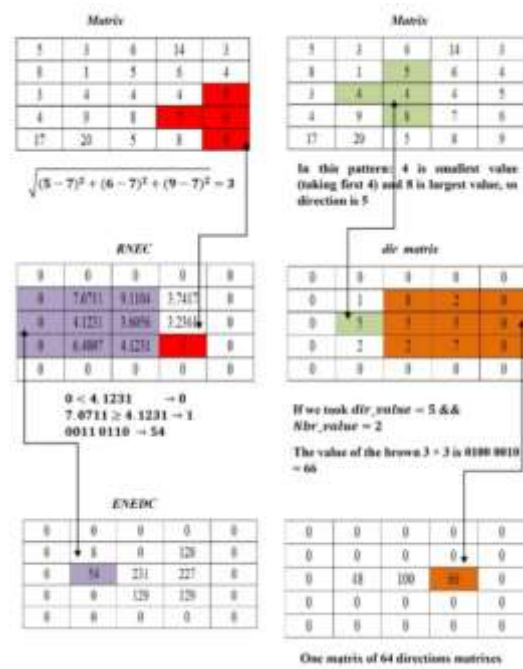


Fig. 5. Example of Calculating RNEC, ENEDC, Direction Matrix, and One Matrix of 64 Directions Matrixes.

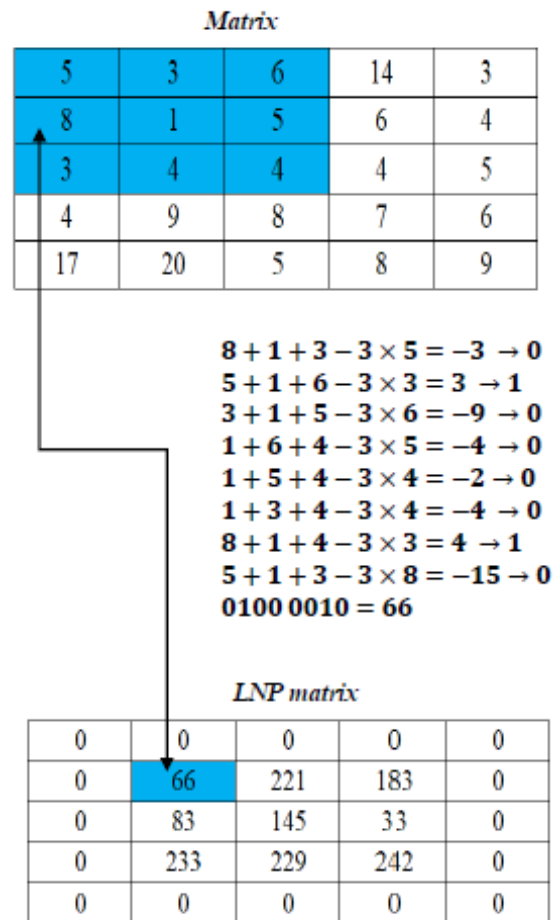


Fig. 6. Example of Calculating Local Neighbors Pattern Matrix.

IV. PERFORMANCE MEASUREMENT

Precision and Recall [50] consider the main performance measures in the image retrieval system, which defined as equations (10-12):

$$P(I_q, n) = \frac{1}{n} \sum_{i=1}^{|DB|} \varphi(\gamma(I_i), \gamma(I_q)) ; Rank(I_i, I_q) \leq n \quad (10)$$

$$\varphi(x, y) = \begin{cases} 1 & ; x = y \\ 0 & \text{else} \end{cases} \quad (11)$$

Where n is the number of retrieved images, $|DB|$ is the size of the database, $\gamma(x)$ is the class of the image x , and $Rank(I_i, I_q)$ returns the rank of the image I_i for the query image I_q among all images in the database.

$$R(I_q, n) = \frac{1}{N_c} \sum_{i=1}^{|DB|} \varphi(\gamma(I_i), \gamma(I_q)) ; Rank(I_i, I_q) \leq n \quad (12)$$

Where N_c indicated the max number of images in the database's class.

Average Retrieval rate (ARR) and the mean Average Precision (mAP) are another performance measures [50], which mathematically reflects the efficiency of CBIR. ARR and mAP defined as equations (13), (14):

$$mAP = \frac{1}{|DB|} \sum_{i=1}^{|DB|} P(I_i, n) \quad (13)$$

$$ARR = \frac{1}{|DB|} \sum_{i=1}^{|DB|} R(I_i, n) ; n \geq N_c \quad (14)$$

A higher value of the previous measures reflects a better efficient retrieving system.

V. EXPERIMENTAL RESULTS AND DISCUSSIONS

A. First Experiment: Image Retrieval using FDLNP

We used two types of databases for evaluating our proposed method that are color databases (Corel 1k and Corel 10k) and Texture databases (Brodatz and Vistex).

Corel 1k database [51] considers as standard database for color image retrieval that contains ten different categories, and each category consists of hundred color images. Some of those categories are African, Beach, etc.

Corel 10 k database [52] used for evaluating the methods that are interested in color features extraction. Corel 10k consists of hundred categories, and each category contains a hundred images. Therefore, it is one of the important large retrieval databases. The images in the same category contain similar semantic information. Some of the categories included in Corel 10 k are flowers, birds, beaches, buildings, etc.

Brodatz texture database [53, 54] used mainly for evaluating the methods of texture image retrieval. Brodatz database consists of 116 grayscale images, 109 images gathered Scale images from the USC database. The dimension of every image is 512×512 , which separated into 16 non-overlapping images of size 128×128 . Thus, the total number of images in this database are 1856.

Vistex database [55] contains 40 images. The dimension of every image is 512×512 , which separated into 16 non-overlapping images of size 128×128 . Thus, the total number of images in this database are 640. Vistex database used for evaluating the methods of color texture retrieval.

For color databases, we are interested in Precision (top 10 images), Recall (top k; where k is the maximum number of images in the database's class, i.e. k=100), and mAP (mean Average Precision). The mAP measure calculated as follows, for each image in the database, we consider top 10, top 20... top 100, then take the average, and repeats this procedure for all images in the database.

For texture databases, we are interested in Precision (top 10 images), Recall (top k; k=16), mAP (mean Average Precision) by taking the average of top 4, top 8, top 10, top 12, and top 16 for all images in the database, and Average retrieval rate (ARR). The ARR calculated by taking the average of top 16, top 32, top 48, top 64, top 80, top 96, and top 112 for all images in the database.

We compared our proposed method with the following methods:

1) Methods that used specifically for texture image retrieval like LDP [56], LTrP [50], LOtP [57], LHDP [57], and LNP [48]. Those methods work on the pixels' values directly and encrypt the relationship between the center pixel and its neighbors.

2) Histogram of oriented gradient method [34], which is interested in the shape of the object, by calculating the gradient orientation for each block in the images, and used mainly in object recognition.

3) Bag of Visual Words method [36], which relies on detecting the interest points and extracts the features from these points.

4) EDBTC [58] and MIFM [59] methods, which depend on extracting both texture and color features. Our proposed method gave better performance than previous methods regarding Precision, Recall, mAP, and ARR for all databases, because it works on extracting the color changes of minimum and maximum intensities of images blocks, in addition to the texture features of the images.

We used Desktop with Intel Core i7 CPU, 8 GB RAM, and Matlab R2020a program to produce those results. The results of the method compared to other methods for both color and texture databases illustrated in table I.

Fig.7 illustrates examples of retrieving similar images using our proposed method, for all the databases, where the top left images are the query images. In the color databases (Corel 1k and Corel 10k), we consider top 20 images as the output, whereas top 16 images as output for texture databases (Brodatz and Vistex). We observe that the precision of those examples are 100%.

TABLE I. COMPARISONS BETWEEN OUR PROPOSED METHOD WITH OTHER METHODS REGARDING PRECISION, RECALL, MAP, AND ARR FOR ALL DATABASES.

Corel 1k	Methods									
Performance Measure	LDP	LTrP	LOtP	LHdP	LNP	HOG	BOW	EDBTC	MIFM	FDLNP
Precision	55.10	57.20	60.80	62.40	61.30	61.24	62.43	79.70	71.20	83.20
Recall	31.20	34.90	36.30	37.42	36.44	37.42	38.45	59.20	57.24	62.80
mAP	42.40	43.60	44.80	47.10	45.20	46.25	47.61	66.50	61.20	73.50
Corel 10k	Methods									
Performance Measure	LDP	LTrP	LOtP	LHdP	LNP	HOG	BOW	EDBTC	MIFM	FDLNP
Precision	31.89	33.41	36.71	37.21	36.39	39.12	43.04	68.24	59.60	74.11
Recall	11.86	12.17	13.22	13.98	13.56	16.20	18.25	45.42	40.24	50.31
mAP	17.11	18.25	19.87	21.21	20.31	22.46	26.16	56.98	49.26	66.27
Brodatz	Methods									
Performance Measure	LDP	LTrP	LOtP	LHdP	LNP	HOG	BOW	EDBTC	MIFM	FDLNP
Precision	81.8	82.8	84.5	86.0	85.8	82.7	83.1	85.6	86.1	88.4
Recall	73.5	75.2	76.9	78.4	77.5	74.4	75.1	80.8	81.4	84.2
mAP	82.8	84.6	85.4	86.7	86.5	83.8	84.4	88.8	89.6	90.9
ARR	86.8	87.8	88.8	89.7	88.8	86.1	86.6	90.2	91.2	93.2
Vistex	Methods									
Performance Measure	LDP	LTrP	LOtP	LHdP	LNP	HOG	BOW	EDBTC	MIFM	FDLNP
Precision	87.9	88.7	90.8	91.8	92.6	89.0	89.4	93.1	93.4	95.8
Recall	77.3	78.8	80.3	81.8	82.5	80.2	81.3	84.7	85.0	87.1
mAP	88.3	89.5	90.7	91.9	92.7	90.2	91.6	94.5	94.7	97.2
ARR	90.6	90.9	91.3	92.1	92.5	91.4	92.7	95.9	96.3	98.8



Fig. 7. CBIR Examples for all Databases using our Proposed Method.

B. Second Experiment: Feature Selection Method

Our proposed method extracts the visual information from the images, and gives an efficient performance for the standard databases. However, the feature vector length considers a bit high. Our aim is to reduce the feature vector dimensions and therefore reducing the complexity of FDLNP. For that, we proposed extended versions of FDLNP by generating partial direction matrixes instead of full direction matrixes via selecting specific directions for generating GLCM and those directions are shown in Fig.8. The extended versions of FDLNP are:

1) *Top Right Direction Local Neighbors Pattern (TRDLNP)*: we take the upper main diagonal directions of *dir_matrix* to get 36 matrixes for each quantizer instead of 64 matrixes. Therefore, the size of feature vector $2 \times (10 + (36 \times 10)) + 256 = 996$.

2) *Down Left Direction Local Neighbors Pattern (DLNLN)*: by taking lower main diagonal directions of

dir_matrix to get 36 matrixes instead of 64 matrixes and the size of feature vector is $2 \times (10 + (36 \times 10)) + 256 = 996$.

3) *Odd Direction Local Neighbors Pattern (ODLNP)*: by taking odd directions numbers from *dir_matrix* to get 32 matrixes instead of 64 matrixes and the size of feature vector calculates as follows: $2 \times (10 + (32 \times 10)) + 256 = 916$.

4) *Even Direction Local Neighbors Pattern (EDLNP)*: by taking even directions number from *dir_matrix* to get 32 matrixes instead of 64 matrixes and the size of feature vector is $2 \times (10 + (32 \times 10)) + 256 = 916$.

5) *Diagonal Direction Local Neighbors Pattern (DDLNP)*: both main and secondary diagonal from *dir_matrix* was taken to get 16 matrixes instead of 64 matrixes and the size of feature vector calculates as follows: $2 \times (10 + (16 \times 10)) + 256 = 596$.

In this experiment, we used the same four databases and mAP and ARR performance measures. We perceive, as shown in table II, that all extended versions of FDLNP gave very good accuracy closed to FDLNP and all the result better than comparing methods.

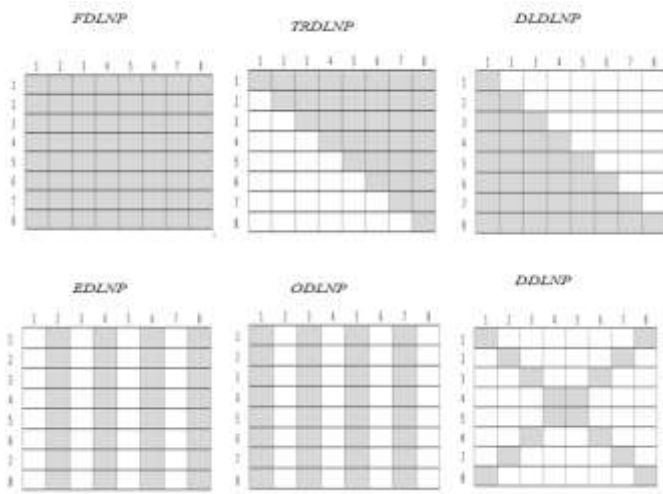


Fig. 8. Illustration Scheme for the Directions of Extended Versions of FDLNP.

TABLE II. COMPARISON BETWEEN EXTENDED VERSIONS OF FDLNP REGARDING MAP AND ARR FOR COREL 1k, COREL 10k, BRODATZ, AND VISTEX DATA

Methods	Databases					
	Vistex		Brodatz		Corel 1k	Corel 10k
	mAP	ARR	mAP	ARR	mAP	mAP
FDLNP	97.2	98.8	90.9	93.2	73.5	66.27
TRDLNP	96.8	98.0	89.1	92.6	73.1	65.9
TLDLNP	96.8	98.2	89.0	92.5	73.2	66.0
EDLNP	97.0	97.6	98.2	91.8	72.6	65.1
ODLNP	96.8	97.7	98.3	91.9	72.4	65.3
DDLNP	96.6	97.2	97.6	91.0	72.0	64.5

C. Third Experiment: Image Retrieval using Machine Learning Classification

In this experiment, we studied the role of machine learning algorithms in the image retrieval system, and its ability for enhancing the retrieval accuracy. We can use the classification algorithms in the CBIR system in two ways:

First, supporting image retrieval outputs, where both classification and content-based image retrieval share in the feature extraction step. Then the retrieval system uses those features for measuring the similarity, whereas in the classification algorithms, we feed those features to the classifier to recognize the class of the query image. In this way, the classification task only provides the class of the query image, alongside the retrieval outputs.

Second, enhancing the image retrieval outputs as following:

Step 1- Extract the features (using the proposed method) from training images to train the classifier.

Step 2- Predict the class of each image using the trainer classifier.

Step 3- When the user inputs the query, the system will extract the feature vector from this image, and then feed it to the classifier, which in its turn predict the class of the query image, let us say *SI*.

Step 4- Measure the similarity distances between the features of the query image and features of all images whose prediction; in the step2, is *SI*, to retrieve top k images.

In this experiment, we used the second way that has the following advantages, enhancing the accuracy of the CBIR as we proved in our previous work [48], reducing the number of comparisons, and make it confined in a specific class. Finally, the output of the classification-based image retrieval system always retrieves similar images, unless the classifier misclassifies the query image, which leads to output completely wrong results, and this is the main disadvantage of this way. For solving this disadvantage, we introduced the *K-Means Based Decision Maker* as shown in Fig.9, which aims to check if the classifier correctly classifies the query image, then it forwards the system to use the classification-based image retrieval, otherwise use the similarity-based image retrieval.

The algorithm of the K means based decision maker summarized with the following steps as shown in Fig. 10:

- Cluster the features database to K clusters using K-Means algorithm [60], where K refers to the number of classes in the database.
- Add label to each cluster's centroid.
- Measure the distances between the features vector of the query image and centroid of each cluster.
- Sort these distances ascendingly.
- If the class of the minimum distance matches with the classifier's label, then use classification-based image retrieval, otherwise use similarity-based image retrieval.

In our work, we use our proposed method FDLNP with different ensemble classification methods, for all databases. The description of used classifiers illustrated in table III.

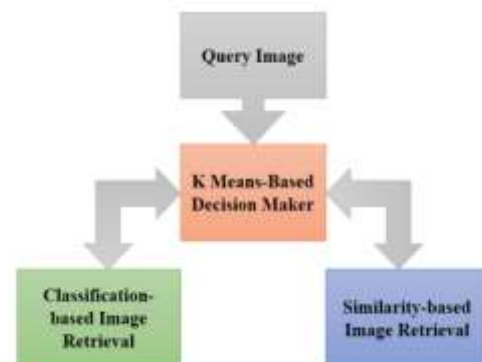


Fig. 9. Illustration Scheme of Decision Maker in Image Retrieval System.

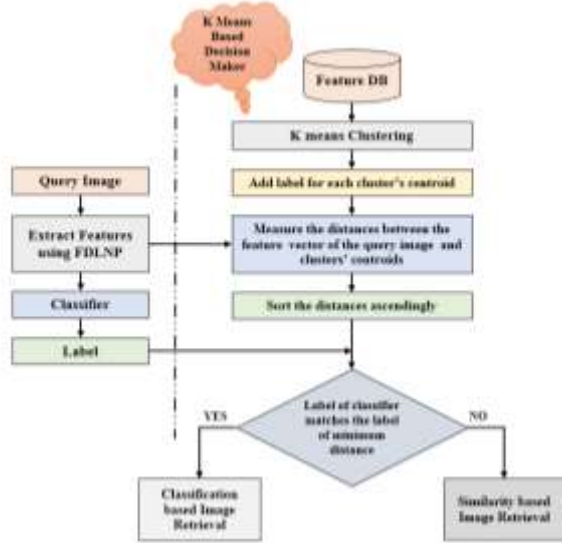


Fig. 10. The Scenario Scheme of the K-Means based Decision Maker in the Retrieval System.

TABLE III. ENSEMBLE CLASSIFIER DETAILS USED IN OUR STUDY

Model Name	Ensemble Method	Learner Type	Number of Learners
Bagged Trees [61]	Bag	Decision Tree	30
Booted Tree [62]	Adaboost	Decision Tree	30
Subspace Discriminant [63]	Subspace	Discriminant	30
Subspace KNN [64]	Subspace	Nearest Neighbors	30

In this experiment, we used our proposed method to train the classifiers with and without PCA (Principal component Analysis) [65], and compared between both methods. For training and testing the classifiers, we used k fold cross-validation [66], and in our work k=10. The results of using FDLNP with ensemble classifiers summarized in table IV.

As we observe from the table IV, FDLNP with Ensemble Bagged Trees classifiers gave the best accuracies for all databases, and we can observe that FDLNP with PCA gave also very good results however, those results are less than using the complete feature vector. The reason for that is being the PCA reduces the feature vector dimension by preserve 95% information from the complete vector.

Using classification based image retrieval system improved the accuracy of the system from (62.80, 50.31, 84.2, and 87.1) to (97.9, 93.2, 99.3, and 99.7) for Core11k, Core10k, Brodatz, and Vistex databases respectively. Moreover, we notice that the enhancements are greater in color databases than texture databases.

D. Fourth Experiment: Image Retrieval using Hadoop Distributed Framework

Hadoop [67-69] has two major layers namely: Processing Computation (Map Reduce), and Storage layer (Hadoop Distributed File System). Our proposed Hadoop framework consists of two phases as shown in Fig.11, off line phase for building the feature database, and online phase for retrieval task.

TABLE IV. CLASSIFICATION ACCURACIES OF ENSEMBLE CLASSIFIERS WITH OUR PROPOSED METHOD FOR BOTH COLOR AND TEXTURE DATABASES

Databases	Classifier	Accuracy without PCA	Accuracy with PCA
Core11K	Bagged Trees	97.9	97.2
	Booted Tree	95.9	93.5
	Subspace Discriminant	97.7	96.7
	Subspace KNN	97.6	96.1
Core10K	Bagged Trees	93.2	92.5
	Booted Tree	91.4	90.8
	Subspace Discriminant	92.8	92.6
	Subspace KNN	92.6	92.1
Brodatz	Bagged Trees	99.3	98.8
	Booted Tree	98.0	97.7
	Subspace Discriminant	99.0	98.6
	Subspace KNN	98.7	98.3
Vistex	Bagged Trees	99.7	99.4
	Booted Tree	98.2	97.4
	Subspace Discriminant	99.4	99.1
	Subspace KNN	99.0	98.6

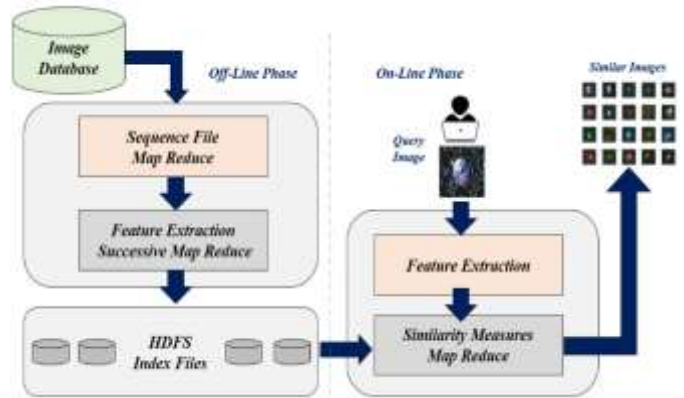


Fig. 11. The Architecture of our Proposed Hadoop Framework.

The aim of the offline phase is converting the image database; that loaded to HDFS, to the features database that stored in the HDFS, using the following steps:

1) *Sequence file map reduce*: The is the first Map Reduce job for converting a large number of small image files into a small number of large files, each containing a number of key-value pairs where the key is an image number and the value is the image data. The size of each large file is 64 MB.

2) *Successive map reduce jobs*: The aim of this step is to distribute our FDLNP method for extracting the features from sequence files by executing successive map-reduce jobs, and building the features database. The function of each job illustrated in the Fig.12. The output of each map reduce job is the input of the next one, and the output of the last job is the feature database in form of <image number, feature vector> that stored in the HDFS.



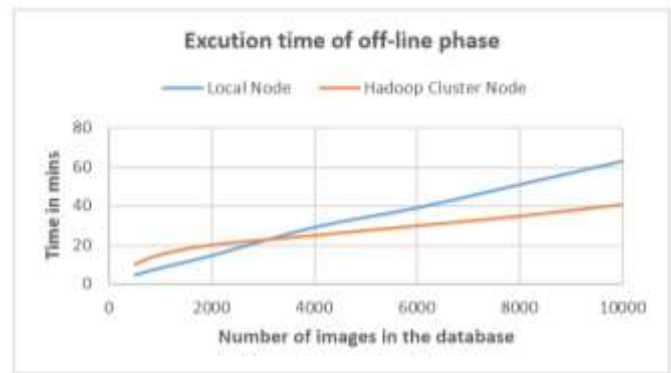
Fig. 12. Our Proposed Method in mAP Reduce Model.

In this experiment, we are interested in measuring the execution time of offline and online phases, on the Hadoop cluster that contains one master node and two slave nodes.

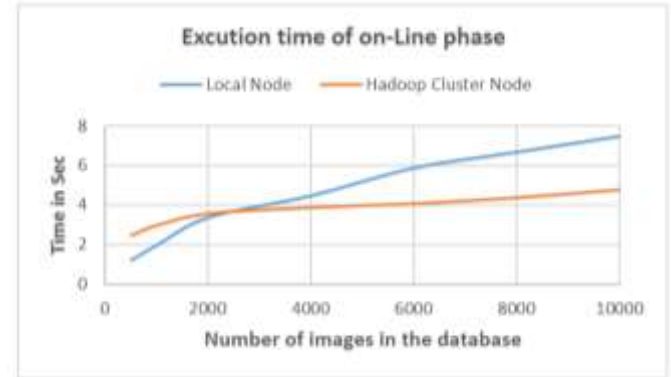
We used partial Corel 10 k database, by taking 5 images from each class, then 10, 20 and so on, for measuring the time of executing the proposed system in the cluster comparing to the time of executing the proposed system in local node.

The Fig.13-a, illustrated the comparisons of executing the proposed method on local and cluster nodes in the offline phase. We noticed that the time of proposed method in the local node is less than cluster for a small number of images (until 3000 images) because the Hadoop starts with a preprocessing step for generating Sequence File. Whereas the Hadoop cluster spends less time for processing a large number of images comparing with the local node.

In the online phase, the aim of the cluster is to calculate the similarity distance, whereas extracting features from the query image is done by the server node. The Fig.13-b, illustrated the time comparison between local and cluster nodes in similarity measuring. As in the offline phase, the local node is better than the Hadoop for a small number of images, whereas the need of the Hadoop is in processing a large number of images for reducing the execution time as much as possible. The online phase connects directly with the user who inputs the query image and waits for similar retrieving images, so we are much interested in reducing the processing time in the online phase, and this is the reason for using map-reduce in measuring the similarity distances.



(a)



(b)

Fig. 13. Comparison of the Execution Time between Local and Cluster Nodes for the Offline and Online Phases in CBIR System.

VI. CONCLUSIONS

In this work, we proposed a novel method for retrieving color and texture images, known as FDLNP that starts with generating the min and max Quantizer, followed by Eight Neighbors Euclidean Decimal Coding matrix and Full Directions Matrixes. After that, we extract GLCM matrix from previous matrixes to derive the features from each GLCM. Finally, we fused those features with the LNP histogram to get the final feature vector, which is a bit long feature vector. For reducing the feature vector length, we proposed five extended versions of FDLNP, by generating partial directions matrixes instead of full directions matrixes. Our proposed methods improved the performance measures in terms of Precision, Recall, mAP, and ARR comparing with some recent works. For enhancing the image retrieval accuracy, we combined our proposed method with machine learning algorithms. Moreover, we proposed a distributed framework to execute our method in map reduce model to get the ability to process a huge number of images in a reasonable time.

VII. FUTURE WORK

In the future, we can enhance our proposed methods to give efficient outcomes for special characterization images as satellite, thermal, and medical images. Moreover, we can use CBIR with the SPARK framework for decreasing the processing time and comparing the spark framework with the Hadoop framework in terms of scalability, fault tolerance, performance, and response time.

REFERENCES

- [1] Y. Rui, T. S. Huang, and S.F. Chang, "Image Retrieval: Current Techniques, Promising Directions and Open Issues," *Journal of Visual Communication and Image Representation*, vol. 10, pp. 39-62, Jan 1999.
- [2] A. Smeulders, M. Worring, S. Santini, A. Gupta, and R. Jain, "Content-based image retrieval at the end of the early years," *IEEE Transactions on Pattern Analysis and Machine Intelligence*, vol. 22, pp. 1349-1380, Dec 2000.
- [3] M. Kokare, B. N. Chatterji, and P. K. Biswas, "A Survey on Current Content based Image Retrieval Methods," *IETE Journal of Research*, vol. 48, pp. 261-271, 2020.
- [4] Y. Liu, D. Zhang, G. Lu, and W.Y. Ma, "A survey of content-based image retrieval with high-level semantics," *Pattern Recognition*, vol. 40, pp. 262-282, 2007.
- [5] R. Datta, D. Joshi, J. Li, and J. Z. Wang, "Image retrieval," *ACM Computing Surveys*, vol. 40, pp. 1-60, 2008.
- [6] Jose Ramos, Thessa T. J. P. Kockelkorn, Isabel Ramos, Rui Ramos, Jan Grutters, Max A. Viergever, "Content-Based Image Retrieval by Metric Learning from Radiology Reports: Application to Interstitial Lung Diseases," *IEEE Journal of Biomedical and Health Informatics*, vol. 20, pp. 281-292, 2016.
- [7] Zegarra, Javier A. Montoya, Neucimar J. Leite, and Ricardo da Silva Torres, "Wavelet-based fingerprint image retrieval," *Journal of computational and applied mathematics*, vol. 227, pp. 294-307, 2009.
- [8] Gavrielides, Marios A., Elena Sikudova, and Ioannis Pitas, "Color-based descriptors for image fingerprinting," *IEEE Transactions on Multimedia*, vol. 8, pp. 740-748, 2006.
- [9] M. Alkhwilani, M. Elmoogy and H. El Bakry, "Text-based, Content-based, and Semantic-based Image Retrievals: A Survey," *International Journal of Computer and Information Technology*, vol. 4, pp. 58-66, 2015
- [10] M. Alrahhah and Supreethi K.P., "Multimedia Image Retrieval System by Combining CNN With Handcraft Features in Three Different Similarity Measures," *International Journal of Computer Vision and Image Processing*, vol. 10, pp. 1-23, Jan 2020.
- [11] G.-H. Liu and J.-Y. Yang, "Image retrieval based on the texton co-occurrence matrix," *Pattern Recognition*, vol. 41, pp. 3521-3527, 2008.
- [12] G.-H. Liu, L. Zhang, Y.-K. Hou, Z.-Y. Li, and J.-Y. Yang, "Image retrieval based on multi-texton histogram," *Pattern Recognition*, vol. 43, pp. 2380-2389, 2010.
- [13] J. Luo and D. Crandall, "Color object detection using spatial-color joint probability functions," *IEEE Transactions on Image Processing*, vol. 15, pp. 1443-1453, 2006.
- [14] D. Xiaoyin, "Image retrieval using color moment invariant," in: *The Seventh International Conference on Information Technology: New Generations (ITNG)*, Las Vegas, NV, pp. 200-203, 2010.
- [15] H. Jing, S.R. Kumar, M. Mitra, W.J. Zhu, R. Zabih, "Image indexing using color correlograms," in: *Proceedings of the IEEE Computer Society Conference on Computer Vision and Pattern Recognition*, pp. 762-768, 1997.
- [16] G.P. Qiu, "Color image indexing using BTC," *IEEE Trans. Image Process*, vol. 12, pp. 93-101, 2003.
- [17] V. Kovalev, M. Petrou, "Multidimensional co-occurrence matrices for object recognition and matching," *Graph. Models Image Process*, vol. 58, pp. 187-197, 1996.
- [18] N. Jhanwar, S. Chaudhuri, G. Seetharaman, B. Zavidovique, "Content based image retrieval using motif co-occurrence matrix", *Image Vis. Comput*, vol. 22, pp. 1211-1220, 2004.
- [19] G. Qiu, "Color image indexing using BTC," *IEEE Trans. Image Process*, vol. 12, pp. 93-101, 2003.
- [20] J. Mathews, M.S. Nair, L. Jo, "A novel color image coding technique using improved BTC with k-means quad clustering," *Advances in Signal Processing and Intelligent Recognition Systems*, pp. 347-357, 2014.
- [21] J.M. Guo, H. Prasetyo, JH. Chen, "Content-based image retrieval using error diffusion block truncation coding features," *IEEE Trans. Circ. Syst. Video Technol*, pp. 99-105, 2014.
- [22] B.S. Manjunath, P. Salembier, T. Sikora, "Introduction to MPEG-7: Multimedia Content Description Interface," Wiley, Chichester, 2002.
- [23] R. Haralick, "Statistical and structural approaches to texture," *Proc. IEEE*, vol. 67, pp. 786-804, May 1979.
- [24] G. Cross, A. Jain, "Markov random field texture models," *IEEE Trans. Pattern Anal. Mach. Intell*, vol. 5, pp. 25-39, 1983.
- [25] D.K. Park, Y.S. Jeon, C.S. Won, "Efficient use of local edge histogram descriptor," *ACM workshops on Multimedia*, ACM, pp. 51-54, 2000.
- [26] E.P. Simoncelli, W.T. Freeman, "The steerable pyramid: A flexible architecture for multi-scale derivative computation," in: *International Conference on Image Processing*, vol. 3, p. 3444, 1995.
- [27] H. Tamura, S. Mori, T. Yamawaki, "Textural features corresponding to visual perception," *IEEE Transaction System, Man Cybernet*, vol. 8, pp. 460-473, 1978.
- [28] X. Wang, Z. Wang, "A novel method for image retrieval based on structure elements' descriptor," *J. Vis. Commun. Image Represent*, vol. 24, pp. 63-74, 2013.
- [29] G.H. Liu, Z.Y. Li, L. Zhang, Y. Xu, "Image retrieval based on micro-structure descriptor," *Pattern Recognition*, vol. 44, pp. 2123-2133, 2011.
- [30] S.A. Chatzichristofis, Y.S. Boutalis, "Fctch: Fuzzy color and texture histogram-a low level feature for accurate image retrieval," *9th International Workshop on Image Analysis for Multimedia Interactive Services*, pp. 191-196, 2008.
- [31] C.C. Lai, Y.C. Chen, "A user-oriented image retrieval system based on interactive genetic algorithm," *IEEE Trans. Instrument. Measur*, vol. 60, pp. 3318-3325, 2011.
- [32] S. Belongie, J. Malik, and J. Puzicha, "Shape matching and object recognition using shape contexts," *IEEE Transactions on Pattern Analysis and Machine Intelligence*, vol. 24, pp. 509-521, 2002.
- [33] D. G. Lowe, "Distinctive image features from scale-invariant key points," *Internatiozal Journal of Computer Vision*, vol. 60, pp. 91-110, 2004.
- [34] N. Dalal and B. Triggs, "Histograms of oriented gradients for human detection," in *Proceedings of the Computer Society Conference on Computer Vision and Pattern Recognition*, pp. 886-893, June 2005.
- [35] H. Bay, T. Tuytelaars, and L. V. Gool, "SURF: speeded up robust features," in *European Conference on Computer Vision*, vol. 1, pp. 404-417, 2006.
- [36] J. Sivic and A. Zisserman, "Efficient visual search of videos cast as text retrieval," *IEEE Transactions on Pattern Analysis and Machine Intelligence*, vol. 31, pp. 591-606, 2009.
- [37] Y. Su and F. Jurie, "Improving image classification using semantic attributes," *International Journal of Computer Vision*, vol. 100, pp. 59-77, 2012.
- [38] L. Wang, L. Zhou, C. Shen, L. Liu, and H. Liu, "A convolutional word-merging algorithm with class separability measure," *IEEE Transactions on Pattern Analysis and Machine Intelligence*, vol. 36, pp. 417-435, 2014.
- [39] H. Lobel, R. Vidal, and A. Soto, "Learning shared, discriminative, and compact representations for visual recognition," *IEEE Transactions on Pattern Analysis and Machine Intelligence*, vol. 37, pp. 2218-2231, 2015.
- [40] A. Babenko, A. Slesarev, A. Chigorin, and V. Lempitsky, "Neural codes for image retrieval," in *European Conference on Computer Vision*, 2014.

- [41] M. Tzelepi and A. Tefas, "Deep convolutional learning for content based image retrieval," *Neurocomputing*, vol. 275, pp. 2467–2478, 2018.
- [42] F. Radenovic, G. Tolias, and O. Chum, "Fine-tuning CNN image retrieval with no human annotation," *IEEE Transactions on Pattern Analysis and Machine Intelligence*, vol. 41, pp. 1655–1668, 2019.
- [43] A. Krizhevsky, I. Sutskever, and G. E. Hinton, "Imagenet classification with deep convolutional neural networks," in *Proceedings of the Advances in Neural Information Processing Systems*, Dec 2012.
- [44] A. Karpathy, G. Toderici, S. Shetty, T. Leung, R. Sukthankar, and L. Fei-Fei, "Large-scale video classification with convolutional neural networks," in *Proceedings of the Conference on Computer Vision and Pattern Recognition*, pp. 1725–1732, June 2014.
- [45] F. Zhao, Y. Huang, L. Wang, and T. Tan, "Deep semantic ranking based hashing for multi-label image retrieval," in *Proceedings of the Conference on Computer Vision and Pattern Recognition*, pp. 1556–1564, June 2015.
- [46] A. Qayyum, S. M. Anwar, M. Awais, and M. Majid, "Medical image retrieval using deep convolutional neural network," *Neurocomputing*, vol. 266, pp. 8–20, 2017.
- [47] A. Alzu'bi, A. Amira, and N. Ramzan, "Content-based image retrieval with compact deep convolutional features," *Neurocomputing*, vol. 249, pp. 95–105, 2017.
- [48] M. Alrahhah and K. Supreethi, "Content-Based Image Retrieval using Local Patterns and Supervised Machine Learning Techniques," in *Proceedings of Amity International Conference on Artificial Intelligence*, Feb 2019.
- [49] M. Islam, K. Kundu and A. Ahmed, "Texture Feature based Image Retrieval Algorithms", *International Journal of Engineering and Technical Research*, vol. 2, pp. 169-173, 2014.
- [50] S. Murala, R. P. Maheshwari, and R. Balasubramanian, "Local Tetra Patterns: A New Feature Descriptor for Content-Based Image Retrieval," *IEEE Transactions on Image Processing*, vol.21, pp. 2874-2886, 2012.
- [51] Corel 1000 image database [Online]. Available: <http://wang.ist.psu.edu/docs/related/>.
- [52] "Content Based Image Retrieval / Image Database Search Engine (SIMPLICity, WIPE, Virtual Microscope)", [Wang.ist.psu.edu](http://wang.ist.psu.edu), 2021. [Online]. Available: <http://wang.ist.psu.edu/docs/related/>.
- [53] P. Brodatz, *Textures: A Photographic Album for Artist and Designers*. New York, NY, USA: Dover, 1996.
- [54] "SIPI Image Database", [Sipi.usc.edu](http://sipi.usc.edu), 2021. [Online]. Available: <http://sipi.usc.edu/database/>.
- [55] "Index of /pub/VisTex", [Vismod.media.mit.edu](https://vismod.media.mit.edu/pub/VisTex/), 2021. [Online]. Available: <https://vismod.media.mit.edu/pub/VisTex/>.
- [56] B. Zhang, Y. Gao, S. Zhao, and J. Liu, "Local Derivative Pattern Versus Local Binary Pattern: Face Recognition With High-Order Local Pattern Descriptor," *IEEE Transactions on Image Processing*, vol. 19, pp. 533-544, 2010.
- [57] U. Raju, Suresh Kumar, K., Haran, P., Boppana, R. and Kumar, N. "Content-based image retrieval using local texture features in distributed environment," *International Journal of Wavelets, Multiresolution and Information Processing*, p.1941001, 2019.
- [58] Jing-Ming Guo, H. Prasetyo and Jen-Ho Chen, "Content-Based Image Retrieval Using Error Diffusion Block Truncation Coding Features," *IEEE Transactions on Circuits and Systems for Video Technology*, vol. 25, pp. 466-481, 2015.
- [59] K. Chu and G. Liu, "Image Retrieval Based on a Multi-Integration Features Model," *Mathematical Problems in Engineering*, pp. 1-10, 2020.
- [60] H. Shen and Z. Duan, "Application Research of Clustering Algorithm Based on K-Means in Data Mining," *2020 International Conference on Computer Information and Big Data Applications (CIBDA)*, 2020.
- [61] E. Ampomah, Z. Qin and G. Nyame, "Evaluation of Tree-Based Ensemble Machine Learning Models in Predicting Stock Price Direction of Movement," *Information*, vol. 11, p. 332, 2020.
- [62] S. Rahman, M. Irfan, M. Raza, K. Moyeezullah Ghori, S. Yaqoob and M. Awais, "Performance Analysis of Boosting Classifiers in Recognizing Activities of Daily Living," *International Journal of Environmental Research and Public Health*, vol. 17, p. 1082, 2020.
- [63] R. K, "Satellite Image Classification based on Ensemble Subspace Discriminant method using Random Subspace Algorithm," *HELIX*, vol. 8, pp. 2714-2718, 2018.
- [64] T. Mokoaleli-Mokoteli, S. Ramsumar and H. Vadapalli, "The Efficiency Of Ensemble Classifiers In Predicting The Johannesburg Stock Exchange All-Share Index Direction," *Journal of Financial Management, Markets and Institutions*, vol. 07, p. 1950001, 2019.
- [65] S. Sehgal, H. Singh, M. Agarwal, V. Bhasker and Shantanu, "Data analysis using principal component analysis", *International Conference on Medical Imaging, m-Health and Emerging Communication Systems*, 2014.
- [66] S. Raschka, "Model Evaluation, Model Selection, and Algorithm Selection in Machine Learning," *arXiv:1811.12808*, 2020.
- [67] Welcome to Apache™ Hadoop®! <http://hadoop.apache.org/>.
- [68] Garry Turkington, "Hadoop Beginner's Guide", *PACKT Publishing, Shroff Publishers and Distributors Pvt. Ltd. Navi Mumbai, India*, 2013.
- [69] Srinath Perera and Thilina Gunarathne, "Hadoop MapReduce Cookbook," *PACKT Publishing, Shroff Publishers and Distributors Pvt. Ltd. Navi Mumbai, India*, 2013.

AUTHORS' PROFILES



Maher Alrahhah was born in Syria in 1992. He received the B.E. degree in computer engineering from Electrical and Electronics Engineering College, Aleppo University, Syria, in 2014, the M.Tech. Degree in Computer Science and Engineering from the National Institute of Technology Warangal, India, in 2018, he is currently pursuing a Ph.D. degree in Computer Science and Engineering at JNTUH College of Engineering, Hyderabad, India. His major fields of interest are content-based image retrieval, biomedical imaging, deep learning, and multimedia systems.



Supreethi K.P. received the Bachelor of Engineering degree in Computer Science and Engineering, Gulbarga University, India, the M.Tech degree in Computer Science in 2004 and a Ph.D. in Computer Science and Engineering from Jawaharlal Nehru Technological University, India, in 2011. She is a professor of CSE at JNTUH College of Engineering, Hyderabad. Her research interests are databases, data mining, medical imaging, and image processing. She is a life member of CSI.

Stanza Type Identification using Systematization of Versification System of Hindi Poetry

Milind Kumar Audichya¹
Computer Science Department
Gujarat Technological University
Ahmedabad, India

Jatinderkumar R. Saini^{2*}
Symbiosis Institute of Computer Studies and Research
Symbiosis International (Deemed University)
Pune, India

Abstract—Poetry covers a vast part of the literature of any language. Similarly, Hindi poetry is also having a massive portion in Hindi literature. In Hindi poetry construction, it is necessary to take care of various verse writing rules. This paper focuses on the automatic metadata generation from such poems by computational linguistics integrated advance and systematic, prosody rule-based modeling and detection procedures specially designed for Hindi poetry. The paper covers various challenges and the best possible solutions for those challenges, describing the methodology to generate automatic metadata for “Chhand” based on the poems’ stanzas. It also provides some advanced information and techniques for metadata generation for “Muktak Chhands”. Rules of the “Chhands” incorporated in this research were identified, verified, and modeled as per the computational linguistics perspective the very first time, which required a lot of effort and time. In this research work, 111 different “Chhand” rules were found. This paper presents rule-based modeling of all of the “Chhands”. Out of the all modeled “Chhands” the research work covers 53 “Chhands” for which at least 20 to 277 examples were found and used for automatic processing of the data for metadata generation. For this research work, the automatic metadata generator processed 3120 UTF-8 based inputs of 53 Hindi “Chhand” types, achieved 95.02% overall accuracy, and the overall failure rate was 4.98%. The minimum time taken for the processing of “Chhand” for metadata generation was 1.12 seconds, and the maximum was 91.79 seconds.

Keywords—Chhand; computational linguistics; Hindi; metadata; poetry; prosody; stanza; verse

I. INTRODUCTION

Hindi (‘हिंदी’) is known as a prevalent language. According to India’s 2011 census, there were 322 million native speakers with Hindi as their first language [1]. The script is required to write any language. For the Hindi language, the writing script is Devanagari (‘देवनागरी’), which is fourth in the world when it comes to the most widely adopted writing systems [2]. With the help of the Devanagari script, more than 120 languages are written all over the world. As per The Unicode Standard, Version 13.0, the Devanagari Unicode range is 0900–097F [3].

Poetries hold an irreplaceable place in the world of literature in every language. Any poem’s creation usually follows some specific patterns or rules known as prosody or poetics. Based on the prosody rules, it can be detected and decided that what kind of poem or part of the poem is, but the patterns may differ from language to language, and even in the

same language, there can be plenty of prosody rules-based patterns [4].

There are two types of language processing approaches in the computational linguistics research domain: the text-based and speech-based approaches [5]. Both methods are required and play a vital role in research in the context of poetry. The text-based system is for working with the significant part of text-oriented rules, and for speech-related practices and patterns, the speech-based approach can be useful to fulfill the research demands. These approaches are adopted and followed based on the need and the nature of the research problem [6].

This research work revolves around Hindi poetry and its different prosody related rules. A significant part of the prosody rules is composed of the order of letters and their frequency. With the text-based approach of computational linguistics, the practices of the composition of stanza were initially systematically classified. Furthermore, the rules were used in the best possible way to carry out the rule-based modeling for the generation of the metadata automatically. In this research work, A proper classification structure will be introduced for Hindi verses. The research will also attempt to detect and identify the Hindi verse based on their appropriate formation rules.

Many verses are written in the Hindi language. This composition of verses in Hindi has been from ancient times. The knowledge hidden behind the rules of the creation of verses has inspired us to do this research work. The authors strongly believe that this research work will prove a milestone to preserve these verses’ composition and give a new direction in computational linguistics research.

The rest of the paper has five major sections: literature review, the knowledge base about the Hindi stanza, Methodology, Results, and Conclusion. One can get a better idea of current research need or gap by going through the literature review first. The next part explains the systematic classification of the stanza specially introduced by this research work. Further, to understand the methodology, formation, and calculation, details of the stanzas are discussed in depth. Based on the various test and experiments, the result section focuses on the outcomes. Finally, based on the complete research work, the overall conclusion is discussed in the last conclusion section, consisting of all significant findings, developments, and results during the research journey.

*Corresponding Author

II. LITERATURE REVIEW

A literature review is a fundamental part of any research work. For the same, best efforts had been given to find out the relevant research works. Research work directly related to the metadata generation, related to the Hindi Prosody, and precisely basis on the Computational Linguistics not found. Some nearby research work related to computational linguistics or metadata generation were seen, which are enlighten here.

Efforts were made to find Indian regional languages related research works to know the research's standing specifically in the Indian languages segment. Moreover, it was found that different research work focusing on the various aspects of problems in Indian language-based studies. Audichya and Saini [7] introduced a way through computational linguistics approach for the automatic metadata generation based on the unified rule-based technique for Hindi poetries. They achieved nearly 98% of correct results. Rest errors were due to some input and provided data-related issues. Joshi and Kushwah [8] did research studies that emphasize the detection of 'चौपाई' (Chaupai – A type of Hindi verses) and achieved more than 85% accuracy in detection. They found the issues because some poets usually increase or decrease the 'Matras' to maintain the rhythm or flow due to some different structured but similar sounding words in the end. They also did some research on another Hindi verse named 'रोला' (Rola – A type of Hindi verses) detection and were able to achieve around 89% of accuracy [9]. The remaining accuracy was not gained due to assumptions of the poets while creating and because of the higher sum value of 'मात्रा' (Matras – Quantity) than the expected threshold.

Bafna and Saini [10] tried to classify the Hindi verses based on the various Machine Learning algorithms. They did a comparative study of SVM, Decision Tree, Neural Network, and Naive Byes on 697 poem classification. In another research work, they did Hindi poetry classification using Eager supervised machine learning algorithms and evaluated using the misclassification error [11]. Research work to predict the Hindi verse class using concept learning done by these researchers in which they found that K-nearest neighbors performed better [12].

Kaur and Saini [13] worked on Punjabi Poems' classification using ten different Machine Learning algorithms. In several other research works, they worked on various Punjabi poems using poetic features, linguistic Features, and Weighting [14-15]. They designed a content-based Punjabi poetry classifier using WEKA using different machine learning algorithms in another research work. They found that the Support Vector Machine algorithm was the best performing accuracy of 76.02% [16-17].

Pal and Patel [18] researched the development of a model based on the nine 'Ras' and tried to classify it using Machine Learning modeling. Saini and Kaur [19] also did emotion detection-based research focusing on 'Navrasa' using machine learning algorithm Naïve Bayes (NB) and Support Vector Machine (SVM), SVM performed better with 70.02% overall accuracy.

Bafna and Saini [20] also worked for the Hindi and Marathi language Prose and Verse application-based researches. Apart from that, research work from the same researchers introduced in which they have given a technique for Hindi Verses and Proses to identify context-based standard tokens [21].

Some research work in the Sanskrit language based on Computational Linguistics was also found [22]. Apart from that, other research works for automatic metadata generation [23], text-based document classification [24-25], and computational linguistics-based metadata building research (CLiMB) works were explored too [26].

The internationally well-known foreign language-based research was analyzed to see the research works, current trends, and progress related to the different language-based works. While reviewing, some excellent foreign language-based research works were found. In a research work of Arabic poetry, emotion classification using machine learning was carried out by Alsharif, AlShamaa, and Ghneim [27]. Hamidi, Razzazi, and Ghaemmaghani [28] researched using Support Vector Machines for the Persian automatic meter classification. In some other research works, researchers have explored Arabic, Bengali, Chinese, English, Hindi, Marathi, Oriya, Persian, Punjabi, and Urdu languages [29-31].

Based on this literature review, it was realized that there is still a lack of essential research for the Hindi poem's automatic metadata generation. Before that, a special effort to structure the combination of the universal unified Prosody ('Chhand') rules systematically is the need of the hour. Furthermore, a robust method based on those rules for metadata generation is the demand of this research wing.

III. IDEA TO SYSTEMATIZE HINDI PROSODY RULES

To know the core idea to systematize the Hindi poetry rules, one needs to know about the Hindi poetry first so let us know about the same in brief. This research work is dealing with the various aspects of Hindi poetry. Let us first know what the essential elements of the construction of the Hindi poems are. There are three necessary parts which are: 'छंद' ('Chhand' - Prosody or Verse), 'अलंकार' ('Alankar' - Figure of speech) and 'रस' ('Ras' - Sentiment). This research work covers the prosody or verse ('छंद') part in-depth, including the proper systematic collection of prosody rules and standardizing the classification for future research purposes. The term 'Chhand' or 'Chhands' is used to address the Hindi verse or stanza in this research paper.

To understand the 'Chhand' better, one must know about the parts of 'Chhands' that need to be taken care of while writing a poem. The six central components for various types of 'Chhand' writing are 1. Stanza ('चरण या पाद'-'Charan ya Pad'), 2. Characters and Quantity ('वर्ण व मात्रा'-'Varn Va Matra'), 3. Flow ('गति'-'Gati'), 4. Pause ('यति'-'Yati'), 5. End of Stanza ('तुक'-'Tuk'), 6. Predefined Sequence of Characters ('गण'-'Gana') [32-34].

These components play a vital role in different rules, and some are having other aspects as well. Let us see each one by one very quickly. Stanzas usually have a fixed number of

characters and quantity based on those characters. There are two types of characters 1. Short ('ह्रस्व'-Hrasva) and 2. Long ('दीर्घ'-Dirgha). 'Hrasva' is denoted from the symbol ('ॐ') while counting quantity is considered one (1). These ('अ', 'इ' (ि), 'उ' (ु), 'ऋ' (ृ)) characters are regarded as 'Hrasva' while calculating quantity. 'Dirgha' holds two (2) quantities at the time of quantity calculation and is represented by the symbol ('ऌ'). These ('आ' (ा), 'ई' (ी), 'ऊ' (ू), 'ए' (े), 'ऐ' (ै), 'ओ' (ो), 'औ' (ौ), 'अं' (ं), 'अः' (ः)) are considered as 'Dirgha'. For which knowledge of quantity calculation rules ('मत्रा गणना नियम')[35-37] is required, that is covered in section 3.1.1 of this paper. The predefined fixed sequence of characters group made up of three character's ('वर्ण'-Varna) combination. There are eight such groups which are known as 'Gana' namely: 1. 'YaGana' ('यगण'), 2. 'MaGana' ('मगण'), 3. 'TaGana' ('तगण'), 4. 'RaGana' ('रगण'), 5. 'JaGana' ('जगण'), 6. 'BhaGana' ('भगण'), 7. 'NaGana' ('नगण'), 8. 'SaGana' ('सगण'). Let us see the quantity calculation's different rules to understand the further analyses better and know more in-depth about the 'Chhands'.

A. Quantity Calculation Rules Simplified

Plenty of poetry rules were tested and authenticated to found appropriate stanza formation rules. Some manual calculations were carried out to know the rules and figure out the facts out of those calculations results. To validate the identified and authenticated rules information from various sources such as advice from some experts, the notes provided by them, some ancient books [32,33,40], online articles, some books which contain some or very minimal parts of 'Chhands' were also considered [38-41]. The research work designed and carried out is a very smooth and systematic way to adopt the new or missing rules if some additional information or practice is found in the future that can also be incorporated easily. Here mentioning the only rules considered for the calculations, and there may or may not be the chance of some new or old rules to be found in the future.

To perform the research work as a researcher or become an influential 'Chhands' writer, one must know the rules for better results to know more about the poems and understand the 'Chhands' from the core. Let us see basic simplified rules of 'Matra Gana' or quantity calculation for Hindi.

The 'Chhand' rules are identified, verified, and modeled in the computational linguistics aspect very first time in this research area. It requires a lot of effort and time to scrutinize and model something that not already standardize. Along with that, the special exceptional rules were incorporated.

1) Common Rules

a) Each 'Hrasva' Vowel ('ह्रस्व स्वर') which are ('अ, इ, उ, ऋ') is counted as one quantity and are called Small ('लघु' - 'Laghu').

b) Each 'Dirgh' Vowel ('दीर्घ स्वर') which are ('आ, ई, ऊ, ए, ऐ, ओ, औ, अं') is counted as two quantity and known as Large ('गुरु' - 'Guru').

c) Each Consonant is also counted as one at the time of quantity calculation and considered 'Laghu'. The following

are the consonants: 'क, ख, ग, घ, ङ, च, छ, ज, झ, ञ, ट, ठ, ड, ढ, ण, त, थ, द, ध, न, प, फ, ब, भ, म, य, र, ल, व, श, ष, स, ह'. Example: चल = 11, नयन = 111, कलरव = 1111.

d) On applying diacritics of 'Hrasva' Vowel ('ह्रस्व स्वर') which are ('ि', 'ु', 'ृ') on any consonant does not change the quantity count and considered as 'Laghu' only so counted as one quantity only. Example: लिख=11, सिल=11, हिन=11, सुध=11, बुलबुल=1111, ऋषि=11.

e) On applying diacritics of 'Dirgh' Vowel ('दीर्घ स्वर') which are ('ा', 'ी', 'ू', 'े', 'ै', 'ो', 'ौ', 'ं', 'ः') on any consonant change the quantity count and considered as 'Dirgh' so counted as two quantity instead of 1. Example: काला=22, चलाना=122, जिला=12, टीला=22, भौर=21, चंदन=211, रखवाना=1122.

2) Special - Exceptional Rules:

a) A special rule of the 'Anunasik' or 'Ardh Chandrabindu' ('ँ') is that if 'Anunasik' ('ँ') is applied to consonants which are considered as 'Laghu' and are not applied with any 'Hrasva' Diacritic than quantity is regarded as one only as it is treated as 'Laghu'. If used on the 'Hrasva', no changes in quantity and considered as two quantities. Example: हँसी=12, चाँद=21.

b) Ligature or Joint Character at the starting of any word is considered 'Laghu' and counted as one quantity only. Example: ज्वर=11, प्रणाम=121, न्याय=21.

c) Ligature or Joint Character at the starting of any word is along with 'Dirgh' Vowel diacritic than considered 'Guru' and counted as two quantities, and Half Characters value becomes 0. Example: भ्राता=22, ज्ञान=21, ध्यान=21.

d) Before ligature, the 'Laghu' characters are considered 'Guru', and quantities become two instead of one. Example: सत्य=21, चक्षु=21, गर्भ=21, वृक्ष=21, अध्यक्ष=221, विनम्र=221.

e) Before the ligature, the 'Guru' characters are considered 'Guru', and quantity is counted as two quantities. Example: आत्मा=22, प्रासांक=221, भास्कराचार्य=21221.

f) If the next character after the ligature is 'ह' and 'Dirgh' Vowel Diacritic, then half the Characters value becomes zero. Example: कन्हैया=121, मल्हार=121, तुम्हारे=122.

g) If the next character after the ligature is 'ह' with 'Laghu' Vowel Diacritic or Laghu Character, there will be no change in calculation rules. Example: दुल्हन=211, अल्हड़=211.

3) Most affecting exceptions: Sometimes at the end of the stanza, if there is 'Laghu', it is considered 'Guru' as per the pronunciation. Also, some poets usually increase and decrease the diacritics to maintain the flow or their own choices. Some poet usually takes references from the existing 'Chhand' creation rules but does not follow those rules completely, which affects the automatic detection. Apart from the poorly formatted and junk characters added by avoiding the formation rules such as emojis, universal special characters,

special characters from other languages considered as the junk characters, and lower down the result accuracy.

After applying these rules, once one gets the allocated quantity, one needs to sum those quantities on a different basis as per the requirement. One example is here for the sum of the word-level quantity sum.

Example: सीताराम = 2221 = 2+2+2+1 = 7, सत्य = 21 = 2+1 = 3

4) 'Gana' Sequence: For 'Varnik' verses the 'Gana' is used in sequence-related rules, one needs to know more about the 'Gana', so Table I will show more about 'Gana'. Table I is representing symbolic representation along with the example of all eight 'Gana'.

That is all about the calculation-related rules and ways, which will help us understand the research work better and surely help future research works. These rules were needed to simplify, and a proper standardized flow by putting massive efforts and experiments were required. It was more challenging to manage everything because no such pertinent standard research-level articles or bases were found.

B. Structure Creation of Hindi 'Chhands' from a Research Perspective

When the authors started finding the information related to the 'Chhands', it was found that only a tiny amount of properly arranged information is available [34], and whatever is available is also having some contradiction at different sources. For instance, Different rules and creation information of 'Bujangi Chhand' were found at various places [42-43]. It has been observed that the available data cannot be used with the research perspectives. With whatever information collected from the different sources which are mentioned in Section 3.1, manually analyzed, validated and once after proper authentication, this decision is made that whatever is available needs to be systemized first and for which an adequate structure creation is required, so this is an effort towards the same.

There are two mainstream types of 'Chhands', which are 'Vedic Chhands' and 'Laukik Chhands'. 'Vedic Chhands' are coming from Vedas' ancient times and mostly written in the Sanskrit language, as mentioned in the 'Agni Purana' [44]. A saint and mathematician named Pingala [45] have written 'Chhandshastra' based on the 'Chhands' only in ancient times. One of the best and trendy examples of 'Vedic Chhand' is a 'Chhand' named 'Gayatri Chhand (गायत्री छंद)'. Gayatri Mantra, written in the Sanskrit language, is the best example of the 'Gayatri Chhand'. 'ॐ भूर्भुवः स्वः तत्सवितुर्वरेण्यं भर्गो देवस्य धीमहि धियो यो नः प्रचोदयात्' ('om bhur bhuvah svah tat savitur varenyam bhargo devasya dhimahi dhiyo yo nah prachodayat' – Let us pray to God who had produced this universe, may He enlighten us with spirituality) [46].

'Laukik Chhands' are the verses written by people and are not a part of Vedas. These are reported in both Sanskrit and the Hindi language. As the research work focuses on Hindi poetry, only Hindi 'Chhands' will be discussed. These verses can be classified into three classes based on the nature of rules of 'Chhand' writing, which are: 1. 'Matrik Chhands (मैत्रिक छंद)', 2. 'Varnik Vrutt/Chhands (वर्णिक वृत्त/छंद)', 3. 'Mukt/Muktak Chhands (मुक्त/मुक्तक छंद)'.

1) 'Matrik Chhands': Hindi verses written with the fixed number of quantities in all the four stanzas based on the different predefined 'Chhand' creation rules are known as 'Matrik Chhand'. In this kind of 'Chhands', the sequence of characters discussed earlier, 'Laghu Varna' and 'Guru Varna' or 'Gana', does not matter. Some most popular 'Matrik Chhands' were managed and structured in systematic classes. There are several classes of 'Matrik Chhands': 1. 'Sam Matrik Chhand', 2. 'Ardh Sam Matrik Chhand', 3. 'Visham Matrik Chhand'. Let us see in a managed and specific structured manner in Table II.

Table II shows the names of 'Chhand', classification type, and subtypes of 'Chhand' along with the 'Matra Counts' used for the detection at the time of rule-based modeling. Apart from these classifications and 'Matra' count, some more rules are associated with the specific verses, and these rules change for every verse. A few 'Sam Matrik Chhand', some 'Ardh Sam Matrik Chhand' and 'Visham Matrik Chhand' are shown in Tables III and IV.

Table III shows the information about the 'Ardh Sam Matrik Chhands' in which it can be seen that 'Matra' count of even and odd stanzas are different. Let's see something about 'Visham Matrik Chhands' as well.

Table IV representing 'Visham Matrik Chhand', the remark of 'Kundliya' says that it can be authored by combining two verses named 'Doha' and 'Rola'. This section was the most about the 'Matrik Chhands'. Let us see the next primary class of 'Chhands'.

TABLE I. 'GANA' WITH THEIR RESPECTIVE EXAMPLES

Sr. No.	Gana	Symbolic Representation	Example
1	मगण	SSS	जारोली
2	नगण	III	शयन
3	भगण	SI	पावन
4	यगण	ISS	हमारी
5	जगण	ISI	जयेश
6	रगण	SIS	राधिका
7	सगण	IIS	अपनी
8	तगण	SSI	दातार

TABLE II. SOME 'SAM MATRIK CHHANDS' WITH THEIR RESPECTIVE MATRA COUNT

Sr. No.	Chhand	Type	Sub Type	Matra Count
1	रोला	मात्रिक छंद	सममात्रिक छंद	24
2	हरिगीतिका / हरगीतिका	मात्रिक छंद	सममात्रिक छंद	28
3	चौपाई	मात्रिक छंद	सममात्रिक छंद	16
4	उल्लाला (सममात्रिक)	मात्रिक छंद	सममात्रिक छंद	26
5	अहीर	मात्रिक छंद	सममात्रिक छंद	11
6	तोमर	मात्रिक छंद	सममात्रिक छंद	12
7	त्रिभंगी	मात्रिक छंद	सममात्रिक छंद	32
8	गीतिका (चंचरी / चंचरी)	मात्रिक छंद	सममात्रिक छंद	26

TABLE III. SOME 'ARDH SAM MATRIK CHHANDS' WITH THEIR RESPECTIVE MATRA COUNT

Sr.No.	Chhand	Type	Sub Type	Even Matra Count	Odd Matra Count
1	दोहा	मात्रिक छंद	अर्द्धसममात्रिक छंद	11	13
2	सोरठा	मात्रिक छंद	अर्द्धसममात्रिक छंद	13	11
3	उल्लाला(अर्द्धसममात्रिक)	मात्रिक छंद	अर्द्धसममात्रिक छंद	15	13
4	बरवै	मात्रिक छंद	अर्द्धसममात्रिक छंद	7	12
5	रूपमाला / मदन	मात्रिक छंद	अर्द्धसममात्रिक छंद	14	10
6	ताटक	मात्रिक छंद	अर्द्धसममात्रिक छंद	16	14
7	कुकुभ	मात्रिक छंद	अर्द्धसममात्रिक छंद	16	14
8	वीर/आल्हा/मात्रिक सवेया	मात्रिक छंद	अर्द्धसममात्रिक छंद	16	15

TABLE IV. SOME 'VISHAM MATRIK CHHANDS'

Sr.No.	Chhand	Type	Sub Type	Remark
1	कुंडलिया	मात्रिक छंद	विषम मात्रिक छंद	दोहा + रोला
2	छप्पय	मात्रिक छंद	विषम मात्रिक छंद	रोला + उल्लाला

2) 'Varnik Chhands': In the creation or writing of 'Varnik Chhands', the 'Gana' plays a vital role as these verses are based on the characters or 'Varnas'. The predefined sequences as per specific rules need to be maintained for each 'Chhand' according to the different arrangements of 'Gana', 'Laghu', and 'Guru' characters. Table V shows some of the 'Varnik Chhands' and the rules and the symbolic representation of the different regulations.

Here it can be seen that the characters' sequence matters the most and is based on those eight 'Gana', 'Guru', and 'Laghu' characters. Here a few 'Matrik' and 'Varnik' verses are included only. Similarly, 'Ardh Sam Varnik' and 'Visham Varnik' information can be managed and organized.

There are plenty of verses available. So, telling how many 'Chhands' exist is impossible now, but that does not mean that the remaining possibilities should left, so the significant rules and classification-related information were added for many 'Chhands', including the 'Chhands' for which examples or information are less available. Fifty-three different verses information were added here, but to add all the verses is does

not seem to be appropriate as the list goes on and on and the remaining 'Chhands' are not having much information available. Managed information consisting of these verses how the relevant information of already written poems and if some new types follow specific rules, such new classes can be organized in systematic management. If research demands new or additional information blocks for each 'Chhand' can also be added, it was not possible until now due to cluttered and unmanaged raw information.

One more point to be noted here is that this information is just the core detailing of the verse creation structures. Along with that, there are still some more things are there which need to be managed and differs from one verse type to another verse type. The conceptual part will be discussed in the methodology section.

TABLE V. SOME 'VARNIK CHHANDS'

Sr. No.	Chhand	Type	Sub Type	Varna Count	Sequence	Symbolic Representation
1	इन्द्रवज्रा	वर्णिक	समवर्णिक	11	मगण, तगण, तगण, गुरु, गुरु	SSSSSISISIS
2	उपेन्द्रवज्रा	वर्णिक	समवर्णिक	11	जगण, तगण, जगण, गुरु, गुरु	ISISISISISIS
3	वसंततिलका	वर्णिक	समवर्णिक	14	तगण, भगण, जगण, जगण, गुरु, गुरु	SSISIIISISISIS
4	मालिनी	वर्णिक	समवर्णिक	15	नगण, नगण, मगण, यगण, यगण	IIIIISSSSISISIS
5	मन्दाक्रान्ता	वर्णिक	समवर्णिक	17	मगण, भगण, नगण, तगण, तगण, गुरु, गुरु	SSSSSIIIIISISISIS

IV. METHODOLOGY

Based on the systemized rules, the best attempts were made to provide the best possible concrete concept for the automatic metadata generation for Hindi poetries by incorporating the rules-based unified modeling. This research work consists of multiple existing Hindi verses and trying to cover up every poetry that has been already written and having a systematic writing rule but is not found or missing until now and will be written in the future.

A. Data Pre-Processing

UTF-8 standard encoded data for Devanagari was chosen to work with as input for automatic metadata generator to use and integrate with the latest technologies will be more comfortable in the future. The automatic metadata generator expects the information in the form of the UTF-8 based complete poems or a few lines or part of poems [3]. These lines are further processed for the pre-processing of the input for passing it for the further calculations after some necessary trimming and cleaning operations. Once the pre-processed data is ready after the cleaning operation, the cleaned data can be passed for the next separation-related operations. There are several levels of the separation-related processes that occur as per the demand of this research work. The first stage of the separation of data is for the line-level break based on the new line character '\n' as the standard delimiter for separating the lines. After separating

the lines, the lines need to be split further into the parts known as 'Charans' or stanzas of the verse. Separation consists of a few delimiters (';', '||', '|'). If there is any remaining delimiter that needs to be used, it can be used too easily. After the 'Charan' separation, the separate stanzas need to chop into the words by performing word-level separation. Each separated word further needs to be divided into the characters and diacritics.

B. 'Chhand' Detection based on the Classification

One might wonder why this much separation is required, so the straight forward answer to the curiosity going on here is that these different separations are needed at different phases. Based on these separated data, the calculative operations can be performed efficiently and in an organized manner. Several kinds of separated data consisting of the line, stanza, words, and character level separation helps in getting so much meaningful information such as word count, character count, diacritic count, stanza count, the sequence of the words and characters, and these pieces of information help retrieve the more meaningful data while processing the data further.

Let us now understand this concept with an example for better conceptual clarity. Here is an example of one of the Hindi verse type 'Doha' from 'Hanuman Chalisa' by a well-known poet-saint Tulsidas [47]: 'पवनतनय संकट हरन, मंगल मूर्ति रूप | राम लखन सीता सहित, हृदय बसहु सुर भूप ||' ('Pavan tanay sankat harana, mangala murati roop. Ram lakhana sita sahita, Hriday basahu soor bhoop - Oh! conqueror of the Wind, Destroyer of all miseries, you are a symbol of Auspiciousness. Along with Shri Ram, Lakshman and Sita, reside in my heart. Oh! King of Gods').

Here if this text is inputted into metadata generation, the separation takes place in different forms after cleaning operations, which are as follow:

Line Separation: (2 Lines)

Line 1: 'पवनतनय संकट हरन, मंगल मूर्ति रूप',

Line 2: 'राम लखन सीता सहित, हृदय बसहु सुर भूप'

Stanza / 'Charan' Separation: (4 Stanzas)

Stanza 1: 'पवनतनय संकट हरन'

Stanza 2: 'मंगल मूर्ति रूप'

Stanza 3: 'राम लखन सीता सहित'

Stanza 4: 'हृदय बसहु सुर भूप'

Words Separation: (14 Words)

1. 'पवनतनय', 2. 'संकट', 3. 'हरन', 4. 'मंगल', 5. 'मूर्ति', 6. 'रूप', 7. 'राम',
8. 'लखन', 9. 'सीता', 10. 'सहित', 11. 'हृदय', 12. 'बसहु', 13. 'सुर', 14. 'भूप'

Stanza Wise Words Separation:

1. i. 'पवनतनय', ii. 'संकट', iii. 'हरन'
2. i. 'मंगल', ii. 'मूर्ति', iii. 'रूप',
3. i. 'राम', ii. 'लखन', iii. 'सीता', iv. 'सहित'
4. i. 'हृदय', ii. 'बसहु', iii. 'सुर', iv. 'भूप'

Character Wise Separation: (53 Characters)

'प', 'व', 'न', 'त', 'न', 'य', 'स', 'ं', 'क', 'ट', 'ह', 'र', 'न', 'म', 'ं', 'ग', 'ल', 'म', 'ूर्', 'ति', 'र', 'ूप', 'र', 'ा', 'म', 'ल', 'ख', 'न', 'सी', 'ता', 'स', 'ह', 'ि', 'त', 'ह', 'ृ', 'द', 'य', 'ब', 'स', 'हु', 'स', 'ुर', 'भ', 'ूप'

These are the type of different separations. Separation of the diacritic count, 'Guru' and 'Laghu' diacritic counts for the

diacritic count stats were done. To add how many times half characters were used the count of the '्' is used. After this, all the main parts come into the implementation, which is the calculation based on all the rules which can be seen under 3.1 Quantity Calculation Rules Simplified. Let us know the calculation mechanism for detecting the verse, type, subtype, and much more. Let us see stanza wise 'Matra' allocation and counting for the given input:

पवनतनय	संकट	हरन,	मंगल	मूर्ति	रूप		
111111	211	111	211	211	21		
1+1+1+1+1+1	2+1+1	1+1+1	2+1+1	2+1+1	2+1		
6	4	3	4	4	3		
	6+4+3= 13			4+4+3= 11			
राम	लखन	सीता	सहित,	हृदय	बसहु	सुर	भूप
21	111	22	111	111	111	11	21
2+1	1+1+1	2+2	1+1+1	1+1+1	1+1+1	1+1	2+1
3	3	4	3	3	3	2	3
	3+3+4+3 = 13				3+3+2+3 = 11		

The 'Matra' allocation and the 'Matra' Count will be used further to detect verse after the rule-based modeling of verse rules automatically. The 'Matra' allocation is also used after a few modifications and merging for character sequence mapping, specifically for 'Varnik' verses.

After this allocation and 'Matra' counting, the input passes through the different set of rule-based methods specifically designed for the specific verse-based rules. Each verse follows its own unique set of rules. The 53 verses were rule-based modeled, which can be detected in a bottom-up approach in which the verse is seen first. Later on, the verse type and subtype can be mapped with the already available and systematically managed list of types and subtypes relationships.

The provided input must follow all the associated rules of that particular verse to detect a verse automatically. Let us see about the given input after the different parts of the processing.

The automatic metadata generator still does not know which kind of verse it is. However, the metadata generator is modeled with rule-based modeling. The rules for the verse named 'Doha' are already available, so once it will process the data, it is capable enough to say that the provided input was 'Doha'. Let us know more about how it can be said automatically. For 'Doha' writing, it is a rule that the odd stanzas 'Matra' count must be 13, and even stanzas 'Matra' count must be 11.

Along with that, even stanzas should end with the 'Laghu' character. Now when the 'Matra' count operation is performed on the 1st and 3rd stanzas, 'Matra' counts are 13,13 and 2nd and 4th stanzas 'Matra' counts are 11, 11 respectively, also you can see that at the end of 2nd and 4th stanza there is 'Laghu' character. After this much modeling, the metadata generator is aware of the input and can say that it is a 'Doha'. A systematically organized hierarchy from which 'Doha' can be mapped as 'Matrik' type and 'Ardh Sam Martik' subtype.

Similarly, for the 'Varnik' verses, there are different character sequence-based rules that work on the sequences related rules specified for the particular verses and are based on the 'Gana', 'Guru' and 'Laghu' sequences only. In 'Varnik' verses, each of the verses has its own unique rule and needs to

be managed separately. Similarly, after detecting each 'Varnik' verse, its type and subtype can be seen from the mapping with the systematically organized hierarchy of verse.

Even after this much processing, if any verses are not found or detected, they are considered the 'Muktak' verses.

C. Advance 'Muktak' Detection

Thought of advancement concerning research computationally means something which does not exist or available yet. During research, the need for this was felt the most, usually whenever the 'Chhand' detection takes place, and the input gets detected as 'Muktak'. In that case, the input gets chopped into several parts again until it is possible to till 'Charan' level separation. Those separated parts are processed again from scratch as separate input and from which the results get recorded. At last, Metadata Generator can tell us that in 'Muktak' verses also it tried to find out if any part of the 'Muktak' verses is using any 'Matrik' or 'Varnik' verse rules than that will also be detected. That can be one or more than one 'Chhand' rules combination.

Apart from this, while processing the individual input, which uses only one type of 'Chhand' rules, some specific part was having some issues. Because of this mechanism, the input first goes into the 'Muktak' part. Except for the faulty/issue part, all remaining parts get detected as the specific 'Chhand', so metadata generator can generate data as the input is having this particular 'Chhand' and is the primary reason for the higher accuracy success rate of this metadata generator.

D. Stop Words Filtering

After this, to add a few more advancements into this metadata generator, detecting stop words from the given input is one of those advancements. Stop words are filtered through the list of already carried out hybrid research work [48], specifically on the stop words for Hindi's stop words. Filtering the stop words is essential because in the next stage, when the terms are processed through wordnet, stop words should not be processed. This filtering gives the metadata generator ability not to process the stop words while getting meanings from the wordnet. It saves a lot of execution time as well as improve the overall efficiency of the metadata generator.

E. Wordnet Integration for Meaning and another Example of Words

Sometimes a user might want to know the meaning of the words used in verse, for which after removing the stop word, the Hindi wordnet named 'pyiwn' for the meaning of the words and the examples were integrated [49]. The wordnet integration makes the metadata generator more worthy because if a beginner wants to learn and understand Hindi Poetry should be aware of the meaning of the poem's words. The user also gets one another similar example of that work, capable enough to make sure that how specific word should be used.

The wordnet integration helps the wordnet advancement too. As it separates, the list of the word does not exist in the wordnet still, or the meaning of the word is yet not incorporated in the wordnet. This list can be considered for the improvement of the ongoing wordnet research works as well.

F. Example Suggestions of Detected 'Chhand'

This mechanism is integrated with keeping the scenario in mind that a user who wants metadata about the input might be interested in the same types 'Chhand' example of the detected 'Chhand' type. It gives the user more ability to know and understand the 'Chhand' formation better by comparing the input with the suggested example. The example sets were stored in key-value pair in the JavaScript Object Notation (JSON) file from which any random example gets populated whenever the specific 'Chhand' type gets detected.

G. Additional Several Utilities

Data collection issues were faced during the research work as the dataset for such research work is not available as of now directly. A systematic approach was required to avoid redundant data, to maintain and manage the collecting data in a decent form. A utility for data collection was also designed to store and check if the entered data already exists or not, and if not, it will add the inputted data. The data collection utility is capable enough to get the single and the multiple inputs from the Comma Separated Value (CSV) files or Text Files.

A utility to generate some random text-based 'Chhand' from the collection of words on the given parameters of the character set was also developed to test the metadata generator's ability to ensure the capacity to handle the 'Chhand' types which do not exist currently or can come up in future. The metadata generator generates the data about the provided input by combining all the mentioned methodology parts, gives robust metadata, and strengthens the metadata performance.

V. RESULTS

Hindi poems can be written using any 'Chhand' or any combination of 'Chhands'. The research work is sufficient enough to help in the automatic generation of the metadata from the Hindi poetries by covering the majority of 'Chhands' already and having the capability to incorporate new kinds of 'Chhands' in a very systematic manner with ease. Along with the detection of 'Chhands', the metadata generator provides several meaningful and useful information. Information includes Word Count, Character Count, Diacritic Count, Quantity ('Matra') Count, Symbolical String Representation, stop words, Meaning of the words, along with an example of the use of the word for better understanding. So, the approach which is followed can be understood better as per this automatically generated metadata. The result is an example of metadata output generated by the metadata generator. The same example discussed in this paper since the beginning for a better understanding of the metadata generator's working.

The metadata generator is modeled based on the rules of the 111 different 'Chhands' classification types, subtypes, and subtypes of subtypes. The 53 different types shown in Table VI, 'Chhands' data were collected for testing and validation. Each class has at least 20 and a maximum of 277 records based on the data's availability, which may vary for different types. Total 3120 records were found from various sources and tested, from which 2992 records were detected successfully. One hundred twenty-eight records were not detected due to some reasons such as poorly formatted data, some grammar-

related issues, manipulated words from regional languages, unnecessary uses of the special symbols, and junk character.

The overall accuracy rate based on the results is 95.02%, and the failure rate is 04.98%. Fig. 1 represents a graph of the 'Chhand' data found, detected, and not found along with the individual accuracy and failure rates of different 'Chhands'. Fig. 1 shows that the various 'Chhands' accuracy rate varies between 84% to 100%, and the failure rate lies between 0% and 16%. Out of all the 53 different types of 'Chhands' data,

only 5 'Chhands' were having an accuracy rate below 90%, and the rest all were between 90 and 100%, and in that also 29 were having 95 or more than 95 and 100% accuracy rate. The lowest accuracy percentage is 84% of 'Chhapay Chhand', which is made up of two different 'Chhands', which makes its construction and detection complex, and due to that, only the error or issues occurs more. The six best performing 'Chhands' with 100% accuracy rate, were 'Aansu', 'Bhujangprayag', 'Janak', 'Mandakranta', 'Muktak' and 'Tilka'.

TABLE VI. PROCESSED 'CHHAND' DATA DETAILS

Chhand	Found	Detected	Not Detected	Success Rate	Failure Rate	Time (Min.)	Time (Avg.)	Time (Max.)
1.Aansu	30	30	0	100.00	0.00	1.35	1.53	1.80
2.Ahir	46	43	3	93.48	6.52	1.23	2.32	16.37
3.Barvai	36	35	1	97.22	2.78	1.28	1.58	6.33
4.Bhujangi	78	77	1	98.72	1.28	1.36	6.50	17.29
5.Bhujngprayag	42	42	0	100.00	0.00	1.44	2.84	19.10
6.Chandrika	34	33	1	97.06	2.94	1.30	1.95	5.60
7.Chaupai	100	98	2	98.00	2.00	1.26	1.67	14.66
8.Chhapay	25	21	4	84.00	16.00	1.72	7.24	36.99
9.Chopaiya	20	17	3	85.00	15.00	1.32	2.20	5.26
10.Dhar	35	34	1	97.14	2.86	1.22	4.57	14.65
11.Digpal	40	37	3	92.50	7.50	1.44	2.25	14.96
12.Dodhak	47	45	2	95.74	4.26	1.36	6.85	31.41
13.Doha	277	265	12	95.67	4.33	1.21	1.62	6.40
14.Drutvilmbit	162	161	1	99.38	0.62	1.20	5.53	25.81
15.Durmil Savaiya	58	56	2	96.55	3.45	1.47	7.36	25.54
16.Harigitika	83	80	3	96.39	3.61	1.46	28.16	76.94
17.Janak	36	36	0	100.00	0.00	1.27	1.53	1.98
18.Krupan Dhanakshari	29	27	2	93.10	6.90	1.29	2.08	5.72
19.Kukubh	35	33	2	94.29	5.71	1.34	2.30	14.08
20.Kundlia	35	33	2	94.29	5.71	1.48	3.57	35.59
21.Madira Savaiya	60	56	4	93.33	6.67	1.45	13.48	91.79
22.Malini	105	103	2	98.10	1.90	1.31	6.45	22.10
23.Mandakrnta	153	153	0	100.00	0.00	1.31	10.60	68.96
24.Manharan Dhanakshari	43	40	3	93.02	6.98	1.27	1.45	2.60
25.Manoram	48	46	2	95.83	4.17	1.40	2.85	13.83
26.Marhatha	25	23	2	92.00	8.00	1.40	2.01	5.45
27.Muktak	58	58	0	100.00	0.00	1.56	11.03	21.65
28.Nidhi	75	72	3	96.00	4.00	1.50	1.90	7.11
29.Nishchal	30	28	2	93.33	6.67	1.36	2.47	14.52
30.Panchamar	43	41	2	95.35	4.65	1.35	5.16	15.94
31.Piyushvarsh	50	49	1	98.00	2.00	1.29	1.70	13.75
32.Pramanika	39	38	1	97.44	2.56	1.27	7.29	18.65
33.Ras	33	31	2	93.94	6.06	1.29	1.70	5.45
34.Rola	147	140	7	95.24	4.76	1.31	3.68	38.87
35.Roopmala	20	19	1	95.00	5.00	1.59	7.58	15.55
36.Sagun	24	22	2	91.67	8.33	1.28	2.68	14.92
37.Sar	28	25	3	89.29	10.71	1.28	5.76	2.08
38.Sarsi	38	36	2	94.74	5.26	1.30	1.68	5.61
39.Shankar	30	26	4	86.67	13.33	1.31	3.28	14.61
40.Shardul Vikridit	32	29	3	90.63	9.38	1.62	17.29	32.02
41.Sindhu	34	32	2	94.12	5.88	1.36	2.62	15.57
42.Sortha	52	51	1	98.08	1.92	1.26	1.49	5.22
43.Sur Dhanakshari	38	37	1	97.37	2.63	1.29	1.63	5.63
44.Swagta	25	23	2	92.00	8.00	1.42	8.32	17.01
45.Tantak	30	27	3	90.00	10.00	1.53	4.60	23.64
46.Tilka	54	54	0	100.00	0.00	1.22	3.65	15.19
47.Tomar	45	41	4	91.11	8.89	1.53	2.82	13.14
48.Tribhangi	27	25	2	92.59	7.41	1.23	4.07	16.86
49.Trotak	52	51	1	98.08	1.92	1.36	3.43	15.37

50.Ullala	31	30	1	96.77	3.23	1.28	1.82	7.45
51.Vanshasth	109	108	1	99.08	0.92	1.28	12.66	55.10
52.VasantTilka	238	222	16	93.28	6.72	1.20	3.99	22.64
53.Vidhata	56	53	3	94.64	5.36	1.25	1.67	5.34
Total	3120	2992	128	5035.21	264.79	71.69	256.45	1020.07
Maximum	277	265	16	100.00	16.00	1.72	28.16	91.79
Minimum	20	17	0	84.00	0.00	1.20	1.45	1.80
Average	58.87	56.45	2.42	95.00	5.00	1.35	4.84	19.25

Chhand Detection Results

Detection Data, Success and Failure rates

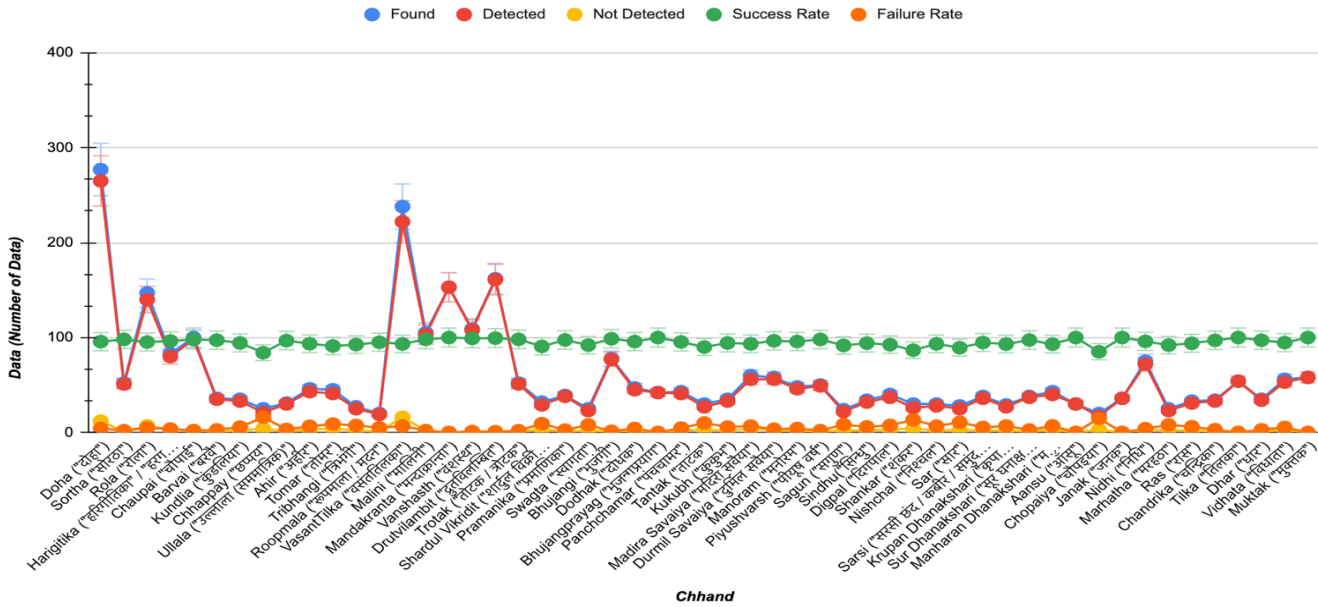


Fig. 1. Graph Showing 'Chhand' Detection Results.

Execution Time Results

Metadata Generation Execution Time

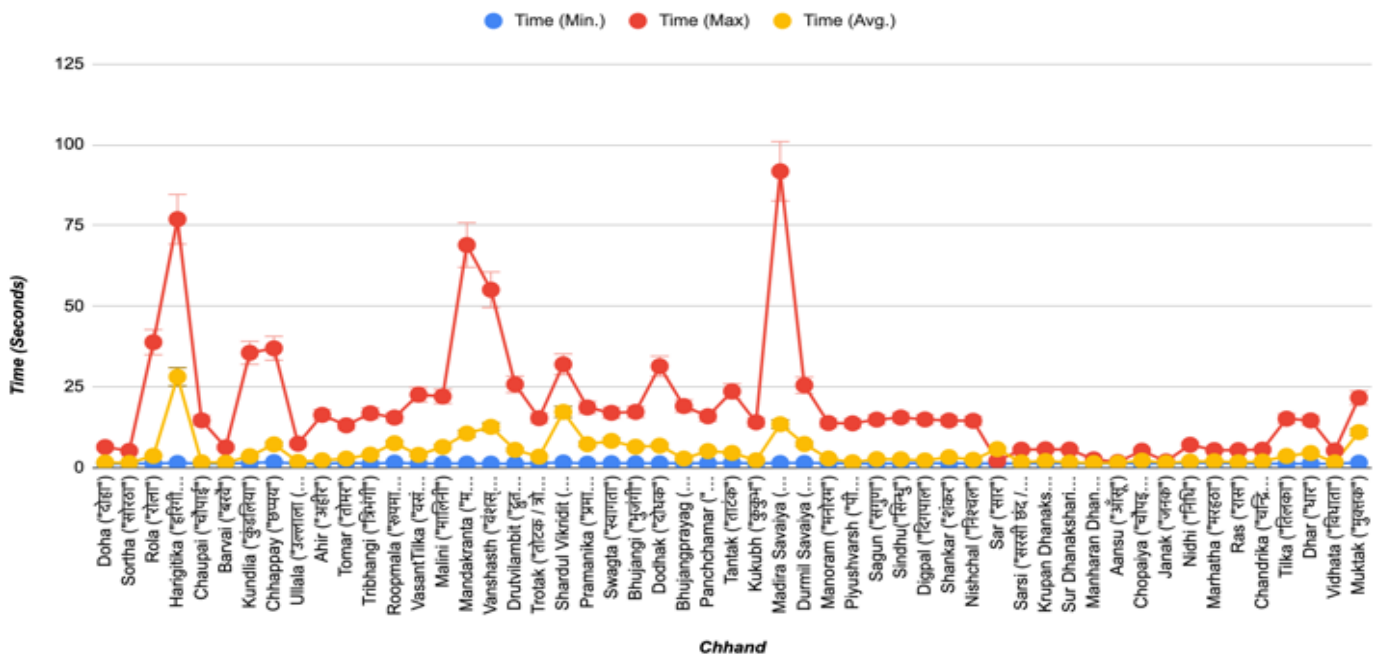


Fig. 2. Graph Showing Execution Time Results.

REFERENCES

- [1] Wikipedia Contributors, "Hindi," *Wikipedia*, May 04, 2019. <https://en.wikipedia.org/wiki/Hindi> (accessed Sep. 18, 2020).
- [2] Wikipedia Contributors, "Devanagari," *Wikipedia*, Sep. 18, 2020. <https://en.wikipedia.org/wiki/Devanagari> (accessed Sep. 18, 2020).
- [3] "Unicode 13.0.0," www.unicode.org, Sep. 18, 2020. <http://www.unicode.org/versions/Unicode13.0.0/> (accessed Sep. 18, 2020).
- [4] Wikipedia Contributors, "Poetry," *Wikipedia*, Sep. 18, 2020. <https://en.wikipedia.org/wiki/Poetry> (accessed Sep. 18, 2020).
- [5] Wikipedia Contributors, "Computational linguistics," *Wikipedia*, Sep. 18, 2020. https://en.wikipedia.org/wiki/Computational_linguistics (accessed Sep. 18, 2020).
- [6] L. Schubert, "Computational Linguistics (Stanford Encyclopedia of Philosophy)," *Stanford.edu*, 2014. <https://plato.stanford.edu/entries/computational-linguistics/> (accessed Sep. 18, 2020).
- [7] M. K. Audichya and J. R. Saini, "Computational linguistic prosody rule-based unified technique for automatic metadata generation for Hindi poetry," *2019 1st International Conference on Advances in Information Technology (ICAIT)*, Jul. 2019, doi: 10.1109/icaity47043.2019.8987239.
- [8] B. K. Joshi and K. Kumar Kushwah, "A Novel Approach to Automatic Detection of Chhanda in Hindi Poems," *IEEE Xplore*, Sep. 01, 2018. <https://ieeexplore.ieee.org/document/8675052> (accessed Sep. 18, 2020).
- [9] K. K. Kushwah and B. K. Joshi, "Rola: An Equi-Matrix Chhanda of Hindi Poems," *Journal of Computer Science Ijcsis*, vol. 15, no. 3, 2017, Accessed: Sep. 18, 2020. [Online]. Available: https://www.academia.edu/32482898/Rola_An_Equi-Matrix_Chhanda_of_Hindi_Poems.
- [10] P. B. Bafna and J. R., "On Exhaustive Evaluation of Eager Machine Learning Algorithms for Classification of Hindi Verses," *International Journal of Advanced Computer Science and Applications*, vol. 11, no. 2, 2020, doi: 10.14569/ijacsa.2020.0110224.
- [11] P. Bafna and J. R. Saini, "Hindi Poetry Classification using Eager Supervised Machine Learning Algorithms," *IEEE Xplore*, Mar. 01, 2020. <https://ieeexplore.ieee.org/abstract/document/9167632> (accessed Sep. 18, 2020).
- [12] P. B. Bafna and J. R. Saini, "Hindi Verse Class Predictor using Concept Learning Algorithms," *IEEE Xplore*, Mar. 01, 2020. <https://ieeexplore.ieee.org/document/9074850> (accessed Sep. 18, 2020).
- [13] J. Kaur and J. R. Saini, "Punjabi Poetry Classification," *Proceedings of the 9th International Conference on Machine Learning and Computing - ICMLC 2017*, 2017, doi: 10.1145/3055635.3056589.
- [14] J. Kaur and J. R. Saini, "Automatic Punjabi poetry classification using machine learning algorithms with reduced feature set," *International Journal of Artificial Intelligence and Soft Computing*, vol. 5, no. 4, p. 311, 2016, doi: 10.1504/ijaisc.2016.081353.
- [15] J. Kaur and J. R. Saini, "Automatic classification of Punjabi poetries using poetic features," *International Journal of Computational Intelligence Studies*, vol. 7, no. 2, p. 124, 2018, doi: 10.1504/ijcistudies.2018.094901.
- [16] J. Kaur and J. R. Saini, "PuPoCl: Development of Punjabi Poetry Classifier Using Linguistic Features and Weighting," *INFOCOMP Journal of Computer Science*, vol. 16, no. 1-2, pp. 1-7, Dec. 2017, Accessed: Sep. 18, 2020. [Online]. Available: <https://infocomp.dcc.ufla.br/index.php/infocomp/article/view/546>.
- [17] J. Kaur and J. Saini, "Designing Punjabi Poetry Classifiers Using Machine Learning and Different Textual Features," *The International Arab Journal of Information Technology*, pp. 38-44, Jan. 2019, doi: 10.34028/iajit/17/1/5.
- [18] K. Pal and B. V. Patel, "Model for Classification of Poems in Hindi Language Based on Ras," *Smart Systems and IoT: Innovations in Computing*, pp. 655-661, Oct. 2019, doi: 10.1007/978-981-13-8406-6_62.
- [19] J. R. Saini and J. Kaur, "Kāvi: An Annotated Corpus of Punjabi Poetry with Emotion Detection Based on 'Navrasa,'" *Procedia Computer Science*, vol. 167, pp. 1220-1229, Jan. 2020, doi: 10.1016/j.procs.2020.03.436.
- [20] P. B. Bafna and J. R., "An Application of Zipf's Law for Prose and Verse Corpora Neutrality for Hindi and Marathi Languages," *International Journal of Advanced Computer Science and Applications*, vol. 11, no. 3, 2020, doi: 10.14569/ijacsa.2020.0110331.
- [21] P. B. Bafna and J. R. Saini, "BaSa: A Technique to Identify Context based Common Tokens for Hindi Verses and Proses," *2020 International Conference for Emerging Technology (INCET)*, Jun. 2020, doi: 10.1109/incet49848.2020.9154124.
- [22] A. Kulkarni and G. Huet, "Google Books," books.google.com, Jan. 15, 2009. https://books.google.com/books/about/Sanskrit_Computational_Linguist (accessed Sep. 18, 2020).
- [23] H. Han, E. Manavoglu, H. Zha, K. Tsioutsoulouklis, C. L. Giles, and X. Zhang, "Rule-based word clustering for document metadata extraction," *Proceedings of the 2005 ACM symposium on Applied computing - SAC '05*, 2005, doi: 10.1145/1066677.1066917.
- [24] X. Yu *et al.*, "Using Automatic Metadata Extraction to Build a Structured Syllabus Repository," *Asian Digital Libraries. Looking Back 10 Years and Forging New Frontiers*, pp. 337-346, 2007, doi: 10.1007/978-3-540-77094-7_43.
- [25] M.-T. Sagri and D. Tiscornia, "Metadata for content description in legal information," *IEEE Xplore*, Sep. 01, 2003. <http://ieeexplore.ieee.org/document/1232110> (accessed Sep. 18, 2020).
- [26] J. L. Klavans *et al.*, "Computational linguistics for metadata building (CLIMB): using text mining for the automatic identification, categorization, and disambiguation of subject terms for image metadata," *Multimedia Tools and Applications*, vol. 42, no. 1, pp. 115-138, Nov. 2008, doi: 10.1007/s11042-008-0253-9.
- [27] N. Ghneim and O. Alsharif, "Emotion Classification in Arabic Poetry Using Machine Learning building a model for gender, dialect and age prediction from Arabic tweets View project Interactive Arabic Dictionary View project Emotion Classification in Arabic Poetry using Machine Learning," *International Journal of Computer Applications*, vol. 65, no. 16, pp. 975-8887, 2013, Accessed: Sep. 18, 2020. [Online].
- [28] S. Hamidi, F. Razzazi, and M. P. Ghaemmaghami, "Automatic meter classification in Persian poetries using support vector machines," *IEEE Xplore*, Dec. 01, 2009. <https://ieeexplore.ieee.org/document/5407514> (accessed Sep. 18, 2020).
- [29] Z.-S. He, W.-T. Liang, L.-Y. Li, and Y.-F. Tian, "SVM-Based Classification Method for Poetry Style," *IEEE Xplore*, Aug. 01, 2007. <https://ieeexplore.ieee.org/document/4370650> (accessed Sep. 18, 2020).
- [30] A. Abbasi, H. Chen, and A. Salem, "Sentiment analysis in multiple languages," *ACM Transactions on Information Systems*, vol. 26, no. 3, pp. 1-34, Jun. 2008, doi: 10.1145/1361684.1361685.
- [31] J. Kaur and J. R. Saini, "A Study and Analysis of Opinion Mining Research in Indo-Aryan, Dravidian and Tibeto-Burman Language Families," *International Journal of Data Mining And Emerging Technologies*, vol. 4, no. 2, p. 53, 2014, doi: 10.5958/2249-3220.2014.00002.0.
- [32] "छंद सारवली," <https://ia601900.us.archive.org/24/items/in.ernet.dli.2015.478241/2015.478241.Chhand-sarawali.pdf>.
- [33] J. Bhanu, "छंदःप्रभाकर," <https://ia801605.us.archive.org/15/items/in.ernet.dli.2015.322488/2015.322488.99999990253040.pdf>, 1935.
- [34] Contributors to Wikimedia projects, "छंद," *Wikipedia.org*, Apr. 16, 2008. <https://hi.wikipedia.org/wiki/%E0%A4%9B%E0%A4%82%E0%A4%A6> (accessed Sep. 18, 2020).
- [35] C. by Admin and V. Groups, "भारतीय छंद विधान," [www.openbooksonline.com](http://www.openbooksonline.com/groups/group/show?groupUrl=chhand&%2F=). <http://www.openbooksonline.com/groups/group/show?groupUrl=chhand&%2F=> (accessed Sep. 18, 2020).
- [36] "छन्द - भारतकोश, ज्ञान का हिन्दी महासागर," <http://bharatdiscovery.org/india/%E0%A4%9B%E0%A4%A8%E0%A5%8D%E0%A4%A6>.
- [37] "kavyakala," *Kavyakala*. <https://kavyakala.blogspot.com/> (accessed Sep. 18, 2020).
- [38] "स्वस्थ हिन्दी समाज," hhindisamaj.blogspot.com. <http://hhindisamaj.blogspot.com/> (accessed Sep. 18, 2020).
- [39] "हिन्दी साहित्य काव्य संकलन - हिन्दी की कविता, लघुगीत, बालगीत, फिल्म गीत, गजल, शायरी, धार्मिक लोकगीत का विशाल संकलन," हिन्दी साहित्य. <http://www.hindisahitya.org/> (accessed Sep. 18, 2020).
- [40] *Hindi Chhandolakshan*. Vani Prakashan.
- [41] Contributors to Wikimedia projects, "वैदिक छंद," *Wikipedia.org*, Dec. 24, 2014. <https://hi.wikipedia.org/wiki/%E0%A4%B5%E0%A5%88%E0>

- A4%A6%E0%A4%BF%E0%A4%95_%E0%A4%9B%E0%A4%82%E0%A4%A6 (accessed Sep. 18, 2020).
- [42] “Chhand In Hindi-छंद की परिभाषा, भेद और उदाहरण,” *hindimeaning.com*, Feb. 06, 2018. <https://www.hindimeaning.com/2018/02/chhand-in-hindi.html> (accessed Sep. 18, 2020).
- [43] “स्वस्थ हिन्दी समाज: भुजंगी छंद (साहिल),” स्वस्थ हिन्दी समाज, May 13, 2018. http://hhindisamaj.blogspot.com/2018/05/blog-post_13.html (accessed Sep. 18, 2020).
- [44] “सं.अमि पुराण | गीताप्रेस, गोस्वपुर.” <https://book.gitapress.org/product-style-5/gitapress-570/> (accessed Sep. 18, 2020).
- [45] “Pingala,” *Wikipedia*, Aug. 26, 2020. <https://en.wikipedia.org/wiki/Pingala> (accessed Sep. 18, 2020).
- [46] “Gayatri Mantra,” *Wikipedia*, Sep. 16, 2020. https://en.wikipedia.org/wiki/Gayatri_Mantra (accessed Sep. 18, 2020).
- [47] “Hanuman Chalisa,” *Wikipedia*, Aug. 02, 2020. https://en.wikipedia.org/wiki/Hanuman_Chalisa.
- [48] V. Jha, M. N, P. D. Shenoy, and V. K R, “Hindi Language Stop Words List,” *data.mendeley.com*, vol. 1, Apr. 2018, doi: 10.17632/bsr3frvvc.1.
- [49] R. Panjwani and P. Bhattacharyya, “pyiwn: A Python-based API to access Indian Language WordNets.” Accessed: Sep. 18, 2020. [Online]

Detection and Recognition of Moving Video Objects: Kalman Filtering with Deep Learning

Hind Rustum Mohammed¹

Faculty of Computer Science and Mathematics
University of Kufa (UoKufa)
Najaf, Iraq

Zahir M. Hussain²

Computer Science and Mathematics, UoKufa, Iraq
Professor, School of Engineering, Edith Cowan University
Joondalup, Australia

Abstract—Research in object recognition has lately found that Deep Convolutional Neuronal Networks (CNN) provide a breakthrough in detection scores, especially in video applications. This paper presents an approach for object recognition in videos by combining Kalman filter with CNN. Kalman filter is first applied for detection, removing the background and then cropping object. Kalman filtering achieves three important functions: predicting the future location of the object, reducing noise and interference from incorrect detections, and associating multi-objects to tracks. After detection and cropping the moving object, a CNN model will predict the category of object. The CNN model is built based on more than 1000 image of humans, animals and others, with architecture that consists of ten layers. The first layer, which is the input image, is of $100 * 100$ size. The convolutional layer contains 20 masks with a size of $5 * 5$, with a ruling layer to normalize data, then max-pooling. The proposed hybrid algorithm has been applied to 8 different videos with total duration of is 15.4 minutes, containing 23100 frames. In this experiment, recognition accuracy reached 100%, where the proposed system outperforms six existing algorithms.

Keywords—Convolution Neural Network (CNN); Kalman filter; moving object; video tracking

I. INTRODUCTION

The problem of detection and recognition of moving objects in deep learning lies in detecting the location of the object and segmentation with removing its background [1]. The recognition model requires object's image without background and a correct categorical label that enables the model to predict the correct location and label the moving object [2].

When addressing the recognition mission, the first important issue to consider is to arrange the class that can be recognized. It is very important to organize knowledge at various levels, and this issue has taken a great interest in Cognitive Psychology, for example in Brown's work, a cat cannot only be thought of as a cat, but a quadruped, boxer, or in general an animated being. Cat is the term in the level of semantic hierarchy that comes to mind most easily, which is by no means accidental [3, 4]. Experimental results revealed that there is a basic level in human categorization. The trouble of object-recognition in digital images have been in the core of computer-vision research a lot of time ago [5]. Past Pascal VOC challenge and ongoing Image-Net wide Scale Visual-Recognition Challenge (ILSVRC) have united significant operations required for the solution of this matter in video

scenes. Growing methods in learning with applications in patient's monitoring and health care such as in [6, 7].

This paper is motivated by the need for higher accuracy in the process of finding objects and components within a video, despite obstacles like the distance being detected by the camera or blurring of the image while the object is moving, where these factors contribute to errors in existing techniques.

This paper is organized as follows: Section 2 deals with related work, while the Section 3 focuses on special details required for theoretical background. Section 4 discusses the dataset, and Section 5 explains the proposed work, with results in Section 6.

II. RELATED WORK

The problem addressed consists of two directions: object localization and object recognition. In [8] (2019) the authors presented a deep neural network algorithm based on the effect of visual variation applied on iLab 20M dataset of toy vehicle objects under variations of lighting, viewpoint, background, and focal setting. The experiment results on 1.751 million images from iLab 20M showed significant improvement in accuracy of object detection: DenseNet: 85.6% to 91.6%, 86.5% to 90.71%, AlexNet: 84.5% to 91.6%). CNN improves variation learning as it is capable of noticing special features and has better learning of object representations, where it decreased detection error rate of ResNet by 33%, Alexnet by 43%, and DenseNet by 42. The author in [9] presented a method for recognizing video objects of interest by applying the global Label Distribution Protocol (LDP) then applying the Speeded up Robust Features (SURF) detector. Finally, the objects in the videos are compared and matched with the objects of interest. In [10] the Authors presented the low performers (developmental prosopagnosics (DP)) by the Cambridge Face Perception Test (CFPT) and Cambridge Face Memory Task (CFMT) as signification methods for detection and matching of human face in real time video based on VG factor in visual domain, where they examined the performance of 14 individuals whom were contacted because they are more experienced than their peers at detection and recognizing faces who scored over 90% correct on the online version of CFMT Aus. In [11] the Authors presented a tool for detection and recognition of new object sample in a video by applying the Hybrid-Incremental Learning method (HIL) with Support Vector Machine (SVM), which can improve the recognition ability by learning new object samples and new object

concepts during the interaction with humans. This hybrid technique improves the recognition quality by minimizing the prediction error. In [12] they worked on removing the background of an image for enhancement of detection and recognition using CNN model of recognition.

III. BACKGROUND

Machine learning is about patterns study that gives computers the capability to learn without being explicitly programmed, where during the training phase the machine learns how to build models and algorithms to predict new data. The most important type of neural networks in deep learning is convolutional neural network (CNN), which is specifically designed for recognition and detection of images.

The author in [13] shows that the performance of various pooling methods used in detecting pictorial objects can be obscured by several confounding factors such as the link between the sample cardinality in the spatial pool and the resolution at which low-level features have been extracted. The authors provide a detailed theoretical analysis of max pooling and average pooling, and give extensive empirical comparisons for object recognition tasks. The author in [14] explains Restricted Boltzmann machines using binary stochastic hidden units, where these can be generalized by replacing each binary unit by an infinite number of copies all having the same weight but have progressively more negative biases. The learning and inference rules for these “Stepped Sigmoid Units” are unchanged. They can be approximated efficiently by noisy rectified linear units (ReLU’s). Compared with binary units, these units learn features that are better for object recognition on the NORB dataset and face verification on the Labeled Faces in the Wild dataset. Unlike binary units, rectified linear units preserve information about relative intensities as information travels through multiple layers of feature detectors.

CNN contains many layers of networks that extract features of an image and detect the class for which it belongs; of course, after it is trained with a set of standard images. The architecture and work of CNN is detailed in [15,16].

CNN contains layers, in every layer we convert one size to another through a differentiable procedure. Three types of layers construct a CNN: Convolutional Layer, Pooling Layer, Fully Connected Layer. The first stage is the convolutional layer which processes the image to extract only salient features in it. Filtering the input image to produce the feature map or activation map [17]. Convolution is pure mathematical method achieved in three stages: the first stage is sliding mask feature and image matching patch, second stage is to multiply each input image part (of size equals the mask size) with mask, third stage is the sum of all these multiplications to find the average, then filling the result in a new matrix of features [18].

The second part in the structure of CNN model is the pool operation to shrink the input image matrix for every feature acquired from previous step (convolutional). This is achieved by first selecting appropriate mask size 2 or 3, then selecting a

stride moving area of image pixels, usually 2, then sliding the mask over convoluted images [19]; and finally, picking the maximum value from every mask. The third part in the structure of CNN model is the ReLU activation function, through which we pass the pooling result where every pixel that is less than zero will be nulled.

The final part in the structure of CNN model is the classification layer, which is a fully connected layer in which we decide the label of the input data, decided based on the highest voted category [20]. The layers of the convolution network can decrease the error of classification using back propagation to produce best prediction. Layers are passed through multiple times (in iterative fashion) [21].

IV. THE DATASET

In this work we build a dataset containing 1000 images from animal and human images from CIFAR-10 database, where each image has the size of 100*100 pixels.

V. THE PROPOSED APPROACH

In this work we build a dataset containing 1000 images from animal and human images from CIFAR-10 database, where each image has the size of 100*100 pixels.

A. Detection of Moving Object with Kalman Filter

The approach uses repetitive prediction and correction to compute the correct location of the object by comparing the current state with previous state of the object recorded in the history of guessing. Kalman filter algorithm is simply the best tool here as it is based on recursive procedure. Kalman filter has a measurement relation and a state model as shown in the following equations:

$$s(t) = O(t-1) s(t-1) + w(t) \quad (1)$$

$$z(t) = H(t) s(t) + v(t) \quad (2)$$

where $v(t)$, $w(t)$ are noise processes of Gaussian distribution with zero average, $H(t)$ is measurement matrix, and $O(t-1)$ is the state transition matrix. After collecting videos of multiple objects, the following Algorithm for detection and tracking of objects is presented. Table I clarifies the details of the steps used in this algorithm.

TABLE I. DETECTION AND BACKGROUND REMOVAL ALGORITHM

Step1:	Prediction and correction by the Kalman filter.
Step2:	A) Compute the variation of intensity between current frame and next frame. B) Select a threshold.
Step3:	If threshold is less than variation between frames, continue.
Step4:	Compute the centroid of object.
Step5:	Create mask of detecting and acquire the position of match and move to analysis.
Step6:	Move the object vertically or horizontally based on certain dimension, where the movements of object in anticlockwise or clockwise.
Step7:	Return the location of object.

The threshold operation helps in separation of foreground and background from the frame, where it is enabled to build a mask for moving objects. It is a requisite to distinguish between noisy clutters motion and real motion of objects. Object to be tracked and detected have features like shape, edge, color, and boundaries. Procedure of tracking movement of object based on observed point in current frame using the previous frame is shown in Fig. 1.

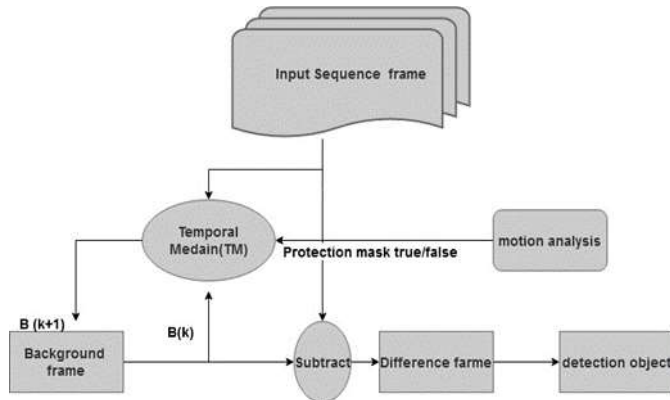


Fig. 1. Detection and Background Removal of Moving Objects.

B. Recognition of Moving Object by CNN

After detecting the object and cropping by Kalman filter, the CNN is applied for training and building a model capable of predicting the new object. In this work each color image consists of three bands (red, green, blue), where the CNN size can be arranged to handle color images; for example, when the color image is of 50*50 size, the hidden layer in CNN model would be of size 50*50*3. When we scale the color image to 100*100, then we need 100*100*3=30000 weights in the hidden layer. CNN input can solve scalability problem. The Layers of CNN have neurons arranged in three dimensions (Height, Width, and Depth) as shown in Fig. 2.

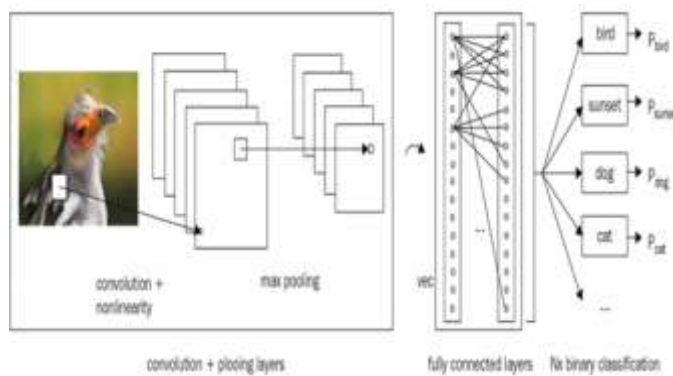


Fig. 2. Operation of CNN.

VI. EXPERIMENTS AND RESULTS

To validate the proposed system, we downloaded 8 different videos from Google, the total video time is 15.4 minutes, each consists of 23100 frames, contains animals and humans. Two basic steps are applied, the first step is for the detection and tracking of the object then removing background by Kalman filtering, the second step is applying the CNN to recognize the object.

A. Detection and Tracking of an Object by Kalman Filter

We apply Kalman filtering for detecting the moving objects. Kalman filter help in three functions: guessing the future location of object, decreasing of noise coming from faulty detections, and facilitating the operation of associating multiple objects to their tracks. The first step is to load the video by using vision.Videoplayer function of MATLAB. After extracting frames of a video, we find the prediction (future position) and correction (error) by the Kalman filtering, then we compute the variation of intensity between current frame and next frame, and select a threshold (the threshold should be less than variation between frames). After that we compute the centroid of object and create a mask of detection and position of matching, move to video components and define object movement, where the object moves vertically or horizontally based on center dimension, where movements are in anticlockwise or clockwise.

B. Recognition of Moving Object by CNN

After detecting the location of object and removing the background of frame, then CNN is introduced for a training model. The size of object is 100*100*3 and the training setup of CNN is as follows. Learning rate is 0.001 and momentum is 0.9. The network architecture consists of four convolutional layers and four pooling layers, followed by two fully connected layers. Each convolutional layer is followed by a ReLU layer, which is an effective activation function to improve the performance of the CNNs. Regularization with the weight decay 5×10^{-4} is used in the network training. The dropout ratio is set as 0.5. The learning rate is initially set as 0.001 and the training is stopped after 1000 epochs. After building the network architecture, then we train CNN model. After building the CNN training model, the video will be processed for detection and background removal. The last process is to classify the moving object using the hybrid technique of Kalman filtering followed by CNN, which achieved (in this experiment) accuracy of 100%. The proposed system has been shown to outperform six other works, as in the Table II.

TABLE II. COMPARISONS WITH EXISTING METHODS

Authors	tools	accuracy
This work	CNN + Kalman filter	100%
Muhammad [22]	SVM classifier	97.95%
Bruno et al. [23]	ANN and k-NN	97%
Tian et al. [24]	Hierarchical Filtered Motion	94%KTH Human Action Dataset
Modarres et al. [25]	Body Posture Graph	94%KTH Human Action Dataset
Sheng et al. [26]	HOG Feature Directional Pairs	94.99 % KTH Human Action Dataset
Kuma et al. [27]	Gabor-Ridgelet Transform	96% KTH Human Action Dataset

VII. CONCLUSIONS

This paper proposed a hybrid system of Kalman filtering and CNN for detection (with background removal) and recognition of moving objects in videos. The algorithm shows an increase in accuracy of guessing new cases when tested using 8 different videos with total video time of 15.4 minutes and 23100 frames. In that test, the rate of accuracy 100% has been reached for identification and recognition of moving objects. Experimental results show the superiority of the proposed detection and recognition approach as compared to existing algorithms, especially in presence of occlusions, making it more appropriate for many applications such as airport control.

REFERENCES

- [1] M. Everingham, et al, The PASCAL Visual Object Classes Challenge: A Retrospective, International Journal of Computer Vision, 2015.
- [2] O. Russakovsky et al, ImageNet Large Scale Visual Recognition Challenge, International Journal of Computer Vision volume, 2015.
- [3] C. Crispim-Junior, et al, Semantic event fusion of different visual modality concepts for activity recognition, IEEE Transactions on Pattern Analysis and Machine Intelligence PP (99) (2016).
- [4] H. Pirsiavash, D. Ramanan, Detecting activities of daily living in first-person camera views, in: IEEE Conference on Computer Vision and Pattern Recognition (CVPR), 2012, IEEE, 2012.
- [5] S. Chaabouni, J. Benois-Pineau, O. Hadar, C. B. Amar, Deep learning for saliency prediction in natural video.
- [6] P. Parker, K. Englehart, B. Hudgins, Myoelectric signal processing for control of powered limb prostheses, J Electromyogr Kinesiol 16 (6) (2006) 541–548.
- [7] L. H. Smith, L. J. Hargrove, B. A. Lock, T. A. Kuiken, Determining the optimal window length for pattern recognition-based myoelectric control: balancing the competing effects of classification error and controller delay, IEEE Trans Neural Syst Rehabil Eng 19 (2) (2011) 186–192.
- [8] Jatuporn ToyLeksut, et al, “Learning visual variation for object recognition”, Image and Vision Computing, 2020.
- [9] M. Gomathy Nayagam, “Reliable object recognition system for cloud video data based on LDP features”, Computer Communications Volume 149, January 2020, Pages 343-349.
- [10] Rebecca K. Hendel, “The good, the bad, and the average: Characterizing the relationship between face and object processing across the face recognition spectrum”, Neuropsychologia, 2019.
- [11] Chengpeng Chen, “Hybrid incremental learning of new data and new classes for hand-held object recognition”, J. of Visual Communication and Image Representation, 2019.
- [12] Fang Wei,” DOG: A new background removal for object recognition from images”, Engineering Applications of Artificial Intelligence, Volume 91, 2020.
- [13] Boureau, Y.-L., ‘A theoretical analysis of feature pooling in visual recognition’, Proceedings of the 27th International Conference on Machine Learning, 2010.
- [14] Nair, V., “Rectified linear units improve restricted boltzmann machines”, in ‘Book Rectified linear units improve restricted boltzmann machines’ (2010, edn.), pp. 807-814.
- [15] Krizhevsky, A., “Imagenet classification with deep convolutional neural networks”, ‘Book Imagenet classification with deep convolutional neural networks’ (2012, edn.), pp. 1098-1106.
- [16] Bottou, L., ‘Stochastic gradient descent tricks’, Neural networks: Tricks of the trade, 2012.
- [17] Christos-Christodoulos, “Hydrophobicity classification of composite insulators based on convolutional neural networks”, Engineering Applications of Artificial Intelligence, 2020.
- [18] T. Shanthi, “Automatic diagnosis of skin diseases using convolution neural network”, Microprocessors and Microsystems Volume 76, July 2020.
- [19] Amin Khatamia, “A weight perturbation-based regularisation technique for convolutional neural networks and the application in medical imaging”, Expert Systems with Applications, 2020.
- [20] Ding-Xuan Zhou, “Theory of deep convolutional neural networks: Downsampling”, Neural Networks Volume 124, April 2020, Pages 319-327.
- [21] The CIFAR-10 dataset.
- [22] Muhammad Ehatisham-ul-Haq, “Continuous authentication of smartphone users based on activity pattern recognition using passive mobile sensing”, J. Network and Computer Applications, 2018.
- [23] Bruno Urbano Rodrigues, “Cachaça Classification Using Chemical Features and Computer Vision”, Procedia Computer Science, Volume 29, 2014, Pages 2024-2033.
- [24] D. K. Vishwakarma, et al, “Unified framework for human activity recognition: An approach using spatial edge distribution and R-transform”, AEU-Int. J. of Electronics and Communications, 2016.
- [25] T. Cover and P. Hart, “Nearest neighbour pattern classification,” IEEE Transactions on Information Theory, vol. 13, no. 1, p. 1967, 21-27.
- [26] Y. L. Tian, L. Cao, Z. Liu and Z. Zang, “Hierarchical Filtered Motion for Action Recognition in Crowded Videos,” IEEE Transactions on Systems, Man, and Cybernetics, Part C, 2012.
- [27] Kumar Vishwakarma, D., “A Two-fold Transformation Model for Human Action Recognition using Decisive Pose,” Cognitive Systems Research, 2020.

Performance Evaluation of Different Mobile Ad-hoc Network Routing Protocols in Difficult Situations

Sultan Mohammed Alkahtani¹, Fahd Alturki²

Electrical Engineering Department, King Saud University, Riyadh, Saudi Arabia

Abstract—Performance evaluation of Mobile Ad-hoc Network (MANET) routing protocols is essential for selecting the appropriate protocol for the network. Many routing protocols and different simulation tools were proposed to address this task. This paper will introduce an overview of MANETs routing protocols as well as evaluate MANET performance by using three reactive protocols—Dynamic Source Routing (DSR), Ad-Hoc On-demand Distance Vector (AODV), and Dynamic MANET On-Demand (DYMO)—in three different scenarios. These scenarios are designed carefully to mimic real situations by using OMNET++. The first scenario evaluates the performance when the number of nodes increases. In the second scenario, the performance of the network will be evaluated in the presence of obstacles. In the third scenario, a group of nodes will be suddenly shut down during the communication. The network evaluation is carried out in terms of packets received, end-to-end delay, transmission count or routing overhead, throughput, and packet ratio.

Keywords—Ad-hoc network; performance evaluation; network simulation; MANET; DSR; AODV; DYMO; routing protocols; Omnet++

I. INTRODUCTION

Wireless networks have reduced the use of wired networks by enabling devices to communicate easily without using cables and wires. The free mobility that is provided by wireless networks has overcome some of the challenges of wired networks such as being difficult, time-consuming, and expensive to install and maintain. These networks have become more popular and secure with new technologies and security protocols [1].

A wireless network is divided into two main types: infrastructure-based and infrastructure-less. An infrastructure-based network is one in which all wireless devices communicate and share information through infrastructure units such as access points, routers, or PCs running access point software [2]. Infrastructure-less or ad-hoc networks are direct connections between wireless devices with no infrastructure units such as a router or access point. Fig.1 compares how devices are connected in an infrastructure network versus an infrastructure-less network. In ad-hoc networks, the network can be set up easily with no aid from infrastructure units, such as access points. In this network, each node has a transmission range. When the destination is out of this range, the connectivity between the transmitter and the receiver will depend on the intermediate nodes. In the aforementioned case, the intermediate node will act as a router. This independence in an ad-hoc network offers free deployment and low cost for the network. Ad-hoc networks

can be classified into three types: Mobile Ad-hoc Networks (MANETs), Wireless Sensor Networks (WSNs), and Wireless Mesh Networks (WMNs).

A MANET is a temporary auto-configuration network that supports users continuously and dynamically changes its network topology. This means the nodes communicate without administration and may connect to the Internet or operate as standalones. In MANETs, routing protocols are essential to finding the right path between the source and the destination. There are many challenging factors for the routing protocols of MANETs. In some situations, the mobility of the nodes may create a significant challenge to the routing protocol because some of the nodes will be out of the transmission range, which will require finding an alternative path to the destination. In a real network, the node is affected by power constraints, as the node is operating with a limited battery, which will affect the lifetime of the nodes [3].

This paper will evaluate the performance of three reactive protocols in three different scenarios. These scenarios are designed to evaluate the network performance under varying situations. The first scenario resembles a standard case, without shutdowns or obstacles. The scenario captures the MANET performs as the number of nodes in the network increases. The second scenario tests the three protocols in the presence of obstacles. The third scenario evaluates protocol performance under random shutdown conditions. In the following sections, the protocols are discussed in more detail and existing literature is reviewed. Following this is a more detailed discussion of the simulation used, the different scenarios, and finally the results and conclusion.

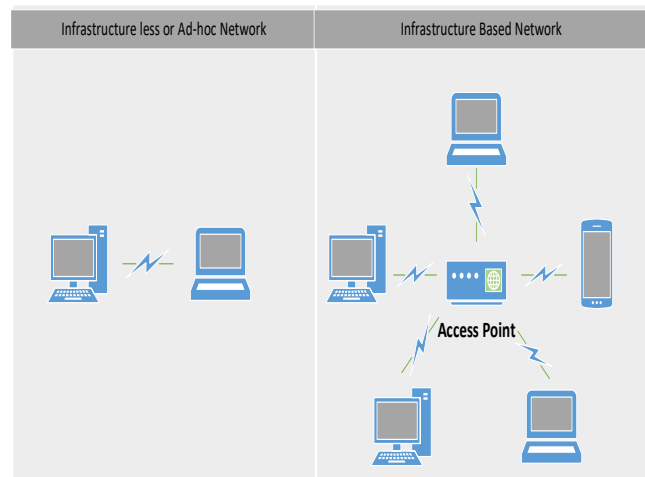


Fig. 1. Ad-hoc Network and Infrastructure Network.

II. MANET ROUTING PROTOCOLS

MANET routing protocols may classify into three categories, as shown in Fig. 2: Reactive (On-demand), Proactive (Table-driven), and Hybrid [4],[5]. This work will focus on evaluating the performance of three types of reactive protocols: Dynamic Source Routing (DSR), Ad-hoc On-Demand Distance Vector (AODV), and Dynamic MANET On-Demand (DYMO).

A. Dynamic Source Routing

The DSR is one of the reactive protocols based on source routing algorithms. The selection of a path is the source's responsibility. It does so by initiating a request packet and sending it to its neighbors. The packet header will contain the information of all intermediate nodes or hops in the route until the destination is reached. The route that was recently discovered will be stored in the cache route of the node. The control message that is periodically exchanged in proactive is no longer used because it relies on the MAC layer to discover the failure of the link. Consequently, it has two advantages over proactive protocols, i.e., in terms of battery consumption and network overhead [6].

Two processes are used in the DSR protocol. The first is to discover the route from the source to the destination. The second is to maintain the route. Route discovery takes place when the source needs to communicate with a specific node. First, the source starts searching in its cache route for the route to the destination. If the source finds the route, it will communicate immediately. If it does not find the route in its cache route, the source will start to discover the route by flooding or broadcasting the route request packet to all neighboring nodes within the transmission range, and the source will add its information in the header of the request packet; the neighbors will search in their caches for the destination node. If one of them finds the path, the replay packet will be created and send to the source. If no such route is found in their cache route, each node will add its address to the request packet and rebroadcast to neighboring nodes within their transmission range until it reaches to the destination or the intermediate node that has information about the route to the destination. If the destination is not found within time to live (TTL), the packet will be expired, and the source will generate a new route request with an increased TTL value. Fig. 3 shows the process of route discovery,

starting with initiation of the Routing Request (RREQ) and broadcasting it to the neighbors, finishing when it reaches the destination [7].

When the Routing Request (RREQ) packet reaches its destination, the destination node will create the Route Reply (RREP) and search for the route information to the source. If the destination finds the route, it will use it in the RREP. If there is no information about the path to the source in its cache route, it will use the same accumulation path in the RREQ. When the RREP reaches the source, it will save the route of the destination in the cache route and start communicating. The RREP could return in various ways and save each route information in its cache route [7].

Fig. 4 illustrates the RREP process. In the second process, which maintains the route, each node in the route is responsible for receiving and sending the data to the next hop. An acknowledgment can confirm the link capability to carry the data. The acknowledgment already exists in MAC protocols such as IEEE 802.11, which is a link layer acknowledgment frame. If no acknowledgment has been received, the sender node will consider the link to be "broken" and will remove this link from its route cache. It will then create the Route Error (RRER) and send it to each node that has sent a packet. Furthermore, the source will start to create RREQ and flood it again to select another path.

Fig. 5 illustrates the broken link between 3 and 6. In this case, node 3 receives the packet and transmits it to node 6; the acknowledgment is still not received in node 3. Thus, node 3 will send an acknowledgment request to node 6. If the acknowledgment is still not received, the node will consider the link broken and create the RRER to send it to the source. The DSR protocol has an advantage over the proactive protocols because it requests the route only when it is needed. This feature will reduce the overhead of the network caused by the control messages and the bandwidth consumption will reduce. However, increasing the number of hops will increase the header of the Routing Request (RREQ) packet. It is possible to have so many routes to the destination in the cache route of the source when the number of nodes in the network is extensive. This may increase collisions of packets, which could cause congestion at the nodes in the case of sending a reply. This problem is called reply storms [8].

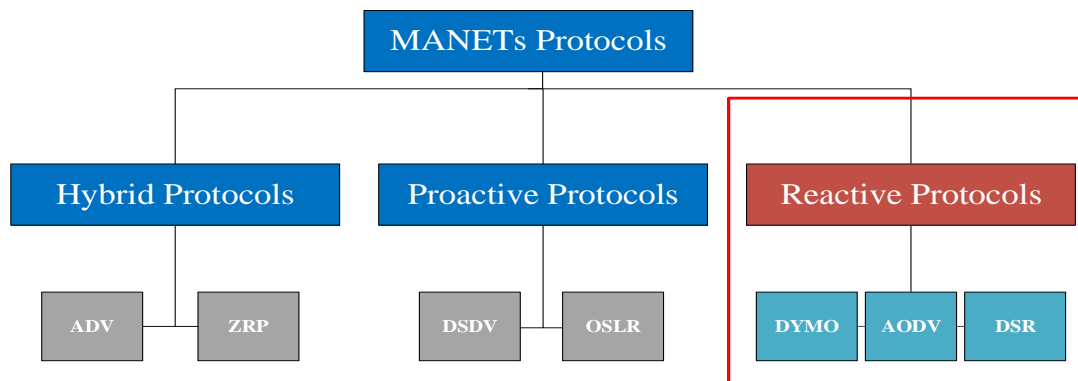


Fig. 2. Protocols Categories of MANETs.

Route Discovery

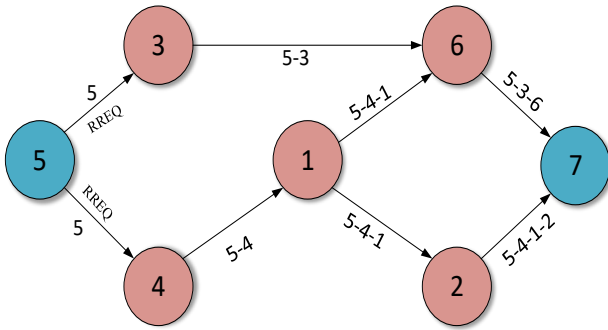


Fig. 3. Route Discovery Process (RREQ).

Route Discovery

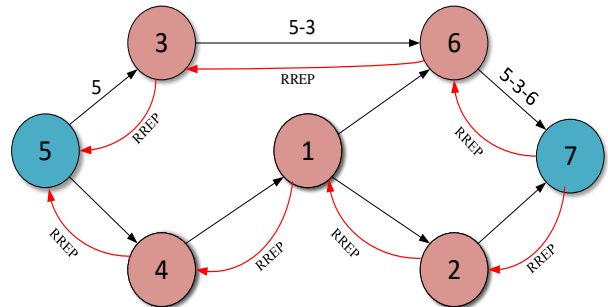


Fig. 4. Route Discovery Process (RREP).

Maintain the route

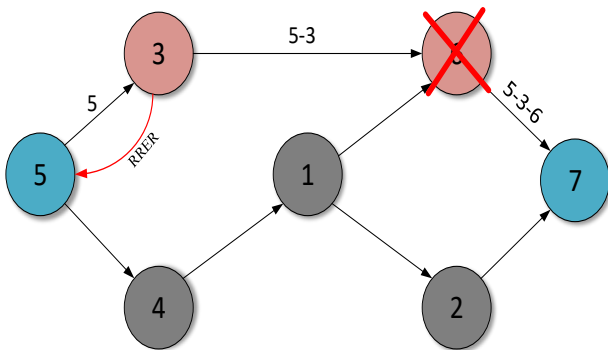


Fig. 5. Maintain the Route Process (RRER).

TABLE I. ROUTING TABLE

Routing Table
Destination Address
Next Hop Address
Destination Sequence Number
Hop Count

The destination sequence number is used to indicate the recent path and is created by the destination once RREQ is reached in the destination [9]. If a route is found in the routing table, then the source will start to send the packets to destination. Otherwise, the source will hold the message in the message queue and initiate RREQ; the RREQ will be flooded within the network until the RREQ reaches the destination. The RREQ contains information as shown in Table II [9].

The destination sequence number used to identify the new path and RREQ ID to avoid the loops. The source sequence number is a unique number used in the new RREQ. When RREQ arrives at an intermediate node, the routing table will be checked for route information. If there is none, the RREQ will continue the process, but the number of hops will be increased one to the previous hops until reach the destination. If the destination is not found within the TTL, the packet will expire and be deleted. The new packet will increase the TTL value. The source sequence number will be higher, and the nodes will update their routing table once they receive a higher source sequence number. In this case, the route is not part of the packet header. When the destination receives the RREQ, the RREP will be generated and sent back to the source. Each intermediate node will store the forward path to the routing table. The destination will be added to the list of active neighbors. Fig. 6 illustrates the route discovery process for AODV [10]. In maintaining the routing process, this process helps to preserve the routes when the topology changes by sending a Hello message between the nodes in the active route to verify the route's validity. When the response is missing, the node reports on the affected node by sending RRER contains unreachable node in the desired route. Then the route replay error will be sent to the source. When the source node receives the RRER, it will compare it with its routing table; the broken route will be deleted from the routing table and the source will generate a new RREQ to discover a new path [11].

TABLE II. ROUTE REQUEST PACKET (RREQ)

Route request (RREQ)
RREQ ID
Source IP Address
Source Sequence Number
Destination IP Address
Destination Sequence Number
Hop Count
Time to Live (TTL)

B. Ad-hoc On-Demand Distance Vector

The AODV is designed to follow the principle of the distance vector algorithm, which means each node has a routing table that is used to store the active paths. The ADOV mechanism is based on the same two processes as DSR, which are route discovery and maintaining the route. Moreover, AODV does not require the node to maintain the idle route. In AODV guarantee loop-free because each request packet has a unique ID number for each packet. This will result in eliminating the distance vector problem counting to infinity. In the route discovery process, the routes are determined when needed. When the source needs to communicate, it examines its own routing table for the route information of the destination. Each routing table consists of information, as shown in Table I.

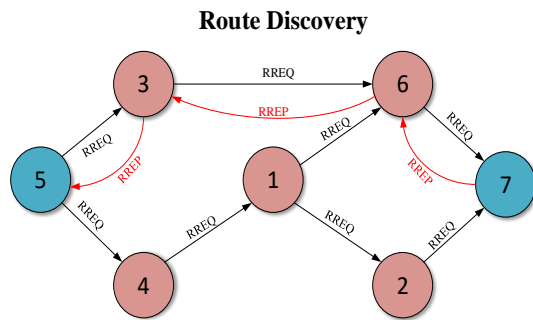


Fig. 6. Route Discovery Process (RREQ and RREP) for AODV.

C. Dynamic MANET On-Demand

The Dynamic MANET On-Demand (DYMO) is a combination of AODV and DSR features. The DYMO has two main processes: route discovery and route maintenance. The route discovery process is used when there is no information about the route between the source and the destination in the routing table of the node. After the path is found, the maintain route process will take place. In route discovery, the source will search for the route information of the destination in the routing table. The routing table contains the destination address, the sequence number of the destination, the next hop address, and the hop count, with the same information as the routing table in AODV. When there is no information about the destination's route, in the routing table of the source, the Routing Request (RREQ) will be generated and broadcast across the network. When the intermediate node receives the RREQ, the node will search in the routing table; if the node did not find the target, will add itself to the RREQ and broadcast it. The idea of adding each node to its information in RREQ is to update the routing table of the next node. This guarantees that each routing table is updated in intermediate nodes. The route reply RREP will be created and sent back to the source once the destination or intermediate node finds the route to the target or the destination, as shown in Fig. 7. In maintaining the route process, DYMO uses the Hello message or beacon message to check the link validity as in AODV if the broken link is detected, the node will create a RERR message, add all the nodes in the broken link, and broadcast back to the intermediate nodes. The nodes that received the RRRER will compare the record list in RRRER with their routing table. If the sequence number of the destination is equal to or higher than the sequence number in the routing table, the information of the route will be deleted [12].

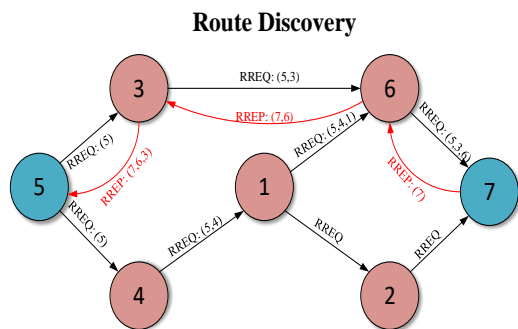


Fig. 7. Route Discovery Process (RREQ and RREP) for DYMO.

III. RELATED WORKS

Many published works have evaluated and tested the performance of MANET protocols in different scenarios and metrics. These works have used different simulation tools. Table III shows the recent research. In [13], two reactive protocols, DSR and AODV, were evaluated using the NS-2.35 simulator. The performance was evaluated under two metrics: packet delivery ratio and remaining energy in two scenarios. The scenarios used were changing the number of nodes in the network from 10,20,30,40, and 50 with increasing node velocity. The performance of DSR is better than that of AODV in both scenarios.

TABLE III. RELATED WORKS

Year	Author	Simulation Tool	Scope of Work
2020	Jamilah, Amnah, and K. Ibrahim	NS-2.35	Comparison between DSR and AODV when the number of nodes changed from 10, 20, 30, 40, and 50 with increasing node velocity
2020	Russell, Nan Wang, and Daniel	NS-3	Comparison between AODV, DSR, OLSR, and DSDV when the velocity of the nodes and the area size increased
2020	Marwan, Salama, Hairulnizam, Aida, Azizul, Mustafa, and Mohammed	NS-2	Comparison between three protocols—AODV, DSDV, and AOMDV—in terms of metrics packet delivery ratio and throughput
2020	A. S. Mustafa, M. M. Al-Heeti, M. M. Hamdi, and A. M. Shantaf	NS-2	Comparison between GPSR and AODV when the size of network varied in terms of packet ratio, end-to-end delay, and throughput.

In [14], the work showed a comparison of four different routing protocols—AODV, DSR, OLSR, and DSDV—in two scenarios. The two scenarios were varying the velocity of the nodes and the area size and comparing their performance in packet delivery ratio and end-to-end delay. The AODV has higher performance in packet delivery ratio in the case of a high velocity of nodes, while DSDV has the lowest packet delivery ratio. In terms of end-to-end delay, DSR has the largest end-end end delay, while the OLSR has the lowest end-to-end delay in both scenarios.

In [15], the authors presented a comparison between three protocols—AODV, DSDV, and AOMDV—in different metrics packet delivery ratios, throughputs, end to end delays, and packet loss ratios. The simulation time was in the range of 600 to 3400 seconds. The AOMDV performs better than the other protocols in terms of metrics packet delivery ratio, throughput, and packet loss ratios. However, the DSDV has the lowest end-to-end delay among the other protocols. Meanwhile, [16] presented a performance evaluation between Greedy Stateless Routing Perimeter (GPSR) and AODV when the size of network varied 500×500, 750×750, 1000×1000, 1250×1250, and 1500×1500 in terms of packet ratio, end-to-end delay, and throughput. The number of nodes was 50, with

a mobility of 20 m/s. GPSR performed better than AODV in terms of all three metrics. AODV suffered from high delay when the size of the network is 1500x1500. However, increasing the network size will degrade the performance of the protocol.

IV. SIMULATION

This work evaluated and compared the performance of three protocols by using OMNET++. OMNET++ is an open-source that provides a free simulation environment for educational use with a wide variety of platforms. It has received a great amount of attention from researchers and developers. OMNET++ has different frameworks, modules, and components based on C++; these are used primarily to build the networks. INETMANET provides modules in various layers that help to build the network and have additional modules and protocols, especially for MANETs, as compared to other frameworks [17].

A. Node Implementation

The node was implemented with a wireless network interface controller that supports 54 Mbps, as shown in Fig. 8. The MANET protocols are in the network layer, and the “manetrouting” module was used as a routing protocols pool with DSR, AODV, and DYMO, which will help to configure the network. In the transport layer, the UDP was used as a transport protocol. The UDPApp is the application providing a data packet that is 512B in size. The node has a transmission range that is coupled with a transmission power of 2mW; the receiving sensitivity is -85dBm.

B. Network Implementation

The network dimensions are 1000m x1000m. The carrier frequency is 2.4GHz and each node has a transmission range that is coupled with the transmission power and receiving sensitivity of the node. The nodes have mass mobility with a velocity varying from 0.01 to 15 meters per second. Table IV summarizes the simulation setup of the network.

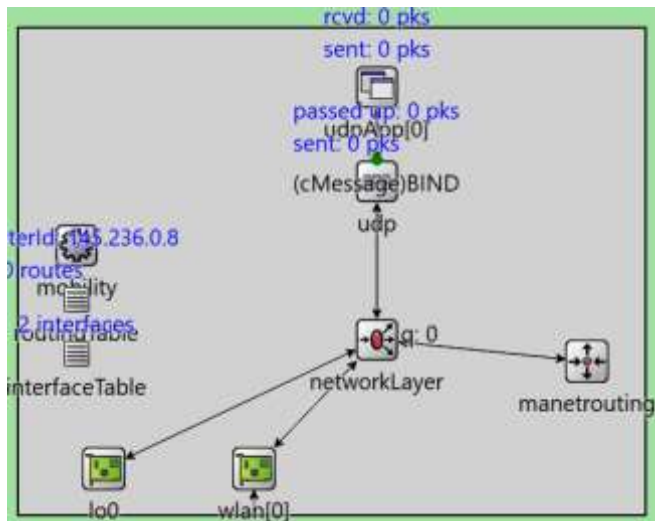


Fig. 8. Node Configuration.

TABLE IV. SIMULATION SETUP

Parameters	Values
Network Dimensions	1000m X 1000m
Carrier Frequency	2.4GHz
Radio Bitrate	54 Mbps
Radio Transmission Power	2mW
Receiving Sensitivity	-85 dBm
Routing Protocols	DSR, AODV, and DYMO
Number of Nodes	25, 45
Message Size	512 Byte
Node Mobility	Mass mobility (0.01 to 15) m/s
Simulation Time	500s

V. SCENARIOS

The simulation setup was applied to three scenarios. These scenarios are designed to evaluate the network performance in different situations. The first scenario is to test the three reactive protocols—DSR, AODV, and DYMO—when the number of nodes increases. The second scenario is to evaluate the performance of the network in the presence of obstacles. The idea of the third scenario is to simulate a real network. A group of nodes will be shut down suddenly during communication.

A. First Scenario

In the first scenario, the network performance was tested by using three reactive protocols, when the number of nodes increased from 25 to 45. The network was implemented in two cases—the first case with 25 nodes and the second case with 45 nodes. Fig. 9 shows the diagram of the network with 25 nodes, which is configured with the specifications listed in Table IV. The source started to send the RREQ to the nodes in its transmission range, where only one node received the RREQ. Fig. 10 shows the network with 45 nodes. The performance of the protocols was evaluated and examined when the number of nodes increased. The idea behind this scenario is to determine which protocol performs well when the number of nodes increases with fast mobility. The network was implemented with a fixed transmitter (sender1) and receiver (reciver1). The rest of the nodes move with a velocity varying from 0.01 to 15 meters per second. Each node has a transmission range coupled with its transmission power and receiving sensitivity.

B. Second Scenario

MANET is a network that is designed to operate in critical situations such as battlefield, emergency, and rescue missions. Thus, it is important to test the network in difficult situations. This scenario implemented three obstacles that were used to block the signal. The obstacles took the shape of black rocks, as shown in Fig.11. The network has 25 nodes with fast mobility varying from 0.01 to 15 meters per second. Each node has a transmission range coupled with its transmission power and receiving sensitivity. The transmitter and receiver network are fixed nodes in the network. The simulation setup in Table IV was used in this scenario to compare the results

with those of the first scenario in the case of 25 nodes. This will indicate how obstacles affect network performance.

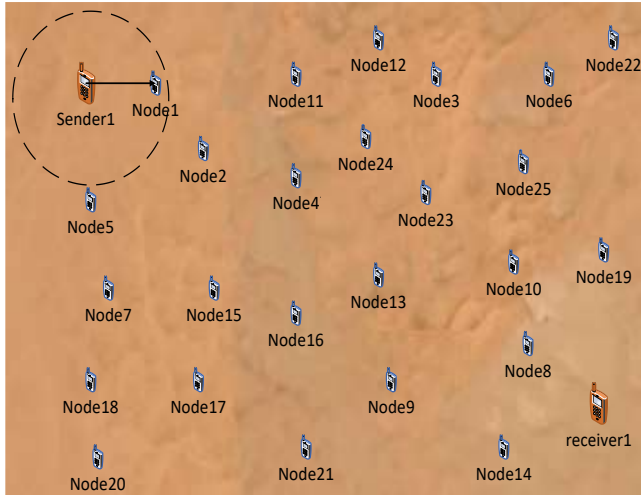


Fig. 9. Network during the Simulation with 25 Nodes.

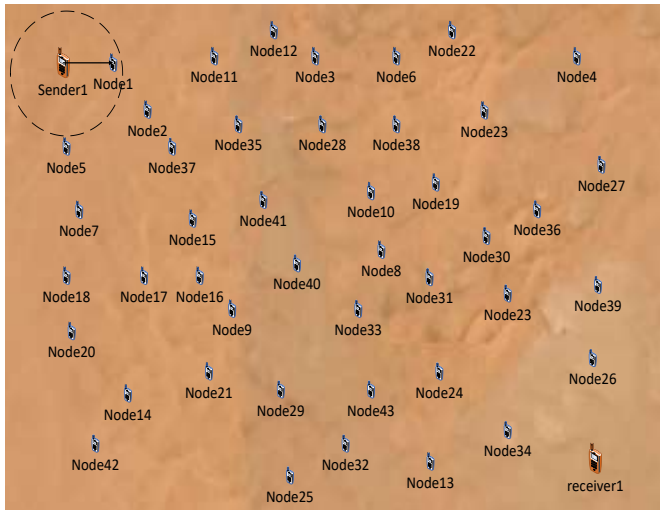


Fig. 10. The Network during Simulation with 45 Nodes.

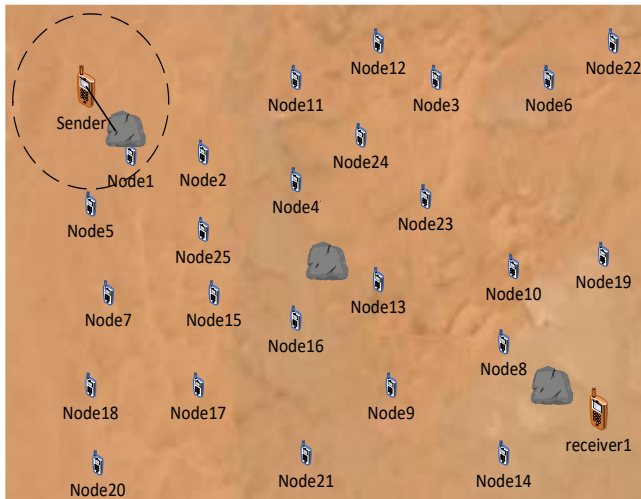


Fig. 11. The Network during Simulation with 3 Obstacles.

C. Third Scenario

In this scenario, the network was tested when a group of nodes is shut down suddenly. In the real network, the nodes have a limited battery, which will shut down the node during the communication. The node will shut down due to the battery or may experience any malfunction. In this scenario, the network has 45 nodes. When the simulation time reaches 250s, the group of nodes (Node [33] to Node [44]) will shut down. Therefore, the network must respond quickly and recover the path between the source and the destination. The transmitter and receiver were fixed in the network. The rest of the nodes move with a velocity varying from 0.01 to 15 meters per second. The simulation setup in Table IV was used in this scenario, as well as the first and second scenarios. Fig. 12 shows the nodes that are shut down at 250s.

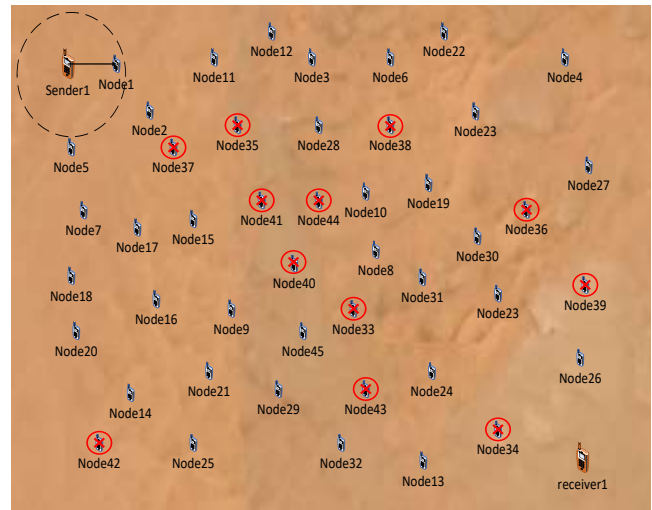


Fig. 12. The Network during Simulation with Shutdown 12 Nodes.

VI. RESULTS

The network evaluation is carried out in terms of packets received, end-to-end delay, transmission count or routing overhead, throughput, and packet ratio.

A. Packet Received

Packets received is the number of packets that the destination successfully received. The higher the number of packets received, indicates the effectiveness of the protocol used. Fig. 13 shows the comparison between the three protocols in the first scenario for two cases when the number of nodes increases from 25 to 45. DYMO is proven to be an efficient protocol when the number of nodes is high, with fast mobility. When the number of nodes is 25, DYMO works better than DSR and AODV. Moreover, when the number of nodes increases to 45, the number of received packets increases in DYMO. The performance of AODV improves when the number of nodes increases as well. DSR performance was degraded when the number of nodes increases, which means DSR did not work well when the network has high-speed mobility nodes resulting in a high packet drop. Fig. 14 shows the results of the second scenario for the three protocols. The network in the second scenario suffered from packet loss for all three protocols; the loss in packets was due to the obstacles. Thus, the three protocols did

not perform efficiently in the presence of obstacles. Compared to the first scenario with 25 nodes, DYMO lost 540 packets more, AODV lost 35 more packets, and DSR lost 138 more packets, and all of this was due to the obstacles. Although DYMO saw the biggest decrease in received packets (compared to the first scenario in case of 25 nodes), it still outperformed its peers in the second scenario.

In the third scenario, as shown in Fig. 15, the network reopened quickly and recovered the path between the source and destination by using DYMO. AODV had a moderate performance. DSR had the worst performance as compared to the other protocols. However, all three protocols experience a performance degradation if one compares their performance to the first scenario with 45 nodes. Since the third scenario was fixed with 45 nodes, comparing the third scenario to the second part of the first scenario shows the effect of dropped nodes on received packets. If the protocol is robust, it should be able to quickly recover the connection, which directly results in more packets successfully received.

B. End-to-End Delay

End-to-end delay is the time interval that it takes to send a packet between the source and destination, including processing and queuing time. A smaller end-to-end delay indicates a fast, high-quality network.

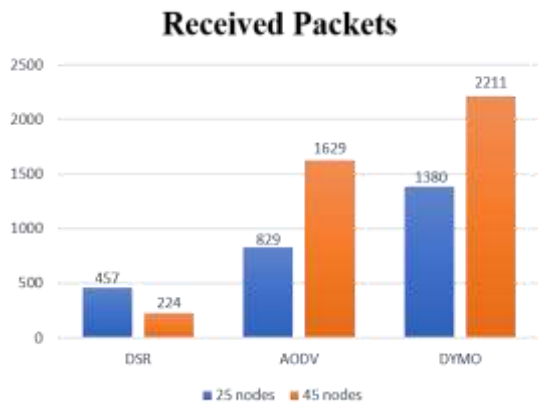


Fig. 13. Received Packets of First Scenario.

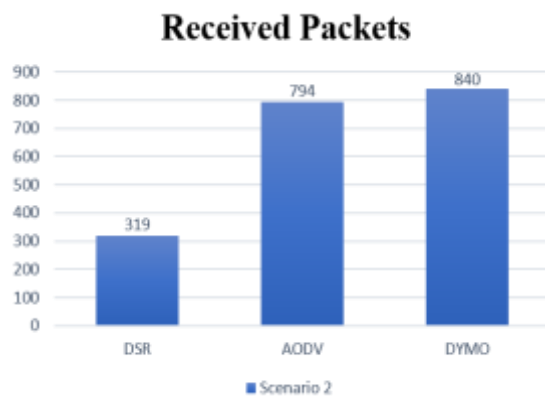


Fig. 14. Received Packets of Second Scenario.

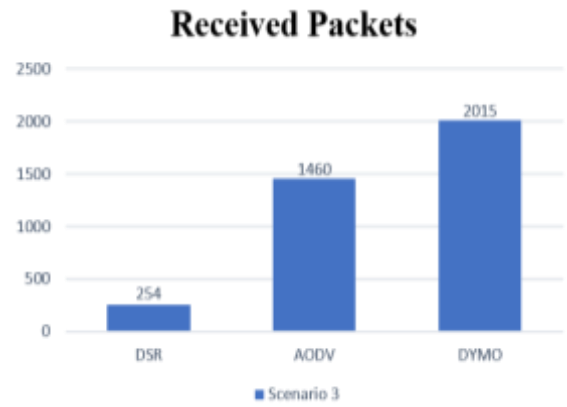


Fig. 15. Received Packets of Third Scenario.

In the first scenario, the three protocols were compared for a varying number of nodes, and the results appear in Fig. 16. In first case, AODV has the smallest end-to-end delay as compared to DYMO and DSR. However, when the number of nodes increases, the end-to-end delay increases by using AODV. DYMO and DSR perform better, in terms of end-to-end delay, when the number of nodes increases.

The second and third scenarios are shown in Fig. 17 and Fig. 18. In the second scenario, AODV has the largest end-to-end delay, while DSR has the smallest end-to-end delay. DYMO maintains the same performance as compared to the first scenario with 25 nodes, which shows that obstacles did not increase the end-to-end delay with DYMO.

In the third scenario, all three protocols experience an increase in the delay as compared to the first scenario with 45 nodes. The number of nodes decreases suddenly, affecting all three protocols performance. However, AODV has the largest end-to-end delay.

C. Transmission Count or Routing Overhead

Transmission count is one of the routing metrics designed for MANETs. It represents the number of transmissions required to send a packet over a link, including the retransmission. A smaller transmission count means less network overhead, which leads to less bandwidth consumption. The results of routing overhead or transmission count are shown in Fig. 19, Fig. 20, and Fig. 21.



Fig. 16. End to End Delay of First Scenario.



Fig. 17. End to End Delay of Second Scenario.

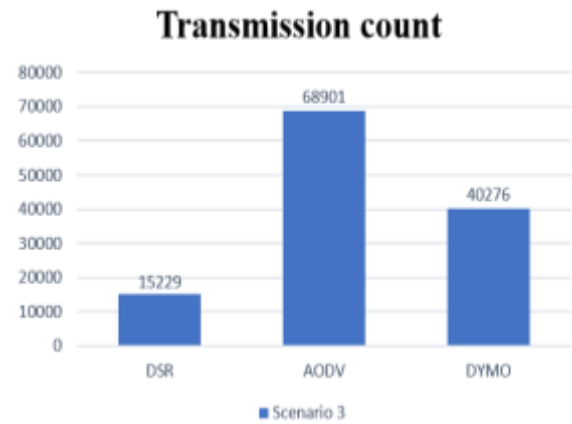


Fig. 21. Transmission Count of Third Scenario.



Fig. 18. End to End Delay of Third Scenario.

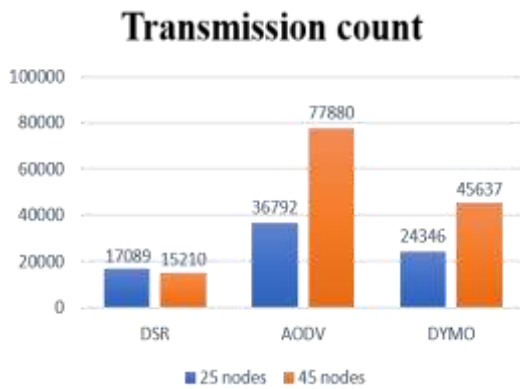


Fig. 19. Transmission Count of First Scenario.

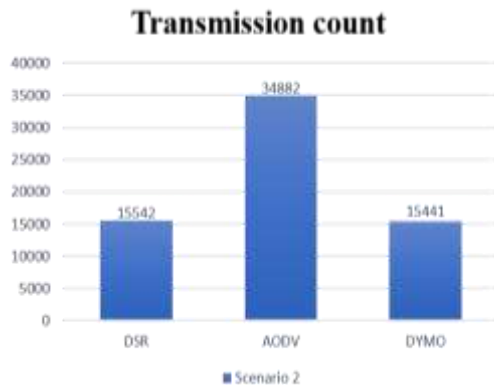


Fig. 20. Transmission Count of Second Scenario.

AODV has the largest transmission count among the three protocols in all three scenarios. AODV uses periodic messages to maintain the routes between the nodes, which increases the routing overhead. DYMO has less routing overhead than AODV, as DYMO uses an accumulation path function. Therefore, DYMO allows the nodes in an active route to use the information of intermediate nodes to the destination to update their routing tables, which helps to reduce the retransmission packets and the RREQ numbers when communication is needed in the future. DSR has the lowest routing overhead except for the second scenario, due to the lack of a periodic message used to maintain the route process. DSR uses an acknowledgment that confirms the link capability to carry the data, which already exists in MAC protocols. This acknowledgement gives DSR an advantage over the other protocols in terms of routing overhead.

D. Throughput

Throughput is the number of packets successfully received at the destination per unit of time and is measured in bits per second.

$$\text{Throughput} = \frac{\sum \text{Number of bit received}}{\text{Simulation time}} \quad (1)$$

Throughput is considered the most important metric identifying the quality of a network. Fig. 22 shows that DYMO is an efficient and reliable protocol when the number of nodes increases and have fast mobility. DYMO has the largest throughput in both cases of the first scenario. AODV has an average performance, but the performance increases when the number of nodes increases. DSR has the worst performance; when the number of nodes increases, the throughput decreases.

The second scenario results are shown in Fig. 23. The network suffered from high packet loss in the presence of obstacles. However, DYMO still has the highest performance, while DSR has the worst performance. In the third scenario, as shown in Fig. 24, the use of DYMO will help the network respond and recover the connection between the nodes faster as compared to DSR and AODV. AODV has average performance, while DSR has the worst performance. This leads to the conclusion that DSR is not suitable for difficult situations.

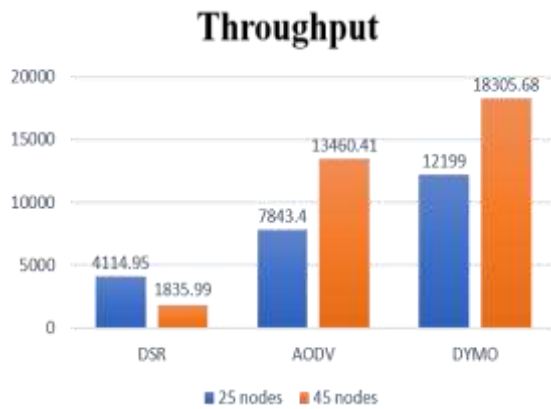


Fig. 22. Throughput of First Scenario.

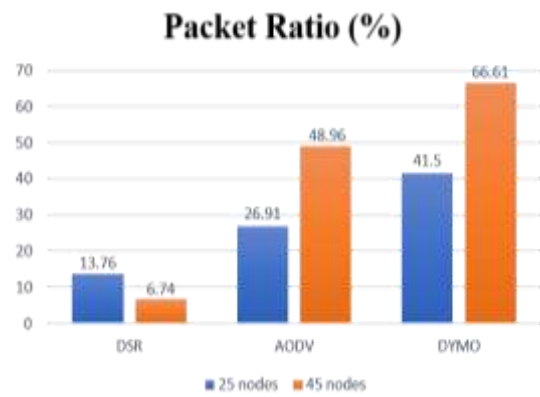


Fig. 25. Packet Ratio of First Scenario.

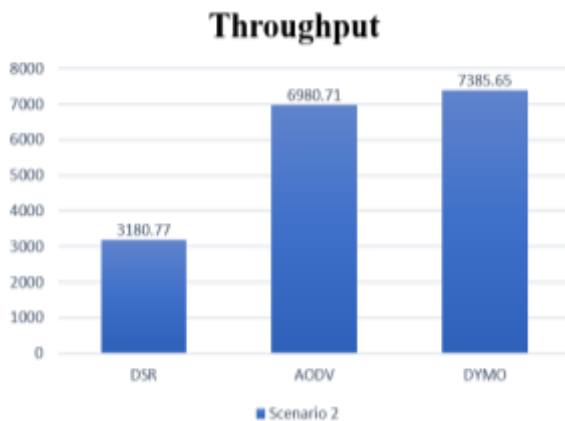


Fig. 23. Throughput of Second Scenario.

In the second scenario, as shown in Fig. 26, DYMO has the highest packet ratio of 25.3%, which means 74.7% of the transmitting packets were lost. AODV received 23.95% packets from the total number of packets sent by the transmitter node means 76.05% of transmitting packets were lost, and DSR received only 9.61% which means 90.39% of the total packets were lost. In summary, all three protocols did not perform well in the second scenario.

In the third scenario, as shown in Fig. 27, DYMO achieved a packet ratio of 60.7%, which is the largest packet ratio as compared to the other protocols. AODV and DSR achieved packet ratios of 43.88% and 7.65%, respectively.

Packet Ratio (%)

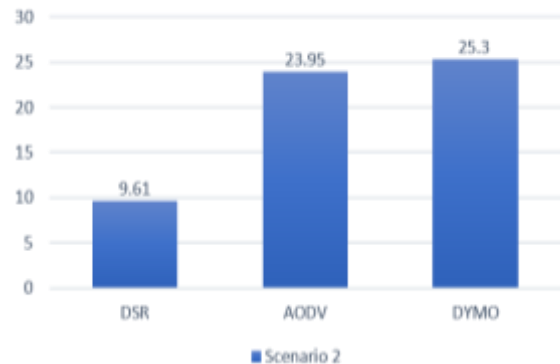


Fig. 26. Packet Ratio of Second Scenario.

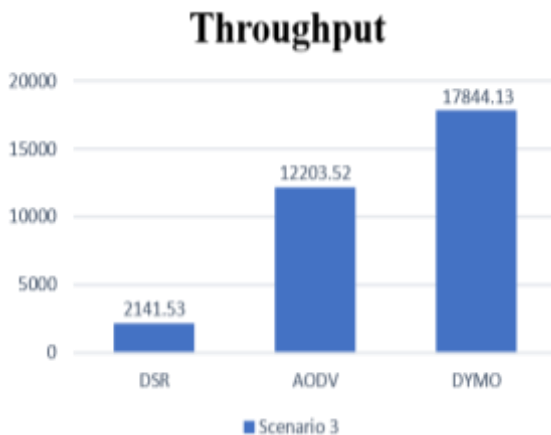


Fig. 24. Throughput of Third Scenario.

Packet Ratio (%)

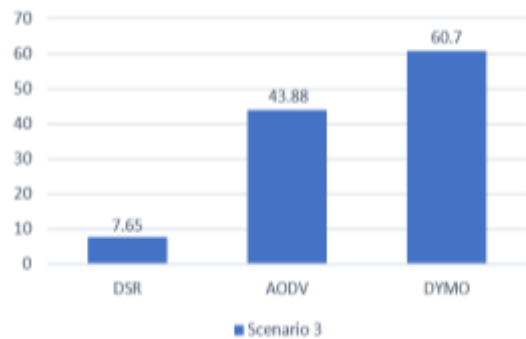


Fig. 27. Packet Ratio of Third Scenario.

E. Packet Ratio

This is the ratio of the number of data packets delivered to the destination and the total number of data packets sent by the source. DYMO has the largest number of delivered packets, as discussed before in Fig. 13, Fig. 14, and Fig. 15. Therefore, DYMO has the highest packet ratio, making it a more reliable protocol among the three in the case of increasing the number of nodes. Fig. 25, shows the comparison when the number of nodes increases from 25 to 45.

VII. CONCLUSION

MANETs are used in different applications, especially in critical applications, due to their features and characteristics that make the networks very flexible. In this paper, DYMO proved to be an efficient and reliable protocol compared to DSR and AODV when the network is large and has fast mobility. DSR performs worst when the number of nodes increases. AODV has average performance, but when the number of nodes increases, the performance increases. Also, AODV has the largest routing overhead due to the periodic messages that are used to maintain the link between the nodes in the active route. Overall, DYMO has the highest performance in the three scenarios and works better under challenging situations than DSR and AODV.

REFERENCES

- [1] H. Valchanov, J. Edikyan, and V. Aleksieva, "An Empirical Study of Wireless Security in City Environment," in Proceedings of the 9th Balkan Conference on Informatics, 2019, pp. 1–4.
- [2] M. A. Jubair et al., "Competitive Analysis of Single and Multi-Path Routing Protocols in Mobile Ad-Hoc Network," Indones. J. Electr. Eng. Comput. Sci., vol. 14, no. 2, 2019.
- [3] A. M. Abdullah, E. Ozen, and H. Bayramoglu, "Energy Efficient MANET Routing Protocol Based on Ant Colony Optimization.," Adhoc Sens. Wirel. Networks, vol. 47, 2020.
- [4] M. Sharma, M. Singh, K. Walia, and K. Kaur, "Comprehensive Study of Routing Protocols in Adhoc Network: MANET," in 2019 IEEE 10th Annual Information Technology, Electronics and Mobile Communication Conference (IEMCON), 2019, pp. 792–798.
- [5] T.-A. N. Abdali, R. Hassan, R. C. Muniyandi, A. H. Mohd Aman, Q. N. Nguyen, and A. S. Al-Khaleefa, "Optimized Particle Swarm Optimization Algorithm for the Realization of an Enhanced Energy-Aware Location-Aided Routing Protocol in MANET," Information, vol. 11, no. 11, p. 529, 2020.
- [6] A. M. Shantaf, S. Kurnaz, and A. H. Mohammed, "Performance Evaluation of Three Mobile Ad-hoc Network Routing Protocols in Different Environments," in 2020 International Congress on Human-Computer Interaction, Optimization and Robotic Applications (HORA), 2020, pp. 1–6.
- [7] V. Kumar, "Improving quality of service in mobile ad-hoc networks (MANETs) using adaptive broadcast scheduling algorithm with dynamic source routing protocol," J. Comput. Theor. Nanosci., vol. 14, no. 9, pp. 4370–4376, 2017.
- [8] P. Nayak and B. Vathasavai, "Impact of random mobility models for reactive routing protocols over MANET," Int. J. Simulation--Systems, Sci. Technol., vol. 17, no. 34, pp. 112–115, 2016.
- [9] I. Nurcahyani and F. F. Laksono, "Performance Analysis of Ad-Hoc On-Demand Distance Vector (AODV) and Dynamic Source Routing (DSR) Routing Protocols During Data Broadcast Storm Problem in Wireless Ad Hoc Network," in 2019 International Seminar on Intelligent Technology and Its Applications (ISITIA), 2019, pp. 29–34.
- [10] R. Rana and R. Kumar, "Performance Analysis Of Aodv In Presence Of Malicious Node," Acta Electron. Malaysia, vol. 3, no. 1, pp. 1–5, 2019.
- [11] Bisoyi, S.K.; Sahu, S. Performance analysis of Dynamic MANET On-demand (DYMO) Routing protocol. Spec. Issue IJCCT 2010, 1, 3.
- [12] U. Yavuz, F. A. Dael, and W. A. J. S. A. Jabbar, "Performance Evaluation of DYMO and OLSRv2 Routing Protocols in VANET," Int. J. Integr. Eng., vol. 12, no. 1, pp. 50–58, 2020.
- [13] Jamilah Alamri, Amnah S. Al-Johani, K. Ibrahim. Ata, "Performance Evaluation of Two Mobile Ad-hoc Network Routing Protocols: Ad-hoc On-Demand Distance Vector, Dynamic Source Routing", IJAST, vol. 29, no. 05, pp. 9915 - 9920, May 2020.
- [14] R. Skaggs-Schellenberg, N. Wang and D. Wright, "Performance Evaluation and Analysis of Proactive and Reactive MANET Protocols at Varied Speeds," 2020 10th Annual Computing and Communication Workshop and Conference (CCWC), Las Vegas, NV, USA, 2020, pp. 0981-0985.
- [15] M. H. Hassan et al., "Mobile ad-hoc network routing protocols of time-critical events for search and rescue missions," Bull. Electr. Eng. Informatics, vol. 10, no. 1, pp. 192–199, 2020.
- [16] A. S. Mustafa, M. M. Al-Heeti, M. M. Hamdi, and A. M. Shantaf, "Performance analyzing the effect of network size on routing protocols in manets," in 2020 International Congress on Human-Computer Interaction, Optimization and Robotic Applications (HORA), 2020, pp. 1–5.
- [17] D. S. Som and D. Singh, "Performance analysis and simulation of AODV, DSR and TORA routing protocols in MANETs," Int. J. Recent Technol. Eng., vol. 1, no. 3, pp. 2277–3878, 2012.

The Design and Implementation of Mobile Heart Monitoring Applications using Wearable Heart Rate Sensor

Umami Namirah Hashim¹, Lizawati Salahuddin², Raja Rina Raja Ikram³
Umami Rabaah Hashim⁴, Ngo Hea Choon⁵, Mohd Hariz Naim Mohayat⁶

Center for Advanced Computing Technology (C-ACT), Fakulti Teknologi Maklumat dan Komunikasi
Universiti Teknikal Malaysia Melaka (UTeM), Durian Tunggal, Melaka, 76100, Malaysia

Abstract—Heart monitoring is important to deter any catastrophic because of heart failure that may happen. Continuous real-time heart monitoring could prevent sudden death due to heart attack. Nevertheless, the major challenge associated with continuous heart monitoring in the traditional approach is to undertake regular medical check-ups at the hospital or clinic. Hence, the aim of this study is to develop a mobile app where patients can real-time monitor their heart rate (HR) and detect abnormal HR whenever it occurs. Caregivers will be notified when a patient is detected with abnormal HR. The mobile app was developed for Android-based smartphones. A wearable HR sensor is used to collect RR data and transmitted to the smartphone via Bluetooth connection. User acceptance test was conducted to comprehend the intention and satisfaction level of the prospective users to use the application. The user acceptance test shows compatibility, perceived usefulness, perceived ease of use, trust, and behavioral intention to use had a high acceptance rate. It is expected that the developed app may provide a more plausible tool in monitoring HR personally, conveniently, and continuously at any time and anywhere.

Keywords—Personalized healthcare; heart monitoring; wearable sensor; mobile; android

I. INTRODUCTION

The heart is one of the most important organs in the human body. Heart monitoring is important to deter any catastrophic because of heart failure that may happen. There are many factors that will cause abnormal heartbeat rhythms such as injury from a heart attack, the healing process after heart surgery, coronary artery disease, and many more. One of the unfortunate incidents that could occur is a sudden heart attack while driving, having chest pain, feeling faint, dizzy, or light-headed feeling faint, dizzy, or light-headed. The number of deaths annually due to heart disease is projected to increase to 22.2 million by 2030 [1]. Hence, continuous heart monitoring and its condition is important to actualize suitable preventive measures. Nevertheless, some individuals are busy with work until they do not have time to undertake annual medical check-ups at the hospital or clinic.

The use of mobile technology and wearable devices focusing on heart disease prevention is rapidly growing [2]. It is expected that 62% of smartphone users use phones to gather health facts and gain knowledge about diseases and health issues [3]. Main technology companies such as Apple Inc.,

Google Inc., and Samsung Group (SAMSUNG, Suwon, South Korea) have incorporated modern styles for health monitoring in designing their smartphones [4], [5]. Mobile technology offers inbuilt applications such as Global Positioning System (GPS) and location-enabled services which is useful for health monitoring. Moreover, current progress in wireless technologies including short-range (Bluetooth) and wide-area (GPRS, UMTS) have made promising progress in the innovative era of health care systems that should offer portable, wearable and flexible health monitoring systems. These systems will empower continuous monitoring of health data and endless access to the patient despite the patient's recent location or activity. Wearable technology is used in HR monitoring, with high levels of accuracy in both smartphone [6] and wrist-based setups [7]. Recently, mobile cloud computing approaches gained huge popularity for real-time heart monitoring and analysis due to the possibility of utilizing the large data storage and abundant computing power [8]–[12].

The aims of this study are to design, develop, and test a Real-Time Mobile Heart Monitoring (RTHM) application. The android-based mobile apps enable HR monitoring by using wearable HR sensors and consequently notify the HR result in smartphones. The app notifies the caregiver or medical center through WhatsApp when an abnormal HR is detected. Moreover, the HR result will automatically save in a cloud database.

II. RELATED WORKS

QardioCore (Qardio®, San Francisco, CA, USA) is a chest strap ECG device targeted for daily continuous ECG monitoring [13]. It is worn below the sternum. In addition to heart data, QardioCore monitors body temperature, stress levels, respiratory rate, and activity tracking. The device is compatible with iOS smart devices only. Cardio App is used to visualize live ECG recorded from QardioCore, view charts, and graphs to analyze the trends of the heart data. Besides, patients can email 30 seconds of ECG records to their doctors.

The AliveCor KardiaMobile ECG device (AliveCor®, Mountain View, CA, USA) is one lead ECG that can be used for 30 seconds to five-minutes of ECG recording [14]. Users are required to lightly place their two or more fingers on the KardiaMobile's electrodes prior to ECG recording. The device uses Bluetooth energy technology to wirelessly transmit the

heart information to the Kardia app installed in iOS or Android smartphone or tablet. Kardia app is used to collect, view, and save ECG recordings. With a minimum of 30 seconds of ECG recording, the device is able to detect atrial fibrillation, bradycardia, tachycardia, or normal heart rhythm. The automatic algorithm has exceptional sensitivity (96.6%) and specificity (94%) for correctly interpreting atrial fibrillation versus physician-interpreted ECGs [15]. KardiaMobile ECG is recommended as an effective and safe device to detect irregular HR [16]. Users shall be notified of their heart status within the Kardia app once the ECG recording is completed.

Zenikor-ECG (Zenikor EKG® thumb, Stockholm, Sweden) is a handheld ECG device aiming for effective cardiac arrhythmias investigation [17]. It enables patients to repeatedly record their ECGs over a long period of time. Registered patients need to place their thumbs on two electrodes of the Zenikor-ECG to record 10 to 30 seconds ECG reading and press a button to transfer the reading to a central ECG database via a mobile network. Zenikor-ECG Doctor System is a web service that enables doctors to store, process, and view their patients' ECG recordings. The system supports ECG interpretation for a quicker and safer diagnosis. Hendrikx et al. [18] conducted a study to compare the efficiency of short ECG recording with 24-hour Holter ECG, in detecting arrhythmias in patients with palpitations and dizziness symptoms. Zenikor-ECG was used to record 30 seconds of ECG recording twice a day during a four-week period. The results proved that short ECG recording at regular time intervals and when having symptoms is more effective than 24-hour Holter ECG in discovering atrial fibrillation and paroxysmal supraventricular tachycardia.

Previous studies showed that handheld and wireless ECG devices are effective and safe for continuous HR monitoring in detecting arrhythmias [15], [16], [18]. However, patients should contact their doctor to review their ECG recordings. Patients may also email or print the ECG recording or doctors may have accessed the recording via the web service provided by the manufacturer. Moreover, the systems do not include a patient's location detection when abnormal HR occurs. On the other hand, an alert notification to the caregiver or medical center is highly important when abnormal HR occurs especially for cardiac patients. Consequently, immediate action or treatment can be taken to save a patient's life. Hence, Real-Time Mobile Heart Monitoring (RTHM) application is designed to notify the caregiver or medical center through WhatsApp when an abnormal HR is detected.

III. SYSTEM DESIGN

Section II explains RTHM system design including system architecture, activities involved in the real-time mobile heart monitoring, and graphical user interface (GUI) design.

A. System Architecture

The system architecture of RTHM is three-tier that consists of (1) HR wearable sensor, (2) android smartphone, and (3) cloud server as illustrated in Fig. 1. The first tier is the user's interface which contains HR wearable sensors. The sensor is used to collect the heart data of the patient. Real-time heart data is transmitted wirelessly from the wearable sensor to

the user's smartphone via Bluetooth Low Energy (BLE). The second tier encompasses android smartphones. HR extraction and detection are done on this tier. The third tier comprises cloud servers. The results of HR monitoring are sent to the cloud server via wireless communication such as Wi-Fi, 4G, and 5G connections. The information saved in the cloud server can be accessed by doctors, patient, and their family members.

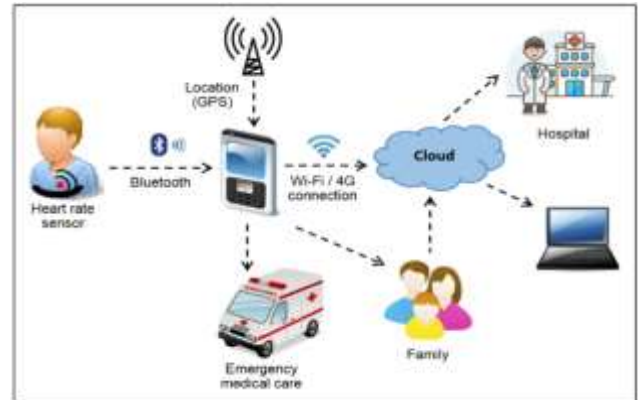


Fig. 1. RTHM Architecture.

B. Activity Diagram of RTHM

The activities involved in the real-time mobile heart monitoring is presented in Fig. 2. A patient is required to create an RTHM account. Then, he is required to edit his profile and caregiver's profile and contact number. An alert notification is sent to the caregiver when abnormal HR is detected. To check or monitor HR, a patient has to wear a wearable HR sensor. The HR sensor needs to be connected to the smartphone via a Bluetooth link prior to the HR monitoring. In the case of an abnormal HR being detected, a permission request to send an alert notification including his location to the caregiver in the contact list will be displayed for 30 seconds. If the patient agrees to send the alert notification or does not respond in 30 seconds duration, the alert notification will be sent to his caregiver via WhatsApp. Finally, the results of the HR monitoring are saved to a cloud database.

C. Graphical User Interface (GUI)

Fig. 3(a) and Fig. 3(b) represent the graphical user interface (GUI) of RTHM. It is an android-based application. Fig. 3(a) shows the login interface. The patient needs to be authorized by entering a username and password to login into the application. If a patient is a new user, he needs to click the create account button to register to the system. Fig. 3(b) shows the main menu. For profile, a patient can update his profile such as phone number and address. The question mark in Fig. 3(b) is the user guideline to use RTHM. The patient needs to wear a Polar H1 Sensor to check HR. Otherwise, no sensor connected will be shown as Fig. 3(b).

Fig. 4 shows the GUI to check HR. The patient needs to touch the start button to check HR or the touch stop button to stop. The default duration to check the reading is three minutes. Fig. 5(a) shows request permission to send abnormal HR alert notification interfaces when abnormal HR is detected. The alert notification will be sent to his caregiver if the patient clicks on the 'OK' button. The request permission interface appears for

30 seconds and automatically sends an alert notification to its caregiver if the patient does not respond. Fig. 5(b) shows the alert notification that is being sent to his caregiver. The message includes the patient's name, his HR, and current location.

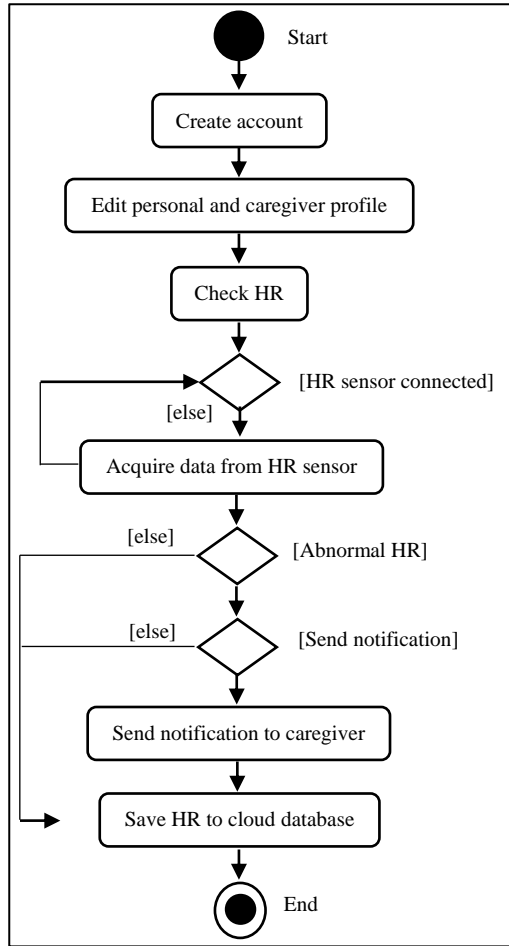


Fig. 2. Activity Diagram.

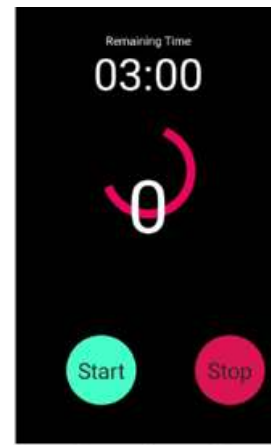


Fig. 4. Check Heart Rate.

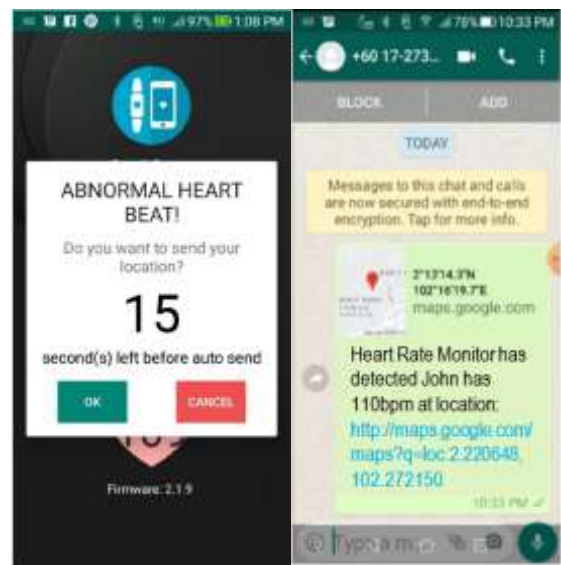


Fig. 5. (a) Request Permission, (b) Alert Notification.

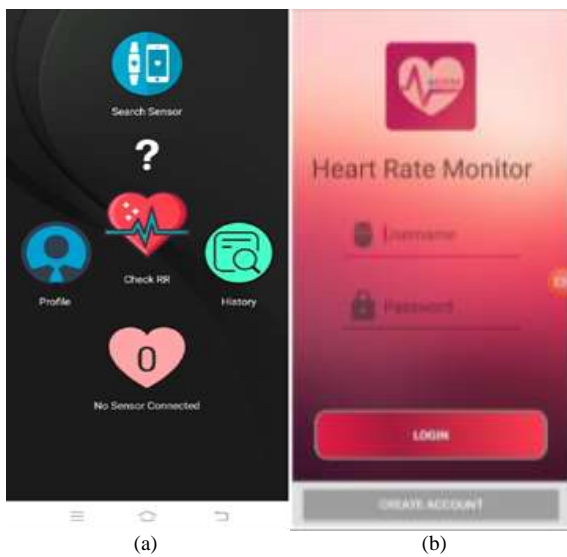


Fig. 3. (a) Login, (b) Menu.

IV. IMPLEMENTATION

The implementation of RTHM including data acquisition and detection of abnormal HR are explained in Section B. Android studio 3.4 or higher was used to develop RTHM.

A. Data Acquisition

Polar H10 (Polar Electro Oy, Kempele, Finland) was used in this study to acquire RR intervals data and then transferred to a smartphone. Polar H10 is a chest-strap HR monitor sensor. The sensor is chosen due to its recording being highly accurate and offers continuous measurement [19], [20]. Polar has implemented wireless Bluetooth Low Energy technology (BLE) for data communication between the sensor and mobile app.

Polar mobile SDK (software development kit) was used to implement the connection between Polar H10 sensor and RTHM app and data acquisition from Polar H10 [21]. Polar H10 transferred RR intervals data (unit of 1/1024 seconds) to a smartphone via Bluetooth communication link. R is the peak of

the QRS complex in the ECG wave and RR is the interval between successive Rs. Fig. 6 shows the implementation to load the default Polar BLE API with only FEATURE_HR enabled and add callback. The code snippet only presents some of the override methods of the PolarBleApiCallback abstract class.

Fig. 7 shows the implementation to automatically connect a nearby Polar device. -50 represents the Received Signal Strength Indication (RSSI) value in dbm. The value is typically from -40 to -60, depending on the used Bluetooth chipset and/or antenna tuning. "180D" represents service in hex string format and null represents any polar device.

B. Detection of Abnormal Heart Rate

RTHM records HR in three minutes. The mean HR and other HRV features such as SDNN, RMSSD, CV, pnn50, VLF, LF, HF and LF/HF ratio is calculated in the RTHM apps based on the RR transferred from Polar H10. Mean HR in beats per minute (bpm) is calculated from RR (ms) as shown in Equation (1) [22].

$$HR = \frac{\sum_{i=1}^n \frac{60 \cdot 1000}{RR_i}}{n} \quad (1)$$

```
PolarBleApi api = PolarBleApiDefaultImpl.  
defaultImplementation (this,  
PolarBleApi.FEATURE_HR);  
  
api.setApiCallback(new PolarBleApiCallback() {  
    @Override  
    public void  
    polarDeviceConnected(PolarDeviceInfo  
    polarDeviceInfo) {  
        Log.d("MyApp", "CONNECTED: " +  
        polarDeviceInfo.deviceId);  
    }  
    @Override  
    public void  
    polarDeviceDisconnected(PolarDeviceInfo  
    polarDeviceInfo) {  
        Log.d("MyApp", "DISCONNECTED: " +  
        polarDeviceInfo.deviceId);  
    }  
    @Override  
    public void hrNotificationReceived(String  
    identifier, PolarHrData data)  
    {  
        //hr is HR in bpm, rrsMs is RRs in  
        milliseconds.  
        Log.d(TAG, "HR value: " + data.hr + " rrsMs:  
        " + data.rrsMs);  
    }  
});
```

Fig. 6. Polar BLE API.

```
api.autoConnectToDevice (-50, "180D",  
null).subscribe ();
```

Fig. 7. Connect to a Polar Device.

An adult HR is normal when the ranges between 60 and 100 bpm. The abnormal HR is below 60 bpm is classified as bradycardia or above 100 bpm is classified as tachycardia [23]. An alert notification is sent to the caregiver when abnormal HR detected via WhatsApp application. The implementation to send an alert notification is shown in Fig. 8.

Google Location Services API is used to get a patient's location. It provides the best accuracy, simplicity, availability, and power-efficiency [24]. The code snippet in Fig. 9 shows the implementation to assess Google API. The Google API Client provides a common entry point to the Location Service API.

Firebase is the cloud database used to save all the patients' data including profile, HR and HRV. The implementation is shown in Fig 10.

```
try{  
    String url =  
    "https://api.whatsapp.com/send?phone="+  
    phoneNo +"&text=" +  
    URLEncoder.encode(message, "UTF-8");  
  
    i.setPackage("com.whatsapp");  
    i.setData(Uri.parse(url));  
  
    if (i.resolveActivity(packageManager) !=  
    null) {  
        this.startActivity(i);  
        finish();  
    }  
} catch (Exception e){  
    e.printStackTrace();  
}
```

Fig. 8. Alert Notification via WhatsApp.

```
mGoogleApiClient = new  
GoogleApiClient.Builder(this)  
    .addConnectionCallbacks(this)  
    .addOnConnectionFailedListener(this)  
    .addApi (LocationServices.API)  
    .build();  
  
locationManager =  
(LocationManager) getSystemService  
(Context.LOCATION_SERVICE);
```

Fig. 9. Google API Location Service.

```
FirestoreDatabase.getInstance().  
getReference("Data").  
child(FirebaseAuth.getInstance().  
getCurrentUser().getUid()).  
child(currentDateTime).setValue(hrv).  
addOnCompleteListener(new  
OnCompleteListener<Void>() {  
  
    @Override  
    public void onComplete(@NonNull  
    Task<Void> task) {  
        if (task.isSuccessful()) {  
            Toast.makeText(RR_Check.this, "Data Saved  
            Successfully", Toast.LENGTH_LONG).show();  
        }  
        else {  
            Toast.makeText(RR_Check.this,  
            "Failed to Data  
            Saved"+task.getException().  
            getMessage(), Toast.LENGTH_LONG).show();  
        }  
    }  
});
```

Fig. 10. Save data to Firebase.

V. USER ACCEPTANCE TEST

A user acceptance test was conducted to comprehend the intention and satisfaction level of the prospective users to use RTHM. An online survey was conducted to test the user's acceptance. The online survey was created using Google Forms.

Table I presents the user acceptance questionnaire items. It consisted of 12 questions, using a 5 point Likert scale. The questionnaire items were adapted from [25], [26]. The questionnaire items were divided into six constructs named compatibility, perceived usefulness, perceived ease of use, trust, perceived financial cost, and behavioral intention to use. Participants were asked to use the RTHM app for five to ten minutes before they answered the questionnaire. Participants wore the Polar H10 sensor while using the app.

TABLE I. QUESTIONNAIRE ITEMS

Constructs	Questionnaire Items
Compatibility	Using RTHM app is suitable for my lifestyle.
Perceived usefulness	Using RTHM app can improve my heart rate.
	Using RTHM app can enhance my heart rate monitoring.
	Using RTHM app can assist me in alerting abnormal heart rates to my caregiver or emergency medical center.
Perceived ease of use	I find that the graphical user interface of RTHM app is clear and easy to understand.
	I find that the display character of RTHM apps is clear and easy to watch.
	I find that the display color of RTHM app is clear and easy to differentiate.
	I find that the information display of RTHM app is not too complex.
Trust	As I understand it, I believe the RTHM app can help me with continuous heart monitoring.
Perceived financial cost	I think a smartphone required to deploy RTHM app is expensive.
Behavioral intention to use	I am willing to keep using RTHM app.
	I would recommend my friends to use RTHM app.

VI. RESULTS

Sixteen participants were involved in the user acceptance test. About 56% of the participants were female. The participant's age was between 18 and 65 years old. More than half of the participants were between 21 and 30 years old as illustrated in Fig. 11. The participants' education level ranged from high school to PhD. A quarter of the participants had bachelor's degrees as shown in Fig. 12.

Table II indicates user acceptance results. Compatibility, perceived ease of use, trust, and behavioral intention to use had more than a 90% satisfaction level. Most of the participants believed that the app is suitable for their lifestyle, easy to use, and useful for continuous heart monitoring. Besides, the majority of the participants had an intention to continuously use RTHM. Nevertheless, half of the participants perceived the financial cost to deploy the app is expensive. They believed that the app required an expensive smartphone.

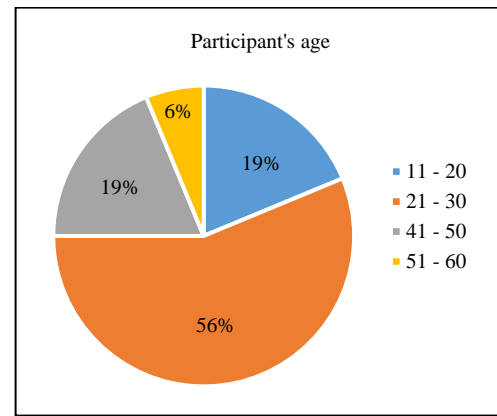


Fig. 11. Patient's Age Distribution.

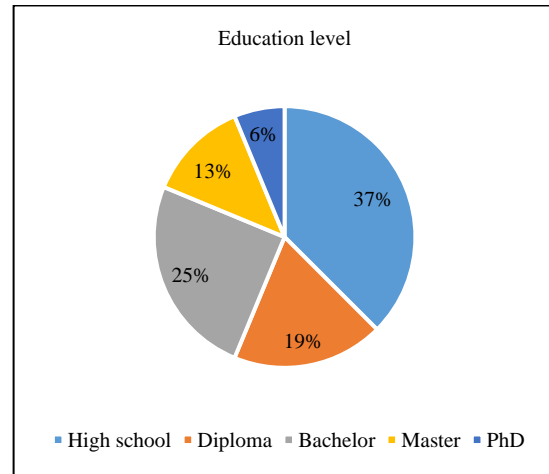


Fig. 12. Patient's Education Level.

TABLE II. USER ACCEPTANCE RESULTS

Construct	Satisfaction (%)
Compatibility	93.75
Perceived usefulness	89.58
Perceived ease of use	95.31
Trust	100.00
Perceived financial cost	50.00
Behavioral intention to use	90.63

VII. LIMITATIONS AND FUTURE WORKS

This study merely focused on the design and implementation of RTHM. System validation and comparison with other similar products should be conducted in the future. The validation includes the accuracy, reliability, efficiency, and energy consumption of the proposed app. Large scale feasibility study involving different age ranges and patients shall be conducted to verify the viability of the app. Besides, the RTHM concentrated on users'/patients' perspectives on continuous heart monitoring. The system can be enhanced in the future by developing a web-based system for doctors to view and diagnose their patients' heart data stored in a cloud database.

VIII. CONCLUSION

A real-time mobile heart monitoring application on android platforms has been proposed to enhance continuous heart monitoring and subsequently reduce death due to heart failure. An alert notification is sent to the caregiver when abnormal HR is detected. The app uses a wearable HR sensor to transfer RR data to the smartphone via a Bluetooth communication link. The HR data is saved to a cloud database and can be accessible to the hospital management system web portal. The user acceptance results showed that compatibility, perceived usefulness, perceived ease of use, trust, and behavioral intention to use had a high acceptance rate. Overall, the results indicated a positive influence on the readiness to use RTHM. The proposed app innovates patient-centered healthcare. It is expected that the RTHM may provide a more plausible tool in monitoring HR personally, conveniently, and continuously at any time and anywhere.

ACKNOWLEDGMENT

This study is supported by the Universiti Teknikal Malaysia Melaka research grant (PJP/2019/FTMK(7B)/S01681).

REFERENCES

- [1] Mozaffarian et al., "Executive summary: heart disease and stroke statistics—2016 update: a report from the American Heart Association," *Circulation*, vol. 133, no. 4, pp. 447–454, 2016.
- [2] N. T. Artinian et al., "Interventions to promote physical activity and dietary lifestyle changes for cardiovascular risk factor reduction in adults: a scientific statement from the American Heart Association," *Circulation*, vol. 122, no. 4, pp. 406–441, 2010.
- [3] A. Smith, "US smartphone use in 2015," Pew Research Center, 2015.
- [4] M. E. Rosenberger, M. P. Buman, W. L. Haskell, M. V. McConnell, and L. L. Carstensen, "Twenty-four hours of sleep, sedentary behavior, and physical activity with nine wearable devices," *Med. Sci. Sports Exerc.*, vol. 48, no. 3, p. 457, 2016.
- [5] S. Marceglia, P. Fontelo, E. Rossi, and M. J. Ackerman, "A standards-based architecture proposal for integrating patient mHealth apps to electronic health record systems," *Appl. Clin. Inform.*, vol. 6, no. 3, p. 488, 2015.
- [6] B. De Ridder, B. Van Rompaey, J. K. Kampen, S. Haine, and T. Dilles, "Smartphone Apps Using Photoplethysmography for Heart Rate Monitoring: Meta-Analysis," *JMIR Cardio*, vol. 2, no. 1, p. e4, 2018, doi: 10.2196/cardio.8802.
- [7] S. E. Stahl, H.-S. An, D. M. Dinkel, J. M. Noble, and J.-M. Lee, "How accurate are the wrist-based heart rate monitors during walking and running activities? Are they accurate enough?," *BMJ Open Sport Exerc. Med.*, vol. 2, no. 1, p. e000106, 2016, doi: 10.1136/bmjsem-2015-000106.
- [8] C. Venkatesan, P. Karthigaikumar, and S. Satheeskumaran, "Mobile cloud computing for ECG telemonitoring and real-time coronary heart disease risk detection," *Biomed. Signal Process. Control*, vol. 44, pp. 138–145, 2018, doi: 10.1016/j.bspc.2018.04.013.
- [9] X. Chen, J. Ji, K. Loparo, and P. Li, "Real-time personalized cardiac arrhythmia detection and diagnosis: A cloud computing architecture," in 2017 IEEE EMBS International Conference on Biomedical & Health Informatics (BHI), 2017, pp. 201–204, doi: 10.1109/BHI.2017.7897240.
- [10] X. Wang, Q. Gui, B. Liu, Z. Jin, and Y. Chen, "Enabling Smart Personalized Healthcare: A Hybrid Mobile-Cloud Approach for ECG Telemonitoring," *IEEE J. Biomed. Heal. Informatics*, vol. 18, no. 3, pp. 739–745, 2014, doi: 10.1109/JBHI.2013.2286157.
- [11] E. M. Fong and W. Y. Chung, "Mobile cloud-computing-based healthcare service by Noncontact ECG monitoring," *Sensors*, vol. 13, pp. 16451–16473, 2013, doi: 10.3390/s131216451.
- [12] H. Xia, I. Asif, and X. Zhao, "Cloud-ECG for real time ECG monitoring and analysis," *Comput. Methods Programs Biomed.*, vol. 110, no. 3, pp. 253–259, 2013, doi: 10.1016/j.cmpb.2012.11.008.
- [13] "Qardicore." <https://www.getqardio.com/qardicore-wearable-ecg-ekg-monitor-iphone/> (accessed Jan. 04, 2021).
- [14] Alivecor, "User Manual for Kardia TM Mobile by AliveCor ®," 2020.
- [15] A. D. William et al., "Assessing the accuracy of an automated atrial fibrillation detection algorithm using smartphone technology: The iREAD Study," *Hear. Rhythm*, vol. 15, no. 10, pp. 1561–1565, Oct. 2018, doi: 10.1016/j.hrthm.2018.06.037.
- [16] M. J. Reed et al., "Multi-centre Randomised Controlled Trial of a Smartphone-based Event Recorder Alongside Standard Care Versus Standard Care for Patients Presenting to the Emergency Department with Palpitations and Pre-syncope: The IPED (Investigation of Palpitations in th)," *EClinicalMedicine*, vol. 8, pp. 37–46, 2019, doi: 10.1016/j.eclinm.2019.02.005.
- [17] "Zenicor-ECG." <https://zenicor.com/zenicor-ekg/> (accessed Jan. 04, 2021).
- [18] T. Hendrikx, M. Rosenqvist, P. Wester, H. Sandström, and R. Hörnsten, "Intermittent short ECG recording is more effective than 24-hour Holter ECG in detection of arrhythmias," *BMC Cardiovasc. Disord.*, vol. 14, pp. 1–8, 2014, doi: 10.1186/1471-2261-14-41.
- [19] D. Jin, H. Adams, A. M. Cocco, W. G. Martin, and S. Palmer, "Smartphones and wearable technology: benefits and concerns in cardiology," *Med. J. Aust.*, no. December, 2019, doi: 10.5694/mja2.50446.
- [20] R. Gilgen-Ammann, T. Schweizer, and T. Wyss, "RR interval signal quality of a heart rate monitor and an ECG Holter at rest and during exercise," *Eur. J. Appl. Physiol.*, vol. 119, no. 7, pp. 1525–1532, 2019, doi: 10.1007/s00421-019-04142-5.
- [21] E. Silvola, "SDK for Polar sensors," Polar Electro, 2018.
- [22] L. Salahuddin and K. Desok, "Detection of acute stress by heart rate variability using a prototype mobile ECG sensor," in Proceedings - 2006 International Conference on Hybrid Information Technology, ICHIT 2006, 2006, vol. 2, doi: 10.1109/ICHIT.2006.253646.
- [23] R. W. Neumar et al., "Part 8: Adult Advanced Cardiovascular Life Support," *Circulation*, vol. 122, no. 18_suppl_3, pp. S729–S767, Nov. 2010, doi: 10.1161/CIRCULATIONAHA.110.970988.
- [24] Danny Gonzalez, "Android Developer's Guide to the Google Location Services API," Toptal, 2016.
- [25] F.-C. Tung, S.-C. Chang, and C.-M. Chou, "An extension of trust and TAM model with IDT in the adoption of the electronic logistics information system in HIS in the medical industry," *Int. J. Med. Inform.*, vol. 77, no. 5, pp. 324–335, 2008, doi: <https://doi.org/10.1016/j.ijmedinf.2007.06.006>.
- [26] M. H. Tseng and H. C. Wu, "A cloud medication safety support system using QR code and Web services for elderly outpatients," *Technol. Heal. Care*, vol. 22, no. 1, pp. 99–113, 2014, doi: 10.3233/THC-140778.

A Survey on Junction Selection based Routing Protocols for VANETs

Dr. Irshad Ahmed Abbasi^{1,*}(Member IEEE), Dr. Elfatih Elmubarak Mustafa²

Department of Computer Science
Faculty of Science and Arts at Belgarn, University of Bisha
P.O. Box 60, Sabt Al-Alaya 61985, Kingdom of Saudi Arabia

Abstract—Objectives: To compare significant position-based routing protocols based on their underlying techniques such as junction selection mechanisms that provide vehicle-to-vehicle communications in city scenarios. **Background:** Vehicular Adhoc Network is the most significant offshoot of Mobile Adhoc Networks which is capable of organizing itself in an infrastructure-less environment. The network builds smart transportation which facilitates deriving in-terms of traffic safety by exchanging timely information in a proficient manner. **Findings:** The main features of vehicular adhoc networks pertaining to the city environment like high mobility, network segmentation, sporadic interconnections, and impediments are the key challenges for the development of an effective routing protocol. These features of the urban environment have a great impact on the performance of a routing protocol. This study presents a brief survey on the most substantial position-based routing schemes premeditated for urban inter-vehicular communication scenarios. These protocols are provided with their operational techniques for exchanging messages between vehicles. A comparative analysis is also provided, which is based on various important factors such as the mechanisms of intersection selection, forwarding strategies, vehicular traffic density, local maximum conquering methods, mobility of vehicular nodes, and secure message exchange. **Application/Improvements:** the outcomes observed from this paper motivate us to improve routing protocol in terms of security, accuracy, and reliability in vehicular adhoc networks. Furthermore, it can be employed as a foundation of references in determining literature that are worth mentioning to the routing in vehicular communications.

Keywords—Position-based; inter-vehicular; urban scenario; algorithms; reliability

I. INTRODUCTION

The Vehicular Adhoc Network (VANET) is a branch of Mobile Adhoc Networks (MANET). It is also called network on wheels which accomplishes communication between vehicles and among nearby vehicles. The vehicular nodes in VANETs are self-organized. They exchange information with each other in an infrastructure less environment [1-7]. VANET is a significant cost-effective tool for building an intelligent transportation system (ITS). It plays a vital role in traffic security and safety enhancement. It advances traffic management, and vehicles control. It is a significant way of providing the most recent applications to the on-wheel community. However, it is an outstanding challenge for the ITS industry to build vehicle to vehicle (V2V) and vehicle to infrastructure (V2I) interactions. The US FCC realises its

intensifying benefits and allotted 75-MHz spectrum for dedicated short-range communications (DSRC) for the deployment or exploitations of WLAN Technology for making vehicular communications a reality [1], [2], [5], [8], [10]. DSRC provides connectivity in a range of about one thousand meter [3], [8]. DSRC is an appropriate and vital technology for building vehicular communication. There are varieties of services that can be accomplished by using VANETs. These include accident avoidance, facilitating internet access inside vehicles, monitoring traffic flow regulations, locating parking lots, finding restaurants, and gas stations [29]. Inside vehicles, it is also useful in managing entertainment applications like playing games, watching movies, and listening music [10], [13].

The afore-mentioned applications cannot be accomplished without a competent routing protocol. The existing literature provides topology-based routing protocols and position-based routing protocols [3]. Topologies based routing protocols are ineffective in VANETs because of intermittent connectivity [13]. The position-based routing category is considered more effective in VANETs [10]. In position-based routing, particularly Junction selection-based routing is considered the most efficient routing mechanisms in city scenarios for addressing routing problems [3], [8], [9], [27], [29]. In the existing literature or surveys [7], [[11], [12], [15], [[17] only certain aspects like forwarding strategies or local optimum and mobility are considered. The study focuses on different methods of junction selection mechanism and their significance along with other aspects. The most prominent features or aspects of efficient routing protocols are tabulated. The working of different routing protocols is described with diagrams. It also provides some missing aspects like security, accuracy, and reliability which if added can further improve the latest junction selection-based routing protocols like DMJSR [28], and RPSPF [29]. Secure, accurate, and reliable exchange of messages is very important in VANETs for a message dissemination routing protocol.

The remaining portion of paper is arranged as follows. The vehicular adhoc network structural paradigm is elaborated in Section II. The detail about the position-based routing approaches particularly junctions selections based working in inter-vehicular communication environment for the urban scenarios is given in Section III. This section is also equipped with brief comparative analysis of position-based protocols from existing literature. The last Section IV concludes the paper and provides the future research directions.

* Corresponding Author

II. ARCHITECTURAL PARADIGMS OF VANETS

In VANETs, each vehicle is equipped with devices called onboard units. Each onboard unit is enabled with wireless communication links and computational capabilities. Vehicles communicate through these wireless links. The vehicular nodes in VANETs act as members and as well as a router of the network. A node communicates directly with other nodes that are present inside its transmission range. The node uses an intermediate node for exchanging information with the nodes that are beyond its transmission range [4], [10], [27]. Due to self-organizing nature of VANET, its structural design categorized into three kinds: i) Pure adhoc networks ii) Pure cellular wireless local area network iii) Hybrid networks [12],[13].

Pure ad-hoc vehicular network design also named as inter-vehicle ad hoc network is presented in Fig. 1. It provides communication between vehicles and nearby vehicles. In this type of architecture, the collection and propagation of road associated information is carried out in the absence of any fixed infrastructure. Due to its infrastructure-less nature, it is cost-effective and easy to deploy [4], [14]. On the other hand, the vehicular nodes are set free to move at high speed. The highly mobile vehicular nodes frequently alter the network topological connections. The frequent topology changes cause network fragmentation [13]. In this kind of architecture, the network fragmentation due to high mobility makes routing of data more challenging [20], [28].

A cellular structural design of VANETs is provided in Fig. 2. It consists of cellular gateways and wireless access points which provide internet access to the vehicular nodes. The cellular architectural paradigm assists in giving information related to traffic jams and traffic flow control. Furthermore, it gives different types of other services which include data downloading, parking information, advertisement, and latest news [10], [24], [28]. It is very difficult to deploy because of the rising cost of cellular towers, geographical restrictions, and wireless access points [12], [14].

The hybrid structural design of VANETs is shown in Fig. 3. It is the mixture of both, infrastructure based domain and pure adhoc based domain. The adhoc domain furnishes V2V interactions. The infrastructure domain provides the V2I communications. This kind of architectural paradigm is supportive in giving more affluent content [8], [9]. It also provides better flexibility in contents sharing [26], [24].

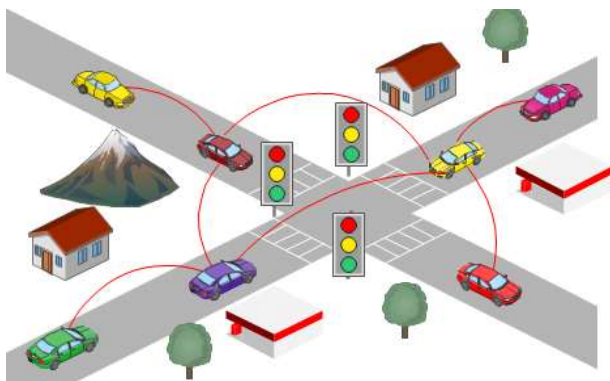


Fig. 1. Ad-hoc Networks Design.

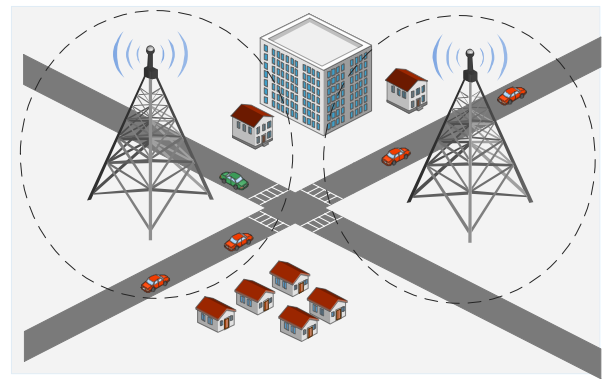


Fig. 2. Pure Cellular Design.

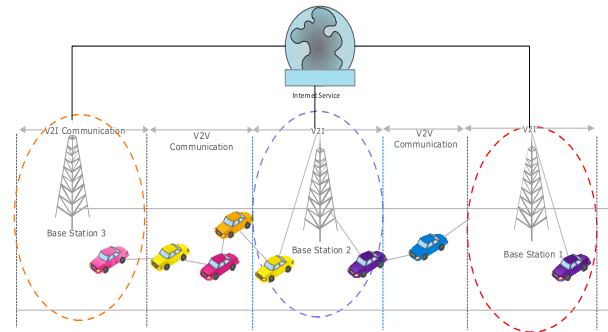


Fig. 3. Hybrid Design of VANETs.

III. POSITION-BASED ROUTING IN VEHICULAR NETWORKS

There are two general categories of baseline routing protocols in vehicular adhoc networks. Topology based routing protocols and position-based routing protocols [1]. The instances of topology based routing protocols include Adhoc On-distance Vector (AODV), Optimized Link State Routing (OLSR), and Dynamic Source Routing (DSR) [3]. In vehicular adhoc communication network, the protocols that belong to this category of routing are not feasible due to their path discovery mechanism [2], [19]. Also, their end to end routing path maintenance mechanism faces difficulties in VANETs. The reason is that irregular distribution of vehicular nodes and their highly mobile nature in adhoc domain cause regular path breakages in these routing protocols [9], [13], [21]. This increases routing overhead and makes VANETs ineffective. The second category of routing is position-based routing.

The existing literature shows that the position-based routing mechanisms are appropriate than topology based routing technique for handling routing problems in vehicular communications [8], [2-4], [13], [6], [17], [18]. The vehicular nodes in this category of routing protocols use their locations for communication. The communication between the source vehicular node and the destination vehicular node is either direct or through intermediate vehicular nodes. Each vehicular node in the network possesses GPS for locating its own position. When the source vehicle desires to interact with the destination vehicle, the source vehicle accomplishes its own position using GPS. The location of destination vehicle is established with the help of location services. The source vehicle or the intermediary vehicle keeps the latest positions of its one hop neighbors in its neighbor table using beacon

exchanges. If the destination vehicle is inside the communication range of source vehicle, in this case, both directly communicate with one another. If the destination vehicle is outside of its direct reach than it relays the packet through an intermediary neighbor vehicle that is nearest to the destination node [8], [2-5], [21], [15]. In this way, the indirect communication between the source vehicular node and the destination vehicle is carried out by intermediate nodes.

Basically, the vehicular adhoc network has two environments. These are highway and urban environments [16]. The highway is composed of mainly straight and curvy roads having no obstacles. On the other hand, the urban environment contains streets with junctions. This environment is rich in impediments such as tall buildings.

The intersection of two or more streets is called junction. The packet passes through a set of junctions and relayed towards destinations. The obstacles around the streets and junction create problems in establishing an optimal routing path connecting source and destination [23]. As both the city and high environments have different structures and characteristics, the researchers designed protocols separately for each environment. In the existing literature, there are different types of position-based routing protocols. Fig. 4 presents the classification of position-based routing protocols. According to the figure, the position-based routing has two main classes i.e. urban environment based routing and highway environment based routing. The protocols are either proposed for V2V communications or V2I communications or for both the environments. This study mainly provides a brief description of routing schemes that are develop for V2V interactions in city scenarios. V2V based routings protocols are classified into two types i.e. static junction selection based routing protocols and dynamic junction selection based routing protocols. The dynamic junction selection based routing protocols are further classified into two classes i.e. dynamic one hop junction selection based routing protocols and dynamic multi hop junction selection based routing protocols [3], [17], [19], [28], [29]. A few of these routing proposals are traffic-aware while others are not. The protocols that are designed on the basis of traffic awareness concepts perform better in terms of packet delivery ratio, end to end delay, routing overhead and hop count as compared to other routing protocols [7], [9], [11], [12]. The description of V2V based routing protocols is given below.

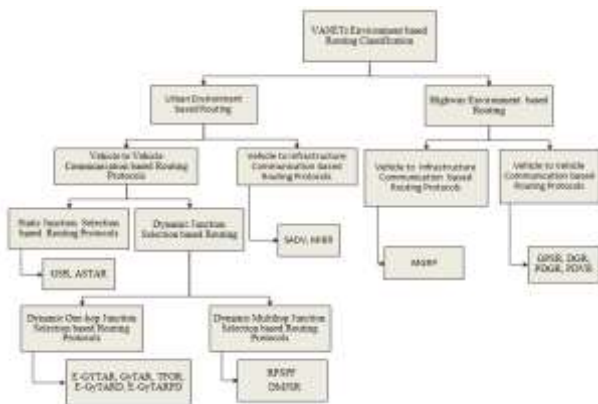


Fig. 4. Classification of Location based Routing Protocols.

A. Greedy Perimeter Stateless Routing (GPSR) [22]

GPSR is proposed for providing vehicle to vehicle interactions in a highway scenario. The description of GPSR provides us facts about the limitation of highway V2V based routing in a city scenario. GPSR finds source vehicle locations with the help of GPS. It locates neighboring nodes with the help of beacons exchange. The location service (likes GLS or HLS) [21] trace the location of the destination in this routing protocol. There are two working phases of GPSR. These are: i) the greedy phase, and ii) the perimeter phase. During greedy phase, the packet sender or forwarding node chooses its one-hop neighbor that is the nearest to the destination for relaying packet towards the destination. The Greedy phase suffers from a local optimum problem that occurs if the forwarding node has no neighbor node that is nearest to the destination node than itself. The working of the greedy phase is presented in Fig. 5.

In this figure, Source vehicle Sv chooses neighbor vehicle Bv among its entire one-hop neighboring vehicles because of its nearest position to the target vehicle Dv and dispatches the packet to it. If GPSR meets the local optimum problem during the greedy mode, it overcomes this situation by using the perimeter phase. There are two steps in the perimeter phase. In the first step, the relative neighborhood graph (RNG) is used to accomplish graph planarization. In the second step, GPSR finds the next forwarding neighbor vehicular node by using right hand rule which is responsible for relaying packet toward destination. GPSR is ineffective in the city environment because of two main reasons. Initially, graph planarization fails due to impediments [3], [29]. Furthermore, the perimeter phase accomplishes long routing paths while dispatching packet towards a destination which causes an increase in the end to end delay. It also generates more routing overhead due to formation of routing loops [19], [18], [25].

Fig. 6 describes the operation of the perimeter phase. The source vehicle S intends to communicate by sending a packet to destination vehicle D. The source vehicle S forwards the packet to the neighbor vehicle A using greedy phase as it is closest to destination vehicle D. At vehicle A, greedy phase stuck in local optimum as A itself is the nearest vehicular node to destination vehicle D as compared to all of its neighbors. The position of destination vehicle lies beyond the direct communication range of vehicle A. Vehicle A uses right hand rule of perimeter phase and overcomes this problem by choosing vehicle X for forwarding packet. In the same way, at vehicle X packet is sent to vehicle Y, GPSR will continue to use perimeter phase until it finds a vehicle to switch back to greedy phase.

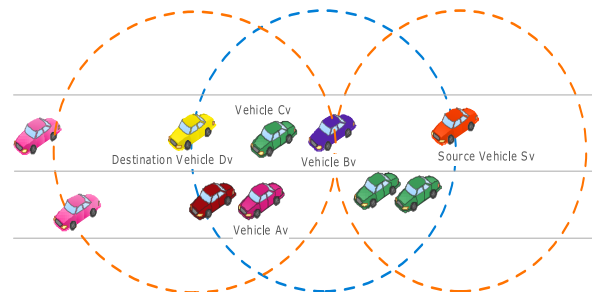


Fig. 5. Function of Greedy Mode.

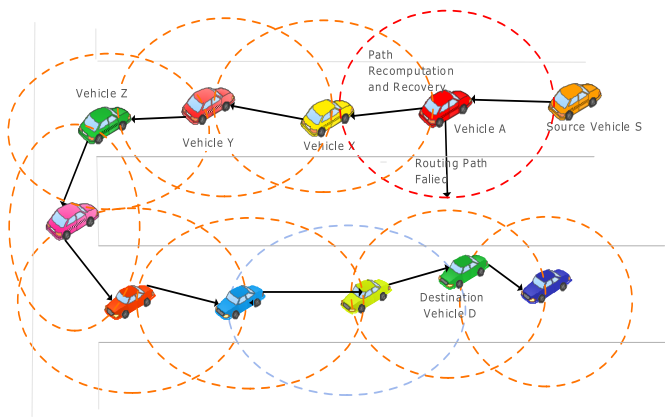


Fig. 6. Perimeter Mode of GPSR.

B. Geographic Source Routing (GSR) Protocol [18]

This protocol is developed for the urban setting to conquer the limitations of GPSR. It is position-based routing protocol. It accomplishes the position of destination vehicular node using reactive location service. It employs the Dijkstra shortest path algorithm to find out the shortest route between source and destinations. The shortest route accomplished by GPSR consists of a sequentially arranged set of intersections. The packet moves from source vehicle to destination vehicle through the set of intersections. In between intersections, greedy forwarding is employed to forward the packet from one node to another node. The simulation results, with reasonable traffic density in city scenarios, shows that GSR outperformed the existing topology based DSR and AODV routing protocols pertaining to end-to-end delay and delivery ratio [9], [19]. This protocol is suffered from one main problem that it chooses intersections statically without the consideration of traffic density. It is not traffic aware. Traffic awareness in between junctions during junctions' selection is necessary, as it provides connectivity for moving packet towards destination [3, 8, 28].

C. Greedy Perimeter Coordinator Routing (GPCR) [25]

It is developed for urban scenarios. This routing protocol is an integration of restricted greedy forwarding phase and perimeter phase. It does not use a digital city map. In the restricted greedy phase, the concept of coordinator node is introduced which is in charge of making routing decisions. The node located at the intersection is named as the coordinator node. Fig. 7 shows the working of the restricted greedy forwarding strategy.

According to this strategy, it is compulsory for the packet carrier node to select a coordinator at the junction for forwarding a packet. It bounds the packet carrier node to avoid packet forwarding to those nodes that are present across the junctions. Restricted greedy forwarding phase sometimes trapped in local optimum problem. GPCR overcomes this issue by applying the perimeter phase. In this phase, it is supposed that the city environment has natural planner graphs. Unlike GPSR, it ignores graph planarization. Making a planer graph in the city environment split the network into parts. The perimeter phase employs right-hand-rule to dispatch packet toward destination. There are certain demerits of this routing protocol. The restricted greedy phase always stops packet at the junction and increase the number of hop counts as compared to simple

forwarding which deteriorate the performance of the network [14]. Fig. 8 shows the ineffectiveness of restricted greedy forwarding. The perimeter phase in GPCR delays in relaying packet towards a destination which diminishes the network performance [8, 2 and 11]. It is also not a traffic-aware routing protocol [3].

Fig. 7 demonstrates that vehicle A receives a packet from vehicle B. If vehicle A uses greedy forwarding, it communicates the packet to vehicular node C that is nearest to the destination. If vehicle A uses restricted greedy forwarding, it sends the packet to a coordinator vehicle, located at the junction instead of vehicle C.

The incompetence of restricted greedy forwarding is demonstrated in Fig. 8. In this figure, the source vehicle is marked with yellow color and the destination vehicle is marked with blue color. In case of simple greedy forwarding, the packet passes just 13 hops while traveling from its source vehicle to the required destination. On the other hand, in case of restricted greedy forwarding, it takes 17 hops for the packet to be transferred to the destination. This proves that restricted greedy forwarding is ineffective in terms of the number of hop counts [10].

D. Anchor-based Street and Traffic-Aware Routing (A-STAR) [23]

This protocol is a position-based routing protocol. It accomplishes an anchor path by using statistically rated maps contain information pertaining to urban bus routes. The anchor path is based on connectivity. The packet passes through the anchors and relayed towards the destination. In the case of local optimum, it uses a route recovery strategy for the formation of a fresh path based on anchors. The outcomes of simulation and analysis indicate that A-STAR gives better performance than GSR and GPSR. The main reason is its competency of establishing an end-to-end route accomplishes connectivity even in low traffic density scenarios. However, its routing paths follow anchor path based on long city bus routes that may not be optimal and result in greater delays [3], [9], [13], [19].

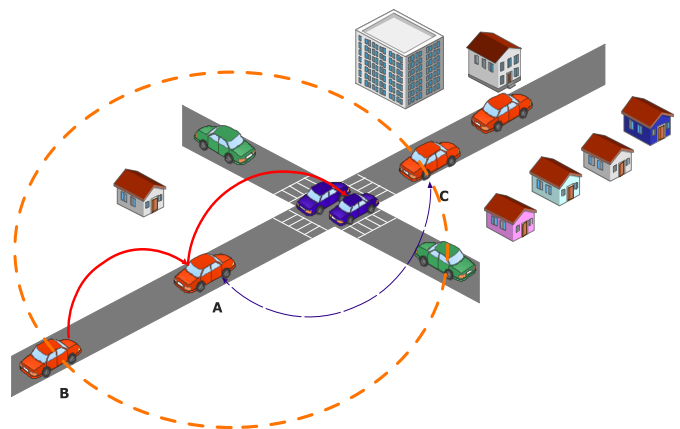


Fig. 7. Restricted Forwarding Mechanism of GPCR.

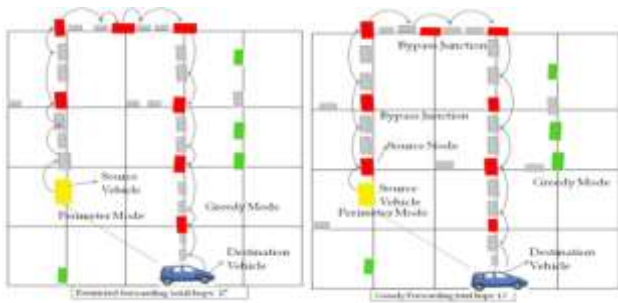


Fig. 8. Ineffectiveness of GPCR.

E. Greedy Traffic-Aware Routing (GyTAR) Protocol [9]

It is a position-based routing strategy that accomplishes optimal routes in city scenarios for relaying packet toward destination. It contains two phases. These are: i) dynamic junction selection method, and ii) an improved greedy forwarding technique for forwarding route in between junctions. In junction/intersection selection method, it decides the subsequent junction considering vehicular traffic density and the shortest distance to the destination. Its dynamic junction selection method moves the packet through city streets providing connectivity and the shortest distance to the destination. GyTAR outperforms the previous routing schemes like GSR and GPSR in terms of end to end delay, routing overhead, and packet delivery ratio. The main drawback of this routing protocol is that during the selection of the next junction, it ignores the vehicular nodes direction. Due to this, it suffers from the local optimum problem in some city scenarios which degrade the network performance [8].

F. Enhanced Greedy Traffic-Aware Routing Protocol (E-GyTAR) [8]

This protocol is an enhancement of GyTAR. It comprises of pair of modes. These are dynamic junction selection mode and an improved greedy forwarding for forwarding packets in between junctions. The dynamic junction selection mechanism selects the subsequent junction based on directional traffic density and the shortest routing path to the destination and thereby route the packet. Sometimes, its improved greedy forwarding stuck in local optimum situation. It exploits carry-and-forward scheme to conquer this problem. The main negative aspect of E-GyTAR is that on multi-lane roads, it ignores non-directional traffic density. In case of absence of directional density, it is unable to select the next junction and the packet cannot be relayed towards the required destination node. The consideration of non-directional traffic density is very important in such scenarios for relaying packet towards the destination [3].

G. Dynamic Multiple Junction Selection based Routing Protocol (DMJSR) [28]

DMJSR is composed of multiple junction selection mechanism. The difference between DMJSR and existing approaches is its new dynamic multiple intersection selection method. Its novel junction selection mechanism establishes route by considering multiple junctions and thereby route data towards the required destination vehicle. It employs an enhanced greedy forwarding that maintains one-hop neighbor information instead of two-hops between the junctions.

DMJSR outperformed the existing one hop junction selection based routing schemes such as TFOR and E-GyTAR in case of packet delivery ratio and the end to end delay. The main dilemma associated with DMJSR is that its forwarding strategy ignores the link reliability while forwarding the packet. It is unable to sustain the frequent link ruptures caused by high speed vehicular nodes which degrade the network throughput [29].

In Fig. 9, the dynamic multiple junction selection technique of DMJSR routing protocol is presented. According scenario presented in the figure, the source vehicle S is present at the current Junction J_1 . J_1 has three two-hop neighbor junctions J_4 , J_5 and J_7 . The source vehicle S selects two hop neighbor junctions J_4 instead of J_5 and J_7 because of its higher traffic density which provides more connectivity and thereby dispatches the packet to the required destination vehicle D.

H. Traffic Flow Oriented Routing Protocol (TFOR) [3]

It is a position-based routing approach for the city surrounding. It accomplishes the routing path based on traffic flows. It has two modes: i) the junction selection mode which is based on the concentration of traffic density and shortest path. ii) A forwarding technique that maintains two-hop neighbor information. It selects the next junction on the basis of directional and as well as non-directional traffic flows. If directional traffic flow on the multi-lanes road is missing, it uses non-directional flow for routing the packet towards the destination. It concentrates on the urban streets containing higher traffic flows because higher traffic flows offer more connectivity in relaying packet towards a destination which enhances the network performance. Simulation results based on a realistic traffic city environment indicate that TFOR achieves higher performance in terms of packet delivery ratio and the end to end delay as compared to GSR, E-GyTAR, and GPSR. The problem with this routing protocol is that its improved greedy forwarding mode suffers from sudden link rupture problem. Also, its dynamic one-hop junction selection mechanism suffers from a local optimum problem at street level [28].

In Fig. 10, the intersection selection technique of traffic-flow oriented routing protocol is presented. According to the figure, the source vehicular node is present at the current intersection J_1 . J_1 has two neighbor intersections J_2 and J_3 . The source vehicle node selects intersection J_3 instead of J_2 because of its higher traffic density and the shortest distance to the destination vehicle and thereby route the packet towards the destination.

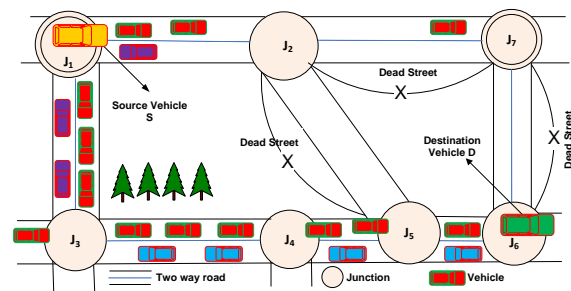


Fig. 9. DMJSR Junction Selection.

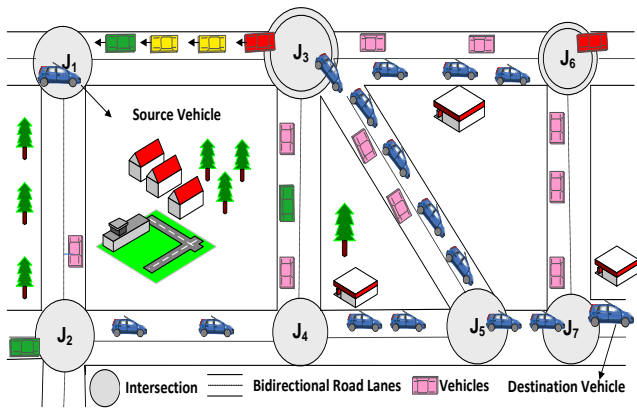


Fig. 10. TFOR Intersection Selection.

I. Reliable Path Selection and Packet Forwarding Routing Protocol (RSPSF) [29]

RSPSF is composed of multiple intersection selection mode and reliable packet forwarding mode. The difference between RSPSF and DMJSR is its novel reliable packet forwarding mechanism. It accomplishes route by considering multiple junctions and thereby route the packet towards destination. Its reliable packet forwarding approach forwards the packets to the next neighbor based on link life-time and link stability to avoid packet-drops because of rapid link ruptures. Simulation outcomes exhibit that RSPSF performs better than the existing one-hop junction selection based routing approaches like TFOR, GPSR, and E-GyTAR in terms of packet delivery ratio, end-to-end delay, and routing overhead. The problem with this routing protocol is that it cannot exchange message securely.

J. Directional Geographic Source Routing (DGSR) [27]

It is an improvement of GSR with a directional forwarding approach. This protocol consists of static junction/intersection selection mechanism of GSR. Instead of simple greedy forwarding, it uses a directional greedy forwarding strategy for forwarding packet in between the junctions. In this routing scheme, the shortest routing path between source and destination is accomplished based on the Dijkstra shortest path algorithm. The shortest routing path consists of a sequence of intersections. The packet passes through the sequence of intersections and reaches the destination. In the situation when this routing scheme suffers from local optimum problem, it uses a carry and forward approach. This protocol suffers from link sudden link rupture problems as its directional forwarding does not consider link reliability while forwarding [29].

K. Enhanced Greedy Traffic-Aware Routing Protocol-Directional (EGyTAR-D) [27]

In this routing scheme, E-GyTAR is enhanced with directional forwarding and named it as EGyTAR-D. It comprises of two phases. These are: i) the intersection selection phase and ii) the directional greedy forwarding phase. This protocol locates the position of destination vehicle using location service. Like E-GyTAR, It chooses the next junction considering directional traffic density and the shortest distance to the required destination. Directional forwarding is used to accomplish the forwarding of packets in between the junctions. Simulations results that consider city scenarios exhibit that E-GyTAR improves packet delivery ratio and reduces the end to end delay as compared to DGSR and E-GyTAR. The directional forwarding of this protocol suffers from sudden link rupture problem [29]. Table I outlines the relative features of all the above mentioned inter-vehicular routing protocols.

TABLE I. COMPARATIVE FEATURES OF SIGNIFICANT POSITION-BASED ROUTING SCHEMES FOR CITY SCENARIOS

Inter-vehicular Position Aware Unicast Routing Schemes	Comparative Features										
	Secure Message Exchange	Traffic Density	Static Junction Selection	Dynamic One hop Junction Selection	Dynamic Multi hop Junction Selection	GPS Require	Digital Map Require	Local Optimum Recovery Technique	Reliability	Hop Count	Realistic Mobility Flows
GPSR[22]	☒	☒	-	☒	☒	☒	☒	Perimeter mode	☒	One-hop	☒
GSR[18]	☒	☒	☒	☒	☒	☒	☒	Switch back to greedy technique	☒	One-hop	☒
A-STAR[23]	☒	☒	☒	☒	☒	☒	☒	Anchor path reconstruction	☒	One-hop	☒
GPCR[25]	☒	☒	-	☒	☒	☒	☒	Right hand Rule	☒	One-hop	☒
GyTAR[9]	☒	☒	☒	☒	☒	☒	☒	Carry and forward	☒	One-hop	☒
E-GTAR[8]	☒	☒	☒	☒	☒	☒	☒	Carry and Forward	☒	One-hop	☒
TFOR[3]	☒	☒	☒	☒	☒	☒	☒	Carry and Forward	☒	Two-hop	☒
DGSR[27]	☒	☒	☒	☒	☒	☒	☒	Carry and Forward	☒	One-hop	☒
D-EGyTAR [27]	☒	☒	☒	☒	☒	☒	☒	Carry and Forward	☒	One-hop	☒
DMJSR[28]	☒	☒	☒	☒	☒	☒	☒	Carry and Forward	☒	One hop	☒
RSPSF[29]	☒	☒	☒	☒	☒	☒	☒	Carry and Forward	☒	One hop	☒

IV. CONCLUSION AND FUTURE RESEARCH DIRECTIONS

In this study, the most vital inter-vehicular communication-based routing protocols designed for urban scenarios are presented. An overview of structural designs of the vehicular adhoc network is presented at the beginning of study. After that, a systematic discussion about the working of various position-based routing protocols along with their limitations is presented. It also presents a qualitative comparative investigation of the above-mentioned routing protocols based on the consideration of several significant parameters. These parameters include vehicular traffic density, forwarding strategies, mobility of vehicles, the mechanisms of junctions' selection which include static junction selection or dynamic one-hop junction selection or dynamic multi-hop junction selection, the techniques to handle local optimum situations, location services, and the ways of accomplishing the shortest routing path. There is a significant impact of all these parameters on the throughput of VANETs.

The designing of an effective optimal routing algorithm for an efficient inter-vehicular communication system faces several technical challenges. Even though, the routing of data for building an efficient ITS through VANETs received a lot of interest from worldwide wireless network research communities and organizations but yet there is a need for further vigilant investigation on some challenges associated with routing. For example, one of them is to design and develop a routing protocol that securely exchanges information in inter-vehicular communication system. The main and crucial component of VANETs is to have a protocol that is capable of quickly and timely disseminating accurate and secure messages about life intimidating incidents like traffic accidents and traffic jams. The dissemination of such critical messages in highly dynamic VANETs in the presence of malicious vehicular nodes is a challenging task. These malicious vehicular nodes normally temper the critical messages which result in devastating consequences in the form of collateral damage to neighboring vehicular nodes and drivers. With security and accuracy of messages, there is a need for reliability and stability of the links through which message travel to other vehicular nodes. In VANETs, high mobility of vehicular nodes makes the network intermittently connected. The intermittent connectivity induces sudden link breaks in the network at the time of forwarding or routing of packets. The induction of sudden link rupture increases packet loss which makes the network unreliable and ineffective. Inter-vehicular communication also needs a scheme of presenting accurate and well-timed information about the vehicular traffic density on the road. An optimal routing protocol that relays the packets considering the shortest distance and vehicular traffic density cannot be accomplished without an effective traffic density estimation mechanism. The traffic density determines the strength of connectivity in VANETs and the accomplishment of such a mechanism is also challenging. The vehicular communication system has two environments, highway, and city. Both have the different architectural designs. Developing a routing protocol that works in both the environment is another research challenge for the research communities.

In conclusion, the way of establishing a most robust routing path to the required destination determined by the mechanism

exists in a protocol. However, for effective inter-vehicular communication, current routing protocols, unable to reflect properly the real-life city scenario characteristics. Therefore, VANETs need a routing protocol that is secure, reliable, stable, and accurately exchange the information between the vehicles. It must incorporate the actual-life urban environment characteristics like high mobility, intermittent connectivity, obstacles, dense and sparse nature of the networks to make VANETs effective in building an efficient transportation system.

REFERENCES

- [1] A. Dahiya, R K. Chauhan, A Comparative study of MANET and VANET environment. *Journal of Computing*. 2010 July, 2 (7), pp. 87–91.
- [2] G. M. T. Abdalla, M. A. Abu-Rgheff, S. M. Senouci, Current Trends in Vehicular Ad Hoc Networks. *Ubiquitous Computing and Communication Journal. UbiRoads*. 2008 Mar, 6 (1), pp. 1-13.
- [3] I. A. Abbasi., B. Nazir, S. A. Madani, A traffic flow-oriented routing protocol for VANETs. *Springer EURASIP J. Wireless Communication and Networking*. 2014 Jul, 121 (2014), pp. 1-17.
- [4] F. Li, Y. Wang, Routing in vehicular ad hoc networks: A survey. *Vehicular Technology, Magazine IEEE*. 2007 Jun, 2 (2), pp. 12–22.
- [5] J. Cheng, J. L. Cheng, M. C. Zhou, F. Liu, Routing in Internet of Vehicles: A Review. *IEEE Transaction on Intelligent Transportation System*. 2016 Aug, 16 (5), pp. 1-20.
- [6] B. T. Sharef, R A. Alsaqour, M. Ismail, Review: Vehicular communication adhoc routing protocols: A survey. *Journal of Network and Computer Applications*. 2014 Dec, 7 (3), pp. 63–96.
- [7] S. A. Shah, J. Zhejiang, Unicast routing protocols for urban vehicular networks: review, taxonomy, and open research issues. *Journal of Zhejiang University-SCIENCE (Computers & Electronics)*. 2014, 15 (7), pp. 489-513.
- [8] S. M. Bilal, S. A. Madani, I. A. Khan, Enhanced junction selection mechanism for routing protocol in VANETs. *International Arab Journal of Information Technology*. 2011 June, 8 (4), pp. 422–429.
- [9] M. Jerbi, S. M. Senouci, R Meraihi, Y. G. Doudane, An improved vehicular ad hoc routing protocol for city environments. *IEEE International Conference on Communication ICC07*. 2007 Jun, pp. 3972–3979.
- [10] S. M. Bilal, C. J. Bernardos, C. Guerrero, Position based routing in vehicular networks: A survey. *Journal of Network and Computer Applications*. 2013 Dec, 36 (2013), pp. 685–697.
- [11] K. C. Lee, U. Lee, M. Gerla, Survey of Routing Protocols in Vehicular Ad Hoc Networks. In: *Advances in Vehicular Ad-Hoc Networks, Developments and Challenges IGI Global*. 2009, pp. 113-175.
- [12] Y. W. Lin, Y. S. Chen, S. L. Lee, Routing Protocols in Vehicular Ad Hoc Networks: A Survey and Future Perspectives. *Journal of Information Science and Engineering*. 2010 May, 26 (3) pp. 913–932.
- [13] R. Sadakale, N. V. K. Ramesh, R. Patil, TAD-HOC Routing Protocol for Efficient VANET and Infrastructure oriented communication networks, *Journal of Engineering*, 2020 Jan, vol. 2020, pp. 1-12.
- [14] J. Liu, J. Wan, Q. Wang, A survey on position based routing for vehicular ad hoc networks. *Journal Telecommunications Systems archive*. 2016 May, 62 (1), pp. 15-30.
- [15] R. Sharma, A. Choudhry, Swami, An Extensive Survey on different Routing Protocols and Issue in VANETs. *International Journal of Computer Applications*. 2018 Nov, 106 (5), pp. 1-20.
- [16] A. C. Silva, Applicability of position-based routing for VANET in highways and urban environment. *Portugal Journal of Network and Computer Applications*. 2013 Jul, 36 (2013), pp. 961–973.
- [17] S. Dhankhar, S. A. Agrawal, Survey on Routing Protocols and Issues. *International Journal of Innovative Research in Science, Engineering and Technology*. 2014 June, 3 (6), pp. 1-15.
- [18] C. Lochert, H. Hartenstein, J. Tian, H. Fubler, D. Hermann, M. A. Mauve, Routing strategy for vehicular ad hoc networks in city

- environments. Proceedings of IEEE Intelligent Vehicles Symposium. 2003, pp. 156 -161.
- [19] A. Husain, R. Shringar, B. Kumar, and A. Doegar, Performance comparison topology based and position based routing protocols in Vehicular network environments. International Journal of Wireless & Mobile Networks (IJWMN), 2019 Aug, 4 (3), pp. 1-16.
- [20] M. M. Bhavani, A. Valarmathi, Smart city routing using GIS & VANET system. Journal of Ambient Intelligence and Humanized Computing, 2020 Jun, 5(4), pp.1-9.
- [21] W. Kieb, H. Fubler, J. Widmer, M. Mauve, Hierarchical location service for mobile ad-hoc networks. ACM SIGMOBILE Mobile Computing and Communications Review. 2004 Oct, 8 (1), pp. 47–58.
- [22] B. Karp, H. T. Kung, and GPSR: Greedy perimeter stateless routing for wireless networks. Proceedings of the 6th annual international Conference on Mobile computing and networking USA. 2019, pp. 243–254.
- [23] C. Lochert, M. H. Mauve, H. Hartenstein, Geographic routing in city scenarios. SIGMOBILE Mobile Computing Communication Review. 2005 Jan, 9 (1), pp. 69–72.
- [24] U. Paranjothi, Y. Tanik, M .S. Khan, "Hybrid-Vehfog: A Robust Approach for Reliable Dissemination of Critical Messages in Connected Vehicles, "Transactions on Emerging Telecommunications Technologies, vol. 30, pp. 1–11,2020
- [25] B. C. Seet, G Liu, B. S. Lee, C.H. Foh, K. Wong, K. Lee, A-STAR: A Mobile Ad Hoc Routing Strategy for Metropol is Vehicular Communications. In Lecture Notes in Computer Science. NETWORKING 2004. International Conference on Research in Networking. 2004, pp. 989–999.
- [26] N. Noorani, and S. A. H. Seno, SDN-and Fog Computing-based Switchable Routing Using Path Stability Estimation for Vehicular Ad Hoc Networks, Peer-to-Peer Networking and Applications, pp. 1–17, 2020.
- [27] S. M. Bilal, A. R. Khan, & S. Ali, Review and performance analysis of position based routing protocols. Springer Wireless Personal Area Communication. 2016 Aug, 1 (3), pp. 1-14.
- [28] I. A. Abbasi, A. S. Khan, S. Ali, Dynamic Multiple Junction Selection Based Routing Protocol for VANETs in City Environment. Applied Sciences. 2018; 8(5):687.
- [29] I. A. Abbasi, A. S. Khan, & S. Ali, Reliable Path Selection and Packet forwarding Routing Protocol for VANETs Springer EURASIP J. Wireless Communication and Networking. 2018 Oct, 218 (2018), pp. 1-18.

Design of a Rule-based Personal Finance Management System based on Financial Well-being

Alhanooif Althnian
Information Technology Department
College of Computer and Information Sciences, King Saud University
Riyadh, Saudi Arabia

Abstract—Financial planning plays an important role in people’s lives. The recent COVID-19 outbreak has caused sudden unemployment for many people across the globe, leaving them with a financial crisis. Recent surveys indicate that financial matters continue as the leading cause of stress for employees. Further, many millennials overspend and make unfortunate financial decisions due to their incapability to manage their earnings, which forbids them from maintaining financial satisfaction. Financial well-being as defined by The American Consumer Financial Protection Bureau (CFPB) is a state where one fully meets current and ongoing financial obligations, feels secure in their financial future, and is able to make choices to enjoy life. This work proposes a Personal Finance Management (PFM) system with a new architecture that aims to guide users to reach the state of financial well-being, as defined by CFPB. The proposed system consists of a rule-based system that provides users with actionable advice to make informed spending decisions and achieve their financial goals.

Keywords—Artificial intelligence; rule-based; deductive reasoning; forward chaining; personal finance; financial well-being

I. INTRODUCTION

Money plays a crucial role in people’s lives. Managing one’s financial life can be challenging due to the increased commitments and spending, hence it may become difficult to achieve the desired financial goals. An employee financial wellness survey that took place in USA in 2020 revealed that 54% of stress is caused by financial matters, and 41% of millennials are unprepared for unexpected expenses [1]. In Saudi Arabia, a recent survey suggests that the average family expenditure is greater than the average family income [2]. Making conscious financial decisions plays a key role in financial well-being. According to Zaltman [3], however, 95% of purchase decisions that people make every day are subconscious. The author suggests that purchase behavior are driven by emotions, and hence may not be logical. Therefore, one may decide to purchase an item as long as he has money to pay for, without considering his overall financial state and future commitments.

The American Consumer Financial Protection Bureau (CFPB) defined financial well-being as “a state of being wherein a person can fully meet current and ongoing financial obligations, can feel secure in their financial future, and is able

to make choices that allow enjoyment of life”[4]. Further, the CFPB identified four main elements of financial well-being, as follows:

- 1) Having control over day-to-day, month-to-month finances.
- 2) Having the capacity to absorb a financial shock.
- 3) Having the financial freedom to make the choices that allow one to enjoy life.
- 4) Being on track to meet your financial goals. [4].

As shown in Fig. 1, these elements span over two dimensions; time (future or present) and goal (security or freedom of choice). The first and second elements pertain securing the present and future, respectively, and the third and fourth elements pertain having freedom of choice in the present and future, respectively [4]. An individual who has control over daily and monthly finances is able to pay bills and all periodical expenses with no delay. Also, an individual, who has the capacity to absorb financial shock, owns personal savings that enable him to deal with future emergencies. One who has the freedom to make financial choices can afford not only what they need but also what they want. Finally, someone who is on track to achieve financial goals has a financial plan and continuously making progress toward achieving their financial goals.

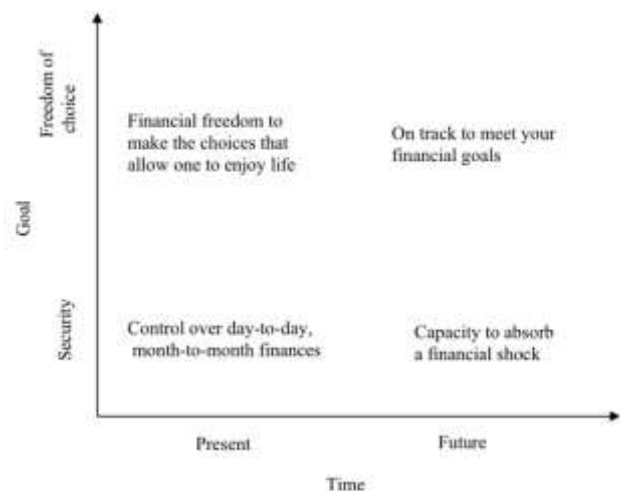


Fig. 1. Elements of Financial Well-being [4].

The aforementioned elements of financial well-being represent the privileges that an individual who reached the state of financial well-being enjoys. However, they do not define how someone may reach that state. In other words, the elements do not answer the question: what are the main practices that one should strive to do in order to reach financial well-being? Many Personal Finance Management (PFM) software are available, but none was designed with the definition of financial well-being in mind, and hence are unable to guide the user to reach the state of financial well-being. This work seeks to fill this gap by proposing three practices and a new architecture for PFM that guides users to adopt them.

The remainder of this paper is organized as follows. Section 2 reviews related work in PFM and financial well-being. Section 3 explains the system model, while Section 4 explains the proposed rule-based system. Finally, a summary with concluding remarks are provided in Section 5.

II. RELATED WORK

A wide range of PFM and budget tracker software exist that help users plan and manage their finances such as Mint [5], Money Pro [6], Wally [7], Wallet [8], Masareef [9], Masareefy Pro [10], Money Coach [11], Spendee [12], Albert [13], Moneyriser [14], Qapital [15], Twine [16], Coin Keeper [17], Moneycontrol [18], and ClarityMoney [19]. We performed an analysis of the main features that these applications offer, and we present our findings below.

All existing applications share three main common features, which are providing current balance, allowing users to categorize their transactions manually into different categories such as family, fitness, and insurance, and providing visualization of user's financial behavior trends using different charts. The next common features are to allow the user to set up and track saving goal, which is offered by Mint [5], Money control [6], Qapital [15], Masareef [9], Money Coach [11], Moneyriser [14], Albert [13], and Twine [16], to present the user's total spending, offered by Money control [18], Money Coach [11], Coin keeper [17], and Masareef [9], Masarify Pro [10], Wally [7], Wallet [8], and ClarityMoney [19], and to allow the user to set up a budget for a specific purpose, which can be found in Mint [5], Wally [7], Money Pro [6], Spendee [12], Wallet [8], Money Coach [11], Albert [13], and Coin keeper [17].

Although important, only some software allow users to set a periodical/recurring transaction such as bills, available in Masareef [9], Masareefy Pro [10], Mint [5], Qapital [15], Money Coach [11], and Moneyriser [14]. In addition, creating multiple accounts and displaying the user's net worth is offered in Mint [5], Spendee [12], and Money Coach [11]. The software Wally [7] and Wallet [8] synch user's account with the bank account and import transactions automatically. Wally [7], Money pro [6], and Moneyriser [14] track user's progress toward paying off their loans. Investment goals are also considered in some software such as Qapital [15], Albert [13], and Twine [16].

Money pro [10] and Qapital [15] offer some unique and exclusive features. The former show the user not only the

current balance, but also his expected balance after paying off all periodical expenses. The latter allows the user to set up customized rules, such as save part of the paycheck automatically each payday or save an amount when you buy what you are trying to resist.

Although many PFM software are available, none was designed with the definition of financial well-being in mind, and hence are unable to guide the user to reach the state of financial well-being for several reasons. First, existing software do not provide actionable advice to users. This is important especially due to the fact that majority of users' purchase decisions are subconscious. Second, some users may have ambitious saving goals that might not fit his financial state, and hence cannot maintain and make progress toward it. This may impact the user's overall attitude toward saving. Further, majority of existing software requires the user to enter every transaction manually, which is not practical.

III. SYSTEM MODEL

A. Definitions

The system uses the following terms.

- *Inflow*: Money going into the bank account.
- *Outflow*: Money going out of the bank account.
- *Periodical expenses*: Monthly outflow transactions such as bills and rent.
- *Budget*: Amount of money saved once and available to spend for a specific purpose with no time frame.
- *Saving amount*: Amount of money to be saved in monthly installments.
- *Saving installment*: a monthly amount to be paid toward a saving goal.
- *Saving plan*: A long-term or short-term plan to save a specific amount of money within a time frame.
- *Commitments*: the total amount of the user's periodical expenses, saving installments, debts monthly installment, and current budgets.
- *Balance*: Total amount of money available in the bank accounts.
- *Available balance*: Amount of money remained after deducting commitments.

B. Financial Well-being Inspiration

As mentioned previously, the definition and elements of financial well-being proposed by CFPB only represent the privileges that one who reached the state of financial well-being enjoys. However, they do not define the main practices that one should strive to do in order to reach financial well-being.

The main goal of this work is to inspire and guide users to reach a state of financial well-being, as defined by CFPB. Therefore, based on the definition and elements of financial well-being mentioned previously, we propose three main

principles that a PFM must follow in order help users reach financial well-being. A PFM shall:

- 1) Build experience by making users aware of their financial activities such as how much they spend or earn over a specific period of time.
- 2) Provide insights into user's finances, i.e. how much, when, and where they spend their money.
- 3) Help users with actionable advice to achieve their financial goals.

The first principle is inspired by the first element of financial well-being, i.e. having control over day-to-day, month-to-month finances. As explained previously, this principle denotes that one is able to pay bills and all periodical expenses with no delay. We argue that one must be first aware of such periodical expenses and their total cost, even before they are paid or deducted from the account. Therefore, allowing the user to set up periodical expenses is an essential requirement for PFM. Further, we propose that periodical expenses are to be deducted from the balance on payday, hence one is well aware of how much he really own, shown in the available balance. These periodical expenses include rent, bills, saving installment, and loan installment. Showing the available balance after deducting periodical expenses supports the third element of financial well-being, i.e. having the financial freedom to make the choices that allow one to enjoy life. Since saving installment is included in the periodical expenses, this principle also supports the fourth element, which is being on track to meet one's financial goals.

The second principle focuses on allowing the user to understand his/her financial behavior. In PFM, this can be achieved by categorizing user's transactions automatically and providing different types of charts that convey spending trends and informative insights. Therefore, the user can see when and what he/she spends his money the most on, which enables him to adjust his behavior to reduce spending. This principle can indirectly contribute the third element of financial well-being that is having the financial freedom to make the choices that allow one to enjoy life. Moreover, based on these insights, a PFM shall be able to evaluate the user's financial performance, i.e. on track or over budget.

The third principle consists of two sub-principles: saving principle and advice principle. The former suggests that a PFM system shall allow the user to set up a saving goal and a saving plan. This supports the fourth element of financial well-being by keeping the user on track to achieve financial goals and continuously making progress toward achieving their financial goals. It also supports the second principle since the user may set up a saving goal for emergency, hence is able to absorb financial shock. The latter sub-principle signifies that a PFM shall also advice the user on different financial issues. For instance, a user may have an overambitious saving goal, which does not fit his current financial situation. Therefore, the user may fail in maintaining and making progress toward it. This may impact the user's overall attitude toward saving if he fails in his first saving plan. Therefore, a PFM shall advice the user on the saving plan and further recommend one that fits his

financial state. This support the second and fourth principles. A PFM shall also advice the user on purchasing decisions, since as explained previously, most of them are subconscious, which supports the third principle.

C. System Architecture

The main goal of this work is to design a PFM system that helps users maintain a healthy financial life and guide them to reach the state of financial well-being. The proposed system uses Artificial Intelligence to achieve this goal and consists of three main modules; awareness module, insight module, and advice module, as shown in Fig. 2. Each module corresponds to one of the proposed principles in the previous sub-section. The following points explain each module in further details.

1) *Awareness Module*: This module supports the first proposed principle; that is to build experience by making users aware of their financial activities such as how much they spend or earn over a specific period of time. This is achieved by offering the following features:

- Tracking user's financial activities (inflow and outflow transactions) automatically by either accessing the SMS messages sent for each transaction or synching with the user's bank account to add the corresponding transactions.
- Allow users to track their spending over a customized period of time, e.g. month or week.
- Allow users to set up periodical expenses.
- Deduct periodical expenses on payday and show both actual balance and available balance.

2) *Insight Module*: This module supports the second principle, which is to provide insights into user's finances, i.e. how much, when, and where they spend their money. The following features are provided by this module:

- Categorize transactions automatically by vendor, location, and time/day to help discover user's spending patterns.
- Allow the user to create custom categories such as education, food, and medical where transactions fall into.
- Create a dashboard for visualizing the user's financial performance using different types of charts.
- Monitor and notify the user of his/her financial performance, i.e. on track or over budget. The aim is to help low-income users avoid situations where they spend most of his income when it is first received, which leaves them with no enough money for the rest of the month, and also help high-income users avoid situations where they spend too much on unnecessary things by setting a limit to his/her spending.

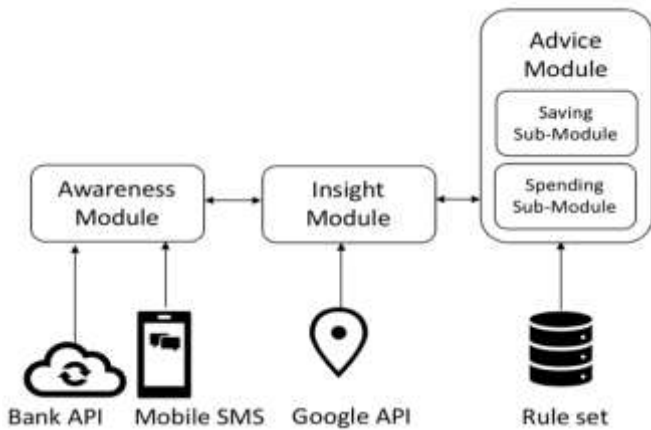


Fig. 2. PFM System Architecture.

3) *Advice Module*: The advice module facilitates the realization of the third principle, which suggests that a PFM shall help users with actionable advice to achieve their financial goals. This module consists of two main sub-modules:

- Spending advice sub-module, where the user can ask the system if he should spend a specific amount of money on an item.
- Saving advice sub-module, where the user may ask about the feasibility of a saving plan, given the amount and target duration of time.

In addition, this module suggests an alternative plan if the current plan is not feasible, by increasing the target duration of time or reducing the target amount of money to be saved. Therefore, the module creates a saving plan according to the user's current financial status and also allows the user to track its progress.

In this work, Rule-Based Reasoning, specifically Forward Chaining, is used to design the two advice sub-modules included in this module. In the sections below, we present the proposed rule-based system for this purpose.

IV. RULE-BASED SYSTEM

Reasoning is a form of deductive learning where rules are provided to the system by a domain expert and the system then reasons about individual cases using the provided rules. Rule-based reasoning relies on facts and rules to solve problems. Deductive reasoning is defined as “the process of inferring conclusions from known information (premises) based on formal logic rules” [20]. The system can use user's information such as his transactions and his standard of living to suggest a spending lifestyle for the user. There are mainly two inference methods; forward chaining and backward chaining. In this work we use Forward Chaining, which starts from then given facts and uses inference rules to produce more facts until the goal is proven.

As shown in Fig. 3, the main component of a rule based system is rule set, working memory, and inference engine. The rule set contains the rules, which will be explained in the following sub-sections. The working memory includes the

facts used by the rules and intermediate results. The inference engine is in charge of performing the forward chaining. The inference starts with matching the rules set with the known facts in the working memory. If there are rules to match, the engine selects a rule and matches its antecedents (left-hand side) with the assertions (facts in working memory) and substitute any variables.

If the match succeeds, the rule is fired and variables in the rule's consequences (right-hand side) are substituted. Then, the result conclusions are added to the patterns. When all rules are matched, the inference engine adds all patterns, if any, to the working memory. If the working memory is updated, another cycle of inference will be performed. This continues until the working memory is not updated after an inference cycle.

In the sub-sections below, we present the proposed rules set for both the spending advice and saving advice components.

A. Saving Advice

This component allows the user to find out if he/she can afford a specific saving goal. The user enters the amount he wants to save (AMOUNT), the saving duration (DUR). The system analyzes the entered values according to the user's financial situation and determines whether the saving goal is feasible or not feasible using the rule-based system explained below.

If the goal is not feasible, the system suggests other feasible saving plans by increasing the value of parameter DUR or decreasing AMOUNT. The proposed solution to give a saving advice to the user works as follows.

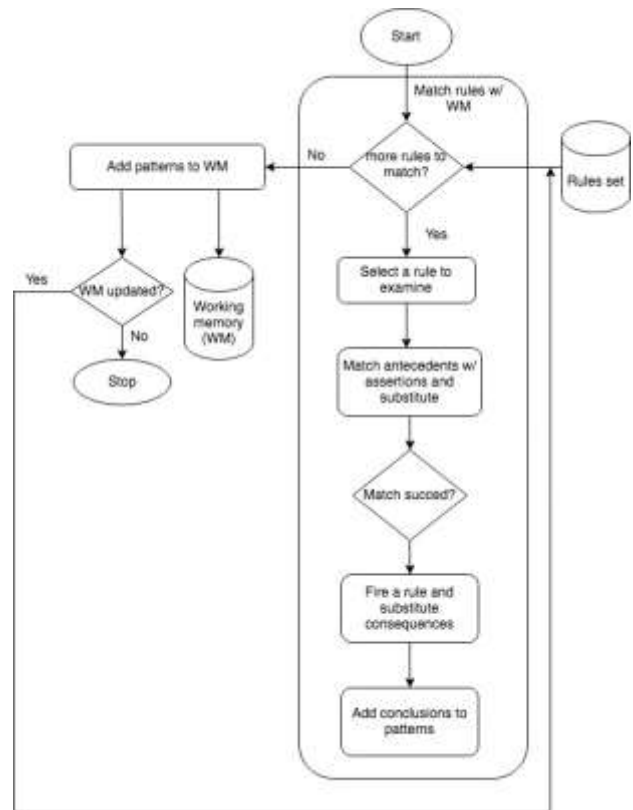


Fig. 3. Forward Chaining Flow Chart.

The monthly saved amount (MAMOUNT) is calculated as the total saved amount (AMOUNT) divided by the duration (DUR), as shown in Eq. (1) below.

$$MAMOUNT = \frac{AMOUNT}{DUR} \quad (1)$$

Where:

AMOUNT = the target amount of money to be saved, entered by the user

DUR = the target duration of time in months

The available user's balance (BALANCE) from which the MAMOUNT will be deducted from is calculated as the subtraction of the total commitments from the current balance, as in Eq. (2).

$$BALANCE = INCOME - COMMIT \quad (2)$$

where:

INCOME = The user's total income

COMMIT = the total amount of the user's total saving plans, current periodical expenses, budgets, and debts.

The values MAMOUNT and BALANCE will be compared as shown in the rule set in Table I.

B. Spending Advice

The spending advice enables the user to ask whether he/she should buy an item. The user enters the price of the item (PRICE), choose whether it is necessary or not. The system infers whether the purchase is needed, advisable, not worth it, or troublesome, according to rule-based system described below.

First, the available balance for the user (ABALANCE) is the current balance of the user (BALANCE) deducted from it the total commitments (COMMIT) associated with the user account, as shown in Eq. (3) below.

$$ABALANCE = BALANCE - COMMIT \quad (3)$$

where:

BALANCE = The current balance of the user

COMMIT = The total amount of the user's total saving plans, current periodical expenses, budgets, and debts.

The system then reasons about the whether the item should be purchased, according to the rule set shown in Table II.

TABLE I. SAVING ADVICE RULE SET

Rule	IF	THEN
R1	$\frac{MAMOUNT}{BALANCE} < 1$	The plan is feasible
R2	$\frac{MAMOUNT}{BALANCE} \geq 1$	The plan is not feasible. An alternative plans is suggested with longer duration and less MAMOUNT that fits the user's current situation.

TABLE II. SPENDING ADVICE RULE SET

Rule	IF	THEN
R1	PRICE < ABALANCE	The user affords the purchase & Calculate percentage of the price to the user's total income PRICE_INCOME_PER = (PRICE/INCOME) *100 & Calculate percentage of the price to the user's available balance PRICE_ABALANCE_PER = $\frac{PRICE}{ABALANCE} * 100$
R2	PRICE > ABALANCE	The user cannot afford the purchase & Calculate percentage of the unaffordable portion of price to the user's total income PRICE_INCOME_PER = $\frac{PRICE-ABALANCE}{INCOME} * 100$
R3	The user cannot afford the purchase & the item is necessary	The purchase is needed & An emergency budget is created by allowing the user to reduce amount allotted to one or more future commitment for the current month, i.e. periodic, budget, or saving plan.
R4	The user cannot afford the purchase & the item is not necessary	The purchase is troublesome
R5	The user affords the purchase & the item is necessary	The purchase is advisable
R6	The user affords the purchase & the item is not necessary & PRICE_INCOME_PER >10	The purchase is not worth it

V. CONCLUSION

The main goal of this work was to propose a personal finance management system with new architecture that builds on the fundamental principles of financial well-being as defined by the American Consumer Financial Protection Bureau (CFPB).

This work has presented the main components of the system architecture and how they guide users to adopt financial practices that help them reach the state of financial well-being. Further, we proposed a rule-based system that provides spending and saving advice that enable the user to make informed spending decisions and achieve their financial goals.

ACKNOWLEDGMENT

The author would like to thank Ghaida Alshdokhi, Shahad Aljubayri, Hala Alntifat, and Nora Alqahtani for their help with this work.

REFERENCES

- [1] PwC's 9th annual Employee Financial Wellness Survey COVID-19 Update, PwC US, 2020.

- [2] The Saudi General Authority for Statistics's Household Income and Expenditure Survey, The General Authority for Statistics Saudi Arabia, 2018.
- [3] G. Zaltman, How customers think: Essential insights into the mind of the market. Harvard Business Press, 2003.
- [4] Consumern Financial Protection Burau (CFPB), Financial well-being: The goal of financial education, 2015.
- [5] Mint: Budget, Bills, & Financial Tracker, Mint.com (Version 7.9.1) [Mobile Application Software]. Retrieved from <https://apps.apple.com/us/app/mint-personal-finance-money/id300238550>
- [6] Money Pro: Personal Finance, iBear LLC (Version 2.6.3) [Mobile Application Software]. Retrieved from <https://apps.apple.com/us/app/money-pro-personal-finance/id918609651>
- [7] Wally – Smart personal finance, Wally Global Inc (Version 3.1.3) [Mobile Application Software]. Retrieved from <https://apps.apple.com/us/app/wally-smart-personal-finance/id1178011327>
- [8] Wallet: Personal Finance, Budget & Expense Tracker, BudgetBakers.com (Version 8.1.291) [Mobile Application Software]. Retrieved from <https://play.google.com/store/apps/details?id=com.droid4you.application.wallet>
- [9] Masareef المصاريف, Al-Masareef App (Version 2.4) [Mobile Application Software]. Retrieved from <https://apps.apple.com/sa/app/%D9%85%D8%B5%D8%A7%D8%B1%D9%8A%D9%81/id463676434>
- [10] مصاريفي برو – إدارة مصاريفك وتنظيم دخلك, Faisal Ammari [Mobile Application Software]. Retrieved from <https://apple.co/38QJfm5>
- [11] MoneyCoach Budget & Spendings, MoneyCoach UG (Version 6.2) [Mobile Application Software]. Retrieved from <https://apps.apple.com/us/app/moneycoach-budget-spending/id989642198>
- [12] Spende Budget & Money Tracker, Cleevio s.r.o (Version 3.16.6) [Mobile Application Software]. Retrieved from <https://apps.apple.com/us/app/spende-budget-money-tracker/id635861140>
- [13] Albert: Budget. Save. Invest., Albert Corporation (Version 5.13.3) [Mobile Application Software]. Retrieved from <https://apps.apple.com/us/app/albert-budget-save-invest/id105771088>
- [14] Moneyriser, Digital Shapes (Version 1.0.25) [Mobile Application Software]. Retrieved from <https://apps.apple.com/sa/app/moneyriser/id1442906284?l=ar>
- [15] Qapital Finance: Budget & Save, Qapital Inc (Version 2.157.0) [Mobile Application Software]. Retrieved from <https://apps.apple.com/us/app/qapital-finance-budget-save/id969977669>
- [16] Twine: Easy Saving & Investing, John Hancock USA (Version 1.18.0) [Mobile Application Software]. Retrieved from <https://apps.apple.com/us/app/twine-easy-saving-investing/id1292080056>
- [17] CoinKeeper: money manager, Disrapp (Version 2.1.16) [Mobile Application Software]. Retrieved from <https://apps.apple.com/us/app/coinkeeper-money-manager/id849747345>
- [18] Moneycontrol - Markets & News, Network18 (Version 7.9) [Mobile Application Software]. Retrieved from <https://apps.apple.com/in/app/moneycontrol-markets-news/id408654600>
- [19] Clarity Money – Budget Manager, Clarity Money (Version 1.73.13) [Mobile Application Software]. Retrieved from <https://apps.apple.com/us/app/clarity-money-budget-manager/id1148133022>
- [20] Ayalon M., Even R. Deductive Reasoning and Learning. In: Seel N.M. (eds) Encyclopedia of the Sciences of Learning. Springer, Boston, MA, 2012. https://doi.org/10.1007/978-1-4419-1428-6_659

Robust Control Approach of SISO Coupled Tank System

Mohd Hafiz Jali^{1*}, Ameelia Ibrahim², Rozaimi Ghazali³, Chong Chee Soon⁴, Ahmad Razif Muhammad⁵
Faculty of Electrical Engineering, Universiti Teknikal Malaysia Melaka, Durian Tunggal, Melaka, Malaysia^{1,3,4}
Department of Electrical Engineering, Politeknik Melaka, Malim, Melaka, Malaysia²
Faculty of Applied Sciences, Ton Duc Thang University, Ho Chi Minh City, Vietnam⁵

Abstract—This paper presents the design principles of sliding mode controller, which is implemented in the coupled tank system. The Sliding Mode Control (SMC) controller exhibited a robust stability which can overcome nonlinearities, reduce disturbances and noise that occur in the coupled tank system. The work start with mathematical modelling the coupled tank system using second order single input single output (SISO) technique. Then, the sliding mode controller design began by deriving the sliding surface according to the second order coupled tank system. The control variables in this system, which are C1 and C2 are manipulated to obtain the best performances of the SMC. From the simulations, the performances characteristic of the SMC is analysed and investigated. The output response is obtained by implementing the SMC on the plant and compared with the proportional, integral, and derivative (PID) controller as a benchmarked controller. The results show that the robust SMC has better output response compared to the PID controller.

Keywords—Sliding Mode Control; PID controller; robustness; coupled tank system

I. INTRODUCTION

Coupled Tank System (CTS) playing important roles in the industrial sector due to the process in the coupled tank which stored, pumped, restored, and pumped the liquid continuously. The industries demand regarding the coupled tank is very high especially in food processing, pharmaceutical industries, mixing process, refilling devices, and the chemical processing. Modern utilization of coupled tanks system (CTS) is broadly utilized as a part of the chemical process. There are a few procedures of CTS, for example, single input single output (SISO) or multiple input multiple output (MIMO) that has been utilized generally as a part of the industrial area. Moreover, the control procedure for multiple input multiple output (MIMO) is more convoluted than SISO in light of the fact that there is a communication between other control circles of MIMO procedures. However, the control structure implemented in the SISO system is less complex as compared to the control of the MIMO system.

However, according to the previous study, it was stated that the problems always occur in controlling the level of the liquid and the flow between the tanks [1],[2], this is due to the industrial demand for the liquid to be pumped, stored, and to be pumped again to another tank. It is very important to monitor the level of the liquid, the flow between tanks and the interaction of the liquid levels. In [3] there are two

configurations of CTS that are single input and single output (SISO) and multiple input multiple output (MIMO) which has different ways of controlling the liquid level.

The Sliding Mode Control (SMC) controller has been introduced and is known as a robust stability which will reduce the external disturbances and eliminates the chattering effect [4]. By referring to the Lyapunov's method, that approach using the lots of variable designs that create sliding mode on the intersection of a few switching surfaces. To ensure that the system trajectory always reaches the sliding surface, the control laws are designed. On top of that, the study shows that for SISO coupled tank system, the 2nd tank act as disturbance while the 1st tank act as a control variable. Meanwhile, a mathematical model for the coupled-tank system and the design of SMC for liquid control in the systems is presented. In this study, it's focussed on the nonlinear SISO mathematical model which is developed in order to use the SMC controller. It was stated that the tracking performances of the SMC controller [5] are tested using different input signals such as step, sinusoidal, and saw tooth. The controller showed that it has a strong robustness when some realistic situations are inserted in the plant. Moreover, the use of SMC can overcome nonlinearities, reduce disturbances and noise. The SMC need to use a suitable sliding surface for the system to slide to its desired final value.

Authors in [6] stated that the SMC controller was initially adopting the concept of variable structure control system which consists of two steps. The first step is to gain a sliding surface for desired stable dynamics and the second step is to get the control law to reach to the sliding surface. In this paper, the comparison between SMC and PID has been made, it shows that the external disturbances will affect the PID controller but not the SMC. The SMC is proven to be robust to parametric uncertainties and external disturbances [7].

Researchers [8] verified that the SMC nonlinear control have a capability to maintain the stability in the control of various different classes of model which are exposed to the disturbances and variations in the system parameters [9]. Thus it has been extensively used in various applications such as active suspension system [10], pneumatic systems [11] and active magnetic bearing systems [12]. Moreover, when a controller designed by the conventional approaches, The SMC controller can be easier to design, to tune and to implement [13] because in [14] it was stated that the Sliding Mode Control controller is the best method for a nonlinear system with uncertainties.

*Corresponding Author

Despite the advantages in various applications of the coupled tank system, it suffers from nonlinearities and parameter uncertainties which cause the performance deterioration. Recently, numerous control techniques have been reported for the coupled tank system in the literature. It can be divided to linear control, nonlinear control and intelligent control [15][16][17]. However, Sliding Mode Controller (SMC) has been proven to be outstanding over other controllers in providing robust performance for the nonlinear dynamic system [18], [19]. Therefore, SMC was chosen for the coupled tank system. The objective is to tune the best controller parameters in SMC in order to get the desired output performance of coupled tank system. According to [20], the tuning problem of controller gains can be considered as an optimization problem.

II. MATHEMATICAL MODELLING

Based on the previous research [1][2], Fig. 1 shows the coupled tank system for the SISO system with the definition of parameters in the coupled tank system.

The area for the SISO coupled tank system can be expressed as,

$$A_1 \frac{dh_1}{dt} = Q_{i1} - Q_{o1} - Q_{o3} \quad (1)$$

$$A_2 \frac{dh_2}{dt} = Q_{i2} - Q_{o2} - Q_{o3} \quad (2)$$

where:

H_1, H_2 = Height of fluid in tank 1 and 2.

A_1, A_2 = Cross-sectional area of tank 1 and 2.

Q_{o3} = The rate flow of fluid between tanks.

Q_{i1}, Q_{i2} = Pump flow rate into tank 1 and 2.

Q_{o1}, Q_{o2} = Flow rate of fluid out of tank 1 and 2.

By using the Bernoulli's equation, the flow between the two tanks is proportional to the square root of the head differential.

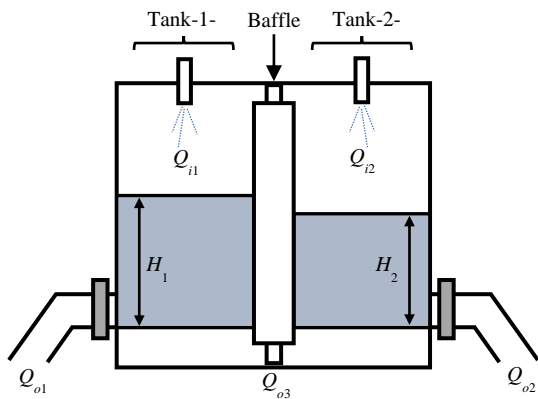


Fig. 1. Coupled Tank System with SISO Structure.

$$Q_{o1} = \alpha_1 \sqrt{H_1} \quad (3)$$

$$Q_{o2} = \alpha_2 \sqrt{H_2} \quad (4)$$

$$Q_{o3} = \alpha_3 \sqrt{H_1 - H_2} \quad (5)$$

where $\alpha_1, \alpha_2, \alpha_3$ are proportional constants that depends on the coefficients of discharge, cross sectional area of each tank and gravitational constant.

By substituting the equations (3), (4) and (5) into equation (1) and (2),

$$A_1 \frac{dH_1}{dt} = Q_{i1} - \alpha_1 \sqrt{H_1} - \alpha_3 \sqrt{H_1 - H_2} \quad (6)$$

$$A_2 \frac{dH_2}{dt} = Q_{i2} - \alpha_2 \sqrt{H_2} - \alpha_3 \sqrt{H_1 - H_2} \quad (7)$$

By linearized perturbation model, consider a small variation in each inflow q_1 in Q_{i1} and q_2 in Q_{i2} . And let the perturbation level be h_1 and h_2 respectively.

$$A_1 \frac{d(H_1 + h)}{dt} = (Q_{i1} + q_1) - \alpha_1 \sqrt{H_1 + h_1} - \dots \dots - \alpha_3 \sqrt{(H_1 - H_2) + (h_1 - h_2)} \quad (8)$$

$$A_1 \frac{d(H_2 + h_2)}{dt} = (Q_{i2} + q_2) - \alpha_2 \sqrt{H_2 + h_2} - \dots \dots - \alpha_3 \sqrt{(H_1 - H_2) + (h_1 - h_2)} \quad (9)$$

For small perturbations,

$$\sqrt{H_1 + h_1} = \sqrt{H_1} \left(1 + \frac{H_1}{2H_1} \right) \quad (10)$$

$$\sqrt{H_1 + h_1} - \sqrt{H_1} \approx \frac{H_1}{2\sqrt{H_1}} \quad (11)$$

$$\sqrt{H_2 + h_2} - \sqrt{H_2} \approx \frac{H_2}{2\sqrt{H_2}} \quad (12)$$

$$\sqrt{(H_1 + h_1) + (h_1 - h_2)} - \sqrt{H_2 - H_1} \approx \frac{h_2 - h_1}{2\sqrt{H_2 - H_1}} \quad (13)$$

Then, assume that

$$h_1 = h_2 = \text{Output}$$

$$q_1 = q_2 = \text{Input}$$

$$A_1 \frac{dh_1}{dt} = q_1 - \frac{\alpha_1}{2\sqrt{H_1}} h_1 - \frac{\alpha_3}{2\sqrt{H_1 - H_2}} (h_1 - h_2) \quad (14)$$

$$A_2 \frac{dh_2}{dt} = q_2 - \frac{\alpha_2}{2\sqrt{H_2}} h_2 - \frac{\alpha_3}{2\sqrt{H_1 - H_2}} (h_1 - h_2) \quad (15)$$

From equation (14),

$$A_1 h'_1 = q_1 - \frac{\alpha_1}{2\sqrt{H_1}} h_1 - \frac{\alpha_3}{2\sqrt{H_1 - H_2}} (h_1 - h_2) \quad (16)$$

And equation (15),

$$A_2 h'_2 = q_2 - \frac{\alpha_2}{2\sqrt{H_2}} h_2 - \frac{\alpha_3}{2\sqrt{H_1 - H_2}} (h_1 - h_2) \quad (17)$$

The manipulated variable is the perturbation to the inflow of tank 1. Assume that, mutually variables are at their steady state value.

$$A_1 h'_1 = q_1 - \left(\frac{\alpha_1}{2\sqrt{H_1}} h_1 + \frac{\alpha_3}{2\sqrt{H_1 - H_2}} \right) \quad (18)$$

$$A_2 h'_2 = q_2 - \left(\frac{\alpha_2}{2\sqrt{H_2}} h_2 + \frac{\alpha_3}{2\sqrt{H_1 - H_2}} \right) \quad (19)$$

where h_1 is the process variable and q_1 is the manipulated variable. The case will be considered when q_2 is zero. The equations (18) and (19) will be expressed between the manipulated variable, q_1 and the process variable, h_2 .

Rewrite the equation (18) and (19),

$$T_1 h'_1 + h_1 = K_1 q_1 + K_{12} h_2 \quad (20)$$

$$T_2 h'_2 + h_2 = K_2 q_2 + K_{21} h_1 \quad (21)$$

where,

$$T_1 = \frac{A_1}{\left[\frac{\alpha_1}{2\sqrt{H_1}} \right] + \left[\frac{\alpha_3}{2\sqrt{H_1 - H_2}} \right]} \quad (22)$$

$$T_2 = \frac{A_2}{\left[\frac{\alpha_2}{2\sqrt{H_2}} \right] + \left[\frac{\alpha_3}{2\sqrt{H_1 - H_2}} \right]} \quad (23)$$

$$K_1 = \frac{1}{\left[\frac{\alpha_1}{2\sqrt{H_1}} \right] + \left[\frac{\alpha_3}{2\sqrt{H_1 - H_2}} \right]} \quad (24)$$

$$K_2 = \frac{1}{\left[\frac{\alpha_2}{2\sqrt{H_2}} \right] + \left[\frac{\alpha_3}{2\sqrt{H_1 - H_2}} \right]} \quad (25)$$

$$K_{12} = \frac{\left[\frac{\alpha_3}{2\sqrt{H_1 - H_2}} \right]}{\left[\frac{\alpha_1}{2\sqrt{H_1}} \right] + \left[\frac{\alpha_3}{2\sqrt{H_1 - H_2}} \right]} \quad (26)$$

$$K_{21} = \frac{\left[\frac{\alpha_3}{2\sqrt{H_1 - H_2}} \right]}{\left[\frac{\alpha_2}{2\sqrt{H_2}} \right] + \left[\frac{\alpha_3}{2\sqrt{H_1 - H_2}} \right]} \quad (27)$$

For SISO (Second order, Single Input), consider $q_2 = 0$. From equation (21),

$$h_1 = \frac{T_2 h'_2 + h_2}{K_{21}} \quad (28)$$

$$h'_1 = \frac{T_2 h''_2 + h'_2}{K_{21}} \quad (29)$$

Substitute equations (28) and (29) into (20),

$$T_1 h'_1 + h_1 = K_1 q_1 + K_{12} h_2$$

$$T_1 \left(\frac{T_2 h''_2 + h'_2}{K_{21}} \right) + \left(\frac{T_2 h'_2 + h_2}{K_{21}} \right) = K_1 q_1 + K_{12} h_2$$

$$T_1 T_2 h''_2 + T_1 h'_2 + T_2 h'_2 + h_2 = K_1 q_1 K_{21} + K_{12} K_{21} h_2$$

$$h''_2 = \frac{K_1 q_1 K_{21} + K_{12} K_{21} h_2 - T_1 h'_2 + T_2 h'_2 + h_2}{T_1 T_2}$$

$$h''_2 = \frac{1}{T_1 T_2} [K_1 q_1 K_{21} + K_{12} K_{21} h_2 - h'_2 (T_1 + T_2) - h_2]$$

$$h''_2 = \frac{1}{T_1 T_2} [-h'_2 (T_1 + T_2) + h_2 (K_{12} K_{21} - 1) + K_2 q_1] \quad (30)$$

III. SLIDING MODE CONTROLLER DESIGN

In this paper, the SMC has been utilized to manipulate the operation of coupled tank system. The block diagram of coupled tank system integrated with SMC implemented in the Simulink environment is demonstrated in Fig. 2. The SMC controller brings a new solution to overcome nonlinearities, disturbances, and measurement noise. The most important characteristics of SMC is to deal with nonlinear and time varying systems.

The sliding surface is designed according to the second order coupled tank system which is expressed as below:

$$s = C_1 h_2 + C_2 h'_2$$

$$s' = C_1 h''_2 + C_2 h'_2$$

When $s' = 0$, assume $C_1 = 1$.

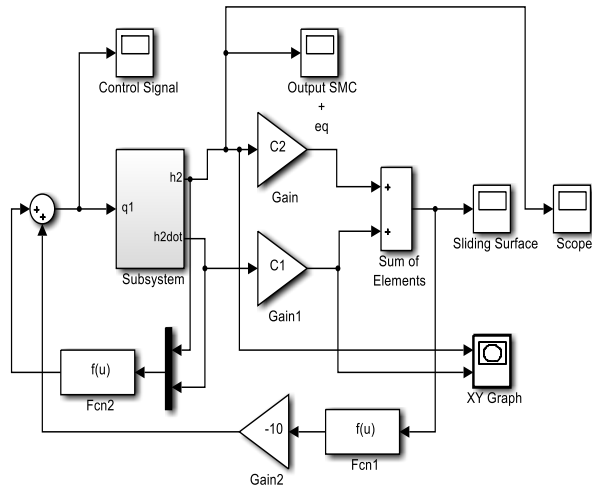


Fig. 2. Simulink Model for Coupled Tank System with the Assistant of SMC.

Generally, the control structure of SMC consists of switching and equivalent control as expressed,

$$U_{smc} = U_{sw} + U_{eq}$$

$$U_{sw} = -K \text{sign}(s) = -K \left(\frac{s}{|s + \xi|} \right)$$

$$U_{eq} = q_1$$

Taking $\xi = 0$,

$$U_{q1} = \frac{h'_2}{K_{21}K_{12}} \left[(T_1 + T_2) - \frac{C_2}{C_1} (T_1T_2) - \dots \right. \\ \left. \dots - \frac{h_2}{K_{21}K_1} (K_{21}K_{12}) \right] \quad (31)$$

Table I and II composed of parameters that will be utilized in the model.

All the parameters in Table I and II will be substituted into the equation (22), (23), (24), (25), (26), (27). Then, the value of T_1 , T_2 , K_{12} , and K_{21} will be substituted into U_{q1} as follow,

TABLE I. THE VALUE OF SELECTED PARAMETERS

Parameters	Value
H_1 (cm)	17.00
H_2 (cm)	15.00
α_1 (cm ^{3/2} /sec)	10.78
α_2 (cm ^{3/2} /sec)	11.03
α_3 (cm ^{3/2} /sec)	11.03
A_1 (cm)	32.00
A_2 (cm)	32.00

TABLE II. THE VALUE FOR THE EQUATIONS (22), (23), (24), (25), (26), (27)

Symbols	Value
T_1	6.15
T_2	6.011
K_1	0.1962
K_2	0.1878
K_{12}	0.749
K_{21}	0.7325

$$0 = -C_1 h'_2 (T_1 + T_2) + C_1 h_2 (K_{21} K_{12} - 1) + \dots \\ \dots + C_1 K_{21} K_{12} q_1 + C_1 K_{21} K_{12} q_1 \quad (32)$$

$$C_1 K_{21} K_{12} q_1 = h'_2 - ((C_2 T_1 T_2 + C_1 (T_1 + T_2) - \dots \\ \dots - C_1 h_2 (K_{21} K_{12} - 1)) \quad (33)$$

$$q_1 = \frac{h'_2}{K_{21} K_{12}} (C_1 (T_1 + T_2) - C_2 T_1 T_2) - C_1 h_2 (K_{21} K_{12} - 1) \quad (34)$$

$$q_1 = 86.469 h'_2 - 262.85 \frac{C_2}{C_1} h'_2 - 3.21 h_2 \quad (35)$$

From the equation (30),

$$h''_2 = \frac{1}{(6.15)(6.011)} [-h'_2 (6.15 + 6.011) + \dots \\ \dots + h_2 (0.7325(0.749) - 1) + (0.7325)(0.192) q_1] \\ = -0.329 h'_2 - 0.0122 h_2 + 3.8 m q_1$$

IV. RESULTS AND DISCUSSION

The analysis of the performances of SMC in the coupled tank system toward disturbances is shown in Figures 3, 4, 5 and 6. The value of C_1 and C_2 are adjusted through two set up. First, the value of C_1 is constant and the value of C_2 is adjusted. Then for the next set up, the value of C_2 is constant and the value of C_1 is adjusted. Both performances are observed to get the best value of C_1 and C_2 which shows the sliding motion and the best performances in term of settling time and percentage of overshoot.

Sliding motion with the best performances. When $C_1 = 1 \text{ cm}^2$ and $C_2 = 2 \text{ cm}^2$. The sliding motion in Fig. 3 with the respected values of C_1 and C_2 show the performances of the sliding motion in the system. It's showing how the system slides across the section of the system until reaching to the zero.

Fig. 4 and Table III show the performances of SMC towards disturbances with a constant value of C_1 and the value of C_2 is adjusted. The settling time increase as the value of C_2 increase. This is due to the area of the orifice that allows the flow of liquid increase which simultaneously increase the disturbance.

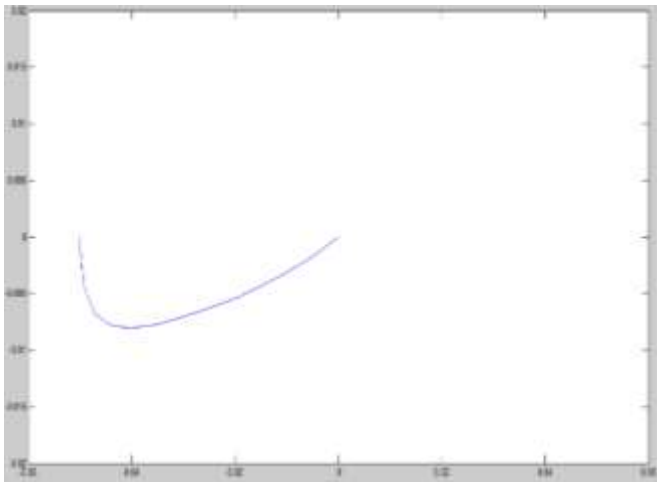


Fig. 3. The Sliding Motion of the System.

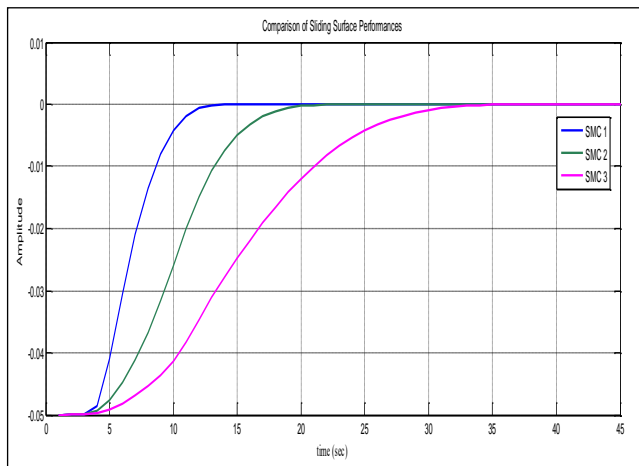


Fig. 4. Comparison of Sliding Surface Performances with a Constant Value of C_1 and the Value of C_2 is adjusted.

TABLE III. COMPARISON BETWEEN SMC WITH CONSTANT VALUE OF C_1

Sliding Surface	$C_1 (cm^2)$	$C_2 (cm^2)$	OS (%)	$T_s(sec)$
SMC 1	2	1	0	23
SMC 2	2	5	0	37
SMC 3	2	10	0	40

Referring to the Fig. 5 and Table IV, the settling time decreased when the area of $C_2 = 2 cm^2$ and $C_1 = 5 cm^2$. However, the settling time increase again when the area of $C_1 = 10 cm^2$. Even though the settling time for $C_2 = 2 cm^2$ and the area of $C_1 = 5 cm^2$ shows better performances compared to settling time when $C_2 = 2 cm^2$ and $C_1 = 1 cm^2$ but the sliding motion for $C_2 = 2 cm^2$ and $C_1 = 1 cm^2$ show better performances when it is slide across the system's normal behaviour to zero.

Then the performances of the Sliding mode control using the best performances are compared with the PID controller using auto tuned method as shown in Fig. 6. The parameters of

the PID controller including $K_p = 14.28289$, $K_i = 0.88983$, and $K_d = 38.21613$, while the best performance of SMC consist of the parameters of $C_2 = 2 cm^2$ and $C_1 = 1 cm^2$.

The SMC response in Fig. 6 shows that it is free from the overshoot unlike the PID controller. The desired level of error correction has been attained by the SMC within short time frame compared to the PID controller. The comparisons between SMC and PID controller are shown in Table V.

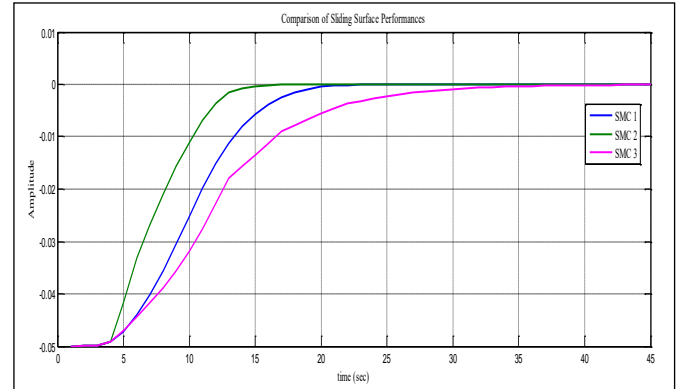


Fig. 5. Comparisons between Sliding Surface with different Value of c_1 and c_2 .

TABLE IV. COMPARISON BETWEEN SMC WITH DIFFERENT VALUE OF C_1 AND C_2

Sliding Surface	$C_1 (cm^2)$	$C_2 (cm^2)$	OS (%)	$T_s(sec)$
SMC 1	1	2	0	23
SMC 2	5	2	0	16
SMC 3	10	2	0	43

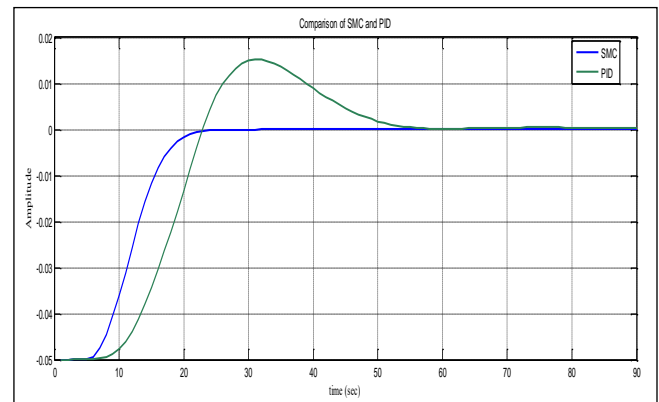


Fig. 6. Comparison between SMC and PID.

TABLE V. PERFORMANCES COMPARISON BETWEEN SMC AND PID CONTROLLERS

Character	SMC	PID
OS (%)	0	1.52
$T_s (Sec)$	23	105

V. CONCLUSIONS

We have successfully demonstrated the sliding mode controller to the coupled tanks system. The mathematical modelling of the coupled tank system has been derived thoroughly. The sliding surface has been designed to suit the second order coupled tank system. The simulation results using MATLAB for the coupled tank system proves that the SMC work very well and is robust to change in the parameters of the system as well as to external disturbances acting on the system. SMC gives a better response than a standard PID controller when applied in the CTS system. This work provides a simple and effective optimization method for selecting the most optimal controller variable of the SMC specifically for the coupled tank system. This method is based on single input and single output coupled tank system. In future multiple input multiple output system could be considered to improve the accuracy. Besides, it could be applied to other industrial applications such as hydraulic, pneumatic and suspension system for future works.

ACKNOWLEDGMENT

The authors would like to thank Universiti Teknikal Malaysia Melaka (UTeM) for the funding thru research grant with code number JURNAL/2019/FKE/Q00045.

REFERENCES

- [1] E. Laubwald, "Coupled Tank System," *Control Syst. Princ.*, pp. 1–8, 2005.
- [2] H. I. Jaafar, S. Y. S. Hussien, N. A. Selamat, M. N. M. Nasir, M. H. Jali, "Analysis of Transient Response for Coupled Tank System via Conventional and Particle Swarm Optimization (PSO) Techniques", *International Journal of Engineering and Technology (IJET)*, vol. 6(5), pp 2002-2007, 2014.
- [3] Y. Muttu, "Design and Implementation of SISO and MIMO Processes using PID Controller for Coupled Tank Process," *Int. J. Innov. Res. Sci. Technol.*, vol. 1, no. 10, pp. 55–62, 2015.
- [4] S. M. Mahmoud, L. Chrifi-Alaoui, V. Van Assche, and P. Bussy, "Sliding Mode Control of Nonlinear SISO Systems with both Matched and Unmatched Disturbances," *Int. J. Sci. Tech. Autom. Control*, vol. 2, no. 1, pp. 350–367, 2008.
- [5] H. Abbas, S. Asghar, and S. Qamar, "Sliding Mode Control for Coupled-Tank Liquid Level Control System," in *International Conference on Frontiers of Information Technology (FIT)*, 2012, pp. 325–330.
- [6] M. T. Alam, P. Charan, Q. Alam, and S. Purwar, "Sliding Mode Control of Coupled Tanks System: Theory and an Application," *Int. J. Emerg. Technol. Adv. Eng.*, vol. 3, no. 8, pp. 650–656, 2013.
- [7] D. Ghodke, B. Parvat, C. Kadu, and B. Musmade, "Robust Stability of Nonlinear Dynamic Systems using Sliding Mode Controller," in *International Conference on Advances in Recent Technologies in Communication and Computing (ARTCom)*, 2013, pp. 164–172.
- [8] R. Ghazali, Y. M. Sam, M. F. Rahmat, D. Hanafi, R. Ngadengon, and Zulfatman, "Point-to-point trajectory tracking with discrete sliding mode control of an electro-hydraulic actuator system," *Proc. - 2011 IEEE Student Conf. Res. Dev. SCOREd 2011*, pp. 148–153,
- [9] C. Edwards and S. K. Spurgeon, *Sliding Mode Control: Theory and Applications*. Taylor and Francis, 1998.
- [10] Y. M. Sam and J. H. S. Osman, "Modeling and control of the active suspension system using proportional integral sliding mode approach," *Asian J. Control*, vol. 7, no. 2, pp. 91–98, 2005.
- [11] Y.-T. Liu, T.-T. Kung, K.-M. Chang, and S.-Y. Chen, "Observer-based adaptive sliding mode control for pneumatic servo system," *Precis. Eng.*, vol. 37, no. 3, pp. 522–530, 2013.
- [12] A. R. Husain, M. N. Ahmad, and A. H. M. Yatim, "Chattering-free Sliding Mode Control for an Active Magnetic Bearing System," *Eng. Technol. World Acad. Sci.*, vol. 39, pp. 385–391, 2008.
- [13] B. B. Musmade, Y. P. Patil, R. K. Munje, and B. M. Patre, "Design of Sliding Mode Control Scheme for Nonlinear Processes for Improved Performance," in *International Conference on Industrial Instrumentation and Control (ICIC)*, 2015, pp. 992–996.
- [14] P. R. Burange, B. Parvat, and C. Kadu, "Design of TSMC for Coupled Tank Process," in *International Conference on Energy Systems and Applications*, 2015, pp. 456–461.
- [15] Saad, M., Albagul, A., & Abueejela, Y. (2014). Performance comparison between PI and MRAC for coupled-tank system. *Journal of Automation and Control Engineering* Vol, 2(3).
- [16] Mrugalski, M., Luzar, M., Pazera, M., Witczak, M., & Aubrun, C. (2016). Neural network-based robust actuator fault diagnosis for a nonlinear multi-tank system. *ISA transactions*, 61, 318-328.
- [17] Jali, M. H., Azhar, A. F., Ghazali, R., & Soon, C. C. (2018). An Intelligent Controller Design Approach for MIMO Coupled Tank System. *International Journal of Robotics and Automation (IJRA)*, 7(1), 8-17.
- [18] Y. Liu and H. Handroos, "Technical Note Sliding Mode Control for A Class of Hydraulic Position Servo," *Mechatronics*, vol. 9, no. 1, pp. 111–123, 1999.
- [19] A. Bonchis, P. I. Corke, and D. C. Rye, "Experimental Evaluation of Position Control Methods for Hydraulic Systems," *IEEE Trans. Control Syst. Technol.*, vol. 10, no. 6, pp. 876–882, 2002.
- [20] M. Y. Kim and C. O. Lee, "An Experimental Study on The Optimization Of Controller Gains for An Electro-Hydraulic Servo System Using Evolution Strategies," *Control Eng. Pract.*, vol. 14, no. 2, pp. 137–147, 2006.

Text Coherence Analysis based on Misspelling Oblivious Word Embeddings and Deep Neural Network

Md. Anwar Hussen Wadud¹, Md. Rashadul Hasan Rakib²

Department of Computer Science and Engineering
Mawlana Bhashani Science and Technology University
Tangail, Bangladesh

Abstract—Text coherence analysis is the most challenging task in Natural Language Processing (NLP) than other subfields of NLP, such as text generation, translation, or text summarization. There are many text coherence methods in NLP, most of them are graph-based or entity-based text coherence methods for short text documents. However, for long text documents, the existing methods perform low accuracy results which is the biggest challenge in text coherence analysis in both English and Bengali. This is because existing methods do not consider misspelled words in a sentence and cannot accurately assess text coherence. In this paper, a text coherence analysis method has been proposed based on the Misspelling Oblivious Word Embedding Model (MOEM) and deep neural network. The MOEM model replaces all misspelled words with the correct words and captures the interaction between different sentences by calculating their matches using word embedding. Then, the deep neural network architecture is used to train and test the model. This study examines two different types of datasets, one in Bengali and the other in English, to analyze text consistency based on sentence sequence activities and to evaluate the effectiveness of this model. In the Bengali language dataset, 7121 Bengali text documents have been used where 5696 (80%) documents have been used for training and 1425 (20%) documents for testing. And in the English language dataset, 6000 (80%) documents have been used for training and 1500 (20%) documents for model evaluation out of 7500 text documents. The efficiency of the proposed model is compared with existing text coherence analysis techniques. Experimental results show that the proposed model significantly improves automatic text coherence detection with 98.1% accuracy in English and 89.67% accuracy in Bengali. Finally, comparisons with other existing text coherence models of the proposed model are shown for both English and Bengali datasets.

Keywords—Coherence analysis; deep neural network; distributional representation; misspellings; NLP; word embedding

I. INTRODUCTION

Text coherence analysis is a very well-known key term in natural language processing for a text with multiple sentences [1]. According to Mann and Thompson (1988), a text is coherent in explaining the role that each paragraph plays in the whole field. Text coherence measures the degree of logical consistency for text which is a key property of any well-

organized text document. With the rapid development of digital communication mediums such as social networks, mobile devices, or online news portals it is more complex to identify which information is consistent or inconsistent. Recently, paperless assessment has increased rapidly and computers have been used to evaluate assessment. It is very difficult to check the consistency of text among sentences with sort time without automatic evaluation. In social networks or mobile communication, users usually use short text for their communication or use their mobile devices for any type of online assessment. During digital communication or online assessment or reporting news sometimes a naive user may misspell some word or couple of words in their whole text [2]. Common errors such as grammatical mistakes, vocabulary, or syntax errors can easily be determined, but finding text coherence between paragraphs is very difficult both in the manual and computerized systems. It is very important to automatically identify which news or information is valid or coherent regarding other information. The following examples show text coherence and news inconsistency. One example is shown in Table I where Text 1 has logical consistency, but in Text 2, the first sentence and the second sentence are logically coherent but the second sentence with the third sentence is not logically consistent.

Text coherence analysis is very important for many reasons. For example, they can be used as the logical bridge between different words, sentences, and paragraphs. Readers easily detect ideas within each sentence and paragraph. Text or paragraph without coherence not only makes it difficult to determine the main idea but also reads the full text. Text coherence checking in a short portion of the text is very easy for humans, but in a large document that has thousands of paragraphs or more is also difficult and time-consuming.

Dealing with text coherence using a machine is very difficult. Foltz in 1998 [3] proposed the first text coherence evaluation method using a machine. Later, many researchers proposed several text coherence methods, but unfortunately, no method is perfect for finding text coherence between words or sentences or paragraphs. Many automatic summarization methods that can extract summaries from a paragraph can also check grammatically correct but are limited for text coherence analysis. Considering coherence needs to check discourse relations [4], finding common patterns during sentence connection [5].

TABLE I. EXAMPLE OF LOGICAL CONSISTENT AND INCONSISTENT AMONG SENTENCES

Bengali	English
জাতীয়দলে খেলতে গিয়ে একজন ফুটবলার তার বাম পা ভেঙে ফেলেন। ডাক্তার তাকে ৩০ দিনের জন্য বিশ্রামের পরামর্শ দিয়েছেন। এজন্যে, তিনি তার নিয়মিত অনুশীলন সাময়িক সময়ের জন্য বন্ধ করেন।	A footballer broke his left leg while playing for the national team. The doctor advised him to rest for 30 days. Because of this, he stopped his regular practice for a while.
Text1: label=1 (coherent)	
জাতীয়দলে খেলতে গিয়ে একজন ফুটবলার তার বাম পা ভেঙে ফেলেন। ডাক্তার তাকে ৩০ দিনের জন্য বিশ্রামের পরামর্শ দিয়েছেন। এজন্যে, তিনি খুব তাড়াতাড়ি বিছানা থেকে উঠেন এবং সকালে নিয়মিত অনুশীলন করেন।	A footballer broke his left leg while playing for the national team. The doctor advised him to rest for 30 days. Because of this, he gets out of bed very early and practices regularly in the morning.
Text2: label = 0 (incoherent)	

Recently, proposed coherence analysis methods [1, 6] have been based on a deep learning framework that uses recurrent and recursive neural networks for computing word vectors in sentences. They capture the interaction between sentences by identifying a set of coherence features and computing the similarity between words which is useful for coherence assessment but the main limitation is finding the right word to measure similarity or interaction between sentences. If we identify misspelling sentences and determine word vectors for correct words from a misspelled word, it is a new dimension for coherence analysis. Here is another example of text coherence with misspelling words shown in Table II.

TABLE II. TEXT IN CONSISTENT WITH MISPELLED WORDS

Bengali	English
টম তার চর্বিযুক্ত শরীর নিয়ে খুব অসন্তুষ্ট (অসন্তুষ্ট)। তিনি চর্বিযুক্ত (চর্বিযুক্ত) খাবার খেতে এবং বিয়ার পান করতে পছন্দ করেন তবে কোনও শারীরিক অনুশীলন করেন না। সুতরাং, আমি মনে করি তার নিয়মিত শারীরিক অনুশীলন করা উচিত।	Tom is very dissatisfied (dissatisfied) with his fat body. He likes to eat fatty food and drink beer but has not done any physical (physical) exercise. So, I think she should do regular physical exercise.

The above example contains some misspelled words such as “অসন্তুষ্ট”, “চর্বিযুক্ত”, “dissatisfied”, “physical” which is logically inconsistent based on existing text coherence analysis methods. The composition is logically consistent between sentences when the correct word is used for each misspelled word such as (অসন্তুষ্ট => অসন্তুষ্ট), (চর্বিযুক্ত => চর্বিযুক্ত), (dissatisfied => dissatisfied), (physical => physical). Existing text coherence analysis methods convert each word into multidimensional word vectors using pretrained word embedding vectors such as Word2vec [7, 8] and Glove [9] and calculate the text set by considering the semantic and syntactic relationship between sentences. However, they did not work on out of vocabulary or misspelled words, and sometimes their results show that any composition is locally inconsistent between the sentences that are logically coherent.

Finding correct word from misspelling word is very challenging work both in Bengali and English language processing task. In Bengali language there have lot of variation in word formation. Changing single character in a word can modify the meaning of a single sentences. In this paper, a modern text coherence analysis method using Misspelling Oblivious Word Embedding Model (MOEM) and deep neural network has been proposed to overcome the above limitation. A set of commonly misspelled words is identified with their correct words to find similarities between sentences and study the coherence problem with a set of coherence features. First, misspelling oblivious word embedding methods generate a sentence matrix with the correct word vector and then apply a deep neural network with a set to cohere to compute the similarity among sentences. Finally, the proposed method estimated the text coherence by combining word vectors and similarity scores. The main contributions of this study are as follows:

- Develop a corpus of 12000 text documents for English and 8000 text documents for Bengali with misspelling words from different social media and newspaper;
- Label each document as coherent and incoherent after performing cleaning, stemming, stop-words removal, normalization and tokenization;
- Identify misspellings with the correct spelling using the MOEM model from the misspelled word dictionary set.
- Design a coherence model to identify English and Bengali documents into coherent and incoherent categories.
- Compare the performance of the proposed text coherence model with the existing models.

The rest of the paper is organized as follows: Section 2 introduces a review of recent work in this field; A detailed explanation about the proposed model is presented in Section 3. Section 3 describes the development of a data corpus for Bengali and English with misspelled word models and calculates their word metrics; Section 4 discusses the experimental setup and performance analysis results of the proposed model; Finally, Section 5 concludes the paper and highlights the importance of text analysis in both English and Bengali, including summaries and future opportunities.

II. RELATED WORK

In this section, the main categories of existing text coherence analysis methods are reviewed and described. In 1998 Flotz [4] proposed the first text coherence evaluation model. In his model, text coherence is defined by checking semantic relatedness between sentences that are adjacent to each other where lexical meaning is used to compute semantic relatedness which is a vector-based representation. Since 1998, many researchers proposed several text coherence analysis models such as entity-based model [10-16], syntactic pattern-based models [17], discourse relation-based models [18], content-based model via Hidden Markov Model [19, 20], coreference resolution-based model [21, 22] and cohesion-driven based model [23]. These models use a supervised learning approach to obtain text coherence by computing the relationship between adjacent sentences based on the lexical chain [13, 24] which is the lexical cohesion structure representation of a text.

The entity-based text coherence analysis model is one of the most popular methods that analyses the grammatical role of words in adjacent sentences and evaluates the local coherence [25] by extracting a pattern from adjacent sentences. Initially, R. Barzilay, M. Lapata [12, 14, 26] proposed the model but in recent years some modern approaches such as neural network models [27] and original bipartite graph [28] models, were proposed to overcome the limitation ability of entity grade to detect consistency in just neighbor sentences [29].

Petersen and Simonsen [30] proposed another novel method based on graph theory and the entropy method for measuring the consistency between sentences in a document. In their model they increased more nouns in the document which increases adverse information in text focusing and is the limitation of the lower score for global coherence analysis. Another graph theory-based novel model was introduced by M. Mesgar [31] for coherence features based on frequent subgraphs where texts are consistent with particular patterns in extracted subgraphs and compare their ability to measure the readability of Wall Street Journal articles [31] using an entity graph coherence model.

Another popular text coherence evaluation [32-34] approach is based on statistical machine translation algorithms such as the EM and IBM Algorithms [12, 24], where the meaning of each word in the target language represents several words and each word establishes a link into multiple sentences and finds coherence using this link word. However, these algorithms cannot overcome semantic feature limitations. Modern approaches such as neural networks [3], deep neural models [1, 3], recurrent neural networks (RNNs) [35, 36], etc. overcome semantic feature limitations and sentence ordering problems by using distributed representation and extracting syntactic representation of discourse coherence [3]. A deep neural network tries to calculate local and global coherence [37] and the RNN network is used to obtain distributed representation [3] of the sentences and sequence modeling tasks [34]. Sennan [42] proposed a text coherence model based on the sentence ordering task, but they did not discuss words outside of vocabulary or misspellings. Nevertheless, there are some limitations because text coherence analysis is a very

challenging task in natural language processing. Different from the above studies, a new text coherence model has been proposed where the deep neural network is to find sentence discourse coherence and Misspelling Oblivious Embeddings [2] used to obtain the correct format and actual meaning of several words in a document.

III. PROPOSED MODEL

The main goal of this work is to develop an architecture based on a deep learning network that can predict text coherence in both Bangla and English text documents. Fig. 1 shows a simple process of the proposed system consisting of four main phases: preprocessing, feature extraction, training, and prediction. The following subsections outline detailed explanations for each level of the proposed system.

A. Collecting Data and Preprocessing

The two most widely used corpora [12, 17, 20, 22, 41], one is a collection of aviation accident reports, and the other corpus is American earthquake-related news has been used for English text coherence analysis. The accident reports-related dataset contains 4500 compositions, where per composition have 11 sentences on average and American earthquake-related news has 3000 compositions, with an average of 10 sentences in each composition.

However, for the Bengali language, no dataset is available to identify the textual consistency of any text document. In this study, data was crawled from several social media, online newspapers, etc. A total of 7121 text documents have been crawled where 3565 texts are consistent and 3556 texts are in inconsistent class. Crowd-sourced data are initially labeled according to coherent and incoherent class. Table III summarizes some of the features of the developed dataset.

Preprocessing is used to convert raw data into a state where the machine can easily parse it. Several techniques were used for data preprocessing. The tokenization technique is used to convert data from sentences to words by dividing the sentence into sets of tokens. The text clear and stop word removal technique is used to remove special characters, punctuation, numbers and unnecessary words. In this research The Natural Language Toolkit (NLTK) is used to complete preprocessing where NLTK provides all text processing libraries, such as tokenization, stemming, parsing, tagging, and semantics reasoning.

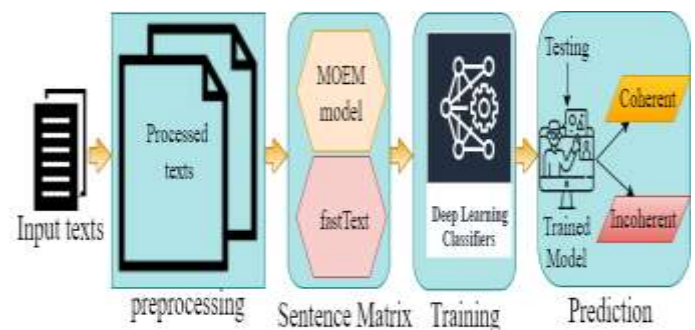


Fig. 1. Simple Process of the Proposed Text Coherence Detection System.

TABLE III. DATASET SUMMARY

Properties	Bengali Data Corpus		English Data Corpus	
	Coherent	Incoherent	Coherent	Incoherent
Total documents	3565	3556	3780	3720
Number of words	122345	233558	148388	225952
Unique words	15450	18490	16735	21687
Avg. words per doc.	34.32	65.68	39.25	60.74
Max. text length	340	2310	510	2690
Min. text length	4	10	1	5
Number of misspelling words	1500	2500	1200	2000

B. Sentence Matrix

Each sentence contains a combination of several meaningful words that must be translated into true-value feature vectors, and the combination of all vectors is used to form a sentence matrix. Some words in a sentence may be misspelled words or even out of vocabulary that cannot be directly translated into feature vectors. The misspellings embedding (MOE) [2] model is used to find the correct word from misspelled words.

C. Word Embedding with Misspelling Word Model

Facebook introduces a new word embedding method named Misspelling Oblivious Embeddings (MOE) [2] which extends fastText [38] architecture to handle out-of-vocabulary (OOV) [2] limitations during natural language processing. fastText was built by extending Word2Vec architecture which uses skip-gram models with negative sampling and the SoftMax activation function.

Popular pretrained word embedding methods such as word2vec [7, 8], GloVe [9], fastText [38], etc. provide word vectors during training but fail to produce word embedding when words are out-of-vocabulary (OOV). MOE word embedding methods work by considering slang, misspellings, or abbreviations. The MOE calculated the weighted sum of two-loss functions which are the semantic loss and spell correction loss functions. The semantic loss function captures the semantic relationship between words denoted by L_{FT} and spell correction loss function map words to find the correct word embedding denoted by L_{SC} . The MOE [2] is defined as follows:

$$L_{MOE} := (1 - \alpha)L_{FT} + \alpha \frac{|T|}{|M|} L_{SC} \tag{1}$$

where α is the hyperparameter, T is the text corpus and M is the misspellings dataset. Define abbreviations and acronyms the first time they are used in the text, even after they have been defined in the abstract.

The misspelling model has a large vocabulary [2] and a set of pairs (misspelling, correction) for the spell correction word. This network model is used to process the first part of our datasets, where there are misspelled words, out-of-vocabulary words, etc. Then we apply the fastText [38] model to obtain word embedding vectors of our corpus.

Fig. 2 shows the word embedding generation process using a fastText model where the N-gram method splits the word into subwords. For example, “orange” word can be split into “ora”, “nge”, “ang”, “oran”, “rang”, “ange”, “orang” and “range” subwords, and the sum of all subword embedding vector is considered as the embedding of “orange” word.

Similarly, Fig. 3 shows the misspelled word embedding generation process where each word consists of pairs (X, C) of a word where X denotes all possible misspelled words as shown in Table IV for a specific correct root word C. If a word is combination of two, three or more root words as shown in Table V then MOE [2] use N-gram method to split the word into all root words then find the correct root word from misspelled word and calculates word embedding by performing dot products between the sum of input vectors of the misspelled word and correct word.

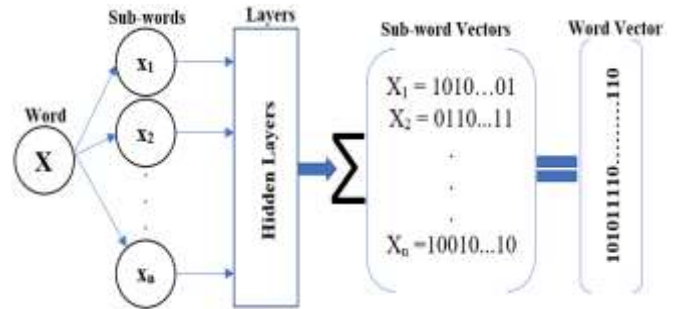


Fig. 2. Generating Word Embedding using FastText.

TABLE IV. SOME ROOT WORD WITH MISPELLED WORD

Misspelled Subword(X)	Correct Spelled Subword(C)
অমন্তুট, অমুলুট, আসন্তুট, অসিন্তুট, অসালুট, etc.	অসন্তুট
দুরি, দুইই, খুর, দরু, দারু, etc.	দূর
ছাকরি, চাকিরি, চাখরি, চাকরী, etc.	চাকরি

TABLE V. SOME COMBINE WORD WITH ROOT WORD

Combine Word	Root words	Combine Word	Root words
বাসস্ট্যান্ড	বাস, স্ট্যান্ড	নিশীথবনবিলাসিনী	নিশীথ, বন, বিলাসিনী
আইনজীবী	আইন, জীবী	অঘটনঘটনপটিয়সী	অঘটন, ঘটন, পটিয়সী
পূর্ণমান	পূর্ণ, মান	উষ্টকন্টকভোজনন্যায়	উষ্ট, কন্টক, ভোজন, ন্যায়

D. Proposed Coherence Detection Architecture

Coherence can be detected by considering all text or paragraphs in a composition or considering two consecutive paragraphs. However, there can be another way to find text coherence that considering any two or three paragraphs makes the whole article semantically coherent which is applied in our model. For example, if one chooses the first sentence and last sentence from multiple sentences in composition and finds coherence then it will be said that the composition is semantically consistent.

1) *Model inputs*: Since this study considers words out of vocabulary, misspelled words, etc. therefore, the input of the proposed coherence model will be the output of the misspelling word embedding model which are word vectors of different types of words. Every time the proposed architecture considers three paragraphs as input into the model from the composition. Then determine the word vector of the selected paragraph and iterate the process until all paragraphs are selected.

2) *Proposed text coherence methods*: A deep learning [1,39,40] network is used to process the current word embedding output and train the model based on a large Bengali and English data corpus. Fig. 4 shows the proposed model where each time processes three paragraphs to find text coherence among three sentences. A word embedding matrix with a 50-dimensional size is formed by concatenating all word vectors in a finite size vocabulary. Convolutional neural networks have been applied to the proposed model and various filters have been used which is a matrix of weights to extract useful patterns from input sentences. The global max pooling layer and rectified linear (ReLU) function defined as $\max(0, x)$, are used to increase the accuracy after the

convolution layer. Then, the first sentence is concatenated with the second sentence and second sentence with the third sentence and third sentence is concatenated with the first sentence to compute sentence-to-sentence similarity. This model used several hidden and softmax layers which are a series of convolutional and pooling operations, to find coherence the probability of these three sentences.

3) *Prediction*: Sigmoid activation function is used to calculate coherence probabilities of three sentence in output layer. This activation function also used as threshold on testing set. The trained classifier model has been used for coherence prediction based on testing set. If the threshold is T_h and predicted probability is P then predicted class C can be defined as:

$$C = \begin{cases} \text{Incoherent, if } P \leq T_h \\ \text{Coherent, if } P > T_h \end{cases} \quad (2)$$

Since the proposed text coherence model classifies coherent and incoherent classes as binary classifications, the sigmoid activation function is used without changing the default threshold value.

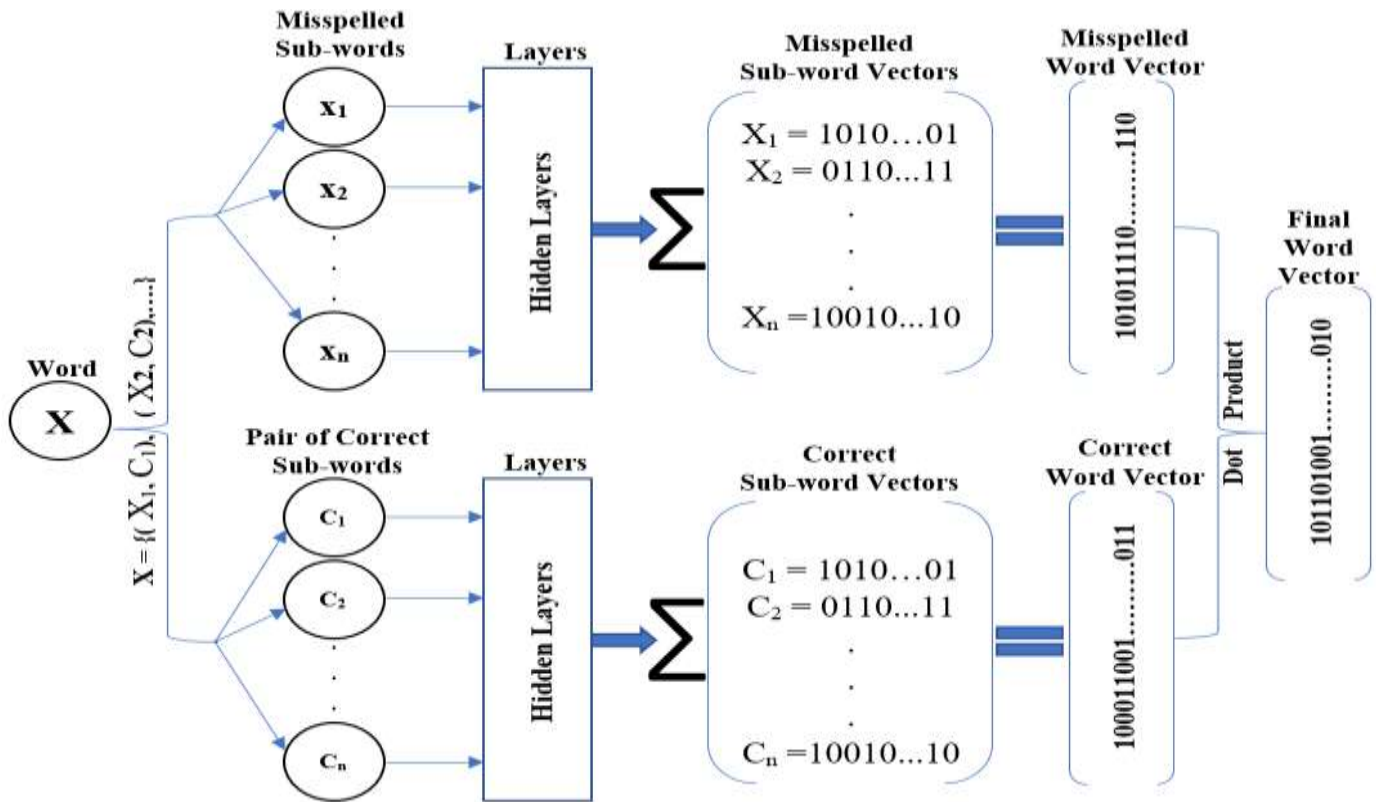


Fig. 3. Misspelling Word Embedding Generation Process using FastText.

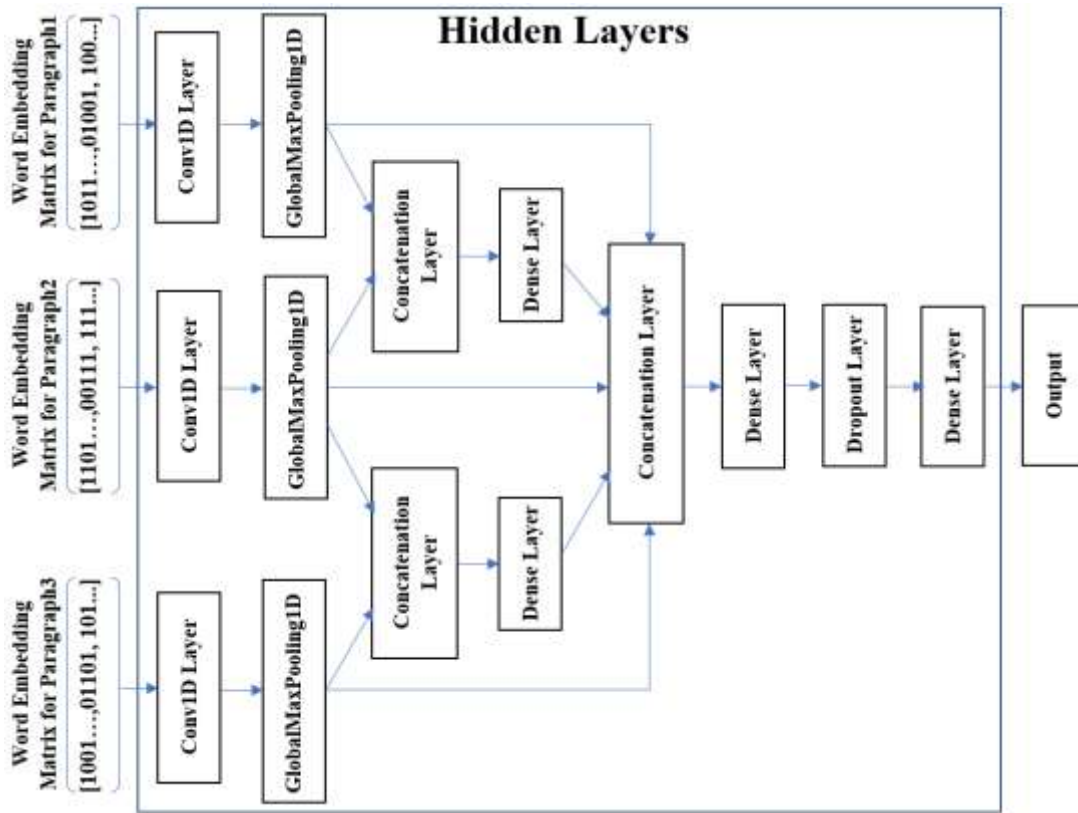


Fig. 4. Proposed Text Coherence Model.

IV. EXPERIMENTAL SETUP

The goal of the experiments is to evaluate the proposed model for two types of datasets and make a comparison between the proposed model and other coherent analysis models. The open-source Google Colab platform was used to conduct the test experiment where the Python version was 3.7, TensorFlow was 2.2.1, Pandas 1.3.3, and Scikit-learn version was 0.22.2. Panda data frame is used for data set preparation and Scikit-learn for training and testing purposes. This study initially examined the dataset from each original document by setting the dimension size of the matrix to 50, the size of the convolution filter to 4, the batch size to 500, and the total number of epochs to 20. Datasets for testing and training, the proposed model uses 80% of the total data for the train and 20% of the total dataset as the test dataset. Every dataset contains misspelled words, out-of-vocabulary words, punctuation, etc. fastText and MOE model used to compute the word embedding matrix for each data corpus. fastText pretrained Bengali word embedding vectors and MOE models are used for misspelling words to construct a word embedding matrix for Bengali text documents. A collection of pairs (misspellings, corrections) with 2,746,061 vocabulary sizes has been used for Bengali and English language datasets to obtain the proper word vector of the misspelled word or out of the vocabulary word in a data corpus. For both the Bengali and English lingual datasets, positive samples are labeled with 1, and 0 is labeled for all negative samples.

A. Measures of Evaluation

Statistical and graphical measure are used to show the performance of the proposed system based on Accuracy, Precision, Recall and F1-score.

1) *Accuracy*: A mathematical measure that indicates that a classifier correctly classifies or prohibits a condition. This is known as the symmetry of the actual results in the amount of samples tested.

$$Accuracy = \frac{TP+TN}{TP+TN+FP+FN} \quad (3)$$

Where, TP = True positive; FP = False positive; TN = True negative and FN = False negative.

2) *Precision*: is the ratio of how many text documents are actually coherent among the whole documents. Precision is defined by.

$$Precision = \frac{TP}{TP+FP} \quad (4)$$

3) *Recall*: is the ratio of how many text documents are classified correctly as coherent among total coherent text.

$$Recall = \frac{TP}{TP+FN} \quad (5)$$

4) *F1-Score*: The weighted average of accuracy and precision. This mathematical assessment metric is used to decide which of these different classifications needs to be chosen.

$$F1\text{-Score} = 2 \times \frac{\text{Precision} \times \text{Recall}}{\text{Precision} + \text{Recall}} \quad (6)$$

B. Result of Proposed Model on English Data Corpus

For the training and evaluation of the English data corpus, positive cliques have been used as coherent documents from the original training document, and other documents contain sentences that were replaced by each other in a set of negative clique datasets. The proposed model has been applied on the English data corpora and made a comparison of proposed results with other existing methods such as DCM [1], Recursive [3], Recurrent [3], Entity Grid [14], HMM [17], HMM + Content [17], Conference + Syntax [14], and Graph [29] as shown in Table VI. According to Table VI proposed model achieves better performance than all other existing coherent frameworks.

TABLE VI. COMPARISON OF DIFFERENT COHERENCE MODELS ON ENGLISH DATA CORPUS

Model Name	Accident	Earthquake	Average
Proposed Model	0.986	0.977	0.981
DCM	0.950	0.995	0.973
Recursive	0.864	0.976	0.920
Recurrent	0.840	0.951	0.895
Entity Grid	0.904	0.872	0.888
HMM	0.822	0.938	0.880
HMM + Content	0.742	0.953	0.848
Conference + Syntax	0.765	0.888	0.827
Graph	0.846	0.635	0.741

Compared with the DCM model, proposed model generates a strong semantic relationship between sentences by using the misspelling oblivious word embedding model which is missing in other text coherence analysis methods. The deep coherence model uses a convolutional neural network for text coherence assessment and word2vec as pretrained word embedding vectors for matrix construction of each sentence so that out of the context word, it cannot calculate and sometimes constructs an incorrect sentence matrix. Proposed model used fastText as pretrained word embedding vectors to compute the word embedding for sentence matrix construction and used the misspelling oblivious word embedding model to calculate out of vocabulary words and produced a better result than the DCM model.

HMM and Entity Grid require manual feature engineering and sentence representation where the proposed model can automatically learn sentence representation. The recursive and recurrent models use syntactic parsers to construct a syntactic tree and then calculate semantic coherence, which requires expensive preprocessing time. Proposed model uses a deep neural network for automatic preprocessing and makes the effort required of feature engineering unnecessary.

Fig. 5 shows the text coherence analysis accuracy result as a pie diagram of accidental data corpus and the accuracy of the text coherence on the earthquake data is shown in Fig. 6. In Fig. 5, proposed model produces 13% accuracy which is higher than other coherence models on accidental data in the English

language. In the accidental data corpus, there are some misspelled words so existing models cannot evaluate these error words. As a result, their accuracy score is lower than the proposed model. However, the proposed model shows 12% accuracy in Fig. 6 which is equal to the accuracy of other models named DCM, recursive, and HMM + content text. Because there is no misspelled word in the test data set. So, the proposed model produces equal accuracy likes other coherence models.

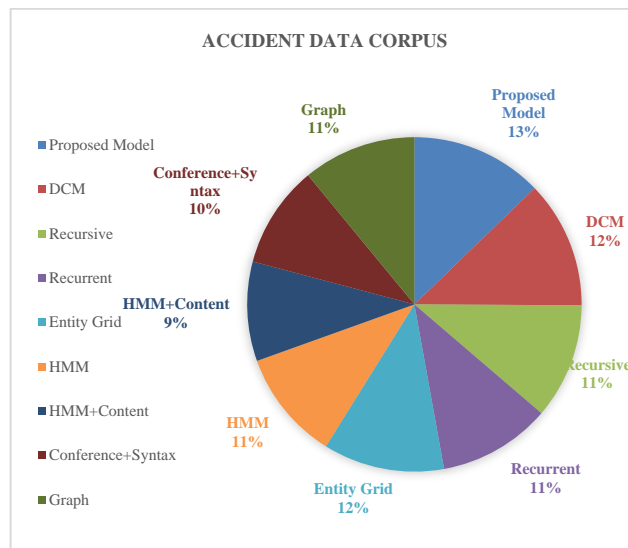


Fig. 5. English Text Coherence Analysis on Accidental Data.

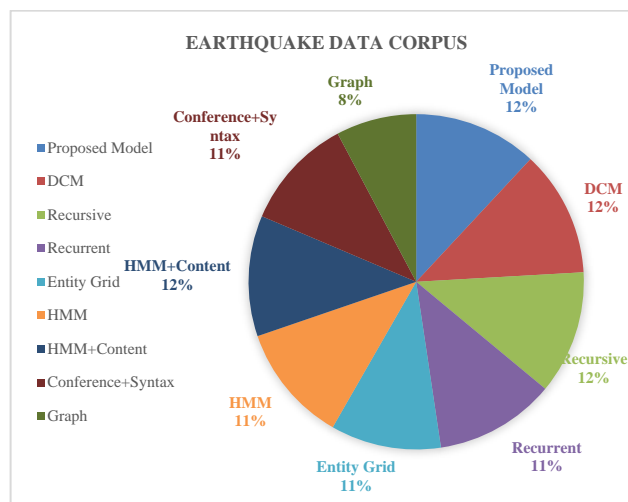


Fig. 6. English Text Coherence Analysis on Earthquake Data.

C. Result of Proposed Model on Bengali Data Corpus

There is no single standard method for analyzing Bengali text consistency. Five separate classification algorithms are used to evaluate the proposed system to find the best method for analyzing Bangla text continuity. To calculate for the best accuracy, the first Bengali dataset was created without considering misspellings and applied the experiment of all text coherence models to the datasets. Table VII reports the results of the proposed model and a comparison of other existing text coherence methods, such as DCM [1], Recursive [3], entity

grid [14], and HMM [17], for the Bengali data corpus. The proposed model has achieved maximum accuracy of 80.46% where the maximum precision value from HMM model is 85.30% and the maximum recall value of 95.87% obtained from the fastText model.

Table VIII shows a comparison of performance between different text coherence models on misspelled words. First, the fast text model has been applied to the Bengali dataset, but the training datasets have a lot of out of vocabulary and misspellings words. Fast text word embedding vectors cannot generate an actual sentence matrix for all Bengali words, and text consistency accuracy is very low in Bengali. Then the proposed model with MOE method has been applied in Bangla data corpus and achieved better results than the fast text model. Using the MOE method, significant changes have been made and more accurate accuracy has been shown for the Bangla data corpus. Other text integrated methods, such as DCM, Entity Grid and HMM models, are applied to the Bangla data corpus and produce lower results than the proposed model.

Fig. 7 depicts the f1-score of different text coherence technique without considering misspelled words where proposed model achieved maximum of 83.38% f1-score and lowest f1-score is 20.37% obtain from HMM text coherence method.

Similarly, Fig. 8 shows the f1 scores of various coherent models applied to the dataset containing misspelled words. The F1 score suggests that the proposed model is more suitable for text consistency analysis than other existing models. This is because the proposed model has achieved the highest F1 score for both coherent (90.06%) and inconsistent (88.57%) classes.

TABLE VII. COMPARISON OF DIFFERENT COHERENCE MODELS ON BENGALI DATA CORPUS WITHOUT CONSIDERING MISSPELLEING WORDS

Model Name	Accuracy (%)	Precision (%)	Recall (%)
Proposed model	80.46	76.29	91.90
fastText Model	79.40	73.66	95.87
DCM	78.67	78.99	80.52
Recursive	73.37	68.41	92.87
Entity Grid	62.47	59.83	89.84
HMM	56.46	85.30	21.54

TABLE VIII. COMPARISON OF DIFFERENT COHERENCE MODELS ON MISSPELLEING WORDS

Model Name	Accuracy (%)	Precision (%)	Recall (%)
Proposed model	89.67	89.68	90.46
fastText Model	78.94	74.28	93.66
DCM	72.24	67.14	93.24
Recursive	75.82	73.84	84.42
Entity Grid	64.08	77.36	45.83
HMM	52.39	93.69	11.43

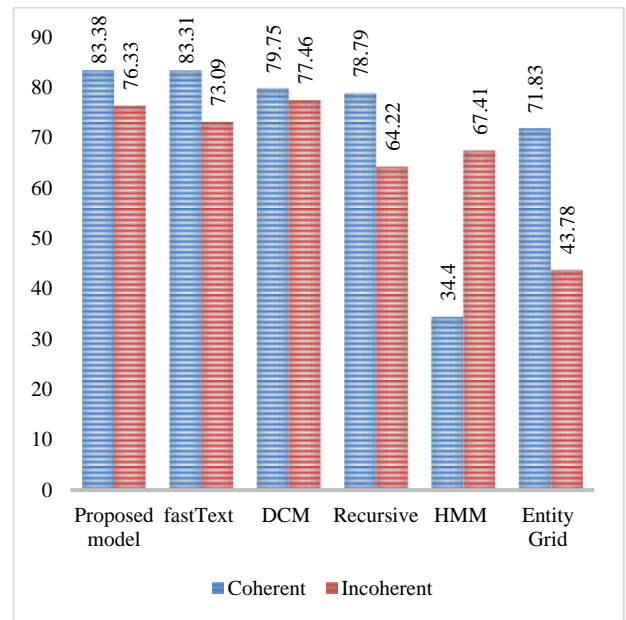


Fig. 7. F1-Score of different Text Coherence Model without Considering Misspelling Words.

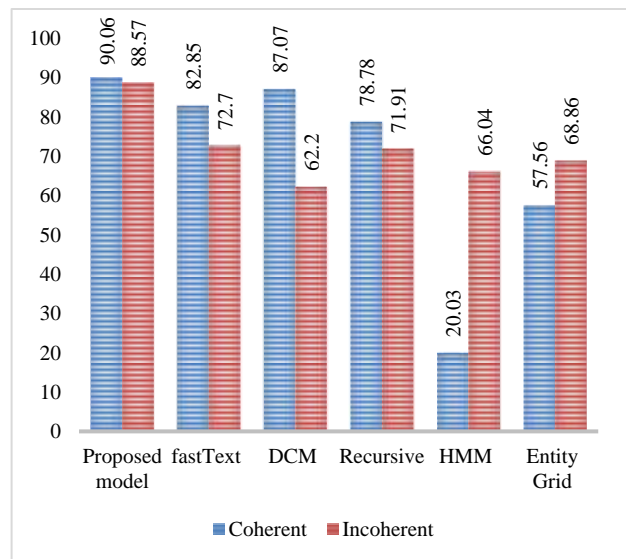


Fig. 8. F1-Score of different Text Coherence Model with Misspelling Words.

The Receiver Operator Characterization (ROC) curve is an important evaluation metric that plots the probability of True Positive Rate (TPR) as opposed to the False Positive Rate (FPR) of different Threshold values and shows the Area Under the Curve (AUC) of various machine learning classifiers. The ROC curve analysis of the various text coherence models shown in Fig. 9 and 10. The ROC curve in Fig. 9 is drawn from a general data set where misspelled words are not considered here. Proposed model obtained the maximum AUC value of 79.7% where the AUC value of other text coherence model is lower than the proposed model. The Fast Text model and the DCM model provide similar AUC values of 78% but HMM Text coherence model shows 58.70% AUC values which is too poor for text coherence classification.

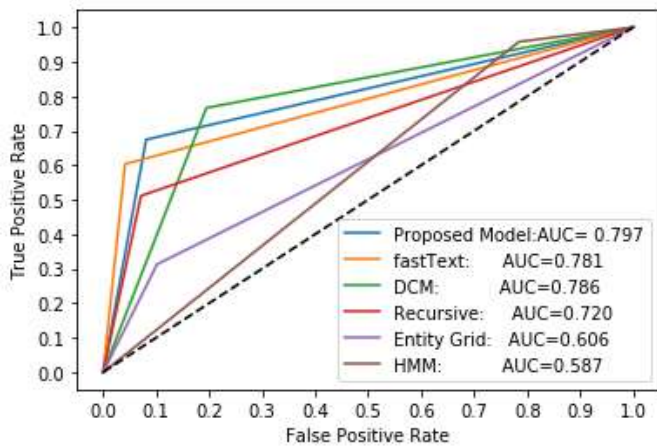


Fig. 9. ROC Curve of different Text Coherence Model without Considering Misspelling Words.

The proposed method gives better results when misspelled words are considered during the test and AUC value is 89.30% as shown in Fig. 10 where accuracy is much higher than the previous AUC value of 79.70% shown in Fig. 9. However, the AUC value of other text-based models remains the same as the previous AUC values. The AOC values of the existing model in Fig. 10 are slightly different but not like the proposed model. This presents that the proposed model performs more accurately during the classification of coherence classes in the dataset.

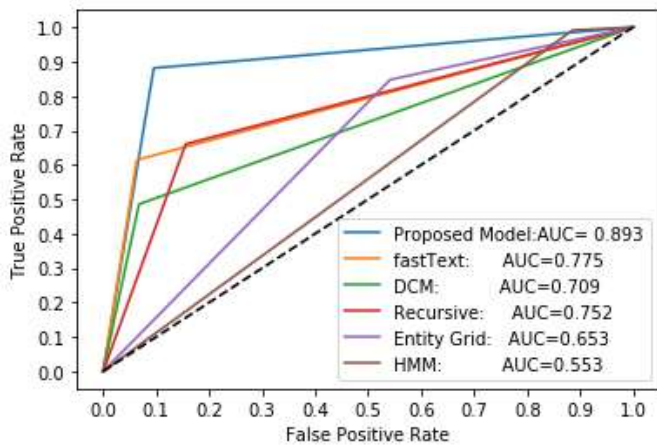


Fig. 10. ROC Curve of different Text Coherence Model with Misspelling Words.

The test data contains some misspelled words and the proposed model gives better results than other text coherence models because other methods may not work on misspelled words which is the main imitation of all other methods. This presents that the proposed model performs more accurately during the classification of coherence classes in the dataset.

V. CONCLUSION

In this research paper, the main objective of this study was to calculate the text consistency with misspelled words in Bengali language. A model has been proposed based on a deep neural network and MOE method for text coherence analysis. For experimental analysis, both Bengali and English data

corpora have been tested and the proposed model shows significant improvement in text coherent assessment. The proposed model shows an average accuracy of 98.1% in English text coherence analysis for datasets considering misspelled words which is higher than the existing models. For the analysis of Bengali text coherent, this study experimented on two types of datasets. One type of dataset contains common words and another type of dataset contains out-of-vocabulary, misspelled words, etc. The proposed model prediction for general datasets shows 80.46% accuracy and misspelled datasets 89.67%. The accuracy of other models is appropriate for general datasets but the accuracy goes down for misspelling datasets. The accuracy of fastText, DCM, Recursive, Entity Grid, and HMM models is 79.40%, 78.67%, 73.37%, 62.47%, and 56.46% respectively for normal dataset but for misspelling dataset accuracy is 78.94%, 72.24%, 75.82%, 64.08% and 52.39% respectively which is less than the normal dataset accuracy. However, the proposed model performs better accuracy for both normal and misspelled datasets and increases the accuracy for misspelling dataset than a normal dataset. Currently, this study uses limited (key, value) pairs for word misspelling but for more accuracy, it requires a huge collection of word pairs for misspelled words which is the main limitation of the proposed model.

REFERENCES

- [1] B. Cui, Y. Li, Y. Zhang and Z. Zhang, Text coherence analysis based on deep neural network, CoRR abs/1710.07770(2017).
- [2] B. Edizel, A. Piktus, P. Bojanowski, R. Ferreira, E. Grave and F. Silvestri, Misspelling oblivious word embeddings, CoRR abs/1905.09755(2019).
- [3] J. Li and E. Hovy, A model of coherence based on distributed sentence representation01 2014, pp. 2039–2048.
- [4] P.W.Foltz, W.Kintsch and T.K.Landauer, The measurement of textual coherence with latent semantic analysis, Discourse Processes 25(23) (1998) 285–307.
- [5] D.Marcu, The rhetorical parsing of natural language texts, in Proceedings of the 35th Annual Meeting of the Association for Computational Linguistics and Eighth Conference of the European Chapter of the Association for Computational Linguistics ACL '98/EACL '98, (Association for Computational Linguistics, USA, 1997), p. 96–103.
- [6] H. Oufaida, P. Blache and O. Nouali, A Coherence Model for Sentence Ordering 062019, pp. 261–273.
- [7] T. Mikolov, K. Chen, G. Corrado and J. Dean, Efficient estimation of word representations in vector space, in 1st International Conference on Learning Representations, ICLR 2013, Scottsdale, Arizona, USA, May 2-4, 2013, Workshop Track Proceedings, eds. Y. Bengio and Y. LeCun2013.
- [8] T. Mikolov, I. Sutskever, K. Chen, G. Corrado and J. Dean, Distributed representations of words and phrases and their compositionality, CoRR abs/1310.4546(2013).
- [9] J. Pennington, R. Socher and C. Manning, Glove: Global vectors for word representation, in Proceedings of the 2014 Conference on Empirical Methods in Natural Language Processing (EMNLP) (Association for Computational Linguistics, Doha, Qatar, October 2014), pp. 1532–1543.
- [10] D. Xiong, M. Zhang and X. Wang, Topic based coherence modeling for statistical machine translation, IEEE/ACM Transactions on Audio, Speech, and Language Processing 23(3) (2015) 483–493.
- [11] C. Petersen, C. Lioma, J. Simonsen and B. Larsen, Entropy and graph based modelling of document coherence using discourse entities: An application (07 2015).
- [12] R. Barzilay and M. Lapata, Modeling local coherence: An entity-based approach, in Proceedings of the 43rd Annual Meeting of the Association

- for Computational Linguistics (ACL'05) (Association for Computational Linguistics, Ann Arbor, Michigan, June 2005), pp. 141–148.
- [13] S. Somasundaran, J. Burstein and M. Chodorow, Lexical chaining for measuring discourse coherence quality in test-taker essays, in Proceedings of COLING 2014, the 25th International Conference on Computational Linguistics: Technical Papers (Dublin City University and Association for Computational Linguistics, Dublin, Ireland, August 2014), pp. 950–961.
- [14] R. Barzilay and M. Lapata, Modeling local coherence: An entity-based approach, *Computational Linguistics* 34(1) (2008) 1–34.
- [15] V. W. Feng and G. Hirst, Extending the entity-based coherence model with multiple ranks, in Proceedings of the 13th Conference of the European Chapter of the Association for Computational Linguistics (Association for Computational Linguistics, Avignon, France, April 2012), pp. 315–324.
- [16] M. Zhang, V. W. Feng, B. Qin, G. Hirst, T. Liu and J. Huang, Encoding world knowledge in the evaluation of local coherence, in Proceedings of the 2015 Conference of the North American Chapter of the Association for Computational Linguistics: Human Language Technologies (Association for Computational Linguistics, Denver, Colorado, May–June 2015), pp. 1087–1096.
- [17] A. Louis and A. Nenkova, A coherence model based on syntactic patterns, in Proceedings of the 2012 Joint Conference on Empirical Methods in Natural Language Processing and Computational Natural Language Learning (Association for Computational Linguistics, Jeju Island, Korea, July 2012), pp. 1157–1168.
- [18] Z. Lin, H. T. Ng and M.-Y. Kan, Automatically evaluating text coherence using discourse relations, in Proceedings of the 49th Annual Meeting of the Association for Computational Linguistics: Human Language Technologies (Association for Computational Linguistics, Portland, Oregon, USA, June 2011), pp. 997–1006.
- [19] M. Elsner, J. Austerweil and E. Charniak, A unified local and global model for discourse coherence, in *Human Language Technologies 2007: The Conference of the North American Chapter of the Association for Computational Linguistics*; Proceedings of the Main Conference (Association for Computational Linguistics, Rochester, New York, April 2007), pp. 436–443.
- [20] R. Barzilay and L. Lee, Catching the drift: Probabilistic content models, with applications to generation and summarization, in Proceedings of the Human Language Technology Conference of the North American Chapter of the Association for Computational Linguistics: HLT-NAACL 2004 (Association for Computational Linguistics, Boston, Massachusetts, USA, May 2 - May 7 2004), pp. 113–120.
- [21] R. Iida and T. Tokunaga, A metric for evaluating discourse coherence based on coreference resolution, in Proceedings of COLING 2012: Posters (The COLING 2012 Organizing Committee, Mumbai, India, December 2012), pp. 483–494.
- [22] M. Elsner and E. Charniak, Coreference inspired coherence modeling, 01 2008, pp. 41–44.
- [23] Z. G. W. M. XU Fan1, ZHU Qiaoming2, Cohesion-driven discourse coherence modeling, 28(3) (2014) p. 11.
- [24] D. Xiong, Y. Ding, M. Zhang and C. L. Tan, Lexical chain based cohesion models for document-level statistical machine translation, in Proceedings of the 2013 Conference on Empirical Methods in Natural Language Processing (Association for Computational Linguistics, Seattle, Washington, USA, October 2013), pp. 1563–1573.
- [25] K. Filippova and M. Strube, Extending the entity-grid coherence model to semantically related entities, in Proceedings of the Eleventh European Workshop on Natural Language Generation (ENLG 07) (DFKI GmbH, Saarbrücken, Germany, June 2007), pp. 139–142.
- [26] M. Lapata and R. Barzilay, Automatic evaluation of text coherence: Models and representations. Proceedings of the 19th International Joint Conference on Artificial Intelligence 01 2005, pp. 1085–1090.
- [27] C. Lioma, F. Tarissan, J. G. Simonsen, C. Petersen and B. Larsen, Exploiting the bipartite structure of entity grids for document coherence and retrieval, CoRR abs/1608.00758 (2016).
- [28] F. Xu, S. Du, M. Li and W. Mingwen, An entity-driven recursive neural network model for Chinese discourse coherence modeling, *International Journal of Artificial Intelligence Applications* 8(03 2017) 1–9.
- [29] C. Guinaudeau and M. Strube, Graph-based local coherence modeling ACL 2013 - 51st Annual Meeting of the Association for Computational Linguistics, Proceedings of the Conference 108 2013, pp. 93–103.
- [30] C. Petersen, C. Lioma, J. Simonsen and B. Larsen, Entropy and graph-based modelling of document coherence using discourse entities: An application (07 2015).
- [31] M. Mesgar and M. Strube, Graph-based coherence modeling for assessing readability, in Proceedings of the Fourth Joint Conference on Lexical and Computational Semantics (Association for Computational Linguistics, Denver, Colorado, June 2015), pp. 309–318.
- [32] M. Abdolahi and M. Zahedi, A new model for text coherence evaluation using statistical characteristics, *Journal of Electrical and Computer Engineering Innovations (JECEI)* 6(1) (2018) 15–24.
- [33] R. Soricut and D. Marcu, Discourse generation using utility-trained coherence models, in Proceedings of the COLING/ACL 2006 Main Conference Poster Sessions (Association for Computational Linguistics, Sydney, Australia, July 2006), pp. 803–810.
- [34] R. Rosenfeld, A maximum entropy approach to adaptive statistical language modeling, *Computer, Speech and Language* 10 (1996) 187–228.
- [35] Y. Pang, J. Liu, J. Zhou and K. Zhang, Paragraph Coherence Detection Model Based on Recurrent Neural Networks 07 2019, pp. 122–131.
- [36] L. Logeswaran, H. Lee and D. R. Radev, Sentence ordering using recurrent neural networks, CoRR abs/1611.02654(2016).
- [37] W. Liang, R. Feng, X. Liu, Y. Li and X. Zhang, Gltm: A global and local word embedding based topic model for short texts, *IEEE Access* 6(2018) 43612–43621.
- [38] A. Joulin, E. Grave, P. Bojanowski, M. Douze, H. Jégou and T. Mikolov, Fasttext.zip: Compressing text classification models, CoRR abs/1612.03651(2016).
- [39] J. Devlin, M. Chang, K. Lee and K. Toutanova, BERT: pre-training of deep bidirectional transformers for language understanding, CoRR abs/1810.04805(2018).
- [40] R. Collobert and J. Weston, A unified architecture for natural language processing: Deep neural networks with multitask learning, in Proceedings of the 25th International Conference on Machine Learning ICML '08, (Association for Computing Machinery, New York, NY, USA, 2008), p. 160–167.
- [41] M. Elsner and E. Charniak, Extending the entity grid with entity-specific features, in Proceedings of the 49th Annual Meeting of the Association for Computational Linguistics: Human Language Technologies (Association for Computational Linguistics, Portland, Oregon, USA, June 2011), pp. 125–129.
- [42] Liu, Sennan, Shuang Zeng, and Sujian Li. "Evaluating Text Coherence at Sentence and Paragraph Levels." arXiv preprint arXiv:2006.03221 (2020).

Comprehensive Multilayer Convolutional Neural Network for Plant Disease Detection

Radhika Bhagwat¹, Yogesh Dandawate²

Department of Technology, Savitribai Phule Pune University Pune, India¹

Department of Information Technology, MKSSS's Cummins College of Engineering for Women, Pune, India¹

Electronics and Telecommunication Engineering, Vishwaskarma Institute of Information Technology, Pune, India²

Abstract—Agriculture has a dominant role in the world's economy. However, losses due to crop diseases and pests significantly affect the contribution made by the agricultural sector. Plant diseases and pests recognized at an early stage can help limit the economic losses in agriculture production around the world. In this paper, a comprehensive multilayer convolutional neural network (CMCNN) is developed for plant disease detection that can analyze the visible symptoms on a variety of leaf images like, laboratory images with a plain background, complex images with real field conditions and images of individual disease symptoms or spots. The model performance is evaluated on three public datasets -Plant Village repository having images of the whole leaf with plain background, Plant Village repository with complex background and Digipathos repository with images of lone lesions and spots. Hyperparameters like learning rate, dropout probability, and optimizer are fine-tuned such that the model is capable of classifying various types of input leaf images. The overall classification accuracy of the model in handling laboratory images is 99.85%, real field condition images is 98.16% and for images with individual disease symptoms is 99.6%. The proposed design is also compared with the popular CNN architectures like GoogleNet, VGG16, VGG19 and ResNet50. The experimental results indicate that the suggested generic model has higher robustness in handling various types of leaf images and has better classification capability for plant disease detection. The obtained results suggest the favorable use of the proposed model in a decision support system to identify diseases in several plant species for a large range of leaf images.

Keywords—Crop diseases; plant disease detection; hyperparameters; deep learning; convolutional neural network

I. INTRODUCTION

Agriculture has a huge impact on the economic development of the country. Factors like climatic changes, the ever-increasing population and the widespread of crop diseases highly affect the contribution made by the agricultural sector [1]. Crop diseases are of profound concern, and hence, to control the corresponding losses, timely and effective solutions are very important. However, plant disease detection using visual symptoms is intricate. Due to the huge variety and diversity in plants and their diseases, diagnosis using visual symptoms can lead to misguided treatments. This traditional method is also time-consuming and costly. In this reference, many researchers along with agriculture professionals have suggested numerous automated plant disease detection techniques [2, 3].

The conventional machine learning procedures for automatic plant disease detection utilize multiple stages like pre-processing, segmentation, feature extraction and classification with various image processing approaches used at each stage [4-9]. One of the major constraints of traditional machine learning methods is that they need domain expertise to extract relevant features. In the past decade, developments in areas of computer vision, computing technology, machine learning, etc. led to accelerated progress in multiple applications and over the last few years, deep learning has given a new advancement to the traditional machine learning techniques to overcome part of the complexities in many domains. Deep Learning algorithms learn the relevant features during training from the raw input data thus eliminating the requirement of domain knowledge for feature extraction.

Deep learning approaches are now being predominantly used in various computer vision and pattern recognition applications like healthcare, text or handwriting generation, image recognition, etc. [10, 11]. In agriculture applications too, deep learning methods have gained huge popularity [12, 13], especially in plant disease diagnosis. Authors in [14] suggested a method for rice disease identification using deep Convolutional neural network (CNN) using infected and healthy leaves and stems. The proposed method could distinguish ten rice diseases to achieve an accuracy of 95.48%. Work in [15] used diseased and healthy leaf images taken under controlled conditions to train deep CNNs. They compared two CNN architectures to identify 26 diseases in 14 plant species. While in [16] the author trained several CNN architectures (VGG, Overfeat, AlexNet, GoogLeNet, and AlexNetOWTBn) to detect and diagnose diseases of plants and found that VGG gave the highest classification of 99.53%. Authors in [17] used transfer learning with VGG16 for disease detection in millet crops. Their proposed approach gave a classification accuracy of 95%, precision of 90.5%, 94.5% recall and 91.75% F1 score. The study in [18] used SVM for segmenting the disease symptoms and used VGG16 along with conditional Convolutional generative adversarial network to get 90% classification accuracy for tea leaf diseases. Authors in [19] suggested an infield wheat disease localization and detection procedure with several instance learning techniques. The suggested model gave higher accuracy as compared with two traditional CNN architectures. Fine-tuning the existing six CNN architectures for analyzing their performance for healthy and diseased images of 38 classes is proposed in [20]. The study suggested DenseNet gives better performance compared to other architectures. The use of the Caffe deep learning

framework for the recognition of plant diseases was done in [21]. Their model discriminated 13 different infections and achieved 91% to 98% precision for different classes with 96.3% overall average classification accuracy.

Most of the models proposed in the literature are either designed for particular crop species [22-24] or are designed for the specific type of images e.g. images captured under controlled laboratory conditions with a plain background[25,26]. In this work, a comprehensive multilayer convolutional neural network (CMCNN) model is proposed for plant disease detection. The work aims on developing a generic model capable of processing a variety of leaf images like, images that are captured under controlled conditions with a plain background, images taken in uncontrolled conditions with real field complex background and images having lone lesions and spots. For this purpose, the use of three public datasets having healthy and infected leaf images is done. The work thereby aims to overcome all the challenges related to these input images. The proposed deep learning architecture is extensively assessed for various hyperparameters and is fine-tuned to process a variety of leaf images. Experimental results give an average classification accuracy of 99.85%, 98.16% and 99.6% for plain background images, complex background images and for images with lone lesions and spots respectively. The model output is also compared against the state of art techniques and the results show that the proposed CMCNN design outperforms other methods in terms of classification accuracy and computational efficiency. The overall experimental results suggest the potential use of the proposed model for handling a huge variety of input images for efficient plant disease detection.

The remainder of this paper is organized in the following manner: Materials and methods used for experimentation are set out in Section II. The results of the experiments and related discussions are presented in Section III and the Conclusion is contained in Section IV.

II. MATERIALS AND METHODS

A. Datasets

The proposed work uses three database repositories. First is the Plant Village [27] repository for laboratory conditions images with plain background, second is Plant Village repository for real field condition images with complex background and third is the Digipathos repository (Database for plant disease symptoms (PDDB)) for images with lone

lesions and spots., ([28]-[30]). The Plant Village database is divided into two categories to study the model performance on the individual type of images.

The Plant Village dataset having plain background images has 38 classes. This dataset has images that have viewpoint and disease severity variations. The Plant Village dataset with complex background images has 11 classes. The images in this dataset have occlusions, variations in shadows, lighting conditions along with viewpoint and disease severity changes. The Digipathos dataset has 53 classes. It has images of individual lesions and spots indicating the disease symptoms. Fig. 1 shows the sample for laboratory condition images with a plain background, real field condition with complex background and images with lone lesions. Table I gives detailed information about the datasets.



Fig. 1. Sample Images for (a) Plain Background, (b) Complex Background, (c) Lone Lesions.

TABLE I. INFORMATION ABOUT DATASETS

Dataset	Type of Image	Background	Crops	Classes	Diseased Classes	Healthy Classes	Images (Number)
Dataset1 (PlantVillage)	Whole Leaf	Plain	14	38	27	11	54,308
Dataset2 (PlantVillage)	Whole Leaf	Complex	3	11	8	3	26,347
Dataset3 (Digipathos)	Disease symptoms	-	15	53	53	0	43,106

B. Proposed Architecture

Convolutional Neural networks belong to the family of deep learning. The major advantage of CNN lies in its ability to learn the best features for given samples during the training process, as compared to the traditional algorithms that require domain knowledge for creating the feature set. CNN models are normally a stack of Convolutional layers, pooling layer and fully connected layer. The CNN architecture can be configured depending upon the utilization. Several CNN architecture variants like AlexNet, GoogleNet, VGG16, VGG19, ResNet, DenseNet, etc. have been suggested in past few years for various applications. These architectures differ in terms of their structural details.

The paper focuses on developing a comprehensive multilayer CNN architecture for plant disease detection optimized for handling a variety of leaf images. Fig. 2 shows the suggested CNN architecture.

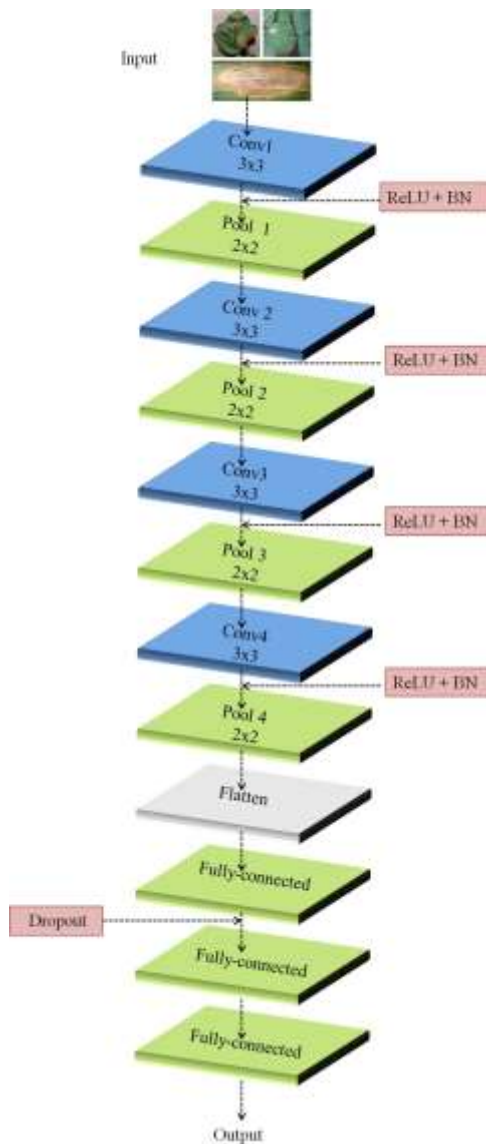


Fig. 2. Proposed CMCNN Architecture.

The model comprises four Convolutional layers each with ReLU activation function, batch normalization (BN) and max-pooling layer and three fully connected (dense) layers with softmax activation for the last dense layer. The convolutional layer is the principal unit of CNN architecture. It is responsible for extracting relevant features from the input data using Convolutional kernels. Initial convolution layers are responsible for capturing the low level features, and the deeper Convolutional layers extract the high level features. This together gives a network that has a detailed understanding of the input images in the dataset. The first convolutional layer used in the proposed work uses 32 filters with a kernel size of 3 while the last convolutional layer uses 192 filters with a kernel size of 3. Thus convolutional layers convolve the input image with several kernels to get various feature maps.

It is then activated by a non-linear activation function that helps to capture complex relations in the data. The convolutional layers in the proposed architecture utilize the ReLU activation function which is represented by:

$$\sigma(x) = \max(0, x) \quad (1)$$

The function returns a zero for any negative value of x , while for any positive input it returns that value. It is the most used activation function as it subdues the vanishing gradient problem and also helps the model to learn fast and give a better performance.

The activation process is succeeded by Batch normalization (BN) and pooling. Batch normalization helps in keeping the input of intermediate layers in the same range throughout the training process to avoid internal covariate shift. Pooling layers lessens the dimensionality of the feature map while retaining the most pertinent features. Two of the most frequently used pooling techniques are Max pooling and Average pooling, however, max-pooling gives better invariant features and helps in convergence [31]. Max-pooling is used in the work with a filter size of 2x2.

After a sequence of Convolutional and pooling layers, the extracted feature map is converted into a 1D array for simple data handling. This is succeeded by fully connected layers where each neuron is attached to every neuron in the next layer. Dropout is used with fully connected layer to avoid overfitting. The final layer in the proposed architecture is the dense or fully connected layer with Softmax classifier whose output is in the form of probabilities representing each class. The expression for softmax function for k classes is as follows:

$$S_j(z) = \frac{e^{z_j}}{\sum_k e^{z_k}} \quad (2)$$

Where z is the input vector to softmax classifier and z_j is the j th element of the vector.

III. EXPERIMENTAL RESULTS

In this work, three database repositories, each with different kinds of images are utilized to assess the generalization capability and performance of the model in handling various challenges (occlusions, illumination variations, viewpoint and disease severity variations) in the input images. The datasets are divided into training, validation and testing sets to better

analyze the model. Table II specifies the train, test and validation ratios used for experimentation.

A. Implementation Details

All the experimentation for the proposed model is executed using the Keras, Scikit-learn and OpenCV library with Tensorflow backend using the python programming language with NVIDIA Tesla K80 GPU.

The model training is done in a supervised method. The initial values of the weights and biases are arbitrarily selected and the new values are updated using back-propagation of the gradient. The loss function used in the work is cross-entropy and the optimizer used is Adam. A batch size of 32 is selected. A learning rate of 1e-4 is selected to improve the model fitting. The training, validation and test sets are shuffled randomly to enhance the model stability. Once the processes of training and validation are over, the trained model is checked for the test dataset. The selected parameters and configuration details are given in Table III.

B. Performance Analysis of Datasets

The performance of the developed model is extensively validated on the three image datasets. Table IV, Table V and Table VI show the precision, recall and F1 score obtained for the test datasets of Dataset1, Dataset2 and Dataset3 respectively. The class name in the tables (Plant_Disease) represents the plant along with the disease or (Plant_Healthy) healthy plant.

The weighted average is considered for evaluation due to the imbalanced datasets. Dataset2 with real field complex background obtained the least overall weighted precision of 0.92 as compared to 0.97 and 0.94 for dataset1 and dataset3 respectively.

TABLE II. TRAINING, TESTING AND VALIDATION RATIOS

Table with 5 columns: Database, Type of images, Training set(70%), Validation set (15%), Testing set (15%). Rows include Plant Village (Dataset 1), Plant Village (Dataset 2), and Digipathos (Dataset 3).

TABLE III. CONFIGURATION AND PARAMETER DETAILS

Table with 2 columns: Parameters, Selected Value. Rows include Convolutional Layers, Max Pooling, Activation Function, Learning Rate, Optimizer, Batch Size, and Dropout.

TABLE IV. EVALUATION FOR DATSET1 (WHOLE LEAF LABORATORY CONDITIONS WITH PLAIN BACKGROUND)

Table with 5 columns: Class, Class Name, Precision, Recall, F1 Score. Rows list 37 classes from P_0 to P_37, including various plant diseases and a final Weighted Average row.

TABLE V. EVALUATION FOR DATASET 2 (WHOLE LEAF REAL FIELD CONDITIONS WITH COMPLEX BACKGROUND)

Class	Class Name	Precision	Recall	F1 Score
C_0	Banana_ Black Sigotaka	0.91	0.9	0.9
C_1	Banana_ Healthy	0.94	0.93	0.91
C_2	Banana_ Speckle	0.89	0.89	0.89
C_3	Corn_ Healthy	0.92	0.91	0.9
C_4	Corn_ Gray leaf spot	0.91	0.89	0.88
C_5	Corn_ lethal necrosis disease	0.92	1	0.92
C_6	Corn_ rust	0.91	0.91	0.9
C_7	Soybean_ downy mildew	0.89	0.89	0.89
C_8	Soybean_ frogeye leaf spot	0.93	0.91	0.91
C_9	Soybean_ healthy	0.91	0.89	0.9
C_10	Soybean_ septorial leaf blight	0.95	0.92	0.91
	Weighted Average	0.92	0.91	0.91

TABLE VI. EVALUATION FOR DATASET3 (LESIONS AND SPOTS)

Class	Class Name	Precision	Recall	F1 Score
L_0	Cabbage_ Alternaria Leaf Spot	1	0.97	0.97
L_1	Cashew_ Algae	0.96	0.86	0.92
L_2	Cashew_ Angular Leaf Spot	0.95	0.94	0.93
L_3	Cashew_ Anthracnose	0.92	0.94	0.85
L_4	Cashew_ Black Mould	0.94	0.78	0.87
L_5	Cassava_ Bacterial Blight	0.91	0.91	0.86
L_6	Cassava_ Green Mite	0.95	0.92	0.93
L_7	Cassava_ White Leaf Spot	0.93	0.87	0.9
L_8	Citrus_ Algae	0.89	0.96	0.91
L_9	Citrus_ Canker	0.95	0.95	0.95
L_10	Citrus_ Greasy Spot	0.96	1	0.96
L_11	Citrus_ Mosaic	0.93	0.92	0.92
L_12	Citrus_ Scab	0.92	0.92	0.92
L_13	Citrus_ Sooty Mold	0.94	0.92	0.93
L_14	Citrus_ Variegated Chlorosis	0.96	0.96	0.96
L_15	Coconut_ Cylindrocladium Leaf Spot	0.91	0.91	0.91
L_16	Coconut_ Lixa Grande	0.92	0.9	0.9
L_17	Coconut_ Lixa Pequena	0.89	0.84	0.83
L_18	Coffee_ Bacterial Blight	0.91	0.87	0.89
L_19	Coffee_ Blister Spot	1	0.84	0.92
L_20	Coffee_ Rust	0.87	0.92	0.91
L_21	Corn_ Northern Corn Leaf Blight	0.85	0.85	0.83
L_22	Corn_ Phaeosphaeria Leaf Spot	0.93	0.86	0.89
L_23	Corn_ Physoderma Brown Spot	0.92	0.91	0.89

L_24	Corn_ Southern Corn Rust	0.89	0.84	0.83
L_25	Corn_ Southern Leaf Blight	0.85	0.84	0.84
L_26	Corn_ Tropical Rust	0.89	0.9	0.87
L_27	Cotton_ Areolate Mildew	0.94	0.92	0.93
L_28	Cotton_ Myrothesium Leaf Spot	0.9	0.94	0.92
L_29	Dry Bean_ Anthracnose	0.9	0.89	0.89
L_30	Dry Bean_ Hedylepta Indicata	0.89	0.9	0.87
L_31	Dry Bean_ Phytotoxicity	0.96	0.96	0.96
L_32	Dry Bean_ Powdery Mildew	0.78	0.85	0.76
L_33	Dry Bean_ Rust	0.89	0.82	0.82
L_34	Dry Bean_ Target Leaf Spot	0.92	0.91	0.89
L_35	Grapevine_ Bacterial Canker	0.89	0.82	0.82
L_36	Grapevine_ Downy Mildew	0.93	0.85	0.88
L_37	Grapevine_ Powdery Mildew	0.79	0.9	0.84
L_38	Grapevine_ Rust	0.87	0.84	0.85
L_39	Passion_ Fruit Bacterial Spot	0.93	0.91	0.92
L_40	Rice_ Blast	0.89	0.89	0.86
L_41	Soybean_ Bacterial Blight	0.94	0.84	0.86
L_42	Soybean_ Brown Spot	0.84	0.89	0.86
L_43	Soybean_ Downy Mildew	0.95	0.98	0.97
L_44	Soybean_ Mosaic Virus	0.94	0.98	0.96
L_45	Soybean_ Phytotoxicity	0.93	0.97	0.78
L_46	Soybean_ Powdery Mildew	0.81	1	0.89
L_47	Soybean_ Rust	0.89	0.89	0.86
L_48	Sugarcane_ Red Stripe	0.88	0.9	0.88
L_49	Sugarcane_ Ring Spot	0.85	0.87	0.87
L_50	Sugarcane_ Rust	0.89	0.88	0.83
L_51	Wheat_ Powdery Mildew	0.84	0.89	0.86
L_52	Wheat_ Rust	0.88	0.78	0.85
	Weighted Average	0.94	0.93	0.93

This could be due to the real field surroundings, which have varied illumination conditions including partial shadows on the leaves, presence of multiple other objects like, fingers, shoes, hand, etc. along with the leaves in the image. In Dataset 3, the images are of lone lesions and spots, thus having very localized areas of the disease symptoms. Few crops like dry bean powdery mildew, grapevine powdery mildew, or crops like sugarcane rust, wheat rust, soybean rust, dry bean rust and coffee rust have relatively similar disease symptoms and can therefore affect the overall performance leading to misclassifications.

C. Comparison with State of Art Architectures

To further access the potential of the suggested model, it was compared with the other popular CNN architectures like GoogleNet, VGG16, VGG19, ResNet, etc. Fig. 3 shows the comparison of the suggested architecture with the state of art architectures.

As illustrated in Fig. 3, the proposed model gives the maximum accuracy and is succeeded by VGG19, ResNet50, VGG16 and GoogleNet. The proposed model gives a notable increase of 5% on Database1 and Database3. It can also be noted that the proposed model outperforms other models on Database2 as well, with an increased classification accuracy of 4%. The results prove that the suggested model performs better on all three datasets.

D. Effect of Model Architecture on Model Efficiency

This subsection demonstrates the impact of the model architecture on the model performance. The experimental results for database 1 are used for the analysis. Table VII shows four model structures for Convolutional and max-pooling layers (M1, M2, M3, and M4) tested for experimental comparison and the classification results for each model. The structure of the M1 model has two convolutional and max-pooling layers.

The overall accuracy and precision achieved with this model are 99.74% and 0.95, respectively. It is clear from

Table VII that as the number of layers is increased the corresponding accuracy and precision increases till we reach a level where there is no further improvement. It has to be noted that the increase in the number of layers makes the model complex and deeper thus increasing the model performance. However, it also increases the computational cost and may also lead to over-fitting. Thus, selecting the number of layers while designing CNN is very critical.

It is evident from Table VII that the maximum accuracy and precision are achieved for the M3 model that has four convolutional and four max-pooling layers, and hence this model is selected as the final model.

The number of filters used for each of the four convolutional layers is 32, 64, 128 and 192, respectively. The number of filters is less initially as they capture the low level features required for differentiating the complex objects in the image while the number increases with the layers to capture more global features.

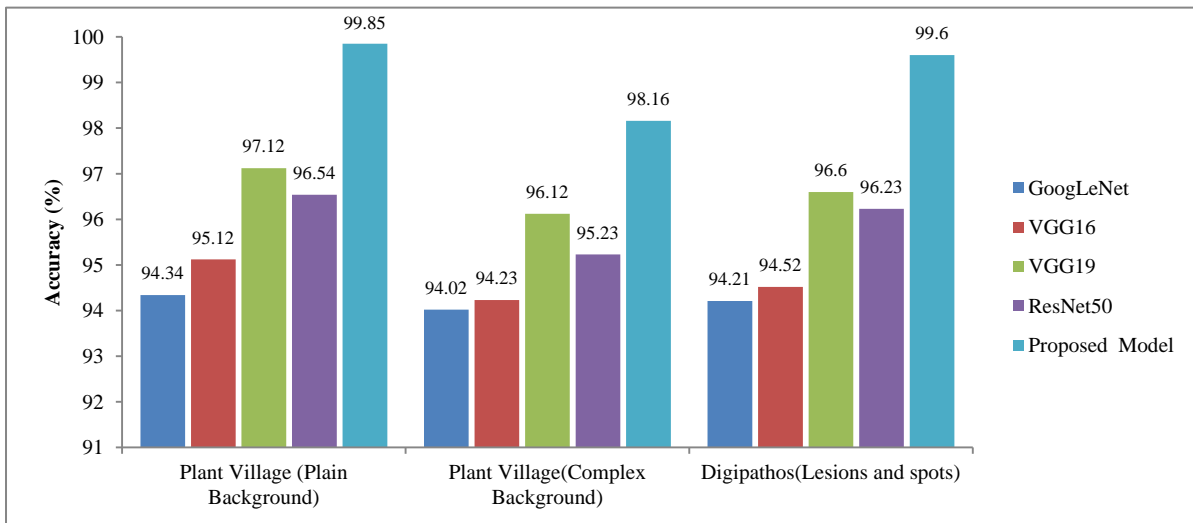


Fig. 3. Comparison of Proposed Architecture with the State of Art Models.

TABLE VII. EFFECT OF MODEL DESIGN ON MODEL PERFORMANCE

Model	Architecture										Accuracy (%)	Weighted Precision
	Conv1	Max-Pool1	Conv2	Max-Pool2	Conv3	Max-Pool3	Conv4	Max-Pool4	Conv5	Max-Pool5		
M1	✓	✓	✓	✓							99.74	0.95
M2	✓	✓	✓	✓	✓	✓					99.77	0.96
M3	✓	✓	✓	✓	✓	✓	✓	✓			99.85	0.97
M4	✓	✓	✓	✓	✓	✓	✓	✓	✓	✓	99.83	0.97

E. Effect of Hyperparameters on Model Efficiency

Hyperparameters play a key role in the model architecture due to their impact on the performance of the learned model. This subsection demonstrates the impact of hyperparameters like learning rate, dropout, and type of optimizer on the model efficiency. Results of Dataset1 are used for the evaluation.

1) *Impact of learning rate:* The learning rate regulates the speed at which the model learns by controlling the adjustments made in the weights of the network. A lower learning rate can provide more accurate results but it takes more time to converge while a large learning rate allows fast learning but the weights might not be optimal. Therefore it is essential to select a proper learning rate for the model.

The proposed model is evaluated for different learning rates as illustrated in Fig. 4. It can be noted that the learning rate of $1e-3$ shows oscillations in performance. The model performs well for the learning rate of $1e-4$ and $1e-5$ with the most stable performance at the learning rate of $1e-4$ while it gives the lowest accuracy for the learning rate of $1e-6$.

2) *Impact of Dropout:* Dropout helps in preventing overfitting of the model. It is a regularization approach and helps the network in learning more powerful distinguishing features. In the experimentation for selecting the best dropout value, the probabilities are varied from 0.2 to 0.8 as shown in Fig. 5. It can be noted that the test accuracy increases with the increase in the dropout values till it reaches the value of 0.5 and then the accuracy starts decreasing for further dropout values. The dropout value of 0.5 which gives the maximum accuracy of 99.85% is selected for the proposed architecture.

3) *Impact of Optimizer:* Optimizers improve the weight parameters to give the most accurate outcome possible by minimizing the loss function. Selecting a suitable optimizer is very important for training deep models [32]. The model performance was verified using several optimizers like SGD, Adagrad, Adadelata and Adam. Fig. 6 shows the performance of the model for these optimizers.

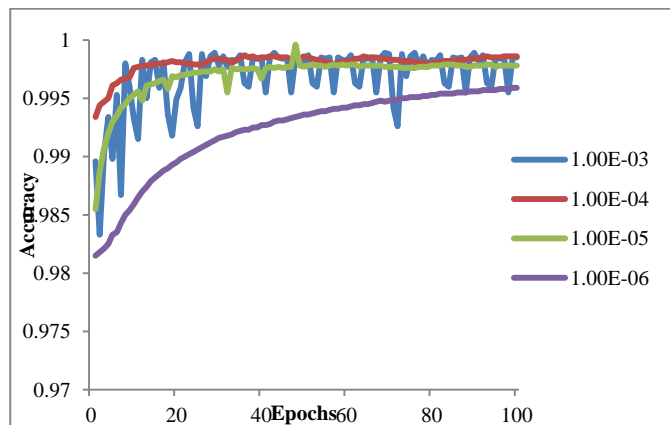


Fig. 4. Impact of Learning Rate on Model Performance.

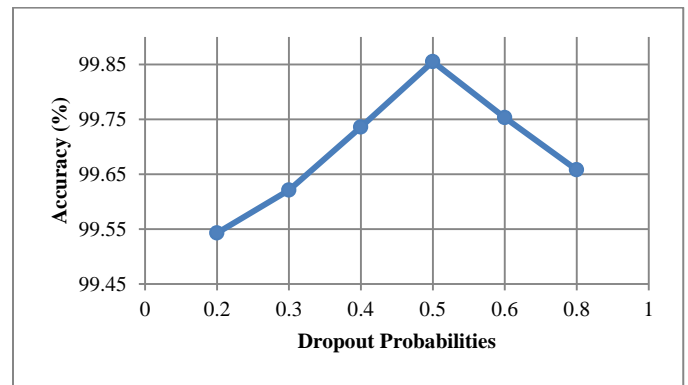


Fig. 5. Impact of Dropout Values on Model Performance.

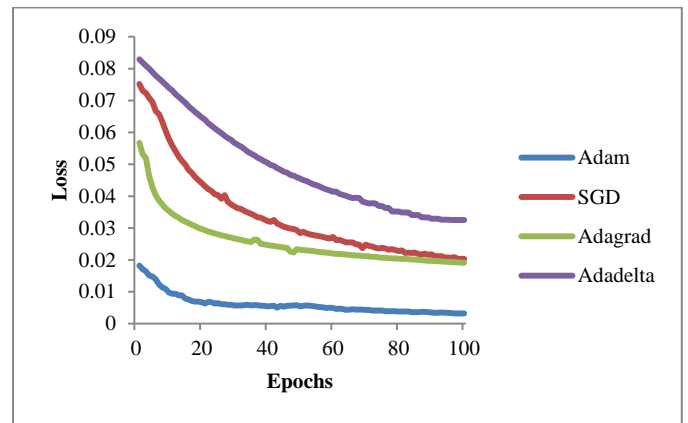


Fig. 6. Impact of Optimizer on Model Performance.

It can be seen that the loss function has a huge gap between Adam and other optimizers and that the Adam optimizer gives the minimum while the Adadelata optimizer giving the maximum loss function. In this work, Adam optimizer was used for training the model.

IV. CONCLUSION

A comprehensive multilayer convolution neural network is proposed in this paper for plant disease detection. To prove the generalization capability and efficiency of the model, three datasets were generated using Plant Village and Digipathos repository, where dataset1 consists of leaf images taken under laboratory conditions with plain background, dataset2 has real field images with complex background while dataset3 has images of lone lesions and spots. The classification accuracy for dataset1, dataset2 and dataset3 achieved is 99.85%, 97.16% and 99.6%, respectively. The model was explored to study the impact of the model architecture and hyperparameters like learning rate, dropout probability and type of optimizer on the model performance. The best hyperparameters were selected for the final optimal architecture. Furthermore, the model is also compared with the state of art techniques. The experimental result proves the superior capability of the proposed CMCNN model in handling various types of leaf images and has better classification efficiency. The obtained results suggest the beneficial use of the proposed model in a decision support system to identify diseases in several plant species for a large range of leaf images.

REFERENCES

- [1] Savary, S., Ficke, A., Aubertot, J. N., & Höllicher, C. (2012). Crop losses due to diseases and their implications for global food production losses and food security. pp.519-537.
- [2] Barbedo, J. G. A. (2013). Digital image processing techniques for detecting, quantifying and classifying plant diseases. *SpringerPlus*, 2(1), 660.
- [3] Sankaran, S., Mishra, A., Ehsani, R., & Davis, C. (2010). A review of advanced techniques for detecting plant diseases. *Computers and Electronics in Agriculture*, 72(1), 1-13.
- [4] Phadikar, S., Sil, J., & Das, A. K. Rice diseases classification using feature selection and rule generation techniques. *Comput. Electron. Agric.* .2013; 90, 76-85.
- [5] Sharif, M., Khan, M. A., Iqbal, Z., Azam, M. F., Lali, M. I. U., & Javed, M. Y. Detection and classification of citrus diseases in agriculture based on optimized weighted segmentation and feature selection. *Comput. Electron. Agric.* .2018; 150, 220-234.
- [6] Singh, V., & Misra, A. K. Detection of plant leaf diseases using image segmentation and soft computing techniques. *Information processing in Agriculture*.2017; 4(1), 41-49.
- [7] Camargo, A., & Smith, J. S. Image pattern classification for the identification of disease causing agents in plants. *Comput. Electron. Agric.* . 2009; 66(2), 121-125.
- [8] A. Camargo, J.S. Smith. "An image-processing based algorithm to automatically identify plant disease visual symptoms," *Biosystems Engineering*, vol. 102, no.1, pp.9-21, 2009.
- [9] Omrani, E., Khoshevisan, B., Shamshirband, S., Saboohi, H., Anuar, N. B., & Nasir, M. H. N. M. Potential of radial basis function-based support vector regression for apple disease detection. *Measurement*.2014; 55, 512-519.
- [10] Dargan S, Kumar M, Ayyagari MR, Kumar G. A survey of deep learning and its applications: A new paradigm to machine learning. *Arch. Comput. Methods Eng.*. 2019;1-22.
- [11] Voulodimos, A., Doulamis, N., Doulamis, A., & Protopapadakis, E. Deep learning for computer vision: A brief review. *Comput. Intell. Neurosci.*, 2018.
- [12] Kamilaris, A., & Prenafeta-Boldú, F. X. Deep learning in agriculture: A survey. *Comput. Electron. Agric.* 2018; 147, 70-90.
- [13] N. Duong-Trung, L.-D. Quach, C.-N. Nguyen, "Learning Deep Transferability for Several Agricultural Classification Problems," *International Journal of Advanced Computer Science and Applications*, 10(1), 2019, doi:10.14569/IJACSA.2019.0100107.
- [14] Lu, Y., Yi, S., Zeng, N., Liu, Y., & Zhang, Y. Identification of rice diseases using deep convolutional neural networks. *Neurocomputing*.2017; 267, 378-384.
- [15] Mohanty, S. P., Hughes, D. P., & Salathé, M. Using deep learning for image-based plant disease detection. *Front. Plant Sci.*.2016; 7, 1419.
- [16] Ferentinos, K. P. Deep learning models for plant disease detection and diagnosis. *Comput. Electron. Agric.* .2018; 145, 311-318.
- [17] Coulibaly, S., Kamsu-Foguem, B., Kamissoko, D., & Traore, D. Deep neural networks with transfer learning in millet crop images. *Comput. Ind.*.2019; 108, 115-120.
- [18] Hu, G., Wu, H., Zhang, Y., & Wan, M. A low shot learning method for tea leaf's disease identification. *Comput. Electron. Agric.* .2019; 163, 104852.
- [19] Lu, J., Hu, J., Zhao, G., Mei, F., & Zhang, C. An in-field automatic wheat disease diagnosis system. *Comput. Electron. Agric.* . 2017; 142, 369-379.
- [20] Too, E. C., Yujian, L., Njuki, S., & Yingchun, L. A comparative study of fine-tuning deep learning models for plant disease identification. *Comput. Electron. Agric.* .2019; 161, 272-279.
- [21] Sladojevic, S., Arsenovic, M., Anderla, A., Culibrk, D., & Stefanovic, D. (2016). Deep neural networks based recognition of plant diseases by leaf image classification. *Computational intelligence and neuroscience*, 2016.
- [22] Iqbal, Z., Khan, M. A., Sharif, M., Shah, J. H., ur Rehman, M. H., & Javed, K. An automated detection and classification of citrus plant diseases using image processing techniques: A review. *Comput. Electron. Agric.* .2018; 153, 12-32.
- [23] Selvaraj, M. G., Vergara, A., Ruiz, H., Safari, N., Elayabalan, S., Ocimati, W., & Blomme, G. (2019). AI-powered banana diseases and pest detection. *Plant Methods*, 15(1), 92.
- [24] Jiang, P., Chen, Y., Liu, B., He, D., & Liang, C. (2019). Real-time detection of apple leaf diseases using deep learning approach based on improved convolutional neural networks. *IEEE Access*, 7, 59069-59080
- [25] Geetharamani, G., & Pandian, A. Identification of plant leaf diseases using a nine-layer deep convolutional neural network. *Comput. Electr. Eng.*.2019; 76, 323-338.
- [26] Ngugi, L. C., Abelwahab, M., & Abo-Zahhad, M. (2020). Recent Advances in Image Processing Techniques for Automated Leaf Pest and Disease Recognition-A Review. *Information Processing in Agriculture*.
- [27] Hughes, D., & Salathé, M. An open access repository of images on plant health to enable the development of mobile disease diagnostics. *arXiv preprint arXiv:1511.08060*.2015.
- [28] Barbedo, J. G. A., Koenigkan, L. V., Halfeld-Vieira, B. A., Costa, R. V., Nechet, K. L., Godoy, C. V., ... & Oliveira, S. A. S. Annotated Plant Pathology Databases for Image-Based Detection and Recognition of Diseases. *IEEE Lat. Am. Trans.*.2018; 16(6), 1749-1757.
- [29] Barbedo, J. G. A. Plant disease identification from individual lesions and spots using deep learning. *Biosyst. Eng.*.2019; 180, 96-107.
- [30] Barbedo, J. G. A., Koenigkan, L. V., & Santos, T. T. Identifying multiple plant diseases using digital image processing. *Biosyst. Eng.*.2016; 147, 104-116.
- [31] Scherer, D., Müller, A., & Behnke, S. Evaluation of pooling operations in convolutional architectures for object recognition. *In International conference on artificial neural networks*. Springer, Berlin, Heidelberg.2010,September; pp. 92-101.
- [32] Kawatra, M., Agarwal, S., & Kapur, R. (2020, October). Leaf Disease Detection using Neural Network Hybrid Models. *In 2020 IEEE 5th International Conference on Computing Communication and Automation (ICCCA)* (pp. 225-230). IEEE.

Personalized Book Recommendation System using Machine Learning Algorithm

Dhiman Sarma^{1*}, Tanni Mittra², Mohammad Shahadat Hossain³

Department of Computer Science and Engineering, Rangamati Science and Technology University, Rangamati, Bangladesh¹

Department of Computer Science and Engineering, East West University, Dhaka, Bangladesh²

Department of Electrical and Electronic Engineering, University of Science and Technology Chittagong, Chittagong, Bangladesh³

Abstract—As the amounts of online books are exponentially increasing due to COVID-19 pandemic, finding relevant books from a vast e-book space becomes a tremendous challenge for online users. Personal recommendation systems have been emerged to conduct effective search which mine related books based on user rating and interest. Most of these existing systems are user-based ratings where content-based and collaborative-based learning methods are used. These systems' irrationality is their rating technique, which counts the users who have already been unsubscribed from the services and no longer rate books. This paper proposed an effective system for recommending books for online users that rated a book using the clustering method and then found a similarity of that book to suggest a new book. The proposed system used the K-means Cosine Distance function to measure distance and Cosine Similarity function to find Similarity between the book clusters. Sensitivity, Specificity, and F Score were calculated for ten different datasets. The average Specificity was higher than sensitivity, which means that the classifier could re-move boring books from the reader's list. Besides, a receiver operating characteristic curve was plotted to find a graphical view of the classifiers' accuracy. Most of the datasets were close to the ideal diagonal classifier line and far from the worst classifier line. The result concludes that recommendations, based on a particular book, are more accurately effective than a user-based recommendation system.

Keywords—Personalize book recommendation; recommendation system; clustering; machine learning

I. INTRODUCTION

Most organizations have their recommendation system when they sell products online. But almost all the websites are not developed of the buyer interest; the organizations' force add-on sells to buyers by recommending unnecessary and irrelevant products. A personalized recommendation system (PRS) helps individual users find exciting and useful products from a massive collection of items. With the growth of the internet, consumers have lots of options on products from e-commerce sites. Finding the right products at the right time is a real challenge for consumers. A personalized recommendation system helps users find books, news, movies, music, online courses, and research articles.

The fourth industrial revolution emerges with a technological breakthrough in the fields like the internet of things (IoT), artificial intelligence (AI), quantum computing, etc. The economic boom improves the living standard of people and elevates the purchasing power of individuals. Nowadays, physical visits to shops and libraries have been

drastically reduced due to their busy schedules and COVID-19 pandemic. Instead, e-marketplaces and e-libraries became popular hotspots. E-book reading platforms and online purchasing tendencies made users discover their favorite books from many items. As a result, users tend to get swift and smart decisions from an unprecedented amount of choices using expert systems. Thus, recommendation systems came into the scene to customize users' searching and deliver the best-optimized results from a multiplicity of options. A personalized recommendation system was initially proposed by Amazon, which contributed to raising Amazon's sales from \$9.9 billion to \$12.83 billion in 2019 (second fiscal quarter) that was 29% more than the previous year [1].

The recommendation systems' algorithms were usually developed based on content-based filtering [2], associative rules, multi-model ensemble, and collaborative filtering. Multi-model ensemble algorithms can be used for personalized recommendation systems, but content-based filtering needs a massive amount of real-world data to train the predictive model. Apriori algorithm is used to find the association rules and degree of dependencies among rules. Multiple classifiers are typical for multi-model based RS. In that case, two different layers can be enforced. In the first layer, a few basic classifiers are trained, and in the second layer, the basic classifiers are combined by using ensemble methods like XGBoost or AdaBoost. A multi-model ensemble algorithm is also used in spatial pattern detection. It can calculate the spatial anomaly correlation with each other and can cluster the anomaly correlations. The clustering technique works as a filter to detect spatial noise patterns [3]. Collaborative filtering filters items based on the similar reactions. It searches a large group of people and can detect a smaller set of users who have a similar taste for collecting items. The similarity measure is a significant component of collaborative filtering. It can find the sets of users who show the behavior to select items [4].

Four main techniques are widely used to developed recommendation systems – collaborative, content-based, hybrid, cross-domain filtering algorithms. Firstly, collaborative filtering uses users' information and opinions to recommend products. It has narrow senses and general senses. It can make automatic predictions based on user preferences by collaborating information from many users in a narrow sense. For example, collaborative filtering could make predictions about a user that television shows a user like or dislike based on partial information of that user. In a general

*Corresponding Author

sense, collaborative filtering involves collaborating large volumes of multiple view-point, agents, and sources. It can be applied in mineral exploration, weather forecasting, e-commerce, and web applications where a massive volume of data needs to be processed to make the predictions. The drawback of collaborative filtering is that it needs a tremendous amount of user data, which is realistic for some applications where we do not use information.

On the other hand, content-based filtering use objects information and recommendation are made based on object similarity. Generally, content-based filtering is useful when we do not have useful information. The Similarity among the products is considered while recommending. Both supervised and unsupervised machine learning algorithms are applied to measure the Similarity among products. The content can be structured, semi-structured, and unstructured, but it must be synchronized into a structured format to calculate the Similarity. A hybrid recommendation system combines two or more filtering techniques to produce the output. The performance of hybrid filtering is better comparing to collaborative and content-based filtering. Collaborative filtering does not consider domain dependencies, and content-based filtering does not consider people's preferences. A combined effort is required from both collaborative and content-based filtering techniques to make better predictions. The combined effort increases the common knowledge in collaborative filtering with content data and content-based filtering with user preferences. Cross-domain filtering algorithms can access information that belongs to different domains. Cross-domain filtering algorithms make predictions by exploring the source domain and increase the prediction in the target domain.

This paper proposed a clustering-based book recommendation system that uses different approaches, including collaborative, hybrid, content-based, knowledge-based, and utility-based filtering. Clustering allows regrouping all books based on the rating and user preference datasets. Such clustering shows remarkable prediction capability for a personalized book recommendation system. The core target of this research is to model an improved approach for customizing the recommendation system.

II. BACKGROUND AND RELATED WORK

Recommendation systems (RSs) or recommendation algorithms are immensely used by personal and corporate entities for searching news and information, pursuing online shopping, engaging in social dating, executing search optimization, etc. [5] [6]. Recommendation systems escalate user adhesion, elevate user experience, and accelerate the use of efficiency of the system. With the rising popularity of e-book reading tendency, and readers increasing demands for finding desired book, book recommendation system plays a significant role [7] while choosing books.

Table I shows a comparison of machine learning-based book recommendation systems with limitations, descriptions,

and used machine learning algorithms. Most of the researcher prefers collaborative filtering to the developed recommendation system. Collaborative filtering requires a vast amount of real-time user data that is not realistic for most recommendation systems. Besides, Table I shows that some researches have low accuracy, and some face overfitting due to small data size. In the paper, we proposed a cosine-distanced recommendation system that uses both user information and preferences.

Collaborative filtering is a very common technique for book recommendation [18] [19] [20]. But the accuracy of this technique was 88% [21] or 89% [22], which is comparatively low. However, a content-based recommendation system needs an enormous amount of training data set, which is not feasible for real-world scenarios [2]. When Jaccard similarity was added with collaborative filtering, it achieved the highest recall. The major drawbacks of a collaborative recommender system are sparsity and cold-start issues. These issues can be removed using a kernel-based fuzzy technique that scored a 95% accuracy rate [23].

The content-based filtering method [2] [24] was used to recommend items based on the Similarity among articles. The major drawback of this method is that it ignores current users' ratings when suggesting new items. But user rating is relevant for recommending new books or journals. As the user rating information is missing in the documents, the content-based filtering has low accuracy in the current book or journal recommendation.

Most of the systems are powered with Artificial Intelligence that search items on popularity, correlation, and content of books [25]. Other popular techniques for RSs are listed as influence discrimination model [26], linear mix model [27], transfer meeting hybrid for unstructured text [28], pseudo relevance feedback [29], fixed effect model [30], natural language processing with sentimental analysis [31], opinion leader mining [32], fuzzy c-mean clustering [33], knowledge graph convolution network, a personal rank algorithm using neural network [34], k-nearest neighbor, and frequent pattern tree [35]. Online search has an abnormal effect on the recommendation system. For example, clicking on high ranking books has no impact but clicking on low ranking books has a positive impact [30]. Data sparsity is another major problem for the traditional book recommendation system, which can be solved using a personal rank algorithm using a neural network [34]. Both k-nearest neighbor and frequent pattern tree are highly efficient for recommending scientific journals for academic journal readers [35]. Moreover, several context-aware rule-based techniques [36], and their recent pattern-based analysis [37] or classification-based techniques [38] [45] [46] or rule-based belief prediction [39] [40] [41] can be used to build the recommendation systems. In this paper, a clustering-based recommendation system was used to achieve the highest accuracy.

TABLE I. COMPARISON OF MACHINE LEARNING-BASED BOOK RECOMMENDATION SYSTEMS

Description	Methods	Limitations	Ref.
* can rank the recommended book * opinion mining technique is used to improve the accuracy of the recommendation system	*opinion mining	* Limited to computer science-related books. * Only recommend 10 books for a particular query	[8]
* combined features from three widely used filtering techniques - content-based filter, association rule, and collaborative filtering	* content-based filtering * collaborative filtering * association rule mining	* These types of filtering techniques need a vast amount of real-time data	[9]
* combined features from two widely used filtering techniques - content-based filter and collaborative filtering	* Content-Based and Collaborative Filtering	* The authors use some unnecessary attributes like name of a registered user, password of the registered user, and email	[10]
* Scraping information is useful for making recommendations. * Consider the temporal aspects while recommending books * Overcome the problems of the content-based and collaborative filtering	* Item-Item Similarity Technique * Web Scraping Process	The authors failed to explain the impact of clustering in the recommendation system Web-based recommendation system needs to be secure	[11]
* Consider scholar reviews, which is helpful library user education * The authors explain how a recommendation system can be applied to grow the interest of the reader to a particular type of books	* problem-based learning (PBL) model intelligent mobile * location-aware book recommendation system	* Only limited to library and e-library book recommendation. * Not suitable for e-commerce-based book recommendation system	[12]
* Positional aggregation based scoring efficiently finds top-ranked books for a university student.	* aggregation based scoring; * fuzzy quantifiers, * Ordered Weighted Averaging	* Limited to university books recommendation system	[13]
* matrix sparsity problem in filtering is solved by the author * Can recommend books to newly admitted university's student with high accuracy	* collaborative filtering algorithm	* Cluster of books did not consider in recommendation; The authors did not consider borrowing the time and length of books	[14]
Use a user-based similarity matrix to increase the accuracy of the collaborative filtering algorithm	* User-Based collaborative filtering	* Cluster can improve the accuracy and performance of the recommendation system	[15]
support-vector machines are used to find the relationships between titles of the books or bibliographic of the authors	support-vector machines	* Dataset contains only 4612 books, which may lead to overfitting problems	[16]
users' behavior-based collaborative filtering recommends a series of books	users' behavior-based collaborative filtering	Low accuracy of the classifier, which is 59%	[17]

III. METHODOLOGY

The proposed system in Fig. 1 used a clustering technique to develop the recommender system. Fig. 1 shows three parts named data acquisition, preprocessing, and clustering techniques. The datasets were collected from the Goodreads-books repository of kaggle in this research. Though Goodreads-books repository of kaggle contains seven datasets, only four datasets (Books.csv, Book_tags.csv, Ratings.csv, and Max_Rating.csv) were considered for this experiment. The preprocessing technique was applied after merging all datasets where we removed the lower-rated books and developed a new dataset for analysis. Finally, the clustering technique was applied for recommending books to those users who stay in proximity to a specific cluster. Besides, a user can then search for a book through a query interface, and results in listing recommended books (Fig. 6).

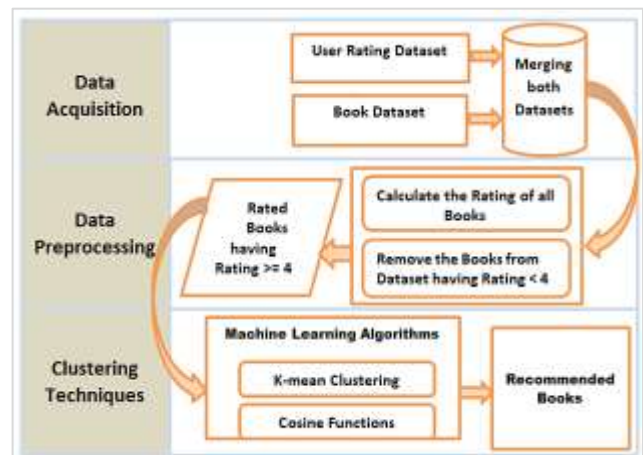


Fig. 1. Proposed Architecture for Book Recommendation.

A. Data Acquisition

The dataset was collected from the GoodReads book dataset repository. It has 10,000 rated data of popular books. This data set consists of 7 tables named Books.csv, Geners.csv, Book_tags.csv, Max_rating.csv, Ratings.csv, to_read.csv, and Tags.csv, where we used Books.csv and Book_tags.csv as book dataset and Ratings.csv and Max_Rating.csv as user rating dataset. The description of the datasets are as follows:

- Books.csv- it has attributes like an author, book_isbn number, rating and contains 10K books.
- Book_tags.csv- it has 596K rows and attributes are goodreader_book_id and tag_id.
- Ratings.csv- it has attributes like user_id,book_id, and rating and contains about 9,00,000 rows.
- Max_Rating.csv- it has similar attributes as Rating.csv. But the number of rows is about 500K.

B. Data Preprocessing

Unstructured noisy text in the data is needed to be preprocessed to make them analyzable. To do the analysis, the dataset needs to be cleaned, standardized, and noise-free. Fig. 2 shows that most of the books were rated 4 or above. We want to recommend only top-rated books. So we remove all the rows having a rating less than 4. It shows us that 68.89% of books were rated 4 and above. Thus our cleaned dataset becomes compact, standardized, and noise-free.

C. Clustering Techniques

K-mean algorithm is used as a cluster partition algorithm where each partition is considered as a k cluster. It is an agile algorithm applied in cluster assessment, feature discovery, and vector quantization. In this experiment, the k-mean algorithm begins with selecting the numbers of k cluster of books. Each book is assigned to the nearest cluster center and moved from the cluster center to cluster average and repeated until the algorithm reaches to convergence state.

Fig. 3 shows the cosine similarity function which calculates the cosine of the angle between two non-zero vectors (vectors A and B). When these vectors align in the same direction then they produce a similarity measurement of 1. If these vectors align perpendicularly then the similarity is 0, whereas two vectors align in the opposite direction will produce a similarity measurement of -1.

Suppose we put a type 'romantic' on the X-axis and 'adventure' on the Y-axis. Then, book B₁ (Sense and Sensibility) in the romantic type creates an angular difference of 90° to the book A₁ (Treasure Island) in the advancer type. Thus,

Cosine similarity between A₁ and B₁ is:
 $\cos 90^\circ = 0$ (1)

Cosine distance between A₁ and B₁ is:
 $1 - \cos 90^\circ = 1 - 0 = 1$ (2)

The angular difference between item A₁ (Treasure Island) and A₂ (Harry Potter) is 0°. Thus,

Cosine similarity between A₁ and A₂ is:
 $\cos 0^\circ = 1$ (3)
 Cosine distance between A₁ and A₂ is:
 $1 - \cos 0^\circ = 1 - 1 = 0$ (4)

where, cosine distance 0 represents that two objects are similar and adjacent, and cosine distance 1 suggests that the objects remain faraway.

The Cosine of two non-zero vectors can be derived by using the Euclidean dot product formula:

$$A \cdot B = \|A\| \|B\| \cos \theta$$
 (5)

Given two vectors of attributes, A and B, the cosine similarity, $\cos(\theta)$, is represented using a dot product and magnitude as

$$\text{Similarity} = \cos \theta = \frac{A \cdot B}{\|A\| \|B\|} = \frac{\sum_{i=1}^n A_i B_i}{\sqrt{\sum_{i=1}^n A_i^2} \sqrt{\sum_{i=1}^n B_i^2}}$$
 (6)

where A_i and B_i are components of vectors A and B respectively [33] [47].

The resulting similarity ranges from -1 meaning exactly opposite, to 1 meaning the same, with 0 indicating orthogonality or decorrelation, while in-between values indicate intermediate Similarity or dissimilarity.



Fig. 2. The Pie Chart of Rating Dataset.

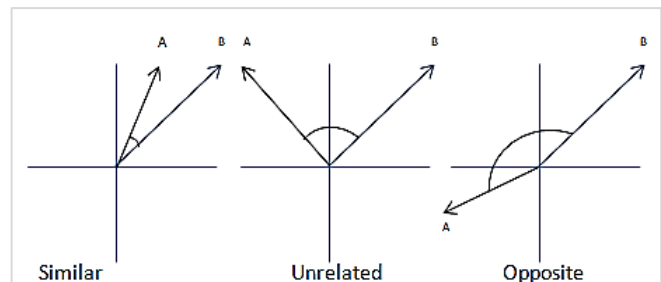


Fig. 3. Cosine Similarity and Cosine Distance Functions.

IV. RESULTS AND DISCUSSIONS

Assessment of predictive accuracy for the book recommendation system is a crucial aspect of evaluation. Receiver operation characteristic (ROC) is widely used for evaluating the accuracy of the classifiers [42][43]. Forecasting is an essential part of every financial department, atmospheric science, and machine learning algorithms. ROC curve gives a visual technique to summarize the accuracy of the classifiers. It is widely used in statistical education and training.

A. Binary Predictor

For the predictions, one of the standard techniques used is binary prediction. It contains beneficial building blocks of a ROC curve. Every classification problem has two classes. Each instance (*I*) belongs to two sets, (*P*) and (*N*), of positive and negative labels of class. A classifier instance has four possible types. If the positive instance is being classified correctly, it is considered as True Positive (TP).

On the other hand, it is regarded as a false negative (FN) if it is classified incorrectly. If the negative instance is classified correctly, it is regarded as true negative (TN). Otherwise, it is considered to be false positive (FP) if it is classified incorrectly. Table II shows performance evaluation results for our proposed system before splitting the training dataset. The test contains 1000 tuples where negative and positive tuples are 610 and 390, respectively. The proposed RS correctly identifies 760 tuples and wrongly classifies 240 tuples. The confusion matrix [44] is widely used to measure the performance of classifiers. Table I depicts the confusion matrix for this research.

We found an FR rate (FPR), FN rate (FNR), TN rate (TNR) or specificity, precision (P), recall (R), and F1 Score by using the following equations:

$$FPR = FP / (TN + FP) \quad (7)$$

$$FNR = FN / (TP + FN) \quad (8)$$

$$\text{Precision (P)} = TP / (TP + FP) \quad (9)$$

$$\text{Specificity or TNR} = TN / (TN + FP) \quad (10)$$

$$\text{Sensitivity or Recall (R)} = TP / (TP + FN) \quad (11)$$

$$F1 \text{ Score} = 2 * (R * P) / (R + P) \quad (12)$$

We extend this definition to include sensitivity =1-FNR and specificity =1-FPR. Sensitivity is known as the true positive rate, and specificity is termed as the true negative rate.

Table III shows Sensitivity, Specificity, F1 Score for the classifier. Sensitivity calculates the proportion of desired books for a user. Specificity calculates the proportion of boring books for an individual user. F1 Score calculates the harmonic mean of the desired and boring books that are correctly identified. The maximum values of the F1 Score can be 1. Table III shows that the highest sensitivity, Specificity,

and F1 Score are 73.14%, 74.28%, and 74.18%. The sensitivity in dataset-1 is higher than other datasets, which means that the prediction probability was high for an exciting book list. Specificity is 65% for dataset -6, which can detect boring books for a reader. F-score is more useful than accuracy. It finds harmonious relation between sensitivity and specificity.

B. ROC Curve

A receiver operating characteristic curve illustrates the trade-off between the five different datasets' sensitivity and specificity in Table III. It can be inferred from Fig. 4; all of our datasets have stayed close to the ideal diagonal line.

Table IV shows Sensitivity, Specificity, F1 Score for the classifier. The sensitivity in dataset-1 is higher than other datasets, which means that the prediction probability was high for an exciting book list. Specificity is 65% for dataset -6, which can detect boring books for a reader. F-score is more useful than accuracy. It finds harmonious relation between sensitivity and specificity.

C. ROC Curve

Fig. 5 presents a ROC curve that was plotted for sensitivity and specificity. Most of the datasets were closed to the diagonal ideal classifier line. None of the datasets crossed the worst classifier line.

D. User Interface

Fig. 6 shows the user interface for the proposed system. The input searching item was 'Sense and Sensibility,' a popular romantic and narrative book. As a result, the system showed all the similar books categorized into the romantic and narrative class.

TABLE II. CONFUSION MATRIX

Hypothesized Class	True Class		
	Positive(P)	Negative (N)	Total
True (T)	490	120	610
False (F)	120	270	390
Total	610	390	1000

TABLE III. SENSITIVITY, SPECIFICITY, AND F1 SCORE FOR 5 DIFFERENT DATASETS

Datasets	Sensitivity (%)	Specificity (%)	F1 Score (%)
1	68.25	67.15	70.57
2	70.25	71.15	73.55
3	48	58	52.52
4	73.14	74.28	74.18
5	55	60	57.39
Average	62.928	66.116	65.642

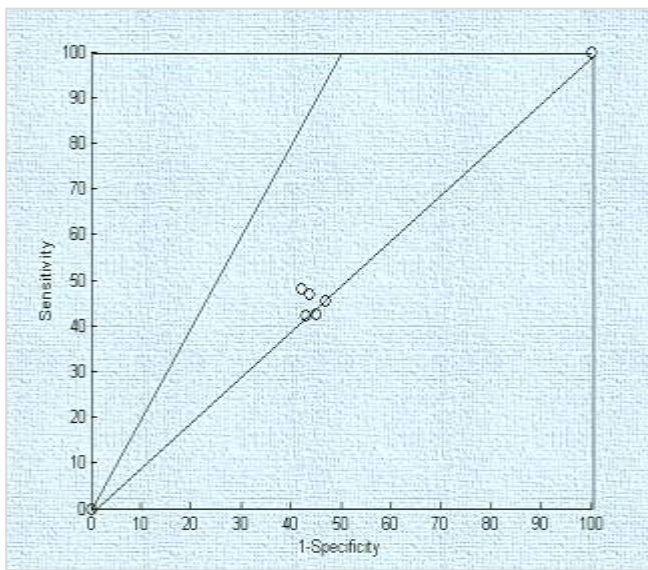


Fig. 4. ROC Curve for Five different Datasets.

TABLE IV. SENSITIVITY, SPECIFICITY, AND F1 SCORE FOR DIFFERENT DATASETS

Datasets	Sensitivity (%)	Specificity (%)	F1 Score (%)
Dataset 1	66	65.15	65.57225
Dataset 2	47	56.25	51.21065
Dataset 3	48	58	52.5283
Dataset 4	45.47	53	48.94709
Dataset 5	55	60	57.3913
Dataset 6	53.5	65	58.69198
Dataset 7	55.5	50	52.60664
Dataset 8	42.17	57	48.47615
Dataset 9	42.47	54.98	47.92202
Dataset 10	42.5	48	45.08287
Average	49.761	56.738	52.84293

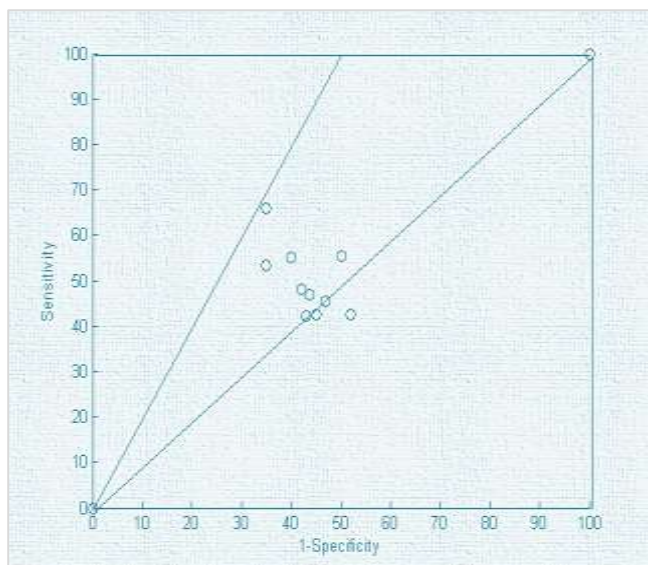


Fig. 5. ROC Curve for Sensitivity vs 1-Specificity (Different Datasets).

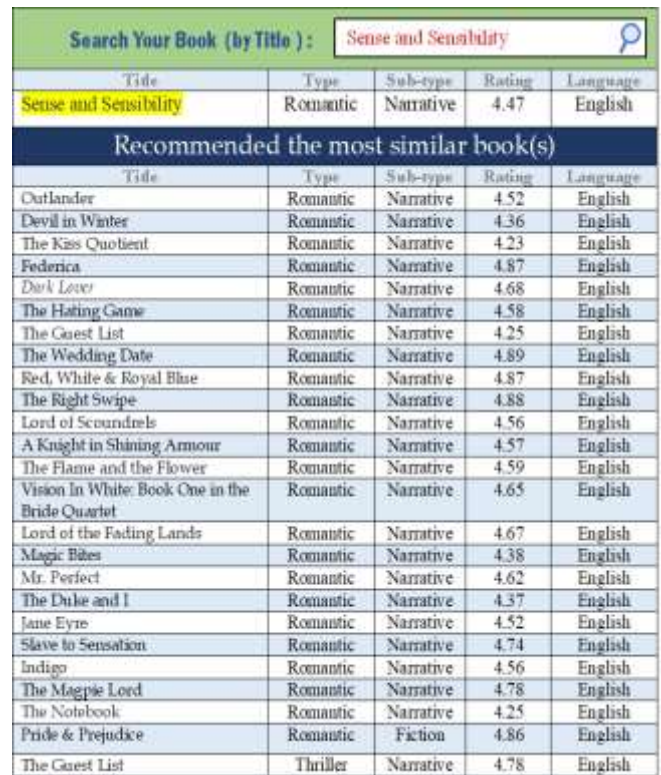


Fig. 6. User Interface for Book Recommendation System.

V. CONCLUSION

This research used clustering algorithms to increase the prediction capacity of the recommendation system. The datasets were collected from the Goodreads-books repository of Kaggle. About 900k ratings of 10k books were processed by using machine learning algorithms (k-means clustering and cosine function). Sensitivity, Specificity, and F1 Score were measured for the algorithms for the proposed model. The average sensitivity and average specificity were 49.76% and 56.74% respectively whereas the F1 Score was 52.84%. These results show that our proposed system can remove boring books from the recommendation list more efficiently. Finally, the ROC curve was plotted for sensitivity and specificity which shows that most of the datasets stay close to the diagonal ideal classifier line.

In our future work, we shall propose a suggestion system for recommending online courses using the convolutional neural network (CNN).

REFERENCES

- [1] N. Grover, "Enabling shift in retail using data: Case of Amazon," 2019.
- [2] Y. Lee, C. Wei, P. Hu, T. Cheng, and C. Lan, "Small Clues Tell: a Collaborative Expansion Approach for Effective Content-Based Recommendations," Journal of Organizational Computing and Electronic Commerce, pp. 1-18, 2020.
- [3] T. Zhao, W. Zhang, Y. Zhang, Z. Liu, and X. Chen, "Significant spatial patterns from the GCM seasonal forecasts of global precipitation," Hydrology and Earth System Sciences, vol. 24, no. 1, pp. 1-16, 2020.
- [4] A. Gazdar and L. Hidri, "A new similarity measure for collaborative filtering based recommender systems," Knowledge-Based Systems, vol. 188, p. 105058, 2020.
- [5] C. Zou, D. Zhang, J. Wan, M. M. Hassan and J. Lloret, "Using Concept Lattice for Personalized Recommendation System Design," in IEEE

- Systems Journal, vol. 11, no. 1, pp. 305-314, March 2017, doi: 10.1109/JSYST.2015.2457244.
- [6] K. Lu, "Research on Intelligent Detection System for Information Abnormal Defect Based on Personalized Recommendation of E-Book," in The International Conference on Cyber Security Intelligence and Analytics, 2019: Springer, pp. 1110-1117.
- [7] T. Y. Tang, P. Winoto and R. Z. Ye, "Analysis of a multi-domain recommender system," The 3rd International Conference on Data Mining and Intelligent Information Technology Applications, Macao, 2011, pp. 280-285.
- [8] S. S. Sohail, J. Siddiqui and R. Ali, "Book recommendation system using opinion mining technique," 2013 International Conference on Advances in Computing, Communications and Informatics (ICACCI), Mysore, 2013, pp. 1609-1614, doi: 10.1109/ICACCI.2013.6637421.
- [9] A. S. Tewari, A. Kumar and A. G. Barman, "Book recommendation system based on combine features of content based filtering, collaborative filtering and association rule mining," 2014 IEEE International Advance Computing Conference (IACC), Gurgaon, 2014, pp. 500-503, doi: 10.1109/IADCC.2014.6779375.
- [10] P. Mathew, B. Kuriakose and V. Hegde, "Book Recommendation System through content based and collaborative filtering method," 2016 International Conference on Data Mining and Advanced Computing (SAPIENCE), Ernakulam, 2016, pp. 47-52, doi: 10.1109/SAPIENCE.2016.7684166.
- [11] S. Kanetkar, A. Nayak, S. Swamy and G. Bhatia, "Web-based personalized hybrid book recommendation system," 2014 International Conference on Advances in Engineering & Technology Research (ICAETR - 2014), Unnao, 2014, pp. 1-5, doi: 10.1109/ICAETR.2014.7012952.
- [12] Chih-Ming Chen "An intelligent mobile location-aware book recommendation system that enhances problem-based learning in libraries, Interactive Learning Environments", Journal Interactive Learning Environments, 2013, pp 469-495, DOI: 10.1080/10494820.2011.593525.
- [13] S. S. Sohail, J. Siddiqui, R. Ali, "OWA based Book Recommendation Technique", Procedia Computer Science, 2015, pp. 126-133, doi: 10.1016/j.procs.2015.08.425.
- [14] J. Qi, S. Liu, Y. Song and X. Liu, "Research on Personalized Book Recommendation Model for New Readers," 2018 3rd International Conference on Information Systems Engineering (ICISE), Shanghai, China, 2018, pp. 78-81, doi: 10.1109/ICISE.2018.00022.
- [15] M. Kommineni, P. Alekhya, T. M. Vyshnavi, V. Aparna, K. Swetha and V. Mounika, "Machine Learning based Efficient Recommendation System for Book Selection using User based Collaborative Filtering Algorithm," 2020 Fourth International Conference on Inventive Systems and Control (ICISC), Coimbatore, India, 2020, pp. 66-71, doi: 10.1109/ICISC47916.2020.9171222.
- [16] K. Puritat and K. Intawong, "Development of an Open Source Automated Library System with Book Recommendation System for Small Libraries," 2020 Joint International Conference on Digital Arts, Media and Technology with ECTI Northern Section Conference on Electrical, Electronics, Computer and Telecommunications Engineering (ECTI DAMT & NCON), Pattaya, Thailand, 2020, pp. 128-132, doi: 10.1109/ECTIDAMTCON48261.2020.9090753.
- [17] R. Rahutomo, A. S. Perbangsa, H. Soeparno and B. Pardamean, "Embedding Model Design for Producing Book Recommendation," 2019 International Conference on Information Management and Technology (ICIMTech), Jakarta/Bali, Indonesia, 2019, pp. 537-541, doi: 10.1109/ICIMTech.2019.8843769.
- [18] C. Sipio, D. Ruscio, and P. Nguyen, "Democratizing the Development of Recommender Systems by means of Low-code Platforms."
- [19] Y. Pan, D. Wu, C. Luo, and A. Dolgui, "User activity measurement in rating-based online-to-offline (O2O) service recommendation," Information Sciences, vol. 479, pp. 180-196, 2019.
- [20] S. B. Shirude and S. R. Kolhe, "Improved Hybrid Approach of Filtering Using Classified Library Resources in Recommender System," in Intelligent Computing Paradigm: Recent Trends: Springer, 2020, pp. 1-10.
- [21] J. Das, S. Majumder, P. Gupta, and K. Mali, "Collaborative Recommendations using Hierarchical Clustering based on Kd Trees and Quadrees," International Journal of Uncertainty, Fuzziness and Knowledge-Based Systems, vol. 27, no. 04, pp. 637-668, 2019.
- [22] S. Parvatikar and B. Joshi, "Online book recommendation system by using collaborative filtering and association mining," 2015 IEEE International Conference on Computational Intelligence and Computing Research (ICCCIC), Madurai, 2015, pp. 1-4, doi: 10.1109/ICCCIC.2015.7435717.
- [23] S. Kanetkar, A. Nayak, S. Swamy, and G. Bhatia, "Web-based personalized hybrid book recommendation system," in 2014 International Conference on Advances in Engineering & Technology Research (ICAETR-2014), 2014: IEEE, pp. 1-5.
- [24] A. Gholami, Y. Forghani, and M. Branch, "Improving Multi-class Co-Clustering-Based Collaborative Recommendation Using Item Tags Improving Multi-class Co-Clustering-Based Collaborative Recommendation Using Item Tags."
- [25] E. Cho and M. Han, "AI Powered Book Recommendation System," in Proceedings of the 2019 ACM Southeast Conference, 2019, pp. 230-232.
- [26] F. Eskandarian, N. Sonboli, and B. Mobasher, "Power of the Few: Analyzing the Impact of Influential Users in Collaborative Recommender Systems," in Proceedings of the 27th ACM Conference on User Modeling, Adaptation and Personalization, 2019, pp. 225-233.
- [27] Y. Gao, C. Huang, M. Hu, J. Feng, and X. Yang, "Research on Book Personalized Recommendation Method Based on Collaborative Filtering Algorithm," in IOP Conference Series: Earth and Environmental Science, 2019, vol. 252, no. 5: IOP Publishing, p. 052099.
- [28] G. Hu, Y. Zhang, and Q. Yang, "Transfer meets hybrid: a synthetic approach for cross-domain collaborative filtering with text," in The World Wide Web Conference, 2019, pp. 2822-2829.
- [29] R. Kumar, G. Bhanodai, and R. Pamula, "Book search using social information, user profiles and query expansion with Pseudo Relevance Feedback," Applied Intelligence, vol. 49, no. 6, pp. 2178-2200, 2019.
- [30] Q. Liu, X. Zhang, L. Zhang, and Y. Zhao, "The interaction effects of information cascades, word of mouth and recommendation systems on online reading behavior: An empirical investigation," Electronic Commerce Research, vol. 19, no. 3, pp. 521-547, 2019.
- [31] C. Musto, P. Lops, M. de Gemmis, and G. Semeraro, "Justifying recommendations through aspect-based sentiment analysis of users reviews," in Proceedings of the 27th ACM Conference on User Modeling, Adaptation and Personalization, 2019, pp. 4-12.
- [32] H. Pasricha and S. Solanki, "A New Approach for Book Recommendation Using Opinion Leader Mining," in Emerging Research in Electronics, Computer Science and Technology: Springer, 2019, pp. 501-515.
- [33] S. Vimala and K. Vivekanandan, "A Kullback-Leibler divergence-based fuzzy C-means clustering for enhancing the potential of an movie recommendation system," SN Applied Sciences, vol. 1, no. 7, p. 698, 2019.
- [34] G. Wen and C. Li, "Research on Hybrid Recommendation Model Based on PersonRank Algorithm and TensorFlow Platform," in Journal of Physics: Conference Series, 2019, vol. 1187, no. 4: IOP Publishing, p. 042086.
- [35] B. Ye, Y. Tu, and T. Liang, "A hybrid system for personalized content recommendation," Journal of Electronic Commerce Research, vol. 20, no. 2, pp. 91-104, 2019.
- [36] Iqbal H. Sarker, "Context-aware rule learning from smartphone data: survey, challenges and future directions," vol. 6, no. 1, p. 95, 2019.
- [37] I. H. Sarker, A. Colman, and J. J. J. o. B. D. Han, "Recencyminer: mining recency-based personalized behavior from contextual smartphone data," vol. 6, no. 1, p. 49, 2019.
- [38] S. Hossain, D. Sarma, and R. J. J. M. L. Chakma, "Machine Learning-Based Phishing Attack Detection," International Journal of Advanced Computer Science and Applications(IJACSA), vol. 11, no. 9, 2020.
- [39] S. Hossain, D. Sarma, F. Tuj-Johora, J. Bushra, S. Sen and M. Taher, "A Belief Rule Based Expert System to Predict Student Performance under Uncertainty," 2019 22nd International Conference on Computer and

- Information Technology (ICCIT), Dhaka, Bangladesh, 2019, pp. 1-6, doi: 10.1109/ICCIT48885.2019.9038564.
- [40] F. Ahmed, et al., "A Combined Belief Rule based Expert System to Predict Coronary Artery Disease," in 2020 International Conference on Inventive Computation Technologies (ICICT), 2020, pp. 252-257.
- [41] S. Hossain, D. Sarma, R. J. Chakma, W. Alam, M. M. Hoque, and I. H. Sarker, "A Rule-Based Expert System to Assess Coronary Artery Disease Under Uncertainty," in Computing Science, Communication and Security, Singapore, 2020, pp. 143-159: Springer Singapore.
- [42] Y. Nieto, V. Gacía-Díaz, C. Montenegro, C. C. González, and R. G. Crespo, "Usage of machine learning for strategic decision making at higher educational institutions," IEEE Access, vol. 7, pp. 75007-75017, 2019.
- [43] J. Chen, X. Luo, Y. Liu, J. Wang and Y. Ma, "Selective Learning Confusion Class for Text-Based CAPTCHA Recognition," in IEEE Access, vol. 7, pp. 22246-22259, 2019, doi: 10.1109/ACCESS.2019.2899044.
- [44] C. Chang, "Statistical Detection Theory Approach to Hyperspectral Image Classification," in IEEE Transactions on Geoscience and Remote Sensing, vol. 57, no. 4, pp. 2057-2074, April 2019, doi: 10.1109/TGRS.2018.2870980.
- [45] M. N. Alam, D. Sarma, F. F. Lima, I. Saha, R. -E. -. Ulfath and S. Hossain, "Phishing Attacks Detection using Machine Learning Approach," 2020 Third International Conference on Smart Systems and Inventive Technology (ICSSIT), Tirunelveli, India, 2020, pp. 1173-1179, doi: 10.1109/ICSSIT48917.2020.9214225.
- [46] I. Saha, D. Sarma, R. J. Chakma, M. N. Alam, A. Sultana and S. Hossain, "Phishing Attacks Detection using Deep Learning Approach," 2020 Third International Conference on Smart Systems and Inventive Technology (ICSSIT), Tirunelveli, India, 2020, pp. 1180-1185, doi: 10.1109/ICSSIT48917.2020.9214132.
- [47] W. Usino et al., "Document similarity detection using k-means and cosine distance," International Journal of Advanced Computer Science and Applications(IJACSA), vol. 10, no. 2, pp. 165-170, 2019.

Learning Management System based on Machine Learning: The Case Study of Ha'il University - KSA

Mohamed Hédi Maâloul¹, Younès Bahou²

Computer Science Department, Community College – University of Ha'il
Ha'il – Kingdom of Saudi Arabia

Abstract—Online learning environments have become an established presence in higher education in the Kingdom of Saudi Arabia, especially with the expected of Covid-19 pandemic. At present, supporting e-learning with interactive virtual campuses is a future aim in education. In order to solve the problems of the interactivity and the adaptability of e-online learning systems in Saudi universities, this paper proposes a module, based on digital learning, and to be used in learning management systems to meet the challenges a future goal in e-online learning. The e-learning system should be intelligent and has the possibility to inspire the specific characteristics (i.e., metadata) of a student used to access to their social media profiles.

Keywords—Learning management systems; blackboard; machine learning; semi-supervised learning; personalization system; SPS System; user profile; social profile

I. INTRODUCTION

In this exceptional pandemic situation related to Covid-19, educational activity was affected to different degrees during containment (closures, activity limitations, reorganizations, etc.). The progressive resumption of activity towards a stabilized situation raises many questions and requires a preparation facilitating its conditions of success.

Therefore, total e-learning has become an obligation for higher education worldwide and particularly in the Kingdom of Saudi Arabia. The Blackboard is the system used at the University of Ha'il to achieve the e-learning aims.

Many types of learning platforms (e.g., Blackboard, Formare, Moodle, Teleformar, WebCT, etc.) have been considered as an opportunity for Saudi universities to provide online courses, tests and evaluations, databases and for online monitor students' progress [1,2].

However, these courses are stored as files on the Learning Management Systems (LMS) server as a single course. These courses do not take into consideration the user's profile (i.e., student's profile) and prerequisites.

This work falls within the framework of improving the performance of learning platforms and the Blackboard platform, and more precisely at the level of the student profile definition module.

Thus, our goal is to experiment with a numerical approach, not currently implemented in the Blackboard platform.

This paper is structured around four sections. This paper is structured around four panels.

The first section presents literature on LMS and the effectiveness of these learning systems, particularly with the expected Covid-19 pandemic.

The second part presents the proposed method for defining a student profile based on the information contained in his social network. The student profile is useful for any learning system that aims to adapt and propose appropriate content that corresponds to a student's specific needs.

The third part presents the Social Profiling of the Student (SPS) system and the process of generating a student's (i.e., social profile).

Finally, the last part focuses on the implementation and evaluation of the proposed method.

II. LITERATURE

Smartphones, tablets, and computers are essential tools in the educational process especially after the spread of Covid-19 all around the world. In the Middle East, and more specifically the University of Ha'il in the Kingdom of Saudi Arabia, the use of IT tools is increasing constantly among students at universities.

Hence, platforms, websites and e-learning Systems are essential and the best way to save the learning process during Covid-19. According to A. N. Alkhalidi, and A. M. Abualkishik, the previous studies mentioned that the Blackboard is a recent technological tool that contributes to sharing knowledge, making quizzes, taking attendance and evaluating students [6].

The earlier study showed that Blackboard “was founded in 1997 by two education advisors, Matthew Pittinsky and Michael Chasen, as a consulting firm to provide technical standards for online learning applications” [17]. They added that the Blackboard witnessed a huge rise until it reached \$752 million in basic stock and become public in June 2004.

In [4] before 2500 years, memorization was the essential method of teaching and the favourable way to preserve knowledge and skills, but the communication was usually oral.

After that, technology has been used in teaching and learning for many years. The results of using technology in teaching represent that there is a positive influence on the education process.

Universities and educational institutions try to improve their own LMSs in order to provide their smart learning online aspects for different groups of learners. The recent studies

define LMSs as the web-based system that provides many benefits for the educational processes [14].

LMS can be used as an effective tool for students belonging to the same University and studying in different campuses [9]. LMS is used to assemble students from a different place and different time zone to join the same lecture, to solve the same problem, to do the same quiz or to sit for the same exam.

According to L. A. Bove and S. Conklin (2020), LMS can simplify and speed the discussions, document sharing, and assignment submission between teachers and their students [13]. Moreover, it helps teachers to better evaluate their students.

Consequently, LMS is helpful and useful for students who witnessed difficulties to move from their home town or home countries to join the lectures at universities. Additionally, LMS is gainful for special needs students.

The cultural aspects of LMS design are of huge importance because it can fit the user's satisfaction which can provide success stories in education for both students and teachers. In addition, learning materials on LMS can respect gender differences. Next, LMS can afford guidelines for students and build a learner-centred educational climate [9].

Today, mobile applications make the use of LMS easier and painless. Students can access their LMS accounts despite the places they are in such as trains, buses, homes, etc.

Mobile Apps are considered as a recent infrastructure that contributes to the spread of LMS. A. W. Bates (2015) in [8] argued that the social media is a significant technology which supports the teaching method since it facilitates the dialogues and strengthens the students' contribution during the lectures.

The Blackboard advances since its foundation until now. The benefits of the Blackboard Learning System are the increased availability, the quick feedback, the improved communication, the tracking, and the skills building [12].

The Digital Report (2020) in Saudi Arabia (<https://datareportal.com/reports/digital-2020-saudi-arabia>) mentioned that the number of social media users rise by (8.7%) between April 2019 and January 2020 (about 2 million users). The report shows that the most used social media platforms are YouTube (76%), WhatsApp (71%), Instagram (65%), Facebook (62%), and Twitter (58%).

However, the statistics show that the preferable social network for students in the University of Ha'il is WhatsApp [7]. Therefore, we build our study on the consideration of the WhatsApp as the first source of data for the User Profile.

Despite the huge number of the users of social media platforms, students cannot access to the Blackboard through their social networking information. Nevertheless, the use of the data from the social network let students better manage their Blackboard accounts.

The previous studies tried to count different drawbacks of the Blackboard. They stated that the Blackboard is hard to learn, its options may be restricted to particular operating

systems, its system inefficiencies, and the cost of the Blackboard is really high [17].

In the past, one of the key limitations of an LMS is the dilemma of how to use new technology in the learning process [5].

There are two challenges in online learning the first is to provide the students with new technological knowledge, the second is to attract their attention to follow the main lecture. The serious obstacle that faces the teacher is that students are not motivated to become expert users of LMS [16].

As a result, in the current study, we try to make the LMS easier for the students at the University of Ha'il through the integration of students' data from social networks.

In defiance of the advances it witnessed, the LMS Blackboard still faces a serious drawback that the previous studies did not deal with it: the user profile, this aspect is the one we will work in in the study in hands.

A. e-Online Learning Challenges

The LMS Blackboard is a standard system; it witnessed some development, but they are not in-depth. Despite the validation of advancement on the Blackboard, the LMS is still incapable to manage the student's metadata from other platforms; it cannot capture student parameters from WhatsApp, Twitter, Facebook, etc.

The present study works on the development of the integration of the student's email used in social networks to access to the Blackboard, instead of using their University Id number (e.g., s20200123). Hence, the student can relate his Blackboard account with their social media profiles.

It is hard for a student to use his preferences; they can forget their Id Number or type it in a wrong way because they use it only to access to the Blackboard or during the exam days. Hence, it is difficult for students to use preferences to access to the Blackboard LMS system, so we are working in the current study to facilitate their access into the LMS by using things which is easy to remember their social media parameters since they use it daily and this step aims to improve the effectiveness of the educational process.

The LMS Blackboard cannot configure student's settings which are fixed by the University technical Unit. Even when the student's name is written in the wrong way, he/she cannot correct it or make any changes. As a result, the University technical unit is supreme power when dealing with the Blackboard, whereas the educational process should be based on the student.

B. Concept of user Profile

The notion of the user profile is widely addressed in user modelling, which can be considered as the process of knowledge extraction in order to identify the information and characteristics of the user or a group of users [3].

The use of the user model in this work improves the quality of human-machine interactions: the deduction of user preferences and contexts from the activities observed in the

social media is used to determine the type of dialogue that the LMS system will have with the user.

Indeed, the user profile is used to adapt and propose appropriate content that corresponds to the user's specific needs [18].

Our work deals with the definition of the student profile which aims to allow the LMS system to adapt to the user. The following section explains this aspect, in the context of information customization systems.

Our study is used to determine, in a first place, the personal data of students that are relatively stable over time, such as their identity (e.g., e-mail, phone number), demographic data (e.g., age, gender, address) and that do not require automatic updates.

Secondly, we consider that preferences and interests tend to change over time and that designate the characteristics of the user such as preferred types of presentation, etc.

In this context, our contribution is to propose a recommendation system that is fundamentally based on a digital learning-based technique (i.e., semi-supervised learning) and that determines the degree of similarity between students, in order to recommend the items corresponding to a student's interest.

The choice of the machine learning technique based on semi-supervised learning is justified by the fact that it allows involving a system with only a small number of labelled items students and a large number of not labelled ones.

The method that we present in this paper aims to process student profiles from the e-learning platform. To do so, we have proposed a digital learning approach [20].

III. PROPOSED METHODOLOGY

Our proposal aims to predict and determine the preferences of the student from the information shared in his different social media. This extracted knowledge allows us to build the student profile that becomes central in any LMS system.

We propose a new method for using the user profile (i.e., student profile) in a referral system to provide a student with resources (i.e., content and items) relevant to his or her interests or specific needs in social media.

Our method is based on a machine learning technique. More precisely, it is based on the semi-supervised learning technique which is composed of two phases: the first one is the learning phase which allows the system to learn how to provide a student with personalized resources [15,21]. We use the J48 algorithm for this phase. The choice of using the J48 algorithm is justified by the fact that it has given the best F-measure scores in comparison with the classification algorithms.

The second phase is the use phase, which allows users to use the learning platforms. Fig. 1 shows the details of the proposed method and the two phases (i.e., the learning phase and the use phase).

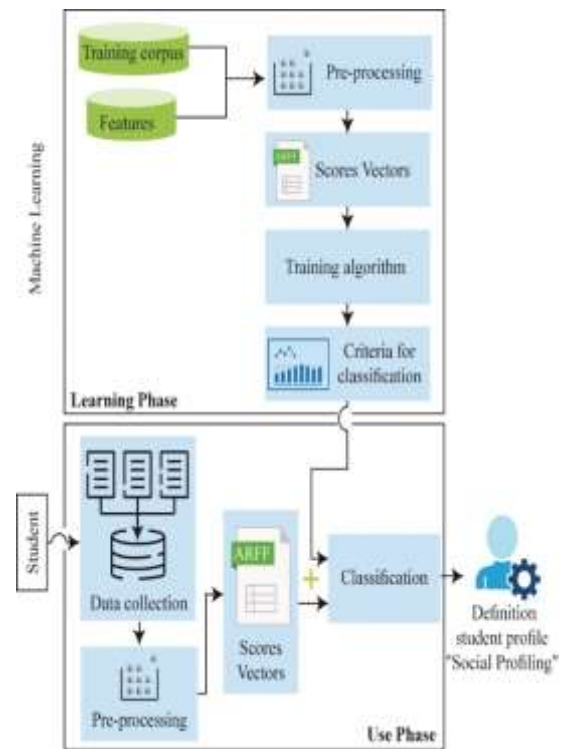


Fig. 1. Principle of the Proposed Method.

A. The Learning Phase

In this phase, we provide a training corpus and metadata features reflecting the student's interests. This information is defined following several studies [7].

The training corpus is composed of the attributes assigned to student information and their profiles. Attributes are assigned to student information and come from different categories: demographic data (e.g., age, gender, address), interests, hobbies, affiliation, preferences [19].

All attributes are initially pre-processed to prepare their segmentations in gender (i.e., male or female), age, description or structured as vectors (e.g., interests). However, some attributes have only one value (e.g., age, gender) while others may have several possible values (e.g., favourite music groups, favourite sports, etc.).

After the pre-processing step, each student entity (i.e., attribute) will be notified according to certain metadata characteristics. This step leads to the construction of a set of V vectors corresponding to the values of the specific characteristics (i.e., metadata) of a student. These vectors are called score vectors. Each vector is associated with classes and indicates the class of the student node.

The score vector has the following structure, $V1 (A1, A2, A3... An)$, where Ai is the score of the metadata criteria from i to n (i.e., the number of criteria).

In the learning phase, the score vectors are combined to associate a score to each characteristic and to generate classification rules.

B. The use Phase

This step is based on the construction of a student profile from the information contained in his or her social network, which we call "social profiling".

The term "social profile" refers to a profile constructed using the student's social network.

A social profile contains metadata reflecting the student's interests extracted from the information shared by the individuals in his or her social network.

Our objective in this phase is to build from this shared information on the student's social network, a score vector based on affinities (e.g., geographical, affiliation, interests, etc.).

Thus, we start this second phase with a step of collecting the student's shared information in his social network. An important point here is data collection problems, which is widely studied in social network analysis. In order to solve this problem, several APIs (Application Programming Interface) tools [11] that allow to query and process very large volumes of data related to public social networks (e.g., Twitter, Facebook, Instagram) have been applied (this is the step of collecting a student attribute).

After the pre-processing step of the collected data, and with the score vectors and the result defined by the learning phase using the J48 learning algorithm, which has proven its efficiency in our proposal, the "social profiling" of the student will be defined in this way.

To justify the choice of our learning algorithm, we tested five best classification algorithms according to the F-measure evaluation metric [10]. We deduced that the J48 algorithm gives the best F-measure. Table I summarizes the test results of the five algorithms.

TABLE I. CLASSIFICATION ALGORITHM TEST RESULTS

Algorithm	Precision	Recall	F-Measure
J48	0.898	0.855	0.876
PART	0.907	0.830	0.867
SVM	0.615	0.609	0.588
BayesNet	0.570	0.566	0.565
NaiveBayes	0.542	0.545	0.538

IV. SPS SYSTEM

The method we proposed for the automatic definition of social profiling of the student was implemented through the SPS system. In this section, we present the implementation details and preliminary results.

A. Implementation Details

Our study corpus consists of 427 student nodes collected from a survey questionnaire that was used to collect data from students at Ha'il University in Saudi Arabia and is accessible to the Blackboard system [7].

Using the study conducted by A. N. Alkhalidi, M. Ali, S. M. Mahmoud, Z. A. Alrefai, and Y. Bahou (2020), we were able to draw up a list of "features" criteria defining the links between students according to their common points or affinities (i.e., geographical, affiliation, interests) [7].

Note that the implementation requires a pre-processing step. This is the preparation of the data. Preparation is the process of collecting, combining, structuring, and organizing data so that it can be analysed in data visualization, analysis, and machine learning applications.

After the data preparation "pre-processing" step, we use nine "features" criteria to classify and define the metadata of each student entity.

Finally, we obtain a file that contains all the score vectors that make up the contribution of each student entity to learning. Table II shows features details.

In the learning phase, we use the J48 algorithm to learn how to classify the student entities. At the end of the learning phase, a score is associated with each element. Some features can have a grade of zero. The J48 algorithm generates a rule by summing the scores associated with each student entity. The system uses the generated rules to calculate the score for each student entity.

Finally, the system combines the classification decisions to obtain a social profile of the student. A social profile contains the metadata reflecting the student's interests extracted from the information shared in their social network and classified by the result generated by the J48 algorithm.

B. Preliminary Results

We used 427 student entities from our corpus to experiment our system (377 student nodes for the learning phase and 50 student nodes for the evaluation phase). The summaries obtained are compared to the expert results.

The main measures for Precision, Recall and F-Measure are 0.943, 0.961 and 0.952, respectively (see Table III).

TABLE II. FEATURES DETAILS

Features	Details
Stu_Sex	Indicates the type of sex (1 = male; 0 = female)
Stu_Diploma	Indicates the type of diploma (Diploma; Bachelor; Master)
Stu_Speciality	Indicates the speciality of the student (Medical and health science; Humanist and social science; Applied science; Natural science)
Stu_Branch	Indicates the geographic location of the student
Stu_Device	Indicates using Blackboard system via (Smartphone; PC; Together)
Stu_Soc_Med	Indicates the social media most used by students (Twitter; Facebook; Instagram; Other)
Stu_Pre_Film	Calculates the tf*idf of the media preference (tf*idf Film)
Stu_Pre_Song	Calculates the tf*idf of the media preference (tf*idf Song)
Stu_Pre_Doc	Calculates the tf*idf of the media preference (tf*idf Document)
Stu_Language	Indicates the interface language

TABLE III. EVALUATION RESULTS

	Precision	Recall	F-Measure
Weighted Avg.	0.943	0.961	0.952

V. CONCLUSION AND FUTURE WORK

In this document, we have proposed a method for defining a social profile that reflects the student's interests. The metadata of the social profile will be useful later on to improve the efficiency of the Blackboard learning process.

Our method is implemented by the SPS system and is based on the technique of machine learning. Indeed, our work focuses on a particular type of student nodes (i.e., Ha'il University students). We believe that the preliminary results are very encouraging. Indeed, the F-measurement is equal to 0.952.

Note, we have used a small corpus for the evaluation and as a perspective, we plan to extend our evaluation to a larger corpus and also to study the effect of other criteria on the definition of student social profiling.

We also plan to enrich our proposal so that it is able to follow the evaluation of the student's social profile with a variety of interests and needs over time. We, therefore, propose to keep the profile up to date through profile updating techniques, which, starting from an already relevant and up-to-date profile, will adjust at each update the interests considered relevant based on the former interests of the previous period [16]. It is thus a question of integrating a temporal factor (a temporal measure in the step of extraction and weighting of student interests).

We could also consider evaluating the social profiles constructed within the framework of our proposal in several LMS, a recommendation system for example the Blackboard.

ACKNOWLEDGMENT

This Research has been funded by Scientific Research Deanship at University of Ha'il – Saudi Arabia through project number RG-191341.

REFERENCES

[1] A. Bartuskova, O. Krejcar, and I. Soukal, "Framework of design requirements for e-learning applied on Blackboard learning system," Computational Collective Intelligence, Springer International Publishing Switzerland, pp. 471–480, 2015. https://doi.org/10.1007/978-3-319-24306-1_46.

[2] A. H. Duijn, and J. Tham, "The current state of analytics: Implications for Learning Management System (LMS) use in writing pedagogy," Computers and Composition, vol. 55, article number 102544, March 2020.

[3] A. Kobsa, Generic user modeling systems, BRUSILOVSKY P., KOBASA A., NEJDL W. (dirs.), The Adaptive Web, Springer Berlin Heidelberg (Lecture Notes in Computer Science), pp. 136-154, 2007.

[4] A. Kukulska-Hulme, E. Beirne, G. Conole, E. Costello, T. Coughlan, R. Ferguson, E. FitzGerald, M. Gaved, C. Herodotou, W. Holmes, C. Mac Lochlainn, M. Nic Giolla Mhichíl, B. Rienties, J. Sargent, E. Scanlon, M. Sharples, and D. Whitelock, Innovating pedagogy 2020: Open

University innovation report 8, The Open University, Milton Keynes, 2020.

[5] A. M. Heirdsfield, S. Walker, M. Tambyah, and D. A. Beutel, "Blackboard as an online learning environment: what do teacher education students and staff think?," Australian Journal of Teacher Education, vol. 36, issue 7, 2011.

[6] A. N. Alkhalidi, and A. M. Abualkishik, "The mobile Blackboard system in higher education: Discovering benefits and challenges facing students," International Journal of Advanced and Applied Sciences, vol. 6, issue 6, pp. 6-14, 2019.

[7] A. N. Alkhalidi, M. Ali, S. M. Mahmoud, Z. A. Alrefai, and Y. Bahou, "Challenges facing students to adopting the Blackboard system: the case study of University of Ha'il in Saudi Arabia," International Journal of Advanced and Applied Sciences - IJAAS, vol. 8, issue 3, 2020.

[8] A. W. Bates, Teaching in a digital age: Guidelines for designing teaching and learning, Vancouver BC, Tony Bates Associates Ltd., ISBN: 978-0-9952692-0-0, 2015.

[9] H. Tinmaz, and J. H. Lee, "An analysis of users' preferences on learning management systems: a case on German versus Spanish students," Smart Learning Environments, vol. 7, 2020. <https://doi.org/10.1186/s40561-020-00141-8>

[10] I. Witten, E. Frank, and M. Hall, "Data mining: Practical machine learning tools and techniques," Morgan Kaufmann Series in Data Management Systems Morgan Kaufmann, pp. 587-605, ISBN: 978-0-12-374856-0 2011. <https://doi.org/10.1016/B978-0-12-374856-0.00023-7>.

[11] J. Cutler, and M. Dickenson, "Application programming interfaces," Computational Frameworks for Political and Social Research with Python, Springer, pp. 87-97, ISBN: 978-3030368258, 2020.

[12] J. R. Hipp, C. Bates, M. Lichman, and P. Smyth, "Using social media to measure temporal ambient population: Does it help explain local crime rates?," Justice Quarterly, vol. 36, issue 4, pp. 718-748, 2019.

[13] L. A. Bove, and S. Conklin, "Learning strategies for faculty during a learning management system migration," Online Journal of Distance Learning Administration, vol. 23, issue 1, pp. 1–10, 2020.

[14] L. Li, Zheng, F. Yang, and T. Li, "Modeling and broadening temporal user interest in personalized news recommendation," Expert Systems with Applications, vol. 41, issue 7, pp. 3168-3177, June 2014. <https://doi.org/10.1016/j.eswa.2013.11.020>.

[15] L. Yao, and Z. Ge, "Deep learning of semi-supervised process data with hierarchical extreme learning machine and soft sensor application," IEEE Transactions on Industrial Electronics, vol. 65, num. 2, pp. 1490–1498, 2018. <https://doi.org/10.1109/TIE.2017.2733448>

[16] M. A. Mohsen, and C. Shafeeq, "EFL teachers' perceptions on Blackboard applications," English Language Teaching, vol. 7, num. 1, pp. 108-118, 2014.

[17] P. Bradford, M. Porciello, N. Balkon, and D. Backus, "The Blackboard learning system," The Journal of Educational Technology Systems, vol. 35, issue 3, pp. 301-314, 2007.

[18] S. Gauch, M. Speretta, A. Chandramouli, and A. Micarelli, "User profiles for personalized information access," BRUSILOVSKY P., KOBASA A., NEJDL W. (dirs.), The Adaptive Web, Springer Berlin Heidelberg (Lecture Notes in Computer Science), pp. 54-89, 2007.

[19] S. On-At, M. F. Canut, A. Péninou, and F. Sèdes, "Time-aware egocentric network-based user profiling," Encyclopedia of Social Network Analysis and Mining, Springer 2nd Ed, pp. 3113-3119, ISBN: 978-1-4939-7131-2, 2020.

[20] V. Aurélien, Intelligence artificielle vulgarisée: Le machine learning et le deep learning par la pratique, Éditions ENI, ISBN: 978-2-409-02073-5, 2020.

[21] Y. C. A. Padmanabha Reddy, P. Viswanath, and B. Eswara Reddy, "Semi-supervised learning: a brief review," International Journal of Engineering & Technology, pp. 81-85, 2018.

Using IndoWordNet for Contextually Improved Machine Translation of Gujarati Idioms

Jatin C. Modh¹

Research Scholar
Gujarat Technological University
Ahmedabad, Gujarat, India

Jatinderkumar R. Saini^{2*}

Professor and Director
Symbiosis Institute of Computer Studies and Research
Symbiosis International (Deemed University), Pune, India

Abstract—Gujarati language is the Indo-Aryan language spoken by the Gujaratis, the people of the state of Gujarat of India. Gujarati is the one of the 22 official languages recognized by the Indian government. Gujarati script was adopted from Devanagari script. Approximately 3000 idioms are available in Gujarati language. Machine translation of any idiom is the challenging task because contextual information is important for the translation of a particular idiom. For the translation of Gujarati idioms into English or any other language, surrounding contextual words are considered for the translation of specific idiom in the case of ambiguity of the meaning of idiom. This paper experiments the IndoWordNet for Gujarati language for getting synonyms of surrounding contextual words. This paper uses n-gram model and experiments various window sizes surrounding the particular idiom as well as role of stop-words for correct context identification. The paper demonstrates the usefulness of context window in case of ambiguity in the meaning identification of idioms with multiple meanings. The results of this research could be consumed by any destination-independent machine translation system for Gujarati language.

Keywords—Contextual information; Gujarati; idiom; IndoWordNet; Machine Translation System (MTS); n-gram model

I. INTRODUCTION

This Machine Translation (MT) is the application of Natural Language Processing (NLP) which is an area of Artificial Intelligence (AI). Machine Translation is the need for the communication between people knowing two different languages. Gujarati language has more than 46 million speakers worldwide making it the 26th spoken native language in the world [1].

Idiom is a common phrase whose meaning is different from its individual literal meaning of word. It is widely used and it has its popular meaning. Gujarati language has approximately 3000 n-gram idioms. Meaning of Gujarati idiom can be understood by the context of the text. Here context refers to the information surrounding that idiom which helps in understanding the meaning of idiom. Dictionary based approach can be used for single meaning idiom unless it has more than one possible meaning. For multiple meaning idioms, the context information before and after the Gujarati idiom appearing in the text has to be looked. Contextual information is nothing but the words surrounding the specific idiom used in the text.

A. IndoWordNet

IndoWordNet is large linked lexical database for Indian languages including Gujarati language. IndoWordNet is the WordNet for Indian languages developed by Center for Indian Language Technology (CFILT) in the Computer Science and Engineering Department at IIT Bombay. Nouns, adjectives, verbs and adverbs are grouped into set. Gujarati WordNet is very important resource for the natural language processing task [2-5].

B. Gujarati Stop-Words

The Stop-words are the most common words in the particular language. They do not add meaning to the text. For natural language processing task, stop-words are generally removed or ignored as pre-processing activity. For phrase searching, stop-words cannot be ignored [6]. Stop-words list is not common for all domains. Example of Gujarati stop-words are અથવા અને આ આથી આદે એ કે કોઈ છતાં છે છો જ જેમ જો તેમ પછી પણ માટે હોય etc. [7].

C. N-gram

N-gram is a contiguous sequence of n items from a given text [8]. N-gram of size 1 is known as 1-gram or unigram; size 2 is referred as 2-gram or bigram; size 3 is referred as 3-gram or trigram; size 4 is referred as 4-gram or four-gram and so on. If input text is “I love my country”, then examples of bigrams are “I love”, “love my” and “my country”; examples of trigrams are “I love my” and “love my country”. N-gram model is used in natural language processing. 1-gram to 8-gram generation sequence will generate first 1-gram, then 2-gram,...8-gram; whereas 8-gram to 1-gram generation sequence will generate first 8-gram, 7-gram, 6-gram,...1-gram respectively.

The rest of the paper is organized as follows: Section II presents the literature review related to context and idiom translation; Section III covers the methodology including idiom data collection and proposed algorithm to find the meaning of idiom. In Section IV, extensive experiments with results and analysis are discussed using IndoWordNet and contextual information; finally conclusion, limitation and future direction are described in Section V.

*Corresponding Author

II. RELATED LITERATURE REVIEW

For the machine translation from one language to other language, several projects have been carried out. For the Machine Translation from Gujarati to English language, Google and Microsoft are the big players in the market. Google Translate [9] supports more than 100 languages, while the Microsoft Translator [10] supports 54 languages. Both support translation from Gujarati to English language. Both do literal translation from Gujarati idioms. Context identification is very important for translation of idioms. Various work related to context identification and idiom translation carried out.

Fortu et al. [11] proposed algorithm for detecting context boundaries and used machine learning model for the detection of subjective contexts using a set of syntactic features. They categorized various types of contexts like Subjective, Time/Space, Domain, Necessity, Planning/Wish contexts.

Turney [12] defined feature relevance definitions like strongly relevance and weekly relevance. He defined various context related definitions like primary feature, contextual feature, context-sensitive feature, strongly context-sensitive features and illustrates these definitions.

Leacock et al. [13] proposed statistical classifier for the identification of word sense. Their proposed classifier is used to disambiguate adjective, verb, and nouns. They combined local clues with topical context. They used general text corpus for training examples. They concluded that the local context is superior to topical context.

Mishra et al. [14] designed hybrid approach to automate Hindi to English idiom translation. They collected idioms in the form of Hindi-English language pair and classified idioms in three categories: (i) similar meaning and similar form (ii) similar meaning and dissimilar form (iii) different meaning and different forms in both languages. They used transfer-based and interlingual-based machine translation of rule based approach.

Pedersen et al. [15] used SenseClusters [16], freely available intelligent system that clusters similar context texts in natural language text. SenseClusters is purely unsupervised and language independent approach. SenseClusters system supports different context representation schemes, feature selection from large corpora, various cluster algorithms and labels for clusters.

Sekiya et al. [17] used Reuters news articles and focused on determining all the senses for every word. They generated conceptual fuzzy sets to express word senses and five statistical measures as relations. They calculated cogency and mutual information by comparing compatibility between each measure and prediction model. They demonstrated the usefulness of the word sequences to identify context. They focused just four words before the target word in experiments.

Salton et al. [18] applied substitution based technique for English/Brazilian-Portuguese language pair. They first substituted original idiom with its literal meaning before translation and again substituted literal meaning with idioms following translation. They indicated improved performance.

Based on this literature review of the most relevant research works found in research community and the analysis based on context identification and Gujarati idiom translation, no researchers have done context identification for Gujarati language idioms. No researchers have experimented window sizes on Gujarati idioms for correct meaning identification. Most of the researchers have applied various techniques for determining word sense; some researchers have applied idiom translation techniques other than Gujarati language.

III. METHODOLOGY

A. Data Collection

Gujarati language idioms are collected from different 11 books and websites. Idioms can be classified as bigram, trigram, four-gram, five-gram, six-gram, seven-gram, eight-gram and so on. Out of 2908 idioms, 1735 idioms are bigrams and 892 idioms are trigrams. Total bigram and trigram idioms are 2627. So 90% of total idioms are bigrams and trigrams. Only 281 idioms are from other category like monogram, four-gram, five-gram, six-gram, seven-gram, eight-gram and so on. So, the analysis of bigram and trigram idioms was done first. Table I shows the classification of Gujarati Idioms. It is based on the work of Modh and Saini [22].

Idioms can be classified further on the base of its meanings like 1-meaning, 2-meanings, 3-meanings, 4-meanings and so on. For example “સંસાર મંડવો” ‘sansar mandvo’ is a Gujarati bigram single-meaning i.e. 1-meaning idiom and its meaning in Gujarati is “પરણવું” ‘paranavu’ only and its translation in English language is “to marry”; where as “અંખ બાતાવવો” ‘aankh batavavi’ is a Gujarati bigram 2-meaning idiom because it has two possible meanings in Gujarati as “ધમકી આપવો” ‘dhamaki aapvi’ and “અંખ બાતાવવો” ‘aankh batavavi’ and so two corresponding possible translations in English language are “to threaten” and “show eyes”. In the collection of overall 2627 bigram and trigram idioms, it was found total 2455 single meaning idioms and 172 idioms are having more than 1-meaning. From bigram and trigram idioms, 172 idioms are having 2-meaning, 3-meaning and 4-meaning idioms [19]. Table II shows the classification of bigram and trigram idioms on the base of meanings of idioms. It is based on the work of Modh and Saini [22].

TABLE I. CLASSIFICATION OF GUJARATI IDIOMS

N-gram Idiom Category	Count
Bigrams (n=2)	1735
Trigrams (n=3)	892
Other N-Gram idioms where n>=4	281
Total	2908

TABLE II. CLASSIFICATION OF GUJARATI BIGRAM AND TRIGRAM IDIOMS ON THE BASE OF MEANINGS

Meanings	Bigram Count	Trigram count	Total Count
1-meaning (single-meaning)	1675	780	2455
n-Meanings where n>=2	60	112	172
Total	1735	892	2627

If idiom has single meaning, then English translation of that particular idiom is very simple and direct, algorithm has to replace its meaning in the place of that idiom. If the idiom has more than one possible meaning, then contextual information comes in the picture. Contextual information is nothing but the collection and study of surrounding words before and/or after the particular idiom. For the correct translation of particular idiom having multiple meanings, algorithm has to examine the surrounding words before and/or after the particular idiom. By removing stop-words from the surrounding words, contextual words are obtained. Fig. 1 and Fig. 2 show the graphical representation of contextual words with bigram and trigram idiom respectively.

So here three options can be considered for contextual words; 1) contextual words before idiom i.e. left window only 2) contextual words after idiom i.e. right window only 3) contextual words before and after idiom i.e. left window and right window collectively. One more concern is about how many surrounding words to be verified from the given input text for the precise meaning identification of particular idiom. Three cases were experimented and results were recorded in order to identify the correct window size for left, right, both and optimum window size for the translation of Gujarati idiom(s) from the given Gujarati input text.

B. Software and Tools used

Following is the list of software and tools that are used to implement the proposed methodology.

- Spyder 4.1.5 (Scientific Python Development Environment) IDE.
- Anaconda3 2019.03 (Python 3.7.3 64-bit).
- pyiwn (Python-based API for IndoWordNet).
- Windows 10 (Operating System).
- XAMP 7.4.11 (cross-platform local web server).
- MySQL (database to store idioms).
- PHP 7.4.11 (scripting language for web development).
- Sublime Text & Visual Studio Code (editors).

C. Algorithm

Table III shows the partial database of Idioms stored in Idiom table. In the database, only bigram and trigram idioms having more than one-meaning are shown. Researchers had already experimented with single meaning idioms [20-22]. “Idiom” field stores the bigram/ trigram/n-gram idiom. “Gujarati meaning” field stores meaning of particular idiom in Gujarati language. “English meaning” field stores the translation of particular Gujarati idiom in English language.

“Gujarati Context Words” field stores the Gujarati context words related to particular idiom record. Gujarati Context Words are collection of all words from manually collected contextual words (from the corpus related to meaning of that idiom) and generated synonyms using Gujarati WordNet. If particular idiom has single meaning then only single record is there in the database. If idiom has n meanings, then n record entries are there in the database. For example, અંખ બતાવવી ‘aankh batavavi’ idiom has two possible meanings in Gujarati language, so two possible translations in English language; ધમકી આપવી ‘dhamaki aapvi’ (to threaten) and અંખ બતાવવી ‘aankh batavavi’ (literally show eyes e.g. for medical checkup). If this idiom has been used in given text, then algorithm has to decide any one meaning from the two possible meanings. “Gujarati Context Words” field is used for the context identification of particular idiom. If surrounding contextual words are related to સોકર તકલીફ દવા અંખ વેખાવું દૂર નજીક અંખ નજર વાંચન સમસ્યા then the translation of idiom અંખ બતાવવી ‘aankh batavavi’ is “show eyes” in English language and “અંખ બતાવવી” in Gujarati language. If surrounding words are related to લસઈ બાળક ઠપકો મૂબાપ સજા ઇોકરો then the meaning of idiom અંખબતાવવી ‘aankh batavavi’ is “to threaten” in English language and “ધમકીઆપવી” in Gujarati language. Gujarati WordNet i.e. IndoWordNet was used for the collection of more contextual words on the base of synonyms of manually collected contextual words. Some words are not found in the Gujarati WordNet. Thus those more words were added in the field “Gujarati Context Words”. For example, words like કકાલાટ ‘kakaalat’, રાજકારણ ‘raajkaaran’, સરોગેટ ‘saroget’, ચોમાસું ‘chomaasun’, ઝગડો ‘zhagado’ વોટીંગ ‘voting’, મધર ‘madhar’ etc. are frequently used words in Gujarati text but are not available in Gujarati WordNet. So these words were added in corresponding field of “Gujarati Context Words”. Gujarati Context Words play very important role in deciding the meaning of particular idiom and so the translation of Gujarati idioms. Algorithm calculated the frequency count of surrounding contextual words for each possible meaning of particular idiom by comparing with “Gujarati Context Words” column; the more count of context words field decide the particular meaning of the idiom. “Popularity” field decides the more frequent meaning of the particular idiom assigned by the Gujarati expert(s) in case of ambiguity. For example, if particular idiom has 3 possible meanings, popularity value 1 is given to that record which meaning is more frequently used in real life. The particular record was decided by studying real life examples as well as with the help of Gujarati language expert(s). Only when there occurs a tie during the process of selection of meanings, the algorithm use “Popularity” field.

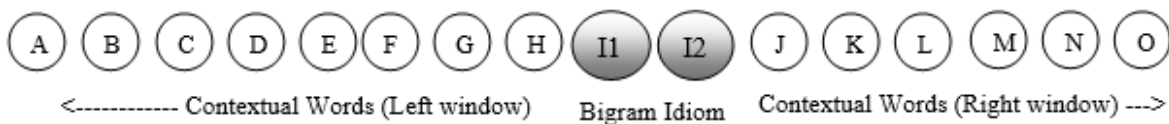


Fig. 1. Graphical Representation of Bigram Idiom with its Contextual Words.



Fig. 2. Graphical Representation of Trigram Idiom with its Contextual Words.

TABLE III. IDIOM DATABASE (PARTIAL) FOR BIGRAM AND TRIGRAM IDIOMS HAVING MORE THAN ONE MEANING

Sr no (1)	Idiom (2)	Transliteration of (2) (3)	Gujarati Meaning (4)	English Meaning (5)	Gujarati Context Words (6)	Popularity (7)
1	આંખ બતાવવી	Aankh batavavi	ધમકી આપવી	To threaten	અંબા અથડામણ અનુશય અપકોશ અપચાર અબ્બા અબ્બાજાન અભિગ્રહ અમ્મા અમ્માજી અમ્મી અર્થદંડ અર્ભ અસ્મૃતિ આત્મજ આત્મસંભવ આયોધન આળ આસ્કંદ આહર આહવ ઉપાલભ ઉલાહના કંકાસ કજિયો કતવ કલહ કલેશ કસૂર કાપાકાપ કિબલા કિબ્લા કિશોર કુમાર ક્ષતિ ખટરાગ ખતા ખામી ખિજાવું ખૂન ખૂનરેજી ખૂનામરકી ગફલત ગિલ્લા ઘર્ષણ ઘસારો ઘાત ચક્રમક ચિરંજીવ ચૂક છેયો છોકરાં છોકરું છોકરો છોરો જંગ જનક જનની જનેતા જન્મદાતા જન્મદાત્રી ઝંઝટ ઝગડો ઝંઘડો ઝપાઝપી ઝાટકણી ટેટો ઠપકારવું ઠપકો ડાંટ તકરાર તનય તનૂજ તાંત દંડ દિકરો દૂંદૂ દૂંદૂ ધમકી ધાત્રી ધિગાણું ધિક્કાર ધુત્કાર નંદન નવજાત શિશુ નવજાતક નાનકું નિંદા પંચાત પિતા પિતાજી પુત્ર પુષ્કર પૂત પૃથુક પ્રતિદારણ પ્રહરણ ફટકાર ફરજદ ફિટકાર બખેડો બચ્યા બચ્યું બટક બાપ બાપા બાલક બાળ બાળક બાળકને બાળકો બેટો ભર્ત્સના ભાંડવું ભૂલ ભૂલકણાપણું મા માં માતા માતારી માતૃ માતૃકા માથાફૂટ માદર માબાપ માયા મારવું મારામારી મૂઠભેડ મૈયા યુદ્ધ રકઝક રણ લડકો લડવું લડાઈ લાડલો લાલ લોયો વટ્ટ વઢવું વત્સ વધ વાદવિવાદ વાલિદ વિગ્રહ વિરોધ વિવાદ વિસ્મરણ વિસ્મૃતિ શિકાયત શિક્ષા શિક્ષા શિશુ સંકુલ સંગ્રામ સંઘર્ષ સંતાન સજા સમર સામનો સુત સ્કંધ સ્મૃતિવિહીનતા હત્યા હિસન હિંસા હુમલો	2
2	આંખ બતાવવી	Aankh batavavi	આંખ બતાવવી	show eyes	અંકુરણ અંકુરણ બિંદુ અંતર અંતરવેદના અંબક અક અઘ અડચણ અધ્યયન અભ્યાસ અરિષ્ટ અર્વાક અલગ અવસન્નતા અવસન્નત્વ અવિદૂર અશર્મ અસુખ અસુવિધા આંખ આંખો આંધું આંધે આદીનવ આપતિ આપદ આપદા આફત આભીલ આર્તિ ઈક્ષણ ઈક્ષિકા ઉતાપો ઉદ્ભેગ ઉપચારક ઉપતાપ એક તરફ એક બાજુ ઓળખ ઓસડ ઔષધ ઔષધિ કને કષ્ટ કુદૃષ્ટિ કલેશ ખ્યાલ ગભરામણ યક્ષુ યશ્મ ચિકિત્સક ચિતવન છેટે છેટે જડીબુટ્ટી જીવ પડવો જોડે ઝળકવું ઝાંખપ ઝાંખું ડીઠ ડોકટર ડોકટરને ડોકટર ડોકટરને તકલીફ તપાસ તસ્દી તેવર તોદન દરદ દરમાન દર્દ દર્શન થવા દવા દવાદાર દાકતર દારુ દુ દુખ દૂર દૂરત્વ દૂરવર્તી દૂરસ્થ દૂરસ્થિત દૃષ્ટિ દૃષ્ટિ પડવી દૃષ્ટિકોણ દેખરેખ દેખાવું દોચન ધૂંધવાઈ ધૂંધવાપણ ધૂંધળાઈ ધૂંધળાપણું ધ્યાન નજર નજર પડવી નજરિયા નજીક નયન નિકટ નિગાહ નિરીક્ષણ નેણ નેત્ર નેત્ર-દૃષ્ટિ નેન પઠન પડવે પડદો પડવું પરખ પરિપ્રેક્ષણ પરે પરેશાની પાથિ પાર્શ્વ પાસે પિઠ પીડા ફણગો ફાસલો બગલ બાજુ ભવાં ભેષજ્ય મનોવ્યથા મુશ્કેલી મુસીબત યંત્રણા યાદ રસાયન રોહજ દંગ લોચન વાંચન વિપતિ વિપદ વિપદા વૃજિન વેગળું વેગળે વેદના વેદ્ય વ્યથા વ્યાકુલતા વ્યાકુલપણું વ્યાકુળતા વ્યાધિ શૂળ સંકટ સંતાપ સંભાળ સમસ્યા સમીપ સુધ સુધિ સોય સ્મૃતિ હકીમ હૂક હેરાનગત	1
3	આંખ માં પાણી આવવું	Aankhma pani avavu	આંખમાં પાણી આવવા	water in the eye	અંકુરણ અંકુરણ બિંદુ અંબક અભિયોગ આંખ આજાર આતપ આમય આરજા ઈક્ષણ ઈક્ષિકા ઈલાજ ઉચરસ ઉપઘાત ઉપચાર કાશ કાસ કેસ ખટલો ખાંસી ગેસ ચક્કર યક્ષુ યશ્મ ચિકિત્સા જર જુખામ જૂવર ટાઢ ઠંડક ઠંડી ઠસક ઠાંસો તખ્તો તરિયો તાપ તાવ ત્રિપાદ દરદ દવા-દવા દારુ-પીનસ પાથિ નેન નેત્ર નેણ નયન દૂ દુખાવો દાવો અરજી ફણગો બિમારી બીમારી બુખાર માથું માવજત મુકદમો મુકદમો મુકદમો રોગ રોગોપચાર રોહજ દંગ લક્ષણ લોચન વિકાર વૈદ્યકી વ્યાધિ શરદી શીત સંભાળગત સરદી સળેખમ સારવાર સારસંભાળ સૂકી ખાંસી હકીમી	1
4	આંખ માં પાણી આવવું	Aankhma pani avavu	દયાની લાગણી થવી	feeling compassion or affection	અંતરવેદના અક અકિંચન અઘ અડચણ અનસ્તિત્વ અનુપલબ્ધિ અનૈશ્વર્ય અપૂર્ણતા અપ્રાપ્તિ અભવ અભાવ અરિષ્ટ અલ્પતા અલ્પત્વ અવસન્નતા અવસન્નત્વ અવસ્થા અશર્મ અસંપન્ન અસમૃદ્ધ અસુખ અસુવિધા આદીનવ આપતિ આપદ આપદા આફત આભીલ આર્તિ આલમ ઉતાપો ઉદ્ભેગ ઉપતાપ કંગાલ કંગાલિયત કકળાટ કમી કષ્ટ કલેશ ખામી ખાલીપણું ખોટ ગતિ ગભરામણ ગરીબ ગરીબાઈ ગરીબી ગેરહાજરી ઠાવાપણું તંગલાલ તકલીફ તસ્દી તોદન દરદ દરિદ્ર દરિદ્રતા દરિદ્રાણ દર્દ દળદર દશા દારિદ્ર દારિદ્ર્ય દીન દીનતા દીનહીન દુ દુખ દૈન્ય દોચન ધનહીન નિધની નિધન નિર્ધનતા પરેશાની પિઠ પીડા ફકીરી બિચારું બેહાલ મનોવ્યથા મુકલિસ મુશ્કેલી મુસીબત યંત્રણા રંક રંકતા રહિતપણું રાંક રાહિત્ય રિક્તતા લાઘવ વિધન વિધનતા વિપતિ વિપદ વિપદા વિપન્નતા વૃજિન વેદના વ્યથા વ્યાકુલતા વ્યાકુલપણું વ્યાકુળતા વ્યાધિ શૂન્યતા શૂળ સંકટ સંતાપ સૂરત સ્થિતિ હાલ હાલત હૂક હેરાનગત	2
5	આંખ માં પાણી આવવું	Aankhma pani avavu	આંખમાં આંસુ આવવા	tears in the eyes	અર્ભ અશ્રુપાત આકંદ આકંદ કરવો આકંદન આત્મજ આત્મસંભવ કલ્પાંત કિશોર કુમાર કંદન ચિરંજીવ છેયો છોકરું છોકરો છોરો તનય તનૂજ દાદા દિકરો નંદન નવજાત શિશુ નવજાતક નાનકું નાના પુત્ર પૂત પૃથુક ફરજદ બચ્યા બચ્યું બટક બાલક બાળ બાળક બેટો માતામહ રડવું રદન રદન કરવું રોધણું રોવું લડકો લાડલો લાલ વટ્ટ વત્સ વિલપન વિલાપ વિલાપ કરવો શિશુ સુત	3

Input text is given in Gujarati language. Input text may contain idiom(s). Entire input text is searched for the idiom(s) using n-gram model. If idiom(s) found in the text, then it may be single meaning or it may be more than one meaning idiom.

For single meaning idiom, the “Gujarati meaning” or “English meaning” column of that idiom can directly be used. But if the idiom has more than one meaning, algorithm has to consider “Gujarati Context Words” column. The algorithm decides the meaning of the particular idiom and substitutes the particular idiom with “Gujarati meaning” column value and produce intermediate output in Gujarati language itself. Output contains Gujarati literal text without any idiom. The algorithm can generate n-gram from the given input text using both the sequence 1-gram to 8-gram or 8-gram to 1-gram.

In the next section, empirical results are shown.

IV. RESULTS AND ANALYSIS

A. Experiments

For the experiments, 150 different Gujarati texts containing 30 different Gujarati idioms having single/multiple meanings from the various Gujarati websites as well as from offline Gujarati content were collected. The collection of various idioms within input texts was performed; like single idiom with single meaning, single idiom with more than one meaning(s), two idioms with single/multiple meaning(s), three idioms with single/multiple meaning(s), four idioms with single/multiple meaning(s) and so on.

L notation for Left window and R notation for Right window were used for simplification. (Ln, Rn) specifies Left window size n, Right window size n; (Ln, R0) specifies Left window size n and Right window size 0; (L0, Rn) specifies Left window size 0 and Right window size n; For example, Fig. 3 shows representation of (L6,R3). (L6, R3) denotes 6 words left side of the idiom and 3 words right side of the idiom. Surrounding words may or may not provide contextual information. Stop-words should be removed to get only contextual words information.

1) *Experiment-1*: Experiment-1 was conducted to decide two things (a) importance of various windows left, right or both for context identification (b) N-gram generation from the input text is possible by two ways; 1-gram to 8-gram generation sequence and 8-gram to 1-gram generation sequence. 1 to 8 gram generation sequence will generate first 1-gram, then 2-gram, 3-gram,...8-gram. 8 to 1 gram generation sequence will generate first 8-gram, then 7-gram, 6-gram,...1-gram. Which sequence is to be selected for better results? 150 Gujarati input texts containing single idiom only for each text was experimented. Idiom within text may have single/multiple meaning(s). Three cases were experimented (1) left window only (Ln,R0) (2) right window only (L0,Rn) and (3) left and right window both (Ln,Rn). Experiments for both the sequences for N-gram generation were conducted: 1-gram to 8-gram and 8-gram to 1-gram generation sequence. The algorithm will generate both the sequences by selection. For simplification and for evaluating importance of windows (left/right/left-right), all surrounding words of idioms were considered as contextual words and for that window size n=30 was applied for the experiment.

- Case-1: Using left window only for contextual information. The left window size was fixed as 30 and right window size was fixed as 0. Overall 150 input texts were tested for (L30,R0). Out of 150 input texts, idioms meaning precisely identified from 111 texts with 1 to 8 gram generation sequence (74% accuracy); idioms meaning precisely identified from 117 texts with 8 to 1 gram generation sequence (78% accuracy).
- Case-2: Using Right window only for contextual information. The right window size was fixed as 30 and left window size fixed as 0. Overall 150 input texts were tested for (L0,R30). Out of 150 input texts, idioms meaning precisely identified from 93 texts with 1 to 8 gram generation sequence (62% accuracy); idioms meaning precisely identified from 99 texts with 8 to 1 gram generation sequence (66% accuracy).
- Case-3: Using fixed left and fixed right window for contextual information. The left window size was set as 30 and right window size 30 i.e. (L30,R30) and tested 150 input texts; Out of 150 input texts, idioms meaning precisely identified from 132 texts with 1 to 8 gram generation sequence (88% accuracy); idioms meaning precisely identified from 138 texts with 8 to 1 gram generation sequence (92% accuracy). Idioms meaning can't be identified from 12 input texts. These 12 input texts were examined and found that the total words in these 10 input texts were less than or equal to 10. Hence out of these 12 input texts, 10 texts have not sufficient contextual information before and/or after idiom.

By comparing Case-1 (left window only), Case-2 (right window only) and Case-3 (left and right window) results of Table IV, Case-3 results are clearly front runner. So it is concluded that only left window or only right window is not useful at all for identifying contextual information. Case-3 (both the left window and right window) i.e. context words before and after the idiom must be considered for collecting contextual information. Also got better results in 8-gram to 1-gram generation sequence compared to 1-gram to 8-gram generation sequence; Particular cases were observed and found that intermediate translation of particular Gujarati idiom will also generate Gujarati idiom; this generated idiom can be found with 8-gram to 1-gram generation sequence. For example, એક ઘાઘે બે કટકા થવા 'ek ghaae be katkaa thavaa' is 5-gram idiom and its meaning is તડ ને ફડ જવાબ થવો 'tad ne fad javaab thavo', તડ ને ફડ 'tad ne fad' is 3-gram idiom and its meaning is સ્પષ્ટ 'spashta' or 'clear answer'; By taking sequence of 1-gram to 8-gram generation, તડ ને ફડ 'tad ne fad' idiom cannot be identified. So 8 to 1 gram generation sequence is preferred over 1 to 8 gram generation sequence.

Results of Experiment-1 in Table IV concluded two things (a) Left Window and Right Window both are required for contextual information. (b) For all N-gram idioms search within input text, 8-gram to 1-gram generation sequence is better one.

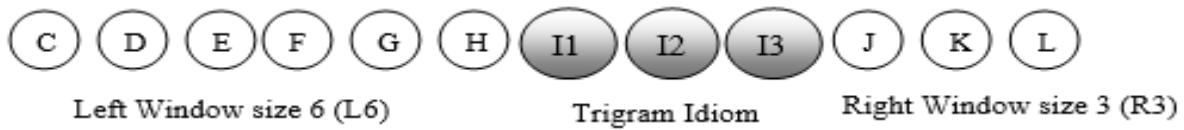


Fig. 3. Graphical Representation of (L6,R3).

TABLE IV. ACCURACY OF CORRECT MEANING IDENTIFICATION FOR SINGLE IDIOM HAVING SINGLE OR MULTIPLE MEANING (S)

Contextual Information and N-gram generation sequence	Case-1 Left Window only (L30, R0)	Case-2 Right Window only (L0,R30)	Case-3 Left & Right Window (L30,R30)
with stop-words and 1-gram to 8-gram generation	74%	62%	88%
with stop-words and 8-gram to 1-gram generation	78%	66%	92%

2) *Experiment-2*: Applying these two settings in the algorithm, experiment-2 was performed in which three things were evaluated: (1) different left and right window sizes for context identification (2) inclusion of stop-words or removing stop-words as contextual information (3) Using Gujarati WordNet words only as contextual information or with added manually collected words in WordNet words as contextual information. Two databases were used, in which first database contains only contextual words supported by Gujarati WordNet as “Gujarati Context Words” column and second database contains WordNet Words of first database + added contextual words in “Gujarati Context Words” column. These added words are not available in IndoWordNet.

For experiment-2, input texts with the sufficient contextual information i.e. input texts with at least ten words surrounding idiom(s) were selected. 8-gram to 1-gram generation sequence was set as it provides better results as per the experiment-1 results. Left window size was set variably from 1 to 20 and right window size was set variably from 1 to 20. Overall 150 input texts containing 30 multiple meaning idiom(s) were experimented. For this experiment input texts containing more than one multiple meaning idiom(s) were selected. The same texts with the inclusion of stop-words as contextual information and without consideration of stop-words as contextual information were experimented. In other words, overall 150 Gujarati input texts for (L1,R1), (L2,R2),

(L3,R3),.....upto (L20,R20) were tested. Only feasible window size(s) were selected for the experiment.

Table V shows the Experiment-2 results. Accuracy was calculated on the base of number of idioms meanings correctly identified. Combination of “Without stop-words and with All words (WordNet+Added Words)” shows the better accuracy for meaning identification for multiple meanings idioms; for (L2,R2) it shows 66.67% accuracy; for (L4,R4) it shows 83.33% accuracy; while for (L7,R7), (L10,R10), (L15,R15) it shows 100% accuracy. In other words, it gives correct translation for (L7,R7) to (L10,R10) and even for (L15,R15); for bigger window sizes (L20,R20) it reduces the performance (83.33% accuracy). More window size is not preferable for meaning identification of multiple meaning idioms. Moreover Table V shows that “without stop-words” option is giving better accuracy than “With Stop-words” option for all windows sizes.

Experiment-2 results concluded three things (1) stop-words should not be considered as contextual information i.e. from the input text stop-words should be ignored (2) All words (WordNet words+Added Words) should be used as “Gujarati Context Words” field for idiom database. Only WordNet words are not giving better results (3) At least Left window size 7 and right window size 7 are required to identify contextual words for the idiom having more than one possible meanings.

TABLE V. ACCURACY OF CORRECT MEANING IDENTIFICATION FOR MORE THAN ONE IDIOM HAVING MULTIPLE MEANING WITH 8-GRAM TO 1-GRAM GENERATION SEQUENCE

Using 8-gram to 1-gram generation sequence	(L2,R2)	(L4,R4)	(L7,R7)	(L10,R10)	(L15,R15)	(L20,R20)
With stop-words and with WordNet words only	16.67	16.67	33.33	66.67	83.33	66.67
Without stop-words and with WordNet words only	33.33	50	83.33	83.33	83.33	50
With stop-words and with All Words (WordNet+Added Words)	16.67	16.67	50	83.33	83.33	66.67
Without stop-words and with All words (WordNet+Added Words)	66.67	83.33	100	100	100	83.33

REFERENCES

If particular Gujarati idiom has more than one possible meaning, then for the translation of that Gujarati idiom into English language, sufficient contextual information is required. Contextual words before the particular idiom and contextual words after the particular idiom must be considered as contextual information for the identification of the precise meaning of multiple meaning idioms. Stop-words should be ignored when considering contextual words before and after multiple meanings idioms.

Gujarati Context Words play very important role in the context identification of multiple meaning idioms. By studying corpus of each multiple meaning idiom used in real life, Gujarati Context Words can be collected. Using Gujarati WordNet, more synonym words can be added in the collection of Gujarati Context Words. Additional words which are not supported by IndoWordNet can be added into the database for collection of Gujarati Context Words collection. The compiled collection of Gujarati Context Words is required source for context identification in the algorithm.

If input Gujarati text has idiom with multiple meanings and if Gujarati text contains overall less than 10 words or 0 context word before idiom or 0 context word after idiom, then the precise meaning identification of that particular idiom is difficult and challenging. As per the experiments, it is suggested that, for correct meaning identification of Gujarati multiple meaning idioms, at least seven contextual words before and seven contextual words after that particular idiom should be verified.

V. CONCLUSION

Based on the results received from the intermediate translations of Gujarati idioms into literal Gujarati text, it is advocated that the proposed machine translation system is promising and worth implementation in real world for the translation of Gujarati idioms. Google Translate and Microsoft Translator also do the literal word to word translation in case of Gujarati idioms. The proposed system can be implemented for translation of Gujarati idioms to any other language translation as it is language independent. Proposed algorithm substitutes idiom with the literal text that can be used for any other language translation from Gujarati language.

Gujarati synonyms were collected from IndoWordNet and from the initially collected context words. Gujarati WordNet provides all the forms of the words in terms of nouns, adjectives, verbs and adverbs. Sometimes it provides additional synonyms not related to idiom meaning; even then it provides better results in terms of contextual words for identifying contextual information. Idiom meaning identification is not possible if idiom used in odd or strange context. In Gujarati, many words adapted from English are used frequently and those words are not included in Gujarati WordNet. So extensive corpus related to multiple meaning idioms is to be examined and used for further improvement.

In future, authors will extend the context identification for the n-gram idioms where $n \geq 9$; variety of window sizes can be tried out in future; experiments of window size with idioms of any language can be done. In future, authors are planning to implement and experiment using lemmatization and stemmer.

- [1] Wikipedia, "Gujarati language", https://en.m.wikipedia.org/wiki/Gujarati_language (accessed December 24, 2019).
- [2] WordNet, "A Lexical Database for English", Princeton University, Available Online: <https://wordnet.princeton.edu/> (accessed December 24, 2020).
- [3] Wikipedia, "IndoWordNet", <https://en.wikipedia.org/wiki/IndoWordNet> (accessed December 24, 2020).
- [4] IndoWordNet, "A wordnet of Indian languages", Center for Indian Language Technology, Indian Institute of Technology, Bombay, Available Online: <http://www.cfilt.iitb.ac.in/indowordnet/> (accessed December 24, 2020).
- [5] Ritesh Panjwani, Diptesh Kanojia, Pushpak Bhattacharyya, 2018, "pyiwn: A Python-based API to access Indian Language WordNets", Proceedings of the GWC 2018 The 9th Global WordNet Conference, Nanyang Technological University (NTU) Singapore, 8-12 January 2018, Available online: http://compling.hss.ntu.edu.sg/events/2018-gwc/pdfs/GWC2018_paper_40.pdf.
- [6] Wikipedia, "Stop word", https://en.wikipedia.org/wiki/Stop_word (accessed December 24, 2020).
- [7] Quanteda/Stopwords, 2019, "A List 210 Gujarati Stop Words", Available online: <https://github.com/quanteda/stopwords/files/2719155/A.List.of.210.Gujarati.Stop.Words.txt> (accessed December 24, 2020).
- [8] Wikipedia, "n-gram", <https://en.wikipedia.org/wiki/N-gram> (accessed December 24, 2020).
- [9] Google Translate, Google Corporation Ltd.; Available Online: <https://translate.google.co.in/> (accessed December 24, 2020).
- [10] Microsoft Translator, Microsoft Limited, Available Online: <https://www.bing.com/translator> (accessed December 24, 2020).
- [11] Ovidiu Fortu and Dan Moldovan, 2005, "Identification of Textual Contexts", International and Interdisciplinary Conference on Modeling and Using Context; Available online: https://link.springer.com/chapter/10.1007/11508373_13.
- [12] Peter Turney, 2002, "The Identification of Context-Sensitive Features: A Formal Definition of Context for Concept Learning"; Available online: <https://arxiv.org/ftp/cs/papers/0212/0212038.pdf>.
- [13] Claudia Leacock, Martin Chodorow, George A. Millers, 1998, "Using Corpus Statistics and WordNet Relations for Sense Identification", Association for Computational Linguistics, Available online: <https://www.aclweb.org/anthology/J98-1006.pdf>.
- [14] Himani Mishra, Rajesh Kumar Chakrawarti, Dr. Pratosh Bansal, 2017, "A New Approach for Hindi to English Idiom Translation", International Journal on Computer Science and Engineering (IJCSE), Vol. 9 No. 07, Jul 2017, Available online: <http://www.enggjournals.com/ijcse/doc/IJCSE17-09-07-024.pdf>.
- [15] Ted Pedersen and Anagha Kulkarni, 2005, "Identifying Similar Words and Contexts in Natural Language Using SenseClusters", Association for the Advancement of Artificial Intelligence (AAAI); Available online: <https://www.aaai.org/Papers/AAAI/2005/ISD05-013.pdf>.
- [16] SenseClusters, 2005, "Cluster contexts and words based on contextual similarity", Available online: <http://senseclusters.sourceforge.net/> (accessed December 24, 2020).
- [17] Hiroshi Sekiya, Takeshi Kondo, Makoto Hashimoto, Tomohiro Takagi, 2007, "Context representation using word sequences extracted from a news corpus", ScienceDirect, International Journal of Approximate Reasoning, 45 (2007) 424-438, Available online: <http://www.science-direct.com/science/article/pii/S0888613X06001125>.
- [18] Giancarlo D. Salton and Robert J. Ross and John D. Kelleher, 2014, "Evaluation of a Substitution Method for Idiom Transformation in Statistical Machine Translation", Proceedings of the 10th Workshop on Multiword Expressions (MWE 2014), pages 38-42, Gothenburg, Sweden, 26-27 April 2014, Association for Computational Linguistics, Available online: <http://www.aclweb.org/anthology/W14-0806.pdf>.
- [19] Gujarati Lexicon, Gujaratillexicon.com, Available online: <http://www.letslearngujarati.com/about-us> (accessed December 25, 2020).

- [20] Modh J. C. and Saini J. R., 2018, "A Study of Machine Translation Approaches for Gujarati Language", *International Journal of Advanced Research in Computer Science*, Volume 9, No. 1, January-February 2018, pages 285-288; Available online: ijarcs.info/index.php/Ijarcs/article/download/5266/4497.
- [21] Saini J. R. and Modh J. C., 2016, "GIdTra: A Dictionary-based MTS for Translating Gujarati Bigram Idioms to English", *Fourth International Conference on Parallel, Distributed and Grid Computing (PDGC) 22-24 December 2016*, pages 192-196, Available online: <https://ieeexplore.ieee.org/document/7913143/>.
- [22] Modh J. C. and Saini J. R., 2020, "Context Based MTS for Translating Gujarati Trigram and Bigram Idioms to English", *2020 International Conference for Emerging Technology (INCET), Belgaum, India, 2020*, pp. 1-6, doi: 10.1109/INCET49848.2020.9154112; Available online: <https://ieeexplore.ieee.org/document/9154112/>.

“iSAY”: Blockchain-based Intelligent Polling System for Legislative Assistance

Deshan Wategama¹, Pasindu S.Silva², Chamika R. Jayathilake³
Kalana Elapatha⁴, Kavinga Abeywardena⁵, N. Kuruwitaarachchi⁶
Faculty of Computing, Sri Lanka Institute of Information Technology, Sri Lanka^{1,2,3,4,5}
Faculty of Technology, University of Sri Jayewardenepura, Sri Lanka⁶

Abstract—“iSAY” is a Blockchain-based polling system created for legislative assistance. Sri Lanka is a democratic country. Country follows a representative democracy and voters in Sri Lanka vote for their preferred government based on their election mandate. However, governments implement legislative decisions that are not stated in the election mandate. People won't get a chance to state their opinion on this legislative matter and the government also doesn't know whether people like this or not. To solve this issue, in this paper the authors propose a blockchain-based intelligent polling application for legislative assistance. “iSay” is an application where blockchain technology gets together with machine learning to add value into the public opinion. The government can create a poll about a legislative decision and people can state their opinion which could be further discussed in the legislature. Adding a significant change to the blockchain based e-voting solutions this paper proposes a novel feature where users can add their idea to a relevant poll. Using machine learning algorithms all these user ideas will be classified and analyzed before presenting to the government. Through this research, it is expected to deploy scalable elections among the general public and get their vote and ideas about specific legislations to generate an overview of general public opinion about legislative decisions.

Keywords—Blockchain; machine learning; distributed systems; e-voting; legislative assistance; liquid democracy; natural language processing

I. INTRODUCTION

In Sri Lanka every five years people vote for their preferred political parties and the political party who wins most votes will govern the country. Government will make legislative decisions and most of the time these decisions will be unchallenged due to less opportunities for the general public to state their opinions on these matters. Social activists will protest against these decisions if they think these legislations are not suitable for the society. Then the government will change this legislation where they can meet activists in a middle ground. However, the government cannot know the general public opinion for sure since there are no methods or tools for that. In this COVID-19 pandemic situation the government took legislative decisions which had a clear impact on society. Because of the Social Distancing and New Normality protests were not allowed. Hence social activists didn't have an opportunity to express their opinion while the government also had no clue about general public opinion. Since “iSay” blockchain based intelligent legislative

polling system solves all these issues this application will be a key application to protect democracy in a post COVID-19 era.

The role played by public opinion in a democracy, particularly as it affects the legislative process, has long been a subject for speculation by political scientists [1]. In Sri Lanka every five years people vote for their preferred political parties and the political party who wins most votes will govern the country. This is called representative democracy and most of the countries follow this [2]. People will look at the mandate of political parties and they will decide which party to vote for. Sometimes governments will implement some Legislative Decisions which were not stated in their election mandates. In the recent past, the Sri Lankan government took a legislative decision to sign an agreement with Millennium Challenging Cooperation of the United States of America [3]. The opposition party debated that voters in Sri Lanka do not want to sign that agreement, however they did not have a way to show this. On the other hand, the government said that this will bring big benefits to the country, nevertheless they also did not have a way to know what people think about this. This is a problem in representative democracy because after election voters do not participate in the legislative decision-making process. Simon Torney stated “Representative Democracy” as a Contemporary Crisis [4] in Australia Parliament paper no 66. To solve this issue specialists introduced a new kind of democracy called Liquid Democracy. In Liquid Democracy voters actively take part in the decision-making process [5].

As found in the preliminary survey of this research, most of the public want a part in the legislative decision-making process. Therefore, authors Introduced “iSay”, a Blockchain-Based Polling System to fill this void created by representative democracy. There was a survey done in Michigan, on smoking in public places in the consideration of non-smoking legislation to measure the opinion of the public [6]. In the study it is reported that the poll results taken from the public helped to restrict smoking in public places.

This system is far different from current blockchain based e-voting solutions. Current blockchain based e-voting applications support only quantitative votes such as 1 (yes) and 0 (no). Since the main aspect of this application is to present an opportunity to the voters to state their ideas on legislative matters, authors added a novel feature which is adding amendments. Since most of these legislations are

A. Liquid Democracy based Considerations

In this proposed system authors are eyeing to achieve Liquid Democracy while helping the government to get a public opinion as well. To achieve this there are few constraints which need to be considered;

- 1) Every voter should have an equal opportunity to vote.
- 2) Every vote should be completely validated.
- 3) Every vote should be protected.
- 4) This voting system should only allow eligible individuals to vote in an election.

In this system all these constraints are satisfied through using blockchain technology. Key to protecting every one of these constraints is protecting users' identity. For every user a pair of private and public keys is generated by the system based on user data and credentials.

B. Create an Election using Smart Contracts

Smart contracts are a binary file or a method which takes the blockchain as input parameter. Since blockchain technology is still in its infancy, there is no exact way to use smart contracts. Consequently most proposed election frameworks authors have studied use smart contracts in various different ways. Most of the proposed systems are using "Elections as a Smart Contract" [19]. Since "iSay" e-voting system is based on a blockchain framework implemented by authors, it is required to use a unique smart contract language as well. Exonum, Quorum and Go-Ethereum blockchain frameworks use Rust and Solidity as their smart contract language. Authors deviated from these existing blockchain frameworks mainly because of storage and computing power related constraints. Unlike most of the other e-voting systems authors decided to run smart contracts in each user node when the user is voting. Therefore, it is proposed to make use of Javascript as the smart contract language due to its lightweight and less resource consuming nature.

C. Validating users in an Election

The ECDSA (Elliptic Curve Digital Signature Algorithm) on secp256k1 curve is used to generate the public key. Authors of this research chose ECDSA over RSA (Rivest-Shamir-Adleman) algorithm because ECDSA uses shorter encryption keys that use fewer memory in CPU resources [17]. The ECDSA equation E over a finite prime number field F_p can be written as follows;

$$E: y^2 = x^3 + ax + b \tag{1}$$

Where

$a, b \in F_p, 4a^3 + 27b^2 \neq 0(mod p)$, and p is a randomly selected large prime number.

The recommended parameters for the secp256k1 curve is as follows in Table I, which is extracted from the Recommended Elliptic Curve Domain Parameters [18].

D. Voting in an Election Blockchain Network.

To achieve the transparency of the poll blockchain needs to be stored in a decentralized network. By doing so it is possible to achieve basic blockchain qualities as well. To achieve these authors, suggest a peer-to-peer distributed network.

As authors found in the literature review most of the proposed blockchain based election systems have static blockchain nodes. Voters have to go to a specific location to cast their votes. Since this system is specially focusing on legislative matters governments cannot ask their voters to go and cast their vote in that specific location several times a month since these legislations are frequently taken out in parliament.

Solve these issues and authors treat all the users as blockchain nodes. So that they can vote from home with proper authorization.

Left hand side of Fig. 2 illustrates a normal blockchain mostly consisting of static nodes. These nodes have computational power to mine the blocks and store them. However, in the proposed network blockchain cannot be stored in every node. To solve this issue through the proposed network authors have created three types of nodes.

- Signaling Node
- Half nodes
- Peer nodes

TABLE I. RECOMMENDED ELLIPTIC CURVE DOMAIN PARAMETERS

Parameter	Value
p	FFFFFFFF FFFFFFFF FFFFFFFF FFFFFFFF FFFFFFFF FFFFFFFF FFFFFFFE FFFFFC2F
a	00000000 00000000 00000000 00000000 00000000 00000000 00000000 00000000
b	00000000 00000000 00000000 00000000 00000000 00000000 00000000 00000007
G	02 79BE667E F9DCBBAC 55A06295 CE870B07 029BFCDB 2DCE28D9 59F2815B 16F81798
n	FFFFFFFF FFFFFFFF FFFFFFFF FFFFFFFE BAAEDCE6 AF48A03B BFD25E8C D0364141
h	01

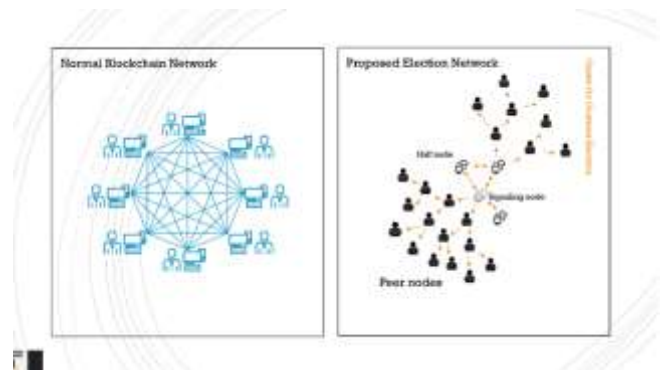


Fig. 2. Blockchain Network Comparison.

Peer nodes are the user nodes which will be voting. In these nodes the blockchain is stored as a hash, hence these can be retrieved in the validation process and recheck the chain. Signaling nodes are the full privilege admin nodes. There will be several signaling nodes with more computational power. These nodes will save the election blockchain. Every other node will be initially connecting to this node when they are restarting. And then these peer nodes will be redirected to another node using Leadership Selection Algorithm. As illustrated in the Fig. 2 every node will act as a client and at the same time as a server.

Admin node will be a privileged user node. It will save the whole blockchain as it is. Giving a novel experience to blockchain based e-voting applications authors propose Clustered Polling. Most of the blockchain based e-voting applications are proposed to handle general elections [19] [20]. Unlike general elections, certain legislative matters may only affect a specific group of participants.

If the legislation added by the government is about farmers, only farmers should be allowed to vote. Otherwise polling results and suggestions will not be accurate as expected. In order to resolve this issue a clustered polling mechanism is used. In the registration process all the voters are classified into clusters using their electorate and profession. Using these clusters government admin can add legislative polls to specific groups. To create this clustered poll authors are using half nodes which were introduced before. When a clustered poll is created they will be disconnected from the main network and they will be connected to a cluster. If this legislation is about farmers the whole cluster consists of farmer nodes.

E. Amendments Adding Feature

If users are satisfied or unsatisfied with the legislation they can just vote 'yes' or 'no'. Or else they want some improvements they can add their opinion on them. However, not all of the opinions are accepted. These suggestions are listed to the other voters and they have to accept them.

F. Amendments Generalization

A main feature of this system is to allow voters to post their own amendment/suggestion to a legislative matter. Since these elections are open to the general public there will be thousands of suggestions and amendments. Anyone whose taking decisions or presenting election results cannot read all the amendments. To solve this issue authors introduced amendments generalization using machine learning algorithms.

A major issue faced by collecting large sets of text data is, it will result in visualizing and managing the voter amendments in an orderly manner. There are amendments which belong to the same groups with similar meaning. Therefore, authors propose a solution of generalizing these amendment text documents using Machine Learning and Deep Learning techniques. This generalization of amendments process will be responsible for partitioning the amendments by taking the inputs as text documents, then cluster into groups and later summarizing the results to give the best generalized output.

ALGORITHM I: The Proposed Algorithm to Generalize Amendments

1. **Input** : Raw amendment text documents
2. **Output** : Clusters of summarized amendments text documents
3. First step
4. Preprocess raw amendments using NLP (Natural Language Processing) pre-processing procedures and return a word corpus.
5. Convert the word corpus into a numerical matrix.
- 6: Second step
7. Calculate the maximum silhouette score to determine the optimal number of clusters of clustering.
8. Apply k-means to selected features and create a model.
9. For each text document
10. Predict the cluster with the model
11. Store cluster text documents.
- 12: Third step
13. Calculate normalized word frequencies of text documents.
14. Calculate the sentence score using normalized word frequencies.
15. Select 30% of sentences with large sentence frequency.
16. Return final clustered and summarized text.

$$JV = \frac{1}{c_j} \sum_{i=1}^c |x_i - v_j|^2 \quad (2)$$

Where,

' $\|x_i - v_j\|$ ' is the Euclidean distance between x_i and v_j points, ' c_i ' is the number of data points in i^{th} cluster, and ' c ' is the number of cluster centers. Since this is an automated process, the real amount of clusters cannot be identified. Therefore this system ran the k-means algorithm for multiple times and created multiple models. Out of all these models, the one with the best Silhouette score is chosen. This chosen k-means model is then stored in the server and the respective cluster for the text document will be predicted.

After the prediction of all these cluster documents, the cluster documents will be combined into single documents. In order to reduce the content of the documents a text document summarization is performed. This is an extractive summarization procedure and the python library Spacy is used. The steps taken for the summarization is mentioned in the above Algorithm 1.

IV. RESULTS AND DISCUSSION

Most of the components of this application are working individually as separate components. Since the rise of Blockchain Technology it has proven that Blockchains are more secure than centralized database systems. However, there were some issues in current blockchain frameworks. One of the main issues was all these frameworks are designed for general purposes. Hence most of them are resource consuming.

Therefore, a new framework is proposed called “iZigma” which is implemented using JavaScript for this system, with multiple chain support and giving freedom for the developer to handle the network according to the system requirement. The framework is created as a node module which allows to use the framework easily in a node project. A platform that gives full customization to the blockchain is needed due to the following two features. In the Table II is a comparison between the proposed framework and the other blockchain frameworks. Fig. 3 illustrates the blockchain framework performance test results.

- 1) The system is designed to have several elections at the same time and each election uses a separate blockchain.
- 2) Network in this system is divided into clusters.

TABLE II. COMPARISON BETWEEN PROPOSED FRAMEWORK AND OTHER BLOCKCHAIN FRAMEWORKS

	Hyperledger Fabric	Go-Ethereum	iZigma
Consensus	PBFT	PoW(Proof of Work), PoS (Proof of Stake) , PoA (Proof of Authority)	PoW
Transactions p/s	3,500 transactions p/s	Depends	Depends (Can be configured)
Private Support	Yes	Yes	Yes
Smart Contract language	Go, Java, Kotlin	Solidity	JavaScript
Programing Language	Go, Java, JavaScript, Python	Go, C, JavaScript	JavaScript
Multiple Chains	No	No	Yes

```

UT-4001_wallet - Operations on New Chain
✓ Read the chain only with genesis block (2ms)
✓ Create a block without any validation (61ms)
✓ Create a a tranasaction (89ms)
✓ Create a a Record (68ms)
✓ Mine transaction (861ms)
✓ Mine record (167ms)
After adding 200 Blocks
✓ Read the chain after 200 blocks (15ms)
✓ Create a block without any validation (245ms)
✓ Create a a tranasaction (78ms)
✓ Create a a Record (66ms)
✓ Mine transaction (802ms)
✓ Mine record (3530ms)
Wallet with SECP256K1 algorithm - Operations on New Chain
✓ Read the chain only with genesis block (1ms)
✓ Create a block without any validation (37ms)
✓ Create a a tranasaction (73ms)
✓ Create a a Record (67ms)
✓ Mine transaction (867ms)
✓ Mine record (89ms)
After 200 Blocks
✓ Read the chain after 200 blocks (15ms)
✓ Create a block without any validation (986ms)
✓ Create a a tranasaction (77ms)
✓ Create a a Record (67ms)
✓ Mine transaction (424ms)
✓ Mine record (467ms)
    
```

Fig. 3. Blockchain Performance Results.

Using this newly created blockchain framework authors were able to create and deploy multiple elections which can run concurrently. As illustrated in Fig. 3 these elections were less resource consuming and more scalable than most of the existing frameworks.

The file size of the blockchain file after doing this process was 2,45 KB. This new Blockchain network was able to do the blocks mining in an improved pace aiding the application to generate real time results.

Using Blockchain the authors were able to hold secure elections. If election results were corrupted by changing a block authors were created validation methods to identify these external changes instantly. If the blockchain was identified as invalid the main application will ask the half node copy of that blockchain and it will be replaced.

Networking part of this blockchain based voting system is important. Here authors faced challenges due to the large number of users connecting concurrently to the application since this application is opened for the general public. To solve this problem, authors propose a distributed network where nodes are loosely coupled.

User nodes can connect and disconnect to the main server anytime they want. Using this approach, blockchain concepts can be protected while allowing thousands of users to connect to the network and vote. Sri Lanka has a population of around 20 million. This approach helps to facilitate a large number of nodes as well. All the nodes will not connect to the main server. Therefore the load to the signalling server is reduced preventing single point of failure due to large amounts of requests. Only oldest nodes will be connected to the signalling server. User nodes are connected with each other and they will contact the signalling server through the oldest nodes in the network.

Fig. 4 represents an image taken from an actual election network. It is clear that all the nodes are creating real time socket connections. Peer node users can install this application and it will run as a local node server. Since authors cannot access the local process of a machine while in the outside world, authors use *ngrok* [21] to tunnel these servers with one another. *Ngrok* creates a random URL each time the node is restarting. This random URL generation will protect the identity of the clients.

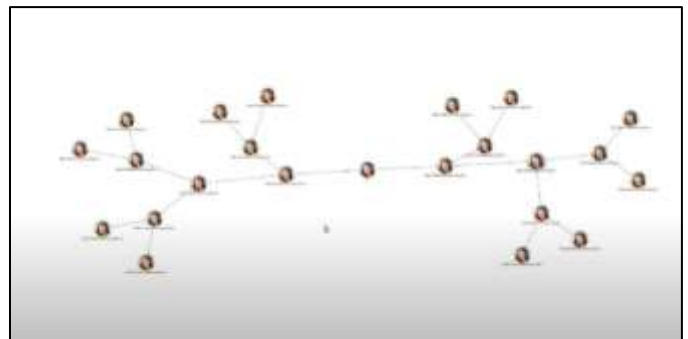


Fig. 4. Actual Blockchain Network.

Voters can connect to this network with proper authentication and add their vote on specific elections. These elections can be clustered elections where the election targets a specific group of people.

When users add their amendments on legislations these amendments will be run through deep learning and machine learning algorithms. This machine learning component is a separate component where this can be used for general purpose as well. Using this amendment generalization component user amendments will be categorized and will be presented with the final election results.

In the amendment generalization as mentioned in the methodology section, authors are using two methods for the numerical representation of text documents. For testing the accuracy of the model authors used live responses from citizens as amendments and suggestions regarding a specific legislative matter. By using the TF-IDF a Silhouette score of 0.012434112109754505 was obtained. With the model created with Doc2Vec, authors were able to calculate a Silhouette score of 0.24956775. Fig. 5 illustrates the Silhouette coefficient against the cluster labels plot for 4 clusters.

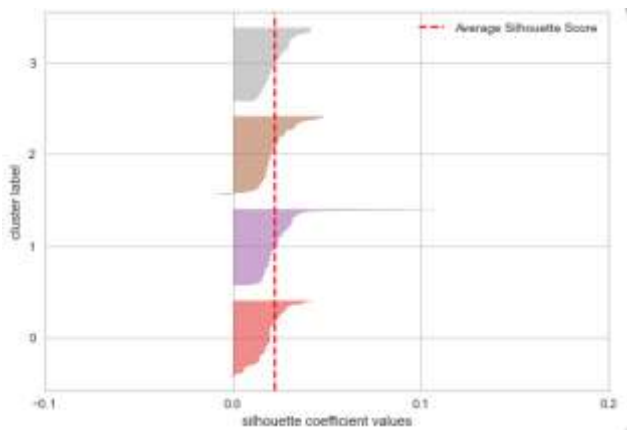


Fig. 5. Silhouette Coefficient Plot.

Therefore, it's clear that Doc2Vec can generate a more accurate k-means model from text documents since Doc2Vec more focuses on the semantic level of the documents [22]. In the proposed extractive text document summarization, only 30% of the sentences from the paragraph with the highest frequency score is taken. Since this is not an abstractive text summarization, it does not focus on the semantic level of the summary. Therefore authors suggest a text summarization implemented using a RNN (Recurrent Neural Network).

V. CONCLUSION

Due to the current COVID-19 pandemic situation "iSay" application now has a value more than ever. In the recent past the general public participated in protests against some legislative decisions. However, the government had no idea about general public opinion about that legislation before presenting that into the parliament. With the current situation there is no chance for protesting and with the "iSay" application both parties, the general public and government can gain benefits since both can express their ideas using this application.

This paper proposes a polling system which will allow the general public to be a part of the legislative decision making process. This polling application will help both government and opposition parties as well. This application will enact liquid democracy while solving the problems of representative democracy. Authors were able to create a stable election network, validate votes real time and give election results real time using the newly proposed blockchain framework and distributed network. As a value addition to the e-voting domain. Authors were able to classify suggestions given by users and run a sentiment analysis on these suggestions.

REFERENCES

- [1] Cantwell, F., 1946. Public Opinion and the Legislative Process. *American Political Science Review*, 40.
- [2] S. Gamage, "Democracy in Sri Lanka: past, present and future," *Asian Studies Review*, vol. 17, no. 1, 1993.
- [3] "Sri Lanka Compact," Millennium Challenge Corporation. [Online]. Available: <https://www.mcc.gov/where-we-work/program/sri-lanka-compact>.
- [4] "Papers on Parliament no. 66 - Parliament of Australia." [Online]. Available: https://www.aph.gov.au/About_Parliament/Senate/Powers_practice_n_procedures/po/Papers_on_Parliament_66/The_Contemporary_Crisis_of_Representative_Democracy.
- [5] Blum, Christian & Zuber, Christina. (2015). Liquid Democracy: Potentials, Problems, and Perspectives. *Journal of Political Philosophy*. 24. 10.1111/jopp.12065.
- [6] Perlstadt, H. and Holmes, R., 1987. The role of public opinion polling in health legislation. *American Journal of Public Health*, 77
- [7] S. Nakamoto, "Bitcoin: A peer-to-peer electronic cash system," 2008. [Online]. Available: <https://bitcoin.org/bitcoin.pdf>.
- [8] Chowdhury, Mohammad & Colman, Alan & Kabir, Ashad & Han, Jun & Sarda, Paul. (2018). Blockchain Versus Database: A Critical Analysis. 1348-1353. 10.1109/TrustCom/BigDataSE.2018.00186.
- [9] M. Hochstein, "Moscow's Blockchain Voting Platform Adds Service for High-Rise Neighbors," *CoinDesk*, 15 Mar. 2018; <https://www.coindesk.com/moscows-blockchain-voting-platformadds-service-for-high-rise-neighbors>, 2018.
- [10] "South Korea Uses Blockchain Technology for Elections," *KryptoMoney*, <https://kryptomoney.com/south-korea-usesblockchain-technology-for-elections>, 2017.
- [11] Andrew Barnes, Christopher Brake and Thomas Perry, "Digital Voting with the use of Blockchain Technology", <https://www.economist.com/sites/default/files/plmouth.pdf>, 2016.
- [12] Agora: Bringing our voting systems into the 21st century Available at: https://agora.vote/Agora_Whitepaper_v0.1.pdf, 2017.
- [13] McCorry, P., Shahandashli, S.F., Hao, F.: A smart contract for boardroom voting with maximum voter privacy. In: *International Conference on Financial Cryptography and Data Security*. pp. 357–375. Springer (2017).
- [14] Zhu, Y., Zeng, Z., Lv, C.: Anonymous voting scheme for boardroom with blockchain. *International Journal of Performability Engineering* 14(10), 2414–2422 (2018).
- [15] Yu, B., Liu, J.K., Sakzad, A., Nepal, S., Steinfeld, R., Rimba, P., Au, M.H.: Platform-independent secure blockchain-based voting system. In: *International Conference on Information Security*. pp. 369–386. Springer (2018).
- [16] Jonathan Alexander, Steven Landers and Ben Howerton, "Netvote: A Decentralized Voting Network", <https://netvote.io/wpcontent/uploads/2018/02/Netvote-White-Paper-v7.pdf>, 2018.
- [17] Mahto, Dindayal & YADAV, DILIP. (2017). RSA and ECC: A comparative analysis. *International Journal of Applied Engineering Research*. 12. 9053-9061.
- [18] *Secg.org*, 2020. [Online]. Available: <http://secg.org/sec2-v2.pdf>.

- [19] F. P. Hjalmarrsson, G. K. Hreioarsson, M. Hamdaqa, and G. Hjalmtýsson, "Blockchain-Based E-Voting System," 2018 IEEE 11th International Conference on Cloud Computing (CLOUD), 2018.
- [20] R. Bulut, A. Kantarci, S. Keskin, and S. Bahtiyar, "Blockchain-Based Electronic Voting System for Elections in Turkey," 2019 4th International Conference on Computer Science and Engineering (UBMK), 2019.
- [21] "Ngrok - secure introspectable tunnels to localhost", *Ngrok.com*, 2020. [Online]. Available: <https://ngrok.com/>.
- [22] D. Kim, D. Seo, S. Cho and P. Kang, "Multi-co-training for document classification using various document representations: TF-IDF, LDA, and Doc2Vec", *Information Sciences*, vol. 477, pp. 15-29, 2019. Available: 10.1016/j.ins.2018.10.006 .

Modeling the Estimation Errors of Visual-based Systems Developed for Vehicle Speed Measurement

Abdulrazzaq Jawish Alkherret¹

Department of Civil Engineering
Faculty of Engineering, Jerash University
Jerash, Jordan

Musab AbuAddous²

Department of Civil Engineering
Hijawi Faculty for Engineering Technology
Yarmouk University, Irbid, Jordan

Abstract—This paper aims to modeling the relationship between the error of visual-based systems developed for vehicle speed estimation (as dependent variable) and each of the detection region length, the camera angle, and the volume-to-capacity ratio (V/C), as independent variables. Simulation software (VISSIM) is used to generate a set of video clips of predefined traffic based on different values of the dependent variables. These videos are analyzed with a video-based detection and tracking model (VBDATM) developed in 2015. Errors are expressed as differences between each of the actual speeds generated by VISSIM and the speeds computed by the VBDATM divided by the actual speed. The results conducted by the forward stepwise regression analysis show that the V/C ratio does not affect the accuracy of the estimate and there are weak relationships between the estimation error and each of camera position and the detection region length.

Keywords—Intelligent transportation systems; image processing; vehicle detection; vehicle tracking; speed estimation; traffic simulation; linear regression analysis

I. INTRODUCTION

Intelligent Transport Systems (ITS) is a most important field of research for traffic planners in recent years. ITS have been developed to improve traffic conditions, detection of anomalous traffic, and secure safe operation of transportation [1]. As a fundamental task in ITS, vehicle detection and tracking aims to provide traffic management centers with necessary information such as traffic volume, traffic speed, etc. Of all parameters, speed is often a critical element in both macroscopic and microscopic traffic analysis [2]. However, the current systems of vehicle speed measurement include induction loop detectors, magnetic strips, laser sensors, ultrasonic technology, video-based technology, and so on [3]. Compared with other technologies, video-based system has a lot of advantages; it is easy to install, operate and maintain, and low cost. Moreover, it has a wide monitoring range, and enables users to obtain rich information with the ability to review recorded tapes whenever needed [4].

Video-based approach or Video Image Processing (VIP) technic has grown rapidly in recent years. Numerous mathematical models were developed to calculate the traffic parameters, especially vehicle speed, from video sequence. In general, the algorithms used to estimate vehicle speed go through three main stages: moving vehicle detection, tracking this vehicle, and then calculating speed.

A. Vehicle Detection

Most common vehicle detection methods in the literature use background subtraction techniques. The background subtraction technique is based on the idea of identifying portions of the image that remain unchanged in successive frames. Subsequently, the background model is subtracted from each frame of the video, and the remaining areas are blobs that indicate the vehicles present in the scene [5]-[15]. In addition to the background segmentation techniques mentioned above, recently, some researchers used the Convolutional Neural Networks (CNNs) approach that is able to precisely detect vehicles present in a single static video frame. This method is based on Machine Learning to analyzing a database and classifies and detects objects by searching for features [16]-[19]. Optical flow technique is also widely used by researchers. The Optical Flow Method is used to extracted moving vehicle from the dynamic background. Based on characteristics of the optical flow information of the moving target changing with time, this method establishes the constraint equation of optical flow in order to detect the target [20]-[23].

B. Vehicle Tracking

Tracking can be defined as estimating the vehicles trajectory in the image texture as they move in the scene and plot the movement path on the road [24]. The literature indicates that the common methods for tracking moving objects are silhouette based tracking, kernel based tracking and point based tracking. Silhouette based approach is used for tracking of complex shapes such as human features (head, hands and shoulders) [25], [26]. In Kernel-tracking methods, the moving object is represented by a geometric shape (a rectangle or an ellipse). Kernel-based tracking methods assign a weight to each pixel in the shape and then the density gradient in the image coordinates is estimated, using these weights, to determine the new position of that object [27]-[29]. The point tracking method has been adopted by most researchers concerned with the calculating speed of moving vehicles [6], [9]-[15], [19], [30] and [31]. This technique recognizes vehicle's features and the marking of points that will be followed, to promote correspondence between different frames, and then connects the positions of the same points of the vehicle in the frame sequence. The choice of points (features) to be followed is essential for tracking accuracy [17]. However, object tracking algorithms allow tracking of the path taken by an object in a set of video

frames. This block, therefore, provides as a result the distance traveled by a vehicle as well as the number of frames that the vehicle took to cover that distance. To ensure temporal consistency, it is preferable that the interval between frames is constant and short, and that there are no sudden changes in the direction of the object [32], [33].

C. Speed Calculation

From a practical point of view, methodologies of calculating speed of moving vehicles can be classified into two categories; Time-based algorithm and Distance-based algorithm. In the first, a specific number of successive frames are used and then the displacement of the tracked point is calculated in pixels between the first and the last frame. Depending on both the frame rate and the dimensions of one of the road features that shown in the video, time and displacement distance can be calculated in metric units [6], [12], [15], and [19].

The Distance-based algorithm allows the user, before starting the processing, to select four points that represent the vertices of the detection area (region of interest, ROI). This area is a quadrilateral with two sides matching both edges of the road and the other two sides are perpendicular to the road axis and represent the entry line and the departure line for this area. The four points are selected based on specific features of the road. Accordingly, the distance (in metric unit) between the entry and departure lines for this area is known. However, based on the video frame rate and the number of frames taken by the vehicle traveled through this ROI, the algorithm calculates the time and thus the speed [8]-[11], [13], [14], [16], [17], and [20].

D. Problem Statement

The review of the literature indicates that most researchers attribute the inaccuracy of the results to weaknesses in the detection and tracking algorithms. Also, most of the research did not address the effect of traffic volume on the accuracy of measuring vehicle speed. On the other hand, a limited number of researches applied the second methodology (Distance-based algorithm) have been concerned with studying the effect of the ROI length on the accuracy of speed measurement. Wicaksono and Setiyono [10] adopted the fact that vehicles traveling at a constant speed and heading towards the camera seem to speed up when they get closer. Based on distance from the camera, the authors divided the captured road into three regions. Moreover, the authors used three different camera angles (45, 50, and 60 degrees) to capture traffic on each region. The authors concluded that the best ROI for 45 and 50 degree was the closest region, while for 60 degree was full region. Al Kherret et al. [13] validated the model they developed for six lengths of ROI (5, 10, 15, 20, 25, and 30 m). The researchers concluded that the best model accuracy is associated with ROI lengths of 10 and 15 m. Javadi et al. [20] adopted four intrusion lines with a spacing of approximately three meters to define three regions of interest (2.87, 5.95, 8.97 m). Results indicated that using cameras with higher frame rates and changing the distances between intercept lines could reduce the error rate in the measurements.

This study aims to provide a new perspective of thinking for other researchers through modeling the relationship

between the error in vehicle speed measurement with video system and each of the length of the detection area, the shooting angle, and the volume of traffic. However, the remaining sections of this paper are structured as follows: Section 2 explains the data collection. In Section 3 statistical data analysis is presented. Section 4 explains the model development and discusses the results. Finally, in Section 5, the conclusions are presented.

II. DATA COLLECTION

Data collection was accomplished in two stages. The first stage achieved using traffic simulation software (VISSIM) to generate visualization of traffic operations (video files) and yield statistical data and save it in text files. The reason behind using simulation software in this research was to ensure the quality of the recorded video of traffic and thus avoid errors that usually result from applying the algorithms used to detect and track moving vehicles, as well as the ability of such programs to provide all the necessary data. In the second stage, a video-based detection and tracking model (VBDATM), developed by Alkherret et al., [13] was used for detecting and tracking moving vehicles in the recorded videos, and collecting traffic data such as traffic count, speed, and headways.

A. The Simulation Software Package

The simulation environment is very important layer for Vision-based approach. VISSIM is a microscopic traffic flow simulation software package used to analyze traffic and transit operations under constraints provided by users and evaluate various alternatives based on transportation engineering and planning measures of effectiveness [34]. Traffic simulation includes: users data inputs, transmission the base input data into analyzed statistical data, and generation of outputs in the form of 2D and 3D animations, and database files [35].

According to VISSIM User Manual [34], the base data provided in VISSIM can be classified into: geometric data of roadway network; traffic control strategies such as speed limit, time gap, vehicle mix rate, vehicle classes and so on; general demands that include initial volume inputs, turning volume, and route choice process; performance data used for model calibration purpose and to minimize difference between simulation data and calibration data; and future demands used for estimation and forecast purposes. The characteristics of VISSIM, such as car following, lane change logic, and making comparisons between the various alternatives in the same scenario, makes it a useful tool in this study.

B. Input Parameters of the Simulation Software

In this research, a one way-two lane road, with lane width of 3.6 m, was created in VISSIM and a 30-meter section has been specified as a region of interest (ROI) to collect traffic data for vehicles as they traversed through it. Within limits of the ROI, twenty-six data collection points were distributed with a uniform spacing of 2.5 meters on the two lanes, as shown in Fig. 1. Furthermore, the models "Car1" to "Car6" were defined and "without lane change" choice was selected using high value for time gap parameter in "Driving Behavior Parameter Sets" dialog box.

On the other hand, three different positions were selected for the camera; in the first position (Pos. I), the camera sight line was parallel with the road's longitudinal axis, in the second position (Pos. II), the camera sight line was perpendicular with the road's longitudinal axis, while in the third position (Pos. III), the horizontal angle between the camera sight line and the road's longitudinal axis (the pan angle) was 45 degrees. The camera height in all positions was set at 30 meters with large focal length to provide a sufficient field of vision. Fig. 2 to Fig. 4 show the viewing field of the three positions.

Using six values to determine the volume-to-capacity ratio (V/C), six video clips were recorded for each of the three previously defined camera locations. The V/C values were: 30%, 50%, 70%, 80%, 90% and 100%. Based on, traffic simulation was run eighteen times. Table I shows the periods of recording video clips (sec) corresponding to each V/C ratio. This table shows that the large values have been selected for the recording period when V/C values are low and vice versa. Selecting multiple values to the simulation's record was to ensure the presence of a sufficient number of vehicles within the monitored section.

As mention above, after each run, VISSIM creates two main file; Audio Video Interleave (AVI) file and text file containing traffic data. VISSIM records AVI files that will be played at a constant rate of 20 frames (pictures) per second. As each simulation time step results in one picture, the actual playback speed of the AVI file depends on the simulation resolution (time steps per simulation second) during the recording; if 10 time steps are chosen (recommended value), the playback speed will be twice as fast as real time. When using only 1 time step, then the resulting playback speed will be 20 times faster than real time.

Data in the text file depends on the parameters defined by the user before running the simulation. In this research, the speeds were attributed to data collection point number, start/end time of the aggregation interval, and vehicle length. This data has been handled and prepared to suit the requirements of this research.



Fig. 2. The Viewing Field of Camera's Position I.

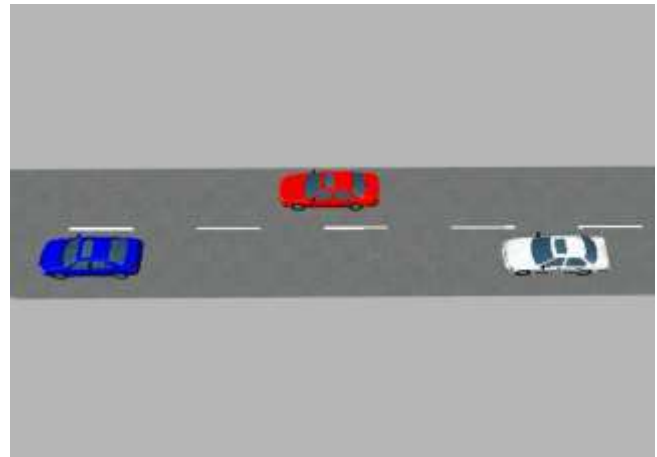


Fig. 3. The Viewing Field of Camera's Position II.

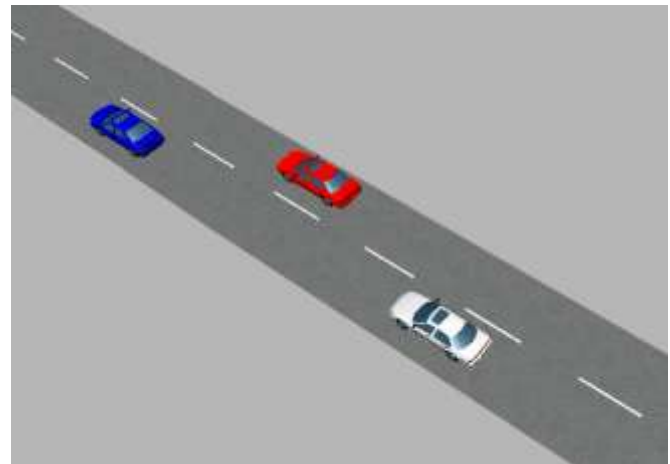


Fig. 4. The Viewing Field of Camera's Position III.

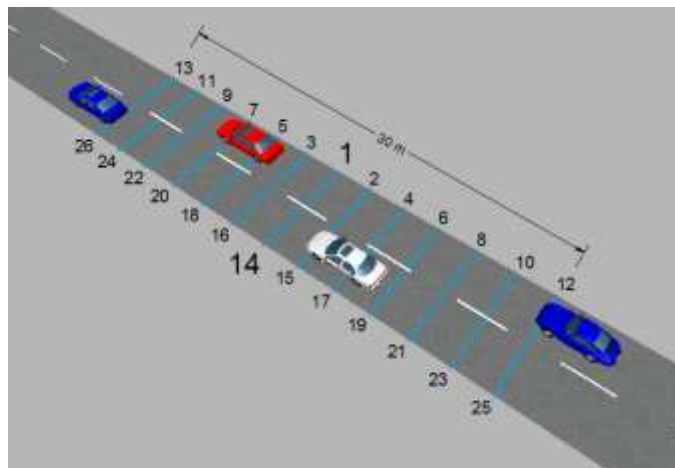


Fig. 1. Distribution of Data Collection Points.

TABLE I. PERIODS OF RECORDING VIDEO CLIPS CORRESPONDING TO V/C RATIO

V/C (%)	30	50	70	80	90	100
Time (sec)	450	450	300	300	150	150

C. Video-based Detection and Tracking Model (VBDATM)

VBDATM was developed using MATLAB Programming Language. This model consists of two sequential phases, namely, detection and tracking moving vehicles, and traffic data collection. However, Gaussian Mixture Models (GMMs) for foreground detection/background subtraction was utilized to formulate code to detect and track moving vehicles in video sequence. The code consists of three main sections:

- The first section was dedicated to initialize system objects for reading the video clip from AVI file, and storing its properties, as well as for read the limits of the region of interest (ROI) that vehicles pass through in the tracking phase. At this stage, the user is instructed to define the limits of the ROI. In this research, six lengths were defined for the regions of interest; 5, 10, 15, 20, 25 and 30 m.
- The second section was devoted to performing three main tasks by external functions: (1) verify the vehicle whether it is inside or outside the ROI, (2) calculate the distance traveled by a vehicle during two given frames, and (3) calculate the total distance that was traveled by the vehicle inside the ROI.
- In the third section, the vehicle is detected using a stream processing loop. The loop aims to read input video frame, convert the colored frame to a binary image, remove small objects (noise), and erode the binary image and generate the final scene. These steps are shown in Fig. 5.

The data collection phase begins with estimating the center's coordinates and bounding box of the blobs in the foreground image using the initialized system object. Then, frame number, the X-center, Y-center, lane, and shortest distance (Short_Dist) are stored in array of six columns and its rows number equals the number of effective frames of the video clip. Effective frames meant only those where the vehicles within the ROI. Table II shows an example of the major output of the processing of the video clip.

These row data used to keep track of already detected vehicles and isolate data of each vehicle. Taking into account value of frame rate of recorded videos, and based on the comparison of data recorded in successive frames, each vehicle was tracked individually and its speed was calculated as it passed through the ROI.

This model validated using speed data collected from video clips recorded with the camera at Position II only. A comparative analysis was established to test whether not the developed model can produce accurate speeds that are close to actual speeds reported by VISSIM for the six lengths of ROI mentioned above. In general, the results of the analysis demonstrated that the VBDATM model is a valuable tool for collecting speed data and other essential traffic data [13].

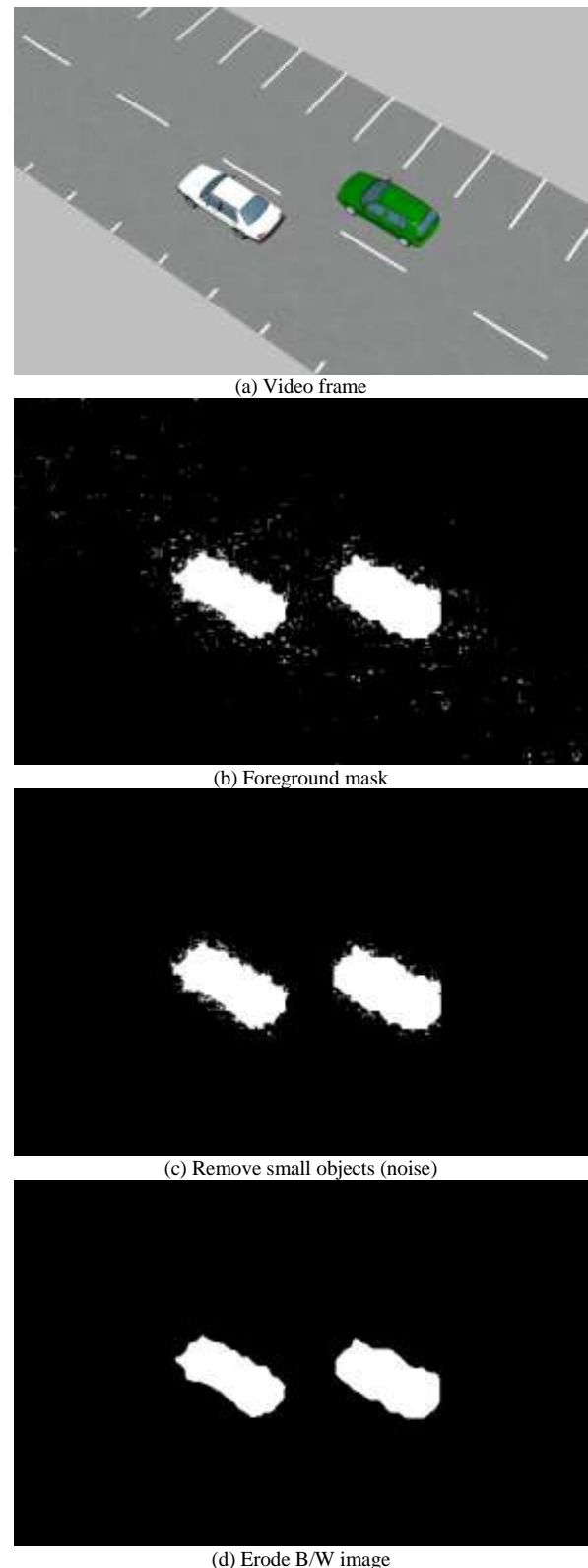


Fig. 5. Foreground Segmentation and Generate the Final Scene.

TABLE II. EXAMPLE OF FRAME BY FRAME OUTPUT DATA

#	Frame	X-Center	Y-Center	Lane	Short_Dist
1	40	859.8890	400.1691	1	24.58260
2	41	475.2345	174.7889	1	470.2743
3	41	823.2294	378.9405	1	66.92720
4	42	452.7923	161.6619	1	496.2658
5	42	788.6323	358.3663	1	107.1734
6	43	430.9909	148.6116	1	521.6720
7	43	755.3047	338.7581	1	145.8319
8	44	406.6719	133.8696	1	550.1092
9	44	723.5303	319.7089	1	182.8753
10	45	382.8607	120.1350	1	577.5845
11	45	691.8086	300.9943	1	219.6980
12	46	657.9541	281.7318	1	258.6226
13	47	626.8792	263.1230	1	294.8395

III. STATISTICAL DATA ANALYSIS

This paper aims to estimate the error value in the measurements of a video-based detection and tracking model, developed for collecting traffic data, and to develop a model that formulates the relationship between the accuracy of the measurements and each of: length of the detection area (i.e. length of ROI), the V/C ratio, and the position of camera as potential influences on this accuracy. For purposes of analysis, the first step was taken to prepare the VISSIM data. The VISSIM database contains speeds values that attributed to data collection point number, start/end time of the aggregation interval and vehicle length as shown in Fig. 6.

Using “FOR” statements loop, a macro was created in MATLAB environment to sort and arrange these data in 26 Excel sheets in three files representing the three camera positions. Each sheet represents the information recorded by one data collection point. Example of final form of the sorted data set is shown in Fig. 7.

Data resulted from the previous procedure were stored in two Excel files. The first file included data of right lane, while the second was devoted to data of left lane. These files used to determine the statistical significant differences between the mean speeds of vehicles for right and left lane. The estimated differences determine whether should study each lane alone or combine in a single database.

A. Descriptive Statistics of Actual and Estimated Speeds Values

Speed data were tested using the “Descriptive Statistics” tool in Excel. Average, standard deviation, maximum and

minimum values of the estimated speeds classified according to the length of the ROI and the camera position with the corresponding values that represent the output of VISSIM. This arrangement is adopted for all V/C ratios. The numbers of observations are included. The descriptive statistics of actual and estimated speeds for right lane are illustrated in Table III and Table IV, and for left lane in Table V and Table VI.

Estimated errors represent the difference between the actual speed (from VISSIM) and the estimated speed (from the VBDATM model) divided by the actual speed. The mean errors in estimating speeds on right and left lane for each of V/C ratios, length of ROI, and camera positions are listed in Table VII.

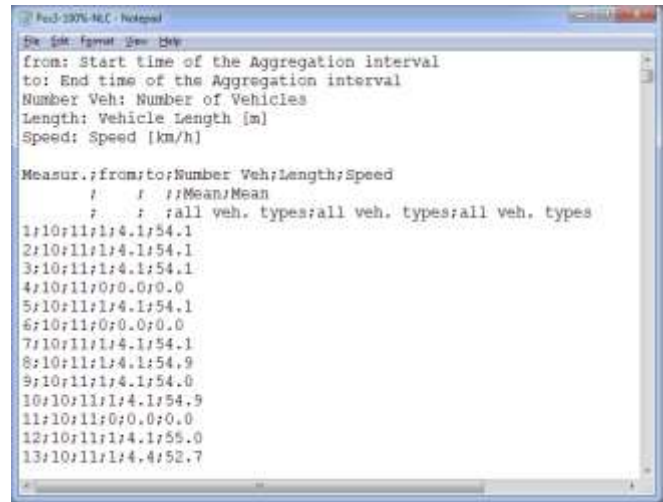


Fig. 6. Example of VISSIM Database.

	A	B	C	D	E	F
1	Measur	from	to	Number_Veh	length	Speed
2	1	0	1	1	4.4	54.1
3	1	0	1	1	4.1	51.8
4	1	1	2	1	4.4	55.3
5	1	1	2	1	4.1	67.0
6	1	2	3	1	4.4	60.1
7	1	2	3	1	4.8	56.1
8	1	3	4	1	4.8	42.0
9	1	4	5	1	4.8	59.6
10	1	4	5	1	4.8	63.1
11	1	5	6	1	4.6	77.1

Fig. 7. Example of Excel Database (Data Collection Point #1; Camera Position III; V/C=100%).

TABLE III. DESCRIPTIVE STATISTICS OF ACTUAL (VISSIM) AND ESTIMATED (MATLAB) SPEEDS FOR RIGHT LANE (ROI = 5, 10, AND 15 M)

	MATLAB (ROI of 5 m)			VISSIM	N*	MATLAB (ROI of 10 m)			VISSIM	N*	MATLAB (ROI of 15 m)			VISSIM	N*
	pos. I	pos. II	pos. III			pos. I	pos. II	pos. III			pos. I	pos. II	pos. III		
V/C = 30%															
Average	69.3	68.5	68.7	69.2	141	71.6	69.9	69.9	68.7	148	70.1	69.4	69.1	68.6	149
St Dev.	10.6	10.6	10.5	10.3		10.7	10.7	10.5	10.3		10.8	10.6	10.7	10.4	
Max	96.9	96.4	96.9	92.4		97.8	95.7	96.3	92.3		95.7	92.4	94.7	92.2	
Min	51.7	50.9	51.3	52.1		54.3	52.5	52.9	52.1		52.3	52.5	52.0	52.0	
V/C = 50%															
Average	68.2	67.5	65.9	66.5	235	68.1	67.5	67.4	66.4	238	66.6	67.1	66.8	66.3	239
St Dev.	9.8	9.8	9.7	9.5		9.8	9.8	9.8	9.6		9.8	9.8	9.8	9.6	
Max	94.9	93.7	93.5	91.6		96.2	95.3	92.9	91.6		92.4	92.8	92.9	91.6	
Min	52.8	52.2	50	51.4		51.7	51.2	51.3	51.4		50.8	51.6	51.2	51.4	
V/C = 70%															
Average	64.4	65	63.1	63.8	215	64.7	64.8	63.9	63.7	218	64.3	63.9	63.7	63.5	219
St Dev.	8.9	8.8	8.9	8.6		8.8	8.9	8.7	8.7		8.8	8.8	8.8	8.6	
Max	89.2	87.7	88.3	86.5		87.9	88.6	86.9	86.5		86.6	87.3	86.4	86.5	
Min	40.2	42.1	38.8	41.6		41.7	41.3	40.5	41.3		41.9	41.0	40.3	42.4	
V/C = 80%															
Average	61.1	62.1	60.2	61.7	240	63.2	62.8	62.1	61.8	246	63.5	62.7	62.6	61.7	248
St Dev.	7.8	7.6	7.4	7.3		7.6	7.5	7.4	7.4		7.6	7.5	7.5	7.3	
Max	86	87.8	83.1	86.5		86.1	88.6	87.5	86.5		88.6	87.5	87.6	86.5	
Min	45.1	49.3	47.9	49.7		47.5	50.3	49.6	49.7		48.4	50.5	50.5	49.7	
V/C = 90%															
Average	60.3	61.8	59.8	60.9	129	62.1	61.4	60.5	60.8	132	62.3	61.3	61.1	60.7	136
St Dev.	7.1	6.9	7.0	6.8		7.1	7	6.9	6.8		7.2	6.8	6.9	6.8	
Max	85.8	87.7	86.9	86.5		88.7	87.8	85.9	86.5		87.5	87.3	86.4	86.5	
Min	49.8	51.5	49.2	51.8		49.4	50.5	50.5	51.4		50.7	51.8	48.6	51.4	
V/C = 100%															
Average	60.5	60.3	58.4	59.7	143	61.3	60.4	59.9	59.6	146	61.2	60.7	60.3	59.7	146
St Dev.	7.5	7.5	7.3	7.3		7.5	7.5	7.3	7.2		7.5	7.4	7.4	7.2	
Max	88.6	90.5	84.1	86.5		88.3	87.8	86.7	86.5		88.5	88.0	87.8	86.5	
Min	49.8	47.4	48.1	50.6		49.5	47.7	48.8	50.6		49.5	51.4	51.1	50.6	

* Number of vehicles

TABLE IV. DESCRIPTIVE STATISTICS OF ACTUAL (VISSIM) AND ESTIMATED (MATLAB) SPEEDS FOR RIGHT LANE (ROI = 20, 25, AND 30 M)

	MATLAB (ROI of 20 m)			VISSIM	N*	MATLAB (ROI of 25 m)			VISSIM	N*	MATLAB (ROI of 30 m)			VISSIM	N*
	pos. I	pos. II	pos. III			pos. I	pos. II	pos. III			pos. I	pos. II	pos. III		
V/C = 30%															
Average	70.7	69.2	69.6	68.6	149	70.0	68.5	70.0	68.6	149	70.0	68.2	70.0	68.5	150
St Dev.	10.7	10.5	10.5	10.4		10.5	10.4	10.7	10.4		10.7	10.3	10.7	10.4	
Max	96.4	92.3	95.2	92.2		94.0	91.9	94.9	92.1		93.4	91.6	93.1	92.0	
Min	52.9	52.5	53.0	52.0		53.5	51.7	53.0	51.8		52.1	51.7	52.6	51.8	
V/C = 50%															
Average	66.2	66.9	67.3	66.3	239	65.7	66.2	67.5	66.2	240	65.8	65.8	67.5	66.2	240
St Dev.	9.7	9.7	9.7	9.6		9.7	9.7	9.8	9.6		9.5	9.6	9.8	9.6	
Max	92.6	93.2	93.5	91.6		91.1	91.9	93.9	91.6		91.2	91.5	94.0	91.6	
Min	50.6	51.4	51.7	51.4		50.5	51.2	49.9	51.4		50.7	50.8	52.2	51.4	
V/C = 70%															
Average	65.1	64.0	64.2	63.6	220	63.8	63.5	65.1	63.5	219	64.9	63.3	65.1	63.5	220
St Dev.	8.9	8.8	8.8	8.7		8.8	8.7	8.8	8.6		8.9	8.7	9.0	8.7	
Max	89.5	87.0	86.9	86.5		87.1	86.8	88.1	86.5		88.1	86.5	87.8	86.5	
Min	41.8	40.7	41.1	40.5		40.9	40.4	41.5	40.5		38.2	40.0	36.2	40.4	
V/C = 80%															
Average	64.0	62.4	62.8	61.7	249	63.0	61.7	63.0	61.7	249	63.4	61.4	63.1	61.7	248
St Dev.	7.8	7.5	7.6	7.3		7.6	7.4	7.5	7.3		7.4	7.4	7.6	7.4	
Max	87.3	87.9	88.0	86.5		86.1	86.5	88.3	86.5		85.7	86.0	88.2	86.5	
Min	50.6	50.1	50.0	49.7		49.5	49.2	50.9	49.7		50.9	49.4	50.6	49.7	
V/C = 90%															
Average	62.4	61.4	61.8	60.8	136	61.7	60.5	61.8	60.7	136	62.5	60.4	62.1	60.7	135
St Dev.	7.0	6.9	6.9	6.8		7.0	6.8	6.9	6.8		7.0	6.9	6.9	6.8	
Max	87.3	87.7	87.9	86.5		85.6	86.7	87.7	86.5		86.1	86.5	88.2	86.5	
Min	49.4	51.2	52.5	51.4		49.9	50.0	49.9	51.4		52.9	50.7	52.6	51.4	
V/C = 100%															
Average	61.2	60.2	60.4	59.6	148	60.3	59.3	60.6	59.6	148	61.4	59.2	61.0	59.6	148
St Dev.	7.5	7.3	7.4	7.2		7.5	7.2	7.3	7.2		7.3	7.2	7.4	7.2	
Max	89.5	88.1	88.2	86.5		87.2	86.3	87.9	86.5		87.5	85.8	88.5	86.5	
Min	51.4	51.0	51.3	50.6		49.6	50.4	51.3	50.6		51.5	49.6	51.7	50.6	

* Number of vehicles

TABLE V. DESCRIPTIVE STATISTICS OF ACTUAL (VISSIM) AND ESTIMATED (MATLAB) SPEEDS FOR LEFT LANE (ROI = 5, 10, AND 15 M)

	MATLAB (ROI of 5 m)			VISSIM	N*	MATLAB (ROI of 10 m)			VISSIM	N*	MATLAB (ROI of 15 m)			VISSIM	N*
	pos. I	pos. II	pos. III			pos. I	pos. II	pos. III			pos. I	pos. II	pos. III		
V/C = 30%															
Average	70.2	69.3	70.2	69.0	125	71.2	68.7	70.8	69.0	125	71.2	70.0	70.3	69.0	125
St Dev.	11.5	11.3	11.5	11.3		11.7	11.2	11.6	11.3		11.6	11.5	11.5	11.3	
Max	94.6	91.6	92.4	90.8		95.6	90.5	93.7	90.8		96.0	92.4	94.5	90.8	
Min	51.4	51.3	52.0	51.4		52.3	50.9	52.3	51.4		52.7	51.8	52.4	51.4	
V/C = 50%															
Average	65.3	66.0	67.0	65.8	233	65.5	65.5	67.5	65.8	233	66.1	66.9	67.2	65.8	233
St Dev.	10.0	9.8	10.0	9.8		9.8	9.8	10.1	9.8		10.0	10.0	10.1	9.8	
Max	89.2	89.6	91.0	89.7		88.9	89.2	91.4	89.7		91.2	91.5	91.9	89.7	
Min	48.8	50.6	50.9	50.7		50.5	50.1	51.2	50.7		50.1	51.3	51.5	50.7	
V/C = 70%															
Average	64.6	63.6	64.8	63.3	217	64.9	63.2	64.8	63.3	217	64.8	63.6	63.9	63.2	217
St Dev.	8.7	8.5	8.7	8.4		8.7	8.5	8.7	8.4		8.7	8.5	8.4	8.4	
Max	91.1	89.9	92.3	89.8		91.2	90.2	92.4	89.8		91.9	89.9	90.9	89.8	
Min	50.9	50.8	51.2	50.5		51.6	50.1	51.4	50.6		50.7	49.1	50.6	50.4	
V/C = 80%															
Average	64.0	62.9	63.9	62.6	249	64.5	62.3	64.1	62.7	248	63.9	62.8	63.0	62.5	250
St Dev.	8.0	7.7	7.8	7.6		7.8	7.6	7.7	7.6		7.9	7.7	7.7	7.6	
Max	93.0	90.0	91.4	89.7		93.4	89.1	91.1	89.7		94.4	90.1	89.8	89.7	
Min	50.4	49.9	50.9	49.6		50.2	49.4	50.7	49.7		50.1	49.7	50.0	49.6	
V/C = 90%															
Average	63.1	62.0	63.1	61.9	135	63.6	61.5	63.4	61.9	135	64.2	62.5	62.8	61.6	134
St Dev.	8.4	8.1	8.2	8.0		8.2	8.0	8.3	8.0		8.4	8.0	8.1	7.9	
Max	92.8	89.6	89.7	89.7		92.1	89.3	91.7	89.7		93.5	91.1	90.0	89.7	
Min	50.7	49.3	51.1	50.1		51.8	49.4	51.3	50.1		52.2	50.7	51.2	50.1	
V/C = 100%															
Average	61.1	61.2	62.2	61.1	152	62.0	60.7	62.5	61.2	151	62.4	61.8	62.1	61.1	151
St Dev.	7.0	6.8	7.0	6.7		6.8	6.7	6.9	6.7		6.9	6.8	6.9	6.7	
Max	86.8	86.9	88.6	86.8		88.5	86.5	88.9	86.8		88.2	87.7	88.2	86.8	
Min	49.9	50.2	50.3	50.2		50.4	49.8	51.0	50.2		51.3	50.8	50.8	50.2	

* Number of vehicles

TABLE VI. DESCRIPTIVE STATISTICS OF ACTUAL (VISSIM) AND ESTIMATED (MATLAB) SPEEDS FOR LEFT LANE (ROI = 20, 25, AND 30 M)

	MATLAB (ROI of 20 m)			VISSIM	N*	MATLAB (ROI of 25 m)			VISSIM	N*	MATLAB (ROI of 30 m)			VISSIM	N*
	pos. I	pos. II	pos. III			pos. I	pos. II	pos. III			pos. I	pos. II	pos. III		
V/C = 30%															
Average	71.1	69.7	70.4	69.0	125	69.9	70.0	69.1	69.1	125	71.3	70.2	69.9	69.0	125
St Dev.	11.9	11.4	11.6	11.3		12.1	11.7	11.3	11.3		12.0	11.4	11.4	11.3	
Max	96.2	91.9	94.1	90.8		95.5	97.2	93.2	90.8		96.1	93.1	93.5	90.8	
Min	52.6	51.5	52.4	51.4		48.3	49.8	49.4	51.4		52.0	51.5	51.5	51.4	
V/C = 50%															
Average	67.6	66.5	67.3	65.8	233	67.0	65.9	64.7	65.8	233	66.7	67.1	66.7	65.8	233
St Dev.	9.9	10.0	10.1	9.8		9.9	9.9	9.8	9.8		9.9	10.0	10.0	9.8	
Max	92.7	91.0	91.5	89.7		92.6	91.8	91.2	89.7		90.9	91.3	91.0	89.7	
Min	50.8	51.1	51.9	50.7		50.9	50.5	49.0	50.7		51.8	51.7	50.0	50.7	
V/C = 70%															
Average	65.2	63.9	64.4	63.3	217	64.4	64.3	64.0	63.2	216	64.7	64.4	63.5	63.3	218
St Dev.	8.7	8.5	8.6	8.4		8.5	8.6	8.7	8.4		8.7	8.5	8.5	8.4	
Max	92.3	90.4	91.7	89.8		88.9	89.1	89.4	89.8		94.9	90.8	90.4	89.8	
Min	51.7	50.5	51.3	50.5		50.7	50.3	50.5	50.3		51.4	50.8	47.1	50.3	
V/C = 80%															
Average	64.9	63.1	63.7	62.6	250	64.1	63.4	63.0	62.5	251	64.8	63.6	63.1	62.5	250
St Dev.	7.7	7.7	7.8	7.6		7.8	7.9	7.9	7.6		7.9	7.8	7.7	7.6	
Max	92.5	90.5	91.1	89.7		90.1	93.4	92.0	89.7		94.3	91.6	90.0	89.7	
Min	52.0	50.2	50.3	49.6		50.4	50.0	49.9	49.6		51.3	50.5	50.6	49.6	
V/C = 90%															
Average	63.9	62.4	63.1	61.9	135	63.4	62.6	62.2	62.2	127	64.2	63.2	62.7	61.8	136
St Dev.	8.6	8.1	8.2	8.0		8.8	8.2	8.1	8.0		8.5	8.2	8.2	8.0	
Max	93.2	90.3	90.0	89.7		95.3	91.5	90.5	89.7		93.5	91.8	89.6	89.7	
Min	52.4	50.5	51.1	50.1		48.7	50.8	50.4	50.1		51.0	51.8	49.9	50.1	
V/C = 100%															
Average	62.7	61.6	62.3	61.1	152	63.0	62.8	62.5	61.0	148	62.2	62.9	62.7	61.1	151
St Dev.	6.9	6.8	6.8	6.7		6.9	7.0	7.1	6.7		7.1	7.0	7.0	6.7	
Max	88.6	87.7	88.3	86.8		89.5	89.6	89.4	86.8		88.8	89.1	90.4	86.8	
Min	51.5	50.6	50.5	50.2		51.9	51.9	50.9	50.2		50.4	51.5	50.8	50.2	

* Number of vehicles

TABLE VII. MEAN ERRORS IN ESTIMATING SPEEDS ON RIGHT AND LEFT LANE

V/C	Right Lane						Left Lane					
	ROI length (m)						ROI length (m)					
	5	10	15	20	25	30	5	10	15	20	25	30
Camera Position I												
30%	2.00	4.32	2.36	3.08	2.33	2.28	3.31	3.36	3.22	3.05	2.00	3.18
50%	3.29	2.60	0.66	0.72	0.90	0.70	2.35	1.66	0.83	2.78	1.72	0.81
70%	2.45	1.96	1.78	2.76	0.72	2.24	2.05	2.56	2.78	3.25	2.26	2.63
80%	2.90	2.81	3.22	3.68	2.32	2.80	2.63	3.73	2.50	3.83	2.38	2.93
90%	2.78	2.96	2.77	2.79	2.02	3.09	2.62	3.85	4.22	3.32	2.14	2.76
100%	2.69	3.08	2.85	2.62	1.89	3.07	3.50	2.10	2.27	2.72	1.44	1.45
Camera Position II												
30%	2.16	1.84	1.12	0.88	0.29	0.43	2.28	1.66	1.37	0.97	0.42	0.50
50%	2.65	1.68	1.21	0.92	0.30	0.64	1.54	2.02	1.71	1.09	0.42	0.58
70%	2.27	1.75	0.85	0.87	0.37	0.50	2.37	1.85	0.73	1.08	0.61	0.85
80%	1.61	1.71	1.56	1.18	0.33	0.63	1.77	1.70	0.50	0.99	0.46	0.57
90%	1.83	1.07	0.93	1.06	0.43	0.58	1.61	2.41	1.34	0.94	0.35	0.62
100%	1.46	1.45	1.72	0.98	0.58	0.79	3.14	2.87	1.06	0.86	0.27	0.70
Camera Position III												
30%	2.00	1.81	1.01	1.57	2.04	2.21	1.81	1.44	1.91	1.96	1.76	2.57
50%	1.93	1.66	1.02	1.53	1.88	1.93	2.32	1.42	2.08	2.24	1.86	2.50
70%	1.72	0.95	0.86	1.30	2.51	2.52	1.69	0.92	1.07	1.89	2.41	2.45
80%	2.65	1.10	1.34	1.70	2.03	2.21	1.52	0.96	0.93	1.89	2.13	2.28
90%	2.05	0.96	0.89	1.74	1.98	2.49	1.82	1.56	1.95	2.02	2.04	2.38
100%	2.31	1.01	1.16	1.41	1.60	2.36	2.68	2.51	1.56	1.97	1.88	2.27

For the right lane, the results showed that the maximum error was 4.32 km/h in speeds estimating at camera position I, while the minimum error was 0.29 km/h. Maximum error estimated when the length of ROI was 10 m and the V/C ratio was 30%. In the video clip recorded at position II, the maximum error was 2.65 km/h corresponding to 5 m for the ROI length and 50% for V/C ratio. The minimum error was 0.29 km/h that estimated when the length of ROI was 25 m and the V/C ratio was 30%. At position III, the maximum error was 2.65 km/h corresponding to 5 m for the ROI length and 80% for V/C ratio, while the minimum error was 0.86 km/h corresponding to 15 m for the ROI length and 70% for V/C ratio.

For the left lane, the results showed that the maximum error was 4.22 km/h, in speeds estimating at camera position I, while the minimum error was 0.81 km/h. Maximum error estimated when the length of ROI was 15 m and the V/C ratio was 90%. In the video clip recorded at position II, the maximum error was 3.14 km/h corresponding to 5 m for the ROI length and 100% for V/C ratio. The minimum error was 0.27 km/h that estimated when the length of ROI was 25 m and the V/C ratio was 100%. At position III, the maximum error was 2.68 km/h corresponding to 5 m for the ROI length and 100% for V/C ratio, while the minimum error was 0.92 km/h corresponding to 10 m for the ROI length and 70% for V/C ratio.

Previous results give an initial visualization that there is no relationship between the speed estimation error and each of

length of ROI, V/C ratio, and the position of camera. However, study the effect of the mentioned factors on the accuracy of estimation involves performing a regression analysis for all data. Before conducting this analysis, the differences between the mean speeds of vehicles for right and left lane should be estimated.

B. Difference between Data of the Two Lanes

One-way classification analysis of variance with interaction (ANOVA) was employed to investigate whether there are differences between speeds values in right lane and left lane. One-way ANOVA tests the equality of population means when classification is by one variable. In other word, one-way ANOVA is used when there is only one way (lane) to classify the populations of interest [36]. In this study, on-way ANOVA was carried out to compare the differences between the mean errors in estimating speeds on right and left lane for each of V/C ratios, length of ROI, and camera positions. However, for the *P-values* less than 0.05, the null hypothesis can be rejected.

The results showed that for most of cases (67% of cases), there was a statistically significant difference (*P-value* < 0.05), at the 95% confidence level, between the mean speeds of vehicles (Table VIII). Accordingly, speeds that estimated on each of the right and left lanes were prepared separately in order to determine the relationship between the measurement accuracy and each of the length of ROI, V/C ratio, and the position of camera.

TABLE VIII. SUMMARY OF ANOVA (P-VALUE): THE DIFFERENCES BETWEEN THE MEAN ERRORS ON RIGHT AND LEFT LANE

V/C	ROI length (m)					
	5	10	15	20	25	30
Camera Position I						
30%	0.000	0.000	0.000	<u>0.769*</u>	<u>0.056*</u>	0.000
50%	0.000	0.000	0.001	0.000	0.000	0.033
70%	0.005	0.000	0.000	0.003	0.000	0.001
80%	<u>0.198*</u>	0.000	0.000	<u>0.205*</u>	<u>0.618*</u>	<u>0.315*</u>
90%	<u>0.667*</u>	0.000	0.000	0.003	<u>0.491*</u>	<u>0.086*</u>
100%	0.001	0.000	0.000	<u>0.792*</u>	0.001	0.000
Camera Position II						
30%	<u>0.523*</u>	<u>0.090*</u>	0.004	<u>0.181*</u>	0.000	<u>0.073*</u>
50%	0.000	0.000	0.000	0.000	0.000	0.047
70%	<u>0.507*</u>	<u>0.162*</u>	<u>0.087*</u>	0.001	0.000	0.000
80%	<u>0.155*</u>	<u>0.917*</u>	0.000	0.000	0.000	<u>0.141*</u>
90%	<u>0.117*</u>	0.000	0.000	0.014	<u>0.315*</u>	<u>0.645*</u>
100%	0.000	0.000	0.000	0.002	0.000	<u>0.191*</u>
Camera Position III						
30%	<u>0.373*</u>	0.031	0.000	0.000	0.012	0.006
50%	0.009	0.009	0.000	0.000	<u>0.906*</u>	0.000
70%	<u>0.849*</u>	<u>0.710*</u>	0.011	0.000	<u>0.228*</u>	<u>0.454*</u>
80%	0.000	0.015	0.000	0.017	<u>0.142*</u>	<u>0.387*</u>
90%	<u>0.219*</u>	0.000	0.000	0.003	<u>0.582*</u>	<u>0.256*</u>
100%	0.040	0.000	0.000	0.000	0.002	<u>0.233*</u>

* P-value > 0.05

IV. MODELS DEVELOPMENT

Statistical Analysis Software (SAS-V8) used to determine the relationship between the estimation error as a dependent variable and each of the length of ROI, V/C ratio, and the position of camera as independent variables. SAS-V8 is statistical analyses software that is capable of handling the multiple regression analysis. In this study, the stepwise regression technique was used in the SAS software so that those independent variables, which are not statistically significant at 95% confidence level, can be automatically removed from the models.

Forward stepwise regression starts with no model variable. At each step it adds the most statistically significant variable into the model until there are none left. However, the dependent variables are defined as the error of speed estimation at right (E_R) and left (E_L) lane. Results of this analysis are shown in Table IX. This table shows that the two models are similar and the V/C ratio does not affect the accuracy of the estimate. Moreover, there are weak relationships (R^2 of 0.1733 and 0.1605) between the estimation error and each of camera position and ROI length.

The two models can be expressed by the following linear equations:

$$E_R = 2.88687 - 0.36183 CP - 0.02332 L_{ROI} \quad (1)$$

$$E_L = 3.04924 - 0.35454 CP - 0.02418 L_{ROI} \quad (2)$$

where:

CP = the camera position.

L_{ROI} = length of the region of interest (m).

In both models, the negative sign of the coefficient for L_{ROI} means that the error of speed estimation (E_R and E_L) decreases with increases in the length of the region of interest.

TABLE IX. RESULTS OF REGRESSION ANALYSIS

Variable	Parameter Estimate	Standard Error	R ²
Dependent Variable: E_R			
Intercept	+ 2.88687	0.25412	0.1733
Camera Position	- 0.36183	0.09300	
ROI Length	- 0.02332	0.00889	
Dependent Variable: E_L			
Intercept	+ 3.04924	0.26560	0.1605
Camera Position	- 0.35454	0.09720	
ROI Length	- 0.02418	0.00929	

V. CONCLUSIONS

The main goal of this study was to present a new perspective of thinking for other researchers through developing a multiple linear regression model of the relationship between the errors of visual-based models used for vehicle speed estimation (dependent variable) and each of the detection region length, the camera angle, and the volume-to-capacity ratio (V/C), as independent variables. Traffic simulation software, VISSIM, was employed to generate a set of videos for virtual traffic according to the following modes: a one way-two lane road, three camera positions, six values for volume-to-capacity ratio, and six distances to measure vehicle speed. These videos were analyzed with a video-based detection and tracking model (VBDATM) developed by Alkherret et al., (2015). Estimated measurement errors were expressed as differences between each of the actual speeds generated by VISSIM and the speeds computed by the VBDATM divided by the actual speed.

In conclusion, regression model showed that the V/C ratio does not affect the accuracy of the estimate and there are weak relationships between the estimated error and each of camera position and the detection region length. The two models clearly indicate that the increase in the length of the region of interest increases the accuracy, in other words, it reduces the amount of error in measurement. Moreover, changing the camera position improves the accuracy of the measurements.

The limitation of the methodology used in this research is to use an ideal environment for traffic visualization generated by a simulation program. The author proposes to apply the methodology and expand it to include real-world traffic, taking into account that, in the real world, camera stability and image clarity cannot be guaranteed, and determine the angle and location of the video camera may not be under control. Furthermore, although the accuracy of the results is affected by the camera location, as is evident in the developed models, the issue of choosing the ideal location for taking the picture remains subject to the costs and capabilities available to the study and implementing authorities.

ACKNOWLEDGMENT

The authors are thankful to Jerash University (Jerash-Jordan) and Yarmouk University (Irbid-Jordan) for their support and for providing their Laboratories and premises.

Our thanks extend to the reviewers for their valuable suggestions that led to enhancement of the quality of article.

REFERENCES

- [1] G. Dimitrakopoulos, L. Uden, and I. Valamis, *The Future of Intelligent Transport Systems*. Elsevier, ISBN: 978-0-12-818281-9, 2020.
- [2] C. Bachmann, B. Abdulhai, M. J. Roorda, and P. Moshiri, "A comparative assessment of multi-sensor data fusion techniques for freeway traffic speed estimation using microsimulation modeling," *Transportation Research Part C: Emerging Technologies*, Vol. 26, 2013, pp. 33–48.
- [3] P. P. Tasgaonkar, R. D. Garg, and P. K. Garg, "Vehicle detection and traffic estimation with sensors technologies for intelligent transportation systems," *Sensing and Imaging*, Vol. 21, 2020, pp. 1–28.
- [4] J. Guerrero-Ibáñez, S. Zeadally, and J. Contreras-Castillo, "Sensor Technologies for Intelligent Transportation Systems," *Sensors*, Vol. 18(4), 1212, 2018, pp. 1–24.
- [5] O. Bourjaa, A. Maacha, Y. Zennayia, F. Bourzeixb, and T. Guerin, "Speed estimation using simple line," *Procedia Computer Science*, Vol. 127, 2018, pp. 209–217.
- [6] M. Khan, M. Nawaz, Q. Nida-Ur-Rehman, G. Masood, A. Adnan, S. Anwar, and J. Cosmas, "Vehicle speed estimation using blob analysis," *Advances in Intelligent Systems and Computing*, Vol. 931, 2019, pp. 303–314.
- [7] A. Gunawana, D. A. Tanjunga, and F. E. Gunawanb, "Detection of vehicle position and speed using camera calibration and image projection methods," in *4th International Conference on Computer Science and Computational Intelligence 2019 (ICCSCI)*, *Procedia Computer Science*, Vol. 157, 2019, pp. 255–265.
- [8] A. Ghosh, M. S. Sabuj, H. H. Sonet, S. Shatabda, and D. M. Farid, "An adaptive video-based vehicle detection, classification, counting, and speed-measurement system for real-time traffic data collection," in *IEEE Region 10 Symposium (TENSYP)*, Kolkata, India, 2019, pp. 541–546.
- [9] F. Afifah, S. Nasrin, and A. Mukit, "Vehicle speed estimation using image processing," *Journal of Advanced Research in Applied Mechanics* Vol. 48(1), 2018, pp. 9–16.
- [10] D. W. Wicaksono, and B. Setiyono, "Speed estimation on moving vehicle based on digital image processing," *International Journal of Computing Science and Applied Mathematics*, Vol.3(1),2017,pp. 21–26.
- [11] P. D. Gulhane, K. R. Nagrale, and P. M. Pandit, "An image processing approach for moving vehicle speed detection by speed camera," *International Journal of Electronics, Communication & Soft Computing Science and Engineering*, Special Issue, 2017, pp. 36–41.
- [12] A. Khan, I. Ansari, M. S. Sarker, and S. Rayamajhi, "Speed estimation of vehicle in intelligent traffic surveillance system using video image processing," *International Journal of Scientific & Engineering Research*, Vol. 5(12), 2014, pp. 1384–1390.
- [13] A. Alkherret, S. Al Sobky, and R. Mousa, "Video-based detection and tracking model for traffic surveillance". Paper No. 15-1465 Presented at the Transportation Research Board 94th Annual Meeting. Washington, DC., United States. 11-15 Jan. 2015.
- [14] B. Makwana, and P. Goel, "Moving vehicle detection and speed measurement in video sequence," *International Journal of Engineering Research & Technology*, Vol. 2(10), 2013, pp. 3534–3537.
- [15] H. A. Rahim, U. U. Sheikh, R. B. Ahmad and A. S. Zain, "Vehicle velocity estimation for traffic surveillance system," *International Journal of Transport and Vehicle Engineering*, Vol. 4(9), 2010, pp. 1465-1468.
- [16] A. Grents, V. Varkentin, and N. Goryaev, "Determining vehicle speed based on video using Convolutional Neural Network," in *XIV International Conference 2020 SPbGASU "Organization and safety of traffic in large cities,"* *Transportation Research Procedia*, Vol. 50, 2020, pp. 192–200.
- [17] V. Barth, R. de Oliveira, M. de Oliveira, and V. do Nascimento, "Vehicle speed monitoring using Convolutional Neural Networks," in *IEEE Latin America Transactions*, Vol. 17(6), 2019, pp. 1000–1008.
- [18] J. Lee, S. Roh, J. Shin, and K. Sohn, "Image-based learning to measure the Space Mean Speed on a stretch of road without the need to tag images with labels," *Sensors*, vol. 19(5, 1227), 2019, pp. 1–19.
- [19] J. Sochora, R. Juráněka, and A. Herouta, "Traffic surveillance camera calibration by 3D model bounding box alignment for accurate vehicle speed measurement," *Computer Vision and Image Understanding*, Vol. 161, 2017, pp. 87–98.
- [20] S. Javadi, M. Dah, and M. I. Pettersson, "Vehicle speed measurement model for video-based systems," *Computers and Electrical Engineering*, Vol. 76, 2019, pp. 238–248.
- [21] H. Dong, M. Wen, and Z. Yang, "Vehicle speed estimation based on 3D ConvNets and Non-Local Blocks," *Future Internet*, Vol. 11(6), 2019, pp. 1–16.
- [22] J. Lana, J. Li, G. Hua, B. Ranb, and L. Wanga "Vehicle speed measurement based on gray constraint optical flow algorithm," *Optik*, Vol. 125(1), 2014, pp. 289–295.
- [23] D. Shukla, and E. Patel, "Speed determination of moving vehicles using Lucas-Kanade algorithm," *International Journal of Computer Applications Technology and Research*. Vol. 2(1), 2013, pp. 32–36.
- [24] P. Craciun, M. Ortner, and J. Zerubia, "Joint detection and tracking of moving objects using spatio-temporal marked point processes," in *IEEE Winter Conference on Applications of Computer Vision*, Jan 2015, Hawaii, United States.
- [25] J. Athanesious, and P. Suresh, "Implementation and comparison of Kernel and Silhouette based object tracking," *International Journal of Advanced Research in Computer Engineering & Technology*, Vol. 2(3), 2013, pp. 1298–1303.
- [26] J. Athanesious, and P. Suresh, "Systematic survey on object tracking methods in video," *International Journal of Advanced Research in Computer Engineering & Technology*, Vol. 1(8), 2012, pp. 242–247.
- [27] Z. Tang, G. Wang, T. Liu, Y. Lee, A. Jahn, X. Liu, X. He, and J. Hwang, "Multiple-Kernel based vehicle tracking using 3D deformable model and camera self-calibration," *arXiv:1708.06831*, 2017.
- [28] K. Lee, J. Hwang and S. Chen, "Model-based vehicle localization based on 3-D constrained Multiple-Kernel tracking," *IEEE Transactions On Circuits And Systems For Video Technology*, Vol.25(1),2015,pp.38–50.
- [29] D. Comaniciu, V. Ramesh and P. Meer, "Real time tracking of non-rigid objects using mean shift," *Proceedings IEEE Conference on Computer Vision and Pattern Recognition. CVPR 2000 (Cat. No.PR00662)*, Hilton Head Island, SC, Vol. 2, 2000, pp. 142-149.
- [30] A. G. Rad, A. Dehghani, and M. R. Karim "Vehicle speed detection in video image sequences using CVS method," *International Journal of the Physical Sciences*, Vol. 5(17), 2010, pp. 2555–2563.
- [31] L. Grammatikopoulos, G. Karras, and E. Petsa "Automatic estimation of vehicle speed from uncalibrated video sequences," Presented at the International Symposium on Modern Technologies, Education and Professional Practice in Geodesy and Related Fields, 3–4 November, 2005, Sofia, Bulgaria.
- [32] M. Fiaz, A. Mahmood, and S. K. Jung, "Tracking Noisy Targets: A Review of Recent Object Tracking Approaches," *arXiv, 1802.03098*, 2018.
- [33] N. K. Kanhere, R. Hall, S. T. Birchfield, R. Hall, and W. A. Sarasua, "Vehicle segmentation and tracking in the presence of occlusions," *Transportation Research Record*. Vol. 1944(1), 2006, pp. 89–97.
- [34] VISSIM 5.30-05 User Manual, PTV Planung Transport Verkehr AG, Karlsruhe, Germany, 2011.
- [35] M. Beaulieu, K. Davis, D. Kieninger, M. Robinson-McCutchen, D. Wright, A. Sanderson, J. Ishimaru, and M. Hallenbeck, "A Guide to Documenting VISSIM-Based Microscopic Traffic Simulation Models," *Washington State Transportation Center (TRAC)*, University of Washington. Report No: WA-RD 678.1. 2007.
- [36] J. R. Evans, and D. L. Olson, *Statistics, Data Analysis, and Decision Modeling*, Volume 1, Upper Saddle River, NJ: Prentice Hall (2000).

Characterization of Quaternary Deposits in the Bou Ahmed Coastal Plain (Chefchaouen, Morocco): Contribution of Electrical Prospecting

Yassyr Draoui¹, Fouad Lahlou²
Laboratory of Energy Engineering
and Materials, Faculty of Sciences
Ibn Tofail University
Kenitra, Morocco

Imane Al Mazini³, Jamal Chao⁴
Laboratory of Natural Resources
Geosciences (NaResGeo) Faculty of
Sciences, Ibn Tofail University
Kenitra, Morocco

Mohamed Jalal El Hamidi⁵
Regional Water Centre of Maghreb
LAMERN, Mohammadia School of
Engineers, Mohammed V University
Rabat, Morocco

Abstract—The Bou Ahmed plain, which is part of the internal area of the Rif, is located along the Mediterranean coast, 30 kilometers of Oued Laou town. This basin is made up by a quaternary filling mainly formed by detrital fluvial facies, channeled conglomerates surmounted by fluvial sand interlayered with pebbles; these facies can be new potential aquifers formations areas. Therefore, the main goal of this study is to build a lithostratigraphic three dimensional model to identify the hydrogeological units and the reservoir geometry of the Bou Ahmed plain. In order to achieve this goal, we have created a database made up by Vertical Electrical Sounding surveys and drilling data integrated into a Geographic Information System. This database allowed us to establish a three-dimensional model of the bottom, geoelectric cross-sections, isopach and isoresistivity maps of new potential aquifers units. This approach allowed us to explain the modalities of deposition for the quaternary deposits of the Bou Ahmed plain and to identify potential hydrogeological reservoirs. These results will also be used to develop a hydrodynamic model based on MODFLOW code in the Bou Ahmed aquifer.

Keywords—Bou Ahmed plain; hydrogeological units; reservoir geometry; vertical electrical sounding surveys; geographic information system; quaternary deposits

I. INTRODUCTION

Covering an area of approximately 12 km², the Bou Ahmed plain is located in northern Morocco between the latitudes 35°15' - 35°25'N and the longitude 5°00' - 4°55'W, and is part of Chefchaouen province (Fig. 1). This plain is materialized by a Plio-Quaternary infill containing new potential aquifers formations. The plain is among the coastal alluvial plains in Morocco, which are highly coveted because of the high population densities and agricultural activities, which can cause overexploitation and/or degradation of the groundwater quality. This situation causes significant drops of the groundwater level and consequently concern the decision makers responsible for the management and planning of water resources.

As a result, the groundwater of Bou Ahmed aquifer was the subject of numerous geological, hydrogeological studies, and reconnaissance geophysical survey [1],[2],[3]. Despite these explorations, the mastery of the bottom geometry and the

deposits that they surmount limit certain interpretations of the phenomena determined for the management of water resources in the region.

The objective of this work aims to specify the structure of the Pliocene bottom, and to identify new potential aquifers intervals, with a view to reasonable management of these hydrogeological reservoirs. To achieve this objective, we used all data collection (geoelectric cross-sections data, hydrogeological drilling data and conductivity analysis data) were processed and led to: (i) Study the lithostratigraphy characteristics of the Bou Ahmed aquifer; (ii) Build a three-dimensional lithostratigraphic model from boreholes data and Vertical Electrical Sounding (VES) surveys data of the Bou Ahmed aquifer; (iii) The production of new potential aquifers levels in terms of thickness and resistivity; (iv) To compare between the conductivity map and the isoresistivity map was performed.

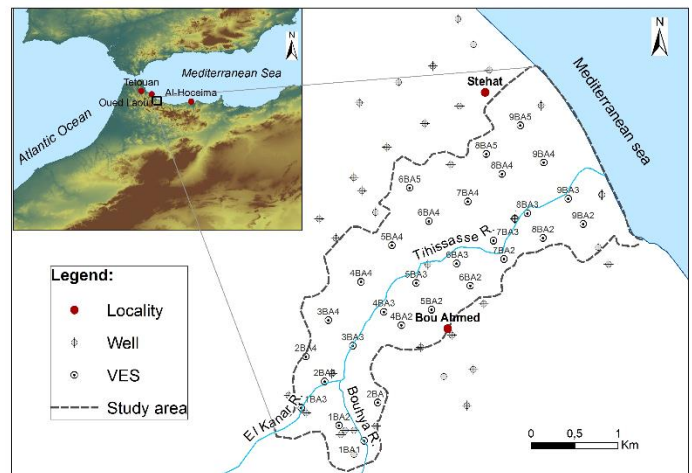


Fig. 1. Geographic Location Map of the Bou Ahmed Aquifer Including the Collected and used Database (Wells/Drilling/VES).

II. GEOLOGICAL SETTING

The Bou Ahmed plain is a geological entity of the internal Rif [4], which is a domain made up by three structural groups piled one on top of the other (Fig. 2): the “Sebtides”, the “Ghomarides”, and the “Calcareous Dorsale” [5]. The

Paleozoic and limestone units form, during the sedimentation of the Rif domain, a shallow in the middle and axial position relative to the "internal" domain ("ultra flyschs" origin) and to the "external" domain [6].

The Bou Ahmed plain is a coastal graben (paleo-golf) which resulted from the Pre-Pliocene subsidence of the Mediterranean basin which was later invaded by the Pliocene Sea ([7], [8] in [3]). This basin has long been considered as a lower Pliocene ria established in ancient Messinian canyons [9], [10].

From the lithostratigraphic standpoint, the study area is in the form of a depression filled from bottom to top with (Fig. 3):

- Palaeozoic basement: the base of the Bou Ahmed basin is materialized by crystallophyllian ("Gneiss" and "Mica-schist") and "peridotite" terrains of the Beni Bousra unit [12]. These formations correspond to the lower "sebtides" which constitute the deepest units of the internal Rif [3].
- Pliocene: in the lower Pliocene the Mediterranean coastal depressions may tend to subside. This allowed the entrance of the Sea and the establishment of a thick marl formation of Pliocene age [3]. This formation is surmounted by coarse conglomerate facies which have become more abundant in the valley of the Tihissasse River [10].
- Quaternary: the basin is covered by quaternary formations formed essentially by purely fluvial detrital facies (channeled conglomerates surmounted by fluvial sand interlayered with pebbles). These more or less coarse detrital formations are poorly classified in the Tihissasse River. At the upstream valley, develops coarse detrital deposits (pebbles and gravels of a schist nature, sandstone, and slightly calcareous). However, towards the downstream medium-grained sandy deposits predominate [2]. This architecture is due to the dynamics of the Tihissasse River from upstream to downstream.

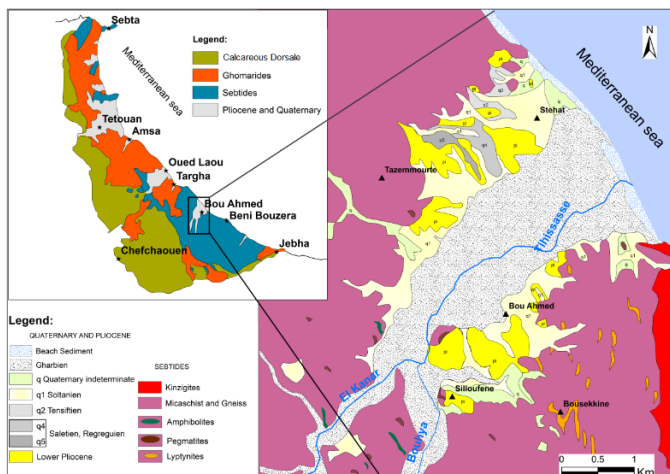


Fig. 2. Location Map of the Bou Ahmed Area in the Internal Rif (Map Simplified from [11]).

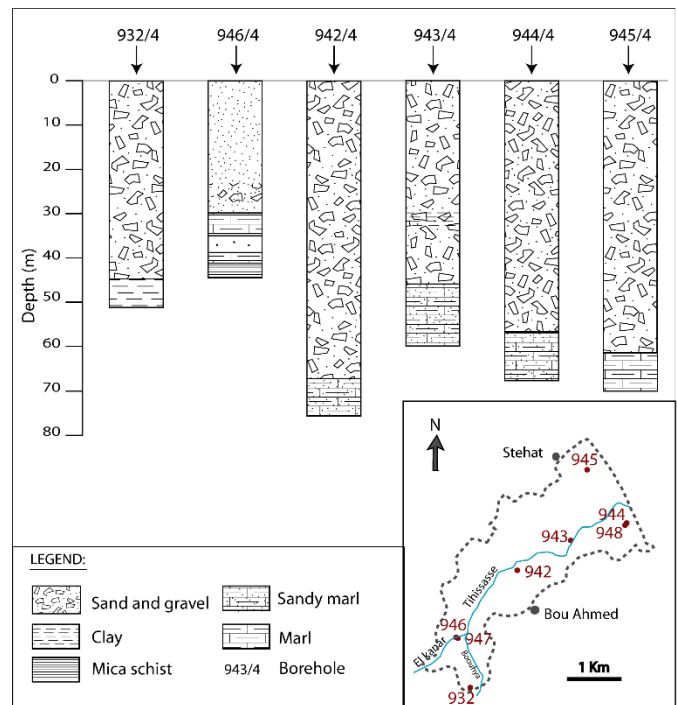


Fig. 3. Synthetic Litho-Stratigraphic Columns in the Study Area.

III. METHODOLOGY

The database used in this work includes hydrogeological and geoelectric drilling data (Fig. 1) hence we used 16 hydrogeological boreholes, six of which reach the lower Pliocene marly bottom.

The electrical data includes six geoelectric cross-sections processed, resulting from the interpretation of 29 VES surveys [1]. The geoelectric method, using electrical survey technique, is one of the first methods used in electrical prospecting in continuous current [13], whose usefulness in the establishment of shallow structures is currently well established [14]. The method is used to characterize the geological formations crossed (thickness and lithological nature) vertical to the measurement point [15] and thus to highlight the stratigraphic evolution of the studied deposits during a lateral correlation [16], [17]. This method is based on the principle of Ohm's law: the injection into the ground of a continuous current at a very low frequency, therefore, the measurement of the voltage allows to reveal the true resistivity of the formations crossed using the Schlumberger array (Fig. 4). In practice, in the field, it uses two steel electrodes for current injection A and B (or C1 and C2), as well as two copper electrodes for the measurement of the potential M and N (or P1 and P2) between which the potential difference ΔV is due to the injection of current by A and B.

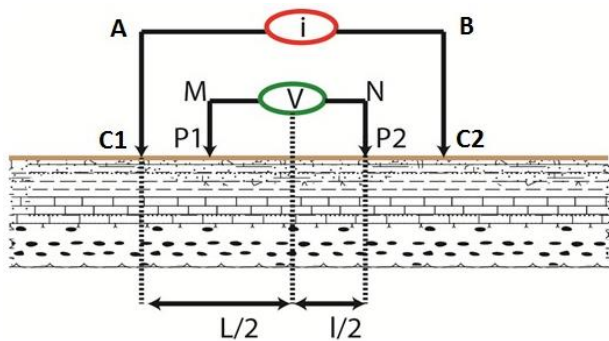


Fig. 4. Electrodes Location for the Schlumberger Array [18].

The three-dimensional representation allows a better understanding of the spatial distribution of the geological structures of the ground. It serves as the basis for a wide range of scientific activities, notably in the area of natural resources assessment and environmental engineering [19], [20], [21]. The three-dimensional (3D) geological modelling is a technology still in development for geological studies used for the exploration of mineral resources, for the quantitative estimation of mineral resources and petroleum exploration [20]. This approach allows 3D modelling of complex and irregular geological objects using geological maps, survey records, geological, geophysical, and data information, etc. [22]. All of this data was integrated into a geographic information system in order to build a 3D geoelectric model and geoelectric correlation sections in different directions.

Knowing that electrical and mechanical surveys are punctual character, and in order to illustrate the characteristics of the various electrical levels, a spatial interpolation method has been used in this work. The Inverse Distance Weighting (IDW) method makes it possible to determine the value of a “node” from a limited number of sampling points [23] in calculating the average values of its points in the vicinity of each processing cell. It is a powerful geostatistical method because it takes into account the spatial variability of the parameters [19], [24]. Currently operating software that is used to model the surface and the sub-surface, includes several spatial interpolation algorithms such as inverse distance weighting, kriging, etc. [25].

Highlighting the relationship between the precision of the Digital Elevation Model (DEM) and interpolation techniques has been the subject of many researches, namely for the creation of a 3D model [19], [20], [23], [26] or for the implementation of the precision of interpolation techniques [24], [27], [28]. The interpolation method thus recommended in the modelling of the sub-surface is the IDW, which, in the estimation of the unknown points, gives more weight to the closest known points instead of the distant ones. The IDW method is very polyvalent, easily programmable, and understandable. In addition, it gives very precise results in data with a wide range of interpretations [28].

IV. RESULTS AND DISCUSSION

A. Bottom Geometry

The three-dimensional model of the blue marl bottom (roof of the lower Pliocene) of the Bou Ahmed basin (Fig. 5) is

established by combining geoelectric data and hydrogeological drilling. The geometry illustrated by this model is mainly characterized by the presence of a large bowl in the NE-SW direction open on the Mediterranean Sea (Fig. 5). This structure is bordered by high areas and affected by a residual relief in the central part of the study area; the growth of this wrinkle seems to be responsible for the separation of two depressions: the first located to the southwest of the basin at the base of the confluence of the El Kanar and Bouhya rivers (depth of about 30 m), and the second located to the northeast of the study area with a depth which increases by about 70 m towards the sea.

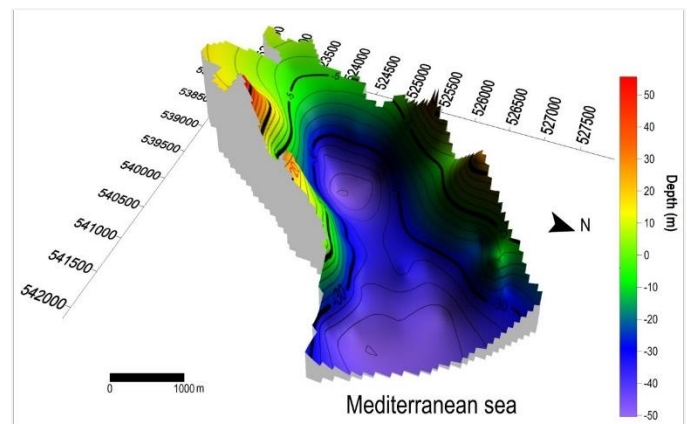


Fig. 5. Three-Dimensional Model of the Blue Marl Bottom (Roof of the Lower Pliocene).

B. Geoelectric Characterization of Quaternary Deposits

The establishment and evolution of the Plio-Quaternary deposits of the Bou Ahmed plain is characterized by the description of the geometry configuration, and the variation of the resistivity values of the geoelectric intervals defined using the geoelectric cross-sections from different directions (Fig. 6 and 7). The geoelectric cross-sections carried out in directions N-S, NE-SW and E-W (Fig. 6 and 7) show that the filling of the quaternary age in the study area is organized into several geoelectric levels: Rs, Cs, R2, C1, R1, and the upper levels (Fig. 6 and 7).

The isometric view, established through two perpendicular sections, highlighted five important geoelectric intervals (Fig. 6). The basal part of the basin is constituted by a geoelectric horizon Rs, which corresponds, according to the boreholes, to mica-schists forming part of the Paleozoic basement.

This horizon is surmounted by the geoelectric conducting interval Cs (limiting an average resistivity interval of 25 Ω .m (Fig. 6 and 7). According to the drilling wells, this horizon coincides with the blue marl bottom of the lower Pliocene (Fig.7). The geometry of its roof is illustrated by the three-dimensional model in Fig. 5, the roof shape of this interval on the cross-sections (Fig. 6 and 7) confirms the geometry in high and low areas. The geometrical configuration of the roof of this geoelectric interval confirms the structuring in high and low zones described in the three-dimensional model of Fig. 5. This interval is surmounted by the relatively resistant geoelectric interval R2 which expressed by resistivity values ranging from

123 to 340 Ω .m. Its correlation to mechanical drilling shows that it consists of coarse detrital formations (coarse sands and gravels) with clayey passages (Fig. 7). This interval is covered by a relatively conductive C1 geoelectric interval (the average resistivity is 35 Ω .m consisting essentially by sedimentation.

The relatively resistant geoelectric interval R1 (123 to 278 Ω .m), its correlation to mechanical drilling shows that it consists of coarse detrital formations (coarse sands and gravels) (Fig. 7).

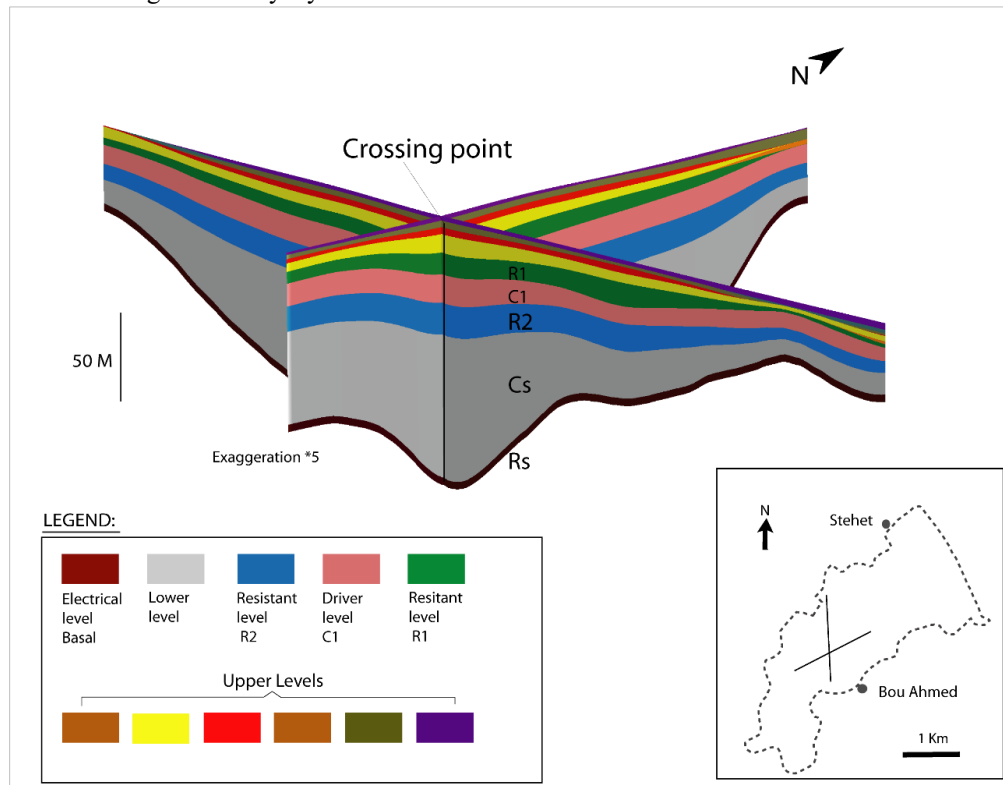


Fig. 6. Fence Diagram Sections (N-S and NE-SW Direction) in the Study Area.

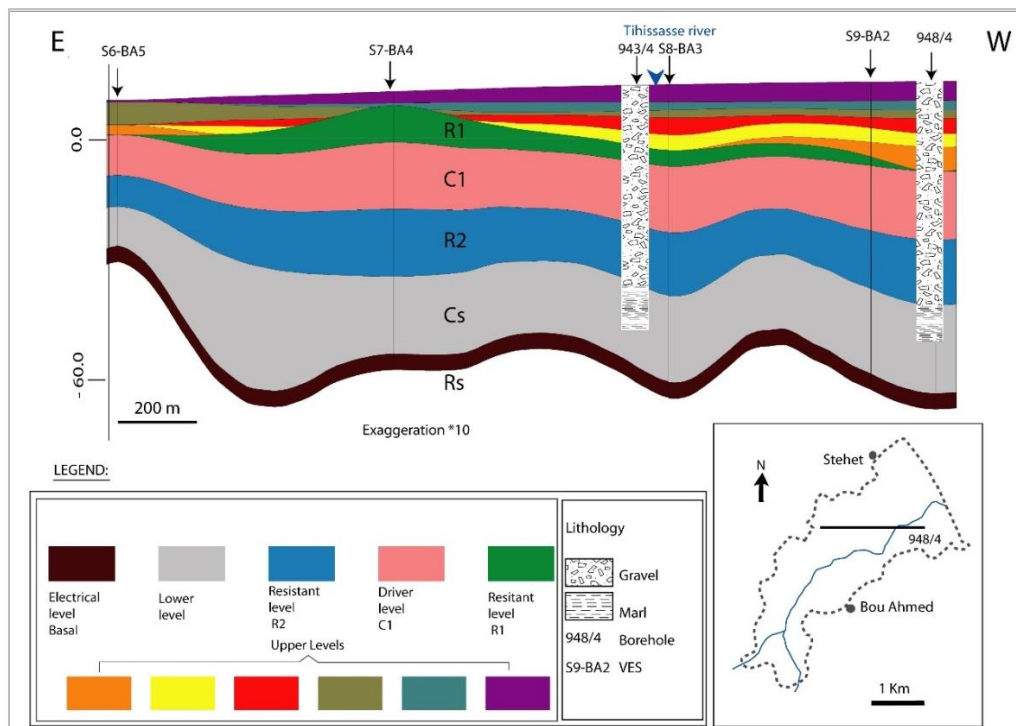


Fig. 7. E-W Direction of Geoelectric Cross-Section in the Centre of the Study Area.

The geoelectric levels end with the alternation of the resistant and conductive levels (Upper levels) of a limited extension (Fig. 6 and 7).

It should be noted that on the scale of the Bou Ahmed plain the filling generally is on a marly bottom. The filling is, sometimes to the west and Northwest of the basin, directly formed on the Paleozoic where the bottom corresponds to mica-schists.

C. Potentially Aquifer Intervals (R2 and R1)

The geoelectric intervals described above, show that the most important levels, in terms of thickness and resistivity, are the R2 and R1 (Fig. 8 and 9) which can be considered as new potential aquifers levels. The spatial distribution of these geoelectric levels is characterized by using maps of isopach and iso-resistivity for each geoelectric interval (Fig. 8 and 9).

1) *The geoelectric interval R2:* The isopach map of the geoelectric interval R2 shows that the largest thicknesses are organized in the form of a NE-SW oriented band (Fig. 8-A). The location of this band in relation to the Tihissasse River shows that the latter has migrated to the Southeast. The comparison between the isopach map of the geoelectric interval R2 (Fig. 8-A) and the roof of the bottom map (Fig. 5) shows that the large bowl is located almost in the same depressions detected on the roof of the Pliocene bottom (Cs). This shows that these bowls function, during the phase of setting up this interval, as sediment traps.

From an electrical standpoint, the spatial distribution of the resistivity values of the geoelectric interval R2 (Fig. 8-B) shows that the zones with high resistivity (340 $\Omega.m$) are located mainly in the East and in the Southwest of the study area (Fig. 8-B). The calibration of these zones to the boreholes shows that this interval consists of coarse sands and gravels. This reflects the fluvio-estuarine environment linked to the paleo-Tihissasse, which dominated in plio-quadernary study area. In the Northwest of the Bou Ahmed town, a decrease in resistivity values is to be observed which goes towards the center of the study area (Fig. 8-B) where the marly bottom is rising (Fig. 5).

2) *The geoelectric interval R1:* The spatial distribution of thickness of the geoelectric interval R1 shows a depression in the center of the plain (14 m) (Fig. 9-A). The comparison of this map with the isopach map of the interval R2 shows that the depression opening on the Mediterranean Sea identified on the geoelectric interval R2 has undergone filling, hence the depression located in the center of the study area continued to play its role as a sediment trap. The placement of this depression, related to the bottom geometry (Fig. 5), shows that there is a continuous subsidence during the quaternary.

The lateral variation of the resistivity values of this interval shows that the zones with high resistivity are very small in the central part of the study area (Fig. 9-B). This can be linked to the clay nature of the layers or to the degradation of the chemical quality of the water.

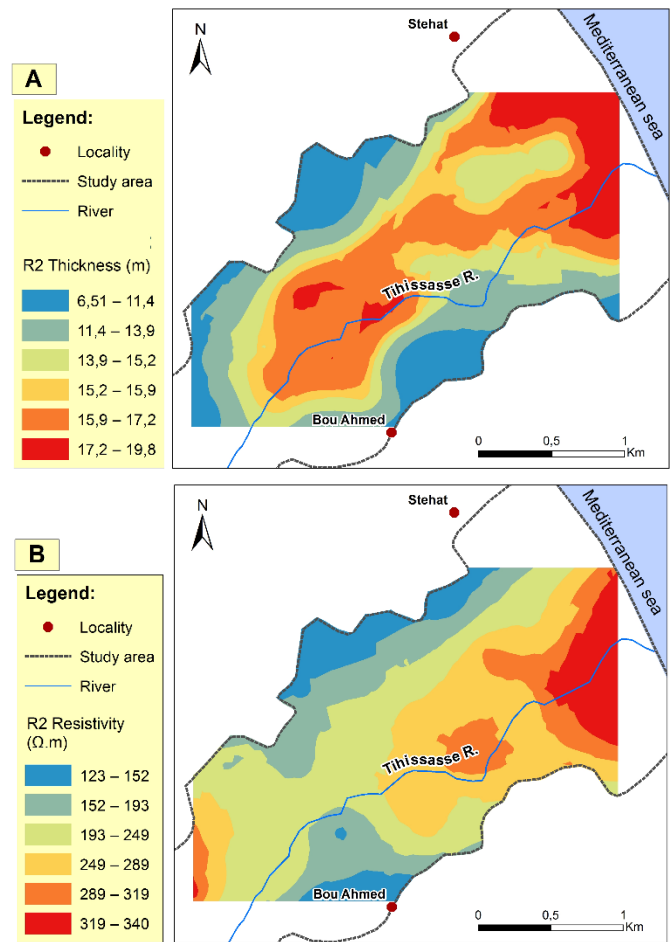


Fig. 8. Maps of the Resistant Level R2 (A- Isopach Map and B- Iso-resistivity Map).

In order to complete the interpretation of the electrical results, we carried out a measurement of the electrical conductivity of the groundwater wells in the study area. Electrical conductivity is the inverse of electrical resistivity, it translates the capacity of an aqueous solution to conduct electric current and the degree of global mineralization, and thus it provides information on the salinity rate.

Spatial distribution of the conductivity measured on the various groundwater wells of the Bou Ahmed plain shows that the values are included in the range [0.5 $\mu s/cm$; 4.3 $\mu s/cm$] (Fig. 10). The conductivity field highlights a spatial variability of this parameter passing from the edges to the central part of the study area (Fig. 9). The most conductive areas ($> 1.46 \mu s/cm$) are located on the eastern and western margins of the plain (Fig. 9). Analysis of the lithological data in these areas reveals that the character of the high conductivity values is related to the flow of groundwater in contact with the bottom, sometimes materialized by marls and sometimes by mica-schist. According to [29], this increase in conductivity can be interpreted as a consequence of the longer contact time with marly sandstones, which has allowed the development of ion exchange processes.

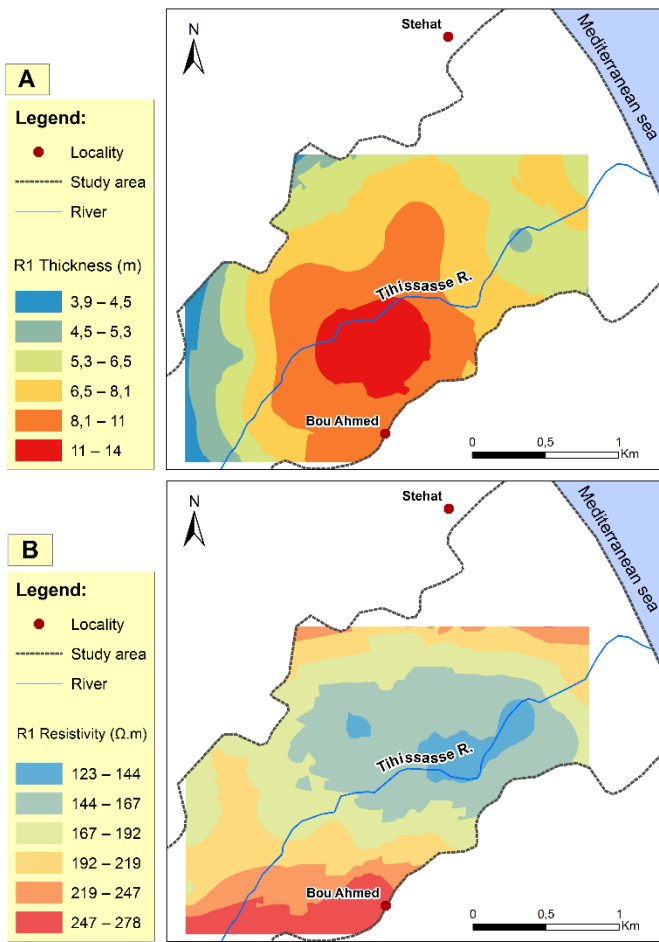


Fig. 9. Maps of the Resistant Level R1 (A- Isopach Map and B - Isoresistivity Map).

Low conductivity values ($< 0.95 \mu\text{s/cm}$) are recorded in the center of the study area. This decrease is related to the surface waters of the rivers supplying the aquifer; El Kanar and Bouhya Rivers. The latter cross terrain characterized respectively by shale formations, carbonate rocks and “Calcareous Dorsale”.

The comparison between the conductivity map (Fig. 10) and the isoresistivity of the geoelectric interval R2 map (Fig. 8-B) shows a reciprocal proportionality between the values whose highest values of conductivity coincide with the low one’s resistivity values (Fig. 10).

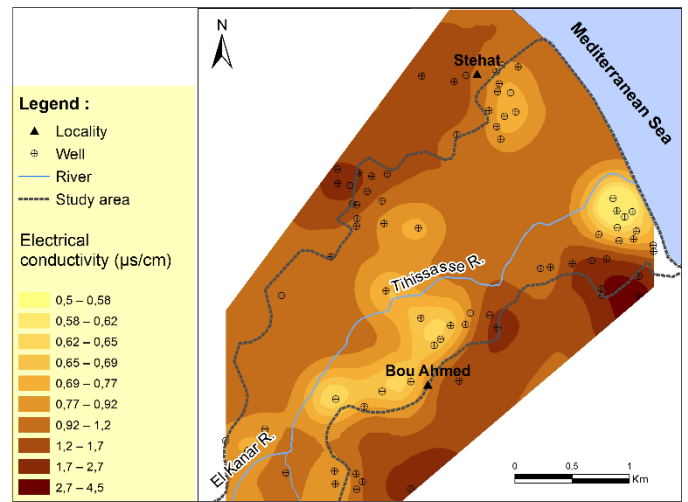


Fig. 10. Distribution Map of the Electrical Conductivity ($\mu\text{s/cm}$) in the Study Area.

V. CONCLUSION

Computer technology and 3D modelling of the subsurface are being increasingly used in different fields of geo-resources. The subsurface data obtained at regular spaces play an important role in the detection of structures of the ground.

At the level of the Bou Ahmed aquifer, the method applied was able to show the complexity of the aquifer. Indeed, it was composed by several levels of different nature and age. The 3D model, the correlation of cross-sections, the fence diagram sections, and the level distribution maps produced clearly show the geometry of the different resistant levels potentially aquiferous in the Bou Ahmed aquifer.

Geophysical reconnaissance by VES of the water table made it possible to show the presence of a depression centered in the Bou Ahmed aquifer. This anomaly corresponds to the confluence zone of the main rivers of the plain (El kanar and Bouhya Rivers).

Tectonic structures were not taken into account in the development of the 3D model of the aquifer due to the lack of data and precision.

The results obtained in this study confirmed previous studies, and carried out new interpretations of the subsurface based on 3D modelling.

Besides, this study allowed us to integrate the 3D lithostratigraphic model of Bou Ahmed aquifer to the layered conceptual model, and prepare the input data such as hydraulic conductivity for groundwater flow model which will be a key decision support system for the decision makers in water resources management.

REFERENCES

- [1] D.G.H, Etude par prospection électrique, nappes d'Oulad Ogbane, Ksar Es-Sghir, Emsa et Azla (Province de Tétouan), nappe de Bou Ahmed et Targha (Province de Chefchaouene), Maroc. 2000.
- [2] DRHL, Synthèse hydrogéologique de la plaine de Bou Ahmed, province de Chefchaouen, Maroc. 1994.
- [3] A. El Attar, « Contribution à l'étude hydrogéologique et hydrochimique des aquifères côtiers d'Amsa et de Bou Ahmed (Maroc Nord Occidental) », 2012.
- [4] J. Thauvin, « Ressources en eau du Maroc, domaine du Rif et du Maroc oriental », Notes Mém. Serv. Géologique Maroc, vol. 231, 1971.
- [5] K. El Kadiri, K. El Kadiri, et A. Rahouti, « Sédimentologie et ichnologie des calciturbidites du Crétacé supérieur-Oligocène inférieur de la série Maurétanienne (nappe des Béni Ider, Rif septentrional, Maroc): implications paléogéographiques », Bull. L'Institut Sci. Rabat, vol. 25, p. 73–91, 2003.
- [6] A. Amraoui, « Hydrogéologie de la dorsale calcaire du Rif (Maroc septentrional) », 1988.
- [7] M. Benmakhlouf, « Genèse et évolution de l'accident de Tétouan et son rôle transformant au niveau du Rif septentrional (Maroc)(Depuis l'oligocène jusqu'à l'actuel) », 1990.
- [8] R. Saji, « Evolution tectonique post Nappes dans le Rif septentrional (Maroc): ses effets sur l'ouverture de la mer d'Alboran », Third Cycle Thesis Univ. Mohammed V Rabat Maroc., 1993.
- [9] J.-L. Morel, « Evolution récente de l'orogène rifain et de son avant-pays depuis la fin de la mise en place des nappes (Rif, Maroc) », 1987.
- [10] J. Rampnoux, J. Angelier, B. Colletta, S. Fudral, M. Guillemin, et G. Pierre, « Sur l'évolution néotectonique du Maroc septentrional », Géologie Méditerranéenne, vol. 6, no 4, p. 439–464, 1979.
- [11] G. Suter, Carte géologique de la chaîne rifaine 1: 500,000. Service géologique du Maroc, 1980.
- [12] O. Saddiqi, I. Reuber, et A. Michard, « Sur la tectonique de dénudation du manteau infracontinental dans les Beni Bousera, Rif septentrional, Maroc », Comptes Rendus Académie Sci. Sér. 2 Mécanique Phys. Chim. Sci. Univers Sci. Terre, vol. 307, no 6, p. 657–662, 1988.
- [13] S. Penz, « Modélisation et inversion de données électriques en courant continu: vers une prise en compte efficace de la topographie », 2012.
- [14] J. Asfahani, Y. Radwan, et I. Layyous, « Integrated geophysical and morphotectonic survey of the impact of Ghab extensional tectonics on the Qastoon dam, Northwestern Syria », Pure Appl. Geophys., vol. 167, no 3, p. 323–338, 2010.
- [15] W. M. Telford, W. Telford, L. Geldart, R. E. Sheriff, et R. Sheriff, Applied geophysics, vol. 1. Cambridge university press, 1990.
- [16] I. Al Mazini, A. Mridekh, M. Kili, B. El Mansouri, M. El Bouhaddioui, et B. Magrane, « Plio-quaternary deposits in the Eastern Rharb (Nw Morocco): Electrosequential characterization », J. Afr. Earth Sci., vol. 138, p. 32–41, 2018.
- [17] M. E. Bouhaddioui, A. Mridekh, M. Kili, B. E. Mansouri, E. H. E. Gasmî, et B. Magrane, « Electrical and well log study of the Plio-Quaternary deposits of the southern part of the Rharb Basin, northern Morocco », J. Afr. Earth Sci., vol. 123, p. 110–122, 2016.
- [18] H. Schlumberger, « Synovial gout in the parakeet. », Lab. Investig. J. Tech. Methods Pathol., vol. 8, p. 1304–1318, 1959.
- [19] S. Akiska, İ. S. SAYILI, et G. DEMİRELA, « Three-dimensional subsurface modeling of mineralization: a case study from the Handeresi (Çanakkale, NW Turkey) Pb-Zn-Cu deposit », Turk. J. Earth Sci., vol. 22, no 4, p. 574–587, 2013.
- [20] O. Kaufmann et T. Martin, « Reprint of “3D geological modelling from boreholes, cross-sections and geological maps, application over former natural gas storages in coal mines”[Comput. Geosci. 34 (2008) 278–290] », Comput. Geosci., vol. 35, no 1, p. 70–82, 2009.
- [21] S. Rziqi, A. Alansari, E. Mouguina, J. Simard, M. Zouhair, et L. Maacha, « Apport du modèle géologique et géophysique 3D dans le développement du gisement polymétallique de Draa Sfar (Massif hercynien des Jebilet centrales, Maroc) », Estud. Geológicos, vol. 68, no 1, p. 29–40, 2012.
- [22] A. Zanchi, S. Francesca, Z. Stefano, S. Simone, et G. Graziano, « 3D reconstruction of complex geological bodies: Examples from the Alps », Comput. Geosci., vol. 35, no 1, p. 49–69, 2009.
- [23] G. Wang et L. Huang, « 3D geological modeling for mineral resource assessment of the Tongshan Cu deposit, Heilongjiang Province, China », Geosci. Front., vol. 3, no 4, p. 483–491, 2012.
- [24] T. Q. Binh et N. T. Thuy, « Assessment of the influence of interpolation techniques on the accuracy of digital elevation model », VNU J. Sci. Earth Environ. Sci., vol. 24, no 4, 2008.
- [25] J. Li et A. D. Heap, « A review of spatial interpolation methods for environmental scientists », 2008.
- [26] A. A. Fazal et M. ATMSH, « 3-Dimensional Analysis and Reserve Estimation of Barapukuria Coal Basin, Dinajpur, Bangladesh », Int Res J Geo Min, vol. 4, no 7, p. 176–187, 2014.
- [27] Y. Gratton, « Le krigeage: la méthode optimale d'interpolation spatiale », Artic. Inst. Anal. Géographique, vol. 1, 2002.
- [28] N. S.-N. Lam, « Spatial interpolation methods: a review », Am. Cartogr., vol. 10, no 2, p. 129–150, 1983.
- [29] A. El Attar, K. El Morabiti, L. Molina, F. Sánchez-Martos, Y. El Kharim, et others, « Consideraciones hidrogeoquímicas sobre el acuífero detrítico costero de Bou Ahmed (Marruecos) », Geogaceta, vol. 46, p. 159–162, 2009.

BiDETS: Binary Differential Evolutionary based Text Summarization

Hani Moetque Aljahdali¹
Ahmed Hamza Osman Ahmed²

Department of Information System
Faculty of Computing and Information Technology
King Abdulaziz University Rabigh, Saudi Arabia

Albaraa Abuobieda³

Faculty of Computer Studies
International University of Africa, 2469
Khartoum, Sudan

Abstract—In extraction-based automatic text summarization (ATS) applications, feature scoring is the cornerstone of the summarization process since it is used for selecting the candidate summary sentences. Handling all features equally leads to generating disqualified summaries. Feature Weighting (FW) is an important approach used to weight the scores of the features based on their presence importance in the current context. Therefore, some of the ATS researchers have proposed evolutionary-based machine learning methods, such as Particle Swarm Optimization (PSO) and Genetic Algorithm (GA), to extract superior weights to their assigned features. Then the extracted weights are used to tune the scored-features in order to generate a high qualified summary. In this paper, the Differential Evolution (DE) algorithm was proposed to act as a feature weighting machine learning method for extraction-based ATS problems. In addition to enabling the DE to represent and control the assigned features in binary dimension space, it was modulated into a binary coded format. Simple mathematical calculation features have been selected from various literature and employed in this study. The sentences in the documents are first clustered according to a multi-objective clustering concept. DE approach simultaneously optimizes two objective functions, which are compactness measuring and separating the sentence clusters based on these objectives. In order to automatically detect a number of sentence clusters contained in a document, representative sentences from various clusters are chosen with certain sentence scoring features to produce the summary. The method was tested and trained using DUC2002 dataset to learn the weight of each feature. To create comparative and competitive findings, the proposed DE method was compared with evolutionary methods: PSO and GA. The DE was also compared against the best and worst systems benchmark in DUC 2002. The performance of the BiDETS model is scored with 49% similar to human performance (52%) in ROUGE-1; 26% which is over the human performance (23%) using ROUGE-2; and lastly 45% similar to human performance (48%) using ROUGE-L. These results showed that the proposed method outperformed all other methods in terms of F-measure using the ROUGE evaluation tool.

Keywords—Differential evolution; text summarization; PSO; GA; evolutionary algorithms; optimization techniques; feature weighting; ROUGE; DUC

I. INTRODUCTION

Internet Web services (e.g. news, user reviews, social networks, websites, blogs, etc.) are enormous sources of textual data. In addition, the collections of articles of news,

novels, books, legal documents, biomedical records and research papers are rich in textual content. The textual content of the web and other repositories is increasing exponentially every day. As a result, consumers waste a lot of time seeking the information they want. You cannot even read and understand all the search results of the textual material. Many of the resulting texts are repetitive or unimportant. It is also necessary and much more useful to summarize and condense the text resources. Handbook summary is a costly and time- and effort-intensive process. In fact, manually summarizing this immense volume of textual data is difficult for humans [1]. The main solution to this problem is the Automated Overview Text (ATS).

ATS is one of the information retrieval applications which aim to reduce the amount of text into a condensed informative form. Text summarization applications are designed using several and diverse approaches, such as “feature scoring”, “cluster based”, “graph based” and other approaches. In the “feature scoring” based approach, some research proposals can be divided into two directions. The first direction concerns proposing features of either novel single feature or structured features. Researchers who are working on this first direction claim that existing features are poorer and not eligible to produce a qualified summary. The second direction is concerned with proposing mechanisms aiming to adjust the scores of already existing features by discovering their real weight (importance) in the texts. This direction claims that employing feature selection may be considered a good solution rather than introducing novel features. Many researchers have proposed feature selection methods, while a limited number of them utilized the optimization systems with the purpose of enhancing the way the features were commonly used to be selected and weighted.

The extractive method extracts and uses the most appropriate phrases from the input text to produce the description. The Abstractive approach represents an intermediate type for the input text and produces a description of words and phrases which differ from the original text phrases. The hybrid approach incorporates extraction and abstraction. The general structure of an ATS system comprises:

1) *Pre-processing*: development by using several linguistic techniques, including phrase segmentation, word tokenization,

stop word deletion, speech marking, stemming and so forth of a standardized representation of the original text [2].

2) *Process*: use one or more summary text methods to transform the input document(s) into the summary by applying one technique or more. Section 3 describes the various ATS methods and Section 4 discusses the various strategies and components for implementing an ATS framework.

3) *Post-processing*: solve some problems in summary sentences generated, such as anaphora resolution, before generating a final summary and repositioning selected sentences.

Generating a high quality text summary implies designing methods attached with powerful feature-scoring (weighting) mechanisms. To produce a summary of the input documents, the features are scored for each sentence. Consequently, the quality of the generated summary is sensitive to those nominated features. Consequently, evolving a mechanism to calculate the feature weights is needed. The weight method aids in identifying the significance of features distinctly in the collection of documents and how to deal with them. Many scholars have suggested feature selection methods based on optimization mechanisms such as GA [3] and PSO [4]. This paper follows the same trend of these research studies and employed the unselected evolutionary algorithm “Differential Evolution” (DE) [5] to act as feature selection scoring mechanism for text summarization problems. For more significant evaluation, the authors have benchmarked the results of those evolutionary algorithms (PSO and GA) found in the related literature.

In this research, the DE algorithm has been proposed to act as a feature weighting machine learning method for extraction-based ATS problems. The main contribution of the proposed method is adopt the DE to represent and control the assigned features in binary dimension space, it was modulated into a binary coded format. Simple mathematical calculation features have been selected from various literature and employed in this study. The sentences in the documents are first clustered according to a multi-objective clustering concept. DE approach simultaneously optimizes two objective functions, which are compactness measuring and separating the sentence clusters based on these objectives. In order to automatically detect a number of sentence clusters contained in a document, representative sentences from various clusters are chosen with certain sentence scoring features to produce the summary. In general, the validity index of the clusters tests in various ways certain inherent cluster characteristics such as separation and compactness. Any sentences from each cluster are extracted using multiple sentence labeling features to generate the summary after producing high quality sentence clusters.

In this study, five textual features have been selected according to their effective results and simple calculations as stated in Section 4.1. To enable the DE algorithm to achieve the optimal weighting of the selected features, the chromosome (a candidate solution) was modulated into a binary-code format. Each gene position represents a feature. If the gene holds the binary ‘1’ this means the equivalent feature is active and should be included in the scoring process,

otherwise ‘0’ means the corresponding features are inactive and should be excluded from the scoring process. Based on active and inactive features, each chromosome is now able to generate and extract a summary. A set of 100 documents was imported from the DUC 2002 [6] and [7]. The summary will be evaluated using the ROUGE toolkit [8] and the recall value would be assigned as a chromosome fitness value. After several iterations the DE extracts weights for each feature and takes them back again to tune the feature scores. Then the new and optimized summary is generated. Section 4 presents deep details on algorithm set-up and configurations.

Referring to the evolutionary algorithm’s competition events, the DE algorithm showed powerful performance in terms of discovering the fittest solution in 34 broadly used benchmark problems [9]. This paper stressed the emphasis to use the unselected “DE” algorithm for performing FS process for ATS applications and established comparative and competitive findings with previously mentioned optimization based methods PSO and GA. The objective of the experimentation that was implemented in this study is to examine the capability of the DE when performing the feature selection process compared to other evolutionary algorithms (PSO and GA) and other benchmark methods in terms of qualified summary generation. The authors used a powerful DE experience to obtain high quality summaries and outperform other parallel evolutionary algorithms. Improving the performance significantly depends on providing optimal solutions for each generation of DE procedures. To do so as recent genetic operators we have taken into account existing developments in Feature Weighting (FW). The polynomial mutations concept is also used to enhance the discovery of the method suggested. The principal drawback in the text summarization, mainly in the short document problem, is redundant. Some researchers exploited the issue of redundancy by selected the sentences at the beginning of the paragraph first and calculated the resemblance to the following sentences to nominate the best. The Maximal Marginal Significance method is then recommended in order to minimize redundancies in multi-documentary and short text summarization, in order to achieve optimum results.

The rest of this study is presented as follows. Section 2 presents the literature review. An overview to the DE optimization method is introduced in Section 3. The methodology is detailed in Section 4. The proposed Binary Differential Evolution based Text Summarization (BiDETS) model is explained in Section 5. Section 6 concludes the study.

II. RELATED WORK

Much research for the functions selection (FS) method has recently been proposed. Because of its relevance, FS affects application quality [10]. FS attempts to classify which characteristics are relevant and which data can reflect. In [11] the authors demonstrated that the device can minimize the problem's dimensionality, eliminate unnecessary data and uninstall redundant features by embedding FS. FS also decreases the quantity of data required and increases thereby the quality of the system results through the machine learning process.

A number of articles on ATS systems and methodologies have been published recently. Most of these studies concentrate on extractive summary techniques and methods, such as Nazari and Mahdavi [12], since the abstract summary requires a broad NLP. Kirmani et al. [13] describe normal statistical features and extractive methods. The surveys of the ATS extractive systems that apply fuzzy logic methods in Kumar and Sharma [14] are given. Mosa et al. [15] surveyed how swarm intelligence optimization methods are used for ATS [15]. They aim to motivate researchers, particularly for short text summaries, to use ATS swarm intelligence optimization. A survey on extractive deep-learning text summarization is provided by Suleiman and Awajan [16]. Saini et al. [17] introduced a method attempting to develop several extractive single document text summarization (ESDS) structures with MOO frameworks. The first is a combination of the SOM and DE (called the ESDS SMODE) second is a multi-objective wolf optimizer (ESDS MGWO) based on multi-objective water mechanism and third a multi-objective water cycle algorithm (ESDS MWCA) based on a threefold approach. The sentences in the text are first categorized using the multi-objective clustering concept. The MOO frame simultaneously optimizes two priority functions calculating compactness and isolation of sentence clusters in two ways. In some surveys, the emphasis is upon abstract synthesis including Gupta and Gupta [18], Lin and Ng [19] for various abstract methods and the abstract neural network methodology methods [20]. Some surveys concentrate on the domain-specific overview of the documents such as Bhattacharya et al. [21] and Kanapala, Pal and Pamula [22], and abstractive deep learning methodologies and challenges of meeting summarization to confront extractive algorithms used in the microblog summarization [23]. Some studies presented and discussed the analysis of some abstractive and extractive approaches. These studies included details on abstract and extractive on resume assessment methods [24, 25].

Big data in social media was re-formulated for the extractive text summarization in order to establish a multi-objective optimization (MOO) mission. Recently, Mosa [26] proposed a text summarization method based on Gravitational Search Algorithm (GSA) to refine multiple expressive targets for a succinct SM description. The latest GSA mixed particle swarm optimization (PSO) to reinforce local search capacities and slow GSA standard convergence level. The research is introduced as a solution of capturing the similarity between the original text and extracted summary Mosa et al. [15, 27, 28]. To solve this dilemma in the first place, a variety of dissimilar classes of comments are based on the coloring (GC) principle. GC is opposed to the clustering process, while the separation of the GC module does not have a similarity dependent on divergence. Later on, the most relevant remarks will be picked up by many virtual goals. (1) Minimize an inconsistency in the JSD method-based description text. (2) Boost feedback and writers' visibility. Comment rankings depend on their prominence, where a common comment close to many other remarks and delivered by well-known writers gives emotions. (3) Optimize (i.e. repeat) the popularity of terms. (4) Redundancy minimization (i.e. resemblance). (5) Minimizing the overview planning. The ATS Single-Focus Overview Method for encoded extractor network architecture

is proposed by Chen and Nguyen [29] using an ATS reinforcement learning algorithm and the RNN sequence model. A selective encoding technique at the sentence level selects the relevant features and then extracts the description phrases. S. N and Karwa. Chatterjee [30] recommended an updated version and optimization criterion for extractive text summarization based on the Differential Evolution (DE) algorithm. The Cosine Similarity has been utilized to cluster related sentences based on a suggested criterion function intended to resolve the text summary problem and to produce a summary of the document using important sentences in each cluster. In the Discrete DE method, the results of the tests scored a 95.5% increase of the traditional DE approach over time, whereas the accuracy and recalls of derived summaries were in all cases comparable.

In text processing applications, several evolutionary algorithms based "feature selection" approaches were widely proposed, in particular text summarization applications. To select the optimal subset of characteristics, Tu et al. [31] used PSOs. These characteristics are used for classification and neural network training. Researchers in [32] have selected essential features using PSO for text features of online web pages. In order to strengthen the link between automated assessment and manual evaluation, Rojas-Simón et al. [33] proposed a linear optimization of contents-based metrics via genetic algorithm. The suggested approach incorporates 31 material measurements based on the human-free assessment. The findings of the linear optimization display correlation gains with other DUC01 and DUC02 evaluation metrics. In 2006, Kiani and Akbarzadeh [34] presented an extractive-based automatic text summarization system based on integration between fuzzy, GP and GA. A set of non-structural features (six features) are selected and used. The reason behind using the GA is to optimize the membership function of fuzzy, whereas the GP is to improve the fuzzy rule set. The fuzzy rule sets were optimized to accelerate the decision-making of the online Web Summarizer. Again, running several rule sets online may result in high time complexity. The dataset used to train the system was three news articles which differed in their topics, while any article among them could be used for the testing phase. The fitness function is almost a total score of all features combined together. Ferreira, R et al. [35] Implemented a quantitative and qualitative evaluation research to describe 15 text summarization algorithms for sentence scoring published in the literature. Three distinct datasets such as Blogs, Article contexts, and News were analysed and investigated. The study suggested a new ways to enhance the sentence extraction in order to generate an optimal text summarization results.

Meanwhile, BinWahlan et al. [36] presented the PSO technique to emphasize the influence of structure of feature on the feature selection procedure in the domain of ATS. The number of selected features can be put into two categories, which are "complex" and "simple" features. The complex features are "sentence centrality", "title feature", and "word sentence score"; while the simple features are "keyword" and "first sentence similarity". When calculating the score of each feature, the PSO is utilized to categorize which type of feature is more effective than another. The PSO had encoded typically

to the number of used features; and the PSO modulated into binary format using the sigmoid function. The score of ROUGE-1 recall was used to compute the fitness function value. The dataset used consisted of 100 DUC 2002 papers for machine preparation. Initialization of the PSO parameters and measurement of best values derived weight from each characteristic. The findings showed that complex characteristics are weighted more than the simple ones, suggesting that the characteristic structure is an important part of the selection process. To test the proposed model the authors published continued works as found in [36]. In addition, the dataset was split into training and testing phases in order to quantify the weights[36]. Ninety-nine documents have been assigned to shape the PSO algorithm while the 100th was assigned to evaluate the model. Therefore, the phrases scored are rated descending, where n is equivalent to a summary duration; the top n phrases are selected as a summary. In order to test the effects, the authors set a human model description and the second as a reference point. For comparison purposes a Microsoft Word-Summary and a first human summary were considered. The results showed that PSO surpassed the MS-Word description and reached the closest correlation with humans as did MS-Word. The authors [37] presented a genetic extractive-based multi-document summarization. The term frequency featured in this proposed work is computed not only based on frequency, but also based on word sense disambiguation. A number of summaries are generated as a solution for each chromosome, and the summary with the best scores of criteria is considered. These criteria include "satisfied length", "high coverage of topic", "high informativeness", and "low redundancy." The DUC 2002 and 2003 are used to train the model, while the DUC 2004 is used for testing it. The proposed GA model had been compared against systems that participated in DUC2004 competition-Task2. It achieved good results and outperformed some proposed methods. Zamuda, Aleš, and Elena Lloret[38] Proposed text summarization method to examine a machine linguistic problem of hard optimization based on multi-documents by using grid computing. Multi-document summarization's key task is to successfully and efficiently derive the most significant and unique information from a collection of topic-related, limited to a given period. During a Differential Evolution (DE), a data-driven resuming model is proposed and optimized. Different DE runs are spread in parallel as optimization tasks to a network in order to achieve high processing efficiency considering the challenging complexity of the linguistic system.

Two text summarization methods: adapted corpus base method (MCBA) and latent semantic analysis based text relationship map (TRM based LSA) have been addressed by [39]. Five features were used and optimized using GA. The GA in this study is so not highly different to the previous work, in which the GA was employed for feature weights extraction. The F-measure was assigned as a fitness value and the chromosome number of each population was set to 1000. The top ten fittest chromosomes shall be selected in the next round. This research introduced a lot of experiments using different compression rate effectiveness. The GA provided an effective way of obtaining features weights which further led the proposed method to outperform the baseline methods.

The GA was also used in the work of Fattah [40]. The GA was encoded and described as similar to [20], but the feature weights were conducted to train the "feed forward neural network" (FFNN), the "probabilistic neural network" (PNN), and "Gaussian mixture model" (GMM). The models were trained by one language, and the summarization performance had been tested using different languages. The dataset is calm of 100 Arabic political articles for training purposes, while 100 English religious articles were used for testing. The fitness value was defined as an average precision, and the fittest 10 chromosomes were selected from the 1000 chromosomes. In order to obtain a steady generation, the researchers adapted the generation number to 100 generations. The GA is then tested using a second dataset. Based on the obtained weights which were used to optimize the feature scores, the sentences were ranked in order to be selected for summary representation. The model was compared against the work presented by [39]. The results showed that the GA performed well compared to the baseline method. Some researchers have successfully modulated the DE algorithm from real-coded space into binary-coded space in different applications. G. Pampara et al. [41] introduced Angle-Modulation DE (AMDE) enabling the DE to work well in binary search space. Pampara et al. were encouraged to use the AM as it abstracts the problem representation simply and then turns it back into its original space. The AM also reduces the problem dimensionality space to "4-dimension" rather than the original "n-dimensional" space. The AMDE method outperformed both AMP SO and BinPSO in terms of required number of iterations, capability of working in binary space and accuracy. He et al. [10] applied a binary DE (BDE) to extract a subset feature using feature selection. The DE was used to help find a high quality knowledge discovery by removing redundant and irrelevant data, and consequently improving the data mining processes (dimension reduction). To measure the fitness of each feature subset, the prediction of a class label along with the level of inter-correlation between features was considered. The "Entropy" or information gain is computed between features in order to estimate the correlation between them. The next generation is required to have a vector with the lowest fitness function. Khushaba et al. [11] implemented DE for feature selection in Brain-Computer Interface (BCI) problem. This method showed powerful performance in addition to low computational cost compared to other optimization techniques (PSO & GA). The authors of this current study observed that the chromosome encoding is in real format but not in binary format. A challenge facing Khushaba et al. was the appearance of "doubled values" while generating populations. To solve this problem, they proposed to use the Roulette-Wheel concept to skip such occurrences of double values.

In general, and in terms of evolutionary algorithm design requirement competition, the researchers are required to design algorithms which provide ease of use, are simple, robust and in line generate optimized or qualified solution [5]. It was found that the DE, due to its robust and simple design, outperformed other evolutionary methods in terms of reaching the optimal and qualified solution [9]. Also, the literature showed that text summarization feature selection methods which were based on evolutionary algorithms were limited to

techniques of Particle Swarm Optimization (PSO) and the Genetic Algorithm (GA). From this point of view, the researchers of this study had been encouraged to employ the DE algorithm for the text summarization feature selection problem.

Although there was successful implementation and high quality results obtained by DE, the literature showed that the DE had never been presented to act as Automatic Text Summarization feature selection mechanism. Section 4 discusses the experimental set-up and implementation in more detail. It is worth mentioning that the DE was presented before for a text summarization problem to handle the process of sentence clustering instead of feature selection [42, 43]. The DE was widely presented to handle object clustering problems such as [44-46] which is not the concern in this study.

III. DIFFERENTIAL EVOLUTION METHOD

DE was originally presented by Storn and Price [5]. It is considered a direct search method that is concerned with minimizing the so-called "cost/objective function". Algorithms in heuristic search method are required to have a "strategy" in order to generate changes in parameter vector values. The Differential Evolution performance is sensitive to the choice of mutation strategy and the control parameters [47]. For the newly generated changes, these methods use the "greedy criterion" to form the new population's vectors. A decision of governing is simple, if the newly generated parameter vector participates in decreasing the value of the cost function then it will be selected. For this use of greedy criterion, the method converges faster. For the methods concerned with minimization, such as GA and DE, there are four features they should come over: ability of processing a non-linear objective function, direct search method (stochastic), ability of performing a parallel computation, and fewer control variables.

This section may be divided by subheadings. It should provide a concise and precise description of the experimental results, their interpretation as well as the experimental conclusions that can be drawn.

The DE utilizes a dimensional vector $x_{i,G}$ with size NP as shown in Formula 1, such that:

$$x_{i,G} = 1, 2, \dots, NP \quad (1)$$

Random selections of the initial vector are rendered by summarizing the values of the random deviations from the nominal solutions $X_{nom,0}$. For producing new parameter vector, DE randomly finds the differences between two population vectors summing them up with a third one to generate what is the so-called Mutant vector. Equation 2 shows how to mutate vector $V_{j,G+1}$ from target vectors $X_{j,G}$.

$$V_{i,G+1} = x_{r_1,G} + F \cdot (x_{r_2,G} - x_{r_3,G}) \quad (2)$$

Where $r_1, r_2,$ and $r_3 \in [1, 2 \dots NP]$ are random index selections of type integer and, $r_1 \neq r_2 \neq r_3$, mutually different and $F > 0$, for $i \geq 4$. F is const and real factor $\in [0, 2]$.

The F is used to govern the augmentation of differential variation as in (3).

$$F \cdot (x_{r_2,G} - x_{r_3,G}) \quad (3)$$

The trail or crossed vector is a new vector merged with a predefined parameter vector "target vector" in order to generate a "trail vector". The goal of crossover is to find some diversity in the perturbed parameter vectors. Equation (4) shows trail vector.

$$(v_{1i,G+1}, v_{2i,G+1}, \dots, v_{Di,G+1}) \quad (4)$$

such that

$$\begin{cases} v_{ji,G+1} & \text{if } (\text{randb}(j) \leq CR) \text{ or } j = \text{rnbr}(i) \\ x_{ji,G+1} & \text{if } (\text{randb}(j) > CR) \text{ or } j \neq \text{rnbr}(i) \end{cases} \quad (5)$$

Where $\text{randb}(j)$ is the j th evaluation of a uniform random number producer with the outcome $\in [0,1]$, CR, is the constant crossover $\in [0,1]$ and can be defined by the user, and $\text{rnbr}(i)$ is a randomly selected value $i \in 1, 2, \dots, D$ computed to guarantee that trail vector $V_{j,G+1}$ will obtain as a minimum one parameter from the mutated vector $V_{j,G+1}$.

In the Selection phase, if the trail vector obtained a lower value of cost function compared with the target vector, it will be replaced with the target vector in the next generation. In this step, the greedy criterion test takes place. If the trail vector $V_{j,G+1}$ yields a lower cost function than a target vector $V_{j,G+1}$ is assigned by selecting the trailed vector, or else nothing is done.

IV. METHODOLOGY

This section covers the proposed methodology (experimental set-up). Firstly, Section 4.1 presents the selected features needed to score and select the "in-summary" sentences and exclude the "out-summary" sentences. The subsequent three Sections 4.2 to 4.4 are about configuring the DE algorithm and show how the evolutionary chromosome has been configured and encoded; how the DE's control parameters were assigned; the suitable assignment of objective (fitness) function when dealing with text summarization problem. The selected dataset and principle pre-processing steps were introduced in Section 4.5. Section 4.6 discusses the sets of the selected benchmarks and other parallel methods for more significance comparison. The last section presents the evaluation measure that was used.

A. The Selected Features

A variety of text summarization features were suggested in order to nominate outstanding text sentences. In the experimental phase, five statistical features were selected to test the model [40, 48]: Sentence-Length (SL) [49], Thematic-Word (TW) [50-52], Title-Feature (TF) [51], Numerical-Data (ND) [40], and Sentence-Position (SP) [51, 53].

1) *Sentence Length (SL)*: The topic of the article may not be a short sentence. Similarly, the selection of a very long

sentence is not an ideal choice because it requires non-informational words. A division by the longest sentence solves this problem to avoid choosing sentences either too short or too long. This normalization informs us equation (6).

$$SL(S_i) = \frac{\# \text{ of words in } S_i}{\# \text{ of words in longest sentence}} \quad (6)$$

Where S_i refers the i^{th} sentence in the document.

2) *Thematic Words (TW)*: The top n terms with the highest frequencies are a list of the top n terms chosen. In the first place, count frequencies in the documents measure the thematic terms. Then a threshold is set for the signing of which terms as thematic words should be chosen. In this case, as shown in equation (7), the top ten frequency terms will be chosen.

$$TW - S_i = \frac{\# \text{ of thematic words in } S_i}{\text{Max number of TW found in a sentence}} \quad (7)$$

Where S_i refers to the i^{th} sentence in the document.

3) *Title Feature (TF)*: To generate a summary of news articles, a sentence including each of the "Title" words is considered an important sentence. Title feature is a percentage of how much the word of a currently selected sentence i match words of titles. Title feature can be calculated using Equation (8).

$$TF(S_i) = \frac{\# \text{ of } (S_i) \text{ words matched title words}}{\# \text{ of Title's words}} \quad (8)$$

Where S_i refers to the i^{th} sentence in the document.

4) *Numerical Data (ND)*: A term containing numerical information refers to essential information, such as event date, money transaction, percentage of loss etc. Equation (9) illustrates how this function is measured.

$$ND(S_i) = \frac{\# \text{ of numerical data in } S_i}{\text{Sentence Length}} \quad (9)$$

Where S_i refers to the i^{th} sentence in the document, and sentence length is the total number of words in each sentence.

5) *Sentence Position (SP)*: In the first sentence, a significant sentence and a successful candidate for inclusion in the summary is considered. The following algorithm is used to measure the SP feature as shown in Equation (10).

For $i = 0..t$ do

$$SP(S_i) = \frac{t - i}{t} \quad (10)$$

Where S_i refers to the i^{th} document sentence, and t is the total number of sentences in document i .

B. Configuring up DE: Chromosome, Control Parameters, and Objective Function

Mainly, this study focuses on finding optimal feature weights of text summarization problems. The chromosome dimension was configured to represent these five features. At the start, each gene is initialized with a real-coded value. To perform feature selection process, the need for modulating these real-codes in binary-codes was emerged. This study follows the same modulation adjustment presented by He et al. [10] as shown in Formula 11.

$$G_{x,y} = \begin{cases} 1, & \text{rand}(r) \geq \exp(-|x|) \\ 0, & \text{otherwise} \end{cases} \quad (11)$$

Where $G_{x,y}$ refers to the current binary status of gene y in chromosome x , $\text{rand}()$ is a random function that generates a number $r \in (1,0)$, and $\exp(-|x|)$ is the exponential value of current gene x . If $\text{rand}(r)$ is greater than or equal to $\exp(-|x|)$ then $G_{x,y} = 1$ else $G_{x,y} = 0$ for each x in y .

If $x=1$ is modulated, it's activated and counted to the final score, or if the bit has zero then it is inactive and is not considered at the final score. The corresponding trait would not be considered. The chromosome structure of the features is shown in Fig. 1. The first bit denotes the first feature "TF", the second bit denotes the second feature "SL", the third bit denotes to the third feature "SP", the fourth bit denotes the fourth feature "ND", and the fifth bit denotes the fifth feature "TW".

A chromosome is a series of genes; their value is status controlled through binary probability appearance. So all probable solutions will not exceed the limit of $2n$ where 2 refers to the binary status $[0,1]$ and n is the problem dimension. Within this limited search space, the DE is suggested to cover all these expected solutions. In addition, it enables DE to assign a correct fitness to a current chromosome. For more explanation check a depiction example of a chromosome shown in Fig. 2. The DE runs real-coded mode ranges between $(0,1)$. To assign a fitness to this chromosome in its current format may become a difficult task; check "row 1" at Fig. 2. From this point of view, a "modulation layer" is needed to generate a corresponding chromosome. Values of Row 1 are $[0.65, 0.85, 0.99, 0.21, 0.54]$, then they will be modulated into binary string as shown at "Row 2" $[0, 1, 1, 0, 1]$; this modulation tells the system to generate a summary only based on the active features $[F2, F3, \text{ and } F4]$ and ignores the inactive features $[F1 \text{ and } F4]$. Then the binary string itself (01101) is modulated into the decimal numbering system, which is equal to (13). Inline to this, the system will store the correspondent summary recall value in an indexed fitness file at position (13). Now, DE is correctly able to assign fitness value to a current binary chromosome of $[0, 1, 1, 0, 1]$.

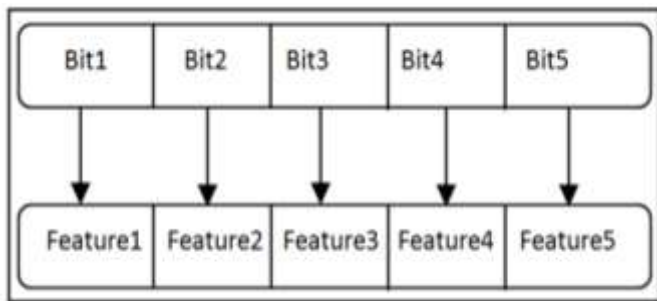


Fig. 1. Chromosome Structure.

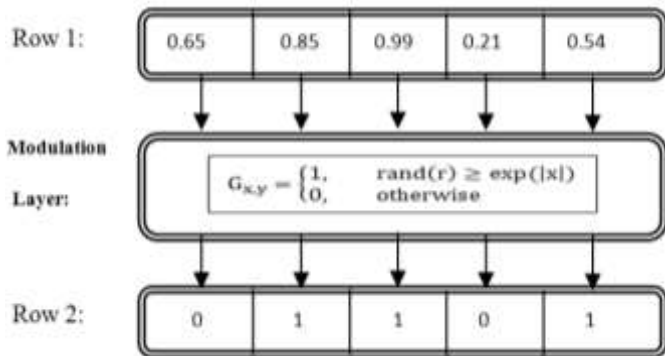


Fig. 2. Gene's Process.

The DE's control parameters were set according to optimal assignments found in the literature as follows. The F-value was set to 0.9 [5, 9, 54-57], the CR was set to 0.5 [5, 9, 54-57] and the size of population NP was set to 100 [5, 9, 54, 57-59]. It is widely known that optimization techniques are likely to run broadly within a high number of iterations such as 100, 500, 1000 and so on. In this experiment it was noted that DE is able to reach the optimal solution within a minimum number of iterations (=100) if the dimension length is so small. Empirically this study justified that when the dimension of the problem is small the number of total candidate solutions cannot be too large. The DE was tested and outperformed many optimization techniques in challenges of high dimension, fast convergence and extraction of qualified solution. To this end, the conducted experiment of this study approved that DE can reach the optimal solution within a very small number of iterations.

The fitness function is a measurement unit for techniques of optimization. These techniques are used to determine the chromosomes achieving the best and best solution. The new population of this chromosome can be restored (survived) in the next generation. This study generates only a probability of $2n$ chromosomes for each input document where n is the dimension or number of features. The system then assigns a fitness value for each chromosome of the resumes it generates. The highest recall value of the top chromosome is selected and the corresponding document will be shown in the dataset. In the literature, a similar and successful work [60] assigned the recall of ROUGE-1 as a fitness value. Equation 12 demonstrates how to measure the recall value in comparison to the reference summary for each summary generated.

C. Selected Dataset and Pre-Processing Steps

The National Institute of Standards and Technology of the U.S. (NIST) created the DUC 2002 evaluation data which consists of 60 data sets. The data was formed from the TREC disks used in the Question-Answering in task TREC-9. The TREC is a retrieval task created by NIST which cares about Question-Answering systems. The DUC 2002 data set came with two tasks single-document extract/abstract and multi-document extract/abstract with different topics such as natural disaster and health issues. The reason for using DUC 2002 in this study is that it was the latest data set produced by NIST for single-document summarization.

The selected dataset is composed of 100 documents collected from the Document Understanding Conference (DUC2002) [7]. These 100 documents were allocated on 10 clusters of certain topics labelled with: D075b, D077b, D078b, D082a, D087d, D089d, D090d, D092c, D095c, and D096c. Every cluster includes 10 relevant documents comprising 100 documents. Each DUC2002 article was attached with two "model" summaries. These two model summaries were written by two human experts (H1 and H2) and were of the size of 100 words for single document summarization.

Often text processing application datasets are exposed to pre-processing steps. These pre-processing steps include, but are not limited to: removal of stop words within the text, sentence segmentation, and stemming process based on porter stemmer algorithm [61]. One of the main challenges in text engineering research is segmenting sentences by discovering correct and unambiguous boundaries. In this study, the authors manually segmented the sentences to skip falling into any hidden segmentation mistakes and guarantee correct results. According to the selected methodology of the specific application sign or resign implementing the pre-processing steps is an unrestricted option. For example, some research of semantic text engineering applications may tend and prefer to retain the stop words and all words in their current forms not in their root forms (stemming). In this study, the mentioned pre-processing steps were employed.

D. The Collection of Compared Methods

This paper diversifies the selection of comparative methods to create a competitive environment. The compared methods had been divided into two sets. Set A includes similar published optimization based text summarization methods: Particle Swarm Optimization (PSO) [60] and Genetic Algorithm (GA) [62]. This set was brought in to add a significant comparison as this study also proposes the Differential Evolution (DE) for handling the FS problem of the text summarization. To the best of the author's knowledge the DE have never been presented before to tackle the text summarization feature selection problem. In the literature, the DE has been proposed before as sentences clustering approach of text summarization problem [42], but not for the feature selection problem. Both works GA and PSO are presented for the problem of feature selection in text summarization. Set B consists of DUC 2002 best system [63] and worst system [64]. Due to source code unavailability of methods in sets A and B, the average evaluation measurement results were being considered as published. In addition, and for a fair

comparison, the BiDETS system had been trained and tested using the same dataset source (DUC2002) and size (100 documents) of comparing methods as well as similar ROUGE evaluation metrics (ROUGE-1, 2, and L). In the experimental part of this paper, summaries found by H1 were installed as a reference summary while summaries found by H2 had been installed as a benchmark method. Thus, H2 is used to measure out which one of all compared methods (BiDETS, set A, or set B) is closest to the human performance (H1).

E. Evaluation Tools

Most automatic text summarization research is evaluated and compared using the ROUGE tool to measure the quality of the system’s summary. Citing such research studies isn’t possible as there are too many to point out here. ROUGE stands for Recall-Oriented Understudy for Gisting. It presents measure sets to evaluate the system summaries; each set of metrics is suitable for specific kind of input type: very short single document summarization of 10 words, single document summarization of 100 words, and multi-document summarization of [10, 100, 200, 400] words. ROUGE-N (N=1 and 2) and L (L=longest common subsequence -LCS) single document measures are being used in this study; for more details about ROUGE the reader can refer to [8]. The ROUGE tool gives three types of scores: P=Precision, R=Recall, and F=F-measure for each metric (ROUGE-N, L, W, and so on). The F-measure computes the weighted harmonic mean of both P and R, see Equation (12):

$$F = \frac{1}{\left(\alpha \times \left(\frac{1}{P} \right) + (1 - \alpha) \times \left(\frac{1}{R} \right) \right)} \quad (12)$$

Where *alpha* is a parameter used to balance between both recall and precision.

For significance testing, to measure the performance of the system using each single score of *n* samples is a very tough job. Thus, the need to find a representative value replacing all *n* items emerged. ROUGE generalizes and expresses all values of (P, R, and F) results in single values (averages) respectively at a 95% confidence interval. Equations 14 and 15 declare how R and P are being calculated for evaluating text summarization system results respectively. For comparison purposes, some researchers are biased in selecting the Recall and Precision values such as [60, 65], and some of them biased behind selecting the F-measure as it reports a balance performance of both P and R of the system [66, 67]. In this study, the F-measure has been selected.

$$Recall = \frac{|System\ Summary| \cap |Human\ Summary|}{|Human\ Summary|} \quad (13)$$

$$Precision = \frac{|System\ Summary| \cap |Human\ Summary|}{|System\ Summary|} \quad (14)$$

V. BINARY DIFFERENTIAL EVOLUTION BASED TEXT SUMMARIZATION (BiDETS) MODEL

The proposed BiDETS model consists of two sub models: Differential Evolution for Features Selection (DEFS) model and Differential Evolution for Text Summarization (DETS) model. The term “Binary” is used here to refer to the current configuration of the system which was modulated into binary dimension space. Each sub model in the BiDETS acts as a separate model and runs independently of the other. The DEFS model is trained to extract the optimal weights of each feature. Then, the outputs of DEFS (the extracted weights) are directed as inputs to the second model. The DETS was designed to test the results of the trained model. Both models were trained and tested using the 10-fold approach (70% for training and 30% for testing). It is important to mention that all models were configured and prepared as discussed in Section 4: pre-processing all documents in the dataset, calculating the features, encoding the chromosome, configuring the DE’s control parameters, and lastly assigning fitness function. Fig. 3 visualizes the whole BiDETS model.

Fig. 3 represent the Inputs and outputs of DEFS and DETS models, where *F* refers features and $W_i * F_i$ refers to a multiplication of the optimized weight *W* by the scored feature *F*.

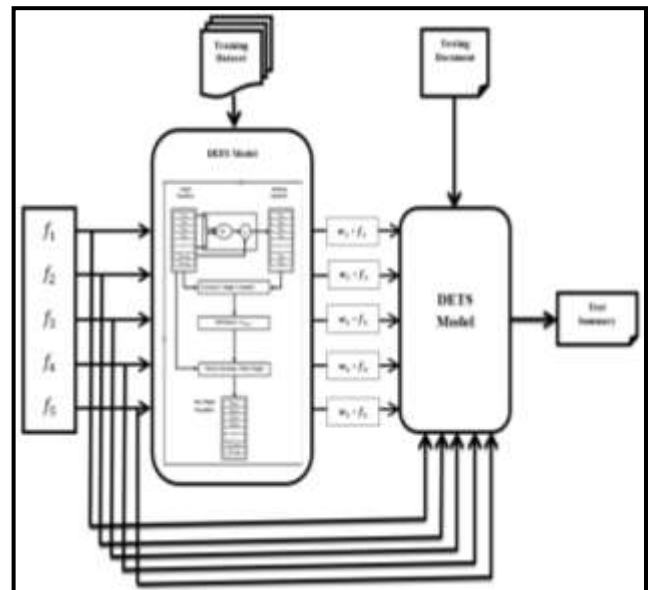


Fig. 3. Inputs and Outputs of DEFS and DETS Models.

A. DEFS Model

To generate a summary, the “features-based” Summarizer computes the feature scores of all sentences in the document. In the DEFS model, each chromosome deals with a separate document and controls the activation and deactivation of the corresponding set of features as shown in Fig. 2. The genes in the chromosome represent the five selected features. The DEFS model has been configured to operate in binary mode; if gene = 1 then the corresponding feature is active and will be included in the final score; otherwise the corresponding feature shall not be considered and will be excluded. In this way, the amount of 2^n probable chromosomes/solutions

(where 2 represents the binary logic and $n = 5 =$ number of selected features) can be obtained, and that is as follows. The model receives document

i (where $1 \leq i \leq nr$, nr is a total number of the documents in the dataset)

, then starts its evolutionary search. For each initiated chromosome a corresponding summary has to be generated for this input document i . The model then triggers the evaluation toolkit ROUGE system and extracts “ROUGE-1 recall” value. Then it assigns this value as a fitness function to this current initiated chromosome. The DEFS continues generating an optimized multiple population and searching for the fittest solution. DEFS stops searching the space, similar to other evolutionary algorithms, when all the 100 iterations have been checked and then picks the highest fitness found. Once the fittest chromosome has been selected, the model stores its binary status into a binary-coded array of size 5×100 , where 5th dimension (features) is and 100 is the length of the array (documents). Then, DEFS receives the next input (document $i+1$). When the system finishes searching all documents and fills the binary-coded array with all optimal solutions, then it computes the averages of all features in decimal format and stores it into a different array. The array is called real-coded array and it is of size $m \times n$, where $m=5$ is the array dimension and $n=100$ is the total number of all runs. DEFS is now considered as finishing the first run out of 10. Then, the aforementioned steps are repeated until the real-coded array is filled and averages have been computed. These averages represent the target feature weights that a Summarizer designer is looking for. To this end, DEFS stops working and feeds those obtained weights as inputs to optimize the corresponding scored features of the DETS model. The DETS model was designed to test the results of the DEFS model as well as being installed as a final summarization application. Fig. 4 shows the obtained weights using DEFS ordered in descending manner for easy comparison.

The weights obtained by the DEFS model are represented in Fig. 3. These weights were organized in descending order for easy comparison. Each weight tells its importance and effect on the text. Firstly, one piece of literature showed that the title's frequency (TF) feature is a very important feature. It is well-known that, when people would like to edit an article, the sentences are designed to be close to the title. From this point of view, TF feature is very important to consider and DEFS supports this fact. Secondly, the sentence position (SP) feature is not less important than the TF as many experiments approved that the first and last sentence in the paragraph introduce and conclude the topic. The authors of this study have found that most of the selected document paragraphs are of short length (between two and three sentences). Then the authors followed to score sentences according to their sequenced appearance, and retain for the first sentence its importance. Thirdly, the thematic word gets an appreciated concern as it owns the events of the story. Take for example this article, the reader will notice that the terms “DEFS”, “DETS”, “chromosome” and “feature” are more frequently mentioned than the term “semantic” which was mentioned only once. These terms may represent the edges of this text. Thus, for the Summarizer it is good to include such feature.

Fourthly, the sentence length feature also has a good effect as follows. In summarization the longest sentence may append with details which are irrelevant to the document topic; also short sentences lack informative information. For this reason, this feature is adjusted to enable the Summarizer to include a sentence of a suitable length. The importance of all mentioned features is ranged from score (0.80 to 0.99) except the last feature. Fifth, according to the definition of numerical feature, this feature is principally very important as it feeds the reader with facts and indications among the lines, for example the number of victims in an accident, the amount of stolen bank balances and so on. DEFS reports that the ND feature importance is acceptable but is the lowest one to weight. This reflects the ratio of presence (weight) of this feature which is (79%) in the documents. The authors have manually checked the texts and found that the presence of the numerical data is not so high. For real verification of these results, the weights are directed as input for the DETS model.

B. DETS Model

The DETS model is the summarization system which is designed with the selected features. The model scores features for each input document and generates a corresponding summary, see Equation (15).

$$Score_F(S_{i \in [1..n]}) = \sum_{j=1}^5 F_j(S_i) \quad (15)$$

where, $Score_F()$ is a function that computes all j^{th} features F for all n document sentences. To optimize the scoring mechanism, DETS is fed with DEFS outputs to adjust the features. The weights can be set in the form of $W = \{w_1, w_2, w_3, w_4, w_5\}$, where w refers to weight. Equation (17) shows how to combine the extracted weights with the scoring mechanism at Equation 16.

$$weighted_Score_F(S_{i \in [1..n]}) = \sum_{j=1}^5 Score_F_j(S_i) \times w_j \quad (16)$$

Where, w_j is j^{th} weight of the corresponded j^{th} feature.

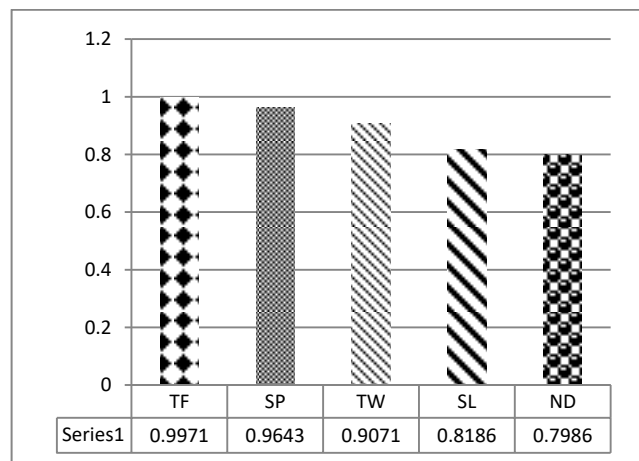


Fig. 4. Features Weights Extracted using DEFS Model.

Tables I, II, and III show a comparison of results between the three methods sets with the proposed method using ROUGE-1, ROUGE-2, and ROUGE-L at the 95%-confidence interval, respectively. The scores of the average recall (Avg_R), average precision (Avg_P), and average F-measure (Avg_F) are generalized at 95%-confidence interval. For each comparison the highest score result was styled in bold font format except the score of H2-H1. It is important to refer to the experimental results of GA published work, only the authors of this work had run ROUGE-1, and this study will depend and use this result through all comparative reviews. Fig. 5, 6, and 7 used to visualize results of the same Tables I, II, and III, respectively.

Two kinds of experiments were executed in this study: DEFS and DETS. The former is responsible for obtaining the adjusted weights of the features, while the latter is responsible for implementing the adjusted weights in a problem of text summarization.

TABLE I. DE, H2-H1, SET A AND B APPROACHES ASSESSMENTS USING ROUGE-1 RESULT AT THE 95%-CONFIDENCE INTERVAL

ROUGE	Method	Avg-R	Avg-P	Avg-F
1	H2-H1	0.51642	0.51656	0.51627
	B_Sys	0.40259	0.50244	0.43642
	W_Sys	0.06705	0.68331	0.1209
	DE	0.45610	0.52971	0.48495
	PSO	0.43028	0.47741	0.44669
	GA	0.45622	0.47685	0.46423

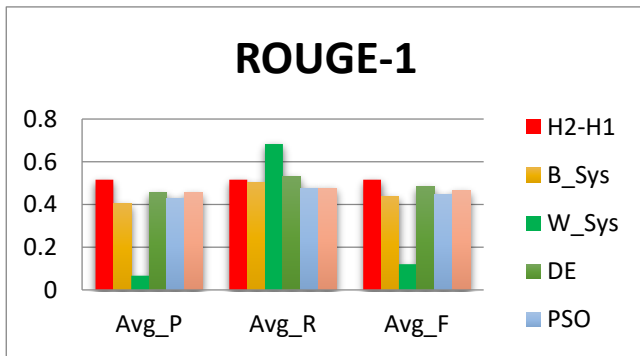


Fig. 5. DE, H2-H1, Set A, B and C Approaches Assessments using ROUGE-1 Avg_R, Avg-P, and Avg_F.

TABLE II. DE, H2-H1, SET A AND B APPROACHES ASSESSMENTS USING ROUGE-2 RESULT AT THE 95%-CONFIDENCE INTERVAL

ROUGE	Method	Avg-R	Avg-P	Avg-F
2	H2-H1	0.23394	0.23417	0.23395
	B_Sys	0.1842	0.24516	0.20417
	W_Sys	0.03417	0.38344	0.06204
	DE	0.24026	0.28416	0.25688
	PSO	0.18828	0.21622	0.19776
	GA	-	-	-

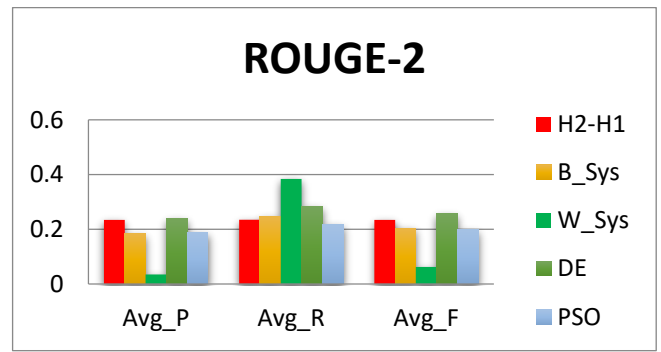


Fig. 6. DE, H2-H1, Set A and B Approaches Assessments using ROUGE-2 Avg_R, Avg-P, and Avg_F.

TABLE III. DE, H2-H1, SET A AND B APPROACHES ASSESSMENTS USING ROUGE-L RESULT AT THE 95%-CONFIDENCE INTERVAL

ROUGE	Method	Avg-R	Avg-P	Avg-F
L	H2-H1	0.48389	0.48400	0.48374
	B_Sys	0.37233	0.46677	0.40416
	W_Sys	0.06536	0.66374	0.11781
	DE	0.42000	0.48768	0.44645
	PSO	0.39674	0.44143	0.41221
	GA	-	-	-

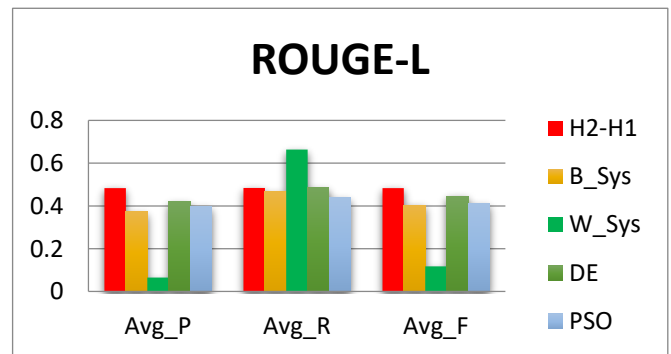


Fig. 7. DE, H2-H1, Set A and B Approaches Assessments using ROUGE-L Avg_R, Avg-P, and Avg_F.

The DETS model was designed to test and evaluate the performance of the DEFS model when performing feature selection for text summarization problems. The DETS model receives the weights of DEFS, as applies Equation 12 to score the sentences and generate a summary. The results showed that qualities of summaries generated using the (DE) are much better than the similar optimization techniques (set A: PSO and GA) and set C: best and worst system which participated at DUC 2002. The comparison of current extractive text summarization methods based on the DUC2002 has been investigated and reported as shown in Table IV.

Table IV demonstrates the comparison of some current extractive text summarization methods based on the DUC2002 dataset. On the basis of the findings generalized, the performance of the BiDETS model is 49% similar to human performance (52%) in ROUGE-1; 26% which is over the human performance (23%) using ROUGE-2; and lastly 45% similar to human performance (48%) using ROUGE-L.

TABLE IV. COMPARISON OF CURRENT EXTRACTIVE TEXT SUMMARIZATION METHODS BASED ON THE DUC2002

Method	Evaluation measure	Results
Evolutionary Optimization [68]	ROUGE-1, ROUGE-2, ROUGE-L	R-1 = 0.4990 R-2 = 0.2548 R-L = 0.4708
Hybrid Machine Learning [69]	ROUGE-1	R-1 = 0.3862
Statistical and linguistic [70]	F-measure	F-measure = 25.4 %
IR using event graphs[71]	ROUGE-1 ROUGE-2	R-1 = 0.415 R-2 = 0.116
Genetic operators and guided local search[72]	ROUGE-1 ROUGE-2	R-1 = 0.48280 R-2 = 0.22840
Graph-based text summarization [73]	ROUGE-1 ROUGE-2	R-1 = 0.485 R-2 = 0.230
SumCombine [74]	ROUGE-1 ROUGE-2	R-1 = 0.3823 R-2 = 0.0946
Self-Organized and DE [17]		20% in R-1 05% in R-2
Discrete DE[30]	Recall Precision F-measure	Recall = 0.74 Precision = 0.32 F-measure = 0.44
BiDETS		52% in R-1 23% in R-2 48% in R-L

This study has approved two contributions: firstly; studying the importance of the text features fairly could lead to producing a good summary. The obtained weights from the trained model were used to tune the feature scores. These tuned scores have a noted effect on the selection procedure of the most significant sentences to be involved in the summary. Secondly, developing a robust feature scoring mechanism is independent of the means of innovating novel features with different structure or proposing complex features. This study had experimentally approved that adjusting the weights of simple features could outperform systems that are either enriched with complex features or run with a high number of features. In contrast of testing phase to other methods classified in set A and B, the proposed Differential Evolution model demonstrated good performance.

VI. CONCLUSION AND FUTURE WORK

In this paper, the evolutionary algorithm “Differential Evolution” was utilized to optimize feature weights for a text summarization problem. The BiDETS scheme was trained and tested with a 100 documents gathered from the DUC2002 dataset. The model had been compared to three sets of selected benchmarks of different types. In addition, the DE employed simple calculated features compared with features presented in PSO and GA models. The PSO method assigned five features that differed in their structure: complex and simple; while the GA was designed with eight simple features. The DE in this study was deployed with five simple features and it was able to extract optimal weights that enabled the BiDETS model to generate summaries that were more qualified than other optimization algorithms. The BiDETS concludes that feeding the proposed systems with many, or complex features, instead of using the available features, may

not lead to the best summaries. Only optimizing the weights of the features may result in generating more qualified summaries as well as employing a robust evolutionary algorithm. The ROUGE tool kit was used to evaluate the system summaries in 95% confidence intervals and extracted results using the average recall, precision, and F-measure of ROUGE-1, 2 and L. The F-measure was chosen as a selection criterion as it balances both the recall and the precision of the system’s results. Results showed that the proposed BiDETS model outperformed all methods in terms of F-measure evaluation.

The main contribution of this research is generate a short text for the input document; this short text should represent and contain the important information in the document. A sentence extraction is one of the main techniques that is used to generate such a short text. This research is concerned about sentence extraction integrate an intelligent evolutionary algorithm by producing optimal weights of the selected features for generating a high quality summary. In addition, the proposed method enhanced the search performance of the evolutionary algorithm and obtained more qualified results compared to its traditional versions. In contrast, It is worth mentioning that, the summary measure basically used to score (document, query) similarity for large numbers of web pages. So, computing the similarity measure is disadvantageous to single document text summarization.

For future works, we assume that compressibility may prove to be a valuable metric to research the efficiency of automated summarization systems and even perhaps for text identification if for instance, any authors are found to be reliably compressible. In addition, this study opens a new trend for encouraging researchers to involve and implement other evolutionary algorithms such as Bee Colony Optimization (BCO) [75] and Ant Colony Optimization (ACO) [76] to draw more significant comparisons of optimization based Feature Selection text summarization issue. In addition and to the optimal of the author’s finding, the literature presented that algorithms such as ACO and BCO have not been presented yet to tackle general text summarization issues of both “Single” and “Multi-Document” Summarization. A second future work is to integrate the results of this study with a technique of “diversity” in summarization. This is to enable the DE selecting more diverse sentences to increase the result quality of the summarization.

ACKNOWLEDGMENT

This project was funded by the Deanship of Scientific Research (DSR) at King Abdulaziz University, Jeddah, Saudi Arabia under grant No. (J:218-830-1441). The authors, therefore, gratefully acknowledge DSR for technical and financial support.

REFERENCES

- [1] G. C. V. Vilca and M. A. S. Cabezudo, "A study of abstractive summarization using semantic representations and discourse level information," in International Conference on Text, Speech, and Dialogue, 2017, pp. 482-490.
- [2] M. Gambhir and V. Gupta, "Recent automatic text summarization techniques: a survey," Artificial Intelligence Review, vol. 47, pp. 1-66, 2017.

- [3] J. H. Holland, *Adaptation in Natural and Artificial Systems: An Introductory Analysis with Applications to Biology, Control and Artificial Intelligence*: MIT Press, 1992.
- [4] R. C. E. J. Kennedy, and Y. Shi, *Swarm Intelligence*. London: Morgan Kaufmann Publishers, 2001.
- [5] R. Storn and K. Price, "Differential Evolution – A Simple and Efficient Heuristic for Global Optimization over Continuous Spaces," *J. of Global Optimization*, vol. 11, pp. 341-359, 1997.
- [6] D. Harman and P. Over, "The DUC summarization evaluations," in *Proceedings of the second international conference on Human Language Technology Research*, 2002, pp. 44-51.
- [7] DUC, "The Document Understanding Conference (DUC).".
- [8] C.-Y. Lin, "ROUGE: A Package for Automatic Evaluation of summaries," presented at the Proc. ACL workshop on Text Summarization Branches Out, 2004.
- [9] J. Vesterstrom and R. Thomsen, "A comparative study of differential evolution, particle swarm optimization, and evolutionary algorithms on numerical benchmark problems," in *Evolutionary Computation*, 2004. CEC2004. Congress on, 2004, pp. 1980-1987 Vol.2.
- [10] H. Xingshi, Qingqing, Zhang, Na, Sun, Yan, Dong, "Feature Selection with Discrete Binary Differential Evolution," in *Artificial Intelligence and Computational Intelligence*, 2009. AICI '09. International Conference on, 2009, pp. 327-330.
- [11] R. N. Khushaba, Al-Ani, A., Al-Jumaily, A., "Differential evolution based feature subset selection," in *Pattern Recognition*, 2008. ICPR 2008. 19th International Conference on, 2008, pp. 1-4.
- [12] N. Nazari and M. Mahdavi, "A survey on automatic text summarization," *Journal of AI and Data Mining*, vol. 7, pp. 121-135, 2019.
- [13] M. Kirmani, N. M. Hakak, M. Mohd, and M. Mohd, "Hybrid text summarization: a survey," in *Soft Computing: Theories and Applications*, ed: Springer, 2019, pp. 63-73.
- [14] A. Kumar and A. Sharma, "Systematic literature review of fuzzy logic based text summarization," *Iranian Journal of Fuzzy Systems*, vol. 16, pp. 45-59, 2019.
- [15] M. A. Mosa, A. S. Anwar, and A. Hamouda, "A survey of multiple types of text summarization with their satellite contents based on swarm intelligence optimization algorithms," *Knowledge-Based Systems*, vol. 163, pp. 518-532, 2019.
- [16] D. Suleiman and A. A. Awajan, "Deep Learning Based Extractive Text Summarization: Approaches, Datasets and Evaluation Measures," in *2019 Sixth International Conference on Social Networks Analysis, Management and Security (SNAMS)*, 2019, pp. 204-210.
- [17] N. Saini, S. Saha, A. Jangra, and P. Bhattacharyya, "Extractive single document summarization using multi-objective optimization: Exploring self-organized differential evolution, grey wolf optimizer and water cycle algorithm," *Knowledge-Based Systems*, vol. 164, pp. 45-67, 2019.
- [18] S. Gupta and S. Gupta, "Abstractive summarization: An overview of the state of the art," *Expert Systems with Applications*, vol. 121, pp. 49-65, 2019.
- [19] H. Lin and V. Ng, "Abstractive summarization: A survey of the state of the art," in *Proceedings of the AAAI Conference on Artificial Intelligence*, 2019, pp. 9815-9822.
- [20] J. Tandel, K. Mistree, and P. Shah, "A review on neural network based abstractive text summarization models," in *2019 IEEE 5th International Conference on Convergence in Technology (I2CT)*, 2019, pp. 1-4.
- [21] P. Bhattacharya, K. Hiware, S. Rajgaria, N. Pochhi, K. Ghosh, and S. Ghosh, "A comparative study of summarization algorithms applied to legal case judgments," in *European Conference on Information Retrieval*, 2019, pp. 413-428.
- [22] A. Kanapala, S. Pal, and R. Pamula, "Text summarization from legal documents: a survey," *Artificial Intelligence Review*, vol. 51, pp. 371-402, 2019.
- [23] F. Jacquenet, M. Bernard, and C. Largeton, "Meeting summarization, A challenge for deep learning," in *International Work-Conference on Artificial Neural Networks*, 2019, pp. 644-655.
- [24] L. Ermakova, J. V. Cossu, and J. Mothe, "A survey on evaluation of summarization methods," *Information Processing & Management*, vol. 56, pp. 1794-1814, 2019.
- [25] A. Mahajani, V. Pandya, I. Maria, and D. Sharma, "A comprehensive survey on extractive and abstractive techniques for text summarization," in *Ambient Communications and Computer Systems*, ed: Springer, 2019, pp. 339-351.
- [26] M. A. Mosa, "A novel hybrid particle swarm optimization and gravitational search algorithm for multi-objective optimization of text mining," *Applied Soft Computing*, vol. 90, p. 106189, 2020.
- [27] M. A. Mosa, A. Hamouda, and M. Marei, "Graph coloring and ACO based summarization for social networks," *Expert Systems with Applications*, vol. 74, pp. 115-126, 2017.
- [28] M. A. Mosa, "Real-time data text mining based on Gravitational Search Algorithm," *Expert Systems with Applications*, vol. 137, pp. 117-129, 2019.
- [29] L. Chen and M. Le Nguyen, "Sentence Selective Neural Extractive Summarization with Reinforcement Learning," in *2019 11th International Conference on Knowledge and Systems Engineering (KSE)*, 2019, pp. 1-5.
- [30] S. Karwa and N. Chatterjee, "Discrete differential evolution for text summarization," in *2014 International Conference on Information Technology*, 2014, pp. 129-133.
- [31] L.-y. C. Chung-jui Tu, Jun-yang Chang, Cheng-hong Yang, "Feature Selection using PSO-SVM," *IAENG International Journal of Computer Science*, vol. 33, pp. 138-143, 2006.
- [32] Y. Liu, Qin, Zheng, Xu, Zenglin, He, Xingshi, "Feature Selection with Particle Swarms," in *Computational and Information Science*. vol. 3314, J. Zhang, J.-H. He, and Y. Fu, Eds., ed: Springer Berlin / Heidelberg, 2005, pp. 425-430.
- [33] J. Rojas-Simón, Y. Ledeneva, and R. A. García-Hernández, "Evaluation of text summaries without human references based on the linear optimization of content metrics using a genetic algorithm," *Expert Systems with Applications*, p. 113827, 2020.
- [34] A. Kiani and M. R. Akbarzadeh, "Automatic Text Summarization Using Hybrid Fuzzy GA-GP," in *Fuzzy Systems*, 2006 IEEE International Conference on, 2006, pp. 977-983.
- [35] R. Ferreira, L. de Souza Cabral, R. D. Lins, G. P. e Silva, F. Freitas, G. D. Cavalcanti, et al., "Assessing sentence scoring techniques for extractive text summarization," *Expert systems with applications*, vol. 40, pp. 5755-5764, 2013.
- [36] M. S. Binwahlan, Salim, N., & Suanmali, L., "Swarm based features selection for text summarization," *International Journal of Computer Science and Network Security IJCSNS*, vol. 9, pp. 175-179, 2009b.
- [37] D. Liu, Y. He, D. Ji, and H. Yang, "Genetic algorithm based multi-document summarization," in *Pacific Rim International Conference on Artificial Intelligence*, 2006, pp. 1140-1144.
- [38] A. Zamuda and E. Lloret, "Optimizing Data-Driven Models for Summarization as Parallel Tasks," *Journal of Computational Science*, p. 101101, 2020.
- [39] J. Y. Yeh, H. R. Ke, W. P. Yang, and I. H. Meng, "Text summarization using a trainable summarizer and latent semantic analysis," *Information Processing & Management*, vol. 41, pp. 75-95, Jan 2005.
- [40] M. A. Fattah and F. Ren, "GA, MR, FFNN, PNN and GMM based models for automatic text summarization," *Computer Speech and Language*, vol. 23, pp. 126-144, Jan 2009.
- [41] G. Pampara, A. P. Engelbrecht, and N. Franken, "Binary Differential Evolution," in *Evolutionary Computation*, 2006. CEC 2006. IEEE Congress on, 2006, pp. 1873-1879.
- [42] R. M. Alguliev and R. M. Aliguliyev, "Evolutionary Algorithm for Extractive Text Summarization.," *Intelligent Information Management*, vol. 1, pp. 128-138, 2009.
- [43] R. M. Alguliev, R. M. Aliguliyev, and N. R. Isazade, "DESAMC+DocSum: Differential evolution with self-adaptive mutation and crossover parameters for multi-document summarization," *Knowledge-Based Systems*.

- [44] Z. Cai, W. Gong, C. X. Ling, and H. Zhang, "A clustering-based differential evolution for global optimization," *Applied Soft Computing*, vol. 11, pp. 1363-1379, 2011.
- [45] R. M. Aliguliyev, "Clustering of document collection – A weighting approach," *Expert Systems with Applications*, vol. 36, pp. 7904-7916, 2009.
- [46] G. Liu, Y. Li, X. Nie, and H. Zheng, "A novel clustering-based differential evolution with 2 multi-parent crossovers for global optimization," *Applied Soft Computing*, vol. 12, pp. 663-681, 2012.
- [47] R. Mallipeddi, P. N. Suganthan, Q. K. Pan, and M. F. Tasgetiren, "Differential evolution algorithm with ensemble of parameters and mutation strategies," *Appl. Soft Comput.*, vol. 11, pp. 1679-1696, 2011.
- [48] M. L. Marina Litvak, Menahem Friedman, "A new approach to improving multilingual summarization using a genetic algorithm," presented at the Proceedings of the 48th Annual Meeting of the Association for Computational Linguistics, Uppsala, Sweden, 2010.
- [49] S. S. C. N. Satoshi, M. Murata, K. Uchimoto, M. Utiyama, and H. Isahara, "Sentence Extraction System Assembling Multiple Evidence," in 2nd NTCIR Workshop, 2001, pp. 319-324.
- [50] H. P. Luhn, "The automatic creation of literature abstracts," *IBM J. Res. Dev.*, vol. 2, pp. 159-165, 1958.
- [51] H. P. Edmundson, "New Methods in Automatic Extracting," *J. ACM*, vol. 16, pp. 264-285, 1969.
- [52] J. L. Neto, Santos, A. D., Kaestner, C. A. A., Freitas, A. A., "Generating text summaries through the relative importance of topics," *Advances in Artificial Intelligence*, vol. 1952, pp. 300-309, 2000.
- [53] P. B. Baxendale, "Machine-made index for technical literature: an experiment," *IBM J. Res. Dev.*, vol. 2, pp. 354-361, 1958.
- [54] S. Rahnamayan and H. Tizhoosh, "Differential Evolution Via Exploiting Opposite Populations Oppositional Concepts in Computational Intelligence." vol. 155, H. Tizhoosh and M. Ventresca, Eds., ed: Springer Berlin / Heidelberg, 2008, pp. 143-160.
- [55] L. Junhong and L. Jouni, "A fuzzy adaptive differential evolution algorithm," in TENCON '02. Proceedings. 2002 IEEE Region 10 Conference on Computers, Communications, Control and Power Engineering, 2002, pp. 606-611 vol.1.
- [56] M. M. Ali, A. T., and M., "Population set-based global optimization algorithms: some modifications and numerical studies," *Comput. Oper. Res.*, vol. 31, pp. 1703-1725, 2004.
- [57] R. Thangaraj, M. Pant, and A. Abraham, "New mutation schemes for differential evolution algorithm and their application to the optimization of directional over-current relay settings," *Applied Mathematics and Computation*, vol. 216, pp. 532-544, 2010.
- [58] L. Chang-Yong and Y. Xin, "Evolutionary programming using mutations based on the Levy probability distribution," *Evolutionary Computation*, *IEEE Transactions on*, vol. 8, pp. 1-13, 2004.
- [59] Y. Xin, L. Yong, and L. Guangming, "Evolutionary programming made faster," *Evolutionary Computation*, *IEEE Transactions on*, vol. 3, pp. 82-102, 1999.
- [60] M. S. Binwahlan, Salim, N., Suanmali, L., "Swarm Based Text Summarization," in *Computer Science and Information Technology - Spring Conference, 2009. IACSITSC '09. International Association of, 2009*, pp. 145-150.
- [61] M. F. Porter, "An algorithm for suffix stripping," in *Readings in information retrieval*, ed: Morgan Kaufmann Publishers Inc., 1997, pp. 313-316.
- [62] L. Suanmali, N. Salim, and M. S. Binwahlan, "Genetic Algorithm Based for Sentence Extraction in Text Summarization," *International Journal of Innovative Computing*, vol. 1, 2011.
- [63] S. H. Finley and S. M. Harabagiu, "Generating single and multi-document summaries with GISTEXTER," in *Proceedings of the workshop on text summarization*, Philadelphia, PA, USA, 2002.
- [64] D. Zajic, B. Dorr, and R. Schwartz, "Automatic headline generation for newspaper stories," in *Proceedings of the workshop on text summarization*, Philadelphia, Pennsylvania, USA, 2002.
- [65] L.-C. Yu, C.-H. Wu, and F.-L. Jang, "Psychiatric document retrieval using a discourse-aware model," *Artificial Intelligence*, vol. 173, pp. 817-829, 2009.
- [66] R. M. Aliguliev and R. M. Aliguliyev, "Experimental investigating the F-measure as similarity measure for automatic text summarization," *Applied and Computational Mathematics*, vol. 6, pp. 278-287, 2007.
- [67] R. Navigli and S. P. Ponzetto, "BabelNet: The automatic construction, evaluation and application of a wide-coverage multilingual semantic network," *Artificial Intelligence*.
- [68] R. M. Aliguliev, R. M. Aliguliyev, and N. R. Isazade, "Multiple documents summarization based on evolutionary optimization algorithm," *Expert Systems with Applications*, vol. 40, pp. 1675-1689, 2013.
- [69] M. A. Fattah, "A hybrid machine learning model for multi-document summarization," *Applied intelligence*, vol. 40, pp. 592-600, 2014.
- [70] R. Ferreira, L. de Souza Cabral, F. Freitas, R. D. Lins, G. de França Silva, S. J. Simske, et al., "A multi-document summarization system based on statistics and linguistic treatment," *Expert Systems with Applications*, vol. 41, pp. 5780-5787, 2014.
- [71] G. Glavaš and J. Šnajder, "Event graphs for information retrieval and multi-document summarization," *Expert systems with applications*, vol. 41, pp. 6904-6916, 2014.
- [72] M. Mendoza, S. Bonilla, C. Noguera, C. Cobos, and E. León, "Extractive single-document summarization based on genetic operators and guided local search," *Expert Systems with Applications*, vol. 41, pp. 4158-4169, 2014.
- [73] D. Parveen and M. Strube, "Integrating importance, non-redundancy and coherence in graph-based extractive summarization," in *Twenty-Fourth International Joint Conference on Artificial Intelligence*, 2015.
- [74] K. Hong, M. Marcus, and A. Nenkova, "System combination for multi-document summarization," in *Proceedings of the 2015 conference on empirical methods in natural language processing*, 2015, pp. 107-117.
- [75] D. Karaboga, "An idea based on honey bee swarm for numerical optimization," *Erciyes University, Kayseri, Turkey*2005.
- [76] M. Dorigo, V. Maniezzo, and A. Colomi, "Ant system: optimization by a colony of cooperating agents," *Trans. Sys. Man Cyber. Part B*, vol. 26, pp. 29-41, 1996.

Semi-Direct Routing Approach for Mobile IP

Basil Al-Kasasbeh

Faculty of Computer Studies
Arab Open University (AOU), Riyadh, Kingdom of Saudi Arabia

Abstract—The Mobile IP (MIP) protocol is used to maintain device connectivity while the device is moving between networks through a permanent IP address and temporary care-of-address (CoA). There are two techniques to implement MIP; these are direct and indirect. The indirect is commonly used in the current industry due to its stability while the mobile host (MH) frequently moves from network to another. However, the indirect technique suffers from the problems of delays and enlargement related to the packet size. The direct technique is more sensitive to frequent mobility, yet it required less transformation overhead with stable mobility. Accordingly, to overcome the disadvantages of both techniques, a semi-direct technique is proposed in this paper. The proposed technique is implemented by minimizing the home agent's interference (HA) with a push notification to the correspondent node (CN) that concerns any modification in the moving MH's CoA. The simulation of the proposed technique, the indirect and the direct routing techniques showed the advantages of the semi-direct routing technique over the conventional approaches. The results showed that the semi-direct approach outperformed the conventional approaches in terms of delay and overhead with frequently moved MH.

Keywords—Mobile IP; direct routing; indirect routing; care-of address; home agent; foreign agent

I. INTRODUCTION

Internet mobility is a crucial aspect of the IP networks that support delivering the data to a moving node [1]. Although different protocols and solutions have been proposed to support mobility, Mobile IP (MIP) protocol is a well-established and commonly utilized protocol [2, 3]. Accordingly, it has been extensively studied and extended to support efficient mobility in network architectures [4]. Mobile IP (MIP) is a communication protocol standardized by the Internet Engineering Task Force (IETF). It is developed to enable connected devices to move from one network to another while maintaining connectivity. The MIP enables the routing of IP packets of a moving mobile node (MN) and enables MN to be location independent [5]. Table I presented the set of abbreviations that are required to discuss the MIP [6].

MIP is focused on the mobility of an MN, a device with a network interface that can move from a network to another and send and receive data packets. MN can communicate with other MN, which in this case is called Correspondent Node (CN). Any node in MIP is identified by three types of addresses based on its location; these are Permanent address (PA), the media access control address, abbreviated as MAC address (MA) and care-of-address (CoA). These addresses can be a source address (SA) or destination address (DA) associated with a transmitted packet. The PA for the MH is a

fixed number assigned by the service provider and allows the MH to be publicly visible. MA is also a unique and permanent address assigned by the manufacturer to be used for communications within a network segment. The CoA is a temporary address used only when the MN is outside the HM [6].

The MIP network architecture consists of essential entities and addressing schemes, as illustrated in Fig. 1. Each network involves the home agent (HA) and the foreign agent (FA) and a set of local MN and possibly visiting MNs that are moved from other networks. For example, in Fig. 1, in network A there is a visiting MN from network B, a visiting MH in network B from network A and a visiting MH in network C from network B.

PA is solely used when the MN is in its HN. On the other hand, when the MN is outside the HN, it is associated with the special CoA. The CoA identifies the current location using an endpoint related to a local tunnel, which leads to the HA. CoA is also responsible for specifying the MN's registration with the HA along with the routing of IP packets through the tunnel. The internet connection is maintained between the stationary and the MN to avoid the negative effects associated with the change of location during the node's mobility. Hence, it keeps the Internet connection in an active mode [7].

TABLE I. DEFINITION OF THE ABBREVIATIONS AND TERMINOLOGY

Term. (Abb.)	Definition
Mobile Node (MN)	A device with a network interface that can move from a network to another
Correspondent Node (CN)	A connected device that is communicating with MN
Permanent Address (PA)	The public IP address that is assigned to an MN
MAC Address (MA)	An address that is used as a unique identifier for MN
Care-of-Address (CoA)	A temporary IP address assigned to a moving MN outside the HN
Source Address (SA)	An address of the MN from which the transmitted packet is originated
Destination Address (DA)	An address of the MN to which the transmitted packet is addressed
Home Agent (HA)	A device that stores information about the locations and addresses of the devices in the MN
Foreign Agent (FA)	A device that stores information about nodes visiting its network and advertise CoA
Home Network (HN)	A network to which an MN belongs and identified through its address
Foreign Network (FN)	A network MN is locating when away from its HN

This work was supported by the Arab Open University, KSA.

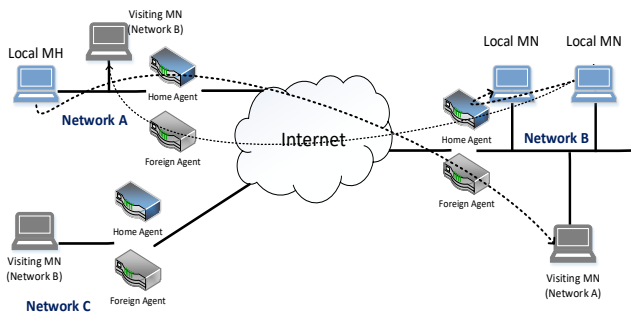


Fig. 1. Mobile IP Architecture.

The data packets transmitted to an MN using MIP are directed into two essential entities: HA and FA. The HA stores the information about the nodes that belong to the home network (HN) through their PA. Additionally, the HA functions as a router at the HN for the MNs and ensures the delivery of packets through a tunnelling process to the MN when the MN is located away from the HN by maintaining the location directory [8, 9]. On the other hand, the FA is responsible for storing information about MNs that visiting the network. The FA is also responsible for the advertisement of the CoA of the visiting nodes. FA also functions as a router on the network that offers different services for routing the registered MN. Moreover, the FA delivers and de-tunnels datagrams to the MN that is tunnelled through the HA. In case there is no FA, the MN has to take the responsibility of addressing and advertising the address by itself [10].

Although HA and FA have predetermined roles in the MIP, these roles change based on the implemented routing technique, indirect or direct. The indirect technique is commonly utilized due to its stability while the MH is moving from network to another frequently. However, it suffers from the problems of delays and enlargement related to the packet size. The direct approach is more sensitive to frequent mobility, yet it required less transformation overhead with stable mobility.

The direct routing technique, also called host-based mobility protocols [11], enables CN to send a packet to MN by using the CoA if the MN located in a visited FN. As illustrated in Fig. 2, the HA is responsible for interacting with a FA of the visiting network to track the mobile station's temporary address (CoA). The CN sends a request to the HA for the CoA of the MA. Packets are sent from the CN to the MN directly based on the CoA as illustrated in Fig. 2. HA has no roles in packet transmissions, and it just enables the CN to send packets directly by providing and tracking the CoA of the MN outside the HN. As the MN frequently moving from a network to another, the communication overhead increased as a result of CoA requesting and packet re-transmission [12, 13].

Indirect routing technique, also called network-based mobility protocols [14], enables a CN to send a packet to MN by using the PA through the HA whether an MN is located in its HN or a visiting an FN. Hence, mobility is completely transparent to its CN. Packets are first forwarded to the HA, as illustrated in Fig. 2. The HA is responsible for interacting with

a FA to track the mobile station's temporary address (CoA). HA also identifies the arriving packets addressed to the MNs whose permanent address is associated with that HA, but currently located in an FN. The HA receives these packets and forwards those to an MN based on two steps. The packet is first forwarded to the correspondent FA by using the MN's CoA and are forwarded afterwards from the FA to the MN. The HA addresses the packet by using the CoA so that the network layer can be able to route the packet through to the FN by applying several conventional routing algorithms. The HA encapsulates the original complete packet within a new larger packet, which is addressed and delivered to the MN's CoA. The FA for which the CoA belongs receives and decapsulates the packet and extracts the correspondent's original packet from the larger encapsulating packet [15, 16].

The growth with the number of connected and moving MN demands for fast and scalable connections with the shortest routing path and minimum handover latency. The existing techniques suffer from delay and overhead problems. For example, in the host-based protocol, as the MN is transmitted from FN to another FN, the transmission could be delivered to the wrong node and lead to communication overhead in re-transmitting the packets. Similarly, as the MN is transmitted from FN to another FN in the network-based protocol, the transmission required a registration processing with overhead communication between the HA and the FA. The gap in the existing techniques embodied in the delay in delivering the transmitted packets and communication overhead with a moving MN. Given the recent advances in software and hardware devices, MNs frequently move with demands to improve delay and overhead and enable intelligent real-time networks [17].

Accordingly, a semi-direct approach is proposed in this paper to reduce the delay and communication overhead with frequently moving MNs. The proposed a semi-direct technique to overcome the problems of both techniques. The semi-directed technique is implemented by minimizing the HA's interference with a push notification to the CN that concerns any modification in the CoA of moving MH. The proposed technique depends on changing the route of the transmitted packets and changes the HA and FA roles compared to the direct and indirect approach. Accordingly, in the semi-direct technique, the HA of the local network and the FA of the visiting network are responsible for verifying the address known to the CN and forwarding the data without encapsulation and decapsulation.

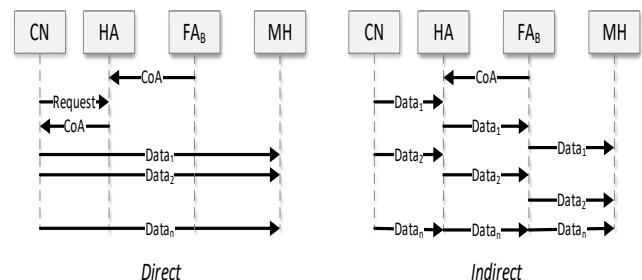


Fig. 2. Direct vs Indirect MIP Techniques.

The rest of this paper is organized as follows: Section 2 gives an overview of the related work that concerns the MIP extensions. In Section 3, the proposed work is presented and discussed in details. Section 4 presents the comparative results of the proposed and the existing techniques, both using analytical and simulation approaches, and finally, Section 5 concludes this paper.

II. RELATED WORK

Various mobile IP routing techniques enable users to be moving through various networks during the reception of support sessions and establishment session requests [18]. In the attempt to minimize the delay and overhead, existing MIP developments have taken different directions, these are: 1) anchor distribution over the networks 2) global dynamic home agent, 3) collector-based location tracking, and 4) predict mobility pattern.

A. Anchor Distribution

The anchor distribution solutions have been developed to eliminate the need for the HA-FA communication overhead and delay with the MN's movement. According to [19] the HA-FA communication overhead can be solved based on "distribution of home agents inside the current Internet topology to reduce distances to end-node". The MN is bind with the closest anchor. The CN can request the address from all available anchors using anycast routing and directly communicating with the MN without the HA's inferencing (e.g., anchor). Similar anchor distribution approaches with different topologies and different network architectures were proposed [20, 21]. In [22] a method for enabling the visiting node to implement a temporary agent within the visited mobile network was proposed. Hence, communication is considered intermediate and is accompanied by the Dynamic Home Agent (DHA) to minimize the risk of encountering a single failure point and deliver a flexible system. In particular, the DHA allocates an impermanent home address for the visiting node for reducing the distance between the HA and the visiting node, and in contrast, reducing the handover latency.

The advantage of anchor distribution approach is reducing the overhead and the delay if the anchor is distributed in the network, which leads to another problem of how to deploy the anchors in the network to avoid the extra signalling cost while avoiding interference of the HA.

B. Global Dynamic Home Agent

In [23] a Global Dynamic Home Agent Discovery (GDHAD) method was proposed, which enables the visiting node to apply the nearest HA within any casting protocol that explores the nearest HA of each node. This method minimizes the cost and delay of the registration process with the original HA. In [24] a different disseminated HA-based method for minimizing the cost and delay of the registration process was proposed. This method relies on a peer-to-peer HA exploration and overlays peer-to-peer networks designed via several home agents. Every home agent contains information regarding other HAs' locations. A mobile station remains to deliver its new location through to the new HA that starts with

an exploration procedure to search for the nearest HA to the MH.

Furthermore, the new HA delivers the MH through to the IP addresses, which found the nearest to their HAs, by connecting to any of these HAs. Similarly, in [25] another method to allocate the nearest HA was proposed. The MH delivers a registration request to the new home agent that preserves the path and historical information about the disseminated HA and MH. Moreover, the new HA searches for the most appropriate one that depends on the history maintained and began with the chosen HA's delegation process. Accordingly, the new HA delivers an acknowledgement through to the HA following the completion of this process. Furthermore, in [26] a mobility management method that can minimize the procedure's cost of a particular communication based on the Markov procedure's use was proposed, which investigates the tracking cost related to the device mobility. A mobile station (MS) grouping and equivalent quadrangular area are applied to minimize the communication overhead and the available stations.

C. Collector-based Location Tracking

Using a software-defined network (SDN), each node in the network can be an anchor for the visiting node. Accordingly, if the MN and the CN are linked to a different anchor, then the communication problem can be eased if the communication between the controllers is within the same administrative domain [4, 27]. The problems with the SDN is not implemented currently on the Internet. Thus, it cannot be generalized in this form.

D. Predicting Mobility Pattern

For predicting the mobility pattern, in [28] a technique for reducing the overhead by predicting and managing the MN location adaptively by estimating the mobility pattern was proposed. Similarly, in [29] a method that relies on the data clustering algorithm to estimate the transferred devices' locations was proposed. The device mobility's history is estimated for predicting the future's movements of any particular node. This algorithm attempts to search for appropriate network topology and identify a suitable routing path automatically.

The adaptive estimation related to a particular moving MN location can only be achieved when the required information's path and speed are existing, and the mobility is taken place at a certain speed on a dedicated path. An adaptive estimation is not applied for the location that belongs to a randomly transferring station. Therefore, before estimating the intended location, the history of mobile activities is exploited for identifying the case of either estimating the location automatically or not. For that reason, adaptive estimation limits the demand for more communications to allocate the transferring device.

An outline summary of this literature is provided in Table II. The direct and indirect techniques and their extensions possess a few drawbacks that are discussed in the literature. In [30] a comparison between the performance of several direct and indirect routing techniques was reported. In [31] and [32] the cost for mobile nodes' mobility throughout

particular networks was estimated. These studies concluded that an appropriate design of the MIP technique is significant for minimizing the processing and signaling overhead for an updated location.

In conclusion, several methods for minimizing the communication overhead within the mobile IP routing are introduced. Yet, a globally optimized technique for the current internet configuration is required.

TABLE II. COMPARISONS AMONG DIFFERENT MOBILE IP ROUTING ENHANCEMENT METHODS

Ref.	Aim	Briefs of the proposed methods	Drawbacks
[19]	Conceals the change in mobile location	Distributes HAs to minimize the distance to end-node. Permits the visiting node to apply an impermanent HA within the visited network	It is hard to deploy the anchors in the network to avoid the extra signaling cost while avoiding the HA's interference.
[20]	Decentralizes communication by deploying agents instead of the HA		
[21]			
[22]			
[23]	Allows the MN to estimate the nearest HA	Permits the visiting node to apply the closest HA for any casting protocol	Required a history of the MN and analyzing such history
[24]		Relies on a peer-to-peer HA exploration through several overlaid peer-to-peer networks	
[25]		Allows the HA to preserves the path and historical information about the disseminated HA and MH to search for an appropriate HA	
[26]		Applies the Markov procedure, which can investigate the tracking cost related to the device mobility, and which can search for the most effective HA	
[4]	Allows the MN to work as HA	Uses the SDN to enable each node in the network to role as an anchor for the visiting node	Cannot be generalized in this form.
[27]			
[28]	Estimates of the location of the nodes' for cost minimization	Adaptively predicts the mobility pattern to identify a suitable location	Required moving MN in a specific pattern
[29]		Estimates the location of the transferring devices by applying an analysis of the network topology	

III. PROPOSED TECHNIQUE

The proposed semi-direct technique for MIP is based on letting the HA of the local network and the FA of the visiting network to forward the data without encapsulation and decapsulation process. Accordingly, both HA and FA are implementing the routing process besides the address

verification process. The HA is responsible for interacting with a FA of the visiting network to track the CoA of the MN. The CN request the CoA of the HM based on the information stored in the HA. Then, the CN sends the packet to MN by using the permanent address and the CoA through the corresponding HA whether a MN is located in its own home network or a visiting a foreign network. Packets are then forwarded to the FA. The second function of the HA is to verify the addresses associated with the arriving packets, which are addressed to the MNs whose permanent address associated with that HA, but that is currently located in a foreign network. Then, the packets are forwarded from the FA to the MN. The FA also verifies the address as the HA did. In case a changing of the CoA occurred, the information is sent back to CN in a back-propagation manner. FA informs HA and HA informs the CN. In turns, the CN will send a new request to the HA for the new CoA of the MN. The verification process at the HA depends on the permanent-to-CoA mapping addresses that took place at the HA. In the verification at the FA, the process depends on the registration information for the COA only. Accordingly, the proposed technique does not depend on the encapsulation-decapsulating processes, which cause a delay. Thus, this way decreases the delay and increases the speed of transmission. This approach provides a new mechanism for delivering packets to a mobile station. In most cases, the mobile station possesses two IP addresses, which comprise the home address within a home network, which is temporarily connectable through a foreign network when having a foreign agent that uses the CoA. The IP packet consists of a header portion that includes the destination address (CoA).

The packet delivery mechanism of the semi-direct approach is discussed based on three potential scenarios. The first scenario is when the MN is currently located within the HN. In this manner, the CN can directly send a packet through to the HA by using different conventional internet routing mechanisms and taking into consideration that the destination IP address of the already sent packet represents permanent address. Because the MN is already located within the HA's scope, it can directly forward the packet through to the intended MH, which receives the packet and replies with a confirmation response should it be required. The second scenario is when the MN is currently located at an FN, and the CN sends a packet through to the HA where the destination IP address of the sent packet represents the permanent address and the CoA, which forward the packet to the corresponding FA. The third scenario is when the MN is moving from an FN to another, the CN sends a packet through to the HA where the destination IP address of the sent packet represents the CoA, the HA verify if there is an update on the destination CoA and, as the HA been informed about the new CoA, the HA response to the CN with a notification of the changes in the CoA. Accordingly, the CN sends new request for the new CoA. The HA replies with the new CoA, and the process starts all over.

In Fig. 3, a flowchart of the three potential scenarios about the packet delivery mechanism that is discussed in this section is illustrated. First, in the DA checking, the HA receives the packet and checks its addressing table to identify the current

temporary IP address (CoA) of the MN. Furthermore, the HA does not perform any encapsulation or header processing. The FA does not implement any processing or decapsulating and thus reduce the processing overhead and the delay. The HA forwards the processed packet through to the FA. When the foreign agent receives the packet, it forwards it directly through to the MN as there is no need for any further header translation. The MN receives the packet, which contains the CoA as its destination address, and recognizes that this packet is sent to its visiting MN. If it is required, the mobile station sends a reply message through to the CN.

It should be noted that the source IP address of the reply message represents the MA, and the destination IP address represents the CN. When the MN is moving from a FN to another before the CN get informed and the packet reaches the FA, the FA verify if there is an update on the destination CoA and, as the FA been recognize the movement of the MN, the FA response to the CN with a notification of the changes in the CoA. The HA response to the CN with a notification of the changes as received by the FA. The CN sends a new request for the new CoA. The HA replies with the new CoA, and the process starts all over.

Mainly, the proposed technique is consists of the following processes: registration, transmission and verification, and notification. These processes are implemented as the MN move from a network to another away from the MN. As the MN return to the HN, only the permanent address is used without the need for the transmission of the data.

A. Registration

In the registration process, FA sends the advertisement message through common protocols, such as Internet Control Message Protocol (ICMP), which are commonly used in diagnostic, error or control purposes. The MH who just moved to the network within the range of the FA sends a request message for forwarding services to the FA. The FA relays the message to the HA. In case HA accept the request, the HA a registration reply to FA. The FA relays the message to the MH. The HA store the CoA with the permanent address of the MH as long as the life-time of the registration expires. This process is illustrated in Fig. 4. Both HA and FA maintain the information about mapping between the permanent address and the CoA for the verification purposes. As a new request is received for CoA of registered MH, the old value is replaced, and the new and old value shall be used for the verification of the transmitted data.

B. Transmission and Verification

Datagram transmission is implemented in a sequence if the MH is located in FN, and the registration has been implemented successfully. In such a case, the MH send the datagram to the HA, which will verify the DA and relay the transmitted packet to the FA, which in turn verify the DA and relay it to the MH. In the verification process, HA stores information about the MA and the CoA of the MH. Similarly, the FA maintain such information to implement his identification purpose. Accordingly, both agents verify the transmission by checking the DA (see Fig. 3).

C. Notification

In the notification process, FA and HA send the notification through common protocols, such as ICMP, when there are modification on the records concerned the MH. In case that the MH get away from the visiting network, the FA sends a notification message for error in the DA. The HA relays the message to the CN. In case that HA recognize such error in the verification process, the notification is sent back to the CN (see Fig. 5). In such a case, the CN send a request for CoA for the HA and start the transmission back when a reply is received for the new CoA.

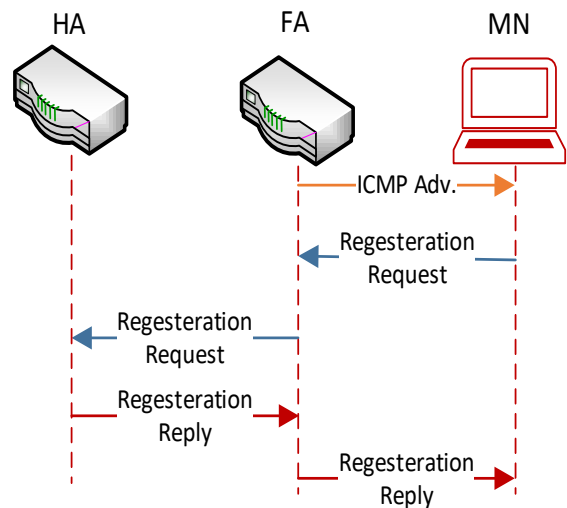


Fig. 4. Registration Sequence.

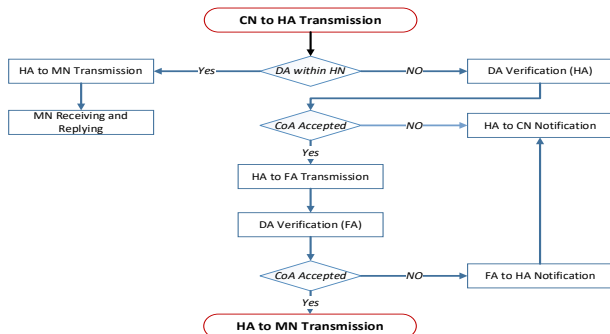


Fig. 3. Flowchart of the Proposed Technique.

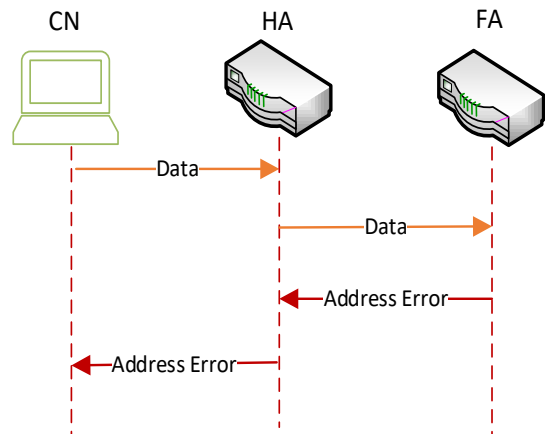


Fig. 5. Notification Sequence.

D. Comparison

Accordingly, the proposed technique is semi-direct in as the HA and the FA intermediate the transmission process for validating processes, yet, there is no header processing nor encapsulating and decapsulating processes. Accordingly, as similar to the indirect technique, the proposed approach keeps track of the MH movement through the verification and updating processes and as similar to the direct technique it minimizes the transmission processes by avoiding the encapsulating and decapsulating processes. The disadvantage of the proposed approach, the location of the MH is not transparent to the CN. A comparison between the proposed and the indirect and direct techniques are given in Table III.

TABLE III. COMPARISONS OF THE PROPOSED TECHNIQUE AND THE EXISTING TECHNIQUES

	Indirect Approach	Direct Approach	Semi-Direct Approach
HA	Receives all the transmitted packets, implements encapsulation and transmission to FA	Receives request for the CoA and replies based on the stored information.	Receives request for the CoA, replies to CN based on the stored information, verifies CoA, receives notification of changes from FA and notifies CN.
FA	Receives all the transmitted encapsulated packets, decapsulates them and transfers them through to the visiting MH	Registers CoA of the visiting MH	Registers and verifies CoA, and notifies HA with CoA changes
MH	Registers the CoA with the FA	Registers the CoA with the FA	Registers the CoA with the FA
CN	Sends all the transmitted packets to the HA	Sends all the transmitted packets to the MH	Sends all the transmitted packets to the HA

IV. ANALYSIS, EXPERIMENTS AND RESULTS

In order to analyze the performance of the proposed technique and the existing techniques in term of the processing overhead and the speed of the transition, delay is used for comparison purpose. Based on the discussed processed for these techniques, there are differences in the total delay based on the location of the MH, and there is different processing that required and causes such delay. The delays that are caused by the discussed techniques is registration delay (DR), encapsulation/decapsulation delay (DCap) and Transmission delay (DT). A numerical analysis and simulation are carried out to provide relevant comparisons among the evaluate techniques. Accordingly, all the scenarios of the connection and transmission between the CN and the MH are analyzed and the total delay at each scenario is calculated. In the numerical analysis, without loss of generality, we assume that the transmission delay is identical regardless of the identity of the sender and the receiver nodes. Accordingly, we also assume that the transmission delay and the CoA registration are identical. Three scenarios depicted these are, MH within the home network (S1), MH is in an FN (S2), and MH moved from FN to another with probability 0.5 (S3). Accordingly, the delay of each of the depicted scenario is calculated as given in Table IV.

TABLE IV. TOTAL DELAY IN THE DIRECT APPROACH AND FOLLOW ME APPROACH

#	Direct		Indirect		Semi-Direct	
	Equation	Unity	Equation	Unity	Equation	Unity
S1	$D_{total} = D_T$	1	$D_{total} = D_T$	1	$D_{total} = D_T$	1
S2	$D_{total} = D_R + D_T$	2	$D_{total} = D_R + 3 * D_T + D_{Cap}$	5	$D_{total} = D_R + 3 * D_T$	4
S3	$D_{total} = \sum_{i=1}^n D_R + D_T$	2n	$D_{total} = D_R + 3 * D_T + D_{Cap}$	5	$D_{total} = D_R + 3 * D_T$	4

Accordingly, the direct technique is good for MH that is not frequently moving through the network, which is not the case in real implementation. Thus, the proposed technique is best compared to the indirect approach. A comparison between the proposed technique and the indirect technique are given in Fig. 6, Fig. 7 and Fig. 8. If five packets with the following payloads (Bytes): 5000, 10000, 15000, 20000 and 25000, are sent from the Correspondent Network (CN) along to a Mobile Station (MS), the results of each scenario are illustrated.

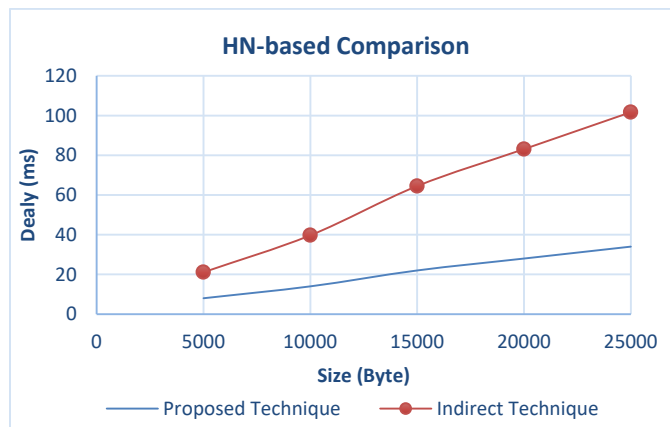


Fig. 6. A Comparison between the Propose and the Indirect Techniques for MH Located within the HN.

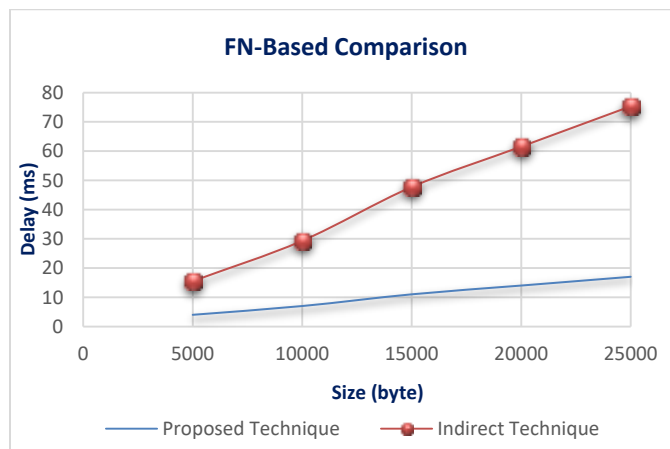


Fig. 7. A Comparison between the Propose and the Indirect Techniques for MH Located in an FN.

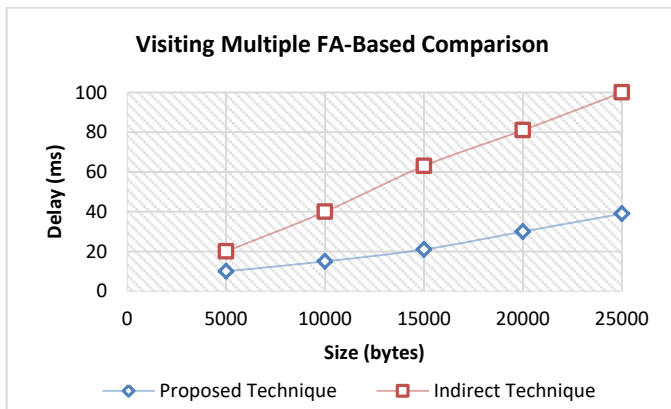


Fig. 8. A Comparison between the Propose and the Indirect Techniques for MH Moving from FA to another.

Based on the previously obtained results, it can be inferred that the delivery of data when using the semi-direct technique for mobile IP is found faster than the delivery of data when using the indirect technique. The reason behind this is that some processes as the encapsulation/decapsulation and additional fragmentation/de-fragmentation are only implemented in the indirect technique of the mobile IP routing technique, and is not implemented in the proposed technique. Thus, any other process requires an additional time. The total checksum time delay is found larger in the conventional indirect routing technique than in the proposed technique due to the fragmentation process in the HA, which uses a conventional approach. This implies that each fragment requires a checksum process. If the HA that uses the encapsulation of the mobile IP receives N packets, the number of output packets represents $2N$ or $2N-1$ packets. The obtained results prove the correctness of the conclusion mentioned above.

V. CONCLUSION

Recently, the encapsulation of packets is the well-known approach of the Mobile IP indirect routing approach, which is still uncommon for using the non-encapsulation approach with the mobile IP indirect routing technique. In this paper, it is inferred from the simulation results for implementing the non-encapsulation approach is found more efficient in comparison with the conventional encapsulation approach. Additionally, the encapsulation process itself increases the transmission delay, and the process of encapsulation for sending packets can enlarge their sizes. Furthermore, the speed of the communication process can be decreased due to the enlarged size of the new packet that should be sent from the home agent's side. Moreover, the de-encapsulation process requires an additional time to return the new packet through to its original structure so that this process can increase the total delay of the communication process. The future work will focus on implementing the semi-direct technique with multiple anchor distribution to further reduce the delay and signalling cost.

REFERENCES

[1] Z. Zhu, R. Wakikawa, and L. Zhang, "A survey of mobility support in the Internet", IETF Request for Comments, 2011, 6301.

[2] C. Perkins, "IP mobility support for IPv4, revised", IETF Engineering Steering Group, 2010.

[3] C. Perkins, D. Johnson, and J. Arkko, "RFC 6275 Mobility Support in IPv6", Internet Engineering Task Force (IETF), 2011.

[4] Y. Wang, and J. Bi, "Software-defined mobility support in IP networks", *The Computer Journal*, vol. 59 (2), pp. 159-177, 2016.

[5] J.M. Opos, S. Ramabhadran, A. Terry, J. Pasquale, A.C. Snoeren, and A. Vahdat, "A performance analysis of indirect routing", in *Book A performance analysis of indirect routing* (IEEE, 2007, edn.), pp. 1-10.

[6] P. Pupatwibul, A. Banjar, A.A. Sabbagh, and R. Braun, "Developing an application based on openflow to enhance mobile ip networks", in "Book Developing an application based on openflow to enhance mobile ip networks" (IEEE, 2013, edn.), pp. 936-940.

[7] A. Boukerche, A. Magnano, and N. Aljeri, "Mobile IP handover for vehicular networks: Methods, models, and classifications", *ACM Computing Surveys, CSUR*, vol. 49 (4), pp. 1-34, 2017.

[8] M.S. Chiang, and C.M. Huang, "A backward fast handover control scheme for mobile internet (BFH-MIPv6)", *Journal of Internet Technology*, vol. 19 (2), pp. 359-367, 2018.

[9] M.H. Rahman, N. Islam, A.I. Swapna, and M.A. Habib, "Analysis of Software Defined Wireless Network with IP Mobility in Multiple Controllers Domain", in *Book Analysis of Software Defined Wireless Network with IP Mobility in Multiple Controllers Domain*, (Springer, 2020, edn.), pp. 529-538.

[10] C.E. Perkins, "Mobile networking through mobile IP", *IEEE Internet computing*, vol. 2 (1), pp. 58-69, 1998.

[11] J.H. Lee, J.M. Bonnin, and X. Lagrange, "Host-based distributed mobility management support protocol for IPv6 mobile networks", in *Book Host-based distributed mobility management support protocol for IPv6 mobile networks*, (IEEE, 2012, edn.), pp. 61-68.

[12] C. Anastasiades, T. Braun, and V.A. Siris, "Information-centric networking in mobile and opportunistic networks", in *Wireless Networking for Moving Objects* (Springer, 2014), pp. 14-30.

[13] J. Lee, and S. Pack, "Mobility management in future wireless networks: Past, present, and future", *IEEE WCNC Tutorial*, 2013.

[14] A. Udagama, M.U. Iqbal, U. Toseef, C. Goerg, C. Fan, and M. Schlaeger, "Evaluation of a network based mobility management protocol: PMIPv6", in *Book Evaluation of a network based mobility management protocol: PMIPv6*, (IEEE, 2009, edn.), pp. 1-5.

[15] T. Clausen, U. Herberg, and J. Yi, "Security Threats to the Optimized Link State Routing Protocol Version 2 (OLSRv2)", in *Book Security Threats to the Optimized Link State Routing Protocol, Version 2 (OLSRv2)* (2017, edn.),

[16] C. Li, M.K. Mukerjee, D.G. Andersen, S. Seshan, M. Kaminsky, G. Porter, and A.C. Snoeren, "Using indirect routing to recover from network traffic scheduling estimation error", in *Book Using indirect routing to recover from network traffic scheduling estimation error*, (IEEE, 2017, edn.), pp. 13-24.

[17] S.H. La, J. Jeong, J. Koo, and U.M. Kim, "On intelligent hierarchical F-PMIPv6 based mobility support for industrial mobile networks", *Procedia Computer Science*, vol. 155, pp. 169-176, 2019.

[18] I. Al-Surmi, M. Othman, and B.M. Ali, "Mobility management for IP-based next generation mobile networks: Review, challenge and perspective", *Journal of Network and computer Applications*, vol. 35(1), pp. 295-315, 2012.

[19] R. Wakikawa, G. Valadon, and J. Murai, "Migrating home agents towards internet-scale mobility deployments", in *Book Migrating home agents towards internet-scale mobility deployments* (2006, edn.), pp. 1-10.

[20] Y. Mao, B. Knutsson, H. Lu, and J.M. Smith, "Dharma: Distributed home agent for robust mobile access", in *Book Dharma: Distributed home agent for robust mobile access*, (IEEE, 2005, edn.), pp. 1196-1206.

[21] Y. Wang, J. Bi, and X. Jiang, "A multi - anchoring approach in mobile IP networks", *Wireless Communications and Mobile Computing*, vol. 16 (18), pp. 3423-3438, 2016.

- [22] R. Zheng, Y. Ge, J.C. Hou, and S.R. Thuel, "A case for mobility support with temporary home agents", *ACM SIGMOBILE Mobile Computing and Communications Review*, vol. 6 (1), pp. 32-46, 2002.
- [23] Y.S. Yen, C.C. Hsu, Y. Chan, and H. Chao, "Global dynamic home agent discovery on mobile IPv6", *2nd International Conference on Mobile Technology, Applications and Systems*, November 2005.
- [24] R. Cuevas, C. Guerrero, A. Cuevas, M. Calderon, and C.J. Bernardos, "P2P based architecture for global home agent dynamic discovery in IP mobility", in *Book P2P based architecture for global home agent dynamic discovery in IP mobility*, (IEEE, 2007, edn.), pp. 899-903.
- [25] G. Motoyoshi, K. Leibnitz, and M. Murata, "Proposal and evaluation of a function-distributed mobility architecture for the future internet", *IEICE transactions on communications*, vol. 94 (7), pp. 1952-1963, 2011.
- [26] K.T. Chen, S.L. Su, and R.F. Chang, "Design and analysis of dynamic mobility tracking in wireless personal communication networks", *IEEE Transactions on Vehicular Technology*, vol. 51 (3), pp. 486-497, 2002.
- [27] A. Bradai, A. Benslimane, and K.D. Singh, "Dynamic anchor points selection for mobility management in Software Defined Networks", *Journal of Network and Computer Applications*, vol. 57, pp. 1-11, 2015.
- [28] W.J. Choi, and S. Tekinay, "An adaptive location registration scheme with dynamic mobility classification", in *Book An adaptive location registration scheme with dynamic mobility classification*, (IEEE, 2002, edn.), pp. 440-444.
- [29] J. Taheri, A.Y. and Zomaya, "Clustering techniques for dynamic location management in mobile computing", *Journal of Parallel and Distributed Computing*, vol. 67(4), pp. 430-447, 2007.
- [30] V.S. Wong, V.C. and Leung, "Location management for next-generation personal communications networks", *IEEE network*, 14 (5), pp. 18-24, 2000.
- [31] J.S. Ho, I.F. and Akyildiz, "A dynamic mobility tracking policy for wireless personal communications networks", in *Book A dynamic mobility tracking policy for wireless personal communications networks*, (IEEE, 1995, edn.), pp. 1-5.
- [32] J. Li, H. Kameda, and K. Li, "Optimal dynamic mobility management for PCS networks", *IEEE/ACM Transactions on Networking*, vol. 8(3), pp. 319-327, 2000.

An Automated Convolutional Neural Network Based Approach for Paddy Leaf Disease Detection

Md. Ashiqul Islam¹, Md. Nymur Rahman Shuvo², Muhammad Shamsojjaman³
Shazid Hasan⁴, Md. Shahadat Hossain⁵, Tania Khatun⁶

Dept. of Computer Science and Engineering
Daffodil International University
Dhaka, Bangladesh

Abstract—Bangladesh and India are significant paddy-cultivation countries in the globe. Paddy is the key producing crop in Bangladesh. In the last 11 years, the part of agriculture in Bangladesh's Gross Domestic Product (GDP) was contributing about 15.08 percent. But unfortunately, the farmers who are working so hard to grow this crop, have to face huge losses because of crop damages caused by various diseases of paddy. There are approximately more than 30 diseases of paddy leaf and among them, about 7-8 diseases are quite common in Bangladesh. Paddy leaf diseases like Brown Spot Disease, Blast Disease, Bacterial Leaf Blight, etc. are very well known and most affecting one among different paddy leaf diseases. These diseases are hampering the growth and productivity of paddy plants which can lead to great ecological and economical losses. If these diseases can be detected at an early stage with great accuracy and in a short time, then the damages to the crops can be greatly reduced and the losses of the farmers can be prevented. This paper has worked on 4 types of diseases and one healthy leaf class of the paddy. The main goal of this paper is to provide the best results for paddy leaf disease detection through an automated detection approach with the deep learning CNN models that can achieve the highest accuracy instead of the traditional lengthy manual disease detection process where the accuracy is also greatly questionable. It has analyzed four models such as VGG-19, Inception-Resnet-V2, ResNet-101, Xception, and achieved better accuracy from Inception-ResNet-V2 is 92.68%.

Keywords—Paddy leaf disease; deep convolutional neural network (DNN); transfer learning; VGG-19; ResNet-101; Inception-ResNet-V2; Xception

I. INTRODUCTION

Toward the start of the 21st century, paddy (*Oryza sativa* species) is as yet the main oat in human food frameworks and the principle wellspring of energy and a critical portion of proteins devoured by very nearly three billion peoples [1]. More than 90% of the world's paddy is produced in the Asia-Pacific Region [2]. In Bangladesh, paddy is the key producing crop food, about 75% of the absolute edited region, and over 80% of the all-out watered zone is planted to rice. As a result, paddy plays an important role in the subsistence of the people of Bangladesh [3].

Most of the time farmers have to face various problems in paddy cultivation such as Damage to arable land, increased population, climate change, pests, and diseases, etc. Due to these various problems, farmers are becoming uninterested in paddy cultivation nowadays. This paper has focused only on the pests and diseases to the various problems of rice cultivation. There are three main types of paddy diseases such as bacterial disease, fungal disease, and miscellaneous diseases. These include subcategories like bacterial blight, bacterial leaf streak, brown spot, leaf smut, leaf scald, panicle blight, bronzing, etc. [4]. Note that the incidence of diseases has of late gotten extreme because of the unfavorable impacts of climate change, especially the ascent in temperature (IPCC, 2007). It is assessed that 4-14% of rice yield in Bangladesh is lost each year by various pests and diseases. Bacterial leaf curse (BLB) and brown spot are currently genuine infections in rice. But the innovations technologies to pests and diseases are still restricted [5].

Generally, the manual recognition of paddy disease is the unaided eye perception of specialists which burns-through additional time, costly on huge homesteads [6]. It is hard to measure and some of the time it delivers a mistake while distinguishing the disease type [7]. Because of the ignorance of appropriate administration to redress paddy plant leaf disease, paddy production is being decreased as of late [8]. To overcome this, appropriate and quick recognition measures are required for the diagnosis of paddy leaf diseases. This work mainly focused on the five most common paddy leaf diseases named Brown spot, healthy leaf, leaf blast, bacterial blight, leaf smut.

The Revolution of Artificial Intelligence has made it easier to maintain a standard of living. Like all other sectors, there is no shortage of AI contributions in the agriculture sector. Technology has made it much easier to solve many problems in agriculture, plant disease is one of them. Currently, it can do a lot of disease detection using machine learning and deep learning. Despite some limitations, it has largely succeeded. As a result, the farmer himself can detect paddy disease in his land without the help of an expert. Technology is going to bring many more revolutions in the agriculture sector in the future.

According to a survey conducted in 1979-1981, 20 diseases of paddy have been reported in Bangladesh were to exist paddy leaf diseases [9], among which 13 diseases were identified as the important ones. In 2019 according to the rice knowledge bank of Bangladesh bacterial leaf blast is one of the most deleterious diseases. In Bangladesh, leaf blast, leaf blight, brown spots are very common diseases in paddy cultivation.

In this paper, it focused on four paddy diseases as Brown Spot, Leaf Blight, Leaf Smut, Bacterial Leaf Blast, and one healthy leaf. This paper selected the Deep Convolutional Neural Network and trained the dataset on the four DNN based pre-trained models named VGG-19, Xception, Inception-Resnet-V2, and Resnet-101.

II. RELATED WORK

Earlier, many studies have been done on various diseases of rice. At present research is being done on various diseases of rice and its cure. Using machine learning techniques by Kawcher Ahmed, et al [10] to detect 3 paddy leaf diseases. They mainly focused on three major leaf diseases of paddy, to complete their work and achieving better accuracy used four machine learning models and 10-fold cross-validation techniques.

Milon Biswas et al. [11] worked on only three paddy diseases and applied one classifier. Firstly, take images, convert to grayscale, image segmentation, apply SVM classifier, and finally predict the result.

Wen-Liang Chen, et al. [12] bacterial blast leaf disease is one of the most paddy diseases. Using the Internet of Things and Artificial Intelligence Technologies they mainly focus on agriculture sensors generating non-image data that can be automatically trained and analyzed by the AI mechanism in real-time. They can detect plant diseases almost efficiently.

Using an Optimized Deep Neural network with Jaya algorithm by S. Ramesh, et al. [13] mainly focuses on recognition and Classification of paddy Leaf diseases. They worked on four paddy diseases like bacterial blight, brown spot, sheath rot, and blast.

At present farmers are facing a lot of losses due to various diseases of paddy. Eusebio L. Mique, Jr. et al. [14] mainly focused on how to measure and control different types of paddy diseases easily using Convolutional Neural Network (CNN) and image processing. Data collected from internet sources and manually captured.

David F. Nettleton et al. [15] compared four models two are operational process-based and two are methods based on machine learning algorithms. They mainly focused on only one plant disease (leaf blast) and details describe it. Process-based and data-driven models can be utilized to give early alerts to envision rice blast and find out its quality, subsequently supporting fungicide applications.

So far a lot of work has been done or is being done on paddy disease detection using AI technology. Jay Prakash Singh et al. [16] focused on how to detect and classify paddy disease using modern image processing and machine learning techniques. They complete their work in four stages like image preprocessing, segmentation, feature extraction, and classification. It's a review analysis based research paper. They have tried to figure out how to better detect rice leaf diseases from various techniques.

When farmers apply pesticides on the land to eradicate various diseases of paddy, it is seen that they have many problems in understanding the severity of the disease or it is very difficult to do it manually. As a result, they apply more pesticides than they need. To solve this problem, Prabira Kumar Sethy et al. [17] has developed a prototype that measures the severity of various diseases in paddy and tells how much pesticide is needed. To develop this prototype they used fuzzy logic of computational intelligence and segmentation techniques of machine learning. Computational Intelligence is a subpart of Artificial Intelligence. They have focused on how to reduce the use of pesticides to reduce pollution.

S. Ramesh et al. [18] proposed a mechanism for rice blast leaf disease detection using KNN and ANN algorithms. They mainly focused on Indian rice crops, one rice leaf disease, and how to detect disease in its early stages. They achieved the best accuracy from ANN is 99%.

Early and proper recognition of any kind of plant disease is an essential step in grain protection. Vimal K. Shrivastava et al. [19] focused on how to solve traditional plant disease detection systems. They work on four classes, three on diseases and one on healthy leaves. To complete their work they used a pre-trained deep CNN model (AlexNet), SVM classifier, and transfer learning, achieving their accuracy of 91.37%.

Dengshan Li et al. [20] proposed a mechanism that detects rice leaf disease from real-time video using deep learning techniques. They used faster-RCNN for image detection from video and also used various deep CNN models like VGG16, ResNet-50, ResNet-101, and YOLOv3.

Gittaly Dhingra et al. [21] mainly focused comprehensive study on various paddy disease detection and classification using image processing techniques. They discussed two issues of rice disease detection and classification.

Junde Chen et al. [34] study five paddy leaf disease using deep learning approach with transfer learning. They used two deep learning models like the Dense-Net and Inception module and achieved accuracy 98.63%.

In Table I, showed many scopes on paddy disease research. This study works on five classes with four diseases and one healthy leaf.

TABLE I. LIMITATIONS OF PREVIOUS WORK

Author Information	Limitations
Kawcher Ahmed, et al. [10]	They have determined that they will work with high-quality datasets in the future and will focus on how to achieve better accuracy using more advanced models.
Milon Biswas et al. [11]	They clarify that their data values are very less in the dataset, they used three paddy diseases and their data values are only 30 images, as a result, they depend on assumption when measuring the performance.
Prabira Kumar Sethy et al. [17]	They worked on just four types of paddy diseases. They will work with other diseases of paddy in the future.
S. Ramesh et al. [18]	They worked on just one rice leaf disease (leaf blast). In the future, they will work on other's rice leaf disease or other crops.
Wen-Liang Chen, et al. [12]	They just focused on only one rice leaf disease
Vimal K. Shrivastava et al. [19]	They declared that their proposed model would give better results if the dataset could be enlarged.
Gittaly Dhingra et al. [21]	The proposed model can be further customized when the two diseases need to be identified and classified together. For achieving better accuracy increase the number of data in the dataset and develop advanced algorithms. For instant solutions can be made mobile-based applications.
Dengshan Li et al. [20]	They declared their proposed system could be applied to other rice disease and pests
S. Ramesh et al. [18]	In the future, to enhance the detection and classification of paddy diseases, any improvement method can be used to get the best performance by decreasing the false prediction.

III. PROPOSED SYSTEM

Previously, much work has been done on paddy disease detection using machine learning and deep learning concepts using different systems. This paper followed a benchmarked approach with a customized deep learning model shown in the flowchart (Fig. 1). After the acquisition of infected paddy leaf images, the image preprocessing term took part. The preprocessed images go through the deep convolutional neural network. Convolutional blocks of the models extract the main features from the input images. Based on the features of the images, the DNN model initiates the weights of each node. The final dense layer of the model contains five neural nodes and the activation function like softmax helps to predict the class of the given data.

The machine inputs the image from the dataset, preprocessing the images like rotates, zoom, flip, shuffle, resize the images. This will apply four deep CNN models: VGG-19, ResNet-101, Inception-Res-NetV2 and Xception where main focused on feature extraction and classification. Finally, predict the result by the best model.

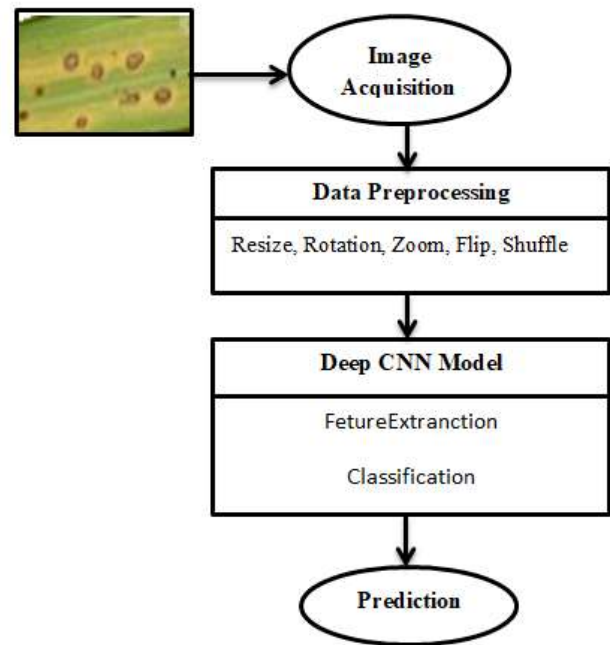


Fig. 1. Proposed Scheme.

IV. SYSTEM OPERATION

This is quantitative applied research based on the deep learning concept. In this section, discuss the methods taken part in this research.

A. Feature Extraction and Segmentation using CNN

Convolutional neural networks (CNN) is a feed-forward artificial neural network [22]. It has convolutional layers that have taken the role of feature extraction [23] shown in Fig. 2. Artificial neural network (ANN) based fully connected layers follow the classification process in a model. Fully connected layers contain multiple nodes and each node is connected to all of the next nodes of the next FC layer. Working with small size visual data, needed less number of neural nodes and in that case, can use only fully-connected layer blocks. In the case of a large image, more parameters needed to execute the process with an artificial neural network [25]. CNN contains neural nodes connected to a small region of neurons of the next convolutional layer. It compares the given visual data with a specific part by part. This specific part is called a feature of the image [24].

The convolutional layer at first lines up the feature from the input images and multiply each input image pixel by the corresponding feature pixel. Then perform summation of the pixel values and divide by the number of the total pixel in the feature. The calculated values are put in the feature map and move the filter throughout the entire image. All the calculated values are reserved in the feature map. In this way, all features go through the process and generate different feature maps. The equation (1) to obtain the convolutional layer is the following,

$$u_{ijm} = \sum_{k=0}^{K-1} \sum_{p=0}^{H-1} \sum_{q=0}^{H-1} z_{i+p,j+q,k}^{(l-1)} + b_{ijm} \quad (1)$$

Where bias is commonly set as b_{ijm} which does not depend on the position of the pixel of the image. h_{pqkm} as an identical value of weight.

Activation function Rectified linear Unit (ReLU) taken part now and remove all negative values from the feature map and replace it with zero. The activation ReLU function formula is shown in Eq. (2),

$$f(x) = \max(0, x) \tag{2}$$

In the pooling layer part, Max pooling layer shrinks the input image size by pooling the maximum value from the feature map, generated by the convolutional layer. The obtained equation (3) of max-pooling layer,

$$u_{ijk} = \max z_{pqk} \tag{3}$$

$$p, q \in P_{i,j}$$

Here, $P_{i,j}$ define a set of pixels including the area. A pixel value, u_{ijk} is gained by using H^2 pcs of pixel value with every k channels.

Finally, the fully connected layer converts the shrink images that come from the last pooling layer of the model, converting them to a single list array vector. The classification task is executed in the fully connected layer.

B. Classification based on Transfer Learning

Transfer learning in the machine learning field is a concept where the gained knowledge is transferred to another model to solve another related problem [27]. Deep CNN based applications of Keras are trained with the ImageNet dataset. ImageNet project which is a large visual database design for visual object recognition research. Deep convolutional neural network-based models are trained with millions of images with thousands of classes [26].

Keras deep learning applications contain multiple convolutional, pooling, and dense layers. The architectures can be separated into multiple blocks of layers shown in Fig. 3, 4 and 5. Convolutional blocks of the network contain multiple convolutional layers that extract features from the input data. Fig. 4 showed a residual inception block [32], a convenient design of convolutional layers. Each inception block followed by a filter expansion layer (1x1 Conv Linear) which was used for scaling up the dimensionality of the filter before the concatenation, shown in Fig. 4.

The parameters of features gained by the model are transferable. Using the pre-trained weights in a new model can solve related problems more effectively than general models [27]. The final block of the Keras applications contains dense layers for classification tasks.

Keras deep learning network architectures are trained with thousands of categories of images and the final dense layer contains thousands of nodes to classify all the categories. Cutting down the top layer of the model and adding a customized fully connected layer to classify the desired classes of images is a novel way when the dataset contains a limited number of data [28].

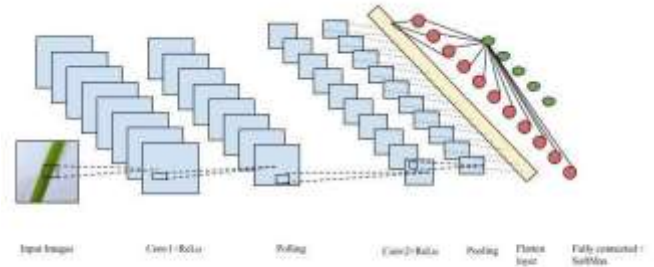


Fig. 2. Schema of the Convolutional Neural Network (CNN) based Model.

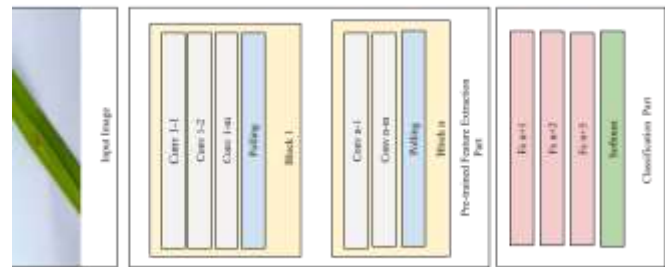


Fig. 3. Schema of VGG Blocks Consist of a Sequence of Convolutional Layers.

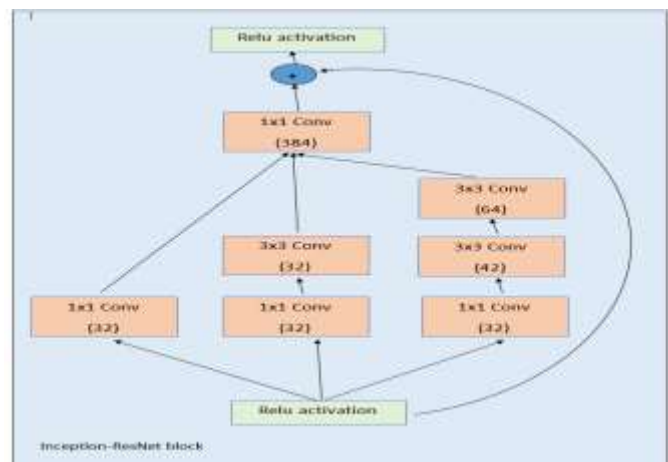


Fig. 4. Schema for Inception-ResNet Block of Inception-ResNe-V2 Network [32]. This is Inception-Resnet block of Fig. 5.

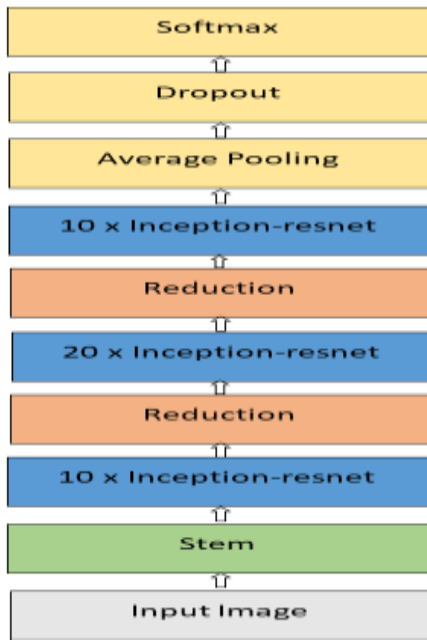


Fig. 5. Schema for Inception-ResNet-V2 Network [32].

V. PADDY DISEASE TYPE AND DATASET DESCRIPTIONS

A. Disease Types

Many food grains are wasted only due to insects and diseases. Research is being done all over the world to eradicate these diseases of rice. Although there were more than 30 rice diseases [9] in total, according to the 1979-81 survey [9], 20 rice diseases were reported in Bangladesh. But 13 diseases are common in all three seasons (Boro, Aus, and Aman), respectively bacterial blight, bacterial leaf streak, sheath blight, sheath rot, leaf blast, brown spot, grain spot, stem rot, leaf scald were as major, Tungro, Bakanae, Cercospora leaf spot, and zinc-deficiency were as minor. Only the diseases that have been dealt with are briefly discussed in section B.

B. Dataset Descriptions

For this work, it has chosen four paddy leaf diseases named brown spot, leaf blast, leaf blight, leaf smut, and one healthy leaf. The dataset contains 984 images. Collected the data from various internet sources: UCI machine learning repository [29] and Kaggle [30]. Table II describes the number of data in the dataset and splits the data for train, validation, and test in detail. Fig. 6 and Fig. 7, describes the classes of the dataset in detail.

1) *Brown spot*: It is one of the most common diseases of paddy leaf which is caused by fungus. At the beginning stage, round, small, dark brown to purple-brown marks can be seen Fig. 6(a). As time passes, big spots on the leaves will increase and can kill the whole leaf.

2) *Leaf blast*: This paddy leaf disease is caused by Magnaporthe oryzae which is a kind of fungus. The primary symptoms of this disease are spots of white to grey-green colour which are spindle-shaped with dark red to brownish borders see Fig. 6(b).

3) *Leaf blight*: This blight disease is a result of being affected by Xanthomonas oryzae which is one kind of bacteria. Infected leaves turn greyish green and followed by yellowing and then it turns straw-coloured and finally the leaf dies as shown in Fig. 6(c).

4) *Leaf smut*: It is caused by the fungus named Entyloma oryzae, which is a widely distributed disease of paddy leaf. The infected leaf will have angular, black spots (sori) on both sides of the leaves seen in Fig. 6(d). The black spots on the leaves are about 0.5 to 5.0 millimetres long and 0.5 to 1.5 millimetres wide.

5) *Healthy leaf*: A healthy paddy leaf will simply be free from every kind of disease. There should not be any sign of diseases and the colour of the leaf should be green.

C. Data Preprocessing

For data preprocessing the Keras ImageDataGenerator function took part. The dataset contains 984 images with three colour channels with different pixel values. Then resize all the images in 256*256-pixel value. Inconstantly rotating the training images in a range of 15 degrees provides the different viewpoint of the visual object. Width and height shift range, zoom and shear range fixed at 0.1. Rescale images is the only common preprocessing technique taken part in both training and testing dataset. For the training dataset batch size is eight and for the test set, it is taken one.

TABLE II. NUMBER OF TRAIN AND TEST IMAGES OF EACH DISEASE

Paddy leaf disease class name	Number of Images	Number of Images Used for Train and Validation	Number of Images used for Test
Brown Spot	166	138	28
Leaf Blast	159	131	28
Leaf Blight	216	188	28
Leaf Smut	216	188	28
Healthy Leaf	227	199	28
Total	984	844	140

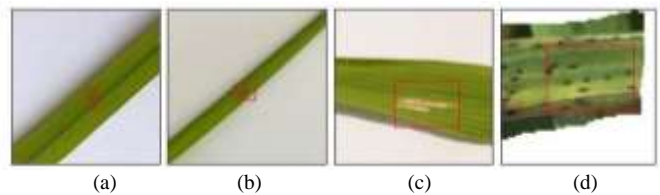


Fig. 6. Paddy Leaf Disease (a) Brown Spot, (b) Leaf Blast, (c) Leaf Blight, and (d) Leaf Smut.

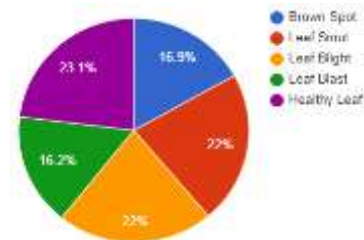


Fig. 7. Data Share Percentages of Classes in the Dataset.

VI. MODEL DESCRIPTIONS

Deep Convolutional Neural Network: Deep CNN models are a kind of feed-forward neural network which are used to adjust the parameters of the network to reduce the value of the cost function. These models have significantly worked in the field of analyzing visual imagery, image or video classification, object detection, natural language processing. THE deep CNN model is based on convolutional neural networks which contain a larger number of layers than a general CNN model. The model generally consists of convolutional layers, activation layers, pooling layers, flatten layer, dropout, batch normalization layers, and dense layers. The dropout is utilized to avoid overfitting. Activation functions like ReLu, Softmax are added to network layers to help the complex patterns exist in the data. Different deep CNN models have shown in Table V that the deep CNN model has great performance for classification and detection. The four models were selected based on the variety of architectural design and depth size of them. In Table III, the Top 5 accuracy refers to the validation accuracy with the ImageNet validation dataset and depth refers to the topological depth of the network.

TABLE III. KERAS BASED DEEP LEARNING CNN MODELS DESCRIPTION [31]

Model Name	Top 5 Accuracy	Parameters	Depth
VGG-19	0.900	143,667,240	26
ResNet-101	0.928	44,707,176	101
Xception	0.945	22,910,480	126
Inception-ResNet-V2[32]	0.953	55,873,736	572

VII. RESULT ANALYSIS

A. Result

This study has worked with four CNN deep learning Keras pre-trained algorithms as mentioned in Table IV to classify and detect the leaf diseases. While analyzing these algorithms, the study found that Inception-ResNet-V2 has obtained the highest accuracy among them which is 0.9286, and similarly, for precision, recall, and F1 score, Inception-ResNet-V2 was ahead of all of them. After Inception-ResNet-V2, Resnet-101 has shown the accuracy of 0.9152. The Xception model has achieved an accuracy of 0.8942 and VGG-19 has the lowest accuracy of 0.8143. Not just in the accuracy but also in the part of precision, recall, and F1 Score it has obtained the lowest results. The number of epochs considered 100 for all training procedures. All of this information is presented in Table III which contains a statistical analysis of these various models. The evaluations metrics (accuracy, precision, recall, f1 score) are defined as following [18].

1) *Accuracy*: Accuracy is calculated from the Confusion matrix. Accuracy is the most instinctive performance measure and it is a general ratio of the correctly predicted data to all the data in the dataset [33]. The formula of accuracy is shown in the Eq. (4) Better accuracy is possible only when the values of false positive and false negative are almost the same in the dataset.

$$\text{Accuracy} = \frac{TP+TN}{TP+TN+FP+FN} \quad (4)$$

2) *Precision*: The precision measurement of the algorithms refers to the ratio of correctly predicted positive values to the total number of positive predicted values [33]. The formula for precision is shown in Equation (5).

$$\text{Precision} = \frac{TP}{TP+FP} \quad (5)$$

3) *Recall*: The recall is the proportion of exactly predicted positive values to the positive actual class in the confusion matrix. Recall calculated formula is given in Eq. (6).

$$\text{Recall} = \frac{TP}{TP+FN} \quad (6)$$

4) *F1 Score*: F1 Score is the weighted mean value of Precision and Recall. That's why this score considers both false positives and false negatives values [33]. In equation (7), the formula of the F1 score is shown. Actually, it is not easy to understand by looking at the accuracy, but F1 is generally more helpful than accuracy.

$$\text{F1 Score} = 2 \times \frac{\text{Recall} \times \text{Precision}}{\text{Recall} + \text{Precision}} \quad (7)$$

Here, TP = True Positive, TN = True Negative, FP = False Positive, FN = False Negative.

As the model Inception-ResNet-V2 has achieved the highest accuracy compared to the other three models, it has created a performance table for this particular algorithm for every class of the dataset and noted the precision, recall, and F1 score of each class. As it can see in Table IV, for the precision, Brown Spot, Leaf Blast, Leaf Blight, Leaf Smut have obtained more than 0.90 but for healthy leaf images, it falls to 0.78. For Recall, for the class leaf blast is 0.71 and for the other classes, it was above 0.90. And finally, for the F1 score, Leaf blast was the lowest which is 0.82 and for Leaf smut class, precision, recall, and F1 score, it is 1.0. All of this information and some other details are presented in Table V.

TABLE IV. STATISTICAL ANALYSIS OF DIFFERENT PRE-TRAINED KERAS MODEL

Models	Accuracy	Precision	Recall	F1 Score
VGG19	0.8143	0.8176	0.8035	0.8041
ResNet-101	0.9152	0.9215	0.9056	0.9056
Inception-ResNet-V2	0.9286	0.9371	0.9262	0.9286
Xception	0.8942	0.8963	0.8865	0.8823

TABLE V. THE PERFORMANCE SCORE FOR EACH CLASS OF INCEPTION-RESNET-V2 MODEL

Classes	Brown Spot	Healthy Leaf	Leaf Blast	Leaf Blight	Leaf Smut
Precision	1.00	0.78	0.95	0.91	1.00
Recall	0.93	1.00	0.71	1.00	1.00
F1 Score	0.96	0.88	0.82	0.98	1

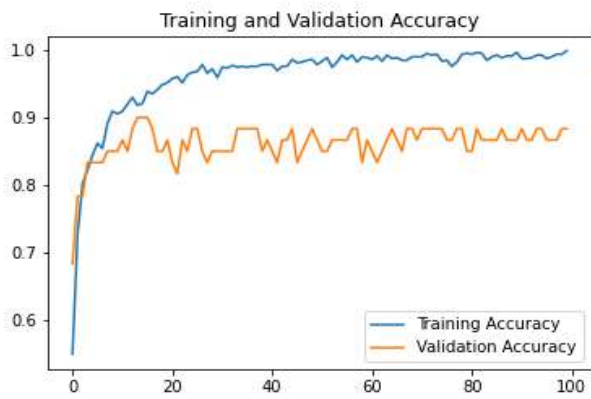


Fig. 8. Training and Validation Accuracy Graph.

Fig. 8 is showing the graph of training and validation accuracy of the model and it can see that for training accuracy, with the blue line, has reached about 1.0 and in the validation accuracy, which is the orange line, it is moving in the range of about 0.80 to 0.90.

B. Error Analysis

Although it is difficult to detect disease manually, technology has made the task much easier for us. But even then technology can't always give perfect results like humans, some limitations remain. The machine sometimes gets confused when it comes to disease detection. After choosing the best model some error has. In Fig. 9, it can see 8 data conflicts between Leaf Blast with Healthy Leaf and 2 data Brown Spot with Leaf Blast and Leaf Blight. Although the number is low.

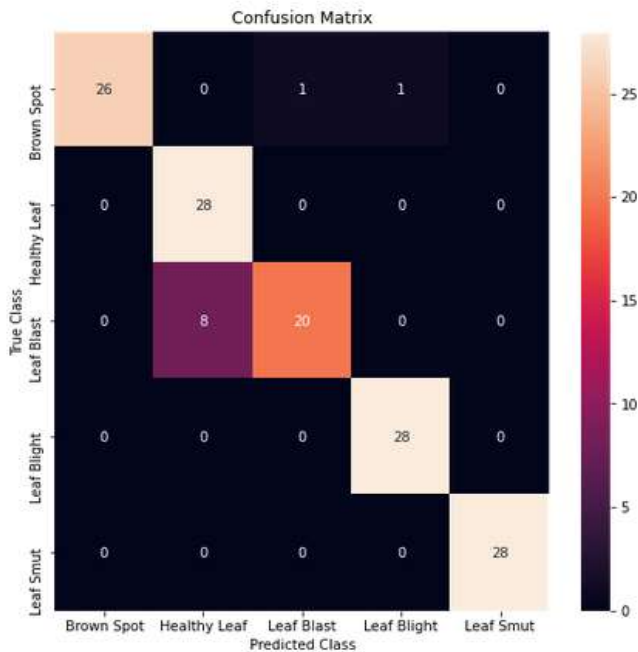


Fig. 9. Confusion Matrix of Inception-ResNet-V2 Model.

VIII. COMPARATIVE ANALYSIS

In this section, it will discuss different methods of identifying and classifying diseases of paddy and its leaves, which can diagnose rice in different ways using different tools and technologies of machine learning and deep learning. Much research has been done on this before and is still ongoing. Some comparisons of previous research are shown in Table VI.

In previous work, it has seen that many researchers worked on one or two or three or four diseases of paddy using machine learning algorithms or deep learning models or computational intelligence concepts.

This study worked on four different diseases (leaf smut, leaf blast, bacterial leaf blight, and brown spot) and one healthy leaf using advanced transfer learning-based deep CNN models.

TABLE VI. COMPARISON OF PREVIOUS RESEARCH ON PADDY DISEASES

References	Diseases	Tools Technologies	Accuracy
Kawcher Ahmed, et al [10]	Leaf smut, bacterial blight, brown spot	KNN, J48, Naive Bayes, Logistic Regression, Decision Tree, 10-fold cross-validation	97%
Wen-Liang Chen, et al. [12]	Leaf blast	CNN, IoT, spore germination	89.4%
Vimal K. Shrivastava et al. [19]	Rice blast, bacterial leaf blast, sheath blight	Deep CNN, SVM, transfer learning, MatConvNet toolbox, AlexNet, NVIDIA GeForce 940M GPU	91.37%
Dengshan Li et al. [20]	Rice sheath blight, rice stem borer, brown spot	deep CNN, faster-RNN, confusion matrix, VGG16, ResNet-50, ResNet-101, YOLOv3, custom DCNN	The better result from custom DCNN
S. Ramesh et al. [18]	Leaf blast	KNN, ANN	99%
Prabira Kumar Sethy et al. [17]	Brown spot, bacterial blight, leaf scald, leaf blast	Fuzzy logic, computational intelligence, SVM, K-means	86.35%

IX. ADVANTAGES

Previously much work has been done on various paddy leaf disease detection and classification using machine learning and deep learning approaches. Since rice is the staple food of most countries in the world, these studies can be used for the development of agricultural sectors in different countries. Since this study focused on four paddy leaf diseases in the perspective of Bangladesh and worked using deep learning models with transfer learning and achieved better accuracy, this study is more helpful for Bangladeshi farmers to easily detect rice leaves.

X. CONCLUSION

Conducting this study, it has evaluated the performance of four benchmark deep learning network architecture and analyzed them in different statistical measures. By analyzing the algorithm's accuracy, precision, recall, and F1 score, the highest achieved a test accuracy of 92.68% from the Inception-ResNet-V2 network architecture. In this paper, the data used for model training and testing collected from different internet sources and local paddy farms. The dataset consists of five classes where four different classes contain four widely infected paddy leaf disease and one class of health leaf images. The unique architecture of the Inception-ResNet-V2 consists of a stem, reduction and inception-resnet blocks with a depth of 571 impacts more than other networks to adapt with Dataset. The ResNet-101 network achieved the second-highest testing accuracy of 91.52%. To achieve a more accurate prediction of the paddy leaf diseases, it was used to transfer learning approaches. This adaptation of transfer learning increased the accuracy and reduced the model training time complexity.

XI. FUTURE WORK

This research can be carried forward with more varieties of paddy leaf diseases and more fine-tuned CNN models with the expectation of finding better accuracy and ensuring faster detection. A detailed comprehensive study is a must to understand the factors affecting the detection of plant diseases, like the classes' datasets, and size of datasets, learning rate, illumination, etc. The basic form of paddy plant diseases changes with the passage of time or the background of the images, images with colour issues, hence, these convolutional neural network models should be modified to enable them to detect and classify diseases during these complex or problematic situations. This study can be extended by considering other types of paddy leaf diseases, with larger data sets and other CNN models can be analyzed too. Shortly, the work will be done along all of these limitations and use this research as a base to detect other plant leaf diseases with greater accuracy. Also, the highest achieved accuracy of Inception-ResNet-V2 is quite motivating for us to explore more about this model and compare it to other CNN models.

REFERENCES

- [1] Trébuil, G., 2011. Rice production systems in Asia: The constant presence of an essential cereal on a continent in mutation.
- [2] Papademetriou, M.K., 2000. Rice production in the Asia-Pacific region: issues and perspectives. *Bridging the rice yield gap in the Asia-Pacific region*, 220.
- [3] Bangladesh Rice Knowledge Bank, available at <<<http://www.knowledgebank-brri.org/riceinban.php>>>, last accessed on 25-11-2020, 08.40 am.
- [4] Wikipedia, list of rice leaf diseases, available at <<https://en.wikipedia.org/wiki/List_of_rice_diseases>>, last accessed on 28-11-2020, 05.10 am.
- [5] Mondal, M. H. (2010). Crop agriculture of Bangladesh: Challenges and opportunities. *Bangladesh Journal of Agricultural Research*, 35(2), 235-245.
- [6] Mohanty, Sharada P., David P. Hughes, and Marcel Salathé. "Using deep learning for image-based plant disease detection." *Frontiers in plant science* 7 (2016): 1419.

- [7] Mahlein, Anne-Katrin. "Plant disease detection by imaging sensors—parallels and specific demands for precision agriculture and plant phenotyping." *Plant disease* 100.2 (2016): 241-251.
- [8] Pinki, F. T., Khatun, N., & Islam, S. M. (2017, December). Content-based paddy leaf disease recognition and remedy prediction using support vector machine. In *2017 20th International Conference of Computer and Information Technology (ICCIT)* (pp. 1-5). IEEE.
- [9] S. Miah, A. Shahjahan, M. Hossain, and N. Sharma, "A survey of rice diseases in Bangladesh," *International Journal of Pest Management*, vol. 31, no. 3, pp. 208–213, 1985.
- [10] Ahmed, K., Shahidi, T. R., Alam, S. M. I., & Momen, S. (2019, December). Rice Leaf Disease Detection Using Machine Learning Techniques. In *2019 International Conference on Sustainable Technologies for Industry 4.0 (STI)* (pp. 1-5). IEEE.
- [11] Biswas, M., Faruqui, N., Siddique, H., Lata, M.A. and Mahi, M.J.N., A Novel Inspection of Paddy Leaf Disease Classification using Advance Image Processing Techniques.
- [12] Chen, W.L., Lin, Y.B., Ng, F.L., Liu, C.Y. and Lin, Y.W., 2019. RiceTalk: Rice Blast Detection using Internet of Things and Artificial Intelligence Technologies. *IEEE Internet of Things Journal*, 7(2), pp.1001-1010.
- [13] Ramesh, S., & Vydeki, D. (2020). Recognition and classification of paddy leaf diseases using Optimized Deep Neural network with Jaya algorithm. *Information processing in agriculture*, 7(2), 249-260.
- [14] Mique Jr, E. L., & Palaoag, T. D. (2018, April). Rice pest and disease detection using convolutional neural networks. In *Proceedings of the 2018 International Conference on Information Science and System* (pp. 147-151).
- [15] Nettleton, D.F., Katsantonis, D., Kalaitzidis, A., Sarafijanovic-Djukic, N., Puigdollers, P. and Confalonieri, R., 2019. Predicting rice blast disease: machine learning versus process-based models. *BMC bioinformatics*, 20(1), p.514.
- [16] Singh, J.P., Pradhan, C. and Das, S.C., 2020. Image Processing and Machine Learning Techniques to Detect and Classify Paddy Leaf Diseases: A Review. In *Machine Learning and Information Processing* (pp. 161-172). Springer, Singapore.
- [17] Sethy, P.K., Negi, B., Barpanda, N.K., Behera, S.K. and Rath, A.K., 2018. Measurement of disease severity of rice crop using machine learning and computational intelligence. In *Cognitive Science and Artificial Intelligence* (pp. 1-11). Springer, Singapore.
- [18] Ramesh, S. and Vydeki, D., 2019. Application of machine learning in detection of blast disease in South Indian rice crops. *Journal of Phytology*, pp.31-37.
- [19] Shrivastava, Vimal K., et al. "Rice Plant Disease Classification using Transfer Learning of Deep Convolution Neural Network." *International Archives of the Photogrammetry, Remote Sensing & Spatial Information Sciences* (2019).
- [20] Li, Dengshan, Rujing Wang, Chengjun Xie, Liu Liu, Jie Zhang, Rui Li, Fangyuan Wang, Man Zhou, and Wancai Liu. "A recognition method for rice plant diseases and pests video detection based on deep convolutional neural network." *Sensors* 20, no. 3 (2020): 578.
- [21] Dhingra, G., Kumar, V. and Joshi, H.D., 2018. Study of digital image processing techniques for leaf disease detection and classification. *Multimedia Tools and Applications*, 77(15), pp.19951-20000.
- [22] G. Bebis and M. Georgiopoulos, "Feed-forward neural networks," in *IEEE Potentials*, vol. 13, no. 4, pp. 27-31, Oct.-Nov. 1994, doi: 10.1109/45.329294.
- [23] T. Kwiatkowski and H. Bölskei, "A Mathematical Theory of Deep Convolutional Neural Networks for Feature Extraction," in *IEEE Transactions on Information Theory*, vol. 64, no. 3, pp. 1845-1866, March 2018, doi: 10.1109/TIT.2017.2776228.
- [24] Zeiler M.D., Fergus R. (2014) Visualizing and Understanding Convolutional Networks. In: Fleet D., Pajdla T., Schiele B., Tuytelaars T. (eds) *Computer Vision – ECCV 2014*. ECCV 2014. Lecture Notes in Computer Science, vol 8689. Springer, Cham. https://doi.org/10.1007/978-3-319-10590-1_53.
- [25] S Agatonovic-Kustrin, R Beresford, Basic concepts of artificial neural network (ANN) modeling and its application in pharmaceutical research,

- Journal of Pharmaceutical and Biomedical Analysis, 2000, Pages 717-727, ISSN 0731-7085, [https://doi.org/10.1016/S0731-7085\(99\)00272-1](https://doi.org/10.1016/S0731-7085(99)00272-1).
- [26] Alex Krizhevsky, Ilya Sutskever, and Geoffrey E. Hinton. 2017. ImageNet classification with deep convolutional neural networks. *Commun ACM* 60, 6 (June 2017), 84–90. DOI: <https://doi.org/10.1145/3065386>
- [27] M. Oquab, L. Bottou, I. Laptev and J. Sivic, "Learning and Transferring Mid-level Image Representations Using Convolutional Neural Networks," 2014 IEEE Conference on Computer Vision and Pattern Recognition, Columbus, OH, 2014, pp. 1717-1724, doi: 10.1109/CVPR.2014.222.
- [28] S. Ghosal and K. Sarkar, "Rice Leaf Diseases Classification Using CNN With Transfer Learning," 2020 IEEE Calcutta Conference (CALCON), Kolkata, India, 2020, pp. 230-236, doi: 10.1109/CALCON49167.2020.9106423.
- [29] UCI Machine Learning Repository, available at <https://archive.ics.uci.edu/ml/datasets/Rice+Leaf+Diseases>, last accessed on 28-11-2020, 04.00 am.
- [30] Kaggle available at <https://www.kaggle.com/vbookshelf/rice-leaf-diseases> last accessed on 28-11-2020, 04.30 am.
- [31] Keras, available at <https://keras.io/api/applications/>, last accessed on 27-11-2020, 8.18 pm.
- [32] Christian Szegedy, Sergey Ioffe, Vincent Vanhoucke, and Alexander A. Alemi. 2017. Inception-v4, inception-ResNet and the impact of residual connections on learning. In *Proceedings of the Thirty-First AAAI Conference on Artificial Intelligence* (AAAI'17). AAAI Press, 4278–4284.
- [33] blog.exsilio.com, Accuracy, Precision, Recall & F1 Score: Interpretation of Performance Measures, available at <https://blog.exsilio.com/all/accuracy-precision-recall-f1-score-interpretation-of-performance-measures> last accessed on 22.01.2021, 09.23 pm.
- [34] Chen, J., Zhang, D., Nanekaran, Y.A. and Li, D., 2020. Detection of rice plant diseases based on deep transfer learning. *Journal of the Science of Food and Agriculture*, 100(7), pp.3246-3256.

Quantification of Surface Water-Groundwater Exchanges by GIS Coupled with Experimental Gauging in an Alluvial Environment

Yassyr Draoui¹, Fouad Lahlou², Jamal Chao³

Lhoussaine El Mezouary⁴, Imane Al Mazini⁵, Mohamed Jalal El Hamidi⁶

Laboratory of Energy Engineering and Materials, Faculty of Sciences, Ibn Tofail University, Kenitra, Morocco^{1,2}

Laboratory of Natural Resources Geosciences (NaResGeo), Faculty of Sciences, Ibn Tofail University, Kenitra, Morocco^{3,5}

Laboratory of Mathematical analysis, N-CG and applications, Faculty of Sciences, Ibn Tofail University, Kenitra, Morocco⁴

Regional Water Centre of Maghreb, LAMERN, Mohammedia School of Engineers, Mohammed V University, Rabat, Morocco⁶

Abstract—Surface water and groundwater are two interrelated components, where the influence of one automatically affects the quantity and quality of the other. These exchange flows are robustly influenced by some mechanisms such as permeability, lithological nature of the soil, landscape, in addition to the difference between the hydrometric height of the river and the piezometric level of groundwater. The study area of Bou Ahmed plain is vulnerable to intensive pumping mainly in the coastal fringe. The increase in water demand, due to demographic development, is accompanied by pressure on groundwater abstraction which causes significant drops of the groundwater level. The main objectives of this study are to develop Geographic Information System database and mathematical models to analyze spatial and temporal hydrogeological characteristics and hydrodynamic functioning of groundwater flow of the Bou Ahmed aquifer. The present work exhibits the characteristics of the river-groundwater exchanges in an alluvial plain. Therefore, we quantified the flows exchanged between a river and its groundwater using GIS tools along with measurements of parameters obtained by the differential gauging, which was carried out in the field, and hydrogeological boreholes data. These quantified flows, moreover, enabled us to eventually estimate the uncertainties related to the use of the GIS method. These results will also be used to support a set of groundwater simulations based on MODFLOW code in the Bou Ahmad aquifer. These models also associated with develop Geographic Information System will help to better plan, manage and control the groundwater resources of this aquifer.

Keywords—Surface water and groundwater; river-groundwater exchanges; geographic information system; differential gauging

I. INTRODUCTION

Generally, the exchanges between surface water and groundwater are complex. The interactions between these two elements take place by lateral subsurface flow in unsaturated soil, and by infiltration or seepage in the saturated spots. Moreover, Surface Water-Groundwater trade can be seen as an important element affecting the underground hydro-systems balance; it also has a significant impact on the quality of the groundwater by means of the solutes flow (contaminant) associated with the hydric transfer [1].

Numerous researchers have focused on the quantification of surface water-groundwater exchanges by estimating conductance [2]–[9] via the McDonald formula [10]. As a matter of fact, other researches dealing with the connections between a groundwater and a watercourse find that the exchanges are controlled by the same type of mechanism as that of drainage through a saturated semi-permeable layer [11], [12].

In a fluvial plain, both the flow and exchange of groundwater are controlled by a number of parameters. The most notable being: Firstly, the allocation and amplitude of the hydraulic conductivities at the river and the associated fluvial plain residues [13]–[15]; secondly the affiliation among the river's stream stage and the adjacent groundwater gradients. Finally, the geometry and position of the stream channel in conjunction with its flow into the fluvial plain [14]. Conductance is a requisite factor for the quantification of the flows exchanged between a river and the groundwater. In this paper, we first attempt to estimate these flow rates, using the conductance parameter attained by a geographic information system-based method only. Then, the assessment of the flows will be made by taking field measurements (differential gauging). The comparison between the two results allowed guesstimating the uncertainties associated with the use of the GIS method solely.

The Bou Ahmed aquifer is defined by the form of a depression filled from bottom to top by the Pliocene and Quaternary deposits on primary grounds. It is the main supplier of water resources for drinking water of several centers of the area (the cities of Bou Ahmed and Stehat). The increase in water demand, due to demographic development, is accompanied by pressure on groundwater abstraction. This situation causes significant drops of the groundwater level and consequently concern the decision makers responsible for the management and planning of water resources. For this purpose, all collected information (relevant technical reports and experimentations in the terrain of the study area) were processed and led to: (i) Study the hydrogeology characteristics of the Bou Ahmad aquifer; (ii) Exhibits the characteristics of the river-groundwater exchanges (watercourse functioning) in an alluvial plain; (iii) Quantification and direction of the flows

exchanged as well as the permeability; (iv) Permeability calibration using data from the GIS.

II. SITUATION AND HYDROGEOLOGICAL BACKGROUND

The location of the study area is in the plain of Bou Ahmed, which is one of coastal basins' alluvial plains of the western Mediterranean, that form part of the Rifain domain allocated in northern Morocco [16] (Fig. 1). The bottom of the plain is characterized by a marly substratum of earlier Pliocene age [17], covered by a Quaternary filling formed mostly by fluvial detrital facies with insertions of pebbles and channeled conglomerates [18]. The examined site is crossed by the Tihissasse River; this latter starts at the convergence point of the Elkanar and Bouhya Rivers (Fig. 1) then reaches the plain with an average slope of 0.45%. The regime of these rivers is irregular with a torrential character during rainy periods [16]. From a hydrogeological standpoint, the study area includes groundwater representing the main source of drinking and agricultural water supply. It is characterized by significant thicknesses in the middle of it which decreases towards the peripherals, on top of a transmissivity that varies between $5.2 \cdot 10^{-4}$ m²/s and $4.5 \cdot 10^{-3}$ m²/s and a storage coefficient of 20% [18].

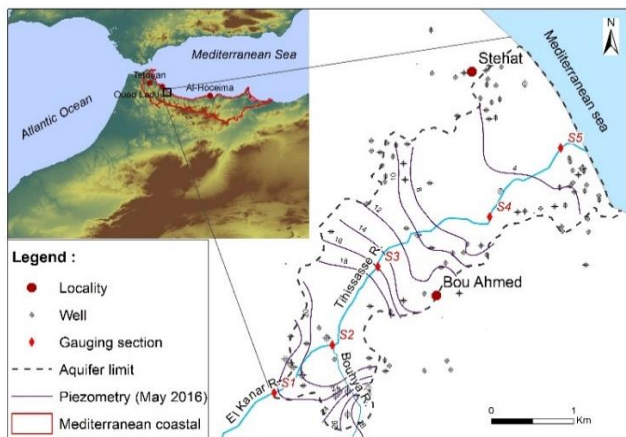


Fig. 1. Geographical Situation and Hydrological / Hydrogeological Background of the Bou Ahmed Aquifer.

III. MATERIALS AND METHODS

A. Differential Gauging

The characterization of the groundwater exchange with the river is generally carried out by initially measuring water levels in wells and piezometers within the streambed and the banks of the channel [15], [19]–[23], afterwards, a gauging (Fig. 2) to a number of cross-sections of the watercourse over a short time period [24].

Furthermore, it is principal to acquire in advance some information on the vertical permeability fields of the material constituting the river bed.

In our examination, we implemented a differential gauging campaign (May-2016), exclusively on the Tihissasse River, and the downstream part of the El Kanar River (Fig. 1) since the Bouhya River was almost dried up during this mission. By subdividing the studied area into five sections of measurements

(Fig. 1), we obtained four parts with a river-groundwater contact width of 6 meters for parts 1, 2 and 8 meters for parts 3 and 4.

B. Calculation of Conductance

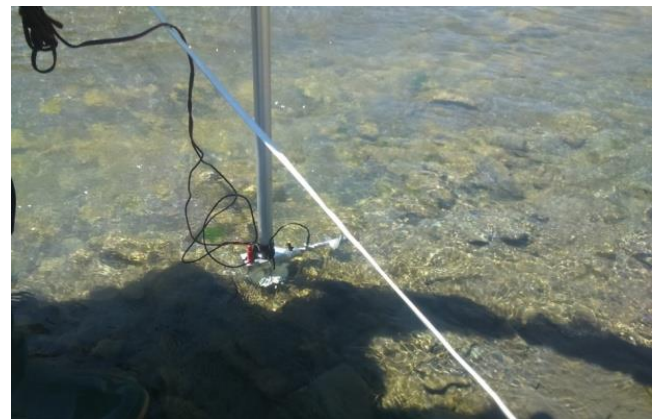
To estimate the surface water-groundwater exchanges as well as facilitating the analysis and spatial computation in the GIS, we have transformed the collected data into thematic raster maps whose pixel values symbolize a measured parameter. In this section, the raster calculator was used to generate raster layers of (2x2 m) dimensions representing thus the value of the difference ($\Delta h = h_a - h_r$) between the hydrometric height of the river and the hydraulic head of the groundwater.

Under the GIS, the calculations of the flows exchanged between the river and the groundwater are based on the permeability values of the four sectioned parts (K_1 (946) = $2.25 \cdot 10^{-4}$ m/s, K_2 (942) = 10^{-5} m/s, K_3 (943) = $3.7 \cdot 10^{-5}$ m/s and K_4 (948) = $8.2 \cdot 10^{-5}$ m/s), [18].

For each segment of the river, the vertical exchange rate is generally modelled by the leakage concept based on the [10] law:

$$Q(\text{m}^3/\text{d}) = C * (h_a - h_r) \quad (1)$$

Where $h_r[L]$ is the water level of the river and $h_a[L]$ is the water level of groundwater.



(a)



(b)

Fig. 2. (a): Reel with a Horizontal Shaft (b): Downstream Part of the Tihissasse River.

C represents the conductance in (m²/d) and it's given by the subsequent formula:

$$C = (K_z * S)/e \quad (2)$$

Where, K_z is the vertical permeability (m/d), S indicates the contact surface river- groundwater (m²).

Thus, e represents the thicknesses clogged in (m). The following figure illustrates some measurements, along the river, of the parameter of the thickness clogged in the approximate way after the drying of the stream and precisely at the end of August, which varies increasingly from upstream to downstream (Fig. 3).

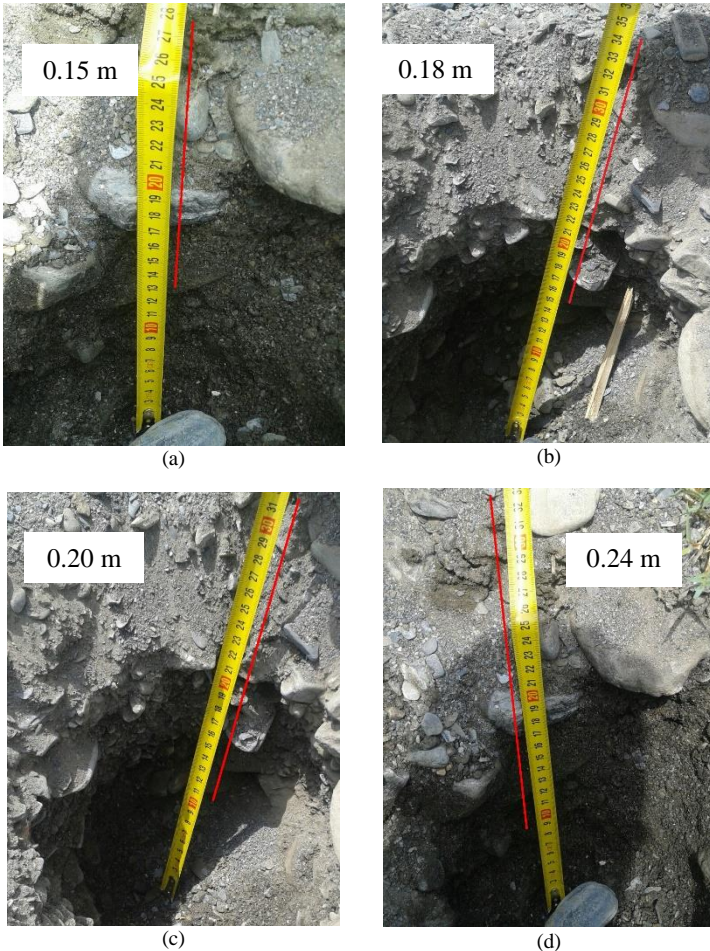


Fig. 3. (a): River Bed in the upstream of Tihissasse River; (b) and (c): River Bed in the Middle Part; (d): River Bed in the Downstream of the River.

IV. RESULTS

A. Quantification of the Exchanged Flows

1) *Quantification by gauging*: The calculated flow rates from the differential gauge (Table I), for the first two parts, with a total length of approximately 2250 m are around -3629 m³/d. Correspondingly, the seized negative values demonstrate that the river supplies the groundwater, which corresponds to a total intake of -1612 m³/d/km. While parts 3 and 4 (3000 m in length) have a flow rate of 15639 m³/d, this indicates that these sections are provided by the groundwater with a total supply of 5213 m³/d/km.

2) *Results obtained by GIS method*: The raster maps generated from (Δh) and the exchange rates (Q) measured for each part of the river (Tab.1) enabled us to approximate the values of the following conductance C_i : $C_1 = 2.7488$ m²/d; $C_2 = 0.7595$ m²/d; $C_3 = 0.7625$ m²/d and $C_4 = 0.0926$ m²/d, which represent the slopes of the linear regression curves in Fig. 4. This helped us deduce the e parameter by equation (2), which will be used later to calculate the flow rates by the GIS method.

The flow values reaped by the GIS method at four parts demonstrate that the lowest flows are located upstream (2 to -4 m³/d/pixel) (parts 1 and 2), whereas the most significant flows are registered downstream of the river with an exchange rate of 63 to -119 m³/d/pixel (parts 3 and 4) (Fig. 5).

B. Calibration and Comparison

To calibrate the permeability values obtained by the GIS method with the experimental ones, we followed a manual calibration methodology; we have systematically modified the permeability values K_z in order to minimize the differences between that of the flows given by the GIS method and the ones observed in the field.

During the calibration phase, it was noticed that the flows calculated by GIS (Fig. 5) tend towards the observed flows (Table I) by reducing the K_z values (Table II).

TABLE I. AVERAGE EXCHANGE RATES RECOUPED BY MEASUREMENTS OF THE FIELD FLOWS

Part	Length (m)	Average width (m)	Average slope (As in %)	Q (m ³ /d) After calibration
Part 1	1000	6	1.1	- 1728
Part 2	1250	6	0.3	- 1901
Part 3	1300	8	0.4	+ 6826
Part 4	1700	8	0.4	+ 8813

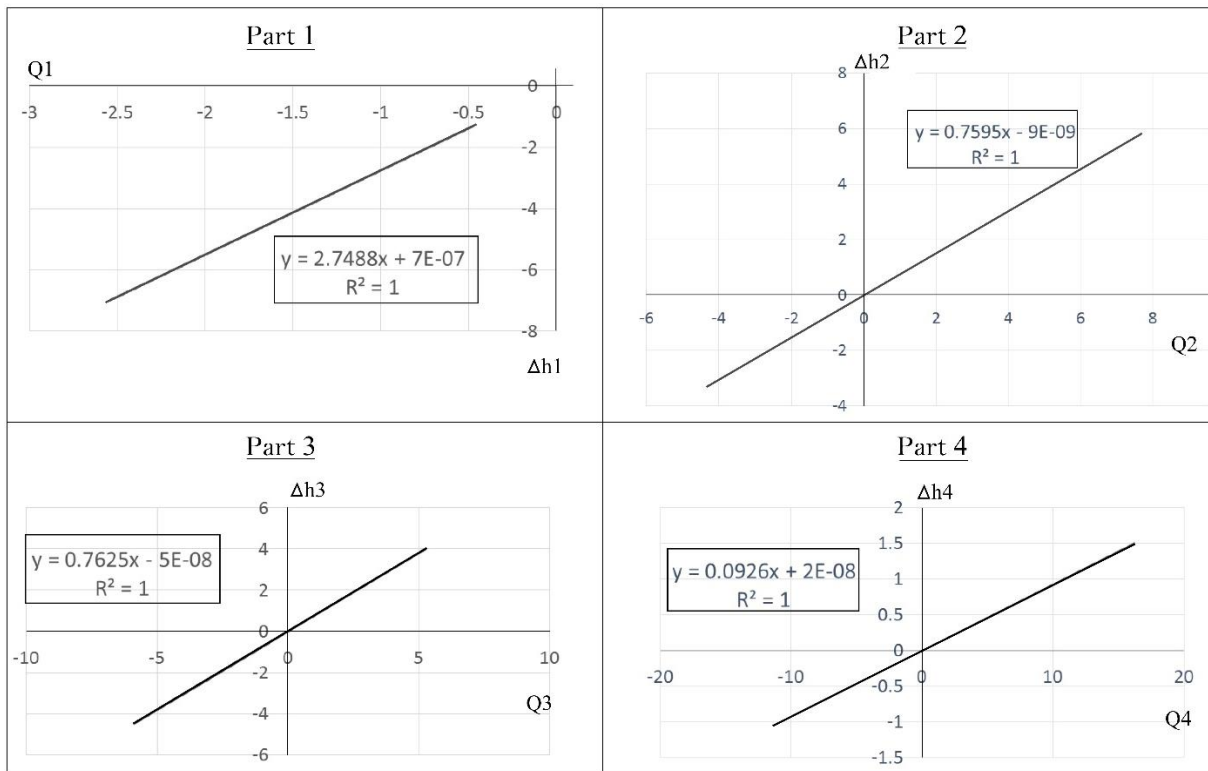


Fig. 4. Illustrations Describing the Flow among the River and Aquifer Q (m^3/s) for each Part as a Function of the difference between the River and Groundwater heads Δh (m).

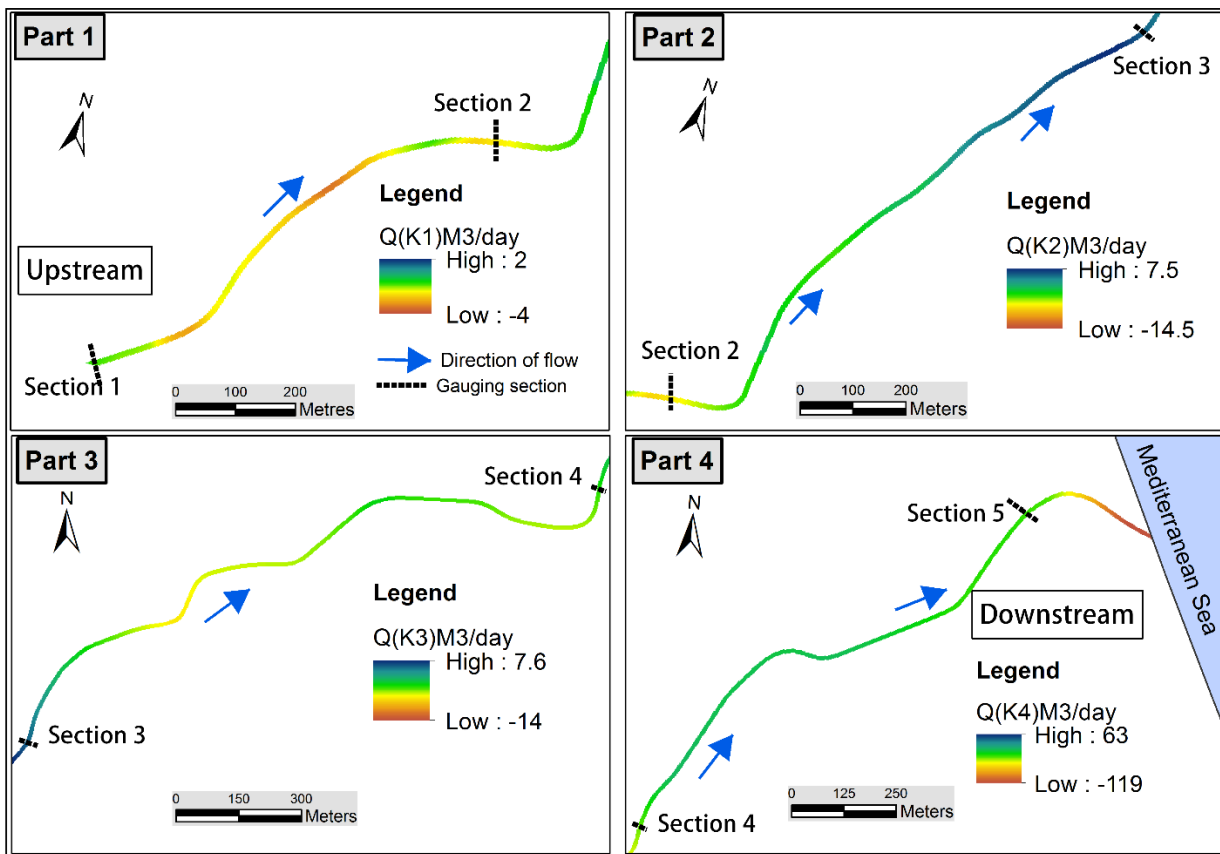


Fig. 5. Maps of Exchanged Flow Values by Parts Obtained from the GIS Method.

TABLE II. VALUES OF THE PARTS PERMEABILITY BEFORE AND AFTER THE CALIBRATION PHASE OF THE FLOW RATES

Part	Length (m)	K_x (m/s) Before calibration	K_x (m/s) After Calibration
Part 1	1000	$2.25 \cdot 10^{-4}$	$1.0 \cdot 10^{-6}$
Part 2	1250	$1.0 \cdot 10^{-5}$	$6.0 \cdot 10^{-7}$
Part 3	1300	$3.7 \cdot 10^{-5}$	$2.8 \cdot 10^{-6}$
Part 4	1700	$8.2 \cdot 10^{-5}$	$2.3 \cdot 10^{-5}$

V. SYNTHESIS AND DISCUSSION

Evaluating and interpreting the boreholes data and gauging measurements allowed us to quantify the surface water-groundwater exchanges in the Bou Ahmed plain. Consequently, the exchange principle used is the one proposed [12] which is based on Darcy's law, whose exchange rate is positive when the groundwater feeds the river ($\Delta h > 0$) and negative when the situation is reversed ($\Delta h < 0$).

The attained results illustrate that in the first part; the exchanges are negative (the river feeds the groundwater) (Fig. 6a) with a low flow rate (Table I). This is explained by the existence of mainly sandy silt formations (Fig. 7).

The crossing towards part 2 is characterized by a $\Delta h = 0$ (Fig. 6b, Fig. 7), which corresponds to a zero exchange between the surface water and the groundwater. While the remaining of the part is characterized by a $\Delta h < 0$ and exchanges that are generally negative (the river feeds the aquifer) (Fig. 6a, Fig. 7). The latter can be explained by a modification in the lithological nature, which changes from

sand to pebbles and gravels accompanied by an increase in the thickness of the groundwater from the upstream all the way to the central part of the Tihissasse River (Fig. 7). This thickening is regulated by the roof geometry of the substratum, which is produced by a depression at the level of the borehole (942/4).

It should be noted that at the downstream fraction of part 2, the collected values of the flows by the GIS method are discordant compared to those obtained experimentally, especially in the direction of the exchanges (Fig. 5). This contradiction can be explained by the effect of the measurement sites choice.

For the third and fourth parts, the exchanges are fundamentally positive (the groundwater supplies the river) with a Δh varying from -1 to 2 m (Fig. 6a and c), this is due to the remarkable effect of the substratum surge which favors the overflow of the groundwater.

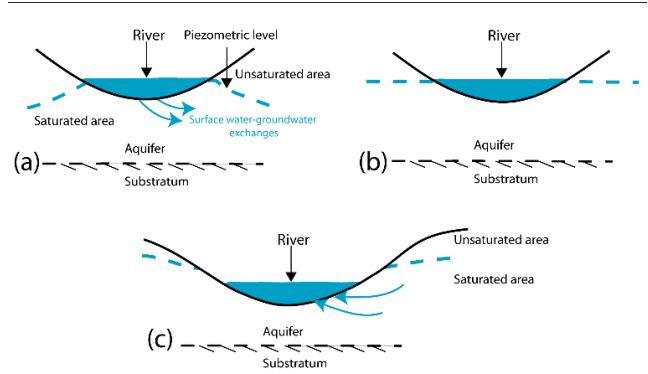


Fig. 6. Possible Situations of Surface Water and Groundwater Exchanges.

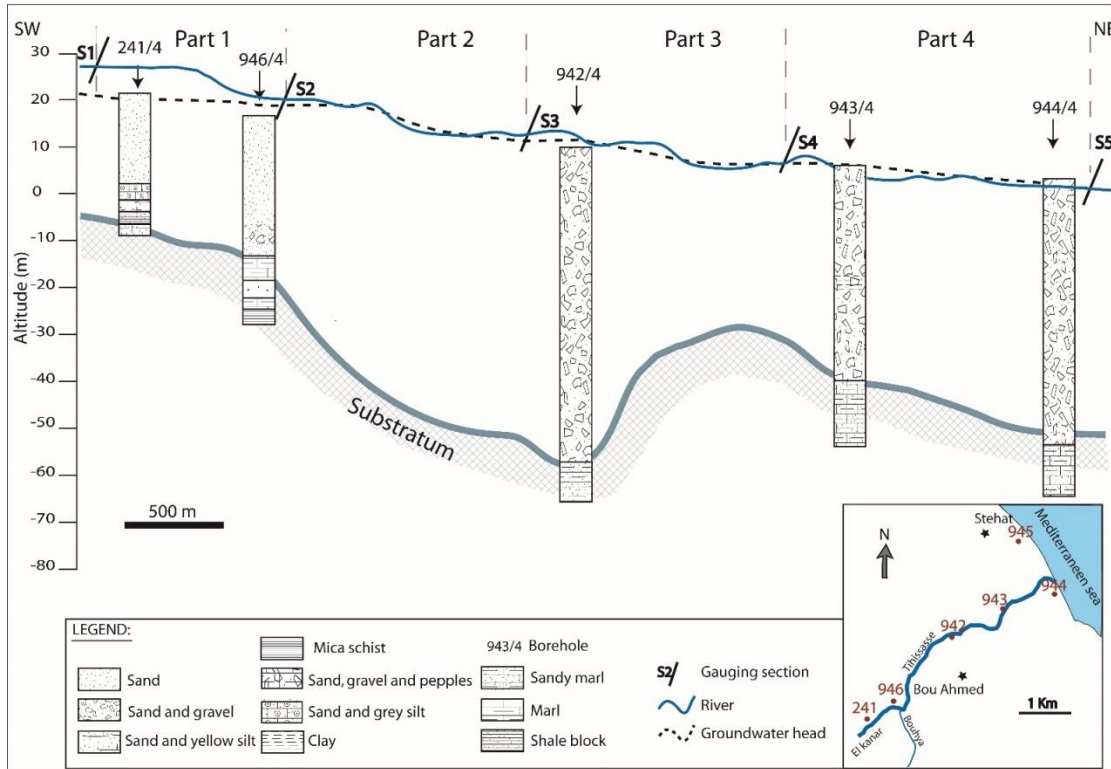


Fig. 7. Synthetic NE-SW Cross-Section along the Watercourse.

VI. CONCLUSION

Computer technologies consisting of geographic information systems and numerical modelling are being progressively employed in different geo-resource domains. The characterization method of surface water-groundwater exchanges, based on GIS tools, made it possible to determine the direction of exchange at each point on top of evaluating the exchanged quantity and estimating a relative average balance.

Nevertheless, the satisfactory results supplied by the GIS method, a degree of uncertainty still triumphs, particularly, in case the hydrodynamic parameters are inconsistent. Hence, the requirement to couple the method by calibration based on measures on the ground is recommended.

Concerning the exchanges with the river, a mathematical groundwater flow model can improve the understanding of the functioning of the alluvial aquifers, and as a result to better manage the water resources. The retrieved results have only enhanced the preceding studies, and have given some new interpretations of the hydro-system's behavior of the studied area based on hydrodynamic modelling. Indeed, these results are of great importance to better represent the conceptual model and prepare the input data for groundwater flow model which will be a key decision support system for the decision makers in water resources management, especially for water supply and protection of the aquifer from seawater intrusion.

ACKNOWLEDGMENTS

The authors would like to thank the Hydraulic Basin Agency of Loukkos-Tetouan (ABHL), who provided us with the necessary database for the fulfilment of this work, and which helped us to realize a campaign of piezometric and gauging measurement.

REFERENCES

- [1] M. Sophocleous, « Interactions between groundwater and surface water: the state of the science », *Hydrogeol. J.*, vol. 10, no 1, p. 52-67, 2002.
- [2] I. Cartwright et H. Hofmann, « Using radon to understand parafluvial flows and the changing locations of groundwater inflows in the Avon River, southeast Australia », *Hydrol. Earth Syst. Sci.*, vol. 20, no 9, p. 3581-3600, 2016.
- [3] L. El Mezouary et al., « Modélisation numérique de la variation saisonnière de la qualité des eaux souterraines de l'aquifère de Magra, Italie », *Houille Blanche*, no 2, p. 25-31, 2015.
- [4] L. Hu, Z. Xu, et W. Huang, « Development of a river-groundwater interaction model and its application to a catchment in Northwestern China », *J. Hydrol.*, vol. 543, p. 483-500, 2016.
- [5] H. J. Morel - Seytoux, C. D. Miller, C. Miracapillo, et S. Mehl, « River Seepage Conductance in Large - Scale Regional Studies », *Groundwater*, 2016.
- [6] X. Sun et al., « Improved simulation of river water and groundwater exchange in an alluvial plain using the SWAT model », *Hydrol. Process.*, vol. 30, no 2, p. 187-202, 2016.
- [7] H. J. Morel-Seytoux, C. D. Miller, S. Mehl, et C. Miracapillo, « Achilles' heel of integrated hydrologic models: The stream-aquifer flow exchange, and proposed alternative », *J. Hydrol.*, vol. 564, p. 900-908, 2018.
- [8] Y. Cousquer, A. Pryet, N. Flipo, C. Delbart, et A. Dupuy, « Estimating river conductance from prior information to improve surface - subsurface model calibration », *Groundwater*, vol. 55, no 3, p. 408-418, 2017.
- [9] R. Valois, Y. Cousquer, M. Schmutz, A. Pryet, C. Delbart, et A. Dupuy, « Characterizing Stream - Aquifer Exchanges with Self - Potential Measurements », *Groundwater*, vol. 56, no 3, p. 437-450, 2018.
- [10] M. G. McDonald et A. W. Harbaugh, « A modular three-dimensional finite-difference ground-water flow model », 1988.
- [11] H. Bouwer, « Theory of seepage from open channels », *Adv. Hydrosci.*, vol. 5, p. 121-172, 1969.
- [12] K. Rushton et L. Tomlinson, « Possible mechanisms for leakage between aquifers and rivers », *J. Hydrol.*, vol. 40, no 1-2, p. 49-65, 1979.
- [13] T. C. Winter, *Ground water and surface water: a single resource*, vol. 1139. DIANE Publishing Inc., 1998.
- [14] W. W. Woessner, « Stream and fluvial plain ground water interactions: rescaling hydrogeologic thought », *Ground Water*, vol. 38, no 3, p. 423-429, 2000.
- [15] G. J. Wroblicky, M. E. Campana, H. M. Valett, et C. N. Dahm, « Seasonal variation in surface - subsurface water exchange and lateral hyporheic area of two stream - aquifer systems », *Water Resour. Res.*, vol. 34, no 3, p. 317-328, 1998.
- [16] J. Thauvin, « Ressources en eau du Maroc, domaine du Rif et du Maroc oriental », *Notes Mém. Serv. Géologique Maroc*, vol. 231, 1971.
- [17] A. El Attar, « Contribution à l'étude hydrogéologique et hydrochimique des aquifères côtiers d'Amsa et de Bou Ahmed (Maroc Nord Occidental) », *Univ. Abdelmalek Essaadi, Faculté des Sciences, Tétouan*, 2012.
- [18] DRHL, « Synthèse hydrogéologique de la plaine de Bou Ahmed, province de Chefchaouen, Maroc ». 1994.
- [19] K. Henry et al., « Ground Water Surface Water Exchange in Two Headwater Streams », 1994.
- [20] D. R. Lee et J. A. Cherry, « A field exercise on groundwater flow using seepage meters and mini-piezometers », *J. Geol. Educ.*, vol. 27, no 1, p. 6-10, 1979.
- [21] E. Modica, « Analytical methods, numerical modeling, and monitoring strategies for evaluating the effects of ground-water withdrawals on unconfined aquifers in the New Jersey Coastal Plain », *US Dept. of the Interior, US Geological Survey; Branch of Information Services [distributor]*, 1998.
- [22] F. J. Triska, V. C. Kennedy, R. J. Avanzino, G. W. Zellweger, et K. E. Bencala, « Retention and transport of nutrients in a third - order stream in Northwestern California: Hyporheic processes », *Ecology*, vol. 70, no 6, p. 1893-1905, 1989.
- [23] S. M. Wondzell et F. J. Swanson, « Seasonal and storm dynamics of the hyporheic zone of a 4th-order mountain stream. I: Hydrologic processes », *J. North Am. Benthol. Soc.*, vol. 15, no 1, p. 3-19, 1996.
- [24] T. J. Buchanan et W. P. Somers, « Discharge measurements at gaging stations », *US Govt. Print. Off.*, 1969.

Simplified Framework for Benchmarking Standard Downlink Scheduler over Long Term Evolution

Srinivasa R K¹

Research Scholar, Visvesvaraya Technological University
Department of Electronics and Communication Engineering
BIT, Bangalore, India

Dr. Hemanth Kumar A.R²

Professor and Principal Investigator (R&D)
Department of Electronics and Communication Engineering
BIT, Bangalore, India

Abstract—Downlink scheduling is one of the essential operations when it comes to improving the quality of service in Long Term Evolution (LTE). With an increasing user base, there will be an extensive challenge in resource provisioning too. A review of existing approaches shows that there is a significant possibility of improvement in this regard, and hence, the proposed manuscript presents a benchmarking model for addressing the issues associated with Best-Channel Quality Indicator (CQI), Round Robin, and Hybrid Automatic Repeat Request (HARQ). The outcome shows HARQ scheduling to offer better performance in higher throughput, higher fairness, and lower delay over different test cases.

Keywords—eNodeB; Scheduler; HARQ; Best-CQI; Round Robin

I. INTRODUCTION

The user-base of mobile communication is increasing rapidly, especially due to internet accessibility with the devices. The internet's capacity for these devices provides a base or a platform to build many applications that can use high dimension data like multimedia, including audio, image, and videos, but these applications are bandwidth-hungry. It demands a very high data transfer rate. The exploration of the finding possibilities of the usage of the spectrum in an optimal ways leads the new standardization of the architecture and communication process to meet the goal of providing adequate resources to the applications, and that shows the evolution of a new generation or era of the wireless communication systems [1]. In every generation of the standard, the data services maximize the high-speed packet access method to achieve a higher data rate, low latency, which is a goal of Long-Term Evolution (LTE) to support a very high demand of the traffic, which aim to evolve the universal terrestrial access network [2].

The typical LTE standard provisions the specifications, as mentioned in Table I. Due to the use of the frequency and time division duplexing, MIMO, and OFDM [3]. In the OFDM, the time-frequency grids are divided into the number of the resource blocks (RB) symbols, and a scheduler operation assigns or allocates the RBs to the users. Every entry in the RBs is known as a resource element (RE). There are two states of the art scheduling algorithm; one is the round-robin scheduling algorithm (RRSA), where every user gets equal privileged ignoring the indications of the quality of the channel, whereas in the second method, namely, best channel quality index(B-CQI), where the users are allocated the RBs

only if it has superior channel quality index. The physical layer characteristics, modulation scheme, and the coding process influence the scheduling algorithm's design [4].

A closer look into the literature shows that there have been various dedicated research attempts towards addressing downlink scheduling issues in LTE. But it is noticed that existing approaches do not meet the demands of the quality-of-service performance that is required in the practical world scenario. It is also noticed that monitoring of the state of memory associated with the end-users is also considered to address this downlink scheduling problem. Still, such an approach doesn't consider various factors that are needed to meet the practical world application. At present, there are more dedicated attempts towards downlink scheduling issues focusing on an advanced version of LTE, i.e., 5G networks, i.e. [5][6][7]. This acts as positive motivation towards carrying out the current work in the proposed system.

The proposed manuscript evaluates two state-of-the-art scheduling algorithms: the best channel quality index (B-CQI) and the round-robin to benchmark its performance with the proposed HARQ-Scheduler as HARQ-S. The contribution of the proposed system is as follows: i) to present a design of novel scheduler using best channel quality indicator, ii) to include investigation using round-robin scheduler and HARQ based scheduler, iii) to develop a localization process for specific users over the base station of the user, iv) to carry out a benchmarking testbed for assessing the potential in downlink scheduling. The organization of the paper is as follows: Section II discusses LTE characteristics followed up by the research trend in Section III. Discussion of standard schedulers subjected to benchmarking is carried out in Section IV, while result discussion of the proposed study is carried out in Section V, while the summary of the proposed study is written in Section VI as a conclusion.

TABLE I. LTE STANDARD PROVISIONS THE SPECIFICATIONS

Downlink peak data rate	300 Mbps
Uplink peak data rate	75Mbps
Latency	≥ 5 ms
Bandwidth Range	1.4 MHz to 20 MHz
MIMO + OFDM	Improves throughput and optimal spectrum sensing

II. LTE CHARACTERISTICS AND ITS INFLUENCE ON THE DESIGN OF SCHEDULER

The LTE and LTE-A and the future evolution of communication standards keep a common goal of optimal spectrum utilization and offer a very high data rate with low latency in lower operating costs, a multi-functional optimization problem.

A. LTE General Architectural Characteristics

LTE's core building blocks collaboratively work to achieve approximately 10Mbps and 50Mbps data rates in downlink and uplink, respectively. The LTE system involves minimal network connections to minimize the latency between User Equipment (UE) and control planes by introducing a mobility management scheme (MMS) that ensures lower operational cost. In LTE, the bandwidth range is between 1.4 MHz to 20 MHz, which operates in pairing and non-pairing of the spectrum to support both time and frequency duplexing, which are TDD and FDD.

LTE adopts spatial multiplexing and multiple antennas to improve the signal power on either side of the transmitter and antenna as the signal power (P_s). The data rate (D) follows the relation as per eq. (1).

$$P_s \propto D \dots \quad (1)$$

The LTE system utilizes all the previous standard spectrum frequency bands (SFB) and additional SFB, making LTE more robust and interoperable. Though the basic architecture of LTE is designed to achieve a coverage of approximately 90 to 100 Km, whereas, at 33% or higher coverage, it suffers degradation into the network's efficiency.

Fig. 1 illustrates a basic architectural building block of an LTE system, where the evolved E-UTRAN collaborates many

numbers of eNodeB and evolved packet core (EPC) supported with OFDM, MMS, FDD, and TDD. The system attains a better data rate at a lower UE speed. The effective scheduling algorithm requires considering these parameters and facts along with the physical layer attributes. Section B below describes the physical layer's essential aspects that impact the effective scheduling algorithm's LTE design aspect.

B. Physical Layer Characteristics

Seamless roaming operation is achieved in LTE by integrating the previous generation frequency band and new frequency bands. The duplex mode FDD operates in 25 combinations of operating frequencies for uplink and downlink in the paired manner. In contrast, TDD's duplex mode uses in 9 varieties of operating frequency band common for uplink and downlink [8]. Both unicast and multimedia broadcast multiple services (BMS) improves the signal-to-noise ratio (SNR) [9]. The channel bandwidth ranges from 1.4 MHz to 20 MHz with varied resource block size ranging in the slots of {6, 15, 25, 50, 75,100}.

C. Technologies and Process of Packet Scheduler in LTE

The supporting technologies such as OFDM, MIMO, and Channel coding, adaptive-link combined functions to fulfill LTE requirements to a greater extent with ease of transmission bandwidth allocation and additional resource optimization using overcoming multipath fading, mapping resource elements with OFDM signal.

The forward error correction (FEC) and Automatic repeat request (ARQ) handle the transmitted data errors. The link adaption is performed using adaptive modulation and coding (AMC); the modulation schemes are decided based on signal to interference noise ratio (SINR). The generation of a signal in the LTE physical layer using appropriate coding and modulation is shown in the Fig. 2.

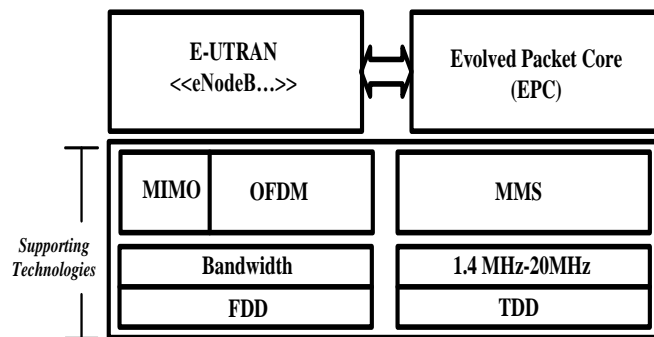


Fig. 1. Architectural backbone of an LTE system

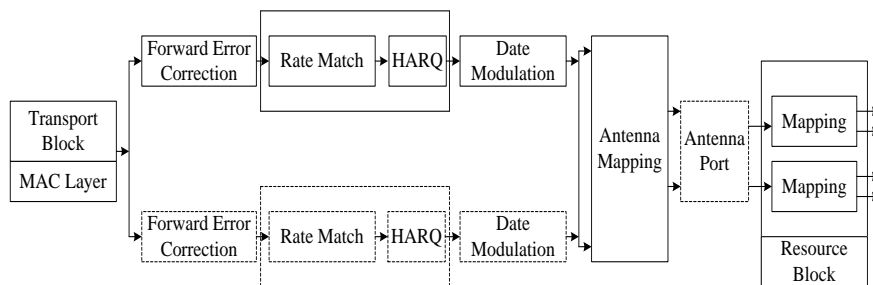


Fig. 2. OFDM Modulated Signal Generation Process.

The mapping of appropriate coding and modulation schemes correlates with channel quality indicator (CQI) measured at UE. The channel quality (CQ): $\rightarrow \{S, C, QR\}$, where $S = \text{SINR}$, $C = \text{Channel}$, and $QR = \text{Receiver's rate}$. The channel or the signal quality is represented by reference symbols and has its placement mechanism in the resource blocks. In this manner, the appropriate resource block and the time slot decision take place based on the value of CQI in a periodic and aperiodic manner using physical uplink control channel (PUCCH) and physical uplink shared channel (PUSCH), respectively. The computation of the number of sub-bands (N_{sb}) takes place using eq. (4), where the total bandwidth (B) is the total sum of N_{sb} sub-band as per eq. (2).

$$B = \sum_{i=1}^N (N_{sb})_i \quad (2)$$

Such that $(N_{sb})_i = \{M_{RB}\}_j$, where 'j' = index of resource blocks and the number of the resource block (M_{RB}) in B , with downlink (DL), is computed using eq. (3).

$$(N_{sb})^{DL/M_{RB}} \quad (3)$$

$$\text{Therefore, } (N_{sb}) = (N_{sb})^{DL/M_{RB}} / (M_{RB}) \quad (4)$$

The core component of traffic management takes place using packet scheduler positions placed in the base station (BS), which is responsible for allocating resources, especially spectrum, to the UE depending upon the channel conditions. There is a trade-off between maximizing the efficiency of spectrum or resources through a useful scheduler or resource allocator that degrades the network's performance by minimizing throughput and fairness. Therefore, the scheduling algorithm's effective design approach considers the intrinsic correlation between CQI, UE data buffer status, and the requirement of the quality of service to map the RBs with appropriate selection of coding and modulation schemes.

III. RELATED WORK

Generally, the delay profile represents more than one version of the transmitted signal at the receiver side. The authors Hani and Samota [10] improvises the base model of the LTE by mapping it to the Rayleigh Fading model for a delay profile in the urban scenario to improve the Delay while accessing the Physical Random-Access Channel (PRACH) using a combined approach of the scheduling and particle swarm optimization. This Model exhibits an approximately 13-14% reduction in the Delay even if the Round Robin Scheduling is not used.

The higher throughput for both uplink and downlink is an essential requirement for better QoS in modern communication systems, which are shared by the multi-users. In contrast, there exists a contradiction of the resource allocation process between pooling and severing as requested. The advanced UMTS Terrestrial Radio Access Network (UTRAN) in LTE facilitates a wide range of scheduling mechanisms to offer users resources. The authors Saxena et al. [11] has performed a critical analysis of the performance metrics, including a) throughput, b) spectral efficiency, and c) fairness for the various schedulers that includes: a) resource fair, b) round-

robin, c) best channel indicator (CQI). It is observed that though the users get more resources, overall network performance degrades.

The authors Minelli et al. [12] evaluates proportional fair (PF) and round-robin (RR) using statistical throughput evaluation model for the context of relay-enhanced LTEA and suggest they are not appropriate methods as both the relay nodes and the backhaul link quality influences the choice of the Scheduler.

The higher data rate demand continues right from the 2G with the introduction of data services, which was improvised in 3G with HSPA and LTE in 4G. The inclusion of OFDM enhances the throughput, but the effective scheduling process can improvise the overall performance. The downlink scheduling plays an important role as the higher data rate from the base station to the user equipment ensures low packet loss. An extensive comparison of downlink scheduling is performed by the authors Ramesh [13], and they list popular algorithms like a) Exponential Rule, b) Proportional Fair, c) Round Robin, etc.

The high data rate in LTE or new radio (NR) for the multimedia applications is achieved through the downlink scheduling like Proportional Fair, round Robin, or by the best Channel Quality. These scheduling approaches have a major limitation: the MAC requires making decisions during every transmission time interval for the allocation of resources for UEs, which is an overhead if there is no change in the channel condition or data scheduling, which increases the processing time overhead. The authors Chilmulwar and Sinha [14] introduces a MAC scheduler using a machine learning approach of namely Autoregressive Integrated Moving Average, that minimizes the resource use of PDCCH along with the time required for the resource allocation to the UE.

In many of the approaches, in the downlink throughput analysis considers a uniform distribution of UEs in the cell, whereas if the proper modeling takes place for this analysis, then many of the effects like spatial distribution of UEs, BS, and network functions can be exploited which affect the throughputs. The authors Olaifa and Arifler [15] use a simulator, namely Vienna, to quantify the throughput analysis and found that if the UEs are in the group near the BS exhibit varied throughput as compared to the uniformly deployed UEs. In real-time strategy, the BS is deployed newer to the dense user bases. Another significant observation was made that the proportional Fair is less advantageous than that of the round-robin in the case of grouped or clustered users surrounding the BS.

The inclusion of the Carrier Aggregation enhances the throughput; therefore, the CA enables down line schedule for eNodeB to ensure higher QoS, but at the same time, the aggregation poses power overhead. The authors Chaudhuri and Das [16] claims a first of its kind of download scheduler, which considers QoS, Resource block, and carrier power. Their algorithm gains twice the throughput in the one hundred cell UEs scenario than the round-robin, Efficient Packet Scheduling, and others.

Thought the objective of the useful Scheduler is to provide better QoS and QoE to UEs. In contrast, the performance is also correlated with the traffic dynamic and resource allocation mechanism. The effect of the TCP variance and combination of the Scheduler on the performance is studied by the authors Adesh and Renuka [17] and observe that the TCP-Westwood performs best out of all combinations. The authors Sundari et al. [18] implement a scheduler to improvise its performance, where they use service class for the bandwidth and resource allocation dynamically with the channel into consideration and offers better understanding as compared to the Round Robin (RR), Best Channel Quality Indicator (BCQI), Proportional Fair (PF) and Opportunistic scheduling. The research of minimizing the energy consumption by the eNodeB is an open research problem in LTE, In the work of Rebekka et al. [19] utilizes the spectrum effectively in reduced energy using the suitably allocate the resource blocks so that even throughput improvise. The Model is benchmarked with the Round robin and Best CQI in terms of the performance metrics like throughput and energy consumption, and fairness.

Yildiz and Sokullu [20] provide consistency in throughput and fairness in the change's mobility pattern compared to the round-robin and best CQI. Another benchmarking by Hayuwidya, Ernawan, and Iskandar [21] uses Monte Carlo simulation and a radio planning software, namely Atoll, and found that proportional fair algorithm for scheduling outperforms as compared to the round-robin. The LTE-sim is used to study the trade-off between the throughput and the fairness of Scheduler Round robin, Maximum throughput, etc., in realistic traffic conditions. Ahmed and AlMuhallabi [22]. The traditional scheduler, including a.) Proportional Fair,

b) Best -CQI and c) Round Robin, lack to meet the real provisioning of the optimal throughput and latency. The authors Kayali et al. [23] formulate the scheduling problem as an optimization problem with the inclusion of the constraints of deadline time for the various packets, a minimum buffer of the UE, and develops an objective function to minimize the packet loss and evaluates their Model with LTE-Sim. The regular scheduler performance is assessed in macro-femtocells Hajjawi et al. [24]. A fair boundary scheduling algorithm is proposed by Rahman et al. [25] to handle the trade-off between throughput and fairness and better fairness concerning the round-robin and Proportional Fair.

The authors Sundari et al. [26] proposes a dynamic multi-traffic scheduler to allocate the bandwidth and the resources dynamically by considering the UE channel status and performs better than a round-robin and Best Chanel quality indicator. The authors Alotaibi and Akl [27] also propose a packet scheduler where both the UE and the physical resource block are considered design parameters and perform better than round-robin. The authors Harkusha et al. [28] proposes a method of frequency and schedule and the security and optimization of the bandwidth allocation to UEs. It is generally observed that the Round-robin balances the fairness issue, whereas the Max Signal to Noise ratio scheduler maximizes the throughput Dadi and Chibani [29]. The performance of the Scheduler gets influence based on the UE mobility as well its density in a cell. Shams et al. [30] have compared the popular round robin and the proportional Fair in the HetNet to ascertain which Scheduler is appropriate in case of very high mobility. The summary of the essential literature from the above discussion is now tabulated in Table II.

TABLE II. SUMMARY OF THE ABOVE-DISCUSSED STUDIES

Cite No	Context	Solution approach	Performance
Hani et al(2018)[10]	Urban Delay profile	Scheduling, PSO	13-14 % delay reduction without round-robin
Saxena et al(2016)[11]	UTRAN and LTE	Performance evaluation of many scheduling algorithms	Resource provision improvise and degrades the network performance
Minelli et al. (2016)[12]	relay-enhanced LTE-A networks	Performance proportional fair (PF) and round-robin (RR)	statistical throughput evaluation model indicates not a suitable approach
Ramesh et al. (2019)[13]	Downlink scheduling in LTE	Exponential Rule, b) Proportional Fair, c) Round Robin, etc	Performance analysis
Chilmulwar et al. (2019)[14]	MAC scheduling	Machine Learning	Reduces the time overhead for resource allocation to UEs
Olaifa, 2016 [15]	Clustered UE near BS	Vienna Simulator for throughput analysis	The proportional Fair provides inferior to Round robin
Chaudhuri, 2016[16]	CA-based Scheduler	RB, Carrier power, QoS in Scheduler design	Provides double throughput as compared to the RR, EPS
Adesh et al., 2017[17]	Traffic Dynamic	TCP variance with schedulers effect	The TCP Westwood performs best with all the schedulers.
Sundari, 2015, [18]	Service Class	Dynamic bandwidth and resource allocation	Improvise the performance with traditional schedulers
Rebekka, 2015,[19]	eNodeB	Optimal resource block allocation	Improves the throughput with lesser energy use.
Yildiz, 2017 [20]	LTE-A with Mobility	Mobility aware downlink scheduling	Robust to mobility
Hayuwidya, 2017[21]	Release 8 LTE	MCS and Atoll 3.2.1	Proportional Fair outperforms
Ahmed,2016[22]	Realistic LTE Traffic condition	LTE-Sim	The trade-off between throughput and fairness
Kayali,2017[23]	LTE	Optimization and LTE-Sim	The decrease in packet loss
Hajjawi,2016[24]	Macro-femtocells over the LTE-A	Effect of Scheduler on Congestion	Minimizes cell congestion in LTE
Rahman et al., 2016[25]	Trade-off fairness and throughput	Fair Boundary	Better fairness

IV. STATE OF THE ART SCHEDULING ALGORITHM

In each time interval, the Scheduler controls the frequency and time resource allocations and the allotment of the resource blocks (RBs), which takes place accordingly, whereas achieving optimal throughput and fairness is an open research problem. The proposed framework evaluates the two popular schedulers, namely Best-CQI and the Round-robin, with the proposed HARQ based Scheduler.

A. Best Channel Quality Indicator Scheduler (BCQI-S)

The eNodeB receives the CQI by the UEs, and the eNodeB, which acts as a base station, sends the reference signal to the UEs, and accordingly CQI based computation of RBs takes place. The UEs with the best CQI get the RBs, whereas the far distant users do not get RBs as their radio links are inferior as a result provides higher throughput and lower fairness.

B. Round Robin Scheduler

This algorithm does not consider the channel quality, and it allocates RBs to the UEs according to the availability of the RBs on an FCFS basis. As a result, it provides better fairness and lower throughput.

C. HARQ Based Scheduler

In both the BCQI-S and RR-S, the packet error overhead is not predominantly considered, which provides inferior performance in the case of very noisy channels. In contrast, LTE's very objective of achieving a high data rate in the robust condition requires a high data rate transfer in a very fast and reliable manner. Therefore, both the eNodeB and the UE adopt the resource block scheduling techniques and the packet error detection and correction mechanism using either ARQ or HARQ.

In HARQ, the packet detection and correction are generally implemented at the PHY layers, and the control mechanism on the MAC layer tries to correct the packets. Some acceptable erroneous packets are forwarded to the upper layer using its buffer mechanism using a hybrid capacity of a forward error correction (FEC) and automatic repeat request (ARR). In ARQ, it discards the packet if it is erroneous. The future generation applications are multimedia data-hungry, where very high throughput, fairness, and low latency only can ensure higher QoS and, finally, better QoE. This is an open research problem to design a schedule that maximizes both the throughput and the fairness to achieve higher network performance. Therefore, the Proposed HARQ-S aims to optimize both the throughput and fairness even in highly noisy channel conditions.

In the proposed HARQ-S, the allocation of the RBs takes place in two ways, in one slot period, RBs are allocated only if it justifies the desired CQI and in another slot based on request priority. The erroneous packets are handled by the FEC and ARR using a buffering technique to handle the erroneous packets. The buffer complements the erroneous packets and continues the NACK till the packet is complete; an ACK is received, as shown in Fig. 3.

The system model-independent variable of HARQ-S is listed in Table III.

The process flow of the HARQ-S is shown in Fig. 4.

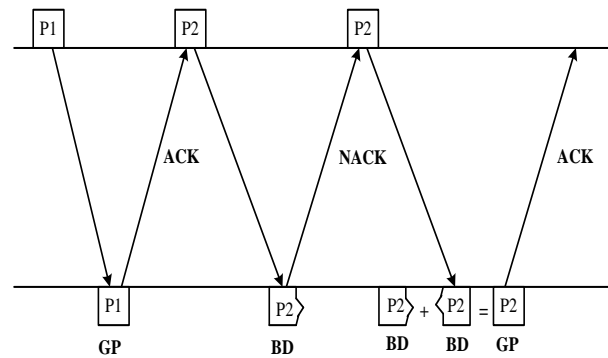


Fig. 3. Packet Error Correction Mechanism in HARQ.

TABLE III. INDEPENDENT VARIABLE OF THE MODEL

Sl. No	System Variable	Symbol	Range
1	Number of user's equipment	nUE	25,75,...225
2	Number of Resource Block	nRB	
3	Time Slots	Ts	
4	System Bandwidth	B	
5	Transmit Power	P	
6	HARQ-Type	HT	

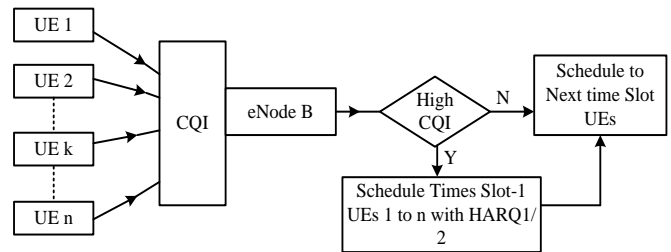


Fig. 4. Process flow of the HARQ-S.

Where the RBs are allotted on the combined basis of CQI, HARQ, and priority.

D. HARQ-S Analytical System Modelling

The designed mathematical Model to imitate the behavior of the scheduling algorithm considers a system with a uni-base station (U-BS) with proximity uniformly with the random deployment of the user's equipment's (UE) in such a way that the localization of the U-BS takes place in the centrality of the cell zone of the dimension of 'L' x 'B' units of the length. The evaluation parameters initialized are listed in Table IV.

TABLE IV. INITIAL PARAMETERS AT THE NODE DEPLOYMENTS

Sl. No	Parameters	Symbols	Initialization
1	No. of Antenna @ U_BS	An	2
2	No. of Antenna @ UE	Au	1
3	System Bandwidth	Bw	1.4 MHz
4	System Noise	Sn	10 dB
5	Noise Spectral Density per Hz	Sdn	174 dBm
6	Transmit Power at U-BS	Pt	0 dBm

1) *Localization of Kth User and Positioning of U-BS:* The localization of all the UEs falls randomly within the proximity of the deployment's region of $L \times B$ in such a way that a uniform random placement takes place within the boundary of the deployment location as UE_x & UE_y using equation (5).

$$UE_x \& UE_y = \sum_{k=1}^{UE_{tot}} f(U_k) \quad (5)$$

Further, with the Euclidian distance computation, the localization vector 'L' is computed for all the user equipment using the equation (6).

$$DUE_{ij} = \sqrt{\sum[(U_{ijx}^2), (U_{ijy}^2)]} \quad (6)$$

The designed concept of HARQ-S evaluates the CQI measures from the UE with two-way slots measurements. According to the justifiable CQI from UE, the primary allocation of RB to the UE in slot-1 takes place. On the other hand, in slot-2, the RB allocation considers the UE's priority and its associative packets. The system evaluates both HARQ1/HARQ2 to deal with erroneous data packets regardless of the channel conditions. A code is utilized for instantaneous error detection and correction from the data packets (pkt) received in this design context. If the code can correct the erroneously received packet (pkt), it will check and validate the (pkt); else, it will provide NACK and discard the packet, and again it will ask for re-transmission. When the re-transmission process occurs and the retransmitted pkt is received at the receiver side, the receiver performs decoding. With an unsuccessful attempt again, the pkt error is encountered. The entire process gets repeated till the system receives successful acknowledgment of the correct pkt receipt. However, this process is quite lengthy due to more parity check bits' computation during the code's error detection and correction. The system optimizes the HARQ1 with scheduling time-slot1 and time-slot2. And in this case, the FEC plays a very significant role in error correction, even if in the presence of bad channel conditions. HARQ1 design accomplishes a higher throughput curve as compared to the traditional ARQ scheme. Fig. 5 exhibits the deployment architecture of the eNodeB with UEs in the formulated HARQ-S based downlink scheduling concept for LTE.

The system also prioritizes HARQ2 for pkt scheduling and promotes delay-sensitive low-queuing to maximize the effective user throughput with fairness index. In the HARQ2 scheme also the re-transmission process is carried out with the same information. The pkts are also encoded with the same channel codes, and the carrier signal comprising the encoded bits is further subjected for decoding with the maximum-ratio-combining (MRC) algorithm. Here the combination process takes place before the decoding process and just after the demodulation. The process of HARQ does not pose any additional redundant bits during the time of re-transmissions.

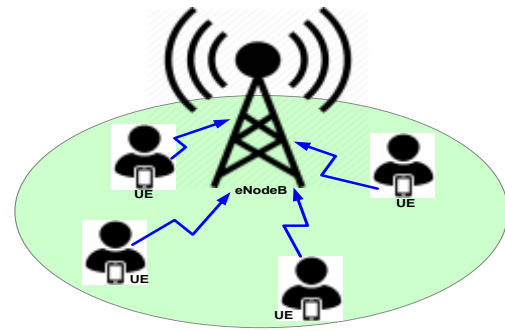


Fig. 5. Deployment of the eNodeB and UEs.

The system employs a flat-architecture of LTE system comprising eNodeBs, which communicates with the core network's respective UEs. The assumption for setting up the channel status metric considers that the smallest RB comprises of $N_{sb} = 12$ where the B is considered 180 kHz with 1 ms of duration. The system designs the formulated HARQ-S based packet scheduling for LTE downlink transmission in a way that aims to attain a higher data-rate and fairness to the UEs, even if in the presence of an erroneous channel. The HARQ-S also targets multi-UEs diversity by mechanizing modulation and coding scheme (MCS), which indicates the channel quality and is frequently reported by the UEs.

The HARQ-S based scheduling algorithm for downlink considers transport block (TB) entity which carries information pkt with headers (h) by interacting variant protocol layers. The MCS associated with RB for each UE influences TB's size and depends on the size of the pkt, which is supposed to be transmitted to the user.

The HARQ-S based pkt scheduling schema considers the UEs at different T_s . The total computation of nUE can be performed with the following mathematical expressions.

$$nUE = ArgMax\{\phi(i) \times pkt_{delay}(Ts)_{UE(i)} \times \frac{T_{bits}(DL)_{UE(i)}}{Avg_{Throughput}UE(i)} \quad (7)$$

Here $\phi(i)$ denotes a maximum probabilistic factor of $pkt_{delay}(Ts)_{UE(i)}$ the head of the line (HOL) pkt delay factor for user i UE(i). and also, $T_{bits}(DL)_{UE(i)}$ here indicates the cumulative number of bits for pkt required for DL transmission. And $Avg_{Throughput}UE(i)$ represents the average throughput for i^{th} UE at T_s slot-1 or slot-2. Here the problem formulation is derived based on selecting the nUE at each T_s to achieve maximum throughput with low-latency of pkt transmission while satisfying the f_i . The problem formulation of the proposed approach is considered as follows from the optimization viewpoint.

To Maximize → nUE with fairness index (f_i)
Subjected to $Avg_{Throughput} UE(i)$ within buffered lesser
Delay (b_d)

Problem condition-1: Subjected to nUE :

$$ArgMax\{\phi(i) \times pkt_{delay}(Ts)_{UE(i)} \times \frac{T_{bits}(DL)_{UE(i)}}{Avg_{Throughput} UE(i)}\}$$

when $i \leftarrow$ non-HARQ users and $p(T) > T_{bits}(DL)_{UE(i)}$

Problem condition-2: Subjected to nUE :

$$ArgMax\{\phi(i) \times pkt_{delay}(Ts)_{UE(i)} \times \frac{p(T)_{UE(i)}}{Avg_{Throughput} UE(i)}\}$$

when $i \leftarrow$ non-HARQ users and $p(T) < T_{bits}(DL)_{UE(i)}$

Problem condition-3: Subjected to nUE :

$$ArgMax\{\phi(i) \times \exp\left(\frac{b_d \times k}{b_d - pkt_{delay}(Ts)_{UE(i)}}\right) \times \frac{p(T)_{UE(i)}}{Avg_{Throughput} UE(i)}\}$$

when $i \in$ both non-HARQ and HARQ users (8)

Here k is constant and $p(T)$ represent the cumulative number of bits in the buffer of $UE(i)$ at time-slot (Ts) 1 or 2.

The study designed an analytical algorithm approach for scheduling packets during LTE down-link transmission with simplified execution steps to address this problem.

Algorithm for down-link packet scheduling for LTE using proposed HARQ-S

Input parameters- nUE , nRB , Ts , B , P , $HT = [HARQ-1$, $HARQ-2]$

Output parameters- resource-aware pkt scheduling in downlink transmission

Start:

1. Initialize: nUE , nRB , Ts , B , P , HT
2. Deploy → UE_1 , UE_2 UEn within the region of $L \times B$
3. Enable proximity of deployment check: using eq. (1)

$$UE_x \& UE_y = \sum_{k=1}^{UE_{tot}} f(U_k).$$

4. Compute Euclidian distance for localization vector (L) computation

$$DUE_{ij} = \sqrt{\sum[(U_{ij}x^2), (U_{ij}y^2)]}.$$

5. Perform connectivity of UE_1 , UE_2 UEn with eNodeB within particular cell j .
7. Enable HARQ-S based scheduling:
8. Compute total bandwidth

$$B = \sum_{i=1}^N (N_{sb})i \dots eq(2)$$

9. eNodeB checks CQI of each $UE(i)$

10. Formulate the optimization problem:

To Maximize → nUE with fairness index (f_i)

Subjected to $Avg_{Throughput} UE(i)$ within

buffered lesser delay (b_d)

11. To solve this approach using HARQ-S:

12. if (CQI = High and Justifiable):

Allocate RBs → $UE(i)s$ in $Ts(1)$

Compute →

$$nUE = ArgMax\{\phi(i) \times pkt_{delay}(Ts)_{UE(i)} \times \frac{T_{bits}(DL)_{UE(i)}}{Avg_{Throughput} UE(i)}\}$$

Use problem-condition-1: to compute nUE

if $p(T) > T_{bits}(DL)_{UE(i)}$ for non-HARQ users

Use problem-condition-2: to compute nUE

if $p(T) < T_{bits}(DL)_{UE(i)}$ for non-HARQ users

Use problem-condition-3: to compute nUE

if $i \in$ both non-HARQ and HARQ users

14. Check pkt error using FEC and ARR

15. End

16. Elseif (Check priority = Req(pkt))

Use HARQ1/HARQ2 for scheduling the pkt in $Ts(2)$ and allocate RBs to required $UE(i)s$

Check pkt error using FEC and ARR

18. Else

19. Schedule to next time slot UEs

20. End

21. Compute $Avg_{Throughput} UE(i)$, $pkt_{delay}(Ts)_{UE(i)}$

End

The proposed downlink packet scheduling combinedly uses the CQI, HARQ, and eNodeB scheduler's strength factors to effectively allocate the RBs to the justified UEs within the LTE network. Initially, the system deploys the eNodeBs and UEs with the optimal mode of deployment so that UEs that belong to a particular cell remains within the proximity of the region of $L \times B$. Further, it can be seen that the scheduling algorithm is designed for both HARQ and non-HARQ UEs. Here the Scheduler operates with eNodeB, which maintains a buffer where pkts wait in the queue for re-transmission to the respective HARQ UEs in downlink and if the RBs are allocated. On the other hand, for non-HARQ users, pkts in eNodeB waits for initial transmission. As highlighted in the above algorithm, the HARQ-S employs both priority-based scheduling and scheduling of pkt based on the CQI computed value. The system allocates RBs to both HARQ and non-HARQ UEs. And similarly, the TBs are correctly received. The throughput and delay calculation is taken place considering the following mathematical expressions.

$$UE_{throughput} = 1/nUE \frac{1}{Ts} \sum \sum Avg_{Throughput} UE(i)_{Ts}$$

Here $1 \leq t \leq Ts$

Here $1 \leq i \leq nUE$ (9)

Average queuing delay $Q_{delay} = 1/Ts \sum 1/nUE \sum$

$$pkt_{delay}(Ts)_{UE(i)} \quad (10)$$

Here $1 \leq t \leq Ts$

Here $1 \leq i \leq nUE$

The next section further discusses the experimental outcome obtained for different stimulation parameter settings within the framework design and execution environment scenario.

V. RESULTS AND ANALYSIS

As the proposed study is a benchmarking model, so the comparison is carried out among existing standard schedulers, e.g., round-robin, Best CQI, and HARQ scheduling. To validate the system model and its benchmarking with the existing RRS and BCQI-S, various combinations of the parameters are taken into consideration, which is having theoretical significance. The simulation parameter combinations are listed in Table V.

The typical performance graph for both HARQ-Type 1 and HARQ-Type-2 is discussed below, wherein both cases the number of resource blocks(nRB), time slot(T), number of user equipment(nUE), system bandwidth(B), and the base station transmit power(P) is taken as 6,2,25,1.4Mhz,23dBm respectively.

A. Performance Graphs of throughput, Fairness, and Delay for HARQ Type I

Fig. 6 illustrates the comparison of the HARQ-scheduling for HARQ type-1 with the RR-S and BCQI-S for Network throughput Vs. Base Station (BS) transmit power.

The throughput pattern increases for all three schedulers with an increment of the base station transmit power. The best CQI-S provides better throughput than the RR-S, whereas the presented concept of HARQ-scheduling yields superior outcomes compared to both BCQI-S and RR-S. The maximum value of network throughput for HARQ-scheduling appeared at the point of 1.8 b/s/Hz for the specific BS transmit power, 45 dBm. On the other, in both BCQI-S and RR-S, when the increased transmit power is set to 45 dBm, then approximately a maximum of 1.7 b/s/Hz and 1.6 b/s/Hz network throughputs are obtained.

Fig. 7 illustrates the comparison of the HARQ-scheduling for HARQ type-1 with the RR-S and BCQI-S for Throughput vs. User's average SNR (dB).

The interpretation illustrates that similarly, in this experimental approach, it is observed that the trend of the curves for Network throughput (b/s/Hz) corresponds to 1. RR-S, 2. BCQI-S, and 3. HARQ-scheduling is progressively increasing for the incremented values ranges between -10 and 35 (dB). However, a closer analysis reveals that for a variable

range of average users SNR (dB), BCQI-S outperforms RR-S in terms of throughput but at that same time found not much superior as compared to the presented HARQ-scheduling approach. HARQ-scheduling in every case of average user SNR (dB) yields superior outcome, and at average users SNR value 35, it produces global maximum value of network throughput, which is approximately 3.9 (b/s/Hz).

Fig. 8 compares the HARQ-scheduling for HARQ type-1 with the RR-S and BCQI-S for Network fairness index Vs. User's average SNR (dB).

TABLE V. SIMULATION PARAMETERS RANGE

Sl. No	System Variable	Symbol	Range
1	Number of user's equipment	nUE	0, 5, 10, 15, 20, 25
2	Number of Resource Block	nRB	6, 15, 25, 50, 75, 100
3	Time Slots	Ts	2
4	System Bandwidth	B (Mhz)	1.4, 3, 5, 10, 15, 20
5	Transmit Power	P	Reference Power (23dbm)
6	HARQ-Type	HT	

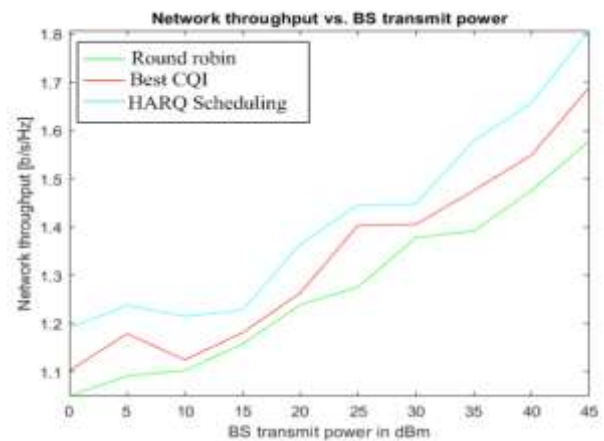


Fig. 6. Network Throughput (bits/Hz) Vs. Base Station Transmit Power.

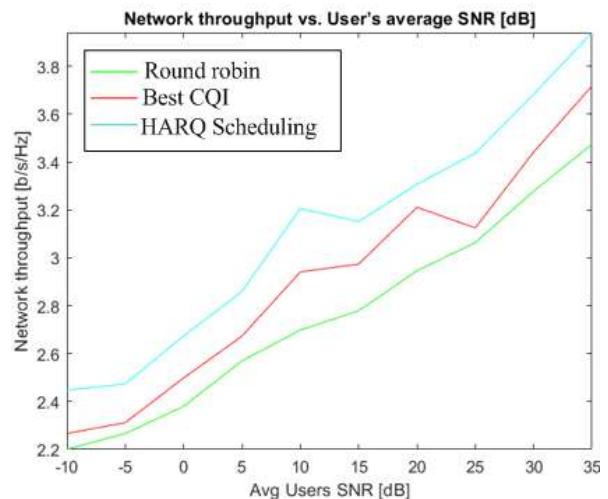


Fig. 7. Network Throughput (bits/Hz) Vs. Average users SNR (dB).

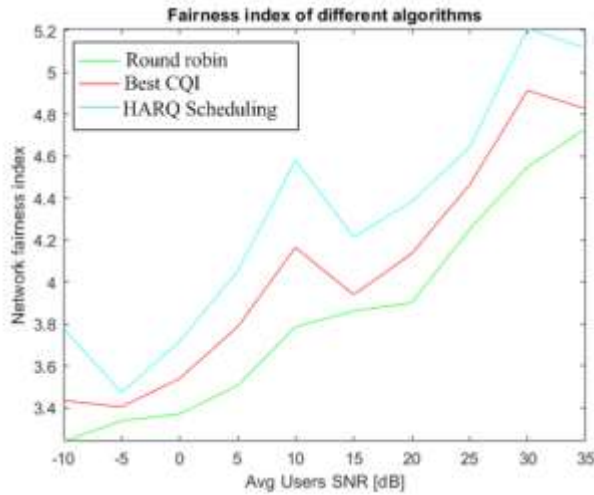


Fig. 8. Network Fairness Index vs. Average users SNR (dB).

The analysis of the network fairness index from the validation of these algorithms such as as: 1) RR-S, 2) BCQI-S, and 3) HARQ-scheduling shows that in this testing scenario, the network fairness index movement trend is quite higher in HARQ-scheduling in contrast with BCQI-S and RR-S. But if we consider the case of both BCQI-s and RR-S, then the BCQI-S outcome for the network fairness index must dominate more as compared to the outcome corresponding to RR-S. The maximum value of network index fairness is obtained in HARQ-scheduling, which is at 5.2 for 30 (dB) average users SNR.

Fig. 9 illustrates the comparison of the HARQ-scheduling for HARQ type-1 with the RR-S and BCQI-S for Delay Vs. BS transmit power in dBm.

With increasing BS transmit power in dBm, it is observed that the amount of Delay computed in the case of RR-S is quite higher, and the impact remains till the value of approximately 1.9 when the BS transmit power is set to 45 dBm. On the other hand, in both the cases of BCQI-S and HARQ-scheduling, the trend of the delay curve movement is found increasing but observed lesser as compared to RR-S. Out of all these three approaches, HARQ-scheduling exhibits consistent and lesser Delay with increasing BS transmit power.

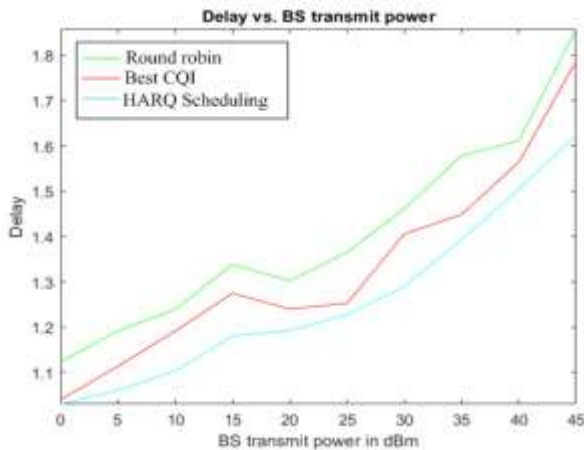


Fig. 9. Delay vs. BS Transmit Power in dBm.

Fig. 10 illustrates the comparison of the HARQ-scheduling for HARQ type-1 with the RR-S and BCQI-S for Delay vs. User's average SNR (dB).

The closer interpretation of the delay analysis outcome is again assessed for the user's average SNR (dB). Here, the pattern of the curve of the delayed movement in each case of 1. RR-S, 2. BCQI-S, and 3. HARQ-scheduling is increasing progressively, but the values of the outcome for Delay in the case of RR-S get negatively influenced when the average user's SNR ranges between -10 to 35 (dB). In this case, also when the delayed outcome is concerned- HARQ-scheduling outperforms the other approaches and significantly minimizes the Delay up to the approximate value of 3.67778.

Fig. 11 illustrates the comparison of the HARQ-scheduling for HARQ type-1 with the RR-S and BCQI-S for Delay of different algorithms vs. User's average SNR (dB).

The Delay analysis in this experimental approach considers the execution of algorithms from the time complexity viewpoint. It clearly outlines that HARQ-scheduling imposes optimized steps of execution. It leads to a scenario where, with an increasing number of average users SNR, the Delay found bounded within a maximum approximate value of 5.4587. In both RR-S and BCQI-S, the delay computation yields an outcome that is quite higher than the presented approach of HARQ-scheduling for increasing value of average users SNR (dB).

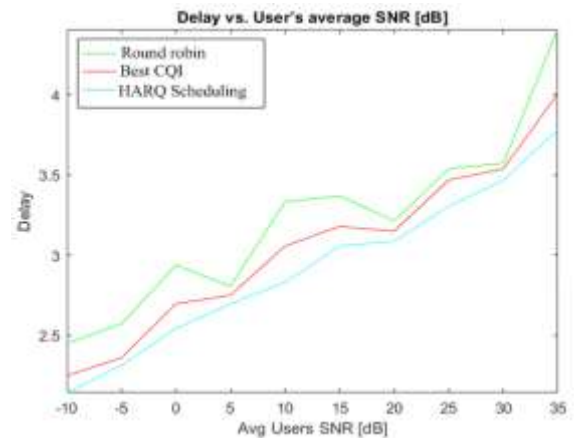


Fig. 10. Delay vs. Average users SNR (dB).

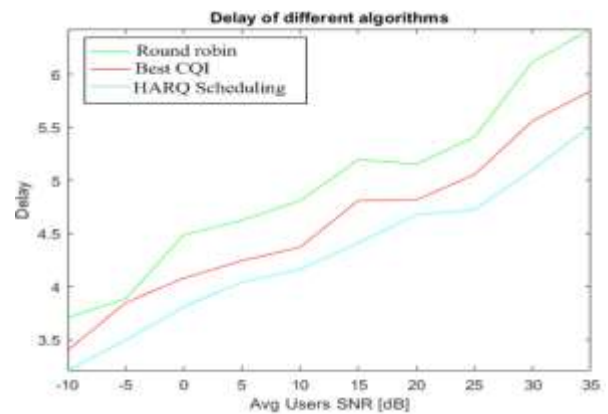


Fig. 11. Delay of different Algorithms vs. Average users SNR (dB).

B. Performance Graphs of throughput, Fairness, and Delay for HARQ Type II

Fig. 12 illustrates the comparison of the HARQ-scheduling for HARQ type-2 with the RR-S and BCQI-S for Network throughput Vs. BS transmit power in dBm.

The analysis of network throughput (b/s/Hz) for HARQ type-2 shows that in comparison with RR-S and BCQI-S, the HARQ-scheduling approach accomplishes superior outcomes increasing values of BS transmit power in dBm, which ranges between 0 to 45. If we consider the cases of RR-S and BCQI-S, then it can be observed that BCQI-S attain better network throughput as compared to RR-S. The maximum value of throughput in the case of HARQ-scheduling appeared at point 2.1 for the BS transmit power of 45 dBm.

Fig. 13 illustrates the comparison of the HARQ-scheduling for HARQ type-2 with the RR-S and BCQI-S for Network throughput Vs. User's average SNR (dBm).

Another experimental approach is assessed to evaluate the network throughput (b/s/Hz) with the increasing amount of Average users SNR (dB) ranges between -10 and 35. The visual representation of the comparable outcome shows that Similarly to the above cases, which is illustrated in Fig. 12, HARQ-scheduling accomplishes superior outcome for the increased values of average users SNR (dB). The visual data representation of the network throughput curves for RR-S and BCQI-S also shows that in contrast with RR-S, the approach of BCQI-S attain a superior outcome where the maximum value of throughput appears at approximately 3.6 b/s/Hz. Fig. 14 illustrates the comparison of the HARQ-scheduling for HARQ type-2 with the RR-S and BCQI-S for Network fairness index Vs. User's average SNR (dBm).

The computed outcome analysis corresponding to the network fairness index for these three algorithms also shows that that index movement is significantly higher and progressive upwards in the case of HARQ-scheduling compared to RR-S and BCQI-S algorithms. For each value of average users SNR, which ranges between -10 and 35, the outcome found superior in HARQ-scheduling and marginally differs from BCQI-S. However, among all these three algorithms, RR-S's performance is quite lower when the parameter network fairness index is concerned with increasing values of average users SNR (dB).

Fig. 15 illustrates the comparison of the HARQ-scheduling for HARQ type-2 with the RR-S and BCQI-S for Delay vs. BS transmit power in dBm.

The Delay's quantified outcome using three different algorithms, such as RR-S, BCQI-S, and the formulated approach of HARQ-scheduling, are visually represented in Fig. 15. It clearly shows that Delay's quantified outcome is significantly lesser in the case of HARQ-scheduling even though the increasing BS transmit power in dBm increases from 0 to 45. The outcome of the HARQ-scheduling in Delay's context is found a maximum of 1.9786, which is significantly lesser than the other baseline scheduling models.

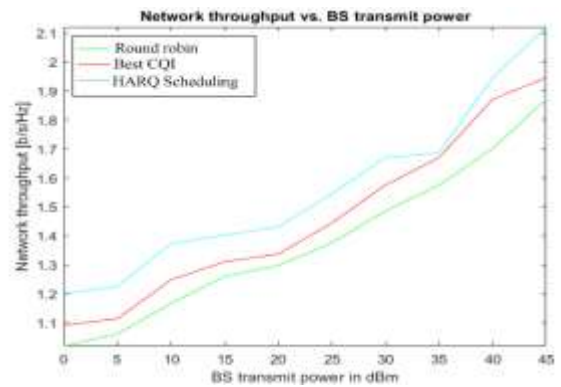


Fig. 12. Network throughput (b/s/Hz) vs. BS Transmit Power in dBm.

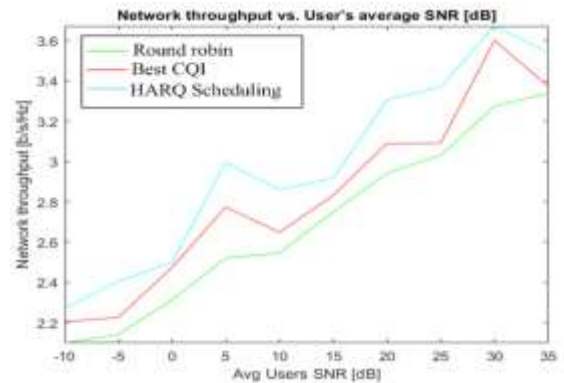


Fig. 13. Network throughput (b/s/Hz) vs. user's Average SNR (dBm).

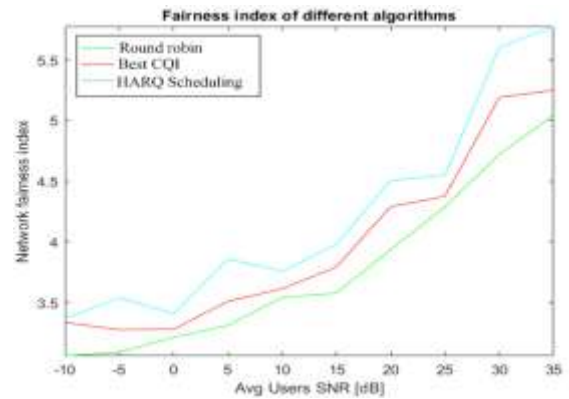


Fig. 14. Extended Analysis of Network Fairness Index.

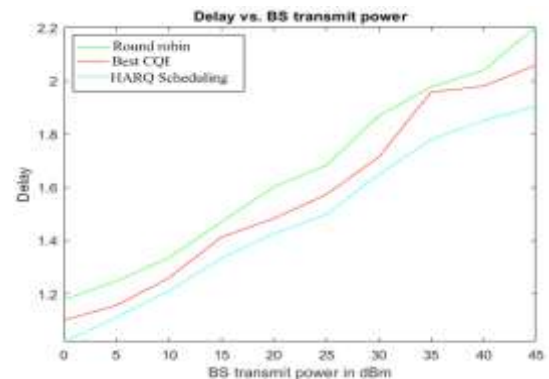


Fig. 15. Extended Analysis of Delay.

Fig. 16 illustrates the comparison of the HARQ-scheduling for HARQ type-2 with the RR-S and BCQI-S for Delay vs. Average users SNR (dB).

The delay performance analysis, in this case, was observed concerning the increased values of Average users SNR (dB), which ranges between -10 and 35. For all three approaches, it is observed that the trend of the delay movement curve increases with the values of average users SNR (dB). However, the BCQI-S attains superior outcome in the context of Delay as compared to RR-S. Still, let's consider the overall performance of the Delay. HARQ-scheduling is superior as it yields a significantly lesser Delay even though the % of the average user's SNR is increased.

Fig. 17 illustrates the comparison of the HARQ-scheduling for HARQ type-2 with the RR-S and BCQI-S for the Delay of different algorithms Vs. Average users SNR (dB).

The delayed outcome here indicates the algorithm performance from a time complexity viewpoint. A closer interpretation reveals that in the presented approach of HARQ-Scheduling, the curve of Delay's curve progressively increases concerning the increasing data points of SNR (dB). Still, if we compare the performance of HARQ-scheduling with RR-S and BCQI-S, then it can be observed that HARQ-scheduling exhibits a superior performance graph among all of these.

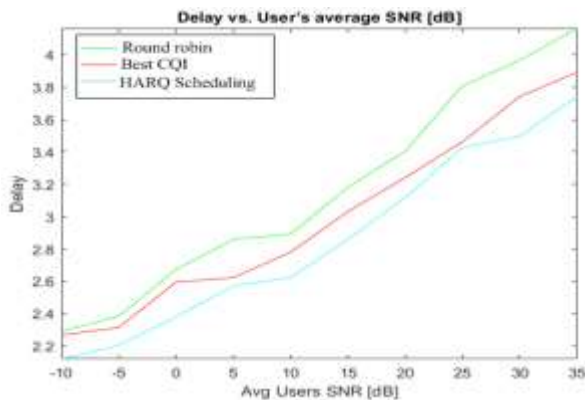


Fig. 16. Analysis of the Impact of SNR on Delay.

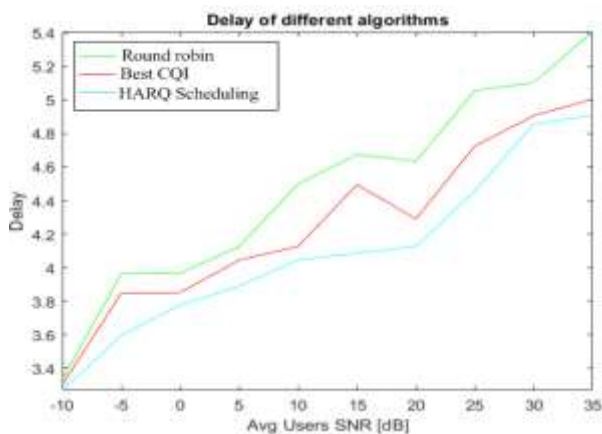


Fig. 17. Delay of different Algorithms vs. Average users SNR (dB).

VI. CONCLUSION

The study outcome of the proposed study shows that the HARQ scheduler offers approximately 37% improvement from Round Robin and approximately 26% improvement from the best CQI algorithm concerning its network throughput in the presence of variable transmit power of the base station. The patterns of network throughput remain nearly the same when evaluated with increasing SNR. HARQ scheduler is also witnessed to offer approximately 40% of reduction in delay from Best CQI and approximately 43% of reduction from Round-robin in the presence of variable transmit power and different SNR values. Similar outcomes are also observed for HARQ type-II algorithms.

Scheduler optimization for balancing the throughput, fairness, and optimal resource allocation is a very active research problem study and significant in the growing UEs density. In this paper, an essential of the general requirements, physical layer characteristics, and the research trend in the scheduling model for LTE /NR is studied, directly impacting the system performance. The OFDM enabled eNodeB to divide the bandwidth into resource element, allocated to the UEs by the schedulers in eNodeB or Base stations (BS). The proposed HARQ-S handles the trade-off issues between the Best CQI and Round Robin to balance optimal throughput and fairness. The time -slot servicing for the RB block takes place on priority dependencies of CQI and HARQ to balance the trade-off between the throughput and the fairness. The benchmarking of the HARQ-S is done with the Best-CQI and Round robin for throughput and fairness and observe optimization in the throughput compared to the RRS and fairness optimization compared to the BCQI. A better scheme of OFDM-MIMO may further claim to have better throughput.

The future work of the proposed study will be to achieving better form of computational efficiency. The present work offers a benchmarking testbed to prove HARQ is the best controller where a distinct section of cumulative memory of HARQ is allocated to each carrier. However, there is a possibility of more increase of incoming HARQ requests by optimizing the computational efficiency. This will be investigated in the upcoming work direction where 5G scenarios can be considered with more approximation cases to leverage throughput.

REFERENCES

- [1] Parameswaran V., Shanmugasundaram M, "Journey of Wireless Communication. In: Ranganathan G., Chen J., Rocha A. (eds) Inventive Communication and Computational Technologies. Lecture Notes in Networks and Systems, Vol 89. Springer, Singapore, 2020.
- [2] Holma H, Lunttila T. LTE-Advanced Evolution. 5 G Technology: 3 GPP New Radio. 2020 Feb 10:477-99.
- [3] I. Pospishny, V. Vasyuk, S. Romanchyk, O. Dovzhenko, O. Dony and V. Shvaichenko, "3GPP long term evolution (LTE)," International Conference on Modern Problems of Radio Engineering, Telecommunications and Computer Science (TCSET), Lviv-Slavske, pp. 192-192, 2010.
- [4] R. Cai, X. Wang, Y. Wang, S. Xiao, C. Wang, and W. Wang, "A Novel and Effective User Scheduling Scheme for Heterogeneous Scenario in LTE-A System," IEEE International Conference on Computer and Information Technology, Xi'an, 2014, pp. 679-683.

- [5] R. B. Abreu, G. Pocovi, T. H. Jacobsen, M. Centenaro, K. I. Pedersen and T. E. Kolding, "Scheduling Enhancements and Performance Evaluation of Downlink 5G Time-Sensitive Communications," in *IEEE Access*, vol. 8, pp. 128106-128115, 2020, doi: 10.1109/ACCESS.2020.3008598.
- [6] G. Femenias, F. Riera-Palou, X. Mestre and J. J. Olmos, "Downlink Scheduling and Resource Allocation for 5G MIMO-Multicarrier: OFDM vs. FBMC/QAM," in *IEEE Access*, vol. 5, pp. 13770-13786, 2017, 10.1109/ACCESS.2017.2729599.
- [7] J. Liang, C. Hsu, J. Chen, K. Wu, and Y. Tseng, "Three-Stage DRX Scheduling for Joint Downlink Transmission in C-RAN," in *IEEE Wireless Communications Letters*, vol. 9, no. 2, pp. 129-133, Feb. 2020, doi: 10.1109/LWC.2019.2943471.
- [8] D. A. Omer, A. B. N. Mustafa, "LTE FDD vs. LTE TDD from a QoS Perspective," *Journal of Electronics and Communication Engineering (IOSR-JECE)*, Vol. 10, Issue. 2, pp. 96-100, 2015.
- [9] Xylomenos, George & Vogkas, Vasilis & Thanos, George. (2008). The multimedia broadcast/multicast service. *Wireless Communications and Mobile Computing*, 8, 255-265. 10.1002/wcm.463.
- [10] U. Hani and K. K. Samota, "Particle Swarm Optimization Algorithm to Improve Access Delay in 5G Technology," 2018 Second International Conference on Advances in Computing, Control and Communication Technology (IAC3T), Allahabad, India, 2018, pp. 23-27.
- [11] A. Saxena and R. Sindal, "Performance Analysis of MAC Scheduler in LTE (EUTRAN) for "ASAR": Resource Allocation," 2016 10th International Conference on Next Generation Mobile Applications, Security and Technologies (NGMAST), Cardiff, 2016, pp. 6-11.
- [12] M. Minelli, M. Ma, M. Coupechoux and P. Godlewski, "Scheduling Impact on the Performance of Relay-Enhanced LTE-A Networks," in *IEEE Transactions on Vehicular Technology*, vol. 65, no. 4, pp. 2496-2508, April 2016.
- [13] T. K. Ramesh, "A Survey on scheduling algorithm for downlink in LTE cellular network," 2019 International Conference on Smart Systems and Inventive Technology (ICSSIT), Tirunelveli, India, 2019, pp. 219-223.
- [14] A. Chilmulwar and V. Sinha, "A Novel Machine Learning-Based MAC Scheduler Algorithm using ARIMA," 2019 16th IEEE Annual Consumer Communications & Networking Conference (CCNC), Las Vegas, NV, USA, 2019, pp. 1-8.
- [15] J. O. Olaifa and D. Arifler, "Using system-level simulation to evaluate downlink throughput performance in LTE-A networks with clustered user deployments," 2016 1st International Workshop on Link- and System Level Simulations (IWSLS), Vienna, 2016, pp. 1-6.
- [16] S. Chaudhuri, I. Baig, and D. Das, "QoS aware downlink scheduler for a carrier aggregation LTE-Advance network with efficient carrier power control," 2016 IEEE Annual India Conference (INDICON), Bangalore, 2016, pp. 1-6.
- [17] N. D. Adesh and A. Renuka, "Impact of traffic burst on the behavior of TCP variants for different LTE downlink schedulers," 2017 3rd International Conference on Applied and Theoretical Computing and Communication Technology (iCATccT), Tumkur, 2017, pp. 18-23.
- [18] K. G. Sundari, R. Gunasundari and K. Jayanthi, "Prioritized dynamic multi traffic scheduler for downlink in LTE," 2015 2nd International Conference on Electronics and Communication Systems (ICECS), Coimbatore, 2015, pp. 1469-1473.
- [19] B. Rebekka, B. V. Kumar and B. Malarkodi, "Radio resource allocation with energy efficiency-throughput balancing for LTE downlink," 2015 2nd International Conference on Electronics and Communication Systems (ICECS), Coimbatore, 2015, pp. 111-115. doi: 10.1109/ECS.2015.7124754.
- [20] Ö. Yildiz and R. Sokullu, "A novel mobility aware downlink scheduling algorithm for LTE-A networks," 2017 Ninth International Conference on Ubiquitous and Future Networks (ICUFN), Milan, 2017, pp. 300-305.
- [21] A. Hayuwidya, M. E. Erwanan, and Iskandar, "Scheduling techniques in release 8 LTE network," 2017 11th International Conference on Telecommunication Systems Services and Applications (TSSA), Lombok, 2017, pp. 1-5.
- [22] R. E. Ahmed and H. M. AlMuhallabi, "Throughput-fairness trade-off in LTE uplink scheduling algorithms," 2016 International Conference on Industrial Informatics and Computer Systems (CIICS), Sharjah, 2016, pp. 1-4.
- [23] M. O. Kayali, Z. Shmeiss, H. Safa and W. El-Hajj, "Downlink Scheduling in LTE: Challenges, improvement, and analysis," 2017 13th International Wireless Communications and Mobile Computing Conference (IWCMC), Valencia, 2017, pp. 323-328. doi: 10.1109/IWCMC.2017.7986307.
- [24] A. Hajjawi, M. Ismail, N. F. Abdullah, M. N. Hindia, A. M. Al-Samman, and E. Hanafi, "Investigation of the impact of different scheduling algorithm for Macro-Femto-Cells over LTE-A networks," 2016 IEEE 3rd International Symposium on Telecommunication Technologies (ISTT), Kuala Lumpur, 2016, pp. 125-128. doi: 10.1109/ISTT.2016.7918098.
- [25] A. A. A. Rahman, A. Man, A. K. Samingan, C. Y. Yeoh and I. Suleiman, "Fair boundary scheduler for LTE system," 2016 IEEE Symposium on Computer Applications & Industrial Electronics (ISCAIE), Batu Feringghi, 2016, pp. 11-15. doi: 10.1109/ISCAIE.2016.7575028.
- [26] K. G. Sundari, K. Jayanthi, and R. Gunasundari, "Prioritized dynamic multi traffic scheduler for downlink in LTE," 2015 2nd International Conference on Electronics and Communication Systems (ICECS), Coimbatore, 2015, pp. 1546-1550. doi: 10.1109/ECS.2015.7124847.
- [27] S. Alotaibi and R. Akl, "Packet scheduling bandwidth type-based mechanism for LTE," 2017 IEEE 8th Annual Ubiquitous Computing, Electronics and Mobile Communication Conference (UEMCON), New York, NY, 2017, pp. 363-368.
- [28] S. Harkusha, O. Harkusha, and V. Olkhovskiy, "Result research model of scheduling block allocation in downlink LTE," 2016 Third International Scientific-Practical Conference Problems of Infocommunications Science and Technology (PIC S&T), Kharkiv, 2016, pp. 92-95. doi: 10.1109/INFOCOMMST.2016.7905345.
- [29] M. Bechir Dadi and R. Belgacem Chibani, "Scheduling performance's study for LTE downlink system," International Conference on Green Energy Conversion Systems (GECS), Hammamet, 2017, pp. 1-4. doi: 10.1109/GECS.2017.8066174.
- [30] A. B. Shams, S. R. Abied and M. A. Hoque, "Impact of user mobility on the performance of downlink resource scheduling in Heterogeneous LTE cellular networks," 3rd International Conference on Electrical Engineering and Information Communication Technology (ICEEICT), Dhaka, 2016, pp. 1-6. doi: 10.1109/CEEICT.2016.7873091.

The Cognizance of Green Computing Concept and Practices among Secondary School Students: A Preliminary Study

Shafinah Kamarudin^{1,*}

Faculty of Computer Science and Information Technology
Universiti Putra Malaysia
43400 UPM Serdang Selangor, Malaysia

Siti Munirah Mohd²

GENIUS Insan College
Universiti Sains Islam Malaysia, Bandar Baru Nilai
71800 Nilai, Negeri Sembilan, Malaysia

Nurul Nadwa Zulkifli³, Rosli Ismail⁴, Ribka Alan⁵

Faculty of Humanities, Management and Science
Universiti Putra Malaysia Bintulu Sarawak Campus
Nyabau Road, P.O. Box 396, 97008 Bintulu, Sarawak
Malaysia

Philip Lepun⁶

Faculty of Agriculture Sciences and Forestry
Universiti Putra Malaysia Bintulu Sarawak Campus
Nyabau Road, P.O. Box 396, 97008 Bintulu, Sarawak,
Malaysia

Muhd Khaizer Omar⁷

Faculty of Educational Studies
Universiti Putra Malaysia, 43400 UPM Serdang, Selangor, Malaysia

Abstract—The use of information communication technology (ICT) is growing and has been a compulsory norm in society. However, the increased use of ICT facilities in all developing countries has contributed to higher energy use and lead to environmental pollution. This study explores the extent of awareness among the younger generation about green computing concepts and practices. In this study, a total of 94 secondary school students were sampled across Selangor state. The data were gathered using a set of questionnaires comprising of 20 items pertaining to the harmful effects of using computers and communication gadgets on the environment, awareness of the concepts and practices of green computing. The findings indicate it reveal that secondary school students are still not aware of the green computing concept. It is observed that 54.35% of students may not realize that computers and communication devices could be disposed of eco-safe. Furthermore, 61.96% of students do not realize that computer hardware can be recycled, and 75% of them do not have experience in disposing of their computers. Surprisingly, they mostly practice green computing when it comes to reducing energy consumption. This study contributes to determining the current level of students' green computing awareness in a sustaining environment. In conclusion, students need to be educated on utilizing ICT resources and practicing green computing mechanisms to boost environmental sustainability.

Keywords—Awareness; energy consumption; green computing; environment pollution; secondary students

I. INTRODUCTION

The utilization of electronic devices, including computers, brings great benefits to human beings. Conversely, this

utilization has led to a rise in energy consumption, electronic waste, as well as to adverse impacts on human health and the environment [1,2]. For example, e-waste generation has been recorded globally, with a volume of 4.18 million metric tonnes in 2014, and e-waste generation exposure human to toxic elements [2,3].

Therefore, the initiatives to foster green computing and energy minimization include low carbon emissions and efficient use of resources, have been highlighted [3, 4]. Green computing is defined as energy-efficient computing practices, eco-friendly, responsible use of computers, and other resources in sustaining environment [5, 6]. Green computing has four major components known as (1) manufacturing and production of computer resources, (2) design of computer system and system resources, (3) usage of computer resource management, and (4) disposal of computer resources and e-waste [7, 8].

The practice of green computing able to reduce energy usage, lower carbon dioxide emissions, conserving resources where less energy is required to produce, use and dispose of products, saving energy and resources, and reducing the risk that might cause health problems and environmental pollution [9]. Green computing encourages recyclability and biodegradability, uses network and computing in proper ways includes promote paperless policies and reduce print volumes, adopting conference calls, use blank screensavers option, and hibernating [6,10].

Then again, green computing requires participation and support from individuals, the community, government, and

*Corresponding Author

private sectors to ensure this effort to sustain a healthy environment. The adoption of green computing practices in sustaining the environment is dependent on green computing awareness and behavior [1,11]. Moreover, the knowledge related to green computing is recommended to be introduced from an early age [12].

Further, the awareness studies on green computing in most countries are conducted for higher institutions. This is due to the massive use of ICT such as digital databases, laptops, LCD, and distance learning programs, and students in the higher institutions are considered a huge segment of ICT users [4, 13]. However, far too little attention has been paid to the awareness of green computing among younger generations, especially among school students.

Besides that, the industrial revolution 4.0 changes the landscape of education, where the concept of Education 4.0 was introduced. Education 4.0 requires primary, secondary, and higher institution students to be digital literate. Therefore, teaching and learning can be conducted in various ways, such as using collaborative software and apps, conducting classes through Google Classroom, using virtual and augmented realities for education [5]. Due to these matters, the research aims at exploring (i) awareness on the impact of using ICT towards environments, (ii) identifying awareness on green computing concepts, and (iii) exploring the green computing practices among secondary school students in urban areas.

Therefore, Section II explained the research background, including the ICT and environment, green computing and its initiative, and the awareness and practices in green computing. Then, the method used in this study is elaborated in Section III and the results are presented in Section IV. Finally, the discussion, concluding remarks and some suggestions for future works are described in Section V.

II. LITERATURE REVIEW

A. ICT and Environment

Since the 1990s, researchers have made a significant contribution to the environmental consequences of ICT. The relationship between ICT and the environment is complex stated in several studies, as ICT leads to positive and negative environmental impacts [14-16,18]. The study of [17] addresses the global consumption of residential electricity by ICT equipment, which increased by almost 7 percent (7%) per year between 1990 and 2008. Even with expected improvements in energy efficiency, electronics consumption is expected to increase by 250% by 2030. Further support is given by [15], which more specifically asserts that ICT decreases CO₂ emissions from developed and developing countries over the period 1990 to 2017 for a complete sample of 91 countries.

Besides, a finding published in [18] stated that ICT influences the environment via three channels, which are:

- **Usage effect** during production, refining, distribution and installation of ICT equipment contribute significantly to CO₂ emissions.

- **Substitution effect** is described as the reorganization of the production process, including decarbonization of dematerialization, demobilization, replacement of physical products with e-books, e-mail and teleconferencing postal mail, smart transport system, GPS, smart camera traffic control system, and reduction of outdoor activities.
- **Cost effect** in which ICT raises the demand for other goods and services due to a drop in prices and a rise in the return of CO₂ pollution.

However, comparative studies have shown that using ICT in developed countries promotes environmental sustainability. It implies that it would be possible to contribute to environmental sustainability and ICT diffusion with greater levels of development of the country. [15,18].

B. Green Computing and its Initiative

The initiative of green computing [19]:

1) *Virtualization*: Virtualization is one such form of technology that provides access from a remote location to servers or users. Nowadays, the green initiative has progressed into the idea of virtualization, in which cloud computing plays an important role.

2) *Power management*: The need for power management in any computer system is highly insisted because of the prolonged battery life, reduction in the cooling requirements, noise also. The hibernate option available in the system is one such kind of power management technique supported comprehensively and efficiently as it will automatically switch off the RAM and CPU of the system, reducing the amount of background working of the system.

3) *Power supply*: Power supplies are also one such factor that will help achieve the green computing concept by implementing the green systems. The drain of more power is supportive in designing a system in an efficient manner. The idea of purchasing and using the power suppliers with “80 plus” certification is considered the best way to save power in the system (State Legislation on E-Waste, 2008). The use of this sort of useful and efficient power supply can probably reduce the wastage of energy consumed and the heat generated in the system.

4) *Displays*: The displays emit heat directly into the device, thereby consuming more fuel. Therefore, the principle of replacing LCD monitors and LED displays with light-emitting diodes are. It's called the best idea. It's because the fluorescence is due to the lamp used consumes more energy and emits elevated heat. Research shows that the LCDs are 66 percent more energy efficient and are also 80 percent highly skilled in growing the system's size and weight. In contrast, the CRT uses about 120W of power, which is twice the power used by the 22-inch LCD. Therefore, any person needs to look for the device components before buying, including the displays, which will probably help reduce the power consumed.

5) *Video cards*: The reduction in the use of video card is considered to be a wise idea as it cannot use the shared terminal, think client or cannot even have desktop sharing properties, which are highly helpful in saving the energy consumed in the system. The reuse of older video cards is considered a wise idea as it will consume only lesser power, thus reducing the heat sinks or fans. The selection of GPU with average wattage or performance per watt is also considered to be a much wiser in the idea of selecting the green system implementation.

C. Awareness and Practices of Green Computing

Theoretically, a "green concept" containing elements of ZEB (Zero Energy Building) and 3R (Reuse, Minimize, Recycle). Green technology's principles include: sustainable, the use of reclaimed natural resources, the manufacture of material that can be reused, the utilization of waste products and chemicals that can be recycled, creative and not adverse to health and environment, the production of practices and products that are environmentally friendly and can protect the earth [20, 22,23]. Green Computing also can be interpreted as "the practices and procedures of using computing resources in a friendly environment way while maintaining overall computing performances" [21]. It has also been stated that green awareness can be divided widely into five community groups [22]:

- 1) Hardware Manufacturer.
- 2) Corporate and Public Consumers.
- 3) Individual Consumers.
- 4) Enforcement Authority.
- 5) Software Designer & Developers.

The most critical aspect of green computing when it comes to practise is the users' attitude towards it and their perceived green computing behavior over green computing's actual behavior. Currently, the major challenge restricting green technology is because the concept itself has not been well socialized to the community. Communication networks are therefore required to promote the adoption of green technology among the general public through communication technology and other communication activities, since the characteristics of network technology and communication affect the implementation of green technology. Communication efforts are also required to spread the value of green technology's position to raise public awareness of environmental issues [20-22].

III. METHODOLOGY

A set of questionnaires was used in this study. The questionnaire is divided into two sections. Section A consists of items related to demographic information. Meanwhile, Section B contained 20 items associated with the impact of using ICT on the environment and the knowledge and practices related to green computing. This section was designed using a dichotomous response scale.

The data were collected using purposive and convenience sampling method. These sampling methods considered the age of respondents ranging from 13 until 17 years old and

conveniently participating in this study. There were 100 questionnaires distributed to secondary school students around Selangor, and 94 questionnaires were returned. Respondents from Selangor are selected as the sampling site because Selangor has the highest enrollment of secondary students in Malaysia with a total number of 364 442 students [24].

However, 92 questionnaires are valid for further analysis. A descriptive analysis was used to analyze the data using Microsoft Excel. The findings of the study are based on the response received through the filled-in questionnaire. This study adapting percentage interpretation from [25] to interpret the level of awareness (Table I).

TABLE I. THE INTERPRETATION FOR AWARENESS LEVEL ON GREEN COMPUTING

Percentage of students' awareness (100%)	The level of awareness of green computing
75-100	High
50-74	Average
25-49	Low
0-24	Very low

IV. RESULT

This section explains the results gain from the survey.

A. Demographic Profile

Table II shows the result of a demographic profile based on gender and age. The demographic distribution shows that 61.0% of respondents were female, and 39.0% of respondents were male who participated in this study. The majority of respondents involved in the study were 16 years old (64.0%), followed by 17 years old (31.0%) and 15 years old (2.0%).

B. Awareness of the Harmful Impact of ICT uses towards Environment

Fig. 1 shows the findings gain on their knowledge and awareness of the harmful impact of ICT Uses on the environment. Question 1 (Q1) aims to know whether secondary school students in Malaysia concern about the environment. This study reveals that 91 (98.91%) respondents agreed that they are concern with the environment. Question 2 (Q2) shows that most respondents (54.35%) did not know that the use of computer hardware can contribute to a harmful impact on environments. Question 3 (Q3) indicates that the majority of respondents (89.13%) know about carbon admission (CO₂). Despite that, findings obtained for question 4 (Q4) show that 55 (59.78%) respondents did not know that computers and IT gadgets can produce carbon emissions. Question 5 (Q5) addressed that electricity usage can contribute to environmental pollution, and 65 (70.65%) respondents agreed with this question. Based on the findings obtained for Question 6 (Q6), 30 (32.61%) respondents know that most of the computer and its gadgets are not biodegradable. Overall, the average knowledge on the impact of ICT use on the environment is only 61.96% and this indicates that the awareness on the impact of ICT uses towards the environment is at the average level.

TABLE II. DEMOGRAPHIC PROFILE OF RESPONDENTS (N=92)

Item	Description	Frequency	Percentage (%)
Gender	Female	56	61
	Male	36	39
Age	17 years old	31	34
	16 years old	59	64
	15 years old	2	2

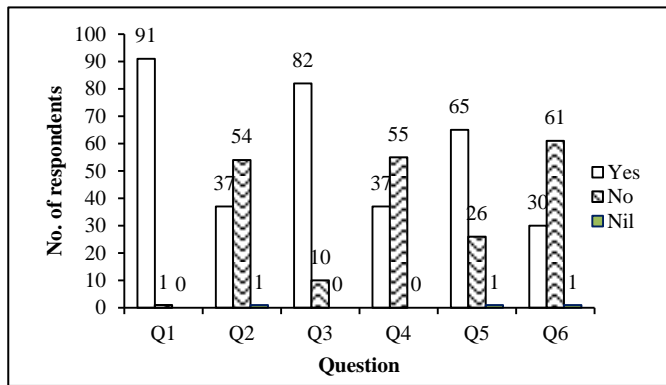


Fig. 1. The Awareness of the Harmful Impact of ICT on Environment.

Therefore, these findings show that students from different level of education remain to have less knowledge and awareness on the impact of ICT to environment [26]. Knowledge on the impact of ICT to environment is commonly being neglected to be exposed to students. Knowledge is a crucial part that should be considered as main priority in raise green computing awareness [7]. Educating students whether from schools and higher education, is vital to encourage them to used ICT in proper techniques while considering the negative impacts on the environment. For example, students are encouraged to use power-saving techniques that present in their computers or other devices. These techniques can reduce electricity consumption and indirectly reduce carbon footprints and other environmental effects [27].

C. Awareness of the Concept of Green Computing

Fig. 2 shows the respondents' awareness of the concept of green computing. Question 7 (Q7) was addressed to know whether the secondary school students aware of any campaign on green computing, question 8 (Q8) was proposed to know the awareness on the definition of green computing and question 9 (Q9) was proposed to identify the awareness on the green computing mission. The findings show a total number of 33 (35.87%) respondents noticed any campaign related to green computing, 40 (43.48%) respondents know the definition of green computing and 53 (57.61%) respondents know that the mission of green computing is to reduce computer hazardous material and to sustain environmental health. The total average of respondents agreed with these three questions is only 45.65%. As a result, this survey showed that the level of students' awareness of green computing is at a low level.

Interestingly, these findings are consistent with a study conducted in 2013 for Malaysian undergraduates [13]. Even though the approach used in accessing the awareness of green

computing concepts is different, both findings show that secondary school students and undergraduate students have little knowledge of the concept of green computing. Therefore, campaigns promoting the concept of green computing such as e-waste or carbon-free computing should be conducted continuously. Furthermore, [13] suggested that future research should be focused on whether students will practice green computing and their intention to embrace the idea.

D. Awareness of the Green Computing Practices

Eleven questions were delivered to identify secondary school students' awareness of green computing practices (Table III). Question 10 until 15 (Q10-15) aims at identifying the secondary school students' awareness of green practices related to recycling and disposing of computers and their gadgets. Based on Q10, it shows that the majority of the respondents (57.61 %) have more than one computer. Q11 shows that 54.35% respondents did not know that computers and their gadgets can be disposed; Q12 reveals that respondents did not know computer hardware can be recycled (61.96%) and Q13 shows 75% respondents do not have experience disposing of their computer hardware. Therefore, there are possibilities that respondents will not manage their e-waste properly. The higher numbers of ownerships for computers and devices means there will be more e-waste generated. Manufactures are recommended to produce computers and their devices are more durable and long lasting to reduce e-waste generation. Furthermore, secondary school students should be equipped with knowledge in discarding or recycling e-waste [2, 28].

Interestingly, Q14 shows that most respondents did not print more than 20 papers per day (82.61%) and Q15 shows that most respondents think that refilling printer cartridge is better (56.53%). According to [27], most printed papers end up as garbage in landfills. Further concern about the use of papers is related to the issues of deforestation where 93% of papers are produced from trees. Regarding the printer cartridge, users are suggested to use certain ink optimization techniques that able to reduce the amount of ink used to print pages. This method is expected to reduce the number of cartridges [27]. Based on findings obtained for Q14 and Q15, it can be concluded that secondary school students contribute less on the paper wastage and have a positive thought in recycling cartridge. Moreover, it is expected that they will continuously use less paper and refill their printer cartridge.

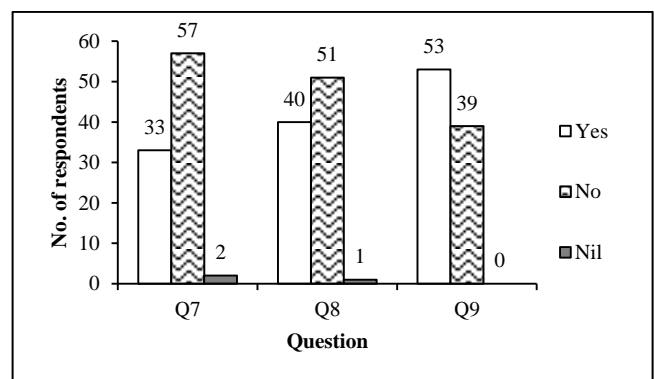


Fig. 2. The Awareness of the Concept of Green Computing.

TABLE III. THE AWARENESS OF GREEN COMPUTING PRACTICES (N=92)

Practice	No.	Question	Yes	No	Nil
Recycling and Disposing	Q10	Do you have more than one computer?	53 (57.61%)	37 (40.22%)	2 (2.17%)
	Q11	Do you know that computer including its gadget (smartphone, tablet, etc.) can be disposed of?	42 (45.65%)	50 (54.35%)	0 (0%)
	Q12	Do you know that computer hardware can be recycled?	35 (38.04%)	57 (61.96%)	0 (0%)
	Q13	Do you have any experience dispose of your computer hardware?	22 (23.91)	69 (75%)	1 (1.09%)
	Q14	Do you print more than 20 pages per day?	16 (17.39%)	76 (82.61%)	0 (0%)
	Q15	Do you think that a refill printer cartridge is better than buying a new cartridge?	52 (56.52%)	37 (40.22%)	3 (3.26%)
Energy Consumption	Q16	Do you use a computer or its gadgets for a long duration?	41 (44.57%)	50 (54.35%)	1 (1.09%)
	Q17	Do you use a computer for more than 5 hours per day?	25 (27.17%)	67 (72.83%)	0 (0%)
	Q18	Do you switch off your computer once you have done your work?	77 (83.70)	13 (14.13%)	1 (1.09%)
	Q19	Do you use a screensaver on your PC?	61 (66.30%)	30 (32.61%)	1 (1.09%)
	Q20	Do you think that using a screensaver can save computer energy?	64 (69.57%)	27 (29.35%)	1 (1.09%)

On the other hand, question 16 until 20 (Q16-20) was delivered to assess the awareness of green computing practices in the context of energy usage. Question 16 shows that 50 respondents (54.35%) did not use a computer and its gadget in a long duration. The findings for question Q17 show that 67 respondents (72.83%) stated that they did not use the computer for more than 5 hours. In response to Q18, most respondents (83.7%) will switch off the computer once they complete their work. Based on these three questions, respondents are considered to have good practices in reducing energy consumption [4]. In contrast, 61 respondents (66.3%) use screensaver and 64 respondents (69.57%) agreed that screensaver could save energy. Findings related to the use of screensavers show that respondents did not aware that screensavers do not save energy [27].

V. DISCUSSIONS, CONCLUSIONS AND FUTURE RESEARCH

The current study found that secondary school students feel concerned about the environment. However, they did not grasp the concept of green computing includes the meaning of the term 'green computing' itself. Although they know that the emission of carbon dioxide can increase in global temperature but they did not know that the computer and their gadgets are part of it. Most of them did not have experience in disposing of the old computer hardware. In general, therefore, it seems that they did not know that computers and their gadgets could be harmful to the environment. This result may be explained by the fact that they are not being exposed to e-waste management.

Nonetheless, they are prone to refill printer cartridge rather than buy a new one; this shows that, they were indirectly practising green computing although they have less understanding of it. Besides, they also printed less than 20 papers per day as this also helps in practising green computing. However, they also believe that by using a screensaver on a computer can reduce energy consumption. These findings suggest that they did not aware that screensavers do not save energy as their knowledge of green computing is low. Therefore, at this point, all the essential stakeholders in Malaysia include parents, teachers, governments and non-profit organisations must play a role to raise awareness of green computing among the younger generations, primarily through formal and informal education.

Several recommendations could be considered in educating and promoting green computing awareness to secondary school students. These followed recommendations are adapted from [6, 10]:

1) The government could establish a green computing master plan for secondary school students. This includes introducing the concept of green computing and practices as well as the advantages of implementing green computing.

2) Provides information green computing to teachers and school staffs.

3) Promotes the idea of recycling computer hardware and IT gadgets and preparing a framework for disposal e-waste in safety ways.

4) Encourage schools to use sustainable energy such as solar, wind and hydro. This example of energy usage will promote students to be more aware of alternative energy besides too dependent on electricity and the ability to reduce energy.

5) Use websites and social media to promote green computing.

6) Encourage schools to purchase and use most "greenest" computers.

7) Encourage and recognize programs for green computing. For example, video competition, posters, slogan or Green-day programs that might bring awareness to secondary school students.

In conclusion, this study gives a brief view of the current state of secondary school students' awareness of green computing. The study reveals that secondary school students'

have an average level of awareness of green computing. Therefore, secondary school students, especially the younger generations, should be informed about the concept of green computing, the practices, and benefits of green computing. Since this study involves a small number of respondents, future research should consider a broader range of respondents to develop an awareness amongst individuals and the community.

ACKNOWLEDGMENT

This research was partially supported by Universiti Putra Malaysia (Research Grant: GP-IPM/2018/9644900).

REFERENCES

- [1] G. Bekaroo, Sungkur, R., Ramsamy, P., Okolo, A. & Moedeen, W., "Enhancing awareness on green consumption of electronic devices: The application of Augmented Reality.," *Sustainable Energy Technologies and Assessments*, vol. 30, issue, pp. 279-291, 2018.
- [2] E.F. Amankwaa, K.A. Adovor Tsikudo, and J.A. Bowman, "'Away' is a place: The impact of electronic waste recycling on blood lead levels in Ghana," *Science of The Total Environment*, vol. 601-602, issue, pp. 1566-1574, 2017.
- [3] B. Debnath, R. Roychoudhuri, and S.K. Ghosh, "E-Waste Management – A Potential Route to Green Computing," *Procedia Environmental Sciences*, vol. 35, issue, pp. 669-675, 2016.
- [4] N. Din, S. Haron, and H. Ahmad, "The Level of Awareness on the Green ICT Concept and Self Directed Learning among Malaysian Facebook Users," In *ASEAN Conference on Environment-Behavior Studies* pp., 2013.
- [5] T.B.T. Ahmad and M.S. Nordin, "University Students' Subjective Knowledge of Green Computing and Pro-Environmental Behavior," *International Education Studies*, vol. 7, issue 2, pp. 64-74, 2014.
- [6] V. Bansal and M.T.M. Khan, "Green computing: A study of perception, approach, and acceptance among faculty members and students of Galgotias University, Greater Noida.," *International Journal of Information Dissemination and Technology*, vol. 9, issue 3, pp. 107-111, 2019.
- [7] N. Samuri, "Making Green IT "Alive" at TVET Institution of Malaysia," In *Proceedings of the Second International Conference on Green Computing, Technology and Innovation (ICGCTI2014)* pp., 2014.
- [8] M. Patel, "Green ICT: A Study of Awareness, Attitude and Adoption among IT/Computer Engineering Students of LDRP-ITR, Gandhinagar," In *11th International CALIBER*, pp., 2017.
- [9] M.V. Sreenandana, Ganesh.B.Nair, and A.S. Aneesh, "Green Computing: Technology as Green Enablers," in *Sustainability, transformation, development in business and management*, J.J. Manohar and S.C.B.S.A. Selvan, Editors. 2020, The American College: Madurai, Tamilnadu, India. p. 206-212.
- [10] S. Wibowo, N.Q. Nada, M. Novita, and S. Budirahardjo, "Exploratory Research on Green Information Technology Knowledge," In *The 1st International Conference on Computer, Science, Engineering and Technology*, pp., 2018.
- [11] H. Sukarman, N.K.S. Putri, and C.H.G. Qing, "Green Information Technology Government Regulation Components: Improving Indonesia Green Information Technology," *Journal of Theoretical and Applied Information Technology*, vol. 97, issue 16, pp. 4467-4477, 2019.
- [12] A.L. Kadiyono, D. Harding, H. Hafiar, Y. Nugraha, T.N. Ma'mun, A.G.P. Siswadi, and H. Wibowo, "The introduction of green technology in increasing green ethos among students," In *The introduction of green technology in increasing green ethos among students*, pp. 1-6, 2019.
- [13] T.B.T. Ahmad, M.S. Nordin, and A. Bello, "The stae of green computing knowledge among students in Malaysian public university," *Journal of Asian Scientific Research*, vol. 3, issue 8, pp. 831-842, 2013.
- [14] J. Houghton, *ICT and the environment in developing countries: a review of opportunities and developments. , What kind of information society? Governance, virtuality, surveillance, sustainability, resilience*. HCC 2010, CIP 2010. IFIP Advances in Information and Communication Technology, ed. H.M. Berleur J, Hilty LM (eds). Vol. 328, Berlin, Heidelberg: Springer, 2010.
- [15] F.N. Khan, A. Sana, and U. Arif, "Information and communication technology (ICT) and environmental sustainability: a panel data analysis," *Environmental Science and Pollution Research*, vol. issue, 2020.
- [16] M. Salahuddin, K. Alam and Ozturk, I. The effects of Internet usage and economic growth on CO2 emissions in OECD countries: A panel investigation. *Renewable and Sustainable Energy Reviews*, 62(C), 1226-1235, 2016.
- [17] I. Røpke and T.H. Christensen, "Energy impacts of ICT – Insights from an everyday life perspective," *Telematics and Informatics*, vol. 29, issue 4, pp. 348-361, 2012.
- [18] K. Danish, "Effects of information and communication technology and real income on CO2 emissions: The experience of countries along Belt and Road", *Telematics and Informatics*, 45, 101300, 2019.
- [19] N.V. Veenaa Deeve, C. Vijesh Joe, and K. Narmatha, "Study on Benefits of Green Computing," *International Journal of Current Research*, vol. 7, issue 4, pp. 14442-14445, 2015.
- [20] A. Lestari Kadiyono, D. Harding, H. Hafiar, Y. Nugraha, T. Nurhayati Ma'Mun, A. Gimmy Prathama Siswadi and H. Wibowo, "The introduction of green technology in increasing green ethos among students," Paper presented at the *Journal of Physics: Conference Series*, 2019.
- [21] A. Abugabah and A. Abubaker, "Green computing: Awareness and practices", Paper presented at the *2018 4th International Conference on Computer and Technology Applications, ICCTA*, 2018.
- [22] S. Singh and S. Gond, "Green computing and its impact Nature-Inspired Computing: Concepts, Methodologies, Tools, and Applications", Vol. 3-3, pp. 1628-1642, 2016.
- [23] I. Semakula and S. Samsuri, "Green computing knowledge among students in a Ugandan University", Paper presented at the *Proceedings - 6th International Conference on Information and Communication Technology for the Muslim World, ICT4M 2016*, 2017.
- [24] Ministry of Education Malaysia, "Bilangan Murid Sekolah Menengah KPM 2019," 2019.
- [25] W.A.S.W. Yunus, M.K.A. Kamarudin, A.S.M. Saudi, R. Umar, S.N.A.M. Bati, N.A. Wahab, and M.K.M. Saad, "Environmentalism among Primary's Students Based on Awareness, Knowledge, and Attitude Study," *International Journal of Academic Research Business and Social Sciences*, vol. 9, issue 12, pp. 1-11, 2019.
- [26] T.A. Shittu, A.I. Gambari, and A.O. Thomas, "Survey of Education, Engineering, and Information Technology Students' Knowledge of Green Computing in Nigerian University," *Journal of Education and Learning*, vol. 10, issue 1, pp. 70-77, 2016.
- [27] S. Agarwal, S. Chakrabarty, A. Bhaumik, and A. Nath, "Trends and Awareness in Green Computing Initiatives: a Comprehensive Study," *International Journal of Advance Research in Computer Science and Management Studies*, vol. 3, issue 4, pp. 1-10, 2015.
- [28] A.K. Awasthi, M. Wang, M.K. Awasthi, Z. Wang, and J. Li, "Environmental pollution and human body burden from improper recycling of e-waste in China: A short-review," *Environmental Pollution*, vol. 243, issue, pp. 1310-1316, 2018.

Recognizing Activities of Daily Living using 1D Convolutional Neural Networks for Efficient Smart Homes

Sumaya Alghamdi¹, Etimad Fadel², Nahid Alowidi³
Faculty of Computing and Information Technology
King Abdulaziz University, Jeddah, KSA

Abstract—Human activity recognition is considered a challenging task in sensor-based monitoring systems. In ambient intelligent environments, such as smart homes, collecting data from ambient sensors is useful for recognizing activities of daily living, which can then be used to provide assistance to inhabitants. Activities of daily living are composed of complex multivariable time series data that has high dimensionality, is huge in size, and is updated constantly. Thus, developing methods for analyzing time series data to extract meaningful features and specific characteristics would help solve the problem of human activity recognition. Based on the noticeable success of deep learning in the field of time series classification, we developed a model called a deep one-dimensional convolutional neural network (Deep 1d-CNN) for recognizing activities of daily living in smart homes. Our model contains several one-dimensional convolution layers coupled with max-pooling technique to learn the internal representation of time series data and automatically generate very deep features for recognizing different activity types. For the performance evaluation, we tested our deep model on the new real-life dataset, ContextAct@A4H, and the results showed that our model achieved a high F1 score (0.90). We also extended our study to show the potential energy saving in smart homes through recognizing activities of daily living. We built a recommendation system based on the activities recognized by our deep model to detect the devices that are wasting energy, and recommend the user to execute energy optimization actions. The experiment indicated that recognizing activities of daily living can result in energy savings of around 50%.

Keywords—Deep learning; one-dimensional convolutional neural networks; time-series classification; Activities of Daily Living (ADLs); smart home; recommendation system

I. INTRODUCTION

In recent decades, internet of things (IoT) applications have been increasing in popularity, and one well-known application is smart homes. These environments relied using sensors to generate large amounts of time series data, which can be analyzed for many purposes, such as monitoring and detecting activities in order to make timely decisions [1]. Recognizing human activities in an automated manner has become essential in many ambient intelligence applications, and a smart home with artificial intelligence (AI) is a great opportunity towards it [2]. Human activity recognition (HAR) in smart homes can be categorized into sensor-based activity recognition and vision-based activity recognition. Sensor-based activity recognition

can be done using two kinds of sensors: wearable sensors, which are placed on a human body to capture frequent motions, such as walking and standing, and ambient sensors, which are used to recognize activities of daily living (ADLs), such as watching television, and cooking. The main difference between these two kinds of sensors is that sensor-based ambient systems have the ability to recognize different behaviors and complex activities by monitoring the interaction between objects and inhabitants in smart homes, while wearable sensors can only capture human physical movements [3]. Recently, increased attention has been given to deep learning in several fields, including speech recognition [4] and image classification [5]. In HAR, deep learning can have a great impact in terms of system performance and flexibility. Deep learning methods can provide efficient tools for high-level feature extraction from multivariable time series data, which is beneficial for many tasks, such as classification. Furthermore, deep learning models have demonstrated significant potential to outperform the state of the art in HAR. They decrease the need for extracting features manually which is usually a time-consuming task and can be error-prone or (at least) a poorly generalizable endeavor. In general, deep learning involves neural networks comprised of several layers that process non-linear information organized hierarchically, where the output of each layer is the input for the next one. Well-known deep learning architectures for time series classification include one-dimensional convolutional neural networks (1d-CNNs) [6] and recurrent neural networks (RNNs) [7]. Since the multivariable time series data of ADLs is high-dimensional data with significant variation, applying feature selection methods on the data before feeding it into a deep learning network would help reduce the complexity of activity recognition and increase the performance of such a system. Indeed, feature selection is a substantial step when dealing with multivariable time series data, allowing for the elimination of variables that are not useful or irrelevant for the model description [8]. In addition, deep learning models (i.e., 1d-CNNs) have been shown to be capable for classifying time series data by automatically capturing local dependencies and preserving feature scale invariance to catch variation in the same class throughout the feature extraction [9]. Thus, combining a feature selection technique with 1d-CNN will result in highly accurate system for recognizing ADLs, which can be then used as a basis for decision making processes, such as those related to energy saving decisions. In fact, recognizing ADLs can increase the energy saving potential of a smart home by using sensory

readings to detect the appliances that are wasting energy and recommend the user to perform energy optimization actions based on the current performed activity [10]. Therefore, daily activity recognition and a learning process in smart homes are necessary and important.

In this work, we take advantage of a feature selection method combined with 1d-CNN to accurately perform activity recognition since, in general, CNNs are good at reducing frequency variations and capturing local dependency. Once our system detects the current performed activity, energy saving recommendations are generated to inform the user of any energy optimization actions. We explored our framework, including the deep model and the recommendation system, on a new large dataset entitled ContextAct@A4H [11] to determine the capacity for activity recognition and study the energy saving potential of recognizing ADLs.

II. RELATED WORK

In this section, we discuss recent research applying deep learning networks to recognize ADLs in ambient-based environments (i.e., smart homes). Then, we review some studies that built model-based activity recognition to increase the energy saving potential in smart homes.

A. Activity Recognition using Deep Learning-based Approaches

In the HAR field, the use of sensors is extremely diverse. As a matter of fact, activity recognition is used in wearable devices to recognize human body movements, such as walking and running, and in ambient sensors to recognize complex daily activities such as taking shower [3]. Among the various activity recognition fields, we are focused on recent studies of daily activity recognition-based ambient intelligent systems, specifically, smart homes. This process can be done by applying ML approaches, which can effectively classify ADLs performed by people. Traditional ML-based approaches are popular in this field, and most of them are supervised learning approaches. Although classical techniques, such as SVM, are simple to use, they require manual feature extraction from the data, which is time consuming and heavily dependent on human knowledge of the domain [12]. Recently, there has been a shift in the use of deep learning techniques in activity recognition to outdo the ML traditional methods by overcoming the need for feature engineering. Many researchers have demonstrated the significant potential of deep learning methods to push the state of the art in HAR. The most frequently used deep learning methods for recognizing ADLs are 1d-CNN, Vanilla RNN, long short-term memory (LSTM), and gated recurrent unit (GRU) [13]. These deep learning methods are summarized in Table I.

In general, the input of the neural network is original raw data, and extracting features from this data tends to maximize the overall performance. Extracting deep information from time series data requires expert knowledge; however, CNNs have been proposed to handle this problem. Therefore, CNNs are one of the most used deep learning approaches in the HAR field not only for extracting features from data but also for activity classification [14]. In ambient-based environments, CNNs have been proposed to extract features from time series

data optioned from ambient sensors for daily activity classification. We introduce these works below.

Recently, [15] exploited CNN to perform activity recognition in smart homes. Specifically, the classification of ADLs, such as cooking and sleeping, were performed using a temporal 1d-CNN model. The proposed deep learning approach contained the input layer, the multiple one-dimensional convolution layers, the fully connected layer, and the softmax classifier. They used 128 filters for each convolution layer with different 1d kernel size. The researchers trained the model with a one-day-left strategy. For the evaluation, they tested their model on the publicly available dataset (Kasteren) and they compared the obtained results with other probabilistic methods, such as naive Bayes (NB) and conditional random fields (CRFs). Their results stated that the 1d-CNN model showed significant improvement in performance in terms of accuracy compared to other classifiers.

A comparison was conducted in [16] to evaluate state of the art ML techniques and the deep learning models for the classification of ADLs in smart homes, including CNNs, LSTM, SVM, and the hidden Markov model (HMM). They used a synthetic dataset for real-life activities and a real-world dataset, which is known as ARAS, to evaluate and compare the performance of the traditional ML techniques and the deep learning models. The performance metrics used for the evaluation were precision, f1 score, and recall metrics. The results of the comparison indicated that the CNN model had the best performance compared to the other evaluated techniques across both datasets in term of F1 score. Since the ADL data consists of sequences recorded by sensors, models based on RNNs have been widely proposed to solve the complexity of sequence lapping problems in daily activity recognition.

A model based RNN was proposed by [17] to learn how to classify daily activities without any prior knowledge. They applied LSTM and evaluated its performance on a publicly available and annotated dataset (Kasteren). For the evaluation, they left one day out of the training and used that data for the testing phase. They compared the performance of their LSTM model and the following common classifiers: NB, HMM, Hidden Semi-Markov model (HSMM). The proposed LSTM model showed a 40% improvement in accuracy compared to the other classifiers.

More recently, paper [18] used vanilla RNN in a learning approach for HAR since human activities generate sequences that contain time-dependent sensor records. Before the training the RNN model phase, they applied dynamic windowing approach in which each window contains the best fitting sensor set for each activity; the obtained windows are then feed the RNN classification model. The proposed RNN model had eight neurons and was trained using a back-propagation algorithm. Their proposed RNN model was testing using 10-fold cross validation. To evaluate their approach, they used three popular datasets for daily activities: Towor, Aruba, and HBMS. The results showed a high overall classification performance for their proposed model based on different evaluation metrics and compared with common classification models, such as SVM and K-Nearest Neighbor (KNN).

TABLE I. THE DEEP LEARNING APPROACHES MOST FREQUENTLY USED FOR RECOGNIZING ADLS

Disadvantage	Advantage	Description	Methods
1d-CNN	It is a multilayer neural network that combines convolution, activation, and pooling layers.	It automatically extracts very deep and discriminative features from sequences of sensory data.	It requires a big dataset and a high number of hyper-parameter tuning to achieve optimal good performance in activity recognition.
Vanilla RNN	It is the classical version of RNN, and it has a temporal layer used to capture sequential information.	It performs well at modelling sequence data and learning changes over time.	It is not good at capturing long-term dependencies on sequences due to the vanishing gradient problem.
LSTM	It is a modern version of RNN that has a memory block (cell state) with many gates to overcome the vanishing gradient problem.	It can capture long temporal dependencies to enable modelling of complex activity details.	LSTMs require too many parameters to be updated during the training time.
GRU	It is an RNN-based model with fewer gates to detect and recognize time complex events.	Same as LSTM except it has fewer parameters and is easy to train.	It only shows good performance on small data.

Meanwhile, [19] studied the problem of activity recognition and abnormal behavior detection among older people with dementia. They investigated three RNN models: LSTM, Vanilla RNN, and GRU. They considered activity recognition to be a sequence labeling problem, making it appropriate for RNNs. To assess RNNs in the activity detection, they followed many steps. First, they segmented the raw dataset into windows by applying the sliding window approach. Then, they fed those instances and their corresponding labels into the RNN-based models to train them to recognize daily activities. To fulfill their purpose, they used a popular dataset gathered by Van Kasteren from three houses to train their models. They divided the dataset into training and testing sets, applying the leave one day out cross-validation approach. To provide an adequate discussion of the performance of the RNN-based models (LSTM, Vanilla RNN, and GRU), they compared them against state-of-the-art classifiers, including SVM, HMM, SHMM, and CRF. Their results showed that the RNNs were very competitive with CRF and much better than the other traditional ML methods.

B. Energy Efficient Smart Home-based Activity Recognition System

In the past decade, researchers have integrated ADLS into the energy management domain in order to increase the energy efficiency of smart homes. Recognizing ADLS could be an excellent way to obtain insights into occupant behavior, which are required for detecting potential energy savings at the smart home [20].

In general, there are two kinds of energy saving systems: the active variant, which directly controls the devices in the smart home, and the passive variant, which is used to increase the awareness of the resident by notify them about the possible energy saving actions [21]. Through the literature, both systems have been integrated in many studies with the process of recognizing ADLS to enhance the potential energy saving in the smart home; we review these works below.

To begin with, paper [10] designed a method called Activity-Appliance-Energy Consumption (AAEC) for energy saving in smart homes based on the relationship between electrical appliances and user activities. In this method, user activity was recognized by analyzing the information gathered from sensors about appliances and how the user interacted with them. The process of activity recognition was performed using two ML techniques: Random Tree (RT) and Logistic

Regression (LR). After detecting the activity, a ranking algorithm was utilized to find a relationship between each activity and the home appliances. Decision Tree (DR) algorithm was then used to define how important each specific appliance is for an activity. Finally, based on the relationship and the importance level between the current performed activity and the appliances, the system sent recommendations to the user whenever it detects a waste of energy. To validate their proposed method, the authors used data obtained from an MIT project. The result showed an average energy savings of about 35%, which was accomplished by applying the AACE method in the smart environment.

Based on the idea that most ADLS at home are related to a number of electrical appliances, researchers in [21] developed a framework called SMARTENERGY.KOM, which aims to achieve energy efficiency in buildings based on recognizing ADLS. For activity recognition, the authors showed how it was possible to recognize user activity by monitoring the energy consumption of appliances to detect which ones were running. To make their activity detections more accurate, they monitored additional information, such as temperature, brightness, and motion in the smart home. The activity recognition performed using random forest classifier. For energy saving, they designed the EnergyAdvisor, which was responsible for directly generating energy saving recommendations once it detected any appliances that were turned on but were not related to the user's current performed activity. The relationship between the activities and the appliances was defined by setting a set of static rules. Using the data they gathered, the authors demonstrated that, by combining power sensors with information obtained from an environment sensor, their system was capable of detecting activity with high level of accuracy and significantly able to save energy.

One work conducted by [22] proposed an activity-aware smart automation system called CASAS activity aware resource learning (CARL). The aim of CARL is to automate a smart building by turning off appliances that are not needed for the current performed activity or any activities that are anticipated to occur within the subsequent 10 minutes. The hypothesis of this work was smart buildings with energy-efficient building automation based activity recognition could realize energy savings while still meeting the needs of the individuals who live there. In their building automation approach, activity learning played two roles. First, activity recognition was applied to identify activities as they were

performed in a smart building environment using SVM. Second, activity prediction was used to predict whether a particular activity would happen within a specific upcoming period of time. Together, these roles provided a basis for building automation that supported the current and upcoming tasks of the residents in the building. CARL's goal was to turn off many devices without interfering with resident tasks. Performance can thus be evaluated in terms of the number of times a device is turned off (to measure energy consumption) and the number of times a user double tapped a switch in order to provide feedback to the system while turning the device back on (to evaluate the accuracy of the event generated). The experiments were run on a smart apartment named Navan, a single-resident apartment with a floor plan equipped with 118 sensors. Using CARAL resulted in reducing device utilization by 56% and an energy savings of up to 50%.

An algorithm based on HMM was proposed by [23] to recognize the activity states of smart home inhabitants and then control the operation of their appliances accordingly. The researchers designed a smart home energy management system (SHEMS), which was based on deploying motion sensors to collect information and actuators to control the appliances in the home. The SHEMS was able to recognize three state of activities: active, sleep, and away. In the active state, the user was at home, and he performed some tasks. In the sleep state, the user was at home but not active, and the away state detected when the user was not at home. Based on the recognized state, the appliances were controlled according to a pre-defined schedule. Each state was identified by monitoring the motion inside the home and the logical status of the main door. HMM was used to estimate the portability for each state to determine which one was occurring. Based on two scenarios, the system was evaluated successfully. The results indicated that the SHEMS could lead to an energy savings of about 18%.

Recently, a work done in [24] aims to recognize daily life activities performed by inhabitants in a smart home in order to save more energy by guaranteeing that the peak demands won't exceed a pre-defined threshold. Their proposed system was able to convert sensory data into meaningful event using a lossy compression algorithm based on minimum description length. Then, from the event sequence, patterns representing activities were extracted and clustered to train a HMM to automatically recognizing activities. Moreover, for each activity, there was a typical consumption model associated with each one identified from the involved appliances. Based on the current detected activity, the system could guarantee that energy consumption won't exceed a predefine threshold to prevent the arising of unwanted peak. Their approach based on delaying the activation of some appliances which were not directly required in the current activity till the demand of energy getting below the giving threshold. Their experiment was performed on three public datasets for ADLs and the results demonstrated that their approach was able to save energy of about 30.

Based on the aforementioned works, we can see that it is possible to design a system that can suggest actions in smart homes based on recognizing ADLs, lowering energy usage without decreasing the comfort levels of the inhabitants. Our work aimed to design deep networks that automatically

recognize daily activities in an ambient-based environment. Model-based RNNs have been widely applied for time series classification. However, those models are hard to train and require a large memory and a long time to update their parameters in each cell state. Moreover, RNN-based models are usually good at predicting what comes next in a sequence, while CNNs can learn to classify a sequence. Thus, building a 1d-CNN to classify time series data for detecting ADLs in ambient-based environment seems to be more logical than building an RNN based model. CNNs can effectively extract very deep features that represent each activity and can be trained faster than RNN-based models with the same or even better results, as shown by [16]. Using the CNN-based model to classify time series data for activity recognition will lead to significant improvements in performance, increase accuracy of the system and provide better results. Moreover, developing a recommendation system that informs inhabitants about potential energy saving actions through ADLs will make their home more efficient, as well as positively will influence their behaviors and make them more aware toward the energy.

III. OVERALL DESIGN

A. Overview

Before analyzing our data, data preprocessing steps were applied. First, data cleaning was implemented, followed by data normalization and splitting (see section 4, subsection B for more detail). Then, a feature selection method was applied to identify the related features from the dataset and remove the less important features (see Section 4, subsection C for more details). After that, a segmentation-based approach was used to obtain sequences from the ambient sensor data in order to feed the input of our deep model. The time series segmentation method we applied was a fixed-sized overlapping sliding window that divided the data into multiple sequences of discrete segments that shared the same length and were assigned to different labels (see Section 4, subsection D for more details). After making the data suitable for analysis, a deep learning model (Deep 1d-CNN) was proposed to classify the time series data for recognizing ADLs. Then, the output of Deep 1d-CNN fed the recommendation system, which was responsible for generating energy saving recommendations to the user. These recommendations were generated when the system detected a waste of energy based on the current performed activity using predefined rules based on the relationships between the activity and the selected energy sensors.

The two main objectives of our work, which were unified in one framework, were: 1) to provide a high level of accuracy in recognizing ADLs by utilizing a deep learning approach and 2) to save energy without decreasing the comfort level of the smart home inhabitant by sending recommendations about the possible energy saving actions based on the current performed activity. The overview of our framework is presented in Fig. 1.

B. Deep 1d-CNN

In this section, we explain in details the architecture of our proposed deep model which represents the third phase in Fig. 1.

Current common algorithms mainly use CNNs for feature extraction and classification; yet, these methods are most common in dealing with image processing. In this work, we propose a deep learning method-based CNN for daily activity recognition, which is able to handle input sequences of time series data obtained from ambient intelligent environments.

Suppose the i^{th} input time series is:

$$C_i = [c_i^{(1)} \cdot c_i^{(2)} \dots \dots c_i^{(t)} \dots \dots c_i^l]. C_i \in \mathbb{R}^d \quad (1)$$

where l is the length of the sequence, $c_i^{(t)}$ denotes the value of time step t , and d represents the input dimension (i.e., the number of input variables).

The main component of the proposed model is the one-dimensional convolutional (1dCnov) layers. Their purpose is to automatically extract deep features from the multivariable time series input. We built our model by stacking multiple convolutional layers composed of convolution operation, activation function, max-pooling, dropout and batch normalization layers. At first, the convolution operations are applied on the sequence input to obtain the feature mapping, as formalized in the equation:

$$f^j = \sigma(b^i + \sum_i k^{ij} * x^i) \quad (2)$$

Then, the ReLU activation function is employed to insure the non-linear behavior of the network. Max-pooling layers are then used to subsample the extracted feature mapping, which

helps eliminate non-maximal values and extract the local dependency characteristics within different regions in the input sequences. After the max-pooling layer, we apply dropout which is a regularization method proposed in [25]. It is mainly used to solve the overfitting problem by randomly selecting a set of activations to be zero at training time. After the dropout, a batch normalization (BN) [26] layer is then added to accelerate the training process and improve the efficiency of our model. All the extracted features from the previous layers are then flattened into a vector to feed the input of the softmax layer (a dense layer with a softmax activation function) in order to generate the classification results. By stacking several convolution operators with the max-pooling technique, the proposed model has the ability to extract the deep features from the input sequence to create a hierarchy of abstracted features that are more robust to noise in order to successfully classify each activity. Both batch normalization and dropout are applied to each convolutional layer to improve the overall performance. Our proposed model is defined according to the network structure presented in Fig. 2.

C. Recommendation System

In this work, we follow the passive system, which seems to be non-intrusive and more satisfying for the user. The main functionality of our system is to promote the saving of energy in smart homes by generating energy saving recommendations based on the user's current performed activity.

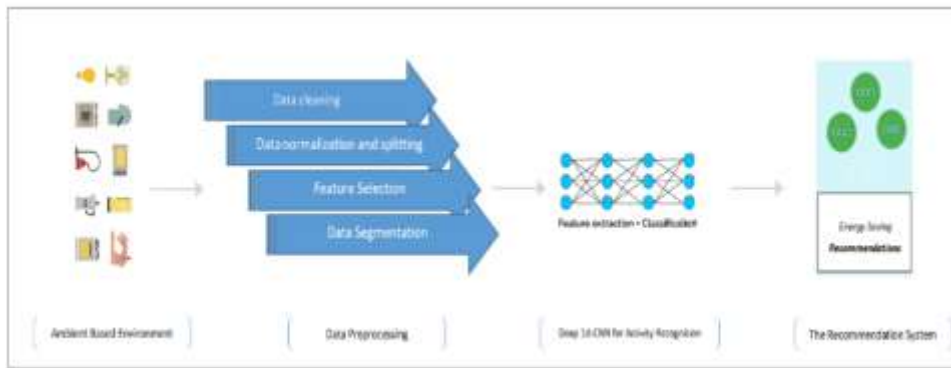


Fig. 1. Overview of our Proposed Framework.

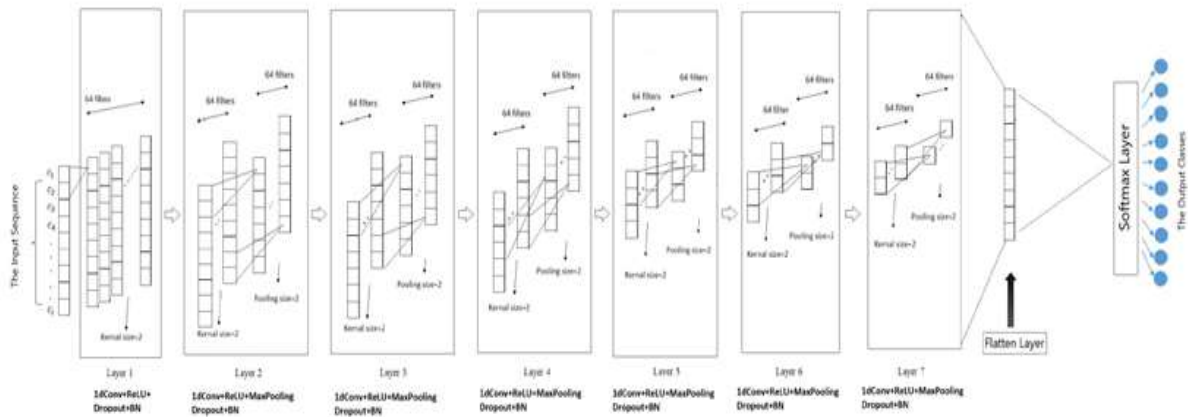


Fig. 2. The Architecture of Deep 1d-CNN for Recognizing ADLs.

At first, we designed our recommendation system to be a rule-based recommendation system. The initial strategy of our recommendation system was to recommend that the user turn off devices that are not needed in support of the current performed activity. We realized this functionality by finding the relationship between each energy-related sensor and the activities and then defining rules to perform a check for conditions in order to generate the energy saving recommendations. The goal of our system is to identify all of the energy sensors that are being used in the current performed activity. Then, for each one, the system must check whether the relationship between that sensor and the current performed activity is exciting or not. If not, energy saving recommendations will be generated to inform the user that this device, which is not needed for the current performed activity, is wasting energy.

IV. IMPLEMENTATION

In this section, we first introduce the dataset we used in our work and the preprocessing steps we implemented to make it suitable for further analyses. Then, we present the implementation details of our deep learning model for classifying time series data to detect ADLs in an ambient environment. Finally, we describe how we implemented our recommendation system for promoting energy saving in smart homes through recognizing ADLs.

A. ContextAct@A4H Dataset

We evaluated our Deep 1d-CNN model on the new real-world dataset, ContextAct@A4H [11]. It contains a large number of sensors that capture many properties related to each activity, measuring not only object interactions but also context features to improve the potential for recognizing ADLs. Although this dataset had been collected for activity recognition purposes, the dataset features many energy-related variables so it can be useful for studying energy saving solutions in smart homes (which is one of our objectives). ContextAct@A4H is a publicly available rich dataset collected using ambient sensors that reflect the context of the environment, as well as annotated ADLs. It is a real-life dataset that was gathered at the Amiquil4Home apartment using 219 of sensors to improve the potential for using the data. Ambient sensors were used to allow the observation of object usage and context conditions in all rooms and the exterior. The following context variables were measured in each room: temperature, carbon dioxide (CO₂) level, noise, humidity, presence, and music information. Weather information was measured for the exterior. Appliance and object usage were measured through electric/water consumption sensors, contact sensors, and state change sensors. Other sensors obtained indirect measures of object usage (e.g., the pressure sensor in the bed). The dataset consisted of one week of captured data during the summer and three weeks in the fall. It contained 10 daily activities, which were annotated by self-reporting in place at the moment of starting and ending each activity. The activities, and their annotated names are listed in Table II.

In Fig. 3, we present an example of activity Travail (working) annotated at the time when it started and the time when it ended along with the information corresponding to the sensor events during this activity.

TABLE II. CONTEXTACT@A4H DATASET

Activity	Annotated as ...	Labelled as ...
Working	Travail	0
Cooking	Cuisine	1
Relaxing	Loisir	2
Using the Toilet	Toilettes	3
Watching TV	TV	4
Washing Dishes	Vaisselle	5
Leaving Home	Sortir	6
Taking a Shower	Douche	7
Eating	Manger	8
Sleeping	Dormir	9

```
"2016-07-30 10:18:28";"current_activity";"Travail_Start"  
"2016-07-30 10:18:29";"Presence_Bureau";"OFF"  
"2016-07-30 10:18:29";"Noise_bureau";"10.73"  
"2016-07-30 10:18:29";"Energie_Totale_Lave_Linge";"424"  
"2016-07-30 10:18:29";"Energie_Partielle_Lave_Linge";"424"  
"2016-07-30 10:18:32";"Status_TGBT";"1"  
"2016-07-30 10:18:32";"I1";"1.29945278"  
"2016-07-30 10:18:32";"PF";"1.36521101"  
"2016-07-30 10:18:32";"VIN";"235.597702"  
"2016-07-30 10:18:32";"P_active";"0.194339529"  
"2016-07-30 10:18:32";"Gaz_Logement";"83363"  
"2016-07-30 10:18:32";"E_active";"1530.326"  
"2016-07-30 10:18:32";"Freq_totale";"49.9864655"  
"2016-07-30 10:18:34";"Noise_bureau";"3.3506"  
"2016-07-30 10:18:35";"Luminosite_Cuisine";"477.76"  
"2016-07-30 10:18:35";"Noise_bureau";"7.74237"  
.  
.  
.  
.  
"2016-07-30 11:16:40";"Puissance_Lave_Vaisselle";"0.0"  
"2016-07-30 11:16:43";"Noise_bureau";"2.48645"  
"2016-07-30 11:16:45";"Noise_bureau";"11.2242"  
"2016-07-30 11:16:46";"Noise_bureau";"1.93088"  
"2016-07-30 11:16:49";"Noise_bureau";"3.94009"  
"2016-07-30 11:16:52";"current_activity";"Travail_End"
```

Fig. 3. An Example of Sensor Events Crossponding to Travail Activity in ContextAct@A4h Dataset.

B. Data Preprocessing

ContextAct@A4H captured about 389 features, those features are measured different type of properties using ambient sensors placed at the smart home. However, some of them are not useful for recognizing ADLs (i.e., music features). Thus, in the preprocessing phase, we removed these unwanted observations from the dataset. Moreover, we converted all needed contextual features to numerical information. For example, binary sensors, such as contact sensors, were given one of two values: open (if a door opened) or closed (if it did not). Hence, we converted the measured unit from contextual information to either 1 or 0. Meanwhile, we cleaned corrupted and repeated data, which could have been caused by hardware failures or problems in the data transfer. After the aforementioned actions were completed, the total number of records was equalled to 642,001.

As with any data pre-processing, we applied data normalization, which is the process of rescaling all feature values in a dataset into a given range. Specifically, we used a min-max scaler, which changed all the features to be between 0 and 1. After data normalization, we split the data randomly into 70% for training and 30% for testing. After making the dataset suitable for further analysis, we applied the feature selection method explained in the next subsection. After making the dataset suitable for further analysis, we applied the feature selection method explained in the next subsection. After making the dataset suitable for further analysis, we applied the feature selection method explained in the next subsection.

C. Feature Selection

In many practical applications of ML algorithms, data that has been pre-processed can result in a large number of features, and it is often necessary to minimize this number during the training phase to allow effective classification. Additionally, supervised learning models that train on data with many features might overfit the model. As we mentioned previously, the dataset contained about 389 features of sensor readings with values ranging from 0 to 1. Our purpose was to reduce the number of features and choose only those that would contribute the most to increase the overall performance of our classification model. Therefore, we applied a common feature selection technique in which we extracted a feature importance rank using different algorithms. Feature importance provides a measure that indicates the value of each feature in the construction of a model. The more an attribute is used to build a model, the greater its relative importance. In scikit-learn, decision tree models and ensembles of trees provide a `feature_importances_` attribute when fitted [27]. The `feature_importances_` attribute used to extract the relative importance of the features from the model. In this work, we compute the relative importance of each attribute in ContextAct@A4H using different algorithms such as Random Forest and AdaBoost since they are support `feature_importances_` attribute (see Fig. 4).

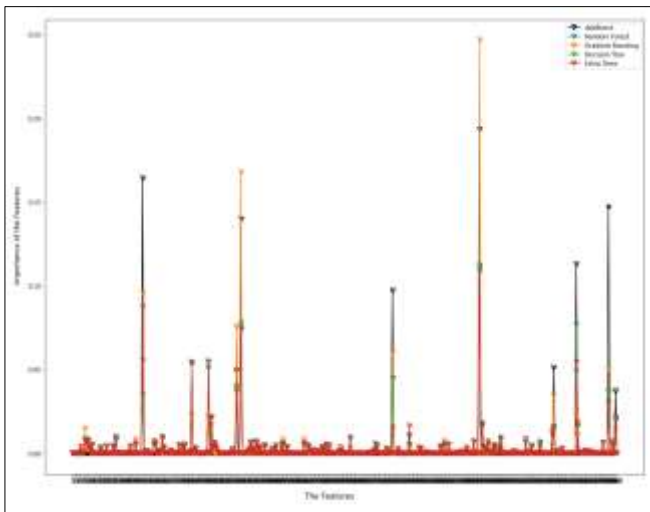


Fig. 4. Feature Importance of Entire Dataset.

After determining the importance of each feature in relation to the activities, we chose the ones with a rank higher than 0.003. Hence, we had a total of 48 features to use in our classification model. Those features are measured different type of properties using ambient sensors at the smart home.

D. Data Segmentation

In activity recognition, data segmentation takes place after the preprocessing step and the feature selection mechanism. For an online deep learning system to effectively classify a particular feature vector representation of the sensor data, the system must include a mechanism for selecting those sensor events from an incoming stream of sensor data. This process is known as segmentation and aims to select the sensor data that lies between activity boundaries. It identifies segments that contain information about the activities to be recognized. Many segmentation methods based on the windowing of streaming data have been used in studies on activity classification, such as time- and sensor-based windowing [28]. Time based windowing breaks the dataset into equal periods of time to segment the data. This approach is favorable when using streamed data where the sensors update continuously in time as in case of our dataset [29]. Thus, we applied time-based segmentation with fixed size and overlapping windows to take the values of the sensors observed in the previous segment. This is because it is generally assumed that, due to the higher number of data points, overlapping sliding windows increase the performance of HAR classifiers compared to non-overlapping ones [30]. In our work, the feature selection is used to reduce the number of features by selecting the most importance ones, while the segmentation step is performed to divided the temporal dimension of the streaming data into windows. All these windows are shared same number of steps, which are vary in time, but they are represented by the same features (which have been selected previously).

In the experiment, we evaluated the effect of varied window sizes and different overlapping sizes on the recognition results of the proposed system. We got the best results when we set the time period of the window to be 80 time steps with overlapping started after a five-step distance while each time step represented by the 48 features. This process yielded 89,971 and 38,398 samples for the training and testing sets, respectively. Each window usually contained time steps associated with different labels. We chose for majority labeling, where the label of each window was specified as the most frequent label in those of the timestamps.

E. Implementation of Deep 1d-CNN

We implemented our deep learning model with Google Colaboratory (also known as Colab), which is a cloud service based on Jupyter Notebook. We used Python runtimes pre-configured with essential libraries, such as TensorFlow and Keras, to build and train our neural networks. The model training and classification were run on an Nvidia Tesla K80 GPU with 2496 CUDA cores and 12 GB RAM. The neural networks were trained in a supervised way by back-propagating the gradients from the softmax layer through to the

convolutional layers. The categorical cross-entropy used was the loss function. For optimization, we used Adam [31] with a learning rate of 0.0001. The training was done on 89,971 samples, and the testing was done on 38,398 samples with a batch size equal to 1,024. To build the topology of Deep 1d-CNN, we performed many experimental studies to define the suitable hyper-parameters for our model. In the end, we decided to have 7 one dimensional convolutional layers, each with 64 kernels, a filter size of 2, and a ReLU activation function. A max-pooling of size two was included in all convolutional layers except in one layer because the temporal dimension of the feature map at the last layer became one; therefore, the max-pooling had to be avoided in any layer. To avoid overfitting, a dropout layer was used in each convolutional layers as a regularization mechanism with a rate equal to 0.2. we also implemented a batch-normalization layer to accelerate the training and improve the overall performance. At the end, all outputs from the previous layers were flattened into a one-dimensional vector, which was then connected to a softmax classifier to defined the output probabilities of the class labels. The hyper-parameters of our deep learning model for the ContextAct@A4H dataset are provided in Table III.

TABLE III. THE RELEVANT PARAMETERS OF EACH LAYER IN DEEP 1D-CNN

Num.	Components	Layer Parameters
Layer 1	1dConv	64*2
	Activation	ReLU
	Dropout	Rate=0.2
	Batch Normalization	-
Layer 2 to Layer 7	1dConv	64*2
	Activation	ReLU
	MaxPool	2
	Dropout	Rate=0.2
	Batch Normalization	-
Layer 8	Flatten Layer	-
Layer 9	Dence Layer	Softmax

F. Implementation of the Recommendation System

Based on the current performed activity predicted by the deep model, our system detected which devices were turned on but not needed for that activity. We realized this functionality by applying rules that checked whether the relation between the current performed activity and the devices that were turned ON existed in the predefined relationships. In another words, our recommendation system used the rules and the relationships to identify appliances that were wasting energy while a certain activity was being performed by the user. To implement this method, we followed several steps:

- First, we extracted the energy sensors from the dataset (all from type switch and electrical outlet). They gave two readings: 0 when the attached device was turned OFF and 1 when it was ON.
- Then, we determined where each device was located.

- After that, we identified the relationship between the sensors and the activities.
- Finally, we defined rules to perform a check for conditions.

Table IV provides examples of what we got after implementing these steps.

Consider the following example, if we assume that our Deep 1d-CNN model predicted the current performed activity is watching TV, the recommendation system would check the value of each energy sensor at the last time period of that activity. If the value of PC10 was ON, then the system would recommend the user to turn it OFF since there are no relationship between this sensor and the watching TV activity.

TABLE IV. IMPLEMENTATION OF THE RECOMMENDATION SYSTEM

Energy-related Sensor ID in the Dataset	Sensor Location	Relation to Activity
PC10 (Smart electrical outlet)	Bedroom	Sleeping
tv_salon_real_status (Switch)	Living Room	Watching TV, Relaxing, and Eating
Defined Rule	If the value of the energy sensor was not equal to 0 and the relationship between this sensor and the current performed activity was false, then a recommendation must send to the user to turn OFF the unattended device.	

V. PERFORMANCE EVALUATION AND DISCUSSION

The results of the performance of our model are presented in this section. We also investigated the performance of our model in case if we removed the max pooling layers in order to see its effectiveness in our network. In addition, to show the advantage of our proposed model, we compared our network with baseline results obtained from deep models. Finally, we show the results of the recommendation system in terms of how much energy savings could be gained through recognizing ADLs.

A. Performance Evaluation of Deep 1d-CNN

1) *Performance measurement:* Classification accuracy is not an appropriate measure of performance since activity datasets collected in natural scenes are often imbalanced between classes. In ContextAct@A4H, some classes (e.g., sleeping and leaving home) contain more number of examples while other classes have less. Therefore, we evaluated the models using other metrics that were suitable for evaluating class-imbalanced problems. Those metrics—precision, recall, and F1 score—have also been used in previous works such as in [16].

Precision determines the ratio of the relevant points chosen by the model to the total selected points, as shown in the following equation, where TP is the number of true positives, and FP is the number of false positives:

$$\text{precision} = \frac{\text{TP}}{\text{TP} + \text{FP}} \quad (3)$$

Recall is the ratio of relevant points selected by the model to the overall total of relevant points, as shown in the following equation, where TP is the number of true positives, and FN is the number of false negatives:

$$\text{recall} = \frac{\text{TP}}{\text{TP} + \text{FN}} \quad (4)$$

The F1 score is defined in terms of both precision and recall as follows:

$$F1 = 2 \times \frac{\text{precision} \times \text{recall}}{\text{precision} + \text{recall}} \quad (5)$$

2) *Experimental results:* The classification results of the proposed method on the ContextAct@A4H dataset are presented in this subsection. We calculated the previously described metrics, namely, precision, recall, and F1 score. We also plotted the accuracy and loss curves during the training and testing process for Deep 1d-CNN.

As shown in Table V, the precision, recall, and F1 score results indicate that applying 1d-CNNs for the time series classification was effective due to their ability to extract very informative deep features from each sequence input to detect the ADLs.

Meanwhile, according to Fig. 5, the training and testing loss of our model kept decreasing until the last epoch, in which both remained in the same range with a slight decrease in training loss. When we stopped the training process, the training loss equaled to 0.21 and validation loss was 0.28. Moreover, the testing accuracy improved until it reached 0.90, while the training accuracy was 0.92. Both then stayed in their same range with no further increases or decreases where we stopped the training process.

The two curves demonstrate that our model did not suffer from an overfitting problem due to add dropout layers in each convolutional layer, which provide regularization and, hence, prevent overfitting. To support our observation, we trained the model without the dropout layers to see how the training process would progress. We observed that the model without the dropout layers started overfitting the data from the beginning, and we had to stop the training at Epoch 30 where the loss function values for the training and testing data were 0.02 and 0.82, respectively. In addition, the gap between training and testing accuracy got bigger, which also indicates that the model overfitted the data. Finally, the results of training our model with BN provided a lower loss function value than the model without BN for both the training and testing data and also resulted in a higher model accuracy rate.

TABLE V. THE CLASSIFICATION RESULTS OF OUR PROPOSED MODEL

Results of Deep 1d-CNN	
Precision	0.91
Recall	0.89
F1 score	0.90
Time Per Epoch	4 sec

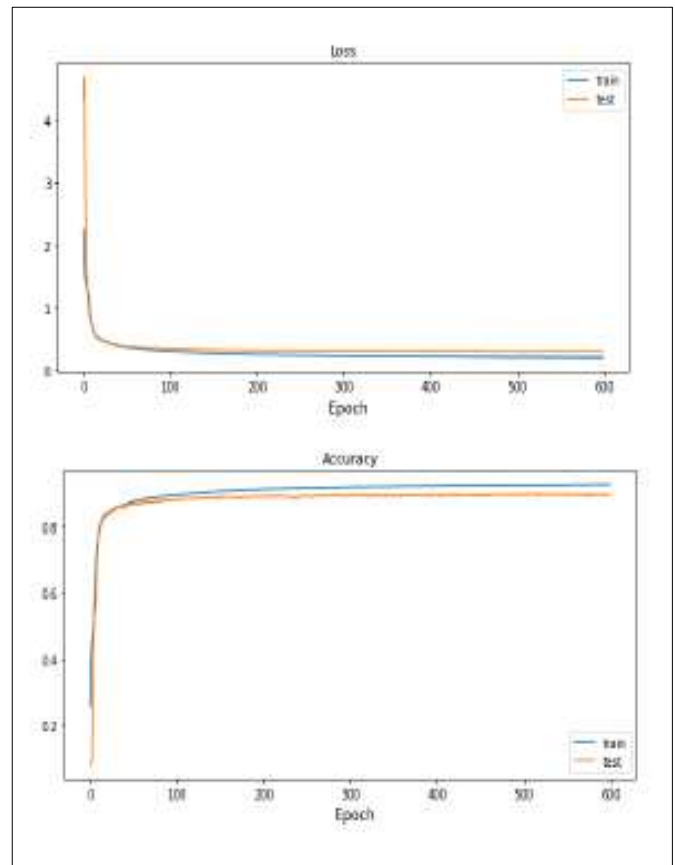


Fig. 5. The Loss and Accuracy Curves of Our Model.

3) *Comparative Results on Deep 1d-CNN with Other Proposed Deep Models:* In this section, we describe the results of our model obtained on the ContextAct@A4H dataset compared to other deep learning approaches proposed for recognizing ADLs using the aforementioned metrics. Since, as said previously, ContextAct@A4H is a newly collected dataset, it has been used in few studies for recognizing ADLs [32,33]. However, non-of them used it along with deep model to solve the complexity of activity recognition, thus, we could not compare our work with them. To overcome such limitation, we chose two deep models proposed in other works for recognizing ADLs and we implemented in our dataset, ContextAct@A4H, to illustrate the advantages of our model Deep 1d-CNN. These two models are 1D-CNN [15] and LSTM [17] and the result of the comparison is presented in Table VI. We train the 1D-CNN model with learning rate equal to 0.0001 while the LSTM model was train with learning rate equal to 0.00001. In both model, we had to stop the training from early epoch (30 epochs for 1D-CNN and for LSTM, we stopped it at epoch 10) since they both started to overfit the training data. In the LSTM model, there was no regularization method used to reduce the overfitting problem, while in the 1D-CNN model, they applied one dropout layer, however, it implemented after the fully connected layer not in the convolutional layers.

TABLE VI. PERFORMANCE COMPARISON OF DEEP 1D-CNN WITH OTHER DEEP MODELS

Model	Precision	Recall	F1
1D-CNN [15]	0.84	0.84	0.84
LSTM [17]	0.81	0.79	0.80
Deep 1d-CNN (Our Model)	0.91	0.89	0.90

B. Energy Savings through Recognizing ADLs

In this section, we evaluate the potential energy savings that could be achieved by our recommendation system in the smart home through recognizing ADLs. We followed an evaluation approach in which we calculated the amount of energy consumed over a period of time with and without the application of our system to find the total percentage of energy savings. As we have mentioned before, the dataset we used consisted of a sequential set of fixed length windows. In this evaluation, we were interested in calculating the energy consumed during each activity by utilizing the last time step of the window before and after applying the system. In this experiment, we followed the assumption that the user was performing one activity at a time.

First, we mathematically calculated the number of energy sensors that were on in the last time period for each predicted activity without applying the energy saving approach. Then, we estimated the total energy consumption per hour using the following equation:

$$totalEC = (TotalEnergyON * time) / 3600 \quad (6)$$

where *totalEC* is the amount of energy consumed before applying the energy saving approach, *TotalEnergyON* is the number of energy sensors that were ON before the energy saving recommendations, and *time* in our case, is the number of samples, since those samples were recorded sequentially over a period of time.

Second, we calculated the number of energy sensors that remained ON in the same time period after applying the energy saving recommendation. Then, we estimated the total energy consumption per hour using the following equation:

$$savingEC = (RemainingEnergyON * time) / 3600 \quad (7)$$

Where *savingEC* is the amount of energy consumed after applying our energy saving system, *RemainingEnergyON* is the number of energy sensors that are kept ON after the energy saving recommendations, and *time* is equal to the number of the samples. Once we determined the energy consumption with and without the energy saving system, we calculated the percentage of energy that have been saved by our system using the following equation:

$$TotalES = totalEC - savingEC / totalEC * 100 \quad (8)$$

Where *totalEC* is the total energy consumption without applying the energy saving system, and *totalEC* represents the amount of consumed energy after applying the system.

As seen in Fig. 6, a significant proportion of energy could be saved by utilizing the recognition of ADLs for an energy saving purpose.

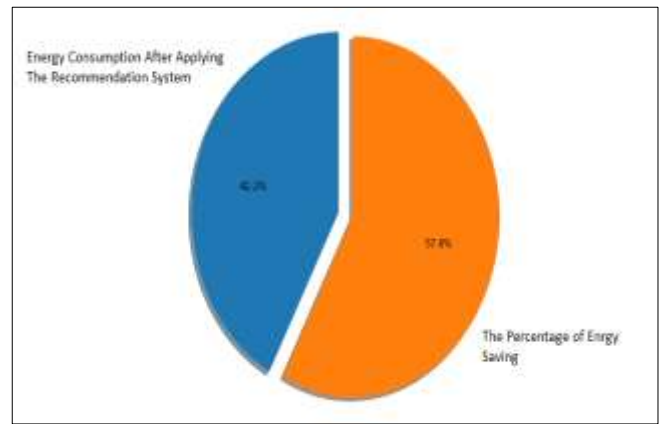


Fig. 6. The Proportion of Energy Saving through Recognizing ADLs.

VI. CONCLUSION

In this work, deep one-dimensional convolutional layers equipped with the max-pooling technique were proposed to deal with time series data to detect ADLs in ambient intelligent environments. Our Deep 1d-CNN unifies feature extraction and classification; it can automatically discover and extract the internal structure of the input time series data and learn deep features to classify ADLs. We evaluated our proposed method on a new real-world dataset, ContextAct@A4H. The results demonstrated that 1d-CNN is one of the most competitive candidates for time series classification owing to its ability to learn more robust deep features. We also expanded our experiment to evaluate the potential energy saving in the smart home by utilizing the recognized activity of our deep model to detect which devices were wasting energy and encourage the user to perform optimization actions. The experiment indicated that recognizing ADLs can achieve an energy savings of around 50%.

The framework proposed in this work has some limitations. They can be seen as extensions and can be addressed in the future. Regarding the proposed deep model, our Deep 1d-CNN achieved good performance in recognizing ADLs, however, we designed our model to only learn single-user activities. Another limitation of our deep model is that most of the parameters were determined through lots of experiments, which is time consuming; so, designing a method of hyper-parameter optimization is ongoing. On the subject of the energy saving recommendation system, the drawback of this approach is that the user might have purposely kept the devices that were detected as wasting energy turned on. However, in using this evaluation approach, we only attempted to show the maximum potential energy savings and demonstrate how recognizing ADLs can have a great impact on energy saving in smart homes.

Regarding directions for future work, we will investigate the problem of recognizing multi-user activities. Moreover, we intend to explore the problem of data imbalance, which is a common problem for real-life HAR. For the recommendation system, we plan to allow the users to send feedback to the system so that it can learn from this feedback in order to enhance its services.

REFERENCES

- [1] Jiang, J., Pozza, R., Gunnarsdóttir, K., Gilbert, N., & Moessner, K. (2017). Using sensors to study home activities. *Journal of Sensor and Actuator Networks*, 6(4), 32.
- [2] Guo, X., Shen, Z., Zhang, Y., & Wu, T. (2019). Review on the application of artificial intelligence in smart homes. *Smart Cities*, 2(3), 402–420.
- [3] Wang, J., Chen, Y., Hao, S., Peng, X., & Hu, L. (2019). Deep learning for sensor-based activity recognition: A survey. *Pattern Recognition Letters*, 119, 3–11.
- [4] Richardson, F., Reynolds, D., & Dehak, N. (2015). Deep neural network approaches to speaker and language recognition. *IEEE Signal Processing Letters*, 22(10), 1671–1675.
- [5] Chan, T. H., Jia, K., Gao, S., Lu, J., Zeng, Z., & Ma, Y. (2015). PCANet: A simple deep learning baseline for image classification? *IEEE Transactions on Image Processing*, 24(12), 5017–5032.
- [6] Albawi, S., Mohammed, T. A., & Al-Zawi, S. (2017). Understanding of a convolutional neural network. In *International Conference on Engineering and Technology (ICET)* (pp. 1–6). IEEE.
- [7] Lipton, Z. C., Berkowitz, J., & Elkan, C. (2015). A critical review of recurrent neural networks for sequence learning. *arXiv preprint arXiv:1506.00019*.
- [8] Oukrich, N. (2019). Daily HAR in smart home based on feature selection, neural network and load signature of appliances (Doctoral dissertation).
- [9] Fawaz, H. I., Forestier, G., Weber, J., Idoumghar, L., & Muller, P. A. (2019). Deep learning for time series classification: A review. *Data Mining and Knowledge Discovery*, 33(4), 917–963.
- [10] Lima, W. S., Souto, E., Rocha, T., Pazzi, R. W., & Pramudianto, F. (2015, July). User activity recognition for energy saving in smart home environment. In *2015 IEEE Symposium on Computers and Communication (ISCC)* (pp. 751–757). IEEE.
- [11] Lago, P., Lang, F., Roncancio, C., Jiménez-Guarín, C., Mateescu, R., & Bonnefond, N. (2017, June). The ContextAct@ A4H real-life dataset of daily-living activities. In *International and Interdisciplinary Conference on Modeling and Using Context* (pp. 175–188). Springer, Cham.
- [12] Ramasamy Ramamurthy, S., & Roy, N. (2018). Recent trends in machine learning for human activity recognition—A survey. *Wiley Interdisciplinary Reviews: Data Mining and Knowledge Discovery*, 8(4), e1254.
- [13] Nweke, H. F., Teh, Y. W., Al-Garadi, M. A., & Alo, U. R. (2018). Deep learning algorithms for human activity recognition using mobile and wearable sensor networks: State of the art and research challenges. *Expert Systems with Applications*, 105, 233–261.
- [14] Sadouk, L. (2018). CNN approaches for time series classification. In *Time series analysis-data, methods, and applications*. IntechOpen.
- [15] Singh, D., Merdivan, E., Hanke, S., Kropf, J., Geist, M., & Holzinger, A. (2017). Convolutional and recurrent neural networks for activity recognition in smart environment. In *Towards integrative machine learning and knowledge extraction* (pp. 194–205). Springer, Cham.
- [16] SEDKY, M., HOWARD, C., Alshammari, T., & Alshammari, N. (2018). Evaluating machine learning techniques for activity classification in smart home environments. *International Journal of Information Systems and Computer Sciences*, 12(2), 48–54.
- [17] Singh, D., Merdivan, E., Psychoula, I., Kropf, J., Hanke, S., Geist, M., & Holzinger, A. (2017, August). Human activity recognition using recurrent neural networks. In *International Cross-Domain Conference for Machine Learning and Knowledge Extraction* (pp. 267–274). Springer, Cham.
- [18] Al Machot, F., Ranasinghe, S., Plattner, J., & Jnoub, N. (2018, March). Human activity recognition based on real life scenarios. In *2018 IEEE International Conference on Pervasive Computing and Communications (PerCom) Workshops* (pp. 3–8). IEEE.
- [19] Arifoglu, D., & Bouchachia, A. (2017). Activity recognition and abnormal behaviour detection with recurrent neural networks. *Procedia Computer Science*, 110, 86–93.
- [20] Nguyen, T. A., & Aiello, M. (2013). Energy intelligent buildings based on user activity: A survey. *Energy and Buildings*, 56, 244–257.
- [21] Alhamoud, A., Ruettiger, F., Reinhardt, A., Englert, F., Burgstahler, D., Böhnstedt, D., & Steinmetz, R. (2014, September). Smartenergy. kom: An intelligent system for energy saving in smart home. In *39th Annual IEEE Conference on Local Computer Networks Workshops* (pp. 685–692). IEEE.
- [22] Thomas, B., & Cook, D. (2016). Activity-aware energy-efficient automation of smart buildings. *Energies*, 9(8), 624.
- [23] Mubdir, B., Al-Hindawi, A., & Hadi, N. (2016). Design of smart home energy management system for saving energy. *European Scientific Journal (ESJ)*, 12(33), 521. *Scientific Journal (ESJ)*, 12(33), 521.
- [24] Cottone, P., Gaglio, S., Re, G. L., & Ortolani, M. (2015). User activity recognition for energy saving in smart homes. *Pervasive and Mobile Computing*, 16, 156–170.
- [25] Srivastava, N., Hinton, G., Krizhevsky, A., Sutskever, I., & Salakhutdinov, R. (2014). Dropout: a simple way to prevent neural networks from overfitting. *The journal of machine learning research*, 15(1), 1929–1958.
- [26] Ioffe, S., & Szegedy, C. (2015). Batch normalization: Accelerating deep network training by reducing internal covariate shift. *arXiv preprint arXiv:1502.03167*.
- [27] Brownlee, Jason . (2014, July 14). Feature Selection in Python with Scikit-Learn. Retrieved April 22, 2020, from <https://machinelearningmastery.com/feature-selection-in-python-with-scikit-learn/>.
- [28] Yala, N., Fergani, B., & Fleury, A. (2015, September). Feature extraction for human activity recognition on streaming data. In *2015 International Symposium on Innovations in Intelligent Systems and Applications (INISTA)* (pp. 1–6). IEEE.
- [29] Quigley, B., Donnelly, M., Moore, G., & Galway, L. (2018). A Comparative Analysis of Windowing Approaches in Dense Sensing Environments. In *Multidisciplinary Digital Publishing Institute Proceedings (Vol. 2, No. 19, p. 1245)*.
- [30] Dehghani, A., Sarbishei, O., Glatard, T., & Shihab, E. (2019). A quantitative comparison of overlapping and non-overlapping sliding windows for human activity recognition using inertial sensors. *Sensors*, 19(22), 5026.
- [31] Kingma, D. P., & Ba, J. (2014). Adam: A method for stochastic optimization. *arXiv preprint arXiv:1412.6980*.
- [32] Molano-Pulido, J., & Jiménez-Guarín, C. (2018). SEABIRD: Adaptable Daily Living Activity Identification from Sensor Data Streams. *Procedia Computer Science*, 130, 939–946.
- [33] Lago, P., Roncancio, C., Jiménez-Guarín, C., & Labbe, C. (2017, August). Representing and learning human behavior patterns with contextual variability. In *International Conference on Database and Expert Systems Applications* (pp. 305–313). Springer, Cham.

A Cryptocurrency-based E-mail System for SPAM Control

Shafiya Afzal Sheikh¹, M. Tariq Bandy²

Department of Electronics and Instrumentation Technology
University of Kashmir, Srinagar, India

Abstract—Sending bulk e-mail is commercially cheap and technically easy, making it profitable for spammers, even if a tiny percentage of recipients falls for the attacks or turn into customers. Some researchers have proposed making e-mail paid so that sending bulk e-mail becomes expensive, making spamming unprofitable and a futile exercise unless many victims respond to spam. On the other hand, the small sending fee is negligible for legitimate e-mail users. Making e-mail paid is a challenging task if implemented using a conventional payment system or developing new cryptocurrencies. Traditional payment systems are challenging to integrate with e-mail systems, and new cryptocurrencies will have challenges in adoption by users on the required scale. This work proposes using cryptocurrency payments to make e-mail senders pay for sending an e-mail without creating a new cryptocurrency or a new blockchain. In the proposed system, the recipients of the e-mail can collect the payments and use the collected revenues to send e-mail messages or even sell them on an exchange. The proposed solution has been implemented using Ropsten, an Ethereum Test Network and tested using enhanced E-mail Client and Server software.

Keywords—E-mail; SPAM; blockchain; cryptocurrency; Ethereum

I. INTRODUCTION

E-mail spamming is one of the critical technical challenges the cyber community faces, causing problems on various fronts. In 2019, 28.5% of total global e-mail traffic was SPAM and was above 45% of total e-mail traffic in 2018 [1]. This huge percentage of SPAM traffic forces e-mail service providers and users to invest hugely in anti-spam technologies and infrastructure, which is a substantial commercial loss globally. These SPAM e-mails take up a considerable amount of storage space on both the e-mail servers and clients. In addition to this, SPAM e-mails pose a multitude of threats to e-mail users by tricking them into visiting malicious websites where they get usually cheated and suffer financial losses. The spammers use phishing, credential phishing, spear phishing, whaling, blackmailing, etc., to harm the recipients in various ways. The SPAM e-mail can also spread and install viruses, rootkits, exploits or other malicious software resulting in data leakage, including passwords, credit card details, etc. and may even compromise the underlying computer software.

Cryptography [2] is being extensively used in securing online communications, including e-mail messaging. Many communication protocols and security features used in the e-mail messaging system rely on cryptographic techniques. These techniques help make e-mail communication safe against the attacks like unauthorized access, spoofing [3],

spamming [4], phishing [5], etc. Cryptographic techniques are also used in various e-mail encryption techniques to send encrypted e-mail to prevent unauthorized access to e-mail message while in transit over a network. The most common protocols and standards which are used for this purpose include GNU Privacy Guard (GPG) [6], Pretty Good Privacy (PGP) [7], Secure Multipurpose Internet Mail Extensions (S/MIME) [8], Privacy-Enhanced Mail (PEM) [9], OpenPGP [10], etc. The Transport Layer Security (TLS) also falls in this category of techniques, which helps encrypt e-mail communication at the transport layer.

Domain Key Identified Mail (DKIM) [11] is a popular cryptography-based e-mail authentication technique which attaches Digital Signatures to outgoing e-mail messages from a domain name. The Digital Signatures are generated by the sending server using Asymmetric Key Cryptographic technique. The recipient can verify them to ensure the incoming e-mail has arrived from the domain name it claims. This helps counter e-mail spoofing, which can result in e-mail SPAM and various email-based phishing attacks.

In combination with blockchain [12] technology, cryptography has revolutionized the payment systems through cryptocurrency. A cryptocurrency is a form of a digital asset that acts as a medium of exchange. The ownership records of assets are stored in a blockchain that is a distributed and decentralized ledger. Cryptocurrencies use modern and secure encryption techniques to secure transactions, verify transactions, and generate new assets. There is no central authority or a trusted party in between the individuals involved in a transaction. The cryptocurrency system works entirely on top of robust cryptographic techniques. Some of the most popular and widely used Cryptocurrencies and blockchain applications are Bitcoin [13], Ethereum [14], Litecoin [15], Chainlink [16], Ripple [17], Stellar Lumens [18] and many more.

Researchers have proposed making e-mail senders pay for sending an e-mail, using tiny amounts, to make sending e-mail for spammers an expensive endeavour. However, there is no robust payment solution to make it possible. Cryptocurrencies can play a vital role in making such proposed system work in reality and can help control e-mail SPAM by making it an expensive and a futile effort for spammers.

A. Contribution

In an attempt to control SPAM by making it expensive, this work proposes the use of existing cryptocurrency and blockchain of payments for sending e-mail messages, without

the need to set up an entirely new payment network. The proposed system has been implemented and demonstrated on Ropsten Ethereum Test Network. It includes implementing a new communication protocol to distribute Wallet Addresses and support creating and verifying cryptocurrency transactions within the existing e-mail infrastructure. The solution's implementation and demonstration include developing a primary E-mail Server with support for the proposed protocol, making and verifying the transaction. The implementation also includes enhancing an open-source e-mail client to create the transactions and attaching them to e-mail messages.

II. LITERATURE REVIEW

Adam Back's Hashcash [19] proposed a proof-of-work-based solution to counter automated abuse of Internet services like e-mail, HTML form submissions, etc. The said solution requires the user to perform some function on the system with moderate CPU requirement before using a service like sending an e-mail. In an e-mail system, this technique ensures that the sender machine has performed some computation and utilized a moderate CPU resource before sending out the e-mail. This computation hardly makes any difference for a legitimate e-mail sender but is extremely expensive for spammers who send many SPAM e-mails within a small-time duration. This technique dramatically reduces the number of e-mails spammers can send within a given amount of time using limited resources. The major drawback to this technique is that spammers will prefer to attack computer users and online servers, control them and use them to process and send e-mails, rather than use their hardware to do the processing. That way, the spammers do not have to invest anything other than hacking into other people's resources and using them for sending their SPAM.

David A. Turner and Ni Deng [20] proposed a solution of payment-based e-mail using Lightweight Currency Protocol. Their proposed solution suggests enhancing the SMTP protocol and includes the payment and payment verification processes into the SMTP protocol. They propose that e-mail service providers will issue their currencies for payments, which will lead to the creation of an unlimited number of currencies that become impossible to manage and lead to problems while performing inter-server mail exchanges. Sending e-mails to different e-mail servers will require purchasing or acquiring a large number of different currencies. Another drawback in their proposed solution is that payments take time to process and verify and including the two processes into the SMTP transaction will make the transaction take too long. This will result in highly reducing the performance of the SMTP servers. Furthermore, changing an existing, widely used protocol is not feasible in a real-world situation. Therefore, the payment transaction and transaction verifications should be independent of the widely used SMTP protocol.

K. Nakayama, Y. Moriyama and C. Oshima [21] have proposed an algorithm named SAGA_{BC}, which uses blockchain technology to control the e-mail SPAM. They propose to make the Sender pay a processing fee to send an e-mail using a new Cryptocurrency which they name as "Mail Send Coin". The fee paid by the senders is later refunded if the

e-mail messages are received correctly by the e-mail recipients. However, their claim to develop and implement an entirely new cryptocurrency for their proposed solution is technically impractical. The cryptocurrency will require mining which should generate returns for the miners. There is no reason why for miners to be interested in investing in mining their proposed cryptocurrency. Another drawback in their proposed system is that refunds are never guaranteed in any cryptocurrency, and it entirely depends upon the recipients to make any refunds. There is no central authority or trusted intermediary in cryptocurrency networks who can guarantee or force a refund in successful e-mail delivery. Furthermore, the authors have not proposed any practical methodology for implementing payment transactions or transaction verification by the recipients.

Likewise, the Credo project's concept is to use Credo Tokens as a payment method for an e-mail service provided by BitBounce. The service makes e-mail senders, who are not in the recipient's contact list, pay for sending e-mails. The non-whitelisted e-mail senders get a payment request when they try to send an e-mail to an e-mail account on the BitBounce Server. However, the credo cryptocurrency is linked directly to the BitBounce e-mail service. There is no information about if any other e-mail service providers can adopt this technology or the cryptocurrency [22].

These researchers and service providers have tried to provide solutions which could help make e-mail messaging paid and control e-mail SPAM. Due to the limitations in their proposed solutions or lack of practical methodology, this work offers a solution that overcomes these shortcomings and proposes a design implemented and tested, using existing cryptocurrency systems without any widely accepted changes e-mail communication protocols.

III. PROPOSED SOLUTION

The work presented in this paper proposes a methodology that uses the existing cryptocurrency as a mode of payment for sending e-mail messages. The Sender of the e-mail, either the E-mail Client or the E-mail Server, makes a payment in advance, for the e-mail message it sends to the recipient. The recipient will get the e-mail message in the inbox, only if the payment is verified successfully. The payment transaction can be made by the sending Mail Transfer Agent (MTA) on behalf the domain users or by the sending Mail User Agent (MUA), depending upon the payment policies and network configuration of the e-mail infrastructure. The proposed solution is comprised of multiple processes viz: (a) Wallet Creation, (b) Wallet Address Distribution, (c) Payment and Stamp Creation, (d) Sending the e-mail, (e) Transaction Verification and (f) Delivering E-mail to MUA.

In the proposed solution, a Cryptocurrency is used for payment processing in which the e-mail sender is required to make a small cryptocurrency payment for sending an e-mail. The small fee is negligible for legitimate users who send a limited number of e-mails. However, the cost will accumulate to form a massive number for spammers who operate by sending out a large number of e-mails in a short time, making spamming expensive and useless. The payment is made using an existing cryptocurrency transaction, and the payment has

been made a prerequisite for delivering the e-mail to the inbox of recipients. The work also proposes a new wallet distribution protocol. With the help of which the Sending MTA or the sending MUA (Email Sender) after opening a connection with the recipient MTA asks for the list of supported cryptocurrencies. The recipient MTA responds with the list of supported cryptocurrencies. The E-mail Sender then requests for the wallet address of the recipient e-mail address on that domain to which the recipient MTA responds with the wallet address of the e-mail address. The E-mail Sender makes a cryptocurrency payment favouring the wallet and attaches the transaction hash of the payment to the e-mail header and sends the e-mail to the recipient MTA. This research names the transaction hash in the e-mail header as "EmailSTAMP". The 'EmailSTAMP' in the e-mail header can be thought of as a postal stamp on a letter's envelope, which implies that the Sender has obtained the stamp by making a payment.

On the receiving side, the 'EmailSTAMP' from the e-mail header is extracted, and the transaction is verified on the blockchain. On successful transaction verification, the e-mail is delivered to the inbox of the recipient e-mail address. If the transaction verification fails or a transaction hash is not found in the e-mail header, the e-mail is categorized as SPAM by the recipient MTA. This proposed solution makes sure that the Sender makes a tiny payment for each e-mail it sends, favouring the recipient or the recipient MTA for successfully delivering e-mails to the recipient's inbox. Fig. 1 show a sequence diagram of the proposed solution.

The various steps and processes involved in the proposed solutions are discussed below in detail.

A. Wallet Creation

The e-mail server creates wallet addresses for all the e-mail accounts present on the e-mail server and stores the private keys securely. The E-mail Server may even create wallets for multiple cryptocurrencies for every e-mail account. The wallets are used to receive payments from the e-mail senders. The wallets can be created immediately when creating the e-mail accounts or whenever an e-mail server requests one. The E-mail Client can request the Private Key from the E-mail Server, after the proper authentication. In an alternate implementation, instead of the E-mail Server, the E-mail Client generates and stores the secret keys and wallet addresses, and shares the E-mail Server's wallet address. In such cases, the payment transaction is made by the E-mail Client itself and attached to the e-mail header before submitting it to the MTA for sending. Fig. 2 shows the flowchart of creating a wallet by the E-mail Server when an E-mail Sender requests a wallet.

As shown in Fig. 2, the Mail Server generates a wallet and returns it to an E-mail Sender for a non-existent e-mail address to counter the problem of e-mail address harvesting. E-mail spammers use various techniques to collect valid and working e-mail addresses to spam them and ensure that most of the e-mail being sent is received by e-mail addresses that exist and are active. One of the methods of collecting e-mail addresses is guessing and cleaning. In this method, the spammers guess e-mail addresses and send them e-mail messages. If the e-mail address is invalid and receives a bounce mail, they remove the e-mail address from the list and keep the ones that did not respond with a bounce mail. This way, they can collect working e-mail addresses and filter out invalid ones. In the proposed technique, if the sending server queries for the wallet address of invalid e-mail addresses, the e-mail server still generates a wallet at runtime and return that to the sending server. This way, instead of returning an invalid-email-address message, the e-mail server will respond positively with a wallet address. If e-mail messages are afterwards received on such, non-existent e-mail addresses, the Server can still collect the payments made and discard the e-mail message silently. This way, the sending e-mail server is made to pay for e-mail address harvesting using guessing and cleaning technique.

B. Identify the Headings

A communication protocol has been proposed, which E-mail Senders and E-mail Recipients use to request and share wallet addresses of e-mail addresses. The sending MTA or the sending MUA (Email Sender) asks the recipient MTA for an e-mail address's wallet address. The recipient MTA responds with a wallet address. The E-mail Sender verifies the wallet address for correct format. If the wallet address is confirmed to be a valid address, the E-mail Sender will use that wallet address to make payment for the e-mail message. Fig. 3 shows an example of the protocol for distribution of wallets against e-mail addresses after establishing a connection. As shown in Fig. 3, R denotes the Recipient Server, and S represents the Sending MTA or MUA. After establishing a connection with the Recipient Server, the E-mail Sender receives a welcome message with a 220-status message. The E-mail Sender issues a command LIST CURRENCY. The Recipient Server responds with a 220-status message and a list of supported cryptocurrencies. The E-mail Sender issues a command WALLETS followed by the cryptocurrency preference, a colon and an e-mail address to send the e-mail. According to the Sender's selected cryptocurrency, the Recipient Server responds with a 220-status followed by a wallet address. After receiving the wallet address, the E-mail Sender closes the connection.

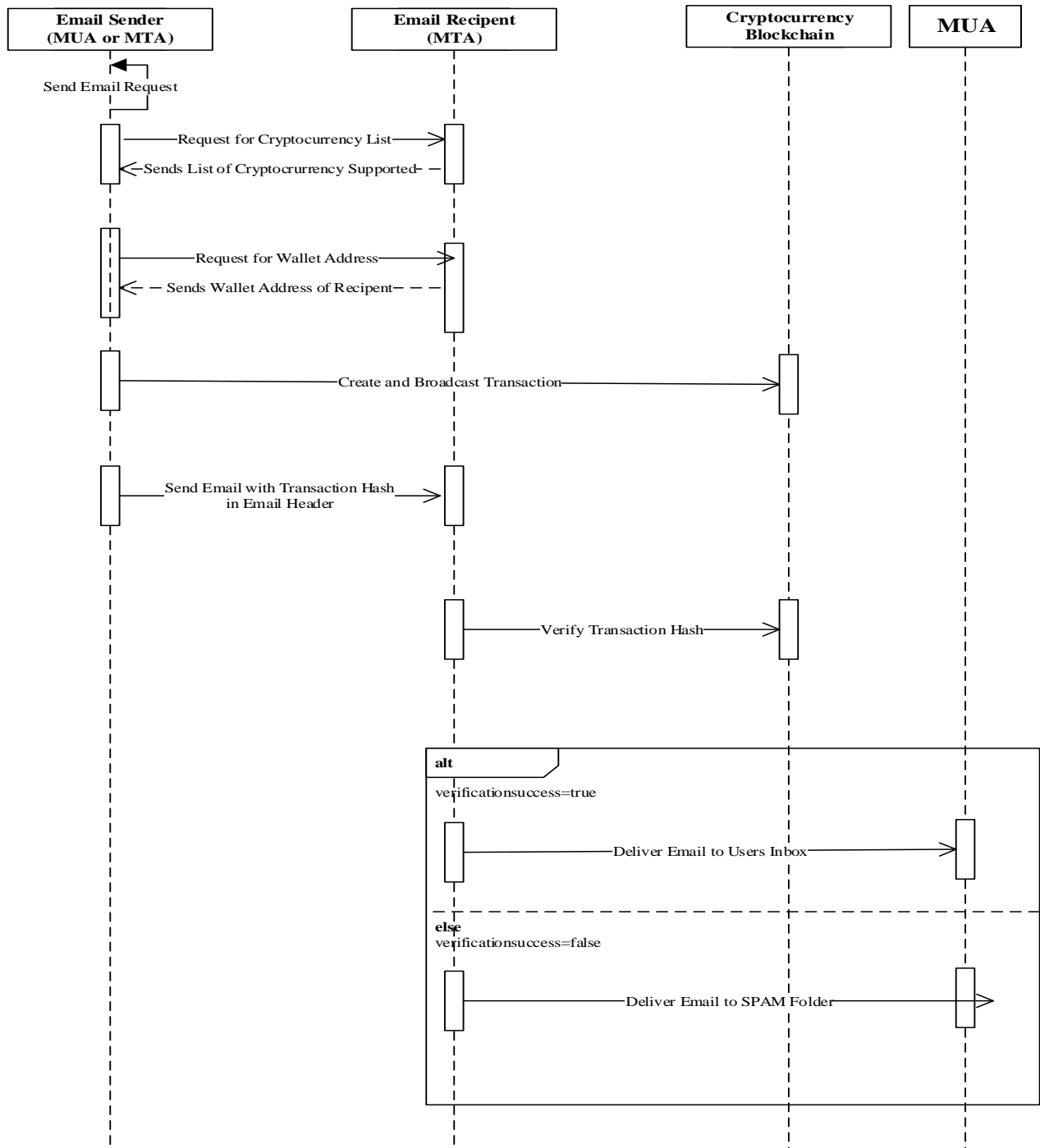


Fig. 1. Sequence Diagram of the Proposed System.

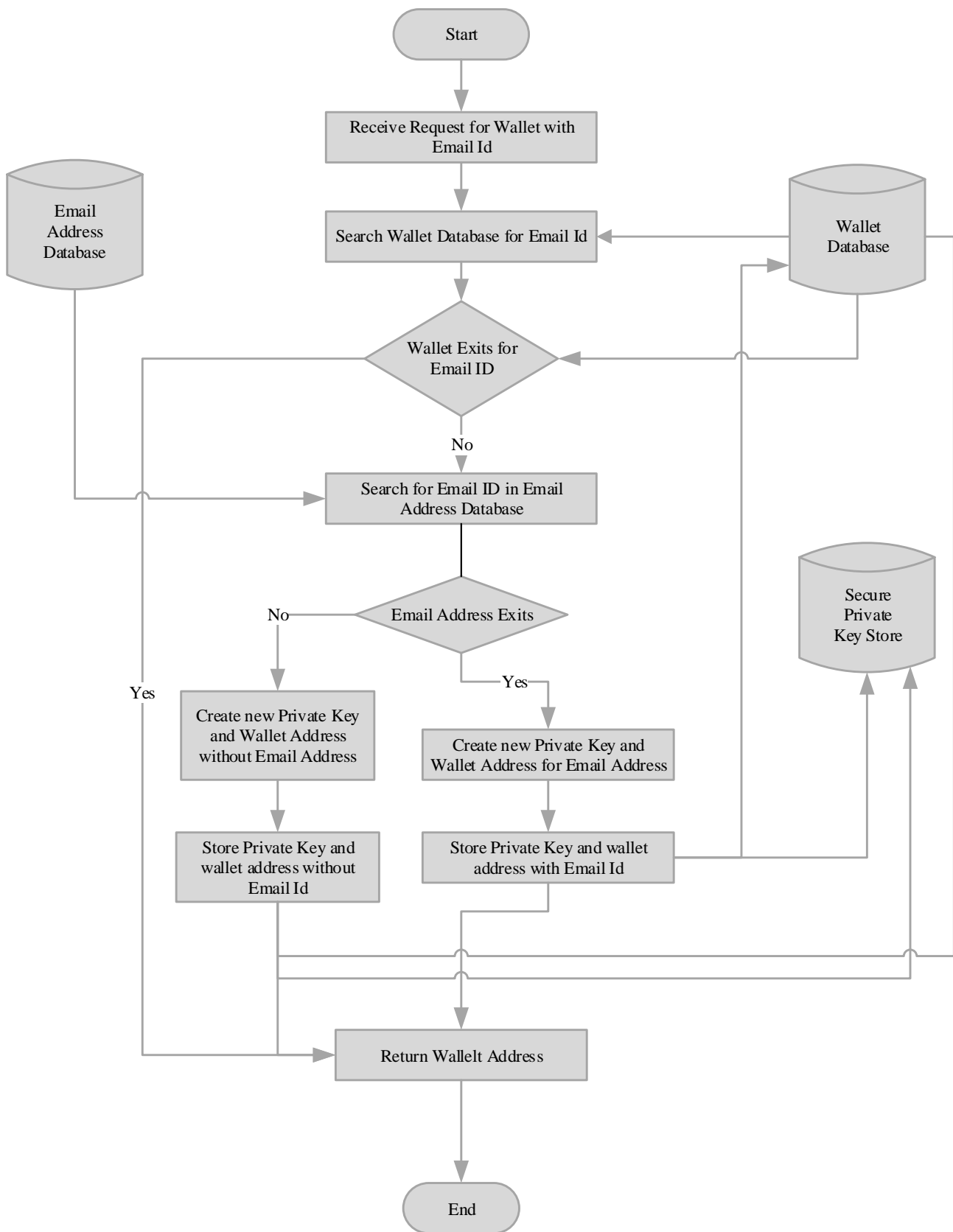


Fig. 2. Flowchart Showing the Creation and Returning of a Cryptocurrency Wallet by the E-mail Sender.

```
R: 220 smtp.recipient-domain.com ESMTP Postfix
S: LIST CURRENCY
R: BITCOIN ETHER DOGE.
S: WALLET DOGE:some-user@recipient-domain.com
R: 220 DB1Xu2kgdkgu83UWxFE3r9hJiG65FaC003D
```

Fig. 3. An Example of a New Wallet Distribution Protocol.

C. Cryptocurrency Payment and 'EmailSTAMP' Creation

In the proposed solution, the Sending MTA or the Sending MUA (Email Sender) is enhanced to generate a cryptocurrency transaction. The transaction is made up of an input wallet address, the wallet address of the e-mail recipient and the amount to be paid. The E-mail Sender concatenates the FROM e-mail address, the recipient e-mail address, the amount and the e-mail subject, together and calculates an md5 hash of the resulting string, named "verification-hash". The verification-hash is then attached to the cryptocurrency transaction and is afterwards used to verify if the payment transaction in the 'EmailSTAMP' applies to the e-mail attached to it re-calculating the verification-hash on the recipient side. The entire transaction is signed by the private wallet key of the E-mail Sender. The transaction hash of the transaction is calculated, and the transaction is broadcasted into the cryptocurrency blockchain network. Fig. 4 shows the structure of a cryptocurrency transaction that can be used as a proof of payment for a given e-mail message. The same transaction cannot be used for any other e-mail messages because of the "verification-hash".

D. E-mail Message Submission

The e-mail server creates the e-mail address in the usual way and adds an extra header, EmailSTAMP, to the e-mail headers. The 'EmailSTAMP' header field contains the cryptocurrency name and the transaction hash, as a proof of payment. The e-mail is then sent to the Recipient Server for delivery.

A sample set of headers is shown in Fig. 5, wherein the 'EmailSTAMP' header field includes the name of the cryptocurrency and the transaction hash. After adding the 'EmailSTAMP' header, the Sending Server can send the e-mail to the Recipient Server in a regular manner. The Recipient Server can use the header information to check for the transaction information on the relevant blockchain.

E. Transaction Verification

The recipient server on receiving the e-mail checks the e-mail header extracts the stamp which contains the transaction hash. It queries the blockchain for the correctness of the transaction hash and gets the information about the transaction. If the transaction is correct and verified by an adequate number of nodes, it is considered successful. The Recipient Server extracts the verification-hash from the transaction details. The Server also calculates the hash of a string resulting from the concatenation of the sender e-mail address, recipient e-mail address and the subject. The calculated hash is compared to the verification-hash obtained from the cryptocurrency transaction details. If the two matches, the Server can be sure that the given transaction has in reality been made for the e-mail message being received. The Recipient Server also compares the transaction date with

the e-mail sending date to ensure that a payment made for an e-mail is not being used again for a similar e-mail the next day. Suppose the E-mail Server cannot verify the transaction for an e-mail message, depending on the policy. In that case, the Server may mark the e-mail message as SPAM or send a bounce e-mail back to the E-mail Sender, explaining that an 'EmailSTAMP' is required for delivering the e-mail message. The transaction verification of 'EmailSTAMP' header in an e-mail message is shown in Fig. 8.

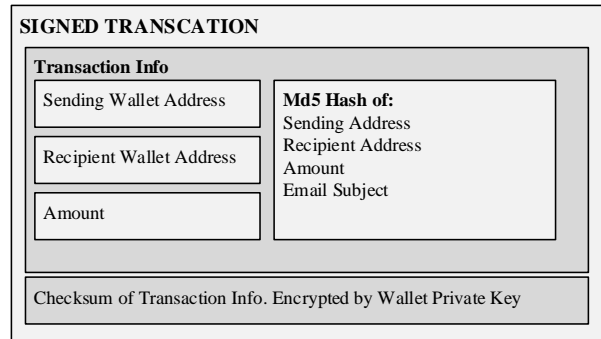


Fig. 4. A Cryptocurrency Transaction showing the Necessary Elements.

```
From: Alice (alice@sending-server.com)
Subject: Offer, Flat 50% of on all products.
Date: December 25, 2020 3:30:58 PM PDT
To: bob@recipient-server.com
Return-Path: <alice@sending-server.com>
Envelope-To: bob@recipient-server.com
Delivery-Date: Fri, 25 Dec 2020 15:31:01 -0700
EmailSTAMP: currency=DOGE; trx-hash=fef584b0bc69af96565cc7541gryhA0af756id8f7rtp0af6daf498ytFDNjH5faf099a
More Headers...
```

Fig. 5. Sample E-mail Headers Containing the Cryptocurrency Payment Information in the 'EmailSTAMP'.

F. E-mail Delivery to the Recipient.

If the Recipient Server can successfully validate the transaction and confirm the payment made for the e-mail being received, it delivers the e-mail message to the user's inbox. The user can then open and read the e-mail message. The E-mail Client is modified to display the amount of cryptocurrency received for the e-mail address, after opening the e-mail message. The E-mail Client also shows the total Cryptocurrency amount available in the user's wallets.

IV. TESTING AND IMPLEMENTATION

The proposed solution has been implemented and tested using an Ethereum Test Network [23]. A Token named "EmailSTAMP" was created on the Ropsten Test Network. The Token is a standard ERC20 token with a fixed number of tokens, and the contract has only standard rules. The agreement was developed using Solidity language and deployed and tested on the Ropsten Test Network. Fig. 6 shows a screenshot of the 'EmailSTAMP'ERC20 Token on the Ropsten Test Network. The screenshot shows the Contract

Address of the 'EmailSTAMP' in the address bar and the Total Supply, which is 100 million. The 'EmailSTAMP' Token was created with support for 18 decimal places. Therefore, a tiny fraction of the Token can also be transferred in transactions.

The Smart Contract was designed such that the users or E-mail Senders can send the verification-hash along with the Token Transfer transaction. The transfer() functions of the Smart Contract accepts an additional string parameter, viz. 'verificationHash', which is meant for sending the verification-hash to the recipient for payment verification.

When calling the transfer() function on the contract, the 'verificationHash' parameter should be supplied. In case the 'verificationHash' parameter is not provided, the contract execution will fail, and the entire cryptocurrency transaction will fail. Fig. 7 shows a screenshot of Remix Ethereum IDE's transfer function, showing the 'verificationHash' parameter, which accepts a string value. Fig. 9 shows the input data of a successful transaction, in which one 'EmailSTAMP' token was transferred. Note that the transaction shows 10^{18} tokens equal to one 'EmailSTAMP' Token because, in the Smart Contract, the number of decimals for the Token was set to 18. This can help send a tiny fraction of the Token in a transaction instead of sending a full Token.

Fig. 9 also shows a value in the 'verificationHash' parameter, the MD5 hash of a string created by concatenating the sender e-mail address, recipient e-mail address, amount and e-mail subject of an e-mail message.

An SMTP Server was written in JAVA and set up on two AWS EC2 Instances, one used for sending e-mail and the other was used as a Recipient. The proposed Wallet Distribution Protocol for requesting and sharing Wallet address was added to the JAVA based E-mail Server. MySQL database server was used to store wallet private keys and wallet addresses. The e-mail server was developed to create transactions on the Ethereum Test Network, create the 'EmailSTAMP' header, and add it to the outgoing e-mail. The e-mail server also verifies transactions on the blockchain, if an 'EmailSTAMP' header is found in the incoming e-mail messages.

An open-source PHP based e-mail client, *SquirrelMail*, was enhanced to work with and support the custom JAVA based SMTP Server. The enhanced E-mail Client was hosted on both the AWS EC2 instances and configured with the respective E-mail Servers. The modified E-mail Client can also create the wallet, store it in MySQL database. On the

Sending Server, the Client can also use the Wallet Distribution Protocol to connect to the Recipient Server to obtain wallet address for an e-mail address. It can create a Transaction and add the transaction hash to an e-mail message 'EmailSTAMP' header before submitting it the E-mail Server.

The E-mail Client was able to create the wallet and store it in the MySQL database. Before sending an e-mail, the E-mail Client successfully obtained the wallet address of an e-mail address on the Recipient Server. It then generated and broadcasted a transaction on the Ropsten Network, created an 'EmailSTAMP' e-mail header, added it to the e-mail and submitted the e-mail to the E-mail Server for Delivery. On the Recipient Server, the e-mail headers were obtained by the SMTP Server. The transaction was extracted, and the transaction was verified on the Ropsten Test Network after which the e-mail was successfully delivered to the recipient's inbox. Another test message, which was sent without adding an 'EmailSTAMP' header, was sent to the Recipient Server which was successfully filtered out and sent to the SPAM folder.

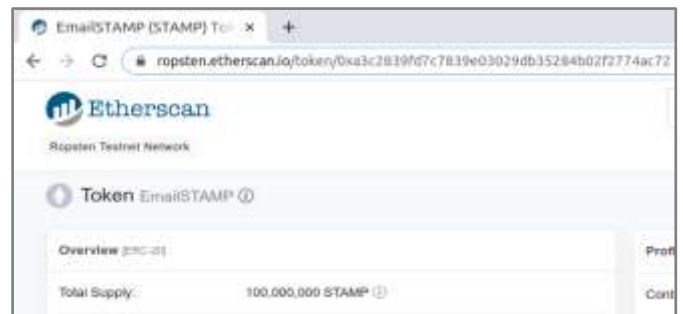


Fig. 6. Screenshot of the 'EmailSTAMP' Token on the Ropsten Test Network.

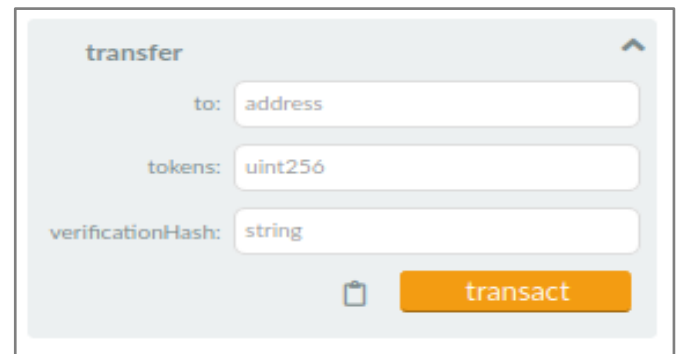


Fig. 7. Screenshot of transfer() function from Remix Ethereum IDE.

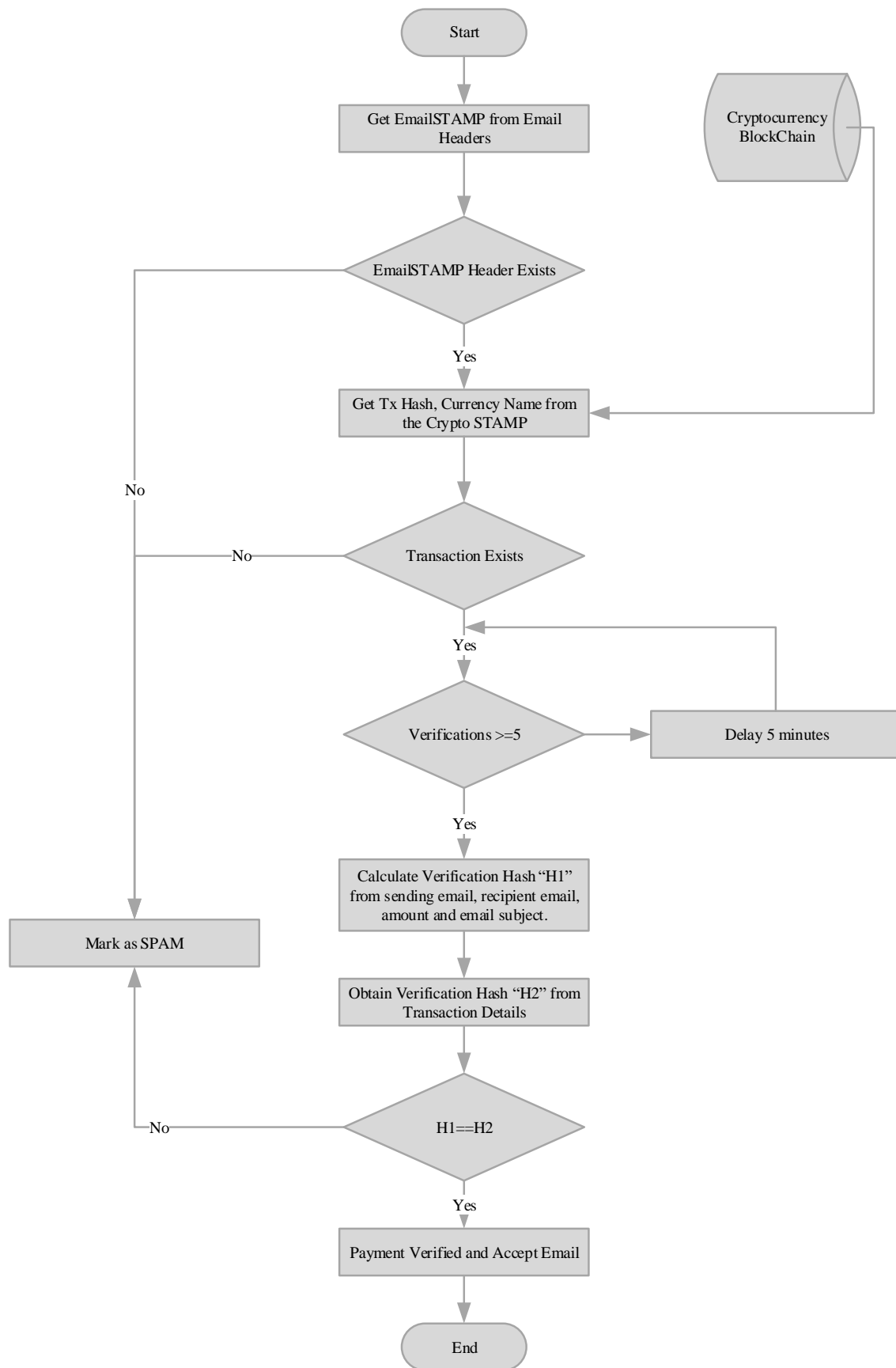


Fig. 8. Verification of the 'EmailSTAMP' Header.



#	Name	Type	Data
0	to	address	af1814ac2f5af18f644e4097add1e2a5d326b60b
1	tokens	uint256	10000000000000000000
2	verificationHash	string	6f30dbc551e420b412d2d583862e4dd0

Decoded input inspired by [Canoe Solidity](#)

Fig. 9. Screenshot of the 'EmailSTAMP' token on the Ropsten Test Network.

V. LIMITATIONS AND FUTURE SCOPE

Although a minimal fee payment per e-mail can serve the purpose of reducing e-mail SPAM, the introduction of a fee for a service which is otherwise free will be an inconvenience for ordinary e-mail users. For such users, large E-mail Service Providers can pay the fee on their behalf. The E-mail Service Providers can make the payments from the amount they collect for incoming e-mails. Therefore, the common users might not even be required to purchase any cryptocurrency at all.

The introduction of extra security measure, no doubt, will have an impact on any process. Likewise, adding a payment system into the e-mail delivery process will introduce some delay in e-mail delivery. Generating and broadcasting a transaction on an Ethereum network will take no more than a second; therefore, sending side will not notice any delays. On the other hand, Ethereum transactions take between 15 seconds and 5 minutes, to complete. Thus, the e-mail recipient will have the e-mail delivered in their inboxes as quickly as within 15 to 20 seconds or may be delayed by about 5 minutes. Time taken to complete and confirm a transaction varies for different cryptocurrency blockchain networks.

There is a need to research various currently available cryptocurrencies regarding their feasibility for implementing the proposed solution. The research can compare and contrast the multiple cryptocurrencies regarding their support for publishing the "verificationHash" and the transaction, transaction verification and processing speed, and transaction fee. The research will help in implementing the proposed solution most effectively.

VI. CONCLUSION

E-mail senders can be made to pay tiny amounts for sending an e-mail negligible for legitimate users but accumulates to form a considerable part for spammers sending bulk e-mail messages. Setting up a payment for such purposes can be extremely difficult using currently available payment infrastructure. It will be costly, if not impossible, for the e-mail recipient to verify if the e-mail sender has paid for incoming e-mail messages. This problem can be solved by using existing blockchains and cryptocurrencies. This will require some modifications to the E-mail Servers and E-mail Clients and implementing an additional communication protocol. In the proposed solution, the E-mail Server can make payments for the outgoing e-mail messages on behalf of its e-mail addresses or the end users can make the payments themselves using their E-mail Clients. At the recipient's end,

these payments can be collected by the e-mail recipients or the E-mail Server and used to send out e-mail messages or be sold on cryptocurrency exchanges.

The work presented in this paper suggests not to create any new cryptocurrency or set up a new blockchain for processing the payments for several reasons. It is tough to use new cryptocurrencies, making it more feasible to use any existing reliable cryptocurrency. Cryptocurrencies need miners to verify transactions and support the blockchain, which is only possible if they find the process profitable. New cryptocurrencies are not attractive for miners at all and are, therefore, challenging to implement. Hence, using an existing cryptocurrency is recommended and demonstrated in this study.

The proposed system is backwards compatible because it does not attempt to modify the basic SMTP protocol or any other established e-mail communication protocols. Existing SMTP servers can receive e-mail from E-mail Senders even if they support the proposed system. In the absence of the payment header, a Recipient SMTP Server which supports the proposed solution will still accept e-mail from the Sender, but it will deliver the message to a SPAM folder instead of inbox.

REFERENCES

- [1] Spam: Share of Global Email Traffic 207-2019, <https://www.statista.com/statistics/420400/spam-email-traffic-share-annual/>, accessed October 2020.
- [2] U. H. Rao, U. Nayak, "Cryptography," An Introduction to Information Security, Springer, September 2014.
- [3] E. Kirda, C. Kruegel, "Protecting Users against Phishing Attacks," The Computer Journal, vol.49, January 2006.
- [4] W. Z. Khan, M. K. Khan, F. T. B. Muhaya, M. Y. Aalsalem, H.C. Chao, "A Comprehensive Study of Email Spam Botnet Detection," IEEE Communications Survey and Tutorials, vol. 4, pp. 2271-2295, June 2015.
- [5] A. Karim, S.Azam, B. Shanmugam, K. Kannoorpatti, M Alazab, "A Comprehensive Survey for Intelligent Spam Email Detection," IEEE Access, vol. 7, November 2019.
- [6] W. Koch, "The GNU privacy guard," <http://www.gnupg.org>, accessed November 2020.
- [7] PGP, "Pretty Good Privacy (PGP)," <http://www.openpgp.org>, accessed November 2020.
- [8] J. Schaad, B. Ramsdell, S. Turner, "Secure/Multipurpose Internet Mail Extensions (S/MIME)," RFC 5751, Version 4.0, April 2019.
- [9] J. Linn, "Privacy-Enhanced Mail (PEM)," RFC1421, February 1993.
- [10] J. Callas, L. Donnerhacke, IKS GmbH, H. Finney, D. Shaw, R. Thayer, "OpenPGP," RFC 4880, November 2007.
- [11] D. Crocker, T. Hansen, and M. Kucherawy, "DomainKeys Identified Mail (DKIM) Signatures," RFC 6376, September 2011.
- [12] Y. Yuan and F.-Y. Wang, "Blockchain and Cryptocurrencies: Model, Techniques, and Applications," *IEEE Trans. Syst. Man Cybern. Syst.*, vol. 48, no. 9, pp. 1421-1428, Sep. 2018.
- [13] S. Nakamoto, "Bitcoin: A Peer-to-Peer Electronic Cash System," 2008. <https://bitcoin.org/bitcoin.pdf>, accessed October 2020.
- [14] V. Buterin, "White Paper- Ethereum," <https://ethereum.org/en/whitepaper/>, accessed November 2020.
- [15] C. Lee, White Paper- Litecoin, <https://litecoin.org/>, accessed October 2020.
- [16] S. Ellis, A. Jules, S. Nazarov, "ChainLink: A Decentralized Oracle Network," URL: <https://link.smartcontract.com/whitepaper>, accessed: October 2020.

- [17] D. Schwartz, N. Youngs, A. Britto, "The Ripple Protocol Consensus Algorithm," https://ripple.com/files/ripple_consensus_whitepaper.pdf, accessed November 2020.
- [18] D. Mazieres, "The Stellar Consensus Protocol," <https://www.stellar.org/papers/stellar-consensus-protocol?locale=en>. Accessed October 2020.
- [19] A. Back, "Hashcash - a denial of service counter-measure," <http://www.hashcash.org/papers/hashcash.pdf>, 2002.
- [20] David A. Turner and Keith W. Ross, "The Lightweight Currency Protocol (LCP)," September 2003. <http://www.ietf.org/internet-drafts/draft-turner-lcp-00.txt>.
- [21] K. Nakayama, Y. Moriyama, C. Oshima, "An algorithm that prevents spam attacks using blockchain," *International Journal of Advanced Computer Science and Applications (IJACSA)*, vol. 9, 2018.
- [22] S. Dennis, "Credo Token-Blockchain Based Spam & E-mail Access Solutions," Turing Technology, Inc., July 2017.
- [23] Ropsten Testnet Explorer, <https://ropsten.etherscan.io/>, accessed December 2020.

Discovery Engine for Finding Hidden Connections in Prose Comprehension from References

Amal Babour¹, Javed I. Khan², Fatema Nafa³, Kawther Saeedi⁴, Dimah Alahmadi⁵

Faculty of Computing and Information Technology

Department of Information Systems, King Abdulaziz University, Jeddah 21589, Saudi Arabia^{1,4,5}

Department of Computer Science, Kent State University, Kent, OH 44240 USA²

Department of Computer Science, Salem State University, Salem, MA 01970 USA³

Abstract—Reading is one of the essential practices of modern human learning. Comprehending prose text simply from the available text is particularly challenging as in general the comprehension of prose requires the use of external knowledge or references. Although the processes of reading comprehension have been widely studied in the field of psychology, no algorithm level models for comprehension have yet to be developed. This paper has proposed a comprehension engine consisting of knowledge induction which connects the knowledge space by augmenting associations within it. The connections are achieved through the automatic incremental reading of external references and the capturing of high familiarity knowledge associations between prose concepts. The Ontology Engine is used to find lexical knowledge associations amongst concept pairs, with the objective being to obtain a knowledge space graph with a single giant component to establish a base model for prose comprehension. The comprehension engine is evaluated through experiments with various selected prose texts. Akin to human readers, it could mine reference texts from modern knowledge corpuses such as Wikipedia and WordNet. The results demonstrate the potential efficiency of using the comprehension engine that enhances the quality of reading comprehension in addition to reducing reading time. This comprehension engine is considered the first algorithm level model for comprehension compared with existing works.

Keywords—Knowledge graph; ontology engine; text comprehension; text summarization; Wikipedia; WordNet

I. INTRODUCTION

Text comprehension is a form of knowledge acquisition whereby readers interact with text and relate the ideas represented to their knowledge and experiences [1]. Generally, reading a single text does not qualify readers to achieve the required level of comprehension. This is because the comprehension process depends largely on reader knowledge or additional knowledge acquired from external sources. A well written text embeds a set of cues to build up a coherent representation of the text. Although the text normally presents a set of related concepts, this does not qualify readers to achieve complete comprehension. In this paper, the focus is on prose comprehension. Prose is a type of text which includes complex concepts manifesting particular meanings of a specific domain with associations among concepts. As prose comprehension is difficult to achieve from a simple reading of the text alone, external knowledge is required to understand the text. The external knowledge readers need is known as

prior knowledge [2]. This prior knowledge is different from one to one comprehension. Sometimes, readers may not even have a minimum level of prior knowledge about a specific topic, making it necessary for them to obtain it by using external sources. Lexicons and external references are two common examples of acquiring additional knowledge. By drawing upon prior knowledge, readers fill the knowledge gap in the prose by connecting the prose contents with their prior knowledge. The process of prose comprehension is flexible to implement and incorporates external information sources into the prose text. An example of such a process is integrating an encyclopedia with linguistic information/ dictionaries.

Although human readers tend to consult external knowledge mediums such as books, Wikipedia, or journal articles to bridge this knowledge gap, such a process is often time consuming and tedious. It requires reading a large amount of text and then finding the relevant portions of the reference to catalyze understanding. While the mental process behind such knowledge induction is intriguing, adopting computational algorithms can help more effective reading comprehension of prose by automatically capturing relevant text pieces from external references and relevant knowledge association of the prose concepts as a summary. This can leverage greater overall comprehension process of a prose text.

The topic of the human reading rate has been widely studied. Carver's reading model identifies the relationship model between reading and comprehension [3]. He defines five reading processes: memorizing, learning, rauding, skimming, and scanning. The reading rate of an individual varies on the basis of material difficulty and reading objective [3, 4]. For example, skimming may be used when a reader requires an overview of the material, whereas learning may be used when a reader requires comprehension of the material. Carver's reading model provides a reading rate that measures how many words are read per minute (wpm) for each of the five processes. For memorization, the rate is 138 wpm, whereas for learning it is 200 wpm, and for rauding the rate is 300 wpm. For skimming, the rate is 450 wpm, and finally for scanning it is 600 wpm. For example, if readers read a text of 2000 words for the purpose of learning, it takes about 10 minutes for them to read and comprehend it.

The previous work focused on generating summarized texts and/or recruiting participants to analyze their level of

comprehension. To the best of knowledge, no existing work proposing an algorithm level model for comprehension. Accordingly, the contribution of this paper can be summarized as follows:

- Develop an algorithm level model comprehension engine to enhance prose comprehension.
- Evaluate the proposed model through set of graph metrics.

The proposed comprehension engine contributes to the reading rate that readers may need to acquire specific knowledge from reference texts. This engine is based on the Knowledge Induction Process which targets increasing knowledge comprehension through two steps: 1) the incremental reading of external reference texts and giving an extractive summary of each by capturing of the highest familiarity knowledge associations amongst prose concepts. One of the distinct features of the proposed algorithm is that it captures the highest familiarity knowledge along with the fewest associations pertaining to prose concepts through a minimum number of external concepts; and 2) using Ontology Engine to find lexical knowledge associations amongst concepts. This can save readers time and increase their efficiency, which are two main advantages of the comprehension engine.

The rest of the paper is structured as follows: Section II provides an overview of the related work. Section III introduces the development of the comprehension engine. Section IV presents an evaluation of the proposed engine. Section V presents the materials used in the experiment and the results, and the final section (Section VI) discusses the conclusion and the future work.

II. RELATED WORK

Considerable research has been done in text summarization and text comprehension in recent years. Some of the research introduced valuable techniques used to produce extractive and abstractive summarization. Extractive summarization summarizes the text by extracting sentences containing salient information from the text itself, while abstractive summarization summarizes the text by paraphrasing the text using words that might not in the text [5]. In recent years, various approaches have been developed for automatic summarization and have been applied widely in different domains.

Van Lierde and Chow [6] combined fuzzy and statistics approaches to obtain extractive summarization. The fuzzy based technique contained manually generated rules where the rules were proceeded based on the length of the sentence. By using these rules, all the sentences were assigned with a weight value ranging from zero to one, where the weight for each sentence was used as a feature in the fuzzy inference system. The authors used such a system to perform the summarization through a number of fuzzy-logic-based analyzers. The work had an advantage of taking into consideration the linguistic variables and human perception.

Hernández-Castañeda et al. [7] proposed a method for extractive automatic text summarization (EATS). The method

based on the conversion of the text into numerical vectors by applying different generation methods. The vectors are grouped into clusters based on measuring proximity among the vectors. Latent Dirichlet allocation (LDA) was used to obtain the key sentences in each cluster that make up the summarized text.

Furthermore, Azadani et al. [8] used graph-based summarization techniques to produce extractive summarization. The technique represented a document as a graph in which a node can correspond to various semantic units including words, phrases, concepts or sentences, whereas an edge demonstrated the relation in connectivity between the nodes. The authors used the frequent itemset mining algorithm to extract the summary.

For summarizing multiple documents, Fuad et al. [9] used two techniques, sentence clustering and neural sentence to produce abstractive summarization. In sentence clustering techniques, they used a deep neural network architecture to represent text. In neural sentence, they applied seq2seq encoder-decoder technique. The proposed method took a related ordered set of sentences and produced a single sentence by merging the input sentence from multiple documents; the output was only one sentence as a summary.

For the purpose of text summarization and comprehension, Ding et al. [10] proposed a text summarization generation model to enrich representing the information of the original text and improve the text comprehension. Their method was based on seq2seq through a dual-encoder, the Gain-Benefit gate for decoding, and the probability distributions of the keywords in the text.

In [11], Caglieroet et al. proposed a method named TESTdriven SUMmarization (TestSumm) to recommend text summarization based on a learner's level of comprehension. The method provides multiple-choice tests to assess the learner's comprehension level of different topics. It performs a Multilingual Weighted Itemset-based Summarizer (MWISum) that relies on frequent itemset mining sentence selection and ranking to generate the material summary. It recommends a personalized summary to learners who did not pass the multiple-choice test.

All the previous text summarization research focused on reducing the volume of the text by capturing or rephrasing the most important sentences that include main keywords and present it to the reader. On the other hand, the current text comprehension research based on recruiting participants and applying descriptive statistics to analyze their performance. Thus, this paper has introduced a text summarization method that may increase the number of concepts in the summary in some cases for the purpose of text comprehension.

III. KNOWLEDGE INDUCTION PROCESS

"Knowledge graph is an emerging technology for massive knowledge management and intelligent services in the big data era" [12]. It provides an ideal technical solution to realize the integration of knowledge sources by incorporating noisy information and connecting the fragmented pieces of knowledge from multiple sources in a consistent way. In this paper, a knowledge graph called the Illuminated Knowledge

Graph (IKG) is proposed to illuminate the relationships among prose concepts using multiple knowledge sources for the purpose of comprehension. These ideas and goals were the inspiration for the graph name.

The IKG is a graph which captures the state of learning process. It shows prose concepts (CL) and associations amongst the concepts. The associations can be found by reading the prose (LTX) and reading some parts relevant to the concepts as a summary from external reference texts (RTX) as well as an Ontology Engine (OE). Beside the CL concepts, the graph could include external concepts belong to RTX or OE in the associations added from them to connect the prose CL concepts. A directed graph presents IKG = (C, E), where C is a concept set and E is an edge set. A concept c_i includes set of senses ($s_{i,1}, s_{i,2}, \dots, s_{i,x}$), where i is the number of concept and x is the number of senses. An edge connects two concepts through a specific sense of each concept. The edge represents a sentential relation between the concepts. It can be a syntactical explicit and/or an Ontology Engine relation, where the latter is one of the six types of word relations: Hyponym, Hypernym, Holonym, Instance, Meronym, or Synonym. Fig. 1(a) illustrates an example of five concepts in IKG. $c_1 = \{\text{Country}\}$, $c_2 = \{\text{State}\}$, $c_3 = \{\text{freedom}\}$, $c_4 = \{\text{Ohio}\}$ and $c_5 = \{\text{Liberty}\}$, where c_1 , c_4 and c_5 are the CL belonging to LTX. c_2 belongs to a RTX. c_3 belongs to an OE.

A Knowledge Path (K) represents the relationship path between two concepts. It is represented as a sequence of edges connecting concepts c_i and c_j in a preserved sense. The concepts c_i and c_j belong to CL. The concepts in the middle may be external to CL. The following are examples of geometric paths:

- 1) $\{c_1-s_{1,1}: \text{Synonym}: s_{2,1}-c_2-s_{2,1}: \text{Instance}: s_{4,1}-c_4\}$.
- 2) $\{c_1-s_{1,1}: \text{Synonym}: s_{2,1}-c_2-s_{2,1}: \text{syntactic explicit}: s_{4,1}-c_4\}$.
- 3) $\{c_1-s_{1,1}: \text{Synonym}: s_{2,1}-c_2-s_{2,2}: \text{Hyponym}: s_{3,1}-c_3-s_{3,1}: \text{Hyponym}: s_{5,4}-c_5\}$.

c_i refers to the i^{th} concept. s_{ij} is the j^{th} sense of the i^{th} concept. For example, c_1 is the first concept and $s_{1,1}$ is the first sense of the first concept. Fig. 1(b, c, d, e) represents examples of geometric paths. The knowledge paths can be derived from geometric paths. For example:

- 1) $\{c_1-s_{1,1}: \text{Synonym}: s_{2,1}-c_2-s_{2,1}: \text{Instance}: s_{4,1}-c_4\}$.
- 2) $\{c_1-s_{1,1}: \text{Synonym}: s_{2,1}-c_2-s_{2,1}: \text{syntactic explicit}: s_{4,1}-c_4\}$.
- 3) $\{c_2-s_{2,2}: \text{Hyponym}: s_{3,1}-c_3-s_{3,1}: \text{Hyponym}: s_{5,4}-c_5\}$.

The three paths that mentioned above are considered knowledge paths, as the incoming and the outgoing senses of each concept are preserved. Fig. 1(b, c, e) represents examples of knowledge paths.

A prose can be often rich with concepts using domain specific terms. While reading such prose, non-specialist readers find these terms difficult to comprehend. They may face these difficulties while reading prose in any domain such as science, medical, finance and technology. Therefore, external knowledge helps the comprehension of prose by the integration with the prose concepts [13, 14]. This is not always

a straightforward process, as readers' prior knowledge may vary. Inexperienced readers may get overwhelmed by the amount of diverse external knowledge sources and types available since the latter can range from reference texts, dictionaries, and papers to conversations with experts. Identifying the right source of knowledge from a vast range of information can be a time consuming and exhausting task.

Therefore, this work proposes the Knowledge Induction Process to enhance prose comprehension. The process is designed to capture knowledge missing in a prose. The external knowledge source is captured through augmenting knowledge associations of prose concepts using reference texts and an Ontology Engine. The proposed solution assumes that concepts are known prior to the process of finding the knowledge associations amongst the concepts. The process reads appropriate parts from relevant reference texts and then captures a summary of the highest familiarity knowledge associations connecting the prose concepts. The Ontology Engine captures lexical knowledge associations for every concept pair. This process is formally presented in the following way: Given a prose LTX for comprehension, a set of prose concepts CL, $CL = \{c_1, c_{i+1}, \dots, c_n\} \in LTX$, a set of reference texts RTX, and an Ontology Engine OE. Find the IKG to represent knowledge associations amongst CL. The IKG is built through two fundamental techniques, namely a generation concepts representation and a reference consultation.

A. Generation of Concept Representation

To understand a prose text, a reader may break it up into a set of concepts and then find knowledge associations amongst these concepts. In order to find new or missing knowledge associations among the prose concepts, this process can be automated by applying a computational representation model. It is assumed that this enhances the prose comprehension. A graph is used to represent the concept and the associations, where each concept is represented by a node and each sentential relation between two concepts is represented by an edge.

A Syntactical Explicit Graph generator function KG() is used to convert a prose text LTX to a knowledge graph G_0 , and a reference text RTX to a reference knowledge graph GR. For each sentence in LTX/RTX, the function searches for pairs of concepts c_i and c_j if a word or a sequence of words found e_b , $b=1,2,\dots,n$ between them in the same sentence, where in LTX, c_i and c_j belong to CL and in RTX, c_i and c_j belong to the reference text noun concepts. The distance between c_i and c_j is $\leq L$, where L is the maximum number of words allowed between c_i and c_j . If it does, the function saves $[c_i, e_b, c_j]$ to be an edge in the graph representing a syntactical relation between c_i and c_j .

To allocate the most familiar knowledge associations that connect the prose concepts, it is crucial to evaluate the familiarity of knowledge associations. These can be calculated through the edge weight in the knowledge graph. Calculating the weight/familiarity value is based on the type of the sentential relation between concepts. The sentential relation types reflect the structures between any pair of concepts. The weight $w_{i,j}$ is calculated by (1) where $f_{i,j}$ is the frequency of the

relation type between concept c_i and c_j attained from the "Gutenberg Project" [15]. The "Gutenberg Project" is an online resource offering over 53,000 free e-books with expired US copyrights. This online archive is a very popular dataset frequently applied in text mining research [16, 17].

$$w_{i,j} = -1 / \left(\frac{1}{\log \left(\frac{f_{i,j}}{10^9} \right)} \right) \quad (1)$$

The familiarity value of a sequence of words between c_i and c_j is calculated based on the lowest weight of words sequence. The log of a word frequency is divided by 10^9 , as word frequencies are in the millions. The result is multiplied by -1 to avoid negative values. High frequency refers to high familiarity of a relation type. An inverse relationship between f and w indicates that the higher the frequency, the less its weight or the less its cost.

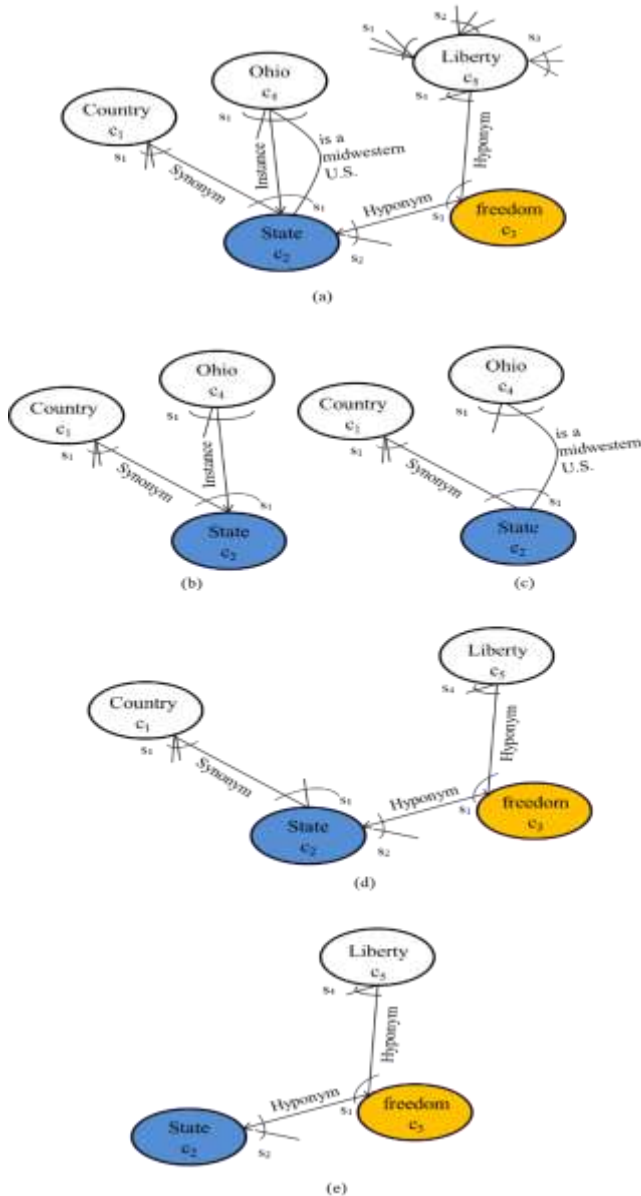


Fig. 1. Example of an Illuminated Knowledge Graph. (b, c, d, e) Exemplifying Geometric Path. (b, c, e) are Examples of Knowledge Paths.

Table I explains five types of the sentential relations between concept pairs. (1) is where a single word e_b appears between c_i and c_j , $b=1$. (i.e. Carbon-Carbon releases carbonization), here $c_i = Carbon-Carbon$, $c_j = carbonization$, and $e_1 = releases$. The weight of the edge is identified by considering the frequency within (1) as the frequency of the word e_1 . (2) is where multiple words e_b appear between c_i and c_j , $b > 1$ (i.e. Ethane is structurally the simplest hydrocarbon), where $c_i = Ethane$, $c_j = hydrocarbon$, $b=2$, $e_1 = structurally$, and $e_2 = simplest$. The weight of the edge is computed by considering the weight of e_1 and e_2 separately and then allocating the minimum weight. (3) is a class/subclass, wherein the sentential relation is either a hypernym or hyponym (i.e. Ethane is a hyponym of hydrocarbon), $c_i = Ethane$, $c_j = hydrocarbon$ and $e = hyponym$. The weight of the edge is determined by considering the frequency within (1) as the frequency of the word class. (4) is a part or subpart, wherein the sentential relation is either a holonym or meronym (Hydrogen is a holonym of water), $c_i = Hydrogen$, $c_j = water$ and $e = holonym$. The weight of the edge is determined by considering the frequency within (1) as the frequency of the word part. (5) is a synonym, if the sentential relation is synonym (Ethane is a synonym for C_2H_6). $c_i = Ethane$, $c_j = C_2H_6$ and $e = synonym$. The frequency of the synonym relation is supposed to be 1. Therefore, the weight of the edge is determined by considering 1 in the frequency given by (1).

To generate an IKG, the Knowledge Induction Process performs six steps as presented in Fig. 2:

- 1) Converting a prose LTX to a prose knowledge graph G_0 representing the syntactical relation between each pair in the prose concepts CL by performing a Graph generator function $KG()$.
- 2) Converting a reference text RTX_i to a reference knowledge graph GR_i representing the syntactical relation between each pair of the RTX_i concepts by performing the same Graph generator function $KG()$ used in step 1.
- 3) Extracting the highest familiarity knowledge path(s) of RTX_i connecting CL from GR_i by performing the Terminal to Terminal Traffic Steiner Tree function $TTTST()$. The extracted path(s) is called a Terminal to Terminal Traffic Steiner tree(s) $TTTST$ and it is represented in a graph called GU_i .
- 4) Joining G_0 and GU_i in a graph called G_{temp} representing the current state of the assimilated knowledge among CL by performing an assimilation function $G_{assmilation}()$.
- 5) Finding OE-Knowledge-Path(s) connecting each pair of G_{temp} concepts by performing the OE-Knowledge-Paths function $KPOE()$. The found paths are represented in a graph called GW_i .
- 6) Joining G_{temp} and GW_i in an Illuminated Knowledge Graph IKG_i representing the current state of the assimilated knowledge amongst CL by performing the assimilation function $G_{assmilation}()$.

Each time the process reads a new RTX_i , it performs steps 2 to 6 where, in step 4, G_0 is replaced with IKG_i . Fig. 3 shows

an example explaining the impact of using reference texts and an Ontology Engine for adding knowledge associations amongst a set of prose concepts about 'Ethane' chemical

compound, where $CL = \{ethane, hydrocarbon, hydrogen, carbon, carbon-carbon \text{ and } carbonization\}$.

TABLE I. TYPES OF SENTENTIAL RELATIONS

Sentential relation type	Sentential relation structure	w_{ij} value
Syntactical Relation		
	(1): Single word: $c_i - s_{i,*} : e_n : s_{j,*} - c_j ; b=1$	$w_{ij} = w(e_1)$
	(2): Multiple words: $c_i - s_{i,*} : e_1 e_2 \dots e_n : s_{j,*} - c_j ; b=1,2,\dots,n$	$w_{ij} = \min(w(e_n))$
OE Relation		
	(3): Class/Subclass: $c_i - s_{i,*} : \text{Hypernym} : s_{j,*} - c_j$ or $c_i - s_{i,*} : \text{Hyponym} : s_{j,*} - c_j$	$w_{ij} = w(e_{class})$
	(4): Part/Subpart: $c_i - s_{i,*} : \text{Holonym} : s_{j,*} - c_j$ or $c_i - s_{i,*} : \text{Meronym} : s_{j,*} - c_j$	$w_{ij} = w(e_{part})$
	(5): Synonym: $c_i - s_{i,*} : \text{Synonym} : s_{j,*} - c_j$	$w_{ij} = w(e_{synonym}) = 1$

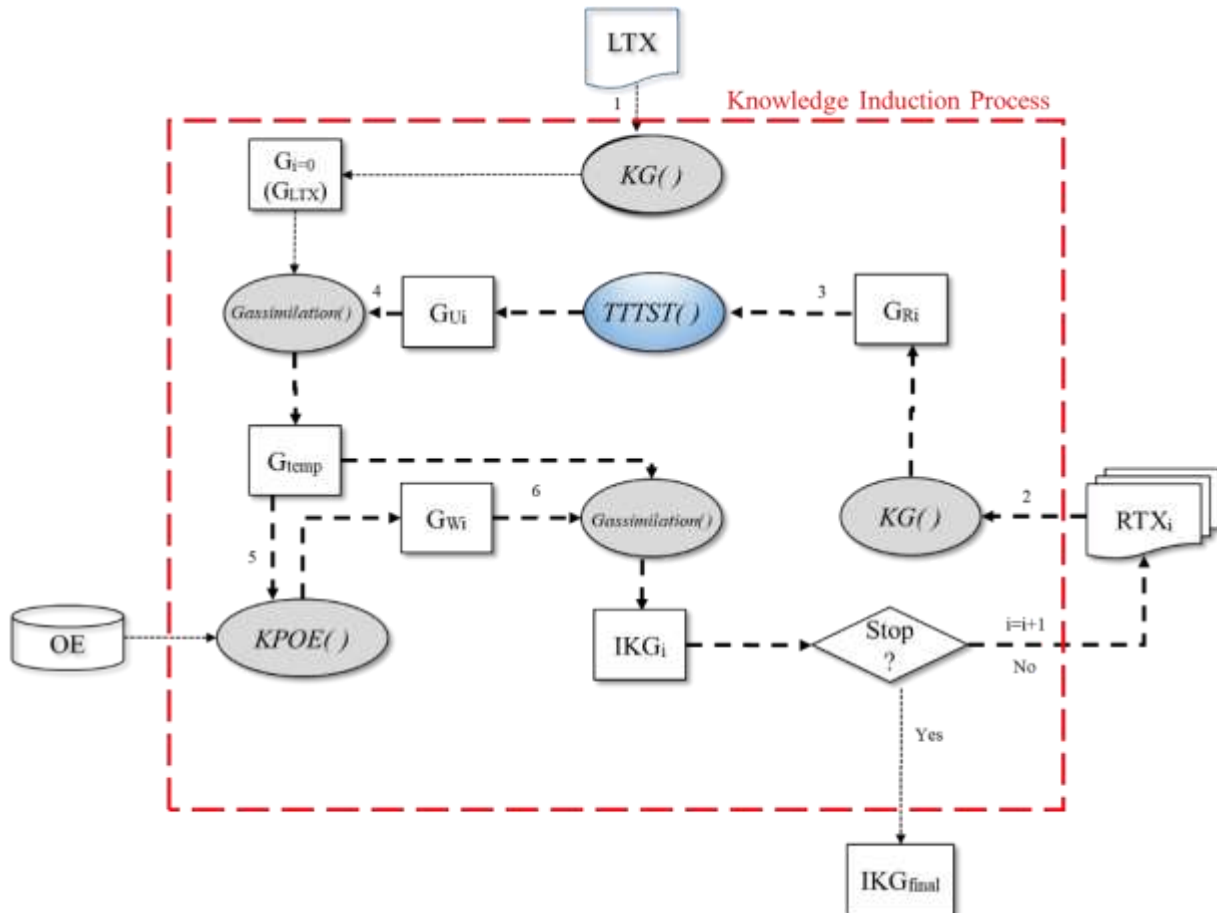


Fig. 2. Comprehension Engine.

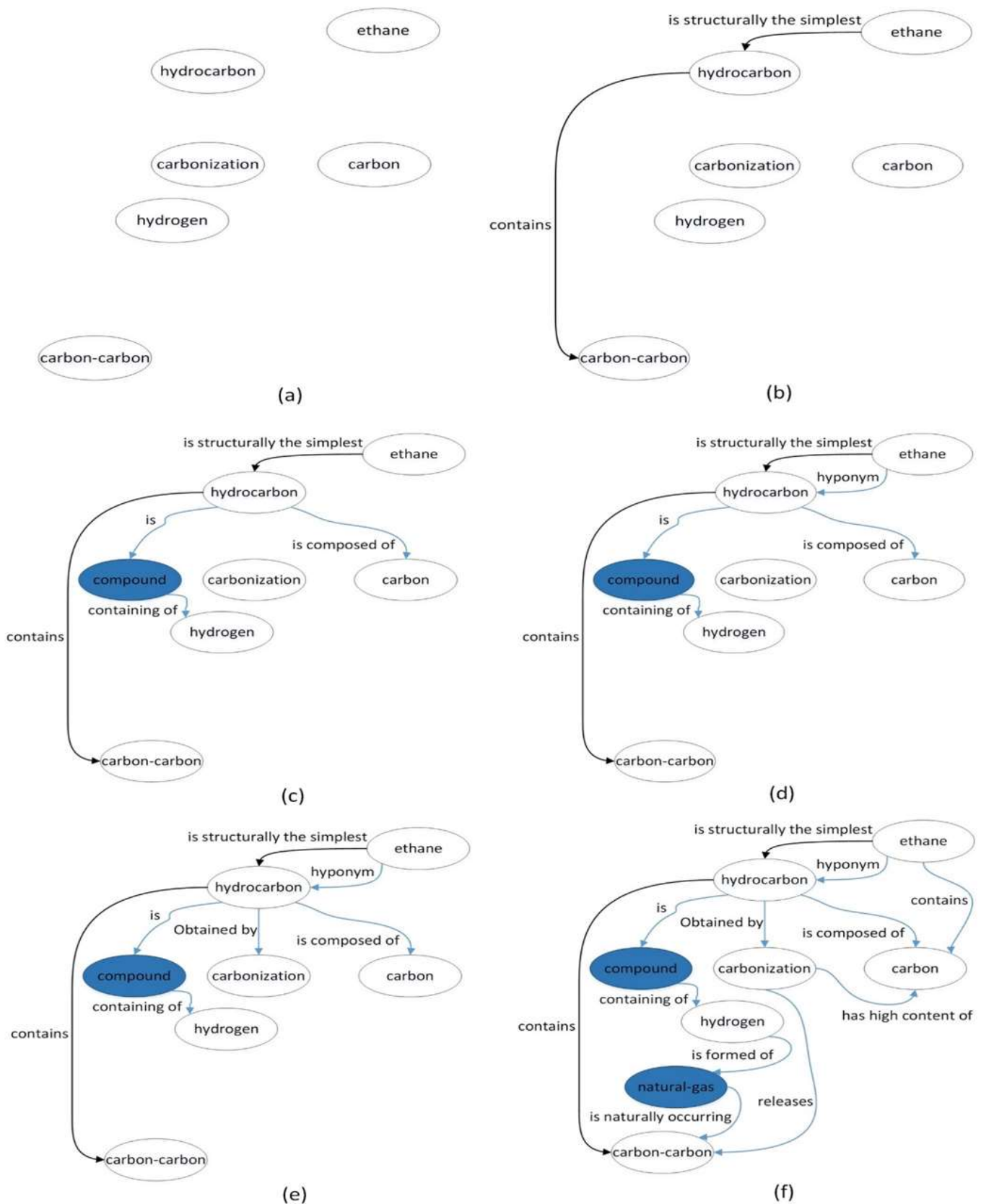


Fig. 3. Connecting CL Process using Reference Texts and Ontology Engine. (a) a set of Prose Concepts at the Initial Prose. (b) Knowledge Path K from the Initial Prose LTX. (c, e, f) Additional Knowledge Path K Extracted from RTX1, RTX2, and RTX3. (d) Additional Knowledge Path K Extracted from Ontology Engine OE.

B. Reference Consultation

1) *Highest familiarity knowledge extraction using a reference text:* Knowledge within a prose is limited, as readers cannot capture the knowledge relevant to all concepts required to comprehend the prose within the prose text only. Therefore, external reference texts are required to capture knowledge association amongst prose concepts. The reference texts are used to fill the knowledge gap of prose.

There are a number of Steiner tree versions that can be useful for identifying knowledge associations amongst the prose concepts [18, 19]. The main role of a Steiner tree in the proposed engine is to capture the highest familiarity knowledge paths amongst the prose concepts CL from each reference text GR_i with a minimum cost and a minimum number of external concepts, where the sentences of the captured knowledge paths are considered the summary of the reference text.

Given a connected, undirected reference knowledge graph $GR_i = (C, E)$, where C is a set of reference text concepts and E is a set of edges representing the relations amongst the graph concepts, the weight for each edge $w_{i,j}$ reflects its cost, where the cost here expresses the familiarity value of the sentential relation between the concepts of the edge ends c_i and c_j as shown in Fig. 4(a). Fig. 4(b) shows the set of prose concepts CL that need to find the highest familiarity knowledge paths amongst them in GR_i . Minimum Steiner Tree (MST) is an approach based on finding knowledge with the minimum cost amongst prose concepts [18]. The cost of MST is calculated by $\sum(w_{i,j})$, where $i, j \in C, i \neq j$. Sometimes, connecting the CL in a MST requires the addition of external concepts to CL. This case can be found in Fig. 4(c), $C = \{A, B, C, D, E\}$, $CL = \{A, C, E, D\}$. The returned Steiner tree is $\{E, D, B, A, C\}$ and it costs 10.

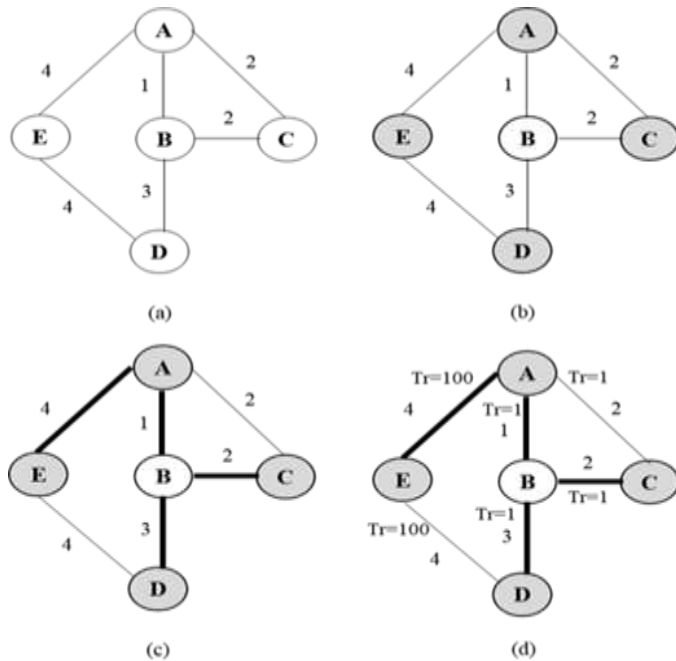


Fig. 4. Example of a Reference Knowledge Graph and different Types of Steiner Trees.

Suppose there is traffic (Tr) between c_i and c_j , where the traffic indicates the comprehension amount of the relation between the two concepts. In this case, the aim of the Steiner tree is to reduce the traffic amongst CL, whereby low traffic means high comprehension. Here, the Steiner tree is called Terminal to Terminal Traffic Steiner Tree (TTTST). Its cost is $\sum(w_{i,j} \times Tr_{i,j})$, where $i, j \in C$ and $i \neq j$. In Fig. 4(d), suppose that the traffic between each two concepts is $Tr_{i,j}=1$ and the traffic between concept E and concept A is $Tr_{E,A}=100$ and between concept E and concept D is $Tr_{E,D}=100$. In this case, the traffic weighted cost for the returned Steiner tree is $((4 \times 100) + (1 \times 1) + (3 \times 1) + (2 \times 1)) = 406$.

Fig. 5 represents the TTTST algorithm in the following way. The algorithm input is GR_i and CL. GR_i is a reference knowledge graph representing the syntactical relation between each pair of RTX_i concepts. The algorithm output is GU_i , which is a tree extracted from GR_i representing the highest familiarity knowledge path(s) connecting CL.

Def TTTST ():

Input: GR_i, CL

Output: TTTST: Terminal to Terminal Traffic Steiner Tree

```

1. //initialization
2. for each co in  $GR_i$ :
3.   if CL!= null:
4.     for each concept c in co
5.       prev[c]= -1
6.       cost[c]=INFINITY
7.       Visited[c]=False
8.       Q=null
9.       s= pick any concept from CL
10.      enqueue(Q,s)
11.     While Q!= null:
12.       c= dequeue(Q)
13.       Visited[c]=True
14.       if c in CL:
15.         cost[c]= 0
16.         add c to M
17.         remove c from CL
18.       for each neighbour  $c_i$  of c:
19.         if  $c_i$  not in Q and Visited[ $c_i$ ]==False:
20.           enqueue(Q,  $c_i$ )
21.           temp= cost[c] +  $w_{c_i,c}$ 
22.           if temp == cost[ $c_i$ ] and c in CL:
23.             prev[ $c_i$ ]=c //a knowledge path with minimum external concepts
                to  $c_i$  is found
24.             cost[ $c_i$ ]=temp
25.             else if temp < cost[ $c_i$ ]:
26.               prev[ $c_i$ ]=c // a less costly knowledge path to  $c_i$  is found
27.               cost[ $c_i$ ]=temp
28. TTTST = getPath(M[ ], prev[ ])
29. return TTTST
    
```

Fig. 5. Terminal to Terminal Traffic Steiner Tree Algorithm.

For each component co in GR_i , the algorithm uses a queue data structure Q to store each visited concept with its neighbors. It initializes Q by picking any concept from CL as the source s . Then, it initializes the cost between s and each concept c in the co to INFINITY and the previous concept $prev$ of each c to -1. In the loop iteration, it dequeues the first concept c in Q , marks it as visited, and checks if c belongs to CL. If so, it updates its cost to 0, adds it to M where M stores the found CL concepts, and removes it from CL. Then, it

enqueues all the neighbors' c_i 's of concept c if they are marked as non-visited, assigns $prev$ and calculates the cost for each of them. If the current c_i cost is equal to the previous one and c belongs to CL that means a knowledge path with minimum external concepts is found. Then, c_i 's $prev$ is updated to the new concept. However, if the current c_i cost is less than its previous one that means a less costly knowledge path to c_i is found wherein less cost means high familiarity. Then, c_i 's $prev$ and cost are updated to the new lesser values and the process is repeated until the queue is emptied. If all items in co are checked, $getPaths()$ constructs the TTTST from M and $prev$. The returned TTTST is represented in GU_i [20]. Suppose the graph shown in Fig. 6 is a reference knowledge graph GR_i . If $CL = \{c_1, c_7, c_8\}$ and the traffic for each edge $Tr=1$, then the TTTST returned by algorithm will be $\{c_1, c_3, c_6, c_7, c_8\}$.

2) *Knowledge extraction using ontology engine*: A useful source of knowledge is the Ontology Engine. An Ontology Engine to provide lexical knowledge associations between any two concepts by using OE-Knowledge-Paths function $KPOE()$ is utilized. This helps in adding a new type of knowledge which can contribute to increasing knowledge and improving comprehension. The OE-Knowledge-Path is a sequence of edges connecting any two concepts in a preserved sense. Each edge represents an ontological relation between its ends, where the ontological relation for each edge is one of the following relations: (1) synonym; (2) hypernym; (3) hyponym; (4) holonym; and (5) meronym.

Fig. 7 represents the $KPOE$ algorithm. It uses an Ontology Engine to search for OE-Knowledge-Path(s) connecting concept s and concept t , where s and t are the first and the last concepts in the path and the length of the path is less than or equal to α . The input of the algorithm is s , t , R , and $relationalGraph$. R is a dictionary that holds all the ontological engine relations in the Ontology Engine, and $relationalGraph$ is a dictionary of all concepts that have any of the ontological relations in R with the last node of the current path. The algorithm does not return the shortest path between s and t because it could be a path of multiple sense concepts. Rather, it searches if the neighbors of s have the same sense of s and have any of the ontological relation in R with s . If so, it searches the neighbors of the neighbors until it reaches t .

$NodeQ$ and $PathQ$ are two queue data structures used in the algorithm. $NodeQ$ keeps the current path that has a concept need to explore its neighbor. $PathQ$ holds the currently created paths. The algorithm starts with s as the current path. The while loop iterates through $PathQ$ paths searching for an OE-Knowledge-Path that connects s and t . In each iteration, it dequeues the first path in $PathQ$ and signs it in $NodeQ$. Then, it checks whether the last concept in $NodeQ$ matches t . If so, it saves the path in $Kpaths$ as an OE-Knowledge-Path between s and t ; otherwise, it checks if the $NodeQ$ length is less than α . If the last concept in $NodeQ$ matches t , for the sense of the $NodeQ$'s last concept, the function gets all of the concepts that have one of the ontological relations in R with the last concept in $NodeQ$, and adds them to $relationalGraph$. A number of paths are created between each $relationalGraph$ concept and

the current path. $PathQ$ saves the newly created paths. If all the paths in $PathQ$ are checked and $Kpaths$ do not exist, the function returns 'Not found' [20].

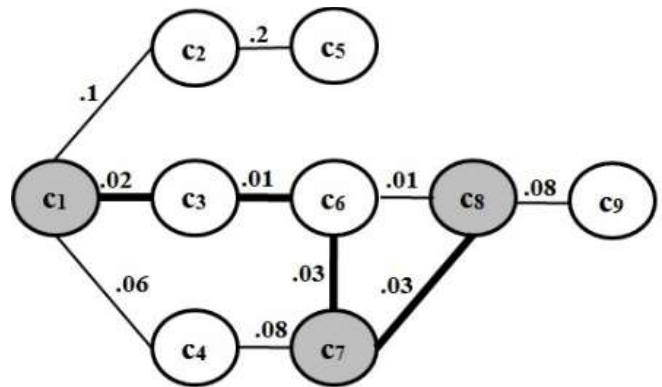


Fig. 6. Terminal to Terminal Traffic Steiner Tree Example.

```

Def KPOE ():
Input: s, t, R,  $\alpha$ 
Output: OE-Knowledge-Paths between s and t
PathQ = [ ]
1. Kpaths = [ ]
2. // push the first path into PathQ
3. PathQ.append([s])
4. for sen in s.sense( ):
5.   while PathQ:
6.     // get the first path from the PathQ
7.     NodeQ = PathQ.pop(0)
8.     // get the last node from NodeQ
9.     node= NodeQ[-1]
10.    // path found
11.    if node == t:
12.      Kpaths.append(NodeQ)
13.    return Kpaths
14.  else:
15.    if len(NodeQ) <=  $\alpha$ :
16.      sl= list( )
17.      for key, value in R.iteritems( ):
18.        re= value
19.        // get all concepts have relations from R with node and have the same sense of node
20.        x= re (node, sen, key)
21.        sl=sl+x
22.        relationalGraph[node] = sl
23.        // enumerate all adjacent nodes, construct a new path and push into the queue
24.      for adjacent in relationalGraph.get(node,[ ]):
25.        new_path=list(NodeQ)
26.        new_path.append( adjacent)
27.        if len(new_path) <  $\alpha$ :
28.          PathQ.append(adjacent)
29.        else:
30.          break
31.      if !(Kpaths):
32.        return 'Not found'

```

Fig. 7. Discovering OE- Knowledge-Paths Algorithm.

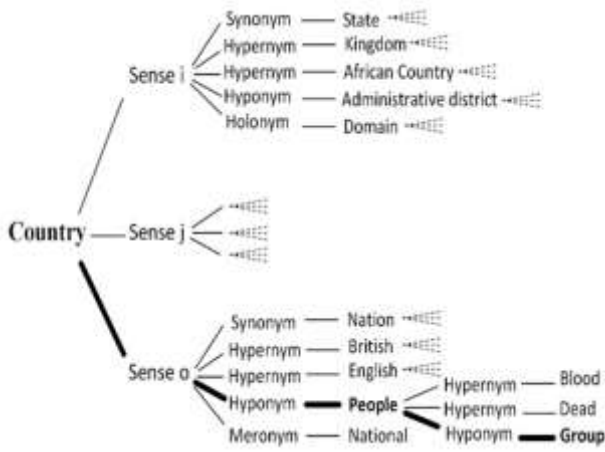


Fig. 8. Example of an OE-Knowledge-Path.

For example, consider $s = \text{"country"}$, $t = \text{"group"}$, and $\alpha = 4$. The returned OE-Knowledge-Path by the algorithm is *country (hyponym) people (hyponym) group*. The process of discovering the OE-Knowledge-Path between “country” and “group” is shown in Fig. 8.

IV. COMPREHENSION MODEL EVALUATION

An evaluation model is needed to assess the comprehension engine. The statistical characteristics of the knowledge obtained by the comprehension engine need to be measured. However, the process of measuring knowledge is still a difficult area that needs to be explored. “The fluid and intangible nature of knowledge makes its measurement an enormously complex and daunting task” [21].

The paper has proposed the use of graph theoretical metrics that provide a natural way to describe the structure and interplay of graph edges. A set of graph metrics presented in this section are divided into two types: quantitative assessment and organizational assessment. The mentioned types are important for the following reasons. (1) Quantitative assessment calculates rare knowledge growth, knowledge overload, and entropy to elaborate different aspects about the amount of knowledge that can be gained from the graph. (2) Organizational assessment calculates the size of the giant component, cluster coefficient and graph density to study the strength of the connections between concepts and their neighbors and the connectedness of the graph where high connectivity means high comprehension. The following section explains the real comprehension model based on all the mentioned graph metrics.

A. Content of Information

Comprehension enhancement is influenced by the size of obtained knowledge in the IKG. The obtained knowledge graph size can be computed by counting the entire number of concepts C and the entire number of relations E in IKG. Based on the Knowledge Induction Process, the graph starts with the prose knowledge graph G_0 . It is transformed into IKG_1 after reading RTX_1 , and then into IKG_2 after reading RTX_2 until it reaches IKG_{final} after reading all the RTX_i . At each state, the size of IKG may be increased and knowledge may be augmented. The knowledge growth rate λ is computed by (2)

where $|IKG_i|$ is the IKG size after reading RTX_i and $|G_0|$ is the prose knowledge graph size.

$$\lambda = \frac{|IKG_i|}{|G_0|} \quad (2)$$

The knowledge overload rate γ may also be increased, and it can be determined by (3):

$$\gamma = \frac{|IKG_i - G_0|}{|G_0|} \quad (3)$$

The amount of information that can be obtained from the knowledge graph can also be calculated by measuring the Entropy δ of the knowledge graph, where high entropy indicates that the knowledge graph has a high amount of information and vice versa. Based on [22], δ can be computed by (4):

$$\delta = - \sum_{i=0}^n p_i \log(p_i) \quad (4)$$

Where p_i is the degree distribution probability of concept c_i in the knowledge graph that can be determined by (5):

$$p_i = \frac{d_i}{2|E|} \quad (5)$$

Where, d_i is the degree of concept c_i and $|E|$ is the entire number of the relations in the knowledge graph. δ is divided by $\log(n)$ to obtain a measure between 0 and 1, where n is the entire number of the knowledge graph concepts.

B. Knowledge Organization

It is obvious that the existence of relationships amongst concepts in the prose influences comprehension. The greater the increase in the relations among the concepts, the higher the understanding of the relations between them. This falls under a graph organization notion that can be calculated by the size of the giant component [23] that can be calculated using (6):

$$GC = \frac{|C|}{|C|} \quad (6)$$

Where $|C|$ is the number of connected concepts forming a giant component and $|C|$ is the total number of concepts in the knowledge graph. The relation amongst the concepts and their neighbors in the knowledge graph can be calculated by the cluster coefficient β [24]. Based on [25], β is obtained by using (7):

$$\beta = \sum_{i=0}^n \frac{2NIC_i}{d_i(d_i-1)} \quad (7)$$

Where NIC_i is the neighbors’ interconnection coefficient of concept c_i , which denotes to the number of the sentential relations between the first neighbors of concept c_i , and d_i is the sentential relations of concept c_i which counts the first neighbors of concept c_i . The graph is considered highly clustered when the value is towards 1. The knowledge graph density ρ is another way to study the Knowledge graph organization to explore the completion and the integrations amongst concepts [26]. A complete knowledge graph contains all possible sentential relations E and density equals 1. The graph density ρ is calculated by (8) [27].

$$\rho = \frac{|E|}{|C|(|C|-1)} \quad (8)$$

Calculating the knowledge growth rate λ , the knowledge overload γ rate, and the cluster coefficient β require a reading of the external consultation to perform their calculations. Thus, their values are zero before reading the external references. The following example explains the influence of reading three reference texts with an Ontology Engine for adding knowledge associations amongst the prose concepts. The comprehension model evaluation for the proposed metrics before using external consultations in Fig. 3(b), and after using them in Fig. 3(f), respectively, is shown in Table II.

TABLE II. EXAMPLE OF THE COMPREHENSION ENGINE EVALUATION BEFORE AND AFTER USING REFERENCE EXTERNAL CONSULTATION

	Before using external consultations	after using external consultations
Growth λ	0	2.5
Overlap γ	0	1.5
Entropy δ	1.5	0.96
Giant Component Size GC	0.5	1
Cluster Coefficient β	0	0.92
Density ρ	0.07	0.21

V. EXPERIMENT

A. Content Material

An experiment was conducted on three prose texts LTX, and eight concepts were selected arbitrarily as the list of the prose concepts CL from each LTX. Wordnet [28] is a reliable Ontology Engine that has been used by many researchers in this area. It is a vast lexical database introduced by George Miller at the Cognitive Science Laboratory at Princeton University that is used as a dictionary of word senses and semantic relations between words [29-31]. This experiment was based on Wordnet Version 1.7 as a general reference text.

The used benchmark reference text articles for this paper were derived from <https://en.wikipedia.org>. Wikipedia articles were employed as RTX. For each LTX, a number of articles are taken from Wikipedia to represent each concept in CL. For the article allocation, the method presented in [32] to automatically select Wikipedia articles was chosen. Table III displays the selected LTX_i, as well as the CL for each prose.

For each LTX_i, the sentential relation among the concepts in its CL is represented in the prose knowledge graph G_0 . Through the Knowledge Induction Process, the system builds a set of Illuminated Knowledge Graphs IKG_i by scanning all of the RTX, where IKG_i is the sentential relation amongst the concepts in CL after reading a new RTX_i. The complete list of the used reference text articles can be found in Appendix Table V. All the references texts were accessed on July 24, 2019.

B. Results

This section presents the analysis of information gained from the Illuminated Knowledge Graph IKG_i of prose LTX_i in the Knowledge Induction Process.

TABLE III. LIST OF THE PROSES USED IN THE EXPERIMENT

	Prose Title	List of prose concepts CL
1 st prose LTX ₁	'Ethane chemical compound'[33]	['Ethane', 'hydrocarbon', 'hydrogen', 'carbon', 'chemical', 'petroleum', 'carbonization', 'coal']
2 nd prose LTX ₂	'New Test for Zika OKed' [34]	['Zika', 'infection', 'dengue', 'chikungunya', 'virus', 'aedes', 'mosquito', 'antibody']
3 rd prose LTX ₃	'Anesthesia gases are warming the planet' [35]	['Anesthetic', 'carbon', 'climate', 'oxide', 'desflurane', 'isoflurane', 'sevoflurane', 'halothane']

The average time needed to read the prose, the eight references attached to the prose and identification of the highest familiarity of sentential relations connecting the prose concepts in each reference are as the following: 4 minutes and 16 seconds for the 1st prose (LTX₁), 5 minutes and 18 seconds for the 2nd prose (LTX₂), and 2 minutes and 7 seconds for the 3rd prose (LTX₃). As noticeable, the machine spends a few minutes to read each prose with its related references.

Fig. 9 displays the information growth λ per knowledge graph in each prose LTX_i. The x-axis represents the prose knowledge graph G_0 and the Illuminated Knowledge Graph IKG_i after reading each reference text RTX_i, whereas the y-axis represents the growth rate λ . In LTX₁, there is a gradual increase in the information after reading reference texts RTX₁ to RTX₆, even though no new information was inserted after reading RTX₇. Interestingly, it started to increase again after reading RTX₈. In LTX₂, the information kept growing gradually from reading RTX₁ to RTX₈. In LTX₃, information increases varied. The information grew after reading RTX₁, while no new information was added after reading RTX₂ to RTX₄. It increased again after reading RTX₅ and RTX₆, although no new information was inserted after reading RTX₇ and RTX₈. This leads to the conclusion that reading references in some cases affect the increase of the knowledge positively, while in other cases these yield no effect.

The information overload rate γ in the knowledge graph is shown in Fig. 10. Here, the x-axis represents the prose knowledge graph G_0 and the Illuminated Knowledge Graph IKG_i after reading each reference text RTX_i, and the y-axis represents the overload rate γ . Similarly, it is clear that information overload varies from being slight to high in the three proses LTX after reading new reference texts RTX_i.

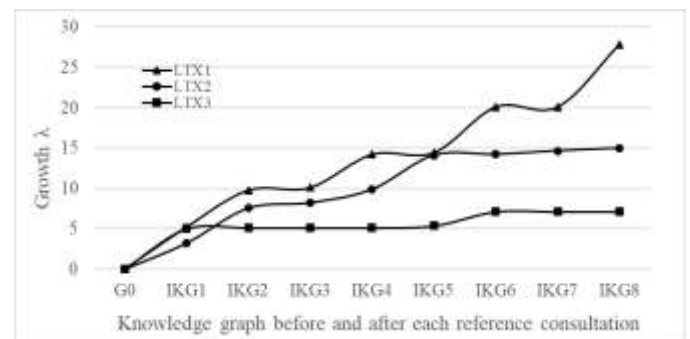


Fig. 9. Information Growth Rate "λ" Per the Knowledge Graphs.

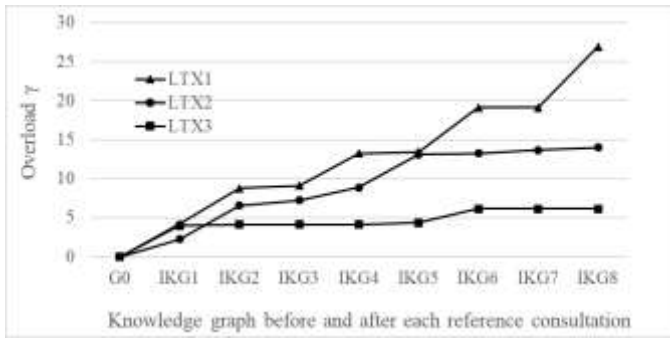


Fig. 10. Information Overload Rate γ Per the Knowledge Graphs.

Fig. 11 represents the entropy δ per each knowledge graph. The x-axis locates for both the prose knowledge graph G_0 and the Illuminated Knowledge Graph IKG_i after reading each reference text RTX_i , and the y-axis is the entropy δ . It was observed that δ in the three proses LTX started with low values, and then it bounced to high values after reading the 1st reference text RTX_1 . This implies that RTX_1 in the three proses LTX contributed to adding a high amount of information. Then, in LTX_1 the entropy value increased a little after having read RTX_2 to RTX_6 and RTX_8 . This means that texts RTX_2 to RTX_6 and RTX_8 inserted a low amount of information, while no new information was inserted when reading RTX_7 . In LTX_2 , there was a little increase in entropy after reading texts RTX_2 to RTX_8 ; thus, a limited amount of information was inserted. In LTX_3 , there was also a slight increase in the entropy after reading RTX_2 and RTX_5 ; a low amount of information was inserted here, and no new information was added after having read texts RTX_3 to RTX_4 , and RTX_6 to RTX_8 . This means that some of the reference texts are highly effective in adding information, while other texts have little effect.

Fig. 12 represents the amount of information that was gained due to contributions of the prose LTX, the reference text RTX, and the Ontology Engine OE concepts in the three proses separately. As shown in Fig. 12(a), for LTX_1 , the entropy value of OE concepts bounced to a greater value than that of the LTX and RTX concepts after reading texts RTX_1 to RTX_8 . This finding suggests that the amount of information inserted by the contribution of OE concepts was higher than the amount inserted by the contribution of the LTX and RTX concepts. In Fig. 12(b), for LTX_2 , the highest entropy value of the LTX, OE, and RTX concepts varied after reading RTX_1 to RTX_8 ; this indicated that the highest amount of information obtained by the contribution of the LTX, OE, or RTX concepts was not concentrated on the contribution of any one of them. In Fig. 12(c), for LTX_3 , the entropy value of the OE concepts was the highest amongst the LTX and RTX concepts after having read RTX_1 to RTX_8 . This means that the amount of information inserted by the contribution of the OE concepts is higher than the amount inserted by the contribution of the LTX and RTX concepts. This explains the importance of the LTX, RTX, and OE concepts when inserting information, showing that none of these concepts show greater gains than any other of these concepts.

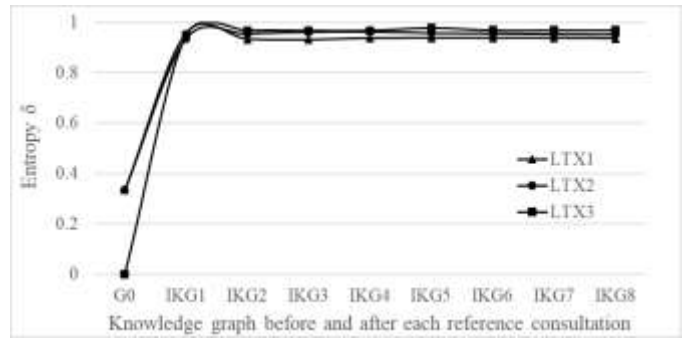
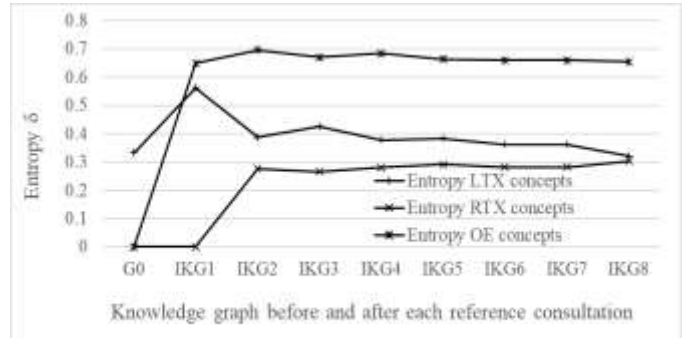
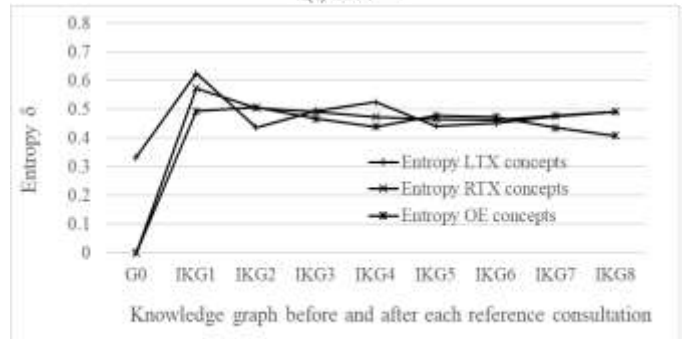


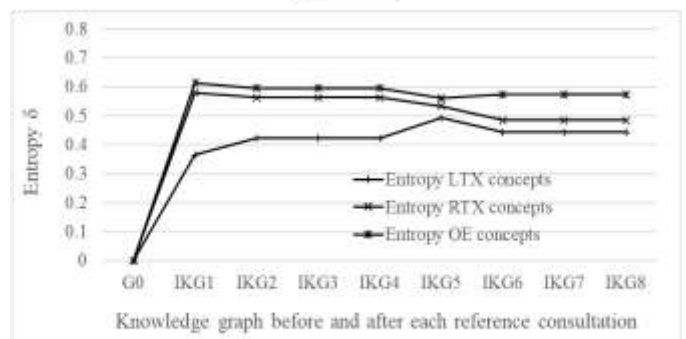
Fig. 11. Entropy and Per the Knowledge Graphs.



(a) LTX1



(b) LTX2



(c) LTX3

Fig. 12. Break Down of the Entropy and Per the Knowledge Graphs for the Three LTX.

Fig. 13 shows the size of the giant component of the knowledge graph both before and after reading the reference texts RTX_i . The x-axis refers to the prose knowledge graph G_0 and the Illuminated Knowledge Graph IKG_i after reading each reference text RTX_i , and the y-axis is the size of the giant

component GC of the knowledge graph. When the process reads a new RTX_i , the size of the giant component increases. It is observable that for LTX_1 , the giant component size moved from 0.25 to 0.85 after reading RTX_1 , and growing to as high as 1 after reading RTX_8 . For LTX_2 , the giant component size was 0.25 in the prose knowledge graph G_0 , and after reading RTX_1 , it reached to 1 and the concepts were fully connected. Meanwhile in LTX_3 , the giant component size bounced from 0 to 0.85 after reading RTX_1 and arrived at 1 after reading RTX_3 . It means that there was an enhancement of prose comprehension by reading reference texts for connecting the prose concepts in a giant component and illuminating sentential relations amongst them.

The breakdown of the total number of concepts C and the number of the sentential relations E in the prose knowledge graph G_0 and the Illuminated Knowledge Graph IKG_{final} for each prose LTX_i are shown in Table IV, wherein the concepts are from the prose LTX , the reference text RTX , and/or the Ontology Engine OE. As can be seen, there is a great variance in the number of concepts and the number of sentential relations between G_0 and IKG_{final} . Increasing the size may affect the information size positively. Therefore, increasing the IKG_{final} size is a significant sign of the overflowing information in the IKG_{final} , which can further support reinforcement of the prose comprehension.

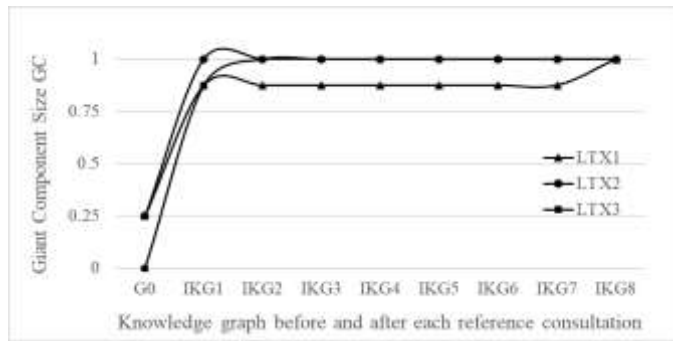


Fig. 13. Giant Component Size GC per the Knowledge Graphs.

TABLE IV. BREAK DOWN OF THE TOTAL NUMBER OF SENTENTIAL RELATION AND CONCEPTS IN THE THREE PROSES

	1 st prose LTX_1		2 nd prose LTX_2		3 rd prose LTX_3	
	G_0	IKG_{final}	G_0	IKG_{final}	G_0	IKG_{final}
Sentential relation	1	168	1	90	0	33
Number of prose LTX concepts	8	8	8	8	8	8
Number of reference concepts	0	12	0	16	0	5
Number of Ontology Engine OE concepts	0	63	0	21	0	11

Moreover, Fig. 14 illustrates the clustering coefficient β obtained in each knowledge graph. The x-axis refers to the prose knowledge graph G_0 and the Illuminated Knowledge Graph IKG_i after reading each reference text RTX_i , whereas the y-axis represents the clustering coefficient β . It is clear that some of the graphs are highly clustered; this is due to the fact that many of the concepts within these graphs are highly related to one another. For LTX_1 , the graph tended to be highly clustered, especially after reading RTX_1 , RTX_4 , RTX_5 and RTX_8 . In LTX_2 , the cluster coefficient bounced to a higher value after reading RTX_2 , lowered slightly after reading RTX_3 , then slightly increased after reading RTX_4 to RTX_8 . In LTX_3 , the cluster coefficient, which was higher when reading RTX_1 became stable after reading RTX_2 to RTX_5 . It increased again after reading RTX_6 and then returned to being steady after reading RTX_7 and RTX_8 . This means that there is enhancement of comprehension when some of the reference texts increase clustering of the concepts. In cases where the texts exercise a limited effect on clustering of the concepts, enhancement of comprehension is not observed.

Fig. 15 gives us a view of the integration amongst the concepts included within each knowledge graph. The x-axis is the prose knowledge graph G_0 and the Illuminated Knowledge Graph IKG_i after reading each reference text RTX_i , and the y-axis is the graph density ρ . As the graph reflects, in the three proses LTX , ρ showed a variance amongst the reference texts when inserting sentential relations amongst the concepts, bringing them close together.

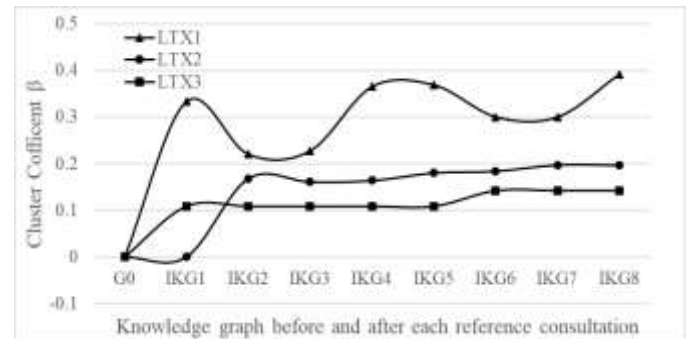


Fig. 14. Cluster Coefficient β Per the Knowledge.

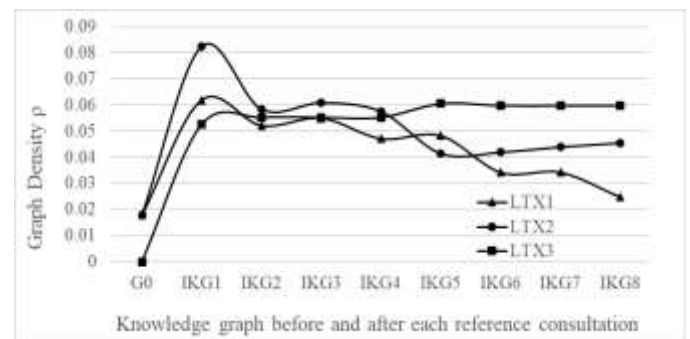


Fig. 15. Density ρ Per the Knowledge Graphs.

VI. CONCLUSION

The objective of this paper was to enhance prose comprehension by reducing the time expended on understanding the text and increasing the quality of comprehension. Accordingly, the comprehension engine was developed to read several reference texts, to allocate a summary of the highest familiarity knowledge amongst a set of target concepts in each reference and to provide lexical associations among the concepts by using an Ontology Engine. The comprehension engine was evaluated through set of graph metrics. The output performance of the comprehension engine demonstrates the efficiency of the compression engine in reducing reading time and increasing the quality of comprehension. Furthermore, the proposed engine can have academic implications on students or academic learners by providing them with the most familiar and lexical knowledge that can help in prose comprehension in a short time. Although the proposed engine may help readers to increase their knowledge and improve prose comprehension, at times this can cause mess and give rise to 'too much knowledge' in prose comprehension, thus challenging preservation and retention by human memory. Future work will be carried out to develop a second phase of the comprehension engine that efficiently select the less difficult to understand knowledge from the augmented knowledge and present it to readers as an enhanced text. In addition, the impact of using the comprehension engine in improving the comprehension through evaluating the comprehension rate on participants and make a comparison between the two-phase results will be studied.

REFERENCES

- [1] R. G. Ortego and I. M. Sánchez, "Relevant parameters for the classification of reading books depending on the degree of textual readability in primary and compulsory secondary education (cse) students," *IEEE Access*, vol. 7, pp. 79044-79055, 2019.
- [2] N. S. Al Madi, "A Study of Learning Performance and Cognitive Activity During Multimodal Comprehension Using Segmentation-integration Model and EEG," Kent State University, 2014.
- [3] R. P. Carver, "Reading rate: Theory, research, and practical implications," *Journal of Reading*, vol. 36, no. 2, pp. 84-95, 1992.
- [4] R. P. Carver, "Reading theory predictions of amount comprehended under different purposes and speed reading conditions," *Reading Research Quarterly*, pp. 205-218, 1984.
- [5] A. P. Widyassari, S. Rustad, G. F. Shidik, E. Noersasongko, A. Syukur, and A. Affandy, "Review of Automatic Text Summarization Techniques & Methods," *Journal of King Saud University-Computer and Information Sciences*, 2020.
- [6] H. Van Lierde and T. W. Chow, "Learning with fuzzy hypergraphs: A topical approach to query-oriented text summarization," *Information Sciences*, vol. 496, pp. 212-224, 2019.
- [7] Á. Hernández-Castañeda, R. A. García-Hernández, Y. Ledeneva, and C. E. Millán-Hernández, "Extractive Automatic Text Summarization Based on Lexical-Semantic Keywords," *IEEE Access*, vol. 8, pp. 49896-49907, 2020.
- [8] M. N. Azadani, N. Ghadiri, and E. Davoudijam, "Graph-based biomedical text summarization: An itemset mining and sentence clustering approach," *Journal of biomedical informatics*, vol. 84, pp. 42-58, 2018.
- [9] T. A. Fuad, M. T. Nayeem, A. Mahmud, and Y. Chali, "Neural sentence fusion for diversity driven abstractive multi-document summarization," *Computer Speech & Language*, vol. 58, pp. 216-230, 2019.
- [10] J. Ding, Y. Li, H. Ni, and Z. Yang, "Generative Text Summary Based on Enhanced Semantic Attention and Gain-Benefit Gate," *IEEE Access*, vol. 8, pp. 92659-92668, 2020.
- [11] L. Cagliero, L. Farinetti, and E. Baralis, "Recommending personalized summaries of teaching materials," *IEEE Access*, vol. 7, pp. 22729-22739, 2019.
- [12] T. Yu, J. Li, Q. Yu, Y. Tian, X. Shun, L. Xu, L. Zhu, and H. Gao, "Knowledge graph for TCM health preservation: design, construction, and applications," *Artificial Intelligence in Medicine*, vol. 77, pp. 48-52, 2017.
- [13] A. Babour, J. I. Khan, and F. Nafa, "Deepening Prose Comprehension by Incremental Free Text Conceptual Graph Mining and Knowledge," in *2016 International Conference on Cyber-Enabled Distributed Computing and Knowledge Discovery (CyberC)*, 2016, pp. 208-215: IEEE.
- [14] J. I. Khan and M. S. Hardas, "Does sequence of presentation matter in reading comprehension? a model based analysis of semantic concept network growth during reading," in *2013 IEEE Seventh International Conference on Semantic Computing*, 2013, pp. 444-452: IEEE.
- [15] M. Hart. (1971). Project Gutenberg. Available: <http://www.gutenberg.org/>, Accessed on: 21 July, 2017.
- [16] A. Agrawal and A. An, "Unsupervised emotion detection from text using semantic and syntactic relations," in *2012 IEEE/WIC/ACM International Conferences on Web Intelligence and Intelligent Agent Technology*, 2012, vol. 1, pp. 346-353: IEEE.
- [17] D. Chandran, K. Crockett, D. Mclean, and Z. Bandar, "FAST: A fuzzy semantic sentence similarity measure," in *2013 IEEE International Conference on Fuzzy Systems (FUZZ-IEEE)*, 2013, pp. 1-8: IEEE.
- [18] H. Takahashi, "An approximate solution for the Steiner problem in graphs," 1980.
- [19] L. Kou, G. Markowsky, and L. Berman, "A fast algorithm for Steiner trees," *Acta informatica*, vol. 15, no. 2, pp. 141-145, 1981.
- [20] A. Babour, "A Computational Mimicry of the Knowledge Augmentation Process in Comprehension based Learning," Kent State University, 2017.
- [21] M. A. Ragab and A. Arisha, "Knowledge management and measurement: a critical review," *Journal of knowledge management*, 2013.
- [22] C. E. Shannon and W. Weaver, *The Mathematical Theory of Communication*, by CE Shannon (and Recent Contributions to the Mathematical Theory of Communication), W. Weaver. University of Illinois Press, 1949.
- [23] R. Hekmat and P. Van Mieghem, "Study of connectivity in wireless ad-hoc networks with an improved radio model," in *Proc. of WiOpt*, 2004, vol. 10.
- [24] P. Drieger, "Semantic network analysis as a method for visual text analytics," *Procedia-social and behavioral sciences*, vol. 79, no. 2013, pp. 4-17, 2013.
- [25] D. J. Watts and S. H. Strogatz, "Collective dynamics of 'small-world' networks," *nature*, vol. 393, no. 6684, pp. 440-442, 1998.
- [26] N. S. Al Madi and J. I. Khan, "Is learning by reading a book better than watching a movie? a computational analysis of semantic concept network growth during text and multimedia comprehension," in *2015 International Joint Conference on Neural Networks (IJCNN)*, 2015, pp. 1-8: IEEE.
- [27] T. F. Coleman and J. J. Moré, "Estimation of sparse Jacobian matrices and graph coloring blems," *SIAM journal on Numerical Analysis*, vol. 20, no. 1, pp. 187-209, 1983.
- [28] G. A. Miller, "WordNet: a lexical database for English," *Communications of the ACM*, vol. 38, no. 11, pp. 39-41, 1995.
- [29] S. Menaka and N. Radha, "Text classification using keyword extraction technique," *International Journal of Advanced Research in Computer Science and Software Engineering*, vol. 3, no. 12, pp. 734-740, 2013.
- [30] J.-M. Chen, M.-C. Chen, and Y. S. Sun, "A novel approach for enhancing student reading comprehension and assisting teacher assessment of literacy," *Computers & Education*, vol. 55, no. 3, pp. 1367-1382, 2010.
- [31] J. Kamps, M. Marx, R. J. Mokken, and M. De Rijke, "Using WordNet to measure semantic orientations of adjectives," in *LREC*, 2004, vol. 4, pp. 1115-1118: Citeseer.
- [32] A. Babour, F. Nafa, and J. I. Khan, "Connecting the dots in a concept space by Iterative reading of Freetext references with Wordnet," in *2015 IEEE/WIC/ACM International Conference on Web Intelligence and Intelligent Agent Technology (WI-IAT)*, 2015, vol. 1, pp. 441-444: IEEE.
- [33] Ethane, *Encyclopaedia Britannica* [Online], 2013, <https://www.britannica.com/science/ethane>, Accessed on: July 24, 2017.

[34] K. Grens. (Mar 22, 2016). New Test for Zika OKed. Available: <https://www.the-scientist.com/the-nutshell/new-test-for-zika-oked-33858>, Accessed on: July 24, 2017.

[35] M. DeMarco. (April 7, 2015). Anesthesia gases are warming the planet. Available: <https://www.sciencemag.org/news/2015/04/anesthesia-gases-are-warming-planet>, Accessed on: July 24, 2017.

APPENDIX

LIST OF THE REFERENCE TEXT ARTICLES USED IN THE EXPERIMENT.

Title	Link
Ethane	https://en.wikipedia.org/w/index.php?title=Ethane&oldid=784178139
Hydrocarbon	https://en.wikipedia.org/w/index.php?title=Hydrocarbon&oldid=797145615
Hydrogen	https://en.wikipedia.org/w/index.php?title=Hydrogen&oldid=794824238
Carbon	https://en.wikipedia.org/w/index.php?title=Carbon&oldid=797606653
Chemical substance	https://en.wikipedia.org/w/index.php?title=Chemical_substance&oldid=797496319
Petroleum	https://en.wikipedia.org/w/index.php?title=Petroleum&oldid=797608302
Carbonization	https://en.wikipedia.org/w/index.php?title=Carbonization&oldid=795078223
Coal	https://en.wikipedia.org/w/index.php?title=Coal&oldid=797262457
Zika fever	https://en.wikipedia.org/w/index.php?title=Zika_fever&oldid=797239605%20130
Infection	https://en.wikipedia.org/w/index.php?title=Infection&oldid=797795424
Dengue fever	https://en.wikipedia.org/w/index.php?title=Dengue_fever&oldid=798056254
Chikungunya	https://en.wikipedia.org/w/index.php?title=Chikungunya&oldid=797661262
Virus	https://en.wikipedia.org/w/index.php?title=Virus&oldid=797985669
Aedes	https://en.wikipedia.org/w/index.php?title=Aedes&oldid=797888558
Mosquito	https://en.wikipedia.org/w/index.php?title=Mosquito&oldid=797321614
Antibody	https://en.wikipedia.org/w/index.php?title=Antibody&oldid=797925412_119
Anesthetic	https://en.wikipedia.org/w/index.php?title=Anesthetic&oldid=796835414
Climate	https://en.wikipedia.org/w/index.php?title=Climate&oldid=797528936
Oxide	https://en.wikipedia.org/w/index.php?title=Oxide&oldid=789414027
Desflurane	https://en.wikipedia.org/w/index.php?title=Desflurane&oldid=797545466
Isoflurane	https://en.wikipedia.org/w/index.php?title=Isoflurane&oldid=797545327_124
Sevoflurane	https://en.wikipedia.org/w/index.php?title=Sevoflurane&oldid=797688679
Halothane	https://en.wikipedia.org/w/index.php?title=Halothane&oldid=797545700

Impact of the Mining Activity on the Water Quality in Peru Applying the Fuzzy Logic with the Grey Clustering Method

Alexi Delgado¹, Anabel Fernandez², Brigitte Chirinos³, Gabriel Barboza⁴, Enrique Lee Huamani⁵
Mining Engineering Section, Pontificia Universidad Católica del Perú, Lima-Perú¹
Facultad de Ingeniería Ambiental, Universidad Nacional de Ingeniería, Lima, Perú^{2,3,4}
Image Processing Research Laboratory, Universidad de Ciencias y Humanidades, Lima-Perú⁵

Abstract—Mining activity in the department of Junín, Peru, is intense, due to the great existing mining-metallic potential that exists in the place, the Yauli and Andaychagua rivers, located in the Yauli Province, belonging to Junín, receive a large volume of discharges causing deterioration in the quality of the water of these rivers. To evaluate this quality in an integral way, fuzzy logic will be applied with the Grey Clustering methodology, defining the central point triangular whitening weight functions (CTWF), having as grey classes the Environmental Quality Standards for water (ECA-Water), Category 3, which were modified for research purposes. Four monitoring points were evaluated, both upstream (point PY-01) and downstream (PY-02) of the Yauli River; as upstream (PA-01) and downstream (PA-02) of the Andaychagua river. From the analysis it was determined that the water quality in PY-01 is 0.7302, 0.8795 in the dry season and 0.5980 in the wet season; in PY-02, 0.5448, 0.6448 in dry season and 0.5628 in wet season were obtained. At point PA-01 it is 0.8213, 0.8691 in dry season and 0.7902 in wet season; In PA-02, 0.8385, 0.8827 in the dry season and 0.8118 in the wet season were obtained, concluding that there is good water quality, decreasing in wet seasons, this due to the influence of the rains in the contact waters. The research provides an integration of the parameters that are considered in the ECA-Water with other international standards allowing to determine a more precise evaluation of the quality status of the Yauli and Andaychagua rivers after receiving the effluents generated by the mining activity, benefiting the relevant authorities for decision making and providing a methodology that improves the analysis of the results obtained by the specific parameters that are evaluated in the environmental monitoring.

Keywords—Mining activity; water quality; grey clustering

I. INTRODUCTION

The department of Junín, in Peru, is divided into 07 metallogenic strips. These strips represent periods of mineralization that extend along regional fault systems and the lithologies that have favored the mineralization of polymetallic mineral deposits of economic interest [1]. This is why it is an ideal place for the exploitation of minerals, a situation that has led many mining companies to grant concessions to a large percentage of this department to carry out the extraction of minerals. In other words, it is an area with great polymetallic mining activity but also with an excessive discharge of acidic waters that contaminate the environment [2].

Based on the above, a particular case will be evaluated regarding the activity of two mining units in the province of Yauli, belonging to the department of Junín, due to the discharge of its effluents affecting, mainly, the rivers that serve as receiving bodies for such effluents, the Yauli and Andaychagua rivers. The Yauli and Andaychagua Rivers are the first to receive the greatest concentration and influence of mining activities in the Junín Region [3], since mining activity is intense, so a large volume of discharges must be evacuated, some of them directly and others in the tailings ponds [4].

The grey system theory is a useful methodology for systems with incomplete information. Grey relational analysis can be used to analyze relationships between one of the main ones, as a reference, and the others to establish a certain comparison [5].

Grey Clustering is a method that can be applied by incidence of grey matrices or grey bleaching weight functions. In this work, we use triangular center-point whitening weight functions (CTWF), since CTWF are applied mainly to test if the observation objects belong to predetermined classes, called grey classes [6], as shown by the decision making studies [7], to determine key indicators [8], for the evaluation of safety management [9], project location selection [10], air quality assessment [11], water resources management. The CTWF could be applied to classify monitoring points in water quality assessment; therefore, in this study 4 monitoring points will be identified, both upstream, and downstream of the Yauli and Andaychagua rivers, taking as standard values the environmental water quality standards, category 3, using the CTWF method.

Based on the information presented, the specific objective is to analyze the impact caused by two mining units when they discharge their effluents into the Yauli and Andaychagua rivers by applying the Grey Clustering methodology, to subsequently compare the water quality of both rivers and determine where the greatest impact is required on the treatment of these effluents, prior to discharge.

In the present work, Section II briefly summarizes the main background taken as reference for the research; Section III shows details about the CTWF method; Section IV describes the case study, followed by the results and

discussion of them in Section V. Finally, the conclusions are presented in Section IV.

II. LITERATURE REVIEW

An investigation on an artificial intelligence model based on grey systems to evaluate the water quality of the Santa River basin is presented [12], in which with the grey grouping method the water quality was evaluated using the artificial intelligence criteria together with the data from twenty-one monitoring points of the Santa River of the National Water Authority of Peru (ANA) in comparison with parameters established by MINAM-Peru (DS No 015-2015). The results showed that 47.6% of the monitoring points had good water quality for the population's consumption, 33.3% of the points had moderate water quality and 19.1% had low water quality for the population's consumption.

The investigation to determine the water quality of five water bodies in the Rimac River Basin [13] which belong to Category 1 A2: "Population and Recreation" with the application of the Grey Clustering analysis methodology and the Prati water quality index. The five bodies of water under study were determined to be uncontaminated, which gives them the characteristics of belonging to Category 1 A2, since they do not represent a risk to human health and can be made drinkable through conventional treatment.

The case of the evaluation of drinking water consumption in the city of Lima is presented using the Grey Clustering method [14]. The evaluation was carried out in 32 districts of Lima, Peru, and resulted in a map of the drinking water consumption situation. These results revealed that the districts that consume the most water are San Isidro, Miraflores, La Molina, San Borja and Lince; and those that consume the least were Ancón, Puente Piedra, Villa el Salvador and Independencia.

On the other hand, an application was made in the integral evaluation of the water environment quality of Zhalong wetland based on the grey grouping method [15], for which the criteria of the water quality classification standard GB 3838-2002 were used, where the degree of contamination is divided into 5 levels. As a result, water pollution was very severe in the area studied, which is caused by the mutual interaction of water scarcity, contaminants above the test standard, and internal pollution, while water scarcity is the main factor of pollution.

There is also an application of the Grey Clustering method for the evaluation of surface water quality [16] and the analysis of results showed that the water quality of Shuangliao was of first degree and slightly contaminated, the water quality of Lanhezha, Liaoyuan, second and fourth degree, while for the water of Erlongshan reservoir, Siping and Yitong were in fifth degree seriously contaminated.

III. METHODOLOGY

For the grey grouping method, m monitoring points and a set of n water quality parameters are taken, being these x_{ij} ($i=1,2,\dots,m;j=1,2,\dots,n$) [6].

The next steps of the method are as follows:

Step 1: First the standard values for each water quality parameter (j) are sized according to Peruvian and foreign regulations for water quality for irrigation of vegetables and drinking of animals

Step 2: The classes of flock on the water parameters taken are plotted as shown in Fig. 1.

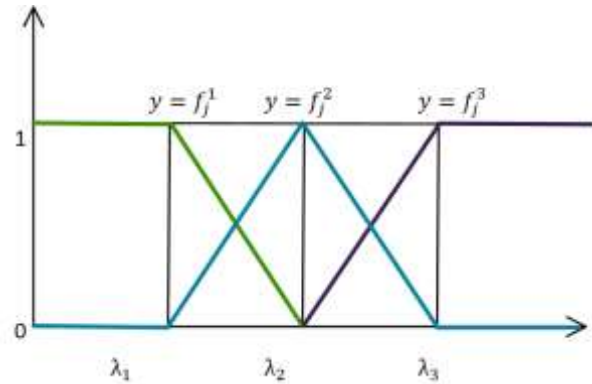


Fig. 1. Clustering Function Chart.

Where:

$y = f_j^1 = A1 = \text{Good quality water for watering}$

$y = f_j^2 = A2 = \text{Moderate water quality for watering}$

$y = f_j^3 = A3 = \text{SPoor quality water for watering}$

Now we present the triangular center-point whitening weight (CTWF) functions for each of the established parameters, for the k-th class grey, $k=1, 2, 3$, of the j-th parameter, $j=1, 2,\dots,n$, for a monitoring value x_{ij} by Eq. 1-3.

$$f_1^1(x_{ij}) = \begin{cases} 1, & x \in [0, \lambda_j^1] \\ \frac{\lambda_j^2 - x}{\lambda_j^2 - \lambda_j^1}, & x \in [\lambda_j^1, \lambda_j^2] \\ 0, & x \in [\lambda_j^2, +\infty] \end{cases} \quad (1)$$

$$f_1^2(x_{ij}) = \begin{cases} \frac{x - \lambda_j^1}{\lambda_j^2 - \lambda_j^1}, & x \in [\lambda_j^1, \lambda_j^2] \\ \frac{\lambda_j^3 - x}{\lambda_j^3 - \lambda_j^2}, & x \in [\lambda_j^2, \lambda_j^3] \\ 0, & x \notin [\lambda_j^1, \lambda_j^3] \end{cases} \quad (2)$$

$$f_1^3(x_{ij}) = \begin{cases} \frac{x - \lambda_j^2}{\lambda_j^3 - \lambda_j^2}, & x \in [\lambda_j^2, \lambda_j^3] \\ 1, & x \in [\lambda_j^3, +\infty] \\ 0, & x \in [0, \lambda_j^2] \end{cases} \quad (3)$$

Step 3: To determine the weights of each established parameter (n_{ij}), the statistical procedure of harmonic mean is established as follows. Eq. 4.

$$n_j^k = \frac{\frac{1}{\lambda_j^k}}{\sum_{j=1}^m \frac{1}{\lambda_j^k}} \quad (4)$$

Step 4: The integral grouping coefficient σ_i^k for each monitoring point $i, i=1, 2, \dots, m$, with respect to the grey classes $k, k=1, 2, 3$, is calculated with the following equation. Eq. 5:

$$\sigma_i^k = \sum_{j=1}^n f_j^k(x_{ij}) \cdot n_j \quad (5)$$

Step 5: We determine the results using the Max clustering coefficient, as shown in Eq. 6, and decide that object i belongs to the k^* grey class. When there are several objects in the k^* grey class, these objects can be sorted according to the magnitudes of their full clustering coefficients.

$$\max_{1 \leq k \leq S} \{\sigma_i^k\} = \sigma_i^{k^*} \quad (6)$$

IV. CASE STUDY

The Yauli and Andaychagua rivers are located in the province of Yauli, department of Junín, where mining activity is intense, so there is a large volume of discharges, some of them directly (mine water, domestic wastewater) and others in the tailing ponds [4].

A. Definition of Objects of Study

Four upstream and downstream monitoring points were analyzed for the Yauli River with respect to mining activity and for the Andaychagua River in the same manner. Upstream of the monitoring points for the Yauli river is the town center of Yauli and downstream is the Pomacocha lagoon. For the Andaychagua river the closest body of water is the Aguascocha lagoon, which is downstream.

Fig. 2 and Fig. 3 show the monitoring points for the Yauli and Andaychagua rivers, respectively.

Points PY-01 and PA-01 belong to the upstream stations of each river in the project and points PY-02 and PA-02 downstream, in addition to each monitoring point was evaluated for wet and dry season. As shown in Table I.



Fig. 2. Monitoring Points in the Upstream and Downstream Yauli River.



Fig. 3. Monitoring Points in the Andaychagua River, Upstream and Downstream.

TABLE I. LOCATION OF MONITORING POINTS

Monitoring points	Location	
	Eastern Coordinated	North Coordinator
PY-01	379109.00 m E	8706069.00 m S
PY-02	380082.00 m E	8706894.00 m S
PA-01	340218.00 m E	8759747.00 m S
PA-02	340450.00 m E	8759243.00 m S

B. Definition of Evaluation Criteria

The evaluation criteria for the study were taken from Peruvian regulations and international standards to obtain a range of specificity regarding water quality, these are.

1) *Dissolved oxygen*: The RCT for water in the Peruvian regulations [17] establishes values >5 mg/L and 4mg/L for irrigation and animal drinking, a more restrictive value taken to consider water quality good was >7.5 mg/L which belongs to the Chilean legislation [18] for water destined for unrestricted irrigation.

2) *Hydrogen potential*: The ECA for water of the Peruvian regulations [17] establishes values of 6.5-8.5 and 6.5-8.4 of pH for irrigation of vegetables and drink of animals. One value taken was from the Water Law [19] with a pH value of 5-9 units.

3) *Arsenic*: The RCT for water in the Peruvian regulations [17] establishes values of 0.1 mg/L and 0.2 mg/L for irrigation of vegetables and drinking water for animals. A more restrictive value was taken from the Regulations for the Control of Water Bodies in Venezuela [20], with a value of 0.05 mg/L of Arsenic for water intended for drinking water for livestock.

4) *Cadmium*: The ECA for water of the Peruvian regulations [17] establishes values of 0.01mg/L and 0.05 mg/L for irrigation of vegetables and animal beverages, a more restrictive value was 0.001mg/L which belongs to the Draft Quality Standard for the Protection of Continental Surface Water in Chile [18], in waters destined to restrictive irrigation.

5) *Coppe*: The ECA for water of the Peruvian regulations [17] establishes values of 0.2 mg/L and 0.5mg/L for irrigation of vegetables and animal beverages, a more restrictive value was 0.002mg/L, which belongs to the Draft Quality Standard for the Protection of Continental Surface Water in Chile [18], in waters destined to restrictive irrigation.

6) *Cobalt*: The RCT for water of the Peruvian regulations [17] establishes values of 0.05 mg/L and 1mg/L for irrigation of vegetables and animal beverages, a value that was taken as an intermediate was 0.1 mg/L which was established in an investigation carried out by the FAO [21].

7) *Iron*: The ECA for water of the Peruvian regulations [17] establishes values of 5mg/L for irrigation of vegetables and animal beverages. Two more restrictive values were chosen: 1 mg/L, established in the General Water Law [19], and 0.3 mg/L, which corresponds to the Draft Quality Standard for the Protection of Inland Surface Water in Chile, for water intended for restrictive irrigation.

8) *Magnesium*: The ECA for water in the Peruvian regulations [17] establishes values of 250 mg/L for irrigation of vegetables and animal beverages. Two more restrictive values were chosen, which were 150mg/L established in the General Water Law [19] and 70mg/L established in the Standard for the Control of the Quality of Venezuelan Water Bodies [20], for water intended for the irrigation of vegetables, legumes consumed raw, cereals and tree crops.

9) *Manganese*: The ECA for water in the Peruvian regulations [17] establishes values of 0.2 mg/L for irrigation of vegetables and animal beverages. Two more restrictive values were chosen, which were 0.05mg/L established in the Draft Quality Standard for the Protection of Inland Surface Water in Chile [18], in waters intended for restrictive irrigation and a value of 0.125 mg/L being a midpoint between the two extremes.

10) *Mercury*: The ECA for water in the Peruvian regulations [17] establishes values of 0.001 mg/L and 0.01mg/L for irrigation of vegetables and animal beverages, a more restrictive value was 0.0002 mg/L in the Standard to Prevent Environmental Contamination in Paraguay [22], in water intended for irrigation of vegetables or fruit plants or crops intended for human consumption.

11) *Nickel*: The ECA for water in the Peruvian regulations [17] establishes values of 0.2 mg/L and 1mg/L for irrigation of vegetables and animal beverages, a more restrictive value was 0.002 mg/L in the General Water Law [19], for irrigation water for raw vegetables and animal beverages.

12) *Lead*: The ECA for water in the Peruvian regulations [17] establishes values of 0.05mg/L for irrigation of vegetables and animal beverages. Two more restrictive values were chosen, which were 0.001mg/L, belonging to the Draft Quality Standard for the Protection of Continental Surface Water in Chile [18], for water intended for restrictive irrigation, and 0.03 mg/L in the Standard to prevent environmental pollution in Paraguay [22], for water intended for irrigation of vegetables or fruit plants.

13) *Selenium*: The ECA for water in the Peruvian regulations [17] establishes values of 0.02 mg/L and 0.05mg/L for irrigation of vegetables and animal beverages, a more restrictive value was 0.005mg/L which corresponds to the Draft Quality Standard for the Protection of Inland Surface Water in Chile [18], in waters destined for restrictive irrigation.

14) *Nickel*: The ECA for water in the Peruvian regulations [17] establishes values of 0.2 mg/L and 1mg/L for irrigation water for vegetable and animal beverages, a more restrictive value was 0.002 mg/L in the General Water Law [19], for irrigation water for raw vegetable and animal beverages.

C. Definition of the Grey Classes

The parameters chosen were based on the ECA category 3 of the Peruvian regulations together with international regulations in order to have a range of 3 types of water quality for the ECA, taking as a basis that the already established Peruvian regulations cannot be exceeded, presenting the final result below.

D. Calculations with Grey Clustering

The calculations in this case study are based on CTWF methods, which are presented as follows.

Step 1: First the parameters chosen for the case study were sized as detailed in Table III.

Points 1 to 6 are from the Yauli River, differentiated by time of year as shown in Table IV. Similarly, points 1 to 7 are from the Andaychagua River.

Then, the dimensioned monitoring data of all points to be studied is shown, Table V.

Points 1 to 6 are from the Yauli River, differentiated by time of year as shown in Table IV. Similarly, points 1 to 7 are from the Andaychagua River.

TABLE II. VALUES TAKEN FOR THE CASE STUDY

Parameters	Unit of measure	Good	Moderated	Bad
OD	mg/L	7.5	5	4
pH	pH	7	7.45	7.75
As	mg/L	0.05	0.1	0.2
Cd	mg/L	0.001	0.01	0.05
Cu	mg/L	0.002	0.2	0.5
Co	mg/L	0.05	0.1	1
Fe	mg/L	0.3	1	5
Mg	mg/L	70	151	251
Mn	mg/L	0.05	0.125	0.2
Hg	mg/L	0.0002	0.001	0.01
Ni	mg/L	0.002	0.2	0.1
Pb	mg/L	0.001	0.03	0.05
Se	mg/L	0.005	0.02	0.05
Zn	mg/L	0.03	2	24

TABLE III. DIMENSIONED CRITERIA

Parameters	Criteria	Good	Moderated	Bad
OD	C1	1.3636	0.9091	0.7273
pH	C2	0.9459	1.0068	1.0473
As	C3	0.4286	0.8571	1.7143
Cd	C4	0.0492	0.4918	2.4590
Cu	C5	0.0085	0.8547	2.1368
Co	C6	0.1304	0.2609	2.6087
Fe	C7	0.1429	0.4762	2.3810
Mg	C8	0.4449	0.9597	1.5953
Mn	C9	0.4000	1.0000	1.6000
Hg	C10	0.0536	0.2679	2.6786
Ni	C11	0.0199	1.9868	0.9934
Pb	C12	0.0370	1.1111	1.8519
Se	C13	0.2000	0.8000	2.0000
Zn	C14	0.0035	0.2305	2.7660

TABLE IV. DESCRIPTION OF POINTS

Monitoring Points	Data	Description
1	PY-01-H	Yauli River upstream, wet season
2	PY-01-S	Yauli River upstream, dry season
3	PY-02-H	Yauli River downstream, wet season
4	PY-02-S	Yauli River downstream, dry season
5	PY-01	Yauli River upstream
6	PY-02	Yauli River downstream
7	PA-01-H	Andaychagua River upstream, wet season
8	PA-01-S	Andaychagua River upstream, dry season
9	PA-02-H	Andaychagua River downstream, wet season
10	PA-02-S	Andaychagua River downstream, dry season
11	PA-01	Andaychagua River upstream
12	PA-02	Andaychagua River downstream

TABLE V. REAL VALUES ARE DIMENSIONED

Points Parameters	1	2	3	4	5	6
C1	1.1197	1.2982	1.4709	4.4655	1.2090	2.9682
C2	1.0948	1.1003	0.0196	1.0865	1.0976	0.5530
C3	1.3527	0.3739	0.0171	0.5314	0.8633	0.2743
C4	0.0344	0.0123	3.7869	0.0984	0.0234	1.9426
C5	0.3393	0.1058	0.0128	0.1026	0.2225	0.0577
C6	0.0048	0.0030	9.9052	0.0052	0.0039	4.9552
C7	1.4577	0.2118	17.4552	0.4733	0.8347	8.9643
C8	0.1866	0.2238	0.0913	0.2987	0.2052	0.1950
C9	21.6917	6.2302	0.0000	145.696	13.9610	72.8480
C10	0.0268	0.0268	0.5357	0.0000	0.0268	0.2679
C11	0.0079	0.0055	1.0728	0.0099	0.0067	0.5414
C12	2.6500	1.0491	0.0370	1.7037	1.8495	0.8704
C13	0.0420	0.0200	43.3200	0.0400	0.0310	21.6800
C14	0.1096	0.0206	0.1244	0.1147	0.0651	0.1195
Points Parameters	7	8	9	10	11	12
C1	1.1462	1.1467	1.1997	1.1582	1.1465	1.1790
C2	1.1003	1.0254	1.1191	1.0686	1.0629	1.0938
C3	0.9139	0.4665	1.4050	0.7886	0.6902	1.0968
C4	0.0190	0.0111	0.0492	0.0123	0.0150	0.0307
C5	0.3409	0.0746	0.1685	0.0760	0.2078	0.1222
C6	0.0013	0.0014	0.0107	15.6569	0.0014	7.8338
C7	0.7506	0.7964	0.8219	0.5008	0.7735	0.6613
C8	0.0696	0.1444	0.0985	0.1137	0.1070	0.1061
C9	4.4819	8.7354	4.4881	5.6736	6.6087	5.0809
C10	0.0268	0.0268	0.0268	0.0268	0.0268	0.0268
C11	0.0043	0.0045	0.0545	0.0263	0.0044	0.0404
C12	1.7737	0.7584	2.2440	1.0481	1.2660	1.6461
C13	0.0280	0.0230	0.0269	0.0240	0.0255	0.0254
C14	0.0263	0.0296	0.0349	0.0104	0.0279	0.0227

Step 2: In the first place, the values presented in Table V. Were substituted in Eq. 1-3, to obtain the CTWF of the three classes of grey. As an example, the results of the first parameter (OD) are shown in Eq. 7-9.

$$f_1^1(x_{ij}) = \begin{cases} 1, & x \in [0, 1.3636] \\ \frac{0.9091-x}{0.9091-1.3636}, & x \in [1.3636, 0.9091] \\ 0, & x \in [0 - 9091, +\infty] \end{cases} \quad (7)$$

$$f_1^2(x_{ij}) = \begin{cases} \frac{x-1.3636}{0.9091-1.3636}, & x \in [1.3636, 0.9091] \\ \frac{0.7273-x}{0.7273-0.9091}, & x \in [0.9091, 0.7273] \\ 0, & x \notin [1.3636, 0.7273] \end{cases} \quad (8)$$

$$f_1^3(x_{ij}) = \begin{cases} \frac{x-0.9091}{0.7273-0.9091}, & x \in [0.9091, 0.7273] \\ 1, & x \in [0.7273, +\infty] \\ 0, & x \in [0, 0.9091] \end{cases} \quad (9)$$

Then, from Table V, the CTWF values were calculated using Eqs. 1-3. As an example, the results of monitoring point 1 and 2, the results are shown in Table VI.

Step 3: From Table II, the weight of each grouping (n_{ij}) of each parameter was calculated by harmonic mean as detailed in Table VII.

Step 4: The values of the clustering coefficients σ_i^k were calculated using equation (5) and are shown in Tables IX, X, XI, XII, XIII and XIV that will be presented in the results and discussions.

Step 5: The maximum values of the clustering coefficient were determined as shown in Table VIII.

V. RESULTS AND DISCUSSION

TABLE VI. CTWF VALUES OF THE FIRST TWO MONITORING

Point 1	C1	C2	C3	C4	C5	C6	C7
f1j(x)	0.0000	0.0000	0.0000	1.0000	0.6092	1.0000	0.0000
f2j(x)	0.5366	0.0000	0.4219	0.0000	0.3908	0.0000	0.4847
f3j(x)	0.4634	1.0000	0.5781	0.0000	0.0000	0.0000	0.5153
Punto 1	C8	C9	C10	C11	C12	C13	C14
f1j(x)	1.0000	0.0000	1.0000	1.0000	0.0000	1.0000	0.5326
f2j(x)	0.0000	0.0000	0.0000	0.0000	0.0000	0.0000	0.4674
f3j(x)	0.0000	1.0000	0.0000	0.0000	1.0000	0.0000	0.0000
Point 2	C1	C2	C3	C4	C5	C6	C7
f1j(x)	0.0000	0.0000	1.0000	1.00	0.8851	1.0000	0.7932
f2j(x)	0.1440	0.0000	0.0000	0.0000	0.1149	0.0000	0.2068
f3j(x)	0.8560	1.0000	0.0000	0.0000	0.0000	0.0000	0.0000
Point 2	C8	C9	C10	C11	C12	C13	C14
f1j(x)	1.0000	0.0000	1.0000	1.0000	0.0578	1.0000	0.9246
f2j(x)	0.0000	0.0000	0.0000	0.0000	0.9422	0.0000	0.0754
f3j(x)	0.0000	1.0000	0.0000	0.0000	0.0000	0.0000	0.0000

TABLE VII. CLUSTERING WEIGHT OF EACH PARAMETER

Parameters	Criteria	Good	Moderate	Bad
OD	C1	0.001	0.044	0.159
pH	C2	0.002	0.039	0.111
As	C3	0.004	0.046	0.068
Cd	C4	0.037	0.081	0.047
Cu	C5	0.212	0.046	0.054
Co	C6	0.014	0.152	0.044
Fe	C7	0.013	0.083	0.049
Mg	C8	0.004	0.041	0.073
Mn	C9	0.005	0.040	0.072
Hg	C10	0.034	0.148	0.043
Ni	C11	0.091	0.020	0.117
Pb	C12	0.049	0.036	0.063
Se	C13	0.009	0.050	0.058
Zn	C14	0.525	0.172	0.042
SUMA		1.000	1.000	1.000

TABLE VIII. MAXIMUM CLUSTERING COEFFICIENT

Yauli upstream		Andaychahua upstream	
Stations	Good	PA-01	Good
Wet season	0.598025423	Wet season	0.79018448
Dry Season	0.879476417	Dry Season	0.86914266
Yauli downstream		Andaychahua downstream	
Stations	Good	PA-02	Good
Wet season	0.562789011	Wet season	0.81181683
Dry Season	0.644790059	Dry Season	0.88265749
Yauli Quality		Andaychahua Quality	
Stations	Good	Stations	Good
PY-01	0.730181309	PA-01	0.82133905
PY-02	0.5448226	PA-02	0.83850656

The analysis of affectation to bodies of water was made by the discharges of the mining company under study. Thus, the analysis was performed in two mining units which discharge into the Yauli and Andaychagua rivers in order to detect which deserves greater attention to water treatment, in order to reduce the impact on water bodies.

The upstream and downstream assessment was performed for each water body. The assessment was separated into wet and dry seasons in order to better assess the mining activity that discharges its waters into the river.

A. About the Case Study

Analysis of the Yauli River upstream and downstream from an industrial discharge point shows that there is no variation in the water quality rating; however, there is a slight decrease in the Clustering value of 25% which shows minimal but acceptable impairment. Table IX shows the Clustering values and the good score at the two sampling points since the values are higher in that score.

As shown in Table X, in the dry season upstream the good water rating is 89% while in the wet season it is 59%.

In the case of Table XI, it shows the results downstream at both times of the year. Decreasing the quality from 64% in dry season to 56% in wet season.

With the criteria in time flooded and low water is evident the affectation by climatic factors even more of the industrial presence of the zone. This variation is due to the increase of contact water generated by the rainy season concentration that although it would not be discharged directly this would be filtered by runoff into the river [23]. This is a consequence of the inadequate disposal of tailings and waste, as well as inappropriate methods for the disposal of industrial effluents that cause leaks and acid drainage [24].

Water quality assessment of the Yauli River at both times of the year shows minimal impact on river quality as the rating is good throughout the analysis. Even though there is a slight variation of 20% between upstream and downstream. On the other hand, it was evident that climatic factors in the low and high seasons influence water quality in the receiving body. Although it is possible that, from a geological point of view, the area has a natural influence on the presence of metals, both mining activity and the existence of mining environmental liabilities in the area are the two main factors that generate alteration of water quality [25].

TABLE IX. YAULI RIVER WATER QUALITY

Seasons	Good	Moderate	Bad
PA-01 (upstream)	0.8213	0.1774	0.2871
PA-02 (Downstream)	0.8385	0.1575	0.3911

TABLE X. PY-01 STATION, UPSTREAM YAULI RIVER

PY-01	Good	Moderate	Bad
Wet season	0.5980	0.1822	0.3839
Dry season	0.8795	0.0756	0.3197

TABLE XI. PY-02 STATION, DOWNSTREAM OF THE YAULI RIVER

PY-02	Good	Moderate	Bad
Wet season	0.5628	0.2346	0.4792
Dry season	0.6448	0.1996	0.3927

The analysis of the Andaychagua River, by another discharge point of the same mining company under study, shows that the quality of its water is of good value as shown in Table XII, since the highest values of clustering are in this category in the two sampling stations. Table XII with the clustering values is shown below.

The analysis of water quality in the Andaychagua River shows a slight improvement in its waters after the industrial discharge. This would indicate that the effluent does not significantly impact the physical-chemical quality of the receiving body; it would also be due to the contributions of tributaries from the Pacchapuquiopampa stream that dilutes the discharge made upstream in a greater proportion.

Over the years, evaluations of this river have shown that it does not exceed the limit values, as indicated in a study conducted by the DGCA-MINAM and DIGEDA in 2009. Similarly, a study of the Mantaro River shows that the receiving bodies of this mine's effluents indicate both upstream and downstream compliance with Environmental Quality Standards [26].

Analysis of the river based on the time of year criteria shows the influence of climatic factors on water quality in the receiving body. Like the Yauli River, water quality in the dry season was better along the entire stretch of the river studied.

Table XIII is shown. With the data of the upstream season, presenting in dry season a value of 87% of good quality, while in wet season a value of 79%.

Table XIV shows the clustering results in the two seasons downstream of the river. The dry season shows an improvement in its waters with a value of 88% in the good classification.

TABLE XII. ANDAYCHAGUA RIVER

SEASONS	Good	Moderate	Bad
PY-01	0.7302	0.1873	0.3604
PY-02	0.5448	0.2935	0.4178

TABLE XIII. STATION PA-01, UPSTREAM ANDAYCHAGUA RIVER

PA-01	Good	Moderate	Bad
Wet season	0.7902	0.1750	0.3339
Dry season	0.8691	0.1632	0.2150

TABLE XIV. PA-02 STATION, DOWNSTREAM OF ANDAYCHAGUA RIVER

PA-02	Good	Moderate	Bad
Wet season	0.8118	0.1338	0.3998
Dry season	0.8827	0.1838	0.3156

The analysis of the Andaychagua River shows an improvement in the quality of its water in both the dry and wet seasons, the rating is good throughout the river, even more so after the discharge slightly improves the quality by 8%. This would indicate that the river is not affected by industrial effluent; however, a better analysis with a greater weighting of critical parameters would be necessary. As was done in a study of the Santa River basin, 21 monitoring points were analyzed, with 47.6% of the points being of good quality and 19.1% of low quality [12].

The evaluation of water quality in the Yauli and Andaychagua Rivers by the dumping of industrial effluents from the same mining company, using the Grey Clustering methodology, gives the rating of good before and after dumping. However, this analysis was carried out with harmonic weighting, which is recommended to be done by experts or by evaluating the criteria of weighting of the parameters according to the impact on each receiving body or by the influence of these on water treatment.

A statistical analysis of all 2019 values was carried out in Yauli and Andaychagua rivers to counteract the results with the Grey Clustering method and compare them with the ECA Water Category 3, vegetables irrigation and animals drink.

The results of the statistical analysis of the Andaychagua river showed that at least 6 chemical parameters (pH, sulphates, Fe, Mn, Pb, Zn) exceeded the ACE for vegetable irrigation and animal drinking, showing its impact on the receiving body. In view of this, for a water evaluation with fuzzy logic, statistical analysis should be taken into account first in order to assess with greater weight these critical parameters and thus evaluate the total quantitative quality of the river.

B. About the Methodology

In the grey grouping method the grouping coefficients are important factors for the final evaluation, which are obtained with the bleaching functions and the weightings, the latter help to obtain reliable results in the evaluation. Being important to highlight the weights, they incur an important effect in the calculations since the greater weight to each criterion this can make us vary the analysis giving us other results that is why it is important to detail the weighting used for the parameters. Likewise, there can be different methods to determine the weighting, not only with the harmonic method. There are also methods such as the Delphy method (based on expert consultation) [27], mixed weighting method [28], weighting of the INSF method [29], etc. These can complement the study to find the appropriate weights for each parameter being analyzed.

There are other methodologies that are also used for the evaluation of water quality such as the INSF methodology, which considers the characteristics that the water body must present for its use as human consumption, this already has established weights for specific parameters, as well as the Water Quality Index in surface currents (ICA), The Prati Index is one of the most commonly used in water quality assessment studies. It characterizes water in five classes, each with a range of established values [30]. This shows us that the

Grey Clustering methodology has a better range of application for water quality since it can be adjusted to the number of parameters with which you want to evaluate and also adds a weighting to each to determine the weighting of the criteria, this weighting can be supplemented with other methodologies already mentioned to improve their effectiveness in the evaluation by adjusting to the place where the study is conducted in terms of conditions and characteristics, compared to existing methodologies which already have weights and parameters which make them a limitation when evaluating water quality.

Based on the review in Section II, the analysis of the Andaychagua River shows an improvement in water quality in both the dry and wet seasons, the rating is good throughout the river, more so after the discharge slightly improves the quality by 8%. This would indicate that the river is not affected by industrial effluent; however, a better analysis with a greater weighting of critical parameters would be necessary. As was done in a study of the Santa River basin, 21 monitoring points were analyzed, with 47.6% of the points being of good quality and 19.1% of low quality [12].

VI. CONCLUSIONS

The Yauli River shows good water quality according to the clustering methodology along the river, even in wet and dry seasons. Although this variation infers a low proportion of water quality being lower in wet periods, this is due to the influence of rainfall on contact water, even so the quality is good. For the Andaychagua River, a good quality rating is shown both upstream and downstream from the industrial discharge. In both rivers there is an alteration of their waters due to climatic factors that slightly modify their water quality. The results with the clustering analysis show that the river is not drastically affected by the industrial mining effluent, however, there is a bias in the analysis since the weighted values were made in a harmonic way to which one could have chosen to recommend to experts, and qualify some parameters that are of greater impact to the receiving body.

The Grey clustering methodology helps to assess water quality in an objective way, based on weights on the parameters that are evaluated, this can be complemented with more restrictive methods for the weights can be found those that are appropriate to the conditions and characteristics of the place of study.

The proposed research is a starting point for the evaluation of water quality, in natural bodies, applying diffuse logic. There are several applications of Grey Clustering; however, water quality assessment is not very widespread. Therefore, taking this research as a reference, the evaluation can be carried out by taking a greater number of monitoring points that show results in greater detail, verifying the impact that mining activity causes not only on rivers, but also on lagoons, and even sediment evaluation could be applied.

REFERENCES

- [1] H. Huisa and I. Rodríguez, "Modelamiento en la evaluación del potencial de recursos minero metálico en la región Junín," XVIII Congr. Peru. Geol., pp. 1–4, 2016.
- [2] C. Meza, P. Luis, and C. Sánchez, "Universidad Nacional Mayor de San Marcos Facultad de Ciencias Biológicas Escuela Académica Profesional de Microbiología y Parasitología Evaluación de hongos resistentes a Cr (VI) y Zn (II) y su capacidad de bioadsorción en solución acuosa, aislados d," 2012.
- [3] J. Cayetano, "Cumplimiento de la normatividad ambiental por el sector minero metalúrgico y su impacto ambiental en el río Mantaro - Región Junín," 2013.
- [4] DIGESA, "Monitoreo del río San Juan - Mantaro y Principales Afluentes," 2008. [Online]. Available: http://www.digesa.minsa.gob.pe/DEPA/rios/2008/SAN_JUAN_MANTARO_2008_ii.pdf.
- [5] W. Y. Chang, "Application of grey clustering approach and genetic algorithm to partial discharge pattern recognition," WSEAS Trans. Syst., vol. 8, no. 12, pp. 1273–1283, 2009.
- [6] S. Liu, J. Forrest, and Y. Lin, Grey Systems: Theory and Applications, Springer, Berlin, 2010.
- [7] L. Ke, S. Xiaoliu, T. Zhongfu, and G. Wenyan, "Grey Clustering Analysis Method for Overseas Energy Project Investment Risk Decision," Syst. Eng. Procedia, vol. 3, no. 2011, pp. 55–62, 2012, doi: 10.1016/j.sepro.2011.11.008.
- [8] W. Liu et al., "Key indices of the remanufacturing industry in China using a combined method of grey incidence analysis and grey clustering," J. Clean. Prod., vol. 168, pp. 1348–1357, 2017, doi: 10.1016/j.jclepro.2017.09.078.
- [9] C. Li, K. Chen, and X. Xiang, "An integrated framework for effective safety management evaluation: Application of an improved grey clustering measurement," Expert Syst. Appl., vol. 42, no. 13, pp. 5541–5553, 2015, doi: 10.1016/j.eswa.2015.02.053.
- [10] Q. Tan, T. Wei, W. Peng, Z. Yu, and C. Wu, "Comprehensive evaluation model of wind farm site selection based on ideal matter element and grey clustering," J. Clean. Prod., vol. 272, p. 122658, 2020, doi: 10.1016/j.jclepro.2020.122658.
- [11] C. Zhu and N. Li, "Study on Grey Clustering Model of Indoor Air Quality Indicators," Procedia Eng., vol. 205, pp. 2815–2822, 2017, doi: 10.1016/j.proeng.2017.09.895.
- [12] A. Delgado and D. Edgar, "Artificial intelligence model based on grey systems to assess water quality from Santa river watershed," Electron. Congr. (E-CON UNI), pp. 1–4, 2017, doi: 10.1109/ECON.2017.8247310.
- [13] A. Delgado, A. Aguirre, E. Palomino, and G. Salazar, "Applying triangular whitening weight functions to assess water quality of main affluents of Rimac river," Proc. 2017 Electron. Congr. E-CON UNI 2017, vol. 2018-Janua, pp. 1–4, 2017, doi: 10.1109/ECON.2017.8247308.
- [14] A. Delgado, J. Soto, and F. Valverde, "Evaluation of the drinking water consumption in Lima city using the grey clustering method," Proc. LACCEI Int. Multi-conference Eng. Educ. Technol., vol. 2019-July, no. July, pp. 24–26, 2019, doi: 10.18687/LACCEI2019.1.1.421.
- [15] L. F. Zhou, S. G. Xu, and W. G. Sun, "Comprehensive evaluation on water environment quality of Zhalong wetland based on grey clustering method," J. Dalian Univ. Technol., vol. 47, no. 2, pp. 240–245, 2007.
- [16] L. Wang, K. Lai, and W. Zhou, "Application of grey clustering method for water quality evaluation in Fenchuan river Yan'an Baota area," ISWREP 2011 - Proc. 2011 Int. Symp. Water Resour. Environ. Prot., vol. 2, pp. 838–841, 2011, doi: 10.1109/ISWREP.2011.5893142.
- [17] Ministerio del Ambiente, "Estándares de Calidad Ambiental para Agua (ECA)," El Peru., pp. 6–9, 2017, [Online]. Available: <http://www.minam.gob.pe/wp-content/uploads/2017/06/DS-004-2017-MINAM.pdf>.
- [18] Chile Sustentable, "Marco Jurídico para Gestión del Agua en Chile: Diagnóstico y Desafíos," pp. 1–16, 2010.
- [19] Ministerio de Agricultura, "Reglamento de la Ley General de Aguas. Decreto Supremo N° 261-69AP," no. 17752, pp. 31–67, 1969.
- [20] R. B. de Venezuela, "Normas para la clasificación y el control de la calidad de los cuerpos de agua y vertidos o efluentes líquidos." Venezuela, p. 24, 1995.
- [21] P. Steduto, T. C. Hsiao, E. Fereres, and D. Raes, Respuesta del rendimiento de los cultivos al agua, vol. 66, 2012.
- [22] SEAM, Resolución 222/2002. Paraguay, 2002, p. 6.
- [23] F. M. Romero, M. A. Armienta, M. E. Gutiérrez, and G. Villaseñor, "Factores geológicos y climáticos que determinan la peligrosidad y el

- impacto ambiental de jales mineros,” *Rev. Int. Contam. Ambient.*, vol. 24, no. 2, pp. 43–54, 2008.
- [24] M. Núñez Aylas, E. Benites Alfaro, and M. Zevallos León, “Evaluación de la calidad del agua asociado al drenaje ácido de mina (DAM), en el río Yauli en época de estiaje distrito de Yauli – Junín, 2013,” *Ucv - Sci.*, vol. 6, no. 1, pp. 25–30, 2014.
- [25] H. Calla, “Calidad del agua en la cuenca del río Rímac-Sector de San Mateo afectado por las actividades mineras,” 2010.
- [26] J. Cayetano, “Cumplimiento de la normatividad ambiental por el sector minero metalúrgico y su impacto ambiental en el río Mantaro - Región Junín,” *Universidad Nacional Del Centro Del Centro De Posgrado*, 2013.
- [27] R. Samboni, Y. Carvajal, and J. Carlos, “Revisión de parámetros fisicoquímicos como indicadores de calidad y contaminación del agua,” *Rev. Ing. e Investig.*, vol. 27, no. 3, pp. 172–181, 2007.
- [28] J. Zonensein, M. G. Miguez, L. P. De Magalhães, and M. G. Valentin, “Flood risk index as an urban management tool. International Conference on Urban Drainage,” *Int. Conf. Urban Drain.*, no. Edinburgh, Scotland, UK., 2008.
- [29] M. Castro, J. Almada, J. Ferrer, and D. Díaz., “Indicadores de la calidad del agua: evolución y tendencias a nivel global. Ingeniería Solidaria,” *Ing. Solidar.*, vol. 10, no. 17, pp. 111–124, 2014, doi: <http://dx.doi.org/10.16925/in.v9i17.811>.
- [30] L. Pratti and R. Pavanello, “Assesment of Surface Water Quality By A single Indx Of Contamination,” *Water Resour. Res.*, vol. 5, pp. 456–467, 1971.

The Role of Electronic Means in Enhancing the Intellectual Security among Students at the University of Jordan

Mohammad Salim Al-Zboun¹, Mamon Salim Al-Zboun², Hussam N. Fakhouri³
School of Educational Science, The University of Jordan, Amman, Jordan^{1,2}
School of Art and Design, The University of Jordan, Amman, Jordan³

Abstract—The study aims to identify the role of electronic means in enhancing intellectual security among students at the University of Jordan. To achieve the objective of the study, a study instrument is developed, and the study sample consists of (525) male and female students. The results show that the response of the university students in assessing the role of electronic means in enhancing the students' intellectual security is with an arithmetic mean of (3.07), and a standard deviation of (1.128), and this score is considered medium. In light of the results of the study, the researchers recommend employing electronic means in activating the intellectual security among the university education students in Jordan.

Keywords—Electronic means; intellectual security; enhancement

I. INTRODUCTION

The information technology sector and electronic means in the eyes of many thinkers, decision-makers and educators represent a golden opportunity for developing countries to achieve development in all its forms if it is properly utilized and employed. Electronic means have recently occupied a prominent place among the measures that indicate the level of civilization and progress in any country in the world, as they constitute an independent strength society. The governments have realized the effective and large role of electronic means due to their influencing power and ability to affect the opinion of the public in society and stimulate them to defend certain standpoints required by them, and thus giving it great attention. Currently, electronic means play an unprecedented role in the issue of enhancing intellectual security. It has a tremendous capacity to educate local citizens, serving as a primary hub in spreading knowledge.

All opinions contribute to the importance of the great role that electronic means occupy in the lives of individuals and groups, and the extent of their influence on their life, economic, social and cultural affairs, and in enriching the knowledge stock and expanding their perception's space. Electronic means are the main source of intellectual, spiritual, educational, and cultural wealth and constitute a large portion of their interest [1].

Hereafter, it is necessary to realize the great and important role of electronic means, especially in light of technical and technological advances, and the information revolution by employing them in a good manner, whether they are readable

or audible. Importantly, the optimal use of electronic means helps clarify visions, provide students with information, facts, and experiences, and qualify them in crystallizing their thoughts and opinions in front of the latest developments to take the appropriate and logical positions that lead to their growth and development [2].

In light of these developments and growths, the importance of intellectual security lies in achieving security and stability in the society by addressing intellectual influences and deviations. Intellectual empowerment becomes one of the priorities that support security planning in Arab society in its current and future stage that protects individuals from intellectual influences which is considered a fundamental necessity in its security, stability, and social and economic prosperity [3].

Therefore, it is essential to pay attention to intellectual security, which aims to make individuals in their society live in full security and reassurance about the components of their personality and the distinctiveness of their culture and their intellectual system stemming from the Holy Qur'an and Sunnah. This means protecting and preserving the Islamic identity from penetration or containment from outside and preserving the security of the nation from the winds of delinquency of the approach of moderation in light of the tremendous momentum of the means of intellectual and cultural invasion. The importance of intellectual security comes from its goal of the integrity of faith, the integrity of behavior, and the proof of loyalty that is the basis of its existence and the reason for its glory and pride [4].

The significance of intellectual security lies in its association with two important matters: security and thought. Security is considered a requirement that all societies strive to achieve, and life is not satisfied without it, while the thought is the beating heart of the civilizations, the more the thought carried by society is healthy and conscious, the more it produces and innovates. Importantly, security and thought do not settle without achieving the intellectual security of the members of society as previously confirmed that no doubt achieving the intellectual security of the individual will ensure an automatic verification of security in all aspects because the mind is the body of the distinctive supreme conscious leadership in the human being and it is the lead agency entrusted with all other types of security. If this leadership is

correct and flawless, then all the members of the security family are correct and flawless [5].

Notably, the issue of intellectual security has become one of the vital and important issues, and the degree of sensitivity it acquires in the lives of peoples and the future of nations necessitates addressing it as it is a basic and contemporary issue and it is inevitable to confront it in light of the facts of the conditions in which the Arab and Islamic nation is living and the tensions that have resulted in the emergence of the two phenomena of cultural alienation and the ideological extremism. It is agreed that intellectual security is the existing or supposed harmony between what societies believe and what they live in the vocabulary of their daily life and what they aspire to. Achieving the said harmony is based on the agreement existing among individuals in relying on a mutual cultural and doctrinal reference that represents the main features of the background in which society believes in its various sects and the multiplicity of its cultural and political textures. Society still needs intellectual security to bring citizens together on one word as achieving intellectual security is the responsibility of society with all its components to unite around one basic idea about the faith and the homeland. Also, it should not be understood that intellectual security means a blockade and a restriction of the mind, but rather an affirmation of freedom of opinion within the framework of respecting the principles of the nation and conserving and protecting its heritage from attempts to defame the identity of the foreign cultural invasion that destroys the foundations and authenticity of society. More importantly, intellectual security is the pillar of the rise of nations and societies and the guarantor of providing the security of people and the country from the dangers of alienation [6].

In light of the above, the electronic means strengthening the intellectual security of university students has become important, especially at present, due to several contemporary international variables such as scientific and industrial development, the globalization of markets, the information revolution, and the development and technological advancement of electronic means.

II. EASE OF THE PROBLEM OF THE STUDY

In light of the aforesaid insight, the problem of the study lies in examining the role that electronic means play in enhancing the intellectual security among students at the University of Jordan students.

III. QUESTIONS OF THE STUDY

In light of the problem of the Study, the following questions are articulated.

- 1) What is the role of electronic means in enhancing the intellectual security of students at the University of Jordan?
- 2) Are there statistically significant differences at the level of ($\alpha \leq 0.05$) in the role of electronic means in enhancing intellectual security among the students at the University of Jordan due to the following variables (gender, specialization, academic level)?

IV. OBJECTIVES OF THE STUDY

The following objectives are formatted to answer the questions of the study.

- 1) Identify the role of electronic means in enhancing the intellectual security of students at the University of Jordan.
- 2) Examine if there are statistically significant differences at the level of ($\alpha \leq 0.05$) in the role of electronic means in enhancing intellectual security among the students at the University of Jordan due to the following variables (gender, specialization, academic level).

V. SIGNIFICANCE OF THE STUDY

The significance of the current study is seen in the results of this study that reveal the reality of the role of electronic means in enhancing intellectual security among students at the University of Jordan. It is also hoped that the results of the current study will contribute to developing the role of electronic means in enhancing the intellectual security of students. Moreover, the current research paper sheds light on an important issue in society, which is intellectual security, where intellectual security is of great importance to ensure the security and stability of society.

VI. TERMS OF THE STUDY

Electronic means: they are the means made through electronic methods such as the Internet, and this type of means is gaining a growing share and status. This is a result of its ease of accessibility, speed of production, development, and modernization. Social networking sites such as Facebook, Instagram, WhatsApp, electronic newsletters, and television are the most important forms of electronic means [7].

Intellectual security: it is the ability and preservation of the integrity of the correct ideas and beliefs of individuals while providing them with research tools, knowledge, and methods of correct thinking, and this is achieved and complemented by the course of literature, education and good communication [8].

VII. LIMITATIONS OF THE STUDY

This study is limited to a sample of students at the University of Jordan during the first semester of the academic year 2019/2020. Concerning the methodological limitations, the results of the study are determined with the validity and reliability of its instrument, and the accurate response of the study sample individuals to the items of the instrument used to collect its data. The results of the study are generalized to the study population from which the study sample is taken.

VIII. PREVIOUS STUDIES

1) *Several studies* have been written on the importance of electronic means and intellectual security in people's life. Jounson (2005) aims at identifying the features of intellectual security for students provided by the Internet in Mankato city in the state of Minnesota in the United States of America. The study indicates that this city can meet security requirements and allow employees and students to enter the greatest sources on the Internet. The study shows that 81% of students have

achieved the intellectual security features in terms of freedom to express opinion objectively via the Internet, use the Internet in education, and search for information and knowledge that provides these students with a tremendous amount of information which leads to achieving the aspired intellectual and information security. Radwan, Ramadan, and Abdulwahab (2010) aim at identifying the role of modern communication technology in developing freedom of expression of opinion among university students. To achieve the above objective, the study has used the descriptive approach and the content analysis method to analyze some of the codes of some student movements. The study shows that tremendous development in communication technology has helped to form a new standard community which is called the virtual community [9][10].

2) *Kuppuswamy and Narayan (2010)* have aimed to examine the impact of social networking sites on youth education. The study shows that young people are attracted to social network sites that have a positive effect on them, but they may lead to students not being interested in their studies. However, these sites can be used in education if they are used in light of sound educational principles and appropriate supervision by teachers [11].

3) *Shaltan (2013)* aims to identify the role of colleges of education in Palestinian universities in enhancing intellectual security for their students and ways to activate it. To achieve this objective, the study has used descriptive and analytical approaches [12]. The results of the study indicate that the students' estimates of the role of colleges of education in Palestinian universities in enhancing intellectual security among their students are (72.23%). The study also shows that there are statistically significant differences between the arithmetic means of the sample responses due to the gender variable (male and female) in the first and second areas, where the differences are in favor of males. The study also shows that there are statistically significant differences between the arithmetic means of the sample responses due to the variable of the university (The Islamic University of Gaza, Al-Aqsa University) in all fields and the total degree in favor of the Islamic University. Also, the study shows that there are no statistically significant differences between the arithmetic means of the sample responses due to the academic level variable (second year, fourth year). Moreover, the study shows there are statistically significant differences attributed to the GPA variable (Pass, good, very good, excellent) for all fields and the total degree in favor of excellence. Abu Khotwa and Baz (2014) have aimed to identify the implications of the social network on the intellectual security of university education students in the Kingdom of Bahrain. The study has used the descriptive approach and a questionnaire applied to a sample of (104) male and female students at the Gulf University in the Kingdom of Bahrain. The results of the study

show that the impact of social media networks on students' intellectual security, in general, is of a medium degree, which confirms the need to work on educating students in the different educational stages of the uses of social networks and work to develop their critical thinking so that they can sort out the ideas and opinions presented to them, and not be misled by the destructive calls that harm the stability and security of society. The study commends presenting a proposed vision for employing the social network to activate intellectual security among university education students in the Kingdom of Bahrain [13][14][15].

In light of the results of previous studies, it is noted that they have generally dealt with many issues about the role of electronic means in developing freedom of opinion and expression and intellectual security without addressing the role of electronic means in enhancing intellectual security among Jordanian university students. The previous studies presented are closely related to the current study, as it aims to enhance the intellectual security of university students by highlighting the need to pay attention to electronic means as one of the means to enhance intellectual security, activate its role in developing students' intellectual security, and increase their knowledge and active participation in the community. Importantly, the current study has benefited from previous studies in several aspects such as identifying the role of electronic means in enhancing intellectual security and in constructing the current study instrument. However, what distinguishes this study from other studies is that it is considered one of the first studies according to the researchers' knowledge that aims to identify the role of electronic means in enhancing intellectual security among Jordanian university students [16] [17].

IX. METHODOLOGY OF THE STUDY

This part of the study includes a presentation of the methodology, study population. The study sample, study instrument, methods for ensuring its validity and reliability, the study procedures followed to attain the results, and the statistical processing used in analyzing the data. This study is considered a descriptive and analytical study. To obtain data related to the role of electronic means in enhancing intellectual security among the students at the University of Jordan, a representative sample of the students of the University of Jordan, which forms the study population, is selected.

1) *Study population:* The study population consists of all undergraduate students at the University of Jordan in the first semester of the academic year 2019/2020.

2) *Study sample:* As for the study sample, it is selected according to the simple random sampling method, which gives everyone in the study population equal opportunities, where the number of sample members is (525) male and female students at the University of Jordan as illustrated in Table I.

TABLE I. FREQUENCIES AND PERCENTAGES ACCORDING TO STUDY VARIABLES

Variable	Category	Number	Percentage
Gender	Male	242	46.0
	female	283	54.0
	Total	525	100.0
Specialization	scientific	249	47.0
	Humanities	276	53.0
	Total	525	100.0
Academic Level	First year	87	16.5
	Second Year	120	22.8
	Third year	143	27.4
	Fourth year	175	33.3
	Total	525	100.0

X. METHODOLOGY OF THE STUDY

This part of the study includes a presentation of the methodology, study population. The study sample, study instrument, methods for ensuring its validity and reliability, the study procedures followed to attain the results, and the statistical processing used in analyzing the data. This study is considered a descriptive and analytical study. To obtain data related to the role of electronic means in enhancing intellectual security among the students at the University of Jordan, a representative sample of the students of the University of Jordan, which forms the study population, is selected.

XI. OBJECTIVE OF THE STUDY

To achieve the objectives of the study, the theoretical literature and previous studies addressing intellectual security such as the study of Abu Khotwa and Baz (2014) and other related studies are reviewed in detail. The questionnaire in its initial form consists of (34) items. The Likert five-level measure is used to (Strongly disagree, Disagree, Neither agree nor disagree, Agree, Strongly Agree).

The five-step Likert scale is used to determine the degree of response of the sample members to the study instrument, where a numerical estimate (1-5) is given for those responses as follows: Strongly agree (5 grades), agree (4 grades), neither agree nor disagree (3 grades), strongly disagree (2 grades), disagree (1 degree). The following measure is adopted to analyze the results:

From 1.00 to 2.33 low

From 2.34 to 3.67 medium

From 3.68 to 5.00 is high

XII. INSTRUMENT VALIDITY

To verify the validity of the study instrument, it is presented to 10 experts and specialists in the fields of education technology, curricula, teaching, measurement, and evaluation to express their opinions on it in terms of the degree of appropriateness of the items in terms of their language, suitability to the field, the degree of their achievement of the objective for which they are set, and the opinions of the validators are taken in terms of deletion, amendment, and addition, and then the final formulation of the questionnaire is articulated.

XIII. INSTRUMENT RELIABILITY

To verify the reliability of the instrument, the test and re-test method is used, where it is applied to a group from outside the study sample consisting of (20) students, and after ten days of applying the questionnaire, the same instrument is applied to the same group. Then, the reliability coefficient is calculated using the Cronbach alpha coefficient equation between the two applications, as the reliability coefficient for the study instrument has reached (0.92). In light of this result, it can be said that the study instrument has high reliability suitable for this type of study.

XIV. RESULTS AND DISCUSSION

This section gives an insight into the study's results and discussion as follows:

Q1. What is the role of electronic means in enhancing the intellectual security of students at the University of Jordan?

To answer this question, the arithmetic means and standard deviations are calculated as illustrated in Table II.

Table II shows that the arithmetic means have ranged (2.35-3.67), where the item (27) which states "The University's web pages encourage obedience to laws and regulations" is ranked first with an arithmetic mean of (3.67) with a medium degree. This may be because those in charge of the university's electronic pages understand the important role that these pages and websites play in achieving intellectual security, which motivates them to create electronic pages capable of meeting the requirements of all students seeking to reach a higher level of the cultural development. It is also attributed to the idea that these electronic pages belonging to the university have awareness of the importance of regulations and laws, which enhance teamwork among students, gain them various skills, and increase their belonging to the society in which they live. These electronic pages also invite students to pay attention to regulations and laws and adhere to them to raise the level of their performance and the mechanism of benefiting from the available means and working to educate students positively so that they are moderate by taking the causes and not neglecting them, and by developing their moral behavior, as they gain virtues and move away from vices, as they destroy society. These values must be encouraged to do good deeds and cooperation and form an open and interactive personality with society and other civilizations.

TABLE II. FREQUENCIES AND PERCENTAGES ACCORDING TO STUDY VARIABLES

Rank	No	Item	AM	SD	Level
1	27	The university's web pages encourage obedience to laws and regulations.	3.67	0.66	Medium
2	16	The university's electronic pages develop sound thinking methods to confront the intellectual invasion.	3.66	0.68	Medium
3	14	The University of Jordan Radio encourages cooperation with community institutions by exchanging visits to achieve national unity.	3.64	0.74	Medium
4	1	Electronic newsletters develop positive and behavioral trends towards community security.	3.62	0.75	Medium
5	5	The University of Jordan pages display activities aimed at protecting students from intellectual deviation	3.60	0.78	Medium
6	17	The University of Jordan Radio develops the skills of scientific research, investigation and problem solving.	3.57	0.80	Medium
7	34	Electronic newsletters help maintain public order and achieve security, reassurance and stability in life.	3.55	0.83	Medium
8	29	The University of Jordan Radio promotes pride in the nation's achievements.	3.53	0.84	Medium
9	28	Facebook for the University of Jordan helps students to become aware of the Kingdom's pivotal role in the religious, Arab, regional and international levels.	3.50	0.89	Medium
9	33	Jordanian radio channels educate the importance of caring for work values in society.	3.50	0.88	Medium
10	11	Facebook of the University of Jordan promotes solidarity and unity.	3.48	0.90	Medium
11	8	Public Security Radio spreads awareness of society's problems and its negative aspects.	3.47	0.92	Medium
12	10	Twitter promotes the collective values of students.	3.44	0.97	Medium
13	4	The University of Jordan Radio provides educational activities to confront intellectual deviation.	3.39	0.99	Medium
14	6	Obtaining scientific knowledge, media and news from Jordanian radio channels.	3.18	1.01	Medium
15	12	Army Radio provides assistance to students in being positive members of society without harming themselves.	3.14	1.03	Medium
16	13	Snapchat helps gain effective communication skills.	3.13	1.04	Medium

17	9	Instagram helps identify students' family problems.	3.09	1.19	Medium
18	24	Radio channels encourage students to engage in dialogue and discussion in resolving political disputes.	3.08	1.10	Medium
19	30	Jordanian radio channels explain the importance of achieving economic security in society.	3.03	1.23	Medium
20	22	Radio University of Jordan promotes pride in the dimensions of human civilization in the Arab and Islamic fields.	3.01	1.26	Medium
21	32	The university's electronic pages provide preventive methods to confront corruption that negatively affects sound thought.	2.89	1.20	Medium
22	21	The university's electronic pages help students to confront the ideological deviations broadcast through the various media.	2.81	1.33	Medium
23	19	The electronic bulletins aim to build positive attitudes and values towards the dimensions of the concept of intellectual security and its practices.	2.83	1.22	Medium
24	18	Jordanian radio channels help create a culture of knowledge about the concepts of intellectual security.	2.62	1.62	Medium
25	3	The television airs examples of educational thinkers to emulate.	2.58	1.69	Medium
26	7	The University of Jordan Radio listens to students' problems and discusses them with them.	2.55	1.23	Medium
27	25	The television airs topics that deepen the concepts of loyalty and belonging to the homeland.	2.54	1.21	Medium
28	20	WhatsApp promotes the security culture.	2.49	1.85	Medium
29	23	Public Security Radio promotes the culture of sacrifice, the presentation of the public interest, and the rejection of deviant cultures.	2.47	1.34	Medium
30	31	Public Security Radio promotes positive economic interaction with society.	2.45	1.32	Medium
31	15	Facebook of the University of Jordan displays examples of positive cultural intellectual currents.	2.43	1.31	Medium
32	26	University of Jordan Radio advises students to stay clear of violence, extremism and terrorism.	2.42	1.31	Medium
33	2	Facebook rejects deviant ideas about society.	2.35	1.13	Medium
	27	Total Degree	3.07	1.128	Medium

However, item (2) which states “Facebook rejects deviant ideas about society”, is the lowest arithmetic means with an arithmetic mean of (2.35) with a medium degree. Then, item (26) which states “The University of Jordan Radio advises students to stay clear of violence, extremism and terrorism is with an arithmetic mean of (2.42), with a medium degree, followed by item (15) with an arithmetic mean of (2.43), and with a medium degree, which states, ‘Facebook of the University of Jordan displays examples of positive cultural intellectual currents’ ”. The general arithmetic mean of the items that measure the role of electronic means in enhancing the intellectual security of Jordanian university students from the students' point of view is (3.07) with a medium degree. This result is in agreement with the findings of the study of Abu Khotwa and Baz (2014), which shows that the effect of social networks on the intellectual security of students, in general, is of medium degree.

Importantly, this is because electronic means in general, including university’s webpages and Facebook, still lack awareness of students in different educational stages of the importance of intellectual security and the development of critical thinking so that they can sort out the ideas and opinions presented to them, and not be misled by destructive calls that harm the stability and security of the society. Also, universities are unwilling to involve themselves in sensitive topics that may contribute to creating future problems, especially since some websites are prohibited from broadcasting not only in the university, but in society, and this certainly reflects on the quality of the programs and the people who are hosted, alongside students' preoccupation with studying and exams, lack of critical thinking skills such as dialogue and discussion, as well as the conviction of their limited role in influencing and changing reality, which affects their understanding of the contents of the programs broadcast by electronic means.

Q2. Are there statistically significant differences at the level of ($\alpha \leq 0.05$) in the role of electronic means in enhancing intellectual security among the students at the University of Jordan due to the following variables (gender, specialization, academic level)?

To answer this question, the arithmetic means and standard deviations are calculated and a 3-way analysis of variance (ANOVA) is applied to reveal the differences in the role of electronic means in enhancing intellectual security due to variables (gender, specialization, and academic level) as illustrated in Table III. The following are the results.

Table III shows that there are apparent differences between the arithmetic means of the role of electronic means in enhancing intellectual security depending on the variables (gender, specialization, and academic level). To reveal the statistical significance of these differences, a 3-way analysis of variance (ANOVA) analysis is applied as illustrated in Table IV.

Table IV shows that there are no statistically significant differences at the level of significance ($\alpha \leq 0.05$) in the role of electronic means in enhancing intellectual security according to the (gender) variable, as the value of (f) does not

reach the level of statistical significance (0.05). It also shows that there statistically significant differences at the level of significance (0.05) in the role of electronic means in enhancing intellectual security according to the variable of specialization, as the value of (f) is (3.432) with statistical significance of (0.058). This is due to the state of awareness formed in Jordanian society as a result of the technological revolution, developments, and the knowledge revolution. The electronic means in offering educational programs neither distinguish between males and females nor based on specialization because intellectual security is a humanitarian necessity for everyone involved in it without exception. It also shows that there are statistically significant differences at the level of significance (0.05) in the role of electronic means in enhancing intellectual security according to the variable of the academic level, as the value of (f) is (3.953) at the level of statistical significance (0.00). To reveal the points of the differences, a Scheffe test is applied as illustrated in Table V.

TABLE III. ARITHMETIC MEANS AND STANDARD DEVIATIONS OF THE ROLE OF ELECTRONIC MEANS IN ENHANCING INTELLECTUAL SECURITY FOR STUDENTS AT THE UNIVERSITY OF JORDAN ARRANGED IN DESCENDING ORDER ACCORDING TO THE VARIABLES (GENDER, SPECIALIZATION, AND ACADEMIC LEVEL)

Variable	Category	AM	SD
Gender	Male	3.48	0.48
	female	3.66	0.44
Specialization	scientific	3.52	0.46
	Humanities	3.38	0.59
Academic Level	First year	3.43	0.56
	Second Year	3.49	0.45
	Third year	3.60	0.43
	Fourth year	3.44	0.55

TABLE IV. RESULTS OF (F) VALUES TO REVEAL DIFFERENCES IN THE ROLE OF ELECTRONIC MEANS IN ENHANCING INTELLECTUAL SECURITY DUE TO VARIABLES (GENDER, SPECIALIZATION, AND ACADEMIC LEVEL)

Source of Variance	Sum of Squares	Degrees of Freedom	Mean of Squares	F	Statistical Sig.
Gender	0.059	1	0.059	0.245	0.512
Specialization	0.781	1	0.781	3.432	0.058
Academic Level	0.944	3	0.944	3.953	0.000
Error	95.363	520	0.18		
Total Adjusted	96.589	525			

TABLE V. SCHEFFE TEST RESULTS TO REVEAL THE POINTS OF DIFFERENCES ON THE ACADEMIC LEVEL VARIABLE IN THE ROLE OF ELECTRONIC MEANS IN ENHANCING INTELLECTUAL SECURITY

Academic Level	AM	First Year	Second Year	Third Year	Fourth Year
First Year	3.43	-	0.05-	0.17-*	0.00
Second Year	3.49		-	0.12-	0.05
Third Year	3.60			-	0.18*
Fourth Year	3.44				-

Table V shows that there are differences in the role of electronic means in enhancing intellectual security according to the variable of the academic level between the two categories (first year and fourth year) on the one hand and the category (third and second year) from the other hand, where the differences are in favor of the category (third year) with an arithmetic mean of (3.60), while the arithmetic mean for the first year is (3.43) and the fourth year is (3.44). This result can be explained by the fact that first-year students are still at the beginning of their university life and have not interacted with electronic means sufficiently, and therefore they have not formed a framework of knowledge that qualifies them to be able to sort out the ideas and opinions presented to them, and they lack many critical thinking skills such as dialogue and criticism. Yet, we find fourth-year students rarely interact with electronic means because of their preoccupation with study and exams, being in the final stages of their university life. However, we find that the differences are in favor of third-year students, and this is explained by the fact that third-year students have the knowledge and intellectual framework that enables them to understand the contents of the electronic means presented to them and participate in it, and their ability to sort out the destructive ideas and opinions that threaten the security of society.

XV. RECOMMENDATIONS

In light of the above results, the study recommends employing electronic means in activating the intellectual security of university education students in Jordan, establishing programs that help students develop critical thinking so that they can sort out the ideas and opinions on electronic means and conducting other similar studies on the role of electronic means to include all public and private universities with the variables of this study and other variables unaddressed by this study.

ACKNOWLEDGMENTS

This Research is supported and funded by the by the Deanship of Scientific Research in The University of Jordan

REFERENCES

- [1] Abu Khotwa, Sayed and Baz, Ahmed. (2014). The social network and its effects on intellectual security for university education students in the Kingdom of Bahrain. The Gulf University in the Kingdom of Bahrain, 7(15) 1-14.
- [2] Abu Arja, Tayseer. (2000). Arab media: Challenges of the present and the future in the information age. Majdalawi Library: Cairo.
- [3] Atribi, Howayda. (2011). The university's role in achieving intellectual security: A suggested concept. *The Arab Journal for Security Studies and Training*, 52 (27) 223-263.
- [4] Danani, Abdul Malik. (2001). The media function of the Internet: A study to identify its uses in the field of media. University Salary House: Beirut.
- [5] Jounson, Doug. (2005). Maintaining intellectual security in the Internet world, *Learning and Leading with technology*, 32 (8) 39-91.
- [6] Kuppuswamy, S. and Narayan, P. (2010). The Impact of social networking websites on the education of youth, *International Journal of Virtual Communities and Social Networking*, 2(1), 67-79.
- [7] Mabrouk, Sobha Bghoura. (2011). Intellectual security. *Journal of Security and Life*, 366 (2), Algeria.
- [8] Rabei, Muhammad Bin Abdulaziz Salih. (2008). The Role of Curricula in Promoting the Concepts of Intellectual Security among University Students in the Kingdom of Saudi Arabia, a paper presented to the First National Conference on Intellectual Security "Concepts and Challenges".
- [9] Radwan, Hanan and Ramadan, Salah, and Abdel-Wahhab, Iman. (2010). The role of modern communication technology in developing freedom of expression of opinion among university students in the light of the postmodern society, research presented to the first scientific conference of the Department of Foundations of Education, Education in Postmodern Society, College of Education, Benha University, 230-295.
- [10] Sajit, Ahmad Mutashar. (2015). The extent to which Islamic education textbooks are included in the higher basic stage of concepts of intellectual security from the viewpoint of teachers in Jordan. [Master Thesis] Al-Bayt University, Jordan.
- [11] Fakhouri, H. N., Hudaib, A., & Sleit, A. (2019). Multivector particle swarm optimization algorithm. *Soft Computing*, 1-19.
- [12] Shehata, Hassan. (2001). University education between theory and practice. Amoun: Nasr City.
- [13] Hamad, F., Al-Fadel, M., & Fakhouri, H. (2020). The effect of librarians' digital skills on technology acceptance in academic libraries in Jordan. *Journal of Librarianship and Information Science*, 0961000620966644.
- [14] Shaltan, Fayez. (2013). The role of colleges of education in Palestinian universities in enhancing intellectual security. *Journal of the Islamic University for Educational and Psychological Studies*, 11(1), 272-312.
- [15] Fakhouri, H. N., Hudaib, A., & Sleit, A. (2019, October). Hybrid Particle Swarm Optimization with Science Cosine Algorithm and Mathematical Equations for Enhancing Robot Path Planning. In *International Conference on Information, Communication and Computing Technology* (pp. 226-236). Springer, Cham.
- [16] Alameri, J., Ismail, H. B., Akour, A., & Fakhouri, H. N. (2019, October). Blended Learning and the Use of ICT Technology Perceptions Among University of Jordan Students. In *International Conference on Information, Communication and Computing Technology* (pp. 271-280). Springer, Cham.
- [17] Shehri, Faiz Bin Ali Bin Abdullah. (2006). The role of secondary schools in spreading security awareness. [Master Thesis] Naif Arab University for Security Sciences, Riyadh.

Enhancement of 3D Seismic Images using Image Fusion Techniques

Abrar Alotaibi¹, Mai Fadel², Amani Jamal³, Ghadah Aldabbagh⁴

Computer Science department, Faculty of Computing and Information Technology

King Abdulaziz University, Jeddah, Saudi Arabia^{1, 2, 3, 4}

Computer Science department, College of Computer Science and Information Technology

Imam Abdulrahman bin Faisal University, Dammam, Saudi Arabia¹

Department of Mechanical Engineering, Massachusetts Institute of Technology (MIT), Cambridge, MA, USA³

Abstract—Seismic images are data collected by sending seismic waves to the earth subsurface, recording the reflection and providing subsurface structural information. Seismic attributes are quantities derived from seismic data and provide complementary information. Enhancing seismic images by fusing them with seismic attributes will improve the subsurface visualization and reduce the processing time. In seismic data interpretation, fusion techniques have been used to enhance the resolution and reduce the noise of a single seismic attribute. In this paper, we investigate the enhancement of 3D seismic images using image fusion techniques and neural networks to combine seismic attributes. The paper evaluates the feasibility of using image fusion models pretrained on specific image fusion tasks. These models achieved the best results on their respective tasks and are tested for seismic image fusion. The experiments showed that image fusion techniques are capable of combining up to three seismic attributes without distortion, future studies can increase the number. This is the first study conducted using pretrained models on other types of images for seismic image fusion and the results are promising.

Keywords—Image fusion; seismic image; seismic attribute; neural networks

I. INTRODUCTION

Seismic images are data gathered during the exploration of the earth subsurface by sending seismic waves to the earth subsurface and recording the reflection. They provide subsurface structural information and allow the modeling and visualization of the earth subsurface [1]. Seismic attributes are quantities derived from seismic data that supplement and emphasize certain information to make the visualization process more informative [2]. To create an accurate representation of the earth subsurface, a geophysicist needs to look at the seismic image and its corresponding seismic attributes, interpreting a large amount of information simultaneously, which is a cumbersome effort. Therein lies the challenge, combining multiple views into a single view that effectively exploits all information contained in all individual views and reduces the duration of the process.

There has been work addressing the challenge of combining seismic attributes such as volume blending, cross-plotting, principal components analysis (PCA) and Octree [3], [4]. The most recent and relevant is the work done by Al-Dossari et al. [4]. They have extended octree color quantization Algorithm, to increase the number of the

combined seismic attributes. The main limitations are the maximum number of attributes is limited to eight, the order of the attributes effects the results and the combined image results have artifacts.

Alfarraj et al. [5] proposed a multiscale fusion technique to enhance the seismic geometric attributes using a Gaussian pyramid to generate different scales of an attribute, which then are fused together to get an enhanced attribute. This technique reduces noise and improves the resolution.

By extending the use of fusion techniques to enhance seismic data instead of enhancing the resolution of a single attribute, these fusion techniques can be used to enhance seismic data by combining multiple attributes, combining multiple images into a single one is a need that is common among several domains such as photography and medical imaging. One of the techniques used to address this need is Image fusion.

Image fusion is used to combine two or more input images containing complementary details of the same scene creating a new image [6]. The input images are taken from the same imaging device with different parameters or from different imaging devices; the resulting fused image will be more informative than any individual input image [7]. Image fusion techniques show incredible benefits in various tasks of image processing that depend on viewing multiple images of the same scene such as object detection and recognition as well as in a variety of fields, for example digital photography, medical imaging and remote sensing [6], [7]. On these types of tasks, combining the significant details of multiple input images into a single fused image can often reduce the difficulty and enhance the outcome of the task [6]. The information enhancement provided by seismic attributes of a seismic image is similar to many image fusions tasks such as medical imaging and remote sensing. Conceptually, we can consider different seismic images and attributes as different types of medical images i.e., the seismic (raw) image as magnetic resonance imaging (MRI); one attribute as positron emission tomography (PET); and another attribute as computed tomography (CT).

Recently, with the rise of Deep Learning (DL) many methods from image fusion using DL have been proposed. DL is a class of Machine Learning algorithms that excel in feature extraction and image representation using neural networks.

Convolutional Neural Networks (CNN) can solve conventional hand-crafted approach issues of designing fusion methods and selecting fusion rules and activity-level metrics as it can learn features implicitly through training on data, since image fusion tasks are very similar to classification tasks which CNN shines in, so it gets better results [8].

In order to achieve our task, in our paper, we propose a deep learning method which is constructed by neural networks. We use the method to extract image features and then fuse them into one. The method receives 3-dimensional (3D) image data; each piece of 3D data represents either the seismic (raw data) image or seismic attributes. Then the method slices the 3D data and forwards the resulting 2-dimensional (2D) images as an input to the fusion model, which extracts the important information from input images using the convolutional layer and creates feature maps. Then we fuse the feature maps to create the output image. Finally, the method constructs the output as 3D data.

We conduct experiments to analyze the proposed method using different fusion models. These models have been pretrained on a dataset belonging to different image fusion tasks and have achieved excellent results compared to other models' performance on the specific task. The reason for using pretrained models is the lack of available datasets for seismic images with ground-truth fusion images, which hinder training process. We are investigating task-specific models' performance on seismic images, trying to find commonality between this task and other tasks, whether due to data similarity or a certain task's model ability to generalize to include seismic images tasks. Thus, the experiments will analyze similarities between the seismic image fusion task and other fusion tasks.

Our paper is structured as follows. In Section II, we briefly review related works. In Section III, the proposed fusion method is introduced in detail. The experiment results are shown in Section IV. The conclusion of our paper and discussion are presented in Section V.

II. RELATED WORK

In this section, we give a briefing of the previous work done by extended octree quantization method and highlight its limitation. Then we review the work done so far in Image fusion, to investigate the most relevant approaches that suites the problem of seismic attributes combination.

Al-Dossari et al. [4], proposed to use octree and its color quantization algorithm to combine groups of attributes onto a single one, by extending octree's color quantization three nodes to eight nodes octree color quantization, this method originated from image processing of compressing colors, it handles eight groups of attributes to form a single attribute. The method was tested on to combine up to eight seismic attributes. The method has the following limitations: The order of the chosen attribute will affect the result and the need to take average of multiple octree sequences to rectify and the method can be applied to up to eight attributes.

A. Overview of Image Fusion

Image fusion is a subfield of image processing. It is the process of combining multiple input images captured from one or more sensors to create a single image [6]. The aim of image fusion is not only to minimize the amount of information, but also to create images that are more suitable and more comprehensible to human and computer perception. It gives the possibility to collect information from multi-source images to generate a high-quality fused image with all spatial and spectral information [7].

The image that has been fused must satisfy the following conditions: (1) include all pertinent information, (2) be clear of all artifacts and anomalies and (3) have all noise and error removed. Major applications of image fusion include remote sensing image fusion, medical image fusion, and multi-focus image fusion [6].

The general image fusion strategy consists of the following steps: acquisition of different input images, image-to-image registration and fusion. Image registration entails feature detection, aligning and matching, estimation of the transformation model, image transformation and resampling. Fusion rules are performed either as a direct mathematical application such as averaging or choosing the maximum pixel value or as a part of the image transformation model [9].

DL-based image fusion has shown a lot of potential in improving image fusion techniques. The basic architecture of CNNs consists of two parts: the feature extractor and the classifier. The feature extractor uses convolutional and pooling layers to extract the salient features of the inputs and represent them using activation maps, which align with the image registration step of image fusion. The classifier can be utilized or changed to apply fusion rules on the maps, which align with the fusion step of image fusion. Also, CNNs have the ability to use multiple fusion rules due to being trained on a large dataset, thus avoiding one of the limitations of classical fusion methods. Fig.1 shows the basic architecture of CNNs.

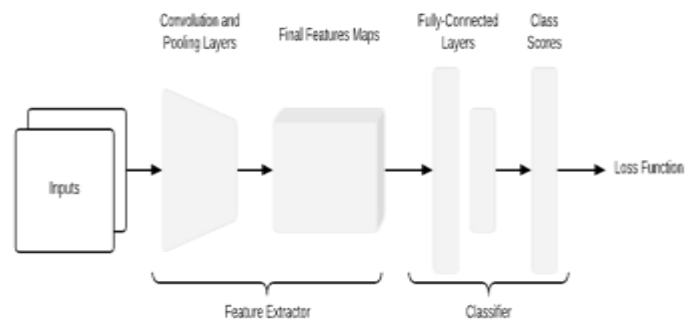


Fig. 1. Basic Architecture of CNNs.

B. Image Fusion Applications

Image fusion can be grouped into multiple classes based on the task it performs. These classes include the following: (1) multi-focus image: it fuses images with different focus depth to create a focused image; (2) Visible/Infrared light image fusion: it fuses images taken using infrared with visible light to create a more informative image; (3) medical image fusion: it fuses images used in the medical field such as MRI

and CT to create a more informative image; and (4) multi-exposure image fusion: it fuses images with different exposure with different lighting to create a superimposed image [10].

For the task of multi-focus image fusion, a CNN is used by Liu et al. [11] to address a binary classification task in the area of multi-focus image fusion in the spatial domain. The Siamese network structure is implemented where two similar networks function together to generate one output. Du and Gao [12] extended the work of Liu et al. [11] with the distinction of adding multi-scale decomposition of inputs before feeding it to the network. The input images are segmented into three overlapping stacks with three different sizes. The network generates three focus maps that are averaged to create a single fused focus map. The work [11] demonstrates that the method benefits from the introduction of the multi-scale strategy in terms of performance but it suffers from the drawback of increased computational cost. Another issue most multi-focus image fusion CNN models face is that although they enhance the decision maps, the initial segmented maps suffer from many errors. To overcome this, Amin-Naji et al. [13] proposed a novel Ensemble of CNN (ECNN) framework to take advantage of ensemble learning, which is used to improve the model's ability to generate decision maps and take advantage of learning from several datasets. The proposed method uses three CNNs trained on three different datasets to create the initial decision maps. The authors used COCO dataset and performed transformation on it to create the additional two datasets. It has the following structure. It has four convolutional layers of sizes $(32 \times 64 \times 64)$, $(16 \times 32 \times 128)$, $(8 \times 16 \times 128)$, $(4 \times 8 \times 256)$ and kernel size (3×3) , stride (1×1) , padding (1×1) , non-linear activation and max-pooling (2×2) for all convolutional layers. For CNN2 and CNN3, they concatenate the output of convolutional layer $(8 \times 16 \times 128)$ as input to convolutional layer $(4 \times 8 \times 256)$, and the output then is concatenated with CNN1 as input to convolutional layer $(4 \times 8 \times 256)$. The output is concatenated and fed to the fully connected layer of size $(4 \times 8 \times 512)$, that classifies each pixel. The novelty of the proposed method lies in its input feeding mechanism; instead of creating branches for feeding focused and unfocused images, the focused and unfocused parts of the image are fed together. As a result, it outperformed all the other models, achieving state-of-the-art results.

For the task of Visible/Infrared light image fusion, Zhong et al. [14] created a model for image fusion and enhanced resolution. First, the input images are upsampled and decomposed, then SR-CNN [15] is used to improve the resolution the high frequency maps. Then they are fused using choose-max rule, while low frequency coefficients are fused using averaging rule. Then the fused image is created by fusing both high- and low-frequency coefficients. This model has produced good results in medical image fusion and multi-focus fusion in addition to Visible/Infrared light image fusion. Li and Wu [16] proposed "DenseFuse," a novel encoder-decoder model for the fusion of infrared and visible images. The model uses a dense block in the encoding part to improve the flow of information between layers and avoid information degradation. It has the following structure: the encoder has two components, a convolutional layer of size $(3 \times 3 \times 1 \times 16)$

and a dense block. The dense block has three cascading convolutional layers of sizes $(3 \times 3 \times 16 \times 16)$, $(3 \times 3 \times 32 \times 16)$ and $(3 \times 3 \times 48 \times 16)$. The output is fed to the fusion layer to fuse the feature maps. The decoder has four convolution layers of sizes $(3 \times 3 \times 64 \times 64)$, $(3 \times 3 \times 64 \times 32)$, $(3 \times 3 \times 32 \times 16)$ and $(3 \times 3 \times 16 \times 1)$. It receives the feature maps from the encoder and constructs the image. The results showed state-of-the-art performance compared to other models and exhibited that the proposed model can be applied to other fusion tasks with appropriate modification.

For the task of medical image fusion, Liu et al. [17] incorporated a multi-scale decomposition framework instead of spatial fusion into the method proposed by [11]. The presented framework decomposes input images using a Laplacian pyramid and also passes the input images into the CNN to acquire the weight map, which is then decomposed using a Gaussian pyramid, using a similarity strategy to adjust fusion rules. The Laplacian and Gaussian decompositions are fused, and then the fused image is created using a Laplacian pyramid reconstruction. In Liu et al. [18] Convolutional Sparse Representation (CSR) was used for image fusion. In their method the proposed input images are segmented into detail layer and base layer. Convolutional Sparse Coding (CSC) is executed on the detail layer to get sparse coefficient maps. After several calculations the "choose max" rule is applied to produce a fused coefficient map that is used alongside dictionary filters to create the fused detail layer. Dictionary filters are a set of filters that are trained on a set of natural scene images. Most medical imagery fusion models cannot preserve the energy levels of the input images in the fused images. Yin et al. [19] proposed a novel model that uses Nonsampled Shearlet Transform Domain with Parameter-Adaptive Pulse Coupled-Neural Network (NSST PA-PCNN) that can maintain the energy level in the fused image. PCNN is an artificial neural network with biological procedures [20]. The paper presented the use of PAP-PCNN to increase the convergence speed and reduce computation. It also uses NSST for enhanced detail extraction. NSST-PAPCNN is a pulse-coupled neural network that takes the following four steps: NSST decomposition, high-frequency band fusion, low-frequency band fusion and NSST reconstruction. NSST decomposition extracts image details using the Shearlet filter, and parameter-adapting pulse coupling trains the neuron in an iterative manner for the fusion process. The model exhibits state-of-the-art performance and outperforms on existing tasks.

For the task of multi-exposure fusion, Kalantari and Ramamoorthi [21] proposed a solution to the motion artifact in dynamic scenery through the implementation of a CNN for High Dynamic Range (HDR) image creation. To generate the HDR image directly, three aligned LDR images are used as the input of the CNN. The authors implemented three different network structures to investigate the output adjustments. For the loss function, the Euclidean interval between tone-mapped ground-truth and approximate HDR images is used. Prabhakar et al. [22] proposed "DeepFuse," a novel model for multi-exposure fusion that takes an unsupervised approach in the fusion process. Also, the authors created and trained the network on a new benchmark dataset, improving the model's

learning rate. The CNN takes an input image pair and segments the image into color channels of YCbCr. The reason for the segmentation is to use luminance channel Y to display fundamental details by using the CNN feature extraction capabilities. Then the remaining Cb and Cr channels for each input are fused respectively using weighted-average fusion rule, generating Cb_{Fused} and Cr_{Fused} channel and they are combined with the outcome of Y channel to generate the fused image. Then the resulting images are converted back into RGB. DeepFuse is an encoder-decoder model and has the following structure: the encoder has two input channels, both of which have two convolution layers of sizes $(5 \times 5 \times 1 \times 16)$ and $(7 \times 7 \times 16 \times 32)$, respectively. A fusion layer using addition rule is used to fuse the feature maps from both channels. The decoder has three convolution layers of sizes $(7 \times 7 \times 32 \times 32)$, $(5 \times 5 \times 32 \times 16)$ and $(5 \times 5 \times 16 \times 1)$. It receives the feature maps from the encoder and constructs the image. The results showed state-of-the-art results compared to other multi-exposure fusion models. Also, results showed that DeepFuse trained on multi-exposure data can perform well on a multi-focus task and that the CNN filters are general enough to be used on other image fusion tasks.

Our studies showed that the pretrained models have not been used for seismic image fusion, and that there are similarities between seismic images and medical images, the data capturing method and the semantic importance of different images used in the fusion process. For data capturing, seismic data and medical image data capture images of a survey line using different kinds of waves to represent a 3D object [23]. Also, seismic and medical image fusion inputs contain different types of information for every image. While there are no similarities between the multi-exposure, Infrared/Visible and multi-focus image fusion tasks, results showed that training models on composite or detailed scenery will allow models to better generalize to other tasks [24].

III. PROPOSED METHOD

The proposed image fusion method supports the fusion of seismic data and one or more seismic attributes as follows: suppose there are M inputs to the method and $M \geq 2$, M are 3D images of identical size that are either seismic data or attributes denoted as I_R and I_{An} respectively, as $I_{An}/n \in \{1, 2, 3, \dots, N\}$ as seen in Fig. 2. The inputs I_R and I_{An} are first sent to a slicing function to convert the 3D data (x, y, z) into 2D data (x, y) with Z number of images. The output of the slicing function is fed as an input to the fusion model. The fusion model accepts a set of images as an input containing one image from each I_R and I_{An} starting by $z = 1$ until Z . After all the fused images are created by the fusion model and the fusion metrics are calculated, the fused images are then made into 3D image data using the reverse of the slicing function.

A. Fusion Model

We chose the models that performs best in their respective fusion task after comparing them in Section II and will compare the performance on the seismic image fusion task. Table I shows a summary of the selected fusion models.

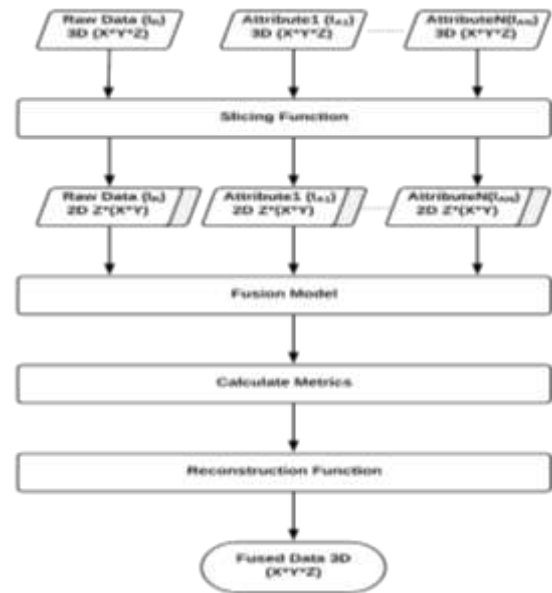


Fig. 2. Schematic of the Proposed Method.

TABLE I. SELECTED FUSION MODELS

Fusion Task	Model Name	Dataset
Multi-Exposure	DeepFuse [22]	EMPA HDR
Multi-Focus	ECNN [13]	MS-COCO
Medical imagery	NSST-PAPCNN [19]	Brain Atlas
Visible/Infrared	DenseFuse [16]	MS-COCO

B. Fusion Metrics

The evaluation performance metrics of image fusion that were used in most of the methods in [10,13,16,18] are used to compare the performance of the models. The assessment of the non-referenced fusion is not direct since the ground truth images are not available, so there is a need to use several non-referenced image fusion metrics to evaluate the models' performance. The metrics formulas can be found in [25]. We used the following metrics:

- 1) Entropy (EN): measure the information content of the fused image.
- 2) Information Transfer ($Q_{AB/F}$): measure the total information transferred from source images to fused image.
- 3) Modified Fusion Artifacts ($N_{AB/F}$): measure artificial artifacts generated by fusion.
- 4) Feature Mutual Information (FMI): measure the dependency between the input images and fused image.
- 5) Mutual Information (MI): measure the similarity of image intensity between the fused and reference images.

IV. EXPERIMENTS AND RESULTS

We conducted experiments on the models discussed in Section II using pretrained models published by [10,13,16,18]. In our study we have designed two experiments. The first experiment takes two inputs and the second one takes three inputs. The first experiment is used to ascertain if the proposed models can combine two different seismic images.

The second experiment is used to show that image fusion can increase the input number limit without distortion, by combining three different seismic images without distorting the resulted image. The common goal of both experiments is to measure and evaluate the performance metrics of running the four selected fusion models on our dataset. Also, conducting the experiments on different numbers of inputs serves the goal of examining the change of measurements as we add more inputs. To evaluate the fusion results, we perform a visual comparison alongside the quantitative comparison, to assess the visual representation such as texture and color etc. of the fused image alongside the structural information.

In the first experiment: the number of inputs M is 2; one input is a seismic image (I_R) and the second is a seismic attribute named skeleton created by a skeletonization algorithm denoted as (I_A) [26]. The size of I_R and I_A is (876,221,271).

In the second experiment: the number of inputs M is 3; in addition to (I_R) and (I_A), another seismic attribute named coherence is used, denoted (I_{Ac}). I_{Ac} has the same size as I_R and I_A .

There are four sets of I_R , I_A and I_{Ac} for the experiments. A sample of these images is shown in Fig. 3. The images are minimized and cropped to accommodate the space limit; experiments are performed on original images.

Experiment 1 and 2's results are presented in Table II and Table III respectively. The average results of the four sets of each experiment are displayed. Results in **bold** signify best performance and results that are underlined signify second best. The results showed the performance of the models with different numbers of available inputs. Experiment 2's fusion had more input, and thus the amount of information in the fusion increased, which can be indicated by larger values of EN and MI , and the amount of artificial fusion noise indicated by $N_{AB/F}$. Thus the discussion below will consider experiment 1's results as it has more information.

The fusion results on two sets of images due to the space limit are shown in Fig. 4 and Fig. 5.

As we can see, the DeepFuse model outperformed all other models. It had the best values in (EN , $N_{AB/F}$, MI) and second-best values in ($Q_{AB/F}$, FMI). Having high EN values denotes that the fused image has a large amount of information and that the model is good for feature extraction. Having high FMI , $Q_{AB/F}$ and MI values denotes that the fused image has maintained structural information and features. Having low $N_{AB/F}$ values denotes less artificial noise due to fusion. When visually comparing the fused image to the input image, the fused image contains all structure information from the inputs; all the edges are clear; the color and texture of the inputs are present and there is no noticeable fusion noise. The performance of the DeepFuse model can be attributed to its filters' adaptability, as it was trained on a large dataset of high-resolution complex images, which allowed the filters to learn and reach a point where they can perform remarkably well on other fusion tasks.

The ECNN model had the best values of FMI and the second-best values of $N_{AB/F}$. This can be attributed to the fusion rules used by the multi-focus task, which chooses the max value of the pixels in the fusion. The fused pixel value is in one of the inputs, and thus there is high dependency between the inputs and the fused images. But, as can be observed in the fusion results example in Fig. 5, ECNN has the worst visual representation of the fused information. The fused image is missing a lot of structural information and the color and texture don't match the input images. This might be as a result of the nature of the multi-focus task, since its aim is to extract the best parts from multiple input images and create a new image from those parts, which in hindsight doesn't match the desired outcome. Thus, it can be inferred that the multi-focus fusion models are not suitable for the seismic data fusion task.

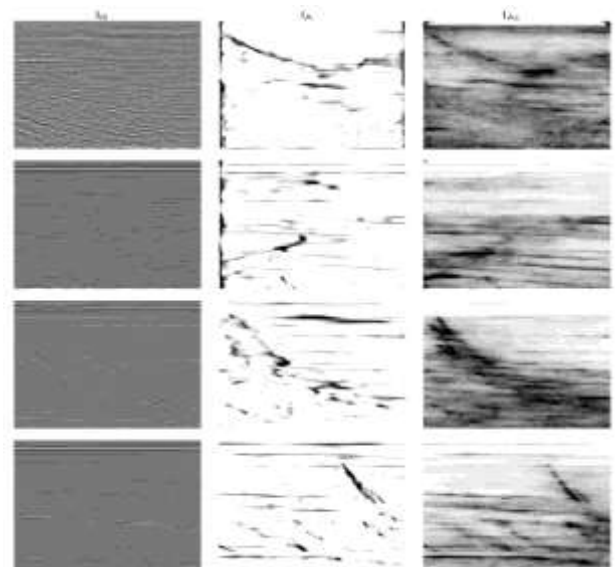


Fig. 3. Four Sets of Source Images. Left Column Contains Seismic Data (I_R) Middle Column Contains Skeleton Attribute (I_A), and Right Column Contains Coherency Attribute (I_{Ac}).

TABLE II. EXPERIMENT 1 FUSION RESULTS AVERAGE OF 4 PAIR

Metric	DeepFuse	ECNN	NSST-PAPCNN	DenseFuse
$EN \uparrow$	6.27397	2.5677	4.74846	<u>5.74016</u>
$Q_{AB/F} \uparrow$	<u>0.40374</u>	0.2435	0.42837	0.40147
$FMI \uparrow$	<u>0.88237</u>	0.8859	0.85902	0.86483
$MI \uparrow$	12.54794	5.1355	9.49692	<u>11.48034</u>
$N_{AB/F} \downarrow$	7.7083e-4	<u>0.0112</u>	0.09243	0.02932

TABLE III. EXPERIMENT 2 FUSION RESULTS AVERAGE OF 4 PAIR

Metric	DeepFuse	ECNN	NSST-PAPCNN	DenseFuse
$EN \uparrow$	6.71435	2.6955	5.5743	<u>6.27537</u>
$Q_{AB/F} \uparrow$	<u>0.60482</u>	0.2468	0.6092	0.50932
$FMI \uparrow$	<u>0.92781</u>	0.9356	0.8978	0.88958
$MI \uparrow$	13.4286	5.3911	11.149	<u>12.5508</u>
$N_{AB/F} \downarrow$	0.00554	<u>0.0108</u>	0.15933	0.03124

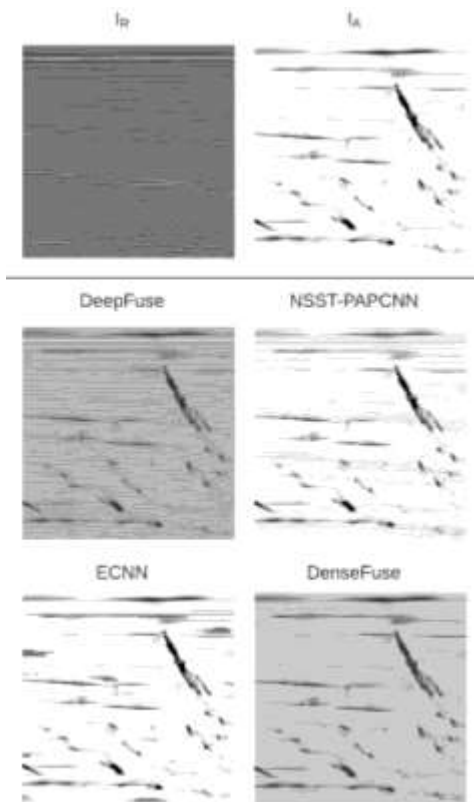


Fig. 4. Fusion Results of Experiment 1, a Test Set is displayed here to Illustrate the Fusion Results. Above-Line: Inputs, Below-Line: Fusion Outputs.

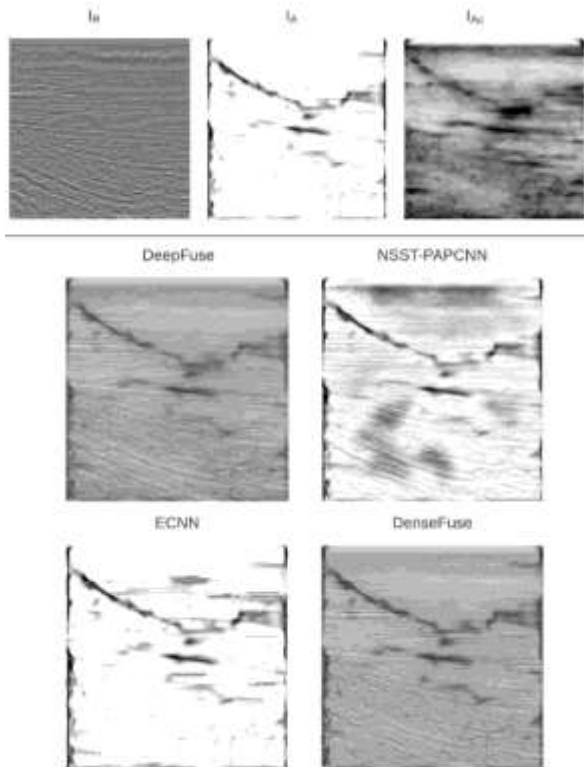


Fig. 5. Fusion Results of Experiment 2, a Test Set is displayed here to Illustrate the Fusion Results. Above-Line: Inputs, Below-Line: Fusion Outputs.

The NSST-PAPCNN model had the best values of $Q_{AB/F}$, which can be attributed to the model's ability to preserve energy levels. Seismic images and medical images are similar in that they are both collected using surveys and that the type of information of every input image is different and needs to be maintained. However, the model suffers from the highest artificial noise having the highest values of $N_{AB/F}$. Visually the fused image emphasizes the edges and lines, but it doesn't capture the color and texture from the input images, and as more inputs are added the fusion noise increases creating a shadow effect on the image.

Finally, the DenseFuse model has the second-best values of EN and MI , indicating the model's ability to extract and maintain the structural information of the input images. This can be attributed to the Dense Block used in the model preserving the images' structure. The model had the second-best overall performance. Visually comparing the fused image to the input image, the fused image contains all structure information from the inputs; all the edges are clear; and there is no noticeable fusion noise. Visually the difference between the best performer DeepFuse and the second-best DenseFuse is the DeepFuse's ability to capture the color and texture of the inputs better with less artificial noise.

In relation to the work done previously, it has combined a limited number of seismic attributes (eight) and cannot add more due to the cluttered results. Our research is work in progress, and we are planning to experiment by adding more attributes. In principle, our work can accept unlimited number of attributes. Also, as can be seen from our experiments, a third attribute improved the results and has not cluttered the images rendering them unreadable.

V. CONCLUSION

In this paper, we investigate enhancement of 3D seismic images using image fusion and deep learning. Fusion technique has been used to enhance the resolution and reduce the noise of a single seismic attributes. The study was conducted to evaluate the feasibility of using image fusion models pretrained on other image fusion tasks for seismic data fusion. We presented a method for the enhancement of 3D seismic images by slicing the 3D data and attributes to images and feeding them to a fusion model. We chose four different models pretrained for different image fusion tasks and tested the method. We used quantitative fusion metrics to evaluate our fusion method. The experimental results show that the DeepFuse model has good fusion results on seismic images; both quantitative metrics and visual representation of the fused images are better than the results of other models. Also, the experimental results show that models pretrained for multi-focus image fusion are not suitable for the task of seismic image fusion. In comparison to previous done work, our results show that the increasing attribute number doesn't distort the image. The experiments showed that image fusion techniques are capable of combing three seismic attributes. In the future, we will conduct studies to increase the number. This is the first study conducted using models pretrained on other types of images for seismic image fusion and the results are promising.

ACKNOWLEDGMENT

The authors would like to express their cordial thanks to Dr. Saleh Aldossary for his valuable advice and providing test data.

REFERENCES

- [1] A. Al-Shuhail, S. A. Al-Dossary, and W. A. Mousa, *Seismic Data Interpretation using Digital Image Processing*, 2017.
- [2] E. L. Galvan Aguilar, "Log property mapping guided with seismic attributes," Sep. 2013.
- [3] S. S. Manral and D. Clark, "Multi Attribute Analysis-An effective visualization & interpretation technique," 2010.
- [4] S. Al-Dossary, J. Wang, and Y. E. Wang, "Combining multiseismic attributes with an extended octree quantization method," *Interpretation*, 2019, doi: 10.1190/int-2018-0099.1.
- [5] M. Alfarraj, H. Di, and G. AlRegib, "Multiscale fusion for seismic geometric attribute enhancement," 2017, doi: 10.1190/segam2017-17750698.1.
- [6] B. Meher, S. Agrawal, R. Panda, and A. Abraham, "A survey on region based image fusion methods," *Inf. Fusion*, vol. 48, pp. 119–132, 2019, doi: 10.1016/j.inffus.2018.07.010.
- [7] B. Ashalatha and M. B. Reddy, "Image fusion at pixel and feature levels based on pyramid imaging," in *2017 IEEE International Conference on Smart Technologies and Management for Computing, Communication, Controls, Energy and Materials, ICSTM 2017 - Proceedings*, 2017, pp. 258–263, doi: 10.1109/ICSTM.2017.8089164.
- [8] S. Li, J. T. Kwok, and Y. Wang, "Multifocus image fusion using artificial neural networks," *Pattern Recognit. Lett.*, vol. 23, no. 8, pp. 985–997, 2002, doi: [https://doi.org/10.1016/S0167-8655\(02\)00029-6](https://doi.org/10.1016/S0167-8655(02)00029-6).
- [9] E. Blasch, Y. Zheng, and Z. Liu, *Multispectral Image Fusion and Colorization*, 2018.
- [10] Y. Liu, X. Chen, Z. Wang, Z. J. Wang, R. K. Ward, and X. Wang, "Deep learning for pixel-level image fusion: Recent advances and future prospects," *Inf. Fusion*, vol. 42, no. September 2017, pp. 158–173, 2018, doi: 10.1016/j.inffus.2017.10.007.
- [11] Y. Liu, X. Chen, H. Peng, and Z. Wang, "Multi-focus image fusion with a deep convolutional neural network," *Inf. Fusion*, vol. 36, pp. 191–207, 2017, doi: <https://doi.org/10.1016/j.inffus.2016.12.001>.
- [12] C. Du and S. Gao, "Image Segmentation-Based Multi-Focus Image Fusion Through Multi-Scale Convolutional Neural Network," *IEEE Access*, vol. 5, pp. 15750–15761, 2017.
- [13] M. Amin-Naji, A. Aghagolzadeh, and M. Ezoji, "Ensemble of CNN for multi-focus image fusion," *Inf. Fusion*, vol. 51, pp. 201–214, 2019, doi: <https://doi.org/10.1016/j.inffus.2019.02.003>.
- [14] J. Zhong, B. Yang, Y. Li, F. Zhong, and Z. Chen, "Image fusion and super-resolution with convolutional neural network," in *Communications in Computer and Information Science*, 2016, vol. 663, pp. 78–88, doi: 10.1007/978-981-10-3005-5_7.
- [15] C. Dong, C. C. Loy, K. He, and X. Tang, "Image Super-Resolution Using Deep Convolutional Networks," *IEEE Trans. Pattern Anal. Mach. Intell.*, vol. 38, no. 2, pp. 295–307, 2016, doi: 10.1109/TPAMI.2015.2439281.
- [16] H. Li and X. Wu, "DenseFuse: A Fusion Approach to Infrared and Visible Images," *IEEE Trans. Image Process.*, vol. 28, no. 5, pp. 2614–2623, 2019, doi: 10.1109/TIP.2018.2887342.
- [17] Y. Liu, X. Chen, J. Cheng, and H. Peng, "A medical image fusion method based on convolutional neural networks," *20th Int. Conf. Inf. Fusion, Fusion 2017 - Proc.*, 2017, doi: 10.23919/ICIF.2017.8009769.
- [18] Y. Liu, X. Chen, R. K. Ward, and Z. J. Wang, "Image Fusion With Convolutional Sparse Representation," *IEEE Signal Process. Lett.*, vol. 23, no. 12, pp. 1882–1886, 2016, doi: 10.1109/LSP.2016.2618776.
- [19] M. Yin, X. Liu, Y. Liu, and X. Chen, "Medical Image Fusion with Parameter-Adaptive Pulse Coupled Neural Network in Nonsampled Shearlet Transform Domain," *IEEE Trans. Instrum. Meas.*, vol. 68, no. 1, pp. 49–64, 2019, doi: 10.1109/TIM.2018.2838778.

- [20] R. Nie, S. Yao, D. Zhou, and H. Deng, "Analyzing of Dynamic Characteristics for Discrete S-PCNN," *Adv. Mater. Res.*, vol. 765–767, Apr. 2013, doi: 10.2991/icsem.2013.53.
- [21] N. K. Kalantari and R. Ramamoorthi, "Deep High Dynamic Range Imaging of Dynamic Scenes," *ACM Trans. Graph.*, vol. 36, no. 4, Jul. 2017, doi: 10.1145/3072959.3073609.
- [22] K. R. Prabhakar, V. S. Srikar, and R. V. Babu, "DeepFuse: A Deep Unsupervised Approach for Exposure Fusion with Extreme Exposure Image Pairs," in *2017 IEEE International Conference on Computer Vision (ICCV)*, 2017, pp. 4724–4732, doi: 10.1109/ICCV.2017.505.
- [23] F. Aminzadeh and S. N. Dasgupta, "Fundamentals of Petroleum Geophysics," in *Developments in Petroleum Science*, vol. 60, Elsevier B.V., 2013, pp. 37–92.
- [24] S. Li, X. Kang, L. Fang, J. Hu, and H. Yin, "Pixel-level image fusion: A survey of the state of the art," *Inf. Fusion*, vol. 33, May 2016, doi: 10.1016/j.inffus.2016.05.004.
- [25] P. Jagalingam and A. V. Hegde, "A Review of Quality Metrics for Fused Image," *Aquat. Procedia*, vol. 4, pp. 133–142, 2015, doi: <https://doi.org/10.1016/j.aqpro.2015.02.019>.
- [26] K. Vasudevan, D. Eaton, and F. A. Cook, "Adaptation of seismic skeletonization for other geoscience applications," *Geophys. J. Int.*, vol. 162, no. 3, pp. 975–993, Sep. 2005, doi: 10.1111/j.1365-246X.2005.02704.x.

AUTHORS' PROFILE

Abrar Alotaibi is a postgraduate student in the Computer Science Department, Faculty of Computing and Information Technology at King Abdulaziz University. She received a bachelor's degree from Imam Abdulrahman Bin Faisal University, Dammam, Saudi Arabia, in 2015. She holds a Teaching Assistant position at the College of Computer Science and Information Technology in the Computer Science Department at Imam Abdulrahman Bin Faisal University. Her research interests are Image Processing and Machine Learning. She is a member of IEEE.

Dr. Mai A Fadel is a lecturer in Software Engineering at the Department of Computer Science, King Abdulaziz University. Her research interest lies in Design Patterns, and software engineering in general, cloud computing and news credibility in social networks and High-Performance Computing (HPC). She has taught courses in software engineering, web development, algorithms and Java programming. Dr. Mai was the Head of the Information System and the Computer Science departments between 2009 and 2016. Dr. Mai received her PhD degree in Computer Science from the Department of Computer Science at the University of Exeter, UK. She is a member of IEEE and ACM.

Dr. Amani Tariq Jamal is an assistant professor at the Computer Science Department, Faculty of Computing and Information Technology at King Abdulaziz University. She received her Master and Ph.D. degrees from Concordia University, Montreal, Canada, in 2009 and 2015 respectively. Her research interests are pattern recognition, artificial intelligence, Natural Language Processing, and document analysis. She is the cofounder and member of the directors' board of Saudi AI Society.



Dr. Ghadah Aldabbagh received her BSc in 1991 in Computer Science, from the College of Engineering at the University of Illinois at Urbana – Champaign, Illinois, United States; she received her MSc in the Data Communication Networks and Distributed System (DCNDS) from the Computer Science Department at the University College London (UCL) in the United Kingdom; received her PhD in 2010 from the Department of Electronic and Electrical Engineering at UCL, UK. Dr. Aldabbagh holds an Associate Professor position at the Computer Science Department at the Faculty of Computing and Information Technology (FCIT) at King Abdul Aziz University (KAU), Jeddah, Saudi Arabia. Her current research interests: 5G, Wireless Communications, Wireless Sensor Networks, Internet of Things (IoT) Platform, Internet of Everything (IoE), Connected Homes, Smart Workspace, Machine Learning, Deep Learning, Deep Reinforced Learning, Artificial General Intelligence, Artificial Intelligence Everywhere, Autonomous Vehicles, providing connectivity of IoT devices and sensors for Smart Cities, Location Awareness. During the summers of 2013 and 2014, Dr. Aldabbagh joined Professor John M. Cioffi's Dynamic Spectrum Management (DSM) Research Group as a visiting professor at Stanford University. She was awarded by KAU four awards of excellence in

scientific publishing for faculty members for the academic year 2015-2016. In March 2016, Dr. Aldabbagh joined the Laboratory for Information and Decision Systems (LIDS) at Massachusetts Institute of Technology (MIT) as a postdoctoral associate and from March 2017 as a visiting scholar to work on the topic of location-aware ad-hoc sensor networks to work with the highly cited Professor Moe Win. In collaboration with Professor Win's research group, her focus is to develop scalable, distributed, and energy-efficient techniques for scheduling and routing in ad hoc sensor networks with

localization-awareness. In November 2019, she participated in the Saudi Think Tank 20 (T20) of the Saudi G20, as a co-author for two policy briefs (PB); the first was in Task Force 10 (TF10): Sustainable Energy, Food and Water Systems and the second PB was TF6: Economy, Employment, And Education In The Digital Age. In April 2020, Dr. Aldabbagh joined the Marconi Society as a member of the Marconi Selection Advisory Committee for the Marconi Prize.

Multi-beam Antenna Array Operating Over Switch On/Off Element Condition

Julian Imami¹, Elson Agastra², Aleksandër Biberaj³
Faculty of Information Technology, Polytechnic University of Tirana
Sheshi Nënë Tereza 1, 1004, Tirana, Albania

Abstract—In this work, is presented the design of a linear multi-beam antenna. The designed procedure is focused on the possibility of switching off a part of antenna array elements, in active antenna systems, in order to preserve resources (power and heat dissipation). The behavior of the original multi beam antenna design is investigated on the radiation pattern alteration due to the switched off elements. The choice of switching on/off antenna elements requires less computational effort from the algorithms incorporated in the active antenna system. Antenna array beam design using progressive phase shifts permits beam orthogonality which is valuable over use multiple beam antenna. In this work, turning off part of antenna elements will inevitably change the beam orthogonality conditions. Despite this, the case presented in this paper, shows beam space discrimination better than 10dB. To rank the behavior of modified antenna, with the turned off elements, are used both Euclidean and Hausdorff distances to measure the changes resulted from the modified array performance. The obtained solutions show the applicability of binary operation on existing antenna array. The metric showed in here can be effectively used as ranking criteria.

Keywords—Multi-beam; phased antenna array; Hausdorff distance; Woodward-Lawson

I. INTRODUCTION

For decades, the mobile telephony system has continually grown, new technologies are continuously applied like the ones of signal processing capabilities and enhanced modulation scheme, also those related to antenna design and operating [1][2][3]. One of the major evolutions of the cellular technology beyond 2G, 3G, 4G up to the 5G, is the antenna sub system with massive MIMO [4] configurations and full digital beam forming capabilities [5].

Combination of massive MIMO with full digital beam forming architecture, especially in the sub-6GHz sub band, permits an increase on the obtained throughput per user [6]. This can be possible by creating orthogonally multiple antenna beams. This configuration can mitigate interferences from nearby user equipment increasing in this way the CNR (Carrier to Noise Ratio) which is proportionally related to user's equipment transmitted throughput [7][8].

The multi-beam antenna feed can be achieved through full digital beam forming network. In this case each antenna element of the array is directly connected to a dedicated RF chain (RF: Radio Frequency) comprising PA/LNA (Power Amplifier/Low Noise Amplifier) [9] and creating so an Active Antenna System (AAS) as shown in Fig. 1. One of the biggest drawbacks of this architecture, rather than its cost, is the

power consumption and high heat dissipation requirements [10] [11].

In this paper we are investigating the possibility of switching off intentionally a part of antenna array elements (corresponding RF chain) to improve power consumption by decreasing its demand for power heat dissipation and extend antenna life span. Switching off some of antenna's element will inevitably change also the original radiation pattern. To quantify the divergences of the modified radiation pattern compared to the desired/required one, will be used a ranking procedure based on Euclidean and Hausdorff distances [12].

In a bed test case, the solution with require three contemporary antenna beams. The proposed test is quite general and is valid for any combination of orthogonal beams. A case presented later in this paper will also investigate when one of the UE (User Equipment) changes its relative position/direction from/to the base antenna. In this case, it is needed to be generated a new beam (among the orthogonal that the antenna array can handle) from the decision making of antenna's internal and the direction of arrival estimation. So the idea of switching off a part of antenna elements, presented by the authors in [12], will be applied to effectively show that the proposed technique is still valid.

The methods for generating antenna array radiation pattern can be found in the scientific literature as in [13] and [14], each of them with relative advantages and disadvantages, mostly they are proprietary algorithms used by antenna's vendor for real case implementation. In this work, without loss of generality, will be applied Woodward-Lawson method for antenna array pattern design [15].

The antenna array used as example for the test scenario is composed by $N = 31$ elements. The original array factor for multi-beam will be designed by using Woodward-Lawson method in each required beam direction. Then the designed feeding network ratio (amplitude and phase) for each beam can be combined linearly as by superposition principle on linear antenna systems. The overall antenna array factor obtained, will be compared with the required masks (one for each beam). As ranking method will be used two distances: Euclidean [16] and Hausdorff Distance [17]. Our aim is to get this array factor by switching off some antenna elements and to compare the obtained pattern with the mask through the use of both methods.

This paper is organized as follows: Section two describes mathematical definitions for the active antenna system and for

multi-beam antenna. It is also introduced the antenna array design based on W-L method followed by definitions of both metrics (Euclidean and Hausdorff) which are used to score how close to required pattern is the designed and modified antenna pattern. Section three describes the antenna array design setup and analysis. Required beam direction and antenna design is analyzed based on beam orthogonality and orthogonality lose when array elements are switched from on to off. Conclusions and recommendations for future work will be emphasized in section four.

II. ANTENNA DESIGN METHODOLOGY

Active antenna systems are a valid option for high performance and speed networks, especially in 4G/5G [13][14][18][19]. Here, the full RF electronics, consisting of RF power amplification, Rx functionality, filtering, and so on, are all integrated in an AAS as shown in Fig. 1.

One of the most valuable features of the AAS is the digital multi-beam forming capability. This configuration allows the AAS to create multiple orthogonal beams which does not interfere with each other. It directs antenna beams to different users in space, so the AAS can simultaneously communicate with multiple users at the same time and same frequency resources with enhanced CNR [20].

In this work, without loss of generality, Woodward-Lawson antenna array design method is being used for pattern design as per predefined (required) pattern distribution. The used method permits to evaluate amplitude and phase for each antenna element composing the array in a way to be feed for creating the required pattern. This method is based on the standard theory of phased antenna array. The complex antenna array can be analyzed as an overlay of different virtual, independent, and superposed arrays. An example of feeding function can be expressed as (1):

$$I_n = I_n^{(1)} + I_n^{(2)} + I_n^{(3)} + \dots + I_n^{(N)}; \quad n = 0, \dots, N-1 \quad (1)$$

The concept is also used for the creation of a second function but in this case is adjusted an uniform progressive phase in order that the maximum main lobe coordinates with the profoundest null of the first step function. So, an excitation in amplitude of this function determines the filling-in of the most profound null of the second function [21]. The third function part of the main function is altered so the maximum of main lobe occurs at the second profound null of the first function and so on. In this way are created one after other all the functions which are part of the sum. In this way all the created (virtual functions) beams are orthogonal to each other as shown in Fig. 2 for the 11 elements on the antenna array design. The presented figure shows the orthogonality of each beam that can be achieved with only phase change.

In real antenna implementation, the required antenna beam number and relative space directions are timely changed due to the number of connected users and antenna usage in space and time. For these cases, artificial intelligence (algorithms for direction finding) implemented in the AAS will evaluate feeding ratio (amplitude and phase) required for each beam and each antenna element.

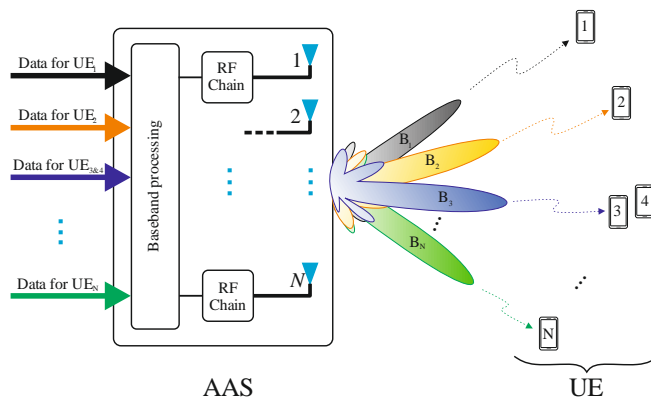


Fig. 1. Active Antenna System and Multi-Beam Concept.

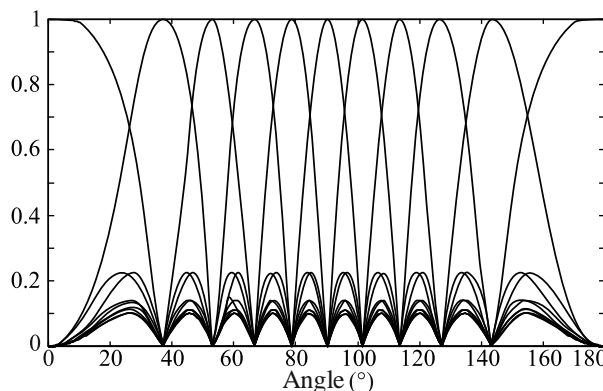


Fig. 2. W-L Antenna Design and Orthogonal Beams for 11 Antenna Elements.

The total number of contemporary beams combinations required in time and space, can lead to a very large definition problem [23][24][25][26]. In this work, without loss of generality, will be considered three different beam directions along with the relative antenna feed. They will be designed using the over-mentioned Woodward – Lawson method as schematically shown in Fig. 3. Those directions can be any of the provided orthogonality conditions.

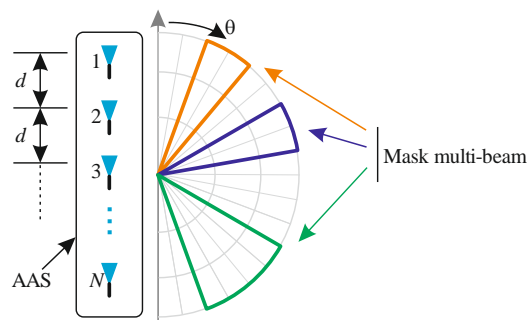


Fig. 3. Multi-Beam Antenna Definition.

It is of crucial importance to keep in mind that the number of orthogonal beams is the same as the number of elements which compose the antenna array. Orthogonality in antenna beam design is one of the biggest advantages which includes less interferences in the directions where other beams (directed to UEs) have their relative maxima. The above advantage increases the CNR and consequently increase the

III. RESULTS

throughput [22]. The array factor (AF) designed through the Woodward-Lawson method will be used as the original antenna pattern (multiple beam). Based on this design, will be investigated the possibility to switch off part of antenna elements. There are being analyzed changes of pattern due to elements switch off, and how it diverges from the desired model (defined as required pattern mask). They will be scored as per Euclidean and Hausdorff distances as per below.

A. Euclidean Distance

The Euclidean distance can be expressed as the straight line between two given points (of course that point can be vectors or matrixes). The length of the straight line represents the shortest distance between the two defined points. It is also used for higher dimensional problems [12][16].

Through this paper we will use the sum of all Euclidean distances (E_k) between array factor (AF_k) and the mask (M_k , the desired model) as given in equation (2).

$$E_k = \sum_{\theta=0^\circ}^{180^\circ} \|AF_k(\theta) - M_k(\theta)\| \quad (2)$$

Where k is the k -th antenna beam designed.

B. Hausdorff Distance

Hausdorff distance can be expressed as the maximum distance of a set, to the nearest point in the other set [12][17].

Through this definition it is easy to understand that the distance expresses the longest distance that it might be forced to travel between two sets of points. Given two sets of points AF_k and M_k , the Hausdorff distance between them can be defined as in (3):

$$H_k(AF_k, M_k) = \max\{h(AF_k, M_k), h(M_k, AF_k)\} \quad (3)$$

Where $h(AF_k, M_k)$ is called direct Hausdorff distance and defined as in (4):

$$h(AF_k, M_k) = \max_{AF(\theta_i) \in AF} \min_{M_k(\theta_j) \in M_k} \|AF_k(\theta_i) - M_k(\theta_j)\| \quad (4)$$

It identifies the point in AF_k that is the farthest from any point in M_k (max definition) and measures the Euclidean distance from that point to the nearest neighbor in M_k (min definition). Likewise, the definition for $h(M_k, AF_k)$ is in (5):

$$h(M_k, AF_k) = \max_{M_k(\theta_i) \in M_k} \min_{AF(\theta_j) \in AF} \|M_k(\theta_i) - AF_k(\theta_j)\| \quad (5)$$

C. Ranking Distances

The above definitions of Euclidian and Hausdorff distances can be directly applied for each antenna beam. In the presented work, the designed pattern are more than one at the same time. In order to have one ranking criteria, a combination of each Euclidian and Hausdorff distances for all the designed contemporary beams is performed as in (6):

$$E = \sqrt{E_1^2 + E_2^2 + E_3^2 + \dots + E_k^2}$$

$$H = \sqrt{H_1^2 + H_2^2 + H_3^2 + \dots + H_k^2} \quad (6)$$

By using Woodward-Lawson design method, is designed a standard linear antenna array with $N = 31$ elements, element intra-distance of $d = \lambda/2$. The required mask is designed to point in space as: M_1 in 43° with 9° width span, M_2 in 82° with 7° width span and M_3 in 125° with 10° width span and zero elsewhere (schematically shown in Fig. 3). The designed antenna array used in sub-6GHz sub band (2100 – 2600 MHz) is approximately 220 cm high.

Designed antenna pattern and relative feeding network by the use of Woodward-Lawson method are shown in Fig. 4.

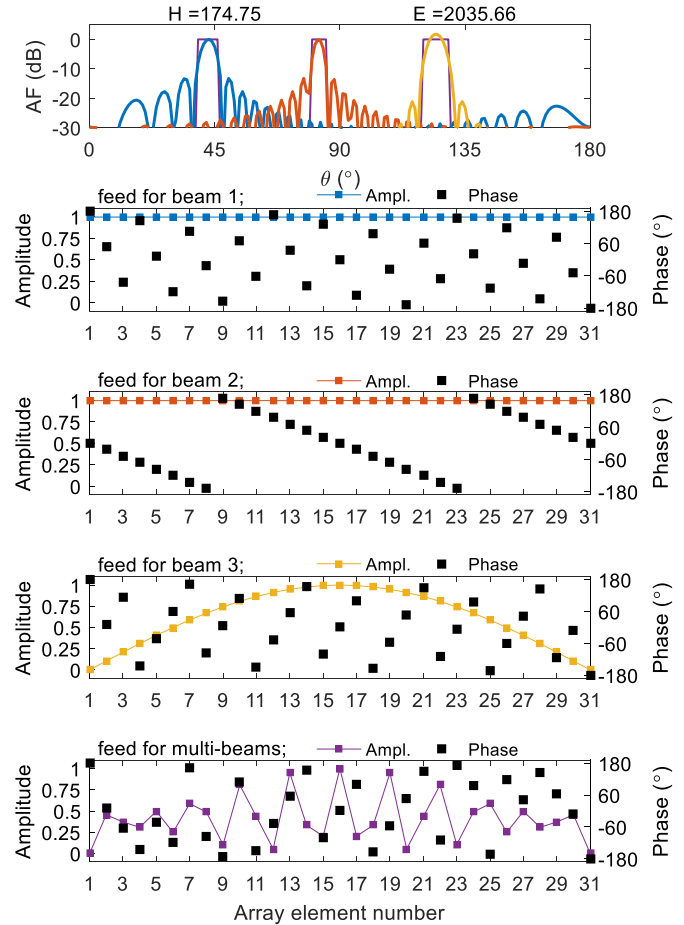


Fig. 4. Multi-Beam Array Pattern and Relative Current at each Element.

The feeding of each virtual array for beam generation is based on progressive phase shift as can be noticed in the graphics feed for beam 1, 2 and 3 in Fig. 4. The overall feeding ratio is not more progressive in phase and amplitude due to the superposition effect. This is the feeding ratio as seen by RF chain at AAS. To recreate the antenna pattern provided, the reader can evaluate radiation pattern from antenna theory based on the current feeding ratio and phase as shown in each sub figure for each beam.

In Fig. 5 are shown the pattern changes and relative feeding ratio from switching off 10 out of 31 antenna elements in the designed multi-beam, shown in the first part of Fig. 4. Sorting criteria for this modified configuration are

respectively $E = 2650.98$ and $H = 223.79$. Both results are increased if compared to the original pattern shown in Fig. 4 ($E = 2035.66$ and $H = 174.75$). What is more evident in this case, is the loose of beam orthogonality, especially for the first and second beam (see Fig. 5) as each beam have not null radiation in the direction of the other beam maxima.

Pattern modification due to turned off antenna elements, despite loos of beam orthogonality, beam discrimination in each space direction (direction of each beam maxima) is better than 10dB. This configuration increases the interference produced by UE₁ to the UE₂ and UE₃ data stream and vice versa, but still the difference in antenna discrimination is better than 10dB.

More antenna element can be switched off, as in the case presented in Fig. 6 where two other elements are turned off if compared to the case presented in Fig. 5. Despite the radiation beam pattern modification, beam discrimination is still better than 10dB in all cases.

The above solution is a good alternative even in time variation of UE position as schematically described in Fig. 7. In this situation, direction of arrival and decision-making algorithms and beam design in AAS configuration will recalculate feeding ratio for a new beam forming to the new UE direction.

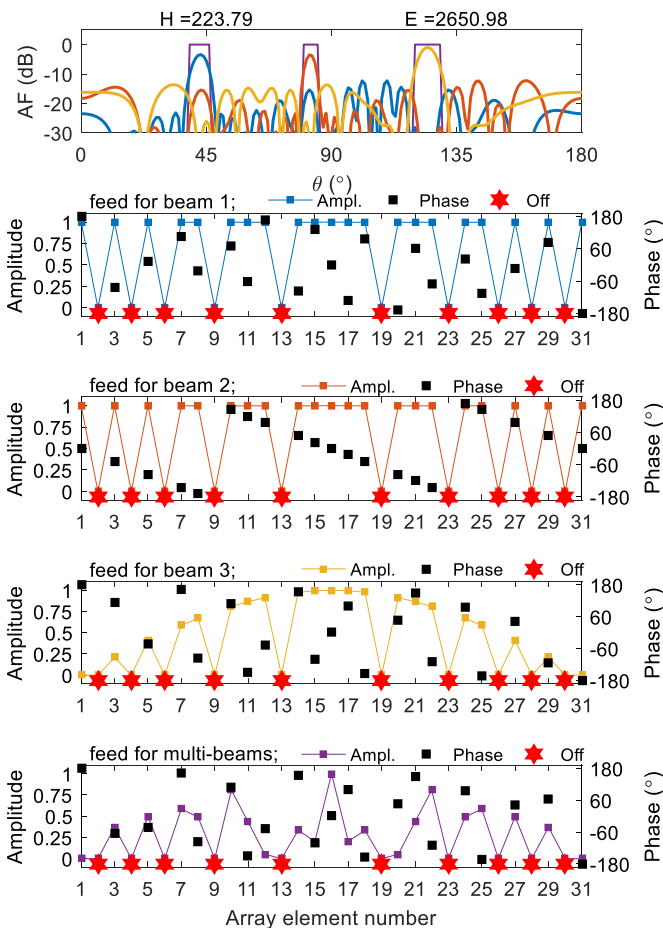


Fig. 5. Multi-Beam Array Pattern and Relative Current for 10 Antenna Elements Switched Off.

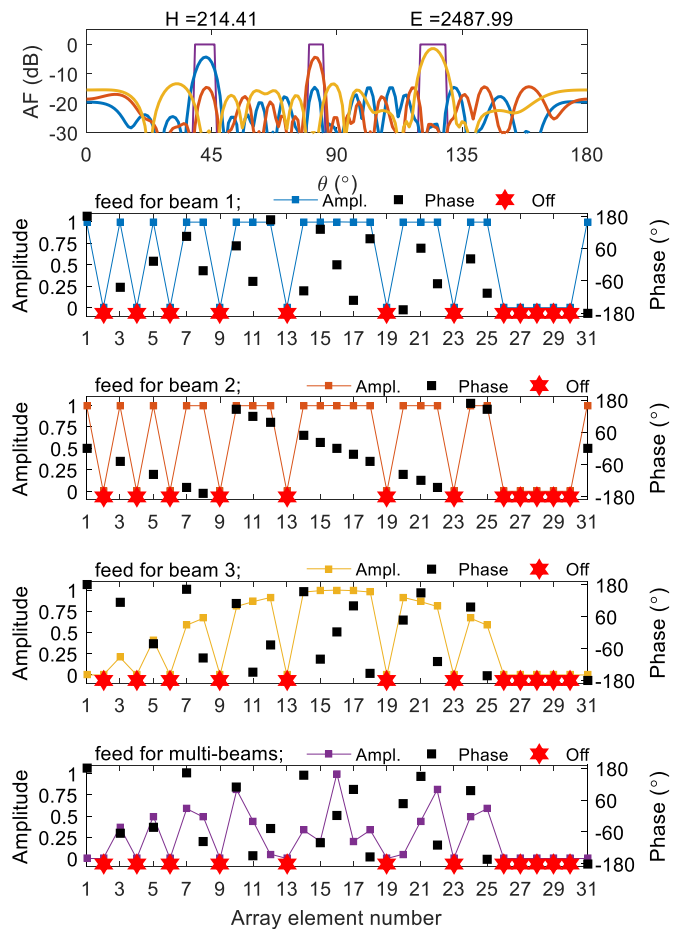


Fig. 6. Multi-Beam Array Pattern and Relative Current for 12 Antenna Elements Switched Off.

Even though the UE changes position in space, the AAS functionality need to reevaluate the antenna elements to turn on/off due to changes in antenna requirements so to follow better and to improve the beam in the new position of UE. Over this position is going to be made the powering OFF of the newly chosen elements like in the first case, but with changed masks.

In Fig. 7 is shown a generic case of a UE that changes relative direction to the cellular antenna. The new direction for beam 2 is from M_2 in 82° with 7° width span in M_2 in 104° with 7° width span and zero elsewhere. The two other beams are maintained at the previous direction as in the first test case. This case is quite general and can be any direction under the original orthogonality condition of beam design.

The result of antenna with the same turned off elements as presented in Fig. 4. The feeding ratio for the new multi beam directions has been designed and the result is presented in Fig. 8. Results show the designed beam patterns for the three directions, maintaining the previous switched off elements. Even in this case, beam discrimination is still better than 10dB in each direction. The solution can be scored based on the provided Ranking criteria, in this case reports Hausdorff and Euclidian respectively $H = 223.77$ and $E = 2601.96$.

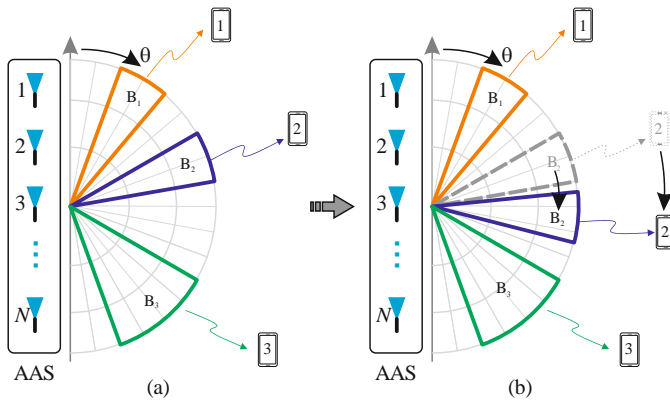


Fig. 7. Multi Beam Directed to UE: (a) Original Problem; (b) UE₂ Changes Position.

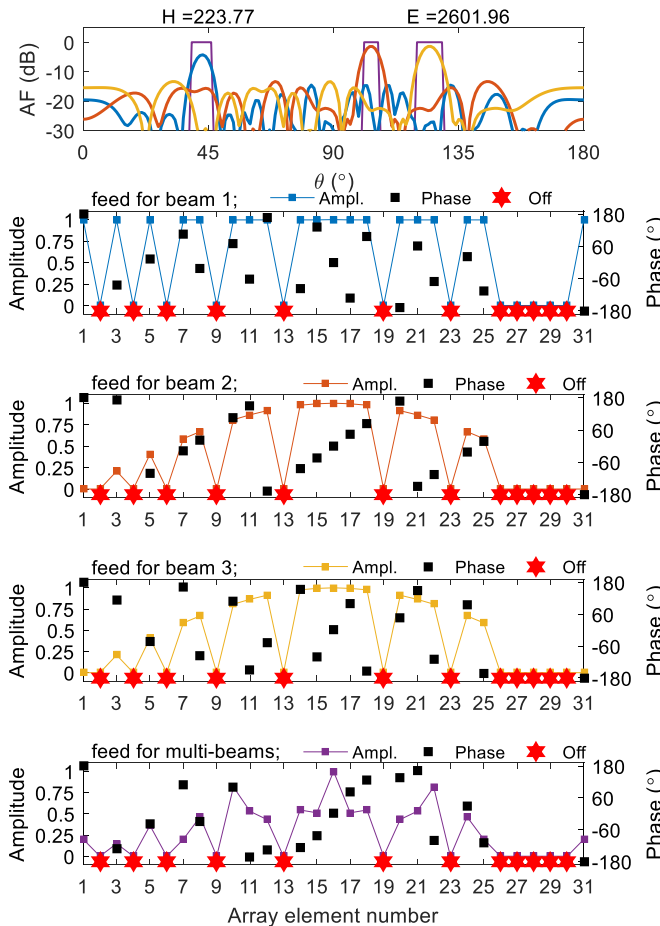


Fig. 8. Multi-Beam Array Pattern for Changed Beam Direction with the Same 12 Elements Turned Off.

Turning on all the antenna elements will bring the orthogonality of all beams due to the original direction orthogonality of the pattern design, as shown in Fig. 9. This is the case, when the antenna will be used in full capacity mode to maintain the maximum CNR over multiple UEs. The metric used in this case is $H = 202.66$ and $E = 2507.65$ which can also be used to evaluate antenna response to the required beam design. Smaller are the E and H values, closer the antenna response is to the required pattern.

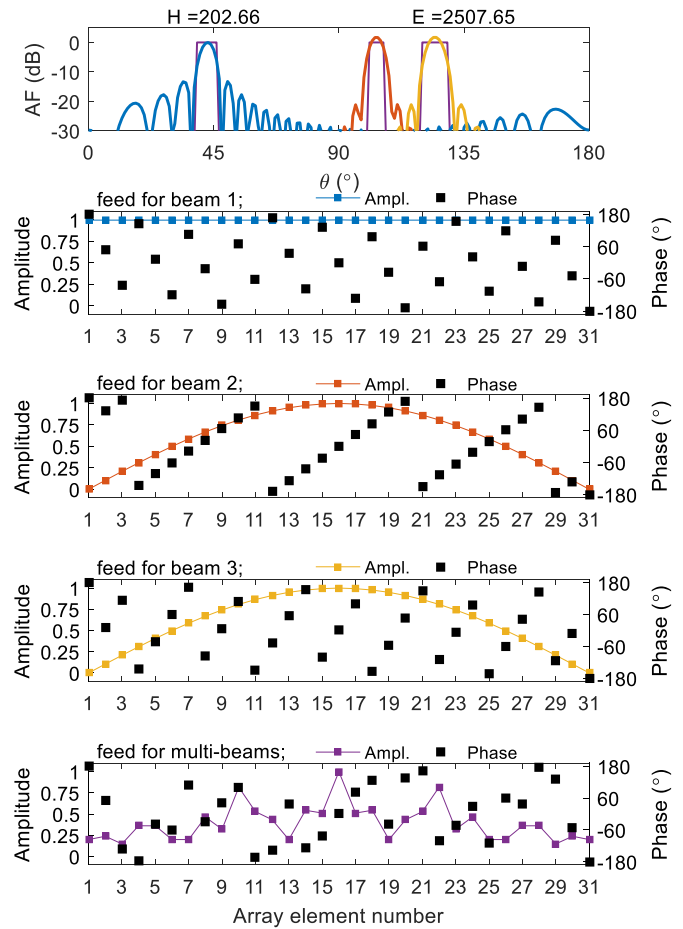


Fig. 9. Multi-Beam Array Pattern and Relative Current for all Elements Turned on for the New Direction of UE₂.

In the analyzed scenario are shown only two cases, but the procedure is quite general and can be applied with more elements switched on/off or/and with more active beams. Since the possibilities for each antenna element are only two (On or Off) there are a finite number of combinations to be tested ($2^N 2^{31} = 2\ 147\ 483\ 648$). With the original antenna array power feeding ratio, designed as by Woodward-Lawson method, analyzing all the above combinations without modifying the feeding ratio between elements but only through changing their state, is not an easy task. Assuming 0.1s computing time to design and rank antenna radiation pattern for each combination, is required more than 7 years of computing time. This is a very huge computing time (in case of calculation of all combinations) but this is not the aim of this work. In this case, can be used more efficient artificial intelligence or optimization algorithms to obtain optimum combinations without making an exhaustive search as in the case of all combinations test.

IV. CONCLUSION AND FUTURE WORK

In this work is presented the analysis of a multi-beam antenna array used with partially switched On/Off antenna elements. The aim of switching off is to preserve energy consumption with less radiation pattern alteration. The presented case shows the applicability of the binary (On/Off)

status change on the antenna elements with a contained impact on the beam orthogonality and relative space discrimination.

The presented analysis is focused on binary format of turning on/off antenna elements which is easier and does not require higher processing capabilities for beam forming evaluating techniques. Modifying antenna array behavior is faster with just powering on/off elements on demand rather than changing power ratio and phase distribution network or beam forming network.

Powering off up to 30% of array elements made possible to have less heat, to save energy without penalizing the radiation pattern and increasing the lifecycle of antenna array. Despite the advantages of the powering off the antenna elements, the major disadvantage is in the beam orthogonality loose, but the space discrimination over multiple-beams remains better than 10dB.

Using both Euclidean and Hausdorff distances as ranking matrix, can be an effective way to the antenna pattern design as close as possible to the required pattern and choose the combination of antenna elements turned on or off which have less deterioration of the radiation models.

REFERENCES

- [1] H. Ji, et al., "Overview of Full-Dimension MIMO in LTE-Advanced Pro," IEEE Communication Magazine, vol. 55, issue 2, Feb. 2017.
- [2] E. Björnson, L. Sanguinetti, H. Wymeersch, J. Hoydis, T.L. Marzetta, "Massive MIMO is a reality—What is next? Five promising research directions for antenna arrays", Elsevier, Digital Signal Processing, Volume 94, November 2019, Pages 3-20.
- [3] E. Westberg, J. Staudinger, J. Annes, and V. Shilimkar, "5G Infrastructure RF Solutions: Challenges and Opportunities" IEEE Microwave Magazine, 2019, 20(12), 51–58.
- [4] B. Yang, Z. Yu, J. Lan, R. Zhang, L. Zhou, W. Hong, "Digital Beamforming-Based Massive MIMO Transceiver for 5G Millimeter-Wave Communications" IEEE Trans. Microw. Theory Tech. 2018, 66, 3403–3418.
- [5] A.F. Molisch, V.V. Ratnam, S. Han, Z. Li, S.L. Nguyen, L. Li, K. Haneda, "Hybrid Beamforming for Massive MIMO: A Survey" IEEE Commun. Mag. 2017, 55, 134–141.
- [6] J. Hoydis, S.T. Brink, M. Debbah, "Massive MIMO in the/DL of cellular networks: How many antennas do we need?", IEEE J. Sel. Areas Commun. 2013, 31, 160–171.
- [7] W. Honcharenko, "Sub-6 GHz mMIMO base stations meet 5G's size and weight challenges," Microw. J., vol. 62, ed. 2, 2019, pp. 40–52.
- [8] A. Prata, J. Sveshtarov, S. C. Pires, A. S. R. Oliveira, and N. B. Carvalho, "Optimized DPD feedback loop for m-MIMO sub-6 GHz systems," in Proc. 2018 IEEE/MTT-S Int. Microwave Symp. (IMS), Philadelphia, PA, 2018, pp. 485–488.
- [9] A. Puglielli, et al. "Design of energy- and cost-efficient massive MIMO arrays," Proc. IEEE, 2016, vol. 104, no. 3, pp. 586–606.
- [10] B. Sadhu et al., "A 28-GHz 32-element TRx phased-array IC with concurrent dual-polarized operation and orthogonal phase and gain control for 5G communications," IEEE J. Solid-State Circuits, vol. 52, no. 12, 2017, pp. 3373–3391.
- [11] D. Liu, X. Gu, C. W. Baks, A. Valdes-Garcia, "Antenna-in-package design considerations for Ka-band 5G communication applications," IEEE Trans. Antennas Propag., vol. 65, no. 12, 2017, pp. 6372–6379.
- [12] E. Agastra, J. Imami and O. Shurdi, "Binary Operating Antenna Array Elements by using Hausdorff and Euclidean Metric Distance" International Journal of Advanced Computer Science and Applications(IJACSA), 11(10), 2020.
- [13] J. Sahalos, "Orthogonal Methods for Array Synthesis: Theory and the ORAMA Computer Tool", 2007, Wiley.
- [14] S. Noh, M. D. Zoltowski and D. J. Love, "Multi-Resolution Codebook and Adaptive Beamforming Sequence Design for Millimeter Wave Beam Alignment," in IEEE Transactions on Wireless Communications, vol. 16, no. 9, 2017, pp. 5689-5701.
- [15] M. D. Migliore, "MIMO Antennas Explained Using the Woodward-Lawson Synthesis Method [Wireless Corner]," in IEEE Antennas and Propagation Magazine, vol. 49, no. 5, 2007, pp. 175-182.
- [16] R. Rajashekar, K. V. S. Hari and L. Hanzo, "Quantifying the Transmit Diversity Order of Euclidean Distance Based Antenna Selection in Spatial Modulation," in IEEE Signal Processing Letters, vol. 22, no. 9, 2015, pp. 1434-1437.
- [17] Gao Y. "Efficiently comparing face images using a modified Hausdorff distance," Image and Signal Processing, IEEE Proceedings, vol. 150, 2003, pp. 346-350.
- [18] Y. Wu, C. Xiao, Z. Ding, X. Gao, and S. Jin, "A survey on MIMO transmission with finite input signals: Technical challenges, advances, and future trends," Proc. IEEE, vol. 106, no. 10, 2018, pp. 1779–1833.
- [19] T. Sowlati et al., "A 60GHz 144-element phased-array transceiver with 51dBm maximum EIRP and $\pm 60^\circ$ beam steering for backhaul application," in Proc. 2018 IEEE Int. Solid-State Circuits Conf. (ISSCC), pp. 66–68.
- [20] T. L. Marzetta, "Non-cooperative Cellular Wireless with Unlimited Numbers of Base Station Antennas," IEEE Trans. Wireless Communications, vol. 9, No. 11, Nov. 2010.
- [21] Comisso, M.; Palese, G.; Babich, F.; Vatta, F.; Buttazzoni, G. "3D multi-beam and null synthesis by phase-only control for 5G antenna arrays", Electronics 2019, 8, 656.
- [22] Y. Wu, S. Med, Y. Gu, "Distributed Non-Orthogonal Pilot Design for Multi-Cell Massive MIMO Systems" In Proceedings of the 2020 IEEE International Conference on Acoustics, Speech, and Signal Processing (ICASSP), Barcelona, Spain, 4–8 May 2020; pp. 5195–5199.
- [23] Z. Jiang, S. Chen, S. Zhou, Z. Niu, "User Scheduling and Beam Selection Optimization for Beam-Based Massive MIMO Downlinks" IEEE Trans. Wirel. Commun. 2018, 17, 2190–2204.
- [24] B. Gopalakrishnan, N. Jindal, "An analysis of pilot contamination on multi-user MIMO cellular systems with many antennas", In Proceedings of the IEEE 12th International Workshop on Signal Processing Advances in Wireless Communications (SPAWC), San Francisco, CA, USA, 26–29 June 2011; pp. 381–385.
- [25] A. Puglielli, G. LaCaille, A. M. Niknejad, G. Wright, B. Nikolic-, and E. Alon, "Phase noise scaling and tracking in OFDM multiuser beamforming arrays," in Proc. 2016 IEEE Int. Conf. Communications (ICC), pp. 1–6.
- [26] D. Nojima, L. Lanante, Y. Nagao, M. Kurosaki, H. Ochi, "Performance evaluation for multi-user MIMO IEEE 802.11ac wireless LAN system", In Proceedings of the 2012 14th International Conference on Advanced Communication Technology (ICACT), PyeongChang, Korea, 19–22 February 2012; pp. 804–808.

A Survey on Image Encryption using Chaos-based Techniques

Veena G¹, Dr. Ramakrishna M²
Dept. of CSE, Vemana Institute of Technology
Bengaluru, India

Abstract—Encryption methods such as AES (Advanced Encryption Standard), DES (Data Encryption Standard), etc. cannot be used for image encryption as images contain a huge amount of redundant data, a high correlation between neighboring pixels and size of the image is very large. Chaos-based techniques have suitable properties that are required for image encryption. The properties include sensitivity to initial conditions, pseudorandom number, ergodicity, and density of periodic orbits. In this paper, a survey of image encryption using chaos-maps such as a logistic map, piecewise linear chaotic map (PWLCM), tent map, etc. is done in order to choose best map for image encryption. Comparison of image encryption using different chaotic maps is done by considering parameters such as key-space and correlation analysis.

Keywords—Chaos theory; image encryption; logistic map; PWLCM; tent map

I. INTRODUCTION

To secure information present in the image from unauthorized user access during transmission and storage, image encryption is used. Image encryption [1][12] can be achieved by changing pixel positions as well as changing contents of pixels as a result the true content of the image is completely changed. Different techniques such as cryptography [28], steganography, compression, and digital watermarking can be used to encrypt the image. Images can be encrypted using chaos-based techniques which are referred to as chaotic cryptography. Chaotic cryptography [1-4] [19-29] is the use of mathematical chaos theory to the cryptography. Chaotic cryptography involves the use of chaotic maps for generating confusion and diffusion. The chaos-based technique has properties that are suitable for image encryption. Sensitivity to initial condition is one property of chaos-based technique in which a minute variation in initial conditions will result in a large variation in behavior of the system, i.e., to decrypt the image, exact initial conditions are very much essential. Numerous chaotic maps are used in encryption. A chaotic map is a function that shows chaotic structure. Chaotic maps are used to generate random numbers. Logistic map, Baker's Map, Tent map, Renyi map [1-4] are a few of the important chaotic maps. Chaotic systems are used to generate the sequence of numbers which can be used as a key in image encryption. Chaotic systems exhibit certain properties required for image encryption and decryption, one such property is sensitivity to initial conditions [5], Fig. 1(a) shows the plot of logistic function for two different initial conditions plotted against time versus the value obtained from logistic function, the red line shows the plot of the logistic map when $x_0 = 0.2$, the green line

shows the plot of the logistic map when $x_0 = 0.200001$. Fig. 1(b) shows the plot of the difference between logistic map values for 2 initial conditions $x_0 = 0.2$ and $x_0 = 0.200001$, it can be seen that the difference between the 2 initial conditions is very small but the difference in values generated by the logistic map is very large this property is known as sensitivity to initial conditions. The sensitivity to initial conditions property of chaotic systems can be used in image encryption. Chaotic systems are used to generate pseudorandom numbers, the numbers generated by the chaotic system exhibit all the properties of random numbers but they are not random since passing the exact initial conditions the numbers can be regenerated. Chaotic systems [18] exhibit a property called ergodicity [10]; a system is said to be ergodic if it shows irreducibility. All the above properties of chaotic systems can be used in effective image encryption and decryption. There exist many techniques to encrypt images using the chaotic maps. This paper surveys different techniques to identify the best chaotic map for image encryption.

The rest of this paper is organized as follows: Section II gives the literature review of image encryption using chaotic maps. Section III gives a comparative analysis of the image encryption using chaotic maps. Finally, Section IV concludes this paper.

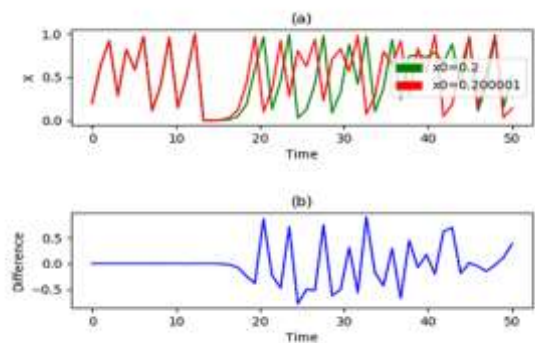


Fig. 1. Logistic Map Plot (a) Logistic Map for 2 Initial Conditions (b) Difference between Logistic Map Values for 2 Initial Conditions.

II. LITERATURE REVIEW

A. DNA Encoding

A combination of DNA encoding and chaos-based logistic map [1] was used to encrypt a color image. In DNA encoding, data encoding will be performed based on DNA sequence.

Bases that are present in single-stranded DNA are Thymine (T), Guanine (G), Cytosine (C), and Adenine (A). T and A are complemented to each other similarly G and C are also complemented to each other. To encode binary data using four bases (T,G,C and A), binary numbers 11, 10, 01, and 00 can be used. Eight coding rules can be used that are shown in Table I.

TABLE I. EIGHT CODING RULES

A	B	C	D	E	F	G	H
00 T	00 A	00 T	00 A	00 C	00 G	00 C	00 G
01 C	01 C	01 G	01 G	01 A	01 A	01 T	01 T
10 G	10 G	10 C	10 C	10 T	10 T	10 A	10 A
11 A	11 T	11 A	11 T	11 G	11 C	11 G	11 C

The logistic map as shown in equation (1) is a simple single-dimensional map that shows the unexpected degree of complexity. Mathematically it is defined as follows.

$$y_{n+1} = \mu x_n(1 - y_n) \quad (1)$$

If the initial values of y_0 and μ is ($0 \leq y_0 \leq 1$) and ($0 < \mu < 4$) respectively then the logistic map produces a sequence of values y_0, y_1, y_2, \dots . The important behavior of logistic map is when μ is ($0 < \mu < 3$) the sequence approaches a fixed value quickly. A different behavior is observed when μ is ($3.56995 < \mu < 4$) the generated sequences are not periodic; they are not convergent and they have sensitivity to initial value.

A Color image [13-15] is split into Red, Green, and Blue components that are transformed into three binary matrixes R, G, and B respectively. DNA encoding is used on each of the matrixes using key1 $\in [1,8]$ after DNA encoding further matrixes are added using mod 2 for increasing the strength of encoding. A chaotic sequence (seq1) is generated by using logistic chaotic map with initial values y_0 and μ_0 . DNA encoded matrixes are complemented using seq1, the complemented result is decoded through DNA decoding using key2 $\in [1,8]$. A chaotic sequence (seq2) is generated using a logistic chaotic map with initial values y_1 and μ_1 . The exclusive-or operation is performed DNA decoded matrix and seq2 and RGB image is recovered. Totally six key parameters used in [1], if the precision used is 10^{-14} the total keys' space will be approximately 10^{56} i.e. ($10^{14} * 10^{14} * 10^{14} * 10^{14}$). The key space is large so it will not be vulnerable to exhaustive attacks. The system is sensitive to initial parameters, with slight variation in initial parameters the decrypted image will be very much different from the original image (avalanche effect). The limitation in the above algorithm is that the speed is not effective, to improve the speed there is a need for DNA chip technology.

B. Tent Map

A chaotic tent map was used to encrypt and decrypt images [2]. Tent map [3] is mathematically defined as in equation 2:

$$x_{j+1} = f(x_j, \alpha) = \begin{cases} f_L(x_j, \alpha) = \alpha x_j, & x_j < 0.5 \\ f_R(x_j, \alpha) = \alpha(1 - x_j), & \text{otherwise} \end{cases} \quad (2)$$

The tent map function [16-17] evaluates to real numbers [0, 1]. α is the control parameter which takes a positive real number and x_0 is the initial condition of equation (2). The behavior of the tent map can be easily studied by the plot of the

bifurcation diagram, which is a plot of the sequence generated by the tent map with the control parameter (α) used for generating the sequence. The following details can be observed from the bifurcation diagram. For $\alpha \in [0,1)$ tent map has one fixed point $x = 0$, i.e., the equation converges to $x = 0$. For $\alpha = 1$ all values of $x \leq 0.5$ are fixed points of the system. For α between 1 and 2, the sequence generated by the system is chaotic which is unstable. Tent map exhibits fixed point-behavior when $\alpha < 1$ and chaotic behavior when $\alpha > 1$. To encrypt the image [2] following procedure is used:

- Read the plane image of size N, initial condition (x_0) as encryption key, and control parameter (α).
- Obtain the sequence of size N using a chaotic tent map as given in equation (2) as array $x(n)$.
- Encrypt image using $x(n)$ to obtain the ciphered image.

To decrypt the image same values of x_0 and α which were used in encryption should be used. Totally two key parameters used in [2] x, α if the precision used is 10^{-16} the total keys' space will be approximately 10^{32} i.e., ($10^{16} * 10^{16}$). The key space is large so it will not be vulnerable to brute-force attacks. The encrypted image showed a correlation coefficient of two adjacent pixels in diagonal, vertical, and horizontal directions as 0.00003, 0.0025, and 0.0016 respectively. The entropy of the encrypted image is 7.999876.

C. 3D cat Map

Equation (3) gives Arnold-cat map, where x and y are representing pixel positions.

$$\begin{bmatrix} x_{n+1} \\ y_{n+1} \end{bmatrix} = \begin{bmatrix} 1 & 1 \\ 1 & 2 \end{bmatrix} \begin{bmatrix} x_n \\ y_n \end{bmatrix} \text{ mod } 1 \quad (3)$$

In equation (3) mod 1 takes care of the fractional part, the linear transform shears unit square, and mod operation folds it back to the unit square. The 3D cat map is given by equation (4) where B is a matrix.

$$\begin{bmatrix} x_{n+1} \\ y_{n+1} \\ z_{n+1} \end{bmatrix} = B \begin{bmatrix} x_n \\ y_n \\ z_n \end{bmatrix} \text{ mod } 1 \quad (4)$$

In [4] following steps are followed to encrypt the image:

- 1) Key generation: 128-bit sequence number is split into $k_{px}, k_{py}, k_{pz}, k_{qx}, k_{qy}, k_{qz}$ that are used in 3D cat map and k_l, k_s are used in logistic map.
- 2) Conversion of the 2D image into 3D: The image is split to form several three-dimensional cubes.
- 3) Apply 3D cat map on the result of step b.
- 4) Apply diffusion process on the result of step c using the logistic map.
- 5) Transform three dimensional cubes to two-dimensional image.

The total key space is 2^{128} [4]. The key space is large so it will not be vulnerable to brute-force attacks. The encrypted image showed a correlation coefficient of two adjacent pixels in diagonal, vertical and horizontal directions as 0.01480, 0.00016, and 0.01183, respectively.

D. Spatiotemporal Chaotic System

In [5] image encryption consists of confusion and diffusion stages. A spatiotemporal chaotic system is used. The chaotic system consists of logistic map and piecewise linear chaotic map (PWLCM). The pseudorandom numbers are produced by the chaotic system which consists of a two-dimensional dynamic map. The two-dimensional dynamic map is as defined in equation (5).

$$\begin{cases} x_{i+1} = (1 - \beta)f_1(x_i) + \beta f_2(y_i) \\ y_{i+1} = (1 - \beta)f_1(y_i) + \beta f_2(x_i) \end{cases} \quad (5)$$

Where f_1 is the logistic map and f_2 is PWLCM. Both f_1 and f_2 are chaotic maps. f_1 and f_2 are defined as in equation (6a, 6b).

$$f_1(x) = \alpha x(1 - x) \quad (6a)$$

$$f_2(x) = \begin{cases} \frac{x}{\gamma}, 0 \leq x < \gamma \\ \frac{(x-\gamma)}{(0.5-\gamma)}, \gamma \leq x < 0.5 \\ f_2(1-x), 0.5 \leq x < 1 \end{cases} \quad (6b)$$

The image encryption consists of a substitution process followed by a diffusion process. In the substitution process S-box is generated and the pixels of the image to be encrypted will be substituted by the contents of the S-box based on the key, substitution process creates confusion i.e., a small change in the key will result in large changes in the ciphered image. The circular S-box is used for the substitution process. Equation (7) is used in the substitution process.

$$\begin{cases} p'_i = S[(header + p_i) \bmod 256] \\ header = p'_i \oplus m \end{cases} \quad (7)$$

Where p_i is pixel in the plane image, p'_i is the cipher pixel corresponding to the original pixel p_i . Usage of circular S-box has an added advantage in which the substitution for a pixel depends on not only on the pixel value itself but also on the value of the previous cipher pixel. The substitution operation is followed by diffusion operation. In the diffusion process a small change in the plane image, will result in large changes in the ciphered image. Key stream buffer is used for the diffusion process. The keys generated by the cypher are stored in key stream buffer. Equation (8) is used in the diffusion process.

$$c_i = [(p'_i \oplus c_{i-1}) + Get(c_{i-1})] \bmod 256 \quad (8)$$

E. Linear Diophantine Equation

In [6] the image encryption is performed based on a chaotic system called piece-wise linear chaotic map (PWLCM) to generate two numbers. The generated numbers are used as coefficient of the Linear Diophantine Equation (LDE) [7]. The set of solutions to LDE is used in the permutation of the image. The image is divided into sub-images of size $N = m \times n$. The solution to LDE is found out only for the first sub-image, for the rest of sub-images the key is altered by replacing d number of values of the key with newly generated d number of values from the chaotic system, since the solution to LDE is not found for each sub-image the encryption is faster. Once all the sub-image is permuted each permuted sub image is diffused. The New initial conditions for the chaotic system are generated that depends on the total encrypted image. The above steps are repeated again to generate the permutation key and the total

encrypted image is permuted again to obtain the cypher image that completes round 1. Depending on the number of rounds the above steps are repeated.

Equation (9) is piece wise linear chaotic map (PWLCM) equation.

$$x(n) = F[x(n-1)] = \begin{cases} \frac{x(n-1)}{r}, \text{if } 0 \leq x(n-1) < r \\ \frac{[x(n-1)-r]}{(0.5-r)}, \text{if } r \leq x(n-1) < 0.5 \\ F[1-x(n-1)], \text{if } 0.5 \leq x(n-1) < 1 \end{cases} \quad (9)$$

The system using PWLCM will behave chaotically when r i.e., the control parameter is within $]0,0.5[$, the initial condition is within $]0,1[$. Equation (10) is LDE equation.

$$ag + bh = c \quad (10)$$

Where a , b and c are constants of natural integers, a and b are generated from PWLCM. The equation (10) can be solved using the equation (11).

$$\begin{cases} g(t) = g_0 + \frac{b}{\wedge} t \\ h(t) = h_0 - \frac{a}{\wedge} t \end{cases} \quad (11)$$

Where \wedge is the GCD of a and b , $t \in \{0,1, 2, \dots, L-1\}$ where L is the permutation length same as the length of sub-image. Once the solutions of LDE are determined as a set of G and H , here G is $\{g(1), g(2), \dots, g(L)\}$ and H is $\{h(1), h(2), \dots, h(L)\}$. The elements of G and H are sorted either in ascending or descending order. If I_G and I_H are index vectors of G and H then the permutation key I_Z is obtained by equation (12). Using I_Z , image is shuffled.

$$I_Z = I_G(I_H) \quad (12)$$

In the above scheme [6] total key space is 2^{256} , which is large for resisting brute force attacks. The entropy using the above scheme [6] is equal to its highest value ($H = 8$). The encryption scheme satisfies zero correlation property.

F. Bidirectional Diffusion

In [8] image encryption is performed using the permutation and diffusion process. Chaos technique is used to generate the key, skew tent map and logistic maps are used in key generation. In the permutation process, the pixel position of the plane image is shuffled as a result the permuted image will be totally different from the plain image. The permutation process is carried out using multiplication operation and insertion operation. In multiplication operation, if P represents a permutation of length l and Q represents a permutation of length m then the multiplication operation produces a permutation of length lm . In insertion operation, if P represents a permutation of length l and let $ins(P, s)$ denote inserting the element l at the position s in P . If S is a sequence of insertion positions of length m , then the $INS(P, S)$ can be computed using the equation (13).

$$INS(P, S) = \begin{cases} P, S = \emptyset \\ INS(ins(P, s_0), S - \{s_0\}), S \neq \emptyset \end{cases} \quad (13)$$

Smaller permutations are combined using multiplication and insertion to generate larger permutations. The entropy using the above scheme [8] is greater than 7.99. Diffusion is a process in which a small change in the plain image should result in large changes in the ciphered image. If a first pixel is altered in the plain image, then because of diffusion all the pixels in the ciphered image will be altered, but if the last pixel is altered in the plain image then only the last pixel in the ciphered image will be altered, hence in [8] the diffusion is carried out in both forward and backward directions. In the above scheme total key space is 2^{312} , that is large for resisting brute force attacks. The entropy using the above scheme [8] is equal to its highest value.

G. Bülban Chaotic Map

In [9] fast image encryption algorithm is implemented using the Bülban chaotic map. A very high chaotic behavior with larger range of parameter values is exhibited by Bülban chaotic map which increases the security level and key space. Bülban chaotic map is a real one-dimensional, simple and discrete chaotic map. Equation (14) defines Bülban chaotic map.

$$x_{n+1} = x_n \times \sqrt{\frac{a}{x_n - b}} \quad (14)$$

The encryption is performed in T rounds, each round consists of confusion and diffusion stages to change the position and values of the pixels. Two sequences (PR, PC) of real numbers are generated using Bülban chaotic map which is converted to unsigned integers. The pixel values of each row are circularly shifted to the right by the number of times as provided by sequence PR. The pixel values of each column are circular shifted down by the number of times as provided by sequence PC. Four real sequences (DR+, DR-, DC+, DC-) are generated using Bülban chaotic map as given in equation (15).

$$\begin{aligned} DR^+ &= \{ DR_j^+ \mid DR_j^+ = DR_j^+ \times 10^5 \text{ mod } 256 \} \\ DR^- &= \{ DR_j^- \mid DR_j^- = DR_j^- \times 10^5 \text{ mod } 256 \} \\ DC^+ &= \{ DC_i^+ \mid DC_i^+ = DC_i^+ \times 10^5 \text{ mod } 256 \} \\ DC^- &= \{ DC_i^- \mid DC_i^- = DC_i^- \times 10^5 \text{ mod } 256 \} \end{aligned} \quad (15)$$

The real sequences are converted to unsigned integers. Equation (16) is used in substitution.

$$\begin{aligned} P_i &= (P_i + (DR^+ \oplus pred(P_i))) \text{ mod } 256 \\ P_{M-i+1} &= (P_{M-i+1} + (DR^- \oplus succ(P_{M-i+1}))) \text{ mod } 256 \\ P_j &= (P_j + (DC^+ \oplus pred(P_j))) \text{ mod } 256 \\ P_{N-j+1} &= (P_{N-j+1} + (DC^- \oplus succ(P_{N-j+1}))) \text{ mod } 256 \end{aligned} \quad (16)$$

Using equation (16) diffusion of pixels is carried out row wise as well as column wise to change the pixel values. Where \oplus operator is bitwise exclusive-or, $pred(P_i)$, and $succ(P_i)$ these functions return the row P_i predecessor and successor respectively. In $pred(P_i)$, if P_i is the first row then the last row will be returned else P_{i-1} row will be returned. In $succ(P_i)$ if P_i is the last row then the first row will be returned else P_{i+1} row will be returned. The above process is repeated for T different rounds. In the above scheme total key space is 2^{360} , which is

large for resisting brute force attacks. The entropy using the above scheme is almost equal to 7.999.

H. Hybrid Chaotic Map

In [10] hybrid chaotic map is used to generate keys required for image encryption. First, the image is subjected to DWT (Discrete Wavelet Transforms). DWT decomposes a digital image into various subbands so that lower frequency subbands have finer frequency resolution and higher frequency subbands have a coarser resolution. DWT here decomposes the image into four subbands LL, LH, HL, and HH. Four different chaotic equations (17-20) are used to generate random sequences.

$$\begin{cases} y_{n+1} = b^2 x_n, \\ x_{n+1} = (x_n)^2 + (y_n)^2 - a.r \end{cases} \quad (17)$$

$$\begin{cases} y_{n+1} = y_n - r.tan(x_n) \\ x_{n+1} = \sin(x_n) + \sin(y_{n+1}) \end{cases} \quad (18)$$

$$\begin{cases} y_{n+1} = y_n - r.tanh(x_n) \\ x_{n+1} = \tanh(x_n) + \sin(y_{n+1}) \end{cases} \quad (19)$$

$$\begin{cases} y_{n+1} = y_n + a.r \cos(x_n) \\ x_{n+1} = \cos(x_n) + \sin(y_{n+1}) \end{cases} \quad (20)$$

The 4 subbands obtained from DWT are subjected to a permutation process. The keys required for permutation is generated using a chaotic system. Different bands use different chaotic equations (H1 to H4). The permuted image is subjected to diffusion. The key required for the diffusion process is generated using one of the four chaotic equations. In the above scheme [10] total key space is 2^{58} , which is large for resisting brute force attacks. The entropy using the above scheme is almost equal to 7.999.

I. Lorenz Chaotic Map

In [11] the pseudorandom numbers required for image encryption are generated by Lorenz chaotic map, the permutation of image rows and columns is carried out by random switch control mechanism. Equation (21) represents Lorenz chaotic map.

$$\begin{cases} \dot{x} = a(y - x), \\ \dot{y} = cx - y - xz, \\ \dot{z} = xy - bz \end{cases} \quad (21)$$

From Lorenz chaotic equation sample sequences $\{x_i\}$, $\{y_i\}$ and $\{z_i\}$ are generated. The generated sequences are used to generate random sequences S1 and S2 as given in equation (22).

$$\begin{aligned} S1_i &= \text{mod}(\text{round}((x_i + y_i) * 10^{12}), 2) \\ S2_i &= \text{mod}(\text{round}(z_i * 10^{12}), 256) \end{aligned} \quad (22)$$

To permute pixels of the image of size M x N, two random sequences R and L are generated using Lorenz chaotic equation, the sequences are represented by the equation (23).

$$\begin{aligned} R &= \{R_1, R_2, \dots, R_M\} \\ L &= \{L_1, L_2, \dots, L_M\} \end{aligned} \quad (23)$$

The sequences R and L are sorted into SR and SL sequences. The positions of each point in the sequences SR and SL in the sequences R and L are marked to get sequences TR and TL. The row and column transformation of the image is performed using the equation (24).

$$\bar{I} = \begin{cases} f_1(I) = if S1_i = 0, \\ f_2(I) = if S1_i = 1 \end{cases} \quad (24)$$

I and \bar{I} represents a plane image and scrambled image respectively. f_1 is a row transformation if $S1_i = 0$ then TR_i row is moved to the i^{th} row. If $S1_i = 1$ then TL_i column is moved to the i^{th} column. After permutation of the image, the pixels of the image will be scrambled and image diffusion will be performed using the equation (25).

$$\bar{I}_i = mod(C_i \oplus S_2 - C_{i-1} - \bar{I}_{i-1}, 256) \quad (25)$$

Where C_i is the ciphered value of the i^{th} pixel. In the above scheme total key space is 2^{128} , which is large for resisting brute force attacks. The entropy using the above scheme is almost equal to 7.99.

III. COMPARISON ANALYSIS AND DISCUSSION

Table II shows different chaotic maps used to encrypt an image. The features like correlation analysis, key spaces are compared. In [1] the algorithm used removes pixel correlation of the RGB image in the spatial domain by using DNA addition, the security of image encryption in [1] depends both on the chaotic systems as well as DNA operation providing the

dual security, the speed performance of the proposed algorithm is not ideal compared to other algorithms. In [2] the pixel values are changed only in one direction hence it is susceptible to entropy attacks. In [4] three-dimensional chaotic map called 3D cat map is used to encrypt the image, the algorithm used in [4] is suitable for real-time Internet image and video encryption. [4] provides very high resistance to statistical attacks as well as differential attacks. In [5] to provide high security the circular S-box is introduced that provides high resistance to common attacks, brute-force attacks, differential attacks, and statistical attacks. In [6] chaotic map is combined with LDE to generate a high speed and more secure image encryption system that is best suited for low-end microprocessors. In [8] image encryption is done using chaotic map with total shuffling and bidirectional diffusion. The key stream used in diffusion depends on both the sequence generated by the chaotic map as well as pixels of the plain image that increases the plaintext security. In [9] Bülban chaotic map is used for image encryption, to provide high security an XOR operation is combined with modulo function, the circular shift is used to shuffle the pixel positions, the proposed algorithm in [9] has very high speed hence can be used in real-time application encryption of images. In [10] DWT and double chaotic function is used to encrypt the image which shows higher NPCR and UACI values 99.6472% and 33.6248% respectively, this method of image encryption is well suited for wireless communications. In [11] pseudorandom sequences are generated using Lorenz chaotic system which shows high entropy.

TABLE II. CHAOTIC MAP COMPARISON ANALYSIS, H – HORIZONTAL CORRELATION, V – VERTICAL CORRELATION AND D – DIAGONAL CORRELATION

Ref.	Chaotic map and Technique used	Correlation Analysis				Key space	Special feature
		Image	H	V	D		
[1]	Logistic map and DNA encoding	Plain	0.9099	0.0059	0.9856	2^{186}	Reduced pixel correlation due to DNA encoding.
		Ciphered	0.0059	-0.0042	0.0180		
[2]	Tent map	Plain	0.9576	0.9362	0.9157	2^{106}	Time taken for encryption and decryption is less. 256 x 256 image with 24 bits takes 0.9-0.95 s for encryption
		Ciphered	0.0016	0.0025	0.0003		
[4]	3D cat map	Plain	0.91765	0.95415	0.90205	2^{128}	Suitable for real rime image encryption and transmission applications.
		Ciphered	0.01183	0.0025	0.0003		
[5]	Logistic map, PWLCM and Spatiotemporal	Plain	0.93348	0.95922	0.91299	2^{280}	Circular S-box is used for substitution operation.
		Ciphered	0.00292	-0.0012	-0.00045		
[6]	PWLCM and LDE	Plain	0.9721	0.9851	0.9595	2^{256}	It can be implemented using low end microprocessors.
		Ciphered	0.0026	0.0034	-0.0019		
[8]	Skew tent map, Logistic maps and Bidirectional diffusion	Plain	0.98498	0.9781	0.96847	2^{312}	The key stream buffer is used in diffusion.
		Ciphered	0.00032	-0.00274	-0.00147		
[9]	Bülban chaotic map	Plain	0.9618	0.9854	0.9618	2^{360}	Circular shift is used to shuffle the pixel positions.
		Ciphered	0.00039	0.0059	-0.0050		
[10]	Hybrid chaotic map and DWT	Plain	0.98453	0.95271	0.97553	2^{58}	The encryption is best suited for applications like wireless communications.
		Ciphered	0.00047	-0.03911	0.00305		
[11]	Lorenz chaotic map and switch control mechanism	Plain	0.9728	0.9281	0.9050	2^{128}	Switch control law is used to realize the pixel permutation of the image.
		Ciphered	-0.0011	0.0014	0.0005		

IV. CONCLUSION AND FUTURE WORK

In this paper nine different techniques are discussed for encrypting the image with the chaotic maps. Chaotic maps are best suited for the image encryption since image has huge amount of redundant data, a high correlation between neighboring pixels and large size. In chaotic maps higher dimensional maps provide higher security compared to lower dimensions. The image encryption system will be highly secure when the key used in substitution and permutation of the image pixels, are both random as well as the key depend on the plain image. Lot of research need to be done in the areas of multimedia encryption and decryption.

REFERENCES

- [1] Lili Liu, Qiang Zhang, Xiaopeng Wei "A RGB image encryption algorithm based on DNA encoding and chaos maps", *Computers & Electrical Engineering*, vol. 38, issue 5, pp. 1240–1248, 2012.
- [2] Chunhu Li, Guangchun Luo, Ke Qin, Chunbao Li "An image encryption scheme based on chaotic tent map", *Nonlinear Dynamics*, vol. 87, no. 1, pp. 127–133, 2017.
- [3] Kanso, A "Self-shrinking chaotic stream ciphers", *Communications in Nonlinear Science and Numerical Simulation* volume 16 issue 2, pp. 822–836, 2011.
- [4] Guanrong Chen, Yaobin Mao, Charles K. Chui "A symmetric image encryption scheme based on 3D chaotic cat maps", *Chaos, Solitons & Fractals*, vol. 21, issue 7, pp. 49–61, 2004.
- [5] Xuanping Zhang, Zhongmeng Zhao, Jiayin Wang "Chaotic image encryption based on circular substitution box and key stream buffer", *Signal Processing: Image Communication*, vol. 29, issue 8, pp. 902–913, 2014.
- [6] J.S. Armand Eyebe Foudaa, J. Yves Effa, Samrat L. Sabat, Maaruf Ali "A fast chaotic block cipher for image encryption", *Communications in Nonlinear Science and Numerical Simulation*, vol. 19, issue 3, pp. 578–588, 2014.
- [7] B. Sroysang, "More on the diophantine equation $8x + 19y = z^2$," *International Journal of Pure and Applied Mathematics*, vol. 81, no. 4, pp. 601–604, 2012.
- [8] Xuanping Zhangas, Zhongmeng Zhao "Chaos-based image encryption with total shuffling and bidirectional diffusion", *Springer Science*, pp. 319–330, 2013.
- [9] Mohamed Zakariya Talhaoui, Xingyuan Wang, Mohamed Amine Midoun "Fast image encryption algorithm with high security level using the Bülban chaotic map", *Journal of Real-Time Image Processing*, 2020.
- [10] Ibrahim Yasser, Fahmi Khalifa, Mohamed A. Mohamed, Ahmed S. Samrah "A New Image Encryption Scheme Based on Hybrid Chaotic Maps", *Hindawi Complexity*, 2020.
- [11] Shenyong Xiao, ZhiJun Yu, and YaShuang Deng "Design and Analysis of a Novel Chaos-Based Image Encryption Algorithm via Switch Control Mechanism", *Hindawi Security and Communication Networks*, 2020.
- [12] P. R. Sankpal and P. A. Vijaya, "Image Encryption Using Chaotic Maps: A Survey", 2014 Fifth International Conference on Signal and Image Processing, Jeju Island, pp. 102–107, 2014.
- [13] Yunpeng Zhang, Fei Zuo, Zhengjun Zhai, Cai Xiaobin, "A New Image Encryption Algorithm Based on Multiple Chaos System", *International Symposium on Electronic Commerce and Security*, pp. 347–350, 2008.
- [14] Shujun L, Xuan Z. "Cryptanalysis of a chaotic image encryption method", *Proceedings of IEEE, International Symposium on Circuits and Systems*, OmniPress. Phoenix-Scottsdale, pp. 87–91, 2002.
- [15] Hongjun L, Xingyuan W. "Color Image encryption based on one-time keys and robust chaotic maps", *Computers and Mathematics with Applications*, pp. 3320–3327, 2010.
- [16] Ye G.D, Huang X.L, "An efficient symmetric image encryption algorithm based on an intertwining logistic map", *Neurocomputing*, pp. 45–53, 2017.
- [17] Lian, S., Sun, J., Wang, Z. "A block cipher based on a suitable use of the chaotic standard map", *Chaos Solitons Fractals*, pp. 117–129, 2005.
- [18] Kurian AP, Puthusserypady S, "Secure digital communication using chaotic symbolic dynamics", *Turk J Elect Eng*, pp. 195–207, 2006.
- [19] Arroyo D, Alvarez G, Li S, Li C, Fernandez V, "Cryptanalysis of a new chaotic cryptosystem based on ergodicity", *Int J Mod Phys B*, pp. 651–659, 2009.
- [20] Alvarez G, Li S, "Some basic cryptographic requirements for chaos-based cryptosystems", *Int J Bifurcations Chaos*, 2129–2151, 2006.
- [21] Kocarev, "Chaos-based cryptography: a brief overview". *IEEE Circ Syst Mag*, pp. 6–21, 2001.
- [22] Yen JC, Guo JI, "A new chaotic key-based design for image encryption and decryption", In: *Proc IEEE Int Conference Circuits and Systems*, vol. 4, pp. 49–52, 2000.
- [23] S. Ahadpour, Y. Sadra, "A chaos-based image encryption scheme using chaotic coupled map lattices", *Int. J. Comput. Appl*, pp.15–18, 2012.
- [24] Mao Yaobin, Chen Guanrong, Lian Shiguo, "A novel fast image encryption scheme based on 3d chaotic baker maps", *Int J Bif Chaos*, pp. 3613–3624, 2004.
- [25] Gao, T., Chen, Z, "Image encryption based on a new total shuffling algorithm", *Chaos Solitons Fractals*, pp. 213–220, 2008.
- [26] Wang X, He G, "Cryptanalysis on a novel image encryption method based on total shuffling scheme", *Optics Communications*, pp. 5804–5807, 2011.
- [27] Musanna F, Kumar S, "A novel fractional order chaos-based image encryption using Fisher Yates algorithm and 3-D cat map", *Multimedia Tools Appl.*, 2018.
- [28] Stallings W, "Cryptography and network security principles and practice", *Int. J. Eng. Comput. Sci.*, pp. 121–136, 2012.
- [29] Wang X, Feng L, Li R, Zhang F, "A fast image encryption algorithm based on non-adjacent dynamically coupled map lattice model", *Nonlinear Dyn*, pp. 1–28, 2019.

Classification of Arabic-Speaking Website Pages with Unscrupulous Intentions and Questionable Language

Haya Mesfer Alshahrani

Lecturer in Information System Department
College of Computer Science and Information
Princess Nourah Bint Abdulrahman University

Abstract—This study aims to put forward a comprehensive and detailed classification system to categorize different Arabic-speaking website pages with unscrupulous intentions and questionable language. The methodology of this is based on a quantitative approach by using different algorithms (supervised) to build a model for data classification by using manually categorized information. The classification algorithm used to construct the model uses quantitative information extracted by Posit or SAFAR textual analysis framework. This model functions with (58) features combined from Posit – n-grams and morphological SAFAR V2 POS tools. This model achieved more than (94 %) success in the level of precision. The results of this study revealed that the best results reaching 94% precision have been achieved by combining Posit + SAFAR + (18 attributes Posit+ SAFAR N-Gram). Moreover, the most reliable results have been achieved by applying a Random Forest classification algorithm using regression. The research recommends working more on this topic and using new algorithms and techniques.

Keywords—Extremism; textual analysis; classification; Posit; SAFAR

I. INTRODUCTION

The last few years have seen a significant increase in the activities of radicalized extremists, launching terrorist attacks around the whole world. They exploit modern technologies such as the Internet and social media, widely used by the public, to plan and maintain contact with their group [1]. Social media like Facebook and Twitter are currently being utilized by extremist groups to create direct contact with their worldwide groups. By the very nature of these applications (i.e., free and unregulated), encouraged extremists to quickly form virtual societies and disseminate their thoughts and their coaching tools without paying attention to the usual means of censorship in the general media [1].

Therefore, social networks have started to intervene by implementing countermeasures against these groups. Twitter was considered the main promotional vehicle for ISIS, so in August 2016, Twitter started taking more stringent measures by closing more than 36,000 feeds that were believed to belong to ISIS [1, 2].

Fundamentally, the benefits of using data collected from social media depend on the factual accuracy of the statements being collected from the users or their groups [3]. However, it was established that additional effective procedures such as utilizing algorithms to uncover clues in the content that points to violence automatically supported this feedback and

improved its performance [4]. Notwithstanding, the feedback resulted in social websites closing a significant number of accounts, however, it was not guaranteed to be accurate, because owners of the pending accounts can create new accounts and resume their activities, or are able to relocate to different social websites. More research needs to be carried out by governments in order to counter the radicalized extremists and stop, or at least reduce their threat [1].

The study seeks to establish a comprehensive system to reveal any publication or entity that has malicious intentions emanating from extremism or seeks terrorism, and that is in various Arabic web pages. Through this study, an individually combined corpus of (5,100) text files, and more than (1,000,000) Arabic words were built. A new enhanced POS (part of speech) from the Posit tool developed by Weir (2007, 2009) was introduced with modifications on the code to deal with Arabic content. Finally, through this study, a classification model that functions with (58) features combined from Posit – n-grams and morphological SAFAR V2 POS tools was developed where this model achieved more than (99 %) success in the level of precision.

This study is divided into an introduction, a literature review of previous work and Arabic morphological classification. Then, the methodology used in this study will be presented beginning with data preparation, compiling, and building of the Arabic corpus, and covering the classification methodology. Part four explains the implementation of this methodology detailing the code used to split the massive corpus into individual text files. Information preparation began by extracting quantitative information from Arabic corpus using Posit and SAFAR frameworks. Part five discusses the experiments and the setup required - starting with the software and ending with WEKA and how it was edited to fit with our approach with the details of POS and SAVAR and the attribute of N-gram. Finally, we tackled the classification results, analysis of the eight hypotheses that have been put forward.

II. RELATED LITERATURE

A. Sentiment Analysis of Arabic Text (Opinion Mining)

Aldayel and Azmi (2016) carried out a study on sentiment analysis that connected various domains of study such as NLP, computational linguistics, and text mining [5]. It concerns the extraction of the given information from textual data. It may be called sentiment analysis or opinion mining as Pang and

Lee (2008) used the Twitter API to collect Twitter data from a specific domain in a specific language [6]. Preprocessing was done by the removal of irrelevant information, tweet cleaning and other preprocessing techniques. The classification technique is based on a Lexicon-based classifier. To extract features used in the classification process, they used the term frequency inverse document frequency (TF-IDF) weighting scheme on the n-grams (1-2-3 gram) and selected the features that have frequencies greater than a certain threshold. They used two measures to evaluate the classification process; namely (The error rate (percentage of misclassification twists) and the accuracy Rate (percentage of correctly classified twists) [6].

The Twitter API for Arabic data collection was used. The data was then passed through data cleaning and attribute extraction using 1-2-gram statistical processing. This is to prepare the data to obtain the feature vector for the main purpose of research, i.e., classification. The machine learning classifiers used are Naive Bayes (NB), and Support Vector Machines (SVM). They apply both classifiers twice. First, they apply both classifiers on features extracted based on unigrams. Then, use the features extracted based on bigram statistics [7].

The SVM classifier was employed as the research classifier and the data collection used the Twitter API. Data cleaning and normalizing, with stemming, and stop words removed were applied to make data suitable for feature extraction. The data sets were organized using 1- Unigrams, 2-Bigrams + Unigrams and 3- Unigrams + Bigrams + Trigrams [7].

The SVM classifier was applied before after applying each stage of the preprocessing to test its effect on the system's performance. Sentiment analysis studies vary in pre-treatment techniques, analysis methods, and review design. Some have used the supervised method, others the unsupervised learning method. A multi-level technique based on semantic orientation (lexical classifier to handling unnamed tweets) and ML (SVM classifier) was suggested by Aldayel and Azmi (2016) to identify the polarity of Arabic tweets. The biggest challenge of this mixed approach, however, is to deal with the application of Twitter in dialectical Arabic [5].

Moraes, Valiati and Neto (2013) compared the execution of SVM (support vector machines) and NN (neural networks) at document-level sentimental Arabic analysis. They have found that NN execution is better than SVM on the same records [8].

Li and Li (2013) have gauged the objectivity and the truthfulness by utilizing SVM as a method [9]. Cherif, Madani and Kissi (2015) worked on the execution of three famous techniques (bagging, boosting and random subspace). This was instituted on five algorithms, which are (Naive Bayes, Maximum Entropy, Decision Tree, K Nearest Neighbor, and Support Vector Machines) for sentiment categorization. The results showed that the random subspace was more accurate [10].

Duwairi and Qarqaz (2014) studied the effects of stemming feature correlation and n-gram models for Arabic text on sentiment analysis. They used Support Vector

Machines, Naive Bayes, and K-nearest neighbor classifiers, while the results of the experiments suggested that choosing the method of preprocessing on the reviews would enhance the performance of the classifiers [11].

B. Classification and Comparing Algorithms on Arabic Text

El Kourdi Bensaïd and Rachidi (2004) categorized Arabic documents on the internet automatically by using an NB classifier with ML algorithms to classify soundless Arabic documents into one of five pre-determined classes. The results of the experiments confirmed the effectiveness of the NB classifier. El Koudri utilized groups of 1500 documents under five categories each with 300 text documents. Through 2000 expressions and roots, the precision of the classification varies in-between categories with an average precision overall for the classifiers of 68.78 %. Moreover, the highest performance of categories in these experiments reached 92.8% [12].

KNN algorithm (K-Nearest Neighbor) is one of the best classifiers for categorizing text documents in English with the SVMs algorithm. This was used by Al-Shalabi Kanaan and Gharaibeh (2006) on the Arabic language for text classification. They utilized the DF (Document Frequency) technique to extract the main words and minimize dimensions. The results proved that the KNN is suitable to categorize Arabic documents [13].

Maximum Entropy (ME) was applied by El-Halees (2015) and Sawaf, Zaplo and Ney (2001) to categorize Arabic news articles. El-Halees pre-processes data, utilizing natural language processing methods such as tokenizing, stemming, and part of speech then uses the maximum entropy method to categorize Arabic documents. The best-reported accuracy was 80.41% and 62.7% when using statistical methods by Sawaf without morphological analysis [14, 15].

Al-Zoghby, Eldin, Ismail and Hamza (2007) proposed a novel system that was developed to determine association rules using similarity measurements based on the derivation of the Arabic language. It also offered the advantage of using the "Frequent Closed Item sets" (FCI) concept when extracting the association rules instead of "Frequent Item sets" (FI) [16].

III. METHODOLOGY

The methodology of this is based on a quantitative approach by using different algorithms (supervised) to build a model for data classification by using manually categorized information. Through this study, a 'seed list' of Arabic words and sentences was used in an input list box and the sketch engine that fetched around one million words per search. The data range was the most likely used words for extremism websites, tweets and any social media website, e.g., the Arabic equivalent of "kill the disbeliever and you enter heaven". Through this process, more than 7000 Arabic text files were collected and processed to form the downloaded corpus of individual files, in which everyone represents pro-extreme text, with associated id and URL. The same approach was followed for Anti-extremism and neutral data.

The research has been divided into several stages, and in each stage, certain methods and tools have been deployed. The following sections will explain these methods and equipment.

A. Data Collection and Preprocessing Stage

The proposed system depends on the analysis of an Arabic dataset but a specific one; it must contain text data for encouraging extremism, anti-extremism and neutral data, in Arabic language. Since such an existing resource proved elusive, we had to develop our own means of gathering such a dataset (using tools like sketch engine). To this end, we used a 'seed list' of Arabic words and sentences in an input list box and the sketch engine will fetch around one million words per search. The data range was the most likely used words for extremism websites, tweets and any social media website, e.g., the Arabic equivalent of "kill the disbeliever and you enter heaven".

Through this process, we collected more than 7000 Arabic text files and processed them to form the downloaded corpus of individual files, in which everyone represents pro-extreme text, with associated id and URL. The same approach was followed for Anti-extremism and neutral data.

The data collection was the first step in this study where it was based on a mixture of locations that considered being antiterrorism, pro-terrorism, and neutral sites to ensure balanced datasets for training and test datasets. Then, preprocessing was performed for the data that include but are not limited to removing non-Arabic text; removing HTML tags; excluding empty files; splitting pages of websites, and adding file ID to each file.

B. Data Analysis Stage

The step following data preprocessing is to apply text analysis toolkits to derive detailed information on the Arabic file content. The result of this process is to generate summary files containing all numeric, quantitative information about the Arabic text files. In addition, an N-Gram file is created to be used for the classification process and prediction calculations.

The main competition among the different data processing tools available lies in the number of distinct features that can be extracted from Arabic text. The more features, the more quantitative information, and, potentially, the more precise will be the classification. We should note the need for an Arabic language expert working side-by-side with the developer to review and audit the results coming out of each tool, to make sure they are semantically correct.

The main operations on the Arabic text should include the following:

- Stem counting,
- Sentence Processing
- Morpho-Syntactic Processing,
- Summarizing,
- Arabic Parsing, and
- Morphological analyzing.

We used the Posit and SAFAR tools, which gave more than 58 features together, to create Summary files. Once we get summary and N-Gram files we are ready for data classification. The classification process is divided into two

main steps; the first step is to ensure that the training data set, which is manually classified, will produce a high-quality model for future use. Then, in the second step, we can test and create the model.

C. Data Classification Stage

The next step is to use the model file that is created in the first step for classification of the unseen dataset to calculate a prediction for each file individually. To calculate prediction and to construct a confusion matrix, we store the extracted quantitative data as well as N-Gram data in a suitable format for training and test datasets. The classification is done by studying the attribute parameters during the training phase, and then considers the hidden files in order to predict the class for each new data item. The classification process can be divided into two main steps.

To perform the classification process for the unseen dataset, we follow these detailed steps:

- Divide the collected corpus into a training dataset and test (unseen) dataset.
- Put all information collected that relates to each file into a suitable format for the classification process (ARFF file format).
- Manually classify the data samples by a high-qualified person for the training dataset. The purpose of the training dataset is to create a classification model used subsequently in the classification of the unseen dataset.
- Examine the training dataset for the quality of classification. We divide the data into 70% and 30% subsets. We use 70% of datasets as a self-training dataset and 30% as self-test datasets.
- Explore the use of different algorithms for classification. To choose the most suitable classification algorithm, we study many classifiers that can be listed under different classification concepts. The results are not selected based on the classifier only but also depend on dataset combinations of the two text analysis toolkits and the use of N-Grams generated by both text analysis toolkits.
- Select the best combination of dataset and classifier, based upon the precision, Recall, and F-Measure.
- We selected WEKA (machine learning environment) as a basis for our classification work because it is rich with a classification environment with attribute processing like attribute selection and a rich library of machine learning algorithms. Moreover, it has an API to be used to throw user-made applications.
- The programming language selected for creating the user interface is JAVA. It can utilize WEKA API to produce an efficient application that can fulfill all research requirements, including classification, and put the results in a suitable form for analysis.

D. Research Tools

In this study, three tools were employed including Posit Toolset that contains POS Profiler, Vocabulary Profiler and Readability Profiler. The second tool was SAFAR (Software Architecture For Arabic language processing) program, which was used in the stage of data processing in the proposed system, as it worked on extracting quantitative information from text file data. Finally, WEKA API was used in the proposed system in order to classify the processed text data into three types (terrorist, anti-terrorist, and neutral).

E. Sample

WEKA API classifier needs training in a pre-categorized dataset to learn how to differentiate between our three categories (pro-terrorism, anti-terrorism, neutral) and the distinct features and words for each category. In this system, a train data set of 300 files of textual data containing the three categories were used to train the classifier, and then this was tested to check its accuracy and effectiveness.

F. Validity and Reliability

Validity and reliability were taken into consideration in each step of the system design and implementation. First, collecting data was done by using several different sources (neutral sources, sources supporting terrorism, and anti-terrorism sources), whether it is on the Internet, social media, and elsewhere.

The manual data classification stage was performed by five different specialized people. Once classified in a category by at least four people the file is considered classified and added to the Corpus, otherwise, it is removed from the Corpus group. In the next stage, a program was used to process the Arabic texts.

The next stage was to train the classifier through a group consisting of 300 text files of the three types. Finally, to ensure the validity of the training, progress and design of the program, the program was tested through a test dataset consisting of 200 text files of the three categories. The 200 files were completely correctly categorized, which demonstrated the validity of the proposed program's work for this message.

IV. RESULTS AND DISCUSSION

In this test, the used ARFF file was created depending on summary files resulting from each of the data sets dataset. Each classification process requires training and test datasets. Fig. 1 shows test classification results obtained by applying desired classifiers on each dataset.

A. Test Results

A review of unseen dataset test only to summarize the results for useful information.

1) Final posit datasets discussion: Table I shows Posit dataset classification best results.

By adding the N-Gram attributes to the Posit attribute, the Random Forest classifier dominated over other classifiers with considerable value (about 5%) for the supervised dataset.

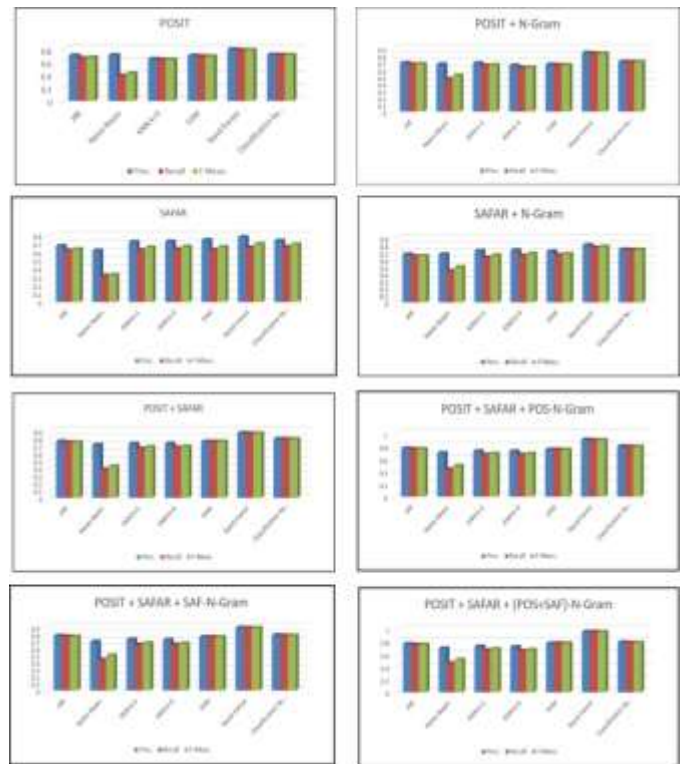


Fig. 1. Shows Test Classification Results Obtained by Applying Desired Classifiers on each Dataset.

TABLE I. POSIT CLASSIFICATION RESULTS

Supervised				
		Prec.	Recall	F-Meas.
Posit	Rand-Forest	0.797	0.785	0.786
Posit+ N-Gram	Rand-Forest	0.840	0.831	0.832

2) Final SAFAR dataset discussion: Table II shows Posit dataset classification best results.

TABLE II. SAFAR CLASSIFICATION RESULTS

Supervised				
		Prec.	Recall	F-Meas.
SAFAR	Rand-Forest	0.778	0.654	0.696
SAFAR + N-Gram	Rand-Forest	0.805	0.771	0.783

The above results show that less precision of 80% for SAFAR + N-Gram dataset. SAFAR dataset without N-Gram attribute offers lower precision by about 3%.

3) Posit + SAFAR dataset discussion: Table III shows Posit + SAFAR datasets classification results.

Results show the minimum precision of 87.2% for (Posit+SAFAR) dataset and best precision by using the Posit+SAFAR + (Posit+SAFAR N-Gram) dataset of value 95.4%.

TABLE III. SHOWS POSIT + SAFAR DATASETS CLASSIFICATION RESULTS

Supervised				
	Classifier	Prec.	Recall	F-Meas.
Posit+SAFAR	Rand-Forest	0.872	0.864	0.867
Posit+SAFAR + (Posit N-Gram)	Rand-Forest	0.904	0.894	0.896
Posit+SAFAR + (SAFAR N-Gram)	Rand-Forest	0.890	0.886	0.887
Posit+SAFAR + (Posit+SAFAR N-Gram)	Rand-Forest	0.954	0.953	0.952

B. Final Results

Here the best results from all tests and achieved the best performance (Precision 95%, Recall = 95%, F-Measure = 95%) by applying Random Forest classifier on (Posit+SAFAR) + (Posit+SAFAR) N-Gram. Table IV shows the classifier results sorted in ascending order of performance.

C. Discussion

Many researchers have tried to obtain the optimum classification algorithm for different languages, especially Arabic. The common toolkit was set up, Posit, to work for the Arabic language. This helped enhance the overall process by finding more than one toolkit to extract meaningful quantum information from Arabic text. The use of N-Gram was another way to process the amount of information used to learn the parameters of attributes and to calculate the prediction of unseen data. WEKA data processing environment is a rich environment for the Random Forest classification algorithm.

1) Comparison: A similar approach to the classification task is reported in the following sections:

Aldayel and Azmi (2016) used a Hybrid approach classifier Algorithm for the Arabic language. The approach is based on using a lexical classifier for training data for the SVM classifier, Lexical classifier. Used for first step classification to produce the training dataset for model creation. Dataset: 1103 tweets (576 positives, 527 negatives). Then the SVM classifier was used for the classification of an unclassified dataset. The hybrid classifier (Lexical + SVM) produce results as follows Table V:

This research uses a lexical classifier for learning datasets rather than manual classification to apply the SVM classifier to classify the unseen tweets dataset. This combination enhances the overall operation.

$$Acc. = \frac{TP + TN}{TP + TN + FP + FN}$$

Shoukry and Rafea (2012) worked to process tweets to provide their sentiments polarity (positive or negative). SVM and Naïve Bayes (NB) used for both training and classification, one by one. Dataset: 1000 tweets (500 positives, 500 negatives). Results obtained were as follows Table VI:

This research use sentiments classification to produce a learning dataset and supervised test for unseen tweets dataset using two different classification algorithms. SVM gave better results over Naïve Bayes by 7.4%.

TABLE IV. ALL DATASETS CLASSIFICATION SORTED RESULTS

Supervised				
	Classifier	Prec.	Recall	F-Meas.
(Posit+SAFAR) + (Posit+SAFAR) N-Gram	Rand-Forest	0.95	0.95	0.95
Posit + SAFAR + (Posit 2-3-4 Gram)	Rand-Forest	0.90	0.89	0.9
Posit + SAFAR + (SAFAR 2-3-4 Gram)	Rand-Forest	0.89	0.89	0.89
Posit + SAFAR	Rand-Forest	0.87	0.86	0.87
Posit + N-Gram	Rand-Forest	0.84	0.83	0.83
SAFAR + N-Gram	Rand-Forest	0.81	0.77	0.78
Posit	Rand-Forest	0.80	0.79	0.79
SAFAR	Rand-Forest	0.78	0.65	0.7

TABLE V. TWEET CLASSIFICATION

		Prec.	Recall	Accuracy
Tweet datasets	Lexical + SVM	0.847	0.838	0.840

TABLE VI. SENTENCE LEVEL ARABIC SENTIMENT (1-2 GRAMS) SVM AND NAÏVE BAYES

		Prec.	Recall	F-Meas.	Accuracy
Tweet datasets (Unigrams and Bigrams)	SVM	0.726	0.728	0.726	0.725
Tweet datasets (Unigrams and Bigrams)	Naïve Bayes	0.652	0.652	0.652	0.652

Its Arabic sentiment considers normalization, stemming, and stop word removal for datasets (during the preprocessing phase) (Shoukry & Rafea, 2012). SVM is used for both training and classification. Dataset: 1000 tweets (500 positives, 500 negatives). The results obtained are as follows in Table VII.

TABLE VII. SENTENCE LEVEL ARABIC SENTIMENT (2-3 GRAMS) SVM (NORMALIZATION, STEMMING, AND STOP WORDS REMOVAL)

Supervised					
Dataset	Classifier	Prec.	Recall	F-Meas.	Accuracy
Unigrams - raw tweets	SVM	0.740	0.740	0.740	0.740
Unigrams – normalized tweets	SVM	0.756	0.756	0.756	0.756
Unigrams + Bigrams + Trigrams stemmed tweets	SVM	0.787	0.787	0.787	0.787
Unigrams + Bigrams + Trigrams after stop words removal	SVM	0.788	0.788	0.788	0.788

Adding 2-3-4 Gram information enriches the training and test datasets. Preprocessing enhances the classification process by different factors.

El-Halees (2015) used a combined approach for Arabic language classification in the beginning; the lexicon-based method is used to classify as many documents as possible. The resultant classified documents are used as a training set for the maximum entropy method, which subsequently classifies some other documents. Finally, the k-nearest method used the classified documents from the lexicon-based method and maximum entropy as a training set and classified the rest of the documents.

Dataset: 949 tweets (415 positives, 534 negatives) belong to "education", "politics" and "sports" categories. Results collected as follows in Table VIII.

A combined classification (Lexical + Maximum Entropy + k-nearest) approach enhances classifier accuracy. Observing the last 4 types of research, the researcher is going forward for the Arabic classification process, which is considered to be an NP-complete problem (nondeterministic polynomial time) [https://www.ics.uci.edu/~eppstein/161/960312.html].

The overview shows that the researcher's results reach an acceptably high level of precision by using different ways of data preprocessing thereby enriching the input data by adding N-Gram or classifying by multiple classifiers. In the following Table IX, a comparison of results to reviewed researches results.

Our approach depends on manual classification for the training dataset (70% + 30% seen dataset) to ensure the best results. Note that the process of manual classification is time consuming, especially if it is carried out on several thousand-text files. This is also influenced by the scientific level and culture of those involved in the process of manual classification. After manual classification, the text-processing toolkit was applied in order to build datasets for the training and classification process. Attribute data is extracted by two different toolkits (Posit & SAFAR), which build information obtained from text files.

2) *Unseen datasets*: The Random Forest algorithm used for creating a classification model employing a carefully and manually classified dataset gives us the best results over other classification techniques, as in Table X.

TABLE VIII. COMBINED APPROACH FOR ARABIC LANGUAGE CLASSIFICATION

	Lexical	Lexical + ME	Lexical +ME + kNN	
Accuracy	50.08	60.73	80.29	
		Prec.	Recall	F-Meas.
Politics Sports Education datasets	Lexical + Maximum Entropy + k-nearest	80.7	79.805	79.895

TABLE IX. COMPARING OTHER CLASSIFICATION RESULTS TO OUR CLASSIFICATION METHODOLOGY

	Dataset	Classifier	Prec.	Recall	F-Meas.	Acc.
1	Tweet datasets	Lexical + SVM	0.847	0.838		0.840
2	Tweet datasets (Unigrams and Bigrams)	SVM	0.726	0.728	0.726	0.725
	Tweet datasets (Unigrams and Bigrams)	Naïve Bayes	0.652	0.652	0.652	0.652
3	Unigrams - raw tweets	SVM	0.740	0.740	0.740	0.740
	Unigrams – normalized tweets	SVM	0.756	0.756	0.756	0.756
	Unigrams + Bigrams + Trigrams stemmed tweets	SVM	0.787	0.787	0.787	0.787
	Unigrams + Bigrams + Trigrams after stop words removal	SVM	0.788	0.788	0.788	0.788
4	Politics Sports Education datasets	Lexical + Maximum Entropy + k-nearest	80.7	79.805	79.895	
5	(POSIT+SAFAR) + (POSIT+SAFAR) N-Gram	Rand-Forest	0.95	0.95	0.95	

TABLE X. RANDOM FOREST CLASSIFIER AGAINST SOME OTHER CLASSIFIERS

Algorithm	Dataset	Prec.	Recall	F-Meas.
Random Forest	Posit + SAFAR + (Posit + SAFAR N-Gram)	0.95	0.953	0.952
RF Via Regression	Posit+ SAFAR + (Posit N-Gram)	0.80	0.79	0.791
J48	Posit+ SAFAR + (SAFAR N-Gram)	0.78	0.768	0.766
SVM	Posit + SAFAR + (Posit + SAFAR N-Gram)	0.77	0.771	0.771
IBk_3	SAFAR + N-Gram	0.73	0.657	0.684
Naïve Bayes	Posit + SAFAR	0.71	0.38	0.42

REFERENCES

The Random Forest algorithm gave the best result against the manually classified dataset (Posit + SAFAR toolkits) and other algorithms with a precision of 0.95. Other algorithms (RF via Regression, J48, SVM, IBk_3, Naïve Bayes) show good results with different datasets, all undergoing manual classification with results of (0.71-0.80).

V. CONCLUSION

This study showed that the classification process can be improved and automated using Random Forest and Random Forest via the Regression classification algorithm, which is integrated into JAVA application using the WEKA machine-learning environment (WEKA API). The used datasets for unseen data classification are different combinations of data extracted using Posit and SAFAR toolkits and N-Gram attributes.

Items in text writing (for example, word or phrase) can be labeled under various tags (Pro extremist – Anti extremist – neutral). This makes it hard to distinguish between different classes of context using the automated classification system. The nature of the text makes it difficult to reach the maximum prediction that is equal to one, but it reduces as much as the uncertainty of determining the item class exists. Moreover, it has been shown from our practical experience that combining different attributes deduced by combined two toolkits for analyzing Arabic text can be used to enhance text categorization using a sufficient set of carefully manually classified files.

This study recommends conducting further studies that are based on the increasing diversity of a collection of data from different site categories (sports – politics – social – food – health, etc.) to get alternative ways of writing and to overcome the lack of sites supporting terrorism. Furthermore, it recommends finding an algorithm that can use in conjunction with manual sorting to reduce the effort and time required for manual classification. Using techniques like attribute selection will have better performance especially with datasets with larger n-gram data. Finally, other future work is to automate the classification process using our produced model and other models for multi-language websites including social media sites, and to propose accepted datasets enhancing the model by re-training to produce a new model file for future use.

- [1] H. Alviri, S. Sarkar, P. Shakarian, Detection of violent extremists in social media, in: 2019 2nd International Conference on Data Intelligence and Security (ICDIS), IEEE, 2019, pp. 43-47.
- [2] T.C. Helmus, E. Bodine-Baron, Empowering ISIS Opponents on Twitter, RAND Corporation, 2017.
- [3] J. Peral, A. Maté, M. Marco, Application of data mining techniques to identify relevant key performance indicators, *Computer Standards & Interfaces*, 54 (2017) 76-85.
- [4] R.K. Bakshi, N. Kaur, R. Kaur, G. Kaur, Opinion mining and sentiment analysis, in: 2016 3rd International Conference on Computing for Sustainable Global Development (INDIACom), IEEE, 2016, pp. 452-455.
- [5] H.K. Aldayel, A.M. Azmi, Arabic tweets sentiment analysis—a hybrid scheme, *Journal of Information Science*, 42 (2016) 782-797.
- [6] B. Pang, L. Lee, Opinion mining and sentiment analysis, *Comput. Linguist*, 35 (2009) 311-312.
- [7] A. Shoukry, A. Rafea, Sentence-level Arabic sentiment analysis, in: 2012 International Conference on Collaboration Technologies and Systems (CTS), IEEE, 2012, pp. 546-550.
- [8] R. Moraes, J.F. Valiati, W.P.G. Neto, Document-level sentiment classification: An empirical comparison between SVM and ANN, *Expert Systems with Applications*, 40 (2013) 621-633.
- [9] Y.-M. Li, T.-Y. Li, Deriving market intelligence from microblogs, *Decision Support Systems*, 55 (2013) 206-217.
- [10] W. Cherif, A. Madani, M. Kissi, A new modeling approach for Arabic opinion mining recognition, in: 2015 Intelligent Systems and Computer Vision (ISCV), IEEE, 2015, pp. 1-6.
- [11] R.M. Duwairi, I. Qarqaz, Arabic sentiment analysis using supervised classification, in: 2014 International Conference on Future Internet of Things and Cloud, IEEE, 2014, pp. 579-583.
- [12] M. El Kourdi, A. Bensaid, T.-e. Rachidi, Automatic Arabic document categorization based on the Naïve Bayes algorithm, in: proceedings of the Workshop on Computational Approaches to Arabic Script-based Languages, 2004, pp. 51-58.
- [13] R. Al-Shalabi, G. Kanaan, M. Gharaibeh, Arabic text categorization using KNN algorithm, in: Proceedings of The 4th International Multiconference on Computer Science and Information Technology, 2006, pp. 5-7.
- [14] A.M. El-Halees, Arabic text classification using maximum entropy, *IUG Journal of Natural Studies*, 15 (2015).
- [15] H. Sawaf, J. Zaplo, H. Ney, Statistical classification methods for Arabic news articles, *Natural Language Processing in ACL2001*, Toulouse, France, (2001).
- [16] A. Al-Zoghby, A.S. Eldin, N.A. Ismail, T. Hamza, Mining Arabic text using soft-matching association rules, in: 2007 International Conference on Computer Engineering & Systems, IEEE, 2007, pp. 421-426.

Cyber Situation Awareness Perception Model for Computer Network

Olofintuyi Sunday Samuel
Mathematical Science Department
Achievers University, Owo, Nigeria

Abstract—With the increase in cyber threats, computer network security has raised a lot of issues among various companies. In order to guide against all these threats, a formidable Intrusion Detection System (IDS) is needed. Various Machine Learning (ML) algorithms such as Artificial Neural Network (ANN), Decision Tree (DT), Support Vector Machine (SVM), Naïve Bayes, etc. has been used for threat detection. In light of the novel threats, there is a need to use a combination of tools to accurately enhance intrusion detection in computer networks, this is because intruders are gaining ground in the cyber world and the side effects on organizations cannot be quantified. The aim of this work is to provide an enhanced model for the detection of threats on the computer network. The combination of DT and ANN is proposed to accurately predict threats. With this model, a network administrator will be rest assured to some extent based on the prediction of the model. Two different supervised machine algorithms were hybridized in this research. NSL-KDD dataset was deployed for the simulation process in WEKA environment. The proposed model gave 0.984 precision, 0.982 sensitivity and 0.987 accuracy.

Keywords—*Situation awareness; intrusion detection system; artificial neural network based decision tree; decision tree; classification*

I. INTRODUCTION

There has been an increase in cyber threats which has caused damages all over the globe, this is not far-fetched from the fact that there is increase in the usage of computer networks and the tremendous applications usage especially after the advent of the internet of things [1]. Data encryption, user's authentication, hardware and software firewalls are some of the approaches used so far for threats detection. Regrettably, these methods may not be able to fully protect cyber threats from computer networks [2]. For example, firewalls can only monitor exchange of data between networks and no signal is given for internal attack. An accurate machine learning algorithm is obviously needed to build a formidable security system. Intrusion Detection System (IDS) helps to identify any form of abnormalities in behavior on a computer network [3]. Based on the user's perspective, IDS are of different types which are Network Based Intrusion Detection System (NIDS) and Host Based Intrusion Detection System (HIDS) [1]. In NIDS, threats are scanned across the networks while in HIDS abnormalities and inconsistency are only checked for in the operating system. Basically, there are two approaches for threat detection which are signature-based IDS and anomaly-based IDS. Signature based IDS helps to detect known threat because of the previous record in the database

while anomaly-based IDS can detect some new set of threats [4]. Recently, there is high demand for protection against the various types of cyber-attacks. This is because the number of users of computer networks are increasing every day. With this, cyber-threats such as Denial Of Service (DOS), probe, User to Root (U2R) and Root to Local (R2L) are also gaining ground in cybersecurity [5]. According to [6], the activity of intruders cost an organization to loss about 8 billion dollars. The security community were able to detect about 50 million malwares in 2010, 100 million unique malwares were also detected in 2010. The number of executable malwares detected in 2019 skyrocketed to about 900 million unique malware and the number keeps increasing everyday, because of this fact, there is a need to build a formidable cybersecurity that can be adopted by organization in order to reduce their loss [7]. The author in [8] in his first work on Situation Awareness (SA), classified SA into three sections which include the following; perception, comprehension and projection. The "perception" which is always the first phase of SA model deals with detecting events (malicious and threat free) in the environment. The second phase of the model is the comprehension phase, this phase is connected to a trained database of various events, after which the perception relays it information to the comprehension, the comprehension phase then judges the event whether it is a malicious event or not. After that, the comprehension phase then relay the information to the projection phase which is finally feedback to the network administrator. This work is set to modify the perception phase by introducing two supervised machines into the perception phase in order to enhance security, this will help the network administrator to forestall attacks. Recently, there has been inspiring attempt at forestalling network attacks using one, two or more hybridized machine learning algorithms. The author in [9] uses ANN for threat detection on a computer network and compares the result with SVM. The author in [10] uses DT for threats classification on the computer networks, [11] adopts SVM and [12] introduces clustering algorithms. The results of these studies have been promising. However, there is still need for improvement. In this work, two supervised machine learning algorithms were used in the perception phase of the SA. The algorithms used are Decision Tree (DT) and Artificial Neural Network (ANN). DT is a classifier that has tree like structure and use historical dataset for its prediction. Artificial neural network is also a classifier which has three layers; input layers, hidden layers and the output layer. The data to be classify are allocated to each neuron in the input layer which feeds the hidden layers and then finally passed to the output layer. The algorithms

were simulated in WEKA environment. WEKA is a simulating tool which contains various machine learning algorithms which are used for classification, data pre-processing, clustering, regression and so on [13]. The remaining section of this paper is as follows: Section II discusses the background to the study, section III discusses the methodology applied with the dataset used. The next section immediately that discusses the simulation results derived from the experiment. The final section talks about the conclusion and the possible future work.

II. LITERATURE REVIEW

In the field of data science and machine learning, one of the best techniques for building prediction models is classification [14]. Various classification algorithms have been proposed by researchers which are used in building a predictive model. Some of the works done so far in machine learning for prediction include the followings: The author in [15] proposed Deep Neural Network (DNN) for the detection of cyber security threats in Internet of Things (IoT) network. The dataset used was obtained from google code jam. After the experimental results, the proposed algorithm showed a better classification performance. The author in [16] deployed a bi-directional recurrent neural network for prediction of cyber-attack. Real world cyber-attack dataset was used to validate the proposed model. The proposed model gave a better prediction accuracy than statistical prediction model. The study by [17] proposed an intrusion detection system based on back propagation neural network. The authors developed an algorithm to classify four types of attacks namely; DOS, Probe, U2R and R2L. The algorithm was evaluated using the KDD99 dataset. The study obtained a detection rate of 0.99 and false alarm rate of 0.03 with a data size of 500. With two hundred increase in data size, the results obtained were still in the range above for detection rate and false alarm rate. The author in [18] proposed C4.5 Decision tree algorithm for the prediction of credit card risk. After data preprocessing and evaluation, the proposed algorithm gave 73.1% accuracy prediction. The accuracy of the C4.5 decision tree was improved to 75.1% by applying bagging ensemble algorithm. The author in [19] proposed a new technique based on soft computing in which a classifier called neuro-fuzzy was used for droppage of packet in MANETS. An Intrusion Detection System (IDS) was used for classification of threats for mobile ad-hoc network, this is because encryption and authentication are not considered as a very good solution to combat with the threat. The proposed IDS use neuro-fuzzy classifier. Matlab toolbox with Qualnet was used as a simulating tool. The result of the simulation showed that the proposed system efficiently detected dropping of packet while attack has low false positive rate and high true positive rate. The author in [20] presented a study on fuzzy rules for intrusion detection system. The work makes use of fuzzy set theory and the analysis of the function of genetic algorithm with fuzzy rule were done for intrusion detection system. In their result, they were able to gain maximum detection of DOS. This approach will be very useful, if the rules can be updated from time to time in order to meet up with the new attacks. The author in [21] presented real time intrusion detection with fuzzy, genetic and Apriori algorithm. The

combination of these approaches was necessitated because several machines learning algorithms have been used for intrusion detection but a satisfactory result was not achieved. KDD 99 dataset was used in implementing the proposed model and their evaluation rate were detection speed, false alarm rate and attack types. After their experiment setup, it was observed that their proposed model gives a better outcome. The author in [22] proposed a work on a system for intrusion detection in which two machines were used which are support vector and genetic network programming. The database used in this work was classified into two namely positive kernel and negative kernel. Where the positive kernel was used in creating the rules. The experimental result shows that the combination of support vector machine and genetic network programming has increase the performance of the detection rate of intrusion detection system and also reduces the false positive rate. In the research conducted by [23], an artificial neural network based sequential classifier was used for the detection of false positive, false negative, true positive and true negative respectively. From the result obtained after the experiment, the introduction of sub classifier increases the accuracy of the proposed algorithm compared to individual model. The author in [24] uses five different classifiers in the proposed model to reduce the incidence of false negative rate. The five classifiers that were used include Naïve baye, multilayer perception, decision tree, random forest and K-nearest neighbor. 90.31% accuracy were achieved after the experimental result.

III. METHODOLOGY

Generally, Situation Awareness model has three phases which this model agrees with, but due to the inaccuracies in detection rate of threats, two algorithms were hybridized in the perception phase. Fig. 1 depicts the proposed model.

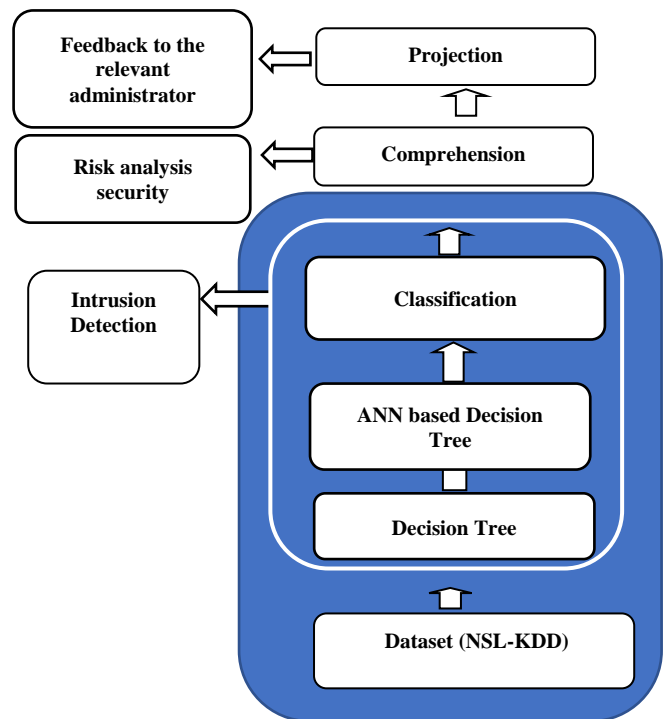


Fig. 1. Proposed Model.

The proposed model has three sections which are the perception phase, comprehension phase and projection phase. The perception phase which deals with detection of events in the environment is made up of two machine algorithms which are Decision Tree and Artificial Neural Network.

A. Dataset

NSL-KDD dataset was used in the simulation of the two algorithms used. The dataset is an online dataset which was derived from the Defense Advance Research Project Agency (DARPA). NSL- KDD dataset has forty-one features as gotten online. The dataset is in numeric form ranging from different numbers. But the dataset was all converted to 0's and 1's. NSL-KDD dataset consists of various categories which are:

1) *Denial of Service (DOS)*: DOS is a group of attack, in which they keep the computing memory busy because of this, the memory no longer has time to attend to legitimate request. Example includes: Apache2, Mail bomb, Process table, Smurf, Udpstorm. Back, Land, Teardrop, Ping of death and SYN Flood.

2) *User to root*: These are group of attacks in which they approach a system as a normal or legitimate user of the system, meanwhile they are intruder. Once they get access to the system, they then explore the system vulnerabilities. Examples are Xterm, perl, loadmodule and fdformat.

3) *Root to local*: These are group of attacks in which they send packet of data to the network which they do not have access to. With this, they tend to gain access and explore the system vulnerabilities. Examples are FTP write, Imap, Xlock, Dictionary, Phf and Guest.

4) *Probing*: are also one of the categories of attack where by an attacker approach a system and then gain access to the system which later explore the vulnerabilities of the system. Examples are Saint, satan, Mscan, Ipsweep and Nmap. Table I below shows the 41 attributes of the dataset.

B. Decision Tree

Decision tree uses historical dataset for it prediction. It is structured as a tree where the node servers as feature and the edges are features value. The dataset used servers as input into the algorithm, it also considers the attribute of the dataset which helps in predicting the classes of threat. As used in the proposed model, decision tree was used to separate the dataset which has 41 attributes into the “attack group” and the normal group”. The main reason why decision tree was firstly used was to classify each of the class of event. All threats are classified as 0 while the normal class was classified as +1. This was done in the excel environment and was then reopened in the notepad which was finally saved in arff format. The dataset must be in arff format so that the simulation tool (WEKA) will accept the dataset for simulation.

C. ANN based Decision Tree Model (Proposed Model)

In the second sub-phase of the model, ANN based decision tree is an excellent approach to resolve the problem of multiclass. Hybridizing different models enhances the performance compared to individual models, this is because

hybridization reduces the weakness of the individual models. ANN based decision tree was used to classify the threat group into the various categories. ANN is a neural network of neurons which are inter-connected. Basically, ANN has three sections which are the input layer, hidden layer and output layer. The input layer takes the output features from decision tree which are then sent to the hidden layer and finally gets to the output layer. Since the classes of threats are classified into four categories from the dataset gotten, once the output gives 0001 it is classified as “user to root” if the output reads 0010 then it is probe. Furthermore, if the output displays 0100 it is classified as “Remote to local” and if it reads 1000 it then means it is “Denial of service”. In this study, the input neurons are represented by each threat feature variables determined by $X_i = \{X_1, X_2, X_3 \dots X_n\}$ where i is the number of variables (input neurons). The effect of the synaptic weights, W_j on each input neuron at layer j is represented by the expression:

$$Z_j = W_{1j}X_1 + W_{2j}X_2 + \dots + W_{3j}X_3 + b \quad (1)$$

TABLE I. LIST OF 41 FEATURES OF THE DATASET

Feature Index	Feature name	types
1	Duration	continuous
2	Protocol type	Symbolic
3	service	Symbolic
4	Flag	Symbolic
5	Scr_bytes	continuous
6	Dst_bytes	Continuous
7	Land	Symbolic
8	Wrong fragment	Continuous
9	Urgent	Continuous
10	Hot	Continuous
11	Num_failed login	continuous
12	Logged_in	Symbolic
13	Num_compromised	Continuous
14	Root_shell	Continuous
15	Su_attempted	Continuous
16	Num_root	Continuous
17	Num_file creation	Continuous
18	Num_shell	Continuous
19	Num_access file	Continuous
20	Num_outbound_cmds	Continuous
21	Is_host_login	symbolic
22	Is_guest_login	symbolic
23	count	Continuous
24	Srv_count	Continuous
25	Serror_rate	Continuous
26	Srv_serror_rate	Continuous
27	Rerror_rate	Continuous
28	Srv_rerror_rate	Continuous
29	Same_srv_rate	Continuous
30	Diff_srv_rate	Continuous
31	Srv_diff_host_rate	Continuous
32	Dst_host_count	Continuous
33	Dst_host_srv_count	Continuous
34	Dst_host_same_srv_rate	Continuous
35	Dst_host_diff_srv_rate	Continuous

36	Dst_host_same_src_port_rate	Continuous
37	Dst_host_srv_diff_host_rate	Continuous
38	Dst_host_serror_rate	Continuous
39	Dst_host_srv_rate	Continuous
40	Dst_host_srv_serror_rate	symbolic
41	Dst_host_serror_rate	symbolic

Equation (1) is sent to the activation function (sigmoid/logistic function) and applied in order to limit the output to a threshold [0, +1]. The difference between the expected output (p) and the actual output (y) is derived using the squared error measure (E):

$$E = (p - y)^2 \quad (2)$$

The output (p) of a neuron depends on the weighted sum of all its inputs as indicated in (1). In this research work, the gradient descent algorithm is applied in order to minimize the error and hence find the optimal weights that satisfy the problem. Derivative of the square error function needs to be calculated with respect to the network's weight. In order to cancel the exponential of 2 when differentiating, 1/2 is required which is used to redefine the square error function.

$$E = 1/2 (p - y)^2 \quad (3)$$

Every neuron j, is defined by the output O_j

$$O_j = Q(net_j) = Q \sum_{k=1}^n W_{kj} X_k \quad (4)$$

The input net_j to a neuron is the weighted sum of outputs O_j of the previous neurons. The number of input neurons is n and the variable W_{ij} denotes the weight between neurons i and j. Table II: The activation function φ is in general non-linear and differentiable, thus, the derivative of the (1) is:

$$\frac{\partial \varphi}{\partial z} = \varphi(1 - \varphi) \quad (5)$$

TABLE II. PATTERN OF THREATS DETECTION

S/N	Attack Group	Different Attacks	Output
1	Denial of service attack	Black, Land, neptune, smurf, teardrop	1000
2	Remote to local attack	ftp write, guess password, imap, multihop	0100
3	user to root attack	buffer overflow, loadmodule, perl, rootkit	0010
4	Probes	satan, ipsweep, nmap, portsweep	0001

The partial derivative of the error (E) with respect to a weight W_{ij} is done using the chain rule twice as follows:

$$\frac{\partial E}{\partial W_{ij}} = \frac{\partial E}{\partial O_j} \frac{\partial O_j}{\partial net_j} \frac{\partial net_j}{\partial W_{ij}} \quad (6)$$

The last term on the left hand side can be calculated from (4), thus:

$$\frac{\partial net_j}{\partial W_{ij}} = \frac{\partial}{\partial W_{ij}} (\sum_{k=1}^n W_{kj} X_k) = X_k \quad (7)$$

The derivative of the output of neuron j with respect to its input is the partial derivative of the activation function (logistic function) shown in (5).

$$\frac{\partial O_j}{\partial net_j} = \frac{\partial}{\partial net_j} \varphi(net_j) = \varphi(net_j)(1 - \varphi(net_j)) \quad (8)$$

The first term is evaluated by differentiating the error function in (3) with respect to y, so if y is in the outer layer such that $y = O_j$, then:

$$\frac{\partial E}{\partial O_j} = \frac{\partial E}{\partial y} = \frac{\partial}{\partial y} \frac{1}{2} (p - y)^2 = y - p \quad (9)$$

Considering E as a function of the inputs of all neurons, receiving input from neuron j and taking the total derivative with respect to a recursive expression for the derivative is obtained:

$$\frac{\partial E}{\partial O_j} = \sum_{i \in L} (\frac{\partial E}{\partial net_i} \frac{\partial net_i}{\partial O_j}) = \sum_{i \in L} (\frac{\partial net_i}{\partial O_j} \frac{\partial O_i}{\partial net_i} W_{ij}) \quad (10)$$

Thus, the derivative with respect to O_j can be calculated if all the derivatives with respect to the outputs O_j of the next layer – the one closer to the output neuron – are known. Putting them all together:

$$\frac{\partial E}{\partial W_{ij}} = \delta_j X_i \quad (11)$$

With:

$$\delta_j = \frac{\partial E}{\partial O_j} \frac{\partial O_j}{\partial net_j} = \left\{ \sum_{i \in L} (O_j - P_j) \varphi(net_j) (1 - \varphi(net_j)) \text{ if } j \text{ is an output neuron} \right.$$

$$\left. \delta_j W_{ij} (net_j) (1 - (net_j)) \text{ if } j \text{ is an inner neuron} \right.$$

Therefore, in order to update the weight W_{ij} using gradient descent, one must choose a learning rate α . The product of the learning rate and the gradient is equal to change in weight added to the old weight.

$$\Delta W_{ij} = \alpha \frac{\partial E}{\partial W_{ij}} \quad (12)$$

Equation (12) is used by the back-propagation algorithm to adjust the value of the synaptic weights attached to the inputs at each neuron in (1) with respect to the inner layer of the multi-layer perceptron. Table II depicts the pattern of threat detection.

D. Event Handler Flowchart

The event handler flowchart in Fig. 2 shows how events are being treated on a computer network with respect to the proposed model and the data used for this research. The output of the data used for this research work are grouped into five categories. The categories include Probe, Denial of Service (DOS), Root to Local (R2L), User to Root (U2R) and Normal. At the third stage of the event handler, the event is being cross-checked whether it belongs to the classes of Root to Local, if it does, it is then disseminated to the network administrator but if the event does fall under root to local, it then moves to the fourth stage. At this stage, it is also being ascertained whether the event belongs to User to Root, if it does, the information is passed to the network administrator and if it is not under User to Root, then it is a normal event.

E. Performance Evaluation

The proposed model was evaluated using the following metrics:

1) *Sensitivity*: Talks about event that are truly positive and are been announced as positive.

$$Sensitivity = \frac{TP}{TP + FN} \tag{13}$$

2) *Precision*: Describe events that are negative and are been announced as negative event.

$$Precision = \frac{TP}{TP + FP} \tag{14}$$

3) *Accuracy*: describes the general effectiveness of the proposed model.

$$Accuracy = \frac{TP + TN}{TP + FP + FN + TN} \tag{15}$$

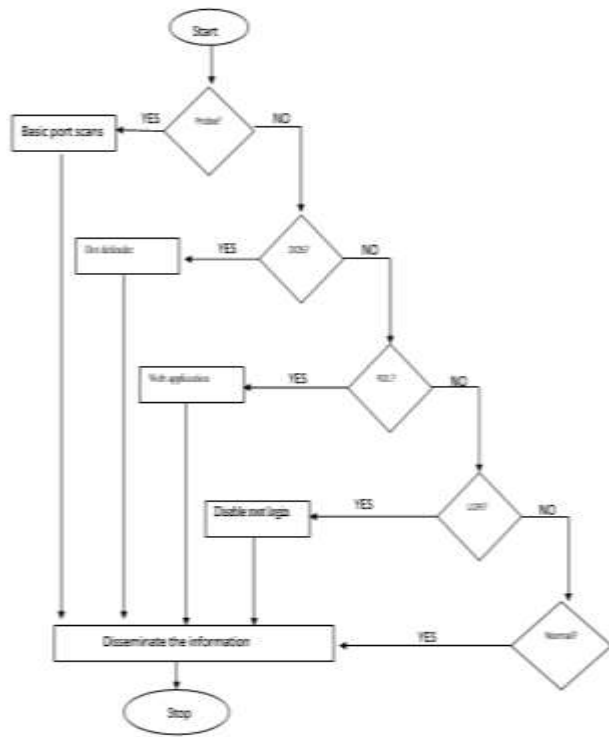


Fig. 2. Event Handler Flowchart.

F. Experimental Setup

In this research work, WEKA simulating tool was used in simulating the proposed model. Two supervised machines were selected and hybridized from the environment. The dataset used was also preprocessed in the excel environment and was then saved in CSV format. For our simulating tool to recognize the dataset, it must be saved in arff format which was done so that the dataset can be recognized. During the experiment process, the dataset was trained and tested. 10-fold cross validation was selected during the process. With the 10-fold cross validation, the dataset was divided into ten different samples where nine out the partitioned dataset was used for training and the testing was done with the remaining one. In a

nutshell, the forty-one features given in the NSL KDD dataset was used during the model training.

IV. RESULT AND DISCUSSION

After the simulation of the models, the two machine algorithms used gave different results for different detection rates. The results show the effectiveness of an ensemble classifier over a single classifier. Decision tree classifier gave 58,119 correctly classified instances where the True Positive (TP) is 32052 and the True Negative (TN) is 26067. The incorrectly classified instances are 1,158 instances where the False Positive (FP) derived is 579 instances and the False Negative (FN) is 579 instances. The artificial neural network-based decision tree gave 58,505 correctly classified instances where the TP is 32052 instances, TN is 26453 instances and 772 were incorrectly classified where the FP is 193 instances and FN 579 instances. Fig. 3 depicts the graph that compares the performance of the two algorithms. Since the strength of both machines are different, and both can detect threats of different kinds, (that is) the group of threats both algorithms can detect varies. Table III depicts the experimental results. It was of great advantage combining the two machines for detection.

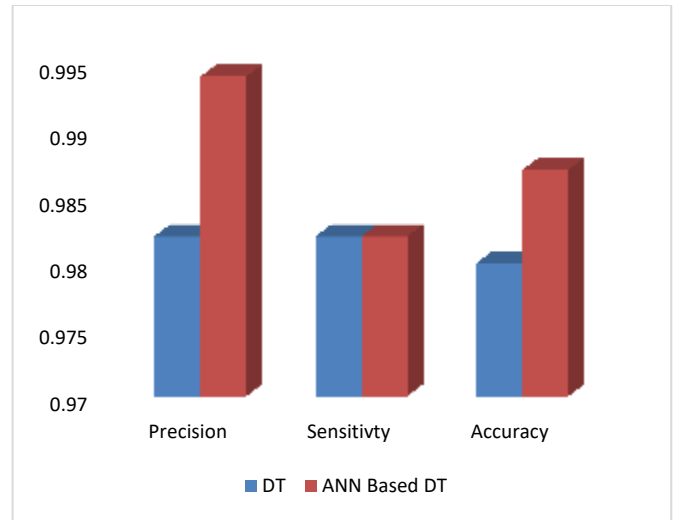


Fig. 3. Performance Compared of the Two Algorithms.

TABLE III. EXPERIMENTAL RESULTS AFTER SIMULATION

Classifiers	No of instances	TP	FP	TN	FN	Precision	Sensitivity	Accuracy
Decision Tree (DT)	59,277	32052	579	26067	579	0.982	0.982	0.980
ANN based DT	59,277	32052	193	26453	579	0.994	0.982	0.987

V. CONCLUSION

The effectiveness and efficiency of a machine learning based intrusion detection system for threats detection to companies and other networks users is of great value. Cyber threats range from one category to another categories, because

of this fact, some machine learning may not be able to detect some of these threats on a computer network. The study proposed a robust cyber situation awareness model which combines the artificial neural network and decision tree as a detector which provided an improved prediction of intrusion on a computer network and enhances cyber security. After the design and simulation of a prediction model for threats detection, the hybridization of the two algorithms in the perception phase suggests a more secured system than a single classifier. Overall, the two classifiers used which are IDS based are data oriented which helps to detect the various patterns in the NSL-datasets. The ANN base decision tree gave a better accuracy of 98.7% than the decision tree classifier. The difference between the results of the proposed algorithm and decision tree may look insignificant but cannot be overlooked. The network administrator will definitely find this system useful for adequate awareness on a computer network. Future work will focus on how to still improve the accuracy of IDS by introducing more than two ensemble algorithms in the perception phase.

REFERENCES

- [1] H.I. Sarker, A.S.M. Kayes, S. Badsha, H. Alqahtani, P. Waters, and N. Alex "Cybersecurity data science: an overview from machine learning perspective" *Journal of Big data*, (2020).
- [2] S. Mohammadi, H. Mirvaziri, M. Ghazizadeh-Ahsae, H. Karimipour, "Cyber intrusion detection by combined feature selection algorithm," *Journal of Information Security Application*, vol. 44, pp. 80–88 (2019).
- [3] Y. Xin, L. Kong, Z. Liu, Y. Chen, Y. Li, H. Zhu, M. Gao, H. HOU and C. Wang "Machine learning and deep learning methods for cybersecurity," *IEEE Access* 6, 35365–35381 (2018).
- [4] I.H. Sarker, Y.B. Abushark, F. Alsolami, I. Khan "Intrudtree: a machine learning-based cyber security intrusion detection model," *Symmetry* 12, 754 (2020).
- [5] B. Gupta, A. Tewari, A. Jain, and D. Agrawal, "Fighting against phishing attacks: state of the art and future challenges," *Neural Computation Application*. 28(12):3629–54, 2017.
- [6] X. Qu, L. Yang, K. Guo, L. Ma, M. Sun, M. Ke and M. Li, "A Survey on the Development of Self-Organizing Maps for Unsupervised Intrusion Detection" *Mobile Network and Application*. 10.1007/s11036-019-01353-0, 2019.
- [7] Z. Hao, Y. Feng, H. Koide, K. Sakurai "A sequential detection method for intrusion detection system based on artificial neural networks" *International Journal of Networking and Computing*, Vol. 10, Number 2, pp. 213–226, July 2020.
- [8] M. Endsley, "Toward a theory of situation awareness in dynamic systems" *In Human Factors Journal*, volume 37(1), pages 32–64, 1995.
- [9] S. S. Olofintuyi, T. O. Omotehinwa, O. H. Odukoya and E. A. Olajubu "Performance comparison of threat classification models for cyber-situation awareness," *Proceedings of the OAU Faculty of Technology Conference*, 2019.
- [10] G.Stein, B. Chen, A. Wu and K. Hau "Decision tree classifier for network intrusion detection with ga-based feature selection," *Proceedings of the 43rd annual Southeast regional conference. ACM*, 2, 2005.
- [11] E.A. Shams and A.A Rizaner "Novel support vector machine based intrusion detection system for mobile ad hoc networks," *Wireless Networks*, 2018.
- [12] W.C. Lin and S.W. Ke "An intrusion detection system based on combining cluster centers and nearest neighbors," *Knowledge-based systems*, 2015.
- [13] S. Hettich, and S.D. Bay, (1999). The UCI KDD Archive. Irvine, CA: University of California, Department of Information and Computer Science.
- [14] J. Han, J. Pei and M. Kamber, "Data mining: concepts and techniques," Elsevier, Amsterdam, 2011.
- [15] F. Ullah, H. Naeem, S. Jabbar, S. Khalid, M. Latif, F. AL-Turjman, and L. Mostarda, "Cyber security threats detection in internet of things using deep learning approach," *IEEE Access*. PP.1-10, 2019.
- [16] X. Fang, M. Xu, S. Xu and Z. peng, "A deep learning framework for predicting cyber-attacks rates," *EURASIP Journal on Information security* 2019.
- [17] M. S. Mehibs, and H. S. Hashim, "Proposed Network Intrusion Detection System In Cloud Environment Based on Back Propagation Neural Network," *Journal of Babylon University, Pure and Applied Sciences*, 26(1), 29-40, 2018.
- [18] M. A. Muslim, A. Nurzahputra, and B. Prasetyo, "Improving accuracy of C4.5 algorithm using split feature reduction model and bagging ensemble for credit card risk prediction," in *IEEE International Conference on ICT (ICOIACT)*, 2018, pp. 141–145, 2018.
- [19] A. Chaudhary, V. N. Tiwari and A. Kumar, "Design an anomaly based fuzzy intrusion detection system for packet dropping attack in mobile ad hoc networks," *IEEE International Conference on Advance Computing (IACC)*, pp. 256-261, 2016.
- [20] P. Sarathi "A Study on Fuzzy Rules for Intrusion Detection" *International Journal of Research Studies in Computer Science and Engineering (IJRSCSE)* Vol 2, Issue 8, pp 1-9, August 2015.
- [21] Rupesh and Balasaheb, "Real Time Intrusion Detection With Fuzzy, Genetic and Apriori Algorithm," *International Journal of Advance Foundation and Research in Computer (IJAFRC)* Vol 1, Issue 11, ISSN 2348 – 4853, 2014.
- [22] P. Kola, C. Suba and A. Kanna, "Network intrusion detection system using genetic network programming with support vector machine," in *Proceeding of the International Conference on Advances in Computing, Communication and Informatics*. Pp. 645-649. Chennai, India, August 3, 2012.
- [23] Z. Hao, Y.Feng, H.Koide and K. Sakurai, "A sequential detection method for intrusion detection system based on artificial neural networks. *International Journal of Networking and Computing*, ISSN 2185-2847 Vol 10, Number 2, pp 213–226, July 2020.
- [24] Wu C Phetlasy S, Ohzahata S et al. A sequential classifiers combination method to reduce false negative for intrusion detection system. *IEICE Transactions on Information and Systems*, 102(5):888–897, 2019.

Visualization of Arabic Entities in Online Social Media using Machine Learning

Khowla Mohammed Alyamani¹, Abdul Khader Jilani Saudagar²
Information Systems Department, College of Computer and Information Sciences
Imam Mohammad Ibn Saud Islamic University (IMSIU)
Riyadh, Saudi Arabia

Abstract—In recent years, the use of social media and the amount of exchangeable data have increased considerably. The increase in exchangeable data makes data mining, analysis and visualization of relevant information a challenging task. This research work assesses, categorizes, and analyzes Arabic entities on social media selected by users at certain time intervals. To accomplish this aim, the authors built a highly efficient classification model to classify entities according to three categories: person, location, and organization. The developed model captures an entity and specific time, collects all the posts on twitter that refer to the entity at this specific time, and then classifies, visualize the entity through three methods. It first starts with classifying the entity through a corpus model that depends on customized corpus. If the entity is not classified through that model, it will be send to an indicators model which uses the pre-indicators or post-indicators for classing. Finally, the entity is passed to a gazetteer model which searches for the entity in three gazetteers (person, location, and organization), and accordingly determines the number of times the entity reference is repeated. This work allows scholars and researchers in different fields to visualize the frequency of entities referenced by a community. It also compares how references to entities change over time. The experimental results show that accuracy of the developed model in classifying the tweets is nearly 90%.

Keywords—Machine learning; classification; visualization; Arabic entities; social media

I. INTRODUCTION

People use social media platforms such as Twitter, Instagram, Snapchat, and Facebook to share details about their daily activities, review products, share comments with their online and offline friends, discuss events, and advertise products. Social media has caused many changes: it has generated new business opportunities, changed advertising methods, provided opportunities to earn a living online, made it possible to make virtual friends, and has changed how news spreads. Web 2.0 allows Internet users to communicate and share information 24/7, with one of its most important facets being social media. Social media platforms include forum, micro blogging, social bookmarking, social administration, and wiki applications and websites. Twitter, started in March 2006 and is considered as one of the well-known social media platforms. It provides services of online news and social networking to its users, with users posting and interacting through messages known as tweets. One tweet is limited to 280 characters, and users can include tags, or hash tags, to

label or categorize their messages according to contextually appropriate tags for every named entity in a text.

When it comes to social media on Arabic platforms using Arabic language which contains more than 12 million words, is one of the most widely spoken languages in the world, with more than 450 million people speaking Arabic as a native language. Moreover, 60 countries use Arabic as the official language or second language, and more than 60 Arabic dialects exist in the Arab countries.

Researchers in the past have identified three types of Arabic language [8, 12, 16]:

1) *Classical Arabic (CA)* is the formal version that has been used incessantly for more than 1,500 years. It is the language of the Holy Quran and most Arabic religious books.

2) *Modern Standard Arabic (MSA)* is the Arabic language of magazines, and education. MSA mirrors the needs of contemporary expression, and CA reflects the needs of older styles. Most Arabic name entity recognition (ANER) systems support MSA.

3) *Colloquial Arabic* dialects are the language used by Arabs in their informal everyday communications, and dialects differ from one region to another.

One of the many challenges in Arabic name entity tagging stems from the prevalence of homographs. For example, اشرف means Ashraf (name) or he supervised (verb). Some homographs have different meanings depending on their vowelization, which refers to the practice of supplying the vowels in a word, that usually are not written. For example, عقد can mean different meaning under the vowelization as shown in Table I.

TABLE I. EXAMPLE OF A DIACRITICIZED ARABIC WORD REPRESENTING 5 VOWELIZATION

Word in Arabic	Transliteration	Meaning
عقد	Egad	Necklace
عقد	Agad	Contract
عقد	Eaqad	Decade
عقد	Oqead	Convention
عقد	Oqad	Knot

One Arabic word may contain one or more prefixes and one or more suffixes in different combinations. For example, “و” means and is pronounced “wa”, “ل” means for and is pronounced “le”. Sometimes و or ل or both are added at the beginning of the word, while “ه”, pronounced as “ha”, is added to the end of the word, for example, و لكتابه (wa le ktabieh) means and for his book. Another problem is that a non-Arabic word can be written in Arabic in many different ways, for example, the word Google can be written in three different ways, as “قولل ووجل ووجل”. Additionally, Arabic letters can be written using different shapes according to their position in the word, for example, the letter alif has four forms, namely ا, آ, إ, and ؤ. Finally, because users typically informally write messages and posts, data scantiness is prevalent on social media [15].

Arabic entity recognition systems still face problems, including a lack of knowledge related to analyzing data, especially data written in colloquial Arabic dialects. Consequently, users are suffering in analyzing references to entities over a selected time interval due to lack of developed systems. Displaying the frequency of references to a particular entity in a selected period demonstrates society's interest in a special event and confirms how that interest changes over time. Besides, showing the frequency of an entity is repeated in different categories (person's name, company, and location) is important, especially for developers and researchers in particular fields such as marketing, advertising, and economics.

The contribution of this research work is to develop a solution to deal with text written in classical Arabic, modern standard Arabic, and colloquial Arabic dialects by classifying the entities referenced into categories, mainly person's name, location, and organization. This research work also helps to understand the use of a machine learning approach in building a system for recognizing entities referenced in Arabic on social media, especially on Twitter, which follows different writing rules than those used in news or formal texts. Furthermore, this work has significant importance in visualizing the frequency of references to entities in a given time, as it is important for researchers in different fields to understand how society's interest in some subjects can change over time.

This paper is organized into five sections. Section 2 provides an overview of several previous systems related to the current study and recent advances in ANER. Section 3 explains how the system used in the current study was built and how it works, while Section 4 contains the results of the research and a discussion of these results. Finally, Section 5 presents the conclusion and a discussion of possible future work.

II. LITERATURE REVIEW

ANER researchers have been developing systems that depend on two approaches: the rule-based approach and the machine learning (ML) approach. Rule-based systems depend on linguistic rules for recognizing named entities (NEs). The advantage of using a rule-based approach for design NER systems is that approach depends on the core of linguistic

knowledge. Additionally, the ruled-based approach is not portable.

Due to these problems, researchers turned their attention to machine learning-based approaches, which involve learning NE tagging decisions from annotated texts. Machine learning-based approaches can be classified into three categories: supervised, unsupervised and semi-supervised. Supervised methods employ tagged corpus to learn the model [4]. Here, sets of features are extracted for each word. The tags of words act as supervisors to tune the model parameters. Unsupervised methods can perform NER in the absence of labeled data. They try to learn representations from the data. Furthermore, the most common approach used in ML for NER is supervised learning (SL). Support vector machines (SVM) and conditional random fields have identified as the most suitable techniques for ANER descend by using the ML approach.

Hybrid technologies use a combination of rule-based and machine learning-based algorithms [2, 6]. The empirical results indicate that the hybrid approach outperforms both the rule-based and the ML-based approaches when they are processed independently because it combines two technologies.

A. Name Entity Recognition Systems

The NERA system developed in [23, 24] generalizes the findings from the Person Name Entity Recognition for Arabic (PERA) system. NERA addresses major challenges posed by NER in the Arabic language. With an architecture optimized for rule-based systems, the NERA system has three components—gazetteers, local grammar in the form of regular expressions, and a filtering mechanism—that uses indicators to formulate recognition rules to solve the lack of capitalization for proper nouns in their system. The researchers built their corpora due to the unavailability of free Arabic corpora for research purposes. Moreover, commercially available Arabic corpora are oriented toward the newswire domain, so the researchers found unequal coverage of the types of named entities involved in their research.

A hybrid approach [22] using decision trees supported by support vector machines and logistic regression classifiers for an ANER system to evaluate the system performance was developed to recognize eleven types of Arabic named entities: person, location, organization, date, time, price, measurement, percent, phone number, ISBN, and file name. Moreover, the authors in [18] developed NERA 2.0 to enhance the coverage and performance of the rule-based NER system. They present a novel methodology for improving the rule-based component (NERA), using gazetteers and Arabic linguistics rules, and also using indicators or keywords for NEs, which assist the detection process via the linguistic rules. The mechanism uses the recognition decisions made by the hybrid NER system to identify the weaknesses of the rule-based component and derive new linguistic rules aiming to enhance the rule base, which helps to achieve more reliable and accurate results.

Furthermore, authors in [25] presented an Arabic information extraction (IE) system used to analyze large volumes of news text every day to extract several NE types: person, organization, location, date, number, and quotations

by and about individuals. Similarly, in [11] the authors developed RenA, an NER for the Arabic language. RenA extracts entities from news articles collected from online resources, and a chunker tokenizes the text based on whitespace. The authors in [3] proposed a rule-based NER system that can be used in Web applications. The system was evaluated using ANERcorp. The researchers conducted two experiments to study the effect of Arabic prefixes and suffixes on the recognition results. The verification process improved the recognition results of NERs across all types, although these improvements were not symmetrical.

Alanazi et al in [4] used features such as corpus, gazetteers, and part-of-speech (POS) tags of words to develop an ANER system for text in the medical domain. The authors in [1] presented an integrated approach between two machine learning techniques, semi-supervised pattern recognition and conditional random fields (CRF) classifier as a supervised technique. Gazetteers and different types of indicators are used for classification. The authors developed an integrated semantic-based ML model [6] for enhancing ANER. The authors' idea was to combine several linguistic features and to use syntactic dependencies to infer semantic relationships between named entities. Accordingly, the model combines internal features that represent linguistic features such as part of speech, gazetteer, indicators, and corpus and external features that represent the semantics of relationships between the three named entities, such as classes, instance, and relations, to enhance the accuracy of recognizing them using external knowledge sources, such as Arabic WordNet (AWN) ontology. They introduced internal and external features to the CRF classifier, which is an effective strategy for ANER [7]. Zayed and El-Beltagy in 2015 [26] focused on the task of Arabic person names recognition. Their model is a combination of rule-based and statistical models, and it uses the unsupervised learning of patterns and clustered dictionaries as constraints to identify a person's name and resolve its ambiguity.

In [10] the author aimed to build a tool for POS tagging and NER using a rule-based technique. The POS tagger contains two phases. In the first phase, words are pasted into a lexicon analyzer and in the second phase morphological information is used to presume the class of the word. The named-entity detector applies the rules to the text and assigns the correct label (tag) for each word. The authors in [2] built a Malayalam NER classifier and in [17] for Vietnamese by using a neural network. Liu and et al. in [14] provided a semi-supervised learning framework to recognize entities in English tweets by combining a linear conditional random fields (CRF) model and K-nearest neighbors (KNN) classifier. Likewise, Patawar and Potey in [19] implemented a semi-supervised algorithm, also by combining the CRF approach with the KNN classifier, to build a NER system for Indian tweets. Finally, in [9] the authors presented TwitterNEED, a hybrid approach for named entity extraction and named entity disambiguation for English tweets.

Researchers have been developing ANER systems [21] based on one of three approaches: the ML, rule-based, and hybrid approaches. The ML approach uses three technologies for classification: supervised, unsupervised, and semi-

supervised. Moreover, common resources on which researchers can draw to build their classifiers and recognition systems include corpus (customized or off-the-shelf), gazetteers, indicators, decision tree, logistic regression, POS tags, and Arabic linguistics.

To the best of author's knowledge, no Arabic entity recognitions systems exist for use with colloquial Arabic dialects. Although some studies have involved Twitter content, but, they did not support Arabic content, thus they cannot be used for the Arabic language because the Arabic language follows different and specific rules, also some work use twitter content but not classify to different classes.

Furthermore, the systems examined do not allow users to search for information about specific entities during selected periods. Consequently, the current study aimed to build an ANER system to fill that gap. The system could be used for Arabic tweets, and it could provide users with the flexibility to search for information about an entity during a specific through tweets.

III. RESEARCH METHODOLOGY

The main goal of the research was to classify and visualize entities frequently referred to on Twitter over a given time. To achieve the research objectives, machine-learning techniques were used to build a system able to visualize Arabic social media content, focusing on Twitter. The system process involves four steps: identifying the entities and time periods, preprocessing or preparing the data, building the classifier model, and performing data visualization of frequency and classification. The steps are discussed in detail below. Fig. 1 shows the system flow chart.

Step 1: Data Collection: The first step was to clarify the difference between "entity" and "named entity" [5]. "Entity" is defined as something that exists by itself, such as locations, humans, or animals. When an entity is given a name, it becomes a "named entity". As an example, Al Riyadh city would be a named entity. In this research, an entity refers to any Arabic word, including adjectives, verbs, and nouns.

The user, in this case the researcher, sets the data collection parameters, the entity reference in Arabic script, and the time and date in a valid format ("DD/MM/YYYY"). The system then retrieves tweets written during the selected time containing a reference to the entity. Subsequently, the system sends the retrieved tweets to pre-processing before saving them to a file.

The code used for retrieving tweets from Twitter by date and/or keyword(s) was originally written by Simon Lindgren. The researcher edited the code to make it suitable for Arabic tweets.

Step 2: Preprocessing: The data (tweets that contain a reference to the given entity posted during the given time) undergo a cleaning process to remove the redundant spaces between words and all symbols such as +, @, \$, and #, punctuation, numbers, non-Arabic letters, and links. White space characters are used to define the words in the text.

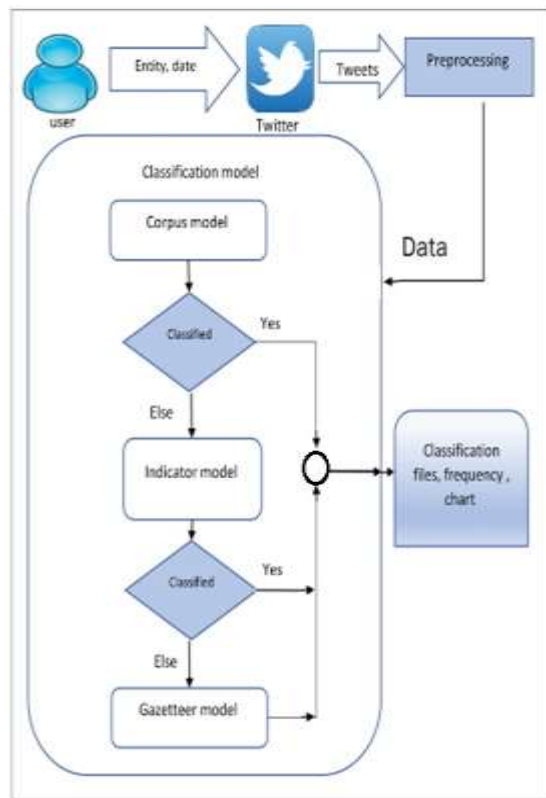


Fig. 1. System Flow Chart.

Step 3: Building the Classifier: Machine learning involves two steps [27, 28]: training, during which the classifier model is built, and testing, during which the classifier model is tested. As in previous works, this classifier does not depend on one feature; it is dependent upon four features and uses both internal and external features to build the model. Internal features include corpus, indicators, and gazetteers. The corpus is an annotated linguistic resource that shows the Arabic grammar, syntax, and morphology for each word. In this model, the corpus was used to show the POS tag for the entity. Indicators are a set of words used to recognize names (NEs). They include preceding indicators (e.g., Mr. "السيد") and post-indicators word (e.g., almotahedah "المتحدة"). Gazetteers can be defined as a list of names of locations, organizations, people, and so forth.

External features were extracted using ontology: "a formal naming" and definition of the types, properties, and interrelationships of the entities that exist for a particular domain of discourse. In this case, the classifier follows three steps to classify the entities: classification based on the corpus model, a model classified by indicators, and using gazetteers.

The works in [1, 3, 4, 23, 24] using a corpus to classifying and recognize in their works. Corpus is a strong method that gives reliable results. It depends on manual tagging by the developer and on context similarity; however, it cannot classify all possible entities because it can only classify the entities found on the corpus vocabulary list. This restriction led to the use of other classification methods. One such method was searching for indicators. Using indicators [1, 6] enhances the accuracy of NER. In the case of failure to

classify through use of indicators, the classification model will refer to gazetteer lists. Many researchers [1, 4, 6, 18] use gazetteers to improve their works.

Ontology is known as a digital repository or a large database that finds connections based on an understanding of the meanings and relationships. Ontology has five components: entity or vocabulary, classes, properties that have attributes for each class, relationships (characterized by their descriptions, names, connotations), and language axioms (including clear rules that restrict the use of concepts, and include confirmed and previously known data). This ordering comes from using ontology rules, which detract from the corpus and indicators methods and depend on linguistic grammar for classification. A description of the three steps follows.

a) *Corpus model*: In the current research, the researcher rebuilt the corpus and made changes to adapt the model to the Arabic language. The first step in this process was building a customized corpus for the classifier, which required that the sentences contain both the entity reference and its POS tag, separated by a forward slash (/). The corpus encompasses samples from tweets during different periods—approximately 250 tweets and more than 2,000 entity references classified as person, location, organization, or non. These entity references could mean a person's name or a location, for example, شام, or Sham. Sham could be a person's name or the geographical area that includes Syria, Lebanon, Palestine, and Jordan. Another example is Hend, which can be a person's name or the Arabic name of India. Additionally, the corpus includes entity references with different purposes, such as Mesk, which could be a person's name or Mesk International Company. Some entity references could refer to all three categories. For example, Najd could be a person's name, a location (Najd Plateau), or the name of a firm. Using these types of entity names allows the system to check the accuracy of classifications.

Using a customized corpus that depends on tweets yields more accurate results than using a corpus that depends on news content, as tweets are written in colloquial Arabic dialects that are used more commonly than formal Arabic [13, 20] found in a study involving the Turkish language that accuracy dropped from 91% to 19% when using NER from news rather than tweets.

The corpus method uses the KNN algorithm for classification. The KNN algorithm is a supervised learning approach; the model contains both entity names and POS tags and based on the similarity approach feature, uses context similarity. In this case $K = 3$. In the corpus for each entity referring to one class, there were about three or four sentences.

Consequently, the model first separates the sentence into smaller parts, with each small part containing an entity reference and its POS tags. It assigns each entity an ID with a normal random number and an ID for POS tags where each node contains the entity reference and the three preceding words. If fewer than three entities are involved, the entity value = unknown word, word ID = 0, POS tag = unknown tag, and POS ID = 0.

The classifications are applied only to entities that are listed in the corpus and that have IDs and POS tags. If an unannotated word appears, the model drops the whole sentence.

For example, in corpus:

جميل/per/الذيبي/per/الفارق/non/بين/non/التخاذل/non/و/non
مقالات/org/عكاظ/non/المواجهة

POS ID = [22 22 7 7 7 7 7 5 7]

جميل الذيبي الفارق بين التخاذل والمواجهة عكاظ مقالات

['جميل']

Word ID =12

[جميل, unknown word, unknown word, unknown word]

Tag = [per, unknown pos, unknown pos, unknown pos]

POS ID = [22,0,0,0]

POS tag=['per']

Node = [(12,22), (0,0), (0,0), (0,0)]

['جميل', 'الذيبي']

Word ID (691 = (الذيبي)

[جميل, الذيبي, unknown word, unknown word]

Tag = [person, person, unknown pos, unknown pos]

POS ID = [22,22,0,0]

POS tag = ['per', 'per']

Node = [(12,22), (691,22), (0,0), (0,0)]

['جميل', 'الذيبي', 'الفارق']

Word ID ('692 = (الفارق)

[جميل, الذيبي, الفارق, unknown word]

Tag = [person, person, non, unknown pos]

POS ID = [22,22,7,0]

POS tag = ['per', 'per', 'non']

Node = [(12,22), (691,22), (692,7), (0,0)]

['جميل', 'الذيبي', 'الفارق', 'بين']

Word ID ('25 = (بين)

[جميل, الذيبي, الفارق, بين]

Tag = [person, person, non, non]

POS ID = [22,22,7,7]

POS tag = ['per', 'per', 'non', 'non']

Node = [(12,22), (691,22), (692,7), (25,7)]

Sending that sentence to the model for classifying entity (عكاظ):

جانب من تجهيزات جناح وزارة التعليم المشارك في الفعاليات واللى يفكر نفسه داخل سوق عكاظ

In corpus model:

[1416,302,41,10] set of word IDs for ['عكاظ', 'سوق', 'داخل', 'نفسه']

[7,7,7,5] set of POS IDs for ['عكاظ', 'سوق', 'داخل', 'نفسه']

Node for entity (10,5), (41,7), (302,7), (1416,7) = (عكاظ)

Classification and KNN chart shown in Fig. 2.

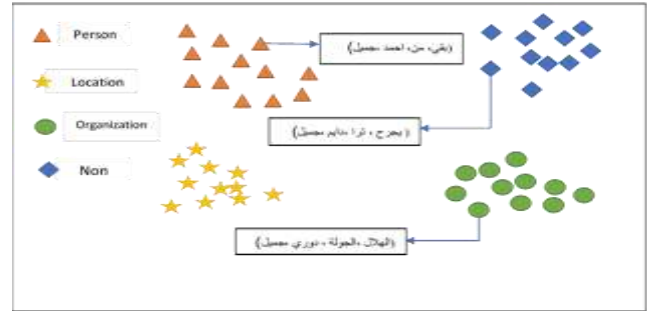


Fig. 2. K Nearest Neighbor Chart for Corpus Model.

b) Indicators model: The second priority for classification is using the indicators model. In this model, a deep neural network was used to classify the entity by using pre- or post-indicators. A neural network "is a series of algorithms that endeavors to recognize underlying relationships in a set of data through a process that mimics the way the human brain operates". Neural networks are powerful tools in the natural language processing of text. The original neural network algorithm used in this research was written by Source Dexter to classify the text into time, age, apology, greeting, or farewell. It was edited to be suited for classifying Arabic entities. This model depends on the unsupervised learning approach for classification. To ensure the reliability of the classification, the tweets that contained entity references were broken down into small parts containing a single entity and the following indicator for each word in the tweet. This approach is known as the n-gram technique. In this case (n = 2). Results were then classified by the order of entities in grams and indicators. The input layer accepts the gram that contains the entity reference, while the hidden layers that contain the indicators and classes classify the sentence. Subsequently, the output layer provides the classification. Fig. 3 shows the layer of the neural network.

Indicators are categorized as pre- and post-indicators for each class: the person, location, and organization classes. Arabic ontology axioms and grammar rules are followed in classifications by using the indicators, specifically by using a bigram, which is a model that looks for the entity and for the previous or next word and the group to which it belongs. It uses only indicators that come directly before or after the word.

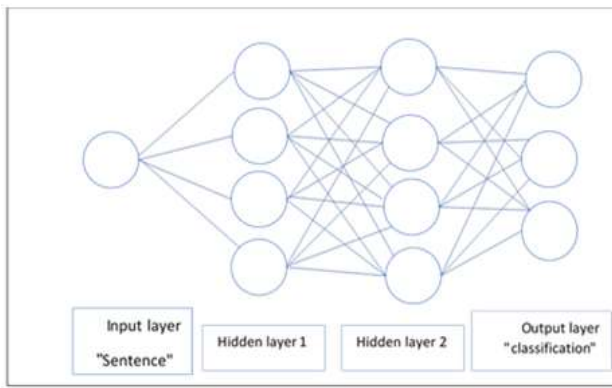


Fig. 3. Neural Network Chart for Indicator Model.

The indicators model attempts to list all possible formal and informal indicators that may contain the following.

- Name title, for example, السيد – mister and باشا – basha
- Job title, for example, الأستاذة – professor
- Relative adjective, for example, المتحدة – united and الأدبي – al Adabi
- Semantic fields, for example, شركة – company
- Interjection articles, for example, يا – oh
- Location indicators, for example, مطار – airport and شارع – street

c) *Gazetteer model*: Liu et al. in [14] and Patawar and Potey in [19] found that using gazetteers significantly improved the accuracy of NER. There are three classes of gazetteers: location, person, and organization. The gazetteers used in the current study include more than 2,000 names of people; more than 2,000 names of locations such as continents, countries, cities, states, political regions, towns, and villages; and approximately 300 names of organizations, including media companies, newspapers, construction firms, banks, insurance companies, airlines, telecommunication companies, and football teams. Entity names that might fall into more than one class were omitted from the gazetteers used in this research to improve the accuracy of the classification. For example, سعيد was omitted because it can be used as a person's name and as the adjective happy, and روما (Roma) was omitted because it is the name of a city and a football team.

The ontology was applied to ordering the gazetteers in the following manner: (1) person's name, (2) location's name, and (3) organization's name. If an entity is identified in one of the gazetteers, it is classified as being in that gazetteer's class.

Step 4: Data Visualization: The human brain tends to process visual information far more easily than written information. Visualization makes the results easier to read and encourage users to explore and even manipulate the data to uncover other factors. This creates a better attitude for use of analytics. Visualization is the act of interpreting visual terms or of putting into visible form.

In this step, the frequency of the entity returns to the user for each class. It displays the results in two ways. One visualizes the results during a given time interval, the other breaks the time intervals down and shows the frequency of each class during these smaller periods. Additionally, the tweets related to classified entities are saved in files depending on their class type and an additional file for tweets that content unclassified entity.

IV. RESULTS AND DISCUSSION

A confusion matrix is a table that describes the performance of a classification model on a set of test data where the true values are known, with rows representing actual classes and columns representing predicted classes.

The accuracy of the model is measured by the overall success rate, calculated using (1).

$$Accuracy = \frac{\text{total correct predicted}}{\text{total sample}} \quad (1)$$

Misclassification, calculated using (2), is the rate of incorrect classifications.

$$Misclassification = 1 - accuracy \quad (2)$$

Precision, a positive predictive value, assesses what percentage of items identified as positive are positive. It can be calculated using (3).

$$precision = \frac{\text{correct entities clasified}}{\text{total entities in acual class}} \quad (3)$$

Recall (sensitivity) is the percentage of relevant instances that have been retrieved correctly from the total number of relevant instances, calculated as follows (4).

$$Recall = \frac{\text{correct entities recognized}}{\text{total entties predeicted in same class}} \quad (4)$$

The researcher used entity references that could refer to a name or a location, that could be the name of a person or an organization, and that could not be classified as any of the three classes (non) and randomly selected tweets posted at different times. Each individual model was measured before combining them.

A. Testing Models

a) *Corpus model*: The researchers used the entity Jamil to test the corpus model.

Entity 1: جميل – Jamil

Jamil can be the name of a person or an organization, or it can mean beautiful. Eighty-four tweets posted between 27/11/2014 and 30/11/2014 that contains a reference to “جميل” was randomly selected. The researcher measured the performance of the algorithm—specifically accuracy, recall, and precision—using the confusion matrix shown in Table II. Fig. 4 shows the frequency of each class in the whole period, while Fig. 5 shows the visualization of classification day by day.

Accuracy = 0.61

Misclassification = 0.39

Recall (organization) = 0.42

Recall (person) = 0.60

Recall (non) = 0.90

Precision (organization) = 0.87

Precision (person) = 0.60

Precision (non) = 0.50

TABLE II. CONFUSION MATRIX FOR JAMIL ENTITY USING THE CORPUS MODEL

N=84	Predicted: Organization	Predicted: Person	Predicted: Non	Total
Actual: organization	20	0	3	23
Actual: person	2	3	0	5
Actual: non	26	2	28	56
	48	5	31	

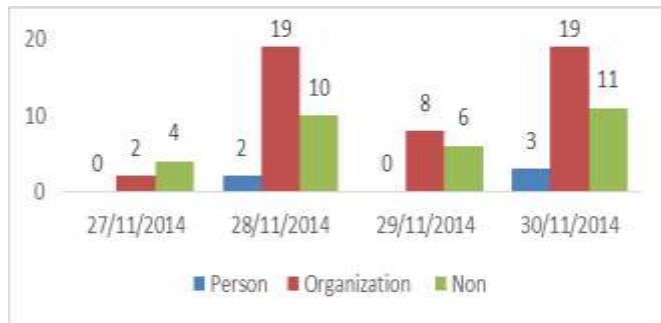


Fig. 4. Visualization of Classification of Jamil Entity Day by Day, using a Corpus Model.

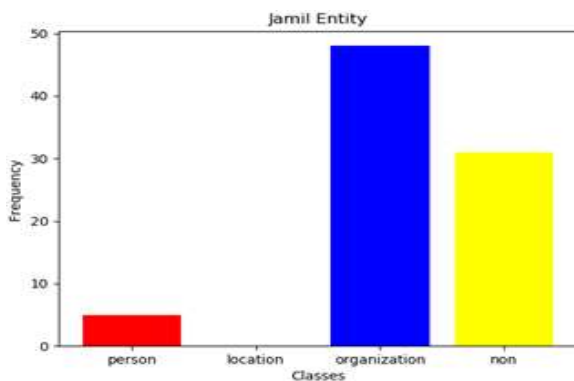


Fig. 5. Visualization of Classification of Jamil Entity as a Whole, Corpus Model.

b) Indicator model: In this model, different indicators were used in one testing sample measure. Some of the tweets contained more than one indicator.

Entity 1: خالد – Khalid.

The Khalid entity can be used with different indicators and classifying in different classes, for example, السيد خالد – Mr. Khalid, دكتور خالد – Dr. Khalid, مطار خالد – Khalid Airport, شارع خالد – Khalid Street, or may mean immortal. Ninety -nine tweets that contain the Khalid entity were used to testing the indicator model, with some tweets containing more than one

indicator, posted between 15/06/2016 and 19/06/2016. Table III shows the confusion matrix for this entity. Fig. 6 is visualized the frequency of each class, while Fig. 7 is the visualization day by day of the prediction classes for the testing sample.

TABLE III. CONFUSION MATRIX FOR KHALID ENTITY USING THE AN INDICATOR MODEL

N=99	Predicted : person	Predicted: location	Predicted: organization	Predicted: non	Total
Actual: person	69	1	0	0	70
Actual: location	12	16	0	0	28
Actual: organization	1	0	0	0	1
Actual: non	0	0	0	0	0
Total	82	17	0	0	

Accuracy = 0.80

Misclassification = 0.20

Recall (person) = 0.77

Recall (location) = 0.94

Recall (organization) = 0

Precision (person) = 0.90

Precision (location) = 0.47

Precision (organization) = 0

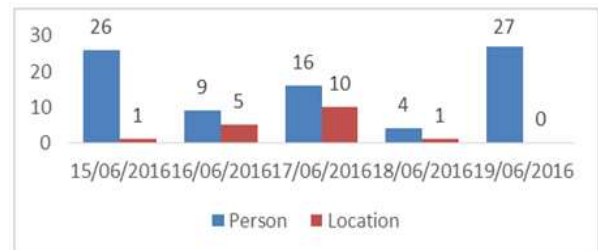


Fig. 6. Visualization of Classification of Khalid Entity Day by Day using Indicator Model.

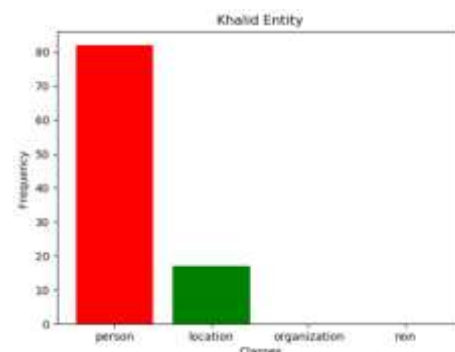


Fig. 7. Visualization of Classification of Khalid Entity as a Whole using an Indicator Model.

c) *Gazetteer model*: For testing the gazetteer model, the researcher chose entities with ambiguous meanings. For the name of an organization, **فورد** – Ford was chosen; for location, **كندا** – Canada; and for a person, **العيسى** – Al Easa was chosen.

Entity 1: **فورد** – Ford.

The researcher selected 57 tweets posted between 12/09/2014 and 16/09/2014 as a testing sample. The Ford entity can be a person or an organization, but the term is most often used in Arabic to refer to the Ford Company.

Table IV shows the confusion matrix for testing this sample. Fig. 8 visualizes the frequency of each class, while Fig. 9 is the daily visualization of the prediction classes for the testing sample.

Accuracy = 0.84

Misclassification = 0.16

Recall (organization) = 0.84

Precision (organization) = 1

TABLE IV. CONFUSION MATRIX FOR FORD ENTITY USING THE GAZETTEER MODEL

N=57	Predicted : person	Predicted: location	Predicted: organization	Predicted: non	Total
Actual: person	0	0	9	0	9
Actual: location	0	0	0	0	0
Actual: organization	0	0	48	0	48
Actual: non	0	0	0	0	0
Total	0	0	57	0	



Fig. 8. Visualization of Classification of Ford Entity Day by Day using a Gazetteer Model.

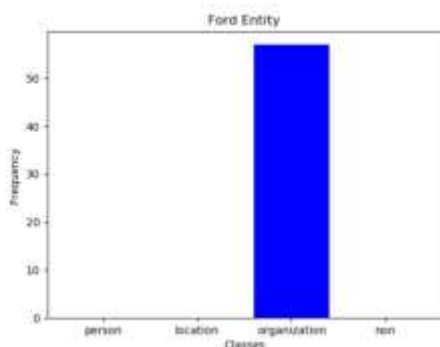


Fig. 9. Visualization of Classification of Ford Entity as a Whole using a Gazetteer Model.

B. Testing the Whole System

The same samples tested using individual models were retested using the proposed system. The tweets that remained unclassified after testing with the corpus model were tested using the indicator model. Those that still remained unclassified were then tested using the gazetteer model. Any tweets that remained unclassified after this were classified as non.

Entity 1: **جميل** – Jamil

The confusion matrix for the test conducted on this entity using the proposed system appears in Table V, with the confusion matrix measuring accuracy, recall, and precision.

Using the corpus method, the researcher classified 34 entities, the remaining 61 tweets being sent to the indicator method. One entity was classified as an organization through the indicator method, and the rest sent to the gazetteer method, where they were classified as non. Fig. 10, Fig. 11, and Fig. 12 visualize the results from each step, while Fig. 13 visualizes a daily classification, and Fig. 14 visualizes the frequency for each class as a whole.

Accuracy = 0.93

Misclassification = 0.07

Recall (organization) = 0.95

Recall (person) = 1

Recall (non) = 0.92

Precision (organization) = 0.87

Precision (person) = 0.60

Precision (non) = 0.98

TABLE V. CONFUSION MATRIX FOR JAMIL ENTITY USING THE WHOLE SYSTEM

N=84	Predicted: organization	Predicted: person	Predicted: non	Total
Actual: organization	20	0	3	23
Actual: person	0	3	2	5
Actual: non	1	0	55	56
Total	21	3	60	



Fig. 10. Visualization of Results from First Step in Testing Jamil Entity through the whole Model.



Fig. 11. Visualization of Results from Second Step in Testing Jamil Entity through the Whole Model.



Fig. 12. Visualization of Results from Third set in Testing Jamil entity through the whole Model.



Fig. 13. Visualization of Classification for Jamil Entity Day by Day using the whole System.

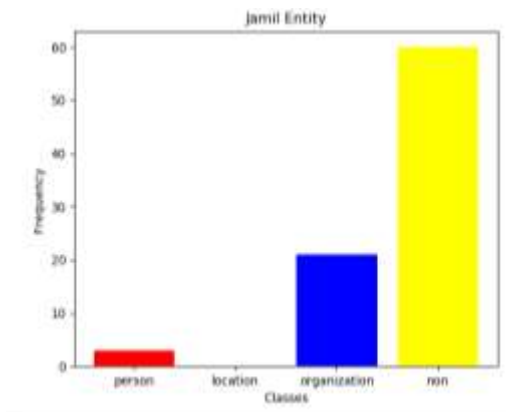


Fig. 14. Visualization of Classification for Jamil Entity as a whole using the whole System.

Entity 2: عكاظ – Aucadh

Out of total (114) as shown in Table VI, a total of 77 entities were classified through the corpus method. The remaining 37 tweets that had unclassified entities were sent to the indicator method. Of these, 16 entities were successfully classified, and the rest were classified using the gazetteer method. Fig. 15, Fig. 16, and Fig. 17 visualize the results from each step, while Fig. 18 visualizes a classification of each day individually in total, and Fig. 19 visualizes the frequency for each class as a whole.

Accuracy = 0.85

Misclassification = 0.15

Recall (location) = 0.71

Recall (organization) = 0.95

Recall (non) = 0

Recall (person) = 0

Precision (location) = 0.81

Precision (organization) = 0.86

Precision (non) = 0

Precision (person) = 0

TABLE VI. CONFUSION MATRIX FOR AUCADH ENTITY USING THE WHOLE SYSTEM

N=114	Predicted: location	Predicted: person	Predicted: organization	Predicted: non	Total
Actual: location	22	0	4	1	27
Actual: person	0	0	0	0	0
Actual: organization	10	2	75	0	87
Actual: non	0	0	0	0	0
Total	32	2	79	1	

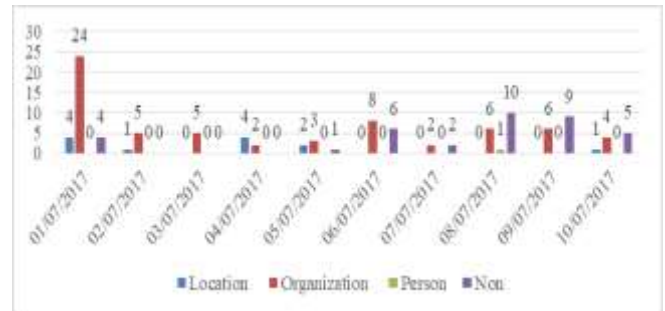


Fig. 15. Visualization of Results from First Step in Testing Aucadh Entity through the whole Model.



Fig. 16. Visualization of Results from Second Step in Testing Aucadh Entity through the whole Model.

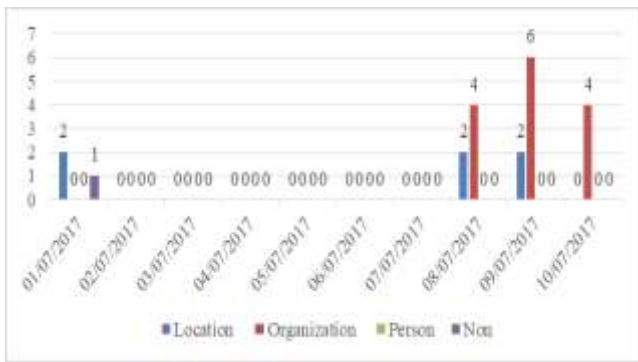


Fig. 17. Visualization of Results from Third Step in Testing Aucadh Entity through the whole Model.

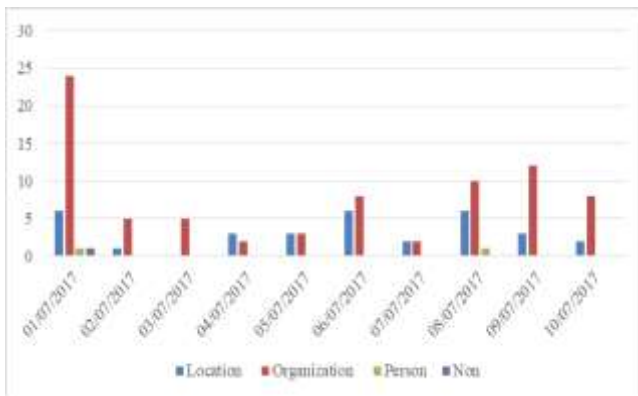


Fig. 18. Visualization of Classification for Aucadh Entity Day by Day using the whole System.

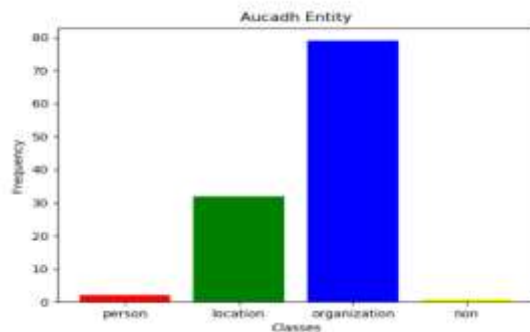


Fig. 19. Visualization of Aucadh Entity as a whole using whole System.

Entity 3: فورد – Ford

Table VII shows the confusion matrix for testing this sample. The corpus method classified 20 entries, with the remaining 37 being classified through the gazetteer method as an organization. Fig. 20 and Fig. 21 visualize the results from each step, while Fig. 22 visualizes a total classification of each individual day, and Fig. 23 visualizes the frequency of each class as a whole.

Accuracy = 0.88

Misclassification = 0.12

Recall (organization) = 0.9

Recall (Person) = 1

Precision (organization) = 0.98

Precision (Person) = 0.33

TABLE VII. CONFUSION MATRIX FOR FORD ENTITY USING WHOLE SYSTEM

N=57	Predicted: person	Predicted: organization	Predicted: location	Total
Actual: person	3	6	0	9
Actual: organization	0	47	1	48
Actual: location	0	0	0	0
Actual: non	0	0	0	0
Total	3	53	1	

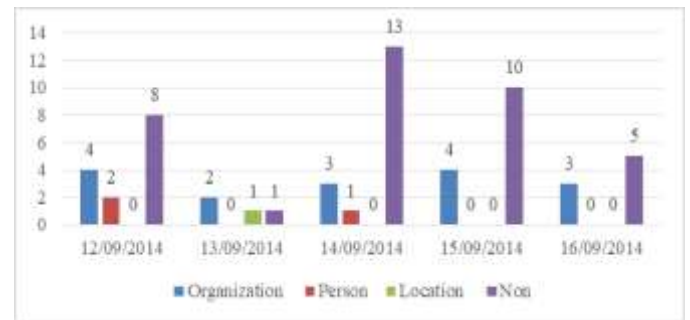


Fig. 20. Visualization the Results from First Step in Testing Ford Entity through the whole Model.



Fig. 21. Visualization the Results from Third Step in Testing Ford Entity through the whole Model.



Fig. 22. Visualization of Ford Entity Classification Day by Day using whole System.

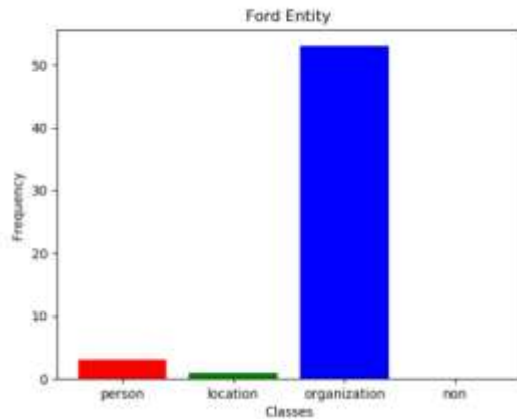


Fig. 23. Visualization of Ford Entity Classification as a whole using whole System.

The accuracy of each model was measured by testing the system and showing the difference between actual classes and the predicted classes of the testing sample using a confusion matrix and then calculating accuracy. The accuracy of testing samples on a single model and the whole system are set out in Table VIII. Using the designed NER system improved the accuracy in some testing samples (Jamil, Aucadh, Khalid, and Ford). The system is 90% accurate, and 10% misclassification.

TABLE VIII. COMPARING ACCURACY OF SINGLE MODEL AND WHOLE SYSTEM

Entity	Testing method	Accuracy
Jamil	Corpus model	61%
	Whole system	93%
Aucadh	Corpus model	71%
	Whole system	85%
Ford	Gazetteer model	84%
	Whole system	86%

V. CONCLUSION

In this research, the researcher developed an Arabic NER system that classifies selected entities mentioned in tweets posted during a specific period as POS (person name, organization, or location). The system uses a machine learning technique to build the classifier, which follows three steps arranged by priority for tagging—using similarity as in customized corpus, using an order of entity and the indicator if found, and, finally, using a list of gazetteers for each class. The system is 90% accurate. One of the main problems encountered during the study was building the customized corpus from tweets. Searching and annotating tweets that contained entity references that can fall into multiple categories depending on their location in the sentence was time-consuming.

In future work, the researcher plans to increase the classification types to more than three types. Furthermore, the researcher aims to make it possible to recognize more than one entity (word) and hopes to solve the limitation problem in retrieving tweets posted after 17/06/2016.

REFERENCES

- [1] Abdel Rahman S., Earnest M., Mandy M., and Filmy A., “Integrated machine learning techniques for Arabic named entity recognition” *International Journal of Computer Science Issues*, vol. 7, no. 4, pp. 27–36, 2010.
- [2] Ages A. P., and Ridicule, S. M., “A named entity recognition system for Malayalam using neural networks” *Procedia Computer Science*, vol. 143, pp. 962–969, 2018.
- [3] Al-Jumaily H., Martínez P., Martínez-Fernández J., and Goot, E., “A real time named entity recognition system for Arabic text mining” *Language Resources and Evaluation*, vol. 46, no. 4, pp. 543–563, 2012.
- [4] Alanazi S., Sharp B., and Stanier, C., “A named entity recognition system applied to Arabic text in the medical domain” *International Journal of Computer Science Issues*, vol. 12, no. 3, pp. 109–117, 2015.
- [5] Alkharashi I., “Person named entity generation and recognition for Arabic language” In *Proceedings of the Second International Conference on Arabic Language Resources and Tools*, Cairo, pp. 205–208, 2009.
- [6] Alsayadi H. A., and Elkorany A. M., “Integrating semantic features for enhancing Arabic named entity recognition” *International Journal of Advanced Computer Science and Applications*, vol. 7, no.3, 2016.
- [7] Benajiba Y., Diab M., and Rosso, P., “Arabic named entity recognition using optimized feature sets” In M. Lapata, H. T. Ng, & X. Wan (Eds.), *Proceedings of the Conference on Empirical Methods in Natural Language Processing – EMNLP 08*, pp. 284–293, 2008.
- [8] Elgibali A., *Investigating Arabic: Current parameters in analysis and learning (Studies in Semitic languages and linguistics)*, Boston, MA: Brill Academic Publishers, 2005.
- [9] Habib M. B., and Keulen M. V., “Twitter NEED: A hybrid approach for named entity extraction and disambiguation for tweet” *Natural Language Engineering*, vol. 22, no. 3, pp. 423–456, 2015.
- [10] Hjouj M., Alarabeyyat A., and Olab I., “Rule based approach for Arabic part of speech tagging and name entity recognition” *International Journal of Advanced Computer Science and Applications*, vol. 7, no.6, pp. 331–335, 2016.
- [11] Kanan T., Kanaan R., Al-Dabbas O., Kanaan G., Al-Dahoud A., and Fox, E., “Extracting named entities using named entity recognizer for Arabic news articles” *International Journal of Advanced Studies in Computers, Science and Engineering*, vol 5, no.11, pp. 78–84, 2016.
- [12] Korayem M., Crandall D., and Abdul-Mageed, M., “Subjectivity and sentiment analysis of Arabic: A survey” In A. E. Hassanien, A. M. Salem, R. Ramadan, & T. Kim (Eds.), *Advanced machine learning technologies and applications, AMLTA 2012, Communications in Computer and Information Science* vol. 322, pp. 128–139, 2012.
- [13] Kucuk D., Jacquet G., and Steinberger, R., “Named entity recognition on Turkish tweets” In N. Calzolari, K. Choukri, T. Declerck, H. Loftsson, B. Maegaard, J. Mariani ... S. Piperidis (Eds.), *Proceedings of the Ninth International Conference on Language Resources and Evaluation, Reykjavik, Iceland: Association for Computational Linguistics (ACL)*, pp. 450–454, 2014.
- [14] Liu X., Wei F., Zhang S., and Zhou, M., “Named entity recognition for tweets” *ACM Transactions on Intelligent Systems and Technology*, vol. 4, no. 1, pp. 1–15, 2013.
- [15] Martínez-Cámara E., Martín-Valdivia M. T., Ureña-López L. A., and Montejo-Ráez A. R., “Sentiment analysis in Twitter” *Natural Language Engineering*, vol. 20, no. 1, pp. 1–28, 2012.
- [16] Monem A. A., Shaalan K., Rafea A., and Baraka, H., “Generating Arabic text in multilingual speech-to-speech machine translation framework” *Machine Translation*, vol. 22, no. 4, pp. 205–258, 2008.
- [17] Nguyen V. H., Nguyen H. T., and Snaes, V., “Named entity recognition in Vietnamese tweets” In M. Thai, N. Nguyen, & H. Shen (Eds.), *Computational Social Networks, Lecture Notes in Computer Science*, pp. 205–215, 2015.
- [18] Oudah M., and Shaalan K., “NERA 2.0: Improving coverage and performance of rule-based named entity recognition for Arabic” *Natural Language Engineering*, vol. 23, no. 3, pp. 441–472, 2016.
- [19] Patwar M., and Potey, M., “Named entity recognition from Indian tweets using conditional random fields based approach” *International*

- Journal of Advanced Research in Computer Engineering & Technology, vol 5, no.5, pp. 1541–1545, 2016.
- [20] Ritter A., Clark S., Mausam., and Etzioni O., “Named entity recognition in tweets: An experimental study” In R. Barzilay & M. Johnson (Eds.), Proceedings of the 2011 Conference on Empirical Methods in Natural Language Processing, pp. 1524–1534, 2011.
- [21] Shaalan K., “A survey of Arabic named entity recognition and classification” Computational Linguistics, vol. 40, no. 2, pp. 469–510, 2014.
- [22] Shaalan K., and Oudah M., “A hybrid approach to Arabic named entity recognition” Journal of Information Science, vol. 40, no. 1, pp. 67–87, 2013.
- [23] Shaalan K., and Raza H., “Arabic named entity recognition from diverse text types” In B. Nordström & A. Ranta (Eds.), Advances in natural language processing. Lecture notes in computer science, vol. 5221, pp. 440–451, 2008.
- [24] Shaalan K., and Raza, H., “NERA: Named Entity Recognition for Arabic” Journal of the American Society for Information Science and Technology, vol. 60, no. 8, pp. 1652–1663, 2009.
- [25] Zaghouni W., “RENAR: A Rule-Based Arabic Named Entity Recognition System” ACM Transactions on Asian Language Information Processing, vol. 11, no. 1, pp. 1–13, 2012.
- [26] Zayed O., and El-Beltagy S., “Named entity recognition of persons’ names in Arabic tweets” Proceedings of Recent Advances in Natural Language Processing, pp. 731–738, 2015.
- [27] AlAjlan, S.A., Saudagar, A.K.J., “Machine learning approach for threat detection on social media posts containing Arabic text” Evolutionary . Intelligence. 2020. <https://doi.org/10.1007/s12065-020-00458-w>.
- [28] AlAjlan S.A., Saudagar A.K.J., “Threat Detection in Social Media Images Using the Inception-v3 Model” Proceedings of Fifth International Congress on Information and Communication Technology. Advances in Intelligent Systems and Computing, vol 1184. 2021. Springer, Singapore. https://doi.org/10.1007/978-981-15-5859-7_57.

Systematic Review of Methodologies for the Development of Embedded Systems

Kristina Blašković¹, Sanja Čandrić²
Department of Informatics
University of Rijeka, Rijeka, Croatia

Alen Jakupović³
Business Department
Polytechnic of Rijeka, Rijeka, Croatia

Abstract—Embedded systems encompass software and hardware components developed in parallel. These systems have been the focus of interest for many scholars who emphasized development issues related to embedded systems. Moreover, they proposed different approaches for facilitating the development process. The aim of this work is to identify desirable characteristics of existing development methodologies, which provide a good foundation for development of new methodologies. For that purpose, systematic mapping methodology was applied to the area of embedded systems, resulting in a classification scheme, graphically represented by a multilayer conceptual network. Afterwards, the most significant clusters were identified, using the k-means algorithm and the squared Euclidean distance formula. Overall, the results provide guidelines for further research aiming to propose a holistic approach for the development of special case of embedded systems.

Keywords—Embedded systems; development; methodology; multilayer conceptual network; cluster analysis; k-means algorithm

I. INTRODUCTION

Embedded systems are systems that encompass software and hardware components. These systems are important due to their wide use in industry, transportation, household, and various specific applications [1]. For development of these heterogeneous systems, standard existing methodologies are not fully applicable, because their phases and activities are oriented only to software or hardware components, or general-purpose hardware usage is implied. The classic approach for development of these systems is very similar to the waterfall process model where software and hardware components are developed separately [2]. Because of this separation, verification of the system occurs later, which leads to the introduction of late changes, as well as time and financial expenses.

Because of that many scientists begun to address this issue and started proposing different approaches and methodologies for development of these systems, with the aim of unifying software and hardware development processes. In this paper, our aim is to identify the characteristics of the proposed methodologies that are suitable for development of these complex systems and adaptable to the challenges of modern trends. Thus, this paper answers following research questions:

Q1: Are there any proposals for improving the development process of embedded systems?

Q2: Given the heterogeneity of the system, what part of the system covers the proposal?

Q3: Is the proposal an entirely new approach or an extension of an existing known approach?

Q4: What problems do the proposed approaches focus on and try to solve?

Q5: What implications are achieved?

To answer these questions, set of relevant articles in the field of embedded systems is reviewed, following systematic mapping methodology steps [3]. Then, the articles are classified based on the following criteria: coverage, type of contribution, thematic focus and implications. Finally, to detect desirable characteristics k-means cluster analysis is conducted, resulting in guidelines for future research.

The focus of authors research are real-time closed-loop control systems, which are considered a special case of embedded systems, comprising real-time close-loop control software, with very specific requirements, firmly tied to specially designed and developed application-specific hardware [1]. RCS Methodology is a development methodology for real-time closed loop control systems that considers software part of the system and implies general-purpose hardware [4], [5].

Hardware and software co-design (HW/SW Co-design) [6] is the most common methodology or set of techniques that define guidelines for the comparative design of software and hardware components. In these systems, most functionalities can be implemented as software or as hardware. If they are implemented as hardware, the system has a better performance and better efficiency, but if they are implemented as software, the system gains flexibility and supports late changes. It is up to the designer to identify the optimal design, from the whole set of possibilities, for the defined application. This set of all possible designs, until implementation, is known as the design space [7].

As these methodologies don't fully cover the specific requirements of the special case of embedded systems in research focus, analysis of the characteristics of existing approaches and methodologies for the development of embedded systems is conducted with the aim to define backbone of the framework which will sustain the development of other new methodologies.

The paper is organized as follows. After background in Section II, in Section III research methodology is presented. Section IV presents research results and the next chapter discussion of obtained results. In the final chapter the paper gives conclusion and announces future work.

II. BACKGROUND

Embedded systems are in the research focus of many scientists. Authors of this paper identified several systematic literature reviews in this field.

Research [8] and [9], considered articles from 2008 to 2014. These papers focused on highlighting appropriate tools for system modeling based on requirements. The same authors [10] performed additional systematic literature review where they analyze the use of UML in modeling of embedded systems. The problem of requirements engineering in embedded systems was studied in [11], where articles from 1970 to 2016 were reviewed. The use of special case of these systems, as well as their requirements, were reviewed in [12] and [13].

Authors also found one systematic review of development methodologies, which considers agile concepts and focuses on the time period from 1990 to 2015 [14].

Considering research questions of this paper and experience of the above-mentioned papers which focus on larger time span, this paper reviews the entire set of papers available, taking into account several classification criteria, as described in the following chapter.

III. RESEARCH METHODOLOGY

A. Systematic Review

First a set of relevant scientific articles needs to be created, focusing on the issues in development process of embedded systems and proposing new or extended approaches to overcome identified problems. For that purpose, Scopus database and Google Scholar service were identified as relevant sources. Preliminary results focused only on the last five years, but this time span was too narrow to get a sufficient number of articles. Therefore, time limit was not applied, i.e., the entire set of articles available in Scopus and Google scholar was considered.

The complexity and importance of the systematic development process of embedded systems, where software modules are directly tied and implemented on hardware modules, have been emphasized by scientists all around the world for quite some time. To create a systematic overview of relevant articles and define the classification scheme, systematic mapping methodology is applied to the field of development of embedded systems. For that purpose, following queries were executed on identified relevant sources:

- 1) Hardware software digital systems simulation.
- 2) "Hardware software" specification and design methodology.
- 3) HW/SW co-design methodology model embedded systems.

- 4) HW/SW "reconfigurable" architectures.
- 5) Integrating hardware (and/) software.
- 6) Integrated hardware software approach framework.
- 7) "HW/SW" synthesis model design partitioning VHDL.
- 8) Hardware software co-design "Very Large Scale Integration".
- 9) ASIC/SoC design.
- 10) Hardware|HW software|SW codesign methodology dynamic reconfiguration +architecture.
- 11) HW/SW codesign rapid prototyping extended finite state machine model.
- 12) VLSI design methodology PLA.
- 13) Hardware software partitioning integrated design automation.
- 14) Platform-based design.
- 15) Mixed "hardware-software" systems co-simulation co-synthesis model.
- 16) Hardware software systems agile.

On the obtained results for each query exclusion criteria evaluation is performed, excluding patents, citations, books and articles not related to the topic. Assuming that sorting algorithm for identified relevant sources sorts results based on importance, for each defined query only first three results were considered. Additionally, multiple appearances of the same article were counted only once. This resulted in the list of 68 articles. Finally, for each article in the resulting list the abstract, conclusion, title, and (if needed and accessible) the entire content were reviewed. Key words along with important concepts were extracted for identification of coverage, type of contribution, base method, thematic focus and achievement.

B. Classification

Once the set of articles was prepared for analysis, it was classified according to the several criteria. The following criteria (as presented in Table I) was used: coverage criterion, type of contribution criterion, thematic focus criterion and implications criterion. As a result, classification scheme is obtained and graphically represented through multilayer conceptual network.

C. Analysis

Finally, set cluster analysis was performed using the k-means algorithm. Each article was assigned to the cluster with the nearest centroid, and the distance was determined with the squared Euclidean distance formula. The algorithm follows these steps:

- 1) Choose a random number of clusters k.
- 2) Choose random k cluster representatives from the analysis set.
- 3) For each article, the distance from every cluster representative is calculated.
- 4) The article is assigned to the cluster with the minimal distance.
- 5) Cluster representatives are updated so that they coincide with the corresponding centroid.
- 6) Steps 1–5 are repeated until there are no updates.

TABLE I. OVERVIEW OF EXISTING APPROACHES TO DEVELOPMENT OF EMBEDDED SYSTEMS

Ref.Num	Article	Coverage	Type of contribution	Base method	Thematic focus	Achievement
1	[15]	E_SY	extension	HW/SW Co-design	TOOLS	SL_SPEC
2	[16]	E_SY	extension	HW/SW Co-design	TOOLS	SL_SPEC
3	[17]	E_SY	extension	HW/SW Co-design	PARTITIONING	PPA
4	[18]	E_SY	new approach	platform-based design	DEV_P	LCS
5	[19]	E_SY	new approach	HW/SW Co-design	TOOLS	FDP
6	[20]	E_SY	new approach	HW/SW Co-design	SYS_MODEL	E_ver
7	[21]	SC	new methodology	new methodology	SPEC_REQ	APPSS
8	[22]	E_SY	new approach	HW/SW Co-design	SYS_MODEL	SL_SPEC
9	[23]	E_SY	extension	HW/SW Co-design	SYS_MODEL	PPA
10	[24]	E_SY	extension	HW/SW Co-design	PARTITIONING	DRA
11	[25]	E_SY	extension	HW/SW Co-design	PARTITIONING	DRA
12	[26]	E_SY	extension	HW/SW Co-design	PARTITIONING	DRA
13	[27]	E_SY	new methodology	new methodology	SYS_MODEL	SL_SPEC
14	[28]	E_SY	new approach	prototyping	TOOLS	E_int
15	[29]	SC	new methodology	new methodology	SPEC_REQ	APPSS
16	[30]	SC	new methodology	new methodology	SPEC_REQ	APPSS
17	[31]	E_SY	new approach	HW/SW Co-design	TOOLS	FWE
18	[32]	E_SY	extension	HW/SW Co-design	TOOLS	SL_SPEC
19	[33]	E_SY	extension	HW/SW Co-design	SYS_MODEL	SL_SPEC
20	[34]	E_SY	extension	HW/SW Co-design	SYS_MODEL	SL_SPEC
21	[35]	E_SY	extension	HW/SW Co-design	PARTITIONING	E_ver
22	[36]	E_SY	extension	HW/SW Co-design	SYS_SIMUL	E_ver
23	[37]	E_SY	new approach	HW/SW Co-design	SYNTHESIS	SL_SPEC
24	[38]	E_HW	new methodology	new methodology	SYS_MODEL	FDP
25	[39]	E_HW	new methodology	new methodology	SYS_MODEL	FDP
26	[40]	E_HW	new methodology	new methodology	SYS_MODEL	FDP
27	[41]	E_SY	extension	HW/SW Co-design	PARTITIONING	DRA
28	[42]	E_SY	new approach	HW/SW Co-design	TOOLS	DRA
29	[43]	E_SY	extension	HW/SW Co-design	SYS_MODEL	FDP
30	[44]	E_HW	new methodology	new methodology	SYS_MODEL	SL_SPEC
31	[45]	E_SY	new approach	platform-based design	SYS_MODEL	LCS
32	[46]	E_SY	new approach	platform-based design	SYS_MODEL	LCS
33	[47]	E_SY	extension	HW/SW Co-design	TOOLS	SL_SPEC
34	[48]	E_SY	extension	HW/SW Co-design	TOOLS	SL_SPEC
35	[49]	E_SY	extension	HW/SW Co-design	TOOLS	FWE
36	[50]	E_HW	new methodology	new methodology	SYS_MODEL	FDP
37	[51]	E_HW	new methodology	new methodology	SYS_MODEL	FDP
38	[52]	E_HW	new methodology	new methodology	SYS_MODEL	FDP
39	[53]	E_SY	extension	HW/SW Co-design	PARTITIONING	FDP
40	[54]	E_SY	extension	HW/SW Co-design	TOOLS	PPA
41	[55]	E_SY	extension	HW/SW Co-design	PARTITIONING	PPA
42	[56]	E_SW	new approach	agile	DEV_P	E_int
43	[57]	E_HW	new approach	agile	DEV_P	E_int
44	[58]	E_HW	new approach	agile	DEV_P	E_int
45	[59]	E_SY	new methodology	new methodology	PARTITIONING	PPA
46	[60]	E_SY	new approach	HW/SW Co-design	SYS_SIMUL	E_ver
47	[61]	E_SY	extension	HW/SW Co-design	PARTITIONING	SL_SPEC
48	[62]	E_HW	extension	HW/SW Co-design	SYS_MODEL	DRA
49	[63]	E_SY	new approach	HW/SW Co-design	SYS_MODEL	DRA

Ref.Num	Article	Coverage	Type of contribution	Base method	Thematic focus	Achievement
50	[64]	SC	extension	HW/SW Co-design	SPEC_REQ	APPSS
51	[65]	SC	extension	HW/SW Co-design	SPEC_REQ	APPSS
52	[66]	E_SY	new methodology	new methodology	DEV_P	FWE
53	[67]	E_HW	new methodology	new methodology	DEV_P	FWE
54	[68]	E_SW	new approach	HW/SW Co-design	SYS_SIMUL	E_ver
55	[69]	E_SY	new approach	HW/SW Co-design	SYS_MODEL	E_ver
56	[70]	SC	new approach	HW/SW Co-design	SPEC_REQ	APPSS
57	[71]	E_HW	new approach	prototyping	PARTITIONING	LCS
58	[72]	SC	new methodology	new methodology	SPEC_REQ	APPSS
59	[73]	SC	new methodology	new methodology	SPEC_REQ	APPSS
60	[74]	E_HW	extension	HW/SW Co-design	PARTITIONING	PPA
61	[75]	E_HW	new approach	HW/SW Co-design	PARTITIONING	FWE
62	[76]	E_HW	extension	HW/SW Co-design	PARTITIONING	DRA
63	[77]	E_SY	new approach	platform-based design	SYS_MODEL	SL_SPEC
64	[78]	E_SY	new approach	platform-based design	SYS_MODEL	SL_SPEC
65	[79]	E_SY	new approach	platform-based design	SYNTHESIS	PPA
66	[80]	E_SY	extension	HW/SW Co-design	SYS_SIMUL	E_ver
67	[81]	E_SY	extension	HW/SW Co-design	SYS_MODEL	PPA
68	[82]	E_SY	new approach	agile	SYS_MODEL	E_ver

In the process of implementation of the k-means algorithm, Excel STANDARDIZE, SUMXMY2 and MIN functions were used.

IV. RESULTS

Results gathered in the process described in the Methodology section are shown in Table I. Obtained results give answer to the research question Q1 as they present proposals for improving the development process of embedded systems. These results are further analyzed in accordance with the selected criteria and research questions set in this paper.

1) *Coverage criterion*: Classification based on the Coverage criterion answers research question Q2.

Articles that consider the system as a whole, were categorized as “embedded system” (or E_SY, as noted in the column Coverage in Table I). If the article covered only part of the system, i.e. only software or only hardware, it was categorized either as “embedded software” (E_SW) or “embedded hardware” (E_HW). The category “special case” (SC) includes articles which cover special cases of hardware-software systems.

The results in Fig. 1 show that most articles focused on the whole system, while eight articles (7,15,16,50,51,56,58,59) focused on solving specific requests of special cases of these systems. Two articles (42,54) focused on the development of embedded software, and 15 articles (24,25,26,30,36,37,38, 43,44,48,53,57,60,61,62) prescribed steps in the development process of embedded hardware.

2) *Type of contribution criterion*: According to this criterion, methodologies presented in the observed articles were further classified. In Table I in the column Type of contribution this classification is shown.

Articles that include existing methodologies (HW/SW Co-design, agile, platform-based design (PLB), and prototyping) were subcategorized in these subcategories: extension (of an existing methodology), a new approach (based on an existing methodology). Understandably, if a methodology was recognized as completely new, it does not have subcategories and therefore it is noted as new methodology.

The results in Fig. 2 show that the HW/SW Co-design methodology is the most common approach for developing these complex systems. Much effort has been invested in proposing extensions of this methodology (1,2,3,9,10,11,12, 18,19,20,21,22,27,29,33,34,35,39,40,41,47,48,50,51,60,62,66, 69).

However, in 23 articles, scientists stated that these heterogeneous complex systems demand novel development methods. Therefore, 12 articles (5,6,8,17,23,28,46,49,54,55, 56,61) proposed new approaches based on HW/SW Co-design methodology, 12 articles (4,14,31,32,42,43,44,57,63,64,65,68) introduced modern concepts in the development process, and 16 articles proposed new development methodologies (7,13, 15,16,24,25,26,30,36,37,38,45,52,53,58,59).

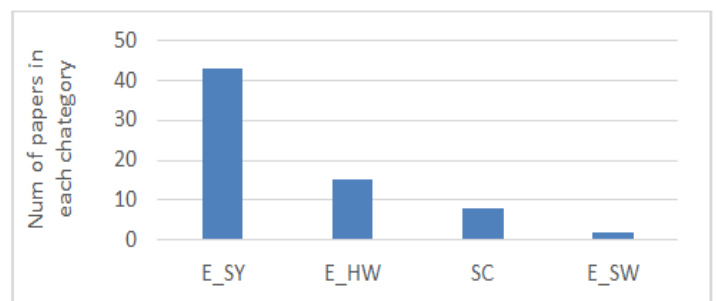


Fig. 1. Graphical Representation of Article Classification based on Coverage.

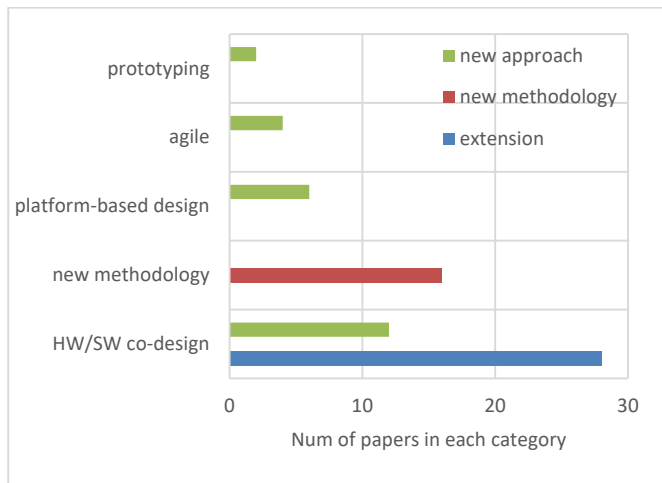


Fig. 2. Graphical Representation of Classification of Articles based on the Type of Contribution.

These results answer the research question Q3.

3) *Thematic focus criterion*: To answer research question Q4 thematic focus criterion was defined. In this criterion articles were first categorized by coverage criterion and then according to their focus on:

- support tools (TOOLS) - programming tools that support the development process,
- partitioning (PARTITIONING) - improvement and automation of the process for choosing appropriate SW/HW components,
- system modeling (SYS_MODEL) - definition of good practices when choosing between software or hardware implementation,
- synthesis of system components (SYNTESIS) - integration of developed SW/HW components, including verification and validation,
- system simulation (SYS_SIMUL) - simulation of the system operation in the absence of sufficiently developed hardware components,
- the entire development process (DEV_P),
- solving specific requirements (SPEC_REQ).

This data is presented in the column Thematic focus of Table I. Graphically, the results are presented in Fig. 3.

Fig. 3 shows that of a total of 43 articles that considered the system as a whole, 11 articles (1,2,5,14, 17,18,28,33,34,35,40) focused on defining the appropriate set of tools that would support the development process. Four articles (22,46,54,66) dealt with system simulation, and two articles (23,65) focused on the integration of developed software and hardware components. Furthermore, 23 articles dealt with the problem of defining the unique system model, of which 15 articles (6,8,9,13,19,20,29,31,32,49,55,63,64,67, 68) considered the whole system, and eight articles (24,25,26,30,36,37,38,48) considered only the hardware part of the system. Additionally, six articles tried to improve the

entire development process. Two of them (4,52) followed the development of the whole system, one article (42) proposed improvements by introducing agile methods in the software development process, and three articles (43,44,53) dealt with the hardware development process. Out of 14 articles that tried to optimize the partitioning process for hardware and software components, ten articles (3,10,11,12,21,27,39,41,45,47) considered the whole system, and four articles (57,60,61,62) the hardware part of the system. Finally, eight articles (7,15,16,50,51,56,58,59) tried to solve problems for special cases of these systems.

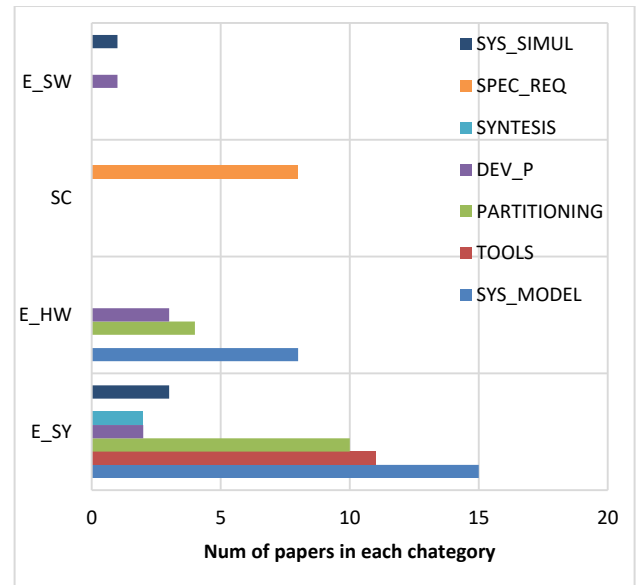


Fig. 3. Graphical Representation of Classification of Articles based on the Thematic Focus.

4) *Implications criterion*: According to this criterion articles were categorized by achieved implications and then by thematic focus criterion, to show how these two criteria are correlated. The following implications were identified:

- system-level specification (SL_SPEC) - software and hardware components are equally specified, and the type of implementation for each component is selected in the implementation phase,
- facilitated development process (FDP) - introduction of improvements in the development process,
- part of process automation (PPA) - introduction of tools or definition of algorithms that automate a certain development phase,
- dynamic reconfiguration architecture (DRA) - flexibility of the hardware part of the system with respect to the implementation of late changes,
- early integration (E_int) - in the case of disagreement with defined requirements, in verification and validation process of the system design, needed changes must be introduced and implementing changes earlier in the development process is less expensive,

- early verification (E_ver) - verification of software and hardware components interaction in the early development stage when the hardware structure is not fully functional,
- late changes support (LCS) - due to the heterogeneous structure of the system, changes can be introduced in software or in hardware and since modification of the hardware part of the system is very difficult in the late development stage the goal is to implement the majority of functionalities as software,
- application-specific solution (APPSS)-solving problems and requirements of application-specific systems,
- framework established (FWE) - defining a set of program tools that support every phase in the development process of these complex systems.

This data is shown in the Achievement column of Table I. The results presented in Fig. 4, give answer to the research question Q5.

14 articles dealt with the problem of system heterogeneity. Of those, five articles (1,2,18,33,34) proposed the introduction of software tools, seven articles focused on system model definition (8,13,19,20,30,63,64), one article (23) proposed improvements in the synthesis phase, and one article (47) examined the partitioning phase. To facilitate the overall development process of these complex systems, seven articles (24,25,26,29,36,37,38) focused on system model definition, one article (39) on the partitioning phase, and one article (5) on defining tools that would support the entire process.

In eight articles, scientists introduced automation of part of the process. Out of these eight, in four articles (3,41,45,60) partitioning was improved by introduction of authors own partitioning algorithms, and in two articles (9,69), the MARTE extension and Web Ontology Language were used to create semantic representations of hardware and software components, from which system model and automatic code were generated, in one article (65), the authors focused on the synthesis phase, and in one article (40), software tools were proposed. Furthermore, eight articles (7,15,16,50,51,56, 58,59) were oriented toward solving application-specific problems. With further development of hardware technology, eight articles proposed the introduction of dynamic reconfiguration architecture as the hardware part of the system. Five of these articles (10,11,12,27,62) proposed improvements in the partitioning phase, two articles (48,49) suggested improved system models, and in one article (28), software tools that allowed selection of dynamic reconfiguration architecture, and thus, variability of the hardware part of the system, were used in the design phase. It is very important to test as soon as possible during the development process does the system in development satisfy preset requirements. For that purpose, eight articles proposed approaches that would allow early verification, out of which three articles (6,55,68) focused on improving system model definition, one article (21) on improved system partitioning, and four articles (22,46,54,66) on the introduction of simulators that would allow verification of the system in early stage. Furthermore, five articles (17,35,52,53,61) contributed

to the establishment of a framework for supporting each development process phase.

In the hardware part of the system, it is very difficult to introduce changes late in the development process. However, as requests for changes are unavoidable, four articles contributed to the introduction of late changes. Of these articles, one (4) tried to ease the entire development process by introducing general-purpose hardware as the hardware part of the system, and application specifics were defined in the software part of the system that supports late changes. The other two articles (32,30) defined the system model on the platform level, where instances from a higher level of abstraction are mapped on lower levels, and each level of abstraction hides implementation details allowing the designer to make compromises in selecting the required components. In one article (57), late changes were supported with the introduction of modern concepts in partitioning. To enable early integration of system components, in three articles (42,43,44), scientists proposed the introduction of modern agile concepts in the entire development process, and in one article (14), support tools were presented, with which mockups of actual software and hardware components were developed, verified, and validated, using an augmented reality (AR) system. If the design is valid, development begins.

As the criteria for classifying the articles were defined, the relationship between them can now be analyzed. For that purpose, a multilayer conceptual network (Fig. 5) is generated to give a better overview of how the criteria affect each other. There are four layers where a single layer is occupied by values for one defined criterion. The values are represented by blue circles. Two layers can be connected, through their values, only if the layers are adjacent. If a single value appears in more than one connection, frequency increases resulting in larger radius circle representation.

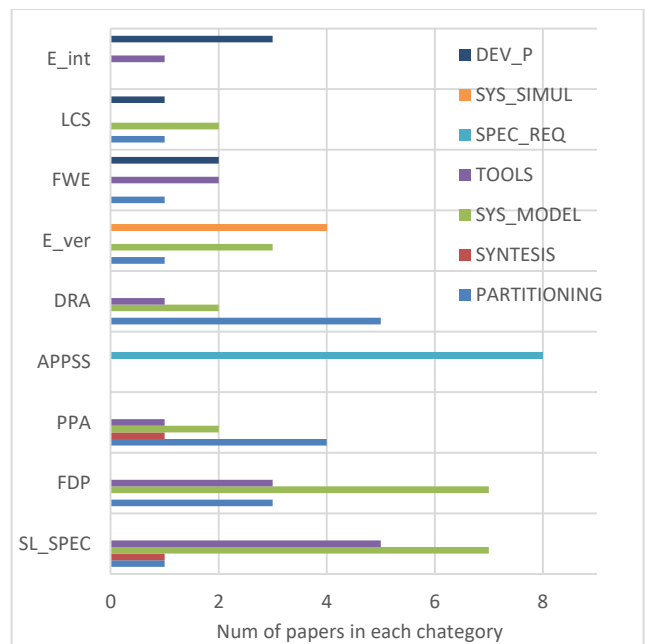


Fig. 4. Graphical Representation of Classification of Articles based on the Implications.

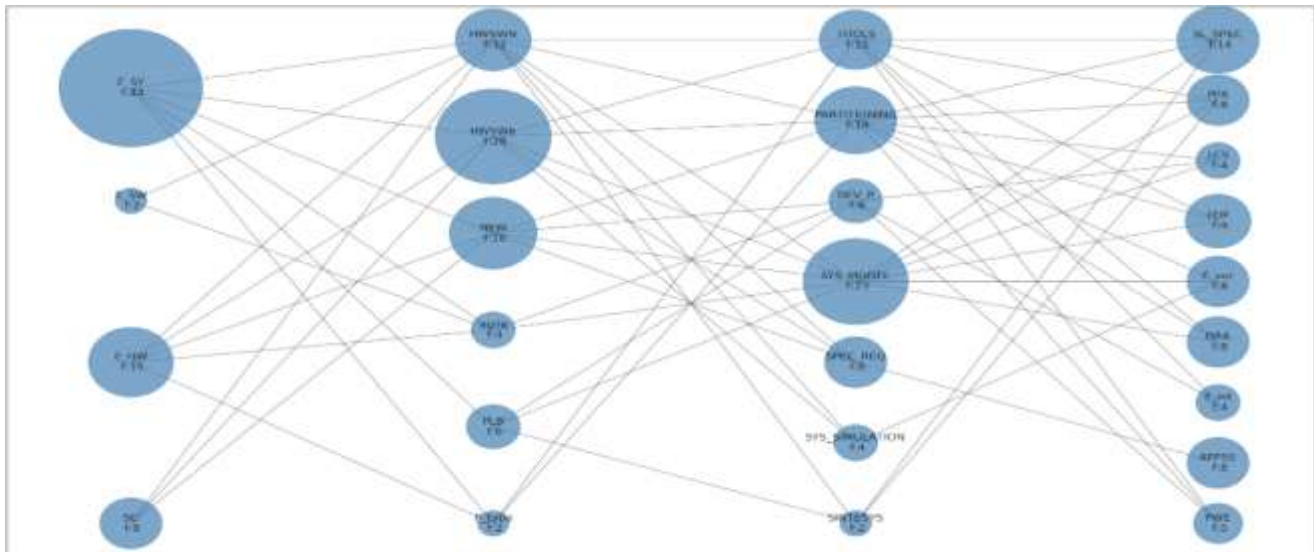


Fig. 5. Multilayer Conceptual Network.

5) *Cluster analysis*: Since k-means algorithm is based on determining the distances from the cluster centroids which implies numerical values, non-numerical values from the analysis set are first assigned to numerical values as shown in Table II.

Next, the mean value and the standard deviation for each criterion were calculated, and data normalized. Afterwards, the desired number of clusters is chosen using the elbow method. In this method first the graphical representation (Fig. 6) is generated where on the y axis the standard deviation of the shortest distances from the cluster centroid is shown, and on the x axis the number of clusters can be found. Finally, the point, where the graph starts flattening, which represents the optimal number of clusters, is chosen (in this case, k = 3).

Once the k random cluster representatives were chosen from the analysis set of data, the distance for each element from each cluster representative was calculated and minimal distance corresponding to assigned cluster identified.

When each element of the analysis set is assigned to a certain cluster, cluster representatives are updated so that their position is in the center of each cluster. For that Excel Solver add-on is used which minimizes the sum of the shortest distances by changing the cluster representatives. As a result, clusters presented in Table III are created.

In Fig. 7 the graphical representation is shown. Here on the x axis the number of clusters is shown and on the y axis distance from cluster centroid for each element of the cluster can be found. If the element coincides with cluster centroid the distance equals 0 and the values increase with distance. If more than one element has the same distance value, the radius of the circle marker increases proportionally.

TABLE II. ASSOCIATING NUMERICAL VALUES TO CLASSIFICATION CRITERIA VALUES

Values for coverage	
Abbreviation	Value
E_SY	1
E_SW	2
E_HW	3
SC	4
Values for type of contribution	
Abbreviation	Value
HWSWE	1
HWSWN	2
NEW	3
agile	4
PLB	5
P_type	6
Values for thematic focus	
Abbreviation	Value
TOOLS	1
PARTITIONING	2
DEV_P	3
SYS_MODEL	4
SPEC_REQ	5
SYS_SIMULATION	6
SINTESYS	7
Values for implications	
Abbreviation	Value
SL_SPEC	1
PPA	2
LCS	3
FDP	4
E_ver	5
DRA	6
E_int	7
APPSS	8
FWE	9

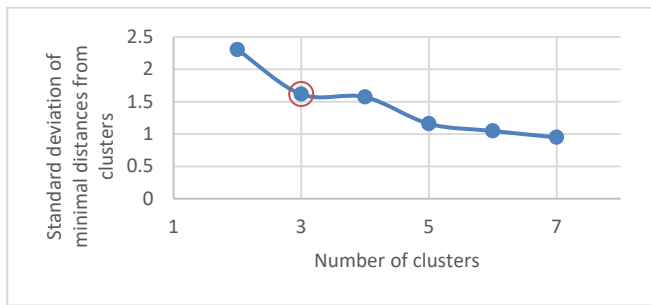


Fig. 6. Determining the Optimal Number of Clusters with the Elbow Method.

TABLE III. CLUSTER ANALYSIS RESULTS

Cluster	Articles	Nr of el.
1	4,13,14,31,32,45,57,63,64,65 and 68	11
2	7,15,16,23,24,25,26,30,36,37,38,42,43,44,46,48,50,51,53,54,56,58,59 and 61	24
3	1,2,3,5,6,8,9,10,11,12,17,18,19,20,21,22,27,28,29,33,34,35,39,40,41,47,49,52,55,60,62,66 and 69	33
Total		68

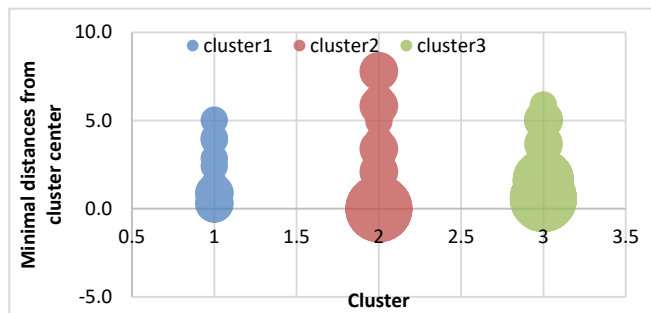


Fig. 7. Graphical Representation of the Cluster Distribution.

V. DISCUSSION

Relevant articles on methodologies for the development of embedded systems were analyzed by applying the systematic mapping methodology. This resulted in classification schema based on several criteria. In terms of coverage, most articles considered the system as a whole. Recently, the number of articles that considered special cases of these systems has increased. In terms of contribution, most articles proposed improvements based on the HW/SW Co-design methodology. Numerous articles also proposed entirely new approaches for facilitating the development process. Furthermore, articles proposed the introduction of modern concepts in the development of software, as well as the hardware part of the system. In terms of thematic focus, most articles focused on defining a system model. Such model unifies hardware and software development processes. Many articles also dealt with the partitioning phase and the definition of adequate software tools that support the development process of embedded systems. In addition, several scholars dealt with specific requirements of special cases of these systems. In terms of implications, the most frequent implication is the definition of system-level specification. This specification provides an overview of the system at a higher level of abstraction. Other most common implications included facilitated development

process, part of the process automation, application-specific solutions, introduction of dynamic reconfiguration architecture, and the possibility of early verification.

Based on this classification schema cluster analysis is performed using k-means algorithm. Analysis resulted in three clusters as shown in Fig. 7 and Table III.

A review of the obtained clusters shows that cluster 3 is the cluster that includes the most elements. The total number (33 elements) accounts for 48.53% of the initial data set. Articles with the following characteristics were found: coverage (the whole system and the hardware part of the system), contribution (extension or a new approach based on hardware/software co-design methodology and new methodology), thematic focus (software tools that support development process, improvements in the partitioning phase of the development process, definition of the optimal system model, system simulation, and the entire development process), and implications (definition of system-level specification, automation of part of the process, facilitated development process, support for early verification, introduction of dynamic reconfiguration architecture, and framework establishment).

The second largest cluster is cluster 2 with 24 elements which is 35.29% of the initial data set. Articles in this cluster have the following characteristics: coverage (special cases of these systems, the whole system, the hardware part of the system, and the software part of the system), contribution (new methodology, new approaches and extensions based on hardware/software co-design methodology, and new approaches based on agile concepts), thematic focus (definition of the optimal system model, solving specific requirements of special cases of these systems, the synthesis phase of the development process, the entire development process, system simulation, and the partitioning phase of the development process), and implications (automation of part of the process, application specific solutions, definition of system-level specification, facilitated development process, support for early integration, support for early verification, introduction of dynamic reconfiguration architecture, framework establishment).

The smallest cluster is cluster 1 with 11 elements which is 16.18% of the initial data set. Articles in this cluster have the following characteristics: coverage (the whole system and the hardware part of the system), contribution (proposals of new approaches based on platform-based design, agile concepts, prototyping and new methodologies), thematic focus (the entire development process, definition of the optimal system model, software tools that support the development process, the partitioning phase of the development process), and implications (support for introduction of changes in a late stage of the development process, definition of system-level specification, support for early integration, part of process automation, and support for early verification).

The results show that for the first criterion (coverage) there are no major deviations between clusters 1 and 3, and special cases of these complex systems appear only in cluster 2. For the second criterion (contribution), new approaches based on modern concepts appear only in clusters 2 and 3. The third

criterion (thematic focus) is similar in all three clusters, but a focus on solving specific requirements appears only in cluster 2. Equally, all clusters are similar in fourth criterion (implications), but application-specific implications can be found only in cluster 2 and support for late changes implications only in cluster 1.

VI. CONCLUSION

Embedded systems are systems that encompass software and hardware components. For the last 50 years, great effort has been invested in proposing improvements and new approaches to the development process. Guided by many researchers who recognized the significance of these complex systems integrated in our everyday lives, in this paper the desirable characteristics of existing approaches to the development of embedded system were detected, which can be used as the foundation for the development of new methodologies.

After extracting relevant scientific articles through systematic review process, based on defined criteria cluster analysis was conducted, implementing k-means algorithm and the squared Euclidean distance. It resulted in three clusters, where cluster 3 and cluster 2 were identified as significant, considering the number of associated elements.

In our previous research we proposed Software development methodology for special case of real-time closed loop control systems. This methodology supports development of application-specific hardware and solves specific requirements.

In our future work a new methodology for development of special case of embedded systems will be designed and proposed. This methodology will unify development process of software and hardware components and will be based on newly developed graphical methods. Furthermore, evaluation procedures will be developed, intended for graphical methods and methodology assessment.

ACKNOWLEDGMENT

This work has been fully supported by the University of Rijeka under the project uniri-drustv-18-140.

REFERENCES

- [1] K. Blašković and S. Čandrić, "DEM4RTS: Software development methodology for special case of real-time closed-loop control systems", *Annals of DAAAM & Proceedings*, vol. 29, 2018.
- [2] M. Chiodo, "Automotive Electronics", In *Hardware/software co-design*, Springer, Dordrecht, pp. 295-310, 1996.
- [3] K. Petersen, R. Feldt, S. Mujtaba and M. Mattsson, "Systematic mapping studies in software engineering", In *12th International Conference on Evaluation and Assessment in Software Engineering (EASE) 12*, pp. 1-10, 2008.
- [4] T. Barbera, M. L. Fitzgerald and J. S. Albus, "Concepts for a real-time sensory-interactive control system architecture", In *Fourteenth Southeastern Symposium on System Theory*, 1982.
- [5] R. Quintero and T. Barbera, "A Real-Time Control System Methodology for Developing Intelligent Control Systems", 1992.
- [6] J. Staunstrup and W. Wolf, "Hardware/software co-design: principles and practice", Springer Science & Business Media, 2013.
- [7] E. Kang, E. Jackson and W. Schulte, "An approach for effective design space exploration", In *Monterey Workshop*, Springer, Berlin, Heidelberg, pp. 33-54, 2010.
- [8] M. Rashid, M. W. Anwar and A. M. Khan, "Toward the tools selection in model based system engineering for embedded systems—A systematic literature review", *Journal of Systems and Software*, vol. 106, pp. 150-163, 2015.
- [9] M. Rashid and M. W. Anwar, "A systematic investigation of tools in model based system engineering for embedded systems", In *2016 11th System of Systems Engineering Conference (SoSE)*, IEEE, pp. 1-6, 2016.
- [10] M. Rashid, M. W. Anwar and A. M. Khan, "Identification of trends for model based development of embedded systems", In *2015 12th International Symposium on Programming and Systems (ISPS)*, IEEE, pp. 1-8, 2015.
- [11] T. Pereira, D. Albuquerque, A. Sousa, F. M. Alencar and J. Castro, "Retrospective and Trends in Requirements Engineering for Embedded Systems: A Systematic Literature Review", In *CIBSE*, pp. 427-440, 2017.
- [12] M. Romero, W. Guédria, H. Panetto and B. Barafort, "Towards a characterisation of smart systems: A systematic literature review", *Computers in industry*, vol. 120, pp. 103224, 2020.
- [13] B. Liao, Y. Ali, S. Nazir, L. He and H. U. Khan, "Security analysis of IoT devices by using mobile computing: a systematic literature review", *IEEE Access*, vol. 8, pp. 120331-120350, 2020.
- [14] R. Hoda, N. Salleh, J. Grundy and H. M. Tee, H. M. (2017). "Systematic literature reviews in agile software development: A tertiary study", *Information and Software Technology*, vol. 85, pp. 60-70, 2017.
- [15] R. K. Gupta, C. N. Coelho and G. De Micheli, "Synthesis and simulation of digital systems containing interacting hardware and software components", In *DAC*, vol. 92, pp. 225-230, 1992.
- [16] G. De Micheli, "Computer-aided hardware-software codesign", *IEEE Micro*, vol. 14(4), pp. 10-16, 1994.
- [17] K. A. Olukotun, R. Helaihel, J. Levitt and R. Ramirez, "A software-hardware cosynthesis approach to digital system simulation. *IEEE Micro*", vol. 14(4), pp. 48-58, 1994.
- [18] A. Sangiovanni-Vincentelli and G. Martin, "Platform-based design and software design methodology for embedded systems", *IEEE Design & Test of Computers*, vol. 18(6), pp. 23-33, 2001.
- [19] D. D. Gajski and F. Vahid, "Specification and design of embedded hardware-software systems", *IEEE Design & Test of Computers*, vol. 12(1), pp.53-67, 1995.
- [20] M. Chiodo, P. Giusto, A. Jurecska, H. C. Hsieh, A. Sangiovanni-Vincentelli and L. Lavagno, "Hardware-software codesign of embedded systems", *IEEE micro*, vol. 14(4), pp. 26-36, 1994.
- [21] J. Vidal, F. De Lamotte, G. Gogniat, P. Soulard and J. P. Diguët, "A co-design approach for embedded system modeling and code generation with UML and MARTE", In *2009 Design, Automation & Test in Europe Conference & Exhibition*, IEEE, pp. 226-231, 2009.
- [22] A. Shaout, A. H. El-Mousa and K. Mattar, "Specification and modeling of hw/sw co-design for heterogeneous embedded systems", In *Proceedings of the World Congress on Engineering*, vol. 1, 2009.
- [23] L. G. Murillo, M. Mura and M. Prevostini, "Semi-automated Hw/Sw Co-design for embedded systems: from MARTE models to SystemC simulators", In *2009 Forum on Specification & Design Languages (FDL)*, IEEE; pp. 1-6, 2009.
- [24] S. Banerjee, E. Bozorgzadeh and N. Dutt, "Physically-aware HW-SW partitioning for reconfigurable architectures with partial dynamic reconfiguration", In *Proceedings of the 42nd annual Design Automation Conference*, pp. 335-340, 2005.
- [25] J. Noguera and R. M. Badia, "HW/SW codesign techniques for dynamically reconfigurable architectures", *IEEE Transactions on Very Large Scale Integration (VLSI) Systems*, vol. 10(4), pp. 399-415, 2002.
- [26] M. Baleani, F. Gennari, Y. Jiang, Y. Patel, R. K. Brayton and A. Sangiovanni-Vincentelli, "HW/SW partitioning and code generation of embedded control applications on a reconfigurable architecture platform", In *Proceedings of the tenth international symposium on Hardware/software codesign*, pp. 151-156, 2002.
- [27] S. Donatelli and G. Franceschinis, "The PSR methodology: integrating hardware and software models", In *International Conference on*

- Application and Theory of Petri Nets, Springer, Berlin, Heidelberg, pp. 133-152, 1996.
- [28] T. J. Nam and W. Lee, "Integrating hardware and software: augmented reality based prototyping method for digital products", In CHI'03 extended abstracts on Human factors in computing systems, pp. 956-957, 2003.
- [29] P. Francesco, P. Marchal, D. Atienza, L. Benini, F. Catthoor and J. M. Mendias, "An integrated hardware/software approach for run-time scratchpad management", In Proceedings of the 41st annual Design Automation Conference, pp. 238-243, 2004.
- [30] A. Shriraman, M. F. Spear, H. Hossain, V. J. Marathe, S. Dwarkadas and M. L. Scott, "An integrated hardware-software approach to flexible transactional memory", In Proceedings of the 34th annual international symposium on Computer architecture, pp. 104-115, 2007.
- [31] S. Kumar, J. H. Aylor, B. W. Johnson and W. A. Wulf, "A framework for hardware/software codesign", Computer, vol. 26(12), pp. 39-45, 1993.
- [32] T. B. Ismail and A. A. Jerraya, "Synthesis steps and design models for codesign", Computer, vol. 28(2), pp.44-53, 1995.
- [33] W. Ecker, "Using VHDL for HW/SW co-specification", In Proceedings of EURO-DAC 93 and EURO-VHDL 93-European Design Automation Conference, IEEE, pp. 500-505, 1993.
- [34] C. A. Valderrama, A. Changuel, P. V. Raghavan, M. Abid, T. B. Ismail and A. A. Jerraya, "A unified model for co-simulation and co-synthesis of mixed hardware/software systems", In Proceedings the European Design and Test Conference. ED&TC 1995, IEEE, pp. 180-184, 1995.
- [35] F. Vahid and D. D. Gajski, "Incremental hardware estimation during hardware/software functional partitioning", IEEE Transactions on Very Large Scale Integration (VLSI) Systems, vol. 3(3), pp. 459-464, 1995.
- [36] G. De Micheli, "Hardware/software co-design: Application domains and design technologies", In Hardware/software co-design, Springer, Dordrecht, pp. 1-28, 1996.
- [37] S. Parameswaran, "Code placement in Hardware Software Co synthesis to improve performance and reduce cost", In Proceedings Design, Automation and Test in Europe. Conference and Exhibition 2001, IEEE, pp. 626-632, 2001.
- [38] J. Henkel, "Closing the SoC design gap", Computer, vol. 36(9), pp. 119-121, 2003.
- [39] R. Puri, L. Stok, J. Cohn, D. Kung, D. Pan, D., Sylvester, D., ... and S. Kulkarni, "Pushing ASIC performance in a power envelope", In Proceedings of the 40th annual Design Automation Conference, pp. 788-793, 2003.
- [40] G. W. Doerre and D. E. Lackey, "The IBM ASIC/SoC methodology—A recipe for first-time success", IBM Journal of Research and Development, vol. 46(6), pp. 649-660, 2002.
- [41] J. Noguera and R. M. Badia, "A HW/SW partitioning algorithm for dynamically reconfigurable architectures", In Proceedings Design, Automation and Test in Europe, Conference and Exhibition 2001, IEEE, pp. 729-734, 2001.
- [42] A. Antola, M. D. Santambrogio, M. Fracassi, P. Gotti and C. Sandionigi, "A novel hardware/software codesign methodology based on dynamic reconfiguration with Impulse C and CoDeveloper", In 2007 3rd Southern Conference on Programmable Logic, IEEE, pp. 221-224, 2007.
- [43] D. E. Thomas, J. K. Adams and H. Schmit, "A model and methodology for hardware-software codesign", IEEE Design & test of computers, vol. 10(3), pp. 6-15, 1993.
- [44] S. Liao, S. Tjiang and R. Gupta, "An efficient implementation of reactivity for modeling hardware in the Scenic design environment", In Proceedings of the 34th annual Design Automation Conference, pp. 70-75, 1997.
- [45] K. Keutzer, A. R. Newton, J. M. Rabaey and A. Sangiovanni-Vincentelli, "System-level design: orthogonalization of concerns and platform-based design", IEEE transactions on computer-aided design of integrated circuits and systems, vol. 19(12), pp. 1523-1543, 2000.
- [46] A. Sangiovanni-Vincentelli, L. Carloni, F. De Bernardinis and M. Sgroi, "Benefits and challenges for platform-based design", In Proceedings of the 41st annual Design Automation Conference, pp. 409-414, 2004.
- [47] K. Buchenrieder, A. Sedlmeier and C. Veith, "HW/SW co-design with PRAMs using CODES", In Computer Hardware Description Languages and their Applications, North-Holland, pp. 65-78, 1993.
- [48] T. Ismail, M. Abid, K. O'Brien and A. Jerraya, "An approach for hardware-software codesign", In Proceedings of IEEE 5th International Workshop on Rapid System Prototyping, IEEE, pp. 73-80, 1994.
- [49] S. Antoniazzi, A. Balboni, W. Fornaciari and D. Sciuto, "A methodology for control-dominated systems codesign", In Third International Workshop on Hardware/Software Codesign, IEEE, pp. 2-9, 1994.
- [50] N. Jayakumar and S.P. Khatri, "A metal and via maskset programmable VLSI design methodology using PLAs", In IEEE/ACM International Conference on Computer Aided Design, 2004, ICCAD-2004, IEEE, pp. 590-594, 2004.
- [51] N. Jayakuma, R. Garg, B. Gamache and S. P. Khatri, "A PLA based asynchronous micropipelining approach for subthreshold circuit design", In 2006 43rd ACM/IEEE Design Automation Conference, IEEE, pp. 419-424, 2006.
- [52] S. P. Khatri, R. K. Brayton and A. Sangiovanni-Vincentelli, "Cross-talk immune VLSI design using a network of PLAs embedded in a regular layout fabric", In IEEE/ACM International Conference on Computer Aided Design, ICCAD-2000, IEEE/ACM Digest of Technical Papers (Cat. No. 00CH37140), IEEE, pp. 412-418, 2000.
- [53] V. Srinivasan, S. Radhakrishnan R. Vemuri, "Hardware software partitioning with integrated hardware design space exploration", In Proceedings Design, Automation and Test in Europe, IEEE, pp. 28-35, 1998.
- [54] R. Ernst, J. Henkel and T. Benner, "Hardware-software cosynthesis for microcontrollers", IEEE Design & Test of computers, vol. 10(4), pp. 64-75, 1993.
- [55] P. Eles, Z. Peng, K. Kuchcinski and A. Doboli, "System level hardware/software partitioning based on simulated annealing and tabu search", Design automation for embedded systems, vol. 2(1), pp.5-32., 1997.
- [56] J. Ronkainen and P. Abrahamsson, "Software development under stringent hardware constraints: Do agile methods have a chance?", In International Conference on Extreme Programming and Agile Processes in Software Engineering, Springer, Berlin, Heidelberg, pp. 73-79, 2003.
- [57] J. Shalf, D. Quinlan and C. Janssen, "Rethinking hardware-software codesign for exascale systems", Computer, vol. 44(11), pp. 22-30, 2011.
- [58] P. M. Huang, A. G. Darrin and A. A. Knuth, "Agile hardware and software system engineering for innovation", In 2012 IEEE Aerospace Conference, IEEE, pp. 1-10, 2012.
- [59] A. Iguider, K. Bouselam, O. Elissati, M. Chami and A. En-Nouaary, "Embedded systems hardware software partitioning using minimax algorithm", In Proceedings of the 4th International Conference on Smart City Applications, pp. 1-6, 2019.
- [60] S. Karthik, K. Priyadarsini and V. Jeanshilpa, "VLSI Systems for Simultaneous in Logic Simulation", In 2018 International Conference on Recent Trends in Electrical, Control and Communication (RTECC), IEEE, pp. 23-27, 2018.
- [61] M. King and N. Dave, "Automatic generation of hardware/software interfaces", ACM SIGARCH Computer Architecture News, vol. 40(1), pp.325-336, 2012.
- [62] P. Zhang, J. Zambreno and P. H. Jones, "An embedded scalable linear model predictive hardware-based controller using ADMM", In 2017 IEEE 28th International Conference on Application-specific Systems, Architectures and Processors (ASAP), IEEE, pp. 176-183, 2017.
- [63] M. Cauwels, J. Zambreno and P. H. Jones, "HW/SW Configurable LQG Controller using a Sequential Discrete Kalman Filter", In 2018 International Conference on ReConfigurable Computing and FPGAs (ReConFig), IEEE, pp. 1-8, 2018.
- [64] D. Sabella, P. Serrano, G. Stea, A. Virdis, I. Tinnirello, F. Giuliano, ... and N. Bartzoudis, "Designing the 5G network infrastructure: a flexible and reconfigurable architecture based on context and content information", EURASIP Journal on Wireless Communications and Networking, vol. 2018(1), pp. 1-16, 2018.
- [65] D. Sabella, P. Serrano, G. Stea, A. Virdis, I. Tinnirello, F. Giuliano,... and N. Bartzoudis, "A flexible and reconfigurable 5G networking

- architecture based on context and content information", In 2017 European Conference on Networks and Communications (EuCNC), IEEE, pp. 1-6, 2017.
- [66] J. R. Stevens, Y. Du, V. Kozhikkott and A. Raghunathan, "ACCLIB: Accelerators as libraries", In 2018 Design, Automation & Test in Europe Conference & Exhibition (DATE), IEEE, pp. 245-248, 2018.
- [67] C. W. Lin and C. Chen, "A processor and cache online self-testing methodology for os-managed platform", IEEE Transactions on Very Large Scale Integration (VLSI) Systems, vol. 25(8), pp. 2346-2359, 2017.
- [68] P. M. Ortega-Cabezas, A. Colmenar-Santos, D. Borge-Diez and J.J. Blanes-Peiró, "Application of rule-based expert systems in hardware-in-the-loop simulation case study: Software and performance validation of an engine electronic control unit", Journal of Software: Evolution and Process, vol. 32(1), 2020.
- [69] C. C. Huang, K. C. Lin, C. H. Huang, H. P. Lin and C. W. Liu, "SoC-based Software-Hardware codesign of intelligent diagnosis", In 2010 International Symposium on Computer, Communication, Control and Automation (3CA), IEEE, vol. 2, pp. 337-340, 2010.
- [70] A. Zemva and M. Verderber, "FPGA-oriented HW/SW implementation of the MPEG-4 video decoder", Microprocessors and Microsystems, vol. 31(5), pp. 313-325, 2007.
- [71] A. Chimienti, L. Fanucci, R. Locatelli and S. Saponara, "VLSI architecture for a low-power video codec system", Microelectronics Journal, vol. 33(5-6), pp. 417-427, 2002.
- [72] C. P. Iatrou, H. Bauer, M. Graube, S. Höppner, J. Rahm and L. Urbas "Hard Real-Time Capable OPC UA Server as Hardware Peripheral for Single Chip IoT Systems", In 2019 24th IEEE International Conference on Emerging Technologies and Factory Automation (ETFA), IEEE, pp. 1631-1634, 2019.
- [73] A. Coelho, N. E. Zergainoh and R. Velazco, "Nocfi: A hybrid fault injection method for networks-on-chip", In 2019 IEEE Latin American Test Symposium (LATS), IEEE, pp. 1-6, 2019.
- [74] J. B. Lim and D. Chen, "Automated Communication and Floorplan-Aware Hardware/Software Co-Design for SoC", In 2019 IEEE Computer Society Annual Symposium on VLSI (ISVLSI), IEEE, pp. 128-133, 2019.
- [75] W. Zuo, L. N. Pouchet, A. Ayupov, T. Kim, C. W. Lin, A. Shiraishi and D. Chen, "Accurate high-level modeling and automated hardware/software co-design for effective SoC design space exploration", In Proceedings of the 54th Annual Design Automation Conference 2017, pp. 1-6, 2017.
- [76] S. Yousuf and A. Gordon-Ross, "An automated hardware/software co-design flow for partially reconfigurable FPGAs", In 2016 IEEE Computer Society Annual Symposium on VLSI (ISVLSI), IEEE, pp. 30-35, 2016.
- [77] M. Lora, S. Vinco and F. Fummi, "Translation, abstraction and integration for effective smart system design", IEEE Transactions on Computers, vol. 68(10), pp. 1525-1538, 2019.
- [78] L. Gauss, D. P. Lacerda and M. A. Sellitto, "Module-based machinery design: a method to support the design of modular machine families for reconfigurable manufacturing systems", The International Journal of Advanced Manufacturing Technology, vol.102(9-12), pp.3911-3936, 2019.
- [79] A. Iannopolo, S. Tripakis and A. Sangiovanni-Vincentelli, "Constrained synthesis from component libraries", Science of Computer Programming, vol. 171, pp.21-41, 2019.
- [80] K. Etzold, T. Fahrbach, S. Klein, R. Scheer, D. Guse, M. Klawitter, M., ... and J. Andert, "Function development with an electric-machine-in-the-loop setup: A case study", IEEE Transactions on Transportation Electrification, vol. 5(4), pp. 1419-1429, 2019.
- [81] A. Perzylo, S. Profanter, M. Rickert and A. Knoll, "OPC UA NodeSet Ontologies as a Pillar of Representing Semantic Digital Twins of Manufacturing Resources", In 2019 24th IEEE International Conference on Emerging Technologies and Factory Automation (ETFA), IEEE, pp. 1085-1092, 2019.
- [82] M. Alhaj, G. Arbez and L. Peyton, "Approach of integrating behaviour-driven development with hardware/software codesign", International Journal of Innovative Computing, Information and Control, vol. 15(3), pp.1177-1191, 2019.

B-droid: A Static Taint Analysis Framework for Android Applications

Rehab ALmotairy¹, Yassine Daadaa²

College of Computer and Information Sciences
Al Imam Mohammad Ibn Saud Islamic University (IMSIU)
Riyadh, Saudi Arabia

Abstract—Android is currently the most popular smartphone operating system in use, with its success attributed to the large number of applications available from the Google Play Store. However, these contain issues relating to the storage of the user’s sensitive data, including contacts, location, and the phone’s unique identifier (IMEI). Use of these applications therefore risks exfiltration of this data, including unauthorized tracking of users’ behavior and violation of their privacy. Sensitive data leaks are currently detected with taint analysis approaches. This paper addresses these issues by proposing a new static taint analysis framework specifically for Android platforms, termed “B-Droid”. B-Droid is based on static taint analysis using a large set of sources and sinks techniques, side by side with the fuzz testing concept, in order to detect privacy leaks, whether malicious or unintentional by analyses the behavior of Applications Under Test (AUTs). This has the potential to offer improved precision in comparison to earlier approaches. To ensure the quality of our analysis, we undertook an evaluation testing a variety of Android applications installed on a mobile after filtering according to the relevant permissions. We found that B-Droid efficiently detected five of the most prevalent commercial spyware applications on the market, as well as issuing an immediate warning to the user, so that they can decide not to continue with the AUTs. This paper provides a detailed analysis of this method, along with its implementation and results.

Keywords—Static analysis; taint analysis; fuzz testing; android applications; mobile malwares; data flow analysis

I. INTRODUCTION

Android’s market share of mobile phones grew to 74.6% in 2020 [1]. However, there remains considerable concern that popular Android apps tend to leak sensitive information about the user, i.e. phone number, the ID of the mobile device, location, and details of the Subscriber Identity Module (SIM) card. In addition to violating the privacy policies of the user, this can potentially lead to the user’s behavior being unknowingly tracked. Even precisely programmed apps may suffer from these leaks. A major contributor to user data leaks is advertisement libraries, included by some applications to earn money, often enabling the applications to be free to use [2]. These libraries permit advertisements to target a user’s private information and identify him or her through unique identifiers (e.g. the MAC-address and IMEI) as well as location or country [3]. However, many app developers are unaware of the scale to which user’s privacy can be compromised and the large amounts of data potentially held by these ad libraries.

A number of steps have been previously undertaken to ensure the security of apps available to users, but this procedure is complex. For example, developers can upload a new app to the Google Play Store, where it is checked by the Google Bouncer [4]. This analyses the security of the app by conducting a time-limited dynamic analysis, with the aim of identifying any malicious content or behavior. This represents welcome progress, but has, offered only limited success. The majority of mobile platforms, including Android, limit the privileges of apps with a permission model, one that should prevent such apps from gaining access to sensitive data. However, this does not always prove effective, resulting in the release of sensitive data [2]. Such data leaks may not only occur in response to malicious apps, but also be due to an app’s failure to adhere to secure coding practices [4]. It is therefore vital to analyze the data flow within the device, ensuring firstly, sensitive data does not cross established boundaries and secondly, that any untrusted aspect is unable to enter trusted data repositories. This type of analysis is known as taint analysis, i.e. any untrustworthy data source is considered to be tainted. Taint analysis has been conducted on Android systems by several researchers.

This current paper focuses on establishing whether data can flow from a sensitive data source to an undesired data sink. For example, a smartphone holds data that should be private to the user, i.e. personal messages, unique identifier and banking details. An undesired sink can be set up to divert the network Application Programming Interface (API) or applications that cannot be trusted. This study’s definition of a data source is one that is external to the app, and from which the app reads data (i.e. a device’s ID, along with contacts, photographs, and current location). A data sink is a resource external to the app to which the app writes data (i.e. the Internet, outbound text messages and the file system).

II. BACKGROUND AND RELATED WORK

In the following sections, we provide some concepts which are relevant to our research and lists previous and related work in the field of static taint analysis.

A. Background

This section provides the theoretical background to the present study, including an overview of Android systems, taint analysis, mobile malwares, and the fuzz testing concept.

1) *Android overview*: This study focuses on Android, which is currently the most popular mobile platform globally,

being ranked as the premier operating system for smartphones in 2020 [1]. Android apps generally use four types of components, either on their own or in combination. Fig. 1 (below) illustrates the possible interactions between these components.

- An Activity refers to the parts of the Android app visible to the user, thus forming the user interface.
- A Service performs tasks that are time intensive but invisible to the user, i.e. they run in the background.
- System events and user-specific events are received by the Broadcast Receiver.
- The Content Provider allows additional apps or components to access unstructured data, functioning as a standard interface.

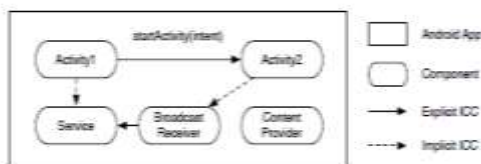


Fig. 1. Overview of Basic Concepts of Android Apps.

2) *Taint analysis overview*: Taint analysis can be either dynamic or static. Static analysis can be described as a method for program analysis in which the source code (or bytecode) is analyzed but not executed. On the other hand, dynamic analysis involves analyzing a code or application by means of its execution, i.e. analyzing an Android app by running it on an Android device.

Examples of dynamic taint analysis include CopperDroid [5], TaintDroid [3], DroidScope [6] and Aurasium [7]. However, it should be noted that the rate of execution of dynamic analysis is less advanced and deficient in code coverage [8] in comparison to static taint analysis.

Static taint analysis lacks runtime overheads, but can detect privacy leaks without running the application [2]. Static taint analyses do not contain the same problems as dynamic taint analyses, but they have their own issues, i.e. they lack the precision required to approximate runtime objects and abstract from the inputs of a program [9]. Much work has been invested in static taint analysis, with over half focusing on points-to-based methods and data flow ([9], [10], [11], [12], [13]). Little research has previously been conducted into analyzing data flows statically in a system comprised of multiple applications. This is significant, as the data's path to a sink might involve passing through one or more components. The advantage of static analysis is that all of the possible execution paths can be explored, not just those invoked during execution. This is beneficial when conducting security analysis, due to breaches of security frequently occurring through unforeseen methods. However, it may not be easy to predict how a program will behave if it is not actually executed. Furthermore, it has been proven that it is

not possible to predict all of the means by which an arbitrary nontrivial program may be executed. Thus, the behavior of programs cannot always be correctly predicted. Nonetheless, static analysis remains valuable, as it provides some approximation of how different parts of a program may behave when executed [14].

3) *Mobile malwares*: Skycure [15] have reported that as many as one in three mobile devices has a medium to high risk of disclosing its user's data. Furthermore, in comparison with iOS devices, Android devices demonstrate almost twice the level of risk of containing malware. This section discusses the most common and damaging malwares impacting on mobile phones.

a) *Trojan*: This is defined as software that works in the background, acting maliciously, but regarded by the user as harmless. A Trojan assists hacker by carrying out actions facilitating attacks by weakening the system security. One example is FakeNetflix, which tricks users into believing they are downloading the official version of Netflix, but instead installs a Trojan on the phone, allowing hackers to access an Android user's credentials for their Netflix account.

b) *Spyware*: This is further common type of malware, consisting of software allowing its author to 'spy' on the user by facilitating unauthorized access to data or collecting information. It runs in the background of the system, where it remains unnoticed by the device user. Two examples of spyware are Nickspy and GPSSpy, both of which run on Android devices. They are able to access the user's confidential information and transmit it to the author of the spyware.

4) *Fuzz testing*: Fuzz testing or fuzzing [16] is an effective technique for finding security vulnerabilities in software or computer systems. It is a technique traditionally used for testing software and can be fully or semi-automated. It supplies unexpected, invalid, or random data as inputs to applications, which can then be monitored to determine whether it engages in unexpected behavior, crashes, or fails built-in code assertions. Applications under fuzz testing fail when they behave in a manner their developers neither intended nor anticipated. There are four categories of failure modes in traditionally applied fuzzing:

- a) Crashes
- b) Endless loops
- c) Resource leaks or shortages
- d) Unexpected behavior

These failure modes vary, based on factors including the type of system or software being tested and the underlying operating system. In this current study, B-Droid was designed and implemented according to the last failure mode category, i.e. unexpected behavior [17]. The consequences depend on the function and purpose of the software, including when and where it is operated. In general, the key to detecting malware is to place it in an ideal environment, followed by providing it with information and monitoring its behavior.

B. Related Work

The literature has suggested that a large body of work is related to static taint analysis approaches, each of which aims to resolve one or more of the many problems facing program analysts when dealing with Android applications. In this section we briefly review some of the existing solutions.

Arzt et al. [9] used the FlowDroid static taint analysis approach to simultaneously evaluate efficiency and precision. This is also the tool we used in our own approach. The results showed that FlowDroid only took a minute to find several security breaches for 500 real world applications, along with 1000 malware samples that were analyzed for 16 seconds per minute.

Bintaint [18] addressed the binary vulnerability mining problem using static taint analysis, so generating the Taint Control Flow Graphs (TCFG). This proposed tool is evaluated employing different compatibility levels of machines using X86 programs for different architecture embedded devices. The outcomes indicated that the proposed Bintaint framework is capable of defeating all the computational overheads of conventional methodologies, as well as addressing all vulnerability issues, without false negativity.

Precise-DF [19] is a novel static analysis method of detecting the taint flow in android apps, through the methodology of reusing the DidFail static analysis tool for fast modular analysis. This approach also uses the Boolean formulas for the DidFail's flow equations, which can help to record the conditions of the flow control for all possible taint flow programs. This approach is novel, as it does not depend on traditional taint flow analysis approaches to evaluate code and using reflection of apps. This method is more involved in providing security to the android apps up to the next level. Taint analysis to GDPR [20] formalizes how taint analysis can be stretched out and enlarged, in order to identify the likely unintended leakage of sensitive data. This study applies the standard static taint analysis methodology to detect any potential data breach, as well as the reconstruction of the flow for the data breach, with the aim of identifying how a breach could take place in relation to the flow. The results demonstrated that flows are not permitted by the privacy policies.

STAR [21] is a prototype designed to address the context-sensitive, flow-sensitive, and multi-source sensitive static taint analysis designed to track the information leaks in android apps. Its novel approach uses two concepts to achieve the performance and scalability of the analysis. The first approach employs the novel summarization technique, beneficial for analyzing the scale for the number of source APIs. The second approach combines techniques in order to establish an efficient propagation of the abstract states, both within and across the method boundaries. FastDroid [22] is a tool proposed as a security measure tool for android apps, being capable of providing efficiency and precision in the detection of sensitive data leaks. Three test suites were used to evaluate the performance of the FastDroid tool, with the results demonstrating high levels of precision and recalls, as well as effective efficiency in the results achieved. FastDroid differs from conventional approaches due to its technique of using

propagation of taint values rather than the data flow values employed in traditional approaches. This resulted in improved efficiency.

COVA [23] this study offers a comprehensive level qualitative analysis for the evaluation of increased precision in static taint analysis. The study used the taint flows reported in FlowDroid [9] in 1,022 real world apps for android, with the results showing some key findings relating to conditions under which taint flows occur.

The analysis showed that specific settings (i.e. environmental setting, user interaction and I/O) are taint flows that are also involved in some specific conditions. BackFlow [24] is a context-sensitive taint flow reconstructor tool that builds paths linking sources to sinks. The results revealed that when BackFlow generates a taint graph for an injection warning, there is empirical proof that such an alert is a true alarm. DepTaint [25] implements a form of static taint analysis that analyzes the taint variables propagated by implicit flows and explicit flows. DepTaint greatly exceeds the static checker of LLVM in both defining taint variables and achieving more fine-grained pathways of taint propagation. ANTaint [26] improves scalability. An experiment involving 60 cases demonstrated that ANTaint is appropriate for 95% of cases, by extending the call graph and applying taint propagation on demand for libraries.

III. ANALYSIS METHOD

When designing and implementing a static taint analysis for detecting malware, it is first vital to consider a robust and native Android anti-malware platform capable of running on smartphones rather than on a third-party device i.e. a computer or laptop. This requires a platform that is efficient modular, automated and static. Our platform consists of three main stages (De-Obfuscation – Data Flow Analysis – Fuzz Testing). During the first stage, we de-obfuscate all Android smartphone-installed applications if their granted permissions touch our privacies, in order to obtain their source code. From this de-obfuscation stage, we go through the static analysis stage using taint analysis, i.e. a special type of data flow analysis. We then integrate the open source FlowDroid tool [9] as a module into our B-Droid platform, followed by double checking the results during the third stage, using a fuzz testing module for the Applications Under Test (AUT). This efficient platform can sandbox any doubtful applications, while instantly testing their leakage by placing them into a real and ideal environment and giving them fake privacy information. The platform then monitors any unacceptable behavior.

The design and implementation of the B-Droid is accomplished in four layers, as shown in Fig. 2.

- Layer 1: Permissions analysis layer:

This is the main module focusing on the following functionalities:

- a) Reading all installed apps' AndroidManifest files.
- b) Searching for permissions of interest inside AndroidManifest files.
- c) Preparing the doubtful apps filter.

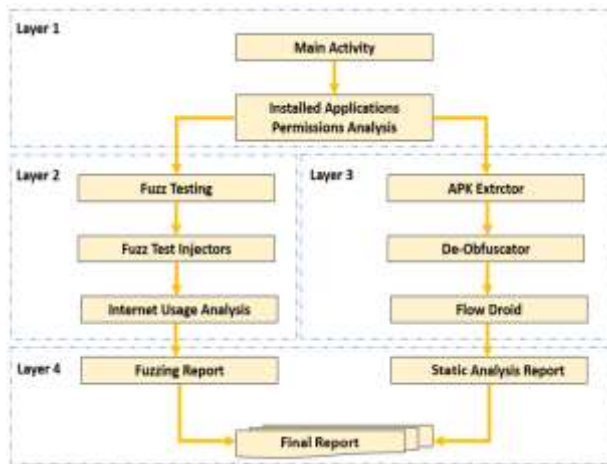


Fig. 2. Proposed Approach.

- Layer 2: Fuzz testing layer:

This layer is comprised of three fuzzing stages:

1) *Fuzz testing*: This is the base class for the fuzzing process, containing the parent attributes and methods of fuzz testing. The main task of the B-Droid is to detect Internet usage that demonstrates unexpected behavior for doubtful applications authorized to access the following permissions:

- a) Receive SMS.
- b) Process outgoing calls.
- c) Read phone state.

These doubtful applications will certainly be authorized to access INTERNET permissions. The B-Droid test case scenario is organized to enable it to detect the misuse of any of the above granted permissions.

2) *Fuzz testing injectors*: This is the base class for the following injector classes:

- a) *Fuzz Received SMS*: This class model is responsible for preparing a well-formatted fake SMS.
- b) *Fuzz Incoming Call*: This class model is responsible for triggering a real incoming call.
- c) *Fuzz Outgoing Call*: This class model is responsible for initiating a real outgoing call [17].

3) *Internet usage analysis*: This is the Internet usage measurement layer, which monitors the sent and received packet changes in a specific period for AUT.

- Layer 3: De-Obfuscator & Static Analysis:

This layer is comprised of three stages:

4) *APK Extractor*: This is the module that we developed to extract the APK file from our doubtful applications list transferred from layer 1.

5) *De-Obfuscator*: This is the module responsible for decompressing the APK file and retrieving its source code [27]:

- a) Resource files (xml, text, icons).
- b) Dex files (JAVA, JAR).

6) *Flow droid*: This is the malware static analysis module [9] that inspects the AUT code, in order to derive information concerning path behavior.

- Layer 4: Final Report Generator:

This layer is comprised of 3 stages:

7) *Fuzzing report*: This is the result obtained after fuzz testing successfully finalizes its mission on AUT and reports whether or not the application carries out malicious behavior.

8) *Static analysis report*: This is the malware analysis decision maker module, which generates a pass/fail report about AUT in response to any identified information leakages or program vulnerabilities.

9) *Final report*: This compares the two previous reports to conclude our work and clearly classify whether or not AUT is malware.

In general, a misinterpretation of a non-malicious activity as an attack by security system results in a “False Positive” error. These errors are a critical issue for today’s cybersecurity. The design of our anti-malware B-Droid platform (which uses both taint analysis and fuzz testing running separately on an AUT) will, as discussed in Section IV, decrease the false positive rate.

IV. IMPLEMENTATION DETAILS

The following subsections discuss the structure and flow chart related to each layer.

A. Permissions Analysis and Filter Layer

This section illustrates the structure and flow chart of the permissions analysis and filter layer. Prior to an examination of the details of the flow chart, we must first note that we have selected a set of dangerous permissions (RECEIVED_SMS, READ_PHONE_STATE, NEW_OUTGOING_CALL) which can be requested to invade the user's privacy and access private data by any malicious application [28].

As shown in Fig. 3, the functionalities of this layer can be divided into two classes: firstly, main activity and secondly, permissions analysis.

The main activity class is the starting point of the B-Droid lifecycle. The main functions of this class are to characterize the application permissions risk and prepare the signatures of application permissions. These are mined in the AndroidManifest files of all installed applications. We then turn to the permissions analysis class functionalities, which appear in the third process. This process enabled us to sequentially read the AndroidManifest files of all installed applications, followed by searching for one or more permission signatures within our area of interest. The application is added to the doubtful list if the signature is found. This layer mechanism resulted in a list of all the installed doubtful applications that are granted one (or more) permissions of interest, in addition to the INTERNET permission.



Fig. 3. Permissions Analysis and Filter Flow Chart.

B. Fuzzing Injector Layer

This section examines the issue from the opposing perspective, i.e. broadcasting fake intents that perform as if real. Although there are an almost infinite number of possible inputs to any given application, our specific inputs or fuzzing injectors focused solely on calls and SMSs. We therefore prepared a real SMS, along with an incoming call and an outgoing call, which we termed injectors. These were then broadcast into the Android application layer to act as bait. B-Droid is able to identify whether AUT takes any of these baits.

Starting from the end of the previous layer, and after filtering all installed applications, the process commences when the user chooses any of the doubtful applications, i.e. AUT. The first process after selecting AUT is to obtain this application's signature, as outlined above. The signature(s) stimulate the B-Droid to prepare the matched injector(s) for the fuzzing process. The following points outline the structures of the three injectors participating in the fuzzing scenario.

1) SMS Injector:

- The received SMS injector is initiated by the previous layer if the AUT permission signature was RECEIVED_SMS. The first process is to create a PDU-formatted SMS [29] with content and other metadata.
- The second process consists of creating an implicit intent to be loaded with the SMS PDU message as additional data. This intent is simultaneously deployed with "android.provider.Telephony.SMS_RECEIVED". This action is used by most malware applications interested in SMSs and is coded in AndroidManifest. The SMS injector is then ready to simulate a real received SMS content, along with its intent.
- The final process in this injection is to broadcast the fake SMS. This is done by broadcasting the prepared intent to the Android application layer, which then informs the Android OS that a new SMS has been received within the message body.

2) *Incoming call injector*: This class implements the incoming call injector with the help of the telephone verification service. This service entails returning a call to a customer on the number provided, in order to verify that: a) the individual placing the order is the same as the owner of the phone and b) that the phone is indeed working. We used this service to perform an automated real incoming call injected into AUT by integrating Cognalys [30] Android API with our project. Cognalys provides a telephone verification service through a multi-platform package that application developers are able to use in their applications to check mobile phone numbers.

- The incoming call injector commences as a response to the AUT permission signature Read_Phone_State.
- The first step in the process was to request Cognalys' API service, by registering with the Cognalys server, then downloading and integrating its Android API with our Android project B-Droid. When registering with Cognalys, the user obtains an API key and an Access Token. These two entities are embedded into the verification call request, in addition to the cell phone number receiving the verification call.
- The second process was to process Cognalys' incoming call, i.e. informing the user that we were waiting for an incoming call by forcing B-Droid to run a waiting view until the incoming call was successfully received.
- Once the verification call had successfully taken place, the role of the third process was to read the response of this verification call, which contained a verification code and the result code. In our case, we were not interested in the verification code (i.e. our main task was to simply receive a real incoming call), but we were concerned with the result code, which informed us whether or not the incoming call was successfully transmitted. If the call is not received (which rarely happens), we would need to resend a new Cognalys request until the response result status code was returned successfully.

3) *Outgoing call injector*: We turn our attention to the final injector, i.e. the outgoing call. The simplest and most efficient means of carrying out a fully automated dynamic real outgoing call is to find a means of forcing the cell phone to call its number. If the user tries to call, then a real outgoing call is made for a period of 4 seconds, which results in the mobile operator giving a response of "busy number" and the call is automatically terminated. This led to our injector simulating a real outgoing call environment for AUT.

- As with previous injectors, the current injector is initiated as a result of the AUT permission signature New_Outgoing_Call.
- The first process is to prepare an implicit intent with the action of calling a phone number and loading it with a bundle of additional data for the dialed mobile phone number.

- The second process is to take the result of the previous process, (i.e. the prepared intent), which then initiates a new process with that intent, i.e. forcing the cell phone to call itself.

C. Internet usage Analysis Layer

This forms the comparator layer for each of the above layers, being considered a monitoring layer in the B-Droid application hierarchy. It is responsible for accounting the transmitted and received internet packets of AUT before, during, and following the injection or fuzz testing lifecycle. The results of this layer directly impact AUT's pass/fail report, i.e. it establishes whether or not this particular AUT is a malware application.

- The starting point is triggered automatically in a synchronous manner when any of the doubtful applications listed is selected by the user, thus entering the fuzzing scenario.
- The first process of this layer is to obtain and store the AUT traffic information (i.e. numbers of transmitted and received packets) prior to fuzzing. This information is comprised of the offset numbers the comparison will use to determine whether, by the end of fuzzing, it increases in number or not.
- During the fuzzing life cycle (approximately 15 seconds for each fuzz test case or injector lifecycle), the second process is run in the background to count any transmitted or received packets related to AUT's internet usage.
- By the end of the fuzz test case(s) life cycle(s), the third process amalgamates the previous process results with the first process offsets, storing them classified by the injectors' internet usage. It will then be fed back into the pass/fail report generator, as discussed in the next section.

D. De-Obfuscator and Static Analysis Layer

The de-obfuscator and static analysis layer inspect the AUT code to derive information about the app's behavior. In general, static analysis can check for programming errors and security flaws. However, our platform uses a taint analysis approach [9], i.e. a special type of data flow analysis. It follows a sensitive "tainted" object from source to sink, tracking the relevant tainted data along the path. Taint analysis can be used to find information leakages and program vulnerabilities, which form the focus of this paper.

1) *APK Extractor*: The Android Application Package (APK) contains the executable application installed on android phones or tablets. We therefore needed to implement a module on our B-Droid platform capable of extracting APK from the installed application. An APK Extractor module was designed and implemented for this purpose, capable of extracting APKs from the AUT list. The APKs thus obtained were stored in the phone's internal memory, ready for the next static analysis stage.

- Initiation of the application leads to processing of a list of all the applications installed on the device. Our APK extractor module employs the built-in classes PackageManager and ApplicationInfo to identify and retrieve all the APK files of the installed app.
- We accessed the AUT public source directory paths through our implemented APKExtractor Class.
- We then converted these paths to an APK File Object, storing them in the phone's internal memory.

2) *De-Obfuscator*: This forms our module to decompile and extract the source code of an Android application (including XML files and image assets), JAR Packages and dex files, which work natively on our Android device. Generally, any Android application consists of 3 main components:

a) *JAVA files*: inside which the developer draws his/her picture.

b) *JAR files*: all external ready-made libraries the developer imports into his/her project to use its built-in classes and functions easily and fairly.

c) *Resources files*: in this case we have all xml files, layouts, media files, drawables and AndroidManifestFile.

From the above main components, we implemented three main decompiler classes in each one: JAVAExtractionWorker Class, JARExtractionWorker Class, and ResourceExtractionWorker Class [27].

3) *FlowDroid*: We used FlowDroid [9] as this implements a special technique for data flow analysis, known as taint analysis. Its procedure is to follow data along the programs' path of execution, which can be performed both forwards and backwards. A taint analysis keeps a record of data and its path from preset data sources to preset data sinks. It is designed with the objective of discovering a range of existing connections between provided sources and sinks. It is frequently used for security-relevant tasks. When the analysis is focused on the integrity of the application, untrusted inputs are specified as sources and should not reach sensitive sinks. Fig. 4 shows the different steps necessary for the analysis of our AUTs. Once the De-Obfuscation module is ready, FlowDroid [9] searches for call-back methods and lifecycles, as well as calls to sources and sinks in the application source code.

This is achieved by parsing different Android-specific files, such as the layout XML files, the dex files including the executable code and the manifest file that specifies the services, activities, content providers and broadcast receivers in the application. Furthermore, from the entry point list, FlowDroid [9] produces the main method. This is the primary approach for producing a call graph and an Inter-procedural Control-Flow Graph (ICFG). This detects all sources capable of being accessed from the given entry points. Starting at these sources, the taint analysis tracks taints by traversing the ICFG. This also introduces a function called Taint Wrapping, which can be used to substitute code unavailable for analysis, so as to

optimize performance. Finally, FlowDroid [9] reports all discovered flows from sources to sinks. The detailed information is provided in the final report module.

E. Final Report layer

The final destination in our approach is the report generator layer, in which we conclude our output results, drawn from the fuzzing and taint analysis modules. It is within this layer that we make and present our decision over whether or not the AUT presents malicious behavior.

1) *Fuzzing report:* The final stage in our fuzzing module is the pass/fail report generator, which is responsible for giving the Android user a clear report concerning AUT. In the case of failure, the report contains the leakage of privacies on which AUT has eavesdropped. In addition, it states whether the AUT passed the test without any leakage.

- The starting point commences automatically following the successful conclusion of the injection life cycle(s) for all injector(s).
- The output of the “Tracking AUT Traffic Information after fuzzing” process is requested from the previous processes to enable a comparison of the traffic information before and after fuzzing, and to calculate these changes for each injector during its lifecycle.
- If the AUT traffic information is found to have increased following the fuzzing lifecycle, it is written in the failure report as spy evidence, tagged by its permission signature. As an example, If the AUT traffic information increased during fuzzing with Received SMS, then it is written in the report as: This App Intercepts Your Received SMS, and the same for the other two properties (Incoming and Outgoing calls). If the traffic information is the same before and after the fuzzing lifecycle, then it will be checked as a clean app.
- The second process stores the results of the pass/fail report, sending them immediately to the user’s notification bar.

2) *Static analysis report:* This analyzes the apps’ bytecode and configuration files to find potential privacy leaks, as follows:

- It searches the application for lifecycle and callback methods, as well as calls to sources and sinks.
- It then generates the dummy main method from the list of lifecycle and callback methods. This is then used to generate a call graph and an inter-procedural control-flow graph (ICFG), as shown in Fig. 4.
- Starting at the detected sources, the taint analysis then tracks taints by traversing the ICFG.
- Finally, Taint Analysis reports all discovered flows from sources to sinks, including full path information.

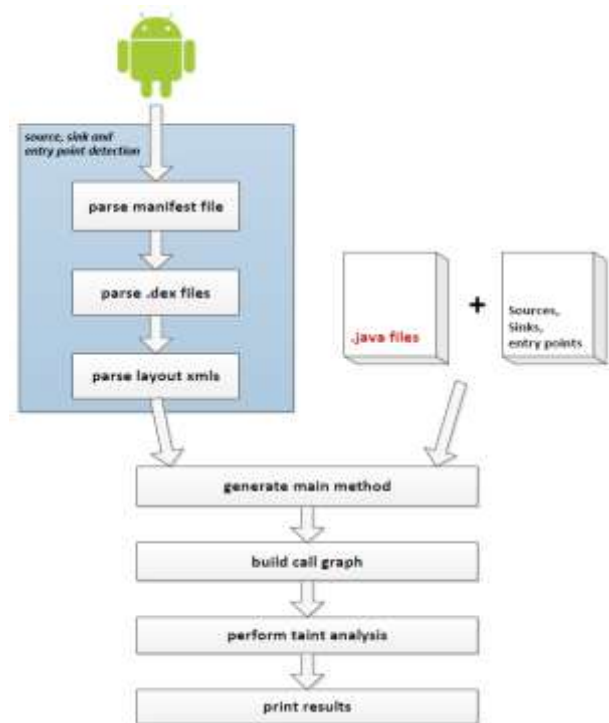


Fig. 4. Overview of Flowdroid.

V. EVALUATION AND RESULTS

A. Results

We tested B-Droid against a dataset of over 100 Android applications uploaded on Google Play (or other third-party Android stores), as shown in Fig. 5. We selected a variety of application categories (Social Media Apps, Chat Apps, Caller Id Apps, and pure Mobile Remote Access Trojans (MRATs Apps)). As show Fig. 8, the results of B-Droid against Social Media Applications and Chat Applications were negative (pass) as well as for the Flowdroid tool. However, for Caller Id and MRATs Applications, the results were positive (fail) in fuzz testing and a few were positive (fail) in Flowdroid. The sample of Social Media and Chat Applications is summarized in Table I and the sample of MRATs and Caller ID Applications are summarized in Table II. These tables show the results of the comparison between B-droid and the prominent taint analysis tool Flowdroid.

- Evaluation 1:

The Caller ID Applications and MRATs we examined changed their Internet usage behavior during the fuzzing lifecycle, employing the available mobile Internet data, i.e. Mobile Data or Wi-Fi. Fig. 7 demonstrates that the number of bytes transmitted during the fuzzing lifecycle differed in AUTs. B-Droid reported that all these applications spied on information related to outgoing calls, incoming calls and received SMSs (see the sample of these results in Table II). Furthermore, the majority of MRAT vendors allowed potential customers to have a free trial of their spy product for 2–7 days. However, B-Droid detected that, even after the ending of the trial period, these free versions continued to transmit private data from the mobile phone.

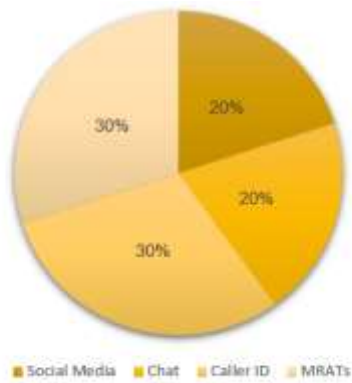


Fig. 5. AUT Flow Chart.

TABLE I. SAMPLE OF TESTED SOCIAL MEDIA AND CHAT APPLICATIONS

App Name	Installed Package	Store/ Provider	B-droid	FlowDroid
Snapchat	com.snapchat.android	Google Play	Pass	0 Leaks
Instagram	com.instagram.android	Google Play	Pass	0 Leaks
Messenger	com.facebook.orca	Google Play	Pass	0 Leaks
Twitter	com.twitter.android	Google Play	Pass	0 Leaks
WhatsApp	com.whatsapp	Google Play	Pass	0 Leaks
Telegram	org.telegram.messenger	Google Play	Pass	0 Leaks

TABLE II. SAMPLE OF TESTED MRATs AND CALLER ID APPLICATIONS

App Name	Installed Package	Store/ Provider	B-droid	FlowDroid
Android Auto	com.system.task	Xnspsy.com	Fail	0 Leaks
Sync Manager	com.android.core.mngp	Snoopza.com	Fail	0 Leaks
Sync Service	com.android.core.mntq	Hoverwatch.com	Fail	0 Leaks
Setting	com.sec.android.as	my.a-spy.com	Fail	1 Leaks
Vibo Caller	com.vibolive	Google Play	Fail	0 Leaks
CallApp	com.callapp.contacts	Google Play	Fail	0 Leaks
True Caller	com.truecaller	Google Play	Fail	0 Leaks

^a NOTE: (Fail= Positive Pass= Negative)

• Evaluation 2:

As shown in Fig. 6, the fuzz testing of the Caller Id Applications gave positive (fail) results for all the permissions of interest to B-Droid (Incoming Call, Outgoing Call, and Received SMS). End users can be sure that the scope of work of this type of application is simply to read incoming and outgoing dialled phone numbers and instantaneously, once it

has access to the Internet, it works outside the phone to retrieve the names matched with those numbers as stored in cloud databases.

• Evaluation 3:

Compared to the popular Flowdroid tool, B-droid is able to detect leaks that the Flowdroid misses. As shown in Table II, static taint (Flowdroid) is insufficiently accurate with the clear malicious applications (MRATs) and the results showed that the majority of these malwares had no leakage (0 Leakage). Our contribution here is B-Droid, which can work hand-in-hand with Flowdroid to correct its weaker points, along with the development team of Static taint (Flowdroid) recommended a dynamic analysis technique work with Flowdroid to review its results. So, we see that static analysis and fuzz testing work hand in hand, such that they further strengthen their respective findings.

• Evaluation 4:

We have transferred our B-Droid model into a form useable by smartphone end users, enabling it to achieve the usability concept as shown in Fig. 9.

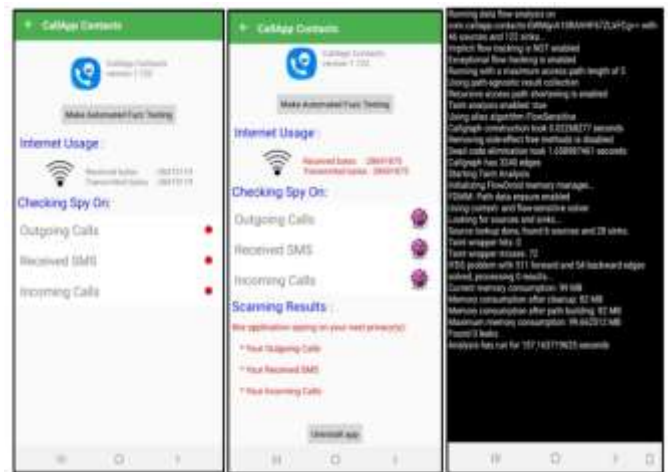


Fig. 6. Sample of Caller Id Apps Report.

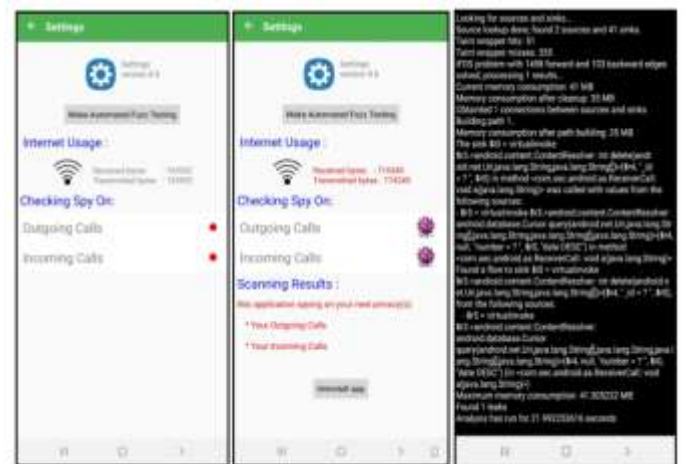


Fig. 7. Sample of MRATs Apps Report.

- [15] B. Amro, "Malware Detection Techniques for Mobile Devices," vol. 7, no. 4, pp. 1–10, 2017.
- [16] A. Labade and H. Ambulgekar, "Fuzzing for Android Application: Systematic Literature Review," 2020.
- [17] M. H. Saad, A. Serageldin, and G. I. Salama, "Android spyware disease and medication," 2015 2nd Int. Conf. Inf. Secur. Cyber Forensics, InfoSec 2015, no. 5, pp. 118–125, 2016, doi: 10.1109/InfoSec.2015.7435516.
- [18] Z. Feng, Z. Wang, W. Dong, and R. Chang, "Bintaint: A Static Taint Analysis Method for Binary Vulnerability Mining," Int. Conf. Cloud Comput. Big Data Blockchain, ICCBB 2018, 2018, doi: 10.1109/ICCBB.2018.8756383.
- [19] W. Klieber, W. Snively, L. Flynn, and M. Zheng, "Practical precise taint-flow static analysis for android app sets," ACM Int. Conf. Proceeding Ser., 2018, doi: 10.1145/3230833.3232825.
- [20] A. Mitras, K. Rannenber, E. Schweighofer, and N. Tsouroulas, Tailoring Taint Analysis to GDPR. 2018.
- [21] W. Choi, J. Kannan, and D. Babic, "A scalable, flow-and-context-sensitive taint analysis of android applications," J. Vis. Lang. Comput., vol. 51, no. October 2018, pp. 1–14, 2019, doi: 10.1016/j.jvlc.2018.10.005.
- [22] J. Zhang, C. Tian, and Z. Duan, "FastDroid: Efficient taint analysis for android applications," Proc. - 2019 IEEE/ACM 41st Int. Conf. Softw. Eng. Companion, ICSE-Companion 2019, pp. 236–237, 2019, doi: 10.1109/ICSE-Companion.2019.00092.
- [23] L. Luo, E. Bodden, and J. Spath, "A qualitative analysis of android taint-analysis results," Proc. - 2019 34th IEEE/ACM Int. Conf. Autom. Softw. Eng. ASE 2019, pp. 102–114, 2019, doi: 10.1109/ASE.2019.00020.
- [24] P. Ferrara, "BackFlow: Backward Context-Sensitive Flow Reconstruction of Taint Analysis Results," 2020.
- [25] R. Ma, X. Wang, and X. Wang, "DepTaint: A Static Taint Analysis Method Based on Program Dependence," 2020.
- [26] Y. Wu et al., "Scaling static taint analysis to industrial SOA applications: a case study at Alibaba," 2020.
- [27] N. Rajendran, "decompiler for android.," pp. 1–9, 2020, [Online]. Available: <https://github.com/niranjn94/show-java>.
- [28] Android Developers, "Manifest.permission," [Online]. Available: <https://developer.android.com/reference/android/Manifest.permission>.
- [29] John Wiley & Sons, "Android Messaging," 2014.
- [30] Cognalys Inc, "Cognalys Android Library (CAL)," [Online]. Available: <https://cognalys.com/>.

HoloLearn: An Interactive Educational System

Human Body Simulation and Allowed User Interaction through Hologram Model and Kinect V2 Sensor for Educational Purpose

Shorooq Alghamdi¹, Samar Aloufi², Layan Alsalea³, Fatma Bouabdullah⁴

Faculty of Computing and Information Technology
King Abdulaziz University
Jeddah, Saudi Arabia

Abstract—The HoloLearn project is a sophisticated interactive educational system that attempts to simplify the educational process in the field of medicine, mainly, through the use of Hologram technology. The Hologram technology has been used in conjunction with the feature of user interaction, to take the whole educational process to a completely new level providing students with a different learning experience. The system is more dedicated to medical students as they must study diverse, complicated structures of the human body anatomy and its internal organs. HoloLearn is aimed at replacing the traditional educational techniques with a new one that involves user interaction with real-sized 3D objects. Based on the interview conducted with medical students from different universities and educational levels in Saudi Arabia, and the questionnaire results, it has been found that traditional learning techniques are insufficient/inefficient as they lack quality and most of the criteria that could qualify them to be highly effective as reliable learning materials. Therefore, there is an increasing need for new learning strategies/methods with enough capabilities to give the students the chance to perceive every concept they study, rather than depending on their imagination to picture what a human body looks like from inside, they need visual learning methods. From another perspective, teachers also face difficulties when explaining medical concepts, especially those related to human body structure and behavior. The currently available materials and sources are mostly theoretical. They promote indoctrination and a result-driven approach instead of engaging the students in a process of sharing knowledge and ideas from both parties i.e., teacher and students. In fact, students have to listen and read instead of practicing and exploring, consequently students are prone to loss of concentration and mental distraction during lessons repeatedly, while from another angle they suffer from long study hours and difficulties in retrieving information. The results of this project indicate that when combining the Hologram technology with the user interaction feature, the educational process can be highly improved, and can be much more creative and entertaining.

Keywords—Interactive educational system; hologram technology; user interaction

I. INTRODUCTION

The world is changing, and technology is contributing to almost everything. Starting with the massive growth of the Internet that connected people from all over the world, the use of mobile applications to simplify daily tasks, and ending with the use of Information Technology in almost every field, industrial, medical, agricultural, and educational. The need to

facilitate the process of education is continuously growing and interactive learning methodologies are becoming an urgent requirement. Every day, people try to find new ways to convey/deliver information in the simplest possible form to enhance long-term memorization while maintaining the information correctness, and here comes the importance of this project. For instance, medical students face daily problems trying to find efficient learning methods and reliable sources of information that simplify the content and provide it in an understandable form. Text-based information, images, videos, models, or even Cadavers, which, according to [1], "remain a principal teaching tool for anatomists and medical educators teaching gross anatomy", are also known as corpses. All these different methods are for the sake of a better understanding of human body structures and different health conditions. Each one of those methods has its own limitations that prevent it from providing enough information, students are still in a continuous search for alternatives. Specifically, medical students from different levels face problems of distinguishing between different body organs and its functions, understanding muscles' movement, body behavior, and how it responds to external stimuli. Memorizing all of these details and applying this knowledge when needed would be a very complicated process if not supported by effective learning methods. Some universities try to simplify the process by using models or corpses. One of the drawbacks of using a corpse is its incapability to demonstrate vital activities. For instance, a corpse will not be able to show blood circulation, heartbeats, or neural flow. On a global scale, it is agreed that the use of corpses in education is not the ideal option. As stated in [2], "The principal disadvantages of the anatomy room embalming solution are the brown discoloration caused by phenol and the irritation to the dissector's eyes and lungs by formalin. Each anatomy department has its own preference for the preparation, concentration of fluids, and the manner in which they are injected. The 'standard' method of preservation outlined is ideal in that bodies can be kept for months at room temperature but on the other hand, it alters the normal color and consistency of the tissues, rendering them less life-like. Most flap dissection workshops last between 2 and 4 days so fresh cadavers are suitable and seem preferable. One should not however forget that fresh cadavers are not sterilized. They must be very carefully selected so that bodies contaminated with HIV, hepatitis, and prions are excluded. Prions or the social". HoloLearn proposes a different method of education that

does not require the use of real corpses, which is learning by interacting with real-sized 3D objects that simulate the human body organs accurately. Our proposed solution aims at facilitating the educational process with the use of the Hologram technology, which is according to [3] is "a photographic method that records the light dispersed from a body and then produces a realistic image identified as three-dimensional Hologram", combined with user interaction. Using the Hologram technology will give the opportunity to display each organ as a 3D object, show its movement, and allow interaction with it, such as selection, rotation, and zooming. Indeed, this method will provide the students with a better and visually appealing experience, ensure full understanding, and enhance long-term memorization. The aim of this project is supported by the fact that auditorial memory is inferior to visual memory according to most research.

HoloLearn project can serve in many fields, including universities and schools to be used by both, teachers, and students as an educational tool where they can see how the actual human body looks from inside and visualize how it behaves under different conditions. Moreover, it can be utilized in hospitals to be used by physicians in surgeries to specify the parts/organs they should work on precisely. Also, can be used by physicians to provide the patient with better visualization of the disease diagnosis.

HoloLearn project is intended to develop an environment with an educational purpose in which users, specifically medical students, can interact with real-sized 3D objects that simulate human body organs. The system consists of three main parts. The first part includes displaying the complex structures of the human body as a Holographic model, including the main systems, such as Muscular, Skeletal, Venous, and Skin. Moreover, it includes the internal organs, such as the heart, lungs, and kidneys. The second part is concerned with the main feature we are interested in, which is the user interaction. This part consists of allowing and capturing some pre-defined movements/gestures made by the user against the model through a specialized sensor (Kinect V2), where a desktop application will be used to process and analyze the received interaction. The third part guarantees that the system reacts in accordance with the gesture made by the user. The reaction is mainly a change in the Hologram model position and appearance to better achieve the interactivity and provide the students with a different visual learning experience.

The project is aimed at contributing to the improvement of the educational process and taking it to a completely different level by replacing traditional educational techniques with a new one that ensures user interaction with real-sized 3D objects, presented using the Hologram technology, where multiple students can participate in the learning process simultaneously and with the least possible number of devices and wear.

This paper is organized as follows: In Section II, an overview of the problem domain and the related work is discussed and followed by the actual implementation of the purposed solution, regarding the hardware and software, in Section III. The obtained results, achieved objectives, and the

shortcoming and challenges are argued in Sections IV and V. finally, the future work is discussed in Section VI.

II. BACKGROUND

The educational methods have evolved rapidly in the past 10 years. In the field of medicine, the students used to depend on paper resources, which may include images to help visualize the structures. These resources could not give the students the ability to understand every concept or visualize the inner structure of the human body comprehensively. The way the human body behaves from inside, the blood flow, the nerve supply, and the way each organ moves, all such important details could not be described sufficiently using books, images, or cadavers. The students were partially, and in some cases totally, incapable of understanding such important details. Later on, the technology started to intervene. 3D videos, animated pictures, and some mobile applications have been developed to serve the purpose of facilitating the educational process. Each one of these methods has its own limitations that increased the need for a new technique. For instance, most of the current mobile applications that are dedicated to medical students either lack interaction or provide objects that can be only displayed in a very small size (usually on mobile screens). Moreover, most of them require a monthly or annual paid subscription. On the other hand, they are not provided by the university as an official source of education or used by teachers in classes, rather, the students themselves are responsible for searching and finding such applications in order to follow up with the lectures and survive the course, as the traditional techniques are no longer useful enough.

Now-a-days, with the simultaneous advancement of technology and education at a time, it has become possible to build a learning environment that gives the students the chance to be more involved. Instead of watching, listening, and receiving information in a unidirectional process, they finally can intervene more in the education, turning the whole process into a bidirectional experience. In the past few years, many technologies have been used in order to provide a high-quality education, such as Augmented Reality (AR), Virtual Reality (VR), and Mixed Reality (MR) technologies.

One of the organizations developed a solution, HoloHuman [4], based on the use of Microsoft HoloLens, where the user has to wear such a lens to become involved in a virtual environment that is built upon Mixed Reality technology. This solution allows users to interact directly with a real-sized 3D model that simulates the actual human body, once the lens is on. Another distinguishing feature of this solution is the ability to accommodate multiple users at once, with the condition of wearing the lens to get involved in the virtual environment. Another interested organization developed a mobile application, called Essential Anatomy 5 [5], to display human body anatomy including the male and female body variations as separated 3D models on screen, where users can carry all the functions at their fingertips. This application contains 11 complete systems that can be accessed from the main screen. "These include Muscular, Skeletal, Connective Tissue, Venous, Arterial (Including the Heart), Nervous (Including the Brain), Respiratory, Digestive, Lymphatic, Urogenital, and Skin" [5]. To support students,

they created a Test-Your-Memory feature, in which a user can use multiple options to evaluate his knowledge. This application works on mobiles with no need for any extra devices, yet it lacks full interactivity and user involvement. Anatomy ARVR is another mobile application with an educational purpose [6]. As the name implies, it uses virtual reality and augmented reality to offer students an interactive learning environment. In this application, the user must position the camera in a certain manner on the ARVR book provided by the same company to visualize the human body organs as 3D objects. This application provides the students with the ability to rotate, zoom and view details, such as the name and function of a selected organ to achieve a better experience. Comparatively, BioDigital, according to [7], is a "software that power's the world understanding of human body anatomy through interactive 3D software platform" for visualizing anatomy, disease, and treatment. In addition to the usual features, such as visualizing human body anatomy in 3D, and allowed interaction, this application has covered the different health conditions, disease diagnoses, and treatment in its scope. The BoneBox™ Skull Viewer is another example of the use of technology to facilitate the educational process in the field of medicine, however, it has a limited scope where it only focuses on the skull anatomy and provides a labeled, detailed description of the type of functions and processes that run inside [8].

The problem of this paper has been addressed multiple times already. However, each of the existing solutions has some limitations that we are trying to overcome in our proposed solution. The need for each user to wear/hold extra devices to finally get involved in the virtual environment has been eliminated by the use of one specialized sensor, Kinect V2, and one projector to display the final Holographic model, which is unlike AR and VR, can be seen by everyone without 3D glasses. This solution makes it possible to place the whole system in one spot at laboratories in schools and universities to be used as an official educational tool. Virtual Reality, Augmented Realty and Mixed Reality technologies have been replaced by Hologram technology to provide a more realistic viewing experience through a large-sized 3D Holographic model. To achieve better interactivity and allow students to take charge of the learning process, reduce the need for an instructor to be present, and promote self-learning, the Kinect V2 sensor has been used. This device will capture and detect any pre-defined gestures made by the user from a reasonable distance, where students can keep in a continuous process of learning through sending and receiving reactions without any manual intervention from a facilitator. From another point of view, the scope of this solution covers the entire human body.

HoloLearn is intended to make a revolution in the field of education. Whether it is the medical, biological, geographical, or engineering school this project will encourage institutes and universities to start allowing technology to intervene more in the evolution of the educational process. Specifically, they will start benefiting from the Hologram technology as it has so many applications and high potential to emulate almost anything.

III. IMPLEMENTATION AND RESULTS

The following subsections discuss the actual implementation of the proposed solution and the individual tools utilized to produce the final working system, including both hardware and software.

A. Hardware Set-up and Installation

In the context of Holographic models, different tools and devices can be suggested to produce a Holographic-like image i.e., Holographic 3D model. The author in [9] defines Holographic displays as "a device that uses light diffraction to create three-dimensional (3D) images in space. When real objects and holographic images are located in the same space, they can be perceived without inhomogeneity". Devices range from low-quality ones, that are capable of producing exclusively small-sized 3D models, that lack flexibility and cannot be extended to incorporate other beneficial features such as user interaction, to high-quality devices that are extremely expensive. Most of the currently available devices are considered to be one-way displays that are incapable of receiving and processing any type of interaction. They do not include any built-in sensors or detectors to recognize human movement. Moreover, they do not consider future scalability and integration with other devices; therefore, they are not physically prepared for such purposes. For instance, there is not any kind of ports or adapters to support possible integration. The traditional basic method of displaying a Holographic model consists of using a pyramid-shaped stage that comes in various sizes in which there is a need for a specific type of tablet to store the 3D objects to be displayed as Holographic images. Other types of Hologram projection devices are "composed of a fan that produces an illusion of 3D objects floating in the air. The fast-spinning fan becomes nearly invisible to the naked eye and the projected object thus gets a see-through background" [10]. Most of the time, these devices are used for advertising and marketing purposes to showcase products in shopping malls and supermarkets. Obviously, the main drawback of the discussed methods is the very small size of the produced models and the questionable quality, thus the incapability to reflect reality precisely or allow users to perceive fairy images without eyestrain. The size of the produced model is one of the most concerned criteria when it comes to selecting a device to display the Holographic model. On the other hand, some of the devices come with a pre-developed mobile application to display only the objects that can be consumed and processed by that application, which prevents any further utilization of such devices. In some rare cases, other devices ship with flash memory that, again, contains all the 3D objects to be displayed as Holographic models.

Hence, none of the above-explained devices fit with the HoloLearn's main purpose, which is being able to output real-sized 3D models while making it possible to receive and analyze user interaction. The main problem of this paper is not focused on displaying Holographic models as this issue has been addressed and solved years ago. On the contrary, it is focused on utilizing this technology and benefiting from the existing studies and tools, i.e., Hologram projectors, to develop a visually appealing environment that adapts the concept of user-engagement in a visual and real learning

experience to help a better understanding and encourage a different method of education.

The reasons and facts showed earlier prove the inadequacy of the existing devices and the increasing necessity of a new customized device that fulfills the new requirements. Our customized display stage is inspired by the related work and previously developed Hologram projectors. It considers their drawbacks and tries to come up with a holistic solution that covers all the aspects and defects.

A Holographic model can be produced through Holographic 3D videos. A 3D video is essentially composed of a 3D object reflected four times. The reflections are made with respect to very precise values of different attributes, such as distance, angle, and tilt to end up with a model displayed correctly in the center. Reflection is a key to produce Holographic models.

Creating a 3D object picturizing each organ, and then reflecting each created object four times on four different sides manually, though various software applications that can accomplish such a task automatically do exist, but the quality is uncertain, to produce a Holographic video would be a long time-consuming process. From another perspective, these videos usually require to be pre-built and ready to be displayed. They cannot be created/delivered on demand. Hence, it would be more complicated to allow interaction with a pre-created set of videos where each video should be displayed according to the gesture/movement done by the user to achieve interactivity, and where there is no time-ordered execution. Especially in those devices where the videos are stored in a flash memory that does not contain any programmed software capable of analyzing the received interaction and selecting the appropriate Holographic video amongst the existing ones to provide a reaction back, i.e., another view of the same Holographic model.

To overcome these obstacles creating a Hologram projection without sacrificing the realistic simulation and the promised quality, we proposed a different solution that uses four replicated projectors, i.e., the usual projectors used in classes to display slideshows, which defined in [11] as "an output device that takes images generated by a computer or Blu-ray player and reproduce them by projection onto a screen, wall, or another surface".

As explained earlier, a Holographic video is composed of a set of reflections of the same 3D object considering very precise measurements. Our proposed solution takes advantage of the pre-designed 3D objects that simulate human body organs provided by the Unity 3D framework, builds the full view of the human body by positioning each organ according to the actual anatomy, and omits the need to reflect each 3D object four times. The exclusion of the reflection step results from the use of four projectors where each one will display a different view of the same 3D object to eventually create the Holographic effect.

The proposed solution is built upon the use of the pyramid-shaped stage, which is the primitive method of displaying Holographic models. To bring realist-looking images to life and allow them to flow in space in real-size, the size of the

stage has been doubled almost 33 times, the measurements have been made in proportion to the small-size Hologram pyramid shown in Fig. 1. With the help of an expert engineer, the stage has been built from scratch to achieve the objective of this project.

The material, size, height, and thickness of the acrylic-made stage have been selected with extreme care to satisfy the requirements of this project. The decision as to which type of glazing should be used has been made upon the need for anti-breaking plates, shatter, and scratch-resistant. Acrylic (PMMA) in comparison to glass is harder to break and can be extremely reflective, which fits the project's purpose of reflecting 3D objects on transparent panels to produce the Holographic model. The degree of slope, the angles between the plates, the angles between the pyramid and the underlying surface are all important factors that have been considered in producing the final Holographic effect.

Indeed, we have omitted the reflection as an editing step during the preparation of the 3D objects before displaying, but the suggested alternative is to use four image projectors, at the production phase, to be positioned at the top corners of the stage. The view angle and the direction of each projector play an important role in outputting each side of the same 3D object correctly on the corresponding plate to form the final model. In other words, the four projectors replace the need for the four digital reflections.

The second part of this system is focused on providing interactivity and encouraging user engagement, which can be achieved through the use of the Kinect V2 sensor that is developed by Microsoft and defined as a "sensor that captures hand and body movements. Kinect can work only with Windows operating systems. Windows Kinect version 2.0 allows developers to create applications that need voice recognition, depth camera or face-tracking to capture the movement of the human body" as explained in [12]. The use of this sensor will allow the system to recognize any gesture/movement made by a human from a reasonable distance. It does not require users to be too close, thus being able to extend the range of detectable gestures and relief the users from the uncomfortableness of being surrounded by devices.

The general architecture of the hardware implementation is shown in Fig. 2.

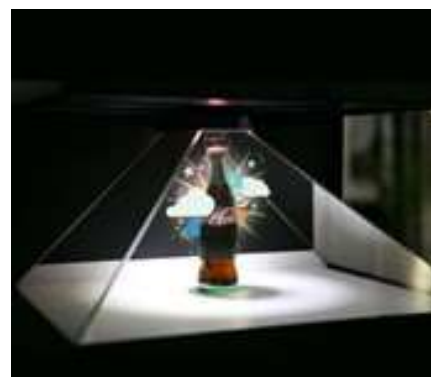


Fig. 1. Hologram Pyramid.

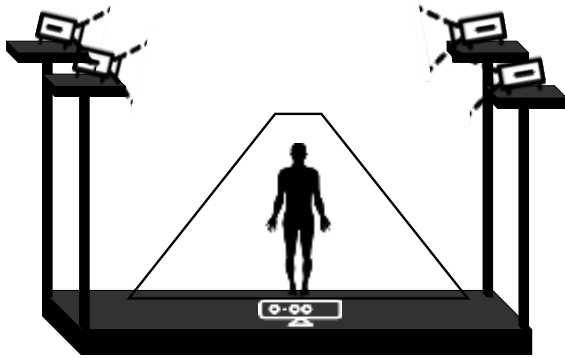


Fig. 2. General Architecture of HoloLearn (HW).

B. Software Implementation and Construction

Given the main requirements of the system, which focus on a realistic simulation of human body anatomy and user engagement obtained through the use of the Kinect V2 sensor, it has been decided to develop a desktop application. This decision is based on the constraint of Kinect V2 devices that require a certain type of port. It only works with USB 3.0 ports and Windows OS. From another angle, the use of four image projectors also requires a connection with a PC/Laptop. Due to the mentioned restrictions, the use of mobiles in this system would be challenging.

As defined in [13], Unity3D Framework is a "cross-platform environment for developing multidimensional Virtual Reality (VR), and AR video games on mobile, desktop, and web platforms". This framework offers developers a set of pre-built 3D objects, in what they call a Unity Asset Store. These objects simulate numerous real-world entities and can be purchased at affordable prices. In our proposed solution we have taken the advantage of this service to build our own complete human body 3D model that composes different systems such as Skeletal, Muscular, Skin, and Venous. Similarly, at the organs level, different internal organs have been simulated, such as the heart and lungs. The internal organs have been placed accurately according to the actual anatomy, taking into consideration depth, distance, and size as our model is not flat.

To accomplish the interactivity, we have made the best use of an open-source pre-developed library, called KinectUnityV.0001. In addition to allowing seamless integration between the sensor and the 3D model, it defines different classes, objects, and functions to facilitate the process of recognizing gestures made by users to be further processed and analyzed. This library gave the chance not only to detect a gesture, e.g., handgrip, but to determine the exact measurements and position of the detected gesture on x, y, and z axes along with other values, such as the angle. This library helped to define detectable gestures and assigning corresponding functions, to be made by users against the model, as follows:

- 1) Right-hand-open for selecting a specific system/organ.
- 2) Right-hand grip for dragging a selected organ.
- 3) Right-hand circulation around the elbow for rotating a selected organ.

- 4) Two hands pinch/apart for zooming a selected organ.
- 5) Right-hand-lasso for switching between functions.

These five functions compose the possible interaction that will allow users to perceive organs from all sides and provide them with a holistic view of the human anatomy. Visual Studio Code has been used as the main environment to analyze the received actions and program reactions accordingly with the help of the C# programming language. C# language is the ideal option for the purpose of this paper, as it is one of the dominant languages in the field of visual systems that may involve technologies like Virtual Reality, Augmented Reality, or Holograms.

The system starts by setting up the environment and getting the Kinect V2 sensor, the projectors, and the desktop application ready to operate. The sensor detects most of the actions and gestures made by the user against the model. On the other side, the application on the backend is waiting to receive one of the five defined gestures. It ignores all other gestures/movements that are not defined in the system. Moreover, it ignores defined gestures that are made outside the boundaries of the defined area/zone. The height in this process plays an important role. For instance, if the user releases his right hand at a very low height, he will be ignored and receive no reaction back.

Once a pre-defined gesture, e.g., right-hand release, at a specific height, i.e., inside the defined area, is detected, the corresponding function is executed. To achieve interactivity, the Hologram model view changes accordingly. Based on the type of gesture and the measurements, such as the position, angle, and height of the hand, the object might be selected, dragged, rotated, or zoomed. The workflow of each function is explained separately in the following paragraphs.

The user begins with selecting a specific body part, e.g., Muscular system or Heart by releasing the right hand and moving it forward to the model; accordingly, each time he continues to move his hand further, the next part will be shown along with the name, while the previous one will be hidden. The body parts are shown sequentially in a pre-defined and certain order. Likewise, the user can follow the same steps to reselect the preceding body part, except that he will have to move his hand back toward his shoulder.

To avoid confusion and keep the user concentrated, the right hand has been nominated to carry most of the functions. To get a closer look at one of the body parts, the user can hold his hand in a grip position to drag the selected organ to a specific point in the space. Relatively, the user can rotate the selected part around the y-axis by moving his right hand in a circular way around the elbow, where the angles of the object will change accordingly, and the object will appear to rotate and float freely. Moreover, a user can pinch and apart his hands to adjust the zooming and view the details of a selected organ as one of the functions provided in HoloLearn.

One of the most concerning issues in this solution is the transitioning between functions. As many functions can be applied to the same object, e.g., an object can be selected, dragged, and then rotated, there has been a need for a distinguishing gesture to define the abortion and transition

from one function to the other. For this purpose, a newly customized gesture, namely lasso, has been developed and programmed so that users can apply multiple functions without ambiguity. For instance, a user can select an organ and then hold his hand in a lasso position to move to the next function, which is dragging, and start dragging that organ. Similar to organs, the functions are ordered in a certain manner that is selection, dragging, rotation and zooming.

IV. DISCUSSION

HoloLearn is an educational system that facilitates delivering medical concepts using Hologram technology incorporated with allowed user interaction. The main targeted users are medical students as they face many problems trying to understand complicated concepts including the different human body structures. The aim of the system is to be able to replace traditional educational techniques with a new one that utilizes technology while adapts visual and interactive methods of learning, which makes a revolution in the field of education and encourage others to innovate new educational methods based on the use of the Hologram technology as it has the potential to make a significant positive impact.

In earlier studies, it was possible to either interact with small-sized 3D objects that are incapable of providing a realistic experience, while wearing and holding many devices or view 3D objects with no interaction at all. Through the architecture proposed in this paper, such problems are solved. Our architecture combines human body simulation and focuses on allowing real-sized simulation as it has been a compromised feature in earlier solutions, with user engagement in one integral system. The implementation of this system has proven to be succeeded to serve the aim intended for the project, which is to engage students in a visual interactive environment that helps students to take the lead of the educational process and start educating themselves, reducing the reliance on teachers.

V. CONCLUSION

This system made it possible to turn education from a tedious process of long classes where students have to listen and write down information, into an entertaining one that allows students to take a bigger part by exploring, practicing, and running an endless loop of failing and trying.

From another point of view, this system has eliminated the need for attending anatomical classes at foul-smelling laboratories full of dead bodies that are reserved at a very low temperature to extend their shelf lives as long as possible.

A. Challenges and Limitations

Finding a Hologram display with enough capabilities to output real-sized 3D models was challenging as most devices are meant for commercial purposes. Besides that, most of these devices are intended only for displaying and cannot be extended to include other advanced features, such as user interaction. The scope of the project commits to offer an atmosphere of interactivity; this requirement has been satisfied through the use of an aided device, i.e., Kinect V2 sensor.

Such a sensor requires exclusively a USB 3.0 port to be connected. On the other hand, mobiles do not fit the purpose of the system as they cannot satisfy the need to capture user interaction and produce the promised results. These shortcomings have been overcome by building a customized Hologram display that allows the incorporation of supplementary devices and is qualified for displaying large-sized models.

VI. FUTURE WORK

Regarding the future work, after implementing all functions included in the scope successfully, the long-term goal is to extend the system by including deeper complex human body structures. Moreover, advanced features can be developed, such as showing the heart pulse, blood circulation, blood supply, nerve supply, and afferent/efferent neurons in order to provide students with a complete guide in the field of medicine. The ultimate goal is to certify the system as an official educational method, where people apply the exact concept that is built upon the use of Hologram technology, in different majors of education.

REFERENCES

- [1] Demiryörek, Deniz, Alp Bayramoğlu, and Şemsettin Ustaçelebi. "Infective Agents in Fixed Human Cadavers: A Brief Review and Suggested Guidelines." *The Anatomical Record* 269, no. 4 (2002): 194–97. <https://doi.org/10.1002/ar.10143>.
- [2] Tolhurst, D.E., and J. Hart. "Cadaver Preservation and Dissection." *European Journal of Plastic Surgery* 13, no. 2 (March 1, 1990): 75–78. <https://doi.org/10.1007/BF00177811>.
- [3] C. R. Ramachandiran, M. M. Chong, and P. Subramanian, '3D Hologram in Futuristic Classroom: A Review', *Periodicals of Engineering and Natural Sciences*, vol. 7, no. 2, pp. 580–586, Jul. 2019, doi: 10.21533/pen.v7i2.441.
- [4] 'HoloHuman – Complete Anatomy', Nov. 02, 2019. <https://3d4medical.com/apps/holohuman> (accessed Nov. 02, 2019).
- [5] 'Essential Anatomy 5 – Complete Anatomy', Nov. 02, 2019. <https://3d4medical.com/apps/essential-anatomy-5> (accessed Nov. 02, 2019).
- [6] 'Anatomy ARVR', Oct. 31, 2019. <https://adonialearn.com/product/anatomy-arvr/> (accessed Oct. 31, 2019).
- [7] BioDigital Human - 3D Anatomy - Apps on Google Play', Oct. 31, 2019. https://play.google.com/store/apps/details?id=com.biodigitalhuman.humanAndroid&hl=en_US (accessed Oct. 31, 2019).
- [8] 'BoneBoxTM - Skull Viewer', App Store, Nov. 02, 2019. <https://apps.apple.com/ca/app/bonebox-skull-viewer/id546232840> (accessed Nov. 02, 2019).
- [9] An, Jungkwen, Kanghee Won, Young Kim, Jong-Young Hong, Hojung Kim, Yongkyu Kim, Hoon Song, et al. "Slim-Panel Holographic Video Display." *Nature Communications* 11, no. 1 (November 10, 2020): 5568. <https://doi.org/10.1038/s41467-020-19298-4>.
- [10] HAMK Unlimited. "Holographic Fan Case Study," January 10, 2019. <https://unlimited.hamk.fi/uncategorized/holographic-fan-case-study/>.
- [11] "What Is a Projector?" Accessed December 31, 2020. <https://www.computerhope.com/jargon/p/projecto.htm>.
- [12] M. A. Almasre and H. Al-Nuaim, 'Comparison of Four SVM Classifiers Used with Depth Sensors to Recognize Arabic Sign Language Words', *Computers*, vol. 6, no. 2, p. 20, Jun. 2017, doi: 10.3390/computers6020020.
- [13] G. Wheeler et al., 'Virtual interaction and visualisation of 3D medical imaging data with VTK and Unity', *Healthcare Technology Letters*, vol. 5, no. 5, pp. 148–153, 2018, doi: 10.1049/htl.2018.5064.

Prototype of Web System for Organizations Dedicated to e-Commerce under the SCRUM Methodology

Ventocilla Gomero-Fanny¹, Aguila Ruiz Bengy², Laberiano Andrade-Arenas³
Facultad de Ciencias e Ingeniería, Universidad de Ciencias y Humanidades, Lima, Perú

Abstract—This research work is based on making a prototype e-commerce system applying the scrum methodology, because currently the systems of many organizations are still developed following traditional methodologies, i.e. the system does not meet the requirements that should provide value to the organization in addition to its poor information security, leading to the organization's data to the vulnerability of loss or theft. That is why this article aims to design a web system for organizations dedicated to e-commerce under the agile SCRUM methodology. The methodology allowed to design the prototype meeting the needs of the organization with frequent retrospectives and continuous communication between stakeholders, in addition to proposing the information security of the company's data. In the results of this research the user stories were analyzed, which allowed the division into 4 Sprint deliverables of the general modules proposed in the article, for which a maximum score of 21 story points per Sprint was placed; in which 16 story points were placed to the first sprint, the second Sprint with 20 story points, the third Sprint with 21 story points and the fourth Sprint with 16 story points. The e-commerce system proposal will be beneficial for the organization and its customers, since it will allow them to have a system according to their requirements and needs in a secure manner.

Keywords—Agile; e-commerce; scrum; sales; user stories; sprint

I. INTRODUCTION

Nowadays, e-commerce is a very important phenomenon that contributes to the technological development of organizations all over the world, since the use of technology has become a transcendental issue in the daily life of a company, because through the use of cell phones it allows a close relationship between the processes of the organizations, then knowing the importance that marks in our days the electronic commerce is necessary to know the concept of it, which is defined as the transaction that is made or produced through the Internet, as the commercial transactions implies the exchange of value across the borders of the companies or individuals in exchange for service or products that are required [1].

In Peru, the use of e-commerce in organizations is becoming increasingly important due to the new era of trade through the Internet [2]. Since the Internet has become part of the lives of the vast majority of citizens, due to reduced costs has been possible to reach many more people, so that organizations both in Peru and in the world, takes advantage of

customer connectivity to a network, being born there the desire to improve the business through the Internet through digital marketing, advertising and others that make possible the mass segmentation of its customers, this is what gives rise to e-commerce order companies dedicated to trade [3].

Also in another research, published by Yadong Huang, Yi Liu, Jianping Shen titled as architecture of next generation e-commerce platform, mentions that, e-commerce has significantly changed the rules in business as they have made e-commerce more intelligent and convenient to perform transactions of all kinds [4]. Also Nayoung Hong, Junbeom Yoo, Sungdeok Cha, mention in their research on customization of Scrum methodology for e-commerce projects, where they analyzed their research by dividing the scrum method into three aspects and showed results of surveys conducted on satisfaction of using scrum methodology components to 18 members where they indicate that 17% are very satisfied, 66% satisfied and 17% indicate that nothing special in using the methodology. Then analyzing the data, we can mention that scrum is a methodology quite used and comfortable for the development of e-commerce projects [5].

The objective of this work is to design a web system for organizations dedicated to e-commerce under the SCRUM methodology.

In the article, in Section II, the literature review of the research is shown, in Section III, the methodology established, in Section IV, the case study of the research, in Section V, the results and discussions reached with the present and finally in Section VI, the conclusions and future work are shown.

II. LITERATURE REVIEW

In addition in another research, published by Yadong Huang, Yi Liu, Jianping Shen In this section are shown important aspects to be addressed, which are related to e-commerce as E-Business, digital marketing, ISO 27001-Annex A9 (as a security issue and information risk prevention for companies and their customers), also clear concepts about scrum the methodology applied in the research and in addition to proposals for development tools for the implementation of the prototype presented.

Then , e-business is understood as the economic activity and business management practices that are carried out through the Internet, in addition to that you can find content editions of images and titles, discussion forums, which make a website

interactive and the user can share ideas and opinions about the products offered; and in addition to providing the advantage of updating and rebuilding a website more easily, exploiting online information, increasing transparency and quality of processes [6].

Digital marketing is understood as the traditional marketing techniques in the digital environment [7]. As for ISO 27001, it is also timely to mention it because it aims to enable organizations to prioritize controls based on their possibility and necessity, i.e., risks in an organization's system, which must be analyzed and managed, and security must be planned, implemented and especially when reviewed must be corrected and improved [8], specifically Annex A9 of ISO 27001, seeks to safeguard the organization's assets, as it could be breached by unscrupulous users with access to an organization's system without any limitation whether it is an internal or external user [9]. Information security in an organization is and will remain the most important asset as this asset could seriously affect a company and even bankrupt a well-positioned organization [10].

Regarding the methodology, SCRUM was used, being one of the most used methodologies in the agile environment that allows continuous communication between stakeholders, so that errors in software delivery are minimized, thanks to frequent sprints and where changes in requirements are also welcomed during the project development [11]. Besides being organized by roles such as the Scrum Master, the development team and the Product Owner, which make possible the development of the system in an agile environment. Then for the development of this research will follow the processes, phases and principles established by the agile methodology SCRUM [12].

For the development of the e-commerce system, it is proposed to be developed in PHP in a development environment such as Visual studio code [13], with the MySQL server database and using the Laravel 7 framework [14].

III. METHODOLOGY

As it has been mentioned above, the methodology that will be applied in this article is the SCRUM agile methodology, due to its agile environment that will allow those involved to interact continuously through the sprint, and then the agile develop [15].

A. Startup Stage

In this phase of the agile methodology, those involved in the research will be described, i.e. the formation of the SCRUM group, the user stories approved by the Product Owner will be described.

B. Planning

Identify applicable sponsor/s here. If no sponsors, delete this text box (sponsors). In this phase we will list the creation of the horses, tasks and requirements which will be estimated by size, following the development we will make a story and user map with the specification of your Product Roadmap [16]. A chart is also made with the planning of the Sprint as well as the determination of the costs or budgets that will be necessary for the implementation.

C. Implementation

In this phase the prototypes of the e-commerce system will be developed, by modules according to the established user stories, prioritized and estimated during planning.

D. Review and Retrospective

In this phase the Sprint is validated, if it is really complying with the established if a change is necessary.

E. Feedback

In this meeting, plans were made and created to improve the execution of the following Sprint, evaluating the development of the feedback given in the previous meetings of the development team.

IV. CASE STUDY

In this section, we will develop the proposed methodology, where in each of the SCRUM phase we will detail the case study applied to carry out the correct development of the agile methodology in this study, with which to provide a proposal for the development of the interactive and feasible e-commerce system that provides value to organizations engaged in trade. To do so, we first show the flowchart of the proposed system in Fig. 1, for a better understanding of the system.

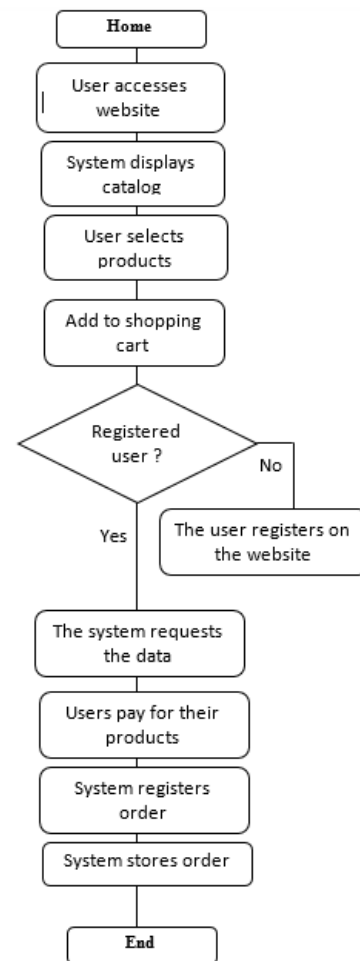


Fig. 1. System Operating Flow.

A. Startup Stage

1) *Identification of those involved:* We mention the people who will be involved in the process of developing the e-commerce system, which in turn will be in constant communication, according to the established in the Scrum methodologies as shown in the following Table I.

2) *Description and prioritization of user stories:* The people who will be involved in the process of developing the e-commerce system are mentioned, (P.1 is developer 01, and P.2 is developer 02) who in turn will be in constant communication, as established in the Scrum methodologies as shown in Table II.

B. Planning Stage

1) *Decomposition of epics to tasks:* In the following one it is shown to decompose the hepicas to simpler tasks to make, as it is observed in Table III.

TABLE I. INVOLVED

ROLE	DESCRIPTION
Product Owner	System owner
Scrum Master	Project members
Development Team	Project members

TABLE II. USER STORIES WITH PRIORITY

USER HISTORY	Nº	P.1	P.2	Priority
As the owner of the organization, I want the system to allow a user role, to have a better access control to the modules.	1	13	13	8
I, as a salesperson of the organization, want the system to be able to divide by category all the products, to have a better control of the stock and to carry out the sales in a more efficient way.	2	13	13	8
I as the Purchasing Manager of the organization require that the system can have a product registration option, in order to maintain stock control of the product.	3	8	8	8
As the organization's distribution manager, I require the system to have ubigeo records for each customer, in order to better serve their orders and generate sectorized promotions.	4	8	8	8
I, as the organization's vendor, require that the system be able to record my order in a timely and detailed manner, for time efficient service.	5	5	5	5
As the organization's purchasing manager, I want the system to be able to record my purchases in detail, in order to have better control of purchases and suppliers	6	5	5	5
As the owner of the organization, I want the system to be able to provide me with reports, by day, month and year, to have a better control of it.	7	5	5	5
I, as the owner of the organization, want the system to be able to give me configuration access, so that I can manage it as I see fit.	8	5	5	5
I, as the owner of the organization, want the system to be able to have a Deshboard area, that is, a report of the most sold and most required products.	9	3	3	3
As a salesperson for the organization, I want the system to be able to have a sales catalog, to have a better overview of the products.	10	3	3	3
As a sales manager, I require the system to detail the products, to have the specific description of each product.	11	3	3	3
As the owner of the organization, I want the system to be able to record the profile of each of our clients, for decision-making purposes.	12	1	1	3
I as an owner require that the system can show me the report of each customer, to have a purchase history of the customers	13	1	1	3

TABLE III. EPIC DECOMPOSITION

REQUIREMENTS	TASKS
Role of users	Add user Delete user Modify user data Save user
Product Category	Add category, delete category, modify category, save category
Product Registration	Add product, remove product, modify product, save product
Ubiquitous registration	Modify ubigeo, delete ubigeo, save ubigeo
Order registration	Consult Product, Add New Product Cancel Sale Modify Product
Purchase record	Register supplier data Register products to buy Cancel purchase , Add new product Make a purchase
Report Registration	Show sales record for day ,month and year Show Stock Generate Commission Reports Report by Seller
Configuration access	Edit configuration area
Deshboard Registration	Add product, remove product, modify product, save product
Product catalog	Add, remove, modify and display product in catalog list
Product detail	Show detail
Customer Profile Registration	Add client Delete customer Modify customer data Save client
Customer Report	Show report

2) *Backlog estimation*: In the next one we will estimate the usury stories using the size estimation, which will allow the requirements to be separated by sprints according to the story points assigned in the estimation as shown in Fig. 2. This was done with the members of the project development and these results were obtained, where we can visualize that 73 points of user history were obtained.

3) *User story map with product roadmap*: In Table IV you can see the map of user history, in addition to the roadmap of products ie the path to be followed for compliance with the sprinst, the top is the most required being the Backbone, followed by the Walkin Skeleton, ie the modules required by the system to operate.

4) *Plamification of deliverables (Sprints)*: The 73 story points observed in the estimation by sizes shown in Table V are then shown. These are broken down by a range of less than 21 story points, to ensure the security of your information.

C. *Implementation Stage*

In this phase, the prototype of the e-commerce System will be designed following the established requirements and will be designed by Sprint as the first version, since they could vary through the retrospective with the Owner products, since in Scrum the changes are welcome.

1) *Initial prototype* : The prototypes were planned based on the requirements previously analyzed and ordered.

a) *Prototype of Sprint 1*: For the development of the first prototype, the decomposition of epics from Table III and Table V of Sprint planning 1 were taken into account, as shown in Fig. 3, Fig. 4 and Fig. 5.

b) *Prototype of Sprint 2*: For the development of the second prototype, the decomposition of epics from Table III and the Sprint 2 planning Table V were taken into account, as shown in Fig. 6, Fig. 7, and Fig. 8.

c) *Initial Prototype of Sprint 3*: For the development of the third prototype the decomposition of epics from Table III and the planning Table V of Sprint 3 were taken into account, therefore in Fig. 9 one of the most important prototypes of this sprint 3 can be seen.

d) *Initial Prototype of Sprint 4*: For the development of the fourth prototype the decomposition of epics from Table III and the planning Table V of Sprint 4 were taken into account, therefore in Fig. 10 one of the most important prototypes of this sprint 10 can be seen.

TABLE IV. PRODUCT ROADMAP

	register products	selling	generate reports	register users
Backbone	Product Registration	Product catalog	Record Report	Role of users
Walking Skeleton	Purchase registration	Order registration		
Less Optional	Product detail	Product Category		Customer Profile Registration
			Customer Report	
Optionalit y	Dashboard Registration	Ubiquitous registration		
More Optional				

TABLE V. PLANNING OF SPRINTS

Nº de Sprint	Description	Value	Sprint points
1	Record Report	5	16 points
	Product catalog	3	
	Product Registration	8	
2	Users' role	13	20 points
	Purchase registration	5	
	Customer Profile Registration	1	
	Customer Report	1	
3	Order registration	5	21 points
	Product detail	3	
	Product Category	13	
4	Configuration access	5	16 points
	Ubiquitous registration	8	
	Deshboard Registration	3	



Fig. 2. Backlog Estimation.

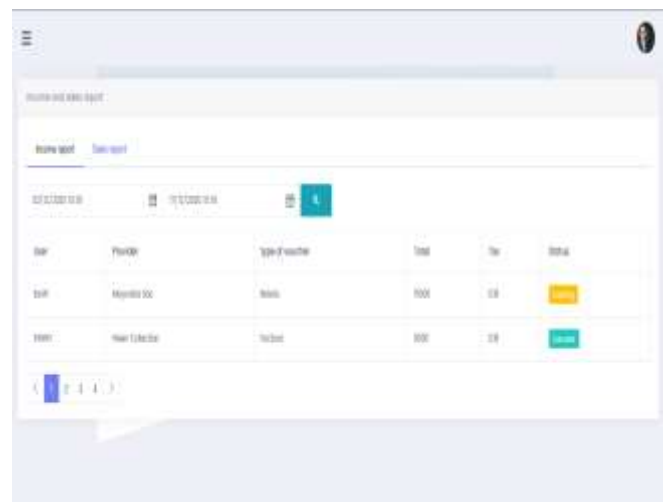


Fig. 3. Reports Module.

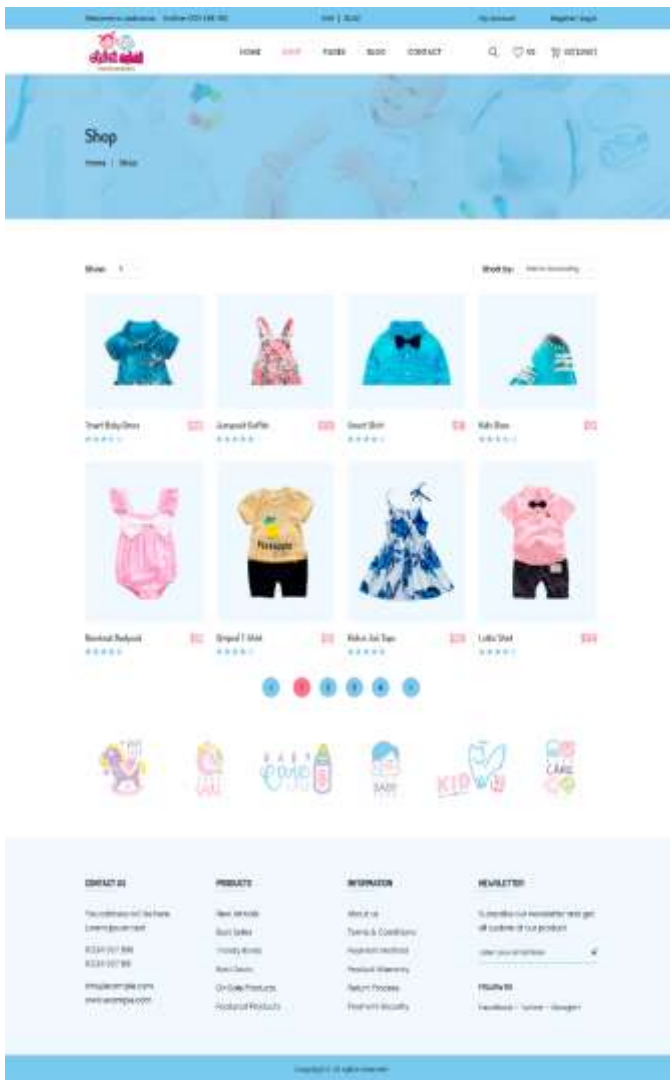


Fig. 4. Product Catalog.



Fig. 5. Register Product.

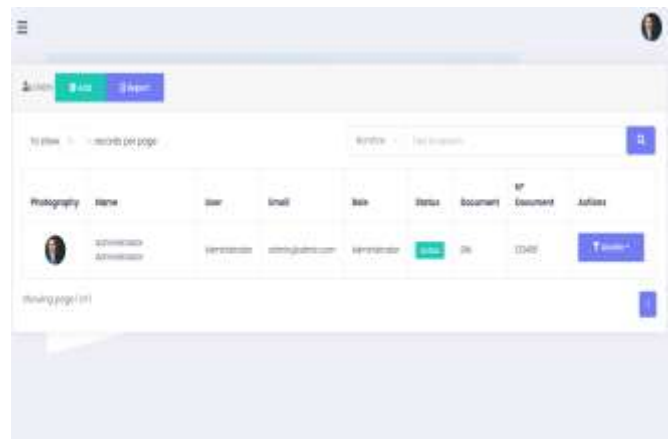


Fig. 6. User Registration.

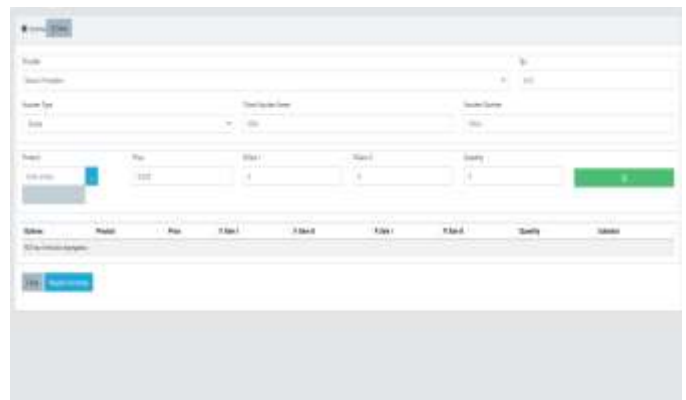


Fig. 7. Shopping Record.

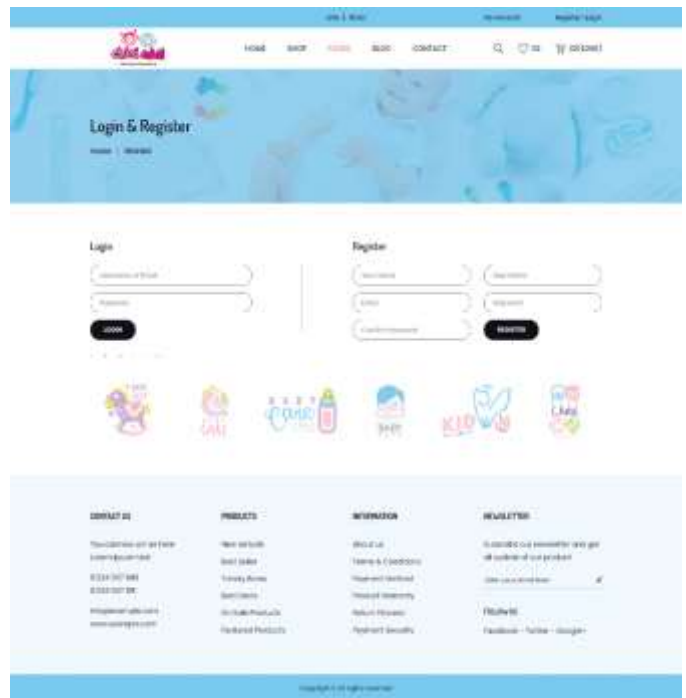


Fig. 8. Customer Profile Registration.

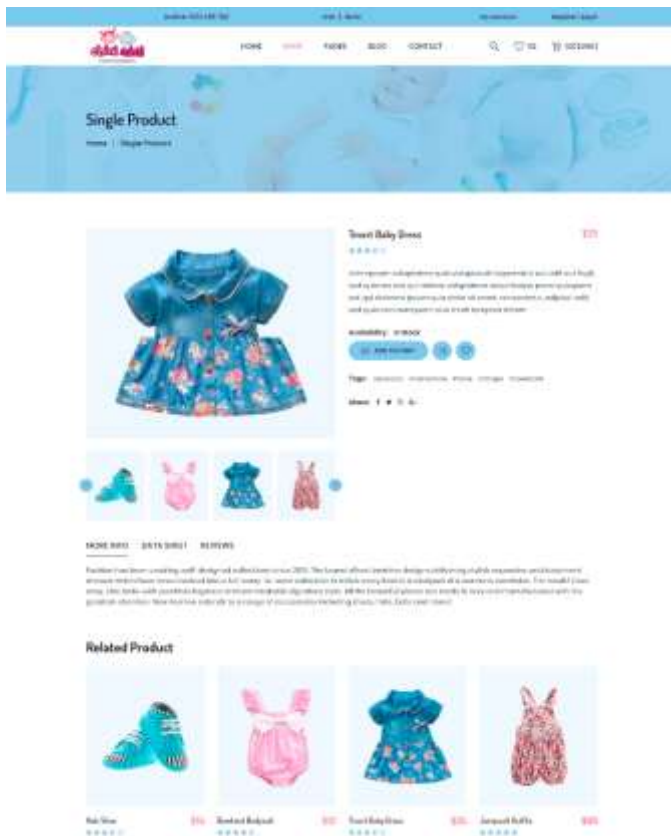


Fig. 9. Product Detail.

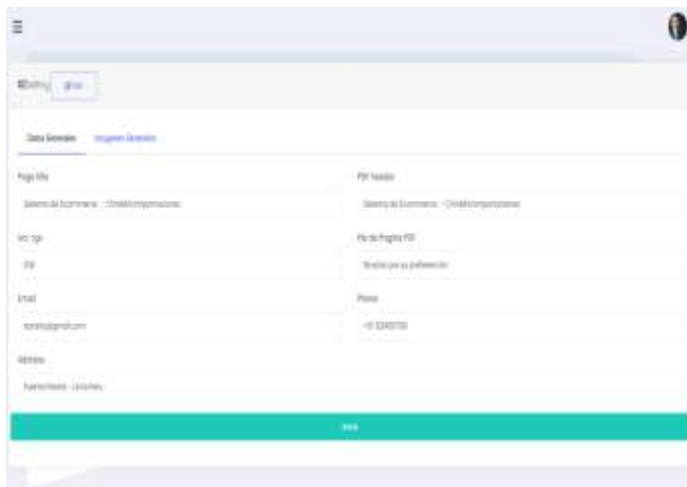


Fig. 10. Page Setup.

V. RESULTS AND DISCUSSIONS

It is shown the results and discussions reached in this article, in the results part it was made the detailed explanation of the operation of each one of the Sprint, and in the discussions part it was made a description of two agile methodologies such as SCRUM and XP, in order to provide the reader with the similarities and differences of these two methodologies.

A. About case Study

We analyzed the 4 Sprint of the general modules proposed in the article for which was placed as a maximum score of 21 points of history by Sprint in which the first sprint has 16 points of history, the second Sprint with 20 points of history, the third Sprint with 21 points of history and the fourth Sprint with 16 points of history. These in turn have a number of 3 to 4 modules according to the score or value evidenced, obviously following (see Table V) the path of the Product Roadmap, where the yellow color represents Backbone, the orange color the Walking Skeleton, the green color the Less Optional and the purple color the Optional (see Table IV). Having mentioned the order of delivery of the Sprint below is to describe each module by Sprint.

1) *For Sprint 1:* It is delivered as a prototype the report registration modules in which the general view of reports by day, month and year is detailed in an infective view; in the product catalog module the products are visualized properly detailed and interactive for the different users and in the product registration module a registration view of the products is visualized so that they are registered in detail. In Fig. 11, it is shown in the sprint 1 burst chart, the path taken by the sprint in a given time of 28 days shown in the X axis and in the Y axis the 16 points of user stories, that is the expected time with the real time of development of the sprint.

2) *For Sprint 2:* In this Sprint are delivered with retrospective the prototype of the user module in which it is observed in detail the different users who will have access to the e-commerce system with certain limitations by type of user, in the module of registration of purchases are observed the very detailed prototype in which it will be possible to register the purchases made for the correct control of stock, in the module of client profile is observed the record of the clients to be categorized later and in the module client report, the clients already registered in the system are visualized. In the Fig. 12, it is observed in the sprint 2 burdow chart, the expected advance of the sprint development and the real way that was taken for the development of the same one, in a time of 28 days as it is shown in the X axis, and in the Y axis the 20 points of history.

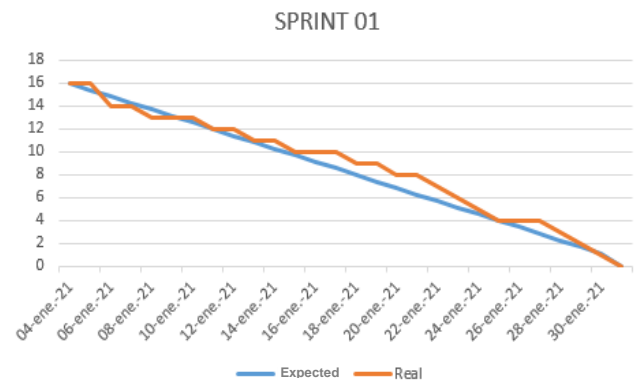


Fig. 11. Development Path for Sprint 1.

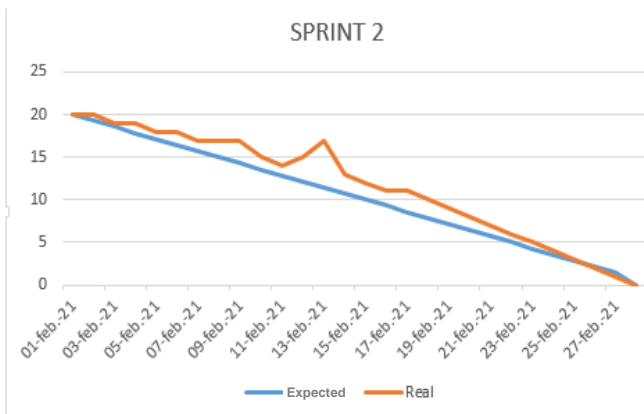


Fig. 12. Development Path for Sprint 2.

3) *For Sprint 3:* The deliverables in this sprint are the prototype of the order registration module which details the registration of orders placed by customers, in the product detail module displays the product more detailed than in the catalog due to the description of each product, in the product category module displays the types of product categorized by texture, shape or others that differentiate them. In Fig. 13, the path taken by the sprint during its development stage is shown in a time of 31 days shown in the Y axis, for its feedback, with 21 points of user history shown in the X axis.

4) *For Sprint 4:* The deliverables in this sprint are the configuration access that is a restricted module only for the user administrator of the e-commerce system, in the registration module of ubigeo are recorded the address by province, district and department of users and addressing of the stores of the organization, and finally in the registration module of Dashboard are the general reports of all made in statistical form for senior management decisions. In Fig. 14, it is shown in the same way the path that the sprint took in its development stage in a period of 16 working days shown in the Y axis, with 16 points of history shown in the x-axis.

B. About Methodology

Scrum and XP (Extreme Programming) are two methodologies of software development very used, the differences between both are firstly in the time of the deliverables or also called sprints or interactions because in scrum a sprint can take between a week and a month, in the course of the development this sprint cannot receive changes ie is not sensitive to changes at least until the sprint has been completed, on the other hand, the time it takes an interaction in XP is one to two weeks, in this methodology changes are welcome i.e. is sensitive to changes, may have concluded some interactions [17], these will be open to change, in scrum the order of priorities are established by the Product owner instead in XP establishes the customer, another very noticeable and important comparison is that Scrum is based on the management of a project, on the other hand XP is focused clearly on the realization of the product [18], while it is true that both methodologies are very good, our project was developed based on the agile methodology of software development scrum for project management, in addition to the

order of priorities we establish based on customer requirements. In the Table VI, we show the sales and disadvantages of these two methodologies compared.

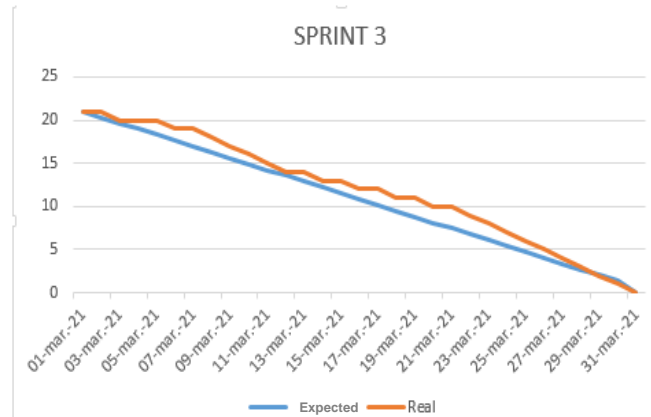


Fig. 13. Development Path for Sprint 3.

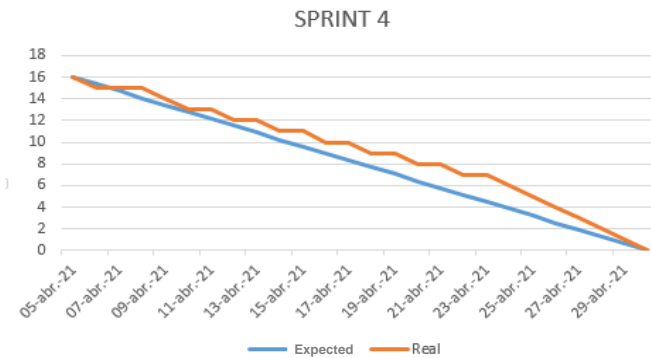


Fig. 14. Development Path for Sprint 4.

TABLE VI. COMPARISON BETWEEN SCRUM AND XP

	Extreme Programming (XP)	Scrum
Advantages	<ol style="list-style-type: none"> 1.- More organized programming. 2.- Continuous improvement of processes and development teams. 3.- Increased communication between clients and development team. 4.- Less error. 	<ol style="list-style-type: none"> 1.- Anticipated results 2.- Flexibility and adaptation of context 3.- Risk management. 5.- shows the progress of the sprints or deliverables. 6.- Se obtains fast results and very short test periods. 7.- Shows a complete vision of the project.
Disadvantages	<ol style="list-style-type: none"> 1.- It is a little difficult to document. 2.- It is recommended to use only in short projects. 3.- if a process there, the costs are high. 	<ol style="list-style-type: none"> 1.- It works more in reduced equipment. 2.- It requires an exhaustive definition of the tasks and their deadlines. 3.- if there are unfinished tasks, the rest of the tasks have to be postponed. 4.- Daily meetings can create stress and frustration among less experienced members

VI. CONCLUSIONS AND FUTURE WORK

In conclusion, the e-commerce systems developed with the agile methodology SCRUM, allowed the system to be based more on the fulfillment of the requirements of the customers, so that it was better adapted to the organization and its needs since the changes in the requirements were welcomed in the agile environment worked, in addition the continuous communication between the stakeholders have made possible the estimation and prioritization of the user stories studied and also gave a path of development in the Product Roadmap to finally be separated by sprint as deliverables. The sprints were separated into 4 deliverables which will be proposed for delivery in a period of 1 to 2 weeks, according to the score of user stories considered in each of the sprints.

It is recommended to further investigate so that sprints can be made with fewer story points, to further detail the requirements and also to implement the e-commerce system in the future with the analysis of the requirements presented in this article.

REFERENCES

- [1] R. Villegas, «La implementación del e-commerce en Flore,» El Capiro SA, Colombia, 2020.
- [2] D. A. Navarro, B. V. D. Lucca y E. V. Gonzabay, «E-Commerce: Un Factor Fundamental Para El Desarrollo Empresarial En El Ecuador,» Revista Científica Ecociencia, p. 17, 2018.
- [3] Q. Wu, J. Ma and Z. Wu, "Consumer-Driven E-Commerce: A Study on C2B Applications," 2020 International Conference on E-Commerce and Internet Technology (ECIT), Zhangjiajie, China, 2020, pp. 50-53, doi: 10.1109/ECIT50008.2020.00019.
- [4] Y. Huang, Y. Chai, Y. Liu y J. Shen, "Arquitectura de la plataforma de comercio electrónico de próxima generación", en Tsinghua Science and Technology , vol. 24, no. 1, págs. 18-29, febrero de 2019, doi: 10.26599/TST.2018.9010067.
- [5] N. Hong, J. Yoo y S. Cha, "Personalización de la metodología Scrum para proyectos de comercio electrónico subcontratados", Conferencia de ingeniería de software de Asia Pacífico 2010 , Sydney, NSW, 2010, págs. 310-315, doi: 10.1109 / APSEC. 2010.43.
- [6] P. Restrepo, « The implementation of E-Commerce in Flores El Capiro, » College of Higher Studies in Administration – CESA, p. 62, 2020.
- [7] C. Y. Yoon, "Measurement systems of individual E-business competency in an E-business management environment," 2017 4th International Conference on Computer Applications and Information Processing Technology (CAIPT), Kuta Bali, 2017, pp. 1-4, doi: 10.1109/CAIPT.2017.8320720.
- [8] PJMAJ Malar, "Tendencias innovadoras de marketing digital 2016", Conferencia internacional de 2016 sobre técnicas eléctricas, electrónicas y de optimización (ICEEOT) , Chennai, 2016, págs. 4882-4888, doi: 10.1109 / ICEEOT.2016.7755648.
- [9] O. F. Mamani y T. G. Málaga, «Evaluación De Madurez De Las Tics Según La Norma Técnica Peruana Ntp-Iso/27001 -2014 En La Oficina De Informática Y Sistemas De La Unjbg, 2016,» Universidad Nacional Jorge Basadre Grohmann, Tacna - Perú, 2016.
- [10] A. P. DAZA, «Diseño De Procedimientos De Gestión De Usuarios Y Gestión Del Cambio En El Sistema Cactus-Hr Aplicando Iso 27001,» Universidad Distrital "Francisco Jose De Caldas", Bogota, 2019.
- [11] P. R. Gómez y G. E. Moraleda, Approach to software engineering, Editorial Centro de Estudios Ramon Areces SA, 2020, 2020.
- [12] A. Srivastava, S. Bhardwaj and S. Saraswat, "SCRUM model for agile methodology," 2017 International Conference on Computing, Communication and Automation (ICCCA), Greater Noida, 2017, pp. 864-869, doi: 10.1109/CCAA.2017.8229928.
- [13] A. A. Maliavko, "The Lexical and Syntactic Analyzers of the Translator for the EI Language," 2018 XIV International Scientific-Technical Conference on Actual Problems of Electronics Instrument Engineering (APEIE), Novosibirsk, 2018, pp. 360-364, doi: 10.1109/APEIE.2018.8545874.
- [14] Á. P. Gómez, J. R. Jalca, J. G. García, O. Q. Sánchez, K. M. Parrales y J. M. Merino, « Database Management Basics,» 3Ciencias, 2017.
- [15] L. B. Angarita and J. A. Guapachá Hernández, "Gamified system for learning of Scrum development process," 2019 14th Iberian Conference on Information Systems and Technologies (CISTI), Coimbra, Portugal, 2019, pp. 1-6, doi: 10.23919/CISTI.2019.8760928.
- [16] M. A. Korimbocus, T. Singh Towokul and S. D. Nagowah, "Scrum Meeting Tool for Knowledge Capture and Sharing," 2019 Conference on Next Generation Computing Applications (NextComp), Mauritius, 2019, pp. 1-6, doi: 10.1109/NEXTCOMP.2019.8883672.
- [17] A. N. Cadavid, J. D. F. Martínez y J. M. Vélez, « Review of agile methodologies for software development,» 04 junio 2013. [En línea]. Available: <https://dialnet.unirioja.es/descarga/articulo/4752083.pdf>.
- [18] J. C. Salazar, A. T. Casallas, J. C. Linares, A. Lozano, and Y. L. Valbuena, "Scrum versus xp: similarities and differences," Technology Research & Academy, vol. 6, no. 2, pp. 29–37, 2018.

Blockchain in Insurance: Exploratory Analysis of Prospects and Threats

Anokye Acheampong AMPONSAH^{1*}
Benjamin Asubam WEYORI³

Department of Computer Science and Informatics
University of Energy and Natural Resources
Sunynai, Sunyani – Ghana

Professor Adebayo Felix ADEKOYA²
Department of Computer Science and Informatics
University of Energy and Natural Resources
Sunynai, Sunyani – Ghana

Abstract—Ever since the first generation of blockchain technology became very successful and the FinTech enormously benefited from it with the advent of cryptocurrency, the second and third generations championed by Ethereum and Hyperledger have explored the extension of blockchain in other domains like IoT, supply chain management, healthcare, business, privacy, and data management. A field as huge as the insurance industry has been underrepresented in literature. Therefore, this paper presents how investments in blockchain technology can profit the insurance industry. We discuss the basics of blockchain technology, popular platforms in use today, and provide a simple theoretical explanation of the insurance sub-processes which blockchain can mutate positively. We also discuss hurdles to be crossed to fully implement blockchain solutions in the insurance domain.

Keywords—Blockchain technology; insurance industry; hyperledger; ethereum

I. INTRODUCTION

Evolving technologies mostly help to change the driving forces underlying economic, social, and business developments [1,2]. Blockchain was developed and introduced in 2008 by a researcher or a group whose identity has remained anonymous even till now [3,4]. It was introduced as a financial application (Bitcoin), to facilitate peer-to-peer electronic cash transfer without requiring a centralized trusted system and for the resolution and prevention of the double payment problem [3,5].

In recent past years, Blockchain has ratcheted up and gained tremendous attention among the academic community [6], industry, and researchers demonstratively placing among the top five technology trends in 2018 [7,8]. According to [9], the output value of Bitcoin per day stands at 4.144 Million and the estimated transaction value of transactions on the blockchain is 158.932k as of September 17, 2020. Blockchain is categorized into three generations. The first generation – blockchain 1.0 was introduced in 2009 and used hardcoded special-purpose systems to focus primarily on digital currency and served potentially malicious public participants [3,10].

The second generation – Blockchain 2.0 commenced in 2014 and emphasized innovative ways of applying Smart Contracts in diverse situations and domains, championed by Ethereum [11] offering user-defined digital assets and partly turing complete functionality [10]. Blockchain 3.0 begun in 2017 with Hyperledger projects (Fabric, Composer, etc.) providing an all-purpose permissioned decentralized application system, mostly associated with user-friendly and highly configurable features. The second generation of blockchain saw significant systems being developed in logistics, certificates, and finance. Recently, the domain applications have expanded to include education, health, agriculture, Internet of Things (IoT), and governance [12,13] Smart Grid, Intelligent Transportation System, Data Center Networking, Electronic Voting System, and more [14,15,16,17]. All three phases are complementary and support one another to formulate the normality of blockchain technology [18].

According to [19,20], in case of an emergency, insurance is one of the essential assistance accessible to populations to neutralize their costs and assist them. The greatest challenge of the sector is how to detect and protect against counterfeit documents and stop the intentions of phoney participants. Consistent with [21], the impact of Blockchain technology has been seen by major insurers and reinsurers, where the majority have begun to invest in trial systems. A vivid example is the Blockchain Insurance Industry Initiative (B3i) launched in 2016 to examine the potential of BC to improve successes in data exchange among insurance and reinsurance enterprises [22]. The insurance companies provide a source of funding for the clients in a state of disaster and as a result, are engraved with enormous paper works and inefficiencies [23]. In the recent past, most insurance companies adopted a centralized architecture for system development as shown in Fig. 1a, and therefore by using a decentralized blockchain as in Fig. 1b, the insurance industry gets an exceptional chance to re-examine its complete value chain, which has continuously depended on utmost good faith and trust and develop novel insurance products for their consumers [24].

*Corresponding Author

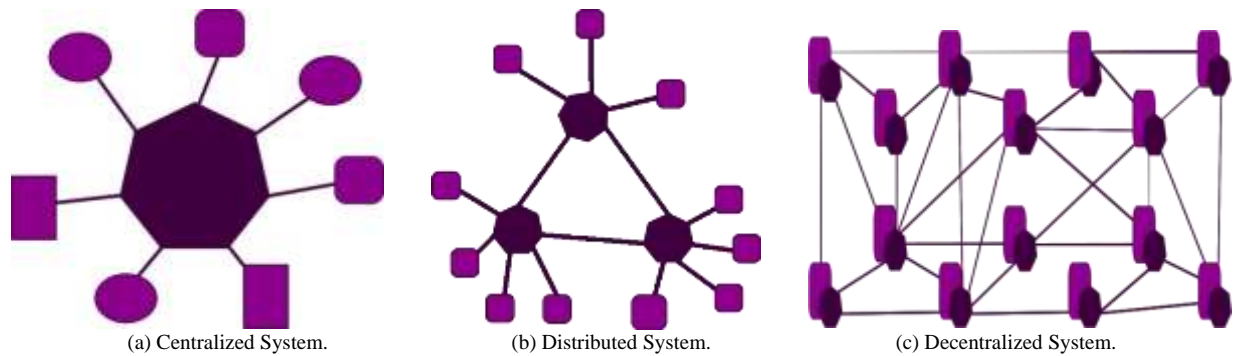


Fig. 1. Architecture of Existing Systems.

II. CONTRIBUTION OF THE PAPER

Currently many researchers have worked on blockchain in different perspectives. As indicated in Tables III and IV in appendix, some authors provided a general understanding of blockchain technology. The author in [10] used a meta survey to provide a strong foundation for their future reference model. The author in [14] built on previous surveys and produced a comprehensive importance of blockchain technology scoping the many different smart communities such as transportation, healthcare, proof-of-work algorithm, smart grid, finance, voting system, data center networking, consensus protocols, and process models, and many more. The author in [12] also provided a snapshot and proposed taxonomy of blockchain applications. There are further surveys for example [25], [26], [27], [28], [29] but they are all geared towards the financial aspects of blockchain and the underlining privacy and security issues. Equally, several surveys exist with a particular focus on other domains. For example, [30] concentrate on blockchain application in the Internet of Things (IoT), [31] authentication and identity management, [32,33] security and privacy, [34] Software Defined Networks (SDN) and a lot more. Closely related to this work as indicated in Table VI (in appendix) are [35], who purposely studied the repercussion of adopting blockchain technology on the operations and regulations of insurance companies with limited depth, and [36], who explained how blockchain can be significant to the insurance sector with the aim of assisting insurance industry players and major stakeholder to be aware of the applicability of blockchain in the sector. Equally, several researchers have reviewed blockchain applications in the insurance sector with a relatively strong introduction and ideas. For instance, as shown in Table IV and Table V [14] surveyed numerous blockchain applications and explained insurance processing using blockchain in the context of the financial sector. Also, [12] similarly acknowledged the application and acceptance of blockchain in insurance and touched on the various incomplete business processes that can be improved or reengineered. Other researchers also concentrated on other peculiar domains. Table VI consists of examples including [37], [2], and [38] with focus on Agric and Food Supply Chain, Business Models, and Construction Management respectively. It is evident that no comprehensive review has been done in assessing the impact or potentiality blockchain technology in the insurance industry. In the light of [14, 12] it is believed that a field like the insurance must have

comprehensive and extensive representation in the literature in terms of blockchain's implications. Therefore, in this work, we fill in the gap by zooming in to review the significant Insurance business processes and how they can be enhanced by utilizing blockchain technology. We subsequently present major insurance sub-domains and how blockchain can be used to create new services and products. We also provide opportunities and describe our future directions.

The remainder of the paper is presented as follows. We first discuss the fundamental concepts of blockchain focusing on features of blockchain, components of blockchain, types of blockchain, and blockchain platforms in Section II. Also, the methodology applied to produce this work is described in Section III. We explain how we augmented systematic and gray literature methods to review the existing literature. There is a presentation of the major types of insurance and how blockchain can be leveraged in Section IV. Also, areas in insurance where blockchain can change are also discussed in Section V. And lastly, we present the limitations of blockchain technology in Section VI.

III. FUNDAMENTAL CONCEPTS OF BLOCKCHAIN

A. Blockchain Technology

Blockchain technology is a publicly verifiable, shared, immutable distributed ledger used for recording the history of transactions. As the name suggests, blockchain is a chain of blocks that contains information inside a block, and each block is connected with a hash of its previous and subsequent blocks to create a chain. Blockchain technology consists of nodes where each node maintains its local copy of the chain and is connected with peer to peer connections. Every block contains a header, an ID of the previous and next blocks, a timestamp, and a series of transactions. As a decentralized technology, blockchain (BC) enables completely new technological systems and business models [39]. BC typically combines previous technologies like digital signature, cryptographic hash, and distributed consensus mechanism [40].

Blockchain is the underlying digital foundation that supports applications such as bitcoin. The technology enhances the process of storing transactions and tracing assets in a cooperate network. Assets can be physical such as a house, car, phone, etc. and virtual like money, titles, bonds, equities, contracts, deeds, and virtually all other kind of assets that can be transferred from a peer to peer and stored securely,

privately, requiring no need for a third-party confirmation. This is so because trust is enforced and the confirmation is done by cryptography, network consensus mechanism, smart code, and collaboration without requiring controlling mediators like governments and banks [41]. Blockchain can be talked of in tandem with other similar algorithms like clustering and complex systems as they can all be described and examined based on the science of data structure serving as the basic building block of present algorithms where nodes are used for data packets and data stores, communicating with one another in consonance with agreed methods of nodes communication [42]. In BC, a transaction is requested which is broadcasted to the peer-to-peer network. Upon validation and verification, the transaction becomes complete when it is added to existing blocks on the blockchain. This is indicated in Fig. 2.

B. Features of Blockchain

Blockchain inherently provides the following features.

- **Immutability and Security:** Immutability makes blockchain a secure and transparent approach to storing and processing data among nodes in the blockchain systems using cryptographic functions [43]. Immutable transactions are sheltered from unauthorized amendments from mischievous users. Participants can create fresh transactions, but cannot remove or edit previous ones, facilitating that all nodes can keep track of all transaction history [44]. Once data is written and stored in the ledger, it can never be changed [45]. If an error exists in a transaction, a different transaction has to be created and the two are available. The distributed ledger diminishes the reliance on a trusted central party and the risk of a single source of a system failure or data manipulation as all nodes have the full information for authentication, verification, and validation [44].

- **Transparency:** By using a consensus mechanism, validation and acceptance rules are enforced in the blockchain network where any party after satisfying the protocols in the blockchain can apparently and publicly initiate and add transactions. The consensus, validation, and acceptance rules in blockchain guarantee trust among participants in the network since all transactions are endorsed by their prospective generators and once a block is accepted, miner nodes broadcast the block to all other nodes in the network [45]. In this case and the case of a public blockchain, all transactions are made available to all participating nodes while in a private blockchain all data are accessible to authorized nodes.
- **Verifiability:** The cryptography and consensus mechanism make the transactions implemented and managed in blockchain technology verifiable by both outsiders and insiders. So, for a transaction to be valid, at least fifty percent plus one participant must agree on its validity.
- **Authenticity:** Using smart contracts in blockchain applications offers the legitimacy of transactions. Also, the transaction in blockchain naturally contains the digital signature of the creator and responder and every block also consists of previous and subsequent hashed IDs.
- **Accountability and Ownership:** The immutability of transactions in the block, the connection among blocks, and the originators' endorsement could enable ownership control as well as accountability in applications powered by blockchain. Also, participants know the provenance of a block or transaction.

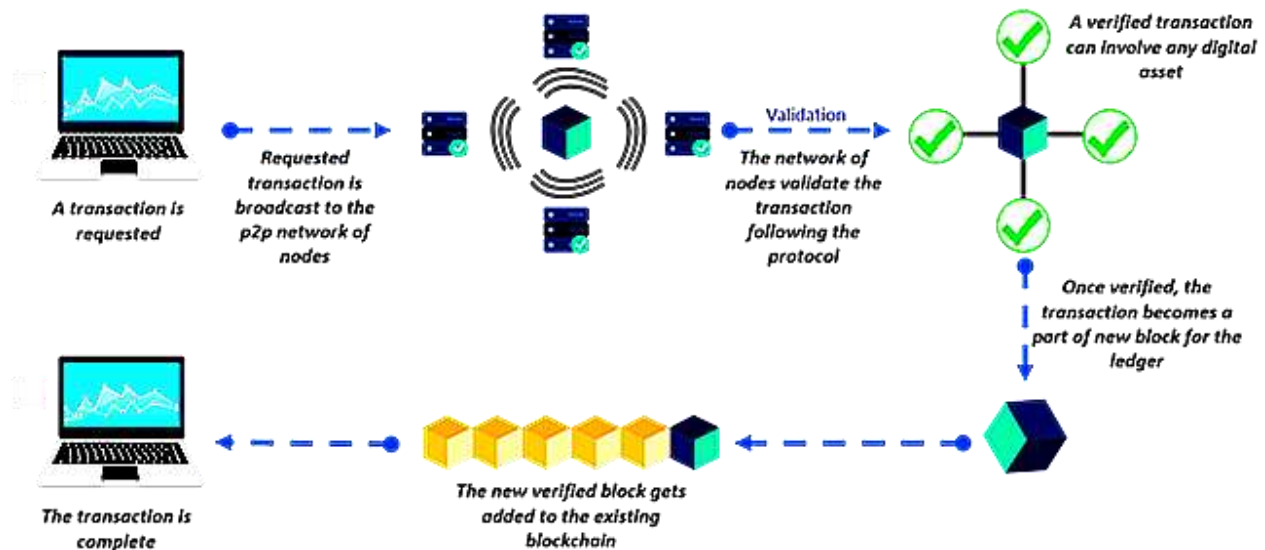


Fig. 2. Graphical view of how Blockchain Works. Source: Edureka.

C. Components of Blockchain

1) *Assets*: An Asset is a thing of value to an organization and by definition, it enables the transfer of nearly everything with economic worth over a blockchain network. Depending on the blockchain system, an asset may be intangible – currency, shares, patents, certificates, personal data, or tangible like food and beverage in a restaurant, properties in real estate, or any other tangible or intangible items. Unlike traditional -assets such as Apple Stock where the right of ownership is paper-based, blockchain asset is purely digital solely owned by the participant and does not require a third-party agent or agency in the case of transfer or sale.

2) *Transactions*: A transaction in blockchain refers to typical time-stamped events that happen to create blocks in the ledger. Transactions are stored using private or public keys giving the participants the option to be unidentified, however, identities can be accessed and verified by third parties. Trust and harmonization in the system are ensured as all transactions and other data are transparently certified before being joined in the ledger using Merkle tree presented by Ralph Merkle in Fig. 3 [46]. Merkle tree is a complete binary tree structure that aids in the verification and assurance of consistency of data [46] thereby helping to haste security authentication in big data systems. Each parent node hashes the value from its corresponding child node.

3) *Consensus algorithm*: In decentralized or distributed systems, a consensus algorithm helps in decision-making [47]. The consensus algorithm is an administrative process in a blockchain network where the majority of the distrustful participants agree upon what rules are used and the decision that is good for them all. The features of the blockchain consensus algorithm include assuring quorum structure, integrity, decentralized governance, authentication, non-repudiation, performance, and byzantine fault tolerance [47].

The decision affects whether a block will be appended to the chain or discarded. The consensus algorithm fulfils its aim by reaching an agreement, supporting collaboration and co-operation, ensuring equal rights and recognition, and also active participation by members. The following are examples of blockchain consensus algorithm. Proof-of-Work, Proof-of-Stake, Delegated Proof-of-Stake, Leased Proof-Of-Stake, Proof of Elapsed Time, Practical Byzantine Fault Tolerance, Simplified Byzantine Fault Tolerance, Delegated Byzantine Fault Tolerance, Directed Acyclic Graphs, Proof-of-Activity, Proof-of-Importance, Proof-of-Capacity, Proof-of-Burn, and Proof-of-Weight. Reference can be made to [14] for a detailed explanation of these algorithms.

4) *Cryptographic functions*: Cryptographic Functions use complex mathematical computations to change the meaning of information into a form that is rendered valueless in the wrong hands. This component of blockchain allows potentially malicious members on a blockchain network to create and append blocks on to the “chain” and engage in secured operations on a network. Every block of the blockchain holds the hash of the previous block which is stored with the transaction data and timestamp. Unlike symmetric encryption, asymmetric (public-key) cryptography employs a public key that is willingly shared for encryption and then a private key for decryption. Hashing is also used to secure the operations of blockchain. Before a transaction is created, data from the previous block is hashed and stored. The transaction creator’s public key is hashed and used to create a transaction identity and the address of the transaction [48, 49, 14]. Examples of hash functions are SHA-256, Ethash, SCrypt, RIPEMD-160, and One-Time Signature, X11, Equihash, Elliptic Curve Digital Signature Algorithm, Edwards-curve Digital Signature Algorithm (EdDSA), Ring, Borromean Ring Signatures and Multi-Signature [14].

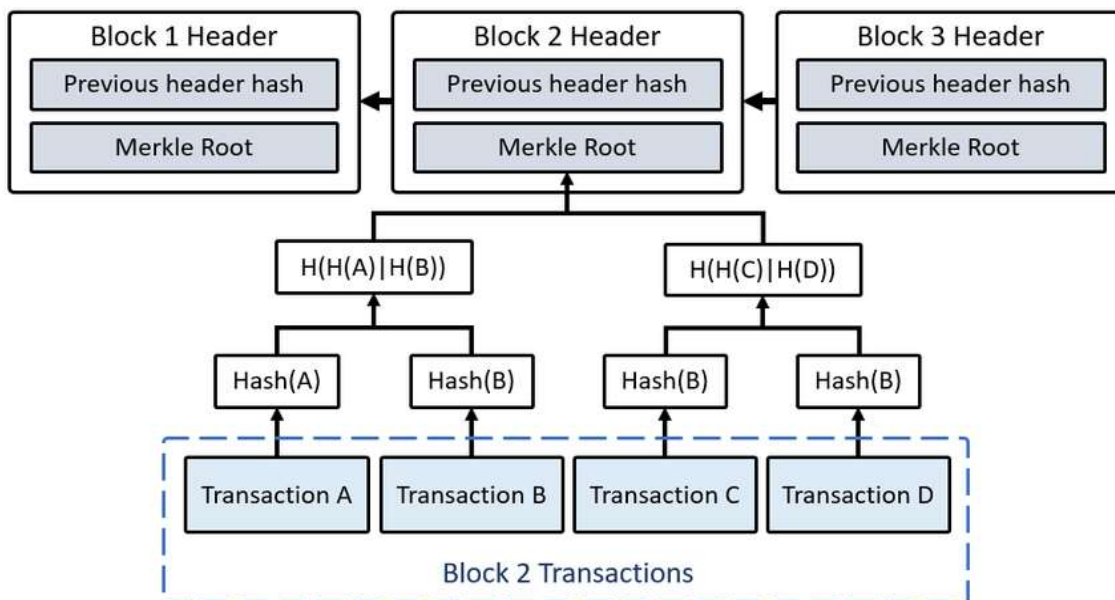


Fig. 3. Block Illustration in Blockchain using Merkle Tree.

5) *Distributed ledger*: A ledger is very crucial in business environments as it contains all transactional records for online and offline operations, users, and their credentials. In a normal business computing environment, a ledger is centralized. However in blockchain, the ledger is decentralized at the core, and depending on the type of blockchain, it is made available to some authorized participants (private) or all participants (public). Distributed ledger together with other characteristics of BC enforces auditability, security, transparency, and accountability.

D. Types of Blockchain

1) *Public blockchain*: Public blockchain uses proof of stake or proof of work to validate transactions before they are added to the block and the chain. This is done in a permissionless manner by allowing everyone to participate in the consensus process. All participants in public blockchain access, read, write, and transact on the network [50,51]. It is decentralized and has no reliance on a sole trusted entity for network control and administration. A public blockchain is protected by verification via cryptography where miners are incentivized. Transactions are consolidated and circulated by miners who can be anyone on the blockchain [50, 51]. Public blockchain uses computing resources and brute force mechanisms to verify transactions because no member on the blockchain is trustworthy and as a result, the miner who finally gets the correct results is given a reward. The most popular public blockchain is Bitcoin and Ethereum [50, 51].

2) *Private blockchain*: A private blockchain is a permissioned blockchain where access control mechanisms are used to restrict network members from accessing parts of the blockchain. This enforces reliance on a centralized control system and permits only a few participants of the blockchain network to write to the blockchain. This type of blockchain is usually useful in the financial sector particularly because it complies with know-your-customer (KYC), anti-money laundering (AML), and Health Insurance Portability and Accountability Act (HIPAA) laws and regulations [51,50]. Hyperledger projects (Fabric, Iroha, Sawtooth, etc.) under the Linux Foundation are examples of the private blockchain.

3) *Consortium blockchain*: A consortium blockchain is a permissioned and semi-decentralized type of blockchain. Unlike a public blockchain, a consortium blockchain requires permission to join, and also network control and administration power are given to a few sets of known nodes. Public participants may be given limited access to the ledger through API and may query the ledger in minimal ways. Consortium blockchain maintains the intrinsic security characteristics of public blockchain but also allows for a better level of regulation over the network. Examples of such platforms are R3, Quorum, Corda [52,50].

E. Blockchain Platforms

The following section discusses some popular blockchain platforms. This is summarized in Table I.

TABLE I. POPULAR BLOCKCHAIN SYSTEMS

Platform	Year Launched	Industry focus	Ledger Type	Consensus Algorithm	Smart Contract	Governance
Hyperledger Composer	2018	Cross-Industry	Permissioned	Pluggable Framework	Yes	Linux Foundation
Ethereum	2013	Cross-Industry	Permissionless	Proof of Work	Yes	Ethereum Developers
Hyperledger Fabric	2015	Cross-Industry	Permissioned	Pluggable Framework	Yes	Linux Foundation
R3 Corda	2016	Financial Services	Permissioned	Pluggable Framework	Yes	R3 Consortium
Quorum	2016	Cross-Industry	Permissioned	Majority Voting	No	Ethereum Developers and JP Morgan Chase
Hyperledger Sawtooth	2019	Cross-Industry	Permissioned	Pluggable Framework	Yes	Linux Foundation
Hyperledger Iroha	2019	Cross-Industry	Permissioned	Chain-based Byzantine Fault Tolerant	Yes	Linux Foundation
OpenChain	2015	Digital Asset Management	Permissioned	Partitioned Consensus	Yes	CoinPrism
Stellar	2014	Financial Services	Both Public & Private	Stellar Consensus Protocol	Yes	Stellar Development Foundation
Tezos	2014	Cross-Industry	Permissionless	Delegated Proof of Stake	Yes	Dynamic Ledger Solutions

1) *Ethereum*: Ethereum allows the blockchain community and developers to create and install blockchain-related systems. It is open-source and supports tokens, cryptocurrency, social apps, wallets and more to be deployed in the Ethereum Distributed Environment. Ethereum does not only support financial applications but also has an architecture that supports the application of distributed ledger technology in other fields. Ethereum supports several networks like Community Test Network, Community Ethereum Network, and other private BC networks.

The components of Ethereum comprises of

- Smart contracts are used to control all the events in Ethereum, written in Solidity programming language.
- Ether is the pillar of Ethereum transactions and cryptocurrency of the Ethereum network.
- Ethereum Clients develop and mine Ethereum blockchain. Examples are Geth, Eth, and Pyethapp.
- Ethereum Virtual Machine (EVM) is the blockchain engine behind Ethereum within which smart contracts run. EVM runs its language of bytecode which has necessitated the development of numerous smart contracts writing languages like Solidity.
- Etherscripter is a graphical user interface used to build smart contracts in Ethereum. In a few and simple steps, the drag and drop mechanism allows the automatic generation of backend codes in LLL, Serpent, and XML.

2) *Hyperledger*: Hyperledger is a worldwide partnership, accommodated by The Linux Foundation, and involves frontrunners in banking, finance, supply chains, Internet of Things, Technology, and manufacturing. Hyperledger is an open-source motivated by a community centered on mounting a collection of reliable bases, libraries, and tools for the development and deployment of enterprise-grade blockchain systems. More blockchain frameworks have been undertaken by Linux Foundation under the Hyperledger project including Fabric, Caliper, Sawtooth, Aries, Besu, Burrow, Cello, Composer, Explorer, Grid, Indy, Iroha, Quilt, and Ursa. Part of these frameworks is P permissioned (private) and others are permissionless (public) [53].

3) *Corda*: Corda was launched by R3 as an open-source blockchain platform in 2016 with provision from a strong community of developers and organizations. Corda is a blockchain with one key differentiator. It is a private blockchain platform that warrants the sharing of data among known participants. Corda was intended to ensure trust, transparency, security, and privacy.

4) *Quorum*: Quorum is a platform for enterprises to use blockchain. It is an enhanced branch of the public Ethereum client ‘geth’ to provide for business essentials. Quorum is also an open-source project and supports the very requirements of businesses – performance, privacy, and access control. The enterprise application requirements which predominantly

include privacy, performance, and permissioning are all provided by Quorum augmenting them with the secrecy of all transactions, scalability, and speed, and ensures authorization.

IV. METHODOLOGY

We employed a methodology used by [12] and [54] and followed some of the steps in PRISMA [55] to allow for the production of reproducibility, transparent, scientific work. The following subsections describe the employed methods in detail. The following research questions were asked before the commencement of the literature search and the question determined the usage of whether gray or systematic literature review.

1) What are the major insurance sub domains that are currently draining the sector?

2) What are the major business processes in insurance that blockchain technology can mutate?

3) What are the current developments of the application of blockchain in the insurance sector?

A. Locating Studies or Data Extraction

To discover the latest papers for the resolution of the research questions, Mendeley Desktop and Google Scholar were used as the main sources for the papers. The search was done with no restricted timeframe. However specific search terms were used. For example, “Blockchain in Insurance”, “Blockchain Insurance”, and “Blockchain Application in Insurance” were used in April 2020. The process was repeated in November 2020. The search term with the highest results is “Blockchain in insurance” and was used to query a total of 578 papers.

B. Data Screening and Selection

As indicated in Table II, exclusion parameters were implemented before accessing the full papers. The types of papers that were included are peer-reviewed papers, book chapters, conference proceedings papers, short surveys, review papers, serials, white papers, official websites, etc. Enormous papers that satisfied any of the exclusion parameters (subject area, document type restrictions, and language) were excluded. Also, some papers were left out because of missing valuable information like authors’ names, and abstracts. The search term fetched numerous articles but, most of them were rejected because their titles portrayed that they belonged to specific domains such as finance, legal, health, etc. All these were done without emphasizing author-specific or journal-specific papers. Other papers were excluded because they were not found although they appeared in the search query. Some papers also duplicated multiple times under different titles and were consequently excluded.

C. Descriptive Analysis

A total of 578 papers were fetched from the search term and a majority of them were excluded using the specified parameters in Table II. From Fig. 5, 455 papers were excluded resulting in the importation of only 123 into the reference manager. Out of the total number of excluded papers, nine papers were rejected after the importation because they appeared multiple times with different titles. Three papers

were included because they provided a strong theoretical foundation of blockchain technology although their titles were not in line with the thematic area. Twenty two papers were excluded because their contents were either unusable or not in line with the theme. Four papers were excluded by title but included by abstract and 15 papers could not be located by Google Scholar or regular Google search. Lastly, 12 papers were written in different languages other than English and

resulted in their exclusion. This resulted in the usage of 80 papers in this review. For the sake of simplicity, only the thematic papers are described and are depicted graphically in Fig. 4. In Fig. 4, it is observed that 6 papers in the area of blockchain technology and insurance were each published in 2016 and 2017. 21 papers were produced in 2018 and 27 papers were published in 2019. Lastly, 20 papers were published in 2020.

TABLE II. EXCLUSION AND INCLUSION PARAMETERS

Parameter	Systematic Review	Grey Literature
Inclusion	<ul style="list-style-type: none"> Peer-reviewed papers Book chapters Conference proceedings papers Short surveys Review papers Serials etc. 	<ul style="list-style-type: none"> Regular Google search Official websites
Exclusion	<ul style="list-style-type: none"> Subject area (other domain-specific papers) Language (Non-English) Missing authors' names Missing abstracts Undiscoverable papers Papers with unusable contents 	

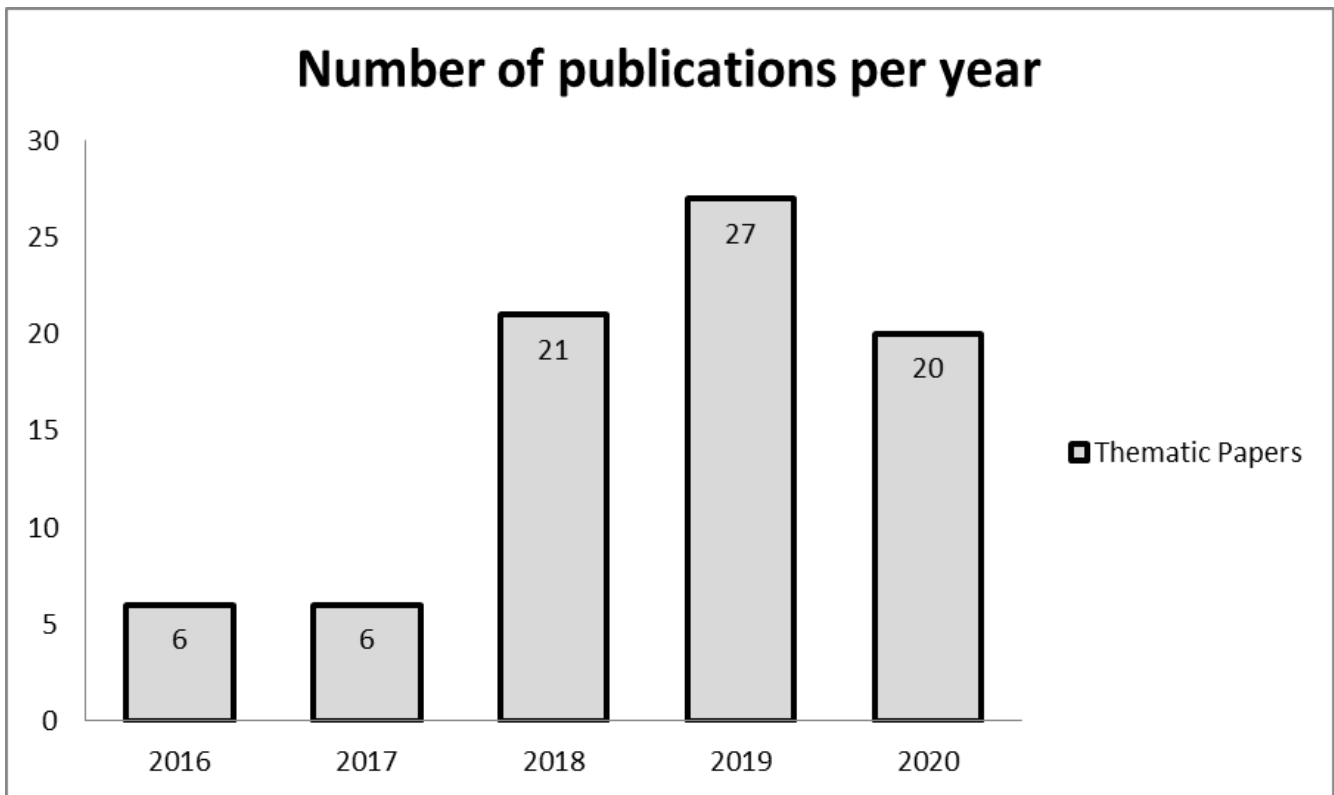


Fig. 4. Yearly Publication of Thematic Papers.

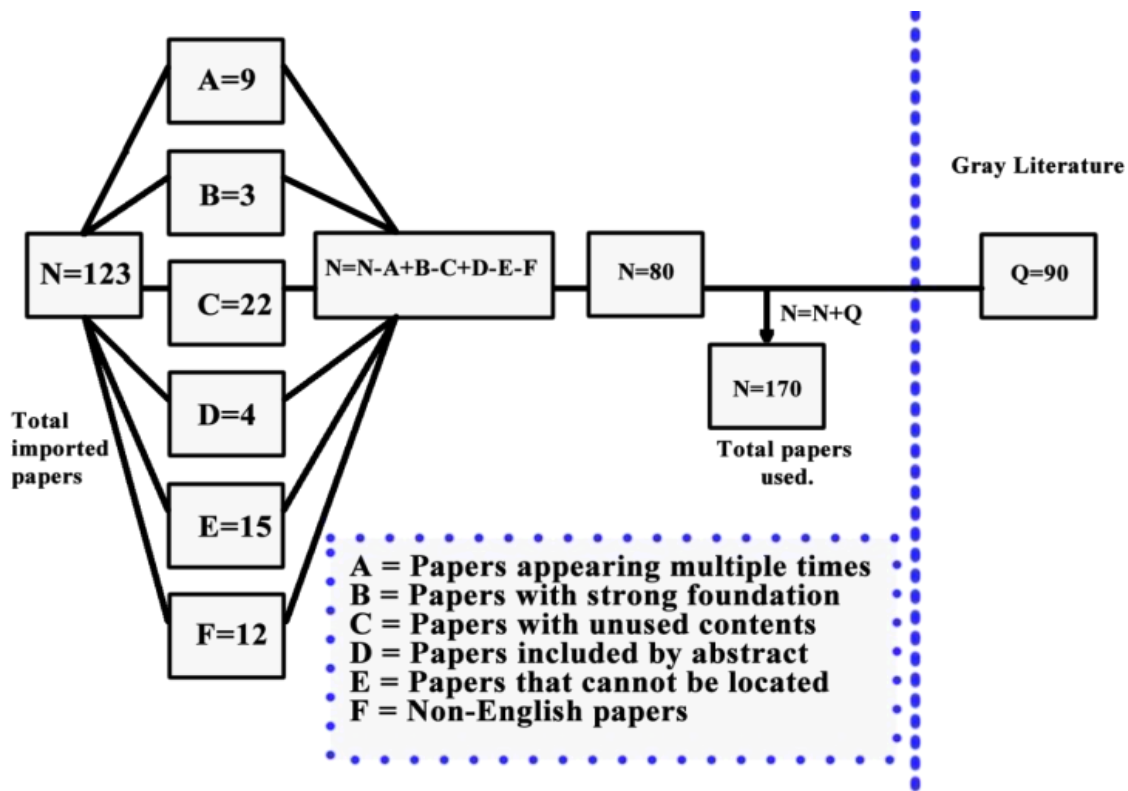


Fig. 5. Graphical view of the Search Strategy.

V. RESULTS AND DISCUSSION

A. Major Types of Insurance

According to [56], although contemporarily found with numerous challenges, insurance is an avenue to provide financial risk mitigation that pays the policyholder in case of the occurrence of an unforeseeable adverse event or loss of property [57]. However, the industry is profoundly reliant on various processes between transacting parties to initiate, maintain, and close different classes of policies. Consequently, the processing time of transactions, settlement, and payment time of claims, and the security of the process execution are major concerns [58].

Futuristically, several existing breakthroughs in computing like Cloud Computing [18], Internet of Things (IoT) [59], Artificial Intelligence (AI), machine learning methods [60], and data analytics [61] will be joined and leveraged to automate and drastically transform the manner in which insurance processes are handled contemporarily. The following are the major types of insurance being provided by modern companies and how blockchain's contribution can be implemented.

1) *Vehicle insurance*: Vehicle insurance is an insurance policy covering motorcycles, trucks, cars, and other vehicles that apply roads. The main purpose of vehicle insurance is to ensure vehicle users' financial fortification against physical or property damage or bodily injury which results from an accidental collision on the road and also against any hostile traffic and vehicular happenings [62]. It was first introduced in

the United Kingdom in August 1930 by an act to regulate traffic motor vehicles on the road and to protect third parties from the dangers associated with vehicular movements [177]. In some cases, vehicle insurance offers a monetary bulwark against vehicle theft and other events like vandalism and natural disasters.

The overwhelming rate of road accidents and related fatalities and injuries necessitates vehicle insurance. Annual road traffic deaths stand at 1.35 million in 2016 [63]. The economic repercussions besides the deaths and injuries are enormous with over \$300 billion annual costs which include travel delays, property damage, medical costs and pain, legal costs, loss of productivity, and loss of quality of life [64]. Without vehicle insurance, injured people would rarely get any recompense in a case of an accident, and motor drivers will mostly cope with considerable charges for injury and destruction of their car and property difficultly or find themselves in an illegal situation, apprehension, or might pay a fine [62]. In most countries, insurance premiums are paid regardless of vehicle usage or not [65]. For efficiency and customer satisfaction, vehicle insurance companies have offered discount programs [66] and designed enhanced business models to reduce the risk of losing revenue [67]. A classic example is the development and institutionalization of Usage-Based Insurance (UBI) [68, 69] which requires customized payable premiums based on vehicle usage to reward good or other driving habits. UBI supports the use of on-board devices [70], and telematics devices to capture relevant information like G-force, speed, mileage, time, location, and trip duration, informing the insurance company

about drivers' driving behaviour [71,69,67,72]. Policies in UBI are categorized as Pay As You Drive and Pay How You Drive [73,74] which makes them economical and precise for drivers [75,76]. Blockchain can be leveraged together with smart contracts to process claims promptly without going through tiresome bureaucracy which mostly results in the rejection of enormous claims. Also, the conditions that must be satisfied before payments can be automated quantitatively, therefore insured drivers or vehicles with rejected claims may accept the rejection and may not lead to further litigations which may also amount to extra costs [77,78]. Again blockchain can be linked with the IoT combined with efficient data capturing devices to collect, store, and process real-time data collected from targeted vehicles resulting in objective monitoring of vehicular movements [45]. This apparently will be particularly useful in usage-based premiums. The author in [65] designed a BC-based system that supports transparent management and analysis of data in a pay-as-you-go car insurance application to allow drivers who rarely use their vehicles to pay premiums on trips of interest. A blockchain system can be combined with smart contracts and sensors installed in customers' vehicles to manually modify policy coverage using environmental conditions for claims settlement and adjudication [79,80].

2) *Home insurance*: Many individuals and societies in the United States have been affected by natural disasters like Hurricane Harvey resulting in the destruction of their homes [81]. Home insurance – building or content insurance insures against events like fire, which destroy homes or domestic properties. In the United States, regular homeowners' insurance policies support costs resulting from hail, wind, and fire, but disregard damages caused by earthquakes and floods [82,81]. Without home insurance, disaster losses are possibly going to impact affected people to live sub-standard lives and in destitution. The wholesale insurance and reinsurance aggregated about 520 billion USD in Gross Written Premiums in 2013 [83]. In areas with great dangers of devastation, governments intervene and take obligation. Countries like the United States, Chile, France, Mexico, Germany, Japan, and the United Kingdom practice this when the risks are considered uninsurable [84].

Blockchain technology can be leveraged to automate claim applications and processing. Once a natural disaster is confirmed by the mandated state institution with the magnitude and level of impact, a smart contract can be triggered to effect payments to the affected communities. The monetary losses incurred by insurance companies from natural disasters ratcheted from \$528 billion (1981–1990) to \$1.6 trillion over the period 2001–2011 [84]. Between 2005 and 2006 the total loss in Europe was about \$1 billion and \$ 400 million in Australia [85]. In 2017 Hurricane Harvey resulted in about \$25 to \$37 billion in flood damage to homes in Texas. Presumably, administrative costs may take a huge chunk of the costs. Consequently, blockchain can be used to cut excessive human involvement and paper works by employing smart contracts [23]. Privacy issues may lead to the adoption of public or private blockchain where exact damage and recompense of individuals are accessed by authorized

users only. An example of such platforms is HurricaneGuard implemented on Etherisc [86].

3) *Life insurance*: Life insurance is a signed bond between an insurer and a policyholder or insured, where the policyholder is required to trade a premium in exchange for an assured amount of money in the case of the death of the insured [87]. A life insurance policy provides for the insured and their dependents in the case of bad events which lead to grief and the seizure of income. The amount to receive or the event to trigger the payment is highly dependent on the investment or the contract which can either be a terminal illness or a critical accident. Insuring oneself against life's uncertainties gives a cover of life risks, death benefits, return on investment, tax benefits, loan options, life stage planning, assured income benefits, and riders. The policies of life insurance are lawful agreements that stipulate the terms and describe the limits of the events insured. For example, some policies may exclude events of suicide, war, fraud, civil commotion, and riot. A major challenge of life insurance perhaps is that the beneficiary of a policyholder is required to present documents like a death certificate and the paper form of the policy [88] which can be destroyed by a natural disaster like flood and other occurrences. Also in the case where the policyholder holds numerous policies, the beneficiary may not be aware of their existence and therefore can also lead to inefficiencies and raise administrative costs unintentionally [89] as is the case in the United States where about 7.4 billion dollars exist in unclaimed life insurance money from insured people [90]. The life insurance industry can leverage blockchain as it helps to ensure information is accurate, secure, and trusted and ensure the transparent sharing of information between two or more parties [91]. Typically, instead of using contracts and agreements in paper form, blockchain-related smart contracts can be programmed to trigger and respond to all predefined services. As a substitute to trusting the insured to keep a copy of the policy, it can be recorded in the distributed ledger of blockchain making it available to the beneficiary, insured, insurer, and other entities (police, deaths and births registry, etc.) and transparently updated when necessary [89]. Smart contracts can also observe already existing platforms like Oracle to confirm and validate the demise of an insured together with other participants on the blockchain network through the consensus algorithm. Real-time clinical information can also be shared and digital proof can be easily amalgamated into insurance underwriting and the anticipation is a prospective mutation in the subdomains of product development and consumer pricing [91].

4) *Disability insurance*: Disability insurance (DI) is a type of insurance that protects the insured against loss of income resulting from disability. It is a social insurance program that provides income and health benefits to people who cannot work because of some form of disability [92]. It covers funded sick leave, temporary disability, and longstanding disability benefits [93]. According to 2015 statistics, the percentage of

people living with disabilities among the civilian population in the United States of America increased from 11.9 to 12.6 in 2014 [94]. Over 51 million (18%) American population stand to be categorized as disabled. Again, in every second and four minutes, incapacitating and deadly incidents occur respectively resulting in 3 out of 10 entry-level workers becoming disabled before retirement [95]. In 2014, the percentage of employed civilians between the ages of 18-64 living with disabilities was 34.4% of US civilians compared to 75.4% for people without disabilities, signifying a difference of 41 percent. The same report indicates that about thirty percent of working-age civilians living with disabilities were living in poverty as of 2014. DI is large and growing faster [92]. In 2012 the DI program in the United States paid beneficiaries about \$136.9 billion. The programs of DI are associated with enormous impediments including a huge number of false rejections and minimal false acceptances [96,92]. With the characteristics of blockchain, numerous problems characterizing the DI programs can be solved. Certainly, there would be a database of civilians with disabilities indicating their level of severity. Smart contracts can also be used to determine the time to disburse payments and the amount to be disbursed to every participant depending on predefined parameters. This can be done transparently and automatically.

5) *Health insurance*: Due to low or loss of income, poor folks and most women in developing countries and all over the world become particularly vulnerable and suffer in the case of sickness because of the overburdened cost of medical expenses [97]. Most people are unable to save, own properties like lands or any valuable ornaments which can be sold to cater for the cost of seeking medical attention if the need be. It is a known case that health-related bills are the cause of depleting personal and family accounts into bankruptcy [97]. Diseases can propel well-living individuals and their families to deplete their accounts and or lead to deteriorating health conditions. Hypothetically, governments are supposed to provide their poor with health insurance schemes and health-related programmes [98]. The reverse is the case in practice [97]. This may be caused by the embezzlement of funds, increased administrative costs, social and political influence, unstructured processes, and mischievous intentions of hospital workers [99]. The process of medical billing is fraught with enormous challenges [99]. It begins when a patient enters the hospital and ends when the patient leaves which involves different stages like arrival, monetary restraints confirmation, coding, and billing, sending the bills to the insurance company, and receiving reimbursement [99]. A major challenge with the medical billing scheme is extreme billing, partly due to the absence of trust and transparency among the parties involved (patients, nurses, doctors, and insurers). Unceasingly, billing and claims are abused in the healthcare zone [99, 100, 101]. This is relatively so because medical bills are prepared on the blind side of the patient but this can easily be resolved by taking advantage of blockchain technology.

For example, by adopting a hybrid blockchain system, patients will be fully aware of the hospital services and prescriptions that lead to the payable amount and they may be required to validate the transaction before committing to the block and the transparency, decentralization, auditability, and immutability of blockchain will make all data in the ledger unchangeably available to all authorized participants [102,99]. Information sharing in the health care sector is extremely important regarding the sensitivity of medical records like patient's health status, medical records ([103]. A patient will be required to see numerous health specialists for a particular treatment or in a lifetime [104]. The manual information-sharing system is fraught with excessive complications and results in unnecessary charges and hassle for the patient [105]. Also, there is a lack of transparency and privacy [106]. Consequently, a cryptographically protected blockchain ensures patient privacy while providing an industry-wide, co-ordinated warehouse of healthcare data, bringing the industry billions in finances a year [105,107]. In this line, [107] and [18] proposed, designed, and implemented a blockchain prototype to ensure verifiability, privacy, and integrity of transactions in a health insurance claim. Medrec and Gem Health are examples of frameworks and blockchain-based systems used for information sharing and administration of medical health records [108]. Also, [109] propose MISTore to provide efficient verification and homomorphic computation, decentralization, and secured data.

6) *Long-term care insurance*: Long-term care insurance protects persons against the cost of receiving regular assistance for chronic disabilities (cognitive or physical). This form of insurance is different from health insurance in the sense that it is not meant for out-patient or specific diseases but to assist insureds in fundamental daily living activities like dressing, eating, and bathing and tasks that are essential for living like cooking, shopping, and any other housework [110]. Long-term care costs are usually covered by state programs (Medicaid, Medicare, etc.), private insurance companies, and the recipients and their families. The cost of long-term medical care is very expensive and as a result, government programs have limited the service coverage. Indeed, most of the expenses are covered by the beneficiaries and their families which exert enormous strain on their finances. For those who satisfy the complex and varying state eligibility rules, Medicaid pays for some amount to cover expenses like domestic health care, nursing home services, and community-based service to enable beneficiaries to remain in their respective communities [110]. Private companies in the domain of long term care insurance remain significantly low, mostly due to sector risks and liabilities. Confidently, support from private and corporate donors, philanthropists, charitable givers, and rich individuals can be very valuable to the beneficiaries and governments in general. An ability of blockchain is the quality of being leveraged to provide financial support for start-up companies and small businesses – Initial Coin Offering (ICO). ICO provides the platform for

company executives and individuals to request funds to start a company or business. One opportunity here is for public programs and private insurers to leverage blockchain to solicit financial support to cater for the substantial cost of seeking long term health care.

7) *Marine insurance*: Voyage transportation is loaded with enormous threats such as piracy, and cross-border shoot-outs as well as natural occurrences that can harm the cargo, ships, terminals, and vessels and cause massive monetary loss to individuals and companies [111]. This has necessitated the development and implementation of marine insurance which protects sea-based transport-related losses. The current initiative by major industry players like EY, Guardtime, Microsoft, A.P. Møller-Maersk, and insurance industry leaders like ACORD, XL Catlin, Willis Towers Watson, and MS Amlin – Insurewave, a built blockchain system to support marine vessel insurance. The initial capacity support is about half a million automated ledger transactions intended to deal with about one thousand vessels [112]. The leverage of blockchain and related distributed ledger helps to bring participants in a single network and ensure efficient execution of processes and maintain an immutable and accurate audit trail.

Since marine insurance is one of the oldest commercial insurance, most of the processes, practices, customs, and policy terms are structured and can be easily translated into programmable lines of code. Consequently, the brokerage purchasing process could be simplified by eliminating financial intermediaries and transparency can be improved among the parties by making quoting, binding coverage, and related activities visible to all participating stakeholders. Marine insurance processes would be greatly enhanced. For example, payments of premiums will be fast and straight into the accounts of the insurer and the policy will be made available upon receipt of funds. With transactions immutably and transparently stored in the blockchain ledger, conflicts will be resolved as quickly as possible [113]. In events of cargo loss, total loss, or products and goods contamination as in pharmaceuticals and food, smart contracts can be developed to trigger payments when the necessary notification and verification have been done and the proof has been submitted to the blockchain ledger.

B. Implementation of Blockchain in Insurance

According to [91], the following are the general blockchain benefits in insurance. Event-triggered smart contracts, increased back-end efficiency, disintermediation, better pricing, and risk assessment, new types of insurance, and reaching the underserved Blockchain-based applications can be very valuable to all insurance companies - travel, agriculture, Assets, medical Insurance, because of the inherent facility to provide long-lasting strategic benefits in terms of lowering operational costs by reducing or eliminating overlapping processes, enhancing automation, reducing counterparty risks and providing secure, transparent and decentralized transactions [114].

Most of the contemporary insurance applications adopt the client-server architecture which has worked well for quite a long time now. However, it must be mutated to enhance security and efficiency [45]. Client-Server Architecture is a computing model in which the server keeps, provides, and controls most of the services and resources to be consumed by the client. Clients request and access resources over a computer network or through an internet connection. Although systems using this architecture perform better and serve the needs of enterprises, their very nature makes them suffer some limitations. Systemic failure can affect all operations that rely on the server. Although safety procedures might be put in place, there is still a higher probability that the data can be manipulated in the server accidentally or deliberately [62]. The following are some key areas in the insurance domain that Blockchain technology can enhance and/or help prevent.

1) *Claim submission and processing*: The author in [114] designed a blockchain-based system that supports quick insurance claim processing. Insurance claim processing can be very tedious, time demanding, inefficient, and susceptible to human errors especially where validation is done through paperwork processes [115, 116]. Also, there is a lack of transparency in the submission of claims and the processing is associated with adverse effects of delays and blunders leading to unsatisfactory customer services [40,45, 117]. Insurance claims is a circulated process involving several entities – insurer, insured, regulators, and third party entities, mostly characterized by inefficiencies and malicious intentions [118].

Blockchain can drastically reduce the claim creation, accepting, and processing time and make it hassle-free, and less costly using smart contracts once the policy conditions for payment are unambiguously clear [119,118,21, 120,121]. Blockchain can be employed to create immutable and auditable statements at the various stages in the insurance claim processing that can be re-accessed by all participants. The benefit would be to reduce the risk and cost of transactions and improve trustless computations. Blockchain has also emerged as impressive technology to provide high efficacy solutions to the problems of contemporary insurance systems (45,122,117). As an example, a novel system is being worked on by ANZ Bank, Suncorp of New Zealand, and IBM to ensure efficient and smooth transmission of data and premium payments between insurers and brokers. By involving blockchain in the storage and update of data, there would exist a single version of truth between insurers and brokers and smart contracts can execute to commence payments automatically [20]. Also, Allianz has employed digital tokens to pay its worldwide affiliates thereby alleviating the challenge of currency exchanges [20]. Also, AXA French insurance company launched a smart contract based flight-delay insurance product to reduce cost, improve customer engagement, and develop new insurance products [123]. InsureETH a startup in UK, and the project of American International Group (AIG) have similar objectives [124]. Fig. 6 shows a theoretical way of handling claims using blockchain as proposed by [125].

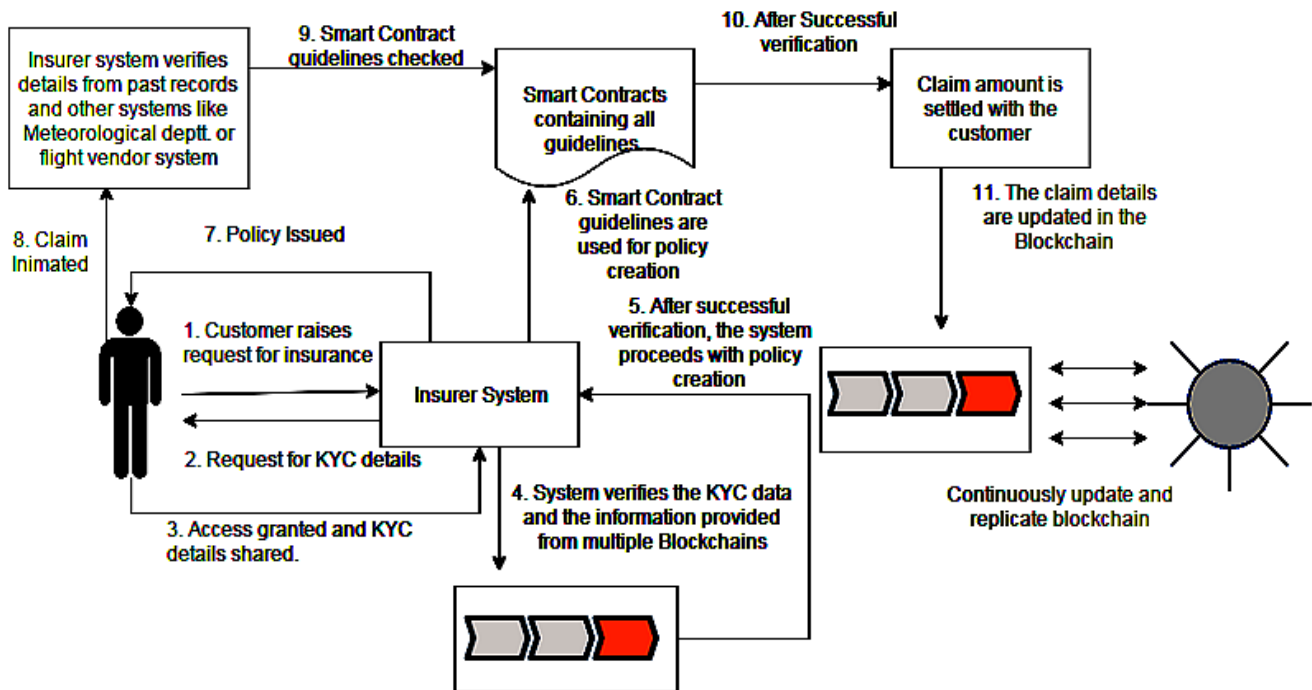


Fig. 6. Claim Submission and Processing using Blockchain.

2) *Fraud detection and prevention:* The insurance companies stand high chances of losing good treasure as a result of claims of fraudulent nature [45,126]. Inadvertently, fraud increases yearly [18] and by estimation, about 5 to 10 percent of all annual claims are fraudulent and the FBI indicates that it costs US non-health insurers over 40 billion every year [127,128] which results in extra costs for policyholders in increased premiums. Similarly, in the UK, claim fraud results in about £3 billion annually [128]. Ditching, Cash for Crash, Double Dipping are some recorded frauds in vehicle insurance [62]. Again the centralized nature of insurance systems affects the integrity and transparency of the data stored in them [45]. Identity theft is another way of fraudulently acquiring and using another person's information thereby impersonating the genuine owner to enjoy unbecoming benefits [129, 130]. An authorized malicious insider can manipulate internal data for financial benefits which can be very detrimental to the company. Blockchain can eliminate the limitations of client-server architecture to prevent fraud. The transactions in Blockchain are visible to all participants and

original statements, policies and contracts are very difficult to mutate [118,62]. The consensus protocol ensures that without any central governing body, any modification to the database happens at an agreeable rate and does not affect the integrity of the data. Again Blockchain can minimize forgery, document or contract alterations, multiple booking [118] as the distributed ledger can be shared among multiple trusted parties like medical doctors and security agencies to create and update [79,130].

The validation of the authenticity, provenance, and ownership of goods and documents is made easy with blockchain. The encryption method applied by blockchain can prevent cyber liability where personally identifiable information can be impaired by third party entities who store such data. Blockchain can eliminate trusted third-party companies whose presence adds value and overheads by authenticating the validity of submitted documents [79]. Fig. 7 demonstrates a framework to detect and eliminate fraud during claim submission and policy issuance as proposed by [125].

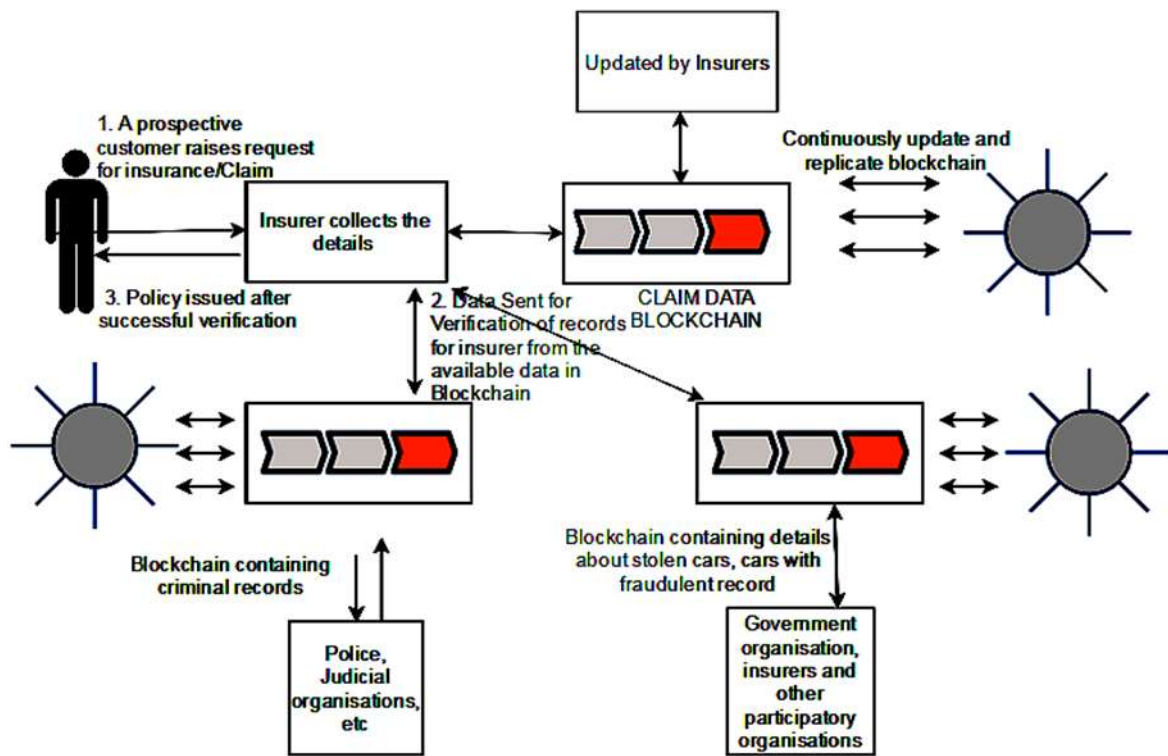


Fig. 7. Framework for Fraud Detection during Claim Submission or Policy Issuance.

3) *Data entry and identification:* A little over sixteen percent of the world's population is without recognized proof that they exist [131]. Consequently, there is a need for virtual identification systems. Fortunately, there exist numerous means to electronically and accurately identify people for who they are and to authenticate their characteristics [132,12,133]. In insurance, the storage of wrong and unverifiable data can have extremely negative effects and support for fraudulent activities [79]. The employment of blockchain in insurance can prevent writers from modifying previously stored data, as data are shared among all participating members in an unchangeable and append-only manner. Immutably hashing the IDs of data originators enforces non-repudiation, data integrity, and authenticity.

4) *Sharing of intelligence data:* Insurance systems face numerous systemic flaws that are exploitable by malicious persons [118]. This results from creating multiple policies and synthetic Identification numbers with the same device. Apparently, insurers invest in public data and subscribe to service providers to get informed about fraud investigation and prevention. In the past, insurers have tried to share intelligence but suffered technological, commercial, and legal roadblocks as a result of confidentiality and national and corporate access control policies [118]. Health records exist in digital formats however communication of such data among healthcare providers remains a challenge [134]. Cyber-insurance has not been widely accepted by insurers and coverage is restricted to business interruption, stolen of digital

assets, and data breach, mainly because of the unavailability of accurate data, legal and procedural approaches for auditing, and assessment of organizational security strength [135; 136]. The comprehensive and palpable benefits of employing blockchain to share insurance-related data will comprise accountability, ledger immutability and transparency, data decentralization, and security [137,138, 139,140]. A group of insurers can team up to initiate a Blockchain network for the system, to host enormous distributed processes on the network, with no single proprietor [118]. The financial sector keeps a record of the credit history of their customers which is accessible to all permitted financial companies and other institutions. Similarly, BC can be used to record insurance premium payments history and other records for access and usage by other insurance companies almost instantly and accurately [21]. [141] propose a scheme to authenticate insurance transactions based on blockchain to solve the problems of security, high cost of data management, and easy data manipulation.

5) *Peer to Peer insurance:* Peer to Peer insurance (P2P) is a new type of insurance that gives like-minded insureds with the same insurance needs and interests the chance to consolidate their funds and manage their private insurance. P2P insurance is different from traditional insurance in the sense that, there is a drastic reduction in the expenses of managing the insurance policy, re-insure insureds when claims surpass the pool and also pay themselves using reserves. This is as a result of bureaucracy bypass, reduction in paper works,

minimal workers, and more [142]. P2P insurance companies make filing a claim and receiving payment less costly, easy, automatic, fast, and transparent mostly by using online service or mobile application. Examples of P2P insurance companies are Tong JuBao in China [143], Guevara in the UK [144], and Friendsurance in Germany [74,145]. Dynamis is a P2P complementary protocol for unemployment insurance that replaces the underwriters with policyholders' social capital and Enigma while ensuring complete privacy, provides the platform for diverse parties to mutually store and perform computations on data [146]. The core characteristics of blockchain have a direct link with the characteristics of P2P insurance – decentralization, speed, automatic, ease of use. A smart contract can be used for claim filing and processing and also automate payouts. Claims are approved by the majority of the blockchain participants before disbursement of the amount after which the reserve is shared among the remaining insureds or given to charity homes [147]. At this point operations research techniques can be applied together with a smart contract running on the blockchain network to ensure the fair and transparent distribution of payouts and reserves.

6) *Getting rid of middlemen:* Middlemen exist in the insurance companies for numerous reasons – for claims data or document preparation and submission on behalf of the claimant, ensuring the right documents are acquired and submitted. The use of middlemen in insurance offers some value for the insurers and the insureds. However, their existence introduces bottlenecks in the process – delay in claims processing and extra cost for the participants involved [148,127].

The architecture of Blockchain eliminates all brokers [6], thereby attributing to each partaking company, the original copy of the ledger. The peer-to-peer nature of blockchain and the consensus algorithm allows the peers to interconnect and transfer data among themselves. The employment of this technique may drastically reduce the approval time of transactions from days to seconds automatically thereby meaningfully improving efficiency at a minimal cost [148,6]. Indeed, by eliminating the need for a middleman, the technology has the potential to disrupt many activities in sub-sectors of the insurance that currently rely on a trusted authority or intermediary operator.

7) *Know-Your-Customer and Anti-Money Laundering (KYC/AML):* Insurers, reinsurers, and brokers perform auditing processes to know their customers and also prevent money laundering and it usually involves multiple entities like individuals and legal personnel [21]. In a case where an insured deals with a broker who works with numerous underwriters which in turn deal with reinsuring brokers, such a transaction will involve multiple participants who have to follow the KYC/AML processes along the value chain. Obviously, this overlay of processes adds to processing cost and time [21]. London's leading commercial think-tank Z/Yen has commenced IDChainZ which is a scalable, globally available, and subject-centered operational proof of concept fabricated using ChainZy mutual distributed ledger technology which allows several parties to add, certify and exchange KYC and AML documentation [149]. IDChainZ is intended to reduce processing time and cost, make time-critical transactions presently uninsured and reduce operational risk [21]. Fig. 8 is a framework for KYC/AML as proposed by [125].

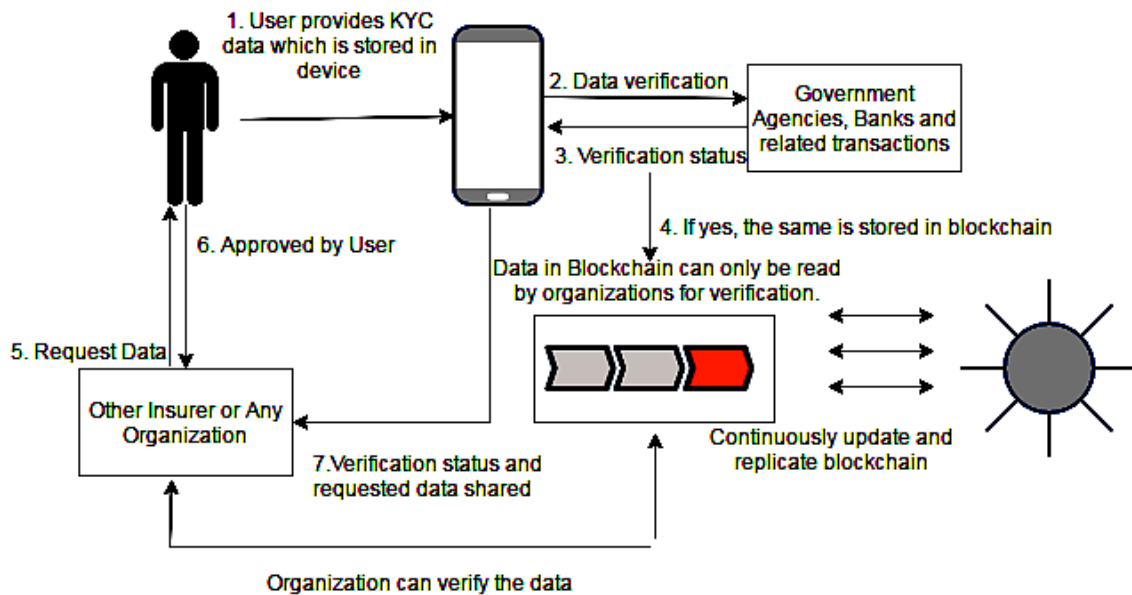


Fig. 8. KYC Compliance Framework using Blockchain.

C. Limitations of Blockchain Technology

Despite blockchain technology's tremendous potential in advancing existing systems with smart contracts, major gaps remain within its implementation as a libertarian-rooted, privacy-minded, decentralized cryptocurrency and a technology stack that fully satisfies business, security, and regulatory requirements [41]. As an emerging technology hurdles exist to impede its wide acceptability and the realization of its full potential. Blockchain is no exception. The following are the challenges of adopting Blockchain in insurance [129,127].

1) *Scalability*: Blockchain is expected to grow in popularity and acceptance and when these are realized, the current infrastructure may not be able to support the growth. Practically, the available computing resources limit the insurance industry from reaching the apogee of implementing blockchain technology. Theoretically, with the current infrastructure, about 1000 transactions should be verified by Ethereum in a second. The number reduces to about 10 which is very small compared to Visa and Paypal, which can verify about 1670 and 193 transactions per second respectively [150]. The current consensus algorithm for permissionless blockchain requires 50 percent plus one participant to agree on the validity and authenticity of blocks and transactions. The case for permissioned blockchain is different with pre-known nodes. In a blockchain, every block has a limited block size, and time interval [150,151]. As the number of network nodes increases, the number of transactions to be processed also increases, however, the scalability decreases. Conceptually, sharding was proposed to enhance blockchain's scalability likewise Super Quadratic Sharding. However, results from implementation may prove otherwise. The decentralization of data and processing capabilities require that individual nodes be possessed with the capability to handle transactions for a growing number of users. At the moment, blockchain works well with a smaller number of participants however, to validate data on a real-time basis and ensure efficiency, the broader as-is nature of the insurance industry needs a different perspective for its larger population. Consequently, there is a need for gargantuan storage space, enhanced consensus algorithms, and robust computing power.

2) *Expertise*: Blockchain technology is a relatively novel innovation and a broad specialization with minimal books and technical knowledge distributed across multiple websites [152]. The technical and technological know-how are other limitations of blockchain systems development. The proficiency and expertise essential to create, apply, and maintain blockchain systems are still at the juvenile stage [129]. There are some successes as few platforms use blockchain without hindrance. However, stability and speed would be required if the technology would be extended to other industries.

3) *Security, Data privacy and management*: Blockchain in its current form has a lot of vulnerabilities and limitations in terms of security privacy and data management [153,154,155]

and a lot of field practitioners and academicians have pointed out that blockchain does not adhere to existing privacy laws such as the EU General Data Protection Regulation [156]. Bitcoin, the famous blockchain application operates the public ledger type and the source code is open which defies privacy and confidentiality [12]. This can be solved by implementing the private type of blockchain [129]. Also, enormous encryption and anonymization techniques can be used successfully but also come with challenges in terms of speed, portability, and scalability [129,12]. In the contexts where the number of nodes is expected to grow tremendously like IoT, implementing such a mechanism can be too challenging [157,12]. Again to prevent the release of sensitive data, secure file sharing protocol methods like telehash, Whisper [158], or content-addressed file system can be used [157].

Although blockchain is 'tamper-proof', the nodes writing to and reading from the blockchain applications can be vulnerable. In case of an attack, the target is not the blockchain application or ledger itself but the external systems such as cryptocurrency wallets. If the data input node is compromised, it will lead to the storage, processing, and usage of inaccurate and misleading information [156]. It is known that the transactions of bitcoin can release massive confidential data [159,12] which confirms the transactional privacy problem of blockchain [160]. In the case of public blockchain applications, the data stored is made available to all involved nodes and it is similar to posts made onto the public Internet [156]. Just like any other computer program, smart contracts also usually comprise bugs that can lead to serious consequences [12]. Decentralized Autonomous Organization (DAO) attack (Siegel, 2016) is an identified weakness in SC which led to a loss of about 47 million dollars and the Parity wallet weakness which also allowed the orchestration of about 280 million dollars [161,12]. Besides the aforementioned susceptibilities of SCs, there are other numerous ones. Solutions have been proposed to mitigate the effects of the identified vulnerabilities [162] and the most encouraging is the approach that attempts to submerge the expressiveness of the underlying programming language [12,158]. Other frameworks exist [163,164], which look for bugs by verifying the correctness and fairness of smart contracts. With Discouragement Attack, [165] propose the use of insurance contract theory to ascertain the withdrawal delay case studying cyber insurance to thwart the attack victims damage.

4) *Regulation, standardization, and taxation*: It is important to note the effective law scheme and the applicable risk management that can be used in public blockchain systems. Nevertheless, in private blockchain systems, the consensus algorithm can be designed to enforce some internal governance scheme and legal framework which will store the rules that will apply to transactions [156]. The conflict resolution process is also required in private blockchain systems. At the moment there is no comprehensive universally acceptable regulatory response to blockchain [166] despite efforts by government and supranational organizations [167]. In a 2018 survey [168], it was discovered that the most

frequent government involvements in blockchain-related issues are the issuance of public educational notices mainly about the vulnerabilities and risks associated with cryptocurrency investments by the central banks. In such cases, the people are warned about the difference between cryptocurrency and actual currency and as such indicate the cryptocurrency is not unregulated and guaranteed by the state. Hence any form of investment in cryptocurrency is perilous [168]. Various countries also issued a warning indicating how cryptocurrency provides a fertile ground for dishonest deeds like terrorism and money laundering. In effect countries like Canada, Australia and the Isle of Man changed their laws to include cryptocurrency and related companies and activities under the laws of financing counterterrorism and money laundering. In countries like Algeria, Vietnam, Nepal ban all events involving cryptocurrencies. Qatar and Bahrain ban and permit their citizens from engaging in cryptocurrency within and outside of their borders respectively. Readers can refer to the [168] for a full report of how countries are regulating cryptocurrency. In particular, understanding who is accountable and legally responsible is a major challenge.

The extension of the existing tax framework to the virtual companies is extremely difficult and has presented enormous challenges globally [156] and taxation of cryptocurrencies is a major question posed by many [168]. Even so, not many countries support the use of cryptocurrency and consequently do not have appropriate taxation structures for cryptocurrencies. As of 2018, only a few countries had instituted measures to tax virtual currency [168]. These countries are indicated in Table III. Taxation of blockchain faces bottlenecks partly because there is a debate Among European Union Member States Cryptocurrency investments are not subject to Value Added Tax (VAT) primarily due to the European Court of Justice ruling in 2015 [168]. No country in Sub Sahara Africa has applied a taxation scheme to cryptocurrency except South Africa. Contemporarily, Ghana has not regulated the employment of blockchain and in effect, blockchain-related systems that intends to take a virtual currency or cryptocurrency payments could be considered illegal when multiple nations participate.

5) *Suitability and compatibility*: The suitability of blockchain in all situations is questionable especially in data management, although the future looks promising and a lot of companies are enthused about the potential of blockchain to transform the virtual infrastructure and solve numerous [12,169]. Because most IT Officers do not understand the basics of blockchain, they hike their interest and predict the use of it in every IT project [12]. In a project where data storage is not required blockchain will probably be of no significance. Furthermore, if only one administrator is needed to read and write content, then blockchain is inappropriate.

Contrarily, blockchain is powerful in a computing environment where trustless entities transact and data need to be permanently stored [12]. Typically blockchain can be very useful when known mistrusting entities will store and change the content of the ledger [170].

6) *Sharding*: Contemporary centralized applications and storage systems may not work efficiently in this age of Artificial Intelligence, IoT, machine learning, Big Data, all running in the cloud [171]. To accommodate scalability, availability, manageability, security, and reliability, existing systems have to be modified [171,50]. The concept of sharding has been around for some time now and works well in database systems providing low-cost high-performance computing. Traditional non-sharded databases usually installed on a single database are prone to a single source of failure leading to the crumbling of the complete business application [171]. AES256-CTR is used to encrypt files at the client-side before they are sharded as in Fig. 9 and the encryption key is completely controlled by the data owner so contents are protected from the company providing the storage space [50].

In blockchain, sharding can be considered a challenge. According to [50], shards can be described as well-designed self-governing blockchain which interconnects with one another. Validators are used to monitor shards and if the total number of shards is $S = O(c)$, where c is the overall number of transactions supported by a shard, then the method can take a maximum of $O(c^2)$ transactions. If the number of shards increases in a composite manner, then the number of transactions will exponentially grow to $O(exp(c))$ [50]. When an application has a shard with minimal interactions or users, then the implementation may be easier and cross-shard communication can be enabled by securely passing information using receipts. Most blockchain systems recently in use are not scalable so most operations can be run on a single shard. However, introducing multiple shards and subsequently implementing cross-shard interaction and asynchronous communication can have serious operational impediments [50].

TABLE III. COUNTRIES WITH BLOCKCHAIN LEGAL FRAMEWORKS AND REGULATIONS

Country	Form of Taxation
Israel	Asset
Bulgaria	Financial Asset
Switzerland	Foreign currency
Argentina	Income tax
Spain	Income tax
United Kingdom	Corporate tax, income tax, capital gains tax

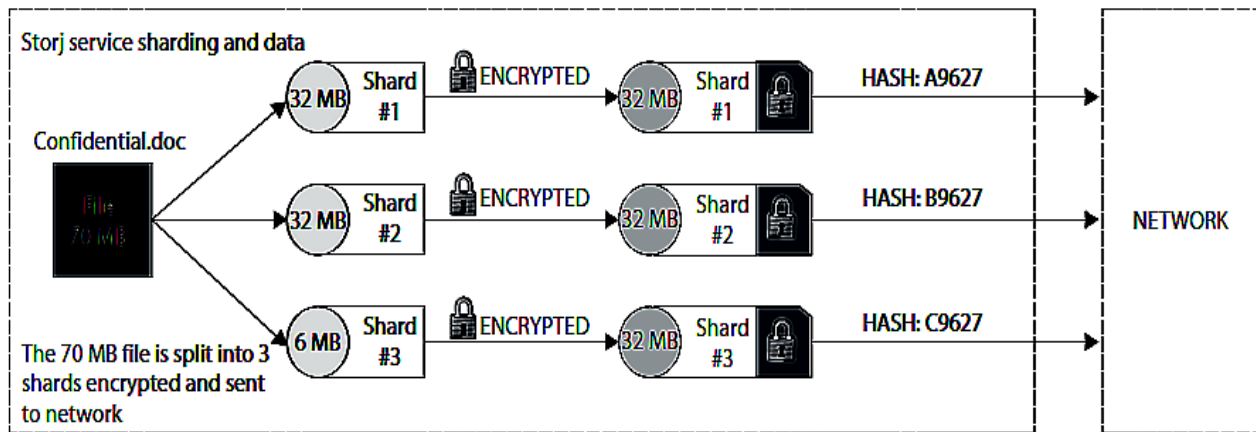


Fig. 9. Sharding Processes. Source:[50].

D. Discussion

Blockchain technology has emerged as contemporary disruptive technology. As indicated in section II, numerous works have been done to expand the applicability of blockchain 3.0 to other domains other than the financial sector. However limited works exist in the insurance industry. Therefore we review various opportunities and threats available in this endeavour. It has been observed by industry and academic researchers that the most important business processes that can be improved or re-engineered in the insurance sector are issues of claims and fraud. The nature of blockchain and its features like cryptography, consensus algorithm, decentralization, etc. make it an ideal solution for the insurance sector. Hashing of the identities of the participant in the blockchain network provides a solution to the problem of data identification and sharing of intelligent data. The blockchain P2P could create a new line of insurance products and get rid of trusted middlemen. This review was done to uncover the prospects to position us well to embark on our future works. At the moment blockchain technology also possesses numerous challenges including security and data privacy, scalability, regulation, and taxation. Although the individual technologies upon which blockchain is mounted is matured, their integration presents some susceptibilities. Blockchain will become a very powerful tool so mitigate many of the technology problem facing the insurance industry.

VI. CONCLUSION AND FUTURE DIRECTION

Ever since blockchain gained public attention, researchers have proposed and developed numerous frameworks, systems, and applications. The financial sector has almost fully benefited from blockchain and so the trend has moved to other domains like supply chain management [175], health, government, law, and more. This work focused on reviewing and producing a simple literature review on blockchain technology with a peculiar interest in the opportunities and threats in the insurance domain. It was discovered that the insurance sector as enormous as it is now can also leverage blockchain technology to enhance core internal processes like claim submission and processing, fraud detection and prevention, etc. Blockchain can also be used to mutate and possibly produce new brands of insurance and also enhance

existing ones. It is also a discovery that BC possesses several challenges including scalability, security, and privacy, taxation and regulation, etc. The Insurance sector has not received the beneficial exploitation of blockchain 3.0. As indicated all initiatives by the insurance industry players are at the beginning stages. Therefore, subsequently, several pieces of research will be conducted to broaden the existing academic literature in terms of leveraging blockchain to enhance the core insurance business processes (Claims submission and processing, fraud detection and prevention, etc.) and mutate existing InsurTechs like Usage Based Insurance in vehicle insurance. We will also employ operations research techniques like game theories to enhance and theoretically create multiple insurance products like the Peer to Peer insurance, health insurance, etc. Again, in private blockchain systems, presumably, not all data are needed by all nodes so decentralization of the full ledger may be technically insignificant and may add to the storage, scalability, and performance issues. Consequently, to increase performance we are going to research how to extract and store the most contextually relevant data especially in a private blockchain.

REFERENCES

- [1] B. Cohen, J. Ernesto Amorós, "Municipal demand-side policy tools and the strategic management of technology life cycles," *Technovation* 2014. <https://doi.org/10.1016/j.technovation.2014.07.001>.
- [2] V. J. Morkunas, J. Paschen, E. Boon, "How blockchain technologies impact your business model," *Bus Horiz* 2019. <https://doi.org/10.1016/j.bushor.2019.01.009>.
- [3] S. Nakamoto, "Bitcoin: A Peer-to-Peer Electronic Cash System," Manubot 2008. [Google Scholar].
- [4] C. S. Wright, "Bitcoin: A Peer-to-Peer Electronic Cash System," (August 21, 2008).
- [5] T. Ahram, A. Sargolzaei, S. Sargolzaei, J. Daniels, B. Amaba, "Blockchain technology innovations". *IEEE Technol. Eng. Manag. Soc. Conf. TEMSCON* 2017, 2017.
- [6] S. Feng, Z. Xiong, D. Niyato, P. Wang, S. S. Wang, Y. Zhang, "Cyber Risk Management with Risk Aware Cyber-Insurance in Blockchain Networks," 2018 *IEEE Glob. Commun. Conf. GLOBECOM* 2018 - Proc., 2018.
- [7] J. Kietzmann, C. Archer-Brown, "From hype to reality: Blockchain grows up" *Business Horizons*. 2019 Jan 1; 62(3):269-71.
- [8] K. Panetta, "5 trends emerge in the Gartner Hype Cycle for emerging technologies," *Gartner*. accessed December 8, 2020 unpublished

- [9] Blockchain.info, "Blockchain Charts" <https://www.blockchain.com/charts/>, accessed September 17, 2020 unpublished.
- [10] E. Kapsammer, B. Pröll, W. Retschitzegger, W. Schwinger, M. Weibenbek, & J. Schönböck, "The Blockchain Muddle: A Bird's-Eye View on Blockchain Surveys", In Proc of the 20th Int Conf on Infor Integ and Web-based App & Ser (pp. 370-374).
- [11] K. Wang, & A. Safavi, "Blockchain is empowering the future of insurance". Available at <https://techcrunch.com/2016/10/29/blockchain-is-empowering-the-future-of-insurance> unpublished.
- [12] F. Casino, T. K. Dasaklis, & C. Patsakis, "A systematic literature review of blockchain-based applications: Current status, classification and open issues". Telemat Informatics 2019.
- [13] J. Mendling, I. Weber, W. V. Aalst, J. V. Brocke, C. Cabanillas, F. Daniel, S. Debois, C. D. Ciccio, M. Dumas, S. Dustdar, A. Gal, "Blockchains for business process management-challenges and opportunities," ACM Trans. on Mgt Inf. Sys (TMIS). 2018 Feb 26;9(1):1-6.
- [14] S. Aggarwal, R. Chaudhary, G. S. Aujla, N. Kumar, K. K. Choo, A. Y. Zomaya, "Blockchain for smart communities: Applications, challenges and opportunities," J of Net & Comp App. 2019 Oct 15;144:13-48.
- [15] K. Yeow, A. Gani, R. W. Ahmad, J. J. Rodrigues, K. Ko, "Decentralized consensus for edge-centric internet of things: A review, taxonomy, and research issues. IEEE Access. 2017 Dec 6;6:1513-24.
- [16] D. E. Kouicem, A. Bouabdallah, H. Lakhlef, "Internet of things security: A top-down survey," Computer Networks. 2018 Aug 4;141:199-221.
- [17] Q. E. Abbas, J. Sung-Bong, "A survey of blockchain and its applications,". In 2019 Int Conf on Art Intel in Inf and Comm (ICAIIIC) 2019 Feb 11 (pp. 001-003). IEEE.
- [18] W. Liu, Q. Yu, , Li, Z., Li, Z., Su, Y. and Zhou, J., "A Blockchain-Based System for Anti-Fraud of Healthcare Insurance," In 2019 IEEE 5th Int. Conf. on Compu. Commun. (ICCC) (pp. 1264-1268). IEEE.
- [19] M. Sharifinejad, A. Dorri, J. Rezazadeh, "BIS-A Blockchain-based Solution for the Insurance Industry in Smart Cities," arXiv, 2020.
- [20] H. Kim, M. Mehar, "Blockchain in Commercial Insurance: Achieving and Learning Towards Insurance That Keeps Pace in a Digitally Transformed Business Landscape," SSRN Electron J 2019.
- [21] M. Mainelli, B. Manson "Chain reaction: How blockchain technology might transform wholesale insurance," How Blockchain Technology Might Transform Wholesale Insurance-Long Finance. 2016 Aug 1. Available at SSRN: <https://ssrn.com/abstract=3676290>.
- [22] L. S. Howard, "Blockchain insurance industry initiative B3i grows to 15 members," Insurance Journal. 2017;6:2017.
- [23] T. Q. Nguyen, A. K. Das, L. T. Tran, "NEO Smart Contract for Drought-Based Insurance," 2019 IEEE Can. Conf. Electr. Comput. Eng. CCECE 2019, 2019.
- [24] Y. Guo, Z. Qi, X. Xian, H. Wu, Z. Yang, J. Zhang, L. Wenyin, "WISChain: An Online Insurance System based on Blockchain and DengLu1 for Web Identity Security," Proc. 2018 1st IEEE Int. Conf. Hot Information-Centric Networking, HotICN 2018, 2019.
- [25] M. Tsukerman, "The Block is hot: A Survey of the State of Bitcoin Regulation and Suggestions for the Future," Berkeley Technol Law J 2016.
- [26] U. Mukhopadhyay, A. Skjellum, O. Hambolu, J. Oakley, L. Yu, R. Brooks "A brief survey of Cryptocurrency systems," 14th Annu. Conf. Privacy, Secur. Trust 2016, 2016.
- [27] M. Conti, E. S. Kumar, C. Lal, S. Ruj, "A survey on security and privacy issues of bitcoin," IEEE Comm. Surveys & Tutorials, 2018 May 31;20(4):3416-52.
- [28] M. C. Khalilov, A. Levi, "A survey on anonymity and privacy in bitcoin-like digital cash systems," IEEE Comm Surveys & Tut. 2018 Mar 26;20(3):2543-85.
- [29] J. Bonneau, A. Miller, J. Clark, A. Narayanan, J. A. Kroll, E. W. Felten, "SoK: Research perspectives and challenges for bitcoin and cryptocurrencies," Proc. - IEEE Symp. Secur. Priv., 2015.
- [30] H. N. Dai, Z. Zheng, Y. Zhang, "Blockchain for Internet of Things: A Survey," IEEE Internet Things J 2019.
- [31] S. Y. Lim, P. T. Fotsing, A. Almasri, O. Musa, M. L. M. Kiah, T. F. Ang, R. Ismail, "Blockchain technology the identity management and authentication service disruptor: A survey," Int J Adv Sci Eng Inf Technol 2018.
- [32] B. K. Mohanta, D. Jena, S. S. Panda, S. Sobhanayak, "Blockchain technology: A survey on applications and security privacy Challenges," Internet of Things 2019.
- [33] Q. Feng, D. He, S. Zeadally, M. K. Khan, N. Kumar, "A survey on privacy protection in blockchain system," J Netw Comput Appl 2019.
- [34] T. Alharbi, "Deployment of blockchain technology in software defined networks: A survey," IEEE Access 2020.
- [35] R. Brophy, "Blockchain and insurance: a review for operations and regulation," J Financ Regul Compliance 2019.
- [36] V. Gatteschi, F. Lamberti, C. Demartini, C. Pranteda, V. Santamaría. Blockchain and smart contracts for insurance: Is the technology mature enough? Futur Internet 2018.
- [37] A. Kamilaris, A. Fonts, F. X. Prenafeta-Boldú, "The rise of blockchain technology in agriculture and food supply chains," Trends Food Sci Technol 2019.
- [38] Ž. Turk, R. Klinc, "Potentials of Blockchain Technology for Construction Management," Procedia Eng., 2017.
- [39] K. Valtanen, J. Backman, S. Yrjola, "Blockchain-Powered Value Creation in the 5G and Smart Grid Use Cases," IEEE Access 2019.
- [40] F. Z. Meskini, R. Aboulaich, "A New Cooperative Insurance Based on Blockchain Technology: Six Simulations to Evaluate the Model," 2020 Int. Conf. Intell. Syst. Comput. Vision, ISCV 2020, 2020.
- [41] A. Tapscott, D. Tapscott, "How Blockchain Is Changing Finance," Harv Bus Rev 2017.
- [42] O. I. Khalaf, G. M. Abdulsahib, H. D. Kasmaei, K. A. Ogudo, "A new algorithm on application of blockchain technology in live stream video transmissions and telecommunications," Int J e-Collaboration 2020.
- [43] N. P. V. Sravan, P. K. Baruah, S. S. Mudigonda, "Use of Blockchain Technology in integrating Health Insurance Company and Hospital," Int J Sci Eng Res 2018.
- [44] S. Ølnes, J. Ubacht, M. Janssen, Blockchain in government: Benefits and implications of distributed ledger technology for information sharing. Gov Inf Q 2017.
- [45] P. K. Singh, R. Singh, G. Muchahary, M. Lahon, S. Nandi, "A Blockchain-Based Approach for Usage Based Insurance and Incentive in ITS," IEEE Reg. 10 Annu. Int. Conf. Proceedings/TENCON, 2019.
- [46] Y. C. Chen, Y. P. Chou, Y. C. Chou, "An image authentication scheme using Merkle tree mechanisms," Futur Internet 2019.
- [47] L. S. Sankar, M. Sindhu, M. Sethumadhavan, "Survey of consensus protocols on blockchain applications," 4th Int. Conf. Adv. Comput. Commun. Syst. ICACCS 2017, 2017.
- [48] J. Lake, Understanding cryptography's role in blockchains 2019. Unpublished.
- [49] D. Puthal, N. Malik, S. P. Mohanty, E. Kougianos, G. Das, "Everything You Wanted to Know about the Blockchain: Its Promise, Components, Processes, and Problems," IEEE Consum Electron Mag 2018.
- [50] J. J. Bambara, P. R. Allen, K. Iyer, R. Madsen, S. Lederer, M. Wuehler, Blockchain: A practical guide to developing business, law, and technology solutions. McGraw Hill Professional; 2018 Feb 16.
- [51] T. K. Sharma, Public Vs. Private Blockchain : A Comprehensive Comparison 2019 unpublished.
- [52] Mycryptopedia, 2018, Consortium Blockchain Explained, unpublished.
- [53] C. Saraf, S. Sabadra, "Blockchain platforms: A compendium," IEEE Int. Conf. Innov. Res. Dev. ICIRD 2018, 2018.
- [54] R. B. Briner, D. Denyer, "Systematic Review and Evidence Synthesis as a Practice and Scholarship Tool," Oxford Handb. Evidence-Based Manag., 2012. Google Scholar.

- [55] D. Moher, A. Liberati, J. Tetzlaff, D. G. Altman, "Preferred reporting items for systematic reviews and meta-analyses: The PRISMA statement," *PLoS Med* 2009.
- [56] O. Mahmoud, H. Kopp, A. T. Abdelhamid, F. Kargl, "Applications of Smart-Contracts: Anonymous Decentralized Insurances with IoT Sensors," *Proc. - IEEE 2018 Int. Congr. Cybermatics 2018 IEEE Conf. Internet Things, Green Comput. Commun. Cyber, Phys. Soc. Comput. Smart Data, Blockchain, Comput. Inf. Technol. iThings/Gree*, 2018.
- [57] H. Mohamed, "Takāful (Islamic insurance) on the blockchain," *Growth Islam. Financ. Bank.*, 2019.
- [58] M. Raikwar, S. Mazumdar, S. Ruj, S. S. Gupta, A. Chattopadhyay, K. Y. Lam, "A Blockchain Framework for Insurance Processes," *9th IFIP Int. Conf. New Technol. Mobil. Secur. NTMS 2018 - Proc.*, 2018.
- [59] M. Vahdati, K. G. Hamlabadi, A. M. Saghiri, H. Rashidi, "A Self-Organized Framework for Insurance Based on Internet of Things and Blockchain," *Proc. - 2018 IEEE 6th Int. Conf. Futur. Internet Things Cloud, FiCloud*.
- [60] N. Dhieb, H. Ghazzai, H. Besbes, Y. Massoud, "A Secure AI-Driven Architecture for Automated Insurance Systems: Fraud Detection and Risk Measurement," *IEEE Access* 2020.
- [61] Z. Li, Z. Xiao, Q. Xu, E. Sotthiwat, R. S. Mong Goh, X. Liang, "Blockchain and IoT Data Analytics for Fine-Grained Transportation Insurance," *Proc. Int. Conf. Parallel Distrib. Syst. - ICPADS*, 2018.
- [62] R. Roriz, J. L. Pereira, "Avoiding Insurance Fraud: A Blockchain-based Solution for the Vehicle Sector," *Procedia Comput. Sci.*, 2019.
- [63] World Health Organization, https://www.who.int/gho/road_safety/mortality/traffic_deaths_number/en/ unpublished.
- [64] S.L. Poczter, L. M. Jankovic, "The Google Car: Driving Toward A Better Future?," *J Bus Case Stud* 2013.
- [65] H. T. Vo, L. Mehedy, M. Mohania, E. Abebe, "Blockchain-based data management and analytics for micro-insurance applications," *Int. Conf. Inf. Knowl. Manag. Proc.*, 2017.
- [66] L. M. Palma, F. O. Gomes, M. Vigil, J. E. Martina, "A Transparent and Privacy-Aware Approach Using Smart Contracts for Car Insurance Reward Programs," *International Conference on Information Systems Security 2019 Dec 16 (pp. 3-20)*. Springer, Cham.
- [67] S. Husnjak, D. Peraković, I. Forenbacher, M. Mumdzjev, "Telematics system in usage based motor insurance," *Procedia Eng.*, 2015.
- [68] P. Handel, I. Skog, J. Wahlstrom, F. Bonawiede, R. Welch, J. Ohlsson, "Insurance telematics: Opportunities and challenges with the smartphone solution," *IEEE Intell Transp Syst Mag* 2014.
- [69] J. Wahlström, I. Skog, P. Händel, "Driving behavior analysis for smartphone-based insurance telematics," *Proc. 2nd Work. Phys. Anal.*, 2015.
- [70] Lin W-Y, Lin FY-S, Wu T-H, Tai K-Y. "An On-Board Equipment and Blockchain-Based Automobile Insurance and Maintenance Platform," *In Int Conf on Broadband and Wireless Comp, Comm & Appl pp. 223-232*, 2020.
- [71] F. Li, H. Zhang, H. Che, X. Qiu, "Dangerous driving behavior detection using smartphone sensors," *IEEE Conf. Intell. Transp. Syst. Proceedings, ITSC*, 2016.
- [72] R. Harbage, "Usage-based Auto Insurance (UBI)," 2011 <https://www.casact.org/community/affiliates/sccac/1211/Harbage.pdf> unpublished.
- [73] A. Kumar, A. Prasad, R. Murthy, "Application of blockchain in Usage Based Insurance," *Int J Adv Res* 2019.
- [74] V. Aleksieva, H. Valchanov, A. Hulyan, "Application of smart contracts based on ethereum blockchain for the purpose of insurance services," *Proc. Int. Conf. Biomed. Innov. Appl. BIA 2019*, 2019.
- [75] H. Qi, Z. Wan, Z. Guan, X. Cheng, "Scalable Decentralized Privacy-Preserving Usage-based Insurance for Vehicles," *IEEE Internet Things J* 2020.
- [76] Z. Wan, Z. Guan, X. Cheng, "Pride: A private and decentralized usage-based insurance using blockchain," *In 2018 IEEE Int Conf Internet of Things IEEE Green Comp & Comm (GreenCom) and IEEE Cyber, Phys Soc Comput (CPSCom) IEEE Smart Data 2018 Jul 30 (pp. 1349-1354)*. IEEE..
- [77] M. Demir, O. Turetken, A. Ferworn, "Blockchain based transparent vehicle insurance management," *6th Int. Conf. Softw. Defin. Syst. SDS* 2019.
- [78] M. B. Abramowicz, "Blockchain-Based Insurance," *SSRN Electron J* 2019.
- [79] F. Lamberti, V. Gatteschi, C. Demartini, M. Pelissier, A. Gomez, V. Santamaria, "Blockchains Can Work for Car Insurance: Using Smart Contracts and Sensors to Provide On-Demand Coverage," *IEEE Consum Electron Mag* 2018. 2816247.
- [80] C. Oham, R. Jurdak, S. S. Kanhere, A. Dorri, S. Jha, "B-FICA: Blockchain based Framework for Auto-Insurance Claim and Adjudication," *Proc. - IEEE 2018 Int. Congr. Cybermatics 2018 IEEE Conf. Internet Things, Green Comput. Commun. Cyber, Phys. Soc. Comput. Smart Data, Blockchain, Comput. Inf. Technol. iThings/Gree*, 2018.
- [81] A. Drexler, A. Granato, R. J. Rosen, "Homeowners' financial protection against natural disasters," *Chicago Fed Lett (409):1* 2019.
- [82] H. Kunreuther, "All-Hazards Homeowners Insurance: Challenges and Opportunities," *Risk Manag Insur Rev* 2018.
- [83] R. Hans, H. Zuber, A. Rizk, R. Steinmetz, "Blockchain and smart contracts: Disruptive technologies for the insurance market," *Am. Conf. Inf. Syst. A Tradit. Innov.*, (AMCIS) 2017.
- [84] B. Hagedorff, J. Hagedorff, K. Keasey, "The Impact of Mega-Catastrophes on Insurers: An Exposure-Based Analysis of the U.S. Homeowners' Insurance Market," *Risk Anal* 2015.
- [85] R. E. Munich, "Natural Catastrophes 2011 Analyses, assessments, positions," 2012 unpublished.
- [86] A. Sheth, H. Subramanian, "Blockchain and contract theory: modeling smart contracts using insurance markets," *Manag Financ* 2019.
- [87] B. Beers, "A Brief Overview of the Insurance Sector," 2020, unpublished.
- [88] S. Lesley, "Life Insurance Industry under Investigation," *CBS NEWS (Apr. 17, 2016)* unpublished.
- [89] A. Cohn, T. West, C. Parker, "Smart after all: Blockchain, smart contracts, parametric insurance, and smart energy grids," *Georgetown Law Technology Review*, 1(2), 273-304.
- [90] D. A. Disparte "Blockchain Could Make the Insurance Industry Much More Transparent," unpublished.
- [91] M. Lounds, "Blockchain and its Implications for the Insurance Industry," 2020 unpublished.
- [92] H. Low, L. Pistaferri, "Disability insurance and the dynamics of the incentive insurance trade-off," *Am Econ Rev* 2015.
- [93] B. Olmsted, "How to Buy Disability Insurance," 2019. unpublished.
- [94] L. Kraus, "2015 Disability Statistics Annual Report. A Publication of the Rehabilitation Research and Training Center on Disability Statistics and Demographics," 2016, Institute on Disability, University of New Hampshire.
- [95] Disability statistics and Facts, https://web.archive.org/web/20110727133227/http://nteu-chapter78.org/documents/member_benefits/Disability%20Statistics.pdf unpublished.
- [96] J. Gera, A. R. Palakayala, V. K. K. Rejeti, T. Anusha, "Blockchain technology for fraudulent practices in insurance claim process," *Proc. 5th Int. Conf. Commun. Electron. Syst. ICCES 2020*, 2020.
- [97] M. K. Ranson, "Reduction of catastrophic health care expenditures by a community-based health insurance scheme in Gujarat, India: Current experiences and challenges," *Bull World Health Organ* 2002.

- [98] G. Saldamli, V. Reddy, K. S. Bojja, M. K. Gururaja, Y. Doddaveerappa, L. Tawalbeh, "Health Care Insurance Fraud Detection Using Blockchain," 2020. In 7th Int. Conf. Soft. Def. Syst. (SDS) 2020 (pp. 145-152). IEEE.
- [99] S. Khezr, M. Moniruzzaman, A. Yassine, R. Benlamri, "Blockchain technology in healthcare: A comprehensive review and directions for future research," *Appl Sci* 2019.
- [100] Z. Chang, "Research of medical insurance based on the combination of blockchain and credit technology," *Proc. 2020 Asia-Pacific Conf. Image Process. Electron. Comput. IPEC 2020*, 2020.
- [101] H. Andre, A. K. Dewi, F. Pangemanan, G. Wang, "Designing blockchain to minimize fraud in state-owned national insurance company (Bpjs kesehatan)," *Int J Emerg Trends Eng Res* 2019.
- [102] V. Dhillon, D. Metcalf, M. Hooper, "Blockchain enabled applications: understand the blockchain ecosystem and how to make it work for you," *Apres*; 2017 Nov 29.
- [103] H. Limin, Y. Jianmin, "Application Research of Blockchain in the Field of Medical Insurance," *Int. Conf. Econs., Mgt. Eng. Edu. Tech (ICEMEET)* 2019.
- [104] H. Gajera, M. L. Das, V. Shah, "Blockchain-powered healthcare insurance system," In *Security and Privacy of Electronic Healthcare Records: Concepts, paradigms and solutions*, *Inst. Eng. Tech.* 2019. 362-410.
- [105] CBInsights. How Blockchain Is Disrupting Insurance. CB Insights 2018 available at <https://www.cbinsights.com/research/blockchain-insurance-disruption/> accessed November 24, 2020 unpublished.
- [106] C. Sandland, D. Schilling, A. Marke, "A Critical Analysis on the Capacity of Blockchain-Based Parametric Insurance in Tackling the Financial Impact of Climatic Disasters," *Strengthening Disaster Resilience in Small States: Commonwealth Perspectives*. 2019 Oct 7:87.
- [107] X. He, S. Alqahtani, R. Gamble, "Toward Privacy-Assured Health Insurance Claims," *Proc. - IEEE 2018 Int. Congr. Cybermatics 2018 IEEE Conf. Internet Things, Green Comput. Commun. Cyber, Phys. Soc. Comput. Smart Data, Blockchain, Comput. Inf. Technol. iThings/Gree*, 2018.
- [108] S. Maganahalli, "Blockchain: The Future of Insurance," *Int J Res Appl Sci Eng Tech*, 8(5), 2020.
- [109] L. Zhou, L. Wang, Y. Sun, "MISStore: A Blockchain-Based Medical Insurance Storage System," *J Med Syst* 2018.
- [110] R. W. Johnson, C. E. Uccello, "Is private long-term care insurance the answer?," (Vol. 29, 2005). Center for Retirement Research at Boston College.
- [111] KaranC, "What is Marine Insurance," 2019 available online at <https://www.marineinsight.com/know-more/what-is-marine-insurance/> accessed November 1, 2020 unpublished.
- [112] EY. World's first blockchain platform for marine insurance now in commercial use, 2018, unpublished.
- [113] C. Reed, "Blockchain and the World of Marine Insurance," 2017. available online at <https://www.marinelink.com/news/blockchain-insurance429260> unpublished.
- [114] P. K. Meduri, S. Mehta, K. Joshi, S. Rane, "Disrupting Insurance Industry Using Blockchain," In *Int. Conf. Intell. Data Comm. Tech. Internet of Things 2018 Aug 7* (pp. 1068-1075). Springer, Cham.
- [115] T. Mohan, K. Praveen, "Fraud detection in medical insurance claim with privacy preserving data publishing in TLS-n using blockchain," *Commun. Comput. Inf. Sci.*, 2019.
- [116] D. Popovic, C. Avis, M. Byrne, C. Cheung, M. Donovan, Y. Flynn, C. Fothergill, Z. Hosseinzadeh, Z. Lim, J. Shah, "Understanding blockchain for insurance use cases," *Br Actuar J* 2020.
- [117] A. Borselli, "Smart Contracts in Insurance: A Law and Futurology Perspective," In: P. Marano, K. Noussia (eds) *InsurTech: A Legal and Regulatory View*. AIDA Europe Res. Ser Insur Law Reg, vol 1. Springer, Cham.
- [118] I. Nath, "Data Exchange Platform to Fight Insurance Fraud on Blockchain," *IEEE Int. Conf. Data Min. Work. ICDMW*, 2016.
- [119] R. Huckstep, "What does the future hold for blockchain and insurance?," Available online at <https://dailyfintech.com/2016/01/14/what-does-the-future-hold-for-blockchain-and-insurance/> unpublished.
- [120] J. Xu, Y. Wu, X. Luo, D. Yang, "Improving the Efficiency of Blockchain Applications with Smart Contract based Cyber-insurance," *IEEE Int. Conf. Commun.*, 2020.
- [121] [1] J. L. Liu, X. Y. Wu, W. J. Yu, Z. C. Wang, H. L. Zhao, and N. M. Cang, "Research and design of travel insurance system based on blockchain," *4th Int. Conf. Intell. Informatics Biomed. Sci.*, 2019.
- [122] A. W. Singer, "Can Blockchain Improve Insurance? Risk Manag 2019.
- [123] S. O. Nam, "How much are insurance consumers willing to pay for blockchain and smart contracts? A contingent valuation study," *Sustain* 2018.
- [124] A. J. Pagano, F. Romagnoli, E. Vannucci, "Implementation of Blockchain Technology in Insurance Contracts against Natural Hazards: A Methodological Multi-Disciplinary Approach," *Environ Clim Technol* 2019.
- [125] A. Sehgal, "Blockchain's Insurance Business Implementation," *Int J Comput Appl* 2017, 174(3):32-7.
- [126] J. Sun, X. Yao, S. Wang, and Y. Wu, "Non-Repudiation Storage and Access Control Scheme of Insurance Data Based on Blockchain in IPFS," *IEEE Access*, 2020.
- [127] N. Lorenz, J. T. Münstermann, B. Higginson, M. Olesen, P.B. Bohlken, "Blockchain in Insurance-Opportunity or Threat? McKinsey & Company Report; McKinsey & Company," *McKinsey Co. Insur.*, 2016.
- [128] J. A. Tarr, "Distributed ledger technology , blockchain and insurance : Opportunities , risks and challenges," *Insur. Law J.*, 2018.
- [129] M. A. Henk and R. T. Bell, "Blockchain: An insurance focus," 2016. Unpublished.
- [130] İ. YILDIRIM and E. E. ŞAHİN, "Insurance Technologies (Insurtech): Blockchain and its Possible Impact on Turkish Insurance Sector," *Uluslararası Yönetim Eğitim ve Ekon. Perspektifler Derg.*, 2018.
- [131] J. J. Roberts. "Microsoft and Accenture Unveil Global ID System for Refugees," 2017 unpublished.
- [132] J. H. Lee, "BIDaaS: Blockchain Based ID As a Service," *IEEE Access*, 2017.
- [133] V. L. Lemieux, "Trusting records: is Blockchain technology the answer?," *Records Manage. J.* 26 (2), 110–139 2016.
- [134] L. Mertz, "(Block) Chain Reaction: A Blockchain Revolution Sweeps into Health Care, Offering the Possibility for a Much-Needed Data Solution," *IEEE Pulse*, 2018.
- [135] I. Vakiliinia, S. Badsha, and S. Sengupta, "Crowdfunding the Insurance of a Cyber-Product Using Blockchain," *9th IEEE Annu. Ubiquitous Comput. Electron. Mob. Commun. Conf. (UEMCON)*, 2018.
- [136] T. Lepoint, G. Ciocarlie, and K. Eldefrawy, "BlockCIS - A blockchain-based cyber insurance system," *Proc. - 2018 IEEE Int. Conf. Cloud Eng. IC2E 2018*.
- [137] P. Tascia, "Insurance Under the Blockchain Paradigm," in *Business Transformation through Blockchain*, 2019, (pp. 273-285). Palgrave Macmillan, Cham.
- [138] L. Zhao, "The Analysis of Application, Key Issues and the Future Development Trend of Blockchain Technology in the Insurance Industry," *Am. J. Ind. Bus. Manag.*, 2020.
- [139] [1] J. Bramblet, "Ultimate Guide to Blockchain in Insurance - Accenture Insurance Blog," *Accenture*, 2018 unpublished.
- [140] L. Xiao, Y. Cheng, H. Deng, S. Xu, and W. Xiao, "Insurance Block: An Insurance Data Security Transaction Authentication Scheme Suitable for Blockchain Environment," In *Int. Conf on Smart Blockchain* (pp. 120-129). Springer, Cham., 2019.
- [141] L. Xiao, H. Deng, M. Tan, and W. Xiao, "Insurance Block: A Blockchain Credit Transaction Authentication Scheme Based on Homomorphic Encryption," *Commun. Comput. Inf. Sci.*, 2020.
- [142] S. Pritzker, "Everything You Need To Know About Peer-To-Peer (P2P) Insurance," 2020, unpublished.

- [143]D. Oleynikova, T. Loac, “P2P Protect – TongJuBao,” unpublished.
- [144]H. Terry, “Guevara Peer to Peer Car Insurance,” 2020 unpublished
- [145]<https://www.friendsurance.com/> unpublished.
- [146]K. Wang, A. Safavi, “Blockchain is empowering the future of insurance,” 2016, accessed December 06, 2020, unpublished.
- [147]fidentiaX, (2018), “Peer-to-Peer Insurance: How Blockchain is challenging the traditional insurance model,” unpublished.
- [148]Norton, S. (February 2, 2016). CIO explainer: What is blockchain? Wall Street Journal. Retrieved May 10, 2020 8:05AM. Unpublished.
- [149]ChainZy. IDChainZ, 2020, unpublished.
- [150]A. Chauhan, O. P. Malviya, M. Verma, and T. S. Mor, “Blockchain and Scalability,” Proc. - 2018 IEEE 18th Int. Conf. Softw. Qual. Reliab. Secur. Companion, QRS-C.
- [151]K. Qin, A. Gervais, “An overview of blockchain scalability, interoperability and sustainability,” Hoch. Luz. Imp. Coll. Lon. Liq. Netw. 2018 May.
- [152]K. Saeedi, A. Wali, D. Alahmadi, A. Babour, F. AlQahtani, R. AlQahtani, R. Khawaja, Z. Rabah, “Building a Blockchain Application: A Show Case for Healthcare Providers and Insurance Companies,” Adv. Intell. Syst. Comput., 2019.
- [153]I. Eyal, E. G. Sirer, “Majority is not enough: Bitcoin mining is vulnerable,” In Int. conf. fin. Crypto. data sec. 2014 Mar 3 (pp. 436-454). Springer, Berlin, Heidelberg.
- [154]J. Yli-Huumo, D. Ko, S. Choi, S. Park, K. Smolander, “Where is current research on blockchain technology?—a systematic review,” PloS one. 2016 Oct 3;11(10):e0163477.
- [155]I. C. Lin and T. C. Liao, “A survey of blockchain security issues and challenges,” Int. J. Netw. Secur., 2017.
- [156]J. Salmon, G. Myers, “Blockchain and associated legal issues for emerging markets,” 2019. [Google Scholar].
- [157]K. Christidis, M. Devetsikiotis, “Blockchains and smart contracts for the internet of things,” IEEE Access. 2016 May 10;4:2292-303.
- [158]D. Chris, Introducing Ethereum and Solidity Foundations of Cryptocurrency and Blockchain Programming for Beginners. Apress, New York. 2017.
- [159]S. Goldfeder, H. Kalodner, D. Reisman, and A. Narayanan, “When the cookie meets the blockchain: Privacy risks of web payments via cryptocurrencies,” Proc. Pri. Enh. Tech. 2018 (4):179-99.
- [160]N. S. bt Abd Halim, M. A. Rahman, S. Azad, M. N. Kabir, “Blockchain security hole: Issues and solutions,” In Int. Conf. Rel. Infor. Commun. Tech. 2017 Apr 23 (pp. 739-746). Springer, Cham.
- [161]Parity Technologies, November 2017. Security Alert, <https://paritytech.io/security-alert-2/>. Unpublished.
- [162]M. Suiche, “Porosity: A Decompiler For Blockchain-Based Smart Contracts Bytecode,” Def Con, 2017.
- [163]S. Kalra, S. Goel, M. Dhawan, and S. Sharma, “ZEUS: Analyzing Safety of Smart Contracts,” DEF con. 2017.
- [164]I. Nikolić, A. Kolluri, I. Sergey, P. Saxena, and A. Hobor, “Finding the greedy, prodigal, and suicidal contracts at scale,” In Proceedings of the 34th Ann. Compu. Sec. Appl. Conf. 2018 (pp. 653-663). 2018.
- [165]J. Li, D. Niyato, C. S. Hong, K. J. Park, L. Wang, and Z. Han, “A Contract-Theoretic Cyber Insurance for Withdraw Delay in the Blockchain Networks with Shards,” Int. Conf. Commun., 2020.
- [166]V. Akgiray, “The Potential for Blockchain Technology in Corporate Governance,” OECD Corp. Gov. Work. Pap., 2019.
- [167]S. Grima, J. Spiteri, and I. Romānova, “A STEEP framework analysis of the key factors impacting the use of blockchain technology in the insurance industry,” Geneva Pap. Risk Insur. Issues Pract., 2020.
- [168]Global Legal Research Center, <https://bravenewcoin.com/insights/regulation-of-bitcoin-in-selected-jurisdictions> 2014. unpublished.
- [169]J. Umeh, “BLOCKCHAIN: DOUBLE BUBBLE or DOUBLE TROUBLE?,” ITNOW, 2016.
- [170]K. Wust and A. Gervais, “Do you need a blockchain?,” In 2018 Crypto Valley Conf. Blockc. Tech. (CVCBT) (pp. 45-54), IEEE 2018, doi: 10.1109/CVCBT.2018.00011.
- [171]S. Bagui and L. T. Nguyen, “Database Sharding,” Int. J. Cloud Appl. Comput., 2015, doi: 10.4018/ijcac.2015040103.
- [172]O. Ali, M. Ally, Clutterbuck, and Y. Dwivedi, “The state of play of blockchain technology in the financial services sector: A systematic literature review,” Int. J. Infor. Manag. 2020.
- [173]F. R. Batubara, J. Ubacht, and M. Janssen, “Challenges of blockchain technology adoption for e-government: A systematic literature review,” ACM Int. Conf. Proc. Ser., 2018.
- [174]X. Wang *et al.*, “Survey on blockchain for Internet of Things,” Comp. Commun.. 2019.
- [175]H. Min, “Blockchain technology for enhancing supply chain resilience,” Bus. Horiz., 2019.
- [176]P. J. Taylor, T. Dargahi, A. Dehghantanha, R. M. Parizi, and K. K. R. Choo, “A systematic literature review of blockchain cyber security,” Dig. Comm. Net.. 2020.
- [177]Road Traffic Act 1930 unpublished.

APPENDIX

TABLE IV. CURRENT BLOCKCHAIN SURVEYS IN INSURANCE AND THEIR LEVEL OF DISCUSSION: A COMPARATIVE SUMMARY

Authors	Year of publication	Level of discussion		
		Low	Medium	High
[14]	2019	*		
[12]	2019	*		
[35]	2019		*	

TABLE V. BLOCKCHAIN TECHNOLOGY GENERAL SURVEYS

Author(s)	Year of Publication	Domains of interest	Other domains
[12]	2019	<ul style="list-style-type: none"> - Financial Application - Integrity and Verification - Governance (Citizenship and user services, Public sector and Voting - Internet of things - Healthcare - Privacy and security - Business and industrial applications (Supply chain management and Energy sector) - Education - Data management 	<ul style="list-style-type: none"> - Crowd-funding - Humanitarian and philanthropy - Intelligent Autonomous transport - Environmental management - social media - grid computing - cloud computing
[14]	2019	<ul style="list-style-type: none"> - Financial system (Insurance processing, Banking system, Enterprise sector and Stock exchange) - Intelligent transportation system (Unmanned Aerial Vehicles, Electric Vehicles, and Vehicular Adhoc Networks) - Internet of Things (Device communication, supply chain management, Access control, Fault tolerance and Energy-efficiency) - Smart grid (Energy trading, Demand response, and Dynamic pricing) - Healthcare networks (Record management, Access control policy, Data sharing and Data storage,) - Voting system (e-voting database manipulation and Tamper-proof vote counting) - Data center networks (Cloud computing, Edge/fog computing, Process models) 	
[32]	2019	<ul style="list-style-type: none"> - Healthcare - Financial - Internet of things - Legal perspective - Government - Power grid - Intelligent transportation systems - Commercial world (digital rights management, production management, copyright management, construction industry, transaction management and users behavior management for network media) - Cloud computing - Reputation system - E-business - Supply chain 	

TABLE VI. BLOCKCHAIN TECHNOLOGY SPECIFIC SURVEYS

Author(s)	Year of Publication	Core Domain	Other Domain(s)
[37]	2019	Agric and Food Supply Chain	
[2]	2019	Business Model	
[38]	2017	Construction Management	
[174]	2019	Internet of Things (IoT)	
[175]	2019	Supply Chain	
[176]	2020	Cyber Security (IoT)	
[173]	2018	e-Government	
[172]		Financial Sector	
[33]	2019	Privacy in blockchain systems	
[36]	2018	Insurance	
[35]	2019	Insurance operations and regulation	

Dual Frequencies Usage by Full and Incomplete Ring Elements

Kamarulzaman Mat¹, Norbahiah Misran², Mohammad Tariqul Islam³, Mohd Fais Mansor⁴

Department of Electrical, Electronic and System Engineering
Faculty of Engineering and Built Environment, Universiti Kebangsaan Malaysia
43600 Bangi, Selangor, Malaysia

Abstract—Full and incomplete ring patch elements antenna can be mixed to generate a variety of responses with respect to the direction of polarization. Dual frequencies requirement in numerous usage like in tracking radar can be achieved by combining the patches. To obtain the favored operating frequency, a straightforward design of a ring patch and also the addition of a gap have been utilized. Various sizes of the gap and the gap's position within a ring have been examined in the study. In order to investigate the element conduct, the surface current distribution, return loss, as well as reflection phase, are monitored. The evaluation revealed that the ring element with a smaller width would offer a sharp gradient of reflection phase that lowers its bandwidth performance. Meanwhile, the element performance was not affected by the gap's placement at the upper and lower part of the ring. However, the gap's size of 0.2 mm placed at the left or right position of the ring has shifted up the resonant frequency from 8.1 GHz to 11.8 GHz. For this study, it was shown that the mixture of full and incomplete ring elements has the potential to be utilized as an antenna to comprehend the operation of monopulse.

Keywords—Incomplete ring; full ring; dual frequencies; polarization-dependent

I. INTRODUCTION

The drawbacks in the parabolic reflector antenna have triggered the reflectarray antenna invention. A mixture of the guided elements mounted on a surface for reflecting radio waves in the favored path forms the reflectarray antenna. In the 1990s, the innovations making use of microstrip elements mounted on a grounded substrate material and arranged in an array became prominent [1].

Since reflectarray elements are printed on a flat surface, getting a phase plane is crucial. Numerous methods have been adapted to get the required phase plane. First of all, various patch element dimensions and a line phase delay were used, which fixed the phase delay in various paths out of the feed [2]. The second method is by utilizing the rectangular bipolar, or ring patch element of different sizes to guarantee the distinct scattering impedances from the elements. In this approach, different phases have to be offset by the delay of various feeds [1]. Finally, different polarization angles are utilized to respond to the variation in the feed's path length [3]. After all, the reflectarray antenna has its own weak point. The significant downside is its modest bandwidth characteristic, which relates to the elements design, focal length, and size of the aperture. In theory, the parabolic reflector has limitless bandwidth. For this

reason, the broadband reflectarray is tough to oppose the parabolic reflector in terms of total performance [4].

A number of techniques have been executed to deal with the concern, such as utilizing microstrip patches in every size and shape, piled microstrip patch, and waveguide [3]. An easy, balanced shape such as square or ring patch element drawing in attraction could be enhanced for several frequency operations and give far better bandwidth [5]-[11]. Some studies state that a ring-shaped microstrip element is uncomplicated to take care of by changing its size. The wanted phase correction essential for reflectarray antenna aperture is acquired in this technique [12].

The source beam in monopulse radar is divided into several sections prior to sending the signals far from the antenna. The transmitted signals then strike an object at a distance and bounced back to the receiving antenna. After that, the received signals are distinguished among them to figure out the position of the object. Due to this, monopulse is often referred to as simultaneous lobe comparison. Monopulse technique has been utilized for overwhelming the lobe switching and conical scan sluggish searching speed, as well as incorrect angle indication discovered in radar tracking systems [13]. Several instances of monopulse applications are tracking radar, automotive radar as well as search and rescue radar. Cassegrain parabolic antennas are rather typical in monopulse radar systems. However, these systems' monopulse comparator is rather heavy, huge, and complicated to install. On the other side, microstrip patch antennas have several fascinating characteristics such as small, low profile, lightweight, and also quite economical to make. Due to the mentioned factors, a microstrip antenna is an excellent option for monopulse operation.

A number of approaches have been suggested to acquire monopulse's mode of operation. A millimeter-wave microstrip monopulse antenna was created by [14], while a bi-directionally-fed microstrip patch array was recommended by [15]. Nonetheless, the comparator network placed in the center of the antenna in the design ended up being a substantial obstruction for the aperture of the antenna. Various other studies include a double layers planar monopulse antenna [16], as well as a compact monopulse microstrip antenna array [17]. The author in [18] had the ability to create an electronically reconfigurable reflectarray antenna by using voltage-controlled liquid crystals as a substrate. However, at microwave frequencies, the readily available liquid crystals have a modest dielectric anisotropy. Subsequently, it limits the dynamic phase range offered [19].

This paper examines the incomplete and full ring element behaviour to validate its reliable use in the monopulse dual-frequencies system. It also features the gap's position and size within a ring concerning the reflection loss and reflection phase performance.

II. METHODOLOGY

A balanced-shape element such as a ring is frequently used in microstrip patch modern technology. The ring element's balanced geometry can be enhanced to obtain several operating frequencies and better bandwidth [20]. In the ring element's periodic arrays, the resonant frequency is established by the element's dimension, electrical properties of the material, and patch periodicity.

In this work, the patch element has been designed using CST Microwave Studio with specific boundary conditions to represent an infinite reflectarray. By adjusting the geometry of the elements, the scattering parameters of the modeled elements were analyzed later. Rogers RT/Duroid 5880 with 1.575 mm thickness, material permittivity ϵ_r of 2.2, and the loss tangent ($\tan \delta$) of 0.0009 was selected as the substrate in the research. Since copper has a 100% electrical continuity rate, it was utilized for ground plane elements and ring patches. The patch and ground plane have 0.035 mm of thickness, while the element's periodicity of 10 mm x 10 mm is chosen. Fig. 1 shows the basics of an antenna design that has been developed. The element's dimension (in terms of internal radius r_{in} and external radius r_{out}), ring's width w , substrate periodicity (a and b), substrate thickness t_s , as well as substrate permittivity ϵ_r established the resonant frequency of the antenna. Table I reveals the specification and its associated symbol made use of in the task.

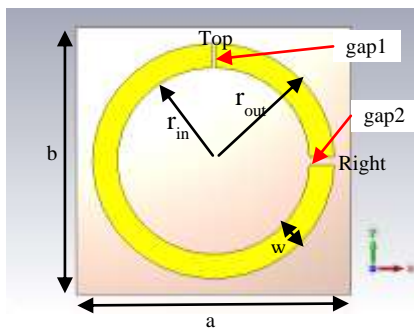


Fig. 1. Patch Antenna Design.

TABLE I. SPECIFICATION AND RELATED SYMBOL

Parameter	Symbol
Internal radius	r_{in}
External radius	r_{out}
Ring's width	w
Gap	$gap1, gap2$
Patch thickness	t_p
Periodicity	a, b
Substrate thickness	t_s
Substrate permittivity	ϵ_r
Ground plane thickness	t_g

A full or complete ring patch responses are independent relative to the incident polarization as a result of their balanced geometry. Nevertheless, the incomplete ring patches are polarization-dependent and produce different responses or reactions. The gap placement in an incomplete ring patch as displayed in Fig. 1 will form an unbalance geometry. In this study, the behavior of full ring, incomplete ring together with the position of the gap are analyzed.

III. RESULTS AND DISCUSSION

A. Full Ring Element

Fig. 2 displays a contrast of surface current distribution between round and ring patches. A round patch can be viewed to possess a nearly consistent surface current distribution. The current distribution for a ring is not uniform, on the other hand. Its current is concentrated at the right and left sections of the ring. In the meantime, the current distribution at the upper and lower part of the ring is practically minimal.

By incorporating an internal radius r_{in} to round patch, the S-parameters have been outlined to investigate its impact on the resonant frequency. Fig. 3 presents the S-parameter for various sizes of the ring. All ring patches in Fig. 3 are noted to make a distinct phase gradient. A thinner size ring (smaller w) will provide a sharp gradient that decreases its bandwidth performance. On the contrary, a thicker size ring (bigger w) will provide a more gradual gradient for the reflection phase curve. For example, the reflection phase gradient for $w = 0.5$ mm is sharper than others, which reduces its bandwidth performance. So, the element with $w = 0.5$ mm ($r_{in} = 3.5$ mm) is not a good option in terms of bandwidth and return loss. These outcomes are in good agreement with previous researchers which says the reduction of reflected surfaces (patch) area will give a steep reflection phase curve [21] - [22]. In other words, a thicker ring performs better than a thin ring in terms of return loss and bandwidth, but a loss in a static phase range.

B. Incomplete Ring Element

Unbalanced or disproportional geometry is created with the existence of a gap in the ring element. As a result, the responses of an incomplete ring patch are actually polarization-dependent. When a gap is placed at a certain position, the patch's response is identical to the full ring. Having said that, at yet another position, its response is rather contrasted, in which the resonant frequency shifted up. This behaviour can be exploited to attain dual operating frequencies by using the same design of the antenna. It can be done by inserting an electronic switch within the gap in the right position. As a result, the patch's current flow or electrical continuity between the upper and lower part of the incomplete ring can be regulated by the switch. The patch's top position gap is required to compel the current to move via the switch when it is switched ON.

In general, the incomplete ring developed in the research is functioning within X-band. As a result, the value of $r_{in} = 3.5$ mm and $r_{out} = 4.4$ mm have been opted for. At this setup, the element gives an 8.10 GHz resonant frequency. In Fig. 4, the incomplete ring geometry, which comprises four sections, i.e., Section A, Section B, Section C, and Section D, is shown. The

angle of 0° is at the bottom, while 90° , 180° , and 270° are at the right, top, and left, respectively. The corresponding resonant frequency for every 15° gap rotation is represented in Table II. From the table, gaps at angles of 0° , 90° , 180° , and 270° will give a single resonant frequency, f_1 . The angle of 0° and 180° produces a resonant frequency of 8.1 GHz, while the angle of 90° and 270° produce a 12.5 GHz frequency. Nevertheless, other angles of the gap will produce two resonant frequencies, f_1 and f_2 . This design approach to produce multiple frequencies using a single ring with a gap is easier than the square ring combination and multiple rings introduced in [10] and [23], respectively. To simplify the design, only the gap angles that give a single resonant frequency, i.e., 0° , 90° , 180° , and 270° were used for further analysis.

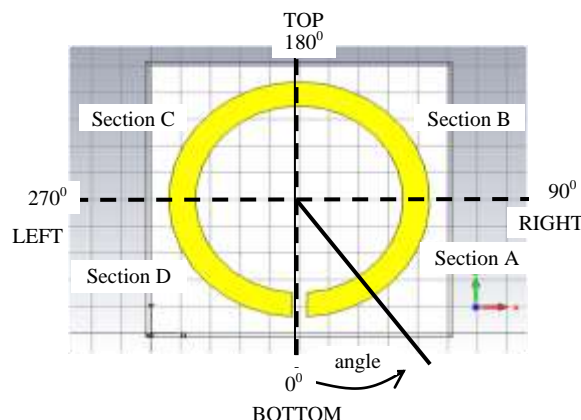


Fig. 4. Four Sections of an Incomplete Ring.

TABLE II. RESONANT FREQUENCY FOR AN ANGLE

Angle ($^\circ$)				Resonant frequency (GHz)	
Sect. A	Sect. B	Sect. C	Sect. D	f_1	f_2
0	180	-	360	8.1	-
15	165	195	345	8.3	13.2
30	150	210	330	8.6	13.1
45	135	225	315	9.0	12.9
60	120	240	300	9.5	12.8
75	105	255	285	10.0	12.6
90	-	270	-	12.5	-

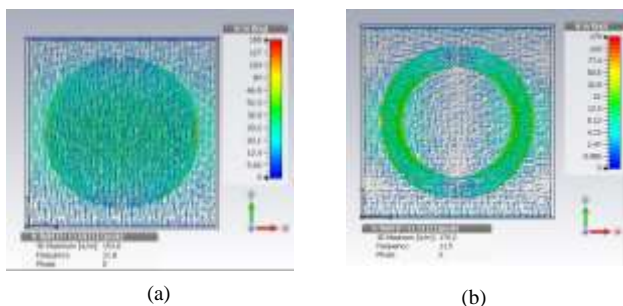


Fig. 2. Surface Current Distribution for (a) Round and (b) Ring Patch.

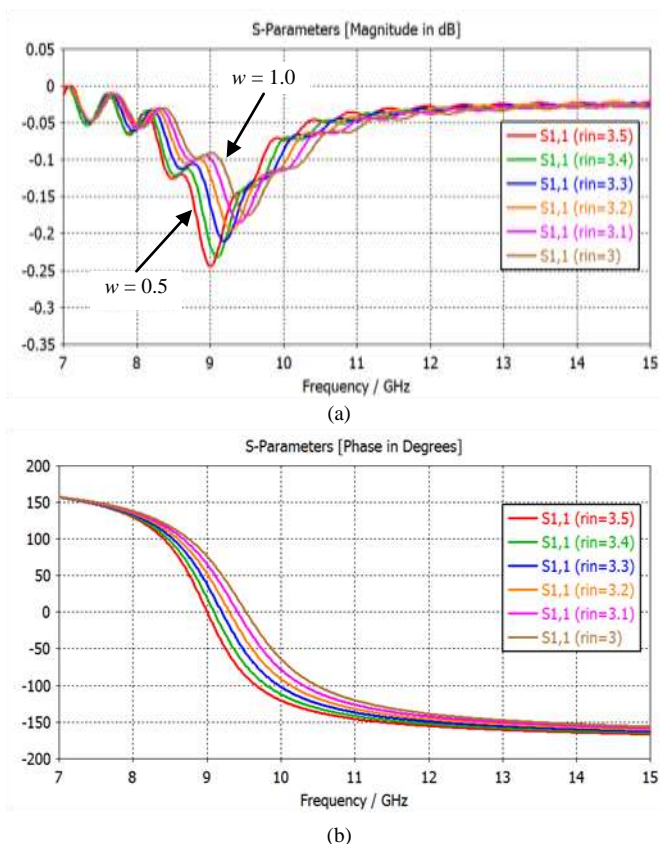


Fig. 3. S-Parameter in (a) Magnitude and (b) Phase for Ring Patch ($r_{out} = 4$ mm) with different width, w .

1) *Gap insertion at the right position:* Fig. 5 presents the incomplete ring element with a gap at the right position (90° angles). At this position, the surface current density is at the highest level. Due to this, the presence of a gap will resist the current flow between the upper and lower part of the incomplete ring. The presence of a gap in the ring will cause its resonant frequency to move higher. For example, the gap's size of 0.4 mm moved the frequency from 8.10 GHz to 12.20 GHz. The bigger the size of the gap, the higher the resonant frequency can be obtained. Fig. 6 highlights the surface current distribution, which is concentrated close to the gap, and minimal at the upper and lower part of the ring. Fig. 7 displays the S_{11} parameter for an incomplete ring patch with a gap at the right position of the ring. It can easily be observed that resonant frequency went up rather significantly from the original frequency (full ring).

2) *Gap insertion at the top:* A gap at this position remains in parallel (180° angle) to the incident field, E . As presented in Fig. 8, the surface current distribution of the ring is rarely affected. The very minimal concentration of surface current can easily be observed at the bottom and on top sectors of the incomplete ring. Fig. 9 shows the S-parameters for the incomplete ring with a gap at the top placement. The reactions of this incomplete ring patch are practically comparable to the response of a full ring. For a gap of 0.2 mm, the resonant frequency went up a little, from 8.10 GHz to 8.12 GHz. The phase slope or gradient is identical for all incomplete rings with various dimensions of the gap.

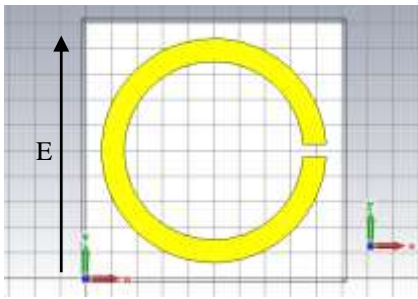


Fig. 5. Incomplete Ring with Right Position Gap.

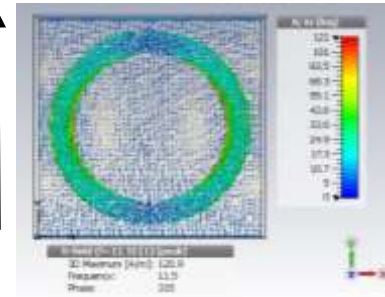


Fig. 8. Surface Current Distribution for an Incomplete Ring with Top Position Gap.

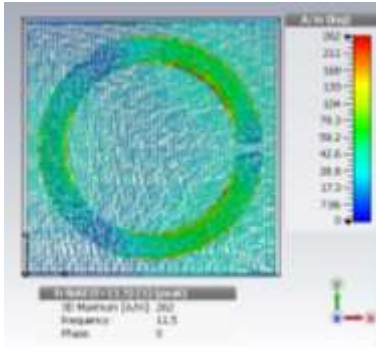


Fig. 6. Surface Current Distribution for an Incomplete Ring with a Gap at the Right Position.

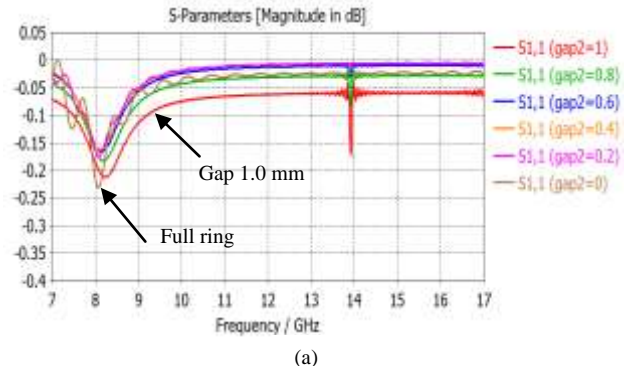


Fig. 9. S-Parameters for Incomplete Ring Patch with a Gap at the Top Position.

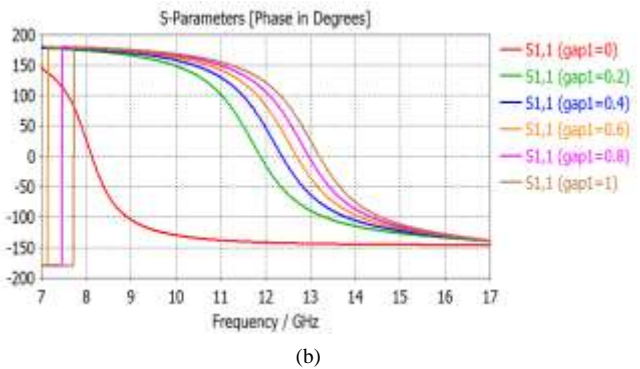
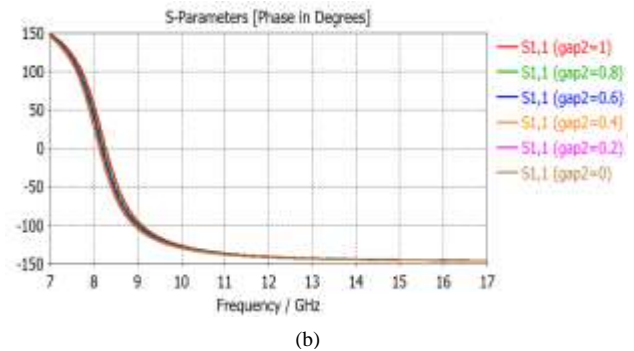
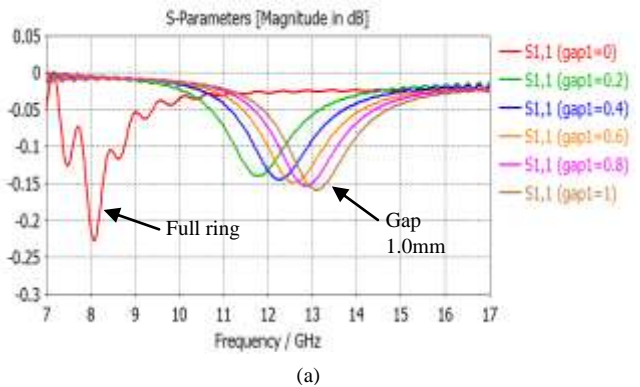


Fig. 7. S-Parameters for Incomplete Ring Patch with Right Position Gap.

3) *Gap insertion at the top and right:* Table III summarizes the resonant frequency obtained for an incomplete ring with gaps at two positions. It was observed that the gap at the top or bottom (or even both) position almost did not affect the resonant frequency. However, the gap at the right or left (or both) position will move up the frequency. For example, the gap's size of 0.6 mm shifted the resonant frequency to 12.7 GHz and 15.9 GHz for single and double gaps, respectively.

To attain dual frequencies, the very same incomplete ring patch element can be enhanced by putting an electronic switching component within a gap [11][24]. The switch aims to provide continuity or discontinuity between the bottom and top sections of the ring. This dual frequencies capability is an excellent attribute in acquiring monopulse mode of sum, Σ and difference, Δ .

The location of an electronic switching within the patch is shown in Fig. 10. When the switch is ON, the upper and lower part of the ring is connected, leaving only a gap at the top position. In this condition, the incomplete ring behaves like a full ring. But if the switch is OFF, the ring will have two gaps at the top and right positions. This will cause the resonant frequency changes to a higher level.

The S-parameters for an incomplete ring with a switch at ON and OFF mode are shown in Fig. 11. During an ON mode, the resonant frequency of 8.10 GHz was achieved. On the other hand, the frequency of 11.8 GHz was obtained during an OFF mode.

TABLE III. RESONANT FREQUENCY FOR DUAL GAP OF INCOMPLETE RING

Gap size (mm)	Resonant frequency, f (GHz)			
	Gap's position			
	Bottom (0°)	Bottom & Top (0° & 180°)	Right (90°)	Right & Left (90° & 270°)
0.0	8.10	8.10	8.1	8.1
0.2	8.12	8.12	11.8	14.3
0.4	8.15	8.15	12.3	15.2
0.6	8.20	8.20	12.7	15.9
0.8	8.25	8.25	13.0	16.5
1.0	8.30	8.30	13.2	17.0

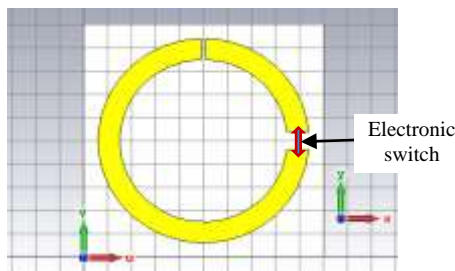


Fig. 10. An Electronic Switch within a Gap.

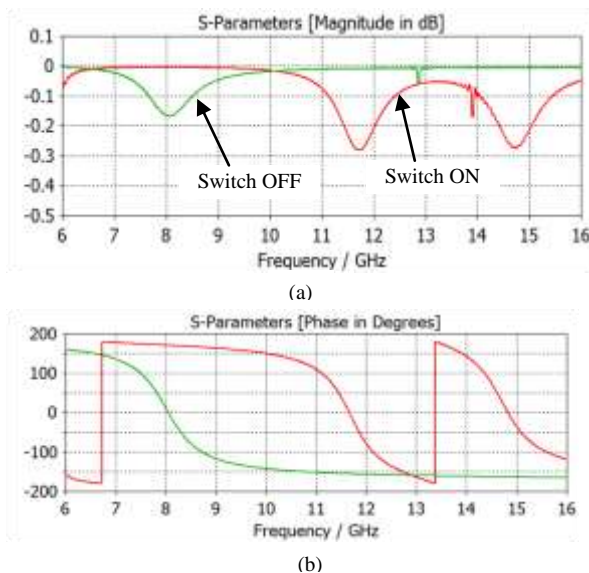


Fig. 11. S-Parameters in (a) Magnitude and (b) Phase for Incomplete Ring Patch with ON and OFF Mode.

IV. CONCLUSION

The balanced geometry of the ring patch is able to be conveniently enhanced to acquire intended resonant frequencies. The research on the incomplete ring patch parameter with the incorporation of the gaps has actually been accomplished to confirm the use of them for dual frequencies operation. Observations from the studies reveal that the higher return loss and higher phase gradient or slope are triggered by the smaller width, w of the ring element, which subsequently lowers its bandwidth performance. Additionally, the incomplete ring is shown to have polarization-dependent reactions. The position of a gap at particular placements of incomplete ring patch can be readjusted to get dual frequencies. As a result, the full and incomplete ring can be put together as an antenna's reflector to accomplish the operation of monopulse radar that requires such frequencies.

ACKNOWLEDGMENT

The authors would like to thank the Universiti Kebangsaan Malaysia under grant number GUP-2019-011 for financial support.

REFERENCES

- [1] D. M. Pozar and T. A. Metzler, "Analysis of a reflectarray antenna using microstrip patches of variable size", *Electronics Letters*, vol. 29, no. 8, pp. 657-658, 1993.
- [2] J. Huang, "Microstrip reflectarray", *Antennas and Propagation Society International Symposium. AP-S. Digest. 2*, pp. 612-615, 1991.
- [3] J. Huang and R. J. Pogorzelski, "Microstrip reflectarray with elements having variable rotation angles", *IEEE AP-S Symposium Digest*, pp. 1280-1283, 1997.
- [4] J. Huang and J. A. Encinar, *Reflectarray Antennas*, Press Wiley-Interscience, 2008.
- [5] A. Smida, "Simulation and analysis of variable antenna designs for effective stroke detection," *Int. Journal of Advanced Computer Science and Applications*, vol. 11, no. 12, pp. 238-244, 2020.
- [6] N. Ramli, S. K. Noor, T. Khalifa and N. H. A. Rahman, "Design and performance analysis of different dielectric substrate based microstrip patch antenna for 5G applications," *Int. Journal of Advanced Computer Science and Applications*, vol. 11, no. 8, pp. 77-83, 2020.
- [7] A. Selamat, M. Ramli, N. Misran, M. F. Mansor and S. H. Zaidi, "A wide bandwidth element of solar reflectarray antenna with scanning ability", *ARNP Journal of Engineering and Applied Sciences*, vol. 13, no. 24, Dec. 2018.
- [8] M. Ramli, A. Selamat, N. Misran, M. F. Mansor and M. T. Islam, "Design of capacitive integrated reflectarray radiating elements for beam scanning reconfigurability", *Journal of Engineering and Applied Sciences*, vol. 11, no. 1, pp. 106-111, 2016.
- [9] M. Ramli, A. Selamat, N. Misran, M. F. Mansor and M. T. Islam, "Superposition of reflectarray elements for beam scanning with phase range enhancement and loss improvement", *ARNP Journal of Engineering and Applied Sciences*, vol. 11, no. 3, pp. 1755-1758, 2016.
- [10] S. H. Yusop, N. Misran, M. F. Mansor, M. T. Islam and M. Abu, "A broadband reflectarray antenna concentric ring square element for dual frequency operation", *Int. Journal of Applied Engineering Research*, vol. 9, no. 24, pp. 26553-26562, 2014.
- [11] M. Ramli, A. Selamat, N. Misran, M. F. Mansor and M. T. Islam, "Dual configurations reflectarray element in improving dynamic phase range and loss", *Int. Journal of Applied Engineering Research*, vol. 9, no. 24, pp. 23707-23716, 2014.
- [12] N. Misran, R. Cahill, and V.F. Fusco, "Reflection phase response of microstrip stacked ring elements", *Electronics Letters*, vol. 38, no. 8, 2002.
- [13] S. M. Sherman, *Monopulse Principles and Technique*, Dedham, MA: Artech House, 1984.

- [14] B. J. Andrews, T. S. Moore and A.Y. Niazi, "Millimeter-wave microstrip antenna for dual polar and monopulse applications," presented at the 3rd Int. Conf. Antennas and Propagation, ICAP 83, Apr. 12–15, 1983.
- [15] S. G. Kim and K. Chang, "Low-cost monopulse antenna using bi-directionally-fed microstrip patch array," *Electronics Letters*, vol. 39, no. 20, 2003.
- [16] P. Rodriguez-Fernandez, A. Guillot-Duran, J. L. Masa-Campos and M. Sierra-Perez, "Planar monopulse antenna with radial line feeding," 2006 IEEE Antennas and Propagation Society International Symposium, pp. 3635-3638, July 2006.
- [17] H. Wang, D. G. Fang, and X. G. Chen, "Compact single layer monopulse microstrip antenna array," *IEEE Trans. Antennas Propagation*, vol. 54, no.2, pp. 503-509, Feb. 2006.
- [18] W. Hu, M. Y. Ismail, R. Cahill, H. S. Gamble, R. Dickie, V. F. Fusco, D. Linton, S. P. Rea and N. Grant, "Tunable reflectarray liquid crystal patch element", *IEE Electronics Letters*, vol. 2, no. 9, pp. 509-511, 2006.
- [19] M. Y. Ismail, W. Hu, R. Cahill, V. F. Fusco, H. S. Gamble, D. Linton, R. Dickie, S. P. Rea and N. Grant, "Phase agile reflectarray cells based on liquid crystals", *Proc. IET IEE Microwaves Antennas and Propagation*, August 2007.
- [20] N. Misran, M. Y. Ismail and M. T. Islam, "Reflectarray antenna with radar cross-section reduction", *Int. Journal of Integrated Engineering (Issue on Electrical and Electronic Engineering)*, vol. 2, no. 3, pp. 17-28, 2010.
- [21] M. Y. Ismail, M. I. Abbasi and M. H. Dahri, "Phase characterization of reconfigurable reflectarray antennas", *Int. Journal on Electrical Engineering and Informatics*, vol. 5, no. 4, pp. 447-453, Dec. 2013.
- [22] M. Y. Ismail, M. I. Abbasi, A. F. M. Zain, M. Amin and M. F. L. Abdullah, "Characterization of loss and bandwidth performance of reflectarray antenna based on lumped components", *Int. Journal on Electrical Engineering and Informatics*, vol. 2, no. 2, pp. 113-122, 2010.
- [23] Y. Zhang, J. Liu, Z. Liang and Y. Long, "A wide-bandwidth monopolar patch antenna with dual-ring couplers", *Int. Journal of Antennas and Propagation*, vol. 2014, pp. 1-6, 2014.
- [24] J. Perruisseau-Carrier and A. Skriverviky, "Monolithic MEMS-based reflectarray cell digitally reconfigurable over a 360 phase range", *IEEE Antennas and Wireless Propagation Letters*, vol. 7, pp. 138-141, 2008.

An Efficient Data Replication Technique with Fault Tolerance Approach using BVAG with Checkpoint and Rollback-Recovery

Sharifah Hafizah Sy Ahmad Ubaidillah¹, A. Noraziah², Basem Alkazemi³

Faculty of Computing, University Malaysia Pahang, Pahang, Malaysia^{1,2}

IBM Center of Excellence, University Malaysia Pahang, 26300 Kuantan, Pahang, Malaysia²

College of Computer and Information System, Umm Al-Qura University, Saudi Arabia³

Abstract—Data replication has been one of the pathways for distributed database management as well as computational intelligence scheme as it continues to improve data access and reliability. The performance of data replication technique can be crucial when it involves failure interruption. In order to develop a more efficient data replication technique which can cope with failure, a fault tolerance approach needs to be applied in the data replication transaction. Fault tolerance approach is a core issue for a transaction management as it preserves an operation mode transaction prone to failure. In this study, a data replication technique known as Binary Vote Assignment on Grid (BVAG) has been combined with a fault tolerance approach named as Checkpoint and Rollback-Recovery (CR) to evaluate the effectiveness of applying fault tolerance approach in a data replication transaction. Binary Vote Assignment on Grid with Checkpoint and Rollback-Recovery Transaction Manager (BVAGCRTM) is used to run the BVAGCR proposed method. The performance of the proposed BVAGCR is compared to standard BVAG in terms of total execution time for a single data replication transaction. The experimental results reveal that BVAGCR improves the BVAG total execution time in failure environment of about 31.65% by using CR fault tolerance approach. Besides improving the total execution time of BVAG, BVAGCR also reduces the time taken to execute the most critical phase in BVAGCRTM which is Update (U) phase by 98.82%. Therefore, based on the benefits gained, BVAGCR is recommended as a new and efficient technique to obtain a reliable performance of data replication with failure condition in distributed databases.

Keywords—Data replication; computational intelligence; fault tolerance; binary vote assignment on grid; checkpoint and rollback-recovery

I. INTRODUCTION

Data replication is a useful technique for a Distributed Database System (DDS) as it can provide high availability and efficient access to required data and can be applied in a grid computation situation to improve the efficiency of the system [1, 2]. Besides, data replication technique can be one of the influential techniques that can expand the usefulness of computational intelligence structure. Data replication involves frequent, incremental copying of data from one database to another database in a continuous manner which can increase availability, provide low response times and allows fast local access of the system [3, 4]. Despite the goodness of data

replication techniques in handling the distributed database, still, it has some weakness when dealing with failure cases.

Handling data replication in the failure cases is very crucial in order to preserve the effectiveness of the systems. The main challenges of data replication are that the replica has to be kept consistent when updates occur despite having any failure during the transaction's running [4]. The only way to solve these problems is by enabling fault tolerance. Fault tolerance approach is a crucial issue in distributed computing; it keeps the transaction in an operational condition in subject to failure. The most important point of it is to keep the transaction working even if any of its part goes off or faulty [5]. Fault tolerance is the dynamic approach that's used to keep the interrelated transaction together, put up with reliability and availability in DDS. Efficient fault tolerance approaches help in detecting of faults and if possible recovers from it [6].

Based on previous studies, the combination of any data replication technique with Checkpoint and Rollback-Recovery (CR) fault tolerance approach in a distributed database is infrequently analyzed irrespectively of its individual promising potential to lessen the total execution time in failure-prone situations [7]. As an example, research done by [7] explored the performance of transaction process using CR only, replication only and the combination of both techniques in linear workflow with the presence of failure. The result obtained reveals that the conditions in which each techniques lead to improved performance. Besides that, paper done by [8] concludes that the CR approach is essential for not only transaction process replication but also for security issues.

Despite good performances, there are only few researchers who had interest in exploring the effectiveness of combining data replication technique with CR fault tolerance approach. It is a common practice to utilize a Checkpoint and Rollback-Recovery (CR) to facilitate an adequate failure recovery for improving transaction reliability [9]. Mainly, the checkpoint is performed to save information linked with the completed portion of a transaction. When a transaction failure occurs, through rollback and information retrievals, the transaction can be resumed from the last successful checkpoint. Instead, without implementing the checkpoint technique, the transaction has to repeat the execution of the entire transaction from the very beginning [10]. Hence, the data replication

transaction might be time consuming without the CR approach if any failure happened.

Therefore, in this study, a data replication technique called as Binary Vote Assignment on Grid (BVAG) is combined with CR with the proposed of evaluating the efficiency of hybridizing data replication technique with fault tolerance approach for a better performance of a single data replication transaction in the presence of failure. The proposed method, BVAGCR is implemented in Binary Vote Assignment on Grid with Checkpoint and Rollback-Recovery Transaction Manager (BVAGCRTM).

The paper is arranged as follows. In the next section, Literature Review is detailing about BVAG data replication technique and CR fault tolerance approach. In Section 3, Methodology describes the procedure of BVAGCR technique which is employed via BVAGCRTM. The Result and Discussion section discussed the outcome obtained from standard BVAG and BVAGCR. Also presented in this section is the comparison of both techniques in terms of execution time while managing data replication transaction with the occurrence of failure. Finally, the conclusion of this research and suggestion for future research are provided in Conclusion.

II. LITERATURE REVIEW

A. Binary Vote Assignment on Grid (BVAG)

The concept of Binary Vote Assignment on Grid (BVAG) is replicating the data from the primary replica to the neighbours' replica which is located at the adjacent sites of the primary replica [11]. Full replication can result in a huge waste of storage space and consume a lot of bandwidth [12]. By using this technique, the execution time of the replication process in a distributed database can be reduced as it only replicates data at the specified sites [12]. The query expansion process involves augmenting initial user query with additional terms that are related to user requirements [13], while BVAG focus challenge to increase write query availability through replication. BVAG is striding a new track in replication that helps to maximize the write availability with little communication cost as a result of minimum number of quorum size needed. Furthermore, the replication is interconnected with transaction procedure [14].

In BVAG, all sites are logically organized in the form of two-dimensional grid structure. For example, if a BVAG consists of nine sites, it will logically organize in the form of 3 x 3 grid structure (Fig. 1) as shown. As can be seen in Fig. 1, site A is neighbours to site B and site D, if A is logically located adjacent to B and D. Hence, four sites on the corners of the grid have only two adjacent sites, other sites on the boundaries have only three neighbours and the site located in the middle of the grid formation has four neighbours [14].

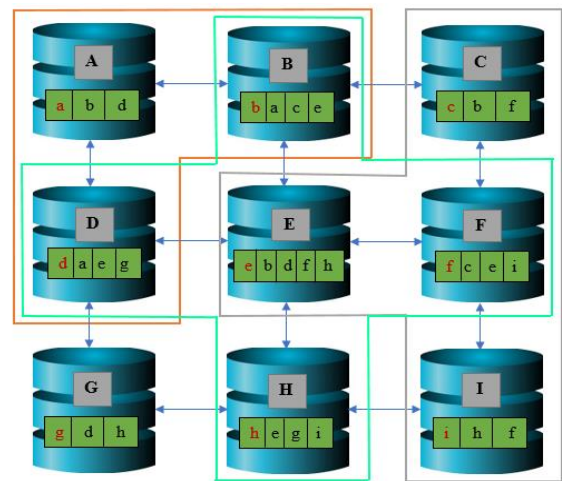


Fig. 1. Binary Vote Assignment on Grid (BVAG).

Each site has a premier data file. Data will be replicated to the neighbours sites from the primary site [11]. For simplicity, the primary site of any data file and its neighbours are assigned with vote one (1) or vote zero (0) otherwise. A neighbour binary vote assignment on grid, B , is a function such that $B(i) \in \{0,1\}, 1 \leq i \leq d$ where $B(i)$ is the vote assign to site i . This assignment is treated as an allocation of replicated copies and a vote assigned to the site results in a copy allocated at the neighbour. Due to the data that will be replicated to neighbours, the possible number of data replication from each site, d , should then be:

$d \leq \text{quorum}$ (the number of neighbours + a data from the primary site itself).

For example, primary data from the site A which is called as 'a' are replicated to site B and site D which are their neighbours. Site E which holds the primary data 'e' has four neighbours, namely, sites B, D, F and H that will get the replicated data of 'e'. As such, the site E has five replicas. Meanwhile, primary data 'f' from site F are replicated to site C, E and I. The number of quorums used are based on the total number of replicated data and the primary data, d , which can be three, four or five [11,14].

The transaction procedure in BVAG is called as Binary Vote Assignment on Grid Transaction Manager (BVAGTM). The BVAGTM is applied to control the transaction of each data replication process. The primary site of any primary data file and its replica are assigned with different votes depends on their condition. There are two types of votes used in this study as shown in Table I. Zero (0) specified that the site is available (free). Meanwhile, one (1) displayed that the site is unavailable (busy). The status of each site is statistically independent of others. The status of each site is statistically independent of others. When a site is available, the copy at the site is available too; otherwise, it is unavailable [11,14].

TABLE I. TYPE OF STATUS

Type of Status	Definition
0	Available (Site is free or not in used)
1	Unavailable (Site is busy or in used)

There are seven main phases involve in BVATM; Initiate Lock (IL), Propagate Lock (PL), Obtain Quorum(OQ), Update(U), Commit (C), Unlock (UL) and Release Lock (RL) [11,14]. IL phase involves locking the primary site if the primary site is in available (0) status. If the primary site is busy (status = 1), then the primary site will be release (RL). After the primary site has been locked, the PL phase determines the status of each neighbours site. All neighbours sites are locked if they are in available (0) status. Otherwise, the neighbours' sites will be release (RL). Then, OQ phase declares that the quorum obtained is enough for the transaction to be continued. Next, the primary data will be updated in the U phase. Afterward, the updated primary data which is also called as new primary data is replicated to the neighbours' sites in C phase. Last but not least, the transaction will unlock (UL) all the sites that are involved in the transaction. The summary of BVAGTM is shown in Fig. 2.

B. Checkpoint and Rollback-Recovery (CR)

Checkpoint with Rollback-Recovery (CR) is a renowned fault tolerance approach. Checkpoint is a process which stores the recent state of a transaction in stable (non-volatile) storage

[9]. It is recognized through the normal execution of a transaction occasionally. The information related to the transaction is saved on a stable storage with the intention of using it in case of site failures. The saved information comprises of the transaction state, its environment, the value of registers, etc. When an error is spotted, the transaction is roll backed to the last saved state [15].

Fig. 3 shows the summary of CR approach. The checkpoint mechanism takes a snapshot of the transaction state and stores the information on some non-volatile storage medium [16]. When failures occur, the restore mechanism copies the last known check pointed state of transaction back into memory and continue processing. The basic idea behind CR is the saving and restoration of transaction state. By saving the current state of the transaction occasionally or before critical code sections, it delivers the baseline information needed for the restoration of lost state in the event of a transaction failure. CR is one of various time efficient fault tolerant approaches [17]. Besides reducing the execution time, CR can also lessen computing resources [18].

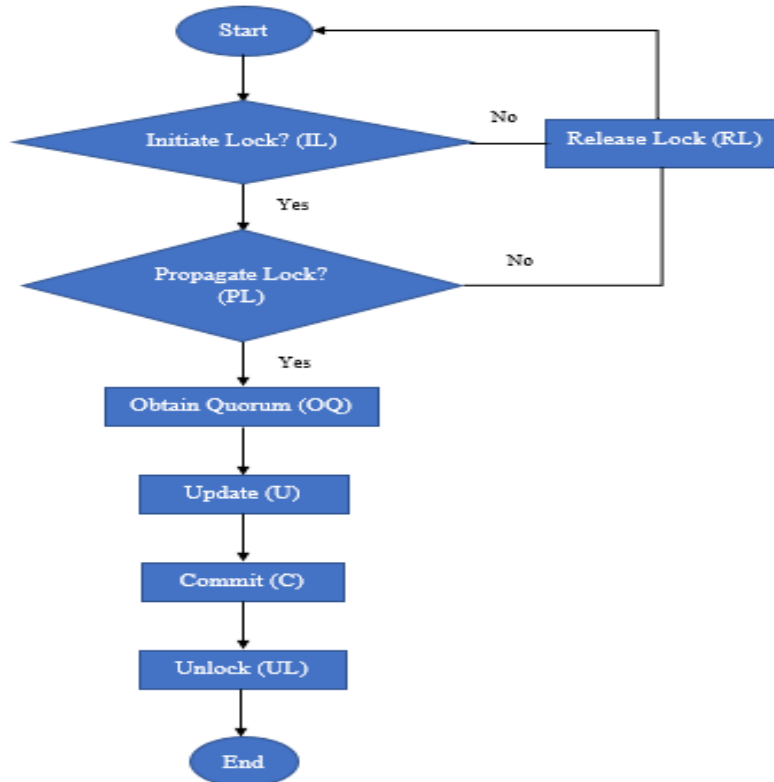


Fig. 2. Binary Vote Assignment on Grid Transaction Manager (BVATM).

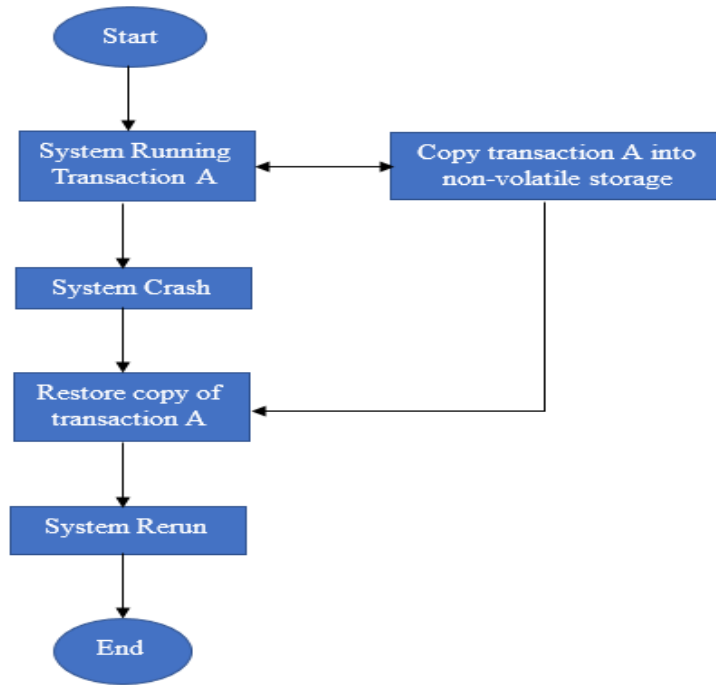


Fig. 3. Checkpoint and Rollback-Recovery (CR).

III. METHODOLOGY

In this section, the methodology of the proposed technique called as BVAGCR is described. Fig. 4 illustrated the algorithm of BVAGCR technique applied in Binary Vote Assignment on Grid with Checkpoint and Rollback-recovery Transaction Manager (BVAGCRTM) for a single data replication transaction.

First, the following notations are defined as:

- 1) T is transaction,
- 2) C is checkpoint transaction,
- 3) λ represents different group of transaction T (before and until get quorum). λ can be either α or β ,
- 4) T_λ is transaction of group λ
- 5) X is the data to be update
- 6) q_i is the number of queue for transaction T_λ . $i = 1, 2, 3, \dots$
- 7) $T_{\lambda x q_1}$ is transaction of λ for data x in queue 1
- 8) $C_{\lambda x q_1}$ is checkpoint transaction of λ for data x in queue 1
- 9) CP is checkpoint file
- 10) $CP_{\lambda x q_1}$ is checkpoint file for transaction of λ for data x in queue 1
- 11) S is the status of the required site
- 12) PR stands for Primary Replica site
- 13) NR stands for Neighbour Replica site
- 14) S_{PR} is status for PR
- 15) S_{NR} is status for NR
- 16) S_{PR_x} is the status of PR which hold data x
- 17) S_{NR_x} is the status of NR which hold data x
- 18) Q is the amount of quorum needed to continue the transaction of $T_{\lambda x q_1}$
- 19) D is database

20) D_{PR} is the database for PR

21) D_{NR} is the database for NR

22) D_{PR_x} is the database of PR that consists of data x

23) D_{NR_x} is the database of NR that consists of data x

A data replication transaction can request to update any data file at any replica. The BVAGCRTM will firstly check whether there is any checkpoint file, $CP_{\lambda x q_1}$ that has been saved in BVAGCRTM. If there is none $CP_{\lambda x q_1}$ file, BVAGCRTM will accept a new data replication transaction.

A new data replication transaction named as $(T_{\lambda x q_1})$ which request to update data (x) is in first queue (q_1) in BVAGCRTM. The transaction will check the status of primary replica (S_{PR_x}) which hold data (x) whether it's status is free (0), busy (1) or having a failure (-1). If the primary replica is free to be used in the transaction, the status will be lock as 1. Else, the primary replica will be released because it is unavailable. The status of (S_{PR_x}) and data (x) are save in the checkpoint file named as $(CP_{\lambda x q_1})$ file. Next, the transaction will request to lock all the neighbours' replicas, (S_{NR_x}) . If all (S_{NR_x}) is in free status, then it will be lock as 1. However, if one or any (S_{NR_x}) is busy, all of it will be released for other transactions. The status of each (S_{NR_x}) is then saved in $CP_{\lambda x q_1}$ file.

Afterward, the total of Q is declared and saved in the $CP_{\lambda x q_1}$ file. After that, the Update and Commit () function is executed. Data (x) will be update at (D_{PR_x}) which is the primary database that hold data (x) . (D_{PR_x}) is then saved in

$CP_{\lambda_{xq1}}$ file. Next, $(T_{\lambda_{xq1}})$ will commit the replication at all neighbours database, (D_{NR_x}) . All (D_{NR_x}) is then saved in $(CP_{\lambda_{xq1}})$ file. Lastly, (S_{PR_x}) and all (S_{NR_x}) will be unlock (status set to 0).

Meanwhile, if there are any $(CP_{\lambda_{xq1}})$ that has been saved in BVAGCRTM, then a transaction called as $(C_{\lambda_{xq1}})$ will retrieve any information saved in $(CP_{\lambda_{xq1}})$. The information that has been saved in $(CP_{\lambda_{xq1}})$ are the status of (S_{PR_x}) and all (S_{NR_x}) , data (x) , (Q) , (D_{PR_x}) and (D_{NR_x}) . (S_{PR_x}) and (S_{NR_x}) is then set as 1 to declare that it is in used for the transaction. Then, the Update and Commit () function is executed based on the information that has been recover.

Finally, all the locks for (S_{PR_x}) and (S_{NR_x}) will be unlock and are sets to 0. This algorithm can be implemented in the case of either primary site or any neighbours' sites are having a failure. The transaction can only be continued if the failed site is back to normal status (0). This is because the proposed algorithm is not constructed to repair the failure but somehow to let the failed transaction to continue running not from the very beginning after the failure is solved.

Main Algorithm

```
{
  If exist  $CP_{\lambda_{xq1}}$  file,
  Begin transaction  $C_{\lambda_{xq1}}$ ,
  Read  $CP_{\lambda_{xq1}}$ ,
  Write  $S_{PR_x} = 1$ ,
  Commit  $S_{PR_x}$ ,
  Write all  $S_{NR_x} = 1$ ,
  Commit  $S_{NR_x}$ ,
  Update and Commit (x),
  Write  $S_{PR_x} = 0$ ,
  Write  $S_{NR_x} = 0$ ,
  Else
  Begin transaction  $T_{\lambda_{xq1}}$ ,
  If  $S_{PR_x} = 0$ ,
  Write  $S_{PR_x} = 1$ ,
  Commit  $S_{PR_x}$ ,
  Save  $S_{PR_x}$  in  $CP_{\lambda_{xq1}}$  file,
  Else
  Write  $S_{PR_x} = 0$ ,
  End
  If all  $S_{NR_x} = 0$ ,
```

```
  Write all  $S_{NR_x} = 1$ ,
  Commit all  $S_{NR_x}$ ,
  Save all  $S_{NR_x}$  in  $CP_{\lambda_{xq1}}$  file,
  Else
  Write all  $S_{NR_x} = 0$ ,
  End
   $Q = \text{majority}$ ,
  Update and Commit (x),
  Write  $S_{PR_x} = 0$ ,
  Write  $S_{NR_x} = 0$ ,
  End
}
```

Function Update and Commit (x)

```
{
  Update  $x$  in  $D_{PR_x}$ ,
  Commit  $x$  in  $D_{PR_x}$ ,
  Save  $D_{PR_x}$ , in  $CP_{\lambda_{xq1}}$  file,
  Commit replication  $x$  in all  $D_{NR_x}$ ,
  Save all  $D_{NR_x}$ , in  $CP_{\lambda_{xq1}}$  file,
}
```

Fig. 4. Algorithm of BVAGCRTM.

In the next section, an experiment considering failure condition has been conducted in order to evaluate the performance of BVAG and BVAGCR. The results obtained and the discussions about the results are also explained in the next section.

IV. RESULT AND DISCUSSION

An experiment of a single transaction with failure condition occurred at the primary replica was conducted in this research using MATLAB simulation. The time between failure and recovery is assumed as 10 seconds. The transaction is continued after failure recovery. In this transaction, the site E is considered as the primary replica holding primary data e. Meanwhile, sites B, D, F, H are the neighbor's replica which will be receiving the copy of data e from site E. In this case, the transaction, $(T_{\lambda_{eq1}})$ requests to update data (e) and replicate the data into the neighbors' replica. A transaction failure is considered to occur in the Update (U) phase seeing that it is the critical phase in BVAG and BVAGCR.

Fig. 5 and Fig. 6 demonstrated the flow of the transaction, $(T_{\lambda_{eq1}})$ with failure condition for BVAG and BVAGCR. As can be seen in Fig. 5 (BVAG), the information related to the transaction in BVAGCRTM was not being saved in a checkpoint file $(C_{\lambda_{eq1}})$. Thus, when a failure occur in T_{10} , the transaction needs to be started all over again as there is no information recovery can be done if failure occurs.

Meanwhile, in BVAGCR (refer Fig. 6), the information related to the transaction is being saved in the checkpoint file

(highlighted with grey) for each phase of BVAGCRTM. Thus, once the transaction ($T_{\lambda_{eq1}}$) failed as in T_{13} , the information can be retrieved from the checkpoint file ($C_{\lambda_{eq1}}$) and the transaction can be resume from the Update phase (U) as the failure occurred in that particular phase.

The execution times for each phase involved in BVAG and BVAGCR methods are recorded before and after failure occurred as shown in Table II and Table III. As presented in Table II, the overall time taken to complete a transaction using BVAG is 15.8574 seconds which include the estimation time duration of failure (10 seconds). The transaction had run four phases which are IL, PL, CQ, OQ that took 0.4931 seconds to be executed before failure occurred. After failure recovery, the transaction needs to be run again from the start due to no checkpoint file, ($C_{\lambda_{eq1}}$) found. The time taken to rerun the transaction is 5.3643 seconds. For the critical phase U, the time needed to finished it is 4.7809 seconds.

As displayed in Table III, BVAGCR need 10.8381 seconds of time to finish a transaction before failure occurred and after failure recovery which also takes account of the estimate time

duration of failure (10 seconds). The transaction had performed four phases same as BVAG which are IL, PL, CQ, and OQ that acquired 0.7443 seconds before failure happened. Once the failure had been recovered, the transaction only needs to rerun at U phase onwards because it had retrieved the information about the transaction which is save in a checkpoint file ($C_{\lambda_{eq1}}$). Based on the ($C_{\lambda_{eq1}}$) file, the last saved information of the current transaction is in phase U. The time used to rerun the transaction from U phase until the data has been replicated to all neighbors' sites is 0.0938 seconds. For the critical phase (U), the time needed to finish it is 0.0516 seconds.

Fig. 7 shows the comparisons of time taken for total time, update phase, execution time before failure and execution time after failure between BVAG and BVAGCR. Based on Fig. 7, the proposed method, BVAGCR used more time (0.7443 seconds) than BVAG (0.4931 seconds) in execution time before failure because it took extra time to save the information about the current transaction into a checkpoint file. However, after failure recovery, BVAGCR spend less time to complete the transaction than BVAG as it does not have to rerun the transaction from the beginning.

REPLICA	E	B	D	F	H
TIME					
T ₁	unlock S_{E_e}	unlock S_{B_e}	unlock S_{D_e}	unlock S_{F_e}	unlock S_{H_e}
T ₂	begin transaction $T_{\lambda_{eq1}}$				
T ₃	initiate lock: S_{E_e}				
T ₄	write lock $S_{E_e} = 1$				
T ₅	get lock S_{E_e}				
T ₆	propagate lock: $S_{B_e}, S_{D_e}, S_{F_e}, S_{H_e}$				
T ₇		write lock $S_{B_e} = 1$	write lock $S_{D_e} = 1$	write lock $S_{F_e} = 1$	write lock $S_{H_e} = 1$
T ₈	get lock : $S_{B_e}, S_{D_e}, S_{F_e}, S_{H_e}$				
T ₉	Obtain majority quorum (Q)				
T ₁₀	update (e) in D_{E_e} and failure occurred				
T ₁₁	unlock S_{E_e}	unlock S_{B_e}	unlock S_{D_e}	unlock S_{F_e}	unlock S_{H_e}
T ₁₂	begin transaction $T_{\lambda_{eq1}}$				
T ₁₃	initiate lock: S_{E_e}				
T ₁₄	write lock $S_{E_e} = 1$				
T ₁₅	get lock S_{E_e}				
T ₁₆	Σ quorum (S_{q_e}) = 1 propagate lock: $S_{B_e}, S_{D_e}, S_{F_e}, S_{H_e}$				
T ₁₇		write lock $S_{B_e} = 1$	write lock $S_{D_e} = 1$	write lock $S_{F_e} = 1$	write lock $S_{H_e} = 1$
T ₁₈	get lock : $S_{B_e}, S_{D_e}, S_{F_e}, S_{H_e}$				
T ₁₉					
T ₂₀	Obtain majority quorum (Q)				
T ₂₁	update (e) D_{E_e}				
T ₂₂	Commit update in D_{E_e}				
T ₂₃		Commit replication in D_{B_e}	Commit replication in D_{D_e}	Commit replication in D_{F_e}	Commit replication in D_{H_e}
T ₂₄	write lock $S_{E_e} = 0$	write lock $S_{B_e} = 0$	write lock $S_{D_e} = 0$	write lock $S_{F_e} = 0$	write lock $S_{H_e} = 0$

Fig. 5. BVAG Transaction's Flow (Failure Occurred While Updating Data).

REPLICA	E	B	D	F	H
TIME					
T ₁	unlock S_{E_e}	unlock S_{B_e}	unlock S_{D_e}	unlock S_{F_e}	unlock S_{H_e}
T ₂	begin transaction				
T ₃	initiate lock: S_{E_e}				
T ₄	write lock $S_{E_e} = 1$				
T ₅	Save S_{E_e} in $C_{\lambda_{eq1}}$ file				
T ₆	get lock S_{E_e}				
T ₇	propagate lock: $S_{B_e}, S_{D_e}, S_{F_e}, S_{H_e}$				
T ₈		write lock $S_{B_e} = 1$	write lock $S_{D_e} = 1$	write lock $S_{F_e} = 1$	write lock $S_{H_e} = 1$
T ₉	save $S_{B_e}, S_{D_e}, S_{F_e}, S_{H_e}$ in $C_{\lambda_{eq1}}$ file				
T ₁₀	get lock $S_{B_e}, S_{D_e}, S_{F_e}, S_{H_e}$				
T ₁₁	obtain majority quorum (Q)				
T ₁₂	Save S_{q_e} in $C_{\lambda_{eq1}}$ file				
T ₁₃	update (e) in D_{E_e} and failure occurred				
T ₁₄	begin transaction $C_{\lambda_{eq1}}$				
T ₁₅	Retrieve information from $CP_{\lambda_{xq1}}$ file				
T ₁₆	write lock $S_{E_e} = 1$	write lock $S_{B_e} = 1$	write lock $S_{D_e} = 1$	write lock $S_{F_e} = 1$	write lock $S_{H_e} = 1$
T ₁₇	update (e) in D_{E_e}				
T ₁₈	Commit update in D_{E_e}				
T ₁₉	Save D_{E_e} in $CP_{\lambda_{xq1}}$ file				
T ₂₀		Commit replication in D_{B_e}	Commit replication in D_{D_e}	Commit replication in D_{F_e}	Commit replication in D_{H_e}
T ₂₁	Save $D_{B_e}, D_{D_e}, D_{F_e}, D_{H_e}$ in $CP_{\lambda_{xq1}}$ file				
T ₂₂	write lock $S_{E_e} = 0$	write lock $S_{B_e} = 0$	write lock $S_{D_e} = 0$	write lock $S_{F_e} = 0$	write lock $S_{H_e} = 0$

Fig. 6. BVAGCR Transaction's Flow (Failure Occurred While Updating Data).

TABLE II. EXECUTION TIME TAKEN FOR BVAG DATA REPLICATION TRANSACTION (A) BEFORE FAILURE OCCUR, (B) AFTER FAILURE OCCUR

PHASES	TIME(SECONDS)
INITIATE LOCK ^A	0.2320
PROPAGATE LOCK ^A	0.2408
OBTAIN QUORUM ^A	0.0203
UPDATE AND FAILURE OCCUR	10.0000
INITIATE LOCK ^B	0.2331
PROPAGATE LOCK ^B	0.2354
OBTAIN QUORUM ^B	0.0300
UPDATE ^B	4.7809
COMMIT ^B	0.0602
UNLOCK ^B	0.0247
TOTAL	15.8574

TABLE III. EXECUTION TIMES TAKEN FOR BVAGCR DATA REPLICATION TRANSACTION (A) BEFORE FAILURE OCCUR. (B) AFTER FAILURE OCCUR

PHASES	TIME(SECONDS)
INITIATE LOCK ^A	0.2390
PROPAGATE LOCK ^A	0.4795
OBTAIN QUORUM ^A	0.0258
UPDATE AND FAILURE OCCUR	10.0000
UPDATE ^B	0.0516
COMMIT ^B	0.0149
UNLOCK ^B	0.0273
TOTAL	10.8381

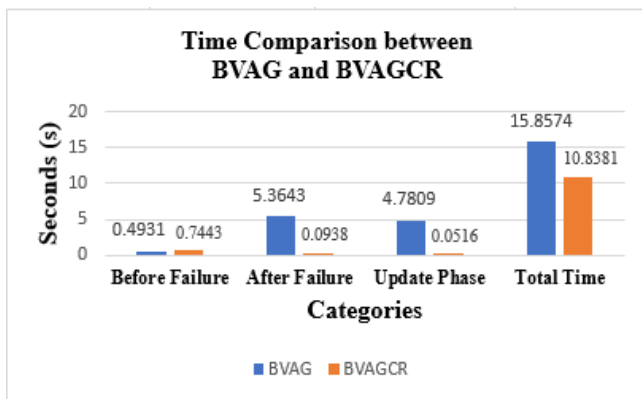


Fig. 7. Time Comparison between Standard BVAG and BVAGCR.

Meanwhile, the total time taken for a single transaction of BVAGCR (10.8381 seconds) is shorter than BVAG (15.8574 seconds). BVAGCR has improved the standard BVAG method by 31.65 % in terms of total execution time. Besides that, the efficiency of BVAGCR can also be seen when it successfully improved the performance of standard BVAG in critical phase which is the Update (U) phase by 98.82%. Thus, based on the results obtained, it can be said that the objective of this study which is to improve the efficiency of standard BVAG by proposing a new data replication technique with fault tolerance approach (BVAGCR) has been successfully achieved.

V. CONCLUSION

This study has explored a new combination of data replication and fault tolerance approach called as BVAGCR. The performance of BVAGCR is tested using a simulation of MATLAB. A comparison between standard BVAG and BVAGCR has been done in order to evaluate the effectiveness of implying the CR fault tolerance approach in BVAG data replication technique. The result gained from this study shows that the proposed BVAGCR has outperformed standard BVAG in terms of total execution time, time taken to execute the U phase and time taken to rerun the transaction after failure recovery.

Therefore, BVAGCR can be proposed as an alternative technique which is efficient and reliable to replicate data in failure condition. To test the robustness of the proposed BVAGCR, future work should explore the application of this proposed method on big data. Besides that, BVAGCR can also be implemented with data mining method in order to get more competent performance of the data replication technique.

ACKNOWLEDGMENT

This study is supported by the Fundamental Research Grant Scheme (RDU190185) with Reference no: FRGS/1/2018/ICT03/UMP/02/3 that sponsored by Ministry of Higher Education Malaysia (MOHE). In addition, this study is also supported by Grant Code: (20UQU0074DSR) under the Deanship of Scientific Research at Umm Al-Qura University. Appreciation is also conveyed to University Malaysia Pahang for project financing under UMP Short Term Grant RDU1903122 and UMP PGRS RDU170329.

REFERENCES

- [1] N. Dogra and S. A. Singh, "A survey of dynamic replication strategies in distributed systems," *International Journal of Computer Applications*, vol. 110, no. 11, Jan 2015.
- [2] S. H. S. A. Ubaidillah and N. Ahmad, "Fragmentation Techniques for Ideal Performance in Distributed Database—A Survey," *International Journal of Software Engineering and Computer Systems*, vol. 6, no. 1, pp. 18-24, May 2020.
- [3] Kumar, Nirmal, and Girish V. Mattur. "Data replication in a database environment." U.S. Patent Application No. 15/813,828.
- [4] B. Kemme, "Data Replication," In: Liu L., Özsu M. (eds) *Encyclopedia of Database Systems*. Springer, New York, NY, 2017.
- [5] A. Sari and E. Çağlar, "Performance Simulation of Gossip Relay Protocol in Multi-Hop Wireless Networks," Owner: Girne American University Editor: Asst. Prof. Dr. İbrahim Erşan Advisory Board: Prof. Dr. Sadık Ülker Assoc. Prof. Dr. Zafer Ağdelen Cover Graphic Design: Asst. Prof. Dr. İbrahim Erşan., pp. 145, 2015.
- [6] A. Sari and M. Akkaya, "Fault tolerance mechanisms in distributed systems," *International Journal of Communications, Network and System Sciences*, vol. 8, no. 12, pp. 471, Dec 2015.
- [7] A. Benoit, A. Cavelan, F. M. Ciorba, V. Le Fevre and Y. Robert, "Combining checkpointing and replication for reliable execution of linear workflows," in *IEEE International Parallel and Distributed Processing Symposium Workshops (IPDPSW)*, 2018, pp. 793-802.
- [8] S. Desai, N. Pendharkar and Veritas Technologies LLC, "Data replication techniques using incremental checkpoints," *United States patent US 9,495,264*. 15 Nov 2016.
- [9] Y. Mo, L. Xing, Y. K. Lin and W. Guo, "Efficient Analysis of Repairable Computing Systems Subject to Scheduled Checkpointing," *IEEE Transactions on Dependable and Secure Computing*, Sep 2018.
- [10] R. Garg and A. K. Singh, "Fault tolerance in grid computing: state of the art and open issues," *International Journal of Computer Science & Engineering Survey (IJCSES)*, vol. 2, no. 1, pp. 88-97, Feb 2011.
- [11] A. Noraziah, A. A. Fauzi, S. H. Ubaidillah, Z. Abdullah, R. M. Sidek, M. A. Fakhreldin, "Managing Database Replication Using Binary Vote Assignment on Grid Quorum with Association Rule," *Advanced Science Letters*, vol. 24, no. 10, pp. 7834-7837, Oct 2018.
- [12] J. P. Yang, "Elastic load balancing using self-adaptive replication management," *IEEE Access*, vol. 22, no. 5, pp. 7495-7504, Nov 2016.
- [13] Muhammad Ahsan Raza, M. Rahmah, A. Noraziah, Mahmood Ashraf, "Sensual Semantic Analysis for Effective Query Expansion", *International Journal of Advanced Computer Science and Applications*, vol. 9, no. 12, pp. 55-60, 2018.
- [14] A. A. Fauzi, A. Noraziah, T. Herawan, Z. Abdullah, R. Gupta, "Managing Fragmented Database Using BVAGQ-AR Replication Model," *Advanced Science Letters*, vol. 23, no. 11, pp. 11088-11091, Nov 2017.
- [15] S. Veerapandi, S. Gavaskar and A. Sumithra, "A Hybrid Fault Tolerance System for Distributed Environment using Check Point Mechanism and Replication," *International Journal of Computer Applications*, vol. 975, pp. 8887, 2017.
- [16] J. Wu. "Checkpointing and recovery in distributed and database systems," 2011.
- [17] D. Poola, M. A. Salehi, K. Ramamohanarao and R. Buyya, "A taxonomy and survey of fault-tolerant workflow management systems in cloud and distributed computing environments," in *Software Architecture for Big Data and the Cloud*, pp. 285-320, Jan 2017.
- [18] T. Sterling, M. Anderson and M. Brodowicz, "High performance computing: modern systems and practices," *Morgan Kaufmann*, Dec 2017.

Evaluation of Water Quality in the Lower Huallaga River Watershed using the Grey Clustering Analysis Method

Alexi Delgado¹, Diego Cuadra², Karen Simon³, Katya Bonilla⁴, Katherine Tineo⁵, Enrique Lee Huamani⁶
Mining Engineering Section, Pontificia Universidad Católica del Perú, Lima-Perú¹
Facultad de Ingeniería Ambiental, Universidad Nacional de Ingeniería, Lima, Perú^{2,3,4,5}
Image Processing Research Laboratory, Universidad de Ciencias y Humanidades, Lima-Perú⁶

Abstract—Currently, the evaluation of water quality is a topic of global interest, due to its socio-cultural, environmental and economic importance, but in recent years this quality is deteriorating due to inadequate management in the conservation, disposal and use of water by the competent authorities, private-state entities and the population itself. An alternative to determine the quality of a water body in an integrated manner is the Grey Clustering Method, which was used in this study taking as an indicator the Prati Quality Index, with the objective of making an objective analysis of the quality of the water bodies under study. The case study is the Lower Watershed of the Huallaga River, located between the region of Loreto and San Martín, along which 12 monitoring stations were established to evaluate its surface water quality, through the analysis of 7 parameters: pH, BOD, COD, Total Suspended Solids (TSS), Ammonia Nitrogen, Substrates and Nitrates. Finally, it was determined that the water quality of eleven monitoring stations in the Lower Huallaga River Watershed are within the "Uncontaminated" category, while one monitoring station is within the "Highly Contaminated" category of the Prati Index, this due to its proximity to a landfill. The results obtained in this study, could be useful for the authorities responsible for the protection and sustainable conservation of the Huallaga River Watershed, in order to propose appropriate measures to improve its quality, additionally, this study could be a reference for future studies since the proposed method allowed to prioritize the quality level of the water bodies and identify critical areas.

Keywords—Water quality; prati index; grey clustering method; protection and sustainable conservation

I. INTRODUCTION

The various activities that have been carried out in the lower watershed of the Huallaga River have motivated the evaluation of water quality [1], since this watershed is used to supply the indigenous communities and surrounding urban areas [2].

The present study is carried out in the lower Huallaga River Watershed, located in the districts of Loreto and San Martín in which twelve monitoring points have been taken from the "Participatory Monitoring Report on Surface Water Quality in the Huallaga River Watershed" [2], which were taken into account due to the proximity of some activity carried out within the area of the lower Huallaga River Watershed. For the calculation of the water quality index, the

Prati index [3] was chosen and for the discussion of results it was compared with the national standard ECA agua [4].

The water quality evaluation was done using the Grey Clustering methodology based on the gray system theory [5], which due to the scarcity of data uses an artificial intelligence approach [6]. This methodology, because it solves problems with scarce data, allows its application to other fields of research [7].

The objective of this study is to evaluate the water quality in the lower Huallaga river watershed using the Grey Clustering methodology [5], which allows us to fully assess the 7 parameters of the Prati index [3] considering 12 monitoring points that cover the area of the lower Huallaga river watershed [2].

This study has the following structure, it begins in Section I with the introduction, in Section II is detailed the literature review, after that is visualized in Section III, the Grey Clustering methodology, continues with Section IV that describes the case study. Section V presents the results and discussions. Finally, Section VI explains the conclusions.

II. LITERATURE REVIEW

In the research work entitled "Evaluation of water quality in a watershed in Cusco, Peru using the Grey Clustering method", they analyzed water quality in an area of mining influence zone located in the Chonta and Milos micro watershed using the Grey Clustering method, for which they established six monitoring stations. The parameters evaluated were pH, OD, STS, iron and manganese. It was concluded that only one monitoring station was contaminated despite being a discharge of treated industrial water from a cyanide destruction plant [8].

In the article entitled "Application of fuzzy logic to determine the quality of water bodies in the Rimac River Watershed", they analyzed the quality of five water bodies in the Rimac River Watershed which belong to Category 1 A2-Population and Recreation using the Grey Clustering method. To select their monitoring points they took data from a Technical Report on Water Quality Monitoring in the Rimac River Watershed prepared by the ANA in 2013. After evaluating the parameters of pH, %O₂, BOD, COD, STS, NH₃

and NO₃, they concluded that the Rimac River Watershed has an unpolluted water quality [9].

In the research paper entitled "Application of Grey Clustering Method Based on Improved Analytic Hierarchy Process in Water Quality Evaluation", they proposed a Grey Clustering method based on an improved analytical hierarchy process to evaluate the water quality of the Qingshui River in Duyun City, by sampling three water periods (periods of abundant, normal and deficient flow) in 4 sections of the river. It was concluded that the water quality of the river belongs to the superclass III according to its regulations, and according to this the contamination is not serious [10].

In the article entitled "Research on Comprehensive Evaluation of Air Quality in Beijing Based on Entropy Weight and Grey Clustering Method", they proposed a Grey Clustering method with entropy weight to evaluate air quality in Beijing, in order to obtain more objective results. The parameters evaluated were PM_{2.5}, PM₁₀, NO₂ and SO₂ for three consecutive quarters. It was concluded that Beijing air quality in the first quarter is better than the second and third quarters and that the entropy weight enriched and improved the Grey Clustering method [7].

In the research work entitled "Environmental conflict analysis using an integrated grey clustering and entropy-weight method: A case study of a mining project in Peru", they proposed an approach for ECA using the Grey Clustering and entropy weighting method to evaluate the social impact of a mining project in northern Peru. Information was collected through interviews with three groups: rural population, urban population and specialists. Three levels of social impact were established in the surveys: positive, negative and normal. It was concluded that for the urban population, rural population and specialists groups, the project would have a positive, negative and normal impact, respectively. In addition, it was concluded that the proposed method showed practical results and potential for application to other types of projects [11].

III. METHODOLOGY

A. Choice of Index

The Patri Water Quality Index was chosen because it considers criteria to evaluate physicochemical parameters, which are relevant to determine contamination in water bodies. Seven of the 13 parameters included in the Prati Index will be evaluated. This index also has ranges for each variable. Table IV shows the range of the Prati index of the seven parameters evaluated and Table II shows the levels of contamination according to the Prati scale [3].

B. Grey Clustering Analysis Methodology

This new methodology focuses on the problems that exist with small and scarce data, thus avoiding uncertain information. The method is based on developing functions of Whitenization of Grey Cluster [5].

It is developed in several areas of research; in this case, the methodology will be used to determine the quality of the water.

Application of Grey Clustering through triangular functions (CTWF) [5].

Step 1: Establish the midpoints of the standard criteria data intervals, obtaining values for: $\lambda_1, \lambda_2, \dots$ and λ_5 .

Step 2: Determine the sized values of the sampling data and the standard criteria data.

Step 3: Determine the triangular functions of Whitenization for each criterion.

The number of triangular functions is related to the water quality index levels for this case. Five functions are proposed since they are five classes on the Prati scale ($\lambda_1, \lambda_2, \dots$ and λ_5), which are obtained from Eq. 1, 2 and 3, and in addition Fig. 1 shows the graph of the triangular functions.

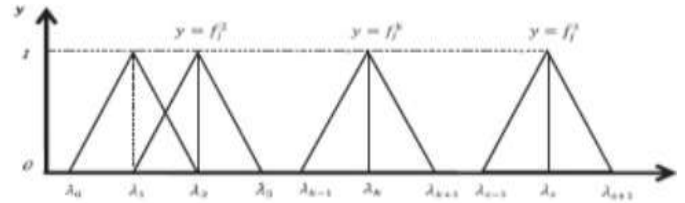


Fig. 1. Graph of the Triangular Functions.

$$f_j^1(x_{ij}) = \begin{cases} 1, x \in [0, \lambda_j^1] \\ \frac{\lambda_j^2 - x}{\lambda_j^2 - \lambda_j^1}, x \in [\lambda_j^1; \lambda_j^2] \\ 0, x \in [\lambda_j^2, \infty) \end{cases} \quad (1)$$

$$f_j^k(x_{ij}) = \begin{cases} \frac{x - \lambda_j^{k-1}}{\lambda_j^k - \lambda_j^{k-1}}, x \in [\lambda_j^{k-1}; \lambda_j^k] \\ \frac{\lambda_j^{k+1} - x}{\lambda_j^{k+1} - \lambda_j^k}, x \in [\lambda_j^k; \lambda_j^{k+1}] \\ 0, x \in [0, \lambda_j^{k-1}] \cup [\lambda_j^k, +\infty) \end{cases} \quad (2)$$

$$f_j^5(x_{ij}) = \begin{cases} \frac{x - \lambda_j^4}{\lambda_j^5 - \lambda_j^4}, x \in [\lambda_j^4; \lambda_j^5] \\ 1, x \in [\lambda_j^5, +\infty) \\ 0, x \in [0, \lambda_j^4] \end{cases} \quad (3)$$

Step 4: Determine the weight of the criteria by using the harmonic mean, which will be calculated with Eq. 4.

$$n_j^k = \frac{\frac{1}{\lambda_j^k}}{\sum_{j=1}^m \frac{1}{\lambda_j^k}} \quad (4)$$

Step 5: Find the clustering coefficients using Eq. 5.

$$\sigma_i^k = \sum_{j=1}^n f_j^k(x_{ij}) n_j \quad (5)$$

Step 6: Find the maximum clustering coefficient to define which class each station belongs to, applying Eq. 6.

$$\max_{1 \leq k \leq s} \{\sigma_i^k\} = \sigma_i^{k^*} \quad (6)$$

IV. CASE STUDY

This study will focus on the evaluation of the surface water quality of the Huallaga lower watershed, located between Loreto region and San Martín as shown in Fig. 2.

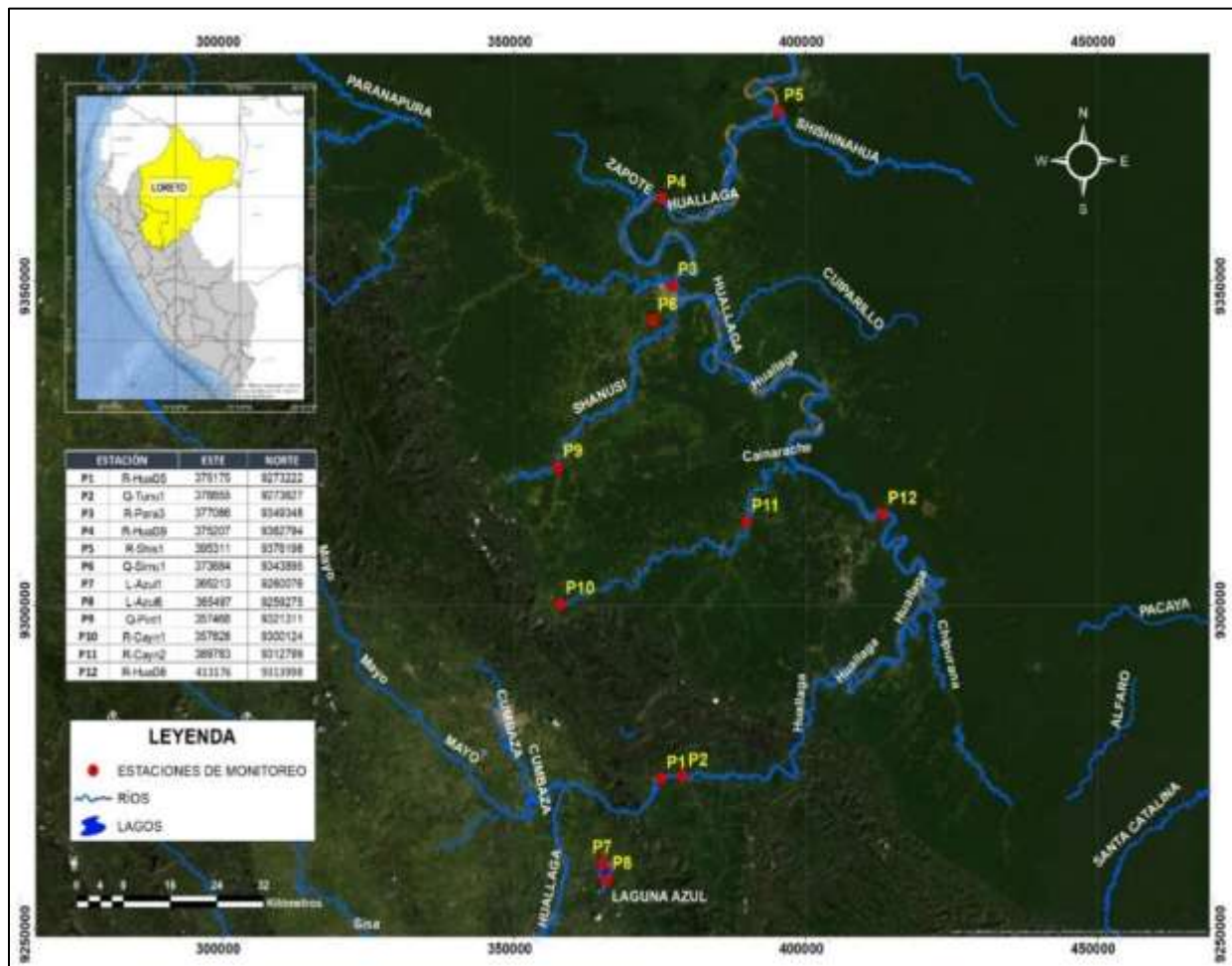


Fig. 2. Monitoring Stations Location Map in the Huallaga Lower Watershed.

In recent years, its water quality has significantly deteriorated, generating conflicts between the population and the responsible authorities. Given this situation, since 2013 the ANA has been identifying the main polluting sources, for subsequent monitoring of water quality with the active participation of the population [3].

The main sources of contamination are associated with the domestic sewage discharge, industrial and untreated municipal wastewater, and also with the bad disposal of solid waste, product of the development of agricultural, energy, industrial activities and Wastewater Treatment Plant (WWTP) [14].

A. Definition of Study Objects

The monitoring points were obtained from the "Participatory Monitoring Report of the quality of surface water in the Huallaga river watershed" carried out in the period February - March 2019 by the National Water Authority [2]. In Fig. 2 shows the location of the monitoring stations.

From the participatory monitoring report that was carried out in the Huallaga river watershed [2], for this case study, 12 monitoring points were chosen, located in the lower Huallaga river watershed, which are shown in Table I.

B. Definition of Evaluation Criteria or Parameters

This study will evaluate 7 water quality parameters of the lower Huallaga river watershed, in the different monitoring stations, previously identified by National Water Authority (ANA by its Spanish acronym). Table II describes these parameters.

The field data were obtained from the "Participatory Monitoring Report of the quality of surface water in the Huallaga river watershed" [2] according to the monitoring stations mentioned in Table I.

Table III details the data of the seven parameters in each monitoring station.

C. Definition of Grey Classes

The water quality of the lower Huallaga river watershed will be evaluated, under the contrast with the regulations of the Environmental Quality Standards for Water (ECA by its Spanish acronym) established in DS 004-2017-MINAM [4] in category 3 and category 4, which corresponds to irrigation of vegetables and drinks of animals and conservation of the aquatic environment, respectively.

TABLE I. LOCATION IN UTM COORDINATES OF MONITORING STATIONS

Stations	Description	Coordinates UTM WGS 84	
		East (m)	North (m)
R-Hual35	Huallaga River - Approximately 200m upstream from embarkation port Chazuta	375175	9273222
Q-Tunu1	Quebrada Tununtunumba - Approximately 400m upstream from embarkation port Banda de Chazuta	378855	9273627
R-Para3	Paranapura River - Approximately 400m before tribute to the Huallaga river	377086	9349348
R-Hual39	Huallaga River - Approximately 700m after tribute to the Paranapura River	375207	9362794
R-Shis1	Shishinahua River - Approximately 180m before tribute to the Huallaga River	395311	9376198
Q-Simu1	Quebrada Simui-Approximately 500m downstream from the Fundo 3 Hermanitos dump	373684	9343895
L-Azul1	Laguna Azul- Approximately 20m from Sauce district wastewater pumping chamber	365213	9260076
L-Azul6	Approximately in the center of the Blue Lagoon	365497	9259275
Q-Pint1	Quebrada Pintuyacu - Approximately 250m before tribute to the Shanusi river	357468	9321311
R-Cayn1	Caynarachi River - Approximately 50m upstream of the carriage bridge (Caynarachi district)	357828	9300124
R-Cayn2	Caynarachi River - Approximately 20m from Santiago de Borja Bridge	389783	9312799
R-Hual36	Río Huallaga - Approximately 200m downstream from embarkation port of the town Papaplaya	413176	9313998

TABLE II. WATER QUALITY CRITERIA

Parameters	Unit
pH	-
DBO	mg / L
DQO	mg / L
Ammonia Nitrogen	mg / L
Total Suspended Solids	mg / L
Chlorides	mg / L
Nitrates	mg / L

TABLE III. FIELD DATA

Stations Criteria	pH	DBO (mg/L)	DQO (mg/L)	NH3 (mg/L)	STS (mg/L)	NO3 (mg/L)	Cl (mg/L)
P1	8.37	1.05	6	6.126	412	16.2	0.631
P2	7.73	1.05	26	0.062	87	0.261	0.512
P3	6.79	1.07	21	0.082	566	13.46	0.493
P4	6.85	1.06	18	0.059	113	2.097	0.951
P5	8.06	3	23	0.003	367	3.263	0.597
P6	7.29	24	97	3.77	12	32.07	0.045
P7	8.4	4	20	0.003	7	112.6	0.076
P8	8.45	2	13	0.03	7	116	0.073
P9	6.93	1.06	1.1	0.115	46	0.43	0.204
P10	8.45	1.08	42	0.08	24	0.005	501
P11	7.7	1.06	11	0.097	79	0.386	824.4
P12	7.8	1.07	15	0.044	152	0.554	19.83

In this sense, the Prati Index will be used, which originally includes 13 parameters, but in this study only 7 parameters will be used.

In addition, this index establishes six levels of water contamination, but due to lack of information, only five levels will be used in this study, which are described in Table IV and the range of criteria in Table V.

D. Calculations using Grey Clustering

1) *Step 1: Determination of center points:* The central point of the semisum of the range of the Prati Index will be determined for the five classes (Not contaminated, Acceptable, Moderately contaminated, Contaminated and highly contaminated) of the parameters pH, BOD, COD, NH₃, SS, NO₃ and Cl (see Table VI).

2) *Step 2: Data dimensioning:* As the evaluated parameters are in different units, the data must be standardized or normalized to homogenize the work. The standard Prati data will be sized and then the sampling data.

TABLE IV. WATER CONTAMINATION LEVELS - PRATI INDEX

CLASS	Contamination level	Quality color
λ_1	Not contaminated	
λ_2	Acceptable	
λ_3	Moderately contaminated	
λ_4	Contaminated	
λ_5	Highly contaminated	

TABLE V. RANGE OF THE PRATI INDEX CRITERIA

Criteria	PRATI INDEX RANGES				
	Class				
	λ_1	λ_2	λ_3	λ_4	λ_5
pH	6.5-8.0	8-8.4	8.4-9.0	9-10.1	>10.1
DBO (mg/L)	0.0-1.5	1.5-3.0	3.0-6.0	6.0-12.0	>12
DQO (mg/L)	0-10	10-20	20-40	40-80	>80
NH ₃ (mg/L)	0-0.1	0.1-0.3	0.3-0.9	0.9-2.7	>2.7
STS (mg/L)	0-20	20-40	40-100	100-278	>278
NO ₃ (mg/L)	0-4	4-12	12-36	36-108	>108
Cl (mg/L)	0-50	50-150	150-300	300-620	>620

TABLE VI. CENTRAL POINTS OF THE PRATI INDEX RANGES

Parámetro Clase	PRATI INDEX STANDARD DATA				
	λ_1	λ_2	λ_3	λ_4	λ_5
pH	7.25	8.2	8.7	9.55	10.4
DBO (mg/L)	0.75	2.25	4.5	9	13.5
DQO (mg/L)	5	15	30	60	90
NH ₃ (mg/L)	0.05	0.2	0.6	1.8	3
STS (mg/L)	10	30	70	189	308
NO ₃ (mg/L)	2	8	24	72	120
Cl (mg/L)	25	100	225	460	695

a) *For Prati Standard Data:* The mean of the standard data is obtained for each parameter, which is detailed in Table VII.

Each value is divided by its respective mean, obtaining Table VIII.

b) *For Sample Data:* In the same way, the sample data is dimensioned. In this case, the data of the parameters are divided by the mean of the data correctly, which were calculated in the dimensioning of the Prati data, obtaining Table IX and Table X.

TABLE VII. MEAN OF THE STANDARDS DATA OF THE PRATI INDEX

Criteria Class	PRATI INDEX STANDARD DATA					MEDIA
	λ_1	λ_2	λ_3	λ_4	λ_5	
pH	7.25	8.2	8.7	9.55	10.4	8.82
DBO (mg/L)	0.75	2.25	4.5	9	13.5	6
DQO (mg/L)	5	15	30	60	90	40
NH ₃ (mg/L)	0.05	0.2	0.6	1.8	3	1.1
STS (mg/L)	10	30	70	189	308	121.4
NO ₃ (mg/L)	2	8	24	72	120	45.2
Cl (mg/L)	25	100	225	460	695	301

TABLE VIII. DATA DIMENSIONING

Criteria Class	DATOS ADIMENSIONADOS				
	λ_1	λ_2	λ_3	λ_4	λ_5
pH	0.8220	0.9297	0.9864	1.0828	1.1791
DBO (mg/L)	0.1250	0.3750	0.7500	1.5000	2.2500
DQO (mg/L)	0.1250	0.3750	0.7500	1.5000	2.2500
NH ₃ (mg/L)	0.0442	0.1770	0.5310	1.5929	2.6549
STS (mg/L)	0.0824	0.2471	0.5766	1.5568	2.5371
NO ₃ (mg/L)	0.0442	0.1770	0.5310	1.5929	2.6549
Cl (mg/L)	0.0831	0.3322	0.7475	1.5282	2.3090

TABLE IX. MEAN OF THE ACTUAL DATA

Station Criteria	pH	DBO (mg/L)	DQO (mg/L)	NH ₃ (mg/L)	STS (mg/L)	NO ₃ (mg/L)	Cl (mg/L)
P1	8.37	1.05	6	6.126	412	16.2	0.631
P2	7.73	1.05	26	0.062	87	0.261	0.512
P3	6.79	1.07	21	0.082	566	13.46	0.493
P4	6.85	1.06	18	0.059	113	2.097	0.951
P5	8.06	3	23	0.003	367	3.263	0.597
P6	7.29	24	97	3.77	12	32.07	0.045
P7	8.4	4	20	0.003	7	112.6	0.076
P8	8.45	2	13	0.03	7	116	0.073
P9	6.93	1.06	1.1	0.115	46	0.43	0.204
P10	8.45	1.08	42	0.08	24	0.005	501
P11	7.7	1.06	11	0.097	79	0.386	824.4
P12	7.8	1.07	15	0.044	152	0.554	19.83
MEDIA	8.82	6.0	40	1.1	121.4	45.2	301

TABLE X. REAL DATA DIMENSIONING

Criteria	REAL DATA DIMENSIONING FROM EACH MONITORING POINT											
	Station											
	P1	P2	P3	P4	P5	P6	P7	P8	P9	P10	P11	P12
pH	0.9490	0.8764	0.7698	0.7766	0.9138	0.8265	0.9524	0.9580	0.7857	0.9580	0.8730	0.8844
DBO (mg/L)	0.1750	0.1750	0.1783	0.1767	0.5000	4.0000	0.6667	0.3333	0.1767	0.1800	0.1767	0.1783
DQO (mg/L)	0.1500	0.6500	0.5250	0.4500	0.5750	2.4250	0.5000	0.3250	0.0275	1.0500	0.2750	0.3750
NH3 (mg/L)	5.4212	0.0549	0.0726	0.0522	0.0027	3.3363	0.0027	0.0265	0.1018	0.0708	0.0858	0.0389
STS (mg/L)	3.3937	0.7166	4.6623	0.9308	3.0231	0.0988	0.0577	0.0577	0.3789	0.1977	0.6507	1.2521
NO3 (mg/L)	0.3584	0.0058	0.2978	0.0464	0.0722	0.7095	2.4912	2.5664	0.0095	0.0001	0.0085	0.0123
Cl (mg/L)	0.0021	0.0017	0.0016	0.0032	0.0020	0.0001	0.0003	0.0002	0.0007	1.6645	2.7389	0.0659

3) *STEP 3: Determination of triangular functions:* The Grey Clustering method is applied to analyze the different criteria and comprehensively evaluate the water body. They are triangular functions and are divided into five classes: λ_1 , λ_2 , λ_3 , λ_4 and λ_5 . The following describes for the criteria "pH" its triangular functions with their respective correspondence rules and their graph (see Fig. 3).

$$f_j^5(x) = \begin{cases} 0, x \in [0, 1.0828] \\ \frac{x - 1.0828}{1.1791 - 1.0828}, x \in [1.0828, 1.1791] \\ 1, x \in [1.1791, +\text{inf}] \end{cases}$$

$$f_j^1(x) = \begin{cases} 1, x \in [0, 0.8220] \\ \frac{0.9297 - x}{0.9297 - 0.8220}, x \in [0.8220, 0.9297] \\ 0, x \in [0.9297, +\text{inf}] \end{cases}$$

$$f_j^2(x) = \begin{cases} 0, x \notin [0.8220, 0.9864] \\ \frac{x - 0.8220}{0.9297 - 0.8220}, x \in [0.8220, 0.9297] \\ \frac{0.9864 - x}{0.9864 - 0.9297}, x \in [0.9297, 0.9864] \end{cases}$$

$$f_j^3(x) = \begin{cases} 0, x \notin [0.9297, 1.0828] \\ \frac{x - 0.9297}{0.9864 - 0.9297}, x \in [0.9297, 0.9864] \\ \frac{1.0828 - x}{1.0828 - 0.9864}, x \in [0.9864, 1.0828] \end{cases}$$

$$f_j^4(x) = \begin{cases} 0, x \in [0.9864, 1.1791] \\ \frac{x - 0.9864}{1.0828 - 0.9864}, x \in [0.9864, 1.0828] \\ \frac{1.1791 - x}{1.1791 - 1.0828}, x \in [1.0828, 1.1791] \end{cases}$$

In the same way, the functions and graphs are proposed for the remaining criteria. Next, Table XI shows the result of the data evaluated in each of the triangular functions of the criteria, for each sampling station.

4) *STEP 4: Determination of the weight of the criteria or parameters:* Objective weights are assigned through the use of "Harmonic Mean".

From the standard dimensioned data, this data is inverted and added for each class (lambda 1, 2, 3, 4 and 5) as a result, Table XII is generated and the weights of each parameter criterion are shown in the Table XIII.

5) *STEP 5: Determination of the clustering coefficient:* Now each value of the parameter is multiplied by its respective weight for each class (lambda 1,2,3,4 and 5) and the total of the function is added. For each point, 5 values will be obtained, one per function and the result is shown in Table XIV.

6) *STEP 6: Results using Max. Clustering coefficient:* The results of each station are evaluated, the highest of the values defines the class and the level of water contamination for the monitoring point from which the sample was obtained. The Classes are related to a Pollution Level, the relationship is the following Table XV.

The results of the maximum clustering coefficient are shown in Table XVI.

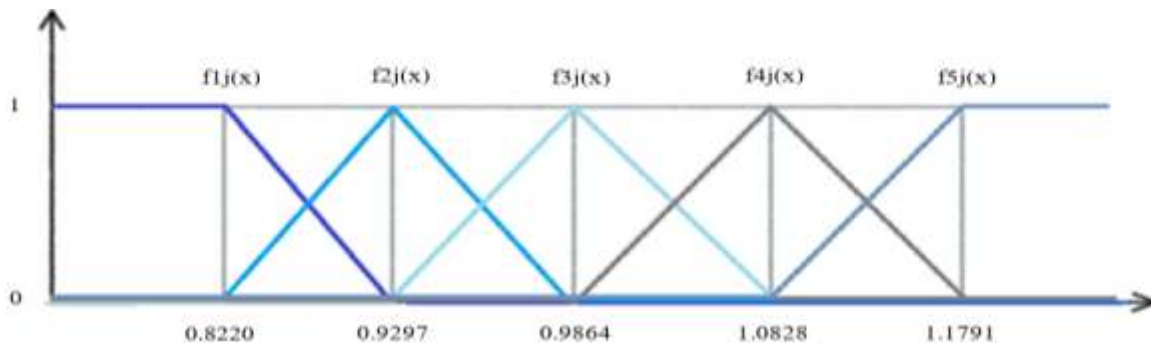


Fig. 3. Graph of the Triangular Functions for the Criterion "pH".

TABLE XI. RESULT OF THE DATA EVALUATED IN THE GREY CLUSTERING FUNCTIONS FOR EACH MONITORING STATION

P1							
CRITERION	pH	DBO (mg/L)	DQO (mg/L)	NH3 (mg/L)	SS (mg/L)	NO3 (mg/L)	Cl (mg/L)
f1j(x)	0,0000	0,8000	0,9000	0,0000	0,0000	0,0000	1,0000
f2j(x)	0,6596	0,2000	0,1000	0,0000	0,0000	0,4876	0,0000
f3j(x)	0,3404	0,0000	0,0000	0,0000	0,0000	0,5124	0,0000
f4j(x)	0,0000	0,0000	0,0000	0,0000	0,0000	0,0000	0,0000
f5j(x)	0,0000	0,0000	0,0000	1,0000	1,0000	0,0000	0,0000
P2							
CRITERION	pH	DBO (mg/L)	DQO (mg/L)	NH3 (mg/L)	SS (mg/L)	NO3 (mg/L)	Cl (mg/L)
f1j(x)	0,4949	0,8000	0,0000	0,9194	0,0000	1,0000	1,0000
f2j(x)	0,5051	0,2000	0,2666	0,0806	0,0000	0,0000	0,0000
f3j(x)	0,0000	0,0000	0,7334	0,0000	0,8572	0,0000	0,0000
f4j(x)	0,0000	0,0000	0,0000	0,0000	0,1428	0,0000	0,0000
f5j(x)	0,0000	0,0000	0,0000	0,0000	0,0000	0,0000	0,0000
P3							
CRITERION	pH	DBO (mg/L)	DQO (mg/L)	NH3 (mg/L)	SS (mg/L)	NO3 (mg/L)	Cl (mg/L)
f1j(x)	1,0000	0,7868	0,0000	0,7861	0,0000	0,0000	1,0000
f2j(x)	0,0000	0,2132	0,6000	0,2139	0,0000	0,6587	0,0000
f3j(x)	0,0000	0,0000	0,4000	0,0000	0,0000	0,3413	0,0000
f4j(x)	0,0000	0,0000	0,0000	0,0000	0,0000	0,0000	0,0000
f5j(x)	0,0000	0,0000	0,0000	0,0000	1,0000	0,0000	0,0000
P4							
CRITERION	pH	DBO (mg/L)	DQO (mg/L)	NH3 (mg/L)	SS (mg/L)	NO3 (mg/L)	Cl (mg/L)
f1j(x)	1,0000	0,7932	0,0000	0,9397	0,0000	0,9834	1,0000
f2j(x)	0,0000	0,2068	0,8000	0,0603	0,0000	0,0166	0,0000
f3j(x)	0,0000	0,0000	0,2000	0,0000	0,6386	0,0000	0,0000
f4j(x)	0,0000	0,0000	0,0000	0,0000	0,3614	0,0000	0,0000
f5j(x)	0,0000	0,0000	0,0000	0,0000	0,0000	0,0000	0,0000
P5							
CRITERION	pH	DBO (mg/L)	DQO (mg/L)	NH3 (mg/L)	SS (mg/L)	NO3 (mg/L)	Cl (mg/L)
f1j(x)	0,1476	0,0000	0,0000	1,0000	0,0000	0,7891	1,0000
f2j(x)	0,8524	0,6666	0,4666	0,0000	0,0000	0,2109	0,0000
f3j(x)	0,0000	0,3334	0,5334	0,0000	0,0000	0,0000	0,0000
f4j(x)	0,0000	0,0000	0,0000	0,0000	0,0000	0,0000	0,0000
f5j(x)	0,0000	0,0000	0,0000	0,0000	1,0000	0,0000	0,0000
P6							

CRITERION	pH	DBO (mg/L)	DQO (mg/L)	NH3 (mg/L)	SS (mg/L)	NO3 (mg/L)	Cl (mg/L)
f1j(x)	0,9582	0,0000	0,0000	0,0000	0,9004	0,0000	1,0000
f2j(x)	0,0418	0,0000	0,0000	0,0000	0,0996	0,0000	0,0000
f3j(x)	0,0000	0,0000	0,0000	0,0000	0,0000	0,8319	0,0000
f4j(x)	0,0000	0,0000	0,0000	0,0000	0,0000	0,1681	0,0000
f5j(x)	0,0000	1,0000	1,0000	1,0000	0,0000	0,0000	0,0000
P7							
CRITERION	pH	DBO (mg/L)	DQO (mg/L)	NH3 (mg/L)	SS (mg/L)	NO3 (mg/L)	Cl (mg/L)
f1j(x)	0,0000	0,0000	0,0000	1,0000	1,0000	0,0000	1,0000
f2j(x)	0,5996	0,2221	0,6666	0,0000	0,0000	0,0000	0,0000
f3j(x)	0,4004	0,7779	0,3334	0,0000	0,0000	0,0000	0,0000
f4j(x)	0,0000	0,0000	0,0000	0,0000	0,0000	0,1541	0,0000
f5j(x)	0,0000	0,0000	0,0000	0,0000	0,0000	0,8459	0,0000
P8							
CRITERION	pH	DBO (mg/L)	DQO (mg/L)	NH3 (mg/L)	SS (mg/L)	NO3 (mg/L)	Cl (mg/L)
f1j(x)	0,0000	0,1668	0,2000	1,0000	1,0000	0,0000	1,0000
f2j(x)	0,5000	0,8332	0,8000	0,0000	0,0000	0,0000	0,0000
f3j(x)	0,5000	0,0000	0,0000	0,0000	0,0000	0,0000	0,0000
f4j(x)	0,0000	0,0000	0,0000	0,0000	0,0000	0,0833	0,0000
f5j(x)	0,0000	0,0000	0,0000	0,0000	0,0000	0,9167	0,0000
P9							
CRITERION	pH	DBO (mg/L)	DQO (mg/L)	NH3 (mg/L)	SS (mg/L)	NO3 (mg/L)	Cl (mg/L)
f1j(x)	1,0000	0,7932	1,0000	0,5663	0,0000	1,0000	1,0000
f2j(x)	0,0000	0,2068	0,0000	0,4337	0,6000	0,0000	0,0000
f3j(x)	0,0000	0,0000	0,0000	0,0000	0,4000	0,0000	0,0000
f4j(x)	0,0000	0,0000	0,0000	0,0000	0,0000	0,0000	0,0000
f5j(x)	0,0000	0,0000	0,0000	0,0000	0,0000	0,0000	0,0000
P10							
CRITERION	pH	DBO (mg/L)	DQO (mg/L)	NH3 (mg/L)	SS (mg/L)	NO3 (mg/L)	Cl (mg/L)
f1j(x)	0,0000	0,7800	0,0000	0,7997	0,3000	1,0000	0,0000
f2j(x)	0,5000	0,2200	0,0000	0,2003	0,7000	0,0000	0,0000
f3j(x)	0,5000	0,0000	0,6000	0,0000	0,0000	0,0000	0,0000
f4j(x)	0,0000	0,0000	0,4000	0,0000	0,0000	0,0000	0,8254
f5j(x)	0,0000	0,0000	0,0000	0,0000	0,0000	0,0000	0,1746
P11							
CRITERION	pH	DBO (mg/L)	DQO (mg/L)	NH3 (mg/L)	SS (mg/L)	NO3 (mg/L)	Cl (mg/L)
f1j(x)	0,5265	0,7932	0,4000	0,6867	0,0000	1,0000	0,0000
f2j(x)	0,4735	0,2068	0,6000	0,3133	0,0000	0,0000	0,0000
f3j(x)	0,0000	0,0000	0,0000	0,0000	0,9244	0,0000	0,0000
f4j(x)	0,0000	0,0000	0,0000	0,0000	0,0756	0,0000	0,0000
f5j(x)	0,0000	0,0000	0,0000	0,0000	0,0000	0,0000	1,0000
P12							
CRITERION	pH	DBO (mg/L)	DQO (mg/L)	NH3 (mg/L)	SS (mg/L)	NO3 (mg/L)	Cl (mg/L)
f1j(x)	0,4206	0,7868	0,0000	1,0000	0,0000	1,0000	1,0000
f2j(x)	0,5794	0,2132	1,0000	0,0000	0,0000	0,0000	0,0000
f3j(x)	0,0000	0,0000	0,0000	0,0000	0,3108	0,0000	0,0000
f4j(x)	0,0000	0,0000	0,0000	0,0000	0,6892	0,0000	0,0000
f5j(x)	0,0000	0,0000	0,0000	0,0000	0,0000	0,0000	0,0000

TABLE XII. INVERSE OF THE DIMENSIONED STANDARD DATAS

Criteria	λ_1	λ_2	λ_3	λ_4	λ_5
	Class				
pH	1,2166	1,0756	1,0138	0,9236	0,8481
DBO (mg/L)	8,0000	2,6667	1,3333	0,6667	0,4444
DQO (mg/L)	8,0000	2,6667	1,3333	0,6667	0,4444
NH ₃ (mg/L)	22,6000	5,6500	1,8833	0,6278	0,3767
STS (mg/L)	12,1400	4,0467	1,7343	0,6423	0,3942
NO ₃ (mg/L)	22,6000	5,6500	1,8833	0,6278	0,3767
Cl (mg/L)	12,0400	3,0100	1,3378	0,6543	0,4331
SUMA	86,5966	24,7656	10,5192	4,8091	3,3175

TABLE XIII. WEIGHTS OF EACH CRITERION OR PARAMETER

Criteria	WEIGHTS OF EACH CRITERION BY WATER QUALITY LEVEL				
	λ_1	λ_2	λ_3	λ_4	λ_5
	Class				
pH	0,0140	0,0434	0,0964	0,1920	0,2556
DBO (mg/L)	0,0924	0,1077	0,1268	0,1386	0,1340
DQO (mg/L)	0,0924	0,1077	0,1268	0,1386	0,1340
NH ₃ (mg/L)	0,2610	0,2281	0,1790	0,1305	0,1135
STS (mg/L)	0,1402	0,1634	0,1649	0,1336	0,1188
NO ₃ (mg/L)	0,2610	0,2281	0,1790	0,1305	0,1135
Cl (mg/L)	0,1390	0,1215	0,1272	0,1361	0,1305

TABLE XIV. RESULTS OF THE FUNCTIONS FOR EACH STATION

P1								Result
CRITERION	pH	DBO (mg/L)	DQO (mg/L)	NH3 (mg/L)	STS (mg/L)	NO3 (mg/L)	Cl (mg/L)	
f1j(x)	0,0000	0,8000	0,9000	0,0000	0,0000	0,0000	1,0000	0,2961
f2j(x)	0,6596	0,2000	0,1000	0,0000	0,0000	0,4876	0,0000	0,1722
f3j(x)	0,3404	0,0000	0,0000	0,0000	0,0000	0,5124	0,0000	0,1245
f4j(x)	0,0000	0,0000	0,0000	0,0000	0,0000	0,0000	0,0000	0,0000
f5j(x)	0,0000	0,0000	0,0000	1,0000	1,0000	0,0000	0,0000	0,2323
P2								Result
CRITERION	pH	DBO (mg/L)	DQO (mg/L)	NH3 (mg/L)	STS (mg/L)	NO3 (mg/L)	Cl (mg/L)	
f1j(x)	0,4949	0,8000	0,0000	0,9194	0,0000	1,0000	1,0000	0,7208
f2j(x)	0,5051	0,2000	0,2666	0,0806	0,0000	0,0000	0,0000	0,0906
f3j(x)	0,0000	0,0000	0,7334	0,0000	0,8572	0,0000	0,0000	0,2343
f4j(x)	0,0000	0,0000	0,0000	0,0000	0,1428	0,0000	0,0000	0,0191
f5j(x)	0,0000	0,0000	0,0000	0,0000	0,0000	0,0000	0,0000	0,0000
P3								Result
CRITERION	pH	DBO (mg/L)	DQO (mg/L)	NH3 (mg/L)	STS (mg/L)	NO3 (mg/L)	Cl (mg/L)	
f1j(x)	1,0000	0,7868	0,0000	0,7861	0,0000	0,0000	1,0000	0,4309
f2j(x)	0,0000	0,2132	0,6000	0,2139	0,0000	0,6587	0,0000	0,2866
f3j(x)	0,0000	0,0000	0,4000	0,0000	0,0000	0,3413	0,0000	0,1118
f4j(x)	0,0000	0,0000	0,0000	0,0000	0,0000	0,0000	0,0000	0,0000
f5j(x)	0,0000	0,0000	0,0000	0,0000	1,0000	0,0000	0,0000	0,1188
P4								Result
CRITERION	pH	DBO (mg/L)	DQO (mg/L)	NH3 (mg/L)	STS (mg/L)	NO3 (mg/L)	Cl (mg/L)	
f1j(x)	1,0000	0,7932	0,0000	0,9397	0,0000	0,9834	1,0000	0,7283
f2j(x)	0,0000	0,2068	0,8000	0,0603	0,0000	0,0166	0,0000	0,1260

f3j(x)	0,0000	0,0000	0,2000	0,0000	0,6386	0,0000	0,0000	0,1306
f4j(x)	0,0000	0,0000	0,0000	0,0000	0,3614	0,0000	0,0000	0,0483
f5j(x)	0,0000	0,0000	0,0000	0,0000	0,0000	0,0000	0,0000	0,0000
P5								Result
CRITERION	pH	DBO (mg/L)	DQO (mg/L)	NH3 (mg/L)	STS (mg/L)	NO3 (mg/L)	Cl (mg/L)	
f1j(x)	0,1476	0,0000	0,0000	1,0000	0,0000	0,7891	1,0000	0,6080
f2j(x)	0,8524	0,6666	0,4666	0,0000	0,0000	0,2109	0,0000	0,2072
f3j(x)	0,0000	0,3334	0,5334	0,0000	0,0000	0,0000	0,0000	0,1099
f4j(x)	0,0000	0,0000	0,0000	0,0000	0,0000	0,0000	0,0000	0,0000
f5j(x)	0,0000	0,0000	0,0000	0,0000	1,0000	0,0000	0,0000	0,1188
P6								Result
CRITERION	pH	DBO (mg/L)	DQO (mg/L)	NH3 (mg/L)	SS (mg/L)	NO3 (mg/L)	Cl (mg/L)	
f1j(x)	0,9582	0,0000	0,0000	0,0000	0,9004	0,0000	1,0000	0,2787
f2j(x)	0,0418	0,0000	0,0000	0,0000	0,0996	0,0000	0,0000	0,0181
f3j(x)	0,0000	0,0000	0,0000	0,0000	0,0000	0,8319	0,0000	0,1489
f4j(x)	0,0000	0,0000	0,0000	0,0000	0,0000	0,1681	0,0000	0,0219
f5j(x)	0,0000	1,0000	1,0000	1,0000	0,0000	0,0000	0,0000	0,3815
P7								Result
CRITERION	pH	DBO (mg/L)	DQO (mg/L)	NH3 (mg/L)	SS (mg/L)	NO3 (mg/L)	Cl (mg/L)	
f1j(x)	0,0000	0,0000	0,0000	1,0000	1,0000	0,0000	1,0000	0,5402
f2j(x)	0,5996	0,2221	0,6666	0,0000	0,0000	0,0000	0,0000	0,1217
f3j(x)	0,4004	0,7779	0,3334	0,0000	0,0000	0,0000	0,0000	0,1794
f4j(x)	0,0000	0,0000	0,0000	0,0000	0,0000	0,1541	0,0000	0,0201
f5j(x)	0,0000	0,0000	0,0000	0,0000	0,0000	0,8459	0,0000	0,0960
P8								Result
CRITERION	pH	DBO (mg/L)	DQO (mg/L)	NH3 (mg/L)	SS (mg/L)	NO3 (mg/L)	Cl (mg/L)	
f1j(x)	0,0000	0,1668	0,2000	1,0000	1,0000	0,0000	1,0000	0,5741
f2j(x)	0,5000	0,8332	0,8000	0,0000	0,0000	0,0000	0,0000	0,1976
f3j(x)	0,5000	0,0000	0,0000	0,0000	0,0000	0,0000	0,0000	0,0482
f4j(x)	0,0000	0,0000	0,0000	0,0000	0,0000	0,0833	0,0000	0,0109
f5j(x)	0,0000	0,0000	0,0000	0,0000	0,0000	0,9167	0,0000	0,1041
P9								Result
CRITERION	pH	DBO (mg/L)	DQO (mg/L)	NH3 (mg/L)	SS (mg/L)	NO3 (mg/L)	Cl (mg/L)	
f1j(x)	1,0000	0,7932	1,0000	0,5663	0,0000	1,0000	1,0000	0,7275
f2j(x)	0,0000	0,2068	0,0000	0,4337	0,6000	0,0000	0,0000	0,2193
f3j(x)	0,0000	0,0000	0,0000	0,0000	0,4000	0,0000	0,0000	0,0659
f4j(x)	0,0000	0,0000	0,0000	0,0000	0,0000	0,0000	0,0000	0,0000
f5j(x)	0,0000	0,0000	0,0000	0,0000	0,0000	0,0000	0,0000	0,0000
P10								Result
CRITERION	pH	DBO (mg/L)	DQO (mg/L)	NH3 (mg/L)	SS (mg/L)	NO3 (mg/L)	Cl (mg/L)	
f1j(x)	0,0000	0,7800	0,0000	0,7997	0,3000	1,0000	0,0000	0,5838
f2j(x)	0,5000	0,2200	0,0000	0,2003	0,7000	0,0000	0,0000	0,2055
f3j(x)	0,5000	0,0000	0,6000	0,0000	0,0000	0,0000	0,0000	0,1242
f4j(x)	0,0000	0,0000	0,4000	0,0000	0,0000	0,0000	0,8254	0,1678
f5j(x)	0,0000	0,0000	0,0000	0,0000	0,0000	0,0000	0,1746	0,0228
P11								Result
CRITERION	pH	DBO (mg/L)	DQO (mg/L)	NH3 (mg/L)	SS (mg/L)	NO3 (mg/L)	Cl (mg/L)	
f1j(x)	0,5265	0,7932	0,4000	0,6867	0,0000	1,0000	0,0000	0,5578
f2j(x)	0,4735	0,2068	0,6000	0,3133	0,0000	0,0000	0,0000	0,1789
f3j(x)	0,0000	0,0000	0,0000	0,0000	0,9244	0,0000	0,0000	0,1524

f4j(x)	0,0000	0,0000	0,0000	0,0000	0,0756	0,0000	0,0000	0,0101
f5j(x)	0,0000	0,0000	0,0000	0,0000	0,0000	0,0000	1,0000	0,1305
P12								Result
CRITERION	pH	DBO (mg/L)	DQO (mg/L)	NH3 (mg/L)	SS (mg/L)	NO3 (mg/L)	Cl (mg/L)	
f1j(x)	0,4206	0,7868	0,0000	1,0000	0,0000	1,0000	1,0000	0,7396
f2j(x)	0,5794	0,2132	1,0000	0,0000	0,0000	0,0000	0,0000	0,1558
f3j(x)	0,0000	0,0000	0,0000	0,0000	0,3108	0,0000	0,0000	0,0512
f4j(x)	0,0000	0,0000	0,0000	0,0000	0,6892	0,0000	0,0000	0,0921
f5j(x)	0,0000	0,0000	0,0000	0,0000	0,0000	0,0000	0,0000	0,0000

TABLE XV. PRATI INDEX LEVELS

CLASS	Contamination level	Quality color
$\lambda_1 \rightarrow$	Not contaminated	
$\lambda_2 \rightarrow$	Acceptable	
$\lambda_3 \rightarrow$	Moderately contaminated	
$\lambda_4 \rightarrow$	Contaminated	
$\lambda_5 \rightarrow$	Highly contaminated	

TABLE XVI. WATER QUALITY RESULTS AT MONITORING STATIONS

Estation Class	λ_1	λ_2	λ_3	λ_4	λ_5
P1	0,2961	0,1722	0,1245	0,0000	0,2323
P2	0,7208	0,0906	0,2343	0,0191	0,0000
P3	0,4309	0,2866	0,1118	0,0000	0,1188
P4	0,7283	0,1260	0,1306	0,0483	0,0000
P5	0,6080	0,2072	0,1099	0,0000	0,1188
P6	0,2787	0,0181	0,1489	0,0219	0,3815
P7	0,5402	0,1217	0,1794	0,0201	0,0960
P8	0,5741	0,1976	0,0482	0,0109	0,1041
P9	0,7275	0,2193	0,0659	0,0000	0,0000
P10	0,5838	0,2055	0,1242	0,1678	0,0228
P11	0,5578	0,1789	0,1524	0,0101	0,1305
P12	0,7396	0,1558	0,0512	0,0921	0,0000

V. RESULTS AND DISCUSSION

It was possible to obtain the results of the evaluation of the water quality in the lower basin of the Huallaga river, which from the monitoring points P1, P2, P3, P4, P5, P7, P8, P9, P11 and P12 shown in Table XVI, have the category level "Unpolluted", these have the lowest water quality rating of the Prati index. However, point P6 shown in Table XVI is in the "Highly contaminated" class, which is why it turns out to be the worst quality monitoring point according to the Prati scale.

In addition, taking into consideration the "Participatory Monitoring Report on the quality of surface water in the Huallaga River Basin" [2], it results in exceeding the ECA 3-subcategory D1 [4], in two parameters (BOD, COD), from which it is concluded that this methodology used is reliable.

E The order of contamination of the 12 monitoring points, from the highest to the lowest according to the results obtained in Table XVI is shown below. $P6 > P12 > P4 > P9 > P2 > P5 > P10 > P8 > P11 > P7 > P3 > P1$.

Furthermore, considering a study conducted in Cuzco [8], which mentions that the anthropogenic activity generated contamination of the surrounding banks through the effluents emitted, in the case of study, and mainly at point P6, there is a landfill of "Fundo 3 hermanitos" and this is probably the cause of the contamination of this study area.

Finally, according to the evaluation of water bodies in the Rimac River basin [9], where 5 representative monitoring points are mentioned "downstream", then, from that, in the case of study, the evaluation of 12 representative points will be carried out, since as more monitoring points the uncertainty about the water quality in the study area decreases considerably and an approximate result of the quality is evidenced. Of the water of the conditions of the section of interest.

A. About the Methodology

Multi-criteria analysis approaches such as Delphi [12] [13] and AHP [14][15], do not consider a degree of uncertainty, because of the importance of the criteria they take into account for the analysis.

In addition, in the assessment of water bodies in the Rimac River [9], they mention that the monitoring points belong to Category 1 A2- Population and Recreation using the Grey Clustering method, so the methodology is similar to the Peruvian RCTs [4]. Therefore, in our study, when the results of the application of the Grey Clustering and the results of the participatory monitoring in the 12 monitoring points were compared, in fact it was evident that they complied with the RCT on water [4] in 11 of the points, and in P6 they did not comply with national standards, thus inferring that the results obtained were much more reliable.

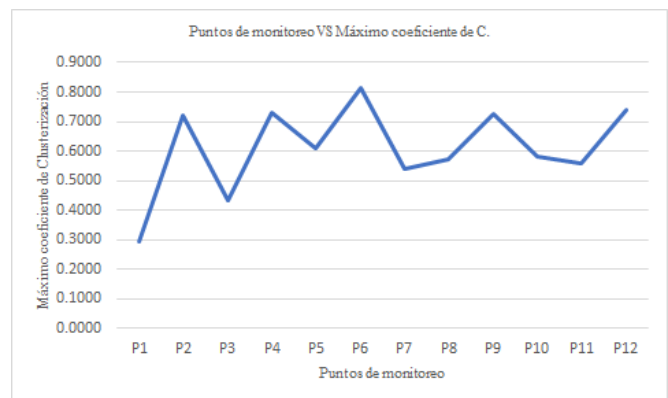


Fig. 4. Displays the Monitoring Points vs the Maximum Clustering Coefficients.

Finally, this method was used because according to the study conducted on the water quality of the Qingshui River in the city of Duyun, China [10], and compared to the results produced by other methods, it turns out to be more scientific and reasonable and can provide a basis for the evaluation of water quality and the management of the water environment in any space where it is carried out.

VI. CONCLUSION

The water quality of eleven monitoring stations in the Lower Huallaga River Watershed is in the "Uncontaminated" category of the Prati Index, according to the following hierarchy from highest to lowest quality: P-12 > P-4 > P-9 > P-2 > P-5 > P-10 > P-8 > P-11 > P-7 > P-3 > P-1, deducing that the development of economic activities surrounding these water bodies is not significantly affecting their quality. While the P-6 monitoring station is in the "Highly contaminated" category, this is due to its proximity to a dump, where domestic, municipal and industrial waste is generally disposed of, the most contaminating being hospital waste.

In this work, the Grey Clustering methodology will be used, since the evaluation of water quality is the result of multiple criteria and in many cases we work with little data and little information, therefore, statistical methods are not suitable for this type of evaluation because they present a certain degree of uncertainty, however, Gray's method works by prioritizing the criteria, that is, it calculates weights to the criteria.

Grey Clustering gives us more reliable results, so it is beneficial to apply this methodology in studies of water quality, air, soil, biodiversity, landscape; as well as the application to other fields of study such as economics, sociology. However, it is laborious to increase the number of monitoring points, so it could be simplified using a programming language.

REFERENCES

- [1] D. G. de aguas y suelos Instituto Nacional de Recursos Naturales, "Monitoreo de la calidad de aguas superficiales," 2000.
- [2] A. A. del A. H. Autoridad Nacional del Agua, "Informe de monitoreo participativo de la calidad de agua superficial en la cuenca del río Huallaga (Febrero -Marzo de 2019)," 2019, [Online]. Available: <https://hdl.handle.net/20.500.12543/3874>.
- [3] CAPITULO III: Índices de calidad(ICAs) y de Contaminación(ICOs) del agua de importancia mundial. 2010.
- [4] MINAM, "Decreto Supremo N° 004-2017-MINAM: Aprueban Estándares de Calidad Ambiental(ECA) para Agua y disponen

- Disposiciones Complementarias," 2017. <https://sinia.minam.gob.pe/normas/aprueban-estandares-calidad-ambiental-eca-agua-establecen-disposiciones>.
- [5] J. Liu, Sifeng; Forrest, "Grey Systems," Springer, 2011, [Online]. Available: <https://www.springer.com/gp/book/9783642161575#:~:text=Authors%3A%20Liu%20Sifeng%20Forrest,and%20models%20with%20practical%20applicability>.
- [6] F. Sifeng, Liu; Yingjie, Yang; Naiming, Xie; Jeffrey, "New progress of Grey System Theory in the new millennium," Emerald, 2015, [Online]. Available: <http://www.tcenter.ir/ArticleFiles/ENARTICLE/3602.pdf>.
- [7] Z. Y. Qi Gao, Baosheng Zhang, "Research on Comprehensive Evaluation of Air Quality in Beijing Based on Entropy Weight and Grey Clustering Method," IEEE Digit. Libr., 2019, [Online]. Available: <file:///C:/Users/PROPIETARIO/Downloads/9491f7fdd2559110a51e516902fbc5e03ac1.pdf>.
- [8] P. I. Alexi Delgado, Acuña M., Justano N., Llanos E., "Water Quality Assessment in a Watershed in Cusco, Peru using the Grey Clustering Method," Int. J. Eng. Adv. Technol., 2019, [Online]. Available: <https://www.ijeat.org/wp-content/uploads/papers/v9i2/B3606129219.pdf>.
- [9] S. G. Aguirre A., Palomino E., "Aplicación de la lógica difusa para determinar la calidad de cuerpos de agua de la cuenca del río Rímac," IEEE Digit. Libr., 2017, [Online]. Available: https://pdfs.semanticscholar.org/fad3/6caddde7ded57f286033bbe51f6e838435d2.pdf?_ga=2.259662211.842781806.1599154288-1675125422.1599154288&_gac=1.174400022.1599154289.EA1aIQobChMIZ_vpv8HN6wIVkIORCh1zaAPvEAAAYASAAEgIBKfD_BwE.
- [10] L. W. Jia Wang, Xu Wang, Xinhua Zhang, Haichen Li, Xiaohui Lei, Hao Wang, "Application of Grey Clustering Method Based on Improved Analytic Hierarchy Process in Water Quality Evaluation," MATEC Web Conf., 2018, [Online]. Available: https://www.mateconferences.org/articles/mateconf/pdf/2018/105/mateconf_ismso2018_02004.pdf.
- [11] I. R. Alexi Delgado, "Environmental conflict analysis using an integrated grey clustering and entropy-weight method: A case study of a mining project in Peru," ELSEVIER, 2016, [Online]. Available: <https://reader.elsevier.com/reader/sd/pii/S1364815215301250?token=B4D89AE8CC485DD8BDAF8FBCB7C80E59928963BBD1393DD4349FDC6A0C5FB7D2DCFA62E876E088816CFBDCCECA1E48751>.
- [12] M. García, Valdés; Suarez, "Delphi method for the expert consultation in the scientific research," Rev. Cuba. Salud Pública, p. 4, 2013, [Online]. Available: <http://scielo.sld.cu/pdf/rcsp/v39n2/spu07213.pdf>.
- [13] P. Quevedo, "Obtención de un índice de calidad de agua (ICA) para las ciénagas que forman parte de la zona inundable del río Magdalena en el departamento del Atlántico - Colombia, a través de la aplicación del Método Delphi," 2017.
- [14] A. Mehdi, Sadeghi; Ahmad, "An AHP decision making model for optimal allocation of energy subsidy among socio-economic subsectors in Iran," ELSEVIER, 2011, [Online]. Available: <https://doi.org/10.1016/j.enpol.2011.12.045>.
- [15] J. Osorio, Juan; Orejuela, "Analytic hierarchic process and multicriteria decision making. Application example," Sci. Tech., 2008, [Online]. Available: <https://www.redalyc.org/pdf/849/84920503044.pdf>.

A Comparative Analysis of Machine Learning Models for First-break Arrival Picking

Mohammed Ayub¹

College of Computer Sciences and Engineering
King Fahd University of Petroleum and Minerals
Dhahran 31261, Saudi Arabia

SanLinn I. Kaka²

College of Petroleum Engineering and Geosciences
King Fahd University of Petroleum and Minerals
Dhahran 31261, Saudi Arabia

Abstract—First-break (FB) picking is an important and necessary step in seismic data processing and there is a need to develop precise and accurate auto-picking solutions. Our investigation in this study includes eight machine learning models. We use 1195 raw traces to extract several features and train for accurate picking and monitoring the performance of each model using well-defined evaluation metrics. Careful investigation of the scores shows that a single metric alone is not sufficient to evaluate the arrival picking models in real-time. Correlation analysis of predicted probabilities and predicted classes of machine learning models confirm that the performance metrics that use predicted probabilities have higher score value than those that use predicted classes. Our study which incorporates comparisons of different machine learning models based on different performance metrics, training time, and feature importance indicates that the approach we developed in this study is helpful and provides an opportunity to determine the real-time suitability of different methodologies for automatic FB arrival picking with clear deep insight. Based on performance scores, we bench-marked the Extra Tree classifier as the most efficient model for FB arrival picking with accuracy and F1-score above 95%.

Keywords—First-break arrival picking; seismology; neural networks; machine learning; feature ranking

I. INTRODUCTION

Detection of the first arrival from seismic phases plays an important role in solving many seismic exploration problems. In fact, picking the first arrivals is the first step in seismic data processing [1], [2]. However, the task is challenging due to the ever-increasing seismic data volume and therefore, manual picking is very time consuming and difficult for human experts. Moreover, in seismology, it is crucial to pick the First Break (FB) for many applications including imaging the subsurface, travel time tomography, understanding near-surface complexities, hydrocarbon and mineral exploration, microseismic monitoring of oil and gas-reservoir, and investigating the earth's crustal structure [3], [4]. Moreover, accurate FB picks help in inverting for a good near-surface velocity model in seismic processing. In fact, many algorithms of FB picking have been proposed including short-term average/long-term average algorithms [5], [6], auto regression with Akaike Information Criterion [7], higher-order statistics [8], [9]. Although these traditional automatic arrival picking algorithms are helpful for many applications and their performance cannot overtake that of manual picks, leaving

them behind would be less useful for seismic imaging. Another problem with traditional methods is that they usually require a threshold, making them difficult to implement in complex seismic regions. On the other hand, manual or interactive FB picking methods can help improve performance in terms of quality and accuracy, requiring longer time and extensive effort, especially when the dataset is large. Due to the availability of huge seismic data and the inclusion of more difficult data acquisition areas, more robust, accurate and better automated first break picking techniques are essential for obtaining subsurface information from seismic data. To that end, the use of machine learning-based picking models bring a significant advantage in terms of cost and time.

Many research works have been in the literature for FB picking using machine learning including recently evolved deep machine learning. Unfortunately, there are many issues that need to be investigated. For example, comparative studies among the different models from the perspective of FB picking are not adequately explored. Different machine learning model exhibits different performance due to their underlying working principles. Again, one single performance metric cannot be used to bench mark the performance of the particular algorithm because scores of evaluation metric vary across the models. More than that, what needs to be emphasized for the efficiency of the FB picking model for real-time usability is an accurate prediction with minimal resources both in terms of time and budget. Hence, the FB picking model that optimize training time with acceptable performance scores of different established metrics needs to be explored. Consequently, we rank features using the automatic feature ranking method. To realize these objectives, we design, develop and evaluate eight machine learning algorithms in addition to three automatic feature selection techniques by which we search the features that reduce the training time, data acquisition and data processing costs.

Our approach involves the following steps to optimize FB picking: (1) Investigate FB picking by deploying eight machine learning models. We analyze the suitability of the same in terms of performance score and training time for real-time deployment of first break arrival picking on noisy and original seismic trace data by using five evaluation metrics. (2) Bench-mark the highest performance score of about 95% for accuracy and F1-score for Extra Tree. Besides, we extract and recommend the most common important features based on experimental results obtained by fitting three powerful ensemble classifiers on noisy data. (3) Correlate/evaluate

machine learning classifiers by means of predicted classes and predicted probabilities.

The rest of the paper is organized as follows: Section II describes the related works and Section III discusses the methods and materials used in this paper. Experiment details and results are given in Section IV followed by discussion and analysis in Section V. The conclusion and future work is given in Section VI.

II. RELATED WORKS

The reference [25] integrated traditional seismic methods and machine learning for picking. Geophysical techniques were first used for preliminary picking and then applied CNN to identify, remove and fix poor picks. In [26], arrival picking problem was studied by formulating it binary image segmentation problem. Arrival was picked using U-net architecture which is based on pixel-wise CNN. Like [26], the authors in [27] proposed FB picking models using deep learning technique. They deployed seven-layered U-Net architecture with skip connection. In [28], U-Net was used for segmentation of seismic image and Recurrent Neural Network (RNN), for arrival picking. Additionally, the authors proposed a simple weight adaptation method for generalization of the model in unseen data.

In SC-PSNET [29], the authors extend 3C seismograms processing with CNN to 1C seismic processing. Their study showed that CNN in combination with RNN is more promising for P- and S- detection when there are not enough training data available. To mitigate high intensive labour and thus high cost of manual seismic picking, the study [30] transferred the PhaseNet model and incorporate it with double-difference tomography. The results showed that the model's prediction was nearly as accurate as the result of a human expert with very low time and cost. The reference [31] proposed a Faster-RCNN based P-wave picking method using local window extracted from seismic waveform to enhance the accuracy of arrival picking. Faster-RCNN is an object localization algorithm based on Regions Proposal Network (RPN) commonly used to detect object of interest in the complex background.

In [10], Chen et al. investigated the automatic seismic waveform classification and arrival time picking using novel anti-noise Convolutional Neural Network (CNN) and K-means Clustering (KC) techniques. The authors used Mean Absolute (MA), Mean Square (MS), Short-Term Average Ratio (STAR) and Long-Term Average Ratio (LTAR) as features. Prior to this, the same first author of [10] in [11] studied FB picking with the same features in an unsupervised machine learning manner where it was showed that the method developed had much better performance than the traditional STA/LTA method in noisy data. In [12], Mezyk and Malinowski proposed a Multi-pattern FB picking method using Deep Neural Net-work (DNN), Support Vector Regression (SVR) and Extreme Gradient Boosting (XGBoost). The models were trained and tested using different features such as STA/LTA, entropy, and fractal dimension and a few others. Their experiment results showed that the DNN classifier outperformed SVR and XGBoost.

Yuan et al. [13] adopted CNN for the classification of seismic waveforms, thereby locating FB using a threshold, first local minimum rule, and median filter in a sequential manner. The experiment results from synthetic and field data showed that the use of CNN using the time-space sub-image as inputs has efficient classification and picking capability.

Another convolutional image segmentation based FB picking was studied by Wu et al. [14]. Their idea was first to convert the microseismic trace into a 1D gray-scale image and pick the first arrival manually. Thereafter, based on that time index, the traces were labeled to train SegNet which was built based on encoder and decoder neural network concept. Similarly, PickNet was introduced in the work of [15] with the inspiration of the VGG-16 image recognition model to pick P and S arrival time. As an overall performance, the model could pick high-quality P and S wave arrival times in real datasets with potential generalization capabilities to other data collected using different seismic networks. Another seismic wave arrival time picking model (PhaseNet) was designed and tested by Zhu and Beroza [17] using a CNN. Their model was adapted from U-net which is a biomedical image processing framework built on Deep Neural Network (DNN).

Different from all the above works, the poor pick identification using a CNN was investigated in the work of [16] with cross-correlation of adjacent traces as the solution to fix the poor picks. P-wave arrival picking using vertical component and classification of first-polarity was explored in [18] by training two different CNNs for picking of P-wave arrival and first-polarity classification, respectively. The model's prediction was much more accurate than that of the analyst with the highest score of classification 95% in terms of precision. Gao et al. studied FB picking using fuzzy C-means, where they first utilize the vertical and horizontal sliding window to determine the first-arrival range and then Particle Swarm Optimization (PSO) to locate cluster centers [19]. Unlike all studies discussed above, the authors of [20] deployed Variational Auto-Encoder (VAE) and a Generative Adversarial Network (GAN) for automatic FB picking using seismic shot gather images as input. In their work [22], Duan and Zhang claimed that seismic traces are correlated with one another and the same is underutilized. They proposed a multi-trace multi-attribute analysis method for FB picking using a Support Vector Machine (SVM) to improve automatic picking. Another image segmentation-based FP picking as in [14] was explored in [21] who used 2D pixel-wise CNN. In their work, raw seismic images were first treated as gray scale images with normalized pixel values between 0 and 255. Then the resulted images were converted into binary images by tagging the pixels before arrival as zero and after arrival as 1. Though the model exhibited the highest accuracy of 96%, it was not suitable for smaller seismic traces. Hollander et al. [23] proposed a five-layered deep neural network composed of one convolutional layer, one pooling layer, one dense layer, and one output layer, for identification of the first break from a seismic trace. The model was trained on augmented data to classify the trace and thereby locating the first break by the use of maximal energy ratio. Transfer learning can save a significant amount of training time by enabling the reuse of the CNN model trained in other domains. The author in [24]

applied the idea for FB identification and arrival time picking using Continuous Wavelet Transform (CWT) as input features for AlexNet, GoogleNet and SqueezeNet. Though the models had superb performance compared to STA/LTA and Adaptive

Multiband Picking Algorithm (AMPA), the accuracy was only about 90%. A summary of all related work is given in Table I. Note that most studies used CNN and the accuracy lies in the range of 78% and 98%.

TABLE I. SUMMARY OF ARRIVAL TIME PICKING METHODS

Problem, Ref.	Features	Algorithm	Datasets	Acc.
Waveform classification and arrival picking[10]	MA, MS, STA/LTA	KC, CNN	Synthetic and real data	98.6%
Event picking [11]	Mean, Power, STA/LTA	FC	Synthetic and real data	-
FB picking [12]	11 features of STA/LTA, entropy, fractal dimension	ANN, SVR, XGBoost	Real data	95%
Waveform classification and FB picking [13]	time-space sub-image	CNN	Synthetic and real data	-
Semi-automatic FB picking[14]	1D seismic trace image	CNN	Synthetic and field data	
Arrival time picking[15]	3C Seismic waveform	CNN (PickNet)	Real-world data	78%
Poor pick identification[16]	Seismic record image	CNN	Real-world data	95%
Arrival time picking[17]	3C seismic waveform	DNN (PahseNet)	NCSN	89.6% (F1)
P-wave picking and First-motion classification[18]	1C seismic waveform	CNN	SCSN	95%(P)
First arrival picking [19]	Seismic trace	Fuzzy C-means	Field data	96.5%
First arrival picking [20]	Seismic image	Deep learning (VAE+GAN)	Field Data	-
First arrival picking [21]	Seismic image	CNN	Field data	96%
First-break picking[22]	advance, multi-trace correlation	SVM	pseudo-synthetic, real	2.4ms-14ms (RMS)
First-break identification[23]	energy ratio	CNN	Private	96%
FB arrival time identification[24]	CWT	AlexNet, GoogleNet, SqueezeNet	Real data	Above 90%
Poor pick identification, remove and fix [25]	Multitrace	CNN	Private	97.8%
Automated arrival picking [26]	Seismic image	CNN (U-Net)	Filed data	-
Automatic FB picking [27]	Seismic image	CNN (U-Net)	Seismic data	-
FB picking [28]	Seismic image	CNN (U-Net), RNN	Synthetic data	-

III. METHODS AND MATERIALS

A. Problem Formulation

We formulate FB picking as a binary classification problem; 1 (True) for the FB event and 0 (False) for the non-FB event. We explain the details of machine learning models used in this study with the metrics used to evaluate performance and automatic feature ranking techniques. An illustration of FB and Non-FB is given in Fig. 1.

B. Machine Learning Models

In this subsection, eight machine learning classifiers are experimented for the classification of first-break arrival picking. These include Feed-forward Neural Network (FNN), K-Nearest Neighbors (KNN), Logistic Regression (LR), Decision Tree (DT), Random Forest (RF), Extra Trees (ET), Gradient Boosting Trees (GB), and XGB Classifier (XGB).

1) *Feed-forward Neural Network (FNN)*: Feed-forward Neural networks are a set of neurons interconnected in the form of layers. The inputs are passed forward by multiplying with certain weights and adding the bias. The neurons in hidden layers and output layers are activated using different activation functions such as linear, tanh, sigmoid, softmax and many others. At the output layer, the error is calculated based on the actual label and is back-propagated to minimize it by the use of some mechanism called gradient descent algorithm. In this manner, all the input samples are trained until a specified number of epochs is reached. The architecture of FNN is designed by including two hidden layers of 32 neurons each, with kernel initializer from normal distribution and activation as ReLU [32], which help in tackling the gradient vanishing problem. As we have two classes to predict, a one-neuron dense layer with Sigmoid activation is put at the end of the architecture.

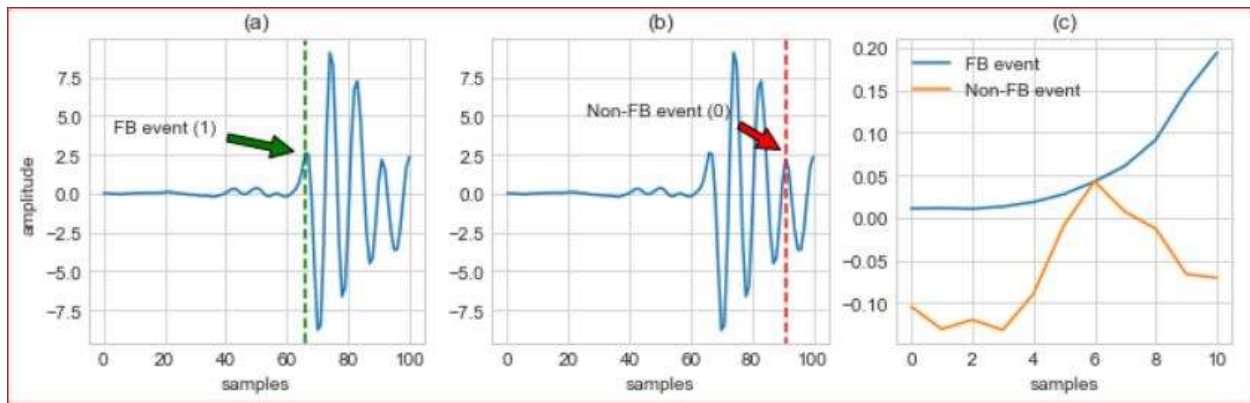


Fig. 1. FB and Non-FB Event; (a) Green Dashed-Line Showing First Break Event, (b) Red Dashed-Line Showing Non-First Break Event, and (c) Illustrative Signal Plot of Normalized Amplitude Values of both Events with 11 Samples.

2) **K-Nearest Neighbor (KNN)**: KNN is a non-parametric algorithm that does not require model learning but makes a prediction on a lazy learning mode, meaning prediction is made just-in-time by calculating the distance between the inputs and training instance. Therefore, KNN requires almost all data while making predictions thereby making a memory burden. Using predefined k along with a new sample, the most common one with new a sample is chosen from the nearest k samples.

3) **Logistic Regression (LR)**: The Logistic Regression (LR) is a probabilistic model that makes a prediction by training data on the logit function. It requires large sample sizes and independent variables need not be correlated with each other. For logistic regression, we tune hyper parameter using random search to get an optimized model which returned 'l2' regularization penalty against 'l1', 'none' class-weight against 'balanced' as the best fits for our problem of classification.

4) **Decision Trees (DT)**: Decision Trees (DT) are flow chart-like diagrams with the terminal node representing the decision. The results of decision tree algorithms are easy to understand and calculate for the human expert and are computationally cheap as well. In DT, some relevant questions are asked at each node and based on how much information a feature provides for the class, the node is branched and this will continue until all the children nodes belong to the same class or the information gain is zero.

5) **Random Forest (RF)**: Random Forest (RF) consists of a set of trees that are built by taking random training samples, where random subsets of features are used when splitting the nodes of decision trees. Then for prediction, the results of all trees are averaged with a technique call bagging, which is bootstrapping aggregating in long-form.

6) **Extra Trees (ET)**: ET is extremely randomized trees and is the same as RF with differences; (1) It uses a random split of a tree, rather than best split as in RF, and (2) It builds multiple trees without bootstrapping, meaning with the replacement of samples. The maximum features considered to branch a given node is calculated based on the square root value of the total features.

7) **Gradient Boosting Trees (GBT)**: GBT are a group of weak learners that are combined to make a stronger predictive model based on weighted minimization. In GBT, new trees are added to the model without manipulating the existing trees, and appending the result of the new tree to that of existing until the loss is minimized or predefined numbers of trees are reached. For our classification problem, GBT is trained on 100 trees with a maximum depth of 3 for each tree.

8) **Extreme Gradient Boosting Tree (XGBT)**: Another boosting tree is designed based on the implementation of GBT but uses an accurate approximation to find fast and robust tree models. This is called XGBT that stands distinctly from other tree-based models with these two properties; (1) unlike other models that use the first-order derivatives of the loss function of the base model to minimize the overall error, XGBoosting finds the second-order derivatives of the loss function for better approximation, (2) It uses advanced regularization techniques such as L1 and L2.

C. Performance Metrics

Normally, we use accuracy for classification problems in machine learning. Sometimes, only the accuracy is typically not enough to evaluate a machine learning model. For example, in a dataset with a large class imbalance, the model will predict correctly the majority class and hence will have a high classification accuracy, which in practicality is misleading. In this case, additional evaluation metrics are required and some of the commonly used ones are explained in this subsection. In order to best explain and understand the metrics, a confusion matrix is shown in Fig. 2.

1) **Precision (P)**: Precision is obtained by dividing the number of True Positives (TP) by the sum of the number of True Positives and False Positives (FP). It can also be called the Positive Predictive Value (PPV) and its mathematical expression is given as:

$$\text{Precision (P)} = \frac{TP}{TP+FP} \quad (1)$$

Precision can be regarded as an indicator of how exactly a classification algorithm will classify a true class as a true. From the equation, it can easily be seen that a low precision value means a large number of False Positives.

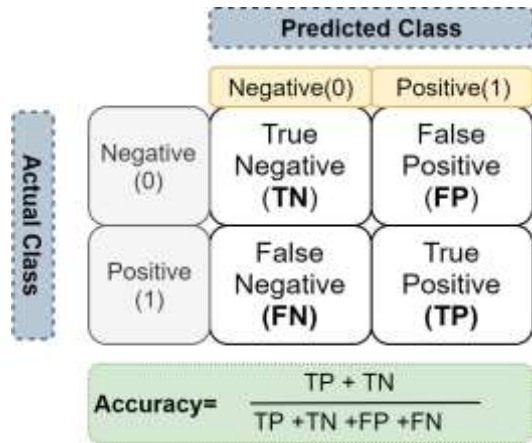


Fig. 2. Confusion Matrix. '1' Represents FB Event '0' Non-FB.

2) *Recall (R)*: Recall is the ratio between the number of True Positives and the sum of the number of True Positives and the number of False Negatives (FN). In the literature, we can see it also as Sensitivity or the True Positive Rate. Its formula is given by:

$$Recall (R) = \frac{TP}{TP+FN} \quad (2)$$

Recall shows the completeness of a classification algorithm, whereas precision shows the exactness of a classification algorithm. A low value of recall testifies that there are many False Negatives.

3) *F1-score (F1)*: The F1 Score is obtained when we divide the product of precision and recall with the sum of the same and again multiplied by 2. It is also termed as the F Score or the F Measure and it shows the balance between the precision and the recall.

$$F1 = 2 \frac{P \cdot R}{P+R} \quad (3)$$

4) *ROC Curve*: It stands for Receiver Operating Characteristics (ROC) curve and is also called AUROC (Area Under the Receiver Operating Characteristics). It is used as one of the most important performance evaluation metrics for the classification model. Using the ROC curve, the performance of any classification model can be measured by setting the thresholds at various points. Mathematically, the ROC is a probability curve and the area under the curve indicates the degree or the measure of separability between classes. We can interpret the ROC as; the higher the AUC, the better the model. That is, the model is predicting True as True and False as False. We can plot the ROC curve putting True Positive Rate (TPR) on the y-axis and False Positive Rate (FPR) is on the x-axis. By analogy, we can say that the model performs better if the ROC is about to touch the left-top corner of the plot.

D. Feature Importance

Machine learning models are largely dependent on high-quality features. The inclusion of irrelevant or less correlated features not only degrades the model performance but also

wastes the computational resources, training time and cost. Therefore, the selection of highly important features contributes towards better performance of the machine learning model. From the perspective of seismic data processing in which a large volume of data is overwhelming due to the availability of high data acquisition technology, the training time of the model for real-time deployment is a crucial factor that is drawing serious attention from business owners and researchers alike. Thus, prioritizing the features or removing the less contributing features is the best acceptable choice among the groups. As such, we deploy the Recursive Feature Elimination (RFE) method in combination with three powerful ensemble estimators such as Random Forest, Extra Trees and Gradient Boosting, one at a time.

IV. EXPERIMENTS AND RESULTS

A. Dataset and Data Preparation

The dataset used in this study is from the published work of Mezyk and Malinowski [12] and is available in Github repository¹. The data preparation steps and extracted features are shown in Fig. 3. For the machine learning model to generalize well, a sufficient number of input samples are required to be trained. Original raw traces of 1195 are perturbed using the Gaussian method to generate more noisy traces. Afterwards, feature matrices are constructed by extracting a total of nine features and appending label '1' for FB and '0' for Non-FB. The extracted features are: (1) raw trace amplitudes, (2) gradient of the absolute trace amplitudes, (3) trace entropy, (4) gradient of the trace entropy, (5) fractal dimension of the trace, (6) gradient of fractal dimension, (7) STA/LTA of the trace, (8) sum of the amplitude spectra of the trace, (9) gradient of the sum of the amplitude spectra. And finally we have a training dataset of 289190 instances that is balanced with true and false first-break events. From the whole noisy dataset, 25% is allotted for validation to measure the learning validity of the model while we use original traces of 5300 for testing purposes in order to check the generalization capability of the learned model.

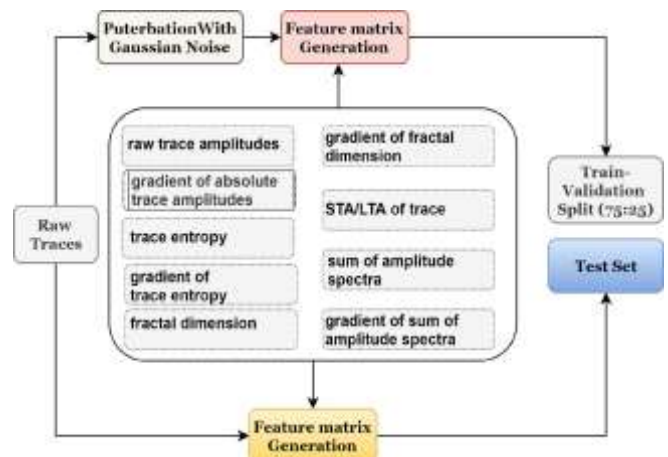


Fig. 3. Data Preparation Pipeline. Train and Validation Sets are Noisy Data. The Test Set Contains Purely Original Traces to Challenge the Generalization Capability of the Models.

¹ <https://github.com/mmezyk/fbpicker/tree/master/data>

B. Experiment Setup

We use Python 3.7.3 (Open source programming with the largest community) and Scikit-learn (Sklearn) machine learning library to implement this work on Keras [41] that use Tensor flow as the back-end. To realize this, we used all-in-one machine learning software package Anaconda 1.9.12 configured in an NVIDIA GEFORCE GTX 950 GPU and four-core i7 6th generation CPU machine with total graphic memory of 16GB and RAM of 16GB. For all experiments, we used Adam and binary cross-entropy as optimizer and loss function, respectively. The experiment results are reported using five best and commonly used metrics such as accuracy, precision, recall, F1-score and ROC score as mentioned in Section III-C. Besides, we also take into account the training time required for each model so that comparative and feasibility analysis can be done.

C. Experiment Results

1) *FNN*: The model is compiled using binary cross-entropy [33] as loss function and Adam [34] (Kingma and Ba, 2014) as the optimizer. The model is trained for 200 epochs with a batch size of 32 on 25% of validation data. The loss, and ROC curves are shown in Fig. 4. From Table II, it is seen that it has a score of accuracy 92.64%, precision 89.18%, recall 97.06% and F1-score 92.95%. From the precision and recall scores it is observed that the neural network model predicts more non-FB events as FB events than first breaks as non-first breaks. This can be clearer we if we analyze the confusion matrix, where there are a total of 312 non-FB events that are predicted as FB (False Positive) in comparison to 78 FB that are predicted as non-FB events (False Negative).

2) *KNN, LR and DT*: We trained KNN keeping the number of neighbors as 3 and, the performance scores as shown in Table II are accuracy 91.68%, F1-score 91.95% and ROC AUC score 96.17%. LR has a precision of 80.55%, recall of 92.38% and accuracy of 85.04%. The rate at which it classifies true first break and false break is significantly lower than KNN, and hence the higher numbers of False Positives and False Negatives. By the DT model, the scores achieved are 89.79%, 92.00% and 90.01, for accuracy, recall and F1-score, respectively. Moreover, False Negatives and False Positives are higher than KNN with lower False Positives than LR. In DT, the quality of the node split is monitored using the Gini impurity measure. Branching of the node is allowed till all leaves becomes pure.

3) *RF, ET, GBT and XGBT*: The hyper parameter tuning using cross-validation random search recommends the deployment of random samples while building each tree and entropy as information gain. It is also observed that the best result is achieved when nodes are split with a minimum number of samples of 9 based on 7 features maximum with having a minimum of 2 samples at the leaf node. The F1-score obtained is 93.39%, with precision and recall 91.19% and 95.70%, respectively. All scores can be seen in Table II.

The maximum features considered to branch a given node in ET is calculated based on the square root value of the total features. In our case, we have nine features and each node is split with 3 features maximum. The branching of the node will stop when all leaves have a number of samples less than 2. The extra tree classifier achieved a precision of 93.07%, accuracy of 95.26% and F1-score of 95.38%.

GBT is trained on 100 trees with a maximum depth of 3 for each tree. Different from other classifiers above, we use Friedman's Mean Squared Error (MSE) to monitor the quality of a split. We have a ROC AUC score of 98.47%, an accuracy of 92.75% and F1-score of 92.94%. XGBT is trained using the maximum depth of each tree with 6 and the precision score is 91.16%. The accuracy and F1-scores are 93.23% and 93.29%, respectively. The ROC curves for all shallow machine learning models are shown in Fig. 5.

4) *Feature Importance*: For feature ranking, we experimented with three estimators using the RFE method. We use an advanced method of REF where the RF estimator is trained using the cross-validation method of StratifiedKFold with a 10 split. We use 100 trees with the replacement of samples while building trees and Giniimpurity is used to calculate information value. For the ET estimator, we use the same parameter as Random Forest except bootstrap equals to false, meaning the subset of samples used for building one tree are not replaced while building subsequent trees. GB Estimator is trained with 100 trees as in previous sections on stratified 10-fold cross-validation of RFE. For calculating the information value, the Friedman Mean Square Error (FMSE) is used. We keep the learning rate 0.1 with the maximum depth of the tree 3, and loss function as deviance.

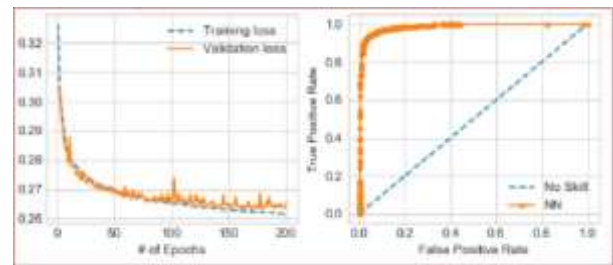


Fig. 4. The Loss and ROC Curves of FNN. The Learning behavior of the Model is good with Little Peak Fluctuation throughout the Epochs.

TABLE II. PERFORMANCE SCORES OF ALL MODELS

Model	Acc.	Pr	Re	F1	ROC	Time (sec.)
FNN	92.64	89.18	97.06	92.95	98.64	1661
DT	89.79	88.11	92.00	90.01	89.79	29
KNN	91.68	89.07	95.02	91.95	96.17	22
LR	85.04	80.55	92.38	86.06	95.23	10
RF	93.23	91.19	95.70	93.39	98.41	160
ET	95.26	93.07	97.81	95.38	99.23	192
GBT	92.75	90.58	95.43	92.94	98.47	534
XGBT	93.23	91.16	95.74	93.39	98.53	163

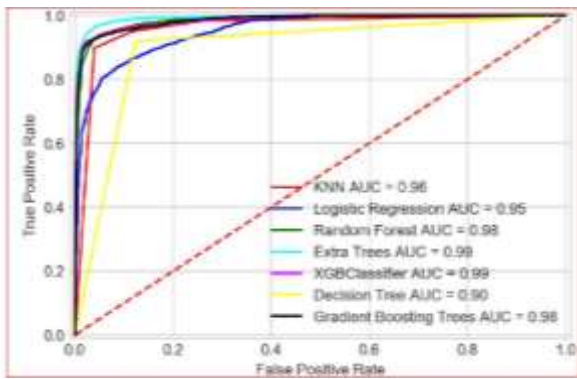


Fig. 5. ROCs of Machine Learning Models. The ET has the Highest Score.

V. DISCUSSION AND ANALYSIS

A. Machine Learning Models

We have evaluated eight different deep machine learning models for picking FB and the performance behavior is monitored using five evaluation metrics. Understanding the real-time deployment and resource requirements for training machine learning models, the training times for each models are also recorded. The FNN has a recall of 97.06%, which is the second-highest in the same category and indicates that it predicts the actual first break event as a non-first break more than the other model does. The training time of machine learning depends on many factors such as the size of the dataset, the number of features used, number of epochs, and many other factors. Furthermore, choosing a larger batch size can make the training faster but with comparatively poor performance.

In general, compared to deep learning models, shallow machine learning models are computationally less sophisticated with less training time and memory requirements than deep learning models. Moreover, traditional machine learning models have limited performance when the data volumes are extremely large. Nonetheless, they can be effectively deployed for real-world problems with the careful granular tuning of the model parameters. In this work, as seen in Table II and Fig. 6, LR and DT have the lowest and second-lowest classification performance in terms of all metrics, respectively. In terms of recall and ROC, LR performs better than DT with scores of 92.38% and 95.23%, respectively. If we scan the scores carefully, we observe that the Extra Tree (ET) performs best in terms of all metrics with an accuracy of 95.25% and ROC 99.23%. GBT has the longest training time with 534 seconds followed by Extra Trees with 192 seconds. LR takes the least amount of training time of 10 seconds among all classifiers. This trend is noticed from the values given in the last column of Table II and Fig. 7.

From the different classifiers we evaluated in this work, Extra Tree clearly outperformed other models in terms of all evaluation metrics. The second highest performers are RF and XGBT with very similar scores if we consider the accuracy, precision and F1-score as evaluation criteria. In terms of recall and ROC, FNN is the second-best performer. If, from all classifiers, the suitable models with less training time and better accuracy are to choose for real-time deployment, ET,

RF and XGBT are the perfect choice because they all need reasonable training time, below 200 seconds. Therefore, for FB arrival classification, traditional machine learning is enough for real-time deployment if ready-made pre-calculated features are to be used, that is if only trace amplitude-based features instead of the seismic image are to be deployed as features.

B. Feature Importance

1) *RFE using Random Forest Estimator*: RFE removes less important features in an iterative fashion. Feature importance is calculated as the coefficient of some estimators such as Random Forest. From the experimental results it is noticed that the highest performance is obtained when all nine features are used. But this method gives STA/LTA, the traditional method, the highest importance and the gradient of trace amplitude (g trc amp) the least importance. The other best five features with decreasing importance are the trace amplitude (trc amp), fractal dimension of the trace (fdm), the gradient of fractal dimension (g fdm), the sum of the amplitude spectra (sum amp spec) of the trace and trace entropy (trc ent). This trend can be seen in Fig. 8.

2) *RFE using Extra Trees Estimator*: As in RF, the best six features according to their importance are the STA/LTA, the fractal dimension of the trace, the trace amplitude, gradient of fractal dimension, trace entropy, and the sum of the amplitude spectra of the trace. As seen in Fig. 9, the fractal dimension of the trace, which is in third place in RF, has now become the second important feature in the Extra Trees estimator. This is due to their handling of input samples while training the different trees.

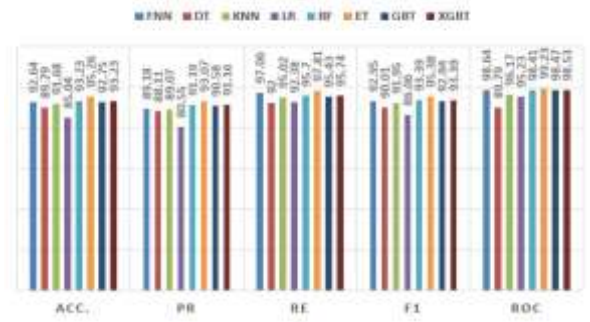


Fig. 6. Performance Scores of Machine Learning Models.

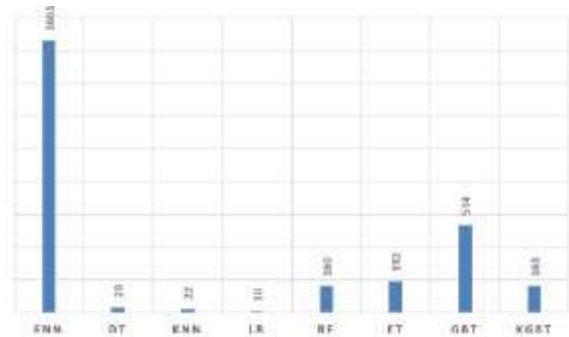


Fig. 7. Training Time (in Seconds) for Machine Learning Models.

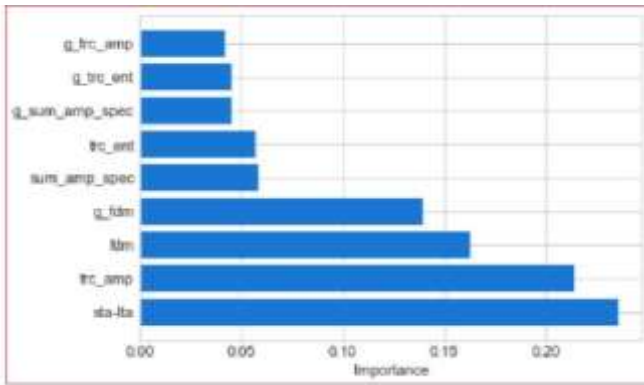


Fig. 8. Feature Ranking using RF Estimator.

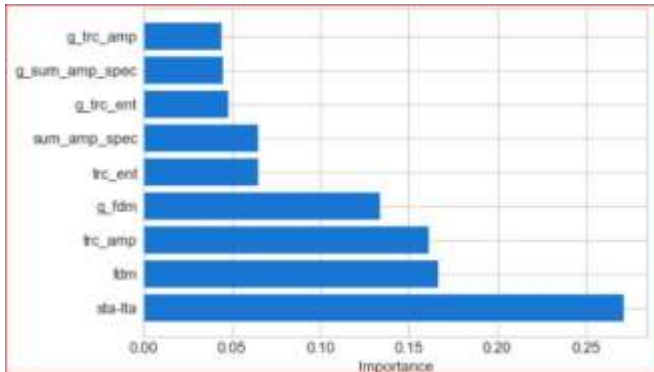


Fig. 9. Feature Ranking using ET Estimator.

models are not suitable enough to handle first-break arrival picking efficiently, compared to other models. Furthermore, as seen in Fig. 12, XGB and GBT have a strong correlation between them with a coefficient of 1.

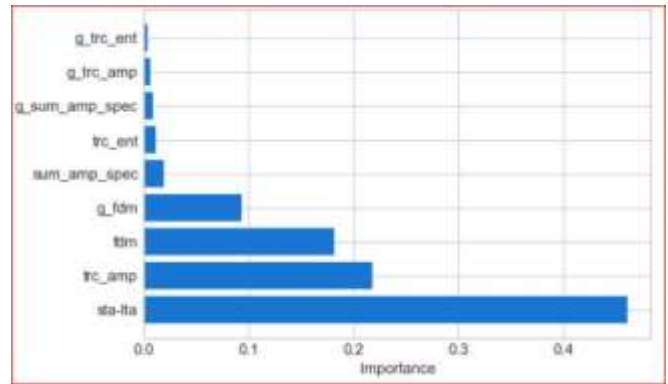


Fig. 10. Feature Ranking using Gradient Boosting Estimator.

3) *RFE using Gradient Boosting Estimator*: Almost like earlier estimators, this estimator selects STA/LTA, the amplitude of the trace, the fractal dimension of the trace, and gradient of fractal dimension as four most significant features as seen in Fig. 10.

From the above experiment results, it is apparent that the STA/LTA, the amplitude of the trace, the fractal dimension of the trace, and gradient of fractal dimension are the most important common features for the classification of FB picking.

C. Prediction Correlation

The machine learning models used in this study provide a prediction for both class labels (i.e. 0 or 1) and probabilities by using a prediction function. Direct class labels are used to calculate accuracy, precision, recall and F1 score, and probabilities are used for calculating AUC, ROCAUC, MSE, MAE, RMSE and many others. In terms of class label prediction, Gradient Boosting Trees and Extreme Gradient Boosting trees have the highest positive correlation with 0.95. The second highest correlation pairs with 0.91 and 0.90 are ET and RF, ET and XGBT, respectively. This can be seen in Fig. 11. If we compare the correlation in terms of prediction probability, we see that almost all classifiers are correlated with values greater than 0.90. This is the reason that ROC scores are higher than those of accuracy and F1 measures. Moreover, we also observed that the correlation of the decision tree and logistic regression with other classifiers are less than that of others in both cases, confirming that both

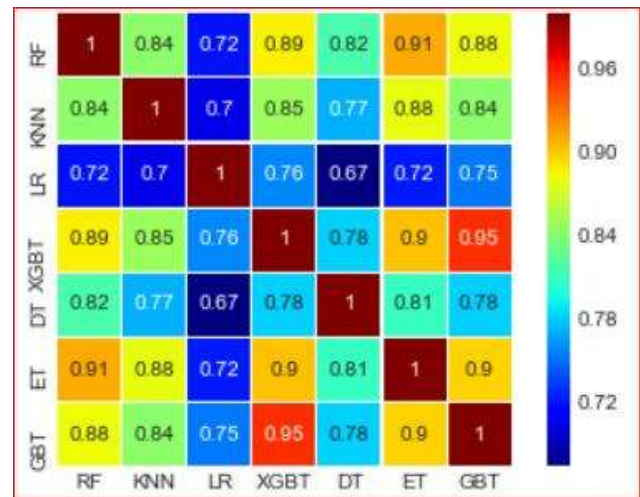


Fig. 11. Pearson Correlation of Machine Learning Classifiers used in this Paper. The Correlation between each Pair of the Classifier is based on Predicted Class (1 for FB Event, 0 for non-FB Event).

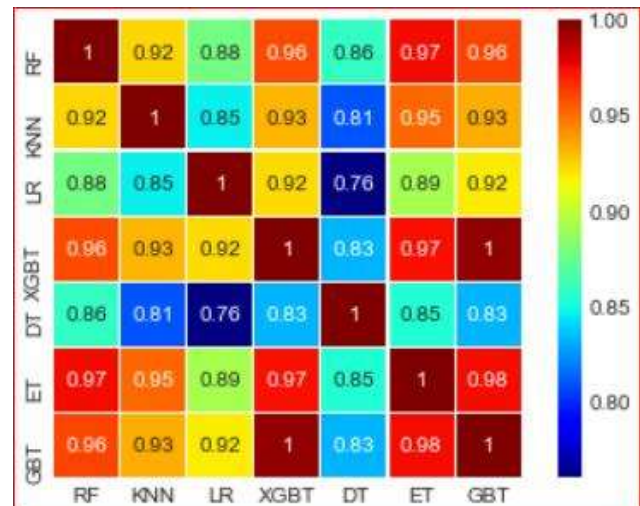


Fig. 12. Pearson Correlation of Machine Learning Classifiers used in this Paper. The Correlation between each Pair of the Classifier is based on Predicted Probability. (1 for FB Event, 0 for Non-FB Event).

VI. CONCLUSION AND FUTURE WORK

A. Conclusion

In this study, we have explored and investigated FB arrival picking by formulating it as a binary classification problem. In that vein, we deploy eight machine learning models. The models are trained on noisy data generated applying Gaussian perturbation using nine features and tested on original data for generalization capability. The models architectures are fine-tuned in line with the first break arrival picking problem by undergoing rigorous experiments. Extra Tree has the highest accuracy of 95.26% and F1-score of 95.38%. All the top performers have acceptable training time and show suitability for the real-time automatic deployment of first break picking. Our deployment of an RFE on nine features using three ensemble classifiers suggests four common important features: the STA/LTA, the amplitude of the trace, the fractal dimension of the trace and gradient of the fractal dimension. Careful investigation of the performance scores proves that a single metric alone is not sufficient to evaluate the FB picking models. As such, other types of measures such as precision, recall and F1-scores are required to further validate the performance of the model. In line with this, we noticed that the use of precision and recall can help experts in obtaining deeper insight into the classification behavior thereby allowing better real-time decisions.

B. Limitations and Future Works

In this paper, we consider only single sample features derived from a single trace using machine learning techniques. Though traditional machine learning techniques are less complicated and require less training time, their performance suffers from degradation when a huge volume of data is involved. Another limitation is that the models are compared using a single dataset. Therefore, as future work, we want to investigate FB picking using features derived from multiple samples on different datasets by deploying hybrid deep learning models.

ACKNOWLEDGMENT

The authors gratefully acknowledge the support provided by King Fahd University of Petroleum and Minerals. This study was supported by the College of Petroleum Engineering and Geosciences start-up grant.

REFERENCES

- [1] J. L. Hardebeck and P. M. Shearer, "A new method for determining first-motion focal mechanisms," *Bulletin of the Seismological Society of America*, vol. 92, no. 6, pp. 2264–2276, 2002.
- [2] P. L. Nelson and S. P. Grand, "Lower-mantle plume beneath the Yellowstone hotspot revealed by core waves," *Nature Geoscience*, vol. 11, no. 4, pp. 280–284, 2018.
- [3] J. Zhang and N. Toksoes, "Monte carlo sampling of solutions to inverse problems," *Geophysics*, vol. 63, pp. 1726–1737, 1998.
- [4] X. Zhu, D. P. Sixta, and B. G. Angstman, "Tomostatics: Turning-ray tomography+ static corrections," *The Leading Edge*, vol. 11, no. 12, pp. 15–23, 1992.
- [5] R. V. Allen, "Automatic earthquake recognition and timing from single traces," *Bulletin of the Seismological Society of America*, vol. 68, no. 5, pp. 1521–1532, 1978.
- [6] P. R. Stevenson, "Microearthquakes at flathead lake, montana: A study using automatic earthquake processing," *Bulletin of the Seismological Society of America*, vol. 66, no. 1, pp. 61–80, 1976.
- [7] R. Sleeman and T. Van Eck, "Robust automatic p-phase picking: an on-line implementation in the analysis of broadband seismogram recordings," *Physics of the earth and planetary interiors*, vol. 113, no. 1–4, pp. 265–275, 1999.
- [8] Z. Ross, M. White, F. Vernon, and Y. Ben-Zion, "An improved algorithm for real-time s-wave picking with application to the (augmented) anza network in southern california," *Bulletin of the Seismological Society of America*, vol. 106, no. 5, pp. 2013–2022, 2016.
- [9] C. D. Saragiotis, L. J. Hadjilentiadis, and S. M. Panas, "Pai-s/k: A robust automatic seismic p phase arrival identification scheme," *IEEE Transactions on Geoscience and Remote Sensing*, vol. 40, no. 6, pp. 1395–1404, 2002.
- [10] Y. Chen, G. Zhang, M. Bai, S. Zu, Z. Guan, and M. Zhang, "Automatic waveform classification and arrival picking based on convolutional neural network," *Earth and Space Science*, vol. 6, pp. 1244–1261, 2019.
- [11] Y. Chen, "Automatic microseismic event picking via unsupervised machine learning," *Geophysical Journal International*, vol. 212, no. 1, pp. 88–102, 2017.
- [12] M. Mezyk and M. Malinowski, "Multi-pattern algorithm for first-break picking employing an open-source machine learning libraries," *Journal of Applied Geophysics*, vol. 170, pp. 103 848–103 860, 2019.
- [13] S. Yuan, J. Liu, S. Wang, T. Wang, and P. Shi, "Seismic waveform classification and first-break picking using convolution neural networks," *IEEE Geoscience and Remote Sensing Letters*, vol. 15, no. 2, pp. 272–276, 2018.
- [14] H. Wu, B. Zhang, F. Li, and N. Liu, "Semiautomatic first-arrival picking of microseismic events by using the pixel-wise convolutional image segmentation method," *Geophysics*, vol. 84, no. 3, pp. V143–V155, 2019.
- [15] J. Wang, Z. Xiao, C. Liu, D. Zhao, and Z. Yao, "Deep-learning for picking seismic arrival times," *Journal of Geophysical Research: Solid Earth*, vol. 124, pp. 6612–6624, 2019.
- [16] X. Duan, J. Zhang, Z. Liu, S. Liu, Z. Chen, and W. Li, "Integrating seismic first-break picking methods with a machine learning approach," in *SEG Technical Program Expanded Abstracts 2018*. Society of Exploration Geophysicists, 2018, pp. 2186–2190.
- [17] W. Zhu and G. C. Beroza, "Phasenet: a deep-neural-network-based seismic arrival-time picking method," *Geophysical Journal International*, vol. 216, no. 1, pp. 261–273, 2018.
- [18] Z. E. Ross, M.-A. Meier, and E. Hauksson, "P wave arrival picking and first-motion polarity determination with deep learning," *Journal of Geophysical Research: Solid Earth*, vol. 123, no. 6, pp. 5120–5129, 2018.
- [19] L. Gao, Z.-y. Jiang, and F. Min, "First-arrival travel times picking through sliding windows and fuzzy c-means," *Mathematics*, vol. 7, no. 3, p. 221, 2019.
- [20] K. C. Tsai, W. Hu, X. Wu, J. Chen, and Z. Han, "Automatic first arrival picking via deep learning with human interactive learning," *IEEE Transactions on Geoscience and Remote Sensing*, 2019.
- [21] Y. Ma, S. Cao, J. W. Rector, and Z. Zhang, "Automatic first arrival picking for borehole seismic data using a pixel-level network," in *SEG Technical Program Expanded Abstracts 2019*. Society of Exploration Geophysicists, 2019, pp. 2463–2467.
- [22] X. Duan and J. Zhang, "Multi-trace and multi-attribute analysis for first-break picking with the support vector machine," in *SEG Technical Program Expanded Abstracts 2019*. Society of Exploration Geophysicists, 2019, pp. 2559–2563.
- [23] Y. Hollander, A. Merouane, and O. Yilmaz, "Using a deep convolutional neural network to enhance the accuracy of first-break picking," in *SEG Technical Program Expanded Abstracts 2018*. Society of Exploration Geophysicists, 2018, pp. 4628–4632.
- [24] X. Liao, J. Cao, J. Hu, J. You, X. Jiang, and Z. Liu, "First arrival time identification using transfer learning with continuous wavelet transform feature images," *IEEE Geoscience and Remote Sensing Letters*, 2019.

- [25] X. Duan and J. Zhang, "Multitrace first-break picking using an integrated seismic and machine learning method," *Geophysics*, vol. 85, no. 4, pp. WA269–WA277, 2020.
- [26] Y. Ma, S. Cao, J. W. Rector, and Z. Zhang, "Automated arrival-time picking using a pixel-level network," *Geophysics*, vol. 85, no. 5, pp. V415–V423, 2020.
- [27] C. Fernhout, P. Zwartjes, and J. Yoo, "Automatic first break picking with deep learning," *IOSR Journal of Applied Geology and Geophysics*, vol. 8, no. 5, pp. 24–36, 2020.
- [28] P. Yuan, S. Wang, W. Hu, X. Wu, J. Chen, and H. Van Nguyen, "A robust first-arrival picking workflow using convolutional and recurrent neural networks," *Geophysics*, vol. 85, no. 5, pp. U109–U119, 2020.
- [29] J. Zheng, J. M. Harris, D. Li, and B. Al-Rumaih, "Sc-psnet: A deep neural network for automatic p-and s-phase detection and arrival-time picker using single component recordings," *Geophysics*, vol. 85, no. 4, pp. 1–64, 2020.
- [30] C. Chai, M. Maceira, H. J. Santos-Villalobos, S. V. Venkatakrishnan, M. Schoenball, W. Zhu, G. C. Beroza, C. Thurber, and E. C. Team, "Using a deep neural network and transfer learning to bridge scales for seismic phase picking," *Geophysical Research Letters*, p. e2020GL088651, 2020.
- [31] Z. He, P. Peng, L. Wang, and Y. Jiang, "Enhancing seismic p-wave arrival picking by target-oriented detection of the local windows using faster-rnn," *IEEE Access*, vol. 8, pp. 141 733–141 747, 2020.
- [32] B. Xu, N. Wang, T. Chen, and M. Li, "Empirical evaluation of rectified activations in convolutional network," *arXiv preprint arXiv:1505.00853*, 2015.
- [33] S. Mannor, D. Peleg, and R. Rubinstein, "The cross entropy method for classification," in *Proceedings of the 22nd international conference on Machine learning*, 2005, pp. 561–568.
- [34] D. P. Kingma and J. Ba, "Adam: A method for stochastic optimization," *arXiv preprint arXiv:1412.6980*, 2014.

Olive Oil Ripping Time Prediction Model based on Image Processing and Neural Network

Mutasem Shabeb Alkhasawneh

Software Engineering Department, Faculty of Information and Technology
Ajloun National University, P.O. Box 43, Ajloun 26810, Jordan

Abstract—The agriculture sector in Jordan depends very much on planting the olive trees. More than ten million of olive trees are planted in the Jordanian soil. Olive fruit are harvested for two purposes; either to produce oil or to produce olive table (pickled olive). Olive fruit harvesting time for extracting the oil from the olive fruit is crucial. Hence, harvesting the olive fruit on ripping time gives the best amount and quality of oil. It also, could lose 15% to 20% of multiple values because of harvesting time. Olive fruit ripping time is varied since it depends on the rainfall, temperature and cultivation. A system to predict the optimal time for harvesting olive fruit for producing oil only is introduced. It based one Digital Image Processing (DIP) and artificial intelligent neural network. Moreover, four features were extracted from the olive fruit image based on the red, green and blue colors. The proposed system tested olive fruits in three stages of ripping time; under ripping, on ripping and over ripping. The classification accuracy achieved in the three stages was 97.51% in under ripping stage 95.10% in ripping stage, and 96.12% in over ripping stage. The proposed system performance was 96.14%.

Keywords—Neural network; image processing; olive ripping time; prediction; classifications

I. INTRODUCTION

Olive tree is the most important tree in Jordan. It represents 70% of the fruit tree in the country [1]. Approximately 560,000 dunums (560,000,000 m²) are planted with more than 10.5 million of olive trees, which represent 72.00% of the agricultures land in the kingdom of Jordan [2]. There are three common kinds of olive trees in Jordan; Nabali olive with high oil content between 28% and 33%. Rasi olive with percentage of oil varies from 15% to 28% and Sori olive for olive table. Furthermore, the investment in the olive sector passed one Billion Jordanian Dinar (JD) in 2018. Also more than 80,000 Jordanian families have benefit from this sector. According to an Agriculture Ministry of Jordan, the olive oil production increases from year to year, where 24,000 tons of olive oil were produced in 2018 with average price varied between 134,880,000 JD to 142,500,000 JD depending on the amount of produced oil in the season and the type of the olive oil. The amount and the quality of olive oil depend on rainfalls, cultivation and the harvesting time. By harvesting the olive trees on the ripping time, the best amount and quality of olive oil can be achieved [3]. Jordan loses 15% to 20% of the amount of olive oil because of harvesting time. By either harvesting the olive fruits before or after the suitable harvesting time [2]. The olive oil characteristics have its own rank among all kinds of oils consumed by human being

because of its pleasant flavor, plat ability, stability and health benefits. Harvesting the olive tree before or after ripping time, reflects the quality grade of oil characteristics, oxidation, stability and nasturtium value of the obtained product [4]. The majority of olive oil (94%) does not have the best commercial quality, because the olive fruit is not picked on the optimal harvesting time [5]. According to [6] harvesting olive fruits must be done when the oil reaches the best quality and the highest amount of oil level [3, 7]. In the Harvesting olive fruit season, the farmers attempt to estimate ripping time based on the color, texture, size and shape of the fruits. This estimation can be done by walking through the olive tree field. Factors such as the size and the shape varied depending on the amount of the rainfall, dryness and cultivation during the year. Also, factors like the color and texture of the fruit are subjective and depend on the farmer experiences. Therefore, farmers need to have additional opinion to determine the harvesting time precisely. As an additional authenticates opinion researchers have proposed different methods like analytical static [7] and intelligent system based on Digital Image Processing (DIP) and Artificial Intelligent (AI) and indeed Artificial Neural Networks (ANN). For instance, in the medical field DIP and ANN were used to classify image breast cancer and detecting brain tumor [8, 9] also new model of neural network was proposed to classify six types of disease; the proposed model has shown very high performance. A convolutional neural network was used in face image manipulation detection [10, 11]. DIP and ANN have shown great potential in managing road traffic system as in [12-14]. In addition, ANN have been widely used to predict the landslide hazard map [15]. Moreover, as a tool of classification ANN and DIP have been widely used in different fields as mentioned in [16-20]. This paper presents a model to determine the optimal time for harvesting olive fruits for oil. The new model relies on Digital Image Processing and Neural Network.

In this section, the aim of this study and general back ground for the proposed system was introduced. In Section 2, the related previous work that used Image Processing and ANN is summarized. Section 3 the data collection and the structure of Cascade Forward Neural Network (CFNN) were explained. Section 4, Image Preprocessing, Section 5, Feature Extraction, Section 6, Classification Model, Section 7, Experimental Methodology, Section 8, Results and discussions and Conclusion in Section 9.

II. RELATED WORKS

Maturities, ripeness, quality and diseases of the fruits have been subject of interest for many studies and included

different types of fruits such as Grape, Apple, Tomatoes, Cucumber, Orange, Palm oil fruits and many other fruits [21-25]. Studies on Olive fruit can be divided into classification the quality of olive fruits for olive table (pickled olive) [26, 27], external damage and diseases of olive fruit [28, 29] and olive fruit ripping time for olive oil [30-32].

To determine the stage of maturity of the olive fruit for oil, various methods were applied [29]. Maturity index (MI) is the common traditional used method to determine the optimal time for harvesting olive fruits for oil. To determine the MI, one KG of olive fruit must be collected randomly from several trees with same variety. Then, 100 olives fruit picked up randomly from 1 KG. Each 100 fruit sample separated into different eight categories of color starting from "0" deep green to "7" purple or black color. Multiply the number of fruits in each color category by the number of that color category (0 to 7) and add up all the numbers and the result divide by 100. When the MI value is 5 it's the optimum time to harvest the olives. The MI method is not accurate since it depends on the human judgment. The work in [33] approves the machine more accurate than the human on the classifying olive table. Thus, finding an automatic system to determine the optimal harvesting olive fruits time has become subject of interest for many studies. In this section, the automatic system based on DIP and ANN will be reviewed.

An automatic model for Ripping Index (RI) based on DIP and ANN introduced by [30]. One KG of olive fruits samples were collected randomly and classified to three classes, then analyzed to measure some chemical parameters; oil, sugar and total phenolic content in the olive fruits. The chemical parameters were compared with color of the fruits. The three chemical inputs and the fruit color were used as input to Multi-Layer Perceptron. The results prove that the proposed system has better results than the traditional used RI.

A study introduced on Arbquina olive fruit type. It aimed to classify the maturity of the olive fruits based on changing the color during the fruits maturity stages; green, yellow green, turning, purple, and black. The study highly recommended using the color of olive fruit as maturity index [34].

A color scale was used to determine the maturity of olive and grape fruits. The color scale generated using the well-known support vector machine based on the multidimensional regression. 250 and 200 samples respectively of grape and olive fruit were used for experimental purposes. The developed color scale can be used in various phenolic states on the fruit [21].

Image analysis was used to determine the maturity of the olive fruits. The system relied on used image segmentations include edge detections and the histogram values for the red, green and blue colors values were calculated. The olive fruit was classified to five categories based on fruit skin color; bright green, greenish yellow, greenish yellow with red black or reddish spots greater than reddish-brown, greenish-yellow with black and/or reddish spots less than reddish-brown and 100% blackish-purple or black [35].

Olive ripping phase was estimated to six phases based on the fruit skin color. The skin color histogram was manipulated in the feature selection phase, and Multi-Layer Perceptron neural network as a classifier. The obtained results showed promising results [36].

A technic was proposed to determine the olive oil based on olive fruit ripening stage using the DIP. The method start by acquiring the olive fruit image then image processing features extraction, features selection and finally the regression mode for classification the oil quality [37].

The quality of the olive oil strongly related to the quality of the collected fruits. A mathematical model based on partial least squares Discriminant Analysis (PLD), and image processing with neural network introduced to classify four type of olive fruits (Mission, Manzanillo, Ascolano, and Sevillan) to four grades (unacceptable, borderline, acceptable, and optimal). 75% and 70% correct classification rates offered by PLD, whereas 93.0% and 90.0% classification rate offered by DIP and neural network [38]. Classifying the olive fruit into different categories are done manually before the oil extraction process. Therefore, an online system that automatically cans categories the olive fruits to their quality level in different class. The study, focused on the olive fruits picked up from the tree or from the ground. In this research, the online system constructed of DIP (image entropy, grey level co-occurrence matrix and statistics like Contrast, Correlation, Energy and Homogeneity) and for classification ANN and Support Vector Machine (SVM) with achieved calcification accuracy 98.8% and 98.4% for the former and later respectively [31].

III. METHODOLOGY

The methodology of this research can be divided into: collecting olive fruit images, image processing, features extraction and classification as shown in Fig. 1.

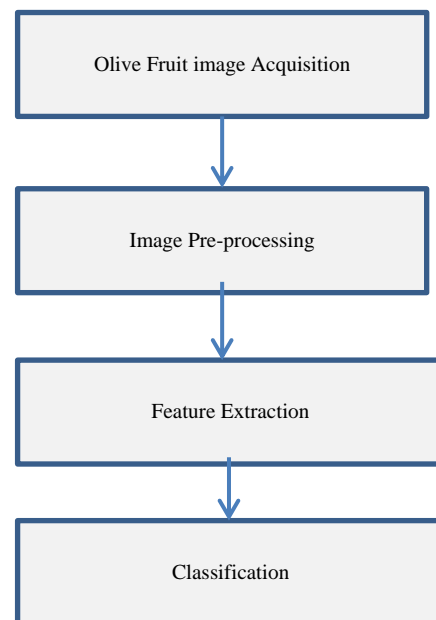


Fig. 1. Flow Chart of the Work Methodology.

A. Olive Samples

The data of the olive fruit were collected during the season 2010 from Rasi olive tree farm in Hawara, Irbid, Jordan. The data were collected between August and December olive fruit color, size and shape change faster than rest of the year. Therefore Olive fruit was randomly picked up and images were taken.

Fig. 2 shows the differences between the olive fruit color between August and December. High temperature and dry weather speed up the change of olive fruit color and vice versa, as mentioned the Sori olive is the subject for this study.

B. Acquisition of Images

Olive fruit images were taken at the farm, the images were taken in day light. Fifty images were taken every week from August to December with totally 1200 images, only ten suitable images were chosen for further process with totally 240 images. The Image acquisition system consists of digital camera Canon EOS 7D, 18 Megapixels, and white sheet of paper was setup in the farm. The deformable durable material was chosen in an attempt to approximate the type that would be available in regular farmers' hands.

1) *Image pre-processing*: In order to have a proper image for extracting information, all images must be with a standard size; thus, olive image were scaled down to 50% of its original size using Image Processing Tool Box in MATLAB Released 2013a. Then, filtering the image and remove any noise. Finally, removing the white back ground from the image, in order to have only the olive fruit as shown in Fig. 3.



(a) From August (b)September (c) November (d) December

Fig. 2. Olive Fruit Color between August and December.



Fig. 3. Olive Fruit after Removing Background.

2) *Feature extraction*: The aim of feature extraction is to achieve some features, which can be used in the classification system. In most cases the color of the fruit is the strongest indication for the fruit maturity. The color of the olive fruits starts changing gradually from dark green to dark black. The image color component Red, Green and Blue (RGB) was used to calculate the mean, median and Standard Deviation (SD) of RGB colors.

IV. CLASSIFICATIONS MODEL

Cascade forward neural network (CFNN) is one of the artificial neural network types. It construct of input, hidden and output layer. Where, input layer connected to one or more hidden layer which also connected to output layer. CFNN also has a connection between the input layer and every layer in the neural network. In addition CFNN also has another connection from each layer to the successive layers in the network Demuth [39]. CFNN has the same principle of work and methodology that multi-layer feed forward neural network do, but the extra two connections [40]. The later connections are introduced to improve the neural network generalizations [41]. Fig. 4. Shows topology of CFNN with three layers; input, hidden and output layer.

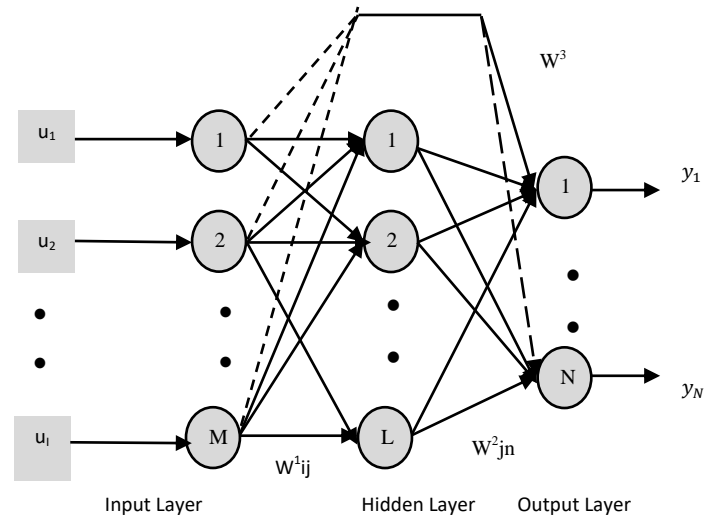


Fig. 4. Cascade Forward Neural Network.

Each neuron in the hidden layer receives input from the input layer. The total input to the hidden layer from all input neurons can be found as in Eq. (1).

$$net_{h_j^{(k)}} = \sum_{i=1}^M w^1_{i,j} u_i^{(k)} \text{ for } 1 \leq j \leq M \quad (1)$$

net_{h_j} is the total of input weights to the hidden layer, where $i = 1, 2, \dots, M$, indexed to the input layer neurons. $w^1_{i,j}$ represent the weight from input layer neuron to hidden layer. k denote to the moment. $u_i^{(k)}$ represent the inputs of neural network.

Eq. (2) shows the total output of the hidden layer at time k $o_{h_j^{(k)}}$. Where $f(*)$ is the linear or nonlinear of hidden layer output function.

$$o_{h_j}^{(k)} = f\left(\text{net}_{h_j}^{(k)}\right) \quad (2)$$

The output of one hidden layer of CFNN can be found as in Eq. (3)

$$y_n^{(k)} = g\left(\sum_{j=1}^L w_{jn}^2 o_{h_j}^{(k)} + \sum_{i=1}^M w_{in}^3 u_i^k\right) \text{ for } 1 \leq n \leq N \quad (3)$$

Where, $y_n^{(k)}$ is the outputs of CFNN, and $n = 1, 2, \dots, N$. is the output neurons.

$g(*)$ is the linear or nonlinear output function of output layer. The connection weight between the nodes in the hidden layer and output layer represented by W_{jn}^2 .

V. EXPERIMENT METHODOLOGY

The experimental process was divided into; preparing the data that will be used for CFNN, the structures of the CFNN and the CFNN performance measurement. Preparing the olive fruit data set includes: normalizing all the features that extracted from olive fruit such RGB color. The later has three different values namely mean, mean Standard Deviation (SD), median and median SD. For each feature the normalization can be varied between 0 and 1 based on the Eq. (7).

$$\text{Normalised value}(i) = \frac{\text{value}(i) - \text{minimum value}(i)}{\text{maximum value}(i) - \text{minimum value}(i)} \quad (7)$$

Where the value (i) is the value to be normalized and (I) is the minimum or the maximum pixels value for every single feature. The intelligent system targets are divided into three classes; before ripping time, on ripping time and over ripping time are represented by 0, 1 and 2, respectively. Moreover, dividing the normalized data before entering the CFNN is a crucial to avoid over fitting during the training process of the CFNN therefore; the normalized data was randomized and then divided to three different sets, 70%, 15% and 15% for training, testing and validation, respectively.

As mentioned, the CFNN with one input, one hidden and output layer structure can solve most of the classifications problems. The number of the neurons in the hidden layer has a high impact on the CFNN performance. For this research, the number of the hidden neurons was tested from 5 to 50 neurons, by increasing the number of the neurons by 5 each time and the accuracy was measured. CFNN with 9 neuron in the hidden layer was found to be the optimal for this study. CFNN Over fitting is another common errors that facing neural network during the training. To overcome this problem, the neural network will stop after 500 epoch, If the performance the neural network could not reach the 0.01 as Mean Square Error (MSE).

The performance of the CFNN classification accuracy was measured during the training and testing stage. The accuracy was calculated by using the Eq. (8).

$$\text{Accuracy} = \frac{\text{Number of olive fruit ripping satge correctly classified}}{\text{Total number of olive fruit sample}} \quad (8)$$

VI. RESULTS AND DISCUSSIONS

In this section and following subsections, the feature extractions and CFNN performance for the olive fruit maturity stages; under ripping time, on ripping time and over ripping time will be evaluated.

A. Under Ripping Stage

The olive fruit color, in under ripping stage, varied between the dark green and yellowish. In this stage the average space of the red color was 66.83% and the Mean SD was 2.56%, while the median and SD median for the red color was 66.71% and 4.50% respectively. The values for green color were 72.30%, 2.08% and 72.15%, 1.50% for the mean, SD mean, median and SD median respectively. Moreover, 1.50%, 40.78%, 3.01%, 39.8% and 2.82% were in orders the values of mean blue, means SD, median blue and median SD blue value. For this stage the red color is considered green color [42] as shown in Table I.

Fig. 5 shows the CFNN classification accuracy for training and testing. The results show that the CFNN classified the olive fruit on under ripping stage with 99.10% for training data and 97.51% for testing data.

TABLE I. FEATURES EXTRACTION VALUES FOR UNDER RIPPING STAGE

Under Ripping Stage	
Mean Red Value	66.83%
Mean SD Red Value	2.56%
Median Red Value	66.71%
Median SD Red value	4.5%
Mean Green Value	72.3%
Mean SD Green Value	2.08%
Median Green Value	72.15
Median SD Green Value	1.5%
Mean Blue Value	40.78%
Mean SD Blue Value	3.01%
Median Blue Value	39.8%
Median SD Blue Value	2.82%

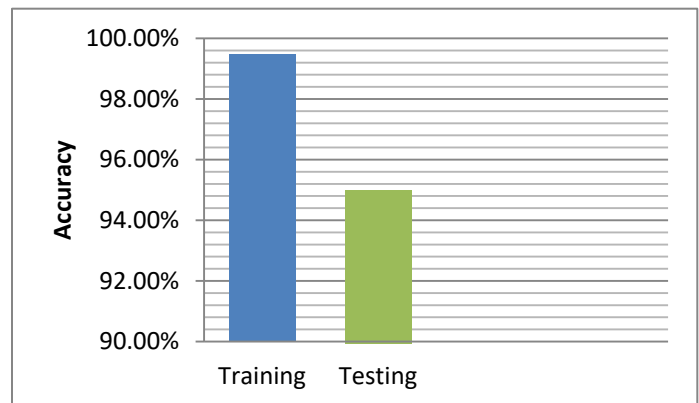


Fig. 5. CFNN Training and Testing Results for under Ripping Olive Fruits Data Set.

B. On Ripping Stage

The olive fruit color on ripping stage is varied between blackish to purple. The red color values for the mean, mean SD, median and median SD in were in ordered 59.71%, 2.5%, 60.12% and 3.08%. The average space of the green was 40.20% and the Mean SD was 1.90%, while the median and SD median for the red color was 38.99% and 2.21% respectively. The values for blue color were 35.90%, 3.56% and 36.79%, 3.31% for the mean, SD mean, median and SD median, respectively as shown in Table II.

98.58% of the olive was correctly classified for training and 95.10% of olive fruits were correctly classified in the testing stage as can be noticed from Fig. 6.

C. Over Ripping Stage

The olive fruit color for over ripping stage is dark black. The values of red, green and blue color as seen from Table III were Mean red 23.65%, mean SD 1.67%, Median red 23.63% and median SD 1.71%. The green color values for the mean, mean SD, median and median SD in were in ordered 21.8%, 1.34%, 21.90% and 1.33%. The values for blue color were 22.23%, 1.11% and 21.97%, 2.10% for the mean, SD mean, median and SD median respectively as shown in Table III.

TABLE II. FEATURES EXTRACTION VALUES FOR ON RIPPING STAGE

Under Ripping Stage	
Mean Red Value	59.71%
Mean SD Red Value	2.5%
Median Red Value	60.12%
Median SD Red Value	3.08%
Mean Green Value	40.20%
Mean SD Green Value	1.90%
Median Green Value	38.99%
Median SD Green Value	2.21%
Mean Blue Value	35.90%
Mean SD Blue Value	3.56%
Median Blue Value	36.79%
Median SD Blue Value	3.31%

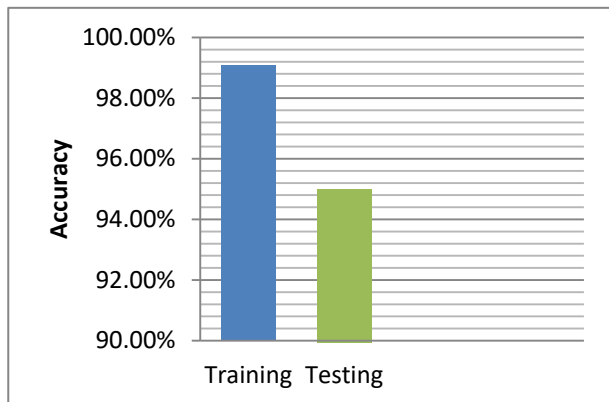


Fig. 6. CFNN Training and Testing Results for on Ripping Olive Fruits Data Set.

TABLE III. FEATURES EXTRACTION VALUES FOR OVER RIPPING STAGE

Under Ripping Stage	
Mean Red Value	23.65%
Mean SD Red Value	1.67%
Median Red Value	23.63%
Median SD Red Value	1.71%
Mean Green Value	21.8%
Mean SD Green Value	1.34%
Median Green Value	21.90%
Median SD Green Value	1.33%
Mean Blue Value	22.23%
Mean SD Blue Value	1.11%
Median Blue Value	21.97%
Median SD Blue Value	2.10%

In Fig. 7, it can be clearly seen that the CFNN achieved 97.00% of accuracy through the training stage and 96.12% accuracy through the testing stage.



Fig. 7. CFNN Training and Testing Results for under Ripping Olive Fruits Data Set.

VII. CONCLUSION

This work introduced a system to predict the optimal time for harvesting olive fruits for extracting oil. The methodology of this work was started by taking pictures for the Rasi olive in different period of time. Then extracting features from olive fruits RGB color. CFNN neural network was used to classify the olive fruits to three levels; under ripe, on ripe and over ripe. In this study an artificial intelligent system was introduced for decision support task of harvesting olive fruits for extracting oil, where the amount and the quality of the olive are increased. Future work should be able to predict the olive ripening time in the real time.

REFERENCES

- [1] Al Rwahnih, M. and M. Al Khasawneh, Jordan, in Production and exchange of virus-free plant propagating material in the Mediterranean region, B. Di Terlizzi, A. Myrta, and V. Savino, Editors. 2001, Bari : CIHEAM. p. 83-85.
- [2] Times, J., Olive trees cover 72% of Jordan’s agricultural land. Jordan times, 2019.
- [3] Zamora, R., M. Alaiz, and F.J. Hidalgo, Influence of cultivar and fruit ripening on olive (*Olea europaea*) fruit protein content, composition, and

- antioxidant activity. *Journal of agricultural and food chemistry*, 2001. 49(9): p. 4267-4270. DOI: 10.1021/jf0104634.
- [4] Gasparini, P., Extra Virgin Olive Oil Production in Jordan. Preliminary overlook on the sector. United nations industrial development organization. , 2001. 1(1).
- [5] Liphshitz, N., et al., Wild Olive (*Olea europaea*) Stones from a Chalcolithic Cave at Shoham, Israel and their Implications. *Tel Aviv: Journal of the Institute of Archaeology of Tel Aviv University*, 1996. 23: p. 135-142. DOI: 10.1179/033443596788138729.
- [6] Stefanoudaki, E., F. Kotsifaki, and A. Koutsaftakis, Classification of virgin olive oils of the two major cretan cultivars based on their fatty acid composition. *Journal of the American Oil Chemists' Society*, 1999. 76(5): p. 623-626. doi:10.1007/s11746-999-0013-7.
- [7] García, J.M., S. Sella, and M.C. Pérez-Camino, Influence of Fruit Ripening on Olive Oil Quality. *Journal of Agricultural and Food Chemistry*, 1996. 44(11): p. 3516-3520. doi.org/10.1021/jf950585u.
- [8] Abdul-Kadir, N.A., et al. Applications of cascade-forward neural networks for nasal, lateral and trill arabic phonemes. in *Information Science and Digital Content Technology (ICIDT)*, 2012 8th International Conference on. 2012.
- [9] S. Giraddi and S. V. Vaishnavi, "Detection of Brain Tumor using Image Classification," 2017 International Conference on Current Trends in Computer, Electrical, Electronics and Communication (CTCEEC), Mysore, 2017, pp. 640-644, doi: 10.1109/CTCEEC.2017.8454968.
- [10] L. Minh Dang, Syed Ibrahim Hassan, Suhyeon Im, Hyeonjoon Moon, Face image manipulation detection based on a convolutional neural network. *Expert Systems with Applications*, Volume 129, 2019, Pages 156-168, ISSN 09574174, <https://doi.org/10.1016/j.eswa.2019.04.005>.
- [11] Guanjun Guo, Hanzi Wang, Yan Yan, Jin Zheng, Bo Li, A fast face detection method via convolutional neural network, *Neurocomputing*, Volume 395, 2020, Pages 128-137, ISSN 0925-2312, <https://doi.org/10.1016/j.neucom.2018.02.110>.
- [12] Zou, X., Y. Fu, and X. Li. Image Feature Recognition of Railway Truck Based on Machine Learning. in *2019 IEEE 3rd Information Technology, Networking, Electronic and Automation Control Conference (ITNEC)*. 2019.
- [13] Jagadamba, G., S. Purohit, and G. Chayashree. *Campus Vehicle Monitoring Through Image Processing*. in *Emerging Research in Electronics, Computer Science and Technology*. 2019. Singapore: Springer Singapore.
- [14] Barreto S.C., Lambert J.A., de Barros Vidal F. (2019) Using Synthetic Images for Deep Learning Recognition Process on Automatic License Plate Recognition. In: Carrasco-Ochoa J., Martínez-Trinidad J., Olvera-López J., Salas J. (eds) *Pattern Recognition. MCP 2019. Lecture Notes in Computer Science*, vol 11524. Springer, Cham. https://doi.org/10.1007/978-3-030-21077-9_11.
- [15] Alkhasawneh, M.S., et al., Intelligent Landslide System Based on Discriminant Analysis and Cascade-Forward Back-Propagation Network. *Arabian Journal for Science and Engineering*, 2014. 39(7): p. 5575-5584. 10.1007/s13369-014-1105-8.
- [16] L. Benali, G. Notton, A. Fouilly, C. Voyant, R. Dizene, Solar radiation forecasting using artificial neural network and random forest methods: Application to normal beam, horizontal diffuse and global components, *Renewable Energy*, Volume 132, 2019, Pages 871-884, ISSN 0960-1481, <https://doi.org/10.1016/j.renene.2018.08.044>.
- [17] Li, D., et al., A novel CNN based security guaranteed image watermarking generation scenario for smart city applications. *Information Sciences*, 2019. 479: p. 432-447. doi.org/10.1016/j.ins.2018.02.060.
- [18] Kelsey A. Ramírez-Gutiérrez, Alejandro Medina-Santiago, Alfonso Martínez-Cruz, Ignacio Algreto-Badillo, Hayde Peregrina-Barreto, RETRACTED: Eggshell deformation detection applying computer vision, *Computers and Electronics in Agriculture*, Volume 158, 2019, Pages 133-139, ISSN 0168-1699, <https://doi.org/10.1016/j.compag.2019.01.036>.
- [19] Chang, Y., Research on de-motion blur image processing based on deep learning. *Journal of Visual Communication and Image Representation*, 2019. 60: p. 371-379. doi.org/10.1016/j.jvcir.2019.02.030.
- [20] Abdollahi, H., et al., Prediction and optimization studies for bioleaching of molybdenite concentrate using artificial neural networks and genetic algorithm. *Minerals Engineering*, 2019. 130: p. 24-35. doi.org/10.1016/j.mineng.2018.10.008.
- [21] Avila, F., et al., A method to construct fruit maturity color scales based on support machines for regression: Application to olives and grape seeds. *Journal of Food Engineering*, 2015. 162: p. 9-17. doi.org/10.1016/j.jfoodeng.2015.03.035.
- [22] Yuri, J.A., et al., Effect of cultivar, rootstock, and growing conditions on fruit maturity and postharvest quality as part of a six-year apple trial in Chile. *Scientia Horticulturae*, 2019. 253: p. 70-79. doi.org/10.1016/j.scienta.2019.04.020.
- [23] Pacheco, W.D.N. and F.R.J. López. Tomato classification according to organoleptic maturity (coloration) using machine learning algorithms K-NN, MLP, and K-Means Clustering. in *2019 XXII Symposium on Image, Signal Processing and Artificial Vision (STSIVA)*. 2019. doi: 10.1109/STSIVA.2019.8730232.
- [24] Ranjan, P., et al., Orange-fleshed cucumber (*Cucumis sativus* var. *sativus* L.) germplasm from North-East India: agro-morphological, biochemical and evolutionary studies. *Genetic Resources and Crop Evolution*, 2019. 66(6): p. 1217-1230. doi.org/10.1007/s10722-019-00778-6.
- [25] Mubin, N.A., et al., Young and mature oil palm tree detection and counting using convolutional neural network deep learning method. *International Journal of Remote Sensing*, 2019. 40(19): p. 7500-7515. DOI: 10.1080/01431161.2019.1569282.
- [26] Hussain Hassan, N.M. and A.A. Nashat, New effective techniques for automatic detection and classification of external olive fruits defects based on image processing techniques. *Multidimensional Systems and Signal Processing*, 2019. 30(2): p. 571-589. DOI: 10.1007/s11045-018-0573-5.
- [27] Ponce, J.M., et al., Automatic Counting and Individual Size and Mass Estimation of Olive-Fruits Through Computer Vision Techniques. *IEEE Access*, 2019. 7: p. 59451-59465.
- [28] Ponce, J.M., A. Aquino, and J.M. Andújar, Olive-Fruit Variety Classification by Means of Image Processing and Convolutional Neural Networks. *IEEE Access*, 2019. 7: p. 147629-147641. doi: 10.1109/ACCESS.2019.2947160.
- [29] Gonzalez-Fernandez, I., et al., A critical review on the use of artificial neural networks in olive oil production, characterization and authentication. *Critical Reviews in Food Science and Nutrition*, 2019. 59(12): p. 1913-1926. DOI: 10.1080/10408398.2018.1433628.
- [30] Furferi, R., L. Governi, and Y. Volpe, ANN-based method for olive Ripening Index automatic prediction. *Journal of Food Engineering*, 2010. 101(3): p. 318-328. doi.org/10.1016/j.jfoodeng.2010.07.016.
- [31] Aguilera Puerto, D., et al., Online system for the identification and classification of olive fruits for the olive oil production process. *Journal of Food Measurement and Characterization*, 2019. 13(1): p. 716-727. doi.org/10.1007/s11694-018-9984-0.
- [32] Diaz, R., et al., Comparison of three algorithms in the classification of table olives by means of computer vision. *Journal of Food Engineering*, 2004. 61(1): p. 101-107. doi.org/10.1016/S0260-8774(03)00191-2.
- [33] Hassan, H., A.A. El-Rahman, and M. Attia. Color properties of olive fruits during its maturity stages using image analysis. in *AIP Conference Proceedings*. 2011. AIP.
- [34] Guzmán, E., et al., Determination of the olive maturity index of intact fruits using image analysis. *Journal of Food Science and Technology*, 2015. 52(3): p. 1462-1470. DOI.org/10.1007/s13197-013-1123-7.
- [35] Mora, M., J. Aliaga, and C. Fredes. Olive Ripening Phase Estimation based on Neural Networks. in *IX Congreso Argentino de AgroInformática (CAI 2017)-JAIIO 46-43 CLEI (Córdoba, 2017)*. 2017.
- [36] Navarro Soto, J.S.M., S.; Martínez Gila, D.; Gómez Ortega, J.; Gámez García, J., Fast and Reliable Determination of Virgin Olive Oil Quality by Fruit Inspection Using Computer Vision. *Sensors*, 2018. 11(18). DOI.org/ 10.3390/s18113826.
- [37] Pariente, E.S., et al., On-site images taken and processed to classify olives according to quality – The foundation of a high-grade olive oil. *Postharvest Biology and Technology*, 2018. 140: p. 60-66. doi.org/10.1016/j.postharvbio.2018.02.012.

- [38] Demuth, H.; Beale, M.H.; Hagan, M.T.: Neural Network Toolbox User's Guide. The MathWorks, Inc., Natick (2009).
- [39] Alkhasawneh, M.S. and L.T. Tay, A Hybrid Intelligent System Integrating the Cascade Forward Neural Network with Elman Neural Network. *Arabian Journal for Science and Engineering*, 2018. 43(12): p. 6737-6749. doi.org/10.1007/s13369-017-2833-3.
- [40] Gao, X.Z.; Gao, X.M.; Ovaska, S.J.: A modified Elman neural network model with application to dynamical systems identification. In: *IEEE International Conference on Systems, Man, and Cybernetics*, 1996 (1996).
- [41] Hassan, H., A. El-Rahman, and M. Attia, Color Properties Of Olive Fruits During Its Maturity Stages Using Image Analysis. *AIP Conference Proceedings*, 2011. 1380.

A New Discretization Approach of Bat and K-Means

Rozlini Mohamed¹, Noor Azah Samsudin²

Faculty of Computer Science and Information Technology
Universiti Tun Hussein Onn Malaysia (UTHM)
Parit Raja, Johor, Malaysia

Abstract—Bat algorithm is one of the optimization techniques that mimic the behavior of bat. Bat algorithm is a powerful algorithm in finding the optimum feature data collection. Classification is one of the data mining tasks that useful in knowledge representation. But, the high dimensional data become the issue in the classification that interrupt classification accuracy. From the literature, feature selection and discretization able to overcome the problem. Therefore, this study aims to show Bat algorithm is potential as a discretization approach and as a feature selection to improve classification accuracy. In this paper, a new hybrid Bat-K-Mean algorithm refer as hBA is proposed to convert continuous data into discrete data called as optimize discrete dataset. Then, Bat is used as feature selection to select the optimum feature from the optimized discrete dataset in order to reduce the dimension of data. The experiment is conducted by using k-Nearest Neighbor to evaluate the effectiveness of discretization and feature selection in classification by comparing with continuous dataset without feature selection, discrete dataset without feature selection, and continuous dataset without discretization and feature selection. Also, to show Bat is potential as a discretization approach and feature selection method. . The experiments were carried out using a number of benchmark datasets from the UCI machine learning repository. The results show the classification accuracy is improved with the Bat-K-Means optimized discretization and Bat optimized feature selection.

Keywords—Classification; discretization; feature selection; optimization algorithm; bat algorithm

I. INTRODUCTION

Bat Algorithm (BA) is a metaheuristic optimization algorithm that is found on echolocation characteristics of microbats where the emission and loudness has a varying pulse rates [1]. BA has been employed to resolve various optimization problems in many application. BA could possibly perform better than Particle Swarm Optimization (PSO) [2]. Further, unlike PSO, the parameter of BA can be varied. Moreover, the BA is capable to zoom the solving space, automatically which eventually allows local exploitation.

In [3] BA was used for classification in medical data. Moreover, this research [4] objective is to improve the classification performance in large data. This objective is achieved by employing BA as feature selection to select important feature in real-life dataset from UCI repository. In [5] hybridization of BA with Weighted Extreme Learning Machine (WELM) known as WELM-BAT was proposed to adjust the parameter for WELM. WELM-BAT was tested on real world medical diagnosis datasets and the result shows the performance of classification is improved.

The classification performance is improved using BA in the large data [6]. In [7] a hybrid Cross-Entropy method (BBACE) with Binary Bat Algorithm is used for feature selection in Big Data. To evaluate the effectiveness of the proposed method, the classifier such as Support Vector Machine and Naïve Bayes is used as a comparison regarding to time processing and accuracy. The results show that BA produced a better result compare to PSO.

Classification aims to assign data into predefined topic correctly. High dimensional, data redundancy and large amount of data are the factors that influence the classification performance. In data mining, classification is one of the popular problems that gets attention from researchers.

In real world datasets, the value of datasets are mixed data (continuous and discrete data), continuous data and discrete data. But some classification approaches require discrete data only. Thus, a process to convert from continuous data into discrete data is required. The process is known as discretization. The discretization task is to convert the continuous values into a small number of range based on the break points and then mapping each continuous value within the range, where each range is assigning to a discrete value. Discretization is needed before performing the feature selection task.

In classification problem, it is challenging to deal with irrelevant features caused by huge size of data [8]. Feature selection aims to select the relevant features and remove the irrelevant features. On the other hand, discretization aims to discretize the continuous value. Data representation in discrete value is easier to understand. Let consider this example, a person's weight has various readings, and it is difficult and ambiguous to interpret whether the reading is light or heavy. Discretization will place the weighted reading within a certain interval and the weight can be easily interpreted as to whether it is light or heavy.

This paper has proposed implementation of optimizing algorithm in discretization and feature selection steps. To implement the steps, BA is hybrid with the K-Means as a discretization approach. Then BA is then used as a feature selection to determine optimum features.

This paper is organized as follows: related works is presented in Section 2. Section 3 discusses the proposed approach based on K-Means and Bat algorithm and the description of the data sets. Section 4 discusses the experiment results and Section 5 presents the conclusion.

II. RELATED WORKS

This section briefly discuss on basic concept of Bat algorithm and reviewed the previous work on classification, discretization, and feature selection.

A. Bat Algorithm

BA is an intelligent optimization algorithm to solve complex engineering problems. The BA is motivated by the emitting sound pulse of bats known as echolocation. The echolocation of bats it used to search prey. In Fig. 1 shows bat will emit the sound to prey or obstacle refers as object. Then the object gives the reflection wave to bat by returning the echo wave to bat. From these echo wave, the bat can differentiate type of object; prey or obstacle event though in the darkness.

In this paper, the rules of bat algorithm are employs as follows:

1) *Rule 1:* The echolocation of bats used to sense the distance and they can recognize object and differentiate the kind object; obstacle or prey.

2) *Rule 2:* Bat randomly flies with varying wavelength, λ and loudness, A_0 , with velocity, v_i at position x_i with a fixed frequency, f_{min} to search for prey. The wavelength (or frequency) is automatically adjusted of their emitted pulses and adjust the rate of pulse emission $r \in [0,1]$, according to distance of target prey.

3) *Rule 3:* The loudness value are varied and can assume a large positive value, A_{max} to a small constant value, A_{min} . Thus based on the above rules, the location x_i^t and velocities v_i^t can be improve regarding to equation as follows;

$$f = f_{min} + (f_{max} - f_{min})\lambda, \quad (1)$$

$$v_i^t = v_i^{t-1} + (v_i^{t-1} - v_*)f_i, \quad (2)$$

$$x_i^t = x_i^{t-1} + v_i^t, \quad (3)$$

where $\lambda \in [0,1]$ is a random vector drawn from a uniform distribution.

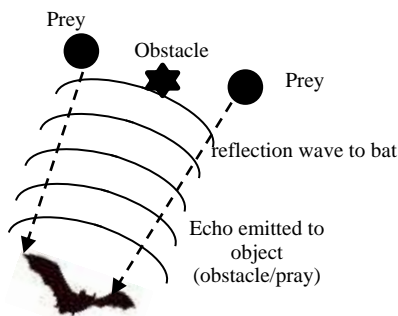


Fig. 1. Echolocation behavior by Bat.

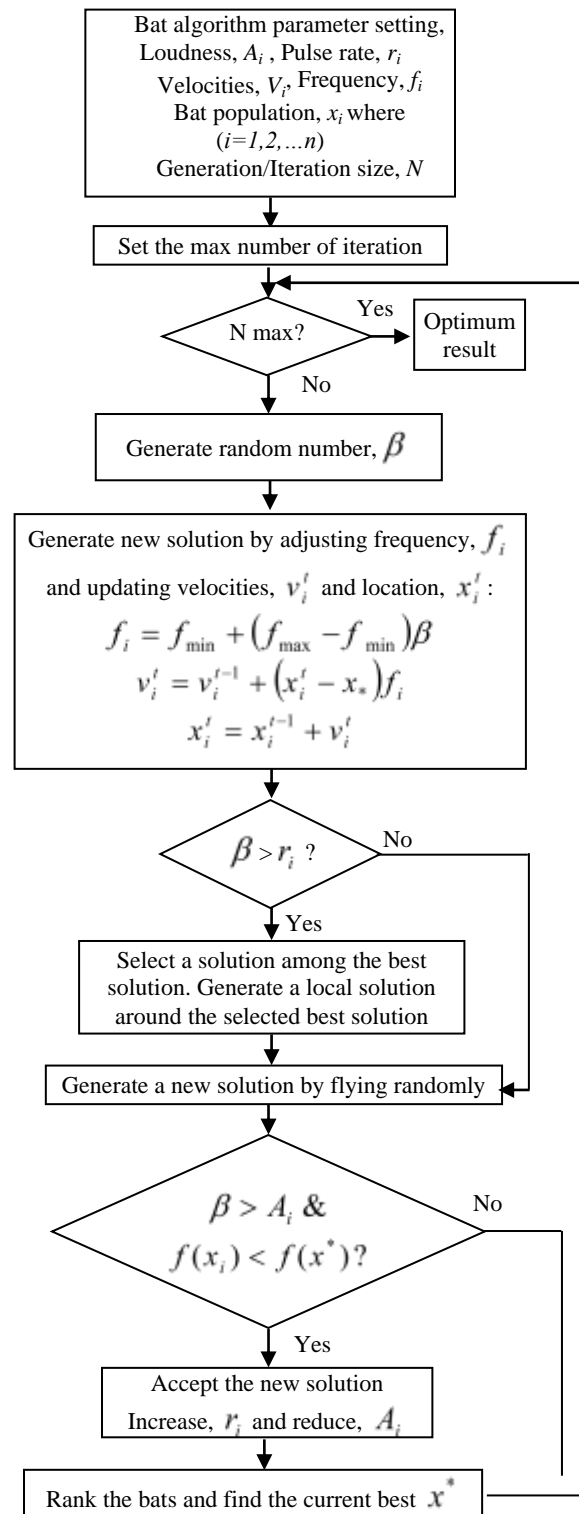


Fig. 2. Bat Algorithm [1].

Fig. 2 shows the flowchart for the Bat algorithm. The algorithm starts with initializing the value of loudness, pulse rate, velocity, frequency, number of bat population and the maximum number of iteration. While the number maximum iteration is not exceeded, the random number is generated to produce a new solution. In this new solution involve adjusting the previous frequency, updating the previous velocity as well

as updating the previous location. The equation 1, 2 and 3 are used to calculate these new frequencies, velocity and location, respectively. The next process is to proceed if the random number is higher than the pulse rate, the local best solution is determined among the solution if not continue to generate the new solution.

Later, if the value of the random number is higher than loudness and frequency in the previous location is lower than the frequency in a new location, accept the new solution otherwise continue to rank the best bat with their frequency. The process is repeated until reach the maximum iteration and when the iteration reaches the algorithm will come out the optimum results.

B. Classification

Various algorithms were designed for supervised data classification which are based on totally different approaches, for example, neural network [9] and text clustering [10]. Cano in 2019 [11] and Shafiq in 2020 [12] presented good review of data classification methods, including their performance measure and comparison.

Ayyagari [13] proposed a new classification algorithm that integrate the CART, k-NN and SVM. The proposed algorithm was used to handle the problem on imbalanced datasets and class overlap that influence the performance of classification algorithm.

One of the approaches can be used for supervised data classification is an optimization algorithm based on swarm. The most influential important factors on the classification performance are discretization and feature selection that occur in data preparation phase. For example, Zhou in their research, employed discretization in feature selection to find relevant feature [14]. In another research, Ucar employed P-Score in feature selection algorithms to improve classification performance [15].

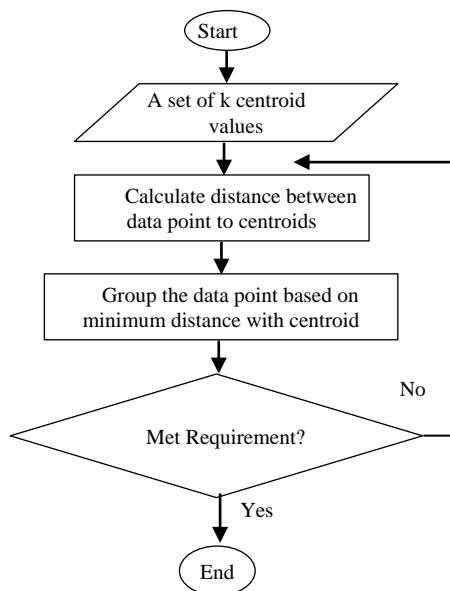


Fig. 3. K-Means Flowchart.

C. Discretization

Discretization can be defined as transforming continuous values into numerical values. In classification, discretization process is employed in data processing step before performing the feature selection process. Data preparation is one of the critical steps in classification problems [16]. The results from preparation is directly incorporated into the model and final results will be obtained. This means a good data source from data processing can increase the accuracy of classification performance.

A discretization approach was proposed to handle a mix of categorical and numeric safety data using fuzzy c means algorithm to discretize values [17]. The research in [18] has employed fuzzy discretization with Random Forest (RF) classifier to enhance labeling accuracy. In [19], Boltzmann machine is used in discretization process.

K-Means was describe by J. MacQueen in 1967 is an iterative algorithms [20]. The K-Means is used as the discretization algorithm [21]. The standard K-Means algorithm as shows in Fig. 3. From Fig. 3, the number k centroid is determined randomly. k is the number of class. Then the distance between data and each k centroid is calculated. The data is grouped into a pre-defined class according to the minimum distance between data and centroid. The process is repeated until the cluster centroid value stop changing.

This study has employed K-Means as pre-treatment method where data is discretized by K-Means before classification process. In [22] K-Means was employed to discretize the mixed data, in which the datasets present both, numerical and categorical attributes. In [23], K-Means is combined with discretization technique and Naïve Bayes to solve the problem in anomaly based intrusion detection for network intrusion detection system.

D. Feature Selection

In classification problem, feature selection is an effective method for dimensional reduction and helps in improving classification performance. Rachman and Rustam [24] in their proposed work researcher have use Fisher's Ratio algorithm to select cancer data. Their experiment reveals that feature selection gives a better result on classification accuracy.

Cheruku and Edla [25] highlight that the problems in medical data classification are redundant and high-dimensional. These problems were solved with improvements in data preparation before classification step. The research has proposed the Branch and Bound algorithm in feature selection step too.

Mithy and KrishnaPriya [26] has employed various feature selection methods in prediction of anemia for pregnant women. The feature selection methods employed rough set base fuzzy threshold in prediction and give promising results.

Reem Kadry and Osama Ismael [27] has improved the K-Nearest Neighbour performance in multidimensional data classification problem. In their work Particle Swarm Optimization (PSO) algorithm is employed to find out the optimum feature on Soybean datasets.

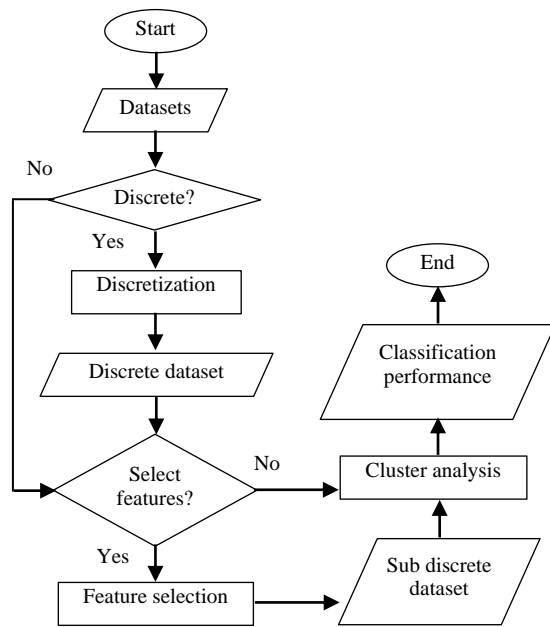


Fig. 4. Research Framework.

III. METHODOLOGIES

The experiments are carried out on nine benchmark datasets from UCI machine learning repository were used as input data and the detail about datasets are shown in Table I. The nine datasets refer as contS dataset and become the initial datasets. Assume the contS consist of the datasets as shown in Table I where,

$$\text{contS} = \{\text{DS1, DS2, DS3, DS4, DS5, DS6, DS7, DS8, DS9}\}$$

In this research, BA is hybrid with K-Means discretization refers as hBA and the hBA is enhance by employ BA as feature selection and refer as hfBA. Fig. 4 shows the framework in this research that involve two main process; 1) discretization process and 2) feature selection process. The implement of hBa and hfBA are explain in the following section.

A. hBA Approach

From Fig. 4, the approach start with the continuous datasets (contS) is convert into discrete data by using Bat-K-Means algorithm (hBA). From Fig. 2, the number k centroid is randomly define, but in hBA dataset, k centroid is according to optimum result from BA as shown in Fig. 3 and generate a new datasets which is optimize discrete dataset refers as hbaS dataset. In this approach, does not used feature selection so the algorithm will continue to the next process which is cluster analysis by using k-Nearest Neighbours. Finally, classification accuracy is measured.

B. hfBA Approach

From Fig. 4, the hfBA approach start in feature selection process. Where, BA algorithm as shown in Fig. 3 is applied to select the optimum feature after discretization with hBA approach. Then a new dataset refer as sub discrete dataset, hfBaS dataset is generated.

In hfBA approach, the size of bat represent by N length, where N is the total number of features in a dataset. The information regarding the instances is given by $I = \{i_1, i_2, \dots, i_n\}$ where n is the number of instance. Each instance is $I_i = \{a_{i1}, a_{i2}, \dots, a_{ik}\}$, where k is the number of attributes for the I_i -th instance in the DS dataset.

For example, it is assumed that DS dataset, has 10 attributes, 25 instances and 50 generations or repetitions. After 50 repetitions, the 10 -th bat or instance number 10^{th} represented by I_{10} is considered the best in the population. The optimum value for 10^{th} instance is $I_{10} = \{a_{10,1}, a_{10,2}, \dots, a_{10,10}\}$. Thus the optimum value for attributes is given by $att = \{a_{10,1}, a_{10,2}, \dots, a_{10,10}\}$. Based on BA, the minimum distance is assume as optimum value, so, in this study only value of $att = 0$ are selected. For example, $att = \{1,0,1,0,1,0,0,0,1,1,1,1,0,1,0\}$, so the attributes 1,3,5,9,10,11,12, and 14 are irrelevant features and will removes from dataset.

This research also employ K-Means discretization to contS datasets refers as discrete datasets (dkS). Besides, BA applied to select optimum feature from dkS and select feature from contS. The approach is follows the algorithm as shown in Fig. 4. The approach and the generated datasets are simplify in Table II.

TABLE I. DATASET INFORMATION

Dataset	No of Instances	No of Attributes
Credit Approval, DS1	690	15
Hill Valley, DS2	606	100
Image Segmentation, DS3	210	19
Libras Movement, DS4	360	90
Plant Species, DS5	1600	64
Steel Plates Faults, DS6	1941	27
Urban Land, DS7	507	147
Automobile, DS8	159	25
Yeast, DS9	1484	8

TABLE II. APPROACH AND DERIVED DATASET

Approach	Experiment	Datasets
	Continuous dataset or original datasets	contS={DS1, ..., DS9}
cfBA	To select feature from contS datasets using BA	cfbaS={cfbaS1, ..., cfbaS9}
dK	To convert contS into discrete dataset using K-Means discretization	dkS={dkS1, ..., dkS9}
dfBA	To select feature from dkS datasets using BA	dfbaS={dfbaS1, ..., dfbaS9}
hBA	To convert contS into discrete dataset using hybrid K-Means classifier with BA	hbaS={hbaS1, ..., hbaS9}
hfBA	To select feature from hBS datasets using BA	hfbaS={hfbaS1, ..., hfbaS9}

IV. EXPERIMENTS AND RESULTS

In this section, the experiments are set up to show Bat algorithm is potential as discretization approach and as feature selection to improve classification accuracy. Four experiments were conducted to show the BA in the discretization process and one experiment to show BA in discretization and feature selection process.

The comparison of hbaS dataset with contS, cfbaS, dkS and df of hfbaS datasets are conducted. The comparison results show in Table III that analyze by k-Nearest Neighbours for all datasets including initial datasets and new datasets. For easier understanding, the results are presented in a graphical form according to the following experiment where involving comparisons between two data sets only.

1) 1st experiment: the experiment is conducted to compare hbaS datasets with contS dataset and the result is shown in Fig. 5.

2) 2nd experiment: the experiment is conducted to compare hbaS datasets with cfbaS dataset and the result is shown in Fig. 6.

3) 3rd experiment: the experiment is conducted to compare hbaS datasets with dkS dataset and the result is shown in Fig. 7.

4) 4th experiment: the experiment is conducted to compare hbaS datasets with dfbaS and the result is shown in Fig. 8.

5) 5th experiment: the experiment is conducted to compare hbaS datasets with hfbaS and the result is shown in Fig. 9.

Fig. 5 presents the comparison between hbaS dataset with contS dataset. The purpose of this experiment is to identify which datasets give the better classification accuracy, either datasets with optimize discretization or continuous (original) datasets. From the results, classification accuracy of 3 datasets are improved by hBA which are DS1, DS5 and DS7. This experiment shows, by using hBA approach on the contS dataset can increase the classification performance results of dataset by 33%.

Fig. 6, presents the comparison between hbaS dataset with cfbaS dataset. The purpose of this experiment is to identify which datasets give the better classification accuracy, either datasets with optimize discretization or continuous dataset with optimize feature selection. The results shows hBA achieve the better performance in 3 datasets; DS3, DS5 and DS7. This experiment shows, hBA approach perform only in 33% from the entire datasets.

In the third experiment, the comparison results between hBA approach with dK approach shows in Fig. 7. The purpose of this experiment is to identify which datasets give the better classification accuracy, either datasets with discretization using optimize discretization or datasets with optimization using original K-Means discretization. Both of the approaches discretize the contS dataset. The results shows hBA achieve the better performance in 3 datasets; DS5, DS7 and DS9. This experiment shows, discretization with dK is better than discretization with hBA. hBA approach perform only in 33% from entire datasets.

In the third experiment, the comparison results between hBA approach with dK approach shows in Fig. 7. The purpose of this experiment is to identify which datasets give the better classification accuracy, either datasets with discretization using optimize discretization or datasets with optimization using original K-Means discretization. Both of the approaches discretize the contS dataset. The results shows hBA achieve the better performance in three datasets; DS5, DS7 and DS9. This experiment shows, discretization with dK is better than discretization with hBA. hBA approach perform only in 33% from entire datasets.

TABLE III. THE EXPERIMENTS RESULTS

Dataset	Accuracy					
	hbaS	contS	cfbaS	dkS	dfbaS	hfbaS
DS1	0.810	0.807	0.816	0.828	0.722	0.842
DS2	0.484	0.584	0.594	0.584	0.498	0.600
DS3	0.864	0.869	0.860	0.895	0.514	0.897
DS4	0.837	0.864	0.866	0.861	0.333	0.880
DS5	0.829	0.754	0.753	0.739	0.262	0.830
DS6	0.683	0.718	0.689	0.718	0.478	0.850
DS7	0.809	0.785	0.768	0.804	0.269	0.817
DS8	0.700	0.788	0.797	0.836	0.745	0.846
DS9	0.551	0.524	0.521	0.522	0.476	0.558

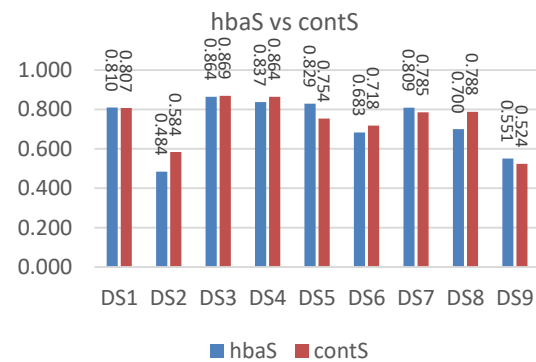


Fig. 5. The Classification Accuracy Comparison for Dataset hbaS with Dataset ContS.

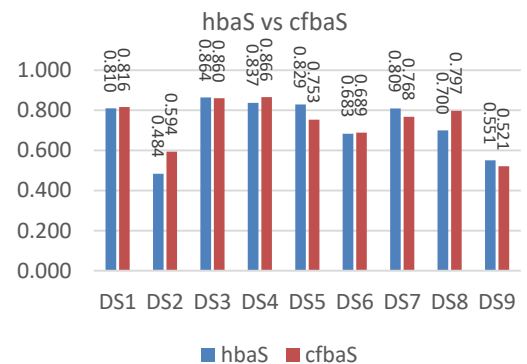


Fig. 6. The Classification Accuracy Comparison for Dataset hbaS with Dataset cfbaS.

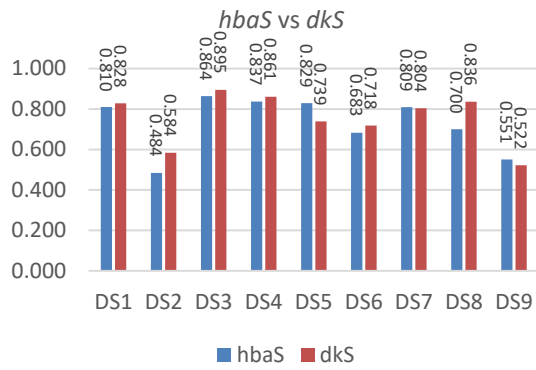


Fig. 7. The Classification Accuracy Comparison for Dataset hbaS with Dataset dkS.

In the fourth experiment, the comparison results between hBA approach with dfBA approach shows in Fig. 8. The purpose of this experiment is to identify which datasets give the better classification accuracy, either datasets with optimize discretization or dataset with K-Means discretization and optimize feature selection. The results shows hBA achieve the better performance in seven datasets; DS1, DS3, DS4, DS5, DS6, DS7 and DS9. This experiment shows, hBA approach perform in 78% from entire datasets.

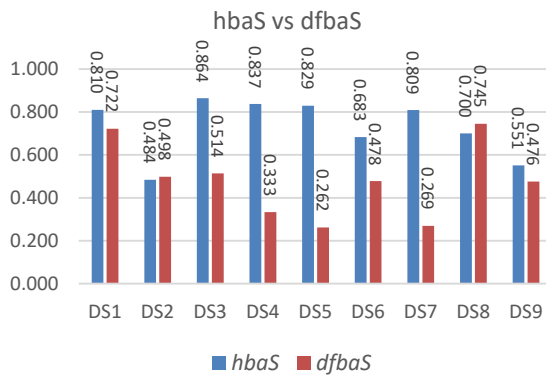


Fig. 8. The Classification Accuracy Comparison for Dataset hbaS with Dataset dfbaS.

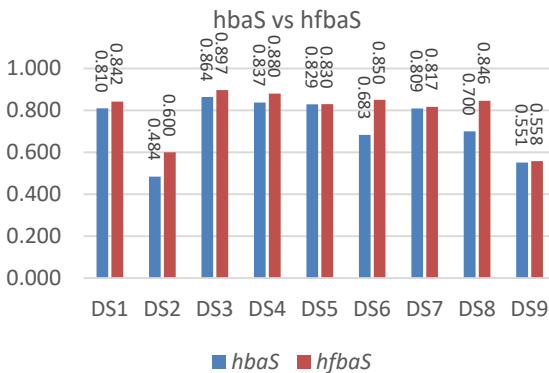


Fig. 9. The Classification Accuracy Comparison for Dataset hbaS with Dataset hfbaS.

Fig. 9 presents the comparison between hBA approach and hfBA. The purpose of this experiment is to identify which one is better in improving classification accuracy either optimize discretization or optimize discretization with optimize feature selection. From the results, hfBA able to improve the classification accuracy in all datasets.

V. CONCLUSION

The Bat algorithm is a powerful algorithm in finding the optimum feature data collection. The algorithm mimic the behavior of bat. Meanwhile, the high dimensional data in classification is interrupt classification accuracy. From the literature, feature selection and discretization is needed to solve. For that reason, this study show the Bat algorithm is potential as a discretization approach and as a feature selection to improve classification accuracy.

In this paper, a new hybrid Bat-K-Mean algorithm is proposed refer as hBA approach that used to convert continuous data into discrete data called as optimize discrete dataset (hbaS). The Bat algorithm is used to select the optimum feature in hbaS dataset for data dimension reduction and the new dataset refer as sub optimize discrete dataset (hfbaS) is created. The experiment was conducted to show the potential BA as discretization approach and feature selection approach to improve classification accuracy. k-Nearest Neighbor is used to evaluate the effectiveness of BA as discretization and feature selection in classification by comparing with dataset without feature selection, discrete dataset without feature selection, and dataset without discretization and feature selection. The experiments were carried out using a number of benchmark datasets from the UCI machine learning repository. The results show the classification accuracy is improved with the Bat-K-Means optimized discretization and Bat optimized feature selection.

The experiment results were present in Table III and Fig. 5 to Fig. 9. From the observation, conventional K-Means is not strong enough to improve classification performance (Fig. 7). If only the optimize discretization used in a continuous dataset is not able to improve the classification accuracy (Fig. 8). Optimize feature selection is required to select the optimum feature in the discrete dataset (Fig. 9). The combination of optimize discretization and optimize feature selection archive the better classification performance compare to continuous (original) in entire datasets.

In conclusion, BA is a powerful optimization technique and potentially to be used in discretization and feature selection. In the future, the research will extend for discretizing the mixed dataset value instead of continuous value only.

ACKNOWLEDGMENT

The authors would like to thank the Ministry of Higher Education, Malaysia for supporting this research under Fundamental Research Grant Scheme Vot K213 (FRGS/1/2019/ICT02/UTHM/02/2) and Universiti Tun Hussein Onn Malaysia for Multidisciplinary Research, Vot H511.

REFERENCES

- [1] X.S. Yang, "A new metaheuristic bat-inspired algorithm," *Studies in Computational Intelligence*, vol. 284, pp.65–74, 2010.
- [2] W. Kongkaew, "Bat algorithm in discrete optimization: a review of recent applications," *Songklanakarin J. Sci. Technol.*, vol. 39, pp. 641–650, 2017.
- [3] Y. Aboubi and H. Drias, N. Kamel, "BAT-CLARA: BAT-inspired algorithm for clustering LARge Applications," *IFAC-PapersOnLine*, vol. 49(12), pp. 243–248, 2016.
- [4] F. Yonis and O. Qasim, "Classification of diseases using a hybrid binary bat algorithm with mutual information technique," *Clinical Oncology and Cancer Biology*, vol. 1(1), pp. 1–5. 2019.
- [5] S. Priya and R. Manavalan, "Tuning the parameters of weighted elm using iwo and bat algorithm to improve the classification performance," in *Proceedings of the 2nd International Conference on I-SMAC (IoT in Social, Mobile, Analytics and Cloud) (I-SMAC)I-SMAC (IoT in Social, Mobile, Analytics and Cloud) (I-SMAC) 2018, 2018*, pp. 547-552.
- [6] D. Gupta, J. Arora, U. Agrawal, A. Khanna, and V. H. C. de Albuquerque, "Optimized Binary Bat Algorithm for classification of White Blood Cells," *Measurement*, vol. 143, pp. 180-190, 2019.
- [7] G. Li and C. Le, "Hybrid binary bat algorithm with cross-entropy method for feature selection," in *Proceedings of the 4th International Conference on Control and Robotics Engineering (ICCRE) 2019, 2019*, pp. 165–169.
- [8] D. Renuka Devi and S. Sasikala, S, "Online feature selection (ofs) with accelerated bat algorithm (aba) and ensemble incremental deep multiple layer perceptron (EIDMLP) for big data streams," *Journal of Big Data*, vol. 6(103), pp. 1-20, 2019.
- [9] Silva J, Borré JR, Piñeres Castillo AP, Castro L, Varela N. Integration of Data Mining Classification Techniques and Ensemble Learning for Predicting the Export Potential of a Company. *Procedia Computer Science*. 2019; 151(2019): 1194–1200.
- [10] A. O. Adeleke, N. A. Samsudin, A. Mustapha and N. Nawi, "Comparative analysis of text classification algorithms for automated labelling of quranic verses," *Int. J. Adv. Sci. Eng. Inf. Technology*, vol. 7(4), pp. 1419, 2017.
- [11] J. R. Cano, P. A. Gutiérrez, B. Krawczyk, M. Woźniak and S. García, "Monotonic classification: an overview on algorithms, performance measures and data sets," *Neurocomputing*, vol. 341(2019), pp. 168–182, 2019.
- [12] M. Shafiq, Z. Tian, A. K. Bashir, A. Jolfaei and X. Yu, "Data mining and machine learning methods for sustainable smart cities traffic classification: a survey," *Sustainable Cities and Society*, vol. 60(2020), pp. 102177, 2020.
- [13] M. R. Ayyagari, "Classification of imbalanced datasets using one-class svm, k-nearest neighbors and CART algorithm," *International Journal of Advanced Computer Science and Applications(IJACSA)*, vol. 11(11), pp. 1-5, 2020.
- [14] Y. Zhou, J. Kang, S. Kwong, X. Wang and Q. Zhang, "An evolutionary multi-objective optimization framework of discretization-based feature selection for classification," *Swarm and Evolutionary Computation*, vol. 60(2021), pp. 1-16, 2021
- [15] M. K. Ucar, "Classification performance-based feature selection algorithm for machine learning: P-Score," *Innovation and Research in BioMedical engineering*, vol. 41(4), pp. 229-239, 2020.
- [16] R. Zhao, Y. Qu, A. Deng and R. Zwiggelaar, "Inconsistency measure associated discretization methods to network-based intrusion detection," in *Proceedings of the 2018 IEEE International Conference on Fuzzy Systems (FUZZ-IEEE)*, 2018, pp. 1–6.
- [17] K. Dhalmahapatra, R. Shingade and J. Maiti, "An innovative integrated modelling of safety data using multiple correspondence analysis and fuzzy discretization techniques," *Safety Science*, vol. 130, pp. 104828, 2020.
- [18] M. Fikri, "The impact of fuzzy discretization's output on classification accuracy of random forest classifier," *International Journal of Advanced Trends in Computer Science and Engineering*, vol. 9, pp.3950–3956, 2020.
- [19] N. Hranisavljevic, A. Maier and O. Niggemann, "Discretization of hybrid CPPS data into timed automaton using restricted Boltzmann machines," *Engineering Applications of Artificial Intelligence*, vol. 95, pp. 103826, 2020.
- [20] J. MacQueen. "Some methods for classification and analysis of multivariate observations." in *Proceedings of the Fifth Berkeley Symposium on Mathematical Statistics and Probability, Volume 1: Statistics*, 1967, pp. 281–297.
- [21] R. Zhao, Y. Qu, A. Deng and R. Zwiggelaar, "Inconsistency measure associated discretization methods to network-based intrusion detection," in *Proceeding of the 2018 IEEE International Conference on Fuzzy Systems (FUZZ-IEEE)*, 2018, pp. 1–6.
- [22] D. Maryono, P. Hatta and R. Ariyuana, "Implementation of numerical attribute discretization for outlier detection on mixed attribute dataset," in *Proceeding of the 2018 International Conference on Information and Communications Technology (ICOIACT)*, 2018, pp. 715–718.
- [23] H. M. Tahir, A. M. Said, N. H Osman, N.H Zakaria, P. N. . M Sabri and N. Katuk, " Oving K-Means Clustering using discretization technique in Network Intrusion Detection System," in *Proceeding of the 2016 3rd International Conference on Computer and Information Sciences (ICCOINS)*, 2016, pp. 248–252.
- [24] A. A. Rachman and Z. Rustam, "Cancer classification using Fuzzy C-Means with feature selection," in *Proceedings of the 12th International Conference on Mathematics, Statistics, and Their Applications (ICMSA) 2016, 2016*, pp. 31–34.
- [25] R. Cheruku and D. Edla, "Bin-BB: Binning with Branch & Bound feature selection for improved diabetes classification," in *Proceedings of the 14th IEEE India Council International Conference (INDICON) 2017, 2017*, pp. 1–4.
- [26] M. D. Mithy and V. KrishnaPriya, "Anemiascreening in pregnant women by using feature selection with data classification algorithms," *Materials Today: Proceedings*, In Press, Corrected Proof, Available online 31 October 2020.
- [27] R. Kadry and O. Ismael, "A new hybrid kNN classification approach based on particle swarm optimization," *International Journal of Advanced Computer Science and Applications (IJACSA)*, vol. 11(11), pp. 291-296, 2020.

Development of a System to Manage Letters of Recommendation

Reham Alabduljabbar
Information Technology Department
College of Computer and information Sciences
King Saud University, Riyadh
Saudi Arabia

Abstract—Letter of Recommendation (LoR) is a letter which describes qualifications, skills, and abilities of the person being recommended. Students need to request a letter of recommendation from their instructors for the purpose of applying for jobs, internships and academic studies. The main obstacle which many students face is that instructors do not respond quickly, especially if the students have graduated. On the other hand, the instructors find it difficult to manage the many requests they receive, especially at the end of the semester. The work in this paper presents the design, development and testing of system that aims to replace the traditional method of requesting/issuing LoRs with a more systematic standardized way. The developed system may be adopted to simplify, unify, and improve the process. The results showed that the developed system enhanced the communication between requesters and issuers, reduced the amount of time and effort comparing with traditional way and achieved the usability requirements.

Keywords—Letter of recommendation; mobile application; letter of reference; android mobile application; LoR; standardized letters of recommendations

I. INTRODUCTION

For many people letters of recommendation are important as they convey an applicant's potential for success, and also highlight an applicant's qualities that cannot always be recognized from a curriculum vitae, test scores, or grades [1], [2]. However, writing a letter of recommendation requires effort from both the requester and the issuer of the recommendation letter. The traditional method of writing letters of recommendation lack standardization [3]—one evaluator's "extremely hard worker" could be another's "typical student." Moreover, as stated in [2] a uniform set of format regarding letters of recommendation does not exist. Normally, both requesters and issuers have little experience in this process and consequently, the letter of recommendation process is random, and the issued LoRs are often shortened. Despite its limitations, many consider these letters essential[2]. Therefore, there is a necessity for a system to guide students in requesting and obtaining a letter of recommendation and for guiding instructors in issuing a letter of recommendation. This work aims at designing, developing and testing a mobile application that offers a communication bridge between requesters and issuers. It aims to simplify the process of requesting, generating, and receiving the LoR. The system will guide its users through the letter of recommendation process. The system utilizes a database of templates for to guide the

issuer in the drafting and issuing of a letter of recommendation. Through the system, the requester can attach curriculum vitae, transcript and track the progress of requests. The requester can pick up her letter of recommendation or received as pdf file. The work in this paper is validated in real world test with students and faculty members from King Saud University, Riyadh, Saudi Arabia.

The remainder of the paper is organized as follows: Section 2 presents the background and discusses related works. Section 3 demonstrates the methodology. Section 4 presents the results and discussion of our system. Finally, Section 5 concludes the paper with future directions.

II. RELATED WORKS

A "Letter of Recommendation", also known as a letter of reference, is a letter that indicate the skills, capabilities, interests, qualifications and abilities of the recommended person to show that persons' ability to perform a particular task, or her academic performance. Furthermore, recommendation letters are used by people for many different purposes such as applying for jobs, internships and academic studies [4]. There are different categories for recommendation letters for example, academic recommendations, employment recommendations [5].

Recommendation letters are letters that are issued by issuers who know the requester. Furthermore, they are supposed to help to get a good picture of the requester. For Example, if the requester says that he/she is hardworking, then the recommendation letters will support him/her. Figure 1 represents a general format of a letter of recommendation for employment or educational purposes.

Usually, the first paragraph of a letter of recommendation is about how the issuer of is connected to the requester. Which includes how the issuer know the requester, also why the issuer is allowed to recommend this requester. The second paragraph of letter of recommendation is about the person that the issuer is writing about. It includes the qualifications of that person and what he/she can do, and why the issuer is recommending that person. More than one paragraph can be written to give more details. If letter of recommendation is for a specific position of a job, it should contain information about how that person skills are matching the position they are applying for it and this can be added in the third paragraph. In the summary section, reasons of why the issuer is recommending that person

can be included. Some phrases can be added like, "strongly recommend", or "recommend without reservation" or "Candidate has my highest recommendation" to strengthen the previous words. In the last paragraph of letter of recommendation has an offer to give extra information. better to write issuers phone number in this paragraph [6].

In order to identify related works, the literature and similar websites have been studied. In addition, a comparison and a discussion between these systems and the proposed system is given. This can be useful for including the best features for the proposed system and finding limitations that require improvements. The work in [7] discussed the importance of having standardized letters of recommendation in residency applications and their relation with objective data. Furthermore, the study in [8] improved the validity of LORs by developing a standardized reference form. The author in [9] argue that letter writing should be a joint opportunity between mentor/supervisor/advisor and trainee/student.

Several websites are available to create a letter of recommendation for a student or employee including Reference-Letter [10] which provides different phrases to build a personalized reference letter. In addition, SampleTemplates[11], which provide many templates for letter of recommendation. Furthermore, FormSwift [12] which helps issuer to write letter of recommendation and exported as doc or PDF file. Indirectly, there are some universities that have their own LoR system such as [13], [14] & [15]. Table 1 shows the comparison of all similar systems to help in visualizing and understanding the developed system.

According to this comparison, only the university systems supports having accounts and a follow up process to generate a letter of recommendation. Other systems are only one time use

which will result in unstructured responses and without any consistency or standardization. University systems do not support having different type of letters or template. Hence, there is a necessity for a system to guide students in requesting and obtaining a letter of recommendation and for guiding instructors in issuing a letter of recommendation. Therefore, based on the comparison and discussion the developed system aims to simplify the process of requesting, generating, and receiving the LoR.

Fig. 1. General Format of a LoR.

TABLE I. COMPARISON OF RELATED SYSTEMS

	Our System	Reference Letter [10]	Sample Templates [11]	Form Swift [12]	Instant Letter Generator [13]	University of Michigan [14]	The University of British Columbia [15]
Log In	✓	✗	✗	✗	✗	✓	✓
Sign UP	✓	✗	✗	✗	✗	✓	✓
Authentication	✓	✗	✗	✗	✗	✓	✓
Upload docs	✓	✗	✗	✗	✗	✓	✓
Write a recommendation by asking questions	✓	✓	✗	✗	✓	✓	✓
Export as PDF	✓	✓	✓	✓	✓	✓	✓
Different templates	✓	✓	✓	✗	✓	✓	✓
Sample Letter of Recommendation	✗	✓	✓	✓	✓	✓	✓
Wizard	✓	✓	✗	✓	✓	✗	✗

III. METHODOLOGY

A. Overview

The identified solution involved the development of an Android application that offers a communication bridge between requesters and issuers. It aims to simplify the process of requesting, generating, and receiving the LoR. Figure 2 shows the process of recommendation letter using the proposed system.

The system has three types of users. Key among them is the Issuer, who will use the system to provide a letter of recommendation to the requester. The issuer normally has a technical skill and has knowledge of mobile application. The second user is the Requester, who will use the system to request letter of recommendation from an issuer. In addition, there is the Admin user, who is responsible for management of the system.

B. Architecture

The system architectural is a model that defines the behavior of a system. The suitable architecture for the proposed system is to be implemented as a client-server model architecture and MVC (see Figure 3). The proposed system needs centralized databases, and many users need to access the server's information at the same time. Since the proposed system requires that different data to be displayed to different users, the MVC architecture was adopted. Not only does MVC support multiple views of the data, but it also allows updating existing ones. Modular decomposition is a decomposition of system into sub-system called modules. There are two modules: object model and data-flow model. Since the proposed system follows object-oriented approach, object model which describe objects, class and relationship between them was adopted [16].

C. Analysis and Design

The system follows an Object-Oriented analysis and design approach instead of structured analysis and design approach as this approach guarantees that the system shall have longer life and less maintenance cost because most of the processes are encapsulated within the system [17]. In order to ensure that the system design fulfills its requirements, a user-centric design method was adopted. A survey was distributed among students and faculty. The results aid in the definition of the requirements and demonstrated the need for the system.

In Figure 4, the use-case diagram of the system is presented, which also shows the main actions that can be performed by the different users of the system. The system provides different interfaces depending on the user. The system utilizes a database of templates for to guide the issuer in the drafting and issuing of a letter of recommendation. The issuer can write the LoR utilizing the templates through the wizard or write her own custom LoR. In addition, the issuers will be notified if they have received a new request and can accept or reject this request. The requester can request academic, employment or general LoR and track the progress of a request. Also, the requester can attach curriculum vitae, transcript and track the progress of requests. The requester can pick up her letter of recommendation or received as pdf file.

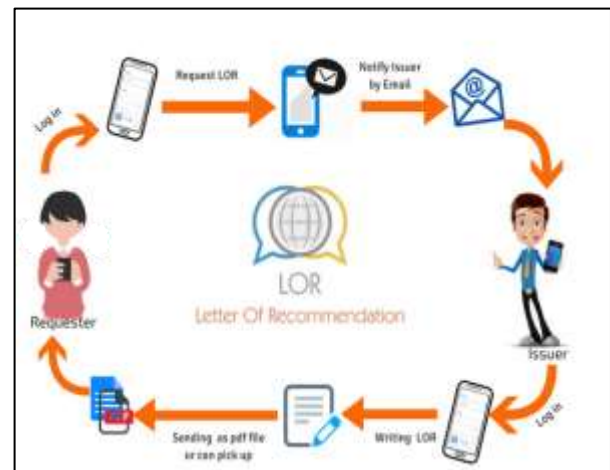


Fig. 2. Letter of Recommendation Process.

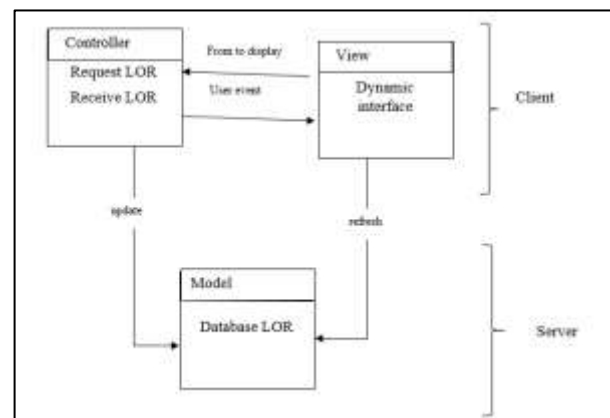


Fig. 3. System Architecture.

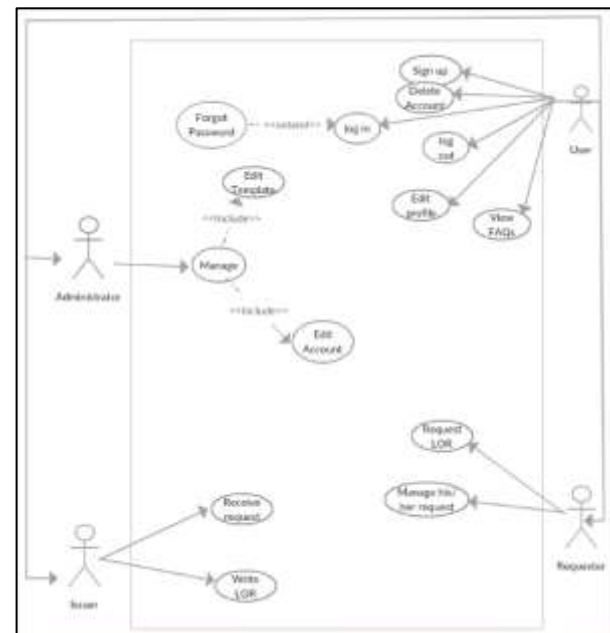


Fig. 4. Use Case Diagram.

Table 2 and Table 3, give descriptions about Request LoR and Write LoR use cases, respectively.

TABLE II. REQUEST LoR USE CASE DESCRIPTION

Use case: Actors: Requestor. Purpose: Allow the requestor to request a letter of recommendation. Overview: The requestor requests a letter of recommendation from a specific issuer. Pre-Condition: Requestor must be logged in.		
Typical course of event	Actor Action	System Response
	1 The use case begins when the requestor chooses to request a LoR.	2 The system presents a form that asks the requestor to write the issuer's email, how to deliver LoR, purpose, upload her CV and transcript and introduce herself in brief information.
	3 The requestor fills the form and uploads files.	
	4 The requestor chooses to submit or cancel the request.	5 The system checks if the issuer's email is not empty.
		6. The system checks if the file is not empty.
		7 The system accepts request and submits it to the issuer.
Alternative(s): Line 4: Requestor chooses to cancel; the system will allow the requestor to continue filling the form. Line 5: The system will ask the user to write issuer's email. Line 6: The system will ask the user to upload new files.		

TABLE III. WRITE LoR USE CASE DESCRIPTION

Use Case: Write LoR. Actor: Issuer. Purpose: The issuer can write the LoR after accepts request. Overview: The issuer writes the LoR using templates, then, the system will show the LoR as pdf file. Pre-Condition: The issuer must be logged. The issuer must accept the request.		
Typical Course of event	Actor Action	System Response
	1 – This use case begins when the issuer wants to write LoR.	2 – The system will display two options (using helpful statement or without helpful statements)
	3 – The issuer selects the option	4 – The system display four steps if the issuer selets helpful statement to write LoR
	5 – The issuer complete steps.	6 – The system display LoR as edit text to make issuer changes and the system will display in this edit text code number
		7 – The system asks the issuer to confirm the request
	8 – The issuer confirms.	9 – The system saves this LoR as pdf file to database and send it to requester.
Alternative(s): Line 8: Issuer chooses to cancel; the system will cancel the request.		

D. Tools

The system is implemented using Android Studio version 2.2.3 and the programming language is java and xml for design. For database, Firebase real-time database was used. Following is a list of the varying hardware and software utilized in the development of the system:

- Android mobile
- Java: It's computer programing language that is object oriented and specially designed to have as dependencies as possible. It's intended to let application developers WORA (Write Once, Run Anywhere) [18].
- Android Studio [19]: is the official integrated development environment it built on JetBrains' IntelliJ IDEA software and designed specifically for Android development.
- Memu Play emulator [20] : is one of the powerful Android emulator. Because it is leading to high performance and unique multiple-Android-kernels support, Memu has more than 15 million users. Memu make the programmers able to Run the application in the pc without using an android mobile by creating a virtual device, you can select the device type tablet or specific mobile phone.
- Notepad++ [21]: is a free source code editor and Notepad replacement that supports several languages.
- Xampp [22]: open source package has been set up to be incredibly easy to install and to use.
- Android SDK [23]: it is a set of development tool used to develop applications for Android platform. IT includes debugging, libraries, Relevant documentation for the Android application program, interfaces and emulator created by Google.

- Extensible Markup Language (XML)[24]: It is a format which is like Hypertext Markup Language (HTML). Both XML and HTML contain markup symbols that describe page contents. The structure of the data is embedded with the data.
- Firebase database [25]: it is a real-time database, cloud-hosted database, Data is stored as JSON., all of your clients share one Realtime Database instance and automatically receive updates with the newest data. Our system has some input fields, such as username, password and more, when the user fills out this information and hits submit, the application will pass the information to our API connector, then it will have submitted by java programming language to the firebase database.
- CPU Monitor Advanced Lite [26]: records historical information about processes running on your device.

E. Navigation and User Interface (UI)

A hierarchy diagram for the main layout of the system is shown in Figure 5.



Fig. 5. The Layout of our System.

The system’s user interface design gives a clear idea of how the system is interacting with its users. The interfaces were designed to be user friendly, simple and consistent. Figure 6 and Figure 7 show snapshot of Requester and Issuer interfaces, while Figure 8 presents how the system guides the Issuer in drafting, organizing and sending the LoR.

IV. RESULTS AND DISCUSSION

This section discusses the system testing which is the most important stage in life cycle of each system. System testing checks if the system is free from bugs and errors. Also, it ensures that the requirements have been met. The system was evaluated through different strategies including Unit testing, Integration testing, Performance, Stress testing and User Acceptance Testing (UAT).

A. System Evaluation

The objective of unit testing is to test the process of each component of the application separately, and to ensure that every component works as expected. Therefore, finding and fixing bugs is easier because we work on small units instead of one large unit [17]. All the components of the system passed this test.

Regression testing is defined as a kind of software testing to make sure that a new code change has not affected the existing work [17].

The system’s functions were divided into components then each function was tested individually. However, before combining all the components, which will form the whole application, they must be tested together, to make sure that they work correctly and fix any bugs or problems that arise when combining the components. This is done by performing the Integration testing. First, component A and component B (Test 1) were tested together. Next, Test 1 was tested with component C and they worked correctly. This process repeatedly continued till all the components were integrated and tested to form the complete application.

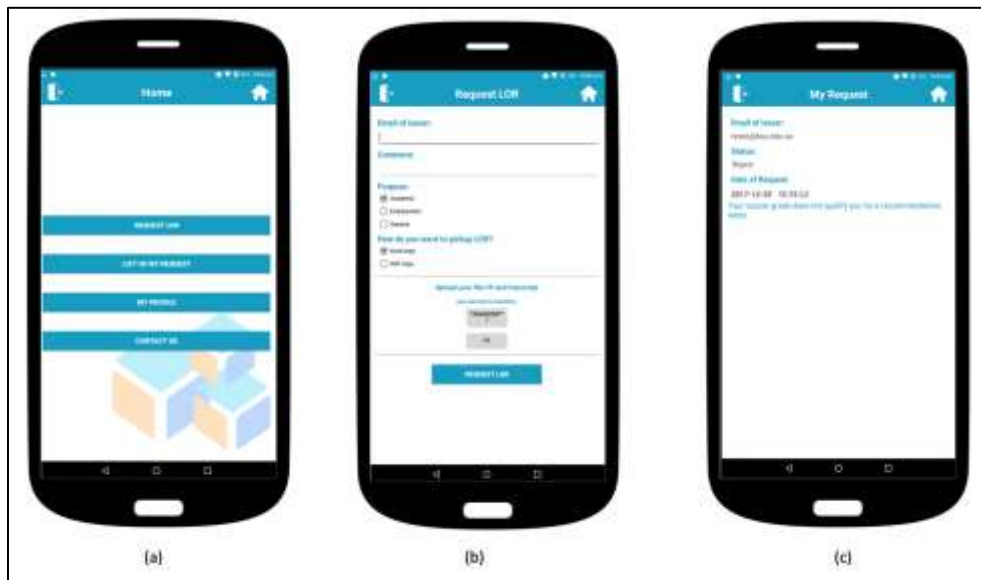


Fig. 6. Snapshot of Some of the Requester Interfaces (a) Main Interface. (b) Request LoR Interface (c) Request Tracking Interface.



Fig. 7. Snapshot of Some of the Issuer Interfaces (a) Main Interface (b) List of Requests (c) Issuing LoR Interface.



Fig. 8. Snapshot of Some of the Issuer Interfaces (a-c) throughout the Process Writing the LoR using the Recommender System (d) Selecting Pick up Date if Chosen Instead of Mailing.

Performance testing is the process of determining the speed or effectiveness of the system. It measures the effects of running the system on the phone. Performance testing was done using CPU Monitor Advanced Lite [26]. Figure 9 displays the CPU usage over the last minute of our system. In the graph CPU utilization rate is 2%, the max use reached 6%.

Stress testing is the process that is used to determine and specify the robustness of the system. Also, it is used to see and observe the response of the system under loading from user [17]. To check the stress testing for the system, the Monkey command line tool [27] was used. The way this tool works is by sending pseudo-random stream of user events to a running emulator to act as a stress test on the system. The system worked as expected after 500 events generation.

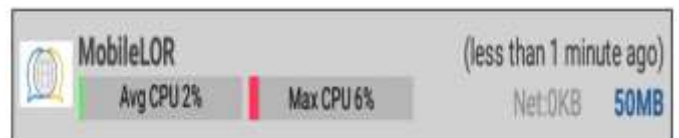


Fig. 9. Performance Testing.

B. User Acceptance Testing (UAT)

The goal of acceptance testing is to approve the system with respect to the requirements that was agreed on it before [28]. The total number of users who participated in the user acceptance testing was seven from the female section of Collage of Computer and Information Sciences, King Saud University. The users were on different level of education and

knowledge. The application's usability was measured based on two criteria:

- Efficiency: by calculating the time that the user took to complete a task.
- Satisfaction: by asking the users to fill a survey to find out how the users actually, feel about the system. The results of the testing are shown on Table 4.

TABLE IV. RESULTS OF THE USER-ACCEPTANCE TESTING

#	Task	Average Time
1	View FAQs	4 Seconds
2	Sign up	30 Seconds
3	Log in	7 Seconds
4	Log out	3 Seconds
5	Reset password	20 Seconds
6	Edit profile	15 Seconds
7	Edit wizard statements	25 Seconds
8	Edit reject reasons	15 Seconds
9	Edit FAQs	18 Seconds
10	View requests	3 Seconds
11	Write the LoR	40 Seconds
12	Delete account	6 Seconds
13	Request LoR	10 Seconds
14	Manage LoR requests	7 Seconds

It is noticed that the task "write the LoR" has the highest average. This can be explained because the user has to go through the process of issuing the LoR via the wizard. On the other hand, tasks "Request LoR", "Manage LoR requests" and "View requests" takes between 3 and 10 seconds only as they need simple clicking. In addition, some tasks that required writing statements like: "Edit wizard statements" and "Edit reject reasons" takes between 15 and 25 seconds. In comparison to traditional method currently being used, a majority of respondents agreed that the proposed system is quicker, easier and more convenient for the letter requesting/issuing.

V. CONCLUSION AND FUTURE WORK

This paper presents an Android based mobile application to manage the process of recommendation letters. The current LoR process is ineffective because it lacks standardization, and it is time and effort consuming for both requesters and issuers. The purpose of the study is to automate and replace the traditional method of requesting and writing LoRs to make the process of recommendation letters easier. The system supports English language only, hence, as future work it is intended to expand the scope of the system to support iOS system and support Arabic language. Moreover, more features will be added such as search for university name to show the list of issuers that are already registered in the system.

ACKNOWLEDGMENT

The author would like to thank Aljazi AlMogern, Aseel AlOmair, Barakah AlHaddad, Mashael AlShiha, and Mashael AlTurki for their contributions in the implementation of the system.

REFERENCES

- [1] G. M. Garmel et al., "Letters of Recommendation," *Journal of Emergency Medicine*, vol. 57, no. 3, pp. 405–410, 2019.
- [2] J. D. Prager, C. M. Myer, and M. L. Pensak, "Improving the letter of recommendation," *Otolaryngology - Head and Neck Surgery*, vol. 143, no. 3, pp. 327–330, 2010.
- [3] A. M. Walters, P. C. Kyllonen, and J. W. Plante, "Developing a Standardized Letter of Recommendation," *Journal of College Admission*, no. 191, pp. 8–17, 2006.
- [4] B. Bodkin and B. Wyskowski, "System and Method to Manage Letters of Recommendation," US 2017/0039665 A1, 2017.
- [5] "Types of Recommendation Letters." [Online]. Available: <https://www.thoughtco.com/recommendation-letters-definition-and-types-466796>. [Accessed: 03-Apr-2020].
- [6] "Letter of Recommendation." [Online]. Available: <https://www.thebalancerecareers.com/recommendation-letter-template-2062919>. [Accessed: 02-Apr-2020].
- [7] A. L. Tang et al., "Are Standardized Letters of Recommendation in Residency Applications Correlated With Objective Data?," *Journal of Medical Education and Curricular Development*, vol. 6, p. 238212051989397, 2019.
- [8] J. M. McCarthy and R. D. Goffin, "Improving the Validity of Letters of Recommendation: An Investigation of Three Standardized Reference Forms," *Military Psychology*, vol. 13, no. 4, pp. 199–222, 2001.
- [9] Z. Master, "A Mentoring Opportunity: A Joint Effort in Writing Letters of Recommendation," *Accountability in Research*, vol. 24, no. 1, pp. 52–59, 2017.
- [10] "Reference-Letter." [Online]. Available: <http://www.reference-letter.com/>. [Accessed: 03-Jul-2020].
- [11] "Sample Templates." [Online]. Available: <https://www.sampletemplates.com/letter-templates/letter-of-recommendation.html>. [Accessed: 07-Sep-2020].
- [12] "Form Swift." [Online]. Available: <https://formswift.com/letter-of-recommendation>. [Accessed: 11-Jun-2020].
- [13] "Instant Letter Generator." [Online]. Available: <https://www.boxfreeconcepts.com/generators/letmasproc.html>. [Accessed: 15-Jun-2020].
- [14] "University of Michigan." [Online]. Available: <https://umich.edu/>. [Accessed: 09-May-2020].
- [15] "The University of British Columbia." [Online]. Available: <https://www.ubc.ca/>. [Accessed: 09-Jul-2020].
- [16] M. Richards, *Software Architecture Patterns*. O'Reilly Media, Inc., 2015.
- [17] I. Sommerville, *Software Engineering*. Pearson Education Limited.
- [18] Wikipedia, "Java (programming language)," 2020. [Online]. Available: [https://en.wikipedia.org/wiki/Java_\(programming_language\)](https://en.wikipedia.org/wiki/Java_(programming_language)). [Accessed: 19-Jul-2020].
- [19] "Android Studio." [Online]. Available: <https://developer.android.com/studio>.
- [20] "MEmu Play emulator." [Online]. Available: <https://www.memuplay.com/blog/about>. [Accessed: 05-Apr-2020].
- [21] "Notepad++." [Online]. Available: <https://notepad-plus-plus.org/>.
- [22] "XAMPP." [Online]. Available: <https://www.apachefriends.org/index.html>. [Accessed: 26-Jun-2020].
- [23] "Android SDK," Techopedia, Oct-2020.
- [24] "XML." [Online]. Available: <https://whatis.techtarget.com/definition/XML-Extensible-Markup-Language>. [Accessed: 04-Aug-2020].
- [25] "Firebase Realtime Database," Firebase, 2020. [Online]. Available: <https://firebase.google.com/docs/database>.
- [26] "CPU Monitor Advanced Lite." [Online]. Available: <https://www.apksum.com/app/cpu-monitor-advanced-lite/com.bigbro.processprofiler>.
- [27] "UI/Application Exerciser Monkey," Android Developers. [Online]. Available: <https://developer.android.com/studio/test/monkey.html>.
- [28] B. HAMBLING and P. VAN GOETHEM, *User Acceptance Testing: A Step-by-step Guide*. BCS Learning & Development Limited, 2013.

Conceptual Temporal Modeling Applied to Databases

Sabah Al-Fedaghi

Computer Engineering Department, Kuwait University, Kuwait

Abstract—We present a different approach to developing a concept of time for specifying temporality in the conceptual modeling of software and database systems. In the database field, various proposals and products address temporal data. The difficulty with most of the current approaches to modeling temporality is that they represent and record time as just another type of data (e.g., values of a bank balance or amounts of money), instead of appreciating that time and its values are unique, in comparison to typical data attributes. Time is an engulfing phenomenon that lifts a system’s entire model from staticity to dynamism and beyond. In this paper, we propose a conceptualization of temporality involving the construction of a multilevel modeling method that progresses from static representation to system compositions that form regions of dynamism. Then, a chronology of events is used to define the system’s behavior. Lastly, the events are viewed as data sources with which to build a temporal model. A case-study model of a temporal banking-management system database that extends UML and the object-constraint language is re-modeled using thinging machine (TM) modeling. The resultant TM diagrammatic specification delivers a new approach to temporality that can be extended to be a holistic monitoring system for historic data and events.

Keywords—*Conceptual modeling; temporal database; static model; events model; behavioral model*

I. INTRODUCTION

In most existing relational database systems, data objects are stored such that when an attribute’s value changes, the new value replaces the old value. Thus, only the latest state of an object resides in the database. However, discarding old information is inappropriate for many database applications (e.g., financial, health-care management, reservation, medical, and decision support system applications). In these cases, time values must be associated with data to indicate the time for which the data are valid. A time dimension is added to a database at either the attribute or the tuple level to maintain a data object’s history. Such a database is referred to as a temporal database [1]. Many temporal extensions of the classical relational database model have been proposed, and some of them have been realized (e.g., [2], [3]).

Conceptual models are essential for describing an application’s requirements, and they facilitate communication between users and designers because they do not require knowledge of the technical features of the underlying implementation platform [4]. A conceptual model provides a notation and formalism, which designers can use to construct a high-level, implementation-independent description of selected aspects of the modeled portion of reality [5].

Time is a source of mystery and sometimes is treated as a philosophical curiosity [6]. In software engineering, modeling

research mostly adopts a “clock-based” mechanistic interpretation of time and ignores the complex, multifaceted, subtle, and socially embedded nature of temporality [7]. Proposals and products have been developed in the database field to address temporal data (e.g., SQL/temporal) [8]. Various time-related concepts exist (e.g., according to Halpin [8]), and three basic temporal data types may be distinguished: instant, interval, and period. Temporal operators (e.g., subtraction) can be defined for each of these types. Temporal database terminology includes many kinds of time values, including valid time, transaction time, snapshot, bitemporal, spun, and time stamp. Extra columns in relational tables often capture some of these times, and the time-as-value sometimes is distinguished from the facts (true propositions). According to Halpin [8], facts are completely devoid of any temporal aspect, and once-only facts correspond to a single event, for which an event seems to be defined as a state of affairs.

A. Related Works

Almost all current approaches to data temporality take the same conceptualization scheme described in the previous paragraph. Surveying more such works would not serve our purposes because what we propose in this paper is not based on their paradigm. Instead, we describe the difference between an example how such approaches conceptualize temporality and our proposed conceptualization of data temporality in our thinging machine (TM) methodology.

B. Difficulties

Over the years, the topic of temporality has been a rich research theme, such as in philosophical essays on time and temporal reasoning. Time is an important notion in many real-world applications. In recent years, research on data temporality has spread to other areas (e.g., the temporal dimensions of semantic Web applications and temporal ontologies). Yet, the field of temporality studies for such applications lacks a common terminology, infrastructure, and conceptual framework, thus reducing the adoption of temporal database technology [9]. According to Lu et al. [10], we have witnessed a major burst of temporal support in conventional database management systems; however, the existing temporal data model is inadequate, and such databases suffer from limited expressiveness [10]. Additionally, notions such as the transaction time in temporal data models are difficult to establish and update [10].

C. Proposed Solution to the Identified Cause

In this paper, we advocate the thesis that the difficulties with current approaches to representing and recording time notion originate from them handling time data as just another value, similar to the number of cars, the length of a tree, or an amount of money. This conception reflects a lack of

appreciation for time as a one-of-a-kind singularity distinct from things such as attributes. In this study, we view time as an engulfing phenomenon that lifts the entire model description from staticity to dynamism. Such movement from staticity converts static description into eventized form (TM machine), injecting activity into the whole system in a way that is analogous to transforming a mere textual narrative into a live theater performance. The text, “Alice comes across a caterpillar sitting on a mushroom”, when converted to a performance in a theater, becomes Alice as a thing knotted in time comes across as an action knotted in time, a caterpillar as a thing knotted in time, sitting as an action knotted in time, on a mushroom as a thing knotted in time. The sentence “Alice comes across a caterpillar sitting on a mushroom”, with its things and action, is a static model, whereas the performance is a dynamic model in which things and actions are transformed into events. Our model captures such a distinction between staticity and dynamism that is not found in most other models (e.g., UML) representing dynamism in a static form (e.g., a UML activity diagram).

The static representation shown in Fig. 1 (adapted from [11]), in which the time is the value of the temporal attribute Date, lacks the key notion that time data are generated at a higher level than that of static descriptions. This idea is adopted in this paper, whereby a static fact (*Employee*, *MoneyAmount*) is at a lower modeling level than time is (Fig. 2). Fig. 2 shows the lower level (dark region) and upper level, along with their respective data (e.g., Date).

D. Outline of the Approach

In this paper, we express the domain involved (i.e., bank-operations management) in terms of a new modeling methodology called TM modeling, which is a conceptual tool that abstractly represents a system at four levels: the static, dynamic, behavioral, and temporal levels. The crucial construction of this multilevel modeling involves a progression from the static representation of a system to a set of compositions that form regions of events. The event chronology defines the system behavior. Lastly, the events are viewed as data sources for a temporal system.

These modeling stages are illustrated in a simplified form using a single decomposition (Fig. 3). Fig. 4 shows the corresponding event. Fig. 5 shows the meta-event that produces salary data and its data of occurrence, which is stored as a record in the temporal salary database. Of course, the record includes other data such as employee names and ID numbers. This record is generated each time the event of updating the salary value occurs.

To provide a self-contained paper, the next section includes a brief summary of the TM model. Section 3 details a full example of TM modeling for understanding the model and its concepts, such as actions, events, and behaviors. Section 4 introduces a temporal database given by El Hayat et al. [12] that extends UML and the object-constraint language (OCL) to produce an elaborate conceptual schema of banking-system management. This temporal database is re-modeled using the TM methodology.

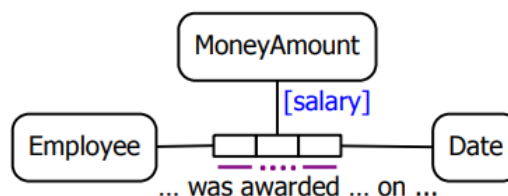


Fig. 1. Model of a Salary with History (Adapted from Balsters et al. [11]).

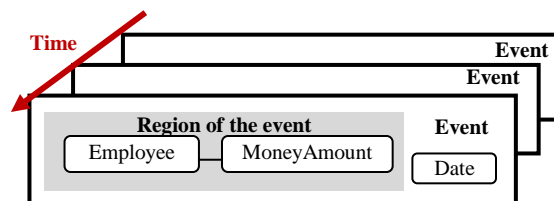


Fig. 2. The Conceptualization of Temporality Adopted in this Paper.

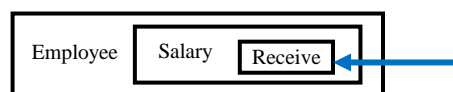


Fig. 3. The Static Model Presented in Terms of a Single Decomposition.

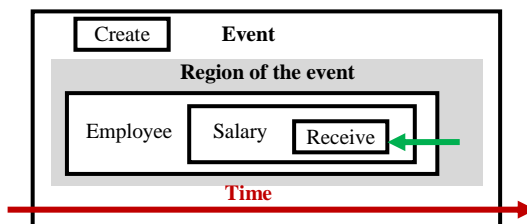


Fig. 4. The Dynamic Model with a Single Event.

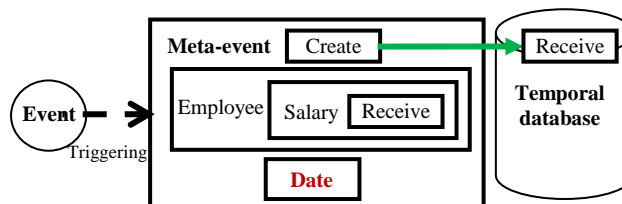


Fig. 5. The Temporal Model Proposed in this Paper.

II. TM MODELING

The TM model articulates the ontology of the world in terms of an entity that is simultaneously a thing and a machine, called a thimac [13-22]. A thimac is like a double-sided coin. One side of the coin exhibits the characterizations assumed by the thimac; on the other side, operational processes emerge, which provide a dynamism that goes beyond structures or things to embrace other things in the thimac. A thing is subjected to doing (e.g., a tree is a thing that is planted, cut, etc.), and a machine does (e.g., a tree is a machine that absorbs carbon dioxide and uses sunlight to make oxygen). The tree thing and the tree machine are two faces of the tree thimac. A thing is viewed based on Heidegger’s [23] notion of thinging. According to Bryant [24], “A tree is a thing through which sunlight, water, carbon dioxide, minerals in the soil, etc., flow. Through a series of operations, the machine transforms those flows of matter,

those other machines that pass through it, into various sorts of cells.” A thing is a machine, and a machine is a thing. A machine facilitates the movement of things; simultaneously, as a machine, it is a thing in its processual mode.

The simplest type of machine is shown in Fig. 6. The actions in the machine (also called stages) are as follows:

- Arrive:** A thing moves to another machine.
- Accept:** A thing enters a machine. For simplification, we assume that all arriving things are accepted; hence, we can combine the arrival and acceptance of the thing into the receive stage.
- Release:** A thing is marked as ready to for transfer outside the machine (e.g., in an airport, passengers wait to board after passport clearance).
- Process:** A thing is changed in form, but no new thing results.
- Create:** A new thing is born in a machine.
- Transfer:** A thing is input into or output from a machine.

Additionally, the TM model includes storage and triggering (denoted by a dashed arrow in this study’s figures), which initiates a flow from one machine to another. Multiple machines can interact with each other through the movement of things or triggering stages. Triggering is a transformation from one series of movements to another (e.g., electricity triggers cold air).

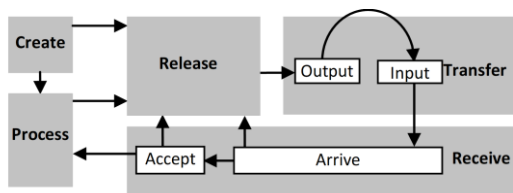


Fig. 6. The Thing Machine.

III. TM MODELING EXAMPLE

Because the subject of temporality in this paper is a fourth-level notion in the TM model, this section builds a solid basis for understanding the model before treating the topic of temporal data.

Etzion and Niblett [25] presented a fast flower-delivery system specification as a case study of an event-processing scheme. The case study involves a consortium of flower stores that have an agreement with local independent van drivers to deliver flowers from the stores to their destinations.

When a store gets a flower delivery order, it creates a request, which is broadcast to relevant drivers within a certain distance from the store, with the time for pickup (typically now) and the required delivery time. A driver is then assigned, and the customer is notified that a delivery has been scheduled. The driver makes the pickup and delivery, and the person receiving the flowers confirms the delivery time by signing for it on the driver’s mobile device. The system maintains a ranking of each individual driver based on his or

her ability to deliver flowers on time. Each store has a profile, which can include a constraint on the ranking of its drivers. The profile also indicates whether the store wants the system to assign drivers automatically or whether it wants to receive several applications and then make its own choice. [21].

Fig. 7 shows the corresponding static TM model. The diagram includes the user (circle 1), the store (2), the driver (3), and the person who receives the flowers (4). The other parts of the diagram model the system. The following occurs accordingly:

- The user creates the order (4), which flows to the store (5), where a minimum ranking requirement (6) is added to the user order to form a delivery order (7).
- The delivery order flows to the system (8) to be processed (9) and is sent to a submachine (10), which extracts a subset of drivers who satisfy the minimum ranking requirement. In this machine, the delivery request is processed (11) to extract the minimum ranking (12), which is compared (13) with driver ranks (14) coming one at a time (15) from the file of all ranked drivers (16). Through this comparison, a file of qualified (minimum ranking) drivers is constructed (17).
- Another machine (18) identifies drivers who are currently in the region by processing:
 - the list of qualified drivers (17);
 - the delivery location, extracted from the delivery request (19); and
 - the current location of the qualified driver (20). The current locations of drivers (21) are updated continuously via satellite (22).
- If a driver is located in a nearby region, then a bid request is constructed (23) and sent to that driver (24).
- Drivers who receive bid requests respond by creating a delivery bid (25), which flows to the system (26) to be collected with other delivery bids (27).
- When bid requests are sent, a timing machine (28) is constructed to set a deadline of 2 minutes (29). At the end of the 2 minutes, the accumulated delivery bids (27) are processed (30). If there are no bids, then an alert is generated (31) and sent to the store (32) and the system manager (33).
- If there are bids and the store policy is to select the assigned driver manually, then a list of top bidders is generated (34) and sent to the store (35), and a deadline for the response is set (36). If there is no response by the deadline, then, as before, an alert is sent to the store and the system manager (37).
- An assignment of a driver is either created by the system (38) or received from the store (39) and sent to the driver (40).

- The driver goes to the store (41) and picks up (42) the flowers (43). A confirmation of this (44) is sent to the system.
- The driver with the flowers (45) drives to the person who ordered the flowers (46), and a confirmation of the delivery is sent to the system (47). Details such as about how the confirmation is sent through signing the driver's mobile device are not included, due to space considerations.

Additionally, the rest of the case study, which involves updating the drivers' ranks, is not modeled, to limit the model to one page. Some other simplifications were also applied, such as lumping all alerts and all confirmations together.

Fig. 8 shows the events in the model, which were developed as a layer over the static model in Fig. 7.

Event 1 (E_1): The user submits an order for flowers to the store.

Event 2 (E_2): The store constructs a delivery request that includes minimum driver rankings.

Event 3 (E_3): The delivery request flows to the system, in which a list of qualified drivers is produced.

Event 4 (E_4): A qualified driver in the nearby region is identified.

Event 5 (E_5): A bid request is generated and sent to the qualified driver in the nearby region.

Event 6 (E_6): A time deadline (2 minutes) is initiated to receive delivery bids.

Event 7 (E_7): The driver formulates a delivery bid, which flows to the system to be stored with all other delivery bids.

Event 8 (E_8): The time deadline (2 minutes) to receive delivery bids expires.

Event 9 (E_9): The list of all delivery bids is processed.

Event 10 (E_{10}): The bid receives no bidders.

Event 11 (E_{11}): An alert is generated and sent to the store and system manager.

Event 12 (E_{12}): There are bidders.

Event 13 (E_{13}): The top delivery bids are selected.

Event 14 (E_{14}): The top delivery bids are sent to the store.

Event 15 (E_{15}): The timing is set for the store to select a driver.

Event 16 (E_{16}): The store selection of a driver passes the deadline.

Event 17 (E_{17}): The system selects a driver.

Event 18 (E_{18}): The store selects a driver.

Event 19 (E_{19}): The selection is sent to the driver.

Event 20 (E_{20}): The driver goes to the store and picks up the flowers

Event 21 (E_{21}): A confirmation is sent to the system.

Event 22 (E_{22}): The driver delivers the flowers to the customer.

Fig. 9 shows the behavioral model of this example. Note that the granularity of events depends on the modeler. For example, Event 3 can be refined further into six events:

Event 3a (E_{3a}): The delivery request is inputted to the submachine.

Event 3b (E_{3b}): The list (file) of ranked drivers is processed.

Event 3c (E_{3c}): A single record of a ranked drivers is retrieved from the file.

Event 3d (E_{3d}): The retrieved record flows for comparison with the requested minimum ranking.

Event 3e (E_{3e}): If the record does not satisfy the minimum requirement, then it is ignored, and the next record is retrieved from the file containing the ranked drivers.

Event 3f (E_{3f}): If the record satisfies the minimum requirement, then it is added to the file of qualified drivers.

The detailed chronology of events for Event 3 can be developed in the same way as in the main model.

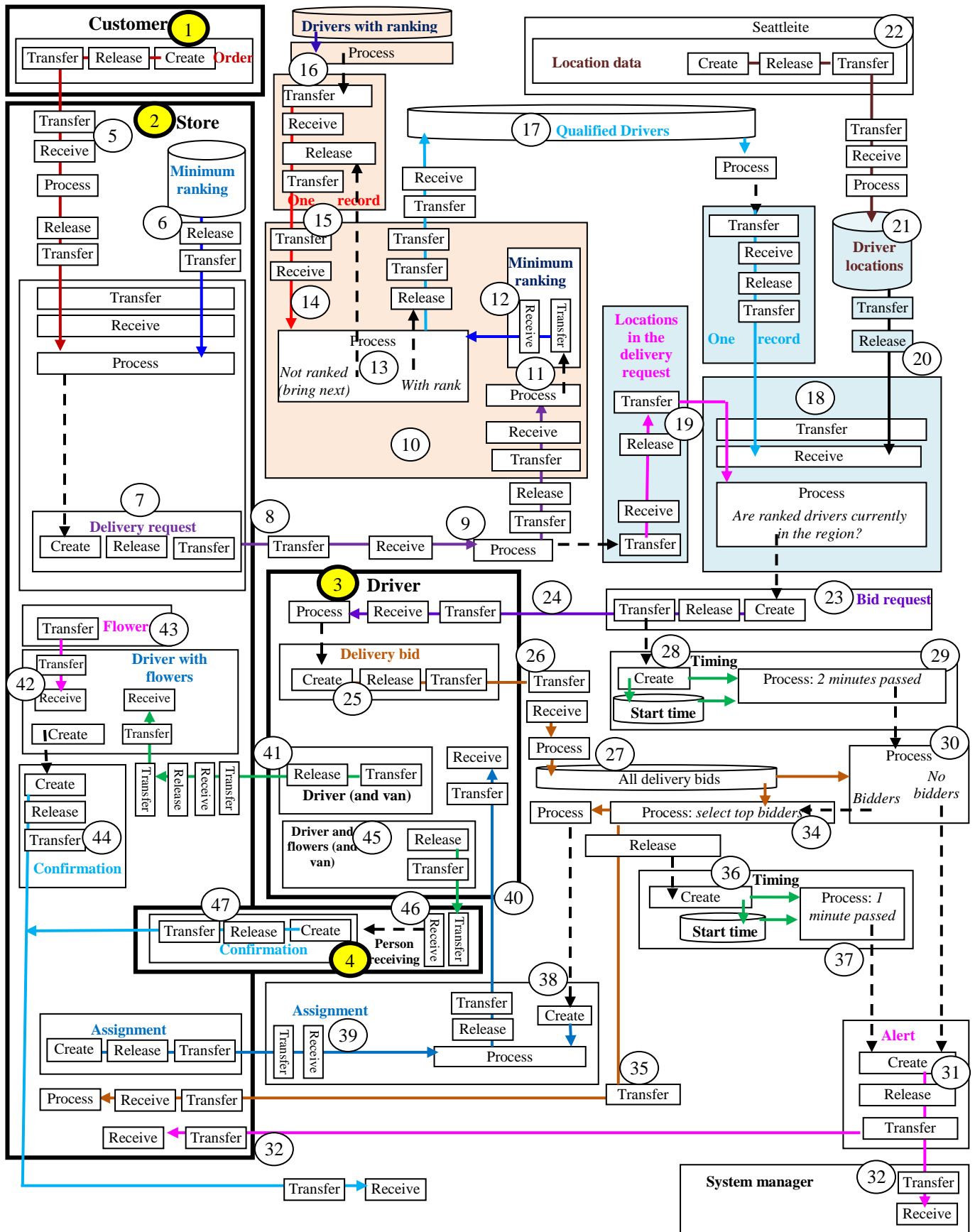


Fig. 7. The Static TM Model of the Consortium of Flower Stores.

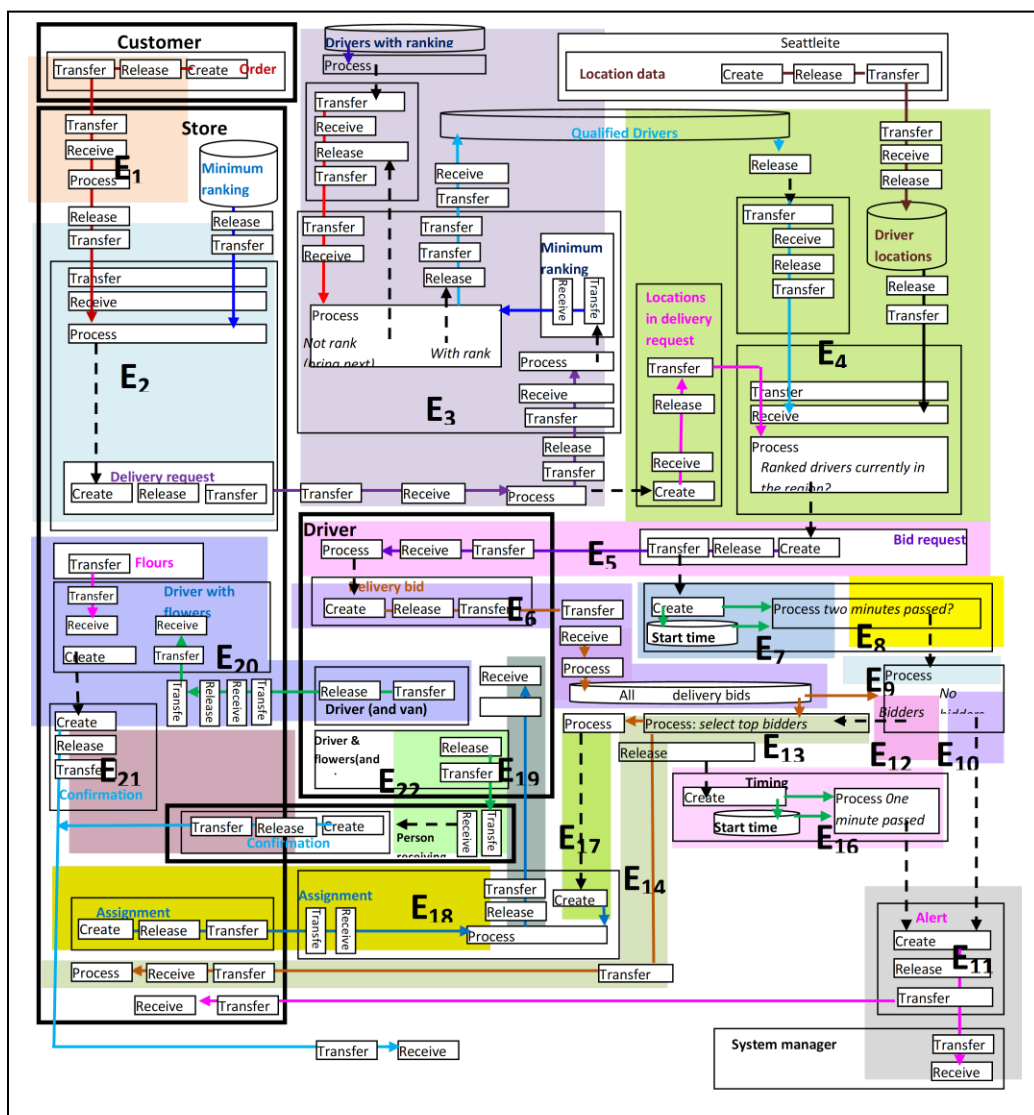


Fig. 8. The Dynamic TM Model of the Flower Store Consortium.

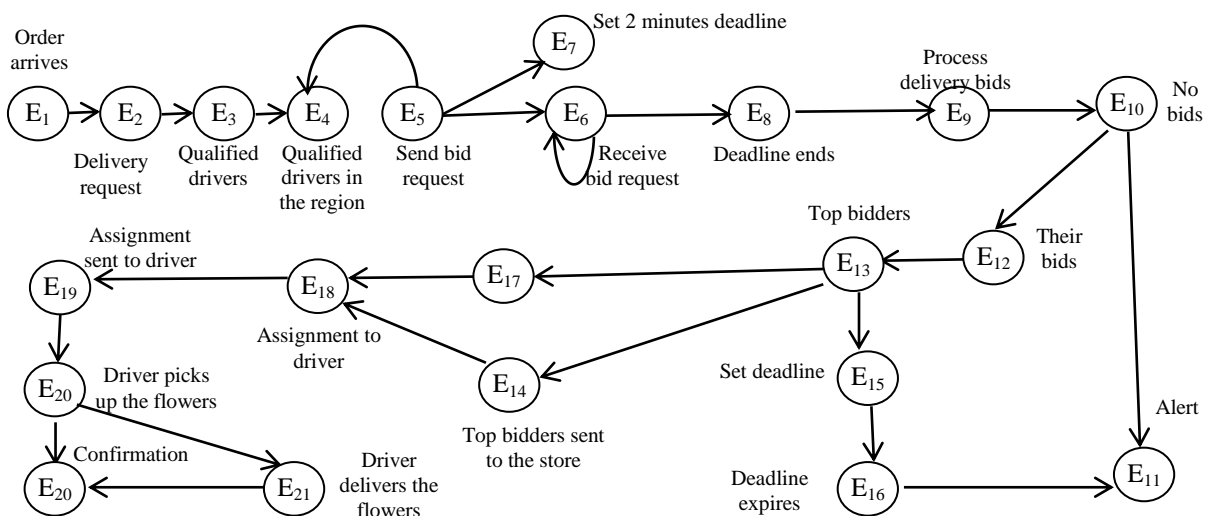


Fig. 9. The Behavioral Model of the Flower Stores.

IV. MODELING A BANK

According to El Hayat et al. [12], the emergence of temporal databases calls for new, efficient visual-modeling techniques to facilitate the design of temporal objects. El Hayat et al. [12] used extended UML and the OCL to produce an elaborate conceptual schema that allows for defining the restrictions and constraints that contain the duplicate and complex expressions in a temporal database. The proposed temporal UML/OCL model is based on bitemporal data, which translate into a temporal object-relational database for tracking historical information efficiently. El Hayat et al. [12] provided the class diagram of a banking system that includes bitemporal data to make records of the history of the data and transaction operations.

A. Static Model

This paper lacks the space to describe El Hayat et al.'s [12] model. We will take their example, with some minor simplifications, as an example of a TM conceptualization of a temporal database. Fig. 10 shows the static TM model of the involved banking system. The simplification of El Hayat et al.'s [12] model involves such changes as eliminating some attributes of the customer's address, such as their city and postal code, while keeping their ID, name, and address. The purpose is to remove redundant types of attributes without changing the kinds of data in the model. Additionally, we will focus on four regions in the model that involve the temporality of data: transfer, withdrawal, deposit, and loan transactions.

In Fig. 10, before a customer (circle 1) requests a service, he or she provides an account number (2), which flows to the system, (3) where it is validated (4) with the account number stored in the system (5 and 6).

a) Loan service: A customer requests a loan (7); hence, the request moves to the system (8 and 9), where it is processed (10). Assuming the loan is approved, the amount is extracted (11) from the request, along with a generated loan number (12) that flows to the loan subsystem (13), where they and the account number (14) are processed (15) to trigger the creation (16) of a loan record, which is stored in the loan database (17).

The temporal data of such activities will be handled in the events model.

b) Transactions (18): A customer requests a transaction (19); hence, the request moves to the system (20 and 21), where it is processed (22). Additionally, the customer provides the transaction request (22), which flows to the system (23). Based on the transaction type (21), the input amount is directed (24) to the transfer (25 and 26), withdraw (27 and 28), or deposit module (29 and 30). The account (31) is updated according to the type of transaction.

c) Transfer: The account is retrieved (32) to be received in the transfer module (33) and is processed along with the input amount (34) to create the new account value (35), which flows as the new account value (36).

d) Withdraw: The account is retrieved (37) to be received in the transfer module (38) and is processed along

with the input amount (39) to create the new account value (40), which flows as the new account value (41).

e) Deposit: The account is retrieved (42) to be received in the transfer module (43) and is processed along with the input amount (44) to create the new value of the account (45) that flows as the new value of the account (46).

In this scenario, we ignore the modeling of processes such as checking whether sufficient funds exist for withdrawal or the mechanism of transferring from the account to the intended destination. These processes can be added easily, but the purpose here is not to demonstrate the TM modeling, which was the purpose of the previous section's example. Rather, the purpose of the current example is to show the temporal features of TM modeling by registering the times of account values for multiple transactions. This will be the function of the TM events model.

B. Dynamic Model

Fig. 11 shows the events model of the bank operations, in which we identify the following events.

Event 1 (E_1): The customer requests a loan.

Event 2 (E_2): The request flows to the system, where it is approved and sent to the loan module.

Event 3 (E_3): The loan amount, number, and account number are processed.

Event 4 (E_4): A record of the loan amount, number, and account number is created and stored.

Event 5 (E_5): The customer requests a transaction service and gives the amount related to the transaction.

Event 6 (E_6): The system determines that the requested service is a transfer and sends the transaction to the transfer module.

Event 7 (E_7): The current balance value is retrieved and is processed along with the transfer amount in the transfer module.

Event 8 (E_8): The new balance value is created in the transfer module.

Event 9 (E_9): The balance value is updated.

Event 10 (E_{10}): The system determines that the requested service is a withdrawal and sends the transaction to the withdraw module.

Event 11 (E_{11}): The current balance value is retrieved and, along with the withdrawal amount, is processed in the withdraw module.

Event 12 (E_{12}): The new balance value is created in the withdraw module.

Event 13 (E_{13}): The system determines that the requested service is a deposit and sends the transaction to the deposit module.

Event 14 (E_{14}): The new balance value is created in the deposit module.

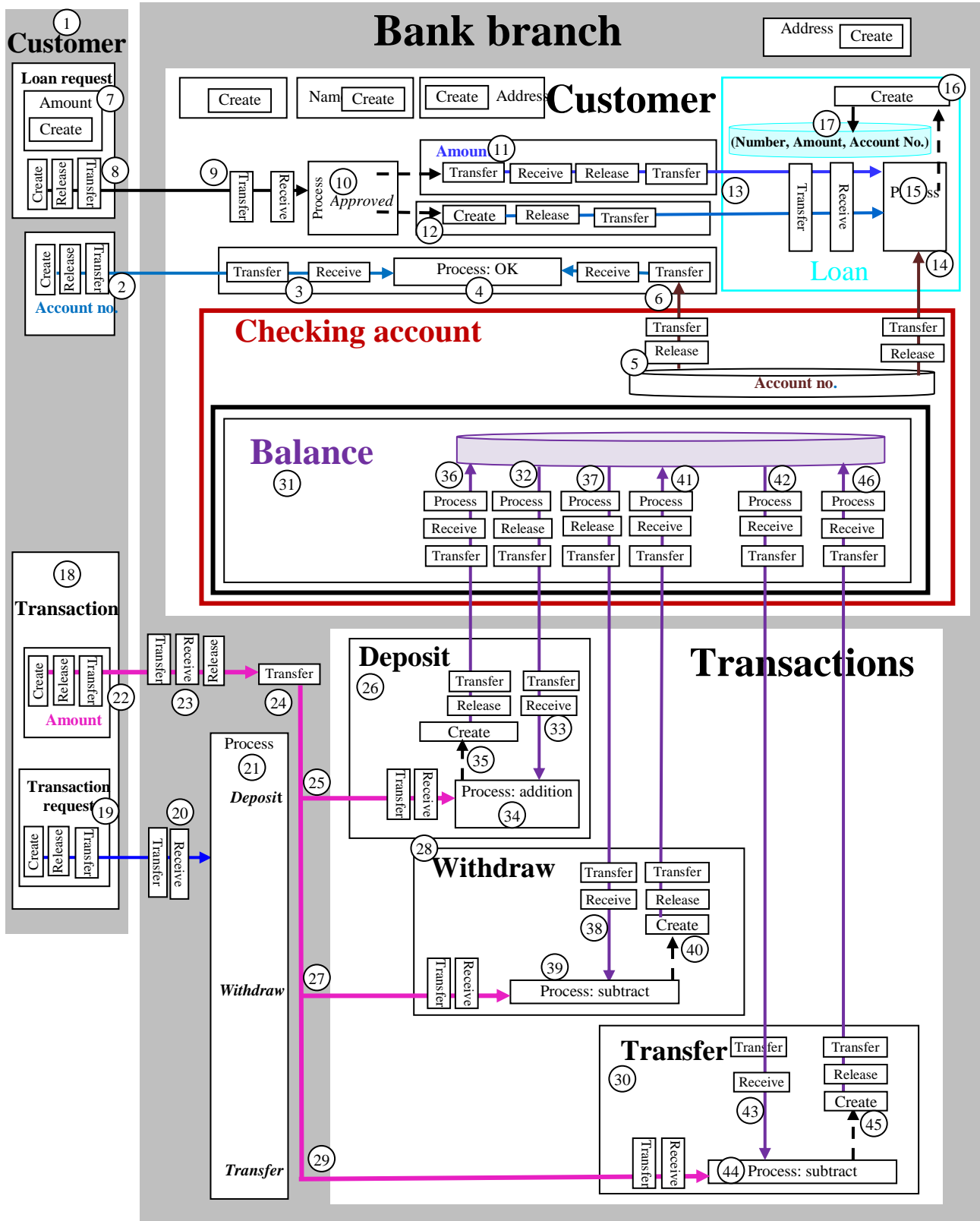


Fig. 10. The Static TM Model of the Bank.

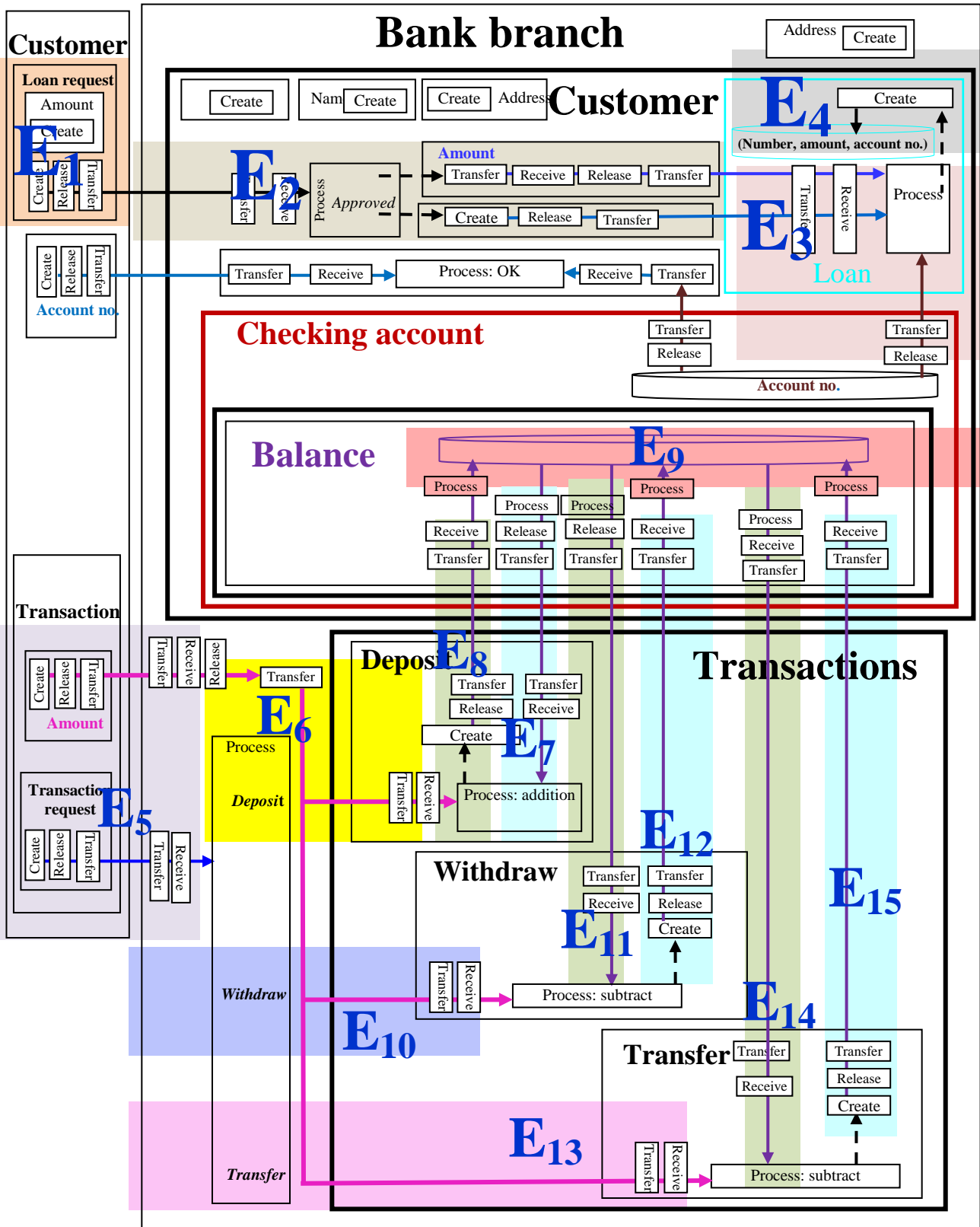


Fig. 11. The Dynamic TM Model for Bank-System Management.

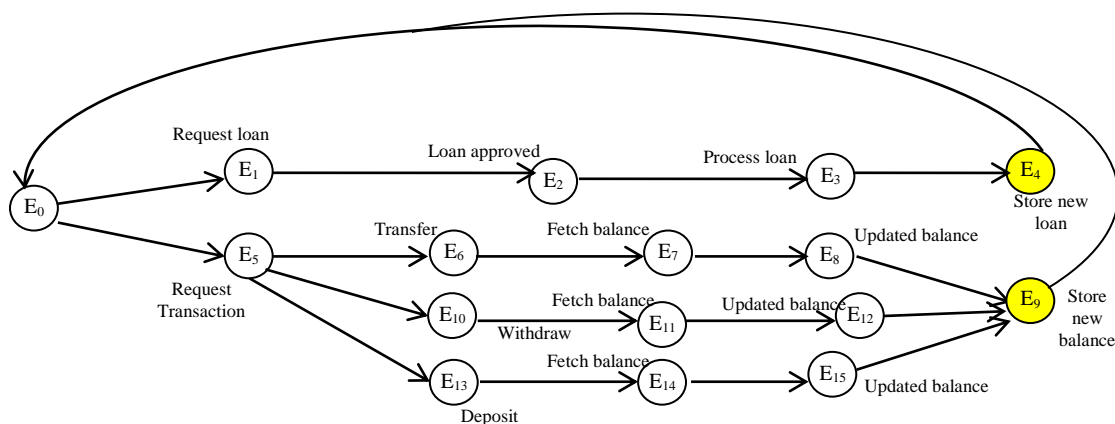


Fig. 12. The TM behavioral of the Bank Services.

Fig. 12 shows the behavioral model of the bank operations.

C. Temporal Model

We will focus on the values of the loans and balances at different times. Fig. 13 shows a file being built for the temporal balance value. This change in the balance value occurs at event E_9 . Accordingly, when event E_9 occurs, it triggers a meta-event (an event that is generated by an event), denoted as ME_9 . ME_9 creates a record of E_9 that contains data about the time of E_9 , the new balance value, and the account number. In general, the event time may include different types of time-related data (e.g., the start time, end time, duration, and urgency). Thus, a temporal file of changes to the customer's balance is updated each time a new value is calculated and stored. A similar file can be constructed for loans.

Such a meta-event notion can be applied not only to collect a history of certain data but also to all events in the behavioral model in order to form a temporal-monitoring system of historic records of all activities. For example, a history record can be generated of the events and data changes for each customer's loan. Fig. 14 shows an expansion of the system to monitor the total activity involved in the loan service. For example, in the loan service, not only are the loan value and loan's time recorded, but also all related activities (e.g., time the customer submitted the request or processing time) are recorded and stored when registering the new loan. We can generalize this model to a complete monitoring system that records all activities and data changes over time, as shown in Fig. 15.

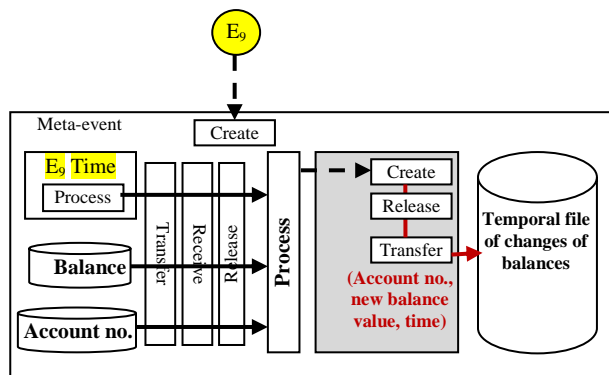


Fig. 13. Generating Temporal Data for Changes in the Balance Value.

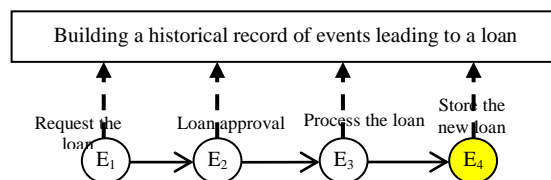


Fig. 14. Historical Record of all Events for a Certain Loan.

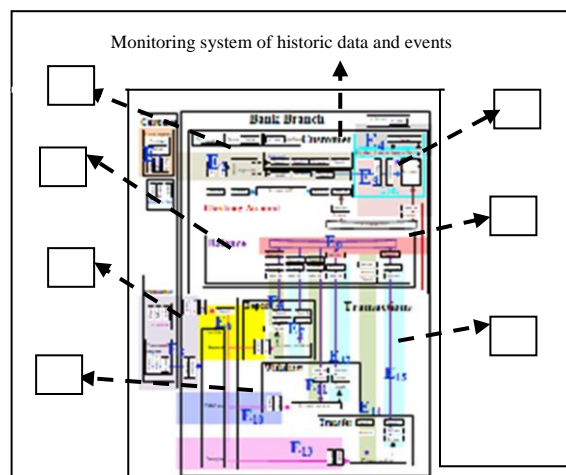


Fig. 15. General Monitoring System for Temporal Data and Changes.

V. CONCLUSION

In this paper, we have examined a model for temporal databases using an example banking-system-management model that extends UML and OCL. The bank system is remodeled using TM modeling. The resulting diagrammatic TM specification delivers a new approach to temporality that can be extended to a holistic monitoring system for historic data and events. In this case, a temporal database can be viewed as a restricted monitoring system. One limitation of TM modeling is the complexity of its diagram. However, this apparent complexity originates from the level of granularity of the description. For example, the actions *release*, *transfer*, and *received* can be eliminated under the assumption that the arrow direction will be sufficient to indicate the direction of flows. Future research can be conducted to develop a general monitoring scheme for an entire organization.

REFERENCES

- [1] A. Shah, F. Fotouhi, W. Grosky, S. H. Shah Khan, and J. Al-Muhtadi, "Operators of the temporal object system and their implementation," *Inf. Sci.*, vol. 158, pp. 37-68, January 2004.
- [2] C. Date, H. Darwen, and N. Lorentzos, *Temporal Data and the Relational Data Model*. San Francisco: Morgan Kaufmann, 2003.
- [3] B. Novikov and E. Gorshkova, "Temporal databases: From theory to applications, programming and computer software," *Programming and Computer Software*, vol. 34, no. 1, pp. 1-6, 2008.
- [4] E. Malinowski and E. Zimanyi, "A conceptual model for temporal data warehouses and its transformation to the ER and the object-relational models," *Data Knowl. Eng.*, vol. 64, pp. 101-133, January 2008. DOI: 10.1007/978-3-540-74405-4_5.
- [5] V. Khatri, "Temporal conceptual models," in *Encyclopedia of Database Systems*, L. Liu and M. Özsu, Eds. New York: Springer, 2017.
- [6] K. Karimi, "A brief introduction to temporality and causality," arXiv preprint, pp. 1007-2449, 2010.
- [7] M. O'Connor, "It's about time: Applying temporality to software development teams," *Proceedings of the 13th International Symposium on Open Collaboration Companion*, pp. 1-8, August 2017.
- [8] T. Halpin, "Temporal modeling (Part 1)," *Business Rules Journal*, vol. 8, no. 2, February 2007. <http://www.brcommunity.com/a2007/b332.html>
- [9] S. de Ridder and F. Frasincar, "Temporally enhanced ontologies in OWL: A shared conceptual model and reference implementation," in *Web Information Systems Engineering*, J. Wang et al., Eds. Springer, 31-45, 2015.
- [10] W. Lu et al., "A lightweight and efficient temporal database management system in TDSQL," *PVLDB*, vol. 12, no. 12, pp. 2035-2046, 2019.
- [11] H. Balsters, A. Carver, T. Halpin, and T. Morgan, "Modeling dynamic rules in ORM," in *On the Move to Meaningful Internet Systems*, R. Meersman, Z. Tari, and P. Herrero, Eds. Berlin: Springer, 2006, pp. 1201-1210.
- [12] S. A. El Hayat, F. Toufik, and M. Bahaj, "UML/OCL based design and the transition towards temporal object relational database with bitemporal data," *J. King Saud Univ. Sci.*, vol. 32, pp. 39-407, 2020.
- [13] S. Al-Fedaghi, "Computer program decomposition and dynamic/behavioral modeling," *Int. J. Comput. Sci. Netw.*, vol. 20, no. 8, pp. 152-163, 2020. DOI: 10.22937/IJCSNS.2020.20.08.16.
- [14] S. Al-Fedaghi, "Modeling the semantics of states and state machines," *J. Comput. Sci.*, 16(7): 891-905, 2020. DOI: 10.3844/jcssp.2020.891.905.
- [15] S. Al-Fedaghi and B. Behbehani, "How to document computer networks," *J. Comput. Sci.*, vol. 16, no. 6, pp. 423-434, 2020. DOI: 10.3844/jcssp.2020.723.434.
- [16] S. Al-Fedaghi, "Conceptual software engineering applied to movie scripts and stories," *J. Comput. Sci.*, vol. 16, no. 12, pp. 1718-1730, 2020. DOI: 10.3844/jcssp.2020.1718.1730.
- [17] S. Al-Fedaghi and E. Haidar, "Thing-based conceptual modeling: Case study of a tendering system," *J. Comput. Sci.*, vol. 16, no. 4, pp. 452-466, 2020. DOI: 10.3844/jcssp.2020.452.466.
- [18] S. Al-Fedaghi and J. Al-Fadhli, "Thing-oriented modeling of unmanned aerial vehicles," *Int. J. Adv. Comput. Sci. Applic.*, vol. 11, no. 5, pp. 610-619, 2020. DOI: 10.14569/IJACSA.2020.0110575.
- [19] S. Al-Fedaghi and J. Al-Fadhli, "Thing-oriented modeling of unmanned aerial vehicles," *Int. J. Adv. Comput. Sci. Appl.*, vol. 11, no. 5, pp. 610-619, 2020. DOI: 10.14569/IJACSA.2020.0110575.
- [20] S. Al-Fedaghi and Y. Atiyah, "Tracking systems as thinging machine: A case study of a service company," *Int. J. Adv. Comput. Sci. Appl.*, vol. 9, no. 10, pp. 110-119, 2018. DOI: 10.14569/IJACSA.2018.091014.
- [21] S. Al-Fedaghi and J. Al-Fadhli, "Thing-oriented modeling of unmanned aerial vehicles," *Int. J. Adv. Comput. Sci. Applic.*, vol. 11, no. 5, pp. 610-619, 2020. DOI: 10.14569/IJACSA.2020.0110575.
- [22] S. Al-Fedaghi and H. Alnasser, "Modeling network security: Case study of email system," *Int. J. Adv. Comput. Sci. Appl.*, vol. 11, no. 3, 2020.
- [23] M. Heidegger, "The thing," in *Poetry, Language, Thought*, A. Hofstadter, Trans. New York: Harper and Row, pp. 161-184, 1975.
- [24] L. R. Bryant, "Towards a machine-oriented aesthetics: On the power of art," *Proceedings of the Matter of Contradiction Conference*, Limousin, France, 2012.
- [25] O. Etzion and P. Niblett, *Event Processing in Action*. Stamford, CT: Manning Publications, 2011.

Towards a Real Time Distributed Flood Early Warning System

EL MABROUK Marouane
CA-GIP, CA, Versailles
France

Abstract—Since the beginning of humanity, floods have caused a lot of damages and have killed many people. So far, floods are causing a lot of losses and damage in many countries every year. When facing such a disaster, effective decisions regarding flood management must be made using real-time data, which must be analyzed and, more importantly, controlled. In this paper, we present a distributed decision support system that can be deployed to support flood management decision makers. Our system is based on Multi-Agent Systems and Anytime Algorithm, and it has two modes of processing: a Pre-Processing mode to test and control the information sent by sensors in real-time and the Main Processing mode, which has three different parts. The first part is the Trigger Mode for monitoring rainfall and triggering the second part, the offline mode, which predicts the flood based on historical data without going through the real-time decision support system. Finally, the online mode predicts the flood based on real-time data and on a combination of communications among different modules, hydrodynamic data, Geographic Information System (GIS), decision support and a remote sensing module to determine information about the flood.

Keywords—Flood; forecasting; distributed decision support system; multi-agent system; anytime algorithm

I. INTRODUCTION

Water, a source of life and, energy, reveals to man his image. When he contemplates, prostrated on the shore of a lake or favorite ocean, a man draws happiness and peace; however, floods are aquatic phenomena that man respects and of which he is afraid. Occurring as a result of heavy rainfall, which is occasionally regular, lasting, intense and violent, floods leave behind desolation, misery and destruction [1].

Based on a report published by the United Nations, floods are considered one of the most damaging natural disasters in the world. Generally, the number of people affected and the economic damages resulting from floods are increasing [2]. In addition, floods are responsible for one-third of all damages caused by natural disasters [3].

The annual damage due to floods worldwide was estimated at 50 billion US dollars per year in the decade from 1990 to 1999, and an increase in costs of 4% per year seems to be emerging [2]. However, despite the constant average number of natural disasters, the number of people affected and the amount of damage recorded is increasing, reflecting not only better identification of disasters but also an increase in the concentrations of people in areas at risk, especially in flood-prone areas [3].

In recent years, Morocco has experienced several floods that caused several deaths and injuries, and serious material and human damages [4]. It is for this reason that flood forecasting has become an important area of research; it is important for national economic planning and saving people's lives. In recent years, flood forecasting technology has begun to use computer science, and the flood forecasting abilities have been greatly improved through database technology, artificial intelligence technology and several decision support systems developed using Web and other technologies [4].

Flood risks cannot be completely eliminated, but with warning systems and decision support systems that can be used to prevent floods, we can reduce their impact. Decision Support Systems (DSSs) are defined as tools that help end users (usually called decision makers) choose from a set of possible decisions or alternatives. In the domain of flood management, DSSs are used for many tasks and are an important part of the decision-making process [5].

DSSs consider three phases of flood management: pre-flood management, operational flood management and post-flood management. DSS tools for floods must provide accurate flood forecast information for the first phase and useful strategies for the second one. This information can be used for warning messages aimed at the general population or towards selected groups and services, such as forest rangers, police forces, fire brigades, military forces and other intervention groups [5].

The rest of the paper is organized as follows: Section 2 introduces proposals for real-time flood monitoring published by other authors. In addition, DSSs and real-time distributed DSSs are presented in Section 2. In Section 3, we introduce our distributed system for flood management that is based on multi-agent systems; it is divided into several parts and modes. In Section 4, we will present the conception, design and implementation of the proposed system. The results and discussion are presented in Section 5. Finally, in Section 6, the conclusion and recommendations are given for further work.

II. STATE OF THE ART

A. Related Work

Since the 1960s, flood forecasting has been the subject of extensive research and has resulted in countless operational developments in many countries because of the human and economic effects associated with these events. Information systems are increasingly used in flood forecasting. Since, several researchers have focused their work on intelligent

systems for decision support for the prediction of floods. In [6], the authors developed a DSS for flood management in urban areas. Their system has several modules, including a module for the analysis of sea level and wind data based on the 48-hour weather forecast. According to the models included (BSM-2010, FMI), the system can calculate the water level in the watershed to trigger the warning.

In [7], the authors proposed a decision support system known as RAMFLOOD DSS that includes several modules and methods for processing the data used in the system, ie, data about land use, topographic data, etc. They also proposed a digital model for hydrodynamic modeling that merged hydraulic methods with soil data using neural networks. The authors in [8] designed and developed DESMOF, a decision support system for the Red River watershed. This system has four components and is able to combine intelligent knowledge with database and model data to support the decisions.

In [9], a real-time flood management system was developed by BCEOM, CS SI and Meteo France. The system includes four parts. The first part is the acquisition and validation of hydrometeorological data (meteorological data and soil data), the second part is for hydrological forecasting calculations, the third is for identifying natural hazard scenarios and the last is to trigger the evacuation plan. The author in [10] developed and proposed an adaptive system based on a multi-agent system using the AMAS approach [11] for real-time flood forecasting. This system is designed to forecast floods in an entire watershed. Its architecture is based on two levels: the first level is for the agents to calculate the water levels. Each agent is designed to provide the variation in the water level for an hour. The second level is for wireless sensors, and each agent in the first level manages these sensors to observe the actual influence of each entry.

B. Real-Time Distributed Decision Support Systems

The growth of the use of computer systems in daily life has pushed the scientific community to focus on improving their reliability. Thus, ensuring proper functioning has become a necessity. To ensure proper operation and the quality of the processing and the results of these systems, we must think in terms of performance, i.e., the processing time, execution time and response time [12]. Hence, using a distributed decision support system is required to ensure resource sharing, fault tolerance, inter-process communication and to facilitate communication between users.

1) *Decision support systems*: Decision support systems increasingly rely on computer systems that are responsible for providing to the decision maker many relevant elements as quickly as possible to support in their decision-making [13].

The concept of the DSS is extremely vast, and its definition often depends on the author's perspective. Simonovic [14] defined a DSS as a system that allows decision-makers to make judgments using computer output based on a user interface that provides the information needed for the decision-making process.

These systems assist with decisions that are related to various problems (structured, semi-structured and

unstructured) using all available information. They use several approaches for processing and responding to the problem requested, such as quantitative models and database elements. They are an integral part of the decision maker's approach when processing and solving a problem.

Decision support systems are often multi-user distributed information systems. Therefore, it is necessary that they rely on distributed computer systems: users in multiple locations who cooperate using computers. That is why, as part of our work, we focused on the conception of a decision support system that is physically and logically distributed using multi-agent systems. First, though, what is a distributed decision support system?

2) *Distributed decision support systems*: The current trend of globalization has transformed the way decisions are made; organizations are now often present at different locations spread around the world. Consequently, data, interfaces and users are often in geographically separate locations. However, before presenting distributed decision support systems, we must first define distributed systems.

Distributed systems includes all of the systems used by several autonomous entities, with each communicating with its neighbors through either communication channels or shared variables. Each entity evolves according to its own state and those of its neighbors. The challenge of distributed algorithms is to succeed in making all of these entities collaborate to achieve a global task [12].

This make distributed systems more powerful. First, they can be more reliable because every function is duplicated several times. When one of the entities fails, another can take over the work and the results of the processing can be stored in several locations. Second, by having several entities, the response and processing times can be kept short by using parallel computation. This property and the fault tolerances of the distributed systems give the systems the potential to be much more powerful than any traditional operating system [15].

It should be noted here that the concept of a DSS is not incompatible with the distribution of knowledge and users but simply that in the classical architecture of a DSS, we have a central synchronization source (often a central database).

The evolution of the concept from the classic DSS to the distributed DSS occurs mainly at the level of the topology used to connect the various components. Gachet [16] defined the Distributed DSS as a set of components and services arranged in a dynamic and unreliable network, whether it is composed of hardware or software services, working together to assist in decision-making.

Many topologies are used in distributed systems, but three main topology types are used for communication: centralized topology, hybrid topology and decentralized topology. Hybrid topology represents an intermediate stage between the other two topologies [16].

3) *Real-Time Multi-Agent system*: The implementation of Anytime Algorithms turns any system into a real-time system.

The necessity of using a distributed system forced us to explore multi-agent systems. Flood disasters require a distributed system that responds quickly because flooding is a disaster that can endanger human lives; thus, using these two approaches is essential. Real-time multi-agent systems are multi-agent systems that account for real-time constraints.

a) *Anytime Algorithm*: An anytime algorithm is an algorithm that exchanges execution time for a high-quality result. Allowing more time to execute a task results in an output of higher quality. Because the execution times are so long, this approach risks increased response times in non-traditional intelligent systems. Fortunately, these algorithms find their places in the field of artificial intelligence because, in this area, the construction of reasoning would occur progressively over time and address some of the deadline needs [17,18].

b) *Multi-Agent System*: From the concept of multi-agent system disengages immediately the idea of a multiple agents system, the concept of agents remains the backbone of it. An agent is a real or virtual entity that evolves in an environment that is able to perceive, act and communicate with other agents, and that exhibits autonomous behavior that can be observed through interactions with other agents and the goals it pursues. Thus, multi-agent systems are very suitable for modeling phenomena in which the interactions between the various entities are too complex to be understood by classical modeling tools [19]. They are increasingly used in disaster management scenarios, especially flood events, because they can represent autonomous entities with behaviors that include cooperating, negotiating and communicating with others.

The approach accounts for the real-time aspect of multi-agent systems and is the approach used most often [20,21], because it enables the design of applications that provide answers in time, even if the results provided are partial or approximate.

Claude Duvallet and Bruno Sadeg [22] proposed a new approach that accounts for the real-time aspect in a multi-agent system: the ANYMAS model, which is a multi-agent system model based on the anytime approach. In this model, the real-time aspect has two levels (agent itself and multi-agent systems).

In the next section, we introduce and present our proposed Distributed Decision Support System for Real-Time Flood Management.

III. PROPOSED DISTRIBUTED DECISION SUPPORT SYSTEMS FOR REAL-TIME FLOOD MANAGEMENT

Our need to design and develop a physically and logically distributed system led us to perform several studies on distributed approaches to choose the most appropriate approach for our case. The advantages that can be provided by the multi-agent approach, namely distributed, parallel, collaborative, hybrid, flexible, recursive, adaptive, cooperative, and intelligent distributed processing and a scalable environment, led us to choose this approach, because it provides us all of the desired advantages in our distributed decision support system.

Our system is a system for flood forecasting and warnings that performs several tasks; the multi-agent approach allowed us to assign agents to specific tasks to perform intelligent, distributed, adaptive and scalable processing to reach cooperative and collective decisions by entering all of the agents into the global processing system.

Our decision support system is a distributed system based on multi-agent systems and Anytime Algorithms for flood disaster management. It is from here that we can see the originality and strength of our proposed system since, in the literature, few examples like this exist.

The coupling of multi-agent systems with Anytime Algorithms makes our distributed decision support system reliable, fast, strong and original compared to other decision support systems for flood disaster management.

Our system is divided into two parts. The first is the pre-processing phase, which aims to:

- Ensure the best functioning of the wireless sensors.
- Test the reliability of data received from these sensors.
- Classify the received data as valid or invalid data.
- Choose the most appropriate data to be saved in the database.

The second part, the main processing phase, aims to:

- Simulate floods and run comparison modules for decisions regarding the occurrence of flooding in the offline mode.
- Support decisions in the online mode using an intelligent distributed architecture based on multi-agent systems in real-time flood forecasting.
- Simulate hydrological data using hydrological modelling modules.
- Use remote sensing to determine land use in areas under surveillance to identify areas at risk.
- Use a GIS module, which allows for the review of all knowledge related to flood risks and provides an overview of the risks to provide support in disaster management.
- Use knowledge bases to determine the constraints for the system to obtain the most intelligent decisions possible.

Fig. 1 shows the general architecture of our distributed decision support system.

Our system is a system based on distributed architecture and client-server architecture with a centralized topology. This topology allows for easy control over data and users and simple implementation [16].

This is, of course, an important factor in the choice of topology for facilitating the implementation of distributed decision support systems. Fig. 2 displays the system's distributed architecture.

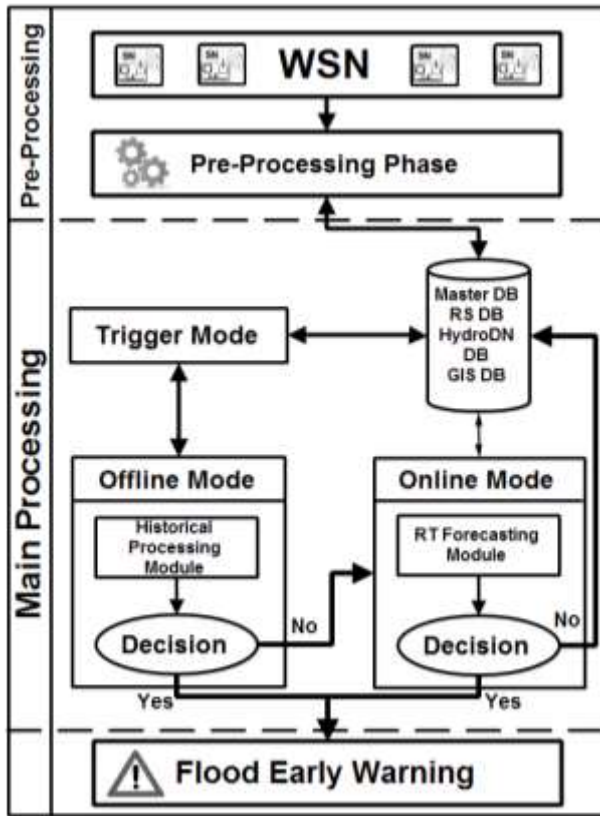


Fig. 1. General Architecture of our Decision Support System.

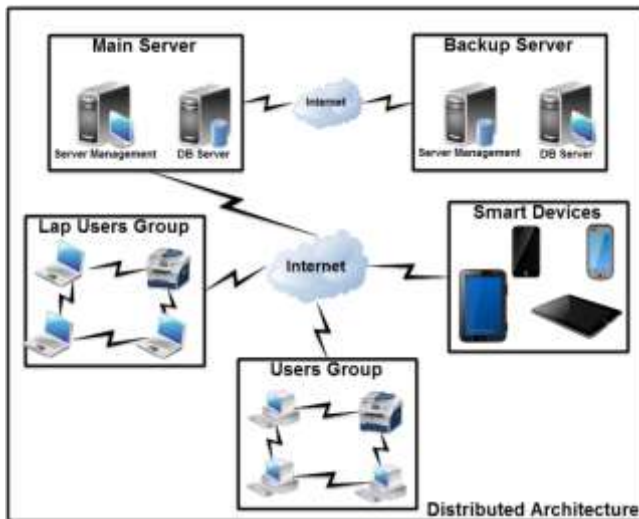


Fig. 2. Proposed Distributed Architecture.

A. Pre-Processing Phase: The Intelligent Proposed Model for Classification and Segregation [23]

The pre-processing phase is used to monitor the function and performance of sensors installed in flood-prone areas. This model is based on multi-agent systems and is used to classify the data received into valid and invalid data. We have proposed three stages with five agents to perform the necessary processing to classify the data to be stored in the database.

Data Aggregation and Classification Stage is the responsible for this data aggregation and classification of data received from the WSN and there are three agents responsible for the classification process, the Rainfall Agent, the Runoff Agent and the Water Level Agent. Each of these agents does a processing according to the following proposition:

$$M(C) = \begin{pmatrix} 0 & & & & & \\ T_{(d_2,d_1)} & 0 & & & & \\ T_{(d_3,d_1)} & T_{(d_3,d_2)} & 0 & & & \\ T_{(d_4,d_1)} & T_{(d_4,d_2)} & T_{(d_4,d_3)} & 0 & & \\ \vdots & \vdots & \vdots & \ddots & 0 & \\ T_{(d_n,d_1)} & T_{(d_n,d_2)} & T_{(d_n,d_3)} & \dots & T_{(d_n,d_{n-1})} & 0 \end{pmatrix} \quad (1)$$

Where

$$T_{(d_i,d_j)} = \left(1 - \frac{\min(d_i,d_j)}{\max(d_i,d_j)} \right) \text{ Where } \begin{cases} i \in [2, n] \text{ Where } n \in \mathbb{N} \\ j \in [1, n-1] \text{ Where } n \in \mathbb{N} \end{cases} \quad (2)$$

The d_i and d_j are a value from the dataset sent by sensors to be processed in the proposed matrix in position i and j . n is the number of lines and columns in the matrix

To range data according to the tolerance specification, we proposed the tolerance percentage and here is its proposed formula:

$$P_{TC} = \frac{(2 \times \Delta_C) + T_F}{100} \quad (3)$$

Where

- Δ_C : Sensor uncertainty designated by the fabrication company.
- T_F : Uncertainty that may be attached to a factor in the study area (Rainfall, Runoff, ...).

Here is the architecture of this proposed Pre-Processing phase presented in the Fig. 3:

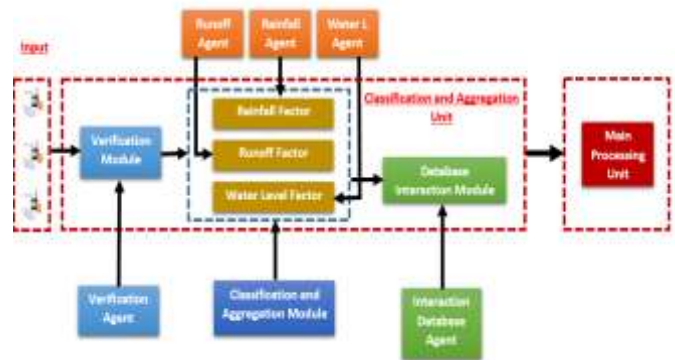


Fig. 3. Pre-Processing Mode Architecture.

B. Main Processing: Trigger Mode

In this sub-mode, we proposed a multi-agent layer responsible for monitoring rainfall and its intensity. When rain is particularly heavy, the agent triggers the double forecasting and warning system (offline and online), sends ACL messages to the system to inform it that rainfall has become stronger, and waits for confirmation from the system. This confirmation allows the server responsible for the online processing to be monitored for proper functioning (Fig. 4).

C. Main Processing (Offline Mode): Proposed Model for Decisions based on Historical Processing

The offline mode is based on similarities between historical data and data received in real time. In this mode, we proposed a model responsible for flood forecasting in the offline mode based on historical data. Our model compares the similarities between two multidimensional objects: historical data and real-time data received from wireless sensors. We proposed an equation that includes all of the factors (rainfall, runoff and water levels). Instead of comparing each factor in the historical data with its corresponding real time data, we compare the result of the proposed equation calculated for the historical and real-time data. In the proposed equation:

$$F(Z) = \frac{aF_1 \times cF_3}{bF_2 \times TSFV} \tag{4}$$

Where

F_1, F_2, F_3 and $TSFV$ represent rainfall (mm), runoff ($\frac{m}{s}$), water levels (m) and the time between the previous forecast value at an instant (t) and the current forecast value at an instant ($t + 1$) in second (s), respectively. For the first record $TSFV = 1$, F_H and F_{RT} are respectively, historical data and real-time data functions for factors that give us values ($V_1, V_2, V_3, V_4, \dots, V_n$) to compare in our Historical Processor Model that has two levels for comparison.

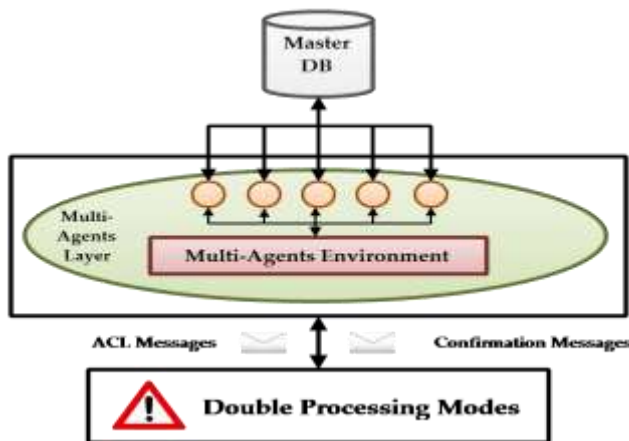


Fig. 4. Trigger Mode Architecture.

(a, b, c) are coefficients and $(a, b, c) \in \mathbb{R}_+^*$. These coefficients are the percentages of influence for each factor that leads to flooding in the affected area.

1) *Proposed model*: Our proposed model is divided into two stages: the splitting stage and the double validation stage.

a) *Splitting Stage*: First, data are loaded from the database, and then the splitting module divides the historical data into categories. The splitting agent calculates the set for all historical data for each record in the database using the equation proposed in the previous section. Next, it divides the historical data into categories depending on the interval (end of flood, beginning of flood). Each distribution includes a set of records beginning with the first record saved directly after the flooding until the next flood event occurred. This distribution then represents one case out of all of the cases of flooding that have occurred in the area. The system compares the real-time data with these distributions to determine if there are any similar cases in the past. The distributions are then saved in the local database. When the agent finishes processing the data, it sends the ACL messages to trigger the Historical Processing Model. Fig. 5 shows how the proposed model divides the data and creates the distributions.

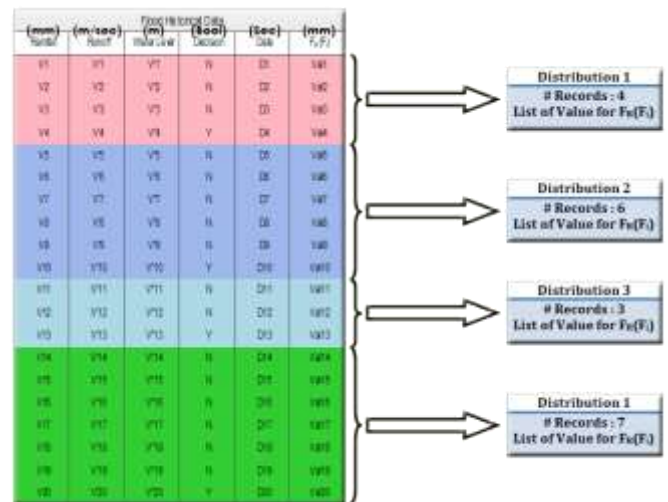


Fig. 5. Splitting Process.

b) *Double Validation Stage*: This stage includes two levels. The first level is for simulation by the variance coefficient, and it has three modules: the first module is the historical data variance coefficient calculation module; it is managed by the variance coefficient calculation agent $AMVCH_i$. This agent calculates the variance coefficient for each distribution that was generated in the previous stage. The second module is the real time data variance coefficient calculation module, managed by the $AMRTC$ agent. This agent calculates the variance coefficient for the real-time data. The third module is the comparison module. The comparator mediator agent allows for comparisons between the historical coefficients and the real-time coefficients. If the coefficients are similar, they will be included in a list of similar

distributions, and it will be sent to the second level. The agent sends ACL messages to inform and trigger the second level. Otherwise, it sends ACL messages to the decision support system to trigger the real-time online forecasting mode for flood disaster management.

The second level is for the Gini index simulation [24]. Our proposed model is based on using inequality measures to perform the comparisons between the generated distributions and the real-time data received from the wireless sensors. The Gini Index is one of the best methods for comparing distributions across different categories because of its easy and simple interpretation using the Lorenz curve diagram. The Gini index also has an important advantage in that it can be used to indicate changes in the distributions. Thus, in this level, there are five modules to validate the similarity of the historical and real-time data. The first module is a module for the interaction with the database. It is managed by the *AMLDDB* agent, which selects the selected distributions already sent by the first level from the database and loads it into the GINI index historical data calculation module. This second module is for calculating the GINI index for historical data. It is managed by the *AMGH_i* agent, which calculates the GINI index for the selected distributions. Additionally, there is a module managed by the *AMGRT* agent responsible for calculating the Gini index for real-time data received from wireless sensors. At the end of the processing, the *AMGRT* agent saves the results in the Master database. The fourth module is used to perform the comparison between the selected distribution and the real-time data based on the results of the two previous modules. During the comparison, the comparator mediator agent of the GINI index is responsible for determining the similarity between the selected distribution and the real-time data using a distance comparison.

If there is a similarity, the system continues to the last module to give the final decision about the likelihood of a flood event occurring, otherwise it proceeds to a real-time decision using the online mode. The final module is the Loopback module managed by the *AMLB* agent. To ensure that there are similarities between the distributions and real-time data, we designed our system to compare 90% of the distribution records with the data received in real time to decide and trigger the early flood warning because if there is 90% similarity, we can be absolutely certain that there will be flooding, and the accuracy of the system's decision will be high. The *AMLB* agent is responsible for testing the number of records in the real-time data. If it reaches 90% of the

number of records of the selected distributions, it triggers the early flood warning. Otherwise, it proceeds to a real-time decision using the online mode.

2) *Architecture of the proposed model:* Fig. 23 (see Appendix) presents the architecture of the offline forecasting mode.

3) *Flow chart of the proposed model:* In this section, we will present the flow chart of the offline forecasting mode.

Fig. 6 presents the flow chart of the first level of validation by the variance coefficient, and Fig. 7 presents the flow chart of the second level of validation by the GINI index.

a) Variance Coefficient Validation Flow Chart

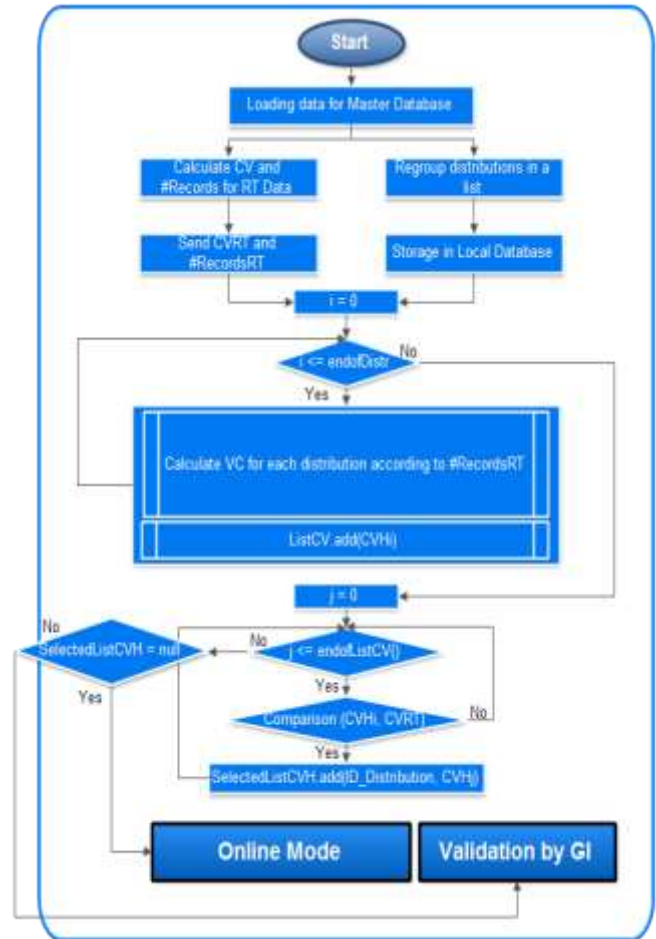


Fig. 6. Variance Coefficient Validation Flow Chart.

b) GINI Index Validation Flow Chart

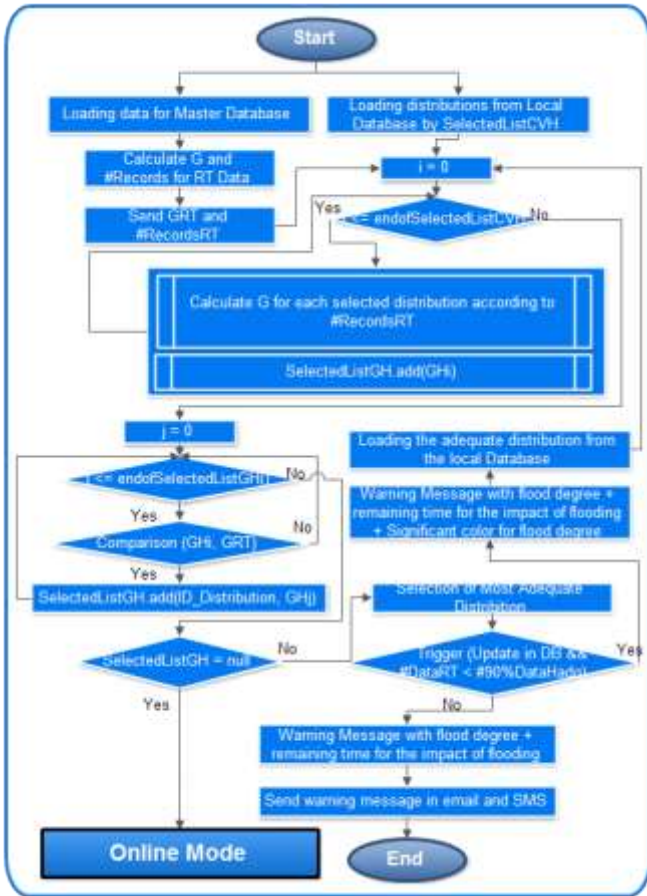


Fig. 7. GINI Index Validation Flow Chart.

4) Validation by GINI Index: We use historical data (Table I) and real-time data (Table II) to make the simulation and the validation with the GINI index. As already mentioned, for a first forecasting of a region, we process its historical data before starting the real-time forecasting in order to calculate the distributions and its variance coefficients and the GINI coefficients and Lorenz curves to be used in comparison with the real-time data during the real-time forecasting. Next, the results are stored in the database.

The validation with the GINI index is triggered only if it found similarity between historical distributions and real-time distributions in the first level of validation by the variance coefficient. The comparison is based on the number of records of real-time data received from sensors. The system gives a decision if and only if 90% the record sum of the historical distribution \geq the record sum of the real-time distribution. If $G \leq 0.1$ so the distributions are similar. Therefore, the system triggers the warning procedure. If there is no similarity with the historical distributions, so the system proceeds to the online mode to make the forecasting and warning. The following are two distributions, with which we will illustrate an example of our system functioning using the validation with the GINI index.

TABLE I. HISTORICAL DATA

Rainfall	Runoff	Water Level	FH(Z)
1	80	0,11	0,001375
2	295	0,33	0,00223729
4	157	0,17	0,00433121
9	221	0,14	0,00570136
6	181	0,26	0,00861878
4	77	0,17	0,00883117
18	186	0,11	0,01064516
12	118	0,20	0,02033898
22	105	0,14	0,02933333
11	86	0,35	0,04476744
12	35	0,22	0,07542857
51	434	0,70	0,08225806

TABLE II. REAL-TIME DATA

Rainfall	Runoff	Water Level	FRT (Z)
1	80	0,01	0,000125
2	120	0,02	0,00033333
4	107	0,09	0,00336449
6	181	0,18	0,00596685
11	106	0,15	0,01556604
12	124	0,19	0,0183871
18	86	0,11	0,02302326
9	50	0,24	0,0432

The Table III (see Appendix) shows the calculated data to plot the Lorenz curve (Fig. 8) for comparison of the historical and real-time distributions.

The Table IV (see Appendix) allows calculating the GINI index of the processed distributions

$$\text{Gini Index} = 1 - (0,531125 + 0,315821) = 1 - 0,846946 = 0,153054$$

It is observed that the real-time distribution and the historical distribution are similar in about 85% and even if it has not reached 90% of the distribution of historical data yet. If G is less than or equal to 0.1 so both of distributions will be similar, therefore the system will trigger the warning. The following curve in the Fig. 8 shows the comparison between the historical and the real-time distributions.

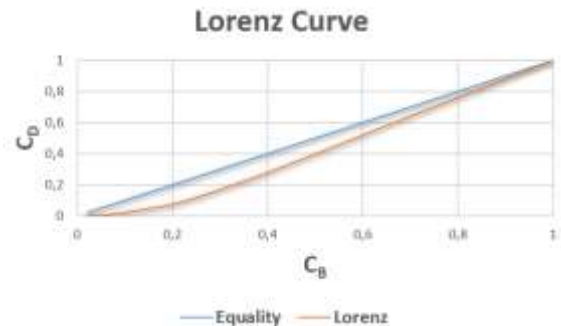


Fig. 8. Lorenz Curve of the Distributions.

Using this technique, the system can decide about the similarity of distributions even if the distributions are different.

D. Main Processing (Online Mode): Decision Support System for Real-Time Flood Management

In this mode, we proposed an expert system based on multi-agent systems and Anytime Algorithms for real-time flood forecasting and warning. Using several modules communicating with each other to provide the best decisions in a short amount of time forced us to design a collaborative system that can quickly determine the likelihood of a flood event. To accomplish this, we used ANYtime Multi-Agent Systems (ANYMAS) [22]. Each anytime agent is responsible for managing a module. The system has four modules in its online mode, which are described below.

1) *Remote sensing module*: This module presented in the Fig. 9 is used to identify the land use in at-risk areas where our system is installed. It has four processing levels. The first level is for receiving satellite images transmitted by the Land 7 satellite, which has as ETM+ sensor. The second level is for mosaicking and super positioning the satellite pictures over each other to obtain the resulting picture. The third level is for the supervised classification of the satellite pictures to analyze and extract the land use of areas under control, and finally, the fourth level is for the generation of the land-use map. This module is surveillance by the *AMRS* Remote Sensing agent. This agent is responsible for all of the data processing inside the module and for communicating with other modules.

2) *Hydrodynamic module* [25]: This module (Fig. 10) is responsible for estimating the risk of flooding, as it allows the hydrological behaviour of the watershed in reference floods to be understood. In Morocco, empirical models are often used to estimate the maximum runoff at the outlet of the watershed. Our module is divided into two levels. The first level is for hydrological modelling using a proposed model for short-term forecasting

Here is the proposed system:

$$(S) = \begin{cases} aX_1 + bY_1 + cZ_1 - Cn = 1 \\ aX_2 + bY_2 + cZ_2 - Cn = 1 \\ aX_3 + bY_3 + cZ_3 - Cn = 1 \end{cases} \quad (4)$$

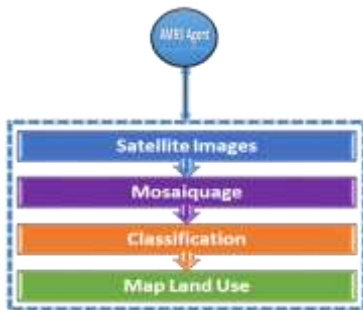


Fig. 9. Remote Sensing Module.

Where

$(X_1, Y_1, Z_1, X_2, Y_2, Z_2, X_3, Y_3, Z_3, Cn) \in \mathbb{R}_+^*$ and (X, Y, Z, Cn) are respectively the rainfall, the runoff, the water level and the evacuation of the area under control.

The solutions of this system are the values with which our expert system detects and makes the flood forecasting and triggers warnings based on the following generic function:

$$F(Z) = aX + bY + cZ - Cn \quad (6)$$

and the empirical model of Hazan-Lazarevic for medium and long-term forecasting.

The runoff is given by the following equation:

$$Q_{(T_1)} = Q_{(T_2)} \times \frac{1 + k \ln T_1}{1 + k \ln T_2} \quad (7)$$

Where:

T_1 and T_2 are respectively the return period and $k \in [0,8, 1,2[$

The second level is for hydraulic modeling using HEC-RAS software. This module is managed by the *AMH* agent, which is responsible for the processing.

3) *GIS Module*: This module introduced in the Fig. 11 aims to provide information about the magnitudes of floods, their causes, and the areas that are at risk. The combination of GIS information layers provides information about the vulnerability of a given area. The layers with which the GIS Module works include occupation records, land-use maps already created in the remote sensing module, urban maps, flood maps, digital ground models and hydrological data. In the ArcGIS software package, we worked with the HecGeoRas module, which is used to model the hydraulic system in a given area to be studied in terms of the rivers and their morphologies so that they can be processed in the hydraulic model using HEC-RAS software.

This module is managed by the *AMS* agent; this agent is responsible for communicating with the ArcGIS software package and other system modules to receive the hydrological data from the watershed morphology to be studied (runoff and the water levels) that are sent by the hydrodynamic module. It also receives the land-use maps sent by the remote sensing module and loads real-time data.

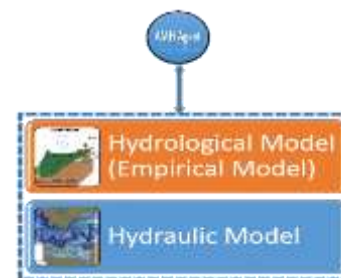


Fig. 10. Hydrodynamic Module.



Fig. 11. GIS Module.

The agent communicates with the remote sensing module and the hydrodynamic module using the Soil and Water Assessment Tool (SWAT) [26], which is a hydrological model linked to the ArcView interface in the ArcGIS software package. It is written in Fortran 90 and can predict the effects of changes in land use on water, sediment and chemical compounds; it also accounts for cultural practices. This is a physically based, semi-distributed model.

4) *Decision support module:* This module is an expert module for decision support capable of accounting for the information received from the other modules and executing the reasoning already developed in the knowledge base. It includes three parts:

- Facts base
- Rule base
- Inference engine

Our inference engine is able to use the facts and the rules from the knowledge base to produce new, partial decisions until the final decision about the impact of the flooding is made. This module also serves to create a custom database to be used in the offline mode and to calculate the forecast parameters that have been proposed and the coefficients of the factors that lead to floods (rainfall, runoff and the water levels). These parameters are the basis of our proposed system for real-time forecasting and are used by the inference engine; we developed the system and rules for testing the impact of flooding based on these parameters. This module is managed by the *AMDSS* agent, which is responsible for receiving the data sent by the other modules and transferring them to this module. After the processing and decision-making, the agent saves all of the processed data in the database to be used in the offline mode in the future. Fig. 12 displays the architecture of the Decision Support module.

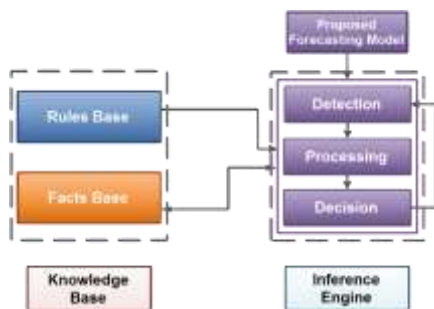


Fig. 12. Decision Support Module.

5) *Architecture of the proposed model:* In this section, we will present the architecture of the real-time flood forecasting model in the online mode. This is displayed in Fig. 13.

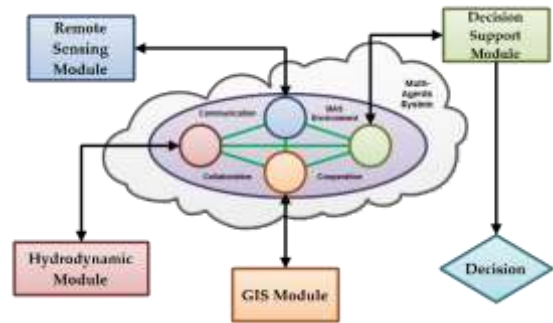


Fig. 13. Architecture of the Proposed Online Model.

The Fig. 14 shows how the different modules communicate in the online mode.

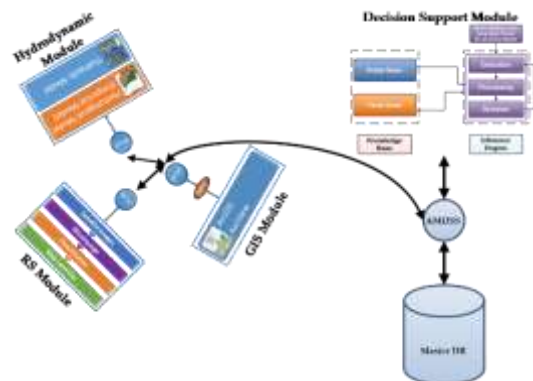


Fig. 14. Modules Communication in the Online Mode.

IV. DESIGN AND IMPLEMENTATION

In the system design phase, we chose visual modelling as a design model for this system because of its many benefits, including simplicity, universality, conciseness and expressiveness. The language used is UML, which is a graphical language for processing and modelling data. The modelling was performed on three levels, structural modelling, behavioural modelling and interaction between objects modelling. [23].

A. Design

1) *Structural and statistical modelling:* The deployment diagram illustrates the distributed architecture dedicated to our decision support system. The decision makers can log in from multiple devices, i.e., PCs, smartphones and tablets, through the Internet or intranet. We use one server for the Database Management System (DBMS) and another server for the decision support system. The deployment diagram is presented in Fig. 15.

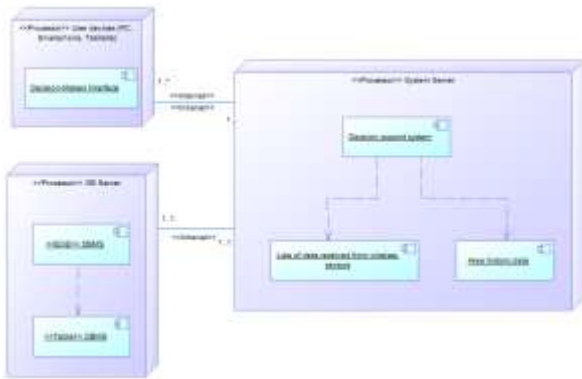


Fig. 15. Deployment Diagram.

2) *Behavioural modelling*: Behavioural diagrams focus on the dynamic behaviour of the system, the behavioural diagrams that we used are the use case diagram and sequence diagram. The main actors in our system are the decision makers who watch over the control and management of floods, responsible and administrators. The use case diagram is shown in the Fig. 16.

The sequence diagram is shown in the Fig. 17.

3) *Interactional and dynamical modelling*: The diagrams of interaction between objects modeling used to model the dynamic behavior of the system, and to indicate how the objects interact at run time. The most interesting diagram of this kind of modeling is the communication diagram. The communication diagram is shown in the Fig. 18.

B. Implementation

In this section, we will present our distributed decision support system for real-time flood forecasting and warning.

1) *Pre-Processing*: In this stage, as already described and shown in [23], the system first verifies the functioning of the wireless sensors installed in the surveillance area to identify the functioning and non-functioning sensors. The system disables the wireless sensors that are broken to remove them from the forecasting process and to have them repaired later.

Fig. 19 presents the classification interfaces of the proposed model for classification and aggregation, where the most appropriate value to be stored in the database is obtained from all of the valid data. In this stage, we also obtain the invalid values and the sensors that sent the erroneous values. The full details and information about this stage is presented in [23].

2) *Main processing (offline mode)*: In this phase, we proposed dividing the historic floods in the area into distributions by calculating the proposed function that includes all of the factors in a single equation.

Then, we proposed comparing these distributions with the data in real time using the double validation process that consists of two levels of comparisons: level 1 for comparisons using the variance coefficient and level 2 for comparisons using the GINI index (Fig. 20).

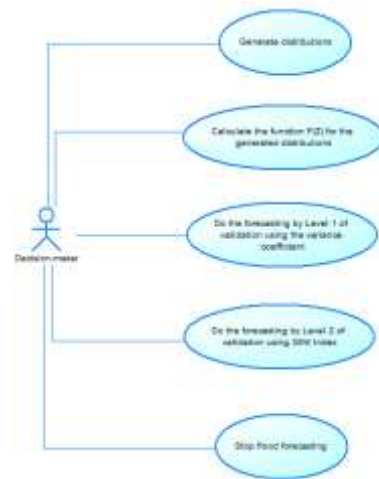


Fig. 16. Use Case Diagram for Main Processing Phase (Offline Mode).

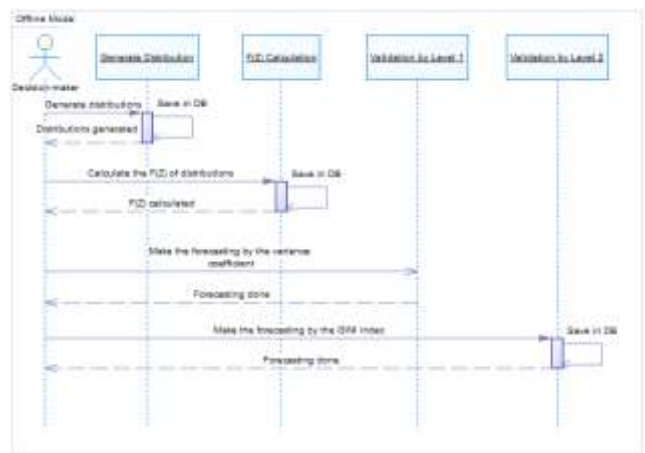


Fig. 17. Sequence Diagram for Main Processing Phase (Offline Mode).

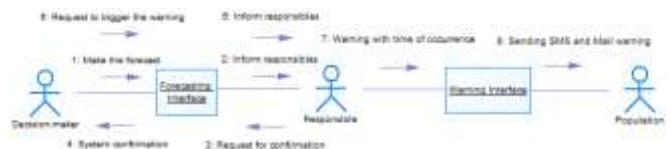


Fig. 18. Communication Diagram for Main Processing phase (Offline Mode).

Fig. 19. Classification and Aggregation Process by the Proposed Model.



Fig. 20. Double Validation Process.

3) *Main processing (online mode)*: In this phase, we can forecast flood in real-time for the short, medium and the long term using a proposed model for short term forecasting and according to a proposed model by Hazan-Lazarevic [25] (Fig. 21). The full details and information about this stage is presented in [25].



Fig. 21. Short-Term Forecasting and Warning.

V. RESULTS AND DISCUSSION

In order to test the performance of our proposed decision support system, we were interested by the response time when dealing with flood events. First, we chose 20 areas in which to experiment where we could perform our experiments using historic data. For each area, we performed four experiments, and in each experiment, we tried to create forecasts and warnings for the areas. For each set of areas, we noted the required response times.

The experiments were first completed using only the online mode. Next, the Pre-Processing mode was used with the online mode, followed by the Pre-Processing mode with the offline and online modes and, finally, the entire distributed decision support system was used.

For all of the experiments, we noticed that the response time increased when the number of areas to be monitored increased, which is normal because that increases the amount of data. Using only the online mode resulted in a long response time for a single area. We noticed that more than five minutes were needed to respond because the amount of data in the database was large and it was not classified, so all of the data had to be processed before the forecasts and warnings could be made, which affected the response time.

In the second experiment, we observed the importance of classifying and aggregating the data before saving it in the

database because the response time decreased compared to the first experiment. In the third experiment, we used the three proposed modes: The Pre-Processing mode for classifications, the offline mode for decisions without the online mode and, of course, the online mode.

It was also noted that the response time decreased significantly compared to the two experiments already conducted due to using the pre-processing mode for classifications and aggregations, and due to the offline mode that helps determine the risk of flooding without using the online mode by comparing the new data with historical data.

Using our entire distributed decision support system, we noticed that the response time decreased by approximately five times compared with the first experiment thanks to the various proposed models and modules, the distributed architecture and the real-time multi-agent environment, which helps the system process data from several locations using several agents where each is responsible for performing a given process. Fig. 22 summarizes what we have just explained.

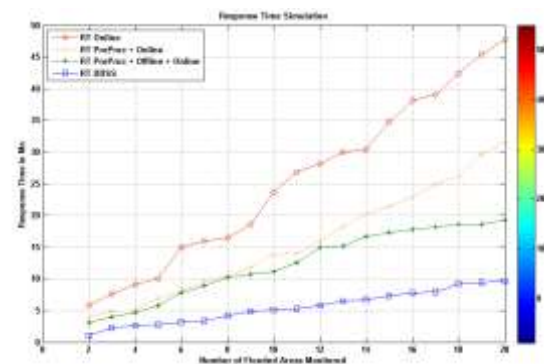


Fig. 22. Simulation of the Response Time of the System.

VI. CONCLUSION AND FUTURE WORK

In this paper, we presented our distributed decision support system for real-time flood forecasting. It has two main parts, the pre-processing part used to monitor the sensors and to classify data received from these sensors so that only the appropriate data are included. Three stages have been proposed for this process: the sensor verification stage, the Data Aggregation and Classification stage and the Database interaction stage.

The second part is the main processing part, and it has three modes:

- **Trigger mode**: This mode is responsible for monitoring rainfall to trigger the proposed systems.
- **Offline mode**: In this mode, we can predict floods without using the online mode by using a proposed model for processing and comparing historical and real-time data. It has two stages, the splitting stage for dividing the historical data into distributions to be used in the double validation stage and the double validation stage for the processing needed to calculate the similarities between the historical and real-time data to determine the likelihood of a flood.

- Online mode: In this mode, we use an expert system based on multi-agent systems and Anytime Algorithms for real-time flood forecasting and warning. This mode has four modules for real-time flood forecasting: the remote sensing module to identify land use, the hydrodynamic module for hydrologic and hydraulic modelling, the GIS module to identify flood-prone areas and, finally, the Decision Support Module for receiving and processing all of the data using a proposed model that manipulates the knowledge base through the inference engine.

Our future work will focus on improving the system by choosing specific criteria to improve. We will also design and develop multi-area forecasting and warning methods to improve our system such that it can monitor several areas at the same time without decreasing the performance and response times.

ACKNOWLEDGMENT

We are so thankful to Mathematics and Applications Laboratory and LIROSA Laboratory, Abdelmalek Essaadi University, Tangier and Tetuan, Morocco for providing support for this research.

REFERENCES

- [1] Jordan F., Modèle de prévision et de gestion des crues. Optimisation des opérations des aménagements hydroélectriques à accumulation pour la réduction des débits de crue, Ph.D. dissertation, Ecole Polytechnique Fédérale de Lausanne, 2007.
- [2] Onu, Guidelines for Reducing Flood Losses. International Strategy for Disaster Reduction. United Nations 2004.
- [3] Doussin N., Mise en œuvre locale d'une stratégie globale de prévention du risque d'inondation : le cas de la Loire moyenne, Ph.D. dissertation, Université De Cergy-Pontoise, 2009.
- [4] Elmabrouk M., Ezziyyani M., and Essaaidi M., Toward an optimal model based on inequality measures for treatment of historical & real time flood's datasets, in Proceeding of the International IEEE Colloquium of International On Information Science and Technology (CIST'14), Tetuan, Morocco, 2014.
- [5] Hernandez J. G., 'Flood management in a complex river basin with a realtime decision support system based on hydrological forecasts', Ph.D. dissertation, Ecole Polytechnique Fédérale de Lausanne, 2011.
- [6] Krzhizhanovskaya V., Melnikova N., Chirkin A., Ivanov S., Boukhanovsky A., and Sloot P., Distributed simulation of city inundation by coupled surface and subsurface porous flow for urban flood decision support system, *Procedia Computer Science*, Vol. 18, pp. 1046 – 1056, 2013.
- [7] Castellet E. B. I., Valentin M. G., Ripolles J. D., Onate E., Piazzese J., And Corestein G., Decision support system for flood risk assessment and management, in Proceeding of the 7th International Conference on Hydroinformatics (HIC'06), Nice, France, 2006.
- [8] Ahmad S. and Simonovic S., An intelligent decision support system for management of floods, *Water Resources Management*, Vol. 20, No. 3, pp. 391 – 410, 2006.
- [9] Raymond M., Peyron N., Bahl M., Martin A., and Alfonsi F., Espada : Un outil innovant pour la gestion en temps réel des crues urbaines, *NOVATECH*, pp. 793 – 800, 2007.
- [10] George J. P., Gleizes M. P., Glize P., and Rgis C., Real-time Simulation 'for Flood Forecast: an Adaptive Multi-Agent System STAFF, in Proceeding of the Symposium on Adaptive Agents and Multi-Agent Systems (AISB). University of Wales, Aberystwyth: Society for the Study of Artificial Intelligence and the Simulation of Behaviour, pp. 109–114, 2003.
- [11] George J. P., The AMAS Theory for Complex Problem Solving based on Self-Organizing Cooperative Agents. First European Workshop on Multi-Agent Systems (EUMAS'03). Oxford, UK, 2003.
- [12] Messika S., Méthodes probabilistes pour la vérification des systèmes distribués, Ph.D. dissertation, Ecole Normale Supérieure de Cachan, 2004.
- [13] Levine P. and Pomerol J. C., Systèmes interactifs d'aide à la décision et systèmes experts, *Traite des nouvelles technologies*, Paris, Hermes, 1989.
- [14] Simonovic S. P., Decision support system for flood management in the red river basin, Report to the Int. Joint Commission Red River Basin Task Force, Ottawa, Washington D.C, Tech. Rep. 1999.
- [15] Mullender S. J., 'Introduction to distributed systems', in Proceeding of the CERN School of Computing (CERN'92), Italy, 1992.
- [16] Gachet A., A new vision for distributed decision support systems, in Proceeding of the DSIage 2002 Conference, Ireland, pp. 341–352, 2002.
- [17] Boddy M. and Dean T., Solving time-dependent planning problems, in Proceeding of the 7th National Conference of Artificial Intelligence, Minneapolis, Minnesota, pp. 979–984, 1989.
- [18] Horvitz E. J., Reasoning about beliefs and actions under computational resource constraints, in Proceeding of the 1987 Workshop on Uncertainty in Artificial Intelligence, 1987.
- [19] Oufella S., Hamdadou D., and Bouamrane K., Conception d'un système interactif d'aide à la décision collective en localisation spatiale, in Proceedings of the 2nd Conference Internationale sur l'Informatique et ses Applications (CIIA'09), Saida, Algeria, 2009.
- [20] Salvant T. and Brunessaux S., Multi-agent based time-critical decision support for c31 systems, in Proceeding of the Practical Applications of Intelligent Agents and Multi-Agents, PAAM, London, 1997.
- [21] Salvant T., CAAM, un modèle d'agent Anytime coopératif pour l'aide à la décision en temps critique, Ph.D. dissertation, ENST, Paris, 1998.
- [22] Duvallet C. and Sadeg B., Des systèmes multi-agents Anytime pour la conception de systèmes d'aide à la décision, *Technique et Science Informatiques*, Vol. 23, No. 8, pp. 997 – 1025, 2004.
- [23] Elmabrouk M. and Gaou S., Proposed Intelligent Pre-Processing Model of Real-Time Flood Forecasting and Warning for Data Classification and Aggregation, *International Journal of Online Engineering (iJOE)*, Vol 13, No 11, pp 4 – 24, 2017.
- [24] Gini C., Measurement of Inequality of Incomes, *the Economic Journal*, Vol. 31, No. 121, pp. 124 – 126, 1921.
- [25] Elmabrouk M., Ezziyyani M., Sadouq Z. A., and Essaaidi M., New expert system for short, medium and long term flood forecasting and warning, *Journal of Theoretical and Applied Information Technology (JATIT)*, Vol. 78, No. 2, pp. 286 – 302, 2015.
- [26] Baker T. J. and Miller S. N., Using the soil and water assessment tool (SWAT) to assess land use impact on Water Resources in an East African watershed, *Journal of Hydrology*, Vol. 486, pp. 100 – 111, 2013.

APPENDIX

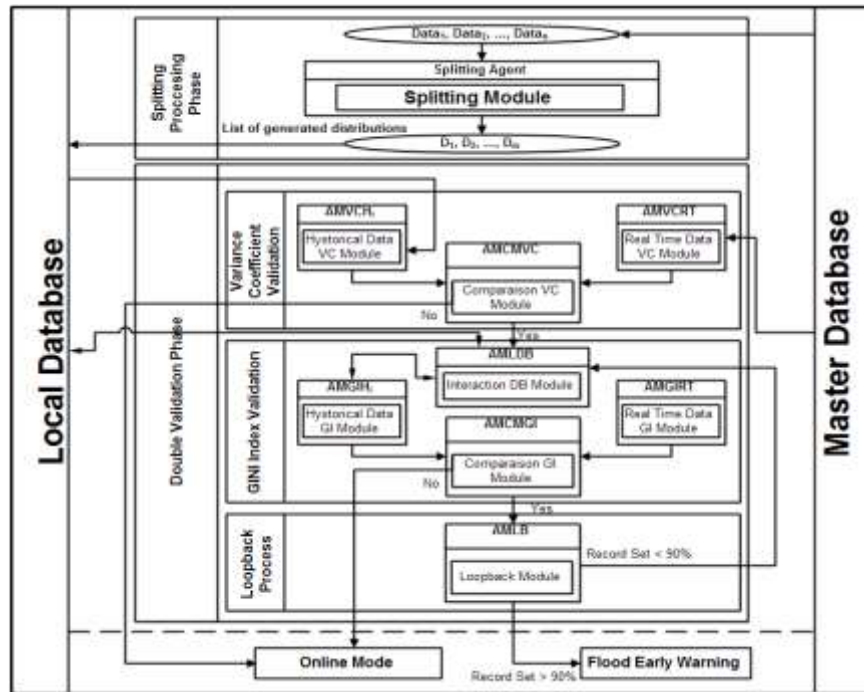


Fig. 23. Simulation of the Response Time of the System.

TABLE III. LORENZ CURVE TABLE

	B	D				
	FH(Z) / TotalFH(Z)	FRT(Z) / TotalFRT(Z)	D / B	CB	CD	 B - D
1	0,02214921	0,00113671	0,05132075	0,02214921	0,00113671	0,0210125
2	0,03603943	0,00303121	0,08410809	0,05818865	0,00416792	0,03300822
3	0,06976938	0,03059571	0,43852631	0,12795803	0,03476363	0,03917367
4	0,09184047	0,05426083	0,59081609	0,2197985	0,08902446	0,03757964
5	0,13883579	0,14155312	1,01957225	0,35863429	0,23057758	0,00271733
6	0,14225708	0,16720703	1,17538637	0,50089136	0,39778461	0,02494995
7	0,17147777	0,20936694	1,22095676	0,67236914	0,60715155	0,03788917
8	0,32763086	0,39284845	1,19905812	1	1	0,06521759
Total	1	1				0,26154808

TABLE IV. GINI INDEX CALCULATION

	B			
	$F_H(Z) / Total F_H(Z)$	C_D	B * CD_i	B * CD_{i-1}
	0	0	0	0
	0,02214921	0,00113671	0,000026	0,000041
	0,03603943	0,00416792	0,000151	0,000291
	0,06976938	0,03476363	0,002426	0,003193
	0,09184047	0,08902446	0,008177	0,01236
	0,13883579	0,23057758	0,032013	0,032802
	0,14225708	0,39778461	0,056588	0,068212
	0,17147777	0,60715155	0,104113	0,198922
	0,32763086	1	0,327631	0
Total			0,531125	0,315821

This section presents all the abbreviations used in this article.

TABLE V. ABBREVIATIONS

Abbreviation	Full explanation
ACL	Agent Communication Language
AMAS	Adaptive Multi-Agents System
AMDSS	Agent Mobile for Decision Support System
AMGHi	Agent Mobile Gini Historic data
AMGRT	Agent Mobile for Real Time data
AMH	Agent Mobile for Hydrodynamic module
AMLB	Agent Mobile for LoopBack module
AMLDDDB	Agent Mobile for Loading Data from DataBase
AMRS	Agent Mobile for Remote Sensing
AMRTCV	Agent Mobile Real Time Coefficient of Variance
AMS	Agent Mobile for Geographic Information System Module
AMVCHi	Agent Mobile Variance Coefficient Historic data
ANYMAS	ANYtime Multi-Agent Systems
Bool	Boolean
CVH	Coefficient of Variance of Historic data
DBMS	DataBase Management System
DSS	Decision Support System
FH(Fi)	Function of Historic data for Factor i
G	Gini
GI	Gini Index
GI Module	Gini Index Module
GIS	Geographic information system
GIS DB	Geographic information system DataBase
Hi	Historic data
HydroDN DB	HydroDyNamic DataBase
m/s	Meter/Second
m	Meter
mm	Millimeter
MAS	Multi-Agents System
RT	Real Time
s	Second
Sec	Second
SD	Standard Deviation
SWAT	Soil and Water Assessment Tool
VC	Variance Coefficient
VC Module	Variance Coefficient Module
Water L	Water Level
WSN	Wireless Sensors Network

Modelling Health Process and System Requirements Engineering for Better e-Health Services in Saudi Arabia

Fuhid Alanazi¹, Valerie Gay²
Faculty of Engineering and Information Technology
University of Technology Sydney, Australia

Mohammad N. Alanazi³
College of Computer and Information Sciences
Al Imam Mohammad Ibn Saud Islamic University (IMSIU)
Riyadh, Saudi Arabia

Ryan Alturki⁴
Department of Information Sciences
College of Computer and Information Systems
Umm Al-Qura University, Makkah, Saudi Arabia

Abstract—This systematic review aimed to examine the published works on e-health modelling system requirements and suggest one applicable to Saudi Arabia. PRISMA method was adopted to search, screen and select the papers to be included in this review. Google Scholar was used as the search engine to collect relevant works. From an initial 74 works, 20 were selected after all screening procedures as per PRISMA flow diagram. The 20 selected works were discussed under various sections. The review revealed that goal setting is the first step. Using the goals, a model can be created based on which system requirements can be elicited. Different research used different approaches within this broad framework and applied the procedures to varying healthcare contexts. Based on the findings, an attempt has been made to set the goals and elicit the system requirements for a diabetes self-management model for the entire country in Saudi Arabian context. This is a preliminary model which needs to be tested, improved and then implemented.

Keywords—e-health; e-health systems; e-health modelling and e-health modelling system requirements

I. INTRODUCTION

Healthcare is a necessity globally. A common adage says a healthy nation is a wealthy nation. This realization has called for massive investments in healthcare in many nations of the world (Alanezi, 2020). However, healthcare remains a luxury for many populations across the globe, and correcting that anomaly requires strategic interventions, including the adoption of technologies. Information and Communication Technologies (ICTs) have opened up possibilities for virtually all aspects of human endeavour. Everything is going digital. A common example that comes to mind is e-Commerce. For many years, research and health practitioners have toyed with the idea of developing e-health models for health systems across the world. An effective e-health system will ensure the effective coverage of multiple health interventions such as telemedicine, telehealth, mobile health, health records, big data and even artificial intelligence.

In the words of Adhikari (2019), e-Health will also encourage equity, ethical standards among practitioners and

promote healthcare education among patients and consumers. While the immense potential benefits for man is well covered, developing a holistic model and modelling system requirements has proven difficult. As Salah, Omran and Lari (2018) suggests, the vision has met with challenges relating to the complexities of the healthcare sector, compatibility issues and the issues of security and unification of eHealth frameworks [20].

Therefore, attempts to incorporate a holistic model requirement in the universal health system has not yielded much success. Efforts aimed at arriving at operationalizing e-Health and enabling its implementation in healthcare practice, education, research and policy have often lacked sufficient conceptual clarity. This has led to the widespread call for a conceptual and practical model of e-Health which adequately captures potential overlaps and complexities (JMIR). In Saudi Arabia, the need to adopt sustainable health issuance strategies and break the barriers limiting the adoption of e-Health has been widely written about. Several e-Health modelling requirements have also been provided by healthcare management experts and scholars around the world, but adopting such within the context of Arabian healthcare would call for comprehensive studies.

This paper, therefore, undertakes a systematic review of e-Health modelling system requirements to explore the possibility of suggesting them for Saudi Arabian healthcare.

The methodology followed for this review is given next.

II. METHODOLOGY OF SELECTING LITERATURE FOR THIS REVIEW

The Preferred Reporting Items for Systematic Reviews and Meta-Analyses (PRISMA) method was followed for search, screen and selection of literature for this review. Search terms, “e-Health”, “e-Health systems”, “e-Health modelling” and “e-Health modelling system requirements” were used to search for research work in Google Scholar using anytime and 2015 and beyond as the time frames. Totally, 74 works were obtained. Out of these, 12 duplicates and works on the same

aspects reported twice and in two sources were removed. Six (6) works, done by the same set of authors on the same aspect over a few years were removed after selecting the most important latest works covering earlier results. When closely similar repetitive points coming from different sources were seen, only one or two representative ones were selected from them. This resulted in not including another 12 papers. Another 24 works were not relevant to the topic and hence excluded. Thus, 20 papers were finally selected for this review as shown in the PRISMA flow diagram in the APPENDIX.

III. WHAT IS E-HEALTH AND ITS IMPORTANCE

Information and Communication Technology (ICT) has several applications in various sectors like agriculture, industry and transportation. The health sector also can immensely benefit from application of ICT. When these technologies are applied to healthcare, such as improving quality of care, electronic patient records- EPR, self-management of chronic diseases through access to information and remote care or accessibility of remote communities (telemedicine) and other fields of healthcare, it becomes e-health. It is where electronic (digital) technologies meet health. The WHO briefly defines e-health as “the use of information and communication technologies (ICT) for health.” (WHO, 2019).

On his part, Eysenbach (2001) defined e-health as “an emerging field in the intersection of medical informatics, public health and business, referring to health services and information delivered or enhanced through the Internet and related technologies. He adds that the term also takes on a broader meaning as it characterises not only a technical development, but also a state-of-mind, a way of thinking, an attitude and a commitment for networked, global thinking, to improve health care locally, regionally and worldwide by using information and communication technology”. This definition seems to suggest that e-Health, when adopted, should not remain an innovation, but should become a way of live, deeply entrenched in the psyche and attitudes of people.

IV. MAIN COMPONENTS OF E-HEALTH

Despite its simple definitions, e-Health is a broad and complex arrangement with several components under its wings. As Alanezi (2020) [11] puts it, these components include;

- *Electronic Medical Coverage:* These are also called electronic health records and refer to real-time health records of patients with clear access to decision-support tools which can aid clinicians in decision making. It also refers to patient and population health information, collected and stored systematically and electronically in a digital format (Gunter & Terry,2005).
- *Electronic Medical Records:* This has quite a simple definition. This component refers to digital records kept by doctors for recording and tracking the health data and metrics of their clients and patients. The Morsani College of Medicine at the University of South Florida calls it the equivalent of charts and paper records that

you’d otherwise find in a clinician’s office or the hospital’s registry.

- *Telemedicine:* The WHO report on the second e-Health global survey of 2010 describes telemedicine simply as “healing at a distance”. At closer look, the global health body posits that it is a way to improve patient outcomes through increased access to medical information and care by use of ICT (WHO, 2010). Here, they say, “distance is a critical factor” and erasing the barriers of distance is the essence of telemedicine.

Others like Picture Archiving & Communication Systems (PACSs) are also worthy of note. But it doesn’t end there, Eysenbach (2001) suggests there are business concepts that also form components of e-Health and which must be considered. The author added that the business concepts of B2B, B2C and C2C are applicable in the case of e-Health in the following manner:

B2C- the capability of patients for online interaction with their healthcare systems.

B2B- improved possibilities for institution-to-institution transmissions of healthcare data for common benefit as evidence-based medicine.

C2C- new possibilities for communication and cooperation among similarly placed patients, especially with respect to self-management of chronic diseases.

The term “e” in e-Health does not stand for electronic alone, but many more e’s. The author briefly described 10 e’s related to e-Health: efficiency, enhancing quality, evidence-based, empowerment, encouragement, education, enabling, extending, ethics and equity [10].

V. CONTEXTS OF E-HEALTH APPLICATIONS

In an interview, Swedish e-Health strategist Henrik Ahlen expressed that currently, e-Health is used for meeting the challenges of growing healthcare needs from aging populations, increasing costs and staff shortages against increasing demands for faster and more personal access to healthcare (Widén & Haseltine, 2015) [22]. Currently, most e-Health applications are used for fitness activities and self-care. This, experts say, is commendable but a far cry from where the world needs to be. To emphasize, e-Health is most beneficial in chronic patients. Available data shows that more than 75% of healthcare costs of countries are incurred by this group of patients. Therefore, cost reduction and efficiency and quality improvement will have a significant impact on national dimensions. Many e-Health initiatives have targeted this group patients already and e-Health is slowly finding its way into the way things are done.

VI. THE RELEVANCE OF E-HEALTH IN SAUDI ARABIA

Saudi Arabia is a fast-developing nation. As the largest exporter of Crude Oil in the world and the centre of religious tourism globally, it wields quite a significant economic power among the comity of nations. When it comes to health, the nation is yet to fully come of age. Altuwaijri (2008) [6] noted that significant progress has been achieved in Saudi Arabia with respect to health care and some hospitals are now

internationally recognised. However, its progress in e-Health had been very slow [10].

Almalki, FitzGerald & Clark (2011) explain that e-Health and electronic information systems are already being implemented in hospitals and healthcare organisations like the King Faisal Specialist Hospital and Research Centre, the National Guard Health Affairs, Medical Services of the Armed Forces and the University Hospitals. Still e-Health systems are being implemented very slowly [5]. In MOH institutions, a number of information systems are operating in the regional directorates and the central hospitals. However, lack of coordination seriously affects the effectiveness of these systems.

From the previously discussed points, it would appear that some barrier exists for promoting e-Health in a big way. One possibility is that there is not enough knowledge about identifying system requirements and modelling of e-Health services to put into practice. This review tries to examine modelling and system requirements for e-Health services and how to adapt them to the Saudi conditions. Since e-Health is more relevant for care situations of chronic diseases, this review will make more references to discussions on e-Health models and requirements for chronic diseases care.

VII. MODELLING E-HEALTH SYSTEM REQUIREMENTS

Different authors have proposed many e-Health frameworks/systems. The components of these frameworks can be considered as the requirements of e-Health. Otherwise, the framework will not work. Some of the frameworks more relevant to Saudi Arabia are discussed below.

The chronic care model of Wagner (1998) given in Fig. 1 and the Innovative Care for Chronic Conditions Framework of WHO (WHO, 2002) given in Fig. 2 may be regarded as the most basic frameworks for e-Health systems dealing with chronic diseases. The WHO model is for universal applications, especially for developing countries, where healthcare is at a low level. The micro, meso and macro levels of the WHO model are the patients at the centre, the healthcare team and community partners, the broader healthcare organisation and community and the positive policy environment respectively. The self-management aspect comes under the micro level which is the patient.

The need to define the business goals of e-Health in a bid to identify system requirements of e-Health was emphasized by Alahmadi, Soh, and Ullah (2014). Most e-Health systems are successful in the pilot stage to the satisfaction of end users with regards to their initial objectives in terms of service quality. But very rarely do they proceed further to robust methods of daily practice. The excessive focus on technology in these models is not helpful in developing the kind of understanding needed between stakeholders and developers for success to be achieved. This had been the cause for failure of many e-Health projects. Besides system requirements and value propositions, what is required or expected to provide the particular service needs to be clearly stated. Different stakeholders may require varying e-Health goals and values as needs and objectives differ. This complicates the goal-setting task. Therefore, it becomes increasingly necessary to identify

and reconcile all the system and stakeholder requirements in the very beginning. This is where requirement engineering comes to play. The term “requirements engineering” is the software engineering aspect that has to do with the processes of identifying, documenting, recording and maintaining the system through the identification of stakeholders and their needs, which can, then, be analysed, communicated and implemented subsequently. The three main categories of requirements engineering are (i) real-world goals (ii) functions, and (iii) constraints. These axes determine the development of the system based on the description of “what” and “why”. There are four steps in system requirements engineering. These are (i) requirements elicitation (ii) requirements negotiation (iii) requirements specification, and (iv) requirements validation. The author provides a methodology to understand the e-Health business environment and come up with system requirements based on organisational goals. Without a clear understanding of the environment, it may be difficult (if not impossible) to efficiently arrive at business goals. It is these goals that will then aid the identification of e-Health system requirements. There are two main phases to this methodology, as illustrated in Fig. 3.

Phase 1 of this framework deals with the well-known and accepted business/IT alignment approach. There are three levels in this phase;

Level 1- e-Health organisation. This makes up the decision level for any e-Health business environment. It describes the details of the aims and objectives of the organisation, the available resources to achieve those objectives and the executives.

Level 2- e-Health business strategy. Once you have identified the objectives and resources, this level goes on to provide a definite, practical and responsive strategy and plan for the e-Health business. This must be encompassing though, and should involve major stakeholders and sectors. The health goals and targets, vision and evaluation, and general objectives of the e-Health strategy are clearly defined here.

Level 3- e-Health business infrastructure. This is where operations take place. It forms the foundations for services and the exchange of information beyond geographical and sectoral boundaries for the e-Health programme. Various dimensions of operations include the physical infrastructure, core services, processes and activities. While Phase 2 dealt with the e-Health business goals modelling methods as they concern e-Health system requirements, this phase elicits the e-Health system requirements using the business goals identified in Phase 1.

The author used a routine patient visit to a healthcare unit in Australia as a case study to illustrate the model of the e-Health system environment using business process modelling symbols. Registration, doctor allocation, consultation, examination as well as discharge are the four processes and activities within the e-Health model. From this model, the method of eliciting system requirements as given in Fig. 4.

In another related paper, the same authors (Alahmadi, Soh, & Ullah, 2014) proposed a model of automated e-Health

system for a patient visit to the hospital in Australia. To elicit the requirements for such system, first tiers of the system were used [1]. Tier 1 consists of e-Health environment in which goals, subgoals and activities exist. In Tier 2, automated e-Health system requirements are derived. These are diagrammatically explained by the authors as given in Fig. 5. Clearly, it is more convenient to elicit system requirements as an end-product of activities in Tier 2.

To address privacy issues, an accountable e-Health system (AeH) was designed by Gajanayake, Iannella, Lane, and Sahama (2012) in Australia. The model is reproduced in Fig 6. In this model, there are three types of users: a central health authority, patients, and healthcare providers (HCP). The accessibility for each user is determined by the need and justification separately. The governing body of HER determines the levels of its employees who can access the patient records in a role-based manner. The patients may

access his/her data or nominate anyone else [12]. These two access policies are combined by a pre-determined protocol between the patient and the HCP. The patient can question the HCP if any misuse occurs. The authors presented the same system as a use case diagram.

A business continuity model for e-Health systems was proposed by Rejeb, Bastide, Lamine, Marmier, and Pingaud (2012) so that the system remains operative even in unexpected conditions. A protected backup system is used for this purpose [17].

A quality of experience (QoE)/quality of service (QoS) model was proposed by Rojas-Mendizabal, Serrano-Santoyo, Conte-Galvan, and Gomez-Gonzalez (2013) based on an e-Health ecosystem consisting of human, technological and economic contexts. The QoE/QoS model is reproduced in Fig. 7.

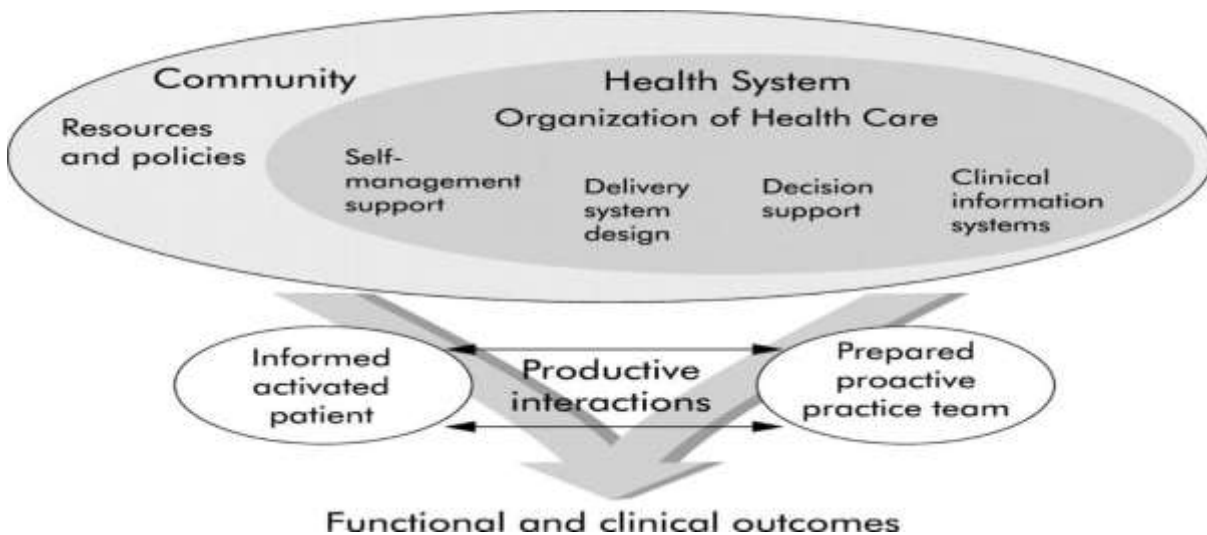


Fig. 1. The Chronic Care Model of Wagner (1998).

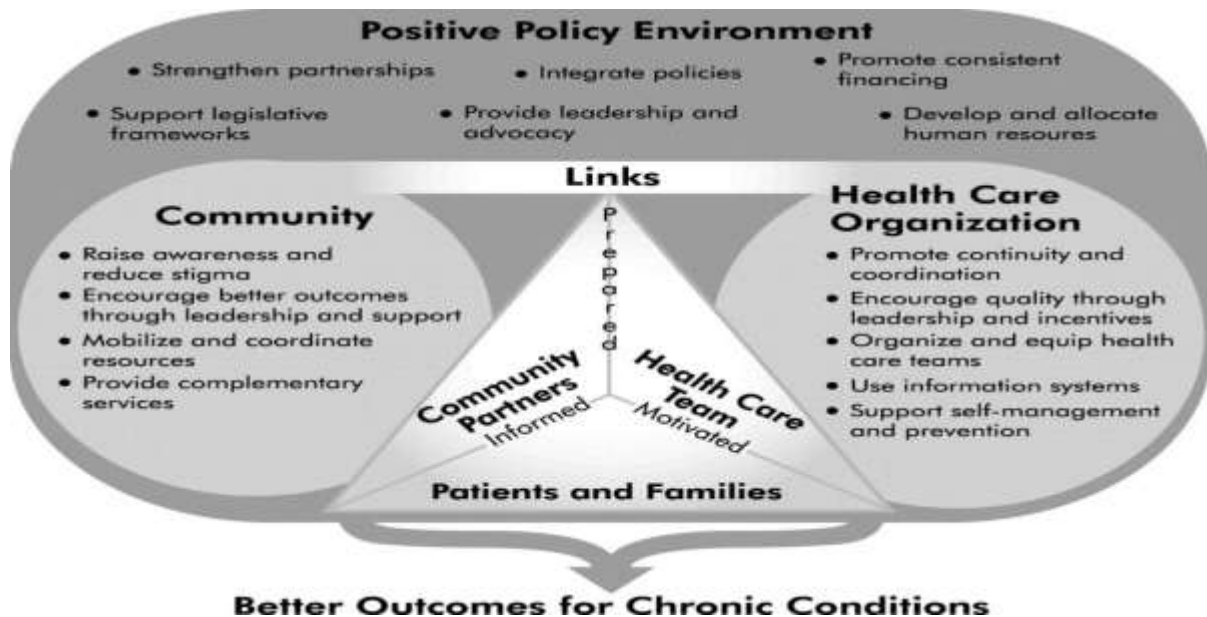


Fig. 2. Innovative Care for Chronic Conditions Framework (WHO, 2002) [21].

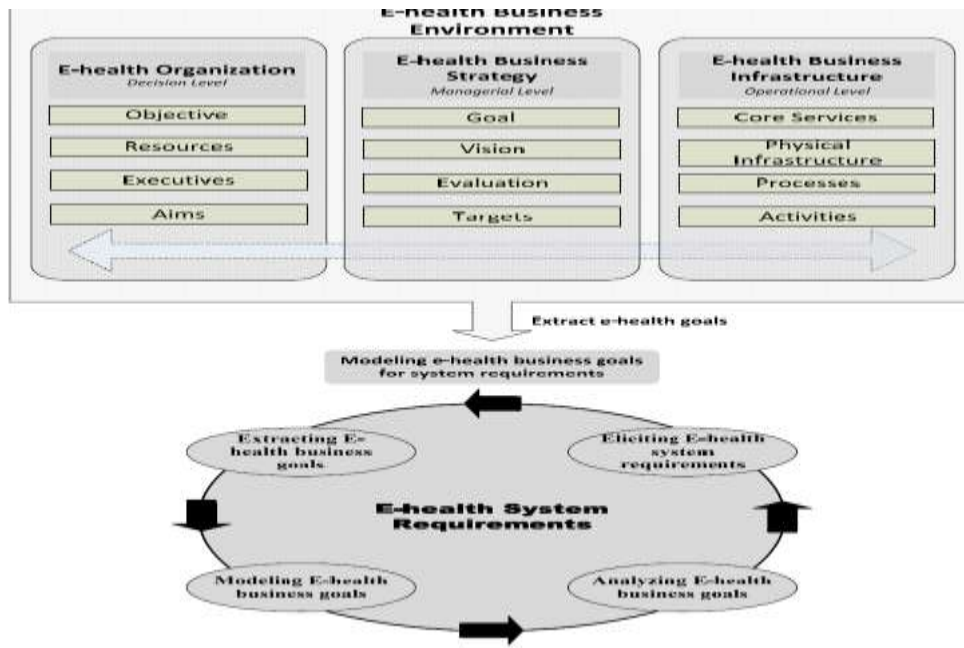


Fig. 3. Methodology of Deriving System Requirements from Business Goals in an e-Health Environment (Alahmadi, Soh, & Ullah, 2014) [2].

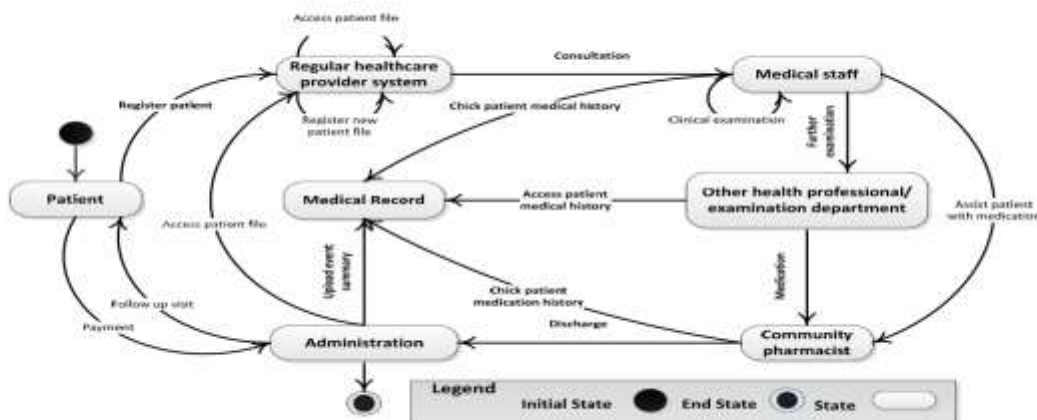


Fig. 4. Method of Extracting e-Health System Requirements based on e-Health Environment Modelling (Alahmadi, Soh, & Ullah, 2014).

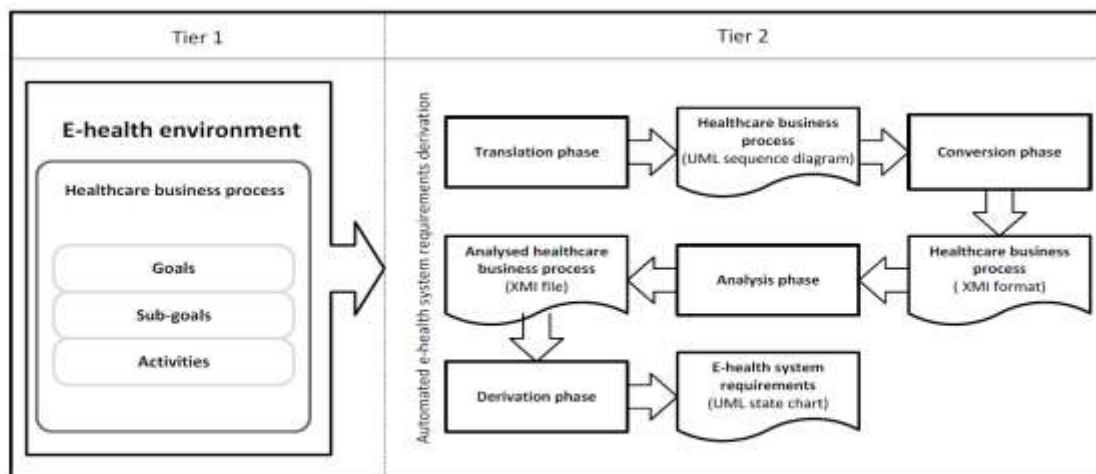


Fig. 5. Automatic e-Health Modelling Approaches (Alahmadi, Soh, & Ullah, 2014).

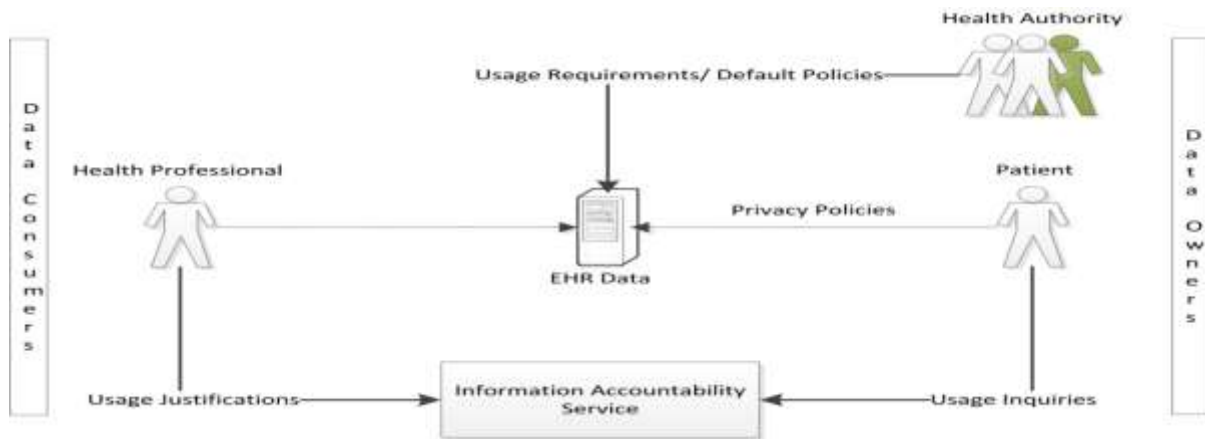


Fig. 6. An Accountable e-Health Model (Gajanayake, Iannella, Lane, & Sahama, 2012).

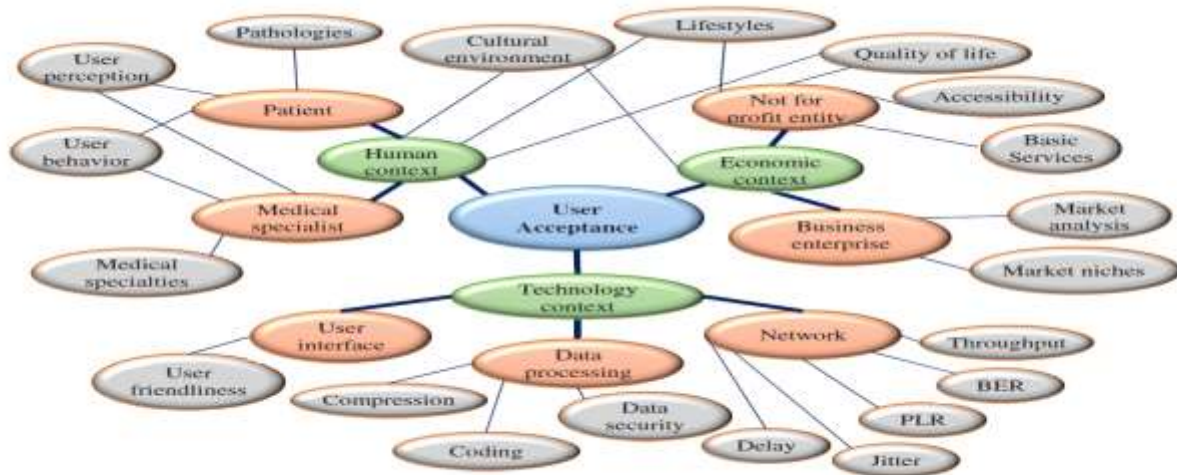


Fig. 7. A QoE/QoS e-Health Model Proposed by (Rojas-Mendizabal, Serrano-Santoyo, Conte-Galvan, & Gomez-Gonzalez, 2013) [19].

A behaviour intention technology (BIT) model for e-Health and mobile e-Health (m-health) applications was proposed and applied to a fitness case by Mohr, Schueller, Montague, Burns, and Rashidi (2014) [16]. The basic model is reproduced in Fig. 8. BIT models use a variety of technologies such as sensors, mobile phones and the web to support users to change behaviours and cognitions of physical health, mental health and wellness problems and interventions to reduce them. The basic requirement is effecting a behavioural change to promote a change from current state of health to a better state of health for the user. Preparation of workflows of such models will be useful to determine when the intervention should be applied. Predetermined or adaptive technological systems can be used depending upon the context.

A service-oriented boundariless e-Health architecture was proposed and applied to an application, CardioNet by Mircea, et al. (2010). It is a patient-centric model, in which, all hardware, software and medical activities are services and patients are customers. This is a truly business model as well. Remote interactions are possible between patients, doctors, providers, labs and authorities. The possible range of interactions is depicted in Fig. 9. Data exchange between the

interacting elements occurs through XML format. How it is implemented in the CardioNet is shown in Fig. 10 reproduced from the work. In CardioNet, boundaryless information flow occurs at the levels of patient, provider, operational centres, home care units and data storage devices.

An RFID based rural e-Health service model was proposed by Chia, Zalzal, Zalzal, and Karim (2013). The hierarchical structure constitutes rural inhabitants (patients), community health workers and the central healthcare facility. The goal of such an e-healthcare system is to facilitate easy and reliable identification of each patient, maintain more precise medical records, provide better healthcare and improve the quality of life in communities that are remote from a central medical facility. It also reduces the pressure on the central healthcare facility [9]. The patient base of the central facility is broadened towards remote localities. The value chain stakeholders are the patients, other inhabitants of the rural area, physicians, administrators of the central facility and providers of equipment, e-Health recorder and communication facilities. The actual rural e-Health system is reproduced in Fig. 11.

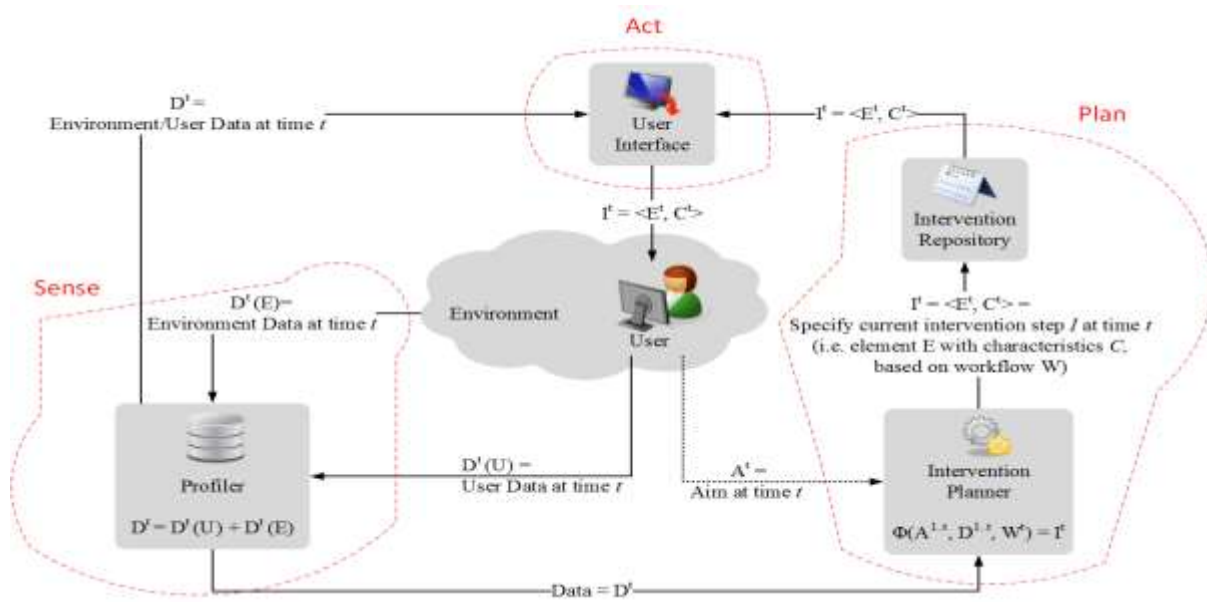


Fig. 8. A basic BIT e-Health Model (Mohr, Schueller, Montague, Burns, & Rashidi, 2014).

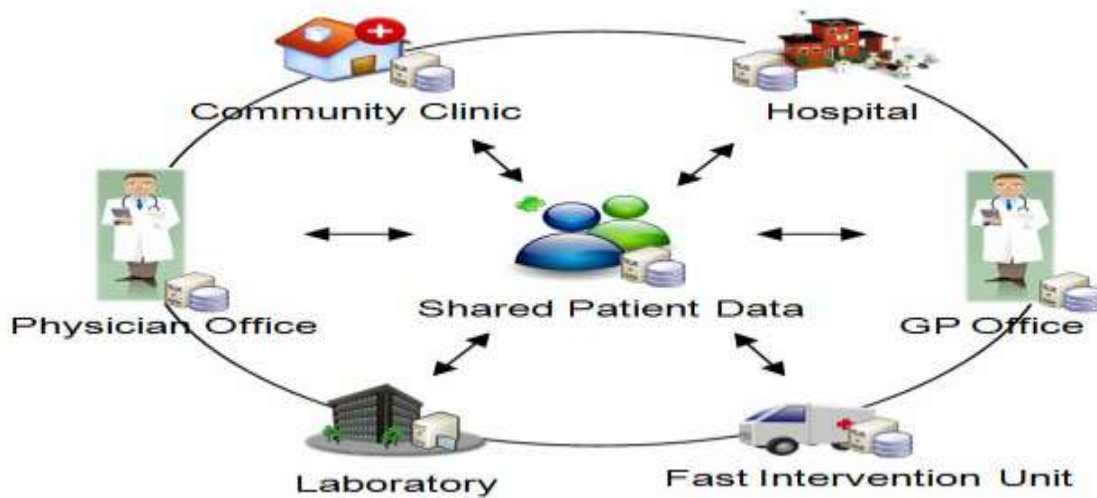


Fig. 9. Boundaryless Information Flow (Mircea, et al., 2010) [15].

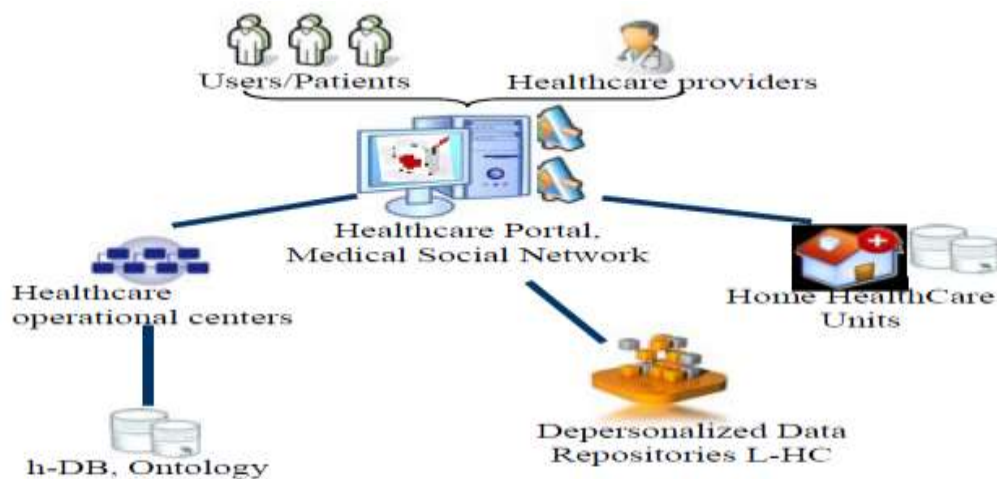


Fig. 10. Application of Boundaryless Information Flow in CardioNet (Mircea, et al., 2010).



Fig. 11. RFID-based Rural e-Health System (Chia, Zalzal, Zalzal, & Karim, 2013).

The system model and security requirements of a secure patient-centric e-Health model was defined by Barua, Liang, Lu, and Shen (2011). The proposed model has the e-Health care service provider working as a trusted party where a patient is registered. The encrypted data is stored in centralised storage, a sort of health-cloud from where future access is possible. The proposed scheme has four major steps: (i) the patient health information (PHI) is collected (ii) the secure encrypted data is transmitted from PHI to e-healthcare provider (iii) at the e-Health provider, the PHI data are processed. Then it classifies the PHI data based on the patient-preferred attributes. Access to the data is based on different privacy levels of requesters like general users, doctors etc. by assigning a different set of attributes to the different levels, and (iv) the processed PHI is transferred to the cloud for future use [7]. The security requirements were defined based on the goals: patient-centric access control, integrity of the message using authenticated sources and non-repudiation, prevention of attacks by cyphertext only methods, provision of patient safety, resistance to collusion attack and resistance to DoS attacks. For each of the security goals, requirements and technologies were developed and integrated into the e-healthcare system.

In his work on implementation of a cloud-based e-Health services in an Indian state, (Joshi, 2016) diagrammatically presented the following requirements-

1) *Software as a service (SaaS)* to citizens through government portals, mobile phones, computers, self/start architecture and m-health applications. These are public services.

2) *Public/private services of Platform as a Service (PaaS)* for database, reporting, multitenancy and programming languages. These provide PaaS for SaaS development.

3) *Infrastructure as a Service (IaaS)* for local units state-wide and servers for database, web and applications are provided with the virtual environment for users to operate. SWAN can be used for connecting various health departments [14].

This list can be used as the basic system requirements of e-Health projects in general. The authors also suggested some challenges and solutions.

A. Discussion

The different e-Health models and requirements discussed above focus on salient issues that often come up when the subject of e-Health is brought up. Take Wagner's Chronic Care model for instance, it is a framework for chronic diseases that focuses on the patient, healthcare team and community partners in developing countries where access to quality healthcare is still a major challenge. Focusing on micro, meso and macro approaches, the primary aim of this model is to ensure that healthcare delivered electronically is supported by a wide coordinated approach cutting across levels of government. The Innovative Care for Chronic Conditions Framework introduced by the WHO in 2002 follows virtually the same approach.

To address privacy issues which are likely to come up when dealing with medical records, an Accountable e-Health System was proposed. As clearly explained above, this addresses the issues of who has access to what; should a patient's medical records be left out in the open? How do you determine who can see them? What about protecting them from just anybody? In many countries, including Saudi Arabia, there is still the long-drawn debate about how Patient-Doctor confidentiality will be maintained in an e-Health system. This model answers that question with a proposition that involves determining access based on need and justification. It is also a flexible system that allows a patient to nominate anyone that can access his health information. For health providers, employees are categorized according to levels and access are granted to only those who truly "need" such access.

Chia et al (2013) proposed a Radio Frequency Identification (RFID) rural e-Health model that seeks to have a common database of residents in an area based on their health status. This is quite a model because of its focus on rural health. Rural settlers across the world have been at the wrong side of access to healthcare for decades. These

residents often encounter barriers that prevent them from getting the healthcare they need (Rural Health Information Hub, 2020). To change this, there is need to provide access to appropriate and necessary healthcare services for rural residents. With this proposed model, this goal can be achieved. This model fails, however, to consider availability of RFID systems in rural communities and whether residents have the tools and knowledge required for such a model to work.

The other models highlighted in this study may focus on several other specifics, but the bottom line is the search for model requirements for e-Health application across the world.

VIII. LIMITATIONS

As a contribution to the existing body of research that seeks an efficient solution to implementing e-Health in societies, this study, and specifically, to identify an e-Health system modelling requirement that suits the Saudi Arabia health system, this study relies heavily on previous works of literature on the subject. However, in the area of a truly specific model for Saudi Arabia, this is a virgin attempt. Not many scholars (if any at all) have attempted a study of e-Health modelling requirements in a bid to find one that suits the Saudi Arabian experience. Furthermore, much of the literature and technologies studied are not peculiar to Saudi Arabia as not much has been done in that regard. The author only sought to examine how, learning from the experiences and models proposed for other climes, a model and its requirements can be developed for the Saudi Arabian nation, which is what this study attempts to do.

IX. WHAT ARE THE MODELLING SYSTEM REQUIREMENTS FOR E-HEALTH IN SAUDI ARABIA?

The above review shows the possibility of multiple contexts and models of e-Health using technologies like cloud, RFID and mobile phones. Evidently, these varied contexts, models and technologies have different system requirements. Also, chronic health conditions seem to be the best contexts for e-Health application according to some of the proponents.

In the case of Saudi Arabia, diabetes and obesity are the most serious chronic health conditions even within the younger demographics due to lifestyle habits of food and nutrition as well as physical activity. In Saudi Arabia, as per the International Diabetes Federation, out of the population of 20.77 million, 3.852 million adults (18.5%) had diabetes in 2017 (IDF, 2019) [13]. News (2019) cited Colliers Report of 17.9% diabetes and another 35.4% obese adults in Saudi Arabia. As the prevalence rapidly increases through an increase in the incidence rates among children and adolescents, especially Type 1 diabetes (Robert, Al-Dawish, Mujammami, & Al Dawish, 2018) [18], proper data collection systems in regular frequencies need to be put in place.

The high prevalence rate of diabetes in Saudi Arabia shows that management of diabetic patients and control of the disease is a serious problem. The average annual cost of diabetes treatment without complications is \$2600 for each Type 1 Diabetes (T1D) patient and about \$2000 per Type 2 Diabetes (T2D) patient, according to an estimate given by the

Saudi Ministry of Health. The country cost burden for diabetes treatment may reach \$6.5 billion by 2020. Presenting these statistics, Alanzi (2018) noted that policy deficits and scarce research on e-Health systems for diabetes have resulted in its poor implementation at hospital level. The e-Health initiatives of the Saudi Ministry of Health were limited to creating silos of health records and some service facilitations [3]. There had been only some very recent works on this issue in Saudi Arabia like those of Aldahmash, Ahmed, Qadri, Thapa, and AlMuammar (2019) and Belcher, Vess, and Johnson (2019) [4] [8].

It is often better to resort to self-management of these problems after initial stages of medical consultations. This will help to reduce the pressure on care hospitals in terms of resources and human power. In self-management, it is possible to obtain the help of community health workers, paramedical professionals and diabetes educators to help from time to time to ensure that the correct procedures are followed. The system does not preclude consultation with specialists if things go out of hand. However, this cannot be effective without a proper e-Health system in place that provides the information resources and monitoring mechanisms needed for self-management.

As many of the reviewed works above show, goal setting is the first step to model the system, based on which the requirements can be derived. In determining the modelling system requirement for patient self-management of diabetes, these steps will be discussed below.

A. Goal setting

1) Self-management goals-

- a) Patient health records before self-management start.
- b) The doctor gives the advice for self-management of blood glucose, medication, diet control, obesity (BMI), exercise and any other activity.

2) Self-management process-

- a) Self-monitoring of blood glucose, diet and physical activity as per the schedule and methods prescribed by the doctor. Assistance of local community health worker can be sought.

- b) The observed values are entered in the patient's page of the e-Health website for further processing, cloud storage and access as per requirement.

- c) The website sends alert signals to the doctor for advice to the patient if any entered value is out of control.

- d) Whether the patient complies with the advice can be known from the subsequent monitoring values.

3) National goals-

- a) Nationwide screening of population for diabetes and obesity based on WHO criteria.

- b) Maximum coverage of diabetic and obese people across the country for e-Health applications.

- c) Creation of electronic health records of all affected persons, whose records are not already available.

- d) Processing of the electronic data and storing in a PHI.

- e) Data encrypted and stored in cloud.

f) Access to data to stakeholders as per their privacy levels, determined based on role and necessity.

g) Adequate security of the data.

h) System requirements

4) Based on the above goals, the system requirements are as follows-

a) Infrastructure- Website, hardware, software, servers, cloud systems, networking of hospitals and communities, remote access, as well as fast and efficient internet service throughout the country.

b) Resources- Finance, buildings and related equipment. Supplies of medication including insulin injection, monitoring devices, exercise outfits, and other needed materials.

c) Human power- Healthcare professionals in hospitals and community health workers, diabetes educators at community levels also required.

d) Technology- Hardware and software, servers, Internet, cloud, PaaS, SaaS, IaaS, cybersecurity and other required technology.

e) Administration and management- Coordination by a dedicated team of MOH management.

f) Regular monitoring and evaluation of the e-Health system for effectiveness by the management and coordination team.

X. CONCLUSIONS

An examination of some selected literature revealed the essential steps to be followed for identification of modelling system requirements for e-Health systems. Based on these steps, a preliminary attempt has been made for identification modelling system requirements for e-Health application for the serious chronic problem of diabetes (and obesity) self-management by patients in Saudi Arabia. These modelling system requirements were arrived at based on identified goals for managing diabetes and obesity in Saudi Arabia. The model is only a skeletal approach and an attempt based on available information. It will require subsequent studies for refinement and testing before large scale implementation can be considered and carried out.

REFERENCES

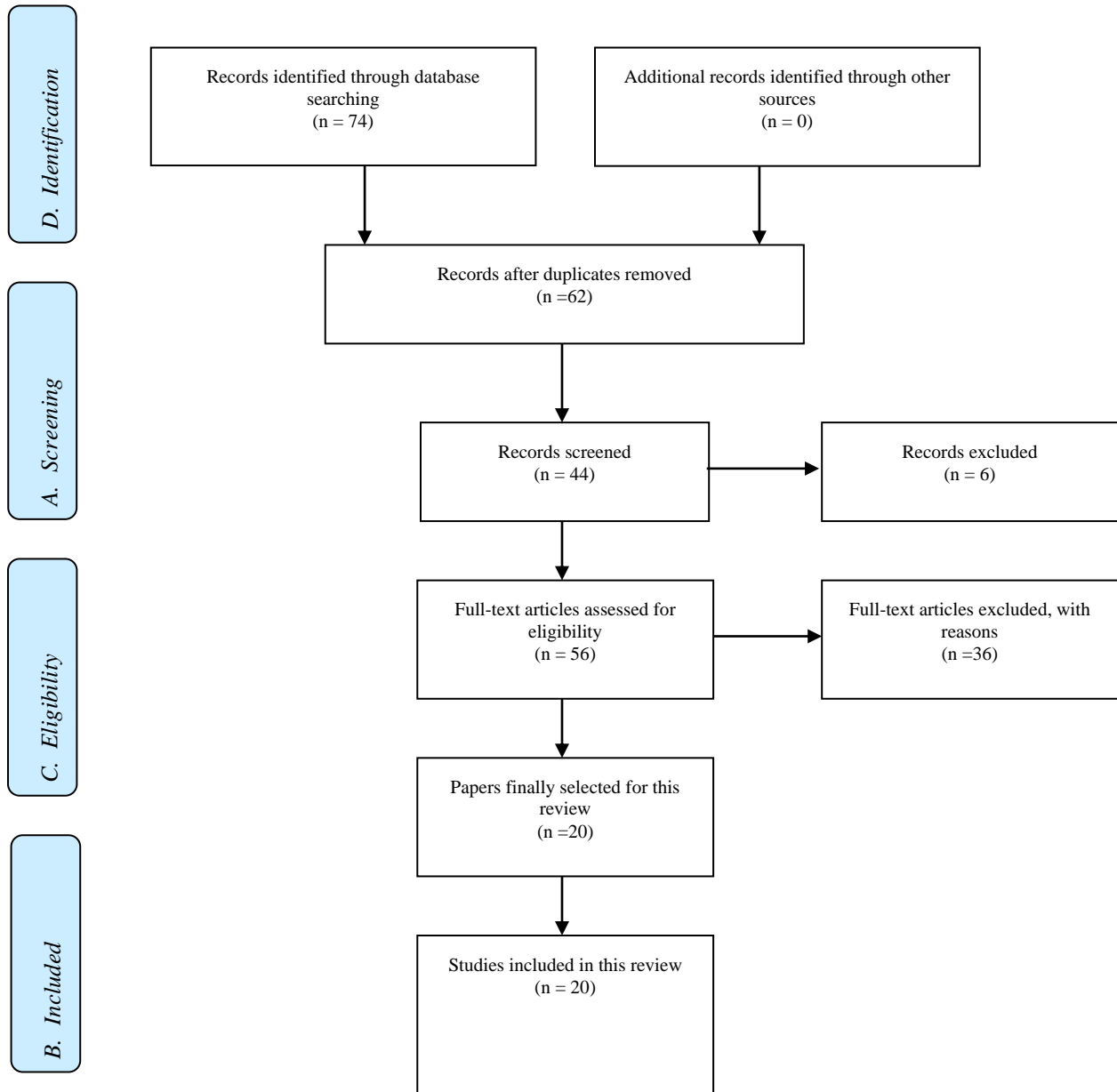
- [1] H. Alahmadi, B. Soh, and A. Ullah, (2014). "Automated health business process modelling and analysis for e-health system requirements elicitation". Pacific Asia Conference on Information Systems (PACIS) 2014 Proceedings (p. 13 pp). AIS Electronic Library (AISeL). Retrieved October 30, 2019, from <https://pdfs.semanticscholar.org/1e3d/d7fc30aec3c3fcac6e41ece710413fc291bf.pdf>.
- [2] A. H. Alahmadi, B. Soh, and A. Ullah, (2014). Improving e-Health Services and System Requirements by Modelling the Health Environment. *Journal of Software (JSW)*, 9(5), 1189-1201. doi:10.4304/jsw.9.5.1189-1201.
- [3] T. Alanzi, (2018). mHealth for diabetes self-management in the Kingdom of Saudi Arabia: barriers and solutions. *Journal of Multidisciplinary Healthcare*, 11, 535-546. doi:10.2147/JMDH.S174198.
- [4] A. M. Aldahmash, Z. Ahmed, F. R. Qadri, S. Thapa and A. M. AlMuammar, (2019). Implementing a connected health intervention for remote patient monitoring in Saudi Arabia and Pakistan: explaining 'the what' and 'the how'. *Globalisation and health*, 15(1), 20. doi:10.1186/s12992-019-0462-1.
- [5] M. Almalki, G. FitzGerald and M. Clark, (2011). Health care system in Saudi Arabia: an overview. *Eastern Mediterranean Health Journal*, 17(10), 784-793. Retrieved October 29, 2019, from https://apps.who.int/iris/bitstream/handle/10665/118216/17_10_2011_0784_0793.pdf.
- [6] M. M. Altuwajjri, (2008). Electronic-health in Saudi Arabia. Just around the corner? *Saudi medical journal*, 29(2), 171-178. Retrieved October 29, 2019, from <https://europepmc.org/abstract/med/18246222>
- [7] M. Barua, X. Liang, R. Lu and X. Shen (2011). Peace: An efficient and secure patient-centric access control scheme for health care system. *IEEE Conference on Computer Communications Workshops (INFOCOM WKSHPS)*, 10-15 April 2011, Shanghai, China (pp. 970-975). IEEE. doi:10.1109/INFCOMW.2011.5928953.
- [8] T. Belcher, J. Vess and E. Johnson (2019). Using patient portal messaging to improve glycemic control in adult patients with diabetes in Saudi Arabia. *Online Journal of Nursing Informatics (OJNI)*, 23(1). Retrieved June 21, 2019, from <https://www.himss.org/library/using-patient-portal-messaging-improve-glycemic-control-adult-patients-diabetes-saudi-arabia>.
- [9] S. Chia, Zalzal, L. Zalzal and A. Karim, (2013). Intelligent technologies for self-sustaining, RFID-based, rural e-health systems. *IEEE Technology and Society Magazine*, 32(1), 36-43. Retrieved October 30, 2019, from <http://lifesciences.embs.org/wp-content/uploads/sites/53/2013/05/06479445.pdf>.
- [10] G. Eysenbach, (2001). What is e-health? *Journal of medical Internet research*, 3(2), e20. doi:10.2196/jmir.3.2.e20
- [11] F. Alanezi, Factors affecting the adoption of e-health system in the Kingdom of Saudi Arabia, *International Health*, , ihaa091, <https://doi.org/10.1093/inthealth/ihaa091>.
- [12] R. Gajanayake, T. Alannella, B. Lane and T. Sahama, (2012). Accountable-ehealth systems: The next step forward for privacy. *Proceedings of the 1st Australian eHealth Informatics and Security Conference*, held on the 3rd-5th December, 2012 at Novotel Langley Hotel, Perth, Western Australi (pp. 22-28). Edith Cowan University. doi:10.4225/75/5796fa8940a98.
- [13] IDF. (2019). Middle East and North Africa. Retrieved June 20, 2019, from *International Diabetes Federation*: <https://www.idf.org/our-network/regions-members/middle-east-and-north-africa/members/46-saudi-arabia.html>.
- [14] M. Joshi, (2016). Proposed cloud based Framework for Implementing E-Health Services in Uttarakhand. *Proceedings of International Conference on Advanced Computing (ICAC-2016)* (pp. 367-371). College of Computing Sciences and Information Technology (CCSIT), Teerthanker Mahaveer University , Moradabad. Retrieved October 30, 2019, from <http://tmu.ac.in/college-of-computing-sciences-and-it/wp-content/uploads/sites/17/2016/10/ICAC-1604227.pdf>.
- [15] R. U. Mircea, G. Saplacan, G. Sebestylen, N. Todor, L. Krucz and C. Lelutiu, (2010). eHealth: towards a healthcare service-oriented boundary-less infrastructure. *Applied Medical Informatics*, 27(3), 1-14. Retrieved October 30, 2019, from <https://ami.info.umfluj.ro/index.php/AMI/article/view/28>.
- [16] D. C. Mohr, S. M. Schueller, E. Montague, M. N. Burns and P. Rashidi, (2014). The behavioral intervention technology model: an integrated conceptual and technological framework for eHealth and mHealth interventions. *Journal of medical Internet research*, 16(6), e146. doi:10.2196/jmir.3077.
- [17] O. Rejeb, R. Bastide, E. Lamine, F. Marmier and H. Pingaud, (2012). A model driven engineering approach for business continuity management in e-Health systems. *6th IEEE International Conference on Digital Ecosystems and Technologies (DEST)*, 18-20 June 2012, Campione d'Italia, Italy (pp. 1-7). IEEE. doi:10.1109/DEST.2012.6227931.
- [18] A. Robert, A. Al-Dawish, M. Mujammami and M. A. Al Dawish, (2018). Type 1 diabetes mellitus in Saudi Arabia: a soaring epidemic. *International journal of pediatrics*, ID 9408370, 9 pages. doi:10.1155/2018/9408370.
- [19] V. A. Rojas-Mendizabal, A. Serrano-Santoyo, R. Conte-Galvan and A. Gomez-Gonzalez, (2013). Toward a Model for Quality of Experience and Quality of Service in e-health Ecosystems. *Procedia Technology*, 9, 968-974. doi:10.1016/j.protcy.2013.12.108.

[20] Salah, Al-Sharhan, Omran, Esraa and K. Lari, (2018). An integrated holistic model for an eHealth system: A national implementation approach and a new cloud-based security model. International Journal of Information Management, 47 (pp.121-130). Retrieved January 9, 2021 from <https://www.sciencedirect.com/science/article/abs/pii/S0268401217305273>.

[21] WHO. (2019). eHealth at WHO. Retrieved June 20, 2019, from WHO: <https://www.who.int/ehealth/en/>.

[22] S. Widén and W. A. Haseltine, (2015). eHealth Technologies and the Future of Healthcare: Interview with Henrik Ahlen. Access Health International, . Retrieved June 20, 2019, from <https://accessh.org/wp-content/uploads/2015/12/Henrik-Ahlen1.pdf>.

APPENDIX



PRISMA 2009 Flow Diagram

Comparison of Deep and Traditional Learning Methods for Email Spam Filtering

Abdullah Sheneamer

Faculty of Computer Science & Information Technology
Jazan University
Jazan, Saudi Arabia

Abstract—Electronic mail, or email, is a method for communicating using the internet which is inexpensive, effective, and fast. Spam is a type of email where unwanted messages, usually unwanted commercial messages, are distributed in large quantities by a spammer. The objective of such behavior is to harm email users; these messages need to be detected and prevented from being sent to users in the first place. In order to filter these emails, the developers have used machine learning methods. This paper discusses different methods which are used deep learning methods such as a Convolutional Neural Network (CNN) and Long Short-Term Memory (LSTM) models with(out) a GloVe model in order to classify spam and non-spam messages. These models are only based on email data, and the extraction set of features is automatic. In addition, our work provides a comparison between traditional machine learning and deep learning algorithms on spam datasets to find out the best way to intrusion detection. The results indicate that deep learning offers improved performance of precision, recall, and accuracy. As far as we are aware, deep learning methods show great promise in being able to filter email spam, therefore we have performed a comparison of various deep learning methods with traditional machine learning methods. Using a benchmark dataset consisting of 5,243 spam and 16,872 not-spam and SMS messages, the highest achieved accuracy score is 96.52% using CNN with the GloVe model.

Keywords—Spam filtering; machine learning; deep learning; LSTM; CNN

I. INTRODUCTION

Email is an inexpensive, effective, and fast way to exchange messages using the Internet. Spam email is a type of email where unwanted messages [1], [2], [3], [4], usually related to unwanted commercial messages, are sent in huge quantities by a spammer. Spam email can contain malicious content, such as a phishing attack and/or malware. Despite considerable cybersecurity improvements and continuous development, spam email and malware damage caused by spam emails can prevent communication, create increased traffic, and waste users' time where the spam emails must be manually deleted. It is also possible to miss important email messages that are accidentally deleted when manually removing large numbers of spam messages.

Cybersecurity is now a hot topic in industrial information and operational technologies. The definition of cybersecurity is technologies and processes which are built to protect computer hardware, software, networks, and data from unauthorized access, vulnerabilities, terrorists, and hackers. Cybersecurity is the protection of the internet, information, and network-based digital equipment from unauthorized access and amend-

ment [5]. For many years, machine learning classifiers have had a prominent role in intelligent system development.

Machine learning methods are more robust and have greater flexibility; consequently, there has been an expansion in security execution and improved defense systems from growing and advanced cyber threats. Machine learning is a technique used in different areas of information security. The aim of this paper is to develop the proof of concept for shallow machine and deep learning for spam datasets. We make a comparison between shallow machine and deep learning methods and the most accurate algorithm capable of distinguishing the spam emails which have the lowest error rate. To summarize, the main points this paper achieves are:

- We propose a CNN model with(out) a GloVe deep learning-based model framework to classify spam email.
- We propose an LSTM model with(out) a GloVe deep learning-based model framework.
- We provide a comparison between traditional machine learning and deep learning algorithms on spam datasets.

In this section, we introduce the various types of spam email. Related works are highlighted in Section 2. In Section 3, we discuss our methodology. In Section 4, we present an evaluation and comparison of our proposed method and report results. Finally, Section 5 presents our conclusion.

A. Types of Email Spams

We have defined spam as any unwanted message which may or not be malicious, that is, a scam or a fraud. Spams can be bulk messages, reaching millions of people daily.

- **Ads.** This is one of the most common types of spam, usually, several unwanted emails offering services or products are received.
- **Chain Letters.** Chain letters usually take the form of exciting stories such as "something bad will happen to you" and encourage the recipient to respond to the message so that the bad event will not occur.
- **Email Spoofing.** Spoof emails are related to phishing scams. This happens when the spammers or phishers attempt to trick the recipient by impersonating someone he/she knows.

- **Hoaxes.** The email spams offer and miracle promises, such as “get rich in less than a week”. The spammer tries to direct the recipient’s email spam to a malicious website.
- **Money Scams.** The spammers send spam email promising easy money. This involves asking for money for poor families who have suffered losses as a result of a natural disaster.
- **Malware Warnings.** These types of email warn the recipient about a malware infection on his device, such as a virus. Spammers send an email which states that they have a solution to the problem and that the recipient must provide some information or download an attached file.
- **Porn Spam.** The spammer sends emails containing pornography. This is very common as the pornography market is very profitable. Spammers can create malicious emails using lustful images and videos.

II. RELATED WORKS

Drucker *et al.* [6] compared the support vector machine (SVM) algorithm with Ripper, Rocchio, and boosting decision tree algorithms to classify an email as spam, or not. They performed experiments on datasets and chose the best 1000 features; one dataset contained over 7000 features. SVM accuracy was good and required less training time. However, extra time was needed to search for the best features in the training algorithm.

Banday and Jan [7] studied the design of common statistical spam filters, including Naive Bayes, Term Frequency-Inverse Document Frequency, K-Nearest Neighbour, Support Vector Machine, and Bayes Additive Regression Tree. They performed experiments on e-mail datasets to evaluate each classifier for accuracy, recall, precision, etc. Additionally, they studied the effectiveness and limitations of various types of statistical filter to discern spam from legitimate emails.

Radhakrishnan and Vaidhehi [8] proposed email spam classification using the Naive Bayes and J48 Decision Tree which has a feature size of 400 attributes. Their results do not achieve maximum efficiency.

Suleiman and Naymat [9] used a method for detecting SMS and email spams using deep learning, Na Bayes, and Random Forest while they used the H2O platform in Weka. In addition, they showed that the Naive Bayes classifier has the best runtime but the is the in regard to performance. Random Forest is the best in precision, recall, F-measure, and accuracy.

Singh *et al.* [10] presented the solution and classification processes and combining classification technique of spam filtering to obtain improved spam filtering results. They used machine learning and engineering knowledge and applied the NB, KNN, SVM, Artificial Neural Network classification methods.

Kumar *et al.* [11] suggested a deep learning-based approach for detecting spam images using convolutional neural networks (CNN), which used a dataset with 810 natural images and 928 spam images.

Jain. *et al.* [12] suggested a system for detecting spam social media texts by using a hybrid technique; combining Convolutional Neural Network (CNN) and Long Short Term Memory (LSTM) network architectures. They use pre-trained embeddings. CNN extracts the n-gram features from the text, whereas LSTM detects the long-term dependencies. The model has better performance than the shallow neural network.

III. METHODOLOGY

A. Preprocessing

This is the first stage and processes incoming mail to the user in several sub-steps, as shown below.

1) *Tokenization:* This stage divides incoming emails into a sequence of representative meaningful words by removing punctuation, known as tokens.

2) *Noise Removal:* The data usually features an increased amount of noise and unwanted symbols and characters, e.g. stop words, numbers, alphanumeric words, white spaces, punctuation, etc. An example of stop words is “a”, “an”, “is” and “it”. While the example of punctuation is “?”, “!”, “,” and “;”. The procedures usually are removed, converting all letters into lower/upper case and the removal of numbers, punctuation, white spaces, and stop words.

3) *Stemming:* Stemming is one method by which to normalize the word form. For example, go, went, going are considered the same word in the feature matrix. In addition, stemming removes suffixes from words such as (“ing”, “ly”, “es”, “s”, etc.).

4) *Lemmatization:* Lemmatization is a method by which to normalize the word form. This is similar to stemming, however, lemmatization converts the word to its root form and morphological analysis using vocabulary or a dictionary. For example, the lemma word “better” is “good”.

B. Feature Extraction

The input must usually be integers or floats for machine and deep learning algorithms. Here some approaches are used to convert words to integers or floats.

1) *Count Vectorizer:* First, all email data is inputted into the Count vectorizer algorithm; the Count vectorizer keeps a dictionary of all words and their respective *ID*, which represents the count of the word.

2) *TF-IDF Vectorizer:* The TF-IDF Vectorizer is used to calculate word frequencies and is known as the TF-IDF. Term Frequency (TF): this summarises the frequency of a specific word appearing in a document. Inverse Document Frequency (IDF): this downscales words that frequently appear across documents. It tokenizes files, learns the vocabulary and inverse document frequency weightings, as well as encoding new files.

3) *Word Embedding:* Word embedding converts words to a vectorized format, which then represents the word’s position in a higher-dimensional space. The cosine distance of the two-word vectors is shorter and closer to each other if those two words have a similar meaning. For example, *King – Man + Woman = Queen*.

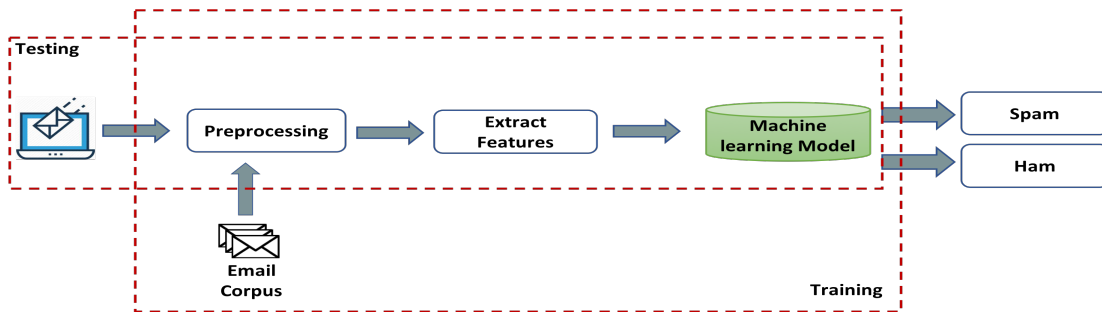


Fig. 1. General Traditional Machine Learning Model

TABLE I. BRIEF DESCRIPTION OF SOME ENRON EMAIL AND SMS SPAM COLLECTION DATASET

Dataset	# Total	# Ham (Not Spam)	# Spam
Enron1	5,172	3,672	1,500
Enron2	5,857	4,361	1,496
Enron3	5,512	4,012	1,500
SMSSpamCollection	5,574	4,827	747
All Emails	22,115	16,872	5,243

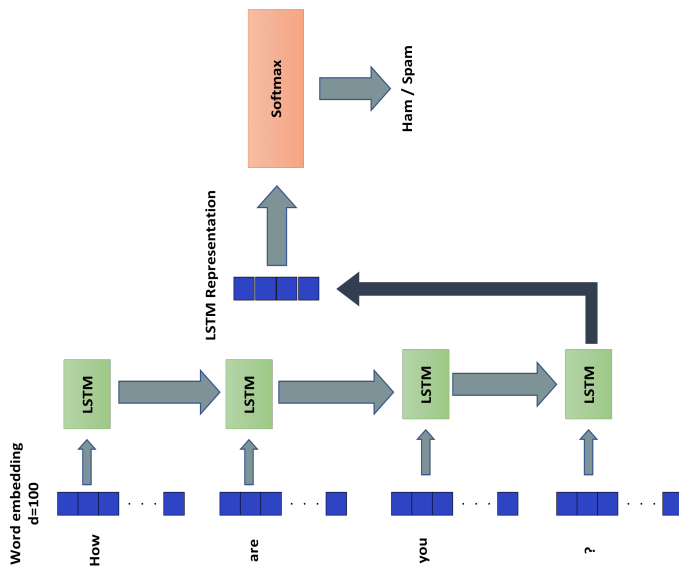


Fig. 2. LSTM Deep Learning Model

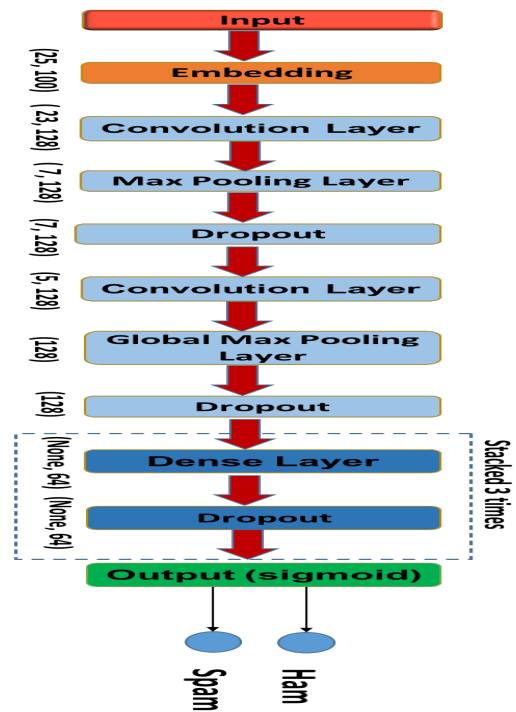


Fig. 3. CNN Deep Learning Model

C. Machine Learning Classifiers

In subsection 3.3.1 we discuss the shallow or traditional machine learning classifiers. In Section 3.3.2. we discuss deep learning classifiers.

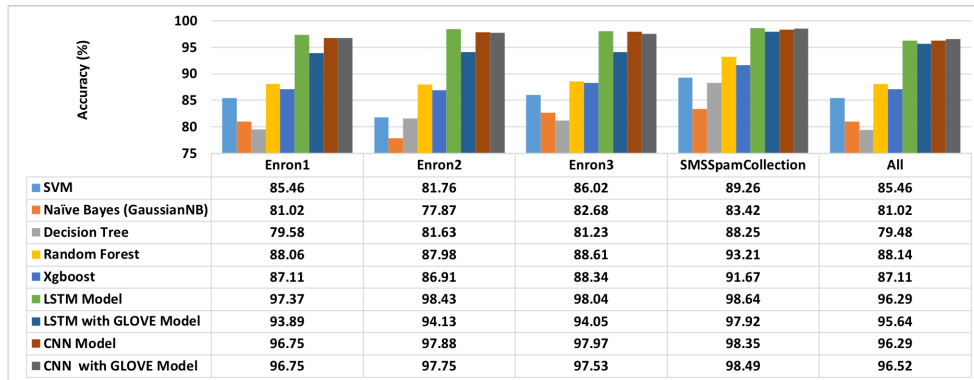
1) *Traditional Machine Learning*: After the pre-processing stage, we extracted occurrence words as features and used TF to select the features. The term frequency (TF) of each word in a document is weight dependent upon the distribution of each word in the files [13]. This represents the importance of each word in the file. These important features are added to a feature matrix which is used for classifying the email into Spam and Not-Spam classes, as shown in Fig. 1 using classifiers such as Random Forest (RF) [14], Support Vector

Machine (SVM) [15], Decision Tree [16], Gaussian Naive Bayes (GaussianNB) [17] and XGboost (XGB) [18].

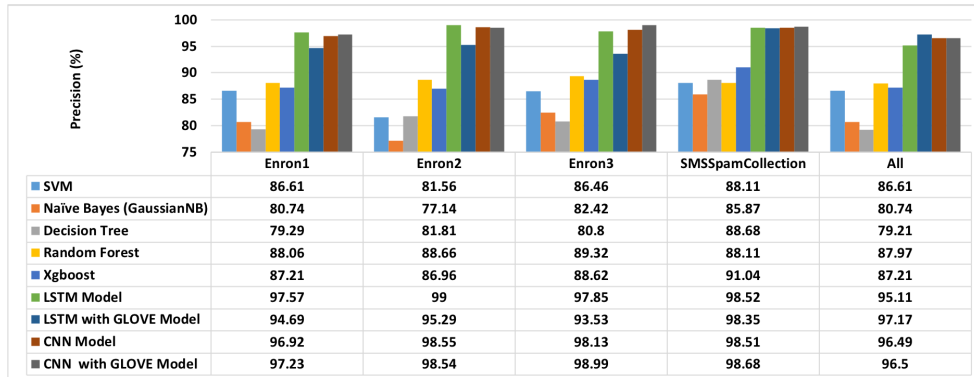
2) Deep Learning Classifiers:

- Long Short-Term Memory (LSTM) Model

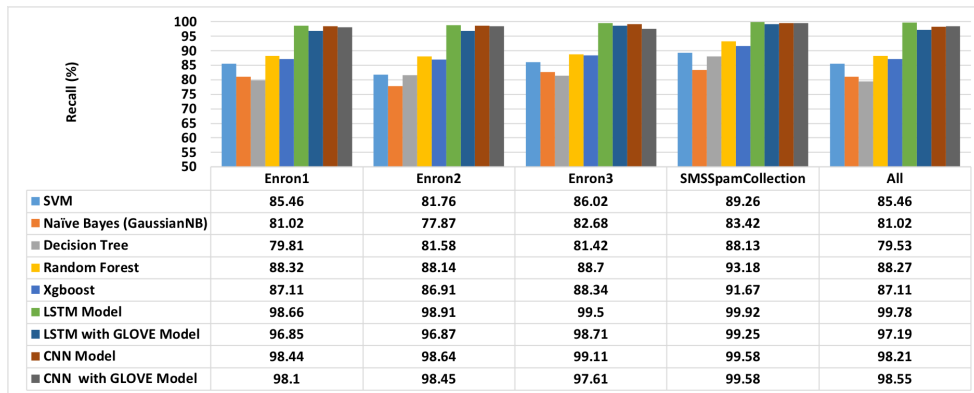
The Recurrent Neural Networks (RNN) can learn long-term dependencies. Hochreiter Schmidhuber (1997) introduced these [19]. LSTMs are widely used and operate effectively on large difference problems. All RNNs can sequence repeating



(a) Accuracy Assessments



(b) Precision Assessments



(c) Recall Assessments

Fig. 4. Performance Comparison of Different Machine and Deep Learning Methods with respect to Different Assessment Metrics on all Enrons and SMS Spam Collection Datasets.

modules of the neural network, for instance, a single tanh layer. The LSTM network can remember the long text sequences ¹.

The first layer maps each word to an N-dimensional vector of real numbers and is known as a pre-trained embedding layer. The second layer is an RNN with LSTM units. The final layer is the output layer, with two neurons corresponding to “spam” or “ham” with sigmoid activation functions, as indicated in Fig. 2. We use Global Vector (GloVe) and 100-dimensional vectors. We use *softmax* since it provides better results than

using *sigmoid* in LSTM with GloVe model. The *softmax* function constructs the whole model.

- Convolutional Neural Network (CNN) Model

A Convolutional Neural Network (CNN) has become a popular algorithm in machine learning. A CNN [20], [21] is a neural network where the input is stored in arrays. A CNN has hidden layers, known as convolutional layers, and is used to process 2D arrays of images or audio spectrograms; and for three-dimensional (3D) arrays such as images and videos, pooling layers, and classification layers which is the output

¹<https://easyai.tech/en/ai-definition/lstm/>

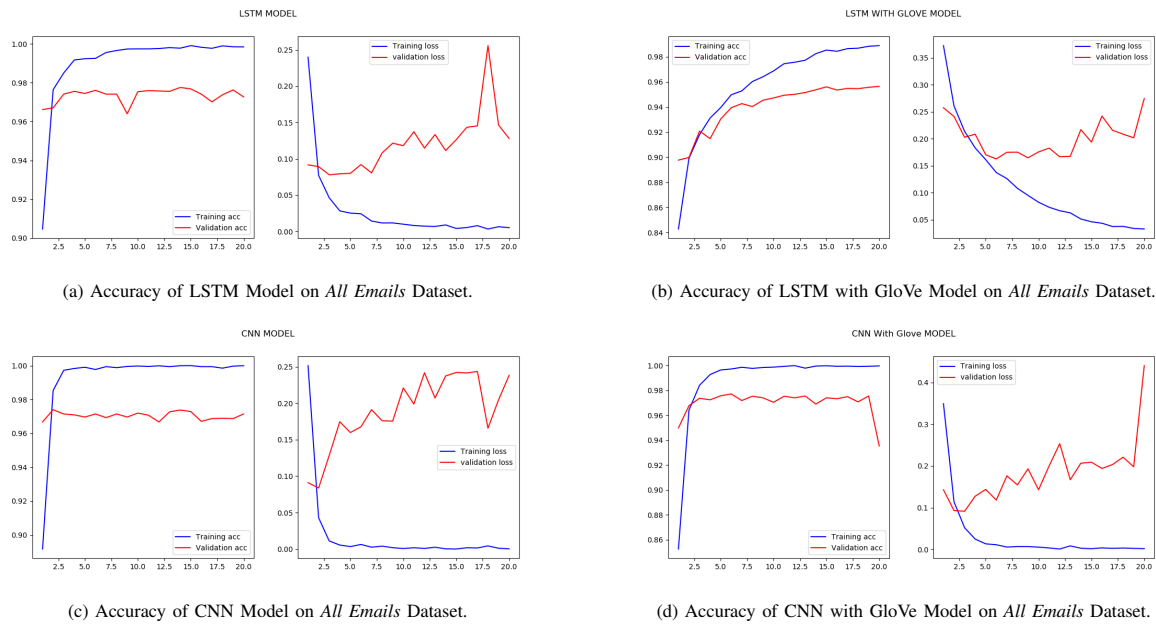


Fig. 5. Accuracy of All Models on All Emails Dataset.

layer and have two neurons each corresponding to “spam” or “ham” with a sigmoid activation function. Because we have applied the CNN model so that it filters spam emails as texts we use an embedding layer with(out) GloVe, as illustrated in Fig. 3, two dimensions convolutional layers *Conv1D*, one max pool *MaxPool1D* layer, four dropout *Dropout* layers, one *GlobalMaxPooling1D* layer, and three *Dense* layers. *Conv1D* layer consists 128 filters, kernel size is 3 and activation method is *relu*. *MaxPool1D* layer size is 2, *Dropout* rate is 0.2, and *Dense* layer activation method is *relu* and *sigmoid* methods.

D. Data Collection

Every machine learning model requires a training set for training the model. We use open datasets from the community, Enron datasets as shown in Table I. and Enron email as the standard dataset, including spam emails and 10K ham. The Enron company is a bankrupt American firm, once a major player in the energy, commodities, and services industries in the United States². After it had gone bankrupt, the company’s secret emails were distributed across the Internet. In the test phase, we have a 10-folds cross-validation mode. Therefore, we have used the Enron email dataset on both the training and testing phases. We used only email subject and body text. The SMS Spam Collection³ is a public set of SMS labelled messages collected for research into mobile phone spam. It contains 5,574 ham and spam messages in English as shown in Table I.

IV. RESULTS AND DISCUSSION

We use email spam data, including 22,115 messages for each of ham and spam from Enron’s and SMS spam collection

datasets. Our baseline uses traditional machine learning algorithms, including five classifiers. We trained and tested each of the classifiers by adding occurrence words as features. Next, we built spam email detection models to compare the impact of shallow machine learning with deep learning models. We performed nine experiments for each of the datasets. Classifier models are produced and tested using cross-validation with 10 folds, using python where to make sure the ratios between spam and not spam classes are identical in each of the folds and the same as in the overall dataset. The results in Fig. 4 show the different machine learning methods of different assessment metrics on all Enron’s and SMS spam collection datasets. Fig. 4 shows the accuracy, recall, and precision of the spam email filtering experiments. The highest accuracy, precision, and recall of the nine classifiers are shown in bold. Deep learning classifiers produce improved results over traditional machine learning classifiers of approximately 10-14%. Random Forest and Xgboost classifiers give better results than the traditional classifiers. The LSTM model is ranked first amongst traditional and deep learning classifiers, however, when all datasets are combined and classifier models built, all deep learning classifiers results are almost identical. The results of all email datasets are provided in Fig. 5a, 5b, 5c and 5d using deep learning algorithms. The figures illustrate the accuracy, loss of training, and validation for all four deep learning classifiers using Embedding word with GloVe or without GloVe. The CNN model is ranked first among deep learning classifiers in regard to accuracy and loss of training and validation curve, such as in Fig. 5c. In Fig. 5a, LSTM mode ranks second in regard to accuracy and loss of training and validation curve.

We use email spam data include 22,115 messages for each of Ham and Spam from Enrons and SMS spam collection datasets. Our baseline uses traditional machine learning algorithms which include five classifiers. We train and test

²EnronDatasetofCarnegieMellonUniversity,SchoolofComputerSciencehttps://www.cs.cmu.edu/~enron/

³https://github.com/mohitgupta-omg/Kaggle-SMS-Spam-Collection-Dataset-

each classifier by adding occurrence words as features. Then, we build email spam detection models to compare the impact of shallow machine learning with deep learning models. We conduct nine experiments for each dataset. Models of the classifiers are produced and tested using cross-validation with 10 folds, using python where we ensure that the ratio between spam and not spam classes is the same in each fold and the same as in the overall dataset. Results for different machine learning methods concerning different assessment metrics on all Enrons and SMS Spam Collection datasets are given in Fig. 4. Fig. 4 shows the accuracy, recall, and precision of email spam filtering experiments. The highest accuracy, precision, and recall of the nine classifiers are shown in bold. Deep learning classifiers produce much better results than traditional machine learning classifiers about 10% to 14%. Random Forest and Xgboost classifiers produce the best results among the traditional classifiers. While the LSTM model ranks first among traditional and deep learning classifiers. But when we combine all datasets and build the models of classifiers, all deep learning classifiers results are almost the same. The results of all email datasets are given in Fig. 5a, 5b, 5c and 5d using deep learning algorithms. These figures show the accuracy and loss of training and validation for all four deep learning classifiers using Embedding word with GloVe or without GloVe. CNN model ranks first among deep learning classifiers based on accuracy and loss of training and validation curve such as Fig. 5c. In Fig. 5a, LSTM mode ranks second based on accuracy and loss of training and validation curve.

V. CONCLUSION

Email is an inexpensive, effective, and fast way to exchange messages using the internet. Spam email is annoying to end-users, financially damaging, and can be a security risk. The objective of spam email is to collect sensitive personal information about users. The majority of emails in internet traffic contain spam. This work uses deep learning methods, such as CNN and LSTM models with(out) GloVe model, to classify Spam and Not-Spam messages. We have compared our proposed technique to other shallow techniques using machine learning algorithms. The work presented in this paper, based on machine and deep learning algorithms, shows that including more datasets and deep learning models considerably increases the accuracy detection rate, from 85.46% to almost 97.52% after including all datasets (All Emails). Future work can be improved by using a combination of deep learning classifiers based on text and image spams.

REFERENCES

- [1] M. Basavaraju and D. R. Prabhakar, "A novel method of spam mail detection using text based clustering approach," *International Journal*

- of Computer Applications*, vol. 5, no. 4, pp. 15–25, 2010.
- [2] G. V. Cormack, *Email spam filtering: A systematic review*. Now Publishers Inc, 2008.
- [3] B. Owen and J. Steiner, "Email filtering system and method," Aug. 25 2009, uS Patent 7,580,982.
- [4] S. J. Delany, M. Buckley, and D. Greene, "Sms spam filtering: Methods and data," *Expert Sys. with Appl.*, vol. 39, no. 10, pp. 9899–9908, 2012.
- [5] E. Blanzieri and A. Bryl, "A survey of learning-based techniques of email spam filtering," *Artificial Intelligence Review*, vol. 29, no. 1, pp. 63–92, 2008.
- [6] H. Drucker, D. Wu, and V. N. Vapnik, "Support vector machines for spam categorization," *IEEE Transactions on Neural networks*, vol. 10, no. 5, pp. 1048–1054, 1999.
- [7] M. T. Banday and T. R. Jan, "Effectiveness and limitations of statistical spam filters," *arXiv preprint arXiv:0910.2540*, 2009.
- [8] A. Radhakrishnan and V. Vaidhehi, "Email classification using machine learning algorithms."
- [9] D. Suleiman and G. Al-Naymat, "Sms spam detection using h2o framework," *Procedia computer science*, vol. 113, pp. 154–161, 2017.
- [10] V. K. Singh and S. Bhardwaj, "Spam mail detection using classification techniques and global training set," in *Intelligent Computing and Information and Communication*. Springer, 2018, pp. 623–632.
- [11] A. D. Kumar, S. KP *et al.*, "Deepimagespam: Deep learning based image spam detection," *arXiv preprint arXiv:1810.03977*, 2018.
- [12] G. Jain, M. Sharma, and B. Agarwal, "Spam detection in social media using convolutional and long short term memory neural network," *Annals of Mathematics and Artificial Intelligence*, vol. 85, no. 1, pp. 21–44, 2019.
- [13] G. Forman, "Bns feature scaling: an improved representation over tf-idf for svm text classification," in *Proceedings of the 17th ACM conf. on Info. and knowledge management*, 2008, pp. 263–270.
- [14] L. Breiman, "Random forests," *Machine Learning*, vol. 45, no. 1, pp. 5–32, 2001.
- [15] J. A. Suykens and J. Vandewalle, "Least squares support vector machine classifiers," *Neural processing letters*, vol. 9, no. 3, pp. 293–300, 1999.
- [16] J. R. Quinlan, "Induction of decision trees," *Machine Learning*, vol. 1, no. 1, pp. 81–106, 1986.
- [17] G. H. John and P. Langley, "Estimating continuous distributions in bayesian classifiers," in *Proceedings of the Eleventh Conference on Uncertainty in Artificial Intelligence*. Morgan Kaufmann Publishers Inc., 1995, pp. 338–345.
- [18] T. Chen and C. Guestrin, "Xgboost: A scalable tree boosting system," *arXiv preprint arXiv:1603.02754*, 2016.
- [19] S. Hochreiter and J. Schmidhuber, "Long short-term memory," *Neural computation*, vol. 9, no. 8, pp. 1735–1780, 1997.
- [20] Y. LeCun, B. E. Boser, J. S. Denker, D. Henderson, R. E. Howard, W. E. Hubbard, and L. D. Jackel, "Handwritten digit recognition with a back-propagation network," in *Advances in neural info. processing sys.*, 1990, pp. 396–404.
- [21] Y. LeCun, L. Bottou, Y. Bengio, P. Haffner *et al.*, "Gradient-based learning applied to document recognition," *Proceedings of the IEEE*, vol. 86, no. 11, pp. 2278–2324, 1998.

Mobile Application Design with IoT for Environmental Pollution Awareness

Anthony Ramos-Romero¹, Brighitt Garcia-Yataco², Laberiano Andrade-Arenas³
Facultad de Ciencias e Ingeniería
Universidad de Ciencias y Humanidades

Abstract—In the present study, we have seen that many people are affected by environmental pollution, so we proposed a mobile application prototype to facilitate awareness of this environmental problem. The methodology that will help us make this application will be the Scrum methodology, since it is adaptable to the constant changes in the mobile application development process. We will also use an Internet of Things and Fire based technology to collect data from the various air pollution sensors. Since users require a visualization of the contamination in real time. The mobile application to which users will automatically register will have easy access for use in monitoring and controlling atmospheric pollution, whose reception data will be through sensors. The result that has been obtained is that it was achieved with the implementation of the application that people are aware of the damage that these pollutants cause to the environment.

Keywords—Environmental pollution; internet of things; scrum; mobile app

I. INTRODUCTION

We are currently in a world immersed in environmental pollution and the negative effect it causes is evident, this is the cause of the continuous pollution that each of the people who live on planet earth do, throwing garbage, polluting rivers, seas without knowing the consequences that such actions can cause, which is why many developed and developing countries have a large number of people who get sick in a certain place and period of time. This makes environmental pollution one of the most relevant problems in the world, pollution levels grow causing serious consequences for health and the environment, air quality is getting worse, this causes major health problems. Being a great problem for the inhabitants of the planet, some countries use the IoT (internet of things) as a way of measuring the level of contamination of the environment but it is very limited since it is not very accessible for the inhabitants of the same [1].

According to the World Health Organization, air pollution around the world kills approximately 7 million people a year, either from vascular strokes, heart disease, lung cancer, as well as acute and chronic respiratory diseases [2].

In developed countries such as Russia, Turkey, South Korea, Japan and the United States, they have agricultural emissions that contain ammonia, which is one of the main sources of environmental pollution [3].

In China, it has reached such a degree that the fine PM (Particulate Material) in its air is PM 2.5, which means that there is a lot of pollution, therefore its inhabitants wear masks to prevent diseases that can cause such pollution [4].

In addition, its annual average concentrations of fine particles in the world vary between 8000 and 19,500 PM 2.5 particles, they are penetrated and can lodge deep in the lung tissue [5].

Likewise, in Latin America there are many countries with poor air quality, among them are Peru, Chile, Mexico, Brazil and Colombia as the main polluting countries because they are the countries with the highest oil production, also due to the number of vehicles that circulate. . emitting various polluting gases such as: carbon monoxide, carbon dioxide and methane [6].

From a closer point of view in Peru; Lima is the department with the highest rate of environmental pollution, due to the large number of vehicles that release carbon monoxide and PM 2.5 hydrocarbons and also due to the excess of waste dumped on the streets [6].

Currently some of the awareness solutions are based on processing data and converting it into information through stations at fixed points, capturing different types of gases in the environment, but only in established areas and many of these results are not available to all people. so they are not responsible for the great damage we are causing to the environment [7].

The IoT is a technology that consists of obtaining data from our environment through the use of electronic components, having various applications that can provide great benefit. One of these applications is the collection of data on the quality of the environment using sensors that have the ability to collect data on the levels of certain gases around us. These data, being interpreted in a correct way, will become a reliable source of information that can be displayed through a mobile application or web interfaces in real time to be seen by the general public, having a great impact on people's mentality, raising awareness about the quality of the environment that surrounds us, the same ones that being committed to their environment will pollute less, use less chemical products, this will result in a decrease in pollution rates [8].

Therefore, the objective of this research work is to carry out a mobile application with integration of the IoT that aims to make people aware of the damage they currently cause to the environment, demonstrating the level of air quality and gases that may be present, to Based on the data grouping analysis of the different electronic components that will be presented through a mobile application, the SCRUM methodology is proposed in turn with the implementation of emerging technologies such as IoT, Cloud Computing (Fire Base), Fog Computing (Mobile Devices) and reactive programming.

The present work is structured as follows, in Section II the methodology used with respect to development will be described. In Section III the technologies to be used as well as the IoT, Cloud Computing, the mobile application, among others, will be detailed. In Section IV the case study will be evidenced, forming friendly prototypes for better understanding, finally, in Section V the results will be discussed and finally in Section VI the conclusions.

II. METHODOLOGY

This section will detail the steps that will be followed for the development of the mobile application and IoT, using the Scrum Methodology, since the work rules it has are perfectly suitable for software development projects, in addition to being an organized process it consists in good practices, allowing teamwork and is open to change, giving this added value since emerging technologies are constantly changing (IoT) [9].

A. Analysis

Scrum is defined in three main roles which are the Scrum Master, the Product Owner and the development team.

The role of the scrum master is to ensure that the team is adopting the methodology, its practices, values and norms. He is the team leader, but he does not manage development. The Product Owner is a single person and represents the stakeholders, is responsible for maximizing the value of the product and the work of the development team; Its functions include managing the list of required functionalities or Product Backlog.

For its part, the development team is responsible for converting what the client wants, the Product Backlog, into functional iterations of the product; the development team does not have hierarchies, all its members have the same level and position: developer. The optimal team size is between three and nine people [10].

This process flow of the Scrum methodology consists in that users identify the system requirements (needs to have information about the environment in a mobile application) that are the user stories, then the development team orders and prioritizes these user stories for your prompt development [11].

In Fig. 1, we can see the steps that must be carried out to make an adequate use of the Scrum methodology.

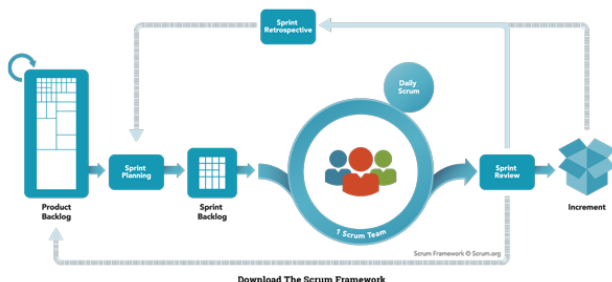


Fig. 1. Scrum.

To better understand the methodology, we find the main Scrum stages in which they are based on sprints, which the

team proposes to generate a deliverable product. In each of them, mini projects are developed that serve to improve the effectiveness of the project, this being of great impact for software development projects and IoT [10].

These are the main stages of the scrum:

1) *Sprint planning*: This stage takes place in the Sprint Planning meeting where your work plan is defined: what will be delivered and how it will be accomplished. That is, the design of the system and the estimate of the amount of work. This activity lasts eight hours for a one-month Sprint. If the Sprint has a shorter duration, the time is allocated proportionally [12].

2) *Development stage*: At this stage, sprint managers must ensure that last minute changes are not generated that affect the objectives. In addition, they must ensure that they meet the established deadlines [13].

3) *Sprint Review*: The Sprint Review occurs at the end of the Sprint and lasts for four hours for a one-month project (or a proportion of that time if the duration is shorter). At this stage: the project owner reviews what was done, identifies what was not done, and analyzes the Product Backlog; the development team tells what problems they found and how they were solved, and shows the product and how it works [12].

Fig. 2 provides an overview of the development flow of a Sprint.

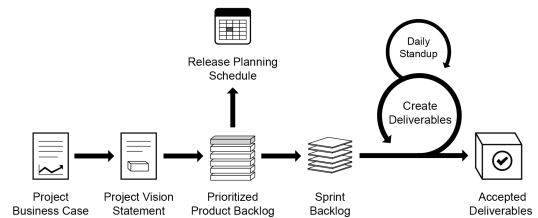


Fig. 2. Scrum Flow for a Sprint.

For the implementation the following steps will be carried out:

I. *Product Backlog*: It consists of identifying the user stories that become the user requirements and giving them a priority level, the backlog comes from a hundred of the list of user stories ordered and prioritized [14].

II. *Sprint portfolio*: It is a segmentation of the prioritized and ordered user stories, where the development team determines the increments that will be developed throughout the project[15].

III. *Sprint planning meeting*: It is the Sprint planning meeting based on the Product Backlog and they participate: Product Owner (responsible for the subject) who prioritizes the tasks to be included in the Sprint Backlog, the Scrum Master and the Development Team [15].

III. TECHNOLOGY

A. Internet of Things

The internet of things is changing the world and this because it helps us obtain data from nature or even from electronic devices that have electronic components capable of capturing data and converting it into information. In this present investigation we will make use of it, we will use IoT technology to capture the data of gases or substances that may exist in the air, we will proceed to analyze them and convert them into information to be able to visualize them [16].

1) *Architecture*: In Fig. 3, we can visualize an architecture that consists of a section where the IoT devices are located that connect to the cloud computing through a gateway to the internet, said cloud computing has multiple services that are used to process the data obtained from the sensors, turning them into information that can be viewed from a web portal and even a mobile application.

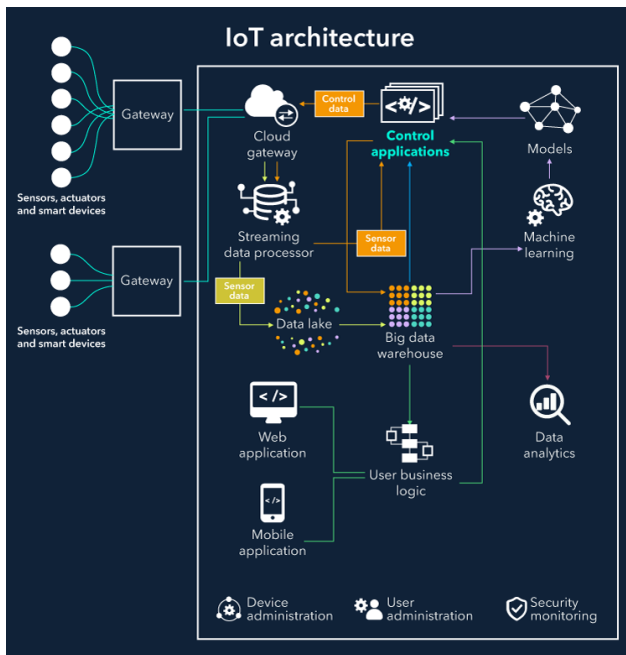


Fig. 3. Architecture IoT.

Next, the following layers belonging to the architecture of IoT technology will be described.

- Perception Cloak: This layer is responsible for collecting all kinds of information through sensors that capture and represent the information [16].
- Network layer: This layer is responsible for the transmission of information through various basic networks, which are the internet, mobile communication network, wireless network, satellite networks, network infrastructure and communication protocols [16].
- Physical layer: This layer is in charge of intelligent computing in which it is organized through the network and the cloud [16].
- Application layer: This layer ensures that users can

access the Internet of Things through the use of a cell phone or computer. [16].

The sensors in charge of obtaining data from the environment cannot manipulate or treat them, so we will use Arduino. The communication of the Arduino and the mobile device will be via Bluetooth. There is a module for Arduino that meets this objective [17]. Likewise, the mobile application will be in charge of communicating with the cloud services by sending the data obtained by the sensors. The development will be carried out on the official development platform for projects made with Arduino [18].

Sensors capable of capturing and emitting data on the different polluting gases that exist in the air, as shown in Table I where we list the electronic components that meet the established requirements.

TABLE I. SENSORS

Electronic components	
1. MQ-7	Carbon monoxide
2. MQ-2	Methane, Butane, Smoke
3. MQ-6	Butane
4. MQ-8	Hydrogen
5. MQ-131	Ozone

These sensors are electrochemical and vary their resistance when exposed to certain gases, internally it has a heater in charge of increasing the internal temperature and with this the sensor can react with the gases causing a change in the resistance value [19].

- MQ-7: Its function is to detect carbon monoxide in the air, since it has a high sensitivity.
- MQ-2: Its function is to detect LPG, propane, methane, alcohol, hydrogen and smoke.
- MQ-6: Its function is to detect LPG, butane, propane and methane.
- MQ-8: Its function is to detect hydrogen concentrations in the air.
- MQ-131: Its function is to detect ozone gas concentrations in the air.

B. Mobile App

Currently most people have a mobile device, so for the research topic we will develop a mobile application that will be in charge of displaying the information processed by the FireBase services, information such as the level of pollutants found in the air anywhere in the world.

The interaction between the Arduino and the mobile application will be making use of consumption by the Arduino and exposure of Rest services (API) by the mobile application, all of this using reactive programming. The development will be carried out with the Kotlin programming language, using FireBase services among other technologies [20].

C. FireBase

It is a platform for the development of mobile applications that offers us a wide variety of services as well as hosting, Real-time database, authentication, among others. The application will use some of the services offered by FireBase such as a real-time database, hosting, among others [21].

D. Prototype

For the realization of the prototypes, the moqups tool will be used, which provides us with a great variety of modern components that can be used for their realization [22].

IV. CASE STUDY

In this section we will see the construction of an air quality control and administration system through IoT and the planning of the sprint of each of the prototypes with the estimates of the times in which it is being carried out in the mobile development.

Fig. 4 represents the operation of the IoT architecture in the hands of the mobile application integrated in air quality through sensors.

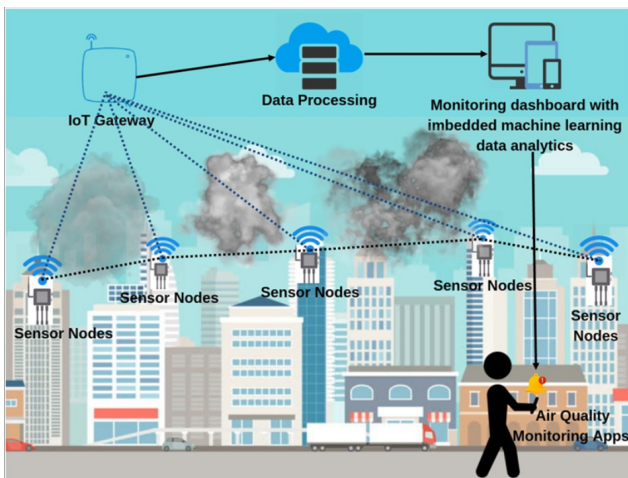


Fig. 4. IoT-based Air Monitoring System.

A. Sprint Planning

- As a user, I need to be able to create a user account to enter the application.
- As a user, I would like to be able to link my mobile device with the sensors via Bluetooth to establish a data collection point in my house to also be able to configure the data reading time and if the information travels to the server.
- As a citizen, I would like to know the gases that surround me to become aware of my actions against the environment.
- As a citizen, I would like to visualize the areas of my city with their respective pollution rates.

B. Development Stage

1) *Time estimate:* In this phase we will see the duration of each of the sprints as shown in Table II.

TABLE II. DURATION OF SPRINTS

Name	Duration	Sprint
Mobile app	4 Month	
Login screen	2 weeks	1
Sensor Integration with Arduino	2 weeks	1
Navigation menu	2 weeks	1
Registration Screen	2 weeks	1
Configuration screen	2 weeks	2
Arduino integration with Mobile device	2 weeks	2
Gas Dashboard screen	2 weeks	2
Location Dashboard screen	2 weeks	3

2) *Product scope:* It is the estimate of the time it takes for the team to have the points of the user stories, for which the estimates of the team's scope will be detailed in the following graph.

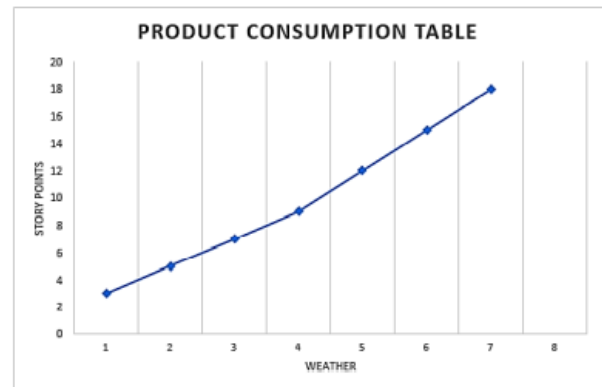


Fig. 5. Product Definition.

3) *Mobile app prototypes:* In this stage we will see the creation of the design of the mobile application that we will carry out and we will detail the functions that each of the modules will have as we see Fig. 6, Fig. 7, Fig. 8, Fig. 9, Fig. 10 and Fig. 11.

4) *Mobile app prototype increases:*

- Increment 1 - Login, Register and Menu. As shown in Fig. 3 to 5, this section is used to enter and register to the system by email or a social network, in turn we show the navigation screen, which has a user-friendly aspect.
- Increment 2 - Configuration and Monitor of gases in the air. The increment consists of two screens (Fig. 6 and 7), one of them is used to configure both the Bluetooth, the time interval to read the data from the sensors and send them to the server and the dashboard screen that is completely informative, we will show the different types of gases that we have around us, the user will be able to view graphs with percentages by type of gas and in turn a list of sensor reading data records.

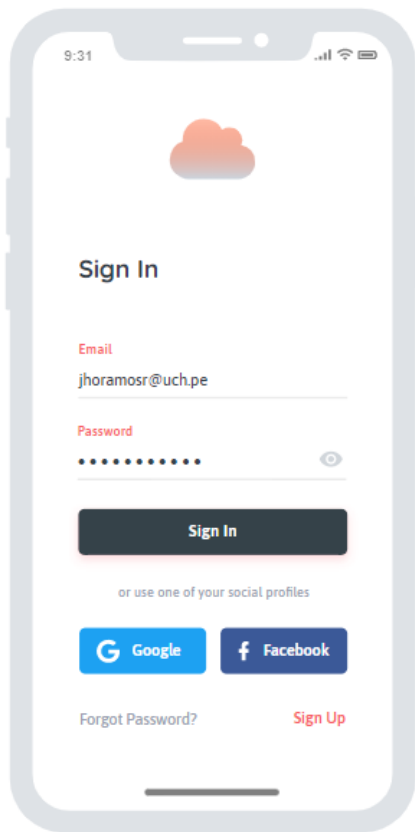


Fig. 6. Login Screen.

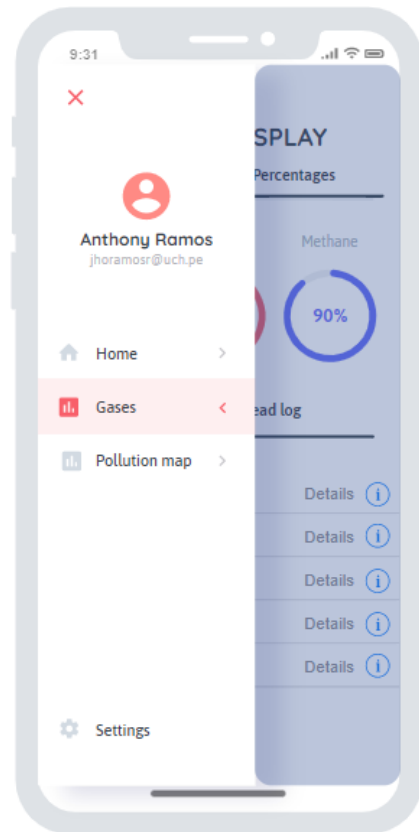


Fig. 8. Navigation Menu.

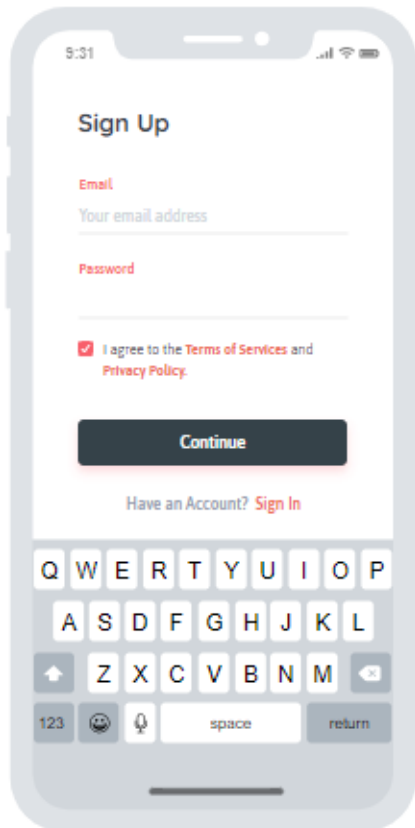


Fig. 7. Registration Screen.

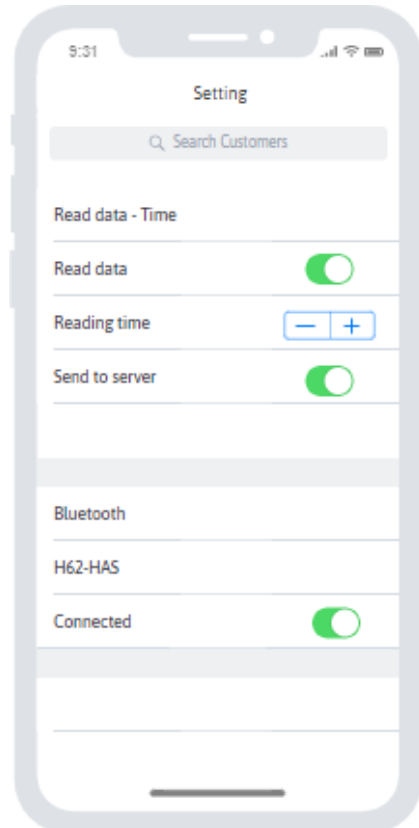


Fig. 9. Setup Screen.

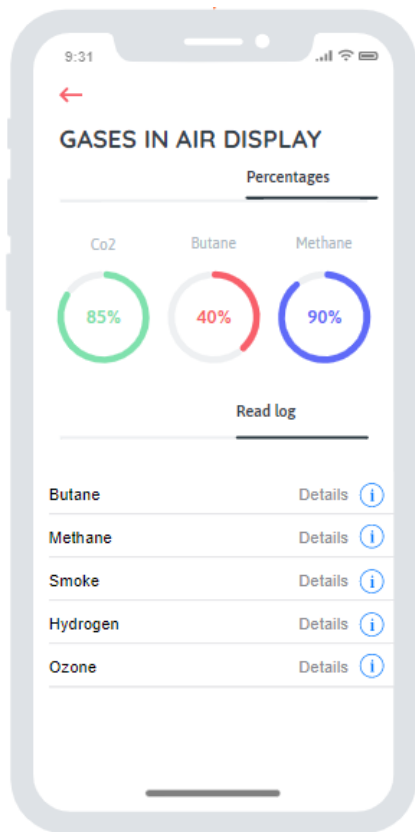


Fig. 10. Dashboard of Gases in the Air.

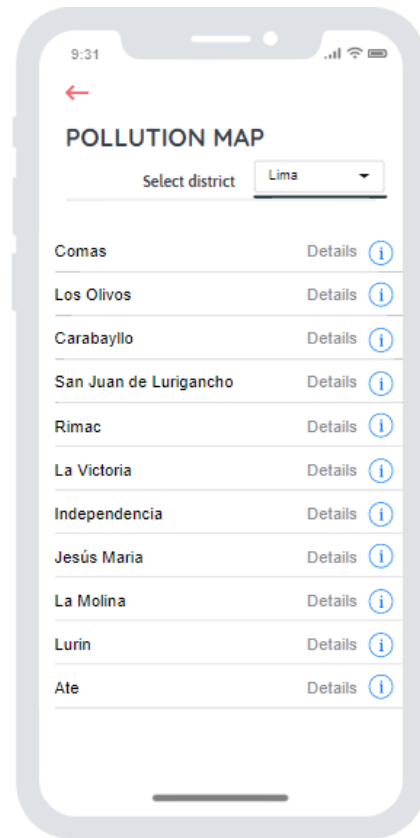


Fig. 11. Dashboard of Gases by Geographic Location.

- Increment 3 - Pollution by Geographical Location. In this section, statistical data will be displayed that can be viewed by departments and districts (Fig. 8).

5) Increments IoT:

- Increment 1 - Sensor Integration with Arduino. The increase consists of the development of the electronic system that will be in charge of reading the environmental data through the electronic components mentioned in the Technologies section and the Arduino.
- Increment 2 - Integration of Arduino with Mobile device. The increase consists of integrating the Bluetooth module to the electronic system in order to be able to make the connection between the Bluetooth system and the mobile application.

V. RESULTS AND DISCUSSIONS

This section presents the results obtained with respect to the methodology, technologies and case study, divided into two parts, which are the following:

A. About the Case Study

The results regarding the case study were highly favorable, the use of the Scrum methodology was proposed due to its Agile nature that allows the development of software quickly and in addition to that, some technologies that meet the proposed purpose were proposed.

As a result of the application of the case study, we obtained the following scheme where the IoT devices communicate with the cloud (Fire Base) that has a great diversity of services for data analysis, additionally provides a hosting for the application. As shown in Fig. 4, through sensors that are located in the upper part of the buildings, they obtain data on the indices of different polluting gases found in the environment that are sent to the server for analysis and interpretation, transforming into information that will be seen through the mobile application, allowing people to perceive in a simplified way the pollution rates around them.

The end user will be able to access the dashboard where they will view the types of polluting gases in the air as shown in Fig. 10 where we see detailed percentage graphs that explain the amount of butane, methane, smoke, etc. that exists in the environment where you are.

Likewise, you can see another board in Fig. 11 where you can search by geographical location for the types of pollutants that exist.

The results in relation to the technologies used were perfectly efficient and effective for the implementation, since the electronic sensors read the data of the medium accurately, the services provided by Fire Base are greatly used as it is a project related to emerging technologies.

B. About the Methodology

The Scrum methodology was a great choice for the development of the research since its way of working allowed us to implement the solution in an agile way, open to the recurring change that was presented, unlike other methodologies such as RUP (Traditional methodology) [10].

In Scrum methodology, "Product Owner" will work closely with the team to detect and prioritize the functionality of the system [11].

Differences in methodologies: this part will detail the differences of using the agile methodology, as opposed to using other methodologies that exist. Table III will detail the differences that each methodology will have.

TABLE III. TRADITIONAL METHODOLOGY VS. AGILE METHODOLOGY

Traditional methodologies	Agile methodologies
Predictive	Adaptive
Rigid process	Flexible process
Process-oriented	People-oriented
Little communication with the client.	Constant communication with the client.
Software delivery at the end of development.	Constant software deliveries
Extensive documentation.	Little documentation.
It is conceived as a project.	A project is subdivided into several smaller projects.

VI. CONCLUSIONS

Finally we can conclude that the proposed objective was achieved, which is to carry out the mobile application with integration of the IoT to make people aware of the damage they cause to the environment. The scientific contribution provided by this research work is very important in the science environment since it is the basis for future projects that will have a great impact on society, projects that will be totally necessary to reduce environmental pollution and thus to save the planet. For future work it is proposed to improve the subject, apply technologies such as artificial intelligence or some other that makes the idea evolve. There are other alternatives to this solution to make people aware of the state of the environment, however those that exist are not available to people.

REFERENCES

[1] Q. Di, Y. Wang, A. Zanobetti, Y. Wang, P. Koutrakis, C. Choirat, F. Dominici, and J. D. Schwartz, "Air pollution and mortality in the medicare population," *New England Journal of Medicine*, vol. 376, no. 26, pp. 2513–2522, 2017.

[2] T. Bourdrel, M.-A. Bind, Y. Béjot, O. Morel, and J.-F. Argacha, "Cardiovascular effects of air pollution," *Archives of cardiovascular diseases*, vol. 110, no. 11, pp. 634–642, 2017.

[3] A. Combes and G. Franchineau, "Fine particle environmental pollution and cardiovascular diseases," *Metabolism*, vol. 100, p. 153944, 2019.

[4] J. Xu, Y. Hu, and E. Miyoshi, "A consideration of media environment regarding air pollution problems in china: Based on the content analysis of the reports of "people's daily" from jan. 1,1970 to nov. 30,2011," in *2018 International Joint Conference on Information, Media and Engineering (ICIME)*, 2018, pp. 211–214.

[5] J. Park, Y. Oh, H. Byun, and C. Kim, "Low cost fine-grained air quality monitoring system using lora wan," in *2019 International Conference on Information Networking (ICOIN)*, 2019, pp. 439–441.

[6] B. Barazandeh and M. Rafieisakhaei, "A data analytics based approach for modeling the effects of a carbon market on the sustainable control of co2 emissions in latin america," in *2017 IEEE Conference on Technologies for Sustainability (SusTech)*, 2017, pp. 1–5.

[7] S. Pal, A. Ghosh, and V. Sethi, "Vehicle air pollution monitoring using iots," in *Proceedings of the 16th ACM Conference on Embedded Networked Sensor Systems*, 2018, pp. 400–401.

[8] S. Dhingra, R. B. Madda, A. H. Gandomi, R. Patan, and M. Daneshmand, "Internet of things mobile-air pollution monitoring system (iot-mobair)," *IEEE Internet of Things Journal*, vol. 6, no. 3, pp. 5577–5584, 2019.

[9] V. Sachdeva and L. Chung, "Handling non-functional requirements for big data and iot projects in scrum," in *2017 7th International Conference on Cloud Computing, Data Science & Engineering-Confluence*. IEEE, 2017, pp. 216–221.

[10] A. Srivastava, S. Bhardwaj, and S. Saraswat, "Scrum model for agile methodology," in *2017 International Conference on Computing, Communication and Automation (ICCCA)*, 2017, pp. 864–869.

[11] B. L. Romano and A. Delgado Da Silva, "Project management using the scrum agile method: A case study within a small enterprise," in *2015 12th International Conference on Information Technology - New Generations*, 2015, pp. 774–776.

[12] A. Alhazmi and S. Huang, "A decision support system for sprint planning in scrum practice," in *SoutheastCon 2018*, 2018, pp. 1–9.

[13] G. Koç and M. Aydos, "Trustworthy scrum: Development of secure software with scrum," in *2017 International Conference on Computer Science and Engineering (UBMK)*, 2017, pp. 244–249.

[14] N. R. Darwish and S. Megahed, "Requirements engineering in scrum framework," *International Journal of Computer Applications*, vol. 149, no. 8, pp. 24–29, 2016.

[15] F. M. Fowler, "The sprint backlog," in *Navigating Hybrid Scrum Environments*. Springer, 2019, pp. 67–70.

[16] G. Jia, G. Han, J. Du, and S. Chan, "Pms: Intelligent pollution monitoring system based on the industrial internet of things for a healthier city," *IEEE Network*, vol. 33, no. 5, pp. 34–40, 2019.

[17] M. M. Rahman, M. A. H. Rimon, M. A. Hoque, and M. R. Sammir, "Affordable smart ecg monitoring using arduino bluetooth module," in *2019 1st International Conference on Advances in Science, Engineering and Robotics Technology (ICASERT)*, 2019, pp. 1–4.

[18] K. Arasu, "Automated experimental procedure using sensors and arduino," in *2017 International Conference on Inventive Computing and Informatics (ICICI)*, 2017, pp. 383–387.

[19] S. Dhingra, R. B. Madda, A. H. Gandomi, R. Patan, and M. Daneshmand, "Internet of things mobile-air pollution monitoring system (iot-mobair)," *IEEE Internet of Things Journal*, vol. 6, no. 3, pp. 5577–5584, 2019.

[20] S. Dhingra, R. B. Madda, A. H. Gandomi, R. Patan, and M. Daneshmand, "Internet of things mobile-air pollution monitoring system (iot-mobair)," *IEEE Internet of Things Journal*, vol. 6, no. 3, pp. 5577–5584, 2019.

[21] W. Li, C. Yen, Y. Lin, S. Tung, and S. Huang, "Justiot internet of things based on the firebase real-time database," in *2018 IEEE International Conference on Smart Manufacturing, Industrial Logistics Engineering (SMILE)*, 2018, pp. 43–47.

[22] G. A. Amagsila, M. E. Cabuhat, J. E. Tigbayan, E. Uy, and E. Ramirez, "A framework for mobile application of flood alert monitoring system for vehicle users using arduino device," in *2017IEEE 9th International Conference on Humanoid, Nanotechnology, Information Technology, Communication and Control, Environment and Management (HNICEM)*, 2017, pp. 1–6.

An Integrated Imbalanced Learning and Deep Neural Network Model for Insider Threat Detection

Mohammed Nasser Al-Mhiqani¹,
Rabiah Ahmed^{2*}, Z Zainal Abidin³
Center for Advanced Computing Technology
Faculty of Information Communication Technology
Universiti Teknikal Malaysia Melaka
Melaka, Malaysia

Isnin, S.N⁴
Faculty of Technology Management and Technopreneurship
Center for Technopreneurship Development CTeD
Universiti Teknikal Malaysia Melaka
Melaka, Malaysia

Abstract—The insider threat is a vital security problem concern in both the private and public sectors. A lot of approaches available for detecting and mitigating insider threats. However, the implementation of an effective system for insider threats detection is still a challenging task. In previous work, the Machine Learning (ML) technique was proposed in the insider threats detection domain since it has a promising solution for a better detection mechanism. Nonetheless, the (ML) techniques could be biased and less accurate when the dataset used is hugely imbalanced. Therefore, in this article, an integrated insider threat detection is named (AD-DNN), which is an integration of adaptive synthetic technique (ADASYN) sampling approach and deep neural network technique (DNN). In the proposed model (AD-DNN), the adaptive synthetic (ADASYN) is used to solve the imbalanced data issue and the deep neural network (DNN) for insider threat detection. The proposed model uses the CERT dataset for the evaluation process. The experimental results show that the proposed integrated model improves the overall detection performance of insider threats. A significant impact on the accuracy performance brings a better solution in the proposed model compared with the current insider threats detection system.

Keywords—Security; insider threat; insider threats detection; machine learning; deep learning; imbalanced data

I. INTRODUCTION

Information systems are facing a security challenge, which comes from outside or inside of an organization. The outside security challenge involves malware and cyber-attack penetrating the network from remote sites. The inside security issue comes from the “trusted” employee within the organization. In which this issue involves both a behavioral and a technical nature [1][2]. Insider threat is commonly known as a problem of utmost importance for information system security management [3].

The malicious insider threat has been defined in the technical report [4] by Cappelli mentioned “a current or former employee, contractor or business partner who has or had authorized access to an organization’s network, system, or data and intentionally exceeded or misused that access in a manner that negatively affected the confidentiality, integrity, or availability of the organization’s information or information systems”. The insider threat activity was conducted by the intentional insiders; such as sabotage of information system, classified information disclosure and theft of intellectual property, or by

an unintentional insider, such as losing external devices that contain sensitive information about the organization. Unlike the tasks of the traditional intrusion detection, several insider threat detection challenges come from the nature of the insider where the insider has the authorization to access the computer systems of the organization and has more knowledge about the security levels of the organization [5][6]. Cybersecurity reports show that 63% think insider attacks have become more frequent in the past 12 months. In a recent survey, 53% of the responders believe that detecting insider attacks has become significantly to somewhat harder [7].

The detection of the insider threat is very difficult task; this is because of many challenges. Firstly, as security mechanisms of an organization are not mainly designed for the people who are already inside the organization’s network, this brings a chance for the motivated malicious insider with authorized access to carry out the malicious actions without triggering alerts. Secondly, majority of the attacks initiated by insider are carried out in several phases over a long time. For this reason, effective detection systems for insider threat have to be designed with consideration of long-term monitoring and wide audit data sources range [8][9].

Despite the good performance demonstrated by the current insider threat detection approaches, the traditional machine learning techniques are not able to utilize all the data of user behavior because of the complexity, high-dimensionality, sparsity, and heterogeneity of the data. ML algorithms normally assuming that the used data are balanced in their nature. However, imbalanced data usually produce high accuracy in detecting the majority class, while the accuracy of the minority class is very low. This type of result is not suitable in the situation of insider threats, where the minority class is the important in detection [10][11].

Hence, to deal with the abovementioned challenge, this article proposes an integrated insider threat detection model, called (AD-DNN), which is based on adaptive synthetic sampling approach (ADASYN) and deep neural network (DNN). The proposed of AD-DNN model contains two main parts. Firstly, the ADASYN oversamples the low-frequency samples of insider threats adaptively for increasing these samples, which will lead in helping the machine learning classifiers to learn the low-frequency insider threats attack samples characteristics. Secondly, The DNN is used to classify the samples to

normal or malicious insider based on the generated new dataset from the first stag. To evaluate the AD-DNN performance, an experiment is conducted on the CERT 4.2 insider threats dataset [12].

The rest of this paper is organized as follows. The related works is discussed in Section 2. Section 3 presents the methodology. Section 4 discuss the Implementation and Results. Finally, Section 5 concludes the work.

II. RELATED WORK

The importance of machine learning in the domain of insider threats is growing [13]. In several earlier researches, the use of machine learning algorithms has been used to build a classifier that can identify threats from insiders [14][15].

A significant work have been done for the propose of insider threats detection. The Hidden Markov Model (HMM) is used by Wang et al. in [16] to develop an insider threat detection approach. The HMM modeled the normal users' behavior to identify any abnormal behaviors which may differ from the normal behaviors. By utilizing the HMM in modeling the insider threats, the states number of HMM have an high impact on the effectiveness of the method. When the number of states increases the HMM computational cost increases.

ML algorithms have a high powerful ability in improving the insider threats detection performance and self-adaptive capabilities in handling the environment changes of insider threat. Nevertheless, these techniques of ML are still influenced from the effect of imbalanced data in the insider threats domain as well as the lack of in depth knowledge of the insider's behavior patterns [17].

Parveen et al. in [18] utilized the use of one-class support vector machine (OCSVM) technique to model the time series of the daily log, that conceptualizes the insider threat detection issue as a stream mining problem.

Lin et al. [19] proposed a hybrid insider threat detection model using the CERT dataset. The Deep Belief Network (DBN) and OCSVM have been used to build the insider threats detection model. Firstly, the unsupervised DBN is applied to extract the raw data hidden features. And then, the OCSVM is applied for the training of the model utilizing the extracted features.

In recent years, DNN and RNN techniques are widely used in the development of the detection systems of insider threat, Tuor et al. [20] proposed an online unsupervised deep learning approach based on DNN and RNNs to detect anomalous insider activities in real-time from the system logs. Their approach is containing three main parts, firstly the feature extractor, secondly the batcher/dispatcher, and finally the number of Recurrent Neural Networks (RNNs) or DNNs. Long short-term memory (LSTM) techniques have been used to model the user behaviors either alone or in combination with other techniques, Yuan et al. [14] applied the LSTM and Convolutional Neural Network (CNN) based model on user behavior to model the normal users behavior and detect anomalous user behavior. They have dealt with user activities like the natural language modeling. Similar with the previous work, Zhang et al. in [17] employed the LSTM for modeling the log activity of the insider and treat these activities same

like the natural language sequences, the proposed solution is worked by extracting the features and detecting the malicious activities when the patterns of the log differ from the training samples. The proposed model evaluation was carried out on a small group of users, only eight users were selected randomly from the CERT experimental dataset. Another work by Sharma et al. [21] also utilized LSTM based Autoencoder using the similar concept to the previous work which models the user behavior using session activities and therefore detect the abnormal data points.

A great efforts have been made by the researchers in the previous literature, however, we believe that there are still way to improve the insider threats detection performance by considering the issue of imbalanced data, and deal with the issue before proceeding the classification task.

III. METHODOLOGY

In this part, the basic concepts and methodology components of the proposed AD-DNN model is discussed as shown in Fig. 1.

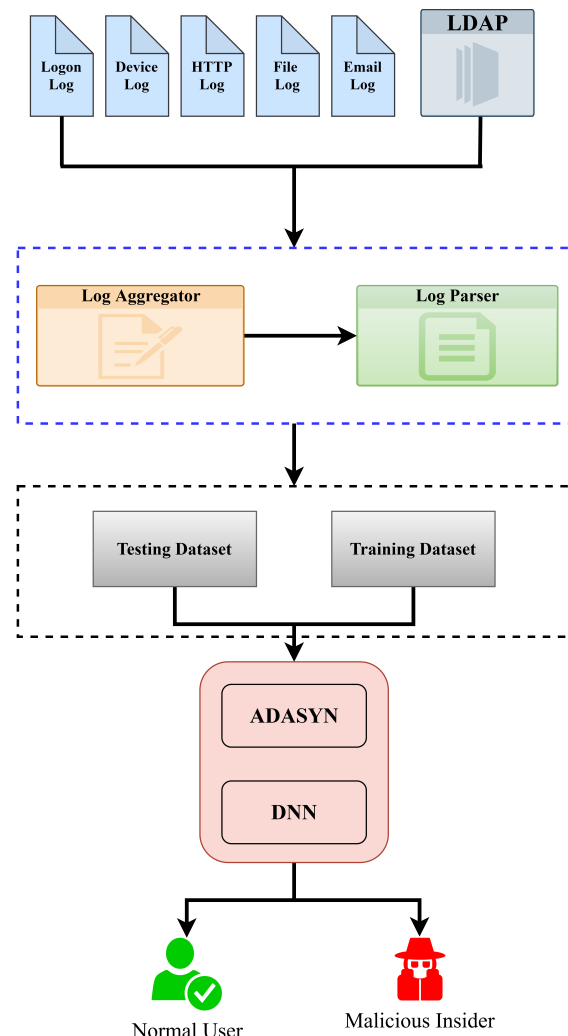


Fig. 1. Proposed Model.

A. Dataset

In this article the CERT r4.2 dataset is used to evaluate the proposed model this is due to the fact that this dataset contains several types of users' event activities, including logon/logoff, device, email, HTTP and files which capture the activities of 1000 employees in an organization for the period of 17 months. Additionally, CERT r4.2 have more instances of malicious insider compared to the other CERT datasets version. The dataset contains 32,770,222 event records generated by the 1000 normal and anomalous users. 7323 of the generated activities are malicious insider instances that were manually injected by experts, representing 3 different scenarios of insider threat. The dataset is divided into two sets: the first subset is used for training and second subset for testing. 80% of the datasets is used to train the proposed model, the remaining 20% is utilized for the evaluation of the model performance.

B. Log Aggregator and Parser

Firstly, the process of log aggregation starts with the collection of all insider data activity from multiple applications to the main-storage in order to prepare it for the processing task. After the combination of this data done by log parser, it can be saved as a new master dataset. Secondly, to make the data is compatible with machine learning algorithms the log parsing or the parsing engine is created. As the CERT data that has been aggregated in the first stage is mostly in text strings format, which is not readable by the DNN algorithms that we are applying here, the aggregated data need to be transformed to the applicable formats. To transform the data for our model the MaxAbsScaler is used to scales the data between the $[-1,1]$ range automatically based on the absolute maximum.

C. AD-DNN

The idea of sampling methods is either increasing or decreasing the number of samples in the evaluation dataset. The oversampling approach increases the records' frequency, which is a lower sample while under-sampling decreases the records' frequency, which is in a higher sample.

In this article, the oversampling method is used, since the focus on the insider threats, where the minority class is the important in detection, the method used called ADASYN. ADASYN approach is an algorithm that generates synthetic data, the ADASYN main idea is to use a weighted distribution for different examples of minority class according to their difficulty level in learning, the more synthetic data is mainly generated for the examples of minority class which is difficult to learn when it is compared to the other examples of minority classes that are easy to learn [22].

The ADASYN firstly calculates the minority class' K-nearest neighbors of every record in the sample class. Moreover, it draws a line between the neighbors and newly generated random points on that line. Then, it adds some small values randomly on the new point, which makes them similar to the real point. Therefore, these added sample points have more variance than the samples that are taken from their parent samples.

Deep learning (DL): is another machine learning techniques that is based on the learning concept of multi-level

representations. The DL creates a hierarchy of features where the lower the level is defining the higher levels and the features of the lower the level helps features are defined at a higher level. The structure of DL is extending the traditional neural networks where more hidden layers are added to the network architecture between the two layers of input and output for modeling the nonlinear and complex relationships. In recent years, this area of research has gained the concern of the researchers due to its great performance for becoming one of the best solutions in many problems. Many DL architectures are existing nowadays, currently, one of the common DL architectures is the convolutional neural networks (CNN), which can carry out complex tasks by using convolution filters. A CNN architecture is a feed-forward layers sequence where the convolutional filters and pooling layers are implemented. CNN adopts many fully-connected layers after the final pooling layer, which work on converting the previous layers 2D feature maps to 1D vector for the classification process. Despite the advantages of the CNN architecture where the feature extraction process is not required before the CNN being applied but the process of CNN training from scratch difficult and time-consuming because it requires large labeled dataset samples to build and train the model before it is prepared for classification. DNN is another type of DL architecture, which is widely utilized and succeeded in both regression and classification in various areas. DNN is a typical feed-forward network where the input flows to the output layer from the input layer using two or more hidden layers. Fig. 2 present the architecture of DNN.

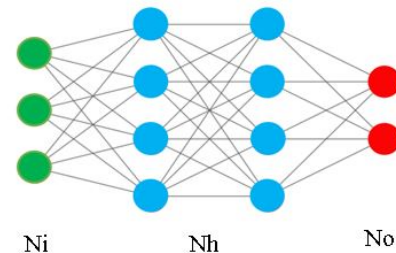


Fig. 2. DNN Architecture.

Fig. 2 shows the typical DNNs architecture where Ni is representing the input layer containing neurons for the input features, the Nh illustrates the hidden layers, and the No is the output layer classes.

IV. IMPLEMENTATION AND RESULTS

We have implemented the proposed system on Python with Tensorflow as the backend. The experiment environment is a Ubuntu 18.04.5 LTS operating system runs on a machine with an NVIDIA 1660Ti GPU on a 3.7GHz Intel Core i7-8700HQ, 16GB RAM.

Model Parameters: The proposed model parameters in this article includes the following: (a) The hidden layer of the DNN network, learning rate, number of epochs, and batch size. (b) The ADASYN algorithm oversampling rate and the number of nearest neighbors. We tuned our model with 20 hidden layers, $1e-3$ learning rate, 50 epochs, $1024 * 16$ batch size, and the Adam optimizer is used.

Metrics: To evaluate the proposed model performance, the parameters used are the average accuracy, average false positive rate, average F-Score, average true-negative rate and average false-negative rate. The performance of the proposed model was compared with other classifiers using the same parameter measurements.

$$Accuracy = \frac{TN + TP}{TN + TP + FN + FP} \quad (1)$$

$$F - score = 2 \cdot \frac{Precision \cdot Recall}{Precision + Recall} \quad (2)$$

$$FPR = \frac{FP}{FP + TN} \quad (3)$$

$$TNR = \frac{TN}{TN + FP} \quad (4)$$

$$FNR = \frac{FN}{FN + TP} \quad (5)$$

where TP (True Positive), TN (True Negative), FN (False Negative), and FP (False Positive). Additionally, to consider the problem of class imbalance where the insider attacks often carried out by the malicious insiders during the normal work time, which scatters the abnormal insider behavior in large amount of normal employees' behavior, we use the Area Under-Curve (AUC) measurement for evaluating the proposed model. The AD-DN produces a better result compared to the other single classifiers, as shown in Fig. 3 the best result that the AD-DNN gets is AUC = 95%.

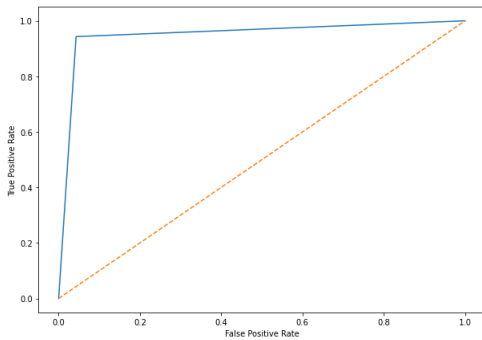


Fig. 3. AD-DNN AUC

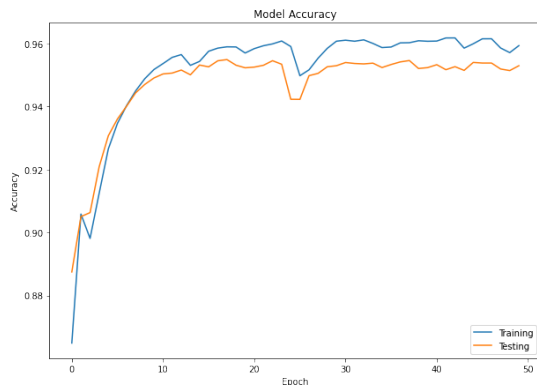


Fig. 4. AD-DNN Accuracy

Fig. 4 presents the average accuracy of the proposed AD-DNN, which shows the accuracy versus the number of epochs. It plots the training and testing performances. As shown in the figure, the proposed AD-DNN obtain good accuracy with average of 96% and there is no major problems indicated with the model since the training and testing curves are very similar to each other and there is no possibility of overfitting.

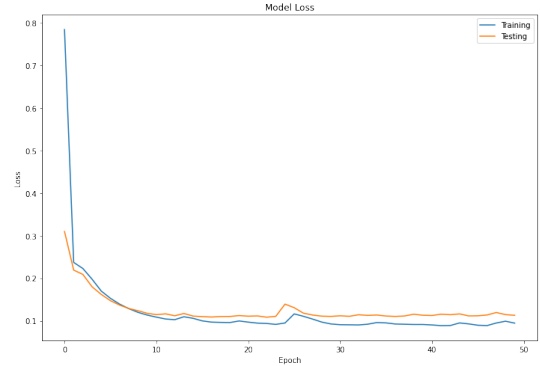


Fig. 5. AD-DNN Loss

Fig. 5 presents the loss of the training and testing in every epoch. In this experiment, the model was stopped after 50 epochs when there is no high testing loss was seen between successive iterations.

Finally, in this article, the designed AD-DNN model is compared with three common methods machine learning techniques (SVM, DNN and LSTM), which have been used in the field of insider threats. The Scikit-Learn library has been implemented to execute three techniques. Additionally, for evaluating the effectiveness of the proposed model using all evaluation matrices, the AD-DNN is compared with some of the recent works as shown in Table I.

TABLE I. COMPARISON SUMMARY OF PROPOSED MODEL

Model	Accuracy	F-Score	AUC	FPR	FNR	TNR
SVM	70%	60%	44%	23.8%	89.10%	76%
LSTM	75%	30%	68%	23.6%	40%	76%
DNN	86%	48%	80%	12.9%	27%	87%
OCSVM based on DBN[19]	87.79%			12.18%		
LSTM Autoencoder[21]	90.17%		95%	9.84%		91%
AD-DNN	96%	95%	95%	4%	5%	96%

On comparative analysis of the well-known classifiers and some of the recent works on detection of the insider threat using the CERT v4.2 dataset, AD-DNN produces a good and promising results. Table I shows that AD-DNN gives the highest accuracy with 96% and the highest F-score, AUC and TNR with 95%, 95% and 96% respectively. Additionally, the AD-DNN achieves the least false rate with 4% FPR and 5% FNR only. It can be seen that AD-DNN is superior to other

methods in almost all the evaluation metric, for example the DNN without ADASYN that gives 86% accuracy, 48% F-score, 80% AUC, 87% FNR, 12.9% FPR and 27% FN. This is because AD-DNN consider and solve the imbalance data problem before start training the classifier, and our method can effectively improve the performance of detection.

V. CONCLUSION

In this article, an integrated insider threat detection model is introduced called as AD-DNN for solving the current challenges in the insider threat detection constructed by employing the theory of machine learning. Firstly, the ADASYN algorithm is used to solve the imbalanced data problem in the situation of insider threats, where the minority class is important in detection. Then, the DNN classifier is designed as the anomaly insider threat detection. The results of the experimental on the CERT dataset shows that the ADASYN algorithm solves the machine-learning algorithms imbalanced the fitting trend of the low-frequency and high-frequency insider data and improves the detection accuracy of the low-frequency insider attack by generating fewer new samples. Furthermore, compared with other recent research works and machine learning techniques used for insider threats detection, the proposed AD-DNN makes the insider threats detection obtains superior and satisfactory results in all the evaluation metrics.

ACKNOWLEDGMENT

Thank you to Research Group of Information Security Forensics and Computer Networking, Center for Advanced Computing Technology (C-ACT), Fakulti Teknologi Maklumat dan Komunikasi, Universiti Teknikal Malaysia Melaka (UTeM). This project is funded by the Ministry of Higher Education Malaysia under the Transdisciplinary Research Grant Scheme (TRGS) with project Number TRGS/1/2016/UTeM/01/3. Its reference is TRGS/1/2016/FTMK-CCT/01/D00006.

REFERENCES

- [1] M. Kandias, A. Mylonas, N. Virvilis, M. Theoharidou, and D. Gritzalis, "An insider threat prediction model," in *International Conference on Trust, Privacy and Security in Digital Business*, S. Bilbao, Ed., vol. 6264 LNCS. Information Security and Critical Infrastructure Protection Research Group, Dept. of Informatics, Athens University of Economics and Business, 76 Patission Ave., GR-10434, Athens, Greece: Springer, 2010, pp. 26–37. [Online]. Available: <https://www.scopus.com/inward/record.uri?eid=2-s2.0-78049354490&doi=10.1007%2F978-3-642-15152-1%2F3&partnerID=40&md5=9bdad27630b10aae5b5e10b2f4c87ea2>
- [2] M. Al-Mhiqani, R. Ahmad, K. Abdulkareem, and N. Ali, "Investigation study of Cyber-Physical Systems: Characteristics, application domains, and security challenges," *ARPN Journal of Engineering and Applied Sciences*, vol. 12, no. 22, 2017.
- [3] M. Theoharidou, S. Kokolakis, M. Karyda, and E. Kiountouzis, "The insider threat to information systems and the effectiveness of ISO17799," *Computers and Security*, vol. 24, no. 6, pp. 472–484, 2005.
- [4] D. M. Cappelli, A. P. Moore, and R. F. Trzeciak, *The CERT guide to insider threats: how to prevent, detect, and respond to information technology crimes (Theft, Sabotage, Fraud)*, 2nd ed. Boston, MA, USA: Addison-Wesley, 2012.
- [5] D. C. Le, N. Zincir-Heywood, and M. I. Heywood, "Analyzing Data Granularity Levels for Insider Threat Detection Using Machine Learning," *IEEE Transactions on Network and Service Management*, vol. 17, no. 1, pp. 30–44, 2020.
- [6] N. Ameer, N. Mohammad, W. M. Yassin, R. Ahmad, A. Hassan, and M. N. Al-mhiqani, "An Insider Threat Categorization Framework for Automated Manufacturing Execution System," *International Journal of Innovation in Enterprise System*, vol. 3, no. 01, pp. 31–41, 2019.
- [7] H. Schulze, "Insider Threat: 2020 Report," Cybersecurity Insiders, Tech. Rep., 2020. [Online]. Available: <https://www.cybersecurity-insiders.com/wp-content/uploads/2019/11/2020-Insider-Threat-Report-Gurucul.pdf>
- [8] L. Liu, C. Chen, J. Zhang, O. De Vel, and Y. Xiang, "Insider Threat Identification Using the Simultaneous Neural Learning of Multi-Source Logs," *IEEE Access*, vol. 7, pp. 183 162–183 176, 2019.
- [9] M. N. Al-Mhiqani, R. Ahmad, Z. Z. Abidin, W. Yassin, A. Hassan, K. H. Abdulkareem, N. S. Ali, and Z. Yunos, "A review of insider threat detection: Classification, machine learning techniques, datasets, open challenges, and recommendations," *Applied Sciences (Switzerland)*, vol. 10, no. 15, 2020.
- [10] A. Azaria, A. Richardson, S. Kraus, and V. S. Subrahmanian, "Behavioral analysis of insider threat: A survey and bootstrapped prediction in imbalanced data," *IEEE Transactions on Computational Social Systems*, vol. 1, no. 2, pp. 135–155, 2014.
- [11] S. Yuan and X. Wu, "Deep Learning for Insider Threat Detection: Review, Challenges and Opportunities," *arXiv*, 2020. [Online]. Available: <http://arxiv.org/abs/2005.12433>
- [12] The CERT Division, "Insider Threat Test Dataset," <https://resources.sei.cmu.edu/library/asset-view.cfm?assetid=508099>, November 2016. (Accessed on 01/16/2021).
- [13] S. Walker-roberts, M. Hammoudeh, A. L. I. Dehghantaha, and S. Member, "A Systematic Review of the Availability and Efficacy of Countermeasures to Internal Threats in Healthcare Critical Infrastructure," *IEEE Access*, vol. 6, pp. 25 167–25 177, 2018.
- [14] F. Yuan, Y. Cao, and Y. Shang, "Insider Threat Detection with Deep Neural Network," in *International Conference on Computational Science*, vol. 10860. Springer International Publishing, 2018, pp. 43–54. [Online]. Available: <http://link.springer.com/10.1007/978-3-319-93698-7>
- [15] M. N. Al-Mhiqani, R. Ahmad, Z. Z. Abidin, W. Yassin, A. Hassan, and A. N. Mohammad, "New insider threat detection method based on recurrent neural networks," *Indonesian Journal of Electrical Engineering and Computer Science*, vol. 17, no. 3, pp. 1474–1479, 2019.
- [16] C. Wang, G. Zhang, and L. Liu, "A detection method for the resource misuses in information systems," in *Advances in Intelligent and Soft Computing*, vol. 137 AISC. Springer, 2012, pp. 545–552.
- [17] D. Zhang, Y. Zheng, Y. Wen, Y. Xu, J. Wang, Y. Yu, and D. Meng, "Role-based Log Analysis Applying Deep Learning for Insider Threat Detection," in *Proceedings of the 1st Workshop on Security-Oriented Designs of Computer Architectures and Processors*, 2018, pp. 18–20. [Online]. Available: <http://doi.acm.org/10.1145/3267494.3267495>
- [18] P. Parveen, Z. R. Weger, B. Thuraisingham, K. Hamlen, and L. Khan, "Supervised learning for insider threat detection using stream mining," in *23rd IEEE International Conference on Tools with Artificial Intelligence Supervised*, 2011, pp. 1032–1039. [Online]. Available: <https://www.scopus.com/inward/record.uri?eid=2-s2.0-84855784162&doi=10.1109%2FICTAI.2011.176%2F&partnerID=40&md5=c556f156272fbd56c9375b1c021e6380>
- [19] L. Lin, S. Zhong, C. Jia, and K. Chen, "Insider Threat Detection Based on Deep Belief Network Feature Representation," in *2017 International Conference on Green Informatics (ICGI)*, 2017, pp. 54–59.
- [20] A. Tuor, S. Kaplan, B. Hutchinson, N. Nichols, and S. Robinson, "Deep learning for unsupervised insider threat detection in structured cybersecurity data streams," *AAAI Workshop - Technical Report*, vol. WS-17-01 -, no. 2012, pp. 224–234, 2017.
- [21] B. Sharma, P. Pokharel, and B. Joshi, "User Behavior Analytics for Anomaly Detection Using LSTM Autoencoder-Insider Threat Detection," in *ACM International Conference Proceeding Series*, 2020, pp. 1–9.
- [22] S. He, H. Bai, Y. Garcia, E., & Li, "ADASYN: Adaptive synthetic sampling approach for imbalanced learning. In IEEE International Joint Conference on Neural Networks, 2008," *IJCNN 2008. (IEEE World Congress on Computational Intelligence) (pp. 1322– 1328)*, no. 3, pp. 1322– 1328, 2008.

A Systematic Study of Duplicate Bug Report Detection

Som Gupta¹
Research Scholar
AKTU Lucknow

Sanjai Kumar Gupta²
Associate Professor
Computer Science Engineering Department BIET Jhansi

Abstract—Defects are an integral part of any software project. They can arise at any time, at any phase of the software development or the maintenance phase. In open source projects, open bug repositories are used to maintain the bug reports. When a new bug report arrives, a person called “Triager” analyzes the bug report and assign it to some responsible developer. But before assigning, has to look if it is duplicate or not. Duplicate Bug Report is one of the big problems in the maintenance of bug repositories. Lack of knowledge and vocabulary skills of reporters sometimes increases the effort required for this purpose. Bug Tracking Systems are usually used to maintain the bug reports and are the most consulted resource during the maintenance process. Because of the Uncoordinated nature of the submission of bug reports to the tracking system, many times the same bug report is reported by many users. Duplicate Bug Reports lead to the waste of resources and the economy. It creates problems for triagers and requires a lot of analysis and validation. Lot of work has been done in the field of duplicate bug report detection. In this paper, we present the researches systematically done in this field by classifying the works into three categories and listing down the methods being used for the classified researches. The paper considers the papers till January 2020 for the analysis purpose. The paper mentions the strengths, limitations, data set, and the major approach used by the popular papers of the research in this field. The paper also lists the challenges and future directions in this field of research.

Keywords—AUSUM; feature-based; deep learning; semantic; unsupervised

I. INTRODUCTION

Bug Report is one of the artifact which is produced during the software development, testing and the maintenance phase of the software process. It has been found that in any normal software development process, maintenance phase accounts for about two-thirds of the total efforts [1]. Mainly bug reporting systems are used for maintaining the bug reports of large software projects like Bugzilla. Nowadays, with the increasing competition and rapid development with quick time to release, it is common among the software community. But this quick time to release also leads to a lot of issues and the remaining features that make the users submit their expectations and issues. Also, these bugs lead to the release of another version of the software. As software defects add to the cost to the testing process. It is very important to detect them as soon as possible. As the software teams are usually geographically distributed, for the collaboration purpose web-based systems are used [2]. Bug Tracking Systems also allows users to report the bug they encounter. It has been found that finding whether the bug report is duplicate or not is more expensive than creating the new bug report.

In a paper by [3] they performed an exploratory study of 8 open-source projects and 1 private company project to analyze what percentage of the corpus consists of the duplicate bug reports, how much time a submitter spends in identifying the duplicate bug report before opening the new bug report, how the time is spent in resolving the duplicate bug report and the valid bug report, the average frequency of duplicate bug reports coming up in the repository on daily basis, how much vocabulary the master and duplicate bug report shares, how the type of bug report impacts the frequency of duplicate bug reports and why the duplicate bug report problem arises. They found that the submitter productivity is impacted by the duplicate bug reports problem as many times almost 48 man-hours need to be spent daily for performing this activity. The same study was later conducted by [4] where their focus was to predict the effort required by developers to identify the duplicate bug reports. They used Peers, Workload, Bug Report, Working Habits, and Triager experience to predict their effort. In another paper by Xie et al. [5], they also analyzed the percentage of duplicate bug reports in various popular platforms like Mozilla Core, Firefox, Thunderbird, Eclipse Platform, JDT, Hadoop, etc. They found that for these popular projects, on an average 12 percent bug reports are duplicate. The statistics of nine famous projects in terms of bug reports and the number of duplicate bug reports are mentioned in Table I. From the table, it is clear the duplicate bug reports comprises of almost 20 percent of the total bug reports.

Because of the following issues, the duplicate bug reports exist in a large number in these bug tracking systems.

- 1) free availability to the users to report the defect
- 2) Millions of users exists for the large projects
- 3) Bug Reports are submitted by both the developers and the users
- 4) Frequent release of software versions
- 5) User Inexperience
- 6) Poor Search Functionality in the Bug Tracking Systems

Many times even if the bug report is duplicate, it gets attached to the master report which is also known as triaging.

Bug Triaging is a process in which the person assigns the bug to a particular person for the resolution. But before assigning, has to go through these bug reports to find which one is duplicate and which one is not. Along with this, the triager has to look whether the bug report is related to the problem or the modification to the software. Because if the same problem is assigned to more than one person, it leads to

TABLE I. DATASET INFORMATION [6]

Project Name	No of Issue per day	Unique Components	No of Duplicates	Duplicate Percentage
Mozilla Core [7]	33	130	44691	21.8
Firefox22		52	35814	30.9
ThunderBird	23	7	12501	30.9
Eclipse Platform [8]	19	21	14404	16.9
JDT [9]	10	6	7688	17
Cassandra [10]	4	24	2083	14.8
MapReduce [11]	2	63	977	13.9
HDFS [12]	3	71	1659	13
Spark [13]	8	29	3077	13.6

the waste of resources. It has been found that many times more than 300 [14] bugs on a day are reported. Not only this but duplicate bugs are also there. This makes the finding of a duplicate bug report a challenging task. They lead to redundancy in the work and thus increase the workload for engineers. For a large project, bug triaging increases the cost to software maintenance, and manually doing this process is almost impractical. Thus there is a need to find the automatic approach which can help find the duplicate bug reports among all.

Because of the above-mentioned problems, need for assistance in detecting duplicate bug reports eases the task of bug triager. In a paper by [15], they observed that detecting duplicate bug reports consume a lot of time. Even though lot of approaches have been proposed but getting the full score for precision is very difficult. The reasons for these results is the diversity of natural language text in the bug reports and the diversity of the features in large software. The poorly written content in the bug reports by the users also poses another challenge to the triager.

Many authors [16] claim that the duplicate bug reports also help find more information. Thus many have proposed the techniques which finds the top-k most duplicate bug reports for the triager to have the additional information also. From our survey we have observed that following techniques are very popular among the research community in this field:

- 1) Natural language based Researches [17] [18]
- 2) Execution Trace Based Researches [19]
- 3) Clustering based models with similarity measures[14] [20]
- 4) Classifier-based machine learning approach [2]
- 5) Convolutional and LSTM Based Deep Learning Models [1]

In most of the projects, the first step to further process the bug report for any analysis is feature vector representation. For the Feature vector representation following natural language processing techniques are mainly used by various researchers: Word Embedding, Bag of Words, Skip-Gram, CBOW (Continuous Bag of Words), Latent Semantic Analysis, Latent Dirichlet Analysis, N-Gram.

On the Basis of above based information, we divide our work into three parts mainly Information-Retrieval, Machine Learning and Natural Language Processing based, according to the approach being used.

The main contributions of the paper are as follows:

- The paper presents the classification of duplicate bug report approaches.

- Paper gives a brief overview to almost all the famous researches in this field till early 2020.
- Paper gives the comparative results of various approaches being used in this field.
- Paper also mentions the various data-sets which have been used by various researchers.
- Paper also mentions the Strengths and Limitations of the works.
- Paper also discusses the Evaluation Measures being used for various approaches.
- Paper also lists down the challenges and the directions for future research.

The paper is organized as follows: Section 2 gives a brief overview of existing approaches which is further divided into Information-Retrieval Based, Natural Language Processing Based and Machine Learning Based. Section 3 discusses the Methodology that we opted for carrying out this research. Section 4 discusses the various evaluation measures being used for measuring the efficiency of Detecting duplicate bug reports detection techniques. Finally we discuss the future directions in this field and the conclusion of the paper.

II. EXISTING APPROACHES

Bug Report is an artifact which is produced during the software testing or software maintenance phase. It contains three types of data in it:

- Textual Data: It consists of Title, Description and comments. Title is a brief introduction about the bug. Description is the detailed overview along with the steps to reproduce to clearly indicate about the bug. Comments are the text that the other users or developers write against the bug in order to either given a suggestion or improvement or solution.
- MetaData: It consists of miscellaneous information about the bug in terms of its classification like product name, component field, assignee, version, priority, reporter, create time, status and resolution. Component refers to the component of the project where the bug has occurred. Status means whether it is duplicate or not. Status means whether the bug report is “open”, “in-progress”, “resolved”, “closed”, “reopen”, “wont fix”, “not a bug”, etc. Version means in which version of the software, the bug has occurred.
- Attachment: It is the screen shot of the issue in order to give better clarity about the bug report. It may also include the execution trace.

Bug Reports not only contains the resolution for the bug but also enhancements, ideas and the change requests. Analyzing bug reports help in change management, software evolution, traceability and also during effort estimation [3]. Many researchers observed that around 10 to 30 percent of the bug reports are duplicate in these open bug repositories. Having no duplicate bug report is also a big problem as it will lead to less information. In research by [16], he observed that duplicate bug reports help improve the knowledge by adding more information bug having large number of duplicate bug reports creates problem.

Many researchers [2] stated that duplicate bug report literature can be classified into two categories: one which finds the relevant bugs and one which aims to find the duplicate bug report. Thus the process can be classified into:

- Prevention of duplicate bug reports while submitting.
- Identification of top-k bug reports during bug report triaging.

Even though the approaches are classified into the mentioned two categories but in a paper by [21] they mentioned that the former approaches can only delete 8 percent of the duplicate bug reports but 92 percent bug reports still remains in the system. Thus leading to no such good benefit to the triager. More than this preventing the duplicate bug reports is a very expensive process also.

We observed the first main research in this field started with [17] where they used the log based weighing techniques along with the NLP Based approaches to identify the duplicate bug reports. The work was extended by [19] where along with the natural language text, execution traces were also used. The shortcomings of these approaches were taken into consideration by [22] where they used SVM model after creating the features using NLP techniques. In the same year [18] used the n-grams for the same purpose. In 2010, [21] used the BM25F to calculate the correlation between the bug reports. In year 2012 the same work of [21] was extended by [23] to calculate the effectiveness of BM25F for duplicate bug report detection. After these works, we observed that most of the works involve deep learning techniques for the same.

By analyzing all the works, we classified the approaches into following categories:

A. Information-Retrieval based

Information Retrieval techniques aim to find out the structure from the unstructured data. IR Based Models are generally divided into two approaches: word-based and topic-based models. Vector Space Model (VSM) is one example which gives the weights to the words and helps identify the main themes out of the document. Mainly Logarithms, IDF and Entropy are common weighing models which are used with these word-based models.

Topic models are one of the very famous approach which is used in IR field to find the latent topics of the text. They help find the similarity scores between the documents. Topic models help capture the semantic information from the bug report. It includes approaches like Latent Dirichlet Allocation

(LDA), Latent Semantic Analysis (LSA), Random Projections and their variants. In topic-based models, the term-document distribution and the word-topic distribution are obtained. These document-topic representation are converted into the vector form. Few hyper parameters are used with the LDA to get the cluster of relevant topics. For those hyper-parameters setting, many researchers have used techniques like Genetic Algorithms, Differential Evolution, Particle Swarm Optimization, Simulated Annealing, Random Search. Similarity between documents is usually calculated by using cosine similarity. General Steps which are used for using Information Retrieval Techniques are: first the pre-processing of the document to extract the relevant words from the document. This step includes stemming and removal of stop words. Then either the Term-by-document matrix or the probabilistic models are generated which are then used to calculate the textual similarities [24]. Term-by-Documents matrix includes vocabulary which is also referred to as Terms as rows and the documents as the columns. Weights are assigned to the terms in the documents by either TF-IDF or their variants.

The author in [19] used the Vector Space Model to transform the execution trace into the vector form for getting the information from the execution trace of a bug report for duplicate bug report detection. The author in [25] used the VSM in their information retrieval module in the JDF server to represent the document for the further similarity calculation.

The author in [26] compared the word-based model VSM with the topic-based model over the Firefox and Eclipse Project. They also analyzed how different weighing models work with the VSM. They found that for the task of duplicate bug report identification, VSM models outperformed the Topic-Based models and Log-Entropy outperformed among the weighing schemes. In the paper of [26], they compared the Vector Space Model with the topic models and observed that the Vector Space Model was performing better than the topic models.

The author in [2] in their paper, used the LDA along with the gibbs sampling to extract the topics. They used the comments to find whether the two bug reports are same or not. Their notion was that many times when the title and description are vague, comments supplement the information and help find out the similarity of bug reports. First they classified the comments into useful and un-useful. For the classification of comments, they used SVM along with the RBF kernel. For the the classification, they used four features namely IDF, bug status, length of comment and unigrams to create the vectors for training purpose. They found the weighted comment similarity to find the similarity between the comments and the bug report title and description. They used LDA topics along with the gibbs sampling to find the main topics of the bug report. Then they used topic distance models like Jensen-Shannon and symmetric KL-Divergence to find the distance between the topic distributions. They also used the knowledge about the issuing author to determine the duplicate bug report. Their notion behind checking the issuing author is that because of some specific way of writing, there can be high similarity between the two bug reports from the same author but chances of being duplicate will be very less.

The author in [27] used the information retrieval model to find the top-k similar bug reports for BlackBerry Systems.

They first preprocessed the bug report then important features were extracted for indexing purpose. The indexing was specified in terms of Term-Vectors. Indexed data was fed to searching and ranking module. They used the Lucene features for finding the similar documents. The ranked documents were then fed to the selection and filtering module to find the top-k similar bug reports.

The author in [28] used the topic model LDA implemented in MALLET along with the machine-learning based approaches to identify the duplicate bug report. In their paper, they first paired the bug reports using metrics like difference of words in the summary and description respectively, number of shared words between the summaries and descriptions respectively, number of shared identical topics between summary and description, priority field, time between two submissions, component field, type of bug report severity, etc. In order to find these metrics, they used LDA with alpha value as 50 and beta value as 0.01 in the Weka.

The author in [29] used vector space model to detect the duplicate bug reports by considering the title and the description.

The author in [30] used the topic-based model LDA for identifying the topics from the bug report which were further used for the feature vector construction for the purpose of training the model. The author in [31] along with the NLP used the SVM to analyze whether the Expected Behavior and steps2reproduce are missing or not. They also trained their model with 10 fold SVM after finding the discourse patterns, N-grams and Part Of Speech.

The author in [32] considered the domain-specific information of the bug report to identify the duplicate bug reports. They utilized the power of IR techniques along with the contextual keywords which includes architectural words, non-functional words, topic words extracted using LDA and labeled LDA, and random dictionary words.

The author in [33] classified the duplicate bug reports as one which shares the vocabulary and one which does not share the vocabulary. They proposed an approach which deals with both type of duplicate bug reports. For the first type of bug reports where the vocabulary is shared, they used the Vector Space Model and Clustering techniques. They used the cross product between the vectors and the vector lengths were computed using euclidian distance. They used the concept that smaller the angle between the two vectors, higher is the similarity. They used the TF-IDF weighing scheme to assign the weight to each term of the vector. For clustering, they used K-Means technique. For finding the dissimilar bug reports, first they identified the dissimilar duplicate bug reports by vector space model with TF-IDF where they analyzed the angle between the bug reports. After finding dissimilar reports, they created the word co-occurrence model. After creating the co-occurrence model, they computed the similarity using BM25 and language modeling techniques like Jelinek-Mercer smoothing and Dirichlet smoothing.

The author in [34] in their mentioned how powerful the word embeddings and the LDA approach is while calculating the similarity between two documents. [35] used the LDA and LSI approaches to find how continuously querying the bug

report like how it happens in Google Search Engine helps find the duplicate bug reports.

The author in [24] in their paper compared five meta-heuristics GA, DE, Particle Swarm Optimization, Simulated Annealing and Random Search, to analyze how the LDA works when applied.

B. Natural Language Processing based

The author in [17] used the natural language text of bug reports, performed the pre-processing by tokenization, stemming and stop word removal, and then converted the text into bag of word models and modeled as feature vectors. For the features calculation, Term frequency was used. Similarity of the bug reports is calculated by calculating the similarity between the features vectors by using cosine, Jaccard and dice similarity measures. The word was extended by [19] where they used the execution information along with the natural language information and in the bug report to compare it with the other reports. For the feature vector construction, they used Inverse Document Frequency (IDF) along with the Term Frequency (TF). They used the cosine similarity measure to calculate the similarity between the feature vectors. They detected the top-k similar bug reports with their approach.

The author in [36] used the event-component similarity approach to find the duplicate bug reports for the bugs having their component as GUI. In their approach they transformed the report into event, component and requirements. They used the Longest Common Subsequence approach for estimating the similarity between the two event, component and requirements.

N-Gram models have been used to analyze the title and the description of the bug report. The author in [18] et al. have used n-gram characters to identify the top-N similar bug reports. They used the number of shared n-gram characters and the number of character-n grams of title present in the other report's description to find the similarity between the two bug reports.

Extending this work, [25] used the above approach to create a tool for Jazz bug repository to identify the duplicate bug reports. They used Natural Language Based Similarities(NL-S) and Execution-information based similarities(E-S) too calculate the similarity of new bug report with the existing bug reports. The author in [21] extended the concept of BM25F to calculate the textual similarity accurately. For BM25F, they used the property of weight of terms in the query. The author in [37] used the bag of diagrams of title and description along with the extension of BM25F to compute the similarity to find the top-k similar bug reports. The author in [38] used the N-grams to find the scores for 25 features for the bug text for finding the semantic similarity between the two texts.

The author in [39] also used the features and textual similarity to help assist in the duplicate bug report detection while writing the bug report so that user also does not continue writing the bug report. In their approach they have used some fixed amount of word to calculate the features. In their paper, they first pre-processed the titles and descriptions by picking only few important words from them. Then they chosen few bug reports which are non duplicate and few which are

duplicate for creating the training set. TakeLab tool is used to calculate the features of the bug report. And then using machine learning classifier approach, they detect whether the bug report is duplicate or not.

The author in [32] used the textual, categorical and contextual similarity measures by calculating the similarity between the title, description, product feature, component feature, bug type, priority and version to find the whether the bug report is duplicate or not. For comparison, cosine similarity measure is being used by them. They used the dictionary having the architectural words which they extracted from project documentation, non-functional requirements which they classified into they efficiency, functionality, maintainability, portability, reliability and usability; LDA-topic words which they extracted by using Vowpal Wabbit online learning tool; and Random English words. For the comparison purpose, they used seven comparison features which includes BM25F with unigram and bigram characters, product, component, difference in versions and priorities, and type of bug report which includes enhancement or defect.

The author in [31] used the discourse based analysis of observed behavior, expected behavior, steps2reproduce to analyze the semantic and syntax of the bug report. They used the part of speech tagging and dependency parsing for finding the discourse patterns. They used Stanford CoreNLP to perform these tasks at the sentence and the paragraph level.

The author in [40] proposed an approach which they called as DURFEX where they used the feature extraction technique by analyzing the stack trace and converting them to a particular format. N-Grams were used to map the stack traces to generate feature vectors. TF-IDF was used to generate the package names. Along with the stack trace, they also used severity and component information of bug report to identify if the bug report is duplicate or not.

The author in [41] used the Longest Common Subsequence approach to find out the most similar substring between the two bug reports to create the feature vector for bug report. The author in [42] used the Hidden Markov Models (HMM) to classify the bug reports as duplicate or not. Their approach included first identifying the stack traces from bug reports. These stack traces were splitted into the duplicate groups. Each group was then separately trained by using HMM. The incoming bug reports were then compared with the trained HMM models to find the scores.

C. Machine Learning based

Machine Learning techniques involve the supervised, unsupervised and semi-supervised approaches. Supervised approaches involve the use of classifiers to either predict binary class problems or multi-class problems. Unsupervised approaches involves the use of clustering or associations where the data is unlabeled. Here we divide the works according to the approaches used:

1) *Supervised approaches*: The author in [21] proposed a new machine learning model after applying textual similarity to fine tune the parameters of BM25F which not only consider

the natural text but also product, component, priority and other aspects of the bug report as well. Similar to this work, [37] also used the SVM approach to learn the REP parameters. In order to address the issues of imbalancing of data, for the training purpose they reduced the number of non-duplicates. The author in [2] used the SVM along with the RBF kernel for the classification of comments of the bug reports. They classified the comments describing the root cause or solution or the bug phenomena as the useful class and rest are classified as less useful. For the classification purpose, they used the idf, status of bug, length of text and unigram features of the comments to create the vector for the learning purpose. The author in [15] in the same year conducted the research where they used the stack trace along with its structure to train the machine learning model. They used the Eclipse project, found that roughly 10 percent of the total corpora contained stack traces but they observed that it was very easy to detect if the bug report is duplicate or not for those 10 percent bug reports in comparison to others where the text needed to be analyzed for the same. They identified the duplicates even before the complete bug report writing was over. The author in [28] used the machine learning classifiers after applying the topic models to pair the bug reports according to the duplicate metrics and used ten-fold cross validation to test their classifiers. Along with ZeroR, NaiveBayes, Logistic Regression, C4.5, K-NN; they also used BootStrap Aggregating Technique to understand how their approach is working. [38] also uses the supervised learning approaches to find the semantic similarity between two texts after finding the feature sets in the vector form. For the binary classification, supervised learning they used the following methods for K-NN(K Nearest Neighbor, Linear SVM, RBF, SVM, Decision Tree, Random Forest and Naive Bayes.). The author in [39] used LibSVM after finding the features to find whether the bug report is duplicate or not.

The author in [32] first created the feature vector by finding the comparison between various features of the bug report and then undersampled the training data and used the Naive-Bayes, K-NN, Logistic Regression and C4.5 for the classification purpose.

2) *Unsupervised approaches*: In the supervised approaches, as it involves the training and the prediction of model depends upon the training data. Thus there is a need of large and good quality data. The author in [43] used the clustering based weighing approach to improve the performance of SVM Based approaches.

3) *Deep learning approaches*: Deep Learning is the part of machine learning which involves neural networks with the hidden layers involving the use of activation functions, max-pooling to train and test the bug reports. They also help extract the non-linear features. Deep Learning techniques in the context of duplicate bug report detection involves first the conversion of text into the numerical terms. Though there a number of ways to do so like One-Hot Encoding, Word Embedding, Vocabulary set creation, etc but word embedding is one of the most famous approach for this purpose.

The author in [1] used Siamese style Neural Network which used CNN and LSTM Based approach to detect whether the Bug Report is duplicate or not and find the top-k similar

bug reports. They considered 3 parts of the Bug Report for the purpose namely structure information like Component, Title and Description. They used Vanilla single layered neural network for the structured information.

$$\sigma(W.b)$$

They used Bi-LSTM for Title and CNN for Description so as to convert it to small text. For Description, they used Filters and Max-pooling layer. For finding top-k similar bug reports they used Max margin training loss objective function along with backpropagation and stochastic gradient. For Classification purpose, they used two layer neural network along with the softmax function. They used Adam optimizer and cross entropy as the loss function for finding the accuracy of the model.

The author in [5] used the word embedding and the convolutional neural networks(CNN) to find the similarity of bug reports and in turn to identify the duplicate bug reports. Word Embedding is the part of language modeling where the words and phrases are converted into features and vectors. Mainly Randomly-generated embedding, Glove and word2vec are used for word embedding. Convolution Neural Networks are feed-forward neural network. They used these techniques to capture both the syntactic and semantic features of the bug report to increase the performance of Natural language processing. Along with the CNN, they used the domain-specific features of the bug reports. For the activation function, hyperbolic tangent function is used by researchers.

The author in [34] proposed a tool POSTER which uses the high precision property of word-embedding and the high recall property of LDA to capture the semantic and syntactic information about the words in the text. Word-embedding was used to convert the text of bug report into the vector form and then the deep learning model was applied to learn the distribution of duplicate and non duplicate bug reports.

After studying the research work in this field, we find the strengths and limitations of the individual papers. Table II and Table III gives the tabular representation of strengths and limitations of the papers.

III. METHODOLOGY

We use the keywords and the citations of the searched papers to find out the relevant documents. We have used IEEE Xplore [50] Elsevier [51], ACL Anthology [52], Cornell University library, Springer [53], ACM [54] and Google Scholar [55] for finding out the concerned research papers. We have used only top 50 research articles for consideration as we observed after these searches the relevance of papers with the query started declining. Table IV describes the searching done to find the important papers in this field.

Table V gives the number of papers which we selected from various libraries for the inclusion into this paper.

Table VI gives the distribution of papers year-wise. The statistics help understand how the evolution of the research in this field has taken place by the research community.

After finding the Papers selected for the literature purpose, we divide them into categories according to the Approach they have used. Table VII gives the summary of papers in

terms of which approach was used, what type of Bug Report Categorization was done and the Corpus used for the purpose.

IV. EVALUATION MEASURES

For the evaluation how effective the approach is in terms of identifying the duplicate bug report,

- True Positive Rate: It is the number of actual duplicate bug reports which are classified as duplicate.
- True Negative Rate: It is the fraction of number of non-duplicate bug reports which are classified as non-duplicate.
- Accuracy: It is the proportion of true results to the total number of observations. It is not a very stable metrics. It works well for balanced-set of data only. In case of bug reports, the ratio of duplicate to non-duplicate bug reports is very skewed as number of duplicate bug reports are very less than the total number of non-duplicate bug reports.
- AUC (Area Under Curve) or ROC (Area Under Receiver Operating Characteristic Curve): It measures the capability of machine classifiers to discriminate between instances of certain class. It is the plotting between the True Positive Rate and False Positive Rate. It describes the trade-off between these two. It is also known as specificity. Closer the curve is to 0, lesser is the trade-off. It helps tell what is the probability that the classifier will choose the positive instances over the negative instances.
- Kappa Statistics: It tells how the model fits the data. It is the statistical measure which calculates the inter-rated agreement. If the judges are completely agreeing to one condition, the kappa value comes to 1 and if complete disagreement is there, the value becomes zero. It is used for agreement between the gold set summaries and the machine learning classifier.
- Precision: It is the ratio of number of bug reports which are duplicate and are classified as duplicates to the total number of bug reports which are classified as duplicates. $\text{Precision} = \frac{\text{True Positives}}{\text{True Positives} + \text{False Positives}}$
- Recall: It is the ratio of number of bug reports which are duplicate and are classified as duplicate to the number of duplicate bug reports available in the repository. $\text{Recall} = \frac{\text{True Positives}}{\text{True Positives} + \text{False Negatives}}$
- F-Measure: It is the harmonic mean of Precision and Recall. $\text{F Score} = \frac{2 * \text{Precision} * \text{Recall}}{\text{Precision} + \text{Recall}}$
- Fisher Score: It is one of the very popular measure of statistics. It is used to find out the effectiveness of different features for distinguishing between duplicate and non-duplicate bug reports. Here mean and standard deviation for the feature values of a particular class are used.

TABLE II. SUMMARY OF STUDIES: STRENGTHS AND LIMITATIONS

(Table Continues in Table III)

Author	Pros	Cons
[17]	Approach does not require training data. Thus can be used for any project.	Their approach could not achieve good results.
[19]	First available approach where the execution trace is also included along with the textual and categorical features of a bug report.	Considered only Recall as the evaluation Measure. More Evaluation measures would have helped give better insights. Their approach depends upon the external tools to collect the execution trace. The approach suffers from privacy issues also.
[20]	They analyzed how the individual feature performs. Thus gives the important features for further research.	Their approach requires the training data. Constructing the training data with large sample size is not an easy task. Very few datasets are available to be used for training for duplicate bug report detection.
[36]	First Paper for analyzing the GUI Bugs by transforming them into Event, Component and Requirement.	Approach does not consider the semantic information of the Bug Report.
[18]	Utilized the word-level information, handled super word features, expansion of short forms, and hyphenated phrases	N-grams introduces the unessential noisy features.
[22]	They used 54 features of bug report title and description along with the SVM to detect the duplicates.	Requires the computation of lot of features.
[21]	Use of BM25 approach along with the stochastic Gradient Descent helped introducing control weights to the features.	Lot of hand-crafted features need to be considered.
[37]	Introduced the concept of relative similarity among the Bug Reports. Approach also addressed the imbalancing problem for Machine Learning .	Only SVM is considered for learning from features.
[44]	They used the longest common subsequence approach which helps preserve the word order. Word ordering is usually neglected by IR approaches.	As the approach is based upon the word ordering, the presence of synonyms and alternate spellings create the problem
[23]		They did not considered the clustering information to their approach.
[2]	First paper where along with just the information from Bug Report, comments and user profile are also considered.	Evaluated only on Naive Bayes, Decision Tree and SVM. More Classifiers can also be considered. More Similarity Measures can be used to improve the feature scores.
[27]	Approach is generic and thus can be used for any software repository.	Their approach does not display the results in ordered manner.
[15]	They used only Stack Traces to find the duplicate Bug Reports. Thus even if the Bug Report is not written properly, it will not impact the performance of the approach.	Very few Bug Reports contain the stack Trace. Thus limiting the approach.
[45]	Achieved the good results with very simple approaches LSI and VSM	Their approaches are experimented on small dataset. Thus results can not be taken as for benchmark.
[46]	They added the contextual information to create the topics which improved their results a lot.	More features can be included for improving the results.
[14]	The approach uses clustering, thus requires no training data	Synonyms and phrases with similar meaning needs to be considered to improve the accuracy of the approach.
[43]	They used the cluster information to their TF-IDF weighing mechanism.	
[29]	The approach does not require training data and can be easily generalized to any project. Rather than just proving their approach, they integrated their approach to the existing bug tracking system and observed the results.	Their approach only used conventional Vector Space Model (VSM) when their exists many other approaches which give better results than the VSM.
[28]	Along with the contextual information and the existing approaches till their time, their approach also used another metric known as Bootstrap Aggregation which gave better results than previous ones.	The approach does not consider for Top-k duplicate bug reports.
[47]	The approach used the contextual information of software engineering for the duplicate bug report detection. The approach reduced the time and effort to detect the duplicate bug report	The contextual information used was software-level specific not the project-specific.
[30]	They involved the use of both the Classification and the Clustering to detect the duplicates. Classification helps get the topic definition while Clustering helps evaluate the degree of correlation between the topics.	Pre processing requires the intervention of experts. Approach first use classification then clustering, Classification requires the goo
[33]	Their paper not only included the techniques to find the Bug Reports which resembles the textual similarity but also those which do not exhibit textual similarity.	The approach needs the properly labeled triaged dataset as it involves the machine learning approach.
[31]	Discourse Based analysis to explore the Observed Behavior, Expected Behavior and Steps to Reproduce helped improve the NLP Based Techniques	Noisy data and typographical mistakes imposes the challenge
[48]	Reduced the machine learning bias by inclusion of Fidelity Loss Function.	Only includes statistical and textual Similarity Features. Semantic Information is not included. Considered the VSM approach. Approach can be evaluated over other models also.

- Mean Reciprocal Rank: This approach is used by [35] to find the rank of correct answer. As mentioned in their paper, as this approach supports only one correct result, this evaluation measure is not very appropriate for duplicate bug report context. The reason is that for a bug report, many duplicate bug reports can exist. It has no lower limit. This metric gives the mean of reciprocal ranks of the correct results. If the rank of correct result is low, then a problem appears.
- Mean Average Precision: It is based on the ranks of correct results. Here the multiple matches are allowed. Average Precision is calculated for each query and then mean is taken for all the queries.

Table VIII gives the tabular representations of various metrics being used by researchers for evaluating the effectiveness of their approach.

V. FUTURE DIRECTIONS

- Need of testing the approaches with large and different dataset: Almost in all the papers of duplicate bug report detection, few includes [38] [25] [34] [37], mentioned the need of testing their approach with the large dataset to find the reliability of the approaches. They also mentioned the need to extensively train the approaches on various types of software projects.
- Extensive Training and Tuning for Deep Learning models: In a paper by [1], they mentioned the need of performing the extensive training for Deep Learning models by involving the use of various approaches like batch normalization. As in DL Based Models, hyperparameters need to be trained for the learning process. Thus need to fine tune the parameters is also required. For ML and DL Based Models, the

TABLE III. SUMMARY OF STUDIES: STRENGTHS AND LIMITATIONS: CONTINUATION OF TABLE 6 SUMMARY

Author	Strengths	Limitations
[1]	Use of LSTM and CNN Models helped achieve highly accurate duplicate bug reports. No handcrafted features were used by them.	The approach needs to be tested with large training set and the attention mechanism should also be added for improving the results.
[34]	Inclusion of word embedding with deep learning improved the results significantly very high.	The approach only uses simple Deep Learning Model along with the Word Embedding while the RNN and CNN gives better results in terms of syntax and semantic aspects. The model includes two step training.
[5]	Simple Convolutional Model is used for learning the long descriptions of the Bug Report.	Domain-specific features are not used for the approach which limits its results.
[35]	Instead of giving the top-k results, their approach continuously queries the similar bug reports and help be alerted before submitting the bug report. Thus the approach helps users stop at any time.	As the approach uses the words for retrieving the results, many times because of the use of synonyms and other similar words, the results do not come effectively.
[24]	Usually the approaches which have used LDA, used number of topics as the paramter. But in their paper,they studied the parameter tuning techniques which included Genetic Algorithms, Differential Evolution, Particle Swarm Optimization, Simulated Annealing and Random Search. Thus it opens the area of improving LDA to achieve better results.	There are many more meta heuristics which are available which can be explored further to see how the LDA models works with them.
[42]	The approach not only helps in detecting the similar bug reports but also helps assign the new bug report to the appropriate group of previous Bug Reports.	Their approach does not work for those bug reports which do not have prior duplicates in the repository. Their approach involves the analysis of Stack Trace Information but only few bug reports contain Stack Trace, thus impacts the validation of efficiency of the approach.
[49]	Query reformulation Strategy used by them is independent of other bug reports other than itself.	Query Reformulation does not consider the description of Bug Report. It only considers the Title and Observed Behavior for finding the duplicates.
[41]	They included all the temporal, categorical, textual and contextual information of the bug report to detect the duplicates. It is the first paper where they used the Manhattan Distance Similarity Measure and found that the accuracy has improved because of this measure.	Use of domain-specific knowledge can improve the accuracy of the model. More work on reducing the search space for feature calculation is also needed.

TABLE IV. KEYWORDS USED FOR SELECTING THE RESEARCH PAPERS

Application	Strings Used
Duplicate Bug Report: NLP	Duplicate bug report detection using Natural Language Processing, Duplicate Bug Report, Duplicate Bug Report NLP, Bug Report
Duplicate Bug Report: Information Retrieval	Duplicate Bug Report Detection: Information Retrieval, Duplicate Bug, Bug Report
Duplicate Bug Report: Machine Learning	Duplicate Bug Reports Machine Learning, Duplicate Bug, Bug Report, Bug Report Duplicate
Duplicate Bug Report: Deep Learning	Deep Learning for Duplicate Bug Reports, Duplicate Bug Report

TABLE V. PAPER DISTRIBUTION: SOURCE WISE

Link	No of Papers	Duplicate Detection: NLP	Duplicate Detection: IR	Duplicate Detection: ML	Duplicate Detection: DL	Total Used in Paper
IEEE	28	11	9	3	2	28
Springer	7	1	3	2	0	7
ACM	6	2	1	2	1	6
ACL Anthology	2	1	0	1	0	1
Elsevier	2	0	0	2	0	2
Total Papers found	45	15	13	10	3	45

TABLE VI. PAPER DISTRIBUTION: YEAR WISE

Year	No Of Papers
2008	3
2009	2
2010	2
2011	2
2012	6
2013	6
2014	6
2015	3
2016	5
2017	3
2018	3
2019	4
Total	45

approaches need to be trained on large datasets for finding their efficiencies.

- The author in [3], mentioned the following things to take care of for avoiding bug reports duplication:
 - Analyze the submitter profile while analyzing the bug report.
 - Use of controlled vocabulary for the bug report writing.

- Initial display of Related Search Results
- Automatic Duplicate Bug Report analysis for the display of only top few duplicate bug reports
- Visualization of bug reports
- The author in [26] mentioned the need to reformulate and expand the queries to get the better results for duplicate bug report detection.
- Even though lot of works have been done in the field of machine learning, properly addressing the issue of imbalanced data is also very important. The author in [37] modified the training set by reducing the number of non-duplicate instances in the training dataset.
- Need to integrate the approaches to the bug reporting management system is also the need of time to reduce the efforts of Triager.
- Most of the works have used Title and Description for identifying the duplicate bug reports, in a paper by [2], they used the comments also to identify the potential duplicate bug reports. There is a need to include all the

TABLE VII. SUMMARY OF STUDIES

Author	Major Approach Used	Type of Duplicate Bug Report Categorization	Corpus	Main Techniques Use
[17]	Natural Language Based	Top-k	Sony Mobile Ericsson Mobile Communications	Similarity Measures, TF
[19]	NLP Based	Top-k	Eclipse, Firefox	Similarity Measures, TF-IDF
[20]	NLP Based	Top-k	Mozilla [56]	Cosine Similarity, TF
[36]	NLP	Top-k		Event Extraction, Longest Common Subsequence(LCS)
[18]	NLP Based	Top-k	Eclipse	Unigram and Bigrams
[22]	Machine Learning Based	Prevention	Openoffice, Firefox, Eclipse	SVM
[21]	Information Retrieval	Top-k	Eclipse, Mozilla, Openoffice	BM25F, Gradient Descent
[37]	Machine-Learning Based	Top-k	Mozilla	SVM
[44]	NLP	Top-k	Eclipse, Firefox	Longest Common Subsequence
[23]	NLP	Top-k	Apache, AgroUML, SVN	BM25
[2]	ML(SL)	Top-k	MeeGo	SVM with RBF Kernel, LDA, Jensen-Shanon, symmetric KL Divergence
[27]	NLP	Top-k	BlackBerry	BM25F+ Smoothing techniques
[15]	NLP	Top-k	Eclipse	TF-IDF
[45]	IR	Top-k	Google Chrome Browser	VSM, LSI
[46]	IR	Prevention	Android [57]	BM25F, LDA
[14]	ML	Top-k	Eclipse, Mozilla, Open Office	K-Means
[43]	ML(USL)	Top-k	Apache, AgroUML,SVN	
[29]	IR	Top-k	-	Vector Space Model
[28]	IR+ ML	Prevention	Android	ZeroR, Naive Bayes, Logistic Regression, C4.5, K-NN, Bagging: REP Tree
[47]	NLP + ML	Top-k	Eclipse, OpenOffice, Mozilla	BM25F
[30]	IR+ML	Top-k	Apache, Eclipse, Mozilla	Naive Bayes, LDA
[33]	IR + ML	Top-k	Chrome Dataset	Vector Space Model, Cosine Similarity, TF-IDF, K-Mean Clustering, Nearest Neighbor Classifier
[48]	IR	Top-k	Eclipse	LDA, Similarity Calculation(Cosine)
[31]	NLP	Top-k	9 different software projects from Github and Jira	SVM+Discourse-Based+Dependency Parsing
[1]	ML(DL)	Top-k, Classification	Open Office, Eclipse, NetBeans	CNN+LSTM +Word Embedding+Feed Forward Neural Network
[34]	DL	Top-k	Firefox, Openoffice	Word Embedding, Deep Learning Feed Forward Neural Network
[5]	DL	Top-k	Hadoop, HDFS, MapReduce, Spark	Word Embeddings, Convolutional Neural Networks
[35]	IR+NLP	Prevention	[58]	LDA, LSA, TF-IDF, BM25F
[24]	IR	Top-k	Bench4BL	LDA with GA, DE, PSO,SA,Random Search
[42]	NLP	Top-k	Firefox and Gnome	Hidden Markov Model
[49]	NLP	Top-k	Accumulo,Ambari, ActiveMQ, Cassandra, Cordova, Continuum, Drill, Eclipse, Groovy, Hadoop, Hbase, Hive, Maven, Firefox, My Faces, OpenOffice, PDFBox, Spark, Wicket, Struts	Ontology
[41]	NLP	Top-k	Android,Mozilla Eclipse, Open Office	LCS , N-gram

aspects of a bug report including comments to solve this problem.

- The author in [4] observed that finding those reports which are textually similar requires less effort by developers but the reports which does not exhibit similar textual similarity are more difficult to be identified by developer. Thus more work is required to identify the approach where the automatic techniques identify the issue reports which do not or exhibit less textual similarity.

VI. CONCLUSION

Duplicate Bug Report Detection is one of the very important and frequent task that is performed on the daily-basis by a person called triager. It is a tedious and a time-consuming activity apart from the main software development and other

tasks. In this paper, we have identified the main works that have been performed for this problem. We classified the works into the Natural Language Processing Based, Information-Retrieval Based, Machine Learning Based and Deep Learning Based. We systematically mentioned all the works in the classified manner. We also present the statistics about this work which gives an insight about how much work has been done in this field. We have mentioned almost all the popular evaluation measures which have been used by various researchers. We have also mentioned the Strengths and Limitations of all the major works in this field along with their experimental results. This will enable the researchers to easily identify the gaps and compare their results. Apart from mentioning just the works done, we also present the challenges and pointers for the future research in this field.

TABLE VIII. RESULTS FROM RESEARCHES

Author	Extension of Re-search	Evaluation Measure1	Evaluation Measure2	Any Other
[20]: Mozilla		TPR: 8 %	TNR: 100 %	Harmonic: 15%
[37]: Mozilla		TPR: 24%	TNR: 91%	Harmonic: 39%
[14]: Mozilla		TP Rate: 27%	TN Rate: 86%	Harmonic: 41%
[21]		MAP(BM25Fext): OpenOffice-45.21 %, Mozilla-46.22%, Eclipse-53.21%, Large Eclipse-44.22%	Recall: Top-1: 37%, Top-20: 71%	
[44]		Recall: Firefox- 73% (Top-20), Eclipse - 85%		
[5]: Spark Dataset		F Measure: Random: 0.964, GloVe: 0.944, word2Vec:925	Accuracy: Random: 0.951, GloVe: 0.935, word2Vec: 0.920	
[18]		Recall Rate: 0.2 (Top-1), 0.35 (Top-5), 0.49 (Top-20)		
[23]		Recall Rate:0.112(Top-1), 0.2 (Top-5), 0.3 (Top-20)		
[34]		Recall Rate: 0.25 (Top-1), 0.5 (Top-5), 0.7 (Top-20)		
[1]		Recall: 80% (Top-20)	Accuracy: 90 % (Top-20)	
[30]: Classification +LDA		Accuracy: Naive Bayes: 38.74(T-1), 46.39 (T-2), 60.52 (T-3) Bayesian Network: 27.93(T-1), 36.98 (T-2), 47.43(T-3) C4.5: 41.31(T-1), 48.5 (T-2), 60.52 (T-3) SVM: 22.96(T-1), 41.33 (T-2), 43.72 (T-3)		
[22] Textual and Categorical		Accuracy: 80%(ZeroR), 79.655% (Naive Bayes), 88.125% (Logistic Regression), 92.105% (C4.5), 91.55 %(K-NN)	AUC: 0.500(ZeroR), 0.904(Naive Bayes), 0.788(Logistic Regression), 0.888(C4.5), 0.7561%(K-NN)	Kappa: 0.0(ZeroR), 0.3508(Naive Bayes), 0.5967(Logistic Regression), 0.7553(C4.5), 0.0.7561(K-NN)
[46]: Textual, Categorical and Labeled-LDA	[22]	Accuracy: 80%(ZeroR), 79.655% (Naive Bayes), 88.125% (Logistic Regression), 92.105% (C4.5), 91.55 %(K-NN)	AUC: 0.500(ZeroR), 0.904(Naive Bayes), 0.788(Logistic Regression), 0.888(C4.5), 0.7561%(K-NN)	Kappa: 0.0(ZeroR), 0.3508(Naive Bayes), 0.5967(Logistic Regression), 0.7553(C4.5), 0.0.7561(K-NN)
[47]: Labelled LDA, Android Textbook	[46]	Accuracy: 80%(ZeroR), 87.01% (Naive Bayes), 94.22% (Logistic Regression), 92.75% (SVM), 94.22 %(C4.5)	Kappa: 0.0(ZeroR), 0.583(Naive Bayes), 0.753(Logistic Regression), 0.750(SVM), 0.799(C4.5)	
[28]	[46]	Accuracy: 80%(ZeroR), 93% (Naive Bayes), 94.5% (Logistic Regression), 94.7% (C4.5), 94.75 %(K-NN), 95.17 (Bagging)	AUC: 0.5(ZeroR), 0.958(Naive Bayes), 0.972(Logistic Regression), 0.941(C4.5), 0.955 %(K-NN), 0.977(Bagging)	Kappa: 0.0(ZeroR), 0.77(Naive Bayes), 0.824(Logistic Regression), 0.832(C4.5), 0.830(K-NN), 0.845(Bagging)
[49]		Recall: Observed Behavior: 56.6 %, Bug Title: 59.6%, Title +Observed: 78%		
[41]		Precision: Mozilla-97.14, Android-99.12, Eclipse-96.86, Open Office-98.45	Recall: Mozilla-97.78, Android-99.45, Eclipse-90.12, Open Office-97.59	Accuracy: Mozilla-97.14, Android-99.47, Eclipse-96.58, Open Office-97.10 %

REFERENCES

[1] J. Deshmukh, A. M. S. Podder, S. Sengupta, and N. Dubash, "Towards accurate duplicate bug retrieval using deep learning techniques," 09 2017, pp. 115–124.

[2] L. Feng, L. Song, C. Sha, and X. Gong, "Practical duplicate bug reports detection in a large web-based development community," in *Web Technologies and Applications*, Y. Ishikawa, J. Li, W. Wang, R. Zhang, and W. Zhang, Eds. Berlin, Heidelberg: Springer Berlin Heidelberg, 2013, pp. 709–720.

[3] Y. C. Cavalcanti, P. A. da Mota Silveira Neto, D. Lucrédio, T. Vale, E. S. de Almeida, and S. R. de Lemos Meira, "The bug report duplication problem: an exploratory study," *Software Quality Journal*, vol. 21, no. 1, pp. 39–66, Mar 2013. [Online]. Available: <https://doi.org/10.1007/s11219-011-9164-5>

[4] W. S. Mohamed Sami Rakha and A. E. Hassan, "Studying the needed effort for identifying duplicate issues." *Empir Software Eng*, vol. 21, pp. 1960 – 1989, 2016.

[5] Q. Xie, Z. Wen, J. Zhu, C. Gao, and Z. Zheng, "Detecting duplicate bug reports with convolutional neural networks," in *2018 25th Asia-Pacific Software Engineering Conference (APSEC)*, Dec 2018, pp. 416–425.

[6] A. Lamkanfi, J. Perez, and S. Demeyer, "The eclipse and mozilla defect tracking dataset: a genuine dataset for mining bug information," in *MSR '13: Proceedings of the 10th Working Conference on Mining Software Repositories, May 18–19, 2013. San Francisco, California, USA*, 2013.

[7] [Online]. Available: <https://bugzilla.mozilla.org>

[8] [Online]. Available: <https://bugs.eclipse.org/bugs/describecomponents.cgi?product=Platform>

[9] [Online]. Available: <https://bugs.eclipse.org/bugs/describecomponents.cgi?product=JDT>

[10] [Online]. Available: <http://issues.apache.org/jira/browse/CASSANDRA>

[11] [Online]. Available: <http://issues.apache.org/jira/browse/MAPREDUCE>

[12] [Online]. Available: <http://issues.apache.org/jira/browse/HDFS>

[13] [Online]. Available: <http://issues.apache.org/jira/browse/SPARK>

[14] R. P. Gopalan and A. Krishna, "Duplicate bug report detection using clustering," in *Proceedings of the 2014 23rd Australian Software Engineering Conference*, ser. ASWEC '14. Washington, DC, USA:

- IEEE Computer Society, 2014, pp. 104–109. [Online]. Available: <https://doi.org/10.1109/ASWEC.2014.31>
- [15] J. Lerch and M. Mezini, “Finding duplicates of your yet unwritten bug report,” 03 2013, pp. 69–78.
- [16] J. He, N. Nazar, J. Zhang, T. Zhang, and Z. Ren, “Prst: A pagerank-based summarization technique for summarizing bug reports with duplicates,” *International Journal of Software Engineering and Knowledge Engineering*, vol. 27, pp. 869–896, 06 2017.
- [17] P. Runeson, M. Alexandersson, and O. Nyholm, “Detection of duplicate defect reports using natural language processing,” in *29th International Conference on Software Engineering (ICSE’07)*, May 2007, pp. 499–510.
- [18] A. Sureka and P. Jalote, “Detecting duplicate bug report using character n-gram-based features,” in *2010 Asia Pacific Software Engineering Conference*, Nov 2010, pp. 366–374.
- [19] X. Wang, L. Zhang, T. Xie, J. Anvik, and J. Sun, “An approach to detecting duplicate bug reports using natural language and execution information,” in *2008 ACM/IEEE 30th International Conference on Software Engineering*, May 2008, pp. 461–470.
- [20] N. Jalbert and W. Weimer, “Automated duplicate detection for bug tracking systems,” in *2008 IEEE International Conference on Dependable Systems and Networks With FTCS and DCC (DSN)*, June 2008, pp. 52–61.
- [21] C. Sun, D. Lo, S. Khoo, and J. Jiang, “Towards more accurate retrieval of duplicate bug reports,” in *2011 26th IEEE/ACM International Conference on Automated Software Engineering (ASE 2011)*, 2011, pp. 253–262.
- [22] C. Sun, D. Lo, X. Wang, J. Jiang, and S. Khoo, “A discriminative model approach for accurate duplicate bug report retrieval,” in *2010 ACM/IEEE 32nd International Conference on Software Engineering*, vol. 1, May 2010, pp. 45–54.
- [23] C. Yang, H. Du, S. Wu, and I. Chen, “Duplication detection for software bug reports based on bm25 term weighting,” in *2012 Conference on Technologies and Applications of Artificial Intelligence*, 2012, pp. 33–38.
- [24] A. Panichella, “A systematic comparison of search algorithms for topic modelling—a study on duplicate bug report identification,” in *Search-Based Software Engineering*, S. Nejati and G. Gay, Eds. Cham: Springer International Publishing, 2019, pp. 11–26.
- [25] Y. Song, X. Wang, T. X. L. Zhang, and H. Mei, “Jdf: Detecting duplicate bug reports in jazz,” 2010.
- [26] N. Kaushik and L. Tahvildari, “A comparative study of the performance of ir models on duplicate bug detection,” in *2012 16th European Conference on Software Maintenance and Reengineering*, March 2012, pp. 159–168.
- [27] M. Amoui, N. Kaushik, A. Al-Dabbagh, L. Tahvildari, S. Li, and W. Liu, “Search-based duplicate defect detection: An industrial experience,” in *2013 10th Working Conference on Mining Software Repositories (MSR)*, 2013, pp. 173–182.
- [28] N. Klein, C. S. Corley, and N. A. Kraft, “New features for duplicate bug detection,” in *Proceedings of the 11th Working Conference on Mining Software Repositories*, ser. MSR 2014. New York, NY, USA: ACM, 2014, pp. 324–327. [Online]. Available: <http://doi.acm.org/10.1145/2597073.2597090>
- [29] F. Thung, P. S. Kochhar, and D. Lo, “Dupfinder: Integrated tool support for duplicate bug report detection,” 2014.
- [30] C. Jingliang, M. Zhe, and S. Jun, “A data-driven approach based on lda for identifying duplicate bug report,” in *2016 IEEE 8th International Conference on Intelligent Systems (IS)*, 2016, pp. 686–691.
- [31] O. Chaparro, “Improving bug reporting, duplicate detection, and localization,” in *2017 IEEE/ACM 39th International Conference on Software Engineering Companion (ICSE-C)*, 2017, pp. 421–424.
- [32] A. Hindle, A. Alipour, and E. Stroulia, “A contextual approach towards more accurate duplicate bug report detection and ranking,” *Empirical Software Engineering*, vol. 21, no. 2, pp. 368–410, Apr 2016. [Online]. Available: <https://doi.org/10.1007/s10664-015-9387-3>
- [33] P. Anjaneyulu, G. Sarbendu, A. Gopichand, P. B. Satya, and P. Srinivas, “An Analytics-Driven Approach to Identify Duplicate Bug Records in Large Data Repositories.” Cham: Springer International Publishing, 2016, pp. 161–187. [Online]. Available: https://doi.org/10.1007/978-3-319-31861-5_8
- [34] A. Budhiraja, K. Dutta, R. Reddy, and M. Shrivastava, “Poster: Dwen: Deep word embedding network for duplicate bug report detection in software repositories,” in *2018 IEEE/ACM 40th International Conference on Software Engineering: Companion (ICSE-Companion)*, May 2018, pp. 193–194.
- [35] A. Hindle and C. Onuczko, “Preventing duplicate bug reports by continuously querying bug reports,” *Empirical Software Engineering*, vol. 24, no. 2, pp. 902–936, Apr 2019. [Online]. Available: <https://doi.org/10.1007/s10664-018-9643-4>
- [36] N. K. Nagwani and P. Singh, “Bug mining model based on event-component similarity to discover similar and duplicate gui bugs,” in *2009 IEEE International Advance Computing Conference*, 2009, pp. 1388–1392.
- [37] Y. Tian, C. Sun, and D. Lo, “Improved duplicate bug report identification,” in *2012 16th European Conference on Software Maintenance and Reengineering*, March 2012, pp. 385–390.
- [38] A. Lazar, S. Ritchey, and B. Sharif, “Improving the accuracy of duplicate bug report detection using textual similarity measures,” in *Proceedings of the 11th Working Conference on Mining Software Repositories*, ser. MSR 2014. New York, NY, USA: ACM, 2014, pp. 308–311. [Online]. Available: <http://doi.acm.org/10.1145/2597073.2597088>
- [39] A. Tsuruda, Y. Manabe, and M. Aritsugi, “Can we detect bug report duplication with unfinished bug reports?” in *2015 Asia-Pacific Software Engineering Conference (APSEC)*, Dec 2015, pp. 151–158.
- [40] K. K. Sabor, A. Hamou-Lhadj, and A. Larsson, “Durfex: A feature extraction technique for efficient detection of duplicate bug reports,” in *2017 IEEE International Conference on Software Quality, Reliability and Security (QRS)*, 2017, pp. 240–250.
- [41] B. S. Neysiani and S. Morteza Babamir, “Improving performance of automatic duplicate bug reports detection using longest common sequence : Introducing new textual features for textual similarity detection,” in *2019 5th Conference on Knowledge Based Engineering and Innovation (KBEI)*, 2019, pp. 378–383.
- [42] N. Ebrahimi, A. Trabelsi, M. S. Islam, A. Hamou-Lhadj, and K. Khanmohammadi, “An hmm-based approach for automatic detection and classification of duplicate bug reports,” *Information and Software Technology*, vol. 113, pp. 98 – 109, 2019. [Online]. Available: <http://www.sciencedirect.com/science/article/pii/S095058491930117X>
- [43] M. Lin and C. Yang, “An improved discriminative model for duplication detection on bug reports with cluster weighting,” in *2014 IEEE 38th Annual Computer Software and Applications Conference*, 2014, pp. 117–122.
- [44] S. Banerjee, B. Cukic, and D. Adjeroh, “Automated duplicate bug report classification using subsequence matching,” in *2012 IEEE 14th International Symposium on High-Assurance Systems Engineering*, 2012, pp. 74–81.
- [45] I. Chawla and S. K. Singh, “Performance evaluation of vsm and lsi models to determine bug reports similarity,” in *2013 Sixth International Conference on Contemporary Computing (IC3)*, 2013, pp. 375–380.
- [46] A. Alipour, A. Hindle, and E. Stroulia, “A contextual approach towards more accurate duplicate bug report detection,” 05 2013, pp. 183–192.
- [47] K. Aggarwal, T. Rutgers, F. Timbers, A. Hindle, R. Greiner, and E. Stroulia, “Detecting duplicate bug reports with software engineering domain knowledge,” in *2015 IEEE 22nd International Conference on Software Analysis, Evolution, and Reengineering (SANER)*, 2015, pp. 211–220.
- [48] J. Zou, L. Xu, M. Yang, M. Yan, D. Yang, and X. Zhang, “Duplication detection for software bug reports based on topic model,” in *2016 9th International Conference on Service Science (ICSS)*, 2016, pp. 60–65.
- [49] O. Chaparro, J. M. Florez, U. Singh, and A. Marcus, “Reformulating queries for duplicate bug report detection,” in *2019 IEEE 26th International Conference on Software Analysis, Evolution and Reengineering (SANER)*, 2019, pp. 218–229.
- [50] [Online]. Available: <https://ieeexplore.ieee.org/>
- [51] [Online]. Available: <https://www.elsevier.com>
- [52] [Online]. Available: <http://aclweb.org/anthology/>
- [53] [Online]. Available: <https://link.springer.com>
- [54] [Online]. Available: <https://dl.acm.org/>

- [55] [Online]. Available: <https://scholar.google.co.in/>
- [56] [Online]. Available: <https://bugzilla.mozilla.org/buglist.cgi?quicksearch=Mozilla>
- [57] [Online]. Available: <https://source.android.com/setup/contribute/>
- [58] [Online]. Available: <https://archive.org/details/2016-04-09ContinuousQuery/report-bugs>

A Blockchain-based Crowdsourced Task Assessment Framework using Smart Contract

Linta Islam¹, Syada Tasmia Alvi², Mafizur Rahman³, Ayesha Aziz Prova⁴,
Md. Nazmul Hossain⁵, Jannatul Ferdous Sorna⁶, Mohammed Nasir Uddin⁷
Dept. of CSE, Jagannath University, Dhaka, Bangladesh^{1,2,5,7}
Dept. of CSE, East West University, Dhaka, Bangladesh^{3,6}
Dept. of CSE, Central Women's University, Dhaka, Bangladesh⁴

Abstract—In today's world, crowdsourcing is a highly rising paradigm where mass people are engaged in solving a problem. Though this system has a lot of advantages, yet people are not interested in working on this platform. Thus, we survey people to find out the constraints of this platform and the main reason behind their unwillingness. 59% of people think that security and privacy is the major challenge of a crowdsourcing platform. Therefore, we propose a blockchain-based crowdsourced system which can provide security and privacy to the user's information. We also have used a smart contract to verify the task so that the users get the exact output that they have wanted. We implemented our system and compared the performance with the existing systems. Our proposed approach outperforms the current methods in terms of cost and properties.

Keywords—Blockchain; crowdsourcing; task allocation; smart contract

I. INTRODUCTION

Crowdsourcing is a marketing platform where a large task is distributed into a collection of small pieces and providing those pieces into a large group of workers [1]. It is one kind of sourcing model where individuals or organizations get services, goods, and ideas from a huge group of participants. Therefore, the workers get some incentives based on their respective work [2]. Crowdsourcing can be done by using smartphones, wearables, computers, etc. devices. Among them, mobile crowdsourcing is one of the powerful approach that can consolidate the wisdom of humans into mobile computations for solving the problem [3]. For collecting data ambient light, proximity, location, movement, noise, etc. sensors are needed and every smartphone has now those sensors like GPS, accelerometer, microphone, etc. Therefore, mobile crowdsourcing can be utilized for collecting unstructured data from heterogeneous sources, industrial applications as well as for subjective assessments with the help of mobile sensors [4].

Blockchain is known as a distributed database system that can store financial transactional records of the people in a linear set of blocks [5]. Each of the blocks is linked with the previous blocks. As it is a decentralized system, therefore there will be no central administrator or third party organization for necessary work. The participants can decide as there is no intermediary in the system [6]. Users have the capability of controlling their transactions. They can delete, rewrite, or change their information easily. As there will be a unique id for each user, hence there is no chance of data losing or hacking [7]. Blockchain has a crypto contract or a smart contract script that included unique addresses, executable functions,

and variables. Therefore, there is a controlling over the digital currency transactions. It is one kind of computer code that runs on the blockchain system as an agreement among two people. Based on the agreement the transactions will happen in the smart contract. Thus, it will be added to the public database which can't be changed. Then the blockchain will process the transactions that happen in the smart contract.

As crowdsourcing is getting popular day by day, still the users have to face numerous problems like resource limitation, privacy and security, spatio-temporal issues, etc. [8]. The main problem is there is no confidentiality [9]. Hence, crowdsourcing with blockchain can be a useful system to resolve those problems fruitfully. As the smart contract will increase the sustainability of the information with a data-centric approach [10]. It can endure the people accountable not only for front end performance but also for back end sustainability. Hence, the user's privacy will be maintained and they can get all the facilities in a useful manner.

Our work aims to implement a crowdsourced task management model employing blockchain to provide security and privacy of the participants along with the task. We have used the smart contract for fairness of the task assessment. The participants can also submit rating points, which helps the coordinator to select the task contributors. As we are storing the task information in the blockchain network, it is difficult for malevolent users to modify any stored information.

The remainder of the paper is organized as follows. Section II overviews the related works. Section III illustrates the motivating scenario of this work. Section IV presents an overview of the system model and defines the problem. Section V describes the details of the proposed blockchain-based crowdsourcing framework. Sections VI and VII evaluates the approach by property analysis and shows the experiment results. Section VIII concludes the paper and highlights some future work.

II. RELATED WORKS

The insufficient amount of research has been done in the field of the blockchain-based crowdsourced system. Feng and Yan [11] presented a distributed blockchain-based system called MCS-Chain that uses consensus mechanism for block generation. This system also has less computational overhead, and it solves the centralization problems. CrowdBC [12] is a decentralized crowdsourcing framework which is developed using the blockchain network. This framework can provide a

user's privacy with a low service fee. CrowdSFL [13] used a re-encryption algorithm to preserve the privacy of the users. The authors also used blockchain-based crowdsourcing in this model. Lu et al. proposed a decentralized crowdsourcing system named ZebraLancer [14]. This system can also provide confidentiality and anonymity alike CrowdSFL. BPTM [15] is a blockchain-based task matching system that provides data confidentiality and anonymity. It also offers a secure and reliable task matching protocol using a smart contract. However, each of these models has several limitations. Some of them did not mention reputation values like other models, and others did not provide any security analysis. Thus, we tried to mitigate the problems of the existing works in our proposed model.

III. MOTIVATION SCENARIO

Before implementing this system, we asked 362 students of Jagannath University and East-West University that whether they are comfortable to use online task participation system and whether they are facing any difficulties while using them. They also have been asked to note down the issues that need to be solved to provide an efficient task participation framework. In this survey, around 59% of people chose the security and privacy of their data as a significant issue. Less than 25% of people believe that the quality of the system and lack of knowledge to use the system as the latter issue. Several people consider that limited resource and location of the task participation is another issue for their unwillingness to participate in this task provisioning. A few numbers of people also believe that online task participation systems are less beneficial than onsite ones. The survey result is represented by a pie chart in Fig. 1.

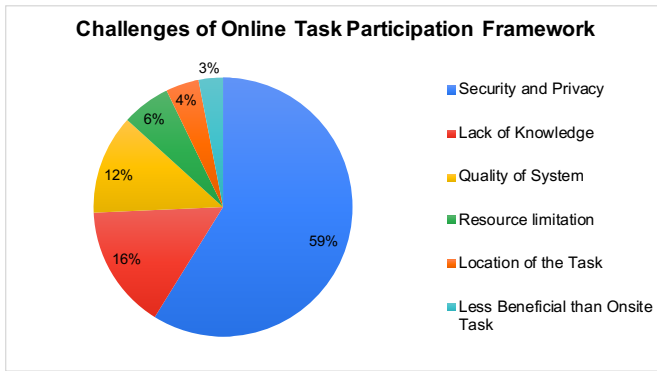


Fig. 1. Challenges of Online Task Participation Framework.

IV. SYSTEM OVERVIEW

This section represents a novel formal model for blockchain based crowdsourcing. In this framework, the crowdsourcing tasks could be irregular and dynamic based on both location and time. We discuss the fundamental concepts of the proposed system and illustrates the workflow diagram briefly.

A. Components of the System Model

In this section, we describe the components of our proposed system. As shown in Fig. 2, the system is composed of

four basic components. These are user block, crowdsourced marketplace, smart contract and blockchain. We will discuss each components thoroughly in this section.

Definition 1. User Block: A mobile crowdsourcing system is consists of several types of participants. In our previous work, we have classified the participants into three categories namely contributors, task requesters, and coordinators [16]. However, in this research work, we have included all the users in the user block of our system model. The users can reside in this block if they own any smart devices, including smartphone, smartwatch, notebooks. All of the users will have to take the authorization power to use this system. This procedure can be accomplished efficiently by registering themselves in the system. We denoted a user by u which is a tuple of $\langle uid, loc_u, t_u, sts_u, urts_u, Q_u \rangle$ where

- uid is a unique user ID
- loc_u is the latest recorded location of the user u
- t_u is the latest time at which the user u participated in any crowdsourced task
- sts_u is the current availability status of the user u
- $urts_u$ is the registration time of the user u
- SKL_u is a tuple $\langle skl_1, skl_2, \dots, skl_n \rangle$, where each skl_i denotes a skill of the user u (e.g. video editing, photo tagging, content writing, website development).
- Q_u is a tuple $\langle q_1, q_2, \dots, q_n \rangle$, where each q_i denotes a QoS property of the user u (e.g. bandwidth, reputation value, coverage distance, latency).

In this user block, there can be two types of users according to their role in this proposed system, namely, task requester and contributor. In our previous paper [17], we have defined these two types of users briefly. The user who posts a task request to the crowdsourced marketplace is called task requester. Any user who will accomplish the task by fulfilling all the requirements is called contributor. Thus, in the crowdsourced marketplace, the task requester act as a buyer, and the contributor act as a seller. Their analytical definition is as follows:

Definition 2. Task Requester: When a user u send a crowdsourced task request crt to the crowdsourced marketplace, then the marketplace consider that user as a task requester $treq$ which is a tuple of $\langle treqid, uid_{treq}, nocrt, rptr_{treq} \rangle$ where

- $treqid$ is a unique task requester ID
- uid_{treq} is a unique user ID of the task requester $treq$
- $nocrt_{treq}$ is the total number of tasks requested by task requester $treq$
- $rptr_{treq}$ is the current rating points of the task requester $treq$

The information mentioned above will be stored at the blockchain only for further references. This way of data storing will reduce the amount of redundant data in the system.

Definition 3. Contributor: When a user u is eligible to perform a crowdsourced task request crt to the crowdsourced

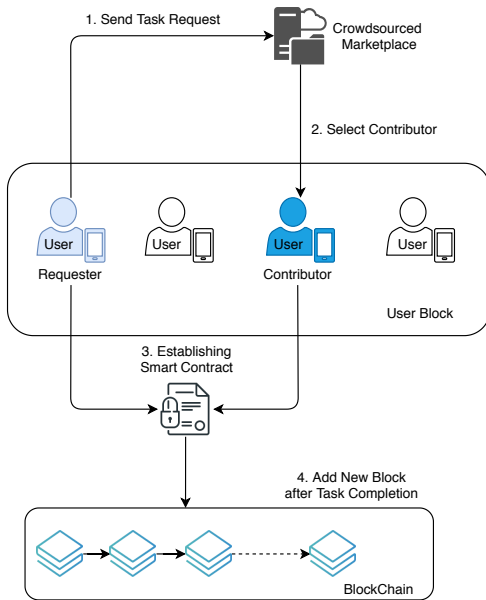


Fig. 2. System Model.

marketplace, then the marketplace consider that user as a contributor con which is a tuple of $\langle conid, uid_{con}, no_{ctr_{con}}, tearn_{con}, rp_{con} \rangle$, where

- $conid$ is a unique contributor ID
- uid_{con} is a unique user ID of the contributor con
- $no_{ctr_{con}}$ is the total number of sub-tasks performed by contributor con
- $tearn_{con}$ is the total earning of the contributor con
- rp_{con} is the current rating points of the contributor con

The aforementioned information will also be stored at the blockchain solely for additional references which will reduce the quantity of redundant data in the system.

Definition 4. Request: When a task requester $treq$ wants to perform a task and requires more workers to achieve that, the task requester then demands one or more contributors by posting a task request to the crowdsourced marketplace. This request is called the crowdsourced task request ctr which is a tuple of $\langle ctrid, loc_{ctr}, t_{ctr}, no_{con_{ctr}}, cost_{ctr}, des_{ctr}, ty_{ctr}, SUBT_{ctr}, SUBDES_{ctr}, Q_{ctr} \rangle$ where

- $ctrid$ is a unique crowdsourced task request ID
- loc_{ctr} is the location where the task ctr needed to be performed
- t_{ctr} is the last time within which the task ctr should be completed
- $no_{con_{ctr}}$ is the number of contributor needed to complete the task ctr
- $cost_{ctr}$ is the total cost of the task ctr that a task requester is ready to pay
- ty_{ctr} is the type of the task ctr

- des_{ctr} is the text description of the task ctr
- $SUBT_{ctr}$ is a tuple $\langle subt_1, subt_2, \dots, subt_n \rangle$, where each $subt_{ctr}$ denotes the type for each subtask of each component which is constitutes of ty_{ctr} . Task requester can provide this information while requesting for a task.
- $SUBDES_{ctr}$ is a tuple $\langle subdes_1, subdes_2, \dots, subdes_n \rangle$, where each $subdes_{ctr}$ denotes the text description for each subtask of each component of ty_{ctr} . Task requester can provide this information if he/she added the sub-task types while requesting for a task.
- Q_{ctr} is a tuple $\langle q_1, q_2, \dots, q_n \rangle$, where each q_{ctr} denotes the minimum requirement for each QoS property of the selected contributor to do the task ctr .

Definition 5. Crowdsourced Marketplace: Crowdsourcing marketplace is a platform which brings the set of contributors CON and the set of task requesters $TREQ$ under the same network and connects them to each other through a task. There might be several tasks which are easier to do if it is distributed among other people. Crowdsourced marketplace receives such kind of task requests CTR and finds the suitable contributors who can accomplish the tasks. In this research, we have used an online cloud-based platform as our crowdsourced marketplace.

Definition 6. Blockchain: Blockchain is a distributed transaction ledger which can store a collection of blocks through establishing a chain. In our proposed model, a block stores information related to an accomplished task and adds it to the blockchain network. Each block bc_n is a tuple of $\langle bcid_n, bcid_{n-1}, bct_n, ctr, uid_{treq}, uid_{CON} \rangle$ where

- $bcid_n$ is the unique block ID. Here, block ID is the hash value of the block.
- $bcid_{n-1}$ is the previous block's ID. Here, the previous block's ID is the hash value of the previous block.
- bct_n is the time when block bc_n is created.
- ctr is the crowdsourced task request.
- uid_{treq} is the unique user ID of the task requester who posted the crowdsourced task request.
- uid_{CON} is the unique user ID of the set of contributors that participated in the crowdsourced task.

Definition 7. Smart Contract: A smart contract is a contract which contains previously defined terms and conditions written by the blockchain network. In our system, the smart contract sc is a tuple of $\langle scid_{ctr}, ctr, uid_{treq}, uid_{CON}, scp, sca_{sc} \rangle$ where

- $scid_{ctr}$ is the unique smart contract id for the task ctr
- ctr is the crowdsourced task request
- uid_{treq} is the unique user ID of the task requester who posted the crowdsourced task request
- uid_{CON} is the unique user ID of the set of contributors that participated in the crowdsourced task

- scp is the protocol or rules that is used to create the smart contract
- $scac_{sc}$ is the account balance of the smart contract sc .

B. Work Flow of the System Model

The workflow of our proposed system is presented in Fig. 3. This system performs the following actions are illustrated subsequently:

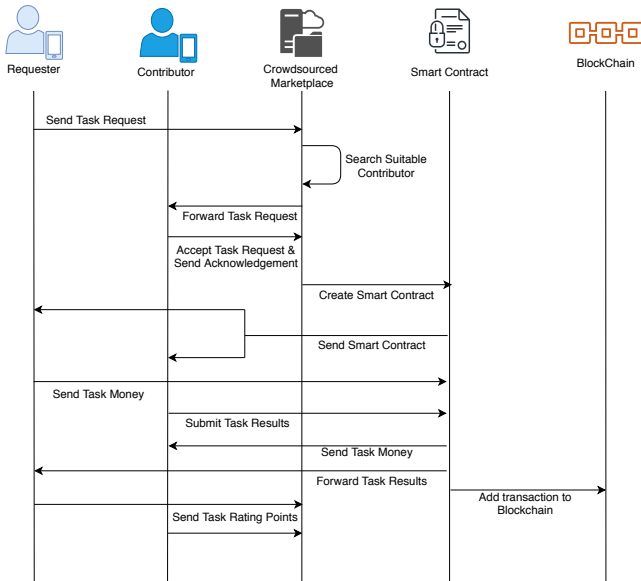


Fig. 3. Work Flow Diagram of Blockchain-based Mobile Crowdsourcing Framework.

Step 1: The task requester $treq$ posts a task request ctr in the crowdsourced marketplace with his intended budget and minimum requirements of the contributors to do that specific task.

Step 2: The crowdsourced marketplace explores the set of contributors CON and retrieves eligible contributors according to the task request ctr . Later, the request is forwarded to the selected contributors only.

Step 3: When a contributor con agrees to do the task, then he/she conveys an acknowledgment message to the marketplace.

Step 4: The crowdsourced marketplace triggers the smart contract upon receiving the acknowledgment from the contributor con . The smart contract will be designed based on the task request ctr .

Step 5: The smart contract is sent to the task requester $treq$ and the contributor con . After receiving the smart contract, the contributor con starts working on the task ctr , and the task requester $treq$ transfers the task money.

Step 6: After finishing the task ctr , the contributor con forwards the output to the smart contract. If the output satisfies the task requirements, the smart contract transfers the task money to the contributor con and forward the output to the task requester $treq$.

Step 7: The task requester $treq$ and the contributor con will give a rating point to each other and submit the rating points to the crowdsourced marketplace. Eventually, the crowdsourced marketplace will add the information related to the task ctr , task requester $treq$ and contributor con to the blockchain by creating a block bc as a transaction for further references.

V. PROPOSED MODEL

In this section, we propose a novel blockchain-based crowdsourcing framework using smart contract. Our crowdsourced model is segmented into seven steps. We explain each step in each subsection.

A. User Registration to the System

The crowdsourced marketplace mainly permits the authorized user to operate the system. To post a task or to receive a task request, a user must have a smart device through which he/she can register himself/herself to the system. After completion of the registration process, the crowdsourced marketplace will provide a unique user identity (User ID) to the user. However, there might be several malicious users who can exploit the system by creating fake user identities. This kind of intrusion is called the Sybil attack [18].

The most common way to prevent this attack is to take the registration fee from the user while registering into the system. Nevertheless, this will increase the cost of the user, and they might be unwilling to pay additionally for the registration [19]. Thus, the user has to submit any identification card (e.g. Student ID, Office ID, National ID, Passport, Driving Licence) to prove his/her identity. In this way, we can prevent sybil attack [20].

Fig. 4 illustrates the process of user registration in the system. Initially, the user will submit his/her profile information including his/her identification card and smart device information to the crowdsourced marketplace. The crowdsourced marketplace will forward the information to the identity verification centre for user authentication. If the user is legitimate, then the crowdsourced marketplace will send a unique user ID to the user, and it will add the user in the particular position in the user block so that the user can gain a remarkable advantage of the system. The users are stored in a sorted form according to their smart device information in the user block. This sorting will help the marketplace to choose contributors from the user block.

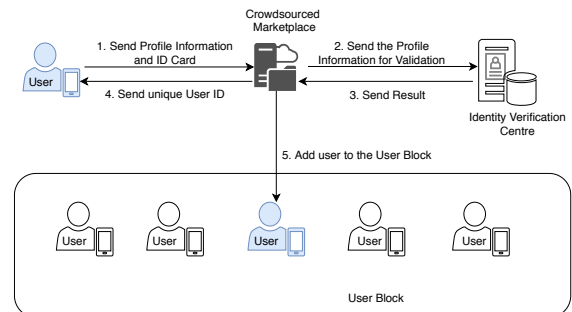


Fig. 4. User Registration Process.

B. Task Request Placement

The task requesters can place a task request at the crowd-sourced marketplace irrespective of time and place. However, to post a task, he/she must specify the task request precisely to such an extent that the marketplace finds suitable contributors for that task without any issue. In the previous section, we have formally defined a task request. The requester must provide the following information while posting a task request.

- **Task Location:** The task requester should clearly define the area where the task should be carried out. The task location can be an area, a city or even a country. If the task requester keeps this field blank, then the task can be performed at any places.
- **Task Finishing Time:** One of the essential criteria of a task request is the finishing time of the task. The task requester must provide a deadline within which the contributor should complete the task.
- **Number of Contributors:** There are various tasks where we need only one person to complete it. For example, to write an article for a blog needs only one person. Additionally, there are several tasks where we need many people to finish it. In particular, if we want to collect data from several places of Dhaka city, we need more people. The task requesters should specify the number of contributors to perform the task.
- **Budget:** The task requesters also necessitate estimating the cost needed to execute any task. Moreover, he/she have to pay to use the services of the marketplace, smart contract and the blockchain network. The service charge of the marketplace, contract and the network is constant. Thus, the task requester has to make a budget considering all these costs. The budget of the task can be defined using equation 1:

$$cost_{ctr} = cost_{con} + cost_{mkt} + cost_{sc} + cost_{bc} \quad (1)$$

Here, $cost_{ctr}$ is the budget of the task which is the total cost to execute the task. The budget includes four types of cost:

- $cost_{con}$ is the cost of the contributor. This amount will be transferred to the contributor after the successful task completion.
 - $cost_{mkt}$ is the cost of the crowdsourced marketplace. The crowdsourced marketplace will charge a few amount to maintain the task placement, task distribution and more.
 - $cost_{sc}$ is the cost of smart contract. To maintain the feasibility of the smart contract, a fixed amount will be cut from the task budget.
 - $cost_{bc}$ is the cost of blockchain. A certain amount will be fixed for the maintenance of the blockchain network.
- **Task Type:** Different types of task can be implemented using crowdsourcing. The example includes photo tagging, video editing, content writing, website or application development. The most popular task, according to the paper [21], is content creation. This task type selection will be helpful for the marketplace

to find a suitable contributor who has expertise in this field.

- **Task Description:** The task requester also should describe the task according to the context. For example, a task requester needs an article writer for his/her blog. This information is not sufficient to understand the task. Thus, the requester must explain the task clearly by setting the article types, word limits, font style and size and more. By reading the task description, the contributors will understand the task thoroughly.
- **Sub-Task Type:** Occasionally, a complex crowd-sourced task is consists of several simple subtasks. For example, a task requester requests for a website for his/her organisation. This website development task is consists of several subtasks such as user interface designing, database designing, connecting interface with the database, testing the system and so on [22]. The task requester may choose the types of subtask for a better product.
- **Sub-Task Description:** The task requester also may provide a text description for the betterment of their product. If a task requester asks for a website for his/her company, he/she might address the specifications for several sub-tasks. For example, the user interface should contain a plethora of blue colour; the database should be built using MySQL and so on. This description will help the contributor to study and implement the small details provided by the task requester.
- **Minimum Requirement of the Contributor:** The task requester can also outline the requirements of the contributor that he/she wants to perform the task. For example, he/she can prefer a contributor who has a mobile device with at least 4 GB of RAM, have a rating point more than four and completed at least ten tasks in the platform. Thus, the marketplace promptly finds a contributor as the requester has already minimized the search list.

Algorithm 1 illustrates the process of task request placement in the crowdsourcing marketplace. The above-explained elements are the input of this algorithm. The output is a successful task request which will be posted in the marketplace with the unique ID $ctrid$. In the beginning, we investigate whether the task requester is a posting for the first time or not. If he/she is a new task requester, then the system will provide them with a unique task requester ID $treqid$ using `createTaskRequester()` function. This function creates a new task requester's ID. The task requester $treq$ is assigned a threshold value θ_{rp} as rating point. (Line 1 ~ 3). Next, the algorithm will check whether the rating point of the $treq$ is greater than or equal to the threshold value θ_{rp} (Line 4). Otherwise, $treq$ will be ineligible to post a task in the marketplace (Line 15 ~ 16). Both of the threshold values θ_{rp} and θ_{cost} will be decided by the marketplace based on the task type ty . Then, we will compare the budget of the task. If the budget of the task $cost_{ctr}$ is higher than the total cost of the task, then it will proceed in the next step. Contrarily, it will return an insufficient budget error message. In the sixth line, we calculate the number of available contributors

Algorithm 1: Task Request Placement

```
Input: Input for Task Request, In =  
{ treqid, rptreq, locctr, tctr, noconctr, costctr, desctr, tyctr, Qctr }  
Output: ctrid  
1 if newTaskRequester() then  
2   | treqid = createTaskRequester()  
3   | rptreq =  $\theta_{rp}$   
4 if In.rptreq  $\geq \theta_{rp}$  then  
5   | if In.costctr  $> (\theta_{cost} + cost_{mkt} + cost_{sc} + cost_{bc})$   
6   |   then  
7   |   | availCon = checkAvailableContributors();  
8   |   | if In.nocon  $\leq availCon$  then  
9   |   |   | Create task request ctr along with a unique ID  
10  |   |   |   | ctrid  
11  |   |   |   | Update CTR  
12  |   |   |   | noctr ++  
13  |   |   | else  
14  |   |   |   | return "No Available Contributors" message  
15  |   | else  
16  |   |   | return "Insufficient Task Budget" message  
17 return "Successful Task Placement" message with ctrid
```

who are interested in participating in the crowdsourcing task. We use checkAvailableContributors() functions and store the result in *availCon*. Then, we compute if the number of contributors required to perform the task is less than *availCon*. If affirmative, then a task request ID *ctr_{id}* is created, and the task is posted to the marketplace. The set of all the task *CTR* is updated, and the number of tasks posted by the task requester *noctr* is incremented (Line 7 ~ 10). Contrarily, the task request is refused due to the lack of contributors (Line 11 ~ 12).

C. Task Request Arrival and Distribution

Suppose there is *noctr* number of task requests posted by *notreq* number of task requesters. To distribute the task request among the contributors, we first divide the time period *TP* to *i* slots as $TP = \{t_1, t_2, t_3, \dots, t_i\}$. In each slot, the task requests have been posted randomly. Thus, we use the Poisson process [23] with the arrival rate λ as the task types are heterogeneous. If the crowdsourced marketplace starts searching suitable contributors for a task immediately after the task posting, it will increase the cost as well as decrease the utility of the marketplace. Therefore, the crowdsourced marketplace distribute the tasks among the contributors using the Algorithm 2.

The marketplace will push all the incoming task requests *crt* in the task buffer *tbfr_{ty}* based on task types. The buffer *tbfr_{ty}* will be used as a input of the Algorithm 2 and the *taskReleaseFlag* is the output of this algorithm. The *taskReleaseFlag* is initialized to false for all *tbfr_{ty}*. By applying Algorithm 2, the marketplace will wait for λ amount of time to distribute the task (Line 8 ~ 9). After the completion of waiting time *wt_{tbfr}*, the marketplace starts searching for the contributor to assign all the task requests (Line 6 ~ 8). If *tbfr_{ty}* is full before the completion of waiting period, the

Algorithm 2: Task Request Distribution

```
Input: {crtid,  $\lambda$ , wttbfr, tbfrty}  
Output: taskReleaseFlagtbfr  
1 foreach crtid in tbfrty do  
2   | taskReleaseFlagtbfr = false  
3   | if tbfrty is full then  
4   |   | taskReleaseFlagtbfr = true  
5   |   | return taskReleaseFlagtbfr  
6   | else if wttbfr  $\leq \lambda$  then  
7   |   | taskReleaseFlagtbfr = true  
8   |   | return taskReleaseFlagtbfr  
9   | else  
10  |   | waitforRelease()
```

contributor starts releasing the task for distribution (Line 3 ~ 5).

D. Contributor Selection

When the *taskReleaseFlag* is true, the system proceeds to the next step and initiates Algorithm 3. In our previous work [17], we used the reverse-auction method to select the contributor. This method was used to find whether the users are interested in performing any task. In this proposed model, we used a flag to find the availability status of each user. The availability status *sts* of a user will be true by default which means he/she is willing to perform a task. If a user is already assigned any task, his/her *sts* will be false. A user can also change his/her *sts* from true to false manually for a definite amount of time, according to his/her choice if he/she is not interested in performing any task. The function *findAvailableUser()* is used to determine the list of interested users *availableuser*.

To become a contributor, users have to pass through several requirements. At first, we verify whether their current location is in the task location or not (Line 5). Then, we examine whether the task type is similar to their skills (Line 6). Finally, we review each QoS parameters (Line 8 ~ 10). If the user passes all of these requirements, then the algorithm chooses him as a contributor. This process is continued until we find all the contributors needed to perform the task (Line 11 ~ 14). Ultimately, the algorithm returns the list of contributors to the marketplace (Line 15 ~ 16). If the number of recognised contributors is less than the required number of contributors, then we call for a reverse auction which was proposed in [17] and include all the contributors in the list (Line 17 ~ 21). This method will help the marketplace to collect all the eligible contributors to perform the task.

E. Smart Contract Implementation

The smart contract *sc* is an agreement between the task requester *treq* and the contributor *con*. The contract runs automatically according to predefined rules and protocols. The crowdsourced marketplace will initiate the smart contract for both task requester and contributor. The Algorithm 4 depicts the specific actions of the smart contract.

Firstly, the crowdsourced market place will accept the task money *taskMoney* from the task requester *treqid* based on

Algorithm 3: Contributor Selection

Input: $\{crt, tbfr, U\}$
Output: $conlist$

```

1 count = 0
2 need = 0
3 foreach crtid in tbfrty do
4     availableuser = findAvailableUser(U)
5     foreach user u in availableuser do
6         if locu in locctr then
7             if tycrt in SKLu then
8                 if each qu ζ = qctr then
9                     conlisti = u
10                    count ++
11                    if count ζ = noconctr then
12                        break
13                    else
14                        continue
15                if count ζ = noconctr then
16                    return conlist
17                else
18                    need = noconctr - count
19                    conAuction = reverseAuction(crt, need, θi)
20                    append conAuction in conlist
21                    return conlist

```

Algorithm 4: Smart Contract Implementation

Input: $\{crt, treqid, con\}$
Output: $taskResult$

```

1 taskMoney = ReceiveMoney(treqid, costctr)
2 conMoney = taskMoney - (costmkt + costsc + costbc)
3 SignContract(treqid, con, ctrid, conMoney)
4 taskResult = ReceiveTaskResult(con)
5 if ResultValidation(taskResult) then
6     if currentTime < tctr then
7         TransferMoney(con, conMoney)
8         return taskResult
9     else
10        TransferMoney(treqid, taskMoney)
11        return "Task Incomplete" message
12 else
13     TransferMoney(treqid, taskMoney)
14     return "Task Invalid" message

```

the task request ctr (Line 1). The cost of the marketplace $cost_{mkt}$, smart contract $cost_{sc}$ and blockchain $cost_{bc}$ will be deducted before the contract creation (Line 2). Then, the marketplace will create a smart contract for the budget of $conMoney$ based on the predefined protocols. The task requester $treqid$ and the contributor con will sign the contract for the task completion using $SignContract$ function (Line 3). After receiving the task result $taskResult$ from the contributor, the contract will verify the result. If the result is valid and submitted on due time, then the smart contract will transfer the money to the contributor (Line 4 ~ 8). Otherwise, the money will be transferred to the task requester (Line 9 ~ 14).

F. Rating Point Computation

After receiving the task result, the task requester bestows a rating point to the contributors based on their satisfaction level. On the other hand, the requester also gets a rating point from the contributors. These rating points will define the reputation of the users. There are several ways to compute reputation scores including Mean-based reputation [24], Bayesian reputation [25], Fuzzy reputation [26] and so on. We modify the following equation to calculate the reputation score of the users which has been proposed in [27].

$$rp = \sum_{i=1}^n \sum_{j=1}^{qos} tr_i \times tw_j \quad (2)$$

We calculate the reputation score rp in equation 2 using weighted average for each rating points. Here, tr_i is the task rating for each task, tw_j is the task weight for each QoS (e.g. bandwidth, reputation value, coverage distance, latency).

G. Addition of Transaction Block

After computing the rating points, the crowdsourced marketplace will add the task details in the blockchain. We will not use any miner competition to add any transaction to the blockchain. The miner competition executes very time-consuming calculations. This miner competition also wastes a lot of resources where the mobile devices have resource constraints [28]. Thus, the marketplace will choose a miner using the miner selection algorithm proposed in [29]. The transaction block is illustrated in the Fig. 5.

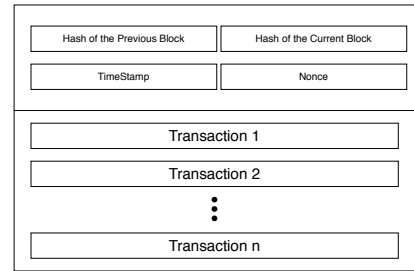


Fig. 5. Structure of Transaction Block.

Each transaction block in the blockchain is consists of two parts: block header and block body. The block header contains the hash value of the current and previous block, timestamp and nonce. Each block is encrypted using a hash algorithm, and the hash is stored in the block header. The block header also contains the hash of the previous block for security purpose. The timestamp is applied to retain the time for each transaction. A nonce is a number which is employed for hashing in the blockchain. The block body comprises of a list of transactions. Each transaction is consists of task requester's information, contributor's information, and task request's information.

VI. SECURITY ANALYSIS

A blockchain-based model should address several security properties. Our proposed framework also provides these properties as it is established based on blockchain. In this section, we discuss several properties that our system offers.

A. Concusses in the Blockchain

With decentralized frameworks, particularly in blockchain-based, a concussion problem can arise. This problem happens when various miner compete to make a block around the same time [30]. Here each miner chooses the same block's hash as a parent hash and creates a block. These types of blocks are not accepted into the blockchain network. In the case of bitcoin, these types of blocks are called orphan block [31] and in the case of ethereum, we call it uncle block [32]. As shown in Fig. 6, when a miner creates a block, it will be linked to create a chain that neither corruptible nor changeable.

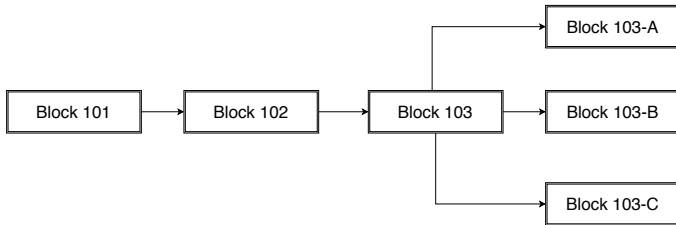


Fig. 6. Concusses in Blockchain.

In the proposed system, there is no concusses problem as all the task-related transaction maintained by the smart contract. Thus, each block's information will be sent to the miner after a specific time interval, as shown in Fig. 7 and, there is no chance for missing any block.

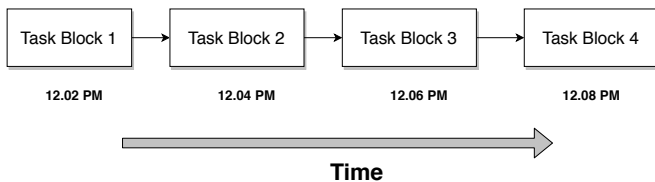


Fig. 7. Solution of Concusses.

B. Anonymity

The identity information of contributors and requesters are protected by anonymity which is essential for crowdsourcing platforms. The anonymity of contributor indicates the inter-connectivity between the retrieval and the privacy of workers [15]. Similarly, anonymity of requesters can be defined as the submission unlinkability between task submission and identity information. In the proposed system uid_{req} is the unique user ID of the task requester and who posted the crowdsourced task request and uid_{CON} is the unique user ID of the set of contributors that participated in the crowdsourced task. From these ID it is not possible to find the relation between task requester, task request and contributors.

C. Efficiency

The computing cost should be minimal enough to guarantee the equivalent services can be provided by the smart contract. The cost of the associated operation must not cross the gas limit [15]. The efficiency of the proposed system is shown in Section VII.

D. Integrity

Blockchain technology implements a Merkle tree to guarantee the integrity of the data [33]. In ethereum, the principle of Merkle tree was introduced to allow for a lightweight, and adequate verifiable proof that assures a transaction is added into a block. The hashes of the child nodes in this data structure are merged into the header of a parent node. This strategy for connecting headers of children's nodes and linking them to the header of the parent node goes on until the last node, right above the root node. This process implies that the root node holds information of all nodes. The Merkle tree includes a hash of all transactions in a block. Thus, if a node wishes to check if a transaction has been modified or not, nodes need to create the Markle Block using entire block transactions [34]. This tree makes validating or invalidating a task effortless.

E. Security

The proposed method ensures protection by preventing unauthorised access and misuse of task-related information. Due to the immutable attribute of Blockchain, it is difficult to alter the documented information on Blockchain. If someone changes a transaction, all block information from that block to the new block would have to be re-mined. A unique hash value is contained by each block using a hash function and the hash of the previous block. If one tries to modify a block's data, the different hash value will result out from this modification. New hash value will conflict with the next block's value. For this reason, re-mined will be needed for the next block. For all the blocks in the chain, the same process of re-mining is required. When the miner is involved in re-mining old blocks, new blocks would be attached to the chain, making it incredibly impossible to exploit a single block. This method requires a massive computing capacity, which is practically impossible in reality [34]. Blockchain, shown in Fig. 8 assures us the information is tamper-proof, and it is quite impossible to manipulate data in our proposed system.

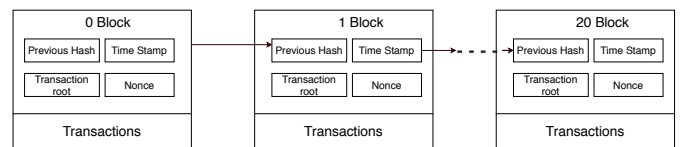


Fig. 8. Security in Blockchain.

F. Privacy

For widespread deployment and acceptance of crowdsourcing, privacy considerations must involve both task requester and contributors [35]. As task requester and contributor are registered into the system, and they use the unique identifier into the blockchain, this provides anonymity and privacy of requesters and contributors.

G. Fairness

Fairness in crowdsourcing refers to a fair sharing in labour results and rewards between the task requesters and the contributors who have given the right solutions [36]. In the proposed system, the task management process is done by smart contracts where the two party's agreement makes the

contracts. Smart contracts are responsible for checking the task results after submitted by the contributors. If the results match the requirements, then the reward money will be sent to the contributors to ensure fairness.

H. Decentralization

The blockchain is a decentralized distributed ledger system built into a network of multiple interconnected nodes. All the network nodes get a distributed ledger, which includes the transaction history known in the blockchain [37]. Compared to conventional systems that depend on crowdsourcing networks, the proposed scheme guarantees that transaction details of requesters and contributors are recorded in the blockchain.

I. Comparative Analysis of Property

In Table I, we have presented the comparison between existing systems and our proposed system based on several security properties which are discussed in this section. From this table, we can observe that the concuss solutions, integrity, efficiency are missing in [38], [15], [13], [39]. Moreover, [38] do not provide anonymity and privacy. In our proposed system, we have solved the concuss problem and provided all the properties.

TABLE I. COMPARISON BETWEEN EXISTING SYSTEMS AND PROPOSED SYSTEM

Properties	BPTM [15]	CrowdSFL [13]	WorkerREp [39]	Ours
Concuss	✓	✓	✓	×
Anonymity	✓	✓	✓	✓
Integrity	×	×	×	✓
Privacy	✓	✓	✓	✓
Security	✓	✓	✓	✓
Decentralization	✓	✓	✓	✓
Efficiency	×	×	×	✓

VII. EXPERIMENT RESULTS

The name of one of the most popular blockchain communities is Ethereum [40]. Ethereum facilitates smart contract functionality in such a way that any Ethereum wallet owner can implement their smart contract on the Ethereum network to benefit their specific business rules. To deploy a blockchain-based crowdsourcing framework in Ethereum, we need to set up the environment first.

A. Environment and Tools

For the implementation of our system prototype, Truffle, Ganache and Metamask are used.

1) *Truffle*: Truffle is primarily able to compile solidity-written smart contracts, executing migration on different contracts, and producing ABI (Application Binary Interface) [41].

2) *Ganache*: Ganache is a local RPC blockchain server which is embedded into Truffle. Ten initial accounts are

provided by it to pre-fund with 100 Ether including a 12 words seed sentence to restore them.

3) *MetaMask*: MetaMask is a browser plug-in that can be used by a user on Chrome, Firefox, Opera and Brave. It adds an API to the browser that makes the read-write requests from standard websites in the Ethereum blockchain, which is a JavaScript library built by the Ethereum core team named web3.js. It enables users to transact Ethereum via traditional websites, communicate to an Ethereum node locally or remotely, via an HTTP or IPC connection[15].

B. Cost Analysis of the System

The cryptocurrency in the Ethereum chain is known as Ether (ETH). Computing cost is payable in ETH within the blockchain and EVM. The execution fee is measured in gas terminology. The Ethereum transaction specifies the data signed by the party initiating the exchange and includes a message sent from the client to some other blockchain client. Contracts can also transfer information to all other contracts when function calls have been formulated for each contract. There is a *gasPrice* sector in a transaction, reflecting the fee that the sender is expected to pay for gas. A notification or another transaction causes the execution of a contract. Every command is then executed on every network node. For every executed operation there is a specified cost, expressed in several gas units and each transaction has a maximum ether cost that is then equal to $gasLimit \times gasPrice$ [42].

TABLE II. COMPARISON OF SMART CONTRACT DEPLOYMENT

Contract	Gas Used	Actual Cost (Ether)	USD
BPTM [15]	973093	0.0194619	6.77274
CrowdSFL[13]	455416	0.0091083	3.16969
WorkerRep[39]	247863	0.0049573	1.72514
Proposed System	156290	0.0031258	1.08778

In Table II, we show the gas costs and the corresponding prices in \$ for the deployment of the agreement contract between existing and proposed systems. At the time of carrying out the experiments, September 2020, the ether exchange rate was 1 ETH = 348.28\$, and the median gasPrice was approximately 0.0000002 ETH (20 Gwei). The comparison between different blockchain-based system is also illustrated in Fig. 9.

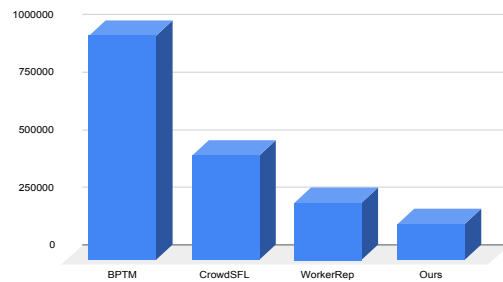


Fig. 9. Comparison Analysis.

VIII. CONCLUSIONS AND FUTURE WORKS

Privacy of the user's data is still a significant issue nowadays. As it is difficult to breach the confidentiality of data stored in a blockchain, we proposed a blockchain-based crowdsourcing model in this paper. The coordinator distributes the tasks in this model, so the fairness of the system prevails. Additionally, the tasks are assessed by the smart contract; therefore, it is possible to prevent any failure in the output. Through adopting blockchain, this model can provide anonymity, integrity, security and efficiency. We have analysed our model with a few existing models. Our model performs adequately well, and it consumes less gas and ether than other models. In future, we will add an incentive mechanism to our proposed model; hence, the users will be more interested in using this platform.

REFERENCES

- [1] J. Howe, "The rise of crowdsourcing," *Wired magazine*, vol. 14, no. 6, pp. 1–4, 2006.
- [2] X. Zhang, Z. Yang, Z. Zhou, H. Cai, L. Chen, and X. Li, "Free market of crowdsourcing: Incentive mechanism design for mobile sensing," *IEEE transactions on parallel and distributed systems*, vol. 25, no. 12, pp. 3190–3200, 2014.
- [3] J. Phuttharak and S. W. Loke, "A review of mobile crowdsourcing architectures and challenges: Toward crowd-empowered internet-of-things," *IEEE Access*, vol. 7, pp. 304–324, 2018.
- [4] V. Pilloni, "How data will transform industrial processes: Crowdsensing, crowdsourcing and big data as pillars of industry 4.0," *Future Internet*, vol. 10, no. 3, p. 24, 2018.
- [5] S. Nakamoto and A. Bitcoin, "A peer-to-peer electronic cash system," *Bitcoin*.—URL: <https://bitcoin.org/bitcoin.pdf>, 2008.
- [6] J. Golosova and A. Romanovs, "The advantages and disadvantages of the blockchain technology," in *2018 IEEE 6th Workshop on Advances in Information, Electronic and Electrical Engineering (AIEEE)*. IEEE, 2018, pp. 1–6.
- [7] M. Crosby, P. Pattanayak, S. Verma, V. Kalyanaraman *et al.*, "Blockchain technology: Beyond bitcoin," *Applied Innovation*, vol. 2, no. 6–10, p. 71, 2016.
- [8] L. Islam, S. T. Alvi, M. N. Uddin, and M. Raham, "Obstacles of mobile crowdsourcing: A survey," in *2019 IEEE Pune Section International Conference (PuneCon)*. IEEE, 2019, pp. 1–4.
- [9] H. Simula, "The rise and fall of crowdsourcing?" in *2013 46th Hawaii International Conference on System Sciences*. IEEE, 2013, pp. 2783–2791.
- [10] R. Hull, "Blockchain: Distributed event-based processing in a data-centric world," in *Proceedings of the 11th ACM International Conference on Distributed and Event-based Systems*, 2017, pp. 2–4.
- [11] W. Feng and Z. Yan, "Mcs-chain: Decentralized and trustworthy mobile crowdsourcing based on blockchain," *Future Generation Computer Systems*, vol. 95, pp. 649–666, 2019.
- [12] M. Li, J. Weng, A. Yang, W. Lu, Y. Zhang, L. Hou, J.-N. Liu, Y. Xiang, and R. H. Deng, "Crowdbc: A blockchain-based decentralized framework for crowdsourcing," *IEEE Transactions on Parallel and Distributed Systems*, vol. 30, no. 6, pp. 1251–1266, 2018.
- [13] Z. Li, J. Liu, J. Hao, and H. Wang, "Crowdsff: A secure crowd computing framework based on blockchain and federated learning," *Electronics*, vol. 9, p. 773, 05 2020.
- [14] Y. Lu, Q. Tang, and G. Wang, "Zebralancer: Crowdsourcing knowledge atop open blockchain, privately and anonymously," *arXiv preprint arXiv:1803.01256*, 2018.
- [15] Y. Wu, S. Tang, B. Zhao, and Z. Peng, "Bptm: Blockchain-based privacy-preserving task matching in crowdsourcing," *IEEE Access*, vol. 7, pp. 45 605–45 617, 01 2019.
- [16] L. Islam, M. A. Islam, and M. N. Uddin, "Three-layered incentive framework for mobile crowdsourcing," in *2018 10th International Conference on Electrical and Computer Engineering (ICECE)*. IEEE, 2018, pp. 153–156.
- [17] —, "A quality-aware reverse auction-based incentive model for mobile crowdsourcing," in *2019 IEEE 5th International Conference for Convergence in Technology (I2CT)*. IEEE, 2019, pp. 1–5.
- [18] J. R. Douceur, "The sybil attack," in *International workshop on peer-to-peer systems*. Springer, 2002, pp. 251–260.
- [19] M. Hossain, "Crowdsourcing: Activities, incentives and users' motivations to participate," in *2012 International Conference on Innovation Management and Technology Research*. IEEE, 2012, pp. 501–506.
- [20] S. Kim, Y. Kwon, and S. Cho, "A survey of scalability solutions on blockchain," in *2018 International Conference on Information and Communication Technology Convergence (ICTC)*. IEEE, 2018, pp. 1204–1207.
- [21] D. E. Difallah, M. Catasta, G. Demartini, P. G. Ipeirotis, and P. Cudré-Mauroux, "The dynamics of micro-task crowdsourcing: The case of amazon mturk," in *Proceedings of the 24th international conference on world wide web*, 2015, pp. 238–247.
- [22] R. Yulius, F. Neta, M. F. A. Nasrullah, and M. F. A. Rambe, "Implementation of task-centered design in a web-based catalogue," in *2nd International Media Conference 2019 (IMC 2019)*. Atlantis Press, 2020, pp. 381–386.
- [23] T. Xie and X. Qin, "Stochastic scheduling with availability constraints in heterogeneous clusters," in *2006 IEEE International Conference on Cluster Computing*. IEEE, 2006, pp. 1–10.
- [24] S. Wang, Z. Zheng, Q. Sun, H. Zou, and F. Yang, "Evaluating feedback ratings for measuring reputation of web services," in *2011 IEEE International Conference on Services Computing*. IEEE, 2011, pp. 192–199.
- [25] H. T. Nguyen, W. Zhao, and J. Yang, "A trust and reputation model based on bayesian network for web services," in *2010 IEEE International Conference on Web Services*. IEEE, 2010, pp. 251–258.
- [26] S. Liu, H. Yu, C. Miao, and A. C. Kot, "A fuzzy logic based reputation model against unfair ratings," in *Proceedings of the 2013 international conference on Autonomous agents and multi-agent systems*, 2013, pp. 821–828.
- [27] A. Abdel-Hafez, Y. Xu, and A. Jøsang, "A normal-distribution based rating aggregation method for generating product reputations," in *Web Intelligence*, vol. 13-1. IOS Press, 2015, pp. 43–51.
- [28] A. Dorri, S. S. Kanhere, and R. Jurdak, "Blockchain in internet of things: challenges and solutions," *arXiv preprint arXiv:1608.05187*, 2016.
- [29] M. A. Uddin, A. Stranieri, I. Gondal, and V. Balasubramanian, "Continuous patient monitoring with a patient centric agent: A block architecture," *IEEE Access*, vol. 6, pp. 32 700–32 726, 2018.
- [30] A. B. Ayed, "A conceptual secure blockchain based electronic voting system," *International Journal of Network Security & Its Applications*, vol. 9, pp. 01–09, 2017.
- [31] P. Tasatanattakool and C. Techapanupreeda, "Blockchain: Challenges and applications," in *2018 International Conference on Information Networking (ICOIN)*. IEEE, 2018, pp. 473–475.
- [32] S.-Y. Chang, Y. Park, S. Wuthier, and C.-W. Chen, "Uncle-block attack: Blockchain mining threat beyond block withholding for rational and uncooperative miners," in *International Conference on Applied Cryptography and Network Security*. Springer, 2019, pp. 241–258.
- [33] B. Rogers, S. Chhabra, M. Prvulovic, and Y. Solihin, "Using address independent seed encryption and bonsai merkle trees to make secure processors os- and performance-friendly," in *40th Annual IEEE/ACM International Symposium on Microarchitecture (MICRO 2007)*, 2007, pp. 183–196.
- [34] R. Bosri, A. R. Uzzal, A. A. Omar, A. S. M. T. Hasan, and M. Z. A. Bhuiyan, "Towards a privacy-preserving voting system through blockchain technologies," in *2019 IEEE Intl Conf on Dependable, Autonomic and Secure Computing, Intl Conf on Pervasive Intelligence and Computing, Intl Conf on Cloud and Big Data Computing, Intl Conf on Cyber Science and Technology Congress (DASC/PiCom/CBDCom/CyberSciTech)*, 2019, pp. 602–608.
- [35] J. Phuttharak and S. Loke, "A review of mobile crowdsourcing architectures and challenges: Towards crowd-empowered internet-of-things," *IEEE Access*, vol. PP, pp. 1–1, 12 2018.

- [36] J. Zhang, W. Cui, J. Ma, and C. Yang, "Blockchain-based secure and fair crowdsourcing scheme," *International Journal of Distributed Sensor Networks*, vol. 15, p. 155014771986489, 07 2019.
- [37] S. Gao, D. Zheng, R. Guo, C. Jing, and C. Hu, "An anti-quantum e-voting protocol in blockchain with audit function," *IEEE Access*, vol. PP, pp. 1–1, 08 2019.
- [38] J. Fan, G. Li, B. C. Ooi, K.-l. Tan, and J. Feng, "icrowd: An adaptive crowdsourcing framework," in *Proceedings of the 2015 ACM SIGMOD International Conference on Management of Data*, 2015, pp. 1015–1030.
- [39] G. K. Bhatia, S. Gupta, A. Dubey, and P. Kumaraguru, "Workerrep: Immutable reputation system for crowdsourcing platform based on blockchain," *arXiv preprint arXiv:2006.14782*, 2020.
- [40] G. Wood *et al.*, "Ethereum: A secure decentralised generalised transaction ledger," *Ethereum project yellow paper*, vol. 151, no. 2014, pp. 1–32, 2014.
- [41] Y. Rosasooria, A. K. Mahamad, S. Saon, M. A. M. Isa, S. Yamaguchi, and M. A. Ahmadon, "E-voting on blockchain using solidity language," in *2020 Third International Conference on Vocational Education and Electrical Engineering (ICVEE)*, 2020, pp. 1–6.
- [42] C. Braghin, S. Cimato, S. R. Cominesi, E. Damiani, and L. Mauri, "Towards blockchain-based e-voting systems," in *International Conference on Business Information Systems*. Springer, 2019, pp. 274–286.

Fake Reviews Detection using Supervised Machine Learning

Ahmed M. Elmogy¹, Usman Tariq², Atef Ibrahim⁴
College of Computer Engineering and Sciences
Prince Sattam Bin Abdulaziz University, KSA^{1,2,4}
Faculty of Eng., Tanta University,
Egypt¹

Ammar Mohammed³
Department of Computer Science
Misr International University, Egypt
Faculty of Graduate Studies of Statistical Research
Cairo University, Egypt

Abstract—With the continuous evolve of E-commerce systems, online reviews are mainly considered as a crucial factor for building and maintaining a good reputation. Moreover, they have an effective role in the decision making process for end users. Usually, a positive review for a target object attracts more customers and lead to high increase in sales. Nowadays, deceptive or fake reviews are deliberately written to build virtual reputation and attracting potential customers. Thus, identifying fake reviews is a vivid and ongoing research area. Identifying fake reviews depends not only on the key features of the reviews but also on the behaviors of the reviewers. This paper proposes a machine learning approach to identify fake reviews. In addition to the features extraction process of the reviews, this paper applies several features engineering to extract various behaviors of the reviewers. The paper compares the performance of several experiments done on a real Yelp dataset of restaurants reviews with and without features extracted from users behaviors. In both cases, we compare the performance of several classifiers; KNN, Naive Bayes (NB), SVM, Logistic Regression and Random forest. Also, different language models of n-gram in particular bi-gram and tri-gram are taken into considerations during the evaluations. The results reveal that KNN(K=7) outperforms the rest of classifiers in terms of f-score achieving best f-score 82.40%. The results show that the f-score has increased by 3.80% when taking the extracted reviewers behavioral features into consideration.

Keywords—Fake reviews detection; data mining; supervised machine learning; feature engineering

I. INTRODUCTION

Nowadays, when customers want to draw a decision about services or products, reviews become the main source of their information. For example, when customers take the initiation to book a hotel, they read the reviews on the opinions of other customers on the hotel services. Depending on the feedback of the reviews, they decide to book room or not. If they came to a positive feedback from the reviews, they probably proceed to book the room. Thus, historical reviews became very credible sources of information to most people in several online services. Since, reviews are considered forms of sharing authentic feedback about positive or negative services, any attempt to manipulate those reviews by writing misleading or inauthentic content is considered as deceptive action and such reviews are labeled as fake [1]. Such case leads us to think what if not all the written reviews are honest or credible. What if some of these reviews are fake. Thus, detecting fake review has become and still in the state of active and required research

area [2].

Machine learning techniques can provide a big contribution to detect fake reviews of web contents. Generally, web mining techniques [3] find and extract useful information using several machine learning algorithms. One of the web mining tasks is content mining. A traditional example of content mining is opinion mining [4] which is concerned of finding the sentiment of text (positive or negative) by machine learning where a classifier is trained to analyze the features of the reviews together with the sentiments. Usually, fake reviews detection depends not only on the category of reviews but also on certain features that are not directly connected to the content. Building features of reviews normally involves text and natural language processing NLP. However, fake reviews may require building other features linked to the reviewer himself like for example review time/date or his writing styles. Thus the successful fake reviews detection lies on the construction of meaningful features extraction of the reviewers.

To this end, this paper applies several machine learning classifiers to identify fake reviews based on the content of the reviews as well as several extracted features from the reviewers. We apply the classifiers on real corpus of reviews taken from Yelp [5]. Besides the normal natural language processing on the corpus to extract and feed the features of the reviews to the classifiers, the paper also applies several features engineering on the corpus to extract various behaviors of the reviewers. The paper compares the impact of extracted features of the reviewers if they are taken into consideration within the classifiers. The papers compares the results in the absence and the presence of the extracted features in two different language models namely TF-IDF with bi-grams and TF-IDF with tri-grams. The results indicates that the engineered features increase the performance of fake reviews detection process.

The rest of this paper is organized as follows: Section II Summarizes the state of art in detecting fake reviews. Section III introduces a background about the machine learning techniques. Section IV presents the details of the proposed approach. Conclusions and future work are introduced in Section VI.

II. RELATED WORK

The fake reviews detection problem has been tackled since 2007 [6]. Two main categories of features have been exploited

in the Fake reviews detection research; textual and behavioral features. Textual features refer to the verbal characteristic of review activity. In other words, textual features depend mainly on the content of the reviews. Behavioral features refer to the nonverbal characteristics of the reviews. They depend mainly on the behaviors of the reviewers such as writing style, emotional expressions, and the frequent times the reviewers write the reviews. Although tackling textual features is challenging and crucial, behavioral features are also very important and cannot be ignored as they have a high impact on the performance of the fake review detection process. Textual features have extensively been seen in several fake reviews detection research papers. In [7], the authors used supervised machine learning approaches for fake reviews detection. Five classifiers are used which are SVM, Naive-bayes, KNN, k-star and decision tree. Simulation experiments have been done on three versions of labeled movie reviews dataset [8] consisting of 1400, 2000, and 10662 movie reviews respectively. Also, in [9], the authors used Naive Bayes, Decision tree, SVM, Random forest and Maximum entropy classifiers in detecting fake reviews on the dataset that they have collected. The collected dataset is around 10,000 negative tweets related to Samsung products and their services. In [10], the authors used both SVM and Naive base classifiers. The authors worked on yield dataset which consists of 1600 reviews collected from 20 popular hotels in Chicago. In [11], the authors used the neural and discrete models with Average, CNN, RNN, GRNN, Average GRNN and Bi-directional Average GRNN deep learning classifiers to detect deceptive opinion spamming. They used dataset from [12] which contains truthful and deceptive reviews in three domains; namely hotels, restaurants and doctors. All the above research works have only considered the textual features without any effort towards the behavioral features.

Other articles have considered behavioral features in the fake reviews detection process. In [13], some behavioral features have been considered on Amazon reviews such as average rating, and ratio of the number of reviews that the reviewer wrote. In another work [14], the authors investigated the impact of both textual and behavioural features on the fake review detection process focusing on the restaurant and hotel domain. Also, In[15], an iterative computation framework plus (ICF++) is proposed integrating textual and behavioral features. They detected fake reviews based on measuring the honesty value of a review, the trustiness value of the reviewers and the reliability value of a product.

From the above discussion and to the best of our knowledge, no approaches have dived deeply in extracting features that reflect the reviewers' behaviors. These features will highly influence the effectiveness of the fake reviews detection process. In this paper a machine learning approach to identify fake reviews is presented. In addition to the features extraction process of the reviews, the presented approach applies several features engineering to extract various behaviors of the reviewers. Some new behavioral features are created. The created features are used as inputs to the proposed system besides the textual features for fake reviews detection task.

III. BACKGROUND

Machine learning is one of the most important technological trends which lies behind many critical applications. The main power of machine learning is helping machines to automatically learn and improve themselves from previous experience [16]. There are several types of machine learning algorithms [17]; namely supervised, semi supervised and unsupervised machine learning. In the supervised approach, both input and output data are provided and the training data must be labeled and classified [18]. In the unsupervised learning approach, only the data is given without any classification or labels and the role of the approach is to find the best fit clustering or classification of the input data. Thus, in unsupervised learning, all data are unlabeled and the role of the approach is to label them. Finally, in the semi supervised approach, some data are labeled but the most are unlabeled. In this part, we introduce a summary of the supervised learning algorithms as they are the main focus of this paper.

Several classification algorithms are developed for supervised machine learning. The main objective of these algorithms is to find a proper model that disseminates the training data. For example, **Support Vector Machines (SVM)** is a discriminated classifier that basically separates the given data into classes by finding the best separable hyper-plane which categorizes the given training data [19]. Another Common supervised learning algorithm is **Naive Bayes (NB)**. The key idea of NB relies on Bayes theorem; the probability of event A to happen given the probability of event B which is formed as $P(A|B) = P(B|A) * P(A) / P(B)$ [20]. NB calculates a set of probabilities by counting the frequency and the combined values in a given dataset. NB has been successfully applied in several application domains like text classification, spam filtering and recommendation systems.

The K-Nearest Neighbors algorithm (or KNN) [21] is one of the most simple yet powerful classification algorithms. KNN has been used mostly in statistical estimation and pattern recognition. The key idea behinds KNN is to classify instance query based on voting of a group of similar classified instances. The similarity is usually calculated using distance function [22]

Decision-tree [23] is another machine learning classifier that relies on building a tree that represents a decision of instances training data. The Algorithm starts to construct the tree iteratively based on best possible split among features. The selection process of the best features relies on a predefined functions like, entropy, information gain, gain ratio, or gini index. **Random Forest** [24] is a successful method that handles the overfitting problems that occur in the decision tree. The key essence of random forest is to construct a bag of trees from different samples of the dataset. Instead of constructing the tree from all features, Random forest generates small random number of features while constructing each tree in the forest. **Logistic regression** [25] is another simple supervised machine learning classifier. It relies on finding a hyperplane that classifies the data.

IV. PROPOSED APPROACH

This section explains the details of the proposed approach shown in figure 1. The proposed approach consists of three basic phases in order to get the best model that will be used

for fake reviews detection. These phases are explained in the following:

A. Data Preprocessing

The first step in the proposed approach is data preprocessing [26]; one of the essential steps in machine learning approaches. Data preprocessing is a critical activity as the world data is never appropriate to be used. A sequence of preprocessing steps have been used in this work to prepare the raw data of the Yelp dataset for computational activities. This can be summarized as follows:

1) *Tokenization*: Tokenization is one of the most common natural language processing techniques. It is a basic step before applying any other preprocessing techniques. The text is divided into individual words called tokens. For example, if we have a sentence (“wearing helmets is a must for pedal cyclists”), tokenization will divide it into the following tokens (“wearing”, “helmets”, “is”, “a”, “must”, “for”, “pedal”, “cyclists”) [27].

2) *Stop Words Cleaning*: Stop words [28] are the words which are used the most yet they hold no value. Common examples of the stop words are (an, a, the, this). In this paper, all data are cleaned from stop words before going forward in the fake reviews detection process.

3) *Lemmatization*: Lemmatization method is used to convert the plural format to a singular one. It is aiming to remove inflectional endings only and to return the base or dictionary form of the word. For example: converting the word (“plays”) to (“play”) [29].

Several approaches have been developed in the literature to extract features for fake reviews detection. Textual features is one popular approach [31]. It contains sentiment classification [32] which depends on getting the percent of positive and negative words in the review; e.g. “good”, “weak”. Also, the Cosine similarity is considered. The Cosine similarity is the cosine of the angle between two n-dimensional vectors in an n-dimensional space and the dot product of the two vectors divided by the product of the two vectors’ lengths (ormagnitudes)[33]. TF-IDF is another textual feature method that gets the frequency of both true and false (TF) and the inverse document (IDF). Each word has a respective TF and IDF score and the product of the TF and IDF scores of a term is called the TF-IDF weight of that term [34]. A confusion matrix is used to classify the reviews into four results; True Negative (TN): Real events are classified as real events, True Positive (TP): Fake events are classified as fake, False Positive (FP): Real events are classified as fake events, and False Negative (FN): Fake events are classified as real.

Second there are user personal profile and behavioral features. These features are the two ways used to identify spammers Whether by using time-stamp of user’s comment is frequent and unique than other normal users or if the user posts a redundant review and has no relation to domain of target.

In this paper, We apply TF-IDF to extract the features of the contents in two languages models; mainly bi-gram and tri-gram. In both language models, we apply also the extended dataset after extracting the features representing the users behaviors.

C. Feature Engineering

Fake reviews are known to have other descriptive features [35] related to behaviors of the reviewers during writing their reviews. In this paper, we consider some of these feature and their impact on the performance of the fake reviews detection process. We consider caps-count, punct-count, and emojis behavioral features. *caps-count* represents the total capital character a reviewer use when writing the review, *punct-count* represents the total number of punctuation that found in each review, and *emojis* counts the total number of emojis in each review. Also, we have used statistical analysis on reviewers’ behaviours by applying “groupby” function, that gets the number of fake or real reviews by each reviewer that are written on a certain date and on each hotel. All these features are taken into consideration to see the effect of the users behaviors on the performance of the classifiers.

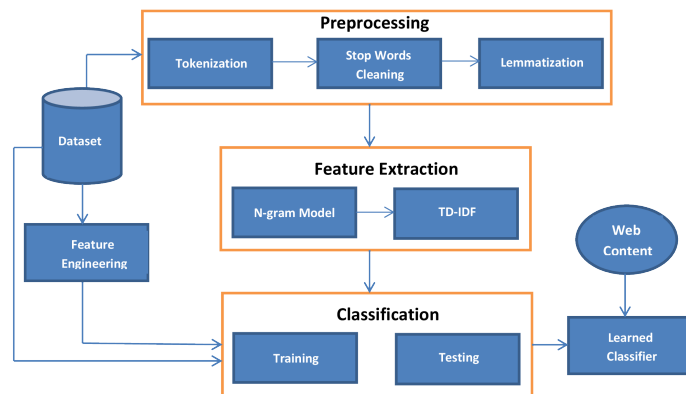


Fig. 1. The Proposed Framework.

B. Feature Extraction

Feature extraction is a step which aims to increase the performance either for a pattern recognition or machine learning system. Feature extraction represents a reduction phase of the data to its important features which yields in feeding machine and deep learning models with more valuable data. It is mainly a procedure of removing the unneeded attributes from data that may actually reduce the accuracy of the model [30].

V. EXPERIMENTAL RESULTS

We evaluated our proposed system on Yelp dataset [5]. This dataset includes 5853 reviews of 201 hotels in Chicago written by 38,063 reviewers. The reviews are classified into 4,709 review labeled as real and 1,144 reviews labeled as fake. Yelp has classified the reviews into genuine and fake. Each instance of the review in the dataset contains the review date, review ID, reviewer ID, product ID, review label and star rating. The statistics of dataset is summarized in Table I. The maximum review length in the data contains 875 word, the minimum review length contains 4 words, the average length

of all the reviews is 439.5 word, the total number of tokens of the data is 103052 word, and the number of unique words is 102739 word.

TABLE I. SUMMARY OF THE DATASET

Total number of reviews	5853 review
Number of fake reviews	1144 review
Number of real reviews	4709 review
Number of distinct words	102739 word
Total number of tokens	103052 token
The Maximum review length	875 word
The Minimum review length	4 word
The Average review length	439.5 word

In addition to the dataset and its statistics, we extracted other features representing the behaviors of reviewers during writing their reviews. These features include *caps-count* which represents the total capital character a reviewer use when writing the review, *punct-count* which represents the total number of punctuation that found in each review, and *emojis* which counts the total number of emojis in each review. We will take all these features into consideration to see the effect of the users behaviors on the performance of the classifiers.

In this part, we present the results for several experiments and their evaluation using five different machine learning classifiers. We first apply TF-IDF to extract the features of the contents in two languages models; mainly bi-gram and tri-gram. In both language models, we apply also the extended dataset after extracting the features representing the users behaviors mentioned in the last section. Since the dataset is unbalanced in terms of positive and negative labels, we take into consideration the precision and the recall, and hence and hence f1-score is considered as a performance measure in addition to accuracy. 70% of the dataset is used for training while 30% is used for testing. The classifiers are first evaluated in the absence of extracted features behaviors of users and then in the presence of the extracted behaviors. In each case, we compare the performance of classifiers in Bi-gram and Tri-gram language models.

Table II Summarizes the results of accuracy in the absence of extracted features behaviors of users in the two language models. The average accuracy for each classifier of the two language models is shown. It is found that the logistic regression classifier gives the highest accuracy of 87.87% in Bi-gram model. SVM and Random forest classifiers have relatively close accuracy to logistic regression. In Tri-gram model, KNN and Logistic regression are the best with accuracy of 87.87%. SVM and Random forest have relatively close accuracy with score of 87.82%. In order to evaluate the overall performance, we take into consideration the average accuracy of each classifier in both language models. It is found that the highest average accuracy is achieved in logistic regression with 87.87%. The summary of the results are shown in Fig. 2.

On the other hand, Table III summarizes the accuracy of the classifiers in the presence of the extracted features behaviors of the users in the two language models. The results reveal that the classifiers that give the highest accuracy in Bi-gram is SVM with score of 86.9%. Logistic regression and Random forest have relatively close accuracy with score of 86.89% and 86.85%, respectively. While in Tri-gram model, both SVM, and logistic regression give the best accuracy with score of

TABLE II. ACCURACY OF BI-GRAM AND TRI-GRAM IN THE ABSENCE OF EXTRACTED FEATURES BEHAVIORS

Classification Algorithm	Accuracy% Bigram	Accuracy% Trigram	Average Accuracy
Logistic Regression	87.87%	87.87%	87.87%
Naive bayes	86.76%	87.30%	87.03%
KNN (K=7)	86.34%	87.87%	87.82%
SVM	87.82%	87.82%	87.82%
Random Forest	87.82%	87.82%	87.82%

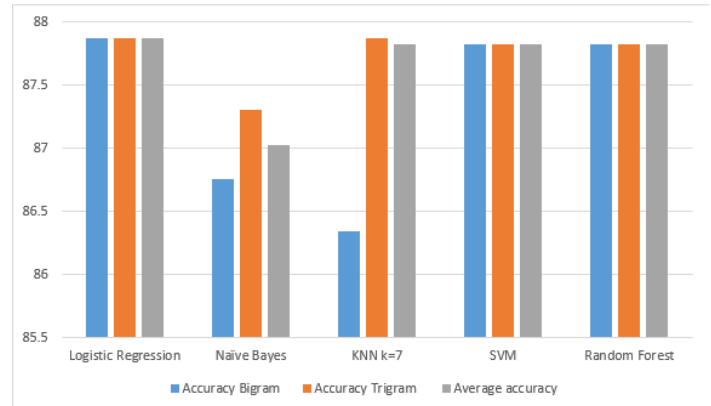


Fig. 2. Accuracy, and Average Accuracy in Absence of Extracted Behavioral Features.

86.9%. The Random forest gives a close score of 86.8%. The summary of the results are illustrated in Fig. 3. Also, it is found that the highest average accuracy is obtained with SVM classifier with score of 86.9%.

TABLE III. ACCURACY OF BI-GRAM AND TRI-GRAM IN THE PRESENCE OF EXTRACTED FEATURES BEHAVIORS

Classification Algorithm	Accuracy% Bigram	Accuracy% Trigram	Average Accuracy
Logistic Regression	86.89%	86.9%	86.89%
Naive bayes	85.82%	86.34%	86.08%
KNN (K=7)	86.56%	85.9%	86.23%
SVM	86.9%	86.9%	86.9%
Random Forest	86.85%	86.8%	86.82%

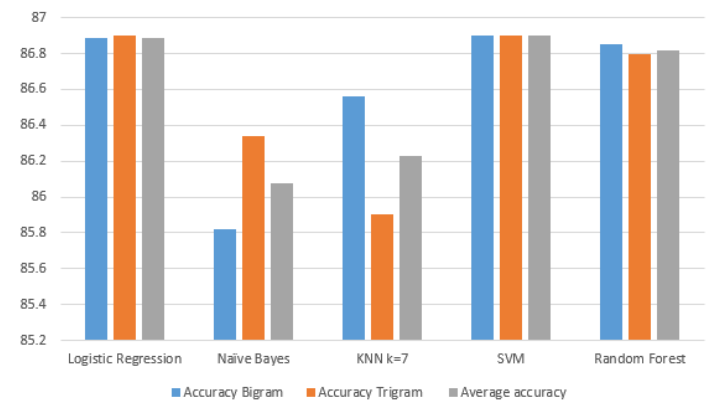


Fig. 3. The Accuracy, and the Average Accuracy after Applying Feature Engineering.

Additionally, precision, recall and f1-score are taken into consideration as evaluation metrics. Actually, they are key

indicators when the data is unbalanced. Similar to the previous, Table IV represents the recall, precision, and hence f1-score in the absence of the extracted features behaviors of the users in the two language models. For the trade-off between recall and precision, f1-score is taken into account as the evaluation criterion of each classifier. In Bi-gram, KNN(k=7) outperforms all other classifiers with f1-score value of 82.40%. Whereas, in Tri-gram, both logistic regression and KNN(K=7) outperform other classifiers with f1-score value of 82.20%. To evaluate the overall performance of the classifiers in both language models, the average f1-score is calculated. It is found that, KNN outperforms the overall classifiers with average f1-score of 82.30%. Fig. 4 depicts the the overall performance of all classifiers.

TABLE IV. RECALL, PRECISION, AND F1-SCORE IN ABSENCE OF EXTRACTED BEHAVIORAL FEATURES

	Bi-gram			Tri-gram			Avg F-score
	Recall	Precision	F-score	Recall	Precision	F-score	
Logistic Regression	87.87%	77.22%	82.20%	87.87%	77.20%	82.20%	82.20%
Naive Bayes	86.79%	78.23%	81.86%	87.30%	78.97%	82.12%	81.99%
KNN(K=7)	86.34%	80.20%	82.40%	87.87%	77.22%	82.20%	82.30%
SVM	87.82%	77.21%	82.17%	87.82%	77.21%	82.17%	82.17%
Random Forest	87.82%	81.29%	82.28%	87.82%	77.21%	82.17%	82.22%

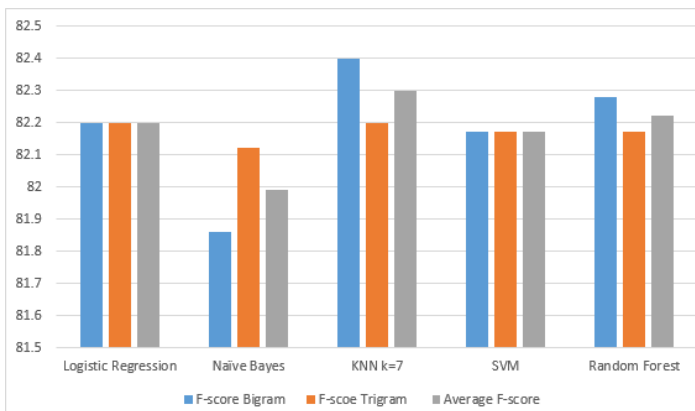


Fig. 4. f-score, and Average f-score in Absence of Extracted Behavioral Features.

Similarly, Table V summarizes the recall, precision, and f1-score in the presence of the extracted features behaviors of the users in the two language models. It is found that, the highest f1-score value is achieved by Logistic regression with f1-score value of 82% in case of Bi-gram. While the highest f1-score value in Tri-gram is achieved in KNN with f1-score value of 86.20%. Fig. 5 illustrates the performance of all classifiers. The KNN classifier outperforms all classifiers in terms of the overall average f1-score with value of 83.73%.

The results reveal that KNN(K=7) outperforms the rest of classifiers in terms of f-score with the best achieving f-score 82.40%. The result is raised by 3.80% when taking the extracted features into consideration giving best f-score value of 86.20%.

VI. CONCLUSION

In this paper, we showed the importance of reviews and how they affect almost every thing related to web based data.

TABLE V. RECALL, PRECISION, AND F1-SCORE IN PRESENCE OF EXTRACTED BEHAVIORAL FEATURES

	Bi-gram			Tri-gram			Avg F-score
	Recall	Precision	F-score	Recall	Precision	F-score	
Logistic Regression	86.90%	75.53%	82%	86.90%	75.53%	80.82%	81.41%
Naive Bayes	85.82%	76%	80.38%	86.34%	76.59%	80.64%	80.51%
KNN(K=7)	86.56%	80%	81.26%	85.30%	78.50%	86.20%	83.73%
SVM	86.90%	75.50%	80.82%	84.90%	75.53%	81.82%	81.32%
Random Forest	86.85%	75.50%	80.79%	87.90%	74.53%	81.90%	81.34%

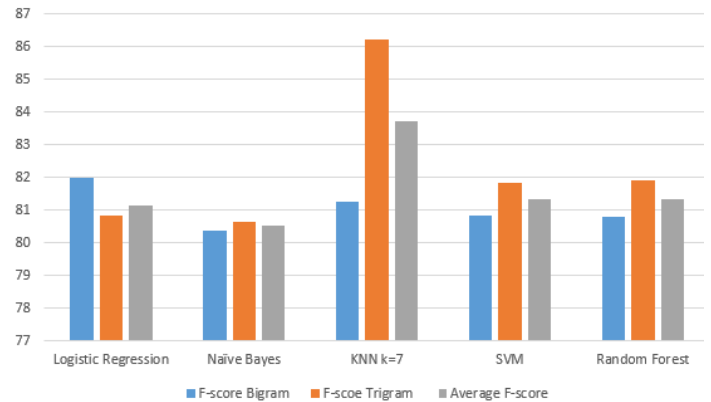


Fig. 5. f-score, and Average f-score in Presence of Extracted Behavioral Features.

It is obvious that reviews play a crucial role in people’s decision. Thus, fake reviews detection is a vivid and ongoing research area. In this paper, a machine learning fake reviews detection approach is presented. In the proposed approach, both the features of the reviews and the behavioral features of the reviewers are considered. The Yelp dataset is used to evaluate the proposed approach. Different classifiers are implemented in the developed approach. The Bi-gram and Tri-gram language models are used and compared in the developed approach. The results reveal that KNN(with K=7) classifier outperforms the rest of classifiers in the fake reviews detection process. Also, the results show that considering the behavioral features of the reviewers increase the f-score by 3.80%. Not all reviewers behavioral features have been taken into consideration in the current work. Future work may consider including other behavioral features such as features that depend on the frequent times the reviewers do the reviews, the time reviewers take to complete reviews, and how frequent they are submitting positive or negative reviews. It is highly expected that considering more behavioral features will enhance the performance of the presented fake reviews detection approach.

ACKNOWLEDGMENTS

The authors would like to thank the Deanship of Scientific Research in Prince Sattam Bin Abdulaziz University, KSA for his support during the stages of this research.

REFERENCES

- [1] R. Barbado, O. Araque, and C. A. Iglesias, “A framework for fake review detection in online consumer electronics retailers,” *Information Processing & Management*, vol. 56, no. 4, pp. 1234 – 1244, 2019.

- [2] S. Tadelis, "The economics of reputation and feedback systems in e-commerce marketplaces," *IEEE Internet Computing*, vol. 20, no. 1, pp. 12–19, 2016.
- [3] M. J. H. Mughal, "Data mining: Web data mining techniques, tools and algorithms: An overview," *Information Retrieval*, vol. 9, no. 6, 2018.
- [4] C. C. Aggarwal, "Opinion mining and sentiment analysis," in *Machine Learning for Text*. Springer, 2018, pp. 413–434.
- [5] A. Mukherjee, V. Venkataraman, B. Liu, and N. Glance, "What yelp fake review filter might be doing?" in *Seventh international AAAI conference on weblogs and social media*, 2013.
- [6] N. Jindal and B. Liu, "Review spam detection," in *Proceedings of the 16th International Conference on World Wide Web*, ser. WWW '07, 2007.
- [7] E. Elmurungi and A. Gherbi, *Detecting Fake Reviews through Sentiment Analysis Using Machine Learning Techniques*. IARIA/DATA ANALYTICS, 2017.
- [8] V. Singh, R. Piryani, A. Uddin, and P. Waila, "Sentiment analysis of movie reviews and blog posts," in *Advance Computing Conference (IACC)*, 2013, pp. 893–898.
- [9] A. Molla, Y. Biadgie, and K.-A. Sohn, "Detecting Negative Deceptive Opinion from Tweets," in *International Conference on Mobile and Wireless Technology*. Singapore: Springer, 2017.
- [10] S. Shojaee *et al.*, "Detecting deceptive reviews using lexical and syntactic features." 2013.
- [11] Y. Ren and D. Ji, "Neural networks for deceptive opinion spam detection: An empirical study," *Information Sciences*, vol. 385, pp. 213–224, 2017.
- [12] H. Li *et al.*, "Spotting fake reviews via collective positive-unlabeled learning." 2014.
- [13] N. Jindal and B. Liu, "Opinion spam and analysis," in *Proceedings of the 2008 International Conference on Web Search and Data Mining*, ser. WSDM '08, 2008, pp. 219–230.
- [14] D. Zhang, L. Zhou, J. L. Kehoe, and I. Y. Kilic, "What online reviewer behaviors really matter? effects of verbal and nonverbal behaviors on detection of fake online reviews," *Journal of Management Information Systems*, vol. 33, no. 2, pp. 456–481, 2016.
- [15] E. D. Wahyuni and A. Djunaidy, "Fake review detection from a product review using modified method of iterative computation framework." 2016.
- [16] D. Michie, D. J. Spiegelhalter, C. Taylor *et al.*, "Machine learning," *Neural and Statistical Classification*, vol. 13, 1994.
- [17] T. O. Ayodele, "Types of machine learning algorithms," in *New advances in machine learning*. InTech, 2010.
- [18] F. Sebastiani, "Machine learning in automated text categorization," *ACM computing surveys (CSUR)*, vol. 34, no. 1, pp. 1–47, 2002.
- [19] T. Joachims, "Text categorization with support vector machines: Learning with many relevant features." 1998.
- [20] T. R. Patil and S. S. Sherekar, "Performance analysis of naive bayes and j48 classification algorithm for data classification," pp. 256–261, 2013.
- [21] M.-L. Zhang and Z.-H. Zhou, "Ml-knn: A lazy learning approach to multi-label learning," *Pattern recognition*, vol. 40, no. 7, pp. 2038–2048, 2007.
- [22] N. Suguna and K. Thanushkodi, "An improved k-nearest neighbor classification using genetic algorithm," *International Journal of Computer Science Issues*, vol. 7, no. 2, pp. 18–21, 2010.
- [23] M. A. Friedl and C. E. Brodley, "Decision tree classification of land cover from remotely sensed data," *Remote sensing of environment*, vol. 61, no. 3, pp. 399–409, 1997.
- [24] A. Liaw, M. Wiener *et al.*, "Classification and regression by random-forest," *R news*, vol. 2, no. 3, pp. 18–22, 2002.
- [25] D. G. Kleinbaum, K. Dietz, M. Gail, M. Klein, and M. Klein, *Logistic regression*. Springer, 2002.
- [26] G. G. Chowdhury, "Natural language processing," *Annual review of information science and technology*, vol. 37, no. 1, pp. 51–89, 2003.
- [27] J. J. Webster and C. Kit, "Tokenization as the initial phase in nlp," in *Proceedings of the 14th conference on Computational linguistics-Volume 4*. Association for Computational Linguistics, 1992, pp. 1106–1110.
- [28] C. Silva and B. Ribeiro, "The importance of stop word removal on recall values in text categorization," in *Neural Networks, 2003. Proceedings of the International Joint Conference on*, vol. 3. IEEE, 2003, pp. 1661–1666.
- [29] J. Plisson, N. Lavrac, D. Mladenić *et al.*, "A rule based approach to word lemmatization," 2004.
- [30] C. Lee and D. A. Landgrebe, "Feature extraction based on decision boundaries," *IEEE Transactions on Pattern Analysis & Machine Intelligence*, no. 4, pp. 388–400, 1993.
- [31] N. Jindal and B. Liu, "Opinion spam and analysis." in *Proceedings of the 2008 international conference on web search and data mining*. ACM, 2008.
- [32] M. Hu and B. Liu, "Mining and summarizing customer reviews." 2004.
- [33] R. Mihalcea, C. Corley, C. Strapparava *et al.*, "Corpus-based and knowledge-based measures of text semantic similarity," in *AAAI*, vol. 6, 2006, pp. 775–780.
- [34] J. Ramos *et al.*, "Using tf-idf to determine word relevance in document queries," in *Proceedings of the first instructional conference on machine learning*, vol. 242, 2003, pp. 133–142.
- [35] G. Fei, A. Mukherjee, B. Liu, M. Hsu, M. Castellanos, and R. Ghosh, "Exploiting burstiness in reviews for review spammer detection," in *Seventh international AAAI conference on weblogs and social media*, 2013.

An Adaptive Genetic Algorithm for a New Variant of the Gas Cylinders Open Split Delivery and Pickup with Two-dimensional Loading Constraints

Anouar Annouch¹

Information Technology and Management
ENSIAS-Mohammed V University in Rabat

Adil Bellabdaoui²

Information Technology and Management
ENSIAS-Mohammed V University in Rabat

Abstract—This paper studies a combination of two well-known problems in distribution logistics, which are the truck loading problem and the vehicle routing problem. In our context, a customer daily demand exceeds the truck capacity. As a result, the demand has to be split into several routes. In addition, it is required to assign customers to depots, which means that each customer is visited just once by any truck in the fleet. Moreover, we take into consideration a customer time windows. The studied problem can be defined as a Multi-depots open split delivery and pickup vehicle routing problem with two-dimensional loading constraints and time windows (2L-MD-OSPDTW). A mathematical formulation of the problem is proposed as a mixed-integer linear programming model. Then, a set of four class instances is used in a way that reflects the real-life case study. Furthermore, a genetic algorithm is proposed to solve a large scale dataset. Finally, preliminary results are reported and show that the MILP performs very well for small test instances while the genetic algorithm can be efficiently used to solve the problem for a wide-reaching test instances.

Keywords—Vehicle routing problem; split delivery and pickup; multi-depot; two-dimensional loading; genetic algorithm

I. INTRODUCTION

LPG logistics transportation, in particular the distribution of the Liquefied Petroleum Gas (LPG) cylinders is considered among the basic building blocks in the Oil and Gas downstream supply chain and also known to be a very complex supply chain [11]. A typical LPG downstream supply chain consists of filling plants, distribution locations, fleet of trucks and customer's depots. The filling plant is an industrial unit composed of several processes in order to fill a broad range of gas cylinders. It should also be noted that the production and storage capacity is different from one filling plant to another. Therefore, each filling plant has an attached distribution location which is a cylinder's storage unit supplied from the production unit, then serves a set of customers by using a fleet of trucks. Moreover, due to the flammable nature of the gas, it is usually stored in liquid form under a specific pressure, in steel or composite plastic gas cylinders carefully checked and protected against deterioration. In general, the companies do not sell the gas cylinders but just the gas contents inside and the packaging remains their property. This type of packaging management system is called consignment.

Motivated by a case of a Moroccan petroleum company, our paper considers a real-life application in the LPG distribution industry. The objective is to deal with a problem

which corresponds to current industry practice and also to give solution methods able to solve real large-scale instances in very fast computation times. The current distribution policy of our case study links two main entities: the gas filling plants and customers depots. Furthermore, each customer depot is served fully by only one truck. So, deliveries are very difficult to manage and generates a huge cost related to the production capacity and the use of trucks. Thus, the GPL Company faces a real problem which is serving customers in a way to optimize both loading and vehicle routing.

Through this document, we will propose a new distribution policy which will remove the dependency constraint between customer depots and filling plants. Those customers can be served by a fleet of heterogeneous trucks based in multiple filling plants. We note that all customers are visited just once by the truck in the same route. Every truck visits a number of customers in a certain order along its route. Thus, the new approach requires the assignment of customers to filling plants. In addition, a fleet of trucks is based at each filling plant, then, each truck originates from one filling plant serves the customers assigned to that plant. The objective of this policy is therefore to offer a global distribution model at minimal cost. This model concerns both the operation of loading cylinder racks into each truck and the construction of the trucks routes.

The remainder of this paper is organized as follows: Section 2 presents the loading and distribution problem considered in our case study. In Section 3, we explore a related literature review. In Section 4, we present a mathematical formulation of our problem based on a mixed integer programming model. Then, we present and discuss computational results. Section 5 presents a developed genetic algorithm (GA). Finally we conclude this paper by discussing results obtained by the GA and compare it with Cplex results, pointing out a few remarks of practical relevance and giving some perspectives of our further researches.

II. PROBLEM DESCRIPTION

The distribution problem studied in this paper includes two sub-problems: a two-dimensional loading vehicle problem and an open multi-depot split delivery and pickup routing problem with time windows (MD-OSPDTW).

A. Two-dimensional Loading Problem

As customer requests are in the form of a set of two-dimensional and rectangular racks, the goal is to find an optimal combination to load it into a set of dissimilar rectangular trailers of height H and width W , without overlapping. The two-loading vehicle problem can be described as a loading of a limited fleet of heterogeneous trucks of capacity P_k and a loading surface with length L_k and height H_k . During loading, racks have a prefixed orientation with respect to the trailers. In addition, all of them should occupy the entire surface width of the truck. We note that in our studied problem three types of trucks are considered.

We consider N racks of several types of gas cylinders to be shipped to r customers. Each rack c is characterized by a width $w_c < L_k$, a height $h_c < H_k$ and a weight q_c known. A problem instance includes a fleet of heterogeneous trucks, initially distributed among filling plants and may differ in term of their cylinders loading capacities. Furthermore, each truck can pull two types of trailers: flatbed trailer and lowboy trailer. Since, the order of each customer is a combination of different types of racks in which we put specific types of gas cylinder; we assume that the loading racks combinations of each truck are known. In addition, the loading surface in each truck can be represented on a rectangular coordinate system (x,y) with origin $(0,0)$, in which the height represents the y -axis and the length represents the x -axis. To summarize, the truck loading is feasible if and only if all racks are placed completely inside the tray surface, two different types of racks cannot overlap and all racks are placed vertically parallel to the truck head.

B. The MD-OSPDTW Problem

The problem considered in our paper can be defined on a directed graph $G = (V,A)$ in which $V = V_1, \dots, V_n, \dots, V_{n+r}$ represent the vertices and $A = (V_i, V_j)$; $i \neq j$ represent the arcs. The set of arcs comprises: $V_c = V_1, \dots, V_n$ as vertices corresponding to the filling plants and $V_e = V_{n+1}, \dots, V_{n+r}$ as vertices representing customer's depots. We indicate by c_{ij} the transportation cost between two vertices i and j . Moreover, customers have a daily requirement D_i of cylinders, a service time S_i and an associated time window. We have to take into account the trucks service time in filling plants $s = (t + w)$ which represent both, the duration t of the trucks processing and the loading or unloading time w . Furthermore, the requirement of each customer may exceed the capacity of the truck, so it has to be split into several routes and each customer can be visited several times by different routes. In addition, each depot has a specific time window and should not be visited outside of this interval time. The objective is to determine for each truck the loading combinations and the set of routes to achieve in order to minimize the total transportation costs.

The problem in our paper is illustrated in Figure 1 and can be considered as an open vehicle routing problem (OVRP). It is a generalization of VRP in which a truck may not return to its departure depot after shipping the last customer on a route. Moreover, instead of the single-depot, deliveries are made from several multi-depots. The considered transportation problems include also more constraints: The time window restriction (OVRPTW), the multi-depots constraints, the fleet of trucks

is assumed to be heterogeneous (HOVRP); the consideration of multi-types of products (MPOVRP). In this paper the transportation problem as a whole can be named as: open split delivery and pickup routing problem with multi-depot, multi-Product, time windows, using a heterogeneous fleet of trucks and obviously with consideration of Two-dimensional loading constraints. To the best of our knowledge, the OVRP as we present it has not been considered in the literature.

III. LITERATURE REVIEW

The vehicle routing problem (VRP) is the most studied combinatorial optimization problem in transport and logistics. It was firstly presented in the literature by [1] as the truck dispatching problem. It can be defined as the determination of an optimal set of routes for a fleet of vehicles which needs to serve a set of customers. Few years later, a considerable number of variants have been considered by researchers: Capacitated vehicles, multi-depots, time-windows, pickup and delivery, heterogeneous fleet, etc. In view of the problem statement, the main purpose of this paper is to focus on the combination of loading constraints and vehicle routing problems. Both problems belong to the NP-hard type of optimization problems. Thus, the combination of these two NP-hard problems gives us a more complicated problem.

In this section, we review only the closely related works which deal with the multi-depots open split pickup and delivery routing problems with time windows and with two-dimensional loading constraints.

The variant of OVRP was firstly introduced in 1981 by [3]. Since then, it has gained much attention from researchers mostly in the studies addressing companies that avoiding being charged for the return trip of the vehicles to their departure depots. So, the important feature of the OVRP problem is that the vehicles are not required to return to the starting depot, but if they do, it must be through visiting customers in reverse order [10]. Authors in [6] presented the first heuristic algorithm to solve the OVRP. They developed a method based on a minimum spanning tree with penalties procedure. Afterwards, a tabu search algorithm was presented in [8] in which authors explore the structure of the OVRP problem and compare its performance with results obtained by other heuristics methods. One year later, the same heuristic was proposed by [10] for finding the routes that minimize both total travelling cost and operating cost while satisfying vehicle capacity and route length constraints. Many researchers have developed various heuristic approaches to efficiently solve the OVRP, such as ant colony optimisation by [19], simulated annealing by the researchers in [9] and genetic and evolutionary computing in [20].

To address the real-world business issues, the OVRP can be combined with more complicated constraints, such as split delivery (SDVRP). The SDVRP was introduced in the first time in [5]. The Authors studied this problem to prove that it can generate savings by allowing divisible deliveries. In [21] a study of the maximum possible savings achieved by enabling divisible deliveries is presented. Authors analyse the SDVRP algorithmic complexity with small capacity vehicles. Another work in which two hybrid genetic algorithms are used to solve a split delivery problem with respect to the total travel

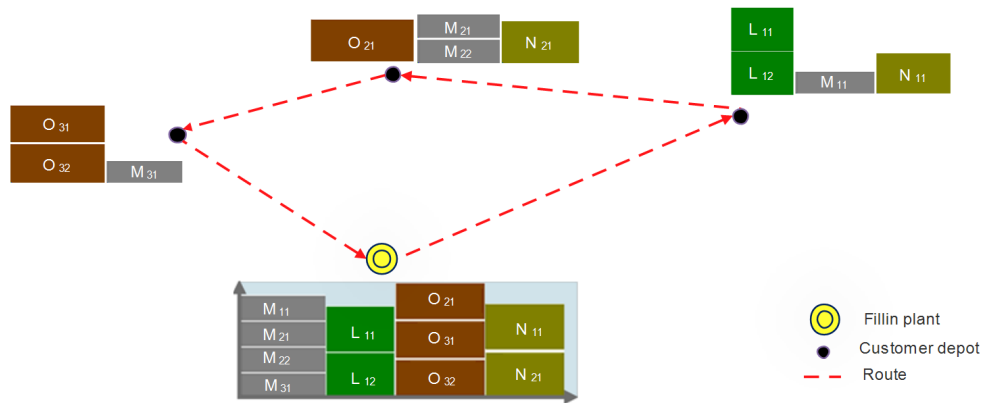


Fig. 1. Illustration of 2L-MD-OSPDTW.

distance is presented by [22]. In regards to the SDOVRP, we find only one interesting paper [30]. Authors developed a mathematical model of the OVRPSD that minimize both total fixed cost of vehicles and delivery workers and total transportation cost. Other features are also considered such as delivery and pickup (DPRP). This problem has received continual attention in transportation logistics field. The early work on the VRPPD was in [2], it was conducted for dial-a-ride scenarios. Later, researchers in [7] provided a lower limit where a demand of each customer does not exceed the vehicle capacity. In the VRPSPD, the vehicles are not only required to deliver goods to customer, but also pickup goods at customer locations. A general assumption in the VRPSPD is that all delivered goods must be originated from the depot and all pickup goods must be transported back to the depot. Very recently an iterated local search metaheuristic and a branch-and-price algorithm are proposed to solve the multi-vehicle one-to-one pickup and delivery problem with split loads [27]. Moreover, Authors in [31] studied a barge transportation of maritime containers between a dry port and a set of sea port terminals. They develop a hybrid local search metaheuristic algorithm, combined with a branch-and-cut method to solve the VRPSPD problem. The objective is to find the best allocation of containers to barges in order to guarantee on-time delivery and meet capacity restrictions. In a previous paper we have introduced the split delivery and pickup vehicle routing problem with two-dimensional loading constraints. We attempt to give solutions for small instances in order to validate the model [26].

Customer's time window is also an important characteristic of the studied OVRP. The modeling of such problems requires consideration of the arrival time of each customer, which requires the integration of time windows constraints of each customer. The first paper introduced the open vehicle routing problem (OVRPTW) was studied by [15] Authors studied a real-world cases such as the delivery of school meals, school bus routing, the plans of passing through tunnels of trains, etc. The problem variants are extended to include the case where more than one depot is considered. The multiple depots open routing problem (MD-OVRP) is a variant of the capacitated vehicle routing problem CVRP in which a fleet of vehicles is based at each depot and customers are assigned to depots.

Recently, [29] proposed a two-phase algorithm to solve a low-carbon multi-depot open vehicle routing problem with time windows (MDOVRPTW) with minimum total costs. In the literature, several papers have studied OVRP and VRPSPD with times windows and multi-depots constraints [8] [28] [29].

Another complicated problem presented in this paper which is the two-dimensional loading constraint. In recent years, a problem of loading customer items into vehicles has become a fertile ground for researchers in the field of combinatorial optimization. Nevertheless, the combination of the loading constraints and vehicle routing problems has received a little attention in the literature. The first work related to transportation problem with loading constraints was introduced by [4]. They address the Pickup and Delivery Traveling Salesman with LIFO Loading where a single rear-loaded vehicle serves a set of customer orders with LIFO policy. Next, [12] addressed the Two dimensional Capacitated Vehicle Routing Problem with Loading Constraints (2L-CVRP) using an Ant Colony Optimization (ACO). In another work they present an exact approach based on branch-and-cut for solving the same problem [14]. Researchers in [17] resolved a two dimensional Capacitated Vehicle Routing Problem using a tabu search algorithm. The 2L-VRP is combined to various VRP variants, such as time windows [16] [23][24], Pickup and delivery [13] [18] and heterogeneous fleet [25].

IV. MATHEMATICAL FORMULATIONS

Two virtual plants are considered to formulate our distribution problem: a departure plant and an arrival one. We suppose that the transportation cost is null between these plants and the other considered plants. We define our problem as an oriented graph $G = (V, A)$ with $V = V_0, V_1, \dots, V_{n+1}, \dots, V_{n+r}, V_{n+r+1}, \dots, V_{2n+r}, V_{n+r+1}$ and $A = (V_i, V_j) ; i \neq j$. The arcs A comprises: a virtual starting plant V_0 , a filling departure plants $V_c = V_1, \dots, V_{n+1}$, a set of customers to be visited $V_e = V_{n+1}, \dots, V_{n+r}$, the arrival filling plants $V_{c'} = V_{n+r+1}, \dots, V_{2n+r}$, and the arrival virtual plant V_{2n+r+1} (Figure 2).

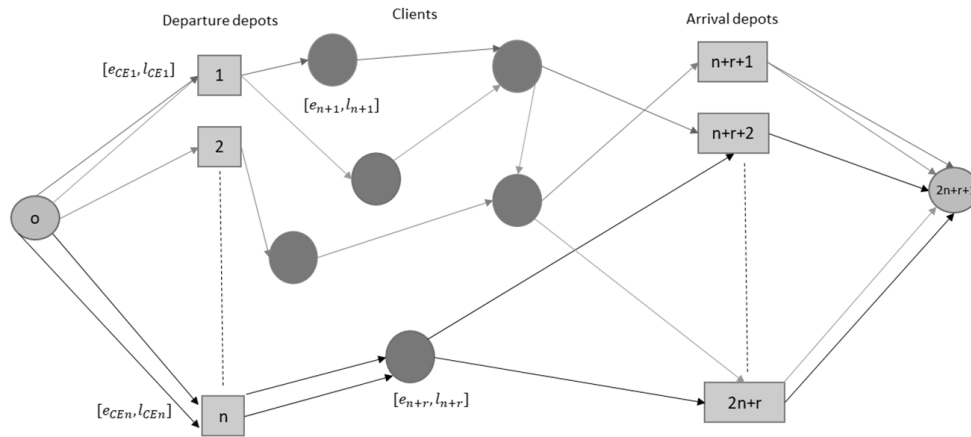


Fig. 2. Illustration of the Solution Method.

A. Assumptions.

- A truck cannot leave or arrive at customer depots outside a specific time window;
- Each filling plan has a determined service time corresponding to unload racks of the empty cylinders and to load racks of the filled cylinders;
- Each customer depot has a determined service time corresponding to unload racks of the filled cylinders and to load racks of the empty cylinders;
- The travel time and the distance between the gas filling plants and the customer depots are well known;
- At the beginning, all trucks are empty and supposed parked at the plants where it belongs;
- The starting location of each tour which is the filling plant can never be a pickup location;
- The last pickup location of the tour is the last served customer;
- Each customer may be served one or more times;
- We suppose the use of heterogeneous and limited fleet of trucks;
- The racks should occupy the entire surface width of the truck;
- The capacity of each truck is well known.

B. Parameters.

In order to formulate the above problem and solve it, we define the complete nomenclature and then state the model. The nomenclature is divided into parameters, sets and variables:

- o : Virtual starting plant;
- n : Number of Plants;
- r : Number of customers;
- $2n+r+1$: Virtual arrival plant;

- K : Number of trucks in the fleet;
- C_{ijk} : Truck k transport cost between vertex i and j ;
- P_k : Truck capacity;
- H_k : Maximum height of truck k ;
- L_k : Maximum length of truck k ;
- C : Number of racks types;
- Max_{ck} : Maximum number of racks with type c on truck k ;

$$\text{Max}_{ck} \leq \frac{H_k}{h_c} < \text{Max}_{ck+1}, \forall k \in 1, \dots, K \forall c \in 1, \dots, C$$

- D_{ic} : Customer requirement of cylinders of the type of rack c .
- D_i : Customer requirement of cylinders:

$$D_i = D_{ic}, \forall c \in 1, \dots, C, i \in 1, \dots, r$$

- n_c : Max number of cylinders in rack c ;
- h_c : Rack c height;
- l_c : Rack c length;
- q_c : Rack c weight when it is full;
- t_{ij} : Travel time between vertex i and j ;
- d_{ij} : Distance time between vertex i and j ;
- M : Large number;
- (e_i, l_i) : Time windows
- w : Time to load / unload a rack in a truck
- s_i : Service time $s_i = 2w * \text{Number of racks}$.
- V_{ik} : Binary parameter

$$V_{ik} = \begin{cases} 1 & \text{if truck } k \text{ was parked in plant } i. \\ 0 & \text{otherwise} \end{cases}$$

- λ : Filling plant waiting time

$$\lambda_i = \begin{cases} \lambda & \text{if } i \in (1, \dots, n). \\ 0 & \text{if } i \in (n+1, \dots, n+r) \end{cases}$$

C. Decision Variables.

Five decision variables are used in our mathematical model as follow:

$$x_{ijk} = \begin{cases} 1 & \text{if truck } k \text{ visits } i \text{ from } j. \\ 0 & \text{otherwise} \end{cases}$$

$$i, j \in (0, \dots, 2n+r+1)$$

$$y_{ik} = \begin{cases} 1 & \text{if truck } k \text{ visits } i. \\ 0 & \text{otherwise} \end{cases} \quad i \in (0, \dots, 2n+r+1)$$

a_{ik} : The arrival time of truck k at customer i .

b_{cik} : Number of racks c delivered to customer i by truck k .

z_{ck} : Number of piles c occupied in the truck k .

$$z_{ck} = \sum_{i=n+1}^{n+r} \sup\left(\frac{b_{cik}}{Max_{ck}}\right)$$

D. Objective and Constraints.

Using the above notation, the problem can be presented as follows.

1)

$$\text{Minimize} = \sum_{i=1}^{2n+r+1} \sum_{j=1}^{2n+r+1} \sum_{k=1}^K C_{ijk} x_{ijk}$$

Subject to:

2)

$$\sum_{j=0}^{2n+r} x_{ijk} = \sum_{j=1}^{2n+r+1} x_{ijk} = y_{ik}$$

$$\forall i \in (0, 1, \dots, 2n+r+1), i \neq j, k \in (1, \dots, K)$$

3)

$$\sum_{j=1}^{2n+r+1} \sum_{k=1}^K x_{ijk} = 0 \quad \forall j \in (0, \dots, n)$$

4)

$$\sum_{i=0}^{2n+r} \sum_{k=1}^K x_{ijk} = 0 \quad \forall j \in (n+r+1, \dots, 2n+r+1)$$

5)

$$\sum_{j=n+1}^{n+r} x_{ojk} = \sum_{j=n+1}^{n+r} x_{j(2n+r+1)k} = 0 \quad \forall k \in (1, \dots, K)$$

6)

$$y_{ok} \leq \sum_{j=n+1}^{n+r} y_{jk} \leq M y_{ok} \quad \forall k \in (1, \dots, K)$$

7)

$$y_{(2n+r+1)k} \leq \sum_{j=n+1}^{n+r} y_{jk} \leq M y_{(2n+r+1)k} \quad \forall k \in (1, \dots, K)$$

8)

$$y_{ok} = \sum_{j=1}^n y_{jk} = y_{(2n+r+1)k} = \sum_{j=nr+1}^{2n+r} y_{jk} \quad \forall k \in (1, \dots, K)$$

9)

$$b_{cik} \leq \frac{D_{ic}}{n_c} y_{jk}$$

$$\forall i \in (n+1, \dots, n+r), c \in (1, \dots, C), k \in (1, \dots, K)$$

10)

$$\sum_{i=n+1}^{n+r} \sum_{c=1}^c (b_{cik} Q_c) \leq P_k \quad \forall k \in (1, \dots, K)$$

11)

$$\sum_{k=1}^K b_{cik} = \frac{D_{ic}}{n_c} \quad \forall i \in (n+1, \dots, n+r), c \in (1, \dots, C)$$

12)

$$a_{ik} + \lambda_i + S_i + t_{ij} \leq a_{jk} + M(1 - x_{ijk})$$

$$\forall i, j \in (1, \dots, 2n+r+1), i \neq j, \forall k \in (1, \dots, K)$$

13)

$$a_{ik} \geq e_i y_{ik} \quad \forall i \in (1, \dots, n+1, \dots, r+n), \forall k \in (1, \dots, K)$$

14)

$$a_{ik} \leq l_i + M(1 - y_{ik})$$

$$\forall i \in (n+1, \dots, r+n, \dots, 2n+r+1), \forall k \in (1, \dots, K)$$

15)

$$\sum_{c=1}^C \sum_{i=n+1}^{n+r} b_{cik} h_c l_c \leq H_k L_k + b_k c_k \quad \forall k \in (1, \dots, K)$$

16)

$$\sum_{c=1}^C z_{ck} l_c \leq L_k \quad \forall k \in (1, \dots, K)$$

17)

$$z_{ck} - 1 + \frac{1}{M} \leq \frac{\sum_{i=n+1}^{n+r} b_{cik}}{Max_{ck}} \leq z_{ck}$$

$$\forall k \in (1, \dots, K), \forall c \in (1, \dots, C)$$

18)

$$x_{ojk} \leq V_{jk} \quad \forall k \in (1, \dots, K), \forall j \in (1, \dots, n)$$

19)

$$a_{ik} \geq 0$$

20)

$$b_{cik}, z_{ck} \in \mathbb{N}$$

21)

$$x_{ijk}, y_{ik} = 0, 1$$

The objective function (1) minimizes the total transportation cost. Constraints (2) impose the continuity of a tour; $x_{ijk} = 1$ indicates that the truck k visits j after i and $y_{ik} = 1$ indicates that the truck k visits i . So if a truck k visits a vertex it should necessarily leave it except for the vertex $2n + r + 1$. Constraints (3) assure that the virtual departure plant 'O' can never be a destination, and the departure filling plant can only be a destination for this virtual plant. Constraints (4) enforce the virtual arrival plant $2n+r+1$ to never be a provenance and the arrival filling plant to be a provenance only for the virtual arrival plant $2n+r+1$. Constraints (5) ensure the passage by a departure filling plant and an arrival filling plant. Constraints (6) require the truck to leave the virtual departure plant if it is used. Constraints (7)-(8) enforce the truck to finish its tour at the virtual arrival plant and pass necessarily by the virtual departure plant. Constraints (9) assure that the quantity b_{cik} delivered to customer i cannot exceed the requirement of this customer. Constraints (10) limit the overall load to not exceed the truck capacity. Constraints (11) impose the satisfaction of customer's demands. Constraints (12) determine the arrival time and represent subtour elimination constraints. Constraints (13)-(14) enforce the respect of time windows. Constraints (15) ensure that the total surface occupied by racks on each truck is less than the total surface of the tray space. Constraints (16) ensure that the sum of the widths of racks loaded in the tray is less than the length of the truck. Constraint (17) determines the number of piles occupied by each type c of racks. Constraint (18) indicates that each truck can only be started at initial parked filling plant.

V. RESULTS

In this section we start by describing the problem instances used within the computational experiments. The test instances considered in our paper are derived from a real-life dataset provided by a major petroleum company in Morocco. For the exact resolution, the dataset consists of 4 problem classes; each problem class is divided into 3 dispersed configurations of different sizes and the model was tested on all 12 instances. In our problem settings we have at most fifteen customer's depots $C = C1...C15$ supplied from four gas filling plants $D = D1...D4$ and using at most forty trucks of three different configurations.

Exact solutions are obtained by implementing the model using the commercial solver IBM ILOG CPLEX 12.5 and tested on a workstation with Intel(R) Core(TM) i7 CPU @ 2.60Ghz (8 CPUs) and 16 GB RAM. Our goal is to determine how large an instance could be solved to optimality in a reasonable amount of time.

Furthermore, the requirement for each customer for three different types of gas cylinders (B03, B06 and B12), the transport costs between each vertex and the dimensions of the storage racks are all known

Furthermore, in the latest test class CL4 in which we have used the real volume of customers' demand, we use four filling plants and limiting the number of customers to be fifteen and the number of vehicles to be forty. Having discussed the savings generated by recovering the packaging, racks should return charged by empty cylinders. Thus, let us now consider the following decision rules: The delivered depot of order

D_i represent the pickup location of the same number and types of racks. In what follows, we detail our findings for each input setting.

Table I reports also the result for each instance. It shows the instances characteristics, the obtained objective value, the best bound, the real gap percentage and the CPU time. We observe that for instances of small size (CL1-01, CL1-02 and CL1-03) the resolution does not take too much time to obtain an optimal solution at less than the 107th iteration. Furthermore, when we increase the number of customers to be served, CPLEX reaches good feasible solutions for medium size instances (CL2-01 to CL3-01). After ten tests, we tried to solve problem instances (CL4-02 and CL4-03); the execution took more than one hour without obtaining results. So, the solver can be stopped sooner without significantly finding a feasible solution. Moreover, we observe that both, the number of iterations and the time of resolution increase extensively with the number of customers affected by the volume of requirement.

Summing up, the MILP model solves the small-size problems (1 gas filling plant and 1 customer) optimally within seconds. When the number of customers increases to 7 (instance CL3-02), MILP could not prove the optimality of solutions within time limits. We note also that the customers' demands used in our first test instances are in the order of a hundred cylinders only, while the actual demand varies between 2000 and 11000. By testing the model of distribution with actual customers' demands (instance CL4-02), the solver ran for a long time without generating any results. Solving our problem requires examining a very large number of combinations. If there are few customers to visit, the number of combinations to explore is low and the problem is resolved quickly. However, adding only a few clients can dramatically increase the number of combinations to explore so that the resolution time becomes excessively long; this phenomenon is called the combinatorial explosion.

An example of an optimal solution to the routing, as well as to the loading problem with five customers and two gas filling stations is depicted in Figure 3. It represents the test instance CL2-3 in which six vehicles spread over the two filling stations. As we have considered in the problem formulation two virtual stations (0 and 0') with transport cost between these virtual stations and the other stations is equal to zero. In the MILP formulation we consider that all vehicles are initially located at depot O.

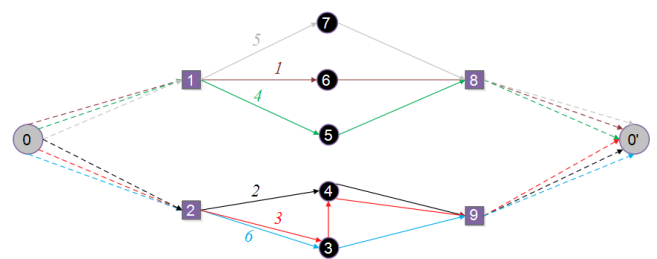


Fig. 3. Illustration of the CL2-03 Solution.

In Table II we report the visited sequence of each tour and the related loading characteristics. As customers' order in the

TABLE I. RESULTS USING ILOG IBM WITH CPLEX AS SOLVER.

I: Number of filling plant J: Number of customers K: Number of trucks R: Number of racks											
Instances	I	J	K	R	Variables	Constraints	Iterations	Objective	Bound	Rel. Gap	CPU (S)
CL1-01	1	1	2	1	75	90	107	1456	1456	0.00	0.02
CL1-02	1	2	3	2	163	208	2382	5983	5983	0.00	0.55
CL1-03	1	3	5	2	356	459	80	21403.47	21403.47	0.00	0.75
CL2-01	2	3	5	2	536	439	993	20045.57	18787.68	6.28	0.22
CL2-02	2	4	6	2	781	794	7175	10392.69	10123.23	2.59	0.42
CL2-03	2	5	6	3	967	1072	110786	14694.68	12435.76	15.37	1.86
CL3-01	3	5	7	2	1450	1293	113050	13224.71	13016.11	1.58	6.58
CL3-02	3	6	7	3	1716	1673	184771	16853.72	16424.73	2.55	105.92
CL3-03	3	10	12	3	5896	5961	17902486	30634.29	30609.29	0.08	1006.78
CL4-01	4	10	15	3	7096	6354	30136529	35215.265	32564.23	7.53	1869.53
CL4-02	4	13	20	3	14461	10980	52413896	-	-	-	>3600
CL4-03	4	15	40	3	25576	16866	52213264	-	-	-	>3600

test instance CL2-03 are small sizes in which total demand for each type of cylinder do not exceed 1000, the distribution of orders is balanced between all vehicles. Thus, we get the optimality for this test instance.

The addressed model is considered to be a NP-hard combinatorial problem. Thereby, the use of exact optimization method to solve this problem may be difficult in an acceptable CPU times, mostly when the problem involves large data sets. Therefore, the exact method is used only for small size problems.

TABLE II. CL2-03 SOLUTION WITH LOADED RACKS.

Truck	Tour	Loaded racks
1	0→1→6→8→0'	Type 1 = 5 racks Type 2 = 8 racks Type 3 = 8 racks
2	0→2→4→9→0'	Type 1 = 7 racks Type 3 = 10 racks
3	0→2→3→4→9→0'	Type 1 = 3 racks Type 2 = 2 racks Type 3 = 10 racks
4	0→1→5→8→0'	Type 1 = 5 racks Type 2 = 8 racks Type 3 = 8 racks
5	0→1→7→8→0'	Type 1 = 7 racks Type 2 = 10 racks Type 3 = 12 racks
6	0→2→4→9→0'	Type 1 = 6 racks Type 2 = 7 racks Type 3 = 3 racks

VI. GENETIC ALGORITHM FOR THE DISTRIBUTION PROBLEM

By drawing inspiration from the mechanisms of the natural evolution of living beings, many optimization problems are resolved successfully by using genetic algorithms. The GA

is a metaheuristic, introduced for the first time by [32]. The main concern is to find approximate solutions for these problems in a reasonable computation time. To implement our GA, it is necessary to have a solution coding, parameters, a fitness function to evaluate the solutions and a mechanism to obtain the initial population. In addition, we need a method of selecting individuals to reproduce and genetic operators adapted to the problem.

In this section we detail our solution approach based on a genetic algorithm (GA) for the resolution of the gas cylinder distribution problem. We present the adopted coding, the initialization as well as the different genetic operators.

A. Solution Encoding

In our genetic algorithm we represent a coding based on a permutation representation for the adopted solution of the studied distribution problem. Each solution is represented in the form of a one-dimensional table in which a sequence represents the departure plant, the order of the visited customer's depots and the arrival plant. However, this representation poses a problem of delimitation between the filling plants and the customers. Therefore, we use a number $n-2$ of permutations in which n represents the number of customers in the tour, then we assume that the filling plants start from $c = a + 1$ with $n \leq a$ (in our study we take $a = 1000$). An example of this encoding for the vehicle routing problem is given in [33]. Authors propose a permutation which contains both customers and route separators with a set $[0, \dots, 9]$ represents the customers while $[10, \dots, 12]$ are the route separators.

Figure 4 represents an example of routes made by 3 trucks (K1, K2 and K3) in which a sequence of visited customers is assigned to them. In the first route made by truck K1, the departure plant represented by 1001, visited customers 4-1-6-2-3-5 (in that order), and the arrival plant as 1001. In the second route, truck K2 starts at same filling plant 1001 to serve customers 1-6-2-4 but this time it terminates at another filling center 1002. In the third route, truck 3 starts its route at plant 1002, visits customers 2-5 -3-1-6 and returns to the same departure plant. Furthermore, this representation makes it possible to represent trucks to which no route is assigned,

when the number of trucks in the problem is fixed and greater than 1. This case is represented by the last empty route of the truck K4.

Truck	Departure station	Visited customers						Arrival station
K1	1001	4	1	6	2	3	5	1001
K2	1001	1	6	2	4			1002
K3	1002	2	5	3	1	6		1002
K4	1002							

Fig. 4. Chromosome Representation.

B. Initial Population Construction

To generate an initial population of our distribution problem we decided to make a mix between two techniques, by generating in a completely random way a half of the population and the rest with a priori good solutions. To build a solution using the random method, we assign randomly selected customers to each truck until all trucks reach their maximum loading capacity. It should be noted that this assignment is made while respecting the various constraints of the problem (time windows, two-dimensional loading constraints, satisfaction of the customer's requirement, etc.). In addition, while building the solution, if the generated route cannot be added to the under construction solution since one of the constraints of the problem will be violated, the route will be rejected. On the other side, if no route can be added to the solution under construction or there is a risk that the random method will turn around the unfeasible routes, we risk that the algorithm will run infinitely without finding a feasible solution. Therefore, we introduce a stop criterion defined by the elapsed CPU time, so the GA stops when this variable reaches the defined limit. To add a randomly generated route to the solution under construction, we have to know the filling plants, the truck that will make the trip and its maximum capacity and the customers who will be visited. The rest of the tour characteristics, in particular the start time, end time and number of racks assigned to each customer, will be calculated based on the solution method. In addition, the calculation of the start and end time of each route must take into account that the truck cannot move for another route until after the end time of its last one.

To generate an initial population of our distribution problem we decided to make a mix between two techniques, by generating in a completely random way a half of the population and the rest with a priori good solutions. To build a solution using the random method, we assign randomly selected customers to each truck until all trucks reach their maximum loading capacity. It should be noted that this assignment is made while respecting the various constraints of the problem (time windows, two-dimensional loading constraints, satisfaction of the customer's requirement, etc.). In addition, while building the solution, if the generated route cannot be added to the under construction solution since one of the constraints of the problem will be violated, the route will be rejected. On the other side, if no route can be added to the

solution under construction or there is a risk that the random method will turn around the unfeasible routes, we risk that the algorithm will run infinitely without finding a feasible solution. Therefore, we introduce a stop criterion defined by the elapsed CPU time, so the GA stops when this variable reaches the defined limit.

Algorithm 1: Random Population Initialization

Input: Population size PS , Filling plants D , Customers C , Trucks K , Racks Cr , Maximal truck capacity CK_{max}

Output: Initial population P_i

```

1 while  $p \leq PS$  do
2   for  $d \in \{1, \dots, D\}$  do
3     Random select of truck  $k$  from  $K$ 
4     while  $Loaded\ capacity \leq CK_{max}$  do
5       Random select of customer  $c$  from  $C$ 
6       Random select of rack  $cr$  from  $Cr$ 
7       Add rack  $cr$  to  $k$ 
8       if All constraints are respected then
9         Add customer  $c$  to route
10    Add route of  $k$  to  $P_i$ 
11   $p \leftarrow p + 1$ 

```

To add a randomly generated route to the solution under construction, we have to know the filling plants, the truck that will make the trip and its maximum capacity and the customers who will be visited. The rest of the tour characteristics, in particular the start time, end time and number of racks assigned to each customer, will be calculated based on the solution method. In addition, the calculation of the start and end time of each route must take into account that the truck cannot move for another route until after the end time of its last one.

Algorithm 2: Greedy Randomized Algorithm

Input: Population size PS , Filling plants D , Trucks K

Output: Initial population P_i

```

1 while  $p \leq PS$  do
2   for  $d \in \{1, \dots, D\}$  do
3     Random select of truck  $k$  from  $K$ 
4      $V \leftarrow$  List of potential routes of  $k$ 
5     Sort  $V$  according to the Fitness
6     while  $V \neq \emptyset$  do
7       if All constraints are respected then
8         Add route of  $k$  to  $P_i$ 
9         Delete route from  $V$ 
10   $p \leftarrow p + 1$ 

```

The Random routes generator operates in a way that at each time it produces a random potential route that can be added to the solution under construction. On the other hand, if this route is not feasible the generator reproduces another one randomly which is different from the first until a feasible potential route is found. Otherwise, this mechanism cannot continue, so it has failed to find a feasible solution randomly. The greedy random method is similar to the random method except we

do not generate the routes randomly. In fact, we associate a fitness with each route in order to be able to compare them.

C. Mutation and Crossover Operators

In the case of our adopted genetic algorithm we will try to reproduce the same mechanism of changing in the sequence as in biology. As a result, the proposed mutation operators should allow us to guarantee the homogeneity of the population and thus avoid too rapid convergence towards a local optimum. In addition, the developed mutation operators in this paper do not apply to all individuals in the population and in each generation. Indeed, we will define a mutation rate P_m which indicates what average proportion of the population must undergo a mutation.

Moreover, the use of completely free mutations allows a better exploration of the solution space. However, as in the case of population initialization, if we have a priori information about our problem, we can restrict the possibilities in order to achieve faster convergence. In this case, there is always the risk, if the information is not relevant, of guiding the GA towards a local optimum. Furthermore, the mutation operator behaves in a completely random manner in choosing the individuals subject to the mutation. As a result, we have the guarantee of the quality of the solutions obtained. In this paper, we propose a mutation operator, based on the local improvements illustrated in Figure 5.

The proposed crossover operator in this paper ensures the mixing and recombination of parental genes to form descendants with new potential. It corresponds to form two new chromosomes (children) based on an exchange of genes between two reproducers (parents). However, we apply a single point crossover operator proposed by [34], which consists in randomly choosing a crossing point. The first child is obtained by taking the first sequence from the first parent, while the rest of the genes are taken from the second parent, so that the genes which have already been taken from the first parent cannot be considered again. It should be noted that the genes from the second parent remain in the same order (Figure 6). Since the crossover operator is random, it occurs with a probability P_c , where we set the rate at 75%.

D. Fitness Function

Because of the variation of trucks capacity in the fleet the crossover and mutation operators can build solutions that do not respect the constraint of satisfying customer needs. On the other hand, our problem is an OVRP where the trucks are not attached to any filling plant at the end of their route. This possibility allows them to end their route at any other plant. Therefore, we encounter a problem of balancing the number of trucks between filling plants at the end of the day which generates a cost that we must consider in our fitness function. Thus, to obtain solutions which respect all the constraints resulting from our problem and after having applied the crossover and mutation operators we are facing a development of very complex mechanisms. Therefore, the best solution is to evaluate each individual by construct a penalization function.

In order to balance the number of trucks between filling centers at the end of the day, we make the least expensive

routes, respecting the following criteria: A truck can move for the second time after all truck are used in the filling plant; a truck cannot move without a load.

Algorithm 3: Genetic Algorithm

Input: P_i : Initial population, P_c : Crossover rate,
 P_m : Mutation rate

Output: Best solution with minimum travelling cost

```
1
2  $P_i \leftarrow$  Generate 50% using the random algorithm
3  $P_i \leftarrow$  Generate 50% using the greedy random
  algorithm
4
5 Evaluate the population using fitness function
6
7 while  $s \leq MaxSteps$  do
8
9   Random select two parents from  $P_i$ 
10  Crossover operator(Parents,  $P_c$ )
11  Mutation operator(Parents,  $P_m$ )
12
13  Evaluate solution using the fitness function
14
15   $s \leftarrow s + 1$ 
```

We adopt the following indicator parameter: "The lower the fitness value, the better the individual". The fitness function is equal to the objective function plus the trucks balancing costs.

$$Fitness = \sum_{i=1}^n \sum_{j=1}^r \sum_{k=1}^K C_{ijk} x_{ijk}$$

A selection operator used in our paper is based on Tournament method in which we select two individuals from the population in a randomly way, we compare their fitness function and we select the one how has the lower value.

E. Computational Experiments of the AG

In this section, we present the statistics and numerical results from the developed genetic algorithm. A heuristic was implemented using the Java language which is an object oriented programming language. In addition, the tests are performed on a machine with an Intel (R) Core (TM) i7 processor at 2.60 GHz (8 processors) and 16 GB of RAM.

To test the performance of our genetic algorithm as well as the power of the mutation and crossover operators used, we present an illustration of the statistics obtained during the tests carried out. For this, we will use a larger instance than the one presented in the exact resolution. The test instance considered in this part is derived from actual data provided by the same oil company. It is made up of 120 customers $C = C1...C110$ supplied by 16 filling centers $D = D1...D16$ and using at most 50 trucks of three different configurations.

We associate with each filling plant a number of heterogeneous trucks in terms of capacity. It should be noted that the tests are carried out for customer needs for a single day, but these needs influence either the number of trucks used

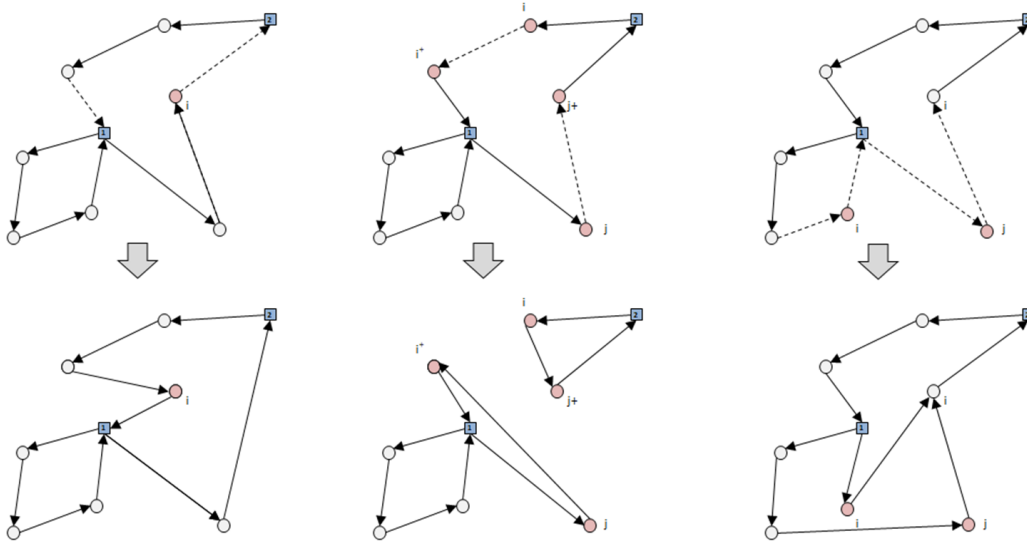


Fig. 5. Example of the Mutation Proposed Operators.

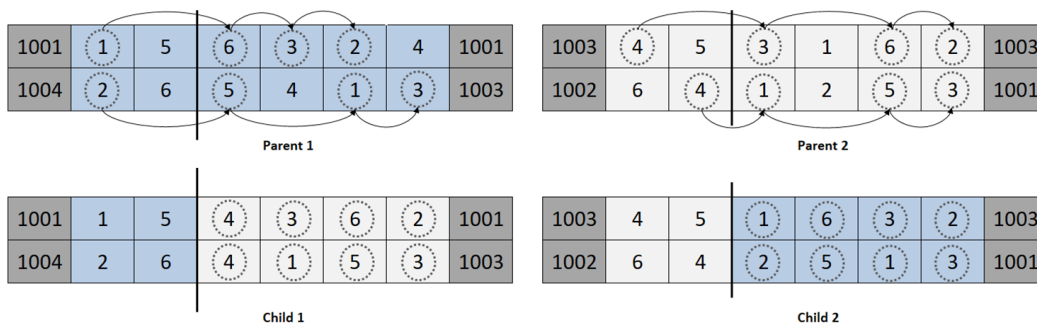


Fig. 6. An Example of the Single Point Crossover.

or the number of customers visited by the trucks or both. The solution obtained with the genetic algorithm depends on a number of parameters which are: population size, mutation rate and crossover rate. To study the influence of the population size we set the stop criterion at 100 iterations, crossover rate at $P_c = 0.85$ and mutation rate at $P_m = 0.50$. Figure 7 shows that the quality of the fitness function improves with the increase in the population size. In addition, we find a positive linear relationship between population size and the computation time.

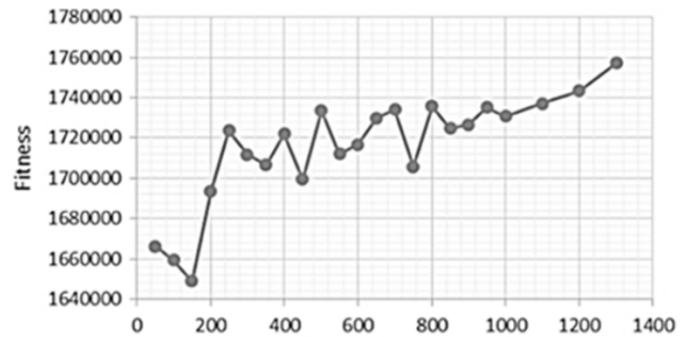


Fig. 7. Influence of the Population Size on the Fitness Value and CPU Time.

The graph illustrated in Figure 8 represents the distributions of the solution values over 37 iterations: the algorithm goes from a population very dispersed solution at the beginning to a population more centered on the optimum found at the end, thus the improvement of the population is very fast at the start (global search) and becomes slower and slower as time

passes (local search).

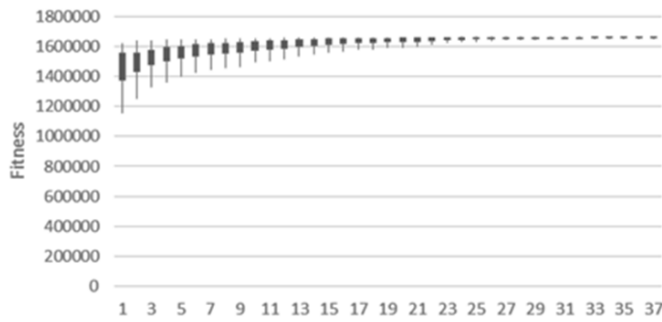


Fig. 8. Variation and Dispersion Fitness Value.

Throughout the evolution of the genetic algorithm the crossover and mutation operators can build solutions that do not respect the problem constraints. However, in most cases these solutions are rejected by the algorithm mechanisms. With the aim of observing this behavior we define a reproduction error rate according to the number of iterations.

$$\text{Error rate} = \frac{\text{Number of invalidate individuals}}{\text{Total number of individuals}}$$

The point cloud in Figure 9 shows an absence of connection between reproduction error and number of iterations. Moreover, the percentage of reproduction error varies between 2% and 8%, so the choice of the crossover and mutation operators is good depending on the probability of reproducing valid individuals. On the other hand, a good choice of the parameters of a method is very important, the adjustment of the parameters is crucial and conditions the quality of the results obtained. However, optimal tuning remains a difficult task.

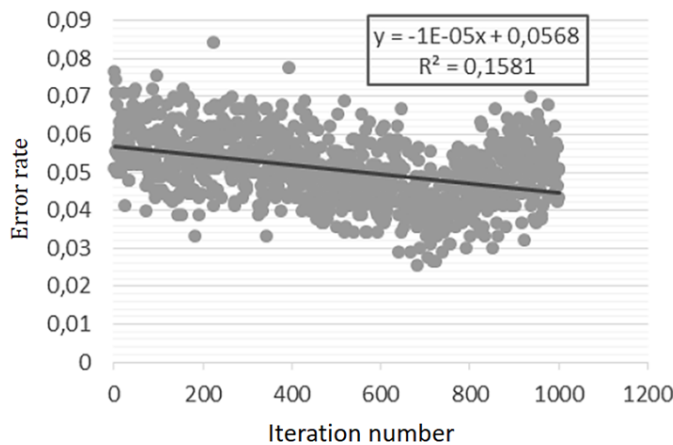


Fig. 9. Error Rate According to the Number of Iterations.

As described above, appropriate adjustment of parameters in genetic algorithms can make a significant difference in

terms of performance. Some values can provide very high performance in specific instances while giving premature convergence in others, even over the same kind of problems. The parameters used in the comparison tests between the proposed GA and the exact method are listed as flow:

- The population size equal to 1400
- The number of iteration equal to 100
- The crossover rate $P_c = 0.85$
- The mutation rate $P_m = 0.50$

Table III shows computational results of the developed genetic algorithm, which also makes comparisons with the exact method illustrated in table I. This table reports the configuration of each instance, the objective and CPU obtained from CPLEX running, solution and CPU obtained with GA and percentage Gaps. Based on results reported in table III we remark that both methods could find optimal solution for the four first test instances. The CPU time performs better in the case of GA for all test instances. In addition, the results obtained from the GA are not too far from those obtained by Cplex. This is justified by the choice of the crossover and mutation operators. Unlike the exact resolution of the studied open split delivery and pick up problem, the developed genetic algorithm gives ambitious results. We have performed tests for real instances of a large scale and in each time we obtain good solutions in a good CPU time. An example of a solution with five customers and two gas filling plants is depicted in Figure 10. It represents the test instance CL2-3 in which six trucks spread over the two filling plants. For example, we have the first truck which leaves from station 1, serves customers 3 and 4 and returns to the station 1 while the second truck which leaves from the same center, serves customer 5 and finishes its trip in the station 2. This is explained by the fact that the trip is open. On the other hand, the first truck which leaves from station 2, serves customers 1 and 3 and returns to the station 2 while the second truck which leaves from the same center, serves customer 1 then customer 2 and finishes its trip in the station 1.

Regarding the loading of each truck, it is clear that the combination is in the form of stacks of n racks of type L, M and N. For example, the truck which leaves from station 1 to serve customer 4 is loaded with five racks of type L, eight racks of type M and eight racks of type N.

VII. CONCLUSIONS

In this paper, we have addressed the open multi-depot split delivery and pickup routing problem with two-dimensional loading constraints in the case of a real-world problem of an LPG distribution company with its real-life assumptions and data. First, we have formulated our problem as a mixed integer linear programming (MILP), then we have tested the problem for 12 tests instances grouped in 4 classes in which we have proved optimality for 10 instances. Also, we have discussed the effect of changing the setting of the input data on the quality of the solutions obtained and on the running time.

TABLE III. COMPARISON BETWEEN RESULTS FROM CPLEX AND FROM THE PROPOSED GA.

Instances	I: Number of filling plant J: Number of customers K: Number of trucks R: Number of racks				CPLEX		GA		Gaps(%)	
	Configuration				Objective	CPU(S)	Solution	CPU(S)	Obj. Gap(%)	CPU Gap (%)
	I	J	K	R						
CL1-01	1	1	2	1	1456	0.02	1456	0.01	0	50
CL1-02	1	2	3	2	5983	0.55	5983	0.01	0	98.18
CL1-03	1	3	5	2	21403.47	0.75	21403.47	0.01	0	98.67
CL2-01	2	3	5	2	20045.57	0.22	20045.57	0.04	0	81.82
CL2-02	2	4	6	2	10392.69	0.42	11023.92	0.13	6.07	69.05
CL2-03	2	5	6	3	14694.68	1.86	14918.11	0.08	1.52	95.7
CL3-01	3	5	7	2	13224.71	6.58	14036.06	1.03	6.14	99.54
CL3-02	3	6	7	3	16853.72	105.92	14564.65	1.56	13.58	98.53
CL3-03	3	10	12	3	30634.29	1006.78	31256.36	3.09	2.03	99.69
CL4-01	4	10	15	3	35215.265	1869.53	36952.47	4.7	4.93	99.75
CL4-02	4	13	20	3	-	>3600	43625.24	4.33	-	-
CL4-03	4	15	40	3	-	>3600	61452.87	6.87	-	-

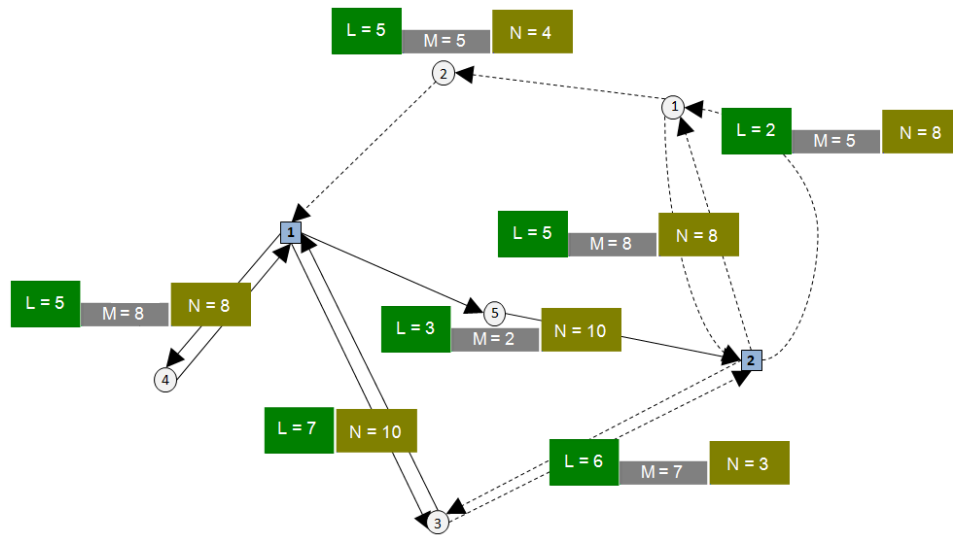


Fig. 10. An Example of Solution.

Due to the difficulty in solving the combination of two NP-hard problems, such as vehicle routing and two-dimensional loading; efficiently, feasible solutions for large instances can be obtained only by developing a metaheuristic method like genetic algorithm. We developed a genetic algorithm and execute it for large data by increasing the size of instances which we are not capable of solving exactly within reasonable computational times. Finally, we gave some statistics and results for the developed GA and discuss obtained results.

REFERENCES

[1] G. B. Dantzig and J. H. Ramser, *The Truck Dispatching Problem*, Management Science, vol. 6, pp 80-91, 1959.

[2] H. Wilson, J. Sussman, H. Wang, B. Higonnet, *Scheduling algorithms for dial-a-ride systems.*, Massachusetts Institute of Technology, Urban Systems Laboratory, Technical Report USL TR-70-13, 1971.

[3] L. Schrage, *Formulation and Structure of More Complex-Realistic Routing and Scheduling Problems.*, Networks, vol. 11, pp 229–232, 1981.

[4] S. Ladany, A. Mehrez, *Optimal routing of a single vehicle with loading and unloading constraints.*, Transportation Planning and Technology, vol 8, pp 301–306, 1984.

[5] M. Dror, G. Laporte, P. Trudeau, *Vehicle Routing with Split Deliveries.*, Discrete Applied Mathematics, vol. 50, pp 239-254, 1994.

[6] D. Sariklis, S. Powell, *A heuristic method for the open vehicle routing problem.*, Journal of the Operational Research Society, vol. 51, pp 564–573, 2000.

[7] J. M. Belenguer, M. C. Martinez, E. A. Mota, *Lower Bound for the Split Delivery VRP.*, Operational Research, vol. 48, pp 801-810, 2000.

[8] J. A. Brandão, *tabu search algorithm for the open vehicle routing problem.*, European Journal of Operational Research, vol. 157, pp 552-564, 2004.

[9] C. D. Tarantilis, G. Ioannou, C. T. Kiranoudis, G. P. Prastacos, *A threshold accepting approach to the open vehicle routing problem.*, RAIRO Operations Research, vol. 38, pp 345-360, 2004.

[10] R.W. Eglese, Z. Fu, L. Li, *A tabu search heuristic for the open vehicle routing problem.*, Journal of the Operational Research Society, vol. 56, pp 267–274, 2005.

- [11] R. Hussain, T. Assavapokee, B. Khumawala, *Supply Chain Management in the Petroleum Industry: Challenges and Opportunities.*, International Journal of Global Logistic Supply Chain Management, vol. 1, pp 90-97, 2006.
- [12] F. Guenther, K. F. Doerner, R. F. Hartl, M. Iori, *Ant colony optimization for the two-dimensional loading vehicle routing problems.*, Computers and Operations Research, vol. 36, pp 655-673, 2007.
- [13] F. Carrabs, J. Cordeau, G. Laporte, *Variable neighborhood search for the pickup and delivery traveling salesman problem with LIFO loading.*, INFORMS Journal on Computing, vol. 19, pp 618-632, 2007.
- [14] M. Iori, J. Salazar-González, D. Vigo, *An exact approach for the vehicle routing problem with two dimensional loading constraints.*, Transportation Science, vol. 41, pp 253-264, 2007.
- [15] P. P. Repoussis, C. D. Tarantilis, G. Ioannou, *The open vehicle routing problem with time windows.*, Journal of the Operational Research Society, vol. 58, pp 355-367, 2007.
- [16] A. Attanasio, A. Fuduli, G. Ghiani, C. Triki, *Integrated shipment dispatching and packing problems: a case study.*, Journal of Mathematical Modelling and Algorithms, vol. 6, pp 77-85, 2007.
- [17] M. Gendreau, M. Iori, G. Laporte, S. Martello, *A tabu search heuristic for the vehicle routing problem with two-dimensional loading constraints.*, Networks, vol. 51, pp 4-18, 2008.
- [18] G. Erdogan, J. Cordeau, G. Laporte, *The pickup and delivery traveling salesman problem with first-in-first-out loading.*, Computers and Operations Research, vol. 36, pp 1800-1808, 2009.
- [19] X. Li, P. Tian, S. C. Leung, *An ant colony optimization metaheuristic hybridized with tabu search for open vehicle routing problems.*, Journal of the Operational Research Society, vol. 60, pp 1012-1025, 2009.
- [20] S. Yu, C. Ding, K. Zhu, *A hybrid GA-TS algorithm for open vehicle routing optimization of coal mines material.*, Expert Systems With Applications, vol. 38, pp 10568-10573, 2011.
- [21] F. Archetti, I. Giordani, G. Mauri, E. Messina, E. *A new clustering approach for learning transcriptional modules.*, International Journal of Data Mining and Bioinformatics, vol. 6, pp 304-23, 2012.
- [22] J. H. Wilck, T. M. Cavalier, *A genetic algorithm for the split delivery vehicle routing problem.*, American Journal of Operational Research, pp 207-216, 2012.
- [23] L. Martinez, C. Amaya, *A vehicle routing problem with multi-trips and time windows for circular items.*, Journal of the Operational Research Society, vol. 64, pp 1630-1643, 2012.
- [24] S. Khebbache-Hadji, C. Prins, A. Yalaoui, M. Reghioui, *Heuristics and memetic algorithm for the two-dimensional loading capacitated vehicle routing problem with time windows.*, Central European Journal of Operations Research, pp 307-336, 2013.
- [25] S. Leung, Z. Zhang, D. Zhang, X. Hua, M. K. Lim, *A meta-heuristic algorithm for heterogeneous fleet vehicle routing problems with two-dimensional loading constraints.*, European Journal of Operational Research, pp 199-210, 2013.
- [26] A. Annouch, A. Bellabdaoui, J. Minkhar, *Split delivery and pickup vehicle routing problem with two-dimensional loading constraints.*, 11th International Conference on Intelligent Systems: Theories and Applications, 7772277, 2016.
- [27] M.N. Haddad, R. Martinelli, T. Vidal, S. Martins, L. S. Ochi, M.J.F. Souza, R. Hartl, *Large neighborhood-based metaheuristic and branch-and-price for the pickup and delivery problem with split loads.*, European Journal of Operational Research, vol. 270, pp 1014-1027, 2018.
- [28] Y. Niu, Z. Yang, P. Chen, J. Xiao, *Optimizing the green open vehicle routing problem with time windows by minimizing comprehensive routing cost.*, Journal of Cleaner Production, vol. 171, pp 962-971, 2018.
- [29] S. Ling, T. Fengming, W. Songyi, *Multi-depot open vehicle routing problem with time windows based on carbon trading.*, International Journal of Environmental Research and Public Health, vol. 15, 2018.
- [30] R. Tarit, C. Phanchita, P. Panurut, V. Rapeeporn, *An Optimization for Split Delivery Open Vehicle Routing Problem with Manual Materials Handling.*, 2nd International Conference on Engineering Innovation (ICEI), 2018.
- [31] F. Stefano, J. C. Fransoo, V. W. Tom, V. Woensel, D. Jing-Xin, *A variant of the split vehicle routing problem with simultaneous deliveries and pickups for inland container shipping in dry-port based systems.*, Transportation Research Part E: Logistics and Transportation Review, vol. 142, 102057, 2020.
- [32] J. H. Holland, *Adaptation in natural and artificial systems.*, Ann Arbor: The University of Michigan Press, 1975.
- [33] E. Alba and B. Dorronsoro, *The exploration/exploitation tradeoff in dynamic cellular evolutionary algorithms.*, IEEE Transactions on Evolutionary Computation, vol. 9, pp 126-142, 2005.
- [34] S. Hartmann, *A competitive genetic algorithm for resource-constrained project scheduling.*, Naval Research Logistics, vol. 45, pp 733750, 1998.

Study of Post-COVID-19 Employability in Peru through a Dynamic Model, Between 2020 and 2025

Richard Ronny Arias Marreros¹, Keyla Vanessa Nalvarte Dionisio², Luis Alberto Romero Tuanama³,
Juber Alfonso Quiroz Gutarra⁴, Laberiano Andrade-Arenas⁵
Facultad de Ciencias e Ingeniería
Universidad de Ciencias y Humanidades

Abstract—The research work is focused on the sector of the population that will have a job, taking into account that the pandemic was a problem that resulted in many people losing their jobs due to the economic crisis that affected all countries because the first half of the year 2020 the equivalent of 400 million full-time jobs were lost and there was a 14% drop in working hours worldwide, also in Lima 1.2 million people were left without work. For this reason, a dynamic analysis was developed for the projection of post-COVID19 employability in Peru from 2020 to 2025 to obtain an approximate knowledge of the population's labor outlook, implementing system dynamics as a methodology since it includes this recommendation, given that any model built through its application will be based on the opinion of those involved in the system to be represented. In this work, system dynamics is presented as a very useful methodology for the analysis of complex problems, developing the Forrester and causal diagram with the help of Vensim software. As a result, the approximate number of jobs that will be available was visualized, and it was observed that the future of employability will be at risk, which is why a good government strategy is necessary so that this does not happen since people need to satisfy their professional, economic and development needs.

Keywords—Employability; forrester diagram; population; system dynamics; vensim

I. INTRODUCTION

In the month of December 2019, there were a large number of cases of severe pneumonia that started in the City of Wuhan in China. Initial epidemiological studies showed that the disease was spreading rapidly, affecting more people aged 39 and 79 with an overall lethality [1]. The outbreak spread rapidly in number of cases and in different regions of China during the months of January and February 2020. The disease, which is now called COVID-19, continued to spread in other Asian countries and then to other continents [2].

On March 11, 2020, the World Health Organization (WHO) issued a statement on the occurrence of the pandemic, calling on all countries to take action and increase control efforts in what appears to be the greatest global public health emergency of modern times [3]. However, as of April 2020, more than 2.6 million cases have been confirmed worldwide, with an estimated 180,000 deaths and more than 700,000 patients recovered, numbers that change daily today, and can be monitored in real time on the Johns Hopkins University website [4].

Currently Peru has 32,162,184 inhabitants and up to November 25, 2020 there are 35,685 people who died from COVID-19, in the last day 44 people have died, a lower figure

than the previous day, in addition there are 952,439 people confirmed to have been infected. In 2019, 515 people died per day, a figure that this year could be increased by the number of deaths from coronavirus. The death rate (deaths compared to confirmed) is 3.75% [5].

Meanwhile, that is why the effect it is having on the world's labor markets is unprecedented. In the United States, 16.8 million people have applied for unemployment benefits during the last 3 weeks (from March 19 to April 9), a number that has never been presented in American history[6].

Consequently, the unemployment rate in Peru has only exceeded 10% of the economically active population. This shows that the main problem of the Peruvian labor market is not the number of unemployed, but rather the quality of employment. Therefore, according to data from the National Institute of Statistics (INEI), employment in the country implies the loss of more than 6 million jobs in the second quarter of the year [7]. So the whole world of work is deeply affected by the global pandemic virus. In addition to being a threat to public health, the economic and social uncertainty jeopardizes the long-term livelihoods and well-being of millions of people. It has generated distrust, collective fear, uncertainty and has further evidenced the high level of poverty and informality, especially the lack of protection in some jobs [8].

To know what a System Dynamic is in the first place, we will start by system. This term is used frequently, although with different exceptions. In the same way we talk about a system, as a way of doing, so we say that we have a system to solve a problem or to reach an objective. This means, that formally we talk about a system as an object with some complexity, formed by coordinated parts, so that the whole has a certain unity, which is precisely the system [9]. Systems Dynamics is based on the use of two types of diagrams, Causal Diagrams and Forrester Diagrams, which have their origin in General Systems Theory and are in fact like two sides of the same coin [10].

The importance of the research is to obtain a future vision of the post-pandemic labor outlook so that the state and the population can take measures in this regard, however, there are limitations such as obtaining accurate information on the rates (employability, birth rate, mortality, etc.) that are important parameters for the projection of employability and the lack of articles related to the subject.

The objective of the article is to carry out a dynamic

modeling of the post-COVID-19 employability projection in Peru during the years 2020 to 2025.

The rest of the document was organized as follows, section II the literature review of the problem, methodology and tool, section III the System Dynamics methodology, section IV the discussions, V the results and finally section VI the conclusion and future work.

II. LITERATURE REVIEW

The author [11] indicates that the Peruvian population is at risk, not only because of the pandemic but also because of job layoffs.

But the level of unemployment depends on several factors. Also, the reactions of labor market indicators to changes in these factors are different in each country. The situation of the population concerning education, demographics, changes in social norms, and preferences for participation in the labor market are important factors, but in the long term, according to the author [12].

The author [13] mentions that the type of economic disruption likely to affect unemployment and inflation would be a supply shock (a negative supply shock would cause an explosion of inflation so, people would expect higher inflation).

Many of the discussions on inflation start with the Phillips curve, which describes the relationship between unemployment and inflation and also takes into account possible changes in the inflation rate in the future depending on the author [13]. Therefore, the inflation factor is also important for the projection of employability, because it has a close relationship with unemployment.

The author [14] mentions that Dynamic Systems was developed by Forrester, and is useful in the study of the continuous dynamic system, which he applied mainly to the simulation of management and social systems.

The author [15] defines Dynamic Systems as a computer-driven approach to policy analysis and design. The approach uses easy-to-use software that produces mathematical models and is described by sets of differential equations. System dynamics models are flows, accumulation of flows in stocks, feedback between stocks, which is also represented as time delays and flows.

Causal diagrams are directed acyclical charts that encode qualitative assumptions about the causal processes that generate the data. Also, the representation of the causal hypotheses in the graph and the assumptions that allow us to evaluate how these causal hypotheses relate to the observed data according to the author's explanation [16].

For the author [17], the most used software for the simulation of continuous and dynamic processes is Vensim, developed by Window Systems, and it can be used to solve management problems. It has the advantage of being able to be programmed in any programming language and also has the

possibility of importing models developed in other software used in modeling and simulation.

Moreover, with Vensim you can check this large amount of data in a simple or complex way depending on the research topic, which can be used by researchers, students, companies and thus improve the output of a proposed system, as explained [18].

III. METHODOLOGY

The methodology that will be used is the system dynamics that is a powerful tool that allows translating the problem situations of the systems and projecting conceptual models to give a solution to such problems in which there is high participation of the human being [19].

A. Description of the Problem

Unemployment in Peru between April and June of this year rose to 8.8 percent, reported the National Institute of Statistics and Information, a period that was strongly marked by the national confinement ordered by the Peruvian government to prevent the spread of COVID-19 in the country.

B. Causal Diagram Design

Fig. 2 shows the causal diagram, which details the variables and their behavior, within the diagram there are two level variables, the first is population which shows as a result the number of future inhabitants within the country. The population is obtained from a calculation between death, birth, migration and emigration, deaths refer to deaths, if these increase, the population will decrease, this relationship results in a negative loop, on the other hand, if births increase the population will do so in the same way, this is a positive loop, migration refers to the arrival of new inhabitants to the country, if this increases the population will also increase this equally gives us a positive loop; finally, emigration refers to inhabitants leaving the country, if this increases the population decreases, this leaves us a negative loop.

The other level variable is the employed population, this is calculated with contracts, layoffs and population; the more population there is the more possibilities of contracts and this leads to an increase in the employed population, from another point if there is more population there will be more layoffs and this will result in less employed population.

C. Forrester Diagram Design

Fig. 1 shows the Forrester diagram, indicating the behavior between various variables categorized in the following aspects:

- **Level variables:** They are those elements that show us in each instant the situation of the model, present an accumulation, and vary only according to other elements called "flows". The "clouds" within the flow chart are levels of inexhaustible content [21], just like the variable population and currently employed population.
- **Flow variables:** These are elements that can be defined as temporary functions. It can be said that they collect

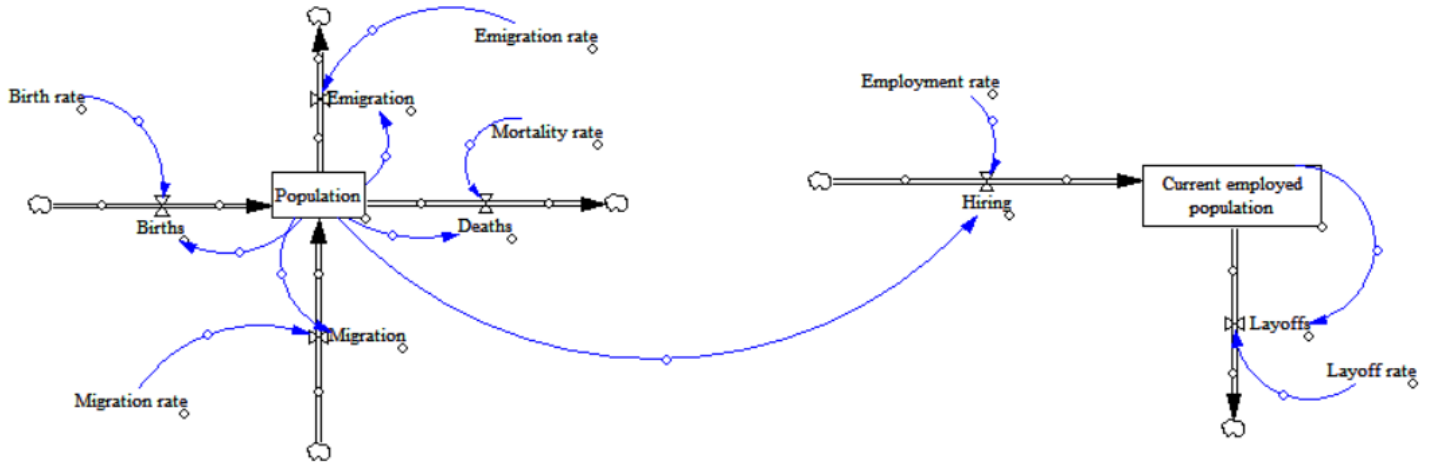


Fig. 1. Forrester Diagram [20].

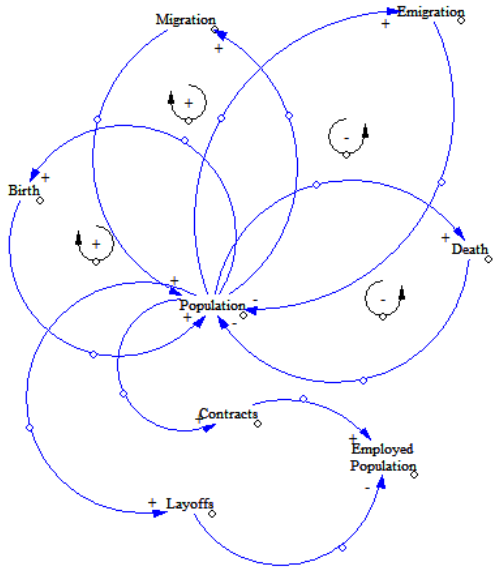


Fig. 2. Causal Diagram [20].

the actions resulting from decisions made in the system, determining the variations in levels [22], as well as the variables births, deaths, migration, emigration, hiring, and firing.

- Parameters:** These are the ones that allow better visualization of the aspects that condition the behavior of the flows [23], such as the variables of birth rate, mortality rate, employment rate, and dismissal rate.

D. Equations

Table I shows the main level variables which are the population and current employed population. The variation of the main population level will depend on the auxiliary variables or parameters of the birth rate, mortality rate, migration and

emigration rate. In the same way, the variation of the main level of the current employed population will depend on the auxiliary variables of the hiring rate and the dismissal rate.

TABLE I. FORMULAS

Num.	Formulas
1	population = emigration + births - migration - deaths
2	population current employee = recruitment - dismissals
3	births = population * birth rate
4	deaths = population / mortality rate
5	emigration = population * emigration rate
6	migration = population * migration rate
7	dismissals = population current employee*(redundancy rate/100)
8	hiring = population*(employment rate/1000)

E. Data

Table II shows the data entered in the Forrester diagram. The initial population is approximately 32 million, the current employed population is 10 million, the mortality rate is 81.8 per 10000 people, and the birth rate is 17.16 per 1000 born in Peru.

TABLE II. DATA ENTERED IN THE FLOW CHART

Num.	Data
1	population (initial value) = 32.162.184
2	Current Employed Population(initial value) = 10.272.400
3	mortality rate = 81.8
4	birth rate = 17.16
5	emigration rate = 4.7
6	migration rate = 2.43
7	redundancy rate = 8.8
8	employment rate = 53.8

IV. DISCUSSIONS

The dynamic systems development method was used, because it focuses on providing functionalities that correspond to the needs of the problem posed, all changes made during the project are reversible, tests are performed throughout the project's life cycle and quality verification occurs throughout

the development process and not only at the end of the project [24].

TABLE III. DSDM - SCRUM COMPARISON

Dynamic Systems Development Method (DSDM)	SCRUM
Product quality is improved throughout the project cycle.	Knowledge needed to achieve a goal.
Ensures rapid developments.	Involves from the beginning and gives a role to everyone.
It allows changes to be made easily.	Reduces the cost of change at all stages.
Allows reuse of application through existing modules.	Visible, transparent by the specialist team

On the other hand, if we compare it with the Scrum framework it only works with small teams and short projects, it requires an exhaustive definition of the tasks and their deadlines, also a risk that this agile methodology has is having to go back to the rhythm of work after the abandonment of some member of the team during the development [25], all this is detailed in Table III.

TABLE IV. VENSIM - STELLA COMPARISON

Vensim	Stella
Make a synthesis of a complex problem.	Simple interface allows us to create convincing models close to reality.
To diagnose the evolution of the analyzed system.	It is not possible to do mathematics or very complex programming.
Create a model of the system and enter it into the computer.	Create versatile models in terms of their possible modification and adaptation to systems.
Perform simulations with the model, aimed at making proposals for action	Tests can be easily performed in different scenarios.

For the development of the Forrester diagram, the Vensim program was used, since it is currently the most versatile, intuitive, and simple program for simulating dynamic models, it also allows building models through causal diagrams or text version, and in any of the modalities, it allows easily comparing the results of different experiments, superimposing graphs of different variables, changing scales, study periods, among other things [26]. On the other hand, the author [27] mentions the Stella software that is also used to model dynamic systems, however, it has a deficit that only allows it to use little sophisticated mathematics and little programming knowledge, all this is further detailed in Table IV.

V. RESULTS

For the results section, statistical tables are shown for the next five years based on the Forrester diagram, both of which give increasing statistical results. These results put the stability of the country at risk and should therefore be carefully evaluated.

Fig. 3 shows that Peru's current population will grow by approximately 2.5 million people between 2020-2025, due to various factors, but the main one is immigration. Peru is a country of transit and reception of Venezuelan migrants, therefore the number of Venezuelan immigrants has grown during the last decade, these are considered the largest group

of foreigners in the country[28], due to this excessive immigration, the birth rate increases and the population does the same, if these variables are not maintained or decrease the population in the country would become double of what was predicted.

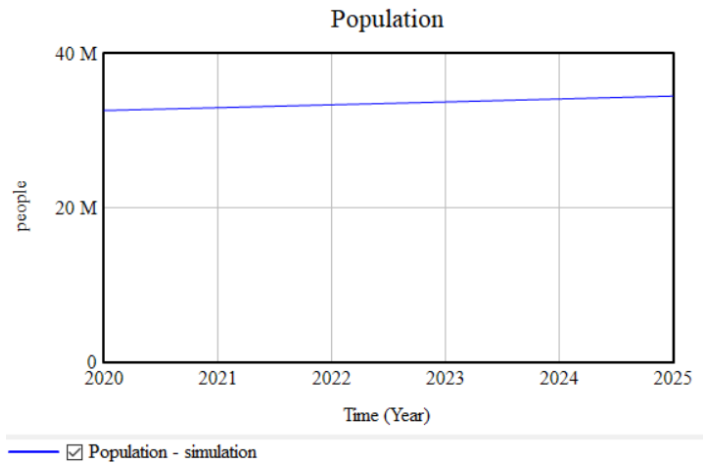


Fig. 3. Population.

Fig. 4 shows that the currently employed population is approximately 10 million people, this will suffer a small growth (compared to the population) of approximately 4 million between 2020-2025, therefore the future of employability is at existential risk, so it is necessary a public policy that benefits Peruvians without harming foreigners since work is the basic and primordial condition of every human being and we can even say that work is an indispensable role in the development of man.

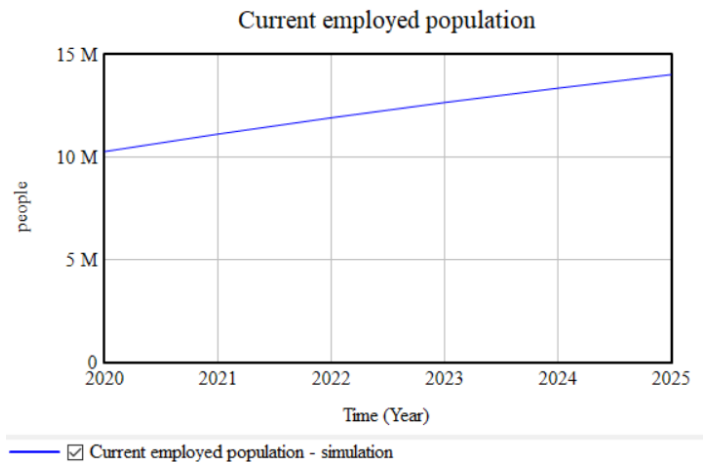


Fig. 4. Current Employed Population.

VI. CONCLUSIONS AND FUTURE WORK

In conclusion, the dynamic systems model for the projection of post-COVID19 employability in Peru between 2020-2025 was performed, and the results were that the Peruvian population will increase by 2.5 million until 2025 due to immigration, and therefore the birth rate also increased. Concerning employability, during the first months of the pandemic, the

layoff rate increased, but the projection of the dynamic systems model performed showed that employability will grow slowly, which puts at risk the availability of work for the population that is also growing. Therefore, a public policy that benefits the entire working population would be necessary, since work is indispensable for a person's livelihood. Therefore, the importance of this research work focuses on the decisions that the state and the population itself will make with the results obtained from the projection.

The dynamic methodology of systems that were implemented in the research work is important because it helps to analyze data, visualize through diagrams and understand how systems behave, and also allows the creation of simulation models for the future projection of systems.

As future work it is planned to improve the model of dynamic systems of work, adding more level variables such as inflation, being the auxiliary variable the inflation rate, among other variables more level and auxiliary, however, this would make the dynamic model more complex, but the results of the projection will be more accurate, and thus the model can be implemented in other countries or provinces.

REFERENCES

- [1] Z. Wu and J. M. McGoogan, "Characteristics of and important lessons from the coronavirus disease 2019 (covid-19) outbreak in china: summary of a report of 72 314 cases from the chinese center for disease control and prevention," *Jama*, vol. 323, no. 13, pp. 1239–1242, 2020.
- [2] Y.-R. Guo, Q.-D. Cao, Z.-S. Hong, Y.-Y. Tan, S.-D. Chen, H.-J. Jin, K.-S. Tan, D.-Y. Wang, and Y. Yan, "The origin, transmission and clinical therapies on coronavirus disease 2019 (covid-19) outbreak—an update on the status," *Military Medical Research*, vol. 7, no. 1, pp. 1–10, 2020.
- [3] F. J. Díaz-Castrillón and A. I. Toro-Montoya, "Sars-cov-2/covid-19: el virus, la enfermedad y la pandemia," *Medicina y Laboratorio*, vol. 24, no. 3, pp. 183–205, 2020.
- [4] C. Courtemanche, J. Garuccio, A. Le, J. Pinkston, and A. Yelowitz, "Strong social distancing measures in the united states reduced the covid-19 growth rate: Study evaluates the impact of social distancing measures on the growth rate of confirmed covid-19 cases across the united states." *Health Affairs*, pp. 10–1377, 2020.
- [5] Expansión, "Perú - covid-19 - crisis del coronavirus." url:<https://datosmacro.expansion.com/otros/coronavirus/peru/>, 2020.
- [6] A. A. Montoya, "¿qué efectos tendrá la covid-19 sobre el empleo de américa latina y el caribe?." url:<https://blogs.iadb.org/trabajo/es/que-efectos-tendra-la-covid-19-sobre-el-empleo-de-america-latina-y-el-caribe/>, 2020.
- [7] M. Murialdo, "Durísima informe: Desempleo es la pandemia colateral del Perú." url:<http://miningpress.com/coronavirus/332697/durissimo-informe-desempleo-es-la-pandemia-colateral-del-peru/>, 2020.
- [8] A.-L. Moreno-Huamanchumo, "Plan de comunicación interna para el retorno a oficinas de colaboradores post covid-19 del banco corporativo americano," 2020.
- [9] L. R. Izquierdo, J. M. Galán, J. I. Santos, and R. Del Olmo, "Modelado de sistemas complejos mediante simulación basada en agentes y mediante dinámica de sistemas," *EMPIRIA. Revista de Metodología de las Ciencias Sociales*, no. 16, pp. 85–112, 2008.
- [10] J. M. García, "Aplicaciones prácticas de la dinámica de sistemas en un mundo complejo." url:<http://www.dinamica-de-sistemas.com/revista/0307a.html>, 2006.
- [11] S. L. R. Vela, "Análisis de riesgo existencial y el futuro de la empleabilidad," *Phainomenon*, vol. 19, no. 1, 2020.
- [12] M. Orlishevych and I. Lukianenko, "European unemployment nonlinear dynamics over the business cycles: Markov switching approach," *Global Business and Economics Review*, vol. 22, no. 4, pp. 375–401, 2020.
- [13] O. Shibistiuk, "Modelling inflation and unemployment by using system dynamics," 2018.
- [14] W.-T. Yang, "A technique for improving readability of forrester diagram in system dynamics," *Yugoslav journal of operations research*, vol. 13, no. 1, 2016.
- [15] T. Nguyen, S. Cook, and V. Ireland, "Application of system dynamics to evaluate the social and economic benefits of infrastructure projects," *Systems*, vol. 5, no. 2, p. 29, 2017.
- [16] T. R. Cortes, E. Faerstein, and C. J. Struchiner, "Use of causal diagrams in epidemiology: application to a situation with confounding," *Cadernos de saude publica*, vol. 32, no. 8, 2016.
- [17] G. O. Bernardo, J. R. T. Santos, and C. G. M. Miranda, "Aplicação da dinâmica de sistemas na gestão de processos de construção civil—utilização do software vensim/application of systems dynamics in the management of civil construction processes—use of vensim software," *Brazilian Journal of Development*, vol. 5, no. 7, pp. 7886–7902, 2019.
- [18] J. L. Díaz-Martínez, E. GUERRA ALEMAN, H. R. NEIRA MOLINA, J. García-Restrepo, L. Londoño-Lara, and A. VALLE-OSPINO, "Análisis de la dinámica de sistemas en el software vensim," <https://www.revistaespacios.com/a19v40n38/19403819.html>, 2019.
- [19] C. R. Cadenas Anaya, "Modelo basado en dinámica de sistemas para pronóstico de resultados de planificación-inversión y ejecución de proyectos industriales," 2020.
- [20] M. Rojas, C. , Pantoja, J. Henao, and R. Murillo, "Dynamic behavior analysis of the gross domestic product in a city in the center of the valle del cauca," *ENCUENTRO COLOMBIANO DE DINÁMICA DE SISTEMAS*, pp. 93–98, 2017.
- [21] J. M. Redondo, G. Olivar, D. Ibarra-Vega, and I. Dyer, "Modeling for the regional integration of electricity markets," *Energy for sustainable development*, vol. 43, pp. 100–113, 2018.
- [22] J. J. Cardiel-Ortega, R. Baeza-Serrato, and R. A. Lizarraga-Morales, "Development of a system dynamics model based on six sigma methodology," *Ingeniería e Investigación*, vol. 37, no. 1, pp. 80–90, 2017.
- [23] J. Fernandez, N. Aguilar, R. Fernandez de Canete, J. C. Ramos-Diaz *et al.*, "Causal modeling of the glucose-insulin system in type-i diabetic patients," 2017.
- [24] F. M. Y. Roxas, J. P. R. Rivera, and E. L. M. Gutierrez, "Locating potential leverage points in a systems thinking

- causal loop diagram toward policy intervention,” *World Futures*, vol. 75, no. 8, pp. 609–631, 2019.
- [25] M. Kuhrmann, P. Diebold, J. Münch, P. Tell, V. Garousi, M. Felderer, K. Trektene, F. McCaffery, O. Linssen, E. Hanser *et al.*, “Hybrid software and system development in practice: waterfall, scrum, and beyond,” in *Proceedings of the 2017 International Conference on Software and System Process*, 2017, pp. 30–39.
- [26] E. A. Lagarda-Leyva, “Collection and distribution of wheat, dynamic of the process of shipping to international markets: Case study,” *Int. J. Sup. Chain. Mgt Vol*, vol. 8, no. 1, p. 43, 2019.
- [27] C. Sbughea, “Simulation of the production process dynamics using vensim and stella,” *Annals of the University Dunarea de Jos of Galati: Fascicle: I, Economics & Applied Informatics*, vol. 22, no. 1, 2016.
- [28] A. Hernández-Vásquez, R. Vargas-Fernández, C. Rojas-Roque, and G. Bendezu-Quispe, “Factores asociados a la no utilización de servicios de salud en inmigrantes venezolanos en Perú,” *Revista Peruana de Medicina Experimental y Salud Publica*, vol. 36, pp. 583–591, 2020.

Topic based Sentiment Analysis for COVID-19 Tweets

Manal Abdulaziz¹, Mashail Alsolamy³
The Department of Information Systems
King Abdulaziz University Jeddah,
Saudi Arabia

Abeer Alabbas⁴
Technical and Vocational Training Corporation
Najran College of Technology Najran,
Saudi Arabia

Alanoud Alotaibi²
The Department of Information Systems
Imam Mohammad Ibn Saud Islamic University
Riyadh, Saudi Arabia

Abstract—The incessant Coronavirus pandemic has had a detrimental impact on nations across the globe. The essence of this research is to demystify the social media's sentiments regarding Coronavirus. The paper specifically focuses on twitter and extracts the most discussed topics during and after the first wave of the Coronavirus pandemic. The extraction was based on a dataset of English tweets pertinent to COVID-19. The research study focuses on two main periods with the first period starting from March 01,2020 to April 30, 2020 and the second period starting from September 01,2020 to October 31, 2020. The Latent Dirichlet Allocation (LDA) was adopted for topics extraction whereas a lexicon based approach was adopted for sentiment analysis. In regards to implementation, the paper utilized spark platform with Python to enhance speed and efficiency of analyzing and processing large-scale social data. The research findings revealed the appearance of conflicting topics throughout the two Coronavirus pandemic periods. Besides, the expectations and interests of all individuals regarding the various topics were well represented.

Keywords—Social media analysis; COVID-19; topics extraction; sentiment analysis; LDA; spark; twitter

I. INTRODUCTION

The Coronavirus outbreak has been a severe disruption to the global economy and this has affected most, if not all, nations. In fact, ever since the World Health organization (WHO) declared the pandemic a Public Emergency of International Concern (PEIC) [1], the subsequent restrictions to curb the spread of the virus continue to do more damage than good. These restrictions include but are not limited to travelling restrictions and closure of non-essential businesses[2]. In light of these measures, most people have resorted to social media to express their views regarding everything that is going on in the world [3]. The impact of social media platforms is becoming more noticeable than ever before. Social networking sites are considered the global big data center because people use their applications and invest much time in these media outlets [4].

The usefulness of these social media platforms is attributable to their ability to highlight valuable insights on varying perceptions of issues that are happening in real-time [5]. Furthermore, social networking has a remarkable impact

and is one of the most increasingly growing social information structures.

A predominant social media platform is one of the most common social networking sites. According to research, an analysis of Twitter data, especially people's emotions, can be useful in many areas such as the stock market, election vote, management of disaster, and crime [5]. Analyzing tweets during and after Coronavirus could be worthy as the condition and people's reactions are changing every instant during this critical period. This study motivated by examining how human emotions and concerns changing with respect to COVID-19 from the start of the pandemic and till now. We have attempted to use PySpark for improving the sentiment of topic modeling analysis and relies on a lexicon-based algorithm that is applied using big data and Machine Learning techniques. Researchers contributed to an opensource of textual datasets. To achieve this aim, a dataset of tweets about COVID-19 created by Christian et al. [6] is selected for this work since it is the only dataset covering the period from January to October, and is considered big data. The contribution of this work is to analyze the COVID-19 tweets dataset from January to October and compare the changes in people's feelings by applying machine learning methods and answering the following two research questions:

Question 1

What are the most traded topics in the COVID-19 pandemic in the course of two different periods, the first period from March to April (first pandemic wave), and second period from September to October (second pandemic wave)?

Question 2

How have people concerns change during the COVID-19 from the start of the pandemic and till now?

The rest of the paper is structured as follows: The second section presents the related works for sentiment analysis and topic modeling. Section three presents the content analysis methods. Section four shows the proposed model of this research while the data analytic and implementation of the model present in section five and six respectively. Section

seven discusses the work's results. Finally, this paper ends with conclusion and future work.

II. RELATED WORK

The vast majority of research studies that cover tweets' sentiment analysis are more inclined towards machine learning algorithms [7]. An apt example is the analysis of the negative connotations that revolve around the Coronavirus related tweets. The researchers often utilize exploratory and descriptive methodology as well as the visual and textual data to get valuable insights based on Naïve Bayes Classifier (NBC) and logistics regression (LR) classification method of machine learning.

The findings showed 91% accuracy of tweets with Naïve Bayes while 74% with the logistic regression classification method [8] made prediction for the feelings of people on Twitter through building a model to explore the real sentiment of people about COVID-19. They made a comparison between five classifiers, which are logistic regression, multinomial Naive Bayes, Decision Tree, Random Forest, XGBoost, and Support Vector Machine (SVM) over n-gram for feature extraction along with bi-class and multi-class setting. The results showed that SVM and Decision Tree outperform the other classifier. However, the SVM classifier is stable and reliable in all tests. Nonetheless, most classifiers were better done with unigram and bigram in the bi-class setting. In addition, the maximum accuracy of the proposed model was 93%, indicating that the model has the ability to analyze the emotion of people within COVID-19 tweets. K- Chakraborty [9] presented all tweets relevant to COVID-19 and WHO were unsuccessful in guiding people across this pandemic outbreak. They analyzed twenty three thousand re-tweeted tweets over the timeframe from 1 January 2019 to 23 March 2020. The results showed that the highest number of tweets indicated neutral or negative emotions. On the other hand, a dataset comprising 226,668 tweets gathered between December 2019 and May 2020 were analyzed and revealed that there were a maximum number of positive and neutral tweets. Analysis reveals that while people tweeted mainly positively about COVID-19, Internet users were busy re-tweeting negative tweets and that no useful terms could be found in WordCloud. The accuracy reached up to 81% when using deep learning classifiers while 79% when using the formulated model based on a fuzzy rule to identify sentiments from tweets.

Regarding to topic modeling, B.Dahal [10] analyzed large datasets of geotagged tweets containing several keywords related to climate change using topic modeling and sentiment analysis. LDA was used for topic modeling to extract the topics in the text, and Valence Aware Dictionary and sentiment Reasoner (VADER) were applied to assess the general emotions and behaviors. Analysis of sentiments indicated that the general discussion is negative, especially when users respond to political or extreme weather events while Topic modeling reveals that the numerous subjects of climate change discussion are diverse, but that some topics are more prominent than others. The debate on climate change in the United States in particular is less focused on political topics than other nations. Kaila and Prasad [11] focused on the flow of Twitter's information during the spread of the Coronavirus. Tweets

associated with Coronavirus are analyzed using sentiment analysis and topic modeling by using LDA.

The study concluded that the flow of information is correct and consistent with minimal misinformation in relation to corona virus outbreak. The LDA identified the most important and reliable topics relating to the epidemic of Coronaviruses while sentiment analysis verified the dissemination of negative sentiments such as fear along with positive sentiments such as confidence [12]. A developed topic modeling LDA methodology, to classify the interesting topics from large-scale tweets connected to two well-known Indian county officials. Spark performed the topic modeling method with R language to improve the speed and performance for large-scale real time social data processing and analysis. In addition, tweet sentiment analysis is conducted in this study by using a lexicon-based approach to classify people's sentiment against these two leaders.

III. CONTENT ANALYSIS

The essence of content analysis is to define trends, themes or ideas within such qualitative data (i.e., text). Using content analysis allows researchers to find out about the aims, messages and impacts of communication content.

A. Sentiment Analysis

Sentiment analysis, one of the most promising methods for content analysis in social media, known as emotion AI or opinion mining, leads to natural language processing (NLP) and text analysis to systematically, quantify, extract, identify, and study effective states and personal information [9].

Sentiment analysis is widely applied in the voice of the customer materials such as survey responses and reviews. Analysis of sentimental peoples can be achieved by millions of likes and retweets, but this vast interaction with such a post does not reflect the importance of the feelings toward those posts [9]. This is because there are several factors, such as happiness, irony, satisfaction, sadness and anger among others. The aforementioned factors can have an impact on the nature of posts. However, broad extractions of human feelings from social media networks are important and strongly affect international public trends, market decisions as well as policy development [13].

This gets to show the importance of sentiment analysis in the interpretation of human feelings. An analysis of peoples' sentiments can be classified in different ways. The first one is text classification and this is also referred to as text categorization or text tagging which is the main process in sentiment analysis. It entails the classification of texts into organized groups and the calculation of sentiment analysis depending on the number of occurrences of positive and negative words in each document. Each document has both negative and positive scores. When calculating the sentiment document score, each negative word is denoted by -1, each positive word as +1, and neutral word is denoted by Zero as neutral word [14].

The three main classification levels are: Sentence, document, and aspect levels [9]. The last of the most common sentiment analysis classifications are based on the rating level. There are three main steps to show how sentiment analysis works [13]:

- **Data Collection:** This entails the use of certain keywords or hashtags to access the information users want depending on their interests. This information has various forms (e.g. tweets, posts, news, texts).
- **Preprocessing:** The collected information is processed during this step in order to prepare the data for the next phase. This phase includes three main stages. First, the cleaning stage contains the removal of repeated letters, text correction, normalization, stop word removal, and language detection. Next, the Tokenization method focuses on converting text into tokens until it becomes vectors. Lastly, the extraction of features such as grammatical structures and mining characteristics.
- **Data analysis:** In this stage, all data should be processed and then identified based on the main purpose of research, such as polarity identification, sentiment analysis, or frequency analysis. Processed identified the main purpose of research, such as polarity identification, sentiment analysis, or frequency analysis.

B. Topic Modeling

Topic modeling analyzes “bags” or groups of words together—instead of counting them individually—in order to capture how the meaning of words is dependent upon the broader context in which they are used in natural language. Topic modeling is not the only method that does this—cluster analysis, latent semantic analysis, and other techniques have also been used to identify clustering within texts. There are many techniques to implement topic model such as Latent Dirichlet Allocation (LDA), Latent Semantic Allocation (LSA), and Non Negative Matrix Factorization (NNMF). One of the most popular topic models is LDA, which generates latent topics in whole corpus [10]. It is a probability distribution of the topics over every word found in the corpus. So, the number of topics and the words in each topics must be determined before LDA is run. The main assumptions of the model are that each document in the corpus is a probabilistic mixture of topics, and each topic is a probabilistic mixture of terms. Topic model requires a word topic matrix and a dictionary as the main inputs. Before running the LDA model, it should create a dictionary, filtered the extremes, and create a corpus object, which is the document matrix LDA model needs as the main input [10]. The most important parameter of LDA is the number of topics the model should infer from the corpus, k . It is not clear how many topics the dataset should be divided into. Too few topics could lead to an incomplete analysis while multiple distinct topics could theoretically be mixed together. Actually, too many topics could lead to multiple topics reflecting a coherent subject together but becoming individually confusing [10]. To address this problem, authors [10], [12] suggested running LDA with different number of K or such as, 5 topics, 20 topics, and 80 topics, then comparing the content of the inferred topics to decide the optimum number of topics. This method was preferred by many researchers to check the suitable number of K that can be used to generate effective result.

The basic premise of topic modeling features entities: words, documents, and Corpora. Word is regarded as the primary unit of discrete data in a document, described as vocabulary items indexed for each uncommon word. The

document is an organization of N words. Corpus is a set of M documents, and corpora are the plural shape of the corpus [15]. Today, one of the most common themes of modeling and analysis is LDA. As text data may have a mix of topics and insights, LDA tries to find a probability of hidden distributions in the input data. LDA is a “bag of words” words order is not essential. However, it assumes that documents that have related words customarily have the same topic. Moreover, documents that have collections of words frequently happening together customarily have the same topic. LDA contains two parts; the first part relates to a document, and this is already known. The second part is unknown because it entails words that relate to a topic or the probability of terms relating to a topic that the paper need to determine. Observations in LDA are pointed to as tweets content, the feature collection is meant to as words/vocabulary, and the resulting classifications are referred to as topics.

IV. PROPOSED MODEL

This section sums up the research methodology that has been implemented in this study. The methodology depends on two algorithms: the LDA to extract the most of the ‘ K ’ Topics from a tweet’s text and lexicon-based approach to identify tweet’s sentiment. LDA needs to train several times to adjust its parameters while lexicon-based approach uses directly. Therefore, there are training phase and runtime phase as shown in Fig. 1.

In training phase, the model starts with the preprocessing step, which is a crucial step to give the model valuable results and success. Preprocessing consists of four primary processes: text cleaning, tokenization, removing stop words, lemmatization and stemming. All these steps will be described in detail in the next section. Then, extract specific features from the tweet’s text that should be in a well-defined format to be used directly as an input to the classification algorithms. There are several methods that can be applied in the extraction of features. In this study, TF-IDF will be used to construct a bag of words where tweets can be divided into words and generate a vector [8]. If one word is introduced, the method is called “unigram,” “bigram” for two words, and “trigram” for three words, respectively [9]. So, this model extracts the feature vector based on the “unigram” method. Some parameters should be determined before running the LDA model. The number of topics (k) and the number of iterations, which controls how many times LDA will execute over each document, are the most critical values that should be selected carefully. Besides, selecting the number of topics depending on the chosen dataset is also essential. Therefore, executing the model and changing the values of K until generating the best result will perform this process. This model works based on NLP and will train with 80% of the dataset and test with 20%. After getting the topics, the paper will identify each sentiment. Since the dataset is not labeled by sentiment, a Vader lexicon model, which is a lexicon-based approach that considers a pre-trained model [16], will be used to identify tweet’s sentiment. It takes a word and classifies its sentiment to positive, negative, or neutral. This can be performed with polarity calculation of sentiment words; there are three main steps to fulfill this analysis [8].

- **Step (1):** This step involves categorizing words as

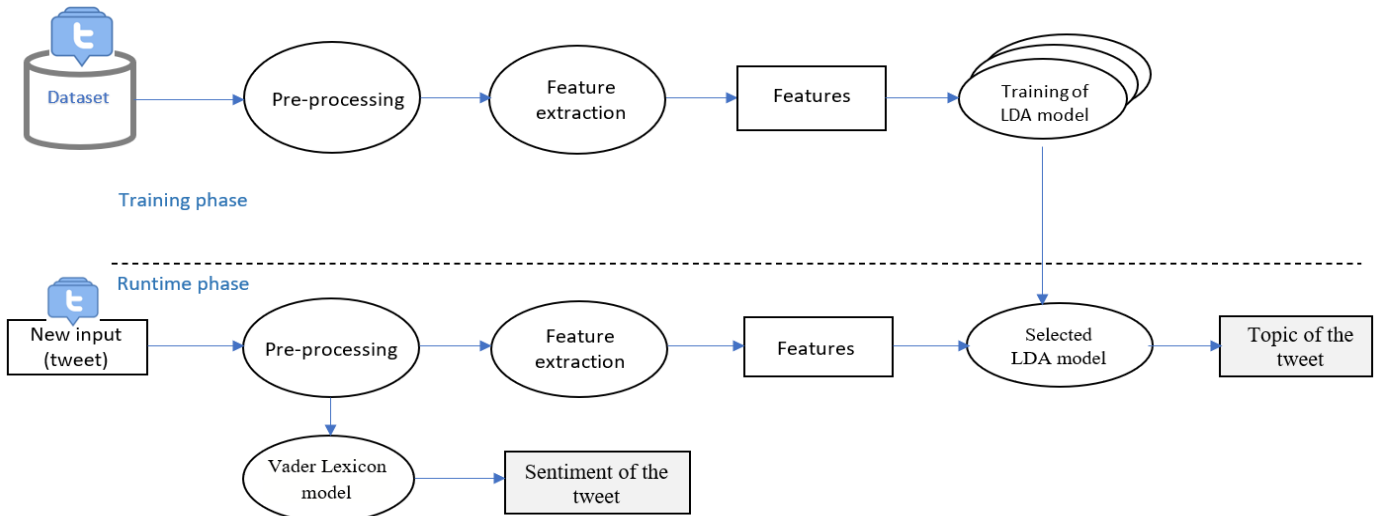


Fig. 1. The Proposed Model.

negative or positive in two groups, based on the frequency of negative or positive words. Then the polarity score for each tweet can be conveniently determined.

- Step (2): The tweet polarity is determined by summing the tweet value of each selected feature. Each tweet is scored using the following formula:

$$PolarityScore(tweet) = \sum featurevalue(tweet_i) \quad (1)$$

where n is the number of features in $tweet_i$.

- Step (3): To conclude a tweet’s feeling, the following rules are established based on its polarity [8].
 Polarity Score < 0, Negative
 Polarity Score = 0, Neutral
 Polarity Score > 0, Positive

In the runtime phase, we will follow the same process of preprocessing step and feature extraction. After that we will execute the trained model with this feature to get the topic of a new tweet. However, considering the Vader lexicon method only deals with words, it will be necessary to first send the processed tweet to obtain its sentiment.

V. DATA ANALYTICS

This section presents information about the dataset using in this research including the description of it and sampling phase.

A. Dataset Description

In order to examine human emotions and concerns with respect to COVID-19, researchers contributed to an opensource of textual datasets. To achieve our objective, a dataset of tweets about COVID-19 created by Christian et al. [6] is selected for this work since it is the only dataset covering the period from March to October, and it considers big data.

The selected dataset is an open-source dataset available for research purposes. It has been collected continuously since 22 January 2020 using the Standard Twitter API. The total of obtained tweets were 942,149,169 tweets on 25 October 2020 for many languages. The English language represented 67.59% of the total tweets. The authors have dedicated more computational resources to pandemic-related tweets as the influence of COVID-19 rises around the world. This is one of the reasons why the number of tweets at some times has risen considerably. They used trending topics on Twitter and some keywords such as coronavirus, ncov19, ncov20, stay-at-home, covid, and virus to collect tweets. According to Twitter Service Terms and Conditions, this dataset contains Tweet ID only. Therefore, “rehydrate” the tweets is applied to obtain all information of tweets using the code available by the authors. Because the dataset’s size is enormous, the paper presents its explanation and preprocessing (incoming section) on the file of 1September. As shown in Fig. 2 using Jupyter notebook, there are 33 attributes having different data types (Boolean, float, integer, object). In this study, four attributes were used and these are presented in Table I.

TABLE I. DESCRIPTION OF SELECTED ATTRIBUTES

Attribute Name	Description
Text	Unique identifier of the tweet as integer
Lang	The language of the Tweet text
Retweet_count	Indicates how many times the tweet was retweeted
Created_at	The date and time in (UTC) of creating a tweet

B. Dataset Sampling

This research worked on English tweets only, so there were 636,798,623 tweets. Since this work runs on personal computer with limited processing capacity, the dataset was decreased to approximately 600,000 tweets. The assumption is that highly retweeted tweets are more critical. For that assumption, we will select tweets having the highest retweet_count per month. Since the number of tweets varies per month, as shown in Fig. 2, a specific percent will apply to each month to track people’s

```

<class 'pandas.core.frame.DataFrame'>
RangeIndex: 415748 entries, 0 to 415747
Data columns (total 34 columns):
#   Column                                Non-Null Count  Dtype
---  ---                                -
0   coordinates                            166 non-null    object
1   created_at                            415748 non-null object
2   hashtags                               85184 non-null  object
3   media                                  31361 non-null  object
4   urls                                   121246 non-null object
5   favorite_count                        415748 non-null int64
6   id                                     415748 non-null int64
7   in_reply_to_screen_name                17158 non-null  object
8   in_reply_to_status_id                 15963 non-null  float64
9   in_reply_to_user_id                   17170 non-null  float64
10  lang                                   415748 non-null object
11  place                                  1697 non-null   object
12  possibly_sensitive                    134811 non-null object
13  retweet_count                         415748 non-null int64
14  retweet_id                            320323 non-null float64
15  retweet_screen_name                   320323 non-null object
16  source                                 415659 non-null object
17  text                                   415748 non-null object
18  tweet_url                             415748 non-null object
19  user_created_at                       415748 non-null object
20  user_screen_name                      415748 non-null object
21  user_default_profile_image            415748 non-null bool
22  user_description                      337442 non-null object
23  user_favourites_count                 415748 non-null int64
24  user_followers_count                  415748 non-null int64
25  user_friends_count                    415748 non-null int64
26  user_listed_count                     415748 non-null int64
27  user_location                         273131 non-null object
28  user_name                             415726 non-null object
29  user_screen_name.1                    415748 non-null object
30  user_statuses_count                  415748 non-null int64
31  user_time_zone                        0 non-null     float64
32  user_urls                             114107 non-null object
33  user_verified                         415748 non-null bool
dtypes: bool(2), float64(4), int64(8), object(20)
memory usage: 102.3+ MB

```

Fig. 2. Description of Dataset's Attributes

Twitter activity about COIVD19. At the end, the processed dataset will save in a new dataset file of type CSV.

VI. IMPLEMENTATION

The implementation was done on two separated parts: preparation the dataset to be ready to use for the proposed model and implementation the model.

A. Dataset Preparation

Each month has 30 files, file per day, so we have 120 files. For each file, the paper applies the following steps using Python Jupyter notebook, tweet here means record or row of data: (file of September 1).

- 1) Remove non-English tweets according to “lang” attribute.
- 2) Remove duplicated tweets according to “text” attribute. As seen in Fig. 3, most tweets are retweeted tweets. And this explains why we do not determine a specific number of tweets from each day.

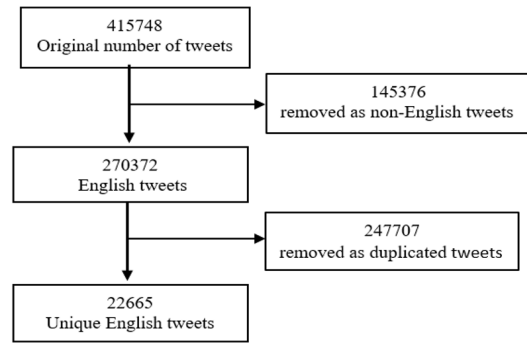


Fig. 3. Changing in the Total Number of Tweets over Preparation.

- 3) Keep the attributes “created_at”, “text”, and “tweet_count” and remove the rest.
- 4) Convert the date format from (Tue Jan 21 22:45:27 +0000 2020) to this format (1/21/2020) .
- 5) Sort tweets in descending order according to “retwee_count” attribute.
- 6) Save the result in a CSV file.

We got 567064 tweets after applying previous processes and the distribution of these tweets over each day is shown in Fig. 4 while Fig. 5 show them per months.

Finally, all prepared files are collected together in one CSV file, the sample from this dataset is presented in Fig. 6. As in text attribute, the text includes hashtag, mention, punctuation, symbols, etc. which need to be removed before entering the text to the model- the next section focuses on cleaning tweets.

B. Model Implementation

The model was executed on Google Colaboratory that provides a web based interactive computing platform. And PySpark programming language was used in writing the code. The implementation was done through several steps starting from preprocessing to getting the optimal model.

1) *Data preprocessing:* In this phase, the raw text of the tweet goes through several stages of cleaning it. This phase is significant in NLP, good cleaning leads to good results. Natural Language Toolkit (NLTK) is a package building in Python to process language. It contains a lot of libraries for text processing. implemented this cleaning was done in five steps using NLTK, as presented in Fig. 7, that gave excellent result.

Step 1: eliminating punctuations, URLs, numbers, hashtags, mention, and symbols from the text; if a symbol associates with a word, the word will also remove which achieves removing of hashtag and mention. Then, converting tweets into lower text. The result of this stage is shown below

Step 2: Applying tokenization that split a text into a list of words using the tokenization methods available in the NLP library. This step is essential to remove unwanted words, as done in the next step.

Step 3: eliminating stopwords located in the stopword library in NLTK. This library includes 179 stopwords of the English language as listed below.

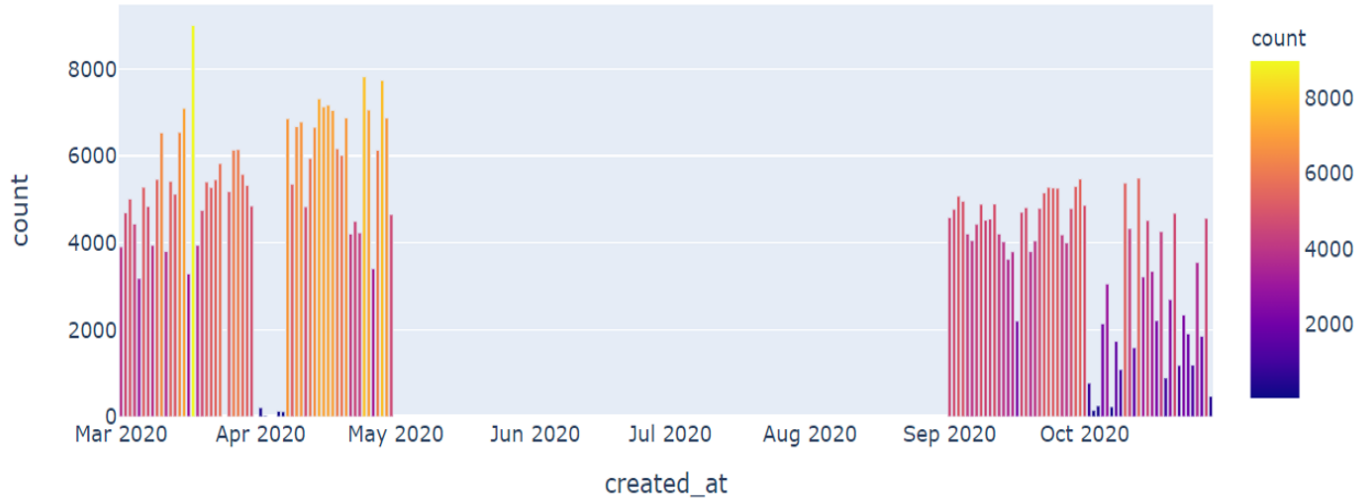


Fig. 4. Distribution of Tweets per Day over 4 Months.

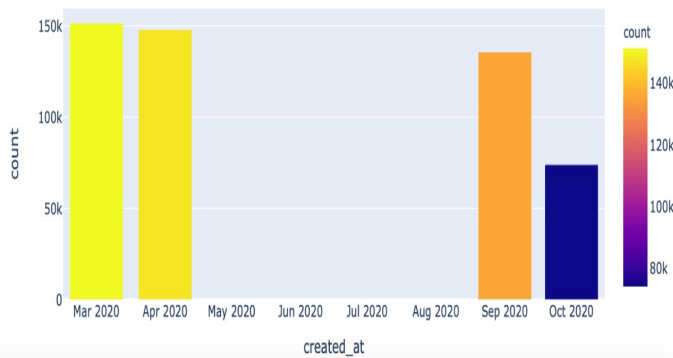


Fig. 5. Distribution of Tweets per Month.

```
0 rt what coronavirus symptoms look like day by day
1 rt llins 900 people get coronavirus and the wh...
2 rt we airing their shows w o a crowd because ...
3 rt when i found out the coronavirus could last...
4 rt this was the start of the coronavirus idc idc
Name: text, dtype: object
```

	created_at	retweet_count	text
250480	2020-09-01	188715	RT @techinsider: What coronavirus symptoms loo...
23823	2020-09-01	152401	RT @Pog_llins: 900 people get Coronavirus and ...
21983	2020-09-01	150231	RT @NoahbyNature: WWE airing their shows w/o ...
255924	2020-09-01	66385	RT @FantasyTweeting: When I found out the Coro...
256634	2020-09-01	40751	RT @williscj_: this was the start of the Coron...

Fig. 6. Sample of the Prepared Dataset.

'nor',	'i',	'its',	'do',	'below',	'our',
'not',	'me',	'itself',	'does',	'to',	'ours',
'only',	'my',	'they',	'did',	'from',	'wasn',
'own',	'myself',	'them',	'doing',	'up',	'wasn't',
'same',	'ourselves',	'their',	'a',	'down',	'weren',
'so',	"should've",	'theirs',	'an',	'in',	'weren't",
'than',	'themselves',	'what',	'the',	'out',	'have',
'too',	'you',	'which',	'and',	'on',	'has',
'very',	"you're",	'who',	'but',	'off',	'had',
's',	"you've",	'whom',	'if',	'over',	'didn',
't',	"you'll",	'this',	'or',	'under',	'didn't",
'can',	'you'd',	'that',	'because',	'again',	'doesn',
'will',	'your',	"that'll",	'as',	'further',	'doesn't",
'just',	'yours',	'these',	'until',	'then',	'shouldn',
'don',	'yourself',	'those',	'while',	'once',	'shouldn't",
"don't",	'yourselves',	'am',	'of',	'here',	'mightn',
'should',	'he',	'is',	'at',	'there',	"mightn't",
'now',	'him',	'are',	'by',	'when',	'isn't",
'd',	'his',	'was',	'for',	'where',	'ma',
'll',	'himself',	'were',	'with',	'why',	"needn't",
'm',	'she',	'being',	'about',	'how',	'aren',
'o',	'she's",	'having',	'against',	'all',	'aren't",
're',	'her',	'hadn',	'between',	'any',	'couldn',
've',	'hers',	"hadn't",	'into',	'both',	'couldn't",
'y',	'herself',	'hasn',	'through',	'each',	'wouldn',
'shan',	'it',	"hasn't",	'during',	'few',	'wouldn't",
"shan't",	'it's",	'haven',	'before',	'more',	'rt',
'we',	'ain',	"haven't",	'after',	'most',	'rts',
'be',	'mustn',	'isn',	'above',	'other',	'retweet']
'been',	'needn',	'no',	'won',	'some',	"mustn't",
			"won't",	'such',	



Fig. 7. Preprocessing of Tweet.

As seen, these words do not give meaning when we need to extract information from a text. Therefore, we removed from the tweet to become the text as follow:

Step 4: The target of this step is to convert words to their root to get distinguishing words. This process is called Stemming and Lemmatization. There are many methods in the NLTK package to implement them. We applied all of them to decide which one is better. Stemming methods are

```
0 coronavirus symptoms look like day
1 llins people get coronavirus whole world w...
2 wwe airing shows w crowd coronavirus gave us q...
3 found coronavirus could last july august
4 start coronavirus idc
Name: text, dtype: object
```

not preferred to use because they remove the letter ‘s’ from the end of the original word; for example, “previous” become “previous” as explained in Table II, row 4.

On the other hand, using the general lemmatization method did not solve the problem because it does not convert verbs to their root; for example, “running” became “running” without change. To overcome these issues, we proposed approach which is apply the lemmatization method three times with change ‘Postag’ parameter each time in a certain order. The order of execution and effectiveness of this approach are explained in Table II, from 1 to 3. In row 1, all plural nouns converted to their root, while adjective words converted bypass ‘a’ to Postag parameter in row 2. And all verbs converted to their root by set Postag = ‘v’ in row 3.

Step 5: The last step is to remove words of length 1 and 2, because they do not imply any meaning, especially ‘rt’ from retweet words that appear in each retweeted text. The final processed data are shown below.

```
0 coronavirus symptom look like day day
1 llins people get coronavirus whole world w...
2 wwe air show crowd coronavirus give quite po...
3 find coronavirus could last july august|
4 start coronavirus idc idc
5 people hometown siena sing popular song house ...
6 light discovery count infant suffocation towar...
Name: clean_text, dtype: object
```

TABLE II. THE RESULT OF LEMMATIZATION APPROACH

Used Method	Result
Original Text	['running', 'presents', 'wives', 'better', 'paid', 'previous', 'cats']
1 Lemmatize method without set pos parameter	['running', 'presents', 'wives', 'better', 'paid', 'previous', 'cats']
2 Lemmatize method with set pos parameter to ‘a’	['running', 'present', 'wife', 'good', 'paid', 'previous', 'cat']
3 Lemmatize method with set pos parameter to ‘v’	['run', 'present', 'wife', 'good', 'pay', 'previous', 'cat']
4 Stemme method	['run', 'present', 'wive', 'better', 'paid', 'previou', 'cat']

2) *Feature extraction:* The next step of implementation is extracting the suitable features from the processed text. The paper applied TF-IDF method to generate a bag of words, then applied “unigram” approach to get the feature vector [8]. TF-IDF consists of two mathematically multiplied parts: TF and IDF. TF (Term Frequency)= frequency of word in the tweet / total words in the tweet. IDF(Inverse Document frequency)=log(total number of tweets/number of tweets that the word belongs to)

$$TF - IDF = TF * IDF \quad (2)$$

So, it produces a feature matrix of size number of tweets * number of unique words in all tweets, which then converts to one vector.

Here is example for one of the tweets:

```
processed_text = ['drop', 'combat', 'look'], It calculate the frequency of
features=SparseVector(5000, {49: 4.5975, 249: 5.5715, 254: 5.5934}))
```

This method also is a built in method in machine learning library of PySpark that used by importing it as:

```
from pyspark.ml.feature import IDF
```

3) *Training model:* The LDA model was used to generate the topics. It is built model located in machine learning library under PySpark that can be used by import it as: from pyspark.ml.clustering import LDA The quality of the model’s result connected with two important parameters: k and the number of iterations. To adjust these parameters, this executed the LDA model many times with change these values each time. The result of each time was evaluated to decide which values are the best, evaluation strategies of these parameters were presented in the next section. Then, the model was built depending on the best parameters, which can use with a new tweet.

4) *Sentiment model:* This paper used Vader-lexicon as a model for sentiment. It is a pre-trained model that can use immediately by importing it from NLTK library as: from nltk.sentiment.vader import SentimentIntensityAnalyzer After obtaining the final topics we sent them to Vader-lexicon to get the sentiment of each topic. Also, the paper used this model to pick up the sentiment of a new tweet after processing this tweet, as mentioned in data preprocessing section.

C. Evaluating the Topics

This section presents the evaluation strategies for selecting the appropriate topics, which depend on two parameters: number of topics and number of iterations.

1) *Deciding the number of topics:* As previously mentioned, large number of topics can lead to wasted topics and in contrast, small number of topics can hide useful topics. Therefore, deciding the number of topics depends on the size and the general subject of the documents. For the documents, the paper implemented LDA with K =5-10 and 15 and evaluated the quality of the outputs manually. The paper focused on the weight of words and the meaning of words in each topic. This paper found that an increase the words more than 10 words to each topics causes sharing some words between the topics as well as words with low weight. In addition, this paper found that 8 topics for our model gave satisfied result.

2) *Deciding the number of iterations:* Giving good topics depends also on the number of iterations. A the number of iterations is affected by the size of the documents and experiment, so LDA was executed with iteration = 50, 100, 150, 200, 300 , 1000 and evaluated the results manually in each time as done in selecting topics. The paper found that there is no significant difference in range 100 to 200 iterations. Therefore, the paper picked 150 iteration for our model.

VII. RESULT AND DISCUSSION

This work divided the dataset described in previous section into two periods. The first period covers from March 01,2020

TABLE III. TOP WORDS IN TOPICS USING LDA

Topic 1(Drug Research)	Topic 2(news)	Topic 3(Losses)	Topic 4(Economy)	Topic 5(Lockdown)	Topic 6(Updated Cases)	Topic 7(School Closures)	Topic 8(Rules)
vaccine	records	business	economy	minister	hospital	school	hand
study	everyone	worker	nation	question	number	student	thing
community	hour	fund	anyone	travel	confirm	stay	johnson
administration	member	look	rate	update	country	force	child
control	vote	service	return	cover	increase	march	rule
bill	fight	Italy	border	face	person	cancel	information
symptom	India	employee	system	watch	issue	press	post
talk	staff	market	supply	lockdown	patient	distance	result
drug	America	support	advice	message	action	event	change
research	measure	relief	read	warn	official	brief	medium

till April 30,2020 while the second period covers from September 01,2020 till October 31,2020. To analyze and identify the most topics traded in the COVID-19 pandemic during the two periods, it used LDA with K=8 (number of topics) and performed in 150 iterations. Table III and Fig. 8 answer to the research question 1 and shows the most traded topics in the two periods and the top words in each topic.

Fig. 8 shows the distribution of topics among documents with high weight for the third topic, Losses, than other topics. COVID-19 is affecting the world and causing a loss in the economy and humanity. Stop most of the markets and services were affected on employment. Most of the employees and other workers stayed without any work. There was a need for financial support to perform their business. These workers don't sense relief and need more support by providing a fund to eliminate the effect of Coronavirus. Italy is one of the countries affected by this epidemic. The number of registered infections with Coronavirus has increased. In addition, there is an increased number of deaths in the first pandemic. The drug researches and updated cases are two topics were presented with little difference in the weights. In drug researches, the Ministry of health and all its administrations were talked about the latest researches that tried to find vaccines and drugs. They studied the current symptom and how can control this virus to avoid dissemination. When this vaccine is ready, it will bill it to all countries in the world to face this virus. Updated cases is topic discusses how the official websites in each country issued updated number of the confirmed cases that effect with COVID-19. Several actions were performed in each hospital to be ready to receive persons who confirmed affected with COVID-19.

In addition, school closure was the most topic present due to increase the number of active cases. Many schools and universities in the world have already had to isolate classrooms or close entire schools due to the outbreak of Corona infection. Most schools cancel students' attendance and allow them to stay at home and study through distance learning to complete their courses. Topic 8 discuss the Rules published by the official website and in social media. These websites posted the updated information and current results what is the most changes that happen. In March, British Prime Minister Boris Johnson conducted a test for the Coronavirus, and the result of this test was that he was infected with the Coronavirus, and he has published this information across the sites. In addition, these rules were focused on the children and it necessary to clean hands and follow the necessary information. One of the ways to reduce the number of Coronavirus infections is a lockdown. Most of the world's countries have banned travel

to another country. During the outbreak of the Coronavirus, a meeting of health ministers was held virtually by watching through a video conference to answer the most important questions and issues. The Ministry of Health confirmed to stay at home, and published warning messages that include not going out or traveling to another country, and not leaving your face uncovered. These messages have been updated based on new events.

Economy is also another topic present in our research. The nations expected shrink of the world's economy due to Coronavirus and the closure of borders, and their relations with other countries. Public health, people's trust in the instructions they read, and state support for them can contribute to restoring the economy. The least visible topic in the Fig. 8 is News, the news during the COVID-19 pandemic show that India becomes the second country most affected by the epidemic, after America. Additionally, there is a significant rise in casualty numbers in hours, which made India fight this epidemic by implementing a set of measures and enforcing everyone in the country to apply them. Also, other staff and other members help in fighting COVID-19.

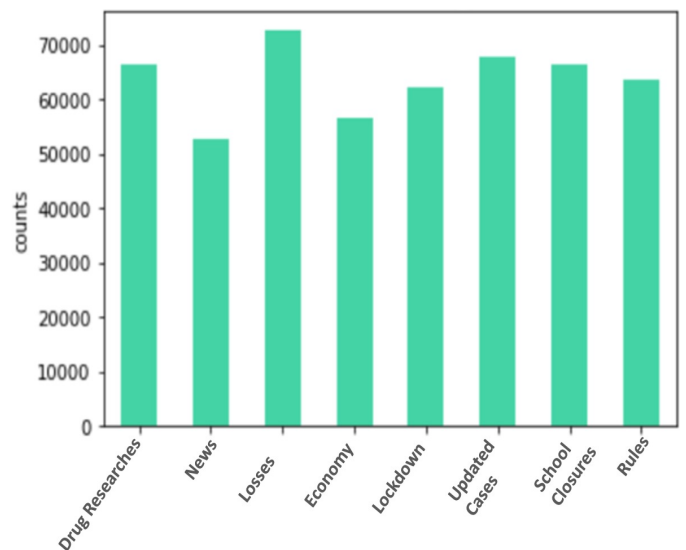


Fig. 8. Topics Distribution among Documents

A. Analysis of COVID-19 Trends

After the discussion of the most topics traded in the pandemic of COVID-19, this section analyzes the topics during

the periods. The study is divided into two main periods according to the outbreak of the Coronavirus around the world. The first period covers March and April (Pandemic revolution), the second period along the months of September and October (Epidemic stabilization). The topics were appeared at different rates in each period according to the strength of the epidemic and its appearance during the period. Fig. 9 and Table IV below show the topic distribution during the two periods.

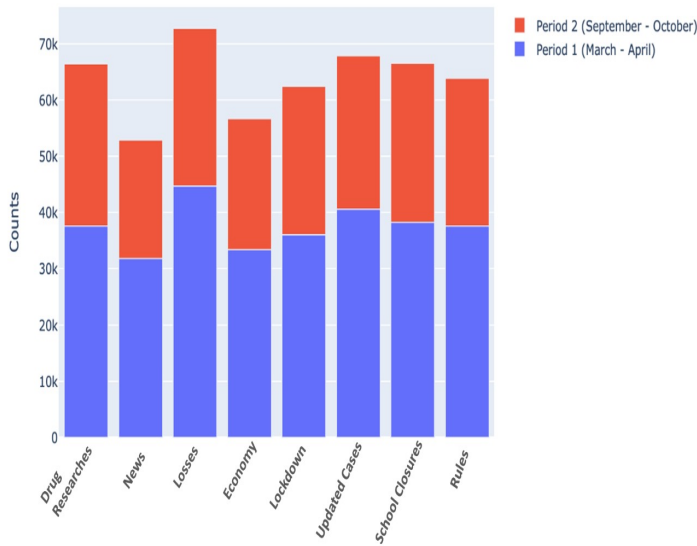


Fig. 9. Topic Distribution during the Months

TABLE IV. DISTRIBUTION OF THE TOPICS THROUGH THE PERIODS

Topic	1st period	2nd period
Drug Research	0.5658	0.4341
news	0.6003	0.3996
Losses	0.6134	0.3865
Economy	0.5883	0.4117
Lockdown	0.5558	0.4242
Updated Cases	0.6073	0.3966
School Closures	0.59001	0.4023
Rules	0.5887	0.4218

In general based on the information in Fig. 9 and Table IV, all of the topics were distributed between the two periods in close proportions. “losses” is the most topic with high percentage than others while “drug research” is the most in the second period. This is a natural state because COVID-19 is affecting the world and causing a loss in the economy and humanity. Stop most of the markets and services were effected on business. “Lockdown” got a high percentage in the first period and then decreased slightly to 42%. Most activities have been curtailed during the Coronavirus outbreak.

Currently, there is an increasing number of cases after a recession in previous months, which could lead to a return to lockdown again. In the same way the 7th topic “School Closures” decreased little bit because until now all schools and universities perform most of educational learning online without student’s attendance. The learning process that performed in the first period is similar in the second one but may much effective now. Furthermore, “updated cases” topic

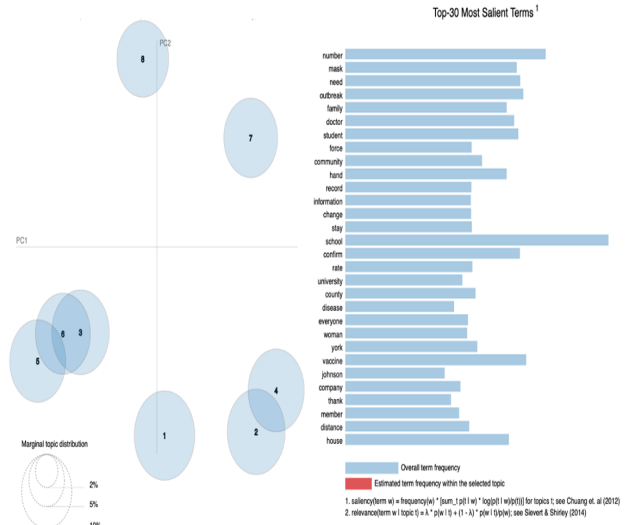


Fig. 10. Top Eight Clusters Representation

was decreased in the second period to reach about 39% . This happen due to some change in the situations in the two periods. Today, people have adapted to the current situation, and the number of cases decreased than it was at the beginning of the period, as the number of confirmed cases reached a high percentage compared to what is happening today. In addition, the “news” topic was also decreased for the same reasons mentioned before in the ”updated case” topic. At the beginning of the pandemic there was high percent of posted news regarding COVID-19 in each minute or second. Most people were good followers of this news with continuous in watching the updated cases and number of infection but it decres in the month of September and October.

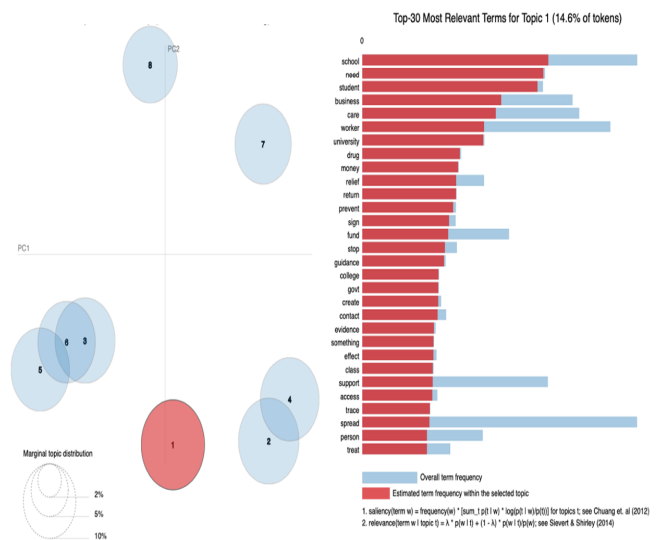


Fig. 11. Term Frequency of First Cluster/Topic Representation

Fig. 10 and 11 display the interactive topics chart by using LDAvis, which is a web based tool to visualize the topics using LDA [17]. It provides an interactive and global view of the most chosen topic. This is executed by Spark and

with the value of K=8. The two figures display LDA plot visualization for the top eight topics discussed in the previous. They demonstrate the general view of the topic model and the interaction between topics. The total term frequency is defined by the light blue color, while the red one reflects the approximate term frequency within the chosen topic. Fig. 10 indicates the average word frequency across all topics while Fig. 11 reflects the cluster of topics match with the frequency of words within the a selected topic. For example in topic1, the most words frequencies were schools, students, need and business. Each circle in the figures matches a topic, the right panel has the horizontal bar plot reflecting the relevance of currently selected topic for words indicating the top 30 words in the topic separately.

B. Textual Data Sentiment Analytics

In this paper, the eight topics were identified from each of the categories: neutral, positive, and negative. Topics are visualized with word cloud shown individually. These tasks are not easy since many pre-processed words have no semantic meaning. However, it can be difficult to understand the relationship between various tokens/words in these subjects, and these meanings can differ significantly from other forms of reviews. Fig. 12, 13, and 14 shows the most positive, neutral, and negative words for each topics. Therefore, the second research question can be answered in this section as it will appear in the following paragraph.

Fig. 12 shows the most positive words for each topics. For the positive cases, “agreement”, “ability”, “advantage”, “appreciate”, “accept”, “authority”, “assure”, “benefit”, “admit”, “asset” and, “allow” are the most frequent words. Those words denote a positive aspect, which is people accepting the COVID-19 pandemic and trying to live with and accept it.

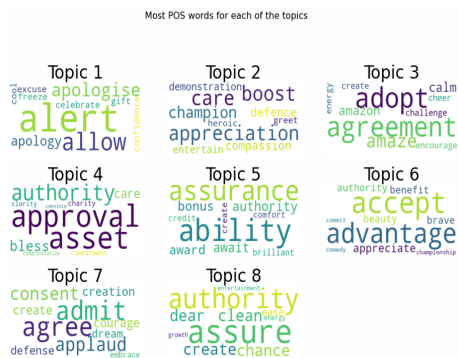


Fig. 12. The Most Positive Words for each Topics

Fig. 13 shows the most neutral words for each topic which are “accord”, “adult”, “adviser”, “access”, “academy”, “absence”, “abundance”. The neutral category is typically more representative and appeared the blend of positive and negative topics which displays the most frequent topics in recent times. Even though they do not mean a specific emotion, they shed light on subjects that are important to users.

Fig. 14 shows the most negative words for each topic which are “cancel”, “attack”, “avoid”, “burden”, “anxiety”, “abuse”, “accident”, “anger”, “absentee”. These words denote

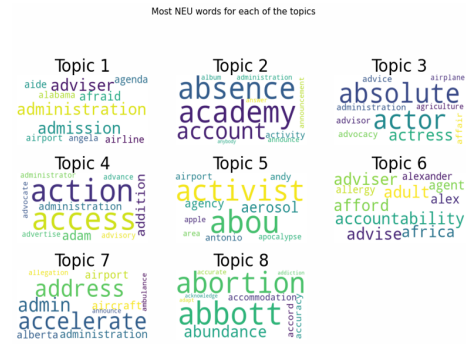


Fig. 13. The Most Neutral Words for each Topics

a negative aspect, of people’s anxiety, fears, and surrounding circumstances during the COVID-19 pandemic.

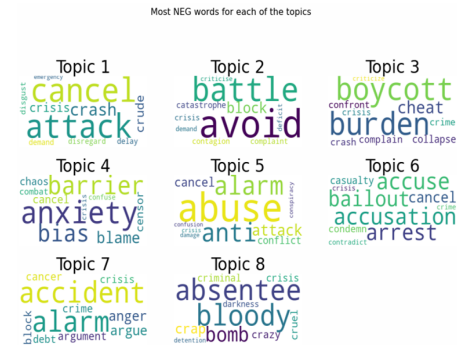


Fig. 14. The Most Negative Words for each Topics

VIII. CONCLUSION AND FUTURE WORK

Social media allows people to not only share their opinions but also express their feelings. A widely used social media platform is Twitter. The research conducted in this paper entailed developing a model that can extract the most topics traded in the Coronavirus pandemic and then analyze the sentiment of these topics during two different periods, from March to April and September to October. For this study, the dataset of English tweets about COVID-19 was selected. 567,064 tweets were processed and analyzed. The implementation was done through several steps starting from pre-processing to getting the optimal model. This work has performed lemmatization step three times to get the best result and overcome the problems of converting word to its right root. So, this approach is the best and delivers the best result. Additionally, this research used LDA model for finding the topics and produced the eight most important topics related to the Coronavirus, which are presented and discussed. This model works based on NLP and will train with 80% of the dataset and test with 20%. Furthermore, this paper presented the sentiment analysis of the collected tweets using lexicon-based approaches to classify people’s feelings based on most of the traded topics. The experiment of this research conducted on the Spark platform with Python to enhance the analysis and processing large set of related tweets.

The challenges of this research were in the dataset preparation phase. The dataset contains tweet-ID only, therefore, it got more time to rehydrate it and then extract all information of tweets using the code available by the dataset's authors. This study has some limitation, it appeared when working with a big data volume, the research spent much time to do that comparing to the time given to finish this research. Furthermore, separating tweets of each day in a file caused long time to collecting them and merge in one dataset. In the future, the plan to label the prepared dataset with its sentiment and use other machine learning algorithms like supervised algorithms, and then comparing the result of the labeled dataset with the result of sentiment analysis that performed in this research.

REFERENCES

- [1] "A Joint Statement on Tourism and COVID-19 - UNWTO and WHO Call for Responsibility and Coordination." [Online]. Available: <https://www.who.int/news/item/27-02-2020-a-joint-statement-on-tourism-and-covid-19-unwto-and-who-call-for-responsibility-and-coordination> (accessed Jan. 21, 2021).
- [2] S. Al-Saqqa, G. Al-Naymat, and A. Awajan, "A large-scale sentiment data classification for online reviews under apache spark," in *Procedia Computer Science*, 2018, vol. 141, pp. 183–189, doi: 10.1016/j.procs.2018.10.166.
- [3] E. Alomari, I. Katib, and R. Mehmood, "Iktishaf: a Big Data Road-Traffic Event Detection Tool Using Twitter and Spark Machine Learning," *Mobile. Networks Appl.*, 2020, doi: 10.1007/s11036-020-01635-y.
- [4] L. DeNardis and A. M. Hackl, "Internet governance by social media platforms," *Telecomm. Policy*, vol. 39, no. 9, pp. 761–770, 2015, doi: 10.1016/j.telpol.2015.04.003.
- [5] M. Y. Kabir and S. Madria, "CoronaVis: A Real-time COVID-19 Tweets Data Analyzer and Data Repository," 2020, [Online]. Available: <http://arxiv.org/abs/2004.13932>.
- [6] C. E. Lopez, M. Vasu, and C. Gallemore, "Understanding the perception of covid-19 policies by mining a multilanguage twitter dataset," pp. 3–6, 2020.
- [7] J. Samuel, G. G. M. N. Ali, M. M. Rahman, E. Esawi, and Y. Samuel, "COVID-19 public sentiment insights and machine learning for tweets classification," *Information*, vol. 11, no. 6, pp. 1–22, 2020, doi: 10.3390/info11060314
- [8] M. Sethi, S. Pandey, P. Trar, and P. Soni, "Sentiment Identification in COVID-19 Specific Tweets," in *Proceedings of the International Conference on Electronics and Sustainable Communication Systems, ICESC 2020*, pp. 509–516, doi: 10.1109/ICESC48915.2020.9155674.
- [9] K. Chakraborty, S. Bhatia, S. Bhattacharyya, J. Platos, and R. Bag, "Sentiment Analysis of COVID-19 tweets by Deep Learning Classifiers — A study to show how popularity is affecting accuracy in social media," *Appl. Soft Comput. J.*, vol. 97, p. 106754, 2020, doi: 10.1016/j.asoc.2020.106754.
- [10] B. Dahal, S. A. P. Kumar, and Z. Li, "Topic modeling and sentiment analysis of global climate change tweets," *Soc. Netw. Anal. Min.*, pp. 1–20, 2019, doi: 10.1007/s13278-019-0568-8.
- [11] R. P. K. Kaila and A. V. K. P. Prasad, "Informational Flow On Twitter - Corona Virus Outbreak – Topic Modelling Approach," *Int. J. Adv. Res. Eng. Technol.*, vol. 11, no. 3, pp. 128–134, 2020.
- [12] P. Monish, S. Kumari, and C. Narendra Babu, "Automated Topic Modeling and Sentiment Analysis of Tweets on SparkR," in *2018 9th International Conference on Computing, Communication and Networking Technologies, ICCCNT 2018*, 2018, pp. 1–7, doi: 10.1109/ICCN-T.2018.8493973.
- [13] A. H. Alamoodi et al., "Sentiment analysis and its applications in fighting COVID-19 and infectious diseases: A systematic review," *Expert Syst. Appl.*, pp. 1–13, 2020.
- [14] A. Assiri, A. Emam, and H. Al-Dossari, "Real-time sentiment analysis of Saudi dialect tweets using SPARK," *2016 IEEE International Conference on Big Data*, pp. 3947–3950, 2016, doi: 10.1109/Big-Data.2016.7841071.
- [15] E. S. Negara, D. Triadi and R. Andryani, "Topic Modelling Twitter Data with Latent Dirichlet Allocation Method," *2019 International Conference on Electrical Engineering and Computer Science (ICE-COS)*, Batam Island, Indonesia, 2019, pp. 386–390, doi: 10.1109/ICE-COS47637.2019.8984523.
- [16] Gilbert, C. H. E., & Hutto, E. "Vader: A parsimonious rule-based model for sentiment analysis of social media text". In *8th International Conference on Weblogs and Social Media(ICWSM-14)*,p.216-225.
- [17] C. Sievert and K. Shirley, "LDAvis: A method for visualizing and interpreting topics," in *Proceedings of the Workshop on Interactive Language Learning, Visualization, and Interfaces*, 2015, pp. 63–70, doi: 10.3115/v1/w14-3110

Building a Personalized Fitness Recommendation Application based on Sequential Information

Manal Abdulaziz¹, Bodor Al-motairy², Mona Al-ghamdi³, Norah Al-qahtani⁴
Department of Information Systems,
Faculty of Computing & Information Technology,
King Abdulaziz University,
Jeddah, Saudi Arabia

Abstract—Now-a-days sports plays a very important role in the life of the human being and it allows to keep him healthy and make him always active. Sport is essential for people to have a healthy mind. However, the practice of a sport can have negative effects on the body and human health if it is practiced incorrectly or if it is not adapted to the body or the human health. This is why, in this paper, we have proposed a recommendations system that allows the selection of the right person to practice the right sport according to several factors such as heart rate, speed and size. The implementation was applied to the FitRec dataset with the help of SPARK tool, and the results show that the proposed method is capable of generating the appropriate training for different groups according to their information, where each group gets the appropriate training. The grouping of this data was done by the k-means method.

Keywords—Big data; big data processing; recommendation system; sport analysis; K-means

I. INTRODUCTION

Sport is an important healthy behavior for improving public health, superior utilization of energies, and it constitutes excellent protection for the human being. In the 21st century, Activities of Sport are modern phenomena to make everybody keep healthy [1]. It's referred to a normal physical effort or skill practiced under agreed rules with the aim of entertainment, competition, pleasure, distinction, developing skills or strengthening self-confidence. No two people disagree on the importance of sport to both physical and psychological health. However, despite this, it has been proven that some sports can have negative results at times parallel to their positive effects on those who practice them. It is difficult for people who have not previously practiced sports to know the correct way to practice some exercise, which makes the possibility of injuries greater. Therefore, it is best to use a sports coach to design a special program and see the appropriate sports for the person in proportion to the individual's capabilities and health so that the latter does not suffer any possible injuries in the future or negatively affect the body health. And because we saw that every person who practices sports needs to know what sport is appropriate for his body and health, we have proposed in this paper a recommendation approach, which recommends the appropriate sport for the person based on several parameters such as heart rate, speed, and height. These parameters are recorded by smart wearable devices (ex. Apple Watch) as shown in Fig. 1. Improving wearable technology enables people to measure and control their behaviors via mobile devices such as Fitbit and Apple watches [2].

The remainder of the paper is ordered as follow, Second Section provide a background of the big data analytic and processing, the third section related work to a spotlight on relevant work that has been conducted in this field. Fourth section concentrates on description of data set. Discussion the methodology and tools that used to build recommendation approach will be in the fifth section, and then the rest sections will be for implementation and results and conclude this paper with conclusion and references.

II. BACKGROUND

A. Big Data Analytics Definition and Importance

The big data analytics (BDA) term was defined for the first time in 2012 by Gantz and Reinsel [3]. They stated that BDA includes three main dimensions, they are the huge data, the technologies used to analyze the data, and the valuable insights delivered from the data to create business values. Some researchers used the term BDA to refer to applying advanced analytic technologies against huge, heterogeneous, and diverse data that coming from different sources to extract values [4]. In Fact, big Data analytic is a revolution in the data science area. The organizations' need to big data analytics are increased, since their data are becoming bigger and heterogeneous. However, this huge amount of data does not provide any value in its raw nature [5]. Organizations have to employ advanced technologies to gain new values, enable smarter decisions, solve economic and social issues. Big data analytics assist process to be more efficient and facilitate in growing the organizations' profitability. As stated in the literature, there are also substantial advantages to performing big data analytic, they are [6][7].

- Enhancing decision makers: big data analytics enhance decision makers since it facilitates a understanding holistic data, creates predictive model, detects data trends and associations, and discovers data patterns.
- Predicting results: big data analytics tools able to model scenarios and then predicts results for each scenario, allowing decision makers to take a right action at the right time.
- Detecting Fraud: big data processing helps to quickly detect and correct deviations and outliers in data.
- Increasing data transparency: big data analytics expand the volume of exchange data between users while

preserving privacy. This therefore allows to access more valuable information.

- Improving organization productivity: big data analytics are considered an essential productivity driver since it provides opportunities for managing change and encouraging workers to be more conscious of their job patterns and practices.
- Improving customer service: big data analysis offers a rich knowledge of both customer issues and sentiment. It helps organizations to incorporate approaches to mitigate customer problems efficiently and proactively.
- Improving market intelligence: big data analysis provides insights into both the current and future state of the market and environment.
- Saving cost: big data tools are cost-effective since a huge amount of data can be processed and stored in commodity servers quickly.
- Developing new products: big data analytics allow organizations to develop new products according to consumers' needs based on analytics results of consumers' pattern and loyalty.

B. Type of Big Data Analytics

There are four major forms of BDA:

- Descriptive analysis: It is also known as data mining. It is the simplest and most common form of data analysis. It translates the immense volume of data into a statistical number that describe the data. Usually, findings of descriptive analysis are visualized in dashboards [8].
- Diagnostic analysis: it is used to detect the data patterns. Actually, diagnostic analysis assist to recognize the problems from their roots and understand reasons behind them [8].
- Predictive analysis: The organizations use predictive analysis to expect what may occur in the future based on both historical and current data [8].
- Prescriptive analysis: it is the most sophisticated form of data analysis as it makes a recommendation and recommends what actions can be taken. [8].

C. Big Data Processing

With the quick expansion of emerging applications such as, sensor networks, semantic web, LBS and social network applications, a variety of data to be processed continues to expand rapidly. Data processing is a collection of mechanics or models of programming to arrival large-scale data to elicit beneficial information for propping and providing decisions active handling of large-scale data (big data) poses an interesting but crucial challenge.

The ability to handle and process continuous data streams is becoming an essential part of building a data-driven organization. Data streams are sequences of unbounded tuples generated continuously in time. Unlike traditional batch processing

which involves processing of static data [9], below sections illustrate the difference between them.

1) *Batch processing*: Batch processing has a long background in the field of big data. This processing includes operating over a huge, constant dataset and generating the result when the computation is complement later in time [10]. The sets of data in batch processing are:

1. Confined: datasets of batch are a limited data collection [10].
2. Continual: data is almost ever support by some kind of constant storage [10].
3. Huge: Often, batch operations are the only way to handle large data sets [10].

2) *Stream processing*: Streaming includes processing continuous or dynamic data [11]. The capability to manage and process continued data streams is becoming a major portion of constructing a data-driven organization [9]. Instead of determining operations to using to a whole set of data, stream processors realize operations that will be utilized to each singular data element as it push through the system [10]. The data set here considered "unbounded", this has a few major consequences:

1. Only the amount of data that has entered the system so far is known as the total dataset.
2. Perhaps the working dataset is more important and is restricted at one time to a single object.

Processing is event-based and unless expressly stopped, does not "end". Results are available instantly and will be revised constantly as new data arrives.

D. Recommendation Systems

Recommendation systems are tools that support the interaction with information spaces that are large and complex, by providing a personalized view of the information space through the prioritization of items that the user may find interesting [12]. The recommender systems' field was first identified in 1995 but became popular in the last decade [13]. According to [14], recommender systems are tools that provide the user with the appropriate recommendations. The definition provided during the inception of the field has been evolved [12]. In its early years, it was defined as a system in which people will provide the recommendations in the form of inputs, which will then be aggregated by the system and directed to the proper recipient. According to this definition, some cases depended primarily on aggregation for transformation while in different instances, the system's value depended on its ability to match recommenders and those in need of recommendations efficiently. This definition was based on collaboration among users. A recommendation system is therefore a system that will produce an output with an individualized recommendation. It can also be a system that can provide a user with personalized guidance to objects that are interesting or useful found in a large space with many possible options. Based on the evolved definition, which can also be formulated into a formal definition, two principles are identified about a recommender system. One is that it is personalized, meaning it caters to the needs of one user and not a group. Secondly, it offers assistance

to the user where discrete options are available, and the user has to make a selection [12]. In developing recommender systems, search needs were the main address point in addition to the selection of relevant products within Big Data from the internet, which is considered to be the biggest marketplace [15]. Recommendation systems are important because they provide customers with a direct connection to the products which they desire minimizing the browsing time used by the user. With the highest level of accuracy, a recommender system will predict a user's interests and provide a recommendation of the product that is perfectly matched to the user's interests [13]. With the assistance of recommendation systems, it is possible to recognize the tastes of a person and automatically find new content that would be desirable to them [16]. This means that the identification of a person's patterns, regardless of their variation in tastes. Recommendation systems are also important to the business using it since it can enhance its sales. This is made possible through the presentation of a variety of items that can match the user's interests since a recommended outcome is dependent on the commercial interests in addition to how ambiguous the customer is in formulating a request or query [15]. If a user or customer makes purchases of more items than they were looking for, through their search request, then the business makes a profit. They eliminate information overload by providing personalized recommendations [17].

1) *Types of recommendation systems:* The two major types of recommendation systems are content-based recommender systems and collaborative recommender systems. Also, there are hybrid recommender systems. A content-based recommender system uses a content-based filtering technique. A system model built using this approach is based on the representation of the product (item description) and the user preference (the customer's preference profile) [15][16]. In this approach, the products have features that are similar to products previously examined by the user or are currently being searched. The products or items are usually identified based on the user properties and the item properties. Other evaluations from the customers are not considered for this approach. The items recommended in this case are usually those that best match the items that have previously been rated. This approach has its drawbacks such as the system's is not able to provide suggestions for a variety of products. Another drawback is where the customer is required to rank several products beforehand so that they can get useful recommendations [16]. The collaborative recommender system uses collaborative filtering. This approach uses the knowledge of the relationship between the user and the item, product or service. It uses past behaviors (like previous purchases) or feedbacks (like ratings) by a customer in addition to decisions that are similar to this made by other customers [15][16]. This information and the relationship between the customer and the product help in predicting the recommended product. This approach has its drawbacks as well which include the need for extensive information on the customer's evaluation in order to achieve computations whose correlations and predictions are precise [15]. Another drawback is the fact that newly added customers or products are not included in the calculations. The hybrid recommender system applies the hybrid filtering technique [16]. This approach is a combination of the content-based and collaborative approaches while allows for the optimization of features from both approaches while



Fig. 1. The Amount of Data that Collected from Smart Watch.

minimizing the drawbacks associated with the two [15],[16]. In this research, the collaborative filtering approach has been adopted since it promotes building the model based on a user's past behavior and similar decisions made for other users to anticipate the most appropriate sport that the user needs.

2) *Applications of recommendation systems:* The online market is one example where a third-party seller can trade their product on online marketplaces. The online market operator processes the transactions happening on the online marketplaces and the customers have a service that allows them to search for products using description or other properties in their knowledge [15]. Travel Industry is another application where customers are able to book hotels, purchase flight tickets directly as well as acquire holiday packages just from the mobile applications or from web pages without any additional costs that would otherwise be presented if the transaction was carried out physically. Recommender systems are being used in different places and for different purposes. It is being used in e-commerce companies such as Amazon to recommend items that a user can buy. Also, it is used for e-learning and e-library where users can get books and research documents in entertainment for movie suggestions, for instance, Netflix and YouTube. E-government is also using recommender systems [15].

III. RELATED WORK

This research focuses sport recommendation and prediction (Fig. 1). We present the associated research from each related field as follows:

A. Context-aware Modeling

In several fields with ample contextual knowledge, context-aware models have been successfully adopted such as in recommender systems[18]. Naturally, like the other context-aware models, fitness and workout information has a heterogeneous input structure. Recommendation systems for tourism play a crucial role in supplying visitors with helpful trip planning. Recently researchers have been working to develop recommendation systems for routes. Users have been widely accepting such kind of systems [18]. Mehmood et al. (2019) [18] proposed a recommendation system to lead tourists in in South Korea.

The proposed system is based on the statistical analysis of user preference. Plus, the popularity of the sites, distance, traffic, weather and time are considered to recommend the routs. The system used Naïve Bayes classifier to calculate the probability of tourists to visit sites, and Haversine formula to measure the distance between the locations. The model evaluated using dataset that contains the patterns of tourist activity, obtained in the years 2016-2017 from tourists' smartphones. This real-time data was gathered from Wi-Fi routers distributed in 149 sites. The results show that, the tourists become able to visit more famous locations conveniently.

B. Sensor Data Mining

Ubiquitous computing combine technologies of processing data that collected from wearable devices, embedded devices and mobile applications [19]. Recently, there is a growing trend to model a recommendation system using these devices. Chowdhury et al. (2018) [20] proposed AdaBoost-based classifier to predict suitable exercise types in real-world contexts based on a limited data for training. First, the system extracts some features from the data such as the distance and heart rate. Then, the system mixes the extracted features with other features that related to each exercise like exercise duration. Finally, the system applies a 5-fold cross validation approach to classify the users. The experiment applied on a dataset contains 22 persons, who performed diverse exercises. The total of the sessions was 40.

Ni et al. (2019) [2] proposed a sequential context-aware model to extract the temporal patterns and personalized fitness data. The model gathers the specific activity data using wearable sensors. It also uses data from user's activity history. The model measures the average heart rate for each exercise, then it directs the user to a suitable exercise based on this biased. The model was evaluated on 250,000 records of workout and millions of measurements collected from the wearable devices.

C. Personalized Recommendation

Nowadays, academia and industry researchers have developed systems to recommend users based on their personalized behavior [21] [22]. Zhang et al. (2016) [21] proposed personalized travel recommendations system that aim to recommend tailored routes based on users' needs and available time. The travel time volatility and point of interest opening hours are also considered to recommend the optimal rout. The model was evaluated on a real-time dataset. The results show that, the SE-SR algorithm helps in increasing performance but lesser quality than the optimal solutions, while PDFS algorithm is the most effective one. Loepf et al (2017) [22] proposed a system to provide runners to the optimal route based on their environment, goals and preferences. Of course, each route must be independently recommended, considering several distinct factors that decide whether a recommendation would eventually serve the runner. The system was evaluated on total of 11 runners from different ages and both genders.

Kushal Bafna, Durga Toshniwal [23] proposed a dynamic framework for a feature-based overview of the views of customers on online products, which operates according to the product domain. When they elicit online feedback on a periodic basis for a product, they conduct the following work

any time after extraction; firstly, it is done to define the characteristics of a product from the opinions of customers. Next, their corresponding views are extracted for each feature and their orientation or polarity (positive / negative) is identified. It calculates the final polarity of the feature-opinion pairs. Feature-based summaries of the reviews are then created by extracting the related excerpts for each pair of feature opinions and placing them in their respective feature-based cluster. Results show that in carrying out their tasks, the proposed methods are highly productive and successful. Now it has become much simpler for users to digest the data found in large numbers of products review corpus by making use.

Klavdiya Hammond and Aparna S. Varde in [24] represent study the predictive model implementation on cloud utilizing Hadoop and MapReduce programming notion. They suggest predictive analytics prototypes for text classification, recommendation framework and decision support using open-source cloud-based solutions, using open source software packages, specifically Apache Hadoop, Hive and Mahout, all of which are designed to be scalable to big data.

Jai Prakash Verma et al. [25] proposed system that offers review or summary of text data obtainable on web for an educational foundation. The suggested method generates the group of choose reviews as a summary of all feedback of big data set. In this system, Sequential Pattern Mining Framework (SPMF) has been used and Elki tool for clustering analysis. In comparison with manually selected reviews and feedback, the results produced by these tools are shown in the various graphs that introduced in paper and considered satisfactory.

Li Chen and Feng Wang [17] have identified that there was a problem with the identification of preference similarity among reviewers. They recognized that for an accurate recommendation to be generated for the buyer, there was a need to identify the essential preference similarities between the buyer and the product reviewers. To try and resolve this issue, Chen and Wang proposed a novel clustering method. The method is founded on the LCRM (Latent Class Regression model). This model makes it possible for reviewers' preference similarity to be identified through the consideration of the overall ratings as well as the feature-level opinion values as they are presented in the textual reviews. Using the model, they derived the cluster-level preferences and reviewer-level preferences, which is compared against active buyer's recommendations. They then used an experiment, applying two data sets from the real world to test the proposed recommender algorithm. The laptop dataset and digital camera dataset were used. The outcome from the experiments was the superior performance of the LCRM based on accuracy which used specifically included; the reviewer-level preferences that were derived were very stable, reviewers clustering were performed effectively and the recommendations generated for the buyer were more accurate regardless of how complete the buyer's preferences were [17].

Hongyan Liu and others [26] identified the low accuracy problem that traditional recommendation methods experienced due to the sparseness of data. They proposed a novel recommendation algorithm, called PORE. The proposed method identified the user's preferences by analyzing the difference between the user's ratings and opinions. It considers implicit opinion and explicit ratings, which helps in addressing the issue with data sparseness. The adverb-based opinion-feature

extraction method is used for the extraction of opinions and the features from the user reviews online. This method would enhance the accuracy of extraction. To evaluate the algorithm's performance, the researchers conducted an empirical study, which is based on the extraction methods. The study would be carried out on a real dataset of an online restaurant review and it would be in Chinese. The purpose of the study is to create a recommendation system for the restaurant as well as demonstrate the proposed method's effectiveness. The results from the experiments carried out show that in comparison to the already existing methods, the extraction method used here has a better performance and it can extract the most features and opinions. The results also show the capabilities of the recommender algorithm in dealing with data sparseness as well as its better accuracy and efficiency in making predictions [26].

Sandra Esparza and others [27] identified that Real-time web (RTW) services usually provide its users with a chance to put across their interests and opinions. RTW data is unstructured and is therefore not recognized in recommender systems. However, they recognized that RTW data can contain consumer reviews that are very useful with regards to the reviewed services, products and brands. Therefore, they proposed an approach that could utilize RTW data (Twitter-like short-form messages) for a product recommendation, where the RTW data is the source for retrieval information and indexing. The approach proposed making recommendations through the use of micro-blogging information. The researchers used four datasets of different products retrieved from the Blippr service to evaluate the micro-blog reviews. The results indicate that despite their use of language being inconsistent and messages being short form, the micro-blogging messages are capable of providing useful recommendations. The approach also proved, from the evaluation and based on accuracy and coverage, that the approach outperforms the traditional collaborative filtering approach [27].

Our contribution: previous studies have considered activity and fitness models from different aspects, but still there is a gap in term of modeling fitness applications based on sequential information such as heart rate. This inspires us to propose a fitness recommendation model based on as heart rate sequential information.

IV. DATA DESCRIPTION

A. FitRec Datasets Description

Datasets of FitRec [28] include sports records of user from Endomondo. Data contains several sources of sequential sensor data like rate of heart, GPS, speed, as well as type of sport, weather condition (such as humidity and temperature) and gender of user. These sets of data are collected from wearable devices (e.g. Apple Watch, Fitbit, etc.) and such data are heterogeneous, noisy, diverse in scale and resolution, and have complex interdependencies. To clean these data, heuristics are utilized by filtering out those unnatural workout samples like too large magnitude, timestamps which are mismatching, sudden changes in coordinates of GPS. We also derive several variables such as distance and speed from the measurements.

Type of Data:

- Measurements data like timestamps, distance, speed, and heart rate,

- Contextual data like altitude, latitude, longitude, sport, user identity, and gender

Table I describe the datasets features, it contains 5 columns. The "variable" column represent the names of the features, while the type of each feature is represented in the "data type" column and the measurement unit is represented in "Unit" column. The Definition column describe the features. As shown in the table, the features is categorized into Measurement and Contextual.

B. Exploratory Data Analysis (EDA)

Table II shows the statistics of the dataset in respect of the total number of sports, workouts, genders, speed, and heart rate. As shown in the table, the majority of participants is males, while the minority is females. There are also **1185** unknown gender participants. The speed mean \pm SD = (20.962 \pm 8.483 MPH) and the speed range is (min =0.0, max=74.859 MPH). The speed standard deviation is small, meaning that speed values of the participants are centralized around the mean. The min value of speed rate illustrates that there are sports that do not require fast movement. The heart rate mean \pm SD = (138.7 \pm 18.961 BPM) and the heart rate range is (min = 0.0, max = 239.0 BPM). The large value of the standard deviation of the heart rate indicates that the heart rates values are scattered, meaning there are a notable difference between the users' heart rates. This could be due to their gender, weight, diseases, etc. Table III clarifies the differences in heart rate between male and females for each sport. These differences confirm that, the heart rates do not follow a specific pattern and they are varying from participant to another according to his/her personalized health. Therefore, the heart rate issues should be considered during the workouts for each participant alone, this is the value of our proposed recommendation system. There are a markable differences between the heart rates and speed rates between the females and males as shown in Table 3, Fig. 2, and 3. The females heart rates are usually higher than the males specially when they skate or play gymnastics. At the same time, the standards show that males are much faster than the females.

Fig. 4 and 5 shows that, generally, males' and females' heart rates are positively correlated with the altitude; this is natural phenomena since climbing heights takes great efforts. However, their heart rates are negatively correlated with the speed due to athletic heart syndrome [3]. It is a phenomenon that explains the natural changes that take place in the hearts of people participating in vigorous athletic training. Eventually, our recommendation model will address these two issues, it recommends participants the suitable sports. Plus, the participant's heartbeat will be observed during the workout to notify him if his heartbeat reach dangers threshold to take suitable action, such as slowing done or changing his path if there are altitudes.

V. THE PROPOSED FRAMEWORK

First when person open the application at first time, there is some information must record it in app, like gender, and ID (id may be generated by app), and app then will join with watch. Participants wear smart watch and start to do workout. During workout, some important data will be generated like speed,

TABLE I. FITREC DATA DESCRIPTION

	Variable	Data type	Unit	Definition
Measurement	Heart Rate	Array<bigint> _i	Beat per Minute (BPM)	The speed of heartbeats for a specific user.
	Timestamp	Array<bigint> _i	Unix Timestamp	Tracking the time of the specific event occurred in form of seconds
	Distance	Array<double> _i	Mile	Measured by calculating the haversine formula which considers longitudes and latitudes to determine the distance among certain points.
	Speed	Array<double> _i	Mile per Hour(MPH)	Measures the movement of an object which is calculated by dividing the distance over time.
Contextual	ID	Bigint	-	The ID for a specific workout.
	UserID	Bigint	-	The user's national ID
	Sport	String	-	The user makes physical exertion and practicing different sports such as bike riding, walking, running, skating, and so on.
	Gender	String	Male,Female	The user can be male or female.
	Altitude	Array<double> _i	Meter	The perpendicular distance from the specific object to the earth's surface.
	Longitude	Array<double> _i	Degree	The geographic coordinations which determine the exact location on the earth's surface.
	Latitude	Array<double> _i	Degree	
	URL	String	-	The link of the user's account

TABLE II. EDA

Feature	Measures	
Sport	43	
Workout	167,783	
Gender	Male	156717
	Female	9881
	Unknown	1185
Speed	Max	74.859
	Min	0.0
	Mean	20.962
	Standard Deviation	8.483
Heart Rate & Standard Deviation & 18.961	Max	239.0
	Min	0.0
	Mean	138.7

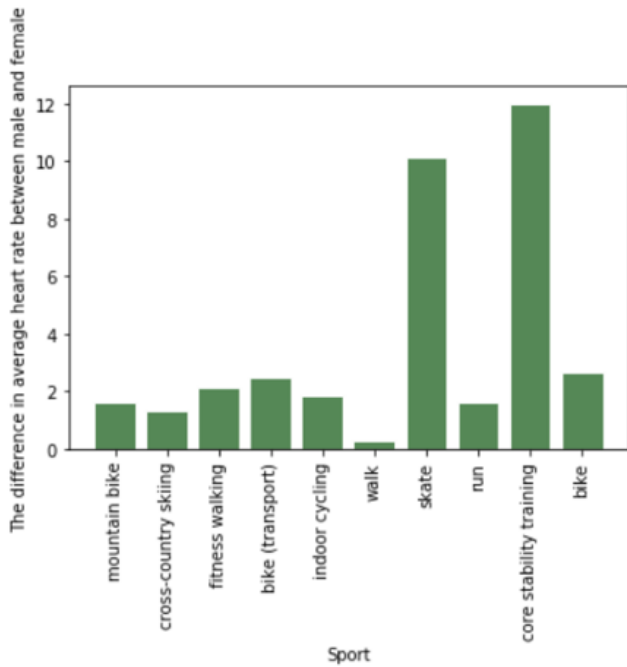


Fig. 2. The Differences in Average Heart Rate between Males and Females.

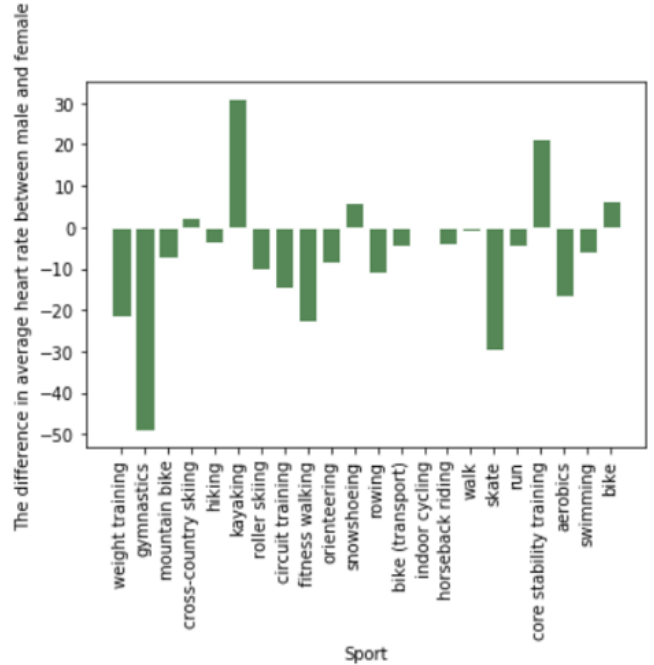


Fig. 3. The Differences in Average Speed Rate between Males and Females.

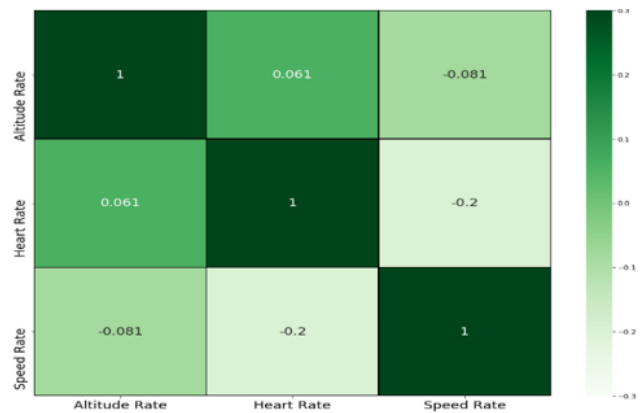


Fig. 4. Male Pearson Correlation of Features.

heart rate and altitude depend on place of person (longitude and latitude). Based on some processes in sequential steps (explained in framework) the application will recommend the suitable workout for person. Fig. 6 shows the system overview. Framework is divided into three layers:

A. Application Layer

1) Data gathering: The data was collected by first: registering in the application, second through workout where data is measured by wearable device (smart watch). These data will

TABLE III. INFORMATION FROM THE DATASET ABOUT SPEED AND HEART RATE FOR EACH SPORT

Sport	Heart Rate			Speed		
	Male	Female	Diff_Heart	Male	Female	Diff_Speed
Mountain bike	135.334108	142.596029	-7.261921	20.403874	18.785404	1.618470
Cross-country skiing	138.137305	135.610060	2.527246	14.566997	13.248498	1.318498
Citnness walking	104.853535	127.391624	-22.538089	9.420005	7.262868	2.157137
Bike (transport)	126.564361	131.209013	-4.644652	23.519709	21.048684	2.471026
Indoor cycling	133.235132	133.297185	-0.062054	27.456905	25.587658	1.869247
Walk	102.351934	103.368996	-1.017062	6.477019	6.214970	0.262049
Skate	118.626881	148.212842	-29.585961	29.880860	19.772502	10.108359
Run	146.752812	151.428408	-4.675596	11.681297	10.079193	1.602104
Core stability training	131.464555	109.941488	21.523067	17.818819	5.822604	11.996215
Bike	133.692914	127.367465	6.325449	27.192178	24.523801	2.668377
Weight training	107.399738	129.021000	-21.621262	—	—	—
Gymnastics	104.550400	153.598000	-49.047600	—	—	—
Hiking	110.213909	114.032450	-3.818541	—	—	—
Kayaking	123.132933	92.156000	30.976933	—	—	—
Roller skiing	129.653974	139.967600	-10.313626	—	—	—
Circuit training	118.425579	133.212308	-14.786729	—	—	—
Orienteering	146.885183	155.238818	-8.353635	—	—	—
Snowshoeing	127.474727	121.362000	6.112727	—	—	—
Rowing	131.076264	142.158111	-11.081847	—	—	—
Horseback riding	138.429000	142.704000	-4.275000	—	—	—
Aerobics	141.228800	157.691000	-16.462200	—	—	—
Swimming	118.511500	124.460667	-5.949167	—	—	—

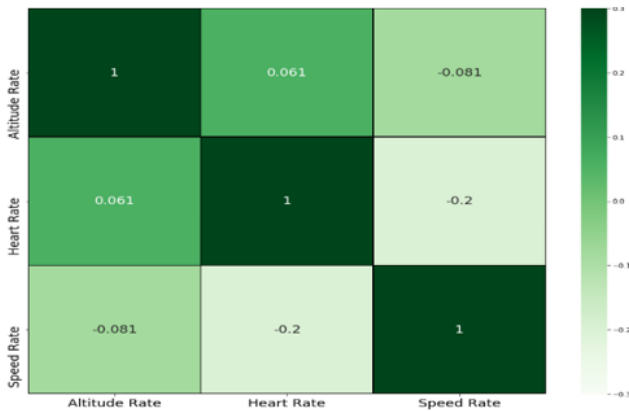


Fig. 5. Female Pearson Correlation of Features.

store in in Repository Layer.

B. Processing Layer (Pre-processing, comparison, prediction, clustering and recommendation)

1) *Recommendation*: depending on the characteristics of person, app will recommend a suitable workout for him to reach the goal of workout without any bad effects on participant’s heart.

2) *Clustering*: The system will proceed with K-means clustering which is the most straightforward and well-known unsupervised machine learning algorithm. The purpose of applying K-means is to aggregate similar data points into a set of clusters. There are several advantages behind using this technique which are simplicity of its implementation as it has only two steps. Also, scaling to big data sets as well as the algorithm works in high speed. Furthermore, the technique ensures convergence and the ease to adjust to new examples [29]. In essence, the similar participants are clustered based on their recorded measures of heart rate speed and altitude of all their previous workouts per sport.

3) *Comparison (stream processing)*: The system check the participants’ heart rate and altitude. It sends an alarm when detecting unusual heart rate and recommend the participant with the suitable action.

4) *Feature selection*: The only workouts that have speed, altitude and heart rate are selected. So, from the overall type of workout, 15 workouts are selected. Average speed, average heart rate, and average altitude are selected to develop the cluster model.

5) Pre-processing: Encoding

- Timestamp encoded into 4 periods, here we will divide 24 hours into 4 period [0 from 12:00 a.m. to 5:00 a.m.], [1 from 6:00 a.m. to 11; 00 a.m.] , [2 from 12:00 p.m. to 9:00 p.m.] and last period [3 from 6:00 p.m. to 11:00 p.m.] . We chose to divide the day into four periods that came from our knowledge of some of the current clubs with high competence in dividing the sport periods into 4 periods.
- Encoding is the process of converting categorical variables into numerical. Binary encoding technique was used to encode the verified and official features, ‘0’ represents the account which is not verified or official the account. Gender data will convert to 0 and 1 (Male =0, female=1).
- The sport feature was encoded using one-hot encoding; it is a type of encoding method [30]. It points to dividing the column which includes numerical categorical data to multiple columns basing on the categories number existing in that column, each column contains “0” or “1” matching to which column it has been placed. The sports which recorded with (speed, altitude and heartrate) only considered. So, the overall total of workout is 15.

Aggregation

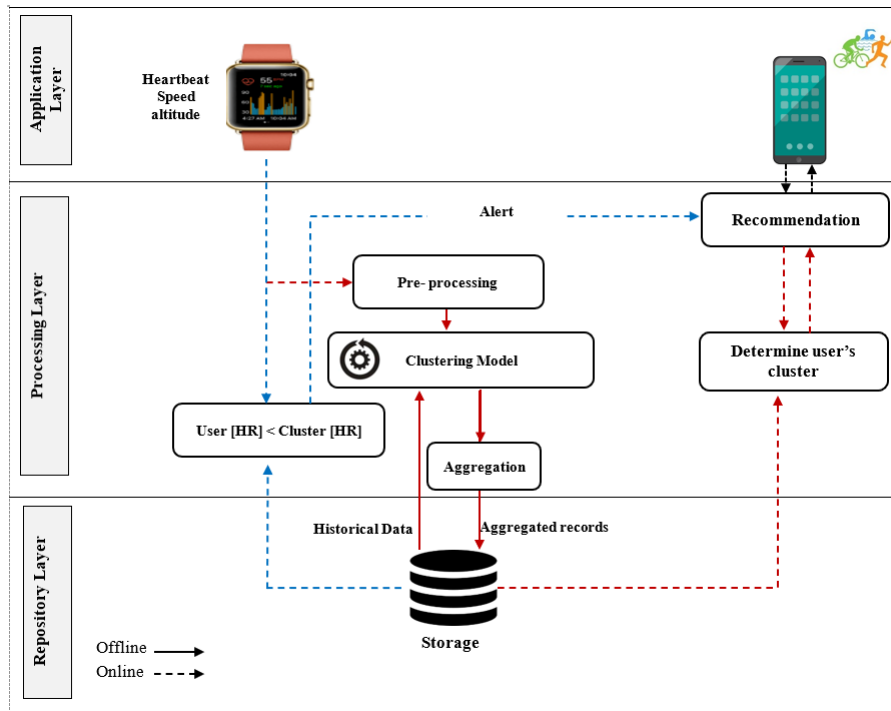


Fig. 6. System Overview.

To implement this step, there is a need first to understand the nature of inputted data for different attributes like heart rate, speed and altitude which each of them is taken as an array of successive values. First, the system will calculate the average heart rate, speed and altitude for each user per workout. Then, it will aggregate all these averages and calculate the overall average for each participant's record per sport.

Missing value

The real-world data often has a lot of missing values. The cause of missing values can be data corruption or failure to record data. The handling of missing data is very important during the preprocessing of the dataset as many machine learning algorithms do not support missing values. The missing values will be replaced by the average values of its feature, depending on the gender.

Vectorization

It is the way to represent the data set into a set of vectors. Many different techniques are available, the simplest one is count vectorizer. This process aims to discover some patterns or relationships within the targeted data [31]. The system will set up co-ordinate vectors for each user prior implementing the K-mean. In detail, these co-ordinate vectors will be assembled dependent on the marks which express an hour period that is divided into 4 marks with values of (0,1,2,3). Each of these marks will have a count for each user Id and it will be updated constantly but the mark that has not existed will be assigned with zero. Also, gender is taking 0 for a male and 1 for a female. Furthermore, calculating the average of different attributes such as speed, heart rate and altitude grouping by workouts in order to constitute vectors of m sports.

Scaling

The dataset consists of various independent variables. The value ranges for those different variables are almost certain to vary widely and to have their own scale. The value ranges of all variables should have a similar scale to promote each variable in contributing proportionately to the ultimate result [32]. The scaling feature is almost confined between 0 and 1 which are viewed as the minimum and maximum values. Accordingly, the min-max scaling methods will be used.

C. Repository Layer (Historical Data)

The dataset will be stored in MongoDB in JSON format. MongoDB is an open source NoSQL database system built for storing semi-structured data. Plus, the data will be stored on the MongoDB after the clustering process. This structure provides flexibility and adaptability in a way that enables the programmer to create classes and objects instead of having a traditional row/column model [33].

VI. EXPERIMENT, RESULTS AND EVALUATION

A. Clustering

The k-mean cluster was used to split the similar participants together according to their heart rate, speed rate, and altitude. One of the properties of the k-mean clustering algorithm is that the optimal number of clusters can be defined before the clustering process. The well-known elbow method was applied to determine the optimal clusters number [1]. The elbow method assumes that the optimal clusters number must produce small inertia, or total intra-cluster variation. To identify the optimal number, the k must be selected at the "elbow" point, after the inertia /distortion begins decreasing in a linear fashion. Fig. 7 shows the optimal number to cluster the data is $k=5$. Table IV shows the elbow points' value in k (2:10).

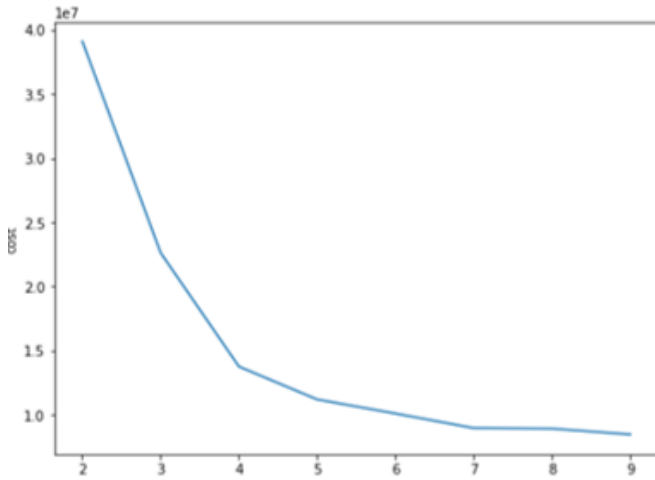


Fig. 7. The Changes on Elbow Values of k (2:10).

TABLE IV. THE ELBOW VALUES OF K (2:10)

K	elbow
2	0
3	0
4	22627014.820202056
5	39113248.973619014
6	13754284.605939962
7	11188781.682890285
8	10090998.661182716
9	8957156.883945007
10	8911367.440781211

The k-mean algorithm was trained on 70% of the data, then it was used to predict the remaining 30% sets of data. The algorithm performance is 0.73128 based on Silhouette Coefficient score. Silhouette Coefficient is a metric used to evaluate the clustering technique [2]. Its value varies between -1 and 1, where 1 indicates that clusters are distinct and clearly differentiated from each other, while -1 indicates the clusters are allocated in the wrong way, and 0 indicates that the clusters are indifferent [2]. Table V shows the properties of each cluster. As shown on the Table V, each cluster was given a name. The majority of the participants are belonged to the Moderate fit athlete cluster (the the account of the participant equal 16989), while the minority to the Unusual (the the account of the participant =176). In General, there is a big discrepancy between the number of participants in the Moderate fit athlete cluster and the other clusters. The Unusual cluster which has a very few participants may contain unusual observations. This appear when comparing its very high-altitude average which equal (1510.427) with other clusters altitude average. The participants who belongs to the Most fit athlete cluster achieved much higher altitude rate than the participants in the Moderate fit athlete cluster. At the same time, they recorded 130.553 which considered close to the normal heart rate. For adults, the average resting heart rate varies between 75 and 170 beats per minute during exercises [3]. A lower heart rate at rest usually means more successful heart function and greater cardiovascular health [3]. So, the participants included in Most fit athlete cluster are the most trained athlete. The participants who belong to the cluster Above-average fit and Adventurers recorded high altitude and heart rates, this metrics

seems normal as most of them practiced hiking, mountain bike, and cross-country skiing as shown in Fig. 8. It seems that the participants in cluster Adventurers reached much higher peaks than those belonged to cluster Above-average fit, increasing their heart rate. Finally, there is no markable differences between the average speed of all the five clusters, all the users' speed rates are ranged in (17.35 and 19.66).

B. Comparison

Based on the center of disease control and prevention [4], and The Heart Foundation charity organization [5], the intensity of exercises can be measured using heart rate measures. The heart rate should be 50% to 70% of the estimated maximum heart rate for exercising at a low to moderate intensity, but during robust exercises it's about 70-85% of maximum. Table VI shows a heart rate measures according to the different ages. For example, if the participant is 20 years old, the maximum estimated heart rate for exercising is 140 in case of intensity exercises and 170 in case of robust exercises. Because of the dataset is limited in term of the age, we will consider the average of all the heart rates as the heart rate threshold, resulting in 122.5 for intensity exercises and 149 for robust exercises.

According to the average altitude which achieved by participant for each cluster. The altitude of the Moderate fit athlete cluster (55) is consider as threshold of the altitude when the participant does not join to one of the robust sports since it represents the majority of the participants. On the other hand, the altitude of the Most fit athlete cluster (213) is consider a threshold of the altitude when the participant joins to one of the robust sports since it represents a high portion of the participants who exercise robust sports. The robust sports are mountain bike, cross-country skiing, hiking, orienteering, run, and bike. Fig. 9 represent the flowchart of the comparison phase. To implement the comparison phase of the system, the streaming data was simulated using pyspark. Fig. 9 shows the flowchart of the recommendation system.

VII. CONCLUSION

This research aimed at building a personalized fitness recommendation application based on sequential information such as heart rate. Specifically, the proposed application will recommend a proper workout type for the one who care to avoid the negative consequences that may affect his health. This target has been achieved through learning the historical workout sequences that is integrated in our proposed framework and applied K-means clustering algorithm to group similar users according to their heart rate, speed rate, and altitude. After the elbow method was applied to determine the optimal clusters number, the result shows that the optimal number to cluster the data is k=5. Furthermore, this clustering algorithm has been trained on 70% of the chosen dataset and then it was utilized to predict the remaining 30% sets of data. The performance of the applied algorithm is 0.73128 based on Silhouette Coefficient score which is indicated that that clusters are distinct and clearly differentiated from each other. This research aimed at building a personalized fitness recommendation application based on sequential information such as heart rate. Specifically, the proposed application will recommend a proper workout type for the one who care to avoid the negative

TABLE V. THE OVERVIEW INFORMATION OF ALL THE FIVE CLUSTERS

Cluster	Cluster Name	Count	%	Avg(speed)	Avg(heart)	Avg (Altitude)	Sport
1	Moderate fit athlete	16989	67.4	19.31756492094167	136.92687567988688	55.29274236638334	mountain bike, cross-country skiing, hiking, kayaking, roller skiing, fitness walking, orienteering, bike (transport, indoor cycling, horseback riding, walk, skate, run, core stability, bike.
2	Unusual	176	0.0069	17.59108255126259	133.46338172392413	1510.426606091586	mountain bike, indoor cycling, walk, run, bike
3	Most fit athlete	5872	23.3	17.35909711437589	130.5529807309039	213.9624622595631	mountain bike, cross-country skiing, hiking, roller skiing, orienteering, bike (transport), indoor cycling, walk, skate, run, core stability, bike.
4	Above-average fit	1592	2.5	17.8432634544732	133.93142304348586	360.10695197968624	mountain bike, cross-country skiing, hiking, roller skiing, fitness walking, orienteering, bike (transport), indoor cycling, horseback riding, walk, skate, run, core stability, bike.
5	Adventurers	568	2.2	19.66543325571946	139.49961339923698	822.0379459052019	mountain bike, cross-country skiing, roller skiing, indoor cycling, core stability, run, bike

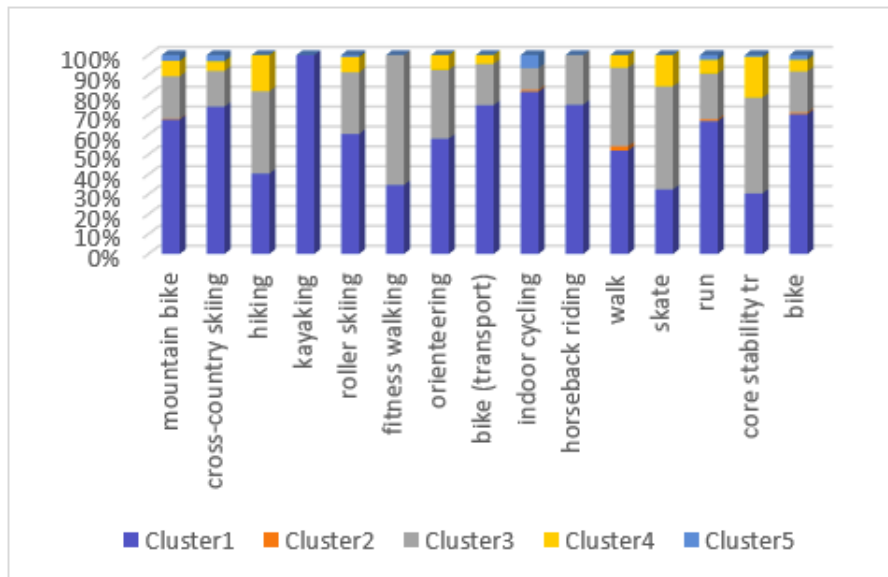


Fig. 8. The Distribution of Sports in each Cluster.

TABLE VI. ESTIMATED HEART RATES FOR EXERCISING

	Intensity Exercises	Robust Exercises
70	75 - 105 bpm	75-128 bpm
60	80 - 112 bpm	80-136 bpm
50	85 - 119 bpm	85-145 bpm
40	90-126 bpm	90-153 bpm
30	95-133 bpm	95-162 bpm
20	100-140 bpm	100-170 bpm

consequences that may affect his health. This target has been achieved through learning the historical workout sequences that is integrated in our proposed framework and applied K-means clustering algorithm to group similar users according to their heart rate, speed rate, and altitude. After the elbow method was applied to determine the optimal clusters number, the result shows that the optimal number to cluster the data is k=5. Furthermore, this clustering algorithm has been trained on 70% of the chosen dataset and then it was utilized to predict

the remaining 30% sets of data. The performance of the applied algorithm is 0.73128 based on Silhouette Coefficient score which is indicated that that clusters are distinct and clearly differentiated from each other. Furthermore, this research is achieved a comparison for the recommendation system by simulating the streaming data using pyspark. In near future, some extra work can be done by integrating a third party that recommends the most appropriate path for the user instead of giving him a general message to change his route. Also, the research needs to employ more features or characteristics related to chronic diseases to have more logical reasons for grouping the clusters.

REFERENCES

- [1] Y. G. Wibowo and B. Indrayana, "Sport: A review of healthy lifestyle in the world," *Indonesian Journal of Sport Science and Coaching*, vol. 1, no. 1, pp. 30–34, 2019.

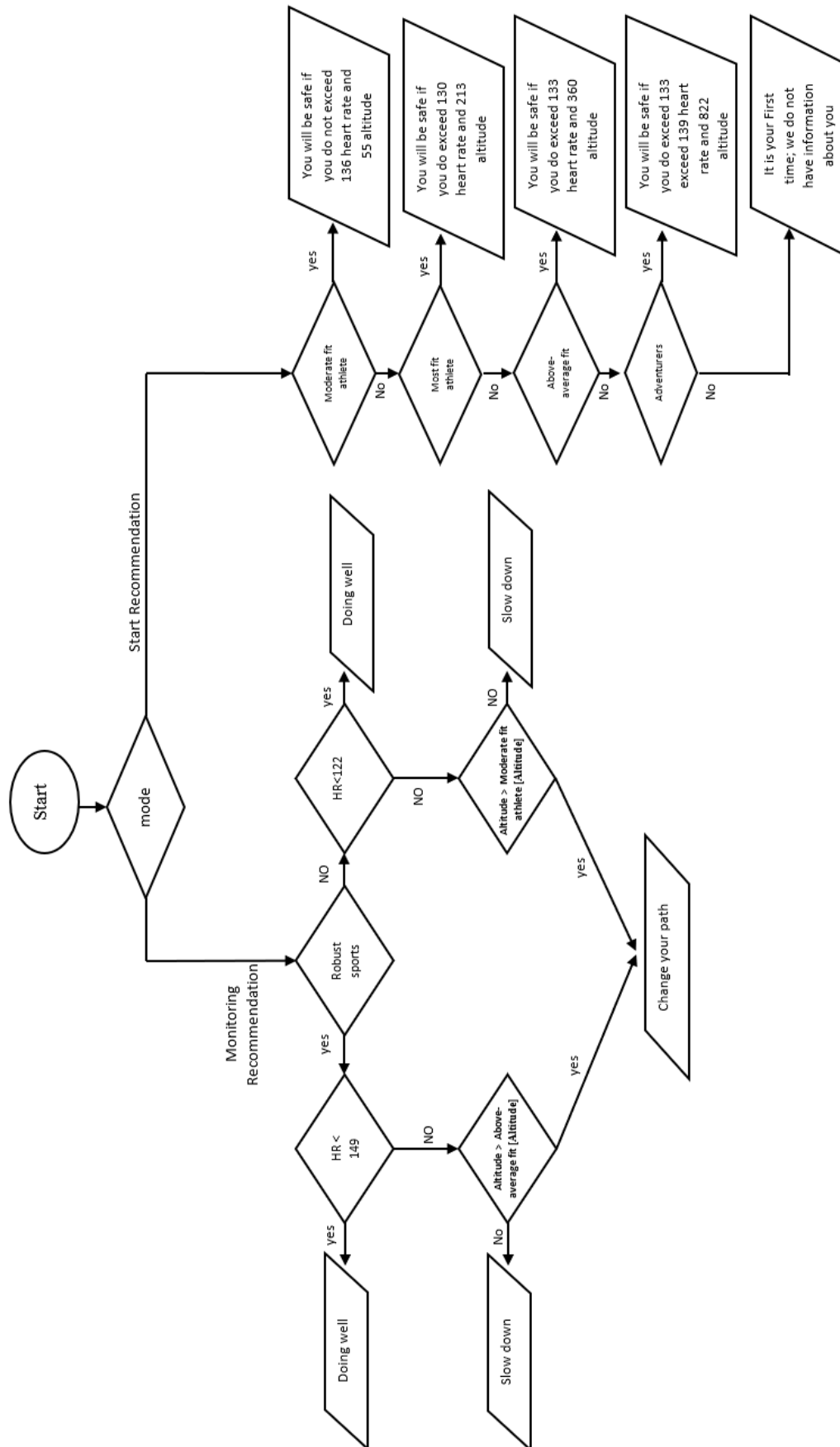


Fig. 9. Flowchart of the Recommendation Phase.

- [2] J. Ni, L. Muhlstein, and J. McAuley, "Modeling heart rate and activity data for personalized fitness recommendation," in *The World Wide Web Conference*, 2019, pp. 1343–1353.
- [3] J. Gantz and D. Reinsel, "The digital universe in 2020: Big data, bigger digital shadows, and biggest growth in the far east," *IDC iView: IDC Analyze the future*, vol. 2007, no. 2012, pp. 1–16, 2012.
- [4] G. George, E. C. Osinga, D. Lavie, and B. A. Scott, "Big data and data science methods for management research," 2016.
- [5] P. Maroufkhani, M.-L. Tseng, M. Iranmanesh, W. K. W. Ismail, and H. Khalid, "Big data analytics adoption: Determinants and performances among small to medium-sized enterprises," *International Journal of Information Management*, vol. 54, p. 102190, 2020.
- [6] S. Guha and S. Kumar, "Emergence of big data research in operations management, information systems, and healthcare: Past contributions and future roadmap," *Production and Operations Management*, vol. 27, no. 9, pp. 1724–1735, 2018.
- [7] P. Mikalef, I. O. Pappas, J. Krogstie, and M. Giannakos, "Big data analytics capabilities: a systematic literature review and research agenda," *Information Systems and e-Business Management*, vol. 16, no. 3, pp. 547–578, 2018.
- [8] B. M. Balachandran and S. Prasad, "Challenges and benefits of deploying big data analytics in the cloud for business intelligence," *Procedia Computer Science*, vol. 112, pp. 1112–1122, 2017.
- [9] H. Isah, T. Abughofa, S. Mahfuz, D. Ajera, F. Zulkernine, and S. Khan, "A survey of distributed data stream processing frameworks," *IEEE Access*, vol. 7, pp. 154 300–154 316, 2019.
- [10] V. Gurusamy, S. Kannan, and K. Nandhini, "The real time big data processing framework: Advantages and limitations," *International Journal of Computer Sciences and Engineering*, vol. 5, no. 12, pp. 305–312, 2017.
- [11] S. Shahrivari, "Beyond batch processing: towards real-time and streaming big data," *Computers*, vol. 3, no. 4, pp. 117–129, 2014.
- [12] R. Burke, A. Felfernig, and M. H. Göker, "Recommender systems: An overview," *Ai Magazine*, vol. 32, no. 3, pp. 13–18, 2011.
- [13] S. Vinodhini, V. Rajalakshmi, and B. Govindarajalu, "Building personalised recommendation system with big data and hadoop mapreduce," *International Journal of Engineering Research and Technology*, vol. 3, no. 4, pp. 2310–2316, 2014.
- [14] R. M and K. R. R. Raman, "Recommendation system: A big data application," *International Journal of Emerging Trends in Science and Technology 2348-9480*, vol. 3, pp. 39–46, 09 2016.
- [15] W. Serrano, "Intelligent recommender system for big data applications based on the random neural network," *Big Data and Cognitive Computing*, vol. 3, no. 1, p. 15, 2019.
- [16] J. P. Verma, B. Patel, and A. Patel, "Big data analysis: recommendation system with hadoop framework," in *2015 IEEE International Conference on Computational Intelligence & Communication Technology*. IEEE, 2015, pp. 92–97.
- [17] L. Chen and F. Wang, "Preference-based clustering reviews for augmenting e-commerce recommendation," *Knowledge-Based Systems*, vol. 50, pp. 44–59, 2013.
- [18] F. Mehmood, S. Ahmad, and D. Kim, "Design and development of a real-time optimal route recommendation system using big data for tourists in jeju island," *Electronics*, vol. 8, no. 5, p. 506, 2019.
- [19] C. Anderson, I. Hübener, A.-K. Seipp, S. Ohly, K. David, and V. Pejovic, "A survey of attention management systems in ubiquitous computing environments," *Proceedings of the ACM on Interactive, Mobile, Wearable and Ubiquitous Technologies*, vol. 2, no. 2, pp. 1–27, 2018.
- [20] A. K. Chowdhury, A. Farseev, P. R. Chakraborty, D. Tjondronegoro, and V. Chandran, "Automatic classification of physical exercises from wearable sensors using small dataset from non-laboratory settings," in *2017 IEEE Life Sciences Conference (LSC)*. IEEE, 2017, pp. 111–114.
- [21] C. Zhang, H. Liang, and K. Wang, "Trip recommendation meets real-world constraints: Poi availability, diversity, and traveling time uncertainty," *ACM Transactions on Information Systems (TOIS)*, vol. 35, no. 1, pp. 1–28, 2016.
- [22] B. Loepp and J. Ziegler, "Recommending running routes: framework and demonstrator," in *Workshop on Recommendation in Complex Scenarios*, 2018.
- [23] K. Bafna and D. Toshniwal, "Feature based summarization of customers' reviews of online products," *Procedia Computer Science*, vol. 22, pp. 142–151, 2013.
- [24] K. Hammond and A. S. Varde, "Cloud based predictive analytics: text classification, recommender systems and decision support," in *2013 IEEE 13th International Conference on Data Mining Workshops*. IEEE, 2013, pp. 607–612.
- [25] J. P. Verma, B. Patel, and A. Patel, "Web mining: opinion and feedback analysis for educational institutions," *International Journal of Computer Applications*, vol. 84, no. 6, 2013.
- [26] H. Liu, J. He, T. Wang, W. Song, and X. Du, "Combining user preferences and user opinions for accurate recommendation," *Electronic Commerce Research and Applications*, vol. 12, no. 1, pp. 14–23, 2013.
- [27] S. G. Esparza, M. P. O'Mahony, and B. Smyth, "Mining the real-time web: a novel approach to product recommendation," *Knowledge-Based Systems*, vol. 29, pp. 3–11, 2012.
- [28] [Online]. Available: <https://sites.google.com/eng.ucsd.edu/fitrec-project/home>
- [29] A. automaticaddison, "Advantages of k-means clustering," Aug 2019. [Online]. Available: <https://automaticaddison.com/advantages-of-k-means-clustering/>
- [30] L. Yu, R. Zhou, R. Chen, and K. K. Lai, "Missing data preprocessing in credit classification: One-hot encoding or imputation?" *Emerging Markets Finance and Trade*, pp. 1–11, 2020.
- [31] G. Goel, "Why data is represented as a 'vector' in data science problems?" Jul 2020. [Online]. Available: <https://towardsdatascience.com/why-data-is-represented-as-a-vector-in-data-science-problems-a195e0b17e99>
- [32] S. Yıldırım, "Data preprocessing with scikit-learn: Standardization and scaling," Jun 2020. [Online]. Available: <https://towardsdatascience.com/data-preprocessing-with-scikit-learn-standardization-and-scaling-cfb695280412>
- [33] "What is mongodb? introduction, architecture, features & example." [Online]. Available: <https://www.guru99.com/what-is-mongodb.html>

Inventory Management Analysis under the System Dynamics Model

Shalóm Adonai Huaraz Morales¹
Faculty of Sciences and Engineering
Universidad de Ciencias y Humanidades

Laberiano Andrade-Arenas²
Faculty of Sciences and Engineering
Universidad de Ciencias y Humanidades

Abstract—In this work, the modeling of the system dynamics concerning inventory management has been carried out, this was done to achieve a correct analysis on said management, and thus make decisions that benefit the company. Knowing that the problem lies in the mismanagement of inventories, which are managed by certain companies with little or vast knowledge about inventory management, for which, it is desired to make use of the system dynamics modeling, so that this, achieves a correct analysis of the management, but is focused on the dynamics of system. The result obtained, from the development of the methodology applied in this work, was a correct and adequate analysis of the dynamics modeling of system in inventory management, which was achieved, using the simulation software known as Vensim, and a methodology based on three stages that are the Causal Diagram, the Forrester Diagram, and the mathematical equations.

Keywords—Causal diagram; dynamics of system; forrester diagram; inventory management; Vensim

I. INTRODUCTION

The systems dynamics model [1] in these days that we live are very useful since this helps in understanding the processes that real systems have, some of these being complex and difficult to understand, that is why the system dynamics model helps us in decision-making in the strategic and tactical field, all this is done by making use of simulation.

This system dynamics model [2] can show different states of difficulty, therefore, it is convenient to know well what you want to analyze, for which we have to select the topic (It has to be oriented to the problem that you want to address), identify the variables, determine the limit (In the future how far we want to go in the behavior of the system and in the past to know what were the ultimate causes that originated the irregular behavior), build the causal diagram (To observe the relationships of the variables), construct the Forrester diagram and finally enter the equations so that a correct analysis can be carried out that gives us the ability to have a clear idea of the system in question [3].

As we already have a clear idea of what the system dynamics model is, in that case, it can be said that the word “system dynamics model” is a kind of “important” instrument that can be used correctly an endless number of systems [4]. It can also be added, as mentioned previously, that the system dynamics model gives a clear idea of complex systems, this is done using the computer as a means, by which the simulations of the systems are carried out [5], for these formulas are created that are entered into the system dynamics model, to later learn from the results obtained, and thus, be able

to predict the behavior of the system over time. According to the article [6] in Cape Town in the country of South Africa, a study was carried out to determine the effectiveness of inventories managed by SMEs (Small and medium-sized enterprises), this study focused on the manufacturing industry, where Questionnaires were collected from 21 SMEs (Small and medium-sized companies), the results obtained were that most of these 21 SMEs (Small or medium-sized companies) knew the inventory management systems, but did not use it to its full capacity.

According to [7] in the City of Piura in Peru, there is underused land, which can be an option for urban farmers, where these lands could be used for urban agriculture, this is based on the risk management of Urban agriculture should complement new policies, based on clear issues, such as mismanagement of their inventories, which consequently results in the poor quality of products.

The objective of this work is to analyze the system dynamics model corresponding to inventory management using Vensim software that allows us to make causal diagrams and simulation through scenarios.

In Section II the literature will be reviewed, in Section III the methodology that will be used, in Section IV the results and discussions, and finally in Section V the conclusions.

II. LITERATURE REVIEW

In this section, the fundamental material for the resolution of this paper is explained, citing articles that have to do with inventory management, as well as model articles with system dynamics that are related to the topic to be treated in this paper.

It started with the article [8], which tells us about the inventory inspection, it mentions its importance, which is to help know the availability of the goods using the “count”, it is like that, what could be said that the inventory is the “products that are acquired”, and these may be raw materials (Trade companies and manufacturing companies), products in the process (Manufacturing companies), finished products (Manufacturing companies) and consumables (Service companies); He also comments on inventory management, which seeks to optimize sales and lower the cost of inventories.

Another article [9], makes a mention of the scarce demand that hospitals have, which generates economic consequences and consequently havoc in the care provided to patients, that is why here it is noted that there is a shortage of medicines (Mismanagement of inventories), it will occur, that the process

of recovery of patients is delayed, for which it will have to place an order for emergency delivery, which will cause the cost to increase; He also mentions their use of the system dynamics model, where they developed their diagrams of causal loops, their graphs, tables and equations, of which they mention that they obtained positive results.

There is also an article [10], which writes about the benefits obtained by applying the system dynamics model, it mentions that the model is used to observe behavior over time, where alterations can occur, implying that the system dynamics model solves complex challenges; here they also generate their causal diagram, Forrester diagram, equations, tables, and graphs; but concerning the manufacturing industry.

Finally, there is an article [11], where they talk about the use of the system dynamics model, but to use it as an examiner, which means that they have used the system dynamics model to analyze the returned products. It should also be mentioned that these returned products generate reverse logistics, which is responsible for analyzing what is going to be done with this “product return” and deciding when and how certain “actions” will be applied, among its “actions”, We have restoration, partial remanufacturing, recycling of raw materials and disposal; They are also using the analysis under the system dynamics model to know which parts of this returned product will be accepted for the production of a new product, in turn determining which parts of this returned product are subjected to another type of control; your causal loop diagram, Forrester diagram, tables, and graphs were also generated here.

III. METHODOLOGY

In this section, the systems dynamics methodology that was carried out in the model carried out in Vensim is explained, a methodology based on the causal diagram was used, followed by the Forrester diagram and at the end, the equations were shown, achieving thus the objectives, thanks to the support of this methodology.

As mentioned, the model is made in Vensim, which is a simulation software that has modeling capabilities, the model based on Vensim, takes the real systems as a base to perform the simulation, and in this way show the dynamics model systems that are very beneficial, since it solves the needs for understanding the “processes” that real systems have, that is why the system dynamics model is an important instrument, since it is correctly accommodated with the system. What Vensim did is carry out the simulations of the systems, but to achieve this development correctly, formulas were added that were entered into the Forrester model so that when executing this model, the knowledge that it provides can be assimilated when generating the tree and graph of causes, as well as graph and table by selected variables; and in this way achieve a forecast of the behavior of the system based on a certain period.

A. Causal Diagram or Dynamic Hypothesis

A causal diagram said colloquially is based on variables that are linked by arrows that represent the causal relationships between the variables, to these “arrows” a positive (+) or negative (-) sign is added, to indicate the change that occurs in the dependent variables at the time the independent variables

change, this can be seen in Fig. 1, where the arrow represents the causal relationship between the independent variable “Purchase Order” and the dependent variable “Supply Line”, Which tells us “the more purchase order, the more supply line”, but if we generate the change in the independent variable and say “the less the purchase order” would result in “less supply line”, which makes change the sign of the arrow representing the causal relationship to the negative sign (-).

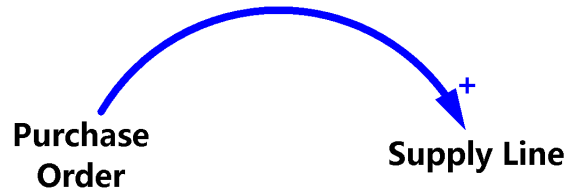


Fig. 1. Causal Diagram

It can also be said that a causal loop diagram, within each loop, has a type of loop that rotates in the same sense of the loop to which it belongs, this sense can be clockwise or counter-clockwise; Likewise, this type of loop is divided into two types, the first known as “Snowball or reinforcing feedback loop (positive)” which is a process in which a “variable a” reinforces a “variable b”, and in turn, this “variable b” reinforces the “variable a”, doing this in an unlimited way, we can see this in Fig. 2 and the second known as “Balance or compensating (negative) feedback loop” that It is a process that tries to obtain an equilibrium, this can be observed in Fig. 3, it is worth mentioning that a causal loop diagram applied correctly allows the creation of a beneficial model for the study of a real system, since it can to assertively assist in the planning and process of the system operations in question, this will later be used to develop the Forrester diagram. One point to highlight is that, for the resolution of this paper, the causal diagram of the reference [12] will be used, which we can see in Fig. 4.

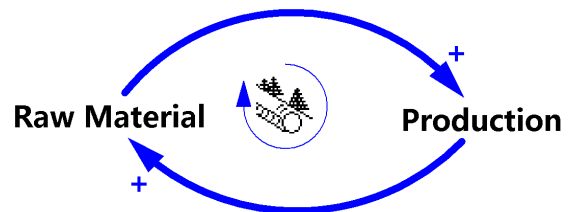


Fig. 2. Reinforced Feedback Diagram

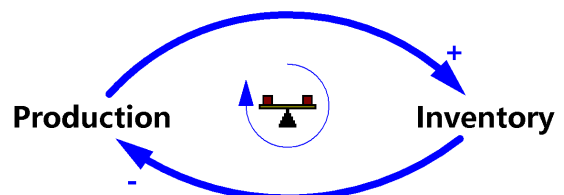


Fig. 3. Compensating Feedback Diagram

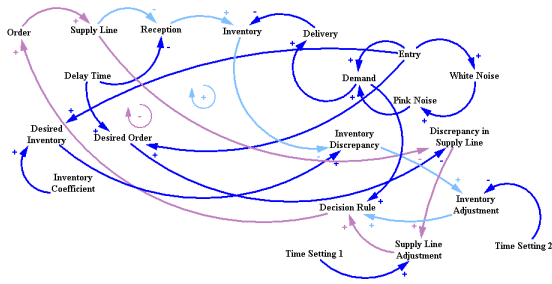


Fig. 4. Inventory Model Causal Loop Diagram

Fuente: [12]

B. Forrester Diagram

In this section, the causal loop diagram in Fig. 4 was used to make the Forrester diagram, as mentioned previously, for this, the variables and the “arrows” were copied identically since the “arrows” represent the causal relationships between the variables. In this Forrester diagram, the types of variables were identified, to which the variables are shown in Fig. 4 belong, that is why in this section the types of variables were known, the first known as a level of stock variable, which it will only change through the flow, if the inflow is higher than the outflow the level will increase, otherwise the level will decrease, it should be noted that the data in a level or stock variable always changes over time; the second known as the exchange rate or flow variable (inflow and outflow), which is in charge of filling the level or stock variable, as the level of the stock variable was mentioned, it can only be changed by the variable flow (Flow in and flow out); and finally the auxiliary or converter variable, which serves as a support for the model and the exchange rate or flow variables (inflow and outflow), making the model more understandable. One point to highlight is that for the resolution of this paper, the Forrester diagram of reference [12] will be used, which we can see in Fig. 5.

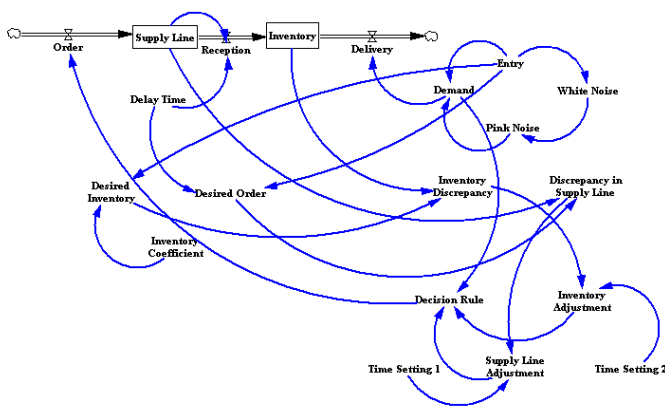


Fig. 5. Forrester Diagram of Inventory Model

Fuente: [12]

C. Mathematical Equations

This section shows the inventory model system but represented by mathematical equations, these mathematical equations are the ones that were entered in each of the variables established in the Forrester diagram, both in the level or stock variables and in the exchange rate or flow variables (inflow and outflow); it should be noted that each of these variables was set their data types corresponding to each of them, this in the simulation software known as Vensim is done through functions, the functions that were used for the inventory model system (Not to mention data type functions) can be seen in (6), (21) and (22).

$$Inventory(t) = Inventory(t - dt) + \left(\frac{Reception}{-Delivery}\right)dt \quad (1)$$

Where:

$$Inventory = Inventory\ Coefficient \times Entry \quad (2)$$

$$Reception = \left(\frac{Supply\ Line}{Delay\ Time}\right) \quad (3)$$

$$Delivery = Demand \quad (4)$$

In (2) the initial value of the level or stock variable known as Inventory is established, in (3) the equation of the exchange rate or flow known as Reception is established and in (4) the equation of the outflow is established known as Delivery; This initial value and these two equations are key for the Inventory level variable since to know the value of the Inventory variable that represents the “state of the system’s inventory”, it is necessary to know both the initial value of the Inventory as well as the equations of the flows that are “connected” to the Inventory variable.

$$Inventory\ Coefficient = 3 \quad (5)$$

$$Entry = 20 + STEP(20, 5) - STEP(20, 30) \quad (6)$$

The common + STEP ({height}, {stime}) function represents the increment in the value of the stream variable known as Input, but since time 5; while the common - STEP ({height}, {stime}) function represents the decrease in the value of the flow variable known as Input, but since time 30. Since it is known how the common function works STEP ({height}, {stime}), it can be said that (6) starts and continues with a value of 20, but when reaching time 5 to that 20, 20 more are added because the common + STEP ({height}, {stime}) function, which gave us a Continuous Input of 40, which changed when it reached time 30, which made that value of 40 be subtracted 20 less because the common - STEP ({height}, {stime}) function was used.

$$Supply\ Line(t) = Supply\ Line(t - dt) + (Order - Reception)dt \quad (7)$$

$$\text{Supply Line} = 50 \quad (8)$$

$$\text{Delay Time} = 1 \quad (9)$$

$$\text{Order} = \text{Decision Rule} \quad (10)$$

$$\begin{aligned} \text{Decision Rule} = & \& \text{Demand} + \text{Inventory Adjustment} \\ & \& + \text{Supply Line Adjustment} \end{aligned} \quad (11)$$

$$\text{Inventory Adjustment} = \left(\frac{\text{Inventory Discrepancy}}{\text{Time Setting 2}} \right) \quad (12)$$

$$\begin{aligned} \text{Inventory Discrepancy} = & \text{Desired Inventory} \\ & \& - \text{Inventory} \end{aligned} \quad (13)$$

$$\text{Desired Inventory} = \text{Inventory Coefficient} \times \text{Entry} \quad (14)$$

$$\text{Time Setting 2} = 2 \quad (15)$$

$$\left(\frac{\text{Supply Line}}{\text{Adjustment}} \right) = \frac{\left(\frac{\text{Discrepancy in}}{\text{Supply Line}} \right)}{\text{Time Setting 1}} \quad (16)$$

$$\left(\frac{\text{Discrepancy in}}{\text{Supply Line}} \right) = \left(\frac{\text{Desired Order}}{-\text{Supply Line}} \right) \quad (17)$$

$$\text{Desired Order} = \text{Entry} \times \text{Delay Time} \quad (18)$$

$$\text{Time Setting 1} = 3 \quad (19)$$

$$\text{Demand} = \text{Entry} + \text{Pink Noise} \quad (20)$$

$$\text{Pink Noise} = \text{SMOOTH}(\text{White Noise}, 2, 0) \quad (21)$$

The common function SMOOTHI ({in}, {stime}, {inival}) represents exponential smoothing (Predicts demand in a set time), where the first parameter is the input value, which in this, In this case, it is the White Noise variable, the second parameter is the delay ti value, which in this case is 2, and the third parameter is the initial value, which in this case is 0.

$$\text{White Noise} = \text{RANDOM NORMAL}(0, 67779, 0.15 \times \text{Entry}, 0) \quad (22)$$

The common RANDOM NORMAL ({min}, {max}, {mean}, {stdev}, {seed}) function returns a random value

from a normal distribution, where the first parameter is the minimum value, which in this case is 0, the second parameter is the maximum value, which in this case is 67779, the third parameter is the mean, which in this case is 0, the fourth parameter is the standard deviation, which in this case is 0.15 X Input and the fifth parameter is for the control of the pseudo-random number generator, which in this case is 0 since it is a value recommended by the Vensim simulation software.

IV. RESULTS AND DISCUSSIONS

In this section, the scenario and the methodology that was applied for the preparation and resolution of this paper are shown, which is focused on the system dynamics model.

A. On Stage

In this graph in Fig. 6, you can see the status of the system inventory for a time expressed in months, this inventory started at 40, and then it decreased and increased until it reached 100 months, this can be seen in Table I, this decrease and increase in inventory are due to the Inventory X Input Coefficient, which was established in (5) and (6).

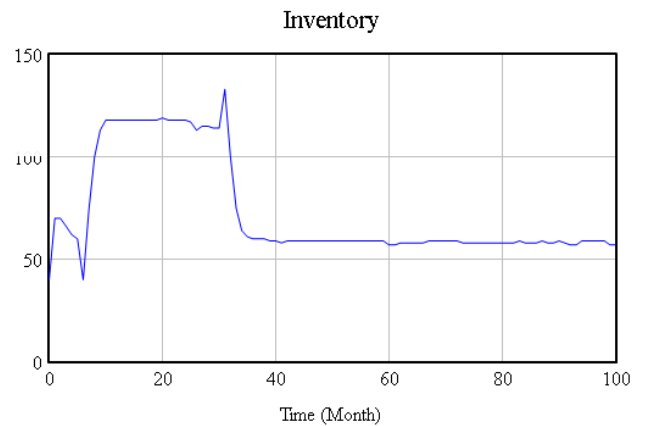


Fig. 6. Graph of the Inventory Level Variable

TABLE I. TIME DOWN OF THE INVENTORY LEVEL VARIABLE

Month	Inventory
0	40
1	70
2	70
3	66
4	62
5	60
6	40
7	74
8	100
9	113
10	118

B. About the Methodology

The systems dynamics methodology [13], was very helpful, since it guided us, in the development of the model analysis, to begin with, it helped us to understand and develop the Causal Loop Diagram necessary for the system dynamics Concerning inventory management, besides, it also helped us

to understand and develop the Forrester Diagram since it was easier to perform because it had the Causal Loop Diagram, it also helped us to establish the mathematical equations that the Forrester Diagram has, which was achieved, thanks to the fact that the Forrester Diagram in the simulation software known as Vensim [14], allows us to add these mathematical equations in a friendly way since if we want to use a function, this simulation software gives us a brief description of what will be entered in each of its parameters.

1) *Advantages:* The advantages offered by the systems dynamics methodology [15] are varied since thanks to its use it was possible to develop the analysis of inventory management under the system dynamics model, for which, we will begin by mentioning the Causal Loop Diagram, which thanks to this methodology allowed us to know the causal relationships between its variables [16], in addition to having an arrow to indicate the change that occurs in the dependent variables at the time the independent variables change. Also, thanks to this methodology, it was possible to develop the Forrester Diagram, where the types of variables were identified (variable level or stock [17], exchange rate variable or flow, and the auxiliary variable or converter), thus generating knowledge “good”, since the identification of these types of variables help us to classify the variables found in the Causal Loop Diagram, another advantage of this methodology is the mathematical equations since this helps us to analyze the model of system dynamics, based on the operations and functions that were entered in the variables of the Forrester Diagram, thus achieving the fulfillment of the objective.

2) *Disadvantages:* One of the disadvantages of this methodology is the development of the system dynamics model of complex systems since an extensive study has to be carried out, so that this system works correctly in the system dynamics model, and not on the contrary, affect the project where the dynamics of the system is being carried out.

V. CONCLUSIONS AND FUTURE WORK

This model of inventory management systems dynamics has gone through a series of successive states so that it progresses satisfactorily, and it is thus that it will help in the analysis of inventory management, since this analysis, produced through simulation software known as Vensim, it is suitable for designing causal models and Forrester models. Vensim simulation software was the tool used for the development of this system dynamics model, which managed to be efficient and valuable, both for the inventory management system that was used, as well as for the developer of this paper, already that this simulation software known as Vensim, helps to introduce a different view than the usual one since it shows us a model in Causal Diagram, a model in Forrester Diagram and mathematical equations, as well as a tree of causes, a document where the variables and values entered, are shown, a graph of the causes, a graph for selected variables and a table for selected variables. To make it clear, well understood and better perceived, it is noted that the methodology used performed and fulfilled its work and function perfectly, which served for a good development of the inventory management analysis under the dynamics model of systems, this being a set of successive key phases, to get to where you want in the intended objective in order to carry out the proposed,

and thus guarantee and give security to the development of the system dynamics model. In future research, the system dynamics model could be implemented in other simulation software, such as Ithink or Stella, so that system dynamics researchers can know how each simulation software is used and when it is appropriate to use the simulation software in specific systems, and thus achieve a better understanding in the field of system dynamics.

REFERENCES

- [1] A. Sapietová and V. Dekýš, “Dynamic analysis of rotating machines in msc. adams,” *Procedia Engineering*, vol. 136, no. 143-149, p. 12, 2016.
- [2] S.-B. Chen, H. Jahanshahi, O. A. Abba, J. Solís-Pérez, S. Bekiros, J. Gómez-Aguilar, A. Yousefpour, and Y.-M. Chu, “The effect of market confidence on a financial system from the perspective of fractional calculus: Numerical investigation and circuit realization,” *Chaos, Solitons & Fractals*, vol. 140, p. 110223, 2020.
- [3] T. Rebs, M. Brandenburg, and S. Seuring, “System dynamics modeling for sustainable supply chain management: A literature review and systems thinking approach,” *Journal of cleaner production*, vol. 208, pp. 1265–1280, 2019.
- [4] Z. Jiang, D. Fang, and M. Zhang, “Understanding the causation of construction workers’ unsafe behaviors based on system dynamics modeling,” *Journal of Management in Engineering*, vol. 31, no. 6, p. 04014099, 2015.
- [5] R. R. P. Langroodi and M. Amiri, “A system dynamics modeling approach for a multi-level, multi-product, multi-region supply chain under demand uncertainty,” *Expert Systems with Applications*, vol. 51, pp. 231–244, 2016.
- [6] N. Ngubane, S. Mayekiso, S. Sikota, S. Fitshane, M. Matsoso, and B. Juan-Pierré, “Inventory management systems used by manufacturing small medium and micro enterprises in cape town,” *Mediterranean Journal of Social Sciences*, vol. 6, no. 1, p. 382, 2015.
- [7] S. Liu and P. Teng, *Subsistence Urban Agriculture: Key Externalities and Way Forward*. S. Rajaratnam School of International Studies., 2017.
- [8] I. H. Parpia and G. Singh, “Automated inventory management,” Mar. 8 2016, uS Patent 9,280,757.
- [9] C. G. Kochan, D. R. Nowicki, B. Sauser, and W. S. Randall, “Impact of cloud-based information sharing on hospital supply chain performance: A system dynamics framework,” *International Journal of Production Economics*, vol. 195, pp. 168–185, 2018.
- [10] I. J. Orji and S. Wei, “An innovative integration of fuzzy-logic and systems dynamics in sustainable supplier selection: A case on manufacturing industry,” *Computers & Industrial Engineering*, vol. 88, pp. 1–12, 2015.
- [11] C. Sy, “A policy development model for reducing bullwhips in hybrid production-distribution systems,” *International Journal of Production Economics*, vol. 190, pp. 67–79, 2017.
- [12] D. A. A. Serna and Y. M. L. Rivera, “Dinámica de sistemas en la gestión de inventarios,” *Ingenierías USBMed*, vol. 9, no. 1, pp. 75–85, 2018.
- [13] Y. Fang, K. H. Lim, Y. Qian, and B. Feng, “System dynamics modeling for information systems research: Theory development and practical application,” *MIS Quarterly*, vol. 42, no. 4, 2018.
- [14] L. S. K. Abadi, A. Shamsai, and H. Goharnejad, “An analysis of the sustainability of basin water resources using vensim model,” *KSCE Journal of civil engineering*, vol. 19, no. 6, pp. 1941–1949, 2015.
- [15] A. Dehdarian, “Scenario-based system dynamics modeling for the cost recovery of new energy technology deployment: The case of smart metering roll-out,” *Journal of Cleaner Production*, vol. 178, pp. 791–803, 2018.
- [16] F. Andrade-Chaico and L. Andrade-Arenas, “Projections on insecurity, unemployment and poverty and their consequences in lima’s district san juan de lurigancho in the next 10 years,” in *2019 IEEE Sciences and Humanities International Research Conference (SHIRCON)*, 2019, pp. 1–4.
- [17] N. Abdelkafi and K. Täuscher, “Business models for sustainability from a system dynamics perspective,” *Organization & Environment*, vol. 29, no. 1, pp. 74–96, 2016.

Cuckoo-Neural Approach for Secure Execution and Energy Management in Mobile Cloud Computing

Vishal¹

Department of Computer Science
and Engineering, IKG Punjab
Technical University,
Kapurthala, Punjab, India

Bikrampal Kaur²

Department of Computer Science
and Engineering, Chandigarh
Engineering College, Landran, Punjab, India

Surender Jangra³

Department of Computer Science, GTBC,
Bhawanigarh, Punjab, India

Abstract—Along with an explosive growth in mobile applications and the emergence of the concept of cloud computing, in mobile cloud computing (MCC) has been familiarized as a potential technology for mobile users. Employing MCC to enable mobile users to realize the benefits of cloud computing in an environment friendly way is an effective strategy to meet today's industrial demands. With the ever-increasing demand for MCC technology, energy efficiency has become extremely relevant in mobile cloud computing infrastructure. The concept of mobile cloud computing offers low cost and high availability to the mobile cloud users on pay-per-use basis. However, the challenges such as resource management and energy consumption are still faced by mobile cloud providers. If the allocation of the resources is not managed in a secure manner, the false allocation will lead to more energy consumption. This article demonstrates the importance of energy-saving mechanisms in cloud data centers and elaborates the importance of the “energy efficiency” relationship to promote the adoption of these mechanisms in practical scenarios. The utilization of resources are being maximized by minimizing the energy consumption. To achieve this, an integrated approach using Cuckoo Search (CS) with Artificial Neural network (ANN) is presented here. Initially, the Virtual Machines (VMs) are sorted as per their CPU utilization using Modified Best Fit Decreasing Approach (MBFD). This suffers from the increase in Service Level Agreement (SLA) violation along with many VM migrations. If the migration is not done at an appropriate host, which can hold the VM for long, Service Level Agreement Violation (SLAV) will be high.

Keywords—Mobile cloud computing; VM migration; energy consumption; SLA violation; VM selection; overloading; under loading

I. INTRODUCTION

Mobile Cloud Computing (MCC) is the development of numerous internet-based technologies that allow mobile users to take advantage of cloud computing while using their mobile devices and achieve green computing [1,2]. The MCC technology mainly the combination of three techniques, including mobile computing (MC), mobile internet and cloud computing systems. By taking the advantages of all these techniques, MCC allows user to upload data and stored into the MCC cloud server [3]. The MCC offered advantages like as increase the storage capacity and provide virus scan facility to enhance the safety as well as reliability of mobile device. It's also minimizes the loss of data risk for mobile users. This is possible by sending data to the mobile cloud [4]. Although, MCC facilitate mobile user with a number of advantages, but still facing some challenging [5]. In this modern era, the

population of smart phone users has increased intensely by some billions (see Fig. 1). In addition to the advantages and features of MCC, some issues like resource limitation, energy consumption, and cost of computation on the mobile, network and server side occurs in MCC [6]. In previous years, mobile users used MCC only to transmit text messages and requested only text information from the cloud server. Gradually, the requirements have changed and now most users prefer to transmit video data over cloud instead of text and images [7]. Compared to text or image data, video data required more

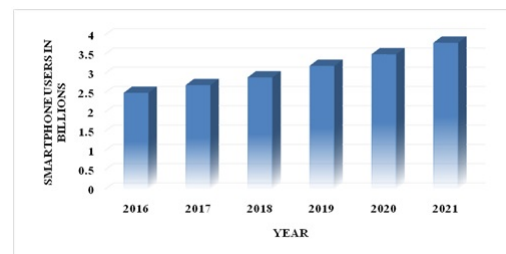


Fig. 1. World-Wide Growth of Smartphone Users

energy to upload as well as to access data from the cloud. The data transfer using video data over the network consumes more energy that the results of pool quality of services. Therefore, the minimization of energy becomes a serious problem to the researchers. This requires mechanism to expand the energy efficiency of MCC data centers while maintaining the specified level of operations [8].

To minimize the power consumption, large scale computer system process is performed by using virtualization technology. Using this approach, a number of servers are consolidated into a single physical node, In other words one can say that the same copy of the software is created to perform several tasks such as storage, task allocation, to execute tasks and many more. This results in minimization of IT cost, whereas increasing the flexibility and efficiency of the system [9]. The recently emerging Mobile cloud computing paradigm employs virtualization and provides an on-demand resource on the internet to the mobile users.

This will allow mobile users to reduce the cost of maintaining their computing environment and move their computing needs onto the mobile cloud [10]. In the Virtual Machine (VM) migration policy, the VMs are migrated from one host

to another in such a way that the idle host can be switched off and save the power consumed during its idle mode. The different parameters such as CPU utilization, overutilization and underutilization have been considered while migrating VMs [11]. Mainly two approaches are used to minimize energy named VM placement approach and VM consolidation approach. The VM placement is used while mapping VMs to PMs in a dynamic environment so that the utilization of resources can be optimized. After that, VM consolidation is employed to enhance the usage of resources by positioning under-loaded resources in idle state. This is performed by combining isolated VMs over a minimal active PMs by turning off the entire idle servers and hence saving the energy [12]. During the VM placement and consolidation process, the developer faces several challenges. The first one is related to time and resource-consuming nature of VMs. Another problem is related to the energy consumption of system. To resolve these problems, if one can turn off a few PMs, then the VMs are enabled to obtain resources at their peak time period. This results in the degradation of reliability and availability of the system that lower the desired QoS of mobile cloud service provider [13-14]. Therefore, to minimize the energy consumption by employing the VM consolidation technique, it leads to decrease the performance of the system. Hence, the SLA violation with the mobile user demand increases [15]. Therefore, to resolve the problem of VM placement and energy consumption, algorithms used such as Modified best Fit Decreasing (MBFD) and Artificial Neural Network (ANN). The aim of this paper is to reduce the power consumption and the SLA violation in the mobile cloud server.

Contribution of the paper is as follows:

1. To minimize energy consumption of resources.
2. To maximize the usage of resources in corporate with desired migration and allocation.
3. To provide satisfactory services to the cloud user.

The rest of the paper is organized as: the related work based on energy-aware and related to minimization of SLA violation is described in Section 2. The detailed description of the proposed work, along with their algorithms, is defined in Section 3. The results and discussion with comparison are demonstrated in Section 4. The overall conclusion of the entire article is presented in Section 5, followed by references.

II. RELATED WORK

The VM allocation in the mobile cloud server is a two-way procedure. The first one is to admit new requests for VM placement on a stationary host. The second one is used to reallocate and find the best allocation for VM on a reliable host. The VM allocation has mainly two foremost goals. The first one is that the mobile cloud servers must utilize power in an efficient way and the other one is to provide maximum QoS to mobile cloud users. The present allocation of VM can be optimized through VM migration process that has been performed on the basis of pre-described constraints. The entire migration procedure is performed in three phases: a selection of best VM, destination host selection and selection of VM migration. The VM placement is an NP-hard problem that can be deliberated as a bin packing dilemma with different bin

sizes in which bin represents the mobile cloud servers and VM is used as an object.

Wang et al. (2015) have formulated the problem occurs during the offloading process in MCC. As a result, energy consumption is minimized and increase the life time of mobile devices. The researchers have used polynomial-time optimal solution that works on bi-partite matching issues [16]. A traffic aware cross site as VM migration system has been proposed by Liu [17]. Using this model, multiple VMs are required to be migrated, which provides a wide range of cross site link that minimizes the count of successful VM migration. The authors have used heuristic algorithm to overcome this problem and obtained optimal results [17]. Halabi have provide security to the mobile cloud users by maintain the security service level agreement. By using the designed system, the preferences of mobile user as well as service providers has been evaluated during the process of resource allocation. By using Gale/Shapley algorithm, the problem is solved and rectified that delivers data with high stability and efficiency [18]. The algorithms such as first fit, next fit and random fit are the simplest VM allocation algorithms and they have not taken the capacity of resources into account while placing VMs. These techniques have not considered the capacity of the physical machine's resource consumption. Therefore, the power-aware algorithm has been initially presented. In which the problem of dynamic VM placement has been resolved with less power requirement and with smaller SLA violations. A p-mapper algorithm has been presented by Verma et al. [19] to resolve the power consumption and SLA violation problem, this technique mainly consists of three controlling units such as a power management unit, performance and migration management unit. This technique has performed both VM placement as well as VM reallocation to achieve an optimized allocation. The test results show that about 25 % of power has been saved using p-mapper algorithm compared to individual first fit and random fit placement algorithm. The energy in mobile cloud server can be saved by employing VM consolidation scheme.

Sharifian, S., & Barati (2019) have presented an integrated prediction scheme to address the issues scalability and resource allocation. Three level (3-L) wavelet transform has been used to decompose the time of workload series into multiple resolution of time and frequency scales. For classification of workload, support vector regression (SVR) has been used as prediction approach. The optimization of SVR parameters has been again refined using chaotic particle swarm optimization (PSO) algorithm as optimization approach. Again, the classification of high frequency data has been performed using generalized auto regressive conditional heteroskedasticity (GARCH) model. At last ensemble model has been applied to predict workload and the performance of the model has shown accuracy of 24.53 % of improvement. The drawback of this model is that the use of multiple approaches to identify workload is very complex process [20]. Mukherjee have presented a decision-making model whether the mobile data is offloaded or not. By using the presented strategy, if the power consumption of the device is decreases below the defined limit only then the data will be offloaded. The energy consumption of the device has been evaluated based on parameters such as computation time and deadline of the task. By using designed algorithm, the energy consumption has been reduced upto 3% to 32 % [21].

Gai et al.(2016) have presented a dynamic energy aware cloud let based MCC approach to optimize the power efficiently with reduced latency period[3]. This approach mainly focused to reduce the problem of energy consumption in MCC. Boukerche et al. (2019) have examined the presently used energy aware offloading schemes, architecture and balancing approaches that have been utilized to balance load and contributed towards green MCC[22]. Mohammed and Tapus (2017) have rectified the issues related to resource management and energy consumption in MCC. The designed model has worked into two phases initially; enthalpy has been calculated using task loss, transmission loss and delay in the second phase. The cuckoo search (CS) algorithm has been utilized to improve and arrange resources as per their priority that results in minimization of energy and cost [23].

Guo et al. [24] have presented an energy efficient based dynamic offloading scheme along with resource scheduling (edors) to minimize the energy consumption as well as decrease the task completion time. To overcome the problem, a new edors algorithm has been designed. The designed model comprises of n number of Smartphone's that are positioned in different regions each consist of an intensive mobile application that must be completed. In proposed model, the mobile application is divided into m number of tasks that have been completed by the mobile device in an MCC environment.

Tang et al. [25] have designed an MCC model specifically to resolve the issues of inadequate battery energy, less storage space. The system is mainly divided into two portions (i) the mobile user and (ii) the mobile cloud. To upload data into the mobile cloud (MC) an access point (AP) link is used. The upcoming tasks in MC have been arranged in a queue. Also, a control action has been performed to check the availability of the computing resources. Also, the tasks have been executed on the basis of the directed acyclic graph (DAG) model, in which the child task cannot be executed before the completion of the parent task. At last, the performance in terms of make span has been measured. The work has been completed for a few numbers of tasks that are only for 20 numbers of tasks, which is very less to check the efficiency of the designed network.

Problem Formulation

To manage energy in Mobile cloud data center is a challenging task. The around 70 to 80 percentage of power is misused by the cloud data center from total available power. Thus, proper monitoring and resource utilization need to be measured. To decide when and which VMs must be migrated to avoid the performance interferences. To select a correct destination host for migration is required for optimizing the VM migration because aggressive VM consolidation can cause performance interferences if the fluctuations on VM footprint rise at an unexpected rate which can lead to congestion. Thus, there is a need to select a correct host and reduce the congestion on the network to optimally utilize the network bandwidth.

III. PROPOSED WORK

Usually, mobile users change their position due to the mobility of mobile nodes. However, the nodes in the system consume higher energy and hence restricted to their energy

resources. While the user changes its location, the chances of energy consumption will be increased, that will result degradation of QoS parameters of the system. Therefore, the allocation of available resources to the mobile users with optimal power and improved QoS parameters becomes a great challenge to the MCC service providers. In this research, an optimized based ANN approach is used to overcome the challenge. The optimization has been performed by using CS as an optimization algorithm and distribution among loads has been determined using neural network algorithm.

This section deals with the methods and the techniques used to migrate the VMs with minimum energy and less SLA violation.

A. Power Model

In a mobile cloud environment, VMs, PMs, and Servers are the main sources of power consumption in terms of CPU utilization and MIPS of VMs and PMs are directly proportional to the CPU utilization which is calculated by the below formula:

$$P_{Consumed}(S) = Idle(P_{Consumed}) + S * (Max(P_{Consumed}) - Idle(P_{Consumed})) \quad (1)$$

Where:

S:It is servers active state CPU utilization

(P_{Consumed}(S)): It is the total consumption of power by the data centre.

Idle(P_{Consumed}): It is the consumption of power by servers in idle condition, which is considered as approximately 70% of Max(P_{Consumed}).

Max(P_{Consumed}): It is the maximum consumption of power by servers.

In the proposed model, CPU utilization of servers, VMs, and PMs may vary with respect to the time due to workload variation. So, the total consumption of power is a function of varying time based on demand and it is an integral of power consumed by active servers in the mobile cloud over a particular time period (Mukherjee et al. 2016). The formula of power calculation is written as:

$$P_{Total} = \int_0^t P_{Consumed}(S(t))dt \quad (2)$$

Mainly three different steps are performed by the proposed approach. Initially, the VMs are allocated to PMs using MBFD algorithm. Secondly, the VM selection using CS algorithm is performed from all over and under-utilized hosts. At the end, the selected VMs are placed on the host to minimize energy consumption and SLA violation as well (see Fig. 2).

B. VM Placement

The problem of VM allocation is subdivided into two segments: (i) To take requests from the users and then place the VMs on the host. (ii) To perform optimization of the present VM allocation. The first one issue is resolved by using the modified best fit decreasing order (MBFD) algorithm, in which

the VMs are allocated to each host as per their CPU utilization. This is advantageous, when the resources are distributed in the heterogeneous mobile cloud environment and hence select the most efficient node to assigned (Gai et al. 2016). By using MBFD algorithm, all VMs are sorted in decreasing order as per their CPU utilization. These sorted VMs are then allocated to each host that offers the minimum power consumption after the allocation. This allows the heterogeneity of resources to be utilized by first selecting the most energy-efficient node. The algorithm in its pseudo code is written below. This algorithm faces $n \times m$ type of problem where n and m are the numbers of allocated VMs and the number of hosts, respectively.

MBFD Algorithm:

-
- 1 Start
 - 2 Input: host list and VM list
 - 3 Sort VM list as per CPU utilization in decreasing order
 - 4 For each user
 - 5 Calculate, $Minpower < -max$
 - 6 Allocated VM $< -[null]$
 - 7 For each VMs
 - 8 Power, $P < -Estimated\ Power\ (VMs,\ Users)$
 - 9 If $P < mean(P)$ then
 - 10 Allocate PM $< -VM$
 - 11 $Min(P) < -P$
 - 12 if Allocated server $\neq null$ then
 - 13 Allocate VM
 - 14 Sort VMs according to P
 - 15 Return: Sorted VMs based on power utilization
 - 16 End
-

C. VM Selection for Secure Placement and Better execution (Cuckoo Search)

In the optimization process, the present VM allocation is performed in two different steps as shown in Fig. 2: (i) firstly, those VMs are selected which are demanded to be migrated, (ii) Secondly, the selected VMs are allocated to the host by utilizing the ANN algorithm. We have applied artificial intelligence technique to know which VMs are integrated and what time. The Cuckoo search is a nature-inspired optimization algorithm which is applied here to resolve the $n \times m$ type problem of MBFD. This algorithm is inspired by a lazy bird named ‘‘Cuckoo’’. The bird cuckoo lays eggs on the nest of other birds that lay similar eggs. This feature increases the production of mature cuckoos, but sometimes the cuckoo’s eggs are identified by the other host bird and hence removed from the nest. Usually, the increase in the number of alive eggs in the nest results into better benefits and that particular area is selected for optimization by the bird cuckoo. Therefore, the persisted cuckoo that survives and lay eggs on the other host’s

nest migrates or changes their position with maximum profit value. Here, the migration has been performed on the basis of the range covered by the bird to lay eggs. The process of laying eggs by the matured cuckoo is continued until the position with the maximum profit value can be attained.

Since CS is a fast and effective algorithm, it helps to resolve the optimization problem of VM selection with minimum energy. Initially, a few numbers of hosts are selected on a random basis. The features of hosts are presented in an array, which is known as habitat. The habitat of Cuckoo is represented by the following equation (3) which indicates the initial position of cuckoos.

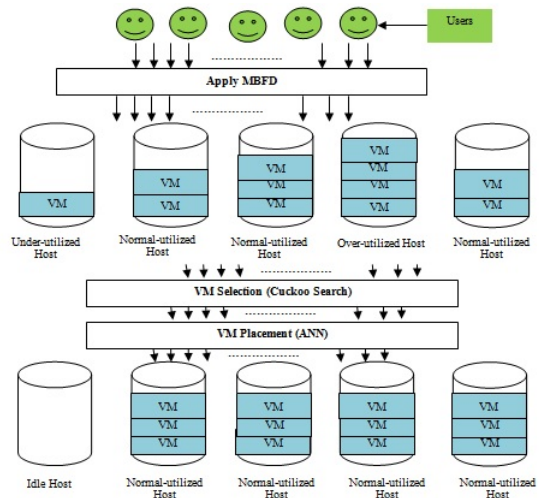


Fig. 2. Flow of Work

$$Habitat = [y_1, y_2, y_3, \dots, y_{nvar}] \quad (3)$$

After population initialization, (number of eggs represented by $y_1, y_2, y_3, \dots, y_{nvar}$), the next is to calculate the CPU utilization that is the profit value of hosts, it is computed using the following formula:

$$Profitvalue = f_{fit}(habitat) = f_{fit}(y_1, y_2, y_3, \dots, y_{nvar}) \quad (4)$$

$$f_{fit} = \begin{cases} TRUE & \text{if attained maximum profit value}(f_s > f_{th}) \\ False & \text{otherwise} \end{cases} \quad (5)$$

Where f_s is the random change in egg and f_{th} is the threshold which should be achieved by host birds.

Using equation (4)(5), the maximum profit value is determined. Afterword’s, each selected host is represented by a cuckoo and random eggs have been generated having upper and lower values. The eggs laying rage is calculated using formula written in equation (7) After population initialization, the nest is to calculate the CPU utilization that is the profit value of hosts, which is computed using the following formula:

$$Profitvalue = f_p(habitat) = f_p(y_1, y_2, y_3, \dots, y_{nvar}) \quad (6)$$

Using equation (6), the maximum profit value is determined. After that of each selected host represented by a cuckoo, random eggs have been generated having upper and lower

values. The eggs laying range is calculated using formula written in equation (7):

$$R_{egg} = \beta(I_{eggs}) / (Tot_{eggs}(a_{high} * a_{low})) \quad (7)$$

Where, a_{high}, a_{low} are the highest and lowest selected eggs for next generation. The I_{eggs} and Tot_{eggs} are the number of current cuckoo's eggs and total number of eggs, respectively. Now,

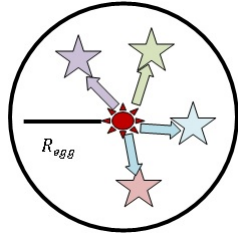


Fig. 3. Egg Laying Range [22]

based on the above-defined egg-laying range, the cuckoos lay eggs randomly, this concept is shown in Fig. 3. In Fig. 3, the red star denotes the random egg lying range, which is an initial cuckoo nest and the other random nests are represented by different color stars. It is assumed that a single egg consists of each individual host and then profit is determined. If the count of cuckoos is higher than the maximum available count of cuckoos, then the cuckoos with low profit are evacuated so that one can reach to the maximum cuckoo number. For this, the CS algorithm has used, K means clustering policy. Therefore, the set of cuckoos with maximum profit value has been selected and considered as a final point around which cuckoo has to revolve around. The cuckoos have not gone directly to the destination, but have moved with a deviation of (θ) the radius with an angle between -60° to $+60^\circ$. After little iteration, the larger portion about 95% is moved towards the best habitat that provides the maximum profit value. The following of the above-mentioned process helps CS algorithm to appropriate selection of the host to which VMs can be migrated. Now, the next process is to migrate VM from the over-utilized host to the underutilized host. It utilizes the space properly and hence leads to energy consumption.

Cuckoo Search Algorithm:

1. Start
2. Initialize CSA operators and parameter – Iterations (ITR) – Number of Egg (EN) – Number of Variables (Nvar)
3. Calculate Size of VM, $S_i < \text{Size (VM)}$
4. Fitness function f_{fit}

$$f_{fit} = \begin{cases} TRUE & \text{if attained maximum profit value}(fs > f_{th}) \\ False & \text{otherwise} \end{cases}$$

Where fs is the random change in egg and f_{th} is the threshold which should be achieved by host birds

5. For each ITR & S_i in respect of j

6. $fs = \sum_{j=1}^s VM_{energy} = E_N$
7. $f_{th} = \sum_{j=1}^s Energy(VMs) / s_j$
8. f_{fit} = fitness function // which is define above
9. $VM_{allocation} = CSA(EN, Nvar, f_{fit})$
- Return: Allocated VMs
- 10 End
- 11 Return: Allocated VMs
- 12 End

D. VM Validation to Cross Check the Allocation

Based on the received optimized properties of host, ANN is trained to find out over-utilized and under-utilized hosts. The trained structure of ANN is shown in Fig. 4 consisting of three-layered architecture that predicts the load based on the error estimation. The problem of over and underutilized

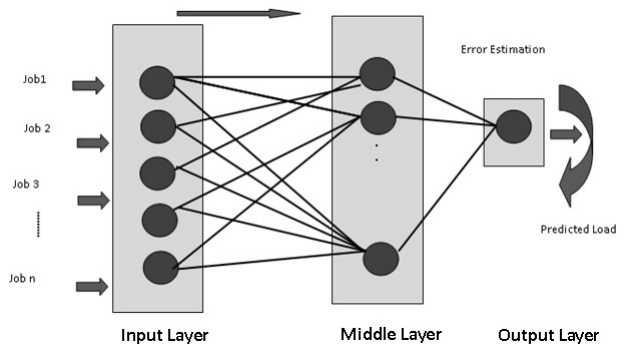


Fig. 4. ANN Structure

hosts is resolved using the ANN technique. Here, a number of jobs are provided at the input layer on the basis of jobs properties such as CPU utilization RAM, ANN is trained. In the hidden layer, a number of neurons are passed to hidden layer in order to adjust the properties according to the weight. Hence, the output in terms of load prediction for over and underutilized host is provided. Since the over and underutilized hosts have not provided services to the entire incoming requests from the user. This increases response time and hence leads to SLA violation. Therefore, for every mobile cloud service provider, it becomes necessary to manage over and under hosts. To overcome this situation, the ANN algorithm is used. For the CPU utilization of each and every host that has been determined using equation-5, ANN has been trained and then over or underutilized host is determined.

ANN Algorithm:

- 1 Start
- 2 Initialize ANN and define the essential parameters using VM properties as training data (T-Data), No. of VMs as a Target (T_R) and Neurons (N).
- 3 Set, Mobile cloud-Net = Newff (T-Data, T_R , N)

```

4 Mobile cloud-Net.TrainParam.Epoch = 1000
5 Mobile cloud-Net.Ratio.Training = 70%
6 Mobile cloud-Net.Ratio.Testing = 15%
7 Mobile cloud-Net.Ratio.Validation = 15%
8 Mobile cloud-Net = Train (Mobile cloud-Net, T-Data,
TR)
9 Current VM = Properties of current VM in Mobile cloud-
Net
10 VM Allocation=simulate(Mobile cloud-Net,Current
VM)
11 If (VM Allocation = True)
12 VM = Not migrated
13 Else
14 VM = Need of migration
15 End
16 Return: VM as a allocation and migrated list of VMs
17 End

```

E. New Vendor Registration

When the cloud is expanding, new vendors will definitely aim to join the existing cloud management architecture to share the profit. In such a scenario, poor vendor selection will always lead to high energy consumption and more SLA violation. The proposed work incorporates Lagrange's interpolation for the appropriate placement of a new PM into the existing cloud architecture. The architecture of interpolation is as follows. The paper proposes two hypotheses for the registration of new node.

Null Hypothesis: The node is capable of serving the Cloud network.

Alternate Hypothesis: There are issues with the registration of node in the network and will consume high energy in the network with a large number of violations.

Proposed work aims to prove the null hypothesis wrong and uses The Lagrange polynomial $S(X)$ containing *degree* $\leq (n-1)$ that demands n number of SN containing public shares of network with co-ordinates $(x_1, y_1=f(x_1)), (x_2, y_2=f(x_2)), \dots, (x_n, y_n=f(x_n))$ is given by

$$S(X) = \sum_{k=0}^n P_k(X) \quad (8)$$

Where P_k is given by

$$S(x) = Y_k \frac{(x - x_l)}{(x_j - x_l)} \quad (9)$$

where $l \geq 1$ and $l \leq n$ and $l \neq k$

If written explicitly for $n=3$ nodes, Lagrange polynomial is represented as follows:

$$S(X) = Y_1 \frac{(x - x_2)(x - x_3)}{(x_1 - x_2)(x_1 - x_3)} + Y_2 \frac{(x - x_1)(x - x_3)}{(x_2 - x_1)(x_2 - x_3)} + Y_3 \frac{(x - x_1)(x - x_2)}{(x_3 - x_1)(x_3 - x_2)} \quad (10)$$

The separate polynomial can also be formulated as per Szego(1975) which was later called Lagrange's fundamental interpolation:

for first node

$$S(X_1) = Y_1 \frac{x_2 * x_3}{(x - x_2)(x - x_3)} \quad (11)$$

for Second node

$$S(X_2) = Y_2 \frac{x_1 * x_3}{(x - x_1)(x - x_3)} \quad (12)$$

for third node

$$S(X_3) = Y_3 \frac{x_1 * x_2}{(x - x_2)(x - x_3)} \quad (13)$$

The key which is generated by the integration of separate polynomials is represented as

$$G_K = \sum_{k=0}^n S(K) \quad (14)$$

If G_K matches the network key only then the null hypothesis is proved to be wrong.

Pseudo Code for Share Verification:

```

1) Order=2; // Interpolation order
2) MYVALUE=[ ] // Initializing the key values to be Empty
3) For i =1:3 // For 3 nodes
a)counter=1;
b)Current1=NodeID1 // Taking the first node as initial reference
4) for j=1:Nodes;
a)Current=Vehiclesj; // For each interpolation, there would be 2 Rest Nodes
b) if Current1 ≈ Current // If nodes are not same
c) Rest(counter)=current;
d) counter=counter+1;
e) End If 5) End For 6) Deno=0 7) Deno=Current1-Rest1*Current1-Rest2// The denominator value
8) Num=Rest1*Rest2
9) Myvalue [i]=Num/Deno
10) Sharedkey=ShareCurrent1*Myvalue[i]
11) End For

```

In order to keep the data secure on the network, this paper also presents a dual encryption algorithm which stores the information of the migration and other attributes of the physical machine and virtual machine. This makes the communication secure and more reliable. The data security is achieved with the involvement of an advanced encryption. The AES algorithm employs three important parameters, namely, key length, number of rounds and the block size. During the encryption processes, bytes in the form of cipher state are used where input bytes are processed to state array that result into output bytes. Additionally, all round keys are also generated. The encryption steps involved in AES consist of five main operations described in following algorithm.

Advanced Encryption Standard (AES) Algorithm:

1. Input: P_{t_b} // P_{t_b} plain text box
 S_k is secret keys and N_r is number of rounds
2. Determine State
 $state_{var}=(P_{t_b}, S_k)$ //state variable
3. AddRoundKey($state_{var}, S_k(0)$)
4. For_{each} I in (N_r-1)
 - a. SubBytes($state_{var}$) // performs byte substitution transformation
 - b. ShiftRows($state_{var}$) //performs shift transformation to rows except first row
 - c. MixColumns($state_{var}$) //performs MixColumns transformation
 - d. AddKey($state_{var}, Key_{textsubscript i}$)//Adds a RoundKey to the $state_{var}$
- End_{for}
5. SubBytes($state_{var}$)
6. ShiftRows($state_{var}$)
7. AddRoundKey($state_{var}, Key_{nr-1}$)
8. Return: ($state_{var}$) // AES state variable

The above encryption algorithm performs the secure VM allocation. However, decryption is performed by reversing the above operations. A small set of example is demonstrated in Table I. Once the encryption is performed, a random shuffling order is created in order to rotate the generated index structure. The pattern of rotation is stored in a semi-storage cache memory which is used to decrypt the pattern once required. The cache memory is refreshed once a new combination is generated.

IV. RESULTS AND DISCUSSION

During the test, the parameters such as energy consumption, SLA violation and number of VM migrations are evaluated and compared with the existing techniques. Table II

TABLE I. VM MIGRATION AND ENERGY CONSUMPTION WITH IMPLEMENTATION OF AES ENCRYPTION

VM ID	PM Number	Migrated To	Energy Consumption (KWh)
22	1	4	0.78
15	2	7	0.32
8	5	9	0.45
32	12	15	0.57
23	6	10	0.38
18	3	11	0.76

represents the computed results simulated in CloudSim tool. The table shows that energy consumption is minimal as compared to the individual MBFD approach. Also, the numbers of migrations are less, which indicates that the application runs at a higher speed. Due to this, the mobile cloud data center consumes less energy to execute the requested application from the user. Also, the decrease in the number of hosts and SLA violations results in minimized energy consumption.

Fig. 5 shows the numbers of hosts to which number of

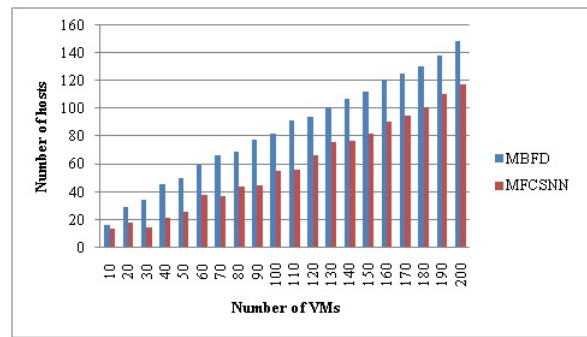


Fig. 5. Number of hosts vs VMs

VMs are allocated with MBFD integrated with CS as well as ANN techniques named as MFCSNN. The results show that with increase in the number of VMs, the number of hosts also increases but the allocation rate is less while utilizing the optimization algorithm with artificial machine learning technique.

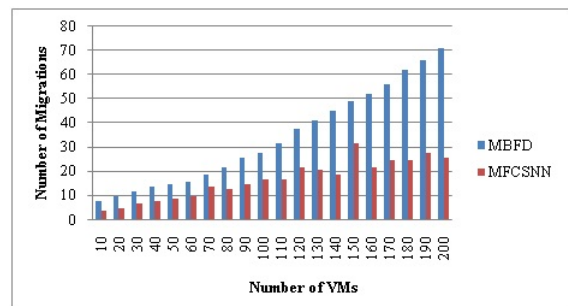


Fig. 6. Number of Migrations vs VMs

Fig. 6 indicates the graph for a number of migrations performed while executing the application using 200 numbers of VMs. The graph indicates that the number of migrations using the proposed MFCSNN approach is less compared to the existing MBFD approach. This is due to the proper selection of host. It also provides applications to the host, which is

TABLE II. COMPUTED RESULTS

Number of VMs	Number of hosts		Number of Migrations		Energy Consumption (KWh)		SLA Violation		Average Response Time (s)	
	MBFD	MFCSSNN	MBFD	MFCSSNN	MBFD	MFCSSNN	MBFD	MFCSSNN	MBFD	MFCSSNN
10	16	14	8	4	0.3	0.2	9	7	1021	1011
20	29	18	10	5	0.4	0.3	8	6	1123	1094
30	35	15	12	7	0.5	0.25	11	10	3751	2574
40	46	22	14	8	0.7	0.48	13	11	5697	4875
50	50	26	15	9	0.7	0.38	14	9	7258	6527
60	60	38	16	10	0.9	0.65	15	10	7236	6851
70	67	37	19	14	1.0	0.87	18	13	8536	7142
80	69	44	22	13	1.3	0.85	22	15	8827	7892
90	78	45	26	15	1.4	1.02	24	19	9364	8538
100	82	55	28	17	1.4	1.09	25	21	10415	9456
110	92	56	32	17	1.7	1.14	27	24	11425	10752
120	94	67	38	22	1.9	1.15	29	26	12578	11364
130	101	76	41	21	2.2	1.35	31	27	12694	11687
140	107	77	45	19	2.3	1.48	35	30	12831	12015
150	112	82	49	32	2.4	1.78	39	34	13984	12675
160	121	91	52	22	2.9	1.75	44	42	14057	13624
170	125	95	56	25	3.1	2.05	46	43	14267	13965
180	131	101	62	25	3.4	2.38	48	45	14428	14025
190	138	111	66	28	3.6	2.67	50	47	14495	14270
200	149	118	71	26	3.8	2.66	53	50	14567	14396

under loaded and hence saves the energy consumption, which is unnecessarily utilized by the ideal host. The average VM migrations performed using MBFD and proposed MFCSSNN approach are 32.15 and 16.95 respectively. The average value is considered as the mean of number of migrations obtained for different number of VMs varies from 10, 20, 30, 40 ...200. Hence, approximately 47.28 % reduction is attained by utilizing the CS with the ANN approach.

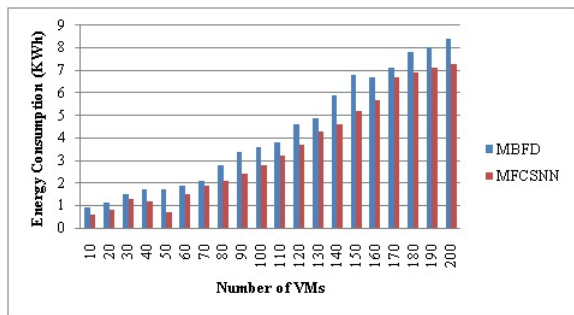


Fig. 7. Energy Consumption vs VMs

Fig. 7 shows that the energy consumption is the main parameter which must be minimized to obtain a green computing environment. It has been known that the ideal computer consumes about 70 % of total power without performing any operation. Therefore, it must be necessary to turn off those hosts which are not performing any operation. To achieve this goal, we have used ANN algorithm to distinguish among the ideal, underutilized and over-utilized host. Therefore, applications are forwarded to that host which is under-utilized and hence save energy. Using the proposed MFCSSNN approach and simple MBFD approach, the average energy consumed is computed as 4.23 KWh and 3.5 KWh respectively. Thus, there is a reduction of about 17.26 %.

The SLA violation is an essential parameter that must be fulfilled by mobile cloud providers to ensure better delivery of mobile cloud services to their users. Along with the energy saving policy, it is essential to meet the SLA parameter of cloud. It indicates the agreement between the user and the cloud service

TABLE III. COMPARATIVE VALUES

Energy Consumption(KWh)		Number of Migrations	
MFCSSNN	Karda and Kalra (2019) [23]	MFCSSNN	Karda and Kalra (2019) [23]
3.5	5.59	16.95	40

provider. The higher SLA indicates better services are provided to the cloud user by the cloud providers and vice versa. The graph drawn in Fig. 8 indicates that the proposed technique provides a better series to their mobile cloud users. The average of SLA violation obtained for MBFD and proposed MFCSSNN approach are 28.05 and 24.45, respectively. Therefore, there is a deterioration of 12.83 % while utilizing the CS with the ANN approach. The results based on the average response time

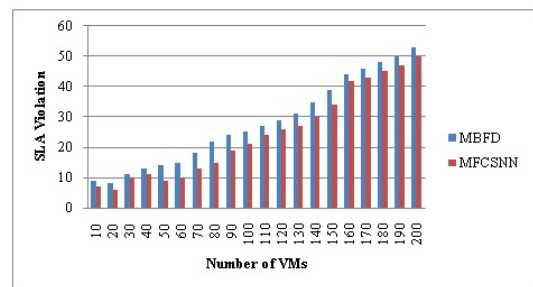


Fig. 8. SLA Violation vs VMs

with respect to the number of VMs are shown in Fig. 9. From this figure, it is clear that the designed MFCSSNN algorithm outperforms as it required less time for migrating VMs to the host. Using traditional approach, the state of the jobs is restored if appropriate resources are not allocated and later allocate jobs whenever find available resources. But by using the proposed approach, time has been saved and therefore according to the demand, the resources are allocated. In addition to this, the computation overhead is also calculated for a new vendor to be added to the network. It is observed that when a new vendor is added into the network, every node not always provided the best outcome, which is desired. Hence to overcome the failure, a new vendor is also searched. Table IV presents the

TABLE IV. COMPUTATION OVERHEAD

Total registration of vendor	Computation Overhead
10	0.4
20	0.33
30	0.28
40	0.24

computation overhead, which is calculated by using equation 15.

The unsuccessful vendor is calculated by the observation of power consumption. If the node is consuming power which is higher than that of the average power consumption of the network for a given time interval, the vendor is unsuccessful.

To Show the comparative analysis comparison with the proposed and existing technique is presented in Table III. Here, the comparison of proposed MFCSNN approach is compared with the BAT and NN approach presented by Akki and Vijayarajan [8].

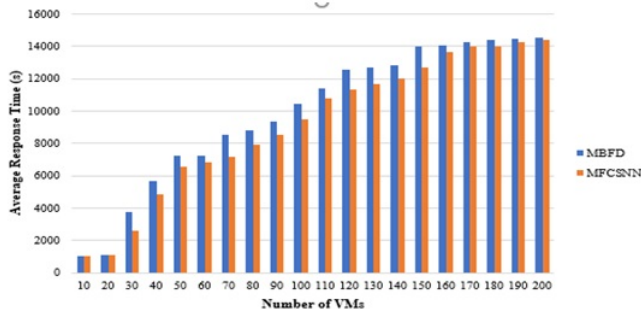


Fig. 9. Average Response Time

$$CO = \frac{(Total\ unsuccessful\ vendors)}{(Total\ added\ vendors)} \quad (15)$$

Fig. 10 and Fig. 11 represent the comparison graph drawn

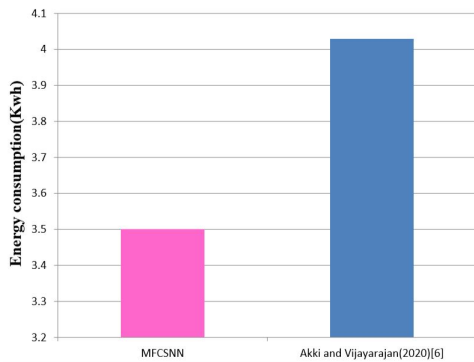


Fig. 10. Comparison of Energy Consumption

from energy consumption and number of migrations as given in Table III. The comparison has been made with the existing work performed by Akki and Vijayarajan (2020) [8] using BAT with ANN approach to optimize the power by selecting the best value among the available values of the generated solution. The aim of the researchers is to route mobile users

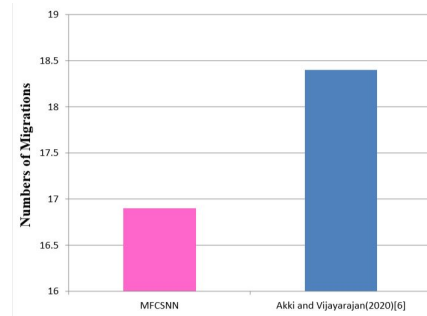


Fig. 11. Comparison of Number of Migrations

to the server without interruption in services as well as with minimum power consumption. From the graph, it is clear that the integrated technique of CS with ANN performs well compared to an individual optimization scheme. Thus, there is an improvement of about 13.15 % and 8.23 % in the energy consumption, and the number of migrations respectively. This is because of the advantages of CS algorithm, as CS works on three parametric values. Therefore, the probability to providing optimized data is high. Also, the CS is able to detect a very small change in the result value so that appropriate solution can be obtained with small optimized time.

V. CONCLUSION

Power consumption has become a critical problem in the mobile cloud computing environment. The continuous growth in power consumption produces carbon dioxide. It has a negative impact on the green environment and hence raises the operating costs. In near future, there will be many scopes to improve load balancing by various techniques to minimize energy consumption within a secure mobile cloud computing environment.

In this article, we have suggested a load balancing technique called MFCSNN to minimize energy consumption in a mobile cloud computing environment. In addition to this, Lagrange's interpolation is incorporated with the existing modification of allocation and migration scheme for a new physical machine registration in the network. The parameters such as energy consumption, VM migration, number of hosts, and SLA violations are evaluated. As per the test results performed with MBFD and proposed MFCSNN, the performance of the designed system has been improved to offer secure VM allocation using AES. Hence it has been analyzed that the proposed model is a green solution with the minimum generation of carbon dioxide. Also, in order to show the effectiveness of the proposed method, comparison with the existing technology has also been presented. Here, as compared to the existing BAT-ANN approach, the proposed approach has minimized energy consumption up to 13.15 %.

REFERENCES

- [1] Sabharwal, M., Agrawal, A., &Metri, G. (2012). Enabling green it through energy-aware software. IT Professional, 15(1), 19-27.
- [2] Bonino, D., De Russis, L., Corno, F., & Ferrero, G. (2013). JEERP: energy-aware enterprise resource planning. IT Professional, 16(4), 50-56.

- [3] Gai, K., Qiu, M., Zhao, H., Tao, L., & Zong, Z. (2016). Dynamic energy-aware cloudlet-based mobile cloud computing model for green computing. *Journal of Network and Computer Applications*, 59, 46-54.
- [4] Ge, Y., Zhang, Y., Qiu, Q., & Lu, Y. H. (2012). A game theoretic resource allocation for overall energy minimization in mobile cloud computing system. In *Proceedings of the 2012 ACM/IEEE international symposium on Low power electronics and design* (pp. 279-284).
- [5] Dinh, H. T., Lee, C., Niyato, D., & Wang, P. (2013). A survey of mobile cloud computing: architecture, applications, and approaches. *Wireless communications and mobile computing*, 13(18), 1587-1611.
- [6] Eshratifar, A. E., & Pedram, M. (2018, May). Energy and performance efficient computation offloading for deep neural networks in a mobile cloud computing environment. In *Proceedings of the 2018 on Great Lakes Symposium on VLSI* (pp. 111-116).
- [7] Jo, B., Piran, M. J., Lee, D., & Suh, D. Y. (2019). Efficient computation offloading in mobile cloud computing for video streaming over 5G. *Comput. Mater. Contin.*, 61, 439-463.
- [8] Akki, P., & Vijayarajan, V. (2020). Energy Efficient Resource Scheduling Using Optimization Based Neural Network in Mobile Cloud Computing. *Wireless Personal Communications* 114, 1785-1804
- [9] Akki, P., & Vijayarajan, V. (2019). An efficient system model to minimize signal interference and delay in mobile cloud environment. *Evolutionary Intelligence*, 1-9.
- [10] Psannis, K. E., Stergiou, C., & Gupta, B. B. (2018). Advanced media-based smart big data on intelligent cloud systems. *IEEE Transactions on Sustainable Computing*, 4(1), 77-87.
- [11] Shiraz, M., Abolfazli, S., Sanaei, Z., & Gani, A. (2013). A study on virtual machine deployment for application outsourcing in mobile cloud computing. *The Journal of Supercomputing*, 63(3), 946-964.
- [12] Shiraz, M., & Gani, A. (2012). Mobile cloud computing: Critical analysis of application deployment in virtual machines. In *Proc. int'l conf. information and computer networks (ICCN'12)* (Vol. 27).
- [13] Abd, S. K., Al-Haddad, S. A. R., Hashim, F., Abdullah, A. B., & Yussof, S. (2017). Energy-aware fault tolerant task offloading of mobile cloud computing. In *2017 5th IEEE International Conference on Mobile Cloud Computing, Services, and Engineering (MobileCloud)* (pp. 161-164). IEEE.
- [14] Krishna, P. V., Misra, S., Nagaraju, D., Saritha, V., & Obaidat, M. S. (2016). Learning automata based decision making algorithm for task offloading in mobile cloud. In *2016 International Conference on Computer, Information and Telecommunication Systems (CITS)* (pp. 1-6). IEEE.
- [15] Yadav, R., & Zhang, W. (2017). McReg: Managing energy-SLA tradeoff for green mobile cloud computing. *Wireless Communications and Mobile Computing*.
- [16] Wang, X., Wang, J., Wang, X., & Chen, X. (2015). Energy and delay tradeoff for application offloading in mobile cloud computing. *IEEE Systems Journal*, 11(2), 858-867.
- [17] Liu, J., Li, Y., Jin, D., Su, L., & Zeng, L. (2015). Traffic aware cross-site virtual machine migration in future mobile cloud computing. *Mobile Networks and Applications*, 20(1), 62-71.
- [18] Halabi, T., Bellaiche, M., & Abusitta, A. (2019). Toward secure resource allocation in mobile cloud computing: A matching game. In *2019 International Conference on Computing, Networking and Communications (ICNC)* (pp. 370-374). IEEE
- [19] Verma, A., Ahuja, P., & Neogi, A. (2008) pMapper: power and migration cost aware application placement in virtualized systems. In *Proceedings of the 9th ACM/IFIP/USENIX International conference on middleware*. pp. 243-264. Springer-Verlag New York, Inc
- [20] Sharifian, S., & Barati, M. (2019). An ensemble multiscale wavelet-GARCH hybrid SVR algorithm for mobile cloud computing workload prediction. *International Journal of Machine Learning and Cybernetics*, 10(11), 3285-3300.
- [21] Mukherjee, A., & De, D. (2016). Low power offloading strategy for femto-cloud mobile network. *Engineering Science and Technology, an International Journal*, 19(1), 260-270.
- [22] Boukerche, A., Guan, S., & Grande, R. E. D. (2019). Sustainable offloading in Mobile cloud computing: algorithmic design and implementation. *ACM Computing Surveys (CSUR)*, 52(1), 1-37.
- [23] Mohammed, M. A., & TÁPUS, N. (2017). A novel approach of reducing energy consumption by utilizing enthalpy in mobile cloud computing. *Studies in Informatics and Control*, 26(4), 425-434.
- [24] Guo, S., Liu, J., Yang, Y., Xiao, B., & Li, Z. (2019). Energy-Efficient Dynamic Computation Offloading and Cooperative Task Scheduling in Mobile Cloud Computing. *IEEE Transactions on Mobile Computing*, 18(2), 319-333.
- [25] Tang, C., Xiao, S., Wei, X., Hao, M., & Chen, W. (2018, January). Energy Efficient and Deadline Satisfied Task Scheduling in Mobile Cloud Computing. In *2018 IEEE International Conference on Big Data and Smart Computing (BigComp)* (pp. 198-205).

An Improved Biometric Fusion System of Fingerprint and Face using Whale Optimization

Tajinder Kumar¹

Department of Computer Science
& Engineering
IKG Punjab Technical University
Kapurthala, Punjab, India

Shashi Bhushan²

Department of Computer Science
and Engineering, Chandigarh
Group of College, Landran,
Punjab, India

Surender Jangra³

Department of Computer Science,
GTBC, Bhawanigarh, Punjab, India

Abstract—In the field of wireless multimedia authentication unimodal biometric model is commonly used but it suffers from spoofing and limited accuracy. The present work proposes the fusion of features of face and fingerprint recognition system as an Improved Biometric Fusion System (IBFS) leads to improvement in performance. Integrating multiple biometric traits recognition performance is improved and thereby reducing fraudulent access. The paper introduces an IBFS comprising of authentication systems that are Improved Fingerprint Recognition System (IFPRS) and Improved Face Recognition System (IFRS) are introduced. Whale optimization algorithm is used with minutiae feature for IFPRS and Maximally Stable External Regions (MSER) for IFRS. To train the designed IBFS, Pattern net model is used as a classification algorithm. Pattern net works based on processed data set along with SVM to train the IBFS model to achieve better classification accuracy. It is observed that the proposed fusion system exhibited average true positive rate and accuracy of 99.8 percentage and 99.6 percentage, respectively.

Keywords—Biometric fusion; face recognition; fingerprint recognition; feature extraction; feature optimization; classifier

I. INTRODUCTION

The unimodal biometric systems are prone to the inconsistencies scores and outliers [1]. However, fusion biometric systems or multi model systems play a crucial role in providing accuracy, security, universality and cost-effectiveness. Various research papers has focused on the face and fingerprint-based fusion system, but classification accuracy has not been achieved so far. This work aims to present a new biometric system that overcomes the problem of authenticity and employs fusion of faces and fingerprint traits [2]. The paper organizes in following sections: Section 2 defines the existing work in fingerprint and face biometric traits in the form of related work. Section 3 presents the formulation of multimodal fusion system. In Section 4, experimental results are considered, and Section 5 states the vital conclusions.

II. RELATED WORK

Nagar et al. had studied the fusion of three biological features (fingerprint, face and iris). It has been proved that multi-biometric systems show a great similarity check and possess high security although it requires a large storage space to save multiple templates of the input data. Here fuzzy vault and fuzzy commitment model was used to form a biometric encryption system framework [3]. A lot of work has

been implemented in the fields of biological key using uni-model biometric system in which algorithm utilized user-key and biometrics authentication [4]. The Dialog Communication Systems developed BioID which is a multimodal identification system that uses three different features: voice, face and lip movement-to recognize people [5]. The present work involves the design of new soft biometric database with a human face, body with clothing attributes at three different distances for investigates indirect influence on the soft biometric fusion [6]. Thereafter authors has been designed multimodal biometric approach and validated on three chimeric multimodal databases such as face, fingerprint and Iris. The performance of this work has been analyzed in terms of Decidability Index (DI), Equal Error Rate (EER), and Recognition Index (RI). Present approach outperforms existing methods by achieved an accuracy of 99.5%, an EER of 0.5% [7]. A novel multi-modal biometric system based on face and fingerprint resolves the issues like noise sensor data, non-universality, susceptibility to forgery and deficiency of invariant representation. The fingerprint matching has been performed through alignment-based elastic algorithm. To get the improved feature extraction, extended local binary patterns (ELBP) has been utilized. This work has been examined on FVC 2000 DB1, FVC 2000 DB2, ORL (AT&T) and YALE databases and accomplished 99.59% of accuracy [8]. The authors have introduced and examined the concepts of dual authority with authentication-based scheme on the basis of biometric along with its influencing factors of recognition rate in biometrics. However the singular model authentication approach does not guarantee the security of jurisdictions in a common regulatory area. By increasing the number of experiments, the average time for face recognizing reduces and leading to the stable value and the rate of recognition to be 92.2%. The authors has explored the ways to enhance the performance of rank identification in Automated Fingerprint Identification Systems (AFIS) while only a partial latent fingerprint has been made available. The preset work approach exploits extended fingerprint features (unusual/rare minutiae) not commonly considered in AFIS. This novel approach has combined with existing minuate-based matcher. A realistic forensic fingerprint casework database comprising of rare minutiae features obtained from Guardia Civil, the Spanish law enforcement agency has been utilized here [9]. The authors have presented a novel multimodal biometric fusion system using three different biometric modalities such as face, ear and gait based on speed-up-robust-feature (SURF) descriptor including genetic algorithm (GA). ANN has been utilized to

classify the biometric modality. The work has been observed on three databases namely AMI ear, Georgia Tech face and CASIA Gait database. Before fusion, SURF features have been optimized through GA and further cross-validated using ANN [10]. The authors have presented two level score level fusion method for the merger of scores being obtained from the cancel-able template of various biometric characteristics. The framework has been run on two virtual databases. The results have shown that the proposed amalgamation have optimized better performance than the uni-biometric system [11].

III. PROPOSED MULTI-MODAL FUSION SYSTEM

This section covers the architecture of the proposed biometric system which is based on fingerprint and face. The simulation of proposed work includes the improved finger print recognition system, frame work of improved biometric fusion system and improved face recognition system is as follows:

A. Database

Quality data mining is the first and the most key aspect of any prediction model. The data sets used in the proposed work represents the collection of face and fingerprint images. Fingerprint images have been collected from FVC fingerprint database and face images were collected from Georgia Tech face database . Fingerprint data corresponds to high resolution gray scale images in *.tif format. Face images are found in *.jpeg format and are represented by 150 pixels square matrix. Database has collection of images with variation of lighting and scale.

B. Framework of IBFS

The multi-modal bio-metric system deals with improvement of the performance by using enhancement of quality of the input data. It is employed to enhance the accuracy and security of the bio-metric recognition systems. Thus, multi-modal fusion systems has proved to be more accurate . Multi-modal systems also provide knowledge about the sample being entered by applying liveness detection techniques. Spoofing is thus far easily detected.

There are various ways to measure the efficiency of IBFS.

- 1) Collectability: Provides the manner in which the person's trait is measured and processed.
- 2) Uniqueness: Determines the uniqueness of the user through the recognition of bio-metric system.
- 3) Performance: It provides the Robustness, accuracy, speed and fault handling achieved using system.
- 4) Universality: The requirements for unique characteristics of each person in the world is known. These cannot be reproduced.
- 5) Permanence: Provides the time frame for recording the personal trait in the database

In this work, IBFS fusion architecture taken into consideration. More information is contained in the feature set about the input bio-metric data than the matching score or the output decision of a matcher. When fusion is done at the feature level better recognition results are generated. To do this first step requires pre-processing of the data. However, there is difficulty in pre-processing which is to acquire a better quality

of input image for bio-metric system. This paper proposes a new method to increase the accuracy of IBFS and optimizes the accuracy of bio-metric traits, which is disturbed in case of noisy data. It uses the fusion levels algorithms between face and fingerprints recognition system [12] [13]. The first system is created combining the fingerprint verification with the Atmospheric Light Adjustment (ALA). It uses Whale Optimization based on minutiae feature extraction technique. The second system used in the multi-modal makes use of face verification by employing Whale optimization based on Maximally Stable Extremal Region (MSER) extraction technique. Both the systems together are then trained using pattern net. Fingerprints are considered and accepted mostly for the identification of person due to their uniqueness and nature of immutability. Even stored and classified using SVM for better accuracy. In this work, the traits of face and finger are considered. Fig. 1 shows the framework of proposed IBFS.

1) *Framework of Proposed IFPRS*: A fingerprint refers to the assortment of furrows and ridges found on the tip of a finger. In local parlance ridge pattern is known as oriented texture pattern comprising of orientation and dominant frequency. Capturing the orientation and dominating frequency of ridges in fingerprint, leads to a distinct representation of this texture [14]. These are commonly categorized into five different types: whorl, left loop, right loop, arch, and tented arch. Fingerprints are considered and accepted mostly for the identification of person due to their uniqueness and nature of immutability. Laptops and smart phones are using this technology in the form of a password to unlock the screen. It is used in residential system for attendance and time. For most recognition systems, problems arise for identifying fingerprints of same type. In general recognition systems employ neural networks to detecting the minutiae's, and the ridge ends in fingerprints. This helps in matching the fingerprint. The problem lies in feature extraction as extracted features vary in length. The second difficulty is due to irrelevant noise caused while obtaining the fingerprint in the online mode from the biometric sensor. A lot of noise is added in the fingerprint images. This results difficulties in formulating a classification system. These difficulties are overcome by using pre-processing, feature extraction, optimization before using classification of biometric features.

Fingerprint Pre-processing: In case of image analysis fingerprint pre-processing provides great results. The main features used in fingerprint pre-processing are subdivided into two types local and global features. The Local features use the minutiae information whereas the secondary features employ the local area information which does not vary with global transformation. The global features include type, number, and the position containing the singularities that includes geometrical and spatial relationship of attributes of size, ridge lines, and shape of the fingerprints [15]. The pre-processing steps applied on the uploaded fingerprint images for enhancing the quality is described below:

Conversion using Color: Color conversion helps in finding the luminance of the fingerprint image which further used in extraction process [16].

$$GrayIm = 0.299 * R_1 + 0.587 * G_2 + 0.114 * B_3 \quad (1)$$

Where GrayIm: Gary image

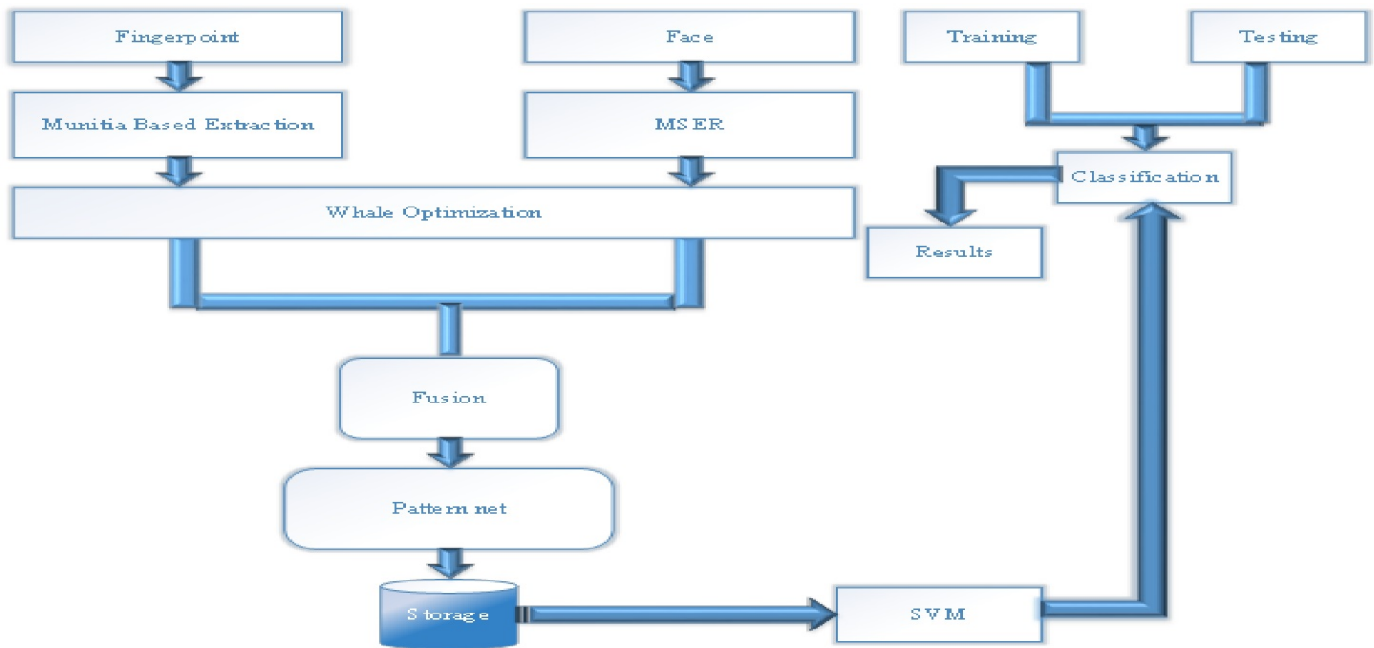


Fig. 1. Framework of Proposed IBFS.

R₁: Red image component
G₂: Green image component
B₃: Blue image component

Image Enhancement: To fix specific pixel points in the image enhancement is used. For improving the quality of fingerprint ALA image enhancement technique is used. This algorithm helps to find the exact minutiae feature of fingerprint.

Algorithm 1: ALA Algorithm

1. Input: Image_{gray}
2. Define variable: Img = double(Image_{gray})
3. Determine: [Image_{height}, Image_{width}, Image_{plane}] = size(Image_{gray})
4. Assign Variables: patch_{size} = 15 // here parts of images are considered
5. pad_{size} = 7 // it demonstrates the extra boundary
6. Determine: P_{mask} = padarray(I, [pad_{size}, pad_{size}]) // generates empty mask of pad_{size}
7. For each j value in Image_{width}
8. For each i value in Image_{height}
9. Construct: patch_{matrix} = pmat(i_{value}:(i_{value}+ patch_{size}- 1), (j_{value}+ patch_{size}- 1), All)
zmat(i_{value}, j_{value}) = min(patch_{matrix} (:))
10. end for
11. end for
12. Apply: A = atmosLight(double(Img), zmat, plane) //applies Atmospheric Light adjustment
13. Image_{Opt} = 1 - zmat

14. Image_{enhance} = Zeros(size(Img)) //creates an empty matrix of size of I

15. for each ind_{value} inplane

16. Image_{enhance}(:,:,ind) = (A(ind) + (Img(:,:,ind) / (max(Image_{opt}, 0.1))))
//where 0.1 is the lightening coefficient

17. end for

18. Output: Image_{enhance}

Fingerprint Feature Optimization (FOP): FOP results in optimizing and reducing the number of features in the data set. It includes selection of features, variable and attributes . These selection techniques are employed for simplifying the models for easy understanding and interpretation by the users.



Fig. 2. Whale Optimized Algorithm Inspired by Behavior of Whales.

There is another technique that is similar to FOP and used

for dimensionality reduction .The difference lies in creating new combination of features whereas feature optimization only excludes and includes the features. The Whale algorithm is used as feature optimization technique. Fig. 2 depicts the inspiration taken from the biological behavior of the whales which corresponds to the typical path followed by Whale Algorithm to achieve an optimized solution.

There are two phases of the algorithm, exploitation and exploration phase. In the exploitation phase whale follows the spiral path to encircle the prey as shown in Fig. 2. In the second phase, prey is randomly searched.

Mathematical explanation of Exploitation Phase:

Prey encircling: It works on two assumptions, firstly, that the target prey is the principal candidate for achieving the most favorable solution. Secondly, other search mediators continuously change their positions in response to search agent. This behavior is represented as follow:

$$Pw_{(itr+1)} = Pp_{itr} - A_{coeffvect} * D_{vect} \quad (2)$$

$$D_{vect} = |B_{coeffvect} * Pp_{itr} - Pw_{itr}| \quad (3)$$

Where, Pp_{itr} is the whale's last position at iteration 'itr' also corresponding to the prey position, $Pw_{(itr+1)}$ is the whale's present position, distance between prey and whale is represented by D_{vect} , $A_{coeffvect}$ and $B_{coeffvect}$ are coefficient vectors represented as follows:

$$A_{coeffvect} = 2 * A_{vect} * r_{vect} + A_{vect} \quad (4)$$

$$B_{coeffvect} = 2 * r_{vect} \quad (5)$$

In order to shrink the search space corresponding to the spiral path followed by the whale, the value of A_{vect} is reduced thereby decreasing the oscillating range of A

Updating Spiral Path Position: Let us consider the whale position coordinates as (Pw,Qw) and prey position coordinates as (Pp,Qp). The spiral path followed by the whales is represented as follows:

$$Pw_{(itr+1)} = exp^{CR} * cos(2\pi R) * Dp_{vect} + Pp_{itr} \quad (6)$$

$$D_{vect} = |B_{coeffvect} * Pp_{itr} - Pw_{itr}| \quad (7)$$

Where, C represents the constant that determines the logarithmic shape of the spiral path and R is the random variable lie between -1 and +1. There always lies a 50% chance that the search mechanism will follow a spiral or shrinking encircling design. The selection is done as follows:

$$Pw_{(itr+1)} = \begin{cases} Pp_{itr} - A_{coeffvect} * D_{vect} & \text{if } R < 0.5 \\ exp^{CR} * Dp_{vect} + Pp_{itr} & \text{if } R \geq 0.5 \end{cases} \quad (8)$$

Mathematical explanation of Exploration Phase. In search phase, position of the search agent is determined in respect to the randomly selected search gents and not with respect to the best search agent. This mechanism corresponds to the strengths of WOA to deal with the shortcoming associated with the local optimization problems. The model is represented as follows:

$$Pw_{(itr+1)} = Pw_{rand} - A_{coeffvect} * D_{vect} \quad (9)$$

$$D_{vect} = |B_{coeffvect} * Pw_{rand} - Pw_{itr}| \quad (10)$$

Where, Pw_{rand} represent the position of a random whale within the population. The Whale optimization algorithm is as follows:

Algorithm 2: Whale Optimization Algorithm

1. Input: F_{points} //Feature points of fingerprint Image_{enhance}
2. Output: Image optimized //optimized feature points
3. Initialize parameters: Itr // Search agents, L_{BN} //lower bound of "N" variables

U_{BN} //upper bound of "N" variables

F_{fit} //fitness function

4. Calculate: $T=size(F_{points})$ // size of the input image

5. for each i value in T

6. Calculate: $F_{pointsselected} = \sum_{i=1}^T F_{points}(i_{value})$

// value for selected F-point in terms of N

7. Calculate:

$$F_{pointsthreshold} = \frac{\sum_{i=1}^T F(i)}{Length(F_{points})}$$

$F_{pointsthreshold}$ is threshold which should be achieved by supervisor N with respect to threshold F-Points

8. Calculate: Fitness

$$F_{fit} = \begin{cases} False, & F_{pointsselected} < F_{pointsthreshold} \\ True, & F_{pointsselected} \geq F_{pointsthreshold} \end{cases}$$

Calculate: $Opt_{value} = WOA(F_{fit}, N, L_{(BN)}, U_{BN})$

end for

While Itr \neq max(T)

Assign: $F_{points} = Opt_{value}$

End while

Output: Image optimized = optimize(F-points) //optimized fingerprint image

2) *Framework of Proposed IFRS:* Face recognition helps in contributing to the IBPS. Bio-metrics of face help in identifying persons of interest and are used to verify their identities. It also helps in gathering the demographic data on large amount of people [17]. This has led to increase in demand for retail marketing. Fig. 3 describes the framework of proposed IFRS. Face is a complex multidimensional structure. There is a need to enhance the input data and computing it with better recognition techniques. Pre-processing of data helps in the feature extraction and optimization and overcome the difficulties faced during face recognition.

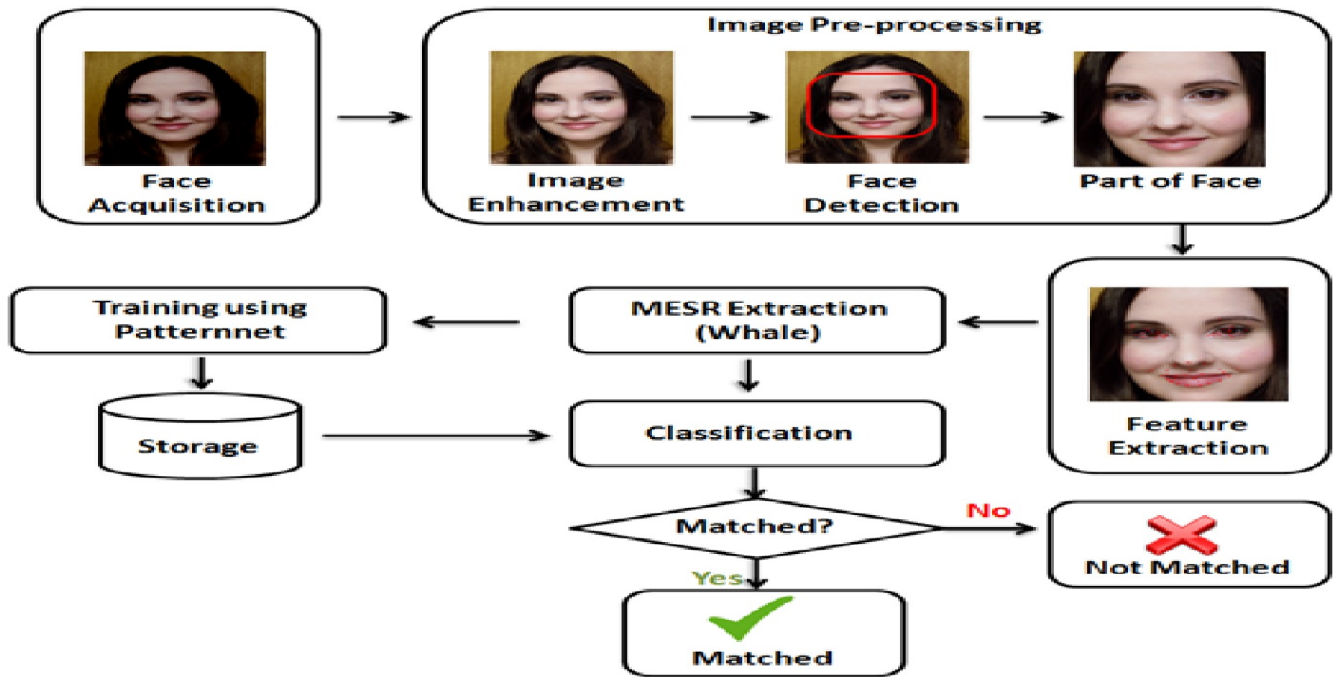


Fig. 3. Framework of Proposed IFRS.

3) *Face image pre-processing*: Facial feature point detection provides many applications such as recognition of face, tracking hallucination, animation and 3D analysis [18]. The first process of pre-processing includes Face data acquisition (FDAQ) which includes uploading the captured face images. FDAQ Algorithm extracts the Region of Interest (RoI). The pre-processing algorithm is given as:

Algorithm 3: Pre-Processing for IFRS

1. Input: $Image_{face}$ //upload image for face recognition
2. for each i_{value} in $Image_{face}$
3. Apply: $Image_{resize}=Resize(Image_{face}(i))$
4. Apply: $image_{detect}=FaceDetector(image_{face}(i))$
5. Calculate: $Image_{bound}=boundary(Image_{detect})$ //find boundary of face detection image
6. Calculate: $Image_{th}=Threshold(Image_{detect})$ //calculate threshold
7. Calculate: $Image_{gray}=GrayConversion(Image_{detect},Image_{th})$
8. Calculate: $Image_{RoI}=crop(Image_{gray},Image_{bound})$
9. end for
10. Output: $image_{RoI}$ //pre-processed face image

This procedure helps to obtain the pre-processed RoI image. MSER Extraction applied after pre-processing helps in finding optimized features.

4) *MSER extraction*: MSERs are used to detect blobs in images. The blobs can be a symbol, text character and content that the MSER algorithm identifies. It reduces the computational overhead by identifying the regions of the image that contains text as to determine whether a region is a true

character or not [19]. Having the property of performing well on homogeneous regions it works well in this case. It provides robustness for large scale images and helps in improving matching performance. In such a case, it performs best when applied in proper strategy. This works as one of the fastest region detectors. Algorithm 4 provides the steps needed to implement MSER.

Algorithm 4: MSER Algorithm

1. Input: $Image_{RoI}$ // upload image
2. Calculate: $[R.C]=size(Image_{RoI})$
3. for each r_{value} in R
4. for each c_{value} in C
5. Calculate: $Image_{intensity}=intensity(Image_{RoI}(r,c))$
6. Calculate: $Image_{components}=component(Image_{intensity}(r,c),8)$
7. $Image_{th} = stable(Image_{components})$
8. $Filter_{points} = filter(Image_{th})$
9. Check: if $Image_{th} == True$
10. $MSER_{points} = Filter_{points}$
11. end if
12. end for
13. end for
14. Assign: $F_{points} = MSER_{points}$
15. Output: F_{points}

5) *Optimization of features of face:* To generate the unique feature sets optimization is applied. Optimization generates best features which are used for face detection. Using Whale algorithm, MSER points are optimized.

C. Training of Proposed Model

The training of the system is done using pattern net. To train the proposed system, Pattern net is used with the optimized feature set. Both systems fuse together to provide the training data for the model. This is called Optimized Pattern net, which is used to leverage the filters in the last convolution layer of a convolution neural network. This helps to find locally consistent visual patches. The visual patterns are discovered efficiently due to Pattern net. To enhance the classification accuracy of the system SVM is used along with Pattern net in the recognition system.

IV. RESULTS

Table I summarizes the images and the stages of image processing in IFPRS and IFRS bio-metric fusion model. Column 2 labels the image processing stages and column 3 and column 4 corresponds to the respective image processing results of IFPRS and IFRS

Experimental evaluation of performance of bio-metric fusion model: The Precision, Recall, F-measure, and Accuracy are calculated while considering confusion matrix parameters for evaluating the performance of machine learning in our proposed model using following formulas:

- 1) Precision

$$Precision = \frac{T_{positive}}{T_{positive} + F_{positive}} \quad (11)$$

- 2) Recall

$$Recall = \frac{T_{positive}}{T_{positive} + F_{negative}} \quad (12)$$

- 3) $F_{measure}$

$$F_{measure} = \frac{precision * recall}{precision + recall} \quad (13)$$

- 4) Accuracy

$$Accuracy = \frac{T_{positive} + T_{negative}}{T_{positive} + T_{negative} + F_{positive} + F_{negative}} \quad (14)$$

Table II summarizes the performance parameters obtained for the bio-metric fusion system over a range of image samples. It is observed that with the increase number of image samples, there is an increase in the number of true positive results which predicts the better performance of classification model.

The parameters, namely, TP, TN, FP, FN are essential for predicting the performance of machine learning classification. Fig. 4 represents the number of image samples used in the bio-metric fusion model. These are plotted on X-axis against the measurements of confusion matrix parameters in percentiles on Y-axis. It is observed that with increase in the number of image samples increases in the number of TP and corresponding reduction in the number of TN, FP and FN values. Initially when 10 image samples are used the TP observed is 70% with

TN, FP and FN as 10% each. As the sample size increases to 100, TP rises to 95% and TN, FP and FN falls to 2%, 1% and 2% respectively. Further it is observed that when the sample size increases to 500, the system achieved improved TP of 99.2% with traces of TN, FP and FN corresponding to 0.4%, 0.2%, and 0.2% respectively. In other words, the plot implies the prevalence of least error in the proposed bio-metric fusion model. Fig. 5 evaluates the precision, sensitivity and accuracy

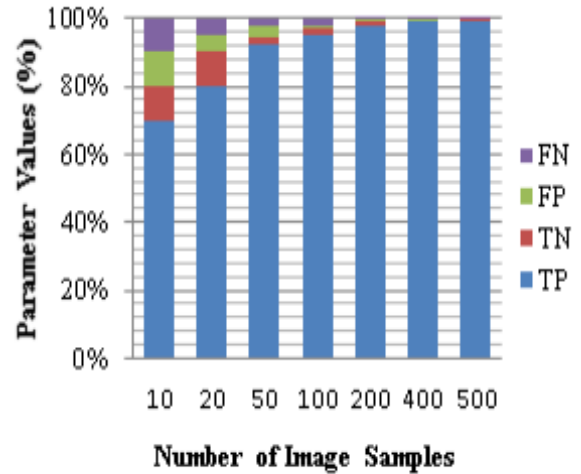


Fig. 4. Confusion Matrix Parameters Expressed in Percentiles.

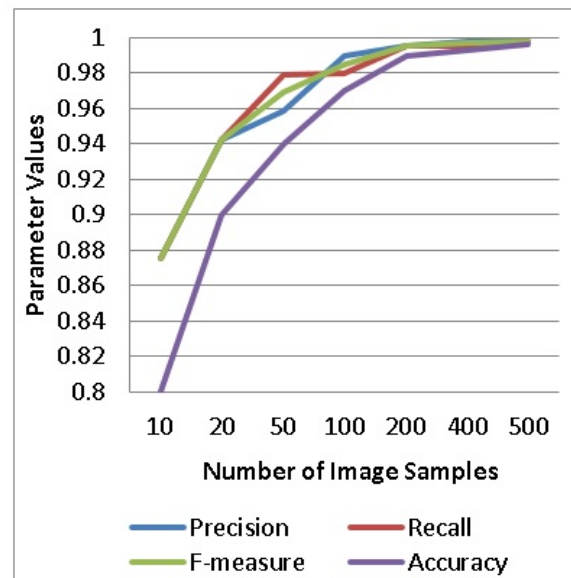


Fig. 5. Parametric Plot of Precision, Recall, Fmeasure and Accuracy.

of sampling and classification in the proposed model over the range of image samples. The plots shows that for a sample of 10 images, the precision is only 0.875. Further, as the sample size is increased to 50, 200 and 500 the precision also increases from 0.95 to 0.995 and 0.998. This trend shows a improvement of 12.3% in precision. Similar trend is observed in case of recall value or the true positive rate. The recall for a sample

TABLE I. IMAGES AT VARIOUS STAGES IN IFPRS AND IFRS.

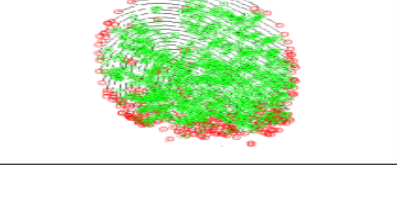
S.No	Stages of Images	IFPRS	IFRS
1.	Original Uploaded Image		
2.	Pre-Processed Image		
3.	ROI Recognition Image		
4.	ROI Enhanced Image		
5.	Optimized Image		

TABLE II. COMPUTED RESULTS.

Number of Image Samples	TP	TN	FP	FN	Precision	Recall	F-measure	Accuracy
10	7	1	1	1	0.875	0.875	0.875	0.800
20	16	2	1	1	0.942	0.942	0.942	0.900
50	46	1	2	1	0.959	0.979	0.969	0.940
100	95	2	1	2	0.990	0.980	0.985	0.970
200	196	2	1	1	0.995	0.995	0.995	0.990
400	396	1	1	2	0.998	0.995	0.997	0.993
500	496	2	1	1	0.998	0.998	0.998	0.996

of 10 images is only 0.875. But as the sample size is increased to 50, 200 and 500 the recall value also increases from 0.979 to 0.995 and 0.998. Hence the system sensitivity increases with increase in the number of input sample images. In case of F-measure, the observed value for 10 images is 0.875. As the number of image samples increases to 50, 200 and 500, this leads to increases the accuracy to 0.969, 0.995 and 0.998. The results show that the system achieved on average precision, recall and f-measure of 99.8% each. Accuracy is an important parameter to predict the correctness of results predicted by the proposed model. The plots show that the initial accuracy of the system is only 0.80 which record a step rise till the sample size is 200 and system attains an accuracy of 0.97. This further

gets accentuated to 99 % for a sample size of 500 images. The performance of the bio-metric fusion system is also evaluated against similar literature cited hybrid approaches. Kumar and Zhang had evaluated the effectiveness of SVM, NN and FFN for feature extraction and classification and conclude SVM to be best approach among others employed in the study [20]. Similar work was also carried on by Kremic and Subasi who employed Random Forest Tree (RFT) with SVM to enhance the performance of their proposed approach [21]. The authors in the current study considered these existing studies for the evaluation of the proposed system in terms of accuracy. Table III and Fig. 6 shows that the recognition accuracy of 89% was achieved by Kumar and Zhang using

SVM classifier [20] and maximum face recognition accuracy of 97.94% was attained when SVM classifier was powered with the employment of RFT by Kremic and Subashi [21]. In comparison to these prediction results, our proposed biometric fusion model demonstrated an average accuracy of 99.6% when a combination of WOA and SVM is used.

TABLE III. ACCURACY EVALUATION WITH EXISTING WORK

Reference Work	Approach used	Accuracy
Proposed Work	WOA + SVM	99.60%
Kumar and Zhang, 2006	SVM	89%
Kremic and Subasi, 2016	RFT + SVM	97.94%

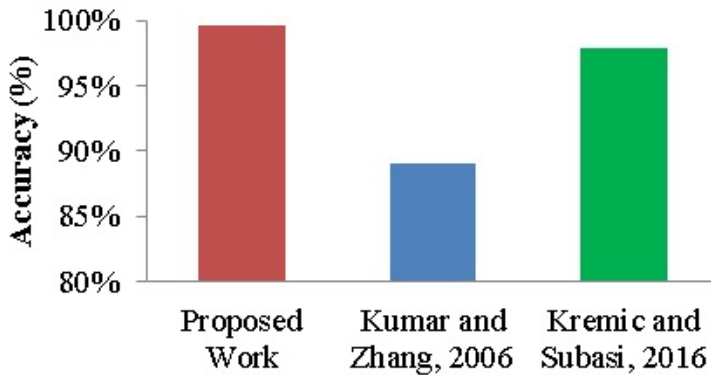


Fig. 6. Accuracy Comparison with Existing Work.

V. CONCLUSION

The authors propose an Improved Bio-metric Fusion System for face and fingerprint recognition in the present work. The system makes use of WOA approach as an optimization technique along with MSER for extracting feature points of the images. Pattern net has been used along with SVM to enhance the accuracy of classification in the proposed fusion system. The resultant recognition system shows an instrumental TP value of 99.2% with minor TN, FP and FN values of 0.4%, 0.2%, and 0.2% respectively. It is also observed that the proposed system demonstrates an average precision, recall and f-measure of 99.8% each with an average recognition accuracy of 99.6%. The overall result achieved an improvement of 12.3% for precision, recall and f-measure and an outstanding enhanced accuracy of 91.6% when a larger data set of images is employed for training the proposed system.

REFERENCES

[1] Dwivedi, R. and Dey, S., 2018. Score-level fusion for cancellable multi-biometric verification. *Pattern Recognition Letters*.

[2] Connor, P. and Ross, A., 2018. Biometric recognition by gait: A survey of modalities and features. *Computer Vision and Image Understanding*, 167, pp.1-27.

[3] Nagar, A., Nandakumar, K. and Jain, A.K., 2011. Multibiometric cryptosystems based on feature-level fusion. *IEEE transactions on information forensics and security*, 7(1), pp.255-268.

[4] Wu, Z., Tian, L., Li, P., Wu, T., Jiang, M. and Wu, C., 2018. Generating stable biometric keys for flexible cloud computing authentication using finger vein. *Information Sciences*, 433, pp.431-447.

[5] Frischholz, R.W. and Dieckmann, U., 2000. BioID: a multimodal biometric identification system. *Computer*, 33(2), pp.64-68.

[6] Nixon, M.S., Guo, B.H., Stevenage, S.V., Jaha, E.S., Almodhahka, N. and Martinho-Corbishley, D., 2017. Towards automated eyewitness descriptions: describing the face, body and clothing for recognition. *Visual Cognition*, 25(4-6), pp.524-538.

[7] Gupta, K., Walia, G. S., & Sharma, K. 2020. Quality based adaptive score fusion approach for multimodal biometric system. *Applied Intelligence*, 50(4), pp.1086-1099.

[8] Aleem, S., Yang, P., Masood, S., Li, P., and Sheng, B. 2020. An accurate multi-modal biometric identification system for person identification via fusion of face and fingerprint. *World Wide Web*, 23(2), pp.1299-1317.

[9] Krish, R. P., Fierrez, J., Ramos, D., Alonso-Fernandez, F., & Bigun, J. 2019. Improving automated latent fingerprint identification using extended minutia types. *Information Fusion*, 50, pp.9-19.

[10] Mehraj, H., & Mir, A. H. 2020. Feature vector extraction and optimization for multimodal biometrics employing face, ear and gait utilizing artificial neural networks. *International Journal of Cloud Computing*, 9(2-3), pp.131-149.

[11] Hussein, I.S., Sahibuddin, S.B., Nordin, M.J. and Sjarif, N.B.A., 2019. Multimodal palmprint technology: A review. *Journal of Theoretical and Applied Information Technology*, 97(11), pp.2882-2896.

[12] Dwivedi, R. and Dey, S., 2019. A novel hybrid score level and decision level fusion scheme for cancellable multi-biometric verification. *Applied Intelligence*, 49(3), pp.1016-1035.

[13] Jain, L.C., Halici, U., Hayashi, I., Lee, S.B. and Tsutsui, S. eds., 1999. *Intelligent biometric techniques in fingerprint and face recognition* (Vol. 10). CRC press.

[14] Zewail, R., Elsafi, A., Saeb, M. and Hamdy, N., 2004, July. Soft and hard biometrics fusion for improved identity verification. In *The 2004 47th Midwest Symposium on Circuits and Systems*, 2004. MWSCAS'04. (Vol. 1, pp. 1-225). IEEE.

[15] Maltoni, D., Maio, D., Jain, A.K. and Prabhakar, S., 2009. *Handbook of fingerprint recognition*. Springer Science & Business Media.

[16] Sing, J.K., Dey, A. and Ghosh, M., 2019. Confidence factor weighted Gaussian function induced parallel fuzzy rank-level fusion for inference and its application to face recognition. *Information Fusion*, 47, pp.60-71.

[17] Saini, M. and Kapoor, A.K., 2016. *Biometrics in Forensic Identification: Applications and Challenges*. *J Forensic Med*, 1(108), p.2.

[18] Wang, N., Gao, X., Tao, D., Yang, H. and Li, X., 2018. Facial feature point detection: A comprehensive survey. *Neuro computing*, 275, pp.50-65.

[19] Natarajan, P., Sikka, A. and Prasad, R., Amazon Technologies Inc, 2016. *Image processing using multiple aspect ratios*. U.S. Patent 9,418,283.

[20] Kumar, A. and Zhang, D., 2006. Personal recognition using hand shape and texture. *IEEE Transactions on image processing*, 15(8), pp.2454-2461.

[21] Kremic, E. and Subasi, A., 2016. Performance of random forest and SVM in face recognition. *Int. Arab J. Inf. Technol.*, 13(2), pp.287-293.

Implementation of an e-Commerce System for the Automation and Improvement of Commercial Management at a Business Level

Anthony Tupia-Astoray¹
Facultad de Ciencias e Ingeniería
Universidad de Ciencias y Humanidades
Lima, Perú

Laberiano Andrade-Arenas²
Facultad de Ciencias e Ingeniería
Universidad de Ciencias y Humanidades
Lima, Perú

Abstract—At present micro and small businesses engaged in the production and marketing of products and have a single means of sale, whether stalls or physical stores, have been affected by the current crisis that is happening due to the pandemic, which came in early 2020 to Europe and different countries in Latin America, which is causing terrible damage to the economy of enterprises, since it does not have a means of virtual sales, where they can offer and market their products so that trade continues to operate during the pandemic. In this way, we designed a prototype e-commerce system meeting the requirements required by the organizations. Where it was based on the Scrum methodology as an agile development framework for the realization of the project. The use of the Marvel design tool allowed the creation of web platform prototypes. Obtaining as a result, prototypes according to an e-commerce system complying with the development procedures established by the Scrum team, which gives you a novel proposal and a productive approach to start implementing e-commerce within the sales processes of each business area. Therefore, this e-commerce system prototype proposal can be implemented by the different micro companies that wish to have a new online sales method and improve their commercial area process, allowing the increase of their client portfolio, as well as their production.

Keywords—Agile development; e-commerce; scrum methodology; prototype; system

I. INTRODUCTION

Currently, e-commerce is becoming a technological solution for the various problems that arise within companies in relation to their sales processes or business management.

e-Commerce is a growing phenomenon in Latin America and the world, so the study of its technological acceptance is high [1]. Having a virtual business tool favors and gives you a series of advantages such as: having access from any geographical area, being accessible 24 hours a day, having a favorable increase of customers and start to be competitive in the market, having information and control of customers accessing the system, in addition to reducing costs and minimizing service times and product deliveries.

For small and micro-enterprises, the use of the Internet and the development of e-commerce is an opportunity because it allows them to increase their capacity to disseminate products, make distance sales and make their cost structure more flexible [2]. e-Commerce drives advances in security and payment systems, marketing strategies and advertising, media distribution,

business-to-business commerce and retailing [3]. People today use e-commerce constantly to make purchases of all kinds and rely on the security they offer when making an online transaction or payment. Businesses also have the ability to be more connected with their shoppers [4].

With the development of the Internet and other technologies, the efficiency of transactions will constantly improve [5]. Therefore, companies need to implement an e-commerce system to improve and automate the commercial management and can undertake a new business direction and provide a solution to their problems. It requires a system that provides a catalog of the company's products, has a reliable database to store the information that is generated from a customer purchase. All this opens you to have new sales opportunities and obtain new customers and therefore more production and sales. However, you will be able to manage a record of customers and sales made, have updated products and also with an adequate control.

The objective of the research work is to implement an e-commerce system that allows to automate and improve the processes of commercial management at the enterprise level, where companies have and count with new business opportunities.

The structure of the article consists of five sections: in Section II is the literature review, Section III details the methodology of the research study, in Section IV the case study will be visualized, in Section V, will consist of the results and discussions; finally in Section VI the conclusions are mentioned.

II. REVIEW LITERATURE

The development of technology and information has spread to various sectors, especially to the sector of product marketing and product transactions. The presence of e-commerce brings new changes in the world of production and business marketing [6]. This situation undoubtedly contributes to the optimization of processes and expands opportunities for companies in e-commerce. Clear and concise communication between the company and the consumer provides security and allows the identification of needs that, when met in a timely manner, enhance service and efficiency in the management and design of information [7].

The new information and communication technologies have revolutionized at the international level broad sectors of knowledge and human activities, fostering the emergence of new ways of doing business [8]. In this regard, it should be noted that the implementation of e-commerce and payment by credit card or cell phone via the Internet is vital for Guinea-Bissau's development.

Globalization requires countries and producers to innovate their ways of marketing in order to remain competitive in the market [9]. One alternative is to incorporate producers and micro and medium-sized enterprises into e-commerce successfully and analyze the results they have obtained by applying it, with the objective of improving their income. To this end, it is necessary to formulate models for the adoption of this form of business, which will allow agroindustrial companies to incorporate it into their daily activities so that they can be more productive.

e-Commerce in the level of sales of micro, small and medium-sized enterprises (MSMEs) of some key sectors of the city of Ibagué (Industry, Commerce and Services), for which we seek to know the current status of e-commerce and its importance, the causes of its use and non-use, and the positioning it has in the strategic plans of these organizations [10].

III. METHODOLOGY

A. Scrum

The Scrum methodology is an iterative process and evokes moments of feedback in a systematic way [11]. Accordingly, it was decided to develop the research work with the Scrum methodology. The technical framework of scrum, is formed by a set of practices and rules that respond to the following agile development principles: Evolutionary product management, instead of the traditional or predictive [12].

Scrum is an agile, lightweight framework that provides steps to manage and control the software and product development process [13]. Quality of the result based on the tacit knowledge of people, rather than on the explicit knowledge of the processes and technology used. Incremental development strategy through iterations (Sprint). scrum methodology is much more than group work. Therefore, it is encouraged to work according to their personal interests [14]. As shown in Fig. 1, the Scrum process scheme was made, which under its work techniques will execute the research development through the daylin scrum, retrospective, sprint review and taking into account the creation of the product backlog, sprint backlog and finally have a release.

1) *Phase 1: Start:* In this first phase, the project objectives will be analyzed to obtain product requirements and from there create the user stories.

2) *Phase 2: Planning:* In this phase the planning of the deliverables (Sprint) will be established, where sets of tasks to be performed by the development team will be established and meetings will be held to determine and discuss.

3) *Phase 3: Implementation:* The sprint is planned by means of a GANT diagram, where start and end dates of its development are established.

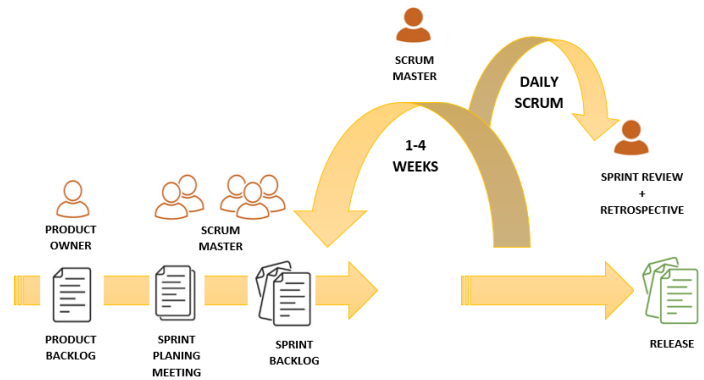


Fig. 1. Scrum Process

4) *Phase 4: Review and Retrospective:* In this phase, sprint retrospective meetings will be held to evaluate and discuss the sprint performed, taking into account the internal evaluation of the team's work.

5) *Phase 5: Launch:* This phase is the final part of the whole process where the complete and functional deliverables are reported for release.

B. Prototype Tool

The development of prototypes is the design vision of the system and how it is required to implement it in the future applying the requirements established by the client, that is why the following software will be used for the development.

1) *Marvel:* This tool allows you to develop or shape your design ideas through its work platform and generate design prototypes quickly.

IV. CASE STUDY

In this section the research study was developed applying the methodology processes, fulfilling all the development of the prototype by executing the phases mentioned above.

1) Phase 1: Start:

a) *Requirements:* The requirements are part of the requirements established by the product owner who is in charge of collecting as much information as possible about how the system is intended to work and how it is visualized. Table I, shows the requirements that were made and that are functional.

TABLE I. REQUIREMENTS

Requirements	
Nº	Item
1	The system must be able to display the company's product catalog
2	The system should allow you to manage the shopping cart, add products, delete products and cancel shopping cart
3	The system must allow the customer to purchase the products added to the shopping cart
4	The System must allow to register the information of the clients as natural person or company
5	The system shall allow adding new products, modifying and deleting existing products
6	The system must allow to display a sales report. The data to be displayed are: date, sale number, customer name, product code, product name, product quantity, unit price, total Sales

b) *Backlog Product*: The backlog is the ordered list of all the requirements previously established by the customer. In Table II, we observe the functional user stories and also the estimation and priority that helps to evaluate each user story.

TABLE II. BACKLOG PRODUCT

Backlog Product			
N°	Item	Priority	Estimate
H1	As a user, I want to see the catalog of the products in the system	High	2
H2	As a user, I need to manage the purchase of the products added to the shopping cart	High	1
H3	As a user, I want to register to the system as a natural person or company	High	2
H4	As a user, I wish to enter the system through a login	High	2
H5	As an administrator, I want to enter the administrator module through a login	Medium	1
H6	As an administrator, I want to add new products, modify and delete existing products	Medium	3
H7	As an area manager, I would like to see the sales reports for the day	Under	1

c) *Estimate - Planning Poker*: The planning poker was used to estimate the user stories and determine the effort it will take to develop each one, depending on its difficulty, which is why it was decided to use this technique. As shown in Table III.

TABLE III. PLANNING POKER

Planning Poker		
Item	Estimate	Time
1	2	2 days
2	1	1 day
3	2	2 days
4	2	2 days
5	1	1 days
6	3	3 days
7	3	1 days
Total	14	12 days

2) Phase 2: Planning:

a) *Sprint Planning*: The necessary activities were carried out to develop a new version of the product (Increment) of functional type, according to the specifications for the Sprint [15]. It was determined what will be the Sprint (Deliverables), by means of a tactical planning of work it was decided that it will be 4 sprint, for this work the sprint counted with two stories of users fully identified previously, as it is shown in Table IV.

b) *Product Roadmap*: In this section the Product Roadmap is established, which is a high-level plan that allows us to see how our product will evolve by launching the deliverables that were established, it is like our roadmap, which allows you to describe how to achieve the objectives or vision of the product to be delivered. All this can be seen in Fig. 2.

3) Phase 3: Implementation:

a) *Sprint Planning Meeting*: In this section the development of the tasks was organized based on a sprint chronogram where the dates of each deliverable were determined. It will help the work team to maintain an order when developing the

TABLE IV. SPRINT PLANNING

Sprint Planning		
N°	User History	N° Item
Sprint 1	H1 As a user, I want to see the catalog of the products in the system H2 As a user, As a user, I want to see the product catalog in the system	1
Sprint 2	H3 As a user, I want to register to the system as a natural person or company H4 As a user, I want to enter the system through a login	2
Sprint 3	H5 As an administrator, I want to enter the administrator module through a login H6 As an administrator, I want to add new products, modify and delete existing products	3
Sprint 4	H7 As an area manager, I would like to see the sales reports for the day.	4

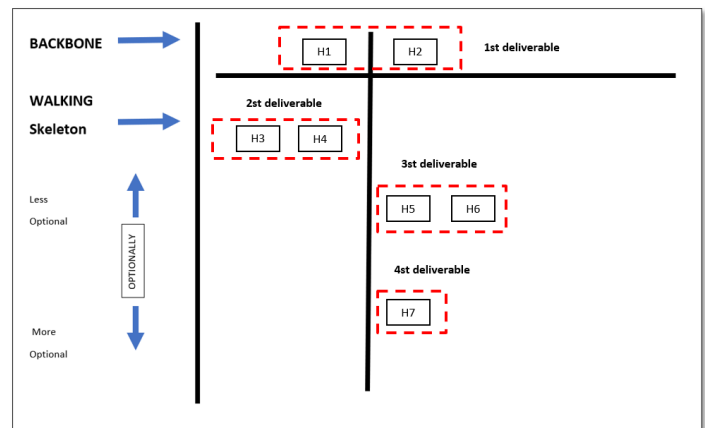


Fig. 2. Product Roadmap

Commercial Management Web System Project					
Inicio: Jue 01/10/20					
Jun 01/10/20 - Lun 14/12/20					
	Modo de	Task name	Duration	Start	End
0		Commercial Management Web System Project	53	mon01/10/20	mon14/12/20
1		Spring 1	3 days	mon12/10/20	wed14/10/20
2		Catalog Interface	2 days	mon12/10/20	tue 13/10/20
3		Shopping Cart	1 day	wed 14/10/20	wed 14/10/20
4		Spring 2	4 days	tue 24/11/20	fri 27/11/20
5		Login registration	2 days	tue 24/11/20	wed 25/11/20
6		System Access	2 days	thu 26/11/20	fri 27/11/20
7		Spring 3	4 days	mon07/12/20	thu 10/12/20
8		Administrator Login	1 day	mon07/12/20	mon07/12/20
9		Administrator module	3 days	tue 08/12/20	thu 10/12/20
10		Spring 4	1 day	mon14/12/20	mon14/12/20
11		Sales Reports	1 day	mon14/12/20	mon14/12/20

Fig. 3. Sprint Timeline

product. The schedule with the items established in the sprint planning is shown in Fig. 3.

4) Phase 4: Review and Retrospective:

a) *Daily Scrum*: All the people involved in the project will meet daily to review the sprint and determine if there is any inconvenience that can be improved or solved. The people involved in the meetings rotated daily every day, with the sole purpose of ensuring that the objective was met and developed normally and without problems. They analyzed what was done wrong, what was done right and what difficulties were encountered that did not allow the project to continue as planned [16].

5) Phase 5: Launch:

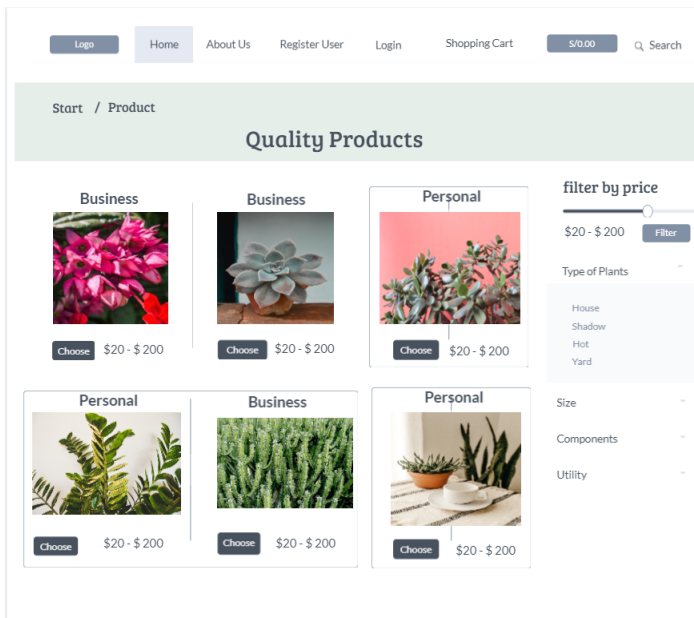


Fig. 4. Product Catalogue

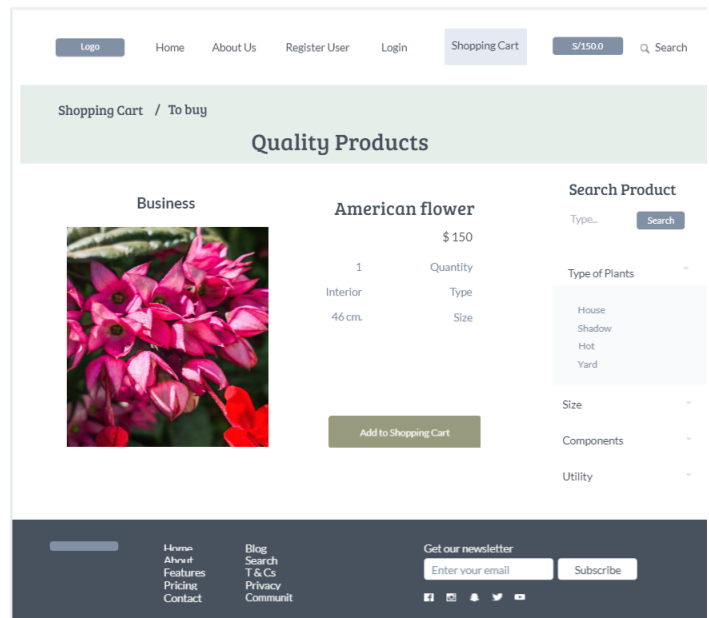


Fig. 5. Purchase Prototype

a) *Sprint 1*: It is based on the first deliverable of the system, where the company's product catalog is displayed, and apart from that, the shopping cart is displayed, which will serve to complete the system's purchase flow. These two are important functionalities for the management of the e-Commerce, that is why it was determined to be the first deliverable because it provides value and functionality to the system, as shown in Fig. 4, the user will be able to visualize the product catalog, then the product will have a main window, where the main characteristics will be shown and also the item can be added to the cart, all this is shown in Fig. 5. Then, we have the shopping cart interface where it will detail how the purchase will be made and what will be the type of payment to be made, as shown in Fig. 6.

b) *Sprint 2*: This is the second deliverable of the system, it consists of two interfaces that will be used for the user to log in to the system after he/she has registered, therefore, an interface for the creation of new users was also created, as shown in Fig. 7. The user registration prototype was also added, where new clients who are interested in having some interaction with the web system can be registered (Fig. 8).

c) *Sprint 3*: It is the third deliverable of the system, it is about the interfaces to the access of the administrator module as shown in Fig. 9, so that the administrator can enter the module, before he must log in, previously registered in the system and have the user data registered in the database, then, he must fill in the fields shown in the interface of email and password, then he will be directed to the administrator module shown in Fig. 10. Where he can manage the products according to the criteria of the company, in sum, he will have administrator permissions to different actions such as deleting, viewing and updating the product.

d) *Sprint 4*: It is the fourth deliverable of the system, the interface was made to show all the reports of the sales that

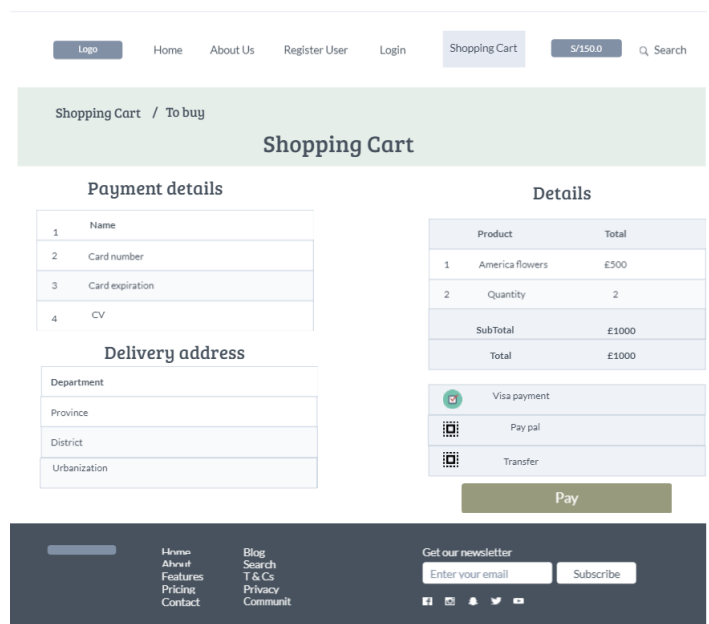


Fig. 6. Shopping Cart Prototype

are made daily, where the area manager can view the items that were part of the purchase of customers, also showing the name and image of the product that was purchased. The area manager can also perform different actions on the product, as shown in Fig. 11.

V. RESULTS AND DISCUSSIONS

A. About the Case Study

The main objective of the study is to develop an e-commerce web system, which is capable of allowing companies to have new sales opportunities through internet com-

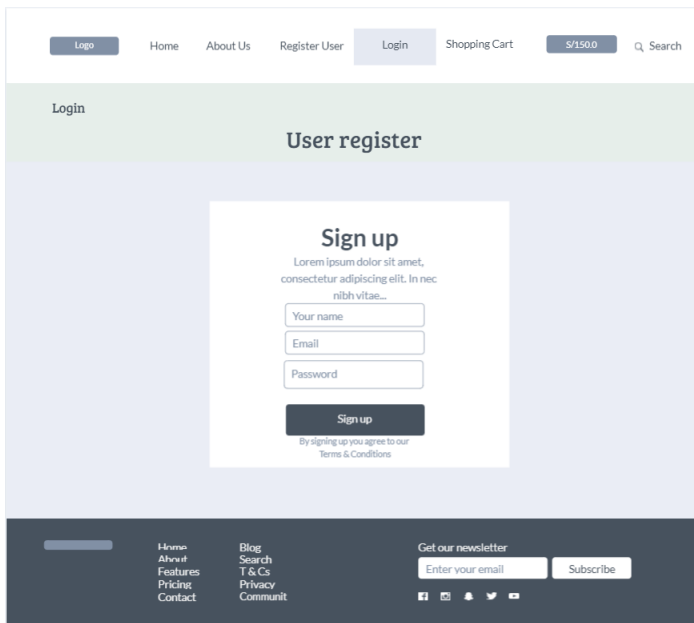


Fig. 7. Registration Prototype

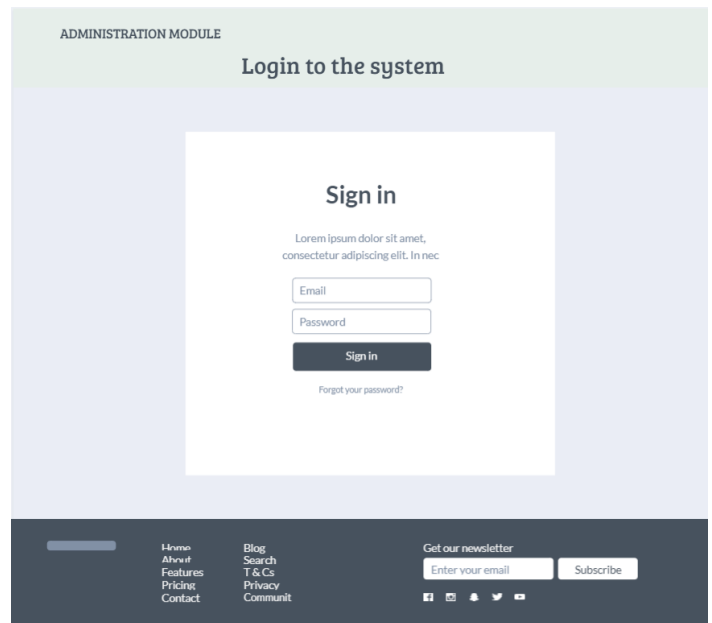


Fig. 9. Admin Login Prototype

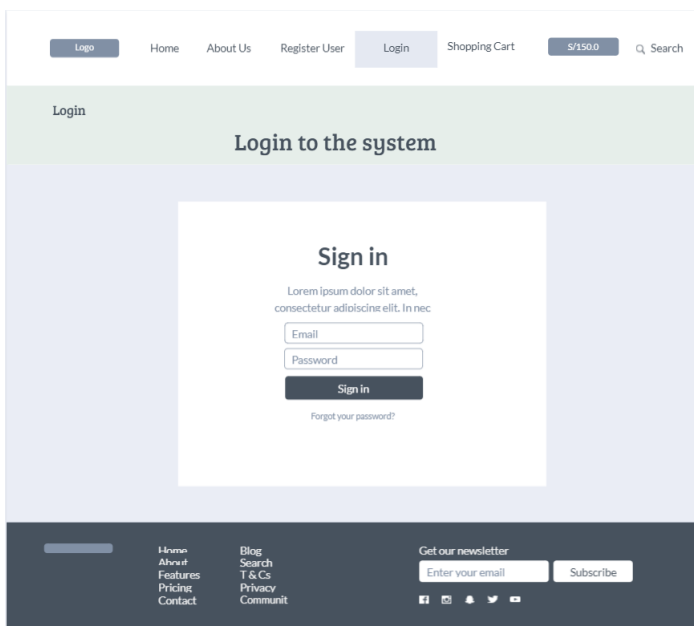


Fig. 8. Login Prototype

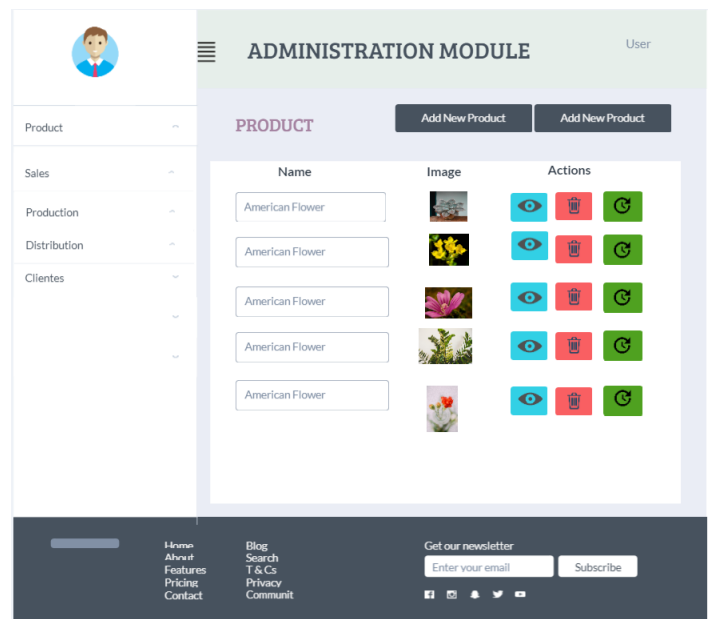


Fig. 10. Product Management Prototype

merce. The implementation of new commercial methods aimed primarily at meeting the needs of consumers should include the monopolization of sales markets, global competition and active development of information technologies [17].

It is a good way to take advantage of new technologies and be able to solve the problems that arise in organizations. The development of the prototypes presented was elaborated by a tool called Marvel, it is a web tool that allows you to transform your design ideas into digital products, which gives you a series of components that facilitate the creation of it, apart from being unique. Eight prototypes were made within this tool, each one with different functionalities which will be

explained below.

1) *Sprint 1*: Sprint 1, has the development of 3 prototypes which are: Product catalog prototype, is the face of the web system, not to say, the presentation and the first thing the user will see, therefore, components were implemented which will make it look interesting and novel. The shopping cart prototype was developed with the functionality to start the purchase flow starting from the product selection. The shopping cart prototype is the final part of the flow, where the payment method and product details are detailed.

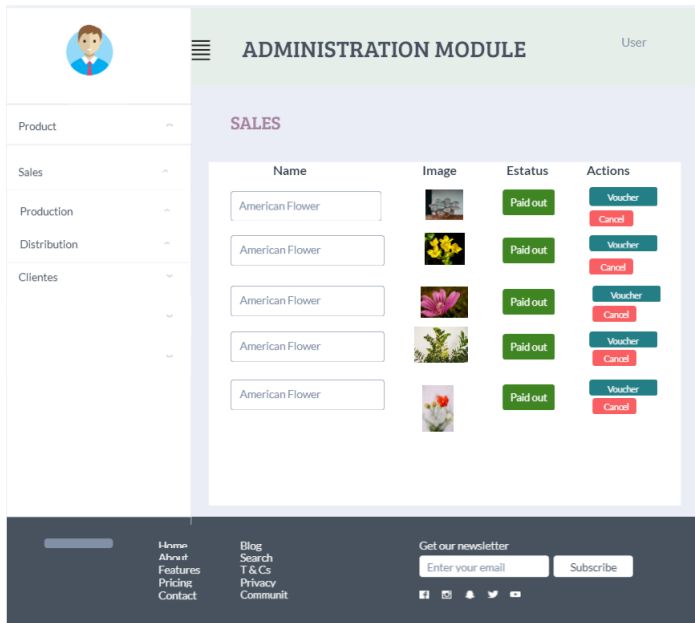


Fig. 11. Sales Record Prototype

2) *Sprint 2*: Sprint 2, has developed 2 prototypes which are: User Registration Prototype which was determined to create this interface for the registration of persons or companies that wish to register to the system and can have records within it. A basic form was added with three fields to fill out and a button to confirm the registration. Prototype of Login to the system, is where the user will log in that allows you to have access to more features and to buy within the page, has two fields of email and password.

3) *Sprint 3*: Sprint 3 has developed 2 prototypes that are part of the administrator page and does not involve the client: Administrator Module Login Prototype, which has a form with two text fields and a Login button. Product Management Prototype, which is the administrator module. This interface shows details of the products published in the e-Commerce which can be modified, deleted, updated, as well as adding new products.

4) *Sprint 4*: Sprint 4 has 1 development prototype, which is the Sales Registration Prototype. A field was created where the daily sales reports are shown, where the products are detailed with their respective images and status of the items, in addition, actions were added so that the area manager has access to modify any sale if necessary.

B. About the Methodology

1) *Advantages*: One of the advantages of Scrum is to provide organization and collaborative work of the team members and is adaptable to the changes that can be generated in the construction of the project [18]. As well as having deliverables periodically and not at the end of the project [19].

2) *Disadvantages*: One of the disadvantages of Scrum is that it requires people capable of managing large projects and who have adequate academic training. Another negative circumstance is that this methodology is misused in development

teams, as it does not comply with the values and principles that Scrum proposes [18].

3) *Comparisons*: The agile methodology that we have used for the development of the project is Scrum, one of the agile methodologies that is currently being widely used and consequently is becoming one of the best, bringing benefits to companies, in addition to the fact that Scrum is capable of managing difficult projects. Scrum is basically an agile and lightweight framework that provides the steps to manage and control the process of software and product development. This is why we are going to make a comparison with a traditional Cascade methodology. Cascade makes a procedural and rigid evaluation, which sometimes does not allow the interaction between processes and techniques, because of its rigorous disposition, does not allow an adequate flow of information that allows to know in an integral way the needs of the client [20]. With everything mentioned above in Table V, the comparison of these two methodologies already mentioned was made, where the important characteristics of each one were named.

TABLE V. COMPARISON CASCADE - SCRUM

Traditional Methodology (Waterfall)	Agile Methodology(Scrum)
It has different stages	consists of periodic deliverables (Sprint)
Does not accept any kind of change	Is able to accept changes
Cost is determined during planning	Cost is determined during the project
The development team is flexible with limited creative capacity	The development team is flexible with unlimited creative capacity
Sequential	Overlay

VI. CONCLUSION AND FUTURE WORK

Finally, in this research, the whole prototyping of the interfaces of the web system that was developed to improve the commercial management, as well as to have new sales opportunities and to face the problems that the company is facing. And to do it now by means of the electronic commerce that is a window that the new technologies allow you to use. All this was carried out thanks to the Marvel tool that has interesting mechanisms and components that made the design ideas take shape as they are, and can be visualized in a realistic way. The methodology used for the good development of the web system was Scrum, which allowed us to carry out the project in a more orderly and efficient way at the time of its development. In my article, as future work, I recommend that the prototypes presented and designed be implemented and put into development. Where micro and small companies have the opportunity to undertake and have a new sales method for their business.

REFERENCES

- [1] J. F. T. Mesías, J. C. S. Giraldo, and B. B. Díaz, "Aceptación del e-commerce en Colombia: un estudio para la ciudad de Medellín," *Revista Facultad de Ciencias Económicas: Investigación y Reflexión*, vol. 19, no. 2, pp. 9–23, 2011.
- [2] G. A. Barrera, "Relación de capacitación con adopción de internet y e-commerce: Diferencias entre microemprendedores de Chile," *Información tecnológica*, vol. 28, no. 6, pp. 61–70, 2017.
- [3] K. C. Laudon, C. G. Traver et al., *E-commerce: business, technology, society*, 2016.
- [4] P. Barrientos Felipa, "Marketing+ internet= e-commerce: oportunidades y desafíos," *Revista Finanzas y Política Económica*, Vol. 9, no. 1 (ene.–jun. 2017); p. 45–56. <http://dx.doi.org/10.14718/revfinanzpoliticon.2017.9.1.3>, 2017.

- [5] Y. Huang, Y. Chai, Y. Liu, and J. Shen, "Architecture of next-generation e-commerce platform," *Tsinghua Science and Technology*, vol. 24, no. 1, pp. 18–29, 2019.
- [6] D. S. Islamiati, D. Agata, and A. R. Anom Besari, "Design and implementation of various payment system for product transaction in mobile application," in *2019 International Electronics Symposium (IES)*, 2019, pp. 287–292.
- [7] H. Chaparro Cuartas *et al.*, "Implementación de una plataforma e-commerce para la compañía promo electric."
- [8] V. L. Sanabria Díaz, L. A. Torres Ramírez, and L. M. López Posada, "Comercio electrónico y nivel de ventas en las mipymes del sector comercio, industria y servicios de ibagué," *Revista EAN*, no. 80, pp. 132–154, 2016.
- [9] D. E. SEPULVEDA ROBLES, D. SEPULVEDA JIMENEZ, F. PEREZ SOTO, E. FIGUEROA HERNANDEZ *et al.*, "Propuesta de modelo para adopción del comercio electrónico en empresas del sector agroindustrial en México," 2014.
- [10] S. Lin and X. Wenzheng, "E-commerce personalized recommendation system based on web mining technology design and implementation," in *2015 International Conference on Intelligent Transportation, Big Data and Smart City*, 2015, pp. 347–350.
- [11] J. Vogelzang, W. F. Admiraal, and J. H. van Driel, "Effects of scrum methodology on students' critical scientific literacy: the case of green chemistry," *Chemistry Education Research and Practice*, 2020.
- [12] J. P. I. Alexander Menzinsky, Gertrudis López, "Scrum master," *Scrum*, pp. 2–94, 2016.
- [13] A. Srivastava, S. Bhardwaj, and S. Saraswat, "Scrum model for agile methodology," in *2017 International Conference on Computing, Communication and Automation (ICCCA)*, 2017, pp. 864–869.
- [14] A. Jurado-Navas and R. Muñoz-Luna, "Scrum methodology in higher education: Innovation in teaching, learning and assessment," *International Journal of Higher Education*, vol. 6, no. 6, pp. 1–18, 2017.
- [15] J. C. A. Becerra and C. E. D. Vanegas, "Propuesta de un método para desarrollar sistemas de información geográfica a partir de la metodología de desarrollo ágil-scrum," *Cuaderno Activa*, vol. 10, pp. 29–41, 2018.
- [16] D. X. Sarango Yunga, "Desarrollo de plataforma web para la evaluación de software basado en la metodología scrum," B.S. thesis, Machala: Universidad Técnica de Machala, 2020.
- [17] A. Kwilinski, R. Volynets, I. Berdnik, M. Holovko, and P. Berzin, "E-commerce: Concept and legal regulation in modern economic conditions," *Journal of Legal, Ethical and Regulatory Issues*, vol. 22, pp. 1–6, 2019.
- [18] D. R. Garcia Cercado, "Factores que afectan la productividad del equipo scrum: Una revisión sistemática de la literatura," 2019.
- [19] A. Srivastava, S. Bhardwaj, and S. Saraswat, "Scrum model for agile methodology," pp. 864–869, 2017.
- [20] F. González González, S. L. Calero Castañeda *et al.*, "Comparación de las metodologías cascada y ágil para el aumento de la productividad en el desarrollo de software," Ph.D. dissertation, Universidad Santiago de Cali, 2019.

Heuristic Evaluation of Peruvian Government Web Portals, used within the State of Emergency

Platforms: Aprendo en casa and Covid19-Minsa

Flores Quispe Percy Santiago¹, Mamani Condori Kevin Alonso²
Paniura Huamani Jose Maykol³, Anampa Chura Diego David⁴
Escobedo Quispe Richart Smith⁵
Escuela Profesional de Ingeniería de Sistemas
Universidad Nacional de San Agustín
Arequipa, Perú

Abstract—The development of web platforms is very abundant at present, this event has developed exponentially due to the state of emergency. Therefore, there is a need to evaluate the quality of these platforms to ensure a good user experience, especially if these platforms are governmental. Currently, there are several platforms that have been developed by governments of different nations, which are related to the theme of covid-19; which should be evaluated from a heuristic perspective to detect usability problems that can occur when users interact with a product and identify ways to solve them. This article presents a heuristic evaluation of Peruvian government web portals, used within the state of emergency; for this purpose, a heuristic evaluation is carried out using a list of 15 heuristic principles, proposed by Toni Granollers, from two government platforms: Aprendo en casa and Covid19 Minsa. In this way, it was identified that the Peruvian platform Aprendo en casa has fewer usability problems compared to the Covid19 Minsa platform. Therefore, there is a need to renew or update the Covid19 Minsa platform using the results of the heuristic evaluation performed; on the other hand, although a heuristic evaluation of these Peruvian government platforms is being carried out, it is recommended to continue with a research that uses other usability evaluation methodologies for other platforms of daily use, such as the S/ 380 bonus platform, Bonus for independent or AFP withdrawal.

Keywords—*heuristic evaluation; usability; heuristic principles; government web portals; Covid-19*

I. INTRODUCTION

Given the world scenario of 2020 and the current situation that Peru is experiencing in the face of the Covid-19 pandemic, as well as the obvious need to develop web platforms that meet the new requirements that the state needs to address the obvious needs that have arisen because of what happened, such as being able to provide statistical information about the development and growth of the new disease throughout the national territory or being able to carry out distance learning for students of regular basic education in this situation [20], lead us to ask ourselves if these developed platforms comply with the standards of usability that all web applications should comply with, governing us and basing our evaluation on the principles of heuristic evaluation as proposed by Jakob Nielsen's [9].

Being the heuristic evaluation [9] a technique for a faster and less difficult analysis, it can be easily used by any user

more than anything else in these times where the increase of users in the network has been increasing massively, to the point that we all depend on different websites to exercise our responsibilities being the state the one that has implemented different websites for the needs of the population that cannot be exercised in person. It could be said that users are becoming more demanding and the needs are increasingly higher, which encourages to evaluate and project a website with an interesting, efficient and convenient format, so Kim demonstrated that there are two criteria to evaluate the interface being the usability and the user experience [18].

The paper to be presented is the production made at the end of the Human Computer Interaction course with motivation in a Human Computer Interaction event at the Catholic University of Santa Maria; which was the motivation to focus on an application. In this way, the proposed paper tries to demonstrate that the heuristic evaluation model, proposed by Toni Granollers [22], meets the basic standards so that any user without previous computational knowledge is able to evaluate web pages identifying general problems compared to other methodologies. For this, the sources in which the development of the paper is supported are reliable; for example: the paper by Toni Granollers, Usability Evaluation with Heuristics, Beyond Nielsen's List [22]; we also rely on quality videos such as the one made by Gonzales, Workshop: Heuristic Usability Evaluation[9], from the Catholic University of Santa Maria. Finally, the expected result is to demonstrate that the Peruvian platform Aprendo en casa has fewer usability problems compared to the Covid19 Minsa platform.

This paper under a methodology uses fourteen heuristics recommended by the literature to perform the evaluation of two important websites especially during the state of emergency for the Peruvian state, allowing to measure the quality of interaction by the interested population, discovering criteria to be considered in the improvement and above all is evidence that developers and designers should consider and not miss.

II. RELATED WORKS

Heuristic evaluation is proposed for the identification of usability problems in a web platform which are difficult to see with the naked eye. In the paper by Thewes, Herrmann and Kluge [1] they examine socio-technical systems where they

prove that the evaluators do not necessarily have to be experts to handle the heuristic test, this is reinforced in the experiment of the authors Paz, Villanueva and Pow [4] who evaluated the HotelClub.com web portal, divided between two novices and three experts, giving results with minimal differences and more specific details on the part of the experts.

On the other hand, Lam and Sajjanhar [3] emphasize the importance of knowing the basics of the topic covered in the web page, making the evaluation more effective. In the research of Botella, Alarcón and Pealver [5] propose a new approach to improve the results of heuristic evaluation done by novices, in addition to the fact that expert evaluators give simple solutions to a recurring problem which are usually not very good contributions. Yusoh and Matayong [6] make use of a public health web portal by surveying the public about usability and evaluated with Jakob Nielsen's 10 heuristic principles which discard 43 sub-factors and prioritize the main usability factors. The wide field of study of heuristic evaluation, can be addressed for web portals, where Borovina, Bošković, Dizdarević, Bulja and Salihbegović described a context of development of the web portal BH Telecom Mobile Services, this same integrates redesign proposals using such evaluation [2].

Likewise, the hotel industry has not received great importance in terms of usability. Yeung and Law present a heuristic evaluation study to calculate usability hazard indices of hotel websites in Hong Kong [7]. Agustinho de Melo and Boaventura-Netto propose a multicriteria evaluation scheme for heuristic algorithms of the classical Condorcet ranking technique. Five criteria and one function were used for natural number ranking. Each algorithm was used with its same structure, applying the same techniques [8]. Thus, the mention of these papers will allow us to have a broad vision to analyze and use new approaches to heuristic evaluation allowing us to make a more effective evaluation of the usability of governmental web portals.

III. THEORETICAL FRAME

A. Usability

The term usability has several connotations on the part of several authors; for example, from the perspective of Computer Engineering [18], usability refers to the level of usability of a given software product or technological tool; furthermore, Paz [18] maintains that as part of the process of interaction between the user and a computer product, the concept of usability is defined as an indispensable requirement to ensure user satisfaction and a pleasant experience in an environment where labor factors also affect.

On the other hand, usability, according to the ISO 9241-11 standard, is defined as "the degree to which a product can be used by specific users to achieve specific objectives with effectiveness, efficiency and satisfaction in a specific context of use" [16]. In this sense, the design of the usable interface is closely related to the terms of effectiveness, degree to which the users making use of the product manage to obtain precisely the desired results; efficiency, level of quality of the results achieved by the product in relation to the resources required for its execution, and satisfaction, degree of comfort that the product has on the part of the users after it has been used.

To measure the degree of usability, there are usability evaluation methods, which according to Fernández et al. [17] can be defined as "systematic procedures composed of a series of well-defined activities that allow the collection of data related to the interaction between the end user and the software product, with the purpose of determining how the specific properties of this system contribute to achieving specific user objectives.

It should be noted that there are different taxonomies to classify the usability evaluation methods; in this opportunity we describe the classification according to the type of participants that are required to perform the usability evaluation [18]: First, the Inspection Methods, which involve the participation of specialists in the area of HCI as the heuristic evaluation, the cognitive journey and the review of checklists; second, the Testing Methods, which involve the participation of representative users of the software product to be evaluated, as the tests with users, the pencil and paper test and the co-discovery.

B. Heuristic Evaluation

In this document, we will go deeper into a usability evaluation method: Heuristic evaluation, according to Sánchez [15] is an evaluation method that aims to measure the quality of an interface so that a group of users can test it in a specific context; therefore, it is carried out by expert juries that make use of inspections based on or guided by previously established principles called heuristics.

On the other hand, heuristic evaluation is a method developed by Jakob Nielsen and Rolf Molich in 1990 to evaluate the level of usability of software products to replace regular user testing [14]; it is important to note that over time, heuristic-based usability evaluation has proven to be an effective method, so there are many studies in the literature that report on its use, especially as part of the process of developing software products [18].

C. Heuristic Evaluation Method

There are different lists of principles that can be used for the realization of a heuristic evaluation; for example, [10] the 10 Nielsen heuristic principles, the 8 golden rules of Ben Schneiderman, the checklist of items of Deniese Pierotti, etc. In this opportunity we describe a list of 15 heuristic principles, proposed by Toni Granollers [11], director of the HCI GRIHO research group at the Escuela Politécnica Superior of the University of Lledia, who is also a member of the Association for Human-Computer Interaction (AIPO) and of the Collaborative Network to support teaching-learning processes in the area of Human-Computer Interaction at the Ibero-American level (HCI-collab), the first ten of which are by Nielsen [9]:

- 1) Visibility and system status: Appropriate information for the user
 - Does the application include a title page, section or visible site?
 - Does the user always know where he is?
 - Does the user always know what the system or application is doing?
 - Are the links clearly defined?
 - Can all actions be displayed directly? (No other actions required)

- 2) Connection between the system and the real world, use of metaphors and human objects: To approach the system with the language of the user but not of the programmer
 - Does the information appear in a logical order for the user?
 - Does the design of the icons correspond to everyday objects?
 - Does each icon do the action you expect?
 - Does the system use phrases and concepts familiar to the user?
 - 3) User control and freedom: The user to do and undo system actions.
 - Is there a link to return to the initial state or home page?
 - Are the “undo” and “redo” functions implemented?
 - Is it easy to return to a previous state of the application?
 - 4) Consistency and standards: Maintain a single style on the website and good structure that is attractive to the user
 - Do the link tags have the same names as their destinations?
 - Do the same actions always have the same results?
 - Do icons have the same meaning everywhere?
 - Is the information displayed consistently on all pages?
 - Are the link colors standard? If not, are they suitable for use?
 - Do the navigation elements follow the standards? (Buttons, checkbox, ...)
 - 5) Recognition instead of memory, learning and anticipation: The user can easily identify certain server action.
 - Is it easy to use the system for the first time?
 - Is it easy to locate information that has already been searched?
 - Can you use the system at all times without remembering previous screens?
 - Is all the content necessary for navigation or the task on the screen?
 - Is the information organized according to a familiar logic to the end?
 - 6) Flexibility and efficiency of use: Facilitate navigation through shortcuts
 - Are there keyboard shortcuts for common actions?
 - If so, is it clear how to use them?
 - Is it possible to easily perform an action that was done before?
 - Does the design adapt to changes in screen resolution?
 - Is the use of accelerators visible to the normal user?
 - 7) Helps users to recognize, diagnose and redo errors: Validate the error before performing an action.
 - Do you show a message before performing irreversible actions?
 - Are errors displayed in real time?
 - Is the error message easy to interpret?
 - Is any code also used to refer to the error?
 - 8) Error prevention: Communicate errors and propose a possible solution to users.
 - Does a confirmation message appear before the action is taken?
 - Is it clear what information should be entered in each box of a form?
 - Does the search engine tolerate typographical and spelling errors?
 - 9) Aesthetic and minimalist design: Highlighting the important:
 - Is a design without information redundancy used?
 - Is the information brief, concise and accurate?
 - Is every piece of information different from the rest and not confused?
 - Is the text well organized, with short sentences and quick interpretation?
 - 10) Help and documentation: The system offers relevant help that is easy to search.
 - Is there a “help” option?
 - If so, is it visible and easily accessible?
 - Is the help section aimed at solving problems?
 - Is there a FAQ section?
 - Is the help documentation clear, with examples?
- It also takes into consideration the principles of interaction design being the author Bruce Tognazzini who makes a proposal of 16 principles in which for this heuristic evaluation Granollers makes mention of 5 which will be a complement for a better evaluation [10]:
- 11) Save the status and protect the work: All information must be auto saved whenever the client wishes which will be stored in the server having the freedom to disconnect and be able to reconnect in another place.
 - Can users continue from a previous state (where they had been or from another device)?
 - Is “AutoSave” implemented?
 - Does the system have a good response to external failures? (Power failure, Internet not working, ...)
 - 12) Color and readability: High contrast text: ideally black on white. Readable font sizes.
 - Are the fonts properly sized?
 - Do the fonts use colors with enough contrast to the background?
 - Do the images or background patterns allow the content to be read?
 - Do you consider people with reduced vision?
 - 13) Autonomy Controlled freedom to the user: Being the users who are informed about the state of the system while the administrators manage their variables.
 - Do you keep the user informed of the status of the system?
 - Also, is the system status visible and updated?
 - Can the user make his own decisions? (Personalization)
 - 14) Default values: Easy detection of user defects and easy correction
 - Does the system or device offer the option to return to factory settings?
 - If so, does it clearly indicate the consequences of the action?
 - Is the term “default” used?
 - 15) Latency reduction: Elimination of load states
 - Is the execution of the heavy work transparent to the user?
 - While performing heavy tasks, is the remaining time or any animation shown?

To obtain an accurate answer and an appropriate score for the web pages we will analyze each question in each section of the heuristic evaluation, a score will be given with respect to the four options observed in Table I that the evaluator must mark and thus organize the data in a better way.

TABLE I. SCORING ACCORDING TO OPTION CHOSEN BY THE EVALUATOR.

Options	Score
Yes	1 point
Neither yes, nor no	0.5 points
No	0 points
Not applicable	—

IV. METHODOLOGY

A study [12] has shown that this technique produces results comparable to a laboratory test of the same application. While this technique potentially saves some travel and installation costs, it is still a time- and labor-intensive task, as well as processes, with observers involved full-time for each test and user session.

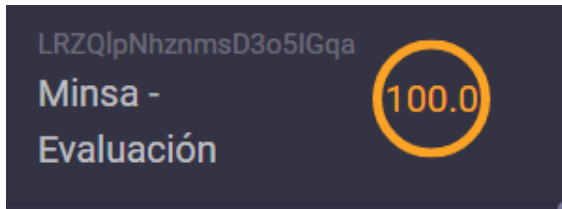


Fig. 1. Pie Chart of Real-time Survey Progress.

Likewise, there is a platform to adequately perform the usability evaluation. This is called Remote Testing Lab. In the same way, usability tests could be carried out. For example, Vividence Corporation [13] offers a type of remote usability test in which test users must download and use an instrumented browser that can capture user click streams, as well as screen shots, and transmit them to the host site for analysis.



Fig. 2. Adding Comment to Question.

One of the main features of the tool is the percentage of progress shown in the upper right hand side, which is in real time and you can check which sections have been advanced and in percentages, as shown in Fig. 1. Also, the comment option is very useful due to the ambiguity of some questions, which can clarify some answers by the user (Fig. 2).

The platform has a suitable interface for easy user understanding. Within this, the percentage of evaluation that is carried out in real time stands out, showing a small pie chart in the upper left part; in the same way, there is the internationalization, with three languages: Spanish, English

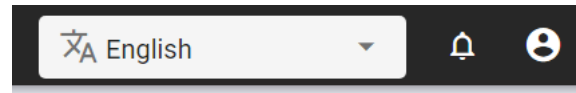


Fig. 3. Language, Notifications and Profile.

and Portuguese (Fig. 3); besides allowing to receive comments from the respondent in each question of each item. Also, a notification icon is shown to inform about some news from the person in charge; and finally, to register the answer, there is a pop-up in the lower right side with the options to save and send, which disappears once the survey is finished (Fig. 4).



Fig. 4. Save and Send Option.

Finally, the tool has striking transitions for the user, which is complemented by the ease of understanding of the platform. The colors, the font size, among other aspects help the permanent attention of the user.

V. GOVERNMENT PLATFORMS

The two case studies chosen for this article were selected from different websites that had purposes such as providing information about bonuses for self-employed workers, withdrawing AFP funds, applying for a work or transit pass, official statistics on infections according to the Minsa, infected areas in Peru, self-testing by the Covid-19 of both the Minsa and the medical school, access to virtual classrooms, and coronavirus results [19]. Among all these web pages with different purposes, we have selected and seen the importance of making a heuristic evaluation of two of them.

First of all, we have Aprendo en casa, a website created in this pandemic to continue with basic and regular education through virtual classes, the importance and the challenge that this website has is colossal according to Eduardo Leon, since the public school in its face-to-face mode has failed to teach children to read and write and to be able to carry out this education from a distance poses a great challenge [20], the same author of the commentary tells us that this website focuses all its offerings on the written text, which for the student represents a great barrier, apart from the fact that he also mentions that many of his workbooks do not respond to the logic of distance education, seen already one of the many problems that this page presents and the great challenge that it supposes we have seen convenient to take it as a case study for our heuristic evaluation, since to better fulfill its purpose

it will have to possess a good user interface and adequate for the people that it is directed as the children are.

On the other hand, we have the Minsa’s Covid-19 infection statistics website, which is of great importance in the current pandemic, since it fulfills the important function of informing the population of the progress of the disease in Peru in terms of those infected at the national and regional level, the number of tests performed, including rapid and molecular tests, the number of deaths from the disease, the mortality rate, hospitalizations, and the availability of ICU beds, among others [21]. In view of all the functions that this website should have and its importance, we have found it convenient to carry out a heuristic evaluation of the website, since the level of usability will determine, to a certain extent, how well a user can navigate to get information on this page.

VI. RESULTS

The evaluation of the Aprendo en Casa and Covid19-Minsa platforms has been carried out by the authors of this article; it is worth mentioning that for this purpose the platform described in the Methodology section is used, within the Theoretical framework. For this, the four evaluators, before starting the evaluation of the platforms had an interaction with these platforms of a duration of 10 minutes.

Fig. 5 and Fig. 7, show the final scores of all evaluators for each principle (this is shown in the Answers section of Remote Testing Lab. In this table, the important values are those in the second column, where the usability percentages are stored. Analyzing these results, it can be seen that, in general, the Aprendo en Casa web platform has a good level of usability.

Evaluator	Usability Percentage	Applicable Question	No Applicable Question
Ev1	76.0%	48	12
Ev2	69.2%	52	8
Ev3	64.6%	41	19
Ev4	41.7%	60	0

Fig. 5. Final Scores of the I Learn at Home Platform Evaluation

On the other hand, Fig. 6 summarizes all the evaluations, showing the average of all the evaluations, which is 62.9%, which means a slightly good level of usability; it is worth noting that when analyzing each principle, it can be seen that the principles “11 - Save the state and protect the work”, “14 - Default values” and “15 - Reduction of latency” show the lowest values; then, it is concluded that the aspects already mentioned should be improved.



Fig. 6. Average Final Scores of the I Learn at Home Platform Evaluation.

On the other hand, in the Covid19-Minsa platform we can see as shown in Fig. 8 and Fig. 10 the final scores of the evaluators for each principle where analyzing the results we can say that the COVID19-Minsa platform has a level of usability above 50%.

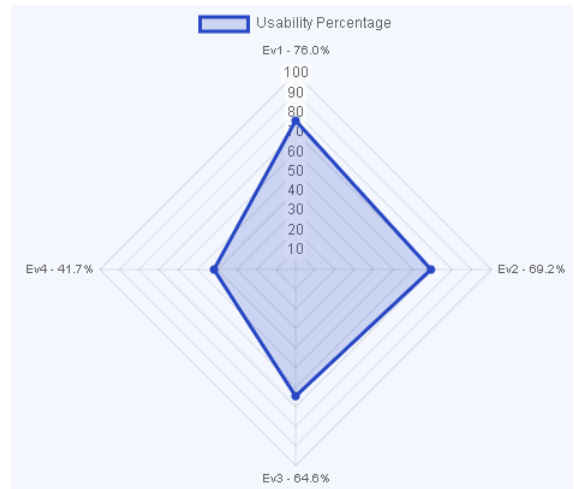


Fig. 7. Final Score Chart for the I Learn at Home Platform Evaluation.

Evaluator	Usability Percentage	Applicable Question	No Applicable Question
Ev1	58.3%	42	18
Ev2	67.9%	56	4
Ev3	43.2%	44	16
Ev4	51.8%	55	5

Fig. 8. Final Scores of the COVID19-Minsa Platform Evaluation.

Fig. 9 summarizes all the evaluations, showing the average of all the evaluations, which is 55.3 %, which means a level of usability neither so good nor so bad; it is worth noting that when analyzing each principle, it can be seen that the principles “11 - Save the state and protect the work”, “13 - Autonomy” and “14 - Default values” show the lowest values; then, it is concluded that the aspects already mentioned should be improved.

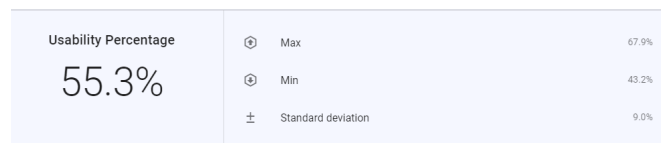


Fig. 9. Average Final Scores of the COVID19-Minsa Platform Evaluation.

VII. CONCLUSIONS

Using the proposed methodology, it was identified that the Peruvian platform Aprendo en casa presents less of a usability problem compared to the COVID-19-Minsa platform. Therefore, it is necessary to renew or update the COVID-19-Minsa platform using the results of the heuristic evaluation carried out, identifying the critical points or making a report on the problems presented by the page and send it directly to the administrators of the same.

Furthermore, it is demonstrated that the heuristic evaluation model, proposed by Toni Granollers, meets the basic standards so that any user without previous computer knowledge is able to evaluate web pages by identifying general problems in comparison with other methodologies.

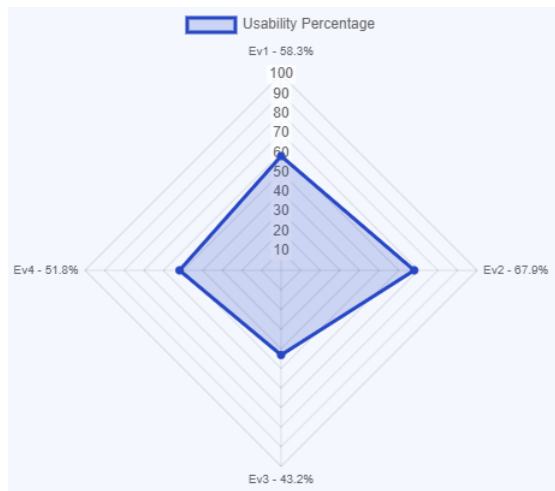


Fig. 10. COVID19-Minsa Platform Evaluation Final Score Chart.

On the other hand, given the existence of several methodologies for the heuristic evaluation of a web page interface, then it is proposed as a possible continuation of the research approach the implementation of other types of methodologies. On the other hand, during the development of the research, although a heuristic evaluation of the Peruvian government platforms, Aprendo en Casa and Covid19-Minsa, is carried out, it is recommended to continue with a research that evaluates other platforms that are used continuously, such as the S/ 380 bonus platform, Bonus for independent or AFP funds withdrawal, which could be the object of another research or be acquired later as an option for other researchers who wish to evaluate the mentioned platforms.

REFERENCES

[1] F. Thewes, T. Herrmann, and A. Kluge, "Validating a Heuristic Evaluation Method An Application Tes", In Proceedings of Mensch und Computer 2019, pp. 593-597, doi: 10.1145/3340764.3344465

[2] N. Borovina, D. Bošković, J. Dizdarević, K. Bulja and A. Salihbegović, "Heuristic based evaluation of mobile services web portal usability", 2014 22nd Telecommunications Forum Telfor (TELFOR), pp. 1150-1153, doi: 10.1109 / TELFOR.2014.7034611

[3] D. Lam and A. Sajjanhar, "Heuristic Evaluations of Cultural Heritage Websites," 2018 Digital Image Computing: Techniques and Applications (DICTA), Canberra, Australia, 2018, pp. 1-6, doi: 10.1109/DICTA.2018.8615847.

[4] F. Paz, F. A. Paz, D. Villanueva and J. A. Pow-Sang, "Heuristic Evaluation as a Complement to Usability Testing: A Case Study in Web Domain," 2015 12th International Conference on Information Technology - New Generations, Las Vegas, NV, 2015, pp. 546-551, doi: 10.1109/ITNG.2015.92

[5] F. Botella, E. Alarcon, and A. Palver, "A new proposal for improving heuristic evaluation reports performed by novice evaluators," ACM Int. Conf. Proceeding Ser., pp. 72-75, 2013, doi: 10.1145/2535597.2535601

[6] S. Yusoh and S. Matayong, "Heuristic evaluation of online satisfaction survey system for public healthcare service: Applying analytical hierarchical process," Proc. - 2017 2nd Int. Conf. Inf. Technol. Inf. Syst. Electr. Eng. ICITISEE 2017, vol. 2018-January, pp. 462-467, 2018, doi: 10.1109/ICITISEE.2017.8285551

[7] T. Au Yeung, R. Law, "Extending the modified heuristic usability evaluation technique to chain and independent hotel websites," 2014 Associate Professor of Information Technology at the School of Hotel & Tourism Management, USA, 2016, pp. 1-14, doi: 10.1016/j.ijhm.2003.03.001

[8] V. Agostinho de Melo, P. O. Boaventura-Netto, "METAHEURISTICS EVALUATION: A PROPOSAL FOR A MULTICRITERIA METHODOLOGY," 2015 ACOPPE/Programa de Engenharia de Produção, Universidade Federal do Rio de Janeiro, RJ, Brasil, 2017, pp. 1-5, doi: 10.1590/0101-7438.2015.035.03.0539

[9] T. Granollers. M. Gonzales. (2020, Sep. 20) Taller: Evaluación de usabilidad heurística Available [Video]: <https://www.youtube.com/watch?v=YAwrcpVaw6I&t=15s>

[10] Galinus. (2012, Feb. 2) Principios de diseño de interacción de Bruce Tognazzini [Online]. Available: <https://usabilidadcss.wordpress.com/2012/02/02/principios-diseno-interaccion-bruce-tognazzini/>

[11] T. Granollers (2018, abr. 20) Evaluacion heuristica, «beyond Nielsen heuristics» [Online]: <https://mpiua.invid.udl.cat/evaluacion-heuristica-una-nueva-propuesta/>

[12] Hartson, H. R., Castillo, J. C., Kelso, J., and Neale, W. C. Remote evaluation: The network as an extension of the laboratory. Proceedings of CHI'96 Conference, pp. 228-235.

[13] Vividence Corporation, 1850 Gateway Drive, San Mateo, CA. <http://www.vividence.com>.

[14] Nielsen, J. and Molich, R., 1990. Heuristic evaluation of user interfaces. Presented at the Proceedings of the SIGCHI Conference on Human Factors in Computing Systems, Seattle, Washington, USA.

[15] Sánchez Alvarez, J., Zapata Jaramillo, C. and Jiménez Builes, J., 2017. Evaluación heurística de la usabilidad de software para facilitar el uso del computador a personas en situación de discapacidad motriz. Revista EIA, [online] 14(27), pp.63-72. Available at: http://www.scielo.org.co/scielo.php?script=sci_arttext&pid=S1794-12372017000100006&lang=es; [Accessed 20 November 2020].

[16] Ergonomic requirements for office work with visual display terminals (VDTs). Geneva: ISO, 1998, p. 44.

[17] Fernandez, A., Insfran, E. and Abrahão, S., 2011. Usability evaluation methods for the web: A systematic mapping study, Information and Software Technology, vol. 53, pp. 789-817.

[18] Paz Espinoza, F., 2017. Método para la evaluación de usabilidad de sitios web transaccionales basado en el proceso de inspección heurística. Doctorado. Pontificia Universidad Católica del Perú.

[19] D. Ayma, "Coronavirus en Perú: COVID-19: Estas son las 15 plataformas web que debes conocer para afrontar el estado de emergencia," RPP, 24-Apr-2020. [Online]. Available: <https://rpp.pe/politica/gobierno/coronavirus-en-peru-covid-19-estas-son-las-15-plataformas-web-que-debes-conocer-para-afrontar-el-estado-de-emergencia-noticia-1260604?ref=rpp>. [Accessed: 22-Nov-2020].

[20] E. L. Zamora, E. León, and Z. — Educación, "Evaluación de sistema, alfabetización inicial y 'Aprendo en casa,'" Educacionperu.Org, pp. 1-9, 1972, [Online]. Available: [www.educacionperu.orgdialogoinformadosobrepolicaspublicashttps://www.educacionperu.org](http://www.educacionperu.org/dialogoinformadosobrepolicaspublicashttps://www.educacionperu.org).

[21] Covid19.minsa.gob.pe. 2020. Covid 19 En El Perú - Ministerio Del Salud. [online] Available at: https://covid19.minsa.gob.pe/sala_situacional.aspx; [Accessed 22 November 2020].

[22] T. Granollers. M. Gonzales (2018) Usability Evaluation with Heuristics, Beyond Nielsen's List [Artículo]: https://www.thinkmind.org/index.php?view=article&articleid=achi_2018_4_10_20055

k -Integer-Merging on Shared Memory

Ahmed Y Khedr¹, Ibrahim M Alseadoon²

College of Computer Science and Engineering, University of Ha'il, Ha'il, KSA¹
Systems and Computers Department, Faculty of Engineering, Al-Azhar University, Cairo, Egypt¹
College of Computer Science and Engineering, University of Ha'il, Ha'il, KSA²

Abstract— The k integer-merging problem is to merge the k sorted arrays into a new sorted array that contains all elements of $A_i, \forall i$. We propose a new parallel algorithm based on exclusive read exclusive write shared memory. The algorithm runs in $O(\log n)$ time using $n/\log n$ processors. The algorithm performs linear work, $O(n)$, and has optimal cost. Furthermore, the total work done by the algorithm is less than the best-known previous parallel algorithms for k merging problem.

Keywords—Merging; parallel algorithm; shared memory; optimality; linear work

I. INTRODUCTION

The problem of merging has many applications in computer science and used as a subroutine for solving many problems such as sorting [1], database management systems [2], information retrieval [3], memory management, scheduling [1], and reconstruction of the tree [4][5]. Most of these applications based their solutions on the merging problem. For example, the optimal algorithm for sorting an array A of size n can be done as follows. (1) Partition the array A into two subarrays of equal size, A_1 and A_2 . (2) Sort recursively for A_1 . (3) Sort recursively for A_2 . (4) Merge A_1 and A_2 .

The merging problem is defined as follows [10]. Given two sorted arrays $A = (a_0, a_1, \dots, a_{n-1})$ and $B = (b_0, b_1, \dots, b_{m-1})$. The merging of two sorted arrays is a new sorted array $C = (c_0, c_1, \dots, c_{n+m-1})$ such that:

- 1) $c_i \in A$ or $c_i \in B, \forall 0 \leq i \leq n + m - 1$; and
- 2) a_i and b_j appear exactly once in $C, \forall 0 \leq i < n$ and $0 \leq j < m$.

On the other side, some applications of computer science such as external sorting and information retrieval systems require to merge k sorted arrays of different lengths. In such a case, the problem is known as a k merging problem. For example, the external sorting (sorting a file of large data) problem can be done by the following steps [1]: (1) Dividing the file into small blocks to fit into main memory. (2) Applying the fast sorting algorithm on each block. (3) Merging the sorted blocks into sorted bigger blocks, until the file is sorted.

The merging problem of k sorted arrays is defined as follows.

Given k sorted arrays of lengths n_i 's, $A_i = (a_{i0}, a_{i1}, \dots, a_{in_i-1})$, such that $\sum_{i=0}^{k-1} n_i = n, 0 \leq i < k, 0 \leq j < n_i$, and $2 \leq k \leq n$. The merging of k sorted arrays is a new sorted array $C = (c_0, c_1, \dots, c_{n-1})$ such that:

- 1) c_j belongs to one of $A_i, \forall 0 \leq j < n$; and
- 2) a_{ij} appear exactly once in $C, \forall 0 \leq i < k$ and $\forall 0 \leq j < n_i$.

In sequential computation, the problem of merging two arrays of sorted elements is solved in linear time, $O(n)$, where $n \geq m$ [1][7], while the problem of k merging required $\Omega(n \log k)$, where $2 \leq k \leq n$ [17].

In parallel computation, different algorithms solve the problem of computation based on different strategies and parallel computational models. The two main types of parallel models are shared memory and interconnection networks. Our paper focuses only on the type of shared memory that is the Parallel Random Access Machine, PRAM. PRAM consists of p identical processors that operate p synchronously and communicate through large shared memory. There are three main models for PRAM based on memory access conflicts in shared memory. (1) Allowing read or write operations to memory location that is called Exclusive Read Exclusive Write (EREW). (2) Allowing only read operations to a memory location that is called Concurrent Read Exclusive Write (CREW). (3) Allowing read or write operations to a memory location that is called Concurrent Read Concurrent Write (CRCW).

In case of merging two sorted arrays [9] [10] [11][12] [13] [14] [15], the optimal parallel algorithm uses $p \leq n/\log n$ processors to run the algorithm in $O(n/p)$ time. The algorithm is based on EREW PRAM [12]. In case of CREW, Kruskal [13] shows that the merging problem can be solved in $O(\log \log n)$ time using $O(n)$ work.

In case the elements of the two arrays are taken from integer domain $[1, m]$, then the problem of merging is called integer merging [6][16][17][18][19]. The problem of integer merging needs further investigation. In case of EREW PRAM, Hagerup and Kutyloushi [19] presented $O(\log \log n + \log \min\{n, m\})$ algorithm with total space $O(n)$, where $m =$

$O(n)$. The total number of operations done by the algorithm is $O(n)$. Additionally, Bahig [16][17] reduced running time to constant, by considering some properties for the elements of the input. These properties are: (1) each element has a constant number of repetitions and (2) the difference between two successive elements is bounded by a constant. In case of CREW PRAM, Berkman and Vishkin in [6] proposed an algorithm that uses $n/\log \log \log m$ processors and has running time $O(\log \log \log m)$, when $m = n^k$. Also; they have proposed $O(\alpha(n))$ algorithm by using $n/\alpha(n)$ processors, where $\alpha(n)$ is the inverse of Ackermann's function and $m=n$. Furthermore the author in [18] proposed a constant-time deterministic algorithm, $O(1)$, for merging on CREW. The proposed algorithm is optimal in case of the values of input elements are less than or equal to the size of the inputs and the number of processors is equal to size of the inputs.

In case of k merging problem, PRAM is the main used algorithm. In [19], the algorithm is based on repeated pairwise merging of k sorted arrays. The algorithm is not working optimally and it is running in $O(\log n \times \log k)$ time. In [20], the author proposed an algorithm based on CREW PRAM. The algorithm has $O(\log n)$ parallel time using $(n \log k)/\log n$ processors with total work $O(n \log k)$. The algorithm based its solution on pipelining strategy and optimal work. In [8], the authors proposed two optimal parallel algorithms on PRAM with work $O(n \log k)$. Previous two algorithms are based on sampling scheme. The first algorithm runs in $\Omega(\log n)$ under EREW, while the second algorithm runs in $\Omega(\log \log n + \log k)$ under CREW. Recently, the authors in [24] proposed a lazy-merge algorithm, have running time equal to $O(k \log(n/k) + \text{merge}(n/p))$, where k and $\text{merge}(n/p)$ are the number of segments and the time needed to merge n/p elements respectively by the used in-place merging algorithm. Also, the authors in [21] presented two parallel algorithms for k integer merging, when no repetition occurs in the elements. The running time for both algorithms are $O(\log n)$ and $O(1)$ under EREW and CREW PRAM respectively.

The paper studies the k integer merging problem on PRAM and shows that the k integer merging problem can be solved in total work $O(n)$, even though the elements number of repetitions is extreme. The proposed algorithm uses $n/\log n$ processors of type EREW PRAM to run the algorithm in time $O(\log n)$.

The paper is organized as follows: an introduction and five sections. In Section 2, we give foundations and subroutines that is needed for proposed algorithm. Proposed algorithm for k integer merging is explained in Section 3. In Section 4, we calculate the complexity analysis of the proposed algorithm. In Section 5, we show how the proposed algorithm works by tracing the algorithm on an example. Finally, in Section 6, we show the conclusion of our work.

II. PRELIMINARIES

In this section, we give the fundamental definitions and subroutines related to k integer merging problem.

Definition 1 [10][22]: Given a problem Q of size n . The cost of the parallel algorithm for Q is equal to the product of the number of processor used and the running time for the parallel algorithm.

Definition 2 [10][22]: Given a problem Q of size n . The cost of parallel algorithm for Q is optimal if it matches with the time complexity of the best-known sequential algorithm for Q .

Definition 3 [8][10][22]: The work of a parallel algorithm is the total number of operations that the processors perform.

Definition 4 [9][10]: The prefix sums of the array $A = (a_0, a_1, \dots, a_{n-1})$ is an array $S = (s_0, s_1, \dots, s_{n-1})$, where $s_i = a_0 \oplus a_1 \oplus \dots \oplus a_i$, and \oplus is a binary operator, $\forall 0 \leq i < n$.

Proposition 1 [23]: An EREW PRAM algorithm for computing the prefix sums of an array of n elements runs in $O(n/p)$ time using p , $p \leq n/\log n$.

The technique used to solve the prefix sum is called binary tree strategy and it can be used to solve many related problems [9][23].

Proposition 2 [1][9][10]: Given an array A of n integers. The integer sorting algorithm runs in $O(n)$ sequential time and $O(\log n)$ using $n/\log n$ time under EREW PRAM.

III. NEW PARALLEL ALGORITHM

In this section, we show that the k integer merging problem on exclusive read exclusive write shared memory model can be solved in total work $O(n)$ instead of $O(n \log k)$, which is the total work for the best-known algorithm for k merging on the same shared memory model. Without loss of generality, assume that the elements of the k sorted arrays, a_{i_j} , are taken from the integer domain $[0, n-1]$, $\forall 0 \leq i < k, 0 \leq j < n_i, 2 \leq k \leq n$, and $n = \sum_{i=0}^{k-1} n_i$. The elements of the k sorted arrays are uniformly distributed over the integer domain. We also assume that the number of processors used to design the parallel algorithm is $n/\log n$.

The main idea behind the proposed algorithm is how to partition the k sorted arrays into $n/\log n$ independent lists. Then, the proposed algorithm assigns each list to a processor to merge it sequentially. The algorithm consists of the following stages.

A. Stage 1: Partitioning

The partitioning stage is the first stage to merge k sorted arrays of integer elements. The goal of this stage is to divide the elements of the k sorted arrays into $n/\log n$ lists. The lists have the following properties.

- P1: The lists are independent which means that the elements of the list number i are different from the elements of the list number j , $\forall i \neq j$.
- P2: The lists are relatively ordered which means that the elements of the list number i is less than the elements of the list number j , $\forall i < j$.
- P3: A small integer range called bounded range, BR., bound the difference between the elements in a list.

To verify the three properties of the $n/\log n$ lists, we define the value of BR by the following equation:

$$BR = \begin{cases} \log n & \text{if } n/\log n \text{ is perfect integer} \\ \log n + 1 & \text{otherwise} \end{cases}$$

To construct the independent lists, we will use two phases to partition the k sorted arrays. These two phases are called *local* and *global* partitioning.

B. Local Partitioning Phase

The main objective of the local partitioning phase is to partition each sorted array A_i into many subarrays based on the values of the elements of A_i . The elements of the i th subarray belong to the range $[(i-1)BR, iBR-1]$, $\forall 1 \leq i \leq n/\log n$.

The input of local phase is k sorted arrays A_0, A_1, \dots, A_{k-1} of lengths n_0, n_1, \dots, n_{k-1} , respectively. By the end of the local partitioning phase, we construct a list, AL_i , of l_i elements for each sorted array A_i , $\forall 0 \leq i < k$. The list contains the boundary indices for each partition in the sorted array A_i . Each element in the list AL_i , $AL_i[j]$, consists of four fields, aNo , pNo , $start$ and end . The component aNo represents the array number, while the component pNo represents the partition number. The fields $start$ and end represent start and end indices for the partition number pNo in the sorted array A_i , respectively.

To construct the elements of AL_i , we have two cases. The first case is when the size of each sorted array is approximately equal to BR . The second case is when the sizes of the sorted arrays are different.

In the case, the size of each sorted array A_i is approximately equal to BR , we do Subroutine 1 to construct the local partition. In the subroutine, we can compute the component of each element for the list AL_i by the following steps.

Initially, the number of elements in the list AL_i is equal to 0, and the first element in the array A_i , a_{i0} , determines the first partition belong to the list AL_i , see lines 1-2 in Subroutine 1.

The first three components of $AL_i[0]$ are as follows:

$$AA_i[\lambda_i] \cdot \alpha No = i$$

$$AA_i[\lambda_i] \cdot \pi No = \alpha_0 \Delta i \varpi BP$$

$$AA_i[\lambda_i] \cdot \sigma \tau \alpha \rho \tau = 0$$

The partition number, pNo , is determined by using the Div operator to return the quotient of division. The fourth component will be determined later when the algorithm determines the start of a new partition. Then, the algorithm scans the elements of the array A_i from the second to the last elements to determine the end of the current partition and the

start of a new partition (see line 3 in Subroutine 1). The end and the start of the current and new partitions, respectively, can be determined by testing if the quotients for the two successive elements, $a_{i,j-1}$, and $a_{i,j}$, on BR are different. When, the result of comparison is different, then, the partition number, pNo , is equal to $a_{i,j} \text{ Div } BR$. In such case, the element $a_{i,j}$ represents the first element of a new partition and the index j represents the start index of current partition. On the other side, the element $a_{i,j-1}$ represents the last element of the current partition and the index $j-1$ represents the last index of the current partition.

In case, the sizes of the k sorted arrays are different; we can compute $AL_i \forall i$, using two steps. The first step include that, we take each array of size greater than or equal to BR and do the following:

- 1) Determine the number of processors required for the array A_i which is equal to $np_i = \lfloor n_i/BR \rfloor$.
- 2) Each processor, p_j , will do the same process as in Subroutine 1 on the i th partition of AL_i , $\forall 0 \leq j < np_i$.
- 3) Combine all the sublists, AL_{ij} , to the list AL_i by using the binary tree paradigm.

After finishing from all arrays of sizes greater than or equal to BR , we execute the second step. The second step includes that, we assign one processor to each of the remainder arrays and do the same process as in Subroutine 1.

Subroutine 1:

Each processor do the following:

1. $l_i=0$ // number of elements in AL_i
 2. $AL_i[l_i]=(i, a_{i0} \text{ Div } BR, 0,)$
 3. for $j=1$ to n_i-1 do
 4. if $a_{i,j} \text{ Div } BR \neq a_{i,j-1} \text{ Div } BR$ then
 5. $AL_i[l_i]=(, , j-1)$
 6. $l_i=l_i+1$
 7. $AL_i[l_i]=(i, a_{i,j} \text{ Div } BR, j,)$
 8. end if
 9. end for
 10. $AL_i[l_i]=(, , n_i-1)$
-

C. Global Partitioning Phase

The main objective of the global partitioning phase is to partition the k sorted arrays into $n/\log n$ lists. Each list satisfies the three previous properties (mentioned in Stage1).

The input of global phase is a collection of k lists $AL_0, AL_1, \dots, AL_{k-1}$, of lengths l_0, l_1, \dots, l_{k-1} , respectively. By the end of this phase, we have an array, AP , of $n/\log n$ elements. The element $AP[i]$ consists of three fields. The first two fields, $start$ and end , represent the start and the end indices for the elements of the k sorted arrays that belong to the partition number i . The third field, no , represents the number of elements in the partition i , for all k sorted arrays. We can construct the array AP as follows:

- 1) Apply the parallel integer sort algorithm [24] on the elements of k lists, $AL = \cup_{i=0}^{k-1} AL_i$, according to the second

component of AL_i , pNo , using $n/\log n$ processors. If there are two elements in AL having the same value of the second component, then the elements are ordered according to the first component. The output of the first step is an array AL of length $l = \sum_{i=0}^{k-1} l_i \leq n$.

2) Divide AL into $n/\log n$ partitions of approximately equal size, $(l * \log n)/n$.

3) Initially, compute the start and the end of the first and the last partitions, respectively, as follows:

$$AP[AL[0] \cdot pNo] \cdot start = 0$$

$$AP[AL[l-1] \cdot pNo] \cdot end = l - 1$$

4) Determine the start and the end of each list that satisfies our proposed three properties, by applying Subroutine 2 on each partition.

5) Each processor, p_i , determines the third component of the partition, $AP[i]$, by scanning the array AP from $AL[i] \cdot start$ to $AL[i] \cdot end$ and calculates the total number of elements using the following formula:

$$AP[i] \cdot no = \sum_{j=AP[i] \cdot start}^{AP[i] \cdot end} AL[j] \cdot end - AL[j] \cdot start + 1$$

Subroutine 2

Each processor p_i do the following test on its partition as follows: $0 \leq i < p$ and $i[l/p] \leq j < (i+1)[l/p]$, except $i=0$ and $j=0$.

1. if $AL[j] \cdot pNo \neq AL[j-1] \cdot pNo$ then
2. $AP[AL[j] \cdot pNo] \cdot start = j$
3. $AP[AL[j-1] \cdot pNo] \cdot end = j - 1$

Note that in case $i=p-1$, the value of j is less than n .

D. Stage 2: Merging

The main objective of the merging stage is to merge elements of each partition. In other words, the goal is to merge the sorted subarrays that belong to the i th partition, $AP[i]$.

To merge sorted subarrays that belong to the i th partition, we have two cases based on the number of elements in each partition. In the first case, the size of each partition is approximately equal to BR , while in the second case the size of each partition is different.

In the first case, we do the process of merging by using Subroutine 3, which uses the idea of counting sorting algorithm [25]. To verify our goal, we use an array CA_i of length BR to merge the subarrays that belong to the partition number i , $\forall 0 \leq i < n/\log n$. Each element in this array consists of two fields. The first component, val , represents the value of the element, while the second component, $count$, represents the number of repetitions of the element val . The first step of Subroutine 3 is to initialize the two fields of the array CA_i with $i \log n + j$ and 0, respectively as in lines 1-3 in Subroutine 3. In the second step we compute the number of repetitions for each element by traversing the elements of the partition $AP[i]$

in lines 4-7 in Subroutine 3. In the third step, we reallocate the elements of the auxiliary array CA_i to the array C_i .

In case that the size of each partition is different, we can construct CA_i by the same method that is described in local partitioning step.

Subroutine 3

Processor p_i do the following

1. for $j=0$ to $BR-1$ do
2. $CA_i[j] \cdot val = i \log n + j$
3. $CA_i[j] \cdot count = 0$
4. for $j = AP[i] \cdot start$ to $AP[i] \cdot end$ do
5. for $x = AL[j] \cdot start$ to $AL[j] \cdot end$ do
6. $y = AL[j] \cdot aNo$
7. $CA_i[A_y[x] \bmod \log n] \cdot count =$
 $CA_i[A_y[x] \bmod \log n] \cdot count + 1$
8. $x=0$
9. for $j=0$ to $BR-1$ do
10. while $CA_i[j] \cdot count \geq 1$ do
11. $C_i[x] = CA_i[j] \cdot val$
12. $CA_i[j] \cdot count = CA_i[j] \cdot count - 1$
13. $x = x + 1$

IV. COMPLEXITY ANALYSIS

In this section, we analyze the proposed parallel algorithm for k integer merging problem according to the following criteria: running time, total number of work, optimality, and storage.

To compute the running time of the parallel proposed algorithm, the algorithm consists of three main stages: local partitioning, global partitioning, and merging.

The running time for the local partitioning stage can be computed as follows. In case that the size of each A_i is approximately equal to BR , each processor p_i will execute a sequential loop on an array of length $O(BR)$ approximately.

Therefore, the running time of this step is $O(BR)=O(\log n)$. In case of the size of A_i is different, the running time can be computed as follows. Determining the number of processors that is required for A_i equal to constant time. The running time for step 2, execution of Subroutine 1, and step 3, combine all the sublists, are $O(BR)$ and $O(\log np_i)$, respectively. The overall time for the local partitioning phase is $O(BR + np_i) = O(\log n)$.

The running time for the global partitioning stage can be computed as follows. The running time for applying the parallel integer sort algorithm on AL is bounded by $O(\log n)$, because the maximum length of the list AL is n . The running time for the substep 2.1 is constant. The running time for the substep 2.2 is $O(\log n)$, because $\frac{l * \log n}{n} \leq \log n$. The running time for the substep 2.3 is $O(\log(n/\log n))$. Therefore, the overall running time for global partitioning is $O(\log n)$.

The running time for the merging phase can be computed as follows. In case of the size of each $AP[i]$ is approximately

equal to BR, the running time for Step 3.1 and 3.3 in Subroutine 3, are $O(BR)$. The running time for Step 3.2 in Subroutine 3 depends on the size of the partition, which is equal to $O(BR)$. So, the overall time for Subroutine 3 is $O(BR)$. In case the size of each partition is different, then, the running time can be computed by a similar way which is equal to $O(\log n)$. The overall running time of the algorithm is $O(\log n)$.

It can be seen from previous calculation that the total number of work done by each processor p_i is $O(\log n), \forall 0 \leq i < n/\log n$. Hence, the algorithm has a total work of $O(n)$.

Therefore, the proposed algorithm has optimal work and cost. Also, the storage required by the proposed algorithm is $O(n)$.

Finally, it is clear that no step in the algorithm requires concurrent read or write. So, proposed algorithm based its work on exclusive read exclusive write shared memory.

V. EXAMPLE

Assume that we have six sorted arrays of total lengths equal to 32 as in Fig. 1.

It is clear that $k=6, n=32, n_0=5, n_1=11, n_2=6, n_3=1, n_4=7,$ and $n_5=2$. Therefore, the number of processors required is $p = \lceil n/\log_2 n \rceil = 6$ and $BR=5+1=6$.

Now, we apply the first stage (local partitioning) on the six sorted arrays as follows. For the sorted array A_0 , the details of constructing the list AL_0 are as follows. Initially, $l_0=0$ and $AL_0[0]=(0,0,0,)$ because $i=0$ and $2 \text{ Div } 6 = 0$. For $j=1$, no updating for AL_0 because $5 \text{ Div } 6 = 2 \text{ Div } 6$. For the next iteration, $j=2, AL_0$ will be updated as $AL_0[0]=(0,0,0,1), l_0=1$ and $AL_0[1]=(0,2,2,)$ because $13 \text{ Div } 6 \neq 5 \text{ Div } 6$. For next iteration, $j=3$, no updating for AL_0 because $13 \text{ Div } 6 = 13 \text{ Div } 6$. For last value of $j=3$, the updating values of AL_0 are as follows. $AL_0[1]=(0,2,2,3), l_0=2$ and $AL_0[2]=(0,3,4,)$ because $23 \text{ Div } 6 \neq 13 \text{ Div } 6$. Finally, the last component of the final element in AL_0 become $AL_0[2]=(0,3,4,4)$. Hence, the elements of AL_0 are $(0,0,0,1), (0,2,2,3)$, and $(0,3,4,4)$. The results of applying the first stage on all sorted input arrays are as in Fig. 2.

Next, the algorithm starts to execute the global partitioning stage by sorting the elements of all lists, $AL_0, AL_1, AL_2, AL_3, AL_4,$ and AL_5 to obtain a sorted list AL of $l=17$ elements as in Fig. 3.

Initially, the processor p_0 determines the start and the end of the first and last partitions, respectively, as follows:

$$AP[0] \cdot start = 0$$

$$AP[16] \cdot end = 16$$

After that, each processor assigned to three elements, except the last processor has two elements, to determine the first two components, *start* and *end* in the array *AP*. For more details, the first three elements, $(0,0,0,1), (1,0,0,1)$ and $(4,0,0,1)$, are assigned to the processor p_0 . The second three elements, $(1,1,2,4), (2,1,0,1)$, and $(4,1,2,3)$, are assigned to the processor p_1 , while the last two elements, $(5,4,1,1)$ and $(1,5,10,10)$, are assigned to the processor p_5 .

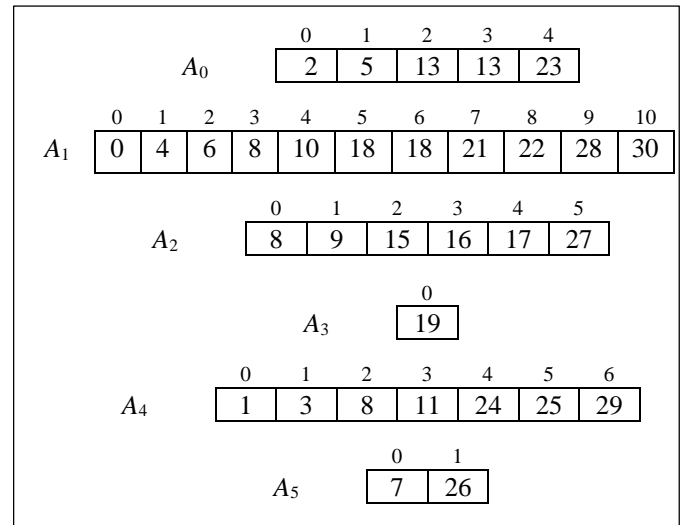


Fig. 1. Input Data.

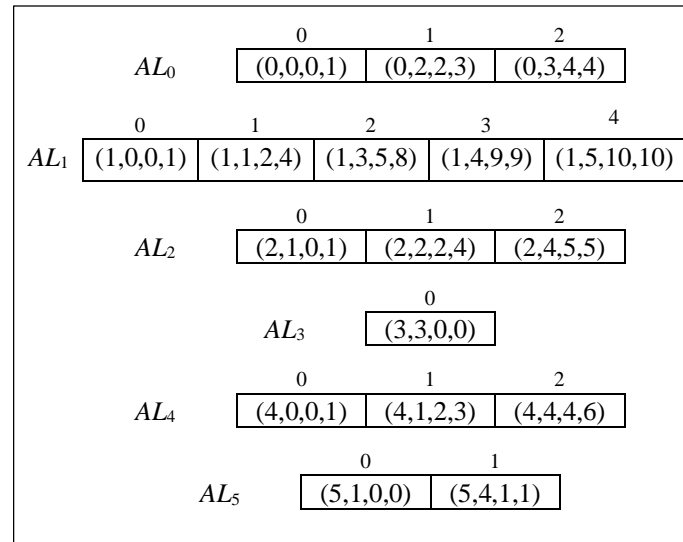


Fig. 2. Execution of Local Partition.

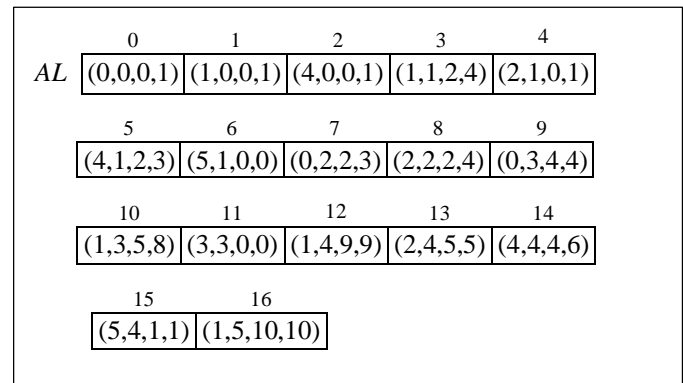


Fig. 3. First Step of Global Partition.

The processor p_0 does not determine any components because $AL[1] \cdot pNo \neq AL[0] \cdot pNo$ and $AL[2] \cdot pNo \neq AL[1] \cdot pNo$ are false. The processor p_1 determines the start of the second partition and the end of the first partition because

$AL[3] \cdot pNo \neq AL[2] \cdot pNo$ is true. So, $AL[1] \cdot start = 3$ and $AL[0] \cdot end = 2$. On the other side, the two other elements do not lead to new partition because $AL[4] \cdot pNo \neq AL[3] \cdot pNo$ and $AL[5] \cdot pNo \neq AL[4] \cdot pNo$ are false. The last processor p_5 determines the start of the fifth partition and the end of the fourth partition because $AL[16] \cdot pNo \neq AL[15] \cdot pNo$ is true. So, $AL[5] \cdot start = 16$ and $AL[4] \cdot end = 15$. The array AP is shown in Fig. 4(a).

By applying Step 5 of the global partition phase, each processor p_i computes the number of elements in each partition. For the processor p_0 , $AP[0] \cdot pNo = 2 + 2 + 2 = 6$, while p_1 computes $AP[1] \cdot pNo = 3 + 2 + 2 = 7$. The array AP becomes as in Fig. 4(b).

In the last stage, each processor, p_i , merges the different subarrays of the i th partition. The results of implementing the last stage consist of two steps. In the first step, each processor computes the repetition of each element as shown in Fig. 5. The results of the second step are shown in Fig. 6. The output array is $C=(C_0, C_1, C_2, C_3, C_4, C_5)=(0, 1, 2, 3, 4, 5, 6, 7, 8, 8, 8, 9, 10, 11, 13, 13, 15, 16, 17, 18, 18, 19, 21, 22, 23, 24, 25, 26, 27, 28, 29, 30)$.

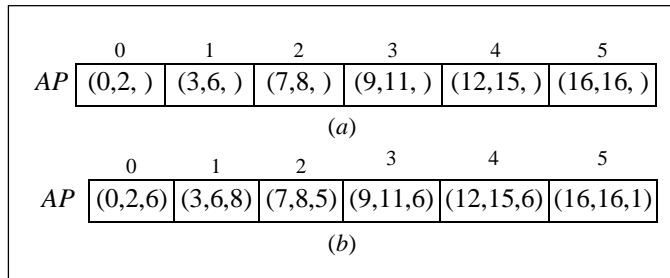


Fig. 4. Result of Global Partition.

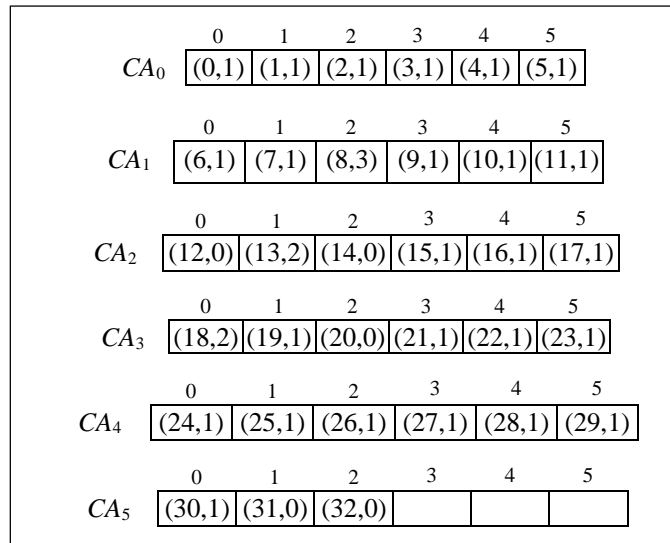


Fig. 5. First Step of Merging Phase.

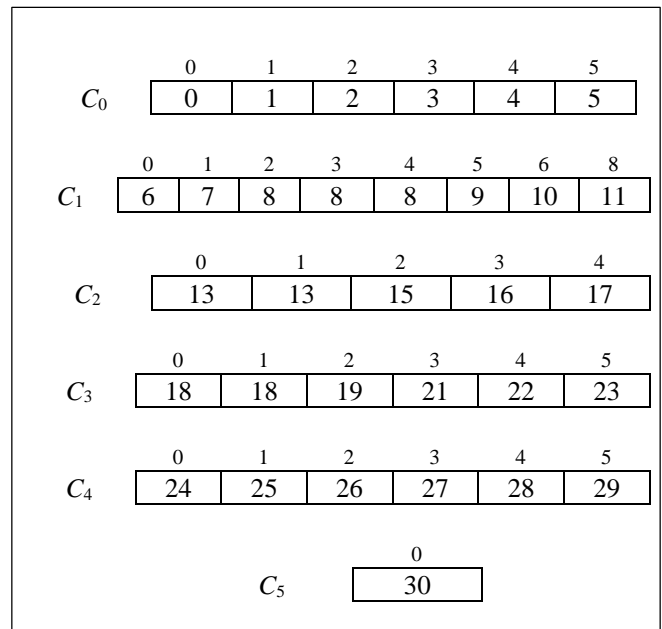


Fig. 6. Results of the Second Step of Merging Phase (Output).

VI. CONCLUSION

The paper addresses the problem of merging when the number of input sorted arrays is k , $2 \leq k \leq n$. The output of the merging is a new sorted array that contains all elements of the input. Our main contribution is solving the k integer merging problem under exclusive read exclusive write shared memory. The proposed algorithm runs in $O(\log n)$ time using $n/\log n$ processors. Additionally, the total work done by the proposed algorithm is $O(n)$, which is less than the best-known k merging parallel algorithm that perform $\theta(n \log k)$ work.

REFERENCES

- [1] D. Knuth. The art of computer programming: sorting and searching. Addison-Wesley, Reading, 1973.
- [2] P. Valduriez, G. Gardarin. "Join and semijoin algorithms for multiprocessors database machines". ACM Transaction Database System Vol. 9, pp. 133-161, 1994.
- [3] T. Merrett. Relational information systems. Reston Publishing Co., Reston, 1984.
- [4] J. Bang-Jensen, et al. "Recognizing and representing proper interval graphs in parallel using merging and sorting". Discrete Applied Mathematics, Vol. 155, No. 4, pp. 442-456, 2017.
- [5] S. Olariu, et al. "Reconstructing binary trees in doubly logarithmic CREW time". Journal of Parallel and Distributed Computing, Vol. 27, 1995, pp. 100-105.
- [6] O. Berkman, U. Vishkin. "On parallel integer merging". Information and Computation, Vol. 106, pp. 266-285, 1993.
- [7] Th. Cormen, et al. Introduction to algorithms. MIT, Cambridge, 1990.
- [8] T. Hayashi, et al. "Work-time optimal k-merge algorithms on the PRAM". IEEE Transaction on Parallel and Distributed Systems, Vol. 9, No. 3, pp. 275-282, 1998.
- [9] S. Akl. Parallel sorting algorithms. Academic Press, Orlando, 1985.
- [10] S. Akl. Parallel computation: models and methods. Prentice Hall, Upper Saddle River, 1997.
- [11] A. Borodin, and J. Hopcroft. "Routing, merging, and sorting on parallel models of computation". Journal of Computer System Science, Vol. 30, pp. 130-145, 1995.

- [12] T. Hagerup, and C. Rub. "Optimal merging and sorting on the EREW PRAM". Information Processing Letters, Vol. 33, pp. 181–185, 1989.
- [13] C. Kruskal. "Searching, merging, and sorting in parallel computation". IEEE Transaction on Computers, Vol. 32, No. 10, pp. 942–946, 1993.
- [14] S. Nagaraja, et al. "A parallel merging algorithm and its implementation with JAVA threads". In: The Mid-Atlantic student workshop on programming languages and systems, IBM Watson Research Centre, 27 April 2001, 2001.
- [15] A. Salah, et al. "Lazy-Merge: A Novel Implementation for Indexed Parallel K-Way In-Place Merging". IEEE Transaction on Parallel and Distributed Systems, Vol. 27, No. 7, pp. 2049-2061, 2016.
- [16] H. Bahig. "Parallel merging with restrictions". The journal of Supercomputing, Vol. 43, No. 1, pp. 99-104, 2018.
- [17] H. Bahig. "Integer Merging on PRAM". Computing, Vol. 91, No. 4, pp. 365-378, 2011.
- [18] H. Bahig. "A new constant-time parallel algorithm for merging". The journal of Supercomputing, Vol. 72, No. 2, 968–983, 2019.
- [19] T. Hagerup, M. Kutylowski. "Fast integer merging on the EREW PRAM". Algorithmica, Vol. 17, pp. 55–66, 1997.
- [20] Z. Wen. "Multi-Way Merging in Parallel". IEEE Transaction on Parallel and Distributed Systems, Vol. 7, No. 1, pp. 11–17, 1996.
- [21] B. Hazem and K. Ahmed. "Parallelizing K-Way Merging". International Journal of Computer Science and Information Security, Vol. 14, No. 4, pp. 497-503, 2016.
- [22] R. Karp, V. Ramachandran. "Parallel algorithms for shared-memory machines". In: Van Leeuwen J (ed) Handbook of theoretical computer science, Vol A: Algorithms and complexity. Elsevier, Amsterdam, 869–941, 1990.
- [23] G. Blelloch. "Prefix sums and their applications". TR CMU-CS-9-190, Carnegie Mellon University, 1990.
- [24] S. Albers, T. Hagerup. "Improved Parallel Integer Sorting without Concurrent Writing". Information and Computation, Vol. 136, No. 1, pp. 25-51, 1997.
- [25] H. Bahig. "Complexity analysis and performance of double hashing sort algorithm". Journal of the Egyptian Mathematical Society, 27, Article number 3, 2019.

An Accessibility Evaluation of the Websites of Top-ranked Hospitals in Saudi Arabia

Obead Alhadreti

Department of Computer Sciences, Computing College
Umm Al-Qura University, Al-Qunfudah, Saudi Arabia

Abstract—Hospital websites offer the potential to improve healthcare service delivery. They can provide up-to-date information and services to patients, at low cost and regardless of their level of abilities. This, in turn, can reduce overcrowding in hospitals and reduce spread of disease, especially in circumstances like the current COVID-19 pandemic. It is, therefore, imperative for designers to ensure the accessibility of hospital websites to the widest possible range of people. This study aims to evaluate the accessibility of the websites of top-ranked hospitals in Saudi Arabia using AChecker. The sample included the websites of the top ten hospitals from each of the public and private sectors. The results show that only 20% of the evaluated websites conformed fully to the Web Content Accessibility Guidelines 2.0. No significant difference was found in terms of the accessibility compliance between the websites of the public and private hospitals. The most frequently observed accessibility errors were related to the structure of information, non-text content, labels and instructions, headings, and keyboard access. The study concludes that Saudi hospitals are not doing an adequate job of meeting accessibility guidelines, thereby denying many of their web customers the ability to fully use their websites.

Keywords—Accessibility; hospital websites; Saudi Arabia

I. INTRODUCTION

The use of information and communication technologies (ICT) to provide services related to health, known as e-health, has been introduced to facilitate equal access to healthcare services to all patients regardless of their abilities and disabilities, and to reduce healthcare delivery costs, hospital overcrowding and spread of diseases [1]. Indeed, people tend to use the Internet to find a wide range of information related to health, for consultations with health practitioners, and to participate in support groups [2]. According to a study of trends in consumer health, four out of five adults with an Internet connection use digital health technology in some form [3]. However, whilst there is valuable healthcare information on the Internet, there are also potential dangers from outdated, inaccurate, and even harmful medical information on-line [4].

An important quality attribute of hospital websites is accessibility, which directly impacts the use of websites by disabled people. In other words, web accessibility is the process by which interfaces are made more user-friendly and inclusive, and capable of operation by any user, in varied situations and under diverse conditions. If hospital websites are not accessible, patients with disabilities may have difficulty finding and understanding health information [5].

Hence, evaluating the accessibility of hospital website is critical.

The healthcare system in Saudi Arabia is one of the largest and most complex sectors. It serves a diverse population, of varied socio-economic backgrounds and in different geographical settings. Furthermore, according to Census of Saudi Arabia in 2017, 7.1% of the total population are suffering from some disability [6]. It is, therefore, important to have hospital websites that are accessible to a wide range of users. The current study examines the accessibility of the websites of the top-ranked hospitals in Saudi Arabia. The study has numerous implications related to hospital website accessibility. It is believed to be the first evaluation of the accessibility of Saudi hospital websites. The findings will be helpful for the Saudi hospital policy-makers such as ministry of health, hospital top management, in designing the policies and programs on e-health success in the country.

The structure of this paper is as follows: Section II reviews the existing literature and states the research questions of the study. Section III presents the evaluation methodology used. Section IV presents and discusses the results obtained. The final draws the conclusions of the study.

II. RELATED WORK

Several studies have considered the evaluation of hospital website accessibility worldwide. Mira et al. [7] assessed and compared hospital websites from and the USA, Great Britain and Spain in terms of ease of use, accessibility, and content quality. The results of their study showed that only ten of 32 websites analysed met accessibility standards. Kurniawan and Zaphiris [8] analysed health websites using an accessibility evaluation tool called 'Bobby', which only approved 28% of them. The researchers emphasised that government websites must be subject to stricter government regulations with the U.S. Telecommunications Act, Section 255, which requires websites of US Federal agencies to be as accessible and usable as possible.

A 2009 study evaluated 53 websites from public-sector hospitals in Greece and found that most lacked key features of good practice in site accessibility [9]. Another study performed in 2010 examined the application of the Korean Web Content Accessibility Guidelines (WCAG) on the websites of 80 hospitals. It found that while many hospitals had attempted to achieve web accessibility, success required the aggressive implementation of the guidelines [10]. A 2016 study of Catalan private hospitals evaluated their websites'

characteristics and quality in terms of usability, accessibility, interactivity, content, quality references, content updates, privacy policies and web 2.0. The results indicated that accessibility evaluations are critical in the development of a website [11]. An additional study of the usability, accessibility and security of Indian hospital websites concludes that evident accessibility problems could be explained by the lack of application of the WCAG 2.0 standard [12].

In 2017, another study investigated the factors influencing the quality and visibility of the websites of private hospitals. The results showed the importance of presenting information with quality-accredited web accessibility [13]. O'Grady assessed 49 Canadian healthcare websites with WCAG 1.0 Priority 1 level. Only approximately 40% of pages examined were free of errors [14]. A study of 108 sites related to general health, by Zeng and Parmanto, found that none of them satisfied the WCAG Priority 1 guidelines [15]. A study in 2014 assessed the websites of 2785 hospitals in the USA, concluding that they lacked accessibility, scoring an average of 5.08 out of a possible ten [16]. Llinás et al. carried out a qualitative study of hospital web-portals. Of the 32 sites studied, twelve were Spanish, ten British and ten American. Only ten met the specified accessibility criteria [17]. A study by Maifredi et al. considered every Italian hospital that had a functional website. Quality ranged widely and most had severe limitations [18]. Mira et al.'s study of the accessibility and readability of Spanish hospital websites revealed that none satisfied accessibility requirements [19].

Whilst there has been an increase in the use of the Internet and particularly for health purposes in Saudi Arabia [20], no study has been carried out to assess the accessibility of the websites of Saudi hospitals. It should be mentioned that the Government of Saudi Arabia has established legislation covering disability in terms of skills development and employment, although the specifics of web accessibility are not addressed [21].

A. Web Content Accessibility Guidelines

The WCAG 2.0 includes a range of recommendations designed to improve the accessibility of website content. This is for the benefit of a people with a broad spectrum of disabilities, individually or in combination, such as visual (reduced sight, blindness), auditory (loss of hearing, deafness), physical (restricted movement), speech impairment, learning and cognitive difficulties, and photosensitivity. It is made up of four general principles and twelve guidelines, as follows below [22].

Principle 1: Perceivable

The user interface's information and elements must be presented so that users can perceive them. There are four guidelines under this principle, related to alternative text, time-based media, distinguishability, and adaptability [22].

Principle 2: Operable

It must be possible to operate the user interface and the navigation sections. There are four guidelines under this principle, related to keyboard accessibility, allowing sufficient time, navigability, and seizures [22].

Principle 3: Understandable

The user interface's content and operation must be comprehensible. Here, there are three guidelines related to readability, predictability, and assistance with input [22].

Principle 4: Robust

The content must be sufficiently robust to allow a wide range of user applications, which use assistive technology, to interpret it reliably. This principle has one guideline, related to compatibility [22].

All the guidelines incorporate success criteria, which comprise levels of conformity relating to the effect of accessibility. To fit the needs of varying situations and diverse users, the guidelines have three levels of conformity [22]:

- 1) A: Lowest level
- 2) AA: Middle level
- 3) AAA: Highest level.

Websites implementing WCAG 2.0 normally apply the 'AA level'. Website accessibility problems can be detected using a combination of automatic tools and criteria set by experts in web accessibility. That said, this process can consume long time and be subjective, as a website's quality is not necessarily apparent to the expert. Software tools are capable of detecting HTML code and CSS structure errors, assessing browser compatibility, checking links and website performance, and generating warnings [23].

B. The Research Questions

As mentioned earlier, it appears that no study has inspected the accessibility of the hospital websites in Saudi Arabia. Given that it is extremely important that websites provided by healthcare institutions are fully accessible for all, and that there are more than half a million Saudi citizens with some form of disability [6], it seemed appropriate to evaluate the level of accessibility of websites provided by Saudi healthcare institutions. The evaluation covered the highest ranked Saudi hospitals, as of 2020, and attempted to answer the following three research questions.

Research Question 1 (RQ1): How accessible are the websites of top-ranked public and private hospitals in Saudi Arabia?

Research Question 2 (RQ2): Do the websites of top-ranked public and private hospitals in Saudi Arabia differ significantly in their accessibility compliance?

Research Question 3 (RQ3): What are the most common types of errors that affect the accessibility of hospital websites in Saudi Arabia?

The following section explains the evaluation methodology. It includes details of the process of selecting sites and the tool of evaluation employed to rate the accessibility of the websites of the selected hospitals.

III. METHODOLOGY

The evaluation procedure comprised three stages: 1) definition of the websites to be targeted for evaluation, the tool to be used for evaluation, as well as the accessibility

guidelines against which the sites would be tested; 2) evaluation of the targeted websites against WCAG 2.0; and 3) analysis and discussion of the results obtained.

A. Targeted Websites

The 'Ranking Web of World Hospitals', developed by Webometrics, was used as the basis for selecting the targeted websites for the evaluation process. It ranks healthcare institutions around the world on various factors [24]. The sample included the hospitals ranked highest (as of 2020) in Saudi Arabia, and the top ten hospitals from each of the public and private sectors (see Tables I and II). The websites were assessed between September and October 2020. The study specifically evaluated the accessibility of the home page of each hospital's website. When it comes to accessibility, the home page is considered the most important part of a site. If there are accessibility problems that prevent the home page from being inclusive, then it is very likely that users will encounter access difficulties with the website's other pages. The home pages of most hospital websites in Saudi Arabia are bilingual, with the content, design and services near-identical in both Arabic and English. Therefore, the researcher decided to evaluate only the Arabic version of the homepages because the Arabic language is the official language in Saudi Arabia.

B. The Evaluation Tool

Out of several tools, AChecker was used for the evaluation process in this study [25]. It was deemed the best evaluation tool for the current study as it is widely used for accessibility assessment and can be applied to individual web pages. It also accepts Arabic websites. AChecker generates a report listing all the accessibility problems found, according to the guidelines selected, in three categories of error: known, likely, and potential. 'Known errors' are definite accessibility barriers that are identified. 'Likely errors' are issues identified as probably being barriers, but where human input is required for a final assessment. 'Potential problems' are issues where AChecker cannot tell if they would have an impact, requiring a human decision [25]. Fig. 1 shows an example of evaluation process in AChecker.

For this study, the criteria in AChecker were set to identify how many errors on each homepage detract from the AA level of conformity in WCAG 2.0. The AA level of WCAG 2.0

guidelines was chosen because, as mentioned earlier, websites implementing WCAG 2.0 mostly apply the 'AA level'. The first step of the second stage of evaluation procedure is to enter the Home page's URL into the tool. The page is then scanned and analysed. The software then displays the results of the analysis, showing the type and numbers of errors and violations encountered. Data collection involved extracting the HTML source code of the web pages of the targeted hospitals (see Fig. 1).

The next section presents and discusses the results obtained.

TABLE I. THE TOP-RANKING PUBLIC HOSPITALS IN SAUDI ARABIA

#	Name
1	King Faisal Specialist Hospital & Research Centre (KSSH)
2	Military Hospital (MH)
3	National Guard Health Care Service (NGHC)
4	Royal Commission Hospital in Jubail (RCHJ)
5	Security Forces Hospital (SFH)
6	King Fahad Medical City (KFMC)
7	King Khaled Eye Specialist Hospital (KKESH)
8	King Fahad Specialist Hospital Dammam (KFSHD)
9	Sultan Bin Abdulaziz Humanitarian City (SBAHC)
10	King Abdulaziz University Hospital (KAUH)

TABLE II. THE TOP-RANKING PRIVATE HOSPITALS IN SAUDI ARABIA

#	Name
1	Magrabi Hospitals & Centers (MHC)
2	Al Moosa General Hospital (AGH)
3	Saudi German Hospitals Group Jeddah (SGHJ)
4	Adama Hospital (AH)
5	Dallah Hospital (DH)
6	Dr Sulaiman Al Habib Medical Group (SAMG)
7	Al Mouwasat Hospitals & Clinics (AH)
8	International Medical Center (IMC)
9	Dama Center Thuriah Ferti Clinic (DCTFC)
10	Almana General Hospital (AGH)

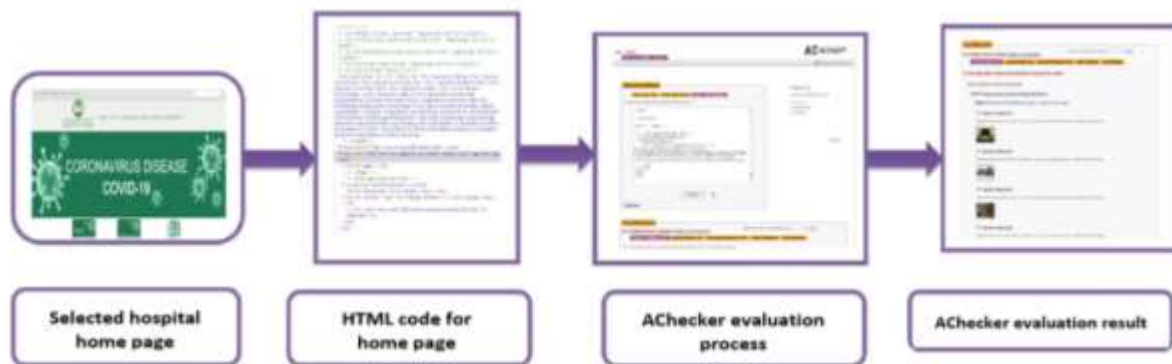


Fig. 1. An Example of the AChecker Evaluation Process.

IV. RESULTS AND DISCUSSION

Fig. 2 illustrates the number of known errors found in all the hospital websites evaluated. A total of 476 known errors were identified in the home pages of the public hospitals (44%), compared to 609 errors discovered in the home pages of the private hospitals (56%), making a grand total of 1085. One of the sites, KFMC had the most amongst the public hospitals. Of the 20 pages evaluated, the mean of the numbers of known errors was 64.7, 47.6 for public hospitals and 60.9 for private ones.

Fig. 3 shows the number of likely errors extracted in the home pages of the targeted websites. A total of 14 likely errors appeared in the home pages of the public hospitals (47%), and 16 issues in the private ones (53%). The grand total of likely errors across the pages assessed is thus 30. SAMG has the largest number of likely errors, across all the targeted hospitals, and KFMC had the most amongst the public institutions. Of the 20 pages evaluated, the mean of the numbers of likely errors was 1.4. This was also the separate mean for each category, private and public.

Fig. 4 displays the number of potential errors. 4992 potential errors were identified in the home pages of the public

hospitals (49%) and 5289 in the websites of the private hospitals (51%), making a grand total across the assessed pages of 10,281. KAUH had the most potential errors of all the hospitals and SAMG had the most amongst the private institutions.

The mean was 514 potential errors across the 20 pages, with 499.2 for the public institutions and 528.9 for the private hospitals. According to the results, there are clearly more potential errors than known errors across the websites examined, while likely errors occur least frequently.

Fig. 5 shows the total number of the accessibility errors detected in all the websites: 5482 errors in the home pages of the public institutions (48%) and 5912 for the private ones (52%). The grand total of errors across the pages evaluated, from public and private institutions is thus 11,394. Saudi Arabia's top-ranked hospitals' websites have a global average number of WCAG 2.0 errors in their home pages of 569.7, with 548.2 for public institutions and 591.2 for the private ones. Once again, SAMG had the greatest number of errors of all the hospitals and KFMC had the most amongst the public institutions. Only four hospitals (20%), KFSH and KKESH (public sector), and MHC and DH (private sector), showed no errors and fully conformed to the WCAG 2.0 standard.

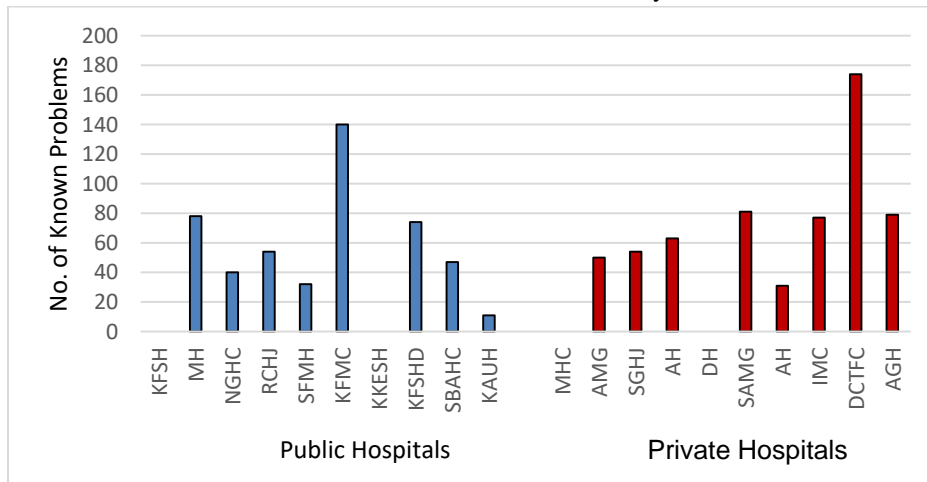


Fig. 2. Number of Known Problems.

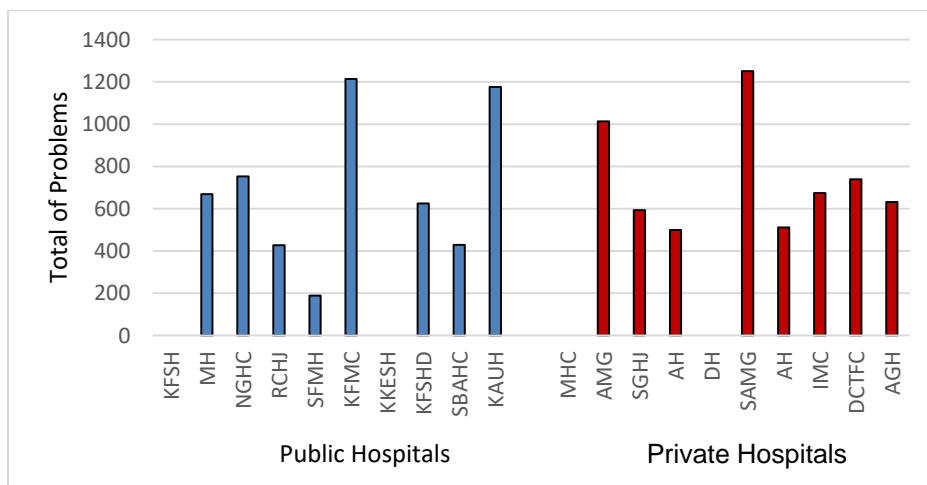


Fig. 3. Number of Likely Problems.

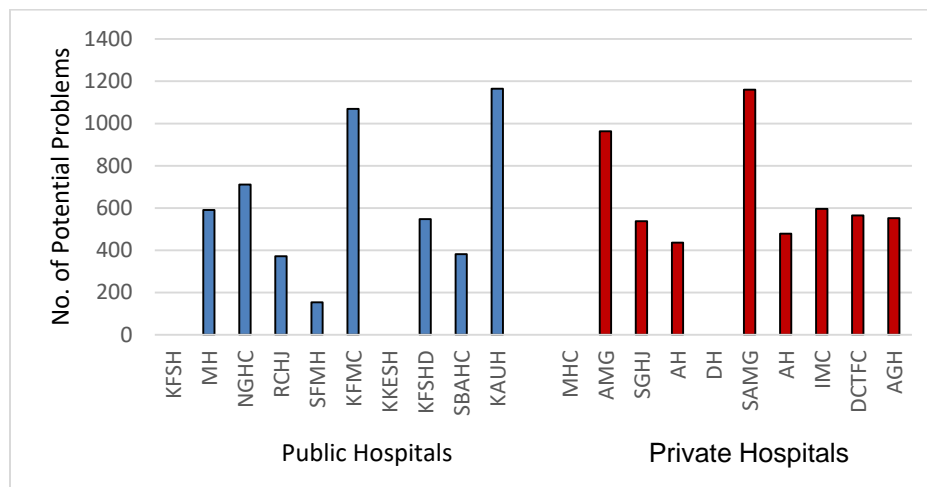


Fig. 4. Number of Potential Problems.

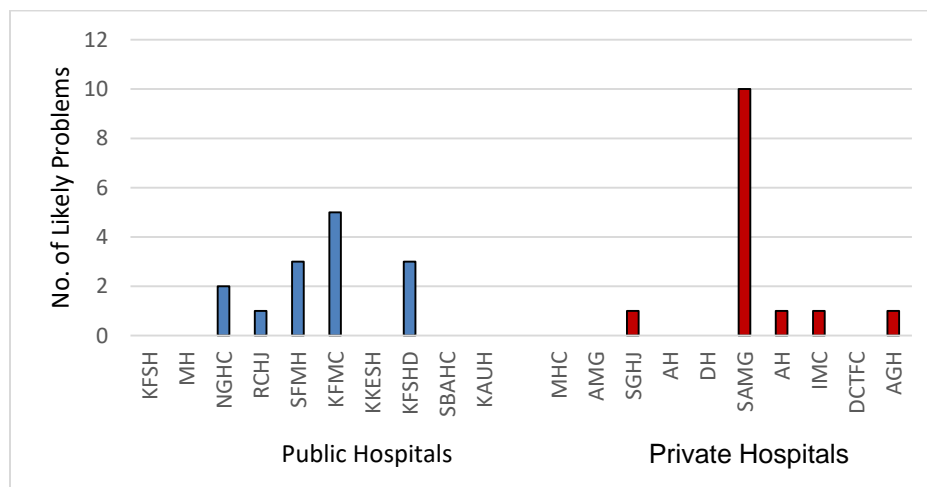


Fig. 5. Total Number of Problems.

As mentioned earlier, the first research question was formulated to identify the accessibility level of the websites of the top-ranked public and private hospitals' websites in Saudi Arabia. The results obtained clearly show that most hospitals' homepages suffer from accessibility issues. The average number of errors for all homepages was 569.7. This result reveals a serious issue for the attainment of even a minimal conformity with web accessibility guidelines. Only 20% of the evaluated sites has passed the WCAG 2.0 conformance test. It should be noted that the AChecker analysis tool looked for WCAG 2.0 compliance errors at Level AA. If AChecker to be set to search at Level AAA, the expected error numbers would increase by 30% [15].

The second research question was designed to determine if there is a significant difference in the accessibility compliance between the top-ranked public and private hospitals' websites. Table III presents the average number of errors for the websites of the two institution types. Using an independent Mann-Whitney test, no significant difference was found between the websites of the two sectors for any accessibility error type, nor for the total errors.

TABLE III. STATISTICAL ANALYSIS OF THE ERRORS IDENTIFIED IN THE WEBSITES OF THE TWO SECTORS

	Public hospitals		Private hospitals		P-value
	Mean	SD	Mean	SD	
Known problems	47.6	42.6	60.9	49.7	.593
Likely problems	1.4	1.7	1.4	3.0	.853
Potential problems	499.2	404.2	528.9	359.5	.684
Total problems	548.2	429.3	591.2	388.3	.739

The third research question was set to identify the most common types of errors that affect the accessibility of hospital websites in Saudi Arabia. To answer this question, the AChecker reports were scrutinised. The most common issue by far in hospital sites was related to 'Info and Relationships'. This error concerns content that it would not be possible to present differently without loss of structure or information. Of the websites analysed, 80% have this issue. The second most common error was 'Non-text Content'. Here, non-text content

such as images lack alternative text that describes it. Alternative text is important as it can enable people with visual disabilities to take on board the non-text content's essence. The third most commonly found error concerned 'Labels or Instructions', which often arises when content requiring user input lacks instructions or labels. The fourth most common issue was that the headings or labels of the targeted websites were not adequately descriptive. The fifth most common issue was 'No Keyboard Access'. Users with mobile disabilities who rely on the keyboard to access a website will be largely affected by this issue.

Overall, the results show that the hospital websites in Saudi Arabia are largely affected by accessibility issues, and to the same extent regardless of whether the institutions are in the private or public sectors. These results are in line with the findings of [12] for Indian hospital websites, which have ongoing accessibility issues and a low rate of compliance with the WCAG 2.0 guidelines. Two specific concerns arise from these findings. Firstly, people with disabilities can encounter difficulties with access to hospital websites. This means they are excluded, whereas people without disabilities are included. Secondly, there is the question of why so few websites follow accessibility standards.

V. CONCLUSION AND FUTURE WORK

The accessibility of any website is a key quality factor. This study aimed to evaluate the accessibility of the websites of the top-ranked public and private hospitals in Saudi Arabia. The results obtained clearly show that most hospitals pay minimal attention to their on-line content's accessibility. Failure to attain even a minimum degree of conformity to accessibility standards is likely to deprive many disabled people of the benefits provided by a website. Of the websites considered, no significant difference was found in the accessibility compliance between those in the public and private sectors. Furthermore, the findings of the study show that several accessibility errors are being made with respect to the structure of information, non-text content, labels and instructions, headings, and keyboard access. These results can be attributed to a lack of established legislation and guidance related to web accessibility in Saudi Arabia. It is clearly incumbent on the Saudi Government either to set formal web accessibility regulations, appropriate to its national context, or to adapt existing international guidelines and enforce them with legal and other, complementary mechanisms.

It is likely that this study still underestimates the accessibility issues with Saudi hospital websites, as further problems may lie beyond the home pages. Future work could make use of different automated tools and test for more pages. Researchers could also focus on identifying accessibility barriers that appear in the experience of disabled patients in their interaction with hospital websites, rather than simply assessing the compliance of those sites against accessibility guidelines or their ability to pass the scrutiny of evaluation tools. This requires the involvement of end-users to perform comprehensive evaluations for such sites. A further topic for research in the future would be the reasons for so many hospital websites not conforming to the available accessibility guidelines. It would also be worth considering a longitudinal

study of hospital websites in Saudi Arabia in order to track progress with web accessibility.

ACKNOWLEDGMENT

The author would like to thank the anonymous reviews for their invaluable comments.

REFERENCES

- [1] Patsioura, Kitsiou, S. and A. Markos. "Evaluation of Greek Public Hospital Websites,." In International Conference on e-Business. pp. 223-229, 2009.
- [2] A. Smith, M. Bensink, N. Armfield, J. Stillman, and L. Caffery, "Telemedicine and rural health care applications," Journal of postgraduate medicine., vol. 51, no. 4, pp. 286-93, Jan. 2006.
- [3] R. Cline, "Consumer health information seeking on the Internet: the state of the art", Health Education Research, vol. 16, no. 6, pp. 671-692, 2001.
- [4] M. Benigeri, "Shortcomings of health information on the Internet", Health Promotion International, vol. 18, no. 4, pp. 381-386, 2003.
- [5] Kaur, D. Dani and G. Agrawal, "Evaluating the accessibility, usability and security of Hospitals websites: An exploratory study," In Proceedings of the 7th International Conference, Cloud Computing, Data Science & Engineering-Confluence. IEEE, pp. 674-680, 2017.
- [6] 'Disability Survey'. [Online] Available at <https://www.stats.gov.sa/en/904>, Accessed November 2020. 2017.
- [7] J. Mira, G. Llinás, D. Rodríguez-Inesta, S. Lorenzo, and C. Aibar, "A comparison of Websites from Spanish, American and British hospitals", Methods of Information in Medicine, 2008.
- [8] Kurniawan, S. and Zaphiris, P. Usability and Accessibility of Aging/Health-Related Websites. Proceedings of the Human Factors and Ergonomics Society 45th Annual Meeting. 206-210. Minneapolis, MN, USA.F. 2001.
- [9] F. Patsioura, Kitsiou, S. and A. Markos. "Evaluation of Greek Public Hospital Websites,." In International Conference on e-Business. pp. 223-229, 2009.
- [10] Y. S. Kim, and K. S. Oh, "A study on current state of web content accessibility on general hospital websites in Korea," Journal of Internet Computing and Services, vol. 11, no. 3, pp. 87-103, 2010.
- [11] J. Creixans-Tenas, and N. Arimany-Serrat, "Calidad de las web de los hospitales privados web quality of private hospitals". In Proceedings of the 11th Iberian Conference on Information Systems and Technologies. IEEE, pp. 1-6, 2016.
- [12] K. Kaur, D. Diksha, and A. Gaurav. "Evaluating the accessibility, usability and security of Hospitals websites: An exploratory study." In 2017 7th International Conference on Cloud Computing, Data Science & Engineering-Confluence, pp. 674-680. IEEE, 2017.
- [13] Creixans-Tenas, J., & Arimany-Serrat, N. Influential factors in the visibility and quality of the websites of private hospitals. In 2017 12th Iberian Conference on Information Systems and Technologies (CISTI) (pp. 1-7). IEEE.Conference on Information Systems and Technologies. IEEE, pp. 1-7, 2017.
- [14] O'Grady, L. Accessibility compliance rates of consumer-oriented Canadian health care Websites. Medical Informatics and the Internet in Medicine. 30(4), pp. 287-295. 2005.
- [15] Zeng X. and Parmanto B. Web content accessibility of consumer health information Web sites for people with disabilities: a cross sectional evaluation. Journal of Medical Internet Research. 6(2), e19.2004.
- [16] Huerta, T., Hefner, J., Ford, E., and McAlearney, A. Hospital website rankings in the United States: expanding benchmarks and standards for effective consumer engagement. Journal of Medical Internet Research. 16(2), pp. e64. 2014.
- [17] Llinás G, Rodríguez-Iñesta D, Mira JJ, Lorenzo S, Aibar C... A comparison of websites from Spanish, American and British hospitals. Methods of Information in Medicine. 47(2), pp. 124-30. 2008.
- [18] Maifredi, G., Orizio, G., Bressanelli, M., Domenighini, S., Gasparotti, C., Perini, E., Caimi, L., Schulz, P.J., and Gelatti, U. The Italian hospitals

- in the web: a cross-sectional analysis of the official websites. *BMC Medical Informatics and Decision Making*. 10:17. 2010.
- [19] Mira, J., Llinás, G., Tomás, O., and Pérez-Jover, V. Quality of websites in Spanish public Hospitals. *Medical Informatics and the Internet in Medicine*. 31(1), pp. 23-44. 2006.
- [20] Internet World Stats. Internet usage in the Middle East. Miniwatts Marketing Group. [Online] Available at <https://www.internetworldstats.com/stats5.html>, [Retrieved October, 2020], 2020.
- [21] Al-Khalifa, H. S., Baazeem, I., & Alamer, R. Revisiting the accessibility of Saudi Arabia government websites. *Universal Access in the Information Society*, 16(4), 1027-1039. 2017.
- [22] W3C, “Web Content Accessibility Guidelines (WCAG) 2.0,” [Online] Available: <https://www.w3.org/TR/WCAG20/> [Retrieved 14/10/2020], 2008.
- [23] P. Acosta-Vargas, S. Luján-Mora, and L. Salvador-Ullauri, “Quality evaluation of government websites,” In *Proceedings of the 4th eDemocracy & eGovernment*. IEEE, pp. 8-14, 2017.
- [24] Cybermetrics Lab. (2016). About Us Page [Online] Available from: http://hospitals.webometrics.info/en/About_Us, Accessed 3-June 2020.
- [25] AChecker. [Online] Available at <https://achecker.ca/checker/index.php> , Accessed 12-June 2020.